ASBMR ABSTRACTS KEY

1001-1222	Oral Presentation
F001-F488	Friday Plenary Poster Presentation
SA001-SA491	Saturday Poster Presentation
SU001-SU461	Sunday Poster Presentation
M001-M461	Monday Poster Presentation
WG01-WG26	Working Group Abstracts
*(asterisk) by author's name	denotes ASBMR Non-Membership

DISCLOSURE/CONFLICT OF INTEREST

The Federation of American Societies for Experimental Biology (FASEB) requires that audiences at FASEB-sponsored educational programs be informed of a presenter's (speaker, faculty, author, or contributor) academic and professional affiliations, and the existence of any significant financial interest or other relationship a presenter has with the manufacturer(s) of any commercial product(s) discussed in an educational presentation. This policy allows the listener/attendee to be fully knowledgeable in evaluating the information being presented. The Program will note those speakers who have disclosed relationships, including the nature of the relationship and the associated commercial entity.

All authors of submitted abstracts completed the disclosure statement in the online submission program. Invited speakers who are not required to submit an abstract received a form in the mail that they completed and returned.

Disclosure may include any relationship that may bias one's presentation or which, if known, could give the perception of bias. These situations may include, but are not limited to:

DISCLOSURE KEY

1. stock options or bond holdings in a for-profit corporation or self-directed pension plan
2. research grants
3. employment (full or part-time)
4. ownership or partnership
5. consulting fees or other remuneration
6. non-remunerative positions of influence such as officer, board member, trustee, or public spokesperson
7. receipt of royalties
8. speaker's bureau

For full-time employees of industry or government, the affiliation listed in the *2002 Program and Abstracts* will constitute full disclosure.

Disclosures for invited speakers and abstract presenters are provided at the end of the session listing for invited speakers and directly after the body of an abstract for abstract submissions. If there is no conflict of interest or disclosure listed, this means that the invited speaker and/or abstract presenter indicated no conflicts to disclose.

The disclosure information will correspond to the key above. If disclosures are given, the company name, along with the respective disclosure relationship number will be listed (for example: Company Name, 2, 8.).

1001

Targeted Disruption of Secreted Frizzled-Related Protein (SFRP)-1 in Mice Leads to Decreased Osteoblast and Osteocyte Apoptosis and Increased Trabecular Bone Formation. P. Bodine[1], W. Zhao[1], Y. Kharode[1], L. Borella[1], F. Bex[1], A. Lambert*[2], M. Goad*[2], G. Stein[3], J. Lian[3], B. Komm[1]. [1]Women's Health Research Institute, Wyeth Research, Collegeville, PA, USA, [2]Investigational Pathology, Wyeth Research, Andover, MA, USA, [3]Department of Cell Biology, University of Massachusetts Medical School, Worcester, MA, USA.

SFRP-1 is a secreted Wnt antagonist. We have previously reported that overexpression of SFRP-1 in human osteoblasts antagonizes Wnt-signaling and accelerates apoptosis. In order to determine if SFRP-1 affects osteoblast function in vivo, we generated a knockout (-/-) mouse line that contained the lacZ coding sequence in place of exon 1 of the SFRP-1 gene. SFRP-1 mRNA was expressed in kidneys, bones and other tissues of wild-type (+/+) mice, while beta-galactosidase activity was detected in the same tissues and in osteoblasts and osteocytes of -/- animals. Overall, the -/- mice appeared normal when compared to the +/+ controls. Prior to reaching peak bone mineral density (BMD), the skeletons of the -/- and +/+ mice were similar. However, beginning at 20 weeks of age and extending until 40 weeks, the -/- mice exhibited large increases in trabecular BMD and bone volume when compared to the +/+ controls. Volumetric trabecular BMD, as determined by peripheral quantitative computed tomography, was 24% higher in tibias of the -/- males at 35 weeks of age. Likewise, trabecular bone and mineralized areas determined histologically increased up to 143% in femurs from the -/- males and females at 35 weeks of age. At the same time, the mineral apposition rate as determined by calcein labeling increased up to 8% in femoral trabecular bone of the -/- mice. Femoral trabecular bone volume, number, thickness and connectivity density as determined by high-resolution micro-computed tomography also increased up to 91% in the -/- males and females at 26 and 35 weeks of age. Additionally, lumbar vertebral trabecular bone volume and number as seen by histomorphometry increased up to 61% in the 40-week old female -/- mice. As predicted from in vitro studies, apoptosis of calvarial osteoblasts and osteocytes as determined by TUNEL staining decreased by as much as 56% in the 33-week old -/- females. Finally, in vitro differentiation of bone marrow osteoprogenitors to alkaline phosphatase positive colonies increased up to 5-fold in cells from 26- and 40-week old -/- females. These results indicate for the first time that SFRP-1 is a negative regulator of osteoblast and osteocyte survival, osteoblast differentiation and bone formation in mice. Moreover, deletion of SFRP-1 results in a temporal delay of age-related trabecular bone loss.

Disclosures: ***P. Bodine****, Wyeth Research 1, 3.*

1002

Wnt-mediated Signaling via LRP5 and Beta-catenin Induce Osteoblast Differentiation and Mediates the Effects of BMP2. S. Roman Roman[1], B. Vayssière*[1], D. Shi*[2], F. Dunn*[3], R. Baron[1], G. Rawadi*[1]. [1]Proskelia, Romainville, France, [2]CNRS, Paris, France, [3]Aventis Pharma, Romainville, France.

LRP5 deficiency in human results in deficient trabecular bone volume leading to a severe osteoporosis. Furthermore, a mutation in the extracellular domain of LRP5 is genetically associated with higher bone mass in humans. LRP5 functions as a Wnt coreceptor in the canonical signaling pathway that employs β-catenin as a downstream effector. LRP5 is expressed in osteoblasts both during embryonic development and postnatally. We have investigated the involvement of Wnt/LRP5 cascade in osteoblast function by using the pluripotent mesenchymal cell lines C3H10T1/2, C2C12 and ST2 and the osteoblast cell line MC3T3-E1. Wnt1, 2, and 3a induced the expression of alkaline phosphatase (ALP) activity in the pluripotent cells. In contrast, Wnt4 and 5a failed to exhibit the same activity. Unlike Wnt1, 2 and 3a , activation by Wnt4 and 5 does not affect the β-catenin pathway. Confirming a key role of β-catenin, overexpression of a β-catenin stable mutant or treatment with LiCl, which stabilizes cytoplasmic β-catenin by inhibiting GSK3β, mimicked the effect of Wnt1, 2, and 3a. Taken together, this data indicates that ALP induction by Wnt is mediated by β-catenin signaling. We then assessed the involvement of LRP5 in Wnt-mediated ALP induction. Overexpression of either LRP5 dominant negative forms or the LRP5/6 selective inhibitor dickkopf 1 (dkk1) inhibited the induction of ALP by Wnt, indicating that LRP5 is required for this Wnt activity. Using Noggin, a BMP inhibitor, or cyclopamine, an Hedgehog inhibitor, revealed that the induction of ALP by Wnt is independent on the expression of these morphogenetic proteins known to induce ALP. In contrast, blocking Wnt/LRP5 signaling inhibited the ability of both BMP2 and Shh to induce ALP in mesenchymal cells. Unlike BMP2 and Shh, de novo synthesis of proteins is not required for Wnt to induce ALP mRNA. Moreover BMP2 is able to increase Wnt expression in our cells. Altogether these data strongly suggest that the capacity of BMP2 and Shh to induce ALP relies on Wnt expression and the Wnt/LRP5 cascade. Although Wnts did not affect ALP activity displayed by MC3T3-E1 cells, antagonizing the Wnt/LRP5 pathway decreased ALP expression in these cells. Finally, over-expression of dkk1 in MC3T3-E1 inhibited mineralization in a BMP-2-dependent assay. Thus, LRP5-dependent control of ALP expression and bone mineralization could constitute one of the molecular mechanisms leading to the phenotypes displayed by OPPG and HBM patients. In conclusion our data demonstrate a crucial role of Wnt-mediated signaling via LRP5 in osteoblast function.

1003

An Osteoblast-Specific Transcription Factor Required for Osteogenesis In Vivo But Transcribed from a Ubiquitous Gene. X. Yang, T. Schinke, G. Karsenty. Molecular and Human Genetics, Baylor College of Medicine, Houston, TX, USA.

OSE1 and OSE2 are two osteoblast-specific cis-acting elements present in the promoter of Osteocalcin, the most osteoblast-specific gene. To identify the factor binding to OSE1, provisionally called OSEBF1, we used a biochemical approach and eventually isolated a cDNA encoding it. OSEBF1 is a leucine zipper-containing protein present only in nuclear extracts of osteoblasts. Transient expression of OSEBF1 in non-osteoblastic cells, but of no other leucine-zipper proteins, increases the activity of the Osteocalcin promoter via the OSE1 element, whereas OSEBF1 fails to transactivate reporter constructs containing binding sites for other leucine-zipper proteins. OSEBF1-deficient mice were generated and most of them die perinatally, however the ones surviving beyond birth are dwarf throughout life. Histologic analysis of the OSEBF1-deficient mice showed fewer osteoblasts than in wild-type littermates, a marked decrease in bone mass, and a delayed ossification, demonstrating the biologic importance of this protein. OSEBF1-deficient osteoblasts proliferate 50% slower than wild-type osteoblasts in vitro, indicating that OSEBF1 is a regulator of osteoblast proliferation. Surprisingly, given the osteoblast-specific synthesis of OSEBF1 and the selective bone phenotype of OSEBF1-deficient mice, this protein is transcribed from a ubiquitously expressed gene as demonstrated by Northern blot analysis. Treatment of non-osteoblast cells with a proteasome inhibitor induced OSEBF1 accumulation, its binding to OSE1, transactivation of Osteocalcin promoter, and expression of endogenous Osteocalcin. Furthermore, endogenous inactivation of a specific ubiquitination-conjugating enzyme by RNA interference in NIH3T3 fibroblasts induced the accumulation of OSEBF1 otherwise absent from these cells. In summary, our results identify a novel transcription factor required for osteoblast proliferation and differentiation and present the first example of a cell-specific transcription factor whose expression pattern is regulated post-translationally. The fact that OSEBF1-deficient mice have osteoblasts, albeit a decreased number, suggests that OSEBF1 acts downstream of Cbfa1 or in a Cbfa1-independent pathway.

1004

Cbfb, a Well-Known Regulator of Hematopoiesis, Cooperates with Cbfa1 and Plays a Critical Role in Bone Development. M. Kundu*[1], A. Javed[2], Y. Yang*[1], G. Nuckolls*[3], M. Muenke*[1], J. Lian[2], G. Stein[2], P. Liu*[1]. [1]National Human Genome Research Institute, National Institutes of Health, Bethesda, MD, USA, [2]Department of Cell Biology, University of Massachusetts, Worcester, MA, USA, [3]National Institute of Arthritis, Musculoskeletal and Skin Diseases, National Institutes of Health, Bethesda, MD, USA.

Cbfa1 is essential for bone development in mouse models, and mutations in CBFA1 are found in 65-80% of patients with cleido-cranial dysplasia (CCD), a developmental syndrome characterized by a variety of skeletal and dental defects. Although all Cbfa family members (encoded by Cbfa genes can interact with Cbfb (encoded by Cbfb) and form heterodimeric transcription complexes, a role for Cbfb in bone development has not been demonstrated. Cbfb-/- embryos die during mid-gestation at 12.5 dpc due to severe hemorrhage and absence of definitive hematopoiesis, precluding the evaluation of Cbfb function at later time points. We fused the gene encoding green fluorescent protein (GFP) with the Cbfb gene by homologous recombination in murine embryonic stem (ES) cells. Heterozygous Cbfb-GFP mice had normal life spans and appeared normal. However, homozygous pups died within the first day after birth. While no major defects in hematopoiesis were detected and no bleeding diathesis was apparent, homozygous embryos exhibited a delay in endochondral as well as membranous ossification that was especially evident in the cranial and pelvic bones. The phenotype of these mice was similar to and more severe than that of Cbfa1+/- mice. In situ hybridization and GFP detection showed Cbfb expression in the developing bones. In addition, we demonstrated that Cbfb interacts with Cbfa1 and enhances its transactivation ability. Biochemical studies suggest that Cbfb-GFP represents a hypomorphic allele that maintains sufficient function in hematopoietic cells to bypass the early embryonic lethality, but uncovers a novel role for Cbfb in bone development. Thus, this study provides the first conclusive evidence that Cbfb plays a critical role in bone development and raises the possibility that mutations in CBFB may be responsible for some of the cases of CCD that are not linked to CBFA1 mutations.

1005

Dmp1-Deficient Mice Develop Dwarfism, Chondrodysplasia, and Exhibit Disorganized Bone Mineralization During Postnatal Development. J. Q. Feng[1], L. Ye*[1], D. Chen[2], H. Huang*[1], J. Zhang*[1], Y. Lu*[1], G. Li[3], S. L. Dallas[1], S. E. Harris[1], L. Bonewald[1], Y. Mishina*[4]. [1]Oral Biology, School of Dentistry, University of Missouri-Kansas City, Kansas City, MO, USA, [2]Molecular Medicine, UTHSCSA, San Antonio, TX, USA, [3]Trauma, The Queen's University of Belfast, Belfast, United Kingdom, [4]NIEHS/NIH, Research Triangle Park, NC, USA.

Dmp-1, initially identified in dentin, is an acidic non-collagenous matrix protein that is expressed in osteoblasts and highly expressed in osteocytes. In addition to bone cells, we have also found expression in hypertrophic chondrocytes in both primary and secondary ossification centers. To determine the role of this matrix protein in dentin, cartilage and bone, Dmp1 null mice were generated. These mice appeared normal at birth, but began to exhibit a dwarfism phenotype by three weeks of age that became more profound by 3 months. Bone radiographs revealed skeletal abnormalities such as shortening of the long bones, widening of the metaphysis, kyphosis and delay of secondary ossification. A dramatic reduction in bone mineral density in both the appendicular and craniofacial skeleton was observed using pQCT and verified by von Kossa staining of histological sections. Histological examination of the long bones revealed an extremely disorganized growth plate in which the columnar organization of the hypertrophic zone was disrupted and replaced with clusters of hypertrophic chondrocytes. This disorganized growth plate appeared to be responsible for the presence of an under-mineralized, hyperostotic matrix in place of the normal trabeculae. Cortical bone was undermineralized and disorganized, especially endosteally and there were many discontinuities in the cortex where mineral was absent. By three months of age, the animals exhibited osteoarthritic changes including narrowing of the joint spaces, the formation of bony cysts, and erosion of the joints. Preliminary studies suggest that the disorganized hypertrophic chondrocytes are undergoing increased cell death. Based on these initial analyses, these mice express multiple skeletal abnormalities analogous to the human conditions of dwarfism, chondrodysplasia, and possibly osteoarthritis and conditions of reduced bone mineral density. Therefore, Dmp1 expression is critical for growth plate formation and function leading to the coupling of chondrogenesis with osteogenesis. Dmp1 also appears to play an essential role in mineralization and subsequently, bone remodeling.

1006

Deficiency of CIZ, A Novel Negative Regulator of BMP, Enhances Osterix Gene Expression in Bone, Osteoblastic Differentiation in Culture and BMP- as Well as Ablation-Induced Bone Formation in vivo. M. Morinobu[1], T. Nakamoto*[2], K. Tsuji[1], Z. Shen[1], A. Nifuji[1], H. Yamamoto*[3], H. Hirai*[2], M. Noda[1]. [1]Dept of Molecular Pharmacology, Tokyo Medical and Dental University, Tokyo, Japan, [2]Dept of Hematology and Oncology, University of Tokyo, Tokyo, Japan, [3]Ehime University, Matsuyama, Japan.

CIZ (Cas interacting zinc finger protein) is a nucleocytoplasmic shuttling protein, which localizes at cell adhesion complex in culture, binds to p130CAS and binds to DNA to act as a transcriptional factor to regulate expression of genes such as those encoding MMPs. CIZ is expressed in osteoblasts in culture and regulates proliferation and type-I collagen gene expression. However, function of CIZ in bone in vivo has not been known. The aim of this study is to elucidate the function of CIZ in bone in vivo. For this purpose we examined the bones in CIZ-deficient (CIZ-KO) mice. The skeletal structures of CIZ-KO mice appeared normal. However, the levels of alkaline phosphatase (ALP) and Osterix mRNA detected by RT-PCR analysis using total RNA from whole long bone were enhanced in CIZ-KO mice. Bone marrow cells obtained from the femora of CIZ-KO mice formed more mineralized nodules than wild-type cells, when cultured in the presence of ascorbic acid and beta-glycerophosphate. These bone marrow cells from CIZ-KO mice also revealed higher basal level ALP activities than the cells from wild-type mice. The ALP activity was enhanced by BMP treatment in wild-type bone marrow cells. Such BMP enhancement was significantly augmented in the bone marrow cells from CIZ-KO mice. To test the hypothesis that CIZ suppresses bone formation activity in vivo, bone marrow ablation was performed. New bone formation was observed after ablation in wild-type mice. In CIZ-KO mice, such new bone formation was significantly enhanced compared to that in wild-type mice. To test whether CIZ deficiency enhances bone formation through augmentation of BMP-effects on bone formation in vivo, BMP-2 was injected every other day for 10 days onto the calvaria to induce orthotopic bone formation. BMP induced bone formation on the calvaria of wild-type mice. CIZ deficiency significantly enhanced BMP induced new bone formation on the calvaria compared to that in wild-type mice. These results indicate that CIZ acts as a novel type inhibitor of BMP-2 signaling in bone in vivo and plays a critical role in the regulation of osteoblastic differentiation and bone formation.

1007

Effects of Parathyroid Hormone, Alendronate, or Both on Bone Density in Osteoporotic Men. J. S. Finkelstein, A. Hayes*, A. Rao*, R. M. Neer. Endocrine Unit, Massachusetts General Hospital, Boston, MA, USA.

Once daily parathyroid hormone (PTH) administration increases bone turnover and bone mineral density (BMD) and reduces vertebral fracture incidence in osteoporotic men. Because PTH increases both bone formation and bone resorption, it is possible that combining PTH with an anti-resorptive agent will enhance its effects of BMD. To test this hypothesis, we randomly assigned 83 men, age 46-85, whose lumbar spine and/or femoral neck BMD was at least 2 SD below the mean of normal young men to receive: alendronate 10 mg orally daily (ALN, n=28), PTH 40 ug sc daily (PTH, n=27), or both (B, n=28) for 30 months. PTH therapy was begun at month 6. All men had normal serum PTH, 25-OH D, TSH, and testosterone levels at entry and none had disorders or had been treated with medications known to affect bone metabolism. Calcium intake was maintained at 1000-1200 mg/day and serum 25-OH D levels were maintained at or above 15 ng/mL. BMD of the posterior-anterior lumbar spine, proximal femur, total body (without head region), and radius shaft were measured every 6 months by DXA (Hologic 4500A). To date, 36 men (n=13, 9, and 14 receiving ALN, PTH, and B) have completed at least 18 months of therapy. Mean (+SD) changes in BMD and alkaline phosphatase to month 18 are shown in the table:

Group	Lumbar spine	Total hip	Radius Shaft	Total Body	Alk Phosphatase
ALN	6.1 + 2.7*	2.2 + 3.2	0.3 + 2.4	2.9 + 3.7	-18 + 8+
PTH	13.7 + 4.3**	2.6 + 5.5	-0.3 + 2.5	-0.4 + 4.3***	74 + 72++
BOTH	10.7 + 2.9	4.0 + 4.0	1.0 + 2.5	4.0 + 4.0	5 + 38

*P<0.001 vs PTH and B; **P=0.06 vs B; ***P=0.07 vs ALN and P=0.02 vs B; +P=0.07 vs B; ++P<0.001 vs ALN and B

When measured 24 hours after the last PTH dose, 0 of 97 serum calcium determinations were elevated in men treated with PTH alone and 1 of 119 were elevated in men treated with PTH and ALN. When measured 4 hours after the last PTH dose, 4 of 99 serum calcium determinations were elevated in men treated with PTH alone and 2 of 119 were elevated in men treated with PTH and ALN. These data suggest that combining PTH and ALN is superior to PTH alone for total body BMD but that ALN may diminish the anabolic effect of PTH on spine BMD. Moreover, ALN appears to block the ability of PTH to increase alkaline phosphatase production. Combining an anabolic and an anti-resorptive agent has complex effects on BMD, the clinical consequences of which are unknown.

Disclosures: ***J.S. Finkelstein****, Eli Lilly and Co. 2, 8; Merck 8.*

1008

An Activating Calcium Sensing Receptor Mutation Associated with Normocalcemic (Idiopathic) Hypercalciuric Nephrolithiasis. P. T. Christie[1], A. J. Curley*[1], B. Harding*[1], M. R. Bowl*[1], J. J. O. Turner*[1], F. P. Cappuccio*[2], C. B. Langman[3], A. K. Saggar*[2], T. Taylor*[4], R. V. Thakker[1]. [1]Nuffield Department of Medicine, University of Oxford, Oxford, United Kingdom, [2]Clinical Genetics, St George's Hospital Medical School, London, United Kingdom, [3]Northwestern University Medical School, Chicago, IL, USA, [4]Department of Paediatrics, St Richard's Hospital, Chichester, United Kingdom.

Calcium sensing receptor (CaSR) mutations are associated with 4 clinical phenotypes: familial hypocalciuric hypercalcemia (FHH), neonatal primary hyperparathyroidism and familial hypercalcemia with hypercalciuria, which are due to loss of function mutations; and autosomal dominant hypocalcemia with hypercalciuria (ADHH), which is due to gain of function mutations. It has also been suggested that some gain of function CaSR mutations may result in idiopathic hypercalciuria (IH) but to date these have not been detected. We reasoned that such CaSR mutations would lead to an early onset of IH and have sought them in 12 unrelated children (10 males and 2 females) who were normocalcemic and developed IH nephrolithiasis early in life, before the age of 4 years. In addition, all 12 of the probands had a family history for IH. Leukocyte DNA samples from the probands were used to search for CaSR mutations. This revealed, in one proband, an abnormality that consisted of a C to T transition at codon 994 (CAC to TAC) which predicts the substitution of the wild type (WT) histidine residue for a tyrosine in the cytoplasmic tail of the CaSR. This His994Tyr missense mutation was demonstrated to co-segregate with IH in the proband's family and to be absent in 110 alleles from 55 unrelated normal individuals. Expression of the mutant and WT CaSRs in HEK293 cells together with an assessment of their responses, as measured by changes in intracellular calcium concentration [Ca] to alterations in extracellular [Ca], revealed the Tyr994 mutant CaSR to have a left-ward shift in the dose-response curve (Tyr994 EC_{50} = 1.43 mM +/- 0.22 versus WT (His994) EC_{50} = 2.74 mM +/- 0.22, $p<0.02$), thereby demonstrating a gain of function. An examination of the mutant sequence indicated that it resulted in a tyrosine kinase phosphorylation consensus sequence and Western blot analysis using transiently-transfected HEK293 cellular extracts and the p-Tyr (PY99) antibody, which detects phosphorylated tyrosine groups in proteins specifically, demonstrated a significantly increased ($p<0.02$) phosphorylation of the mutant CaSR. Thus our results, which report the first CaSR mutation in IH nephrolithiasis, reveal a novel cytoplasmic mutation that increases phosphorylation and activity of the CaSR.

1009

Role of RANK Ligand (RANKL) in Mediating Increased Bone Resorption in Early Postmenopausal Women. G. Eghbali-Fatourechi[1], S. Khosla[1], W. J. Boyle*[2], D. L. Lacey[2], B. L. Riggs[1]. [1]Mayo Clinic, Rochester, MN, USA, [2]Amgen, Thousand Oaks, CA, USA.

Based on studies in rodents, a number of cytokines have been implicated as paracrine mediators of the increased osteoclastogenesis during estrogen (E) deficiency. However, RANKL, the final effector of osteoclastogenesis, has not been shown to be altered by E deficiency, and in vivo studies have not as yet been made on changes in RANKL producing cells in human bone marrow. We have developed a method for isolating bone marrow cells that express RANKL on their surfaces using flow cytometry with fluorescent-labeled osteoprotegerin as a probe. Bone marrow aspirates are passaged through a Ficoll-gradient and 2-color flow cytometry is employed to categorize cells expressing RANKL as marrow stromal cells (MSC), T-cells or B-cells using antibodies against alkaline phosphatase, CD3, and CD19, respectively. Isolated MSC were shown to express bone-related genes and to form mineralized nodules when cultured in a differentiating medium. Thus, we studied 12 premenopausal women (Premps), 11 early (<10 yrs after menopause) postmenopausal women (Postmps), and 13 postmenopausal women (matched for years after menopause) receiving long-term estrogen therapy (Postmps + E). Serum carboxyl-terminal telopeptide (CTx), a marker of bone resorption, was 4366, 6725, and 3192 pM in the Premps, Postmps, and Postmps +E women, respectively (P<0.001). MSC were decreased by 55% (P<0.001, Student-Newman-Keuls test) in the Postmps as compared with the Premps group (consistent with a rapid throughput kinetic model whereby these pre-osteoblastic cells are depleted by the increased demand for osteoblasts on bone surfaces). Values in the Postmps + E women were also higher than in Postmps women but were not different from Premps women. T-cells and B-cells expressing RANKL did not differ among groups. Based on fluorescence intensity, RANKL surface concentration per cell in the Postmps women was increased over that in the Premps women in MSC by 304% (P<0.001), in T-cells by 248% (P<0.01), in B-cells by 238% (P<0.01), and in total RANKL positive cells by 254% (P<0.01). Moreover, in these women, the bone resorption marker, serum CTx, was correlated (P=0.005) with RANKL expression per cell in MSC (r=0.52), T-cells (r=0.46), B-cells (r=0.57), and total RANKL positive cells (r = 0.46), attesting to the biological relevance of our assessment of RANKL expression by bone marrow cells. Although these findings do not exclude contributions by other cytokines, they indicate that upregulation of RANKL on bone marrow cells is a major determinant of increased bone resorption during E-deficiency and that MSC, T-cells and B-cells participate, apparently to a similar extent, in RANKL-mediation of estrogen action.

*Disclosures: **G. Eghbali-Fatourechi**, Guitty Eghbali-Fatourechi, Amgen Inc. 2; W.J. Boyle, D.L. Lacey, Amgen, Inc. 3.*

1010

Absence of Estrogen Receptor α Inhibits the Osteogenic Response to Mechanical Loading. K. C. L. Lee, A. S. Davies*, L. E. Lanyon. The Royal Veterinary College, London, United Kingdom.

Evidence that estrogen receptor α (ERα) is involved in osteoblasts' proliferative response to mechanical strain in vitro led to the hypothesis that the inadequate bone architecture characteristic of post-menopausal osteoporosis reflects less effective adaptation to mechanical loading due to decreased ERα number in bone cells.[1] To ascertain whether ERα is required for adaptive bone (re)modelling in vivo, we loaded the left ulnae of 21 to 24 week old female estrogen receptor α knock out (α ERKO) mice and their wild type (WT) littermates, by non-invasive dynamic axial compression via the flexed carpus and olecranon as previously published for the rat.[2] Forty 3.6N load cycles, engendering peak strains of 2900με and maximum strain rates of 0.1/s at the lateral ulnar midshaft, were applied to the ulna over 10mins, 3 days/wk for 2wks. Right ulnae served as non-loaded controls. Mice were sacrificed 3 days after the last loading day. The response of the cortical bone 3.5mm distal to the midshaft was assessed histomorphometrically using double calcein labels administered on days 3 and 12 of the loading period. The osteogenic response to loading was greatest at this site. In non-loaded control ulnae cortical bone area was the same in α ERKO and WT mice (0.22± 0.01mm^2) and periosteal new bone formation was undetectable. Endosteal bone formation rate (BFR) was 0.10± 0.10 μ m^2/μ m/day in α ERKO controls, significantly lower than 0.51± 0.07μ m^2/μ m/day in WT controls (p<0.05). In WT mice loading stimulated significant increases in both periosteal and endosteal bone formation, resulting in a 10± 1% increase in cortical bone area, compared to 0.3± 0.1% in non-loaded controls (p<0.01). This increase in cortical bone area was due to significant increases in periosteal and endosteal mineralising surfaces (MS), mineral apposition rates (MAR) and BFR (p<0.01). In α ERKO mice the loading-related increase in cortical bone area was 3± 0.6%, which was significantly lower than in WT mice (p<0.01). This was due to failure of the endosteal loading response in α ERKO mice; and 50% and 20% lower loading-induced increases in periosteal MAR and MS respectively in α ERKO mice compared to WT mice. These data show that in mice the absence of functional ERα substantially diminishes bones' osteogenic response to mechanical loading in vivo.

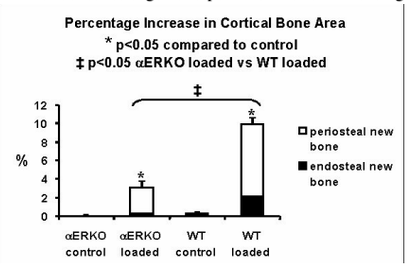

1) JBMR 2001; 16:1937-47. 2) Bone 1997; 20:191-8

*Disclosures: **K.C.L. Lee**, Wellcome Trust 2.*

1011

TNAP and PC-1 Control Bone Mineral Deposition by Directly Regulating Pyrophosphate Levels. L. Hessle*[1], K. A. Johnson*[2], H. C. Anderson*[3], R. Terkeltaub*[2], J. L. Millán[1]. [1]The Burnham Institute, La Jolla, CA, USA, [2]VAMC/UCSD, San Diego, CA, USA, [3]University of Kansas Medical Center, Kansas City, KS, USA.

A variety of human skeletal disorders develop due to abnormal levels of inorganic pyrophosphate (PP_i) in bone matrix. Deposition and propagation of hydroxyapatite crystals is suppressed by PP_i, but the metabolism and the proteins responsible for the regulation of this mineralizing inhibitor are poorly known. To address this topic, we have investigated the role of two osteoblast enzymes; Tissue-Nonspecific Alkaline Phosphatase (TNAP) and Plasma Cell glycoprotein-1 (PC-1). Both proteins are present in the membrane-limited matrix vesicles (MVs) that are responsible for the primary seed of hydroxyapatite in the process of ossification. Deleting the TNAP gene (*Akp2*) in mice results in hypophosphatasia characterized by poorly mineralized bones, spontaneous fractures and elevated extracellular concentrations of PP_i. PP_i is primarily produced by the nucleoside triphosphate pyrophosphohydrolase activity of a family of isozymes, with PC-1 being the only member present in MVs. Mice null for the PC-1 gene (*Enpp1*) display hypermineralization abnormalities similar to cartilage calcification in osteoarthritis and ossification of the posterior longitudinal ligament of the spine. We have found that mice lacking both TNAP and PC-1 show the respective correction of the bone mineralization abnormalities that are found in single knockout mice. Morphological normalization of the tibial growth plate in the double null mice was also observed. Furthermore, each allele of *Akp2* and *Enpp1* was found to exhibit a measurable influence on the mineralization status *in vivo*. Unlike primary cells from single knockout mice, *ex vivo* experiments using double knockout osteoblasts and their MVs demonstrate restored levels of PP_i and normalized mineral deposition. Our data identify TNAP and PC-1 as key regulators of the extracellular PP_i concentrations required for controlled bone mineralization. Our results also suggest that inhibiting PC-1 function is a viable therapeutic strategy for hypophosphatasia, a disease that to-date remains an incurable condition. Conversely, interfering with TNAP activity may be used in the treatment of pathologic cartilage calcification and hyperostosis due to local and systemic PC-1 deficiency.

1012

Frzb1, an Inhibitor of Wnt Signaling, is Over-expressed in Chondrocytes from Low Bone Mass Mice. R. F. Klein[1], R. J. Turner*[1], A. S. Carlos*[1], K. A. Vartanian*[1], D. A. Olson*[1], J. N. Kansagor*[1], J. K. Belknap*[2], E. S. Orwoll[1]. [1]Bone and Mineral Unit, Oregon Health & Science University, Portland, OR, USA, [2]Department of Behavioral Neuroscience, Oregon Health & Science University, Portland, OR, USA.

The role of low bone mineral density (BMD) in determining fracture risk is well established and the peak BMD level achieved in early adulthood is a highly heritable trait. In previous studies, using complementary mapping populations derived from C57BL/6 (B6) and DBA/2 (D2) inbred mouse strains, we identified four quantitative trait loci (QTLs) that contribute to BMD variation between these two strains. To explore the genetic architecture of peak BMD, reciprocal congenic strains were developed. QTL regions from Chr 1, 2, 4, & 11, defined by chromosomal molecular markers, were transferred from B6 to D2 and vice versa by 10 cycles of backcrossing. Peak whole body BMD (determined by DEXA in vivo) was significantly increased by D2 alleles on Chr 1 (2%; $p < 0.001$), Chr 2 (2%; $p < 0.02$) and Chr 4 (5%; $p < 0.001$) and by B6 alleles on Chr 11 (5%; $p < 0.0001$). To establish functional links between genotype and phenotype, we used high density oligonucleotide arrays (Affymetrix MG-U74Av2) to measure the relative expression levels of ~ 12,500 genes and ESTs in costal chondrocyte RNA isolated from Chr 2 congenic and D2 background mice. A total of 26 known genes and 7 ESTs reproducibly exhibited at least a 2-fold difference between the two genotypes. Among these candidates, only one - secreted frizzled related protein-3 (sfrp3 or Frzb1) – was located within the Chr 2 QTL (delineated by chromosomal markers D2Mit91 at 37cM and D2Mit164 at 71cM). The Frzb1 gene was up-regulated 4.1 ± 0.2 fold in the low BMD congenic mice. Frzb1 encodes a secreted antagonist of Wnt signaling. The recent identification of mutations in low-density lipoprotein receptor-related protein 5 (LRP5) in humans and now Frzb1 in mice suggests that the Wnt signaling pathway likely plays an important, and previously unrecognized, role in the attainment of peak BMD. Interestingly, the expression levels of a number of muscle-specific genes (myosin, actin, troponin) and proteinases (MMP-3, MMP-13, cathepsin G) were reduced (2 – 6 fold) in the congenic chondrocytes, indicating possible adaptive mechanisms to the increased Frzb1 expression. We suggest that microarray analyses of congenic strains have utility in identifying putative target genes underlying a given BMD QTL and may also elucidate other associated developmental pathways.

*Disclosures: **R.F. Klein**, Merck 8; Procter & Gamble 8; Aventis 8; Eli Lilly 8.*

1013

PTH-mediated Control of Proteasome-Mediated Degradation of Runx2/Cbfa1: A Pivotal Determinant of the Longevity of PTH-Initiated Anti-Apoptosis Signaling in Osteoblastic Cells. T. Bellido, L. I. Plotkin, C. A. O'Brien, S. C. Manolagas, R. L. Jilka. Endo/Metab. Center for Osteoporosis and Metabolic Bone Diseases, Central Arkansas Veterans Healthcare System, University of Arkansas for Medical Sciences, Little Rock, AR, USA.

The ability of intermittent PTH administration, but not sustained elevation of the hormone, to elicit an anabolic effect on the skeleton may be accounted for by the short-lived nature of PTH-induced anti-apoptosis signals in osteoblasts, a phenomenon demonstrated earlier using cultured osteoblastic cells and time course analysis. Specifically, it was previously shown that PTH causes transient protein kinase A (PKA)-mediated phosphorylation

and thereby inactivation of the pro-apoptotic Bad. As shown elsewhere in this meeting, Bad phosphorylation, as well as CREB- and Runx2/Cbfa1-mediated transcription, are required for the anti-apoptotic effect of PTH. Based on these observations, and evidence that PTH stimulates ubiquitin/proteasome-dependent degradation of Runx2/Cbfa1 in osteoblastic cells, and that cAMP promotes proteasome-mediated degradation of CREB in other cell types, we hypothesized that PTH-induced degradation of Runx2/Cbfa1 and/or CREB contributes to the short-lived nature of anti-apoptosis signaling. We now report that 10 μM lactacystin, an irreversible inhibitor of proteasomal-dependent proteolysis, prolonged by at least four-fold (from 6 to 24h) the duration of the anti-apoptotic action of PTH in OB-6 osteoblastic cells. Moreover, this effect of lactacystin was completely abrogated by expression of dominant negative Runx2/Cbfa1. On the other hand, expression of a dominant negative CREB did not influence the effect of lactacystin. Consistent with the critical role of Runx2/Cbfa1 level as a determinant of the longevity of the survival effect of PTH, overexpression of wild type Runx2/Cbfa1 prolonged the anti-apoptotic effect of PTH to the same extent as lactacystin. These results indicate that PTH upregulation of proteasome-mediated degradation of Runx2/Cbfa1 contributes to the short-lived nature of anti-apoptosis signaling. Moreover, they show that the stability of Runx2/Cbfa1 is a pivotal determinant of the longevity of the PTH-initiated survival signaling; and hence, of the ability of PTH to deliver repeated and self-limiting anti-apoptotic signals when administered in a pulsatile fashion, but not when elevated in sustained fashion.

1014

Unsuspected Megakaryocyte-Osteoblast Interaction Results in Increased Bone Formation in Mice Deficient in the Transcription Factors GATA-1 and p45 NF-E2. M. A. Kacena[1], K. M. Wilson*[1], M. L. Bouxsein[2], M. C. Horowitz[1]. [1]Orthopaedics, Yale University School of Medicine, New Haven, CT, USA, [2]Orthopedic Surgery, Beth Israel Deaconess Medical Center, Boston, MA, USA.

GATA-1 and p45 NF-E2 are transcription factors required for megakaryocyte (MK) differentiation and ultimately platelet formation. Loss of GATA-1 and p45 NF-E2 results in a developmental arrest of MK differentiation with an accumulation of MKs in the spleen and bone marrow. An unanticipated, marked 250% increase in osteoblast number and trabecular and cortical bone volume was also observed in these mice. A 4500% increase in trabecular bone volume was measured for the entire femoral medullary canal. The strikingly similar bone phenotype in both animal models led us to explore the novel interaction between osteoblasts and MKs from GATA-1 and p45 NF-E2 mutant mice. When calvarial osteoblasts from either wild-type or mutant mice were co-cultured with mutant MKs, osteoblast proliferation was increased up to 6 fold. To determine whether osteoblasts were activated by MK derived soluble factors, osteoblasts were cultured with and without conditioned medium (CM) from mutant MKs. MK CM failed to enhance osteoblast proliferation. To define the requirement for cell-to-cell contact, osteoblasts were separated from the MKs by a cell impermeable membrane in transwell cultures. As a control, MKs and osteoblasts were cultured in direct contact. No osteoblast proliferation occurred when the membrane separated the cells. Osteoblast proliferation was similarly enhanced when cultured in direct contact with either irradiated or mitomyicin-C treated mutant MKs. The wealth of evidence points to a mutant MK-osteoblast mediated response that enhances osteoblast proliferation. This proliferation should result in increased bone formation. Indeed, adoptive transfer of mutant spleen cells into irradiated recipients caused increased bone formation, supporting this idea. This mechanism would account for the increased number of osteoblasts seen in vivo and the bone phenotype in both GATA-1 and p45 NF-E2 deficient mice. A MK-osteoblast interaction of this type represents a novel anabolic pathway for new bone formation.

1015

Signaling via β-catenin Directs Osteogenic Lineage Allocation Independent of cbfa1. G. Mbalaviele, S. Sheikh*, S. Cheng, J. P. Stains, R. Civitelli. Div. Bone and Mineral Diseases, Washington University, St. Louis, MO, USA.

β-catenin, a component of adhaerens junctions, is also part of the *wnt* signaling system, modulating the activity of Tcf/Lef transcription factors. Mutations of critical components of this pathway, including LRP5, profoundly affect skeletal development or bone mass acquisition, and transcriptionally active β-catenin prevents adipogenesis. To test the hypothesis that β-catenin signaling is involved in mesenchymal lineage allocation to osteogenic cells, we generated a retroviral vector carrying a β-catenin mutant lacking the N-terminal moiety of the molecule (ΔN151). This truncation removes the domain required for proteolytic cleavage, resulting in a stable, transcriptionally active β-catenin. Transduction of ΔN151 in the uncommitted, multipotential C3H10T1/2 cells resulted in a 2-fold increase in osteocalcin mRNA abundance (assessed by real time RT-PCR), without significant effects on other markers of osteogenic differentiation. However in cells expressing ΔN151, BMP-2 (50 ng/ml for 7 days) produced greater increases in alkaline phosphatase activity (12- vs. 6-fold) and mRNA abundance for osteocalcin (16- vs. 2-fold) and bone sialoprotein (1.8- vs. 0.9-fold), relative to control cells, suggesting a synergism between β-catenin signaling and BMP-2. Intriguingly, cbfa1 mRNA was, if anything decreased by ΔN151 expression and its abundance after BMP-2 stimulation was not different than that of unstimulated control cells, indicating that β-catenin enhancement of BMP-2 response is independent of cbfa1. One week post-confluence, ΔN151 expressing C3H10T1/2 cells formed multilayered, nodular "domes", a few of them alizarin red positive. In the presence of BMP-2, massive calcification occurred, covering >50% of the tissue culture dishes. No such changes were seen in cells transduced with an empty vector, even in the presence of BMP-2, indicating that activation of the canonical β-catenin pathway is necessary to fully commit C3H10T1/2 to the osteogenic pathway. Consistent with this hypothesis, transfection with a β-catenin mutant lacking the armadillo repeats domain, which accumulates in the nucleus and inhibits β-catenin signaling, almost completely (>90%) prevented BMP-2 induced stimulation of alkaline phosphatase in both C3H10T1/2 cells and the undifferentiated but committed MC3T3-E1 cells. Therefore, β-catenin directs osteogenic lineage allocation, enhancing uncommitted cell responsiveness to osteogenic factors, such as BMP-2. Signaling via β-catenin is a fundamental component of the osteoblast phenotype, acting independently or downstream of cbfa1.

*Disclosures: **G. Mbalaviele**, Pharmacia Corporation 3.*

1016

Opposing Roles of Osterix and TGFß Inducible Early Gene in Osteoblast Differentiation Downstream of Cbfa1/Runx2. S. A. Johnsen*, M. Subramaniam, T. J. Ruesink*, T. C. Spelsberg. Biochemistry & Molecular Biology, Mayo Clinic & Foundation, Rochester, MN, USA.

Cbfa1/Runx2 has been shown to play an important role in skeletal formation and the differentiation of osteoblasts. However, emerging evidence suggests that additional factors are necessary for the formation of mature osteoblast cells. The Krüppel-like zinc finger transcription factors Osterix (Osx) and TGFß inducible early gene (TIEG) are induced at different points following bone morphogenetic protein (BMP)-2 treatment in pre-osteoblastic cells and regulate the transcription of differentiation markers. Osx was recently cloned and identified as a BMP-2 inducible gene that is required for skeletal development and the formation of mature osteoblasts in vivo. Osx binds to an Sp1 element and functions downstream of Cbfa1/Runx2 to activate transcription of the osteoblast specific gene osteocalcin. Interestingly, like Osx, TIEG appears to regulate osteoblast differentiation downstream of Cbfa1/Runx2 since TIEG overexpression does not affect Cbfa1/Runx2 expression. However, in contrast to Osx, TIEG is a transcriptional repressor and down-regulates osteocalcin secretion and gene expression. We now show evidence that TIEG directly represses the osteocalcin promoter. This repression appears to be independent of Cbfa1/Runx2 since the promoter region regulated by TIEG is upstream of the OSE2 (Cbfa1/Runx2 binding site). Furthermore, Cbfa1/Runx2 overexpression does not reverse the repression by TIEG. However, we now show that TIEG binds to an Sp1 element and may thus compete with Osx for binding to the same sequences in target gene promoters. Thus we propose a model in which TIEG and Osx play differing roles at distinct points in osteoblast differentiation. In our model TIEG is rapidly induced following BMP-2 treatment and may serve to restrict the expression of late genes in osteoblast differentiation (i.e., osteocalcin). However, later in the differentiation pathway, Osx is expressed and displaces TIEG at target gene promoters thereby activating transcription of the late osteoblast differentiation markers. This new model provides insight into the regulation of osteoblast differentiation downstream of Cbfa1/Runx2.

1017

Four And A Half Lim Protein 2 (FHL2) Stimulates Osteoblast Proliferation And Differentiation. C. F. Lai[1], L. R. Halstead[1], P. McLoughlin*[2], B. W. Schafer*[2], P. H. Chu*[3], J. Chen*[3], X. Cao[4], D. A. Towler[1], S. L. Cheng[1]. [1]Division of Bone and Mineral Diseases, Washington University, St. Louis, MO, USA, [2]University of Zurich, Zurich, Switzerland, [3]University of California, La Jolla, CA, USA, [4]University of Alabama, Birmingham, AL, USA.

Integrin αvβ5 is one of the most abundant integrins expressed by human osteoblasts (HOB). This integrin governs osteoblast interaction with bone sialoprotein, osteopontin, and vitronectin. It has been well established that the cytoplasmic domain of integrin β subunit is essential in transmitting the signals induced by integrin-matrix interaction. In order to elucidate the function of αvβ5, we employed the yeast two-hybrid screening using an U2OS cDNA library as prey to identify proteins interacting with the cytoplasmic domain of β5. Out of 36 clones sequenced, one was identical to the full length FHL2. Immunoprecipitation and Western blotting confirmed the interaction of αvβ5 with FHL2 in HOB. Immunostaining and confocal examination indicated that FHL2 co-localized with αvβ5 at the focal adhesion sites. FHL2 was also detected in the nuclei. Employment of FHL2 deletion constructs and the Lim domain mutants in yeast two-hybrid assays indicated that the whole molecule of FHL2 was required for interaction with β5. To gain insight into the role of FHL2 in osteoblast function, we generated an MC3T3-E1 osteoblastic cell line overexpressing FHL2 by using a Flag-tagged FHL2. The Flag-tagged FHL2 was localized at the focal adhesion sites and in the nuclei. Cell adhesion to fibronectin and vitronectin were enhanced in FHL2 cells, which could derive, in part, via the higher β3 and β5 integrin levels in these cells. Cell proliferation, alkaline phosphatase activity, and osteopontin and bone sialoprotein levels were also elevated in FHL2 cells. Matrix mineralization and the upregulation of osteocalcin by Cbfa1 were enhanced in these cells. Examination of the calvarial sections derived from FHL2 deficient, with concomitant LacZ knock-in, mice indicated that FHL2 was expressed in osteoblasts and cells in the osteogenic front. Since this expression pattern was similar to that of FGF receptors and FHL2 expression was upregulated by FGF2, we analyzed the relationship between FHL2 and FGF2. FHL2 potentiated the stimulatory effects of FGF2 on osteocalcin expression and AP-1 and CRE activities. FHL2 also enhanced the FGF2-induced cell migration on type I collagen. In conclusion, FHL2 is expressed in osteoblasts and the osteogenic front. In osteoblasts, FHL2 co-localizes with αvβ5 at the focal adhesion site and is present in the nuclei. FHL2 upregulates osteoblast growth and differentiation and synergizes Cbfa1 and FGF2 activities. Thus, FHL2 may play an important role in bone formation.

1018

New Insights into Calcineurin Aα Function and Signaling. E. Abe[1], X. B. Wu[1], M. Lu*[1], X. Zhang*[1], B. S. Moonga[1], S. Epstein[1], H. C. Blair[2], L. Sun[1], M. Zaidi[1]. [1]The Mount Sinai Bone Program and Bronx VA GRECC, New York, NY, USA, [2]University of Pittsburgh, Pittsburgh, PA, USA.

Calcineurin Aα, a ubiquitously expressed Ca^{2+}/calmodulin-sensitive phosphatase, is a target for two of the most widely used immunosuppressants, cyclosporine (CsA) and tacrolimus (FK506). We found that calcineurin Aα and Aβ are expressed in both osteoblasts and osteoclasts. Deletion of the calcineurin Aα gene resulted in dramatic osteoporosis evident from a decrease in bone mineral density at the femur, tibia and lumbar spine. This was associated with reduced cortical thickness and a ~40% reduction in bone formation in tetracycline double labeling studies. Osteoblast progenitors, measured as colony-forming units-fibroblasts (CFU-Fs), in bone marrow cultures of calcineurin $Aα^{-/-}$ mice showed no decrease when compared to wild type littermates. Likewise, the inhibition of calcineurin Aα by CsA and FK506 resulted in unchanged CFU-F counts. In contrast, there was a marked reduction in osteoclast formation from hematopoetic progenitor cells in calcineurin $Aα^{-/-}$ mice, as well as in wild type cultures treated with CsA or FK506. An action of calcineurin Aα on osteoblast differentiation was evident from a dramatic increase in alkaline phosphatase activity of MC3T3.E1 cells transduced with a TAT-calcineurin Aα fusion protein. Together, the results provide compelling evidence that calcineurin Aα has a key role in bone formation without affecting the osteoblast progenitor pool. In parallel, chemical cross-linking studies, immunoprecipitation experiments, and phosphatase activity assays revealed that calcineurin Aα bound to and dephosphorylated not only the transcription factor, NFATc, but also the transcription inhibitor, IκBβ. This interaction resulted in the modulation of a variety of genes. Most notably, cells transfected with calcineurin Aα displayed a dramatic increase in NFATc1 and type 1 ryanodine receptor expression and a decrease in the phosphorylated form of IκBβ. Likewise, deletion of the calcineurin Aα gene in the $Aα^{-/-}$ mouse resulted in a marked reduction in NFATc and NFκB (p50, p65 and c-Rel) expression and an increased expression of phosphorylated IκBβ. The results suggest that calcineurin, through its phosphatase activity, not only dephosphorylates NFATc, but also dephosphorylates IκBβ to enhance its binding to the NFκB members thus preventing their nuclear localization. Taken together, our results demonstrate that calcineurin Aα is a key regulator of osteoblastic bone formation, and that this effect may be exerted not only through the traditional NFATc pathway, but also *via* the dephosphorylation of IκBβ, an interaction that we demonstrate for the first time in any eukaryotic cell.

1019

Structure/Function Study of the RANK Cytoplmasic Domain in Osteoclast Differentiation and Function Using a Chimeric Receptor Approach. H. Yang[1], P. Patel*[1], D. Hoang*[1], S. L. Teitelbaum[2], F. Ross[2], S. Takeshita[2], K. Chennareddy*[1], X. Feng[1]. [1]Pathology, University of Alabama at Birmingham, Birmingham, AL, USA, [2]Pathology, Washington University School of Medicine, St Louis, MO, USA.

RANKL, a member of the TNF-α superfamily, plays a pivotal role in osteoclast (OC) differentiation and function. RANKL exerts these effects by binding to its receptor RANK expressed on OC precursors and mature OCs. As a member of the TNF receptor superfamily, RANK may transduce intracellular signaling by recruiting intracellular signaling molecules such as TRAFs. Several groups have previously characterized the RANK functional domains that may interact with TRAFs. However, the data from these studies are conflicting. Furthermore, these studies were performed in cells unrelated to OCs, thus, the relevance of these data to OC biology remain unknown. We have developed a tool that permits us to carry out a detailed structure/function study of the RANK cytoplasmic domain in OC differentiation and function using authentic OCs. Using a retroviral technology, we expressed a chimeric receptor containing the extracellular domain of TNFR1 linked to the transmembrane and cytoplasmic domains of RANK in authentic OC precursors isolated from TNFR1/R2 double knockout mice. Treatment of the chimera-expressing OC precursors with TNF-α, as a RANKL surrogate, plus M-CSF, generates OCs, indistinguishable from those induced by RANKL and M-CSF. Most importantly, OCs generated using the chimeric receptor approach are fully capable of resorbing bone. Previously, several studies suggested that six putative TRAF-binding sites (pTRAF1, ILLMTREE at a.a.286-293; pTRAF2, PSQPS at a.a.349-353; pTRAF3, PFQEP at a.a.369-373; pTRAF4, VYVSQTSQE at a.a.537-545; pTRAF5, PVQEET at a.a.559-564; pTRAF6, PVQEQG at a.a.604-609) and two tyrosines (Y345 and Y468) in the RANK cytoplasmic tail may be involved in transducing RANK intracellular signaling. To investigate the role of the putative TRAF sites and two tyrosine residues in OC differentiation, we mutated these six putative TRAF sites and two tyrosine residues individually in the chimeric receptor constructs. The mutant chimeras were used to repeat the osteoclastogenesis assays described above. Our data indicate that all 8 mutant chimeras were still capable of mediating OC formation. In summary, we have developed a chimeric receptor strategy for identifying the RANK functional domains involved in OC differentiation and function. Moreover, using this chimeric receptor approach, we have demonstrated that six putative TRAF binding sites and two tyrosine residues, which have been suggested to be implicated in RANK signaling, are not essential for OC formation.

1020

Targeted Overexpression of Osteoprotegerin (OPG) in Osteoblasts Provides In Vivo Evidence for a Direct Role of Periosteal Osteoclasts in Normal Bone Growth. F. J. Asuncion*[1], D. M. Danilenko*[2], J. Li[1], D. Hill*[2], S. Kaufman*[2], C. R. Dunstan[1], D. L. Lacey[1], W. S. Simonet[1]. [1]Metabolic Disorders, Amgen, Thousand Oaks, CA, USA, [2]Pathology, Amgen, Thousand Oaks, CA, USA.

OPG was first characterized as a functional in vivo osteoclast inhibitor through the analysis of mice that expressed OPG under control of the human ApoE promoter (Cell 89:309-319 (1997)). ApoE-OPG transgenic mice, which express OPG predominately in the liver, exhibit increased trabecular bone density with total occlusion of the bone marrow space in high-expressing animals. However, apoE-OPG mice lack club-shaped bones, impaired tooth eruption and retarded bone growth typical of osteopetrotic mouse models. Both endosteal and periosteal osteoclasts are present in apoE-OPG mice in areas that express RANKL (OPG ligand) by in situ hybridization, but only endosteal osteoclasts show reduced numbers and activity. There are sufficient numbers of functional osteoclasts to allow for normal bone growth and modeling but are not sufficient to allow for remodeling of the primary spongiosa resulting in the observed phenotype. The unique features of this osteopetrotic model were hypothesized to be a result of hepatic OPG expression which resulted in high circulating levels of OPG that may not have sufficient access to all bone compartments. To test this hypothesis, transgenic mice overexpressing OPG in functional osteoblasts, the site of endogenous OPG expression, have been generated utilizing a rat Collagen1a1 promoter. In contrast to the apoE-OPG mice, the rCol1a1-OPG mice have undetectable levels of circulating OPG, yet exhibit more typical, severe osteopetrosis with impaired tooth eruption, retarded growth, and club-shaped, sclerotic long bones. The numbers of osteoclasts both on the periosteum and endosteum in the rCol1a1-OPG are markedly reduced compared to the apoE-OPG mice being most reminiscent of the phenotypes of RANK and RANKL KO mice. In summary, the apoE-OPG and rCol1a1-OPG mouse studies describe two phenotypically distinct osteopetrotic mouse models which result from OPG-mediated differential inhibition of subpopulations of osteoclasts on the surfaces of hypertrophic growth plate cartilage, trabecular and cortical bone, likely due to the cellular source of transgenic OPG expression.

Disclosures: ***F.J. Asuncion****, Amgen 1, 3.*

1021

Systemic TNFa Promotes Erosive Bone Resorption by Increasing the Number of CD11b+ Osteoclast Progenitors in the Periphery Which Are Dependent on RANK Signaling for Osteoclastogenesis. P. Li*, E. M. Schwarz, R. J. O'Keefe, B. F. Boyce, L. Xing. University of Rochester, Rochester, NY, USA.

TNFa, a potent osteoclastogenic factor, has been shown to act directly on cells in the osteoclast lineage, or indirectly by affecting the production of the essential osteoclast differentiation factor RANKL by osteoblasts. The mechanism by which TNFa increases osteoclastogenesis in vivo is unknown. Furthermore, there is controversy in this field as to whether TNFa induces osteoclastogenesis in the absence of RANKL. To elucidate the mechanism of TNFa-mediated osteoclastogenesis in vivo, we used TNFa transgenic (hTNF-Tg) and RANK knockout mice, and studied the effects of chronic TNFa exposure on osteoclast (ocl) precursor differentiation and the requirement of RANKL/RANK in this process. Splenocytes from hTNF-Tg mice 1) formed more ocls (#ocl/well 432+14 vs 55+28 in wt mice); 2) had an increase in the frequency of CD11b+ (10.7% vs 1.2% in wt mice) and CD11b+/c-Fms+ cells (4.0% vs 0.4% in wt mice). Only CD11b+ cells sorted by FACS formed ocls, indicating that CD11b can be used as a marker of ocl progenitors in spleen. Enhanced osteoclastogenesis and increased CD11b+ cells in hTNF-Tg mice were prevented by in vivo administration of the TNFa antagonist, Etanercept. Treatment of hTNF-Tg mice with a RANK antagonist, RANK:Fc (10 mg/kg, ip, daily for 2 weeks) dramatically reduced ocl numbers in arthritic joints (2.3+1.4/tibia and 0.3+0.2/erosion surface vs 138.3+13.8/ tibia and 5.3+0.6/erosion surface in PBS group), but did not decrease CD11b+ ocl progenitor frequency. Consistent with these findings, hTNF-Tg mice in a RANK null background have severe osteopetrosis and no ocl, but increased CD11b+ ocl precursors. Thus, chronic TNFa increases osteoclastogenesis through two distinct mechanisms in vivo: 1) it increases the pool of CD11b+ osteoclast progenitors through a RANKL/RANK independent mechanism; and 2) it stimulates osteoclast formation via a RANKL/RANK dependent mechanism.

1022

Unoccupied $\alpha_v\beta_3$ Integrin Transmits a Positive Death Signal in Osteoclasts. H. Zhao, F. P. Ross, S. L. Teitelbaum. Department of Pathology, Washington University School of Medicine, St. Louis, MO, USA.

Cell/matrix detachment is a general inducer of programmed cell death, an event mediated by loss of integrin/ligand association. Because $\alpha_v\beta_3$ is the major integrin expressed by the osteoclast (OC) we asked if its occupancy promotes survival of the resorptive cell. Thus, we generated wild type (WT) pre-OCs by treating bone marrow macrophages (BMMs) with M-CSF and RANKL for three days at which time they express TRAP, and as assessed by western blot, the β_3 integrin. The cells were lifted and placed on selective matrix proteins. Consistent with the posture that $\alpha_v\beta_3$ occupancy promotes survival, OCs plated on native collagen, a protein not recognized by the integrin, undergo apoptosis, as detected by ELISA, four fold faster that OCs plated on the $\alpha_v\beta_3$ ligand, vitronectin ($p<.001$). To further explore the role of $\alpha_v\beta_3$ in OC apoptosis, pre-OCs generated from WT and $\beta_3^{-/-}$ mouse BMMs were placed in suspention and apoptosis determined, with time. Surprisingly, $\beta_3^{-/-}$ pre-OCs, in suspension, undergo a rate of apoptosis only 40-60% of that of their WT counterparts ($p<.01$) indicating that unoccupied $\alpha_v\beta_3$ transmits a positive

death signal. Supporting this conclusion, activation of the activator caspase, caspase-8, and the executioner caspase, caspase-3, both of which mediate OC apoptosis, is blunted in suspended $\beta_3^{-/-}$ pre-OCs. We have shown that the resorptive defect of $\beta_3^{-/-}$ OCs can be rescued by transduction of WT β_3 cDNA but not one bearing a $S^{752}P$ mutation. To determine if the same holds as regards OC apoptosis, we constructed lentivirus vectors encoding GFP, WT β_3 or β_3 $S^{752}P$. $\beta_3^{-/-}$ BMMs were transduced with each viral construct at an efficiency of 60-90%. Pre-Ocs were generated and placed in suspention culture. Once again, $\beta_3^{-/-}$ cells were protected against apoptosis, as were those bearing the GFP construct ($p<.001$). Similar to its effect on bone resorption, transduced WT β_3 normalized the apoptotic rate of $\beta_3^{-/-}$ pre-OCs. Unexpectedly, however, β_3 $S^{752}P$ transductants also died at a rate indistinguishable from WT. In conclusion, 1). Deletion of $\alpha_v\beta_3$ protects OCs from apoptosis, 2). Cell death in non-matrix attached OCs is due principally to positive death signals transmitted by unoccupied $\alpha_v\beta_3$ integrin, 3). β_3 $S^{752}P$, which is essential for OC function, does not participate in $\alpha_v\beta_3$-derived death signals.

1023

RANK-TRAF6 Interaction: A New Target for Therapeutic Intervention of Osteolytic Disease. A. Poblenz*[1], M. Kalidas*[2], N. K. Shevde*[3], B. Lamothe*[4], K. Du*[1], S. Singh*[5], H. Wu*[6], J. E. Price*[7], J. W. Pike[3], B. G. Darnay[1]. [1]Bioimmunotherapy, University of Texas MD Anderson Cancer Center, Houston, TX, USA, [2]Medical Breast, Baylor College of Medicine, Houston, TX, USA, [3]Biochemistry, University of Wisconsin-Madison, Madison, WI, USA, [4]Pharmacology, Yale University, New Haven, CT, USA, [5]Imgenex, Inc., San Diego, CA, USA, [6]Biochemistry, Weill Medical College of Cornell University, New York, NY, USA, [7]Cancer Biology, University of Texas MD Anderson Cancer Center, Houston, TX, USA.

Breast cancer-induced osteolytic lesions are associated with increased morbidity secondary to pathologic fractures, hypercalcemia, and nerve compression syndromes. Elucidating the exact interaction between breast cancer cells and the bone microenvironment would aid in the development of new therapeutic agents. Receptor activator of NF-kB (RANK) and its ligand (RANKL) are essential mediators of osteoclastogenesis. RANK signals through tumor necrosis factor receptor-associated factors (TRAFs), and we have previously identified a unique TRAF6-binding motif in RANK which is distinct from the interaction domains for the other TRAFs. Furthermore, a peptide from RANK (residues 342-349) has been co-crystallized with the TRAF-C domain of TRAF6 and its structure indicates distinct molecular interactions. The importance of TRAF6 in osteoclastogenesis, like that of RANK and RANKL, is highlighted by null mice, which develop severe osteopetrosis and lack osteoclasts. Since TRAF6 appears to be the critical adaptor molecule, we developed a novel, cell-permeable TRAF6 decoy peptide (T6DP), which specifically targets the interaction of TRAF6 with RANK. We demonstrate that T6DPs inhibit RANKL-mediated signaling and osteoclast differentiation of RAW264.7 cells and primary mouse monocytes. In co-culture assays of RAW264.7 cells with breast cancer cell lines T47D or MDA-MB-468, T6DP treatment abolished their ability to induce osteoclast differentiation. To examine whether T6DPs could inhibit bone destruction associated with bone metastasis, we have developed an in vivo mouse model, in which the breast cancer cell line SUM 149 is injected into the proximal tibia of a nude mouse, and after 4 weeks, the mice develop osteolytic lesions. Preliminary results indicate that treatment of these mice with wild-type T6DP, but not mutant T6DP, prevents osteolysis induced by the breast cancer cell line. Thus, disruption of the RANK-TRAF6 interaction may prove useful as a novel target for the development of therapeutic agents for diseases of the bone.

1024

C-Fos Over-expression Induces Osteoclastogenesis Independent of RANK Signaling. T. Yamashita[1], L. Xing[1], P. Li*[1], E. M. Schwarz[1], W. C. Dougall[2], B. F. Boyce[1]. [1]Univ of Rochester Med Ctr, Rochester, NY, USA, [2]Immunex Corporation, Seattle, WA, USA.

Neither RANKL nor RANK knockout mice form osteoclasts due to a cell autonomous defect downstream from RANKL/RANK interaction, which activates a number of signaling pathways and leads to gene transcription. Analysis of c-fos knockout and NF-kB p50/p52 double knockout (dKO) mice has identified an essential role for AP-1 and NF-kB transcription factors in osteoclastogenesis, but the relative roles of these molecules that mediate RANK signaling in osteoclastogenesis remain poorly understood. To address this issue, we prepared splenocytes derived from 3-5 week-old RANK-/- and NF-kB dKO mice as a source of osteoclast precursors and determined by FACS analysis that cells from both types of mice express the osteoclast precursor antigen, CD11b. We cloned the gene for each subunit of the transcription factor families, AP-1 (c-Fos, Fra-1) or NF-kB (p52, p105 (the p50 precursor) and p65) into the pBabe vector and transfected these into the packaging cell line, Plat-E. We then infected spleen cells with retrovirus supernatants from the virus producing cells. Ten days after virus infection, cells were fixed and stained for TRAP to evaluate TRAP+ cell numbers. TRAP+ cells formed only in the wells containing RANK-/- splenocytes infected with the c-Fos expressing virus (102+/-21 per cm2). In particular, unlike the findings in similar published experiments using c-fos-/- splenocytes, Fra-1 expression did not rescue the defect in osteoclastogenesis in RANK-/- or NF-kB dKO splenocytes. Almost all of the cells formed in response to c-Fos retroviral expression were mononuclear. c-Fos-induced TRAP+ cell formation from RANK-/- splenocytes was not enhanced by co-infection with NF-kB p65, p52 or p105, or with Fra-1. Thus, only c-Fos over-expression appeared to induce osteoclast precursor formation in the absence of RANK dependent signaling, but this was insufficient to induce their fusion to form functional mature osteoclasts.

1025

Osteoblast Specific Expression of 11β-HSD2 in Transgenic Mice Abrogates Steroid-Induced Apoptosis and Attenuates Loss of BMD and Strength. R. S. Weinstein, C. A. O'Brien, J. A. Crawford*, S. C. Manolagas. Div. of Endo/Metab, Center for Osteoporosis and Metabolic Bone Diseases, Central Arkansas Veterans Healthcare System, Univ of Ark for Med Sci, Little Rock, AR, USA.

Studies in rodents and humans have elucidated that the adverse effects of glucocorticoid (GC) excess on the skeleton result from decreased osteoblastogenesis and osteoclastogenesis, increased prevalence of osteoblast and osteocyte apoptosis, as well as an extension of the life span of osteoclasts at the early stages of hypercortisolemia. Decreased intestinal calcium absorption, urinary calcium losses, secondary hyperparathyroidism and hypogonadism have also been implicated as mechanisms of the deleterious effects of GC excess on bone. To dissect the contribution of the effects of GCs on osteoblastic/osteocytic cells from effects on osteoclasts or extraskeletal actions, we generated a transgenic mouse in which GC action on osteoblastic/osteocytic cells was blocked by overexpression of 11ß-HSD2. As previously shown, 11ß-HSD2 overexpression under the control of the osteocalcin gene promoter (OG2) resulted in rapid pre-receptor inactivation of GCs and thereby spared osteoblastic cells from the pro-apoptotic effects of GCs in vitro. Northern blot analysis of RNA prepared from various tissues indicated that the transgene is specifically expressed in bone. We now report that after 35 days of prednisolone administration (2.1 kg/mg/day) to 6-month-old mice overexpressing the 11ß-HSD2 gene, loss of spinal BMD was reduced by 40% ($p<0.02$), as compared to administration of the same dose of prednisolone to wild-type litter mates. In a second experiment, 28 days of prednisolone administration decreased vertebral compression strength by 45% in wild-type animals while strength was maintained in the transgenic mice ($p<0.02$). These findings suggest that GC -induced loss of compression strength may principally result from abnormal bone quality rather than quantity. In support of this contention, the expected increase in osteoblast and osteocyte apoptosis due to GC excess, as noted in wild-type mice, did not occur in 11β-HSD2 transgenic animals. Moreover, cancellous osteoblast numbers were maintained in the transgenic animals receiving prednisolone. Based on this and evidence that GCs prolong osteoclast survival, we conclude that direct effects of GCs on osteoblastic/osteocytic cells account for as much as 40% of their negative effect on bone mass; the remaining probably resulting from increased osteoclastic resorption. Furthermore, direct effects of GCs may account for practically their entire deleterious effects on osteoblast/osteocyte viability and the ensuing loss of bone strength.

1026

Transgenic Expression of 11ß-hydroxysteroid Dehydrogenase in Osteoblasts Reveals an Anabolic Role for Endogenous Glucocorticoids in Bone. L. B. Sher[1], H. W. Woitge[1], J. R. Harrison[2], D. J. Adams*[3], B. E. Kream[1]. [1]Medicine, University of Connecticut Health Center, Farmington, CT, USA, [2]Orthodontics, University of Connecticut Health Center, Farmington, CT, USA, [3]Orthopaedic Surgery, University of Connecticut Health Center, Farmington, CT, USA.

In humans, glucocorticoid excess leads to bone loss, primarily by decreasing bone formation. Yet, glucocorticoids promote osteogenesis in a variety of bone organ and cell culture models. The relation of the anabolic effect of glucocorticoids in vitro to the physiological actions of glucocorticoids in vivo is a long-standing question in bone biology. To elucidate the role of endogenous glucocorticoids in bone, we previously developed transgenic mice in which a 2.3 kb Col1a1 promoter fragment drives 11β-hydroxysteroid dehydrogenase (11β-HSD2) expression in mature osteoblasts. 11β-HSD2 metabolically inactivates endogenous glucocorticoids, thereby reducing glucocorticoid signaling. Two phenotypic assessments of bone of wild-type (WT) and transgenic (TG) littermates were made: collagen synthesis rates in organ cultures of six- to eight-day old calvariae, and trabecular bone morphometric parameters of 7- and 24-week old vertebrae and femurs. To measure collagen synthesis rates, calvariae were cultured in the presence or absence of cortisol for 96h and labeled with [^{3}H] proline for the final 2h of culture. The inhibitory effect of 300 nM cortisol on percent collagen synthesis was blunted in TG calvariae, demonstrating that the transgene was active. The baseline percent collagen synthesis was 32% lower in TG calvariae (n=28) compared to WT (n=37): 18.7±0.9 vs. 27.4±0.9, mean±SEM, $p<0.0001$. A similar difference was seen in an additional TG line. Trabecular bone, as measured by microcomputed tomography at 7- and 24- weeks of age, was effected in L3 vertebrae, but not in distal femurs, of Tg (n=10) females compared to WT (n=10). At both time points, bone volume (BV/TV) was decreased, although this difference was not significant ($p=0.066$ & 0.055, respectively). At both time points, trabecular number (TbN) was significantly lower in TG compared to WT females, (3.14±0.12 vs. 3.87±0.17 & 2.97±0.12 vs. 3.74±0.20, mean±SEM, $p<0.003$) respectively. These changes were not seen in males. Trabecular thickness was unchanged in both males and females. Our data demonstrate that endogenous glucocorticoids are required for normal levels of collagen synthesis in neonatal calvariae, suggesting that disruption of glucocorticoid signaling in vivo impairs osteoblast differentiation and/or function. Moreover, our data suggest that endogenous glucocorticoids may exert site- and sex-specific anabolic effects in bone.

1027

A Selective Androgen Receptor Modulator (SARM) Displays Dissociated Activity on Bone and Seminal Vesicles in Mice. C. Robin-Jagerschmidt*[1], P. Clément-Lacroix[1], D. Minet*[1], V. Hippomène*[2], M. Gaillard-Kelly[2], R. Baron[1], M. Resche-Rigon[1]. [1]Proskelia, Romainville, France, [2]Aventis, Romainville, France.

Both androgens and estrogens are essential for skeletal development and maintenance in men. However the determination of age-associated hypogonadism in men (andropause) is not as clear as it is in women, partly due to the slow and gradual decrease of testosterone level over time. The protective effects of androgen replacement therapy (ART) on bone mass and muscle strength in males are nevertheless well recognized. Testosterone has been shown to normalize bone mineral density and biochemical parameters of bone turnover in hypogonadal men. However, increased risk of clinically progressive prostate carcinoma as well as precipitation or exacerbation of benign prostatic hyperplasia compromise the prolonged utilization of androgens. Searching for tissue selective compounds, we have previously shown that cyproterone acetate, initially an anti-androgen used in the treatment of prostate cancer, behaves as an androgen receptor agonist in osteoblasts, decreasing IL-6 secretion similarly to DHT (Robin-Jagerschmidt et al. 1999, ASBMR, F460). In order to test its effects *in vivo*, we used a model of osteopenia in male mice. Twelve week-old C57Bl/6 mice were orchidectomized and treated with pTesto, or DHT (2.5mg/kg/d, pellet), for 4 weeks. Orchidectomy induced a significant (30 ± 4%) trabecular bone loss in long bones (tibia), and increased bone turnover. Serum osteocalcin (OC) and urinary deoxypyridinolin (D-Pyr) were increased 2 weeks after orchidectomy and remained elevated for two additional weeks. DHT and pTesto treatment normalized OC and (D-Pyr) levels to sham control. Both compounds fully prevented the decrease in seminal vesicle weight induced by orchidectomy. Cyproterone acetate (30mg/kg/d s.c.) was also able to prevent the ORX-induced bone loss at both trabecular and cortical sites, but did not increase seminal vesicle weight of ORX mice. More interestingly, when administrated in combination with DHT (2.5mg/kg/d), cyproterone acetate antagonized at least 85% of the DHT effects on the seminal vesicles, but did not counteract the bone sparing effects of DHT. These results demonstrate that cyproterone acetate displays *in vivo* tissue selective agonist activity. Such SARMs are promising drugs for the prevention of osteoporosis in aging men.

1028

Constitutive Expression of 25-Hydroxyvitamin D3 1 alpha-Hydroxylase in a Human Melanoma Cell Line: Autocrine Regulation by Endogenous PTHrP Production. D. C. Huang[1], R. L. Horst[2], D. Goltzman[1], R. Kremer[1]. [1]Medicine, Mcgill University, Montreal, PQ, Canada, [2]USDA, Agriculture Research Svc., National Animal Disease Center, Ames, IA, USA.

Tumoral expression of 25-hydroxyvitamin D3 1 α-hydroxylase has previously been reported in a human small cell lung cancer cell line. Here we report a human melanoma cell line which can synthesize 1,25-dihydroxyvitamin D3 [1,25-(OH)2D3] from its inactive precursor 25-hydroxyvitamin D3 (25-OHD3). This cell line also expresses PTHrP and was used as a model to examine the autocrine regulation between 25-hydroxyvitamin D3 1 α-hydroxylase and PTHrP. 1,25-(OH)2D3 and PTHrP expression and production were identified and quantified by Northern blot analysis, radioimmunoassays and HPLC. Normal human melanocytes were also examined for PTHrP and 1 α-hydroxylase expression. Northern blot analysis revealed high levels of 1 α-hydroxylase gene expression in this melanoma cell line. Cloning and sequencing of 1 α-hydroxylase cDNA from the melanoma cells identified a transcript identical to that observed in human renal cells and keratinocytes. Enzyme kinetic studies revealed a Km for 1 α-hydroxylase of 500 nmol/litre, with a maximum velocity of 3.5 ng/h/ml/10exp6 cells. This activity was inhibited following transfection with 1 α-hydroxylase antisense cDNA. Addition of substrate 25-OHD3 significantly inhibited cell growth, PTHrP expression and production, and induced morphological changes similar to the effect observed with 1,25-(OH)2D3. Targeted disruption of the PTHrP gene in this cell line totally eliminated PTHrP production and resulted in a drastic reduction of 1 α-hydroxylase activity by over 80% as compared to the parent cell line. Although normal human melanocytes expressed low levels of PTHrP no detectable expression or activity of 1 α-hydroxylase was found. This is the first report of 1 α-hydroxylase expression by human melanoma cells and its autocrine regulation by PTHrP in a reciprocal positive/negative feed back loop.

1029

Comparison of Mice with Deletions of the 25OH Vitamin D_3-1α Hydroxylase (1αOHase), of the Vitamin D Receptor (VDR), and of Both, Suggest an *In Vivo* Role for VDR-Dependent and Independent Regulation of Calcium and Skeletal Homeostasis. D. K. Panda[1], D. Miao[1], R. Huo*[1], G. N. Hendy[1], D. Goltzman[2]. [1]Medicine, McGill University, Montreal, PQ, Canada, [2]Medicine, McGill University Health Centre and McGill University, Montreal, PQ, Canada.

We compared calcium and skeletal homeostasis in mice homozygous for targeted disruption of the 1α(OH)ase gene [1αOHase$^{-/-}$], the VDR gene [VDR$^{-/-}$], and both genes [1αOHase$^{-/-}$; VDR$^{-/-}$]. All mice were fed normal chow (1% calcium, 0.9% phosphorus) with high calcium (15%) in drinking water and were analyzed at 9 weeks. Serum calcium was: 10.8 ± 0.3 mg/dl in wild-type (WT) littermates; 8.8 ± 0.4 mg/dl in 1α(OH)ase$^{-/-}$ mice, 7.1 ± 0.5 mg/dl in VDR$^{-/-}$ mice; and 6.4 ± 0.2 mg/dl in 1α(OH)ase$^{-/-}$; VDR$^{-/-}$ mice. Serum 1,25$(OH)_2D_3$ concentrations were 64.2 ± 10.4 pg/ml in WT, 498 ± 36.7 pg/ml in VDR$^{-/-}$, and were undetectable in both mutants deficient in 1α(OH)ase. Parathyroid glands were enlarged in all 3 mutants. Radiologic analysis revealed a progressive reduction in long bone size and extent of mineralized bone from WT to 1αOHase$^{-/-}$ to VDR$^{-/-}$ to 1α(OH)ase$^{-/-}$; VDR$^{-/-}$. Animal size also was progressively reduced from WT (23 ± 1.4 g) to 1α(OH)ase$^{-/-}$ (21 ± 0.9 g) to VDR$^{-/-}$ (16.4 ± 0.8 g) to 1α(OH)ase$^{-/-}$; VDR$^{-/-}$ (12.3 g). Histological analysis revealed a very widened, disorganized cartilaginous growth plate in the two models deficient in 1α(OH)ase; in contrast, in VDR$^{-/-}$ mice, the growth plate was only slightly thickened compared to WT and was better organized. Trabecular bone was reduced in the VDR$^{-/-}$ mice with increased TRAP-positive osteoclasts and was poorly mineralized. Trabecular bone was increased in both 1α(OH)ase$^{-/-}$ models with increased osteoblast numbers and decreased TRAP-positive osteoclasts but was poorly mineralized in the compound mutants. Trabecular mineralization therefore seemed dependent on ambient calcium levels. In these models, therefore, hypocalcemia correlated better with VDR than with 1α(OH)ase status; normalization of the cartilaginous growth plate occurred in the absence of VDR but not in the absence of 1α(OH)ase; and increased trabecular bone volume, increased trabecular osteoblasts and decreased TRAP-positive osteoclasts correlated with the absence of 1,25$(OH)_2D_3$ rather than with VDR deficiency. These *in vivo* results suggest that in regulating skeletal and calcium homeostasis, vitamin D can exert effects that may be dependent on or independent of the VDR.

1030

Rickets in VDR Null Mice Is Secondary to Decreased Apoptosis of Hypertrophic Chondrocytes. M. M. Donohue*, M. B. Demay. Endocrine Unit, Massachusetts General Hospital, Harvard Medical School, Boston, MA, USA.

The absence of a functional VDR in mice and humans leads to hypocalcemia, hyperparathyroidism, hypophosphatemia, rickets and osteomalacia. By 24 days of age, VDR knockout mice have an expansion in the layer of hypertrophic chondrocytes, characteristic of rickets; however, prevention of abnormal mineral ion homeostasis by instituting dietary therapy by 18 days prevents rickets, demonstrating that the VDR is not required for normal growth plate maturation. We, therefore, hypothesized that rickets, in the absence of a functional VDR, is a consequence of impaired mineral ion homeostasis. Analyses of rachitic growth plate morphology demonstrated normal resting and proliferating chondrocyte layers in the VDR knock-out mice; however a 2.1 fold expansion of the hypertrophic chondrocyte layer was present at 24 days of age. Recent studies have demonstrated that extracellular calcium plays a role in chondrocyte maturation. We, therefore, examined markers of chondrocyte differentiation in the rachitic VDR null growth plate. In situ hybridization analyses revealed normal expression of hypertrophic chondrocyte markers in the tibial growth plate of 24 day old VDR knock out mice suggesting that the increase in hypertrophic chondrocyte layer was not secondary to impaired differentiation. Furthermore, expression of VEGF was not altered in the VDR null growthplate. We then addressed whether the expansion of the hypertrophic chondrocyte layer in the VDR null mice was secondary to increased proliferation or decreased apoptosis. BrdU labeling failed to demonstrate a difference in proliferation between VDR knock-out and control animals in both the proliferating chondrocytes (42.1% vs. 42.0%) and hypertrophic chondrocytes (1.2% vs. 4.7%). The lower percent BrdU incorporation in the hypertrophic chondrocytes of the VDR null mice is due to an increase in the total number of hypertrophic chondrocytes rather than a decrease in the number of proliferating cells. Apoptosis was evaluated following in vivo labeling with Annexin-V-biotin. In contrast to control littermates, no detectable annexin-V biotin was seen in the growth plate of the VDR null mice, suggesting that an impairment in programmed cell death led to expansion of the hypertrophic chondrocyte layer. Normalization of the growth plate phenotype in VDR null mice with normal mineral ions is consistent with in vitro studies demonstrating that inorganic phosphate induces chondrocyte apoptosis. Thus, our data support the hypothesis that impaired mineralization in the region of the hypertrophic chondrocytes, in the setting of abnormal mineral ion homeostasis, markedly attenuates apoptosis, leading to the characteristic findings of rickets.

1031

Improved Survival Rate and Bone Status in Senile Female Mice Lacking Estrogen Receptor-beta. H. Z. Ke[1], H. Qi[1], D. T. Crawford*[1], H. A. Simmons[1], Q. Zhang*[2], T. A. Brown[1], D. N. Petersen[1], W. S. S. Jee[2], D. D. Thompson[1]. [1]Pfizer Global Research and Development, Groton, CT, USA, [2]University of Utah, Salt Lake City, UT, USA.

The purpose of this study was to compare the differential response to long-term aging and ovariectomy (OVX) between estrogen receptor-beta (ER-b) knockout (BERKO) senile female mice and wild-type littermate controls (WT) in survival rate and bone status. Fourteen WT and 14 BERKO mice were necropsied at 13 months of age and served as basal controls. The remaining WT and BERKO mice were sham-operated or OVX, and were necropsied at 8 months post-surgery. By 21 months of age, only 5 of 14 (35.7%) mice survived in the WT-sham group, while 14 of 16 (87.5%) survived in the BERKO-sham group. There were 9 of 13 (69.2%) survivors in the WT-OVX group, and 10 of 15 (66.7%) in the BERKO-OVX group. These results indicate that the survival rate in senile female mice lacking ER-b is increased as compared with WT. OVX increased the survival rate in WT but not BERKO senile female mice. At 13 months of age, PQCT analysis showed that BERKO mice had significantly higher total content (+30%), cortical content (+32%) and trabecular density (+48%) at the distal femoral metaphysis (DFM) and significantly higher total content (+19%) and cortical content (+17%) at the femoral shafts (FS) as compared with WT mice. The higher bone mass was accompanied with a lower bone resorption and bone turnover in BERKO mice. There was a significant decrease in total content (-34%), cortical content (-30%) and trabecular density (-19%) at the DFM and a significant decrease in total content (-15%) and cortical content (-13%) at the FS in WT mice from 13 to 21 months of age. In BERKO mice, there was no significant difference in total content, cortical content and trabecular density at the DFM, while there was a significant increase in total and cortical content at the FS from 13 to 21 months of age. Micro-CT analysis of the DFM showed that the trabecular bone volume decreased significantly from 13.6% at 13-month-old to 5.0% at 21-month-old in WT mice, while this parameter increased from 25.6% to 33.4% during this period in BERKO mice. These results indicate that ER-b knockout completely protected against age-related cancellous and cortical bone loss between 13 to 21 months of age. At 8 months post-OVX, cancellous and cortical bone mass significantly decreased to the same levels in WT-OVX and BERKO-OVX mice, despite BERKO mice had higher bone mass at the time of OVX. These results indicate that ER-b knockout does not protect against bone loss induced by OVX. In summary, our data showed that ER-b knockout improved the survival rate and completely protected against age-related bone loss, but failed to protect against OVX-induced bone loss in these senile female mice.

Disclosures: ***H.Z. Ke****, Pfizer 3.*

1032

Interchangeable Ligand/Receptor Interactions Mediate ERK Activation and the Pro- and Anti- Apoptotic Effects of Estrogens and Androgens on Murine Osteoclasts and Osteoblasts from Females and Males: A Molecular Explanation of the In Vivo Equivalence of their Skeletal Actions in either Sex. J. R. Chen[1], S. Kousteni[1], L. Han[1], A. M. Vertino[1], L. K. McCauley[2], A. A. Ali[1], T. Bellido[1], R. S. Weinstein[1], C. A. O'Brien[1], R. L. Jilka[1], S. C. Manolagas[1]. [1]Division of Endocrinology and Metabolism, Center for Osteoporosis & Metabolic Bone Diseases, Central Arkansas Veterans Healthcare System, U/sity of Arkansas for Medical Sciences, Little Rock, AR, USA, [2]School of Dentistry, U/sity of Michigan, Ann Arbor, MI, USA.

Estrogens restore bone mass in males with androgen deficiency, whereas nonaromatizable androgens can protect the female skeleton against the adverse effects of estrogen deficiency. Based on this and evidence, reported elsewhere in this meeting, that estradiol (E_2) or dihydrotestosterone (DHT) administration to gonadectomized mice results in equivalent effects on osteoclastogenesis, osteoblastogenesis and BMD irrespective of the sex of the replaced animal, we investigated the specificity of the ligand/receptor interaction in murine bone cells from females and males. The sex of the donor mice in these experiments was determined by Southern blot analysis of genomic DNA isolated from livers, using a cDNA probe specific for the Y chromosome. Osteoblasts or osteoclasts from females and males exhibited indistinguishable levels of ERα, ERβ or AR expression, as determined by semi-quantitative RT-PCR or staining with specific receptor antibodies. E_2 or DHT (10^{-11} - 10^{-7} M) prevented etoposide-induced apoptosis of calvaria osteoblasts and stimulated osteoclast apoptosis in a dose dependent manner and with identical efficacy, in cells from females and males. The identical potency of E_2 and DHT on the lifespan of osteoblasts and osteoclasts resulted from the ability of the ER (α or β) or the AR to transmit ERK-activated signals with similar efficiency irrespective of whether the ligand was an estrogen or an androgen. Indeed, all the effects of E_2 or DHT on osteoblasts or osteoclasts were blocked by either the ER antagonist ICI 182,780 or the AR antagonist flutamide; and this phenomenon was reproduced in HeLa cells transiently transfected either with ERα, ERβ or AR alone. Strikingly, E_2 stimulated ERK phosphorylation, prevented osteoblast, and stimulated osteoclast apoptosis in cells obtained from mice lacking both ERα and ERβ (DERKO), provided by P. Chambon. As in the wild type control, all the effects of E_2 in the DERKO cells could be prevented by either ICI 182,780 or flutamide. These results suggest that the equivalence of the bone protective effects of estrogens and androgens in males and females results, at least in part, from interchangeable ligand/receptor interactions in bone cells from either sex.

1033

Prevention of Ovariectomy-Induced Bone Loss in β_3 Integrin Knockout Mice. H. Zhao*, F. P. Ross, S. L. Teitelbaum, D. V. Novack. Department of Pathology, Washington University School of Medicine, St. Louis, MO, USA.

Both blocking and β_3 knockout mouse studies have established that $\alpha_v\beta_3$ integrin is essential for optimal osteoclastic bone resorption. However, the role of $\alpha_v\beta_3$ in the pathogenesis of postmenopausal osteoporosis had not been explored. In this study, 2-month old female wild type (WT) and β_3 integrin knockout (KO) mice were ovariectomized (OVX) or sham-operated (sham). Thirty days after operation bone mineral density (BMD, mg/cm^2) was measured by DEXA (Pyximus). As shown in Table 1, ovariectomy induced a 7% decrease ($p< 0.05$) in whole body BMD in WT mice, while KO mice showed a statistically insignificant rise in BMD. BMD was 12-15% lower in WT mice at the femoral neck and lumbar vertebrae following OVX, while these parameters remained unchanged in KO mice. Isolated tibiae were subjected DEXA, then processed for histomorphometric analysis of TRAP-stained sections. Tibial BMD was unaffected by OVX in KO mice, compared to a 12% drop in OVX WT mice. Consistent with this, KO mice fail to show the OVX-induced increase in osteoclast surface (OCS/BS) and decrease in trabecular bone volume (BV/TV) seen in WT mice (Table 2). We conclude that the absence of $\alpha_v\beta_3$ confers protection against OVX-induced osteoporosis. These findings confirm the critical role of $\alpha_v\beta_3$ integrin in bone resorption and indicate that inhibitors of this integrin may be useful in preventing postmenopausal osteoporosis.

Table 1.

	Whole body	Femoral neck	Vertebrae	Tibia
WT/sham (n=7)	50.3±2.8	70.6±5.5	56.0±4.4	54.7±4.5
WT/OVX (n=8)	46.8±1.1*	60.9±2.6**	47.5±2.7**	48.1±4.8***
KO/sham (n=4)	47.7±3.0	65.4±3.7	53.3±4.7	49.6±5.1
KO/OVX (n=6)	49.1±4.4	67.4±4.5	54.3±7.6	52.3±5.5

BMD (mg/cm^2) represented as mean ± SD. n, number of mice per group. *, $p<0.05$, **, $p<0.01$; ***, $p<0.001$ by unpaired, two-tailed t test, compared to WT/sham.

Table 2

	OCS/BS (%)	BV/TV (%)
WT/sham	15.7±4.3	4.2±1.6
WT/OVX	20.5±6.7 *	2.3±1.4**
KO/sham	17.7±3.2	4.3±2.3
KO/OVX	18.7±4.2	4.7±1.8

*, $p<0.05$; **, $p<0.01$ by unpaired, two-tailed t test, compared to WT/sham.

1034

Tob-Deficiency Prevents Ovariectomy-Induced Bone Loss through the Enhancement of Osteoblastic Differentiation in Bone Marrow Stromal Cells to Augment Bone Formation (BFR/MAR) In Vivo. M. Usui*[1], Y. Yoshida*[2], K. Tsuji[1], I. Ishikawa*[3], A. Nifuji[1], T. Yamamoto*[2], M. Noda[1]. [1]Molecular Pharmacology, Medical Research Institute, Tokyo Medical and Dental University, Tokyo, Japan, [2]Tokyo University, Tokyo, Japan, [3]Periodontology, Tokyo Medical and Dental University, Tokyo, Japan.

Tob(Transducer of ErbB2) is a member of novel antiproliferative family. Tob-deficient mice reveal high levels of bone mass in adult, due to increase in bone formation without major alteration in bone resorption. Furthermore, Tob acts as an inhibitor against BMP-induced Smad signaling (Cell, 2000). We recently observed that Tob-deficiency preserves bone mass even after the bone loss due to ovariectomy (OVX). However, the mechanisms underlying this phenomenon have not been known. The aim of this paper was to elucidate the cellular mechanism, which causes Tob-deficiency effects on OVX-induced bone loss. In vitro nodule formation (NF) assay conducted using bone marrow cells (BMCs) obtained 14days after OVX revealed about 5-hold enhancement in NF in BMCs from ovariectomised (OVXed) mice compared to sham-operated (Sh-) mice in wild type (WT) group. In the case of Tob-deficient (TD) BMCs, the levels of NF in Sh-group were similar to those in the Sh-WT group. However, OVX-induced enhancement of NF was significantly more in the BMCs from TD mice compared to the BMCs from OVXed WT mice. The number of osteoclast (OC) developed in the bone marrow cultures treated with dexamethasone and vitamin D was enhanced by about 80% in OVXed group compared to Sh-WT mice. In contrast to Tob-deficiency enhancement of NF, OC development induced by OVX was similar between TD and WT mice. Based on such enhancement in the osteoblastic (OB) activity in BMCs in culture, we evaluated OB activity in vivo based on histomorphometry. Mineral apposition rate (MAR) was enhanced by OVX in WT mice as reported previously. In TD mice basal levels of MAR in Sh-mice was high and comparable to the high levels of MAR in OVXed WT mice. Interestingly, OVX in TD mice enhanced MAR significantly compared to the Sh-group in TD mice. Similarly bone formation rate (BFR) was enhanced by OVX in WT mice and the basal levels of BFR in TD mice in Sh-group was comparable to that in OVXed WT mice. OVX further enhanced BFR significantly compared to the Sh-mice in TD background. OVX increased the spleen weight (SW) in WT mice. In Sh-TD mice, SW was similar to the corresponding SW in OVXed WT mice. Intriguingly, however, OVX did not further enhance SW in TD mice. These data indicate that Tob-deficiency prevents OVX-induced bone loss through the enhancement of OB differentiation in bone marrow environment and this results in the augmentation in BFR and bone mass gain in vivo.

1035

Local Glucocorticoid Activation Mediates the Effect of Glucocorticoids on Bone. M. S. Cooper[1], A. Blumsohn[2], P. E. Goddard*[1], W. A. Bartlett*[1], C. H. Shackleton*[3], R. Eastell[2], M. Hewison[1], P. M. Stewart*[1]. [1]Medical Sciences, University of Birmingham, Birmingham, United Kingdom, [2]Bone Metabolism Group, University of Sheffield, Sheffield, United Kingdom, [3]Children's Hospital Oakland Research Institute, Oakland, CA, USA.

Glucocorticoid excess decreases bone formation and BMD, and increases fracture risk but these effects are difficult to predict in any given individual. We recently described expression of 11β-hydroxysteroid dehydrogenase type 1 (11β-HSD1) in osteoblasts where this enzyme generates active cortisol (or prednisolone) from inactive cortisone (or prednisone). In vitro, this enzyme regulates glucocorticoid action in osteoblasts and thus we hypothesized that this enzyme modulates the clinical effects of glucocorticoids on bone. We have now defined the determinants of variation in the response of bone markers to glucocorticoid therapy. 20 healthy males (age 31±8; mean±SD) took 5mg prednisolone twice daily orally for 7 days. 24hr urinary steroid metabolites (by GC/MS), BMD and biochemical bone markers (osteocalcin (OC), N-terminal propeptide of type I collagen (PINP), serum C-telopeptide of collagen cross-links (βCTx) and PTH) were measured before steroids and repeated at days 4 and 7. Prednisolone absorption, prednisone generation and steroid half-lives were subsequently determined (by HPLC) post oral prednisolone (5mg at 0900). OC and PINP both decreased at days 4 and 7 (29±11ng/ml vs 18±8 and 19±8 for OC; 67±24ng/ml vs 52±19 and 52±16 for P1NP; all $p<0.001$) but βCTx and PTH did not change significantly. There was a negative correlation between 11β-HSD1 activity (measured as the urinary (THF+alloTHF)/THE ratio) at baseline and OC at days 4 and 7 (r=-0.58 and -0.56; both $p<0.01$) and PINP at day 4 (r=-0.51; $p<0.05$). There was no correlation with measures of glucocorticoid inactivation (11β-HSD2 activity: urinary cortisol/cortisone ratio), total steroid metabolites, BMD, peak prednisolone or prednisone level, or prednisolone half-life. The relationship between 11β-HSD1 activity and bone formation markers could reflect either systemic or osteoblastic steroid generation. 11β-HSD1 activity did not predict increased prednisolone area under the curve or circulatory half-life thus it is unlikely that systemic activity mediates the observed relationship. Urinary 11β-HSD1 activity predicts the response of bone formation markers to glucocorticoids, explaining approximately a third of variability between individuals. This appears to reflect increased local generation of active glucocorticoids within osteoblasts. Measures of 11β-HSD1 activity predict the skeletal response to glucocorticoids and may form the basis of a test to predict individual susceptibility.

1036

Down-regulation of Interleukin-11 may be Involved in the Pathogenesis of Glucocorticoid-induced Osteoporosis. S. Kido, D. Inoue, S. Kato*, Y. Ito*, T. Matsumoto. Department of Medicine and Bioregulatory Science, University of Tokushima, Tokushima, Japan.

We have reported that Fos family transcripton factors including deltafosB, and an AP-1 target interleukin (IL)-11, are induced by mechanical stress and PTH in an ERK-dependent manner. Conversely, marrow stromal cell AP-1 activity and IL-11 expression is reduced by aging. Importance of IL-11 is underscored by recent observations that transgenic mice over-expressing IL-11 exhibit high bone mass due to enhanced bone formation and are protected from aging-associated bone loss. In the present study, we investigated a role for IL-11 in the pathogenesis of glucocorticoid (GC)-induced osteoporosis, characterized by suppressed bone formation. As we have already shown, fluid shear stress (FSS) as well as treatment with PTH, dibutylyl cAMP, TPA and calcium ionophore all induced fosB/deltafosB and IL-11 mRNA expression by primary osteoblasts (POB) obtained by sequential digestion of newborn mouse calvariae. In vivo treatment of mice with PTH also resulted in two to three fold induction of IL-11 mRNA expression in tibiae and femurs as assessed by quantitative real-time PCR analysis. Interestingly, the induction of IL-11, both in vitro and in vivo, was almost completely abolished by pretreatment with dexamethasone (Dex), while induction of fosB/deltafosB remained intact. Furthermore, Dex treatment of ST2 cells stably transfected with an IL-11 promoter-luciferase construct almost completely suppressed both basal and induced luciferase activities. These results are consistent with an idea that Dex inhibits IL-11 transcription by blocking AP-1 activities. In order to further elucidate a role for IL-11 in GC-induced osteoporosis, we next examined its effects on osteoblast apoptosis. As previously reported, Dex and etoposide induced POB apoptosis as evidenced by DNA ladder formation. Calvarial cell fractionation revealed that Dex-induced apototosis occurs mostly in fraction V representing mature osteoblasts. We found that IL-11 inducers such as FSS and PTH as well as IL-11 itself strongly blocked the apoptosis. Furthermore, anti-apoptotic effects of PTH was partially reversed by an anti-IL-11 neutralizing antibody. Both PTH and IL-11 blocked DEX-induced down-regulation of Bcl-2 while levels of Bax stayed the same. Finally, in vivo analysis using IL-11 transgenic mice suggested that over-expression of IL-11 partially suppressed Dex-induced OB apoptosis. We therefore conclude that IL-11 is an osteogenic cytokine which not only promotes early osteoblastogenesis but also enhances osteoblast survival and that down-regulation of IL-11 may be associated with osteoblast apoptosis and thereby contributes to bone loss induced by GC excess.

1037

Resolution of Effect Following Alendronate: Six-Year Results from the Early Postmenopausal Interventional Cohort (EPIC) Study. M. McClung[1], R. Wasnich[2], M. Omizo*[1], C. Christiansen[3], P. Ravn*[3], D. Hosking[4], M. Wu*[5], A. Kaur*[5], A. M. Mantz*[5], S. Snodgrass[5], A. Santora[5]. [1]Oregon Osteoporosis Center, Portland, OR, USA, [2]Radiant Research / Honolulu, Honolulu, HI, USA, [3]CCBR, Ballerup, Denmark, [4]City Hospital, Nottingham, United Kingdom, [5]Merck Research Laboratories, Rahway, NJ, USA.

Alendronate[1] (ALN) is indicated for the prevention of osteoporosis to maintain bone mass and reduce the risk of future fracture.[2,3] Women who received ALN 5 mg for 6 years experienced significant, persistent gains in mean lumbar spine and hip BMD, that were maintained. In contrast, BMD steadily decreased in the placebo (PBO) group. The objective of this report is to assess the effect of discontinuation. We now report the change in BMD after treatment was discontinued following 2-4 years of therapy with ALN or estrogen/progestin (E/P). Healthy postmenopausal women (n=1609), aged 45-59 years, mean T-score spine BMD -0.8 were initially randomized to ALN 2.5 or 5 mg daily, or PBO (stratum 1 and 2), or E/P (stratum 1 only). After 2 or 4 years, ALN was switched to PBO in a portion of women. E/P women were off therapy in Years 5 and 6. BMD was measured at the lumbar spine, hip, forearm and total body at baseline, and then annually. Percent change during Years 5 and 6 was used to assess the resolution of effect. Women in stratum 1 who previously received E/P for 4 years generally had significantly greater mean BMD loses at the lumbar spine (-8.3%), hip sites (TH, -5.5%; FN, -6.1%; T, -7.9%), and forearm (-2.8%) during Years 5 and 6 which were greater losses than in those who had received ALN 5 mg for 4 years.

Mean Percent Change in BMD during Years 5 & 6

Treatment	**Lumbar Spine†**		**Total Hip**		**Femoral Neck**		**Trochanter**		**Distal one-third forearm**	
Yr 1-2/3-4/**5-6**	**n**	**%**	**n**	**%**	**N**	**%**	**n**	**%**	**n**	**%**
PBO/PBO/**PBO**	139	-0.72*	138	-0.43	138	-0.88**	138	-0.67*	138	-1.34***
ALN 5/5/**5**	96	0.02	94	0.14	94	0.34	94	0.57	95	-0.45
ALN 5/5/**PBO**	88	-2.07***	89	-1.85***	89	-1.58***	89	-1.71***	89	-1.93***

Within Group: * p≤ 0.05 ** p≤ 0.01 *** p≤ 0.001; PBO, Placebo daily; ALN 5, Alendronate 5 mg daily

Bone loss resumes when ALN 5 mg daily is discontinued after 4 years albeit at a rate slower than that following E/P therapy. BMD at the end of 6 years remained significantly higher in women who previously received alendronate 5 mg for 4 years than in those who were never treated with alendronate.

[1]Manufactured by Merck & Co., Inc., Whitehouse Station, NJ
[2]Hosking et al. NEJM 338:485-92, 1998.
[3]Ravn P, et al. Ann Intern Med 131:935-42, 2000

Disclosures: ***M. McClung****, Merck & Co., Inc. 2, 5.*

1038

Non-Vertebral Fracture Benefit from Oral Ibandronate Administered Daily or with a Unique Drug-Free Interval: Results from a Pivotal Phase III Study in postmenopausal osteoporosis (PMO). R. Recker[1], J. A. Stakkestad*[2], T. Weber[3], S. Cohen[4], P. Delmas[5], R. Schimmer*[6], P. Mahoney*[6], J. Kilbride*[6]. [1]Creighton University School of Medicine, Omaha, NE, USA, [2]CECOR AS, Haugesund, Norway, [3]Duke University Medical Center, Durham, NC, USA, [4]Metroplex Clinical Research Center, Dallas, TX, USA, [5]Hôpital Edouard Herriot, Lyon, France, [6]F. Hoffmann-La Roche Ltd, Basel, Switzerland.

Although effective, current oral bisphosphonates are associated with relatively stringent dosing requirements that may be inconvenient to some patients, potentially reducing compliance and jeopardizing therapeutic outcome. Intermittent oral dosing may provide a more convenient option. Recent results from a large double-blind, multinational study (BONE: Bonviva® Osteoporosis Trial in North America and Europe) demonstrated that oral ibandronate, given daily or intermittently with a dosing interval of >9 weeks, significantly reduces vertebral fracture (VF) risk in women with established PMO (Delmas P, et al. IOF World Congress on Osteoporosis 2002; abstract O37). In this study, 2,946 patients (aged 55-80 years, at least 5 years since menopause) with PMO (1-4 prevalent VFs, lumbar spine bone mineral density [BMD] T-score<-2.0 SD) were randomized to oral ibandronate either daily (2.5mg) or intermittently (20mg every other day for 12 doses at the start of each 3-month cycle) or placebo for 3 years. All patients received daily oral calcium (500mg) and vitamin D (400IU). Both ibandronate regimens provided significant BMD increases at the lumbar spine and hip versus placebo and reduced markers of bone turnover to within the range of premenopausal levels. VF risk was significantly reduced by 62% (p=0.0001) and 50% (p=0.0006) with the daily and intermittent regimens, respectively, over 3 years. No statistically significant reduction was seen in non-VFs. However, the study population was at low risk for such fractures, with a minority of women (30.5%) having low femoral neck BMD at baseline (T-score ≤-2.5 SD), and >30% of patients having a femoral neck BMD T-score >-1.6 SD. Daily and intermittent oral ibandronate reduced the incidence of clinical fractures by 66% (p=0.0058) and 50% (p=0.0461) and non-VFs by 69% (p=0.013) and 37% (p=0.22), respectively, relative to placebo in a higher-risk subgroup (femoral neck BMD T-score >-3.0 SD). Thus, daily and intermittent oral ibandronate significantly reduced the risk for new morphometric and clinical VFs. The daily regimen provided significant reduction in the incidence of non-VFs in a higher-risk subgroup, even though the overall population was at low risk for non-VFs. These results support the potential of ibandronate to become an important alternative to current treatments in PMO.

1039

Effects of Parathyroid Hormone, Alendronate, or Both on Bone Density in Osteoporotic Postmenopausal Women. R. Neer, A. Hayes*, A. Rao*, J. Finkelstein. Endocrine Unit, Mass. General Hospital, Boston, MA, USA.

Once-daily parathyroid hormone (PTH) administration increases bone formation and bone mineral density (BMD) and reduces vertebral and non-vertebral fractures in osteoporotic postmenopausal women, but does not eliminate fragility fractures. Because PTH also increases bone resorption, combining it with an anti-resorptive agent may enhance its effectiveness. To test this hypothesis, we randomly assigned 93 such women whose lumbar spine and/or femoral neck BMD T-score was ≤ minus 2.0 to receive alendronate 10 mg orally daily (ALN, n=31), PTH 40 ug sc daily (PTH, n=31), or BOTH (n=31) for 30 months. PTH treatment started at month 6. All women had normal serum PTH, 25-OH D, and TSH levels at entry. None had other disorders that (or took medications that) affect bone metabolism or BMD. Calcium intake was maintained at 500-1500 mg/day and serum 25-OH vitamin D was maintained >15 ng/mL. BMD of the posterior-anterior lumbar spine, proximal femur, radius diaphysis, and total body (without head region) were measured every 6 months by DXA (Hologic 4500A). To date, 53 women (n=19, 19, and 15 receiving ALN, PTH, or BOTH, respectively) have completed at least 12 months of therapy. Mean (±SD) percent changes in BMD and serum alkaline phosphatase to month 12 are:

Group	Vertebrae	Total Hip	Radius Diaphysis	Total Body	Alk P'tase
ALN	4.7 ± 3.3	0.9 ± 5.3	2.2 ± 2.9	2.1 ± 2.8	- 18 ± 15
PTH	7.5 ± 5.0	0.1 ± 7.5	- 2.2 ± 3.1 *	0.5 ± 4.1	96 ± 61 **
BOTH	7.3 ± 2.3	3.6 ± 6.2	0.1 ± 3.0	2.5 ± 2.9	6 ± 25

* p < 0.05 vs. ALN * * p < 0.01 vs. ALN

Adding ALN reduced the PTH-induced increase in serum alkaline phosphatase, reduced the incidence of PTH-induced mild, transient, hypercalcemia, and did not alter PTH's effects on vertebral BMD (substantially trabecular bone). The superior changes in total hip, radius diaphysis, and total body BMD suggest that ALN prevents PTH-induced losses of cortical bone mineral. Co-administration of PTH+ALN illuminates bone resorption-formation interactions; prolonged co-administration is likely to improve the treatment of postmenopausal osteoporosis.

Disclosures: ***R. Neer****, Eli Lilly, Inc. 5, 8; Merck, Inc. 5, 8.*

1040

Combination Therapy for Prevention/Treatment of Osteoporosis in Elderly Women: A Randomized, Double-Blind, Placebo-Controlled, NIH-Sponsored Clinical Trial. S. L. Greenspan[1], N. M. Resnick*[2], R. A. Parker*[3]. [1]Osteoporosis Prevention & Treatment Center, University of Pittsburgh, Pittsburgh, PA, USA, [2]Division of Geriatric Medicine, University of Pittsburgh, Pittsburgh, PA, USA, [3]Biometrics Center, Beth Israel Deaconess Medical Center and Harvard Medical School, Boston, MA, USA.

Although antiresorptive agents have been shown to increase bone mass, there are few head to head comparisons of single agents, combination therapy, or their impact on unselected community-dwelling, elderly women with or without a uterus. Four-hundred-eighty-five women age 65 or older (65-91 years, mean 72±5 years) from the Boston area with a low bone mass entered a 3-month, open-label run-in with hormone replacement therapy (HRT). Three-hundred-seventy-three completers were randomized into a double-blind, placebo-controlled, 3-year trial with 1) Prempro® or Premarin® (HRT), 2) alendronate (ALN) 10 mg/day, 3) HRT + ALN (COMB), or 4) placebo (PLB). All received supplementary calcium and vitamin D. Results are presented as mean±SEM of percent changes at 3 years analyzed on an intention to treat basis.

Percent Bone Mineral Density (BMD) Increase from Baseline

	Total Hip***	Trochanter**	Femoral Neck***	PA Spine***	Lateral Spine***
HRT	3.0±0.5#	4.0±0.7#	1.8±0.5#	6.8±0.6#	7.1±0.8#
ALN	4.1±0.4#	5.4±0.6#	2.6±0.5#	7.4±0.6#	8.4±0.8#
COMB	5.4±0.4#	6.9±0.6#	3.6±0.5#	9.2±0.7#	10.3±0.8#
PLB	-0.8±0.5	-1.0±0.6	-0.7±0.6	0.9±0.5#	1.2±0.7
COMB vs. HRT	2.4±0.6***	2.9±0.9***	1.8±0.7*	2.3±0.9**	3.3±1.1**
COMB vs. ALN	1.3±0.6*	1.5±0.8	1.0±0.7	1.8±0.9*	2.0±1.1

# P < 0.05 vs baseline * P < 0.05, ** P < 0.01, *** P <0.001 between all groups or between pairs of groups

There were no statistically significant differences between those who discontinued during run-in and those who were randomized. Baseline clinical characteristics, adverse events and compliance were similar across groups, with 90% retention at 3 years. BMD increased at all sites in all treatment groups, with the greatest increase in the COMB group. Although the BMD gain in the ALN group was greater at all sites compared to HRT, there were no statistically significant differences between these two groups. BMD at the spine and hip were higher in women in the COMB group compared with women in the HRT or ALN groups. We conclude that: 1) unselected elderly women do well on HRT, ALN, or COMB, 2) after 3 years, gains in BMD in women on HRT or ALN were similar, and 3) COMB provides a significantly greater increase in BMD than does HRT or ALN alone. These data support the need for a large trial powered to assess the relative efficacy in fracture reduction with combination therapy.

1041

Improved 3-Dimensional Microstructure of Cancellous and Cortical Bone in a Multicenter, Double-Blind, Randomized and Placebo Controlled Study of Teriparatide [rhPTH(1-34)]. Y. Jiang[1], J. Zhao[1], E. F. Eriksen[2], O. Wang*[2], H. K. Genant[1], B. H. Mitlak[2]. [1]Osteoporosis and Arthritis Research Group, University of California, San Francisco, CA, USA, [2]Lilly Research Laboratories, Eli Lilly and Company, Indianapolis, IN, USA.

Teriparatide injection (rDNA origin) [rhPTH(1-34)] significantly increased areal bone mineral density (aBMD) at the lumbar spine and proximal femur, had no effect or decreased aBMD at the distal radius, and decreased both vertebral and nonvertebral fractures in a Fracture Prevention Trial of postmenopausal women with osteoporosis (Neer et al., NEJM 2001). In this study, the effects of teriparatide were measured on cancellous and cortical bone from iliac crest bone biopsies from a subset of women enrolled in the Fracture Prevention Trial. For the 3-dimensional micro-computed tomography (3DμCT), paired biopsies were obtained from women in the placebo group (n=19) and the combined teriparatide treated group [20 μg (n=18) and 40 μg (n=14)] at baseline and after 18 ± 5 months (mean ± SD) (range 12-24 months). The 3D cancellous and cortical structural parameters were measured directly using a Scanco μCT with isotropic resolution of 17 μm^3, without stereological model assumptions as in 2D histomorphometry. These parameters provide an estimate of bone biomechanical properties and mechanical competence of bone. All specimens underwent blinded assessment. Compared to placebo, teriparatide treatment significantly increased cancellous bone volume fraction (BV/TV; mean ± SEM) (60% ± 26% vs. -2% ± 10%, P=0.075; ΔBV/TV, 0.025 ± 0.014 vs. -0.024 ± 0.015, P=0.033), decreased the cancellous structure model index (-12% ± 7% vs. 25% ± 15%, P=0.016), and increased cancellous connectivity density (40% ± 13% vs. -5% ± 9%, P=0.021) and cortical bone thickness (29% ± 9% vs. -2% ± 7%, P=0.029), teriparatide vs placebo, respectively. There was no significant difference in cortical porosity between placebo and teriparatide-treated groups. In summary, teriparatide treatment resulted in an increase in cancellous bone volume and connectivity, shifted the trabeculae towards a more plate-like structure, and increased the thickness of cortical bone without increasing cortical porosity. These changes in cancellous and cortical bone morphology contribute to the increased biomechanical competence and may explain the reduced vertebral and nonvertebral fracture incidence demonstrated after teriparatide treatment.

Disclosures: ***Y. Jiang****, Eli Lilly and Company 2.*

1042

Prevention of Bone Loss After Cardiac Transplantation with Alendronate or Calcitriol: Efficacy and Safety. E. Shane[1], V. Addesso*[1], P. Namerow*[1], S. Maybaum*[1], R. Staron*[1], S. Lo*[1], M. Zucker*[2], S. Pardi*[2], D. Mancini*[1]. [1]Columbia University, New York, NY, USA, [2]Beth Israel Medical Center, Newark, NJ, USA.

The first year after cardiac transplantation (CTX) is characterized by high rates of bone loss and vertebral fracture (VF). Bone mineral density (BMD) declines 5% -10% at the spine (LS) and femoral neck (FN); VF incidence ranges from 18% - 35%. To prevent this important complication of CTX, we conducted a 1-year, double-masked, randomized clinical trial (RCT) in which the efficacy and safety of alendronate (ALN; 10 mg QD) and calcitriol (1,25D; 0.25 μg BID) were evaluated. Subjects (n=149) were randomized to ALN (n=74) or 1,25D (n=75), 21 +/- 11 days after CTX. Bone loss was compared between treatment groups and to a nonrandomized group of subjects (CON; n=25) who declined to participate in the RCT. All participants received daily calcium (Ca; 1000 mg) and vitamin D (1000 IU) and immunosuppressive therapy (prednisone, cyclosporine). Baseline BMD was similar at the LS (ALN, 1.047 ± 0.15; 1,25D, 1.059 ± 0.17; CON, 1.087 ± 0.17 g/cm2), FN (ALN, 0.837 ± 0.16; 1,25D, 0.836 ± 0.15; CON, 0.819 ± 0.12 g/cm2) and total hip (TH; data not shown). The 3 groups were similar with respect to gender, race, age, renal function, serum /urine Ca. Bone loss (% change from baseline at 1 year +/- S.E.M.) was analyzed by intent-to-treat (ITT) and on a subset (n=104) verified to have completed the RCT on study medications (VC). Bone loss was minimal in treated groups and did not differ between ALN and 1,25D. Both sustained significantly less bone loss than CON (Table 1).

Table 1

SITE/ANALYSIS	ALN	1,25D	CON
LS/ITT	-0.7 +/- 0.5	-0.9 +/- 0.7	-2.7 +/- 1.0
LS/VC *	+0.7 +/- 0.5	+0.5 +/- 1.2	-2.7 +/- 1.0
FN/ITT **	-1.4 +/- 0.6	-2.0 +/- 0.8	-5.9 +/- 1.0
FN/VC ***	-1.2 +/- 0.8	-0.3 +/- 0.9	-5.9 +/- 1.0
TH/ITT *	-1.4 +/- 0.4	-2.2 +/- 0.6	-4.1 +/- 1.0
TH/VC **	-0.8 +/- 0.5	0.9 +/- 0.5	-4.1 +/- 1.0

*p≤.04; **p≤.002; ***p≤.0001 compared to CON

The 3 groups did not differ by prednisone or cyclosporine dose, hospitalizations, infections, rejections or GI symptoms. However, elevated urine Ca (> 300 mg/g), serum creatinine (> 3 mg/dl) and low creatinine clearance (< 30 ml/min) were more frequent in 1,25D than ALN (p=0.04 to 0.02). In summary, subjects randomized to ALN or 1,25D did not sustain significant bone loss, nor did rates of bone loss differ between ALN and 1,25D groups at any site or time. In contrast, CON subjects sustained significant bone loss at all sites. We conclude that both ALN and 1,25D prevent bone loss after CTX. However, the potential for deleterious effects of 1,25D on urine Ca excretion and renal function and the need for biochemical monitoring makes ALN a more convenient and safer choice in this setting.

Disclosures: ***E. Shane****, Merck 2.*

1043

Cumulative Effects of Calcium Supplementation and Physical Activity on Bone Accretion in Prepubertal Period: A Randomized Double-Blind Placebo-Controlled Trial. D. Courteix[1], C. Jaffré*[1], E. Lespessailles[2], C. Benhamou[2]. [1]Inserm ERIT-M 0101 and LPM University of Orléans, Orléans, France, [2]Inserm ERIT-M 0101, Orléans, France.

High calcium intake (Ca+) during childhood has been suggested to increase bone mass accrual. Physical activity (PA) has been shown to improve the bone mineral density especially during the circumpubertal period of growth. The combined effects of Ca+ and PA are not identified in prepubescent subjects. In a double-blind, placebo-controlled study, 115 healthy prepubertal girls aged 9.9 ± 1.2 yr were randomly allocated two powder products containing either 800 mg of calcium phosphate (Ca+) or not (placebo, Ca-) on a daily basis for 1 yr. The group was composed of 63 sporty (PA+, 7.3 ± 4 $hr.wk^{-1}$) and 50 non active (PA-, 1.2 ± 0.8 $hr.wk^{-1}$) children. The final experiment concerned 4 groups : [PA+,Ca+] n=12, [PA+,Ca-] n=41, [PA-,Ca+] n=10 and [PA-,Ca-] n=21. Areal bone mineral density (BMD) at 6 skeletal sites and body composition were determined by dual-energy x-ray absorptiometry. Bone age was calculated and the daily spontaneous calcium intake was assessed in each subject by a frequency questionnaire. All the tests were performed at baseline and 1yr by the same person. The 1-year bone gain was assessed by a 2 factors (PA and Ca) ANOVA with repeated measures (baseline, 1yr) analysis. At each investigation there was no difference between groups for bone age, height and weight. Spontaneous Ca intake was the same in each groups at baseline then the Ca+ groups had a significant greater intake for the period of investigation (1783 ± 499 vs. 972 ± 313, $p<0.001$). The sporty girls were found leaner than the controls at each test. BMD gains were significantly greater in [PA+,Ca+] than in other groups at the Total body (+6.3 %, $p<0.05$), lumbar spine (+11 %, $p<0.05$), Femoral neck (+8.2 %, $p<0.02$), Ward's triangle (+9.3 %, $p<0.01$). There was no difference between the other groups. In conclusion these data suggest that 1) the calcium supplementation increases the effect of physical exercise on bone mineral acquisition in prepuberty, 2) the calcium supplementation without physical activity is unable to improve the BMD acquisition during this period. Physical exercise that is known to stimulate the bone accretion needs a high calcium intake to be completely efficient. By contrast calcium supplementation without physical activity is unable to stimulate the BMD gain. In such a situation it has been shown that only the subjects characterised by a low spontaneous calcium intake can draw benefit from the calcium supplement. These results indicate that both physical activity and calcium intake should be encouraged at a prepubertal age in order to increase bone density.

1044

Microarray Analyses Identified NF-kB to Be the Target of Osteopontin-Dependent Regulation of Gene Expression in the Bone of Mice Subjected to Tail-Suspension. M. Ishijima[1], Y. Ezura[2], K. Tsuji[1], S. R. Rittling[3], H. Kurosawa*[4], D. T. Denhardt[3], M. Emi*[2], A. Nifuji[1], M. Noda[1]. [1]Molecular Pharmacology, Tokyo Medical and Dental University, Tokyo, Japan, [2]Nippon Medical School, Kawasaki, Japan, [3]Rutgers University, Piscataway, NJ, USA, [4]Juntendo University, Tokyo, Japan.

Osteopontin-null (OPN-/-) mice showed resistance to unloading-induced bone loss (J Exp Med 2001, J Bone Miner Res 2002). However, molecular mechanisms underlying the phenomenon have not been known. To obtain further insight into the role of OPN in mediating mechanical stress effect on bone, we carried out microarray analyses on the genes expressed in bone marrow in the hindlimbs of mice subjected to tail-suspension for 1 week. After tail-suspension, mRNA was obtained from bone marrow cells of the femora. Complementary DNA pools obtained based on the RNA obtained from bone marrow cells of the femora were subjected to microarray analysis. Genes regulated by tail-suspension in both wild type and OPN-/- mice were identified and the specific gene expression pattern due to the presence or absence of OPN in response to tail-suspension was investigated. Unloading induced reduction in bone mass in wild type, while such reduction of bone mass in response to unloading was not observed in OPN-/- mice, used for the microarray analyses. Transcription of ten genes was enhanced by tail-suspension in wild type but not in OPN-/- mice. On the other hand, transcription of 4 genes was enhanced by tail-suspension in OPN-/- but not in wild type mice. Among these genes, expression levels of NF-kB p105 subunit gene in bone marrow cells of the femora were enhanced by tail-suspension in wild type mice. In contrast, they were not altered in OPN-/- mice. Furthermore, expression levels of Bax gene were enhanced by tail-suspension in bone marrow cells of the femora in OPN-/- mice, however such enhancement was not observed in wild type mice after tail-suspension. These observations were confirmed by RT-PCR analyses in both wild type and OPN-/- mice. Expression levels of bone sialoprotein (BSP), which is also one of the bone matrix proteins containing an RGD-sequence, were enhanced by tail-suspension in both wild type and OPN-/- mice. However, the enhancement rate was significantly more in OPN-/- mice compared to that in wild type mice. While p53 mRNA expression was up regulated in bone marrow cells by tail-suspension in wild type mice as reported previously, this up-regulation of p53 gene expression by tail-suspension was no longer observed in OPN-/- mice. In conclusion, OPN plays a crucial role in mediating signals of mechanical stress in bone marrow cells through the regulation of NF-kB and apoptosis related genes.

1045

Osteoprotegerin Mitigates Spaceflight-Induced Changes in Mouse Bone Mass, Density and Mineral Composition. T. A. Bateman[1], S. Morony[2], V. L. Ferguson[1], S. J. Simske*[1], D. L. Lacey[2], K. S. Warmington*[2], Z. Geng[2], H. L. Tan[2], V. Shalhoub[2], C. R. Dunstan[2], P. J. Kostenuik[2]. [1]BioServe Space Technologies, University of Colorado, Boulder, CO, USA, [2]Metabolic Disorders, Amgen Inc., Thousand Oaks, CA, USA.

The effects of microgravity on mouse bone have not been previously studied. This experiment characterized the effects of spaceflight (SF) on the skeleton of mice treated with or without OPG, a protein that blocks osteoclast formation and activity. 10-week-old female C57/B6J mice (n=12/group) received a single injection (SC, 24 h pre-launch) of either OPG (20mg/kg) or vehicle (VEH). Mass and age-matched ground control (GC) mice received similar treatments. An age-matched group was sacrificed at launch and served as baseline (BL) controls. 24 SF mice spent 12-days in orbit on Space Shuttle flight STS-108. Upon landing, SF/VEH femur dry mass was lower compared to GC/VEH mice ($p<0.001$: 7%). OPG significantly increased femoral dry mass in both SF and GC conditions ($p<0.001$: 12% 9%, respectively). Compositional analysis of these femurs indicated that both SF and OPG had significant effects on the mineral mass of bone (Min-M). Whole bone Min-M and percent mineral composition (%Min) were lower in SF/VEH mice compared to GC/VEH ($p<0.01$: 10% 3%, respectively). SF/OPG had a greater Min-M and %Min than SF/VEH ($p<0.001$: 15% 3%, respectively). Organic bone mass (Org-M) was less influenced by SF and OPG. SF decreased Org-M by a non-significant 3% (vs. GC/VEH) and OPG increased Org-M by 6% (vs. SF/VEH: $p<0.05$). SF/VEH had lower epiphysis %Min compared to BL ($p<0.01$: 3%), suggesting a decline in material properties from pre-flight conditions. From a structural perspective, femur mid-diaphysis cross-sectional area was reduced for SF/VEH compared to GC/VEH ($p=0.05$), though changes in principle moments of inertia were not significant. pQCT analysis of the lumbar vertebra (L5) revealed a relative deficit in both total and cortical BMD in SF/VEH mice compared to GC/VEH ($p<0.01$). OPG blocked these SF-induced changes ($p<0.01$). Serum and mRNA (humeral diaphysis) analyses suggest relative changes in bone formation and resorption that may have contributed to the SF-induced osteopenia. A significant decline in mRNA expression of osteocalcin combined with a trend towards lower serum osteocalcin levels indicates a reduction in bone formation. Increased bone resorption in SF mice was suggested by a trend towards increased mRNA expression of the pro-resorptive cytokine RANK ligand with no changes in OPG mRNA expression. These data demonstrate that spaceflight causes a relative osteopenia in mice that alters bone material properties to a greater degree than structural properties. A single OPG treatment prevented these changes.

Disclosures: ***T.A. Bateman****, Amgen Inc. 2.*

1046

Rest-Inserted Loading: A Mild Yet Potently Osteogenic Stimulus for the Aged Skeleton. S. Srinivasan, S. C. Agans*, N. Y. Moy*, S. L. Poliachik*, T. S. Gross. Orthopaedics and Sports Medicine, University of Washington, Seattle, WA, USA.

Mechanical loading has the potential to be perceived as an intensely anabolic stimulus by bone cells and tissue. However, the osteogenic response to mechanical stimuli is markedly suppressed in the aged skeleton and, in particular, mild and low-magnitude forms of physical activity have proved ineffective in building bone mass in the elderly. We recently found that inserting rest (or unloaded) intervals between mechanical loading cycles transformed non-stimulatory low-magnitude regimens into potent osteogenic stimuli in young animals. Here, we extend our observations and test the hypothesis that low-magnitude rest-inserted mechanical loading is osteogenic in the aged skeleton. The right tibiae of aged C57BL/6 mice (21 Months, n=18) were subject to a 50 cycle/day, 2-week loading protocol utilizing the non-invasive murine tibia model. Animals were randomly assigned to one of three groups: a) low-magnitude repetitive loading (inducing peak normal strain of 900 με at the tibia mid-shaft), b) high-magnitude repetitive loading (inducing 2200 με at the mid-shaft), and c) rest-inserted loading wherein a 10-s rest interval was inserted between each of 50 low-magnitude (900 με peak strain) load cycles. Activation of periosteal bone formation at the tibia mid-shaft was examined via calcein incorporation. The contralateral control tibiae in the aged animals exhibited minimal mean (± S.E.) periosteal bone formation (0.03 ± 0.01 $\mu m^3/\mu m^2/d$) and was not different between groups ($p=0.49$). While exposure to 50 cycles/d of high-magnitude loading (almost 2.5 fold the strain magnitude induced via low-magnitude loading) was sufficient to enhance bone formation compared to controls (0.12 ± 0.03 $\mu m^3/\mu m^2/d$, $p = 0.03$), low-magnitude repetitive loading (similar in magnitude to that encountered during mild functional activity) did not significantly enhance bone formation (0.075 ± 0.04 $\mu m^3/\mu m^2/d$, $p=0.12$). In contrast, inserting10-s of rest between each of 50 low-magnitude load cycles significantly enhanced bone formation compared to controls (0.14 ± 0.04 $\mu m^3/\mu m^2/d$, $p=0.05$), an 87% increase compared to low-magnitude repetitive loading. Our results suggest that rest-inserted loading provides a subtle yet potently osteogenic stimulus that enables sustained activation of the aged periosteum despite the limited availability of osteoprogenitor cells and the increased propensity for fully differentiated osteoblasts in aged bone tissue to undergo apoptosis. Given the ease of implementation of this novel stimulus (inserting an unloaded rest interval between load cycles), low-magnitude rest-inserted loading holds promise for building bone mass in the frail elderly.

1047

A Genetic Compensatory Mechanism for Preventing Disuse Related Bone Loss. S. Judex[1], R. Garman*[1], M. Squire*[1], L. Donahue[2], C. Rubin[1]. [1]Biomedical Engineering, SUNY Stony Brook, Stony Brook, NY, USA, [2]The Jackson Laboratory, Bar Harbor, ME, USA.

Despite the clear impact of subtle genetic variations on achieving and retaining bone quantity and quality, it is less clear to what extent the genome influences the response of the skeleton to catabolic pressure. We have recently demonstrated a genetic basis for the sensitivity of trabecular bone to the removal of its mechanical environment; hindlimb suspension significantly reduced bone formation rates (BFR) in the proximal tibia of genetically distinct BALB/cByJ (BALB) mice but not in C57BL/6J (B6) or C3H/HeJ (C3H) mice. Here, we used micro-computed tomography (μCT) to assess the structural impact of this catabolic stimulus in three strains of mice. Adult (16wk) B6, BALB, and C3H mice were subjected to either hindlimb suspension or free cage activity (n~10 per group) in protocols up to 3wk. Upon sacrifice, distal femurs were scanned at a resolution of 11μm and indices of bone quantity and architecture were computed for both metaphyseal trabecular bone and its surrounding cortical shell. Mechanical disuse severely reduced fractional trabecular bone volume by 57% ($p<0.001$) in BALB mice while no significant amount of trabecular bone tissue was lost in either C3H or B6 mice. This large decrease in bone quantity was accompanied by compromised bone architecture as indicated by a 35% decrease in connectivity density ($p<0.03$). In contrast to the genetically dependent sensitivity of trabecular bone, the endocortical envelope significantly increased in size in all three strains of mice (between 9% and 18%, $p<0.05$). The larger endocortical envelope led to a significant smaller cortical bone volume in B6 (-8%, $p<0.008$) and BALB (-18%, $p<0.001$) mice as their periosteal envelopes were not affected by disuse. In C3H mice, however, disuse concomitantly increased the volume of the periosteal envelope by 10% ($p<0.02$), leaving cortical bone volume unchanged in this strain. These data indicate that the efficacy of a strongly catabolic stimulus heavily relies on genetic makeup, both for trabecular and cortical bone. C3H mice displayed a unique genetic mechanism that was able to compensate for the loss of bone at the endocortical surface with increased bone formation at the periosteal surface, demonstrating bone's ability to orchestrate a complex response to the loss of functional weigthbearing. Extrapolated to the genetically heterogeneous human population, our data may explain the large individual variability in bone loss observed during bedrest, spaceflight, or aging. Current work is exploiting the differences in mechanosensitivity between these three strains of mice to identify the genetic basis of bone's adaptive response to the loss of functional weightbearing.

1048

Effect of Gender and Estrogen on the Skeletal Sensitivity to Mechanical Loading. T. L. N. Jarvinen*[1], P. Kannus*[2], I. Pajamaki*[1], T. Vuohelainen*[1], J. Tuukkanen[3], M. Jarvinen*[1], H. Sievanen*[2]. [1]Dept. of Surgery, University of Tampere, Tampere, Finland, [2]UKK Institute, Tampere, Finland, [3]University of Oulu, Oulu, Finland.

The aim of this study was initially to evaluate whether there is any difference in the skeletal responsiveness to mechanical loading between female and male rats. In experiment #1, 5-week-old littermates of 25 male and 25 female rats were randomised into either free-cage activity (CTR) or treadmill training (EX) for a period of 14 weeks. Using peripheral quantitative computed tomography (pQCT) and mechanical testing of the femoral neck, we observed that the skeletal responsiveness to external loading was clearly lower in females than in males. Also, relative to the mechanical demands placed on the skeleton, the bones of the young female rats were considerably denser (>50%) than those of the males. To ensure that the observed changes (growth/puberty-related condensation of female bones and the lower responsiveness to loading) were not restricted only to the rapid period of growth, we repeated the first experiment with 33-week-old rats and observed virtually identical responses in these mature rats. To follow these findings further, we hypothesized that if estrogen was attributable for the observed deposition of extra stock of mineral into female bones and the subsequent lower responsiveness to mechanical loading, then withdrawal of estrogen should not only result in a reduced bone density, but also an increased response to loading. Accordingly, in experiment #3, 60 littermates of 3-week-old female rats were first SHAM-operated or ovariectomized (OVX) and then further randomized to EX- or CTR-groups, respectively. At the end of a 16-week intervention, our pQCT and mechanical testing analysis showed not only the anticipated effect of reduced bone density in the OVX rats (~ -20% vs. SHAM), but also the hypothesized better response to mechanical loading in these estrogen-depleted rats. In conclusion, our series of three experiments suggest that as such estrogen has very little primary effect on the sensitivity of female bone to mechanical loading, but rather deposits extra stock of mineral into female bones in puberty. This estrogen-driven extra condensation of the female skeleton persists into adulthood, simultaneously damping the responsiveness of the female skeleton to loading.

The skeletal responsiveness (EX vs. CTR, in %) of rats to mechanical loading in experiments #1-3.

	CSA	BMC	vBMD	Fmax
Female, young	+3.0	+4.2	-0.6	+4.7
Male, young	+25**	+27***	+10	+28**
Female, mature	+2.1	+3.4	+2.5	-1.1
Male, mature	+10	+18	+23**	+27*
SHAM	-3.5	-0.4	+4.4	-4.2
OVX	+9.1	+12*	+9.6	+16*

1049

Novel Role of Vitamin D in Electrolyte, Volume and Blood Pressure Homeostasis: 1,25-Dihydroxyvitamin D3 Is a Negative Endocrine Regulator of the Renin-Angiotensin System. Y. Li[1], J. Kong*[1], M. Wei*[1], Z. Chen*[2], S. Liu*[3], L. Cao*[1]. [1]Medicine, University of Chicago, Chicago, IL, USA, [2]Anesthesiology, Washington University, St. Louis, MO, USA, [3]Biomedical Engineering, Northwestern University, Evanston, IL, USA.

The renin-angiotensin system plays a central role in the regulation of blood pressure, electrolyte and volume homeostasis. Inappropriate activation of the renin-angiotensin system has been implicated as one major potential risk factor for hypertension, heart attack and stroke. Clinical studies have revealed an inverse relationship between plasma 1,25-dihydroxyvitamin D3 [1,25(OH)2D3] concentrations and the blood pressure and/or the plasma renin activity in both normotensive men and patients with essential hypertension, and vitamin D treatment has been shown to reduce blood pressure as well as plasma renin activity and angiotensin II (Ang II) levels in hypertension patients. However, the mechanism is unknown. To explain these observations we hypothesize that vitamin D is a negative regulator of renin expression in vivo, and have tested this hypothesis in animal models and cell cultures. We found that renin expression and plasma Ang II production were increased several fold in vitamin D receptor (VDR) null mice, leading to hypertension, cardiac hypertrophy and increased water intake. The elevation of blood pressure in VDR null mice was abolished by captopril, an angiotensin-converting enzyme inhibitor, confirming that the rise in blood pressure is indeed due to elevation of Ang II. However, the high basal renin level does not abrogate the salt- and volume-sensing mechanisms that control renin synthesis. In wildtype mice, inhibition of 1,25(OH)2D3 biosynthesis also led to an increase in renin expression, whereas injection of 1,25(OH)2D3 reduced renin expression. We further showed that the vitamin D regulation of renin expression is independent of calcium metabolism, since the renin up-regulation was still detected in pre-weaned normocalcemic VDR null mice as well as in adult VDR null mice whose serum calcium had been normalized by dietary treatment, but not in hypocalcemic Gcm2 null mice. Furthermore, we demonstrated that 1,25(OH)2D3 markedly suppressed renin mRNA expression as well as renin gene promoter activity in cell cultures by a VDR-mediated mechanism. These data provide the first direct evidence that 1,25(OH)2D3 is a novel and potent negative endocrine regulator of the renin-angiotensin system, and plays a critical role in maintaining the homeostasis of electrolytes, volume and blood pressure. They also have implications for the potential use of vitamin D analogues as preventive or therapeutic anti-hypertension agents.

1050

WINAC(WSTF Including Nucleosome Assembly Complex) Is a Novel Chromatin Remodeling Complex Modulating Vitamin D Receptor(VDR)Transactivation. H. Kitagawa[1], J. Yanagisawa*[2], R. Fujiki*[1], D. Matsui*[1], T. Matsumoto[3], S. Kato[2]. [1]Nuclear Information, IMCB, Tokyo, Japan, [2]Nuclear Information, IMCB,CREST, Tokyo, Japan, [3]First Department of Internal Medicine, University of Tokushima school of Medicine, Tokushima, Japan.

Many complexes interact with nuclear receptors for their ligand-dependent transactivation through modulating chromatin structure in the promoters of a set of target genes. Distinct classes of co-regulator complexes like DRIP/TRAP complex, p160 family complex, and TRRAP/GCN5 complex are shown to interact with nuclear receptors in a ligand-dependent way. But still other unknown complexes are assumed to support VDR transactivation in different ways. Using GST fused VDR ligand binding domain (LBD) as a bait, we purified nuclear complexes associated with liganded VDR-LBD from HeLa nuclear extracts, and identified WSTF(Williams syndrome transcription factor) as one of the interactants. WSTF has been reported to be one of the candidate genes causing Williams syndrome, which often accompanies infantile hypercalcemia. To examine WSTF function in VDR transactivation, we purified a VDR interacting WSTF complex using Flag-tagged WSTF stably expressing cells. Using MALDI TOF-MS and Western blotting, we found that the complex designated 'WINAC' is a novel SWI/SNF related ATP dependent chromatin remodeling complex composed of at least 12 components. In vitro chromatin reconstitution and disruption assay showed that this complex modifies chromatin configuration through recognizing VDR in a ATP-dependent way. A ChIP analysis showed that this complex is recruited on some VDR target gene promoters in a ligand- independent way and regulates vitamin D metabolism through VDR-mediated target genes expression. Some components of the WINAC are shared with those of other complexes involved in DNA replication, suggesting that this complex has multiple functions by bridging multiple complexes. Finaly we confirmed that VDR transactivation is abnormal due to low expression of WSTF in Willliams syndrome patients using primary culture cells of their skin fibroblasts. These results provide a new insight into the transcriptional mechanism of VDR ,the calcium metabolism through VDR transactivation, and the target gene therapies of Williams syndrome.

1051

Activation of PKC by Gαq Results in Osteopenia by Blocking Osteoblast Differentiation. N. Ogata[1], S. I. Roth*[2], H. Kawaguchi[3], G. V. Segre[1]. [1]Endocrine Unit, Massachusetts General Hospital, Harvard Medical School, Boston, MA, USA, [2]Department of Pathology, Massachusetts General Hospital, Harvard Medical School, Boston, MA, USA, [3]Orthopaedic Surgery, University of Tokyo, Tokyo, Japan.

To examine the role of Gαq-mediated signaling in bone, we generated two independent lines of transgenic (TG) mice that overexpress constitutively-active Gαq (mutation of Q209L) in osteoblasts with a hemagglutinin tag, driven by the 2.3-kb osteoblast-specific, mouse pro-α 1 (I) collagen promoter. Specific expression of the TG was determined by RT-PCR of mRNA extracted from bones of TG mice, but not from other tissues. TG mice were indistinguishable from wild-type (WT) mice at birth. However by 2 weeks of age, they exhibited progressive shortening of their limbs and lower weights (60% of WT), and reduced bone mineral density at 8 weeks (70% of WT). Both long bones and calvariae of TG mice had thinner cortices, consisting predominantly of woven bone, and increased osteocytes with irregular spacing and rounder lacunae. Trabecular bone was markedly reduced and long-bone fractures were common, but osteoid seams were not widened. Bone volume/total volume and bone formation rate/bone surface were reduced to 40% and 10%, respectively, at both 4 and 8 weeks of age compared to WT mice. Neither osteoclast number nor activity (eroded surface/bone surface) were abnormal. In situ hybridization demonstrated reduced expression of osteoblast-related mRNAs and slightly increased expression of Gαq in the bones of TG mice. In vitro, both primary osteoblasts derived from TG neonatal calvariae and bone marrow stromal cells flushed from TG long bones showed significantly reduced collagen synthesis and ALP activity and virtually no mineralization, compared to WT osteoblasts. Osteocalcin gene expression in TG osteoblasts was nearly absent, while type I collagen and osteopontin expression were slightly decreased, indicating that differentiation of TG osteoblasts was blocked. Addition of the PKC inhibitor, GF109203X, to both WT and TG osteoblasts in culture increased ALP activity to nearly the same absolute level. However, [^{3}H]-TdR incorporation by WT and TG osteoblasts was indistinguishable. Overexpression of Gαq in osteoblasts results in severe osteopenia with immature bone and fractures. We propose that Gαq-mediated activation of PKC in WT and TG osteoblasts plays a crucial role in bone formation by inhibiting differentiation of osteoblasts.

1052

Conditional Knockout of *PTHrP* in Osteoblasts Leads to Premature Osteoporosis. D. Miao, B. He*, X. K. Tong*, D. Goltzman, A. C. Karaplis. Medicine, McGill University, Montreal, PQ, Canada.

Intermittent administration of parathyroid hormone-related peptide (PTHrP) in vivo has an anabolic effect on bone. The precise molecular and cellular bases for the anabolic action of PTHrP, however, remain unclear and efforts to elucidate these mechanisms in PTHrP knockout mice have been compromised by the perinatal lethality of these animals. To overcome this obstacle, we have used cell-specific, Cre-mediated recombination in mice to selectively disrupt PTHrP expression only in osteogenic cells, while maintaining normal expression levels of the protein in all other tissues. Toward this objective, PTHrP$^{+/flox}$ (exon 4 of PTHrP flanked by loxP sites) mice carrying the *Cre* recombinase transgene under the control of the 2.3-kb fragment of the murine pro-α1(I) collagen gene promoter (Col I), were crossed with mice homozygous for the floxed PTHrP allele to generate mice with osteoblasts lacking the PTHrP gene (PTHrP$^{flox/flox}$;cre$^{col\ I}$). Serum calcium, PTH and 1,25-dihydroxy vitamin D_3 levels were normal in 6-week-old PTHrP$^{flox/flox}$;cre$^{col\ I}$ mice, compared to PTHrP$^{flox/flox}$ sex-matched littermates (controls). On the other hand, bone density at the femur and tibia, as measured by PIXImus densitometer, was decreased by 6.4% and 9.0%, respectively, in PTHrP$^{flox/flox}$;cre$^{col\ I}$ mice compared to control animals. Trabecular bone volume was also affected, and was decreased by 33% and 36% in femurs and tibiae, respectively, from newborn, and 34% and 47% from 6-week-old PTHrP$^{flox/flox}$;cre$^{col\ I}$ mice. Histomorphometric analysis revealed that osteoblast number and surface, osteoid thickness, and trabecular thickness were all decreased significantly in 6-week-old PTHrP$^{flox/flox}$;cre$^{col\ I}$ mice. This was further substantiated by immunohistochemistry, as areas positive (immunoreactivity in bone matrix and/or osteoblasts) for type I collagen, osteocalcin, and osteopontin staining in the metaphysis of femurs of 6-week-old PTHrP$^{flox/flox}$;cre $^{col\ I}$ mice were reduced compared to their wild type counterparts. Bone formation rate was also reduced, as assessed by histomorphometry following double-calcein labeling. Furthermore, osteoclast number and surface were also significantly reduced. These results unequivocally demonstrate that osteoblast-derived PTHrP exerts anabolic effects in bone by promoting osteoblast function and identify it as a key factor to be targeted in the therapeutic intervention for osteoporosis.

1053

Expression of a Constitutively Active PTH/PTHrP Receptor in Bone Marrow Stromal Cells Leads to Expansion of Hematopoietic Stem Cells in vivo and in vitro. L. M. Calvi[1], G. B. Adams*[2], D. P. Olson*[2], M. C. Knight*[1], F. R. Bringhurst[1], E. Schipani[1], P. Divieti[1], H. M. Kronenberg[1], D. T. Scadden*[2]. [1]Endocrine Unit, Massachusetts General Hospital and Harvard Medical School, Boston, MA, USA, [2]Partners AIDS Research Center and MGH Cancer Center, MGH, Boston, MA, USA.

In severe cases of primary hyperparathyroidism, fibrosis of the bone marrow cavity has been reported, and is associated with anemia in some cases. We recently described transgenic mice (col1-caPPR) in which a constitutively active PTH/PTHrP receptor (caPPR) is expressed under the control of the alpha1(I) collagen promoter. These transgenic mice have increased trabecular bone volume and an expanded stromal-like cell population with a fibrotic appearance. In situ hybridization identifies these stromal-like cells as preosteoblasts at different stages of differentiation. Our goal was to use this transgenic model to study the role of the activated PPR in modulating the ability of bone marrow stromal cells to support hematopoiesis. While the hematocrit of col1-caPPR mice was decreased, as in cases of hyperparathyroidism with marrow fibrosis, the number of hematopoietic stem cells as assessed by both flow cytometric analysis and long-term culture initiating cell (LTC-IC) analysis was surprisingly increased in the bone marrow from transgenic vs normal littermates. In primary bone marrow stromal cell cultures from adult transgenic mice and normal littermates, expression of the transgene was confirmed by Northern blot analysis and in situ hybridization. When normal hematopoietic cells were cultured in the presence of transgenic stromal cells in LTC-IC assays, the frequency of hematopoietic stem cells was significantly increased. In addition, treatment of normal stromal cells with rPTH(1-34) was sufficient to reproduce the enhanced support of the hematopoietic stem cell population. Interestingly, bone marrow stromal cell cultures from transgenic mice had an increased proportion of alkaline phosphatase positive cells, reproducing the increased osteoblastic population seen in vivo. In conclusion, PTH treatment of bone marrow stromal cells increased their ability to support hematopoietic stem cells. Since stromal cells isolated from mice expressing the caPPR only in the osteoblastic lineage also increased support of hematopoietic stem cells, this action of PTH was probably mediated by activation of the PPR in the stromal cell compartment. This surprising effect of activation of the PPR on bone marrow stromal cells points out a novel role of PTH in mediating stroma-hematopoietic cell interactions, and may have important therapeutic implications for the expansion of hematopoietic stem cells in bone marrow transplantation and recovery.

1054

Dramatic High Turnover Osteoporosis and Focal Sclerosis in a TSH (Thyrotropin) Receptor Null Mouse Reveals a Critical Role for TSH as a Negative Regulator of Bone Remodeling. M. Zaidi[1], R. Marians*[1], X. B. Wu[1], S. Dolgilevich*[1], Y. Li*[2], H. Blair[2], T. F. Davies*[1], E. Abe[1]. [1]The Mount Sinai Bone Program and Bronx VA GRECC, New York, NY, USA, [2]University of Pittsburgh, Pittsburg, PA, USA.

We report, for the first time, that TSH receptors (TSHRs) negatively regulate bone remodeling. TSHR null mice generated by disrupting exon 1 of the TSHR gene were profoundly osteoporotic with a marked reduction in bone mineral density at the femur, tibia and lumbar spine. Histological analysis revealed focal sclerosis, woven bone, and disorganized collagen: hallmarks of rapid bone turnover that are reminiscent of pagetic bone. Tetracycline double labeling showed an increased bone formation rate. Osteoblast progenitors in bone marrow cell cultures counted as fibroblastoid and osteoblastoid colony forming units (CFU-F and CFU-OB) were also markedly elevated. Likewise, hematopoetic stem cell cultures showed enhanced TRAP-positive osteoclast formation. Together, the results argue strongly for the TSHR as a negative regulator of osteoblast and osteoclast formation and function. Notably, all of these effects were equally profound in TSHR heterozygotes as in homozygotes indicating a surprising but profound effect on bone of halving the TSHR content. That the bone phenotypes of thyroxine-replete and hypothyroid homozygotic mice were virtually undistinguishable attests further to a direct action of TSHRs on bone remodeling that was not exerted through thyroid hormone action. We next explored the localization of TSHRs to bone cells by following the expression of GFP integrated at the TSHR deletion site. Both CFU-Fs and osteoclast precursors in bone marrow cell cultures derived from TSHR deficient mice showed intense GFP fluorescence. Dual photon confocal scanning microscopy of the inner table of the skull likewise confirmed GFP localization to osteoblasts *in situ*. That TSHRs were expressed in wild type bone tissue and marrow cell cultures was further confirmed by real time RT-PCR and (or) immunoblotting. The functional significance of the TSHR in negatively regulating osteoclast formation was further confirmed by demonstrating a marked inhibition of TRAP-positive osteoclast formation from TSHR-overexpressing RAW264 cells. Likewise, recombinant TSH inhibited osteoclast formation in wild type mouse marrow cell cultures as well as osteoblast differentiation in progenitor cell lines. Overall, therefore, the localization of the TSHR to bone cells, its direct regulation of osteoclast and osteoblast formation and function, and the significant impact on bone of its absence, when taken together, reveal a *hitherto* yet uncharacterized role for the TSHR and its ligand, TSH, in the negative regulation of bone remodeling.

1055

Mutations In Type 2a Sodium-Phosphate Co-Transporter (NPT2a) Gene Cause Renal Phosphate Leak Associated With Osteoporosis Or Urolithiasis In Human. D. P. Prié*[1], V. Huart*[1], G. Planelles*[2], G. Friedlander*[1], B. Grandchamp*[3], C. M. Silve[1]. [1]Hôpital Bichat, Inserm U426, Explorations Fonctionnelles, Paris, France, [2]Faculté Necker, Inserm U467, Paris, France, [3]Hôpital Bichat, Biochimie B, Paris, France.

Epidemiologic studies have identified familial aggregation for both bone demineralization and renal calcium stone formation, findings compatible with the influence of genetic factors in these disorders. The search for gene variants predisposing to these common diseases, however, has generally yielded negative results. Both of these disorders are likely to be genetically heterogeneous, in which case a variety of different biological abnormalities may contribute in producing the clinical phenotype in individual patients. Low serum phosphate concentrations due to a decrease in renal phosphate reabsorption have been reported in some patients with urolithiasis or bone demineralization suggesting that genetic factors leading to a decrease in renal phosphate reabsorption can contribute to these diseases. In the kidney, phosphate is reabsorbed in the proximal tubule by the type 2a sodium-phosphate co-transporter (NPT2a). We tested the hypothesis that mutations in the NPT2a gene may account for renal phosphate leak associated with urolithiasis or bone demineralization. We sequenced the coding region of the NPT2a gene from 20 hypophosphatemic patients. Two non-synonymous mutations were found at the heterozygous state, one in a male patient with urolithiasis and one in a female patient with severe bone demineraliza-

tion (bone mineral density: at the lumbar spine 0.639 g/cm2, Z-score-4.3; at the femoral neck 0.679 g/cm2, Z-score –2,7). Both patients exhibited an increase in urinary calcium excretion and calcitriol serum concentration. These mutations were absent in 200 alleles from control subjects. The function of the mutated proteins was analyzed by the injection of increasing concentrations of wild type or mutated NPT2a RNA in Xenopus laevis oocytes. These experiments demonstrated a decrease in Na-dependent phosphate uptake and phosphate-induced currents in oocytes expressing the mutated NPT2a proteins. These results provide the first evidence that mutations in the NPT2a gene are responsible for hypophosphatemia and urinary phosphate leak in humans. The identification of functional variants of the NPT2a gene in patients with hypophosphatemia associated with urolithiasis or bone demineralization also provides genetic evidence that a defect in renal phosphate reabsorption may indeed be one of the multigenic components that contribute to the pathogenesis of these two common diseases.

1056

Mutations in the Gene Encoding Osteoprotegerin Cause Idiopathic Hyperphosphatasia. B. Chong*[1], M. Hegde*[1], M. Fawkner*[1], J. Seidel*[2], B. Tuysuz*[3], B. Yuksel*[4], M. Coker*[5], H. Cassinelli*[6], C. Tau*[6], D. Love*[7], T. Cundy[7]. [1]Molecular Genetics Laboratory, Auckland Hospital, Auckland, New Zealand, [2]International Hyperphosphatasia Collaborative Group (IHCG), Jena, Germany, [3]IHCG, Istanbul, Turkey, [4]IHCG, Adana, Turkey, [5]IHCG, Izmir, Turkey, [6]IHCG, Buenos Aires, Argentina, [7]University of Auckland, Auckland, New Zealand.

Idiopathic hyperphosphatasia (MIM 239000) is a rare bone disease characterised by progressive deformity, a propensity to fracture and very high bone turnover. We studied a family with 3 affected siblings and established linkage of the disorder to a locus on 8q24, using a genome-wide scan. The gene *TNFRSF11B* encoding osteoprotegerin (OPG), which lay within this locus, was an obvious candidate, given the critical role of OPG in regulating osteoclastogenesis. We examined genomic DNA of 10 subjects with hyperphosphatasia (from 8 families) for mutations in *TNFRSF11B* and its promoter. The subjects ranged in age from 2 to 29 years. All had long bone deformity and short stature (≤3rd centile). Plasma alkaline phosphatase activity was 4 to 13 times the upper limit of age-appropriate normal ranges. Mobility was significantly impaired in 7/10 subjects, and 6/10 had enlargement of the skull (≥98th centile). Primers were designed to amplify the promoter region and 5 exons of the OPG in order to screen for deletion/insertion and splicing mutations. Mutations were detected in two of the four families reporting parental consanguinity. The first family had three affected subjects with a homozygous in-frame 3bp deletion in exon 3, resulting in the loss of an Asp residue at position 182. This mutation lies within the region crucial for OPG function, and is predicted to cause disruption of the loop structure necessary for correct folding of the molecule. The second family had a much larger 20bp homozygous deletion, also in exon 3. This 20bp deletion, which lies outside the region crucial for OPG function, is expected to result in aberrant transcript splicing and premature termination of translation. No mutations in *TNFRSF11B* or its promoter region were identified in the six other families. This study demonstrates that mutations in the gene for OPG can cause autosomal recessive idiopathic hyperphosphatasia; however, this syndrome is apparently genetically heterogeneous.

1057

A Novel Mutation in OPG That Causes Familial Idiopathic Hyperphosphatasia Impairs OPG Capacity to Inhibit Bone Resorption. C. A. Middleton-Hardie, T. Cundy, T. Banovic*, I. R. Reid, J. Cornish, D. Naot. Medicine, University of Auckland, Auckland, New Zealand.

Genetic analysis of a large family with Familial Idiopathic Hyperphosphatasia, a rare autosomal recessive bone disease, identified linkage to a region of chromosome 8q that contains the gene for OPG. (See Abstract by B. Chong et al. for details.) Sequencing of this gene in members of the family identified an in-frame 3 base pair deletion resulting in the deletion of an aspartate residue at position 182, within the critical TNF-receptor like region. The aim of our study was to determine whether this mutation causes loss of function of OPG, and could therefore be the cause of the highly accelerated bone turnover seen in the patients. Wild-type and mutant OPG cDNA were cloned into pcDNA3.1(-)/myc-HisA vector and expressed in HEK293 cells. The conditioned media containing the recombinant proteins were collected, concentrated and tested for their ability to inhibit bone resorption in a neonatal murine calvarial organ culture. We demonstrated that conditioned medium containing wild type OPG inhibited bone resorption, whereas the conditioned medium containing the mutant protein had no effect (%45Ca release, means±SEM: control, 23±1.2; wild type OPG 14±0.83; mutant OPG 24±1.9, p<0.0001, Student's t test). We also investigated altered post-translational modification of the mutant protein. Western blot analysis demonstrated that the mutant protein had a lower electrophoretic mobility than the wild type. Following deglycosylation with N-glycosidase F, both proteins appeared to be of similar size, suggesting that the mutant protein is hyper-glycosylated. The importance of glycosylation to OPG's biological activity is being elucidated. These data indicate that the absence of functional OPG protein in the patients results in the severe phenotype. It is possible that the bone deformities of these patients could be alleviated by administration of recombinant wild-type OPG, similar to the effects shown in studies of OPG administration to OPG knockout mice.

1058

Dissociation of the Skeletal from the Reproductive Effects of Sex Steroids with an Activator of Nongenotropic Estrogen-Like Signaling (ANGELS), in Both Females and Males: A Lead to a Bone Anabolic, Sex Neutral Hormone Replacement Therapy. S. C. Manolagas, L. Han, A. M. Vertino, J. R. Chen, A. A. Ali, T. Bellido, R. S. Weinstein, C. A. O'Brien, R. L. Jilka, S. Kousteni. Division of Endocrinology and Metabolism, Center for Osteoporosis & Metabolic Bone Diseases, Central Arkansas Veterans Healthcare System, U/sity of Arkansas for Medical Sciences, Little Rock, AR, USA.

Certain synthetic non-phenolic ligands of the estrogen (ER) or androgen (AR) receptor can activate cytoplasmic kinases, without affecting classical transcription. To elucidate the mechanism of action and the spectrum of the biologic activities of such class of compounds on bone and reproductive tissues, we examined a) downstream consequence of ERK activation, b) in vitro effects on the life span of murine osteoblasts and osteoclasts, and c) in vivo effects on bone and reproductive tissues of female and male mice, using a prototypic ANGEL, designated ABX102. We report that like classical estrogens, activation of a Src/Shc/ERK pathway or downregulation of JNK by ABX102 led to potent downstream modulation of the activity of Elk-1/SRE and AP-1 respectively. Also like estrogens, ABX102 dose dependently (10^{-12} - 10^{-7} M) attenuated osteoblast and stimulated osteoclast apoptosis, with identical efficacy in cells from female and male mice. For the in vivo studies, we administered ABX102 to ovariectomized (OVX) or orchidectomized (ORX) 8 month-old Swiss Webster mice, and compared its effects, at a dose of 7.6 mg per 60 day release pellet, to a replacement dose of either 17β-estradiol (E_2) or dihydrotestosterone (DHT): 0.025 mg or 10 mg per 60 day release pellets, respectively. The dose for ABX102 was chosen based on its lower binding affinity (~300-fold) for the ER, compared to E_2. At 6 weeks, the gonadectomy-induced loss of BMD was restored by E_2 replacement in females and DHT replacement in males, as expected. OVX females receiving ABX102 exhibited greater BMD than those receiving E_2, in both the femur and the spine; and greater compression strength of the lumbar vertebrae. ABX102 also prevented the bone loss induced by orchidectomy, and was superior to DHT at the spine. In sharp contrast to E_2, ABX102 did not suppress the OVX-induced increase in serum osteocalcin. Unlike E_2 or DHT, ABX102 had no effect on the uterus or the seminal vesicles of the gonadectomized mice. Hence, ligands that can activate only the nongenotropic function of the ER (or AR) represent an advantageous class of pharmacotherapeutic agents (true anabolic as opposed to antiresorptive) and sex neutral for the management of osteopenic states; and perhaps a rational therapy for sex hormone deficiencies in postreproductive life, at large.

Disclosures: ***S.C. Manolagas****, ANABONIX 4; Eli Lilly 8; Procter and Gamble 8; Wyeth 8.*

1059

Ten-Year Efficacy and Safety of Alendronate in the Treatment of Osteoporosis in Postmenopausal Women. R. Emkey[1], I. Reid[2], A. Mulloy[3], R. Correa-Rotter[4], M. Favus[5], H. Bone[6], J. Gupta*[7], A. LaMotta*[7], A. Santora[7]. [1]Radiant Research, Wyomissing, PA, USA, [2]Auckland Hospital, Auckland, New Zealand, [3]Medical College of Georgia, Augusta, GA, USA, [4]Instituto Nacional de la Nutricion Salvador Zurian, Tlalpan, Mexico, [5]University of Chicago, Chicago, IL, USA, [6]Michigan Bone and Mineral Clinic, Detroit, MI, USA, [7]Merck Research Labs, Rahway, NJ, USA.

Alendronate sodium* (ALN), a specific inhibitor of osteoclastic bone resorption, reduced the risk of vertebral fractures and progressively increased BMD over 3 yrs in a study of 994 postmenopausal osteoporotic women. We reported 7 yr results from 350 women who, after 5 years of continuous ALN treatment, participated in a double-blind 2 yr extension (Yrs 6-7), and now report the results for 247 women who entered an additional 3 yr extension (Yrs 8-10). During Yrs 6-10, patients in the ALN 5 and 10 mg groups remained on their prior ALN dose. Patients in the ALN 20/5/placebo (A-PBO) group (20 mg for 2 yrs, 5 mg for 3 yrs) received placebo in Yrs 6-10. A significant increase in spine BMD of 2.25 % for ALN 10 mg and 1.60 % for 5 mg groups was found during Yrs 8-10. At the hip and total body, prior increases in BMD were maintained during Yrs 8-10. Forearm BMD was stable with 10 mg but decreased slightly with 5 mg. Women in the A-PBO group who had not been treated with ALN since the end of Yr 5 showed no significant change in BMD at both spine and total body, but small decreases in hip and forearm BMD occurred during Yrs 8-10. Cumulative 10 yr spine BMD increases were 13.7 % with ALN 10 mg and 9.8 % with 5 mg. After the initial 18 mo, each additional yr of treatment with ALN 10 mg increased spine BMD by 0.73 % vs. 0.57 % with ALN 5 mg. The safety and tolerability profiles of ALN 5 and 10 mg were similar to placebo during both Yrs 8-10 and Yrs 6-10. The 3 yr incidences of non-vertebral fractures during Yrs 8-10 were 8.1, 11.5, and 12.0 % in the ALN 10 mg, 5 mg and A-PBO groups. The 3 yr incidences in the original cohort during Yrs 1-3 were 8.5 % (pooled ALN) and 10.7 % (placebo). Although patients were older in Yrs 8-10, the expected age-related increase in fracture risk was not observed. Neither stress fractures nor fracture malunion were reported. We conclude that ALN treatment is effective for 10 yrs and is generally well tolerated. Spinal BMD continues to increase over 10 yrs and other skeletal benefits are maintained. Non-vertebral fracture data indicate no change in risk over time, and suggest that fracture risk reduction is maintained during continued treatment. Discontinuation of ALN after 5 years leads to bone loss at non-spine sites, and continued treatment with ALN through 10 years yields sustained skeletal benefits.

* Manufactured by Merck & Co., Inc., Whitehouse Station, NJ

Disclosures: ***R. Emkey****, Merck & Co., Inc. 2, 5, 8.*

1060

Interleukin-6 Genetic Variation and the Effects of Estrogens and Dietary Calcium on Bone Mass: The Framingham Osteoporosis Study. S. L. Ferrari[1], D. Karasik[2], J. Liu*[3], S. Karamohamed*[3], A. G. Herbert*[3], A. L. Cupples*[4], D. P. Kiel[2]. [1]Div. of Bone Diseases, University Hospital, Geneva, Switzerland, [2]Div. of Aging, Harvard Medical School, Boston, MA, USA, [3]Framingham Heart Study Genetics Laboratory, Boston University School of Medicine, Boston, MA, USA, [4]Dept of Epidemiology and Biostatistics, Boston University School of Public Health, Boston, MA, USA.

Genetic factors make an important contribution to peak bone mass, but their influence on bone mass in the elderly remains poorly appreciated. IL-6 is a pleiotropic cytokine playing a central role in bone remodeling. We have previously reported two G>C variants at position –174 and –572 in the IL-6 promoter which influenced IL-6 expression and were associated with levels of bone resorption in postmenopausal women. In this study, we examined interactions between IL-6 polymorphisms and non-genetic factors, including estrogen status, physical activity, smoking, dietary calcium, vitamin D and alcohol intake, on femur BMD (neck, FN, trochanter, FT, and Ward's area) in unrelated women (n=817, mean age ±sd =60.3 ±9.4 yrs) and men (n=737, 59.6 ±9.3 yrs) from the Framingham's Offspring Cohort. IL-6 promoter haplotypes were directly determined by allele-specific PCR and genotypes confirmed by DNA mass spectrometry. Frequency of the GG, GC and CC genotypes was, respectively, 36%, 50% and 14% at –174, and 89%, 11% and <0.5% at –572 positions. Significant interactions (p = 0.009 to 0.09) affecting age-adjusted BMD were found in women between IL-6 –174 genotypes and estrogen status, calcium intake, and years since menopause. Thus, BMD was higher in CC compared to GG women with calcium intake below 940 mg/d (n=383, percentage difference=10.6%, pANOVA=0.002, 6.7%, p=0.05 and 5.6%, p=0.024, at Ward's, FT and FN, respectively); in postmenopausal women not receiving ERT (n=408, 9.4%, p=0.02, 6.6%, p=0.05 and 5.2%, p>0.05); and in women who were >15 years past menopause (n=309, 12.6%, p=0.016, 10,2%, p=0.025 and 8.4%, p=0.017). In contrast, no significant association was observed in models that considered only the main effects of IL-6 polymorphisms, nor in women who were either estrogen-repleted, or less than 15 years since menopause, or whose calcium intake was above 940 mg/d, nor in men (n = 737). In summary, the IL-6 gene promoter variant –174C is associated with preserved hip BMD in subjects at increased risk of osteoporosis, such as older women, postmenopausal women without ERT and those with low calcium intake. Considering the role of estrogens and calcium on regulating IL-6 expression and bone turnover, it is plausible that interactions between these factors and variants in the IL-6 gene regulatory region contribute to bone mass determination in aging women.

1061

The Anabolic Effect of Parathyroid Hormone Is Impaired in Bones of Fgf2 Null Mice. M. M. Hurley[1], Y. Okada[2], T. Sobue[1], X. Zhang[1], L. Xiao*[1], Y. Tanaka*[2], M. Ito*[3], N. Okimoto*[4], T. Nakamura*[2], J. Coffin[5], C. J. Rosen*[6], T. Doetschman*[7]. [1]Medicine, Univ of CT Hlth Cntr, Farmington, CT, USA, [2]Univ of Occ & Environ Hlth, Kitakyushu, Japan, [3]Univ of Nagasaki, Nagasaki, Japan, [4]Univ of Occ & Environ Hlth, Kitakyushu, Japan, [5]Univ of Montana, Missoula, MT, USA, [6]Jackson Lab, Bangor, ME, USA, [7]Univ of Cincinnati, Cincinnati, OH, USA.

Intermittent administration of parathyroid hormone (PTH) stimulates new bone formation in mice, aged rats and humans. However, the mechanism by which PTH increases bone formation is not established. Basic fibroblast growth factor (FGF-2) is a potent bone anabolic agent when administered intermittently to young and aged rats in vivo and Fgf2-/- mice develop low bone mass with aging. Since PTH increased FGF-2 mRNA and protein expression in osteoblasts and the acute hypercalcemic effect of PTH is diminished in Fgf2-/- mice, we assessed whether the anabolic effect of PTH was impaired in Fgf2-/- mice. Eight week old Fgf2+/+ and Fgf2-/- male mice were weighed and injected s.c. once daily with vehicle or PTH 1-34 (8 µg/kg body wt) for 30 days. Mice were injected with calcein (0.6 mg/kg) on day 18 and day 24 to assess new bone formation. There were no significant differences in body wt pre and post PTH in either genotype. Serum calcium obtained 24 h after the last injection was similar in vehicle and PTH treated mice of both genotypes. Micro-CT and dynamic histomorphometry of the distal femoral metaphysis is shown below. PTH significantly increased parameters of bone formation in Fgf2+/+ mice but the changes were smaller and not significant in Fgf2-/- mice. Similar results were obtained in 6 week old male and 15 month old female mice. Bone mineral density (BMD) was measured in femurs excised from Fgf2+/+, Fgf2+/- and Fgf2-/- mice that were treated with PTH (16 µg/kg body wt) for 10 days. BMD was increased by 18% (p<0.05) in PTH treated bones from Fgf2+/+; 3% in Fgf2+/- mice and reduced by 3% in bones from Fgf2-/- mice. Serum IGF-1 was not significantly different between vehicle and PTH treated mice of each genotype. We conclude that endogenous Fgf2 is a critical mediator of the anabolic effect of PTH, on bone in mice.

Parameters of bone formation in femoral metaphysis of Fgf2+/+ and Fgf2-/- mice

	Fgf2+/+ Vehicle	Fgf2+/+ PTH	Fgf2-/- Vehicle	Fgf2-/- PTH
BV/TV	27.0 (2.4)	37.1 (2.1)*	19.9 (2.9)	25.4 (3.4)
TbN	5.7 (0.3)	6.6 (0.1)*	4.7 (0.4)	5.2 (0.4)
Tb Sp	130.0 (9.3)	95.0 (4.9)*	185.0 (31.8)	150.0 (21.3)
D-LSBS	7.0 (0.6)	14.0 (0.8)*	5.3 (0.4)	5.5 (0.5)
BFR/BS	24.8 (1.6)	47.6 (2.6)*	17.8 (1.3)	21.0 (1.9)
Ob S/BS	10.4 (0.7)	21.4 (1.6)*	8.4 (1.1)	10.8 (1.1)
Oc S/BS	6.0 (0.4)	8.0 (0.9)	5.1 (0.6)	5.6 (0.4)

N=6, Values are means with (SE) in parenthesis. * P<0.05.

1062

Intermittent PTH Fails to Restore Deficient Bone Mass and Microarchitecture in Male Mice Null for ß-Arrestin2. M. L. Bouxsein[1], D. Sternlight*[1], V. Glatt*[1], D. Pierroz*[2], S. L. Ferrari[2]. [1]Orthopedic Biomechanics, Beth Israel Deaconess Medical Center, Boston, MA, USA, [2]Division of Bone Diseases, University Hospital, Geneva, Switzerland.

ß-arrestins are cytoplasmic molecules which mediate the internalization and desensitization/resensitization of the parathyroid hormone (PTH)/PTH-related protein receptor. We previously reported that 6 month-old female mice null for ß-arrestin2 (ß-arr2 KO) had normal skeletal morphology, but decreased bone mass and altered trabecular architecture compared to wild-type (WT) littermates. To investigate whether this was due to a deficiency in peak bone mass acquisition and/or accelerated bone loss, we evaluated bone mass longitudinally by pDXA in 4 to 24 wk-old ß-arr2 KO and WT mice (n=84 females and 86 males). In addition, to study the role of PTH in this process, 12 wk-old male and female mice were matched for weight and either sacrificed immediately, or received intermittent PTH (80 µg/kg/d, sc) or vehicle (VEH) for 4 wks (n=6-12/group). Changes in bone mass and microarchitecture were analyzed in vivo by pDXA, and ex vivo by µCT, respectively. Both male and female KO had a modestly lower bone mass at all skeletal sites by 8 wks, which persisted until peak bone mass was achieved (ie, Total Body BMC: -5.5% for males, -8.4% for females, p<0.005 for both). KO also had a lower body weight at all timepoints (-1.4 g in males, p<0.005; -1.2 g in females, p=0.03). In the PTH study, VEH-WT females had higher total body BMC (+8.4%, p=0.01), cortical thickness (+14%, p=0.003) and vertebral trabecular BV/TV (+10%, p=0.18) after 4 wks compared to baseline, with similar trends seen in VEH-WT males. In contrast, these variables did not increase in VEH-KO females, and in KO-males, vertebral trabecular BV/TV and trabecular number actually declined (-18% to -20%, p<0.005 for both). Intermittent PTH significantly increased total body BMC, as well as cortical and trabecular bone parameters in WT males and females (+9 to 30%). A similar anabolic response was seen in PTH-KO females. In contrast, in KO males, PTH failed to increase trabecular and cortical BV/TV, resulting in a persistent decline in bone mass. Compared to VEH, osteocalcin levels were significantly increased (+50%) by PTH treatment and positively correlated to changes in total body BMC in all groups (r= 0.46 to 0.63, p<0.01), except for KO males (r=0.14, ns). Taken together, these data indicate that ß-arr2 is important in regulating both acquisition and maintenance of bone mass. Altered PTH bioactivity in the absence of ß-arr2 may be implicated in the premature bone loss observed in KO males. The mechanism(s) by which ß-arrestins influence peak bone mass acquisition remains to be elucidated.

1063

Mammary Epithelial Cell PTHrP Secretion During Lactation: Regulation by a Calcium Sensing Mechanism In Vitro and In Vivo. J. N. VanHouten*[1], P. R. Dann*[1], M. C. Neville*[2], E. M. Brown[3], J. J. Wysolmerski[1]. [1]Yale University School of Medicine, New Haven, CT, USA, [2]University of Colorado Health Sciences Center, Denver, CO, USA, [3]Brigham and Women's Hospital, Boston, MA, USA.

During lactation, the breast mediates the transfer of large quantities of calcium from the maternal circulation into milk. This process is associated with marked increases in bone turnover and significant bone loss in lactating mothers. Furthermore, it has been suggested that PTHrP, secreted by mammary epithelial cells may participate in the regulation of bone turnover and bone loss during lactation. Therefore, we wondered if the breast was a calcium-sensing organ and if mammary epithelial cells regulated PTHrP secretion in response to changes in extracellular calcium concentration. In order to address these questions, we first examined the expression of the calcium sensing receptor gene in normal breast tissue in mice. By RT-PCR and by Affymetrix gene profiling, we have found that the CaSR gene is expressed in lactating, but not pregnant or virgin breast tissue. Immunohistochemistry for the CaSR demonstrated that it is expressed on epithelial cells within the lactating breast. When mammary epithelial cells from normal mice are cultured in lactogenic media, PTHrP secretion is suppressed in a linear fashion by raising extracellular calcium concentrations from 0.5 through 10mM. Increasing concentrations of neomycin also progressively suppress PTHrP secretion by primary cultures of mammary epithelial cells, suggesting that the effect of calcium on PTHrP secretion is mediated by the CaSR. Finally, placing lactating mice on a low calcium diet (0.01%) induces relative hypocalcemia and increases PTHrP levels in milk. These data suggest that the lactating breast senses calcium and that mammary epithelial cells adjust PTHrP secretion in response to changes in extracellular calcium concentration. Interestingly, the effects of raising the extracellular calcium concentration on PTHrP secretion by lactating mammary epithelial cells mirror the effects of raising calcium concentrations on PTH secretion by parathyroid cells, and are the opposite of the effects described in breast cancer cell lines. The regulation of PTHrP secretion by the CaSR is likely to contribute to the overall regulation of calcium metabolism during lactation and the transfer of calcium from mother into milk.

1064

The Transcription Factor GCMB Induces Expression of PTH in HEK 293T Cells. C. Ding, A. Maret*, M. A. Levine. Pediatric Endocrinology, Johns Hopkins University, Baltimore, MD, USA.

The *GCMB* gene, a human ortholog of the Drosophila gene glial cells missing (*gcm*), is expressed exclusively in parathyroid cells and regulates parathyroid gland development. Involvement of *GCMB* in parathyroid cell embryogenesis has been demonstrated by "loss of function" studies, wherein human subjects or transgenic mice lacking *GCMB/Gcm2* fail to develop parathyroid glands. Here we have used a "gain of function" approach to test whether *GCMB* could endow HEK293 cells with parathyroid cell characteristics. Transient transfection of 293T cells with green fluorescent protein (GFP) fusion constructs contain-

ing either *Drosophila* (d)GCM or human (h)GCMb showed intense fluorescence in the cell nucleus, confirming expression and appropriate nuclear localization of these proteins. Co-transfection of 293T cells with a luciferase reporter plasmid containing six tandem copies of the GCM-binding site plus plasmids containing dGCM or hGCMb produced 200- and 10-fold increases in luciferase activity, respectively, confirming that dGCM is a much stronger transactivator than hGCMb. To test transactivation of endogenous genes, we transfected 293T cells with either vector alone or plasmids containing dGCM or hGCMb and after 48 hours isolated total RNA. RNA was analyzed by RT-PCR using oligonucleotide primers that spanned introns in order to distinguish amplification of mRNA from contaminating genomic DNA. Cells that had been transfected with hGCMb expressed mRNA encoding for PTH, but not for the calcium sensing receptor. By contrast, cells that transfected with dGCM or vector alone did not express either PTH or calcium sensing receptor. To determine whether PTH mRNA was effectively translated into protein, we performed immunocytochemistry with a monoclonal antibody to the amino-terminus of human PTH. 293T cells transfected with hGCMb showed strong cytoplasmic staining, confirming ectopic expression of immunoreactive PTH in these cells. In conclusion, our data show that expression of hGCMb is sufficient to induce PTH production in 293 cells. By contrast, expression of dGCM, a stronger transactivator than hGCMb, did not induce PTH expression in these cells, suggesting that naturally occurring transcription factors in 293T cells may act in concert with ectopic hGCMb but not with dGCM to induce PTH expression. Finally, ectopic expression of PTH but not calcium sensing receptors in 293 cells expressing hGCMb suggests that under our present conditions acquisition of parathyroid cell characteristics is incomplete. Additional studies, including microarray analysis and regulated PTH secretion, of stably transfected 293 and other cell lines will be required to characterize more fully the transactivation potential of hGCMb.

1065

In Vivo Role of Stimulatory G Protein (Gs) in Cartilage Development. M. Bastepe[1], L. Weinstein*[2], H. M. Kronenberg[1], H. Juppner[1], U. Chung[1]. [1]Endocrine Unit, Mass. Gen. Hosp., Boston, MA, USA, [2]Niddk, NIH, Bethesda, MD, USA.

Stimulatory G protein (Gs) transduces signals from various cell-surface receptors to intracellular adenylate cyclases, which generate the second messenger, cAMP. The α subunit of Gs (Gsα) is encoded by GNAS1 (mouse homolog encoded by Gnas). Heterozygous inactivating mutations in one of the 13 exons of GNAS1 encoding Gsα cause Albright's Hereditary Osteodystrophty (AHO) and related disorders. The in vivo role of Gs signaling in skeletal development is still largely unknown, due to early embryonic lethality of mice homozygously missing the Gnas exon 1 ($Gnas^{E1/E1}$) or exon 2 ($Gnas^{E2/E2}$) and due to absence of easily detectable phenotypes in growth plate chondrocytes heterozygous for the mutations. We have generated chimeric mice containing wild-type and $Gnas^{E2/E2}$ cells. Exon 2 of the Gnas gene not only encodes Gsα but also contributes to other alternatively spliced transcripts such as XLα s, NESP55 and A/B. $Gnas^{E2/E2}$ chondrocytes phenocopy PTH/PTHrP receptor $(PPR)^{-/-}$ cells in the growth plate by ectopically undergoing hypertrophy. Heterozygous mutant cells also ectopically hypertrophy in the growth plate, but to a lesser extent than $PPR^{-/-}$ cells and $Gnas^{E2/E2}$ cells. XLαs mRNA is expressed at very low levels even in the wild-type growth plate. However, heterozygous cells with a mutant paternal allele ($Gnas^{+/pat\ E2}$) have more severe phenotypes than cells with a mutant maternal allele ($Gnas^{+/mat\ E2}$), suggesting that XLαs expressed only from the paternal allele may play a role similar to that of Gsα in chondrocyte differentiation. Introduction of rat Gsα cDNA into $Gnas^{E2/E2}$ ES cells as a CMV promoter-driven transgene and generation of chimeras with these transfected cells lead to a complete reversal of ectopic hypertrophy in chimeras, when cAMP response to cholera toxin in the transfected ES cells is completely restored in vitro. In other lines, in which the cAMP response is partially restored, a partial reversal similar to that found using $Gnas^{+/E2}$ cells is seen. Thus, Gs is sufficient to mediate signaling through the PTH/PTHrP receptor in the growth plate. In conclusion, these data strongly suggest that signaling through the PTH/PTHrP receptor is mediated mainly by Gs in growth plate chondrocytes. Furthermore, they also suggest that $Gnas^{+/E2}$ cartilage has haplo-insufficiency of Gs signaling.

1066

Distinct Roles of Individual Signaling Pathways Activated by the PTH/PTHrP Receptor in Endochondral Development Ex-Vivo. J. Guo, U. Chung, R. F. Bringhurst, H. M. Kronenberg. Massachusetts General Hospital and Harvard Medical School, Boston, MA, USA.

Chondrocyte differentiation in the endochondral growth plate is delayed in mice expressing exclusively a mutant form of the PTH/PTHrP receptor ("DSEL') that activates adenylyl cyclase normally but not phospholipase C (PLC). This phenotype in DSEL homozygous (PTHRD/D) mice is quite distinct from that observed in mice lacking the PTH/PTHrP receptor, in which chondrocyte diffferentiation is accelerated during endochondral development. To further analyze how specific signals generated by the PTH/PTHrP receptors may affect chondrocyte differentiation, PTHR+/- and PTHRD/- were mated, and E14.5 metatarsal and tibia rudiments from the resulting litters were cultured in serum-free medium in vitro. Mineralization of cartilage, as viewed serially with a dissecting microscope, gradually expanded distally from the center of the metatarsal rudiments of PTHR+/- embryos during 7 days in culture. In previous studies in vivo, hemizygous PTHR+/- mice exhibited normal growth plates. In rudiments from PTHR-/- mice, mineralization was more extensive and extended much farther toward the articular surfaces, whereas the appearance of mineralized cartilage was greatly delayed in hemizygous PTHRD/- rudiments during this period of culture. As shown by in situ hybridization analysis, the domain of chondrocytes expressing collagen type X and osteopontin was dramatically decreased in size by treatment with hPTH(1-84) for 3 days in both PTHR+/- and PTHRD/- rudiments, whereas no effect of hPTH (1-84) on PTHR-/- rudiments was observed. This inhibitory effect was mimicked by treatment with forskolin, a stimulator of adenylyl cyclase, and [Gly1, Arg19]hPTH(1-28), a PTH analog that cannot activate PLC. In contrast, hypertrophy of chondrocytes was augmented by incubation of rudiments with active phorbol ester. These findings indicate that in mediating the action of PTHrP or PTH, the PTH/PTHrP receptor exerts both an inhibitory and a stimulatory effect on differentiation of growth plate chondrocytes, depending on the specific signal generated by the receptor. We have further observed that treatment with 100 nM PTH for either 6 hr or 3 days caused dramatic down-regulation of Cbfa-1 in both PTHR+/+ and PTHRD/D rudiments, as shown by in situ hybridization analysis. These results suggest that PLC-independent signaling via the PTH/PTHrP receptor may retard chondrocyte differentiation, at least, in part, via the Cbfa-1 transcriptional activation pathway, since mice lacking Cbfa-1 exhibit a delay in chondrocyte differentiation during endochondral development.

1067

Biglycan Is Essential for BMP-4 Stimulated Osteoblast Differentiation. X. Chen, T. Xu*, M. Young. Craniofacial and Skeletal Diseases Branch, National Institutes of Dental and Craniofacial Research, NIH, Bethesda, MD, USA.

Biglycan (bgn) is a small leucine rich proteoglycan that is enriched in extracellular matrices of skeletal tissues. Previously, we reported that bgn-deficient (knockout, KO) mice developed age-related bone lose with a phenotype that resembled osteoporosis, that is due to a defect in the proliferation and differentiation of osteoblast precursors. It was also found that osteoblasts obtained from bgn-KO mice accumulated less mineral than those from wild type (wt) mice in the presence of BMP-2/4 in vitro. In the present study, our hypothesis was that biglycan plays a role in BMP-4 stimulated osteoblast differentiation. To test this hypothesis, we examined how bgn-KO osteoblasts responded to BMP-4 in the regulation of Cbfa1, and whether the BMP-4 signaling transduction pathway was involved. Cells were harvested from newborn animals by repeated digestions with collagenase and cultured until 80% confluent. The cells were treated with BMP-4 for 48 hours, and Cbfa1 was detected in the lysed cells by Western blot analysis. The data showed that the bgn-KO cells produced a significantly lower level of Cbfa1 with or without BMP-4 treatment compared to wt cells. To further study the decreased production of Cbfa1 in the bgn-KO cells, we transfected the cells with a promoter that contains 6 copies of the consensus sequence (OSE2) for Cbfa1 linked to a luciferase promoter. Based on the data of the luciferase assay, BMP-4 did not elevate the level of activity in the bgn-KO cells (0.28 ± .05 vs. 0.29 ± 010). In contrast, the wt cells significantly increased the activity level from 0.35 ± 0.05 to 0.56 ± 0.17 ($p = 0.03$, $n = 5$) after BMP-4 treatment. This indicated that bgn-KO cells did not respond to BMP-4 in the production and function of Cbfa1. To further understand why there was the differential response to BMP-4 in the bgn-KO cells, we examined the signaling pathway, particularly the active phosphorylated Smad1 (p-Smad1) and BMP type I receptor by Western blot analysis. The data showed that p-Smad1 was lower in bgn-KO than wt cells after the cells were treated with BMP-4 for 30 minutes. Surprisingly, we found that bgn-KO cells over expressed the type I receptor in both the untreated and treated cells with BMP-4 compared with wt cells. Overall, the results suggested that bgn-KO cells responded poorly to BMP-4, which in turn causes a reduction in Cbfa1 production. It may also explain our previous observation that bgn-KO cells reduce the expression of BSP, osteopontin, osteocalcin, and accumulate less mineral during the differentiation process. We propose that biglycan is required for BMP-4 stimulation, and may act by modulating BMP-4 or other growth factors in control of osteoblast function.

1068

Biglycan and Decorin Have Overlapping Roles in the Commitment, Proliferation, Differentiation, and Survival of Osteoblasts and Their Precursors. Y. Bi*[1], X. Chen[1], T. Xu*[1], R. V. Iozzo*[2], M. F. Young[1]. [1]NIH, Bethesda, MD, USA, [2]Thomas Jefferson University, Philadephia, PA, USA.

Small leucine-rich proteoglycans (SLRPs) are extracellular molecules that bind to collagens and growth hormones to regulate cell growth and matrix assembly. Biglycan (BGN) and decorin (DCN), two members of class I SLRPs, are predominantly expressed in bone. Because the functions of BGN and DCN in bone formation may, at least partially, be compensated by each other in single knockout animals, we created BGN and DCN double-knockout (DKO) mice. DKO mice exhibit osteopenia earlier and more severely than the BGN or DCN single knockout mice. In this study, we examined the cellular and molecular mechanisms that underline the accelerated bone loss in DKO mice. To assess the number of osteogenic stem cells, we compared the colony forming efficiency (CFU-F) in DKO bone marrow stromal cells (BMSCs) with wild type (WT) cells. We previously reported that the number of CFU-F was only significantly decreased at 12 (24%) and 24 weeks (52%) of age in BGN KO cells compared to WT cells. In the present study, we found that the number of CFU-F in DKO cells was decreased by 66 ± 6 % (n=6) compared to WT cells as early as two months of age. Thus, the CFU-F decreases earlier and is more pronounced in DKO than in BGN KO, which is consistent with their skeletal phenotypes. To better understand the mechanisms of the decreased number of CFU-F in the DKO, we examined the expression of over 100 genes related to apoptosis. Interestingly, several genes of the TNF receptor family (TNFR1, TNFRSF11A, and DR6) and a potential ligand (LT-b) of TNF receptors were highly expressed in the DKO osteoblast precursors, indicating that BGN and DCN may protect cells against apoptosis via TNF-induced pathways. Next, we determined the potential of BMSCs differentiating into functional bone forming cells using a mineralization assay. The results showed that calcium accumulation was significantly lower (47.5 ± 1.5%) in the cultures of DKO BMSCs compared to WT BMSCs after normalization for protein content. The DKO cultures were observed microscopically to have greater cell numbers than WT cultures. This led us to speculate that the DKO cells may have a higher proliferation rate than WT cells. To confirm this, we determined the proliferation of osteoblast precursors using the MTT assay. The proliferation rate of osteoblast precursors from DKO mice was 25 ± 5% (n=5) higher than cells from WT mice. Taken together, we postulate that the small leucine-rich proteoglycans, BGN and DCN, have overlapping functions in regulating the commitment, proliferation, differentiation, and survival of osteoblasts and their precursors.

1069

The Matricellular Protein, Thrombospondin-2, Has Opposing Effects on Osteogenic and Adipogenic Differentiation of Marrow-derived Mesenchymal Stem Cells. K. D. Hankenson. Department of Orthopaedic Surgery, University of Michigan, Ann Arbor, MI, USA.

Matricellular proteins (MP) are a functional group of extracellular matrix molecules that modulate structural matrix formation and function, growth factor/cytokine activity, and cell physiology. Mice with targeted deletions of MP genes show abnormalities in bone modeling and remodeling. Specifically, thrombospondin-2 (TSP2)-null mice show an increase in endosteal bone formation that occurs coincident with an increased number of marrow-derived mesenchymal stem cells (MSC). TSP2 functions as an autocrine inhibitor of MSC cell-cycle progression and may contribute to maintaining MSC quiescence. The purpose of this study was to determine whether TSP2 can also affect MSC differentiation. The ability of MSC to support osteoclastogenesis (TRAP+, multinucleated cells), form mineral (Alizarin red), and develop into adipocytes (Oil red O) was studied. WT spleen cells and RAW 264.7 cells (neither of which produce appreciable TSP2) were cultured on confluent MSC monolayers in the presence of vitamin D and dexamethasone (DEX). TSP2-null and WT MSC supported osteoclastogenesis equivalently. An examination of osteoblastogenesis in the presence of beta-glycerophosphate showed that recombinant TSP2 expedited mineralization of both TSP2-null immortalized MSC and ST2 cells, in addition to limiting proliferation. Whereas mineralization in TSP2-null immortal cells was not observed until d 28, in the presence of TSP2, mineral was observed on d 21. When TSP2 was added to TSP2-null and ST2 cells that were induced to form adipocytes (DEX/insulin/IBMX treatment), the proportion of lipid containing cells was substantially decreased (15% of control). To determine the domain of TSP2 that imparts the positive osteogenic and negative adipogenic effects, four recombinant TSP2 fragments were studied in comparison to full-length TSP2. The three type I repeats were required for inhibition of proliferation and promotion of mineralization; however, the type I repeats were not required for inhibition of adipogenesis. These results demonstrate that the effect of TSP2 on MSC behavior is not monotrophic, as was originally proposed. We postulate that TSP2 in vivo, in addition to modulating the proliferation of early-stage MSC, promotes bone formation and inhibits adipogenesis. In the TSP2 knockout mice these alternative roles may be masked by the dominant effect of increased MSC number. Furthermore, based on the study of TSP2 fragments, we conclude that the promotion of mineralization and inhibition of adipogenesis are not linked events, and that inhibition of adipogenesis does not occur secondary to inhibition of proliferation.

1070

Targeted Expression of a Constitutively Active Mutant of MEK1 in Chondrocytes Inhibits Endochondral Ossification and Rescues the Phenotype of FGFR3 Deficient Mice. S. Murakami*[1], S. McKinney*[1], D. Givol*[2], B. de Crombrugghe*[1]. [1]Department of Molecular Genetics, U.T.M.D.Anderson Cancer Center, Houston, TX, USA, [2]Weizmann Institute of Science, Rehovot, Israel.

In order to examine the role of the MAPK pathway in chondrocyte differentiation, we generated transgenic mice that overexpress a constitutively active mutant of MEK1 (S218/222E, Δ32-51) in chondrocytes using 6 kb promoter/intron sequences of *Col2a1*. Three lines of transgenic mice that show cartilage specific expression of the transgene were established. All three lines exhibited a dwarf phenotype similar to human achondroplasia, a dwarfism syndrome caused by activating mutations in FGFR3. Skeletal preparations showed shortened axial and appendicular skeletons, mid-facial hypoplasia, and dome-shaped cranium. Histological examination of the growth plate of long bones revealed incomplete hypertrophy of chondrocytes and narrower hypertrophic zone in transgenic mice compared to wild-type littermates. In addition, formation of secondary ossification centers and ossification of carpal bones were delayed in transgenic animals. Since these mice showed mid-facial hypoplasia at birth, we examined the endochondral ossification process in the cranial base during embryonic development. Histological examination of the head at E15.5 to E17.5 revealed a delay in hypertrophic differentiation of chondrocytes in the cranial base. Ossification of basisphenoid and basioccipital bones was delayed, and morphologically smaller chondrocytes persisted in these transgenic mice. Immunohistochemical analysis showed reduced staining for collagen type X and persistent expression of Sox9, a master transcription factor that inhibits hypertrophic differentiation of chondrocytes. These observations indicate that the MAPK pathway inhibits hypertrophic differentiation of chondrocytes and negatively regulates bone growth. In order to test the hypothesis that skeletal overgrowth in FGFR3 deficient mice is caused by the reduced activity of the MAPK pathway, we crossed these transgenic mice with FGFR3 deficient mice. Expression of a constitutively active mutant of MEK1 in chondrocytes of FGFR3 null mice inhibited skeletal overgrowth, indicating activation of the MAPK pathway is sufficient to overcome the growth promoting effects of FGFR3 deficiency. Since the MAPK pathway is a major component of FGF signaling, our observations strongly suggest that regulation of bone growth by FGFR3 is at least in part mediated by the MAPK pathway. Increased activity of the MAPK pathway could account for the dwarf phenotype in achondroplasia and thanatophoric dysplasias, two human genetic diseases that are caused by activating mutations in FGFR3.

1071

The Transcription Factor Sox9 Has Essential Roles in Successive Steps of the Chondrocyte Differentiation Pathway and Is Required for Expression of Sox5 and Sox6. H. Akiyama[1], M. C. Chaboissier*[2], J. F. Martin*[3], A. Schedl*[2], B. de Crombrugghe*[1]. [1]Molecular Genetics, MD Anderson Cancer Center, Houston, TX, USA, [2]Institute of Human Genetics, University of Newcastle, Newcastle, United Kingdom, [3]Alkek Institute of Bioscience and Technology, Texas A&M System Health Science Center, Houston, TX, USA.

To examine whether Sox9 is essential during the sequential steps of chondrocyte differentiation, we have used the Cre/loxP recombination system to generate mouse embryos in which either Sox9 is missing from undifferentiated mesenchymal cells of limb buds or the Sox9 gene is inactivated after chondrogenic mesenchymal condensations. Mice harboring a conditional ("floxed") allele of Sox9, in which exons essential for Sox9 function were flanked by loxP recombination sequences, were intercrossed with transgenic mice that expressed Cre recombinase under control of either Prx1 or Col2a1 regulatory sequences. Prx1-Cre deletion of Sox9, which occurred in undifferentiated mesenchymal cells of limb buds, resulted in very short limbs completeyly lacking chondrogenic mesenchymal condensations and limb skeleton formation. Expression of transcripts for a series of patterning proteins that mark the different axis of limb buds was comparable in mutants and wild-type limb buds. In contrast, expression of Sox5 and Sox6, as well as that of bone morphogenetic protein receptor-1b, was completely downregulated, and expression of Runx2/Cbfa1 was severely inhibited in mutant limb buds. Embryos harboring Col2a1-Cre, in which Sox9 was deleted after chondrogenic mesenchymal condensations were established, exhibited a severe generalized chondrodysplasia, similar to that in Sox5; Sox6 double-null mutant mice. In these Sox9-/- mutants, most cells were arrested as condensed mesenchymal cells and did not undergo overt differentiation into chondrocytes. Furthermore, chondrocyte proliferation was severely inhibited, and characteristic columns of proliferating chondrocytes were absent. The presence of hypertrophic chondrocytes suggested that some cells underwent overt chondrocyte differentiation but that as soon as the Sox9 gene was inactivated they were promptly converted into hypertrophic chondrocytes. Moreover, expression of Indian hedgehog, Patched1, parathyroid hormone-related peptide (Pthrp), and Pth/Pthrp receptor were downregulated in mutant embryos. We conclude that Sox9 is needed during successive steps of the chondrocyte differentiation pathway and is required for Sox5 and Sox6 expression during chondrogenesis.

1072

Mutation in cGMP-dependent Protein Kinase 2 Causes Dwarfism in a Novel Rat Mutant, MRI, through Uncoupling of Proliferation and Differentiation of Chondrocytes. H. Chikuda[1], K. Hoshi[1], T. Shimoaka[1], T. Akune[1], H. Kawano[1], K. Kawano[1], K. Nakamura[1], U. Chung[1], K. Komeda*[2], H. Kawaguchi[1]. [1]Orthopaedic Surgery & Tissue Eng., Univ. of Tokyo, Japan, [2]ARC, Tokyo Medical College, Japan.

The miniature rat Ishikawa (MRI) is a naturally occurring mutant which exhibits longitudinal growth retardation caused by an autosomal recessive mutation. Limbs and trunk of MRI (*mri*/*mri*) are 30-40% shorter than those of wild-type (WT or +/+) and +/*mri* littermates, although the mutant is healthy and fertile without major organ abnormalities. To identify the mutation, we performed positional candidate cloning. The *mri* locus was mapped to a genomic region between D14rat76 and D14rat6, in which several candidates were identified by comparative mapping. By sequencing them, we found a 220-bp deletion in the cGMP-dependent protein kinase 2 (cGK2) transcript in MRI, which resulted in a frame shift and a premature stop codon, predicting a truncated product that lacks the kinase domain. cGK2 is an intracellular signaling molecule of C-type natriuretic peptide, an important regulator of endochondral bone formation. Histomorphometric analysis of MRI at 10 weeks showed normal bone density and turnover; however, height of its growth plate was about 2.5-fold that of WT with a thick layer of small and flattened chondrocytes between the proliferative and hypertrophic zones. BrdU labeling and immunohistochemistry / in situ hybridization for differentiation markers (PTH/PTHrP receptor, Ihh, ALP and COL X) revealed that these chondrocytes were abnormal cells that had stopped proliferation but had not started differentiation into hypertrophic chondrocytes. Although the hypertrophic zone was irregular and narrow in MRI, mineralization and blood vessel invasion were normal. Similar impairment of endochondral bone formation was observed during the fracture healing process after osteotomy in the MRI tibiae. We further examined the functions of cultured primary growth plate chondrocytes. Cellular proliferation was similar between MRI and WT; however, differentiation of MRI chondrocytes determined by alcian blue and ALP staining was markedly suppressed compared to that of WT cells. Differentiation of WT chondrocytes was impaired when cocultured with MRI chondrocytes in a double chamber dish separated by a porous membrane, although that of MRI cells was not rescued by WT cells. This suggests that there is an autocrine / paracrine factor(s) which is stimulated by cGK2 dysfunction and prevents chondrocyte differentiation. In conclusion, a mutation in cGK2 causes growth retardation in MRI due to impaired endochondral bone formation. cGK2 may play an important role in the coupling of proliferation and differentiation of chondrocytes.

1073

Interleukin-11 Receptor Signaling Is Required for Normal Bone Remodeling in Male and Female Mice. N. A. Sims[1], B. J. Jenkins*[2], J. M. W. Quinn[3], K. W. Ng[1], T. J. Martin[3], M. T. Gillespie[3], L. Robb*[4], M. Ernst*[2]. [1]Department of Medicine at St. Vincent's Hospital, University of Melbourne, Fitzroy, Australia, [2]Ludwig Institute for Cancer Research, Melbourne, Australia, [3]St. Vincent's Institute of Medical Research, Fitzroy, Australia, [4]Walter and Eliza Hall Institute, Melbourne, Australia.

Interleukins 6 and 11 have been implicated in bone loss in estrogen deficiency due to their ability to stimulate osteoclastogenesis in vitro and to reduced production of IL-6 and IL-11 by stromal cells in the presence of estradiol. Furthermore, the roles of these two cytokines have been linked, with the suggestion that each may compensate for the absence of the other to maintain trabecular bone volume and turnover. To determine whether IL-11 is required for normal bone turnover, we examined the bone phenotype of mature male and female IL-11 receptor knockout mice (IL-11Rα KO). IL-11Rα was disrupted such that no full-length or truncated transcripts were expressed (Robb et al, Blood, 1997). Tibiae from intact 16 week old male and female mice were collected and studied by dynamic bone histomorphometry. In both male and female IL-11Rα KO mice, trabecular bone volume was approximately double that of wild type littermate controls (mean BV/TV ± SEM: female wild type: 6.0 ± 0.9; female IL-11Rα KO: 12.2 ± 1.4, male wild type: 8.9 ± 0.4; male IL-11Rα KO: 14.3 ± 0.5). This high bone volume was associated with a high trabecular number and a low level of bone turnover. For example, osteoblast surface was reduced to less than 50% of wild type levels, osteoclast surface was reduced by 20% and bone formation rate was reduced by 40% compared with wild type littermates. The low bone turnover and high trabecular bone volume in these mice indicate that IL-11Rα signaling is required for normal bone turnover in both male and female mice. Since it has been suggested that IL-6 and IL-11 play similar and complementary roles, with the ability to compensate for the absence of the other, we also examined the bone phenotype of IL-6 KO mice, and mice lacking both IL-6 and IL-11Rα (compound knockouts). As previously reported, the bones of IL-6 KO mice were not significantly different to wild type mice; neither trabecular bone volume nor bone turnover were altered. However, compound IL-6 KO/ IL-11Rα KO mice demonstrated an identical bone phenotype to the IL-11Rα KO, with a high trabecular bone volume and low bone turnover, indicating that normal bone mass and turnover in IL-6 knockouts does not relate to IL-11 compensation. Furthermore, reduced bone turnover and increased bone volume in IL-11Rα null mutants is not mediated by changes in IL-6, nor worsened by its absence.

1074

TGF-b2 Regulates Chondrocyte Differentiation and Proliferation During Embryonic Development. J. Alvarez-Pinera*, A. Mukherjee*, R. Serra. Molecular and Cellular Physiology, University of Cincinnati, Cincinnati, OH, USA.

Indian hedgehog (Ihh) and Parathyroid Hormone related Peptide (PTHrP) regulate the rate and extend of endochondral bone growth through the establishment of a negative-feedback loop in which production of Ihh by prehypertrophic chondrocytes induces PTHrP expression in the periarticular perichondrium which in turn inhibits hypertrophic differentiation. We have shown that PTHrP also acts downstream of transforming growth factor b (TGF-b) in a common signaling cascade to regulate hypertrophic differentiation in embryonic mouse metatarsal cultures. Transgenic mice that express a dominant-negative mutation of the TGF-b type II receptor in skeletal tissue demonstrated increased terminal differentiation and persistent expression of Ihh in growth plate chondrocytes. Since Ihh normally acts as an inhibitor of chondrocyte differentiation it was proposed that TGF-b was required for Ihh-mediated inhibition. Previously we showed that Sonic hedgehog (Shh) a functional substitute for Ihh, stimulates expression of TGF-b2, TGF-b3 and PTHrP in the perichondrium of metatarsal organ cultures. In this study we propose a model where TGF-b acts downstream of Ihh and upstream of PTHrP to regulate hypertrophic differentiation. First, we show using adenovirus mediated gene transduction into the organ cultures that TGF-b signaling in the perichondrium is required for Shh-mediated stimulation of PTHrP expression. We also show that the effects of Shh are specifically dependent on TGF-b2, as metatarsal cultures from TGF-b3 null embryos respond to Shh but cultures from TGF-b2 null embryos do not. The data suggest that TGF-b2 acts as a signal relay between Ihh and PTHrP in the regulation of hypertrophic differentiation. Next, we tested the effect of TGF-b2 treatment in intact and perichondrium free cultures. TGF-b2 treatment inhibited chondrocyte growth and differentiation as well as dramatically enhanced PTHrP expression in the perichondrium. Removal of the perichondrium blocked the ability of TGF-b2 to inhibit bone growth and hypertrophic differentiation. Next the role of TGF-b2 on chondrocyte proliferation and differentiation in vivo was tested using 17.5 day embryos from crosses of TGF-b2+/- mice. TGF-b2-/- embryos showed higher levels of chondrocyte proliferation when compared to wild type littermates. Long bones of TGF-b2-/- embryos also demonstrated higher levels of type X collagen expression than that observed in wild type embryos. These data suggest that TGF-b2 signaling not only plays a main role in the regulation of chondrocyte differentiation acting as a signaling relay between Ihh and PTHrP but also regulates chondrocyte proliferation during embryonic development.

1075

Dramatic Low-Turnover Osteoporosis in a Noggin-Overexpressing Mouse Establishes the Essential Role for Noggin in the Negative Regulation of Osteoblast Differentiation and Bone Formation. X. B. Wu, A. Schneider*, M. Zaidi, E. Abe. The Mount Sinai Bone Program and Bronx VA GRECC, New York, NY, USA.

Here we provide evidence that establishes noggin, a BMP antagonist, as a negative regulator of osteoblast differentiation and bone formation. Mice overexpressing noggin at ~10-fold higher levels in mature osteoblasts under the control of the osteocalcin promoter, OG-2, became overtly osteoporotic at 8 months. This was accompanied by radiological osteopenia coupled with significantly reduced bone mineral density at the lumbar spine, femur and tibia. Histological analysis revealed a marked loss of trabecular bone in the face of modest cortical thinning. Osteoblast differentiation in *ex vivo* bone marrow cell cultures, determined by counting early fibroblastoid and late mineralizing osteoblastoid colony forming units (CFU-Fs and CFU-OBs), was diminished by ~40%. In contrast, TRAP-positive osteoclast formation in hematopoetic stem cell cultures was only marginally reduced indicating a weak effect of noggin-overexpression *in vivo* on osteoclastogenesis. In 4 month-old mice, the bone phenotype remained subtle with histological evidence of disorganized endochondral bone formation and reduced CFU-OB formation in *ex vivo* marrow cell cultures. Bone mineral density, CFU-F counts, and osteoclast formation remained largely unaffected. In parallel *in vitro* studies, we over-expressed noggin or the constitutively activated BMP receptor 1A, ca-ALK-3, in pre-osteoblastic UAMS-33 cells using a retrovirus. Ca-ALK-3 is known to trigger BMP signaling in the absence of ligand, and is thus expected to be insensitive to the BMP antagonist, noggin. We found that noggin-overexpressing osteoblasts displayed decreased differentiation, measured both as alkaline phosphatase activity and osteocalcin expression. The pro-differentiation effects of BMP-2 were expectedly dampened in these cells compared with those infected with empty vector. Osteoblast proliferation, however, remained unaffected. Furthermore, co-culture of noggin-overexpressing cells with hematopoetic osteoclast precursors resulted in a marked reduction in osteoclast formation, consistent with our earlier observation for reduced RANK-L expression in, and hence, the diminished osteoclast-supporting function of osteoblasts treated with recombinant noggin. Ca-ALK-3 over-expressing pre-osteoblasts, in contrast, showed a pronounced enhancement of osteoblast differentiation that was, as expected, mostly insensitive to inhibition by noggin. Together, the results argue strongly for noggin, acting through disruption of BMP action, as a negative regulator of osteoblast maturation and function during adult skeletal remodeling.

1076

Impaired Osteogenic Response of *Bmp6* Null Mice. K. E. McDougall*[1], M. J. Perry[2], T. Whitworth*[2], S. M. Colley*[1], E. J. Robertson*[3], J. H. Tobias[1]. [1]Rheumatology Unit, University of Bristol, Bristol, United Kingdom, [2]Department of Anatomy, University of Bristol, Bristol, United Kingdom, [3]Department of Molecular and Cell Biology, Harvard, Cambridge, MA, USA.

In a recent study of the role of regulatory factors in bone formation, BMP-6 was found to be up-regulated during the osteogenic response of long bones to high-dose estrogen in female mice. To explore the role of BMP-6 in new bone formation induced by estrogen, we investigated whether this response is impaired in *Bmp6* null mice. Other than delayed ossification of the sternum in late gestation embryos, the latter have previously been reported to have a normal skeletal phenotype. A breeding colony of *Bmp6* null mice was established in our animal facility, crossed with resident C57Bl/6 animals. F1 heterozygotic offspring produced were interbred to generate homozygous knockouts and wild-type littermate controls as identified by PCR genotyping. Ten-week-old female wild-type and *Bmp6* null mice were subsequently separated into groups of 7-8, and administered 17beta-estradiol 0, 4, 40, 400, 4000microg/kg/day for 28 days. These doses were selected based on previous studies to identify the full dose-response range for estrogen-induced osteogenesis in mouse long bones. Animals were subsequently sacrificed, long bones removed, and DXA analysis performed on the proximal tibial metaphysis and distal femoral metaphysis using a Lunar PIXI with dedicated mouse software. In line with previous studies where we correlated histological measures of bone formation following estrogen with DXA analysis at these sites, we found a highly significant increase in BMD at the tibial and femoral metaphyses in response to estrogen ($p<0.0001$). However, the response to higher doses of 17beta-estradiol was significantly reduced in *Bmp6* null mice compared to controls (results show mean +/- SEM g/cm^2; *$p<0.01$ versus wild-type mice by one-way ANOVA). We conclude that the osteogenic response of female mouse long bones to high-dose estrogen is impaired in in *Bmp6* null mice, suggesting that BMP-6 plays a non-redundant role in this response that is not fully compensated for by other regulatory pathways.

	Tibial Metaphysis		Femoral Metaphysis	
	Wild-type	*Bmp6* null	Wild-type	*Bmp6* null
Vehicle	102+/-5	110+/-3	118+/-4	117+/-2
E4	122+/-3	130+/-7	138+/-5	134+/-7
E40	142+/-8	142+/-6	146+/-7	140+/-4
E400	163+/-9	141+/-5*	164+/-8	155+/-3
E4000	165+/-5	141+/-3*	168+/-5	146+/-7*

1077

Sclerostin: An Osteocyte-expressed BMP Antagonist that Inhibits Bone Formation by Mature Osteoblasts. R. L. Van Bezooijen[1], D. Winkler*[2], T. Hayes*[2], M. Karperien[1], A. Visser*[1], L. van der Wee-Pals*[1], H. Hamersma*[3], S. E. Papapoulos[1], J. A. Latham[2], C. W. G. Lowik[1]. [1]Endocrinology, Leiden University Medical Center, Leiden, Netherlands, [2]Celltech Inc., Bothell, WA, USA, [3]Florida Park, Roodepoort, South Africa.

Sclerosteosis is a sclerosing skeletal disorder characterized by generalized progressive bone overgrowth due to loss of the SOST gene product sclerostin. Bone formation is systemically increased, while bone resorption is generally not affected. Sclerostin belongs to the DAN family of BMP antagonists and preferentially binds and inhibits BMP-5 and 6. SOST mRNA expression is restricted to mineralized osteoblastic cultures and, in vivo, to mineralized bone of fetal and neonatal mice. In the present study, using in situ hybridization, we identified osteocytes as the only cells expressing SOST in bone of young adult mice. By immunochemistry, sclerostin protein expression was found to be restricted to osteocytes in human bone specimen of a 22-week-old fetus, a 6-month-old baby, and 16 adults. Interestingly, osteocyte canaliculi and/or lacunae stained positive for sclerostin, suggesting that the protein is transported to neighboring osteocytes or osteoblasts at the bone surface. Specificity of the sclerostin signal was shown by the absence of any signal in bone biopsies of 4 patients with sclerosteosis. Sclerostin treatment of mouse pre-osteoblastic KS483 cell cultures only slightly suppressed alkaline phosphatase activity, an early osteoblast differentiation marker. This is in contrast to other BMP antagonists, such as noggin, that block differentiation of these cells. Sclerostin treatment (1 microg/ml and higher) during specific stages of osteoblast differentiation strongly reduced calcium deposition only when added before onset of mineralization, i.e. before induction of SOST expression. Addition of sclerostin during only the early stages of osteoblast development had no effect. In contrast, noggin blocked calcium deposition when added during only these early stages. In conclusion, sclerostin is a unique BMP antagonist and the first to be associated with a human bone disorder. In contrast to other BMP antagonists, it is specifically expressed by osteocytes and inhibits BMP activity on mature osteoblasts rather than the progenitors and precursors. Sclerostin may be the osteocyte-derived factor controlling the active bone-forming phase of mature osteoblasts as suggested in Marotti's theoretical model. Its absence, as in sclerosteosis, keeps osteoblasts in a state of continuous bone deposition and, as a consequence, increases bone formation.

1078

Targeted Deletion of the TGF-ß type II Receptor in Cartilage. R. Serra, E. Slattery*, P. Sohn*, J. Alvarez*, A. Mukherjee*. Molecular and Cellular Physiology, University of Cincinnati, Cincinnati, OH, USA.

Members of the TGF-ß superfamily are secreted signaling proteins that regulate many aspects of skeletal development. Previously, we demonstrated that dominant-negative interference of TGF-ß signaling in the periosteum/perichondrium of transgenic mice results in increased hypertrophic differentiation in growth plate chondrocytes suggesting a role for the perichondrium in regulating differentiation in the growth plate. Recently, we demonstrated that TGF-ß1-mediated inhibition of growth and hypertrophic differentiation in mouse embryonic metatarsal organ cultures is dependent on the perichondrium. To address the question of the role of TGF-ß signaling directly in chondrocytes, we generated mice with targeted deletion of the TGF-ß type II receptor in cartilage using the cre/lox recombinase system. Mice expressing cre under the control of the type II collagen promoter (Col IIcre) were crossed to mice in which the type II receptor gene was flanked with bacterial loxP sites (TgfbrloxP/loxP). Newborn offspring as well as embryos at 17.5 and 13.5 days of gestation were genotyped to determine the actual versus the expected ratio of each genotype. The ratio of newborn mice with the ColIIcre+/-;TgfbrloxP/loxP genotype was far below expected (7% versus 25%). The ratio of ColIIcre+/-;TgfbrloxP/loxP embryos 17.5 and 13.5 days of gestation were as expected suggesting mice with the ColIIcre+/-;TgfbrloxP/loxP survived until late in gestation but did not survive birth. Next alizarin red/ alcian blue stained skeletons were prepared from embryos at 17.5 days of gestation. Skeletal preparations from ColIIcre+/-;TgfbrloxP/loxP embryos were compared to those from ColIIcre-/-;Tgfbr+/loxP embryos. ColIIcre+/-;TgfbrloxP/loxP embryos were smaller than control embryos. However, no dramatic differences were detected in the length or hypertrophic area of the long bones of the limbs suggesting TGF-ß signaling directly in chondrocytes does not regulate these processes and supporting our model where TGF-ß signals to the perichondrium to regulate development of the long bones. The most dramatic phenotype was observed in the vertebrae. Specifically, each vertebrae was shorter than control and the neural arch and dorsal spine were either absent or not well developed. While the vertebral bodies were only moderately affected, the intervetebral discs were either missing or incomplete. Defects in the connection between the thoracic vertebrae and the ribs were also detected. The data suggest that TGF-ß signaling is critical for proper development of the axial skeleton and we are currently testing hypotheses regarding the mechanism of this regulation.

1079

Quantitative Trait Loci for Spine bone Mineral Density are Linked to Chromosome 19q in Men and Women and to 21q in Women Less Than 50 Years Old. C. M. Kammerer[1], B. D. Mitchell[2], J. L. Schneider*[3], S. A. Cole*[3], J. E. Hixson*[4], R. Perez*[5], R. L. Bauer[5]. [1]University of Pittsburgh, Pittsburgh, PA, USA, [2]University of Maryland School of Medicine, Baltimore, MD, USA, [3]Southwest Foundation for Biomedical Research, San Antonio, TX, USA, [4]University of Texas Health Science Center at Houston, Houston, TX, USA, [5]South Texas Veterans' Health Care Systems, San Antonio, TX, USA.

The San Antonio Family Osteoporosis Study was designed to detect and locate genes that affect bone mineral density (BMD) using data on 34 large, Mexican American families. We performed a genome scan using variance components linkage analysis to detect quantitative trait loci (QTLs) that affect bone mineral density of the spine. Genotypic data on 389 microsatellites (a 9.9 cM map) were available on 657 individuals aged 20 years and older from the largest 23 families. Spine BMD was measured using dual x-ray absorptiometry. Previous analyses of these families revealed that residual heritability of spine BMD was 0.51 overall, but differed between men and women (0.53 vs 0.77), and between women <=50yo and >50yo (0.84 vs 0.56). Therefore, we performed genome scans overall and separately in men (n=258), women (n=399), and women <= 50yo (n=287). Overall, we found suggestive evidence that a QTL on chromosome 19q near locus D19S433 (at 47 cM pter) affects spine BMD (multipoint lod =2.3, nominal p =0.0005). We obtained no evidence for QTLs in men or women analyzed separately (all lods < 1.9), but in women <= 50yo, we obtained significant evidence for a QTL on chromosome 21q near marker D21S1446 at 62cM pter (multipoint lod =3.2, nominal p =0.00006). We also observed suggestive evidence for linkage to 19q in these women (multipoint lods =1.8). Our detection of an additional QTL on 21q in women <=50yo, but not in the other groups, may not be surprising given that heritability of spine BMD was highest among this group. This QTL may also have sex-specific effects on spine BMD. We conclude that QTLs affecting variation in spine BMD may be located on chromosomes 19q and 21q.

1080

Gender Sensitivity for an IGF-I Quantitative Trait Locus (QTL): Defining the Interaction of Estrogen and IGF-I in Peak Bone Acquisition. C. J. Rosen[1], R. Klein[2], E. Orwoll[2], M. L. Bouxsein[1], L. R. Donahue[1], C. Ackert-Bicknell*[1], K. L. Shultz*[1], W. G. Beamer[1]. [1]The Jackson Laboratory, Bar Harbor, ME, USA, [2]Oregon Health Sciences University, Portland, OR, USA.

The strongest quantitative trait loci (QTL) for serum IGF-I in female C3HxB6 F2 mice is located in a 20cM region on Chr 6. This epistatic QTL reduces serum IGF-I and accounts for 8% of the variance among F2 mice. Female N10F2 congenic(6T) mice were constructed so that *c3* alleles from Chr 6 were backcrossed into B6 (N10); female 6T mice have serum and hepatic (but not bone) IGF-I expression 20-25% lower than B6 throughout puberty with smaller femorae and reduced trabecular connectivity. Male 6Ts differ from females by having low serum IGF-I but only at 16 weeks;although femoral BMD is reduced in males, femoral length and area are identical to B6. Hence,based on this gender difference we hypothesized that estrogen might modulate the action of gene(s) contained within this QTL.To test that tenet, we first wanted to establish that the QTL on Chr 6 was gender specific. We measured serum IGF-I in > 300 male and female 16 week mice from 23 BXD RI strains and performed whole genome scanning. An IGF-I QTL for female mice only on Chr 6 (p= 2.3 $x10^{-3}$) mapped to a region identical to the QTL for the C3B6 F2 female mice. In the RIs, there was strong gender x strain effect (p=1.0x 10^{-4}). Next, to test the role of estrogen in modulating IGF-I in the congenic, we ovariectomized 4 month 6Ts and compared them with ovariectomized congenics on B6 carrying a QTL from C3H for BMD but not IGF-I (4T)and ovx'd B6 littermates. Femoral BMD and IGF-I were measured 6 weeks after ovx. Despite similar rates of bone loss post ovx, serum IGF-I increased in 6Ts but not 4Ts or B6;this increase (249 $\pm$ 12 to 289 $\pm$11 ng/ml;p=0.003)brought serum IGF-I levels close to basal sham B6 and ovx B6 levels (IGF-I sham B6:300 $\pm$ 10;ovx B6:306$\pm$30ng/ml). In conclusion the Chr 6 QTL for serum IGF-I: 1) contains an important gene that down-regulates IGF-I expression in several strains of mice; 2) is gender sensitive and exerts it effect on IGF-I during early phases of rapid linear growth and bone acquisition in females; 3) is regulated by endogenous estrogen concentrations. Identifying the gene within this QTL may elucidate the interaction between estrogen, IGF-I and bone acquisition.

Congenic Strain	4-T (n=21)	6-T (n=19)	P: 6-T vs 4-T
% decrease in Tot Fem BMD (ovx vs sham-ovx)	-5.9 +/- 2.3%	-5.2 +/- 1.3 %	0.800
% increase IGF-I (ovx vs sham-ovx)	+0.00 +/- 2.0%	+16.2 +/- 4.1%	0.0003

1081

Characterization of Mutations in the Chloride Channel 7 (ClCN7) Gene That Cause Autosomal Dominant Osteopetrosis, Type II. S. G. Waguespack[1], K. E. White[2], D. L. Koller[3], G. Carn*[2], K. A. Buckwalter*[4], W. E. Evans*[2], M. L. Johnson*[2], M. Kocisko*[2], T. Foroud[3], M. J. Econs[5]. [1]Medicine and Pediatrics, Indiana University, Indianapolis, IN, USA, [2]Medicine, Indiana University, Indianapolis, IN, USA, [3]Medical and Molecular Genetics, Indiana University, Indianapolis, IN, USA, [4]Radiology, Indiana University, Indianapolis, IN, USA, [5]Medicine and Medical and Molecular Genetics, Indiana University, Indianapolis, IN, USA.

Autosomal dominant osteopetrosis, Type II (ADO2) is an uncommon sclerosing bone disorder with a distinct radiographic appearance and unique clinical characteristics. We currently present the results from genetic studies designed to identify the ADO2 gene through a positional candidate approach. Initially, linkage studies were undertaken in our 7 largest kindreds and a summed maximum LOD score of 15.91 was observed at marker D16S521 on chromosome 16p13.3. Critical recombinations in affected subjects further narrowed the putative gene region to a 7.6 cM (3.5 Mb) region between markers D16S521 and D16S3027. Multiple candidate genes were identified in this region, including ATP6L and ClCN7. Mutational analysis of the 3 exons of the ATP6L gene revealed no mutations in affected subjects from 13 different families. Concomitantly, ADO2 was reported to result from mutations in the chloride channel 7 (ClCN7) gene (Cleiren et al. 2001 Hum Mol Genet 10:2861-7). Direct DNA sequencing of ClCN7 exons revealed one novel and two known missense mutations in 5 kindreds, three of which were large families that had previously been linked to this area. Families EOP2, EOP17, and EOP19 shared the same mutation (R286W) in exon 10, family EOP10 had a mutation (R767W) in exon 24, and

EOP8 was found to have a novel mutation (R762L) in exon 24. The latter mutation, which occurred in a sporadic yet typical case of ADO2, was confirmed through repeat sequencing of the proband and RFLP analysis of the proband plus 82 control subjects. In families with non-sporadic cases (EOP2, EOP10, and EOP17), the known ADO2 mutations segregated with the disorder in at least three generations and were not detected in a minimum of 50 control subjects. Mutation analysis of the ClCN7 gene continues in our other osteopetrosis families, including 4 kindreds with suggestive linkage to chromosome 16p13.3. In summary, we report the results of our positional candidate studies to identify the ADO2 gene. In five osteopetrosis families we have identified one novel and two known missense mutations in the ClCN7 gene. Furthermore, our data, in concert with that of others, suggests that genetic heterogeneity does not exist in ADO2. We conclude that mutations in the ClCN7 gene are responsible for the sclerotic bone disorder, ADO2.

1082

Novel Polymorphisms in the Promoter of the 24-Hydroxylase Gene Alter Transcriptional Activity. N. Schuetze[1], O. Poeppelmeier*[2], B. Mentrup*[3], C. Schohe-Reiniger*[2], F. Jakob*[2]. [1]Molecular Orthopaedics, Orthopaedische Universitaetsklinik, Wuerzburg, Germany, [2]Orthopaedische Universitaetsklinik, Wuerzburg, Germany, [3]Abteilung Molekulare Innere Medizin, Medizinische Poliklinik, Wuerzburg, Germany.

24-hydroxylase (24OHase) is involved in controlling local and circulating levels of 1,25-dihydroxyvitamin D3 (1,25(OH)2D3) by inactivating the active hormone to 1,24,25(OH)3D3. Additionally, this enzyme also generates 24,25(OH)2D3 from 25(OH)D3. This metabolite locally plays an important role and signals via a specific membrane receptor. A region within the promoter of the gene 24OHase containing two A-stretches was analyzed by fragment analysis and sequencing using an ABI 310 sequencer. PCR products from genomic DNA were subcloned into the pGL3 basic plasmid. Plasmids were transiently transfected into osteoblasts and chondrocytes by electroporation and promoter activity was measured in triplicate and expressed as luciferase units per µg protein. 24OHase promoter sequences were amplified from 72 human DNA samples. Performing fragment analysis 27 PCR products displayed variations in peak patterns indicative for polymorphisms of the respective genomic DNA. Variations in the length of the oligo-A stretches in the 24OHase promoter were found in 1/3 of the samples and a 5bp insertion was detected in 4 cases. Promoter constructs containing up to 580nt´s downstream of the transcriptional start site representing the published promoter of the 24OHase gene as well as constructs with the detected polymorphisms were transfected into human osteoblasts (hFOB-cells) and chondrocytes (T/C 28-1cells). Marked differences in promoter activity were observed reproducibly in both cell lines (n=7 independent experiments). Addition of 1 or 2 A-residues within the A-stretches enhanced promoter activity 2.5fold and 3fold, respectively, compared to the wild type promoter. The plasmid containing an insertion within the A-stretch displayed a 1.5fold reduced promoter activity. These altered transcriptional activities were obtained at basal conditions (no treatment of cells) and were maintained under conditions of 4-6fold promoter activation due to treatment with 10nM 1,25(OH)2D3. In summary, several new polymorphisms were detected in the promoter of the human 24OHase gene. These sequences markedly influenced promoter activty in vitro. Therefore, the detected novel polymorphisms within the promoter might correspond to altered enzyme activity of 24OHase in vivo within the human population. We conclude that altered transcriptional activities of the alleles of the 24OHase gene in vivo might influence vitamin D metabolism as well as local signaling of 24,25(OH)2D3.

1083

Dissociation of the Genetic and the Epigenetic Defect at the *GNAS1* Locus in Pseudohypoparathyroidism 1b. S. M. Jan de Beur, C. Ding, J. Y. Cho*, M. A. Levine. Medicine and Pediatrics, Johns Hopkins University, Baltimore, MD, USA.

Subjects with pseudohypoparathyroidism 1b (PHP 1b) have renal resistance to PTH and lack Albright hereditary osteodystrophy. By contrast to PHP 1a, levels of Gsα protein are not reduced, and the 13 exons of *GNAS1* that encode Gsα are normal. *GNAS1* has 3 upstream alternative first exons (NESP55, XLαs, and exon A) that are bidirectionally imprinted. The recent demonstration that subjects with PHP 1b have defects in methylation of maternally inherited *GNAS1* alleles suggests that an imprinting defect that affects expression of *GNAS1* in the proximal renal tubule is the basis for this disorder. The specific genetic mutation(s) that accounts for this epigenetic defect is unknown, however. To understand the relationship between the genetic defect and the epigenetic defect in PHP 1b, we studied five multigenerational PHP 1b families. Using linkage analysis, we found that the genetic defect causing PHP 1b maps to a 5.7 cM interval on chromosome 20q13 that includes part of *GNAS1* and regions telomeric to *GNAS1*. Based on this analysis, disease-associated haplotypes were identified. In addition, we analyzed allelic expression and methylation of CpG islands within exon A of *GNAS1* in these five PHP 1b kindreds. cDNA transcribed from total RNA from mononuclear cells or transformed lymphoblasts was amplified with a downstream primer in exon 6 and an upstream primer in exon A of *GNAS1*. PCR products were directly sequenced and allelic expression was determined using polymorphisms in exon 5 or exon A. The methylation status of exon A was determined by sequencing bisulfite-treated genomic DNA or by restriction endonuclease analysis with *NgoM*IV, a methylation-sensitive enzyme. In the PHP 1b kindreds investigated, all subjects with PTH resistance showed loss of methylation of the exon A region on the maternal *GNAS1* allele and/or biallelic expression of exon A-containing transcripts. Moreover, affected subjects had a maternally-inherited, disease-associated haplotype, whereas unaffected subjects who were obligate gene carriers had inherited the same haplotype paternally. Remarkably, analysis of one pedigree demonstrated a novel dissociation between inheritance of the disease-associated locus and the epigenetic *GNAS1* defect as members of the same sibship showed either PTH resistance or PTH responsiveness despite having inherited the same *GNAS1* haplotype from their mother. The absence of the epigenetic defect in subjects who have inherited a defective maternal *GNAS1* allele yet lack hormone resistance indicates that the genetic mutation may be incompletely penetrant, and implies that the epigenetic defect and not the genetic mutation is the cause of renal resistance to PTH in PHP 1b.

1084

The Osteopetrotic Mutation toothless (tl) Is a Loss-of-Function Mutation in the Rat CSF-1 Gene, Confirming a Crucial Role for CSF-1 in Osteoclastogenesis and Endochondral Ossification. W. Van Hul[1], P. R. Odgren[2], L. Van Wesenbeeck*[1], F. F. Safadi[3], S. N. Popoff[3], S. C. Marks[2]. [1]Medical Genetics, University of Antwerp, Antwerp, Belgium, [2]Cell Biology, University of Massachusetts Medical School, Worcester, MA, USA, [3]Anatomy and Cell Biology, Temple University School of Medicine, Philadelphia, PA, USA.

The biology and actions of the monocyte/macrophage colony stimulating factor CSF-1 (mCSF) have been elucidated by numerous studies that utilise the naturally occurring CSF-1 frameshift mutation in the osteopetrotic (op) mouse. Along with many abnormalities in the immune and reproductive systems, the op mouse is deficient in bone-resorbing osteoclasts, which over the first few months of life corrects itself. Another rodent osteopetrotic mutation, the toothless (tl) mutation in the rat, has been well-characterized phenotypically, but the genetic lesion has remained unknown. tl is an autosomal recessive mutation whose skeletal consequences include severe osteopetrosis with profound-, unresolving osteoclastopenia, growth deficiency, progressive growth plate chondrodysplasia and abnormal angiogenesis, among other pathologies. Some, but not all, of these benefit from injections of recombinant CSF-1. To evaluate the causal role of the CSF-1 gene in the tl phenotype, we looked for the chromosomal localization of the phenotype-causing gene. Based on the analyses of polymorphic markers in outcrossed animals, evidence was obtained for the assignment of the tl-causing gene to the region of chromosome 2 harboring the CSF-1 gene. Subsequent mutation analysis of the CSF-1 gene in tl rats identified a 10-base-pair duplication in exon 1 resulting in a frameshift mutation and an early stopcodon. The mutated sequence is also present in tl CSF-1 cDNA. The phenotype of the op mouse, caused by a frameshift mutation in exon 4, is far milder than the tl rat: op mice have some osteoclasts, they don't develop the growth plate chondrodystrophy seen in tl rats, and they spontaneously recover over the first few months of life. This difference might be explained if the tl rat represents a genuine CSF-1 loss-of-function mutation and the op mouse is a "leaky" mutation, perhaps due to alternative splicing, as previously proposed. Our findings suggest that a critical re-assessment of studies that have assumed a complete loss of CSF

1085

Rate of Hip Bone Loss Is Greater Among Caucasian vs. African-American Women. J. A. Cauley[1], L. Lui[2], K. L. Stone[2], K. E. Ensrud[3], T. Hillier[4], M. C. Hochberg[5], S. R. Cummings[2]. [1]University of Pittsburgh, Pittsburgh, PA, USA, [2]University of California, San Francisco, CA, USA, [3]University of Minnesota, Minneapolis, MN, USA, [4]Kaiser Center for Health Research, Portland, OR, USA, [5]University of Maryland, Baltimore, MD, USA.

African-American women have higher bone mineral density (BMD) and experience lower fracture rates than Caucasian women. Little is known, however, about the racial/ethnic differences in the rate of bone loss. In the current study, we tested the hypothesis that the rate of hip bone loss is greater in Caucasian women compared with African-American women and in both groups, the rate of bone loss increases with age. We compared 6,007 Caucasian women (mean age 73 yr) with 482 African-American women (mean age 75 yr) enrolled in the Study of Osteoporotic Fractures. Total hip and femoral neck BMD was measured by DXA (QDR 1000 or 2000, Hologic Inc., Bedford, MA). The type of scanner was the same across visits. The average interval between DXA scans was 3.5 years ± 0.4, Caucasians and 2.0 years ± 0.1, African-Americans. Stepwise linear regression was used to compare differences in the rate of bone loss between ethnic groups adjusting for factors previously shown to predict bone loss in Caucasians including age, weight change, smoking, grip strength, estrogen, diabetes and pulse rate. The African-American women had a greater body weight, grip strength, initial BMD and a higher prevalence of diabetes than Caucasian women. There was no difference in current smoking or use of estrogen. The multivariate-adjusted average annualized percent rate of change in bone density among Caucasian and African-American women respectively was -0.57% and -0.33% ($p< 0.0001$) at the total hip and -0.51% and -0.31% ($p=0.04$) at the femoral neck. The annualized rate of bone loss was higher among women age ≥75 compared with women < age 75 in both ethnic groups but within each age group, African-American women lost less bone (Table).

Table: Annualized % Bone Loss in African-American and Caucasian Women by Age

	African-American		Caucasian	
Total Hip	(n)	Mean ± SD	(n)	Mean ± SD
Age < 75	(255)	-0.08 ± 1.9	(4188)	-0.44 ± 1.4
Age ≥ 75	(227)	-0.61 ± 2.1	(1819)	-0.89 ± 1.6
Femoral Neck				
Age < 75	(255)	-0.09 ± 3.1	(4188)	-0.45 ± 1.7
Age ≥ 75	(227)	-0.42 ± 3.5	(1819)	-0.65 ± 1.9

In conclusion, the rate of bone loss was greater among Caucasian than African-American women. But, within each race, the rate of bone loss increased with advancing age, especially among African-American women.

1086

Volumetric Femoral Neck Bone Density as a Single Measure of Hip Fracture Risk in Men and Women. J. R. Center, T. V. Nguyen, J. A. Eisman. Bone and Mineral Research Program, Garvan Institute of Medical Research, Sydney, NSW, Australia.

Proximal femur bone density T-scores are widely used to indicate fracture risk based on epidemiological and non randomized controlled trial data in women. An equivalent cut-off value for men has not been determined although - 2.5 SD is commonly used clinically without adequate supportive evidence, particularly considering areal BMD is higher for men than women. Areal bone density does not account for bone depth, such that a larger bone will generally have a greater areal BMD for the same true volumetric density. The aim of this study was to examine whether volumetric BMD, calculated using estimated mean femoral neck width, may be a more appropriate measure to determine hip fracture risk between men and women. Of 925 women and 658 men followed prospectively for 10.4 ± 2.7 years (mean ± SD) from the Dubbo Osteoporosis Epidemiology Study, 73 women and 23 men had a hip fracture following or within 3 months of a DXA scan. Hip fracture subjects were older than their non-fracture counterparts (77 ± 8 vs 70 ± 7 years, p = 0.0001). Areal BMD was lower in women than men for both hip fracture (0.63 ± 0.11 vs 0.76 ± 0.14 g/cm2, p = 0.0001) and non-fracture subjects (0.81 ± 0.12 vs 0.93 ± 0.15 g/cm2, p = 0.0001). In contrast, although volumetric BMD was also lower in the hip fracture subjects it did not differ between sexes. Volumetric BMD was 0.25 ± 0.04 g/cm3 and 0.26 ± 0.04 g/cm3 for women and men, respectively with hip fractures and 0.31± 0.06 g/cm3 for both women and men without fractures. The sensitivity of a T-score for hip fracture prediction was similar in women for both areal (73%) and volumetric (78%) BMD. However, a volumetric BMD T-score was more sensitive than an areal BMD T-score in men (70% vs 43%) with similar specificity for women (77% vs 75%, men and women, respectively). These data indicate that, with a volumetric estimate of hip BMD, the differences between men and women disappear and that men and women with hip fractures have a similar but lower volumetric BMD than non-fracture men and women. The similar sensitivity of volumetric T-scores in hip fracture prediction between men and women suggest that volumetric femoral neck BMD could be used as a single measure of hip fracture risk in both sexes.

1087

Elderly Long Term Care Residents Continue to Lose Bone, but not Uniformly. K. E. Broe[1], M. T. Hannan[2], C. E. Stewart*[1], D. P. Kiel[2]. [1]Hebrew Rehab Ctr for Aged, Boston, MA, USA, [2]Hebrew Rehab Ctr for Aged & Harvard Med Sch, Boston, MA, USA.

Elderly long-term care (LTC) residents are at high risk of morbidity and mortality due to complications from osteoporotic fracture. Maintaining bone mineral density (BMD) remains a strategy to prevent future fracture in this population. Although longitudinal studies of community-dwelling older persons have shown that bone loss continues into the eighth and ninth decades, the pattern of bone loss among elderly LTC residents has not been clearly established. Therefore, we examined BMD change over two years among residents of a LTC facility in Boston, MA. Participants included 170 residents (123 women, 47 men) aged 69 to 100 years (mean: 88 yrs ±6) who had baseline BMD measured between 1992 and 1997 and at least one annual follow up exam. BMD was measured in g/cm^2 using a Hologic, QDR 1000W at the femoral neck, trochanter, total femur, radial shaft, ultra distal radius and whole body. Rate of BMD change was calculated as sex-specific annual percent change in BMD for each skeletal site. Participants were split into three groups (≤ 85 yrs, 86-91 yrs, and ≥ 92 yrs) and rates of change were compared among age-groups separately by gender. Both women and men had bone loss at all sites. In women, the greatest amount of bone loss occurred at the radial shaft with women losing on average 1.8% per year followed by the total hip site with losses averaging 1.6% per year. In men, the greatest bone loss occurred at the femoral neck with an average loss of 2.3% followed by the total femur (1.5% per year). The whole body site showed the least amount of loss for both women and men. Bone loss did not appear to differ between age-groups at any of the BMD sites (p-trend ≥0.21) except the whole body for which the oldest women (≥ 92 yrs) had significantly increased whole body losses compared with those women in the younger age-groups (mean annual change: ≤ 85 yrs =(+0.3%), 86-91 yrs=(-0.1%), ≥ 92 yrs=(-1.6%), p-trend=0.0005). While all BMD sites, on average, showed bone losses, there was much variability in BMD change. Across all BMD sites, at least 45% of participants had no change (less than ±1%) or actually had an increase in BMD. At the femoral neck site, 28% of participants had no change while an additional 17% had an increase of 1% or more. We conclude that bone loss occurs among elderly LTC residents, but the magnitude of loss does not appear to increase with age. In fact, some residents lost significant amounts of bone while others maintained or even gained BMD. Further understanding of the factors that contribute to BMD change will help in developing additional strategies to care for LTC residents most at risk for bone loss.

1088

Maternal History of Osteoporosis Is Related to Femur Bone Density and Geometry in Men and Women. A. C. Looker[1], T. J. Beck[2]. [1]Natl Ctr Health Stats, CDC, Hyattsville, MD, USA, [2]Johns Hopkins University, Baltimore, MD, USA.

Results from previous studies suggest that family history may affect fracture risk via skeletal factors other than bone density. To address this question, we examined differences in femur neck areal BMD values collected from 5371 non-Hispanic whites ages 20+ years in the third National Health and Nutrition Examination Survey (NHANES III, 1988-94) by reported maternal history of osteoporosis (OP HX). We supplemented the conventional areal BMD data (Hologic QDR 1000) with measurements of areal BMD and geometric properties (subperiosteal width, section modulus, cortical thickness and buckling ratio) made on the same scan data at narrow "cross-sectional" regions traversing the femoral neck and the proximal shaft using a structural analysis program. 221 men and 331 women reported a positive OP HX (e.g., their biological mother had sustained a hip fracture after age 50 years or had a physician's diagnosis of osteoporosis). Differences in bone density and geometry by OP HX were examined after adjusting for potential confounding variables (age, body weight, smoking, personal diagnosis of osteoporosis, health status and hormone use). Several bone parameters differed by OP HX in both sexes at the femur neck, but none differed at the femur shaft. At the neck, those with a positive OP HX had values that differed by ~3-4% (lower for BMD, BMC, cross sectional area, section modulus, and cortical thickness; higher for buckling ratios) from those with a negative OP HX ($p < 0.05$). The relationship between OP HX and these variables did not differ significantly by age in either men or women. In conclusion, regardless of age, both men and women with a positive maternal history of osteoporosis may be at greater risk of femur neck fracture due to thinner cortices and less bone mineral content, which in turn results in potentially less bending strength (section modulus) and greater cortical instability (buckling ratio) at this skeletal site.

1089

The Impact of Magnesium Intake on Fractures: Results from the Women's Health Initiative Observational Study (WHI-OS). R. D. Jackson[1], T. Bassford*[2], J. Cauley[3], Z. Chen[2], A. LaCroix[4], A. Sparks*[4], J. Wactawski-Wende[5]. [1]The Ohio State University, Columbus, OH, USA, [2]University of Arizona, Tucson, AZ, USA, [3]University of Pittsburgh, Pittsburgh, PA, USA, [4]WHI Coordinating Center, Seattle, WA, USA, [5]University of Buffalo, Buffalo, NY, USA.

Magnesium (Mg) deficiency has been associated with the development of parathyroid hormone resistance. Previous studies have suggested that higher Mg intakes may be associated with a higher bone mass but there are no data regarding the role of magnesium intake on fracture risk. We examined the relationship between Mg intake and hip, wrist/lower arm and other clinical fractures in 89,717 postmenopausal women age 50-79 years enrolled in the WHI-OS. Total daily Mg intake was defined as the sum of dietary Mg intake ascertained from Food Frequency Questionnaire and supplement use through direct observation by interviewers, coded using the Medispan database. The average daily Mg intake for the cohort was 320.4 mg/day: 246.9± 98.7 mg/d from diet and 73.5± 154.7 mg/d from supplement. During 4.4 years of follow-up, there were 321 hip, 1582 wrist/lower arm and 4712 other clinical fractures. Incidence of hip and other clinical fractures were similar across the quintiles of Mg intake (0.96 hip fractures and 17.94 other fractures/1000 person-years respectively). In contrast, rates of wrist/lower arm fractures increased in participants with the highest Mg intake relative to the four lower quintiles of Mg intake (5.50 fractures versus 4.56 fractures/1000 person-yrs). Using Cox proportional hazards analyses (with adjustment for age, BMI, smoking, alcohol, exercise, current estrogen use, calcium and history of fracture), the relative hazard (RH) associated with the highest quintile of Mg intake (>431 mg/day) was 1.05 (95% confidence interval 0.77-1.43) for hip fracture, 1.21 (1.06-1.38) for wrist/lower arm fracture and 1.02 (0.96-1.10) for other clinical fractures. The relationship of high Mg intake and wrist/lower arm fracture was stronger in women age 50-64 [RH 1.4 (1.11-1.77)] and with current HRT use [RH 1.57 (1.16-2.14)]. Although there was a relationship between higher Mg intake and higher calcium intake, stratification based on calcium intake did not reveal any significant associations. These findings indicate that high Mg intake does not confer a protective effect against fracture and in fact, may increase the risk of wrist/lower arm fractures in the large WHI-OS cohort.

1090

How Many Deaths from Hip Fracture Might Be Prevented. J. A. Kanis[1], H. Johansson*[2], A. Oden*[2], B. Jonsson*[3], O. Johnell*[4], C. De Laet*[5]. [1]WHO Collaborating Centre for Metabolic Bone Diseas, University of Sheffield Medical School, Sheffield, United Kingdom, [2]University of Stockholm, Stockholm, Sweden, [3]Stockholm School of Economics, Stockholm, Sweden, [4]Malmo General Hospital, Malmo, Sweden, [5]Institute for Medical Technology Assessment, Rotterdam, Netherlands.

Excess mortality is well described after hip fracture. They are in part related to co-morbidity and in part causally related to the hip fracture event itself. The aim of this study was to examine the quantum and pattern of mortality following hip fracture. We studied 160,000 hip fractures in men and women aged 50 years or more in 28.8 million person years from the patient register of Sweden using Poisson nmodels applied to hip fracture patients and the general population. At all ages the risk of death was markedly increased immediately after the event. After a period of declining risk, the risk increased at a rate that was higher than that of the general population. The latter function was assumed to account for deaths related to comorbidity and the residuum assumed to be causally related deaths. Causally related deaths comprised 17-32% of all deaths associated with hip fracture (depending on age) and accounted for more than 1% of all deaths in the population aged 50 years or more. Hip fracture was a more common cause for mortality than pancreatic or stomach cancer. Thus, interventions that decreased hip fracture rate by say 50%, would avoid 0.5% or more of all deaths. This conclusion depends critically upon our assumptions concerning avoidable deaths, but to test this assumption on hip fracture mortality would require an intervention trial of more than 2,000,000 patients.

1091

Monitoring Progression of Breast Cancer Cells in Bone/Bone Marrow by Optical Imaging: Bisphosphonates do not Suppress Tumor Growth Rate and Tumor Burden. G. van der Pluijm[1], B. Sijmons*[1], I. Que*[1], J. Buijs*[1], M. Cecchini*[2], C. Löwik[1], S. Papapoulos[1]. [1]Endocrinology, Leiden University Medical Center, Leiden, Netherlands, [2]Urology, University Hospital, Berne, Switzerland.

Bone metastases are common in patients with breast and prostate cancer and cause considerable morbidity and deterioration of the quality of life. Bisphosphonate (Bp) treatment reduces skeletal-related events by inhibiting tumor-induced osteolysis. In addition, local anti-tumor effects of Bps have been reported in vitro and in an in vivo model of metastatic bone disease. In the latter model, however, evaluation of tumor burden was assessed by measuring lytic bone lesion areas (radiographs) and histomorphometric analyses of tumor areas within the bone collar. In most studies, therefore, the suggested reduction in tumor burden is based primarily on the osteoprotective properties of Bps. Recently, we established an extremely sensitive, non invasive, optical imaging method to detect, monitor and quantify luciferase transfected tumor cells (MDA-MB-231/luc+) in vivo. Optical imaging also enables continuous monitoring in the same animal of growth kinetics for each metastatic site and allows the measurement of the overall tumor burden by photon counting (Am. J. Pathol. 160:1143,2002). We applied this model to determine the effects of different Bps on the local progression of human breast cancer cells in the bone/bone marrow microenvironment. One week after intraosseous injection of MDA-MB-231/luc+ cells into the tibiae of nude mice, the animals were treated with various high doses of bisphosphonates (clodronate, pamidronate, olpadronate) previously shown to completely inhibit osteoclastic bone resorption. Bps were either given continuously (mini-osmotic pumps) or by daily s.c. injections for 28 days. As expected, all tested Bps significantly inhibited cancer-induced bone destruction measured by osteolytic bone areas. In contrast, however, the tested Bps did not inhibit tumor progression when quantified by optical imaging (photon counting after 1-2-3-4 weeks) confirmed by histomorphometrical analysis at the end of each experiment. Our data, therefore, provide no evidence of an anti-tumor effect by Bps despite the observed protection of bone integrity.

1092

OPG Inhibits the Progression of Bone Destruction and Skeletal Tumor Burden in Mice With Established Osteolytic MDA-231 Breast Cancer Metastases. S. Morony, K. Warmington*, H. Tan, V. Shalhoub, G. Chow*, C. R. Dunstan, D. L. Lacey, P. J. Kostenuik. Metabolic Disorders, Amgen Inc., Thousand Oaks, CA, USA.

OPG, a RANKL decoy receptor, inhibits osteoclast formation and activation by preventing RANKL-RANK interactions on osteoclasts and their precursors. We previously demonstrated that OPG treatment started at the time of MDA-231 cell inoculation inhibited tumor-associated osteolysis and reduced skeletal tumor burden (Morony et al, Cancer Res 61: 4432, 2001). The present study tested whether OPG treatment would prevent the progression of osteolysis and skeletal tumor burden after MDA-231 lesions were already established in bone. Nude female mice were inoculated in the left ventricle with MDA-231 tumor cells. Three weeks later, digitized radiographs of all mice were analyzed to quantify the area of osteolytic lesions. Mice without radiographic evidence of osteolysis were excluded from the study. The remaining mice were allocated to groups that had similar average baseline areas of osteolysis. At baseline, group means for area of osteolysis ranged from 0.88 to 0.99 mm2/mouse (n=13-15/group). One group of tumor-bearing mice was sacrificed prior to treatment for the histological determination of baseline skeletal tumor burden (1.87 ± 0.6 mm2/mouse). Mice were treated with PBS (vehicle) or with OPG (3 mg/kg, SC) on days 23, 24, 27, 29, and 31 post inoculation, and were sacrificed on day 31. The radiographic area of osteolysis increased by 400% during PBS treatment (3.31 ± 0.44 mm2/mouse, p<0.01) and decreased by a non-significant 19% (0.81 ± 0.19 mm2/mouse) during OPG treatment. Histologically, skeletal tumor burden increased 210% (5.79 ± 1.32 mm2/mouse, p<0.01) during PBS treatment, while the increase during OPG treatment was a non-significant 32% (2.47 ± 0.82 mm2/mouse). The differences in osteolysis and skeletal tumor burden between OPG and PBS treated groups were statistically significant (p<0.01). OPG treatment also reduced the number of osteoclasts per mm2 of skeletal tumor area by 96% vs. PBS treated mice (p<0.01). The inhibitory effect of OPG on skeletal tumor burden might be related to the inhibition of bone resorption. A direct effect of OPG on tumor cells was not supported by cell culture studies. Neither OPG nor RANKL had any effect on MDA-231 cell number during 48 h of culture with various concentrations of fetal bovine serum. These data support the hypothesis that OPG indirectly inhibits MDA-231 tumor burden in bone via its potent antiresorptive effects. The ability of OPG to suppress the bone destruction and the skeletal tumor burden associated with established osteolytic lesions underscores the potential utility of OPG as a therapeutic option for the treatment of metastatic bone disease.

1093

Gene Transfer of Osteoprotegerin-Fc Inhibits Osteolysis and Disease Progression in a Murine Model of Multiple Myeloma. P. Doran[1], S. J. Russell*[1], D. Chen*[2], S. M. Greiner*[1], J. Ludvigson*[1], S. Khosla[1], B. L. Riggs[1]. [1]Mayo Clinic, Rochester, MN, USA, [2]Amgen Inc., Thousand Oaks, CA, USA.

Multiple myeloma has major adverse skeletal effects, including bone pain, pathologic fractures, and hypercalcemia, that are only transiently and incompletely reversed by currently available therapy. Osteoprotegerin (OPG) potently inhibits osteoclast differentiation and activation, but, if used therapeutically, it or the more prolonged-acting OPG-Fc-fusion protein analog require repeated subcutaneous injections. Gene therapy has shown promise in the treatment of various malignancies. Thus, as proof-of-principle for antiresorptive gene therapy of osteolytic bone disease, we evaluated the effect of *ex vivo* OPG-Fc gene transfer in a murine model of multiple myeloma. In this model, injection of human ARH-77 cells into 6-week-old SCID mice results in severe osteolytic lesions. In the therapeutic group, the injected ARH-77 cells were stably transduced with the OPG-Fc-fusion protein gene using a replication-incompetent lentiviral vector (OPG-Fc, n=18). Effects were compared with those in positive control mice (PC, n=19) injected with the same number of ARH-77 cells that were similarly transduced with a non-expressing control vector, and with those in negative control mice (NC, n=20) that did not receive ARH-77 cells. The mean ± SEM level of serum OPG-Fc levels obtained at sacrifice was undetectable (<0.02 ng/mL) in the control groups but was 966 ± 239 ng/mL at sacrifice (P<0.001) in the OPG-Fc expressing group. None of the NC mice developed any disease manifestations. The median time for onset of partial paraplegia was 22 days in the PC as compared to 30 days in the OPG-Fc mice (P<0.001), and complete paraplegia occurred in 84% of PC as compared to 39% of OPG-Fc mice (P<0.001). Total body BMD was greater at 4 weeks in the OPG-Fc mice (0.0404 ± 0.0004 g/cm^2) than in the PC and NC mice (0.0394 ± 0.0003, P=0.05 and 0.0393 ± 0.0003, P=0.04, respectively). Osteolytic radiographic lesions developed in 78% of PC mice, but in only 17% of the OPG-Fc expressing mice (P<0.001). There were similar differences when osteolytic lesions were quantified by number, diameter, and the sum of diameters (all P<0.001). Finally, median survival time was 32 days compared with 37 days in the PC and OPG-Fc groups, respectively (P=0.005). In conclusion, our finding that *ex vivo* OPG-Fc gene transfer dramatically attenuates the skeletal manifestations of murine multiple myeloma suggests that therapeutic gene transfer using this or other genes offers considerable promise as a novel therapy for neoplastic bone disorders, either alone or in combination with conventional therapies.

Disclosures: ***P. Doran****, David Chen, Amgen Inc. 3.*

1094

Bisphosphonates Induce Apoptotic Prostate Cancer Cell Death in Vitro. J. C. Dumon*[1], F. Journé*[1], N. Khedoumi*[1], L. Lagneaux*[2], J. J. Body[1]. [1]Lab. of Endocrinology and Breast Cancer Research, Inst. J. Bordet, Free University of Brussels, Brussels, Belgium, [2]Lab. of Hematology, Inst. J. Bordet, Free University of Brussels, Brussels, Belgium.

Bone tissue is the most common site of distant metastases in breast and prostate cancers. Bisphosphonates have been shown to reduce the morbidity rate of metastatic bone disease from breast cancer and, quite recently, also from prostate cancer. These effects are attributed to their powerful inhibitory activity on osteoclast-mediated bone resorption. We have shown that bisphosphonates also induce human breast cancer cell death in vitro (Fromigué et al., JBMR 2000). We have now investigated their effects on the survival, growth and death of prostate cancer cells (PC3) in vitro after 1, 2, 4 and 6 days of incubation. We tested four bisphosphonates at doses ranging from 10-8 to 10-4M: clodronate (Clod), ibandronate (Iban), pamidronate (Pam), and zoledronate (Zole). The inhibitory effects on PC3 cells viability (evaluated by the MTT test) were maximal at 10-4M and this concentration was used for further experiments. The MTT results are summarised below as % of control cell survival (mean±SEM). Total DNA content was also decreased at day 6: to 46±6% for Clod, to 31±3% for Iban, to 46±2% for Pam, and to 4±0.2% for Zoledronate. FACS experiments showed that, at day 1, there was already a marked decrease (except for clodronate) in the number of cells in "Synthesis and Mitosis" phases (decreases of 24% for Iban, 57% for Pam, and 43% for Zole). At day 4, according to the bisphosphonate, 50% to 90% of the cell population was apoptotic. In conclusion, bisphosphonates caused an early inhibition of prostate cancer cell proliferation followed by cell death, essentially through apoptosis. Zoledronate was the most potent compound with an almost complete cell death at day 6. Such effects could contribute to the beneficial role of bisphosphonates in the treatment and the prevention of prostate cancer-induced bone disease.

	Clod	Iban	Pam	Zole
Day 1	100±5	95±5	85±12	89±5
Day 2	101±12	90±3	67±5	71±7
Day 4	80±5	75±12	56±15	71±6
Day 6	77±7	70±6	49±9	16±6

1095

Apomine, a Novel Bisphosphonate Ester, Is a Potent Antiproliferative Drug: A Comparison with Risedronate. N. Lameloise*, Y. Guyon-Gellin*, S. Nolli*, P. Villemin*, P. Latin*, D. Masson*, E. J. Niesor. Biosciences and Pharmacology, Ilex Oncology Research, Versoix, Geneva, Switzerland.

Apomine, a novel bisphosphonate ester, increases HMG-CoA reductase degradation *in vitro*, thus depleting the isoprenoid pool generated by the mevalonate-isoprenoid-cholesterol (MIC) synthetic pathway. On the other hand, risedronate has been shown to inhibit farnesyl-PP synthase, another enzyme of the MIC pathway. Therefore, Apomine and risedronate may act on cell proliferation by decreasing Ras/Rho isoprenylation. Apomine has been shown to inhibit bone metastasis *in vivo* after intracardiac injection of breast cancer cells (MDA-MB-231) in mice. The aim of this study was to assess the antiproliferative activity of Apomine *in vitro* and *in vivo* in comparison to risedronate. *In vitro* studies were performed in breast cancer MDA-MB-231 cells mutated for K-ras and in H-ras-transfected 3T3 fibroblasts (PAP-2 cells). Both cell lines were incubated in the presence of Apomine (0.1-20 µM) or risedronate (1-200 µM) for 6, 24, and 48 hours. Cell number and apoptosis rate were measured. In MDA-MB-231 cells, Apomine inhibited cell proliferation (IC50 = 5 µM) and risedronate had no effect on cell growth even at the highest concentration (200 µM). In PAP-2 cells, Apomine inhibited cell proliferation (IC50 = 8 µM), whereas risedronate showed only a mild antiproliferative activity (IC50 = 80 µM). *In vivo*, tumours were induced by s.c. injection of MDA-MB-231 or PAP-2 cells in a nude mice xenograft model. Animals were treated either with Apomine or risedronate (50 mg/kg in diet), and tumour growth was then evaluated twice weekly. In MDA MB-231 injected mice, Apomine inhibited tumour growth by -31% and -25% after 6 and 17 days of treatment, respectively. In PAP-2 injected mice, Apomine inhibited tumour growth by -59% and -39% on days 8 and 14, respectively. Risedronate did not show any antiproliferative effect with either cell line in this xenograft model. The present study shows that Apomine, which enhances HMG-CoA reductase degradation, is antiproliferative *in vitro* and *in vivo* in two different Ras-dependent cell lines (MDA-MB-231 and PAP-2). In direct comparison, risedronate has no significant antiproliferative activity.

Disclosures: ***N. Lameloise****, Ilex Oncology Research 3.*

1096

Bone Microenvironment Triggers IGF-I Release from Prostate Carcinoma. J. Rubin[1], L. Chung*[2], X. Fan[1], L. Zhu*[1], T. C. Murphy*[1], M. S. Nanes[1], C. J. Rosen[3]. [1]Medicine, VAMC & Emory University, Decatur, GA, USA, [2]Winship Cancer Center, Emory University, Atlanta, GA, USA, [3]Jackson Laboratory, Bar Harbor, ME, USA.

Prostate carcinoma has a propensity to metastasize to the skeleton, inducing a characteristic osteoblastic response from the local cell population. The cancer cell itself takes on characteristics of bone cells, expressing RUNX2/cbfa1, osteocalcin and RANKL. Interestingly, OPG infusion has been shown to prevent bone metastasis in a nude mouse model (Wang 2001). Clinical data has suggested that IGF-I levels may be related to the advancement of disease in the bone compartment. We recently reported that IGF-I both upregulated bone cell RANKL expression, and downregulated OPG expression (Rubin ASBMR 2001). This suggested that IGF-I might have multiple influences on prostate metastatic disease, e.g., increasing bone turnover through alteration of RANKL/OPG and influencing osteoblast proliferation and function. In the study presented here we used human prostate carcinoma cell lines: LNCaP originating from lymph node (LN) metastasis, C4-2 which was derived from chimeric prostate tumors derived from co-inoculation with LNCaP and a bone stroma cell line (MS) in castrated nude mice, and C4-2B which was passed in castrated mice and derived from bone metastases (Thalmann 1994, 2000). LNCaP expressed very low levels of RANKL mRNA while C4-2 and C4-2B had high levels as assessed by RT-PCR. 24-h treatment of cell lines with 100 ng/ml IGF-I stimulated RANKL expression in LNCaP, as expected, but had no effect on the constitutively high expression of the highly metastatic C4-2 and C4-2B lines. We next measured IGF-I secretion by these lines using a sensitive RIA that detects as low as 0.2 ng/ml IGF-I. Serum-free conditioned media of LNCaP contain no measurable IGF-I in 24 or 48 hours. IGF-I secretion elevated substantially in C4-2 cells which was measurable at 24 h, doubling at 48 h, but was 1/10 the levels secreted by C4-2B line at 0.5 ng/ml at 24 h, and 0.92 ng/ml at 48 h (or 2.5 ng/mg protein). IGF-BP3 was not detectable in the conditioned media thus increasing the potential bioavailability of IGF-I. In sum, our results suggest that interaction of prostate carcinoma with the bone microenvironment results in a stably upregulated IGF-I axis which includes elevated RANKL and bone remodeling. Whether this is a pre-selected trait, i.e., an a priori requirement for bone anchorage and growth, or a result of "adaptive" events leading to aberrant signals in the bone environment which upregulate IGF-I expression in metastatic cells, will be important to understand in an effort to treat aggressive androgen-independent prostate carcinoma.

1097

DeltaFosB Isoforms Are Able to Interact with the Osteoblast Transcription Factor Runx2 and Synergistically Regulate its Promoter Activity. M. Wu[1], G. Rowe*[1], M. Kveiborg[1], G. Rawadi[2], P. Ducy[3], W. Horne[1], R. Baron[1], G. Sabatakos[1]. [1]Yale University, New Haven, CT, USA, [2]Aventis Pharma, Paris, France, [3]Baylor College of Medicine, Houston, TX, USA.

ΔFosB, an alternative splice form of the *fosb* transcript, is a member of the AP-1 family of immediate-early transcription factors that have been implicated in the regulation of bone metabolism. Previous work showed that overexpression of ΔFosB in transgenic mice under the control of the NSE promoter results in osteosclerosis. This effect was shown to be cell autonomous to the osteoblast lineage since *ex vivo* studies demonstrated that increased levels of ΔFosB and Δ2ΔFosB, an N-terminally truncated isoform of ΔFosB, led to increased expression of osteoblast markers (collagen type 1, osteocalcin, osteopontin, and Runx2), and increased mineralization. In order to explore the mechanism by which ΔFosB and Δ2ΔFosB regulate bone formation and osteoblast differentiation, we used a gal-4 based yeast two-hybrid screen to identify novel binding partners of ΔFosB and Δ2ΔFosB. ΔFosB strongly autoactivated the reporter, and therefore only Δ2ΔFosB was used in the screen. Three independent clones isolated in the screen were identified as Runx2, a transcription factor that has been shown to be required for skeletogenesis. The interaction of Δ2ΔFosB with Runx2 in yeast was confirmed by directed two-hybrid activation of beta-galactosidase activity. In addition, transient co-transfection experiments in C3H10T1/2 cells showed that both ΔFosB and Δ2ΔFosB interacted with Runx2. Thus, Δ2ΔFosB and Runx2 both interact with each other and upregulate Runx2 expression. To determine the mechanism of transcriptional regulation of the Runx2 promoter by ΔFosB isoforms and Runx2, we performed transient co-transfections of Runx2 with a human Runx2 promoter luciferase reporter. As previously shown, Runx2 can activate its own promoter. ΔFosB and Δ2ΔFosB alone are not able to activate the Runx2 promoter; however, co-transfection of Runx2 with ΔFosB resulted in a synergystic increase in promoter activity. Deletion analysis of the Runx2 promoter revealed region-specific differences in the synergistic activities of ΔFosB and Δ2ΔFosB with Runx2 on OSE2 elements in the distal and proximal Runx2 promoter. In conclusion, ΔFosB isoforms are not only able to interact with Runx2, but also regulate the transcriptional activity of the Runx2 promoter in a synergistic manner. These mechanisms may be, at least in part, responsible for the increased bone formation in ΔFosB transgenic mice.

1098

Severe Osteopenia with Increased Osteoclast Progenitors in Pax5 Deficient Mice. M. C. Horowitz[1], Y. Xi[1], D. L. Pflugh*[1], D. G. T. Hesslein*[1], D. G. Schatz*[1], J. A. Lorenzo[2], A. L. M. Bothwell*[1]. [1]Yale University School of Medicine, New Haven, CT, USA, [2]University of Connecticut Health Center, Farmington, CT, USA.

Recent evidence demonstrates a relationship between B lymphopoiesis and osteoclastogenesis. The Pax5 gene encodes for the transcription factor B cell lineage specific activation factor (BSAP) which is required for B lymphocyte development. Mice deficient in Pax5 have a developmental arrest of B cell differentiation at the pro-B cell stage, which results in the absence of mature B lymphocytes and the presence of multipotential pro-B cells in the bone marrow. Pax5 deficient mice are severely runted and rarely live past 20 days. We characterized the bone phenotype of Pax5 wild-type (+/+), heterozygous (+/-) and homozygous mutant (-/-) mice to examine if Pax5 -/- mice had an altered bone phenotype. Mice were analyzed by histomorphometry and biochemistry. Spleen and bone marrow cells were used as sources of osteoclast precursors. Bones from Pax5 -/- mice were strikingly osteopenic 15 days after birth (BV/TV 66% less than +/+ controls), with increased numbers of osteoclasts (>100% increase), and decreased trabecular number (>50% loss). The number of osteoblasts in Pax5 -/- bones and their function in vitro were not different from +/+ controls. In addition, Pax5 was not expressed by primary wild-type osteoblasts in Northern analysis. To investigate the origin of the in vivo increase in osteoclasts, Pax5 -/- or +/+ spleen cells were cultured with M-CSF and RANKL and multinucleated, $TRAP^+$ cells counted. Cells from Pax5 -/- spleen produced 5-10 times more osteoclast-like cells (OCL) than did controls. Culture of Pax5 -/- but not +/+ spleen cells resulted in the development of cell lines that when stimulated with M-CSF and RANKL formed large, multinucleated OCLs. The OCLs were functionally mature as they produced abundant resorption pits when cultured on bovine cortical bone slices. Pax5 -/- cell lines could also be sustained in culture for up to 6 weeks without added growth factors. Essentially all cells in these long-term cultures expressed the monocyte markers CD11b/Mac-1, CD115/c-fms (the M-CSF receptor), and CD16/32 (FcRγIII/II) as assessed by flow cytometry. These data imply that the markedly decreased bone mass in Pax5 -/- mice resulted from an increase in the number of osteoclast precursors and were not due to insufficient or defective osteoblasts. Because Pax5 is expressed exclusively in the B cell lineage, the data imply that cells in the B cell lineage ($B220^+$, $c\text{-}kit^+$) regulate osteoclast progenitor differentiation and/or may be capable of differentiating into osteoclast precursor cells.

1099

RAIN, A Novel Intracellular Molecule that Associates with RANK and Negatively Regulates Osteoclastogenesis. A. Poblenz*[1], K. Du*[1], B. Lamothe*[2], N. K. Shevde[3], J. W. Pike[4], B. G. Darnay[1]. [1]Bioimmunotherapy, University of Texas MD Anderson Cancer Center, Houston, TX, USA, [2]Pharmacology, Yale University, New Haven, CT, USA, [3]Biochemistry, Univerisity of Wisconsin-Madison, Madison, WI, USA, [4]Biochemistry, University of Wisconsin-Madison, Madison, WI, USA.

Receptor activator of NF-kB (RANK) and its ligand (RANKL) are essential mediators of osteoclastogenesis. RANK utilizes tumor necrosis factor receptor-associated factors (TRAFs) to activate signal transduction pathways. In an effort to identify other factors that interact with the cytoplasmic domain of RANK, we screened a human thymus library with the RANK cytoplasmic domain using a yeast two-hybrid approach. Of the 13 clones we identified in this screen, five clones encoded the C-terminal region of TRAF2. One other clone specifically interacted with RANK. Based upon its function in osteoclastogenesis, this clone was termed RAIN (RANK Associated Inhibitor). We cloned both the mouse and human homologues which contain 241 and 242 residues, respectively. RAIN is a novel protein with no identifiable domains or motifs. To demonstrate interaction of RAIN with endogenous RANK, we transfected RAW264.7 with FLAG-tagged RAIN and it coprecipitated with endogenous RANK. Furthermore, RAIN was demonstrated to interact with TRAF2, TRAF5, and TRAF6. To understand the function of RAIN, we established RAW264.7 cells stably expressing RAIN. In these stable clones, RAIN appeared to block 50% of NF-kB activity induced by RANKL, but did not have any adverse effects on ERK or JNK activation. In addition, in the RAIN stable clones, RANKL was not able to induce

osteoclast differentiation. Thus, it appears that RAIN is a negative regulator of osteoclast differentiation. Furthermore, RANKL treatment of RAW264.7 cells caused induction of RAIN mRNA and protein, which begins on day 2 and continues through day 5. Next, we established RAW264.7 cells stably expressing anti-sense RAIN to knock out the function of RAIN. Surprisingly, we observed increased osteoclast differentiation, which was observed as early as day 2. Thus, we have identified a novel protein that interacts with RANK and TRAFs and negatively regulates RANKL-mediated osteoclastogenesis.

1100

Bone Specific DeltaFosB Induced Osteosclerosis Is Independent of Adipogenesis. M. Kveiborg, G. Sabatakos, R. Chiusaroli, M. Wu, W. Grant*, W. C. Horne, W. M. Philbrick, R. Baron. Yale University School of Medicine, New Haven, CT, USA.

The AP-1 family of transcription factors plays important roles in bone cell function. Previous findings demonstrated that transgenic mice overexpressing ΔFosB, a splice variant of FosB, under the control of the neuron-specific enolase (NSE) promoter develop a progressive and severe osteosclerosis, shown to be, at least in part, due to autonomous effects of ΔFosB on cells of the osteoblastic lineage. In addition, adipogenesis is inhibited in the NSE-ΔFosB mice, with decreased abdominal fat and decreased number of bone marrow adipocytes. Given that the NSE promoter directs expression of ΔFosB to several different tissues, including bone and adipose tissue, it is not clear if the fat phenotype is due to direct autonomous effects on cells of the adipocyte lineage. To further understand the mechanisms of ΔFosB action in osteoblast versus adipocyte differentiation, we have generated transgenic mice expressing ΔFosB under the control of the mouse osteocalcin promoter (OG2), which directs transgene expression specifically to osteoblastic cells beyond the branching point of adipocyte versus osteoblast commitment. Complete histomorphometric analysis of two independent founder lines showed that targeting the ΔFosB transgene to osteoblasts results in a significant increase in bone formation. At 10 weeks of age, trabecular bone volume was more than doubled (16.2±5.1 vs. 7.9±2.3 BV/TV, $p<0.05$), and the dynamic parameters of bone formation were also significantly increased (mineralizing surface: 43.2±1.7 vs. 32.5±5.2 MS/BS, $p<0.05$, mineral apposition rate: 1.6±0.1 vs. 1.2±0.2, $p<0.05$, and bone formation rate: 255.2±18.1 vs. 141.8±33.9 BFR/BS, $p<0.005$). Similar to NSE-ΔFosB transgenic mice, no changes in bone resorption parameters, such as osteoclast surface and osteoclast number were observed. These results clearly demonstrate that ΔFosB-induced osteosclerosis is a direct effect of ΔFosB overexpression in osteoblasts. In contrast to the recurrence of the osteosclerotic phenotype, no differences were observed in either abdominal fat or number of adipocytes in the bone marrow of OG2-ΔFosB transgenic mice. Thus, these findings indicate that when ΔFosB is induced specifically in osteoblasts and at late stages of differentiation, osteosclerosis can be mediated independent of decreased adipogenesis.

1101

Endothelial Nitric Oxide Synthase Is an Important Regulator of Osteoblast Growth and Differentiation. F. Afzal*[1], M. Nohadani*[2], P. L. Huang*[3], J. M. Polak*[2], L. D. K. Buttery[2]. [1]Cell Biology, UMASS, Worcester, MA, USA, [2]Cell Biology and Tissue Engineering, Imperial College, London, United Kingdom, [3]Cardiovascular Research Center, Harvard Medical School, Charlestown, MA, USA.

We have previously reported that the nitric oxide (NO) signaling pathway contributes to osteoblast function. However, the mechanisms underlying the NO-mediated effects on osteoblast lineage cells are yet to be determined. In this study, we evaluated the contribution of NO and specific NOS enzymes involved in the control of osteoblastic bone formation in vivo using rat and eNOS-null mice models. Our results show that in rat calvarial osteoblasts, inhibition of endogenous NO synthesis by NΩ-Nitro-L-Arginine (L-NNA) significantly delayed the osteoblast differentiation process as evidenced by reduction of alkaline phosphatase activity (ALP) and mineralized bone nodule formation. Growth and differentiation assays using eNOS KO-derived osteoblasts revealed a significant decrease in both their proliferation and their differentiation compared to their WT littermates. In addition, RT-PCR analyses revealed significant reductions in osteocalcin (OCN) and core binding factor (Cbfa1) gene expression in osteoblasts from eNOS KO mice. Rescue experiments ex-vivo showed that this impaired growth and differentiation could be totally restored to WT levels after addition of the exogenous NO donor S-nitroso-N-acetyl-DL-penicillamine (SNAP) to eNOS KO-derived osteoblasts. Mechanical properties of long bones from 8 and 12 week old eNOS KO mice and their corresponding WT controls were also assessed. The eNOS KO mice at 8 weeks had significantly reduced bone elasticity and strength, and reduced bone hardness. Furthermore, our results show that total bone mineral density (BMD) as well as calvarial, pelvic/femoral, spinal BMD is also significantly reduced in the eNOS KO mice at 8 weeks. These parameters were modestly reduced at 12 weeks. The bone abnormalities were completely prevented after treatment of 4 week old eNOS KO mice with the NO donor glyceryl trinitrate as determined by DEXA, microhardness tests and osteocalcin levels. Taken together, our studies demonstrate that the eNOS enzyme is a major regulator of NO-mediated osteoblast cell signalling. Our in vivo data clearly show that the bone abnormalities in the eNOS KO mice are age-dependent suggesting an implication of this second messenger during early stages of bone formation and periods of rapid growth in postnatal mice.

1102

Adenoviral Gene Therapy Using an Anti-Proliferative Mutant of PTHrP Completely Prevents Arterial Re-Stenosis. N. M. Fiaschi-Taesch*, K. K. Takane*, S. Masters*, A. F. Stewart. Endocrinology, University of Pittsburgh School of Medicine, Pittsburgh, PA, USA.

Coronary and peripheral vascular disease are increasingly treated using angioplasty approaches. Re-stenosis results in late failure in approximately 20-50% of patients undergoing angioplasty. PTHrP is produced in the arterial wall, is upregulated by vascular injury, by balloon distention and by vasoconstrictors, and acts as a vascular smooth muscle (VSM) relaxant. These effects of PTHrP are believed to be principally paracrine and/or autocrine. PTHrP also has a nuclear/nucleolar localization signal (NLS) in the 88-106 region. In cultured A-10 VSM cells, stable expression of PTHrP lacking an NLS (delta-NLS) markedly inhibits proliferation in VSM cells. These observations suggest that gene delivery of delta-NLS-PTHrP might be effective in preventing arterial re-stenosis is following angioplasty. Methods: Male Sprague-Dawley rats (450-600 g) underwent left common carotid balloon injury followed by local arterial delivery of: 1) buffer alone with no virus; 2) recombinant adenovirus encoding beta-galactosidase (Ad-lacZ); or, 3) delta-NLS (Ad-delta-NLS). The right carotid was left undisturbed and used as a normal control. Two weeks following surgery, the rats were sacrificed, both carotids were fixed, and quantitative histomophometric analysis was performed on the injured and contralateral non-injured carotid arteries. Results: As can be seen in the Table, and as expected, angioplasty alone (no adenovirus) resulted in marked neointimal hyperplasia (re-stenosis). Angioplasty followed by Ad-lacZ resulted in indistinguishable findings, indicating that adenovirus neither worsened nor ameliorated the re-stenosis (neointima formation). In dramatic contrast, Ad-delta-NLS resulted in striking and essentially complete inhibition of arterial re-stenosis, with complete patency of the lumen. These results were highly statistically significant. In summary, local treatment of the arterial lumen wall at the time of angioplasty with Ad-delta-NLS dramatically and completely inhibits arterial re-stenosis in rats. This approach may be useful in treating human coronary and peripheral arterial disease.

	Neointima Area (mm2)	Media Area (mm2)	Neointima/Media Ratio
Control Carotid, No Angioplasty (n=28)	0.00	0.145 +/-0.011	0.00
Angioplasty with No adenovirus (n=9)	0.099 +/-0.018	0.142 +/-0.010	0.68 +/-0.17
Angioplasty with Ad-lacZ (n=9)	0.098 +/-0.020	0.209 +/-0.042	0.50 +/-0.12
Angioplasty with Ad-delta-NLS-PTHrP (n=10)	0.006* +/-0.002	0.181 +/-0.017	0.03** +/-0.01

* = $p < 0.0025$
** = $p < 0.0001$

1103

Fracture Risk Following Bilateral Oophorectomy in Elderly Women: A Population-Based Study. L. J. Melton[1], S. Khosla[2], G. D. Malkasian*[3], S. J. Achenbach*[1], A. L. Oberg*[1], B. L. Riggs[2]. [1]Health Sciences Research, Mayo Clinic, Rochester, MN, USA, [2]Internal Medicine, Mayo Clinic, Rochester, MN, USA, [3]ObGyn, Mayo Clinic, Rochester, MN, USA.

Estrogen (E) deficiency is largely responsible for age-related bone loss in elderly women, and those with the lowest serum E levels are at greatest risk of bone loss and fractures. It is controversial, however, whether the postmenopausal ovary is an important source of the androgens that are the substrate for endogenous E production after menopause or whether they are mainly adrenal in origin. Therefore, it is unclear whether bilateral oophorectomy in postmenopausal women might have unexpected adverse effects on the skeleton. To assess the practical significance of this potential problem, we estimated long-term fracture risk among the inception cohort of Olmsted County, MN, women who underwent bilateral oophorectomy (median age, 62 yr) for a benign condition in 1950-87 following a natural menopause (median, 50 yr). In a population-based retrospective cohort study, these 338 women were followed for 5627 person-years (median, 16 years per subject) during which 192 women experienced 511 fractures (72% from moderate trauma). Compared to expected rates among community women, statistically significant increases were seen for fractures at most axial sites, such as the vertebrae (standardized incidence ratio [SIR], 3.01; 95% CI, 2.46-3.66), as well as the proximal femur (SIR, 1.51; 95% CI, 1.15-1.96) and distal forearm (SIR, 1.47; 95% CI, 1.06-1.99). Overall, there was a significant increase in the risk of any osteoporotic fracture (moderate trauma fracture of the hip, spine or distal forearm: SIR, 1.54; 95% CI, 1.29-1.82) but almost as big an increase in any other fracture (SIR, 1.33; 95% CI, 1.11-1.57). In multivariate analyses, the independent predictors of overall fracture risk were age, anticonvulsant or anticoagulant use ≥ 6 months and a history of alcoholism or prior osteoporotic fracture; obesity was protective. Risk factors for any osteoporotic fracture included age, anticonvulsant use, history of prior osteoporotic fracture or kyphosis and more recent year of oophorectomy, while thiazide use was protective. Hormone replacement therapy was associated with a 10% reduction in overall fracture risk (hazard ratio [HR], 0.90; 95% CI, 0.64-1.28) and a 20% reduction in osteoporotic fractures (HR, 0.80; 95% CI, 0.52-1.23) but neither was statistically significant. Our demonstration of a 50% increase in osteoporotic fracture risk among women who underwent bilateral oophorectomy following natural menopause is consistent with the hypothesis that androgen production by the postmenopausal ovary is protective against fractures induced by estrogen deficiency.

1104

Femoral Neck Bone Loss Predicts Risk of Hip Fracture in Elderly Women. T. V. Nguyen, J. R. Center*, J. A. Eisman. Bone and Mineral Research Program, Garvan Institute of Medical Research, Sydney, Australia.

In postmenopausal women, measurement of femoral neck bone mineral density (FNBMD) predicts hip fracture risk, and improvement in BMD with antiresorptive therapy are associated with decreased fracture rate. However, it is not clear whether short-term bone loss is an independent risk factor for hip fracture. To address this question, 724 elderly women of the Dubbo Osteoporosis Epidemiology Study were studied. The women aged 60+ years (as at June 1989), had been followed for a median of 8.6 years, and had had at least two FNBMD measurements prior to the fracture event. During the follow-up period, 43 women suffered a hip fracture, who had multiple measurements of BMD prior to the event. Apart from lower baseline BMD and higher age, the [mean ± SD] annual rate of bone loss for fracture women was -2.1 ± 4.2 %, significantly greater than in non-fracture women (-0.76 ± 2.8%; p = 0.005). Lumbar spine (LS) BMD among hip fracture women also decreased at a significantly higher rate than among those without a fracture (-1.1 ± 3.4% vs. +0.1 ± 2.02%; p <0.01). In Cox's proportional hazards model (univariate analysis), each 5% decrease in FNBMD and LSBMD was associated with a 1.8-fold (1.2 - 2.8) and 2.8-fold (1.5 - 5.4) increase in hip fracture risk, respectively. In multivariate analysis, after adjusting for age in a proportional hazards model, each 0.1 g/cm^2 loss of FNBMD was associated with a relative risk (RR) of 3.1 (95% CI: 1.6 - 6.1) for fractures at the hip, comparable to a 0.1 g/cm^2 difference in baseline hip fractures (RR 3.6, 95% CI: 2.7 - 4.8). These results suggest that bone loss at the femoral neck is an independent predictor of hip fracture risk in elderly women, and help explain why a modest improvement in BMD induced by antiresorptive therapy is associated with greater reduction in fracture risk that is predicted from cross-sectional BMD studies.

1105

Effects of Olpadronate on Children with Osteogenesis Imperfecta: A Double-blind Randomized Clinical Study. D. Kok*[1], C. Uiterwaal*[2], R. Engelbert*[3], A. Van Dongen*[4], M. Jansen*[5], H. Pruijs*[1], A. Verbout*[1], D. Schweitzer[6], R. J. B. Sakkers[1]. [1]Orthopedic Surgery, UMCU, Utrecht, Netherlands, [2]Julius Centre, UMCU, Utrecht, Netherlands, [3]Pediatric Physiotherapy, UMCU, Utrecht, Netherlands, [4]Nuclear Medicine, UMCU, Utrecht, Netherlands, [5]Pediatrics, UMCU, Utrecht, Netherlands, [6]Internal Medicine, Reinier de Graaf Groep, Delft, Netherlands.

The purpose of this study was to evaluate the effects of Olpadronate (dimethyl-APD) on children with osteogenesis imperfecta (OI) in a double-blind randomized placebo-controlled study of two years. Thirty-four children of at least 4 years old participated in this study. To be able to measure a difference in functional outcome, only children with a restricted level of ambulation were included. Excluded were those children with prior or current use of bisphosphonates. Half of the children were treated with Olpadronate tablets in a dose of 10mg/m2/day, the others received placebo tablets. The whole group was treated with calcium and vitamin D in a dose of respectively 500mg/m2/day and 400 I.U./day, as recommended for growing children. Lumbar BMD was measured at the beginning of the study and at one and two years of follow-up with DEXA (Hologic QDR 2000W, Waltham, MA). Functional parameters were measured every six months. Level of ambulation was assessed using the criteria of Bleck (non-walker, therapy or exercise walker, household walker, neighbourhood and community walker with or without the use of crutches). Community walkers were not included in the study. The Pediatric Disability Inventory (PEDI) was used to assess self care, mobility skills, social skills, caregiver assistance and the use of modifications. Thirty-two children completed the two-year follow-up period of the study, 15 of them in the Olpadronate and 17 in the placebo group. The mean ages were 10.4 (SD 2.8) and 10.6 (SD 4.0) years, respectively, in both groups. In the complete study group, spinal BMD increased significantly during the two years of follow-up (p<.0001), but the level of BMD accretion per year in the Olpadronate group was higher than in the placebo group (p<.0155). No differences in changes in functional outcome (Bleck, PEDI) were observed. No side effects of the medication were noted during this study. The two children that did not complete the study were on Olpadronate. It can be concluded that Olpadronate proved to be effective in this first double-blind randomized placebo-controlled study on the effects of bisphosphonates in children with OI, as demonstrated by a greater annual increase in BMD, independent from the effects of increase of age and calcium and vitamin D supplementation. No favorable effects on functional outcome were noted during these two years of follow-up.

1106

Defining Candidate Genes for a Major IGF-I QTL that Affect Bone Mass: Use of In Silico and Micro-array Technology. C. L. Ackert-Bicknell*, K. L. Shultz*, W. G. Beamer, L. R. Donahue, G. Churchill*, J. D. Stockwell*, C. J. Rosen. The Jackson Laboratory, Bar Harbor, ME, USA.

Changes in serum and skeletal IGF-I, a key regulator of bone remodeling, can profoundly affect bone formation and mineralization. We found that differences in hepatic IGF-I expression between C3H/HeJ (C3H) and C57BL/6J (B6) mice are due to enhanced transcription from the P2 promoter. Using whole genome scanning to look for QTLs controlling serum IGF-1 levels, we found a strong QTL on Chr 6. A congenic strain for this locus, B6.C3H-6T (6T), has low serum IGF-I, plus markedly reduced trabecular and cortical BV/TV (Bouxsein, et al. JBMR, 2002). The QTL region is about 20cM in size and contains many genes. To find candidate genes in the Chr 6 QTL region, we performed a dye-flip microarray experiment using mouse 15K microarray chips from the Ontario Microarray Center. Total RNA was isolated from the livers of 6 wk old, fasted female B6 and 6T mice, then converted to cDNA. B6 cDNA was labelled with Cy3 and 6T cDNA with Cy5 for two arrays and then dye labeling reversed for two additional arrays. Gene chips were hybridized with labeled cDNA at 42º C overnight and scanned. Each EST was spotted on the chips twice, giving 8 data points/EST. We used ANOVA, (Kerr et al, JCB, 2000) and bootstrapping to identify genes that were significantly different in expression. Of the 15K EST's analyzed on these chips, 48 were down regulated and 8 were up regulated in 6T vs. B6 (p< 1.0 x10^{-7}). 23 differences were linked to known genes and the remaining additional differences were found for EST's not associated with characterized mouse genes. 22 additional differences were identified in the UniGene databases and by BLAST searching the Celera mouse genome, allowing putative transcripts for these genes to be predicted. In addition, by using domain, structure and human homology databases, putative protein function could be predicted for some of these genes. Three ESTs mapped to our region of interest on Chr 6. These genes were *p23,* human hypothetical protein FLJ22405*,* and *Lsm-3.* A fourth gene, *Gata-2*, located within the 6T region, was down regulated by 65%, but was only suggestively significant (p< 1.0X10^{-6}). Using the VISTA comparative alignment package, we found four regions of high nucleotide conservation between human and mouse in the P2 promoter of the IGF-I gene. These regions bind several transcription factors, including *GATA-2,* enhancing its potential as a candidate gene. In summary, by using the 6T congenic mouse, along with traditional bench top experimentation and in silico data-mining, we have been able to considerably narrow the list of candidate genes for this QTL and gained further insight into the biological differences embodied by this strain.

1107

P2X7 Receptor Regulates Bone Formation and Bone Resorption. H. Z. Ke[1], H. Qi[1], D. T. Crawford*[1], Q. Zhang*[2], W. A. Grasser[1], V. M. Paralkar[1], M. Li[1], L. P. Audoly*[1], C. A. Gabel*[1], M. Su*[2], W. S. S. Jee[2], D. D. Thompson[1]. [1]Pfizer Global Research and Development, Groton, CT, USA, [2]Univ. of Utah, Salt Lake City, UT, USA.

The P2X7 receptor (P2X7R) is an ATP-gated ion channel expressed by monocytes, macrophages, osteoclasts and subpopulation of osteoblasts. However, the role of P2X7R in bone is not known. The purpose of this study was to elucidate the role of P2X7R in regulating bone formation and resorption by characterizing the bone phenotype of male and female mice that had been genetically modified to delete the P2X7R (KO). Femoral length did not differ between KO and wild-type (WT) littermates at 2, 5 and 9 months of age in either male or female mice, indicating that P2X7R does not regulate longitudinal bone growth. PQCT analysis of the distal femoral metaphysis (DFM) and femoral shafts showed that KO male or female mice had significantly lower total bone area (up to -39%), cortical content (up to -36%) and periosteal circumference (up to -20%) as compared with WT controls at 2, 5 and 9 months of age. Histomorphometric analysis of tibial shafts showed that KO mice had significantly lower periosteal bone formation at all ages. These results demonstrated that P2X7R deficiency decreases periosteal bone formation, radial bone growth and cortical bone mass. In cancellous bone, PQCT analysis of DFM showed that trabecular content was significantly lower at 2- and 5-month-old KO male mice as compared with WT controls. Histomorphometric analysis of proximal tibial metaphysis indicated that a lower cancellous bone mass and bone formation and a higher bone resorption was found at 2-month-old KO male mice as compared with WT. Cancellous bone resorption remained higher in KO than in WT at 5 and 9 months of age. A significant decrease in serum osteocalcin was found in both male and female KO mice at 2, 5 and 9 months of age as compared with WT controls. Results from the bone marrow culture study showed that cells derived from either male or female KO mice expressed a significant decrease in alkaline phosphatase activity compared with WT controls. Number of TRAP-positive multinuclear cells in bone marrow culture was no difference in either male or female KO mice. These results demonstrate that P2X7R deficiency decreases cancellous bone formation and increases bone resorption. Increased osteoclast number in vivo but unchanged number of TRAP-positive multinuclear cells in bone marrow culture in KO mice suggests a possible role of P2X7R in osteoclast apoptosis. Our data reveal that P2X7R plays a stimulating role in periosteal and cancellous bone formation, and an inhibiting role in cancellous bone resorption. Thus activation of the P2X7R provides a therapeutic potential for prevention and treatment of osteoporosis.

Disclosures: ***H.Z. Ke****, Pfizer 3.*

1108

Elevated Fibroblast Growth Factor 23 Concentrations in Humoral Hypercalcemia of Malignancy and Primary Hyperparathyroidism. C. M. Preissner*[1], R. Singh*[1], R. Kumar[2]. [1]Pathology and Laboratory Medicine, Internal Medicine, Mayo Clinic, Rochester, MN, USA, [2]Biochemistry and Molecular Biology, Mayo Clinic, Rochester, MN, USA.

Fibroblast growth factor 23 (FGF 23) causes hypophosphatemia and rickets. Both humoral hypercalcemia of malignancy (HHM) due to excessive amounts of parathyroid hormone-related peptide and primary hyperparathyroidism (1º HPT) are also associated with decreases in the serum inorganic phosphorus concentrations. To ascertain whether increases in circulating FGF 23 might contribute to the hypophosphatemia seen in these disorders, we measured FGF 23 in the serum of patients with HHM and 1º HPT. FGF 23 levels were measured in an ELISA kit from Immutopics, Inc. The 2-day assay utilizes two affinity-purified goat antibodies, one coated onto a microtiter plate and the other biotinylated, and a horseradish peroxidase-avidin conjugate. Twenty-one patients with HHM diagnosed on the basis of increased parathyroid hormone related peptide concentrations (PTHrP > 2 pmol/L) and a concomitant malignancy, 13 patients with 1º HPT diagnosed on the basis of hypercalcemia and increased parathyroid hormone concentrations (PTH > 5 pmol/L) and twenty-one normal subjects were examined. All patients had normal renal function as assessed by the measurement of serum creatinine concentrations. In normal subjects FGF 23 concentrations were 48.5+/-7.3 RU/ml. In patients with 1º HPT FGF 23 concentrations were 90.4+/-19.3 eq/ml (p < 0.027 vs normal). In patients with HHM the concentrations of FGF 23 were 677.4+/-149.5 RU/ml (p < 0.001 vs normal and p < 0.004

vs, 1° HPT). These data show that FGF 23 concentrations are elevated in both 1° HPT and HHM and could contribute to the hypophosphatemia seen in these disorders. Additionally, the higher FGF 23 concentrations in HHM relative to 1° HPT, could explain the smaller increases in 1,25-dihydroxyvitamin D concentrations in HHM compared to 1° HPT. The precise reason for elevated FGF 23 concentrations in these disorders remains to be determined but causes include stimulation of FGF 23 synthesis by PTHrP or PTH, or the mobilization of FGF 23 from bone by PTHrP and PTH. In conclusion, FGF 23 levels are elevated in patients with 1° HPT and HHM; however, the increases are of much greater magnitude in HHM compared to 1° HPT. These findings are of relevance in the clinical interpretation of FGF 23 assays and in the pathophysiology of hypophosphatemia in both 1° HPT and HHM.

1109

LIP, a Natural Truncated Isoform of the Transcription Factor C/EBPβ, Promotes Osteoblastogenesis and Inhibits Adipogenesis in the Mesenchymal Stem Cells. K. Hata*[1], F. Ikeda[1], K. Yamashita*[1], F. Ichida*[1], T. Matsubara*[1], T. Nokubi*[1], A. Yamaguchi[2], R. Nishimura[1], T. Yoneda[1]. [1]Department of Biochemistry, Osaka University Graduate School of Dentistry, Osaka, Japan, [2]Department of Oral Pathology, Nagasaki University School of Dentistry, Nagasaki, Japan.

C/EBPβ belongs to a large family of basic leucine zipper transcription factors. Recently several natural truncated isoforms of the C/EBPβ have been identified and one of them named LIP which lacks the transactivation domain is found to function as a dominant-negative repressor of C/EBPβ activity. Since C/EBPβ is known to play an important role in adipogenesis in the mesenchymal stem cells which also give rise to osteoblasts, we hypothesized that LIP was involved in osteoblastogenesis and adipogenesis. Consistent with this hypothesis, we found distinctive LIP expression in primary mouse calvarial osteoblasts. To define the role of LIP in osteoblastogenesis, we overexpressed LIP in the C3H10T1/2 mouse pluripotent mesenchymal cells using an adenovirus system. Since the C3H10T1/2 cells did not express Cbfa1 which is an essential transcription factor for osteoblastic differentiation in non-stimulated condition, overexpression of LIP alone did not cause osteoblastogenesis. However, when LIP and Cbfa1 were co-introduced, LIP significantly enhanced Cbfa1-induced osteoblastic differentiation. Co-immunoprecipitation experiments demonstrated that LIP physically associated with Cbfa1. Furthermore, we found that LIP directly bound to the osteocalcin gene promoter and transactivated the osteocalcin gene in cooperation with Cbfa1 despite that LIP lacked the transactivation domain. Consistent with these results, LIP together with Cbfa1 promoted osteoblastic differentiation in the C2 mouse mesenchymal cells that were deficient in Cbfa1 gene. Of note, LIP inhibited adipogenesis and suppressed the transcriptional activity of the PPARγ gene promoter in C3H10T1/2 cells. In contrast to LIP, C/EBPβ itself promoted osteoblastic differentiation and also adipocytic differentiation with an up-regulation of PPARγ expression in C3H10T1/2 cells. In summary, our results show that LIP enhances Cbfa1-induced osteoblastogenesis, suggesting that LIP is a co-activator of Cbfa1. On the other hand, LIP can inhibit adipogenesis in dominat negative fashion. These results suggest that LIP has different roles in osteoblastogenesis and adipogenesis from C/EBPβ and may direct the differentiation of the mesenchymal stem cells toward osteoblasts in collaboration with Cbfa1.

1110

Runx1(Cbfa2/AML1) Is Expressed in Tissues Supporting Osteogenesis and Temporally Regulated During Chondrocyte and Osteoblast Differentiation. E. Balint[1], A. Javed[1], H. Drissi*[1], R. Vitti*[1], E. Quinlan*[1], L. Zhang*[2], T. North*[2], A. J. van Wijnen[1], J. L. Stein*[1], G. S. Stein[1], N. A. Speck*[2], J. B. Lian[1]. [1]Department of Cell Biology, University of Massachusetts Medical School, Worcester, MA, USA, [2]Department of Biochemistry, Dartmouth Medical School, Hanover, NH, USA.

Runx2/Cbfa1 has an essential role in formation of a mineralized skeleton. Here we provide evidence that the hematopoietic transcription factor Runx1/AML1 contributes to early events in formation of the skeleton. Expression of Runx1 during embryonic development was characterized in a $Runx1^{+/lz}$ mouse model in which the LacZ gene was inserted in the C terminus. Thus the resulting Runx1-LacZ fusion protein allowed detection of Runx1 gene expression in its native context by monitoring β-gal activity. Although homozygous mice die at 10.5 dpc due to a lack of definitive hematopoiesis, heterozygous mice develop normally. We find that Runx1 expression in the skeleton is initiated at 12.5 dpc predominantly in mesenchymal condensations that will form bone and in dorsal root ganglia. Runx1 expression continues in all periosteal and perichondrial membranes of bone in the axial and appendicular skeleton. In perichondrium contributing to appositional growth of the epiphysis, Runx1 expression is observed in chondroblasts, but is downregulated in mature hyaline cartilage of the skeleton. By 15.5 dpc Runx1 expression was observed in the suture lines of the calvarium. Runx1 is expressed in osteoblasts at sites of new bone formation, but not in osteocytes of mature bone. In post-natal mice and in adults (up to 1 yr), Runx1 expression is retained in the calvarial sutures and periosteum and in hyaline cartilage of the trachea, but not in the vertebrae or limbs. Ex vivo cultures of cells from suture lines, periosteum, or marrow stroma show Runx1 positive colonies distinct from alkaline phosphatase positive colonies, as well as cells expressing both markers. In osteoblasts from the central bone of calvariae, an induction of Runx1 expression was observed during differentiation. These findings indicate a spatial and temporal role of Runx1 in the early events of osteochondroprogenitor cell maturation and in supporting the properties of periosteal and sutural membranes. We propose that Runx1 has functions beyond hematopoiesis and contributes to early skeletal development.

1111

Loss of a Half Cbfa1 Gene Dosage Sharply Blocks Cancellous Bone Regeneration after Bone Marrow Ablation in Aged Adult Mice Due to the Reduction in Osteoblastic Cell Population in the Stromal Cells. K. Tsuji[1], T. Komori[2], M. Noda[1]. [1]Mol. Pharmacol., Med. Res. Inst., Tokyo Med. and Dent. Univ., Tokyo, Japan, [2]Osaka Univ., Osaka, Japan.

Cbfa1/Runx2, a transcription factor which belongs to Drosophila runt family, is required for bone development as shown by the knockout experiments. Retinoblastoma protein(pRb) induces G1 phase arrest during cell cycle by negatively regulating the transcriptional activity of E2F and also binds to Cbfa1 to co-operatively enhance osteocalcin promoter activity. Therefore, Cbfa1 interaction with pRb may play a pivotal role, and in this regard the dosage levels of Cbfa1 gene product to interact with pRb could influence the maintenance of the population of differentiated osteoblasts in bone. However, heterozygote Cbfa1 mutation ($Cbfa1^{+/-}$) has only been reported to exhibit cleidocranial dysplasia. Thus, the aim of this paper is to examine the effects of Cbfa1 gene dosage on osteoblastic differentiation in vivo and in vitro. First, we conducted bone marrow ablation experiments. In wild type mice, new bone formation to fill the ablated bone marrow space was observed within the first seven days and after that bone resorption followed during the next seven days in the bone marrow either in young(8 week old) or aged(over 20 week old) mice. In young $Cbfa1^{+/-}$ mutant mice, the amounts of regenerated cancellous bone formed within the first seven days in the bone marrow cavity in tibia were similar to those in wild type mice. In contrast, in the aged $Cbfa1^{+/-}$ mutant mice, regeneration of cancellous bone in femora after operation was sharply blocked(80% reduction compared to wild type). Bone volume levels in the non-operated femora were similar between aged wild type and $Cbfa1^{+/-}$ mutant mice. This block of cancellous bone regeneration in the $Cbfa1^{+/-}$ mutant mice was not simply due to delay in bone formation since new bone formation was not observed even fourteen days after bone marrow ablation in the $Cbfa1^{+/-}$ mutant mice. To examine cellular mechanisms underlying this observation in the aged $Cbfa1^{+/-}$ mutant mice, bone marrow cells were cultured in the presence of beta-glycerophosphate and L-ascorbic acid. The development of alkaline phosphatase positive cells in bone marrow cells after culture (7 days) was significantly reduced when cells were prepared from aged $Cbfa1^{+/-}$ mutant mice compared to wild type. Furthermore, mineralized nodule formation was completely blocked even after longer period of culture (21 days) in $Cbfa1^{+/-}$ mutant cells while abundant nodule formation was observed in wild type. These results indicate that full Cbfa1 gene dosage is required for osteoblastic differentiation in bone marrow cells in vitro and cancellous bone regeneration in vivo in aged mice.

1112

Cell Growth Regulatory Role of Runx2 During Proliferative Expansion of Pre-osteoblasts. J. Pratap[1], M. Galindo*[1], S. K. Zaidi[1], D. Vradii*[1], J. A. Robinson[2], B. M. Bhat[2], J. Choi*[3], T. Komori[4], J. L. Stein*[1], J. B. Lian[1], G. S. Stein[1], A. J. van Wijnen[1]. [1]Department of Cell Biology, University of Massachusetts Medical School, Worcester, MA, USA, [2]Bone Metabolism/ Osteoporosis, Wyeth Research, Collegeville, PA, USA, [3]Department of Biochemistry, School of Medicine, Kyungpook National University, Daegu, Republic of Korea, [4]Department of Molecular Medicine, Osaka University Medical School, Suita, Osaka, Japan.

The Runx2 (CBFA1/AML3/PEBP2αA) transcription factor promotes skeletal cell differentiation by activating bone phenotypic genes in post-proliferative osteoblasts. The presence of Runx2 in actively dividing osteoprogenitor cells indicates a dual regulatory role in control of osteoblast growth and differentiation. The genetic contribution of Runx2 to bone cell proliferation was directly addressed analyzed by monitoring ex vivo growth of calvarial osteoblasts. Cells were derived from wild type mice, Runx2 null (-/-) mice or Runx2 ΔC/ΔC mice which contain a mutation in the Runx2 gene that eliminates the normal C-terminus of the protein. The data show that calvarial cells from Runx2 -/- and ΔC/ΔC mice exhibit significantly higher cell growth rates. In contrast, mouse embryonic fibroblasts that do not express Runx2 protein did not display genotype-dependent alterations in cell growth. Therefore, Runx2 is essential for normal proliferation of osteoblasts and the C-terminal region, that integrates several cell proliferation related signaling pathways (e.g., Smad, Yes/Src, MAPK, pRB), is required for the cell growth regulatory functions of Runx2. Western blot analysis reveals that Runx2 (-/-) calvarial cells contain elevated levels of G1/S phase related regulatory factors (e.g., cyclin E and pRB/p105). Thus, increased cell growth rates of Runx2 (-/-) cells may be mechanistically linked to changes in cell cycle markers. Treatment of wild type osteoblasts with cell cycle inhibitors that block cells in G1 or S phase reveals that Runx2 levels are elevated when cells stop dividing. Hence, Runx2 acutely responds to cessation of cell growth. Calvarial cells from wild type but not Runx2 (-/-) or ΔC/ΔC mice are capable of differentiating into mature osteoblasts. Re-introduction of Runx2 into Runx2 -/- cells using an adenoviral vector does not restore the defect in osteoblast differentiation unless BMP2 is also present at early stages. These data show that cessation of proliferation and/or onset of differentiation in osteoblasts are both BMP2 and Runx2 dependent. We propose that Runx2 promotes osteoblast maturation at a key developmental transition by simultaneously supporting exit from the cell cycle and activating genes that promote skeletogenesis.

1113

Regulation of *TWIST* Gene Expression by *Wnt* 11 in Human Osteoblasts: *Wnt* Signaling Pathway in Osteoblast Differentation. T. Yan*[1], S. D. Flanagan*[2], A. Kudo[3], C. A. Glackin[1]. [1]Molecular Medicine, Beckman Research Institute of the City of Hope, Duarte, CA, USA, [2]Neurosciences, Beckman Research Institute of the City of Hope, Duarte, CA, USA, [3]Tokyo Institute of Technology, Yokohama, Japan.

The purpose of this study is to examine the role of the *Wnt* signaling pathway in osteoblast differentiation. *Wnt* is a family of secreted cysteine-rich glycoproteins that are expressed in a wide variety of organ systems in developing embryos. They are thought to play an important role in cell proliferation and differentiation. Recently, a newly isolated human *Wnt* gene, *Wnt*-11, has been shown to be highly expressed in perichondrium of developing human skeleton; however, its role in the human skeletal system is largely unknown. *TWIST* is a basic helix-loop-helix (b-HLH) transcription factor that is important for cell type determination and differentiation. We have shown that *TWIST* is an important regulator in osteoblast differentiation. In order to find the target genes that are regulated by *TWIST*, microarray studies were performed using RNA from stable osteoblast cells that over (TS) or under (TAS) expresses *TWIST*. We found that periostin, a known target of Wnt signaling, was up-regulated 23 fold in HSaOS-2 cells that overexpress *TWIST* as compared with controls. Furthermore, LM-PCR *in vivo* footprinting, gel-shift and super-shift analyses indicate that *TWIST* binds specifically to the "E-box" of the periostin promoter. Transient transfection studies further demonstrated that *TWIST* overexpression *trans*-activates the periostin promoter. These studies showed that *TWIST* binds specifically to the periostin promoter and is an important activator of periostin gene expression. Since *Wnt*-11 is highly expressed in the developing human skeletal system, and periostin is known to be a target of the *Wnt* signaling pathway, we have undertaken studies to examine the role of *Wnt*-11 in the regulation of periostin and *TWIST* expression. RT-*PCR* studies show that HSaOS-2 cells express *Wnt*-11. TS cells treated with *Wnt*-11 conditioned medium show a significant reduction of *TWIST* expression (74%). Interestingly, a dramatic decrease of periostin expression after *Wnt*-11 treatment (93%) was also observed. These results demonstrate that the *Wnt* signaling pathway is important for regulating genes critical for osteoblast differentiation. We propose that *Wnt*-11 reduces *TWIST* expression leading to the down-regulation of periostin expression. Our studies, for the first time, demonstrate that *Wnt* signaling is important for regulating genes critical to osteoblast differentiation. Future studies will explore the paracrine/autocrine effects of *Wnt* signaling on osteoblast differentiation.

1114

Msx2 Suppresses Osteocalcin Gene Expression via Interactions with a Novel Ku Antigen Complex and Runx2/Cbfa1/Osf2. D. M. Willis*, S. L. Cheng, N. Charlton-Kachigian*, A. P. Loewy*, J. S. Shao*, D. A. Towler. Division of Bone and Mineral Diseases, Washington University, Saint Louis, MO, USA.

The homeoprotein Msx2 exerts a minimum of two distinct actions in MC3T3E1 calvarial osteoblasts: (1) Cell-autonomous enhancement of cellular proliferation/DNA synthesis; (2) Inhibition of terminal differentiation, including suppression of osteocalcin (OC) gene expression. The rat OC promoter fragment –154 to –113 confers both basal and FGF responsiveness to the OC gene, and is a target for Msx2-dependent transcriptional suppression. Two elements, the OC FGF response element (OCFRE) and osteoblast specific element 2 (OSE2) are encoded in this region and recognized by the heterotrimeric OCFRE binding complex (Ku70, Ku80, and Tbdn100) and Osf2, respectively. We wished to study the functional interactions between these proteins supporting OC promoter activity via this region. In co-transfection assays, Osf2 upregulates 7-fold the transcription driven by multimerized OC[-154/-113] placed upstream of the unresponsive RSV minimal promoter. Co–expression of Ku70 and Ku80, the DNA binding constituents of the OCFRE complex, enhance Osf2-dependent transcription an additional 2 to 4-fold. Under basal conditions, the transcriptional adapter molecule Tbdn100 marginally enhances Ku–dependent transcription, with no effect on basal Runx2-dependent activity. Remarkably, in the presence of activated FGF receptor 2 signaling, Tbdn100 triples Osf2-dependent transcription. By contrast, Msx2 completely abrogates transcription activated by Osf2 and the Ku complex via this element in MC3T3E1 cells. Suppression is not reversed by the histone deacetylase (HDAC) inhibitor trichostatin A, indicating that suppression is not HDAC dependent. Chromatin immunoprecipitation (ChIP) assays confirm the association of Osf2/Runx2, Ku, and Tdbn100 with the endogenous OC chromatin in MC3T3E1 cells. Stable expression of Msx2 in MC3T3E1 cells suppresses OC gene expression and diminishes the association of Osf2, and to a lesser extent Ku, with OC chromatin. In pull-down assays, Msx2 associates strongly with Ku70 and Ku80, but only weakly with Osf2, suggesting that the Ku complex represents a primary target of inhibition. In culture, Ku70 -/- calvarial osteoblasts exhibit profound deficiency in OC gene expression though Runx2 is readily detected, consistent with a role for Ku in facilitating osteoblast terminal differentiation. In toto, these data indicate that Osf2 and the Ku antigen transcriptional complex functionally interact to support OC transcription in calvarial osteoblasts. Msx2 inhibits OC transcription by antagonizing the assembly of specific protein-DNA interactions in the proximal OC promoter.

1115

Difference of Bone Mineral Density Between Both Hips. Influence of Body Weight and Age. J. L. Mansur, M. C. Cianciosi*. Center of Endocrinology and Osteoporosis La Plata, La Plata, Argentina.

Although Bone Mineral Density (BMD) of both sides are highly correlated in same reports, it is not described how many people have significant differences. We prospectively study the BMD of both hips (Lunar Prodigy) of 150 postmenopausal women. The presence of scoliosis in the image of spine scans, and previous treatments with drugs that affect bone metabolism were exclusion criteria. We report the difference between both sides in 1) % and 2) T-Score, in four regions: A) Femoral neck (FN), B) Ward area (W), C) Trochanter (Troch), and D) Total Hip (TH). We study the group as a whole, and divided in tertils of age and weight. Results: n:150. Age: x: 58.6 (SD: 9.0) years. Weight: 68.9 (SD:14.0) Kg. Difference mean: 3.84 % in FN, 3.75 % in W, 4.11 % in Troch, and 3.08 % in T.H. I) % of patients with difference between both sides; II) Dividing them in tertils, women with more weight (> 71 Kg) have more difference between both sides in all regions , and there were no difference in tertils of age. Conclusions: although BMD of both hips are correlated, a significant number of postmenopausal women without scoliosis have difference between both sides. Bilateral DXA-measurements of hips are recommended, specially in obese women.

Difference of BMD between both hips

	Femoral N.	Ward	Troch	Total hip
> 3 %	44.6 %	44.6 %	48.7 %	34.0 %
> 5 %	23.3 %	20.0 %	26.0 %	12.7 %
>10 %	4.0 %	4.7 %	2.7 %	1.3 %
>0.5 SD	18.7 %	8.7 %	12.7 %	6.7 %
> 1 SD	1.3 %	0.7 %	0.7 %	0.7 %

1116

Influence of Double Deficiency of Estrogen and Androgen in Bone Mass in Castrated Aromatase-knockout Mice. C. Miyaura[1], C. Matsumoto*[1], K. Toda*[2], A. Ito*[1]. [1]Department of Biochemistry, Tokyo University of Pharmacy and Life Science, Tokyo, Japan, [2]Kochi Medical School, Kochi, Japan.

Aromatase is the sole enzyme able to convert androgen to estrogen. We have reported that estrogen deficiency induces bone loss by increased bone resorption not only in female aromatase-knockout (ArKO) mice but also in male ArKO mice, suggesting the essential roles of estrogen in bone metabolism in both genders. However, the possible role of androgen in bone mass in males, and the relationship between estrogen and androgen in bone metabolism remain unclear. To clarify these issues, we induced the double deficiency of estrogen and androgen by orchidectomy in ArKO male mice. ArKO mice were born phenotypically normal, and the growth of ArKO mice after birth was similar to that of wild-type siblings. At 7 weeks of age, male ArKO and wild-type mice underwent sham-operation or orchidectomy (ORX). At 4 weeks after operation, in ORX mice, the weight of seminal vesicles decreased in both ArKO and wild-type mice, indicating that the mice were deficient in androgen. Femoral bone mass was measured by DEXA, and trabecular bone of femoral metaphysis and cortical bone in the middle position of the femur was analyzed by pQCT and histological analysis. Sham-operated ArKO mice showed a significant loss of cancellous bone in femoral metaphysis due to increased bone resorption in comparison with that in sham-operated wild-type mice. ORX/wild-type mice showed significant bone loss compared with that in sham/wild-type mice. The bone mass in sham-operated ArKO mice was similar to that in ORX/wild-type mice. In ORX/ArKO mice, femoral bone mass was further decreased compared with that in sham/ArKO mice not only in cancellous bone but also in cortical bone due to the deficiency of both estrogen and androgen. Most of metaphysial cancellous bone disappeared, and the cross-sectional area of cortical bone at the midshaft of the femur was severely decreased in ORX/ArKO mice. Deficiency of both sex steroids may induce bone resorption and suppress bone formation, resulting in a scant skeletal structure. To examine the anabolic function of androgen, we used weaning wild-type mice in the next experiment. When 3-week-old wild-type mice underwent ORX, periosteal bone formation was severely suppressed in cortical bone and bone resorption was elevated in the metaphysial trabecular bone. At puberty, the cortical thickness and BMD in both cortical and trabecular bone were markedly decreased by ORX. These results suggest that estrogen maintains cancellous bone mass and androgen stimulates cortical bone formation. Sex steroids may share the work of regulating bone metabolism in males.

1117

Increased Wnt-Frizzled Gene Expression in Cortical Bone from Transgenic Mice with Elevated Osteoblastic VDR Expression. W. Zhu*, G P. Thomas*, L. E. Worton*, P. A. Baldock*, R. F. Enriquez*, S. U. K. Baker*, C. M. Alles*, Y. Shi*, J. A. Eisman, E. M. Gardiner. Bone and Mineral Research Program, Garvan Institute of Medical Research, Sydney, Australia.

Wnt secreted glycoproteins, signaling through frizzled (Fzd) transmembrane receptors, regulate cell growth and polarity, and have been shown to be involved in osteoblastic differentiation and bone formation. We have found that OSVDR transgenic mice, overexpressing vitamin D receptor (VDR) in mature osteoblastic cells, exhibit elevated periosteal bone formation on long bone diaphyses. Transcript profiling was conducted to identify changes in gene expression associated with this anabolic bone phentoype. Long bones

were collected from OSVDR and FVB wildtype mice 6 hours after treatment with 1,25-dihydroxyvitamin D3 (1,25-D) or vehicle. Wnt-Fzd gene expression changes were detected in whole tibial midshafts using Atlas cDNA filter arrays (Clontech). These changes were corroborated by real time RT-PCR analysis of femoral diaphyses with periosteum intact but marrow removed. Cellular localization of Wnt-Fzd gene expression and osteoblast differentiation markers (osteocalcin and alkaline phosphatase) was examined in femurs by in situ hybridization (ISH). In cluster analysis of Atlas array data, several genes of the Wnt-Fzd regulatory cascade were changed in OSVDR bone. In real time RT-PCR, there were OSVDR-associated increases in expression of Wnt5b, Fzd7 and Fzd8 genes (9-, 2- and 3-fold) but not Wnt4, in cortical bone from vehicle-treated mice. Interestingly, 1,25-D treatment reduced expression of Wnt5b, Fzd7 and Fzd8 genes by 90%, 47% and 60% in OSVDR but not FVB cortical bone. By contrast, Wnt4 expression was reduced by 1,25-D treatment in both OSVDR and FVB bones (68% and 56%). Cell-specific Fzd8 expression was confirmed to be abundant in mature osteoblasts on OSVDR and FVB periosteal surfaces (ISH), consistent with the observed differences between OSVDR and wild-type mice. However, Wnt4 expression was only observed in a few immature osteoblasts in the periosteum on the posterior aspect of the distal metaphysis and in mature trabecular osteoblasts of the secondary spongiosa. These findings indicate that expression of Wnt5b, Fzd7 and Fzd8 is up-regulated in association with elevated VDR in mature osteoblastic cells of OSVDR mice, but acute 1,25-D treatment reduced expression of these genes as well as Wnt4. The acute negative 1,25-D response may relate to direct effects on gene transcription, whereas the Wnt-Fzd differences in vehicle-treated mice could relate to effects of OSVDR at late stages of differentiation in the osteoblastic lineage. These data support a role for the Wnt-Fzd pathway in vitamin D regulation of cortical bone formation.

1118

Gene Repression Mediated by the Liganded VDR Is Exerted by the Concomitant and Vitamin D-dependent Recruitment of DNA-PK, HDAC2 and VDR. T. Okazaki[1], E. Ogata[2], T. Fujita*[1]. [1]Endocrine Unit, Internal Medicine, University of Tokyo School of Medicine, Tokyo, Japan, [2]Cancer Institute Hospital of Japan, Tokyo, Japan.

(Background) By using chromatin immunoprecipitation (ChIP) assay, we previously demonstrated that vitamin D-dependent recruitment of VDR and HDAC2 (histone deacetylase 2) to the nVDREm, the half site of DR-3 DNA element originally found in the human PTHrP gene, was necessary for hypoacetylation of the nVDREm-containing chromatin region. Further, this assay revealed a vitamin D-dependent interaction between HDAC2 and VDR. On the other hand, we had suggested that the VDR phosphorylated by DNA-dependent protein kinase (DNA-PK) in the presence of vitamin D led to a weaker interaction with the nVDREm. We postulated that both HDAC2 and DNA-PK were crucially involved in this type of gene repression by vitamin D. (Purpose and methods) To clarify the effect of vitamin D on the recruitment of DNA-PK and its regulatory subunit, Ku antigen, to the chromatinized nVDREm, we performed ChIP assay. MCF7 cells and human lymphocyte MT2 cells, in which VDR and PTHrP genes are endogenously expressed, were transiently transfected with the nVDREm-TK reporter gene. Chromatin was immunoprecipitated from these cells treated with no or 10 nM of vitamin D for 40 hours. DNA-PK, Ku antigen, VDR and acetylated histone3 were immunoprecipitated with the respective antibody. These chromatin immunoprecipitates were then analyzed for the presence of the nVDREm in the introduced reporter or endogenous PTHrP gene by PCR. (RESULTS) We found that these two cell lines gave identical results and both types of PCR showed similar tendency. Vitamin D treatment decreased the degree of histone H3 acetylation, while it recruited VDR and DNA-PK to the nVDREm in the chromatin. However, Ku antigen was recruited to the nVDREm only in the absence of vitamin D. Therefore, Ku antigen as a DNA-binding protein constitutively recruited to the chromatinized nVDREm was replaced by its catalytic subunit, DNA-PK, after vitamin D treatment. To better define the manner of the interactive recruitment of DNA-PK and VDR, similar ChIP assay was carried out after introduction of the AF2-only domain of VDR, which by itself was not recruited to the nVDREm, along with the nVDREm-TK reporter into MCF7 cells. In these cells, we observed no recruitment of DNA-PK to the chromatinized nVDREm even in the presence of vitamin D, suggesting that DNA-PK interacts with the AF2 domain of VDR in the presence of vitamin. D. (Conclusion) Because the recruitment pattern of DNA-PK and VDR coincided well with that of HDAC2, we postulate that the concomitant recruitment of these three molecules is a prerequisite for this type of gene repression by vitamin D.

1119

MET, a Novel Stimulator of Estrogen-induced Transcription Isolated from Mouse Bone Marrow. S. M. Colley*[1], A. Flynn*[2], M. Norman*[2], D. Wynick*[2], J. H. Tobias[1]. [1]Rheumatology Unit, University of Bristol, Bristol, United Kingdom, [2]Urcn, University of Bristol, Bristol, United Kingdom.

High-dose estrogen is known to stimulate osteoblast activity in postmenopausal women and rodent models. To investigate the molecular mechanisms which mediate this action, subtractive hybridisation analysis was employed to compare the gene expression profiles of mRNA isolated from tibiae of adult mice treated with vehicle or high-dose estrogen for 4 days. A gene fragment showing no significant homology to previously characterised sequences was subsequently isolated and found to detect a single 3.8Kb transcript by northern analysis. A full length cDNA homologous to this gene, which we refer to as MET, was generated by EST directed Rt-PCR using bone marrow cDNA as the source of template. Sequence analysis of the cloned product revealed it coded for a 1031 amino acid protein. This peptide contains a SAF Box DNA binding motif, an RNA binding domain and shares an overall identity of 34% with the estrogen suppresser SAF-B/HET/HAP (HET). MET cDNA was subsequently expressed as a fusion product with enhanced yellow fluorescent protein and, consistent with a role as a regulator of transcription, found to localise to the nucleus of mammalian cells. To explore its cellular actions, we then compared the effects of MET and HET over expression on estrogen-induced ERE-luciferase reporter gene transcription in MCF-7 breast, HepG2 liver and a range of human and rodent bone cell lines. Consistent with previous reports, HET over expression was found to suppress the actions of estrogen on reporter gene expression. In contrast, MET co-transfection increased estrogen-induced reporter activity by 50-100% in all cell lines studied. Taken together, our results indicate that MET represents a novel SAF Box-containing nuclear protein which, in contrast to a related protein HET, serves to stimulate rather than suppress estrogen-induced gene transcription. Whether MET plays a significant role in regulating the response of the skeleton and other tissues to estrogen, and represents a useful target for novel therapies designed to manipulate these actions, is currently under study.

1120

A Novel Vitamin D Analogue Exhibits Selective Anabolic Actions in Osteoblasts that Result in Enhanced Bone Formation. N. K. Shevde, H. Yamamoto, M. Clagett-Dame*, L. Plum*, H. F. DeLuca, J. W. Pike. Biochemistry, University of Wisconsin- Madison, Madison, WI, USA.

Adult bone remodeling is achieved through the coordinated activity of bone-resorbing osteoclasts (OC) and bone-forming osteoblasts (OB). While many factors regulate the OB and the OC, the actions of 1,25-dihydroxyvitamin D_3 ($1,25(OH)_2D_3$) on OB proliferation, maturation, differentiation and function are well recognized. These actions are mediated by the vitamin D receptor (VDR), a transcription factor that regulates patterns of gene expression not only in the OB but in other tissues as well. High levels of $1,25(OH)_2D_3$, however, strongly induce the expression of RANKL by the OB, stimulating OC activity and recruitment in turn. This homeostatic imbalance leads to elevated bone resorption, hypercalcemia and weight loss. A novel series of $1,25(OH)_2D_3$ analogues was recently discovered that exhibit a 30 to 50 fold increase in calcium mobilizing activity in the rat, suggesting a selective activity on the OB. These analogues modified by either an alpha methyl or a methylene substitution on carbon 2, bind to the vitamin D receptor (VDR) with a affinity constant similar to that for $1,25(OH)_2D_3$. One of these analogues, 2-methylene-19-nor-(20S)-$1,25(OH)_2D_3$ (2MD), was evaluated further for its selective activity on osteoblasts in vitro. We explored the ability of 2MD to stimulate 1) OB-specific expression of RANKL, 2) OB-mediated OC formation in cocultures and 3) OB differentiation and mineralized nodule formation in vitro. 2MD was found to be 100x more potent than $1,25(OH)_2D_3$ in stimulating RANKL production and OC formation in cocultures in vitro. Surprisingly, 2MD markedly stimulated both mouse and human osteoblast cultures to form bone nodules at concentrations as low as 10^{-12} to 10^{-10} M. $1,25(OH)_2D_3$ showed little or no activity at the highest concentrations tested (10^{-7} M). This effect was absent in osteoblasts derived from VDR null mice, demonstrating that the molecular actions of 2MD are mediated by the VDR. Importantly, 2MD stimulated these potentially anabolic activities in OBs at concentrations well below those that favor OC formation in vitro. These results suggest that 2MD is a potent vitamin D analogue with VDR-selective bone forming anabolic actions in the OB in vitro. Moreover, our results are fully supported by current studies in ovariectomized rats that indicate that 2MD strongly induces bone formation in the absence of hypercalcemia. This analogue should prove therapeutically useful in bone diseases such as age- and sex steroid-related osteoporosis, cancer-induced osteolysis or perhaps to accelerate bone formation during fracture healing.

1121

Fragmentation of Insulin-Like Growth Factor Binding Protein (IGFBP) 5 Is Required to Induce Osteoblastic Differentiation. D. Durant, R. M. R. Pereira*, E. Canalis. Research, Saint Francis Hospital and Medical Center, Hartford, CT, USA.

Insulin-like growth factors (IGF) have important anabolic effects in bone and their actions are modulated by IGFBPs. Of the six IGFBPs secreted by bone cells, IGFBP-5 has been reported to enhance the stimulatory effects of IGF-I in bone cells. However, the mechanisms of this effect and the specific molecules involved remain unclear. Transgenic mice overexpressing IGFBP-5 under the control of the osteocalcin promoter develop osteopenia due to decreased bone formation, suggesting that intact IGFBP-5 in excess is not anabolic and binds IGF-I, preventing its stimulatory actions on bone formation. However, IGFBP-5 secreted by osteoblasts is rapidly fragmented by the activity of metalloproteases, likely matrix metalloprotease (MMP) 13 or collagenase 3. We postulated that IGFBP-5 fragments have distinct activity. Initially, we used amino acid analysis and mass spectroscopy to determine the cleavage sites of IGFBP-5 by collagenase 3 and define the fragments formed. We demonstrated cleavage at glu162 - meth163, ala193 - val194, and glu235 - tyr236. Based on this information we created retroviral vector constructs to express intact IGFBP-5 1-252 and its fragments, IGFBP-5 1-162, IGFBP-5 1-193, IGFBP-5 1-235, and IGFBP-5 163-252. For this purpose, the indicated fragments, preceded by the signal peptide, were cloned into the retroviral vector pLPCX, transfected into PT67 or Phoenix packaging cells and the supernatant used to transduce MC3T3-E1 mouse osteoblastic cells. MC3T3-E1 cells were cultured for 0 to 4 weeks following confluence in alpha-MEM in the presence of 5mM beta-glycerophosphate and 100 ug/ml ascorbic acid. Overexpression of IGFBP-5 and each individual fragment was confirmed by reverse transcription polymerase chain reaction using specific primers to identify the recombinant transcript and by Northern blot analysis. Cells transduced with IGFBP-5 1-193 displayed accelerated maturation and enhanced mineralization, as determined by alizarin red staining, when compared to MC3T3 cells and to cells transduced with pLPCX vector. In contrast, intact IGFBP-5 1-252 impaired cell differentiation and the fragments IGFBP-5 1-162, 1-235, and 163-252 had little impact on cell maturation. In conclusion, intact IGFBP-5 impairs osteoblastic maturation, whereas the IGFBP-5 1-193 fragment induces the differentiation of cells of the osteoblastic lineage.

1122

Rescue of the Osteopetrotic Defect in op/op Mice by Osteoblast-specific Targeting of Membrane-bound CSF-1. S. L. Abboud, K. Woodruff*, N. Ghosh-Choudhury. Pathology, University of Texas Health Science Center at San Antonio and South Texas Veteran's Health Care System, San Antonio, TX, USA.

Soluble (s) and membrane-bound (m) forms of macrophage colony-stimulating factor (CSF)-1 are synthesized by osteoblasts in the bone microenvironment. In the op/op mouse, absence of osteoblast-derived CSF-1 leads to decreased osteoclasts and osteopetrosis. Systemic administration of recombinant sCSF-1 to op/op mice corrects the osteopetrotic defect. However, osteopetrosis relapses one month following cessation of CSF-1 therapy and it cannot be reversed if sCSF-1 is administered after 7 days of age, suggesting that early and sustained postnatal CSF-1 expression in the bone is required for complete remission. Our recent studies show that sCSF-1, selectively expressed in the bone of op/op mice, stimulates normal tooth eruption and rescues the osteopetrotic defect by 5 wks, with this effect persisting for over l2 mo. To determine if mCSF-1 alone can reverse the defect, transgenic mice harboring the human mCSF-1 cDNA under the control of the osteocalcin (OC) promoter were generated and crossbred with heterozygous op/wt mice to establish op/op mutants expressing the transgene (op/opT). The op/op genotype and transgene expression were confirmed by PCR and Southern blot analysis, respectively. mCSF-1 protein was detected in bone extracts (382 pg/mg protein), but not in other tissues or plasma. Op/opT mice showed tooth eruption of upper and lower incisors, albeit delayed, 25 days after birth. The abnormal body weight and skeletal abnormalities observed in op/op mice were significantly improved in 5-10 wk old op/opT mice. By x-ray, op/opT mice showed radiolucent marrow spaces in the iliac crest, caudal vertebrae, tibial and femoral diaphysis comparable to wt mice, although mild metaphyseal sclerosis persisted. Continuous resolution of osteopetrosis in op/opT mice is being evaluated at later time points using pQCT scanning and histomorphometry. These findings indicate that mCSF-1 is almost as effective as sCSF-1 in correcting the osteopetrotic defect, suggesting a redundant role of membrane-bound and soluble CSF-1 in regulating osteoclastogenesis and normalization of bone turnover. Moreover, the osteocalcin promoter provides an efficient tool for delivering CSF-1 and other cytokines to osteoblasts that, in turn, express these factors in a physiologic manner throughout development. Osteoblast-specific targeting of mCSF-1 may provide a useful therapeutic approach for regulating osteoclast development and function in a variety of bone disorders.

1123

gp130 Regulates Bone Turnover and Bone Size by Distinct Downstream Signaling Pathways. N. A. Sims[1], B. J. Jenkins*[2], J. M. W. Quinn[3], T. J. Martin[3], M. Glatt*[4], M. T. Gillespie[3], M. Ernst*[2]. [1]Department of Medicine at St. Vincent's Hospital, University of Melbourne, Fitzroy, Australia, [2]Ludwig Institute for Cancer Research, Melbourne, Australia, [3]St. Vincent's Institute of Medical Research, Fitzroy, Australia, [4]Novartis Pharma, Basel, Switzerland.

IL-11, IL-6 and LIF are bone-active cytokines of the same family; their actions are transduced by interaction of their ligand-specific receptors with the gp130 signaling receptor subunit. gp130 signaling is itself mediated through at least two intracellular pathways including the SHP2/ras/Erk and STAT1/3 pathways. To further delineate the pathways through which gp130 regulates bone mass, we have analyzed the bone phenotypes of two gp130 knock-in mutant mice. The first mutant (gp130ΔSTAT) harbors a COOH-terminal truncation deleting all STAT signaling (Ernst et al, JEM 2001). The second mutant (gp130Y757F) contains a phenylalanine substitution of tyrosine 757 to abolish the SHP2/ras/Erk signaling pathway (Ernst et al, submitted). In male and female gp130Y757F mice, trabecular bone volume was reduced by approximately 50%, detected by histomorphometry and microCT. This reduction in bone volume was associated with high bone turnover. In male mice, osteoclast surface (OcS/BS) was 70% greater, osteoblast surface (ObS/BS) was doubled and osteoid volume (OV/BV) was three times that of control mice. Similarly, in vitro RANKL-driven osteoclastogenesis was elevated in cultures of bone marrow cells from gp130Y757F mice compared to wild type controls, indicating that this phenotype does not relate to alterations in systemic hormones. High bone turnover in these mice indicates that gp130 signaling through SHP2/ras/Erk is required for normal bone turnover. This result is comparable with elevated osteoclastogenesis in the gp130 knockout mouse previously described, and suggests that gp130-mediated effects on osteoclastogenesis and trabecular bone volume are mediated through the SHP2/ras/Erk pathway. In contrast, bone turnover and trabecular bone volume were normal in gp130ΔSTAT mice, suggesting that the STAT1/3 pathway is not required for gp130-mediated regulation of trabecular bone volume. However, in gp130ΔSTAT mice, longitudinal bone growth was reduced. Tibial and femoral length were significantly lower than in wild type mice, and growth plate closure was observed as early as 12 weeks of age, indicating that while gp130 signaling through STAT1/3 is not required for normal bone turnover, it is required for continued longitudinal bone growth. In conclusion, gp130 signaling is required for normal longitudinal bone growth and regulation of trabecular bone mass, but these two activities are mediated by distinct downstream signaling pathways.

1124

Protein Kinase D Induced Activation of the Stress-sensitive MAP kinases JNK and p38 is a New Signaling Pathway Involved in BMP-2 Induced Osteoblastic Cell Differentiation. J. Lemonnier*, C. Ghayor*, J. Caverzasio. Division of Bone Diseases, University Hospital of Geneva, Geneva, Switzerland.

BMP-2 is a critical morphogenetic protein for the development of osteoblastic cells. However, the cellular mechanisms by which BMP-2 induces this process remains uncompletely understood. Recent finding suggest that, in addition to the SMAD pathway, BMP-2 may also signal via protein kinase C (PKC) and/or the mitogen-activated protein kinases (MAPKs). In this study, we investigated the molecular mechanism by which BMP-2 activates JNK and p38 and the role of these pathways in the differentiation of osteoblastic cells. In MC3T3-E1 osteoblastic cells, the activation of JNK and p38 by BMP-2 (23-25 x at 3h) was not affected by overnight pretreatment of the cells with PMA suggesting that conventional PKC isoforms are not involved in this signaling response. In contrast, the PKC and protein kinase D (PKD) inhibitor Go6976 (10 μM) completely blocked BMP-2-induced activation of JNK and p38 without influencing SMAD1,5 phosphorylation. Interestingly, Go6976 also completely blunted the stimulation of alkaline phosphatase (ALP) activity (3-5x) induced by BMP-2. PKD, which is the mouse homologue of the human PKC mu, is a newly described diacylglycerol-sensitive protein kinase with homology to PKCs and unknown function. Among various PKCs expressed in MC3T3-E1 cells, BMP-2 only induced phosphorylation/activation of PKD with a maximal effect (3.3x) after 1 h incubation and this response was completely prevented by Go6976. To further determine the role of PKD in mediating activation of JNK and p38 by BMP-2, we constructed a MC3T3-E1 cell line stably expressing PKD antisens oligonucleotide (AS-PKD). In this cell line, PKD expression was lowered by 50-60% compared with vector transfected cells (V-PKD). Interestingly, activation of JNK and p38 as well as the stimulation of ALP induced by BMP-2 were markedly impaired in AS-PKD compared to V-PKD transfected cells suggesting a functional role of activation of JNK and p38 by PKD in osteoblast-like cells. In conclusion, our data describe a new signaling pathway activated by BMP-2 in osteoblastic cells. This pathway involves PKD-dependent activation of JNK and p38 which, in addition to SMADs, appears to be essential for the effect of BMP-2 on osteoblastic cell differentiation.

1125

Neuropeptide Y Y4 and Y2 Receptors Act Synergistically in Neuroregulation of Bone Mass. P. A. Baldock*[1], A. Sainsbury-Salis*[2], N. Ueno*[3], M. Couzens*[2], R. F. Enriquez*[1], A. Inui*[3], H. Herzog*[2], E. M. Gardiner[1]. [1]Bone and Mineral Research Program, Garvan Institute of Medical Research, Sydney, Australia, [2]Neurobiology Program, Garvan Institute of Medical Research, Sydney, Australia, [3]Clinical Molecular Medicine, Kobe University Graduate School of Medicine, Kobe, Japan.

Neuropeptide Y (NPY) Y2 receptor has previously been shown to regulate bone mass, with knockout resulting in increased cancellous bone formation. Pancreatic polypeptide (PP) a member of the NPY family was elevated in these mice, suggesting a mechanism for this effect. Further, PP is the major ligand for NPY Y4 receptor, implicating Y4 in the Y2 KO bone phenotype. This study compared the effect of NPY Y2 KO with Y4 KO, Y2/Y4 double KO and PP transgenic overexpression in the regulation of bone mass. Bone structure was examined in the distal femoral metaphysis and mid-femoral diaphysis of 4 month old male knockout, transgenic and wild type mice. PP overexpression did not affect bone mass, as cancellous bone volume (BV/TV) in PP mice was not different from wild type mice (10.4 ±1.9 vs 9.0 ±1.2%), with no differences in trabecular number or thickness observed. Similarly, there was no difference in cortical area (0.81 ±0.04 vs 0.80 ±0.03 mm2). Unlike Y2 KO, deletion of the Y4 receptor did not affect bone mass. BV/TV in Y4 KO mice did not differ from wild type mice (8.2 ±1.2 vs 6.6 ±1.4%), and there were no microarchitectural differences. These values were significantly lower than in Y2 KO mice (12.4 ±1.7%). Cortical area was also unaffected by Y4 knockout (1.12 ±0.04 vs 1.17 ±0.14 mm2) and values did not differ from Y2 KO mice (1.09 ±0.5 mm2). Despite the lack of skeletal phenotype in Y4 KO mice, deletion of both receptors in Y2/Y4 KO mice had a synergistic effect on bone mass. BV/TV was elevated compared to Y4 KO (17.4 ±2.1 vs 8.2 ±1.2%) and Y2 KO (12.4 ±1.7%), although the latter 40% difference was not significant (p=0.055). Trabecular number was also elevated (4.9 ±0.4 vs 3.2 ±0.3 /mm) and (4.0 ±0.3 /mm). Trabecular thickness was elevated compared to Y4 KO (34.4 ±2.6 vs 24.7 ±1.9 um) but not Y2 KO (29.9 ±2.0 um). In contrast to cancellous increases, cortical area was reduced in Y2/Y4 KO compared to both Y4 KO (0.91 ±0.03 vs 1.12 ±0.04 mm2) and Y2 KO (1.09 ±0.05 mm2), associated with reduced cortical thickness (203 ±4 vs 239 ±5 and 237 ±6 um). These data suggest that PP is not involved in the Y2 KO bone phenotype. Furthermore, although the Y4 receptor pathway does not independently regulate bone mass, synergistic interaction between Y2 and Y4 elevates cancellous bone mass over Y2 KO levels, and produces a reduction in cortical bone not present in either KO. In conclusion, this study suggests neuroregulation by these two receptors to reduce cancellous and increase cortical bone.

1126

Mim-1, an Osteoclast Secreted Chemokine, Stimulates Differentiation, Matrix Mineralization and Increased Vitamin D Receptor Binding to the VDRE of Osteoblastic Precursor Cells. L. V. Ponomareva*, W. Wang*, N. J. Koszewski, J. P. Williams. Internal Medicine, University of Kentucky, Lexington, KY, USA.

Osteoclasts are terminally differentiated cells of hematopoietic origin. Mechanisms coordinating bone degradation by osteoclasts and new bone synthesis by osteoblasts are poorly defined. We have identified an osteoclast-secreted chemokine, mim-1, that stimulates concentration dependent increases in migration and differentiation of osteoblastic precursor cells. The signaling pathways mediating these effects have not been identified. We have reported that mim-1 stimulates concentration dependent changes in protein tyrosine phosphorylation and activation of ERK in human mesenchymal cells as determined by Western analysis with phospho-specific antibodies. In this study we demonstrate that mim-1 stimulates concentration dependent increases in differentiation and matrix mineralization of MC3T3 E1 cells and human mesenchymal cells as determined by total calcium measurements and VonKossa staining. The effects of mim-1 on early signaling events in osteoblast differentiation were examined. Mim-1 stimulates time and concentration-dependent increases in binding of the osteoblast-specific transcription factor, *cbfa1,* to the proximal transcription-factor binding site in the osteocalcin promoter. Increased *cbfa1* binding is evident at 30 minutes and maximal by 2 hours treatment with 15 nM mim-1. Binding is stimulated by as low as 0.3 nM mim-1. We examined the effect of mim-1 in vitamin D receptor (VDR) binding and demonstrate that mim-1 also stimulates increased VDR binding to the VDRE of osteocalcin with 10 minutes treatment in the absence of added hormone as determined by electrophoretic mobility shift assays and confirmed in supershift assays. VDR binding to the VDRE is maximal at 1 hour. These hormone-independent effects of mim-1 on VDR binding to the VDRE consistently preceded the *cbfa1* binding (n=3). In conclusion, the osteoclast derived chemokine stimulates migration, differentiation and matrix mineralization of osteoblastic precursors suggesting that mim-1 is an important signaling molecule regulating recruitment and differentiation of osteoblastic precursor cells to areas of recent bone resorption, and may represent an endogenous anabolic agent in bone.

1127

The Effect of Monitoring on Adherence and Persistence with Raloxifene Therapy and the Impact on the Effectiveness of Treatment. J. A. Clowes, N. F. A. Peel, R. Eastell. Clinical Sciences (North), University of Sheffield, Sheffield, United Kingdom.

Long-term adherence and persistence with antiresorptive therapy is poor, this limits the effectiveness of treatment. Monitoring techniques may improve adherence or persistence and potentially increase the therapeutic response. The aims of the study were to determine if 1) monitoring by medical staff could enhance adherence and persistence with an antiresorptive agent, 2) providing information on biochemical response to therapy resulted in additional benefit and 3) different rates of adherence to therapy altered treatment efficacy. Seventy-five healthy postmenopausal women (age 50-80 years) with osteopenia (T score < -1 SD and > -2.5 SD), recruited from general practice surgeries, were treated with 60 mg raloxifene and 500 mg elemental calcium. Subjects were randomized in an open label study to one of three arms involving 1) marker monitoring, 2) nurse monitoring or 3) no monitoring. At each visit nursing staff followed a standard interview. Subjects in the monitoring (nurse and marker) protocols attended for visits at 12, 24 and 36 weeks. All subjects were evaluated at 1 year. In the marker protocol results of urine N-telopeptide of type I collagen (uNTX) measurements collected prior to each visit were given to subjects. Adherence was assessed using electronic event monitors, which record the date and frequency a prescription bottle is opened. Persistence with therapy was defined as continuing to take tablets for greater then 7 out of any 14 days prior to the 1-year visit. Cumulative adherence was the number of tablets actually taken divided by the number of expected tablets taken at each time point expressed as a percentage. The hazard ratio for persistence was 0.81 with a trend for monitored subjects to persist with therapy for longer (Log rank test; P = 0.07). This was seen for both nurse-monitored (Wilcoxon (Gehan) test; P = 0.06) and marker-monitored (P = 0.26) subjects. The hazard ratio for cumulative adherence to therapy (> 75%) was 0.64 with monitored subjects 36% more likely to adhere to > 75% therapy (Log rank test; P = 0.039) than non-monitored subjects. There was a trend for greater cumulative adherence to therapy (> 75%) in the nurse-monitored and marker-monitored subjects (P = 0.05 and P = 0.15). Adherence at 1 year was strongly correlated with % change in hip BMD (r = 0.34, P = 0.003) and % change in uNTX (r = - 0.46, P = 0.0001). We conclude that the monitoring of patients increases adherence to therapy by 36% over 1 year. Furthermore increased adherence to therapy increased the effectiveness of raloxifene therapy determined using surrogate end points.

1128

Acute Androgen Deprivation Causes Early Rapid Bone Loss: A Longitudinal Study. P. S. Coates, J. Wagner, J. Ribich, D. L. Trump*, J. B. Nelson*, S. L. Greenspan. University of Pittsburgh Medical Center, Pittsburgh, PA, USA.

Androgen deprivation therapy, the most effective systemic therapy for prostate cancer, is a major risk factor for osteoporosis in men. To investigate the effects of androgen deprivation over time, we studied 120 men prospectively over 6 months. We compared men with prostate cancer; 1) not on androgen deprivation (No AnDep), N=27; 2) following acute (<6 months) androgen deprivation (Acute AnDep), N=23; and 3) following chronic (>6months) androgen deprivation (Chronic AnDep), N=32; with 4) healthy controls, N=38. The men did not differ in age, height, weight or BMI. Men with acute AnDep lost BMD at the radius, total hip and total body, gained body fat and had increased markers of bone turnover acutely over 6 months, compared to men on no AnDep, chronic AnDep or controls who remained stable (data shown in table, mean ± SD). Urine N-telopeptide (NTX) at 6 months was inversely related to the 6-month change in bone density at the radius (R=-0.43, p<0.01), total body (R=-0.54, p<0.001) and trochanter (R=-0.39, p=0.02), with a similar trend at the total hip. We conclude that AnDep causes an early rapid bone loss that slows over time. These longitudinal data suggest future studies are needed to target preventive strategies for this population.

% change in 6 months

	No AnDep	Acute AnDep	Chronic AnDep	Controls
Total radius BMD	0.63 ± 3	-1.46 ± 2[a]	-0.35 ± 3	0.04 ± 1
Total hip BMD	0.36 ± 1.3	-1.9 ± 3 [a]	1.7 ± 6	-0.27 ± 2
Total body BMD	-0.52 ± 2	-2.4 ± 2[b]	-0.16 ± 2	-0.15 ± 2
PA spine BMD (L1-L4)	0.58 ± 2	0.01 ± 3	1.41 ± 3	-0.22 ± 2
% body fat	2.1 ± 6	8.0 ± 7[c]	1.2 ± 6	1.1 ± 3

[a]p<0.05, [b]p<0.01, [c]p<0.001 compared to baseline

Bone turnover markers (6 months)

	No AnDep	Acute AnDep	Chronic AnDep	Controls
NTX (nM BCE/nM Cr)	37 ± 17	74 ± 30 [c†]	34 ± 15	30 ± 13
Osteocalcin (ng/ml)	15.4 ± 4	27.9 ± 7 [b‡]	15.3 ± 9	14.5 ± 8
ALP (IU/L)	77 ± 17	93 ± 21 [a†]	95 ± 35	77 ±20

[a]p<0.05, [b]p<0.01, [c]p<0.001 compared to controls
†p<0.05, ‡p<0.001 compared to -AnDep

1129

The Relationship Between Prospective Height Loss and Multiple Vertebral Fractures. K. Siminoski[1], J. D. Adachi[2], G. Cline*[3], C. B. M. B*[4], V. E. R. T Study Group*[3]. [1]Radiology, Univ of Alberta, Edmonton, AB, Canada, [2]Medicine, McMaster Univ, Hamilton, ON, Canada, [3]Procter & Gamble Pharm, Mason, OH, USA, [4]Bone Alliance, Toronto, ON, Canada.

We have analyzed the relationship between height loss during prospective monitoring and the occurrence of multiple new vertebral fractures. Subjects were women in the placebo arms of the VERT MN/NA risedronate studies (average age 69 yrs; range: 38-85 years) who had post-baseline data for both variables. Height loss was determined as the difference between the baseline measurement and the subsequent measurement using a stadiometer. Lateral vertebral radiographs were performed at the same times and were analyzed by digital morphometry from T4 to L4. Vertebral fractures were determined using both quantitative and semiquantitative methods. New fractures occurred in 18.1% of the 985 subjects over 3 years of observation. The odds ratios (OR) for detecting 1 or more fractures increased with the amount of height loss, as shown in the figure. In comparison to subjects with no height loss, height loss in the range of 0 to 1 cm produced an OR of 2.0; for height loss > 4 cm, OR was 25.1. For detecting two or more fractures, the OR increased from 2.0 for height loss in the range of 0 to 1 cm to 60 for height loss of > 4 cm. Odds increased further for detection of three or more fractures: OR was 3.9 when height loss was 0 to 1 cm, and rose to 117 for height loss > 4 cm. Two relationships are revealed by these analyses. First, for a specific number of vertebral fractures, the OR rises sharply as the amount of prospective height loss increases. Second, at a specific level of observed height loss, the OR increases for greater numbers of fractures. We conclude that (1) the greater the amount of height loss, the greater the likelihood that an incident vertebral fracture has occurred, and (2) the greater the height loss, the greater the likelihood of multiple fractures. Height loss > 2 cm during prospective monitoring substantially increases the probability that one or more vertebrae have fractured.

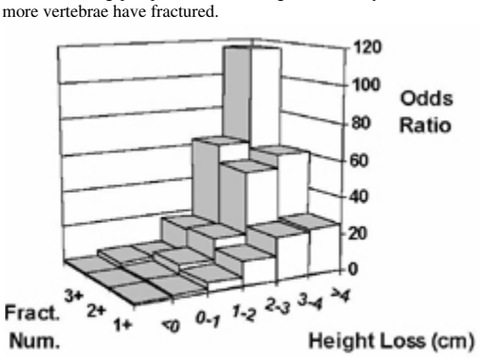

Disclosures: ***K. Siminoski****, Procter & Gamble 2, 5, 8.*

1130

Comparison of 3 Bone Ultrasounds for Determining Osteoporotic Fracture Risk over 3.5 Years in 7487 Elderly Women: The SEMOF study. M. A. Krieg, J. Cornuz*, P. Burckhardt. Internal Medicine, University Hospital, Lausanne, Switzerland.

The SEMOF study group : Büche D, Dambacher MA, Hartl F, Häuselmann HJ, Kraenzlin M, Lippuner K, Neff M, Pancaldi P, Rizzoli R, Tanzi F, Theiler R, Tyndall A, Wimpfheimer K. The Swiss Evaluation of the Methods of Measurement of Osteoporotic Fracture Risk (SEMOF) study is a prospective multicenter study which compares 3 bone ultrasounds (QUS), Achilles+ (GE-Lunar), Sahara (Hologic), and DBM sonic 1200 (IGEA) for the assessment of osteoporotic fracture risk in elderly women, under strict quality control conditions. 7487 women aged 75.3 ± 3.1 years (mean±SD) were assessed using the following QUS parameters : "SI" for Achilles+, "QUI" for Sahara, and "ADSOS" for DBM Sonic 1200 (DBM). In addition, 80% of the measurements with DBM (n=6017) were analyzed in order to calculate the "UBPI". During the mean 3.5-year follow-up, 569 osteoporotic fractures (469 for UBPI) were reported. Age-adjusted relative risks (RR and 95% confidence intervals) were calculated for the QUS parameters, and expressed per decrease of 1 SD of the respective parameter (table). To compare the different devices, areas under the ROC curve (AUC) were calculated. Only Achilles+ and Sahara predicted hip fracture risk. However, all 3 QUS predicted other osteoporotic fracture risks, such as for vertebral or forearm fractures. For hip and forearm fractures, AUC (and by that prediction power) of Achilles+ and Sahara (AUC 0.59-0.70) were both higher ($p<0.01$) than AUC of ADSOS and UBPI (AUC 0.51-0.59). For clinical vertebral fractures, there was no significant difference between AUC of the 3 devices (AUC 0.57-0.64). These results of the SEMOF study show that QUS of the heel (Achilles+ and Sahara), and to a lesser degree QUS of the phalanges (DBM sonic 1200), are predictors of osteoporotic fractures in a cohort of elderly Swiss women.

Type of fracture	Hip	Clinical vertebral	Forearm
Nb of fractures	74	95	181
	RR (95%CI)	RR (95%CI)	RR (95%CI)
Achilles+ (SI)	1.8 (1.4 - 2.3)	1.5 (1.2 - 1.8)	1.4 (1.2 - 1.6)
Sahara (QUI)	2.1 (1.6 - 2.8)	1.7 (1.3 - 2.2)	1.8 (1.5 - 2.1)
DBM (ADSOS)	0.9 (0.8 - 1.2)	1.2 (1.0 - 1.5)	1.2 (1.0 - 1.3)
DBM (UBPI)	1.0 (0.8 - 1.3)	1.4 (1.1 - 1.9)	1.2 (1.0 - 1.5)

1131

QCT Spine BMD, Hip BMD, and Risk of Fractures in Elderly Black and White Men and Women. S. R. Cummings[1], F. Harris[1], T. Lang[1], T. Harris[2], D. Taaffe[3], F. Tylavsky[4], J. A. Cauley[5], D. M. Black[1]. [1]University of California, San Francisco, San Francisco, CA, USA, [2]National Institute on Aging, NIH, Bethesda, MD, USA, [3]University of Queensland, St. Lucia, Australia, [4]University of Tennessee, Memphis, TN, USA, [5]University of Pittsburgh, Pittsburgh, PA, USA.

The predictive accuracy of volumetric BMD (vBMD) of the spine has never been tested or compared with areal BMD (aBMD) of the hip by DXA. Additionally, the predictive accuracy of hip BMD has never been prospectively compared for women (W), men (M), African-Americans (AA) and Caucasians (C). We measured hip aBMD (Hologic 4500) in 846 CW, 929 CM, 724 AA W and 544 AA M age 70-80 years and trabecular vBMD by QCT in half of this cohort and then validated clinical fractures during a mean 3.7 years follow-up. All analyses are age-adjusted and exclude participants taking bone active drugs. Adjusting for gender and race, each SD decrease increased the risk of clinical fracture 1.8-fold (95% CI:1.2, 2.5) for spine vBMD and 2.1 (1.6 to 2.8) for total hip DXA. In the whole cohort, one SD decrease in total hip aBMD increased risk of clinical fractures in all race and gender groups: from 1.6 to 2.9 per SD. This was statistically significant for all groups except for black men who suffered only 4 fractures. We conclude that aBMD by hip DXA might be a somewhat stronger predictor of clinical fractures than vBMD of the spine. Hip DXA predicts clinical fractures in women of both races and in white men.

1132

Serum OPG and Bone Turnover in Human Pregnancy and Lactation. K. E. Naylor*[1], N. Wilde*[1], A. Rogers[1], C. Smith[1], R. B. Fraser*[2], R. Eastell[1], A. Blumsohn[1]. [1]Bone Metabolism Group, University of Sheffield, Sheffield, United Kingdom, [2]Department of Obstetrics and Gynaecology, University of Sheffield, Sheffield, United Kingdom.

Osteoprotegerin (OPG) is an osteoblast derived decoy receptor, which inhibits osteoclastogenesis and bone resorption by neutralising RANKL. Animal studies have indicated that serum OPG is increased in pregnancy and might prevent excessive maternal bone resorption. The role of OPG in human pregnancy has not been studied. We assessed serum OPG in a longitudinal study of planned human pregnancy and lactation, and in human neonates. Fasting morning blood samples and 24 hour urine samples were collected before conception, at 16, 26 and 36 weeks gestation, and at 2 and 12 weeks postpartum in 17 Caucasian women (ages 20 to 36). Samples were also collected from 22 neonates. Reference data were obtained from an additional 35 healthy pre-menopausal women (ages 20 to 39). OPG was measured using an immunometric ELISA assay. Markers of bone turnover included serum βCTX (Roche Diagnostics), urine NTX (Ostex International), and bone ALP. Serum OPG increased to 151%±13SEM ($P < 0.001$) of pre-conception values at 26 weeks gestation, and to 251%±16 ($P< 0.001$) by 36 weeks gestation. By 2 weeks postpartum maternal OPG was not significantly higher than pre-conception values. Serum OPG was lower in neonates than in premenopausal women (289±91SD pg/mL vs. 420±167 pg/mL; $P<0.001$). Bone turnover was also markedly increased during pregnancy (increase vs pre-conception: βCTX 176%±17, UNTX 319%±41, bone ALP 206% ±18 by 36 weeks gestation; all $P<0.001$). There was however no correlation between the change in OPG and bone turnover. The tissue source of circulating OPG in pregnancy is uncertain, but the rapid postpartum decline in maternal OPG, and low levels of OPG in neonates suggest that the breast and fetus are unlikely sources. These findings may be consistent with a placental source.

1133

Preservation of Osteocyte Viability by Bisphosphonates Contributes to Bone Strength in Glucocorticoid-Treated Mice Independently of BMD: An Unappreciated Determinant of Bone Strength. R. S. Weinstein, C. C. Powers*, A. M. Parfitt, S. C. Manolagas. Div. of Endo/Metab, Center for Osteoporosis and Metabolic Bone Diseases, Central Arkansas Veterans Healthcare System, Univ of Ark for Med Sci, Little Rock, AR, USA.

Osteocyte viability and thereby integrity of their mechanosensory network, seems to be a critical determinant of bone strength. For example, glucocorticoid excess, in mice and humans, is known to increase osteoblast and osteocyte apoptosis and may alter the BMD threshold such that fractures may occur at higher lumbar BMD values than those found in sex steroid-deficiency or involutional osteoporosis. To investigate whether osteocyte viability contributes to bone strength independently of bone mineral density (BMD), we examined the relationship between spinal BMD and vertebral compression strength in adult Swiss-Webster mice receiving prednisolone pellets (n=47) compared to mice receiving placebo (n=153). We report that glucocorticoid administration significantly alters the correlation between vertebral strength, determined by compression of L5, and spinal BMD, determined by live DEXA. Specifically, the slope of the relationship between vertebral strength and spinal BMD found in the control animals was significantly different in the prednisolone group ($p<0.001$), indicating a glucocorticoid-induced deterioration in bone quality. In a second experiment with mice receiving prednisolone (2.1 mg/kg/d), placebo, alendronate (0.75 mg/kg/day) or prednisolone together with alendronate for 10 days (n=10 per group), the prevalence of osteocyte apoptosis was indirectly related to vertebral strength ($r = -0.38$, $p<0.03$). Moreover, preservation of cortical osteocyte viability in mice receiving both prednisolone and bisphosphonate ($p<0.01$) was associated with increased bone strength ($p<0.05$) as compared to mice receiving prednisolone alone, even though loss of BMD was similar between the two groups at this time point. These lines of evidence strongly suggest that osteocyte viability is a heretofore unappreciated determinant of bone strength.

1134

Systemic Lentiviral Delivery of Osteoprotegerin-Fc Fusion Protein Increases Bone Mass in Mice. P. Doran[1], S. J. Russell*[1], D. G. Fraser*[1], C. R. Dunstan[2], B. L. Riggs[1], S. Khosla[1]. [1]Mayo Clinic, Rochester, MN, USA, [2]Amgen, Inc., Thousand Oaks, CA, USA.

Osteoprotegerin (OPG) is a potent suppressor of osteoclast development and activity, but therapeutically must be administered subcutaneously, and has a relatively short half-life. With the availability of safe lentiviral vectors that provide sustained expression of proteins, we explored the possibility of delivering OPG systemically in mice over an extended period. To prolong the circulating half-life of the OPG protein, we engineered replication-incompetent lentiviral vectors expressing an OPG-Fc fusion protein. Since murine immune responses can neutralize human OPG, 10-week old female SCID mice (n = 12) were used. The mice (n = 6 per group) were injected with either a control lentivirus vector or with a similar vector expressing the OPG-Fc construct. Serial determinations of BMD (using a PIXImus densitometer) and serum levels of human OPG-Fc protein (by ELISA) at baseline and after 2, 10, and 16 weeks were obtained. The table shows the % changes from baseline BMD (mean ± SEM) at the tibia and vertebrae in the 2 groups.

	Tibia			Vertebrae		
	2 weeks	10 weeks	16 weeks	2 weeks	10 weeks	16 weeks
Control vector	+0.7 ± 0.4	+5.9 ± 2.1	+8.3 ± 2.0	+4.1 ± 2.3	+11.8 ± 2.6	+21.3 ± 3.8
OPG-Fc vector	+6.2 ± 1.2**	+13.6 ± 1.7*	+15.4 ± 2.0*	+16.2 ± 3.3*	+28.6 ± 5.2*	+36.0 ± 7.9

*, $P < 0.05$ and **, $P < 0.01$ versus control vector

The OPG-Fc lentivirus injected mice had 4 to 9-fold greater increases in BMD at 2 weeks than did the control mice. By 16 weeks, the differences between the increases in BMD in the 2 groups were less marked (~2-fold). Circulating OPG levels were undetectable (< 0.040 ng/ml) in all but one of the control mice. By contrast, the OPG-Fc lentivirus injected mice had serum OPG levels of 78.7 ± 10.7 ng/ml, 24.2 ± 3.3 ng/ml, and 17.6 ± 2.8 ng/ml at 2, 10, and 16 weeks, respectively (compared to normal circulating levels in humans of 0.1-0.2 ng/ml). This "proof of concept" study thus demonstrates that systemic lentiviral delivery of OPG results in increased BMD in mice. These data also indicate that with continued improvements in viral delivery systems, OPG (or other proteins with anti-resorptive or anabolic efficacy) could be delivered systemically or locally in bone, opening up novel therapeutic approaches to the treatment of osteoporosis and other metabolic bone diseases.

Disclosures: ***P. Doran****, Amgen Inc. 3.*

1135

Gene Array Analysis of the Bone Effects of Raloxifene and Alendronate Show that Alendronate Strongly Inhibits the Expression of Bone Formation Marker Genes. J. E. Onyia, E. Dow*, C. Adams*, F. Lawrence*, K. Bemis*, D. L. Halladay*, R. R. Miles*, S. Huang*, P. Chen*, S. Chandrasekhar, C. A. Frolik, M. Sato, L. Ma, H. Bryant, L. Gelbert*. Eli Lilly and Company, Indianapolis, IN, USA.

The selective estrogen receptor modulator, raloxifene (Ral), and alendronate (ABP) are therapies currently used to treat osteoporosis. In an effort to ascertain the molecular/genomic events regulated by these agents in vivo, we characterized the pattern of bone gene expression in 6 months old ovariectomized rats treated with Ral or ABP. Rats were orally administered fully efficacious doses of Ral (1.0 mg/kg/day po) or ABP (8 µg/kg/day sc) starting from 5 days post-ovariectomy for 5 weeks. At study termination, total RNA was isolated from the proximal femoral metaphysis, labeled by in vitro transcription, and hybridized to a Affymetrix microarrays containing 8500 rat genes. To enable statistical validation of data, total RNA from bones of biological replicates (n=5 animals/group) were not pooled and each sample was analyzed on duplicate chips. Gene expression analysis ($P < 0.05$) demonstrated that 850 genes (10%) changed following ovariectomy. Treatment with ABP and Ral regulated 954 (11.2%) and 930 (10.9%) genes, respectively, indicating regulation of a comparable number of genes. Of the 850 genes induced by ovariectomy, approximately 23 % (195 genes) were regulated by ABP, while 30% (252) were regulated by Ral. A comparison of genes regulated by ABP vs. Ral showed that 793 genes were unique to ABP and 769 genes were unique to Ral, while 161 were common to both treatments. An analysis of the bone formation and bone resorption pathway genes identified novel potential differences in ABP and Ral action. ABP strongly inhibited the expression of bone formation marker genes -osteocalcin, collagen type1, alkaline phosphatase, collagen binding protein, SPARC, biglycan, decorin, IGF-I & -II. By contrast, Ral had no effect on any of the bone formation markers except for reductions in expression of decorin and IGF-I. Of the resorption pathway genes on the chip, ABP inhibited carbonic anhydrase II & III but stimulated cathepsin K, calcitonin receptor C 1b, and cortactin isoform C. Ral inhibited colony stimulating factor-1 (CSF-1), but stimulated carbonic anhydrase IV, and cortactin isoform C. These results demonstrate both similarities and differences in the molecular fingerprint of ABP and Ral that may give insights into the mechanistic differences in their skeletal actions in vivo. The strong suppression of osteoblast genes shown for ABP is consistent with the strong suppression of bone formation activity observed for ABP by histomorphometry in vivo.

Disclosures: ***J.E. Onyia****, Eli Lilly & Company 3.*

1136

Early Response of Bone Turnover Markers and Bone Mineral Density to Teriparatide [Recombinant Human Parathyroid Hormone (1-34)] in Postmenopausal Women Previously Treated with an Antiresorptive Drug. B. Ettinger[1], J. A. San Martin[2], G. Crans*[2], I. Pavo*[2]. [1]Division of Research, Kaiser Permanenete Medical Care Program, Oakland, CA, USA, [2]Lilly Research Labs, Eli Lilly & Company, Indianapolis, IN, USA.

To determine if prior use of an antiresorptive affects the response to teriparatide (TPTD), we are measuring changes in bone mineral density (BMD) and bone markers in postmenopausal women who stopped long-term antiresorptive therapy and switched immediately to TPTD 20 ug/day. Eligible patients were identified from pharmacy and bone density databases of the Kaiser Permanente Medical Care Program in Northern California. Patients included women who had regularly used either alendronate (ALN) 10mg/day or raloxifene (RLX) 60mg/day for at least 18 months and whose prescription data indicated ≥ 70% compliance in the prior year. A prior spinal or total hip BMD T-score must have been < -2.5, and at study entry the T-score had to be < -2.0. At baseline, ALN and RLX were similar in age (71.5±7.1 vs 69.4±5.7 y, mean±SD, respectively) and treatment duration (27.8±5.0 vs 27.8±6.0 mo), while each bone marker was significantly lower in ALN. After one month of TPTD, markers of bone formation (OC, PINP, BSAP) and resorption (CTX, NTX) increased above baseline, but RLX had a 2-3 times greater increase in formation markers than ALN.

Bone markers	Previous therapy	Baseline (median)	1 month (median)	Change after 1 mo (median)
OC (µg/L)	RLX	18.7	42.0	21.2[a,b]
	ALN	10.2	20.2	7.5[a]
PINP (µg/L)	RLX	38.8	93.5	48.5[a,b]
	ALN	13.6	37.3	22.5[a]
BSAP (µg/L)	RLX	9.3	17.5	5.1[a,b]
	ALN	4.7	6.8	1.2[a]
NTX (nMBCE/L)	RLX	11.3	13.7	2.9[a]
	ALN	7.6	9.4	1.5[a]
CTX (pmol/L)	RLX	2424.0	2921.5	370.0[a]
	ALN	980.5	1880.5	854.0[a]

[a] P<.05 within group, [b]P<.05 vs ALN (controlling for baseline differences); n=33 (ALN), n=26 (RLX). OC=serum osteocalcin, PINP=serum procollagen type I N propeptide; BSAP=serum bone-specific alkaline phosphatase; CTX=serum C-telopeptide type I collagen; NTX= serum N telopeptide

Early bone marker changes indicate that patients previously treated with either ALN or RLX have an appropriate initial response to TPTD. The magnitude of the initial response for bone formation markers was greater in patients previously treated with RLX. We will present 3 and 6 month BMD and bone marker data from this open label, prospective study.

Disclosures: ***B. Ettinger****, Eli Lilly and Company 2, 5, 8.*

1137

Vitamin D and Calcium Treatment and Environmental Adjustment in the Prevention of Falls and Osteoporotic Fractures among Elderly Danish Community Residents. E. R. Larsen*[1], L. Mosekilde*[1], A. Foldspang*[2]. [1]C, Aarhus Amtssygehus, Aarhus University Hospital, Aarhus, Denmark, [2]Institute of Epidemiology and Social Medicine, Aarhus University, Aarhus, Denmark.

Falls and fractures among elderly people living in the community constitute a major public health problem, as falls are the leading cause of mortality due to unintentional injury in elderly aged 65 and over. In January 1995, 9,605 community dwelling residents aged 66 and over (females 5,771, males 3,834; median age, 74.0 years; range, 66-103 years) in the municipality of Randers were identified in the Danish Central Population Registry. For the present purpose, the municipality was divided into four blocks each comprising 2-3 public social service centres, which took care of the data collection. The four blocks were randomly allocated to three different fall and fracture prevention programmes. Participants in the first block were offered a home safety inspection by a community nurse in order to identify and remedy possible hazards. Furthermore, they were offered identification and correction of potential health or dietary problems. Finally, their prescribed medication was evaluated by the nurse in order to identify eventual errors or needs for dose adjustment. Participants in the second block were offered a daily supplement of 1,000 mg of elemental calcium as calcium carbonate and 400 IU (10 µg) of vitamin-D_3 (Calcichew D®, Nycomed DAK). Furthermore, they were offered an evaluation of their prescribed medication, as mentioned above. Participants in the third block were offered a combination of the two programmes. Residents in the last block served as controls. Information was achieved on actual health problems, medication, falls and fractures, exercise habits, dietary supply of vitamin D and calcium, social background and environment. Information on falls and fractures in the study population was achieved by use of the Danish Hospital Registration Database. The overall acceptance of a home visit was 51%. When offered the calcium and vitamin D programme, elderly female residents seemed to fall more rarely (RR, 0.9, $p<0.05$), whereas both males and females had a reduced risk of osteoporotic fractures (RR, 0.8, $p<0.025$) during the 3½ years of follow-up. The present factorial intervention study support that vitamin D and calcium supplementation may prevent falling in elderly females and osteoporotic fractures in both genders in an European region known to be deficient in vitamin D.

1138

Daily Oral Ibandronate Prevents Bone Loss in Postmenopausal Women Without Osteoporosis. M. McClung[1], R. D. Wasnich*[2], R. Recker[3], J. A. Cauley[4], K. Ensrud[5], A. Burdeska*[6], P. Mahoney*[6], C. Hughes*[6], C. Chesnut[7]. [1]Oregon Osteoporosis Center, Portland, OR, USA, [2]Radiant Research, Honolulu, HI, USA, [3]Creighton University School of Medicine, Omaha, NE, USA, [4]University of Pittsburgh, Pittsburgh, PA, USA, [5]V.A. Medical Center, Minneapolis, MN, USA, [6]F. Hoffmann-La Roche Ltd, Basel, Switzerland, [7]Osteoporosis Research Center, University of Washington Medical Center, Seattle, WA, USA.

A previous phase III trial (Delmas P, et al. IOF World Congress on Osteoporosis 2002; abstract O37) demonstrated the effectiveness of oral ibandronate, a potent nitrogen-containing bisphosphonate, in preventing vertebral fractures in women with postmenopausal osteoporosis (PMO). The objectives of this phase II/III dose-finding study were to investigate the efficacy, tolerability and optimal dose of oral daily ibandronate in the prevention of bone loss. In this multicenter, double-blind, placebo-controlled study, 648 postmenopausal women were allocated to one of four strata based on time since menopause (TSM) and baseline lumbar spine (L1-L4) bone mineral density (BMD); stratum A, normal BMD, TSM up to 3 years; stratum B, osteopenic, TSM up to 3 years; stratum C, normal BMD, TSM >3 years; and stratum D, osteopenic, TSM >3 years. Women were randomized to receive placebo (n=159) or ibandronate 0.5mg (n=161), 1.0mg (n=165) or 2.5mg (n=163) as once-daily oral treatment for 2 years. The primary endpoint was the percent change in lumbar spine BMD with ibandronate compared with placebo. All women received calcium supplementation (500mg daily). Baseline characteristics were similarly distributed across the four treatment groups. After 2 years, oral daily ibandronate produced a dose-related and consistent increase in BMD at the lumbar spine and hip (total hip, femoral neck, trochanter), together with a dose-dependent decrease in bone turnover (as indicated by serum as well as urinary CTx and osteocalcin levels). The results were consistent across the four enrolment strata. The greatest increases in lumbar spine BMD were observed with the 2.5mg dose, which produced statistically significant BMD gains compared with placebo at 6 months and all subsequent time points (+1.9% vs baseline [$p \leq 0.0001$] after 24 months). Lumbar spine BMD in the placebo group decreased by -1.2%. The largest lumbar spine BMD gain with ibandronate relative to placebo was observed in stratum D, where the change from baseline in the 2.5mg ibandronate group was 3.5% greater than that with placebo after 2 years. Oral daily ibandronate was well tolerated and no safety concerns were identified. In summary, oral daily ibandronate dose-dependently increases BMD and reduces bone turnover in postmenopausal women without osteoporosis, with the 2.5mg dose being the most effective. Furthermore, daily oral ibandronate is well tolerated.

1139

FGF-23 Is a Circulating Factor that Is Elevated in Oncogenic Osteomalacia and X-linked Hypophosphatemic Rickets. K. B. Jonsson[1], R. Zahradnik*[2], T. Larsson*[1], K. E. White[3], G. Hampson[4], A. Miyauchi[5], Ö. Ljunggren[1], H. Koshiyama*[6], T. Sugimoto*[7], K. Oba*[8], T. Yamamoto*[9], Y. Imanishi*[9], M. Econs[3], J. Lavigne*[2], H. Jueppner[10]. [1]Dept of Medical Sciences, University of Uppsala, Uppsala, Sweden, [2]Immutopics, Inc, San Clemente, CA, USA, [3]Indiana University School of Medicine, Indianapolis, IN, USA, [4]St Thomas Hospital, London, United Kingdom, [5]Kobe University Graduate School of Medicine, Kobe, Japan, [6]Amagasaki Hospital, Hyogo, Japan, [7]Kobe University, Kobe, Japan, [8]Kyushu University, Fukuoka, Japan, [9]Osaka University, Osaka, Japan, [10]Endocrine Unit, Massachusettes General Hospital, Boston, MA, USA.

Mutations in FGF-23 are responsible for autosomal dominant hypophosphatemic rickets (ADHR). Furthermore, FGF-23 mRNA is abundantly expressed in tumors that cause oncogenic osteomalacia (OOM) and recombinant FGF-23 leads, when injected into mice, to urinary phosphate wasting and hypophosphatemia, indicating that this growth factor is directly or indirectly involved in regulating phosphate homeostasis. The clinical and laboratory findings in ADHR or OOM are similar to those in X-linked hypophosphatemic rickets (XLH), suggesting that all three disorders may have a common pathway possibly involving FGF-23. To determine whether FGF-23 is secreted by OOM tumors, and whether its secretion and/or metabolism is abnormally regulated in different phosphate-wasting disorders, an assay for human FGF-23 was developed. Affinity purified antibodies against [Tyr-223]FGF-23(206-222)amide and [Tyr-224]FGF23(225-244)amide were used to develop an enzyme-linked immunosorbant assay (ELISA), which detects equivalently recombinant human FGF-23(1-251) and [R179Q]FGF-23(1-251), and synthetic human FGF-23(207-244)amide. Healthy individuals revealed FGF-23 concentrations of 55.6±50.6 RU/mL (mean±SD). Four OOM patients had concentrations ranging from 426.1 to 7970.0 RU/mL, which returned to normal after successful surgical tumor removal; other patients with suspected OOM showed levels of 481.4±159.2 RU/mL (mean±SEM). FGF-23 concentrations were elevated in 9 of 14 patient with XLH (range: 169.5 to 2335.0 RU/ml). Since circulating FGF-23 is readily detectable in healthy individuals, it could have a physiological role in phosphate regulation. FGF-23 measurements are likely to gain importance for establishing the diagnosis of OOM, for localizing OOM tumor, and for long-term monitoring of affected patients. Our findings furthermore suggest that PHEX may be involved in FGF-23 degradation indicating that urinary phosphate wasting in XLH could also be caused by elevated circulating concentrations of this growth factor.

1140

Chronic Kidney Disease (CKD) Directly Produces an Adynamic Bone Disorder Which Can Be Successfully Treated With BMP-7. R. J. Lund*[1], M. R. Davies*[1], N. Huq*[1], K. A. Hruska[2]. [1]Medicine, Washington University, St. Louis, MO, USA, [2]Pediatrics & Medicine, Washington University, St. Louis, MO, USA.

An adynamic bone disorder (ABD) is an increasingly important complication of CKD that is associated with high rates of bone fractures and perhaps calcification of the vascular media. The ABD is produced in patients with end-stage CKD on dialysis when PTH levels are aggressively suppressed. This has lead to the hypothesis that CKD directly affects skeletal remodeling and perhaps is a state of inadequate bone anabolism. The ABD is characterized histomorphometrically by very reduced active osteoblast number and surfaces, and by very reduced bone formation and mineral apposition rates. Here we report successful production of an animal model of the ABD demonstrating direct production of an osteodystrophy by CKD in the absence of secondary hyperparathyroidism, and its successful treatment with BMP-7. Twelve week old C57Bl6 mice were subjected to electrocautery of the right kidney followed in two weeks by left nephrectomy to create CKD. Animals were randomized into 5 Groups: Sham operated fed normal mouse chow (0.6%Pi, 0.8%Ca) n=7; Sham operated fed low phosphate chow (0.2% Pi, 0.5% Ca) and calcitriol (20 ng/kg tiw sq) n=12; CKD mice fed normal mouse chow n=11; CKD mice fed low phosphate chow and treated with calcitriol n=8; CKD mice fed low phosphate chow and treated with calcitriol and BMP-7 (10 mcg/kg q week) n=12. All groups were maintained on their regimens for 12 wks prior to calcein labeling of mineralization fronts, sacrifice and histomorphometry of distal femurs and proximal tibial metaphyses. BUN levels were elevated equally in all of the CKD groups, iPTH levels were elevated only in the CKD/chow fed group. Ca and PO_4 levels were normal in all groups until 12 weeks when the sham/low Pi and Calcitriol and the CKD/low Pi, calcitriol and BMP-7 groups had reduced PO_4 levels compared to the other groups. Osteoblast number and perimeters, mineralizing surfaces, bone formation rates, mineral apposition rates and activation frequency were all significantly depressed in the CKD/low Pi and Calcitriol group (ABD group) ($p<.01$) compared to the sham/chow group (normal group). The changes were all reversed to normal or greater levels in the BMP-7/low Pi and Calcitriol group ($p<.01$ vs the ABD group). In addition, BMP-7 lowered serum PO_4 by increasing its deposition into the skeleton in the rapidly exchangeable pool of the mineralization fronts. We conclude that CKD in the absence of hyperparathyroidism directly produces an ABD which we have successfully reversed by BMP-7 therapy.

1141

Late Low Dose Steroid Withdrawal in Renal Transplant Recipients Increases Bone Formation and Bone Mineral Density Without Altering Renal Function: A Randomised Controlled Trial. C. K. T. Farmer*[1], G. Hampson*[2], S. Vaja*[2], I. C. Abbs*[1], R. M. Hilton*[1], G. Koffman*[1], J. Watkins*[1], S. H. Sacks*[1], I. Fogelman[3]. [1]Nephrology and Transplantation, Guy's and St. Thomas' Hospital, London, United Kingdom, [2]Chemical Pathology, Guy's and St. Thomas' Hospital, London, United Kingdom, [3]Nuclear Medicine, Guy's and St. Thomas' Hospital, London, United Kingdom.

Glucocorticoid-induced osteoporosis is a major cause of secondary osteoporosis. Over 70% of renal transplant recipients remain on long-term steroid therapy despite clinical evidence showing the safety of late steroid withdrawal. However data on the effects of steroid withdrawal on bone metabolism in renal transplant patients on long-term low dose glucocorticoids (5-7.5 mg/day) are lacking. The aim of this study was to assess the effect of late low dose corticosteroid withdrawal for 12 months on bone mineral density (BMD) at the spine and hip, and humoral markers of bone metabolism in stable renal transplant recipients. We studied 52 patients mean 9.5 (3.4 SD) years post renal transplantation. They were randomised to 2 groups. The control group remained on their maintenance dose of prednisolone. The prednisolone dose was reduced by 1 mg per month in the patients in the withdrawal group. BMD (DXA) and biochemical markers of bone formation (serum osteocalcin ng/ml) and resorption (serum C-terminal telopeptides of type 1 collagen, CTx, pM) were measured at baseline and at 12 months. The clinical data and results are shown below.

	Control	Withdrawal
Number of Patients	29	23
Males n (%)	20 (68%)	14 (61%)
Mean Age (SD)	47.2 (12.4)	44.6 (15.3)
Femoral Neck BMD % Change (p)	-0.1	3.1 (<0.02)
L1-L4 BMD % change	-0.7	1.7 (<0.01)
% change in osteoclacin (range) (p)	3.7 (-63-325)	131.3 (-30-499) (<0.01)*
% change in CTx (range) (p)	-5.7 (-67-143)	10.1 (-79-211) (ns)

*Significant difference between groups and within groups

There was no significant difference in renal function following steroid withdrawal, mean serum creatinine 124umol/l. Late steroid withdrawal, even at low dose, results in a significant increase in BMD in renal transplant recipients with no detrimental effects on renal function. This is attributable to a positive effect on bone formation without any change in bone resorption.

1142

Effect of the Acute Infusion of Frizzled Related Protein 4 (FRP-4), a Protein Highly Expressed in Tumors Associated with Osteomalacia, on Phosphate Excretion In Vivo. T. J. Berndt*[1], J. Vassiliadis*[2], D. Reczek*[2], S. C. Schiavi*[2], R. Kumar[1]. [1]Medicine, Biochemistry and Molecular Biology, Mayo Clinic, Rochester, MN, USA, [2]Genzyme Corporation, Framingham, MA, USA.

Frizzled related protein-4 (FRP-4) is over expressed in human tumors associated with osteomalacia, hyperphosphaturia and hypophosphatemia. The present studies were performed to determine whether infusion of biosynthetic FRP-4 protein increases renal phosphate excretion *in vivo*. Phosphate and inulin clearance studies were performed in 10-12 week old mice with intact parathyroid glands. The mice were anesthetized with Inactin (150 mg/kg). Catheters were placed in the carotid artery for measuring blood pressure and for blood sampling, and in the jugular vein for infusions. Mice were infused with a solution of 1% inulin and 0.1% BSA in isotonic saline at a rate of 2% BW/hr. After a ninety-minute equilibration period, phosphate and inulin clearances were determined during a control 30-minute clearance period. Following the control clearance period, FRP-4 (0.05 µg/120 min, n=7) was infused. Control mice received vehicle alone (n=3). Following a 45-minute stabilization period, fractional excretion of phosphorus and glomerular filtration rate were determined during two consecutive 30-minute clearance periods.

Fractional Excretion of Phosphate (%)

Clearance period	C_1	C_2	C_3
Vehicle infusion	0.02 ± .02	8.1 ± 6.7	9.2 ± 3.2
FRP-4 infusion	3.0 ± 1.5	21.3 ± 6.6*	26.3 ± 6.6*

*Indicates a significant difference from C_1, $p < 0.05$ paired T test.

Infusion of FRP-4 (0.05 µg/120 min) significantly increased fractional excretion of phosphate (FE_P) and was associated with a decrease in blood pressure from 102 ± 4 to 84 ± 5 mm Hg. Glomerular filtration rate decreased from 0.28 ± .09 to 0.16 ± .04 ml/min, ($p < .05$). Despite this decrease in glomerular filtration rate, FE_P increased significantly. We conclude that FRP-4, decreases renal phosphate reabsorption in intact mice *in vivo* and that FRP-4 is a "phosphatonin' like molecule.

Disclosures: ***T.J. Berndt****, Genzyme Corporation 2.*

1143

FGF-23 Protein is Present in Normal Plasma and Is Increased in Patients with Tumor-Induced Osteomalacia. Y. Yamazaki*[1], M. Shibata*[2], R. Okazaki[2], Y. Takeuchi[3], T. Fujita*[3], T. Yamashita[1], S. Fukumoto[4]. [1]Pharmaceutical Research Labs, KIRIN Brewery Co., Ltd., Takasaki, Japan, [2]Department of Medicine, Teikyo University, Ichihara, Japan, [3]Department of Medicine, University of Tokyo School of Medicine, Tokyo, Japan, [4]Department of Laboratory Medicine, University of Tokyo Hospital, Tokyo, Japan.

Tumor-induced osteomalacia (TIO) is a paraneoplastic syndrome characterized by hypophosphatemia and osteomalacia. Recently FGF-23 was identified as a causative factor of TIO. Recombinant FGF-23 induced hypophosphatemia with increased renal phosphate excretion and overexpression of FGF-23 in experimental animal models reproduced osteomalacia. In addition, abundant expression of FGF-23 has commonly been demonstrated in responsible tumors for TIO. However, it has not been shown that circulatory level of FGF-23 is actually elevated in patients with TIO. In addition, it has been unclear whether FGF-23 has some physiological role in healthy people, either. Therefore, to further investigate physiological and pathophysiological role of FGF-23, we developed the quantitative sandwich ELISA for FGF-23. BALB/c mice were immunized with purified recombinant human FGF-23. Because the substantial amount of cleavage between Arg^{179} and Ser^{180} of FGF-23 protein occurs in cell culture systems and affects the biological activity, two monoclonal antibodies, NA1 and CA1, that recognize N-terminal (25-179) and C-terminal (180-251) polypeptide of FGF-23, respectively, were selected to construct the sandwich ELISA. The assay range was between 15 and 500 pg/ml of standard full-length FGF-23. Plasma concentrations of FGF-23 in 25 healthy adults were detectable but below 50 pg/ml. In contrast, plasma FGF-23 was clearly high in a patient with TIO (270 pg/ml). The presence of uncleaved FGF-23 in plasma of the TIO patient was also confirmed by immunoprecipitation followed by Western blotting. After the removal of the responsible tumor, the elevated plasma FGF-23 concentration rapidly decreased to the normal range within a few hours. This change of FGF-23 level preceded the increase of 1,25-dihydroxyvitamin D and phosphate, and decrease of 24,25-dihydroxyvitamin D, which were first detected at 3, 6 and 9 hours, respectively. Thus, we demonstrated the presence of FGF-23 in circulation of healthy subjects and the elevation of FGF-23 in a patient with TIO. These results support the notion that TIO is caused by overproduction of FGF-23 and also suggest that FGF-23 plays an important role in physiological phosphate metabolism.

1144

Endocrine Response to Escalating-Dose Phosphate Supplementation in Men: Is FGF-23 Phosphatonin? H. C. Allen, A. Whybro*, M. E. Barker*, R. Eastell, A. Blumsohn. Bone Metabolism, University of Sheffield, Sheffield, United Kingdom.

Recent studies have shown that fibroblast growth factor 23 (FGF-23) is the probable mediator of hypophosphatemia and hyperphosphaturia in oncogenic osteomalacia, X-linked hypophosphatemia and autosomal dominant hypophosphatemic rickets. It is uncertain whether FGF-23 is a physiologically relevant phosphate regulating hormone, 'phosphatonin'. The aim of this study was to examine the effect of escalating dose phosphate supplementation in healthy adults. Twelve healthy men (ages 19 – 38 years) were studied for 5 weeks. For the first week, participants were studied on their habitual diet. Participants were then studied for 4 weeks on a standardised diet containing 1000mg/d phosphate and 1000mg/d calcium. No supplement was given for one week, followed by 1000mg/d, 1500mg/d and 2000mg/d elemental phosphate on successive weeks (total dose 1000mg/d, 2000mg/d, 2500mg/d, 3000mg/d respectively). Blood and urine samples were collected before breakfast at the end of each week. Serum FGF-23 was measured by ELISA (Immutopics, Inc., San Clemente, CA). Renal phosphate excretion increased with escalating phosphate intake from 34.2±3.4mmol/d at 1000mg intake to 61.4±3.6mmol/d at 3000mg intake (repeated measures ANOVA, $P<0.001$). As expected, calcium excretion decreased from 4.9±0.5mmol/d to 2.5±0.4mmol/d ($P<0.001$). There was a small but non-significant increase in PTH and no significant change in fasting serum calcium or phosphate. Fasting FGF-23 increased significantly in response to phosphate loading (40.5±1.9U/mL to 53.6±6.7U/mL; repeated measures ANOVA P=0.015). We conclude that serum FGF-23 does respond to altered phosphate intake within the physiological range, and the direction of effect is consistent with its possible role as a phosphate regulating hormone.

1145

Development of a Novel Bone-Targeted Src Tyrosine Kinase Inhibitor AP23451 Having Potent In Vitro and In Vivo Anti-Resorptive Properties. B. F. Boyce[1], W. Shakespeare*[2], L. Xing[1], Y. Wang*[2], R. Sundaramoorthi*[2], T. Keenan*[2], C. Metcalf*[2], R. Bohacek*[2], M. R. van Schravendijk*[2], D. Dalgarno[2], J. Iuliucci*[2], T. Sawyer[2]. [1]Pathology, University of Rochester, Rochester, NY, USA, [2]ARIAD Pharmaceuticals, Cambridge, MA, USA.

Genetic knockout studies have shown src -/- mice develop a bone-specific phenotype known as osteopetrosis resulting from defective remodeling. At the cellular level, these activities have been correlated to osteoclast (ocl) mediated bone resorption and osteoblast (obl) mediated bone formation. Recently, Src tyrosine kinase has been implicated in several examples of tumor proliferation, angiogenesis and metastases to bone. We have developed a novel bone-targeted Src tyrosine kinase inhibitor AP23451 having potent in vitro and in vivo activities, including: 1) low nM inhibition of Src tyrosine kinase and demonstrating high selecitvty against a panel of >30 protein kinases; 2) dose-dependent inhibition of ocl resorption in vitro (pit area and number); 3) dose-dependent inhibition of PTH induced hypercalcemia in mice (1-10 mg/kg/d s.c.) and inhibition of in vivo bone resorption (osteoclast number/mm calvarial bone surface: 14.4 +/- 3.3 PTH alone vs 1.7 +/- 1.7 PTH + AP23451 at 10 mg/kg b.i.d.); and 4) prevention of Ovx-induced vertebral (DEXA: .070+/-.0011 vs .0572+/-.0016 g/cm2) and femoral metaphyseal (pQCT: 660+/-13 vs 455+/-17 g/cm3) bone loss, with associated decreased ocl activity determined histomorphometrically. Our findings provide evidence that AP23451 is a novel bone-targeted Src tyrosine kinase inhibitor having potent in vitro and in vivo anti-resorptive properties for use in treating bone metastases and malignant hypercalcemia.

Disclosures: ***B.F. Boyce****, ARIAD Pharmaceuticals 2, 5.*

1146

CSF1, TNFα and RANKL Promote Osteoclast Survival by Signaling Through mTOR/S6 Kinase. H. Glantschnig*, G. A. Rodan, A. A. Reszka. Bone Biology and Osteoporosis Research, Merck & Co., Inc., West Point, PA, USA.

Survival signaling by growth factors and cytokines in osteoclasts (OCL) is known to involve at least two anti-apoptotic signaling pathways including the effector molecules PI3K/PDK1/PKB and IKK/IκB/NF-κB, most likely followed by the synthesis of anti-apoptotic proteins. We report here a third anti-apoptotic pathway involving mTOR/ S6 Kinase (S6K) that is activated by CSF1, TNFα and RANKL and is essential for osteoclast survival *in vitro*. This pathway was investigated since we observed that inhibition of translation rapidly induces caspase activation and apoptosis in the OCL. OCL were generated by coculture of mouse bone marrow cells and MB1.8 osteoblasts. MB1.8 cells were removed by collagenase and purified OCL were further cultured in the presence of 15 ng/ml CSF1. OCL were then treated either with CSF1 (40 ng/ml), TNFα (50ng/ml) or RANKL (100 ng/ml) for various times in 0.5% FBS. Thereafter cell lysates were analyzed by western blotting with phospho-specific antibodies, and caspase-activities were determined fluorometrically. We found that CSF1 strongly induced PKB activation in OCL by phosphorylation at T308 and S473, but did not induce IκB phosphorylation. TNFα and RANKL only marginally induced PKB phosphorylation but strongly stimulated phosphorylation of IκBα at S32/36 and activation of NFκB. Interestingly, two mTOR substrates, S6K (T389) and 4E-BP1 (S65) were highly phosphorylated in OCL after treatment with any of these three pro-survival cytokines. Consistent with this observation, cytokine treatment led to phosphorylation of ribosomal protein S6, which was inhibited by rapamycin, a PKB-inhibitor or a MEK inhibitor. To test if mTOR is essential for survival, we treated differentiated OCL with rapamycin (1-100 nM) for 20 hr. This dose dependently induced morphological changes consistent with apoptosis and increased caspase-3 and -9 activities and (consequently) 34 kDa Mst1 kinase activity up to ca. nine-fold. Rapamycin also significantly suppressed the generation of TRAP+ OCLs from mouse bone marrow in the coculture system or when induced by CSF1 and RANKL, pointing to a role of mTOR in OCL differentiation. In summary we show in OCL distinct signaling by CSF1 via PKB and by TNFα / RANKL via IκB. However, all three osteoclastogenic survival factors induce the mTOR/ S6K signaling cascade. Upstream activators of mTOR and S6K include but are not restricted to PDK1 and PKB, thus creating an intersection of CSF1/ TNFα /RANKL signaling pathways. This demonstrates for the first time the existence of a survival pathway, common to seemingly divergent pro-survival cytokines, involving mTOR/S6K activation.

1147

PYK2 Regulation of Osteoclast Ruffled Border Formation During Bone Resorption. P. T. Lakkakorpi[1], G. A. Rodan[2], L. T. Duong[2]. [1]Inst. of Biomed., Dept. of Anatomy, Univ. of Turku, Turku, Finland, [2]Dept. of Bone Biology & Osteoporosis Res., Merck Res. Labs., West Point, PA, USA.

Osteoclast $\alpha_v\beta_3$ integrin engagement leads to PYK2 tyrosine phosphorylation, tyrosine kinase activation, association with c-Src and cytoskeletal reorganisation. PYK2 localises to podosomes during osteoclast (OC) attachment and to the sealing zone in bone resorbing OCs. Using adenovirus expressing PYK2 mutants, we have shown that the PYK2 autophosphorylation site Y402, but not its kinase activity, is necessary for adhesion-induced association with c-Src, which further leads to the phosphorylation of tyrosines Y579/Y580 and Y881 in the PYK2 C-terminal domain. In this study we examined the effects of the PYK2 kinase-dead mutant *(K457A)* and the mutant lacking the autophosphorylation site *(Y402F)* on osteoclastic bone resorption, determined by light and electron microscopy. Infection of osteoclast-forming co-cultures with HSV-tagged PYK2*(wt)* or its mutants for 3-days resulted in 3-4 fold higher expression in purified pre-fusion osteoclasts (pOCs) of the exogenous constructs, relative to endogenous PYK2. OCs expressing PYK2(*wt)* or the mutants produced the same number of resorption pits per bone slice as uninfected cells. However, relative to controls OCs expressing PYK2(*wt)* or PYK2*(K457A)* formed smaller F-actin rings and deep resorption pits, whereas cells expressing PYK2*(Y402F)* mutant formed large F-actin rings, but very shallow resorption pits (by SEM). Interestingly, both mutants as well as PYK2*(wt)* were recruited to the sealing zone, based on the co-localisation of HSV-tag and F-actin. However, while β_3 integrin and cathepsin K were abundant (by immunolocalization) in the ruffled border of OCs expressing PYK2(*wt*) or PYK2 kinase dead*(K457A)*, they were absent from this region in cells expressing PYK2*(Y402F).* These findings suggest that the latter could have defective ruffled borders and reduced secretion. TEM confirmed that ruffled borders were almost completely lacking in OCs expressing PYK2*(Y402F)*, while cells expressing PYK2(*wt*) or kinase dead PYK2*(K457A)* showed deep convoluted ruffled borders. Thus, while overexpression of PYK2 or kinase-dead PYK2*(K457A)* seems to alter the dynamics of cell polarisation, expression of PYK2*(Y402F)* resulted in severe disruption of ruffled border formation, without significantly affecting formation of the osteoclast sealing zone. Since Src(-/-) or β_3(-/-) osteoclasts were previously found to have reduced ability to form ruffled borders on bone, we suggest that the adhesion-induced recruitment of c-Src to PYK2 via its autophosphorylation site Y402, but not PYK2 kinase activity, is important for the formation of ruffled border in osteoclasts during bone resorption.

1148

Osteoclast Differentiation by RANKL Is Mediated by Inhibition of Cyclin-dependent Kinase 6 as a Downstream Effector of NF-κB Pathway. T. Ogasawara[1], M. Katagiri[1], A. Yamamoto[1], S. Tanaka[1], D. Chikazu[1], T. Takato*[1], K. Nakamura[1], H. Okayama*[2], H. Kawaguchi[1]. [1]Sensory & Motor System Medicine, University of Tokyo, Tokyo, Japan, [2]Molecular Biochemistry, University of Tokyo, Tokyo, Japan.

Cell cycle arrest at the G1 phase is a prerequisite for cell differentiation, so that it is possible that cell cycle molecules such as cyclins, cyclin-dependent kinases (CDKs) and CDK inhibitors (CKIs) may possibly regulate not only proliferation but also differentiation of cells. The regulation of osteoclast differentiation by cell cycle molecules was studied by looking at the involvement of these molecules in the action of receptor activator of nuclear factor-κB ligand (RANKL) on a murine monocytic cell line RAW 264.7 (RAW cells), known as osteoclast progenitor cells. We initially investigated the regulation of cell cycle molecules known to affect the G1 phase: cyclin D1, D2, D3, E, CDK2, 4, 6, and CKIs (p18, p21 & p27). Western blot analysis revealed that only the CDK6 level was markedly decreased by soluble RANKL (sRANKL, 100 ng/ml) in advance of the appearance of TRAP-positive multinucleated osteoclasts, while those of other cell cycle molecules were not significantly affected by sRANKL throughout the culture period up to 7 days. When NF-κB pathway was inhibited by overexpression of a dominant negative mutant of IκB kinase 2 gene ($IKK2^{DN}$) in RAW cells using an adenovirus vector, neither the inhibition of CDK6 nor the induction of osteoclastogenesis by sRANKL was seen, while the control LacZ adenovirus infection did not affect the sRANKL actions. To further investigate the contribution of CDK6 to osteoclast differentiation, we established stable clones of RAW cells transfected with *cdk*6 cDNA, and selected several of them with high expression and low expression on Western blotting. sRANKL induced osteoclastogenesis in low expressing clones and parental cells, whereas these effects were markedly suppressed in high expressing clones. sRANKL inhibited DNA synthesis determined by BrdU uptake and decreased the cell population in the G2/M phase determined by FACS; however, these proliferation parameters were similar among high expressing clones, low expressing clones, and parental cells both in the presence and absence of sRANKL. This indicates that the inhibitory effect of CDK6 on osteoclast differentiation is independent of its effect on the proliferation. We therefore conclude that CDK6 is a key molecule determining the differentiation rate of osteoclasts as a downstream effector of NF-κB pathway. Since we previously reported that osteoblast differentiation is also associated with CDK6 inhibition, CDK6 might possibly play a role in the coupling of bone formation and resorption.

1149

The Functions of c-Cbl and Cbl-b Are Different in Osteoclasts: Cbl-b Deletion Leads to Increased Osteoclast Activity and Osteopenia. R. Chiusaroli[1], H. Gu*[2], R. Baron[1], A. Sanjay[1]. [1]Orthopaedics and Cell Biology, Yale University School of Medicine, New Haven, CT, USA, [2]Immunology, NIH, Bethesda, MD, USA.

The mammalian members of Cbl family of proteins, c-Cbl and Cbl-b are predominantly expressed in hematopoietic cells and function as ubiquitin ligases mediating down-regulation of both receptor- and non-receptor tyrosine kinases. We have previously shown that c-Cbl lies downstream of the vitronectin receptor and Src and forms a trimolecular complex with Src and Pyk2 in a signaling pathway that regulates cell adhesion and motility. We have also shown that deletion of the c-Cbl gene altered the ability of osteoclasts (OCs) to migrate in vitro and in vivo during development, delaying resorption and ossification of cartilage in long bones. However, detailed histomorphometric analysis of long bones from c-Cbl-/- adult mice failed to demonstrate any change in bone volume or in bone resorption parameters. Even though c-Cbl and Cbl-b are highly homologous in their phosphotyrosine binding domain and RING finger, there are significant differences between the two proteins in their C-terminal proline rich and acidic regions. To further investigate the role of Cbl family of proteins in osteoclast function we undertook a detailed bone histomorphometric analysis on adult Cbl-b-/- mice. In contrast to c-Cbl-/- mice, 12 week old Cbl-b-/- mice had decreased trabecular bone volume (wt, 7.7 ± 1.1; c-Cbl-/-, 7.4 ± 2, p = n.s. vs. wt; Cbl-b-/-, 4.6 ± 1.6, p <0.01 vs. wt; BV/TV mean ± SD), while no changes in osteoblast as well as in osteoclast surface and number were observed. Dynamic parameters of bone formation were also unaffected. In vitro pit assay revealed that in contrast to OCs derived from c-Cbl-/-mice, or to c-Cbl antisense-treated OCs whose bone resorption ability was reduced, the pit area resorbed by Cbl-b-/- OCs was 2.5 fold higher than wt control OCs (wt, 0.044 ± 0.017; c-Cbl-/-, 0.039 ± 0.009, p = n.s. vs. wt; Cbl-b-/-, 0.110 ± 0.02, p<0.01 vs. wt; pit area/total area/number of OCs, mean ± SD). Furthermore stimulation of the wt and c-Cbl-/- OCLs with IL-1 (10 ng/ml), a potent stimulator of osteoclastic bone resorption, led to a substantial increase (1.5 fold) in pit resorption area, whereas Cbl-b-/- mice-derived OCLs did not exhibit any further increase in pit resorption area in response to IL-1 stimulation. Collectively these data suggest that Cbl-b-/- osteoclasts display a cell autonomous defect, which results in increased bone resorption activity, and consequently in an osteopenic phenotype observed in Cbl-b-/- mice.

1150

The Small GTP-Binding Protein Rac1 Is Involved in Signal Transduction of Osteoclast Survival. A. Fukuda*, Y. Kadono, T. Akiyama, A. Yamamoto, H. Oda*, K. Nakamura, S. Tanaka. Department of Orthopaedic Surgery, Faculty of Medicine, The University of Tokyo, Tokyo, Japan.

Although recent findings suggest that osteoclast survival is regulated through interactions of various cytokines and molecules, the precise molecular mechanism is not fully understood. We previously reported that small GTP-binding protein (G-protein) Ras plays an important role in osteoclast survival by regulating ERK activation. Rac1 is a member of Rho family small G-proteins, which is known to be involved in the cytoskeletal organization. Recent studies, however, have revealed that Rac1 also mediates anti-apoptotic signals in some types of cells. In the present study, we examined the role of Rac1 in osteoclast survival using adenovirus vector expression system. We constructed the adenovirus vector carrying either cDNA of fusion protein of EGFP and dominant negative Rac1 ($Rac1^{DN}$) or constitutively active Rac1 ($Rac1^{CA}$) gene, and osteoclast-like cells (OCLs) generated in mouse co-culture system were infected with these viruses as well as the control virus (EGFP virus). Clear induction of these molecules in OCLs was demonstrated by green fluorescence and Western blot analysis. To examine the role of Rac1 in osteoclast survival, OCLs were purified by removing the osteoblasts 24 hrs after infection. After 24 hrs of osteoblast removal, almost 100% of control virus-infected OCLs became apoptotic in the absence of stimulatory cytokines such as macrophage colony-stimulating factor (M-CSF). M-CSF has strong anti-apoptotic effects on OCLs, which was suppressed by overexpression of $Rac1^{DN}$. Overexpression of $Rac1^{CA}$ dramatically enhanced OCL survival in the absence of survival cytokines, and more than 30% of the cells survived after 24 hrs. The pro-survival effect of $Rac1^{CA}$ was completely abrogated by the treatment with phosphatidylinositol 3-kinase (PI3-kinase) inhibitor, LY294002 or wortmannin. Rapamycin, mTOR inhibitor also had a potent inhibitory effect, while MEK inhibitor PD98059 showed only partial inhibition. These data suggest that Rac1 lies downstream of M-CSF receptor signaling, and mediates survival signal of OCLs mainly via PI3-kinase pathways. Further study will be required to elucidate the role of Rac1 in osteoclast survival.

1151

Osteonectin Supports Osteoblast Maturation and Survival. A. M. Delany, E. Canalis. Research, Saint Francis Hospital and Medical Center, Hartford, CT, USA.

Osteoblasts synthesize osteonectin (SPARC, BM-40), a glycoprotein important for the maintenance of bone mass. Osteonectin-null mice develop osteopenia due to decreased osteoblast number and bone formation rate. We used primary cultures of osteoblasts and stromal cells from wild type (WT) and osteonectin-null mice, and osteoblast cell lines established from these mice, to determine how osteonectin regulates cell number and bone formation. Although osteonectin is suggested to regulate cell proliferation, osteoblasts from calvaria of osteonectin-null mice did not have altered cell replication. However, our data suggest increased apoptosis in stromal cells from osteonectin-null mice. To determine whether osteonectin-null cells are more susceptible to stress, the ability of osteoblastic cell lines from osteonectin-null and WT mice to survive serum deprivation was assessed. After 2 days of serum-deprivation, ~60% of osteonectin-null cells survived, compared to ~85% of WT cells. When cell lines were transduced with retrovirus expressing full length osteonectin under the control of the CMV promoter, the ability of the osteonectin-null osteoblasts to survive serum deprivation was identical to that of wild type cells. Thus, osteonectin regulates osteoblast number by enhancing tolerance to stress. Further, osteonectin-null osteoblasts do not achieve a fully mature phenotype. Osteoblast cultures from osteonectin-null mice form fewer mineralized nodules, however transduction of osteonectin-null osteoblast cell lines with retrovirus constitutively expressing full length osteonectin or a C-terminal fragment containing the EF hand domain of osteonectin appeared to rescue this differentiation/mineralization defect. WT and osteonectin-null osteoblast cultured for up to 3 weeks post-confluence had similar levels of transcripts for osteopontin, type I collagen and bone sialoprotein. In contrast, expression of osteocalcin RNA was delayed and attenuated in osteonectin-null osteoblasts. Surprisingly, osteonectin-null cultures contained increased numbers of adipocytic cells. While the osteonectin-null mutation did not affect RNA for PPAR gamma 2, an early adipocytic marker, transcripts for adipsin, a marker of mature adipocytes, were increased. The C/EBP family of transcription factors functions in the differentiation of adipocytes and osteoblasts; and osteonectin-null cells had increased RNA for C/EBP delta, a stimulator of adipogenesis. In conclusion, osteonectin functions to maintain bone mass by increasing cell survival and by contributing a matrix that enhances osteoblast maturation, possibly at the expense of adipogenesis, through mechanisms that could involve C/EBP delta.

1152

The Tumor Suppressor Gene VHL Is a Critical Modulator of Cell Proliferation and Cell Growth in the Mammalian Growth Plate. E. Schipani[1], T. Kobayashi[1], H. E. MacLean[1], M. C. Knight*[1], R. S. Johnson*[2], V. Haase*[3]. [1]Endocrine Unit, MGH-Harvard Medical School, Boston, MA, USA, [2]Division of Biology, Molecular Biology Section, UCSD, San Diego, CA, USA, [3]Renal-Electrolyte and Hypertension Division, University of Pennsylvania, Philadelphia, PA, USA.

It has been previously reported that the transcription factor HIF-1alpha (or Hypoxia Inducible Factor-1alpha) plays an essential role in chondrocyte survival and growth arrest. The ubiquitously expressed tumor suppressor gene VHL (or Von Hippel Lindau) negatively regulates HIF-1alpha levels and transcriptional activity in various tissues. We therefore explored the possibility that VHL could be a modulator of growth plate development. Mice nullizygous for VHL die at about E9.5. In order to study the role of VHL in chondrocyte activity, we conditionally inactivated the VHL gene in the murine growth plate by using the Cre-loxP system. Mutant mice lacking VHL in chondrocytes were viable, but smaller than control littermates and with short limbs. Their growth plates were remarkably hypocellular both in the round proliferative and in the columnar layers. In addition, the round proliferative layer appeared to be mainly occupied by "atypical" chondrocytes that were larger than wild-type cells. These "atypical" chondrocytes expressed collagen type II but not collagen type X, as shown by in situ hybridization, and they were not Tunel-positive, excluding therefore the possibility that their presence would be due to ectopic and/or premature hypertrophy. Furthermore, BrdU incorporation revealed that, in comparison to control chondrocytes, proliferation was dramatically inhibited both in the round proliferative and in the columnar layers of the mutant growth plate. Tunel assay did not show any significant difference between mutant and wild-type growth plates. The mutant phenotype

was already evident at E15.5, and persisted in postnatal life. Interestingly, viable chondrocytes lacking HIF-1alpha display an increase in proliferation rate. Further investigations will be now necessary in order to determine whether the VHL mutant phenotype is, at least in part, HIF-1alpha-dependent. In summary, the tumor suppressor gene VHL is, paradoxically, a critical positive modulator of chondrocyte proliferation in vivo; furthermore our model suggests the lack of VHL has a different effect on cell proliferation and cell growth, respectively, in the mammalian growth plate.

1153

RANKL/RANK/NF-kB Signaling Regulates Chondrogenesis. L. Xing[1], T. Yamashita[1], L. Childs*[1], E. M. Schwarz[1], R. J. O'Keefe[1], W. C. Dougall[2], B. F. Boyce[1]. [1]University of Rochester, Rochester, NY, USA, [2]Immunex, Inc., Seattle, WA, USA.

Recent studies have indicated that RANKL-/- and RANK-/- mice are dwarfed and have thickened growth plates. We observed similar abnormalities in NF-kB p50;p52 double knockout (dKO) mice, which have disorganized growth plates and an extended hypertrophic chondrocyte zone, suggesting that RANK/NF-kB signaling may regulate chondrocyte function. To study this possibility further, we examined growth plates in wild-type (wt) and RANK-/- (KO) mice of different ages. Growth plate thickness is increased in young, and to a lesser extent in older RANK-/- mice (age 2w: 0.73+/-0.12 mm vs 0.35+/-0.04 in wt; 3w: 0.38+/-0.01 vs 0.35+/-0.03; 6w: 0.27+/-0.01 vs 0.2+/-0.03), due predominantly to an increase in the hypertrophic zone thickness. The number of BrdU+ve proliferating chondrocytes (assessed using BrdU-labeling) was significantly decreased in the KO mice (29+/-4 vs 64+/-21 in wt), while the number of TUNEL+ve apoptotic hypertrophic chondrocytes was reduced (2.3+/-1.5 vs 8.3+/-1.5 in wt), suggesting a role for RANK/NF-kB signaling in chondrocyte and proliferation. To further examine the role of RANK signaling in chondrogenesis, cells from wt embryonic mouse limb buds (E11.5) were treated in vitro to produce micromass cultures of chondrocytes, using established methods. RANKL increased chondrocyte nodule formation alone (nodule area: 0.42+/-0.06 vs 0.17+/-0.04 mm2) and synergistically increased BMP2-mediated chondrocyte nodule number and area (3.2+/-0.4 mm2 vs 1.5+/-0.2 in BMP2-treated cultures). RANKL+BMP2 also increased the expression of chondrocyte-related genes (sox9 by 4-fold and type II collagen by 13 fold), as assessed by Real Time PCR analysis. To assess the role of RANK signaling in cartilage formation during fracture repair, tibiae of RANK-/-, Op/Op (a control osteopetrotic mouse) and wt mice were fractured and stabilized with an intra-medullary pin, using a standard method. Fracture healing was impaired in the RANK-/- animals (75% non-union rate) and they had reduced cartilage formation compared with the Op/Op and wt control animals, all of which healed their fractures. Our findings indicate that RANKL/RANK/NF-kB signaling plays an important regulatory role in endochondral ossification during embryogenesis, and in cartilage formation during fracture repair.

1154

Influence of Gli2 Deficiency on Endochondral Bone Formation and the Indian Hedgehog Signaling Pathway. D. Miao[1], M. Niu*[1], R. Huo*[1], C. Hui*[2], D. Goltzman[1], J. E. Henderson[1]. [1]Medicine, McGill University, Montreal, PQ, Canada, [2]Molecular and Medical Genetics, University of Toronto, Toronto, ON, Canada.

Signaling by hedgehog family members is mediated in part by members of the Gli family of transcriptional regulators. Mice homozygous for targeted disruption of the gene encoding Gli2 (Gli2-/-) die at birth with a variety of developmental defects, which include short-limbed dwarfism. The current studies were undertaken to characterise the defects in endochondral bone formation in the axial and appendicular skeleton of Gli2-/- mice. A delay in endochondral bone formation was evident at E16.5 and E18.5, which was associated with longer cartilaginous growth plates, reduced bone tissue, and failure to develop intervertebral disks and primary ossification centres in the vertebral bodies by E18.5. The growth plates of tibiae and vertebrae exhibited increased chondrocyte proliferation, as determined by immunostaining for proliferating cell nuclear antigen, with no change in chondrocyte apoptosis, as shown by TUNEL assay. The increased number of proliferating chondrocytes was also reflected by an increase in type II collagen staining and was associated with increased FGF2 production. The zone of hypertrophic cartilage was also expanded in Gli2-/- mice, as evidenced by an increase in type X collagen expression, but revealed no defect in mineralization when stained with silver nitrate (von Kossa). Immunostaining for the angiogenic factors vascular endothelial growth factor (VEGF) and angiopoietin-1 (Ang-1) were reduced in the upper hypertrophic zone of Gli2-/- growth plates compared with those of wild type mice. This was associated with a reduction in TRAP positive cells at the chondro-osseous junction and with decreased numbers of osteoclasts and osteoblasts in metaphyseal bone. Indian hedgehog (IHH), its receptor patched (PCT) and parathyroid hormone related peptide (PTHrP), which play central roles in chondrocyte proliferation and maturation, were down-regulated in the growth plates of Gli2-/- mice. In contrast, hedgehog interacting protein (HIP) and the receptor smoothened (SMO), which inhibit hedgehog action, were increased. Taken together our observations suggest that Gli2 regulates endochondral bone formation by inhibiting chondrocyte proliferation by a PTHrP-independent pathway, by enhancing neo-vascularisation of mature cartilage and by recruiting osteoblasts to bone. Furthermore, Gli2 regulates the expression of PTHrP and components of the hedgehog signaling pathway.

1155

NF-kB Mediates Inflammatory Bone Erosion in Autoimmune Rheumatoid Arthritis. C. Biondo*, Y. Abu-Amer. Washington University School of Medicine, St. Louis, MO, USA.

Rheumatoid arthritis (RA) is an immune-inflammatory response associated with a joint inflammation, which often leads to matrix degradation and focal bone erosion. In this study, we set out to investigate molecular events that contribute to exacerbation of bone lesions in RA. We utilized a mouse model of T-cell transgenic K/BxN mice, which develop spontaneous joint RA. Serum-transfer from these mice triggers a rapid autoreactive Ig response in host mice that results in a highly joint-specific inflammatory arthritis. The onset of joint arthritis in serum-induced mice was within 48 hours. Swelling and limb deformation progressed thereafter. Histological examination of joint and ankle sections revealed a dramatically eroded bone surfaces. Bone erosion was maximal as early as 7 days post-serum transfer and was sustained thereafter. Next we examined osteoclast recruitment in long bones, ankles and joints. The data indicate a striking increase of osteoclast number and size in cortical and trabecular bone of arthritic mice compared to controls, with osteoclasts present throughout the arthritic cartilage. Articular cartilage and subchondral bone thickness in arthritic mice was reduced to approximately third of that in controls. We next turned to examine molecular events that mediate this inflammatory osteolysis. Given that NF-kB and p38 MAP kinase are central to inflammatory processes and both are essential for osteoclast development, activity of these two factors was investigated. Nuclear extracts from healthy or diseased joint tissue were subjected to DNA binding assays using specific probes. The data indicate that DNA binding activity of NF-kB and p38 was significantly increased within 48 hours post serum-induction of arthritis and maximal at 7 days. Thus, we reasoned that inhibition of NF-kB and/or p38 may reduce severity of the disease. Indeed we find that administration of dominant-negative form of IkB significantly reduced NF-kB DNA-binding activity and recruitment of osteoclasts in vivo. We also observed reduced clinical signs such as joint swelling and ankle thickening in the presence of the inhibitor. P38 inhibition studies are under investigation. In summary, our study describes a rapid and sustained autoimmune RA confined to joints. Development and progression of the disease are rapid and highly reproducible. More importantly, we document that severe osteolysis and bone erosion in this model is mediated, at least in a major part, by NF-kB and p38 activities. This conclusion was based on the fact that in vivo blockade of NF-kB by a dominant-negative form of its inhibitory protein IkB diminished the severity of inflammation and bone erosion.

1156

Osteopontin-Deficiency Suppresses TNF-alpha-Mediated Cytotoxicity in Chondrocytes to Protect Joints Against Destruction in Anti-Type II Collagen Antibody-Induced Arthritis in Mice. K. Yumoto[1], M. Ishijima[1], S. R. Rittling*[2], K. Tsuji[1], Y. Tsuchiya*[3], S. Kon*[3], A. Nifuji[1], T. Uede*[4], M. Noda[1]. [1]Dept of Molecular Pharmacology, Tokyo Medical and Dental University, Tokyo, Japan, [2]Rutgers University, Piscataway, NJ, USA, [3]IBL, Gumma, Japan, [4]Hokkaido University, Sapporo, Japan.

OPN is an extracellular matrix protein containing Arg-Gly-Asp (RGD) sequence which interacts with integrins, promotes cell attachment, cell migration and is expressed in synovia and joint cartilage in rheumatoid arthritis patients. We recently demonstrated that osteopontin-deficiency suppressed joint swelling, chondrocyte apoptosis and joint destruction in mice rheumatoid arthritis (RA) model induced by injection with a mixture of anti-type II collagen monoclonal antibodies and lipopolysaccharide (mAbs/LPS). (PNAS 99:4556, 2002). The levels of angiogenesis in synovia estimated by the presence of CD31-positive vessels and the levels of bone resorption based on urinary deoxypyridinoline (D-Pyr) in this RA model were also suppressed in the absence of OPN even after mAbs/LPS injection. To understand the mechanism of OPN-deficiency induced resistance against joint destruction in the arthritis model mice, we examined the cellular basis for such protection. We found that the release of lactate dehydrogenase (LDH), a cytotoxic marker, from wild-type chondrocytes in culture, was induced by the treatment with TNF-alpha, a cytokine responsible for the pathogenesis of RA and for cytotoxicity and apoptosis in chondrocytes. TNF-alpha-induced LDH release from chondrocytes was observed in a dose-dependent manner. In contrast, LDH release by TNF-alpha treatment was significantly suppressed in chondrocytes derived from OPN-deficient mice. To explore the systemic components underlying the OPN-deficiency-induced resistance to joint destruction in arthritis model mice, we examined the levels of serum TNF-alpha induced by LPS injection. Serum TNF-alpha levels was very low in saline-injected mice, but was elevated by LPS injection. In OPN-deficient mice, similar elevation of serum TNF-alpha levels was observed after LPS injection. Thus, TNF-alpha production as a response to LPS was normal in OPN-deficient mice. Finally, toluidine blue staining revealed that more than 60 % of proteoglycan-positive cartllage surface was lost in the joint of wild-type mice after mAbs/LPS injection. In contrast, OPN-deficient mice did not show such loss of proteoglycan even after mAbs/LPS injection. These data indicated that OPN plays a critical role in TNF-alpha-mediated cytotoxicity in chondrocytes and OPN-deficiency protects joint cartilage against destruction at least in part through this mechanism.

1157

Identification of Smurf1 as the E3 Ubiquitin Ligase Responsible for Degradation of the Bone-Specific Transcription Factor Runx2/Cbfa1. M. Zhao, M. Qiao*, G. R. Mundy, D. Chen. Molecular Medicine, University of Texas Health Science Center at San Antonio, San Antonio, TX, USA.

The osteoblast-specific transcription factor Runx2/Cbfa1 plays a central role in osteoblast differentiation and bone formation. Regulation of its activity has not been fully characterized. Since Runx2/Cbfa1 turnover is controlled by the ubiquitin-proteasome pathway, we have identified the specific E3 ubiquitin ligase responsible for this process. Protein ubiquitination involves a sequential cascade of enzymatic reactions catalyzed by E1, E2 and E3 enzymes. Among these, E3 ubiquitin ligases play a specific and crucial role in defining substrate specificity and subsequent protein degradation by 26S proteasomes. It has been reported that Smad1, the downstream mediator of BMP receptor signaling, directly interacts with Runx2/Cbfa1 and Smad1 undergoes ubiquitin-proteasome degradation mediated by E3 ubiquitin ligase, Smurf1. In the present studies, we examined the effect of Smurf1 on Runx2/Cbfa1 degradation in myoblast/osteoblast precursor C2C12 cells. We found that Smurf1 interacted with Runx2/Cbfa1 and mediated Runx2/Cbfa1 degradation in a dose-dependent manner. In contrast, unrelated F-box E3 ligase FWD1 has no significant effect on Runx2/Cbfa1 degradation. The Smurf1-mediated degradation of Runx2/Cbfa1 is ubiquitin and proteasome-dependent. A ubiquitinated protein ladder of Runx2/Cbfa1 was observed when the Runx2/Cbfa1 protein was immunoprecipitated in the presence of Smurf1. Treatment with the proteasome inhibitors epoxomicin or PS-I completely abolished the effect of Smurf1 on Runx2/Cbfa1 degradation. The interaction domain of Runx2/Cbfa1 with Smurf1 has been mapped. Smurf1 lost its ability to degrade Runx2/Cbfa1 when the C-terminal 153 amino acid residues of Runx2/Cbfa1 is deleted. In this C-terminal domain, a PY motif, the potential binding site for Smurf1, was identified. Smurf1-mediated Runx2/Cbfa1 degradation caused functional changes in Runx2/Cbfa1. Transfection of Runx2/Cbfa1 significantly increased luciferase activity of a specific reporter gene, 6xOSE2-OC-luc. Co-transfection of Smurf1 with Runx2/Cbfa1 completely inhibited Runx2/Cbfa1-induced luciferase activity of this reporter gene. Consistent with these findings, transfection of Smurf1 in osteoblasts significantly decreased alkaline phosphatase (ALP) activity. In contrast, transfection of ΔSmurf1 (C710A), which lacks catalytic activity, increased ALP activity and osteocalcin production. Our findings show mechanisms by which Runx2/Cbfa1 is regulated in osteoblasts during bone formation, and provide a new potential molecular target for drug discovery.

Disclosures: ***M. Zhao****, OsteoScreen Ltd 3.*

1158

Osteoblast Specific Connexin43 (Cx43) Gene Deletion in Mice Leads to Reduced Bone Mass and Osteoblast Dysfunction. C. Castro[1], S. Sheikh*[1], L. Halstead[1], V. Szejnfeld[2], R. Civitelli[1]. [1]Div. Bone and Mineral Diseases, Washington University, St. Louis, MO, USA, [2]Div. Rheumatology, UNIFESP, Sao Paulo, Brazil.

Interference with Cx43 expression or function alters osteoblast gene expression, and genetic deficiency of Cx43 *in vivo* causes developmental defects of the craniofacial skeleton and impaired osteoblast differentiation and function. To determine the role of Cx43 in adult bone mass achievement and maintenance, we developed a mouse model of selective Cx43 gene deletion in osteoblasts using a Cre/*lox*P approach, thus overcoming the perinatal lethality of the conventional knock out strategy. In this model, Cre mediated recombination replaces the entire Cx43 reading frame with the *Lac*Z reporter cassette. Homozygous $Cx43^{fl/fl}$ mice were crossed with mice expressing Cre driven by the OG2 promoter in a heterozygous Cx43-null background (OG2-Cre;$Cx43^{+/-}$). The recombination event was demonstrated exclusively in osteoblasts by X-gal staining of sections of tibia as well as calvarial cell cultures from OG2-Cre;$Cx43^{-/fl}$ mice. Cx43 mRNA (by Real Time RT-PCR) and protein abundance progressively declined in OG2-Cre;$Cx43^{-/fl}$ calvaria cells with time in culture compared to $Cx43^{+/fl}$, OG2-Cre;$Cx43^{+/fl}$ and $Cx43^{-/fl}$ controls, and disappeared after 3 weeks, concomitant to an increase in X-gal staining. Alkaline phosphatase activity was reduced in cells isolated from calvaria of OG2-Cre;$Cx43^{-/fl}$ mice compared to control $Cx43^{+/fl}$, OG2-Cre;$Cx43^{+/fl}$ and $Cx43^{-/fl}$ littermates, and this reduction was inversely correlated with Cx43 mRNA abundance. Matrix mineralization was also lower in OG2-Cre;$Cx43^{-/fl}$ calvarial cells compared to controls after 2 and 3 weeks in the presence of ascorbic acid and β-glycerophosphate. Accordingly, OG2-Cre;$Cx43^{-/fl}$ calvarial cells also exhibited lower abundance of Cbfa1 and type I collagen mRNA compared to control cells. Total body bone mineral density, monitored monthly by DEXA (PIXImus™, GE-Lunar), was consistently lower in OG2-Cre;$Cx43^{-/fl}$ mice compared to all control littermates up to 6 months of life, with maximum difference of 8% (OG2-Cre;$Cx43^{-/fl}$: 59±1.6mg/cm^2, $Cx43^{+/fl}$: 64.3±3.6mg/cm^2, $Cx43^{-/fl}$: 63.3±4.1mg/cm^2, $p<0.05$, at 5 months) without gender differences. Weight and percent body fat were similar among all groups at all times. Thus, Cx43 gene deletion *in vivo* disrupts the normal function of differentiated osteoblasts, leading to reduced bone mass. These results support the notion that Cx43 gap junctional communication is critical for bone formation in adult animals, contributing to achievement of peak bone mass.

1159

Gene Network Regulated by the Immediate Early BMP2 Responsive Gene, Dlx5, in Osteoblasts. S. E. Harris[1], D. Guo*[1], A. Krishnaswamy*[1], A. C. Lichtler[2], M. A. Harris[1]. [1]Oral Biology, UMKC, Kansas City, MO, USA, [2]Genetics and Developmental Biology, UCONN Health Center, Farmington CT 06030, CT, USA.

The Dlx5 homeobox gene has been shown to be important in osteoblast growth and differentiation by analysis of null mutations of the Dlx5 locus in mice (Acampora et al, 1999; Depew et al, 1999). Dlx5 plays a role in regulating Col1a1, Runx2, and Msx2 genes (Pan et al, 2002; Shibuya et al, 2001; Tadic et al, 2001). We have shown that Dlx family members are also important in regulating BMP2 transcription in primary rat calvarial osteoblasts and that Dlx5 is an immediate early BMP2 responsive gene in both primary osteoblasts and 2T3 mouse osteoblasts. Dlx 5 is induced at 30 min and stays elevated for 3-5 days after BMP2 addition. To better understand the genetic network of BMP2 regulated genes, we are using several genomic approaches to identify early and late genes that are directly regulated by Dlx5. Using microarray analysis of immediate early (30 min to 1hr) and early (1hr to 8hr) BMP2 responsive genes, we selected a set of 48 genes that are induced a minimum of 2.5 fold by 100ng/ml of BMP2 in the 2T3 osteoblast model. This data was derived from 2 independent culture experiments and analyzed by Significance Analysis of Microarrays (SAM) (Tuscher et al, PNAS, 2001) for significance. As expected, Dlx5 was a member of this set and this was confirmed by Northern analysis. Of the 48 genes, 30 are unknown or poorly annotated genes and the other 18 well annotated. To derive additional information, we searched the Celera mouse genome and obtained the coding region, exon/intron structure and 10 kb of 5' and 3' flanking region of all 48 genes. Next, the equivalent human genes were obtained and mouse/human homology studies initiated using VISTA and Family Relations programs which identify islands of conserved nucleotide sequences (CNS) in the cis-regulatory regions of the respective genes. Then, candidate Dlx response elements were mapped in all 48 genes which are co-induced by BMP2 in this model. A criteria was set that at least two TAAT or one TTAATG sequence(s) had to be in the CNS motif of a given gene. Using this analysis, a provisional virtual gene network of candidate early genes that are directly regulated by Dlx5 or similar family members was built. To test components of this network experimentally, we have designed a Dlx5 expression virus vector in which the strong repressor domain of engrailed is fused to Dlx5. Upon infection of 2T3 cells with this vector, we will be able to identify genes directly regulated by Dlx5 using several microarray approaches. Thus, by using both computational and experimental approaches, we can derive a provisional regulatory gene network of early BMP2-Dlx5 functions in osteoblasts.

1160

Marked Synergistic Interaction Between the Homeodomain Protein Nkx 3.2 and the Serum Response Factor (SRF) Transcription Factors on the Human α2 Type I Procollagen (hCol1A2) Promoter: A Key Stimulatory Mechanism for Osteoblast Collagen Expression. W. Zimmer*[1], K. Moses*[1], T. Linkhart*[2], D. Dean*[3], C. Stivers*[2], D. D. Strong[2]. [1]Univ South Alabama, Mobile, AL, USA, [2]Musculoskeletal Disease Center, J.L. Pettis VAMC, Loma Linda, CA, USA, [3]Northwestern Univ, Chicago, IL, USA.

Our goal was to identify a minimal set of control elements in an osteoblast specific promoter that would drive high expression in osteoblasts for development of retroviral skeletal targeting vectors for gene therapy that would not adversely affect viral titer. We found that the minimal hCol1A2 promoter (-267 to +1) was highly expressed in osteoblasts comparable to the rat 2.3 rat Col1A1 promoter and not in fibroblasts, marrow stromal cells or chondrocytes. While many control elements in the rat and mouse Col1A1 promoter for high osteoblast expression have been identified, much less is known about the required elements in the hCol1A2 promoter. Using deletion and mutation analysis, the hCol1A2 promoter was mapped for elements conferring high basal activity in ROS 17/2.8 cells and mouse calvarial osteoblasts and a complex stimulatory element containing a serum response element (CArG Box) and Nkx binding sites was identified. A similar complex Nkx-CArG element in the γ-actin promoter bound Nkx 3.1, a homeodomain transcription factor, and SRF to synergistically activate this promoter in smooth muscle cells. Furthermore, mouse Nkx gene family deletion studies indicate that loss of Nkx 3.2 resulted in serious skeletal defects (loss of bones & reduction in bone and cartilage size). We found by RT-PCR that Nkx 3.2 was expressed in osteoblasts. These results prompted us to test the effect of Nkx 3.2 and SRF overexpression alone and in combination on hCol1A2 promoter activity. Both SRF and Nkx 3.2 increased (2-6 fold of control) hCol1A2 promoter activity. More importantly, the combination of Nkx 3.2 and SRF synergistically increased hCol1A2 promoter activity up to 47 fold of control. Mutation of the CArG-Nkx complex abrogated the synergism. Nkx 3.1 did not significantly stimulate promoter activity or synergise with SRF. Gel shift analysis was conducted and Nkx 3.2 and SRF bound to the complex CArG-Nkx element. Mutation of each site eliminated the gel shift using purified proteins. In conclusion, these studies have identified a novel 47 fold stimulatory mechanism for transcriptional activation of the type I collagen gene in osteoblasts. These studies also suggest that the skeletal phenotype of the Nkx 3.2 knock-out mouse may be caused, in fact, by a reduction in type I collagen expression. Project sponsor: Dept Army (C/A 2000-65-LLVARE-Strong). Information not reflective of Gov/NMTB policies/positions. No official endorsement inferred.

1161

CRM1/Exportin1-Mediated Nuclear Export is Required for the Pro-Survival Effect of Bisphosphonates on Osteocytes: Evidence for Cytoplasmic-Restricted Signaling by ERKs. L. I. Plotkin, B. Laska*, S. C. Manolagas, T. Bellido. Div. Endo/Metab. Center for Osteoporosis and Metabolic Bone Diseases, Central Arkansas Veterans Healthcare System, University of Arkansas for Medical Sciences, Little Rock, AR, USA.

Prevention of osteocyte and osteoblast apoptosis by both bisphosphonates (BPs) and estrogens (E) requires activation of the extracellular signal regulated kinases (ERKs). However, whereas E activate ERKs via a non-nuclear function of the estrogen receptor, BPs induce ERK activation by a novel, gap junction-independent effect initiated by opening of connexin43 hemichannels followed by Src activation. Using MLO-Y4 osteocytic cells and specific inhibitors of ERKs (PD98059 and U0126), PI3K (wortmannin), or PKA (H-89), we now report that, unlike in the case of E, ERKs are the only survival kinases required for BP anti-apoptotic effect. ERKs could inhibit apoptosis by transcription-dependent or independent mechanisms. The anti-apoptotic effect of BPs was not blocked by inhibition of RNA or protein synthesis with actinomycin D or cycloheximide. Moreover, dominant negative (dn) forms of the ERK-activated transcription factors Elk1, Stat3, Runx2/Cbfa1, C/EBPβ/NF-IL6, fos, jun, or CREB did not affect BP-induced anti-apoptosis. In contrast (as shown elsewhere in this meeting), the anti-apoptotic effect of E required gene transcription, and it was abolished by dn forms of several ERK-activated transcription factors. Further, whereas E increased Elk1-driven luciferase transcription, BP did not. On the other hand, the anti-apoptotic effect of BPs was abolished by a catalytic inactive dn mutant of the known ERK cytoplasmic substrate $p90^{RSK}$ or by a dn Bad mutated at Ser^{112}, the site specifically phosphorylated by $p90^{RSK}$. Taken together, these results indicate that BP-induced anti-apoptosis depends on cytoplasmic but not nuclear substrates of ERKs. Because the ability of ERKs to activate particular targets depends on their subcellular localization, we examined whether exclusion of activated ERKs from the cytoplasm abolished BP-induced anti-apoptosis. We restricted ERKs to the nuclear compartment by inhibiting the nuclear exporter CRM1/Exportin1 with its specific ligand leptomycin B. When the nuclear export of proteins was inhibited, BPs did not prevent apoptosis and, as expected, did increase Elk1-dependent transcription. These results indicate that cytoplasmic localization of activated ERKs is required for the survival effect of BPs and that activation of ERK nuclear targets is not sufficient for survival. Our findings provide evidence for cytoplasmic-restricted ERK signals triggered by BPs and suggest that BPs and E inhibit apoptosis by activating distinct pools of ERKs.

1162

Cell Autonomous Inhibition of Osteoblast Differentiation in Transgenic Mice with Targeted Overexpression of p20C/EBPß, a Truncated C/EBP Isoform. J. Y. Lee*[1], P. L. Kelly*[1], D. Harrison*[2], J. R. Harrison[1]. [1]Department of Orthodontics, University of Connecticut Health Center, Farmington, CT, USA, [2]Department of Medicine, University of Connecticut Health Center, Farmington, CT, USA.

We reported previously that Col1a1 promoter-targeted overexpression of p20C/EBPß in transgenic (TG) mice causes osteopenia. These mice, in which the 3.6 kb Col1a1 promoter/first intron directs expression of a p20C/EBPß transgene to bone, show decreased trabecular bone volume and cortical thickness. Dynamic histomorphometry showed a decrease in the mineral apposition and bone formation rates, consistent with an inhibition of bone formation in this model. Long bones and calvariae of TG mice showed reduced COL1A1 and osteocalcin (OC) mRNA levels in vivo. To test the hypothesis that p20C/EBPß inhibits osteoblast differentiation, we used an ex vivo bone marrow stromal cell culture model. In some experiments, heterozygous p20C/EBPß mice were crossed with a homozygous pOBCol2.3-GFP mouse so that all progeny were heterozygous for the GFP transgene, an established marker of the differentiated osteoblast. Both male and female mice were used, with the sex ratio held constant for WT and TG groups. Stromal cells were cultured in MEM containing 10% FCS; half the medium was replaced on day 3. On day 7 and alternate days thereafter, cells were fed with differentiation medium containing ß-glycerolphosphate (8 mM) and ascorbic acid (50 µg/ml). At various times, cultures were stained for alkaline phosphatase (AP) activity and mineralized colonies were visualized by transmitted light. GFP fluorescent colonies were imaged at the macroscopic level using a fluorimager and at the cellular level by fluorescence microscopy. RNA was extracted for determination of transgene and osteoblast marker gene expression by Northern analysis. Bone marrow stromal cells from WT and TG mice showed similar AP staining patterns at 14 and 21 days of culture. However, both the number of mineralized colonies and the degree of mineralization was reduced in TG cultures. In WT cultures, GFP fluorescence in the nodules became apparent by day 14, and nodules showed intense GFP fluorescence at 17 and 21 days. In contrast, TG cells showed a reduction in both the number and intensity of GFP fluorescent nodules. Levels of osteopontin and bone sialoprotein mRNA were reduced in TG cells in 2 of 3 experiments, whereas OC mRNA levels in TG cells were dramatically reduced in all experiments. These data indicate that osteopenia in pOBCol3.6-FLp20C/EBPß transgenic mice may result from a cell autonomous inhibition of osteoblast differentiation and suggest that C/EBP transcription factors might function as key regulators of osteoblast lineage progression and bone mass.

1163

Decreased Postmenopausal Bone Strength due to Bone Loss Is Compensated by Increased Bone Size, and a Strength Index Including both Bone Mass and Size, Predict Future Fractures - A 19 Year Population Based Prospective Study in 108 Women. H. G. Ahlborg*[1], O. Johnell[1], C. H. Turner[2], M. K. Karlsson[1]. [1]Department of Orthopaedics, University Hospital MAS, Malmo, Sweden, [2]Departmentt of Orthopaedics, The Biomechanics and Biomaterial Research Center, Indiana University, Indianapolis, IN, USA.

Bone strength depends on material properties, as bone mass, and structural characteristics, as bone size. The bone loss at menopause (MP) reduce bone strength, but a compensatory mechanism may occur by improving the skeletal geometrical properties. Additional, if a Strength Index, taking both bone mass and skeletal geometry in account, better predict fragility fractures than a bone mass measurement, is unclear. This prospective study evaluated bone loss and geometrical changes following MP in 108 women, all premenopausal at age 47, during a 19 years period. Bone mineral content (BMC) and bone mineral density (BMD) was estimated by single-photon absorptiometry (SPA) of the distal radius every second year. Skeletal geometry, cross sectional moment of inertia (CSMI) and Strength Index was calculated from the graphical tracing of the scans. Data is presented as mean with 95 % confidence interval (95% CI). BMD decreased with 1.7 %/year (95% CI 1.5%-1.8%), medullary width increased with 1.0 %/year (95% CI 0.8%-1.2%) and periosteal width by 0.6 %/year (95% CI 0.5%-0.7%). CSMI increased as a result with 2.8 %/year (95% CI 2.3%-3.2%) while Strength Index decreased with 0.7 %/year (95% CI 0.5%-0.8%). The quartile of women with the largest medullary expansion had compared to the quartile of women with the least medullary expansion the greatest BMC loss [mean 1.6 %/year (95% CI 1.3-1.9) vs. 0.8 %/year (95% CI 0.5-1.1)] but a larger subperiosteal apposition [mean 0.9 %/year (95% CI 0.7-1.1) vs. 0.3 %/year (95% CI 0.2-0.5)]. Thus, the quartile of women who lost most bone also increased skeletal size most. Also, annual changes in medullary and subperiosteal width correlated ($r=0.5$, $p<0.001$). A -1 SD reduction in Strength Index at baseline conferred a risk ratio (RR) of 3.8 (95% CI 1.8-8.0) and a -1 SD reduction in BMD by 1.5 (95% CI 0.9-2.6), to sustain a distal radius fracture during the study period. The decreased bone strength due to demineralisation of the distal radius following MP is compensated by a subperiosteal apposition, partly preserving bone strength. A Strength Index, including both bone mass and skeletal geometry, is an important predictor of distal radius fractures.

1164

Low Levels of Serum Estradiol Contribute to the Rate of Bone Loss in Postmenopausal Elderly Women. P. B. Rapuri[1], J. C. Gallagher[2], G. Haynatzki[3]. [1]Bone Metabolism, Creighton University, Omaha, NE, USA, [2]Bone Metabolism Unit, Creighton University, Omaha, NE, USA, [3]Osteoporosis Research Center, Creighton University, Omaha, NE, USA.

There are conflicting data on the effect of low levels of endogenous estradiol on bone. In the Study of Osteoporotic Fractures, elderly women with serum estradiol levels of <5 pg/ml had increased bone loss at the hip and higher risk of hip and spine fractures. However, in the EPIDOS study of elderly women, no relationship was observed between serum estradiol and the occurence of hip fractures. In another study, administration of an aromatase inhibitor reduced serum estradiol levels from 5 to 1 pg/ml and caused a significant increase in bone resorption markers. To explore the relationship between low estradiol and bone further, we examined the relationship between the total/bioavailable estradiol and the rate of bone loss at the spine, total body and femoral neck. The study population consisted of 98 women (mean age 71±3 years) assigned to the placebo group of an osteoporosis intervention study for 3 years. Serum total estradiol was determined by RIA (DSL Inc) and the fraction of bioavailable estradiol was determined as the difference between the total and SHBG bound estradiol. The rate of change in BMD over 3 years was determined at multiple skeletal sites by DEXA. Statistical analysis was performed using Pearson's correlations and independent sample t test. There was a significant correlation between serum total estradiol and bioavailable estradiol ($r=0.89$, $p<0.001$) and between serum estradiol and body mass index ($r=0.31$, $p<0.001$). Women were divided into higher or lower serum estradiol groups using the median value. The median value for serum bioavailable estradiol was 3.3 pg/ml and for serum total estradiol it was 11.4 pg/ml. The group with serum bioavailable estradiol below 3.3 pg/ml had significantly faster bone loss at the spine ($p<0.01$) and total body ($p<0.01$) but not the hip. Similar results were obtained for serum estradiol above and below 11.4 pg/ml. In conclusion,these results show that very low levels of estradiol play a contributing role in the pathogenesis of bone loss in the elderly women.

Effect of endogenous estrogen levels on the rate of bone loss

	percent change over baseline		
estradiol levels (pg/ml)	spine (L1-L4)	femoral neck	total body
bioavailable estradiol			
<3.3 (47)	-2.58±0.75	-0.59±0.68	-2.75±0.34
>3.3 (49)	-0.23±0.55**	-0.40±0.76	-1.31±0.44**
Total estradiol			
<11.4 (49)	-2.43±0.73	-0.05±0.71	-2.47±0.38
>11.4 (49)	-0.32±0.56*	-0.93±0.70	-1.61±0.42

values are mean ± SEM

* $p<0.05$ and ** $p<0.01$ compared to <3.3 (for bioavailable) and <11.4 (for total estradiol)

1165

Effect of Octreotide on Bone Turnover and Parathyroid Hormone after Oral Glucose: Evidence for a Novel Endocrine Interaction between the Gastrointestinal Tract and Bone. J. A. Clowes, H. C. Allen, D. Prentis, R. Eastell, A. Blumsohn. Clinical Sciences (North), University of Sheffield, Sheffield, United Kingdom.

Feeding results in the acute suppression of bone turnover markers, an effect which is also seen with oral glucose. We have shown that insulin does not mediate this effect, but several other gastrointestinal hormones (e.g. glucose dependent insulinotropic peptide, GIP) appear to modulate bone turnover in vitro and may mediate the effect. The purpose of this study was to inhibit the production of gastrointestinal hormones using octreotide (a long acting analogue of somatostatin) to identify if the glucose-mediated suppression in bone turnover could be blocked. Fifteen volunteers (9M, 6F, age 27 ± 1.5 SEM) were each studied on 4 occasions in a randomised single blind crossover study to receive either 1) placebo (oral water, iv saline), 2) oral glucose (75g), 3) oral glucose + iv octreotide (50 µg/hr) and 4) iv octreotide alone. We measured serum C-terminal telopeptide of type I collagen (sβCTX), urine N-terminal telopeptide (uNTX), osteocalcin (OC), procollagen type I N-terminal propeptide (PINP), PTH, insulin, ionised calcium and glucose over 4 hours following the oral load. All bone turnover markers decreased significantly following oral glucose (repeated measures ANOVA; all $P < 0.001$). At 120 min sβCTX decreased by 45% ± 2, uNTX by 31% ±7, OC by 16% ± 1 and PINP by 6% ± 1. Octreotide completely abolished the bone turnover response to glucose for all markers (Figure sβCTX; legend glucose (G), octreotide (S); AUC analysis all $P < 0.01$ except uNTX (AUC; $P = 0.05$). Octreotide alone resulted in a significant increase in all bone turnover markers (AUC; $P < 0.05$) as well as an increase in PTH (AUC; $P < 0.01$), which was not explained by changes in ionized calcium. We conclude that octreotide completely abolishes the bone turnover response to glucose intake and increases PTH secretion. This suggests that the apparent bone turnover response to feeding is likely to be mediated by an octreotide-inhibitable endocrine factor.

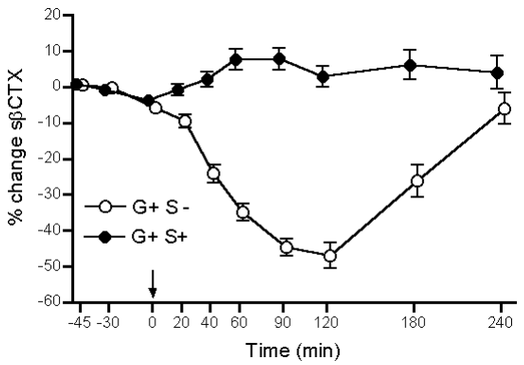

1166

Bone Mass and Bone Loss at Trabecular and Cortical Sites are Differently Regulated by Sex Hormones in Elderly Men. L. Gennari[1], D. Merlotti*[2], S. Gonnelli[2], G. Martini[1], A. Montagnani*[2], M. B. Franci*[2], S. Campagna*[2], R. Nuti[1], C. Gennari[2]. [1]Metabolic Disease Unit, University of Siena, Siena, Italy, [2]Institute of Internal Medicine, University of Siena, Siena, Italy.

Sex steroid hormones play an important role in regulating bone turnover and bone mass in males, as well as in females. However, the exact mechanism of bone loss in men remains unknown. In this study 300 elderly men (age range 50-85 yrs) were recruited and followed for three years to evaluate the relationships between hormone levels, bone turnover, bone mineral density (BMD), and bone loss at different skeletal sites. Femoral and Lumbar BMD (DEXA), bone ultrasound parameters at the os calcis and phalanxes, serum dehydroepiandrosterone sulphate (DHEAS), serum testosterone (T), serum estradiol (E), sex hormone binding globulin (SHBG), gonadotropins (LH and FSH) and bone turnover markers (urinary CTX and bone alkaline phosphatase, BALP) were evaluated at the enrollment and after three years. The free androgen index (FAI) and free estrogen index (FEI) were calculated as the ratios between total hormone levels and SHBG. In the total population, T, DHEAS, FAI and FEI but not E decreased significantly with age while LH, FSH, and SHBG increased significantly. A significant effect of estrogen on bone was observed, particularly at trabecular sites. Subjects with FEI or E below the median showed lower baseline lumbar BMD values as well as higher rates of bone loss at the lumbar spine and Ward's triangle with respect to men with FEI or E above the median. Serum basal BALP was significantly higher and increased significantly after three years in men with FEI or E below the median than in men with FEI and E above the median. By contrast, androgens but not estrogen significantly affected ultrasound parameters at phalanxes. Subjects with FAI below the median showed lower AD-SOS values with respect to subjects with FAI above the median, with a difference in T-score of about 1SD (-2.8 vs –1.9). Moreover, the time frame, a graphic trace parameter related to the cortical thickness of the phalanxes, was significantly lower in subjects with FAI below the median than in subjects with FAI above the median. In conclusion, results from the present study indicate a different regulation of bone mass and loss by sex hormones at different skeletal sites, in males.

1167

Racial Differences in Hip Fracture Risk Are Established During Growth: Structural and Biomechanical Determinants of Strength at the Proximal Femur in Asians and Caucasians. X. F. Wang*[1], T. J. Beck[2], Y. Duan[1], E. Seeman[1]. [1]Department of Medicine, Austin & Repatriation Medical Centre, Melbourne, Australia, [2]Radiology, The Johns Hopkins University School of Medicine, Baltimore, MD, USA.

The lower areal BMD (aBMD) in Asians than Caucasians is largely due to their smaller bone size so that the lower hip fracture rate in Asians is unlikely to be attributed to racial differences in aBMD. To determine the structural and biomechanical differences at the femoral neck at peak between Asians and Caucasians, we used DXA derived bone mass and dimensional data (width) to estimate endosteal diameter, mean cortical thickness, cross-sectional moment of inertia (CSMI) and section modulus at the mid-point of the femoral neck (FN) and calculated the buckling ratio, an estimate of the relative cortical thickness (subperiosteal radius/cortical thickness) in 42 healthy Asian men and 63 Asian women (Chinese ancestry), 101 healthy Caucasian men and 264 Caucasian premenopausal women aged 18 to 43 years. We hypothesized that Asians have a narrow bone with a thicker cortex at peak conferring a lower risk of hip fracture than Caucasians. FN width and cortical thickness were 11% and 10% narrower in Asian than Caucasian men, and 16% and 7% narrower in Asian women than Caucasian women. Section modulus was 29%-36% lower in Asians than Caucasians before, and after, adjusting for total body lean mass. There was no difference in buckling ratio between Asian and Caucasian men (8.0 ± 0.2 vs. 8.1 ± 0.2, NS), but buckling ratio was lower in Asian than Caucasian women (7.1 ± 0.2 vs. 7.8 ± 0.1, $p < 0.01$). Sex differences in FN width were greater than those in cortical thickness (Asians, 20% vs. 6%; Caucasians, 13% vs. 9%). Section modulus (an estimate of bending strength) was 57% higher in Asian men than women, and 43% higher in Caucasian men than women, but adjusting for sex differences in height and total body lean mass the difference disappear. We concluded that: (i) despite the larger bone size and greater bone strength in Caucasians than Asians, the relatively thicker cortices within the narrower FN in Asian women at peak may produce a more structurally stable femoral neck in old age. (ii) FN strength is greater in men than women in both racial groups due to the differences in lean body mass.

1168

Inhibin B is a Marker of Diminished Ovarian Function and Increased Bone Turnover in Peri-menopausal Women. D. Gaddy-Kurten[1], S. E. Bledsoe*[1], S. J. Achenbach*[2], S. Khosla[2]. [1]Physiology and Biophysics, University of Arkansas for Medical Sciences, Little Rock, AR, USA, [2]Mayo Clinic and Foundation, Rochester, MN, USA.

Clinical indices of increased bone turnover are first detected in peri-menopausal women, and correlate best with elevated serum FSH levels, rather than decreases in estradiol. Other studies in peri-menopausal women have demonstrated that the mechanism responsible for the rise in FSH levels is a selective decrease in ovarian Inhibin B. These data led to our hypothesis that a selective loss of Inhibin B in peri-menopausal women, independent of changes in sex steroids, may have a direct effect on osteoblast and osteoclast development, thereby increasing bone turnover. In support of this hypothesis, our previous results in murine bone marrow cultures demonstrated that Inhibin B suppresses both osteoblast and osteoclast development. The current study was designed to determine if Inhibins could suppress human osteoblastogenesis, and if decreased serum Inhibin B in peri-menopausal women was associated with increases in markers of bone turnover. Human mesenchymal stem cells were grown for 21 days under osteoblastic conditions in the presence or absence of 50 ng/ml Inhibin A or Inhibin B. Mineralization of the developing osteoblasts was determined by alizarin red staining, normalized to total protein content per well. Both Inhibin A and Inhibin B suppressed osteoblastogenesis; Inhibin B was a more potent suppressor than Inhibin A. To determine if serum levels of Inhibin B were correlated with markers of bone turnover, a cohort of pre- and post-menopausal women (n = 188, age range 21-85 yrs) were analyzed by decade. Serum and urine samples were collected during the follicular phase of the cycle for pre-menopausal women. Samples were excluded if the women were obtaining estrogen through the use of oral contraceptives or hormone replacement therapy. Consistent with our hypothesis, in the cohort of women of peri-menopausal age (45-54 yrs) but not in any of the other age groups, Inhibin B was inversely correlated with Bone Alkaline Phosphatase (BAP; $R=-0.36$, $p<.05$), with a similar but non-significant trend for serum osteocalcin. These novel findings in human samples, along with our published suppressive effects of inhibins on both osteoblast and osteoclast development in murine cells, indicate that selective changes in Inhibin B alter human bone marrow cell differentiation in vitro and may also be doing so in vivo. Further studies and larger patient cohorts are required to validate the hypothesis that Inhibin B changes are significantly correlated with the increased bone turnover observed during the peri-menopausal transition.

1169

A Double Blind Randomized Placebo Controlled Trial of Alendronate in Primary Hyperparathyroidism. A. A. Khan[1], J. P. Bilezikian[2], A. W. C. Kung*[3], M. M. Ahmed*[1], S. J. Dubois*[1], A. Y. Y. Ho*[3], Z. Motagally*[1], M. Rubin*[2], S. J. Silverberg*[2], T. I. Standish*[1], Z. A. Syed*[1]. [1]Medicine, McMaster University, Hamilton, ON, Canada, [2]Columbia University College of Physicians and Surgeons, New York, NY, USA, [3]University of Hong Kong, Hong Kong, China.

A randomized, double blind, placebo-controlled trial was conducted to determine if alendronate 10mg daily (ALN) maintains or improves bone mineral density (BMD) in patients with primary hyperparathyroidism (PHPT). Eligible patients were asymptomatic and did not meet surgical guidelines. Forty-four patients randomized to placebo or active treatment arms were stratified for gender. At 12 months, patients taking placebo crossed over to active treatment. All patients were on active treatment in year 2. Assessments were made at baseline, 3, 6, 9, 12, 15, 18, 21 and 24 months. The primary outcome index, BMD at the lumbar spine (LS), femoral neck, total hip and distal one-third radius, was measured at baseline, 6, 12, 18 and 24 months with dual energy X-ray absorptiometry (DEXA). Indices of bone metabolism - calcium, phosphate, PTH (IRMA), bone specific alkaline phosphatase, urinary calcium, urine N-telo peptides were obtained. Data are provided for 35 patients who completed 24 months of the protocol. Paired t-tests were conducted for groups A (active years 1 and 2) and B (placebo year 1, active year 2) second year mean differences for total hip, LS, and distal 1/3 radius BMDs; total and ionized calcium and phosphorus levels. Blinded analysis of year 1 data showed significant increases in the mean treatment group LS BMD by 5.4 % and total hip by 3.0% from baseline. Radial BMD showed no statistically significant change. Treatment with ALN over two years was associated with a significant increase in LS BMD by 6.85%(0.05 grams/cm2, 95% CI: 0.037,0.067, t=7.3, p< .001), a 2.9% increase in the BMD total hip (0.02 grams/cm2, 95% CI: -0.003,0.043,t=1.79,p= .09) and distal 1/3 radial sites remained stable (0.012 grams/cm2, 95% CI: -0.003,0.015, t=1.4, p= .19) compared to baseline. Group B mean LS and total hip BMD significantly increased from years 1 to 2 by 3.6% (0.87 grams/cm^2, 95% CI: 0.01, 0.05, t=3.4, p= .004) and 2% (0.73 grams/cm^2, 95% CI: 0.00,0.03,t=2.6,p=0.017) respectively. The distal 1/3 radial site remained stable (0.005 grams/cm2, 95% CI: -0.002,0.01, t=1.4, p= .17). Preliminary analyses of biochemical data demonstrated no significant change in total or ionized calcium, or phosphate. This is the first randomized placebo-controlled trial evaluating the effect of ALN on BMD in men and women with PHPT. ALN significantly increases BMD at the lumbar spine after 12 and 24 months of therapy from baseline. ALN may be an alternative to surgery in some patients with PHPT.

Disclosures: ***A.A. Khan****, Merck and Company 2.*

1170

Effect of Anastrozole on Bone Density and Bone Turnover: Results of the 'Arimidex' (Anastrozole), Tamoxifen, Alone or in Combination (ATAC) Study. R. Eastell[1], R. A. Hannon[1], J. Cuzick*[2], G. Clack*[3], J. E. Adams[4]. [1]University of Sheffield, Sheffield, United Kingdom, [2]Cancer Research UK, London, United Kingdom, [3]AstraZeneca, Macclesfield, United Kingdom, [4]University of Manchester, Manchester, United Kingdom.

The ATAC Study is a randomised, double blind trial of anastrozole (1 mg/day, A), tamoxifen (20 mg/day, T) or their combination (A+T) in 9366 postmenopausal women with early breast cancer (adjuvant therapy). The initial results from this study show that disease-free survival (DFS) was significantly improved in the A group compared with the T group (p=0.013), and the incidence of new (contralateral) primary breast tumours was reduced in the A group compared with the T group. After a median duration of 2.5 years, the fracture rate in the A group (5.8%) was higher than in the T group (3.7%). This could be a consequence of either the complete suppression of oestrogen levels by anastrozole or the partial oestrogen-agonist effect of tamoxifen on bone. We measured bone mineral density (BMD) by DXA at the lumbar spine (LS) and total hip (TH) in a subset of 308 women from the ATAC study, and 46 unrandomised control patients with breast cancer but receiving no hormone therapy. Bone resorption, by urinary N-telopeptide (NTX) and free deoxypyridinoline (DPD), and bone formation, by bone alkaline phosphatase (bone ALP), were also measured. The table shows the estimated percentage changes at one year in those patients completing the first year, following Analysis of Variance on log transformed data.

	A (n=80)	T (n=87)	A+T (n=82)	Controls (n=39)
LS-BMD	-2.59 (-3.41 to -1.77)	1.01 (0.15 to 1.88)	0.21 (-0.69 to 1.12)	-0.36 (-1.51 to 0.82)
TH-BMD	-1.68 (-2.36 to -0.98)	0.48 (-0.23 to 1.20)	0.78 (0.02 to 1.55)	-0.13 (-1.09 to 0.83)
NTX	12.2 (2.1 to 23.4)	-34.5 (-40.2 to -28.1)	-33.7 (-39.8 to -27.0)	-8.8 (-19.7 to 3.5)
DPD	-2.2 (-10.4 to 6.7)	-31.2 (-36.8 to -25.1)	-22.4 (-29.0 to -15.3)	-9.9 (-20.2 to 1.8)
Bone ALP	20.8 (13.3 to 28.6)	-14.0 (-19.3 to -8.2)	-9.6 (-15.4 to -3.5)	4.6 (-4.7 to 14.8)

Estimated Percentage Change (95% Confidence Interval).

Thus, at one year A therapy was associated with bone loss at the spine and hip and an increase in markers of bone resorption and formation, and T therapy with an increase in BMD and a decrease in markers of bone turnover; A+T had a similar effect on BMD and bone turnover as T alone. We conclude that the administration of A is probably associated with an increase in bone remodelling and that any consequent bone loss may be associated with a small increase in the risk of fractures. These data need be balanced against the overall efficacy and tolerability benefits observed in the main ATAC trial.
Submitted on behalf of the ATAC trialists

Disclosures: ***R. Eastell****, AstraZeneca 2, 5.*

1171

NSAIDs Impair Fracture Healing. M. Haberland*, M. Gesicki*, C. K. Nguyen*, J. Tibba*, F. T. Beil, M. Amling, J. M. Rueger*. Trauma Surgery, Hamburg University School of Medicine, Hamburg, Germany.

NSAIDs belong to the most widely used drugs in Europe and the USA. Their main action is to inhibit cyclooxygenase II and thereby reducing the synthesis of proinflammatory cytokines. Some of the most important inflammatory signals which are reduced by NSAIDs belong to the prostaglandin family, which has recently been shown to be important for skeletal homeostasis. We therefore hypothesized that NSAIDs might influence skeletal repair mechanisms, e. g. fracture healing. To test this hypothesis, fracture healing was studied in 100 mice treated with the NSAID diclofenac or placebo. Drugs or vehicle were administered via osmotic pumps or subcutaneously implanted pellets. Diclofenac was given in doses (per kg) similiar to the ones used in humans and for different periods of time to mimic chronic or acute use of these drugs. To make mouse models accessible to fracture modulation studies that also allow biomechanical analysis, we modified the Einhorn tibia fracture model and developed a standardized close femur fracture model. Analysis included biomechanics, contact-radiography, microCT analysis and undecalcified histology. In normal, control mice, the fractured femur reaches a biomechanical stability comparable to the contralateral intact femur after 20 days. Therefore the radiological, histological and biomechanical findings at 20 days in controls were defined as the physiologic reference. In sharp contrast, mice treated with diclofenac showed a significant delay in fracture healing. Callus size as assessed by contact-radiography and microCT was significantly reduced. Furthermore, not only radiological and histological data demonstrated a morphological interference of diclofenac with the fracture healing process, but also the functional competence of bone, as assessed by three-point-bending tests, was dramatically compromised at day 10 (Force to failure: 6,2 N in controls vs. 2,5 N in diclofenac treated mice, p< 0,05) and at day 20 (Force to failure: 15,2 N in controls vs. 9,1 N in diclofenac treated mice, p< 0,05). This study shows that NSAIDs impair the fracture healing process in vivo, leading to significantly reduced biomechanical stability. As these drugs are widely used in patients with fractures, it seems important that further experimental and clinical studies clarify the role of these drugs in fracture healing.

1172

"Incipient" Primary Hyperparathyroidism: A "Forme Fruste" Of An Old Disease. S. J. Silverberg, J. P. Bilezikian. Medicine, Columbia University College of P&S, New York, NY, USA.

Recently, we have become increasingly aware of individuals with elevated levels of PTH in the absence of hypercalcemia. They have been carefully evaluated for other causes of elevated PTH. None have been found. These patients may represent the "forme fruste" of primary hyperparathyroidism (PHPT). The group includes 17 women (3 premenopausal, 14 postmenopausal; mean age: 60 ± 2 years), with normal renal function, no evidence for liver or gastrointestinal disease, no medications that could alter PTH or calcium levels. All have normal serum calcium levels (9.7 ± 0.1 mg/dl; nl: 8.4-10.4), with elevated PTH (118 ± 19 pg/ml; nl: 10-65). Urinary calcium is 182 ± 24 mg/24 hours (nl: 50-300), and bone density is normal compared to age and sex-matched controls at all sites (Z-Scores: spine: -0.4 ± .4; hip: -0.8 ± .2; radius: -0.3 ± .2). 25-hydroxyvitamin D levels are normal (34 ± 10 ng/dl; nl: 9-52), and well within the physiological range (>20 ng/dl). They do not have Familial Hypocalciuric Hypercalcemia (no family history of hypercalcemia; no hypocalciuria). They do not show evidence for the cortical demineralization that is characteristically seen when patients with hypercalcemia and PHPT are first evaluated. In one patient who fits this description, ^{99}Technetium-labeled Sestamibi imaging revealed a parathyroid adenoma that was removed and confirmed histologically. The existence of these patients satisfies many expectations about the disorder. Many of the clinical manifestations of PHPT are already present when the disorder is diagnosed; studies monitoring bone density and biochemical indices confirm that in most patients there is little evidence for disease progression. The pathophysiological construct calls for a biphasic disease course, in which the disorder is not clinically recognized when it begins (Phase 1) followed by the appearance of its biochemical hallmark, hypercalcemia (Phase 2). If one had insight into the earlier stage of the disorder, it would be characterized first by elevated PTH levels in the absence of hypercalcemia. Such patients would represent the earliest manifestation of PHPT, the elusive Phase 1 of the disease. The patients we describe have been referred for a screening evaluation of skeletal health. If our hypothesis is correct, hypercalcemia will develop as these patients are followed; we would then see the emergence of the typical pattern of bone loss as well as histomorphometric characteristics of PHPT. Information from the study of patients who represent this earliest form of PHPT could fill important gaps in our understanding of the development of the clinical features of modern PHPT.

Disclosures: ***S.J. Silverberg****, Eli Lilly 2.*

1173

Three Dimensional Assessment of Trabecular Architecture in Mild Primary Hyperparathyroidism (PHPT). D. W. Dempster[1], N. J. Caldwell*[2], S. A. Goldstein*[2], M. Parisien*[3], S. J. Silverberg[4], E. Shane[4], L. A. Fitzpatrick[5], R. Lindsay[6], J. P. Bilezikian*[7]. [1]Regional Bone Center, Helen Hayes Hopital, West Haverstraw, NY, USA, [2]Orthopaedic Research Laboratory, University of Michigan, Ann Arbor, MI, USA, [3]Department of Pathology, Columbia University, New York, NY, USA, [4]Department of Medicine, Columbia University, New York, NY, USA, [5]Department of Medicine, Mayo Clinic, Rochester, MN, USA, [6]Regional Bone Center, Helen Hayes Hospital, West Haverstraw, NY, USA, [7]Departments of Medicine and Pharmacology, Columbia University, New York, NY, USA.

We and others have previously reported maintenance of cancellous bone volume and trabecular number and connectivity in patients with mild PHPT. However, all studies to date have been performed in two dimensions. In the present study we have extended the analysis to the third dimension using microcomputed tomography. We studied biopsies from 10 premenopausal women and 15 men with primary hyperparathyroidism. The results were compared with biopsies from 14 normal women and 15 normal men. The average age of the men was the same in both groups (Normal, 48±3; PHPT, 49±3 years, p=NS). The women with PHPT were an average of five years older than their controls (Normal, 38±1; PHPT, 43±3 years, p<0.03). The results are given in the table.

	Men		Women	
	PHPT	Normal	PHPT	Normal
Cancellous bone volume (%)	23.3±1.7	21.4±1.8	30.8±2.2	30.2±2.1
Trabecular number (mm^{-1})	1.78±0.11	1.56±0.09	2.04±0.08	1.98±0.06
Trabecular thickness (μm)	131±6	135±8	151±8	152±7
Connectivity density (/mm^3)	4.17±0.69*	2.55±0.84	5.01±0.55	3.34±0.88

* p<0.05 by Wilcoxon's Rank Sum test

There were no significant differences between patients and controls in cancellous bone volume, trabecular thickness, and number. Trabecular connectivity density was significantly higher than controls in men with PHPT and there was a similar trend (p<0.06) in the women, especially noteworthy considering that the women with PHPT were significantly older by 5 years than their respective controls. This is the first study to analyze the three-dimensional structure of cancellous bone in patients with PHPT. The results confirm and extend our previous assessment, based on two-dimensional histomorphometric analysis, that cancellous bone volume is preserved in men and women with PHPT, and trabecular connectivity may be improved.

1174

Long-term Effects of Primary Hyperparathyroidism on Trabecular Bone Density. P. L. Selby[1], M. Davies[1], C. Alsop*[2], J. E. Adams[2]. [1]Musculoskeletal Research Group, University of Manchester, Manchester, United Kingdom, [2]Clinical Radiology, University of Manchester, Manchester, United Kingdom.

Primary hyperparathyroidism is a common disorder which is frequently asymptomatic. There remains controversy as to the long-term implications of the disease and the indications for surgical treatment. Recent evidence has indicated that parathyroidectomy leads to an increase in lumbar spine bone mineral density (BMD) which has led to suggestions that surgery should be offered to preserve bone density. However there are few data examining the long-term effects of primary hyperparathyroidism on trabecular bone density during conservative management and following parathyroidectomy. We studied 50 patients (16 male) aged 55 (SD 10) years with mild primary hyperparathyroidism (mean plasma calcium 2.76mmol/l, SD 0.11mmol/l). All had been followed with Quantitative Computed Tomography (QCT) bone densitometry of the lumbar spine for at least five years. Mean volumetric trabecular vBMD was measured in mg/cm^3 in 10mm slices in the mid-plane of four vertebrae (generally T12-L3) using K_2HPO_4 bone equivalent phantom. The median follow-up was 7.2 years and maximum 13.0 years. 16 patients underwent parathyroidectomy during follow-up. The effects of time and parathyroidectomy upon bone density were assessed using analysis of variance. Mean vBMD was 102.0 (SE 0.6) mg/cm^3 in those patients who did not undergo parathyroidectomy and 109.2 (SE 1.3) mg/cm^3 following surgery (mean difference 7.2 mg/cm^3 p<0.0001). Although there was a steady decline in vBMD with time (-2.3 mg/cm^3/y 95%CI -1.9 – -2.6), this was no greater than would be expected with age, and there was no change in Z score with time (mean change 0.00/y 95%CI -0.001 - +0.002). Furthermore, the relationship between bone loss and time was unchanged by parathyroidectomy. This study represents the longest follow-up of changes in trabecular bone density in patients with primary hyperparathyroidism. It indicates that parathyroidectomy does not alter the rate of trabecular bone loss in the long term, although surgery is associated with an initial quantal increase in bone density. We conclude that parathyroidectomy is of limited value in prevention of trabecular bone loss in patients with mild primary hyperparathyroidism..

1175

Homozygous Deletion of the Murine Calcitonin Receptor Gene Is an Embryonic Lethal. C. Laplace*, X. Li*, S. R. Goldring, D. L. Galson. NEB Bone & Joint Institute, Dept. of Medicine, Beth Israel Deaconess Medical Center & Harvard Medical School, Boston, MA, USA.

The calcitonin receptor (CTR) has multiple ligands. It is the receptor for both calcitonin (CT) and amylin (requiring in the latter case, a RAMP accessory protein). CTR is expressed in a variety of tissues at different times during development from embryonic through adult, suggesting a role in morphogenesis. To study the consequences during development of a complete ablation of the murine CTR (mCTR) gene, we generated two ES cell lines that have a targeted deletion of exons E6 and E7 in one allele of the mCTR gene. Deletion of these exons should effectively disable all mCTR isoforms as splicing of exon E5 to exon E8a is out of phase. Therefore, any protein that could be generated would encode no more than a portion of the first extracellular domain. Although we have generated 17 chimeric mice from the two ES cell lines, only one male chimera has sired mCTR (–/+) heterozygous mice. Our heterozygous breeding pairs have produced 69 mCTR (+/+) wild type mice (29%), 170 mCTR (–/+) heterozygous mice (71%) and no mCTR (–/–) homozygous mice (0%). These results indicate that, although CTR is known to be expressed in sperm at various stages of differentiation, male heterozygous CTR knock-out mice are not sterile and do produce CTR-negative sperm. Therefore, expression of CTR is not necessary for sperm differentiation or function. However, the absence of CTR knock-out mice suggests that lack of CTR expression results in a lethal embryonic defect. Pregnant females from mCTR (–/+) heterozygous intercrosses were sacrificed at different times of gestation and the embryos genotyped by PCR. Analysis of 25 embryos at 9.5 days post coitum (dpc) shows that there is a concordance between the observed (7:12:6; +/+, –/+, –/– , respectively) and expected (1:2:1) distributions. These data indicate that there is no deleterious effect of the homozygous CTR deletion up to this point of development. Therefore, these data exclude the possible theory that blastocyst expression of CTR is necessary for implantation. This is a critical observation as uterine CT has been suggested to have a key regulatory role during blastocyst implantation and CTR has been demonstrated on mouse preimplantation embryos. The observed ratio of embryos at 10.5 dpc (11:38:5) suggests that some homozygous null embryos are dying between 9.5 and 10.5 dpc. We have not observed any homozygous null embryos after 10.5 dpc. The 66 embryos analyzed from 11.5 through 14.5 dpc have an observed ratio of 1:2.7:0. We have not observed any obvious differences in gross anatomy between the homozygous null and heterozygous or wildtype embryos. Further analysis of the lethal developmental defect due to ablation of the CTR gene is underway.

1176

Runx2/Cbfa1 Is Essential for the Anti-apoptotic Effect of PTH on Osteoblasts. L. I. Plotkin[1], T. Bellido[1], A. A. Ali[1], Q. Fu[1], I. Gubrij[1], L. K. McCauley[2], C. A. O'Brien[1], S. C. Manolagas[1], R. L. Jilka[1]. [1]Endo/Metab. Center for Osteoporosis and Metabolic Bone Diseases, Central Arkansas Veterans Healthcare System, University of Arkansas for Medical Sciences, Little Rock, AR, USA, [2]School of Dentristy, University of Michigan, Ann Arbor, MI, USA.

PTH inhibits osteoblast apoptosis *in vivo* and *in vitro*, but the molecular mechanism of this effect has not been fully elucidated. It has been previously reported that activation of protein kinase A (PKA), but not protein kinase C or ERKs, is required for this action; and that PKA phosphorylates, and thereby inactivates, the pro-apoptotic protein Bad. Nonetheless, it is known that PKA also phosphorylates and activates the cAMP response element binding protein (CREB) and possibly Runx2/Cbfa1; and that CREB increases AP-1 activity by stimulating expression of AP-1 family members such as c-fos. To investigate whether CREB and/or Runx2/Cbfa1 play a role in the anti-apoptotic effect of PTH, we have utilized chemical transcription inhibitors as well as dominant negative (dn) mutants of these and other transcription factors. We report that actinomycin D abolished the survival effect of PTH on osteoblastic OB-6 cells, indicating the requirement for transcription. More specifically, dn CREB and dn Runx2/Cbfa1, completely abrogated the anti-apoptotic effect of PTH; but dn c-fos or dn c-jun were ineffective. The dispensability of c-fos was confirmed independently by the observation that osteoblastic cells obtained from *fos* null mice still exhibited the anti-apoptotic effect of PTH. We attempted to identify PTH-regulated genes involved in anti-apoptosis using an Affymetrix DNA microarray chip containing 12,000 genes (U74A). RNA was prepared from triplicate OB-6 cultures maintained under basal conditions, or treated with 50 nM PTH for 30, 60, or 120 minutes. Using Significance Analysis of Microarray software (Stanford University), we found that PTH caused statistically significant changes in the expression of several hundred genes, 8 of which have a known role in apoptosis. Of these, the best characterized is the anti-apoptotic protein Bcl-2, which was increased 2-fold at 1 hour following exposure of OB-6 cells to PTH. This response was confirmed by Western blot analysis using OB-6 and murine calvaria cells. Stimulation of Bcl-2 synthesis by PTH is consistent with the presence of one CREB binding site and several putative Runx2/Cbfa1 binding sites in the promoter region of the Bcl-2 gene. These findings demonstrate for the first time that, in addition to its essential function in osteoblast differentiation, Runx2/Cbfa1 is indispensable for the anti-apoptotic action of PTH on osteoblasts; and perhaps for osteoblast survival in general.

1177

Effects of PTH/PTHrP Receptor-Generated Signals on RANKL/RANK-Induced Osteoclastogenesis : Analyses I*n Vitro, In Vivo and Ex Vivo*. H. Kondo[1], J. Guo[2], U. Chung[2], S. Kasugai[1], H. M. Kronenberg[2], F. R. Bringhurst[2]. [1]Masticatory Function Control, Tokyo Medical and Dental University, Tokyo, Japan, [2]Endocrine Unit, Massachusetts General Hospital and Harvard Medical School, Boston, MA, USA.

PTH is one of the major regulators for osteoclast formation and activation in bone metabolism. It has been previously reported that the PTH-supported osteoclastogenesis is also accompanied by reciprocal up- and down-regulation of RANKL and OPG, respectively. However, it is not yet clear how the downstream signals generated by PTH/PTHrP receptor - cAMP/PKA and PLC/PKC- are involved in osteoclastogenesis. To address this issue, we conducted the following experiments. Cyclic AMP accumulation, mRNAs expression of RANKL, OPG, and M-CSF, and osteoclast formation were examined in an established murine marrow stromal cell line (MS1) or in primary bone marrow stromal cells (BMSC). MS1 and BMSC supported osteoclast formation in response to PTH(1-34), stimulating RANKL and inhibiting OPG mRNA expression. Northern blot analysis dem-

onstrated expression of RANKL was stimulated by [G^1R^{19}]PTH(1-28), a PKA selective PTH analogue, which exerted similar effects to PTH(1-34) and other PKA stimulators on reciprocal regulation of RANKL and OPG, and on osteoclast formation. On the other hand, PMA, a direct PKC stimulator, did not stimulate RANKL, and up-regulated OPG rather than down-regulated it. Furthermore, PMA inhibited PTH(1-34)-dependent osteoclast formation. These results suggest that cAMP/PKA signaling controls RANKL-induced osteoclastogenesis, and that PLC/PKC may exert inhibitory effects on it. To further elucidate the mechanism whereby PTH promotes osteoclastogenesis, we generated PLC/PKC signaling defective PTH/PTHrP receptor knock-in mice. EKKY sequence, located in the second intracellular loop of the intact PTH/PTHrP receptor, was replaced by DSEL. As previously shown, this mutation selectively abolished PLC activation downstream of PTH/PTHrP receptor, preserving intact AC/cAMP signaling. Histological observation in tibiae of 8 week-old mice indicated that phenotype in PLC defective mutant mice was similar to wild type except larger marrow space in mutant mice, suggesting that PLC/PKC signaling is not required for osteoclasotgenesis. Moreover, primary bone marrow cells from both mutant and wild type mice support osteoclasts by PTH(1-34), and the number of osteoclasts from the mutant mice is greater than wild type. These *in vivo* and *ex vivo* findings, coupled with *in vitro* analysis, revealed that cAMP/PKA signaling plays a major role for osteoclastogenesis, and PLC/PKC is not required. Furthermore, PLC/PKC signaling may play a negative role for PTH-dependent osteoclastogenesis.

1178

Inhibition of Osteoclast Formation by Human PTH(7-84) Involves Direct Actions on Hematopoietic Cells. P. Divieti, O. Lotz*, A. Geller*, H. Jüppner, F. R. Bringhurst. Endocrine Unit, Mass General Hospital and Harvard Medical School, Boston, MA, USA.

Intact parathyroid hormone, PTH(1-84), regulates formation and activity of cells in bone via interaction of its amino-terminus with the G protein-coupled PTH/PTHrP receptor (PTHR). Osteoblasts and osteocytes derived from PTHR-null mice express additional receptors for PTH that specifically recognize the carboxyl(C)-terminal region of the hormone. These C-terminal PTH receptors (CPTHRs) are highly expressed on osteocytes, where they can induce cell death, an action opposite to that reported for PTHR activation in these cells. Recently, large carboxyl-terminal fragments of PTH, with chromatographic properties similar to synthetic hPTH(7-84), were detected in plasma of normal subjects and, at much higher levels, in plasma of patients with advanced renal failure. Synthetic hPTH(7-84) blocked the calcemic actions of PTH(1-84) and PTH(1-34) in parathyroidectomized rats in vivo. These actions appear to result from direct effects of hPTH(7-84) via CPTHRs in bone, as this peptide, which neither activates nor antagonizes PTHRs in vitro, inhibits both osteoclast formation in murine bone marrow cultures and resorption of intact murine calvarial bone in vitro. The cellular target(s) of these antiresorptive actions of hPTH(7-84) are unknown, although osteoblasts and marrow stromal cells are known to express CPTHRs. To determine if the antiresorptive actions of hPTH(7-84) might be mediated by activation of CPTHRs on cells of the hematopoietic lineage, we first sought effects of hPTH(7-84) on osteoclast formation induced by M-CSF and RANKL in murine whole bone marrow (WBM) and in purified bone marrow macrophage (BMM) cultures. As expected addition of RANKL(40ng/ml) and M-CSF (10ng/ml) induced osteoclast formation in both in vitro systems, as assessed by TRAP staining and TRAP solution assay. Addition of hPTH (7-84) (300nM), reduced osteoclast formation induced by combined RANKL and M-CSF treatment by about 40% in both systems, suggesting a direct effect of hPTH(7-84) on the hematopoietic compartment. We then performed CPTHR radioligand binding analysis using BMM and 125I- [Tyr34]hPTH(19-84) and observed that 1) BMM expressed specific CPTHRs and 2) the CPTHR expression in these cells was further reduced by treatment with RANKL, suggesting that CPTHR expression may decrease during osteoclast maturation. We conclude that CPTH fragments may act upon both the stromal/osteoblast and hematopoietic compartments, and that inhibition of bone resorption by hPTH(7-84) involves, at least in part, a direct effect of the hormone via CPTHRs expressed on osteoclasts or their precursors.

1179

Teriparatide (rhPTH (1-34)) Skeletal Efficacy Is not Affected by Longterm Pretreatment with Alendronate, Estrogen, or Raloxifene in Ovariectomized Rats. Y. L. Ma, Q. Q. Zeng*, A. Schmidt*, J. L. Hoover*, H. W. Cole*, H. U. Bryant*, M. Sato. Endocrine, Lilly Research Labs, Indianapolis, IN, USA.

Because of the ready availability of other therapies, teriparatide (rhPTH (1-34)) may be administered to osteoporotic women who have already been treated with other agents, such as alendronate (ABP), estrogen (EE2), or raloxifene (RA). The latter agents suppress bone turnover, by inhibiting resorption and secondarily reducing bone formation; and so, could interfere with the skeletal efficacy of teriparatide which increases bone turnover, as it stimulates mineral apposition. To probe this question, ovariectomized (Ovx) rats (3 months old) were pretreated with ABP (28µg/kg/2xwk sc), EE2 (0.1mg/kg/d po), or RA (1mg/kg/d po) for 10 months, before switching to PTH 30µg/kg/d sc for 2 months. All 3 agents prevented ovariectomy induced bone loss after 10 months, but were mechanistically distinct as shown by histomorphometry. For example, ABP preserved the primary spongiosa by preventing remodeling, because the primary spongiosa was considerably reduced compared to baselines for all other groups (13 months of age). ABP strongly suppressed activation frequency, eroded surface, and bone formation rate to below other treatment groups after 10 months, whereas these parameters were not different from Sham for EE2 and RA. Trabecular area for ABP, EE2 and RA were greater than Ovx controls, but trabecular number was greater for ABP compared to all other groups, while EE2 and RA had trabecular number that were between Ovx and Sham controls. RA tended to increase trabecular thickness, whereas ABP and EE2 had trabecular thickness that were not different from Sham. After 2 months of sequential teriparatide (PTH) treatment, trabecular area was increased by 105%, 113%, 36% and 48%, for vehicle/PTH, ABP/PTH, EE2/PTH and RA/PTH, respectively, compared to 10 month levels. The trabecular area of ABP/PTH resulted from the greater primary spongiosa which was preserved with the 10 month ABP treatment. PTH induced significant increases in mineralizing surface, mineral appositional rate, and bone formation rate in all the groups. Biomechanical testing of vertebra in compression showed that PTH improved peak load, stiffness and toughness in all groups to a proportionately similar extent compared to 10 month levels. These data showed a surprising ability of the rat skeleton to respond to PTH, despite extensive pretreatment with ABP, EE2, or RA and even when activation frequency was suppressed by more than 90% with ABP before switching to PTH. The mature skeleton of ovariectomized rats remained vigorously responsive to the appositional effects of PTH, regardless of pretreatment status in terms of bone turnover or trabecular bone area.

Disclosures: ***M. Sato****, Eli Lilly & Co. 3.*

1180

The Effect of Aging on the Skeletal Response to Intermittent Treatment with Parathyroid Hormone. E. A. Knopp*[1], B. Sun[1], N. Troiano*[1], K. Wilson*[1], C. Coady*[1], K. Lostritto*[1], C. M. Gundberg[1], M. L. Bouxsein[2], K. Insogna[1]. [1]Yale University, New Haven, CT, USA, [2]Beth Israel Medical Center, Boston, MA, USA.

Although proposed for therapeutic use in the elderly, little is known about the modifying effects of age on the skeletal response to intermittent treatment with PTH. We therefore compared the response to intermittent PTH treatment in aged and mature mice. In each of two identical experiments, 30 18-month old and 30 3-month old male C57BL/6 mice were randomly divided into PTH- or vehicle-treated groups. Treated mice received s.c. injections of h(1-34)PTH at 95 ng/g body weight once daily for 4 weeks. Serial bone density measurements by DEXA demonstrated a time- and PTH-dependent increase in bone density at all skeletal sites. The increase in total body density as compared to vehicle-treated animals was equivalent in aged and mature mice (+6.0% vs. +6.5%, combined data from both experiments). Surprisingly in each experiment, the aged animals demonstrated a greater increase in spinal BMD than their younger counterparts whether expressed as percent increase (+13.6% vs. +5.4%, $p<0.001$) or as an absolute increment in BMD (51×10^{-4} vs. 34×10^{-4} gms/cm^2, $p<0.045$). MicroCT analysis confirmed these findings and demonstrated a greater increase in L5 trabecular bone mass in the PTH-treated aged animals again whether measured by percent increase (+40.1% vs. +19.7%, BV/TV) or absolute increment. By contrast, the mature animals showed a significantly greater increase in femoral BMD when compared to the aged group (8.5% vs. 4.5%, combined DEXA data, $p<0.04$). This was confirmed by pQCT data from the two experiments which showed a 21% increase ($p<0.0002$) in mature adult tibial cortical content vs. a non-significant 5% increase in aged animals. Osteocalcin levels rose more significantly in the aged mice (157% vs. 83%), suggesting a greater sensitivity of osteoblasts to PTH in the aged group. Consistent with this latter finding, initial L-spine histomorphometric data demonstrated a significantly greater increase in NOb/TAR in the aged animals than in the mature ones (414% vs. 241%). The number of alkaline phosphatase positive and Von Kossa positive colonies in cultured marrow were unaffected by PTH treatment in either group. In summary, the trabecular-rich lumbar spine appears to be more responsive to PTH with aging while the response in the more cortically enriched femur declines. Differential effects on osteoblast progenitor recruitment do not seem to be the cellular mechanism underlying these changes. The occurrence of such effects on osteoblast apoptosis is being investigated currently. We conclude that aging differentially effects the regional skeletal response to PTH.

1181

Transfer of *CasR* Deficiency Onto the *GCM2* Null Background Rescues the Perinatal Lethality and Skeletal Abnormalities in *CasR*-Deficient Mice. Q. Tu*[1], M. Pi[1], G. Karsenty[2], L. D. Quarles[1]. [1]Center for Bone and Mineral Disorders, Duke University Medical Center, Durham, NC, USA, [2]Molecular and Human Genetics, Baylor College of Medicine, Houston, TX, USA.

The calicum sensing receptor *(CasR)* plays a predominant role in regulating parathyroid gland function, but its independent function in the skeleton is uncertain. Targeted deletion of *CasR* results in severe hyperparathyroidism resulting from the absence of CasR in the parathyroid glands and in an unexpected impairment of bone and cartilage mineralization resulting from excessive PTH levels and/or the absence of CasR in bone and cartilage. Ascertaining the contribution of excess PTH to the bone phenotype by surgical removal of the parathyroid gland has not been feasible, because of the high perinatal mortality in CasR deficient mice. *Glial cells missing2* (*Gcm2)*-deficient mice that lack parathyroid glands but produce auxiliary PTH in the thymus provide a genetic approach to achieve parathyroid gland ablation in *CasR* deficient mice. We crossed F2 double heterozygotic $Gcm2^{+/-}CasR^{+/-}$ mice to generate double knockout $Gcm2^{-/-}CasR^{-/-}$mice. We compared survival rates, serum calcium and PTH, and bone mineral density (BMD) in $Gcm2^{-/-}CasR^{-/-}$double knockouts, $Gcm2^{-/-}CasR^{+/+}$ double knockout, $Gcm2^{+/+}CasR^{-/-}$ single knockouts, and wild-type ($Gcm2^{+/+}CasR^{+/+}$) littermates. Consistent with previous reports, the mortality rates at 6-weeks in *CasR*-and *GCM2*-deficient mice were 100% and 30%, respectively. Serum calcium (mg/dl) and PTH (pg/ml) were 13.9± 0.8 and 456.98± 69 in 1 week-old *CasR*-deficient mice, compared to 6.3± 0.4 and 17.02± 3.0 in 6-week old *GCM2*-deficient mice, and 8.1± 0.2 and 23.6±4.0 in wild-type mice. The mortality rate (29%), calcium (6.1±0.3), and PTH (11.5+1.3) in $Gcm2^{-/-}CasR^{-/-}$ double knockout mice were not different from *Gcm2*-deficient littermates. Bone ashed weights (% dry wt) and BMD (g/cm^2) also were not different between $Gcm2^{-/-}CasR^{-/-}$, *Gcm2*-deficient, and wild-type mice. These findings indicate that genetic ablation of the parathyroid glands by intercrossing *CasR*- and *Gcm2*-deficient mice rescues the perinatal lethality of *CasR*-deficiency, and prevents the development of hypercalcemia, hyperparathyroidism, and low bone density in *CasR*-deficient mice. Further characterization of the phenotype of $Gcm2^{-/-}CasR^{-/-}$ should provide insights into the extra-parathyroid functions of *CasR*.

1182

Targeted Ablation of FGF-23 Causes Hyperphosphatemia, Increased 1,25-dihydroxyvitamin D Level and Severe Growth Retardation. T. Shimada*[1], M. Kakitani*[1], H. Hasegawa*[1], Y. Yamazaki*[1], A. Ohguma*[1], Y. Takeuchi[2], T. Fujita*[2], S. Fukumoto[3], K. Tomizuka*[1], T. Yamashita[1]. [1]Pharmaceutical Research Labs, KIRIN Brewery Co., Ltd., Takasaki, Japan, [2]Department of Medicine, University of Tokyo School of Medicine, Tokyo, Japan, [3]Department of Laboratory Medicine, University of Tokyo Hospital, Tokyo, Japan.

Previous investigation revealed that transgenic mice for FGF-23 and mice carrying tumor expressing FGF-23 showed hypophosphatemia and low serum 1,25-dihydroxyvitamin [1,25$(OH)_2$D]. These results indicated that excess actions of FGF-23 decrease serum phosphate and 1,25$(OH)_2$D levels. However, it has been unclear whether FGF-23 has any physiological role in mineral metabolism. In the present study, we generated FGF-23 null (-/-) mice to address this issue. A 5.2 kb fragment containing 5'-untranslated region and 1.8 kb fragment encoding a part of exon 1 and the following intron of FGF-23 gene were isolated from C57BL/6 genomic BAC library and subcloned into 5' and 3' of a neomycin resistance gene, respectively, to construct a targeting vector. Using this targeting vector, ES clones carrying a targeted allele were selected and FGF-23 (+/-) mice were established from them. The phenotypes and biochemical parameters of FGF-23 (+/-) mice were indistinguishable from those of wild-type mice. When FGF-23 (+/-) mice were interbred, FGF-23 (-/-) mice were born according to Mendelian frequency, indicating that ablation of FGF-23 did not cause embryonic lethality. Body size of FGF-23 (-/-) mice was not different from that of wild-types or heterozygotes at birth. However, remarkable growth retardation in FGF-23 (-/-) mice was observed at 10 days and thereafter. Body weight of FGF-23 (-/-) mice was significantly less than that of heterozygotes both at 10 days and 9 weeks (10 days: 3.8 +/- 0.3 vs. 5.6 +/- 0.3 g, $p < 0.01$, 9 weeks: 6.5 +/- 0.5 vs. 20.7 +/- 0.4 g, $p < 0.001$). Life span of FGF-23 (-/-) mice was short and the survival of them more than 12 weeks has never been observed. Serum phosphate of FGF-23 (-/-) mice was significantly increased at 10 days compared to that of heterozygotes (16.9 +/- 2.6 vs. 10.8 +/- 0.2 mg/dL, $p < 0.001$), but serum calcium was not different (10.5 +/- 0.2 vs. 10.1 +/- 0.2 mg/dL). In contrast, serum phosphate, calcium and 1,25$(OH)_2$D of FGF-23 (-/-) mice were elevated at 9 weeks compared to those of heterozygotes (Pi: 14.7 +/- 0.5 vs. 8.58 +/- 0.42, $P<0.001$; Ca: 10.7 +/- 0.3 vs. 8.9 +/- 0.2, $p < 0.01$; 1,25$(OH)_2$D: 378 vs. 129 pg/ml). These results indicate that FGF-23 is not necessary during fetal development, but indispensable for normal growth after birth. Furthermore, FGF-23 plays physiological roles in maintaining serum phosphate, calcium and 1,25$(OH)_2$D levels.

1183

Effects of Secreted Frizzled-Related Protein (sFRP)-3 on Osteoblasts In Vitro: sFRP-3 Is a Stimulator of Osteoblast Differentiation. Y. Chung, D. J. Baylink, A. K. Srivastava, Y. Amaar, Y. Kasukawa, S. Mohan. J.L. Pettis VAMC, Loma Linda, CA, USA.

The Wnt gene family represents a large and diverse group of signaling molecules involved in the proliferation and differentiation of a variety of cell types. The involvement of Wnt signaling in regulating bone formation is evident from recent studies demonstrating that mutations in LDL-receptor-related protein 5 gene influences bone accretion via alterations in Wnt-mediated signaling. Based on the findings that sFRP family members bind Wnt proteins and antagonize Wnt signaling, and that activation of Wnt signaling stimulates osteoblast differentiation, we proposed that sFRP is an inhibitor of osteoblast differentiation. To test this hypothesis, we evaluated the effect of sFRP-3 (Frzb1), originally identified in cartilage, on osteoblast proliferation and differentiation. Serum-free cultures of MC3T3-E1 mouse osteoblasts were incubated with various doses of recombinant sFRP-3 (1, 10, 100, 1000 pM) and cell number determined by alamarBlue assay. sFRP-3 inhibited cell number in a dose-dependent manner with a maximal inhibition of 53% ($P<0.001$) at 1 nM dose. At a dose of 10 pM, sFRP-3 caused a 33% inhibition ($P<0.001$). sFRP-3 inhibition of MC3T3-E1 cell proliferation is not specific to this cell type since sFRP-3 also decreased cell number significantly in mouse bone marrow stromal cells. To evaluate the effects of sFRP-3 on osteoblast differentiation, mouse bone marrow stromal cells or MC3T-3 E1 cells were incubated with varying doses of sFRP-3 for 6 days and its effect on ALP activity and osteocalcin production determined under serum-free conditions. Surprisingly, sFRP-3 caused a dose-dependent increase in ALP specific activity with a maximal increase of 2-fold over control (79.7±12 vs 38.1±6.6 mU/mg protein, $P<0.001$) at 100 pM dose. This increase in ALP activity was higher than that obtained with a combination of 1 ng/ml TGFβ and 10^{-8}M 1,25 D (62±11 mU/mg protein) under identical culture conditions. Consistent with the ALP data, osteocalcin level, which was undetectable in the culture media of control cultures (<1 ng/ml), was increased to 15±5 and 24±8 ng/ml respectively at 10 and 100 pM doses of sFRP-3. Summary: 1) sFRP-3 inhibits osteoblast cell proliferation. 2) sFRP-3 stimulates ALP activity and osteocalcin production in osteoblasts. 3) sFRP-3 is active at extremely low doses (1-10 pM). Conclusions: 1) Our findings demonstrate for the first time that sFRP-3 is a potent stimulator of osteoblast differentiation. 2) Based on these and other findings, the concept that sFRP acts exclusively to inhibit Wnt is probably oversimplified; instead, we propose that sFRP-3 may act as a novel ligand for an as-yet unidentified receptor in osteoblasts.

1184

In Vivo **Expression of a Dominant Negative Cadherin Increases Adipogenesis and Delays Achievement of Peak Bone Mass.** C. Castro[1], C. Shin[2], S. Sheikh*[1], S. Cheng[1], R. Civitelli[1]. [1]Div. Bone and Mineral Diseases, Washington University, St. Louis, MO, USA, [2]Internal Medicine, Seoul National University, Seoul, Republic of Korea.

A null mutation of cadherin-11 or single allele deletion of Ncad cause mildly decreased bone mass, suggesting overlapping roles of these two cell adhesion molecules in skeletal development. To overcome the redundancy of cadherins and understand their biologic function in bone, we generated a mouse strain expressing a truncated Ncad mutant derived from an in-frame deletion of most of the extracellular domain of *Xenopus* Ncad, driven by the mouse OG2 promoter (OG2-NCadΔC), which functions as a dominant negative cadherin. The transgene was selectively expressed in calvarial and bone marrow stromal cells, its abundance increasing with osteoblast differentiation and upon BMP-2 stimulation. Alkaline phosphatase activity was reduced in cells isolated from newborn calvaria of transgenic mice compared to wild type controls, although matrix mineralization was similar after 4 weeks in the presence of ascorbic acid and β-glycerophosphate. Total body bone mineral density (BMD) and percent body fat (%BF) were monitored monthly by DEXA. During the first 3 months of life – when bone mass accumulates – BMD was reduced in transgenic animals compared to wild type littermates, with maximal difference of 10% at age 3 months (51.54±2.01mg/cm^2 vs. 57.3±2.45mg/cm^2; $p<0.001$; respectively). By contrast, %BF was 27% higher in OG2-NCadΔC than in wild type mice (29±5.7% vs. 22.8±2.3%, respectively; $p=0.011$). During this time, body weight and food intake were also higher in mutant vs. wild type animals. At age 4 months and higher, BMD, %BF, and body weights were no longer different between mutant and normal animals. There were no gender differences at any time. At the cellular level, the number of colony forming unit-adipocytes (CFU-AD) in bone marrow cells from OG2-NCadΔC mice was 3-fold higher compared to wild type cultures (7.9±1.5 vs. 1.6±0.6 CFU-AD/10^6 cells, respectively; $p<0.01$) after induction by hydrocortisone and indometacin. Accordingly, adipsin and PPAR-γ mRNA abundance – assessed by real-time RT-PCR - were increased in OG2-NCadΔC bone marrow cultures compared to wild type controls (2.3- and 10-fold, respectively), whereas cbfa1 mRNA was decreased 40%. These results suggest that *in vivo* disruption of cadherin function hinders full osteoblast differentiation, thus favoring, indirectly, bone marrow progenitor cell commitment to the alternative adipogenic lineage, and resulting in delayed acquisition of maximal bone mass. Since NcadΔC binds β-catenin, depletion of transcriptionally active β-catenin pools may cause a shift from osteogenesis to adipogenesis in these animals.

1185

Use of GFP-Marked Primary Osteoblast Culture to Assess the Effect of PTH on the Osteoprogenitor Lineage. Y. H. Wang, K. M. Buhl*, D. W. Rowe. University of Connecticut Health Center, Farmington, CT, USA.

Transgenic mice harboring green fluorescent protein (GFP) marker genes driven by various promoter fragments can be used to identify the level of osteoblastic differentiation in real time in primary bone cell culture. This study was initiated to demonstrate the utility of these reagents for studying an agent that alters osteoblastic differentiation, in this case PTH. An inverted fluorescent microscopic workstation has been assembled that allows 63% of a 35 mm culture well to be reproducibly imaged over time from a series of 25 adjacent pictures that are tiled into a single image of the plate. Three fluorescent markers were used: pOBCol3.6GFP which is activated in preosteoblastic cells; pOBCol2.3GFP which is restricted to mineralized nodules; and xylenol orange (XO) which stains the mineralized nodules. The tempo and staining pattern was established at multiple time points in mouse calvarial osteoblast cultures. Preosteoblastic cells were evident at day 7 and markers of osteoblastic differentiation (accentuated expression of pOBCol3.6GFP, activation of pOBCol2.3GFP and XO staining) were evident by day 14 and became more intense by day 21. Continuous exposure to 25 nM PTH blocked expression of osteoblastic differentiation resulting in a cell population enriched for preosteoblastic cells. Addition of PTH for day 1-7 of culture delayed the appearance of osteoblastic markers but ultimately resulted in a culture with a greater number of osteoblastic nodules, while PTH given between day 7-14 delayed osteoblastic differentiation that had not fully recovered by day 21. In contrast, exposure of the culture to PTH between day 14-21 caused the pOBCol2.3GFP-positive cells to revert from a strongly fluorescent cuboidal cell to one with weaker fluorescence and more fibroblastic shape. pOBCol2.3 cells with these characteristic have not been previously appreciated and may represent dedifferentiated osteoblastic cells. Unlike pOBCol2.3, the high osteoblastic-associated expression in pOBCol3.6 cells was not lost while low fibroblastic-associated expression increased in the PTH treated cells. The analysis suggests that PTH acts on early progenitor cells to expand their number and maintain their ability to differentiate when PTH is removed, while the mature osteoblastic cells dedifferentiate into cells whose differentiation capacity is yet to be characterized. Thus the model has the sensitivity to reveal subtle alterations of the differentiation pathway, and when combined with FACS sorting, to define the molecular profile of a PTH directed cell subpopulation and their potential for subsequent osteoblastic differentiation.

1186

Use of a Col1a1-GFP Retroviral Marker System to Monitor In Vitro Differentiation of ES Cells into Osteoblastic Cells. U. Chung[1], M. Stover*[2], I. Kalajzic*[2], D. W. Rowe[2], A. C. Lichtler[2]. [1]Endocrine Unit, Massachusetts General Hospital, Boston, MA, USA, [2]Department of Genetics and Developmental Biology, University of Connecticut Health Center, Farmington, CT, USA.

Embryonic stem (ES) cells are pluripotent stem cells that can contribute to all cell types of the embryo. Recently, there has been intense research on development and tissue engineering of ES cells, since they have been shown to differentiate in vitro into many cell types, and they can proliferate almost indefinitely. Although they were shown to differentiate into osteoblastic cells in vitro, the efficiency and duration of the differentiation protocol is still not good enough to replace or substantially complement in vivo experiments or to be applied to clinical settings. To develop better protocols, it is necessary to have an easy and precise monitoring system for osteoblastic differentiation. For this purpose, a retroviral vector was constructed, which contains a 2.3 kb Col1a1 promoter driving green fluorescent protein (GFP) and the neomycin resistance gene. The 2.3 kb Col1a1 promoter was previously shown to confer specific expression in osteoblasts. The LTR of this retrovector was designed to self-inactivate upon integration, so that the viral promoter would not interfere with the inserted promoter. The vector was then packaged in a VSV-G pseudotyping sys-

tem. Wild-type ES cells were infected with the retrovirus containing the vector. Infected cells were selected, and single clones were isolated. Infected ES cells were then differentiated into osteoblastic cells by allowing formation of embryoid bodies, then culturing them in medium containing ascorbic acid, dexamethasone, and b-glycerophosphate. As bone nodules form, cuboidal cells in the nodules that accumulate calcium matrix start to show fluorescence. The nodules were positive by von Kossa stain as well as Alizarin Red S. Spindle-shaped cells surrounding the nodules show weaker fluorescence, suggesting that they may be osteoblastic precursors. On the other hand, fluorescence was not detected in other cell types such as trophoplastic, adipocytic and chondrocytic cells. Since it detects fluorescence, live cells can be monitored over time repeatedly, and a great number of samples can be tested easily and rapidly. We think that this method of monitoring differentiation is useful in developing and refining the differentiation protocol, and we are currently optimizing osteoblast differentiation by changing all parameters in the existent protocols. If successful, the establishment of the protocol may facilitate some aspects of in vitro studies of osteoblast differentiation as well as help open up possibilities for use of ES cells in tissue engineering of bone.

1187

A Novel Bone-specific Secreted Protein Which Regulates Osteoblast Differentiation. C. Lanctot, M. Bessette*, M. Gaumond*, R. Gingras*, É. Godin*, P. Moffatt*, P. Salois*, K. Sellin*, N. St-Amant*, G. Thomas. Phenogene Therapeutics, Montreal, PQ, Canada.

Screening of a mouse embryonic calvarial cDNA library using a signal trap strategy has identified a novel secreted protein referred to as PGTI0306. The protein is synthesized as a 130 amino acid precursor encoded by a 1280bp mRNA. The protein is well conserved across species (mouse to human 74.6%, mouse to rat 90.2%), but shares no homology with known genes. However, 2 conserved dibasic cleavage sites present the possibility that the protein is synthesized as a prohormone-like precursor and downstream proteolytic processing maybe necessary for activation. A cleavable signal peptide is located at the N-terminus of the molecule. Expression of this gene is highly specific. Northern blot analysis of 52 fetal and adult tissues revealed detectable expression only in bone tissues. A different sized mRNA species was evident in adult rat spleen, possibly arising through differential splicing. Interestingly, expression of PTGI0306 decreased with age in both long bones and calvaria. In situ hybridization on sections of developing embryos demonstrated expression in bones to be confined to the inner layer of the periosteum, co-localising with a subset of Cbfa1-positive cells that did not express osteocalcin. Expression of PGTI0306 was also demonstrated in primary rat osteoblastic cultures where the gene was down-regulated by 1,25 dihydroxyvitamin D3 treatment. The secretory nature of this protein was established via immunofluorescence and Western blotting utilising a specific antibody. Analysis was performed on HEK293 cells transiently transfected with an expression vector for PGTI0306. The bulk of the protein was found in the culture medium. Intracellularly, the protein was concentrated in the Golgi apparatus. Treatment of primary rat osteoblasts with conditioned media from transfected HEK293 cells resulted in an inhibition of osteoblast differentiation as indicated by reduced alkaline phosphatase levels and osteocalcin expression. The expression pattern and functional effects of PGTI0306 in vitro is suggestive of an autocrine/paracrine role for this prohormone-like molecule at an early stage in osteoblast differentiation, possibly to maintain the pool of osteoblast precursors.

1188

The Effects of Modulating Osteoactivin Function on Osteoblast Differentiation. A. Selim*[1], S. M. Abdelmagid*[1], S. L. Smock*[2], T. A. Owen[2], S. N. Popoff[1], F. F. Safadi[1]. [1]Anatomy and Cell Biology, Temple University School of Medicine, Philadelphia, PA, USA, [2]Cardiovascular and Metabolic Diseases, Pfizer Global R&D, Groton, CT, USA.

In a study examining differential gene expression in bone from normal and *osteopetrotic* (*op*) rats, we isolated a novel cDNA, termed osteoactivin (rOA), that was over-expressed in *op* when compared to normal bone. Subsequent *in situ* hybridization and immunohistochemical localization demonstrated that rOA mRNA and protein are expressed by osteoblasts. In primary osteoblast cultures, rOA mRNA levels exhibited a temporal pattern of expression being expressed at highest levels during the later stages of matrix maturation and mineralization. Furthermore, the protein is synthesized by osteoblasts and secreted into the medium. In this study we attempted to block rOA expression and function using an rOA anti-sense oligonucleotide or an anti-rOA antibody. Using an rOA anti-sense oligonucleotide, we were able to block rOA expression in primary osteoblast cultures resulting in decreased alkaline phosphatase activity, osteocalcin production, nodule formation and matrix mineralization. Using the Chariot protein transfection reagent as a vehicle to deliver the anti-rOA antibody inside the cells, we demonstrated that anti-rOA antibody treatment also showed a dose-dependent inhibition of alkaline phosphatase activity, osteocalcin production, nodule formation and mineralization. Conversely, a CMV-rOA construct was generated and used to examine the effect of rOA over-expression on osteoblast development and function in MC3T3-E1 osteoblast-like cells. rOA over-expression in cells transiently transfected with CMV-rOA increased nodule formation, alkaline phosphatase activity, osteocalcin production and matrix mineralization compared to cultures following transfection with an empty vector or treated with transfection reagent alone. These data suggest that rOA plays a major role in the regulation of osteoblast differentiation and function.

Disclosures: ***A. Selim****, Pfizer, Inc. 2.*

1189

Molecular Mechanisms by which Osteoblast Differentiation Is Dependent on Microtubule Assembly. D. Chen, G. Rossini*, M. Zhao, M. Qiao*, G. Gutierrez, G. R. Mundy. Molecular Medicine, University of Texas Health Science Center at San Antonio, San Antonio, TX, USA.

Osteoblast differentiation and bone formation are regulated by a number of important signaling molecules involved in BMP/Smad and wnt/β-catenin signal transduction pathways. Smad1 and β-catenin bind to and form a complex with microtubules and upon dissociation translocate from the cytoplasm to the nucleus where they are responsible for transactivation of genes involved in osteoblast differentiation. To determine if the state of microtubule assembly may regulate osteoblast differentiation by controlling nuclear translocation of these transactivating factors, we examined whether inhibition of microtubule assembly activates these signaling pathways and induces bone formation. A series of microtubule inhibitors were examined in BMP/Smad1 (12xSBE-OC-luc) and wnt/β-catenin (11xTCF-TATA-luc) reporter assays. Inhibitors of microtubule formation (depolymerization), namely nocodazole, colchicine, TN-16 and vincristine, stimulated luciferase activity of these reporters in myoblast/osteoblast precursor C2C12 cells and osteoblast precursor 2T3 cells. These compounds bind to both the colchicines and vinca sites on microtubules. In contrast, the microtubule stabilizers taxol and epothilone had no effects on these reporter genes. We then examined the effects of the microtubule inhibitor TN-16 on nuclear translocation of Smad1 and β-catenin by immunostaining. We found that TN-16 increased nuclear translocation of both proteins. To examine the effects of these microtubule inhibitors on bone formation *in vivo*, we injected 0.1-10 mg/kg/day for 2 days of these inhibitors into subcutaneous tissue over calvarie of mice and found that all microtubule depolymerizers, that stimulated luciferase activity in the reporter assays described above, also stimulated new bone formation in a dose-dependent manner. Also consistent with the reporter assays, microtubule stabilizers had no effects on bone formation. In separate experiments, systemic administration of TN-16 into 3-month old intact Sprague-Dawley rats (1-12 mg/kg/day for 5 days) or 2-month-old intact mice (2-8 mg/kg/day for only 2 days) substantially increased bone mineral density (6-12%), bone volume (26-46%) and bone formation rates (1.8-2.7 fold) in a dose-dependent manner when examined one month later. These results demonstrate that microtubule inhibitors have anabolic effect on bone formation and this effect is at least in part through activating BMP/Smad and wnt/β-catenin signaling pathways and facilitating nuclear translocation of critical signaling molecules.

Disclosures: ***D. Chen****, OsteoScreen Ltd 1, 3.*

1190

Nongenotropic Regulation of CREB-, C/EBPβ-, as well as Elk-1- and AP-1 - Mediated Transcription by Estrogens: Downstream Effects of ERK and JNK Kinase Modulation Required for Anti-apoptosis. S. Kousteni, L. Han, L. I. Plotkin, T. Bellido, C. A. O'Brien, R. L. Jilka, S. C. Manolagas. Division of Endocrinology and Metabolism, Center for Osteoporosis & Metabolic Bone Diseases, Central Arkansas Veterans Healthcare System, U/sity of Arkansas for Medical Sciences, Little Rock, AR, USA.

Estrogens or androgens activate a Src/Shc/ERK signaling cascade via a non-genotropic action of their classical receptors. It was shown previously that this action leads to activation of the transcription factor Elk-1 which in turn binds to the serum response element (SRE) present in the promoter of many genes and rapidly induces their transcription; and that kinase-initiated transcriptional events are indispensable for the anti-apoptotic action of estrogen. In the studies reported here, we searched for the signaling pathway that leads to AP-1 downregulation and investigated the effects of AP-1-dependent transription, as well as the contribution of CREB or C/EBPβ, in the anti-apoptotic effects of sex steroids. To this end, HeLa cells were transiently transfected with either ERα or AR, together with a reporter construct in which binding of c-jun/c-fos to the AP-1 site drives the expression of secreted human alkaline phosphatase (SEAP) and with or without a dominant negative (dn) JNK1. Fifteen-minute exposure to 10^{-8} M 17β-estradiol (E_2) or dihydrotestosterone (DHT), followed by removal of the steroid from the culture media, downregulated AP-1-SEAP activity. This effect was blocked by the dn JNK1, indicating that sex steroids decrease AP-1-dependent transcription via the JNK signaling pathway. In agreement with this finding, in ERα transfected HeLa cells, expression of dn constructs for JNK1 or AP-1 abolished the anti-apoptotic effect of E_2. This effect was also abrogated by a dn CREB or a dn C/EBPβ but not dn mutants of STAT3, c-fos, or Cbfa-1/Runx2. The dn C/EBPβ selectively blocks the transcriptional activity of C/EBPβ without interfering with its phosphorylation by ERKs or its ability to form complexes with procaspases 1 and 8. The effects of the dn mutants were reproduced in osteocytic MLO-Y4 cells. Elucidation of the effect of estrogens or androgens on the regulation of not only Elk-1 but also CREB and C/EBPβ, through Src/Shc/ERK, raises the possibility that these are only few of probably several transcription factors regulated by the nongenotropic, sex nonspecific, mechanism of gene transcription described herein. Hence, the existence of kinase-initiated routes by which the ER or AR can exert transcriptional control provides the means of regulating a range of genes much wider than the ones that are regulated by the classical transcriptional mechanisms that depend on protein/DNA or protein/protein interactions.

1191

The Anabolic, but Not Anti-Resorptive, Effect of Mevastatin In Vivo Is Dependent on Endothelial Nitric Oxide Synthase. R. J. van't Hof, K. J. Armour*, M. H. Helfrich, S. H. Ralston, K. E. Armour*, C. E. Clarkin*, M. J. Rogers. Medicine & Therapeutics, University of Aberdeen, Aberdeen, United Kingdom.

Statins have both anti-resorptive and bone anabolic effects in vitro and in vivo. Statins inhibit resorption by preventing the prenylation of small GTPases in osteoclasts. The mechanisms underling the anabolic effect are less clear. However, the prenylated GTPase Rho can negatively regulate eNOS levels in endothelial cells, whilst eNOS itself is required for osteoblast differentiation and function. It is therefore possible that statins affect osteoblasts in vivo by enhancing eNOS function due to inhibition of Rho prenylation. We examined the importance of eNOS for the anti-resorptive and anabolic effects of mevastatin using mice with targeted inactivation of eNOS. 10mg/kg mevastatin or PBS was injected twice daily over the calvaria of four-day old wild-type or eNOS-null mice for 5 days. One day or 11 days after the final injection, (i.e. on day 6 or day 16) the mice were euthanised and the calvariae dissected for histomorphometric and pQCT analysis. In wild-type mice 1 day after the final injection of mevastatin, osteoclast number and erosion surface were decreased but calvarial width and bone volume were unchanged, suggesting anti-resorptive effects on osteoclasts. However, 11 days after the final injection we observed an increase in bone remodelling, associated with significantly increased osteoclast number, increased calvarial width and bone volume, and the presence of large medullary spaces. pQCT analysis also confirmed a significant increase in bone area and mineral content in the calvariae of wild-type mice. This apparent anabolic effect on day 16 was blunted in eNOS-null mice. Treatment with mevastatin did cause an increase in erosion surface and the appearance of medullary spaces, but calvarial width and bone volume were not significantly altered. Mevastatin treatment did not affect the number of calvarial osteoblasts in wild-type or eNOS-null mice. In calvarial organ cultures in vitro, 10nM or more mevastatin significantly inhibited resorption (45Ca release) in wild-type and eNOS-null calvariae. Histomorphometric analysis also demonstrated that 1μM mevastatin decreased osteoclast number and erosion surface in both wild-type and eNOS-null calvariae. Together, these observations demonstrate that the anti-resorptive effect of mevastatin is not dependent on eNOS. However, the apparent anabolic effect and increase in calvarial width in vivo is eNOS-dependent. It remains to be determined whether the anabolic effect is due to direct stimulatory effects of mevastatin on osteoblast activity or to an eNOS-dependent response following withdrawal of mevastatin treatment.

1192

Id1/Id3 Double Gene Knockout Reasults in Defects in Angeogenesis in Fracture Callus and Suture Development. Y. Maeda*[1], R. Benezra*[2], M. Noda*[1]. [1]Dept of Molecular Pharmacology, Tokyo Medical and Dental University, Tokyo, Japan, [2]Cell Biology, Memorial Sloan -Kettering Cancer Center, New York, NY, USA.

Angiogenesis plays an important role during bone development and regeneration. Id proteins belong to helix-loop-helix transcription factors and expression of Id genes in osteoblasts is under the control of calciotropic agents such as BMP and vitaminD. Recently, Id1 and Id3 were demonstrated to be required for tumor angiogenesis. However, the function of Id1 and Id3 during bone formation in vivo has not yet been elucidated. The purpose of this paper is to elucidate the role of Id1 and Id3 in regulation of bone metabolism. We first examined fracture healing which requires angiogenesis. Histological examination of the callus formed after the fractures maded in the ribs of wild type mice revealed abundant angiogenesis. In contrast, Id1-/+Id3-/- double knockout mice revealed suppression of such angiogenesis in the fracture callus. Quantification of CD31 positive vessels in the tissue sections revealed more than two-fold reduction in the number of vasculatures ($p<0.05$). This was associated with delayed remodeling process in the callus in the Id1-/+Id3-/- double knockout mice including new bone formation compared to the fractrue callus in wild type mice. We further examined calvarial bones to obtain insights into the Id function in bone cells. The calvarial sutures were clearly observed on the soft X-ray films in wild type mice. In contrast, such sutures in Id1-/+Id3-/-double knockout mice were unclear and almost fused in part compared with those in wild type mice. Quantification of the suture width revealed more than 50% reduction in Id1-/+Id3-/- double knockout mice compared to wild type. To obtain cellular basis for the mechanism of such defects, we examined proliferation and differentiation activities of the primary calvaria-derived osteoblasts. Proliferation was significantly reduced in Id1-/+Id3-/- double knockout osteoblasts compared to wild type cells. Alkaline phsphosphatase activity induced by BMP treatment was also significantly reduced in osteoblasts derived from Id1-/+Id3-/- double knockout mice compared to wild type cells. These results indicated that Id1 and Id3 are required for angiogenesis during fracture healing and the development of calvarial sutures.

1193

MyoD/Myf5 Null Mice Cannot Move actively *in utero* and Have Thin Weak Long Bones and No Rib Development. T. M. Skerry, N. M. Peet*. Veterinary Basic Sciences, Royal Veterinary College, London, United Kingdom.

Mechanical loading influences skeletal mass profoundly and is more effective in early than adult life. This suggests that modelling is more influenced by loading than is remodelling, and raises the question: how early in skeletal development do mechanical events influence bone development? To explore this question we bred mice lacking genes for muscle proteins MyoD and Myf5, hypothesising that the consequent demonstrated lack of functional skeletal muscle would prevent active movement in utero and affect bone development. While MyoD null mice are apparently normal, Myf5 nulls are poorly viable, so we bred double heterozygotes and crossed those to produce double knockouts (KOs). The predicted ratio of these offspring to heterozygotes and wild types should have been 1:4, but was ~1:40. There were striking differences between knockout and wild type (WT) pups. The long bones of the KOs were smooth, featureless and straight in contrast to the curved bones in the WT, which had recognisably adult proportion and shape. Specifically traction epiphyses where major muscles attached were absent or very much reduced. QCT analysis revealed that the shafts of the bones of KOs had cortices that were thinner (by 19%) than WT and less mineralized (by 24%)($p<0.001$). However, the most remarkable and striking difference between the KO and WT animals was that the KOs lacked ribs and the middle and medial parts of the clavicles. This was not due to a lack of thoracic contents, which were present. Osteoblasts isolated from both KO and WT calvariae were cultured on plastic strips and subjected to mechanical loading in vitro (1500 microstrain of bending at 1Hz) and showed identical responses as determined by NO release and proliferation. These data show that the KO animal's osteoblasts are not incapable of responding to mechanical stimuli, but that the absence of active movement in utero has profound consequences on the shape, mass and density and therefore strength of the bones. Since active movement in utero in humans can be affected by speech or music, there may be means by which it is possible to obtain high bone mass in babies at birth. The ratio of double null offspring of double heterozygote matings suggests that deletions in the KOs lead to a significant loss of viability, perhaps because of a problem with implantation or early embryonic mortality. The unexpected and remarkable lack of rib development of the KOs implies that some areas of the skeleton rely crucially on the expression of specific genes that have only lesser and indirect consequences on the rest of it. Should similar patterning be specified for vertebral trabeculae or the femoral neck, this would provide a means to target anabolic modalities in a radically new way.

1194

Biglycan Deficiency Interferes with Ovariectomy-induced Bone Loss. K. L. Nielsen*[1], M. R. Allen*[2], S. A. Bloomfield*[2], I. A. Timm*[3], X. D. Chen*[4], M. F. Young[4], A. Heegaard[1]. [1]Nordic Bioscience A/S, Herlev, Denmark, [2]Department of Health and Kinesiology, Texas A&M University, College Station, TX, USA, [3]CCBR, Ballerup, Denmark, [4]Craniofacial & Skeletal Disease Branch, NIDCR, Bethesda, MD, USA.

Biglycan is a small extracellular matrix proteoglycan enriched in skeletal tissues. Biglycan deficient mice suffer from osteopenia with decreased trabecular bone mass and bone strength as compared to wild type (wt) mice. The osteopenic phenotype has been shown to involve defects in the bone marrow stromal cells and in bone formation. The purpose of this study was to investigate the effect of estrogen depletion (ovariectomy) on the bone phenotype of the biglycan deficient mice. The ovx or sham operations were performed on 21 weeks old mice divided into four groups: wt sham (n=7), wt ovx (n= 9), biglycan deficient sham (n= 10) and biglycan deficient ovx (n=10). Six and two days prior to sacrifice the mice were injected with calcein and tetracyclin, respectively. The mice were sacrificed 4 weeks post surgery. Bone mass and bone turnover were analysed by periferal quantitative computed tomography (pQCT), biochemical markers, and histomorphometry. The results revealed that the biglycan deficient mice were resistant to the ovariectomy induced trabecular bone loss at the proximal tibia, and also did not show an increase in serum osteocalcin levels in response to ovx. The wild type mice responded as expected with an ovx induced bone loss and increased bone turnover. Similar, but less pronounced results were also found when using younger mice (6-8 weeks old). Analyses of the bone resorption marker deoxypyridinoline in the urine showed a delayed, but eventually equally strong induction in response to ovx for the biglycan deficient mice as compared to the wild type mice. These data support the previous findings indicating that biglycan deficiency leads to a defective bone formation, and show that even a strong stimulus such as estrogen deficiency cannot overcome this. Furthermore, we show that biglycan deficiency protects against increased bone turnover and bone loss in response to estrogen deficiency. Taken together these data support the concept that biglycan has dual roles in bone where it may modulate both formation and resorption ultimatively influencing the bone turnover process.

1195

Absence of TACE, but not of ADAM-9 or 15, Prevents the Formation of the Primitive Marrow Cavity that Is Required for the Development of Long Bones. P. Boissy*[1], T. R. Lenhard*[1], T. Kirkegaard*[1], C. P. Blobel*[2], J. Peschon*[3], R. A. Black*[3], C. Christiansen[4], J. M. Delaisse[1], M. C. Ovejero*[1]. [1]Nordic Bioscience A/S, Herlev, Denmark, [2]Sloan-Kettering Institute, New-York, NY, USA, [3]Immunex Corp., Seattle, WA, USA, [4]CCBR, Ballerup, Denmark.

ADAMs (A Disintegrin And Metalloprotease domain) belong to a rapidly growing family of membrane-anchored cell surface proteinases, and they have been shown to modulate proteolysis, cell adhesion, cell fusion and signalling in a variety of tissues. Some ADAMs have been previously detected in bone cells. There is, however, little information on the actual function of ADAMs in bone physiology. In order to address this question, we investigated developing metatarsals of mouse embryos that were made deficient or not for a specific ADAM. We focused on the developmental stage where the primitive marrow cavity is about to be formed, because it is likely to give information on basic events of bone development like osteoclast (OC) differentiation, migration and resorption, as well as angiogenesis and ossification of cartilage. We found that the absence of ADAM 9 and 15 did not affect the metatarsal development, whereas in ADAM 17 (TACE) knockout bones, migration of OCs into the core of the diaphysis was impaired, thereby impeding the formation of the marrow cavity. Because TACE has been implicated in shedding of members of the TNF family including RANKL, and because RANKL is important for OC recruitment, we performed immunohistochemistry of RANKL in developing metatarsals. The signal was found at a very high concentration at the interface between the periosteum and the osteoid of the bone collar, i.e. exactly at the site of OC differentiation. We could however not relate this signal to TACE activity. Next, we investigated systematically in which bone cells

ADAM 9, 15, 17, and others are expressed by using northern blot (NB) and RT- PCR on both mouse and rabbit bone cells and tissues. NB was performed on 1-day rabbit long bones which permit a high purification of each bone cell type, and showed that ADAM 9 was expressed by both OCs and osteoblasts whereas ADAM 17 was restricted to the osteoblast population. By RT-PCR on OC progenitor and osteoblastic cell lines (MOCP-5 and MC-3T3, respectively) as well as on primary rabbit OCs, we have found ADAM 1, 6, 8, 9, 12, 15, 17, 19 and TS-1. NB was performed on RNA prepared from E18-mouse calvaria, which exhibit a strong remodeling activity at this stage. mRNAs of ADAM 8, 9, 12, 15, 17, 19 and TS-1 were found in this tissue. From this study we couldn't show any essential role of ADAM 9 and 15 in bone. In contrast, TACE proves to be indispensable for OC recruitment into the developing marrow cavity of long bones.

1196

Transcriptional Regulation of Osteopontin Production by TGF-beta in Breast Cancer Cells: Implications in Metastasis and Tumorigenicity. N. Hashimoto, T. Yoneda. Div Endocrinol, Univ of Texas Hlth Sci Ctr, San Antonio, TX, USA.

Osteopontin (OPN), a secreted phosphoglycoprotein, is found to be expressed in many of human primary breast cancers, indicating that breast cancer cells produce OPN. Since OPN has been implicated in tumorigenesis and metastasis in a variety of cancers, elucidation of the mechanism by which OPN production is regulated in breast cancer cells is important. Here we studied this by examining the effects of TGFb, a well-known stimulator of OPN production, in the 4T1 mouse mammary cancer cells which constitutively produced large amounts of OPN. RT-PCR analysis and luciferase reporter assay showed that TGFb increased OPN mRNA expression and OPN gene promoter activity in 4T1 cells, respectively. Of note, Smad6 and Smad7, which are natural antagonists of the TGFb signaling molecule Smad, inhibited the TGFb-stimulated OPN promoter activity and TGFb failed to activate the OPN promoter lacking the Smad-binding element (SBE). Moreover, a homeobox gene Hoxa-9, which is known to bind to the Hox-binding element (HBE) in the OPN promoter and work as a repressor, inhibited TGFb-stimulated OPN promoter activity. In addition to 4T1 cells, we also found that TGFb stimulated OPN mRNA expression in the MDA-435, MCF-7 and MDA-231 human breast cancer cells. Since elevated plasma levels of OPN has been correlated with increased distant metastases in breast cancer patients, we next studied the role of OPN in the metastasis of 4T1 cells which spontaneously spread to bone and lung following orthotopic inoculation in the mammary fat pad in syngeneic female Balb/c mice. To approach this, 4T1 cells were stably transfected with a firefly luciferase gene for quantification of the tumor burden in lung and with an anti-sense OPN gene (4T1/luc.ASOPN cells). The 4T1/luc.ASOPN cells showed reduced OPN production and anchorage-independent growth in soft agar. These cells exhibited diminished frequency of bone metastases and histological examination showed reduced metastatic tumor burden in bone compared with empty vector-transfected 4T1/luc cells. Lung metastases determined by luciferase activity were also decreased. Tumor formation at the orthotopic site was also reduced. Consistent with these results, a neutralizing antibody to OPN inhibited the colony formation of 4T1/luc cells in soft agar and tumor formation at the orthotopic site. In conclusion, our results suggest that OPN production is regulated by TGFb at a transcriptional level in breast cancer cells and that OPN plays a critical role in controlling the distant metastasis and tumorigenicity of breast cancer. Thus, suppression of OPN production is a potential new adjuvant therapy for OPN-positive breast cancers.

1197

Loss of Function of Matrix Metalloproteinase-13 (MMP-13) Affects Collagen Accumulation and Bone Formation. M. Inada[1], Y. Wang[1], M. H. Byrne*[1], C. Miyaura[2], S. M. Krane[1]. [1]Department of Medicine, Harvard Medical School, Mass General Hospital, Boston, MA, USA, [2]Biochemistry, Tokyo University of Pharmacy and Life Science, Tokyo, Japan.

To determine possible roles of collagenases in bone development and remodeling and the specific role of MMP-13 (collagenase-3), we targeted a null mutation in mice in the MMP-13 gene splicing out Exon 5 which encodes the critical catalytic, Zn-binding domain. Previously we presented preliminary results indicating that homozygous mutant mice (MMP-13 -/-) had increased width and delayed maturation of the growth plates and increased bone mass. Here we show using histomorphometry (microCT) an increased bone vol/tissue vol ($p<0.001$), trabecular number ($p<0.001$) and trabecular thickness ($p<0.03$) but decreased trabecular separation ($p<0.001$) in 3 month-old MMP-13 -/- vs. MMP-13 +/+ mice. Evidence for increased bone formation in vivo in MMP-13 -/- mice includes increased osteocalcin-expressing cells(in situ hybridization) on bone surfaces and increased osteoblast proliferation (uptake of BrDU). To investigate further potential roles of type I collagen synthesis and degradation in the absence of MMP-13, we used bone marrow culture (BMC) with cells obtained from 1 month-old mice. In early phases of BMC (~ 1 week) osteoblast proliferation (MTT analysis, $p < 0.001$) and expression of alkaline phosphatase ($p < 0.01$) were increased in BMC from MMP-13 -/- vs. MMP-13 +/+ mice; differences were potentiated by addition of ascorbic acid (0.1mM) and/or parathyroid hormone (PTH), 0.1 microM. By Realtime PCR (Exon 5 primers), no MMP-13 mRNA was detected in MMP-13 -/- BMC but abundant MMP-13 was expressed in BMC from MMP-13 +/+ mice (2.6 x 106 molecules/50 ng RNA) and levels were increased ~ 6 fold in BMC treated with PTH. In longer term BMC (3 weeks), bone nodule formation (Alizarin red) and collagen accumulation (Sirius red) were evident and were increased in the BMC from MMP-13 -/- vs. MMP-13 +/+ mice. In the presence of the collagen synthesis inhibitor, dehydroproline (DHP) 0.01mM, bone nodule formation and collagen accumulation were abolished. Thus, type I collagen deposition continues as a result of osteoblast function in wild type BMC despite collagenase expression and is increased in MMP-13 -/- BMC suggesting that absence of MMP-13 and decreased collagenase-mediated collagen degradation are negative regulators of bone formation. This suggestion is consistent with other studies (Xiao et al., J Biol Chem 273:32988, 1998) indicating that an alpha2-integrin-collagen-interaction is required for activation of Osf2/Cbfa1 and induction of osteoblast-specific gene expression.

1198

Characterization of Collagenase-3 Binding to the Collagenase-3 Specific Receptor and LRP1. I. Choudhury*[1], S. Williams*[1], L. J. Raggatt*[1], M. H. Byrne*[2], S. M. Krane[2], N. C. Partridge[1]. [1]Department of Physiology and Biophysics, UMDNJ-Robert Wood Johnson Medical School, Piscataway, NJ, USA, [2]Department of Medicine, Harvard Medical School and Arthritis Unit, Massaschusetts General Hospital, Boston, MA, USA.

Previously we have shown that in rat osteoblast-like cells and mouse embryo fibroblasts, a specific receptor for collagenase-3 (MMP-13) associates with the endocytotic receptor, the LDL receptor related-protein (LRP1) in binding, internalization and degradation of MMP-13. The purpose of this study was to investigate the nature of the interaction of MMP-13 with the specific collagenase-3 receptor and the LRP1. This has involved purification and sequencing of the specific collagenase-3 receptor in addition to whole cell and solid phase binding studies. Sequencing by LC-MS of the affinity-purified 170 kDa specific collagenase-3 receptor from primary rat osteoblastic cells showed that the molecule had no homology with any protein in the database. Solid phase binding assays showed that 125I-MMP-13 binds to the specific collagenase-3 receptor but not to LRP1 alone. However, in the presence of LRP1, there is enhanced binding of 125I-MMP-13 to the specific receptor. These results suggest one of two possibilities: that LRP1 associates with the specific receptor thus enhancing the latter's affinity for MMP-13. Alternatively, the binding of MMP-13 to the specific receptor induces a conformational change in the ligand which exposes the binding domain of MMP-13, allowing it to bind to LRP1. We have used a series of human MMP-1/MMP-13 chimeric proteins to identify the regions of MMP-13 that bind to the specific receptor and LRP1 (human MMP-1 does not compete). Binding experiments showed that the chimeric construct H(1-228)/M(229-472) does not bind to the specific receptor indicating that the MMP-13 binding site lies within the amino acid region 1-228. The chimera containing MMP-13 amino acid residues 141-228 did not compete as effectively, however the construct in which exon 5 (amino acid residues 213-267) was deleted competed almost as well as the wild-type form of MMP-13. These results indicate that the domain for MMP-13 binding lies within residues 1-228. The fact that residues 141-228 do not compete as well suggests that the receptor binding site lies more specifically within the region 1-141. However, it is possible that residues 141-228 are necessary to create the correct protein conformation for MMP-13 binding to its specific receptor. The data confirm and support our previous observations that binding and removal of MMP-13 from the extracellular milieu requires initial binding to a specific receptor and internalization by LRP1.

1199

Children and the Risk of Fractures due to Oral Corticosteroids. T. P. van Staa[1], C. Cooper[2], H. G. M. Leufkens*[1], N. Bishop[3]. [1]Pharmacoepidemiology and Pharmacotherapy, Utrecht Institute for Pharmaceutical Sciences, Utrecht, Netherlands, [2]Environmental Epidemiology Unit, Medical Research Council, Southampton, United Kingdom, [3]Sheffield University, Academic Child Health, Sheffield, United Kingdom.

Oral corticosteroids are known to increase the risk of fracture in adults. Whether the effects of oral corticosteroids are similar in children is unknown. The medical records of general practitioners in the UK (from the General Practice Research Database) were used to estimate the incidence rates of fracture of children aged 4 to 17 years taking oral corticosteroids and of control children. Within those cohorts, each child with a fracture was subsequently matched by age, sex, practice, and calendar time to one child without a fracture, in order to adjust for risk factors for fracture. There were 37 562 children taking oral corticosteroids. The average duration of treatment was 6.4 days (median 5 days). The figure shows the fracture incidence in children using oral corticosteroids (squares) and control children (diamonds). The risk of fracture was increased in children with a history of frequent use of oral corticosteroids: children who received four or more courses of oral corticosteroids had an adjusted OR for fracture of 1.32 (95% CI 1.03-1.69). There was also a trend towards higher fracture risks in children using high daily doses. The adjusted OR for fracture was 1.22 (CI 0.99-1.50) in children using 30 mg prednisolone or more per day. Children who stopped taking oral corticosteroids had a comparable risk of fracture to those in the control group. Frequent use of oral corticosteroids was associated with an increased risk of fracture. Our findings suggest that children who receive more than four short-term courses of oral corticosteroid have an increased risk of fracture.

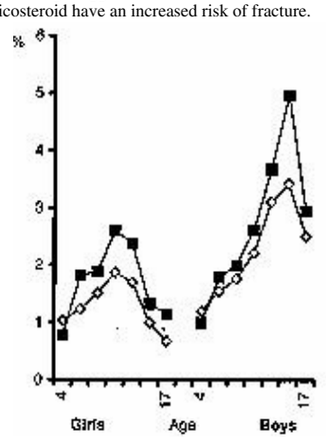

Disclosures: ***T.P. van Staa****, Procter & Gamble Pharmaceuticals 1, 3.*

1200

Long Term Effect of Calcium Supplementation and Dairy Products on Bone Mass of Young Females. V. Matkovic[1], N. Badenhop-Stevens*[1], J. Landoll*[1], P. Goel*[2], B. Li*[2]. [1]Bone and Mineral Metabolism Laboratory, The Ohio State University, Columbus, OH, USA, [2]Statistics, The Ohio State University, Columbus, OH, USA.

The purpose of this investigation was to evaluate the long-term effect of Ca supplementation (Ca-s) and dairy product (DP) consumption on bone mass (BM) of young females (YF) through modeling (M-p) and consolidation phases (C-p) of skeletal development. The study was conducted among 456 healthy Caucasian YF (age 10.8±0.8 y) in pubertal stage 2 and with Ca intake (Ca-i) below/above threshold (T) level (1480 mg/d) at baseline. 354 YF with Ca-i below the T (mean 937±215 mg/d) were recruited and randomized into a double-blind, placebo-controlled clinical trial (CT) with Ca citrate-malate (Procter & Gamble Co.) at 1000 mg Ca/d. 102 YF with Ca-i above T (dairy group, DG) were followed as an observational study (OS). 179 YF completed the 7-y CT and 85 DG individuals finished 7-y OS. Anthropometry, BM of the forearm & total body (TB) by DXA (GE-Lunar, DPX-L), and nutritional and activity records were obtained every 6 months (m) (DG every 12 m); while blood and 24-hr urine for Ca, hormones, and biomarkers were collected every 12 m. Hand X-rays for bone age and radiogrammetry were obtained at ages 11, 15, 18 y. Hip and spine measurements were measured by DXA every 6 m (DG every 12m) after age 15 y. The results of the study show a positive influence of Ca-s and DP consumption on BMD of the TB and various skeletal regions. This influence is more pronounced during bone M-p (ages 11-15 y). The "catch-up" phenomenon in BM acquisition exists and proceeds in the control individuals (accustomed to Ca-i of ~850 mg/day/7 y) by the C-p of skeletal development when Ca requirement (Ca-r) declines. A permanent deficit in peak BM, as a result of inadequate Ca-i during M-p, is expected at the hip and metacarpals, and at other sites among certain subgroups of the population based on body size and activity. The DG subjects maintained their behavior with regard to DP intake and had higher BM throughout. The results of this research indicate that Ca-r are size dependant, however, understanding difficulties in predicting body size, current high dietary Ca-i standards for growth should be implemented to meet the demand of all young Americans. In addition, establishing healthy lifestyles (nutrition, activity) during early childhood should be initiated as a part of primary prevention programs for osteoporosis.

1201

Protein Intake Modulates the Effect of Calcium Supplementation on Bone Mass Gain in Prepubertal Boys. T. Chevalley[1], S. Ferrari[1], D. Hans[2], D. Slosman[2], M. Fueg*[1], J. P. Bonjour[1], R. Rizzoli[1]. [1]Division of Bone Diseases, Dept Internal Medicine, University Hospitals Geneva, Switzerland, [2]Division of Nuclear Medicine, Dept of Radiology, University Hospitals Geneva, Switzerland.

Calcium (Ca) and proteins are important nutritional determinants of bone growth. To what extent dietary protein intake can modulate the beneficial effect of calcium supplementation (Calsup) in healthy children is not known. In a one-year prospective double-blind placebo-controlled trial we examined in prepubertal boys whether the gains in areal bone mineral density (aBMD) in response to Calsup were modulated by protein intake at several skeletal sites. 235 healthy prepubertal boys aged 7.4±0.1 yrs (mean±SEM, range 6.5-8.5 yrs) were randomized into a group (Calsup, n=116) consuming 2 food products providing 850 mg of Ca daily, and into a placebo control group. The latter (Placebo, n=119) consumed similar products in terms of energy and protein but without added Ca. aBMD was determined by DXA using Hologic QDR 4500 at 6 skeletal sites: radius (distal metaphysis=Rmet; diaphysis=RDia); hip (femoral neck=FN; trochanter=FT); femoral diaphysis (FDia) and L2-L4 vertebrae (LS). Spontaneous Ca and protein intakes were assessed by frequency questionnaires at baseline, 6 and 12 months and the mean of the 3 records was taken into account. In an intention-to-treat analysis, the gain in aBMD (mg/cm2±SEM) was significantly higher at Fdia in the Calsup (n=114) as compared with the Placebo (n=117) group (76±3 vs 65±3, p=0.008). At the 5 other sites the Calsup effect was not statistically significant, even in the subgroup having spontaneous Ca intake below the median (727 mg/d). In these subjects with a relatively high spontaneous protein intake (1.8±0.1 g/kg/d), baseline BMD values at all sites were better positively correlated with protein than Ca intakes. Over the one year study, mean aBMD gain in the placebo group was higher with protein intake above than below the median (1.7 g/kg/d) (25±2 vs 17±1 mg/cm2, p<0.0012) at the 5 sites (Rmet, Rdia, FN, FT, LS). At these 5 sites, there was a significant (p=0.012) interaction between protein intake and Calsup effect on aBMD gain. Thus, in boys with a spontaneous protein intake below the median, mean gain in aBMD was significantly higher in the Calsup than in the Placebo group (24±2 vs 17±1 mg/cm2, p=0.007). In conclusion, our study strongly suggests a positive relationship between protein intakes and bone mass gain in prepubertal boys. In addition, the response to Ca supplementation appears to be modulated by protein intake.

1202

Interpretation of Whole Body DXA in the Assessment of Cortical Bone Health in Children: Validation with Peripheral QCT. M. B. Leonard[1], J. Shults*[2], V. A. Stallings[1], B. S. Zemel[1]. [1]Pediatrics, Children's Hospital of Philadelphia, Philadelphia, PA, USA, [2]Center for Clinical Epidemiology and Biostatistics, University of Pennsylvania School of Medicine, Philadelphia, PA, USA.

The confounding effects of bone size on traditional DXA measures of areal bone mineral density (areal-BMD, gm/cm2) are well-recognized. An alternative strategy has been proposed to determine if decreased whole body (WB) DXA bone mineral content (BMC) for age is due to short stature (decreased height for age), narrow bones (decreased bone area adjusted for height) or decreased density (decreased BMC adjusted for bone area). Although this approach has been adopted in studies of healthy and ill children, this approach has not been validated. The purpose of this study was to compare WB DXA results (which consist of predominantly cortical bone) with peripheral quantitative CT (pQCT) measures of cortical bone geometry and volumetric density (gm/cm3). WB DXA scans (Hologic QDR 4500) and pQCT scans of cortical bone at the 20% distal tibia (Stratec XCT-2000) were completed in 150 healthy children (75 female), 6 to 21 years of age. Bone results were log-transformed and standardized residuals (z-scores) were created for the following WB DXA measures: bone area for height and BMC for bone area; and for the following pQCT measures: cross sectional area (CSA) for tibia length, and bone strength (cross-sectional moment of inertia) for tibia length. Cortical volumetric BMD, as measured by pQCT, was not associated with tibia length. The correlations (R) between DXA and pQCT measures are summarized below. (NS = $p > 0.05$) These data demonstrate that decreased WB DXA bone area for height is significantly associated with decreased bone cross-sectional area for bone length, suggesting WB DXA bone area adjusted for height provides a valid measure of cortical bone geometry. Decreased breadth is associated with decreased strength since periosteal dimensions are a critical determinant of bone strength. However, WB DXA BMC adjusted for bone area is not significantly associated with cortical bone volumetric density, size or strength, suggesting this is not a valid measure of cortical bone mineralization. Decreased WB DXA BMC for bone area may give the false impression of decreased cortical bone density and strength.

Correlations between DXA and pQCT Z-Scores

	WB DXA Bone Area for Height	WB DXA BMC for Bone Area
pQCT CSA for Tibia Length	R = 0.45, p < 0.0001	NS
pQCT Bone Strength for Tibia Length	R = 0.53, p < 0.0001	NS
pQCT Volumetric Density (gm/cm3)	NS	NS

1203

Removal of Unremodelled Growth Plate in the Metaphysis after Bolus Zoledronic Acid in Growing Rabbits. E. J. Smith[1], A. McEvoy*[2], R. A. Peat*[2], J. N. Briody[2], J. A. Eisman[1], D. G. Little*[2], E. M. Gardiner[1]. [1]Bone and Mineral Program, Garvan Institute of Medical Research, Sydney, Australia, [2]Orthopaedic Research Unit, Childrens Hospital Westmead, Sydney, Australia.

Use of bisphosphonates in children suffering severe osteogenesis imperfecta or for prevention of fracture in patients undergoing distraction osteogenesis for correction of limb length discrepancy has major clinical benefits in terms of increased bone strength, leading to patient mobility and participation in normal childhood activities. However, there are concerns about the impact of bisphosphonates on the growth plate, metaphyseal modeling and consequent growth in long bones. This study examined bisphosphonate effects on metaphyseal histology and tibial length of 12 contralateral non-operated tibias in a growing male NZW rabbit model of distraction osteogenesis. At 8 weeks of age, 6 animals received IV saline, 6 received IV 0.1mg/kg zoledronic acid at 8 and 10 weeks. DXA scans and x-rays were taken at 10, 12, 14, 26, 40 and 52 weeks of age. For histology tibias were collected from other studies using the same model. X-rays of treated bones had radiolucent lines in the metaphysis that corresponded to number of doses. Histologically, lines contained chondrocytes in columnar formation from the hypertrophic zone surrounded by calcified matrix. Resorption of these lines at later times was evident in x-rays and histology. Tibial length in both groups increased by 14% from week 10 to 26 at a rate of 0.9mm/wk. Between 26 and 52 weeks there was no increase in length, consistent with normal cessation of rabbit growth at 25 weeks of age. Tibial length was 3-7% shorter at 14, 26, 34, 40 and 52 weeks in the treated groups ($p<0.05$) and a similar trend (2-5%) was seen at 12 weeks. The decrease in bone length at 14 weeks was still evident at 52 weeks. As shown with other bisphosphonates in animal models, zoledronic acid caused loss in tibial length but did not impact on growth rate. This study shows that zoledronic acid causes transient retention of growth plate remnants in the metaphysis, in association with transient inhibition of growth. It provides histological insights into the nature and persistence of growth inhibition by bisphosphonates, not otherwise seen with continuous dosing used in other studies. Removal of growth plate remnants may be important for resumption of normal bone ultrastructure and quality.

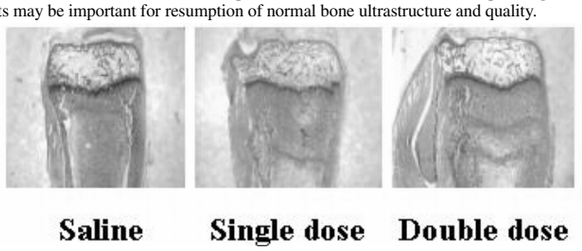

1204

Sprouty2 Induced by Constitutively Active FGF Receptor 3 Suppresses the Chondrocyte Proliferation through Inhibition of IGF-1 Signaling. Y. Yamanaka[1], H. Tanaka[1], K. Ueda*[1], E. Yamagami*[1], R. Nishimura[2], Y. Seino[1]. [1]Pediatrics, Okayama University Graduated School, Okayama city, Japan, [2]Biochemistry, Osaka University Faculty of Dentistry, Osaka, Japan.

Achondroplasia, the most common form of short-limb dwarfism, and its severe type, thanatophoric dysplasia (TD) are caused by constitutively activated mutations in FGFR3. The excessively activated FGFR3 appears to suppress the proliferation of chondrocytes, resulting in disturbing the growth of long bones. However, little is known how these mutations suppress proliferation of chondrocytes. To address this, we determined whether Sprouty2, which mediates FGFR3 signals, is involved in this process, using a chondrogenic cell line, ATDC5. BrdU incorporation assay demonstrated that the cells expressing TDII-mutated FGFR3 (TDII cells) showed the decreased DNA synthesis by 40%, compared with wild-type FGFR3 expressing cells (WT cells). In contrast, the expression of Sprouty2 mRNA is significantly increased in TDII cells. GH-IGF axis is an important system in bone growth. Especially, IGF-1 has a potent stimulator of chondrocyte proliferation. Of note, overexpression of Sprouty2 in WT cells markedly decreased IGF-1 dependent-DNA synthesis by 30% of WT cells. Furthermore, overexpression of dominant-negative Sprouty2 recovered DNA synthesis in TDII cells. These data suggest that Sprouty2 negatively regulates the mitogenic effects of IGF-1. To further investigate the mechanism, by which TDII FGFR3 mutation suppressed the IGF-1-dependent proliferation, we examined the effect of Sprouty2 on the MAP kinase since IGF-1 exhibits the mitogenic activity through MAP kinase pathway. In WT cells, IGF-1 increased MAP kinase activity as well as proliferation. Overexpression of Sprouty2 suppressed the IGF-1-induced MAP kinase activity. In conclusion, these results collectively suggest that excessive activation of FGFR3 by TDII mutation suppressed MAP kinase by up-regulating the Sprouty2 expression, consequently inhibiting the proliferation of chondrocytes. Our data suggest that excessive expression of Sprouty2 may account for the disturbance of endochondral bone formation in FGFR3-related skeletal dysplasia.

1205

The *Hyp* Mutation in Mice Reduces, but does not Eliminate, the Genomic Response of the Kidney to Low Phosphate Diet. M. H. Meyer, R. A. Meyer. Department of Orthopaedic Surgery, Carolinas Medical Center, Charlotte, NC, USA.

The genes active in the regulation of phosphate reabsorption in the kidney are not well understood. It is also not clear whether mutations of the *Phex* gene block renal adaptation to low phosphate diets. To investigate this, 5-week-old normal and *Hyp* mice were fed a control (1.0% P) or low phosphate (0.03% P) diet for five days. The kidneys were then collected, and the RNA was extracted and pooled between three animals to create each sample. Two microarrays were done for each diet for normal mice and three microarrays for each diet for the *Hyp* mice for a total of 10 arrays (30 mice). cRNA was prepared and hybridized to Affymetrix U74Av2 GeneChip microarrays with probes for 12,473 genes. Binomial tests were done to identify genes affected by diet or genotype. An average of 5,178 genes were scored as present. Of this number, 92 genes were scored as increased in both normal mouse samples on low P diet ($P < 0.001$). Of these, only 11 genes were also increased in the *Hyp* samples on low P diet, but this remained a significant overlap with the normal mice ($P < 0.001$). Three genes, calbindin-D9K, 25-hydroxyvitamin D-1alpha-hydroxylase, and glutathione reductase 1, were increased in normal mice on low P diet, but decreased in *Hyp* mice on low P diet. Diphor-1 (AW046638) was decreased in *Hyp* mice and not significantly affected by low P diet. The type IIb sodium/phosphate transporter was scored as absent in all samples. In contrast to the increased genes, 85 genes decreased in the two samples from normal mice on low P diet ($P < 0.001$). Of these, only 16 decreased in the *Hyp* mice ($P < 0.001$). On the control diet *Hyp* mice differed from normal mice by having 65 genes decreased ($P < 0.001$) and 53 genes increased ($P < 0.001$). In addition, we tested whether genes affected by low dietary P in normal mice were the same genes as those altered by the *Hyp* mutation under the control diet: No significant overlap was found between them. In conclusion, low phosphate diet led to significant alteration in mRNA expression of specific genes in the mouse kidney. The *Hyp* mutation reduced the number of affected genes, but did not totally eliminate this adaptation. The renal response to changes in dietary phosphate involves both *Phex*-dependent and *Phex*-independent mechanisms.

1206

C-type Natriuretic Peptide Elongates the Dwarfing Bones in Mice Model of Achondroplasia by Increasing the Extracellular Matrix of Growth Plate Chondrocytes. A. Yasoda*, Y. Komatsu, H. Chusho*, A. Ozasa*, T. Miyazawa*, N. Tamura*, Y. Ogawa*, K. Nakao*. Medicine and Clinical Science, Kyoto University Graduate School of Medicine, Kyoto, Japan.

Achondroplasia is the most common genetic form of dwarfism of which no efficient therapy has been established so far. Recently, we have demonstrated that C-type natriuretic peptide (CNP) is a novel skeletal growth factor regulating endochondral ossification. Here we report the therapeutic efficacy of CNP for achondroplasia using mice model of achondroplasia with targeted overexpression of the activated FGFR3 in cartilage ($FGFR3^{ach}$-Tg), which develop dwarfism with shortening of bones formed through endochondral ossification. To investigate the direct effect of CNP on longitudinal bone growth of $FGFR3^{ach}$-Tg mice, we performed organ culture experiments using tibiae from 16.5-G.D. fetal $FGFR3^{ach}$-Tg mice. Fetal $FGFR3^{ach}$-Tg tibiae were significantly shorter than non-Tg tibiae throughout the 4-day culture period, and 10^{-7}M CNP elongated the cultured $FGFR3^{ach}$-Tg tibiae to the level of vehicle treated non-Tg tibiae at the end of the culture period. Histological analysis revealed that CNP elongated the short cartilagenous primordia of $FGFR3^{ach}$-Tg tibiae, both in the proliferative and hypertrophic chondrocyte layers, with a characteristic picture of the enlarged extracellular space there. The decreased extracellular matrix synthesis of $FGFR3^{ach}$-Tg tibiae estimated by $^{35}SO_4$ incorporation was recovered by 10^{-7}M CNP up to just the same extent to that of non-Tg tibiae treated with vehicle. Then we achieved targeted overexpression of CNP using typeII collagen promoter in cartilage of $FGFR3^{ach}$-Tg mice to observe the effect of CNP for achondroplasia in vivo, and exhibited that CNP substantially rescued the shortening of bones formed through endochondral ossification. Histological analysis showed that CNP recovered the narrowed growth plate of $FGFR3^{ach}$-Tg mice with increased extracellular space, as was observed in organ culture experiments. On the other hand, decreased proliferation of the growth plate chondrocytes in $FGFR3^{ach}$-Tg mice shown by the BrdU staining was not recovered. CNP overexpressed in cartilage did not alter the intensity of type II and X collagens shown by in situ hybridization, or the delayed formation of the secondary ossification center in $FGFR3^{ach}$-Tg mice. These results exhibit that the mechanism by which CNP could rescue the shortening of bones of $FGFR3^{ach}$-Tg mice is to increase the extracellular matrix with little alteration in the proliferation and the differentiation of the growth plate chondrocytes, followed by the substantial recovery in the bone length, indicating the efficacy of CNP for the treatment of human achondroplasia.

1207

Differences in Measures of Femoral Neck Strength between Japanese-American and Caucasian-American Women. A. S. Karlamangla*, J. T. Young*, M. Huang*, G. A. Greendale. Division of Geriatrics, UCLA, Los Angeles, CA, USA.

Japanese women have fewer hip fractures than Caucasian women, despite having lower bone mineral density. Differences in hip geometry might be at the root of this difference in hip fracture risk. However, previous studies have not consistently found hip axis length (HAL) to be disproportionately longer in Caucasian women. The objective of this study is to compare structural measures of femoral neck strength in Japanese-American and Caucasian-American women, relative to the loads that they bear. Under the assumption that mineralization of the femoral neck is mostly in its cortical rim, the ability of the femoral neck to withstand compressive and bending forces proportional to body weight is given by Compressive Strength = BMD * FNW / Weight, and Bending Strength = BMD * $(FNW)^2$ / (HAL * Weight), where BMD refers to the projected (areal) bone mineral density of the femoral neck and FNW is the femoral neck width. Similarly, the ability of the neck to absorb the energy of impact in a fall from standing height is given by Impact Strength = BMD * FNW * HAL / (Height * Weight). We measured BMD, HAL, and FNW from dual energy x-ray absorptiometry scans and calculated the above 3 strength measures in 267 Japanese and 199 Caucasian women residing in the Los Angeles area, who participated in the Study of Women's Health across the Nation (SWAN) at the University of California at Los Angeles site. Though Caucasian women had higher mean BMD (p=.0003) than Japanese women, the means of each of the 3 strength measures was 12-13% higher in Japanese women than in Caucasian women (p<.0001 for each comparison).

Femoral Neck Strength Measures (in gm/ kg.meter)	**Mean**		**p value for t-test**
	Caucasian (N=199)	**Japanese** (N=267)	
Bending Strength	0.490	0.556	< .0001
Compressive Strength	2.49	2.78	< .0001
Impact Strength	0.161	0.180	< .0001

Relative to the forces that they have to withstand in weight bearing, and relative to the energy that they have to absorb in an impact from a fall from standing height, the femoral necks of Japanese American women are substantially stronger than those of Caucasian American women. This finding is consistent with the observed difference in hip fracture risk between Japanese and Caucasian women.

1208

Thoracic Kyphosis and Rate of Incident Vertebral Fracture. K. M. Shipp[1], H. A. Guess*[2], K. E. Ensrud[3], M. C. Nevitt[4], D. M. Kado[5], S. R. Cummings[4]. [1]Duke University, Durham, NC, USA, [2]Merck Research Laboratories, Blue Bell, PA, USA, [3]University of Minnesota, Minneapolis, MN, USA, [4]University of California, San Francisco, CA, USA, [5]University of California, Los Angeles, CA, USA.

Biomechanical evidence supports the theory that hyperkyphosis may increase the risk of new vertebral fractures (VFs). When the spine is in a flexed (kyphotic) position, the vertebral bodies sustain sufficiently high loads for usual daily activities potentially to result in a fracture in the osteoporotic spine. This cohort study examined whether baseline severity of thoracic kyphosis (TK) was associated with subsequent risk of new radiographically-detected VF, over 2 to 4 years of follow-up in 3,038 women, between 55 and 81 years of age with baseline femoral neck BMD $\leq$ 0.68 g/cm^2, enrolled in the placebo arms of the Fracture Intervention Trial. TK, measured by Debrunner kyphometer, was the primary exposure variable. VFs were assessed by quantitative morphometry using standard definitions. Our goal was to evaluate TK as an independent predictor of new VFs. Crude new VF rates follow:

TK (quartiles)	Person-years	#	Rate/1,000 p-yrs
7.0º -- 40.0º	3,150	45	14.3
40.1º -- 47.0º	2,701	43	15.9
47.1º -- 55.5º	2,854	54	19.0
55.6º -- 80.0º	2,680	79	29.5

Over 20 reported risk factors for osteoporotic fracture were evaluated as potential effect modifiers or confounders of the TK -- VF relationship. Controlling for age and BMD, TK > 36º was linearly related to incident VF, rate ratio [per 10º > 36 º] 1.22 (1.07, 1.39), giving the following predicted values:

TK	Rate Ratio	95% CI
60º vs. 36º	1.62	1.18, 2.22
70º vs. 36º	1.98	1.27, 3.09
80º vs. 36º	2.42	1.36, 4.32

With previous VFs added to this model, there was no independent effect of TK on risk of VF, rate ratio [per 10º > 36º] 1.03 (0.91, 1.18). Women with hyperkyphosis are at increased risk for new VFs, independent of age and BMD. This association is explained by a greater number of existing VFs among women with hyperkyphosis. Measurement of kyphosis may be useful for predicting vertebral fracture risk when spine radiographs are not available.

1209

Increased Risk of Falls, Increased Bone Resorption and Decreased Bone Mineral Density in Elderly Men with Hypogonadism. The MINOS Study. P. Szulc[1], F. Munoz*[1], B. Claustrat*[2], P. Garnero[1], F. Marchand*[3], P. D. Delmas[1]. [1]INSERM 403 Research Unit, Lyon, France, [2]Hôpital Cardiologique, Lyon, France, [3]SSMB, Montceau les Mines, France.

The goal of the study was to identify the clinical and biological pattern of hypogonadism in a large cohort of men. In that cohort of 1066 men aged 19 to 85 years, serum concentrations of free testosterone (fT) and of bioavailable testosterone (bioT) decreased with age (r = -0.39 and r = -0.43, respectively, p=0.0001). Hypogonadism was defined as concentration of fT more than 2 SDs below the mean in young healthy men. After adjustment for age and body weight, hypogonadal men had a lower bone mineral density (BMD) at the level of total hip (-5.8 %, p<0.005), ultradistal radius (-6.3 %, p<0.04), whole body (-3.9 %, p=0.002) and higher levels of the bone resorption markers (total deoxypyridinoline - +35 %, p=0.0001, urinary beta-isomerized C-terminal telopeptide of collagen type I [betaCTX–I] - +41 %, p=0.0001, serum betaCTX–I - +28 %, p=0.001). The same pattern was observed when hypogonadism was defined by the level of bioT. In contrast, serum concentrations of bone formation markers (osteocalcin, bone alkaline phosphatase, N-terminal extension propeptide of type I collagen) did not differ between groups. Hypogonadal men had a lower lean body mass (-3.1 %, p<0.002). In men aged more than 49 years, hypogonadism was associated (after adjustment for age and body weight) with an impairment of several clinical tests of muscle strength and balance such as standing up 5 times from a sitting position (O.R. = 5.0, p<0.005), maintaining equilibrium for 10 sec with open eyes (O.R. = 3.4, p<0.05) and for 5 sec with closed eyes (O.R. = 2.5, p<0.05), walking forwards 10 steps on a line drawn on the floor (O.R. = 4.1, p<0.001). In men aged more than 69 years, hypogonadism was a risk factor for falls (O.R. = 2.7, p<0.03). In conclusion, elderly men with hypogonadism have two groups of risk factors for osteoporotic fractures: decreased BMD and increased bone resorption on the one hand and, on the other hand, lower muscle strength, impaired balance, and increased risk for falls.

1210

Low Plasma Vitamin B12 Is Associated with Lower Bone Mineral Density: The Framingham Osteoporosis Study. K. L. Tucker[1], M. T. Hannan*[2], P. Jacques*[1], J. Selhub*[1], I. Rosenberg*[1], P. W. F. Wilson*[3], D. P. Kiel*[2]. [1]USDA Human Nutrition Research Center, Tufts University, Boston, MA, USA, [2]Hebrew Rehabilitation Center, Harvard Medical School, Boston, MA, USA, [3]Boston University, Boston, MA, USA.

Osteoporosis has been previously associated with pernicious anemia and vitamin B12 is thought to be important to osteoblast activity. In one case report, a man with pernicious anemia showed marked improvement in bone density over two years of vitamin B12 treatment. However, few studies have examined vitamin B12 and BMD. We therefore assessed the relationship between plasma vitamin B12 and BMD in 1144 men and 1487 women in the Framingham Offspring Study. In 1995-99, participants (30-87y) had BMD measured with Lunar DPX-L at hip (femoral neck, trochanter, Wards area, total hip) and lumbar spine. Plasma from the same examination was analyzed for vitamin B12 by radioassay, (Ciba-Corning). We divided subjects based on standard cutoffs for vitamin B12: 200-250, >250-350, and >350 pg/mL. BMD measures were each regressed onto this categorical variable by sex, adjusting for age, BMI, height, smoking, alcohol use, calcium intake, vitamin D intake, physical activity score and season of measurement and least squares means were obtained. We also regressed BMD onto each of the three higher categories relative to the lowest, separately for men and women. 5% of men and 4% of women had B12 <=200 pg/mL. These subjects had significantly (p<.05) lower BMD than at least two of the three higher categories as follows: Men: fermoral neck, Ward's area and total hip, but not spine or trochanter; Women: trochanter, Ward's area, spine and total hip, but not femoral neck. As an example, for men, the LS means for total hip BMD for the 4 categories were 0.98, 1.02, 1.03, 1.03 g/cm2, suggesting that vitamin B12 <=200 pg/mL was associated with BMD about 5% lower than those above this cut point (p< .05 with the 3rd and 4th). For women, corresponding total hip BMD LS means were 0.676, 0.705, 0.703, 0.700 g/cm2, p<.05 for 1st vs. 3rd and 4th. Patterns were similar for other BMD sites. These results support the hypothesized association between vitamin B12 deficiency and low BMD for both men and women in a population sample. Future studies should focus on B12 effects on bone biology, including the possibility that B12 effects are mediated directly or possibly through homocysteine metabolism.

1211

Long-Term Fracture Risk Following Renal Transplantation: A Population-Based Study. L. Vautour[1], L. J. Melton[1], B. L. Clarke[2], S. J. Achenbach*[1], A. L. Oberg*[1], J. T. McCarthy*[3]. [1]Health Sciences Research, Mayo Clinic, Rochester, MN, USA, [2]Endocrinology, Mayo Clinic, Rochester, MN, USA, [3]Nephrology, Mayo Clinic, Rochester, MN, USA.

While abnormalities in bone metabolism are well recognized in patients with end-stage renal disease, the overall risk of fracture following renal transplantation has not been well quantified. The 86 Olmsted County, MN residents who underwent a renal transplant between 1965 and 1995 were followed for 911 person-years in a retrospective cohort study. Risk factors and fracture outcomes were assessed through review of each subject's complete (inpatient and outpatient) medical records in the community. There were 59 men (69%) and 27 women, of whom 7 were postmenopausal. During follow-up extending to 33 years (mean 10.6±7.4 years), 117 fractures were observed. The cumulative incidence at 15 years of one or more fractures was 68% compared to 22% expected in the general population (p<0.001). Renal transplantation was associated with a significantly increased risk of any fracture (standardized incidence ratio [SIR] 4.8, 95% CI 3.6-6.4), but these patients had a particular risk of vertebral (SIR 23.1, 95% CI 12.3-39.6), rib (SIR 15.0, 95% CI 9.5-22.5), pelvic (SIR 17.1, 95% CI 4.7-43.8), and foot fractures (SIR 8.4, 95% CI 5.1-12.9). By univariate analysis, increasing age at transplantation, diabetes, peripheral neuropathy, peripheral vascular disease and blindness were significant predictors of fracture risk. In multivariate analysis, however, only age at first transplant and diabetic nephropathy were independent predictors of risk, while higher activity level had a protective effect. Diabetes was the only independent predictor of lower limb fractures, and duration of dialysis was the only predictor of vertebral fractures in multivariate analyses. An increase in cumulative glucocorticoid dosage was not correlated with increased fracture risk. Thus, renal transplantation among unselected patients in the community is associated with a significant increase in the risk of fractures (especially those of the vertebrae, ribs, pelvis and lower limbs) even up to 15 years post-transplant. Diabetics, in particular, seem to suffer a great number of lower limb fractures, possibly secondary to peripheral neuropathy, and perhaps should receive greater attention to ambulatory problems post-transplantation.

1212

Are Traumatic Fractures Osteoporotic? S. R. Cummings[1], K. L. Stone[1], L. L. Lui[1], T. A. Hillier[2], D. C. Bauer[1], H. K. Genant[1], S. T. Harris[1], J. A. Cauley[3]. [1]University of California, San Francisco, San Francisco, CA, USA, [2]Kaiser Center for Health Research, Portland, OR, USA, [3]University of Pittsburgh, Pittsburgh, PA, USA.

It is widely believed that fractures that occur during excessive trauma, such as motor vehicle accidents, are not related to osteoporosis. Traumatic fractures are ignored in assessment of risk and excluded as outcomes in trials. We tested two hypotheses: first, that there would be an inverse relationship between BMD and risk of subsequent traumatic fractures and second, that women with traumatic fractures would have an increased risk of subsequent non-trauma fractures. We tested these hypotheses in the prospective Study of Osteoporotic Fractures, a cohort of 9,704 women ≥ age 65 who had peripheral and central BMD measures and more than 15 years of subsequent follow-up for incident fractures. 218 women suffered fractures as a result of severe trauma (83% due to car crashes) during 11.6 years of follow-up after baseline measurement of calcaneal BMD. Of these, 144 occurred during the 10.0 years after measurement of total hip BMD (Hologic QDR 1000). Adjusting for age, the risk of traumatic fracture increased 1.3-fold with each SD decrease in calcaneal BMD (95% CI: 1.1 to 1.5) and 1.6-fold with each SD decrease in total hip BMD (1.3 to 2.0). This remained significant after adjustment for alcohol use. After age-adjustment, women with a traumatic fracture had a 1.7-fold (1.2 to 2.3) risk of suffering a future 'low trauma' fracture. We conclude that, as conventionally defined in SOF, traumatic fractures are osteoporotic fractures. Fractures that occur during trauma should be counted as risk factors for future fractures and as outcomes in trials.

1213

Oral Corticosteroids and the Relationship between Dose and Bone Mineral Density and Fracture: A Systematic Review of Literature. T. P. van Staa[1], H. G. M. Leufkens*[1], C. Cooper[2]. [1]Pharmacoepidemiology and Pharmacotherapy, Utrecht Institute for Pharmaceutical Sciences, Utrecht, Netherlands, [2]Environmental Epidemiology Unit, Medical Research Council, Southampton, United Kingdom.

We conducted a meta-analysis to examine the effects of oral corticosteroids (CS) on bone mineral density (BMD) and fracture risk. It included 66 BMD and 23 fracture studies (with 1 very large and 22 smaller fracture studies). Multiple linear regression analysis was used to estimate BMD change by cumulative CS dose (across-study range of 6.5 to 58.4 g). It was found that all BMD studies reported reduced lumbar spine and hip BMD in CS users (across-study average of 89.4% and 88.8% of normal, respectively). Cumulative dose was strongly correlated to BMD loss at the spine and hip (Pearson correlation coefficients p-values < 0.05). Using the regression analysis, the BMD loss was estimated to be 4.7% at the spine and 6.1% at the hip at a cumulative dose of 13.9 g (mean dose across the smaller fracture studies). This correlated to an expected RR of 1.48 for vertebral and 1.41 for hip fracture (based on published data on the relationship between BMD and fracture risk). The observed RRs of vertebral fractures at this cumulative dose were 3.05 in the largest fracture study and 2.86 in the other fracture studies. For hip fractures, the observed RRs were 2.34 and 2.01, respectively. Longitudinal BMD studies reported a rapid onset of bone loss after start of CS therapy. The risk of fracture was found to be correlated to daily dose and to rapidly increase after the start of CS therapy (within 3 to 6 months) and decrease after stopping therapy. We conclude that fractures may occur at much higher rates than expected on the basis of BMD changes.

Relationship between BMD changes and risk of fracture

Cumulative dose	Estimated BMD change as % normal	Expected fracture RR	Observed fracture RR (95% CI) -largest study	Observed fracture RR (95% CI) - smaller studies
1.5g	-0.5% Spine	1.04	2.40 (1.88-3.07)	-
13.9g	-4.7% Spine	1.48	3.05 (2.51-3.70)	2.86 (2.56-3.16)
1.5g	-0.7% Hip	1.04	1.54 (1.28-1.85)	-
13.9g	-6.1% Hip	1.41	2.34 (1.94-2.81)	2.01 (1.74-2.29)

*Disclosures: **T.P. van Staa**, Procter & Gamble Pharmaceuticals 1, 3.*

1214

Anticonvulsant Use in Elderly Women Increases the Rate of Hip Bone Loss. K. E. Ensrud[1], T. L. Blackwell*[2], P. J. Bowman*[1], T. S. Walczak*[3], E. R. Ensrud*[4], K. L. Stone[2]. [1]Medicine & Epidemiology, VA Medical Center & University of Minnesota, Minneapolis, MN, USA, [2]Medicine, Epidemiology & Biostatistics, University of California, San Francisco, San Francisco, CA, USA, [3]Minnesota Comprehensive Epilepsy Program, Minneapolis, MN, USA, [4]Noran Neurological Clinic, Minneapolis, MN, USA.

Anticonvulsant use may be directly detrimental to bone by resulting in osteomalacia or secondary hyperparathyroidism. To test the hypothesis that elderly women with continuous anticonvulsant use have increased rates of hip bone loss, we assessed current use of anticonvulsants using an interviewer-administered questionnaire at the 4th, 5th, and 6th exams in a cohort of 4202 elderly women participating in the Study of Osteoporotic Fractures. Hip bone mineral density (BMD) was measured at the 4th exam and an average of 4.4 yrs later at the 6th exam. We verified use from medication containers and classified type of medication from product brand or generic names obtained from containers using a computerized medication dictionary. We categorized women according to their reported anticonvulsant use as continuous users (use at all 3 exams), partial users (use at 1 or 2 exams), or non-users (no use at any exam). Individual drug use within the continuous user category included phenytoin, carbamazepine, valproic acid, divalproex sodium, and primidone. The mean annual percent change in total hip BMD (THBMD) and its 4 subregions was calculated by category of anticonvulsant use. All results were adjusted for the following characteristics measured at the 4th exam: age, health status, total calcium intake (dietary plus supplemental), vitamin D supplement use, estrogen use, body mass index, and THBMD. The average rate of decline in THBMD in the overall cohort steadily increased from -0.70%/yr in non-users to -0.94%/yr in partial users to -1.17%/yr in continuous users (p for trend =0.006). Findings were similar at subregions of the hip, though results reached significance only at the intertrochanteric region.

Category of Anticonvulsant Use	Mean Annual % Change in THBMD (95% CI)
Non-users (n=4094)	-0.70 (-0.74 to -0.66)
Partial users (n=68)	-0.94 (-1.25 to -0.63)
Continuous users (n=40)	-1.17 (-1.58 to -0.77)

Anticonvulsant use in elderly women is associated with increased rates of hip bone loss; continuous users have the highest rates of loss. Assessment of anticonvulsant use should be included in the clinical evaluation of osteoporosis risk in older women.

*Disclosures: **K.E. Ensrud**, Pfizer Global Research and Development 2; Merck & Company, Inc. 2; Eli Lilly & Company, Inc. 2; Roche Global Research & Development 2.*

1215

Spondyloepimetaphyseal Dysplasia, Missouri Variant, Is Located on Chromosome 11q22.3 and Is Caused by a Mutation of Matrix Metalloproteinase 13 (MMP13). A. M. Kennedy*[1], P. T. Christie[1], B. Harding*[1], A. A. J. Pannett*[1], A. Dearlove*[2], M. P. Whyte[3], R. V. Thakker[1]. [1]Nuffield Department of Medicine, University of Oxford, Oxford, United Kingdom, [2]MRC HGMP Resource Centre, Cambridge, United Kingdom, [3]Shriners Hospitals For Children, St. Louis, MO, USA.

Spondyloepimetaphyseal dysplasias (SEMDs) are a genetically heterogeneous group of skeletal disorders characterised by defective growth and modelling of the vertebrae and long bones. Genetic defects in two of the six autosomally inherited SEMDs have been identified, and involve abnormalities of the collagen type II gene, located on chromosome 12q12-q13.2, and an ATP sulfurylase/APS kinase gene, located on 10q23-34. These abnormalities are not the cause of the Missouri variant ($SEMD_{MO}$), which is an autosomal dominant trait in a four-generation kindred with 14 affected and 11 unaffected members. In order to identify the gene causing $SEMD_{MO}$ we first determined its chromosomal location by performing a genome wide search using chromosome-specific sets of fluorescently labelled microsatellite marker loci (400 primer pairs) at an average intermarker distance of 10 cM. Linkage was established between $SEMD_{MO}$ and loci from an approximate 30 cM region on chromosome 11q14.3-q23.2 (peak LOD score = 4.92, at 0% recombination, with D11S898). Analysis of this region using the ENSEMBL database revealed 234 genes including a cluster of 8 matrix metalloproteinase (MMP) genes (*MMP-1*, *-3*, *-7*, *-8* -*10*, *-12*, *-13* and *-20*) located in 11q22.3. We reasoned that MMP13, which is known to preferentially degrade collagen type II and is specifically expressed in fetal chondrocytes and osteoblasts, was the best candidate gene for $SEMD_{MO}$, and searched for mutations in the 1416 bp coding region, which is encompassed by 10 exons, in an affected family member. This revealed a T to C transition at residue 56 (TTC to TCC). This abnormality, which predicts an alteration of the wild type phenylalanine residue to a serine, co-segregated with $SEMD_{MO}$ and was absent in 110 unrelated normal individuals. This MMP13 missense mutation (Phe56Ser) resides in the pro-region domain and the alteration of a non-polar phenylalanine to a polar serine residue predicts a significant structural change in the enzyme that is likely to affect its processing and activity. Thus, our results have elucidated the molecular defect causing $SEMD_{MO}$ and an important role for MMP13 in skeletal development.

1216

A Genome-wide Screening of N-Ethyl-N-nitrosourea (ENU) Mutagenized Mice for Musculoskeletal Phenotypes. A. Srivastava, S. Mohan, J. E. Wergedal, D. J. Baylink. Musculoskeletal Disease Center, Jerry L. Pettis Memorial VA Medical Center, Loma Linda, CA, USA.

We describe a mouse ENU mutagenesis program incorporating a genome-wide screen of dominant as well as recessive mutations affecting musculoskeletal disorders in C3H/HeJ mice. In a primary screen, progeny of one-generation dominant mutations (F1) and three generation recessive (F3) mutations were screened at ten weeks of age for abnormalities in total BMD, bone mineral content (BMC), bone area, muscle mass, and femoral bone density using DEXA. Biochemical markers, such as osteocalcin, C-telopeptide (type-I collagen), and skeletal ALP were evaluated to detect defects in bone turnover. Abnormal phenotypes were identified as ±2.5 SD different from baseline data collected from age and sex matched non-mutagenized control mice. A secondary screen at 16-week of age incorporating pQCT was used to confirm the abnormal phenotypes observed in the primary screen. Inheritability of mutations was tested in multiple litters and in at least two generation using wild type C3H/HeJ strain. We have screened about 600 mice (with dominant mode of inheritance) and were able to identify six mice with quantitative abnormalities in BMD, BMC, bone size, or bone turnover. 4 of the abnormal phenotypes are shown in the following table:

Mouse ID	BMC (DEXA)	BMD (DEXA)	Tibia Perimeter (pQCT)	Confirmed in Inheritance Test
5.37.5.C.F	-26%	-2%	-14%	Confirmed
6.5.5.A.M	-20%	-10%	-10%	Testing
6.9.5.B.M	+17%	+1%	+14%	Testing
6.5.3.B.M	-22%	-3%	-15%	Testing

Mutant 5.37.5.C.F showed statistically significant lower tetracycline labeled perimeter and decreased periosteal bone formation in the preliminary histological analysis. This mutant is ready for genotyping. In addition to the above phenotypes, two outliers were identified with abnormal C-telopeptide and skeletal ALP serum levels. In addition to quantitative phenotypes, several binary phenotypes were observed such as syndactyly, dominant spotting, albino, and kinky tail. In summary, we demonstrate feasibility of large scale screening of ENU-mutagenized progeny for musculoskeletal phenotypes. The precision of the screening procedures was an important factor in identifying quantitative skeletal phenotypes and less number of outliers was identified with low precision screens such as, bone turnover markers. In conclusion, this program has identified ENU mutants with genes contributing significant differences in BMD, BMC and bone size and will facilitate future discovery of major gene(s) that regulate BMD and other relevant skeletal phenotypes.

1217

B6.C3H Congenic Mouse Strains Exhibit Site-Specific Alterations in Femoral and Vertebral Trabecular Bone Mass and Microarchitecture. M. L. Bouxsein[1], P. Solanki*[1], R. Müller[2], C. H. Turner[3], K. L. Schultz[4], C. Ackert-Bicknell[4], L. R. Donahue[4], C. J. Rosen[4], W. G. Beamer[4]. [1]Orthopedic Biomechanics, Beth Israel Deaconess Medical Center, Boston, MA, USA, [2]ETH, Zurich, Switzerland, [3]Indiana Medical School, Indianapolis, IN, USA, [4]the Jackson Laboratory, Bar Harbor, ME, USA.

We previously identified several quantitative trait loci (QTL's) for total femoral and vertebral BMD, assessed by pQCT, from the F2 intercross of female C57Bl/6J (B6) and C3H/HeJ (C3H) mice (Beamer et al, JBMR 2001). The strongest of these QTLs mapped to Chr 1, 4, 13 and 18 for femurs, and to Chr 1, 4 and 18 for vertebrae. Chr 1 and 4 were also identified as major regulators of vertebral trabecular architecture (Bouxsein et al, ASBMR 2001). To test the effect of these QTLs in vivo, we generated congenic strains by backcrossing the QTL chromosome regions from C3H onto the B6 background for 9 generations. We used high-resolution micro-computed tomography to assess bone volume fraction (BV/TV) and trabecular microarchitecture in the femur and 5th lumbar vertebrae (34 and 12 um resolution, respectively) from 4 mo. old female congenics, and compared them to B6 controls (n=7-10/group). Trabecular thickness (Tb.Th.), number (Tb.N.) and separation (Tb.Sp.) were computed using a direct 3-D approach (Hildebrand et al, JBMR 1999). For the intact femur, bone volume was similar in Chr 1, 4, and 18 congenics and B6 controls, but was 8% lower in Chr 13 congenics ($p=0.05$). In the distal femur, Chr 1, 4, 13 congenics had 2 to 4 fold higher trabecular BV/TV, and increased Tb.Th. (16-40%) and Tb.N. (27-54%) compared to B6 controls ($p<0.01$ for all). Chr 18 congenics also had increased femoral BV/TV (103%, $p<0.05$) and Tb.Th. (+16%, $p=0.01$), but had similar Tb.N. as B6 controls. Cortical thickness at the femoral mid-shaft was unaltered in Chr 4, 13 and 18 congenics, but was 7% higher in Chr 1 congenics ($p=0.05$) compared to B6 controls. In the vertebral body, Tb.Th. did not differ, but BV/TV and Tb.N. were 10-19% lower in Chr 1, 13 and 18 congenics ($p<0.06$ for all). In contrast, in Chr 4 congenics, vertebral trabecular BV/TV and Tb.Th. were higher (17% and 9%, respectively, $p<0.01$), while Tb.N. was similar to B6. Thus, interestingly, C3H alleles of the genes defined by the QTL regions from Chr 1, 13 and 18 were associated with increased femoral, but decreased vertebral trabecular BV/TV, whereas C3H alleles from Chr 4 were associated with increased trabecular BV/TV at both the femur and spine. Together these observations provide evidence that: 1) the BMD QTLs are indeed important regulators of trabecular bone mass and microarchitecture in both the femur and spine, and 2) genetic regulation of trabecular bone is skeletal site-specific.

1218

Hip Bone Mineral Density (BMD) Is Linked to Chromosomes 14 and 15. M. Peacock[1], D. L. Koller[2], S. L. Hui[1], C. C. Johnston[1], P. M. Conneally*[3], T. Foroud[1], M. J. Econs[1]. [1]Medicine, Indiana University School of Medicine, Indianapolis, IN, USA, [2]Medicine, Indiana University School of Medicine, Indianapolis, IN, USA, [3]Medicine, Indiana School of Medicine, Indianapolis, IN, USA.

A major determinant of osteoporotic hip fracture risk is peak BMD. In an initial autosomal genome screen using 279 micro-satellite markers in 429 pre-menopausal white sister pairs, there was suggestive linkage of hip BMD to chromosome 14. The aim of this study was: to corroborate these findings in an independent sample of pre-menopausal white sister pairs; to examine the effect of utilizing these two samples to further localize the linkage finding; to test whether black sister pairs demonstrate linkage to the same chromosomal regions as white sister pairs. A second genome screen using 392 micro-satellite makers was performed in 570 white pre-menopausal sister pairs, of which 281 pairs overlapped with the initial sample, and in 204 black sister pairs. BMD at femoral neck, Wards and trochanter were measured by DXA. Non parametric quantitative trait sibling pair linkage analysis was performed using Map maker/SIB and chromosomal regions with evidence of linkage to the three hip BMD phenotypes identified. Chromosomal positions are reported using Marshfield map coordinates. At chromosome 14 the initial sample (n=429 pairs) had a LOD score of 2.0 (106cM) for trochanter BMD. In the second independent sample (n=289 pairs) LOD score was 1.8 (71 cM), 35cM centromeric to linkage in the initial sample. Analyses performed combining 281 pairs from the initial sample and 289 pairs from the second sample (n=570 pairs) yielded a LOD score of 1.8 (71cM). Analysis of the 204 black sister pairs yielded a LOD score of 1.6 (80cM). When these were analyzed with the 570 white sister pairs (n=774 pairs) the LOD score increased to 3.5 (72cM). At chromosome 15 the initial sample (n=429 pairs) had a LOD score of 1.8 (56cM) for neck BMD. In the second independent sample (n=289 pairs) the LOD increased to 2.2 (62cM). In the enlarged sample of white pairs (n=570 pairs) the LOD score increased to 3.2. Analysis of the 204 black sister pairs produced a LOD score of 1.5 (72cM). When the black sister pairs were analyzed with the enlarged sample of white sister pairs (n=570 pairs) the LOD score increased further to 4.2 (62cM). The study corroborates our initial finding that hip BMD is linked to a region on chromosome 14. It also shows significant linkage to a region on chromosome 15, which in the initial sample was below significance. The study provides strong evidence that regions on chromosome 14 and 15 harbor genes that affect peak BMD at the hip in both blacks and whites and illustrates the importance of replication of initial findings of linkage.

1219

Age-dependent Effect of Bax Deficiency on Bone Quality in Mice. L. M. Wise*[1], M. D. Grynpas[1], A. Jurisicova*[1], S. J. Korsmeyer*[2], G. I. Perez*[3], J. L. Tilly*[3]. [1]Mount Sinai Hospital & University of Toronto, Toronto, ON, Canada, [2]Dana-Farber Cancer Institute, Harvard Medical School, Boston, MA, USA, [3]Massachusetts General Hospital, Harvard Medical School, Boston, MA, USA.

Bax is a pro-apoptotic member of the Bcl-2 gene family. Increased *Bax* expression has been correlated with ovarian cell death in both mice and humans. Moreover, young *Bax*-null female mice have 3 times as many primordial follicles in their ovarian reserves as do their wild-type (WT) sisters, and this follicle supply is maintained in advanced chronological age. Given that *Bax* deficiency thus prevents ovarian failure with age, these animals may serve as useful models to study menopause and its relation to the skeleton. Accordingly, *Bax*-null (knockout, KO) female mice and WT littermates were generated and euthanized after 2.5 months (young group), 7 months (mature group) and 22 months (old group). Dual energy x-ray absorptiometry (DEXA) using a PIXImus™ mouse densitometer was performed on all mice to determine bone mineral content (BMC), bone mineral density (BMD), and overall tissue lean and fat mass. To evaluate mechanical properties of the bones in these mice with age, unilateral compression was performed on the 6th lumbar vertebrae, while 3-point bending and torsion testing were performed on the femurs. The results were normalized to determine the elastic modulus, maximum stress, toughness, and post-yield behavior. Bone architecture and mineralization were evaluated using μCT, histomorphometry, backscattered electron imaging (BSE) and x-ray diffraction. The following figure displays the whole mouse BMD results among the 3 age groups.

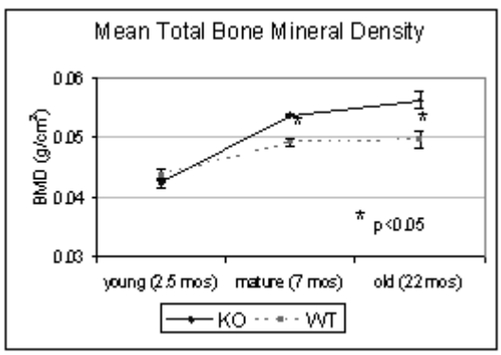

For the 7- and 22-month age groups, the KO mice were found to have significantly higher BMD and BMC when compared to WT females. The 7-month old KO mice also had significantly higher values for total lean mass than the WT mice. When analysing the bones independently, the 22-month old KO mice had significantly higher vertebral BMD values than the WT mice, while the 7-month old KO mice had significantly higher femoral BMD

values when compared to WT mice. These findings suggest that *Bax* plays a significant role in preventing both age-related and post-menopausal bone loss. Current ovariectomy studies are now determining whether the effect of *Bax* gene disruption is due to indirect effects via a maintenance of ovarian function or a direct effect on the skeleton.

1220

Femoral Response to Ovariectomy by C57BL/6J (B6), C3H/HeJ (C3H), and B6.C3H Congenic Strain Female Mice Carrying Quantitative Trait Loci (QTLs) for Volumetric BMD. K. L. Shultz*[1], A. B. Silva*[1], L. G Horton*[1], L. R. Donahue[1], M. L. Bouxsein[2], C. J. Rosen[1], W. G. Beamer[1]. [1]The Jackson Laboratory, Bar Harbor, ME, USA, [2]Beth Israel Deconess Ctr., Boston, MA, USA.

Loss of bone mineral density (BMD) following withdrawal of gonadal steroid support is a well documented and mechanistically complex problem in skeletal biology. Unexpectedly, ovariectomy of 4 month old nulliparous and 8 month old retired breeder B6 and C3H mice showed that B6 lost bone after 6-8 wks, whereas C3H did not. Given that BMD is a polygenic trait with at least 10 independent regulatory loci in B6C3HF2 mice (Beamer et al. JBMR 2001), we hypothesized that c3h alleles at one or more BMD QTLs may block bone loss due to steroid-deficiency. To test this, we developed B6.C3H congenic strains of mice wherein B6 serves as the recipient background strain and C3H as the strain donating 1 of 5 different chromosomal segments. Each segment carries a BMD QTL accounting for 2 to 10% of the BMD variance identified in B6C3HF2 mice. Each congenic strain has significantly altered femoral BMD by pQCT: B6.C3H-1T, 4T, 13T, & 18T increased, whereas B6.C3H-6T decreased BMD. At 4 months of age, littermates from each congenic strain were assigned to control or treatment groups, then subjected to sham surgery or ovariectomy and held for 6 additional weeks. At necropsy, skeletal specimens were preserved in 95% EtOH, then femurs were assessed for changes in femoral density and cross-sectional phenotypes. A highly significant reduction in uterine wt/body wt confirmed completeness of ovariectomy. pQCT data showed that ovariectomized B6.C3H-1T, 4T, 6T, and 13T strain had significantly decreased femoral BMD (5 to 9%) and significantly decreased mid-diaphyseal cortical thickness (4 to 12%). Mid-diaphyseal periosteal circumfernces were unchanged. The B6.C3H-18T congenic strain was exceptional in that ovariectomy did not significantly decrease either femoral BMD or mid-shaft cortical thickness. These findings indicate: 1) genetic differences in response to ovariectomy exist among inbred mouse strains; and 2) c3h alleles for the Chr 18 BMD QTL may provide insight to why C3H female bone is resistant to loss of estrogen support.

1221

Insulin-Like-Growth-Factor I (IGF-I) Gene Promoter Polymorphism And The Risk Of Fracture In The Elderly: The Rotterdam Study. F. Rivadeneira*[1], J. Houwing-Duistermaat*[1], H. A. Pols[2], C. M. Van Duijn*[1], A. G. Uitterlinden[2]. [1]Epidemiology & Biostatistics, Erasmus Medical Center, Rotterdam, Netherlands, [2]Internal Medicine, Erasmus Medical Center, Rotterdam, Netherlands.

Previously, we have found a polymorphism in the promoter region of the IGF-I gene associated to bone mineral density (BMD) levels and rate of bone loss in post-menopausal women. We examined the role of this polymorphism in relation to frailty and site-specific risks of fracture within the Rotterdam Study, a population-based cohort study of determinants of chronic disabling diseases in the elderly. Genotyping was performed in 7012 (87.8%) of the 7983 respondent participants. Genotype relative risks were estimated as odds ratios from logistic regressions and as hazard ratios from Cox regressions, both adjusted for age, sex and body mass index. The mean follow-up period was 6.3 (*SD* 2.5) years. The distribution of incident fractures in genotyped individuals (n=905) was 26.6%, 10.3%, 4.3%, 25.9% and 32.9% for hip, proximal humerus, pelvis, wrist and other type of fracture, respectively. All genotype frequencies were in Hardy-Weinberg equilibrium proportions. When taking all frailty fractures into account (Figure 1), non-carriers of the wild type (*192-bp*) allele had a higher risk of fracture (*OR* 1.4 *95%CI* 1.0-1.9) than individuals carrying the allele, suggesting a recessive effect of the gene on the phenotype. This effect was consistent (although not significant) for the risk of hip fracture (*HR* 1.3 *95%CI* 0.9-1.9) evidencing a higher incidence in non-carriers of the allele (Figure 2). An allele dose effect was observed at the proximal humerus (Figure 3), where non-carriers (*HR* 2.2 *95%CI* 1.2-4.2) and heterozygotes (*HR* 1.8 *95%CI* 1.1-2.9) had a higher risk of fracture, as compared to homozygotes for the *192-bp* allele. None of these effects were observed at the pelvis, wrist or other type of fractures. When we adjusted for femoral neck BMD our point estimates did not essentially change. Our findings suggest that this promoter polymorphism or another polymorphism in linkage disequilibrium may be a genetic determinant of osteoporosis, including fractures. These results are consistent with our earlier findings on BMD and serum IGF-I levels. Based on this, we suggest that absence of the wild type allele (*192-bp*) has a deleterious effect on BMD and possibly on bone quality.

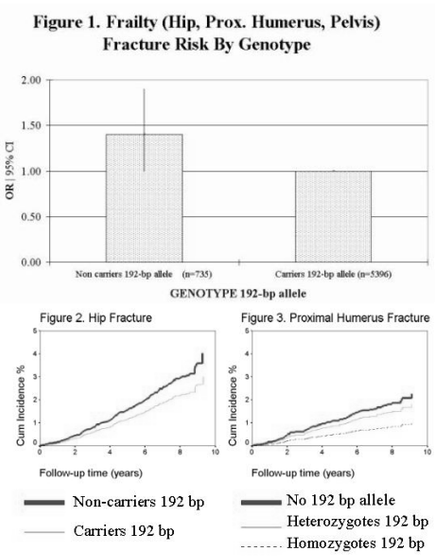

1222

Association of Polymorphisms in the Sclerosteosis/vanBuchem Gene Region with Bone Mineral Density in Elderly Subjects. A. G. Uitterlinden[1], P. P. Arp*[1], J. B. J. van Meurs[1], B. W. Paeper*[2], S. Proll*[2], P. Charmley*[2], T. B. Britschgi*[2], J. A. Latham*[2], R. C. Schatzman*[2], H. A. P. Pols[1], M. E. Brunkow*[2]. [1]Internal Medicine, Erasmus University Rotterdam, Rotterdam, Netherlands, [2]Celltech R&D, Bothell, WA, USA.

Osteoporosis has a strong genetic component but the genes involved are poorly defined. In this study we examine the association between the gene encoding sclerostin (SOST) and BMD in order to ascertain whether SOST can be considered an osteoporosis candidate gene. Sclerostin is an important regulator of bone density, and mutations in SOST result in sclerosteosis (MIM 269500), a rare recessive sclerosing bone dysplasia. We sequenced >90 kb of the SOST gene region in 90 ethnically diverse individuals, and used a set of 8 polymorphisms thus found to genotype 1927 men and women (55-80 years) from a large population-based prospective cohort study of elderly Dutch Caucasians. We analyzed genotype effects on BMD and on risk of vertebral and non-vertebral fractures (n=270) during 7 years of follow-up. We found no SOST gene coding polymorphisms but identified 3 variants within 8 kb upstream of the coding sequence, and 3 variants within a far downstream 52 kb interval recently found to be deleted in van Buchem disease, a monogenic bone disorder very similar to sclerosteosis. A 3 bp GGA-insertion in the SOST promoter region (SOST3; allele frequency 39%) was shown to be associated with decreased BMD in women at the femoral neck (p=0.05) and at the lumbar spine (p=0.01) with evidence for an allele-dose effect. We found genotype differences at the lumbar spine to strongly increase with age (Figure 1). In addition, we found a G-variant in the van Buchem deletion region (SOST9; allele frequency 41%) to be associated with increased BMD in men at femoral neck (p=0.006) and at lumbar spine (p=0.01) with evidence for an allele-dose effect. In both cases, overall differences between extreme genotypes amounted to 0.2 SD and we observed no genotype effects on fracture risk. In conclusion, 2 common variants in the SOST gene region were associated with BMD differences and the relations were found to be modified by gender (SOST 3 and 9) and by age (SOST3). The effect-size we observed on BMD was too small to be detected as genotype-dependent differences in fracture risk. The mechanism underlying the BMD differences is unclear but is likely to involve modulation of expression of sclerostin.

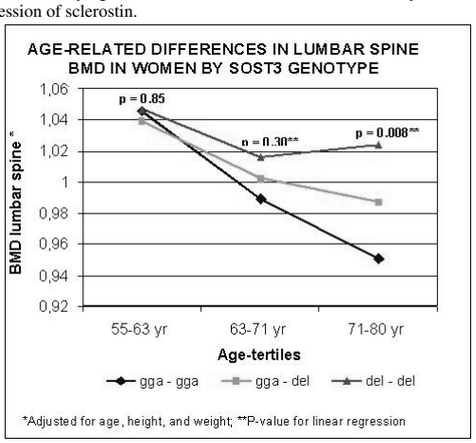

Disclosures: ***A.G. Uitterlinden****, Celltech R&D 2, 5.*

F001

Bone Response to Maternal vs Therapist Administered Physical Activity in Premature Infants. L. J. Moyer-Mileur[1], S. D. Ball*[1], V. L. Brunstetter*[2]. [1]Pediatrics, University of Utah, Salt Lake City, UT, USA, [2]Occupational and Physical Therapy, University of Utah Hospital, Salt Lake City, UT, USA.

Background: Preterm infants are at risk of developing osteopenia due to limited in-utero bone accretion and increased ex-utero bone nutrient needs. We have previously reported greater bone mass and body weight gains in preterm infants who received daily physical activity (PA) from a trained occupational therapist (J Peds 1995 and Pediatr 2000). We wondered if a daily PA program administered by the infant's mother would elicit a similar response. Purpose: To compare bone and body weight changes in infants who received a maternal versus therapist-administered PA program. Design: Preterm infants (n=32) were randomized to the maternal (MT; n=16; 6M/10F) or therapist (OT; n=16; 10M/6F). PA consisted of range of motion against passive resistance to all extremities for 5-10 minutes each day for a 4-week period. The therapist provided PA training to mothers of MT infants at study entry. Infants were fed 24Kcal/oz mother's milk with fortification or preterm infant formula (Mead Johnson Nutritionals, Evansville, IN) to achieve an average daily intake of 120 Kcal/kg/day. Body weight and nutrient intake were recorded daily. Forearm measurements by pDEXA (Norland, Fort Atkinson, WI) and serum and urine markers of bone and anabolic activity were obtained at study entry and 4 weeks. MT and OT infant results were compared to age and weight-matched infant controls (n=16; 10M/6F) from the previous study. Body weight at entry and completion, energy intake, and study days were treated as covariants in the statisitical analyses. Results: The MT and OT groups experienced similar gains in bone mass and body weight. Despite similar nutrient intakes, bone mineral content (BMC; mg), area (BA; cm^2), and density (BMD, mg/cm^2) gains were greater for both MT and OT versus controls while OT infants had greater weight gain than controls ($p < 0.05$; Table). Bone alkaline phosphatase (BAP) levels increased ~15% in MT and OT infants and decreased ~20% in controls from baseline ($p < 0.05$). Urine calcium/creatinine excretion was similar and within normal limits for all groups. Conclusion: A daily PA program administered by the infant's mother or a trained therapist is equally effective in promoting greater bone mass in premature infants.

Forearm Bone Mass and Body Weight Changes During the 4-Week Study Period

	MT	OT	Control	p
BMC(mg/d)	9.3 ± 4.8	9.3 ± 5.4	4.3 ± 5.0	0.004
BA(cm^2/d)	0.08 ± 0.06	0.09 ± 0.05	0.05 + 0.05	0.05
BMD(mg/cm^2/d)	0.4 ± 0.4	0.3 ± 0.2	0.1 ± 0.4	0.03
Weight (g/kg/d)	14.5 ± 2.9	16.2 ± 2.4	14.2 ± 1.9	0.03; OT>Control

F003

Impact of Calcium Supplementation on Markers of Bone and Calcium Metabolism in 16-18 Year Old Boys. F. Ginty[1], S. J. Stear*[1], S. C. Jones*[1], D. Stirling*[1], J. Bennett*[1], A. Laidlaw*[1], T. J. Cole*[2], A. Prentice[1]. [1]MRC Human Nutrition Research, Cambridge, United Kingdom, [2]Department of Paediatric Epidemiology and Biostatistics, Institute of Child Health, London, United Kingdom.

The impact of increased Ca intake on markers of bone and Ca metabolism in older adolescent boys has not been previously investigated. To address this, we analysed samples from 143 boys, aged 16-18 years, who took part in a 12 month randomised, double-blind, placebo-controlled calcium intervention study (see Prentice et al, ASBMR Annual Meeting 2002). Randomisation was stratified according to physical activity level (less or greater than 9h of sport per week) and subjects were then assigned to either a Ca supplement (1000 mg of Ca/day (as CaCO3)) or matching placebo. Ca supplementation resulted in significant increases in skeletal size and bone mineral content (BMC). To identify the underlying mechanisms for these changes, first morning urine and non-fasting blood samples were collected at baseline and after 5 months (interim) and 12 months (final) supplementation. Urine was analysed for Ca, deoxypyridinoline (DPD) and N-terminal telopeptides of type I collagen (NTX-I), phosphate (P), and creatinine. Plasma was analysed for parathyroid hormone (PTH), intact osteocalcin (OC[1-49]), bone-specific alkaline phosphatase (Bone ALP), albumin-adjusted Ca (Ca-alb) and phosphate (Pi). In the Ca supplemented group at interim, there was a non-significant increase in urinary Ca excretion (+12%, p=0.26), a significant reduction in PTH (-16.2%, p=0.03) and DPD was reduced in the higher compliers (-11.5%, p=0.03). Non-significant reductions were also observed for NTX-I (-15%, p=0.08) and OC[1-49] (-10%, p=0.30), in the higher compliers. Only marginal changes were found for Bone ALP, Ca-alb, Pi and urinary P (ranging between -1 and +1%). By the end of the study, urinary Ca was 21% higher (p=0.04) in the Ca group and 34% higher (p=0.02) in the higher compliers. Both OC[1-49] and NTX-I were lower in the higher compliers (-11.4%, p=0.04 and -15.4%, p=0.08, respectively). Little effect of the supplement on PTH and DPD was observed (-4% and -2%, respectively, ns) and, again, the remaining markers only marginally changed. No interaction was found between the supplement and physical activity level. The results of this study suggest that the observed increases in BMC may have been due to a transient decrease in PTH, resulting in a lower rate of bone turnover. The varying responses of the markers demonstrates the importance of measuring more than one formation and resorption marker, at more than one timepoint, in order to fully elucidate mechanisms. Further analysis is underway to determine the mechanisms that led to increases in skeletal size.

*Disclosures: **F. Ginty**, Shire Pharmaceuticals 2; Nycomed Pharma 2.*

F006

Patterns and Pitfalls in pQCT Measurements of the Tibia in Children. B. S. Zemel, R. Ittenbach*, V. Stallings*, S. Kaup*, M. Gomelsky*, M. B. Leonard. Pediatrics, The Children's Hospital of Philadelphia, Phila, PA, USA.

Peripheral quantitative computed tomography(pQCT) measurements of the tibia have been proposed for assessment of bone density, dimensions and strength in children. Recommended measurement parameters were developed at a Pediatric User's Group Meeting in 2000. Following those guidelines, we assessed bone health in well children as part of a study to establish reference data on bone health and body composition in children. 152 (77 female) healthy children, ages 6 to 21 years enrolled. 35% of children were African-American ethnicity. All pQCT measurements were taken with a Norland-Stratec XCT2000 using a voxel size of 0.4mm and slice thickness of 2.3 mm. The medial aspect of tibia length (TL) was measured anthropometrically. The reference line was placed at the distal end of the epiphyses on the scout view scan. Measurements were obtained at the 4% (trabecular assessment), 20% (cortical assessment) and 66% (muscle assessment) sites. An additional region of interest (ROI) within the cortical bone envelope was defined at the 20% site to minimize partial volume effect. Cross-sectional moment of inertia (CSMI) was derived from the 20% site. Cross-sectional muscle area was derived from the 66% site(MA66%). All scans were reviewed for scan quality by two investigators. Results were evaluated in relation to age, gender, TL, ethnicity, and MA66%, by regression analysis. The major difficulty with scan quality occurred at the 4% site where variability in epiphyseal size resulted in glancing the metaphysis. This usually occurred on the bone periphery, so trabecular analysis was restricted to the inner 45%. There were no age or size trends in trabecular density. Girls had significantly greater trabecular density than boys, with a significant interaction between gender and ethnicity (r2=0.07). Overall cortical density was significantly associated with age, TL, gender, ethnicity (r2=0.63); however, cortical ROI density was associated with age and gender (r2=0.29). Cortical thickness was associated with MA66% and TL (r2=0.78). CSMI was associated with MA66%, TL and gender (r2=0.79). This measurement protocol had limitations due to variability in epiphyseal size and shape. Consequently, the interpretation of trabecular bone density is uncertain. There were no age trends in trabecular density, which may be related to the problems in the measurement protocol. Cortical density was strongly related to age, size and ethnicity, but the ROI analysis demonstrated weaker associations, which may be due to partial volume effect. New measurement strategies are necessary to further develop this tool for bone health research in children.

F009

Intervertebral Disc Degeneration Increases Load-bearing by the Neural Arch and Reduces BMD in the Anterior Vertebral Body. P. Pollintine*[1], J. H. Tobias[1], D. S. McNally*[2], G. K. Wakley[1], P. Dolan*[1], M. A. Adams*[1]. [1]University of Bristol, Bristol, United Kingdom, [2]University of Nottingham, Nottingham, United Kingdom.

Introduction: Bone mineral density (BMD) of the whole vertebra is conventionally used to diagnose spinal osteoporosis. However, recent evidence suggests that bone loss can be more pronounced in the anterior vertebral body (1). We hypothesise that age-related degeneration of intervertebral discs increases neural arch compressive load-bearing, causing pronounced anterior vertebral body bone loss and weakening. Materials and Methods: Fifteen cadaveric thoraco-lumbar motion segments (aged 72-92 yrs), comprising 2 adjacent vertebral bodies and intervening disc and ligaments, were compressed to 1.5 kN while positioned to simulate the erect standing posture. The distribution of compressive stress was measured within the intervertebral disc by pulling a miniature pressure transducer along its mid-sagittal diameter. “Stress profiles” were integrated over area to give the compressive force acting on the anterior and posterior halves of the vertebral body (2). These were subtracted from the 1.5 kN to determine the force on the neural arch. Compressive strength of each motion segment was measured in flexion to simulate forwards stooping. DXA was used to measure bone mineral content (BMC) of the anterior vertebral body, and of the whole vertebra (including the neural arch). Volumetric BMD of the anterior vertebral body, and of the whole vertebra was then calculated from BMC. Results: In the simulated erect posture, the neural arch resisted 12-86% of the applied 1.5 kN, while the anterior vertebral body resisted only 4-32%. Compressive strength in flexion correlated negatively with load-bearing by the neural arch in erect posture ($r^2 = 0.51$, $p = 0.006$). Anterior vertebral body BMD was consistently lower than whole vertebra BMD ($p < 0.002$). Anterior vertebral body BMD was a better predictor of compressive strength than whole vertebral BMD ($r^2 = 0.82$ and $r^2 = 0.72$, respectively). Discussion: Age-related degenerative changes cause intervertebral discs to lose height, increasing neural arch compressive load-bearing in erect postures. This unloads the disc, particularly its anterior half, reducing the compressive force on the anterior vertebral body. Habitual unloading causes bone loss that is pronounced in the anterior vertebral body, making it vulnerable to fracture when the spine is loaded in flexion. Anterior vertebral body BMD measurement may be of greater diagnostic value in predicting vertebral fracture risk than whole vertebra BMD.

1. Simpson EK et al (2001) JBMR 16: 681-7
2. Pollintine P et al (2001) Paper No. 872. 47th Ann. Meet. Orthop. Res. Soc. San Francisco, USA

F011

Young-old Differences in Vertebral and Proximal Femoral Bone Density and Size: The Mr Os Study. T. F. Lang*[1], J. Li*[1], A. Yu*[1], K. Ensrud[2], M. Nevitt[3], E. Orwoll*[4]. [1]Radiology, University of California, San Francisco, CA, USA, [2]VA Med Ctr, University of Minnesota, Minneapolis, MN, USA, [3]Epidemiology, University of California, San Francisco, CA, USA, [4]Medicine, Oregon Health Sciences University, Portland, OR, USA.

Bone size is thought to increase to compensate for the age-related decrease in bone mineral density. To address this issue we imaged the proximal femorae and L1-L2 vertebrae of 30 young Caucasian-American (mean age 39±3 years) and 800 elderly (mean age=75±7 years) men with volumetric quantitative computed tomography (vQCT). The young men were residents of the San Francisco Bay Area and had no known conditions affecting bone metabolism. The elderly subjects were healthy community-dwelling males recruited by the Pittsburgh and Minneapolis clinics of the Study of Osteoporotic Fracture in Men (Mr Os). VQCT images were processed to obtain measurements of integral (iBMD) and trabecular (tBMD) bone density and integral cross-sectional area (CSA) as well as indices of bending (BSi) and compressive strength (Csi) in the hip and spine respectively. Spine measures included tBMD, iBMD, CSA and CSi (CSi=iBMD2*CSA). Hip measures included iBMD and tBMD in the femoral neck. We also calculated the minimum CSA of the femoral neck and the polar moment of inertia (J) at this location. BSi was calculated by dividing J by sqrt(2*CSA/p). To adjust for differences in height and weight, we used ANACOVA to compare between young and elderly males. Elderly men had lower BMD but larger CSA than young men at both the spine and the hip. CSi was smaller in older men. BSi was also smaller in the elderly men, but the difference was not statistically significant. Results are tabulated below. Compared to younger men, older males have larger vertebral and femoral neck cross-sectional areas but lesser BMD. The increase in cross-sectional area appears to preserve BSi in the femoral neck. However, despite the increase in vertebral CSA in the elderly men, the CSi was significantly reduced in this group.

Results

		Spine		
	iBMD	tBMD	CSA	CSi
Y	0.188***	0.162***	10.2***	0.36***
O	0.150	0.114	12.5	0.28
		Hip		
	iBMD	tBMD	CSA	BSi
Y	0.324***	0.147***	12.4**	2.15
O	0.288	0.097	13.9	2.11

*p<0.05, **p<0.01, ***p<0.001

F013

Assessment of Densitometric Criteria for the Diagnosis of Osteoporosis in Men and Women with Vertebral Fractures. L. del Rio[1], N. Guañabens[2], P. Bassa*[1], P. Peris[2], A. Monegal*[2], L. Jover*[3]. [1]Densitometria Osea, CETIR Centre Medic, Barcelona, Spain, [2]Servicio de Reumatologia, Hospital Clinico, Barcelona, Spain, [3]Departamento de Salud Publica, Facultad de Medicina, Barcelona, Spain.

The aim of this study was to investigate the relations between bone mineral density (BMD) and vertebral fractures in men and women who attended our facility for their osteoporosis work-up. BMD and anthropometric data of lumbar spine and proximal femur were obtained from a total of 71093 patients (68007 women, 3086 men). There were 2860 patients (2428 women and 432 men) with at least one vertebral fracture/deformity with no relationship with a significant trauma, and confirmed by conventional anterior and lateral X-ray of lumbar spine or vertebral morphometry using dual X-Ray absorptiometry (MXA). Mean age of women and men with vertebral fractures was 63.6 years (9.9 SD), and 61.1 (11.4 SD), respectively. BMD values in lumbar spine and proximal femur were obtained using LUNAR equipment (DPX-L and EXPERT), and results in spine were expressed as density by area (g/cm2) and apparent density (g/cm3), T-score and Z-score. Accumulated frequency for vertebral fracture was calculated for every parameter studied. Our results showed that BMD values in patients with spine fractures were significantly lower than in patients with no fracture, independently of sex. T-score in both regions was very similar for women and men with vertebral fractures (median value in lumbar spine, T, -2.2 vs 2.3). We found vertebral width differences (p<0.0001) between patients groups, with and without fractures, in both sexes. Vertebral height was not determinant for categorizing patients according to the fracture status, however, values were significantly lower in patients with fractures, irrespective of sex, in comparison with non-fractured patients. By using the WHO criteria, 50.92% of men and 51.02% of women with vertebral fractures were categorized within the osteoporotic range. Apparent BMD (g/cm^3) did not contribute with additional data in this study. These results suggest that WHO criteria for the identification of caucasian women with osteoporosis may also be applied to men, standing from the vertebral fracture strategy.

F016

Specific Regulation of BMP-2 Gene Expression by NF-κB in Growth Plate Chondrocytes. D. Chen[1], J. Q. Feng[2], J. Zhang*[2], M. Zhao[1], D. Horn*[1], J. Chan*[1], S. E. Harris[2], G. R. Mundy[1], B. F. Boyce[3], L. Xing[3]. [1]Molecular Medicine, University of Texas Health Science Center at San Antonio, San Antonio, TX, USA, [2]Oral Biology, University of Missouri, Kansas City, MO, USA, [3]Pathology, University of Rochester, Rochester, NY, USA.

It has been well documented in osteopetrotic null mice that NF-κB p50 and p52 proteins are essential for osteoclastogenesis. What has not been previously appreciated is that in two-week-old NF-κB p50/52 double knockout (dko) mice, the architecture of the endochondral growth plate is disorganized with a significantly expanded hypertrophic zone. Since this is not a feature of src-/- osteopetrosis, we hypothesized that NF-κB may play an important specific role in chondrogenesis. In *drosophila*, the dpp gene, a homologue of BMP-2, is regulated by *dorsal*, a homologue of mammalian NF-κB. BMP-2 has been shown to play important roles in chondrocyte proliferation and maturation. We hypothesized therefore that NF-κB regulates chondrogenesis via effects on BMP-2. We firstly examined BMP-2 mRNA expression in NF-κB p50/52 dko mice by in situ hybridization. BMP-2 mRNA was detected predominantly in hypertrophic and articular chondrocytes in wild-type and NF-κB p50/52 dko mice but its expression in hypertrophic chondrocytes in the dko mice was greatly reduced. We then investigated mechanisms by which NF-κB may regulate BMP-2 expression in chondrocytes. Two NF-κB response elements were found in the -2712/+165 region of the BMP-2 gene. Mutations in the NF-κB cis-DNA response elements of the BMP-2 gene or transfection of mutant I-κBα expression plasmids with the BMP-2 promoter into TMC-23 chondrocytes suppressed BMP-2 transcription. Gel shift assays demonstrated that TMC-23 cell nuclear preparations bind these two NF-κB response elements in the BMP-2 gene. The supershift assays revealed that the NF-κB proteins, which bound to NF-κB response elements in the BMP-2 gene, were NF-κB subunits p50 and p65. To determine if there are functional changes in growth plate chondrocytes of p50/p52 dko mice, cell proliferation following *in vivo* BrdU labeling and apoptosis with TUNEL staining were analyzed. In the NF-κB p50/52 dko mice, chondrocyte proliferation was dramatically reduced (BrdU+ve cells: 14.0 ± 2.1 in wt Vs 3.5 ± 2.4 in dko) and apoptosis of chondrocytes at chondrocyte/hypertrophic chondrocyte junction area of growth plate were also reduced in NF-κB p50/52 dko mice (apoptotic cells: 12.3 ± 0.5 in wt Vs 6.3 ± 1.9 in dko). Type X collagen mRNA expression was also reduced in the hypertrophic chondrocyte area in NF-κB p50/52 dko mice. These findings indicate that NF-κB regulates chondrocyte maturation in postnatal murine growth plates by directly activating BMP-2 gene expression.

Disclosures: ***D. Chen****, OsteoScreen Ltd 1, 3.*

F018

Transplantation of Fibroblasts Expressing BMP-2 Promotes Bone Repair More Effectively Than That Expressing Cbfa-1. K. Hirata*[1], T. Tsukazaki[1], Y. Shibata*[1], A. Mizuno*[2], T. Komori[3], A. Yamaguchi[1]. [1]Oral Pathology, Nagasaki University School of Dentistry, Nagasaki, Japan, [2]Oral and Maxillofacial Surgery, Nagasaki University School of Dentistry, Nagasaki, Japan, [3]Osaka University, Osaka, Japan.

To explore new therapeutic approach to repair large bone defect, a new strategy, including cell transplantation and gene therapy, has to be established. Recently, an ex vivo gene therapy using adenoviral BMP-7 expression in fibroblast has been demonstrated to regenerate rat calvarial defect. However, it is so far unclear whether gene expression of bone-specific transcription factor also transduces nonosteogenic cells to osteoblastic lineage, and eventually forms bony tissue in vivo. In this study, we investigated the osteogenic potential of skin fibroblasts that transduced BMP-2 or Cbfa-1, an essential transcription factor for osteoblast, by transplantation into critical-sized bone defect. Skin fibroblasts isolated from newborn GFP transgenic mice (provided by Dr. Okabe) were transfected with adenovirus encoding hBMP-2 (provided by Dr. Bessyo) or mCbfa-1. These cells were trypsinized, immersed in a carrier of poly D,L lactic-co-glycolic acid gelatin sponge (PGS) and transplanted into bony defects with 4mm diameter that created on parietal bone of 8 weeks old mice with the identical genetic background. This calvarial defect was not repaired until at least 6 weeks when PGS was transplanted. Expression of BMP-2 and Cbfa-1 in vitro persisted at least 5days after transfection, as evaluated by ELISA and fused EGFP fluorescence color image analysis, respectively. Transfection of Cbfa-1 remarkably induced alkaline phosphatase (ALP) activity in vitro, but failed to stimulate bone formation even after 6 weeks of implantation. In contrast, BMP-2 transfected fibroblasts induced bone formation from 2 weeks in all cases, and more than 50% of PGS was replaced by newly formed bone at 4 weeks. This bone formation was initiated within PGS, and bone marrow tissue was also reconstructed. Immunofluorecence analysis of the regenerated tissue revealed that a part of the bony tissue contained EGFP-positive osteocytes and osteoblasts. These indicate that overexpression of BMP-2 in fibroblast promotes bone repair, and such fibroblasts have a potential to differentiate into osteoblastic lineage. In contrast, Cbfa-1 expression is insufficient to induce bone formation despite intense activity to induce osteoblast differentiation in vitro. Taken together, our results suggest that expressing several osteogenic growth factors is more suitable for fibroblast-based gene therapy to large bone defect than expressing osteogenic transcription factors.

F020

αv-Containing Integrins Colocalize with BMP-2 Receptors and Are Essential in BMP-2 Function. C. F. Lai, S. L. Cheng. Division of Bone and Mineral Diseases, Washington University School of Medicine, St. Louis, MO, USA.

It is well established that integrins and BMP-2 regulate osteoblast growth and differentiation. Integrin-matrix interactions and BMP-2 also share overlapping signal transduction by activating MAPK cascade. Therefore, there appear to have intimate relationship between integrins and BMP-2 in osteoblast function. Indeed, collagen integrin receptors (α1β1 and α2β1), FAK, and Ras/Erk have all been implicated to play important roles in BMP-2 induction of osteoblast differentiation (JBMR14:1075, 1999; JBMR16:1772, 2001; JBMR17:101, 2002; and JBMR17:240, 2002). Conversely, BMP-2 has been shown to up or down regulate the expression of integrins depending on the cell types analyzed. In addition to collagen, osteoblasts also express several non-collagenous proteins such as osteopontin, bone sialoprotein, and fibronectin, which are important for matrix mineralization. These proteins can interact with the αv-containing integrins (αvβ) and their expression is upregulated by BMP-2. We examined the effects of BMP-2 on integrin expression and the role of αvβ integrins in BMP-2 regulation of normal human osteoblast function. BMP-2 elevated the levels of αvβ integrins, including αvβ3, αvβ5, αvβ6, and αvβ8, on osteoblast surface. The surface level of β1-containing integrins (αβ1) was also increased by BMP-2. Consistent with the increase in integrin levels, osteoblast adhesions to osteopontin and vitronectin, which were dependent on the αvβ integrins, were enhanced by BMP-2. Immunoprecipitation with specific integrin antibodies followed by Western blotting for BMP-2 receptors indicated that both type I and type II receptors of BMP-2 co-localized with αvβ integrins (αvβ3, αvβ5, αvβ6, and αvβ8) and αβ1 integrins. Immunostaining and confocal examination confirmed the co-localization of BMP-2 receptors with these integrins. To analyze the role of αvβ integrins in BMP-2 function, we employed the function-blocking anti-αv antibody, L230. BMP-2 reduced the proliferation of normal human osteoblasts and this inhibition was reversed by L230. L230 lessened the stimulation of alkaline phosphatase activity and abrogated the increase in osteopontin and bone sialoprotein levels by BMP-2. Incubation of osteoblasts with L230 prevented BMP-2 from inducing matrix mineralization. We conclude that BMP-2 and integrin share close relationship in their regulation of osteoblast function. BMP-2 increased the surface levels of αv- and β1-conatining integrins, resulting in an enhanced osteoblast adhesion to bone matrix proteins. Perturbation of αvβ integrin function inhibits BMP-2 regulation of osteoblast activity. Thus, the αv-containing integrins are essential in BMP-2 function.

F024

Increased Root Cementum in ANK-Mutant Mice – Developmental and Regenerative Implications. F. H. Nociti, Jr.*[1], J. E. Berry*[1], B. L. Foster*[1], K. Gurley*[2], D. M. Kingsley*[2], M. J. Somerman[1]. [1]Periodontics, Prevention, Geriatrics, University of Michigan, Ann Arbor, MI, USA, [2]Developmental Biology, Stanford University, Stanford, CA, USA.

Ank is a multipass transmembrane protein that appears to control the transport of intracellular pyrophosphate (PPi) into extracellular matrix. Mice carrying a mutation in the *ank* gene exhibit an extracellular PPi deficiency and develop excess mineralization of articular surfaces and synovial fluid with eventual death due to joint immobilization. These mice have been used as a model for arthritic-like crystal deposition. We hypothesized that *ank/ank* mutant mice would develop ectopic hydroxyapatite crystals within the developing periodontium resulting in a compromised dentition. Studies designed to test this hypothesis were performed in compliance with guidelines of the University of Michigan Unit for Lab Animal Medicine and Stanford University Institutional Animal Care and Use Committee. In order to investigate the effects of this gene mutation on the periodontium, an initial *in situ* hybridization and immunohistochemical screen for ank expression in normal mice was performed. The results indicated that ank is highly expressed in cells involved in the developing tooth from day 21 to 33 (where day 19 is the date of birth), and that expression is weaker and relatively non-specific at later times. Subsequent experiments were done in which mandibular tissues in the first molar region of *ank/ank* mutant mice, at sequential stages of root development, were analyzed by routine H&E staining, *in situ* hybridization and immunohistochemical methods. H&E staining of the tooth root region of a fully developed molar revealed an enormous amount of cementum, predominantly cellular, on the root surface, approximately 10-fold greater than wild type littermates. No ectopic mineral formation was noted within the periodontal ligament region, and the surrounding alveolar bone appeared comparable to that observed in the wild type mice. Examination by H&E of mutant mice at earlier ages revealed that this striking overproduction of cementum is apparent from the onset of cementogenesis. Further investigations by *in situ* hybridization showed a 2-3 fold increase over wild type of mRNA levels of both type I collagen and also of osteopontin, a molecule consider to regulate crystal growth and whose expression has been shown to be sensitive to phosphate. These remarkable findings suggest that cementum production and cells within the periodontal region are highly responsive to changes in ANK activity and pyrophosphate metabolism. These results may have important clinical implications in the formulation of regenerative therapies for periodontal disease.

F026

A Functional Feedback Loop Comprising Stanniocalcin 1, the Type III NaPi Transporter (Pit1) and Pi Transport Regulates Bone Matrix Mineralization In Vitro and In Vivo. Y. Yoshiko[1], G. A. Candeliere[2], N. Maeda*[1], J. E. Aubin[2]. [1]Oral Growth and Developmental Biology, Hiroshima University, Hiroshima, Japan, [2]Anatomy and Cell Biology, University of Toronto, Toronto, ON, Canada.

In diseases such as X-linked hypophosphatemic rickets/osteomalacia, a dysfunction intrinsic to osteoblasts appears to be related to aberrant transport of inorganic phosphate (Pi), but little is known about how Pi transport is regulated and contributes to bone formation. To assess the role of the osteoblast sodium-dependent Pi (NaPi) transporter(s) in bone formation, we injected foscarnet, a selective inhibitor of NaPi transport, subcutaneously over the newborn rat calvaria. We observed a mineralization defect in the calvaria, without any detectable change in other bones or in serum levels of Pi, Ca, ALP and $1,25(OH)_2D_3$. The mineralization defect was also exhibited in the fetal rat calvaria (RC) cell culture model treated with foscarnet. To address the NaPi transporter(s) in osteoblasts, we analyzed RNA from discrete RC osteoblast colonies and Pit1 was found to be the predominant transporter expressed. To dissect the role of Pit1 in mineralization, we over- and underexpressed this transporter in RC cells using plasmid transfections and antisense (AS) oligonucleotides; mineralization positively correlated with Pit1 expression levels. To identify soluble proteins expressed in osteoblasts that may regulate their NaPi transport, we searched for genes responding to foscarnet in RC cells and identified stanniocalcin 1 (STC1). STC1 has been suggested not to be the putative phosphaturic substrate of PHEX (the phosphate-regulating gene with homologies to endopeptidases located on the X chromosome), because it is thought to stimulate renal NaPi transport and not to be cleaved by PHEX. However, to address further the role of STC1 and its relationship to NaPi transport and/or mineralization, we treated RC cells with STC1 AS oligonucleotides or recombinant STC1 (rSTC1) with or without Pit1 AS oligonucleotides. STC1 was found to stimulate NaPi uptake and mineralization and positively correlated with expression of Pit1 and osteopontin (OPN), a gene reported to be responsive to NaPi transport in an osteoblastic line. Concomitant with these findings in vitro, we confirmed that injections of rSTC1 over the neonatal rat calvaria hastened the mineralization process as indicated by decreased osteoid area and increased Pit1 and OPN expression in the calvaria without other systemic changes. Thus, we conclude that osteoblast-mediated NaPi transport is an essential process for bone matrix mineralization and have identified a new pathway regulating this process, which consists of a functional loop of STC1, Pit1 and Pi transport.

F029

Targeted Inactivation of the Integrin-Linked Kinase (ILK) in Mouse Chondrocytes Reduces PKB/Akt Phosphorylation, Diminishes Chondrocyte Proliferation and Adhesion, and Impairs Growth Plate Development. L. Terpstra*[1], J. Prud'homme*[1], A. Arabian*[1], S. Dedhar*[2], R. St-Arnaud[3]. [1]Genetics Unit, Shriners Hospital for Children, Montreal, PQ, Canada, [2]BC Cancer Research Centre, University of British Columbia, Vancouver, BC, Canada, [3]Genetics Unit, Shriners Hospital for Children and McGill University, Montreal, PQ, Canada.

Chondrocyte proliferation and differentiation requires their attachment to the collagen type II-rich matrix of developing bone. This interaction is mediated by the integrin family of transmembrane proteins and their cytoplasmic effectors, such as the integrin-linked kinase (ILK). To understand the role of integrin signaling in these processes, we have specifically inactivated the ILK gene in growth plate chondrocytes using the Cre-lox methodology. Mice carrying an ILK allele flanked by loxP sites (ILK-fl) were crossed to transgenic mice expressing the Cre recombinase under the control of the collagen type II promoter. Inactivation of both copies of the ILK-fl allele lead to a disorganization of growth plate architecture and to dwarfism. Chondrocyte proliferation, assessed by BrdU or PCNA labeling, was reduced. Apoptosis and differentiation of growth plate chondrocytes were not affected, however. Integrin-mediated adhesion of primary cultures of chondrocytes from mutant animals to collagen type II was severely impaired. At the molecular level, ILK inactivation in chondrocytes reduced phosphorylation of PKB/Akt on serine 473 and inhibited cyclin D1 expression. These results confirm that PKB/Akt is a physiologically relevant substrate of ILK and show that ILK inactivation in chondrocytes has dramatic consequences for chondrocyte proliferation and growth plate development.

F031

CTGF/Hcs24, a Hypertrophic Chondrocyte-Specific Gene Product, Stimulates Proliferation and Differentiation but Not Hypertrophy of Cultured Articular Chondrocytes. T. Nishida*[1], S. Kubota*[1], T. Nakanishi*[1], T. Kuboki*[2], G. Yosimichi*[1], S. Kondo*[1], M. Takigawa[1]. [1]Department of Biochemistry and Molecular Dentistry, Okayama University Graduate School of Medicine and Dentistry, Okayama, Japan, [2]Department of Oral and Maxillofacial Rehabilitation, Okayama University Graduate School of Medicine and Dentistry, Okayama, Japan.

Connective tissue growth factor/hypertrophic chondrocyte-specific gene product 24 (CTGF/Hcs24), which is specifically expressed in hypertrophic zone of growth plate, plays a key role in the proliferation and differentiation of growth cartilage cells. Such effects on the cells suggest that CTGF/Hcs24 might also play a role in the function and maintenance of articular cartilage cells as well. However, the effects of CTGF/Hcs24 on articular cartilage cells have not been studied yet. In this study, we investigated the effects of CTGF/Hcs24 on the proliferation and differentiation of rabbit articular cartilage (RAC) cells in vitro. RAC cells transduced by recombinant adenoviruses generating mRNA for CTGF/

Hcs24 synthesized more proteoglycan than the control cells. Also, treatment of RAC cells with recombinant CTGF/Hcs24 (rCTGF/Hcs24) increased DNA and proteoglycan syntheses in a dose-dependent manner. Northern blot analysis revealed that the rCTGF/Hcs24 stimulated the gene expression of type II collagen and aggrecan core protein, which are markers of chondrocyte maturation, in both rabbit growth cartilage (RGC) and RAC cells. However, the gene expression of type X collagen, a marker of hypertrophic chondrocytes, was stimulated by rCTGF/Hcs24 only in RGC cells, but not in RAC cells. Oppositely, gene expression of tenascin-C, a marker of articular chondrocytes, was stimulated by rCTGF/Hcs24 in RAC cells, but not in RGC cells. Moreover, rCTGF/Hcs24 effectively increased both alkaline phosphatase (ALPase) activity and matrix calcification of RGC cells, but not of RAC cells. These results indicate that CTGF/Hcs24 promotes the proliferation and differentiation of articular chondrocytes, but does not promote their hypertrophy or calcification. Taken together, the data show that CTGF/Hcs24 is a direct growth- and differentiation factor for articular cartilage and suggest that it may be useful for the repair of articular cartilage.

F033

Regulation of Chondrogenesis by Nuclear Factor of Activated T Cells (NFAT) and p38 MAP Kinase. M. Tomita*, M. C. Naski. Pathology, University of Texas Heailth Science Center at San Antonio, San Antonio, TX, USA.

Elevation of intracellular calcium triggers cell growth and differentiation in many cell types. Calcium signals lead to the activation of the phosphatase calcineurin. Calcineurin, in turn, dephosphorylates the transcription factor family, nuclear factor of activated T cells (NFATs). Dephosphorylation of NFATs results in translocation from the cytoplasm to the nucleus and subsequently regulation of gene expression. We report here that the calcium/calmodulin-dependent phosphatase calcineurin and NFATs, contributes to early chondrogenesis using two different culture systems. In the chondroblast clone RCJ 3.1C5.18 (C5) the calcium ionophore, ionomycin, induced aggrecan gene expression. Additionally, induction of aggrecan expression was inhibited following the addition of the calcineurin inhibitor; cyclosporineA. A physiological inhibitor of calcineurin, CAIN, also inhibited the induction of aggrecan by ionomycin. Using the mouse limb bud culture assay, we showed that ionomycin augments chondrogenesis as demonstrated by increased numbers of alcian blue staining cartilage nodules. Furthermore, cyclosporine A blocked the differentiation of limb bud mesenchyme. These data indicate that ionomycin induces chondrogenesis and aggrecan expression through a calcineurin-dependent pathway. Because calcineurin can regulate NFAT activity, we hypothesized that NFATs may contribute to aggrecan gene expression. To test this we overexpressed NFATc3 and NFATc4 in C5 cells. We found that NFATc3, but not NFATc4, can induce aggrecan gene expression. NFATs frequently regulate gene expression cooperatively with other transcriptional regulators, such as AP1, GATA, etc. In addition, while an activated form of calcineurin A upregulated aggrecan gene expression, the magnitude of gene induction was not as great as that observed with ionomycin, suggesting that other calcium-dependent regulatory pathways, in addition to NFATs, may contribute to aggrecan expression. Consistent with this we observed that the p38 MAP kinase inhibitor, SB203850, inhibited ionomycin-induced aggrecan expression in C5 cells. Furthermore, SB203850 diminished the number of alcian blue staining cartilage nodules in the limb bud culture system. Taken together, we conclude that intracellular calcium activates both the calcineurin/NFAT and MAP kinase-signaling axis during chondrogenesis.

F036

Increased Bone Mass in Proline-Rich Transcript of the Brain (prtb)-Deficient Mice. D. W. Sommerfeldt[1], M. Priemel[1], X. Wang*[2], M. Amling[1], T. Schinke[1], M. Hadjiargyrou[3], S. L. Mansour*[2], J. M. Rueger[1]. [1]Trauma and Reconstructive Surgery, Hamburg University Hospital, Hamburg, Germany, [2]Human Genetics, University of Utah, Salt Lake City, UT, USA, [3]Biomedical Engineering, State University of New York at Stony Brook, Stony Brook, NY, USA.

Prtb (Proline-rich transcript of the brain) is a recently discovered gene encoding a novel protein expressed in the brain of adult mice. Using differential display-PCR we found that prtb is also expressed in osteoblasts where its expression is upregulated during serum exposure and adhesion to various substrates. To determine whether prtb plays a physiologic role during bone remodeling in vivo, we analyzed the bones of prtb-deficient mice using static and dynamic histomorphometry. Initial contact radiography of 10 week-old prtb-/- mice, which have no gross pathological abnormalities, demonstrated an increase in bone density. Static histomorphometry confirmed a 41%-increase in bone mass within the spine of prtb-/- mice as compared to wildtype controls (17.85 ± 1.12 % vs. 12.7 ± 2.01 %, $p<0.001$). Surprisingly, bone cell number and bone cell surface indices were nearly identical between the two groups. In contrast, dynamic histomorphometry after fluorochrome labeling revealed a significant increase in bone formation rate in prtb-/- mice compared to wildtype littermates (223.79 ± 76.42 mm3/mm2/y vs. 144.61 ± 39.08 mm3/mm2/y, $p<0.05$). These findings suggest that the bone phenotype in prtb-deficient mice is due to a functional change of osteoblast activity and not due to an effect on bone cell differentiation and/or survival. Taken together, our data demonstrate that in adult mice the prtb gene is selectively expressed in brain and bone and that prtb-deficiency leads to an increased bone mass in mice due to increased bone formation.

F038

Temporospatial Expression of BIG-3 During Endochondral and Intramembranous Ossification. F. Gori, M. B. Demay. Endocrine Unit, Massachusetts General Hospital, Harvard Medical School, Boston, MA, USA.

Osteoblastic differentiation is a complex process controlled by a wide variety of factors including the family of the bone morphogenetic proteins (BMPs). We recently identified a novel BMP-2 induced gene, named BIG-3 (BMP-2 Induced Gene 3kb), that dramatically accelerates the program of osteoblastic differentiation in stably transfected MC3T3E1 cells. BIG-3 encodes a protein that belongs to the WD-40 family of proteins. The members of this family of proteins contain 4-17 WD repeats that form a characteristic beta-propeller structure that forms a scaffold for protein-protein interactions required for a wide variety of cellular functions including signal transduction, mRNA processing, gene regulation and the cell cycle. BIG-3 contains seven WD repeats, a C-terminal region of 3 amino acids, and a N-terminal domain of approximately 40 amino acids. We postulate that the N-terminal domain serves to determine the subcellular localization of the BIG-3 protein and thus regulates its function. Thus, we undertook studies to examine the subcellular localization of BIG-3 by immunohistochemistry and confocal microscopy. We have raised antibodies to an epitope that includes the sequences in the seventh WD repeat of BIG-3. Following affinity purification of serum on a peptide column, the purified anti-BIG-3 antibody recognized a single band of the correct size on Western analyses. Confocal microscopy using MLB13MYC clone 17 cells and MC3T3E1 cells showed that BIG-3 has a punctate cytoplasmic distribution. To further characterize this novel protein, we investigated the temporospatial expression of BIG-3 during endochondral and intramembranous bone formation from 13.5 to 18.5 days post coitus (dpc) embryos. In the developing tibia, BIG-3 was first detected at 13.5 dpc. By 16.6 dpc, BIG-3 was highly expressed in the proliferating and hypertrophic chondrocytes as well as in the cortical osteoblasts. BIG-3 was also present in osteoblasts of calvaria from embryonic day 14.5 to 18.5. Our data demonstrate that BIG-3 is a cytoplasmic protein and is developmentally expressed in cartilage and osteoblasts during endochondral and intramembranous ossification, suggesting that this novel WD-40 protein plays a developmental role in both endochondral and intramembranous bone.

F040

Haploinsufficiency of NF1 Tumor Suppressor Gene, Increases Osteopontin Expression snd Impairs Bone Strength, but Not Bone Mass in a Mouse Model of Neurofibromatosis Type 1. X. Yu*[1], O. Potter*[2], J. Milas[1], S. Murthy*[1], S. Chen*[3], D. W. Clapp*[3], J. M. Hock*[1]. [1]Anatomy & Cell Biology, Indiana University, Indianapolis, IN, USA, [2]Biology, Purdue University, West Lafayette, IN, USA, [3]Pediatrics, Indiana University, Indianapolis, IN, USA.

Impaired bone healing and osteoporosis occur in up to 50% of humans with Neurofibromatosis Type 1 (NF1). The loss of neurofibromin, which negatively regulates *p21*-ras, in NF1 results in constitutive activation of ras signal transduction in targeted cells. To better understand how NF1 affects bone homeostasis, we studied the skeletal biology of *Nf1* heterozygote mice (*Nf1* +/-), which model several features of human NF1. The skeletal phenotype was defined by bone mass, bone strength and bone histomorphometry. Cell biology was characterized as proliferation, apoptosis, osteoblast commitment (ALP+ CFU-f) of metaphyseal bone cells and diaphyseal bone marrow stromal cells, and ex vivo induction of osteoclasts (TRAP+ multinucleated cells) from spleen or bone marrow cells exposed to RANKL and M-CSF. Molecular characterization was based on RT-PCR of selected proteins in whole bone, metaphyseal bone cells and bone marrow stromal cells. Bone mass (BMD, BMC, XA and ash weight) and trabecular bone histomorphometry were equivalent in *Nf1*+/- and intact control mice. Biomechanical properties of strength (ultimate force and stiffness) were altered in female *Nf1*+/- mice; cortical bone formation was decreased in *Nf1*+/- males but with no detrimental effects on male bone strength. Osteoprogenitor proliferation, apoptosis and osteoblast commitment were all significantly impaired in *Nf1* +/- mice, while ex vivo induction of osteoclasts was increased and further enhanced by PTH and 1,25(OH)2D3. Osteopontin (OPN) expression increased in bone marrow stromal cells, but was equivalent to intact controls in whole bone, metaphyseal bone cells and osteoclasts. Immunohistochemistry showed OPN in bone marrow stromal cell cultures and increased OPN in epiphyseal bone of *Nf1*+/- mice. Expression of type I collagen, alkaline phosphatase, PTH1-receptor, RANKL and osteoprotegerin was equivalent in whole bones and primary bone cells from *Nf1* +/- mice and intact controls. In summary, haploinsufficiency of NF1 increased OPN expression in bone marrow cells, altered osteoprogenitor and osteoclast induction in vitro, and, in vivo, impaired biomechanical strength properties, in the absence of effects on bone mass. As bone marrow stromal cells support bone cell homeostasis, altered OPN may perturb bone cell functioning, resulting in detrimental effects on biomechanical properties of bone strength.

F042

β-Catenin Directly Activates Bone-Specific Genes in Osteoblasts and Chondrocytes. M. Zhao[1], J. Zhang*[2], J. Q. Feng[2], B. Oyajobi[1], S. E. Harris[2], G. R. Mundy[1], D. Chen[1]. [1]Molecular Medicine, University of Texas Health Science Center at San Antonio, San Antonio, TX, USA, [2]Oral Biology, University of Missouri, Kansas City, MO, USA.

Recently, several lines of evidence have implicated the role of β-catenin in osteoblast differentiation and bone formation. Wnt/LRP5 signaling has been associated with bone mass and LRP5 activates downstream β-catenin, which is likely involved in this process. However, the precise molecular mechanism by which β-catenin stimulates osteoblast differentiation is unknown. Thus, we examined the effects of β-catenin (constitutively active form) on the transcription of bone-specific genes. The sequences of Runx2/Cbfa1, type I collagen, osteopontin, dentin matrix protein 1, BMP-2 and type X collagen promoters were analyzed and putative TCF response elements were found in these promoters. When these promoters were co-transfected with β-catenin and TCF-4 expression plasmids in pluripotent fibroblast C3H10T1/2 cells, myoblast/osteoblast precursor C2C12 cells, osteoblast precursor 2T3 cells and chondrocyte TMC-23 cells, β-catenin/TCF-4 stimulated transcription of all these genes 3-8 fold. Co-transfection of an expression plasmid of Inhibitor of β-catenin (ICAT) completely blocked promoter activity induced by β-catenin/TCF-4. Mutation of the TCF response element in the osteopontin promoter reduced basal promoter activity over 50% and β-catenin/TCF-4 failed to activate the osteopontin promoter with the mutated TCF response element. Co-transfection of an F-box deleted dominant-negative mutant of the murine E3 ligase FWD1, which protects the proteasome degradation of β-catenin, greatly enhanced the activity of wild-type β-catenin to activate these bone-specific genes. Transfection of β-catenin and TCF-4 increased ALP activity in C3H10T1/2 and TMC-23 cells. We also examined the expression pattern of β-catenin in bone tissues by in situ hybridization. Strong expression of β-catenin mRNA in growth plate chondrocytes and articular chondrocytes and expression in trabecular and cortical bones were observed in 2-week-old mice. Our findings demonstrate that β-catenin stimulates transcription of Runx2/Cbfa1, but in addition also directly stimulates the transcription of a number of other osteoblast and chondrocyte-specific genes.

Disclosures: ***M. Zhao****, OsteoScreen Ltd 3.*

F044

COX-2 Dependent PGE2 Cooperates with BMP-2 to Enhance Osteoblast Differentiation Through the Induction of CBFA-1 and Osterix. X. Zhang, E. Schwarz, E. Puzas, R. Rosier, R. O'Keefe. Orthopaedics, University of Rochester Medical Center, Rochester, NY, USA.

We have previously demonstrated an important role of COX-2 in fracture repair and bone healing. To elucidate the mechanism we utilized bone marrow stromal cells from wild type and COX-2 -/- mice and examined the expression of CBFA-1 and Osterix, by real time PCR analysis. We found that CBFA-1 was slightly reduced in COX-2 -/- cells, whereas Osterix gene expression was reduced by about 49+12% ($p<0.05$). Accordingly, osteocalcin gene expression was reduced by about 72+15% ($p<0.05$). The COX-2 -/- cultures had a defect in nodule formation and this was completely restored by addition of PGE2. In these COX-2 -/- cultures with PGE2, CBFA-1 gene expression was increased 2.5 fold and Osterix gene expression was restored to the wild type levels. To examine whether BMP-2 is regulated by COX-2, we examined BMP-2 mRNA expression in these cultures. We found that BMP-2 expression in the knockout and wild type cells was similar, however, exogenous PGE2 stimulated BMP-2 mRNA expression in COX-2-/- cells by 2.1 fold. In comparison with wild type cells, COX-2 -/- cells also had an increased induction of CBFA-1 by BMP-2, indicating that a compensatory mechanism may have developed in the COX-2 -/- mice with increased BMP-2 responsiveness. Exogenous PGE2 has been reported to increase bone nodule formation in low density cultures of rat bone marrow cells. In our experiments with low density mouse marrow stromal cells culture (0.5-1X106/10cm2), we found that PGE2 increased the total cell number and the number of alkaline phosphatase positive colonies in both wild type and knockout cultures by about 2 fold on day 10. However, in these experiments, PGE2 induced CBFA-1 and Osterix expression only after 17 days of cultures. On day 13, no significant changes in CBFA-1 and Osterix gene expression were noted in both COX-2-/- and wild type cultures with PGE2. In contrast, if BMP-2 was added with PGE2, a 5-10 fold synergistic induction of CBFA-1,Osterix and Osteocalcin gene expression was observed. This result demonstrated that PGE2 can cooperate with BMP-2 to enhance osteoblast differentiation through the induction of CBFA-1 and Osteix. Taken together, we propose that PGE2 is capable of regulating osteoblastogenesis by regulating BMPs and/or by cooperating with BMP-2 in the local milieu. Our data support a model in which the role of COX-2 is limited in skeletalogenesis, but is required for mesenchymal stem cell differentiation in bone healing process in which COX-2 and its metabolites are highly expressed.

F046

Chondromodulin-I Is a Positive Regulator of Bone Remodeling. Y. Nakamichi*[1], C. Shukunami*[2], T. Yamada[1], K. Aihara*[1], H. Kawano[3], Y. Nishizaki*[2], T. Sato*[1], Y. Yamamoto*[1], M. Shindo*[1], K. Yoshimura*[1], H. Kawaguchi[3], Y. Hiraki*[2], S. Kato[1]. [1]Laboratory of Nuclear Signaling, Institute of Molecular and Cellular Biosciences, University of Tokyo, Tokyo, Japan, [2]Institute for Frontier Medical Sciences, Kyoto University, Kyoto, Japan, [3]Orthopaedic Surgery, University of Tokyo, Tokyo, Japan.

Chondromodulin-I (ChM-I) is a 25 kDa glycoprotein generated from a larger typeII transmembrane precursor protein after post-translational modification and proteolytic cleavage at the processing signal site. ChM-I is mainly expressed in proliferating and prehypertrophic zone of cartilage and also ,to a lower extent, in eye and thymus. In vitro analyses of ChM-I have shown growth promoting activity of chondrocyte and inhibitory activity of angiogenesis. ChM-I also stimulated osteoblast proliferation and reduced ALPase activity of osteoblasts. ChM-I is a multifunctional growth regulator depending on the target cell type and seemed to be implicated in both cartilage growth and endochondral bone formation. To investigate the biological roles of ChM-I in vivo, we have generated ChM-I Knockout (KO) mice. ChM-I KO mice grew normally with no discernible physical defects and with normal fertility. ChM-I KO mice also exhibited no overt aberrations in cartilage development and endochondral bone formation at various pre- and post-natal stage. However, a significant increase (10%) in radiological bone mineral density was observed in 12-week-old ChM-I KO mice. Histomorphometric analysis showed trabecular bone volume (BV/TV) in ChM-I KO mice were 2.5-fold higher than in wild-type mice. Both bone formation (Ob.S/BS, MAR & BFR) and bone resorption indicators (Oc.N/B.Pm , Oc.S/BS & ES/BS) were reduced in ChM-I KO mice compared to wild-type mice. Reduced (20%) serum marker levels (ALPase activity and osteocalcin) and no alteration in serum minerals (Ca, P) in ChM-I KO mice supported the hypothesis that bone formation activity was reduced by ChM-I inactivation. The increased bone mineral density in ChM-I KO mice appeared to be due to lowered bone resorption with respect to bone formation. These results demonstrated that ChM-I is likely to be a positive regulator of bone remodeling through control of osteoclast and osteoblast functions rather than being involved in cartilage development.

F048

Functional Role of Acetylcholinesterase in Cranial Development. C. A. Inkson[1], T. Evron*[2], H. Soreq*[2], E. Duysen*[3], O. Lockridge*[3], P. Genever[1]. [1]Biology, University of York, York, United Kingdom, [2]Hebrew University of Jerusalem, Jerusalem, Israel, [3]University of Nebraska, Omaha, NE, USA.

Although best known for its role in cholinergic neurotransmission, Acetylcholinesterase (AChE) is a multifunctional protein that plays fundamental roles in cell differentiation, proliferation and adhesion in a variety of tissues including bone. The AChE gene undergoes complex translational and post translational modifications resulting in 3 different AChE isoforms, AChE-S (synaptic), AChE-E (erythrocytic) and AChE-R (readthrough). Previously we identified expression of all AChE isoforms in bone and demonstrated that AChE can function as a bone matrix protein and regulate osteoblast differentiation and adhesion. Here we provide evidence of a fundamental role for AChE in murine cranial development. By immunohistochemistry using a pan-specific antibody to AChE, we have shown that AChE is expressed in the condensing mesenchyme of developing calvaria during rat embryogenesis and is present in periosteal osteoblasts and throughout the midsutural mesenchyme in neonatal rat calvaria. Using ex-vivo cultures of primary osteoblasts extracted from neonatal rat calvaria, we demonstrated that application of bFGF and TGF-beta 1, key regulators of cranial development, caused marked increases in AChE expression. Four lines of transgenic mice were used to determine the functional role of AChE during skull development in vivo: mice overexpressing two different isoforms of AChE (AChE-S and AChE-R); mice expressing antisense for AChE (AChE-AS) and AChE knock out mice (AChE-KO). Whole mount skeletal staining with alizarin red and alcian blue on postnatal day 3 transgenics revealed delayed closure of sagittal and lambdoidal sutures in AChE-R, AChE-AS and AChE-KO mice compared to wild-type controls. Furthermore, histological analysis of calvariae from AChE-KO mice of various ages demonstrated reduced calvarial width compared to wild-type littermates. These observations were supported by radiographic analyses of AChE-KO mice, which indicated a reduced bone density throughout the skeleton but most significantly in the skull. Immunolocalisations for homeobox proteins involved in craniofacial patterning, Msx2 and Dlx5, using sections taken from AChE-KO mice calvariae indicated apparent normal expression patterns when compared to wild type mice. These data demonstrate a significant role for AChE in mammalian cranial development and may identify a previously unrecognised component of suture patterning and formation.

F052

Bone Sialoprotein (BSP) Promotes Invasion by Osteotropic Cancer Cells Through an RGD Dependant Mechanism. A. Karadag[1], A. Jain*[2], N. S. Fedarko[2], L. W. Fisher[1]. [1]Nidcr, National Institutes of Health, Bethesda, MD, USA, [2]Department of Medicine, Johns Hopkins University, Baltimore, MD, USA.

BSP is a member of the SIBLING (Small Integrin-Binding LIgand, N-linked Glycoproteins) family of proteins that also include, osteopontin, MEPE, DMP1 and DSPP. Each contains the integrin-binding tripeptide, Arg-Gly-Asp (RGD), as well as several conserved phosphorylation and N-glycosylation sites. We and others have previously reported that BSP levels are elevated in both the tissues of many tumors and in the serum of patients with breast, prostate, and thyroid cancers. In order to investigate whether the increased BSP levels are associated with metastatic ability of these cancer cells, we have modified the Boyden-chamber invasion assay and investigated the ability of a number of cancer lines to invade through Matrigel, an artificial basement membrane. The cells treated with BSP (4-20μg/ml), BSP with its RGD modified to KAE (Lys-Ala-Glu), or vehicle were placed on the upper chamber of transwell inserts and media conditioned by NIH-3T3 cells were placed at the lower chamber as a chemoattractant. After incubation for 6-24h, the cells that had migrated through the Matrigel layer were labeled with calcein and quantified using a fluorescence plate reader. Both prostate cancer cell lines treated with BSP, PC-3 and DU-145, showed a 3.5-fold increased invasion level over that of the untreated cells ($p<0.01$). Interestingly, the invasion level is 5.5-fold higher when compared to the cells treated with BSP-KAE ($p<0.01$). Breast cancer cell lines, MDA-MB-231, MDA-MB-435S, LCC-15, and MCF-7, showed a 12.6-, 3.1-, 17.6- and 31.6-fold increases respectively when compared to vehicle alone ($p<0.01$), and all of the values were higher when compared to the same cells treated with BSP-KAE ($p<0.01$). Similarly, a lung cancer cell line (NCI-H520) and a thyroid cancer cell line (SW-579) showed a 3.1- and 6-fold increase in invasive activity (over vehicle) with BSP ($p<0.01$) and 10.5- and 17.7-fold increase

respectively when compared to the BSP-KAE treated cells ($p<0.01$). In conclusion, many tumor cell lines are made more aggressive by the addition of recombinant BSP and less aggressive if the BSP has its RGD mutated to KAE. We have previously shown that BSP caused the release of proMMP-2 from marrow stromal fibroblasts and that it could bind and activate proMMP-2. Therefore, we propose that the BSP made in many types of tumors may be accentuating the invasive properties of the cells by releasing and activating MMP-2 through an RGD-dependent mechanism. Furthermore, this mechanism can be foiled by the addition of recombinant BSP-KAE that can bind proMMP-2 but not its integrin.

F054

Osteopontin-deficiency Not Only Suppresses Bone Destruction by the Invasion of Melanoma Cells But Also Preserves Newly Formed Marrow Bone After Ablation. Y. Ohyama*[1], Y. Nemoto[1], S. Rittling[2], K. Tuji[1], D. T. Denhardt[2], A. Nifuji[1], M. Noda[1]. [1]Molecular Pharmacology, Medical Resarch Institute, Tokyo Medical & Dental University, Tokyo, Japan, [2]Piscataway, Rutgers University, New Jersey, NJ, USA.

Osteopontin is an RGD-containing protein and is recognized by integrin family members. Osteopontin promotes cell attachment to bone, which is abundant in this protein. As osteopontin levels were reported to be elevated in patients bearing highly metastatic tumors, osteopontin has been implicated in the metastasis of tumors. However, the effect of osteopontin on the invasion of tumor cells in bone microenvironment has not been clear. The purpose of this paper is to elucidate the role of host osteopontin in the invasion of tumor cells in bone. Bone marrow ablation was conducted in the femora of mice and B16 melanoma cells were injected directly into the ablated bone marrow space of the osteopontin-deficient and wild type mice to examine the behavior of the tumor cells in bone. Invasion foci of B16 melanoma cells in the cortical bone were observed seven weeks after tumor cell implantation. The number of the foci was five-fold less in osteopontin-deficient mice compared to that in wild type. Trabecular bone was formed within a week of ablation. However, in wild type mice, tumor cells occupied the marrow and the remaining trabecular bone was destructed and not observed. In contrast, a significant amount of trabecular bone was remained in osteopontin-deficient mice as these trabecular bone was not resorbed compared to wild type mice. These observations indicated that the absence of osteopontin prevented tumor cell invasion after implantation of tumor cells into the bone marrow space. To examine cellular mechanisms of these observations, cocultures of bone marrow cells using B16 cells and bone marrow cells were conducted. While the presence of B16 cells promoted TRAP positive cell development in wild type bone marrow cells, varying levels in the enhancement of TRAP-positive cell formation by B16 cells were observed in the case of bone marrow cells from osteopontin-deficient mice. Thus, bone resorbing function of osteoclasts in response to tumor cell invasion in the local environment is impaired in osteopontin-deficient mice.

F056

Identification of Proteolytic Cleavage Sites in Latent TGFβ Binding Protein-1 that may be Responsible for Release of TGFβ During Bone Matrix Degradation. S. L. Dallas*[1], L. F. Bonewald[1], C. Barley*[2], Q. Chen*[1], J. Guthrie*[3]. [1]Oral Biology, University of Missouri, Kansas City, Kansas City, MO, USA, [2]Biochemistry, University of Manchester, Manchester, United Kingdom, [3]Midwest Research Institute, Kansas City, MO, USA.

Latent TGFß binding proteins (LTBPs) are large extracellular glycoproteins that bind to TGFßs and regulate their activity. We have previously shown that LTBP1 targets latent TGFß to bone extracellular matrix (ECM) for storage and that proteolytic cleavage of LTBP1 by osteoclasts and by osteolytic bone metastatic breast cancer cells provides a mechanism for release of latent TGFß from bone ECM. To determine the protease cleavage sites important for release of LTBP1 from bone ECM, a recombinant protein expression approach was used. LTBP1 fragments spanning the complete molecule were expressed using a modified pCEP4 episomal mammalian expression vector, engineered with a BM40 signal sequence and a 6 or 10 His epitope tag. Using this vector system, milligram amounts of recombinant fragments were obtained. Our previous studies suggested the involvement of serine proteases and matrix metalloproteinases in release of LTBP1 from bone matrix by osteoclasts and breast cancer cells. We therefore performed proteolytic cleavage studies using purified plasmin, MMP2 and MMP9. An LTBP1 fragment spanning 413 to 545 (termed the "hinge domain" due to its predicted flexibility) was cleaved by both plasmin and MMP2. A recombinant fragment spanning amino acids 526 to 1014, consisting of a long stretch of epidermal growth factor-like repeats, proved to be very resistant to cleavage with any of these proteases. A C-terminal fragment, 1008 to 1394, was cleaved by plasmin. Western blotting showed that the larger proteolytic fragment from this plasmin cleavage no longer expressed the His tag. By MALDI-TOF mass spectroscopy of a tryptic peptide mass map, it was determined that all peptides after residue 1285, including the His tag were missing. Edman sequencing confirmed that the N-terminus was still intact, suggesting that the cleavage site is located between 1285 and 1394. Edman sequencing of the smaller plasmin proteolytic fragment confirmed that plasmin cleavage occured on the carboxy side of Arg1285. These studies show that plasmin specifically cleaves the carboxy terminal fragment of LTBP1 at position 1285 and that amino acids 526 to 1014 of LTBP1 are protease resistant, which may protect latent TGFß from inappropriate activation. Specific cleavage of the hinge fragment 413 to 545 by plasmin and MMP2 may play a role in release of latent TGFß from bone ECM, potentially the first step in the pathway by which ECM-bound TGFß is rendered active.

F058

Mechanism of Mechanical Stress-induced Activation of AP-1/IL-11 Transcriptional Cascades. D. Inoue, S. Kido, T. Matsumoto. Department of Medicine and Bioregulatory Science, University of Tokushima, Tokushima, Japan.

Mechanical stress to bone plays a critical role in maintaining bone mass and strength. We have shown that deltafosB, a fosB splicing variant, and an AP-1 target interleukin (IL)-11, both of which have been shown to stimulate bone formation in vivo when overexpressed in transgenic mice, are rapidly induced by reloading in tail-suspended mouse tibiae and femurs as well as by fluid shear stress (FSS) in cultured primary osteoblasts (POB). The induction of deltafosB and IL-11 expression was dependent on an intracellular calcium rise and ERK activation but independent of prostaglandin synthesis. In the present study, we further attempted to delineate the mechanism of AP-1/IL-11 induction. Pre-treatment with an transcriptional inhibitor, DRB, completely abolished the induction of deltafosB and IL-11 mRNA by FSS in POB, suggesting a requirement for ongoing transcription. We then cloned and analyzed the upstream regulatory region of the mouse fosB gene. Analysis with luciferase reporter assays revealed that FSS indeed increased transcriptional activity of a 1 kb fosB promoter fragment by two to three fold and that SRE at -428 and juxtaposed AP-1 like sequences are mainly responsible for the response to FSS. We also confirmed that IL-11 transcription is induced by FSS in both transient and stable transfection experiments using IL-11 promoter-luc constructs. The results indicated that the two tandem AP-1 sites, playing a critical role in both basal and TGF-beta-induced IL-11 transcription, conferred the response to FSS. Furthermore, although all the four fos family members were induced by FSS in vitro, we found that only c-fos and fosB/deltafosB preceded IL-11 in kinetic studies and that c-fos was dispensable for FSS-induced fosB/deltafosB and IL-11 mRNA expression using c-fos gene-deleted mouse osteoblasts, supporting a critical role for fosB/deltafosB in IL-11 induction. Interestingly, we observed that BMP increased IL-11 promoter activity in ST2 cells stably expressing luciferase under the control of 1.7 kb long IL-11 promoter fragment and endogenous IL-11 expression by C3H10T1/2 cells. Consistent with a cross-talk between Smads and AP-1, we found that FSS induced Smad1 phosphorylation and Smad4 nuclear translocation within 30 min in POB and that deltafosB, but much less (long)fosB, co-immunoprecipated with Smad1 when overexpressed in Cos cells. Collectively, our results suggest that mechanical stress activates an AP-1(deltafosB)/IL-11 transcriptional cascade contributing to enhanced bone formation, and participation of Smad signaling in this cascade may explain its bone specificity.

F061

Microcrack Matrix Strain Is 15 Times Greater than Average Global Strains; Implications for Osteocyte Signaling. D. P. Nicolella*[1], L. F. Bonewald[2], J. Lankford*[1]. [1]Materials Engineering, Southwest Research Institute, San Antonio, TX, USA, [2]Department of Oral Biology, University of Missouri at Kansas City, Kansas City, MO, USA.

Microdamage in bone occurs naturally as a result of normal functional in-vivo loading. In healthy bone, microdamage is repaired via the bone remodeling process, whereby osteoclasts specifically target regions of damaged bone matrix. Although the underlying mechanisms controlling this process are unknown, osteocytes are hypothesized to be essential in initiating and controlling this process. Several current theories link bone remodeling to biochemical signaling by the osteocyte in response to strain generated through deformation of the bone matrix or through fluid flow induced shear stresses. In-vivo bone matrix strains have been measured to be approximately 2,000 microstrain during rigorous physical activity. However, when applied in-vitro to osteoblastic cells via substrate stretching, this level of strain does not induce a significant biological response, whereas significantly higher levels of in-vitro substrate strain do. Alternatively osteoblastic and to a greater extent, osteocytic cells are more responsive to fluid flow induced shear stress than substrate strain in-vitro. However, fluid flow induced shear stress levels in bone in vivo have not been directly measured and are unknown. We hypothesize that compared to undamaged bone, microdamage results in a substantial increase in bone matrix strain in the surrounding area of the microcrack thus resulting in an altered mechanical signal to nearby osteocytes. We directly measured bone matrix strain in microdamaged bovine cortical bone at the microstructural level. The bone specimen was loaded in a specially designed microscopy load frame to specific levels of global mechanical strain while observed and imaged at high magnification using an optical microscope (Axioscope 2, Carl Zeiss Inc., NY). Strain fields associated with the microcrack and nearby osteocyte lacuna were measured by comparing loaded vs. unloaded image pairs using a custom image correlation system. Matrix strains at the tip of the microcrack reached 30,000 microstrain (3.0%) locally, up to 15 times greater than the average global strains measured in-vivo. Matrix strain in intact bone away from the microcrack was on the order of 2,000-3,000 microstrain. These results indicate that tissue strains acting on osteocyte lacunae associated with microdamage can be much greater than strain in undamaged bone and it is this high level of matrix strain that may cause osteocytes to initiate a remodeling response.

F064

A Novel Cathepsin K Inhibitor with Oral Activity in Rat and Monkey. M. Missbach[1], J. A. Gasser[1], K. Toriyama*[2], J. R. Green[1], T. Buhl*[1], H. Ishihara*[2], M. Kometani*[2], E. Altmann*[1], N. Teno*[2], R. Gamse[1], C. P. Jerome[3], R. Lattmann*[1], C. Betschart*[2]. [1]Novartis Pharma AG, Basel, Switzerland, [2]Novartis Pharma KK, Tsukuba, Japan, [3]SkeleTech Inc., Bothell, WA, USA.

The cysteine protease cathepsin K has been shown to be highly expressed in osteoclasts and to play an essential role in bone matrix degradation. The effects of a novel class of reversible inhibitors of cathepsin K on in vitro and in vivo assays of bone resorption have been examined. Inhibitors were identified based on a substrate analogue approach and further optimized to reveal potent compounds showing excellent specificity against cathepsins B, L and S. Compound 1 inhibits cathepsin K with Ki values of 3.3 nM (rabbit), 30 nM (rat) and 0.5 nM (human). It is highly specific with an IC50 of 2.5 nM for human cath K versus 4400 nM (cath B), 3700 nM (cath L) and >10,000 nM (cath. S). Cellular activity in vitro was demonstrated by the reduction of the total pit volume produced by rabbit osteoclasts on ivory slices (IC50 63±3.6 nM; mean±S.E., n=3). In vivo activity on bone resorption was tested in ovariectomised (OVX) rats treated orally with 50 mg/kg bid. Compound 1 reduced urinary deoxypyridinoline excretion by 85% after 2 weeks of treatment. In a separate experiment over 4 weeks, bone protection at the proximal tibia was 51% measured as cross-sectional BMD by pQCT. To confirm the ~60-fold higher potency on the human/monkey over the rat enzyme, compound 1 was evaluated in cynomolgus monkeys rendered estrogen deficient by a depot GnRH agonist. After administration of 5 mg/kg bid p.o. two serum markers of bone resorption, CTx and NTx, were reduced far below levels of the non-GnRH treated control group already at day 1. They remained depressed throughout treatment over 4 weeks and returned to normal within one day after the end of dosing. This is the first demonstration that an orally administered inhibitor of cathepsin K is able to potently and effectively reduce bone resorption markers in rats and monkeys and to partially protect BMD after ovariectomy in rats. Such compounds could represent a novel therapeutic approach for metabolic bone diseases like osteoporosis.

F066

Involvement of Collagenase-3 (MMP-13) in the Collagen Breakdown Required for the Excavation of the Cartilaginous Epiphysis of the Developing Rat Long Bone. E. R. Lee[1], L. Lamplugh*[1], B. Kluczyk*[1], J. S. Mort*[2], G. Murphy*[3], C. P. Leblond*[1]. [1]Electron Microscopy Unit, Shriners Hospital for Children, Montreal, PQ, Canada, [2]Joint Diseases Laboratory, Shriners Hospital for Children, Montreal, PQ, Canada, [3]School of Biological Sciences, University of East Anglia, Norwich, United Kingdom.

The formation of a secondary ossification center in the cartilaginous epiphysis of long bones requires the excavation of canals and marrow spaces and, therefore, the resorption of cartilage. On the assumption that the resorption requires the lysis of the major cartilage component, type II collagen, it was noted that this collagen was cleaved with high efficiency *in vitro* by collagenase-3. Such cleavage took place within the triple helix at the Gly^{775}- Leu^{776} bond to produce two fragments of itself at ¾ and ¼ the length of the original molecule. To find out if collagenase-3 produced the same cleavage in the epiphysis of the developing rat tibia, two affinity purified peptide antibodies were prepared; one against the amino acid sequence LAGQR… ending the N-terminus of the ¼ fragment of the cleaved collagen; the other against the sequence YNVFP…corresponding to the N-terminus of activated enzyme. With the aid of these antibodies we report here that the cleavage of type II collagen by collagenase-3 is localized to newly developed sites of cartilage erosion. Thus at 6 days of age, canals allowing the entry of capillaries are dug from the surface of the epiphysis (stage I), while immunostaining, indicative of the activated collagenase-3 enzyme or collagen cleavage fragments, appears at the blind end of each canal. By 8 days of age, the canal blind ends fuse to create a marrow space in the epiphysis (stage II), where the immunoreactivity produced by the two anti-peptide antibodies continues to coincide along the walls of the space. By 10 days of age, clusters of hypertrophic chondrocytes are scattered along the marrow space wall to initiate the formation of the secondary ossification center (stage III), where resorption sites are reactive to the anti-LAGQR but are unreactive to the anti-YNVFP antibodies. From 10-15 days the center keeps on enlarging and, as the secondary growth plate advances (stage IV), it is intensely immunostained with the anti-LAGQR but not the anti-YNVFP antibodies, indicating that the collagen has been cleaved, but not by collagenase-3. We conclude that collagenase-3 contributes to the lysis of collagen, but only at some sites and stages in the development of the tissue, particularly at early phases of excavation (stages I and II). This result implies that more than one collagenase is required to complete the excavation of a secondary center.

F069

Impaired In Vitro Osteogenesis and Defective Runx2 Activity in Multiple Myeloma Patients. J. J. Westendorf[1], K. Evenson*[2], R. A. Kahler*[3], X. Li*[1], A. M. Masellis*[2]. [1]Orthopaedic Surgery and Cancer Center, University of Minnesota, Minneapolis, MN, USA, [2]Virginia Piper Cancer Institute, Minneapolis, MN, USA, [3]Graduate Program in Cancer Biology, University of Minnesota, Minneapolis, MN, USA.

The bone marrow stroma contains a reservoir of mesenchymal progenitor cells (BMPCs) capable of osteogenesis in response to environmental cues such as growth factors/cytokines, cell to cell interactions and cell to extracellular matrix interactions. In individuals with the plasma cell malignancy multiple myeloma, there is evidence that bone formation rates are reduced and that increased ostoeclastic bone resorption is associated with impaired osteoblast function. The central hypothesis of our study is that impaired osteogenesis, resulting in defective mature osteoblast function, contributes to the formation of osteolytic bone lesions in multiple myeloma patients. Our data indicate that myeloma BMPCs exhibit decreased in vitro osteogeneic differentiation as compared to normal donors. BMPCs were cultured in osteogenic induction medium and assessed for bone alkaline phosphatase (ALP) expression and mineralization by immunohistochemistry, and for osteoblast specific markers by immunohistochemistry and Rt-PCR. Normal BMPCs showed a ten-fold increase in ALP levels, an induction of the osteocalcin transcript and a high degree of mineralization by day 21 in osteogenic induction medium. In contrast, myeloma BMPCs showed only a 1.3 fold increase in ALP and minimal mineralization at day 21. Because osteogenesis was impaired in myeloma-derived BMPCs, we analyzed Runx2 expression and activity in these cells. Runx2 (Cbfa1) is a transcription factor required for osteoblast formation. Immunoblot analysis indicated that Runx2 was expressed in both normal and myeloma-derived BMPCs. Runx2 DNA binding activity was easily detected in normal BMPCs; however it was significantly reduced in myeloma-derived BMPCs. Thus decreased Runx2 activity in BMPCs is directly correlated with decreased osteogenesis in myeloma patients. These data suggest that Runx2 activity is deregulated in BMPCs from myeloma patients. These studies provide novel cellular and molecular insights into the deregulation of bone formation in myeloma patients.

F071

Molecular Mechanisms by which Proteasome Inhibition Reduces Myeloma Burden in Bone. B. O. Oyajobi, P. Williams*, A. Gupta*, A. Trauernicht*, M. Zhao, D. Chen, I. R. Garrett, G. R. Mundy. Molec Medicine, UTHSC, San Antonio, TX, USA.

Multiple myeloma (MM) is characterized by extensive tumor-induced osteoclastic bone destruction. Recently there have been reports that a proteasome inhibitor has striking therapeutic benefit in this disease and its bony complications. To determine mechanisms by which inhibition of the ubiquitin (Ub)-proteasome system reduces myeloma burden, we used the peptide aldehyde Z-Ile-Glu(OtBu)-Ala-Leu-CHO (Proteasome Inhibitor-1; PSI) as a tool. In syngeneic C57BL mice bearing subcutaneous 5TGM1 plasmacytomas, daily intratumoral injections of PSI (1mg/kg), after tumors were established significantly reduced tumor growth and induced dramatic regression of tumors in 50% of mice with marked apoptosis (assessed by standard morphological criteria) in PSI-treated tumors. In separate experiments, parenteral administration of PSI (5mg/kg/day; 28 days) prolonged time to onset of paraplegia in 5TGM1 MM-bearing mice inoculated via the tail vein. Flow cytometry of PSI-treated 5TGM1 and human RPMI 8226 MM cells revealed marked time- and dose-dependent induction of apoptosis (60-80%, Annexin V+/Propidium iodide-). In this regard, PSI was more potent (IC_{50} < 0.1μM) than other compounds with known proteasome inhibitory activity tested (MG132, epoxomicin, lactacystin, lovastatin) and was 2 log orders more potent than Risedronate. NF-κB activation promotes growth/survival of MM cells and since IκB degradation and consequently NF-κB activity, depends on proteasome function, we reasoned that proteasome inhibitors work through this transcription factor. Although parthenolide, an IκB kinase (IKK) inhibitor, also induced myeloma cell apoptosis it is unlikely that PSI acts by inhibiting IKK since TNFα (5ng/ml) still enhanced phospho-IκB levels in 5TGM1 and RPMI cells pretreated with 1μM PSI. Protein ubiquitination is mediated by an enzymatic cascade with substrate specificity due to E3 Ub protein ligases. As proteasome inhibitors have multiple potential targets, to directly assess the role of NF-κB blockade in myeloma apoptosis, the murine IκB-E3 ligase FWD1 and an F-box deleted dominant-negative mutant (FWD1ΔF), were transiently expressed in 5TGM1 cells. FWD1 expression in 5TGM1 cells reduced basal apoptosis levels compared to empty vector (EV) cells and there was no difference between them in response to TNFα. In contrast, apoptosis was increased in FWD1ΔF transfectants and TNFα further increased apoptosis (>30% vs untreated FWD1ΔF cells). Together, our data suggest that MM growth and behaviour in bone is dependent on nuclear translocation of NF-κB, and that inhibition of the Ub-proteasome pathway by PSI and other proteasome inhibitors works through this mechanism.

Disclosures: ***B.O. Oyajobi****, OsteoScreen 5.*

F073

AML-1B Down-Regulates Macrophage Inflammatory Protein-1α (MIP-1α) Expression in Multiple Myeloma (MM) Cells. S. J. Choi*[1], T. Oba*[2], N. S. Callander*[3], D. Jelinek*[4], G. D. Roodman[2]. [1]Medicine/Hematology, University of Pittsburgh, Pittsburgh, PA, USA, [2]Medicine, University of Pittsburgh, Pittsburgh, PA, USA, [3]University of Texas Health Science Center at San Antonio, San Antonio, TX, USA, [4]Mayo Clinic, Rochester, MN, USA.

High concentrations of MIP-1α are produced by MM cells in about 70% of patients and MIP-1α levels correlate with their disease activity and a poor prognosis. Furthermore, blocking MIP-1α expression in an in vivo model of human MM profoundly decreases both tumor burden and bone destruction, suggesting that MIP-1α is an important mediator of MM bone disease. To further analyze the regulation of MIP-1α production in MM, we cloned the hMIP-1α promoter and characterized its transcription factor (TF) motifs. The proximal region of hMIP-1α promoter was composed of two sets of identical transcription regulatory regions consisting of GATA-2+AML-1+C/EBPα sites. Since two alternatively spliced variants of the AML-1 class of TFs can bind the AML-1 region, AML-1A and AML-1B, we examined the relationship between the expression levels of AML-1A or AML-1B in MM cells with their capacity to express MIP-1α. AML-1A, AML-1B and MIP-1α mRNA expression levels were analyzed by RT-PCR using AML-1A, AML-1B, MIP-1α and GAPDH specific primers. AML-1A mRNA was relatively over-expressed compared to AML-1B in MM cell lines that produced high levels of MIP-1α (>1ng/ml / 10^6 cells / 72 hrs), but AML-1A was not increased in MM cell lines that expressed less than 200 pg/ml of MIP-1α. Furthermore, AML-1B mRNA levels were also decreased in marrow samples from MM patients that expressed increased amounts of MIP-1α. In contrast levels of AML-1A mRNA did not differ significantly between MM patients and normals. The average ratio of AML-1A to AML-1B mRNA in MM patients was 8-fold higher than in normals. To test the effects of AML-1A and AML-1B on MIP-1α expression in

MM cells, AML-1A and AML-1B cDNA constructs were transfected into ARH-77 MM cells. AML-1B totally blocked MIP-1α production by ARH cells, while AML-1A did not affect MIP-1α expression. Taken together, these data demonstrate that the relative levels of AML-1B are decreased in MM patients that produce increased concentrations of MIP-1α, and that transduction of AML-1B into MM cells totally blocks MIP-1α expression. These data further suggest that increasing AML-1B levels in MM cells may have beneficial effects on the bone destruction and tumor burden in MM patients.

F075

Beta 3 Integrin -/- Mice are Protected From Osteolytic Bone Invasion. S. J. Bakewell*[1], N. R. Dowland*[2], K. N. Weilbaecher[2]. [1]Physiology and Biophysics, University of Arkansas for Medical Sciences, Little Rock, AR, USA, [2]Medicine and Pathology, Washington University School of Medicine, St. Louis, MO, USA.

Skeletal metastases are the cause of significant morbidity and mortality. Drugs that inhibit osteoclast (OC) function ameliorate both osteolytic and osteoblastic metastatic bone disease suggesting that OCs are involved in the pathogenesis of bone metastases. The beta 3 integrin subunit (β3) has been hypothesized to influence the development of metastases because of its critical role in osteoclastic bone resorption (αvβ3), tumor/platelet interactions (αIIbβ3 and αvβ3), and in tumor associated angiogenesis (αvβ3). To examine the role of the β3 integrin in skeletal metastases we utilized mice with a germline-targeted disruption of the β3 subunit gene ($\beta3^{-/-}$). The $\beta3^{-/-}$ mouse has diminished platelet aggregation mediated by αIIbβ3, and dysfunctional osteoclast resorption mediated by αvβ3. We established an in vivo model of bone metastasis using the B16 murine melanoma cell line (F10), which induces osteolytic bone metastases after tumor cell injection in the cardiac left ventricle (LV). After LV injection of B16 cells into β3 wild-type and heterozygous mice, extensive osteolytic bone lesions, pathologic bone fractures, spinal cord compression and histologic tumor invasion of the bone are observed in 87% of mice (n=46) after 14 days. However, after injecting $\beta3^{-/-}$ littermates (n=24), there is no evidence of osteolytic lesions or histologic evidence of tumor invasion in the bone. In fact, 23/24 $\beta3^{-/-}$ mice showed no histologic evidence of any tumor growth in the marrow cavity, and only 1/24 B16 injected $\beta3^{-/-}$ mice had a small focus of tumor cells growing in the marrow cavity. 18-fluorodeoxyglucose (18-FDG) Positron Emission Tomography (PET) of in vivo tumor activity/growth demonstrates extensive tumor activity in the spine of wild type mice at day 7 and 14 after B16 LV injection. In contrast, little 18-FDG tracer uptake was observed in saline injected wild type or tumor injected $\beta3^{-/-}$ littermates at days 7 and 14. In summary, osteolytic metastases are significantly impaired after LV injection of B16 tumor cells in $\beta3^{-/-}$ mouse compared to wild type littermate controls. Our data suggest that host cell β3 integrin expression facilitates the process of tumor cell metastasis to bone.

F079

Interleukin 8 Regulation of RANKL Is a Mechanism for the Metastatic Potential of Human Breast Cancer Cells. M. Bendre, T. Mon*, D. Gaddy-Kurten, L. J. Suva. Orthopaedics and Physiology and Biophysics, UAMS, Little Rock, AR, USA.

Metastasis is the process by which tumor cells spread from their site of origin to distant sites after gaining access to the circulatory system. An understanding of the factors contributing to the metastatic potential of breast cancer cells may enhance the prospect of developing new therapies. Using an in vivo selection scheme involving left cardiac ventricle injection into nude mice we previously identified a highly metastatic human breast cancer cell line (MDA-MET) from a less metastatic parental cell line (MDA-231). Complete microarray analysis identified the molecular fingerprint of gene expression in the metastatic (MDA-MET) versus non-metastatic (MDA-231) cells. An important molecular difference between MDA-MET and MDA-231 cells was the over expression by MDA-MET cells of the proangiogenic cytokine IL-8. Both RT-PCR and ELISA confirmed the increased expression of IL-8 in MDA-MET cells. The relevance of IL-8 expression in metastasis was demonstrated by its elevated expression in a variety of human cancer cell lines with an enhanced metastatic phenotype in vivo. Mining of the microarray data confirmed a lack of TGF-b-regulated PTHrP expression, no RANKL mRNA expression, and revealed the absence of IL-8 receptor (CXCR1 and 2) expression in MDA-MET cells. These experiments suggested that expression of other factors like IL-8 (and not PTHrP) by MDA-MET cells was related to their enhanced metastatic potential in vivo. As a result, we speculated that IL-8 expression by tumor cells in the bone marrow could directly regulate osteoclastogenesis by altering the RANKL:OPG ratio in osteoclast support cells. Testing this hypothesis, RT-PCR analysis of RANKL and OPG mRNA expression in murine osteoblastic MC3T3E1 cells showed that IL-8 markedly upregulated RANKL mRNA expression (within 6 hours), with no effect on OPG expression. Similarly, levels of RANKL protein were also increased after 24 hours of IL-8 treatment. These data suggest that in the early stages of the colonization of bone by breast cancer cells, the expression of cytokines such as IL-8 may be critical for tumor growth and the initial phase of tumor-activated bone resorption. Once osteoclastic bone resorption is increased, the normal products of bone resorption (such as TGF-b) would serve to further enhance osteoclast formation and bone resorption. These data implicate IL-8 (and potentially other unidentified factors) as important mediators of the process of breast cancer metastasis to bone.

F081

Over-expression of Native OPG by Breast Cancer Cells Enhances Tumor Growth in Bone. J. L. Fisher*[1], R. J. Thomas*[1], J. Elloitt*[1], C. R. Dunstan[2], P. F. M. Choong*[3], T. J. Martin[1], M. T. Gillespie[1]. [1]St. Vincent's Institute of Medical Research, Melbourne, Australia, [2]Amgen Corporation, Thousand Oaks, CA, USA, [3]Department of Orthopaedics, St. Vincent's Hospital, Melbourne, Australia.

Osteoprotegerin (OPG) acts as a decoy receptor for RANKL (receptor activator of NF-kB ligand), preventing it binding to its receptor, RANK, thereby inhibiting osteoclast formation and activation. We have previously demonstrated that OPG-Fc (22 – 194 aa) inhibits in vitro osteoclast formation stimulated by MCF-7 breast cancer-derived PTHrP. OPG-Fc also reduced the establishment of osteolytic lesions in a mouse model of tumor cell growth in bone following intratibial injection with MCF-7 cells over-expressing PTHrP. Since the local production of OPG may also be a means to limit tumor expansion in bone by preventing osteoclastogenesis, we transfected MCF-7 parental cells and MCF-7 cells overexpressing PTHrP with full-length cDNA for OPG (1 – 401 aa) in pCEP4. In vitro analysis demonstrated that over-expression of OPG in MCF-7 cells resulted in increased cell growth, in the presence or absence of PTHrP. Parental, vector control and MCF-7 cells over-expressing PTHrP, OPG or PTHrP plus OPG were injected into the proximal tibiae of athymic nude mice. The animals were monitored for 2.5 weeks, after which they were sacrificed and their limbs were assessed by radiology and histology. No osteolysis was observed radiologically following inoculation of the MCF-7 parental cells or the MCF-7 cells over-expressing OPG, although small intramedullary tumors were evident histologically in the latter group. Surprisingly, the MCF-7 cells over-expressing PTHrP and OPG developed larger tibial tumors than the MCF-7 cells over-expressing PTHrP alone (18.6 ± 3.1 % osteolysis as determined by radiology, compared with 9.0 ± 2.2 %, $p < 0.05$). The tumors overexpressing OPG also exhibited a change in histology, which was reflective of a less differentiated phenotype compared with MCF-7 cells over-expressing PTHrP. This increased tumor growth afforded by the over-expression of OPG was abrogated by treatment with OPG-Fc (2.5 mg/kg/day, subcutaneous) resulting in inhibition of tumor growth (2.5 ± 0.3 %, $p < 0.001$ compared with control). These results indicate that full-length native OPG exerts dramatically different actions on tumor behavior than OPG-Fc. These differences may relate to the death domains of native OPG or its intracellular expression.

F083

Clodronate Decreases the Incidence of Skeletal Metastases in Primary Breast Cancer - A Randomised, Placebo-Controlled Study. T. Powles*[1], E. McCloskey[2], A. Paterson*[3], J. Kanis[2], S. Ashley*[1], A. Tidy*[1], K. Rosenqvist*[4], I. Smith*[1], L. Ottestad*[5], S. Legault*[6], M. Pajunen*[7], A. Nevantaus*[1], S. Atula*[4], J. Nevalainen*[4], L. Pylkkänen*[4]. [1]Royal Marsden Hospital, London, United Kingdom, [2]Univ. of Sheffield, Sheffield, United Kingdom, [3]Tom Baker Cancer Centre, Calgary, AB, Canada, [4]Leiras, Helsinki, Finland, [5]Norwegian Radium Hospital, Oslo, Norway, [6]Montreal General Hospital, Montreal, PQ, Canada, [7]Central Hospital, Jyväskylä, Finland.

The development of bone metastases depends at least in part on tumour-induced osteoclastic resorption of bone. We wished to determine if the bisphosphonate, clodronate, could reduce the subsequent incidence of bone metastases when given to patients with primary breast cancer. This double blind, multicentre, trial accrued 1069 evaluable patients with primary operable breast cancer between 1989 and 1995. All patients received surgery, radiotherapy, chemotherapy and tamoxifen as required. Patients were randomised to receive oral clodronate 1600 mg/day or placebo for 2 years, starting within six months of primary treatment**.** The primary endpoint was relapse in bone, analysed on an intent-to-treat basis, during the medication period and during the total follow-up period (median follow-up 2007 days). Secondary endpoints were relapse in other sites, mortality and toxicity. During the total follow up period, there was a non-significant reduction in occurrence of bone metastases (63 clodronate, 80 placebo, HR 0.77, 95% CI 0.56 to 1.08, p=0.127). During the medication period there was a significant reduction in the occurrence of bone metastases (clodronate 12, placebo 28, HR 0.44, 95% CI 0.22 to 0.86, p=0.016). The occurrence of non-osseous metastases was similar (clodronate 112, placebo 128**,** p=0.257) but there was a significant reduction in mortality (clodronate 98, placebo 129, p=0.047) during the total follow up period. Clodronate, given to patients with primary operable breast cancer, reduces the occurrence of bone metastases, although this reduction was only significant during this medication period. There was a significant 23% reduction in mortality. The optimal duration of therapy needs to be addressed in future studies.

Disclosures: ***E. McCloskey****, Leiras 2, 8.*

F085

Prostate Cancer Cells Induce Osteoblastogenesis through Bone Morphogenetic Proteins (BMPs) and BMP-Mediated Autocrine Production of Vascular Endothelial Growth Factor (VEGF). J. Dai[1], J. Zhang[2], A. Mizokami*[3], E. T. Keller[2]. [1]Pathology/ULAM, University of Michigan, Ann Arbor,, MI, USA, [2]Pathology/ULAM, University of Michigan, Ann Arbor, MI, USA, [3]Department of Urology, University of Occupational & Environmental Health, Kitakyushu, Japan.

Advanced prostate carcinoma (CaP) is associated with osteoblastic bone metastases. Many factors are involved in osteoblast differentiation, including bone morphogenetic proteins (BMPs) and vascular endothelial growth factor (VEGF). The goal of this study was to determine if there is a relation between BMP and VEGF in prostate cancer-induced osteoblastogenesis. Using the C4-2B prostate cancer cell line, an androgen-independent bone metastatic cell line, we measured the effect of BMPs on VEGF expression. We first determined that C4-2B cells expressed BMP-2, BMP-6 and BMP-7 and VEGF. To determine if BMPs regulate VEGF expression in C4-2B cells, BMPs-2, -4, -6 and -7 were added to C4-2B cell cultures for 24 hours, all BMPs had increased VEGF in the culture supernatants as measured using ELISA. To determine if BMPs promote VEGF expression in C4-2B cells through an autocrine mechanism, the C4-2B cells were cultured in the serum-free medium plus Noggin, a BMP inhibitor. At 24 hours, Noggin had decreased VEGF expression in a dose-dependent manner. To determine if BMP controls VEGF expression through transcription, we transfected the VEGF promoter driving the luciferase reporter gene into the C4-2B cells then treated with BMPs and Noggin. BMP-2, -4, -6, and -7 induced promoter activity by 5-fold compared to basal levels. Noggin decreased basal luciferase activity by 70%. To determine if BMPs or VEGF could mediate prostate cancer-induced osteoblastogenesis, $SaOS_2$ cells and primary human osteoblast-like cells (HOB) were treated with C4-2B conditioned media (CM) plus Noggin or neutralizing anti-VEGF antibody. Alkaline phosphatase (ALPase) activity and osteocalcin (OCN) level in the supernatants was measured as indices of osteoblastogenesis. CM increased ALPase and OCN production by the $SaOS_2$ and HOB cells. Noggin decreased CM-induced ALPase and OCN levels by approximately 50-65% and 40-45%, respectively. Anti-VEGF antibody decreased CM-induced ALPase and OCN levels by approximately 27-32% and 26-39%, respectively. Combining Noggin and anti-VEGF antibody had no greater effect than Noggin alone. These findings indicate that C4-2B cells stimulate osteoblastogenesis through BMPs and VEGF secreted from C4-2B cells. Furthermore, the data demonstrate that VEGF expression is increased in C4-2B cells through autocrine activity of BMPs. These data suggest that BMPs play an important role in the development of prostate cancer osteoblastic metastases.

F087

NF-κB Mediates the Production of Osteoclastogenic Factors by Breast Cancer Cells. C. Menaa[1], J. Turbov*[1], C. J. Froelich*[1], M. Fujishiro*[2], T. Asano*[2], S. M. Sprague[1]. [1]Evanston Northwestern, Evanston, IL, USA, [2]Yamaguishi University, Yamaguishi, Japan.

Breast cancer cells are resistant to apoptosis and capable of migrating to bone, causing osteolysis. Tumor cells acquire this potential by expressing osteoclastogenic factors (OF). Osteoclast (OC) formation is identified as a key step in bone metastasis, however the mechanism is poorly understood. To determine how breast cancer cells support OC formation, MCF7 and MDA-231 were used. Both MCF7 and MDA-231 cells induced osteoclast formation when incubated with purified primary murine OC precursor cells, CFU-GM, or RAW 267.4 cell line. This effect did not require physical contact between tumor cells and OC precursors. Condition media (CM), harvested from tumor cell culture, dose dependently induced OC formation by a mechanism independent of RANKL and TNF-α production. Amounts of OPG and of neutralizing antibody against TNF-α that were sufficient to block, respectively 100 ng/ml of RANKL and 100 ng/ml of TNF-α were not able to block OC formation induced by CM. Utilizing MCF7 cells over-expressing the pro-apoptotic gene, caspase 3 (C3), not just abolished their resistance to apoptosis, but also totally blocked the breast cancer cells from supporting OC formation, suggesting that resistance of cancer cells to apoptosis and their osteolytic capacity are mechanistically linked. To analyze how C3 affects the production of OF, we examined NF-κB activity as this transcription factor is known to control protein expression and secretion. NF-κB has also been proposed to be directly linked to the pro-apoptotic effects of C3. Compared to wild type MCF7, Western blot showed that IκB, the inhibitory compound of NF-κB, was not degraded in MCF7-C3 cells. These results indicate expression of C3 blocks IκB degradation which, in turn, reduces NF-κB activation, an outcome crucial for OF production. To verify whether NF-κB mediates the control of OF by C3, we developed a MCF7 cell line over-expressing a mutated IκB that acts as a super repressor of NF-κB activation even upon stimulation with TNF-α (10 ng/ml). The super repressor IκB abolished the tumor cells' ability to support OC formation similar to the C3 effect, while the empty vector or the wild type IκB had no effect. These data suggest that NF-κB is the downstream signaling pathway of C3 effect that controls both cell resistance and OF production by breast cancer cells. In summary, we found that breast cancer cells regulate OC formation by a mechanism that is independent of RANKL and TNF-α. The production of OF is modulated by C3 expression through an NF-κB dependent pathway suggesting that apoptosis and OF production may converge at NF-κB. Thus, the NF-κB pathway could be an appropriate target for treatment of breast cancer.

F091

Digital X-ray Radiogrammetry Indices,Particularly MCI, Can Predict Vertebral Fracture Risk in Osteoporotic Women. S. Vasireddy*[1], C. Haigh*[2], L. Reaney*[1], J. Adams*[2], P. L. Selby*[2], S. K. Bal*[1], R. Ashford[1], D. Charlesworth*[1], J. A. Kanis[1], T. Jalava*[3], M. Beneton*[1], E. V. McCloskey[1]. [1]University of Sheffield, Sheffield, United Kingdom, [2]University of Manchester, Manchester, United Kingdom, [3]Leiras Oy, Helsinki, Finland.

It is not yet clear whether combined measures of skeletal strength are of more value in the prediction of fracture risk than a single measurement alone. We wished to determine the predictive ability of two new simple measurements, derived from hand radiographs, for future vertebral fractures in women with osteoporosis. We also wished to compare their performance with that of DXA measurements at the spine and hip. 538 women fulfilling the WHO criteria for osteoporosis (spine or hip T-score <-2.5) and/or with at least one prevalent vertebral fracture were recruited to a 3-year double-blind, controlled study. The women received either clodronate 800mg daily by mouth (Bonefos®) or an identical placebo and all patients received a calcium supplement of 500mg daily. Bone density (BMD) was measured at the spine and hip by DXA at baseline. Prevalent and incident vertebral fractures were identified by morphometric evaluation of lateral spine radiographs obtained at baseline and annually thereafter. Hand radiographs obtained at baseline were analysed using the Pronosco X-posure system^{TM} to derive DXR-BMD and metacarpal cortical index (MCI). The present analysis is blinded to the study treatment. 90 women (17%) experienced one or more incident vertebral fractures during the study. At baseline, these women were significantly older and had significantly lower mean values of BMD at the spine, hip, DXR-BMD and MCI (P≤0.001 for all). In univariate analysis, the gradients of risk per 1SD decrease (Odds Ratio, 95%CI) for incident vertebral fractures were identical for MCI and spine BMD (1.8, 1.4-2.4 for a 1SD decrease in either) and were slightly higher than that for DXR-BMD and total hip BMD (1.6, 1.2-2.0 and 1.5, 1.2-1.9 respectively). In a multivariate forward conditional regression model, the baseline presence of vertebral fracture, spine BMD and MCI were all significant independent predictors of future vertebral fracture with odds ratios of 6.8 (3.7-12.8) for prevalent vertebral fracture, 1.6 (1.2-2.1) for spine BMD and 1.5 (1.0-2.1) for MCI. We conclude that DXR-BMD and MCI are indicators of vertebral fracture risk in women with osteoporosis that are as good as that provided by spine or hip BMD. Moreover, MCI may capture a component of risk for incident vertebral fractures that is not accounted for by other measures of BMD. These simple measures may have wide applicability in the management of osteoporosis since hand radiographs are relatively inexpensive and involve low doses of radiation.

Disclosures: ***E.V. McCloskey****, Pronosco, Denmark 2.*

F094

Fractures of the Distal Forearm, Humerus, Hip and Vertebrae: Association with Peripheral and Axial Densitometry Measurements. J. A. Clowes, N. F. A. Peel, R. Eastell. Clinical Sciences (North), University of Sheffield, Sheffield, United Kingdom.

We have examined whether the strength of association between different types of osteoporotic fracture and measurement of the peripheral skeleton are similar to those of the central skeleton. We consecutively recruited women (age 55 - 80 years) who had sustained a distal forearm (n = 78), humeral (75), hip (53) or vertebral (73) fracture. These were compared to a population-based sample of 500 women (age 55 - 80 years) from the Sheffield center of the osteoporosis and ultrasound study (OPUS study). All subjects had measurements of spine and total hip DXA (Hologic QDR4500A), distal forearm DXA (Osteometer DTX 200), distal forearm pQCT (Stratec XCT 2000) and QUS of the heel (Lunar Achilles+, Osteometer DTU One, Metra QUS 2, and DMS UBIS 5000). Measurements were made on the side contralateral to the site of fracture for the fracture cohorts. We examined the association of these measurements with fracture by calculating age adjusted standardized odds ratios per one SD decrease of population variance.

Age Adjusted sOdds Ratio (95% CI)

Parameter	Forearm #	Humeral #	Hip #	Vertebral #
DXA spine	1.74 (1.33-2.29)	1.96 (1.48-2.60)	2.25 (1.59-3.17)	4.67 (3.24-6.71)
DXA total hip	1.74 (1.32-2.30)	1.76 (1.32-2.36)	3.40 (2.30-5.04)	4.29 (2.99-6.15)
DXA forearm	2.05 (1.53-2.75)	1.62 (1.22-2.17)	1.81 (1.27-2.60)	2.91 (2.11-4.00)
pQCT forearm	2.02 (1.44-2.81)	1.85 (1.33-2.56)	1.93 (1.30-2.85)	3.51 (2.37-5.20)
Achilles BUA	1.77 (1.36-2.31)	1.82 (1.38-2.40)	2.89 (2.01-4.17)	3.08 (2.21-4.30)
DTU One BUA	1.81 (1.42-2.30)	1.75 (1.37-2.23)	2.46 (1.79-3.36)	3.23 (2.43-4.29)
QUS 2 BUA	2.01 (1.50-2.69)	1.85 (1.38-2.49)	3.44 (2.31-5.12)	3.67 (2.61-5.17)
UBIS 5000 BUA	1.65 (1.26-2.15)	1.67 (1.26-2.22)	2.70 (1.88-3.87)	4.03 (2.86-5.69)
Achilles SOS	1.54 (1.18-2.01)	1.46 (1.10-1.94)	2.41 (1.66-3.50)	2.68 (1.94-3.70)
DTU One SOS	2.01 (1.50-2.67)	1.66 (1.24-2.20)	3.17 (2.08-4.83)	3.20 (2.26-4.52)
UBIS 5000 SOS	1.36 (1.03-1.80)	1.33 (1.00-1.78)	2.28 (1.53-3.39)	2.73 (1.96-3.80)

The association of peripheral devices with fracture is site specific with hip and vertebral fractures more closely associated with BMD than upper limb fractures. This is consistent with the observation that prevalent vertebral fractures are stronger predictors of incident osteoporotic fractures than upper limb fractures. The performances of heel BUA, heel SOS and peripheral BMD are comparable with DXA in discriminating different types of osteoporotic fracture.

F099

In vivo Non-Invasive Monitoring of Changes in Structural Cancellous Bone Parameters with a Novel Prototype MicroCT in Rats. J. A. Gasser, J. Yam*. Arthritis & Bone Metabolism, Novartis Pharma AG, Basel, Switzerland.

At present, obtaining information on changes in structural parameters of cancellous bone is only possible after necrospy of animals followed by histomorpometric analysis or time intensive measurements on dedicated microCT systems ex vivo. In our study we tested a novel prototype micoCT scanner from SCANCO Medical (Bassersdorf, Switzerland) which allows for the first time to monitor such changes repeatedly in anaesthetised animals at 26µm resolution with an acquisition time of less than ten minutes for mapping of the entire proximal tibia metaphysis. Skeletally mature, 8 month old virgin Wistar rats (n:10 / group) were treated the following way to induce known specific changes in cancellous bone architecture: 1. Sham OP + placebo s.c., 2. hPTH(1-34) (25µg/kg/day s.c.), 3. OVX + placebo p.o., 4. OVX + zoledronic acid (5µg/kg s.c. 2.inj/week) or 5. OVX + 17-alpha ethinylestradiol (aEE, 0.3mg/kg/day p.o.). Cancellous bone structure was assessed by microCT at baseline as well as 1, 2, 4, 8, 12, and 16 weeks after surgery. Sham operated animals did not show any significant change in trabecular number (TbN), thickness (TbTh), bone volume/tissue volume (BV/TV), connectivity density (ConnD) or the Structure Model Index (SMI). As expected, administration of hPTH(1-34) increased BV/TV, TbTh significantly at 2 weeks with the effect starting to plateau at 4 weeks. TbN did not change significantly but tended to be lower than in Sham OP rats. The SMI dropped dramatically and even assumed negative values in the PTH group indicative of the development of a plate-like structure. In OVX-rats BV/TV, TbTh and TbN dropped to reach statistically significant differences from Sham OP animals at two weeks already. The increase in the SMI indicated development of rod-like characteristics. ConnD also decreased significantly at 8 and thereafter. Rats treated daily with aEE were not different from Sham OP rats at any time-point or parameter. A tendency towards an increase in TbTh and BV/TV was observed in rats treated with zoledronic acid. Our results demonstrate for the first time that this protoype micro-CT scanner has a great potential to investigate the effects of known and novel therapeutic agents on 3D-trabecular microarchitecture accurately, repeatedly, reliably and quickly in anaesthetised rats. Furthermore it is capable to pick up the structural changes induced by OVX, anabolic and antiresorptive treatment and to distinguish between them.

F104

Optimizing the Biological Diagnostic Tools in Primary Hyperparathyroidism. C. Cormier[1], E. Lawson-Body*[2], C. Kindermans[2], B. Lacour*[3], E. Sarfati*[4], J. Souberbielle*[2], A. Kahan*[1]. [1]Rheumatology Cochin Hospital, APHP, Paris, France, [2]Physiology Necker Hospital, APHP, Paris, France, [3]Biochemistry Necker Hospital, APHP, Paris, France, [4]Surgery Saint Louis Hospital, APHP, Paris, France.

The diagnosis of primary hyperparathyroidism (PHP) may be difficult when serum calcium and / or serum PTH are within the normal range. We recently proposed (Souberbielle et al. J Clin Endocrinol Metab 2001, 86: 3086-90) that reference values for serum PTH should be established in healthy subjects without vitamin D insufficiency. By doing this, the reference range for serum PTH obtained with a widely used PTH assay, the Allegro Nichols assay, becomes 10-46 pg/mL instead of the usually accepted range (10-65 pg/mL). Furthermore, choosing to measure serum ionized calcium (iCa++) or total calcium corrected for albumin (alb corr tCa) is debated. We thus aimed to clarify 1) whether serum iCa++ may be more informative than alb corr tCa and 2) whether normative PTH values which take vitamin D status into account are more efficient than usual PTH reference values to diagnose PHP. We reviewed the charts of 42 consecutive patients with surgically proven PHP. These patients had been addressed to our calcium metabolism unit because of osteoporosis in order to eliminate secondary causes. Only one patient (2.4 %) had normal iCa++ (<1.31 mM), whereas 25 (61%) had normal alb corr tCa (<2.58 mM). Serum PTH was below 66 pg/mL in 17 patients (40.5%) and below 47 pg/mL in 5 patients (12%). It is noteworthy that 10 patients (24 %) had both normal alb corr tCa and serum PTH <66 pg/mL whereas only two (4.9 %) of them had PTH <47 pg/mL. For these 2 patients iCa++ was high. In conclusion, we found that using normative PTH data which take vitamin D status into account and iCa++ instead of alb corr tCa allowed to reduce the number of normal pre-surgery biological results in patients with surgically proven PHP.

F106

Reduction in Bone Turnover Predicts Hip, Non-spine, and Vertebral Fracture in Alendronate Treated Women: The Fracture Intervention Trial. D. C. Bauer[1], D. M. Black[1], P. Garnero[2], M. Hochberg[3], S. Ott[4], D. L. Schneider[5], J. Orloff[6], D. Thompson[6], S. Ewing*[1], P. D. Delmas[2]. [1]University of California, San Francisco, San Francisco, CA, USA, [2]INSERM, Lyon, France, [3]University of Maryland, Baltimore, MD, USA, [4]University of Washington, Seattle, WA, USA, [5]University of California, San Diego, San Diego, CA, USA, [6]Merck, Rahway, NJ, USA.

Short-term changes in biochemical markers of bone turnover with bisphosphonate therapy are weakly associated with subsequent changes in bone mass, but the relationship between change in markers and non-spine fracture is unknown. In the Fracture Intervention Trial (FIT), we measured BMD of the spine (BMDsp), and used stored serum (non-fasting) to measure bone specific alkaline phosphatase (BAP, Hybritech), C-terminal telopeptide (CTX, Crosslaps), and terminal propeptide (P1NP, Orion) at baseline and after 1 year of alendronate (ALN), 5 mg/d (n=3005), or placebo (PBO)(n=3081). During a mean follow-up of 3.6 years, 72 hip and 786 non-spine fractures were confirmed by central review of x-ray reports, and 336 women with incident vertebral fracture were identified from paired lateral spine x-rays. We used separate age-adjusted hazard models in the ALN and PBO groups to examine the relationship between percent change in marker or percent change in BMDsp and hip (n=45) or non-spine fracture (n=515) occurring after the 2nd marker or BMD measurement. Incident vertebral fractures were analyzed with logistic regression and odds ratios (OR) were calculated. We found no significant associations in the PBO group, but change in one or more biochemical marker was associated with the risk of hip, non-spine, and vertebral fracture in the ALN group (Table). Further adjustment for baseline BMD and prevalent vertebral fracture, or limiting the analysis to women with osteoporosis, had little effect on the results. We conclude that greater reductions in bone turnover with ALN therapy are associated with fewer hip, non-spine and vertebral fractures, and the effect is at least as strong as that observed with change in BMD.

Change in Marker (Per SD Reduction) or BMD (Per SD Increase) and Fracture Risk (*p<0.05)

	Mean % Change (SD)	Hip Fx RR (95% CI)	Non-spine Fx RR (95% CI)	Vertebral Fx OR (95% CI)
BAP	-31.1 (22.1)	0.61 (0.46, 0.80)*	0.89 (0.78, 1.00)*	0.74 (0.63, 0.87)*
CTX	-59.2 (31.1)	0.89 (0.61, 1.31)	0.94 (0.84, 1.06)	0.83 (0.73, 0.95)*
P1NP	-50.9 (30.7)	0.78 (0.51, 1.19)	0.90 (0.80, 1.03)	0.77 (0.66, 0.90)*
BMDsp	4.1 (3.9)	0.94 (0.56, 1.59)	1.05 (0.93, 1.20)	0.92 (0.76, 1.11)

Disclosures: ***D.C. Bauer****, Merck 2, 5; Pfizer 5; Astra Zeneca 5.*

F109

Diurnal Rhythm of Serum-based Markers of Bone Turnover: Impact on Monitoring Response to Risedronate in Osteoporosis. A. C. Eagleton[1], N. Hoyle*[2], A. Blumsohn[1], R. Eastell[1]. [1]Bone Metabolism Group, Division of Clinical Sciences (North), University of Sheffield, Sheffield, United Kingdom, [2]Roche Diagnostics GmbH, Penzberg, Germany.

Bone turnover markers show a diurnal rhythm with a peak in the early morning. This variability influences interpretation of marker measurement and requires defined sample collection procedures. The aims of this study were to assess the diurnal variability of serum-based markers of bone turnover in osteoporosis and after treatment with the bisphosphonate risedronate, and to determine an optimal sampling time for monitoring response to therapy. Measurements of procollagen type I N-terminal propeptide (PINP), osteocalcin (OC), and C-terminal telopeptide of type I collagen (CTX (β-Crosslaps™ assay)) were made using the Elecsys® 2010 (Roche Diagnostics GmbH) automated system. Diurnal profiles were determined at baseline and week one in postmenopausal women (n = 14, mean age 62 years, range 54,67) with osteoporosis (T<-2.5, Z<-1). Bisphosphonate therapy was begun and profiles re-determined at twelve and thirteen weeks. Diurnal profiles at a one week interval were determined in healthy controls (n = 15, mean age 62 years, range 53, 69). Study conditions were strictly controlled with meals at 10am, 11am, 1pm, and 4pm. Blood samples were taken at 8.30am, 9am, 9.30am, 11am, 12pm, 2pm, 3pm, 5pm, 6pm and 7pm. Time of measurement was significant for all the markers (ANOVA repeated measures P<0.05). CTX and OC measurements were significantly higher in the osteoporosis group pre-treatment compared to the controls (unpaired t test P<0.05). The shape of the profile was similar for all markers in the osteoporosis (pre- and post-treatment) and control groups with a peak in the morning before breakfast and nadir in the afternoon. The 'peak to trough' was minimal for PINP and OC (PINP 13%, OC 12%, CTX 129%). The post-treatment mean decrease in marker level varied between timepoints from 55% to 61% in PINP, 74% to 99% in CTX and 25% to 32% in OC. The least significant change (P<0.05) at each time-point was used to define response. The highest number of responders identified using PINP (n = 13) was at 8.30am and 6pm, at 8.30am for CTX (n = 12) and at 5pm, 6pm and 7pm for OC (n = 12). The signal to noise ratio was calculated at each timepoint. For PINP this was highest at 12pm (range 6.3, 12.7), for CTX at 9am (range 2.2, 6.8) and for OC at 6pm (range 3.2, 6.9). In conclusion, the serum markers of bone metabolism PINP, CTX, and OC have a diurnal rhythm. The rhythm has the greatest amplitude in CTX. The rhythm is not altered by osteoporosis or bisphosphonate therapy. PINP has the highest signal to noise ratio. The optimal sampling time for monitoring response to therapy would appear to vary according to the marker used.

F111

Prospective Evaluation of Hip-Fracture Risk in Institutionalized Elderly by Measurement of Ultrasonic Velocity at the Radius and Phalanx. H. Dobnig, A. Fahrleitner*, C. J. Piswanger-Sölkner*, B. Obermayer-Pietsch*, G. Leb*. Internal Medicine, Karl Franzens University, Graz, Austria.

Fractures constitute a major clinical problem in institutionalized elderly. Here, annual incidence rates for hip fractures usually range between 3% to 5%. Since bone mass or -density constitute an important factor of bone strength and DEXA measurements are limited in the majority of these patients (restricted mobility of patients and DEXA availability) we sought to investigate whether bone ultrasound measurements would help to characterize patients at very high risk for hip- and other non-vertebral fractures. A total of 1085 female patients above 70 years of age who lived in 95 homes for elderly in the southern and eastern part of Austria were followed for an average of 1 year. We excluded patients with hypercalcemia and renal or hepatic dysfunction. Speed of sound (SOS) was measured with a portable quantitative ultrasound device (Sunlight Omnisense Ultrasound Bone Sonometer) at the distal one-third of the radius (RAD) and at the proximal phalanx of the third finger (PLX). So far a total of 147 non-vertebral fractures have occurred, 78 of these being hip fractures. Correlations between age and PLX- or RAD-SOS measurements were comparable (r=-0.20 and -0.19, both p<0.0001). Over the 8th, 9th and 10th decade there was a significant decrease in mean SOS values of 0.84 SD (RAD) and 0.60 SD (PLX). RAD- and PLX-SOS values were correlated with each other (r=0.45, p<0.001). Using Cox-regression analysis and adjusting the data for age, body mass index and measurement device we found a significant increase in the relative risk of hip fracture for each standard deviation decrease in SOS: OR 1.51 (1.16-2.0) for the radial and OR 1.50 (1.16-1.93) for the phalangeal measurement. When all non-vertebral fractures were considered the odds ratios were 1.47 (1.22-1.8) for the radial and 1.19 (1.00-1.42) for the phalangeal measurements. Combining both radial and phalangeal measurements did not result in further improvement of fracture risk prediction. We conclude that measurements of both phalangeal and radial SOS in a large high-risk patient cohort significantly predicted hip-fractures and other non-vertebral fractures. Compared to published data on prediction of hip fractures (neck bone mineral density (OR 2.1/SD decrease); calcaneal SOS and BUA (OR 1.5-1.7/SD decrease) peripheral bone ultrasound measurements may present an attractive screening tool for identification of institutionalized individuals at very high risk of fractures.

F113

Population-Based Calcaneal Quantitative Ultrasound Reference Data: Results from the OPUS Study. R. Barkmann[1], R. John*[1], R. Eastell[2], D. Felsenberg[3], D. Reid[4], C. Roux[5], C. C. Glüer[1]. [1]University Hospital Kiel, Kiel, Germany, [2]University of Sheffield, Sheffield, United Kingdom, [3]Free University Berlin, Berlin, Germany, [4]University of Aberdeen, Aberdeen, United Kingdom, [5]René Descartes University, Paris, Germany.

Population-based reference data are essential for accurate assessment of bone status using quantitative ultrasound (QUS) approaches. We generated such data for four different QUS calcaneus devices and compared them to manufacturer-provided reference data. In the Osteoporosis & Ultrasound (OPUS) study a population-based sample of 2837 women (463 of ages 20 to 39, 2374 of ages 55 to 79 years) has been recruited in 5 European cities. QUS was obtained on the GE/Lunar Achilles+ (n=2246), OSI/Osteometer DTU-one (n=2769), Quidel/Metra QUS-2 (N=1858) and DMS UBIS 5000 (n=2503). We calculated mean values and standard deviations SD for age 20 to 39 years and in 5-year age groups for ages 55 to 79. Manufacturers' reference data for broadband ultrasound attenuation (BUA) and speed of sound (SOS) for DTU-one and UBIS 5000; for stiffness for Achilles+ and for BUA for QUS-2 were evaluated. Differences among devices are expressed as OPUS-based T-scores calculated from the 20-39 year group. Differences between OPUS and manufacturers' reference data are expressed in OPUS-based Z-scores (dZ-sc) and as percent difference for the standard deviation of population variance (%dSD). Comparing OPUS based T-scores among devices and QUS variables (see figures), postmenopausal age-related slopes are similar in all devices and variables, however SOS T-scores are slightly lower than BUA T-scores. The Achilles+ BUA and SOS decrease in each age-group and are lower in postmenopausal women compared to the other devices. Comparing OPUS and manufacturers data, differences in premenopausal women are small in mean (dZ-sc<0.25) and SD (%dSD<11%) except for BUA of UBIS 5000, where OPUS mean and SD values are higher (dZ-sc=0.35 and %dSD=31%). In postmenopausal subjects, differences for SOS of UBIS 5000 and BUA of QUS-2 are small (dZ-sc 0.2, %dSD<15%). For all other variables OPUS data are higher than manufacturer data (dZ-sc=0.17 - 0.75, %dSD=-19 to 31%). We propose that the OPUS reference data is used in place of the manufacturers' reference data. There are differences among devices and QUS variables even when a common population-based reference database is used.

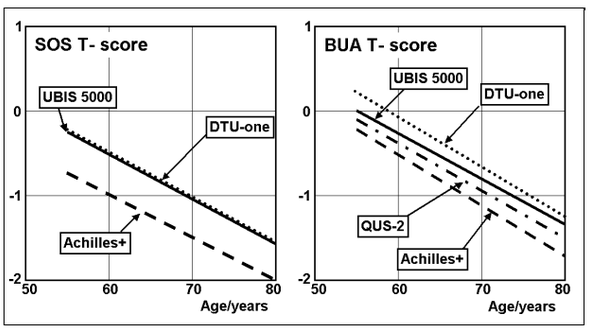

F115

Fracture History and Other Factors Associated with Calcaneal QUS in Men: The MrOS Study. D. C. Bauer[1], D. L. Schneider[2], J. A. Cauley[3], S. Ewing*[1], E. S. Orwoll[4]. [1]University of California, San Francisco, San Francisco, CA, USA, [2]University of California, San Diego, San Diego, CA, USA, [3]University of Pittsburgh, Pittsburgh, PA, USA, [4]University of Oregon, Portland, OR, USA.

Quantitative ultrasound (QUS) has been widely studied in women, but there are few studies of older men. In this cross-sectional study we measured calcaneal QUS (Hologic Sahara) and femoral neck BMD (Hologic QDR 2000) in 5112 men age >65 (mean±SD, 73.7±5.9) recruited from 6 US centers. Duplicate QUS measurements with repositioning were obtained; if the first two BUA results differed by at least 10 dB/MHz, or if either were non-linear (defined as Chi square >50 when frequency is plotted against attenuation), a 3rd measurement was obtained. Medical history (including previous hip and other non-spine fractures), medication use, health habits and total calcium intake (food frequency) were collected by questionnaire. Factors associated with QUS were analyzed with linear regression; QUS and fracture history were analyzed with logistic regression (Table) and are presented as odds ratios (OR) and 95% confidence intervals per SD reduction in QUS or BMD. 16.2% of BUA measurements were non-linear and not analyzed, leaving 4738 men (93%) with at least one valid measurement. The mean BUA (±SD) was 79.0±16.8 dB/MHz and the mean BMDfn was 0.78±0.12 gm/cm2. 2458 men reported previous non-spine fracture, including 83 hip fractures. In multivariate analyses lower age, greater BMI, greater grip strength, and increased physical activity were independently associated with higher BUA (p<0.05), while previous fracture and smoking were associated with lower BUA. Calcium intake and use of medication were not associated with BUA (p>0.05). Results were similar for other QUS parameters (SOS and QUI). After adjustment for age and clinic, men were 39% more likely to report a history of hip fracture and 19% more likely to report non-spine fractures with each SD reduction in BUA (Table). Femoral neck BMD was also associated with fracture history. We conclude that non-linear BUA measurements are common in older men, but at least one valid measurement is obtained in a high proportion of subjects. QUS in men is influenced by body habitus, strength, and health habits. The association between QUS and non-spine fracture is similar to that observed with BMD.

QUS, BMD and Fracture History (OR and 95% CI)

Fracture	BUA	SOS	QUI	BMDfn
Hip	1.39 (1.12, 1.74)	1.46 (1.15, 1.85)	1.44 (1.15, 1.81)	1.85 (1.46, 2.35)
Non-spine	1.19 (1.12, 1.26)	1.21 (1.14, 1.29)	1.21 (1.14, 1.29)	1.22 (1.15, 1.29)

F119

Skeletal Phenotype of Mice Expressing the Human High Bone Mass Gene. F. Bex[1], P. Babij*[2], W. Zhao[1], Y. Kharode[1], C. Small*[2], P. Reddy*[3], P. Yaworsky*[3], P. Bodine[1], B. Bhat[1], J. Robinson[1], M. Bouxsein[4], R. Moran*[1]. [1]Women's Health Research Institute, Wyeth Research, Collegeville, PA, USA, [2]Genomics Division, Wyeth Research, Andover, MA, USA, [3]Genomics Division, Wyeth Research, Cambridge, MA, USA, [4]Musculoskeletal Sciences Division, Wyeth Research, Cambridge, MA, USA.

A mutation (G171V) in the low-density lipoprotein receptor related protein 5 (LRP5) has been shown to cause high bone mass (HBM) in an extended kindred. To validate and investigate the G171V substitution as being the cause of the HBM phenotype, we created transgenic mice expressing the human LRP5 G171V mutation in bone. Immunohistochemistry of calvaria and long bone revealed strong transgene expression in the pre-osteoblasts and osteoblastic cells lining the periosteum and in osteocytes present in mineralized bone. Measurement of volumetric BMD (vBMD) by pQCT analysis showed significant increases (p<0.01) in both total femoral vBMD (30-55%) and trabecular vBMD (103-250%) of the distal femoral metaphysis in male and female transgenics at 5, 9, 17, 26 and 52 weeks of age over their non-transgenic littermates. Diaphyseal cortical vBMD proximal to the metaphysis was slightly but not significantly increased (2-8%), whereas cortical thickness at the mid-diaphysis increased by 21-42% (p<0.01) due to an increase in periosteal circumference (7-17%; p<0.05). High resolution microCT analysis of the distal femorae from the transgenics revealed an increase (125-232%) in trabecular bone volume fraction due to both increased (41-53%) trabecular number and increased (43-46%) trabecular thickness resulting in greater (121-344%) connectivity density (p<0.01). There were no differences in osteoclast number at 17 weeks of age (controls: 21.41 ± 1.65 /mm2 vs. transgenics: 20.66 ± 1.07 /mm2). Fluorescent micrographs of calcein labeled bone revealed a 33% increase in actively mineralizing bone surface in the transgenic animals and an 11% increase in mineral apposition rate. There was enhanced alkaline phosphatase staining in osteoblasts and a significant reduction in the number of TUNEL positive osteoblasts and osteocytes. Taken together these results indicate that the increased BMD in the transgenics is due to increased osteoblast number and activity, which could in part be due to their increased functional lifespan. Importantly, increased bone density in the transgenics was associated with significant increases in vertebral compressive and femoral bending strength. The similarity of the bone density and architectural changes in the transgenic mice, together with the increased strength of the bone, suggest that the skeletal effects of LRP5 (G171V) transgene expression in the mouse closely mimic the human HBM phenotype.

Disclosures: ***F. Bex****, Wyeth Research 3.*

F122

Lumbar Spine BMD is Linked to Genetic Markers on Chromosome 1q. M. J. Econs[1], D. L. Koller[2], S. L. Hui*[1], P. M. Conneally*[2], C. C. Johnston[1], M. Peacock[1], T. Foroud[2]. [1]Medicine, Indiana University School of Medicine, Indianapolis, IN, USA, [2]Medical and Molecular Genetics, Indiana University School of Medicine, Indianapolis, IN, USA.

BMD of the spine is a major risk factor for fracture and has a high heritability. We previously performed an autosomal genome screen in 429 pre-menopausal Caucasian sister pairs and found significant evidence of linkage to markers on chromosome 1q (JCEM 85:3116, 2000). The maximum LOD score was attained at the 170 cM position of the Marshfield chromosome 1 map (Am J Human Genetics 63:861-689). The goal of the current study was to replicate this linkage finding in an independent sample of sister pairs. BMD for L2-4 was measured using a Lunar DPXL densitometer. A genome wide screen was performed using 392 microsatellite markers in 289 premenopausal, Caucasian sister pairs. Multipoint, nonparametric linkage analysis was performed using the maximum likelihood variance components method (Mapmaker/SIBS) yielding a LOD score of 3.2 approximately 18 cM distal to the previously reported linkage finding (at position 188 cM on the Marshfield map). We subsequently performed linkage analysis in an expanded sample of 570 white and 204 black sister pairs, which has partial overlap (281 white pairs) with the previously reported genome screen sample (JCEM 85:3116, 2000). The resulting maximum LOD score in this sample of 774 sibling pairs was 4.5 at position 188 cM. Due to the known racial differences in BMD, the sample of 204 black sister pairs was independently analyzed and yielded a maximum LOD score of 1.85 approximately 30 cM distal to the peak LOD score reported in the combined black/white analyses (at position 217 cM). Analyses of only the 570 white sister pairs demonstrated the strongest evidence for linkage to chromosome 1q with a maximum LOD score of 6.3 at position 188 cM. In summary, this study provides very strong evidence that a gene on chromosome 1q affects peak BMD of the lumbar spine in premenopausal white women. Further studies will be necessary to determine whether this gene also affects peak spine BMD among black premenopausal women.

F124

Large-Scale Genome-Wide Screen of Female Twin Pairs Confirms Presence of QTLs for BMD at 1p36 and 3p21. S. G. Wilson[1], P. W. Reed*[2], M. Chiano*[2], M. Shi*[2], J. Lichter*[2], M. Langdown*[2], T. D. Spector[3]. [1]Department of Endocrinology & Diabetes, Sir Charles Gairdner Hospital & PathCentre, Nedlands, Australia, [2]Sequenom Inc., San Diego, CA, USA, [3]Twin Research & Genetic Epidemiology Unit, St Thomas' Hospital, London, United Kingdom.

Low bone mineral density (BMD) is a major risk factor for osteoporotic fracture and studies of families and twins have shown that BMD is under strong genetic control. We performed a genome screen of a large cohort of unselected twin pairs to identify regions of the genome that contain quantitative trait loci (QTL) for BMD. Female twin pairs aged 18-80 years, were recruited from the St Thomas' Hospital, UK Twin Registry. Multiple phenotypes were assessed including BMD (Hologic DEXA) at lumbar spine (L1-4), hip (total, trochanter, intertrochanter, femoral neck, Ward's), forearm (1/3, mid and ultra distal) and whole body. Heritability estimates for BMD ranged between 0.66 and 0.82, which are consistent with published data. Genome scans were performed using the DNA extracted from the blood of 1098 twin pairs. Four-hundred highly polymorphic microsatellite markers from the ABI Prism linkage mapping set (ver. 2) and Genethon genetic linkage map were analyzed using PCR and electrophoresis on an ABI Prism 377 sequencer. Statistical analysis of the data was performed using MAPMAKER/SIBS and a non-parametric multipoint linkage (NPL) approach with BMD assessed as a quantitative trait. A nominal cut off of z=2.3 (LOD=1) was chosen for linkages that warranted further consideration. The maximum NPL score defined in this analysis was z=3.5 for spine BMD at 3p21. Fifteen additional regions were highlighted in the results using the $z \geq 2.3$ threshold. Among the results, linkage of hip BMD to 1p36 (z=3.0) was also of particular interest. These studies validate the use of large cohorts of unselected twins in linkage analysis and the search for QTLs that regulate BMD. Twins offer the advantage that they are age matched, have the same parents and generally have shared upbringing and environment. In contrast to the affected sib pair experimental design, multiple phenotypes can be analyzed simultaneously when genome scans are performed on unselected twins. Compelling regions identified in these studies are being validated by fine mapping and taken forward into Sequenom's gene discovery pipeline through large-scale high throughput SNP association analysis using the MassARRAY™ technology platform. This report provides substantial evidence for linkage of BMD to 1p36 and 3p21 and provides a replication of linkage to two regions highlighted from other linkage studies as well as defining numerous other regions that are likely to be important for the study of genes that regulate BMD.

Disclosures: ***S.G. Wilson****, Sequenom Inc. 1.*

F130

Estrogen-metabolizing Gene Polymorphisms but not Estrogen Receptor Gene Polymorphisms Are Associated with the Onset of Menarche and Years of Menstruation in Healthy Postmenopausal Japanese Women. I. Gorai, K. Tanaka*, M. Inada*, H. Morinaga*, Y. Uchiyama*, R. Kikuchi, O. Chaki, F. Hirahara*. Obstetrics and Gynecology, Yokohama City University School of Medicine, Yokohama, Japan.

Both onset and cessation of menstruation have strong genetic inclination. An early onset of menopause is related with higher risks of cardiovascular diseases, osteoporosis and ovarian cancer, increasing the risks of mortality. Delayed menopause, however, increase the risk of endometrial and breast cancer. We aimed to identify genetic factors influencing the onset of menarche and natural menopause in a Japanese population by investigating the polymorphisms of estrogen receptor(ER) and estrogen-metabolizing enzyme genes. Three hundred and seventeen postmenopausal Japanese women aged 46 yr and over were enrolled in this study under informed consent. Genomic DNA was extracted from peripheral leukocytes and PCR-based restriction fragment length polymorphism(RFLP) assays were used to determine ER, *PvuII* and *XbaI*, and *CYP17*; estrogen biosynthesis, *CYP1A1*; hydroxylation and *COMT*; inactivation genotypes. There were no significant differences in ages at menarche and natural menopause, and years of menstruation among each *PvuII* or *XbaI* genotype and seven combinations of *PvuII* and *XbaI* genotypes. We could find ages at menarche in women with A1/A2 (higher activity of *CYP 17*) (13.6+/-1.2 yr) were significantly earlier than in those with A1/A1 (lower activity of *CYP 17*) (14.1+/-1.3 yr). There were no significant differences in ages at natural menopause and years of menstruation among each *CYP17*, *CYP1A1* or *COMT* genotypes. When three RFLPs of the estrogen metabolizing enzymes were classified together, ages at menarche were significantly earlier in women with A1/a2h/Lwt/vt (13.4+/-1.4 yr) genotypes as compared with those with A1/A1H/Hvt/vt (14.4+/-1.4 yr), A1/A1H/Hwt/wt (14.3+/-1.4 yr) and A2/A2H/Lwt/vt (14.7+/-1.5 yr) genotypes (P=0.0223, P=0.0252 and P=0.0155, respectively). Women with A2/A2H/Lwt/vt genotypes (34.0+/-1.8 years) had significantly shorter years of menstruation than those with A1/A1H/Lwt/wt (37.1+/-3.4 years), A1/A2H/Hwt/vt (36.8+/-3.0 years) and A1/A2H/Hwt/wt (37.3+/-3.4 years) genotypes (P=0.0391, P=0.0391 and P=0.0266, respectively). The results suggest that estrogen metabolizing *CYP17* genotype alone influences on ages at menarche and that combinations of three estrogen metabolizing genotypes, *CYP 17*, *CYP1A1* and *COMT*, interdependently have some consequences on the timing of onset of menarche and years of menstruation in healthy postmenopausal Japanese women.

F137

Fibroblast Growth Factor Receptor 2 (FGFR2) Interacts with FGF23 and Type IIa Na-Pi Cotransporter (NaPi Cotransporter) in OK Cells. H. Yokote*, X. Yan*, L. Yao*, S. Liang*, K. Fujita*, X. Jing*, E. Okuno*, K. Sakaguchi. Department of Molecular Medicine, Institute of Advanced Medicine, Wakayama Medical University, Wakayama, Japan.

Autosomal dominant hypophosphatemic rickets (ADHR) is caused by mutation of FGF23, that makes the molecule less susceptible to proteolytic cleavage, while overproduction of FGF23 is the cause of tumor-induced osteomalacia. FGF23 appears to be phosphatonin that is cleaved by PHEX, whose gene mutation is responsible for X-linked hypophosphatemic rickets. Then, how does FGF23 induce hypophosphatemia? To investigate which FGF receptor is involved in the signaling of FGF23 to NaPi cotransporter that is responsible for phosphate reabsorption in the proximal tubule, we examined the following: (1) mRNA expression of FGFRs 1-4 by RT-PCR in OK cells, (2) phosphorylation of FGFRs in OK cells in response to the exogenously added recombinant FGF23 with one of the ADHR mutations and an HA-His epitope at the C-terminus (FGF23[R176Q-HA-His]), (3) the interaction of FGF23[R176Q-HA-His] with extracellular domains of FGFRs, and (4) the interaction of FGFRs with NaPi cotransporter in OK cells. We found mRNA expression of FGFR2, FGFR3 and FGFR4 in OK cells. When all the 4 FGFRs with C-terminal myc-epitope (FGFRs-myc) were separately expressed in OK cells and exposed to FGF23[R176Q-HA-His], only FGFR2 was shown to be phosphorylated further by the immunoblotting study following immunoprecipitation by anti-myc antibody. Since FGFR2 can be divided into two isoforms containing IIIb or IIIc exon according to ligand binding specificity, we constructed the expression vectors for these extracellular domains fused to the IgG-Fc fragment (Ex-FGFR2-Fc), and examined the interaction of the recombinant receptors with FGF23[R176Q-HA-His] by immunoblotting with anti-HA antibody following precipitation of the receptor-ligand complex using GammaBind plus sepharose. Ex-FGFR2-Fc with either IIIb or IIIc exon interacted with the ligand. Finally, we cotransfected FGFRs-myc with NaPi cotransporter tagged with flag epitope (NaPi cotransporter-flag) into OK cells, and examined coimmunoprecipitation of the two molecules by immunoblotting with anti-FGFR antibody after immunoprecipitation by anti-flag antibody. Only FGFR2-myc coimmunoprecipitated with NaPi cotransporter-flag in OK cells. We conclude that FGF23 is likely to exert its effect on NaPi cotransporter through FGFR2 in OK cells representing the proximal tubular cells.

F139

FGF Signaling Regulates Dach1 Expression During Limb Skeletal Development. A. Horner, L. Shum*, J. A. Ayres*, G. H. Nuckolls*. Cartilage Biology and Orthopaedics Branch/NIAMS, National Institutes of Health, Bethesda, MD, USA.

Dach1 is a mouse homologue of the Drosophila dachshund gene, which is a key regulator of cell fate determination during eye, leg and brain development in the fly. Dach1 is expressed in the distal mesenchyme of the early embryonic mouse limb bud and subsequently becomes restricted to the tips of digital cartilages. Since signaling pathways that regulate skeletal patterning in the limb bud also regulate chondrocyte proliferation and maturation during endochondral bone development, we have investigated the expression and growth factor regulation of Dach1 during skeletal development in the mouse limb. Dach1 protein was localized to postmitotic, prehypertrophic and early hypertrophic chondrocytes of prenatal and early postnatal phalanges. Dach1 co-localized with Cbfa1 in chondrocytes but not in the forming bone collar or primary spongiosa. Dach1 also co-localized with cyclin dependent kinase inhibitors p27 (Kip1) and p57 (Kip2) in chondrocytes of the growth plate and in the epiphysis prior to formation of the secondary ossification center. Since fibroblast growth factors (FGF), bone morphogenetic proteins (BMP) and hedgehog molecules (Hh) regulate skeletal patterning of the limb bud and chondrocyte maturation in developing endochondral bones, we investigated the regulation of Dach1 by these growth and differentiation factors. Expression of Dach1 in 11 dpc mouse limb buds in organ culture was upregulated by implanting beads soaked in FGF2, 4, 8, or 9 but not FGF10. BMP4 soaked beads slightly down regulated Dach1 expression while Shh and BSA had no effect. Furthermore, FGF4 or 8 could substitute for the apical ectodermal ridge in maintaining Dach1 expression in the limb buds. Immunolocalization of FGFR2 and FGFR3 revealed overlap with Dach1 expression during skeletal patterning and chondrocyte maturation. We conclude that Dach1 is a target gene of FGF signaling during limb bud outgrowth and patterning, and is co-expressed with FGF receptors that regulate chondrocyte proliferation and maturation in developing endochondral bones. Genetic mutations that disrupt FGF signaling cause frequent, severe skeletal malformations. Therefore, further characterization of the function of Dach1 in FGF signaling during skeletal development will contribute to an understanding of the molecular mechanisms of skeletal morphogenesis and dysmorphogenesis.

F144

Flt-1 Tyrosine Kinase-Deficient Homozygous Mice Result in Decreased Trabecular Bone Turnover and Bone Strength. O. Hajime*[1], S. Uchida[1], M. Watanuki*[1], S. Tanaka*[1], A. Sakai[1], S. Niida*[2], T. Nakamura[1]. [1]Orthopedic Surgery, University of Occupational and Environmental Health, Kitakyushu, Japan, [2]Geriatric Research, National Institute for Longevity Sciences, Aichi, Japan.

Vascular endotherial growth factor (VEGF), a crucial modulator of angiogenesis, recently has been shown to affect directly on osteoblasts and osteoclasts through the expression of tyrosine kinase receptor Flt-1 (VEGFR1). Flt-1 displays higher affinity for VEGF but much lower kinase activity than Flk-1 (another tyrosine kinase receptor for VEGF, VEGFR2). Recent studies have suggested that Flt-1 plays a main role in angiogenesis as ligand-binding molecule, rather than as a signal transducting receptor. However the role of Flt-1 in osseous tissue has not been well characterized. The purpose of this study was to clarify whether the deficiency of Flt-1 tyrosine kinase domain causes abnormal bone metabolism. We examined C57BL/6J mice, aged 9 or 16 weeks, with disruption of the Flt-1 tyrosine kinase domain gene (Flt-1TK-/-) and compared with age matched wild type mice (WT). Dynamic histomorphometry confirmed significant decrease in the values of mineralising surface (MS/BS), mineral apposition rate (MAR), bone formation rate (BFR/BS) and osteoclast surface (Oc.S/BS) in the trabecular bone of the proximal tibiae. However there was no significant differences in the value of trabecular bone volume (BV/TV). Although the values of bone mineral content (BMC) and bone mineral density (BMD) of the femur showed no significant differences, the values of bending load of the femur significantly decrease in Flt-1TK-/- mice. In addition, serum osteocalcin significantly decreased in Flt-1TK-/- mice compared with those in WT mice. These findings demonstrate that Flt-1TK-/- mice show lower bone turnover and bone strength than WT mice, and suggest that VEGF signal pathway through the Flt-1 tyrosine kinase domain could be implicated in bone formation and resorption.

F146

IL-10 Knockout Mice Develop Reduced Bone Formation, Osteopenia and Mechanical Fragility. R. Dresner Pollak[1], N. Gelb*[2], D. Rachmilewitz*[3], F. Karmeli*[3], M. Weinreb[2]. [1]Hadassah University Hospital, Jerusalem, Israel, [2]Goldschleger School of Dental Medicine, Tel-Aviv University, Tel-Aviv, Israel, [3]Shaare Zedek Medical Center, Jerusalem, Israel.

Interleukin 10 (IL10), an anti-inflammatory cytokine, inhibits osteoclastogenesis and osteoblastic differentiation *in vitro*. To evaluate the role of IL10 in bone physiology *in vivo* we studied bone status in 8-12 week-old IL10 -/- mice and their age-matched, wild-type (WT) counterparts (C57BL/J6). IL10 -/- mice had lower body weight, lower femoral length and lower serum albumin, suggesting malnutrition. At 8 weeks of age, IL10 -/- mice exhibited osteopenia, evidenced by significantly reduced femoral ash weight (-9%) and tibial cancellous bone area (-25%). At 12 weeks, osteopenia was more pronounced (-22% and -55% respectively), and included reduced tibial cortical thickness (-25%), lower trabecular width (-30%) and number (-39%). Mid-femoral mechanical strength, tested at 12 weeks by 3-point bending, revealed reduced maximal load (-27%) and stiffness (-29%) in IL10 -/- mice. Using calcein-based histomorphometry, we found that 8-week old IL10 -/- mice had significantly reduced bone formation (35% and 19% reduction in cancellous % double labels and mineralizing surface, respectively, 20% reduction in cancellous mineral apposition rate (MAR), 37% reduction in cancellous bone formation rate and 16% reduction in endocortical MAR). In agreement, serum osteocalcin was reduced by 27% in IL10 -/- mice. There were no significant differences in serum PTH, $25(OH)D_3$ and DPD (deoxypyridinoline) levels. Since IL10 -/- mice develop progressive enterocolitis, we wished to examine whether their developing osteopenia is associated with the colitis. IL10 -/- mice with colitis (based on rectal prolapse and colon weight) had lower body weight, lower bone mass and lower osteocalcin levels compared to IL10 -/- mice with no gross evidence of colitis, suggesting that the two disorders may be associated. In summary, IL10 knockout mice develop a bone disease characterized by diminished bone formation, osteopenia and decreased mechanical bone strength, which may be caused by disregulated cytokine expression and/or malnutrition.

F149

Seven Quantitative Trait Loci (QTL) Contribute to Variation in Serum IGF Binding Protein-5 Levels in F2 Mice (MRL/MpJ X SJL/J): Evidence That Genetic Determinants of IGFBP-5 Are Involved in the Regulation of Peak BMD. S. Mohan[1], G. Masinde[1], X. Li[2], D. J. Baylink[1]. [1]J.L. Pettis VAMC, Loma Linda, CA, USA, [2]Univ of Chicago, Chicago, IL, USA.

Past findings that 1) IGFBP-5 is a growth factor that stimulates bone formation (BF) independent of IGFs, 2) IGFBP-5 production in osteoblasts is regulated by osteorgeulatory agents that regulate BF, and 3) serum IGFBP-5 levels are decreased in hip fracture patients and correlate with bone mineral density (BMD), provide evidence that IGFBP-5 could be an important physiological regulator of BF. Because serum IGFBP-5 levels correlate with BMD, a trait that is largely genetically determined, we proposed that serum IGFBP-5 level has a strong heritable component and that genetic determinants for serum IGFBP-5 levels are involved in the regulation of peak BMD. To evaluate this hypothesis, we intercrossed two inbred strains of mice, MRL/MpJ and SJL, which exhibit a 79% difference in serum IGFBP-5 levels (554±68 vs 309±51 ng/ml respectively, $P<0.001$). Genome wide scan was carried out using 119 polymorphic markers in 633 F2 female mice. Serum IGFBP-5 levels were measured using an RIA, which has been validated for mouse serum samples. Serum IGFBP-5 levels in the F2 progeny showed a normal distribution with an estimated heritability of 74%. Whole genome wide scans for co-segregation of genetic marker data with high or low serum IGFBP-5 levels revealed seven different QTL in chromosomes 1, 6, 9 (two), 10, 11 and X, which together explained 30% of F2 variance. Chromosome 11 QTL exhibited the highest LOD score (6.6). If IGFBP-5 is an important BF regulator, we predicted IGFBP-5 to contribute to BMD variation in F2 mice. Accordingly, we found three of the seven IGFBP-5 QTL (Chr 1, 9 and 11) identified for serum IGFBP-5 phenotype also showed significant association with total body BMD phenotype (DEXA) in the F2 mice. Summary: 1) MRL and SJL mice exhibit extreme differences in serum IGFBP-5 levels. 2) Serum IGFBP-5 level is a highly inherited polygenic trait in mice. 3) Seven genetic loci contribute to approximately 30% of phenotypic variance in serum IGFBP-5 levels in F2 mice (MRL X SJL). 4) IGFBP-5 and BMD phenotypes share three common genetic loci. Conclusions: Our study provides 1) the first identification of QTL regulating serum IGFBP-5 levels and 2) genetic evidence for a growth factor regulating BMD.

F150

Evidence that a Disintegrin and Metalloprotease (ADAM)-9 Is an IGF Binding Protein (BP-5) Protease that Binds to alpha2Macroglobulin (alpha2M) and Exists as a Complex in the Conditioned Medium (CM) of Human Osteoblasts (hOBs). S. Mohan[1], G. Thompson*[1], Y. Amaar[1], G. Hathway*[2], H. Tschesche*[3], D. J. Baylink[1]. [1]J.L. Pettis VAMC, Loma Linda, CA, USA, [2]Calif Inst of Tech, Pasadena, CA, USA, [3]Univ of Bielefeld, Bielefeld, Germany.

Previous studies have shown that BP-5 is a multifunctional protein that acts not only as a traditional binding protein but also as a growth factor independent of IGF to stimulate bone formation. The actions of BP-5 in local areas of bone are controlled in part by BP-5 protease produced by hOBs. Therefore, elucidation of the identity of BP-5 protease produced by hOBs is important for our understanding of the molecular pathways that control the actions of BP-5. In this regard, BP-5 protease purified by various chromatographic steps from a CM of U2 cells migrated as a single band, which comigrated with the protease activity in native PAGE and yielded multiple bands in SDS-PAGE under reducing conditions. N-terminal sequencing of these bands revealed that three of the bands yielded amino acid sequences that were identical to that of ∝2M. Although ∝2M is produced in large quantities by several hOB cell types, it was not found to be a BP-5 protease based on several criteria including failure of ∝2M antibodies to block BP-5 protease in hOB CM. Because ∝2M has been shown to complex with ADAM proteases and because ADAM-12 was found to cleave BP-3 and BP-5, we evaluated if one of the members of ADAM family is the BP-5 protease. The relative expression of various members of ADAMs (9, 10, 12, 17 and TS1) known to contain active proteolytic domain by Northern and Western immunoblot revealed that ADAM-9 is produced and secreted in high abundance by various hOB cell types. In addition, ADAM-9 but not other ADAMs was present in highly purified preparations of BP-5 protease. To determine if ADAM-9 could cleave BP-5, we expressed the metalloprotease domain of recombinant ADAM-9 and evaluated proteolysis of BP-5 and other BPs. Purified ADAM-9 cleaved BP-5 effectively while it did not cleave other BPs or did so with less potency. Because BP-5 protease existed as a complex by binding to ∝2M, we expected ADAM-9 to bind to ∝2M if it were the BP-5 protease. Accordingly, we found that purified ADAM-9 formed a complex with ∝2M. To determine if ∝2M alters the potency of ADAM-9 to cleave BP-5, ADAM-9 was incubated with or without purified native ∝2M prior to BP-5 proteolysis. It was found that addition of ∝2M did not prevent degradation of BP-5 by ADAM-9. Conclusions: Our findings demonstrate for the first time that 1) ADAM-9 is produced by hOBs and forms a complex with ∝2M which exhibits potent BP-5 protease activity, 2) ∝2M binding to ADAM-9 may protect ADAM-9 from degradation, and 3) ADAM-9 degrades BP-5 and thereby may regulate bone formation.

F151

Impaired Adaptation to a Low Dietary Calcium Stress in IGF-I Knockout Mice. S. Mohan, Y. Kasukawa, J. E. Wergedal, Y. Amaar, R. Guo*, D. J. Baylink. J.L. Pettis VAMC, Loma Linda, CA, USA.

Human adaptation to decreased dietary calcium (Ca) intake is impaired with age, resulting in increased serum PTH levels. Based on prior findings that serum IGF-I levels decline with age and correlate with indices of calcium homeostasis, we proposed that a deficiency in IGF-I production contributes to impaired adaptation to low dietary Ca stress. Accordingly, serum PTH was elevated 7-fold (35±3 vs 4.9±2 pg/ml, P<0.001) in IGF-I knockout (KO) mice fed with normal Ca diet compared to wild type (WT) mice. To determine the molecular pathways contributing to increased PTH levels in IGF-I KO mice, we evaluated the effect of Ca deficiency on bone formation (BF) and resorption (BR) processes known to participate in Ca homoeostasis. At 4 weeks of age, IGF-I KO and WT mice were fed with low Ca (0.01%) or normal Ca (0.6%) for 2 weeks and labeled with tetracycline. Two weeks of Ca deficiency did not affect an increase in body wt. or femur length in either IGF-I KO or WT but increased PTH levels significantly in both. Low Ca diet caused a much greater increase in the bone resorbing surface in the tibia of IGF-I KO mice compared to WT (144% vs 46% increase, P<0.05). While resorbing surface was absent in the periosteum of WT mice, approximately 10% of the surface was covered with TRAP positive osteoclasts in IGF-I KO mice. Thus, the magnitude of increase in BR is greater in IGF-I KO mice compared to WT during Ca deficiency. Ca depletion also significantly decreased the endosteal BF parameters in IGF-I KO mice (60%, P<0.05) but not in WT mice (7%). Accordingly, femur BMC and bone area (DEXA) failed to increase significantly during active growth phase in IGF-I KO mice during Ca deficiency while they were increased in WT (40%, P<0.05). Furthermore, periosteal circ. (PQCT) increased in IGF-I KO mice fed with normal Ca but not low Ca while it increased similarly in WT mice fed with normal and low Ca. Serum Ca change due to Ca deficiency was greater in IGF-I KO mice compared to WT mice (11.5% vs 5.3%, p<.05). 1, 25 D was 25% less (P<0.05) in IGF-I KO mice fed with normal Ca compared to WT mice despite 7-fold higher PTH levels, thus suggesting that 1,25 D deficiency contributes to this impaired adaptation. Summary: 1) Serum PTH levels are elevated in IGF-I KO mice compared to WT mice in both normal and low Ca diet. 2) BF is severely compromised while BR is increased in IGF-I KO mice fed with low Ca, resulting in impaired bone growth. 3) Serum 1,25 D levels are significantly lower in IGF-I KO mice compared to WT mice fed with normal Ca diet. Conclusions: 1) Adaptation to low Ca stress is impaired during IGF-I deficiency. 2) IGF-I is a regulator of 1,25 D status, a finding which, together with published data, is strongly suggestive of a cross talk between the IGF and 1,25 D regulatory systems.

F155

Parathyroid Hormone Enhances Mechanically Induced Bone Formation Through Activation of L-type Voltage-Sensitive Calcium Channels. J. Li*[1], R. L. Duncan[2], D. B. Burr[1], C. H. Turner[2]. [1]Anatomy and Cell Biology, Indiana University School of Medicine, Indianapolis, IN, USA, [2]Orthopedic Surgery, Indiana University School of Medicine, Indianapolis, IN, USA.

Intermittent administration of parathyroid hormone (PTH) stimulates bone formation. Cell culture studies show that PTH enhances the intracellular calcium concentration in osteoblastic cells subjected to fluid flow, and the synergistic effect between PTH and a mechanical stimulus can be attenuated by L-type calcium channel blockers, such as verapamil. These data suggest that PTH enhances fluid shear-induced calcium signaling in osteoblastic cells through activation of L-type voltage-sensitive calcium channels (VSCCs). We tested the in vivo effect of the L-type VSCC blocker verapamil on bone formation after PTH injection or mechanical loading using the rat ulnar loading system. Adult rats (6 months old) were divided into 8 groups (n=8 each group): vehicle, verapamil, PTH, or both verapamil and PTH treated groups with loading or without loading. Verapamil was given orally at 100 mg/kg using a gavage 90 minutes before loading, which gives maximal plasma levels of verapamil coincident with loading. PTH was injected subcutaneously at 80 microgram/kg 30 minutes before loading. The relative bone formation rate, indicated by bone formation rate from the left limb (nonloaded control) subtracted from the right limb (loaded ulna) value, is shown in the figure. One bout of loading at 360 loading cycles (2 Hz, 16 N peak force) significantly increased bone formation rate on the periosteal surface of the ulna (p<0.0001). Treatment with PTH increased load-induced bone formation by 76% (p<0.001). Treatment with verapamil decreased mechanically induced bone formation rate by 59% (p<0.01). Furthermore, treatment with verapamil suppressed bone formation in rats subjected to PTH+loading by 66% (p<0.0001). In the groups without loading, both verapamil and PTH treatment did not significantly change any bone parameters. This study indicates that L-type VSCCs mediate mechanically induced bone formation in vivo. It suggests that PTH enhances mechanically induced bone adaptation through activation of L-type VSCCs.

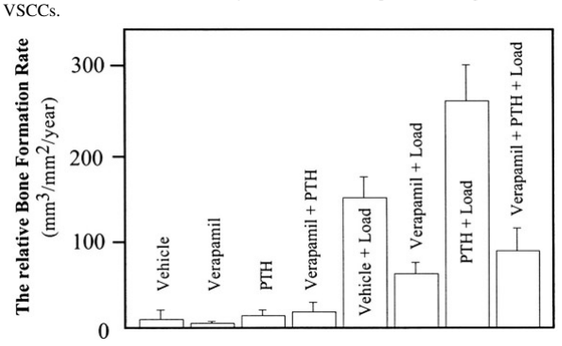

F157

Osteopontin: A Marker of Osteocyte Stress in Response to Loss of Mechanical Loading. T. S. Gross, N. A. Rabaia*, N. Y. Moy*, S. Srinivasan. Orthopaedics and Sports Medicine, University of Washington, Seattle, WA, USA.

Osteopontin (OPN) is a glycoprotein expressed by cells in numerous tissues. Recently, it was observed that the OPN -/- mouse does not lose bone in response to tail suspension, suggesting an integral role for OPN in bone mechanotransduction. Here, we present data at the in vivo and in vitro levels that suggests a mechanism by which OPN expression may modulate disuse induced bone loss. The left ulna diaphysis of four adult turkeys was deprived of mechanical loading via parallel metaphyseal osteotomies. The left and intact right ulnae were recovered following 24 hr of disuse and decalcified sections were obtained from each mid-diaphysis. Sections were incubated with a mouse anti-OPN antibody and detected with a FITC secondary antibody. At 12 equal angle intervals around the cortex, osteocytes were imaged via confocal microscopy (x60) to determine the mean percentage of OPN positive osteocytes. For in vitro studies, MLO-Y4 osteocyte-like cells were plated at 25% confluence and grown for 24 hr in α-MEM supplemented with 2.5% fetal bovine serum (FBS) and 2.5% calf serum (CS). Osteocytes were then challenged by one of two conditions: 1) normal oxygen (19%) with a 90% reduction in serum levels, or 2) hypoxia (2%) and a 90% reduction in serum levels. For three separate experiments, Western blot analysis of OPN expression was performed on extracts at the following time points: 0, 4, 8, 12, 24, and 48 hr. Mean fold elevation of OPN band density was assessed via NIH ImageJ. One day of disuse resulted in a 90% increase in the mean (+S.E.) number of osteocytes staining positive for OPN (16.1 + 4.4% vs 30.6 + 9.9%, p=0.03). During the first 12 hours of serum reduction with normal oxygen, OPN was unchanged compared to zero-time control levels (5% increase). At 24 and 48 hr, OPN expression was substantially elevated (73% increase). In contrast, the OPN expression pattern in response to hypoxia and serum reduction was bimodal, with peaks near 8 to 12 hr (49% increase) and 48 hr (132% increase). At both peaks, OPN expression in hypoxic cells exceeded that observed in cells exposed to serum reduction alone (52% and 28%, respectively). The in vivo data presented here emphasize that loss of loading confers a 'stressful' environment upon the osteocyte, one by product of which is a rapid increase in OPN expression. In vitro, we found that osteocyte OPN expression was elevated by either oxygen and/or nutrient reduction, both of which occur when bone is deprived of loading. Given the known influence of OPN upon osteoclast recruitment, we speculate that this molecule, modulated by altered osteocyte oxygen and nutrient status, plays an important role in the mechanotransduction pathway resulting in disuse induced bone loss.

F159

Skeletal Unloading Induces Resistance to Insulin like Growth Factor-I (IGF-I) by Inhibiting Activation of the IGF-I Signal Pathways. T. Sakata, Y. Wang*, B. P. Halloran, H. Z. ElAlieh*, J. Cao*, D. D. Bikle. Endocrine Unit, Veterans Affairs Medical Center, San Francisco, CA, USA.

We have previously reported that skeletal unloading induces resistance to IGF-I with respect to bone formation. To investigate further the mechanisms underlying this resistance, we first determined the response of bone to IGF-I administration in vivo with respect to osteoblast proliferation and apoptosis during skeletal unloading (hindlimb elevation). We then evaluated the response of osteoprogenitor (BMOp) cells isolated from unloaded bones to IGF-I treatment in vitro with respect to activation (phosphorylation) of the IGF-I receptor and the MAPK (Erk1/2) and PI3K/Akt pathways as well as induction of genes marking osteoblast differentiation. To eliminate the variable of endogenous growth hormone during exogenous IGF-I treatment, we used growth hormone-deficient dwarf (dw-4) rats. For the in vivo experiments, 3 mo old rats were given IGF-I (2.5 mg/kg/day) or vehicle during the 2 week hindlimb elevation period. To evaluate cell proliferation, 5-bromo-2'-deoxyuridine (BrdU) was given to the rats during the first 7 days of the 14 day unloading period. IGF-I significantly increased the number of BrdU positive osteoblastic cells on the bone surface (BrdU(+)Ob./BS). Unloading markedly decreased the BrdU(+)Ob./BS in the vehicle treated rats, and blocked the ability of IGF-I to increase the BrdU(+)Ob. To evaluate apoptosis of the osteoblasts, the TUNEL procedure was used. Unloading for 7 days significantly increased apoptosis of the osteoblasts in both the vehicle-treated and IGF-I treated rats. IGF-I did not significantly alter apoptosis in either loaded or unloaded rats. Phosphorylation of the IGF-I receptor, Erk1/2 and Akt were measured in BMOp cells (8 day culture) isolated from unloaded (7 days) or normally loaded tibiae and femurs following IGF-I treatment (10 ng/ml, for 5 min). IGF-I stimulated the phosphorylation of the IGF-I receptor, Erk1/2 and Akt in the BMOp cells from loaded bones, but these effects were markedly diminished in the BMOp cells from unloaded bones. Furthermore, unloading decreased the protein levels of Erk1/2 and Akt, but not that of the IGF-I receptor. The mRNA levels of collagen (type1), alkaline phosphatase (ALP) and osteocalcin were measured in cultured BMOp cells treated with IGF-I (10 ng/ml, for 12 h) using quantitative real-time PCR. IGF-I increased the mRNA levels of collagen, ALP and osteocalcin in the BMOp cells from loaded bones, but BMOp cells from unloaded bone showed a blunted response. These results indicate that skeletal unloading induces resistance to IGF-I by inhibiting the activation of IGF-I signal pathways leading to altered rates of proliferation and differentiation.

F161

Extracellular Signal-Regulated Kinase (ERK)-1 and ERK2 Are Both Essential in the Mediation of the Flow Shear Strain-Induced Human Osteoblast Proliferation. S. Kapur, S. T. Chen*, D. J. Baylink, K. H. W. Lau. Musculoskeletal Disease Center, Jerry L. Pettis Mem VAMC, Loma Linda, CA, USA.

ERK1 and 2 are key mediators of mitogenic signaling pathways. There is now abundance of evidence that mechanical strain stimulates osteoblast proliferation through multiple signaling pathways, which may involve activation of ERK1 and/or 2. However, it remains unclear whether the activation of either ERK1 or 2 or both is required. Thus, this study sought to test whether the protein kinase activity of ERK1 and/or 2 is essential for the fluid flow shear strain-induced osteoblast proliferation. To test this hypothesis, we prepared MLV retroviral-based vectors that express either the wild type (wt) or kinase-dead (kd) ERK1 and 2. A HA tag was added to the N-terminus of each construct to help to distinguish the overexpressed enzyme from the endogenous enzyme. An MLV-red fluorescent protein (RFP) vector was also included as a control for comparison. Human TE85 osteosarcoma cells were transduced three times with each of the test retroviral vectors with a total MOI of 30. This treatment resulted in an apprxoimately 10-fold and 2-fold overexpression of ERK1 and 2, respectively, in TE85 cells based on Western analyses and protein kinase assays. To determine the effect of overexpression of ERK1 or 2 on fluid flow shear stress-induced cell proliferation, we measured the [^{3}H]thymidine incorporation in each MLV-transduced TE85 cells 24 hr after a 30 min constant flow shear stress at 20 dynes/cm^2. The RFP expressing control TE85 cells showed a 1.7-fold increase ($p<0.01$) in [^{3}H]thymidine incorporation in response to the flow strain. Cells overexpressing wt ERK1 or 2 also showed a mitogenic response to the flow strain with a 2- ($p<0.01$) and 2.7-fold ($p<0.01$) increase, respectively, in [^{3}H]thymidine incorporation, but the flow-induced increase in [^{3}H]thymidine incorporation in cells overexpressing wt ERK1 or 2 was not significantly different from that in control cells. That overexpression of either wt ERK1 or 2 had no further enhancing effect on the cellular mitogenic response to the flow strain suggests that the downstream substrates of ERKs rather than the levels of ERKs are the rate-limiting step of the flow-induced cell proliferation. In contrast, overexpression of an inactive form of either ERK1 or 2 completely abolished the fluid flow-induced bone cell proliferation, since the same flow strain failed to induce an increase in [^{3}H]thymidine incorporation in cells overexpressing either kd-ERK1 or ERK2. In summary, this study demonstrates for the first time that the protein kinase activity of ERK1 and that of ERK2 are both essential for the fluid flow strain-induced osteoblast proliferation

F165

Synergistic Effects of Exercise Plus Alendronate on Bone Mass and Structural Properties in Ovariectomized Rats. R. K. Fuchs[1], M. Shea[2], J. Widrick*[1], S. Stark*[1], B. Hansen*[2], C. M. Snow[1], [1]Oregon State University Bone Research Laboratory, Corvallis, OR, USA, [2]Oregon Health & Science University, Orthopaedic Biomechanics Laboratory, Portland, OR, USA.

We examined the effects of alendronate (Fosamax) therapy plus exercise on bone mass, geometry and biomechanical properties in 7-month old female rats (ovariectomized, n=46; sham-operated, n=13). Ovariectomized rats were randomly assigned to: placebo, n=10 (ovx); Fosamax-treated, n=12 (ovx+fos); exercise-trained, n=12 (ovx+run); and Fosamax-treated plus exercise-trained, n=12 (ovx+fos+run). The ovx+fos and ovx+fos+run groups received 1ml/kg body weight of Fosamax 2x/wk for 15 wks; sham, ovx and ovx+run groups received 1ml/kg body weight of placebo 2x/wk for 15 wks. All exercised rats were run on a motorized treadmill 60 min/day, 5 days/wk, for 15 wks. Total body mass (g) and BMC (g) were assessed by DXA at wks 1 and 15, and BMC of the excised left femur and L4 vertebral body were assessed by DXA at wk 15. The left femur and L4 vertebral body were scanned using μCT for geometric parameters. The left femur was tested to failure in 3-point bending and the L4 vertebral body was compressed to failure using an Instron system. At baseline there were no group differences for total body mass and whole body BMC. After 15-weeks the ovx and ovx+fos groups gained over 50% more body weight than the sham, while the sham, ovx+run and ovx+fos+run groups had similar gains in body weight. At sacrifice the sham had significantly higher BMC at the total femur and L4 vertebral body than the ovx group (+17% and +22%, respectively). Using multivariate analysis of variance for adjusted BMC (dependent variable: BMC/body weight), the ovx+run+fos group had significantly greater total femoral BMC than the ovx (+25%), ovx+fos (+16%), ovx+run (+17%) and sham (+8%) groups, and significantly greater L4 BMC than the ovx (+34%), ovx+fos (+22%), ovx+run (+21%) and sham (+13%) groups. In multivariate ANOVA, the ovx+fos+run group had significantly greater femoral failure load and stiffness compared to ovx (+16% and +19%, respectively) and ovx+run (+15% and +13%, respectively) groups. At L4, the ovx+fos+run group had significantly greater cross-sectional area than the ovx (+16%) and ovx+run (+12%) groups. Femoral and vertebral material properties (strength and modulus) did not differ between groups. Exercise plus Fosamax was synergistic for bone mass, as the combined effects were greater than those of each treatment independently. A synergy was also apparent for femoral failure load and vertebral cross-sectional area. Exercise plus Fosamax may provide the most effective strategy for reducing osteoporotic fractures and also prevent weight gains that may be associated with drug therapy alone.

F168

Evidence for a Skeletal Mechanosensitivity Gene on Mouse Chromosome 4. A. G. Robling[1], K. L. Shultz[2], W. G. Beamer[2], C. H. Turner[1]. [1]Indiana University School of Medicine, Indianapolis, IN, USA, [2]The Jackson Laboratory, Bar Harbor, ME, USA.

Skeletal loading experiments conducted in different inbred strains of mice reveal that bone tissue's sensitivity to mechanical stimulation is partly under genetic control. For the same amount of mechanical strain, C57/BL6 (B6) mice form more bone in response to ulnar loading than do C3H/He (C3H) mice (Fig 1). The genes contributing to skeletal mechanosensitivity have yet to be identified, but the differences in mechanical adaptation observed among the C3H and B6 mice suggest that these two strains can be used to elucidate the genes involved in mechanosensitivity regulation. The C3H and B6 skeletons also differ in bone size. In particular, the femoral width is greater in B6 compared to C3H mice. Several quantitative trait loci (QTL) have been mapped for femoral width. We hypothesized that genes controlling bone size might exert their effect by influencing mechanosensitivity. The hypothesis was tested using the B6.C3H-4T (4T) congenic mouse strain that is 98.4% B6 and carries the C3H Chromosome 4 QTL genomic DNA donated to the B6 background strain by nine cycles of backcrosses. Using a noninvasive in vivo ulnar loading model adapted for the mouse forelimb, we applied 3 different load magnitudes to the right ulnae of the 4T congenic and B6 control strains. Load was applied for 3 consecutive days (60 cycles/day, 2 Hz), followed by calcein labeing on days 5 and 9. After sacrifice (day 18) bone formation rates (BFR/BS) were calculated from histomorphometric measurements collected from midshaft sections of the right (loaded) and left (nonloaded) ulnae. On a set of calibration animals from both 4T and B6 strains, mechanical strain was measured at midshaft using single element strain gauges. When expressed as a function of mechanical strain, the increase in relative (right minus left) BFR/BS was significantly greater in the 4T mice compared to the B6 controls (Fig. 2). These results might explain why 4T mice have wider femora and ulnae than do B6 control mice. In conclusion, mouse Chromosome 4 appears to contain a genetic locus that modulates the mechanosensitivity of bone tissue.

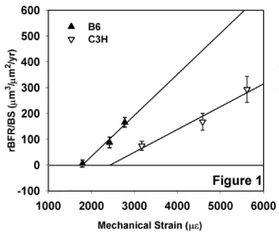

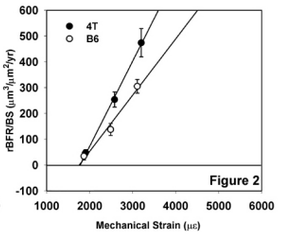

F173

Estrogens Induce Bad Phosphorylation via both ERK and PI3K Activation: A Two Pronged Signal Requirement for their Anti-apoptotic Effects. S. Kousteni, L. Han, T. Bellido, C. A. O'Brien, R. L. Jilka, S. C. Manolagas. Division of Endocrinology and Metabolism, Center for Osteoporosis & Metabolic Bone Diseases, Central Arkansas Veterans Healthcare System, U/sity of Arkansas for Medical Sciences, Little Rock, AR, USA.

Estrogens exert anti-apoptotic effects on osteoblasts via a nongenotropic mechanism of action of the estrogen receptor (ER) α or β, causing activation of the cytoplasmic kinases ERKs and PI3K. It has been reported that inactivation of the pro-apoptotic protein Bad is indispensable for the anti-apoptotic effects of estrogens. Based on evidence that either ERKs or PI3K may induce the phosphorylation, and thereby inactivation, of Bad we investigated here whether the anti-apoptotic effect of estrogens require convergence of these two signaling cascades on Bad. To this end, we employed HeLa cells transiently co-transfected with ERα and wild type Bad. Using Western blot analysis of immunoprecipitated Bad and antibodies specific for serines 112 (Ser-112), 136 (Ser-136) or 155 (Ser-155), we found that short exposure to 17β-estradiol (E_2) induced transient phosphorylation of Ser-136, wich peaked at 30 min. In addition, E_2 induced Bad phosphorylation at both Ser-112 and Ser-155, in a biphasic manner: a first peak occuring at 15 min and a second at 120 min. Pretreatment of the cells with either 50μM PD98059 or with 30nM wortmannin, specific inhibitors of ERKs and PI3K respectively, for 30 min, abrogated the E_2-induced phosphorylation of 112 and 155 serine residues at 15 and 120 minutes. Consistent with this, dominant negative (dn) Bad mutants lacking the ability to undergo phosphorylation at serines 136 or 155 abrogated the anti-apoptotic effect of E_2 in ERα- transfected cells. In contrast, a Ser-112 dn mutant did not. These findings, along with evidence that Ser-112 and Ser-136 are responsible for the recruitment of 14-3-3 proteins which when bound to Bad provoke the release of Bcl-2 from the Bad/Bcl-2 complex, suggests that phosphorylation of Ser-136 and Ser-155, but not Ser-112, is responsible for 14-3-3 recruitment in E_2-treated cells. Finally, a dn Rsk2 abolished phosphorylation of Bad at Ser-155 and blocked the anti-apoptotic effect of E_2 indicating that, at least part of, the estrogen-initiated survival signals that begin with the activation of ERKs and PI3K converge upstream of Bad, at the Rsk2 kinase. In support of this conclusion, Bad phosphorylation in response to simultaneous input from several kinases, like PI3K, PKA and ERKs, has been implicated in the pro-survival signals delivered by growth factors and cytokines in a variety of normal and transformed cells.

F176

gp130-Mediated Signals Are Necessary for Full Activation of Both Osteoblasts and Osteoclasts. H. I. Shin[1], T. Kobayashi[2], U. Chung[2], P. Pajevic[2], N. A. Sims[3], R. Baron[4], F. R. Bringhurst[2], H. M. Kronenberg[2]. [1]Oral Pathology, Kyungpook National University, Daegu, Republic of Korea, [2]Endocrine Unit, MGH, Harvard,, Boston, MA, USA, [3]St. Vincent's Institute, Melbourne University, Melbourne, Australia, [4]Pathology, Yale University, New Haven, CT, USA.

Substantial evidence indicates that gp130-associated cytokines play a role in skeletal homeostasis by stimulating the development of osteoclasts and also by promoting the development of osteoblasts. However, in contrast to widely recognized effects of gp130-associated cytokines on osteoclasts, their roles in osteoblastic function are still incompletely characterized. To address this issue, we analyzed the effect of gp130-mediated signals on bone metabolism by using gp130 knockout mice [gp130 (-/-)] and primary calvarial cells harvested from them. gp130 (-/-) mice showed retarded skeletal development with reduced bone matrix formation and mineralization during embryonic development compared to wild type littermates. In histomorphometric analysis of tibia from wild type and gp130 (-/-) embryos at E18.5 the osteoblast number per total bone area and percentage of osteoblast surface per bone surface were significantly reduced in gp130 (-/-) mice. The osteoblasts in gp130 (-/-) tibiae revealed reduced alkaline phosphatase (ALP) activity and decreased expression of type I collagen and osteocalcin mRNA compared to wild type. In addition, the primary spongiosa was decreased, with markedly increased numbers of large multinucleated TRAP+ cells in that area. However, ultrastructurally, the TRAP+ cells showed poorly developed ruffled border, raising the possibility that these osteoclasts are dysfunctional. Primary calvarial osteoblastic cells from gp130(-/-) mice also showed reduced ALP activity and generated few bone nodules under osteogenic culture conditions, whereas calvarial cells from wild type littermates formed numerous bone nodules after 2 weeks in culture. Primary calvarial osteoblasts from gp130(-/-) mice did not support osteoclastogenesis in co-cultures with wild type spleen cells in the presence of 10^{-7} M hPTH(1-34). These findings suggest that gp130-mediated signals are necessary for full osteoblastic differentiation and function.

F180

Cap- and IRES-Dependent Translational Control of *Cbfa1/Runx2* Expression. Z. Xiao*, L. G. Simpson*, L. D. Quarles. Center for Bone and Mineral Disorders, Duke University Medical Center, Durham, NC, USA.

The *Cbfa1* (*Runx2*) gene has a complex organization giving rise to Type II and Type I isoforms that differ in their N-termini and 5'untranslated regions (UTRs). The 5'UTR (designated UTR1) for *Cbfa1* Type II is complex and contains a "mini-intron", several open reading frames, and sites for generating alternatively spliced products. The distinct 5'UTR for *Cbfa1* Type I (designated UTR2) also has a complex secondary structure. The complexity of the respective 5'UTRs suggests that translational control may play an important role in regulating *Cbfa1* isoform expression. To evaluate potential differences in cap-dependent translation imparted by the 5'UTRs of *Cbfa1*, we created monocistronic SV40-UTR1-Luc and SV40-UTR2-Luc constructs, in which the 5'UTR of Luc was replaced with the UTR1 or UTR2. These monocistronic constructs were tranfected into MC3T3-E1 osteoblasts and NIH3T3 fibroblasts and luciferase activity measured to estimate translational efficiency of the various UTRs. We found that UTR1 and UTR2 imparted 2 to 3 fold greater levels of translation in MC3T3-E1osteoblasts than NIH3T3 fibroblasts. In addition, the UTR2 was translated approximately twice as efficiently as UTR1 in MC3T3-E1osteoblasts. The inclusion of the "mini-intron" in UTR1 significantly suppressed its translation in these cells. More importantly, we observed a 2-fold decline in cap-dependent translation by both UTR1 and UTR2 during culture duration dependent maturation of MC3T3-E1osteoblasts. The complex secondary structures of the 5'UTRs of Type II and I *Cbfa1* also suggest a possible role of internal ribosome entry site (IRES)-dependent translational regulation. To investigate this possibility, we created bicistronic vectors SV40-Rluc-UTR1-Fluc, SV40-Rluc-UTR2-Fluc, and SV40-Rluc-IRES2-Fluc, in which transcription generates Rluc by cap-dependent translation and Fluc is produced only if the intercistronic UTR confers an IRES-dependent translation. These constructs were transfected into MC3T3-E1 osteoblasts and translational control was evaluated in response to cell stress and osteoblastic maturation. We found that both the UTR2 and the UTR1 possess IRES activity similar to the viral IRES2 and this activity increased with serum deprivation and genotoxic stress induced by mitomycin C. In addition, we observed an maturational stage dependent 3-fold increase in IRES-mediated translation by both UTR1and UTR2. These findings suggest that *Cbfa1* UTRs have dual cap-dependent and IRES-dependent translational activities. The alternative IRES translational mechanisms may permit continued *Cbfa1* expression under conditions that may not be optimal for cap-dependent translation.

F182

A CT-rich Element in the Proximal Osteocalcin Promoter Confers Sensitivity to Gap Junctional Communication. J. P. Stains[1], F. Lecanda[2], J. Screen[1], D. A. Towler[1], R. Civitelli[1]. [1]Div. Bone and Mineral Diseases, Washington University, St. Louis, MO, USA, [2]Histology and Pathology, Univeristy of Navarra, Pamplona, Spain.

Disruption of gap junctional communication by overexpression of connexin45 (Cx45) in cells that endogenously express connexin43 (ROS 17/2.8, MC3T3-E1) alters osteoblast gene regulation, including downregulation of osteocalcin gene transcription. Accordingly, osteocalcin expression is markedly decreased in connexin43 null osteoblasts, which are not chemically coupled. To elucidate the molecular mechanisms of gap junction-mediated gene transcription regulation, we systematically analyzed the rat osteocalcin promoter to identify regions affected by changes in connexin expression profiles. Using 5' deletion analysis, we had previously mapped gap junction sensitivity to the -92 to +32 osteocalcin proximal promoter. We now report the identification of a minimal response element mediating this novel regulatory function of gap junctions. By electrophoretic mobility shift analysis (EMSA) of ROS 17/2.8 nuclear extracts, we identified a CT-rich stretch in the -67 to -57 promoter region that form DNA/protein complexes altered in response to Cx45 overexpression. Luciferase reporter assays demonstrated that this CT-rich element can confer gap junction sensitivity to a heterologous RSV minimal promoter, and that deletion of the CT element from the -92 to +32 osteocalcin promoter abrogates this sensitivity in the homologous promoter context. EMSA using radiolabeled CT element revealed two DNA/protein complexes whose binding activities are affected by gap junctional communication. The binding of a slow migrating complex was increased in nuclear extract from ROS 17/2.8 overexpressing Cx45, while the binding of faster migrating complex was decreased. Supershift and mutational analysis identified the low mobility complex as containing Sp1 and Sp3 transcription factors. In co-transfection experiments, we found that Sp1 stimulates transcription specifically via the CT element. Thus, an Sp1/Sp3 complex can bind and regulate the rat osteocalcin proximal promoter via a pyrimidine-rich CT element, a gap junction sensitive transcriptional unit. Since the Sp1/Sp3 ratio in the complex imparts either transcriptional activation or repression, respectively, we postulate that Cx45 overexpression increases the abundance of inhibitory Sp3 and Sp1/Sp3 heterodimers, leading to downregulation of osteocalcin gene expression.

F184

Locally Delivered Transcription Factor Cbfa1 Gene Enhances Periodontal Bone Repair and Regeneration. J. D. Dickson*[1], L. J. James*[1], J. Tang*[1], H. F. Thomas*[1], D. L. Cochran*[2], G. Karsenty*[3], C. A. G. McCulloch*[4], J. Chen[1]. [1]Pediatric Dentistry, University of Texas Health Science Center at San Antonio, San Antonio, TX, USA, [2]Periodontics, University of Texas Health Science Center at San Antonio, San Antonio, TX, USA, [3]Baylor College of Medicine, Houston, TX, USA, [4]University of Toronto, Toronto, ON, Canada.

The runt domain transcription factor, Cbfa1 (core binding factor, also called Runx2) has been identified as a "master gene" in osteogenesis. Bone formation is inhibited in Cbfa1-deficient mice and heterozygotic Cbfa1 deficient mice (Cbfa1+/-) survive but demonstrate many skeletal abnormalities. Using a bone wound healing model we found that bone repair was delayed in Cbfa1+/- mice (Tang et al., J Dent Res 81:A146, 2002). To determine in more depth the effects of Cbfa1 in enhancing bone wound healing and regeneration, we used a gene activated matrix (GAM) method to locally deliver Cbfa1 DNA into mouse periodontal bone wounds. Briefly, sterile and pure Cbfa1 DNA was prepared on a large scale from a CMV-Osf2/Cbfa1 plasmid. A biodegradable, absorbable bovine type I collagen sponge was mixed with the plasmid DNA. Periodontal wounds were created in three 7-week-old mice, and GAM was inserted and packed into the defect sites. Control sponges were collagen without plasmid DNA and were used in two mice. The animals were euthanized at 7 and 14 days, respectively, after transplantation. Tissues in the wound site were dissected, processed and subjected to histological analysis. Implantation of matrix containing Cbfa1 DNA promoted bone formation at the wound sites. We found that compared to controls, there was increased alveolar bone formation that almost filled the wound defect 14 days after surgery. The bone appeared more mature and was characterized by the formation of Haversian systems, compared to controls. In controls, bone formation was minimal and was scattered in the connective tissues. The newly formed bone in controls was poorly organized and weakly stained. In some samples of control tissues at 14 days, there were large amounts of granulation tissue in the wound site. The collagen sponge matrix did not seem to elicit significant foreign body reaction in either experimental or control groups. The results of this gain-of-function study suggest that Cbfa1 DNA, when incorporated into a collagen matrix, can induce tissue repair at osteogenic wound sites. Thus local application of Cbfa1 might promote osteogenic differentiation, trigger extracellular matrix gene expression, and subsequently enhance bone tissue regeneration.

F186

Regulation of Bone Collagenase-3 Gene Expression by the AP-1 and RD/Cbfa sites of the Collagenase-3 Promoter and by Overexpression of Cbfa1/Runx2 In Vivo. S. C. Jefcoat[1], N. Selvamurugan[1], Y. Yang*[1], R. Kowalewski*[1], O. Linton*[1], E. Karagrigoriou*[1], Z. Fung*[1], J. Ricci*[2], N. C. Partridge[1]. [1]Physiology and Biophysics, UMDNJ-RW Johnson Medical School, Piscataway, NJ, USA, [2]Prosthodontics and Biomaterials, UMDNJ-New Jersey Dental School, Newark, NJ, USA.

Previous work in our laboratory has determined that the activator protein-1 (AP-1) and runt domain binding (RD/Cbfa) sites and their respective binding proteins, c-Fos/c-Jun and Cbfa1/Runx2, regulate the collagenase-3 promoter in both parathyroid hormone (PTH)-treated and differentiating osteoblasts in culture. Furthermore, protein-protein interaction studies indicate that Cbfa1/Runx2 and the runt domain of Cbfa1/Runx2 alone interact with c-Fos and c-Jun. Also, co-transfection of Cbfa1/Runx2 in UMR 106-01 cells has been shown to enhance transactivation of the collagenase-3 promoter. In this study, we wished to show the importance of Cbfa1/Runx2 and the AP-1 and RD/Cbfa sites in the expression of collagenase-3 in vivo. To determine the regulatory elements of the collagenase-3 promoter in different tissues, transgenic mice containing either wild-type (-456 or -148) or AP-1 and RD/Cbfa mutated (-148A3R3) collagenase-3 promoters fused with the E. coli lacZ reporter were generated. Immunohistochemical studies show that wild-type transgenic lines express high beta-galactosidase expression in bone and teeth, some expression in skin, and none in heart, liver or lung, compared to the mutant and non-transgenic lines. Based on these data, we investigated if overexpression of Cbfa1/Runx2 regulates collagenase-3 expression in vivo, and whether this causes morphological changes in these animals. Five lines of mice were generated that carry a c-myc tagged rat collagenase-3 promoter (-148) driving expression of the Cbfa1/Runx2 gene. Samples of kidney, liver, stomach and calvariae were immunohistochemically analyzed for collagenase-3. Preliminary results show increased collagenase-3 staining in the calvariae of 14 day transgenic mice compared to wild-type mice, two transgenic lines were affected in their ability to breed, and x-ray analyses of 6 and 16 week old transgenic mice show that overexpression of Cbfa1/Runx2 causes a reduction in the length of the femur compared to the wild-type mice. These data provide evidence that Cbfa1/Runx2 and the RD/Cbfa and AP-1 sites are sufficient to regulate collagenase-3 gene expression in vivo, confirming our in vitro data as well as supporting the importance of the role of Cbfa1/Runx2 in normal bone development.

F191

Colorful Transgenic Mice: New Autofluorescent Marker Genes of the Osteoblastic Lineage. I. Marijanovic, S. Dogan*, A. C. Lichtler, D. W. Rowe. Department of Genetics and Developmental Biology, University of Connecticut Health Center, Farmington, CT, USA.

Osteoblasts are generated from bone marrow osteoprogenitor cells by traversing through many maturational stages. We have demonstrated that promoter-GFP reporter constructs can visually discriminate some of these maturational stages in intact bone of transgenic mice as well as in cell cultures derived from those mice. We used 3.6 and 2.3 kb fragments of rat collagen promoter with 1.6 kb fragment of collagen first intron (pOB Col3.6 and pOB Col2.3). Activity of pOBCol3.6 was detected in early stages of osteoblast differentiation and activity of pOBCol2.3 was restricted to mature osteoblasts. These studies utilized either GFPtopaz or GFPemerald (Clontech) which cannot be visually discriminated. Both genes maintain their activity in histological section of bone after decalcification and paraffin embedding, a property that is not shared by the widely used eGFP (Clontech). Here we report generation of transgenic mice that express autofluoresent transgenes that can be distinguished with proper fluorescent filtering. GFPsaph (Clontech), GFPcyan (Clontech) and DsRed1 (Clontech) were placed under the control of Col2.3 promoter (no intron). Expression from all three transgenes was evident in freshly isolated tail biopsies as distinctly different colors than themselves and GFPtpz. In the cultures derived from the GFPsaph and GFPcyan, cells became GFP positive only in mineralized nodules at day 14 confirming our previous findings. Histology performed on bones derived from GFPsaph and GFPcyan transgenic mice showed GFPsaph does but GFPcyan does not survive paraffin embedding. Analysis of the DsRed1 expressing transgenic line in culture and histological sections is pending. In addition the utility of a dual reporter was assessed. Col2.3CATiresGFPcyan transgenic mice express two reporter proteins translated from same bicistronic mRNA. Expression of CAT was restricted to calvaria, teeth, long bones and tendon (cyan is lost during histological preparation) while both reporters were present during the differentiation phase of primary bone cultures. CAT activity preceded GFP expression in primary culture probably because it is a more sensitive reporter. In conclusion, these experiments demonstrate that it should be possible to develop multicolor (currently 4) and enzymatic (currently 3; CAT, Firefly and Renilla luciferase) reporters marking different stages of osteoblastic differentiation for the simultaneous visual and quantitative analysis of lineage progression in cell cultures.

F197

Fibroblast Growth Factor Receptor 2 with Apert Mutation (S252W) Increase Osteoblast Differentiation and Mineralization. Y. Tanimoto*, M. Yokozeki, K. Hiura*, K. Moriyama. Department of Orthodontics, School of Dentistry, University of Tokushima, Tokushima, Japan.

Apert syndrome characterized by craniosynostosis, hypertelorism, ocular proptosis and syndactyly, is reportedly associated with gain-of-functional mutations (S252W, P253R) in extra cellular domain of fibroblast growth factor receptor (FGFR) 2. This suggests that aberrant FGFR2 signaling might contribute to the establishment of the pathogenesis of this syndrome. Previously, we have reported the increased differentiation and mineralization of osteoblastic cells derived from two Apert syndrome patients with FGFR2S252W mutation. Therefore, in this study, in order to clarify the molecular mechanism of osteoblast heterogeneity caused by Apert FGFR2 signaling, we examined the effect of mesenchymaly expressed FGFR2IIIc with S252W (FGFR2IIIcS252W) on differentiation and mineralization of osteoblastic cells. The full length FGFR2IIIc and its soluble form with or without S252W which we previously isolated by RT-PCR, were subcloned into expression vectors driven by CMV promoter. When FGFR2IIIc and FGFR2IIIcS252W expressing vectors were transiently transfected in COS1 cells, highly autophospholylation were observed in FGFR2IIIcS252W as compared with FGFR2IIIc. For the assessment of dominant negative effects of FGFR2 soluble form, MG-63 osteoblastic cells were treated with conditioned media (IIIc-sup, IIIcAp-sup) from COS1 cells which were transiently transfected by FGFR2IIIc or FGFR2IIIcS252W expression vectors. IIIc-sup and IIIcAp-sup significantly inhibited the endogenous and FGF2 induced proliferation of MG-63 cells and the inhibitory effect were stronger in IIIcAp-sup than IIIc-sup. In order to evaluate the effect of the FGFR2IIIcS252W on osteoblast differentiation and mineralization, we established a stable MG-63 cell line (MG63-Ap) overexpressing the FGFR2IIIcS252W. MG63-Ap highly expressed RUNX2, osteopontin and osteocalcin mRNA as compared with MG-63 and MG-63-mock. MG63-Ap showed massive intensity of matrix mineralization within 6 days of culture and neither MG63 nor MG63-MOCK showed mineralization even in after 28 days of culture. Furthermore, administration of IIIcAp-sup dramatically inhibited the increased mineralization of MG63-Ap cells. These results suggest that FGFR2 signaling with Apert mutation have a critical role in controlling differentiation and mineralization of osteoblasts.

F199

Overexpression of the Notch 1 Receptor Intracellular Domain Inhibits Differentiation in Cells of the Osteoblast Lineage. M. P. Sciaudone*, A. M. Delany, E. Canalis. Research, Saint Francis Hospital and Medical Center, Hartford, CT, USA.

Notch receptors are important for communicating signals that determine the fate of cells in multiple systems. Following activation, Notch receptors are cleaved and the intracellular domain of the receptor translocates to the nucleus where it initiates a regulatory cascade involved in cellular differentiation. Notch signaling inhibits myogenesis and neurogenesis, but its role in osteoblastogenesis is unclear. Osteoblastic cells express the Notch 1 receptor, suggesting a possible function in osteoblast differentiation. Furthermore, cortisol induces Notch 1 mRNA, and it is possible that Notch 1 mediates selected effects of glucocorticoids on osteoblastic differentiation. Notch signaling might have different effects in osteoblastic precursors, such as stromal cells, and in committed osteoblasts. To examine Notch overexpression during osteoblast differentiation, we used a murine stromal cell line (ST-2) and a murine osteoblastic cell line (MC3T3-E1). Cells were transduced with the retroviral vector pLPCX containing the CMV promoter driving the Notch 1 intracellular domain, to generate cell lines constitutively overexpressing active Notch 1. Northern analysis was used to demonstrate expression of retroviral derived Notch 1 mRNA. Following confluence, ST-2 and MC3T3-E1 cells were cultured in the presence of 10% fetal bovine serum, 5 mM beta-glycerophosphate and 100 ug/mL ascorbic acid for up to 4 weeks. ST-2 cells were cultured with or without bone morphogenetic protein (BMP-2) at 1 nM, an inducer of osteoblast differentiation. ST-2 cells overexpressing Notch 1 had reduced levels of alkaline phosphatase activity and mineralized nodules when compared to ST-2 cells transduced with pLPCX alone. This effect was independent of BMP-2 addition and was maintained over the experimental period. Two independently derived ST-2 cell lines overexpressing Notch 1 were examined. Notch 1 inhibited osteoblast differentiation in both lines although the effect was more pronounced in a line expressing higher levels of Notch 1 mRNA, suggesting a dose dependent effect. MC3T3-E1 cells overexpressing Notch 1 had decreased alkaline phosphatase activity and did not form mineralized nodules, whereas MC3T3-E1 cells transduced with pLPCX alone formed mineralized nodules. In conclusion, Notch 1 overexpression inhibits osteoblastogenesis in both early and late stages of osteoblast differentiation and could mediate the inhibitory effects of glucocorticoids on the process.

F201

The Novel Membrane-bound Glycerophosphodiester Phosphodiesterase-like Protein, DD045, Dramatically Promotes Osteoblastic Differentiation. N. Sakurai[1], E. Kawai*[2], N. Yanaka*[2], Y. Imai*[2], H. Akatsuka*[1], T. Takagi*[2]. [1]Discovery Research Laboratory, Tanabe Seiyaku Co., Ltd., Saitama, Japan, [2]Discovery Research Laboratory, Tanabe Seiyaku Co. Ltd., Osaka, Japan.

The osteoblast is the bone-lining cell responsible for the biosynthesis, organization, and mineralization of the bone extracellular matrix. Osteoblast maturation is a multistep series of events characterized by an integrated cascade of gene expression that are accompanied by specific phenotypic alterations. To find new osteoblast-related genes we cloned differentially expressed cDNAs characteristic of specific differentiation stages in the mouse osteoblast-like MC3T3-E1 cells. By a differential display method, we have identified a novel gene, DD045, specifically expressed at the stage of matrix maturation. It encodes a protein of 593 amino acids with seven putative transmembrane regions. Interestingly, one of the extracellular loops is highly homologous to glycerophosphodiester phosphodiesterases (GlpQ). Northern blot analysis revealed that DD045 was also expressed in spleen as well as primary calvarial osteoblasts and femur. Immunofluorescence staining with DD045 antibody and phalloidin in MC3T3-E1 cells indicated that endogenous DD045 might be co-localized with the actin cytoskeleton. We next transfected HEK293T cells with DD045 with green fluorescent protein (GFP) fused to the C terminus (DD045-GFP). DD045-GFP accumulated at the cell periphery, and the transfected cells changed from a spread form to retracted or rounded form with disappearance of actin filaments. This dynamic morphological change seemed to mimic the rounding/retracting of the lining osteoblast involved in the coupling phenomenon of the bone remodeling. Replacement of amino acids of DD045 significantly conserved with GlpQs suppressed the morphological alteration, and the mutated proteins were not localized peripherally. This mutagenesis study suggested that the biological function of DD045 might depend on the putative enzy-

mic activity of the extracellular GlpQ-like motif to mediate the intercellular signal transduction. To identify a role for DD045 in osteoblast differentiation, MC3T3-E1 cells stably expressing the full-length protein were constructed. Pooled MC3T3-E1-DD045 clones showed alkaline phosphatase activity earlier and 10-30-fold higher than cells transfected with the empty vector. In conclusion, we have identified a novel seven transmembrane protein with a GlpQ-like extracellular motif expressed during the osteoblastic differentiation that dramatically accelerates the program of osteoblastic differentiation and involves in the morphological change of cells with the cytoskeletal disintegration.

F203

Androgen Inhibition of Elk-1 Transcription Factor Activity may Mediate Reduced Osteoblast Growth. K. M. Wiren, A. Evans*, X. W. Zhang. Oregon Health & Science University, VA Medical Center, Portland, OR, USA.

Clearly, non-aromatizable androgens have significant beneficial effects on skeletal homeostasis independent of conversion to estradiol, but the mechanisms are not established. The aim of this study is to elucidate the effects of non-aromatizable dihydrotestosterone (DHT) on committed osteoblast growth by characterizing specific signaling cascades using either normal rat calvarial osteoblastic (rOB) cultures, or immortalized clonal calvarial osteoblastic cells (MC3T3-E1 or Py1a). We show that in differentiating rOB cultures treatment with DHT (48h; 10^{-9}M - 10^{-7}M) dose-dependently inhibits osteoblast viability measured by colorimetric MTT assay. DHT treatment also inhibited DNA accumulation measured with Hoechst bisbenzimid H 33258. Since little is known about signaling cascades important in DHT control of osteoblast growth, we interrogated mitogenic pathway-specific cDNA microarrays. Results showed reduced expression of several genes important in MAP kinase-mediated signaling, implicating this pathway as a target of androgen regulation. In both rOB and MC3T3-E1 osteoblast models, DHT treatment (48h; 10^{-8}M) in the presence of charcoal-stripped serum inhibited both ERK-1 and -2 roughly 30% with the most dramatic effect an 80% reduction in Elk-1 expression. Further, MAP kinase activation of the Elk-1/GAL4 transactivator with GAL4/luciferase reporter was reduced nearly 30% by DHT treatment, with a similar reduction in phosphorylated Elk-1 abundance by Western analysis. Since Elk-1 belongs to the ETS-domain family of transcription factors and is a c-*fos* protooncogene regulator, we determined whether DHT treatment also influenced c-*fos* gene expression. Northern analysis revealed a modest reduction in c-*fos* gene expression in DHT-treated rOB cultures. DHT treatment also reduced activation of an AP-1/CAT reporter construct by IGF-I nearly 80%. These results suggest one of the mechanisms by which DHT modulates osteoblast viability is through inhibition of the expression of Elk-1 target genes like c-*fos*. Together these data provide the first evidence that androgen inhibition of the MAP kinase signaling pathway, particularly at the level of Elk-1, is an important mediator of committed osteoblast growth and may be a specific downstream target of DHT in its growth control pathway. Since the AP-1 transcription factor is also a significant regulator of osteoblast development, these findings may provide valuable insight into the molecular mechanisms of androgen action.

F206

Smad1C, a Hoxc-8 interacting Domain of Smad1, Augments Bone Mineral Density in Transgenic Mice. Z. Liu*[1], W. Shi[1], C. Sun*[1], T. Nagy*[1], C. Lu*[1], W. S. S. Jee*[2], X. Ji[3], Y. Wu*[1], X. Shi[1], Q. Li*[1], X. Cao[1]. [1]Pathology, University of Alabama at Birmingham, Birmingham, AL, USA, [2]University of Utah, Salt Lake City, UT, USA, [3]P & G Pharmaceutics, Cincinnati, OH, USA.

Bone morphogenetic proteins (BMPs), members of the TGF-beta superfamily of secreted signaling molecules, bear an obligatory task in the induction of osteoblast differentiation and bone formation. Smads, a group of functional and structural related molecules, mediate signaling initiated by BMPs and regulate cell definite commitment. Previously, we showed that Smad1 activates osteopontin and OPG gene expression in response to BMP through dislodging Hoxc-8, which functions as a transcription repressor associating osteopontin promoter. Smad1C, a domain of Smad1 spanning from the COOH terminal of MH1 to linker region (145-278aa), was characterized as interacting with Hoxc-8 and disabling Hoxc-8 DNA binding ability. Ectopic expression of Smad1C with nuclear localization sequence mimics the Smad1 function in activation of osteopontin gene expression. Furthermore, overexpression of Smad1C in 2T3 osteoblast precursor cells induced osteoblast differentiation by upregulating bone mark gene expression and mineralized bone matrix formation. These data suggest that Smad1C is able to bypass BMP's signals in induction of osteoblast differentiation and bone formation in vitro cell culture. To test the function of Smad1C on osteogenesis in vivo, we generated transgenic mice which express Smad1C exclusively in bone and under control of exogenous induction by utilizing tetracycline inducible system (Tet-on) and bone specific type I collagen α promoter (α1p). We detected mRNA of Smad1C in the binary transgenic mice (α1p-rtTA/ Smad1C) under doxcycline induction. Double-transgenic α1p-rtTA/TRE-Smad1C mice in absence of doxcycline and any single-transgenic mice (either α1p-rtTA or Smad1C) fed with water containing doxcycline did not show any noticeable Smad1C expression. The mice expressing Smad1C showed higher bone density compared with their littermates, including non-transgenic and single-transgenic mice. As a control, double transgenic mice in absence of doxcycline did not display distinct differences in terms of bone density from their littermates. Culturing stromal cells isolated from transgenic mice in the medium supplemented with osteoblast induction reagent and doxcycline, we found that stromal cells isolated from dual transgenic mice displayed higher potential to differentiate osteoblasts than the others. Bone histomorphometric analyses showed that significant trabecular bone was induced. Taken together, the results of this study indicate that ectopic Smad1C mimics BMPs in induction of osteogenesis in vivo.

F208

Role of Hedgehog Signaling in KS483 Osteoblastic Differentiation. G. van der Horst*, H. Sips*, C. Lowik, M. Karperien. Endocrinology, Leiden University Medical Center, Leiden, Netherlands.

Indian hedgehog (Ihh) has been shown to control both chondrocyte and osteoblast differentiation. In the present study, we have analyzed the role of hedgehog signaling in osteoblast differentiation in greater detail using the pre-osteoblastic cell line KS483. This cell line differentiates into mature, mineralizing osteoblasts in a three-week culture period. First, we analyzed expression of hedgehog signaling components at various stages of differentiation, using semi-quantitative RT-PCR. Ihh, the receptors patched1 (ptc), ptc2 and smoothened, as well as the intracellular mediators Gli1, 2 and 3 were all present. Interestingly, Ihh mRNA expression increased during differentiation and peaked during matrix formation and maturation, decreasing thereafter. Furthermore, ISH demonstrated the presence of Ihh in osteoblasts in tissue sections of human prenatal bone. Continuous addition of sonic hedgehog (rShh) significantly increased osteoblastic differentiation of KS483 cells dose-dependently. Modest effects on alkaline phosphatase (ALP) activity were observed, whereas mineralization was strongly affected. In addition, mRNA expression of various markers of osteoblast differentiation, such as osteocalcin, cbfa1 and the PTH/PTHrP receptor, as well as Ihh, Gli1, Ptc1 and smoothened was upregulated. Addition of Shh during the first week of culture only, was sufficient for increasing osteoblastic differentiation. Addition during later phases, i.e. matrix maturation and mineralization, was not effective, suggesting that Hh predominantly affects less differentiated osteoblasts. The stimulatory effects of Hh were blocked by the antagonist cyclopamin, which by itself had no effect on differentiation. It has been suggested that Hh regulates osteoblast differentiation via BMPs. In KS483 cells, the stimulatory effects of Shh were synergistically enhanced by BMP-4. Furthermore, the effects of BMPs were not blocked by cyclopamin. In contrast, the effects of Hh were completely blocked by BMP antagonists. This is in line with the observation that KS483 osteoblastic differentiation strictly depends on autocrine BMP signaling. It has been shown that PTHrP is a negative regulator of Hh expression in chondrocytes. Also in KS483 osteoblasts, PTHrP downregulates Ihh mRNA expression and inhibits differentiation. In addition, immunohistochemistry demonstrated a dramatic increase in Ihh expression in osteoblasts in tissue sections of Blomstrand dysplasia (human PTH/PTHrP receptor knockout), compared to control. These data suggest that PTHrP might be a natural inhibitor of hedgehog expression in osteoblasts. In conclusion, our data suggest a role for osteoblast expressed Hh in bone formation.

F210

CGI-135 Is Part of a New Chromatin Remodelling Protein Complex and It Regulates the Osteoprogenitor Proliferation-Differentiation Transition. G. A. Candeliere, Y. Yoshiko, J. E. Aubin. Anatomy and Cell Biology, University of Toronto, Toronto, ON, Canada.

We isolated CGI-135 based on its high and differential expression during the osteoprogenitor proliferation-differentiation transition and showed that it was part of a new higher-order chromatin remodelling complex. To address the in vivo function of CGI-135 in bone formation, we prepared adenoviral vectors designed to over- and underexpress the protein and injected them subcutaneously over the calvaria sagittal suture of newborn rat pups. Reducing CGI-135 levels for three days resulted in a statistically significant decrease in bone volume at the sagittal sutures, growth retardation at the osteogenic front, and reduced cell numbers over the ectocranial trabecular surface. In contrast, increasing CGI-135 levels for 3 days resulted in an increase in active osteoblasts over the ectocranial trabecular surface. Overexpression for 8 and 12 days resulted in a statistically significant and progressive increase in bone volume with time. These data suggest that CGI-135 is essential for rapid de novo bone formation and that it promotes appositional bone growth in vivo. To address the cellular mechanisms responsible, we infected primary rat calvaria (RC) cells during different proliferation-differentiation time windows. Reducing CGI-135 in confluent RC populations prior to bone nodule formation resulted in dose-dependent death of preosteoblastic cells surrounding bone nodules, while differentiated osteoblasts over mineralizing portions survived. Consistent with this, the number of nodules formed was not different from control-treated cultures, but a dose-dependent and statistically significant decrease in the mineralized area of nodules was seen in antisense virus-treated RC cells. Increasing CGI-135 levels in RC cells during log phase growth resulted in more rapid growth, an increase in the number of alkaline phosphatase-positive cells, and a statistically significant and dose-dependent increase in both mineralized nodule number and mineralized area. Increasing CGI-135 in rapidly proliferating MC3T3-E1 cells resulted in a cell cycle shift from G1 to S and G2 phase (24 hours post infection), but this did not occur in more mature cells. On the other hand, decreasing CGI-135 in rapidly proliferating MC3T3-E1 cells caused a cell cycle shift from S and G2 to G1 phase, followed by cell death and decreased bone formation, while decreasing it in more mature cells had no effect on bone formation or on cell death. These data show that CGI-135, which we had identified as being part of a new chromatin remodelling complex, regulates osteoprogenitor proliferation-differentiation in vivo and in vitro at a specific time during lineage progression.

F214

Constitutive Activation of Wnt signaling through Low-Density Lipoprotein-Related Protein-5 Elevates Expression of TGF-beta, Fibronectin and Osteocalcin in Primary Murine Osteoblasts. G. Yao, K. Yu*, M. Mitnick, K. Insogna. Yale University, New Haven, CT, USA.

Wnt signaling through the low-density lipoprotein receptor-related protein 5 (LRP-5) has been recently identified as an important pathway regulating bone mass. Loss of function mutations in LRP-5 cause the autosomal recessive disorder, osteoporosis-pseudoglioma syndrome. Recently, two families with very high bone density were found to have identical G to T transversions in exon 3 of the LRP-5 gene resulting in a glycine-to-valine change at amino acid 171. It is presumed, but not proven, that this is a gain of function mutation. One of these kindreds was noted to have marked elevations in circulating levels of osteocalcin, transforming growth factor-beta (TGF-beta) and fibronectin. LRP-5 is expressed by osteoblasts and is capable of functioning as a Wnt co-receptor in the canonical signaling pathway that employs beta-catenin as a downstream effector. A truncated version LRP-5, which includes the entire intracellular domain, the transmembrane domain, and a portion of the extracellular domain beginning with residue 1370, has been reported to constituitively activate the Wnt pathway. To examine the response of osteoblasts to activation of the Wnt signaling pathway we constructed a truncated murine LRP-5 beginning with residue 1305 and introduced it into the mammalian expression vector PcDNA4/His-Max. Transient transfection experiments were performed in primary cultures of murine osteoblasts. As compared to vector transfected cells, cells expressing the truncated form of LPR-5 secreted 2-3 fold greater amounts of fibronectin into the condition media. Since fibronectin is a known target of the Wnt signaling pathway in other cells, these data suggest that the increase in circulating levels of fibronectin observed in patients with the G-to-V LRP-5 variant may reflect activation of the Wnt pathway in osteoblasts. Levels of osteocalcin were about 25% higher and levels of TGF-beta were approximately 2-fold elevated in the conditioned media of cells expressing the truncated receptor. We conclude that activation of Wnt signaling in osteoblasts leads to increased expression of proteins consistent with the biochemical profile in one kindred with the G-to-V LRP-5 variant. These data support the conclusion that this variant results in a gain of function in the Wnt pathway in osteoblasts.

F218

Telomerase Accelerates Osteogenesis of Bone Marrow StromalStem Cells by Increasing Proliferation and by Up-regulation of CBFA1, Osterix, and Osteocalcin. S. Gronthos*[1], S. Chen*[2], C. Y. Wang*[2], P. G. Robey*[1], S. Shi*[1]. [1]Craniofacial and Skeletal Diseases Branch, NIDCR/NIH, Bethesda, MD, USA, [2]Department of Biologic and Material Sciences, University of Michigan, Ann Arbor, MI, USA.

Telomerase activity can prevent telomere shortening and replicative senescence in human somatic cells. We and others have demonstrated that forced expression of telomerase in human bone marrow stromal cells (BMSSC-Ts) is able to extend their lifespan. In this study, we found that telomerase was able to accelerate and enhance osteogenesis in vitro and in vivo by osteogenic inductive culture conditions and xenogeneic transplantation, respectively. Furthermore, there is no evidence of malignant transformation. Low density DNA array analysis revealed that telomerase activity increases the expression of genes that regulate progression through G1 of the cell cycle including cyclin D3, cyclin E1, E2F-4, and DP2. Hyperphosphorylation of retinoblastoma (pRb) appears to extend the proliferative capacity of BMSSC-Ts beyond 40 population doublings. Importantly, BMSSC-T transplants showed a higher number of human osteogenic cells surviving at eight weeks post transplantation when compared to the control BMSSCs transplants, coupled with a significantly increased osteogenic capacity. One possible mechanism leading to accelerated osteogenesis by BMSSC-Ts may be attributed, at least in part, to the up-regulation of the important osteogenic genes such as CBFA1, osterix, osteocalcin, and increasing population of STRO-1 positive progenitors. Taken together, these findings show that telomerase can accelerate and enhance osteogenic differentiation of BMSSCs, due to the progression from G1-to-S phase, as well as up-regulation of CBFA1, osterix, and osteocalcin.

F220

Clonal Tendon-derived Cell Lines Behave as Pluripotent Stem Cells to Differentiate into Multiple Cell Lineages Including Bone, Cartilage and Fat Cells. R. Salingcarnboriboon[1], H. Yoshitake*[2], K. Tsuji[1], A. Nifuji[1], T. Amagasa*[2], M. Noda[1]. [1]Dept.of Molecular Pharmacology, Tokyo Medical & Dental University, Tokyo, Japan, [2]First Dept.of Oral and Maxillofacial Surgery, Tokyo Medical & Dental University, Tokyo, Japan.

Ectopic bone formation in tendon under pathological or experimental conditions raises a possibility of the presence of pluripotential mesenchymal stem cells in tendon. However, this has not been directly demonstrated. The aim of this study was to establish and characterize tendon cell lines to be utilized as a model for further studies on tendon biology and also to understand the mechanism that differentiates these cells from the cells in osteoblastic and chondrocytic lineages. Transgenic mice harboring SV 40 large T antigen were used to establish tendon-derived cell clones (E4, G11, and D6). Tendon specific phenotype related genes including Scleraxis, Six1, EphA4, and COMP were expressed in the tendon cell clones. Proliferation of these cells was significantly increased by the treatment with bFGF ($p<0.01$) and TGF-b ($p<0.01$) but not BMP2. Interestingly, these cells expressed the genes of osteogenic (OC, OPN, Col-I, ALP, Osterix), chondrogenic (Sox9, Col-II, Col-X), and adipogenic (aP2, PPAR-g) lineages when examined by RT-PCR. Northern blot analysis indicated the constitutive expression of Scleraxis, OPN, Col-I, and Cbfa1 but not OC and ALP mRNAs. BMP2 treatment increased ALP activity and upregulated ALP and osterix mRNA levels while it downregulated Scleraxis gene expression. The cells differentiated into osteoblasts or adipocytes when they were cultured in respective differentiation medium. Formation of tendon-like connective tissue bands, stained strongly positive for mature collagen and anti-large T antigen antibody, was observed when tendon cell sheets detached from long-term culture were transferred to cultured on chorioallantoic membrane in ovo. Formation of fibrocartilagenous tissue was also observed in vivo when D6 cell sheets were implanted into patella tendon defects in adult mice. These observations indicated that the established tendon cell lines could serve as mesenchymal stem cells. This observation will be the first evidence indicating the existence of stem cells in tendon.

F223

Actin Related Protein (Arp)2/3 Complex in Osteoclasts. I. R. Hurst*, J. Zuo*, L. S. Holliday*. Orthodontics, University of Florida College of Dentistry, Gainesville, FL, USA.

Actin rings are dynamic cytoskeletal structures that are required for forming sealing zones, essential elements of the bone resorptive apparatus of osteoclasts. The Arp2/3 complex is a vital regulator of actin dynamics, suggesting a role for Arp2/3 in the formation of actin rings. Polyclonal anti-Arp2 and anti-Arp3 antibodies were shown to bind specifically to Arp2 and Arp3 from purified platelet Arp2/3 complex and to recognize single bands in mouse osteoclast and OPGL-stimulated RAW 264.7 osteoclast extracts. By confocal microscopy, Arp2/3 complex was most abundant in actin rings and was at highest concentrations where the cell contacted the substrate. Arp2/3 generally co-localized with microfilaments but sometimes sandwiched the zone of microfilaments near the plasma membrane. When osteoclasts were torn free from glass coverslips by shearing force, an actin ring remnant remained that was rich in Arp2/3. Somewhat surprisingly, because of the tremendous enrichment of F-actin in actin rings, the ratio of Arp2/3 to F-actin was lower there than in the network of actin filaments that underlies the ruffled border. Based on the presence of Arp2/3 in actin rings we propose that continuous Arp2/3 complex-triggered actin polymerization pushes the plasma membrane at the base of the actin ring into the bone surface, creating the sealing zone. Integrin-based adhesions between the osteoclast and bone outside of the actin ring-ruffled membrane area counter the force being applied by the polymerization motor at the sealing zone and keep the osteoclast in position on the bone. The enrichment of Arp2/3 in the sub-ruffled membrane actin network may provide a supply of Arp2/3 complex near the region of polymerization that could be mobilized by gelsolin. Such a supply would be necessary because, as Arp2/3 nucleates polymerization near the sealing zone, it would be expected to move basolaterally as the newly formed filaments treadmill. The idea that actin rings are Arp2/3 directed actin polymerization-depolymerization motors would explain the dynamic nature of the actin ring-sealing zone region and the inability to identify an adhesion molecule associated with the sealing zone.

F225

Pyk2-dependent Recruitment of Src to Adhesion Structures Is Important for Osteoclastic Bone Resorption. T. Miyazaki[1], A. Sanjay[1], L. Neff[1], S. Tanaka[2], W. C. Horne[1], R. Baron[1]. [1]Yale University, New Haven, CT, USA, [2]The University of Tokyo, Tokyo, Japan.

Pyk2 is a member of the focal adhesion kinase family, that like Src is highly expressed in osteoclast podosomes and is phosphorylated in response to integrin stimulation upon adhesion. We have previously established that Pyk2 autophosphorylation at Y402 is required for the formation of the Pyk2/Src /Cbl complex, which plays an important role in bone resorption. Osteoclasts derived from mice lacking any of these proteins exhibit decreased migration indicating that all three proteins participate in the regulation of osteoclast motility and, thereby, bone resorption. While Pyk2 autophosphorylation in osteoclasts is not Src-dependent, the two molecules associate by the interaction of Pyk2's phosphorylated tyrosine 402 and the Src SH2 domain. To further investigate the function of Pyk2 in osteoclasts and its relation to Src recruitment and activation, we have used adenovirus encoding Xpress-tagged wild type Pyk2, autophosphorylation site-mutated Pyk2 (Pyk2Y402F) or kinase-dead Pyk2 (Pyk2KD) to express these proteins in osteoclast-like cells (OCLs). Although Pyk2 and Pyk2KD were able to interact with endogenous Src, Pyk2Y402F was not, demonstrating that the Src/Pyk2 interaction requires the binding of Src SH2 to Pyk2 phosphotyrosine 402. Similarly, while Pyk2- and Pyk2 KD-OCLs exhibited the characteristic peripheral actin ring, Pyk2Y402F-OCLs exhibited actin patches and multiple small actin rings located in the center of the cell, a pattern also found in the Pyk2-/- osteoclasts. To investigate the functional consequence of overexpressing Pyk2 mutants, the bone resorbing activity of OCLs was quantified in the pit assay. The pit-forming activity of Pyk2Y402F-OCLs was strongly inhibited (85%), while overexpression of Pyk2 and Pyk2KD had no effect. The interaction between phosphorylated Y402 of Pyk2 and SrcSH2 increases Src kinase activity. To determine whether up-regulation of Src kinase activity is sufficient to rescue the decreased pit-forming activity of Pyk2Y402F-OCLs or whether recruitment of Src to adhesion structures is also required, we co-infected OCLs with Pyk2Y402F and CskKD. Src kinase activity was increased when CskKD was expressed alone or in combination with Pyk2Y402F, but the increased Src kinase activity was not sufficient to rescue the inhibitory effect of AxPyk2Y402F on bone resorption. Thus, high Src kinase activity alone is not sufficient to rescue the decreased bone-resorbing activity in Pyk2Y402F-OCLs. We conclude that Pyk2-dependent recruitment of Src to podosomes is necessary for osteoclastic bone resorption.

F227

Identification of the RGD-Binding Site in the Human Osteoclast alphaVbeta3 Integrin Receptor. A. Wittelsberger[1], D. Yahalom*[1], D. F. Mierke[2], M. Rosenblatt[1], J. M. Alexander[1], M. Chorev[1]. [1]Department of Bone and Mineral Metabolism, BIDMC-Harvard Medical School, Boston, MA, USA, [2]Division of Biology and Medicine, Departments of Chemistry and Molecular Pharmacology-Brown University, Providence, RI, USA.

By combining data obtained by photocross-linking RGD-containing ligands to the intact membrane-bound human $\alpha_V\beta_3$ integrin with the crystal structure of the ectopic domain of this receptor (Xiong et al. *Science*, 2001, 294, 339-345), we have modeled the bimolecular contact interface between the 49-amino acid RGD-containing disintegrin ligand echistatin and $\alpha_V\beta_3$. We synthesized three novel analogs, [Bpa^{21},Leu^{28}]-, [Bpa^{23},Leu^{28}]-, and [Bpa^{28}]echistatin, each of which contains a photoreactive *p*-benzoylphenylalanyl (Bpa) residue in close proximity to the RGD motif present at positions 24-26. The analogs bind with high affinity to the purified recombinant $\alpha_V\beta_3$ integrin, but very poorly to the closely related human $\alpha_{IIb}\beta_3$ platelet integrin. While the echistatin analogs containing Bpa in either position 23 or 28 cross-link specifically and almost exclusively to the β_3 subunit of $\alpha_V\beta_3$, [Bpa^{21},Leu^{28}]echistatin cross-links to both α_V and β_3 subunits, with cross-linking to the former favored. [Bpa^{23},Leu^{28}]echistatin cross-links 10-30 times more effectively than the other two analogs. We identified β_3[109-118] as the domain that encompasses the contact site for [Bpa^{28}]echistatin. This domain is included in β_3[99-118], a contact domain previously identified by our group (Bitan et al. *Biochemistry*, 2000, 39, 11014-11023) for a cyclic RGD-containing heptapeptide with a benzophenone moiety in a position that is similar to the placement of the benzophenone in [Bpa^{28}]echistatin relative to the RGD triad. Recently, we identified β_3[209-220] as the contact site for an echistatin analog with a photoreactive group near the C-terminus of echistatin (Scheibler et al. *Biochemistry*, 2001, 40, 15117-14126). These experimentally identified contact sites where used as constraints when docking echistatin, based on its NMR structure, onto the crystal structure of the ectopic receptor domain. The model obtained after relaxation and molecular dynamics simulations is consistent with the very recently published crystal structure of a cyclic RGD-containing pentapeptide in complex with the extracellular segment of $\alpha_V\beta_3$ (Xiong et al. *Science*, 2002, 296, 151-156) and allows for the first time to gain insights on the bimolecular interface between a large disintegrin ligand and the $\alpha_V\beta_3$ integrin.

F230

WASp Deficiency in Mice Results in Abnormal Assembly of Podosomes in Osteoclasts and Defects in Bone Resorption. Y. Calle*[1], C. Jagger*[2], T. Chambers[2], K. Fuller[2], M. P. Blundell*[3], J. Chow[2], G. E. Jones[1], A. Thrasher*[3]. [1]The Randall Center for Molecular Mechanisms of Cell Function, King's College London, London, United Kingdom, [2]Department of Cellular Pathology, St. George's Hospital Medical School, London, United Kingdom, [3]Molecular Immunology Unit, Institute of Child Health, University College London, London, United Kingdom.

The Wiskott Aldrich Syndrome protein (WASp) is a protein specifically expressed in haematopoietic cells. It belongs to a larger family of more widely expressed proteins that mediate actin polymerisation. In humans, mutation in the gene coding for WASp is the basis of the Wiskott Aldrich Syndrome (WAS), an immune disorder characterised by eczema, thrombocytopenia and severe immunodeficiency. Leukocytes and platelets from WAS patients show abnormal cytoskeletal organisation including lack of podosomes in macrophages and dendritic cells. Podosomes are highly dynamic conical adhesion structures only observed in cells of the monocytic lineage and also in certain tumour cells. They consist of a core of actin filaments and other structural and adaptor proteins, which are linked to adhesion molecules of the integrin family. Podosomes are involved in osteoclast adhesion, migration and in the formation of the actin ring around the osteoclast periphery that defines the resorbing area during bone resorption. WASp is a structural component and plays a key role in the dynamics of podosomes in macrophages and dendritic cells. To our knowledge, no evidence has been provided showing that WASp is a structural component of podosomes in osteoclasts. In addition, no obvious abnormalities in bone development and/or structure have been reported as part of the clinical manifestations in WAS patients. In the present work we aimed to investigate whether WASp was involved in assembly of osteoclast podosomes and if expression of WASp was necessary for bone resorption. Using cultures of bone marrow derived osteoclasts from normal and WASp deficient mice, our results showed that: a) In cultures on glass, WAS osteoclasts failed to assemble migratory podosomes (podosomes not inserted in actin rings) and assembled actin plaques co-localising with vinculin instead. Some punctate actin structures were observed inserted in ring frames although they were significantly fewer than in normal cells and they did not appear evenly arranged in the ring. b) In cultures on bone slices, WAS osteoclasts performing resorption presented a dense plaque of actin surrounded by incomplete and thin actin rings, which were absent in many instances. In contrast, normal cells assembled well-defined actin rings. Migratory osteoclasts with podosomes were absent in WAS cultures whereas they could be detected in normal cells; c) Transduction of WASp deficient osteoclasts with eGFP-WASp rescued the normal phenotype on glass and on bone. In addition, WASp localised to the core of podosomes. Our results provide evidence that WASp is a structural component of podosomes in osteoclasts and suggest an important role of WASp in the dynamics of these actin structures during bone resorption. The differences in bone resorption will be discussed at the conference.

F234

RANKL Renders Pre-osteoclasts Resistant to Interferon-gamma While Preserving JAK-STAT1 Signaling. W. Huang*[1], R. O' Keefe[2], R. Rosier[2], J. E. Puzas[2], E. Schwarz[1]. [1]Orthopedics, University of Rochester, Rochester, NY, USA, [2]University of Rochester, Rochester, NY, USA.

While a number of studies have identified IFN-γ to be a potent inhibitor of osteoclastogenesis *in vitro* and *in vivo*, these findings are inconsistent with the inflammatory bone loss that occurs in patients with psoriatic arthritis and bone infections, which are known to occur in the presence of high levels of IFN-γ. To understand the mechanism of this resistance to IFN-γ we hypothesized that IFN-γ has different effects on early-stage versus late-stage osteoclast precursors. In cultures of RAW264 cells and primary murine splenocytes, pretreatment with RANKL ($\geq$ 50ng/ml) for 48hrs rendered these cells resistant to the anti-osteoclastogenic effect of IFN-γ in a dose dependent manner. Interestingly, these cells were also resistant to the effects of IFN-γ on macrophage activation. Nitric oxide production was completely inhibited by pretreatment with $\geq$ 50ng/ml RANKL ($p<0.01$). Additionally, IFN-γ induced upregulation of Mac-1 (mean fluorescence intensity from 1285 to 1912) was inhibited MFI = 547) by RANKL pretreatment. These data indicate that early administration of RANKL causes a broad inhibition of the cellular effects mediated by IFN-γ. To examine whether RANKL disrupts the JAK-STAT1 pathway used by IFN-γ signaling, western blot analysis of nuclear extracts with antibodies specific for STAT1 and its active-phosphorylated isoform revealed that both phosphorylation and translocation of this transcription factor following IFN-γ stimulation were not inhibited by RANKL pretreatment. This phosphorylated STAT1 was capable of DNA binding, as measured by gel-shift, confirming that RANK signaling does not inhibit IFN-γ signaling upstream of the STAT1 transcription factor. STAT1 inhibitors SOCS1 and SOCS3 were undetectable in cytoplasmic extracts. These results lead us to propose a model of osteoclastic bone resorption at sites of Th1 mediated immune responses in which osteoclast precursors are exposed to RANKL before they reach the site of erosion. In support of this model, immunohistochemistry revealed that monocytes/preosteoclasts from patients with psoriatic arthritis must migrate through the RANKL rich enviroment of the synovial lining before they can be exposed to Th1-produced IFN-γ in the synovial fluid. Thus, these preosteoclasts may be resistant to the anti-osteoclastogenic effects of IFN-γ in the joint and capable of the extensive bone erosion seen in this disease.

F236

Osteopontin-Dependent CD44 Surface Expression Is Stimulated by Association With ROK-α and Is Required for Normal Bone Resorption. M. A. Chellaiah[1], R. S. Biswas[1], D. S. Yuen[1], S. R. Rittling[2], D. T. Denhardt[2], K. A. Hruska[3]. [1]Dept. of OCBS, University of Maryland, Baltimore, MD, USA, [2]Dept. Cell Biology and Neuroscience, Rutger's University Nelsons Labs, Piscataway, NJ, USA, [3]Department of Pediatrics, Washington University, School of Medicine, St. Louis, MO, USA.

Osteopontin (OPN) deficiency reduces plasma membrane CD44 surface expression leading to osteoclast hypomotility and decreased bone resorption both *in vitro* and *in vivo*. OPN stimulates podosome assembly dependent on Rho-A GTPase activation as a key step in osteoclast motility. We demonstrate that Rho kinase (ROK-α) is a critical down stream effector of CD44 bound Rho, and plays a critical role in CD44 phosphorylation and its interaction with the ERM/actin complex. Osteoclasts were transduced with Tat-HA fusion proteins containing constitutively active Rho^{Val-14} and dominant negative Rho^{Asn-19}. A dramatic translocation of ROK-α from cytoplasm to membrane was observed in OPN and Rho^{Val-14} -treated osteoclasts that required ROK-α phosphorylation. Increased phosphorylation of ROK-α enhances its association with CD44 resulting in an increase in the CD44 phosphorylation and its surface expression. Y-27632, a specific ROK-α inhibitor, blocked OPN and Rho^{Val-14} stimulated bone resorption thereby indicating a critical role for ROK-α in the osteoclast function. CD44 surface expression as well as CD44/ROK- α association was markedly diminished in the osteoclasts isolated from OPN-/- mice. Transduction of Rho^{Val-14} rescued the OPN-/- phenotype. Exogenous addition of OPN to OPN-/- osteoclasts augments the association of ROK- α with CD44. Although antibodies against α_v, β_3, or CD44 inhibited osteoclast migration and bone resorption, only antibody to α_v or β_3 blocked OPN- induced phosphorylation of ROK-α, CD44 and ERM proteins. Taken together, these results demonstrate that OPN-dependent $\alpha_v\beta_3$ outside-in signaling pathway is required for the Rho-dependent phosphorylation of CD44 associated proteins, and CD44 surface expression. In the absence of OPN or surface CD44 expression activation of bone resorption by estrogen deficiency, parathyroid hormone or RANKL is incomplete.

F239

AlphavBeta5 Integrin Modulates Osteoclast Generation and Activity–Results from Ovariectomized avb5-Null Mice. N. Lane[1], W. Yao[1], D. Sheppard*[1], X. Huang*[1], G. Wesolowski[2], T. Howard*[3], D. Kimmel[2], F. P. Ross*[4]. [1]Department of Medicine, University of California at San Francisco, San Francisco, CA, USA, [2]Merck Research Laboratory, West Point, PA, USA, [3]Creighton University, Omaha, NE, USA, [4]Department of Pathology, Washington University School of Medicine, St. Louis, MO, USA.

Alphavbeta5 ($\alpha V\beta 5$) is highly expressed in the osteoblasts and osteoclast precursors. The purpose of this study was to examine the role of $\alpha v\beta 5$ in bone remodeling using an $\alpha v\beta 5$ knockout mouse model. Six-weeks-old 129/SvEm wide-type (WT) or $\alpha v\beta 5$-knock-out (KO) mice were either sham-operated or underwent bilateral ovariectomy (OVX) and maintained for 6 weeks. In-life double calcein labeling was completed. At sacrifice, bone histomorphometry was performed on the right proximal tibial metaphysis to determine cancellous bone mass, structure and bone turnover. Bone marrow aspiration of the femur was performed and aspirates were co-cultured with mouse osteoblast cells for 7 days in the presence of vitamin D and then stained for tartrate resistant acid phosphatase (TRAP) activity to determine the number of multinucleated cells. Biochemical assessment of bone resorption (DPD) was evaluated at 0, 3 and 6 weeks by ELISA. Statistical analysis of histomorphometric variables and bone turnover was done within groups as means and standard deviations, and between groups and treatments with a 2-factor ANOVA (genotype and estrogen). Results: BV/TV, BFR/BV, Oc.S., Oc.N, and osteoclast activity are influenced only by estrogen status, and TRAP(+) is influenced by both genotype and estrogen. These findings suggest that this integrin has a role in controlling osteoclast generation following estrogen depletion. Additional studies are now in progress to further evaluate the role of this integrin in regulating osteoclast generation in other conditions of high bone turnover.

Groups	N	BV/TV (%)	BFR/BV (%/yr)	Oc.S (%)	Oc.N (%)	TRAP(+) (#/0.72 cm^2)	DPD/Cr (nM/mM)
WT-Sham	5	11±3	312±85	5±1	2±0.2	11±6	10±1
WT-OVX	5	4±1	367±92	8.±1	3±1	22±6	18±2
KO-Sham	6	10±4	265±113	7±2	2±0.3	70±40	9±1
KO-OVX	6	3±1	608±146	10±3	5±0.5	497±137	19±3
Two-factor ANOVA P values							
Genotype		0.707	0.104	0.104	0.161	0.0001	0.162
Estrogen Status		0.050	0.005	0.029	0.050	0.0001	0.0001
Interactions		0.556	0.073	0.425	0.306	0.0001	0.162

Data are presented as mean±SD. BV/TV, bone volume; BFR, bone formation rate; Oc.S, osteoclast surface; Oc.N, osteoclast number; DPD, Deoxypyridinoline cross-links (6wks); Cr, creatinine.

F241

Cholesterol and Lipoproteins Regulate Osteoclast Formation and Survival. E. B. Luegmayr*, G. A. Rodan, A. A. Reszka. Bone Biology and Osteoporosis Research, Merck & Co., Inc., West Point, PA, USA.

Osteoporosis is associated with both atherosclerosis and vascular calcification. No mechanism yet explains the parallel progression of these diseases. While lipids and lipid-lowering agents are known to affect osteoblast differentiation, little is known about lipid effects on osteoclasts (OCL). We previously observed that OCL synthesize very little sterol, suggesting that internal stores of cholesterol may depend on exogenous sources. In the present study we demonstrate that lipoproteins (i.e. exogenous cholesterol regulation) modulate osteoclast formation and survival. OCL were generated by coculture of mouse bone marrow and MB1.8 osteoblasts in FBS. OCL were purified and then cultured in the presence of M-CSF, RANKL and lipoprotein-deficient FBS (LPDS), containing 90% less cholesterol than FBS. Exogenous lipoproteins were then used to modulate cholesterol levels in OCL. Low-density lipoprotein (LDL), used to deliver cholesterol, increased OCL viability up to 3- fold (vs. controls) at 48 hr. High-density lipoprotein (HDL), used as a cholesterol acceptor, removed dose-dependently up to 70% of labeled cholesterol over 24 hr and increased OCL apoptosis up to 3-fold by 48 hr, as measured by formation of pyknotic nuclei, actin disruption and caspase-3 activation. More rapid effects were observed with methyl-β-cyclodextrin (MBCD), which removed 80% of labeled cholesterol from OCL within one hr and induced massive apoptosis within 6-12 hr. Similar but delayed apoptotic responses to MBCD (over 24 hr) were observed in macrophages (J774, Raw264.7) but not cells derived from mesenchyme (osteoblasts, NIH/3T3). The LDL receptor null mouse (LDLR -/-) was used to further investigate the role of cholesterol delivery in OCL formation and survival. OCL were formed in vitro using bone marrow from LDLR-/- or background (+/+) C57BL6 mice. The OCL from LDLR-/- mice were substantially smaller by comparison to +/+. In males, there was an 8-fold reduction in the proportion of large (i.e. >340 μm) OCL, while in females there was a 2.5-fold reduction. This was accompanied by a significant increase in the number of smaller multinucleated cells, suggesting a defect in spreading rather than in fusion. OCL formation in +/+ could be suppressed by replacing FBS with LPDS during differentiation. Indeed, in LPDS, the size distribution of LDLR-/- and +/+ OCL was identical. In summary these observations show that exogenous cholesterol delivery via the LDL receptor plays an essential role for OCL formation and survival *in vitro*. Conversely, cholesterol removal leads to apoptosis. These effects might contribute to the link between osteoporosis and hyperlipidemia observed epidemiologically.

F243

Localization of a Sequence in TRAP Promoter Mediating RANKL-Induced Transcription of TRAP Gene. Y. Liu*, Z. Shi*, H. Yang, X. Feng. Pathology, University of Alabama at Birmingham, Birmingham, AL, USA.

Osteoclasts (OC), the major bone-resorbing cells, derived from cells of monocyte/macrophage lineage. RANKL is an essential and potent activator of OC differentiation. Despite the critical role of RANKL in OC differentiation has been established, the molecular mechanisms underlying RANKL-induced OC differentiation remain largely unknown. During RANKL-induced OC differentiation, a variety of genes are activated, including the gene for Tartrate-Resistant Acid Phosphatase (TRAP). In this study, we investigated the molecular mechanisms by which RANKL activates TRAP gene. We subcloned 1.8-kb mouse TRAP promoter (-1284 to +552), amplified by PCR based on published sequence, into pGL3-basic to generate a reporter construct named RL(-1284)Luc. RL(-1284)Luc was transiently transfected into RAW264.7 cells and transfected cells were then either untreated or treated with RANKL. The transfection results indicated RANKL up-regulates the TRAP promoter activity about 2-fold. Thus, the 1.8-kb TRAP promoter contains a sequence(s) mediating RANKL-dependent activation of TRAP gene transcription. To locate the sequence(s), we generated 5 deletion mutants of the TRAF promoter: TRAP(-684)Luc, TRAP(-484)Luc, TRAP(-484)Luc, TRAP(-284)Luc, TRAP(+116)Luc. These mutants contain RANKL promoter regions starting from different 5' positions (the numbers in parentheses) and ending at the same 3' site (+552). Transfection data with these mutants demonstrated that a 200-bp promoter region (-684 to -484) contain the sequence(s). To further locate the sequence(s), we prepared 4 more mutants: TRAP(-644)Luc, TRAP(-604)Luc, TRAP(-564)Luc, TRAP(-524)Luc. Transfection assays with these mutants further located the sequence(s) in a 40-bp region (-684 to -644). Gel shift/competition assays showed that 40-bp oligos derived from the 40-bp region specifically binds nuclear proteins from untreated RAW264.7 cells. Consistent with the transfection data, the banding was significantly enhanced in gel shift assays using nuclear extracts from RANKL-treated RAW264.7 cells, suggesting that RANKL activates TRAP transcription through the nuclear proteins binding to the 40-bp sequence. Given that RANKL activates NF-kB or AP1, we determined whether the nuclear proteins binding to this 40-bp sequence are NF-kB or AP1. Super shift assays with antibody against p50, P65, c-fos and c-jun confirmed that the 40-bp sequence binds transcription factors other than NF-kB and AP1. Taken together, we have located a 40-bp sequence in TRAP promoter regulating RANKL-induced TRAP gene transcription. More interestingly, this sequence may regulate TRAP transcription by binding novel transcription factors induced by RANKL.

F246

A Potent Antagonist of $\alpha_v\beta_3$ Integrin Is a Powerful Inhibitor of Bone Resorption In Vivo. S. B. Rodan[1], L. T. Duong[1], M. E. Duggan*[2], J. E. Fisher[1], M. A. Gentile[1], C. Fernandez-Metzler*[3], W. Halczenko*[2], G. D. Hartman*[2], J. H. Hutchinson*[2], C. Leu[1], L. Lipfert*[1], R. M. Nagy*[1], B. Pennypacker[1], T. Prueksaritanont*[3], J. G. Seedor*[1], G. Wesolowski[1], D. B. Kimmel[1], G. A. Rodan[1]. [1]Bone Biology & Osteoporosis Research, Merck Research Laboratories, West Point, PA, USA, [2]Medicinal Chemistry, Merck Research Laboratories, West Point, PA, USA, [3]Drug Metabolism, Merck Research Laboratories, West Point, PA, USA.

The $\alpha_v\beta_3$ integrin was shown to play a major role in bone resorption *in vitro* and *in vivo*. $\alpha_v\beta_3$ is highly expressed in osteoclasts and binds to the RGD sequence in extracellular matrix proteins. We report here the pharmacological properties of a low molecular weight RGD mimetic (compound A) and its *in vivo* activity in several models of bone resorption. ^{3}H-compound A binds with high affinity (Kd 0.33 nM) to purified human $\alpha_v\beta_3$. In cell assays *in vitro* compound A: (i) is a potent inhibitor of osteoclast formation and bone resorption with IC50s of ~ 10 nM; (ii) inhibits attachment to vitronectin of HEK 293 cells, transfected with either $\alpha_v\beta_3$ or $\alpha_v\beta_5$ integrin, with IC_{50}s of 0.6 and 25 nM, respectively; and (iii) inhibits $\alpha_{IIb}\beta_3$-dependent human platelet aggregation with an IC_{50} of 35 μM. In pharmacological assays of *in vivo* bone resorption compound A: (i) increases bone mineral density (BMD) significantly in growing male rats, when administered at 10 and 30 mg/kg P.O., b.i.d. for 10 days; (ii) increases BMD dose dependently in growing male rats by 4.7 to 32%, at increasing steady state concentrations between ~70 and 1550 nM, respectively, obtained by administering the drug S.C. with minipumps; (iii) in 6 month old ovariectomized (ovx) rats (a) increases BMD of distal femur; (b) increases bone volume of proximal tibial cancellous bone determined by histomorphometry; and (c) reduces bone turnover rate, when administered orally at 10 and 30 mg/kg, b.i.d. for 4 weeks, all relative to ovx rats receiving vehicle; and (iv) suppresses urinary N-telopeptide (uNTx) in ovx rhesus monkeys, when administered orally at 5, 15 and 40 mg/kg/day. In conclusion, compound A, a potent and selective $\alpha_v\beta_3$ integrin ligand, is a powerful inhibitor of bone resorption; it prevents bone loss in several animal models when given orally, without eliciting detectable changes in other tissues examined.

Disclosures: ***S.B. Rodan****, Merck & co. 3.*

F248

Generation and Characterisation of Bisphosphonate-Resistant J774 Cells. K. Thompson*, M. J. Rogers. Medicine & Therapeutics, University of Aberdeen, Aberdeen, United Kingdom.

Different cell types exhibit different sensitivities to bisphosphonates (BPs) *in vitro*. To identify possible routes by which cells could become resistant to BPs, we sought to isolate a BP-resistant strain of J774 macrophages. J774 cells were cultured in increasing concentrations of ibandronate (IBA), from 0.1μM to 5μM, which caused extensive (>95%) apoptosis. The surviving cells were further cultured in IBA (5μM) for 3 weeks, until recovery occurred. The resulting cells (J774-RES) were resistant to the cytotoxic effects of BPs in

an MTT assay (IC_{50} >100μM for IBA, vs 59μM in wild-type cells) but grew at a comparable rate to the parental cells, although the protein content of the resistant cells was significantly lower than in the parental strain. J774-RES cells were also found to be cross-resistant to the cytotoxic effects of zoledronic acid (ZOL) (IC_{50} 69μM in J774-RES vs 18μM in parental cells). The resistance of J774-RES cells to BPs was not due to differences in cellular uptake since J774-RES cells did not differ from parental cells in the ability to internalise [^{14}C]IBA or [^{14}C]ZOL. Western blotting for unprenylated Rap1A and metabolic labelling with [^{14}C]mevalonolactone were used to determine the effect of IBA and ZOL on protein prenylation in the resistant cells. IBA and ZOL were markedly less effective at inhibiting protein prenylation in J774-RES cells compared to the parental cells. To determine the mechanism for the resistance of J774-RES cells, we examined the activity of FPP synthase, the molecular target of IBA and ZOL. FPP synthase activity in lysates of the resistant cells was not significantly different to the activity in parental cells and there was no difference in the degree of inhibition by IBA or ZOL. J774-RES cells did not differ from the parental cells in the cytotoxic response to mevastatin, suggesting that changes in HMG-CoA reductase activity do not account for the mechanism of resistance. Western blot analysis also suggested that the level of HMG-CoA reductase did not differ between resistant and parental cells, and IBA and ZOL treatment upregulated the level of HMG-CoA reductase in both strains. This study supports the notion that cells can become resistant to BPs, although the exact molecular basis for this resistance remains to be determined.

Disclosures: ***K. Thompson****, Novartis Pharma AG 2.*

F249

N-Bisphosphonates Stimulate Proliferation of γ/δ-T Cells in Human PBMC Cultures by Inhibiting the Mevalonate Pathway: Clarification of the Acute Phase Response. K. Thompson*, S. A. Gordon*, M. J. Rogers. Medicine & Therapeutics, University of Aberdeen, Aberdeen, United Kingdom.

Several recent studies have suggested that bisphosphonates (BPs) can stimulate proliferation of γ,δ-T cells by acting as non-peptide antigens (such as isopentenyl diphosphate/IPP) that can be presented to the γ,δ-TCR. However, since nitrogen-containing BPs (N-BPs) can disrupt the mevalonate pathway by inhibiting farnesyl diphosphate (FPP) synthase, it is also possible that N-BPs affect γ,δ-T cells by altering the intracellular synthesis of isoprenoid lipids or by preventing protein isoprenylation. We examined the effect of a range of BPs on the proliferation of γ,δ-T cells, using flow cytometry to quantitate the number of CD3+/γ,δ-TCR+ cells after 7 days' culture of human PBMCs in the presence of rhIL-2. 1μM zoledronic acid, ibandronate, alendronate and pamidronate, or 1μM IPP, consistently increased the proportion of γ,δ-T cells in the CD3+ population (from 3-6% in controls to 20-65%). The order of effectiveness of N-BPs was similar to the order of potency for inhibiting FPP synthase (ZOL>ALN~IBA>PAM). Furthermore, minor changes in N-BP structure that affect the potency for inhibiting FPP synthase also affected the ability to stimulate γ,δ-T cell proliferation. Clodronate, which does not inhibit FPP synthase, had no effect. The stimulatory effect of N-BPs on γ,δ-T cell proliferation was abrogated by co-incubation with 1μM mevastatin, but was not affected by 10μM geranylgeraniol. Furthermore, mevastatin alone did not affect the proportion of γ,δ-T cells, suggesting that the stimulatory effect of N-BPs on T cells was not due to inhibition of protein isoprenylation but was related to the accumulation of isoprenoid lipids (eg IPP) upstream of FPP but downstream of mevalonate. Treatment of purified γ,δ-T cells (isolated from PBMCs by negative selection) with N-BPs or IPP in the presence of rhIL-2 did not stimulate T cell proliferation, indicating that accessory cells are required for the stimulatory effect of N-BPs on γ,δ-T cells. Together, these observations demonstrate that N-BPs indirectly stimulate the proliferation of human γ,δ-T cells *in vitro*. This effect is dependent on the ability of N-BPs to inhibit the intracellular enzyme FPP synthase, either in γ,δ-T cells or in other PBMCs. Inhibition of FPP synthase causes the accumulation of isoprenoid lipids (eg IPP) upstream of FPP in the mevalonate pathway. It is likely that the release of isoprenoid lipids can cause activation of γ,δ-T cells via presentation of isoprenoid lipid on antigen-presenting cells. These studies finally shed new light on the mechanism underlying the acute phase response observed in patients treated with N-BPs.

Disclosures: ***K. Thompson****, Novartis Pharma AG 2.*

F252

A New Class of Anti-Resorptives: Inhibitors of Type IIa Sodium/Phosphate Cotransporter. E. Chan*, A. deRosier*, S. Sankuratri*. Roche Bioscience, Palo Alto, CA, USA.

The type IIa sodium/phosphate co-transporter (Npt IIa) is a key player in overall phosphate homeostasis and bone remodeling. In addition to its expression in kidney, previous studies showed that the protein was expressed in osteoclasts and the plasma membrane expression and activity of Npt IIa protein in osteoclasts increased in presence of bone particles. A non-specific inhibitor of Pi transport, PFA reduced Pi uptake in isolated osteoclasts and inhibited pit formation in a dose-dependent manner. Npt IIa-/- mice exhibited reduction in osteoclast number and higher trabecullar volume in 115d or older mice relative to wild-type mice. Hence, it makes Npt IIa an attractive target for developing anti-resorptive agents. We established a stable Npt IIa expressing mammalian cell line, which was then subjected to high throughput screening with Roche's collection of compounds. Several inhibitors have been identified with an IC_{50} as low as 2 μM in Pi transport assays. Specificity and selectivity of the identified inhibitors have been confirmed using a variety of assays. None of the inhibitors showed cytotoxic effects (>100 μM) and were at least 5-fold selective over sodium/sulfate co-transporter. Many of these compounds also showed selectivity over two other related sodium/phosphate cotransporters Npt IIb and a type III transporter. The most potent compounds were tested for their ability to inhibit bone resorption by mouse osteoclasts. The compounds inhibited osteoclast-mediated bone resorption by over 80% at 10 μM. These compounds could be potential leads to develop a more potent anti-resorptive drug.

F254

Non-peptide Small Molecule Compound that Selectively Inhibits RANK-RANKL Interaction. N. Sakurai, H. Akatsuka*, J. Mizukami*, N. Sato*, M. Tsuda*, S. Hashimoto*, E. Koitabashi*, K. Kawano*, J. Kohno*, M. Nishio*. Discovery Research Laboratory, Tanabe Seiyaku Co., Ltd., Saitama, Japan.

Receptor activator of NF-κB (RANK) and its ligand RANKL play crucial roles in osteoclast differentiation and activation. A secreted soluble TNF receptor family member, osteoprotegerin (OPG), a natural decoy receptor for RANKL, has been found to be a potent inhibitor of osteoclast differentiation and activation *in vitro* and *in vivo*. The administration of OPG has been reported to be effective on several animal models for bone diseases characterized by excessive bone resorption including osteoporosis, suggesting that inhibition of RANK-RANKL interaction is a promising avenue to the prevention of bone loss. In this study, we identify a novel non-peptide small molecule compound that blocks the RANK-RANKL interaction. We isolated TMC-315s from a fungal culture extract composed of at least four homologs of molecular weight of about 600 as inhibitors of RANKL function. TMC-315B2, the best of these components inhibited the RANKL-induced NF-κB activation at submicromolar concentrations while it failed to block the TNF-induced activation. TMC-315B2 also inhibited the RANK-RANKL interaction in enzyme-linked immunosorbent assay using soluble forms of RANKL and RANK proteins (IC50=2.1 μM), whereas it did not antagonize the TNF-TNFR1 binding. Biospecific interaction analysis using surface plasmon resonance detection (BIAcore) revealed that TMC-315B2 bound to RANKL but did not bind to RANK. Moreover, the binding of TMC-315B2 to TNF or TRAIL was not detected. We next tested TMC-315B2 for its effect on osteoclastogenesis using the coculture system. Osteoclast formation was inhibited dose-dependently by TMC-315B2. We further examined the effect of TMC-315B2 on bone resorption *in vivo*. TMC-315B2 significantly prevented parathyroid hormone-related peptide (PTHrP)-induced hypercalcemia in thyroparathyroidectomized (TPTX) rats when administered intravenously at 10 mg/kg. In conclusion, we have identified a non-peptide small molecule TMC-315B2 that antagonizes osteoclastogenesis by blocking RANK-RANKL interaction and exerts this effect both *in vivo* and *in vitro*. Derivatives of this compound may have a therapeutic advantage over OPG as they may be orally available.

F256

Zoledronic Acid Modulates Bone Repair through Transiently Delayed Remodelling. E. J. Smith[1], R. A. Peat*[2], A. McEvoy*[2], J. N. Briody[2], P. A. Baldock*[1], J. A. Eisman[1], D. G. Little*[2], E. M. Gardiner[1]. [1]Bone and Mineral Program, Garvan Institute of Medical Research, Sydney, Australia, [2]Orthopaedic Research Unit, Childrens Hospital Westmead, Sydney, Australia.

Distraction osteogenesis for correcting limb length discrepancy can be clinically difficult due to fractures through poorly mineralised regenerate bone in the distraction gap. Bisphosphonates increase regenerate mineral content, size and strength but the mode by which this occurs is unclear. Inhibition of osteoclastic resorption may lead to regenerate retention, but bisphosphonates also stimulate bone formation in vitro. To investigate these possibilities 8 week old male NZW rabbits underwent right tibial osteotomy, 14 days of distraction and consolidation until sacrifice at 2, 4, 6, 18 and 44 weeks post surgery. The intact left tibia was used as internal control. Animals received saline, single dose zoledronic acid (0.1mg/kg at surgery), or double dose zoledronic acid (at surgery and 2 weeks later). X-rays were taken at 6, 18 and 44 weeks. In some animals, BMD and BMC were measured by DXA at 2, 4, 6, 12, 18 and 44 weeks. In others histomorphometry was carried out after sacrifice. Although BMD and BMC increased in all animals between 2 and 4 weeks, this was greater in single and double dose animals (33% and 53%, $p<0.01$). Saline animals lost regenerate bone between 4 and 6 weeks (34%, $p<0.01$) but treated animals did not. Between 6 and 44 weeks BMD and BMC gradually decreased in treated animals and increased in saline group, such that at 18 and 44 weeks there was no difference between groups. Trabeculae and cortical bone ends were still apparent in x-rays of treated groups at 18 and 44 weeks. Trabecular BV/TV was greater in the double dose group at 4, 6 and 18 weeks ($p<0.05$). Similar increases in single dose group were not significant. Trabecular number increased by 26% and 53% in single and double dose groups at 4 weeks and by 28% and 60% at 6 weeks ($p<0.01$). There was no difference in trabecular thickness at 2, 4 or 6 weeks and no change in mineral apposition rate at later times. Osteoblast surface tended to be lower in treated animals (15% at 2 weeks and 11% and 50% in single and double dose groups at 4 weeks, $p<0.05$). There was a decrease in osteoclast surface (63% at 2 weeks in single dose and 20% and 60% at 4 weeks in treated groups, $p<0.05$). Thus these data do not support a bisphosphonate-induced increase in bone formation. Rather, the increase in new bone in the distraction gap appears due to retention as a result of decreased resorption. In this study, the clinically valuable increase in regenerate volume and strength can be explained by bisphosphonate suppression of osteoclastic resorption of bone produced in the exuberant osteoblastic response to fracture and distraction.

F259

Possible Role for TGF-Beta-Induced SOCS Expression in Osteoclast/ Macrophage Lineage Commitment In-Vitro. S. W. Fox*, T. J. Chambers. Dept of Cellular Pathology, St George's Hospital Medical School, London, United Kingdom.

The ligand that induces osteoclast (oc) differentiation has been identified as RANKL, a member of the TNF superfamily. However, only some precursors form oc when incubated with RANKL, suggesting that RANKL alone might not be sufficient to ensure that precursors become oc at sites of resorption. Responses to stimuli from the TNF superfamily are characteristically associated with inputs from other factors such as TGF-beta. Previously, we have shown that TGF-beta augments oc formation. Furthermore, oc formation is abolished by anti-TGF-beta antibodies, suggesting that oc that form without the addition of exogenous TGF-beta are dependent on TGF-beta in the medium or produced by precursors themselves. The mechanism by which TGF-beta facilitates oc formation is unknown. One possibility is that the environment in-vitro is essentially pro-inflammatory, due to the presence of agents such as interferons, and TGF-beta opposes this. Interferons signal via the JAK-STAT pathway, and TGF-beta might therefore block these signals. Recently, a group of STAT-induced factors, termed SOCS (suppressors of cytokine stimulation), have been isolated which form part of the negative-feedback mechanisms that switch off JAK-STAT signalling after cytokine stimulation. Therefore, we proposed to identify those SOCS expressed in oc, and establish if SOCS expression plays a role in the mechanisms by which TGF-beta enables oc formation. To assess the pattern of SOCS1-4 expression in oc and their precursors we performed Northern analysis and quantitative PCR on RNA extracted from macrophages, oc and precursor cells incubated with or without TGF-beta-1. Interestingly, we found that while SOCS1-4 mRNA is not detectable in macrophages, oc express SOCS3 mRNA, and TGF-beta further upregulates this expression. Furthermore, TGF-beta induces SOCS3 expression in uncommitted precursors within 1 hour. To determine if SOCS3 plays a role in the mechanisms by which TGF-beta facilitates oc formation we examined the effect of overexpressing SOCS3 in precursors using retrovirus. We found that oc formation and bone resorption were significantly enhanced in SOCS3-infected cells. This suggests that TGF-beta-induced expression of SOCS3 mRNA may represent a mechanism by which TGF-beta suppresses inhibitory cytokine signalling, priming precursors for oc differentiation.

F261

Cell Swelling Mediates Activation of a Cl^- Channel by Extracellular Ca^{2+} in Murine Osteoclasts. K. Sakuta*[1], H. Sakai[2], H. Mori[1], H. Morihata*[3], M. Kuno[1]. [1]Physiology, Osaka City University Graduate School of Medicine, Osaka, Japan, [2]Orthopedic Surgery, Osaka City University Graduate School of Medicine, Osaka, Japan, [3]Neurology, Osaka City University Graduate School of Medicine, Osaka, Japan.

Bone resorbing activity of osteoclasts is inhibited by high concentrations of extracellular Ca^{2+} ($[Ca^{2+}]_o$) released from the degraded bone matrix in the resorption pit. Osteoclasts possess Ca^{2+}-sensing cellular machineries to regulate their own activity. We have previously shown that exposure to high $[Ca^{2+}]_o$ (≥20 mM) activates a volume-sensitive, outwardly-rectifying Cl^- (OR_{Cl}) channel (Shibata et al., 1997; Sakai et al., 1999). In this study, the Ca^{2+}-sensing mechanisms leading to activation of the OR_{Cl} channel were examined using whole cell current recordings of murine osteoclasts developed from bone marrow cells in the co-culture with ST-2 cells in the presence of vitamin D. The OR_{Cl} current was also activated by Gd^{3+}, Zn^{2+} and a polycation, neomycin, suggesting that osteoclasts respond to di-, tri-, and polycations. Activation of the OR_{Cl} channel by these cations was accompanied by increases in the planar cell area of the cell body, suggesting that swelling is involved in the Ca^{2+}-sensing response. There was a positive correlation between the current density and increment in the cell area. The $[Ca^{2+}]_o$-induced swelling was confirmed in intact (unclamped) cells by three-dimensional analysis using confocal scanning microscopy with a fluorescent dye (BCECF) in the extracellular medium, although the extent of swelling was smaller than that in clamped cells. Either removal of extracellular Na^+ or a blocker for the Na^+-Ca^{2+} exchanger (2'4'-dichlorobenzamil hydrochloride) inhibited both the $[Ca^{2+}]_o$-activated OR_{Cl} current and the accompanying cell swelling. Decreasing intracellular pH from 7.3 to 6.6 enhanced the sensitivity of the OR_{Cl} channel to cations. Amiloride (1 mM), a blocker for the Na^+-H^+ exchanger, prevented the activation and decreased the current once activated at pH 6.6. Intracellular dialysis with an ATP-free pipette solution or application of an actin-destabilizer (cytochalasin D, 0.1 μM) inhibited the $[Ca^{2+}]_o$-activated OR_{Cl} current and the accompanying cell swelling. These results propose a new Ca^{2+}-sensing mechanism in osteoclasts: exposure to high $[Ca^{2+}]_o$ may induce cell swelling by Na^+ influx via Na^+-dependent transporters, such as the Na^+-Ca^{2+} exchanger and the Na^+-H^+ exchanger, which leads to activation of the OR_{Cl} channel. Cell volume may be a second-message in the regulation of osteoclast function.

F263

Association of the Cytoplasmatic Tail of the Calcitonin Receptor with Filamin Prevents its Degradation in Lysosomes. T. Seck, L. Neff, W. C. Horne, R. Baron. Cell Biology and Orthopedics, Yale University, New Haven, CT, USA.

The interactions of G-protein coupled receptors (GPCR) with a variety of intracellular proteins regulate receptor signaling, internalization and recycling. To identify proteins that might interact with intracellular domains of the calcitonin receptor (CTR), we used the carboxy-terminal tail of the receptor as bait to screen a yeast two hybrid library. We isolated a clone encoding filamin, an actin binding protein. The interaction of the CTR and filamin was confirmed by co-immunoprecipitation. However, a CTR mutant lacking the C-terminal tail did not bind to filamin. Confocal microscopy showed partial colocalization of filamin and the CTR at the surface of mouse osteoclast-like cells. Using the directed yeast two-hybrid assay, the binding site on filamin was mapped to amino acids (aa) 2129-2330, and the interacting site on the CTR was mapped to the C-terminal half of the tail (aa 447-474). Overexpression of fragments spanning the interacting site of filamin or the C-terminal tail inhibited the interaction. The functional relevance of the association of the CTR with filamin was tested in M2 melanoma cells that lack filamin and a control cell line (A7) stably transfected with filamin. The production of cyclic AMP and elevation of cytosolic free calcium in response to Calcitonin (CT) were identical in both cell lines. CT-induced Erk1/2 phosphorylation was also intact in filamin-free cells. Thus, filamin is not directly involved in signal transduction from the CTR. However, there was markedly less of the CTR in the filamin-free M2 cells, as determined by Western blots. Moreover, surface expression of the CTR, determined by FACS analysis, was significantly lower in the filamin-free cells. Pulse chase experiments, comparing the rates of degradation of the CTR in the two cell lines, showed a significantly faster ligand-independent degradation of the receptor in the absence of filamin. In contrast, the degradation of another GPCR, the beta2-adrenergic receptor, was identical in both cell lines. The degradation of the CTR was partly inhibited by chloroquine and ammonium chloride, agents which inhibit lysosomal degradation. Thus, the interaction of the cytoplasmatic tail of the CTR with the actin binding protein filamin regulates the level of expression of the CTR at the cell surface by preventing its degradation.

F269

The Effect of Socioeconomic Deprivation on Primary Care Referral to a Direct Access DXA Scanning Service. S. J. Gallacher[1], A. R. McLellan[2], I. Baxter*[3], P. McGill*[4], R. Dargie*[5], C. Morrison*[3]. [1]Medical Unit B, Southern General Hospital, Glasgow, United Kingdom, [2]Western Infirmary, Glasgow, United Kingdom, [3]Greater Glasgow NHS Board, Glasgow, United Kingdom, [4]Stobhill Hospital, Glasgow, United Kingdom, [5]Royal Infirmary, Glasgow, United Kingdom.

Osteoporosis and increased fracture risk is recognised to be a major public health problem. Strategies are required to identify individuals at highest risk in order that interventions can be targeted to this group. Bone densitometry, in particular axial DXA scanning, has been shown to predict individuals both at increased risk of fracture and those who are likely to derive benefit from bisphosphonate therapy. This work describes the outcome of collaboration amongst four hospitals serving the population of the City of Glasgow (population 960,000) to provide Direct Access DXA Scanning to primary care physicians for patients with clear osteoporosis risk factors. These risk factors include history of low trauma fracture over age 50, long term (>3 months) oral corticosteroids, early menopause (<45 years) and radiological osteopenia. Over the past 3 years 3985 patients have been seen through this service. There are 216 primary care practices in Glasgow all of whom were advised of this service. Of these 190 (88%) have used the service. The modal number of referrals per practice was between 2 and 9 but 4 practices have referred over 100 patients. The reason behind this disparity is not clear. One factor might relate to patients' socioeconomic status. To investigate this further all referred patients had their appropriate Deprivation Category (Depcat) (Carstairs 1991) allocated. Depcat is a 7 point score with category 1 being most affluent and category 7 least affluent. The proportion of the total population in each Depcat was related to the proportion of DXA referrals in each Depcat. 17.5% of the population of Glasgow are in Depcat 1 & 2 but this population accounted for 27.6% of referrals. At the other extreme 52.6% of the population are in deprivation categories 6 & 7 and this population accounted for only 38.5% of patients scanned. This variation remained present in each of the age bands 50-59, 60-69 and greater than 70 years and remained constant by year of referral. Overall patients resident in the most deprived area of the city are approximately 8 times less likely to be referred for DXA than those from the most affluent area. As some osteoporosis risk factors (such as cigarette smoking) are more prevalent in populations of lower socioeconomic status, it is reasonable to expect a higher prevalence of osteoporosis in this population. This is another example of the inverse care law where the population most at risk is least likely to receive appropriate medical care.

F275

Low Vitamin K Status Is Associated with Low Bone Mineral Density and Quantitative Ultrasound in Men. S. L. Booth[1], K. E. Broe[2], R. R. McLean[2], D. R. Gagnon*[3], J. W. Peterson*[1], M. T. Hannan[2], L. A. Cupples*[3], D. M. Cheng*[3], P. W. F. Wilson*[3], B. Dawson-Hughes[1], D. P. Kiel[2]. [1]USDA HNRCA at Tufts University, Boston, MA, USA, [2]Hebrew Rehab Ctr & Harvard Med Sch, Boston, MA, USA, [3]BU Sch Public Health, Boston, MA, USA.

Low vitamin K (VK) status, as indicated by low fasting plasma phylloquinone (VK1) and high serum % undercarboxylated osteocalcin (%ucOC), is a potential risk factor for bone loss and hip fracture. Few data exist on the association between VK and bone mineral density (BMD) in men. We examined associations between fasting plasma VK1, serum %ucOC, BMD and quantitative ultrasound (QUS) of the calcaneus. BMD of the hip (femoral neck and trochanter) and spine (L2-4) was measured by Lunar DPX-L in 734 men participating in the Framingham Study Offspring cohort. Broadband ultrasound attenuation (BUA) and speed of sound (SOS) were also measured in 576 of these men using the Sahara bone sonometer (Hologic). Participants had a mean (SD) age of 59 (9) years, with a mean (SD) VK1 of 1.5 (2.0) nmol/L and a mean (SD) %ucOC of 15.8 (16.1). The mean (SD) BMD of the femoral neck, trochanter and spine were 0.982 (0.142), 0.894 (0.144) and 1.328 (0.221) g/cm^2, respectively. The mean (SD) BUA and SOS were 80.6 (17.2) dB/MHz and 1555 (31) m/s, respectively. The associations between VK status, BMD and QUS were evaluated using regression models that adjusted for age, BMI, current smoking, caffeine, alcohol and total calcium intakes, physical activity, and plasma 25(OH)D and triglycerides. Plasma VK1 was positively associated with femoral neck BMD (p=0.03), BUA (p=0.009) and SOS (p=0.03). There was also a non-significant (NS) trend between plasma VK1 and BMD of the trochanter (p=0.07) and spine (p=0.16). Whereas %ucOC was negatively associated with BMD of the femoral neck (p=0.02) and trochanter (p=0.004), with a NS trend at the spine site (p=0.18), %ucOC was not associated with either QUS measure. In conclusion, low vitamin K status is associated with low QUS and low BMD of the femoral neck and trochanter in men. VK supplementation trials are needed to evaluate the role of vitamin K in reducing bone loss.

F277

Prevalence of Vitamin D Depletion Among Subjects Seeking Advice on Osteoporosis: A Five-Year Cross Sectional Study with Therapeutic and Public Health Implications. N. Parikh*, T. Eskridge*, J. Hill*, E. Phillips*, D. Rao. Bone & Mineral Research Laboratory, Henry Ford Hospital, Detroit, MI, USA.

There is continued concern about vitamin D depletion in the U.S. population. We previously reported that a significant proportion of patients seeking advice for osteoporosis are vitamin D depleted. Since then concerted public health education efforts about calcium (Ca) and vitamin D nutrition have occurred. We therefore assessed the impact of such efforts on the prevalence of vitamin D depletion among individuals attending our osteoporosis clinic. The computerized database of all patients seen between January 1997 & December 2001 was reviewed for the prevalence of vitamin D depletion (defined as serum 25-OHD of ≤15 ng/ml). We excluded patients with obvious known causes for vitamin D, and all Hispanics and Asians (n=201). Serum Ca, creatinine (Cr), PTH and 25-OHD were measured in all patients. Three thousand, seven hundred, and ninety new patients were seen during the 5 years; 3343 (88%) were women and 3195 (84%) were whites. The mean age was 65 ± 13 years. For the entire study cohort the prevalence of vitamin D depletion was 20% (748/3790) and remained constant during the 5 years (17%, 21%, 18%, 18%, and 24% respectively). Vitamin D depletion was higher in blacks than in whites (43% vs 16%; p<0.001). Serum 25-OHD correlated with PTH (r= -0.22; p<0.001) but not with age, Ca, or Cr. Age and serum 25-OHD, Ca and Cr all predicted PTH level, but serum 25-OHD and Cr were the strongest predictors (t statistic -13.7 & +17.7 respectively). Based on the differences in slopes of PTH on 25-OHD, black women had a greater increase in PTH than white women (-1.23 vs. -0.79) This is the largest study of its kind in the U.S. and confirms the preliminary findings of our 2-year study. Indeed, we observed a disturbing upward trend (about 2%-5%) in vitamin D depletion over the 5 years despite an explosion of public education efforts. This implies that either these efforts are ineffective, or that foods and supplements contain inadequate amounts of vitamin D, or both. Conclusions: Vitamin D depletion is prevalent among ambulatory patients seeking advice about osteoporosis. Since poor vitamin D nutrition may adversely affect response to specific osteoporotic therapy, greater attention to vitamin D nutrition in addition to Ca is essential. The lack of decline in the prevalence of vitamin D depletion over 5 years implies that current efforts are ineffective and need reexamination.

F279

Dietary Phytoestrogen Intake Is Not Associated With Low Bone Mineral Density in Healthy Caucasian Premenopausal Women. M. R. French*[1], A. C. Blakely*[1], C. C. Chase*[1], L. U. Thompson*[2], G. A. Hawker[1]. [1]Osteoporosis Research Program, Sunnybrook and Women's College Health Sciences Centre, Toronto, ON, Canada, [2]Department of Nutritional Sciences, Faculty of Medicine, University of Toronto, Toronto, ON, Canada.

The consumption of soy products and other dietary phytoestrogens has increased, likely due to perceived potential benefits on menopausal symptoms, postmenopausal bone health and cancer risk. The bone effects of these compounds in premenopausal women is unclear. We evaluated the association between dietary intake of the two major classes of phytoestrogens, isoflavones and lignans, and bone mineral density (BMD) in 557 healthy, Caucasian, premenopausal women aged 21-40 years. Intake of lignans and isoflavones were assessed by quantitative food frequency questionnaire during a detailed standardised interview. Total phytoestrogen intake was a composite value of dietary lignan and isoflavone intakes. BMD was measured at the lumbar spine (L2-L4) and femoral neck using dual energy Xray absorptometry (DXA). Bone mass was classified as low if BMD values (g/cm^2) were in the lowest quintile as measured by DXA. Using multiple logistic regression modelling, independent correlates of low BMD were identified. Variables considered included age, weight, height, dietary factors including phytoestrogen intake (daily lignan, isoflavone and total phytoestrogen intake by quartiles), menstrual and reproductive history, body composition, physical activity and smoking. The mean age of the cohort was 31.9 ± 4.7 years. Mean intake of isoflavones, lignans and total phytoestrogens were 21.6 µmol/day (0-404.9 µmol/day), 4.6 µmol/day (0.1-22.7 µmol/day) and 26.3 µmol/day (0.2-420.4 µmol/day), respectively. At the femoral neck, low BMD was associated with low body weight, lower percent lean body mass and physical inactivity as an adolescent. Younger age, low body weight and lower percent lean body mass were associated with low BMD at the lumbar spine. Low BMD at the femoral neck was not associated with daily intake of isoflavones (OR 1.176, 95% CI 0.952 – 1.453), lignans (OR 1.120, 95% CI 0.901 – 1.393) or total phytoestrogens (OR 1.217, 95% CI 0.995 – 1.490). Nor was there an association between phytoestrogen intake and low BMD at the lumbar spine. In this sample of healthy Caucasian premenopausal women, dietary phytoestrogen intake was not associated with BMD. A prospective study is ongoing to determine whether dietary phytoestrogen intake affects changes in BMD over time.

F282

Inflammatory Bowel Disease and the Risk of Fracture. T. P. van Staa[1], L. S. Brusse*[2], M. K. Javaid[1], H. G. M. Leufkens*[2], C. Cooper[1], N. K. Arden*[1]. [1]Medical Research Council Environmental Epidemiology Unit, Southampton, United Kingdom, [2]Pharmacoepidemiology and Pharmacotherapy, Utrecht Institute for Pharmaceutical Sciences, Utrecht, Netherlands.

Patients with inflammatory bowel disease (IBD), Crohn's disease (CD) and ulcerative colitis (UC), have an increased risk of low bone mass, the pathogenesis of which is multifactorial. There are limited data on fracture prevalence in patients with IBD, with conflicting results. We therefore conducted a primary care based case-control study to determine the risk and major risk factors of fracture in IBD patients. 231,778 patients with a fracture and 231,778 age and sex matched controls were recruited from the General Practice Research Database. The database has been previously demonstrated to be a representative sample of the general population of England and Wales. The IBD diagnosis and risk factors were collected from electronic medical records. Adjusted odds ratios (OR) were estimated from conditional logistic regression. The mean age of cases and controls was 51 years and 52.5% were women. A history of IBD was found in 1134 fracture cases, compared to 896 of the controls (adjusted OR 1.21; 95% CI 1.10-1.32 p<0.001). The risk of fracture was significantly related to disease severity, as assessed by the number of symptoms [OR in IBD patients without symptoms, 1.02 (0.90-1.17); 1 symptom, 1.66 (1.41-1.96); and 2 or more symptoms, 1.74 (1.43-12.12)]. Similarly, severity assessed by medication demonstrated inceasing fracture risks compared to untreated patients:Aminosalicylates use: 1.32 (1.14,1.54), oral corticosteroids 1.46 (1.18-1.82) and disease modifying agents 1.86 (1.15,3.02). IBD patients with a history of small bowel surgery did not have an increased risk of fracture [OR 1.03 (0.84-1.28)]. Use of oral corticosteroids increased with disease severity. The OR in IBD patients was 1.10 (1.00-1.20) after adjustment for oral corticosteroids. For hip fracture, this OR was 1.46 (1.04-2.04). In conclusion, IBD patients have a significantly higher risk of fractures, especially in patients with more severe disease. This increased risk is partially explained by oral corticosteroid usage.

Table 1. Risk of fracture in CD and UC

Disease	All fracture	Hip fracture	Vertebral fracture	Distal forearm fracture
CD	1.32 (1.13,1.53)	1.86 (1.08,3.21)	2.25 (1.13,4.47)	1.38 (0.99,1.93)
UC	1.13 (1.02,1.27)	1.40 (0.92,2.13)	1.42 (0.84,2.40)	1.17 (0.93,1.47)

OR with 95% CI adjusted for age, sex, disease and medication history and body mass index and smoking.

Disclosures: ***T.P. van Staa****, Procter&Gamble Pharmaceuticals 1, 3.*

F284

The Utility of Prospective Height Loss for Detecting Vertebral Fracture Depends on Fracture Incidence. K. Siminoski[1], J. D. Adachi[2], G. Cline*[3], C. B. M. B*[4], V. E. R. T Study Group*[3]. [1]Radiology, Univ of Alberta, Edmonton, AB, Canada, [2]Medicine, McMaster Univ, Hamilton, ON, Canada, [3]Procter & Gamble Pharm, Mason, OH, USA, [4]Bone Alliance, Toronto, ON, Canada.

Our previous analysis of the VERT MN/NA risedronate studies indicated that prospective height loss could not be used to rule in the development of an incident vertebral fracture in that population. Height loss < 2 cm could effectively rule out a new fracture in the VERT population. We have examined the performance of height loss as a clinical test across a range of fracture incidence to determine (1) whether there is any clinically relevant fracture incidence range for ruling in a fracture, (2) the useful incidence range for ruling out a fracture. Sensitivity and specificity were derived from the placebo arms of the risedronate VERT MN/NA trials. Post-baseline height and vertebral radiographs were available in 985 postmenopausal female subjects (average age 69 years, range: 38-85 years). Height loss was determined as the difference between the baseline measurement and the subsequent measurement using a stadiometer. Lateral vertebral radiographs were performed at the same times and were analyzed by digital morphometry from T4 to L4. Vertebral fractures were determined using both quantitative and semiquantitative methods. New vertebral fractures occurred in 18.1% of study subjects. At a cut-off point of 2 cm height loss over 3 years, sensitivity was 38% and specificity was 93%. These parameters were applied over a range of theoretical vertebral fracture incidence to determine positive predictive value (PPV) and negative predictive value (NPV). Fracture can be ruled in when PPV is high. As shown in the figure, PPV is relatively low over much of the incidence range. PPV only rises > 80% at a fracture incidence of 41%, and only becomes greater than 90% when incidence is 61%. Fractures can be effectively ruled out when NPV is high. The negative predictive value is > 90% when fracture incidence is < 14%. NPV is above 80% up to fracture incidence of 27%. This analysis demonstrates that a 2 cm cut-off for height loss during prospective monitoring could only rule in a fracture with high accuracy at extremely high fracture incidence rates (>61%). A 2 cm cut-off can rule out the development of a fracture with high accuracy over the range of vertebral fracture incidence that would be observed in clinical practice (< 14%).

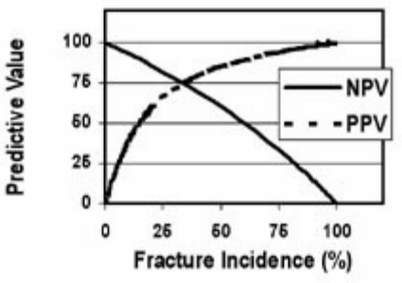

Disclosures: ***K. Siminoski****, Procter and Gamble Pharmaceuticals 2, 5, 8.*

F286

The Global Burden of Vertebral Fracture. C. Cooper[1], O. Johnell[2], P. Lips[3], L. J. Melton[4], J. A. Kanis[5]. [1]MRC Environmental Epidemiology Unit, University of Southampton, Southampton, United Kingdom, [2]Malmo General Hospital, Malmo, Sweden, [3]Vrije Universiteit Medical Center, Amsterdam, Netherlands, [4]The Mayo Clinic, Rochester, MN, USA, [5]Sheffield University Medical School, Sheffield, United Kingdom.

Vertebral fractures are recognised as a hallmark of osteoporosis, yet their global burden has not been characterised. A large number of epidemiological studies have now been performed that use consistent methods for the definition of incident morphometric deformities. We have performed a systematic review of these studies which permit characterisation of the global burden of morphometric vertebral deformity; the proportion of these deformities that come to clinical attention; and estimates of the global cost. The figure illustrates age and sex-specific incidence rates of morphometric vertebral deformities among men and women aged ≥ 50 years from various studies around the world. The application of these incidence rates to the global population suggests that around 4.67 million incident vertebral deformities occur worldwide among men and women aged ≥ 65 years each year; 1.34 million among elderly men, and 3.33 million among elderly women. The rate at which incident vertebral deformities come to clinical attention varies in the literature. Sensitivity analyses suggests that as many as 1.4 million of these deformities may come to clinical attention each year; however, ascertainment levels in some populations vary, such that this number may be as low as 373,000 annually. The minimum annual cost of vertebral fracture worldwide is estimated at $2.4 billion.

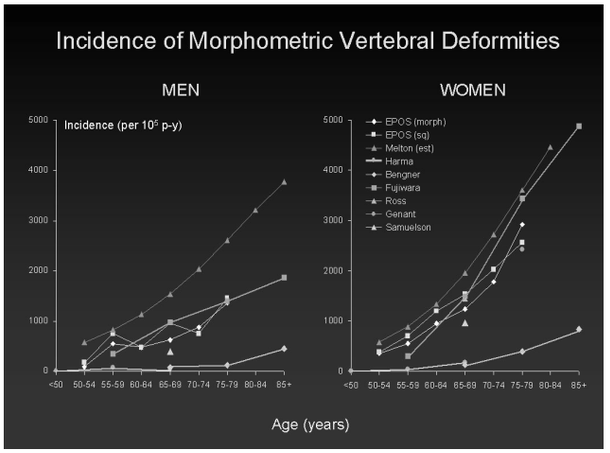

F288

Reducing Risk of Vertebral Fracture Through Specific Back Exercises: A Long Term Follow-up. M. Sinaki[1], E. Itoi*[2], H. W. Wahner*[3], P. Wollan*[4], R. Gelczer*[5], B. P. Mullan*[3], D. A. Collins*[3]. [1]Physical Medicine and Rehabilitation, Mayo Clinic, Rochester, MN, USA, [2]Department of Orthopedic Surgery, Akita University School of Medicine, Akita, Japan, [3]Nuclear Medicine, Mayo Clinic, Rochester, MN, USA, [4]Biostatistics, Mayo Clinic, Rochester, MN, USA, [5]Diagnostic Radiology, Mayo Clinic, Rochester, MN, USA.

The long-term protective effect of strong back muscles on reducing the risk of vertebral fractures in healthy Caucasian postmenopausal women was assessed. Fifty women, aged 58 to 75 years, who had completed a 2-year, randomized controlled trial 10 years earlier, were reassed. Of these, 27 had previously performed progressive, resistive back strengthening exercises for 2 years and 23 had served as controls. Bone mineral density (BMD), spine radiographs, back extensor strength (BES), biochemical marker values, and level of physical activity (PA) were obtained on all subjects at baseline, 2 years, and 10 years. Mean BES in the back exercise (BE) group was 39.4 kg at baseline, 66.8 kg at 2 years (after 2 years of prescribed exercises), and 32.9 kg at 10 years (8 years after cessation of the prescribed exercises). Mean BES in the control (C) group was 36.9 kg at baseline, 49.0 kg at 2 years, and 26.9 kg at 10 years. The difference between the 2 groups was still statistically significant at 10-year follow-up (P = 0.001). PA was not significantly different between the 2 groups at baseline. At 10-year follow-up PA was lower in both groups but still significantly higher in the former BE group (P = 0.0106). The difference in BMD, which was not significant between the 2 groups at baseline and 2-year follow-up, was significant at 10-year follow-up (P=0.0004). The incidence of vertebral compression fracture at 10-year follow-up was 14 fractures in 322 vertebral bodies examined (4.3%) in the C group and 6 fractures in 378 vertebral bodies examined (1.6%) in the BE group (Chi square test, P = 0.0290). The relative risk for compression fracture was 2.7 times greater in the C group than in the BE group. We conclude that strong back muscles can reduce the risk of vertebral fractures in estrogen-deficient women.

F290

Sleep and Nap Habits Predict Falls, Fractures and Mortality in Older Women. K. L. Stone[1], S. K. Ewing*[1], D. C. Bauer[1], J. C. Cauley[2], S. Redline*[3], S. Ancoli-Israel*[4], K. E. Ensrud[5], T. A. Hillier[6], S. R. Cummings[1]. [1]Univ of California, San Francisco, CA, USA, [2]Univ of Pittsburgh, Pittsburgh, PA, USA, [3]Case Western Reserve Univ, Cleveland, OH, USA, [4]Univ of California, San Diego, CA, USA, [5]Univ of Minnesota, Minneapolis, MN, USA, [6]Kaiser Ctr for Health Research, Portland, OR, USA.

Sleep disturbances are very common in the elderly. Insomnia and other sleep disorders have been associated with poor cognitive function and other risk factors for falls, fractures and mortality. Napping is a marker of sleep disorders, such as sleep apnea, that cause daytime sleepiness. Disturbed sleep alters circadian rhythms and hormone levels and may increase the risk of age-related diseases, such as osteoporosis. During the fourth exam (1993-4) of the Study of Osteoporotic Fractures (SOF), we administered a brief questionnaire to assess sleep and nap habits in 8,101 women aged 69 and older. We examined the relationship of self-reported sleep and nap habits with subsequent risk of falls, fractures and mortality. During 6.7 years of follow-up we observed 553 hip fractures and 1,922 deaths. 913 women (11%) reported suffering 2 or more falls during the year after the fourth exam. Daily napping (DN) was reported in 11% of participants, while insufficient sleep (IS) was reported among 26%. Short (< 6 hours) and long (> 8 hours) night-time sleep were reported in 13% and 10% of women, respectively. In multivariable models adjusting for age, BMI, health status, depression, cognitive function, selected medication use, and personal health habits, those who reported DN were 40% more likely to report two or more falls during the year after Exam 4 (Relative Risk=1.4; 95% CI= 1.1 - 1.7), had a 30% increase in risk of hip fracture (RR=1.3; 1.0 - 1.8) and 50% higher mortality risk during follow-up (RR=1.5; 1.3 - 1.7) than others. IS was associated with subsequent risk of falls (RR=1.2; 1.0 - 1.4) but did not predict mortality or fracture risk. Self-reported duration of sleep was not independently associated with any of the outcomes studied. Impaired sleep, marked by daily napping, is a common and often treatable risk factor for falls, hip fracture, and mortality. More objective and comprehensive assessments of sleep patterns are underway in SOF, so that we may further examine the associations of sleep disorders and these outcomes.

F292

Women with Incident Hip Fracture and Baseline BMD T-score >-2.5 Have Fewer Risk Factors than those with Fracture and Lower BMD. S. A. Wainwright*[1], L. M. Marshall*[1], M. T. Vogt[2], T. A. Hillier[3], J. A. Cauley[2], D. M. Black[4], M. C. Hochberg[5], E. S. Orwoll[1]. [1]Oregon Health & Science University, Portland, OR, USA, [2]University of Pittsburgh, Pittsburgh, PA, USA, [3]Kaiser Permanente Center for Health Research, Portland, OR, USA, [4]University of California, San Francisco, CA, USA, [5]University of Maryland, Baltimore, MD, USA.

Many older women who experience hip fracture have baseline BMD T-scores > -2.5. For instance, 54% of women (age 65 and over) with incident hip fracture over 5 years in the Study of Osteoporotic Fractures (SOF) had baseline total hip BMD T-score > -2.5. To establish the characteristics of these women and to test the hypothesis that they have other important risk factors for fracture, we analyzed data from SOF. Baseline demographics, medical history, activity, fall frequency, strength, and vision were assessed and total hip BMD was measured using DXA. Ascertainment of incident, nontraumatic hip fractures began at the time of BMD measurement and continued for five years. Hip fracture cases were divided into a higher BMD group (total hip BMD T-score >-2.5) and a lower BMD group (BMD T-score ≤ -2.5). We compared case characteristics in the higher versus lower BMD groups, using appropriate statistical tests for difference. In 5 years of follow-up, 131 hip fractures occurred in 6667 participants in the higher BMD group and 111 occurred in 1398 participants in the lower BMD group, yielding incidence rates of 4.1/1000 person-years and 17.5/1000 person-years respectively. Hip fracture cases in the higher BMD group were younger (mean 76.3 vs 78.1 yrs); had greater weight (mean 67.3 vs 58.0 kg), knee height, and BMI; better distance depth perception, contrast sensitivity, mental status, grip strength, and knee extension force; and lower frequency of weight loss since age 25 (yes/no) than those in the lower BMD group. There was a tendency toward lower frequency of previous fracture in the higher BMD group. The groups were not different with regard to history of maternal hip fracture, weekly activity, weighted lifetime activity, being on one's feet less than 4 hours each day, inability to rise from a chair without using one's arms for support, and any falls in the last year. In summary, many elderly women with hip fracture have baseline BMD T-scores > -2.5. While we postulated that women with higher BMD and fracture are older, more frail, more likely to fall, and more likely to have a family history of fracture, our results do not support these hypotheses. In fact, many of these risk factors are more common in women with lower BMD (T-scores ≤ -2.5). The pathophysiology of fracture in women with higher BMD is obscure. Understanding more about this group is essential to direct appropriate prevention and treatment strategies.

F295

The Use of Magnetic Resonance Imaging to Diagnose Occult Fractures of the Femoral Neck. K. M. Sanders*. Clinical & Biomedical Sciences, The University of Melbourne, Geelong, Australia.

While increased awareness and treatment of people with osteoporosis will help reduce the occurrence of hip fractures, prompt comprehensive treatment at the time of fracture will help maximise functional recovery. It can be difficult to diagnose a femoral neck fracture on plain radiograph in the elderly due to low bone density or the technique used to take the radiograph. In the acute setting a nuclear bone scan may involve a delay of up to 72 hours. If an occult hip fracture is not detected, displacement can occur with an associated increased risk of prolonged incapacity, avascular necrosis and non-union resulting in escalated health costs and morbidity. Magnetic resonance imaging (MRI) was performed on 76 patients (mean age (years), range; 83.6 {45.1, 101.5}) who presented with clinical features suggestive of a hip fracture but had negative plain radiographs (anterior-posterior and cross-table lateral). Patients were imaged in a flexible phased-array body coil wrapped around the pelvis, with images showing the pelvic girdle, both hips and the proximal femur. Twenty-seven patients (36%) presenting with suspected hip fracture but with negative plain radiographs were subsequently found to have a fractured neck of femur with MRI. This represents 5.6% of all hip fracture cases treated at our acute hospital between July 1997 and February 2000. None of the 49 patients in whom a hip fracture was not detected subsequently presented with this type of fracture within two months of the MRI scan. There was minimal delay in establishing a diagnosis through the use of MRI as 52 patients (68%) had their scan performed within 24 hours of their presentation. Failure to detect an occult hip fracture can lead to disastrous results with subsequent displacement. MRI is an effective means of detecting these fractures allowing early and accurate diagnosis.

F297

Spine, Hip, Wrist and Rib Fractures are Strongly associated with Stiffness Index measurement both in Early and in Late Postmenopausal Women. G. Crepaldi*[1], D. Maugeri*[2], G. Gandolini*[3], B. Frediani*[4], G. D'Avola*[5], G. Iolascon*[6], S. Gatto*[6], R. Giorgino[7]. [1]Internal Medicine, University of Padova, Padua, Italy, [2]Geriatrics, Ospedale Cannizzaro, Catania, Italy, [3]Fondazione Don Gnocchi, Milano, Italy, [4]Rheumatology, University of Siena, Siena, Italy, [5]ASL Catania 3, Catania, Italy, [6]Orthopaedics, Primo Policlinico, Naples, Italy, [7]Procter&Gamble Health Care, Rome, Italy.

A multicenter population based study was conducted in order to relate the prevalence of osteopenia and osteoporosis with personal fracture history in the Italian general female population. Eighty-three University and Hospital centers located over 18 out of 21 Italian peninsular and insular regions participated to the study. Subjects were randomly invited to participate from 1,536 General Practitioners through their own Patients Directory by a specific randomization protocol: reasons of decline were accurately recorded. . Eleven thousands-eleven females aged 40-79 were enrolled for the study: each woman underwent a bone quantitative ultrasound measurement on a Lunar Achilles Express. Personal history for clinical vertebral, hip, rib, wrist and other low-trauma fractures (occurred after the age of 50) was recorded. The table below shows the proportion of 7,441 postmenopausal women who reported an history of fractures according to age and Stiffness T-score categories.

Decade	50-59 years			60-69 years			70-79 years		
T-score	>-1	<-1, >-2.5	<-2.5	>-1	<-1, >-2.5	<-2.5	>-1	<-1, >-2.5	<-2.5
Cases	**1206**	**1366**	**480**	**711**	**1414**	**993**	**176**	**519**	**576**
All Fx	4.4%	9%	13.8%	13.9%	21.1%	28.9%	22.7%	29.1%	34.7%
Spine Fx	0.4%	0.7%	1%	1.4%	2.1%	3.8%	1.1%	3.1%	5.4%
Hip Fx	0.1%	0.1%	0.4%	0.1%	0.9%	1.8%	0.1%	1.7%	4.2%
Rib Fx	0.5%	1.1%	1.5%	1.7%	2.2%	2.8%	2.3%	2.7%	5.7%
Wrist Fx	0.8%	2.5%	3.8%	3.0%	6.0%	9.2%	8.0%	8.9%	12.2%
Other Fx	2.5%	5.3%	8.5%	8.7%	12.8%	16.8%	14.8%	17%	17.4%

The association between Stiffness Index and Fractures history was significant at all sites and in each decade. In particular the proportion of subjects with an history of hip fractures was about 4 times higher in 50-59 years aged osteoporotic subjects (T-score <-2.5) vs normals (T-score>-1), 18 times higher in the 60-69 decade, and 42 times higher in the 70-79 years aged osteoporotic group. This large population-based study establishes that Stiffness Index ultrasound measurements are strongly and significantly related to spine, hip, wrist and rib fractures either in early and in late postmenopausal women.

F300

Racial Differences in Bone Mineral Density in Older Men. A. George*[1], J. K. Tracy*[1], P. D. Wilson*[2], R. H. Flores*[1], M. C. Hochberg[1]. [1]Medicine, University of Maryland School of Medicine, Baltimore, MD, USA, [2]Epidemiology & Preventive Medicine, University of Maryland School of Medicine, Baltimore, MD, USA.

While several studies have examined factors associated with bone mineral density (BMD) in older white men, none have had sufficient numbers of older black men to allow for meaningful comparisons by race. The Baltimore Men's Osteoporosis Study (MOST) is a prospective cohort study designed to identify factors associated with low bone mass and bone loss in older men. 503 white and 191 black men aged 65 and above (mean [SD] 75.1 [5.8] and 72.2 [5.7] years, respectively) were recruited through mass mailings to holders of Maryland drivers licenses; 85% were veterans. All men completed a battery of self-administered questionnaires, underwent a standardized examination, and had BMD measured at the femoral neck (FN), lumbar spine (LS) and total body (TB) using a Hologic QDR-2000 and quantitative ultrasound (QUS) performed at the heel using a Hologic Sahara. Results (mean [SD]) by racial group are shown in the Table; all comparisons by race were significantly different with $P < 0.001$. Forty-three (8.6%) white and only 2 (1.0%) black men had osteoporosis at the FN as defined by WHO criteria. FNBMD was significantly correlated with LSBMD (R = 0.51), TBBMD (R = 0.62) and QUS Index (R = 0.34) when data from both groups of men were combined; correlations did not differ between racial groups. In multiple variable linear regression models, adjusted for age, height, weight, mean quadriceps strength, total calcium and vitamin D intake, alcohol consumption, smoking, physical activity in the past year and use of seizure medications, as well as all potential interactions, black men had significantly higher adjusted FNBMD than white men: mean adjusted difference (95% confidence interval) = 0.09 (0.07, 0.12) g/cm^2. This difference, corresponding to about 0.7 SD, may explain in part the reduced risk of hip fracture in older black compared to white men. Longitudinal measurememt of BMD as well as vertebral radiographs are currently being collected during the first annual followup visit.

BMD and QUS Index by Race in Older Men

Racial Group	Femoral Neck BMD	LumbarSpine BMD	Total Body BMD	QUS Index
White	0.75 (0.13)	1.09 (0.19)	1.18 (0.13)	94.0 (19.7)
Black	0.86 (0.15)	1.16 (0.20)	1.25 (0.13)	101.9 (23.7)

*Disclosures: **M.C. Hochberg**, Department of Veterans Affairs 2, 3.*

F302

Height Loss and Increased Risk of Osteoporosis in Men. E. A. Krall[1], J. J. Anderson*[1], D. R. Miller[2], R. Ferguson*[2], S. E. Rich*[1]. [1]Boston University, Boston, MA, USA, [2]Massachusetts Veterans Epidemiology Resource & Information Center, Boston, MA, USA.

Height loss is a risk factor for fracture, particularly of the spine. Height loss is usually inferred from self-reported height in young adulthood, which may be prone to recall error. We examined height loss in men in relation to osteoporosis status using heights recorded over 4 decades as part of a research study. The subjects are 353 participants in the VA Longitudinal Osteoporosis Research (VALOR) study who also participated in the VA Normative Aging Study (NAS) since 1962 and had >10 years of serial height measurements. Standing height was measured and recorded in tenths of an inch every three years between 1962 and 1998 (mean±SD time period=30±3 years, range=12 to 36) in the NAS. At the NAS baseline, mean age was 40±7 years, range 25 to 57. In 1998-2001, femoral neck, total femur, total radius and total body bone mineral density (BMD) were measured using DXA (model DPX-IQ, Lunar Corp., Madison, WI). Osteoporosis was defined as BMD 2.5 SD or more below the mean value of males age 20-29 years. Mean height loss by BMD status and odds ratios (OR) of osteoporosis were evaluated by analysis of covariance and logistic regression. Odds ratios were adjusted for age, current weight, smoking history, and years of follow-up. Current age of the men was 56 to 89 years (mean ±SD=72±7). Average height declined from 69.4±2.5 inches to 68.4±2.6 inches over the time period, for a mean individual loss of 1.0±0.7 inches. Fourteen percent of men were osteoporotic at any skeletal site, 53% osteopenic, and 33% normal. Prior height loss in men who were osteoporotic was 67% greater than in men who were normal or osteopenic (Table). Per one inch lost, the odds of osteoporosis at any site doubled (OR=2.0, 95% confidence interval, CI=1.2-3.3). Odds of osteoporosis at individual sites were similar: femoral neck, OR=1.9 (CI=1.1-3.4); total femur, OR=2.2 (CI=1.0-4.8); total radius, OR=2.0 (CI=1.1-3.6); and total body, OR=3.1 (CI=1.2-8.1). These results suggest that a relatively small amount of height loss is an indicator of increased risk of osteoporosis in men. Table 1.

Bone status at worst site	N	Mean ± SD Total height loss (inches)
Osteoporotic	49	1.5±0.9*†
Osteopenic	186	0.9±0.6†
Normal	118	0.8±0.5*

*† Means with matching symbols differ, p<0.001.

F304

Bone Mass in Men of African Heritage: Relative Contribution of Serum Androgens and Estrogens. J. M. Zmuda[1], J. A. Cauley[1], A. L. Patrick*[2], V. W. Wheeler*[2], C. H. Bunker*[1]. [1]Epidemiology, University of Pittsburgh, Pittsburgh, PA, USA, [2]The Tobago Regional Hospital, Scarborough, Trinidad and Tobago.

Recent population studies in older Caucasian men suggest that endogenous estrogens may be more strongly correlated with bone mass than androgens. However, the relative importance of sex steroid hormones for bone health among non-white men is less well defined. Thus, we evaluated associations among bioavailable testosterone (BT), bioavailable estradiol (BE) and bone mineral density (BMD) in 367 Afro-Caribbean men (age 40-91 yr; mean±SD, 57±12 yr) who were participants in the Tobago Bone Health Study. Hip and whole body BMD was measured with a Hologic QDR 4500 densitometer. BT and BE were measured in fasting morning serum samples by radioimmunoassay (Esoterix Endocrinology). BT and BE decreased 56% and 41%, respectively, between ages 40 and 80 yrs ($P<0.01$). Total hip BMD increased with increasing BT and was 0.5 standard deviations or 7% greater among men in the highest compared with lowest quartile independent of age, body weight and height (Table). In contrast, we found no significant association between BE and hip BMD. Similar results were observed for the sub-regions of the hip and whole body BMD. We conclude that in contrast to studies in Caucasians, bioavailable testosterone, but not bioavailable estradiol, is correlated with bone density among middle-aged and elderly Afro-Caribbean men. Table.Quartile of Serum Biovailable Sex Hormones and Total Hip BMD (g/cm^2) in Afro-Caribbean Men.

BT(ng/dl)	Hip BMD*	BE (pg/ml)	Hip BMD*
≤ 128	1.09 (.16)	≤ 16	1.13 (.17)
129-168	1.13 (.15)	17-22	1.12 (.15)
169-219	1.13 (.14)	23-28	1.13 (.14)
≥220	1.17 (.15)	≥ 29	1.14 (.14)
P (ANOVA)	0.02		0.62

*Values are mean (SD) and adjusted forage, weight, height.

F307

A Potentially Deleterious Role of IGFBP-2 on Bone Mineral Density in Aging Men and Women. S. Amin, E. J. Atkinson*, L. J. Melton, S. Khosla, A. L. Oberg*, B. L. Riggs. Mayo Clinic and Foundation, Rochester, MN, USA.

Insulin-like growth factors (IGFs) and their binding proteins (IGFBPs) are important regulators of tissue growth and metabolism, but their association with bone mineral density (BMD) is controversial. In an age-stratified, random sample of the adult community population, we assessed serum levels of IGF-I, IGF-II, IGFBP-1, -2 and -3, bioavailable estradiol (Bio E2) and testosterone (Bio T), and sex hormone binding globulin (SHBG); and measured total fat and skeletal muscle mass, and total hip BMD by DXA. The associations between the IGF/IGFBP system and hip BMD were assessed using regression models, before and after adjustment for age, sex steroids, SHBG, muscle and fat mass. Analyses were stratified by sex and by menopausal status in women. We studied 348 men (age range 23-90) and 276 women not on oral contraceptives or hormone replacement (age range 21-93; 166 postmenopausal). In men, lower IGF-I, IGF-II and IGFBP-3 were associated with lower hip BMD (r=0.21, 0.14, 0.12, respectively; $p < 0.04$). In postmenopausal women alone, similar associations were seen with IGF-1 and IGFBP-3 (r=0.23, 0.22; $p < 0.01$). In all men and women, higher IGFBP-2 correlated with lower hip BMD (r=-0.36, r=-0.53, respectively; $p < 0.001$) and was the strongest predictor of hip BMD among the IGFs and IGFBPs studied. In men and women, IGFBP-2 was correlated with age (r=0.55, r=0.45) and SHBG (r=0.60, r=0.53) but inversely correlated with all other covariates (r=-0.24 to -0.53; r=-0.29 to -0.39). IGFBP-2 remained an independent predictor of hip BMD after adjustment for age, Bio E2 and Bio T in both sexes. Both SHBG and muscle mass attenuated the association between IGFBP-2 and hip BMD in men and women, with the association being lost in men following adjustment for muscle mass. In women, but not men, adjustment for fat mass attenuated the effect of IGFBP-2 on hip BMD, particularly in premenopausal women where the association was lost. Associations of other IGFs and IGFBPs with hip BMD in men and postmenopausal women were similarly attenuated or lost with adjustments for age, SHBG, or muscle mass. Thus, among the IGFs and IGFBPs studied, we found IGFBP-2 to be a key negative predictor of total hip BMD in both men and women. Our findings suggest a potential role of the IGF/IGFBP system in regulating bone loss in aging men and women, and identify a previously unrecognized, potentially deleterious role for IGFBP-2, a known inhibitor of IGF action, which increases with age in both sexes. Whether the action of the IGF/IGFBP system on bone is mediated through its effects on fat and muscle mass, or SHBG, deserves further study.

Disclosures: ***S. Amin****, Merck & Co. 2.*

F309

Primary Care Resident Evaluations for Chronic Health Conditions: A Failure to Assess for Osteoporosis. A. Chhabra*[1], T. McNearney*[1], A. J. Shepherd*[1], N. Hussain*[1], N. Goel[2]. [1]University of Texas Medical Branch, Galveston, TX, USA, [2]University of Texas Medical Branch, Procter & Gamble Pharmaceuticals, Galveston, TX, USA.

Primary care residents routinely screen for hypercholesterolemia, hypertension, diabetes, and breast cancer in the at-risk population and institute therapy where appropriate. This prospective, single-blind, longitudinal, observational study tests the hypothesis that primary care residents at a university teaching hospital outpatient clinic evaluate their patients for osteoporosis at a rate less than that for other common diseases in the at-risk female population. The medical records of 122 new female outpatients 45 years or older seen by an internal or family medicine resident in their continuity clinics between 9/01 and 3/02 were reviewed. Data were collected on 1) risk factor assessment, 2) physical findings, 3) diagnostic tests ordered, and 4) treatment initiated for multiple common chronic health conditions. Additional data were obtained regarding the availability of information to the resident at the time of their evaluation which would identify patients for bone density screening by the Osteoporosis Risk Assessment Instrument (ORAI). Data analysis was performed by Fisher's exact test. A p value of < 0.05 was considered significant. Most of the outpatients were evaluated by a first or second year resident (32% and 54%, respectively). The median age of the patients was 58 years with an interquartile range of 14 years. Documented rates of screening, diagnosis, and therapy were 68% for hypercholesterolemia, 67% for breast cancer, 51% for hypertension, and 49% for diabetes mellitus. In marked contrast, screening or evaluation for osteoporosis was documented in only 5% of patients ($p < 0.001$ compared to hypertension or hypercholesterolemia). Risk factors widely considered contributory to osteoporosis were addressed or documented as part of the general work-up with variable frequency: estrogen use 47.2%, postmenopausal 50%, supplemental calcium 22%, prior fracture 5%, smoking 85%, ethanol use 78%, thyroid disease 30%. ORAI scores of 9 or above were obtained in 34.1% (n=41) of the 120 patients with sufficient information for ORAI scoring by an independent evaluator. Among those at-risk patients, only 24.4% (n=10) had a BMD ordered. In conclusion, primary care residents at a university teaching hospital outpatient clinic assess at-risk female patients for osteoporosis at a rate far below the rates for other common health conditions. The impact of specific interventions to increase primary care resident awareness of the diagnosis and treatment of osteoporosis will be determined next.

Disclosures: ***A. Chhabra****, Procter & Gamble Pharmaceuticals 2.*

F311

The Impact of Cyclooxygenase Selectivity on Bone Loss: The Health ABC Study. L. D. Carbone[1], F. A. Tylavsky[2], J. A. Cauley[3], T. B. Harris*[4], D. C. Bauer*[5], K. D. Barrow*[2], S. B. Kritchevsky*[2]. [1]Medicine, University of TN, Memphis, TN, USA, [2]Preventive Medicine, University of TN, Memphis, TN, USA, [3]Epidemiology, University of Pittsburgh, Pittsburgh, PA, USA, [4]National Institute of Aging, Bethesda, MD, USA, [5]Prevention Sciences Group, UCSF, San Francisco, CA, USA.

Nonsteroidal Anti-Inflammatory Drugs (NSAID) could potentially influence BMD by affecting the production of prostaglandins involved in the bone remodeling cycle. Cross-sectional evidence suggests that the relative selectivity of cyclooxygenase (COX) 1 and 2 of NSAIDs may have an impact on BMD, and the use of aspirin (ASA) may blunt the effect of COX-2 selective NSAIDs. The objective of this study was to examine the effects by relative COX selectivity both with and without concomitant aspirin (ASA) use on changes in BMD of the total hip over two years. Participants enrolled in the Health, Aging and Body Composition Study (Health ABC) who consistently reported using NSAIDS, ASA or no use of NSAIDS or ASA at baseline, year 1 and year 2 follow-up visits were included in this analyses. 1134 individuals (40% African- American, 56% Male, Mean age at baseline=73.6 years) were grouped for analysis according the COX selectivity of NSAID used, with or without the use of aspirin. BMD of the total hip by DXA was assessed at baseline and after 2 years of follow-up. After adjustment for potential confounders, those with consistent use of COX-2 showed an increase in BMD compared to little or no change in the other groups. (Table I, Mean +/-SEM).

Analysis Group	Baseline BMD (g/cm2)	Year 3 BMD (g/cm2)	Percent Change (%)
Nonuser (N=658)	0.890 +/- 0.006	0.888 +/- 0.006	-0.28 +/- 0.12*
Relative COX-1 Selective NSAID only user (N=55)	0.902 +/- 0.019	0.902 +/- 0.020	0.14 +/- 0.42
Relative COX-2 Selective NSAID only user (N=14)	0.873 +/- 0.038	0.885 +/- 0.039	1.43 +/- 0.82
Aspirin only user (N=37)	0.901 +/- 0.007	0.899 +/- 0.008	-0.27 +/- 0.16*
Relative COX-1 and Aspirin user (N=21)	0.945 +/- 0.031	0.939 +/- 0.032	-0.57 +/- 0.67
Relative COX-2 and Aspirin user (N=9)	0.914 +/- 0.048	0.916 +/- 0.049	0.28 +/- 1.04

* P<0.05 compared to relative COX-2 selective NSAID only users **Adjusted for gender, race, age at baseline, study site, History of rheumatoid arthritis,

History of osteoarthritis, Womac score at baseline, Vitamin D supplementation, Calcium supplementation, oral estrogen use, and weight change from baseline to year 3 Our results suggest that the consistent use of COX-2 selective NSAIDS may have a small but potential benefit on BMD of the hip. In addition, there is insufficient power to evaluate whether ASA blunts this benefit. These preliminary results will need to be replicated in a larger sample with a longer duration of follow-up.

Disclosures: ***L.D. Carbone****, Merck 8; Proctor and Gamble 8.*

F314

Decreased Osteocyte Density Is Relevant to Fragility Fracture. S. Qiu*[1], D. Rao[2], S. Palnitkar*[2], A. Parfitt[3]. [1]Bone and Mineral, Henry Ford hospital, Detroit, MI, USA, [2]Bone and Mineral, Henry Ford Hospital, Detroit, MI, USA, [3]Division of Endocrinology and Center for Osteoporosis and Metabolic Bone Disease, University of Arkansas for Medical Sciences, Little Rock, AR, USA.

The objective of this study was to test the hypothesis that the decreased osteocyte density is a factor in the etiology of fragility fracture. Iliac bone biopsies were performed in 144 postmenopausal white women, aged 50 to 73 years. Of them, 66 were healthy subjects and 78 suffered from nontraumatic vertebral fracture not just deformity. Conventional bone histomorphometry was conducted for all the subjects. Osteocyte density was measured in 56 of healthy and 44 of fracture subjects due to the fair quality of cell stain in these sections. Receiver operating characteristic (ROC) curve was used to discriminate fractured patients from healthy subjects by cancellous bone volume fraction (BV/TV), trabecular thickness (Tb.Th) and osteocyte density in superficial bone (Ot.N/B.Ar(s)) (<25µm from the bone surface), deep bone (Ot.N/B.Ar(d)) (>45µm from the bone surface) and whole trabecula (Ot.N/B.Ar(w)). The results are shown in table 1 (in p* column: p values are for area comparison with indicated variable numbers; all p values < 0.001). Conclusion: The results suggest that the risk of fragility fracture may be increased in the subjects with deteriorated bone architecture and osteocyte network. According to the area under the ROC curve, a decrease in cancellous osteocytes has a closer relationship with vertebral fragility fracture than decreased cancellous bone volume and trabecular thickness, although both of them have been regarded as major insults to bone strength. Our data indicate that the decrease in osteocyte density contribute to bone fragility independent of bone volume. Moreover, the decrease in osteocytes in superficial cancellous bone may play important role in producing fragility fracture.

Table 1. Data from ROC analysis

Variables	Sensitivity (%)	Specificity(%)	Area (%)	p*
1) BVTV (%)	85.5	56.1	76.9	1 vs 2, 3 & 4
2) Tb.Th (µm)	80.3	50.0	63.8	2 vs 3 & 4
3) Ot.N/B.Ar(w) (/mm²)	74.4	96.3	92.2	3 vs 5
4) Ot.N/B.Ar(s) (/mm²)	90.7	85.2	93.1	4 vs 5
5) Ot.N/B.Ar(d) (/mm²)	53.5	81.5	71.1	

F321

Tumor Necrosis Factor Alpha but not Interleukine-1 Is involved in Protein Undernutrition-Induced Bone Resorption. P. Ammann[1], C. Gabay*[2], G. Palmer*[2], I. Garcia*[3], R. Rizzoli[1]. [1]Department of Internal Medicin, Division of Bone Diseases, Geneva-14, Switzerland, [2]Department of Internal Medicin, Division of Rheumatology, Geneva-14, Switzerland, [3]Department of Pathology, Geneva-14, Switzerland.

Bone loss resulting from protein undernutrition is related to an uncoupling in bone turnover with increased bone resorption and decreased bone formation. Tumor Necrosis Factor Alpha (TNF) and Interleukine-1 (IL-1) could be involved in the increased bone resorption. We studied the effects of isocaloric low (2.5%) or normal (15%) protein diets in 6-month old female transgenic mice (Tg), either expressing high levels of soluble tumor necrosis factor receptor-1 fusion protein (TNFR1) which blocks the actions of TNF or IL-1 receptor antagonist (IL-1Ra) which blocks IL-1. Respective negative littermates TNFR1 and IL-IRa (NegLit) were used as controls. We measured bone strength (integrating all the modifications of bone structures) at skeletal sites containing cortical and trabecular bone (proximal tibia) or mainly cortical bone (midshaft tibia), and bone mineral density (BMD) before and after 12 or 16 weeks of low/normal protein diets, in IL-1Ra or TNFR1 Tg and their Neglit, respectively. Isocaloric low protein diet was associated with similar decreases in IGF-I (-47 to -57%) and osteocalcin (-37 to -51%) in all animals. Whereas proximal tibia bone strength was significantly decreased in NegLit (13.1±1.8* vs 23.3±2.8N) but not in TNFR1 Tg (19.0±3.0 vs 22.2±1.3), it was significantly decreased in both NegLit (8.5±1.0* vs 19.6±0.9N) and IL-1Ra Tg (7.3±1.0* vs 20.1±0.9). Similar trend was observed at the midshaft tibia. BMD decrease (in % of pretreatment values) was less pronounced in TNFR1 Tg (-6.4±3.1* vs +7.9±5.4) than in their NegLit (-19.6±2.6*# vs +7.0±3.6%) (*p<0.05 vs 15%; # vs 2.5% NegLit by ANOVA, x±SEM), but of similar magnitude in IL-IRa Tg (-27.5±3.9* vs -10.9±3.6) and in their NegLit (-20.9±3.2* vs –6.0±1.6). Midshaft diameter was lower in protein-undernourished TNFR1 and IL-1Ra Tg suggesting a reduced periosteal apposition. Thus, blocking TNF attenuated the increase in bone loss and the decrease in bone strength induced by protein undernutrition. In contrast, blocking IL-1 did not modify this response. Decrease IGF-I and osteocalcin, and possible depressed periosteal apposition were observed in TNFR1 and IL-1Ra Tg suggesting a reduced bone formation. This suggests that TNF but not IL-1 might play a role in increased bone resorption caused by an isocaloric low protein diet but not in the depressed bone formation. This underlines the bone catabolic role of TNF during protein undernutrition.

F325

Trial to Predict the Risk of Vertebral Compression Fractures in Patients Treated with Glucocorticoid. M. Yamauchi*, T. Makino*, H. Sowa*, T. Yamaguchi, T. Sugimoto, K. Chihara*. Division of Endocrinology/Metabolism, Neurology and Hematology/Oncology, Kobe University Graduate School of Medicine, Kobe, Japan.

Since vertebral compression fractures associated with glucocorticoid (GC)-induced osteoporosis is one of major problems in patients treated with GC, it would be clinically useful if fracture risk could be predicted. In the present study, anthropometric indices, bone mineral density (BMD) as well as biochemical bone markers were compared between patients with (Fx+) and without vertebral compression fractures (Fx-) and we further tried to predict the fracture risk in patients treated with relatively high dose of GC for the long duration. Subjects were 62 women aged 24 to 74 (mean 48 years) who were treated with predonisolone (PSL) [means of average daily dose and total dose: 13.6mg and 27.3g, respectively] for more than 6 months (mean 87.2 months), because of collagen diseases except rheumatoid arthritis as well as myasthenia gravis disease. 15 patients had more than one vertebral compression fractures. Regional BMD values of lumbar spine (L2-4), femoral neck (FN) and distal one-third of radius (R1/3) were measured by DXA. Mean BMD values (mean Z-scores) of L2-4, FN and R1/3 were 0.827 (-0.7), 0.640 (-0.6) and 0.600g/cm^2(+0.5), respectively, indicating preferential loss of trabecular bone. Z-score of FN was negatively correlated with total PSL dose and positively correlated with serum osteocalcin (BGP) level. Age, serum ALP and urinary deoxypyridinoline levels were significantly higher in Fx+ group, compared with Fx- group, while body height, body weight, handgrip strength as well as Z-score of FN and BGP level were significantly lower. Receiver Operating Characteristic (ROC) and logistic regression analyze were performed to select indices which discriminated Fx+ from Fx- most effectively. In these analyze, handgrip strength, FN BMD and BGP level were selected [sensitivity-specificity and odds ratio (95%CI): 75%, 73%, 65% and 0.37(0.16-0.90, p=0.03), 0.31(0.13-0.75, p=0.009), 0.21(0.07-0.61, p=0.004), respectively]. ROC analysis revealed that cut-off values of BMD that discriminated Fx+ from Fx- were 0.783, 0.599 and 0.592 g/cm^2 for L2-4, FN and R1/3, respectively. These values were all higher, compared with cut-off values obtained from 205 postmenopausal healthy women [48~84 years (mean 64), numbers of Fx+ subjects: 66] (0.691, 0.570 and 0.444g/cm^2). In conclusion, FN BMD, handgrip strength and BGP level are clinically useful to predict the risk of vertebral compression fractures in women treated with GC and bone of GC-treated patients would have severer fragility than estimated from BMD value.

F327

Prevalence of Sex Steroid Deficiency in Men Receiving Systemic Glucocorticoids. S. J. A. Goemaere[1], K. Toye*[1], M. Daems*[1], D. De Bacquer*[2], J. M. Kaufman[1]. [1]Unit for Osteoporosis, Ghent University Hospital, Gent, Belgium, [2]Dpt of Public Health, Ghent University Hospital, Gent, Belgium.

Glucocorticoid excess in men can result in sex steroid deficiency, however also in lower serum sex hormone binding globulin (SHBG) levels, with better preservation of biological active hormone fractions. There have been few systematic evaluations of the prevalence and severity of sex steroid deficiency in men under glucocorticoid therapy. We analysed the sex steroid status of 174 men (median age: 59y; P25-P75:47-68y) receiving long-term glucocorticoid (GC) treatment (prednisolone equivalent dose ≥ 7.5 mg/day) for dermatologic (12%), rheumatologic (54%), pulmonary (18%), gastrointestinal (9%) or other (7%) diseases and participating in a clinical trial on prevention and treatment of glucocorticoid induced osteoporosis (GIOS) with alendronate* (Saag et al, N Engl J Med 339: 292, 1998). Testosterone (T), estradiol (E2) and SHBG were determined by immunoassay in serum obtained at the base-line visit. Free T (FT) and E2 (FE2) were calculated using a validated equation. For comparison we examined a healthy young (n=107, age 20-39y) and an age-matched (n=174) male reference group. The proportion of patients with serum levels below the 5th percentile for young controls was 71 and 68% for T and FT, 19% for SHBG, 25 and 21% for E2 and FE2. Compared to age-matched controls, the median decrease in patients was 34%, 22%, 31%, 19% and 5% , respectively for T, FT, SHBG, E2 and FE2. The prevalence of values below the 2.5 percentile for matched controls was 25%, 14%, 9%,19% and 12%, respectively. The difference between patients and controls increased by increasing actual GC dose for T, FT and E2 (p=0.04 to 0.004; p=0.06 for FE2) and was not significantly affected by the cumulative dose or duration of the GC treatment. Alcohol use and disease category significantly affected the (F)E2 levels. After adjustment for age, BMI, albumin and creatinine the actual dose remained significantly negatively correlated with absolute hormone levels and deviations of patients from controls (r ranging from -.14 to -.34). The observed difference in sex steroid levels did not correlate with biochemical indices of bone turnover, as assessed by urinary NTX and serum BAP. In conclusion, a considerable proportion of patients receiving systemic GC therapy have sex steroid levels ((F)T and (F)E2) below the reference for young men, but the prevalence is lower compared to age-matched controls. The observed effects are dose dependent. These findings constitute the background for the need of prospective data (re)evaluating the contribution of sex steroid deficiency in the pathogenesis of GIOS in men.*Manufactured by Merck & Co., Inc., Whitehouse Station, NJ

F330

Increased T Cell Proliferation and Lifespan through Enhanced Expression of Interferon Gamma and Class II Transactivator Mediate Ovariectomy Induced Bone Loss. S. Cenci, C. Roggia, G. Toraldo, M. N. Weitzmann, Y. Gao, O. Sierra, W. Qian, R. Pacifici. Bone and Mineral Diseases, Washington University School of Medicine, St. Louis, MO, USA.

Expansion of the pool of TNF-producing T cells in the bone marrow (BM) is critical for the bone wasting effect of estrogen deficiency, but the responsible mechanism is unknown. In vivo BrdU incorporation studies in mice revealed that ovariectomy (ovx) increases T cell number by upregulating T cell proliferation and by decreasing T cell apoptosis. Increased T cell proliferation results from enhanced activation induced by an increase in the activity of macrophages as antigen-presenting cells (APC), due to augmented MHCII expression. We also found that ovx decreases T cell apoptosis by suppressing Fas ligand (FasL) expression in response to activation. Class II transactivator (CIITA) is the master regulator of MHCII expression and APC activity in macrophages and of activation-induced FasL expression in T cells. By RT-PCR, CIITA mRNA was found to be increased threefold by ovx both in macrophages and in T cells, thus identifying a key mediator of the control of T cell activity exerted by estrogen in vivo. Production of interferon-gamma (IFN-gamma), the physiologic inducer of CIITA, by T helper cells was found to be higher in ovx mice, as assessed by ELISA and FACS, thus providing a mechanism for increased CIITA expression in target cells. Increased T cell secretion of IFN-gamma was repressed in vitro by a selective inhibitor of the MAP kinase p38, indicating that induction of IFN-gamma by ovx is cytokine-driven. Indeed, ovx was found to stimulate macrophagic production of IL-12 and IL-18, the physiologic inducers of T cell IFN-gamma production, thus defining a mechanism whereby estrogen regulates IFN-gamma in vivo. To assess if enhanced IFN-gamma and CIITA mediate the effects of ovx on T cell and bone homeostasis in vivo, we sought to block both IL-12/18-induced IFN-gamma production, and IFN-gamma induced CIITA expression. As CIITA, IL-12 and IL-18 are all specifically induced by IFN-gamma via IFN-gamma receptor (R) signaling, we utilized IFN-gamma R deficient (-/-) mice. In vivo blockade of IL-12/18 signaling and CIITA induction through silencing of IFN-gamma R resulted in failure of ovx to upregulate CIITA in macrophages and T cells, and to modulate T cell proliferation and apoptosis. As a result, ovx failed to increase the number of TNF producing T cells in the BM and to induce bone loss, as assessed by DEXA and histology, in IFN-gamma R -/- mice. Thus, upregulation of T cell proliferation and lifespan through increased IFN-gamma signaling and CIITA expression is critical for the bone wasting effect of estrogen deficiency.

F333

HIV Protease Inhibitor Indinavir Impairs Osteoblastic Bone Formation, in vivo and in vitro. M. W. H. Wang, S. Wei, S. L. Teitelbaum, F. P. Ross. Pathology, Washington University School of Medicine, St. Louis, MO, USA.

We and others have demonstrated previously that HIV protease inhibitor usage is associated with osteopenia in HIV infected individuals. To investigate the underlying mechanism for this observation, we tested the hypothesis that one or more HIV protease inhibitors block osteoblast differentiation and/or function. Two HIV protease inhibitors, nelfinavir and ritonavir, have no effect on bone nodule formation in vitro. In contrast, we find that indinavir, at a pharmacologically relevant concentration (5 μg/ml), arrests osteoblast bone nodule formation, decreases alkaline phosphatase activity, and impairs type I collagen synthesis. Congruent with the observation of impaired osteoblast maturation, alkaline phosphatase, PTH/PTHrP receptor, and osteocalcin gene expressions are dose dependently decreased with indinavir (1 and 5 μg/ml), while osteopontin, a matrix protein not specific to osteoblasts, is not affected. Confirming that the inhibition is not due to cell toxicity, the drug has no effect on the number, proliferation, or apoptosis of osteoblasts. Furthermore, systemic indinavir administration to mice leads to a ten fold decrease in osteoblast colony forming units ex vivo, indicating that the drug affects early osteoblast differentiation. Consistent with an early differentiation arrest, indinavir downregulates the gene expression of Cbfa1 and Osterix, both critical osteoblast transcription factors. To extend the effect of indinavir to bone in vivo, we administered the drug to 4 week old mice for 5 weeks and analyzed the skeleton. We find that indinavir treatment leads to a 17-20% decrease in bone mineral density by DEXA, a 50% decrease in proximal tibial trabecular bone volume, as assessed by bone histomorphometry, and a decrease in cortical and trabecular bone, as seen by Faxitron radiography. Furthermore, consistent with osteopenia resulting from an osteoblast defect, indinavir treatment dampens the mineral appositional rate (1.05 +/- 0.22 vs. 0.41 +/- 0.09; $P < 0.01$) and bone formation rate (571.9 +/- 60.8 vs. 179.3 +/- 42.3; $P < 0.01$) as determined by double fluorochrome labeling. Consistent with a cell type specific inhibitory effect, indinavir has no effect on osteoclast formation or function in vitro and in vivo. In sum, these findings indicate that the HIV protease inhibitor indinavir can lead to osteopenia by selectively impairing osteoblast maturation.

F337

Maintenance of Increased Bone Mass After Recombinant Human Parathyroid Hormone(1-84) with Sequential Zoledronate Treatment in Ovariectomized Rats. Y. Rhee*[1], S. Kim*[1], R. Namgung[2], R. Hwang*[3], S. Lim[1]. [1]Internal Medicine, College of Medicine, Yonsei University, Seoul, Republic of Korea, [2]Pediatrics, College of Medicine, Yonsei University, Seoul, Republic of Korea, [3]Internal Medicine, College of Medicine, Brain Korea 21 Project, Yonsei University, Seoul, Republic of Korea.

Anti-resorptive agents against osteoporosis have quite a limitation in the aspect of increasing bone mass to only with these agents. Strong anabolic agent such as human parathyroid hormone(PTH) is expected to be helpful. However, as PTH is only injectable, it would be practical to use both anti-resorptives and anabolic agents sequentially. To determine the effectiveness of the respective anti-resorptive agents after anabolic phase with the PTH to prevent the loss of bone mass, the maintenance therapy with estrogen or zoledronate was tested. Thirty 16 weeks-old virgin female Sprague-Dawley rats were used. Ovariectomy was done at 16 weeks of age then 5 weeks were given to have the osteopenic changes in the bones. Then each treatment was started at the age of 21 weeks for 5 weeks of recombinant human PTH(1-84) [rhPTH(1-84)] 100 mcg/kg/d*5 days/wk, then respective sequential therapy for 5 weeks. Groups were as follows ; 1) Ovariectomized rats (OVX) (n=6), 2) Sham operated rats (SHAM) (n=6), 3) PTH treated then withdrawn OVX rats (PTH-Veh) (n=6), 4) PTH maintained OVX rats (PTH-PTH) (n=6), 5) PTH treated OVX rats then treated with 17b-estradiol(E2) [10 mcg/d, SQ *5 days/wk] (PTH-E2) (n=6), 6) PTH treated OVX rats then treated with zoledronate(PTH-ZOL) [12.5 mcg/kg, SQ weekly] (n=6). Bone mineral density(BMD) of rt femurs were measured with dual x-ray absorptiometry(Hologic QDR 4500A, Waltham, MA). The μCT and software used for structural parameter of 2nd lumbar vertebrae are from Skyscan (Antwerpen, Belgium). Three-point bending test was done with material testing machine (Instron LTD, Buckinghamshire, England). The BMD of right femur and bone volume and trabecular thickness of L2 vertebrae were highest in the PTH-PTH and PTH-ZOL groups compared with OVX rats($p<0.05$). There was no significant differences in circumferential diameter, but the significant cortical thickening was observed in PTH-PTH group($p<0.05$). Maximal load at 3-point bending test was highest in PTH-PTH group($p<0.05$). In conclusion, PTH withdrawal resulted in loss of acquired BMD and sequential therapy with zoledronate prevented further loss as much as continuous PTH-treated rats. Therefore, it would be practical and beneficial to administer bisphosphonate after the gaining bone mass with PTH.

F339

Efficacy and Safety of Oral Weekly Ibandronate in the Treatment of Postmenopausal Osteoporosis (PMO). C. Cooper*[1], G. Hawker*[2], R. Emkey[3], R. McDonald*[4], R. Schimmer*[5], P. Mahoney*[5], K. Wilson*[5]. [1]Southampton General Hospital, Southampton, United Kingdom, [2]Sunnybrook and Women's College, Toronto, ON, Canada, [3]Radiant Research, Wyomissing, PA, USA, [4]University of Pittsburgh, Pittsburgh, PA, USA, [5]F. Hoffmann-La Roche Ltd, Basel, Switzerland.

Bisphosphonates are well established in PMO. However, these agents are currently associated with relatively stringent dosing guidelines that may be inconvenient to some patients and potentially result in reduced compliance. Reducing dosing frequency is predicted to increase convenience. The highly potent, nitrogen-containing bisphosphonate, ibandronate, has demonstrated strong reduction (62%) in vertebral fracture risk when administered once daily (Delmas P, et al. IOF World Congress on Osteoporosis 2002; abstract O37). Ibandronate has strong potential for intermittent administration: significant and lasting antifracture efficacy was observed when ibandronate was given with a dosing interval of >9 weeks. A multicenter, double-blind, randomized, non-inferiority study was initiated in 235 women (age 55-80 years; time since menopause at least 3 years) with PMO (lumbar spine bone mineral density [BMD] T-score <-2.0) to compare oral daily 2.5mg and once-weekly 20mg ibandronate. All patients received daily calcium (500mg) and vitamin D (400IU). The primary endpoint was the relative change in lumbar spine BMD after 48 weeks. Baseline characteristics were similar across both treatment arms. The daily and weekly dosing regimens produced similar increases in BMD and reductions in bone turnover. The mean increases in lumbar spine BMD at 48 weeks were 3.47% and 3.54% in the 2.5mg daily and 20mg once-weekly groups, respectively. The mean spine BMD difference (95% CI) between daily and weekly dosing was 0.07% (-0.96, 1.10). The boundary of the one-sided 97.5% confidence interval (-0.96%) of the observed differences in mean spine BMD between the two dosing regimens lay well above the pre-specified margin for non-inferiority (-1.65%) and met also more stringent non-inferiority criteria as subsequently set by Health Authorities (-1.1%). These results indicate that weekly dosing of ibandronate provides the same efficacy as daily dosing in women with PMO based on non-inferiority criteria. In addition, both regimens had similar safety profiles: the incidence of clinical adverse events (AEs), including upper gastrointestinal AEs, was comparable and no drug-related serious AEs were observed. In summary, once-weekly dosing of oral ibandronate is equally efficacious and tolerable as daily dosing, but provides the advantage of greater convenience. This added benefit may enhance compliance and, thus, improve therapeutic outcomes in women with PMO.

F341

Efficacy of Oral Ibandronate in Postmenopausal Osteoporosis: Incidence of Vertebral Fractures by Subgroup. M. Ettinger[1], R. Emkey[2], R. Schimmer*[3], P. Mahoney*[3], J. Kilbride*[3]. [1]Regional Osteoporosis Center of South Florida and Radiant Research, Stuart, FL, USA, [2]Radiant Research, Wyomissing, PA, USA, [3]F. Hoffmann-La Roche Ltd, Basel, Switzerland.

A multinational, randomized, double-blind, placebo-controlled phase III pivotal fracture study (BONE: Bonviva® Osteoporosis Trial in North America and Europe) recently compared daily and intermittent oral ibandronate regimens, which provide similar cumulative doses every 3 months (Delmas P, et al. IOF World Congress on Osteoporosis 2002; abstract O37). A total of 2,946 women with postmenopausal osteoporosis (PMO; at least 1 vertebral fracture [VF] at entry) were enrolled. Baseline characteristics were comparable across the three study arms. After 3 years, treatment with oral daily ibandronate 2.5mg resulted in a significant 62% reduction in the incidence of new VFs in the ITT population ($p=0.0001$). Even when administered intermittently with a dose-free interval of 9-10 weeks (20mg every other day for 12 doses at the start of each 3-month cycle), oral ibandronate significantly reduced the risk of VFs by 50% after 3 years ($p=0.0006$). Similar reductions in VF risk were observed after 2 years (daily, 61% [$p=0.0006$]; intermittent, 56% [$p=0.0017$]), indicating a robust and consistent efficacy without waning of effect over time. Ibandronate is the first oral bisphosphonate that has proven - prospectively, in a full ITT population - to offer antifracture efficacy from a regimen with a dose-free interval of 9-10

weeks. Highly significant risk reduction was consistently demonstrated in subgroups of patients who were at varying fracture risk, based on the number of prevalent VFs at baseline and the history of a previous clinical fracture (see Table). Both regimens of oral ibandronate were well tolerated and there were similar incidences of adverse events across all treatment groups. Thus, oral ibandronate provides clinically significant and lasting reductions in the incidence of new VFs for patients at low and high risk for new VFs, whether given daily or intermittently.

Subgroup	Placebo fracture rate (%) [n=975]	New VF risk reduction (%) 2.5mg (daily) [n=977]	CI	20mg (intermittent) [n=977]	CI
All patients	9.6	62		50	
Zero or 1 baseline VF	7.5	66	(27–84)	42	(–8–69)
≥2 baseline VFs	16.7	61	(34–77)	55	(24–73)
History of clinical fracture within 5 years of study	13.1	67	(24–85)	52	(–3–78)
No history of clinical fracture within 5 years of study	11	60	(33–76)	49	(19–68)

F343

Risedronate Significantly Reduces Moderate and Severe Vertebral Fractures by 70% in One Year. D. Felsenberg[1], D. A. Hanley[2], T. D. Johnson*[3], M. D. Manhart[3], H. K. Genant[4]. [1]Department of Radiology, University Hospital Benjamin, Berlin, Germany, [2]University of Calgary, Calgary, AB, Canada, [3]Procter & Gamble Pharmaceuticals, Mason, OH, USA, [4]University of California San Francisco, San Francisco, CA, USA.

We have analyzed data from the VERT studies to determine the vertebral fracture risk reduction with risedronate treatment on moderate or severe fractures in 1 year using the semi-quantitative assessment method of Genant et al (JBMR 1993; 8: 1137). In the VERT studies both quantitative and semi-quantitative methods were used to determine fractures. If these methods disagreed on the fracture status, adjudication was utilized to determine if a fracture was present. Overall efficacy results with this adjudicated method agreed with the results of semi-quantitative analysis alone. In the present analysis, the semi-quantitative method was used to determine fracture status and only moderate (a change from grade 0 to grade 2) or severe (a change from grade 0 to grade 3) fractures were used. The VERT studies enrolled patients with either low BMD (T-score < -2) and one prevalent vertebral fracture (VERT-NA) or patients with at least two prevalent vertebral fractures (VERT-MN). Patients were randomized to receive either placebo or risedronate 5 mg daily. All patients received 1 g/day calcium supplementation, and up to 500 I.U. vitamin D/day if serum 25-OH vitamin was low at baseline. Kaplan-Meier estimates were used to determine new fracture incidence. During the first year, 46 out of 992 (4.6%) patients experienced a new moderate to severe vertebral fracture in the placebo group compared to 14 out of 1002 (1.4%) in the risedronate-treated group. The risk reduction in moderate and severe vertebral fractures at 1 year was 70.7% (p<0.001). If all incident fractures, i.e., mild, moderate and severe were included in the analysis, there is a vertebral fracture risk reduction of 63.9% (p<0.01) at 1 year. The reductions in vertebral fracture risk were sustained over three years. Treatment with risedronate 5 mg daily results in significant vertebral fracture risk reduction, especially for moderate and severe vertebral fractures.

F345

Alendronate in the Prevention of Osteoporosis. P. N. Sambrook[1], J. P. Rodriguez[2], R. D. Wasnich*[3], M. M. Luckey[4], A. Kaur*[5], A. Lombardi[5]. [1]University of Sydney, Sydney, Australia, [2]Dept. Biologia Celular, Universidad de Chile, Santiago, Chile, [3]Hawaii Osteoporosis Center, Honolulu, HI, USA, [4]St. Barnabas Ambulatory Care Center, Livingston, NJ, USA, [5]Merck Research Laboratories, Rahway, NJ, USA.

In a 3-year study followed by a 2-year open-label extension, alendronate sodium (ALN)* maintained or increased bone mineral density (BMD) in 445 recently postmenopausal women with a spine BMD T-score > -2. In a second 2-year extension, 84 women previously treated with either 5 or 10 mg ALN daily during the first 3 years and 5 mg ALN during the first extension (Group A) were randomized to either 5 mg ALN or placebo (PBO). Another group of 59 women (Group B) received 20 mg ALN during the first 2 years, PBO during Year 3, and were then followed up without treatment during Years 4-7.

Group	Triple-Blind		Open-Label Extension	Triple-Blind Extension
	Years 1 and 2	Year 3	Years 4 and 5	Years 6 and 7 (N = 143)
A	ALN 5 mg	ALN 5 mg	ALN 5 mg	ALN 5 mg (N = 26) or PBO (N = 15)
	ALN 10 mg	ALN 10 mg	ALN 5 mg	ALN 5 mg (N = 29) or PBO (N = 14)
B	ALN 20 mg	PBO	Follow-up without treatment	Follow-up without treatment (N = 59)

Continuous ALN treatment for 7 years increased spine and trochanter BMD by 2.7-4.1% and 3.3-4.2%, respectively, while femoral neck and total body BMD were maintained. Patients switched to PBO during the last 2 years lost femoral neck and total body BMD, while spine and trochanter BMD remained stable. Among women who received ALN 5 mg during Years 4-7, those who had been treated with 10 mg ALN in the first 3 years had slightly greater increases in BMD at all sites at the end of the study, compared with women who received 5 mg ALN during the first 3 years. Women in Group B showed significant loss in BMD at all skeletal sites during Year 4-7, when they received no treatment. In conclusion, ALN 5 or 10 mg daily for up to 7 years prevents bone loss in recently postmenopausal women. Early postmenopausal women who discontinue ALN after 2 years of treatment experience significant bone loss at all skeletal sites. Patients initially started on 10 mg ALN appear to gain more BMD than those initially treated with 5 mg ALN. *Manufactured by Merck & Co., Inc, Whitehouse Station, NJ

Disclosures: ***P.N. Sambrook****, Merck & Co., Inc. 2.*

F348

Effectiveness of External Hip Protectors in Preventing Hip Fractures: A Randomized Clinical Trial. N. M. van Schoor*[1], J. H. Smit*[2], G. Asma*[3], L. M. Bouter*[1], P. Lips[3]. [1]Institute for Research in Extramural Medicine, VU University Medical Center, Amsterdam, Netherlands, [2]Department of Sociology and Social Gerontology, VU University, Amsterdam, Netherlands, [3]Department of Endocrinology, VU University Medical Center, Amsterdam, Netherlands.

The incidence of hip fractures is very high in institutionalized elderly. Hip protectors have been shown to be an effective preventive treatment option, but compliance remains a problem. A randomized clinical trial was performed to examine the effectiveness and compliance of external hip protectors (Safehip, Denmark) in preventing hip fractures. The participants were residents from nursing homes, homes for the elderly or apartment houses for the elderly, aged 70 years and over, with a low bone density and /or high fall risk. The inclusion criteria were: (1) broadband ultrasound attenuation 'BUA' ≤ 40; or (2) 40 < BUA ≤ 60 and two risk factors for falls; or (3) 60 < BUA ≤ 70 and three risk factors for falls. Based on previous research of our institute, we used the following risk factors for falls: fall in the previous half year, dizziness while standing up, stroke with consequences, urinary incontinence, cognitive impairment, low activity, low mobility. A member of the research team performed unexpected visits to assess the compliance at 1, 6 and 12 months after inclusion in the study. During these visits, it was checked whether the participant was wearing the hip protector and whether the hip protector was worn correctly (placed over the greater trochanter and protectors in good state). Furthermore, all participants and /or nurses were interviewed to assess the determinants of compliance. Of the 830 persons that were screened for risk of hip fracture, 561 persons had a high risk. These persons were assigned to the hip protector group (n=276) or control group (n=285) by individual randomization. After exclusion of the persons who died and other persons who could not be visited, the compliance was 61% after 1 month (n=217), 55% after 6 months (n=201) and 61% after 12 months (n=140). About 92% of the participants was wearing the hip protector correctly. By intention to treat, 18 persons from the hip protector group fractured a hip during the study period versus 20 persons from the control group. Only 4 persons from the hip protector group were actually wearing the hip protector while fracturing a hip. Per-protocol and subgroup analysis will be performed. To our knowledge, this is the first large trial, which has used individual randomization to assign persons to the intervention or control group. In this study, hip protectors were not effective in reducing the incidence of hip fractures.

Disclosures: ***N.M. van Schoor****, Praeventiefonds 2.*

F354

Interactive Effects of Hormone Replacement Therapy and Abdominal Fat on Bone Mineral Density: A Twin Study. L. M. Paton*[1], C. Margerison*[1], C. Nowson*[2], L. Lan*[1], S. Kantor*[1], B. Kaymakci*[1], J. D. Wark[1]. [1]Medicine, University of Melbourne, Melbourne, Australia, [2]Deakin University, Melbourne, Australia.

Hormone replacement therapy (HRT) maintains or increases bone mineral density (BMD) in postmenopausal women. In our studies of adult female twins, within-pair differences in BMD were associated with fat mass (FM) and lean mass (LM). Since soft tissue composition may influence the response to HRT, we used a co-twin design to examine interactive effects of HRT use and soft tissue composition as determinants of BMD. Lumbar spine (LS) and femoral neck (FN) BMD, total LM, total FM and abdominal fat mass (AFM) were measured by dual-energy X-ray absorptiometry in 127 pairs of healthy female twins aged 30-65 years (Group 1) and in 39 pairs, aged 42-88 years, reporting within-pair discordance for HRT use (Group 2). The strongest interaction was with total abdominal fat mass: for the FN, the within-pair difference (SE) in BMD increased from 4.7(1.9)%, P = 0.01, per kg of AFM in Group 1 to 14.1(3.1)%, P <0.001, per kg of AFM associated with HRT discordance in Group 2. Similarly, for the LS the within-pair BMD difference increased from 6.2(1.6)%, P <0.001, per kg of AFM in Group 1 to 11.6(3.2)%, P = 0.001, per kg of AFM in Group 2 twins. There was no within-pair difference in FM, AFM or LM in either group. In a multivariate model including age, FM and AFM in Group 2, AFM predicted the within-pair difference in LS BMD (16.7(5.9)%, P = 0.008, per kg) while FM was not associated significantly with BMD. This model explained 37% of the within-pair difference in BMD for Group 2. In Group 1, FM was predictive of the within-pair difference in LS BMD (0.7 (0.3)%, P = 0.035, per kg), while AFM was not associated with the within-pair difference in LS BMD. Further modeling including age, height, LM, FM and AFM supported these findings. Similar results were found for the FN. These finding demonstrate that the association between fat mass and BMD is enhanced in HRT-discordant twin pairs. Abdominal fat mass was identified as a powerful determinant of FN and LS BMD associated with HRT use. These effects suggest novel mechanisms by which HRT may influence bone mass.

F356

The Association between Changes in Bone Mineral Density (BMD) and Biochemical Markers of Bone Turnover at 1 Year with Vertebral Fracture Risk at 3 Years: Results from the Multiple Outcomes of Raloxifene Evaluation (MORE) Trial. S. Sarkar*, G. G. Crans*, M. Wong, K. D. Harper. Lilly Research Laboratories, Eli Lilly and Company, Indianapolis, IN, USA.

Although the association between baseline BMD and new fracture risk is well understood, the relationship between BMD change and fracture risk is less clear. We have previously demonstrated that BMD change was a poor predictor of vertebral fracture risk in raloxifene-treated women, explaining only a small proportion of the drug's efficacy [JBMR 17 (2002): 1-10]. Recently, Bjarnason et al., have shown that changes in bone turnover markers during raloxifene therapy were significantly associated with future fracture risk [Osteopor Int 12 (2001): 922-30]. In the current analysis, we consider prediction of vertebral fracture risk using changes in both BMD and bone turnover simultaneously, while controlling for important baseline variables. MORE was a randomized, placebo-controlled trial of 7705 women with osteoporosis treated with raloxifene 60 or 120 mg/d for 3 years [JAMA 282 (1999): 637-45]. Since markers of bone turnover were measured in one-third of the study population, the present analyses involve only these women. Logistic regression models were constructed utilizing one-year percentage changes in BMD and bone turnover, and relevant baseline demographics to predict the risk of vertebral fracture with pooled raloxifene therapy at 3 years. All covariates were standardized before modeling, to facilitate direct comparisons between changes in BMD and changes in bone turnover. Prevalent vertebral fracture status ($p<0.0001$), baseline lumbar spine BMD ($p<0.0001$), and number of years postmenopausal ($p=0.0005$) were significant. Therapy-by-change in femoral neck BMD interaction ($p=0.02$) and therapy-by-change in osteocalcin (OC) interaction ($p=0.01$) were also significant. These interactions indicate that changes in BMD and OC have different effects on fracture risk for the placebo and pooled raloxifene groups. To further investigate these interactions, models for pooled raloxifene and placebo were fit separately, using the above baseline variables and changes in BMD and OC. The final raloxifene model included each baseline variable and change in OC ($p=0.01$), while change in femoral neck BMD was not significant. In summary, baseline lumbar spine BMD, prevalent vertebral fracture status, and number of years postmenopausal were the most important baseline variables to predict vertebral fracture risk at 3 years. After adjustment of these baseline variables, the percentage change in OC appears to be a better predictor of fracture risk reduction with raloxifene therapy than the percentage change in femoral neck BMD.

Disclosures: ***S. Sarkar****, Eli Lilly and Company 3.*

F358

Endogenous Levels of Estrogen Determine the Response to Treatment with Hormone Replacement Therapy in Elderly Women. P. B. Rapuri*[1], J. C. Gallagher[2], G. Haynatzki*[3]. [1]Bone Metabolism, Creighton University, Omaha,, NE, USA, [2]Bone Metabolism, Creighton University, Omaha, NE, USA, [3]Osteoporosis Research Center, Creighton University, Omaha, NE, USA.

Age related bone loss in elderly women has been attributed to age-related factors such as malabsorption of calcium, vitamin D nutritional status and secondary hyperparathyroidism. There is some evidence to suggest that low levels of endogenous estradiol may influence the age related bone loss. However, it is not known whether endogenous estradiol can influence the response to treatment with estrogen in elderly women. In the present study, we investigated the association between the baseline estradiol levels and the treatment response to estrogen. The study population included 489 elderly women aged 65-77 years randomized to 4 treatment groups, placebo, calcitriol (0.5 mcg/d), estrogen (conjugated equine estrogen (CEE), 0.625mg/MPA2.5 mg) and calcitriol+CEE. Baseline total and bioavailable estradiol, and the percent change in bone mineral density (BMD) after 3 years at spine, femoral neck and total body were determined in 337 women who were adherent to treatment. The rate of bone loss across the tertiles of bioavailable estradiol and total estradiol in the 4 treatment groups was compared by analysis of variance (ANOVA). In the placebo group, women in the lowest tertile for baseline bioavailable estradiol showed significantly higher bone loss at spine ($p<0.05$) and total body ($p=0.08$) compared to that of the highest tertile. No such significant changes were noted in the calcitriol group. In the hormone treatment groups (analyzed by combining both the estrogen groups), women in the lowest tertile for baseline bioavailable estradiol gained a significantly higher BMD at the spine ($p<0.01$) and femoral neck ($p<0.01$) compared to women in the highest tertile. Similar results were observed when the data was analyzed for total estradiol. This is the first observation to show that estrogen therapy causes a larger increase in BMD in elderly women with the lowest serum estradiol, probably because they have higher bone resorption and a larger remodeling space. In conclusion, endogenous estradiol level is an important determinant of bone loss and affects the response to treatment with estrogen, in elderly women.

Response to Treatment according to Bioavailable Estradiol

		percent change in BMD		
treatment group/ tertiles of bioavailable estradiol	bioavailable estradiol (pg/ml)	spine	total body	femoral neck
placebo 1(28) 2(33) 3(35)	1.71±0.10 3.17±0.08 6.09±0.32	-3.59±0.91 - 0.18±0.83** - 0.75±0.66*	-3.02±0.47 - 1.41±0.44** - 1.79±0.52	-0.56±1.01 - 0.14+0.68 - 0.78+0.96
hormone groups 1(47) 2(46) 3(46)	1.78±0.06 3.07±0.51 6.08±0.40	7.74±0.85 5.71±0.66 4.88±0.73**	2.40±0.35 1.37±0.33 2.05±0.33	6.71±0.64 5.11±0.59 2.19±0.64***

* $p<0.05$ ** $p<0.01$ ***$p<0.001$ compared to tertile 1

F360

Longitudinal Changes in Three-Dimensional Trabecular Microarchitecture of Paired Iliac Crest Bone Biopsies before and after Estrogen Replacement Therapy in Postmenopausal Women. J. Zhao[1], Y. Jiang[1], S. Vedi*[2], J. E. Compston[2], H. K. Genant[1]. [1]Oarg, University of California, San Francisco, CA, USA, [2]Department of Medicine, University of Cambridge, Cambridge, United Kingdom.

Postmenopausal bone loss is associated with deterioration of trabecular bone microarchitecture, which has adverse biomechanical effects. Estrogen replacement therapy (ERT) has been shown to prevent menopausal bone loss and reduce fracture risk, but its effects on three-dimensional (3D) trabecular microarchitecture have not been characterized. This study was designed to capture true longitudinal changes in 3D trabecular architecture before and after ERT, which may improve our ability to estimate bone biomechanical properties in terms of fracture resistance, as the mechanical competence of trabecular bone is a function of its apparent density and 3D distribution. During aging and in diseases such as osteoporosis, trabecular plates are perforated and connecting rods dissolved, with a continuous shift from one structural type to the other. These changes can not be evaluated by 2D histological sections in bone histomorphometry based on the parallel plate model assumption. We examined paired bone biopsies from the iliac crest (not a primary weight bearing anatomical site) from 20 postmenopausal women with osteopenia or osteoporosis. Bone biopsies were obtained from one side of the iliac crest before treatment and from the other side after treatment (mean 2 years). The specimens were blindly scanned and evaluated using a micro computed tomography scanner ($\propto$CT 40, Scanco) with isotropic resolution of 15 $\propto m^3$. 3D trabecular structural parameters were directly measured without stereological model assumptions as in 2D histomorphometry. Values of 0 and 3 for the structure model index represent an ideal plate structure and a perfect cylindrical rod structure, respectively, while values between 0 and 3 indicate a structure with both plates and rods of equal thickness, depending on the volume ratio of rods and plates. Compared with pre-treatment, post-treatment biopsies showed significant change in structure model index (-13.7%). Post-treatment changes in 3D trabecular bone volume fraction (+0.3%), trabecular thickness (+2.4%), trabecular number (-13.2%), trabecular separation (+9.0%), connectivity density (-0.4%), and degree of anisotropy (-4.4%) were statistically non-significant. The results indicated that ERT not only preserves existing 3D trabecular bone microarchitecture and connectivity but also is able to reverse the change from rod-like structure to plate-like pattern, which may improve trabecular biomechanical competence in terms of resistance to osteoporotic fragility fractures.

F364

Teriparatide (rhPTH(1-34) Improves the Structural Geometry of the Hip. K. Uusi-Rasi*[1], T. J. Beck[1], T. L. Oreskovic*[1], M. Sato*[2], C. E. Bogado*[3], J. R. Zanchetta*[3]. [1]Department of Radiology, Johns Hopkins University, Baltimore, MD, USA, [2]Eli Lilly and Company, Indianapolis, IL, USA, [3]Fundación de Investigaciones Metabólicas, Buenos Aires, Argentina.

Postmenopausal women administered teriparatide (rhPTH (1-34) showed increased BMD with lower fracture rates, suggesting that bone strength properties were improved. We used the hip structure analysis (HSA) program to clarify possible effects of teriparatide on the hip structural geometry. This program measures BMD and geometric properties within narrow regions across the femoral neck, intertrochanter and femoral shaft from images acquired by DXA. Subjects were participants in a multi-center placebo-controlled clinical trial of teriparatide (Lilly). Data for this pilot study were obtained from the Buenos Aires cohort of patients and included 84 postmenopausal women (mean age 67.6 ± 6.4 years) randomized into those receiving daily injections of placebo (n=26), 20 (n=32) or 40µg (n=26) teriparatide, respectively. Hip DXA scans (Lunar-GE, Madison WI) were performed at baseline and repeated on average at 20.1 months. General linear models were used to assess the effects of teriparatide treatment on bone structure using baseline values as covariates. Adjusted % mean differences (95% CI) from baseline at termination are listed for treatment groups in the table with significant differences ($p<0.05$) noted with asterisks. While not all points reached significance, BMD, cross-sectional area (CSA), and section modulus (Z) an index of bending strength, were higher in 20 or 40 mg groups. Reduction in buckling ratio (BR), an index of cortical instability, may be particularly important since fracture cases in other studies have high BRs and the ability to reduce this parameter may help to explain teriparatide efficacy in reducing non-vertebral fractures. Results of this pilot study are encouraging and should be verified with a larger sample size to further clarify the structural effects of teriparatide treatment.

Percent Mean Difference (95% Confidence Interval) from Placebo Controls

Variable	Narrow Neck		Shaft	
	20 ug	40 ug	20 ug	40 ug
BMD	6.4 (1.1 to 12.0)*	12.5 (6.7 to 18.6)*	8.9 (3.1 to 15.0)*	3.1 (-2.5 to 8.9)
CSA	3.3 (-2.5 to 9.3)	13.4 (6.9 to 20.4)*	7.9 (2.7 to 13.3)*	3.7 (-1.3 to 9.0)
Z	0 (-7.4 to 7.9)	14.8 (6.1 to 24.4)*	6.9 (0.3 to 13.9)*	4.2 (-2.3 to 11.1)
Avg. Cortex	6.8 (1.3 to 12.6)*	12.7 (6.7 to 19.1)*	10.0 (3.4 to 17.1)*	3.3 (-3.0 to 10.0)
BR	-9.1 (-13.8 to -4.3)*	-10.3 (-15.1 to -5.3)*	-10.2 (-17.4 to -2.4)*	-2.6 (-10.4 to 5.9)

F366

The Association of Serum RANKL and OPG Levels with Other Biochemical Markers of Bone Turnover in Glucocorticoid Induced Osteoporosis Patients treated with hPTH (1-34). N. Lane, W. Yao, C. D. Arnaud. Department of Medicine, University of California at San Francisco, San Francisco, CA, USA.

Daily injections with hPTH (1-34) is associated with increase in both biochemical markers of bone formation and bone resorption. In addition, changes in levels of biochemical markers predicted increases in bone mass associated with hPTH (1-34) treatment (Lane, Osteo Inter, 2000). Since osteoclast maturation and activity are influenced by RANKL and OPG, we determined the changes in the serum levels of RANKL and OPG and compared these changes to other biochemical markers of bone turnover in patients treated with hPTH (1-34) for 1 year. All studied subjects (n=51) had post-menopausal osteoporosis, were treated chronically with glucocorticoid + HRT and were randomized to hPTH (1-34) 40 ug/d (n=28) or a control group (n=23). In addition, all study subjects were also treated with 1000mg/d calcium + diet and 800IU/d vitamin D3. Biochemical markers of bone formation (osteocalcin) and bone resorption (Deoxypyridinoline/Cr = DPD), sRANKL and OPG were monitored at the baseline, 1 month and every 3 months for 1 year. Results: In the hPTH (1-34) group, osteocalcin increased by 150% above baseline at 1 month ($p<0.01$ from time 0) and was maintained at this level throughout the treatment period. sRANKL increased > 250% over the baseline level at 3 months and was maintained at 150% above baseline for the next 9 months ($p<0.05$). The ratio of sRANKL/OPG did not significantly change until 3 months of treatment, when it increased > 100% over the baseline level and was maintained at > 60% above baseline throughout the treatment period ($p<0.05$). DPD levels increased at a slower rate than sRANKL and osteocalcin, with an increase of only 70% by 1 month and an increase of 150% above baseline by 6 months ($p<0.01$). In the control group, no significant changes were observed in any of the biochemical markers of bone turnover or sRANKL/OPG ratio evaluated. In summary, we found that daily hPTH (1-34) injections increase sRANKL levels earlier and to a greater degree than DPD levels. These results support the hypothesis that hPTH (1-34) daily injections increases osteoclast activity by stimulating osteoblast production of RANKL. Additional studies are now underway to determine if changes in RANKL/OPG levels are correlated with or predict bone mineral density changes with hPTH (1-34) treatment.

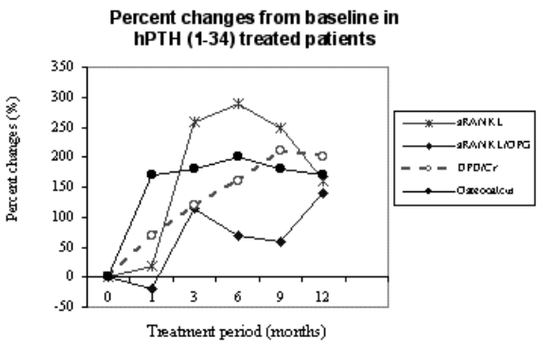

F369

OPG Prevents Relative Osteopenia and Deficits in Skeletal Strength in Mice During a 12 Day Spaceflight. P. J. Kostenuik[1], T. A. Bateman[2], S. Morony[1], K. S. Warmington*[1], Z. Geng[1], S. J. Simske[2], V. L. Ferguson*[2], C. R. Dunstan[1], D. L. Lacey[1]. [1]Metabolic Disorders, Amgen Inc., Thousand Oaks, CA, USA, [2]University of Colorado, BioServe Space Technologies, Boulder, CO, USA.

Bone loss poses a barrier to long-term spaceflight that could be alleviated with a safe and convenient bone-sparing agent. OPG is a protein that causes sustained inhibition of bone resorption after a single injection. We tested the ability of OPG to preserve bone during spaceflight (SF) in mice, a species whose skeletal response to microgravity has not been previously described. 10 week old female C57/B6 mice (n=12/group) were injected once (SC) with OPG (20 mg/kg) or with vehicle (VEH), 24 h prior to launch. Ground control (GC) mice (VEH or 20 mg/kg OPG) were maintained under environmental conditions that mimicked those in the shuttle middeck. A group of age-matched mice was sacrificed at launch to serve as baseline (BL) controls. SF mice were launched into orbit for 12 days on the shuttle Endeavor (STS-108), and were sacrificed within 4 hours of their return. pQCT analysis of the proximal tibial metaphysis revealed that GC/VEH, but not SF/VEH mice, gained BMD during the mission ($p<0.05$ vs. BL). After landing, SF/VEH mice had lower BMD vs. GC/VEH mice ($p<0.05$), while SF/OPG mice had greater BMD than SF/VEH or GC/VEH groups ($p<0.05$). OPG increased tibial cancellous bone volume and BMD in all groups ($p<0.05$ vs. VEH). SF reduced elastic strength at the femoral midshaft in VEH mice ($p<0.05$), while OPG increased elastic strength in SF mice ($p<0.05$). Serum TRAP was elevated in VEH/SF mice vs. VEH/GC mice (p95% in all groups ($p<0.05$). This OPG effect provides a plausible mechanism for the preservation of bone during SF. However, inhibited bone formation appeared a more significant mechanism for SF-induced osteopenia. SF reduced periosteal bone formation rate in the femoral diaphysis ($p<0.05$ vs. GC mice). SF/VEH mice also had lower serum alkaline phosphatase ($p<0.05$ vs. GC/VEH mice), suggesting the suppression of osteoblast activity during SF. OPG did not cause any reversal of the SF-related changes in these bone formation parameters. These observations suggest that the beneficial effects of OPG on mouse bone during SF are due to dramatic and sustained suppression of bone resorption. In growing mice, this effect appears to compensate for the SF-related inhibition of bone formation, while preventing any potential SF-related increase in bone resorption. We have demonstrated that the young mouse is an appropriate model for SF-induced osteopenia. A single pre-flight treatment with OPG effectively prevented the deleterious effects of SF on mouse bone.

F371

Maintenance of Therapeutic Effects of hPTH in Ovariectomized Rats with Established Osteopenia: Evaluation of Bazedoxifene, Raloxifene and Ethinyl Estradiol. Y. P. Kharode, J. T. Marzolf*, P. V. N. Bodine, B. S. Komm, F. J. Bex. Women's Health Research Institute, Wyeth Research, Collegeville, PA, USA.

Intermittent administration of hPTH produces osteogenic effects in both normal and ovariectomized (ovx) rats. The osteogenic effects observed in ovx rats with hPTH regress upon discontinuation of the treatment resulting in a very rapid bone loss and recurrence of osteopenia. The present study was conducted to evaluate the effects of the SERMs bazedoxifene (BZA), and raloxifene (RAL), as well as ethinyl estradiol (EE) on maintenance of the hPTH effects in ovx rats with established osteopenia as outlined below.

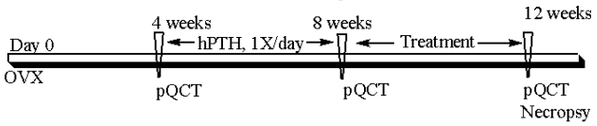

48 female rats were ovx at 12 weeks of age and were found to have developed significant osteopenia compared to eight age matched sham ovx rats after four weeks as judged by proximal tibial (PT) bone mineral density (BMD) using pQCT (total BMD 542 ±4 mg/gm^3 for ovx vs. 709 ± 8 mg/cm^3 for sham, $p<0.01$ and trabecular BMD 353 ± 6 mg/cm^3 for ovx vs. 533 ± 15 mg/cm^3 for sham, $p<0.01$). The ovx rats were then treated daily with hPTH (1-34), 10 µg/kg, sc (n=40) or vehicle (n=8) for four weeks. BMD measurements taken after hPTH treatment, eight weeks after ovx, confirmed a significant hPTH osteogenic effect (total BMD 564 ± 15 mg/cm^3 for ovx + vehicle vs. 686±6 mg/cm^3 for ovx +hPTH, $p<0.01$; and trabecular BMD 256±15 mg/cm^3 for ovx vs. 431 ± 10 mg/cm^3 for ovx + hPTH, $p<0.01$). After stopping PTH treatment the rats were divided in five groups of eight and received daily oral treatment for four weeks as follows: (1) Vehicle (2) BZA, 0.1mg/kg (3) BZA, 0.3 mg/kg (4) RAL, 3 mg/kg and (5) EE, 0.3 mg/kg. After four weeks of treatment, twelve weeks after ovx, the total and trabecular BMD (621±12 mg/cm^3 and 307± 5 mg/cm^3 respectively) decreased significantly in the vehicle group compared to the immediate post-PTH eight week observation but remained significantly higher than the ovx group not receiving PTH. At the twelve week time point, total and trabecular densities between the treatment groups were not statistically different and were not significantly different from the immediate post-PTH eight week time period. We conclude that BZA, RAL and EE were all effective in maintaining the effects of hPTH in the ovx rat with established osteopenia, although potential differences in potency were observed.

F373

Different Effects of Anti-resorptive Agents on Fracture Repair of Ovariectomized Rats. Y. Cao*[1], S. Mori[1], T. Mashiba[1], M. S. Westmore[2], L. Ma[2], M. Sato[2], T. Akiyama*[1], L. Shi*[1], S. Komatsubara*[1], K. Miyamoto*[1], H. Norimatsu[1]. [1]Orthopedic Surgery, Kagawa Medical University, Takamastu, Japan, [2]Lilly Bone Research Laboratories, Indianapolis, IN, USA.

The effects of anti-resorptive agents-estrogen, raloxifene, and alendronate- on the processes of fracture repair were studied in ovariectomized rats. 140 female SD rats were either ovariectomized or sham-operated and divided into five groups: Sham (vehicle), OVX (vehicle), EE2 (0.1mg/kg, estrogen), Rlx (1.0mg/kg, raloxifene) and Aln (0.01mg/kg alendronate) groups. Treatment started from the day of surgery. Four weeks later, pre-fracture controls were euthanized, while bilateral osteotomies were performed on femoral midshafts and fixed with intramedullary wires for all remained animals. Treatment was continued and the rats were sacrificed at 6 and 16 weeks post-fracture for evaluation by x-ray radiography, QCT, biomechanical testing, and histomorphometry. At 6 weeks post-fracture, Aln and OVX had significantly larger callus than other groups. Sham and OVX had significantly higher ultimate load than EE2 and Rlx, while Aln no different from either control. Aln callus contained more mineral (BMC) than all other groups. By 16 weeks post-fracture, OVX callus was significantly smaller than at 6 weeks, while the callus volume for Aln had not changed. Aln had significantly higher BMC and ultimate load than OVX, EE2 and Rlx. EE2 and Rlx had similar biomechanical properties with Sham. Ultimate load normalized by body weight showed no significant difference in strength of the whole callus among the groups at either 6 or 16 weeks post-fracture. However, Aln strongly suppressed the remodeling of callus, resulting in the highest content of woven bone, persistent visibility of the original fracture line, and lowest content of lamellar bone, compared to the other groups. OVX-stimulated bone turnover resulted in the fastest progression of fracture repair that was most delayed with alendronate treatment, consistent with marked suppression of bone resorption and formation activity. Estrogen and raloxifene had similar effects that were generally similar to Sham, indicating that mild suppression of bone turnover with these agents has insignificant effects on the progression of fracture repair.

F381

Effect of Estrogen, Calcitriol or the Combination of Both on Falls and Non Vertebral Fractures in Elderly Women. J. C. Gallagher[1], G. Haynatzki*[2], S. Fowler*[3]. [1]Bone Metabolism, Creighton University, Omaha,, NE, USA, [2]Osteoporosis Research Center, Creighton University, Omaha, NE, USA, [3]Biostatistics, George Washington University, Washington D.C, MD, USA.

Nonvertebral fractures represent 50 percent of total fractures, the majority of which are due to falls. Therefore, reducing falls is a very effective way to reduce fractures. In a prospective study, 489 women were randomized in a double blind placebo trial to treatment with placebo, calcitriol 0.25mcg bid, conjugated equine estrogens (CEE)0 .625mg (ERT or HRT), and a combination of CEE and calcitriol. Women were followed for 3 years and data collected prospectively on falls, non-vertebral fractures due to falls and changes in bone density. Only the data on falls and fractures will be presented. To compare the effect of treatment on falls the cumulative number of falls over 3 years and the incidence rate of falls was performed by recurrent events analysis using a homogeneous Poisson regression model.(SAS GENMOD)Allresults were corrected for body mass index and age . Results: The cumulative number of falls in each group over 3 years was 63 percent on placebo, 56 percent on estrogen, 56 percent on the combination of estrogen and calcitriol and 48 percent on calcitriol; there was a significant decrease in the number of falls in the calcitriol treated group ($p<0.001$). The three-year incidence rate for falls was 0.43 on placebo, 0.39 on ERT/HRT, 0.35 on the combination, and significantly lower on calcitriol 0.29 ($p<0.001$). There was no significant relationship between serum 25 hydroxyvitamin D or serum PTH on fall incidence,caffeine($p<0.09$),but there was a highly significant decrease in the incidence of falls in women who smoked ($p=0.00006$). Overall, 10 percent of women suffered non-vertebral fractures due to falls. There was a significant reduction in fall related fractures in the two groups treated with calcitriol compared to the non calcitriol groups($p<0.052$).There was no significant effect of estrogen on fractures. In conclusion, calcitriol reduces the incidence of falls and fall related fractures.Because falls are one of the most important cause of non-vertebral fractures,this therapeutic approach to preventing fall related fractures may be a useful adjunctive effect to that on bone density.

Disclosures: ***J.C. Gallagher****, Wyeth 2; Roche 2.*

F385

Regulation of PHEX Gene Expression in Bone by Chronic Renal Insufficiency and 1,25-Dihydroxyvitamin D_3. A. J. Brewer*, L. Canaff*, G. N. Hendy, H. S. Tenenhouse. McGill University, Montreal, PQ, Canada.

The PHEX gene (Pi-regulating gene with homologies to endopeptidases on the X chromosome), which is mutated in patients with X-linked hypophosphatemia, is predominantly expressed in bones and teeth. However, little is known about the regulation of PHEX expression. The present study was undertaken to examine the effects of hyperparathyroidism, secondary to chronic renal insufficiency (CRI), and hypoparathyroidism, in response to 1,25-dihydroxyvitamin D_3 (1,25-$(OH)_2$D) administration, on PHEX mRNA and protein expression in rat bone. Rats underwent 5/6 nephrectomy (Nx) or sham operation (control) and were maintained on a high Pi (1.4%) diet for five weeks. In addition, normal rats were injected 48 and 24 hours before sacrifice with either vehicle or 1,25-$(OH)_2$D (10 pmol/gBW). PHEX mRNA abundance, relative to β-actin, was measured by ribonuclease protection assay and PHEX protein abundance, relative to actin, was quantitated by analysis of western blots. When compared to controls, Nx rats exhibited increased serum creatinine (Cr) and urea concentrations, increased serum Pi and urinary Pi excretion, and increased serum PTH (38 ± 2 vs 102 ± 7 pg/ml, $p<0.001$) and urinary cAMP/Cr (23 ± 5 vs 35 ± 5, $p<0.05$). These results indicate that the conditions for CRI and hyperparathyroidism are evident in Nx rats. PHEX mRNA (100 ± 7 vs 168 ± 26, $p<0.05$) and protein (100 ± 11 vs 157 ± 23, $p<0.05$) abundance were significantly increased in tibia of Nx rats when compared to controls. Administration of 1,25-$(OH)_2$D to normal rats had no effect on serum Cr or urea but significantly increased serum Ca and Pi concentrations, and urinary Ca and Pi excretion. Furthermore, both serum PTH (35 ± 2 vs 7 ± 0.5 pg/ml, $p<0.001$) and urine cAMP/Cr (19 ± 2 vs 12 ± 1, $p<0.05$) were significantly decreased in response to 1,25-$(OH)_2$D, indicating that the pharmacological dose was effective in generating hypoparathyroidism. PHEX mRNA (100 ± 12 vs 63 ± 10, $p<0.05$) and protein (100 ± 13 vs 56 ± 11, $p<0.05$) abundance in tibia of 1,25-$(OH)_2$D-treated rats were significantly decreased when compared to vehicle-treated rats. In contrast, tibial mRNA expression of the homologous neutral endopeptidase (NEP) was unchanged in Nx rats and increased in 1,25-$(OH)_2$D rats. The serum concentration of PTH was positively correlated with tibial PHEX mRNA ($p<0.001$) and protein ($p<0.001$) abundance. In summary, we demonstrate that PHEX mRNA and protein expression in rat tibia are significantly increased by Nx, decreased by 1,25-$(OH)_2$D and correlate with the serum concentration of PTH. We also show that PHEX and NEP expression are differentially regulated in rat tibia. Our data suggest that PTH status plays an important role in the regulation of PHEX expression in bone.

F387

Expression of mRNA and Protein for the Stimulatory G Protein Alpha Subunit (Gsα) of Adenylyl Cyclase in Progressive Osseous Heteroplasia (POH) Patients with Inactivating *GNAS1* Mutations. M. Xu*[1], S. M. Jan de Beur[2], C. Li*[1], N. Hebela*[1], S. Fitzgerald*[1], M. A. Levine[2], F. S. Kaplan[1], E. M. Shore[1]. [1]Orthopaedic Surgery, University of Pennsylvania School of Medicine, Philadelphia, PA, USA, [2]Medicine and Pediatrics, Johns Hopkins University School of Medicine, Baltimore, MD, USA.

Progressive osseous heteroplasia (POH) is an autosomal dominant disorder of extensive dermal ossification during childhood followed by disabling ossification of skeletal muscle and deep connective tissue. POH is caused by heterozygous inactivating *GNAS1* mutations. Although most identified cases of POH appear to be due to spontaneous mutations, all known examples of genetic transmission occur by a paternal inheritance pattern. To date, we have identified *GNAS1* mutations in 18 of 27 POH families with one or more affected members. These mutations include small (1-4 nucleotide) insertions and deletions, tandem duplications, and a single nucleotide substitution that disrupts a splice site junction. Each of these mutations predicts a protein reading frame shift. The *GNAS1* gene consists of 12 common exons plus 4 alternative first exons and generates transcripts for XLαs, NESP55, 1A, and Gsα. Although the *GNAS1* gene is reciprocally imprinted, the most well-characterized product, the Gsα protein, is biallelically expressed in most cell types. Examination of Gsα mRNA expression by RT-PCR in cultured lymphoblasts from POH patients with *GNAS1* mutations revealed expression of only normal transcripts if the mutation occurred prior to exon 13, but both normal and mutant transcripts were detected if the mutation affected the last exon. This result was confirmed by RNA blot analyses that detected reduced or normal amounts of hybridizing Gsα mRNA for patients with pre or post exon 13 mutations, respectively. No Gsα transcripts of altered sizes were identified. Immunoblot analysis showed reduced Gsα protein in cultured lymphoblast membranes from POH patients as compared to controls. These data suggest that haploinsufficiency of Gsα protein may be important in directing the clinical phenotype of POH. However, paternal inheritance of *GNAS1* mutations in POH is similar to that observed in pseudopseudohypoparathyroidism, a form of Albright hereditary osteodystrophy (AHO) that is clinically distinct from POH but which is also caused by paternally inherited mutations of the *GNAS1* gene. We conclude that the explanation for differences between these two disorders may not be solely dependent on the level of Gsα expression but may be influenced by the tissue-specific expression of the additional *GNAS1* transcript forms (Nesp55, XLαs, 1A) and/or by involvement of other genes.

F389

Paternal Imprinting of $G\alpha_s$ in the Thyroid as the Basis for TSH Resistance in Pseudohypoparathyroidism type IA. E. L. Germain-Lee*[1], C. Ding[1], J. L. Crane*[1], W. F. Schwindinger*[2], M. Ringel*[3], M. Saji*[3], M. A. Levine[1]. [1]Pediatric Endocrinology, Johns Hopkins University School of Medicine, Baltimore, MD, USA, [2]Weiss Center for Research, Geisinger Clinic, Danville, PA, USA, [3]Medstar Research Institute, Washington, DC, USA.

Albright hereditary osteodystrophy (AHO) is characterized by somatic defects that include brachydactyly, short stature, and obesity and heterozygous mutations in the *GNAS1* gene that lead to reduced expression or function of the alpha chain of G_s, the heterotrimeric protein that couples heptahelical receptors to stimulation of adenylyl cylase. AHO patients with *GNAS1* mutations on maternally inherited alleles also manifest resistance to multiple hormones (*e.g.* PTH, TSH), a variant termed pseudohypoparathyroidism (PHP) Ia, due to presumed tissue-specific paternal imprinting of $G\alpha_s$. Studies of transgenic mice in which one *Gnas* allele has been inactivated by homologous recombination have confirmed these clinical predictions and have demonstrated tissue-specific paternal imprinting of $G\alpha_s$ in renal proximal tubule cells, as well as in fat cells. Similar studies in humans have failed to demonstrate imprinting of $G\alpha_s$, although recent experimental evidence suggests that $G\alpha_s$ may be imprinted in the human pituitary. Because mild hypothyroidism due to TSH resistance occurs in AHO patients and *Gnas* +/- mice that inherit the mutant allele maternally, we sought to determine whether there is imprinting of $G\alpha_s$ in the thyroid. We isolated RNA from normal regions of thyroids that had been removed at surgery from subjects with thyroid nodules. Eight of 12 patients were heterozygous for a known T/C polymorphism in exon 5 of *GNAS1* that allowed us to distinguish between parental alleles. RT-PCR was performed using a common primer in exon 6 and exon-specific upstream primers and demonstrated expected uniallelic expression of NESP55 (maternal), XLαs (paternal), and 1A (paternal). Relative expression of $G\alpha_s$ mRNA was significantly greater from the maternal allele of *GNAS1* than the paternal allele in all 8 cases (0.83 ± 0.03 vs 0.40 ± 0.06). The proportion of paternal $G\alpha_s$ transcripts in these samples ranged from 25-40%. Immunohistochemical analyses of $G\alpha_s$ expression in thyroid tissue showed little or no apparent staining in *Gnas* +/- mice that had inherited the mutant allele maternally and reduced staining in mice that had inherited the mutant allele paternally compared to normal mice. We conclude that $G\alpha_s$ is incompletely paternally imprinted in the thyroid both in humans and in mice. The partial imprinting of the paternal $G\alpha_s$ allele is could explain the development of mild TSH resistance in both patients with AHO and *Gnas* +/- knock-out mice that inherit the mutant allele maternally .

F391

Partial Rescue of the Hyp Phenotype by Osteoblast-Targeted PHEX Expression. X. Bai*[1], D. Miao[1], D. Panda[1], M. D. McKee[2], D. Goltzman[1], A. C. Karaplis[1]. [1]Medicine, McGill University, Montreal, PQ, Canada, [2]Dentistry, McGill University, Montreal, PQ, Canada.

Inactivating mutations and/or deletions of PHEX/Phex are responsible for X-linked hypophosphatemic rickets in humans and in the murine homologue, Hyp. The predominant osteoblastic expression of Phex has implicated a primary metabolic osteoblast defect in the pathophysiology of this disorder. By targeting PHEX expression to osteoblasts in the Hyp genetic background, we aimed to correct the corresponding biochemical and morphological abnormalities and obtain information on their pathogenetic mechanism. When transgene Phex expression, driven by a mouse pro-α1(I) collagen gene promoter, was crossed into the Hyp background, it improved the defective mineralization of bone and teeth but failed to correct the hypophosphatemia and altered vitamin D metabolism associated with the disorder. Ex-vivo bone marrow cultures confirmed the amelioration in the Hyp-associated matrix mineralization defect following Phex expression. These findings suggest that while the Hyp bone and teeth abnormalities partially correct upon PHEX gene transfer, additional factors and/or sites of PHEX expression may be critical for the elaboration of the appropriate molecular signals that alter renal phosphate handling and vitamin D metabolism in this disorder.

F395

Expression of *FGF23* mRNA in Human Cell Lines and Tissues. M. Mirams*[1], B. G. Robinson*[2], R. S. Mason[1], A. E. Nelson[2]. [1]Dept of Physiology, Institute of Biomedical Research, University of Sydney, Sydney, Australia, [2]Cancer Genetics Dept, Kolling Institute of Medical Research, Royal North Shore Hospital, University of Sydney, Sydney, Australia.

The inherited phosphate wasting condition autosomal dominant hypophosphatemic rickets (ADHR) has been found to be associated with missense mutations in *Fibroblast Growth Factor 23* (*FGF23*) (1). Tumors associated with oncogenic osteomalacia (OOM), a tumor-induced phosphate wasting condition with similar features to ADHR, express FGF23 (2). The pathogenesis of OOM is unknown, but FGF23 may be involved. The purpose of this study was to investigate *FGF23* in cell lines established from OOM tumors, other human cell lines and normal human tissue. Sequencing of *FGF23* exons, amplified from genomic DNA, from OOM tumor cell lines revealed no mutations, and specifically not at the RXXR site that is affected by mutation in ADHR. Some evidence of a direct effect of expressed FGF23 on renal OK cell phosphate uptake was detected. Expression of *FGF23* mRNA was detected in OOM cell lines by RT-PCR. A number of other cell lines, including HEK293 and HUH7 cells, were found to express *FGF23* mRNA, and the identity of the product was confirmed by sequencing. In human tissue samples, *FGF23* mRNA expression was detected by RT-PCR in both renal and bone tissues, as well as in liver tissue. Results with human bone cultures suggest that *FGF23* mRNA expression is increased with mineralisation in the presence of beta-glycerophosphate. The lack of mutations in *FGF23* from OOM cell lines indicates that the mechanism of the disease differs from ADHR, and gives weight to the suggestion that overproduction of FGF23, rather than a mutated protein, plays a part in OOM. The expression of *FGF23* mRNA in bone and renal tissues is consistent with a role of FGF23 in regulation of mineral metabolism. This is also indicated by the increased expression of *FGF23* mRNA in mineralised, compared to non-mineralised, bone cells. The significance of *FGF23* mRNA expression in liver is as yet unknown. We conclude that *FGF23* may be a regulator of phosphate metabolism, and that overproduction of FGF23 by OOM tumors contributes to this disorder. (1) ADHR Consortium (2000) Nat. Gen. 26:345-348. (2) White, KE et al. (2001) J Clin. Endocrinol. & Metab. 86:497-500.

F398

Circulating FGF-23 Concentrations in Oncogenic Hypophosphatemic Osteomalacia (OHO) Patients Pre- and Post-surgery. K. E. White[1], W. E. Evans*[1], D. I. Shulman*[2], G. Colussi*[3], S. M. Moe*[1], M. Peacock[1], M. J. Econs[1]. [1]Indiana Univ. Sch. of Med., Indianapolis, IN, USA, [2]Univ. of So. Fl. Coll. Med., Tampa, FL, USA, [3]Niguarda-Ca' Granda Hospital, Milan, Italy.

We determined that FGF-23 is the secreted factor mutated in the heritable renal phosphate wasting disorder autosomal dominant hypophosphatemic rickets (ADHR) and demonstrated that FGF-23 is over expressed by tumors causing the acquired phosphate wasting syndrome oncogenic hypophosphatemic osteomalacia (OHO). ADHR and OHO share similar clinical profiles, and OHO is rapidly resolved upon surgical removal of the tumor, thus we hypothesize that FGF-23 is the factor responsible for the renal phosphate leak present in these disorders. The serum concentrations and clearance mechanisms of FGF-23 in OHO patients are, however, unknown. Therefore, our present goals were: 1) to test whether FGF-23 concentrations are elevated in OHO patients prior to tumor resection; and 2) to assess whether FGF-23 is cleared through the kidneys. Using an ELISA-based serum assay that recognizes C-terminal portions of FGF-23, the mean pre-operative serum concentrations of seven OHO patients was 786.1 RU (Relative Units)/ml ±SE 224.3 compared to 67.9 RU/ml ± 7.9 for normal controls (n=30), P<0.02. In a subset of OHO patients, FGF-23 was assessed pre- and post-tumor resection. For patient 1, FGF-23 was originally 1873.8 RU/ml and fell 91% to 161.0 RU/ml 24 h post-surgery, and 99% to 43.1 RU/ml after 48 h. Serum phosphorus concomitantly rose from 1.7 mg/dl to 2.6 mg/dl. For patient 2, FGF-23 was initially 1248.8 RU/ml, and fell to 91.1 RU/ml; serum phosphorus increased from 1.4 mg/dl to 3.0 mg/dl. Patient 3 had an FGF-23 value of 250.7 RU/ml that decreased to 38.7 RU/ml after surgery. FGF-23 mRNA was readily detectable in available tumors from patients 1 and 2. To test if FGF-23 is cleared by the kidney, pre-operation urine from patient 1 was assayed, and had a 5.8 FGF-23/creatinine ratio vs. 0.4± 0.076 for controls (n=26). In addition, pooled serum from renal failure patients had an FGF-23 level of 25,654.5 RU/ml. In summary, the elevated FGF-23 concentrations in OHO patients rapidly normalize following tumor removal. The presence of FGF-23 in OHO urine indicates that FGF-23 or C-terminal portions may be cleared through the kidneys. This is supported by the high serum levels of FGF-23 in renal failure patients. Our studies indicate that renal function is necessary for FGF-23 and/or C-terminal fragment clearance, or that FGF-23 is secreted in response to hyperphosphatemia. The fact that OHO patient serum phosphorus and FGF-23 concentrations rapidly return to normal after tumor removal further implicates FGF-23 as the phosphate wasting factor responsible for OHO.

F400

CHO-cells Expressing MEPE, PHEX and Co-expressing MEPE/PHEX Cause Major Changes in BMD, Pi and Serum Alkaline Phosphatase in Nude Mice. P. S. N. Rowe*[1], Y. Kumagai[2], R. Garrett[3], R. Blacher*[2], A. Escobada*[3], G. R. Mundy[1]. [1]Molecular Medicine, University of Texas HSC San Antonio IDDW/CTRC, San Antonio, TX, USA, [2]Acologix Inc, Emeryville, CA, USA, [3]Osteoscreen, San Antonio, TX, USA.

MEPE is secreted by tumors causing oncogenic hypophosphatemic osteomalacia (OHO) and increased expression occurs in murine X-linked hypophosphatemic rickets (Hyp). PHEX is a Zn metalloendopeptidase that is mutated in patients with HYP/hyp. Both proteins are developmentally co-expressed in osteoblasts. The effects of MEPE and PHEX over-expression and MEPE/PHEX co-expression *in-vivo* using CHO-cell nude-mouse models were investigated. Measurements were made on BMD, serum alkaline phosphatase (SAP), and serum inorganic phosphate (Pi), over a 21-day period in mice (3 week old female) injected (subcutaneously) with CHO cells. 60 animals divided into 6 experimental and control groups (10 animals per group) were used. The groups consisted of saline control (N), blank CHO cells (CHO-B), CHO cells transfected with empty vector (CHO-V), CHO cells expressing MEPE (CHO-M), CHO-cells expressing PHEX (CHO-P) and CHO cells co-expressing MEPE and PHEX (CHO-MP). BMD measured from days 13 to 21 decreased significantly (-5% to -11%) at the distal-femur in all groups except group CHO-MP and the saline control group-N. Group CHO-MP and N exhibited a significant increase in distal-femur BMD of +5.4% and +2.8% respectively over this period. SAP levels as expected declined steadily in the saline control group N over the 21 days. Surprisingly, all tumor groups except CHO-MP showed a marked and significant decrease (50%) in SAP levels on days 13 and 21 relative to group-N saline control animals. SAP levels in MP tumor-animals were not significantly different to the saline controls on day 13 but did decrease significantly relative to non-tumor controls by day 21 (Group-N; 39.9 IU/l SEM=2.9, group CHO-MP; 17.3 IU/l SEM=3.9). Groups CHO-M and CHO-MP exhibited decreased serum Pi relative to the other groups (including saline control) with group CHO-MP showing a more marked decrease on day 13 (group-N; 10.5 mg/dl SEM=0.3 and CHO-MP; 7.1 mg/dl SEM=0.5). In contrast, all tumor-groups exhibited a marked and significant increase in serum Pi by day 21 including groups CHO-M and CHO-MP relative to the saline controls (group-N; 9.9 mg/dl SEM=0.5 and group-CHO-B; 14.2 mg/dl SEM=2.6)). Finally, addition of purified recombinant MEPE protein (<1 ng/ml) to rat calvaria in bone-organ culture stimulated bone-resorption in a dose dependent manner. Thus confirming a direct *in-vitro* effect of MEPE on bone. In conclusion these studies demonstrate that MEPE and MEPE/PHEX interactions play major roles in bone-renal homeostasis in disease and health.

Disclosures: ***P.S.N. Rowe****, Osteoscreen 5; Acologix 5.*

F403

SHIP Deficient Mice Are Severely Osteoporotic Due to Accelerated Bone Resorption by Pagetic-like Osteoclasts. S. Takeshita[1], N. Namba[1], J. J. Zhao[2], Y. Jiang[2], H. K. Genant[2], M. J. Silva[3], M. D. Brodt*[3], C. D. Helgason*[4], R. K. Humphries*[4], G. Krystal*[4], S. L. Teitelbaum[1], F. P. Ross[1]. [1]Pathology, Washington University, St. Louis, MO, USA, [2]Radiology, University of California, San Francisco, CA, USA, [3]Orthopedic Surgery, Washington University, St. Louis, MO, USA, [4]Terry Fox Laboratory, BC Cancer Agency, Vancouver, BC, Canada.

SHIP is an SH2-containing inositol-5-phosphatase, preferentially expressed in hematopoietic cells. By dephosphorylating its major substrate, phosphatidylinositol-3,4,5-trisphosphate (PIP_3), SHIP blunts phosphatidylinositol-3-kinase (PI3-K) initiated signal transduction. $SHIP^{-/-}$ mice are known to be rich in bone marrow macrophages (BMMs) and we find osteoclasts (OCs), which are derived from these cells, are increased two fold in these mutants. Consistent with the increased number of OCs in $SHIP^{-/-}$ mice, osteoclastogenesis induced by RANKL or M-CSF, occurs at substantially lower concentrations of either cytokine, than WT. Furthermore, the number of apoptotic nuclei and the level of cytoplasmic histones/DNA, the latter measured by ELISA, were decreased 75% in $SHIP^{-/-}$ OCs. Thus, the increased OC number characterizing $SHIP^{-/-}$ mice arises from a combination of an enhanced response to the osteoclastogenic cytokines M-CSF and RANKL and a prolonged lifespan. More strikingly, $SHIP^{-/-}$ OCs are greatly enlarged (2.6 fold), contain upwards of 100 nuclei, and are indistinguishable from those characterizing Paget's disease of bone. Like Pagetic osteoclasts, the capacity of those generated from $SHIP^{-/-}$ mice to generate resorptive pits on dentin slices is enhanced. In contrast to resorption, the rates of bone formation, assessed by calcein double labeling, are indistinguishable in $SHIP^{-/-}$ and WT mice. Consistent with accelerated resorptive activity, 3D trabecular volume fraction, trabecular thickness and trabecular number and connectivity density of $SHIP^{-/-}$ long bones, determined by micro-computed tomography, are all dramatically reduced, resulting in a 22% loss of bone mineral density (BMD) and a 49% decrease in fracture energy, measured by DEXA and three point bending, respectively. Since the SHIP gene co-segregates with a site of loss of heterozygosity for familial Paget's disease, and $SHIP^{-/-}$ and pagetic osteoclasts are indistinguishable, it is possible that SHIP is mechanistically important in some Pagetic patients. Thus, SHIP negatively regulates osteoclast formation and function and absence of the enzyme results in severe osteoporosis, with a pathological state mimicking the resorptive phase of Paget's disease.

F405

Juvenile Paget Disease Caused By Homozygous Deletion Of *TNFRSF11B* Encoding Osteoprotegerin. M. P. Whyte[1], S. E. Obrecht*[2], P. M. Finnegan*[2], J. L. Jones*[2], M. N. Podgornik*[1], W. H. McAlister*[3], S. Mumm[1]. [1]Cntr Metab Bone Dis & Mol Res, Shriners Hosp Child, St. Louis, MO, USA, [2]Div Bone & Min Dis, Wash Univ Sch Med, St. Louis, MO, USA, [3]Mallinckrodt Inst Radiol, Wash Univ Sch Med, St. Louis, MO, USA.

Juvenile Paget disease (JPD), an autosomal recessive osteopathy, features rapidly remodeling woven bone, osteopenia, fractures, and progressive skeletal deformity. If untreated, JPD can be lethal. The molecular basis is not known. *Osteoprotegerin* (OPG) deficiency could explain JPD because OPG suppresses bone turnover, functioning as a decoy receptor for *osteoclast differentiation factor* (ODF). ODF, also called *RANK ligand*, promotes skeletal resorption when it binds on osteoclasts to *receptor activator of nuclear factor-κB* (RANK). Two Navajos with JPD in separate families were studied for defects in the *TNFRSF11B* gene, encoding OPG, by: i) polymerase chain reaction (PCR) with direct sequencing, and ii) Southern blotting. Genetic loci adjacent to *TNFRSF11B* were investigated by PCR. Delineation of the breakpoints of a deletion removing *TNFRSF11B* involved sequence tagged site (STS) content mapping and PCR across the deletion breakpoints. Selective, homozygous deletion of *TNFRSF11B*, with identical chromosomal 8q24.2 breakpoints, affects both JPD patients. The defect spans ~ 100 kb but leaves genes neighboring *TNFRSF11B* intact. Serum levels of OPG and uncomplexed ODF are undetectable and markedly raised, respectively. JPD results from OPG deficiency due to homozygous deletion of *TNFRSF11B*. Consequently, circulating levels of unbound ODF are elevated. OPG importantly suppresses bone remodeling in humans. OPG knockout mice manifest JPD rather than osteoporosis. The JPD literature suggests that OPG protects against arterial calcification. Both "bottleneck" and "founder" effects involving *TNFRSF11B* deletion seem to be emerging in the Navajo population. Prenatal and carrier detection is now possible. OPG administration could be a particularly effective treatment for JPD.

F408

Significance of 7-84 PTH in Primary Hyperparathyroidism: Its Production and Metabolism. H. Yamashita[1], P. Gao[2], T. Cantor[2], S. Noguchi*[1], S. Uchino*[1], S. Watanabe*[1], M. Fukagawa*[3]. [1]Surgery, Noguchi Thyroid Clinic, Beppu, Japan, [2]Scantibodies Laboratory Inc, Santee, CA, USA, [3]Dialysis and Metabolism, Kobe University School of Medicine, Kobe, Japan.

Most current commercial 2nd generation intact PTH (iPTH) assays cross-react with 7-84 PTH and this interference accounts for up to 90% of immunoreactivity in samples obtained from uremic patients. It is reported that 7-84 PTH has an antagonistic action to 1-84 PTH, however, very little is known about the production and metabolism of 7-84 PTH. A new 3rd generation cyclase activating PTH (CAP) novel immunoradiometric assay, was shown to specifically measure 1-84 PTH without any cross reactivity to 7-84 PTH. Using this CAP assay, we studied the production and metabolism of 7-84 PTH in primary hyperparathyroidism (pHPT). This study comprised 63 patients with pHPT caused by a single adenoma who underwent parathyroidectomy. Preoperatively, blood samples were drawn from the bilateral internal jugular vein by ultrasonographic guidance and from the peripheral vein. During surgery, blood samples were drawn after anesthesia (basal level), before excision (pre-excision level) of one enlarged parathyroid gland, and at 5, 10, and 15 minutes post excision. The 7-84 PTH level was calculated by subtraction of the 3rd generation CAP assay value from the 2nd generation iPTH assay value. There were 34 patients whose iPTH assay levels differed by more than 10% between the right and left internal jugular. In those 34 patients, the level of 7-84 PTH levels obtained from the adenoma side was significantly higher than those from the contralateral side (124±18 vs. 44±18 pg/ml, $p<0.05$).The plasma CAP and iPTH value had dropped to 25±10 and 32±11% at 5min, 14±7 and 21±7% at 10 min, and 10±5 and 17±7% 15 min after removal of an enlarged gland of pre-excision value, respectively ($p<0.001$). Interestingly, the 7-84 PTH level after 5 min was higher than that at pre-excision in seven of 63 patients (11%). Further, the level at 10 min was higher than that at 5 min 1n 10 (16%) and the level at 15 min was higher than that at 10 min 1n 15 (24%). Our results suggest that 7-84 PTH may not only be produced by parathyroid adenomas but also may be produced by the metabolism of 1-84 PTH during circulation and the new 3rd generation CAP assay may be a more useful adjunct to parathyroidectomy than the currently used 2nd generation iPTH assay.

F410

The Calcimimetic Compound KRN1493 Suppresses Parathyroid Hyperplasia in Rats with Chronic Renal Insufficiency. M. Wada*, T. Kawata*, Y. Furuya*, N. Kobayashi*, M. Ozai*, S. Miyata*, S. Obana*, N. Nagano. Pharmaceutical Development Laboratories, Kirin Brewery Co., Ltd., Takasaki-shi, Japan.

Secondary hyperparathyroidism is characterized by the elevation of circulating parathyroid hormone (PTH) levels and parathyroid hyperplasia. In this study, we evaluated the effects of the calcimimetic compound KRN1493 on secondary hyperparathyroidism progression using 5/6 nephrectomized rats. Exp.1 Rats were subjected to 5/6 nephrectomy and treated with KRN1493 (1 or 5 mg/kg) for 5 consecutive days. During the treatment, rats were infused with 5'-bromo-2'-deoxyuridine (BrdU) to label S-phase cells. After sacrifice, the parathyroid glands were dissected and subjected to immunohistochemical analysis for BrdU. The number of BrdU-positive parathyroid cells in rats with chronic renal insufficiency (CRI) was about 5-fold larger than that in sham-operated controls. Treatment with KRN1493 (5 mg/kg) reduced the number of BrdU-positive parathyroid cells by 40% compared to the vehicle-treated controls. Exp.2 We evaluated the long-term effect of KRN1493 on the progression of parathyroid cell hyperplasia. Rats were subjected to 5/6 nephrectomy and KRN1493 (3 or 15 mg/kg) was orally given for about 5 weeks daily. Serum PTH levels were measured before and after the last administration. Parathyroid glands were dissected and subjected to quantitative stereologic analyses, unbiased estimations of parathyroid cell number and size. Serum PTH levels in rats with CRI were about 9-fold higher than those in sham-operated controls before the last administration. KRN1493 (15 mg/kg) reduced serum PTH levels significantly 90 min after the last administration. Both the number of parathyroid cells and parathyroid grand volumes in rats with CRI were about 2.5-fold larger than those in sham-operated controls. KRN1493 (15 mg/kg) reduced the number of parathyroid cells by 47% and parathyroid grand volumes by 40%, respectively. The parathyroid cell volumes in rats with CRI were 1.3-fold larger than those in sham-operated controls and were not affected by KRN1493 (15 mg/kg). Serum PTH levels before the last administration positively correlated with the number of parathyroid cells ($r=0.85$, $P<0.01$) and the parathyroid grand volumes ($r=0.83$, $p<0.01$). We conclude that treatment with KRN1493 inhibits the progression of parathyroid hyperplasia by suppressing parathyroid cell proliferation. The present data suggest that KRN1493 would be a useful therapeutic agent for the treatment of secondary hyperparathyroidism.

F412

Elevated expression of RANK in osteoblasts from Pagetic Lesions. D. G. Ammerman*[1], A. M. Desphande*[1], D. Pathmanathan*[1], P. Bhatia[1], K. K. Unni*[2], M. Seton[3], R. J. Leach[4], M. F. Hansen[1]. [1]Molecular Medicine, University of Connecticut Health Center, Farmington, CT, USA, [2]Pathology, Mayo Clinic, Rochester, MN, USA, [3]Rheumatology, Massachusetts General Hospital, Boston, MA, USA, [4]Cellular and Structural Biology, UT-Health Science Center, San Antonio, TX, USA.

Paget's disease of bone (PDB) is a focal disorder of bone metabolism characterized by accelerated bone resorption coupled to bone formation in affected sites. PDB is thought to be driven primarily by osteoclasts (OC), as the initial lesion is lytic, the phenotypic and biochemical abnormalities have been demonstrated in the OC, and it is sufficient to treat the OC to restore normal parameters of bone turnover. Noting both previously reported elevated expression of Receptor Activator of NFkB (RANK) in OC from Pagetic lesions, and recent data suggesting that RANK may play a role in osteoblast growth, we were interested to see if RANK expression was also elevated in Pagetic osteoblasts. We therefore examined osteoblasts for expression of RANK and its' ligand RANKL. We found that while RANKL expression levels remained comparable to those of normal bone, RANK expression was increased in osteoblasts in both the Pagetic bone and osteosarcomas that arose in Pagetic patients. To rule out the possibility that the increased expression was due to infiltrating osteoclasts (or their precursors), we immunostained the samples with Cathepsin K, a marker of osteoclast lineage. This confirmed that the cells examined were not osteoclasts. Elevated expression of RANK in the osteoblasts may induce these cells to proliferate inappropriately, possibly contributing to both PDB and Pagetic osteosarcoma tumorigenesis. Our study is the first to show primary biochemical abnormalities in the Pagetic osteoblasts.

F414

Decrease in Parathyroid Hormone Serum Levels with Age and with Correction of Extracellular Calcium Is Not Associated with a Reduction in Parathyroid Gland Size in Mice with a Nonfunctioning Vitamin D Receptor. K. Weber*[1], U. Zeitz*[1], C. Bergow*[1], D. W. Soegiarto*[2], R. Balling*[2], R. G. Erben[1]. [1]University of Munich, Institute of Animal Physiology, Munich, Germany, [2]GSF National Research Center for Environment and Health, Institute of Mammalian Genetics, Neuherberg, Germany.

Cell proliferation and parathyroid hormone (PTH) secretion in the parathyroid gland is known to be regulated by the vitamin D hormone via the vitamin D receptor (VDR) and by extracellular calcium via the calcium-sensing receptor. In this study, we sought to separate the effects of extracellular calcium from the effects of vitamin D on parathyroid gland function and size using mice with a nonfunctioning VDR. By 10 weeks of age, homozygous VDR mutant mice developed profound hypocalcemia and severe secondary hyperparathyroidism with PTH serum levels beyond 1,000 pg/ml in all animals. The parathyroid glands of 10-week-old VDR mutants were grossly enlarged, as measured by about a 3-fold higher maximum area in serial histological sections. After the rapid growth phase, when calcium demands of the growing skeleton decrease, hypocalcemia was less pronounced, and PTH serum levels declined from 1290 ± 418 in 10-week-old mutants to 45 ± 45 pg/ml in 1-year-old mutants (means ± SD). Northern analysis of total RNA extracted from the larynx region and in situ hybridization with a PTH-specific probe showed variations in PTH gene expression that paralleled those of PTH serum levels. However, the age-related decline in PTH mRNA levels and PTH secretion was not associated with a reduction in parathyroid gland size. In mice fed a rescue diet enriched with calcium, phosphorus, and lactose, beginning from 16 days of age, blood ionized calcium, PTH mRNA levels, PTH serum levels and parathyroid gland size were normal, showing that the absence of vitamin D signaling is not associated with increased chief cell proliferation or increased PTH secretion. When 6-month-old VDR mutants where switched to the rescue diet, PTH serum and mRNA levels declined over the 3-month experimental period. However, the rescue diet was not able to induce a decrease in parathyroid gland size. Also, there was no evidence of an increase in chief cell apoptosis in the parathyroid glands of animals on the rescue diet, as measured by TUNEL staining. We conclude that 1) vitamin D has no essential function in the control of PTH secretion and of cell proliferation in the parathyroid gland, and 2) that normalization of extracellular calcium reduces PTH gene expression and PTH secretion but does not reduce parathyroid gland hyperplasia in the absence of a functioning VDR. Our findings suggest that signaling via the calcium-sensing receptor is not able to reverse parathyroid gland enlargement.

F417

Lymphocytes from FOP Patients Induce Early FOP-like Lesions in Nude Mice. P. C. Billings*[1], Y. Wu*[1], R. Caron*[1], L. Serrano de la Pena*[1], F. H. Gannon[2], B. Young*[3], M. Pacifici[3], F. S. Kaplan[1], E. M. Shore[1]. [1]Orthopaedic Surgery, University of Pennsylvania School of Medicine, Philadelphia, PA, USA, [2]Orthopedic Pathology, Armed Forces Institute of Pathology, Washington, DC, USA, [3]Anatomy and Histology, University of Pennsylvania School of Dental Medicine, Philadelphia, PA, USA.

Fibrodysplasia ossificans progessiva (FOP) is a devastating genetic disease of progressive hetrotopic ossification leading to joint ankylosis throughout the body. While FOP was first described ~300 years ago, the precise genetic defect(s) and pathophysiology remain enigmatic. Progress in understanding FOP has been hampered by the lack of an animal model to study FOP lesion formation. To address this problem, we subcutaneously implanted lymphoblastoid cell lines obtained from FOP patients or unaffected family members into nude mice. As positive controls, upper and lower sternal chick chondrocytes were also implanted. Both types of sternal chondrocytes grow as a solid mass in mice, laying down a cartilage matrix. Cells from unaffected individuals either did not grow or formed small masses with little evidence of a fibrotic or angiogenic response. In contrast, cells from FOP patients gave rise to solid tumor-like masses in the animals. Histopathological evaluation of these lesions indicated that FOP cells induced angiogenesis and a fibrotic response in the host, similar in appearance to early FOP patient lesions (stage 1A-2B). FOP cell-induced lesions were probed for human-specific Alu sequences, confirming that the cellular masses contained human as well as host cells. These results suggest that cells of FOP patient origin produce stimulatory factors that induce changes in cell growth and/or differentiation, and mimic events in early FOP lesions. Hence, implantation of FOP-derived cells in nude mice will provide a useful model for examining the early stages of the disease and ultimately, a better understanding of this catastrophic condition.

F419

Osteoporosis and Fractures in Children with Duchenne Muscular Dystrophy Treated with Glucocorticoids: A Longitudinal Study. G. Chabot[1], N. Alos*[1], Y. Brousseau*[2], J. Dubé*[2], E. Delvin*[1], M. Filiatreault*[2], M. Vanasse*[1]. [1]Hopital Ste Justine, Montreal, PQ, Canada, [2]Hopital Marie Enfant, Montreal, PQ, Canada.

Oral glucocorticoids (OG) are increasingly used to treat Duchenne Muscular Dystrophy (DMD) to preserve muscle function and mobility. Concerns of skeletal complications associated with chronic administration of OG led us to follow at the neuro-muscular diseases clinic a group of 46 boys with DMD treated with deflazacort. Treatment was started between 4 and 11 years of age (mean: 7y 5m) and extended from 4 months to 9 years (mean: 5y 9m). Every patient received vitamin D (400 IU/day) and calcium supplements (750 mg/day). Growth was recorded at regular intervals. Bone mineral content (BMC) of the lower spine was measured and areal bone mineral density (aBMD) was calculated with a Hologic QDR 4500 DXA scanner, and repeated over a period of 4 years. Fractures were recorded and documented by X-ray. During the treatment period, 26 of the 46 patients (52%) suffered from 37 fracture events. Of these, 18 (39%) presented crush fractures of the vertebrae, and 19 episodes of long bone fractures occurred in 17 patients. Delay between treatment onset and the first fracture ranged between 22 months and 71/2 years (Mean 4 1/ 2 years). A total of 106 BMC measurements were performed in 46 patients between the ages of 5 years 11 months and 17 years and 5 months. Over this age span, the aBMD did not increase. The aBMD Z score decreased from a mean of –2 SD at 5 years to reach –5 SD at 17 years of age. Repeated measurements in 37 patients at a mean interval of 2 years allowed us to assess the longitudinal changes of the aBMD. In this subgroup, the aBMD Z score decreased from a mean of –2,59 SD to –3,27 SD ($P < 0,001$, paired T test) and the mean aBMD remained essentially unchanged at 0,480 g/cm2. The mean BMC increased slightly from 15,71 to 16,12 gm but the difference was not statistically significant. Our data allow us to conclude that skeletal complications in patients with DMD treated with OG are frequent and are associated with very low aBMD as calculated with DXA. If glucocorticoids are to be given to these patients, treatment to prevent bone loss should be started early. A study to evaluate the effectiveness and safety of such a preventive treatment should be initiated.

F422

Kaliotoxin Decreases Receptor Activator of NFκB Ligand (RANKL) Expression in Activated T Cells *In Vitro* and Ameliorates Local Inflammatory Bone Resorption in Experimental Periodontal Disease. P. Valverde*[1], T. Kawai*[2], M. A. Taubman*[2]. [1]Oral Biology, The Forsyth Institute, Boston, MA, USA, [2]Immunology, The Forsyth Institute, Boston, MA, USA.

It has been reported that the alveolar bone destruction observed in periodontal infections is partly mediated by microorganism-triggered induction of receptor activator of NFκB ligand (RANKL) expression on T cells and the subsequent activation of osteoclasts. The activation of RANKL in T cells is calcium-dependent and hence can be blocked by the calcineurin-dependent inhibitor cyclosporin A. Therefore, it might be expected that blocking Kv1.3, a T cell-expressing voltage-gated potassium channel that regulates the membrane potential and therefore the driving force for calcium entry through calcium release-activated calcium channels, will decrease the expression of RANKL and hence ameliorate T-cell mediated bone resorption. To test this hypothesis, we first analyzed whether kaliotoxin, a specific blocker of Kv1.3 can decrease the expression of RANKL in human peripheral blood T cells activated *in vitro* with anti-CD3 alone or anti-CD3 and anti-CD28 antibodies. RT-PCR and flow-cytometric analyses indicated that RANKL expression was decreased by more than 50% on T cells activated in the presence of kaliotoxin as compared to the absence of kaliotoxin. Secondly, we tested whether the inflammatory alveolar bone resorption induced by Th1 clone cells in an experimental model of periodontal disease could also be decreased by kaliotoxin. In this rat model, gingival injection of *Actinobacillus actinomycetemcomitans* 29-kDa outer membrane protein (Omp29) and LPS induces bone resorption on the palatal surface of the maxillary molars 10 days after transfer of antigen-specific Th1 clone cells. Subcutaneous injections of 10 μg of kaliotoxin twice a day for 4 days (days 0 to 3), resulted in a decrease of 84% ($p<0.01$, n=7) of the bone loss induced in the control group, injected with saline as placebo. The kaliotoxin group of rats also exhibited 74% lower levels of serum IgG2a antibody levels to Omp29 than the control group as determined by ELISA ($p<0.01$, n=7). Furthermore, the antigen-specific-stimulation index of T cells isolated from the spleens of kaliotoxin-treated animals was 65% lower than that of the control group ($p<0.01$, n=7). Taken together, these data suggest that selective blocking of Kv1.3 by kaliotoxin may decrease local T cell-mediated inflammatory bone resorption and therefore might be a novel therapeutic approach for intervention with periodontal disease and other inflammatory bone resorptive disorders.

F424

Zoledronic Acid Improves Short-Term Outcome in Traumatic Osteonecrosis in Young Wistar Rats. R. A. Peat*[1], A. McEvoy*[1], P. R. Williams*[1], P. A. Baldock[2], E. J. Smith[1], D. G. Little*[1]. [1]Orthopaedic Research Unit, Children's Hospital at Westmead, Sydney, NSW, Australia, [2]Garvan Institute of Medical Research, Sydney, NSW, Australia.

Currently there is no reliable medical therapy for the prevention of femoral head collapse and deformity in patients suffering from osteonecrosis. We hypothesized that the bisphophonate zoledronic acid could preserve femoral head structure while allowing revascularization and new bone formation. To model traumatic osteonecrosis, 24 female Wistar rats had the right femoral head dislocated, ligamentum teres divided, and femoral neck denuded of all soft tissue. Rats were randomized into 3 treatment groups: saline, zoledronic acid (0.1 mg/kg) at 1 and 4 weeks post-operation (post), and zoledronic acid (0.1 mg/kg) given 2 weeks pre-operation and 1 and 4 weeks post-operation (pre-post). Bone scintigraphy revealed revascularization at 6 weeks in all groups, with an observed increase in uptake on the operated side. Radiographs showed collapse of the femoral head in the saline group, with considerable preservation in both treated groups, such that femoral head size was increased 31% and 49% in post and pre-post groups, respectively ($P<0.01$), whereas only 13% and 0% of operated heads in treated groups were aspherical ($P<0.05$). DXA generated BMD was increased by 52% and 73% in the treated groups over saline, and BMC by 111% and 160% ($P<0.01$). Undecalcified histomorphometry showed preservation of femoral head architecture in treated groups, whereas the saline group had collapsed (Fig 1). There were increases of 14% and 20% in BV/TV in treated groups, as well as an increase in trabecular number of 22% and 16% ($P<0.05$). MAR was increased by 51% in the operated limb as compared to the non-operated limb of saline animals ($P<0.05$). MAR was similar in the operated femoral heads of saline and post animals, but reduced to the values of non-operative saline animals in the pre-post group. BFR increased in saline operated femoral heads over treated groups but this was not sufficient to prevent collapse. Zoledronic acid treatment prevented collapse of the femoral head following traumatic osteonecrosis in this rat model at 6 weeks. Pre-treatment with zoledronic acid provided protection from the avascular insult. These data indicate that by retaining femoral head architecture, revascularization can occur, preventing collapse.

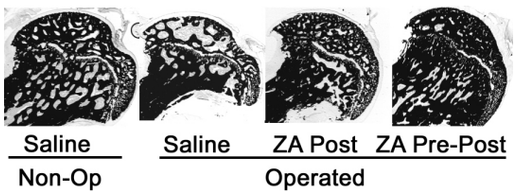

*Disclosures: **R.A. Peat**, Novartis 2.*

F433

Parathyroid Gland Responsiveness to Hypo- and Hypercalcaemic Stimuli in Adult Growth Hormone Deficiency Before and During Growth Hormone Replacement. A. M. Ahmad*[1], J. Thomas*[1], H. White*[1], M. Hopkins*[1], B. Durham*[1], W. D. Fraser[2], J. P. Vora*[1]. [1]Diabetes & Endocrinology, Royal Liverpool University Hospital, Liverpool, United Kingdom, [2]Clinical Chemistry, Royal Liverpool University Hospital, Liverpool, United Kingdom.

Adult GH deficiency (AGHD) is associated with osteoporosis. Alterations in parathyroid gland responsiveness to changes in calcium concentration play a role in the genesis of osteoporosis. We investigated PTH response to hypo- and hypercalcaemic stimuli in AGHD. 12 patients with severe AGHD were hospitalised, prior to GH replacement (GHR), at 0800 h after an overnight fast. Venous cannulae were inserted in each arm and ½ hourly blood sampling commenced at 0900 h. After 5 basal samples, sodium EDTA infusion (50 mg/kg, in 500 ml 5% dextrose with 7 ml 2% lignocaine) was commenced at 1100 h for 2 h to induce hypocalcaemia in 6 patients (group 1). Hypercalcaemia was induced in 6 patients (group 2) by calcium gluconate (6 mg/kg in 500 ml of 5% dextrose) over 2 h. Sampling continued at ½ hourly intervals during the infusions up to 1800 h. PTH, calcium and albumin were measured on all samples. GHR was commenced after baseline visit. The protocol was repeated at 3/12 and 12/12 on GHR. The 5 basal samples (0900-1100 h) were averaged and showed a significant increase in adjusted-calcium (ACa) concentration (mmol/L) at 3/12 and 12/12 ($p<0.001$). PTH concentration (pmol/L) decreased significantly at 12/12 ($p<0.001$), compared to baseline in both groups. In group 1, maximum PTH stimulation occurred at an ACa concentration (percentage drop) of 1.79 (23.8%) at 0/12 . Following GHR, maximum PTH stimulation occurred at an ACa concentration of 1.92 (17.2%) at 3/12 and 2.16 (12.9%) at 12/12 ($p<0.05$). The maximum PTH response was a 365% rise before and 326% rise after 12/12 (p=ns). In group 2, maximum PTH suppression occurred at an ACa concentration (percentage rise) of 2.79 (18.9%) at 0/12 compared to 2.92 (16.7%) at 3/12 (p=ns) and 2.84 (14.7%) at 12/12 ($p<0.01$). The maximum PTH suppression was 75% before and 82% after 12/12 (p=ns). The calcium set point (the calcium concentration at which the rate of PTH secretion is one half of its maximal value) progressively increased from 2.08 ± 0.04 (SEM) at 0/12 to 2.20 ± 0.04 at 3/12 ($p<0.01$) and 2.35 ± 0.04 at 12/12 ($p<0.001$) in group 1, and increased from 2.39 ± 0.04 at 0/12 to 2.59 ± 0.04 at 3/12 ($p<0.05$) and 2.61 ± 0.04 at 12/12 ($p<0.001$) on GHR in group 2. These results suggest increased parathyroid gland sensitivity to significantly smaller changes in serum calcium following GHR. Together with the increase in calcium set-point this may explain the increase in basal calcium and decrease in PTH concentration. Our findings may help explain the genesis of osteoporosis in AGHD patients.

F435

The PTH mRNA 3'-Untranslated Region (UTR) Calcium and Phosphate Responsive Element – Structure and Function. R. Kilav*, O. Bell*, J. Silver, T. Naveh-Many. Nephrology, Hadassah Hospital, Jerusalem, Israel.

Ca^{2+} and Pi regulate PTH gene expression post-transcriptionally by affecting PTH mRNA stability. This is due to binding of *trans* acting factors to a *cis* acting instability element in the 3'-UTR. In hypocalcemia there is increased binding to the element that protects the PTH mRNA from degradation by cytosolic ribonucleases resulting in higher levels of PTH mRNA In hypophosphatemia there is decreased binding, with a subsequent increased degradation of the PTH mRNA resulting in low levels of PTH mRNA. We have identified the sequence of a minimal protein-binding element and have now studied its functionality and structure. The cDNA coding for the 63 nt *cis* element of the PTH mRNA 3'-UTR was inserted into two reporter cDNAs, GFP and growth hormone (GH). The constructs were transiently transfected into HEK293 cells. mRNA levels were measured by Northern blot, and protein levels of GFP by immunofluorescence, and secreted GH by radioimmunoassay. There was a dramatic reduction in the expression of the chimeric genes containing the 63 nt, but not with a truncated PTH 40 nt element, compared to wt genes. The 63 nt transcript, like the full-length PTH RNA, bound PT proteins by REMSA, but the truncated element did not bind PT proteins. These results are consistent with the destabilizing effect of the *cis* element in the PTH mRNA. RNA utilizes sequence and structure for its regulatory functions. To study the structure of the *cis* element, we performed RNase H analysis, and computer modeling of the PTH mRNA. The secondary structure was substantiated by primer extension analysis using a PTH transcript that was partially cleaved by structure specific RNases and the resulting cDNAs analyzed on sequencing gels. Our results indicate that there is a defined loop-stem-loop structure in the 63 nt. This structure is preserved when the full-length PTH mRNA and smaller transcripts including the functional 63 element of the 3'-UTR were studied. This structure was disrupted in a transcript of the truncated element that was not functional in reporter RNAs and in PT protein binding. In addition, point mutations in the PTH element that disrupted structure did not bind cytosolic PT proteins in binding assays. The results demonstrate an important role of the defined structure of the *cis* element. In summary, we have demonstrated a functional instability *cis* element in the PTH mRNA 3'-UTR that also confers instability to reporter genes. The element has a defined structure that is important for its function. Protein-RNA interactions at the element determine PTH mRNA stability. Calcium and phosphate regulate mRNA levels by altering the binding of the *trans* acting parathyroid cytosolic proteins to the *cis* acting PTH mRNA 3'-UTR element.

F437

Role of Cyclooxygenase-2 in the Calvarial Response to Parathyroid Hormone. M. Xu*, G. A. Gronowicz, O. S. Voznesensky, L. G. Raisz, C. C. Pilbeam. Medicine, University of Connecticut Health Center, Farmington, CT, USA.

Cyclooxygenase-2 (COX-2) is necessary for the maximal osteoclastogenic response to parathyroid hormone (PTH) in marrow stromal cell cultures. We injected PTH above the calvariae in 4 month old male COX-2 wild type (+/+) and knockout (-/-) mice to examine the role of COX-2 in osteoclastic responses in vivo. COX-2+/+ and -/- were bred for experiments by mating C57Bl/6x129 COX-2 heterozygote (+/-) mice. Mice were injected once daily for 14 days over one half of the calvaria with vehicle (7 COX-2+/+, 5 COX-2-/-) or with 30 μg/kg of rhPTH 1-34 (7 COX-2+/+, 6 COX-2-/-). Histomorphometric analyses were performed on the injected half of the calvaria. There were no differences in body weights between COX-2+/+ and COX-2-/- mice at the beginning or the end of the experimental protocol. Serum creatinine (Cr) and calcium were measured at time of sacrifice. Cr tended to be higher (although not statistically significantly different) in COX-2-/- mice relative to COX-2+/+ mice. Serum calcium was not elevated in any group at the end of treatment. Calvarial width was significantly increased ($P < 0.05$) in COX-2+/+ mice treated with PTH (212 ± 23 μm) relative to COX-2+/+ mice treated with vehicle (155 ± 9.5 μm). Bone marrow area was increased 18-fold ($P < 0.05$) in PTH-treated COX-2+/+ mice, reflecting a marked increase in porosity of the calvariae after PTH treatment. As a result, the percent bone area relative to total tissue area (TA/TTA) was decreased in COX-2+/+ mice from 98.0 ± 0.8% in vehicle-treated mice to 74.8 ± 9.1% in PTH-treated mice ($P < 0.05$). In COX-2-/- mice, PTH treatment did not increase calvarial width, bone marrow area or TA/TTA. Osteoclast number and osteoclast number per bone marrow perimeter were both significantly increased in PTH-treated COX-2+/+ mice: 17.0 ± 2.9 vs. 1.6 ± 0.9 ($P < 0.01$) and 26.0 ± 2.1 per mm vs. 1.0 ± 0.6 per mm ($P < 0.05$), respectively. Neither parameter was increased by PTH in COX-2-/- mice. We conclude that the absence of COX-2 expression results in resistance to PTH-stimulated resorption in calvariae *in vivo*.

F439

Effect of Low Calcium Diet on Calcium and Skeletal Homeostasis in PTH-Deficient Mice. X. K. Tong*, D. Miao, R. Huo*, A. C. Karaplis, D. Goltzman. Medicine, McGill University, Montreal, PQ, Canada.

We previously reported that targeted disruption of the PTH gene leads postnatally to abnormalities in skeletal development and calcium homeostasis. $PTH^{-/-}$ mice on normal (1.0%) calcium diet developed hypocalcemia, hyperphosphatemia and decreased serum 1,25-dihydroxy vitamin D_3 ($1,25(OH)_2D_3$) levels and exhibited increased trabecular and cortical bone volume compared to wild type littermates. To further investigate the regulation of calcium and skeletal homeostasis in the absence of PTH, 2-month-old PTH deficient mice and wild type littermates were fed either a normal (1.0%) or low calcium (0.005-0.01%) diet for 8 weeks. When placed on a low calcium diet, normocalcemia and hypocalcemia persisted in the wild type and $PTH^{-/-}$ mice, respectively, but serum phosphate rose from 17.9±1.4 to 20.2±1.6 mg/dl in the $PTH^{-/-}$ mice. Serum $1,25(OH)_2D_3$ levels increased from 120 to 587 pmol/L in wild type and from 51 to 305 p mol/L in $PTH^{-/-}$ mice during the transition from a normal to a low calcium diet. Low calcium intake caused marked decreases in trabecular bone volume in both wild type (56%) and $PTH^{-/-}$ (78%) mice. Only in $PTH^{-/-}$ mice, however, did a low calcium diet cause a marked decrease (44%) in cortical bone volume. On a normal calcium diet, the number of TRAP positive osteoclasts was decreased (28.5%) in $PTH^{-/-}$ mice compared to the wild type animals. However, when the animals were changed to a low calcium diet for 3 days, the number of osteoclasts was increased 2-fold in the wild type mice and 6-fold in the $PTH^{-/-}$ mice. These studies show that although $PTH^{-/-}$ mice on a normal calcium intake have hypocalcemia, low $1,25(OH)_2D_3$ levels, low bone turnover and elevated bone mass, on a low calcium intake, $1,25(OH)_2D_3$ increases, accelerates bone resorption and has a negative impact on trabecular and cortical bone. Consequently a low calcium diet can stimulate $1,25(OH)_2D_3$ production even in the absence of PTH.

F440

Monitoring the Skeletal Response to PTH by Analysis of Peripheral Leukocyte Gene Expression. T. E. Hefferan[1], Q. Rehman*[2], N. E. Lane[2], R. T. Turner[1]. [1]Orthopedic Research, Mayo Clinic, Rochester, MN, USA, [2]Rheumatology, University of California - San Francisco, San Francisco, CA, USA.

Rheumatic disease is often treated with low-dose glucocorticoids , which is a risk factor for bone loss and fractures. Presently, several therapies are used to reverse this bone loss, including antiresorptive agents, calcium and vitamin D supplementation. These therapies are able to suppress resorption, but are unable to stimulate bone formation. Parathyroid hormone (hPTH 1-34) has been shown to increase spine trabecular bone density in postmenopausal women undergoing low-dose glucocorticoid therapy. Current methods to evaluate safety and efficacy are highly invasive (histomorphometry), insensitive (densitometry), or nonspecific (conventional biochemical markers). Therefore we wanted to determine a method of monitoring bone changes that was less invasive. We hypothesized that RNA extracted from leukocytes could be analyzed by microarray to examine genes related to bone metabolism that were being regulated with hPTH treatment. To test this hypothesis, RNA was isolated from leukocytes of control subjects and subjects receiving hPTH, 400U subcutaneously per day. One microgram RNA was hybridized to a microarray filter from ResGen that contains approximately 4,000 named genes. The microarrays from the hPTH treated subjects were compared to the microarrays from the control subjects. Many genes involved with bone metabolism were detected in the RNA isolated from the leukocytes, including growth factors, cytokines, bone matrix proteins, and bone morphogenetic proteins (BMPs). Bone matrix proteins including, type I collagen,

alkaline phosphatase, and biglycan were upregulated with PTH treatment. TGF-beta, as well as selective BMPs, -2,-4,-6, were upregulated in leukocytes with PTH treatment. Interestingly, both IGF–I and IGF-II, as well as IGF-binding proteins (IGFBP) –1, -2, and –3 were detected in leukocyte RNA. The microarray analysis showed IGF-I, the most potent IGF in bone, and IGFBP-3 to be upregulated by PTH treatment. Similar gene changes were observed in RNA isolated from the proximal tibial metaphysis of rats treated with hPTH (1-34). Thus, the regulation by PTH of selected genes in leukocytes that are related to bone metabolism reflects a similar regulation seen in bone. Therefore, analysis of gene expression in leukocytes could be utilized as a less invasive technique to assess expression of bone-related genes during disease and treatment.

F442

Osteopontin-Deficiency Augments Parathyroid Hormone Activation of Bone Formation (BFR/MAR) and Mineralized Nodule Formation without Altering PTH Enhancement of Deoxypyridinoline Excretion, in Vitro Osteoclastogenesis and Osterix Gene Expression. K. Kitahara[1], M. Ishijima[1], S. R. Rittling[2], K. Tsuji[1], H. Kurosawa*[3], A. Nifuji[1], D. T. Denhardt[2], M. Noda[1]. [1]Dept of Molecular Pharmacology, Tokyo Medical and Dental University, Tokyo, Japan, [2]Rutgers University, Piscataway, NJ, USA, [3]Juntendo University, Tokyo, Japan.

Treatment of osteoporosis patients at high risk requires not only inhibitors for bone resorption but also stimulators for bone formation. Intermittent parathyroid hormone (PTH) treatment enhances bone volume in osteoporosis patients and thus it is considered to be one of the promising treatments. However, underlying molecular mechanisms are largely unknown. Since PTH regulates expression of osteopontin (OPN) in osteoblasts, OPN could play a certain role in PTH actions in bone. We observed that OPN-deficiency enhanced PTH-dependent increase in bone mass based on micro-CT analyses of trabecular bone volume. To examine cellular and molecular basis for the OPN-deficiency effects on PTH-induced bone gain, we injected 80μg/kg PTH (1-34) daily for 5 days a week for 4 weeks into mice. PTH treatment increased mineral apposition rate (MAR) (by about 30%) as well as bone formation rate (BFR) (by about 30%) in wild type mice. In the OPN-deficient mice, basal levels of the two bone formation parameters were similar to those basal levels in wild type mice. However, OPN-deficiency significantly augmented PTH enhancement in MAR (by about 40%, $p<0.05$) and BFR (by about 100%, $p<0.05$). In vitro cell culture experiments using bone marrow cells obtained from PTH-treated mice indicated that OPN-deficiency clearly enhanced bone nodule formation (by 30%, $p<0.05$) while such augmentation was not significant in the bone marrow cell cultures taken from PTH treated wild type mice. PTH enhanced expression of osterix gene about 3-fold in the wild type long bone and a similar PTH effect on the expression levels of osterix m-RNA expression (3-fold) was observed in the long bone of OPN-deficient mice. In contrast to the OPN-deficiency enhancement of the PTH effects on bone formation parameters in vivo as well as in vitro, the levels of PTH-enhancement on the osteoclast number per area in vivo, TRAP positive cell development in culture, and excretion of deoxypyridinoline in urine were similar in wild type and OPN-deficient mice. These data indicated that OPN deficiency specifically augments the effect of PTH on bone formation in vivo as well as in vitro.

F446

Genetic Rescue of Cardiac Defects in Mice Lacking the PTH/PTHrP Receptor. M. C. Colbert*[1], J. Qian*[2], W. D. Stuart*[2], D. Witte*[3], E. Gruenstein*[4], H. Osinska*[5], B. Lanske[6], H. M. Kronenberg[7], T. L. Clemens[2]. [1]Department of Pediatrics, Children's Hospital Medical Center, Cincinnati, OH, USA, [2]Department of Medicine, University of Cincinnati, Cincinnati, OH, USA, [3]Pathology, Children's Hospital Medical Center, Cincinnati, OH, USA, [4]Department of Molecular Genetics, University of Cincinnati, Cincinnati, OH, USA, [5]Division of Molecular Cardiovascular Biology, Children's Hospital Medical Center, Cincinnati, OH, USA, [6]Department of Oral Pathology, The Forsythe Institute and Harvard Dental School, Boston, MA, USA, [7]Endocrine Unit, Massachusetts General Hospital, Boston, MA, USA.

Parathyroid hormone-related protein (PTHrP) is a key developmental regulatory protein and a potent vasoactive agent. Previous studies have shown that mice lacking either the *Pthrp* or the PTH type 1 receptor (*Pth1r*) gene exhibit severe chondrodysplasia, but in most genetic backgrounds, the receptor null mice die prenatally at mid gestation. We have previously reported that a functional PTH1R is expressed throughout the developing wild type mouse heart at E11 and that mice lacking the *Pth1r* gene die abruptly with massive cardiomyocyte death at gestational day E12. In the present study we further investigated the mechanisms for the heart defects in the PTH1R null mice. Histological and ultrastructural analysis revealed precipitous cardiomyocyte death and striking mitochondrial abnormalities at E11.5 followed by degenerative changes in the liver and massive necrosis of other tissues 24 hr later. No abnormalities were observed in the yolk sac or placenta implicating heart degeneration as the primary cause of death. To further examine the cause of cardiomyocyte death, sections of wildtype and null hearts were examined at E11.5, E12, and E12.5 and processed for TUNEL and caspase 3 staining. Our results suggest that apoptotic rates were not significantly elevated in nulls over those observed in wild-type mice. In order to verify that the lack of the receptor caused cardiomyocyte death, we intercrossed the PTH1R knockout mice with mice carrying a smooth muscle alpha actin PTH1R transgene (SMP-8-PTH1R). These transgenics, which express the receptor in the heart by E9.5, had been backcrossed onto the C57BL/6 background for 9 generations. PTH1R transgenic mice carrying both null *PTH1R* alleles survived until birth with skeletal dysplasia and other phenotypic abnormalities indistinguishable from the PTHrP null mice. Taken together, these findings demonstrate that the PTH1R is required for the development of normal cardiomyocyte function.

F449

Parathyroid Hormone-mediated Activation of MAPK Is Dependent upon NHERF2 in PS120 Cells. M. J. Mahon*[1], G. V. Segre[2]. [1]Endocine Unit, Massachusetts General Hospital, Boston, MA, USA, [2]Endocrine Unit, Massachusetts General Hospital, Boston, MA, USA.

The receptor for parathyroid hormone (PTH1R) binds to the Na+/H+-exchanger regulatory factor 2 (NHERF2) via a PDZ-domain-specific interaction in vitro, in glomerular extracts and when they are expressed in PS120 cells. The purpose of this research was to investigate the downstream actions of PTH1R when bound to NHERF2. NHERF2 contains two PDZ domains and a C-terminal region that interacts with ERM (ezrin, radixin, and moesin) actin-binding proteins. In vitro, PDZ1 and PDZ2 bind PLCbeta1 and PTH1R, respectively, to form a multiprotein complex. PTH treatment of PS120 cells that express both NHERF2 and PTH1R activate Gi/o protein(s) and thus inhibit adenylyl cyclase (AC) and markedly activate phospholipase C (PLC). Introduction of a M591A point mutation at the C-terminus of the PTH1R disrupts the NHERF2 interaction. PTH treatment of PS120 cells expressing NHERF2 and PTH1R, but not PTH1R(M591A), transiently activates extracellular regulated kinases (ERK) 1 and 2. Peak activation occurs after 5 minutes of PTH treatment as demonstrated by ERK1/2-mediated phosphorylation of myelin basic protein (MBP). Importantly, PTH treatment of PS120 cells expressing PTH1R(M591A) and NHERF2 fails to elicit a significant increase in ERK1/2 activation, indicating that signaling via the MAPK pathway is dependent upon the PTH1R-NHERF2 interaction. Neither AC/PKA nor PLC/PKC pathways, however, appear to be involved. Acute treatment of PS120 cells that express PTH1R and NHERF2 with forskolin (10 mM) fails to activate ERK1/2 and treatment with the PKA inhibitor, H89, fails to block the PTH-mediated activation of MAPK. These data suggest that PTH-mediated activation of MAPK is AC-independent. Whereas acute treatment of PS120 cells with phorbol esters (10 nM) activates ERK1/2, 24-hour treatment of PS120 cells with phorbol esters or an acute treatment with calphostin C, a PKC inhibitor, fail to block the PTH-mediated activation of ERK1/2, suggesting that PTH-induced MAPK is not dependent upon PKC activation. Furthermore, herbimycin A, a src-kinase inhibitor, genistein, a non-specific tyrosine kinase inhibitor and wortmannin, a PI-3 kinase inhibitor, fail to block PTH-mediated activation of MAPK. We conclude that PTH stimulation of the NHERF2-PTH1R complex activates the MAPK pathway by a novel mechanism(s).

F451

Arrestin Is Translocated by PTH but not Required for PTH1 Receptor Internalization. W. B. Sneddon*[1], A. Bisello[2], P. A. Friedman[1]. [1]Pharmacology, University of Pittsburgh, Pittsburgh, PA, USA, [2]Medicine, University of Pittsburgh, Pittsburgh, PA, USA.

Arrestins are adapter proteins that target activated G protein-coupled receptors (GPCRs) for endocytosis in clathrin-coated vesicles. Arrestin-dependent endocytosis of GPCRs has been implicated in receptor desensitization, downregulation, and recycling. The type I PTH receptor (PTH1R) is a class B GPCR that desensitizes and internalizes in response to ligand binding. In distal tubules (DT), the nephron site of PTH's calcium sparing action, both the agonist PTH(1-34) and the antagonist PTH(7-34) stimulate PTH1R endocytosis. In contrast, PTH(1-34), but not PTH(7-34), desensitizes the PTH1R in DT cells. PTH(1-34)-induced PTH1R internalization has an associated latency of 10 min, whereas PTH(7-34) internalizes the PTH1R promptly and 50% more extensively. This suggests that the two ligands employ different mechanisms of PTH1R internalization in DT cells. Ligand activated PTH1R internalization and arrestin3 movement were examined in DT cells by real-time confocal fluorescence microscopy. PTH(1-34) induced clustering and endocytosis of a green fluorescent protein (GFP)-tagged PTH1R. Internalization was not inhibited by a dominant negative (319-418) arrestin2, which competitively blocks arrestin's interaction with clathrin. However, this dominant negative arrestin blocked endocytosis of the same PTH1R in HEK293 cells. Internalization of the ß-adrenergic receptor by isoproterenol in DT cells was abolished by the dominant negative arrestin. In normal DT cells co-transfected with the wild-type human PTH1R and an arrestin3-GFP fusion protein, PTH(1-34) mobilized arrestin3 to the plasma membrane within 5 min. Clusters of arrestin3-GFP appeared in the cytoplasm after 15 min. In contrast, PTH(7-34) did not induce arrestin3 mobilization. Co-expression of PTH1R-GFP and an arrestin3-DsRed fusion protein indicated that the PTH1R and arrestin3 traffic together in response to PTH(1-34) but not PTH(7-34). Clathrin depolymerization prevented PTH1R internalization in response to both PTH(1-34) and PTH(7-34). We conclude that the interaction and trafficking of the PTH1R and arrestin3 is opportunistic but not required for PTH1R endocytosis in clathrin-coated vesicles. This interaction may, however, be required for PTH1R desensitization. The differential ability of different PTH peptides to desensitize and internalize the PTH1R underscores the presence of structural determinants within the PTH peptide that direct these processes. Carboxy-terminal PTH fragments that accumulate in renal insufficiency may contribute to PTH resistance through arrestin-independent PTH1R internalization.

F452

PTH Receptor Desensitization Accompanies Receptor Activation and not Internalization. W. B. Sneddon*[1], A. Bisello[2], P. A. Friedman[1]. [1]Pharmacology, University of Pittsburgh, Pittsburgh, PA, USA, [2]Medicine, University of Pittsburgh, Pittsburgh, PA, USA.

The physiological activity of G protein-coupled receptors (GPCRs) is a function of the balance between signal activation and termination. Receptor desensitization and downregulation are two mechanisms that terminate GPCR action. The parathyroid hormone type 1 receptor (PTH1R), a class B GPCR, is activated by the agonists PTH(1-34) and PTH(1-31), but not by the antagonist PTH(7-34). In contrast to their differential effects on receptor activation, both PTH(1-34) and PTH(7-34) internalize the PTH1R by 50% and 80%, respectively, after 15 min in mouse distal tubule (DT) cells, the site of the calcium sparing action of PTH. PTH(1-31), which stimulates cAMP, does not internalize the PTH1R. The present experiments were directed at determining if the separation of PTH1R activation and internalization was associated with a concomitant dissociation of PTH1R desensitization. Mouse DT cells stably expressing the PTH1R fused to enhanced green fluorescent protein (PTH1R-EGFP) were pre-treated with PTH(1-34), 7-34, 1-31, or vehicle at 37C. Cells were rinsed with ice-cold PBS, acid washed, and rinsed again with ice-cold PBS. The cells were loaded with ^{3}H-adenine at 4C and then challenged for 15 min at 37C with PTH(1-34) in the presence of IBMX. cAMP accumulation was measured after the second peptide treatment. Pre-treatment with PTH(1-34) or PTH(1-31) reduced subsequent PTH(1-34)-stimulated cAMP formation by 35% and 30%, respectively. In contrast, PTH(7-34), which robustly internalized the PTH1R did not desensitize the PTH1R. The inverse relation between receptor activation (RA) versus endocytosis (VE) of PTH peptides was analyzed. RA and VE were normalized to the effects of PTH(1-34), which has a value of 1. PTH(1-31) and PTH(7-34) have RAVE values of 6.6 and 0.02, respectively. We conclude that PTH1R desensitization follows the pattern of receptor activation but not the profile of endocytosis, and occurs with peptides having RAVEs >1. Therefore, PTH1R desensitization and internalization proceed by different mechanisms. Both phenomena employ similar structural determinants within the C-terminus of the PTH1R. However, uncoupling of the PTH1R from its cognate G protein may desensitize the PTH1R without necessarily targeting the receptor for internalization.

F456

A Novel Mutation in Helix 12 of the VDR Impairs Coactivator Interaction and Causes Hereditary 1,25-Dihydroxyvitamin D-Resistant Rickets Without Alopecia. P. J. Malloy*[1], R. Xu*[1], L. Peng*[1], P. A. Clark*[2], D. Feldman[1]. [1]Department of Medicine, Stanford University, Stanford, CA, USA, [2]Department of Pediatrics, University of Louisville, Louisville, KY, USA.

Hereditary vitamin D resistant rickets (HVDRR) is a genetic disorder most often caused by mutations in the vitamin D receptor (VDR). The patient in this study exhibited the typical clinical features of HVDRR with early onset rickets, hypocalcemia, secondary hyperparathyroidism, and elevated serum concentrations of alkaline phosphatase and 1,25-dihydroxyvitamin D, [1,25(OH)2D3]. Interestingly, the patient did not have alopecia. Assays of the VDR showed normal high affinity low capacity binding for [3H]1,25(OH)2D3 in extracts from the patient's fibroblasts. However, the cells were resistant to 1,25-dihydroxyvitamin D action as demonstrated by the failure of the patient's cultured fibroblasts to induce the 24-hydroxylase gene when treated with either high doses of 1,25(OH)2D3 or vitamin D analogs. This finding is unique since all other reported cases with complete resistance to 1,25(OH)2D3 action have had alopecia. A novel point mutation was identified in helix 12 in the ligand-binding domain of the VDR that changed a highly conserved glutamic acid at amino acid 420 to lysine (E420K). The patient was homozygous for the mutation. The E420K mutant receptor recreated by site-directed mutagenesis exhibited many normal properties including ligand binding, dimerization with the retinoid X receptor (RXR) and binding to vitamin D response elements (VDREs). However, the mutant VDR was unable to elicit 1,25(OH)2D3-dependent transactivation. Subsequent studies demonstrated that the mutant VDR had a marked impairment in binding the coactivators SRC-1 and DRIP205. Taken together, our data indicate that the mutation in helix 12 alters the coactivator binding site preventing coactivator binding and transactivation. In conclusion, we have identified the first case of a naturally occurring mutation in the VDR (E420K) that disrupts coactivator binding to the VDR and causes HVDRR.

F458

Enhanced Transactivation Activity of Vitamin D Receptor B1 Associated with Focal Nuclear Accumulation and Cofactor Binding. J. L. Flanagan*, K. L. Sunn*, G. M. Leong, C. Fong*, A. P. Kouzmenko*, J. A. Eisman, E. M. Gardiner. Bone and Mineral, Garvan Institute of Medical Research, Sydney, Australia.

Biological responses to 1,25 dihydroxyvitamin D3 are mediated by the vitamin D receptor (VDR), of which there are two protein isoforms. The A/B region of the recently identified VDRB1 isoform is extended at the N-terminus by 50 amino acids producing a 73 amino acid A/B region, compared with the 23 amino acids of the conventional VDRA receptor. As A/B regions of nuclear receptors often contain ligand-independent activation function (AF-1) domains, the functional properties of this region of VDRB1 might differ from those of VDRA. The VDRB1 isoform exhibited greater (144% ± 17%) transactivation of a rat 1,25-dihydroxvitamin D-24-hydroxylase reporter construct than VDRA in transiently transfected COS-1 cells 6 hr post treatment with 10nM 1,25-dihydroxyvitamin D3. This difference was not apparent at 16 hr post treatment. Evidence for AF-1 activity in the VDRB1 N-terminal A/B region was observed in yeast and mammalian one-hybrid experiments. The VDRB1 A/B region exhibited strong AF-1 activity (8-fold ligand-independent activation), compared to the VDRA A/B region (3-fold activation). Similarly, there was stronger interaction between the A/B region of VDRB1 and the VDR ligand binding domain (LBD) in mammalian two-hybrid and GST pull-down assays (3-fold in the presence of ligand, whereas interaction between the VDRA A/B domain and the LBD was weak. Introduction of an E420Q mutation into the LBD, which inactivates C-terminal ligand-dependent transactivation (AF-2) activity by abolishing recruitment of coactivators, markedly reduced but did not abolish ligand-dependent interaction with the VDRB1 A/B domain. This suggests that, as well as cofactor mediated interaction between the VDRB1 A/B domain and the LBD, there may be a direct AF-1/AF-2 interaction. In the absence of ligand, GFP-tagged VDRB1 accumulated in discrete nuclear foci whereas VDRA exhibited a diffuse nuclear signal. VDRB1 foci were not observed with the E420Q mutation, suggesting that speckle formation may be mediated at least in part by A/B domain-LBD interaction or by cofactor recruitment in the absence of ligand. Ligand-independent interaction of p160 co-activator proteins with full-length wildtype VDRB1, but not with the E420Q mutant VDRB1 or wildtype VDRA in GST-pull-down assays, supports the latter concept. Thus, accumulation of VDRB1 in nuclear foci may relate to its differential binding to transcriptional co-activators in the absence of ligand and the physical association of cofactors in the absence of ligand may allow for a more rapid response to ligand leading to the more effective transactivation observed.

F460

Persistent Reduction in Bone Resorption Despite Prolonged Dietary Calcium Restriction in Transgenic Mice with Elevated Osteoblastic Vitamin D Receptor. P. A. Baldock*, J. A. Eisman, G. P. Thomas, E. M. Gardiner. Bone and Mineral Research Program, Garvan Institute of Medical Research, Sydney, Australia.

1,25-Dihydroxyvitamin D3 stimulates both osteoblast and osteoclast activity. In order to amplify its osteoblastic actions, vitamin D receptor (VDR) levels were elevated exclusively in mature cells of the osteoblastic lineage in a transgenic mouse model (OSVDR). As previously reported, bone loss after 1 month of calcium restriction was reduced in OSVDR mice. These observations have now been extended to examine the long-term kinetics of this protective effect. Three month old OSVDR and wild type (FVB/N) mice were divided into 2 dietary groups consuming semi-synthetic High Ca (1% Ca) and Low Ca (0.1%) diets. Groups were collected at baseline (3 months old) and after 1 and 3 months of calcium restriction (4 and 6 months old). The 4th caudal vertebrae were analysed for trabecular architecture and turnover. Cancellous bone volume was greater in OSVDR than FVB/N across the study ($P<0.0001$). This difference (OSVDR vs FVB/N) was evident in High Ca fed groups at both 4 months (27.1 ±1.5% vs 21.5± 2.3%; $p<0.05$) and 6 months (21.1 ±0.9% vs 16.9 ±1.0%; $p<0.05$). In Low Ca groups, OSVDR was greater at 4 months (24.9 ±1.6% vs 17.5 ±1.5%; $p<0.05$) but had returned to FVB/N levels at 6 months (17.6 ±1.7% vs 16.6 ±1.4%). Trabecular thickness changes paralleled those of bone volume. Trabecular number was not different between genetic groups. The decline of OSVDR bone volume to FVB/N levels in the Low Ca group at 6 months was not the result of bone resorption. Osteoclast surface was significantly reduced in OSVDR across the study ($P<0.005$), but this was significant only in the Low Ca groups: 4 months (8.6 ±1.1% vs 13.3 ±0.6%; $p<0.05$) and 6 months (12.8 ±1.8% vs 19.7 ±2.3%; $p<0.01$). The decline in bone volume in the older Low Ca OSVDR group was, however, consistent with changes in bone formation. Bone formation rate was initially higher in OSVDR at 3 months (0.19 ±0.02 um2/um/d vs 0.12 ±0.02 um2/um/d; $p<0.05$) but was reduced in the 6 month groups to be lower than FVB/N ($p<0.005$) on both High Ca (0.09±0.01 vs 0.69±0.01) and Low Ca (0.21±0.01 vs 0.95±0.04) diets. These data suggest that elevation of VDR protein in mature osteoblastic cells results in a permanent reduction in bone resorption that persists despite extended calcium restriction. Furthermore, reduction in bone formation can contribute significantly to net bone loss during calcium restriction.

F463

Functional Characterization of the Intracellular Estradiol Binding Protein in Estrogen Resistant New World Primates. H. Chen[1], B. Hu*[2], M. Sharma*[3], Z. Sun*[3], J. S. Adams[1]. [1]Endocrinology/ Medicine, Cedars-Sinai Medical Center, UCLA School of Medicine, Los Angeles, CA, USA, [2]Pathology, Cears-Sinai Medical Center, UCLA School of Medicine, Los Angeles, CA, USA, [3]Surgery and Molecular Pharmacology, Stanford University School of Medicine, Stanford, CA, USA.

New World primates (NWP) exhibit a compensated form of resistance to gonadal steroid hormones. We recently demonstrated that estrogen resistance in NWP cells was associated with the overexpression of two proteins, one a non-receptor–related, dominant-negative acting-estrogen response element binding protein (ERE-BP) and the other an intracellular estradiol binding protein (IEBP). In order to study the function of IEBP, a 17ß-estradiol (E2) affinity column was used to purify IEBP from the estrogen-resistant NWP cell line, B95-8. N-terminal sequence analysis of tryptic peptides from E2-affinity-purified protein disclosed IEBP to be in the hsp27 family. The full-length cDNA of IEBP was successfully cloned and demonstrated 81% nucleotide homology with human hsp27. When hormone-responsive, wild type Old World primate (OWP) cells were transiently transfected with IEBP cDNA, E2-directed estrogen response element (ERE) reporter luciferase activity was reduced 50% compared to vector alone-transfected OWP cells. When IEBP and ERE-BP were co-transfected, the ERE luciferase reporter activity was further reduced by 60%. Gel shift analysis showed that IEBP neither bound to ERE nor competed with the estrogen receptor (ER) for binding to ERE. However, there was evidence of protein-protein interaction of IEBP and ER alpha; IEBP was coimmunoprecipitated with anti-ER alpha antibody in wild type cells stably transfected with IEBP. Specific interaction between the ER alpha and IEBP was confirmed in GST-pull down assays. Extracts from estrogen–responsive wild type and IEBP-overexpressing cells were incubated with a panel of GST-hormone receptor ligand binding domain fusion proteins representing the ER alpha, VDR

and GR. The GST-ER alpha fusion protein only reacted specifically with the hsp27-related IEBP but not with hsp70 or hsp90. The interaction of ER alpha and hsp27 in IEBP-overexpressing cells was 2-fold greater than in wild type cells. In summary, we have cloned and purified an intracellular estradiol binding protein (IEBP). IEBP is an hsp27-related protein which binds to the ligand domain of the ER alpha and acts to squelch ER alpha-directed ERE transactivation. We conclude that IEBP may collaborate with ERE-BP to cause estrogen resistance.

F465

Estrogen Receptor-β Reduces Estrogen Receptor-α Regulated Gene Transcription in Mice. C. Ohlsson[1], M. K. Lindberg*[1], S. Movérare[1], S. Skrtic*[1], H. Gao*[2], K. Dahlman-Wright*[2], J. Å. Gustafsson*[2]. [1]Div. Endocrinology, Dept. Internal Medicine, Gothenburg, Sweden, [2]Dept. Medical Nutrition and Dept. BioScience, Karolinska Institute, Novum, Huddinge, Sweden.

Estrogen is of importance for the regulation of adult bone metabolism. The aim of the present study was to determine the role of estrogen receptor-β (ERβ) *in vivo* on global estrogen-regulated transcriptional activity in bone. The effect of estrogen in bone of ovariectomized (ovx) mice was determined using microarray analysis including 9400 genes. Most of the genes (89%=289 genes) that were increased by estrogen in wild type (WT) mice were also increased by estrogen in ERβ inactivated ($ER\beta^{-/-}$) mice. The relative magnitude of the effect of estrogen in WT and $ER\beta^{-/-}$ mice was compared for these genes. Interestingly, the average stimulatory effect of estrogen on the mRNA levels of these genes was 82% ($p<0.0001$) higher in $ER\beta^{-/-}$ (472±25% over vehicle) than in WT (260±12% over vehicle) mice, clearly demonstrating that ERβ reduces ERα regulated gene transcription in bone. A similar inhibitory role of ERβ on ERα regulated gene transcription was also seen in liver ($p<0.0001$). The average stimulatory effect of estrogen on estrogen-regulated bone genes in ERα inactivated mice ($ER\alpha^{-/-}$; 169±9% over vehicle) was intermediate between that seen in WT (260±12% over vehicle) and ERαβ double inactivated mice ($ER\alpha^{-/-}\beta^{-/-}$; -7±3% over vehicle), demonstrating that ERβ, in the absence of ERα, is partially able to mediate the effect of estrogen on gene transcription. Thus, ERβ inhibits ERα mediated gene transcription in the presence of ERα, while, in the absence of ERα, it can partially replace ERα. In conclusion, our *in vivo* data indicate that an important physiological role of ERβ is to modulate ERα mediated gene transcription and we propose that ERβ may act as a transdominant repressor of ERα activity in mice.

F468

Real-time Non-Invasive *In vivo* Imaging of Estrogen Receptor Activity in Transgenic Mice. P. Ciana*[1], C. Lowik[2], E. Vegeto*[1], A. Brusadelli*[1], S. Belcredito*[1], I. Que*[2], A. Maggi*[1]. [1]Dept. of Pharmacological Sciences, Center MPL, Milan, Italy, [2]Endocrinology, LUMC, Leiden, Netherlands.

Estrogens exert complex physiological functions extending far beyond the control of reproductive functions. Several reports point to a beneficial role of estrogens with respect to diseases related to bone, mental and cardiovascular systems. Thus an increased understanding of the modalities of estrogen action and estrogen receptor (ER) activation in different tissues, might have relevant implications also from the therapeutic point of view. To date this has been hampered by the lack of suitable model systems. We recently generated transgenic mice expressing a ER reporter gene ubiquitously for direct evaluation of ER state of activation in physiological conditions as well as after treatments with compounds active through ERs. Preliminary results, showed that the luciferase reporter gene is expressed in all the tissues taken under consideration and is significantly induced by ER agonist only in tissues expressing ERs. Pharmacological studies carried out in male and female mice show that in the estrogen target organs the transcriptional activation of ER is regulated by estrogens in a dose- and time-dependent manner. In addition, the ER antagonists ICI 182,780 and Tamoxifen block estradiol action and have partial agonist functions in selected tissues. By the use of a CCD camera we here show that the activity of luciferase can be directly measured in living animals. The CCD camera was mounted on a light-tight specimen box and the bioluminescence emission from the anesthetized transgenic mice previously injected with luciferine was acquired and analyzed by the aid of specialized software. The *in vivo* analysis was initially carried out in adult cycling mice. We show that at at proestrus, when circulating estrogens are highest, lucifease activity is maximal in mammary gland, uterus, ovaries and liver, but not in bone, brain and intestine where luciferase peaks three days later at diestrus. In the absence of detectable levels of circulating estrogens like in ovariectomized and two-week old mice we document that estrogen receptor is transcriptionally active. Theses results demonstrate that the levels of circulating estradiol are not predictive of the state of estrogen receptor activity in each target. This is not the case with exogenous administration of estradiol to ovariectomized mice which induces a synchronous increase of luciferase activity in all the organs tested. The results of the present study underline a so far unsought complexity in the regulation of estrogen receptor activity partly independent from estradiol blood levels and which is not reproduced in hormone replacement therapy.

F473

Tumor Suppressor Smad4/DPC4 as a Differentially Ligand-Regulated Estrogen Receptor Corepressor. L. Wu*[1], S. Bai[1], X. Li*[1], Z. Liu*[1], B. Gathings*[2], C. Lu*[1], X. Cao*[1]. [1]Pathology, University of Alabama at Birmingham, Birmingham, AL, USA, [2]University of Alabama at Huntsville, Birmingham, AL, USA.

Estrogens regulate differentiation and maintenance of reproductive, skeletal, cardiovascular and neural tissues by activating their estrogen receptors (ER). Antiestrogen compounds exhibit a variety of different effects in different tissues, and are widely used for the treatment of osteoporosis, breast cancer and other diseases. Tamoxifen is an ER antagonist in breast tissue but an ER agonist in bone and uterine tissue. Raloxifene is also an ER antagonist in breast tissue and agonist for bone yet without estrogenic effect in uterine tissue. To examine their molecular mechanisms, we have identified that Smad4, a common signal transducer in BMP/TGF-β signaling pathway, functions as a transcription corepressor for human ERα. Smad4 plasmid was cotransfected with human ERα and estrogen response reporter plasmids in MCF-7 cells. Ectopic expression of Smad4 inhibited both estrogen and antiestrogen induced luciferase activity dose-dependently. In comparison with ERα, Smad4 only partially inhibited estrogen induced luciferase activity when human ERβ was coexpressed with Smad4 and the reporter plasmids, and it did not affect antiestrogen-mediated transcription inhibition like in ERα signaling. Yeast two-hybrid assay demonstrated the interaction between Smad4 and ERα. Furthermore, immunoprecipitation showed that endogenous ERα was co-immunoprecipitated with Smad4 and the interaction was only induced by antiestrogen ligands, not by β-estradiol. In addition, Smad4 and ERα formed a complex in gel-shift assays. The complex was further confirmed by super shifts with antibodies against Smad4 or ERα, respectively. As expected, Smad4 was demonstrated to interact with HDAC-3. By using TUNEL assay, we detected that retrovirus-mediated Smad4 expression enhanced antiestrogen-mediated apoptosis of MCF-7 cells. In a similar experiment, Smad4 enhanced antiestrogen-induced cell growth arrest. In summary, we found Smad4 functioned as a human ERα transcription repressor, and Smad4 repression activity was differentially regulated by antiestrogens. Thus, TGF-β may regulate breast cancer cell fate through Smad4-mediated cross-talk with estrogen signaling.

F478

Characterization of Glucorticoid Receptor (GR) Function in Osteoblast Differentiation using GR Deficient Mice. J. P. Tuckermann, B. Stride*, F. Tronche*, M. Kirilov*, G. Schütz*. Division of Molecular Biology of the Cell I, German Cancer Research Centre (DKFZ), Heidelberg, Germany.

An excess of glucocorticoids (GC) leads to net bone loss (osteoporosis) which is a major problem in therapeutic applications of GC. GC exert their effects by binding to the glucocorticoid receptor (GR) which in turn, causes positive or negative regulation of gene expression by binding to GC responsible elements (GRE) in the promoter region of target genes or by interacting with and thus interfering with other transcription factors such as AP-1 and NFkB. In addition GC have also been shown to act via non genomic effects interfering with signal transduction pathways. The role of the GR during differentiation of osteoblasts is at present unknown. Therefore, we analyzed the proliferation and differentiation capacity of primary calvarial osteoblasts derived from mice with abrogated glucocorticoid receptor by gene targeting (GRnull). The synthetic glucocorticoid dexamethasone inhibits the past confluency growth of calvarial osteoblastic cells. This inhibition is abolished in GRnull cells. The differentiation of GR deficient osteoblasts is accelerated in the presence of dexamethasone. The number of alkaline phosphatase positive cells are increased after one week of differentiation in GRnull cultures which results in an earlier onset of mineralized nodule formation. These results demonstrate that the GR is essential for mediating the inhibitory effects of GC in osteoblastic cell differentiation. In order to determine the mechanism by which the GR regulates osteoblastic differentiation we are currently extending our analysis to calvarial osteoblasts derived from GRdim mice. These mice carry a DNA binding defective GR, which is not able to activate GRE regulated gene expression. However, the mutated receptor is still able to interact with AP1 and NFkB to regulate gene expression. Finally, in order to more specifically address the role of GR in osteoblast function we are currently generating mice with an osteoblast specific deletion of the GR using the cre-lox P system. The precize characterization of these mice GR will allow an extended understanding of glucocorticoid induced osteoporosis on the molecular level.

F482

Serum 25 Hydroxyvitamin D Level Required to Minimise Bone Resorption in Postmenopausal Women. A. G. Need[1], P. D. O'Loughlin*[2], D. R. Jesudason*[3], B. E. C. Nordin*[4]. [1]Clinical Biochemistry, Institute of Med and Vet Science, Adelaide, Australia, [2]Clinical Biochemistry, Institute of Medical and Veterinary Science, Adelaide, Australia, [3]Clinical Biochemistry, Instituite of Medical and Veterinary Science, Adelaide, Australia, [4]Institute of Medical and Veterinary Science, Adelaide, Australia.

We have previously reported that serum parathyroid hormone (PTH) is increased in postmenopausal women with serum 25 hydroxyvitamin D (25(OH)D) below 40 nmol/L and that serum PTH becomes critical for maintenance of serum 1,25 dihydroxyvitamin D at these low levels [1]. Elderly patients with vitamin D insufficiency have elevated levels of PTH (which normalise when vitamin D is given), as well as a raised serum alkaline phosphatase (ALP) [2] and increased urinary excretion of c-termninal telopeptide [3] suggesting an increase in bone resorption. There is, however, controversy over the level of 25(OH)D necessary for bone health. We have therefore examined the relationships between serum 25(OH)D, serum ionised calcium, PTH, the formation marker ALP and resorption markers fasting urinary hydroxyproline, pyridinoline and deoxypyridinoline, corrected for creatinine (OHPr/Cr, PYD/CR and DPD/CR) in 486 postmenopausal women of mean age 63 (SD9.5) years attending our osteoporosis and menopause clinics. PTH, OHPr/CR, PYD/CR and ALP were inversely related to serum 25(OH)D. PTH was inversely related to serum ionised calcium. When the patients were divided into two groups with 25(OH)D above or below 20, 30, 40, 50, 60 or 70 nmol/L, we found the most significant differences between groups for all markers at a serum 25(OH)D of 60 nmol/L ($P<0.001$ for all). The most significant difference between groups for serum PTH was found when the patients were divided at a serum 25(OH)D of 50 nmol/L. When the patients with and without vertebral fractures were studied separately, a cut-off of 60 nmol/L of 25(OH)D was again found to give the most significant difference in both groups for all measures of bone turnover. We conclude that rises in PTH, three bone resorption markers and ALP can be detected in postmenopausal women when the serum 25(OH)D level falls below 60 nmol/L. Levels above this may be required for optimal bone health.

1. Need et al, Am J Clin Nutr 2000;71:1577-1581
2. Chapuy et al, N Engl J Med 1992;327:1637-1642
3. Mezquita-Raya et al, J Bone Miner Res 2001;16:1408-1415

F484

Identification of Oncogenic Nucleoporin CAN/Nup214 as a Regulator of Vitamin D Receptor -Mediated Transcription. Y. Miyauchi*[1], T. Michigami[1], K. Ozono[2]. [1]Department of Environmental Medicine, Osaka Medical Center and Research Institute for Maternal and Child Health, Osaka, Japan, [2]Department of Pediatrics, Osaka University Graduate School of Medicine, Osaka, Japan.

Vitamin D receptor (VDR) is one of the ligand-dependent transcription factors and must be localized in nuclei to exert its function. We have previously shown that VDR is located predominantly in nuclei even in the absence of ligand, and that the presence of ligand induces the accumulation of more VDRs in nuclei. In the present study, in an attempt to explore the molecules that can interact with VDR and modulate its function, we screened human kidney cDNA library by yeast two-hybrid system, and have found that VDR can bind to the C-terminal region of an oncogenic nucleoporin, CAN/Nup214. CAN/Nup214 was originally identified through its involvement in two types of acute myeloid or undifferentiated leukemia, and is a component of nuclear pore complex (NPC) that mediates the bidirectional traffic of macromolecules across the nuclear envelope. The binding of VDR with the C-terminal region of CAN/Nup214 was further confirmed by co-immunoprecipitation experiments in mammalian cells. In the region, CAN/Nup214 possess a FG repeat motif, which has been reported to play important roles in the nucleocytoplasmic traffic. We then examined the effect of overexpression of the FG repeat region of CAN/Nup214 on the 24-hydroxylase-gene promoter activity in osteoblastic SaOS-2 cells that possess the endogenous VDR. Treatment with 1,25(OH)2D3 increased the 24-hydroxylase-gene promoter activity, and the overexpression of the FG repeat region of CAN/Nup214 suppressed the 1,25(OH)2D3-induced transactivation in a dose-dependent manner. Similar results were obtained when COS7 cells were utilized with the exogenously expressed VDR. These results suggest that CAN/Nup214 regulate the VDR-mediated gene transcription probably by modulating the nuclear transport of VDR. It is reported that overexpression of CAN/Nup214 induces growth arrest in monocytic cell line U937, and 1,25(OH)2D3 is known as an inducer of differentiation in the cells of macrophage-monocyte lineage. Interaction between VDR and CAN/Nup214 might be involved in 1,25(OH)2D3-induced monocytic differentiation.

F488

Liganded VDR Induces CYP3A4 via DR3 and ER6 VDREs: A Potential Mechanism for Vitamin D-mediated Cellular Detoxification. P. W. Jurutka, P. D. Thompson, G. K. Whitfield, S. M. Myskowski*, K. R. Eichhorst*, C. Encinas Dominguez*, C. A. Haussler*, M. R. Haussler. Biochemistry and Molecular Biophysics, University of Arizona College of Medicine, Tucson, AZ, USA.

The nuclear vitamin D receptor (VDR) mediates the effects of 1,25-dihydroxyvitamin D_3 ($1,25D_3$) to alter gene transcription and achieve bone mineral homeostasis. Additionally, extraosseous actions of $1,25D_3$ are observed in several epithelial cell types, as well as in the immune and central nervous systems. $1,25D_3$ also triggers vitamin D catabolism through induction of 25-hydroxyvitamin D_3 24-hydroxylase (24-OHase), a cytochrome P450-containing (CYP) enzyme encoded by a gene possessing two (proximal and distal) vitamin D responsive elements (VDREs). In the present study, we examined the efficacy of $1,25D_3$ to induce other CYP enzymes. The human CYP3A subfamily consists of four homologous proteins (CYP3A4, -3A5, -3A7 and -3A43) that are collectively expressed in many tissues, including the gastrointestinal tract, liver, kidney and prostate. Exposure of human colorectal adenocarcinoma cells (HT-29) to 10^{-8} M $1,25D_3$ resulted in a 3-fold induction of CYP3A4 mRNA as assessed by quantitative RT-PCR. The effect was specific for VDR since treatment with dexamethasone (a GR and PXR agonist), that normally upregulates CYP3A4 in liver, did not affect expression in HT-29 cells. Examination of HT-29 cell extracts by Western blotting with anti-CYP3A4 mAb confirmed a stimulatory action of $1,25D_3$ at the protein level. Analysis of the promoter region of human CYP3A4 (10.5 kb) revealed the presence of six VDRE-like sequences that were then tested in hormone-dependent gel mobility shift assays using purified human VDR and RXRα along with HT-29 cellular extracts. Each VDRE was also examined for its ability to drive the transcription of a reporter gene in response to 10^{-8} M $1,25D_3$ in HT-29 and Intestine 407 cells. These experiments identified two candidate VDREs that support both significant $1,25D_3$-dependent VDR/RXR binding and marked stimulation of reporter gene expression. The first VDRE is a canonical DR3-type element located in the distal region of the promoter (-7719-GGGTCA gca AGTTCA-7733), and the second is a more proximal, non-classical everted repeat with a spacer of 6 bases (ER6; -169-TGAACT caaagg AGGTCA-152). A similar analysis of the rat CYP3A23 (the kidney-expressed homolog of human CYP3A5) promoter led to the identification of an active DR3-type VDRE (-120-AGTTCA tga AGTTCA-134). These data suggest that $1,25D_3$-dependent, VDR-mediated induction of CYP enzymes may be an important mechanism not only in vitamin D catabolism via upregulation of 24-OHase, but also of more general significance in the cellular detoxification of xenobiotics.

SA001

See Friday Plenary number F001.

SA002

Changes in Bone Geometry and Body Composition during Adolescence: The Penn State Young Women's Health Study. T. L. Oreskovic*[1], K. Uusi-Rasi*[1], M. A. Petit[2], C. Bentley*[2], M. Tulchinsky*[3], T. J. Beck[1], T. Lloyd[2]. [1]Department of Radiology, The Johns Hopkins University School of Medicine, Baltimore, MD, USA, [2]Department of Health Evaluation Sciences, Penn State University, College of Medicine, Hershey, PA, USA, [3]Department of Radiology, Penn State University, College of Medicine, Hershey, PA, USA.

Skeletal bone mass is known to accumulate during growth and reaches a peak in early adulthood. Whether this accumulation of mass corresponds to an increase in mechanical strength has not been established and was the objective of this study. Longitudinal hip scans acquired on a Hologic QDR2000 DXA in the Penn State Young Women's health study were analyzed using the Hip Structure Analysis (HSA) program. The program analyzes narrow regions traversing the femoral neck and proximal shaft to derive BMD, cross-sectional area (CSA), subperiosteal width (W) section modulus (Z) and estimated mean cortical thickness (CT). Changes in BMD and bone structural variables from 16.5y (range 16-17y) to 21.5y (range 21-22y) were compared in 56 participants at the neck and 53 at the shaft (reduced due to shaft cut-off on 3 images). Body composition (lean and fat mass) was taken from DXA total body scans. Paired t-tests were used to assess change in body composition, BMD and bone structural variables over 5 years. On average, weight, total fat mass, total body bone mass (tbBMC) increased from ages 17 to 22, while total lean mass declined ($p < 0.001$). BMD increased at the shaft but remained unchanged at the neck. CSA, W and Z increased ($p < 0.03$) but CT remained unchanged at both regions. After adjusting for change in lean and fat masses, BMD and CT changes were non significant at both regions, but Z, CSA and width all increased significantly ($p< 0.03$). Over the late adolescent period, proximal femur BMD remained unchanged in these young, healthy Caucasian women. The lack of change in BMD was due to an increase in the amount of bone (CSA) as well as in its size, because these changes have opposing effects on BMD. The increases in CSA and Z suggests that axial and bending strength is increasing during this period of life, independent of changing body mass and composition.

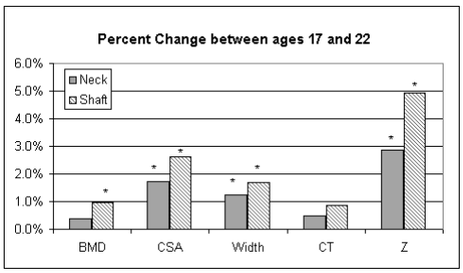

SA003

See Friday Plenary number F003.

SA004

Generalised Osteopenia Associated with Higher Calcium Intake in Adolescent Idiopathic Scoliosis. W. T. K. Lee*[1], C. S. K. Cheung*[1], X. Guo[2], J. C. Y. Cheng*[1]. [1]Orthopaedics & Traumatology, The Chinese University of Hong Kong, Shatin, Hong Kong Special Administrative Region of China, [2]Rehab. Sciences, Hong Kong Polytechnic University, Kln., Hong Kong Special Administrative Region of China.

Adolescent Idiopathic Scoliosis (AIS) is a serious deformity of the spine affecting mostly adolescent girls. Generalised low bone mineral density (BMD) has been observed in AIS patients. Whether low BMD is due to low calcium (Ca) intake is not certain. This study aimed to correlate the habitual Ca intake and BMD in AIS patients and to compare with age-matched normal controls. 788 girls aged 11-16-y (582 AIS patients & 206 healthy control girls) entered the study. Areal BMD (aBMD) of the lumbar spine (L2-L4), femoral neck, Ward's triangle and trochanter were measured by DXA (Norland XR-36). Volumetric BMD (vBMD) of the distal radius and distal tibiae were measured by pQCT (Densiscan 1000). Ca intake was assessed by a food frequency method. Pubertal status was physically examined. Osteopenia and osteoporosis were defined as BMD based Z scores -(1 to 2) SD of, and -2 SD of normal mean BMD values respectively. 20.33% & 22.45% AIS patients were found osteopenic while 2.03% & 2.35% were osteoporotic based on aBMD and vBMD based Z scores respectively. At pre-puberty, no significant differences in aBMD & vBMD were found between AIS and controls. However, as the girls grew from Tanner's stage (breast) 2 to 5, the differentials of aBMD at various sites between the AIS and control group increased from -4.3% to -9.4 % ($P = 0.0033$ to <0.001), whereas those of vBMD between the AIS and control group increased from -5.0% to -9.3 % ($P = 0.09$ to <0.001). Mean Ca intakes of both groups were <500 mg/d. However, mean Ca intake of AIS patients was significantly higher than that of controls (442.6 ± 349.1 mg/d vs. 349.3 ± 224.5 mg/d, $P<0.001$). Furthermore, Ca intake was significantly correlated with BMD at most skeletal sites in AIS from Tanner's stage 3-5 ($P = 0.048$ to < 0.0001). In addition, multiple regression models showed that Ca intake was an independent predictor to predict the variations of aBMD ($P<0.05$) and vBMD ($P<0.05$) at various sites of the girls. To conclude, a large proportion of AIS girls were found osteopenic and even osteoporotic at the critical phase of pubertal bone growth, the disparity of BMD between AIS girls and controls increased when they were becoming sexually matured. Ca intake was positively correlated with BMD in AIS. Despite a relatively higher Ca intake, BMD of AIS was still significantly lower than that of controls suggesting an abnormal Ca homeostasis and bone turnover exists in AIS patients. Further study on the etiology of osteopenia in AIS patients would provide novel approach in the monitoring, prognostication and treatment of AIS.

SA005

Abnormal Bone Turnover in Adolescent Girls with Idiopathic Scoliosis. C. S. K. Cheung*[1], W. T. K. Lee*[1], X. Guo[2], S. P. Tang*[1], S. K. M. Lee*[1], J. C. Y. Cheng*[1]. [1]Orthopaedics & Traumatology, The Chinese University of Hong Kong, Shatin, Hong Kong Special Administrative Region of China, [2]Rehab. Sciences, Hong Kong Polytechnic University, Kln., Hong Kong Special Administrative Region of China.

Declines in axial and peripheral bone mineral density (BMD) during pubertal growth have been observed in adolescent idiopathic scoliosis (AIS). In our ongoing study more than 20% and 2% of AIS girls at age 11-16-y were found osteopenic and osteoporotic respectively based on BMD Z-scores. Bone deposition in growing children is a net result of bone formation and bone remodeling process. Thus, low systemic BMD in growing AIS girls could well be related to disturbance of bone turnover. We attempted in this study to evaluate the bone turnover in AIS patients and compared the results with normal age matched controls. 538 girls aged 11-15-y (AIS, n = 396; normal controls, n=142) entered the study. Serum bone-alkaline phosphatase (bALP) reflecting bone formation activity and urinary deoxypyridinoline (Dpd) reflecting bone resorption activity were assayed by spectrophotometry and ELISA method (Metra Biosystems, USA) respectively. AIS girls had markedly higher serum bALP level at age 11, 13 & 14 year, whereas urinary Dpd level of AIS was marginally lower at age 13-y and were significantly lower than those of controls at age 14-y (P=0.022) and 15-y (P=0.043) (Fig. 1). In conclusion, AIS patients from age 11-15-y had uncoupled bone turnover rates: higher bone formation and lower bone resorption rate during pubertal growth. The significant reduction in BMD in growing AIS as evident in our ongoing research was not a direct result of enhanced bone resorption as reflected in the Dpd level in the present study. This observation is drastically different from that of age related osteoporosis. Further metabolic bone studies are warranted to understand the etiopathogensis of fast linear growth rate and systemic low BMD in growing AIS patients.

Fig.1. Median Levels of bALP and Dpd of AIS *vs.*Control Girls Aged 11-15-y

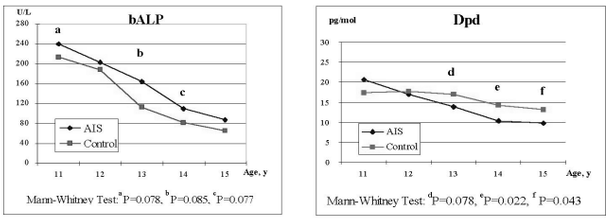

SA006

See Friday Plenary number F006.

SA007

Seasonal Gains in Bone Mineral Content of the Spine during Puberty in Girls. S. S. Sullivan*[1], C. J. Rosen*[2]. [1]Food Science and Human Nutrition, University of Maine, Orono, ME, USA, [2]Maine Center for Osteoporosis Research and Education, St. Joseph Hospital, Bangor, ME, USA.

Puberty is a time of rapid bone mineralization and a critical time for interventions to maximize the peak bone mass acquired. The purpose of this study was to compare gains in bone mineral content (BMC) at the end of summer with those at the end of winter to see if a seasonal pattern in bone mineralization could be detected. We measured BMC of the spine using dual x-ray absorptiometry in 23 girls, age 10 to 13 years, each September and March for two years. The subjects self-assessed their Tanner stage of puberty using photographs. The ratings for breast and pubic hair stages were averaged together. Heights and weights were measured with each bone density measurement. Gains in BMC were stratified according to Tanner stage: Tanner 1.5 to 2 (n=10 measurements), Tanner 2.5-3 (n=28 measurements), and Tanner 3.5-4 (n=26 measurements). The mean ± standard deviation 6-month gain in BMC for girls in Tanner stage 1.5 to 2 was 1.91 ± 0.86 g, in stage 2.5-3 was 2.52 ± 1.59 g, and in stage 3.5-4 was 4.4 ± 1.99 g. Within each Tanner category, there was no significant difference between gains in BMC after summer versus winter seasons. The greatest mean 6-month gain in height (3.56 ± 0.95 cm) occurred in Tanner stage 2.5 to 3 while the greatest mean 6-month gain in weight (3 ± 3.19 kg) occurred in Tanner 3.5-4. A seasonal difference in the rate of gain in BMC or in rate of growth was not apparent.

SA008

In vivo Three-Dimensional Analysis of Trabecular Structure of Human Vertebra Using Image Data from Multi-Detector Computed Tomography-Its Precision Study. M. Takada[1], S. Imai*[2], K. Kikuchi*[2], K. Murata*[1]. [1]Radiology, Shiga Univ. of Med. Sci., Otsu, Japan, [2]Orthopaedic Surgery, Shiga Univ. of Med. Sci., Otsu, Japan.

We developed a system to perform in vivo three-dimensional (3D) analysis of trabecular structure of human vertebra using image data from multi-detector computed tomography (MDCT). Image data of MDCT, which is used clinically, was imported into the software specialized for 3D analysis of trabecular bone architecture. This allowed us to evaluate human vertebra in vivo. The purpose of this study was to evaluate reproducibility of those parameters. The lumbar vertebra of a cadaver (male, 84 years old) was used for this precision study. The L1-5 vertebra with the surrounding soft tissue was scanned by MDCT, Somatom Plus 4 (Siemens, Erlangen, Germany), at 140Kv and 170mAs, by a slice thickness of 0.5mm, and the CT images were reconstructed using a field of volume of 50mm x 50mm with 0.2mm interval, resulting a spatial resolution of 0.097mm x 0.097mm with a thickness of 0.2mm. The image data of the 165 slices was imported into the software of 3D analysis for trabecular structure, TriBON (Ratoc System Engineering, Tokyo, Japan) and a 3D image was constructed. A cubic region of interest (ROI) for analysis was extracted by the following way. The base was the maximum size of a square on the transverse image at the middle portion of the vertebra. Along z-axis, the images containing the upper and lower endoplates were excluded. Finally the size of the ROI for the vertebra was 19 x19 x 17.3 mm3. 3D analysis was performed for the cube, and bone volume (BV), bone surface (BS), trabecular bone volume fraction (BV/TV), trabecular thickness (Tb.Th), trabecular separation (Tb.Sp), trabecular bone pattern factor (TBPf), structure model index (SMI), and number of nodes (N.Nd) were calculated. In order to evaluate reproducibility, the vertebra was scanned 5 times with repositioning, and coefficient variations (CVs) of those parameters were calculated. The CVs for BV, BS, BV/TV, Tb.Th, Tb.Sp, TBPf, SMI, N.Nd were 1.8%, 0.91%, 1.8%, 1.4%, 1.5%, 7.7%, 0.81%, 2.5%, respectively. The results were comparable to those of bone densitometry by dual x-ray absorptiometry except TBPf. This suggests that our method to set ROI would be reproducible, and also a possibility of in vivo 3D analysis of trabecular bone structure of human vertebra.

SA009

See Friday Plenary number F009.

SA010

Aging Increases the Propensity of Osteoblasts to Induce Osteoclastogenesis by Increasing Expression of RANKL and Decreasing Expression of OPG. J. Cao, L. L. Venton*, B. P. Halloran*. Department of Medicine and Physiology, University of California at San Francisco, San Francisco, CA, USA.

With advancing age, the osteoprogenitor pool diminishes, while the osteoclast progenitor pool increases and the balance between formation and resorption necessary to maintain bone mass is lost. Osteoblasts regulate the recruitment and activity of osteoclasts through expression of receptor activator of nuclear factor κB ligand (RANKL) and osteoprotegerin (OPG). To determine whether osteoblasts from marrow stromal cultures of aged animals have a greater tendency to induce osteoclastogenesis than osteoblasts from younger animals we measured: 1) induction of osteoclastogenesis (tartrate resistant acid phosphatase staining) by osteoblasts in a donor-age-mixed cross-over co-culture system, and 2) expression of RANKL and OPG by real-time PCR in whole bone and bone cells in 6 week (young), 6 month (adult) and 24 month (old) old mice. Co-culture of equal numbers of osteoblasts (OB) from young (Y), adult (A) and old (O) mice with equal numbers of osteoclast (OC) precursor cells from young, adult and old mice produced 56±16, 63±12 and 135±31 (Y, A, O-OB x y-OC, respectively); 66±5, 71±18, and 202±38 (Y, A, O-OB x A-OC, respectively); 69±11, 96±17, and 246±77 (Y, A, O-OB x O-OC, respectively) tartrate-resistant acid phosphase-positive osteoclast-like cells. RANKL mRNA levels in whole bone were 2.1- fold and 4.4-fold higher in adult and old mice, respectively, compared to young mice, whereas OPG mRNA levels in whole bone decreased with age. Expression of RANKL was higher and expression of OPG lower in cells from older animals early in culture (day 7). With cell maturation in culture, RANKL mRNA levels in cells from young and adult mice increased significantly while levels in cells from old animals decreased. By 21 and 28 days of culture, no differences were found in RANKL mRNA in osteoblasts among different age groups. These data demonstrate that: 1) osteoblasts from older animals have a greater propensity to induce osteoclastogenesis than oseoblasts from younger animals, and 2) these changes are associated with increased RANKL and decreased OPG expression.

SA011

See Friday Plenary number F011.

SA012

Osteoprotegrin, COLIA1 and VDR Gene Polymorphisms and the Rate of Bone Loss in Postmenopausal Irish Women. F. J. Drummond*, F. Wynne*, M. G. Molloy*, K. A. Quane*. Rheumatology and Medicine, National University of Ireland, Cork, Cork, Ireland.

Genetic factors are known to influence peak bone mass and there is increasing evidence to suggest that they also affect the rate of change in bone density. We investigated the role of polymorphisms in the Osteoprotegrin (OPG), COLIA1 and VDR genes with change in bone mineral density (BMD) by association in a longitudinal study in 134 postmenopausal Irish women (mean age 58.19 ± 7.67 years) over a mean follow-up time of 2.70 ± 1.15 years. Rate of change in bone mineral density (BMD) at the lumbar spine (LS) and femoral neck (FN) was calculated from baseline and follow-up DEXA measurements and expressed as annualised percentage (%/yr) rate of change from initial BMD values. Significant covariates with rate of change of BMD were identified from stepwise linear regression analysis and were used to adjust annualised bone loss. The Fok1 VDR, Hpa1 OPG T950C, Alwn1 OPG G1181C and Sp1 COLIA1 polymorphisms were investigated by RFLP analysis. Association of genotype with change in BMD was analysed in terms of three possible genetic models: the effect of a (A) dominant or (B) recessive allele, tested using an unpaired 2-tailed t-test and (C) allele-dose effect of a "risk/protective" allele, tested by looking for a linear trend going from 0 alleles to 1 to 2 by linear regression analysis. Bonferroni correction factor was used to correct for multiple hypothesis testing ($p<0.01$). Genotype frequencies for each polymorphism were in Hardy-Weinberg equilibrium. Bone loss at the FN was adjusted for weight, age and baseline BMD. There was a relationship between bone loss at the FN and OPG G1181C genotype ($p = 0.03$) such that the CC group lost more bone than the GG group (22.41 %/yr and 17.85 %/yr, respectively). This was not significant following the Bonferroni correction. A significant interaction between age and OPG G1181C genotype ($p = 0.01$) was observed, where women above 60 years with the CC genotype had 25% greater bone loss than women with the GG genotype and heterozygotes had intermediate rates of bone loss. There was a linear allele dose effect ($p = 0.03$). An interaction was also observed between age and VDR genotype, where women older than 60 years with the FF genotype lost more bone than the other two genotypes ($p=0.03$). No association was observed between rate of bone loss and either of these alleles in women below 60 years. Annualised bone loss at the LS was adjusted for weight and baseline BMD. No association was observed between OPG T950C or COLIA1 and rate of bone loss at the FN or between polymorphisms in these three genes and the rate of bone loss at the LS. This data supports the involvement of OPG G1181C and Fok1 VDR polymorphisms in the regulation of postmenopausal change in bone density at the FN.

SA013

See Friday Plenary number F013.

SA014

Long-term Bone Loss in Elderly Women: A 10-year Epidemiological Study. T. V. Nguyen*, J. R. Center*, J. A. Eisman. Bone and Mineral Research Program, Garvan Institute of Medical Research, Sydney, Australia.

Femoral neck bone mineral density (BMD) is known to decline with aging, but the magnitude of decline has been inadequately documented as short-term studies are often confounded by few measurements and relatively small sample size. The present epidemiological, population-based study was designed to assess the long-term changes in BMD in a group of 1030 Caucasian women of Caucasian background, whose age was 70 ± 6.6 years (mean ± SD). The women had been followed for an average of 8.6 years (range: 1.3 to 12.6 years). BMD at the femoral neck and lumbar spine were measured dual energy X-ray absorptiometry using a LUNAR DPX-L densitometer (LUNAR Corporation, Madison, Wisconsin, USA). The median number of measurements per subjects was 4 (range: 2-6). The annual rate of change in femoral neck and lumbar spine BMD, measured by DXA, was -0.6 ± 1.8% and +0.2 ± 1.4% (mean ± SD), respectively. The increase in lumbar spine BMD was presumably confounded by osteoarthritis and degenerative change. At the femoral neck, although there was a wide range of loss, there were no evidence of a distinct "fast loss" group as the rates were normally distributed. During the the entire study period, approximately 54% of women experienced a decrease of at least 1% per year, 14% of women experienced an increase of at least 1% per year, and 32% of women experienced no change in BMD. The rate of loss in femoral neck BMD accelerated with advancing age. There was no significant correlation between baseline BMD and its rate of change. Subjects with only 2 measurements had a significantly higher rate of femoral neck bone loss (-1.1 ± 3.0%; $p < 0.01$) than those with higher frequency of measurements (-0.5 ± 1.4%). However, among subjects with the same number of measurements, those who had been followed for a longer duration had a significantly lower rate of loss than those who had been followed for a shorter duration. While both weight and age were significantly associated with change in femoral neck BMD, they accounted for only 3% of the variance of rates of change in femoral neck BMD. However, the changes in bone mineral content and cross-sectional area explained almost 94% of the variance of femoral neck bone loss. It is concluded that bone loss at the femoral neck in elderly women is highly heterogeous, and increased with advancing age but at a slower rate than previously documented. These results also suggest that a two-measurement method of estimation of bone loss is not reliable, and that an increase in the duration of follow-up (more than 2 years) could yield a more accurate estimate of change in bone mineral density for individual subjects.

SA015

Identification of Placental Growth Factor as a New Early BMP-2 Target Gene in Bone Cells. S. Marrony*, F. Bassilana*, K. Seuwen*, H. J. Keller. Bone Metabolism Research, Novartis Pharma AG, Basel, Switzerland.

The bone morphogenetic proteins (BMPs), and in particular BMP-2, are well known inducers of bone formation both in vitro and in vivo. BMPs are even capable of inducing ectopic bone formation when injected subcutaneously into rodents through a process that resembles endochondral bone formation and fracture repair. Although BMP-2 has been shown to stimulate in vitro osteoblast differentiation and concomitant induction of osteoblastic gene expression, the early gene regulatory events by which these complex effects are induced are unclear. Thus, we have used high-density cDNA microarrays to identify new BMP-2-regulated genes in primary human trabecular bone cells (HTBs). Placental growth factor (PlGF) was found to be an early regulated gene whose induction was already detected after 2h treatment with BMP-2. Microarray tissue distribution analysis of PlGF mRNA in several tissues and cell lines showed a very restricted expression only in BMP-2 treated HTBs and in placenta, as previously described. Induction of PlGF by BMP-2 in HTBs was confirmed by ribonuclease protection assay (RPA). In addition, RPA was used to measure PlGF isoform expression. Two PlGF isoforms (PlGF1 and 2) have been described that differ in a 21 amino acid insert near the C terminus. PlGF-1 was twice as much expressed in HTBs than PlGF-2, whereas placenta showed the reverse ratio as described. Next, we analyzed PlGF expression in two commonly used osteosarcoma cell lines, MG63 and U-2 OS. Interestingly, BMP-2 induced PlGF expression in MG63 but not in U-2 OS cells. PlGF induction appears highly specific as neither vitamin D3, tumor growth factor beta, nor basic fibroblast growth factor were able to stimulate PlGF expression. BMP-2 induced PlGF mRNA expression in MG63 with an ED50 of about 50 ng/ml and expression peaked between 24 and 32 h after treatment. Finally, strong stimulation of PlGF protein release by BMP-2 from MG63 and HTBs was detected by immunoassay. In summary, we have identified PlGF, which is a member of the vascular endothelial growth factor (VEGF) family, as a new BMP-2-regulated early gene in bone cells. This suggests that PlGF may play a role in osteoblast differentiation and bone formation.

Disclosures: ***H.J. Keller****, Novartis Pharma AG, Basel, Switzerland 3.*

SA016

See Friday Plenary number F016.

SA017

OP-1 Induces Bone Formation in the Presence of Bacterial Infection. L. S. Kidder, X. Chen*, A. H. Schmidt*, W. D. Lew*. Midwest Orthopaedic Research Foundation, Minneapolis, MN, USA.

Infection is a common complication of open fractures. Since infection directly hinders the bone healing cascade, it is necessary to effectively treat the infection before significant healing can be appreciated. Treatment usually requires the removal of the fixation device, surgical débridement, and antibiotic therapy, followed by re-fixation. An intervention that accelerates fracture healing without exacerbating the infection would improve the clinical management of these difficult cases. To address this, we have examined whether Osteogenic Protein-1 (OP-1/BMP-7), can be used to stimulate bone formation in the presence of Staphylococcus aureus. In one series of experiments, we assessed BMP-mediated osteoinduction in a mechanically isolated setting with and without the presence of metal. Lyophilized allogenic collagen carrier was combined with 0 or 25 ug OP-1 +/- 5x10E5 CFUs of S. aureus. This bolus was implanted in surgically created pockets in rats thoracic erector spinae muscle. A 1x1mm stainless steel rod was sutured into some pockets, in order to provide a metallic surface for bacterial proliferation. Quantitative radiographic examination and calcium measurements of the intramuscular ossicles revealed that OP-1 induced the formation of mineralized bone by 2 weeks ($p=0.002$). While infection significantly diminished the osteoinductive response ($p<0.01$), 25ug OP-1 initiated significant mineralized bone formation compared with carrier alone ($p=0.015$). The presence of metal did not significantly influence the outcomes. In order to assess osteoinduction in an intraosseus setting, a 6mm mid-diaphyseal segmental defect was surgically created and internally stabilized in the rat femur. These critical defects received implants of either 0, 11, or 50ug of OP-1 mixed with collagen carrier +/- 10E5 CFUs of Staphylococcus aureus. Untreated infection in this model resulted in loss of fixation by 9 weeks. OP-1 (50ug) healed the infected defect, significantly maintaining construct stability. We demonstrate here that OP-1/BMP-7 maintains its osteoinductive capacity in the presence of a clinically significant infection. The controlled application of an osteo-anabolic cytokine (such as a BMP) may permit the earlier removal of stabilizing hardware, thereby allowing more efficacious treatment of osteomyelitis Resources for this project were generously provided by the (US) Orthopaedic Trauma Association and Stryker Biotech Corp.

Disclosures: ***L.S. Kidder****, Stryker Biotech 2.*

SA018

See Friday Plenary number F018.

SA019

Effects of Osteogenic Protein-1 (OP-1, BMP-7) on Medial Collateral Ligament Cells in Culture. A. D. Tsai*[1], L. C. C. Yeh*[1], J. C. Lee[2]. [1]Biochemistry (MC7760), University of Texas Health Science Center, San Antonio, TX, USA, [2]Biochemistry (Mail Code 7760), The University of Texas Health Science Center, San Antonio, TX, USA.

The medial collateral ligament (MCL) is a commonly injured area of the knee joint. Healing of the ligament is a complicated process consisting of cellular proliferation and migration, as well as synthesis and deposition of ligament components. The healing process seems to be affected by growth factors, such as basic FGF, PDGF-B, and TGF-beta. Limited data is currently available on the effects of bone morphogenetic proteins (BMPs) on ligaments. BMPs are members of the transforming growth factor-β superfamily. Osteogenic Protein-1 (OP-1), a member of the BMP family, induces formation of new bone and cartilage. In the present study, we wished to use primary cultures of rat MCL cells as a model to study the effects of Osteogenic Protein-1 (OP-1, BMP-7) on cell proliferation and gene expression. MCLs from young adult male rats were surgically excised from the surrounding connective tissues at the knee joints and cultured in DMEM/F12 with 10% FBS. Treatment with OP-1 resulted in dose-dependent increases in alkaline phosphatase activity and cell proliferation. Northern blot analysis revealed that control cells expressed a high level of type I collagen mRNA. OP-1-treated MCL cells expressed an elevated steady-state mRNA expression level, in a dose- and time-dependent manner. OP-1 stimulated the activity of the cloned promoter of type I collagen. The mRNA expression levels of several BMP receptors as a function of time in culture, in both control and OP-1-treated cells, were also measured by Northern blot analysis. Control cells expressed a significant level of mRNA coding for ActR-I, BMPR-IA, BMPR-IB, and BMPR-II at the beginning of culture. The levels remained relatively constant throughout the 16 days in culture. OP-1 appeared to stimulate mRNA expression of all four receptors examined, though to varying extents. In summary, the present study indicates that the primary culture of MCL cells might be an appropriate cell culture model to study the effects of growth factors on ligament growth and repair. We showed that OP-1 stimulated cell proliferation and mRNA expression of several biochemical markers in this culture model.

SA020

See Friday Plenary number F020.

SA021

Prefabrication of Vascularized Bone Flap Transformed from Fat Vascularized Pedicle Using rhBMP-2 in Rat Femur. M. Hosoya*[1], Y. Maruoka*[1], M. Oda*[2], I. Asahina[1], S. Ichinose*[3], H. Kimura*[2], K. Omura*[1]. [1]Oral Surgery, Department of Oral Restitution, Division of Oral Health Sciences, Graduate School, Tokyo Medical and Dental University, Tokyo, Japan, [2]Dentistry and Oral Surgery, Hirosaki University School of Medicine, Aomori, Japan, [3]Instrumental Analysis Research Center, Tokyo Medical and Dental University, Tokyo, Japan.

In the field of not only oral surgery but also clinical medicines, it is significant to restore bone defect as a result of trauma or tumor. We described a vascularized bone flap transformed from a fat vascularized pedicle (FVP) raised on host using recombinant human bone morphogenetic protein-2 (rhBMP-2). It is enable to increase the survival rate of the subsequently grafted bone, and to form it into the desired shape. Collagen sheet was applied inside of the cylinder shaped silicone mold to deliver impregnated with rhBMP-2. FVP, the same size as lumen of the mold, was raised on the superficial inferior epigastric neurovascular bundle in Wistar rat, and then it was sandwiched between two halves of silicone mold. In the experimental group, 20 ug of rhBMP-2 was used; diluting material alone, in addition, ligation of the neurovascular bundle upstream to the molds for control groups. At 2, 4, and 8 weeks after surgery, bone formation were confirmed radiologically, histologically, and electronmicroscopically. Macroscopically, compared to the control group, new bone was formed with the identical shape as the lumen. In the control groups, bone was not observed. Here, we found out that FVP applied with rhBMP-2 induced a vascularized bone. It was indicated that our model could be a potential approach therapeutically for bone reconstruction effectively.

Fig 1: New Vascularized Bone from FVP

SA022

Bone Morphogenetic Protein-1 Expression During Rat Tibia Bone Formation. P. Manduca, S. Zanotti*, C. Volta*, F. Galmozzi*. Dobig, University of Genova, Genova, Italy.

BMP-1 (procollagenase I) processes trimeric pro-collagens I, II and III and produces carboxyl trimer pro-collagen fragments (C3). The C3 I production occurs in developmentally regulated fashion in osteoblasts cultures differentiating in vitro. C3 I is a powerful chemoattractant for endothelial and breast carcinoma cells, suggesting that it might drive bone vascular invasion and tumor homing to bone. We investigated the expression of BMP-1 in ossifying rats tibiae (from fetal to 10 days after birth) by in situ hybridization and by immunoperoxidase staining with antisera to the C3 I, and levels of BMP-1 mRNA by PCR in rat tibia osteoblasts differentiating in vitro. Expression of BMP-1 mRNA is first detected in limbs in the newly formed bone collar and thereafter increasing with animal age in osteoblasts in trabecular bone under the growth plate and in the diaphyseal collar. Osteocytes are usually negative, occasionally less positive that the osteoblasts. Osteoblasts differentiating in vitro express BMP-1 mRNA, detected by PCR, in a developmentally regulated fashion, with maximal expression in mature osteoblasts. Periosteum and adjacent perichondrium, and osteoclasts are strongly positive. Peroxidase staining with antiserum either to the a1 or to the a2 chains of the C3 I, decorate mostly ECM, in locations consistent with the expression of mRNA by the cells. Bone marrow positive both for mRNA and protein expression is found in patches. In the cartilage, differences in intensity of in situ hybridization in the pre- and hypertrophic chondrocytes are observed between the proximal and distal epiphyses, as if, during growth, a defined pattern of expression in the chondroblast department of tibial epiphyses evolved, expressed differently in the two extremities of the bone. Peroxidase staining with the antiserum to the a1 chain of the C3 I, detected the corresponding fragment from type II pro-collagen in cartilage. In summary, expression of BMP-1 in the cells of the bone compartment suggests that the production of C3 I could enhance endothelial cells mobility towards and within the forming bone. BMP-1 expression is also modulated during osteogenesis in vitro and is a developmental feature of the osteogenic phenotype. The modalities of the expression of BMP-1 in the cartilage department of the forming tibia suggest that both spatial and developmental control of its expression could be acting during chondroblast differentiation. No informations are presently available on a biological role of the C3 II, the BMP-1 product in cartilage. The expression of BMP-1 limited to areas (clones ?) in the bone marrow is a new finding and the nature of the producing cells is presently under investigation.

SA023

Comparison of Aortic Calcification in Hemodialysis Patients between with and without Diabetes Mellitus. H. Taniwaki*[1], T. Tabata*[1], S. Shoji*[1], A. Shioi[2], E. Ishimura*[3], T. Inoue*[1], Y. NIshizawa[4]. [1]Internal Medicine, Inoue Hospital, Suita, Japan, [2]Cardiovascular Medicine, Osaka City University Graduate School of Medicine, Osaka, Japan, [3]Nephrology, Osaka City University Graduate School of Medicine, Osaka, Japan, [4]Metabolism, Endocrinology and Molecular Medicine, Osaka City University Graduate School of Medicine, Osaka, Japan.

Vascular calcification is frequently seen in patients with diabetes and also in patients with chronic renal failure who are undergoing hemodialysis (HD). It is unknown, however, whether there are different factors associated with vascular calcification between diabetic HD patients and non-diabetic HD patients. Thirty-three HD patients were enrolled in the present study. The patients ranged in age from 40 to 85years (19 men and 14 women). They were divided into two groups according to the presence of diabetes mellitus (DM). DM group consisted of 14 patients, and non-DM group of 19 patients. Using computerized tomography (CT), calcification of the abdominal aorta above the bifurcation was evaluated in 10 slices of 1 cm interval, and aortic calcification index (ACI %) was calculated by division of calcified aortic area by total aortic areas (expressed in percent). Blood was drawn for routine analysis before a session of HD. There were no significant differences in age, mean blood pressure (mean BP), total cholesterol, serum calcium, serum phosphrus, and intact parathyroid hormone (i-PTH) between DM and non-DM groups. There was significant difference in the duration of HD between the two groups. The ACI % did not significantly differ between the two groups. Although there was significant correlation between ACI % and age, and between ACI % and mean blood pressure in non-DM group, there were no significant correlation between ACI % and these parameters in DM group. The results suggest that factors affecting calcification of abdominal aorta are different between DM and non-DM hemodialysis patients.

SA024

See Friday Plenary number F024.

SA025

Mineralization and Nano-mechanical Properties of Human Femoral Articular Calcified Cartilage and Subchondral Bone. V. L. Ferguson[1], A. J. Bushby*[1], A. Boyde[2]. [1]Department of Materials, Queen Mary, University of London, London, United Kingdom, [2]Department of Anatomy and Developmental Biology, University College London, London, United Kingdom.

The levels of mineralization and the micromechanical properties of normal and arthritic human femoral head articular calcified cartilage (ACC) are unknown, as is any correlation. We studied the former using quantitative backscattered electron imaging (qBSE) and the latter using nanoindentation. The novel technical combination gave means to study relationships in the thin, complex structure of intact, undecalcified ACC and immediately underlying subchondral bone (SCB). Thick slices of human normal reference post-mortem (PM) and osteoarthritic (OA) femoral heads (n=7/group) were embedded in PMMA, micro-milled, carbon coated, and studied using qBSE, quantified via halogenated dimethacrylate standards. Nanoindentation (3µm diameter, spherical tip diamond indenter; UMIS 2000, CSIRO, Australia) was performed in selected superior (more highly loaded) and medial regions of the joint surface. A partial unloading method gave Young's modulus (E) as a function of indenter penetration depth (40 increments/indent). Each test used an array (5*24 at 20 micron spacing) spanning SCB, ACC and hyaline articular cartilage. Mineralization at each indent site was derived from qBSE data. Elastic modulus and mineralization levels of ACC tended to be higher in superior regions in both PM and OA cases. In keeping with its more recent replacement, OA SCB had greater ductility and lower mineralization than in PM reference cases. In superior regions, elastic modulus in ACC was 16.9% greater than SCB in OA, cf. 2% greater in the PM group. There was no relationship between superior vs. medial sites (loading history) and elastic modulus and mineralization in ACC or SCB in normal PM tissue. However, there was a profound difference in OA, where mean values for elastic modulus and mineralization in superior ACC were both 11% greater than in medial ACC. One extreme case contained superior ACC that was 51% more highly mineralized than medial regions on the same sample. Such hypermineralization occurs as water space, comprising ~70% of normal cartilage, is filled with mineral. This hypermineralization of ACC, which occurred primarily in superior regions of OA samples, implies altered tissue microstructure, where more mineral per unit volume may be present as more or larger crystals. We surmise that the very highly mineralized cartilage component will function as a hard grinding abrasive, thus accelerating wear rates, and whether attached to or fragmented from the eburnated (‘bone‘ to ‘bone‘ contacting) surfaces of OA ACC.

SA026

See Friday Plenary number F026.

SA027

Temporal and Spatial Development of Cholesterol-Induced Atherosclerotic Calcification in Juvenile Rabbits. H. H. T. Hsu, O. Tawfik*, F. Sun*. University of Kansas Medical Center, Kansas City, KS, USA.

Accumulating epidemiological evidence indicates that atherosclerotic calcification can occur in young age of human population, suggesting that the dietary influence is as important as the aging process in the development of atherosclerotic calcification. However, there is a lack of detailed knowledge on morphological and biochemical changes that eventually lead to calcification in the affected aortas responding to high lipid diets in youth. We selected 4-month-old young rabbits as an animal model to study some of these changes during the course of mineral deposition in aortas. Rabbits were fed 0.25% cholesterol and 2% peanut oil for up to 6 months. Several histochemical stains were utilized in the study. These included H & E for morphology, Verhoeff’s van Gieson (VVG) stain for elastin, Masson Trichrome stain for collagen, and Alizarin red stain for calcification. At the end of 3 months of atherogenic diet, rabbits developed the earliest lesions with partial thickening of the intima. VVG staining revealed a focal rupture of the internal elastic laminae. Collagen deposition was noted to accumulate at the same location of elastic disruption. Calcification was barely detected at the same site as well. When animal were sacrificed at 4, 5, or 6 months of high lipid intervention, progressive worsening of the above-mentioned changes was noted. The intima was progressively circumferentially thickened and fibrotic. The media became partially fibrotic. Collagen deposition became more prominent while elastic fibers completely disintegrated at this stage of atherosclerosis. At the 6th month, calcification was predominantly present in the intimal area adjacent to the media. The fatty streaks and calcification areas were frequent in the proximal regions of the aorta and were gradually decreased in the distal part of aortas. The structural irregularity of the proximal aorta as a result of the high lipid dieting may cause earlier occurrence of calcification, since this portion of aortas is subjected to more turbulence and less shearing force of blood flow than the distal part of aortas. Coincidentally, calcifiability of vesicles isolated from proximal aortas was higher than from the distal regions. Likewise, vesicle calcifiability was higher at the 6th month of cholesterol intervention than that at the 3rd month. Thus, it is concluded that atherosclerotic calcification is closely related to the direct effect of cholesterol dieting on aortas besides the expected outcome of the aging process. The correlation of vesicle ability to calcify to the extent of mineralization in aortas further strengthens the role of calcifying vesicles in atherosclerotic calcification.

SA028

CTGF/Hcs24 Induces Chondrocyte Differentiation Through p38 Mitogen-activated Protein Kinase (p38MAPK), and Proliferation Through p44/42 MAPK/Extracellular-signal Regulated Kinase (ERK). G. Yosimichi*[1], T. Nakanishi*[2], T. Nishida[2], T. Hattori*[2], T. Takano-Yamamoto*[3], M. Takigawa[2]. [1]Biodental Research Center, Okayama University Graduate School of Medicine and Detistry, Okayama, Japan, [2]Biochemistry and Molecular Dentistry, Okayama University Graduate School of Medicine and Dentistry, Okayama, Japan, [3]Orthodontics, Okayama University Graduate School of Medicine and Dentistry, Okayama, Japan.

Connective tissue growth factor/hypertrohic chondrocyte specific gene product 24 (CTGF/Hcs24) promotes proliferation and differentiation of chondrocytes in culture. We investigated the roles of two major types of mitogen activated protein kinase (MAPK) in the promotion of proliferation and differentiation by CTGF/Hcs24. Here we report the effects of the MAPKK/MEK 1/2 inhibitor, PD098059, and p38 MAPK inhibitor, SB203580, in a human chondrosarcoma-derived chondrocytic cell line (HCS-2/8) and rab-

bit growth cartilage cells (RGC) treated with CTGF/Hcs24. In the proliferation phase, CTGF/Hcs24 induced about a 5-fold increase in the phosphorylation of p44/42 MAPK/ERK and about a 2-fold increase in that of p38 MAPK in an in vivo kinase assay. These inhibitors of MAPKK and MAPK suppressed phosphorylation of ets-like gene-1 (Elk-1) and nuclear activating transcription factor-2 (Atf-2) induced by CTGF/Hcs24 in a dose-dependent manner, respectively. Western blot analysis showed that phosphorylation of ERK was induced from 10 to 30 min and phosphorylation of p38 MAPK from 3 to 30 min after the addition of CTGF/Hcs24 in confluence HCS-2/8 cells. PD098059 suppressed the DNA synthesis of HCS-2/8 cells and RGC cells, while SB203580 did not. On the other hand, the p38 MAPK inhibitor, SB203580, completely inhibited the CTGF/Hcs24-induced synthesis of proteoglycans in HCS-2/8 cells and RGC cells but the MEK1/2 inhibitor, PD098059, did not. These results suggest that ERK mediates the CTGF/Hcs24-induced proliferation of chondrocytes, and that p38 MAPK mediates the CTGF/Hcs24-induced differentiation of chondrocytes.

SA029

See Friday Plenary number F029.

SA030

Differentiation of Chondrocytes Sensitizes Them to Apoptosis. P. Bruna*. Orthopaedic Research, Thomas Jefferson University, Philadelphia, PA, USA.

Endochondral bone formation is a key pathway in the development of long bones in the vertebrate skeleton. During this process chondrocytes proliferate and exit the cell cycle to mature into hypertrophic chondrocytes. These chondrocytes then undergo apoptosis leaving mineralized cartilage and empty lacunae for blood vessel and osteoblast invasion. The objectives of this study test the hypothesis that the mature chondrocyte exhibits a high sensitivity for matrix apoptogens. Chick cephalic sternal chondrocytes were matured by treatment with 35 nM retinoic acid (RA). Chondrocyte maturation was determined by the expression of collagen type X and by activation of alkaline phosphatase. Chondrocytes were treated with Pi and Ca^{2+} ions. Ion pair treatment of maturing chondrocytes induced cell death in a dose-dependent manner. Chondrocytes maintained in the absence of RA showed a reduced sensitivity to ion pair-induced apoptosis. To probe the mechanism of cell death, Bcl-2 family member expression was measured by western blot analysis. During chondrocyte maturation, protein levels of Bcl-2- and Bcl-xl, both anti-apoptotic proteins, were decreased. In contrast, the protein levels of several pro-apoptotic proteins, including Bax, remained elevated. These results indicate that during chondrocyte maturation there is a significant downregulation of anti-apoptotic factors. This observation suggest that the process of chondrocyte hypertrophy and the ultimate cell death of those chondrocytes may be linked and may share molecular pathways.

SA031

See Friday Plenary number F031.

SA032

Characterization of Collagenase-3 Binding and Internalization by Rabbit Chondrocytes. L. J. Raggatt[1], I. Choudhury*[1], S. Williams*[1], M. L. Tiku*[2], N. C. Partridge[1]. [1]Physiology and Biophysics, UMDNJ-Robert Wood Johnson Medical School, Piscataway, NJ, USA, [2]Rheumatology, UMDNJ-Robert Wood Johnson Medical School, Piscataway, NJ, USA.

Collagenase-3 (MMP-13) is an extracellular matrix metalloproteinase that cleaves type II collagen, the major protein component of cartilage, with high specificity. Several studies have identified increased levels of MMP-13 in arthritic synovial fluid where it may contribute to matrix destruction in this disease. Our laboratory has previously documented a process whereby osteoblastic cells remove MMP-13 from the surrounding milieu by binding the enzyme to a specific receptor. The enzyme is then internalized and degraded through the actions of the endocytotic receptor, the low-density lipoprotein receptor-related protein (LRP). Such a mechanism provides for a controlled elimination of a potentially destructive enzyme from the extracellular environment. The process of MMP-13 internalization also occurs in chondrocytes and is significantly reduced in osteoarthritic (OA) chondrocytes. We are currently characterizing the internalization of MMP-13 in normal rabbit chondrocytes. Primary rabbit chondrocytes were harvested and cultured in monolayers for three passages. RT-PCR was used to assess the cell phenotype during the culture period and the rabbit chondrocytes were found to express the cartilage specific genes aggrecan and type II collagen throughout this time. 125I-MMP-13 was used to determine the ability of the rabbit chondrocytes to bind MMP-13. Appreciable specific cell-association of MMP-13 was detected after 10 min of exposure to the ligand and equilibrium was obtained after 2 h. After identifying the time to equilibrium we determined whether binding was saturable by incubating the chondrocytes with increasing concentrations of 125I-MMP-13 ranging from 0 to 50 nM at 4°C for 2 h. The amount of specifically associated MMP-13 approached saturation at 50 nM, allowing assessment of the receptor kinetics. Finally, we have investigated the ability of rabbit chondrocytes to internalize a single cohort of 125I-MMP-13 over time at 36°C. Internalization of MMP-13 accumulation was evident after 20 min, reached a maximum at 30 min and had returned to baseline by 90 min. Subsequent to internalization the enzyme is released to the cell surface or into the extracellular media as trichloroacetic acid-soluble degradation products. The internalization of MMP-13 by rabbit chondrocytes correlates with that of normal human cartilage cells. We are currently using this accessible rabbit chondrocyte model to explore the receptors involved in the internalization of MMP-13 by chondrocytes as a first step in identifying how this system is impaired in OA cartilage.

SA033

See Friday Plenary number F033.

SA034

The Function of p21 Cip-1/SDI-1/WAF-1 in Chondrogenic Differentiation. Y. Negishi*, N. Ui*, M. Nakajima*, K. Kawashima*. Pharmaceutical Sciences, Teikyo University, Kanagawa, Japan.

Development of skeletal cartilage is characterized with coupling growth arrest and cell differentiation. Here, to know the cyclin-dependent kinase inhibitors involved in the progression of chondrogenic differentiation, we examined changes in the expression levels of CKI members using mouse ATDC5 prechondrocytes as a widely used in vitro model of cartilage differentiation. By a semiquantitative reverse transcriptase-polymerase chain reaction analysis, up-regulation of p21 mRNA and p27 mRNA was observed following a decrease in growth rate of prechondrocytes, and both transcripts subsequently accumulated during chondrogenic differentiation; p15, p18, and p19 mRNA, in contrast, did not change during the differentiation. The increase of p21 and p27 gene expression preceded the up-regulation of gene marker, type(II)collagen, in early chondrogenic differentiation. Only the up-regulation of p21 mRNA during the differentiation was prevented by the continuous treatment of early chondrogenic inhibitor, parathyroid hormone, indicating a close correlation between the differentiation and p21 induction in ATDC5 cells. Furthermore, by immunoprecipitation analysis, we observed that the level of p21 and p21/CDK2 complexes transiently increased during the differentiation, but not in undifferentiated cells, leading to a decrease in CDK2-associated kinase. This down-regulation of CDK2-associated kinase correlated with a reduction in DNA synthesis during the differentiation. Finally, to examine the role of endogenous p21 during chondrogenesis, we established stable-cell lines overexpressing full-length p21 antisense RNA in ATDC5. The reduction of endogenous p21 in these cell lines caused inhibition of the early chondrogenic differentiation in ATDC5.

SA035

Establishing Immortalized Periodontal Ligament Cells from Oncogene Transgenic Rat and Gene Expression of Bone Metabolic Markers. M. Chiba[1], M. Kubota*[1], M. Obinata*[2], H. Mitani*[1]. [1]Division of Orthodontics, Tohoku University, Graduate School of Dentistry, Sendai, Japan, [2]Department of Cell Biology, Institute of Development, Ageing and Cancer, Tohoku University, Sendai, Japan.

It is well known that there are multiple populations of periodontal ligament (PDL) cells and that these maintain PDL homeostasis. Various cell types in the PDL control orthodontic tooth movement. When the PDL is stimulated, cell differentiation is prompted and the cell-component ratios change to suit the new environment. The stimulus of mechanical stress is thought to cause osteoblasts, cementoblasts, and fibroblasts to differentiate from undifferentiated mesenchymal stem cells. However, the process of differentiation is unknown. The purposes of this study were to establish immortalized PDL cell lines derived from the PDL of transgenic rats harboring the temperature-sensitive simian virus 40 T-antigen gene (TG rats), and to compare the characteristics of these cell lines. The PDL was removed from the molar roots of TG-rats and incubated in alpha-MEM supplemented with 10% FBS and antibiotics in a humidified atmosphere of 5% CO_2 in air at the permissive temperature (33ºC). Cells that grew from the PDL were passaged and cloned depending on the shape of colony formation. RT-PCR analysis of the cell lines established was used to examine the expression of genes for Type-I collagen, osteopontin, fibronectin, alkaline phosphatase (bone type), bone sialoprotein, the receptor-activator of NF-kB Ligand, and osteoprotegerin. Furthermore, to examine the capacity of differentiation into mineralized-tissue-forming cells, cells were treated with 1,25 (OH) $_2D_3(10^{-8}M)$(D3) and incubated at 37º C. The formation of mineralized nodules was examined in a mineralized medium. Fifteen cell lines were established. These cell lines could be classified into six groups based on their pattern of gene expression at 33ºC. Calcified nodule formation occurred in two clones. The gene expression patterns also changed when the cell lines were treated with D3 and incubated at 37ºC, enabling the subclassification of the cell lines. In conclusion, differential gene expression in established cell lines was demonstrated in PDL-cell subpopulations. There were cells that had the potential for differentiating into cells found in mineralized tissues, like osteoblasts and cementoblasts, and cells that expressed the molecules that regulate osteoclast differentiation.

SA036

See Friday Plenary number F036.

SA037

Analysis of Gene Expression in Osteoblastic Cell Stimulated by Connective Tissue Growth Factor/Hypertrophic Chondrocyte-Specific Gene Product 24 (CTGF/Hcs24). E. Nakata*[1], T. Nakanishi*[1], T. Nishida*[1], A. Kawai*[2], H. Doi*[1], H. Inoue*[2], M. Takigawa*[1]. [1]Department of Biochemistry and Molecular Dentistry, Okayama University Graduate School of Medicine and Dentistry, Okayama, Japan, [2]Department of Orthopaedic Surgery, Okayama University Graduate School of Medicine and Dentistry, Okayama, Japan.

Connective tissue growth factor (CTGF/Hcs24) belongs to the CCN family which is believed to regulate many biological processes. We reported that recombinant CTGF/Hcs24 (rCTGF/Hcs24) promoted the proliferation and differentiation of osteoblastic cells (Saos2) in culture and increased the expression levels of collagen type I, alkaline phosphatase, osteopontin, and osteocalcin. To investigate the effect of rCTGF/Hcs24 on gene expression levels in Saos2, we used DNA microarrays. Saos2 cells cultured in DMEM containing 10% FBS for 48hs was incubated in DMEM containing 0.5% FBS for 12 hrs. Then, DMEM containing 0.5% FBS or DMEM containing 0.5% FBS and 50 ng rCTGF/Hcs24 was added to the culture. DNA microarrays containing 1091 human genes were used to compare mRNA levels between cultures with or without rCTGF/Hcs24 at 6 and 24 hrs after the addition of rCTGF/Hcs24. Total RNA was isolated from cells cultures with or without rCTGF/Hcs24, and purified mRNA was labeled with Cy3 or Cy5, respectively. These cDNA probes were hybridized to DNA microarrrays. We compared the resulting expression patterns between Cy3 and Cy5, and identified some genes in each time point using a criteria of over 1.5-fold change in expression. After 6hr incubation with rCTGF/Hcs24, several genes such as calcium-activated potassium channel beta, PLC-beta-1, camp response element binding protein, and MCM5 DNA replication licensing factor were up-regulated, and several genes such as hint protein, and IL-10 were down-regulated. After 24hr incubation, several genes such as transforming growth factor beta receptor, Smad4, and integrin beta 7 were up-regulated, and several genes such as phospholipase A2, and cadherin 3 were down-regulated. These results suggest the utility of DNA microarrays to identify the expression patterns of mRNA involved in the cellular response to rCTGF/Hcs24.

SA038

See Friday Plenary number F038.

SA039

Role of the Calcium-Binding Domain in Cartilage Oligomeric Matrix Protein (COMP) on Its Synthesis and Secretion. H. Yusuke*. Dept. of Orthop. Surg., Osaka City University Medical School, Osaka, Japan.

Cartilage oligomeric matrix protein (COMP) is a large pentameric glycoprotein in the territorial matrix surrounding chondrocytes and the fifth member of the thrombospondin (TSP) family and the causal molecule of an autosomal dominantly inherited chondrodysplasia such as Pseudoachondroplasia (PSACH) and multiple epiphseal dysplasia (MED). Beside pentamer-formation and EGF domains, the calcium-binding repeat domain was widely believed to be important because many mutations occurred in this small region. The function of COMP has remained unknown although genetic analyses provided important clues. With the goal of establishing a model to study the mechanisms by which COMP mutations cause these disease, a COMP cDNA was isolated from human synovial cells and a mutation (G1414T) was introduced into the calcium-binding domain that was previously reported for a severe PSACH patient. Both COMP cDNA were transfected in synovial cells or COS cells and their biochemical and morphological changes were examined with an aid of newly prepared antibodies against the bacterial recombinant peptides corresponding the amino-terminal and carboxyl-terminal COMP fragment. A considerable amount of wild COMP but not mutant COMP was detected in the culture medium of transfected cells while mutant COMP was found to accumulate as a full-sized form in cells. This observation indicates that mutant COMP was synthesized as wild COMP but failed to take outside due to reduced secretion process but not increased degradation. A confocal view showed that both COMPS were associated with the rough endoplasmic reticulum (rER) marker molecule such as Bip or Grp78, indicating that COMP is an ER retention or membrane/secretion protein. Increased immunofluorescence was detected in cells transfected with mutant COMP as compared with wild COMP. Moreover such immunofluorescent structures of mutant COMP were strikingly swollen. This was in good agreement with the previous in vivo observation that the characteristic enlarged lamellar appearing rER cisternae were observed in PSACH and MED. The possible occurrence of ER stress as the main mechanism for this mutation was examined. However, little difference in eIF2-a, ER stress marker, was observed between cells tranafected with wild and mutant COMPs. In contrast, we observed a significant TUNEL-reactivity in cells with mutant COMP, suggesting that a secretion process is important for COMP function and secreted COMP itself also plays a surviving role on chondrocyte.

SA040

See Friday Plenary number F040.

SA041

Transcriptional Regulation of Cartilage gene expression by SRF. M. I. Reinhold, M. C. Naski. Pathology, University of Texas Health Science Center, San Antonio, TX, USA.

The differentiation of mesenchymal cells into chondrocytes is a multistep pathway. These steps include the condensation of mesenchymal chondroprogenitor cells into aggregates assembled by intercellular cadherin dependent contacts. Continued differentiation of the condensed mesenchyme into chondrocytes results in the dissociation of the condensed cells, which at this stage surround themselves with an abundant layer of extracellular matrix that is characteristic of cartilage. The actin cytoskeleton is required for intercellular adhesion and its remodeling coincides with the loss of cell-cell contacts during differentiation. Recent studies showed that alterations in actin dynamics activate serum response factor (SRF). We hypothesized that SRF is activated during the dissociation of chondrogenic mesenchyme and that this contributes to chondrocyte differentiation. To investigate SRF during chondrogenisis, we examined i) activation of SRF following dissociation of cadherin-mediated intercellular contacts and ii) SRF-dependent transcription of genes that are key regulators of chondrocyte differentiation. We found that SRF is potently activated following dissociation of calcium-dependent intercellular contacts in the mesenchymal chondrocytic cell-line RCJ3.1C5.18. Activation of SRF was evidenced by the up-regulation of a SRF-dependent reporter gene and coincided with the loss of N-cadherin mediated intercellular contacts. Activation of SRF correlated with increased expression of chondrocyte specific genes, such as aggrecan. Conversely, a dominant-negative form of SRF suppressed aggrecan gene expression. The fibroblast growth factor receptor (FGFR) 3 gene was also specifically regulated by SRF and promoter mapping studies identified a 50 bp sequence element in the FGFR 3 gene that contains a SRE. The transcriptional activity of the 50 bp element is strictly dependent on the SRE and SRF. We conclude i) that SRF is activated following the dissociation of condensed-chondrogenic mesenchyme and ii) that SRF contributes to chondrocytic differentiation by regulating chondrocyte specific gene expression.

SA042

See Friday Plenary number F042.

SA043

Novel *cis*-element TRENDIC that Enhance Connective Tissue Growth Factor (ctgf) Gene Expression in Chondrocytic HCS-2/8. T. Eguchi*[1], S. Kubota*[1], S. Kondo*[1], Y. Mukudai*[1], T. Kuboki*[2], H. Yatani*[2], M. Takigawa[1]. [1]Biochemistry&Molecular Dentistry, Okayama University Graduate School of Medicine and Dentistry, Okayama, Japan, [2]Oral and Maxillofacial Rehabilitation, Okayama University Graduate School of Medicine and Dentistry, Okayama, Japan.

CTGF, which is a multi-functional growth factor, is specifically expressed in hypertrophic zone of endochondral growth plate. HCS-2/8 chondrocytic cells also highly express CTGF. In the previous study, we demonstrated that TGF-β signaling pathway was working through the TGF-β response element (TbRE) in the CTGF promoter in HCS-2/8 cells, and it was thought to be one of the cause of the high expression level of CTGF in HCS-2/8 cells. While continuing to analyze the chondrocyte-specific regulatory mechanism of CTGF gene expression, we subsequently identified a novel *cis*-element in the promoter region, which acts in the HCS-2/8-specific transcriptional enhancement of CTGF gene expression. For functional evaluation, plasmids containing firefly luciferase gene under the control of CTGF promoter, and its deletion/point mutants were constructed to be used in transfection experiment into HCS-2/8 and fibroblasts (NIH3T3 and HeLa cells). On the basis of the results of the luciferase assay, several DNA sequences in the critical region in the promoter were selected for the preparation of the probes for the gel shift assay, and it was performed with nuclear extracts of HCS-2/8 and other types of cells as controls. Comparative luciferase assay of the *ctgf* promoter deletion mutants among HCS-2/8 chondrocytic cells and fibroblastic cells revealed that a110 bp region in the promoter was critical in the HCS-2/8-specific transcriptional enhancement. Subsequent competitive gel shift assay revealed that transcription factors in HCS-2/8 nuclei bound to a 60 bp portion in the corresponding region. Relative luciferase activity from a CTGF promoter with mutant TbRE was 16.9% lower than that from the intact promoter. On the other hand, relative luciferase activity from a CTGF promoter with 4 bp point mutations in the 30 bp upstream of the TbRE was 47.7% lower than that from the intact one. The binding activity of HCS-2/8 nuclear factor(s) to the sequence over the 4 bp was especially higher than any nuclear extract form other cells. Therefore, we entitled the sequence 'TRENDIC', a transcription enhancer dominant in chondrocytes. Further investigation on the TRENDIC-binding transcription factor and the mechanism of its action is currently in progress.

SA044

See Friday Plenary number F044.

SA045

Insight Into the Molecular Complexity of Fracture Repair. F. Lombardo*[1], D. White*[2], J. Joo*[3], H. Ahn*[3], C. T. Rubin[4], M. Hadjiargyrou[5]. [1]Biomedical Engineering, SUNY, Stony Brook, Stony Brook, NY, USA, [2]Metabolic Disease, Millennium Pharmaceuticals, Cambridge, MA, USA, [3]Applied Mathematics and Statistics, SUNY, Stony Brook, NY, USA, [4]Biomedical Engineering, SUNY, Stony Brook, NY, USA, [5]Biomedical Engineering, State University of New York, Stony Brook, NY, USA.

The healing of a fractured bone is, in essence, a recapitulation of embryonic development that involves chondrogenesis, ossification and remodeling. These processes are characterized by an intricate series of events that requires temporal and spatial orchestration of numerous cell types and the expression of thousands of genes. Despite detailed understanding of skeletal repair at the tissue and cellular level, there is surprisingly little known of the scale or complexity of the process at the molecular level. This study was designed to address this issue, by characterizing the global increases in gene expression that occur during the critical phases of bone fracture repair. Previously we reported the construction and analysis of a cDNA library that consisted of transcriptionally induced genes (pooled from RNA isolated from post fracture (PF) 3, 5, 7 and 10 day callus) that were subtracted following hybridization with RNA derived from intact bone. This cDNA library included thousands of known genes that reflected a variety of families with diverse functions in cell cycle regulation, cell-matrix and cell adhesion, ECM construction, inflammation, general metabolism, mitochondria signaling, transcriptional regulation, protein transport, etc. In addition, hundreds of cDNAs showed homology to expressed sequenced tags (EST's). Further, custom microarrays containing all isolated cDNA clones were constructed and screened using RNA derived from intact bone (control) as well as PF day 3, 5, 7, 10, 14 and 21 callus. These experiments confirmed the temporal expression (PF day 3-21) of all genes and also indicated that ~93% of the subtracted cDNAs are upregulated during the repair process. Finally, clustering analysis revealed subsets of genes, both known and unknown, that exhibited distinct expression patterns over 21 days PF, indicating distinct roles in the healing process. In summary, the data demonstrate that the healing process is exceedingly complex, involves thousands of activated genes and indicates that groups of genes rather than individual molecules should be considered if the regeneration of bone is to be accelerated exogenously. Given the strong parallels of mammalian bone regeneration, skeletal development, and wound repair, this information will surely provide great insight towards some of the critical molecular mechanisms involved in a wide array of skeletal processes and dysfunctions.

SA046

See Friday Plenary number F046.

SA047

Phase-Contrast X-Ray Imaging in Investigation of Osseointegration of Craniofacial Implants and Other Hard Tissue Applications. S. L. O'Connell*[1], S. Watson*[1], J. Courtney*[2], J. G. Clement*[1]. [1]School of Dental Science, University of Melbourne, Melbourne, Australia, [2]X-Ray Technologies Pty. Ltd., Melbourne, Australia.

Phase-Contrast X-ray Imaging (PCI) radiographs contain both absorption and phase contrast and thus display enhanced edge definition of objects and their structural features. We compared PCI images with conventional contact radiographs during investigation of the osseointegration of surgical implants in growing pigs. Six 3-week old male piglets were implanted with 'Epitek' craniofacial fixtures. One fixture (12.5 x 12.5mm), anchored by 3mm screws, was placed beneath the periosteum on the left parietal bone. Another (12.5 x 24.5mm) was placed over the left coronal suture, with an extra dummy screw head in each long side. The pigs were sacrificed 9 weeks after surgery. A single section was cut along the coronal plane, spanning both sides of the skull and bisecting one end of the square fixture. Another section dissected one long end of the rectangular fixture in the sagittal plane, with a parallel control section cut from the untreated side. Radiographs were taken using a conventional X-ray unit (Faxitron Series 43805N, Hewlett-Packard, USA) (40kV, 54 mAs) and high resolution film (Agfa Structurix D2), scanned using a UMAX Powerlook 2000 Flatbed scanner (2000dpi/8.5um pixels). Digitised radiographs were obtained for comparison using a phase-contrast unit (X-Ray Technologies Pty. Ltd., Australia) (30um molybdenum filter, 30kV, 2.1 mAs) and Fuji phosphor imaging plates scanned with a BAS-5000 scanner (25um pixels). The anterior ends of the sagittal implants were overgrown with bone, whereas posterior ends were partially overgrown or remained exposed. The control slices were thicker, with more trabecular and cortical tissue. In the coronal sections, the implants were overgrown so as to be effectively translocated to deep within the calvarial bone. Again, bone around the implants was thinner than on the control side. Osseointegration was observed around the attachment screws but not the dummy heads or immediately beneath the connecting bars. In these areas, fibrous connective tissue and granulation tissue were observed, indicating an inflammatory response, later confirmed by histology. Craniofacial implants reduced the amount of new bone formed in the calvarium, probably a response to their force-bearing properties. This was readily observed in the PCI images, which provided greater detail than conventional radiographs. The variable inherent magnification of PCI also permitted closer examination of areas of interest, in addition to digital manipulation. Phase-contrast X-ray imaging appears to have potential for a wide variety of hard tissue research applications.

Disclosures: ***S.L. O'Connell****, X-Ray Technologies Pty. Ltd. 2.*

SA048

See Friday Plenary number F048.

SA049

The Primer Metabolic Processes on the Bone after Xenobiotics Treatment. Z. Valkusz[1], M. Gálfi[2], A. Juhász[3], O. Vetró[2], A. Farkas[2], A. Petri[4]. [1]Dept. of Endocrinology, University of Szeged, Szeged, Hungary, [2]Faculty of Juhász Gyula Teacher Training College, Department of Biology, Environmental Sciences Team, University of Szeged, Szeged, Hungary, [3]Dept. of Psychiatry, University of Szeged, Szeged, Hungary, [4]Dept. of Surgery, University of Szeged, Szeged, Hungary.

From **earlier studies** is known, that on the cellular and higher organization levels the normal neuronal, hormonal, and immune regulation determine the synthesis of bone matrix. The xenobiotics disturb these processes, by the systemic endocrine-immune intra- and extracellular effects of these agents. The xenobiotics change the function of osteoblasts, and osteoclasts, the mineral content, and the fundamental structure of the bone matrix. Our **aim** was investigate the effects of halogenic-hydrocarbones on the changes of bone formation. The hormone levels and calcium level in serum, and calcium content in the bone were measured. Wistar rats (100-120 g b w.; female, male/exp. group) treated with chlorobenzene by stomach-bougie, for10-30 days (hexachlorobenzene: 2,4,6-trichlorobenzene; one-to-one rate each 25µg/bw.kg.) were used in this experiment. **Control system:** normal control (untreated); positive control (1,5% ethanol treated); negativ-1 control (only stomach-bougie); negative-2 control (water treated). After the treatment the steroid hormone levels, the calcium content in the serum and in the bone were measured. The structure of the bone was studied after different histological stains for morphological analysis. **Our results**: The bone structure showed strong morphological deformation in fundamental bone matrix. This destruction in the bone matrix correlates with the changes of the hormone- and calcium levels in the serum and in the bone. (This work was supported by: ETT 06402/2000)

SA050

Bone Parameters In Remnant Kidney Osteopontin Knockout Versus Wildtype Mice. A. R. J. Bervoets*, V. P. Persy*, G. J. S. Behets*, M. E. De Broe, P. C. D'Haese*. Nephrology-Hypertension, University of Antwerp, Antwerp, Belgium.

To further unravel the role of osteopontin in bone remodeling, we induced chronic renal failure in osteopontin knockout and wild type mice. Bone histomorphometric analysis was performed in the "remnant kidney" mouse model (3/4 nephrectomy) of both the osteopontin knockouts (n=13) and wild types (n=18). Four knockout and 6 wildtype mice were sham operated and served as controls for the effect of renal function on bone metabolism. Animals were sacrificed at 12 weeks after installation of the chronic renal failure and tibiae and femora of all animals were transferred and fixed in either Burkhardt or ethanol. Bone was embedded in methylmetacrylate. Bone histomorphometry was performed on Goldner stained sections. We found a lower ($p<0.05$) (mean ± SD) osteoid surface (1.5 ± 1.3% vs 3.3 ± 2.4%) and perimeter (13.0 ± 9.1% vs 25.6 ± 15.1%) in remnant kidney osteopontin knockout mice as was the case for the number of active osteoblasts (3.3 ± 8.4 vs 7.2 ± 7.1) and the number of osteoclasts (0.3 ± 0.9 vs 1.8 ± 1.9) per unit of osteoid perimeter lining the resorption lacunae. There was no statistical difference in sham operated knockout versus wildtype mice. These findings indicate that osteopontin plays a role in the development of renal osteodystrophy. Further experiments and dynamic histomorphometry are needed for a better understanding of the exact role of osteopontin in bone remodelling.

SA051

Immunohistochemical Localization of Lysyl Oxidase and Its 18kDa Pro-Peptide in Endochondral Bone Development and in Differentiating MC3T3 Cells. N. R. Pischon*, A. H. Palamakumbura*, Y. Guo*, R. B. Santana*, P. C. Trackman. Oral Biology, Boston University, Boston, MA, USA.

Endochondral bone formation is a suitable model to study the sequential events of mesenchymal cell differentiation. Limited data suggest that the lysyl oxidase pro-peptide has modulating effects on differentiating bone forming cells. The 18 kDa pro-peptide, is a cationic, arginine-rich protein which is spliced from the 50 kDa pro-lysyl oxidase by procollagen-C-proteinase, a Bmp1 gene product. We investigated the spatial distribution of the pro-peptide and the mature enzyme in the process of endochondral ossification. Upper tibial growth plates, metaphyseal and epiphyseal bone as well as articular cartilage were obtained from 2 week old male mice (CD1). Dissected tissues were fixed in 4% paraformaldehyde and decalcified (7% EDTA, pH 7.4) for 16 days at 4 °C. Serial sections were cut at 6 µm thickness utilizing a cryostat. In addition, in order to determine forms of lysyl oxidase protein expression in osteoblasts, murine calvarial cell cultures (MC3T3) were plated in 4-well chamber slides at a density of 40,000 cells/well. Confluent cell monolayer where treated with differentiation media (10 % FCS, ascorbate, ß-GP) for 6 days and then processed for immunohistochemistry. Primary pro-peptide antibody (Ab), and anti-mature 30 kDa lysyl oxidase Ab, were produced as described earlier[Uzel 2001; Palamakumbura 2002]. Non-immune antisera was used as control. Microscopic images were captured using the Image Processing Solution (IPS) System (Media Cybernetics). Results show strong lysyl oxidase pro-peptide staining in the resting as well as the late hypertrophic cartilage zone. Different from type II collagen, which is expressed in the extracellular matrix, a cell associated accumulation of the lysyl oxidase pro-peptide was detected in vivo. This observation can be confirmed by a discrete cell associated pro-peptide expression in MC3T3 cells. Calcified bone matrix in the primary and secondary ossification zone was highly immunoreactive for the pro-peptide as well as for the mature lysyl oxidase. Little staining for mature 30 kDa lysyl oxidase was seen in resting cartilage, suggesting that the released lysyl oxidase pro-peptide may accumulate preferentially in this area. The observed staining patterns for the lysyl oxidase pro-peptide in vivo and in vitro suggest that it could have a role in chondrocyte and osteoblast differentiation.

SA052

See Friday Plenary number F052.

SA053

The Matrix Extracellular Phosphoglycoprotein OF45 Is Down-Regulated by Growth Factors and Osteotropic Hormones. D. N. Petersen, A. Mansolf*, T. A. Brown. Osteoporosis, Pfizer Global Research and Development, Groton, CT, USA.

OF45, also known as MEPE, is a bone-specific extracellular matrix protein that has been implicated in the process of mineralization. Targeted disruption of MEPE in the mouse was previously reported to increase bone mass. In order to gain further understanding of the role of OF45 in the normal physiology of bone, in this report we determined the regulation of OF45 mRNA by various growth factors, steroid and osteotropic hormones. UMR106 cells were treated with and without 10 nM dexamethasone (DEX) with the following compounds for 7 days: PGE2, PTH(1-34), IGF-I, 1,25 dihydroxyvitamin D3 (VD), retinoic acid, estradiol, dihydroxytestosterone, and progesterone. DEX induced the expression of OF45 mRNA in these cultures. No OF45 mRNA was detected in the absence of DEX treatment under any of the conditions. Therefore, all subsequent determinations were in the presence of DEX treatment. Under these conditions, PGE2, PTH, and VD markedly reduced the expression of OF45. Other treatments had no effect on OF45 expression. In order to further define the time course of expression, UMR106 cells were treated with PGE2, PTH or VD for 4 h, 8 h, 24 h, 72 h, or 7 days. VD reduced OF45 mRNA expression at 24 h and 72 h and no OF45 mRNA could be detected after 7 days of VD treatment. OF45 mRNA expression was reduced with PGE2 treatment at 72 h and completely eliminated with 7 days of treatment. PTH reduced OF45 mRNA expression even more rapidly with a slight reduction by 4 h, marked reduction by 72 h; and complete elimination after 7 days of treatment. Since both PTH and PGE2 can act by increasing cAMP activated pathways, we determined that activation of these pathways with forskolin also had a pronounced effect on OF45 mRNA expression; ~50% reduction by 8 h and total abrogation by 24 h. To further delineate the mechanisms of regulation, the protein synthesis inhibitor cyclohexamide (CHX) was added for 24 h to cultures that had been pretreated for 6 days with 10 nM DEX. CHX dramatically reduced the expression of OF45 mRNA, suggesting that sustained new protein synthesis was necessary for the elevation of OF45 mRNA expression by DEX. In the absence of protein synthesis, neither VD, PTH, PGE2 nor forskolin further reduced OF45 mRNA expression, suggesting that down-regulation by these agents also requires new protein synthesis. In summary, OF45 mRNA expression is markedly reduced by VD, PTH and PGE2, agents known to be important in the regulation of bone formation and bone resorption. These data, combined with the increase in bone mass reported in OF45 knockout mice, suggest that OF45 has a role in the physiological processes regulating bone homeostasis.

SA054

See Friday Plenary number F054.

SA055

Osteocalcin Response to Stress in Lewis and Fischer 344 Rats. P. E. Buckendahl[1], G. Blakley*[1], L. Pohorecky*[1], S. Rao*[2], B. Martin*[2], R. Kvetnansky*[3]. [1]Center of Alcohol Studies, Rutgers University, Piscataway, NJ, USA, [2]University of California, Davis, CA, USA, [3]Institute of Experimental Endocrinology, Bratislava, Slovakia.

Lewis (Lew) and Fischer 344 (F344) rats are histocompatible inbred strains derived from Sprague-Dawley rats selected for the response of the hypothalamic-pituitary-adrenal (HPA) axis to stressful psychosocial and environmental stimuli. Lew are hyporesponsive and have a defective hypothalamic production of corticotropin releasing hormone, while F344 are hyperresponsive. Because of the importance of the HPA axis to bone metabolism we investigated bone and osteocalcin (OC) in male Lew and F344 rats. OC is highly responsive to stressful stimuli, acutely elevated by foot restraint immobilization (IMMO), and slowly decreased by anxiety inducing stimuli. IMMO of 4 mo old and 24 mo old male F344 rats (n=8 each) induced significant elevation of OC ($p < 0.01$) which was greater in old (120%) than young (34%) rats compared with non-IMMO controls after 2 hr. Second, we obtained timed samples via tail cannulae during IMMO of 3 mo old F344 (n=7) and Lew (n=5) rats. Lew rats were higher than F344 at baseline and did not change significantly during 120 min, while F344 increased 43% after 5 min IMMO and remained elevated for at least 60 min ($p< 0.01$). Corticosterone (cort) levels for these rats (previously published Moncek et al, 2001) were elevated in both strains, but lower in Lew than F344 verifying the divergent stress response. Third, we evaluated growth, bone strength, and OC response to social interaction in 6 Lew and 8 F344 rats, beginning at age 2 mo. Intra-strain diad pairs were formed to evaluate dominant and submissive behaviors previously shown to elicit strong cort response. Blood was obtained from tail cuts to establish basal levels of OC and cort. On the following day, rats were paired for 15 minutes and social behaviors recorded, followed by a second tail blood sampling. OC in Lew did not change in spite of clear evidence of dominance or submission, but was decreased by 25% in F344 ($p < 0.01$). Basal cort in F344 was nearly 3 times higher than Lew (243 ± 35 vs 89 ± 18 ng/ml) and was further elevated by social interaction in both strains (666 ± 30 and 370 ± 30 ng/ml, F344 and Lew respectively, $p << 0.001$). At time of arrival in the laboratory, Lew were significantly heavier than F344 (210 ± 2 vs 177 ± 2). This relative difference was maintained until sacrifice at 5 mo (362 ± 10 vs 336 ± 7, $p < 0.05$). F344 femurs were shorter ($p < 0.01$), diaphysis thinner ($p < 0.05$), and bones more fragile ($p < 0.05$) than Lew, consistent with published findings in females of the same strains. We believe these two rat strains will be an excellent model in which to study relationships between the HPA axis and bone in response to stressful stimuli.

SA056

See Friday Plenary number F056.

SA057

Tensile Stress-inducible α-adaptin C Enhances Endocytosis and Osteoblast Differentiation in Calvarial Sutures. J. Shimomura*[1], O. Ishibashi[2], M. Ikegame[3], T. Yoshizawa*[2], S. Ejiri[3], T. Noda*[1], H. Kawashima[2]. [1]Division of Pediatric Dentistry, Course for Oral Life Science, Niigata University Graduate School of Medical and Dental Sciences, Niigata, Japan, [2]Division of Cell Biology and Molecular Pharmacology, Course for Oral Life Science, Niigata University Graduate School of Medical and Dental Sciences, Niigata, Japan, [3]Division of Anatomy and Cell Biology of the Hard Tissue, Course for Oral Life Science, Niigata University Graduate School of Medical and Dental Sciences, Niigata, Japan.

We previously demonstrated that tensile stress- (TS) induced osteoblast differentiation with the increased expression of several genes including bone morphogenetic protein-4 (BMP-4)[1] and tetranectin[2], which eventually led to osteogenesis in an organ culture of mouse calvarial sutures. In the present study, we employed RNA-fingerprinting arbitrary primed polymerase chain reaction to identify α-adaptin C, a component of the endocytosis machinery AP2, as a TS-inducible gene in the sutures. Western blotting revealed that protein production, as well as gene expression, of α-adaptin C was induced by TS as early as 3 hr following the initiation of loading. By *in situ* hybridization we demonstrated that the induction of α-adaptin C occurred not only in (pre)oteoblasts but also in alkaline phosphatase (ALP)-negative fibroblastic cells in the sutures, suggesting that it precedes TS-induced osteoblast differentiation. Overexpression of α-adaptin C in A431 epithelial cells resulted in the enhanced internalization of fluoroscein-labeled epidermal growth factor (EGF), thereby indicating that increased α-adaptin C expression eventually stimulates receptor-mediated endocytosis. Several proteins in TS-loaded and control sutures were differentially tyrosine-phoshorylated by EGF. Among the proteins, extracellular signal-regulated kinases (ERKs) were hyperphosphorylated in the TS-loaded sutures relative to control sutures after EGF stimulation. Since EGF receptor (EGFR) endocytosis has previously been reported to positively rather than negatively regulate EGF-induced ERK phosphorylation, our data raise a possibility that TS activates the endocytosis of growth factor/hormone receptors represented by EGFR. Further, TS-induced ALP activity in the sutures was significantly suppressed when endocytosis was inhibited by potassium depletion. These results, taken together, suggest that TS accelerates osteoblast differentiation and subsequent osteogenesis, at least in part by the induction of α-adaptin C protein and consequent activation of endocytosis.

1) Ikegame et al. J. Bone Miner. Res. 16: 24-32, 2001.2) Shimomura et al. J. Bone Miner. Res. 14 (Suppl. 1): S194, 1999.

SA058

See Friday Plenary number F058.

SA059

Effect of Long-term Skeletal Unloading on Articular Cartilage and Bone of Growing Rats. M. Tomiya*, S. Ichimura*, T. Kikuchi*, Y. Yoshihara*, T. Kobayashi*, K. Fujikawa*. Orthopaedic Surgery, National Defense Medical College, Tokorozawa, Japan.

We investigated the effects of skeletal unloading on articular cartilage. Sixty-four 9-week-old male F344/N rats were randomly divided into two groups: caged control (C) and tail suspended (TS). Hind limbs of the TS rats were subjected to unloading for up to 12 weeks. Animals were injected twice with calcein to label the site of the mineralization front (tidemark) in the articular cartilage. The sequential changes of the patellar cartilage and bone were analysed by pathological findings with hematoxylin-eosin stain and alkaline phosphatase (ALP) stain. Total cartilage area (TCA), calcified cartilage area (CCA)/TCA, and bone volume (BV)/total volume (TV) both in medial and lateral facets and the tidemark mineral apposition rate (tidemark MAR) were analysed in the section of the distal one-third of the patella. The values of cross-linked C-telopeptide of type II collagen (Col2CTx) in 24 h urine were also measured by ELISA. A partial defect of patellar cartilage at the medial facet margin was found in 94% of the TS animals after 9 weeks or more of tail suspension, but no fibrillation was observed in the remaining articular surface. In the medial facet of the patella at 3 and 6 weeks, most of the subchondral bone marrow was in direct contact with the calcified cartilage. TCA in the medial facet was significantly decreased after the first 3 weeks, but no such significant differences were found in the lateral facet. In contrast, CCA/TCA significantly increased after 3 weeks. Bone atrophy was also observed, with significant decreases in BV/TV after 3 weeks, and was more marked in the medial facet than in the lateral at 3 weeks. Tidemark MAR was sequentially reduced in both groups. In the TS group, it was highest at the first 3 weeks and had a tendency to be elevated compared with the C group. The number of ALP-stained chondrocytes in the deep zone in the TS group was greater than in the C group. Urinary Col2CTx excretion in the C group slowly decreased during the experimental period; however, the excretion in the TS group was highest at the first week and was significantly elevated until 9 weeks compared with the C group. This study indicated that skeletal unloading accelerated advancement of not only the tidemark, which was preceded by a high level of ALP expression in chrondrocytes in the deep zone but also the subchondral ossification front. Also, revealed was a full-thickness cartilage defect in the medial margin of the patella without any fibrillation of the remaining articular surface. These results suggested that long-term skeletal unloadings could cause the destruction of the articular cartilage in the different way from that induced by overloading.

SA060

Development of a Model of the Regulation of Bone Strength Based on Data from 29 Genetically Inbred Strains of Mice. J. E. Wergedal[1], M. H. C. Sheng*[1], C. L. Ackert-Bicknell*[2], W. G. Beamer*[2], D. J. Baylink[1]. [1]Musculoskeletal Disease Center, J.L. Pettis VAMC, Loma Linda, CA, USA, [2]The Jackson Laboratory, Bar Harbour, ME, USA.

In order to develop a model of the regulation of bone strength that is based on universal relationships among various parameters contributing to bone strength, we undertook a study of 29 genetically different inbred strains of mice. Each strain was evaluated at 10 weeks of age for femoral volumetric bone density and size by the Norlan pQCT, bending bone strength of the femur by the DynaMite instrument, as well as femoral bone length and body weight. All animals were reared and housed under identical environmental conditions. We selected maximum load as our strength parameter for model development. There was a 26% CV in bone strength in the strains studied, which was only slightly reduced to 21% by dividing by body weight. In our model, bone strength was determined 38% by bone density, 42% by architecture (moment of inertia), and 20% was due to measurement error, plus other unknown factors. Accordingly, the multiple correlation coefficient for bone density and moment of inertia, versus bone strength, was r=.91, p<.001. In the moment of inertia component, 22% of variation was accounted for by growth in femur length, 12% by adaptation (body weight), and 8% was unaccounted for. We next sought to evaluate bone quality. Sigma max is strength corrected for size, is an estimate of bone quality (which includes material bone density) and showed a 19% variation among these inbred strains of mice, suggesting that some of the material properties of bone are variable and genetically determined. By regression analysis, material bone density accounted for 48% of the variation in sigma max. This is surprising and may indicate that material density contributes to the variance in bone strength. We next sought to determine the relationship of two major determinants of bone strength, bone density and bone size (ie moment of inertia), with body weight, since, to some extent, body weight reflects the amount of mechanical stress imposed upon the femur. For bone density, there was only a low correlation with body weight (r=.23), whereas for moment of inertia (even after adjustment for length) there was a stronger correlation, (r=0.56, p<.01). Summary and conclusions: 1) bone size (ie moment of inertia) and bone density are the major determinants of bone strength and both are genetically regulated. 2) Mechanical stress may have more influence on bone size than bone density. 3) Sigma max (bone quality) is genetically regulated.

SA061

See Friday Plenary number F061.

SA062

Interlaminar Discectomy and Selective Foraminotomy in Degenerated Lumbar Lesions. S. Singh*, M. Garg*. Orthopaedics, B.P.Koirala Institute Of Health Sciences, Dharan, Nepal.

Objective: To assess the clinical outcome of interlaminar discectomy in patients suffering with degenerated lumbar disc lesions. **Methods:** We made a prospective study of 50 consecutive patients who underwent limited lumbar discectomy, based on specific objective patient selection criteria. The clinico-radiological parameters, type of surgery performed and the post-operative follow up were assessed. **Results:** Interlaminar discectomy without laminotomy was adequate in 33 cases (66%). Most patients requiring laminotomy (17 cases –34%) for discectomy had associated lumbar canal stenosis, herniation at proximal levels (L3-4) and/or sacralization of L5 vertebra. Selective foraminotomy in addition to discectomy was performed in 28 cases (56%). The post-operative results were good in 43 (86%) fair in 6 (12%) and poor subjective in 1 case (2%). No patient was classified as poor objective. **Conclusion :** Interlaminar discectomy without laminotomy is a safe, effective and reliable surgical technique for treating properly selected patients with herniated lumbar disc at L4-5 and L5-S1 levels.

SA063

Inhibition of Proteolytic Cleavage of MEPE by *Phex*. R. Guo*[1], P. S. N. Rowe[2], S. Liu[1], L. D. Quarles[1]. [1]Center for Bone and Mineral Disorders, Duke University Medical Center, Durham, NC, USA, [2]Institute for Drug Development and Molecular Therapies, The University of Texas Health Science Center, San Antonio, TX, USA.

X-linked hypophosphatemia (XLH) is caused by inactivating mutations of *Phex*, a phosphate regulating endopeptidase predominantly expressed in osteoblasts. Abnormal *Phex* in osteoblasts derived from the *Hyp*-mouse homologue of XLH results in the accumulation of an unknown factor that inhibits mineralization of extracellular matrix *in vitro*. We investigated whether the matrix extracellular phosphoglycoprotein MEPE, which is also increased in *Hyp*-osteoblasts, is a *Phex* substrate using recombinant *Phex* produced in *Sf9* cells. We found that *Phex* did not directly hydrolyze MEPE, but that endogenous cathepsin-like enzyme activity present in *Sf9* cells cleaved recombinant human MEPE into two major fragments of ~50 and ~42 kDA. The expression of mouse recombinant wild-type *Phex* protein (r*Phex*WT) in *Sf9* membrane fractions or pretreatment of *Sf9* membranes with leupeptin prevented the hydrolysis of MEPE by *Sf9* membranes. Moreover, purified Cathepsin B mimicked the effects of *Sf9* membranes to degrade MEPE. In addition, Cathepsin B-mediated MEPE cleavage was blocked by r*Phex*. *Phex* enzymatic activity, however, was not required to inhibit *Sf9* membrane cleavage of MEPE, since EDTA, which inhibited *Phex*WT activity against a chromagenic peptide Z-Ala-Ala-Leu-pNA, failed to prevent *Phex*WT inhibition of MEPE cleavage by *Sf9* membranes. The C-terminal domain of *Phex* was required, since r*Phex*(1-433)3'M, a C-terminal deletion mutant, did not block *Sf9* cleavage of MEPE. These findings suggest that non-ezymatic actions of the *Phex* interfere with the metabolism of MEPE *in vitro*. Whether non-enzymatic actions of *Phex* are involved in the physiologic regulation of MEPE degradation and control of mineralization *in vivo* remain to be established.

SA064

See Friday Plenary number F064.

SA065

Temporal Expression of Metalloproteinases and Angiogenic Factors during Murine Fracture Healing and their Dependence on TNF-alpha. W. Lehmann[1], C. C. Edgar*[2], T. Cho[3], A. W. Tsay*[2], J. M. Rueger*[1], L. C. Gerstenfeld[2], T. A. Einhorn[2]. [1]Department for Trauma and Reconstructive Surgery, University Clinic Hamburg-Eppendorf, Hamburg, Germany, [2]Department of Orthopaedic Surgery, Musculoskeletal Research Laboratory, Boston, MA, USA, [3]Department of Orthopaedic Surgery, Seoul National University College of Medicine, Seoul, Republic of Korea.

The progression of endochondral ossification during fracture healing is dependent on the concurrent processes of proteolytic degradation and ingrowth of new blood vessels that allow osteogenic and osteoclastic cells to facilitate the primary resorption of the calcified cartilage. Thus the expression and activation of selective metalloproteinases (MMP´s) that cleave the extracellular matrix and the expression of specific angiogenic factors are essential for both the remodelling and induction of new bone formation. Our previous investigations have shown that TNF-alpha is a key mediator at multiple steps during fracture healing. The aims of this study were to identify metalloproteinases and important angiogenic factors that are temporally expressed during fracture healing and determine if TNF-alpha functionally affects these processes. RNA expression was examined over a 28-day period following the generation of simple transverse fractures in mouse tibiae of TNF-alpha receptor null (p55-/- p75-/-) and strain matched control mice. The effects of TNF-alpha on the expression of specific MMPs and angiogenic factors was also examined ex vivo in cultures of cells prepared from eight day post fracture callus tissues. Using microarray analysis we examined the expression of 20 MMPs, their associated inhibitors and 23 different angiogenic factors during murine fracture healing. These data identify those MMPs and angiogenic factors that are expressed uniquely during both the period of endochondral resorption and later times during osteogenic tissue formation. Two of the unique findings of these data were the identification of pleiotrophin (OSF) as the quantitatively the highest angiogenic associated gene that showed peak expression during the endochondral phase and MMP8 which was restricted during the osteogenic phase. Both these genes were uniquely expressed by osteogenic lining cells and periosteal cells based on in situ hybridization. However MMP8 was also highly expressed by osteogenic cells infiltrating the areas of cartilage resorption. Multiple members of these two families of factors were delayed and showed altered levels of expression in the absence of TNF-alpha signaling. In summary the pattern of MMP and angiogenic factor expression during fracture repair shows unique temporal spatial and quantitative variations in the expression.

SA066

See Friday Plenary number F066.

SA067

Matrix Metalloproteinase-9 Antisense Oligodeoxynucleotide Inhibits Osteoclastic Pit Formation on MATRIGEL-coated Dentin Slices. S. Niwa*[1], O. Ishibashi[2], T. Inui*[3]. [1]Tsukuba Research Institute, Novartis Pharma K.K., Tsukuba, Japan, [2]Cell Biology and Molecular Pharmacology, Niigata University Graduate School of Medical and Dental Sciences, Niigata, Japan, [3]Tsu City College, Tsu, Japan.

We have previously demonstrated that the inhibitor of matrix metalloproteinases (MMPs), BB-94, inhibited osteoclastic pit formation on dentin slices coated with reconstituted basement membrane, MATRIGEL. On the other hand, the inhibitor had no effect on osteoclastic pit formation on naked dentin slices, indicating that MMPs are necessary for the migration of preosteoclasts and/or immature osteoclasts to bone surfaces through basement membranes, but not for direct bone resorption. However, it still remains to be demonstrated that which MMP in osteoclasts plays the most crucial role in the degradation of basement membranes. Since MMP-9 is a most abundant MMP in osteoclasts, we have investigated the effect of MMP-9 antisense phosphothiorate oligodeoxynucleotide (S-ODN) on the osteoclast-mediated degradation of MATRIGEL-coated dentin slices in the present study. Rabbit osteoclasts were cultured on the dentin slices for 24 h in the presence or absence of the antisense S-ODN in a medium containing 100 nM TfxTM-50, polycationic liposome, as a carrier of the S-ODN. The antisense S-ODN inhibited the osteoclastic pit formation in a concentration-dependent fashion. At 10 microM the antisense S-ODN reduced the total pit volume by approximately 40%. The sense S-ODN of MMP-9, which was used as negative controls, had no effect on the pit formation. The inhibitory effect of the antisense S-ODN similar to that of BB-94 demonstrates that MMP-9 is an MMP playing a major role in the migration of preosteoclasts and/or immature osteoclasts through basement membrane.

SA068

An Altered Bone Microenvironment Can Select a More Aggressive Multiple Myeloma Cell Line. H. Libouban*[1], M. Moreau*[1], M. Baslé*[1], R. Bataille*[2], D. Chappard[1]. [1]LHEA-GEROM, Angers, France, [2]INSERM U463, Nantes, France.

Bone destruction is the main clinical consequence of multiple myeloma (MM). Several cytokines implied in the bone remodeling can promote the tumor growth. Plasma cells are also secreting cytokines that activate bone remodeling leading to a "vicious circle" between bone and MM cells. The graft of 5T2MM mouse plasma cells in the C57BL/KaLwRij mouse mimics bone lesions observed in human. We recently showed that a pre-existing high bone turnover dramatically increases the growth of MM cells in a combined model 5T2MM+OVX (Ovariectomy). The 5THL cell line was naturally selected by the microenvironment in a 5T2MM-OVX mouse. Cells were propagated unchanged in normal C57BL/KaLwRij mice during 5 generations. This study characterized a new plasma cell line 5THL in terms of its morphology, expression of paraprotein, osteolytic activity and proliferative activity. Two groups of mice were injected intravenously with 1.5 106 of 5T2MM or 5THL cells. The development of the disease was monitored from 6 weeks post injection by serum electrophoresis to detect the presence of the paraprotein. Paraproteinemia was detected 6 weeks post injection in 5THL group and after 8 weeks in the 5T2MM group. At 8 weeks, the concentration of the paraprotein was 5 fold higher in the 5THL than in the 5T2MM group. All 5THL mice developed a hind-limb paralysis after 9-10 weeks and were euthanazied due to ethical consideration. Control mice were euthanazied at 16 weeks. Osteolytic lesions were analyzed by numeric radiography and X-ray microtomography. At 10 weeks, we observed the presence of numerous bone lacunae in the long bones of the 5THL mice. No extra osseous lesions were observed. We have euthanazied 3 animals in each group at 6 and 8 weeks post injection. Histological examination of the femur revealed infiltration of MM cells into the marrow cavity at 6 weeks in the 5THL group. Radiological lesions were observed at 8 weeks post injection in the 5THL group and at 10-11 weeks post injection in the 5T2MM group. The proliferative activity was assed by nucleolar organizer regions (AgNOR). Texture analysis of the nuclear DNA revealed marked differences between the 2 cells lines ($p<0.001$). The 5THL MM model closely mimics the human disease with higher and faster bone aggressiveness. This new aggressive cell line, with a preserved phenotype, was selected by an altered microenvironment due to an increased bone remodeling.

SA069

See Friday Plenary number F069.

SA070

2-Methoxyestradiol Inhibits the Osteosarcoma Cell Growth by Inducing a Blockade in Cell Cycle. A. M. Kennedy*, R. T. Turner, A. Maran. Orthopedic Research, Mayo Clinic, Rochester, MN, USA.

Osteosarcoma occurs most frequently in childhood and adolescence. Although the combination of surgery and chemotherapy has led to improved survival rate, the mortality rate remains high and a definite therapy is not yet available. 2-Methoxyestradiol (2-ME), a naturally occurring mammalian metabolite of 17beta-estradiol has been implicated as a physiological inhibitor of tumor cell proliferation. 2-ME did not affect the growth of normal osteoblasts in rats or in cell culture but inhibited the proliferation of osteosarcoma cells and induced programmed cell death. To explore the beneficial effects of 2-ME in controlling osteosarcoma, we have investigated further the molecular mechanisms associated with its growth inhibitory actions. Flow cytometric analysis of 2-ME treated MG63 human osteosarcoma cells showed a 50% increase in the Go/G1 phase population and a 68% decrease in S phase population in the cell cycle compared to the vehicle control. Whereas the parent compound, 17beta-estradiol and other metabolites of estrogen (4 and 16-alpha hydroxyestradiol) did not have any effect on MG63 cell growth. These results demonstrate that 2-ME inhibits osteosarcoma cell proliferation by progression of cells from Go/G1 to S-phase. Thus, a reduction in cell proliferation as well as induction of cell death by apoptosis is responsible for the reduction in osteosarcoma cell number following treatment with 2-ME.

SA071

See Friday Plenary number F071.

SA072

Molecular Characterization of Head and Neck Osteosarcoma Suggests a Distinct Disease Entity. D. Krishnadasan*[1], A. M. Deshpande*[1], D. G. Ammerman*[1], P. Bhatia[1], G. Pringle*[2], M. M. Sanders*[3], K. K. Unni*[4], M. F. Hansen[1]. [1]Molecular Medicine, University of Connecticut Health Center, Farmington, CT, USA, [2]Department of Pathology, Temple University, Philadelphia, PA, USA, [3]Department of Pathology, University of Connecticut School of Medicine, Farmington, CT, USA, [4]Department of Laboratory Medicine and Pathology, Mayo Clinic, Rochester, MN, USA.

Osteosarcoma is the most common primary tumor of bone and the third most common malignancy in adolescents. Osteosarcoma of all sites accounts for approximately 20% of all malignant tumors of bone and approximately 7, 500 new cases annually in the United States. Although a majority of osteosarcomas occur in the long bones of the skeleton, 6-13% of all osteosarcomas occur in the head and neck. Evidence, such as the differences in the degree of cellular atypia, the frequency of local versus distant metastases, the time until metastases, and the median age of onset, suggests that primary osteosarcoma of the appendicular skeleton and primary osteosarcoma of the head and neck represent biologically discrete diseases. To demonstrate this hypothesis we chose to analyze expression patterns of genes implicated in appendicular osteosarcoma tumorigenesis. The expression patterns of these genes differed in head and neck osteosarcomas from those observed in the appendicular osteosarcomas. These results suggest that the mechanism of tumorigenesis in these two forms of osteosarcoma may also be distinct and that primary head and neck osteosarcoma may be a separate disease from appendicular skeletal osteosarcoma.

SA073

See Friday Plenary number F073.

SA074

Inhibition of Renal Cell Carcinoma Growth in Bone by the Receptor Tyrosine Kinase Inhibitor, PKI166. K. Weber*[1], M. Doucet*[2], J. Price*[2], I. J. Fidler*[2]. [1]Surgical Oncology and Cancer Biology, University of Texas M.D. Anderson Cancer Center, Houston, TX, USA, [2]Cancer Biology, M.D. Anderson Cancer Center, Houston, TX, USA.

Purpose: The purpose of this study is to determine the effect of epidermal growth factor receptor (EGF-R) blockade on growth of renal cell carcinoma (RCC) in the bones of nude mice. Methods: Standard proliferation assays, Western blotting, and ELISA assays were used to characterize RBM1-IT4, a novel RCC cell line derived from a human bone metastasis. An experimental animal model was developed where intratibial injection of RBM1-IT4 cells produces lytic destructive lesions similar to those seen in patients with metastatic RCC. Faxitron analysis and immunohistochemical techniques were used to study the bone lesions. A double staining technique for CD31 and TUNEL was used to evaluate the presence of apoptotic endothelial cells. Results: RBM1-IT4 cells express high levels of EGF-R. Proliferation of these cells is increased 2.0-2.3-fold when stimulated with EGF or TGF-alpha. There is inhibition of proliferation from 12-63% when TGF-alpha and PKI166, a novel receptor tyrosine kinase inhibitor in increasing doses from 0.1-3.2 uM/ml, is added compared to TGF-alpha alone ($p<0.05$). Western blot analysis reveals an 11-fold increase in tyrosine autophosphorylation when RBM1-IT4 cells are stimulated with EGF and an 87% decrease when PKI166 (2.5 uM/ml) and EGF are added compared to EGF alone. Murine-derived bone endothelial cells also express EGF-R. They respond similarly to the addition of EGF or PKI166. Mice treated with PKI166 alone or in combination with Taxol show a marked decrease in radiographic bone destruction after 9 weeks. The mean tumor weights were 156 mg in the Control group, 24 mg in the Taxol group, 20 mg in the PKI166 group, and 8 mg in the PKI166/Taxol group ($p<0.05$). There is a decreased incidence of tumors in the PKI166 +/- Taxol groups. No drug toxicity was noted and the effect is maintained at 20 weeks. Immunohistochemical analysis reveals no difference in the presence of EGF, TGF-alpha, and EGF-R in the 4 groups. There is a marked decrease in activated EGF-R in the PKI166 and PKI166/Taxol groups. There is a decrease in tumor cell proliferation and an increase in tumor cell apoptosis as evidenced by PCNA and TUNEL staining in these groups, respectively. There is also an increase in apoptotic endothelial cells in the same groups. Microvessel density (CD31 staining) is decreased in the Taxol and Taxol/PKI166 groups. Conclusions: Blockade of EGF-R signaling with PKI166 causes a decrease in bone destruction and tumor growth in the bones of nude mice. This is due to a direct effect on the tumor cells and an indirect effect on the surrounding endothelial cells.

SA075

See Friday Plenary number F075.

SA076

Bisphosphonate Induce Apoptosis in Stromal Tumor Cells of Giant Cell Tumor of Bone. Y. Y. Cheng*[1], L. Huang*[2], F. M. Lai*[3], M. H. Zheng[4], S. M. Kumta*[5]. [1]Department of Orthopaedics and Tramatology, The Chinese University of Hong Kong, Hong Kong, Hong Kong Special Administrative Region of China, [2]Department of Orthopaedic and Tramatology, The Chinese University of Hong Kong, Hong Kong, Hong Kong Special Administrative Region of China, [3]Department of Anatomical and cellular pathology, The Chinese University of Hong Kong, Hong Kong, Hong Kong Special Administrative Region of China, [4]Department of orthopaedic surgery, University of Western Australia, Perth, Australia, [5]Department of Orthopaedics and Traumatology, Chinese University of Hong Kong, Hong Kong, Hong Kong Special Administrative Region of China.

Giant cell tumor of bone (GCT) is a benign primary neoplasm of bone, but is locally aggressive and produces expansible and lytic lesions. Bisphosphonate has been known to prevent osteoclastic bone resorption by inhibiting osteoclast activity and promoting osteoclast apoptosis. Recent evidence also emerged that bisphosphonate has potent anti-tumor effect by inducing tumor cell apoptosis. Indeed there is level I clinical evidence that bisphosphonate therapy has beneficial effects in preventing the development of skeletal lesions in patients with giant cell tumor of bone. However the molecular mechanism involved remained unclear. We have therefore investigated whether bisphosphonate induce cell death in giant cell tumor of bone. Surgical specimens were collected from patients with GCT before and after clinical treatment with pamidronate. Electron micrographs and TUNEL assay were used to study the morphological changes associated with apoptosis. We demonstrated that pamidronate induce apoptosis in both stromal tumor cells and multinucleated giant cells in GCT. The percentage of apoptotic cells in specimens after pam-

idroate treatment was significantly increased compared with those before pamidronate treatment. Our observation suggests that bisphosphonate may inhibit tumor progression of GCT by inducing cell death in both stromal tumor cells and multinucleated giant cells.

SA077

Cellular Interplays Between Myeloma and Bone Cells Enhance Myeloma Expansion and Bone Resorption While Suppressing Bone Formation. M. Abe[1], T. Hashimoto*[1], T. Oshima*[1], H. Shibata*[1], S. Ozaki*[1], A. Shioyasono*[2], Y. Tanimoto*[2], K. Hiura[2], K. Moriyama[2], S. Kido*[1], D. Inoue[1], T. Matsumoto[1]. [1]Dpt of Medicine and Bioregulatory Science, University of Tokushima, Tokushima, Japan, [2]Dpt of Orthodontics, University of Tokushima, Tokushima, Japan.

We and others have identified and reported that CC chemokines macrophage inflammatory protein (MIP)-1 alpha and beta are among major osteoclast activating factors secreted by multiple myeloma (MM). Since MM cells almost exclusively expand in the bone marrow, close interactions with bone cells may be critical to the develoment of myeloma bone disease. We therefore investigated a role of such cellular interplays in the present study. First, MIP-1 stimulated adhesion of MM cells to stromal cells via VLA-4/VCAM-1, and to OCs as well. The MM cell interactions with stromal cells enhanced MIP-1 secretion. The MIP-1-induced adhesion also promoted IL-6 secretion by stromal cells and to lesser extent by OCs. IL-6 in turn enhanced both MIP-1alpha and beta secretion by MM cells. These results suggest that MIP-1 secretion by MM cells form a positive feedback loop with MM adhesion to stromal cells and OCs, and IL-6 production by these bone cells. As we previously reported, PBMC-derived OCs enhanced survival and growth of MM cells in a partially IL-6-dependent but strongly contact-dependent manner. Even though stromal cells also supported MM cell expansion, the effect was much weaker than that of OCs on the per cell basis. We found that in the presence of IL-6 and osteopontin (OPN) significantly increased the number of MM cells. This effect was blocked by neutralizing antibodies against OPN and IL-6 in combination. We also confirmed abundant expression of OPN receptors including CD44, VLA-4 and vitronectin receptor by MM cells. Importance of OPN was further supported by our observations that OCs secreted a much higher amount of OPN but much lesser IL-6 than stromal cells. Finally, we examined if MM cells affect osteoblast function in long-term primary osteoblast cultures. The results indicated that MM cell-conditioned media, but not MIP-1 itself, suppressed bone nodule formation either in the presence or absence of BMP-2, suggesting MM cells suppress bone formation through unknown mechanism. Consistently, measurements of metabolic bone markers in MM patients revealed that serum osteocalcin levels were relatively suppresed compared to urinary deoxypyridinoline excretion. We therefore conclude that the cellular interplays between MM cells and bone cells result in efficient activation of osteoclastic bone resorption and myeloma expansion as well as impaired bone formation, leading to an uncoupling status of bone turnover which causes rapid and profound loss of bone mass.

SA078

Vitamin D Enhances Caspase Dependent and Independent TNF- Induced Breast Cancer Cell Death - the Role of Reactive Oxygen Species and Mitochondria. R. Koren*[1], G. Weitsman*[2], U. A. Liberman[2], A. Ravid*[2]. [1]FMRC Physiology&Pharmacology, Tel Aviv University, Tel Aviv, Israel, [2]Tel Aviv University, Tel Aviv, Israel.

The in-vivo anti cancer activity of calcitriol (1,25(OH)2D3) may be partially due to potentiation of the activity of immune agents including the major cytotoxic cytokine, TNF. TNF can cause cell death by activating caspase dependent (apoptotic) and independent pathways, and reactive oxygen species (ROS) are thought to play a mediatory role in its action. Our aim was to investigate the role of caspases and the involvement of ROS in the interaction between calcitriol and TNF using MCF-7 human breast cancer cells as the experimental model. Caspase 3-like activity, implicated in the execution phase of apoptosis, was increased 6 hours following exposure of the cells to TNF. This activity was monitored by cleavage of the fluorogenic substrate DEVD-AMC and of the endogenous substrate Poly-(ADP-Ribose)-Polymerase. TNF-induced caspase activation was markedly enhanced by a 24-hour treatment with calcitriol in a dose dependent manner. Under these conditions calcitriol on its own had no effect on caspase 3-like activity or on cell viability. Co-treatment of cells with TNF and the pan-caspase inhibitor zD-cho, at a concentration that abrogated caspase 3-like activity, reduced the cytotoxic effect of the cytokine. However, calcitriol enhanced TNF cytotoxicity by the same extent, in the presence or absence of zD-cho. Pretreatment of MCF-7 cells with the antioxidants N-acetylcysteine, GSH, ascorbic acid and lipoic acid only slightly reduced TNF-induced caspase activity, but markedly inhibited caspase activation in cells co-treated with calcitriol. Antioxidants also inhibited caspase independent TNF-induced cytotoxicity in the presence or absence of calcitriol. These findings indicate that calcitriol enhances both caspase dependent and independent TNF-induced cell death by affecting ROS dependent event(s) in both pathways. Mitochondria are one of the major sites for ROS production in the course of TNF-induced cell death. Thus, we examined the effect of TNF on mitochondrial membrane potential (Dp) using the specific potential sensitive fluorescent probe JC-1. We found a transient increase in Dp, peaking about 9 hours after addition of TNF, which was followed by a marked decrease in Dp to about 80% of control levels after 24 hours. At all time points Dp was lower in cells treated with calcitriol for 24 hours, whereas the hormone on its own did not affect Dp. We conclude that the interaction between TNF and calcitriol at the level of the mitochondria can account for the ROS dependent enhancement of caspase dependent and independent TNF-induced cell death.

SA079

See Friday Plenary number F079.

SA080

The Genotype of Metastatic and Non-metastatic Breast Cancer Cells Provides Insight into Their Phenotype. M. Bendre, T. Mon*, D. Gaddy-Kurten, L. J. Suva. Orthopaedics and Physiology and Biophysics, UAMS, Little Rock, AR, USA.

In order to understand the mechanism(s) that permit human breast tumors to metastasize specifically to the skeleton, a population of human breast cancer cells (MDA-MET) with an enhanced metastatic potential in vivo was isolated from an initial population of poorly metastatic tumor cells MDA-MB-231 (MDA-231). We reasoned that genetically related cell lines with distinct metastatic phenotypes would be useful for the identification of genes involved in the metastasis of breast cancer cells to bone. Having identified the distinct phenotypes of MDA-231 and MDA-MET, the role of PTHrP in the metastatic phenotype of MDA-MET cells was evaluated. Basal PTHrP protein secretion was low in both cell lines, and not increased by the addition of 10 ng/ml TGF-b in MDA-MET. Gene expression profiling validated this specific phenotypic characteristic of MDA-MET cells and revealed a lack of TGF-b type II receptor mRNA. Array comparison between MDA-MET and MDA-231 defined the pattern of genes differentially expressed (greater than 2-fold up- or down regulated). Using a simple reductionist approach to focus attention on the process of bone metastasis, which is significantly different in the two related cell types, all differentially expressed genes was assigned to non-mutually exclusive metastasis-related process categories. A total of (7) process categories: proliferation, transcription and translation, signaling, motility invasion and cytoskeleton, immune surveillance, adhesion, angiogenesis were developed. This rationale assumed that if a gene was represented in multiple metastasis process categories, then that gene was more likely to play a significant role in the aggressive phenotype of the MDA-MET cells. The high rate of assignment of the candidate genes is presumably related to the design of the comparison (using cells with a similar genotype, but distinct metastatic potential) and the bias of the method used to assign the genes (PubMed search). Mining of the array data identified many genes whose expression was altered (e.g.: IL-8, tie-2) or absent (e.g.: CXCR1; RANKL) in MDA-MET cells. On the basis of this metastasis-related characterization, IL-8 was considered a candidate to be associated with the aggressive behavior of MDA-MET compared with MDA-231 cells. The elevated expression of IL-8 by MDA-MET cells was confirmed by RT-PCR. These data suggest that the genotype of MDA-MET cells may explain the functional metastatic phenotype in vivo. An understanding of the factors contributing to the metastatic potential of breast cancer cells will enhance the prospect of developing new therapies that impede the metastasis of breast cancer to bone.

SA081

See Friday Plenary number F081.

SA082

Characterization of C4-2 Bone Metastasis and Its Response to Castration. E. Corey[1], J. E. Quinn*[1], A. M. Odman*[1], J. Zhang[2], E. T. Keller[2], R. L. Vessella*[1]. [1]Urology, University of Washington, Seattle, WA, USA, [2]University of Michigan, Ann Arbor, MI, USA.

Prostate cancer metastasizes with high frequency to bone. Well-characterized pre-clinical models of CaP bone metastases are needed in order to improve our understanding of the nature and development of CaP bone lesions in patients. Moreover, almost all patients with CaP bone metastases undergo hormone ablation, and it is therefore important to characterize models of bone metastasis under hormone-ablated conditions. The objective of this study was to characterize C4-2 bone metastases and their response to castration in a murine model. C4-2 cells were injected directly into tibiae of intact SCID male mice. Group-1 animals were sacrificed 8 weeks after injection of C4-2 cells. In group 2 animals were castrated three weeks after injection of C4-2 cells, and tumors were monitored for an additional 5 weeks. Blood samples were drawn for PSA determination to monitor tumor growth. Bone mineral density (BMD) was determined for all tibiae by Dual X-ray absorptiometry. Bone histomorphometric analysis was performed on un-decalcified tibiae stained with Goldner's stain. Our data showed that C4-2 cells cause a decrease of ~36% in BMD (p=0.0005) and ~74% in BV/TV (p=0.0131) *vs.* contralateral normal tibiae. The numbers of both osteoblasts and osteoclasts were significantly higher in C4-2 tibiae *vs.* normal tibiae (p=0.0370 and p=0.0089, respectively). When animals underwent castration we detected a drop in serum PSA levels in all animals, with a nadir at 14 days post-castration (67.7% of the starting PSA level, p=0.0059), after which PSA levels started to rise again. Tumor volume (TuV) in castrated animals was lower than in intact animals (p=0.0220). Castration decreased the bone destruction associated with C4-2 bone lesions: BMD of tibiae with tumor in castrated animals was ~18% higher than in intact animals but the difference did not reach significance (p=0.0899). However, C4-2 tumors after castration still caused bone destruction: BMD of tibiae with tumor in castrated animals was lower than BMD of normal tibiae (p=0.0006). In three of five castrated animals, %BV/TV was higher in tibiae with tumors than in intact animals, but the other two castrated animals exhibited %BV/TV in the same range as the intact animals. We also detected decreases in BMD and %BV/TV in tibiae without tumor in castrated *vs.* intact animals (p=0.0406 and p=0.0545, respectively). Based on our data, the C4-2 model of bone metastasis recapitulates the response to androgen-deprivation observed in CaP patients with mixed and lytic bone lesions. We conclude that this model is suitable for studying mechanisms associated with CaP bone metastasis and for evaluation of new therapeutic modalities.

SA083

See Friday Plenary number F083.

SA084

Role of Estrogen Receptor Alpha in Aggressiveness and Osteoclastogenic Potential of Human Breast Carcinoma Cells. N. Rucci*[1], M. Brama*[1], E. Ricevuto*[1], A. Teti[1], S. Migliaccio[2]. [1]Experimental Medicine, University of L'Aquila, L'Aquila, Italy, [2]Medical Physiopathology, University La Sapienza, Rome, Italy.

Since a correlation between breast cancer aggressiveness and estrogen receptor alpha (ER) expression has been hypothesized, we chose ER+ and ER- human breast cancer cell lines to address this issue in a culture system. MCF7(ER+) cells and an adriamycin-selected MCF7 clone failing to express ER (ADR) showed no difference in proliferation rate. However, a higher ability to migrate and invade gelatine and matrigel substrates was observed in ADR(ER-) cells. Enhanced invasiveness might result from increased MMP-9 activity and cytoskeletal re-arrangement, since ADR(ER-) cells expressed higher levels of tyrosine kinases involved in cell adhesion and motility, such as c-Src, PYK2 and FAK. In these cells, we also observed significantly higher levels of the alpha and beta2 PKC isoforms and a selective activation of the epsilon PKC isoenzyme. This was at variance with MCF7(ER+) cells, where the most abundant isoforms were beta1 and delta. Given the involvement of PKC alpha, beta and epsilon in cell motility, we believe that the pattern observed in ADR(ER-) cells may further account for their greater aggressiveness. To investigate the ability of the two breast cancer cell lines to induce osteoclastogenesis, mouse bone marrow cultures were treated with MCF7(ER+) or ADR(ER-)-conditioned media (CM). MFC7(ER+)-CM stimulated osteoclast formation and bone resorption. In contrast, ADR(ER-)-CM had no effect. Paracrine factors stimulating (IL-6, IL-1β, TNF-α) or inhibiting (IL-12, IL-18, GM-CSF) osteoclastogenesis were significantly increased in ADR(ER-) relative to MCF7(ER+) cells, raising the hypothesis that the inhibitory cytokines could selectively overwhelm the effects of the stimulatory ones in ER+ cells. Interestingly, treatment of osteoblast primary cultures with MCF7(ER+)-CM induced a selective up-regulation of IL-6 expression, suggesting an indirect stimulation of osteoclastogenesis and bone resorption via the osteoblast lineage. This occurrence was confirmed in vitro by treatment of mouse bone marrow cells with IL-6, which was found to increase both osteoclast numbers and pit formation. In conclusion, we have demonstrated that, despite a more invasive phenotype of ADR(ER-) cells relative to MCF7(ER+), these ER- cells failed to stimulate osteoclastogenesis and osteoclast activity. Therefore, we believe that ER might reduce aggressiveness of breast carcinoma cells but might enhance their osteotropism and consequently facilitate the development of osteolytic metastases.

SA085

See Friday Plenary number F085.

SA086

Tyrosine Kinase Src Inhibitors: Cellular Mechanisms for Potential Therapeutic Applications in Bone Disease. I. Recchia*[1], N. Rucci[1], S. Migliaccio[2], A. R. MacKay*[1], C. Festuccia*[1], M. Bologna*[1], D. Fabbro*[3], M. Susa[3], A. Teti[1]. [1]Experimental Medicine, University of L'Aquila, L'Aquila, Italy, [2]Medical Physiopathology, University La Sapienza, Rome, Italy, [3]Novartis Pharma, Basel, Switzerland.

A variety of cancers are associated with bone. Not only primary tumours can arise in this tissue but also common cancers, such as those of breast and prostate origin, metastasize to bone. The interaction of tumour cells with bone cells, either osteoblasts and osteoclasts, and with the bone local environment is a promising target for the development of new drugs against tumour bone diseases. c-Src proto-oncogene plays a critical role in osteoclast mediated bone resorption and osteoblast differentiation. Moreover, it is known that several tumours show high levels of c-Src expression. On this basis we tested the effects of pyrrolopyrimidine Src inhibitors on bone cell and tumour cell function. Src inhibitors, CGP77675 and CGP76030, exhibited a potent concentration-dependent inhibition of osteoclast maturation and mature osteoclast bone resorption ability. Moreover, they impaired osteoclast adherence and spreading, with a greater effect on mature vs immature cells. Src inhibitors triggered apoptosis, with apoptotic osteoclasts showing marked ERK1/2 activation and reduced expression of $p21^{WAF1/CIP1}$. They also dramatically reduced, concentration- and time-dependently, proliferation, adhesion and spreading of the human, bone metastasis-derived, prostate cancer cell line, PC3. However, the Src inhibitors were scarcely active in promoting cell detachment. When PC3 cells were left to attach to substrate prior to treatment with the inhibitors, cell adherence showed only 15% reduction at the highest concentration (20microM). Nevertheless, cells rounded up, confirming a role of Src in cell spreading. To evaluate the effect of Src inhibitors on the invasive potential, we plated PC3 cells in porous membrane transwells, coated with reconstituted Matrigel or gelatine. Adherent cells were treated with Src inhibitors and allowed to migrate vs chemoattractant (NIH3T3 cell conditioned medium). Results showed a dramatic concentration-dependent inhibition of PC3 cell ability to invade these substrates. These effects appeared merely due to block of cell motility, since changes in secretion and activity of MMP-2, MMP-9, uPA and their inhibitors TIMP1 and 2 were unremarkable. In conclusion, these data demonstrated not only a role for Src activity in the regulation of osteoclast and PC3 behavior, but also highlighted the cellular mechanisms through which Src kinase inhibitors could find an application as therapeutics, particularly in the field of bone and cancer-induced bone metastases.

SA087

See Friday Plenary number F087.

SA088

The Effect of Osteoprotegerin Administration on the Intra-tibial Growth of the Osteoblastic LuCaP 23.1 Prostate Cancer Xenograft. J. A. Kiefer[1], R. L. Vessella*[1], J. E. Quinn*[1], A. M. Odman*[1], J. Zhang*[2], E. T. Keller*[2], E. Corey[1]. [1]Department of Urology, University of Washington, Seattle, WA, USA, [2]Department of Pathology, University of Michigan, Ann Arbor, MI, USA.

Skeletal deposits of metastatic prostate cancer (CaP) frequently cause an increase in bone remodeling which is predominately osteoblastic in nature. Associated with the osteoblastic lesions is a significant resorptive component, which may facilitate CaP growth in bone. Osteoprotegerin (OPG) is a soluble member of the TNF Receptor family, which functions as a decoy receptor for the pro-resorptive cytokine RANKL. Elevated levels of OPG are associated with a decrease in bone resorption. The objective of our study was to investigate the effects of exogenous administration of OPG on CaP growth in the bone, using the osteoblastic LuCaP 23.1 osseous CaP model. LuCaP 23.1 cells were injected intra-tibially and Fc-OPG (6.0 mg/kg) was administered subcutaneously three times a week either starting at the time of cell injection (prevention regimen) or at 4 weeks post-injection (treatment regimen). Administration of Fc-OPG resulted in an increase in bone mineral density (BMD) at tumor site as determined by dual x-ray absorptiometry (DXA). The BMDs of LuCaP 23.1 tibia from the control group (n=8) were 0.102 ± 0.026 g/cm^2, treatment group (n=8) 0.101 ± 0.022 g/cm^2, and prevention group (n=7) 0.130 ± 0.023 g/cm^2 ($p<0.05$ *vs.* control). The increase in bone density was confirmed histologically. In the animals receiving Fc-OPG, serum PSA levels decreased by 80% ($p<0.05$) and 74% ($p<0.05$) in the prevention and treatment regimens, respectively, compared to the untreated animals. Lower levels of PSA are often associated with decreased tumor growth, indicating that OPG may interfere with CaP growth in the bone. Our results suggest a potential role for OPG in the treatment of CaP bone metastases.

SA089

Validation of the ORAI, OST and Body Weight to Aid in the Identification of Women Aged 45 or More Years with Osteoporosis. S. M. Cadarette, S. B. Jaglal, W. J. McIsaac*, G. A. Hawker, L. Jaakkimainen*, A. Culbert*, G. Zarifa*, E. Ola*. University of Toronto, Toronto, ON, Canada.

The purpose of this study was to assess criterion validity of the Osteoporosis Risk Assessment Instrument (ORAI), the Osteoporosis Self-Assessment Tool (OST) and body weight to identify women with osteoporosis. The ORAI is an additive scoring tool based on age, body weight and current estrogen use. The OST is a mathematical equation based on age and body weight (OST=integer(0.2*weight)-integer(0.2*age)). Both tools target the identification of women with primary osteoporosis and recommend that decisions for testing among women at high risk for secondary osteoporosis or with prior fragility fracture be made independently. Body weight of at least 70 kg has also been suggested as a method to selectively exclude women for testing. Chart abstractions from family practices of 3 University affiliated hospitals were completed for women aged 45 years or more with baseline bone mineral density (BMD) testing results by dual energy X-ray absorptiometry. Participants taking bone active medication other than ovarian hormones, or at high risk for secondary osteoporosis were excluded. Receiver operating characteristic (ROC) curve analyses were used to evaluate the identification of women with osteoporosis defined as a BMD t-score ≤-2.5 SD at either the femoral neck or lumbar spine (L1-L4), N=691. Exact binomial 95% confidence intervals (CI) were calculated. At the thresholds of ≥9 (ORAI) and ≤1 (OST), and selecting body weight <70 kg, the sensitivity to identify women with osteoporosis was 92% (95%CI=85.0-95.9) for the ORAI, 91% (95%CI=83.9-95.3) for the OST and 93% (95%CI=87.1-97.0) using the weight criterion. The tools also selected 41% (ORAI, 95%CI=35.2-47.4), 30% (OST, 95%CI=24.5-35.9) and 52% (weight criterion, 95%CI=45.5-57.8) of women with normal BMD (t-score ≥-1.0 SD). Area under the ROC curves to identify women with osteoporosis were significantly better for both the ORAI (0.805, SE=0.02) and the OST (0.819, SE=0.02) compared with body weight (0.749, SE=0.02). Overall, all three methods proved to be good tools to aid the identification of women with osteoporosis. Each identified over 90% of women with osteoporosis yet selected fewer than 48% of women with normal BMD. Our results validate the efficacy of the ORAI and OST at the thresholds of 9 and 1 respectfully, and body weight <70 kg to identify women with primary osteoporosis. The practical application (clinical utility) of the OST equation compared with the additive ORAI or simple body weight to assist the identification of women with osteoporosis should be explored.

SA090

Ultrasound and DXA Bone Mineral Density in Patients with Ankylosing Spondylitis. H. Franck*, T. Meurer*. Center of Rheumatology, Oberammergau, Germany.

Introduction: Patients with ankylosing spondylitis well-known to have osteoporosis / osteopenia dependend on the inflammatory acitivity and immobilisation of the spine. Consequently controll measurements of bone densitometry has to be done more frequently than in the normal population. The aim of our study was to compare the ultrasound densitometry and DXA-measurements in patients with ankylosing spondylitis. Methods: We have incuded 184 patients with ankylosing spondylitis, all fulfilled the modified New York cirtria. We measured the bone mineral density with DXA (QDR 4500) in the right hip and lumbar spine and with ultrasound (UBIS 5000) in the calcaneum. Results: The best correlation was found between DXA of the right hip and ultrasound (tab.) Discussion: The hip total measured by DXA present with significant (p > 0,005) correlations with ultrasound measurements of the calcaneum. In contrast BMD of the lumbar spine did not show significant correlations with the ultrasound measurements. As measurements of BMD of the lumbar spine in patients with ankylosing spondylitis has limitations caused to disease specific changes of the lumbar vertebra, also sound measurement should be considered as an alternative.

Correlation Bmd hip total (BMD LS total) with				
	N =	mean value	r =	p =
Ultrasound BUA	184 (184)	65,32 (65,32)	0,235 (0,135)	0,001 (0,067)
Ultrasound T-Score	184 (184)	0,80 (0,80)	0,205 (0,119)	0,005 (0,108)
Ultrasound Z-Score	184 (184)	0,07 (0,07)	0,203 (0,133)	0,006 (0,072)

SA091

See Friday Plenary number F091.

SA092

Digital X-ray Radiogrammetry Indices are Sensitive to Clodronate Treatment In Women With Osteoporosis. C. Haigh*[1], L. Reaney*[2], J. Adams[1], M. Davies*[1], P. L. Selby[1], J. Robinson[3], R. Francis[4], A. Dey[2], J. A. Kanis[2], J. Bostock*[2], C. Horvath*[5], J. Kenrali*[6], T. Jalava*[6], E. McCloskey[2]. [1]University of Manchester, Manchester, United Kingdom, [2]University of Sheffield, Sheffield, United Kingdom, [3]Crosby Clinical Research Centre, Liverpool, United Kingdom, [4]University of Newcastle, Newcastle, United Kingdom, [5]Simmelweis University, Budapest, Hungary, [6]Leiras Oy, Helsinki, Finland.

A number of new techniques have been developed for skeletal assessment that are more convenient than DXA, but require biological validation. The aim of this study was to determine the utility of DXR-BMD and metacarpal cortical index (MCI), estimated by the Pronosco X-posure system™, to assess responsivity to treatment with the bisphosphonate, clodronate, in a prospective clinical trial in osteoporosis. Women fulfilling the WHO criteria for osteoporosis (spine or hip T-score <-2.5) and/or with at least one prevalent vertebral fracture were recruited to a 3-year double-blind, controlled study. Hand radiographs on standard film were obtained at baseline in 538 women (91% of all participants) and were repeated annually during follow-up. The women received either clodronate 800mg daily by mouth (Bonefos®) or an identical placebo and all patients received a calcium supplement of 500mg daily. Bone density (BMD) was measured at the spine and total hip at 6, 12, 24 and 36 months by DXA. Prevalent and incident vertebral fractures were identified by morphometric evaluation of lateral spine radiographs obtained at baseline and annually thereafter. At entry, no significant differences in DXR-BMD and MCI were observed between the women randomised to clodronate or placebo. Treatment with clodronate was associated with highly significant differences in changes of DXR-BMD and MCI and other skeletal measures over 3 years compared to placebo (Table). The mean changes in DXR-BMD and MCI were of similar magnitude to those observed at the spine when expressed relative to precision errors (CV% for spine BMD, hip BMD, DXR-BMD and MCI of 1.3%, 1.6%, 0.6% and 0.7% respectively.)

% Change from Baseline (±SE)				
	Clodronate	Placebo	P-value*	Mean Diff./CV%
DXR-BMD	-0.68±0.17	-2.80±0.24	<0.0001	3.5
MCI	-0.86±0.17	-3.55±0.27	<0.0001	3.8
Spine BMD	5.14±0.48	0.60±0.46	<0.0001	3.5
Hip BMD	1.03±0.43	-3.33±0.45	<0.0001	2.7

* Using absolute changes

We conclude that DXR-BMD and MCI are sensitive to changes induced by anti-resorptive therapies. These measures have potential applicability in multi-centre clinical trials in osteoporosis and may be of similar utility to spine BMD for monitoring treatment in osteoporosis.

Disclosures: ***E. McCloskey****, Pronosco A/S, Vadbaek, Denmark 2; Leiras Oy, Helsinki, Finland 2.*

SA093

A Comparison of pQCT and DXA for Bone Density Measurements in the Mouse. G. Toraldo*, C. Roggia*, M. N. Weitzmann, Y. Gao, S. Cenci, R. Pacifici. Division of Bone and Mineral Diseases, Washington University and Barnes Jewish Hospital, St. Louis, MO, USA.

In studies with mice, bone densitometry is an established technique for the detection of the bone loss induced by ovariectomy (ovx). Today two different techniques are available for this purpose, peripheral quantitative computerized tomography (pQCT) and dual-energy x-ray absorptiometry (DXA). However, there is no consensus on which is the preferable method for studies in mice. Although used interchangeably, measurements by these methods differ quite considerably as only pQCT measures a true volumetric density and provides selective measurements of both trabecular and cortical bone. To test the diagnostic sensitivity of these methods, we measured BMD 4 weeks after either ovx or sham operation in mature C57BL/6 mice. pQCT measurements were obtained from isolated tibias using an XCT-960M Nordland instrument. Peripheral and central DXA measurements (total body, spine, femurs, limbs) were obtained in vivo using a PIXImus2, Lunar scanner and a Hologic QDR 2000, respectively. All three methods were able to discriminate between the two groups, but the greatest bone loss was detected by pQCT (-16%). Peripheral DXA was less sensitive (-14%) than pQCT but superior to central DXA which detected only a 9% difference between ovx and sham mice. pQCT measurements were highly correlated with peripheral DXA measurements (r = 0.74-0.80), depending on the anatomical site, while no significant correlations were found between pQCT and central DXA measurements. When peripheral DXA was compared to central DXA, significant correlations were found between each site measured using the peripheral device and total body and limbs measured with the central device. The remaining central sites did not correlate with any peripheral measurement. The coefficients of correlation for within-instrumental comparisons with peripheral DXA were >0.9 for all the sites analyzed, with the best correlation between total body and spine (r = 0.98). For central DXA, the best correlation was found between total body and spine (r = 0.81) and the poorest between spine and limbs (r = 0.04). The short term in vivo precision (CV) was 1.7% for peripheral DXA and 2% for both central DXA and pQCT. The precision of pQCT for repeated measures in vivo was ~ 5%. In conclusion, pQCT is the most sensitive method for ex-vivo cross-sectional studies and is the technique of choice when selective measurements of either trabecular or cortical bone are required. However, because of the higher precision, especially for repeated in vivo measurements, peripheral DXA measurements is the technique of choice for prospective in vivo studies.

SA094

See Friday Plenary number F094.

SA095

Validation of a Risk Index to Identify Men with an Increased Likelihood of Osteoporosis. M. C. Hochberg[1], J. K. Tracy*[1], M. van der Klift*[2], H. Pols[2]. [1]Medicine, University of Maryland School of Medicine, Baltimore, MD, USA, [2]Epidemiology, Erasmus University School of Medicine, Erasmus, Netherlands.

The Osteoporosis Self-assessment Tool (OST) was originally developed to classify the risk of osteoporosis (OP), as defined by low bone mineral density (BMD), in postmenopausal Asian women (Koh et al: Osteoporos Int 2001;12:699-705). The OST is easily calculated from just the patient's weight and age: OST = 0.2 (weight [in kg] - age [in years]); the result is truncated to the integer. We previously validated the OST in Caucasian women who were screened for eligibility for the Fracture Intervention Trial and those enrolled in the Rotterdam Study (Geusens et al: Mayo Clin Proc: accepted for publication). In the present analysis, we calculated sensitivity, specificity, positive and negative predictive values, likelihood ratios and post-test odds for the OST using data from two cohorts of older Caucasian men: the Rotterdam study (2445 men aged 55 and over) and the Baltimore Men's Osteoporosis Study (503 men aged 65 and over). BMD was measured in Rotterdam men using a Lunar DPX-L, and in Baltimore men using a Hologic QDR-2000. OP was defined as a BMD T-score of -2.5 or less at the femoral neck using young white male reference data from NHANES III. The OST risk groups were defined using the cutpoints of >2 (low risk), 2 to -2 (moderate risk), and <-2 (high risk). Results are shown in the table. Results were generally similar when OP was defined as a BMD T-score of -2.0 or less, although prevalence and proportions in all risk groups were higher. While there are presently no published guidelines for the assessment and treatment of OP in men, we conclude that this free and simple risk assessment tool could help increase awareness of and encourage the appropriate use of BMD measurements to diagnose OP in men.

Prevalence of OP in Older Men by Risk Group

Cohort	Baltimore	Rotterdam
Overall Prevalence of OP	6.6%	12.2%
Sensitivity (OST=2 or less)	88%	79%
Specificity (OST>2)	32%	51%
Low risk	2.6%	4.0%
Moderate risk	7.7%	16.5%
High risk	14.7%	34.9%

SA096

Radiographic Texture Analysis of Calcaneous Images in Assessing Bone Fragility. T. J. Vokes[1], M. R. Chinander*[2], M. L. Giger*[2], L. B. Dixon*[2], M. J. Favus[1]. [1]Medicine, University of Chicago, Chicago, IL, USA, [2]Radiology, University of Chicago, Chicago, IL, USA.

Radiographic texture analysis (RTA) of spine radiographs has been shown to predict the presence of vertebral fractures elsewhere in the spine. Also, RTA of the hip radiographs predicts bone fragility as measured in the mechanical strength testing of femoral neck specimens excised during hip surgery. The present study examines whether RTA of the heel images obtained using the peripheral densitometer PIXI can differentiate patients with from those without vertebral fractures. The subjects were 121 patients (age 61.7±13.2 years, range 18-92 years; 8 males) referred for densitometry who agreed to participate. BMD of the lumbar spine and proximal femur was measured using Prodigy and BMD and digital radiographic image of the left heel were obtained using PIXI (both from GE Medical Systems). Prevalent vertebral fractures (reduction in vertebral height of at least 25%) were identified using Lateral Vertebral Assessment (LVA) on Prodigy and/or standard radiographs of thoracic and lumbar spine. The PIXI heel images were subjected to computerized RTA yielding Fourier based measures: root mean square variation (RMS - a measure of the magnitude of fluctuation in trabecular texture pattern) and the first moment of the power spectrum (FMP - a measure of the texture pattern's spatial frequency content). 26/121 patients (22%) had vertebral fractures. We performed 3 types of statistical analysis: a) A multivariate logistic regression, which showed that the presence of vertebral fractures was predicted by a combination of texture features, age and T scores of the heel and femoral neck (but not spine). The effect was significant for the texture features (RMS at p=0.032, and FMP at p= 0.019) but not for any of the T scores. When the analysis was restricted to 105 subjects over 50 (21% with vertebral fractures), the results were even more significant (RMS at p=0.02, FMP at p=0.009). b) Receiver operator characteristic (ROC) analysis was used to assess performance of texture features and BMD in distinguishing between patients with and those without fractures. The area under the ROC curve (Az) was 0.56 for heel BMD, 0.51 for RMS and 0.58 for FMP. Combination of the two texture features RMS and FMP yielded an Az of 0.66 while the combination of RMS, FMP and BMD achieved an Az of 0.70. c) Linear regression to examine the relationships between texture features and BMD. A strong correlation was found between the texture features and heel (but not spine or femoral neck) BMD in patients with fractures (R^2 = 0.47, p<0.0001) but not in those without (R^2=0.005, p=0.5). We conclude that RTA may contribute information about bone structure not captured by the BMD measurement alone.

Disclosures: ***T.J. Vokes****, Merck 8.*

SA097

Relation Between Disease Activity and Apparent Trabecular Texture at the Wrist in Individuals with Rheumatoid Arthritis. N. J. MacIntyre[1], C. E. Webber[2], J. D. Adachi[3]. [1]Queen's University, Kingston, ON, Canada, [2]Hamilton Health Sciences, Hamilton, ON, Canada, [3]St. Joseph's Hospital, Hamilton, ON, Canada.

This pilot study characterizes the relation between disease activity and apparent radial bone trabecular texture in individuals with rheumatoid arthritis (RA). RA patients diagnosed within the past 8 years (n = 15) and age-matched controls (n = 15) were recruited. A high-resolution image was acquired at the 4% site of the nondominant radius for each subject using peripheral quantitative computed tomography (XCT 960, Stratec). From this cross-sectional image, indices of apparent trabecular texture (average hole size: H_A, maximum hole size: H_M, connectivity index) were determined using in-house developed software. Volumetric bone density (total: ToBD, trabecular: TrBD), bone mineral content (total: ToBMC, trabecular: TrBMC), and bending strength (Strain Stress Index: SSI) were also evaluated at the same radial site using commercial software. For RA subjects, disease activity was characterized by disease duration, counts of the number of active and damaged joints in both upper limbs, and scores on three subscales of the Arthritis Impact Measurement Scales 2 questionnaire (Physical Function Score, Arthritis Impact Score, and Arthritis Pain Score). Between-group differences and relations between disease activity and bone variables were analyzed using ANOVA and Pearson Correlation Coefficient analysis, respectively. Between-group differences were not detected although RA subjects tended to have higher values for H_A, H_M, and lower values for the connectivity index, density, and mass. Active joint count correlated with H_A (r = 0.57, p = 0.03), ToBMC (r = -0.66, p < 0.01), TrBMC (r = -0.55, p = 0.03), and SSI (r = -0.52, p = 0.04). Disease duration correlated with H_M (r = 0.60, p = 0.02). Damaged joint count correlated with TrBMC (r = -0.64, p = 0.01). Physical Function Score correlated with ToBD (r = -0.58, p = 0.02), ToBMC (r = -0.65, p < 0.01), and SSI (r = -0.74, p = 0.001). Arthritis Impact Score correlated with ToBMC (r = -0.54, p = 0.04), and TrBMC (r = -0.51, p = 0.05). No outcome measures correlated with connectivity index or TrBD. These data show that as the number of active and damaged joints in the upper limb increase, the H_A in the trabecular network increases and the bone mass and bending strength decreases at the ultradistal radius. In contrast, the Physical Function Score is related to bone density, mass, and bending strength but not the mineral organization in the trabecular network.

SA098

In vivo 3D-Evaluation of Bone Structure in the Human Forearm; A Time Saving and Non Invasive Procedure. M. Neff[1], M. A. Dambacher[2], P. Rüegsegger[3]. [1]Center for Osteoporosis, Zurich, Switzerland, [2]Univ. Hospital Balgrist, Zurich, Switzerland, [3]Inst. for Biomedical Engineering Univ. and Swiss Federal Inst. of Technology, Zurich, Switzerland.

Purpose: In vivo, till now only bone mass was available quantitatively. The non invasive evaluation of bone structures, which play an important role in the fracture risk prediction, was made qualitatively using high resolution 2D-CT-images (Densiscan 1000, Scanco Medical). Recently quantitative 3D structure analysis became available in vivo with the help of 3D-QCT (Densiscan 3D). Methods: The new system has a 2-dimensional detector array in combination with a 0.15 x 12mm line-focus x-ray tube (effective energy 40keV), enabling the simultaneous acquisition of a stack of 110 tomograms perpendicular to the bone axis with a maximal diameter of 90mm. The radial resolution is 160µm (10% MTF, isotropic voxel size 90µm) and axial 200µm (10%MTF). The tomograms are taken 7mm proximal from the endplate of the distal radius delivering a coverage of a region of about 10mm. The data acquisition time is about 2 minutes and the local skin radiation dose for a whole examination (scout view included) 2.5mGy. With automatic repositioning the reproducibility is <±1% (for structure elements) in mixed collectives. Results: In praxi it is now possible (see graph) to quantify microarchitectural features as number of trabeculae, trabecular and cortical thickness, trabecular spacing and endosteal surface in addition to the separate volumetric BMD of trabecular and cortical bone. Conclusions: Such a characterization will give better insight in pathogenesis, prevention and treatment of primary and secondary osteoporosis. It also improves individual fracture risk prediction; e.g. with the help of finite element analysis.

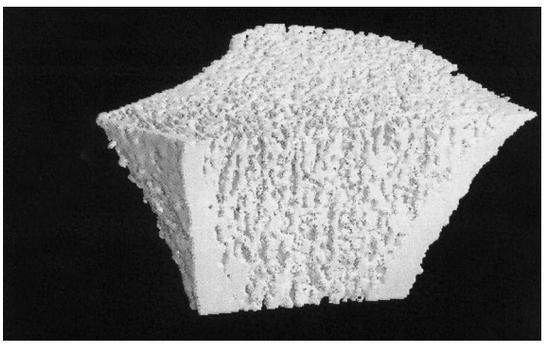

SA099

See Friday Plenary number F099.

SA100

Assessment of the Tibia in Prepubertal Girls Using Ultrasonic Guided Waves. P. Moilanen, P. H. F. Nicholson*, T. Karkkainen*, Q. Wang*, J. Timonen*, S. Cheng. Univ. of Jyvaskyla, Jyvaskyla, Finland.

The purpose of this study was to compare low frequency guided ultrasonic wave measurements with established ultrasound and bone density measurements in terms of their ability to characterize human long bones. Subjects were 12-14 year-old girls (n=106) who participated in a calcium and vitamin D intervention study. A prototype low frequency pulse transmission device consisting of a uniaxial scanning mechanism and low frequency transducers orientated perpendicularly to the limb was used to measure ultrasound velocities in the tibia. This device recorded the velocity of two propagating waves: a lateral mode (V1) travelling at 3300-4400 m/s and an additional slower mode (V2) propagating at 1500-2000 m/s and which has been shown elsewhere to be consistent with the lowest order antisymmetric guided mode. In addition, commercial ultrasound devices (Omnisense, Sunlight Ltd., QUS-2, Quidel Corp) were used to measure the speed of sound (SOS) in the tibia and the radius, and attenuation (BUA) in the calcaneus. Bone mineral content (BMC), volumetric cortical density (BMD) and cortical thickness (CTh) of the tibia were measured using pQCT, site-matched to the ultrasound measurements. Both V1 and V2 correlated significantly with tibial BMC, BMD and CTh, SOS of the tibia and radius, and BUA of the calcaneus. On the other hand, SOS only correlated with BMD and no correlations were found between SOS and CTh. These results indicate that the prototype device using guided waves reflects aspects of tibial cortical bone geometry in addition to bone density, thereby offering the potential of increased diagnostic information compared to existing tibial ultrasound devices.

	V1	V2	SOStibia	SOSradius	BUA
Whole bone					
BMC	.30 **	.28 **	ns	ns	.47 ***
BMD	.37 ***	.39 ***	.43 ***	.40 ***	.19 *
Cortical bone					
BMC	.32 **	.30 **	ns	ns	.48 ***
BMD	.44 ***	.46 ***	.54 ***	.49 ***	.26 **
CTh	.24 *	.28 **	ns	ns	.43 ***

|Values shown are correlation coefficients, r
*, **, ***, p < 0.05, 0.01, 0.001 respectively

SA101

The Discrimination Between Cases of Hip Fracture and Matched Controls Is Improved with a Biomechanic Analysis. P. Mayhew*[1], N. Loveridge*[1], N. Rushton*[1], M. Parker*[2], H. Kroger*[3], J. Reeve[1]. [1]University of Cambridge, Cambridge, United Kingdom, [2]Peterborough District Hospital, Peterborough, United Kingdom, [3]University of Kuopio, Kuopio, Finland.

We tested the hypothesis that measures of bending resistance made ex-vivo would discriminate cases of hip fracture from controls better than BMD (BMC/Area), which in vivo typically produces mean case – control differences of – 0.5 Z score units. Peripheral Quantitative Commuted Tomography (pQCT) cross sectional images of the femoral neck were used. The fracture biopsies (n = 19,F) were from subjects that had suffered an intracapsular hip fracture. The control material (n = 22,F) was from post-mortem subjects, with no history of disease known to affect bone and who died in hospital within 14 days of admission. The biopsies were fixed and embedded in methylmethacrylate without decalcification. Serial 0.5 mm thick pQCT cross-sectional images were obtained using the Densiscan 1000, (Scanco AG) and matched for location along the neck. Assuming that the density of methylmethacrylate was a good surrogate for soft tissue density, this was subtracted from each pixel's density and the remaining pixels showing positive densities were mapped on to 2-D images for calculation of 2-D section modulus (SM) and BMD. SM was calculated with respect to distances from the horizontal neutral axis in stance (0 degrees). As shown in the Table the fracture cases had a considerably lower resistance to bending while there was a much less impressive differences in BMD between cases and controls. To simulate the forces experienced during a sideways fall on to the greater trochanter, the model's neutral axis was rotated by –45 degrees. This imposes the greatest compressive and tensile stresses on the superior-posterior and inferior-anterior aspects of the femoral neck respectively. The results for SM were quantitatively similar to those at 0 degrees. We conclude that measures of hip strength such as SM provided greatly improved discrimination between hip fracture cases and controls when scanning was simulated in the AP plane. Rotation of the femoral neck to align the scanning plane so as to measure SM in the fall-loading configuration did not affect discrimination.

Angle of Rotation (degrees)	BMD/Strength Quantity	Cases (mean)	Controls (mean)	Mean Z score Diff**	P
0	BMD	0.547 gm/cm2	0.606 gm/cm2	0.56	0.08
0	log (SM)	466* mm3	736* mm3	1.54	0.0002
-45	log (SM)	428* mm3	631* mm3	1.28	0.0007

*log normal distribution; **Z : 1 SD unit

SA102

Comparison of BMD and Radiographic Texture Feature Analysis of Spine and Calcaneous in the Prediction of Vertebral Fractures. M. R. Chinander*[1], M. L. Giger*[1], Y. Peng*[1], L. B. Dixon*[1], T. Vokes[2]. [1]Radiology, The University of Chicago, Chicago, IL, USA, [2]Medicine, The University of Chicago, Chicago, IL, USA.

The addition of bone structure information via texture analysis of radiographic images may aid BMD in the assessment of bone strength and fracture risk. While the spine and hip are the anatomic sites of most interest, the assessment of the heel has advantages, namely low dose and efficient scanning in a screening environment. In this study, we compare the performance of BMD and radiographic texture analyses of the heel with those of the spine in terms of predicting the presence of vertebral fracture. Our database consists of fourteen subjects with at least one vertebral fracture and nineteen without a fracture. Spine and calcaneous BMD measurements were performed with Prodigy and PIXI peripheral bone densitometers, respectively. Lateral lumbar spine radiographs were obtained and digitized with 2905 Abe Sekkei (Tokyo, Japan) laser film digitzer to 0.100 mm pixel size. The BMD images from the peripheral bone densitomer were transferred to a Unix workstation for the texture analysis. Regions of interest (ROIs) were selected from the third lumbar vertebra on the digitized spine film and in the central portion of the calcaneous on the PIXI images. Fourier-based texture measures, including the RMS variation and first moment of the power spectrum were computed for each ROI. Receiver operator characteristic (ROC) analysis was used to assess the performance of the features in the task of distinguishing between fracture and non-fracture cases. The combination of the BMD measurements and texture features using linear discriminant analysis was also assessed. Results are summarized in the table. In general, the measurements from the spine performed better than those of the calcaneous. The use of texture analysis to assess bone structure from either the spine radiographs or heel BMD images was able to predict the presence of vertebral fractures about as well as BMD measurements at the same site.

Areas under the ROC curves (Az) for predicting the presence of vertebral fractures

Features	Spine Az	Heel Az
BMD	0.64	0.55
RMS Var., First Moment	0.68	0.58
RMS Var., First Moment, BMD	0.68	0.58

*Disclosures: **M.R. Chinander**, R2 Technology, Inc. 1.*

SA103

Absence of Marked Seasonal Change in Bone Turnover in a Large Multicenter Cross-Sectional Study. A. Blumsohn[1], K. E. Naylor[1], W. Timm*[2], A. C. Eagleton[1], R. Eastell[1]. [1]Bone Metabolism Group, University of Sheffield, Sheffield, United Kingdom, [2]Arbeitsgruppe Medizinische Physik, OPUS Study Group, University of Kiel, Kiel, Germany.

Studies investigating the relationship between season and bone turnover are contradictory. Resolution of this issue is of substantial importance for the use of markers of bone turnover to monitor therapy in routine clinical practice, and for appropriate design of therapeutic and epidemiological studies. No information, is available on seasonality of reliable new serum markers of bone resorption. We investigated the effect of season on serum markers of bone turnover in a large population-based multicenter European study (n=2780 women, Osteoporosis and Ultrasound Study, OPUS). Participants from 5 different European cities (Aberdeen, Berlin, Kiel, Paris, Sheffield) were identified by random selection from registers of local general medical practitioners or lists of the local registry office. Measurements were performed in a randomised order, and included serum β-Crosslaps (sβCTX), procollagen type I N-terminal propeptide (PINP), and osteocalcin (OC). Seasonality was assessed by cosinor analysis with Hotelling's T2-test. Less than one percent of the between person variance was accounted for by seasonality for all markers (n = 2780). There was small but statistically significant summertime increase in OC and PINP in the healthy postmenopausal population after exclusions based on disease or medication use (remaining n = 1226, ages 50 to 80 years; amplitudes 5.6% and 5.4% respectively, $P < 0.001$). There was also a small but statistically significant seasonal trend in PTH with Amplitude 7.1% ($P = 0.038$) and estimated peak on the 9th of March. There was no significant effect of season on serum sβCTX. To assess the practical implications of season for the generation of reference intervals, 95% non-parametric reference limits were calculated by season. There was no major effect of season on reference intervals, but the small summertime increase was statistically significant for OC and PINP (one way ANOVA $P<0.05$), but not for sβCTX. We have been unable to confirm findings of a marked wintertime increase in bone formation and resorption within the general population. The absence of marked seasonality was irrespective of age, menopausal status, or geographical location. The statistically significant summertime increase in bone formation in this and other studies is unlikely to confound clinical interpretation of these measurements.

SA104

See Friday Plenary number F104.

SA105

Biochemical Markers of Type I Collagen Synthesis and Degradation in Monitoring Osteoporosis Treatment with Raloxifene or Alendronate. J. J. Stepan, D. Michalska*, V. Zikan*, J. Vokrouhlicka*. 3rd Department of Internal Medicine, Charles University Faculty of Medicine, Prague, Czech Republic.

The aim of this study was to assess clinical value of biochemical markers of type I collagen synthesis (serum aminoterminal propeptide of type I collagen, S-PINP) and collagen degradation (serum type I collagen cross-linked C-telopeptide beta, S-CTX) in monitoring treatment of postmenopausal osteoporosis with raloxifene or alendronate. The open label study involved 165 postmenopausal women (mean age 63 ± 8 years). Fifty patients were treated for 1 year with raloxifene (60 mg/day), calcium (500 mg/day) and vitamin D (800 IU/day); 65 patients were treated with alendronate (10 mg/day), calcium and vitamin D; and 50 patients received calcium and vitamin D (control group). Premenopausal values were determined in 65 healthy women. S-PINP was measured by a radioimmunoassay (Orion Diagnostica). S-CTX was measured using the Elecsys (Roche). Bone mineral density at the lumbar spine and proximal femur was measured using the QDR 4500A Bone Densitometer (Hologic, U.S.A.). Before treatment, no significant differences in biochemical markers were found between the treatment groups. After one year of treatment with raloxifene, the increase of the spine BMD (1.45 ± 2.56%, n.s.) did not correlate with decrease in S-CTX (-50±16%, $p<0.01$) and S-PINP (-32±20%, $p<0.01$). A significant decrease in S-CTX was observed in 80% of the patients while an increase in BMD exceeding the least significant change was found in only 13/50 patients. After 1 year of treatment, mean S-CTX and S-PINP (345±124 ng/l, and 34±8 ug/l, respectively) was at the range of the premenopausal levels (284±72 ng/l, and 31±9 ug/l, respectively). After 1 year of treatment with alendronate, both S-CTX and S-PINP (99±41 ng/l, and 14±4 ug/l, respectively) were below the premenopausal range ($p<0.01$) and were significantly below the values in raloxifene treated patients. No significant changes of BMD and markers were observed in the control group. In conclusion, after 1 year treatment with raloxifene, markers of type I collagen synthesis and degradation decreased to the mean premenopausal levels. Treatment with alendronate resulted in a significant suppression of both markers below the premenopausal range. Responders to treatment with alendronate could be identified using either BMD or biochemical markers. S-CTX is a candidate marker for monitoring treatment with raloxifene.

SA106

See Friday Plenary number F106.

SA107

Tartrate-Resistant Acid Phosphatase 5b Correlates with Histomorphometric Parameters of Osteoclasts and Bone Resorption in Hemodialysis Patients. P. Chu[1], T. Chao*[1], Y. Lin*[1], A. J. Janckila[2], L. T. Yam*[2]. [1]Medicine, National Defense Medical Center and Tri-Service General Hospital, Taipei, Taiwan Republic of China, [2]Medicine, VAMC, Louisville, Louisville, KY, USA.

Metabolic bone disease is common among patients on chronic hemodialysis (HD). Histomorphometry of bone biopsy is the gold standard for diagnosis and classification of renal osteodystrophy (ROD). Our purpose was to determine if serum tartrate-resistant acid phosphatase (TRACP) 5b activity, an osteoclastic marker of bone resorption, could be used to distinguish HD patients with high turnover hyperparathyroid (HPT) bone disease from other forms of ROD. Fourteen HD patients and six normal males were included for study. All subjects underwent transiliac bone biopsy after dual tetracycline labeling and concomitant biochemical testing for TRACP 5b, intact parathyroid hormone (iPTH), cross-linked C-telopeptides (ICTP), total calcium, phosphorous, and albumin. Bone biopsies were evaluated for static and dynamic histomorphometric parameters of: osteoid volume/bone volume (OV/BV), osteoblast surface/bone surface (OBS/BS), fibrosis surface/bone surface (FbS/BS), erosion surface/bone surface (ES/BS), erosion depth (EDe), osteoclast number/100 mm bone perimeter (NOC/BPM), osteoclast surface/bone surface (OCS/BS), mineral apposition rate (MAR), bone formation rate/bone surface (BFR/MS). Histomorphometry revealed six HD patients to have predominant HPT disease, four to have adynamic bone disease, three to have mixed uremic osteodystrophy, and one to have osteomalacia. All six with HPT had high TRACP 5b (11.97 ± 8.92 U/L) compared to control (3.25 ± 0.59 U/L). All remaining non-HPT cases had TRACP 5b levels at or below the normal mean. iPTH and ICTP levels were also highest in HPT, but were elevated in most other non-HPT patients as well. Significant correlations among histomorphometric and biochemical parameters of bone resorption are shown below: TRACP 5b correlated more strongly with parameters of osteoclastic activity than with evidence of erosion. Further, TRACP 5b correlated more strongly with osteoclasts than did iPTH or ICTP. Serum TRACP 5b is a highly valid biochemical marker for osteoclastic activity in endstage renal disease and, with further study and documentation, may prove to be a useful test to differentiate high turnover HPT bone disease from other ROD.

Spearman's "r" between biochemical and histomorphometric parameters of bone resorption

	NOC/BPM	OCS/BS	ES/BS	EDe
TRACP 5b	.91***	.92***	.50*	.66**
iPTH	.82***	.76***	.59**	.78***
ICTP	.62**	.54*	.42	.65**

SA108

Serum Tartrate-Resistant Acid Phosphatase Isoforms 5a and 5b in Rheumatoid Arthritis. A. J. Janckila[1], D. H. Neustadt*[2], Y. R. Nakasato[2], J. M. Halleen[3], T. Hentunen[3], L. T. Yam*[1]. [1]Medicine, VAMC, Louisville, Louisville, KY, USA, [2]Medicine, University of Louisville, Louisville, KY, USA, [3]Anatomy, Institute of Biomedicine, University of Turku, Turku, Finland.

In many patients with rheumatoid arthritis (RA), total serum tartrate-resistant acid phosphatase (TRACP) protein is elevated while TRACP activity is not. Serum TRACP exists as two related isoforms; non-osteoclastic TRACP 5a and osteoclastic TRACP 5b. Our objective was to determine the significance and source of elevated serum TRACP protein in RA. Thirty-five RA, 32 osteoarthritis (OA) and 16 control subjects were studied. Serum TRACP 5b activity and total TRACP protein were determined by enzyme capture and two-site immunoassay, respectively. TRACP isoforms 5a and 5b were analyzed by non-denaturing polyacrylamide gel electrophoresis (PAGE). Serum bone alkaline phosphatase (BAP), crosslinked N-telopeptides (NTx), and C-telopeptides (ICTP) of type I collagen were estimated as markers of bone turnover. C-reactive protein (CRP) was measured as a marker of chronic inflammation. Macrophages and dendritic cells (DC) were developed from peripheral blood monocytes. Cell lysates and culture supernatants were analyzed for TRACP isoforms by immunoassay and PAGE. In RA, mean TRACP 5b activity was normal (2.55 ± 0.77 U/L vs 2.48 ± 0.71 U/L), but median total TRACP protein was significantly increased (15.81 μg/L vs 9.69 μg/L; $p < 0.001$). In OA TRACP 5b activity and protein were normal. In RA, TRACP 5b activity correlated weakly with ICTP ($r = 0.56$) while TRACP protein levels correlated weakly with NTx ($r = 0.43$). Additionally, TRACP protein, but not TRACP 5b activity correlated significantly with CRP ($r = 0.42$). Macrophage and DC lysates contained TRACP 5b, while tissue culture supernatants contained TRACP 5a. We conclude that elevated total TRACP protein in RA sera was probably due to TRACP 5a and not derived from osteoclasts. Rather, it could be a secreted product of inflammatory macrophages and DC. Serum TRACP 5b activity is further validated as a marker for osteoclastic activity.

SA109

See Friday Plenary number F109.

SA110

Is there a Relationship between Bone Density as Measured by Ultrasound and Foot Loading. I. P. Drysdale, H. J. Hinkley, D. Bird*, N. J. Walters*. British College of Osteopathic Medicine, London, United Kingdom.

Previous studies by the same authors have shown a bilateral difference in Broadband Ultrasound Attenuation (BUA) of the calcaneus, using the McCue Cubaclinical II device, with differences of up to 30 % being reported. Other studies using different equipment and technologies support this. The subjects concerned had no apparent reasons for these differences. The purpose of this study was to further investigate any bilateral differences using different measurement criteria and a new data set. Subjects were excluded if there was previous history of limb disease or bone fracture. The BUA ($dBMz^{-1}$) of 66 subjects was determined for the non-dominant and dominant calcanei, each three times in succession. Both heels were re-positioned between each measurement to allow for anatomical variation and the mean calculated for each foot. Foot pressure was also measured using a Footscan plate (RSscan), with static and dynamic measurements being recorded. In addition leg length, weight and height were recorded. The load of the non-dominant and dominant hindfoot expressed as a percentage of body weight (static), the dynamic pressure load rate in $N/cm^2/ms$ (speed of loading) and the pressure impulse in Ns/cm^2 (total loading over time), were compared to non-dominant and dominant BUA. No significant correlation of BUA with the measured parameters was found except in the case of non-dominant BUA versus non-dominant load rate ($n=54$), $r=0.3$, $P<0.05$.

SA111

See Friday Plenary number F111.

SA112

Quantitative Calcaneal Ultrasound Identifies Men with Prostate Cancer and Androgen Deprivation at Risk for Osteoporosis. P. S. Coates, D. L. Medich*, J. Wagner, J. Ribich, D. L. Trump*, J. B. Nelson*, S. L. Greenspan. University of Pittsburgh Medical Center, Pittsburgh, PA, USA.

Androgen deprivation therapy, the most effective systemic treatment for prostate cancer, is a major risk factor for osteoporosis. Little is known about the use of calcaneal ultrasound to identify bone loss in these men. To identify prostate cancer patients at risk of osteoporosis we measured broadband ultrasound attenuation (BUA) using the Sahara (Hologic, Bedford, MA) and QUS-2 (Metra Biosystems, Mountainview, CA) clinical sonometers and compared this to conventional bone mineral density (BMD) by dual-photon absorptiometry at the PA spine, femoral neck and total hip (Hologic 4500-A, Hologic, Bedford, MA). We studied 95 men in 4 groups; men with prostate cancer 1) not on androgen deprivation, N=23; 2) on androgen deprivation <6 months, N=17; 3) on androgen deprivation >6 months, N=24; and 4) healthy controls, N=31. The groups did not differ in age, height or weight. BUA was lower in men on chronic androgen deprivation using the QUS-2 sonometer than controls ($p<0.01$), with a similar trend using the Sahara. Using both sonometers, BUA was related to BMD at all sites. Duration of androgen deprivation and markers of bone turnover were inversely related to BUA with both instruments. In conclusion, BUA using 2 different instruments is related to BMD, duration of androgen deprivation, and bone turnover markers, and may be useful to identify men on androgen deprivation at risk of osteoporosis. Longitudinal studies are needed to confirm this finding.

	QUS (dB/MHz)	**Sahara (dB/MHz)**
Androgen status		
No androgen deprivation	80.6 ± 22	84.6 ± 22
Acute androgen deprivation (<6 months)	82.9 ± 20	82.1 ± 20
Chronic androgen deprivation (>6 months)	73.2 ± 18†	75.1 ± 24
Controls	87.8 ± 19	84.3 ± 26

†$p< 0.01$ compared to controls

Correlation (R) PA spine (g/cm^2)	0.38**	0.31**
Femoral neck (g/cm^2)	0.52***	0.38**
Total hip (g/cm^2)	0.53***	0.44***
Duration androgen deprivation (months)	-0.28**	-0.26*
NTX (nM BCE/nMCr)	-0.24*	-0.22*
Osteocalcin (ng/ml)	-0.30**	-0.13

*$p<0.05$, **$p<0.01$, ***$p<0.0001$

SA113

See Friday Plenary number F113.

SA114

Relationship of Calcaneal Broadband Ultrasound Attenuation and Osteoarthritis of the Lower Limb. H. J. Hinkley, I. P. Drysdale, D. Bird*, N. J. Walters*. British College of Osteopathic Medicine, London, United Kingdom.

Patients with Osteoarthritis (OA) have been reported to have greater bone density, in most cases measured by techniques other than ultrasound. This study investigates the association using Broadband Ultrasound Attenuation (BUA) of the calcaneus. Forty-three postmenopausal women aged 50 to 78 with OA of the lower limb were scanned with the McCue Cubaclinical II bone densitometer. Two measurements on each heel were taken and the minimum BUA used. OA was graded on the ability to walk less than 100m (1), more than 100m (2), more than 500m (3) and more than 1000m (4). The severity of OA was compared with the BUA Zu score and no significant correlation was found. Of the subjects who had unilateral OA there was no significant difference in bilateral BUA. The minimum BUA measure for the OA group was compared to the BUA for an age matched group of normal female subjects, using the students t test. In this study Caucasian post menopausal women with OA of the lower limb, did not have significantly higher levels of bone density at the calcaneus as measured by ultrasound. This supports the findings of a Japanese study involving women suffering OA of the knee.

SA115

See Friday Plenary number F115.

SA116

Biomechanical Validation of Quantitative Ultrasound. G. Whan*[1], R. J. Runciman*[1], M. B. Hurtig*[2]. [1]School of Engineering, University of Guelph, Guelph, ON, Canada, [2]Ontario Veterinary College, University of Guelph, Guelph, ON, Canada.

Quantitative Ultrasound (QUS) has previously been explored as a clinical tool for assessing bone properties. Results from these studies have been, for the most part, inconclusive. This extensive comparative study focuses on QUS versus biomechanical strength and stiffness in the equine metacarpus (MC3). In isotropic, homogeneous and pure elastic materials, there is a positive relationship between the speed of sound (SOS) in a material with its Modulus of Elasticity (E). This theoretical relationship is more complex in biological materials. Nine potential clinical sites of interest were identified for testing in this study. The diaphysis of the whole bone was divided into three levels, proximal, mid and distal. Each level was also divided into three sites, medial, dorsal and lateral. QUS readings were taken at the nine sites. QUS measurements were made using a Sunlight Omnisense, manufactured by Sunlight Medical Ltd. Previous investigations with this equipment has shown that QUS measurements are repeatable and reliable on the equine MC3 with and without overlying soft tissue and for various sample temperatures. 3D parallelepiped testing samples were prepared from each of the nine sites from the whole bone. Each sample had a constant testing cross sectional area of 25mm2 of cortical bone. Each sample was tested to destruction under tension. Load was applied using an Inston (Model 4204) outfitted with a 50kN load cell at a rate of 6mm/min. Strain was measured using a modular strain measurement clip. All output data was collected using standard A/D equipment and data collection software. Collected data was analysed to find Modulus of Elasticity (E) and Ultimate Tensile Strength (UTS) of each sample. The correlative relationship between QUS, E and UTS was examined using the statistical analysis program, SAS. Independent correlations were studied as well as the interactions between all the parameters. The medial and lateral proximal sites were found to be unreliable in measuring repeatable QUS data due to the external geometry of the bone. Similarly, the internal geometry of the cortical bone on the distal sites has effected the outcome of the biomechanical testing. Our results indicate an identifiable relationship between QUS, E and UTS. Further analysis is required to investigate the significance of this relationship.

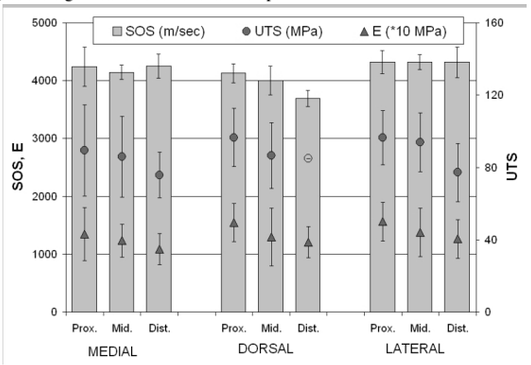

SA117

Bone Mass Phenotypes in Alcohol Preferring Rats. I. Alam*, A. G. Robling, L. G. Carr*, L. Lumeng*, T. K. Li*, C. H. Turner. Indiana University, Indianapolis, IN, USA.

The association between moderate alcohol intake and elevated bone mass has been demonstrated by several epidemiological studies, raising some important issues whether the beneficial effects of alcohol consumption are related to genetics, life style or other factors. It might be that the individuals who are genetically predisposed to drink alcohol also have genetic alleles that promote higher bone mass. Thus, animals selectively bred for alcohol preference might also have higher bone mass even without consuming alcohol. To test this hypothesis, three separate lines of rats [alcohol-preferring (P), high alcohol-drinking 1 & 2 (HAD1, HAD2)] selectively bred based upon high alcohol preference were compared to their non-alcohol preferring control lines [non-alcohol-preferring (NP), low alcohol-drinking 1 & 2 (LAD1, LAD2)] to determine the effects of alcohol preference alleles on bone phenotype. We used growing (3-month old) rats from each of these three lines to characterize volumetric bone mineral density (vBMD), bone mineral content (BMC) and cross sectional area (CSA) at the femoral midshaft and distal metaphysis using pQCT. The P rats exhibited significantly greater (2-12%, $p<0.05$) total and cortical vBMD, BMC, and CSA than the NP rats at the femoral midshaft. At the distal metaphysis, P rats exhibited significantly greater (3-23%, $p<0.05$) values for bone mass in the cortical shell. Conversely, the HAD 1 rats exhibited significantly lower (9-12%, $p<0.05$) total vBMD, total BMC, cortical BMC and cortical area at the midshaft femur than the LAD1 rats. The HAD 1 distal metaphysis exhibited a significantly thinner cortical shell than the LAD1 rats. Similar to the P rats, the HAD2 rats exhibited significantly greater (11-13%, $p<0.05$) total vBMD and cortical area at midshaft and significantly greater (15-27%, $p<0.0001$) total vBMD, BMC and cortical CSA at distal metaphysis than their low-drinking counterparts (LAD2). HAD2 rats also had significantly greater ((5-188%, $p<0.05$) trabecular bone measurements in distal femoral metaphysis, compared to the LAD2 control strain. Our preliminary findings demonstrate an apparent link between alcohol preference and bone mass in some rat strains. P and HAD2 rats have a high bone mass phenotype, while HAD1 rats have a low bone mass phenotype. These findings suggest that P and HAD2 rats have high bone mass genes associated with signals in the brain that make rats prefer alcohol. HAD1 rats do not have high bone mass genes even though they prefer alcohol. Consequently these three different strains of alcohol preferring rats may allow us not only to better understand the association between alcohol preference and bone mass, but potentially to identify new genes linked to BMD.

SA118

Genetic and GH/IGF-I Effects on Vertebral Trabecular Architecture. L. R. Donahue[1], C. J. Rosen[1], R. Muller[2], K. L. Shultz*[1], V. Guido*[1], W. G. Beamer[1], M. L. Bouxsein[2]. [1]The Jackson Laboratory, Bar Harbor, ME, USA, [2]Beth Israel Deaconess Medical Center, Boston, MA, USA.

We demonstrated that vertebral trabecular density and structure are polygenic traits and discovered QTLs for vertebral BMD in F2s from a C57BL/6J (B6-low BMD) X C3H/HeJ (C3H-high BMD) cross. To decompose the vertebral BMD phenotype and to determine which aspects are GH/IGF-I dependent or independent, we are utilizing a spontaneous mouse mutation, *little,* with a non-functional GHRHR. We made a congenic strain by backcrossing the *little* mutation from the original B6 background to C3H. In both B6-*lit/lit* and C3.B6-*lit/lit* mice, circulating GH is undetectable, serum IGF-I is low, and femoral BMD (pQCT), areal BMD (PIXImus), femur length, and body mass are reduced compared to *lit/+* mice. Although C3.B6-*lit/lit* mice are of the same body weight as B6-*lit/lit* mice, C3.B6-*lit/lit* mice have higher whole body, femoral, and vertebral BMD. These data suggest both GH/IGF dependent and independent regulation of BMD and indicate that this phenotype needs to be decomposed to understand mechanisms of genetic and endocrine regulation. We have started with vertebral BMD utilizing high resolution microcomputed tomography (μCT) to characterize trabecular bone in a single lumbar vertebra (L5) in 4 month old *lit/+* and *lit/lit* females (mean±SD). These data show that trabecular BV/TV has a strong genetic regulation whereby B6 alleles impart higher BV/TV in both *lit/lit* and *lit/+* mice compared to C3H alleles. Contributing to overall BV/TV are the number, thickness, and spacing of trabeculae. B6 alleles in both *lit/lit* and *lit/+* mice impart greater numbers of trabeculae that are thinner and closer together than C3H alleles. However, the status of heterozygosity for *little* can be seen to effect trabecular thickness regardless of genetic background, but is strain dependent for trabecular number and spacing. These data emphasize the interaction between genetic background and endocrine status. A QTL analysis of F2s from a B6-*lit/lit* x C3.B6-*lit/lit* cross, coupled with data from our B6C3F2s without the *little* mutation will reveal which loci are responsive to GH/IGF-I regulation and which are not.

Phenotype	C57BL/6J-*lit/+*	C57BL/6J-*lit/lit*	C3.B6-*lit/+*	C3.B6-*lit/lit*
Vert Trab BV/TV (%)	19.3±1.1^	19.2±2.2^	13.6±2.8*^	10.6±1.3*^
Vert Tb. Th (μm)	49±2*^	44±1*^	60±4*^	53±3*^
Vert Tb. N (1/mm)	4.17±0.12*^	4.71±0.47*^	2.61±0.31^	2.89±0.23^
Vert Tb. Sp. (μm)	238±10^	209±27^	402±42*^	351±28*^
IGF-I (ng/ml)	171±25*^	37±7*	209±44*^	44±5*
Body Weight (g)	20.56±1.58*^	14.24±1.75*	22.36±2.16*^	13.71±0.95*
Whole Body BMD g/cm$^{2)}$	.043±.001*^	0.29±.003*^	0.48±.001*^	0.35±.001*^

*between genotypes (*lit/lit* vs *lit/+* within strain), $p<.05$
^between strains (B6 vs C3H within genotype), $p<.05$

SA119

See Friday Plenary number F119.

SA120

Bone Mineral Density in 30 Men with Genetic Hemochromatosis and C282Y Mutation HFE Gene Homozygoty. P. Guggenbuhl, Y. Deugnier*, J. Boisdet*, Y. Rolland*, A. Perdriger*, Y. Pawlotsky*, G. Chalès*. CHU, Rennes, France.

Genetic Hemochromatosis (GH) is a genetic disease of iron overload mainly related to the C282Y mutation on the HFE gene. Bone involvement has been recognised only recently. The aim of the study was i- to assess bone mineral density (BMD) and bone remodeling in males with GH; ii- to discuss the influence of iron overload. Patients admitted between September 1995 and July 1997 in our Rheumatology Unit for GH were included. The diagnosis of GH was ascertained on the association of a plasma transferrin saturation > 45% and homozygoty for the Cys282Y mutation; 23 (76.7%) had a liver biopsy. No other condition could explain iron overload. Among the 52 patients screened, 30 males (aged 47±10 years) with GH were considered for the study. Twenty controls were assessed for biological measurements. The results were (mean±SD) : ferritin level was 1508±1365 ng/ml, transferrin saturation was 70.6±21.1%, the hepatic iron concentration (HIC) was 356.3±164.8 µmoles/g. BMD measured by DXA was 0.94±0.15g/cm2 at lumbar spine (LS) and 0.79±0.16 g/cm2 at femoral neck (FN). Osteopenia at LS (Tscore<-1 SD) was observed in 15/29 (51.7%) patients and in 17/28 (60.7%) at FN ; when either LS or FN were considered, osteopenia was found in 21/30 patients (70%). Osteoporosis (Tscore<-2.5 SD) occurred in 6/29 (20.7%) at LS and in 7/28 (25%) at FN ; when either LS or FN were considered, osteoporosis was found in 7/30 patients (23.3%). Three patients (10%) suffered from a vertebral fracture which occurred in 3 of the 6 (50%) osteoporotic patients. There was no significant relationship between BMD and iron saturation, ferritin, PTH and bone remodelling markers, but a significant negative correlation between HIC and BMD at FN (r = -0.49 ; p = 0.019). BMD was positively associated with testosterone at LS (r = 0.342 ; p = 0.07) and with 25 OH vitamine D at LS (r = 0.365 ; p= 0.056) and at FN (r = 0.44 ; p = 0.021). Five patients (16.7%) were hypogonadic; among the 7 osteoporotic patients, 2 (28.6%) were hypogonadic. When the 21 patients with osteopenia were considered, 4 (19.05%) were hypogonadic. There was an increase of bone specific alkaline phosphatase (20.6 vs 11.7 U/l ; p = 0.001) and osteocalcin (23.36 vs 19.5 ng/ml ; p = 0.017) in GH patients vs controls. Conclusion : in our population of 30 males with genetic hemochromatosis and C282 mutation homozygoty for HFE gene, 70% suffered from osteopenia and 23.3% from osteoporosis; a vertebral fracture occurred in 10%. There was no evidence of hypogonadism in the majority of the GH patients, nor low 25-hydroxycholecalciferol levels or PTH 1-84 dysfunction. Biochemical markers of bone formation were found to be increased compared to control and hepatic iron concentration seemed to influence negatively BMD.

SA121

Bone Mass in Rats Is Highly Heritable. Q. Sun[1], S. J. Warden*[1], D. L. Koller*[2], T. Foroud*[2], C. H. Turner*[1]. [1]Orthopaedic Surgery, Indiana University, Indianapolis, IN, USA, [2]Indiana University, Indianapolis, IN, USA.

Rats are the most common animal model for skeletal research. However, mice are most often used for skeletal genetics studies. With the rapid growth in genetic markers and genome sequence information, genetic studies in rats are now quite feasible. One important question remains: Are bone measurements heritable in rats? We studied first (F1) and second (F2) generation offspring from Fischer 344 (F344) and Lewis (LEW) rats to determine the heritability of peak bone mass. F344 and LEW rat strains were chosen because they have been previously demonstrated to differ considerably in bone mass. The study population included 6 month old female F344 (n=16), LEW (n=16), F1 (n=16), and F2 (n=303) rats. Bone mineral content (BMC) was measured using dual energy x-ray absorptiometry (DXA) for L3-5 spine and the whole femur. In addition, high resolution peripheral quantitative computed tomography (pQCT) was used to measure volumetric bone mineral density (vBMD) for L5 vertebrae and the proximal, mid and distal femur. For each phenotype, the environmental variance was estimated as the pooled variance of F344, LEW and F1 rats. Heritability, or the proportion of the variability due to genetic factors, was then calculated as one minus the ratio of the environmental variance estimate to the total variance in the F2 rats, which would be expected to contain both genetic and environmental contributions. Heritability for body weight (BW) was 77%, and for BMC at L3-5 and the femur was 66% and 71%, respectively. When BMC was normalized by BW, the heritability was 47% and 52% for the spine and femur. This finding suggests that a substantial portion of the genetic variability in BMC is under the control of genetic factors different from those genetic factors contributing to total body weight variability. Heritabilities of vBMD measured at the proximal, mid and distal femur were 82%, 80% and 60%, respectively, and the heritability of L5 vBMD was 80%. Consequently, the heritability of bone mass and vBMD in rats is very high, ranging from 60% to over 80%. The observed heritability values are in agreement with those that have been observed in mice and humans. We conclude that, like mice, selected inbred strains of rats will serve as excellent models for studies of skeletal genetics.

SA122

See Friday Plenary number F122.

SA123

Linkage of Femoral Structure QTLs to Chromosomes 3 and 19. D. L. Koller[1], K. E. White[2], G. Liu[2], S. L. Hui[2], P. M. Conneally*[1], C. C. Johnston[2], M. J. Econs[2], T. Foroud[1], M. Peacock[2]. [1]Medical and Molecular Genetics, Indiana University, Indianapolis, IN, USA, [2]Medicine, Indiana University, Indianapolis, IN, USA.

Femoral structure contributes to bone strength and predicts hip fracture risk independently of BMD. We reported an autosomal genome screen in 309 white premenopausal sister pairs (JBMR 16:985-91, 2001). Pelvic and femur axis lengths, and widths of femur head and midshaft, measured from radiographs, demonstrated linkage to regions of chromosomes 3, 4, 5, 17, and 19. To replicate these initial linkage findings, we collected an independent sample of 246 white premenopausal sister pairs and completed a genome screen using 392 microsatellite markers. Multipoint quantitative linkage analysis was performed using Mapmaker/SIBS. We subsequently performed linkage analysis in an expanded sample of 437 white and 201 black sister pairs, which has partial overlap (191 white pairs) with the previously reported genome screen sample (JBMR 16:985-91, 2001). All chromosomal positions (cM) reported here correspond to the Marshfield map coordinates (Am J Hum Genet 63:861-689, 1998). On chromosome 3, the initial sample gave a maximum LOD score of 1.8 at 130 cM with femur head width. The second sample (n=246 white pairs) showed suggestive evidence of linkage with femur head width (LOD=3.3 at 106 cM). In the enlarged sample of black and white sisters (n=638 pairs), a significant maximum LOD score of 4.7 was obtained at 106 cM. Evidence of linkage was also found in this region of chromosome 3 for a second phenotype, femur shaft width, (LOD=3.9 at 112 cM with n=638 pairs). In similar fashion, the independent sample (n=246 pairs) gave a LOD score of 1.3 with femur axis length on chromosome 19 (75 cM). This is in agreement with the result for femur axis length in the initial sample (LOD=2.0 at 80 cM). The LOD score in the enlarged sample (n=638 pairs) for this region of chromosome 19 was 2.6 at 73 cM. For the remaining regions reported in the initial sample (chromosomes 4, 5, and 17), the LOD scores in the independent sample were low (0.7 or less). These findings emphasize the importance of replication of initial linkage findings, and confirm our previously reported linkages to chromosomes 3 and 19.

SA124

See Friday Plenary number F124.

SA125

Is a Factor Score Combining Dual X-Ray Absorptiometry and Ultrasound a Better Phenotype for Genetic Studies? D. Karasik[1], M. T. Hannan[1], D. P. Kiel[1], M. L. Bouxsein[2], L. A. Cupples*[3]. [1]Hebrew Rehab Ctr, Harvard Med Sch Divis on Aging, Boston, MA, USA, [2]Orthopedic Biomechanics Laboratory, BIDMC & Harvard Med Sch, Boston, MA, USA, [3]Biostat, Boston Uni Sch Public Health, Boston, MA, USA.

Genetic factors substantially contribute to variation in bone mineral density (BMD) and quantitative ultrasound (QUS). Many bone characteristics measured by the two methods are similar, but QUS potentially measures features of bone not assessed by BMD. We hypothesize that a score composed of both BMD and QUS may serve as a single indicator of general bone status and represent a useful phenotype for genetic studies of osteoporosis. BMD, QUS and anthropometric measurements were obtained in 1203 persons in 323 pedigrees from the population-based Framingham Osteoporosis Study, along with data on age, sex, alcohol and caffeine intake, smoking status, physical activity, vitamin D and calcium intake, and estrogen use (in females) during 1995-98. BMDs were measured at lumbar spine, femoral neck, trochanter, and Ward's area using a Lunar DPX-L, and broadband ultrasound attenuation (BUA) and speed of sound (SOS) at the calcaneus with a Hologic Sahara. In each sex and generation, we performed principal component analysis of BMD and QUS measures with Varimax rotation and subsequent regression of the resulting composite score on the covariates. Using SOLAR program, we estimated crude and covariate-adjusted heritability (h^2). Correlations between QUS and BMD ranged 0.34-0.45 in both sexes in Original and Offspring Cohorts. The first of the two resulting factor scores (FS1) explained ~65% of the total variation of all six BMD and QUS measurements. Factor loadings for FS1 ranged 0.7-0.9 for BMD and 0.2-0.3 for QUS measures. Loadings of FS1 were extracted for each individual. Multiple regression of FS1 with the covariates revealed that BMI and height were significant predictors of FS1 variation, with age and estrogen therapy significant in Offspring females only. Crude and covariate-adjusted h^2 of FS1 were higher than these of BMD or QUS (Table), suggesting that the composite score may increase genetic signal to noise ratio by providing higher heritability estimates, which may be beneficial for subsequent genetic analysis than either BMD or QUS measures alone. However, additional studies are needed to determine whether FS1 will be a better predictor of skeletal fragility than BMD or QUS.

	Femoral neck BMD	Lumbar spine BMD	BUA	SOS	FS1
h^2crude	0.52±0.05	0.56±0.07	0.50±0.07	0.37±0.06	0.61±0.07
h^2adjusted	0.54±0.06	0.62±0.06	0.51±0.07	0.38±0.06	0.66±0.07

SA126

Polymorphic Variation in the Human Vitamin D Receptor Gene: An Association with Muscle Strength in Younger Swedish Women. E. Grundberg*[1], E. Ribom*[2], H. Brändström*[1], Ö. Ljunggren*[1], H. Mallmin*[2], A. Kindmark*[1]. [1]Department of Medical Sciences, Uppsala, Sweden, [2]Department of Surgical Sciences, Uppsala, Sweden.

Bone mineral density (BMD) is regulated by both environmental and genetic factors and known to be associated with muscle strength. Furtermore, muscle strength itself is under strong genetic control, demonstrated in both twin studies and genetic association studies. The polymorphisms of the gene for the Vitamin D receptor (VDR) are commonly studied in relation to BMD and several groups have reported a significant association between BMD and VDR alleles. However, little is known about the genetic influence of VDR on muscle strength. The purpose of this study was to investigate two VDR polymorphisms in relation to BMD and muscle strength in 168 Swedish women. The polymorhisms studied were the single nucleotide polymorhism BsmI and the poly A microsatellite, both situated in the 3´end of the VDR gene. The individuals in the study are part of the Swedish T-score cohort, containing a total of 340 women, aged 20-40, where the BMD data will be the basis for the Swedish reference population of bone density in women. BMD has been measured by dual X-ray absorbtiomtery (DXA) at spine, proximal femur, total body and heel and QUS (Quantitative Ultrasound)at the heel. Also, in 168 individuals quadriceps, hamstrings and handgrip muscle strength have been measured by using a modified Cybex II dynamometer and a JAMAR hydracraulic hand dynamometer. The gene fragments of VDR were amplified by PCR from the individual´s leukocyte DNA and analyzed for genotype. The VDR poly A microsatellite were separated on a polyacrylamidegel using ABI 377 sequencer and fragments < 19 repeats were denoted short (S) and repeats ≥ 19 denoted long (L). The VDR fragments containing the BsmI polymorphism were separated on an agarose gel after restriction digestion using the enzyme BsmI. The genotype frequencies were ss 16%, sL 44%, LL 40 % for the poly A repeat and bb 39%, bB 43 %, BB 18 % for the BsmI polymorphism respectively. Both the genotypes were in Hardy-Weinberg equilibrium and in strong linkage disequilibrium. Significant associations between the two VDR genotypes, ss and BB, and hamstrings strength were observed. However, no significant correlations between BMD at spine, proximal femur, total body and heel and VDR genotypes were found when analyzing 168 women out of 340. The results show that younger women, in this Swedish population based cohort, with shorter poly A repeat, ss, (p=0,041) or absence of the BsmI restriction site, BB, (p=0,0049) in the VDR gene, have significantly higher hamstrings muscle strength, which indicate a strong genetic effect on muscle strength.

SA127

Variations Of Aromatase Gene, Peak Bone Mass And Height In Young Women. J. A. Riancho[1], M. T. Zarrabeitia*[2], A. L. Zarrabeitia*[2], J. Gonzalez-Macias[1]. [1]Internal Medicine, Hospital U.M. Valdecilla, Santander, Spain, [2]Unit of Legal Medicine, University of Cantabria, Santander, Spain.

Aromatase, the enzyme responsible for the synthesis of estrogens from C19-steroids, is expressed in the gonads and a variety of other tissues, including bone. The enzymatic complex includes a unique cytochorme P450 aromatase, the product of CYP19 gene. Spontaneous mutations of aromatase gene result in delayed skeletal maturation in male human subjects, and osteoporosis develops in both male and female aromatase-deficient ArKO mice A common tetranucleotide tandem repeat polymorphism in intron 1 of human CYP19 has also been described as associated with the risk of developing breast cancer, as well as vertebral fractures in postmenopausal women. However, it is unclear if it is due to a low peak bone mass or to an accelerated loss later in life. Therefore, we explored the influence of CYP19 allelic variation on peak bone mass and body size in young women. Fifty one healthy women aged 22-34 years were studied. The polymorphic region was amplified by PCR, allele size was determined in an ABI Prism 310 gene sequencer, and designated as suggested by Healey et al. (Carcinogenesis 2000; 21:189). Bone mineral density (BMD) was measured by DXA with a Hologic machine. Women having CYP19 alleles with 7 or more repeats (n=27) were, on average, 3.1 cm taller (CI 0-6.2; p=0.05) than those with 6 or less repeats (n=23). However, there were no significant differences between both subgroups regarding body weight (56 ±6 vs. 57±7 kg), or BMD at the spine (1.020±0.124 vs. 1.059±0.101 g/cm2) or femoral level (0.816±0.102 vs. 0.861±0.098 g/cm2), whether adjusted by height or not. These results suggest that CYP19 allele variants do not influence peak bone mass in women, but may be associated with differences in body size.

SA128

Aromatase Gene Polymorphisms: Association with Bone Mineral Density and Serum Estradiol Concentrations in Post-menopausal Women. J. Somner[1], J. Cheung*[1], Y. T. Mak*[1], E. Prowse*[2], M. Frost*[2], K. Knapp*[2], I. Fogelman*[2], A. S. Wierzbicki*[1], G. Hampson*[1]. [1]Chemical Pathology, St Thomas Hospital, London, United Kingdom, [2]Nuclear Medicine, Guy's Hospital, London, United Kingdom.

Genetic and environmental factors influence estrogen homeostasis and tissue exposure to estrogen. Aromatase catalyses the conversion of androgens to estrogens. The aromatase gene (CYP19) is a candidate for susceptibility to diseases associated with estrogen exposure. As estrogen plays an important role in osteoporosis we investigated the association between the Valine 80 'G' to 'A' polymorphism in exon 3 of CYP19, bone mineral density (BMD) and serum estradiol concentrations in 253 post-menopausal women aged (mean [SD]) 64.5[9.23] years, cases [osteoporosis] n = 139, controls [normal BMD] n = 114. BMD was assessed at the spine, femoral neck and total hip. Data was analysed by multiple regression analysis including relevant factors such as body mass index (BMI), age at menarche/menopause, exercise, calcium intake, smoking, and alcohol intake. Estradiol values were partially normalised by log transformation. No association was observed between BMD values, 'Z' scores and the CYP 19 genotype in the study population. Allele frequencies were similar between cases and controls (cases AA: 22 % GA: 52.5 %, GG : 25 %, controls AA : 28 %, GA : 53.5 %, GG : 18 %; p= 0.36). However in older women (>10 years since menopause [YSM]) an association (p=0.09) was found between total hip and femoral neck BMD and the CYP 19 genotype after adjustment for other risk factors including family history. The CYP 19 genotype was found to be significantly associated with serum estradiol concentrations (p= 0.002) after adjustment for age at menarche, degree of exercise and BMI. The subjects with the 'AA', 'GA' and 'GG' genotypes were matched for age (mean [SD] years) (AA: 64.7 [8.9], GA: 65 [9.5], GG : 63.2 [8.6]), YSM (16.3 [10], 16.9 [9.6], 16.1 [10.3]), menopausal age (48.5 [5], 48.2 [4.9], 47 [5.3]), BMI (kg/m ^{2}) (25[4.1], 24 [4.5], 25 [4.4]). However those women with the 'AA' genotype had significantly higher serum estradiol concentrations than in the 'GA' group (p=0.08) or 'GG' group (p=0.02). Geometric mean (range) estradiol levels were 17 (2.1-52.8) pmol/L in the 'AA' genotype group; 13.0 (0.8-57.0) pmol/L for 'GA' and 10.0 (0.2-164.0) pmol/L for the 'GG' genotype group. A lower incidence of fractures was seen in subjects with the 'AA' genotype (p=0.07). In conclusion, although the 'G' to 'A' polymorphism was not significantly associated with BMD in our study population except in older women, the CYP 19 genotype was clearly associated with serum estradiol concentrations and may thus be useful as a genetic marker of aromatase efficiency and estrogen synthesis.

SA129

A Single Nucleotide Polymorphism at -238 In The TNF Gene Influences Promoter Activity In-Vitro. J. M. Wilkinson[1], A. G. Wilson*[2], R. Eastell[1], E. Kiss-Toth*[3]. [1]Bone Metabolism Group, University of Sheffield, Sheffield, United Kingdom, [2]Division of Genomic Medicine, University of Sheffield, Sheffield, United Kingdom, [3]Cardiovascular Research Group, University of Sheffield, Sheffield, United Kingdom.

Tumor Necrosis Factor (TNF) is a pro-inflammatory cytokine that is thought to play a pivotal role in osteolysis after total hip arthroplasty (THA). We have recently shown that a single nucleotide polymorphism (SNP) at -238 in the TNF gene promoter is associated with development of osteolysis after THA. Possession of the rare 'A' allele at this site is associated with a higher rate of osteolysis after THA versus carriage of the [more common] 'G' allele. The aim of this study was to examine the functional significance of this polymorphism on TNF gene transcriptional activation in a luciferase reporter gene assay. A 691 bp fragment (-585 to +106) of the TNF gene was amplified by polymerase chain reaction and directionally cloned into the PGL3.basic vector (Promega, Madison, WI). Insert sequences were checked using an ABI 377 DNA sequencer (PE Applied Biosystems, Foster City, CA). RAW264.7 murine macrophage-like cells in rapid growth phase were transfected with plasmids containing either the TNF-238G allele or the TNF-238A allele. pTK-RL (Promega), that expresses the Renilla luciferase gene under the control of Herpes Simplex Virus minimal promoter, was used as a transfection control. The cells were then either left unstimulated or were induced using lipopolysaccharide (LPS), phorbol 12-myristate 13-acetate (PMA), human TNF, or LTA (Lypothicaid acid). All transfections were made in triplicate. Luciferase reporter activity was measured after 4 hours and the relative luciferase activity was calculated. Results for unstimulated state and after LPS stimulation are shown in the table below. LTA and TNF stimulation at 0.05µg/mL and 0.2ng/mL, respectively, resulted in greater luciferase expression for -238A versus -238G (P<0.05). Higher concentrations of these agonists, and PMA, did not result in differential luciferase expression between the alleles. The promoter allele TNF-238A results in higher basal and stimulated levels of transcriptional activation in-vitro than the TNF-238G allele. Our data suggest a potential mechanism by which the TNF-238 polymorphism may influence the development of osteolysis after THA.

Mean relative luciferase activity

	TNF-238A Mean (Std.Dev.)	TNF-238G Mean (Std.Dev.)	P-value
Unstimulated	32.1 (2.1)	25.2 (2.4)	0.02
LPS 100ng/mL	43.4 (2.2)	33.0 (1.0)	0.002
LPS 10ng/mL	35.0 (3.7)	31.8 (2.7)	N.S.
LPS 1ng/mL	32.3 (1.6)	27.0 (2.7)	0.04

SA130

See Friday Plenary number F130.

SA131

The MTHFR (*C677T*) Polymorphism and BMD at Menopause: Analysis of the Effects of Bone Size, Body Composition and Physcial Activity. Results from the Danish Osteoporosis Prevention Study. B. Abrahamsen[1], J. S. Madsen*[2], C. L. Tofteng*[3], L. S. Stilgren[1], E. M. Bladbjerg*[4], S. R. Kristensen*[2], K. Brixen[1], L. Mosekilde[5]. [1]Dept. of Endocrinology M, Odense University Hospital, Odense C, Denmark, [2]Dept of Clin. Biochemistry, Odense University Hospital, Odense, Denmark, [3]The Osteoporosis Research Clinic, Hvidovre, Denmark, [4]Dept of Clin. Biochemistry, Ribe C. Hospital, Esbjerg, Denmark, [5]Aarhus University Hospital, Dept of Endocrinology C, Aarhus, Denmark.

We have previously reported an association of the *TT* genotype of the MTHFR polymorphism with a 0.3 SD reduction in BMD at the spine and 0.2 SD at the total hip at the time of menopause, with a normal response to HRT. The mechanism by which this polymorphism affects BMD is unknown, but interference with collagen cross-linking ultimately affecting bone structure has been proposed. Because many inherited disorders of collagen metabolism are associated with reduced growth, the following analysis was undertaken to test for effects on body- and bone size. Body composition and physical activity was also investigated. MTHFR genotyping was done in 1748 healthy post-menopausal Danish women. BMD and body composition was measured using Hologic QDR-1000 and QDR-2000 densitometers. The *TT* genotype was not associated with differences in lean body mass or fat mass. Bone areas did not differ. BMD was lower as previously reported. Participants with the *TT* genotype were very slightly taller, with a trend towards lower BMI but these differences did not reach statistical significance. Physical activity scores were identical in the two groups, with the exception that women with the *TT* genotype spent 35 minutes a week on gymnastics compared with 25 minutes for the rest of the study population (p=0.02).

	TTn=153	CC or CT n=1595	p
Height (cm)	165.3 ± 6.1	164.3 ± 7.2	0.12
Weight (Kg)	64.9	65.7	0.68
BMI (Kg/m2)	23.9	24.2	0.19
L2-L4 area cm2	46.5 ± 4.2	46.1 ± 4.1	0.72
L2-L4 BMD g/cm2	1.00 ± 0.14	1.03 ± 0.14	0.02
Total hip area cm2	37.1 ± 3.5	37.0 ± 3.6	0.72
Total hip BMD g/cm2	0.89 ± 0.11	0.92 ± 0.12	0.01

In conclusion, the significant effects of MTHFR genotype on menopausal BMD are not explained by differences in body composition or bone size. A trend towards greater height and lower BMI in the TT genotype did not reach statistical significance.

SA132

Effect of ER Alpha Gene PvuII-XbaI Polymorpisms on the Development of Hyperthyroidism and Thyroid Hormone-stimulated Bone Loss. E. Bajnok*, I. Takacs, A. Tabak*, C. Horvath, G. Speer*, Z. Nagy, P. Lakatos. 1 st. Department of Medicine, Semmelweis University, Budapest, Hungary.

Genetic background of hyperthyroidism and thyroid hormone-stimulated bone loss have not yet been established. Estrogen is a potent immunomodulatory hormone that may have a role in tumorgenesis as well as in the development of hyperthyroidism. In this study, we investigated the previously described estrogen receptor alpha (ER alpha) gene PvuII-XbaI polymorphisms to test their possible functional contribution to the pathogenesis of hyperthyroidism. Based on former results, we studied the effect of these polymorphisms on bone mineral density (BMD), as well. We genotyped 248 (18-83 years) women: 68 patients with Graves' disease (GD) and 70 with toxic adenoma (TA) and compared the genotype frequencies with 110 healthy controls (C). BMD of 36 GD patients (mean age 49,19 ± 7,15 years), 48 TA patients (mean age 57,52 ± 10,27 years) and 108 control subjects (mean age 54,6 ± 5,4 years) was measured at the lumbar spine and femoral neck. We found the xx genotype to be significantly less frequent in hyperthyroid (HT) patients than in controls. When separating the HT group into GD and TA subgroups, this difference remained significantly only in TA patients (p=0,002). The ER-PvuII genotype distribution was similar in all groups. At the same time, no relationship was seen between these polymorphisms and BMD adjusted for age and BMI at any site in these subgroups. In summary, our data raise the possibility that ER alpha gene XbaI polymorphism might play a role in the development of toxic adenoma.

SA133

Genetic Polymorphisms and Bone Quality in Postmenopausal Women. I. Takacs, C. Horvath, É. Bajnok*, G. Speer*, Z. Nagy, P. Lakatos. 1.st Department of Medicine, Semmelweis University, Budapest, Hungary.

Osteoporosis is a complex disease that is presumably influenced by multiple genes. Part of the genetic effect has been ascribed to the polymorphism in vitamin D receptor gene (VDR), estrogen receptor gene (ER), interleukin-1 receptor antagonist protein gene (IL-1RN) but their genetic implications are still controversial. The majority of studies concentrated on bone quantity rather than bone quality. Recently, bone ultrasound appears to provide non invasive information on bone quality. In this study, we investigated the role of VDR, ER and IL-1RN polymorphisms on bone mineral density (BMD) and bone ultrasound parameters in a group of 53 healthy and 55 hyperthyroid Hungarian postmenopausal women. VDR BsmI., ER, XbaI, and Pvu II. restriction fragment length polymorphisms, as well as IL-1RN variable tandem repeat polymorphism have been determined. BMD was measured at the lumbar spine (L2-4) and femoral neck by DEXA. Women underwent quantitative ultrasonometry (QUS) at the heel. No association could be shown between VDR, ER and IL-RN genotypes and BMD. XbaI. "xx"and PvuII. "pp" alleles were accompanied with ultrasound values reflecting reduced bone quality as compared with other genotypes. Our results raise the possibility that some genetic factors might exert their effects on bone tissue through influencing bone quality.

SA134

Association between Two Types of VDR Gene Polymorphisms and Bone Density in Japanese Women. M. Kubota*[1], S. Yoshida*[2], H. Arai*[3], M. Ikeda*[1], Y. Okada*[1], K. Miyamoto*[3], E. Takeda*[3]. [1]Okayama Prefectural University, Okayama, Japan, [2]Kinki Welfare University, Hyougo, Japan, [3]Clinical Nutrition, Tokushima University, Tokushima, Japan.

[Objective] Bone density is influenced by many factors, which can be broadly divided into genetic and environmental factors. We have previously shown the presence of an M polymorphism at the translation initiation sites in exon 2 of the VDR gene and a polymorphism in the hVD-SIF1 region on the VDR gene promoter. In this study, we analyzed the association of bone density and bone metabolic markers with these two VDR polymorphisms to clarify their usefulness as predisposing genetic markers. [Materials and Methods] 347 healthy Japanese women (20-86 years old) were studied. The polymorphic regions were amplified by the PCR technique; the M genotypes were classified into mm, MM, and Mm by RFLP analysis; and hVD-SIF1 genotypes were classified into WT, MT, and heterozygous type by direct sequencing. The bone mineral density (BMD) (L2-L4) was measured using DXA (QDR-2000). Bone metabolic markers (ALP III and TR-AP activities) were assessed, and body compositions were measured simultaneously. Questionnaires were done on dietary habit and life style. [Results] (1) Subjects were divided by menstrual stage into four groups: pre-menopausal: 153, irregular menopausal: 36, 2-9 years post-menopause: 76, and 10 years post-menopause: 83. The VDR MM, Mm, and mm genotypes frequencies were 12.2%, 52.3%, and 35.5% respectively, while the hVD-SIF1 WT, MT, and hetero type frequencies were 17.6%, 30.5%, and 51.9% respectively. (2) In M polymorphism, the BMD and Z score were significantly higher in the pre-menopausal and irregular group in order of mm>Mm>MM ($p<0.001$). No difference was noted between the 2-9 years and the 10 years group. (3) In hVD-SIF1 polymorphism, the BMD and Z score in the 2-9 years and the 10 years group were high WT > hetero > MT respectively. No changes were observed in the pre-menopause and the irregular group. (4) For BMD, positive correlation with milk ingestion (elementary and junior high school) was observed in pre-menopause and the 10 years group (MM types) and with recent daily product intake was the 10 years group (MM types). In mm types, a positive correlation with BW, body fat mass, BMI. (5) For the BMD relationship, positive correlation with milk ingestion (elementary and junior high school) was observed in irregular group (MT type), and in the 10 years group (WT and hetero types). These results indicate that the association of bone density with two VDR gene polymorphisms varies according to age and menstrual history, and suggest that differential screening for these genetic markers and appropriate nutritional instruction are useful for preventing osteoporosis.

SA135

Novel Polymorphism in the Human Fos Related Antigen-1 Gene Is Associated with Bone Mineral Density in Women from the UK. O. M. E. Albagha*, F. E. McGuigan*, D. M. Reid, S. H. Ralston. Medicine and Therapeutics, University of Aberdeen, Aberdeen, United Kingdom.

Genetic factors are important in the pathogenesis of osteoporosis and regulation of bone mass, but most genes responsible remain to be defined. Linkage studies in families have shown evidence of a quantitative trait locus for regulation of bone mass on chromosome 11q12-13. Fos-related antigen-1 (Fra-1) gene is one of the candidate genes located in this region because of its effect on bone cell function. Recent reports have shown that transgenic mice over-expressing Fra-1 in various organs develop a progressive increase in bone mass leading to osteosclerosis with the observation of enhanced osteoblast differentiation and elevated osteoclastogenesis in vitro (Jochum et al., 2000). We investigated the potential role of the Fra-1 gene in the regulation of bone mineral density (BMD) by screening its coding region for novel polymorphisms and then assessing the potential relationship between the identified polymorphisms and BMD. Mutation screening by DNA sequencing identified a novel C10lT polymorphism located in the first exon (numbers are in reference to GenBank Accession AJ297411). Genotypes were determined by PCR-RFLPs analysis using the EcoRI restriction enzyme. The exon 1 polymorphism was then investigated in relation to BMD in a population-based cohort of 501 perimenopausal women randomly selected from Northeast of Scotland. We found that subjects with the EE genotype (homozygote T variant) had significantly lower lumbar spine BMD (mean Z-score +/- SEM; 0.038 +/- 0.108; n = 82) than subjects without this genotype (0.385 +/- 0.052; n = 419; p = 0.004). A similar trend was observed for the femoral neck BMD but results did not reach statistical significance (p = 0.18). Results for the lumbar spine remained significant (p = 0.007) even after adjustment for confounding factors (such as age, weight, height, menopausal status and HRT use) using general linear model ANOVA analysis. In conclusion, the work presented here is the first to report a significant association between polymorphisms of the human Fra-1 gene and BMD, which suggest that allelic variation at the Fra-1 gene might be important for regulation of BMD, raising the possibility that Fra-1 genotyping could be useful genetic marker for BMD and susceptibility to fractures. However, the exact mechanism by which this polymorphism affects BMD remains to be determined.

SA136

Prostaglandins Increase FGF-2 and FGF Receptor Expression and Nuclear Accummulation in Osteoblasts via Mitogen Activated Protein Kinase. M. G. Sabbieti*[1], L. Marchetti*[2], M. Menghi*[2], S. Materazzi*[3], G. Menghi*[2], L. G. Raisz[4], M. M. Hurley[4]. [1]Dept of Comparative Morphological and Biochemical Sciences, University of Camerino, Camerino, Italy, [2]Dept. of Comparative Morphological and Biochemical Sciences, University of Camerino, Camerino, Italy, [3]Department of Chemistry, University "La Sapienza", Rome, Italy, [4]Medicine/Division of Endocrinology & Metabolism, University of Connecticut School of Medicine, Farmington, CT, USA.

We previously reported that prostaglandin F2a (PGF2a) and the PGF2a agonist fluprostenol (Flup) increased basic fibroblast growth factor (FGF-2) mRNA and protein production in osteoblastic Py1a cells. The present report extends these studies by examining the effects of PGs on FGF receptor (FGFR) mRNA expression, the subcellular localization of FGF-2 and FGFR proteins and the signaling pathway involved. Rat osteoblastic Py1a cells were grown to confluence in Ham's F-12 medium containing 5% fetal calf serum and then serum deprived for 24 h before treatment with PGF2a or Flup for 2 to 24 h. Expression of FGFR mRNA was determined by Northern blot analysis. Py1a cells expressed only one FGF receptor (FGFR2). In the absence of serum, Py1a cells expressed a 4 kb FGFR2 mRNA transcript. Time course experiments revealed that PGF2a caused a 40% and Flup a 60% reduction in FGFR2 mRNA levels at 4 h and both caused an 80 % reduction after 24 h. To investigate in situ localization of FGF-2 and FGFR2 protein, binding patterns of FITC labeled antibodies to FGF-2 and FGFR-2 were examined by confocal laser scanning microscopy (CLFM). Py1a cells expressed low levels of cytoplasmic and nuclear localization for both FGF-2 and FGFR2 protein. Following 24 h of treatment with PGF2a or Flup, FGF-2 and FGFR2 proteins accumulated at the nuclear membrane and were also co-localized in the nucleus of Py1a cells. CLSM studies showed that pretreatment with cycloheximide blocked nuclear labeling for FGF-2 in response to PGF2a. Treatment with SU5402, a specific FGFR tyrosine kinase inhibitor, did not block PG mediated nuclear accumulation of FGF-2 or FGFR2. In contrast, pretreatment with PMA, an activator of protein kinase C (PKC) pathway prevented the nuclear accumulation of FGF-2 and FGFR2 in response to PGF2a. Similar results were obtained by pretreatment with the PKC inhibitor H-7. Cells treated with PGs or PMA showed increased nuclear labeling for the mitogen activated protein kinase, p44/ERK2, compared to control cultures. Pretreatment with PMA blocked both PG and PMA induced ERK2 nuclear labeling. We conclude that PGs stimulate nuclear accumulation of FGF-2 and its receptor by a PKC dependent pathway and suggest a role for p44/ERK 2 in this process.

SA137

See Friday Plenary number F137.

SA138

Glycogen Synthase Kinase-3 (GSK-3) Signaling Is Involved in the Anti-apoptotic Effect of Fibroblast Growth Factor-2 in Human Calvaria Osteoblasts. F. Debiais[1], F. Lasmoles*[1], G. Lefevre*[2], F. Mascarelli*[2], P. J. Marie[1]. [1]INSERM U349, Paris, France, [2]INSERM U450, Paris, France.

Fibroblast Growth Factor-2 (FGF-2) is an important factor controlling osteogenesis. We hypothesized that FGF-2 may control human calvaria osteoblast apoptosis by involving regulation of GSK-3, a component of the APC/axin/beta-catenin complex which is important in determining cell fate. We found that, in both primary human calvaria osteoblasts and immortalized human neonatal calvaria (IHNC) cells, FGF-2 (50 ng/ml, 0-72 hrs) prevented by 50 % ($p<0.05$) DNA fragmentation induced by serum deprivation, as determined by terminal deoxynucleotidyl transferase-mediated nick-end labeling (TUNEL) analysis. This preventive effect of FGF-2 was due to reduction in caspase-2 and effector caspases-3,-6,-7 activity ($p<0.05$) whereas caspases-8 and -9 were unaffected. Western blot analysis of transduction signaling pathways showed that FGF-2 resulted in a rapid (5-15 min) Ser-473 phosphorylation of Akt, a serine/threonine kinase which phosphorylates GSK-3, resulting in phosphorylation and ubiquitin-mediated proteasomal degradation of beta catenin. Accordingly, FGF-2 induced Ser-9 phosphorylation of GSK-3 and beta catenin degradation, suggesting the implication of GSK-3-ß-catenin pathway in the anti-apoptotic effect of FGF-2. In agreement, selective inhibition of GSK-3 phosphorylation by lithium chloride (5-50 mM) or by the GSK-3 inhibitor SB 216763 (1-10 µM) increased caspase-2 and caspases-3, -6, -7 activity and suppressed the inhibitory effect of FGF-2 on caspases activity in serum-deprived IHNC cells. Furthermore, we found that LY 294002 (5-50µM) which inhibits the phosphorylation of phosphatidylinositol-3-kinase (PI-3-K) acting upstream of Akt, blunted the anti-apoptotic effect of FGF-2 and further increased caspase-2 and caspases-3, -6, -7 activity in serum-deprived IHNC cells. In contrast, inhibition of MAPK Erk-1, 2 or MAPK p38 by PD 98059 (25 µM) and SB 203580 (1-10 µM), respectively, did not affect GSK-3 activity or osteoblast survival induced by FGF-2. We conclude that 1) caspase-2, caspases-3, -6, -7 activity and apoptosis induced by serum deprivation are negatively regulated by the PI-3K-Akt-GSK-3 signaling pathway in human osteoblasts 2) FGF-2 reduces caspase-2 and effector caspases activity and apoptosis through selective activation of the PI-3K-Akt-GSK-3 signaling pathway. Thus, GSK-3 plays a critical role in the protective effect exerted by FGF-2 against apoptosis in human osteoblasts.

SA139

See Friday Plenary number F139.

SA140

Parathyroid Hormone Receptor Type 1 (PTHR1)/ Indian Hedgehog (IHH) Expression Is Preserved In The Growth Plate Of Human Fetuses Affected With Fibroblast Growth Factor Receptor Type 3 (FGFR3) Activating Mutations. S. Cormier*[1], A. L. Delezoide*[2], C. Benoist-Lasselin*[3], L. Legeai-Mallet*[3], J. Bonaventure*[3], C. M. Silve[1]. [1]Faculté de Médecine X. Bichat, Inserm U426, Paris, France, [2]Hôpital Robert Debré, Service de Biologie du Développement, Paris, France, [3]Hôpital Necker Enfants Malades, Inserm U393, Paris, France.

Two principal pathways are known to play a key role in regulating endochondral ossification, that mediated by FGFR3 signaling, and that mediated by IHH/PTHR1 signaling. Human chondrodysplasias have been ascribed to mutations in either FGFR3 or PTHR1 genes. However, the involvement of these signaling systems to endochondral ossification has been mostly documented in mouse models. Although both the FGFR3 and IHH/PTHR1 signaling pathways are acting on the same developmental bone process, relatively few studies have evaluated the possible interactions between these two pathways. Analysis of the interplay between these pathways in mouse models expressing different FGFR3 activating mutations has lead to conflicting results owing to the inability of some models to faithfully reproduce the human phenotype. This underlines the importance of studies performed on human tissues. We analysed the femoral growth plates from fetuses carrying activating FGFR3 mutations (9 with achondroplasia, 21 with type 1 thanatophoric dysplasia, and 8 with type 2 thanatophoric dysplasia) and 14 age-matched controls by histological techniques and in situ hybridization using riboprobes for human IHH, PTHR1, type X and I collagen transcripts. We show that bone-perichondrial ring enlargement and increased vascularization of the growth plates in FGFR3-mutated fetuses correlate with the phenotypic severity of the disease. PTHR1 and IHH expression in growth plates, bone-perichondrial rings and vascular canals is not affected by FGFR3 mutations, irrespective of the mutant genotype and age, and is in keeping with cell phenotypes. Our study extends the genotype-phenotype correlation between human growth plate abnormalities and FGFR3 mutations. In addition, our results indicate that in human, FGFR3 signaling does not regulate the main players of IHH/PTHR1 pathway. Furthermore, we show that cells within the bone-perichondrial ring in controls and patients express IHH, PTHR1, and type X and I collagen transcripts, suggesting that bone-perichondrial ring formation involves cells of both chondrocytic and osteoblastic phenotypes.

SA141

Post-natal Defects in Bone Metabolism in Mice Deficient in FGFR3 Signaling. G. Valverde-Franco[1], H. Liu*[1], D. M. Ornitz*[2], R. Poole[3], D. Goltzman[1], J. E. Henderson[1]. [1]Medicine, McGill University, Montreal, PQ, Canada, [2]Molecular Biology and Pharmacology, Washington University School of Medicine, St Louis, MO, USA, [3]Surgery and Medicine, McGill University, Montreal, PQ, Canada.

Bone development and maintenance of the adult skeleton are regulated by conserved signaling pathways, which are linked to multifunctional growth factors and their high affinity receptors. Fibroblast growth factor receptor 3 (FGFR3) is a receptor tyrosine kinase that binds preferentially to FGFs 2, 9 and 18 and is expressed in a restricted pattern in chondrogenic cells during limb development. Recent evidence suggests that FGFR3 is also expressed by cells of the osteogenic lineage in cranial sutures. Point mutations that result in constitutive activation of FGFR3 have been identified as the cause of a variety of human skeletal disorders that are characterised by short limbed dwarfism and bossing of the skull. Conversely, mice homozygous for targeted disruption of FGFR3 are born with longer bones in the axial and appendicular skeleton and develop severe kyphosis and impaired gait by 4 months of age. The hypothesis on which the current studies were based is that FGFR3 signaling mediates post-natal bone metabolism and maintains skeletal integrity. The absence of FGFR3 signaling would therefore result in osteopenia. We used a combination of non-invasive imaging and classic histology to compare the mineral content, micro-architecture and molecular composition of the bones of young adult wild type and FGFR3-/- male mice. Faxitron x-ray analysis consistently demonstrated kyphosis, lengthening of the humerus, femur and vertebra and loss of mineral in 4-month old FGFR3-/- mice compared with wild type littermates, an observation that was confirmed by bone densitometry measurements. X-ray microtomography, performed by Eric Beulens at Skyscan, Belgium, revealed a substantial loss of cortical and trabecular bone, a significant loss of trabecular connectivity and an increase in the SMI from 1.60 to 2.00 in mutant mice compared with control. Histochemical and immunochemical analyses of the proximal tibia demonstrated sparse trabeculae arising from a disorganised region of hypertrophic chondrocytes that stained heavily for type X collagen. This was associated with an increase in periosteal fibrous tissue, significant thinning of the cortices and failure to down-regulate MMP13 activity in the primary spongiosa. Taken together these observations reveal a previously un-identified role for FGFR3 in post natal bone metabolism and identify it as a potential molecular target to prevent disorders such as ostoporosis, which are associated with low bone mass.

SA142

Prenatal Exposure of IL-1 in Male Rats Have Skeletal Effects. D. Swolin-Eide[1], C. Nilsson*[2], J. Dahlgren*[3], A. Holmäng*[2], C. Ohlsson*[1]. [1]Department of Internal Medicine, Research Center for Endocrinology and Metabolism, Gothenburg, Sweden, [2]Wallenberg Laboratory, Sahlgrenska University Hospital, Göteborg, Sweden, [3]Pediatric Growth Research Center, Queen Silvia Children's Hospital, Göteborg, Sweden.

Interleukin-1 (IL-1) is a multifunctional cytokine that is involved in bone metabolism. Different sorts of stress or hormonal influences, during particular periods of pregnancy, may result in persisting or transient changes. Events occurring early in life or prenatally are able to play important roles in the pathogenesis of diseases in adult age. The aim of the present study was to investigate whether exposure to IL-1β during fetal life has any effect on bone tissue in rat offspring. Pregnant rats were given injections intra peritoneal (1 μ g/rat IL-1β) on day 8, 10 and 12 of gestation. Body weight was recorded from birth to 10 weeks of age. Offspring were sacrificed at 10 weeks of age. No effect on body weight or food intake was seen at any time in the IL-1β -injected group compared with controls. The weights of thymus, muscles, adipose tissues, gonads, spleen and heart were unchanged in the IL-1β -injected group. Interestingly, IL-1β -treated offspring showed reduced vertebral heights and tibial lengths. Furthermore, areal bone mineral density and bone mineral content in the spine, as studied by DXA, were reduced in the IL-1β -injected group compared to control rats. In conclusion, prenatal exposure of IL-1β results in reduced skeletal growth in male offspring.

SA143

Differential Expression of Cytokines and Chemokines in the Interface Membrane of Aseptic Loosened Endoprotheses of the Hip. E. A. Kaiser[1], C. Gentzsch*[1], N. Schultz*[1], J. Plutat*[2], R. Sellckau*[2], J. Wodtke*[2], G. Delling*[1]. [1]Bone Pathology, Center for Biomechanics, Hamburg, Germany, [2]Endoklinik, Hamburg, Germany.

Aseptic loosening of hip endoprotheses is the most common reason for implant failure. Between the implant-to-bone interface a synovial-like tissue that contains macrophages, fibroblasts and vascular endothelial cell develops that effects the loosening of prosthesis. The cells of this interface membrane secrete cytokines, chemokines and growth factors, which could stimulate bone resorption and fibrosis as well as reduce bone formation. To investigate the expression profile of the cytokines and chemokines, we subjected interface membrane samples obtained from 6 patients undergoing revision hip surgery to Clontech Atlas™ Nylon cytokine/receptor cDNA Expression Array. As a control, muscle tissue from the same patients was used. Our results indicate that 9 genes are differentially expressed in at least 3 out of the 6 patients. Interleukin-10 (IL-10), Calgranulin A, B, monocyte chemotactic protein-1 (MCP1), Rantes, tumor necrosis factor receptor (TNFR) 2, human teratocarcinoma-derived growth factor (TDGF1), ribonuclease/angiogenin inhibitor (RAI) and Thymosin beta10 mRNA is upregulated in the interface tissue as compared to control tissue. MCP1 and Rantes, C-C chemokines, as well as IL-10 and TNFR have been reported to be associated with the periprosthetic granulomas, whereas Calgranulin A, B, TDGF1, RAI and Thymosin b10 have been detected for the first time. Some of the corresponding proteins of the newly identified genes have been associated with tumor development and wound-healing adding new aspects to the pathological cell associated condition of aseptic loosening. These results suggest that in addition to recruitment, proliferation and activation of inflammatory cells, an inaccurate activation of mesenchymal cells might also contribute to pathological cell associated condition of aseptic loosening.

SA144

See Friday Plenary number F144.

SA145

Roles of Inflammatory Cytokines in Acquisition of Calcifying Phenotype of Vascular Smooth Muscle Cells. A. Shioi[1], A. Kizu*[2], H. Taniwaki*[3], S. Jono*[2], Y. Okuno*[1], H. Koyama*[2], Y. Nishizawa[2]. [1]Cardiovascular Medicine, Osaka City University Graduate School of Medicine, Osaka, Japan, [2]Metabolism, Endocrinology and Molecular Medicine, Osaka City University Graduate School of Medicine, Osaka, Japan, [3]Internal Medicine, Inoue Hospital, Suita, Japan.

Calcification is a common feature of atherosclerotic lesions, especially in advanced stages of plaque formation. Inflammatory cells such as macrophages and T lymphocytes play an important role in the development of atherosclerotic lesions. By using a coculture model, we have identified tumor necrosis factor-α (TNF-α) and oncostatin M (OSM) as major cytokines derived from macrophages responsible for induction of alkaline phosphatase (ALP) in human vascular smooth muscle cells (HVSMC) in the presence of interferon-γ (IFN-γ) and 1α,25-dihydroxyvitamin D_3 ($1,25D_3$). In this study, we investigated the roles of these factors in acquisition of calcifying phenotype of vascular smooth muscle cells. Only in the presence of IFN-γ, $1,25D_3$, TNF-α, and OSM, ALP activity and its gene expression in HVSMC were increased in a time-dependent manner. ALP-positive HVSMC calcified their extracellular matrix in the presence of 10 mM β-glycerophosphate as evidenced by von Kossa staining and calcium quantification. In vitro calcification by HVSMC was dose-dependently inhibited by the treatment with bisphosphonates such as etidronate. Immunoblot revealed that the expression of SMC phenotypic markers such as α-smooth muscle actin and calponin in ALP-positive HVSMC were decreased compared with control HVSMC. Moreover, the expression of osteoprotegerin was also down-regulated in ALP-positive HVSMC. Since signaling through p38 mitogen-activated protein kinase (MAPK) mediates inflammatory responses to cytokines such as TNF-α, the role of p38 MAPK pathway was investigated with a specific inhibitor, SB203580. SB203580 dose-dependently inhibited ALP induction by these factors. Finally, we examined the expression of ALP in atherosclerotic calcified lesions of apoE-deficient mice. ALP activities were detected in smooth muscle cells around calcified plaque lesions. These data suggest that cytokines derived from macrophages and T lymphocytes may contribute to the development of atherosclerotic calcification.

SA146

See Friday Plenary number F146.

SA147

New Small Molecular Weight Peptide Bone Growth Factor for Fracture Repair. D. R. Sindrey, E. Plawinski*, J. Auluck*. Millenium Biologix Inc., Mississauga, ON, Canada.

Various extraction methods have been applied to bone to extract, isolate, test and identify potential new bone growth factors. Most of these extraction methods, like those used for BMP's, have used conditions to preserve the integrity of the proteins extracted from bone. Using cancellous bovine bone, we have enzymatically extracted a bone growth factor that stimulates new bone formation. This factor has been identified as a 9mer fragment of one of the proteins normally present in the matrix of bone. A small molecular weight peptide, easily produced by peptide synthesis, could prove to be a promising factor for use in the systemic treatment of osteoporosis or local bone fracture repair. This study was conducted to investigate the bone forming ability of the synthetically produced BCSP™ (Bone and Cartilage Stimulating Peptide) P30 in a rat tibia assay as a preclinical development candidate for fracture repair. P30 peptide was dissolved in normal saline at 5 mgs per 100 microliter w/v and combined with a carrier of 1 mg of Skelite™ powder, a synthetic bone biomaterial. Male Wistar rats, weighing 125-200 grams, were randomized and then anaesthetized using Isoflurane. Delivery of the test material was made using a 0.5cc Insulin syringe with an integrated 28G1/2" needle. Test material was deposited onto the periosteal surface of the right medial tibia surface proximal to the knee under the Tibialis cranialis muscle group. The control group was injected with saline plus carrier. Animals received one injection. Tibia were dissected out after 7 days and submitted to DEXA scan, micro CT and demineralized histology sectioning. Particular attention was given to the metaphysis region (injection site) to assess the ability of the material to stimulate local bone formation. After 7 days, one injection of BCSP™ P30 peptide increased local bone formation in the tibia by 16% as measured by BMD (bone mineral density) and 22% as measured by BMC (bone mineral content) in the injection region compared to contralateral limb. Skelite™ carrier alone produced a 5.5% and 6.8% increase in BMD and BMC respectively. Micro CT scans and histology showed a marked increase in bone formation at the periosteal surface in the region of the injection. At dissection tibia appeared normal but notably larger than the contralateral limb. There was no evidence of ectopic bone formation, inflammation, muscle atrophy or bone trauma at the site of the injection. Stimulation of the periosteal lining would suggest a similar effect could be achieved on endosteal surfaces if the peptide was introduced into a fracture or trauma site. The rapid onset of the stimulatory effect would make the BCSP™ P30 peptide a potent site-specific candidate for the treatment of bone fracture and trauma.

*Disclosures: **D.R. Sindrey**, Millenium Biologix Inc. 1.*

SA148

Inadequate Copper (Cu) Intake Reduces Serum Insulin-like Growth Factor-1 (IGF-1) and Bone Strength in Growing Rats. Z. K. Roughead, H. C. Lukaski*. Grand Forks Human Nutrition Research Center, USDA-ARS, Grand Forks, ND, USA.

Decreased serum concentrations of IGF-1 are associated strongly with an increased risk of osteoporotic fractures. Although dietary zinc (Zn) has been reported to influence serum IGF-1 directly, the effects of other trace minerals, such as Cu, on serum IGF-1 and bone metabolism have not been elucidated. This study determined the effects of graded intakes (low, marginal and high) of Zn and Cu on serum IGF-1 concentration and measures of bone quality in growing rats. Weanling male Sprague Dawley rats (n=84) were randomly assigned to 12 groups using a 3x4 factorial design and were fed modified AIN-93G basal diets with varying amounts of Cu (0.3, 3, and 10 mg/kg designated as LC, MC, and HC, respectively) and Zn (5, 15, 45 mg/kg designated as LZ, MZ, and HZ, respectively) for 6 wk; a group of rats was pair-fed to each LZ group. No statistical differences were found between the LZ groups and the pair-fed groups in the variables reported. Dietary Zn affected body weights which were highest in the HZ groups ($p<0.0001$). The femur weights were the lowest in the LC groups ($p<0.004$), however, the calcium concentration of the femurs in the LC groups were higher as compared to the HC groups ($p<0.0001$). Dietary Cu influenced femur nitrogen concentration; it was about 10% higher in the LC compared to the HC groups. Although dietary Zn tended to influence serum IGF-1 concentrations ($p = 0.09$), dietary Cu was the primary determinant of this variable ($p<0.0001$). Dietary Cu was also the main determinant of differences in volumetric densities of lumbar vertebras (L4) and femurs, as determined by Archimedes' Principle, and femur breaking strength, as measured by a 3-point breaking test ($p<0.001$) and these variables were the lowest in the LC groups. Compared to the HC groups, serum IGF-1 and femur breaking strength were reduced by 27% and 14%, respectively ($p<0.05$). Serum IGF-1 correlated with both vertebral density and femur breaking strength even after accounting for contributions by body weight (semi-partial $R2 = 0.17$ and 0.15, respectively, $p<0.001$). In summary, low dietary Cu decreased serum IGF-1 concentration and the quality of spinal and long bones in growing rats. The poor quality of bones associated with low Cu intakes may be explained, at least in part, by the decreased serum IGF-1 concentrations. In the presence of graded intakes of Cu, effects of various amounts of dietary Zn were minimal.

*Disclosures: **Z.K. Roughead**, North Dakota Beef Commission 2.*

SA149

See Friday Plenary number F149.

SA150

See Friday Plenary number F150.

SA151

See Friday Plenary number F151.

SA152

Transcription from Promoter 2 of the IGF-I Gene is Increased in Liver of C3H/HeJ Mice that Exhibit Increased Peak Bone Formation. M. L. Adamo[1], C. Ackert-Bicknell[2], L. R. Donahue[2], W. G. Beamer[2], D. Powell*[3], C. J. Rosen[4]. [1]Biochemistry, University of Texas Health Science Center at San Antonio, San Antonio, TX, USA, [2]The Jackson Laboratory, Bar Harbor, ME, USA, [3]Lexicon, The Woodlands, TX, USA, [4]St. Joseph Hospital, Bangor, ME, USA.

Insulin-like growth factor-I (IGF-I) is an important osteotrophic agent. Evidence exists supporting critical roles of both circulating and locally produced IGF-I in the acquisition and maintenance of peak bone mass and bone mineral density. Moreover, variation of serum IGF-I within the normal physiological range correlates with bone mineral density. Genetic, non-growth hormone dependent factors contribute to variations of serum IGF-I. Our groups have determined that inbred mouse strains are useful tools for characterizing genetic regulation of the serum IGF-I and bone mineral density phenotype. The C3H/HeJ mouse exhibits significantly higher serum and skeletal IGF-I content and bone mineral density and strength than the C57/Bl6 strain. The increased serum IGF-I is associated with a 2-fold increase in expression of IGF-I mRNA transcribed from the second promoter (P2) in liver and several other soft tissues. We have utilized an antisense RNA probe complementary to contiguous IGF-I gene sequence consisting of the 3' 126 bp of intron 1, the 72 bp of exon 2 and the first 188 bp of intron 2 in RNase protection assays (RPA) to show that levels of correctly initiated P2 premRNA and P2 mature mRNA transcripts are increased by 2-fold in C3H liver compared to C57 liver ($p < 0.05$). P1 premRNA transcripts are not increased, consistent with the lack of significant increase in mature P1 transcripts. As previously reported for rat liver, there is greater animal-to- animal variability in the abundance of premRNA transcripts than in the abundance of mature transcripts in both mouse strains, presumably reflecting the slower turnover rate of mature transcripts. The P2 promoter region was amplified by PCR from genomic DNA from several C3H and C57 mice and several sequence variations were noted in the region between -1350 and +32 (+1 is the first nucleotide of exon 2). In transiently transfected mc3T3 cells, and OVCAR-3 cells that express high levels of P2 transcripts, C3H P2 exhibited greater promoter activity than C57 P2 when comparing clones in which an A residue in C3H P2 replaced a C residue in C57 P2 at position -28. However, two additional clones each of C57 and C3H P2 all showed an A residue at position -28, and there was no difference in promoter activity. We conclude that P2 transcription in liver is increased in C3H mice and we speculate that differences in trans-acting factors binding to the P2 promoter region play an important role in the different rates of transcription.

SA153

Dexamethasone-induced Osteoprogenitor Proliferation and Differentiation in Rat Bone Cells Are Associated with Increased Insulin-like Growth Factor Binding Protein-4 (IGFBP-4) Proteolysis by Pregnancy Associated Plasma Protein-A (PAPP-A). D. Jia, J. N. Heersche*. Faculty of Dentistry, University of Toronto, Toronto, ON, Canada.

Our previous results clearly indicate that dexamethasone (Dex)-induced rat bone cell differentiation is associated with changes in expression of IGF system components. One of these, IGFBP-4, has been shown to consistently inhibit IGF action in a variety of systems, and we have demonstrated that IGFBP-4 mRNA levels are regulated by Dex. In the present study, we evaluated the effects of Dex on IGFBP-4 peptide levels in differentiating bone cells. Osteoprogenitor-containing cells were isolated from explant cultures of vertebrae of 3-month-old rats, cultured and treated with 10 nM Dex or vehicle for up to 20 days. Cell layer proteins were prepared from 6-, 8-, 14- and 20-day cultures and conditioned media (CM) collected from 14-d cultures. Osteoprogenitor-derived bone nodules were visualized by alkaline phosphatase staining of 20-d cultures. Dex stimulated bone nodule formation as reported previously. Western blots showed that cell layer IGFBP-4 levels were lower in Dex-treated cultures than in controls at all 4 time points. Because IGFBP-4 proteolysis has been observed by others in various human and rat cell cultures, we evaluated degradation of recombinant rat (rr) or human (rh) IGFBP-4 by CM using Western blotting. In the absence of IGF-II, a 2-hour incubation with CM from control (CM-Ctrl) and Dex-treated (CM-Dex) cultures both resulted in a small decrease in intact rrIGFBP-4, accompanied by the appearance of a smaller fragment. In the presence of 10 nM IGF-II, the decrease induced by CM-Dex was 2-5-fold greater than that induced by CM-Ctrl. Similar results were observed using rhIGFBP-4. In human fibroblasts, others have identified PAPP-A as the specific IGFBP-4 protease. To determine whether IGFBP-4 proteolysis induced by CM was related to PAPP-A activity, we pre-incubated CM with an anti-human PAPP-A neutralizing antibody before analyzing IGFBP-4 proteolysis. The antibody, which dose-dependently inhibited human PAPP-A-induced rrIGFBP-4 proteolysis, prevented the rrIGFBP-4 from being degraded by CM. Our results demonstrate for the first time that PAPP-A-like IGFBP-4 proteolytic activity exists in rat bone cell cultures and that the activity is higher in CM-Dex than in CM-Ctrl. The findings suggest that the decreased IGFBP-4 levels in Dex-treated cultures likely result from increased IGFBP-4 proteolysis. Since IGFs have been shown to stimulate osteoprogenitor proliferation and differentiation, increased IGFBP-4 proteolysis resulting in an increase in IGF action may be part of the mechanism by which Dex regulates osteoprogenitor differentiation.

SA154

Intracellular Osteopontin May be Required for OPN-null Bone Cells to Respond to Pulsatile Fluid Flow. D. T. Denhardt[1], C. C. Kazanecki*[1], L. W. Fisher[2], E. S. Sorensen*[3]. [1]Rutgers University, Piscataway, NJ, USA, [2]Csdb, nidcr, National Institutes of Health, Bethesda, MD, USA, [3]Protein Chemistry Laboratory, University of Aarhus, Aarhus, Denmark.

Osteopontin (OPN) is both a component of the bone matrix, mediating cell attachment and migration, and a cytokine, activating signal transduction pathways via integrins and CD44. There is also an intracellular form associated with CD44 and ezrin. OPN-null mice have superficially normal mineralized tissues despite a general defect both in osteoclast function and in bone resorption/remodeling. For example, they do not lose mineral to the same extent as wild-type mice after ovariectomy or when bones are unloaded. The purpose of this study is to understand why osteoblast/osteocyte-like bone cells in culture do not release NO in response to pulsatile fluid flow (PFF) if they cannot synthesize OPN. The question addressed here is whether OPN acts extracellularly or intracellularly. The approach is to expose bone cells (derived by outgrowth from fragments of the long bones of OPN-/- mice) to PFF while providing OPN either as an exogenously added protein or via infection with an OPN-expressing adenovirus vector. Responsiveness to PFF is assessed by the ability of the cells to produce NO in the first few minutes of exposure to PFF. Slides carrying the cells are placed in a fluid flow chamber and exposed to PFF for 20 min at roughly 18 dynes/cm2. At various times, medium is removed and assayed for nitrite. In contrast to wild-type cells, OPN-/- cells are deficient in their ability to produce NO in response to PFF. The results to date suggest that plating OPN-/- bone cells on recombinant OPN does not restore their ability to produce NO in response to a PFF stimulus. Efforts to restore OPN to the OPN-/- cells using an OPN-expressing adenovirus suggest in contrast that when OPN is synthesized endogenously in these cells, some sensitivity to PFF is restored. Mineralization of primary long bone cells isolated from control and OPN-/- mice was also assessed. The OPN-/- cells did not produce as many bone nodules in culture as control cells, although both cultures did stain similarly for alkaline phosphatase. We have generated clonal cell lines from spontaneously immortalized OPN-/- cells and are currently assessing their ability to mineralize and to respond to fluid flow with and without OPN. In conclusion, current evidence suggests that intracellular OPN is required for the osteoblast/osteocyte-like bone cells in culture to respond to a PFF stimulus as measured by the ability of the cells to produce NO in the first few minutes after the initiation of PFF. In the absence of OPN, bone nodule formation in mineralizing bone cell culture is also modified in that nodule formation is much less focused.

SA155

See Friday Plenary number F155.

SA156

Mechano-sensing By Stretch-activated Calcium Influx Pathways In Human Chondrocytes. A. Miyauchi[1], M. Goto[2], K. Notoya[2], T. Sugimoto[3], Y. Takagi[1], K. Jinnai*[1], Y. Yoshimoto[1], K. Chihara*[3], T. Fujita[4], K. Okabe[5], Y. Mikuni-Takagaki[6]. [1]Medicine, National-Hyogo Chuo Hospital, Sanda, Japan, [2]Pharmaceutical Research Division, Takeda Chemical Industries Limited, Osaka, Japan, [3]Division of Endocrinology/Metabolism, Department of Clinical Molecular Medicine, Kobe University Graduate School of Medicine, Kobe, Japan, [4]Calcium Institute, Osaka, Japan, [5]Cellular Physiology, Fukuoka Dental College, Fukuoka, Japan, [6]Oral Biochemistry, Kanagawa Dental College, Yokosuka, Japan.

Mechanical stimuli, both anabolic and catabolic, are essential in maintaining morphology and function of cartilagenous tissues. The mechanisms of mechanosensing in chondrocytes, however, are not well characterized in human cells, in particular. We compared responses of chondrocytes derived from different species to stretch loading. Human, rabbit and bovine articular chondrocytes were cultured, loaded with fura-2, and distributions of subcellular cytosolic Ca^{2+}, $[Ca^{2+}]i$, were monitored using video image analysis. Stretch loading by swelling the cells with hypoosmotic solution (50% osmolarity) induced a rapid and progressive $[Ca^{2+}]i$, increase in either human(65±6 nM above basal, n=14), rabbit(99±15 nM, n=11) and bovine chondrocytes(126±21 nM, n=10). By depleting intracellular Ca^{2+} stores with thapsigargin, 70% of hypotonically induced $[Ca^{2+}]i$ increase was inhibited in rabbit and bovine chondrocytes. In contrast, more than 90% of the $[Ca^{2+}]i$, increased by exposing human chondrocytes to hypotonic solution, was abolished either by adding Gd^{3+} to the solution or by replacing with Ca^{2+} free media. Moreover, preincubation with thapsigargin inhibited the hypotonically-induced increase by less than 20%. It is suggested that a major source of intracellular Ca^{2+} is the influx of extracellular Ca^{2+} but not the release from intracellular Ca^{2+} stores. A larger $[Ca^{2+}]i$ increase was demonstrated by Ca^{2+} imaging in the submembranous region than in the perinuclear cytoplasm in response to the hypotonic exposure. In human cells, the hypotonically-induced [Ca2+]i increase are more likely to be sustained and oscillatory. Taken together, our results indicate that the hypotonically induced $[Ca^{2+}]i$ increase was primarily caused by an influx of Ca^{2+} through stretch-activated Ca^{2+} channels in human chondrocytes. In conclusion, human chondrocytes may be different from rabbit and bovine cells in sensing stress by stretch-activated Ca^{2+} channels. The SA channels may be involved in human chondrocyte volume regulation and mechanotransduction inherent to the human articular physiology.

SA157

See Friday Plenary number F157.

SA158

Different Response of Human Mandibular Bone Osteoblast and Osteocyte to Mechanical Loading. H. Sekiya[1], Y. Mikuni-Takagaki[2], A. Miyauchi[3], T. Kondoh*[1], K. Seto*[4]. [1]1st Department of Oral &Maxillofacial Surgery, School of Dental Medicine, Tsurumi University, Yokohama, Japan, [2]Oral Biochemistry, Kanagawa Dental Collage, Yokosuka, Japan, [3]Internal Medicine, National Hyougo Central Hospital, Kobe, Japan, [4]1st Department of Oral and Maxillofacial Surgery, School of Dental Medicine, Tsurumi University, Yokohama, Japan.

The aim of this study is to characterize mechanical responses of bone cells as underlying mechanisms of bone regeneration. We compared the response of osteocytes and osteoblasts to low-intensity pulsed ultrasound (LIPUS) and stretching. Primary cells were prepared from human mandibular bone chips removed for a certain clinical treatment of patients who gave consent. We analyzed the effect of mechanical loading on message levels of c-fos, osteocalcin and IGF-I by RT-PCR analysis and Western blotting. The experiments gave us contrasting results: in the response of osteocytes to stretching, the steady-state level of osteocalcin mRNA was unregulated at 1h after the initiation of stretching. In the response to LIPUS, however, there was no upregulation of osteocalcin mRNA in osteocyte. While stretching induced calcium influx into the osteocytic cells, their proliferation was decreased. In the response of osteoblast to LIPUS, the steady-state level of osteocalcin mRNA was upregulated also at 1h after the initiation. In osteoblasts, however, mechanical loading by a low frequency stretching stimulus did not result in any such induction. In this study, we have clearly demonstrated that the high-frequency, LIPUS did not induce any significant responses of osteocyte including Ca2+ influx. Our findings support the notion that the osteocytes are sensitive to deformation of bone, sensing even a low strain magnitude through Ca2+ channels and PKA pathways, while osteoblastic cells in the osteogenic lineage are sensitive to another type of strain through different sensing mechanisms and signaling pathways. It is concluded that at least two entirely different types of mechanotranduction pathways are present in mandibular bone.

SA159

See Friday Plenary number F159.

SA160

Fluid Shear Stress Induces Nuclear Translocation of Beta-catenin in Osteoblasts. S. M. Norvell*, F. Pavalko. Cellular and Integrative Physiology, Indiana University School of Medicine, Indianapolis, IN, USA.

Mechanical loading of bone produces movement of interstitial fluid over the surfaces of cells of the osteoblast lineage. The resulting fluid shear stress (FSS) is a potent metabolic stimulus for osteoblasts. The biological response of osteoblasts to FSS involves the conversion of the mechanical signal into a molecular signal. In this study, we investigated whether β-catenin functions as a molecular component of FSS-induced mechanotransduction in osteoblasts. β-catenin is a component of cell-cell adherens junctions where it is associated with cadherins. In response to certain stimuli, β-catenin also functions as a signaling molecule when it translocates to the nucleus and promotes gene expression. To examine whether FSS activates β-catenin signaling in osteoblasts, we subjected MC3T3-E1 osteoblast-like cells and primary rat calvarial osteoblasts to 1 hour of 12-dynes/cm^2 laminar FSS or 1 hour of static conditions and measured β-catenin subcellular localization. Immunofluorescence analysis revealed that 1 hour of FSS induced β-catenin nuclear translocation. To dissect the mechanism for FSS-induced β-catenin nuclear translocation, we examined the phosphorylation/activation state of Glycogen Synthase Kinase-3β (GSK-3β). In un-stimulated cells, β-catenin is phosphorylated by active GSK-3β and is targeted for degradation. The activity of GSK-3β itself is regulated by phosphorylation. Phosphorylation of serine 9 is known to inactivate GSK-3β. Analysis of GSK-3β phosphorylation revealed that 1 hour of FSS induced significant phosphorylation of GSK-3β at serine 9 as compared to static controls, which is consistent with FSS preventing phosphorylation of β-catenin and promoting the signaling capacity of β-catenin. To begin to elucidate pathways that β-catenin may regulate in osteoblasts, we investigated whether β-catenin regulates expression of cyclooxygenase-2 (Cox-2) in osteoblasts. To this end, we established MC3T3-E1 cell lines stably expressing a mutant β-catenin molecule that cannot be phosphorylated by GSK-3β and therefore cannot be degraded. Immunofluorescence analysis revealed that the mutant β-catenin molecule localized both to cell-cell interfaces and the nucleus of MC3T3-E1 cells. Cells expressing the mutant β-catenin molecule consistently showed increased levels of Cox-2 protein compared to control MC3T3-E1 cells, demonstrating a potential role for β-catenin in modulation of Cox-2 levels in osteoblasts. In summary, these data suggest that FSS induces β-catenin signaling via a mechanism that may involve GSK-3β, and also demonstrate that β-catenin regulates Cox-2 expression in osteoblasts.

SA161

See Friday Plenary number F161.

SA162

Neither the Microfilament nor the Microtubule Cytoskeleton Is Required for Fluid Shear Stress Induced Increases in Cyclooxygenase-2 and Prostaglandin Release in MC3T3-E1 Cells. S. Norvell*, S. Ponik, F. Pavalko. Cellular and Integrative Physiology, Indiana University School of Medicine, Indianapolis, IN, USA.

Osteoblasts are mechanosensitive cells that respond to fluid shear stress (FSS) by increasing expression of cyclooxygenase-2 (Cox-2) and increasing prostaglandin release. Additionally, FSS induces reorganization of the actin microfilaments into contractile bundles termed stress fibers. It is thought that the cytoskeleton provides an organized network of fibrils that facilitate the transmission and conversion of mechanical signals into biological responses. In this study, we investigated whether an intact microfilament or an intact microtubule network is necessary for FSS-induced increases in Cox-2 and prostaglandin release in MC3T3-E1 osteoblasts. MC3T3-E1 cells were treated with multiple disruptors of actin filament formation including Cytochalasin B, Cytochalasin D, Latrunculin A and Jasplakinolide or with disruptors of microtubule formation including Nocodozole and Colchicine. Cells were treated with drug for 1 hour prior to the experiment, and were then subjected to 90 minutes of 12-dynes/cm^2 laminar FSS or static conditions in the presence of drug. After cessation of flow, cells were incubated for 30 minutes in 1mL of media in the presence of drug. After 30 minutes, the levels of the prostaglandins PGE_2 and PGI_2 released into the 1mL of media were measured using an enzymeimmunoassay and the cells were lysed in SDS sample buffer for analysis of Cox-2 levels by immunoblot. Neither disruption of the actin cytoskeleton nor disruption of the microtubule cytoskeleton with any drug prevented a significant FSS-induced increase in either PGE_2 or PGI_2 release or Cox-2 protein. These results suggest that neither the microfilament nor the microtubule cytoskeleton is required for FSS-induced prostaglandin metabolism. To rule out the possibility that the presence of either an intact microfilament or an intact microtubule cytoskeleton is sufficient for FSS-induced prostaglandin metabolism, we also disrupted both filament systems and then measured FSS-induced Cox-2 levels and prostaglandin release. Even in the absence of both intact microfilaments and intact microtubules, FSS still induced a significant increase in Cox-2 protein and PGE_2 and PGI_2 release. In summary, neither microtubules nor microfilaments are required for FSS-induced prostaglandin metabolism in MC3T3-E1 cells.

SA163

Osteocyte Formation and Reduced Bone Strength During Rapid Growth. D. Murray*[1], B. Williams*[1], N. Loveridge[2], D. Waddington*[1], C. Farquharson[1]. [1]Roslin Institute, Scotland, United Kingdom, [2]Bone Research Group, Addenbrookes Hospital, Cambridge, United Kingdom.

In response to increased loads during growth, bones increase their diameter by the deposition of circumferential lamellae and the incorporation of primary osteons at the periosteal surface. However, the influence of growth rate on circumferential growth and bone architecture in the immature skeleton is not fully understood. We have compared morphometric and biochemical indices between tibiae from chickens with fast (F) and slow (S) growth potential. Body weight at 42 days was, F=2441g and S=1224g and appositional bone formation rate was F=98.0 and S=68.4 um/day. Bone diameter was greater in the fast growing birds (F=7.16mm, S=5.36mm, P<0.001) and allometric analysis indicated that bone width increased in relation to body weight in both strains. Although bone breaking strength (F=448N, S=270N, P<0.001) and stiffness (F=363N/mm, S=285N/mm; P<0.01) were higher in the fast growing birds after adjustment for body weight the bones were inherently weaker (breaking strength; F=99N, S=181N, P<0.05, stiffness; F=60N/mm, S=220N/mm, P<0.001). To explain these reduced mechanical properties, porosity and ash content were determined. Porosity was elevated periosteally (F=36%, S=27%, P<0.01) but not endosteally. Staining for TRAP and cement lines indicated the increased porosity was not a result of primary osteon remodelling. Increased porosity was due to slower infilling of the primary osteons in the fast strain (F=42.5%, S=27.0%, P<0.01). Osteocyte density within the periosteal interstitial bone was higher in the fast growing strain(F:5.3/mm2, S:1.8/mm2, P<0.01) but unchanged in primary osteons (F:2.73/mm2, S:2.86/mm2, P<0.01).Ash content was reduced in the fast strain (F=45.0%, S=48.0%, P<0.05). In conclusion, fast growth resulted in the expected circumferential expansion to withstand increasing loads. This was accompanied by increased porosity resulting from rapid formation of primary osteons at the periosteal surface and the incapacity of osteoblasts to completely infill the resultant canal. As periosteal interstitial bone of the fast strain had a higher osteocyte density the reduced osteon infilling is unlikely to be due to a decrease in osteoblast numbers. These events suggest that transit through the osteoblast lineage is more rapid at the periosteal surface of the fast strain and while osteoblast precursors are locally available, this has no effect on bone growth. Such increased osteoblast transit times would account for the reduced primary osteon infilling but as osteocyte density within primary osteons was similar in both strains other mechanisms such as increased apoptotic rates may be responsible.

SA164

Low Amplitude Vibration Does Not Induce Osteogenesis in the Mouse Ulna. S. M. Tanaka*, M. I. Alam*, C. H. Turner. Orthopaedic Surgery, Indiana University, Indianapolis, IN, USA.

It is known that the bone strain profile involves not only periodic strain waves at around 1 cycle/s (Hz), but also broad frequency vibration with small amplitude. Others have suggested that low amplitude, high frequency (20-30 Hz) vibration is an osteogenic stimulus for bone tissue. The purpose of this study is to evaluate effects of the broad frequency (0-50 Hz) vibration on new bone formation. Male C57BL/6 mice (16 weeks old) were used for this study. The following types of loading were applied to ulnae of the mice under anesthesia for 30 sec/day for 2 days using a newly developed mechanical stimulator: (1) low

frequency, high amplitude sinusoidal loading at 2 Hz with 3 N peak-to-peak (n=10), (2) broad frequency, low amplitude vibration with 0.3 N of mean amplitude and frequency ranging from 0 to 50 Hz (n=8), and 3) no loading control (n=8). After mechanical loading, new bone formation on the periosteal surface was analyzed histomorphometrically on cross-sections cut from the ulnar midshaft. High amplitude, low frequency (2 Hz) loading significantly increased mineralizing surface (MS/BS, %), mineral apposition rate (MAR, mm/day), and bone formation rate (BFR/BS, mm3/mm2/year) on the right ulnae compared to non-loaded left ulnae. However, no new bone formation was induced by low amplitude, broad frequency vibration. From these results, we conclude that low amplitude vibration does not induce osteogenesis in the mouse ulna even when applied at frequencies of up to 50 Hz.

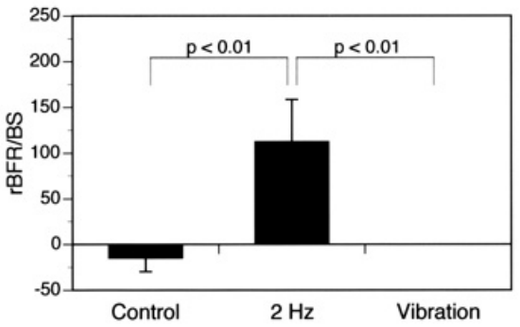

SA165

See Friday Plenary number F165.

SA166

Effect of Long-duration Spaceflight on Integral and Compartmental Bone Density in the Spine and Hip. T. F. Lang[1], H. Evans*[2], N. Rianon*[3], Y. Lu[1], H. Genant[1], A. Leblanc[3]. [1]Radiology, University of California, San Francisco, CA, USA, [2]Wyle Labs, Houston, TX, USA, [3]Medicine, Baylor College of Medicine, Houston, TX, USA.

Bone loss is a well-established medical risk factor for long-duration spaceflight. Recent DXA studies of the MIR crewmembers demonstrated an average bone mineral loss from the spine and hip of 1.1-1.6%/month, with large heterogeneity between subjects and between skeletal sites in the same subject. However, these studies utilized integral measurements and there is little information on how the bone loss distributes three-dimensionally across the trabecular and cortical compartments. To address this issue, we are performing a study of astronauts making long-duration spaceflights (4-6 months) on the International Space Station, using volumetric quantitative computed tomography (vQCT) to measure changes of cortical and trabecular bone in the hip and spine. Five subjects were imaged in the hip and L1/L2 vertebrae using a helical vQCT protocol (GE Hispeed Advantage, 80 kVp, 280 mAs hip, 140 mAs spine, 3mm slice thickness, pitch=1) before and after missions lasting from 120-165 days. For comparison, the subjects underwent DXA of the spine and hip (Hologic QDR-4500) at the same time points. Hip measures included integral (iBMD), trabecular (tBMD) and cortical (cBMD) bone density, as well as cortical bone mass (cBMC), in the femoral neck and total femur regions. Spine measures included iBMD and tBMD in the vertebral centrum as well as iBMD in a region containing the entire vertebra. We tabulated the average percentage change (standard deviation) in these measures and determined the statistical significance using the paired t-test.

QCT-Femoral neck				QCT-Total femur			
iBMD	tBMD	cBMD	cBMC	iBMD	tBMD	cBMD	cBMC
-5.8(1.5) p<0.001	-11.1(5.2) p<0.01	-3.1(2.5) p<0.05	-4.4 (4.4) ns	-7.6(3.9) p<0.01	-10.2(4.3) p<0.01	-3.5(2.3) p<0.05	-8.6(7.3) p<0.05

QCT-Centrum		QCT-Total Vertebra
iBMD	tBMD	iBMD
-3.7(2.2) p<0.05	-1.2 (1.4) ns	-3.8(2.5) p<0.05

For DXA of L1-L4 and the total femur, the percentage changes were -3.3 (SD=3.2, p<0.05) and -5.6 (SD=1.7, p<0.01) respectively. The relatively small changes observed in the vertebrae were offset by larger proximal femoral changes. There was a trend in the hip data for trabecular losses to exceed cortical and integral losses. Our preliminary data indicate that current countermeasure approaches may be insufficient to prevent serious loss of bone mineral in the hip.

SA167

Effect of Nicotine on Distraction Osteogenesis of the Rat Mandible. A. J. M. Schulten*[1], L. B. Kaban*[2], D. Perrott*[2], J. Glowacki[1]. [1]Orthopedic Surgery, Brigham and Women's Hospital, Boston, MA, USA, [2]Oral and Maxillofacial Surgery, Massachusetts General Hospital, Boston, MA, USA.

Distraction Osteogenesis (DO) has gained clinical acceptance as a surgical technique for bone lengthening, but success is unpredictable. There is need for new approaches to study the biology of DO, especially in compromised settings. Nicotine inhibits soft and hard tissue wound healing in several animal models. We assessed the effects of nicotine (NC) on DO in rats undergoing mandibular distraction. We anticipated that NC treatment would diminish osteogenesis and bone elongation. Mandibular body osteotomies were created between the 2nd and 3rd molars in 25 adult male rats; they were fitted with custom distraction devices. Twenty-four animals underwent gradual lengthening of the right hemimandible using a 3-day latency period, 6-day distraction (0.25 mm twice daily), and 4 weeks of neutral fixation. Twelve of these rats received subcutaneous nicotine pellets (153 mg nicotine; NC group), and twelve received placebo pellets (Vehicle group, Ve). A pilot study showed that these slow-release pellets achieved plasma levels of NC at 60.6 ± 1.6 ng/mL (equal to 1.5 packs/day). One animal underwent acute lengthening (3 mm) and fixation, without implantation of NC or Ve. After removal of devices, specimens were analyzed for radiographic bone fill score, amount of bone advancement, and histological features. Although all animals underwent temporary weight loss following surgery and change to soft diet, subsequent weight gain was similar in NC and Ve. Device distraction of 3.2 mm ± 0.2 was achieved. The mean radiographic bone fill score with NC (2.7 ± 0.9) was 75% of that in Ve (3.6 ± 0.7; p=0.0036). Maintenance of elongation (after removal of the device) in NC was 49% of that in Ve, p=0.0008. With NC, distracted hemimandibles were 1.18 ± 0.84 mm longer than contralateral sides (104.2% ± 3.3; p=0.0014); with Ve, distracted hemimandibles were 2.39 ± 0.33 mm longer (108.5% ± 1.0, p<0.0001). Analysis of the relationship between radiographic bone score and hemimandible advancement showed a significant correlation (Spearman r=0.549, p=0.012). Qualitative histological and enzyme analysis demonstrated less bone, and less osteoblastic and osteoclastic activity in NC. Rather, the gaps contained dense, poorly vascularized scar tissue. The animal with acute advancement showed poor bone fill radiographically and fibrosis by histology, as evidence that gradual distraction was needed to repair a gap this size. This study shows that nicotine inhibits osteogenesis, vascularity, and bone lengthening in mandibular DO wounds. This novel model provides the opportunity to evaluate potential means of enhancing impaired osteogenesis.

SA168

See Friday Plenary number F168.

SA169

Effect of Swimming Exercise on Bone Mineral Density and Trabecular Bone Architecture in Ovariectomized Rats. Y. Joo*[1], T. Sone[2], M. Fukunaga[2], S. Onodera*[1]. [1]Health and Sports Sciences, Kawasaki University of Medical Welfare, Kurashiki, Japan, [2]Nuclear Medicine, Kawasaki Medical School, Kurashiki, Japan.

Weight-bearing exercise is traditionally recommended for improving bone health in postmenopausal women. In this study usefulness of swimming exercise as an alternative to weight-bearing exercise was examined in ovariectomized rats. Ovariectomy (OVX) or sham-operation (SHAM) was conducted to Fisher-344 female rats of the 18 weeks old. Rats in a swimming exercise group (SW-OVX, n = 9; SW-SHAM n = 9) swam for 12 weeks, 5 days/week for 60 min per session. A control group (CON-OVX n = 7; CON-SHAM, n = 9) engaged in no structured exercise. After 12 weeks of intervention, femurs and lumber vertebrae (L1-L4) were analyzed for bone mineral density (BMD) by dual energy X-ray absorptiometry. Cancellous bone in distal femoral metaphysis was analyzed for three-dimensional trabecular bone architecture by microcomputed tomography (micro-CT). BMD and geometrical properties of diaphyseal cortical bone were evaluated in the mid-femoral region by micro-CT. Finally, biomechanical properties of the femurs were analysed by three-point bending (Instron). Bone mineral densities were significantly decreased both in femur and lumber vertebra by OVX. These changes were suppressed by swimming exercise. Trabecular bone width, number, and connectivity were decreased by OVX, whereas the structure model index, i.e. the ratio of rod-like to plate-like trabeculae, increased. These changes were also suppressed by swimming exercise. Femurs of the SW group had greater cortical thickness compared with CON. No significant effect of OVX was observed for mechanical properties of femoral diaphysis. In conclusion, data from this study suggest that the swimming exercise would have some beneficial effects on bone mass, structure, and strength.

SA170

The Effects of Weight-Bearing (Running) and Non-weight-bearing (Swimming) Exercise on Bone Development in Growing Rats. R. S. Yang*[1], T. H. Huang*[1], S. S. Hsieh*[2], F. L. Chang*[2], S. H. Liu*[3]. [1]Department of Orthopaedics, National Taiwan University Hospital, Taipei, Taiwan Republic of China, [2]Department of Physical Education, National Taiwan Noraml University, Taipei, Taiwan Republic of China, [3]Institute of Toxicology, National Taiwan University, Taipei, Taiwan Republic of China.

Mechanical loading is an important factor on the bone development. Different exercise will cause various kinds of mechanical loading on bone. In the present study, we investigated the effects of two different exercise modes, swimming vs. running, on rat's bone development.Twenty-nine male Wistar rats (7-wk-old) were randomly divided into three groups: control group (CON, n=10), running group (RUN, n=9) and swimming group (SWIM, n=10). Running exercise was held on the treadmill at a moderate exercise intensity (20m/min in speed) and the swimming trained animals swam with a weight (2% of body weight) attached to their tails. The training protocols were 1hr/day and 5 days/wk for a period over 8 wks. All rats were deeply anesthetized and sacrificed by decapitation after the end of training session. The measured parameters included: 1) wet weight and length of bone; 2) cross-sectional parameters of long bone midshaft; 3) spongy bone histomorphometric analysis; 4) bone mineral density (BMD) and bone mineral content (BMC) by using DEXA (dual energy X-ray absorptiometer). The results showed that exercise training significantly reduced the increment of body weight. Therefore, statistic analysis of one-way ANCOVA was used to correct the effects of body weight on original data and compared the means among groups. In femoral bone mass measurement, two exercise groups (RUN: 1293.4±106.3 mg; SWIM: 1269.5±80.8 mg) showed a higher wet mass than CON rats (1148.3±66.9 mg) (p= .002). Although statistical significance did not reach, SWIM rats were still lower in long-axis values (p= .069) and higher in short-axis values (p= .056) of tibial cross-section. Due to the higher body weight, CON rats were originally higher in BMD and BMC value. After correction of the effects of body weight with covariance analysis, RUN rats had the highest BMD on the proximal tibia and distal femur. The histomorphometric studies showed that exercise groups had a 27% higher bone volume ratio than CON. In addition, RUN rats had a thicker trabecular bone than SWIM rats in proximal tibia, although the significant difference was not found. In conclusion, weight-bearing exercise showed a benefit in increasing BMD on specific sites. Different exercise modes had different adaptation types in tibia cross-sectional geometry and spongy bone. However, swimming training might not provide a sufficient stress for the improvement of BMD and BMC.

SA171

***In vitro* Effects of Ribavirin and Interferon alpha-2b on Primary Human Osteoblasts.** R. O. Moreira*[1], M. L. F. Farias[1], F. J. S. Saboia*[1], A. Balduino*[2], L. Boldrini*[2], H. S. H. Martins*[2], R. Borojevic*[3], M. E. L. Duarte[3]. [1]Division of Endocrinology/HUCFF, Universidade Federal do Rio de Janeiro, RJ, Brazil, [2]Dept. of Histology and Embriology, Universidade Federal do Rio de Janeiro, RJ, Brazil, [3]Dept. of Histology and Embriology and PABCAM/HUCFF, Universidade Federal do Rio de Janeiro, RJ, Brazil.

Hepatitis C is a chronic disease that affects approximately 100 million people worldwide. The treatment of hepatitis C with interferon α-2b (IFNα-2b) and ribavirin has already been related with a significant decrease in bone mineral density. The purpose of this study is to investigate the *in vitro* effects of different concentrations of ribavirin and IFNα-2b on human osteoblasts and thus help to define the mechanisms that contribute to the associated bone loss. Accordingly, we exposed primary human osteoblasts obtained by outgrowth of cells from bone chips discarded after orthopedic procedures to ribavirin and/or IFN-α2b. The cells (2.5 x10^4 - 10^5 cells/ml) were cultured in DMEM medium containing 10% FCS and treated with IFN-α2b (0.1-1000 UI/ml), ribavirin (0.01-50 μg/ml) and IFN-α2b (100UI/ml) + ribavirin (0.01-50 μg/ml) respectively. At regular time points, cultures were harvested for posterior analysis. The level of alkaline phosphatase activity (ALP) was determined at 7 and 14 days and the proliferative potential of the cells was assessed by MTT at 3, 4 and 5 days respectively. Cell cycle analysis and apoptosis were ascertained by flow citometry using propidium iodide (PI) at 24 and 48 hours after incubation. In the concentrations used in this study, IFN-α2b did not affect the viability, ALP expression and osteoblast proliferation capacity. In ribavirin and ribavirin+IFN-α2b treated cultures, ALP activity was diminished within 14 days (P<0.001 and P<0.01 respectively) in comparison with IFN-α2b treated cultures. The number of apoptotic osteoblast cells was increased after 48h of incubation with ribavirin in high concentrations (10 and 50 μg/ml). The reduction in cell proliferation was dose-dependent and was detected as early as day 3 in all cultures treated with ribavirin. In conclusion, our experiments demonstrate that ribavirin reduced in a time and dose dependent manner cell proliferation and the expression of osteoblasts markers. Cell apoptosis is likely to be also accelerated by ribavirin. It is possible that localized increase in the levels of this antibiotic may be disruptive to osteoblast mitogenic potential and function. This action may contribute to the loss of bone reported *in vivo*.

SA172

Leptin Induces Apoptosis via ERK/cPLA2/cytochrome C Pathway in Human Bone Marrow Stromal Cells. G. S. Kim[1], J. S. Hong*[2], S. W. Kim*[2], J. M. Koh*[1], E. S. Kim*[3], C. S. An*[4], J. Y. Choi*[5], S. L. Cheng[6]. [1]Division of Endocrinology and Metabolism, Asan Medical Center, University of Ulsan College of Medicine, Seoul, Republic of Korea, [2]Asan Institute for Life Science, Seoul, Republic of Korea, [3]Department of Internal Medicine, University of Ulsan College of Medicine, Seoul, Republic of Korea, [4]School of Biological Sciences, College of Natural Sciences, Seoul National University, Seoul, Republic of Korea, [5]Medical Research Institute, Kyungpook National University, Taegu, Republic of Korea, [6]Division of Bone and Mineral Disease, Department of Medicine, Washington University, School of Medicine, St Louis, MO, USA.

Leptin, the Ob gene product, has recently emerged as a key regulator of bone mass. However, the mechanism mediating leptin effect remains controversial. Since the action of leptin is dependent on its receptors, we analyzed their expression in osteoblast-lineage primary human bone marrow stromal cells (hBMSC). Both the short and long forms of leptin receptors were detected in hBMSC. Incubation of hBMSC with leptin significantly decreased the cell viability. This cytotoxic effect was prevented by Z-Val-Ala-Asp-fluoromethylketone, a pan-caspase inhibitor, implicating that leptin-induced hBMSC death was caspase-dependent. Further investigation demonstrated that leptin activated caspase-3 and caspase-9, but not caspase-8, and increased the cleavage of poly (ADP-ribose) polymerase (PARP) and the release of cytochrome C into cytosol. Leptin was found to activate ERK, but not p38 and JNK, and up-regulated cPLA2 activity, the latter was abolished by pre-treatment of cells with the MEK inhibitor (PD098059 or U0126) or cPLA2 inhibitor (AACOCF3). PD98059, U0126, and AACOCF3 also diminished the leptin-induced cell death and caspase-3 activation, implicating that leptin induced hBMSC apoptosis via ERK/cPLA2/cytochrome C pathway, which subsequently activated caspase-9 and caspase-3 and cleaved PARP. To our knowledge, this is the first study demonstrating the detrimental effect of leptin on bone cell development.

Disclosures: ***G.S. Kim****, the Korea Health 21 R & D Project, Ministry of Health & Welfare, Republic of Korea 2.*

SA173

See Friday Plenary number F173.

SA174

Crovidisin, a Snake Venom Protein, Selectively Induced Apoptosis of ROS 17/2.8 Osteosarcoma Cells but not of Rat Primary Osteoblasts. C. H. Tang*[1], R. S. Yang*[2], W. M. Fu*[1], C. Z. Liu*[3]. [1]Pharmacology, National Taiwan University, Taipei, Taiwan Republic of China, [2]Orthopaedics, National Taiwan University Hospital, Taipei, Taiwan Republic of China, [3]Pharmacology, Tzu Chi University, Hualien, Taiwan Republic of China.

Apoptosis, a programmed, physiological mode of cell death, is important in tissue homoeostasis. Crovidisin, a collagen-binding protein, prevents platelet-collagen interaction. In addition, crovidisin expresses matrix metalloproteinase I (MMP-1) activity. Here we report crovidisin, purified from *Crotalus viridis* venom, selectively induced apoptosis of ROS 17/2.8 the osteosarcoma cells but not of rat primary osteoblasts. Immunofluorescence showed that osteoblasts and ROS 17/2.8 exert different pattern of fibronectin (Fn) fibrillogenesis, type I collagen (Cn) and α5 integrin. Immunocytochemistry, western blotting and flow cytometric analysis showed that osteoblasts have more abundant expression that ROS 17/2.8, including Fn, Cn, α5, β1, α2 integrin and focal adhesion kinase (FAK). Crovidisin selectively reduced more adhesion activity of ROS 17/2.8 to Fn or Cn than osteoblasts. Treatment with crovidisin for 24 hr selectively caused the detachment of ROS 17/2.8 but not osteoblasts. However, triflavin, a RGD-dependent disintegrin purified form *Trimeresurus flavoviridis,* did not cause the detachment of either osteoblasts or ROS 17/2.8. Treatment with crovidisin for 36 hr caused the mitochondrial membrane potential loss in ROS 17/2.8 but not in osteoblasts, suggesting that crovidisin is also to induce early apoptosis in ROS 17/2.8. Treatment with crovdisin for 48 hr induced apoptosis in ROS 17/2.8 as examined by propidium iodide and DNA fragmentation analysis. These results suggest that primary rat osteoblasts secrete more matrix and have more integrin expression than ROS 17/2.8 cells. Since the cell-matrix interaction is vital for the cell survival, the crovidisin can bind to collagen and cleave Cn may selectively induce apoptosis of ROS 17/2.8 cells.

SA175

Celiac Disease Affects Bone Remodelling: An *in vitro* Study. D. Fortunati*, A. Taranta, M. Longo*, S. Migliaccio, M. L. Bianchi*, M. T. Bardella*, S. Saraifoger*, A. Teti. Experimental Medicine, University of L'Aquila, L'Aquila, Italy.

Gluten intolerance causes celiac disease. This inflammatory disorder of the small bowel is often associated with low bone mass. To assess whether celiac disease directly affected bone formation, human osteoblasts were challenged with sera from three categories of patients: 25 celiac patients on gluten-free diet for at least two years, 17 just-diagnosed, yet untreated celiac patients, and 21 healthy donors. ^{3}H thymidine incorporation revealed that sera from both groups of celiac patients stimulated osteoblast proliferation (p<0.01 vs. controls). Alkaline phosphatase activity and matrix mineralization were mostly increased in osteoblast cultures exposed to sera from untreated celiac patients (p<0.005 vs. controls). These data hint to

an osteoblast stimulation, possibly due to serum factors enhancing their function. However, our observation was not in agreement with those in patients showing reduced bone mass. We therefore hypothesized that osteoclast activity could be increased in celiac patients by serum factors, and that enhanced osteoblast activity could stimulate osteoclast function by released cytokines. Indeed, osteoclast formation and activity was marked increased in human peripheral blood monocyte cultures exposed to sera from celiac patients relative to normal subjects, with a clear-cut acceleration of multinucleated osteoclast differentiation. Notably, RT-PCR analysis of specific cytokines in osteoblast cultures kept in the presence of our sera showed negligible transcriptional expression of TNFalpha and IL-18, and similar mRNA levels for IL-1, IL-6, IL-12 in all conditions, but reduced mRNA levels of osteoprotegerin (OPG) in osteoblasts exposed to sera of celiac patients ($p<0.01$ vs. controls), with consequent alteration of OPG-ligand/OPG ratio. As OPG is a decoy receptor which blocks OPG-ligand stimulatory effect on osteoclasts, we believe that reduction of this factor may contribute to the enhanced bone loss observed in celiac disease.

SA176

See Friday Plenary number F176.

SA177

The RANKL Promoter Is Activated Through Acetylation. J. Rubin[1], T. C. Murphy*[1], L. Zhu*[1], J. W. Pike[2], M. S. Nanes[1], X. Fan[1]. [1]Medicine, VAMC & Emory University, Decatur, GA, USA, [2]Biochemistry, University of Wisconsin-Madison, Madison, WI, USA.

RANKL expression in bone determines the level of osteoclast recruitment and activity. While it is clear that osteoactive substances regulate RANKL mRNA expression, studies of the RANKL promoter have not been particularly informative. For instance, vitD robustly stimulates the endogenous murine gene but has little to no effect on RANKL promoter delivered transiently despite the presence of a vitD consensus sequence. Furthermore, while RANKL expression is restricted to certain cell types, the RANKL promoter appears to be equally active in multiple lineages. This suggests that silencing of an otherwise active promoter might be a predominant control mechanism. To better understand regulatory controls of this important remodeling signal, we first examined endogenous RANKL mRNA levels in ST2 stromal cells. Northern analysis showed that RANKL mRNA was dose-dependently upregulated in the presence of the histone deacetylase inhibitor trichostatin A (TSA). In fact, 6 h TSA treatment raised RANKL mRNA equivalently to that caused by 24 h 10 nM vitD exposure. We next studied the response of five RANKL promoter luciferase constructs of 2020, 1500, 957, 725 and 500 base pairs (bp) from the tsp. Luciferase was measured 48 h after transfection of RANKLpr-luc constructs. There was no apparent tissue specificity (comparing ST2, COS7 and HeLa cells), nor were basal activities different between the five constructs. TSA dose-dependently stimulated -2020bpRANKLpromoter-luc activity maximally to 32 ± 2 fold over basal (basal = promoter activity in absence of TSA). This was significantly higher than TSA's stimulation of a co-transfected SV40-promoter, which peaked at 3-fold over basal SV40 activity. The full TSA effect was present in both the -500bpRANKLpr-luc and the -725bpRANKLpr-luc constructs (34 ± 3 fold and 30 ± 1 fold over basal, respectively). Addition of the next 232 5'-bps (to -957bpRANKLpr-luc) was associated with a significant decrease in TSA effect, to only 20 ± 1 fold over basal. This repression was relieved with inclusion of further 5'-sequence: TSA stimulated the -1500bpRANKLpr-luc construct 31 ± 2 fold. This suggested that the first 500 bp contain a sequence sensitive to acetylation. EMSAs performed with overlapping 150 bp probes representing this RANKLpr sequence revealed numerous bands, none of which was altered by pretreatment with 25 nM TSA. Finally, the -2020bpRANKLpr was extended 3' through the entirety of exon+1: addition of 3'-sequence conferred neither tissue specificity nor response to vitD. Overall, our data suggest that acetylation of histone or transcription factors associated with the endogenous RANKL gene may be involved in its regulation.

SA178

Metabolic Acidosis Stimulates Expression of RANK Ligand RNA. K. K. Frick, D. A. Bushinsky. University of Rochester School of Medicine and Dentistry, Rochester, NY, USA.

Metabolic acidosis increases net calcium efflux from bone, initially through physicochemical and later predominantly through cell-mediated mechanisms. Acidosis decreases bone formation by osteoblasts and increases bone resorption by osteoclasts. Growth and maturation of osteoclasts, which are derived from hemopoietic precursors in the monocyte / macrophage lineage, are dependent on the interplay of a number of factors, including RANKL, M-CSF and OPG produced by osteoblasts. Commitment of precursors to functional osteoclasts is induced by the interaction of the osteoclastic cell-surface receptor RANK with its ligand expressed on the surface of osteoblasts, RANKL. The RANK / RANKL interaction not only initiates a differentiation cascade which leads to mature, bone resorbing osteoclasts but increases their resorptive capacity and survival. To test the hypothesis that metabolic acidosis alters the expression of one or more of these mediators of osteoclastogenesis, we compared RNA expression from neonatal mouse calvariae cultured in acidic (initial pH ~ 7.1 and [HCO3-] ~ 10.6 mM) or neutral (initial pH ~ 7.5 and [HCO3-] ~ 25.1 mM) medium for 24 and for 48 h. Initially using RT-PCR and with subsequent quantitation by Northern analysis we found that metabolic acidosis significantly increased expression of RANKL RNA at both 24 h (2 fold) and 48 h (5 fold) compared to respective controls. There was no alteration of OPG or M-CSF RNA levels with metabolic acidosis. Net calcium efflux from bone was also increased into the acidic, compared to control, medium. At 48 h, net calcium efflux correlated directly with RANKL expression ($r = 0.770$, $n = 15$, $p < 0.001$). The acidosis-induced increase in RANKL would be expected to augment osteoclastic bone resorption and help explain the acidosis-induced increase in cell-mediated net calcium efflux.

*Disclosures: **K.K. Frick**, NIH 2; Renal Research Institute 2.*

SA179

Regulation of Target Genes by TGF-ß Inducible Early Gene Through Specific Binding to an SP-1 Binding Site. M. Subramaniam, S. A. Johnsen*, K. Rasmussen*, T. C. Spelsberg. Biochemistry and Molecular Biology, Mayo Clinic & Foundation, Rochester, MN, USA.

TGF-ß is an important autocrine and paracrine growth factor which plays an important role in human osteoblast growth and differentiation. To understand the role of TGF-ß signaling in human osteoblasts and to study the role of downstream target genes, we cloned a TGF-ß inducible early gene (TIEG) from human osteoblasts which acts as a downstream target for TGF-ß signaling. TIEG transcript is rapidly induced within 60 minutes of TGF-ß treatment. TIEG was shown to be a primary response gene induced by selective members of TGF-ß superfamily in human osteoblasts. TIEG encodes a 480 amino acid nuclear protein and has a unique N-terminal end with several SH-3 binding sites. The C-terminal end has three C2 H2 type zinc finger domains with a high homology to several Krüppel transcription factor family members. Further, TIEG is a phosphoprotein and has two Erk1 phosphorylation sites at amino acid residues 97 and 293. It also has potential GSK3 kinase and PDK1 binding sites at residues 93 and 100, respectively. To characterize this protein further and to understand the transcriptional regulation and DNA binding specificity of TIEG protein to DNA, we performed electrophoretic mobility shift assay (EMSA) using an SP-1 consensus sequence (GGG GCG GGG) and a purified TIEG protein produced by a baculovirus expression system. EMSA analysis demonstrated a specific shift when TIEG was incubated with the SP-1 consensus sequence. Competition experiments with excess unlabeled SP-1 duplex DNA competed for TIEG protein binding to SP-1 sequence, whereas the mutant SP-1 duplex DNA did not have any effect on the shift. Further, we were able to supershift this complex with TIEG specific polyclonal antibody suggesting that TIEG protein binding to SP-1 consensus sequence is highly specific. Using gel shift analyses, TIEG showed minimal to no binding to other known zinc finger binding consensus sequences, suggesting TIEG specifically binds to the SP-1 core sequence. We have previously demonstrated that TIEG down-regulates Smad-7 promoter activity. We now demonstrate that TIEG protein binds to an SP-1-like sequence within the Smad-7 promoter. We are now examining whether this SP-1-like sequence represents the target site for the down-regulation of this promoter. In conclusion, we have identified a DNA binding consensus site for TIEG protein which may be utilized in the transcriptional repression of the target gene promoters.

SA180

See Friday Plenary number F180.

SA181

Dlx5 Is a Direct and Specific Target of BMP-signaling, Which in Turn, Triggers Downstream Transcrption Factors, Runx2 and Osterix. M. Lee*[1], Y. Kim*[1], J. Sung*[2], J. M. Wozney[3], H. Kim[4], H. Ryoo[1]. [1]Biochemistry, School of Dentistry, Kyungpook National University, Daegu, Republic of Korea, [2]Orthodontic Dentistry, School of Dentistry, Kyungpook National University, Daegu, Republic of Korea, [3]Genetic Institute Inc, Cambridge, MA, USA, [4]Pediatric Dentistry, School of Dentistry, Kyungpook National Nuiversity, Daegu, Republic of Korea.

Injection of BMP-2 in muscular tissue induces ectopic bone formation. Likewise, BMP-2 treatment not only blocked myogenic differentiation but also induced osteoblastic transdifferentiotion of myogenic C2C12 cells. Previous reports suggested a clue that BMP-2-stimulated Runx2 could play the pivotal role in the transdifferentiation. However, Runx2 expression was induced also by TGF-b1 which could not support osteoblast differentiation in vitro, and Runx2 overexpression by itself could not support osteoclacin expression that was induced by BMP stimulation. Therefore, the induction of Runx2 is not sufficient to explain the BMP-induced transdifferentiation. Here we demonstrated that Dlx5 was specifically expressed in osteogenic cells, and was specifically induced by BMP-2 or BMP-4 signaling but was not by other osteogenic signals including TGF, GDF, FGF, glucocorticoid and Vit.D. Forced expression of constitutive active BMPR-I or BMP R-Smads also stimulated Dlx5 expression even in the absence of BMP-2. Since key transcription factors related to osteoblast differentiation, Dlx5, Runx2 and Osterix, are induced by BMP signaling, the hierarchical regulatory relationship between them would be the next question. Dlx5 induction by BMP was immediate and did not require de novo protein synthesis in C2C12 cells. In contrast, Runx2 or Osterix did require new protein synthesis. Antisense-blocking of Dlx5 completely abrogated both of Runx2 and Osterix expression induced by BMP-2. Dlx5 overexpression strongly enhanced osteogenic marker genes, such as alkaline phosphatase, type I collagen, bone sialoprotein, osteocalcin, even in the absence of BMP-2. On the contrary, neither Runx2- null mutation nor Runx2-overexpression influeced on the Dlx5 or Osterix induction by BMP-2 treatment. Taken together, these results strongly suggest that Dlx5 is the proximal target of BMP signaling that triggers Runx2 and Osterix independently, which in turn, resulted in the bone marker gene expression.

SA182

See Friday Plenary number F182.

SA183

Heterogeneous Nuclear Ribonucleoprotein K Represses Transcription from a CT Element in the Osteocalcin Promoter. J. P. Stains[1], F. Lecanda[2], D. A. Towler[1], R. Civitelli[1]. [1]Div. Bone and Mineral Diseases, Washington University, St. Louis, MO, USA, [2]Histology and Pathology, University of Navarra, Pamplona, Spain.

Heterogeneous nuclear ribonucleoprotein K (hnRNP K) was biochemically purified from a screen of proteins that co-purify with binding activity to the osteocalcin proximal promoter. HnRNP K is a unique member of the heterogenous ribonucleoprotein (RNP) family. Unlike other RNPs, hnRNP K preferentially binds single stranded DNA rather than RNA via 3 repeats of a KH motif. HnRNP K has been implicated as a transcription factor that can transactivate via interaction with a pyrimidine-rich CT element. Because a nearly identical CT-rich element is present in the rat osteocalcin proximal promoter, we tested the ability of hnRNP K to affect osteocalcin promoter activity. Electrophoretic mobility shift analysis (EMSA) of binding of recombinant hnRNP K to a CT-rich element in the -76 to -55 region of the rat osteocalcin promoter reveals that hnRNP K binds single stranded, rather than double stranded oligonucleotide probes. Additionally, hnRNP K antibody can supershift a binding activity present in ROS 17/2.8 nuclear extract using single stranded sense, but not antisense or double stranded -95 to -47 oligonucleotides. Addition of recombinant hnRNP K to ROS 17/2.8 nuclear extract disrupts formation of a DNA/protein complex on double stranded CT element oligonucleotides. The identity of the affected protein/DNA complex is currently unknown, but is under investigation. Luciferase reporter assays demonstrate that overexpresssion of hnRNP K in ROS 17/2.8 cells can repress transcription from the -92 to +32 osteocalcin promoter, which includes the CT element, as well as from a single CT element placed upstream of a RSV minimal promoter. In summary, we have identified hnRNP K as a novel transcriptional repressor acting on the osteocalcin promoter. HnRNP K inhibits osteocalcin gene transcription via two possible mechanisms, 1) modulation of protein-protein interactions that inhibit the formation of a transcriptional complex on the CT element; or 2) binding single stranded CT element *in vivo*, where hnRNP K may act directly as a repressor of transcription.

SA184

See Friday Plenary number F184.

SA185

Identification by cDNA Microarray of Genes Involved in human Mesenchymal Stem Cells Osteogenesis and Mineralization. M. Doi[1], A. Nagano*[2], Y. Nakamura*[1]. [1]Laboratory of Molecular Medicine, Institute of Medical Science, The University of Tokyo, Tokyo, Japan, [2]Department of Orthopaedic Surgery, Hamamatsu University School of Medicine, Shizuoka, Japan.

Using a culture system that facilitates osteogenic differentiation of bone marrow-derived human mesenchymal stem cells, we analyzed gene-expression profiles during the mineralization process by means of a cDNA microarray system consisting of 23,040 genes. We compared expression profiles of the cells at days 3, 15, and 27 of incubation in media containing either a combination of 0.1mM dexamethasone (Dex), 0.05mM ascorbic acid-2-phosphate (AsAP), and 10mM beta-glycerophosphate (bGP), Dex only, AsAP plus bGP, or medium with no osteogenic supplements. Histochemical detection of alkaline phosphatase and staining by alizarin red S revealed osteogenic differentiation of cells incubated in the presence of all three agents, but not in the other cultures. Comparison of the expression profiles disclosed transcriptional stimulation of 55 genes and repression of 82 genes among more than 20,000 examined. Some of the differentially expressed genes had already been cited for involvement in synthesis of extracellular matrix, in cell differentiation, and in proliferation. For example, within 3 days of incubation, the osteogenesis-inducing medium repressed expression of latent transforming growth factor beta binding protein 2, matrix methalloproteinase 14, myosin regulatory light chain 2, and other genes known to be associated with maintenance of extracellular matrix and muscle structure. After 15 and 27 days, a negative regulator of helix-loop-helix protein called “inhibitor of DNA binding 4” was down-regulated, and we detected up-regulation of methallothionein 2A, osteoprotegerin, and S100 calcium-binding protein A10, all known to have roles in osteogenesis. The set of differentially expressed genes we report here should contribute to a better understanding of the process of mineralization in the matrix surrounding human mesenchymal stem cells.

*Disclosures: **M. Doi**, the Japan Society for the Promotion of Science 2.*

SA186

See Friday Plenary number F186.

SA187

Characterization of Dexamethasone-Induced Glutamine Synthetase Expression in Human Osteoblastic Cells. A. Olkku*[1], P. V. N. Bodine[2], A. Linnala-Kankkunen*[3], A. Mahonen[1]. [1]Medical Biochemistry, University of Kuopio, Kuopio, Finland, [2]Women´s Health Research Institute, Wyeth-Ayerst Research, Radnor, PA, USA, [3]Biochemistry, University of Kuopio, Kuopio, Finland.

Recently, it has become clear that glutamate signalling is also functional in non-neuronal tissues including bone. Several reports show that human osteoblasts and osteoclasts express diverse glutamate receptors similar to those expressed in the central nervous system. In addition, osteoblasts express a glutamate transporter, GLAST, that is responsible for the cellular glutamate uptake. However, the importance of glutamate and its metabolism in bone cells is currently unknown. Previously, we showed that dexamethasone (Dex), a synthetic glucocorticoid, powerfully induced 12-fold increase in glutamine synthetase (GS) expression in human MG-63 osteosarcoma cells. The glucocorticoid receptor mediated induction needed partly new protein synthesis and was modulated by another potent regulator of osteoblasts, $1,25(OH)_2D_3$. In further characterization of GS in MG-63 cells, the activity of the enzyme was about 15 times higher in 100 nM Dex-treated cells (24 h) compared to the control. A 5-fold increase in GS mRNA level by Dex (3 h) was identified with RT-PCR. Furthermore, the role of GS on glutamate action in these cells was explored by using riluzole, an inhibitor of glutamate release. In our experiments, riluzole-induced accumulation of glutamate alone did not stimulate GS expression implying that the elevated level of substrate is not enough to stimulate GS expression in MG-63 cells. However, given both Dex and riluzole for 24 h, the GS expression was elevated and at the same time, the growth suppressive action of riluzole was diminished. This may indicate that Dex-induced GS expression during riluzole-treatment was able to increase the survival rate of MG-63 cells. The Dex-induction of GS was characterized also in other human osteoblastic cells: in conditionally immortalized preosteoblasts, HOB-03-C5, and mature osteoblasts HOB-03-CE6. In these cells, the Dex-response was slower and weaker than in MG-63 cells, but the induction was determined both on transcriptional and translational levels. Also the enzyme activity was elevated accordingly. GS is an enzyme catalyzing the conversion of glutamate and ammonia to glutamine. In bone, the role of GS is unknown but based on the recently characterized glutamate receptors and transporters, this enzyme may have a central role in glutamate signalling system. Therefore, GS as a regulator of intracellular glutamate concentration can be important in controlling osteoblast proliferation and differentiation, and thereby the development of glucocorticoid-induced osteoporosis.

SA188

Human Osteoblasts Express Functional CXC Chemokine Receptors 3: Their Ligand CXCL10 Induces Alkaline Phosphatase And N-Acetyl-β-D-Glucosaminidase Release. G. Lisignoli*[1], S. Toneguzzi*[1], A. Piacentini*[1], L. Cattini*[1], M. Tschon*[1], S. Cristino*[1], F. Grassi[1], A. Facchini*[2]. [1]Laboratorio di Immunologia e Genetica, Istituti Ortopedici Rizzoli, Bologna, Italy, [2]Laboratorio di Immunologia e Genetica, Istituti Ortopedici Rizzoli, Dip. Medicina Interna e Gastroenterologia, Università degli Studi di Bologna, Bologna, Italy.

Osteoblasts (OBs) represent a bone cell population that contributes to the maintenance of bone homeostasis, and directly or indirectly regulates bone remodeling, growth and mineralization .OBs are not only responsible for matrix deposition, but they also support the differentiation of immune system cells. Chemokines are key mediators of leukocytes recruitment and activation to site of inflammation. These factors interact with specific receptors, thus eliciting different responses (i.e. immunological, enzymatic) in situ. In particular, in the bone tissue they favour the degradation of extracellular matrix and bone remodelling. We investigated the expression of the CXC chemokine receptors in isolated human OBs from post-traumatic patients by RT-PCR and flow cytometry. OBs express high levels of CXC chemokine receptor 3 (CXCR3) and 5 (CXCR5), intermediate level of CXCR1 and CXCR4 but not CXCR2. Functional assays to evaluate the engagment of CXCR3 to its ligand CXCL10 demonstrate that significantly induce the release of N-acetyl-β-D-glucosaminidase, an enzyme involved in endochondral ossification and bone remodelling able to degrade important extracellular matrix components. Moreover, alkaline phosphatase activity, a useful index of matrix formation was also upregulated by CXCL10. Both Bordetella pertussis toxin and neutralizing anti-CXCR3 monoclonal antibodies block CXCL10 induction. We also demonstrated the expression of CXCL10 and CXCR3 in human bone tissue biopsies from post-traumatic patients. These results indicate that CXCR3/CXCL10 receptor-ligand pair may play an important role in OB activity through the specific upregulation of two enzymes which are involved in the bone remodeling process.

SA189

Spatial and Temporal Expression of the Tyrosine Phosphatase, OST-PTP, During Osteogenesis. L. A. Yunker*[1], C. S. Carlson*[2], L. J. Mauro[3]. [1]Grad Program in Molecular Veterinary Biosciences, U of MN, St. Paul, MN, USA, [2]Veterinary Diagnostic Medicine, College of Vet Med, St Paul, MN, USA, [3]Animal Science-Physiology, U of MN, St. Paul, MN, USA.

Osteotesticular Protein Tyrosine Phosphatase (OST-PTP) is the only tyrosine phosphatase currently being studied that appears to be specifically expressed by osteoblasts, is hormonally regulated and is necessary for osteoblast differentiation. Previous studies have examined the in vitro regulation of OST-PTP in primary osteoblasts or cell lines, but little is known about its expression in vivo. To better characterize the regulation of OST-PTP in bone and to further our understanding of its function in osteogenesis, in vivo expression patterns and levels were determined by in situ hybridization and Northern blot analysis. The spatial and temporal expression of the murine OST-PTP (mOST-PTP) gene was compared to markers of bone formation during embryogenesis as well as in tissues formed by endochondral vs. intramembranous ossification. Adjacent paraffin-embedded tissue sections of embryos 11, 12.5, 14,16 and 19 days post-coitum (dpc) as well as neonatal calvaria and long bones were incubated with 35S-labeled riboprobes encoding mOST-PTP as well as Cbfa1, alkaline phosphatase (ALP) and osteocalcin (OC). Northern analysis was performed on embryo, limb and calvarial mRNA. During embryonic development, mOST-PTP mRNA is first detected at 12.5 dpc in the mesenchyme of the skull and several other cranio-facial bones. This highly restricted expression overlaps with that of Cbfa1 mRNA, a transcriptional regulator of osteoblast commitment, which localizes to the mesenchyme of the skull, cranio-facial bones, the clavicle and ribs. By 14 dpc, mOST-PTP expression expands to include most of the cranio-facial

bones, the clavicle, ribs, vertebrae, hip and hindlimb. The relative level of mOST-PTP expression increases at 16 dpc in the ossification centers of the embryo. By 19 dpc, this gene is only observed in the perichondrium of the ribs on the ventral side but continues to be expressed in other areas of ossification. During endochondral ossification, mOST-PTP mRNA is observed in the perichondrium, the periosteum, the surface of the trabecular bone, and along the chondro-osseous junction. Adjacent long bone sections show OC expression restricted mainly to the surfaces of trabecular bone and the periosteal surface of cortical bone. Northern analysis confirms that temporal expression of OST-PTP overlaps with Cbfa1, ALP and OC expression. These results suggest that the OST-PTP gene is expressed in osteoprogenitor cells and that this expression is highly regulated and site-specific in the skeleton during embryogenesis and ossification.

SA190

Analysis of DMP1 Expression During Osteoblast Lineage Differentiation. I. Kalajzic*[1], A. Braut*[1], M. Stover*[1], A. Narayanan*[2], A. George*[2], M. Mina[1], D. Rowe[1]. [1]University of Connecticut Health Center, Farmington, CT, USA, [2]University of Illinois, Chicago, IL, USA.

The osteoprogenitor lineage passes through a number of proliferation and differentiation stages in the process of producing differentiated osteoblasts and osteocytes. Our previous studies have demonstrated that promoter-green fluorescent protein (GFP) transgenes can be used to identify and isolate populations of cells at the preosteoblastic stage (pOBCol3.6GFP positive cells) and at the mature osteoblastic stage (pOBCol2.3GFP) in real time in primary bone cell cultures derived from mice bearing these marker transgenes. This strategy forms the basis for appreciating the cellular heterogeneity of lineage and relating gene function to cell differentiation. Lacking in our model system has been a selective marker at the osteocytic level of differentiation. Based on previous studies in chicken and rat that dental matrix protein 1 (DMP1) exhibits an osteocyte-restricted pattern of expression, we monitored the expression of this protein in murine primary marrow stromal and calvarial osteoblast cultures and in developing bone, calvaria and teeth. In both culture models, a strong DMP1 mRNA signal was detected after the onset of mineralization, 2-4 days after the onset of osteocalcin (OC) mRNA expression. Using in situ hybridization, we confirmed a restricted pattern of DMP1 expression in osteocytes of mouse calvaria and long bones. Osteoblasts on the endosteal and perisoteal surface were negative for DMP1 expression. This data indicate that DMP1 should be a good candidate for identification of living osteocytes using DMP1 promoter-GFP as a marker. Therefore we utilized a 3.0 kb rat DMP1 promoter to drive the coral autofluorescent marker, DS2-red, in a VSV-G pseudotyped retroviral vector. The mature vector contains inactivated LTRs allowing the inserted promoter to drive the marker gene expression in response to its cellular environment. We are currently evaluating DMP1 promoter expression after retroviral infection of neonatal calvarial osteoblast cultures relative to pOBCol2.3GFP and OC-GFP activation. The characterization of DMP1-Red positive cells will be necessary to confirm the value of the DMP1 promoter currently in hand as an osteocyte marker prior to generating transgenic mice expressing the construct.

SA191

See Friday Plenary number F191.

SA192

Developmental Stages of Murine Heterotopic Bone, a Model for Assessing Bone Formation in vivo. Z. Kalajzic*, J. He*, R. Gu*, B. Kream, D. Rowe. University of Connecticut Health Center, Farmington, CT, USA.

Assessing the intrinsic capacity of the osteoprogenitor pathway to form bone in vivo as a consequence of a genetic manipulation or altered gene function is an essential component in somatic gene therapy and functional genomics. We have previously characterized transgenic mice harboring the green fluorescent protein (GFP) gene fused to different fragments of the Col1a1 promoter that activate at defined stages of cell differentiation as judged by its expression pattern in primary cell culture and in intact mouse bone. The pOBCol3.6GFP transgene initiates low-level expression in AP+ fibroblastic shaped cells in culture and within the periosteum (preosteoblastic stage of differentiation) and becomes much stronger in cuboidal shaped cells of the developing nodules and in lining osteoblasts of bone (early osteoblastic cells). The pOBCol2.3GFP transgene expression is restricted to the mineralized nodule in culture and surface osteoblasts on the surface and within bone (mature osteoblast and osteocyte). This study was initiated to determine if the pattern of expression was recapitulated in newly formed heterotopic bone from implanted marrow stromal cells (MSC), a source of cells likely to be available for genetic engineering and functional genomic studies. An FGF-expanded population of MSCs derived from either transgenic mouse were suspended in a neutral collagen solution, heat gelled at 37C and implanted into the dorsal subcutaneous space of C.B-17 Hsd Scid/bg immunodeficient mice. Recipients were sacrificed at days 8, 11, 14, 19 and 24 and the vascularized implant examined in paraffin embedded sections. At day 8 and day 11, the tissue was richly invested with capillaries and cells with a fibroblastic morphology. The pOBCol3.6GFP transgene was activated as elongated, “fibroblast-like” cells which in some regions included a tissue “envelope”. No strong pOBCol3.6+ or any pOBCol2.3+ cells were present at this time. However by day 14, the morphology of pOBCol3.6+ cells in areas of primitive osteoid had became rounded and strongly positive cells, and by at day 19, these areas had well-developed bone with accompanying marrow elements. These same areas are also positive for the pOBCol2.3+ cells but by day 25 when the mature module is formed, the distributions of the two transgenes differ. Strong pOBCol3.6+ cells line the bone surface while the pOBCol2.3+ cells are more prominent within the osteoid. This is the typical pattern of expression in normal bone in these two transgenic lines. This model should be useful to study osteoblast lineage in vivo as well as to examine donor and recipient participation in the process of the new bone formation.

SA193

BMP-2 Inducible Kinase (BIKe) Inhibits Cbfa1 Action on the Osteocalcin Promoter. B. Sanyal*, A. E. Kearns. Division of Endocrinology, Mayo Clinic, Rochester, MN, USA.

BIKe is a novel kinase whose expression is increased during BMP-2 induction of osteoblast differentiation. Overexpression of BIKe in MC3T3-E1 cells attenuates differentiation of these cells to osteoblasts. The mechanism of this effect is not known. Since Cbfa1 is a critical transcription factor for osteoblast differentiation, we investigated whether BIKe can alter Cbfa1 action on the osteocalcin promoter. ROS 17/2.8 cells were transiently transfected with an osteocalcin promoter-luciferase reporter plasmid, a Cbfa1 expression plasmid or control, and either pCMV/BIKe expression plasmid or control pCMV plasmid. BIKe overexpression did not affect luciferase activity generated from endogenous transcription factor action on the osteocalcin promoter. However, BIKe overexpression decreased by 40% the luciferase activity from co-transfection of the Cbfa1 expression plasmid. OSX is a recently discovered transcription factor that is downstream of Cbfa1 in the program of osteoblast differentiation and also is critical for osteoblast differentiation. Analogous transient transfection experiments were performed to assess the effects of BIKe expression on OSX action on the osteocalcin promoter. A pcDNA4.1/OSX expression plasmid or pcDNA4.1 control were transfected into ROS 17/2.8 cells with the osteocalcin promoter-luciferase reporter, and with pCMV/BIKe or pCMV control. Preliminary results indicate no effect of BIKe expression on luciferase activity generated from OSX action on the osteocalcin promoter. Our experiments suggest that BIKe may either directly regulate Cbfa1 action on the osteocalcin promoter, or indirectly by, for example altering interaction with repressors or inhibiting other factors downstream of Cbfa1. Additional experiments are underway to further address these possibilities.

SA194

Thiazide-Sensitive Sodium Chloride Co-Transporter (NCC) in Cryosections of Rat and Human Bone. M. M. Dvorak[1], H. Carter*[2], D. Riccardi*[1]. [1]Physiology, Pharmacology & Toxicology, University of Manchester, Manchester, United Kingdom, [2]Oral Pathology, University of Manchester, Manchester, United Kingdom.

Thiazide diuretics act by inhibiting the activity of the thiazide-sensitive sodium chloride co-transporter (NCC) in the kidney. Such therapy is also associated with an increase in bone mineral density, however, the mechanism for these effects in bone is still unclear. Recent studies have demonstrated the presence of NCC-related transcripts in a rat osteogenic cell line, suggesting that thiazides may have a direct effect on bone cells. To further examine the role of this transporter in bone, expression of NCC was examined by immunocytochemistry, using biochemically intact cryosections of rat bone and biopsies of human mandible. Undecalcified sections from freshly frozen adult rat femora (n = 6) and freshly frozen human mandible (n = 3) were stained using affinity-purified polyclonal antibodies raised against a 110 amino acid segment from the amino terminus of rat NCC. Comparisons were made with known distributions of the bone-specific proteins osteopontin and bone sialoprotein. Our results showed that there was clear NCC-specific immunofluorescence, present in a characteristic punctuate pattern, predominantly in the osteoblasts and osteocytes. In the extracellular matrix of mature lamellar bone, strong immunofluorescence was evident in the regions of reversal lines, while a more general distribution was present in the matrix of primary woven bone. This pattern of expression was confirmed using decalcified paraffin embedded sections of rat femur. We conclude that NCC is present in the cells of osteoblastic origin and in the extracellular matrix of bone. These results suggest a role for this molecule in bone cell function and provide evidence that the effects of thiazide diuretics on bone mineral density may be mediated via direct effects on bone cells. The extracellular distribution of NCC in bone suggests an as yet unkown function for this molecule as an extracellular protein. Further studies characterising the role of NCC in bone metabolism and bone disease are in progress.

SA195

Identifying the ‘Secretome’ of Bone Cells. C. Lanctot, P. Moffat*, P. Salois*, M. Gaumond*, N. St-Armant*, E. Godin*, K. Sellin*, G. Thomas. Phenogene Therapeutiques Inc, Montreal, PQ, Canada.

Secreted and membrane-bound proteins are key players in bone biology. In an effort to discover new bone anabolic agents, we have developed a novel functional genomics tool to identify the subset of cDNAs encoding secreted and membrane-bound proteins (the ‘secretome’). Libraries of cDNA fragments are expressed in mammalian cells from conditionally-defective viral genomes that can be packaged and exported in the culture medium only if the cDNA fragment encodes a secretory signal. Thus, this technology allows the selective retrieval of cDNAs encoding secreted and membrane-bound proteins by simply analyzing the content of viral particles collected from the culture medium of transfected cells. Libraries were constructed from various developing and adult bones as well as from osteoblastic cell models. A total of 9 libraries were screened. 2546 inserts that were retrieved were sequenced; 2473 (97%) contained a putative secretory signal. These encoded 419 unique cDNAs, of which 325 (77%) were previously annotated and 32 specifically associated with skeletal biology. As expected, the known secretome of bone cells was characterized by an abundance of cDNAs encoding proteins involved in secretory processes and matrix deposition. Interestingly, the secretome also included a number of molecules involved in Wnt signaling, consistent with the recently proposed importance of this pathway in osteoblast function. Of the 94 cDNAs encoding proteins of unknown function, 23 (24%) either had no match in databases or contained a secretory signal that could not be predicted from database mining. Expression profiles of these novel cDNAs were determined by Northern analysis on a panel of 52 embryonic and adult tissues. Expression of 9 clones was found to be bone-specific or greatly enriched in bone. Our screening effort has thus identified a number of novel secreted and membrane-bound molecules that may play a role in osteoblast function.

SA196

Differential Regulation of Cbfa1 (Runx2) Protein and Activity by Bone Morphogenetic Protein-2 (BMP-2) in Osteoblastic Cell Lines at Various Stages of Differentiation. C. Halleux, B. Fournier*, N. Zamurovic*, H. Keller*, M. M. Susa. Arthritis and Bone Metabolism Therapeutic Area, Novartis Pharma Research, Basel, Switzerland.

Cbfa1 (Runx2) is a master gene regulator of osteoblastic differentiation, as shown by gene deletion and dominant negative construct overexpression in mice. BMP-2 is a known inducer of osteoblast differentiation and was also reported to up-regulate Cbfa1 mRNA levels. However, the exact role of Cbfa1 in the differentiation process remained elusive. Here we examined in detail the steps on BMP-2-induced Cbfa1 pathway in two murine cell lines at various stages of osteoblast differentiation: pluripotent C2C12 cells and pre-osteoblastic MC3T3-E1 cells. Both C2C12 and MC3T3-E1 cell lines responded to BMP-2 by an increase in markers of osteoblast differentiation (alkaline phosphatase, osteocalcin), and by the activation of expected signaling pathway (Smad1, but not Erk phosphorylation). MC3T3, but not C2C12 cultures, also formed mineralized bone nodules. In both cell lines, BMP-2 did not stimulate Cbfa1 type II promoter, but induced its mRNA after 3 days, suggesting an indirect, post-transcriptional regulation. Cbfa1 type I mRNA was expressed, but not regulated. The proteins for Cbfa1 type II (starting with MASNS) and for Cbfa1 type I (starting with MRIPV) were detected by Western blotting in both cell lines. However, BMP-2 induced Cbfa1 type II protein only in MC3T3 cells, but not in C2C12 cells. BMP-2 increased Cbfa1 DNA binding activity in both cell lines, albeit to higher levels in MC3T3 cells. By contrast, the activity of luciferase driven by Cbfa1 response element OSE2 was increased by BMP-2 in C2C12, but not in MC3T3 cells. These findings unravel the unexpected complexity in Cbfa1 regulation by BMP-2: often reported mRNA regulation does not translate into protein up-regulation in C2C12 cells and the protein binding to OSE2 element does not increase reporter gene activity in MC3T3 cells. These data suggest that Cbfa1 OSE2 transcriptional activity can be regulated independently of protein levels at early stages of differentiation, while higher levels of Cbfa1 protein may have OSE2-unrelated functions at later stages of differentiation.

Disclosures: ***M.M. Susa****, Novartis Pharma Research 1, 3.*

SA197

See Friday Plenary number F197.

SA198

Noggin Arrests Stromal Cell Differentiation In Vitro. E. Gazzerro[1], S. Rydziel[1], L. Priest[1], A. N. Economides*[2], E. Canalis[1]. [1]Research, Saint Francis Hospital and Medical Center, Hartford, CT, USA, [2]Functional Genomics, Regeneron Pharmaceuticals, Inc., Tarrytown, NY, USA.

The activity of cytokines present in the bone microenvironment can be regulated by binding proteins. Noggin is a bone morphogenetic protein (BMP) dependent glycoprotein secreted by cells of the osteoblastic lineage and characterized by binding BMPs specifically, and antagonizing their activity. To define the role of noggin and BMPs in stromal cell differentiation, ST-2 cells were transduced with a retroviral vector (pLPCX) or a vector driving noggin (pLPCX noggin) under the control of the CMV promoter, and cultured for 4 weeks in the presence of beta- glycerophosphate and ascorbic acid. Only ST-2 cells transduced with pLPCX noggin expressed detectable levels of noggin mRNA and protein by Northern and Western blot analyses. The cellular phenotype of wild type, nontransduced cells was not affected by pLPCX alone. ST-2 cells expressed alkaline phosphatase, Cbfa-1, and type I collagen mRNA in the early stages of the culture, and this was followed by the appearance of mineralized nodules. In the presence of cortisol, ST-2 cells did not display osteoblast gene markers, but expressed peroxisome proliferator-activated receptor gamma 2 and adipsin transcripts, indicating a shift towards the adipocytic pathway. pLPCX noggin delayed the expression of osteoblastic gene markers, and prevented the expression of osteocalcin and the development of mineralized nodules. In addition, pLPCX noggin prevented the adipocytic phenotype induced by cortisol. These results indicate a generalized arrest of stromal cell differentiation. ST-2 cells expressed constant levels of type I and type II Cbfa-1/runx-2 mRNA throughout the 4 week culture period and they were not modified by pLPCX noggin. Confirming previous observations, differentiating control cells underwent apoptosis. This event was prevented by pLPCX noggin, indicating survival of undifferentiated cells. Despite a decrease in apoptosis there were fewer cells in pLPCX noggin cultures indicating a decrease in cell replication. In conclusion, noggin overexpression causes arrest of stromal cell differentiation. Since noggin effects may be due to the binding of locally produced BMPs, the results suggest that BMPs are required for overall stromal cell differentiation.

SA199

See Friday Plenary number F199.

SA200

Overexpression of Fra-1 in Primary Human Mesenchymal Stem Cells Induces Osteoblastic Differentiation and Decreases Molecular Markers of Adipogenic Differentiation in vitro. A. Dickason, P. Stevens*, D. Ebert*, N. Jaiswal, A. Houghton. Discovery, Procter & Gamble Pharmaceuticals, Mason, OH, USA.

Fos family members Delta FosB and Fra-1 have both been demonstrated to induce osteosclerosis when overexpressed in transgenic mice. Subsequent data has demonstrated that overexpression of Delta FosB decreases the adipocytic differentiation of pluripotent osteoblast precursors suggesting that this might be one of a number of possible mechanisms by which Delta FosB increases bone formation. However to date the effects of Fra-1 on the adipogenic differentiation of pluripotent human osteoblast precursors has not been described. We therefore performed experiments to determine the effects of Fra-1 on both the osteogenic and adipogenic differentiation of primary human mesenchymal stem cells (MSCs). Myc tagged Fra-1 cDNA was adenovirally packaged by Galapagos Genomics and crude Ad-Fra-1 or control adenovirus used to infect cultures of MSCs at various multiplicities of infection (MOI). MSCs were infected with Ad-Fra-1 at various MOIs and alkaline phosphatase activity measured after 6 days. At higher MOIs of Ad-Fra-1 clear changes in cell morphology were apparent within 3 days, with nodule-like structures composed of cuboidal cells being formed. Alkaline phosphatase assays clearly demonstrated that overexpression of exogenous Fra-1 significantly increased osteoblast differentiation at MOIs as low as 500. MSCs are also able to differentiate into adipocytes when cultured in presence of rabbit serum and 10^{-7}M dexamethasone, as indicated by changes in morphology, increased cellular staining with oil-red O and elevations of mRNAs for the adipocyte marker genes aP2 and lipoprotein lipase (LPL). To determine the effects of Fra-1 on MSC adipocyte differentiation, Ad-Fra-1 and control infected MSCs were cultured in the presence of rabbit serum and Dexamethasone. After 7 days, Ad-Fra-1 infected cells were stained with oil-red O, and aP2 and LPL mRNA measured by Taqman. Microscopic analysis showed no significant difference between control cells and Ad-Fra-1 infected cells in the number of oil-red O stained cells however, both LPL and aP2 mRNA expression levels were decreased in Ad-Fra-1 infected cells compared to control, demonstrating that whilst overexpression of exogenous Fra-1 did not decrease the number of oil-red O stained cells it did inhibit the expression of markers of adipocytic differentiation. In conclusion these data clearly demonstrate that in primary human populations of MSCs, overexpression of Fra-1 induces osteoblast differentiation and decreases the expression of molecular markers of adipocytes, suggesting inhibitory effects on adipogenic differentiation in human cells.

Disclosures: ***A. Dickason****, Procter & Gamble 3.*

SA201

See Friday Plenary number F201.

SA202

Stage-Restricted and Distinct Expression of Estrogen and Androgen Receptors Requires Osteoblast Differentiation. K. M. Wiren, A. E. Evans*, X. W. Zhang. Oregon Health & Science University, VA Medical Center, Portland, OR, USA.

Both estrogens and non-aromatizable androgens have significant beneficial effects on skeleton homeostasis, but the mechanisms are unclear. Most biologic responses to steroids are mediated through binding to their cognate receptor proteins, and the magnitude of response may reflect the level of expression of the receptor itself. We have investigated the relative expression of both estrogen receptor (ER) isoforms (ERα, ERβ) and androgen receptor (AR) during osteoblastic differentiation. Normal rat primary osteoblastic cultures derived from calvaria by collagenase digestion were grown for up to 35 days either in the presence of ascorbic acid and organic phosphate (differentiation medium) for normal differentiation and without differentiation medium to examine the dependence of receptor expression on osteoblast phenotype. Total RNA or protein was isolated at various timepoints during proliferation, matrix maturation phase, mineralization and late mineralization stages in differentiation medium, and at the same time points in non-differentiating cultures. AR, ERα and ERβ receptor expression was determined by semiquantitative relative RT-PCR and by Western analysis. Stage-specific and distinct patterns for each of the sex steroid receptors were observed throughout normal differentiation. Relative to GAPDH, AR mRNA levels were elevated during proliferation, dropped slightly during matrix maturation, and were again elevated in the mineralization stage. In general, AR protein levels corresponded to the RNA patterns with greater than two-fold elevation in mature osteocytic cultures at day 35. In contrast, ERα expression increased during differentiation and dropped in late mineralizing cultures, but ERβ expression was relatively constant throughout differentiation. Again, protein levels roughly corresponded to these patterns. Interestingly, when osteoblast cultures did not proceed through normal differentiation (in the absence of ascorbic acid), AR, ERα and ERβ mRNA levels did not exhibit these differences in expression. Thus, normal osteoblast differentiation modulates expression of the sex steroid receptors. These results are consistent with the observation that both sex steroids play significant but distinct roles in regulating function and are an important component of osteoblast differentiation.

SA203

See Friday Plenary number F203.

SA204

Proliferation of Serial Passaged MC3T3-E1 Preosteogenic Cells: Effect of Altered Cell Cycle Distribution and ECM Interaction, and Increased Sensitivity to Cell Population Density. W. J. Peterson[1], K. H. Tachiki*[2], D. T. Yamaguchi[3]. [1]GRECC 691/11g, Greater Los Angeles Healthcare System and UCLA School of Medicine, Los Angeles, CA, USA, [2]Research Searvice, Greater Los Angeles Healthcare System and UCLA School of Medicine, Los Angeles, CA, USA, [3]Research Service, Greater Los Angeles Healthcare System and UCLA School of Medicine, Los Angeles, CA, USA.

Many studies have demonstrated that increasing cell passage number or population doubling decreases cell function suggesting that diminished replicative potential of osteoblast progenitors may depress bone formation. While the mechanism of this process is unknown, changes in the cell cycle and characteristics of ECM and/or the ability of cells to respond to growth stimulants may be contributing factors. MC3T3-E1 cells were selected to study proliferation because (a) these cells undergo a complete developmental sequence of proliferation and differentiation in vitro; and (b) we and others have shown that serial passage of these cells leads to dysfunctional proliferative activity, including decrease in the rate of cell proliferation, production of C Fos and incorporation of tritiated thymidine. Cells from passage 25-65 were used to study population doubling, cell cycle distribution, change in cell size and growth on plastic and ECM surfaces. Data are expressed as the mean±SE. Results show: (1) the proliferative potential of MC3T3-E1 cells is determined by the quality of FBS, the number of population doubling or cell passage number and ECM; (2) ECM from low passage (LP) cells fail to stimulate proliferation in LP and high passage cells (HP); (3) ECM from HP cells stimulates proliferation in both LP and HP cells; (4) Increased cell population density decreases the proliferative potential of HP cells but not LP cells; and (5) decreased proliferation of HP cells is associated with an increase in both the percentage of cells in the G2+M phase of the cell cycle and cell size. These results suggest that the decreased cell number in cultures of HP cells may be due to impaired proliferation caused by the high percentage of cells in the G2+M phase of the cell cycle and the sensitivity of HP cells to culture density.

SA205

Activation of PPARgamma Is Involved in Osteoblastic Differentiation. Y. Takeuchi[1], M. Fujita*[1], M. Suzawa*[2], K. Nakayama[1], S. Watanabe*[1], S. Kato[2], S. Fukumoto[3], T. Fujita*[1]. [1]Department of Medicine, University of Tokyo School of Medicine, Tokyo, Japan, [2]Institute of Molecular and Cellular Biosciences University of Tokyo, Tokyo, Japan, [3]Department of Laboratory Medicine, University of Tokyo School of Medicine, Tokyo, Japan.

PPARγ is an essential transcription factor for adipocytic differentiation. Osteoblasts and adipocytes derive from common mesenchymal precursor cells, and differentiation of both cells is tightly coordinated. It is shown that activation of PPARγ in common precursor cells promotes adipocytic differentiation. However, it is yet uncertain how PPARγ influences osteoblastic differentiation. The present study was undertaken to address this issue by inhibiting PPARγ actions in common precursor cells for osteoblasts and adipocytes. cDNA for dominant negative mutant of PPARγ (P467L) reported previously was constructed and cloned into pcDNA3 expression plasmid. Mouse stromal ST2 cells, which can differentiate into either osteoblasts or adipocytes, were transfected with P467L or wild type (WT) PPARγ expression plasmid. Several stable transfectants of ST2 cells were selected with G418. In the presence of a PPARγ ligand, troglitazone, the number of Oil-Red O-positive adipocytic cells was higher in WT-ST2 cells and lower in P467L-ST2 cells than that in parental ST2 cells. Alkaline phosphatase activity, an osteoblastic marker, was suppressed in WT cells compared with that in parental cells in the presence and absence of BMP-2. Unexpectedly, ALP activity was also lower in every clone of P467L cells than parental cells. In mouse osteoblastic MC3T3-E1 cells, troglitazone failed to induce adipocytic differentiation but increased ALP activity. All cells examined expressed PPARγ mRNA. These observations indicate that PPARγ activation is involved in osteoblastic differentiation, although it preferentially promotes adipogenesis in common precursor cells for adipocytes and osteoblasts. In particular, PPARγ may stimulate osteoblastic differentiation once their precursors lose potential of adipogenesis. Hence, it is suggested that PPARγ not only plays a pivotal role for adipogenesis if a set of adipogenic genes are transcriptionally responsive to PPARγ but is required for osteoblasts when adipogenic genes are inert.

SA206

See Friday Plenary number F206.

SA207

GFP Expressing Cells Are Useful Tools for Tracing the Fate of Osteoblastic Cells *in vivo*. A. Kadowaki*[1], T. Tsukazaki[1], Y. Shibata*[1], N. Yoshida*[2], A. Yamaguchi[1]. [1]Oral Pathology, Nagasaki University School of Dentistry, Nagasaki, Japan, [2]Orthodontics, Nagasaki University School of Dentistry, Nagasaki, Japan.

Mechanism of differentiation process of osteoblasts from mesenchymal stem cells remains poorly understood *in vivo*, due to lack of suitable experimental models. To establish such experimental models, we employed cell transplantation systems using GFP (Green fluorescent protein)-expressing immortalized cells, which were isolated from GFP transgenic mice (provided by Dr. Masaru Okabe). Osteoblastic cells were isolated from calvariae of newborn GFP transgenic mice. These cells were passaged until 26th, then two kinds of single cell-derived clonal cell lines (GFP-C1, GFP-C3) were established. Characterization of these cell lines was investigated *in vitro*. In addition, we transplanted these cells into back subfascia with rhBMP-2/carrier complex as well as bone defects created on diaphysis of femur in wild type mice (C57 Black6), and monitored the fate of the transplanted cells by detecting GFP fluorescence. Incubation of these cells with rhBMP-2 in culture increased alkaline phosphatase activity with a concomitant expression of mRNAs for osteocalcin and osterix by a dose- and time- dependent manner, though the expression levels of these markers in the cells without rhBMP-2 were under detectable levels. These stimulatory effects of rhBMP-2 on osteoblast phenotypes were more prominent in GFP-C3 than GFP-C1 cells. BMP-2 treatment failed to induce expression of aggrecam mRNA in these cell lines. These results indicated that GFP-C1 and GFP-C3 are osteoblast lineage cells. *In vivo* experiments demonstrated that many GFP-positive cells surrounded mineralized bones and some GFP-positive cells were embedded into mineralized bone matrices when these cell lines were transplanted with rhBMP-2/carrier complexes into back subfascia of wild type mice. Observation by serial sections clarified that GFP-positive cells surrounding mineralized bones retained alkaline phosphatase activity, indicating that the transplanted cells differentiated into osteoblasts *in vivo*. Furthermore, when these cells were transplanted into cortical bone defects, these cells also differentiated into osteoblasts and osteocytse in the newly formed cancellous bones from a relatively early stage. These results indicate that our cell lines are capable of differentiating into bone forming osteoblasts and terminally differentiated osteocytes *in vivo* without exclusion from the regenerative process in the recipient mice. Thus, our osteoblastic cell lines stably expressing GFP are useful tools for analyzing the process of osteoblast differentiation during bone formation as well as bone regeneration.

SA208

See Friday Plenary number F208.

SA209

Effects of Iridoid Glucosides on Osteoblast-like Cell Proliferation and Osteoclast Inhibition. H. Ha[1], J. Ho*[2], C. Kim[1]. [1]Korea Institute of Oriental Medicine, Seoul, Republic of Korea, [2]Graduate School of East-west Medical Sciences, Kyunghee University, Seoul, Republic of Korea.

Bone is a tissue maintaining itself through continuous osteogenesis and osteolysis by osteoblast and osteoclast, respectively. Iridoid glucosides such as geniposidic acid (GA), geniposide (GP), and aucubin (AU) were tested for analyzing their therapeutic efficacy on osteoporosis. The proliferation of osteoblast-like cells (MG-63 and Saos-2) induced by iridoid glucosides was analyzed using a tetrazolium (MTT), alkaline phosphatase (ALP) activity, and [^{3}H]-proline incorporation assays. The inhibition on osteoclast was studied using the coculture method of mouse bone marrow cells and mouse stromal cells (ST-2). As a result, the GA, GP, and AU induced cell proliferation on MG-63 (135% of control) and Saos-2 (153%, 122%, and 131% of control). The ALP activity of AU on Saos-2 was 129% of control, while GA and GP had no effect on the increase in ALP activity. The proline incorporation activities of GA on MG-63 were 120% of control, while GP and AU were not different from that of the control. In addition, GA (IC_{50}: 4.43×10^{-7} M), GP, and AU had an excellent inhibition on osteoclast. In summary, GA participates in stimulation of osteoblast to osteogenesis and suppression of osteoclast activity to inhibit osteolysis.

SA210

See Friday Plenary number F210.

SA211

Overexpression of CHOP, a Dominant-negative C/EBP, Accelerates and Enhances Osteoblastic Differentiation in Stromal Cells. R. C. Pereira, A. M. Delany, E. Canalis. Research, Saint Francis Hospital and Medical Center, Hartford, CT, USA.

CHOP, or GAPD 153 (C/EBP zeta), is a member of CCAAT/enhancer binding protein (C/EBP) family of transcription factors, which play a role in cellular proliferation and differentiation. CHOP is unlike others C/EBPs in that it cannot bind DNA; rather it heterodimerizes with C/EBP alpha and beta and serves as a dominant negative inhibitor by preventing their binding to DNA. C/EBPs alpha, beta, and delta are necessary for adipogenesis, and CHOP overexpression inhibits adipogenesis. CHOP is expressed at relatively low levels in preadipocytes but at high levels in the murine stromal cell line ST-2. Recent studies indicate that the C/EBP family of transcription factors plays a role in osteoblast differentiation. We showed that cortisol enhanced the expression of C/EBP beta and delta, and together they down regulate IGF-I transcription in osteoblasts. Conversely, bone morphogenetic protein (BMP) 2 induces osteoblastic differentiation and induces the transcription of CHOP in stromal cells. We hypothesize that CHOP expression aids in the development of the osteoblastic phenotype by antagonizing the activities of C/EBPs important in adipocyte differentiation. Therefore, we examined the role of CHOP in osteoblast differentiation by transducing ST-2 cells retrovirus overexpressing CHOP. Three separate cells lines, consisting of pooled antibiotic resistant cells, were generated and CHOP overexpression was confirmed by Northern blot analysis. Cells were cultured for up to 30 days post-confluence, in the presence or absence of BMP-2. All CHOP over expressing cell lines had higher levels of alkaline phosphatase and accelerated differentiation towards the osteoblastic pathway, as determined by the appearance of alizarin red positive mineralized nodules. This effect was intensified by treatment with BMP-2. These data indicate that CHOP overexpression stimulates osteoblast differentiation. This effect may be due to the dominant-negative effect of CHOP on other C/EBP family members, most importantly C/EBP beta and delta, which contribute to the differentiation of adipocytes.

SA212

Protein Kinase D Mediates Activation of Stress-sensitive MAP Kinases p38 and JNK Induced by Gq Protein-coupled Receptors in Osteoblast-like Cells. J. Caverzasio, J. Lemonnier*, C. Ghayor*. Division of Bone Diseases, University Hospital of Geneva, Geneva, Switzerland.

G protein-coupled receptors (GPCRs) are transducers of the anabolic effect of potent osteotropic factors such as parathyroid hormone, fluoride, prostaglandins and the recently described Wnt glycoprotein. The signaling pathways involved in activation of osteoblasts by GPCRs remains largely unknown. Recent studies reported that GPCRs can induce activation of several mitogen-activated protein kinases (MAPKs) and that the stress-sensitive MAPKs JNK and p38 are probably involved in the regulation of osteoblastic cell differentiation. In this study, we investigated the effect of PGF2alpha (PGF2a), a GqPCR agonist, on activation of MAPKs in MC3T3-E1 osteoblast-like cells and the molecular mechanism by which PGF2a induces activation of JNK and p38. PGF2a (1 microM) activated the three MAPKs Erk, JNK and p38 with different kinetics. Erk activation was rapid, maximal at 5 min and lasted about 10 min whereas activation of JNK and p38 was apparent after 15 min, maximal at one hour and lasted about 3 h. Activation of JNK and p38 but not of Erk was completely blunted by Go6976, a protein kinase C (PKC) and protein kinase D (PKD) inhibitor. PKD is a newly described diacylglycerol-sensitive protein kinase with homology to PKCs and unknown function. To determine the role of PKD in mediating activation of JNK and p38 by PGF2a, we constructed a MC3T3-E1 cell line stably expressing a PKD kinase dead mutant (K612W). In this MC3T3-E1-K612W cell line, activation of JNK and p38 induced by PGF2a was markedly impaired (80-90% inhibition) whereas cell proliferation and Erk activation were normal. Kinetic analysis of PKD activation in normal MC3T3-E1 cells indicated that PGF2a induces a rapid translocation of PKD from the cytosol to a membrane fraction wherein it becomes phosphorylated on several serine residues (p-PKD). Then p-PKD returns in the cytosol. Interestingly, the return of p-PKD in the cytosol correlated with activation of JNK and p38 by PGF2a. This return was blocked by Go6976 likely explaining the blunting effect of this compound on activation of JNK and p38 by PGF2a. In conclusion, GqPCRs in osteoblast-like cells can stimulate Erk, JNK and p38 by different mechanisms. In this study, we demonstrate for the first time that PKD mediates activation of stress-sensitive MAPKs JNK and p38 by GqPCRs in osteoblast-like cells, an observation not yet reported in mammalian cells. The molecular mechanism by which PKD activates JNK and p38 is complex. It involves the translocation of PKD from the cytosol to a membrane fraction for its phosphorylation and activation. Then, activated PKD returns in the cytosol for the stimulation of JNK and p38 pathways.

SA213

Is PKIγ Responsible for Termination of Immediate-Early Gene Expression after Induction by PTH? X. Chen*[1], J. Dai[1], S. A. Orellana*[2], E. M. Greenfield[1]. [1]Orthopaedics, Case Western Reserve University, Cleveland, OH, USA, [2]Pediatrics, Case Western Reserve University, Cleveland, OH, USA.

We have previously shown that rapid termination of immediate-early gene expression following induction by PTH is due to mechanisms that act downstream of receptor desensitization and cAMP degradation. PTH receptor desensitization was blocked with either G protein-coupled receptor kinase 2 (GRK2) antisense transfection or oligonucleotides. However, neither of these approaches increase the time courses of PKA activation, CREB/ATF-1 phosphorylation, and expression of immediate-early genes (IL-6 and *c-fos*) that occurs after induction by PTH in ROS 17/2.8 osteoblastic cells. Moreover, IBMX blocks cAMP degradation but also does not alter the time course of the downstream effects. Since forskolin (FSK) directly stimulates adenyl cyclase, we have now compared the effects of FSK and PTH on ROS 17/2.8 cells. While PTH rapidly and transiently elevates cAMP, FSK acts in a slower but sustained fashion with maximal cAMP levels observed beginning at 30 min and lasting for the 24 h duration of the experiment. Despite this sustained elevation of cAMP, FSK transiently induces the downstream effects with time courses that are indistinguishable from those induced by PTH. Similar results were also observed in osteoblastic MC3T3-E1 cells treated either with FSK or with IBMX plus PTH as well as in fibroblastic NIH3T3 cells treated either with FSK or with IBMX plus isoproterenol. These results further support our conclusion that mechanisms downstream of cAMP degradation are primarily responsible for the termination of immediate-early gene expression in ROS 17/2.8 cells and suggest that this is a general feature of cAMP signaling in mesenchymal cells. One mechanism that may explain the rapid termination of the downstream effects is inactivation of PKA and its translocation out of the nucleus by the protein kinase inhibitor (PKI) family. Consistent with this possibility, western blotting of nuclear extracts showed that the catalytic domain of PKA rapidly translocates into and out of the nucleus. Thus, nuclear levels of PKA are maximal 15-30 min after exposure to PTH and return to baseline levels by 2 h. RT-PCR assays employing positive control mRNAs from murine tissues that express each isoform and sequencing of the PCR products to confirm their identity showed that PKIγ mRNA is strongly expressed in ROS 17/2.8, MC3T3-E1, and NIH3T3 cells, while little or no mRNA encoding the other family members (PKIα and PKIβ) is expressed. These results are consistent with the possibility that PKIγ is involved in termination of PKA activation, CREB/ATF-1 phosphorylation, and expression of immediate-early genes following induction by PTH.

SA214

See Friday Plenary number F214.

SA215

Isolation, Characterization, and Functional Regulation of the CD38 (ADP-ribosyl cyclase) Gene Promoter. L. Sun, M. Lu*, X. Zhang*, E. Abe, M. Zaidi. The Mount Sinai Bone Program and Bronx VA GRECC, New York, NY, USA.

CD38 (ADP-ribosyl cyclase), an enzyme that cyclizes NAD^+ to cyclic ADP-ribose, plays a key role as an NAD^+ sensor in coupling cellular metabolism to Ca^{2+} signaling in both osteoclasts and osteoblasts (J. Cell Biol, 146: 1161, 1999; FASEB J, 16: 302, 2002). Thus, CD38 null mice display an osteopetrotic phenotype characterized by increased bone mineral density, enhanced bone strength, dramatically reduced osteoclastic resorption, and increased osteoblastic bone formation. To study the transcriptional control of the CD38 gene, we examined the regulation of its promoter by Ca^{2+}, protein kinase C (PKC) and cAMP. A 1.8 kb genomic fragment was cloned from a rabbit genomic DNA library using, as a probe, the 280 bp CD38 cDNA fragment that we had cloned previously. Primer extension analysis indicated two transcription start sites consistent with the absence of a TATA box. Sequence analysis revealed several AP-1, AP-4, myo-D, GATA, and SP-1 sequences. MC3T3.E1 cells were then transfected with the CD38 promoter ligated to the luciferase reporter gene. We constructed 9 deletion fragments all of which, except the shortest 41 bp fragment, showed significant luciferase activity. Additionally, there was a marked stimulation of basal activity in the 93 bp fragment. This fragment, containing a GC box and SP1 site, was then analyzed further for its sensitivity to Ca^{2+} (using ionomycin) and PKC (using TPA, H7, and staurosporine). Ionomycin (1 and 10 μM) potently inhibited promoter activity, while PKC activation by TPA (10 and 100 nM) was stimulatory. In contrast, H7 and staurosporine, both potent and specific PKC inhibitors, prevented transactivation of the 93 bp fragment. Notably, H7 or staurosporine did not reverse the ionomycin-induced inhibition of promoter activity suggesting that separate sequences likely mediated the opposing effects of PKC and Ca^{2+}. That the short 41 bp fragment was insensitive to both Ca^{2+} and PKC modulation indicated that the respective regulatory elements resided between –41 and –93 bp upstream of the transcription start site. Furthermore, using forskolin (100 μM), we identified two inhibitory cAMP-sensitive sequences, one between –41 and –93 bp and another between –722 and –931 bp. Finally, neither the full-length promoter nor its shorter fragments responded to interleukin-6 or interleukin-11, both of which utilize the gp130 pathway. Thus, modulation of the expression of the NAD^+-sensing enzyme, CD38, by Ca^{2+}, PKC and cAMP may contribute to the physiological coupling of the intense metabolic activities of the osteoclast and osteoblast to their respective bone-resorbing and bone-forming functions.

SA216

PTHrP Transactivates RANKL Gene through PKA and PKC Pathways on Mouse Stromal Cells. R. Kitazawa, S. Kitazawa. Division of Molecular Pathology, Department of Biomedical Informatics, Kobe University, Kobe, Japan.

Parathyroid hormone-related protein (PTHrP) is thought to act on the osteoblastic cell lineage to promote osteoclastogenesis by increasing RANKL gene expression through the PTH/PTHrP receptor. In a coculture of ST2 cells and bone marrow macrophages, PTHrP (1-34) promoted the formation of TRAP-positive multinucleated cells. Northern blotting demonstrated that PTHrP increased the expression of 2.8 kb transcripts of the mouse RANKL gene by elevating the gene transcription rate assessed by nuclear run-on studies. To identify the post-receptor mechanism conducting PTHrP signaling for RANKL gene expression, we analyzed the mouse RANKL promoter by transient transfection and electromobility shift assay (EMSA). Although the promoter lacked canonical CRE and AP-1 binding sites, a CRE-like sequence (TGAGGTCA -940) and three putative AP-1 binding sites (TGTCTCA -880, TGCCTTCA -730 and TGGCTCA -560) were located upstream of the basic promoter. ST2 cells were transfected with a series of nested deletion constructs of the promoter ligated to a luciferase gene and then treated with human PTHrP (1-34), agonists and antagonists for either PKA or PKC. When transfected with 1.0-2.3 kb constructs, 6 to12-hour treatment with PTHrP increased the promoter activity up to 180%. Forskolin, but not TPA, enhanced the promoter activity; furthermore, H89 abolished the inductive effect of PTHrP and forskolin. When the cells were transfected with a -724-luc lacking a CRE-like sequence, no effect was observed by 6 to12-hour treatment with PTHrP and forskolin. By EMSA, a CRE-like sequence (-940) showed specific binding to the nuclear extract from PTHrP-treated ST2 cells and the supershift with anti-CREB-1 and ATF-2 antibodies. Taken together, TGAGGTCA (-940) could act as a functional CRE. On the other hand, 24 to 48-hour treatment with PTHrP and TPA, but not with forskolin, showed the inductive effect on 1.0-2.3 kb constructs; calphostin C reduced the effect of PTHrP. Neither PTHrP nor TPA showed the inductive effect on -523-luc lacking AP-1 binding site-like sequences. Furthermore, two of the putative AP-1 binding sites, TGTCTCA (-880) and TGGCTCA (-560), showed specific binding to the nuclear protein; the bindings were supershifted with anti-Jun-D and -Fra-2 antibodies. No shifted band was observed with anti- c-Jun, Jun-B, c-Fos, Fos-B or Fra-1 antibodies. We therefore speculated that PTHrP promotes RANKL transcription through the PKA pathway in the early phase and through the PKC pathway (the binding of Fra-2 and Jun-D heterodimer to AP-1 sites) in the later phase.

SA217

Osteoblastic Differentiation of Human Bone Marrow Stromal Cells Is Associated with Increased Runx2/Cbfa1 Activity and Phosphorylation without a Change in mRNA or Protein Levels. C. Shui*, T. C. Spelsberg, B. L. Riggs, S. Khosla. Mayo Clinic, Rochester, MN, USA.

Runx2/Cbfa1 has been identified as a "master gene" controlling osteoblast differentiation. However, its role in inducing the osteoblast phenotype has been characterized primarily in rodent systems. Thus, we examined Runx2/Cbfa1 mRNA, protein, and activity levels during osteoblastic differentiation of human bone marrow stromal (BMSC) cells. The human BMSC cells (hMS2-15) were cultured in differentiation medium (DM) [(α-MEM medium plus 10% FBS, 10^{-8} M dexamethasone (Dex), 50 μg/ml L-ascorbate, and 10 mM β-glycerophosphate] for up to 14 days, or in DM with various doses of Dex for 7 days. Semi-quantitative RT-PCR analysis demonstrated that the expression of alkaline phosphatase and osteocalcin mRNAs increased in a time-dependent manner in these cells, and histochemical (alizerin Red-S) staining revealed extensive mineralization at day 14. Type-II Runx2/Cbfa1 mRNA was found to be constitutively expressed in hMS2-15 cells and not altered following incubation in DM; there was no detectable expression of the type-I Runx2/Cbfa1 transcript. Interestingly, despite the absence of any change in Runx2/Cbfa1 mRNA levels during osteoblastic differentiaion of these cells, the activity of Runx2/Cbfa1, as assessed by binding to the osteoblast-specific *cis*-acting element 2 (OSE2), increased markedly at all time-points examined, with the highest activity level seen at day 7. Furthermore, incubation of hMS2-15 cells with 10^{-10}-10^{-7} M Dex for 7 days increased Runx2/Cbfa1 DNA binding activity, but not mRNA levels, in a dose-dependent manner. Similar results were observed in the less differentiated human marrow-derived mesenchymal stem cells (Clonetics, Inc.) following incubation in DM for 7 days. Immunoprecipitation and Western blot analysis revealed that while there was no increase in Runx2/Cbfa1 protein levels with differentiation in hMS2-15 cells, there was an increase in Runx2/Cbfa1 phosphorylation, as detected by specific antibodies against phosphorylated threonine, tyrosine, and serine residues. We conclude that, in contrast to most rodent systems where osteoblastic differentiation is associated with clear increases in Runx2/Cbfa1 mRNA and protein levels, osteoblastic differentiation of human BMSC is associated primarily with increases in Runx2/Cbfa1 activity, without a change in mRNA or protein levels. Our findings also demonstrate that the increase in Runx2/Cbfa1 activity occurs through a post-translational mechanism involving phosphorylation of key residues.

SA218

See Friday Plenary number F218.

SA219

Morphology of the Marrow Sac in Human Bone. An Electron Microscopic Study. L. X. Bi[1], N. Ding*[2], Y. Zhang*[2], R. T. Throndson*[1], W. L. Buford*[1], E. Mainous*[1]. [1]Depts. Orthopaedics & Surgery, University of Texas Medical Branch, Galveston, TX, USA, [2]Hebei Medical University, Shijiazhuang, China.

It is well-known that endosteal osteoblasts are largely recruited from the mesenchymal cells in bone marrow. While clonal technique have shown that bone marrow stromal cells are not all equally osteogenic, those studies do not reveal the anatomical distribution and relative frequency of these populations. One would anticipate that the putatively osteogenic stromal cells would be those that lay closest to the lining of endosteal osteoblasts, and we believe that this population constitutes the sac of epitheleoid-like cells which divides the myeloid and osteoblast populations. TEM/SEM studies show the ubiquity of marrow sacs in laboratory animals, but the situation in man has never been visualized. That was the objective of the present study. Discarded tubular segments of femoral diaphyseal bone were obtained from healthy young (4- 6 yr) male and female patients undergoing femoral shortening surgeries. The specimens were examined by scanning (SEM) and transmission electron microscopy (TEM). The bone was completely covered by a hexagonally packed layer of plump osteoblasts. Their surfaces were studded with many tiny microvillar-like projections, and they displayed numerous intercellular cytoplasmic processes. No osteoclast-like cells were identified. Marrow myeloid elements were always invested in and separated from the endosteal osteoblast lining by a continuous of sac of flattened cells. In the SEM, the sac presented a very distinctive pattern of large flat overlapping auricular-like, lobulate cells which were easily distinguished from the larger populations of medullary hemopoietic cells and the endosteal osteoblasts. TEM studies showed that the marrow sac was 1 or 2 cells thick, that the cells were attenuated with elongated nuclei, and appeared to display intercellular tight junctions. The cells contained few small round mitochondria, few lysosomal bodies and filaments, and sparse rough endoplasmic reticulum. The sac cells lacked basal laminae, but concentrations of collagen fibrils were found in association with their deep medullary surfaces. We conclude that humans share with laboratory animals a broadly similar cellular organization at the bone-marrow interface, but differ interalia in the morphology of the marrow sac cells which envelop the medullary hemopoietic space.

SA220

See Friday Plenary number F220.

SA221

In Search of Blood-Borne Mesenchymal Stem Cells (MSCs) in The Peripheral Blood of Patients Following Long Bone Fractures. G. Li[1], D. Shirley*[2], G. Burke*[2], D. Marsh*[2]. [1]Department of Orthopaedic Surgery, Queen's University of Belfast, Belfast, United Kingdom, [2]Department of Orthopaedic Surgery, Queen's University Belfast, Belfast, United Kingdom.

It is well known that the MSCs reside among the bone marrow can differentiate into functional osteoblasts. The presence of primitive haematopoietic cells in adult peripheral blood has been recognized for long, but there is a controversy as to whether bone marrow MSCs can migrate through the circulation. Few recent studies have suggested the existence of rare numbers of MSCs in normal adult human peripheral blood. This study was to investigate whether the number of MSCs in the peripheral blood changes in the patients with fractures. 15 mls peripheral blood sample was taken from 8 patients (male, age 20-50) with long bone fracture at day 2-3, 5-10, and 14-20 post-fracture. One blood sample was also taken from 4 aged-matched healthy volunteers as controls. The peripheral blood mononuclear cells (PBMNCs) were isolated by centrifugation over a density gradient (1.077 g/ml, Nycomed). Half PBMNCs were immediately spanned onto glass slide and fixed, subject to immunocytochemistry (ICC) with various antibodies of osteoblast-related markers. The remaining PBMNCs were cultured in standard osteogenic medium in 8 well chamber slides. The medium was changed at day 7 and twice weekly thereafter. After 3 weeks, the cells were fixed and used for ICC examinations. The PBMNCs in about two thirds of all the blood samples from fracture patients showed the presence of positive staining for Cbfa-1, BMP-2, BMPR-I or II, Endoglin, Collagen type I, and Vimentin. There was little or no staining of these markers in the PBMNCs from the normal controls. In the fracture patients' PBMNCs culture, numerous fibroblastic cells adhered to the flasks at the first week. The greatest number of adherent cells was found in the blood samples taken at 14-20 days post-fracture. At 3 weeks, these cells were in spindle or round shapes, but did not form colonies. ICC examinations confirmed that some of these cells were positive for all the markers mentioned above, but negative for alkaline phosphatase. We did not observe any fibroblastic cell formation in the PBMNC cultures from the controls. This study has confirmed for the first time that patients with a recent fracture have an increase in the number of circulating MSCs in their peripheral blood. However, it is uncertain where these circulating MSCs come from. Further study is on the way to clarify the links between trauma stimuli and the release of MSCs in circulation. Understanding this phenomenon may provide exciting alternative methods for harvesting skeletal progenitor cells for the treatment of fracture and other skeletal diseases, such as osteoporosis.

SA222

Possible Role of Monocytes in the Retraction of Cells Covering a Bone Surface. S. Perez*[1], W. Beertsen[1], V. Everts[2]. [1]Periodontology, Academic Centre for Dentistry, Amsterdam, Netherlands, [2]Cell Biology, Academic Medical Centre, Amsterdam, Netherlands.

Prior to attachment of osteoclasts to a bone surface, cells covering this surface have to withdraw. The processes involved in this phenomenon are not clear. As a model to study how pre-osteoclasts invade a layer of cells, we added blood monocytes to confluent layers of osteoblasts or fibroblasts. Osteoblasts were isolated by sequential enzymatic digestion from rabbit calvariae, and fibroblasts were isolated from the periosteum of these bones. The cells were cultured until confluence after which isolated rabbit blood mononuclear cells were seeded on top of them. The co-cultures were maintained for up to 15 days. The cultured cells were stained for TRAP activity and the actin filament distribution pattern was visualized by FITC-conjugated phalloidin. In addition we analysed the effect of conditioned media obtained from cultured monocytes or osteoblasts. The following sequence of events was found in the co-cultures: (I) A limited number of monocytes strongly attached to the confluent layer of osteoblasts or fibroblasts (days 1-3). (II) The osteoblasts and fibroblasts then retracted, thus forming cell-free areas (day 4). (III) The monocytes invaded these areas and attached to the surface of the well (days 4-8). (IV) These attached monocytes fused and formed multinucleated TRAP-positive osteoclast-like cells (days 8-15). Osteoblast/fibroblast-free areas were only formed when monocytes were attached to the osteoblast/fibroblast cell layer. The addition of monocyte-conditioned media had no effect on this event. Conditioned media from cultured osteoblasts added to monocyte cultures, however, induced attachment of monocytes and in some instances the appearance of binuclear cells that proved to be TRAP-negative. Multinucleated cells within the cell-free areas showed a dot-like pattern of actin staining, resembling podosomes of osteoclasts. By comparing the co-cultures of osteoblasts with those of fibroblasts, we found that in the osteoblast co-cultures the cell-free areas were 3-4 times larger. Also the number of attached monocytes and multinucleated TRAP-positive cells proved to be much higher (18-fold). Our in vitro observations indicate that cell-cell interactions between monocytes and osteoblasts (or fibroblasts) result in an active retraction of the latter cells. Within the thus formed cell-free areas monocytes adhere, fuse and form osteoclast-like cells. We propose that due to specific cell-cell contacts between both cell types, yet unknown signals are transduced which activate bone-covering cells to withdraw.

SA223

See Friday Plenary number F223.

SA224

Parathyroid Hormone Activates Adhesion in Bone Marrow Stromal Precursor Cells. J. Davies*, T. J. Chambers. Dept of Cellular Pathology, St George's Hospital Medical School, London, United Kingdom.

Bone mass can be increased by parathyroid hormone (PTH), but the mechanisms underlying this phenomenon remain unknown. Osteoblasts derive from multipotential bone marrow stromal precursor cells that form colonies of fibroblastic cells (CFU-F) upon culture ex-vivo. Activation of such stromal precursors is likely to be an early event in the anabolic response of bone to PTH, and indeed induction of c-fos expression occurs in stromal cells adjacent to bone surfaces within an hour of PTH administration. We therefore tested the notion that an early component of the anabolic response of bone to PTH is the activation of CFU-F. To test this, we measured the number of CFU-F that could be extracted from bone marrow soon after administration of an anabolic dose of PTH. We found that a very early response to the administration of PTH to mice is a dramatic reduction, within 3 hrs, in the number of CFU-F that could be extracted from their bone marrow. We then tested whether PTH similarly stimulates adhesion of CFU-F in-vitro. To do this, bone marrow cells were incubated in PTH for varying times. Non-adherent cells were then removed and the adherent cells were incubated for 14 days in PTH-free medium, to assess the number of precursors of CFU-F that had adhered. We found incubation in PTH for 24 hrs caused a substantial increase in the number of CFU-F that formed. This did not seem to be mediated through a PTH-induced increase in Interleukin-6, since Interleukin 6 had no effect on CFU-F numbers when substituted for PTH. Similarly, adhesion was unaffected either by incubation in dibutyryl cyclic AMP, or by inhibitors or donors of nitric oxide. However, CFU-F formation by PTH was strongly inhibited by indomethacin. Our results suggest that a crucial component of the anabolic response of bone to PTH is the activation of previously quiescent osteoblastic precursors.

SA225

See Friday Plenary number F225.

SA226

PYK2-Mediated Signaling Is Involved in Calcitonin-Induced Sealing Zone Detachment in Resorbing Osteoclasts. J. Shyu[1], S. Chung[1], J. Wang*[1], C. Lin*[2]. [1]Biology and Anatomy, National Defense Medical Center, Taipei, Taiwan Republic of China, [2]Microbiology and Immunology, National Yang-Ming University, Taipei, Taiwan Republic of China.

Bone resorption is initiated by adhesion of osteoclasts to the bone surfaces through interactions between the integrin (avb3) and RGD-containing extracellular matrix proteins, such as vitronectin, followed by cytoskeletal rearrangement and formation of the sealing zone, which polarize the cell. Previous results have demonstrated that calcitonin treatments appeared to decrease the motility of isolated osteoclasts, resulting in retraction of the cells from their spread morphologies. It has been shown that adenyl cyclase and phospholipase C might be involved in calcitonin-mediated activities; however, detailed signaling cascades, especially those regarding osteoclast activities, are not well characterized. In the present study, we address the role played by proline-rich tyrosine kinase 2 (PYK2), a cytoplasmic kinase related to the focal adhesion kinase, as a potential effector downstream of the calcitonin pathways. Calcitonin treatments caused retraction and detachment of cultured osteoclasts from the substrates. These detachment events were accompanied by decrease of phosphorylation levels of PYK2. Our results demonstrated that PYK2 might play an important role in mediating calcitonin-induced bone remodeling.

SA227

See Friday Plenary number F227.

SA228

Regulation of the Formation of Osteoclastic Actin Rings by PYK2 Interacting With Gelsolin. W. C. Xiong*[1], Q. Wang*[2], Y. Xie*[1], Q. Du*[1], X. Wu[3], X. Feng*[1], L. Mei*[2], J. M. McDonald[1]. [1]Pathology, University of Alabama at Birmingham, Birmingham, AL, USA, [2]Neurobiology, University of Alabama at Birmingham, Birmingham, AL, USA, [3]Pathology, University fo Alabama at Birmingham, Birmingham, AL, USA.

Osteoclast activation is important for bone remodeling and is altered in multiple bone disorders. It requires cell adhesion and extensive actin cytoskeletal reorganization. Proline-rich tyrosine kinase 2 (PYK2), a major cell adhesion activated tyrosine kinase in osteoclasts, plays an important role in regulating this event. The mechanisms by which PYK2 regulates osteoclastic activation remain largely unknown. In this paper, we provide evidence that PYK2, but not its related focal adhesion kinase (FAK), interacts with gelsolin, an actin binding, severing, and capping protein essential for osteoclastic actin cytoskeletal organization. The interaction is mediated via the focal-adhesion-targeting domain of PYK2 and a LD motif in gelsolin's C-terminus. PYK2 phosphorylates gelsolin at tyrosine residues and regulates gelsolin bioactivity including increasing gelsolin binding to phosphatidylinositol lipids and decreasing gelsolin binding to actin. In addition, PYK2 activates phosphatidylinositol 4-kinase, a kinase critical for generation of phosphoatidylinositol lipids. Furthermore, PYK2 increases actin polymerization at the fibroblast cell periphery, which requires gelsolin protein. Finally, PYK2 activation is required for the formation of actin rings in osteoclasts. Taken together, our results suggest that PYK2 is a negative regulator of gelsolin's actin severing and capping activities, revealing that gelsolin is an important mediator by which PYK2 regulates osteoclastic actin cytoskeletal organization.

SA229

Osteoclasts Express Kca Channels Involved in Cell Spreading and Bone Resorption. L. G. Paret*, L. Espinosa*, C. Ojeda*, C. Chenu. Inserm Unit 403, Lyon, France.

Cell movement and spreading involve calcium-dependent processes and ionic channel activation. We previously showed that osteoclast spreading is correlated with spontaneous and oscillatory activation of a calcium-dependant potassium current (Ik_{ca}). We have now characterised the channel involved in this process and investigated its role in osteoclast activity. Rabbit osteoclasts were isolated from long bones and electric recordings were performed using patch-clamp techniques in whole cell and single channel configurations. Three different families of K_{Ca} channels have been described: big conductance channels (BK), small conductance channels (SK1, SK2, SK3) and intermediate conductance channels (IK1 = SK4). The Ik_{ca} was identified as a current generated by a channel with a unitary conductance of approximately 30 pS, within the range of SK4 channels. Pharmacological studies performed in whole cell configuration have shown a high sensitivity of Ik_{ca} to charybdotoxin (specific blocker of BK and SK4 channels), and a lower one to apamin (targeting SK channels). Specific inhibitors of BK channels, iberiotoxin and low concentrations (<5mM) of tetramethylammonium, had no effect on Ik_{ca}. Using RT-PCR analysis, we demonstrated the expression by osteoclasts of mRNA for alpha subunit (Slo) of BK channels and mRNA for SK3 and SK4 channels. The presence of SK4 was further confirmed in mouse osteoclasts and RAW 264 cells differentiated as osteoclasts under the influence of Rank Ligand. Altogether, our results are in favor of an Ik_{ca} generated by SK4 channels. However, we cannot presently exclude that osteoclasts contain nonclassical BK channels with properties modulated by beta regulatory subunits, or SK/BK chimera channels. Blockade of Ik_{ca} by charybdotoxin and apamin significantly inhibit osteoclast spreading and *in vitro* bone resorption, demonstrating a physiological role for this current in osteoclast activity. Using single channel recordings in a cell attached configuration, we showed that extracellular Ca^{2+} regulates K_{Ca} channel activation. This suggests that a Ca^{2+} influx, may be triggered by ryanodine or calcium-sensing receptors, generates a cytosolic Ca^{2+} increase which activates K_{Ca} channels. Our results clearly demonstrate the presence in osteoclasts of K_{Ca} channel, whose activation is involved in the control of membrane spreading and bone resorption, and which may be an SK4 type channel. Work is in progress to investigate the signals that induce Ik_{ca} activation and the interactions of K_{Ca} channels with proteins involved in the regulation of osteoclast spreading.

*Disclosures: **L.G. Paret**, INSERM 2.*

SA230

See Friday Plenary number F230.

SA231

Calpain Contributes to the Regulation of Osteoclast Attachment and Spreading. M. Marzia*, L. Neff, R. Baron, W. C. Horne. Orthopaedics and Cell Biology, Yale University School of Medicine, New Haven, CT, USA.

Rapid podosome assembly and disassembly is thought to be critical for the high motility of osteoclasts. Calcitonin (CT) inhibits motility, induces marked cellular retraction, and disrupts the actin ring of osteoclasts (OCs), suggesting that CT regulates at least some of the mechanisms responsible for podosome function. Calpains are Ca2+-dependent proteases that catalyse the limited cleavage of specific proteins during regulatory signaling and they are thought to promote cell spreading and locomotion by modifying adhesion sites and by facilitating rear-end detachment. CT receptor (CTR) stimulation leads to an increase in intracellular Ca2+, which might in turn activate calpains. We therefore examined whether calpains might be associated with adhesion structures in OCs and if CT might affect calpain activity. Immunofluorescence analysis of rabbit OCs showed that high levels of mu-calpain were associated with the actin ring. CT treatment induced the rapid (1-3 min) dispersion of the actin ring and the associated mu-calpain, followed soon after by cell retraction (5 min). The actin ring, again with associated mu-calpain, reappeared 20-60 min after the addition of CT. In OCs treated with the calpain inhibitor calpeptin, the actin ring was more prominent and the staining of both F-actin and mu-calpain was more intense than in untreated cells. A second inner ring of individual podosomes was also present in many of the calpeptin-treated OCs. CT still induced the loss of the actin ring in the calpeptin-treated OCs, but the recovery occurred more rapidly than in the control OCs (3-5 min). In addition, CT induced little or no retraction in the presence of calpeptin. Two known substrates of calpain, filamin A and talin were also associated with the OC actin ring, and treatment with CT induced the dispersion of both filamin and talin in parallel with that of the actin ring. The full length forms of both filamin A and talin and as well as high MW cleavage products of both proteins were detected by Western blotting of lysates of untreated OC. The cleavage products were not detected in lysates of calpeptin-treated OCs, suggesting that filamin and talin may be continuously cleaved by calpain in untreated OCs. CT treatment also transiently reduced the amounts of filamin A and talin fragments, with minimum amounts detected at 5 min and recovery to basal levels by 10-20 min. The demonstration that a calpain inhibitor blocks the cleavage of two podosome-associated proteins, filamin and talin, and affects the stability of the actin ring suggest that calpain is involved in the regulation of podosome assembly and/or disassembly. Our results also suggest that calpain contributes to the retraction of OCs in response to CT.

SA232

Dynamin- and Cbl-containing Molecular Complexes Are Present in Podosomes and Are Dissociated by Src Kinase Activation. A. Bruzzaniti, A. Sanjay, L. Neff, R. Baron. Yale University School of Medicine, New Haven, CT, USA.

Osteoclasts grown on bone or dentin develop dynamic actin-containing attachment structures known as podosomes which form the sealing zone and encircle the resorptive space. In osteoclasts derived from transgenic mice lacking c-Src or Pyk2, podosome ring formation is completely abolished, osteoclast migration is inhibited, and the mice exhibit an osteopetrotic phenotype. Following engagement of the vitronectin receptor, the adaptor protein Cbl forms a trimolecular complex with the non-receptor tyrosine kinases Src and Pyk2, and signaling from this complex plays a role in osteoclast attachment and motility. Directly relevant to osteoclasts, a functional link between Src activation, dynamin and the actin cytoskeleton at podosomes was previously demonstrated in BHK cells transformed with v-Src, strongly suggesting a role for dynamin in signaling downstream of integrins. In addition, since dynamin is a multi-domain protein essential for endocytosis and membrane remodeling, it may play a role in osteoclast resorption and in the formation of the ruffled border where endocytosis is a key functional event. In this study, we established that dynamin constitutively participates in functional complexes with Cbl in osteoclasts and when over-expressed in HEK-293 cells stably expressing the vitronectin receptor. Using GST-purified proteins we further show that the proline-rich domain (PRD) of dynamin and the C-terminal domain of c-Cbl, most likely its PRD or acidic domain, are necessary for the two proteins to co-immunoprecipitate in the same molecular complex. Interestingly, while over-expression of activated Src led to the tyrosine phosphorylation of both dynamin and Cbl, Src kinase activity had a dominant negative effect on dynamin-Cbl complex formation. In support of this, dynamin-Cbl association was enhanced following treatment with PP1 (a Src family kinase inhibitor), genistein (a non-specific kinase inhibitor), or by over-expression of a kinase dead c-Src mutant (K295M). The disruptive effects of Src kinase activity on dynamin-Cbl association were abrogated when the known Src SH3 binding site in Cbl was mutated. Thus, phosphorylation of Cbl by Src destabilizes Cbl's association with dynamin, most likely via a similar mechanism to that proposed for the association of UbcH7 with Cbl (Yokouchi et al., JBC, 274:31707, 1999). We propose that dynamin and Cbl coordinately participate in a process that regulates podosome turnover and, thereby, cell motility.

SA233

Thyroid Hormones and Vitamine D Coordinately Stimulate Osteoclast Formation Through RANKL Induction. M. Miura*[1], Y. Komatsu[1], K. Tanaka[2], M. Suda*[1], A. Ozasa*[1], K. Nakao*[1]. [1]Medicine and Clinical Science, Kyoto University Graduate Shool of Medicine, Kyoto, Japan, [2]Nutirition Science, Koshien University, Takarazuka, Japan.

Thyroid hormones enhance osteoclast formation and their excess is an important cause of secondary osteoporosis. Using the northern blot analysis, 3,5,3'-Triiodo-L-thyronine (T3) (10^{-8}-10^{-5} M) induced mRNA expression of receptor activator of nuclear factor-kappa B ligand (RANKL), which is a key molecule in osteoclast formation, in primary osteoblastic cells (POB). RANKLmRNA expression was 1.3-1.8 times higher after 24 hours and 2.5-3.0 times higher after 48 hours than the basal expression. In contrast, the mRNA expressions of OPG and M-CSF were unaltered with T3. This effect was amplified in the co-presence of 10^{-8} M of 1-alpha, 25-dihydroxyvitamin D_3 (1,25(OH) $_2D_3$). Although T3 alone did not induce osteoclasts in coculture of bone marrow cells with POB, T3 enhanced 1,25(OH) $_2D_3$-induced osteoclast formation, detected as TRAP-positive multinuclear cells. Thyroxine (T4) (10^{-7}-10^{-5} M) also enhanced 1,25(OH) $_2D_3$-induced osteoclast formation. These data suggested that T4 was locally metabolized to T3 for its action, since T4 was a prohormone with little hormonal activity. Northern blot analysis revealed that the mRNA expression of type-2 iodothyronine deiodinase (D2), which is responsible for maintaining local T3 concentration, was induced by 1,25(OH) $_2D_3$ (10^{-9}-10^{-7} M) dose- and time-dependently until 48 hours in POB and ST2 cells, although the mRNA expression of D2 was undetectable at basal condition. Treatment with 1,25(OH) $_2D_3$ did not show any obvious change in the mRNA expression of ALP. The mRNA expression of D2 was negligible after stimulation by other bone-resorbing cytokines, TNF-alpha or IL-1alpha. Either stimulation of Bt^2cAMP or PTH did not induce the mRNA expression of D2. As treatment with 10 microgram/ml of cycloheximide attenuated the induction of D2 by 1,25(OH) $_2D_3$, this induction mechanism may require de novo synthesis of transacting regulatory proteins. Our data would facilitate our understanding of the mechanism of osteoclast formation by thyroid hormones and suggest a novel interaction between thyroid hormones and 1,25(OH) $_2D_3$.

SA234

See Friday Plenary number F234.

SA235

Contribution of Terminal Prostaglandin E_2 Synthase (PGES) to Bone Resorption. M. Saegusa[1], M. Murakami*[2], K. Matsuda*[1], K. Nakamura[1], I. Kudo*[2], H. Kawaguchi[1]. [1]Orthopaedic Surgery, Univ. of Tokyo, Tokyo, Japan, [2]Showa Univ., Tokyo, Japan.

Prostaglandins (PGs) are potent regulators of bone metabolism. Among the prostanoids that are known to be produced in bone, PGE_2, $PGF_{2\alpha}$, PGI_2 and thromboxane B_2, we confirmed that only PGE_2 has the potency to stimulate osteoclastogenesis and resorbed pit formation on a dentine slice in the coculture of mouse marrow cells and osteoblasts. The major enzymes in the synthesis of PGE_2 are phospholipase A_2, cyclooxygenase-1 or -2 (COX-1, -2), and PGE_2 synthase (PGES) which is the terminal and specific enzyme for PGE_2 biosynthesis. We and another group recently identified two isoforms of PGES, cytosolic PGES (cPGES) and membrane-associated PGES (mPGES). Cotransfection of cPGES and mPGES with COX-1 and COX-2 into HEK293 cells indicated that cPGES was functionally coupled with COX-1 and mPGES was coupled with COX-2 for PGE_2 biosynthesis. Both cPGES and mPGES were shown to be expressed in mouse long bones *in vivo* and cultured primary osteoblasts from mouse calvariae by RT-PCR. In cultured mouse primary osteoblasts, Northern and Western blot analyses revealed that both mPGES and COX-2 were induced by bone resorptive cytokines such as IL-1α, TNF-α and FGF-2. Induction of the mPGES mRNA level peaked at 3-6 h and decreased thereafter, while the maximal protein level was seen at 12 h and maintained up to 48 h. These were later than the COX-2 induction that was transiently seen from 1 to 6 h. mPGES and COX-2 mRNA levels were also shown by RT-PCR/Southern blotting to be induced in mouse long bone and bone marrow *in vivo* by intraperitoneal injection of lipopolysaccharide (0.5-5 mg/kg) dose dependently with maximal effects at 3 h. cPGES and COX-1, however, were expressed constitutively both *in vitro* and *in vivo* without being affected by these stimuli. To determine the contribution of mPGES to bone resorption, we treated coculture of mouse marrow cells and osteoblasts with an antisense oligonucleotide that was confirmed to block mPGES expression. The antisense oligonucleotide not only blocked PGE_2 production measured by ELISA, but also 80-90% reduced osteoclastogenesis and pit formation stimulated by bone resorptive cytokines, while the control oligonucleotide had no effect. Addition of exogenous PGE_2 reversed the inhibition. In conclusion, since mPGES is induced by and mediates effects of bone resorptive stimuli, it may play an important role in physiological and pathological bone resorption. Unlike NSAIDs which inhibit COX activity and suppress not only PGE_2 but also other essential PGs maintaining physiological homeostasis, an inhibitor of this PGE_2 specific enzyme, mPGES, could be a highly selective treatment for bone resorptive diseases with low side effects.

SA236

See Friday Plenary number F236.

SA237

Effects of TNF Alpha on Osteoblasts and Osteoclasts. S. Wada*, S. Suda*, M. Kogawa*, S. Kitahama*, S. Yasuda*, M. Iitaka*, S. Katayama*. Internal Medicine IV, Saitama Medical School, Iruma-gun, Japan.

Recent epidemiological surveys have revealed that diabetes is a risk factor for fractures. This mechanism would be associated with various factors accompanied by diabetes (e.g., insulin deficiency or resistance and/or continuous hyperglycemia). We, therefore, studied the effects of high glucose and TNF alpha on osteoblasts (OBs) and osteoclasts (OCs); TNF alpha has been shown to be a key factor responsible for insulin resistance. The high glucose concentrations (60 mM) did not affect alkaline phosphatase (ALP) activity in mouse primary OBs, whereas treatment with TNF alpha significantly decreased ALP activity and bone formation assessed by von-Kossa staining. Flow cytometric analysis using fluorescein labelled Annexin V revealed that treatment with TNF alpha increased the number of apoptotic OBs but not OC progenitors. When mouse OBs and bone marrow cells were cultured in the presence of PGE2 and 1,25(OH)2D3, OCs were formed under high glucose concentrations (5.6-60 mM), while TNF alpha attenuated PGE2- and 1,25(OH)2D3-stimulated OC formation in the co-cultures. Since this effect was inhibited by antibody against TNF alpha receptor (p55), it seemed that TNF alpha acted on the type 1 receptor. When mature OCs were studied on bone resorbing function, it was found that bone resorption was inhibited by exposure to high glucose (15-60 mM). TNF alpha also inhibited bone resorbing capacity. The effects of decreased bone resorption were, at least partly, due to the deranged actin ring formation of OCs. Although OCs formation and function were modified, treatment with high glucose and TNF alpha did not influence the expression of RANKL and OPG in OBs nor the expression of RANK in OC progenitors. These results indicate that the functions of OBs and OCs could be modified by the factors associated with diabetes. This study suggests that multiple factors or cytokines produced in the microenviroment of bone could affect the cellular function of OBs and OCs, which would be related, to some extent, to low turnover of bone observed in diabetes.

SA238

Transgenic Mice Overexpressing Soluble RANKL Exhibit Severe Osteoporosis. H. Yasuda[1], A. Mizuno*[2], T. Kannno*[3], M. Hoshi*[4], O. Shibata*[5], K. Yano*[6], N. Fujise*[7], M. Kinosaki*[8], K. Yamaguchi*[5], E. Tsuda*[6], A. Murakami*[5], K. Higashio*[9]. [1]Institute of Medical Science, Univ. of Tokyo, Tokyo, Japan, [2]Department of Pharmacology,, Jichi Medical School, Tochigi, Japan, [3]Mitsubishi Chemical Safety Institute, Ibaraki, Japan, [4]Iwate Pharmaceutical Plant, Snow Brand Milk Products, Iwate, Japan, [5]Proteome Research Laboratory, Daiichi Pharmaceutical, Tochigi, Japan, [6]Biological Research Laboratories, Sankyo, Tokyo, Japan, [7]Pharmaceutical Division, Snow Brand Milk Products, Saitama, Japan, [8]Pharmaceutical Technology Laboratory, Chugai Pharmaceutical, Shizuoka, Japan, [9]Research Center for Genomic Medicine, Saitama Medical School, Saitama, Japan.

Osteoclast differentiation factor, RANKL, also called ODF, TRANCE, or OPGL, is a key molecule for osteoclast differentiation and activation, and is thought to act as a membrane-associated molecule in bone remodeling. Recent study suggested that soluble RANKL (sRANKL) released from T cell has also some roles in bone resorption. To investigate the physiological and pathological function of sRANKL, we generated two types of transgenic mice overexpressing sRANKL. Mice overexpressing sRANKL ubiquitously from the early developmental stage died at the late fetal stage. Another type of mice, expressing sRANKL only in the liver after birth, grew to be matured with normal body size and weight. However, they exhibited a marked decrease in bone mineral density with aging compared with the non-transgenic littermates. In addition, strength of their femurs was extremely lowered. Histological analysis showed that the trabecular bone mas was decreased at 6 weeks old and was sparse at only 3-4 months old. The number of osteoclasts was significantly increased, while the number of osteoblasts was not altered on the surface of young trabecular bone. These results indicate that excessive production of sRANKL causes osteoporosis by accelerated osteoclastogenesis. The transgenic mouse overexpressing sRANKL in the liver would serve as a useful animal model for studying bone remodeling and evaluating therapeutic agents for osteoporosis.

SA239

See Friday Plenary number F239.

SA240

Transcriptional Program of Mouse Osteoclast Differentiation Governed by the Macrophage Colony-Stimulating Factor and the Ligand for the Receptor Activator of NF{kappa}B. D. Cappellen*[1], N. Luong-Nguyen*[1], S. Bongiovanni*[2], O. Grenet*[2], C. Wanke*[2], M. M. Susa[1]. [1]Arthritis and Bone Metabolism Therapeutic Area, Novartis Pharma Research, Basel, Switzerland, [2]Pharmacogenomics Area, Novartis Pharma Development, Basel, Switzerland.

Cytokines macrophage colony stimulating factor (M-CSF) and the receptor activator of NF{kappa}B ligand (RANKL) induce differentiation of bone marrow hematopoietic precursor cells into bone-resorbing osteoclasts without the requirement for stromal cells of mesenchymal origin. We used this recently described mouse cell system and oligonucleotide microarrays representing about 9,400 different genes to analyze gene expression in hematopoietic cells undergoing differentiation to osteoclasts. The ability of microarrays to detect the genes of interest was validated by showing expression and expected regulation of several osteoclast marker genes. In total 750 known transcripts were up-regulated by more than 2-fold, and 91% of them at an early time in culture, suggesting that almost whole differentiation program is defined already in pre-osteoclasts. As expected, M-CSF alone induced the receptor for RANKL (RANK), but also, unexpectedly, other RANK/NF{kappa}B pathway components (TRAF2A, PI3-kinase, MEKK3, RIPK1), providing a molecular explanation for the synergy of M-CSF and RANKL. Furthermore, interleukins, interferons and their receptors (IL-1{alpha}, IL-18, IFN-{beta}, IL-11R{alpha}2, IL-6/11R gp130, IFN{gamma}R) were induced by M-CSF. Although interleukins are thought to regulate osteoclasts via modulation of M-CSF and RANKL expression in stromal cells, we showed that a mix of IL-1, IL-6, and IL-11 directly increased the activity of osteoclasts by 8.5-fold. RANKL induced about 70 novel target genes, including chemokines and growth factors (RANTES, PDGF{alpha}, IGF1), histamine and {alpha}1A-adrenergic receptors, and three waves of distinct receptors, transcription factors and signaling molecules. In conclusion, M-CSF induced genes necessary for a direct response to RANKL and interleukins, while RANKL directed a three-stage differentiation program and induced genes for interaction with osteoblasts, and immune and nerve cells. Thus, global gene expression suggests a more dynamic role of osteoclasts in bone physiology than previously anticipated.

Disclosures: ***M.M. Susa****, Novartis Pharma Research 1, 3.*

SA241

See Friday Plenary number F241.

SA242

Carbohydrate Binding Specificity of Osteoclast Inhibitory Lectin. C. Gange*[1], V. Kartsogiannis[2], H. Zhou[2], J. M. W. Quinn[1], M. T. Gillespie[1], K. W. Ng[2]. [1]St. Vincent's Institute of Medical Research, Fitzroy, Australia, [2]Department of Medicine, The University of Melbourne, St. Vincent's Hospital, Fitzroy, Australia.

Osteoclast Inhibitory Lectin (OCIL) is a predicted type II membrane-bound molecule of 207aa containing a C-lectin domain in its extracellular domain which shows structural homology with the type II transmembrane proteins of natural killer (NK) cell receptor group of the C-type lectin super-family. Recombinant protein to the extracellular domain of murine OCIL (mOCIL) inhibits osteoclast formation in vitro. mOCIL, like the NK cell receptors (e.g. Ly49A/C and CD69), does not contain conserved residues for calcium binding however, we report here that mOCIL does exhibit calcium-independent carbohydrate binding with specificity for high molecular weight sulfated sugars. mOCIL bound to high molecular weight sulfated glycosaminoglycans (GAGs) with binding to carrageenan being 3 fold greater than dextran sulfate and 2.3 fold greater than fucoidan. Dose-dependent binding was observed showing saturation at 25ng mOCIL per pmol fucoidan. No significant binding was seen for unsulfated dextran, suggesting that the presence of anionic sulfate groups was important for interaction. Independence of anionic charge alone was observed, since mOCIL did not bind to hyaluronic acid. The low molecular weight sulfated GAGs, chondroitin sulfate A, chondroitin sulfate C, dermatan sulfate, heparan sulfate, heparin, and keratan sulfate showed no specific affinity for mOCIL, while only weak interactions were observed for some monosaccharides. This is consistent with the sugar binding specificity for Ly49A/C and CD69. mOCIL inhibited osteoclast formation in murine bone marrow macrophage precursor (BMMP) cells cultured with M-CSF and RANKL. In BMMPs treated with fucosidase (to remove terminal fucose residues) osteoclast formation was enhanced. mOCIL inhibition of osteoclast formation from such fucosidase treatment was reduced to approximately 50%. In BMMPs treated with neuraminidase as a control (to remove sialic acid residues), the inhibitory action of mOCIL was not ablated and complete inhibition was noted, suggesting that this inhibitory action may be mediated by specific sugar binding. In summary, mOCIL exhibited binding to high molecular weight GAGs that contain anionic sulfate groups. Fucosidase treatment of BMMP cells partially ablated subsequent mOCIL inhibitory action on osteoclast formation, suggesting a role for specific sugar binding in mOCIL inhibition of osteoclastogenesis.

Disclosures: ***H. Zhou****, Pfizer Global Research and Development 2.*

SA243

See Friday Plenary number F243.

SA244

Implication of Cyclooxygenase-2 in Human Osteoclast Differentiation. M. Lora*, R. Samadfam*, S. I. Briand*, A. J. De-Brum Fernandes. Rheumatic Diseases Unit, Université de Sherbrooke, Sherbrooke, PQ, Canada.

We have developed a model of osteoclastogenesis from marrow obtained from human fetal liver that does not require glucocorticoïds, $1,25(OH)_2$ vitamin D_3 or support cells, as other models described in the literature. This model is therefore ideal for studying the roles of cyclooxygenases (COX) in osteoclast development. By determining the number of tartrate resistant acid phosphatase (TRAP) colored cells in the preparation ($TRAP^+$ cells/field of view, corresponding to the surface of a circle of 1 mm diameter), we observed that the inhibition of both COX by indomethacin (100 µM, 58.2 ± 6.2) or ibuprofen (100 µM, 54.1 ± 3.0) as well as the inhibition of COX-2 by DFU (100 nM, 54.5 ± 5.6) or NS-398 (100 nM, 53.0 ± 1.8) doubled the number of $TRAP^+$ cells in our culture when compared to the control (29.6 ± 1.5). The COX-1 specific inhibitor valeryl salicylate (100 µM) had no effect on $TRAP^+$ cell counts when compared to control. Furthermore, we have demonstrated that anti-OPG antibody increased the number of $TRAP^+$ cells just as well as indomethacin (CTRL 17.4 ± 1.8, Indo 30.6 ± 2.5 and anti-OPG 26.4 ± 3.3 $TRAP^+$ cells/field of view). We now know that the RANKL-OPG-RANK system is implicated in our model. We therefore investigated the possibility that the inhibition of COX-2 blocked OPG accumulation in the supernatant which might be responsible for the increase of $TRAP^+$ cells when COX-2 is inhibited. With a sandwich ELISA technique, we have shown that COX-2 inhibition by either NS-398 (100 nM) or indomethacin (100 uM) decrease OPG accumulation in the supernatant and this effect could be reverse by adding exogenous prostaglandins. These results suggests that prostaglandins produced by COX-2 are implicated in osteoclastogenesis (TRAP decrease) and that prostaglandins produced by COX-1 do not seem important for this phenomenon. We can therefore conclude that the prostaglandins produced by COX-2 activity are osteoclastogenesis inhibitors in our system. Pinpoint pharmacological intervention with specific inhibitors of COX may be important elements in understanding and eventually controlling osteoclast differentiation.

SA245

Inhibition of Tumor-Induced Osteolysis by Minodronic Acid (YM529) in Nude Mice with Bone Metastases. K. Shibasaki*, S. Tanaka*, N. Katou*, H. Yuyama*, H. Koutoku*, K. Miyata*. Institute for Drug Discovery Research, Yamanouchi Pharmaceutical Co., Ltd., Tsukuba, Ibaraki, Japan.

The effects of minodronic acid (YM529) on osteolysis due to bone metastases of breast cancer were investigated and compared with other bisphosphonates. Metastases were induced by intracardiac injection of the human breast cancer cell line MDA231 into BALB/c nu/nu mice. Test compounds were intravenously given to mice after osteolytic metastases were radiologically defined. Histological examination confirmed that numerous

TRAPase-positive (osteoclastic) cells appeared on the bone surface near the tumor in the breast cancer metastases model. Intravenous administration of minodronic acid or zoledronic acid reduced the number of osteoclasts and the ratio of osteoclast surface to bone surface at each tumor site in a dose dependent manner. The effects of these two compounds were statistically significant at doses of 0.1 mg/kg i.v. In contrast, a dose of 10 mg/kg i.v. was necessary for pamidronate, a currently available bisphosphonate, to cause a significant decrease in the number of osteoclasts and the ratio of osteoclast surface to bone surface. In conclusion, minodronic acid inhibited osteolysis caused by bone metastases of MDA231 cells. Consequently, minodronic acid holds promise as an intravenous treatment for bone lesions arising from metastases of breast cancer to bone. In this model, minodronic acid has the same potency as zoledronic acid and is more potent than pamidronate.

SA246

See Friday Plenary number F246.

SA247

The Promotion Effects Of Sodium Fluoride On Osteoclast Apoptosis Of Adult Intact And Ovariectomized Wistar Rats*. Y. Li[1], Y. Sun[1], F. Yang[1], M. zhu[2], B. Lu[2], M. Qiu*[2]. [1]Biology, Institute of Radiation Medicine, Chinese Academy of Medical Sciences, Tianjin, China, [2]Endocrinilogy, Tianjin Medical University, Tianjin, China.

Fluoride has been shown to increase bone density, possible by reduce the solubility of hydroxyapatite crystals, though the mechanism for this remains unclear. Bone density reflects the comparative rates of osteoclast-mediated bone resorption (bone mineral loss) and osteoblast-mediated new bone formation. The mechanism by which sodium fluoride (NaF) modulates osteoclastic bone resorption also remains unclear. Purpose It has been built a method of osteoclast culture and observation of its' apoptosis in vitro in order to unveil the mechanisms of endemic fluorosis and osteoporosis treatment by fluoride on cellular level. Method Intact and ovariectomized (OVX) rats drank 5mg/L or 15mg/L NaF water desirably. It has been carried out the investigations of osteoclast-like cell (OLC) formation and its' apoptosis in vitro of adult rat modulation by fluoride administrated in vivo and the effects of 5, 10, 15mg/L NaF in culture media on OLC formation and its' apoptosis in vitro. Results [1] The number of OLC in OVX rats was found to be increased, compared to intact rats, two weeks after OVX and still present 6 months after OVX. [2] Both 5 and 15mg/L NaF inhibit intact and OVX rats OLC formation in vitro after fluoride administration of 5 months although the inhibition effect of 5mg/L group was less than latter. However, the inhibition effect of 15mg/L group was obviously even from 2 months after NaF administration. [3] 2 weeks after NaF administration, Fluoride could promote OVX rat OLC apoptosis. From 2nd month after NaF administration both 5 and 15mg/L NaF could promote intact and OVX rat OLC apoptosis. The promotion effects were getting stronger with the time and 15mg/L group's was stronger than that of 5mg/L group. [4] The effects of 5, 10, 15mg/L NaF in culture media on OLC formation inhibition and its' apoptosis promotion were dose-dependent. Conclusion The evidence presented in this paper may explain the reason that the observed reduction in osteoclast numbers is sodium fluoride reduce osteoclast formation and induce its apoptosis.

*This work was supported by NSFC (39770668, 30070828)

SA248

See Friday Plenary number F248.

SA249

See Friday Plenary number F249.

SA250

A TNF-α Peptide-antagonist W9 Inhibits the Soluble RANKL-induced Osteoclastogenesis Stronger Than that Induced by Membrane-bound RANKL. Y. Suzuki*[1], K. Aoki[2], I. Ishikawa*[1], K. Ohya[2]. [1]Section of Periodontology, Department of Hard tissue Engineering, Graduate school, Tokyo Medical and Dental University, Tokyo, Japan, [2]Section of Pharmacology, Department of Hard tissue Engineering, Graduate school, Tokyo Medical and Dental University, Tokyo, Japan.

Therapeutic peptidomimetics that interfere with the TNF/TNF receptor(I) interaction have been developed based on atomic structures deduced from the crystal structures of TNF-α and the TNF-β/TNF receptor(I) complex (Nature Biotechnology 15: 1266-1270, 1997). The cyclized peptidomimetic WP9QY (Tyr-Cys-Trp-Ser-Gln-Tyr-Leu-Cys-Tyr) which engineered to mimic the most critical TNF-α recognition site on the TNF receptor(I) efficiently antagonized the effects of TNF-α binding to the TNF receptor(I). We have already given a presentation at the 21st annual meeting that this TNF-α peptide-antagonist blocks vitamineD_3/PGE_2- and soluble RANKL(sRANKL) - induced osteoclastogenesis *in vitro* (J. Bone Miner. Res. 14: S178, 1999). Recently it was reported that the sRANKL derived from activated T cells might induce osteoclastogenesis under the inflammatory condition. On the other hand, it has already known that vitamin D_3 and PGE_2 iuduce osteoclastogenesis via the trimeric membrane-bound RANKL on osteoblasts, that is supposed to be relevant for the physiological bone resorption. These raised the question whether the inhibitory effect of W9 might be different depending on the stimulants for inducing osteoclasts. To address this question, we performed a standard co-culture experiment using bone marrow cells from ICR mice and primary osteoblasts isolated from calvaria comparing the bone marrow culture stimulated by sRANKL and macrophage-colony stimulating factor. We found that W9 inhibited the sRANKL-induced osteoclastogenesis stronger than that induced by vitamin D_3 and PGE_2. These results suggest that W9 could inhibit the T cell-mediated bone resorption more than the physiological bone resorption which contributes a normal remodeling cycle.

SA251

The Mechanism Of Inhibition Of Farnesyl Diphosphate Synthase By Nitrogen-Containing Bisphosphonates. J. E. Dunford*[1], F. H. Ebetino*[2], M. J. Rogers[1]. [1]Medicine and Therapeutics, University of Aberdeen, Aberdeen, United Kingdom, [2]Procter & Gamble Pharmaceuticals, Mason, OH, USA.

We and others have recently shown that farnesyl diphosphate synthase (FPP synthase), an enzyme of the mevalonate pathway, is the major molecular target of nitrogen-containing bisphosphonates such as risedronate (RIS). FPP synthase catalyses the condensation IPP and DMAPP to form GPP, then the condensation of GPP with IPP to form FPP. The exact mechanism by which bisphosphonates inhibit FPP synthase are unknown, although the enzyme has 2 binding sites for isoprenoid lipids (IPP and either DMAPP or GPP). Using recombinant human FPP synthase in vitro, we have investigated the mechanism for inhibition of the formation of FPP from GPP+IPP. Enzyme kinetic analysis showed that low concentrations of RIS (<75nM) caused uncompetitive inhibition with IPP but competitive inhibition with GPP, suggesting that RIS binds to the GPP binding site, but also influences the binding of IPP at the other site. At higher concentrations of RIS (>75nM), the inhibition was partially competitive with IPP and noncompetitive with GPP, suggesting that RIS does also bind to the IPP binding site. Further kinetic analysis suggested that more than one molecule of RIS binds to the enzyme, and that this binding occurs in a cooperative manner. We therefore propose that RIS inhibits FPP synthase by binding at the GPP binding site of the enzyme. This then facilitates the binding of RIS at the IPP binding site. The potency for inhibiting FPP synthase may therefore depend on the affinity of the enzyme for the bisphosphonate and the ability of the bisphosphonate to bind to both substrate binding sites in a cooperative manner.

*Disclosures: **J.E. Dunford**, Procter and Gamble Pharmaceuticals 2.*

SA252

See Friday Plenary number F252.

SA253

Effects of Membrane Potential on Acid-extrusion via Proton-translocating Subunit (c) of a Vacuolar Type H+-ATPase from Murine Osteoclasts. H. Sakai[1], H. Mori*[2], H. Morihata*[2], J. Kawawaki*[3], A. Shioi[4], M. Kuno[2]. [1]Orthopedic Surgery, Osaka City University, Osaka, Japan, [2]Department of Physiology, Osaka City University, Osaka, Japan, [3]Central Laboratory, Osaka City University, Osaka, Japan, [4]Cardiovascular Medicine, Osaka City University, Osaka, Japan.

A vacuolar type H+-ATPase (V-ATPase) enriched in the ruffled membrane of osteoclasts is a principal H+ secreting mechanism responsible for bone resorption. Although the molecular basis for the V-ATPase is revealed, mechanisms regulating the H+ transport in osteoclasts are yet to be defined well. The membrane potential of osteoclasts could switch between two levels, that is, around –60 and 0 mV. Considering that V-ATP is an electrogenic pump, the acid secretion may be affected by the membrane potential. V-ATPase possesses a trans-membrane domain that contains subunit c (16 kDa) for H+ translocation and subunit a3 (116 kDa) required for localization. In this study, we investigated how the membrane potential affected H+ transport with the two subunits in COS 7 cells transfected with cDNAs encoding the genes. The PCR products of subunit c and a3 were subcloned into pcDNA3.1(+) expression vector and used to transfect COS7 cells. Intracellular pH (pHi) in transformed cells was measured by a co-expressed, pH-dependent marker, GFP. Single-cell RT-PCR analysis confirmed that more than 90% of the GFP-expressing cells overexpressed subunit c and/or subunit a3. Confocal microscopy revealed that the chimeric protein subunit c-GFP and/or subunit a3-RFP (Ds-red) were localized in the cellular and subcellular membranes. In the Na+-free, high-K+ solution, pHi recovered from acid-load induced by washings of NH4Cl in cells transfected with subunit c cDNA, although not in non-transfected cells. The pHi recovery was also brisk even in the Na+- and K+-free solution containing 50 mM TEA-Cl, a K+ channel blocker that could depolarize cells. This pHi recovery was not enhanced by co-transfection with subunit a3 and was not induced in cells transfected with subunit a3 only, suggesting that subunit c, but not subunit a3, was responsible for the depolarization-dependent pHi recovery. Transfection with cDNA for either subunit c or a3 did not alter the resting pHi in the standard extracellular solution. The Na+-independent pHi recovery was not inhibited by bafilomycin A1 (200 nM) in cells transfected with subunit a3 and c. These results suggest that H+ extrusion via subunit c is enhanced by membrane depolarization, which would modify bone-resorbing functions of osteoclasts under different membrane potentials.

SA254

See Friday Plenary number F254.

SA255

Molecular Modeling of the Bisphosphonates (BPs) in Farnesyl Diphosphate (FPP) Synthase. Proposed New Mechanism of Inhibition by Potent Nitrogen Containing Bisphosphonates (NBPs). F. H. Ebetino[1], M. Rogers*[1], J. Dunford*[1], X. Liu*[1], R. Phipps*[1], R. G. G. Russell*[2], G. Mieling*[1], B. Barnett*[1]. [1]Procter & Gamble Pharmaceuticals, Mason, OH, USA, [2]Oxford University, Oxford, United Kingdom.

Although BPs have been successfully utilized clinically for a number of years, only recently has our understanding of the exact antiresorptive mechanism of action of these agents developed. FPP synthase has been shown to be the key biochemical target for the nitrogen containing (N-BPs). To provide improved opportunities for drug design in this field, and to offer clinicians more insight into the potential differences among members of this drug class, we have continued to study the precise chemical and biochemical mechanisms of action of BPs. Minor changes in the side chains of these compounds result in varying potency for FPP synthase inhibition and antiresorptive activity, which suggests that N-BPs interact with their target via a stereochemical recognition event. The relative potency for inhibiting FPP synthase correlates with the known acute *in vivo* potencies of BPs (zoledronate > risedronate > alendronate > pamidronate). These potential interactions in the enzyme can be visualized via molecular modeling techniques, therefore we can now examine the inhibitory interactions that may take place within this enzyme in order to explain exactly how the structure of N-BPs relates to potency. For example, Martin *et al* recently proposed that BPs may inhibit FPP synthase by acting as transition state analogues at the geranyl diphosphate (GPP) binding site. On close analysis of active and inactive structurally-related pairs of BPs, we propose a potentially more specific inhibition due to binding at a predicted isopentenyl diphosphate (IPP) binding site in the enzyme. Docking potent N-BPs such as risedronate in the IPP binding site enables the nitrogen of the N-BP to form a salt bridge with either the diphosphate of GPP or with a N-BP in the GPP site. In the putative IPP binding site, the conformationally restricted, potent N-BP NE-58025 (IC_{50}=110nM, rhFPP) appears to bind in a similar manner to risedronate, whereas the inactive, conformationally-restricted N-BP NE-58086 (IC_{50}=3850nM) is unable to form the salt bridge. In the IPP site, zoledronate appears to form two salt bridge interactions at the imidazole nitrogen, thus explaining its enhanced IC_{50} vs. other N-BPs, whereas alendronate displays greater solvent (water) accessible surface, potentially explaining its lower propensity for FPP synthase inhibition. Work continues to further validate these hypotheses, utilizing enzyme purification and crystallography, but many of the intricacies of the mechanism of action of N-BPs are now becoming clear.

Disclosures: ***F.H. Ebetino****, Procter & Gamble Pharmaceuticals 3.*

SA256

See Friday Plenary number F256.

SA257

A TNF-α-Related Peptide Inhibits Both Bone Resorption and Inflammation in Collagen-Induced Arthritis. T. Kojima*[1], K. Aoki[2], K. Nonaka[2], R. Murali*[3], M. I. Greene*[3], T. Amagasa*[1], K. Ohya[2], W. C. Horne[4], R. Baron[4]. [1]Section of Maxillofacial Surgery, Tokyo Medical and Dental University, Tokyo, Japan, [2]Pharmacology, Tokyo Medical and Dental University, Tokyo, Japan, [3]University of Pennsylvania, Philadelphia, PA, USA, [4]Yale University, New Haven, CT, USA.

The peptidomimetic WP9QY (YCWSQYLCY), which was designed to mimic the most critical TNF-α recognition site on the TNF receptor(I), efficiently antagonizes the effects of TNF-α binding to the TNF receptor(I) (Nature Biotechnol. 15: 1266, 1997). We previously reported that this peptide inhibits bone resorption induced by RANKL *in vitro* or by a low calcium diet *in vivo* . Osteoprotegerin, which is a strong antagonist of RANKL but not of TNF-α, has been reported not to inhibit inflammation in the rat arthritis model. Since WP9QY antagonizes both TNF and RANKL in *in vitro* assays, we sought to determine if this peptide would antagonize both cytokines *in vivo* by examining the effect of WP9QY on the inflammatory bone destruction in the collagen-induced arthritis (CIA) model. Male 7 week-old DBA/1J mice were immunized intradermally with bovine type II collagen and boosted similarly at day 21. Mice were divided into three groups; non-immunized control group, immunized group with vehicle injections, and immunized group with peptide injections. The WP9QY peptide (24mg/kg x 8/ day) was administered by SC injections starting before the onset of paw swelling (at day 22, 24, and 26). The arthritis score began to increase in the vehicle-injected group starting at day 25 and reached an average score of 9.6 (12.0 is a full score using this evaluation) at day 38. In contrast, the average score in the peptide-injected group at day 38 was 5.7, indicating that the WP9QY peptide inhibited inflammation. The trabecular bone density of tibial metaphysis, measured by pQCT, was significantly reduced from 261 mg/cm ^{3} in the control group to 210 mg/ cm ^{3} in the vehicle-injected group, and this decrease of bone mineral density was significantly inhibited by the peptide injections (19.6% decrease in the vehicle-injected group vs 6.7% decrease in the peptide-injected group). Histological analysis revealed that WP9QY both blocked the invasive pannus tissue formation in the knee joint and prevented the increase in the number of osteoclasts in the joint area that occurred in the vehicle-injected group. Furthermore, WP9QY reduced the amount of anti-collagen II antibody in serum by 64%. Although the amount of the injected peptide is very high, these results clearly prove the concept that WP9QY peptide inhibits both inflammation and bone destruction that characterizes CIA.

SA258

Expression of EP_3 and EP_4 Prostaglandin Receptors in Mature Human Osteoclasts. P. Sarrazin*, I. Fortier*, S. I. Briand*, A. J. De-Brum Fernandes. Rheumatic Diseases Unit, Université de Sherbrooke, Sherbrooke, PQ, Canada.

Prostaglandins are potent, multifunctional and complex regulators of bone metabolism that may increase both bone formation and resorption. PGE_2 is the major prostaglandin produced in bone. Cellular effects of PGE_2 are mediated through specific receptors named EP_1, EP_2, EP_3 and EP_4. Little is known on the distribution of PGE_2 receptors in bone cells, although this knowledge could be important to understand the complex actions of PGE_2 on bone. The objective of the present work was thus to study the distribution of the EP receptors in human osteoclasts and to determine their effects on the presence of lamellipodia and actin rings, cytoskeleton structures necessary for osteoclast motility and bone resorption, respectively. *In situ* hybridization showed that human mature osteoclasts in culture expressed mRNA for the EP_3 and the EP_4 prostaglandin receptors. The presence of the EP_3 and EP_4 receptor proteins was also demonstrated using immunohistochemistry. EP_1 and EP_2 mRNA and proteins were not detected in these cells. We also investigated the expression of the EP receptors in human bone sections. The EP_3 and EP_4 polyclonal antiserum stained osteoclasts from human foetal, osteoporotic and pagetic bone tissues. A concentration dependant decrease of the number of TRAP positive cells with actin ring was observed with increasing PGE_2 concentration (EC_{50} of 1.09 +/- 1.2 nM). Incubation with 11-deoxy-PGE_1, an EP_2 and EP_4 agonist, showed a concentration dependant decrease in the percentage of TRAP positive cells with actin ring (EC_{50}: 14.3 +/- 2.8 nM) and a concentration dependent increase in the percentage of TRAP positive cells with podosomes (EC_{50}: 1.6 +/ - 1.9 nM). 11-deoxy-PGE_1 had no effect on TRAP positive cells with lamellipodia. Butaprost, a selective agonist for the EP_2 receptor, induced no changes in the actin cytoskeleton. Misoprostol, an EP_2 and EP_3 specific agonist, had no effect on the percentage of TRAP positive cells with actin ring but significantly increased the percentage of TRAP positive cells with podosomes (EC_{50}: 1.7 +/- 2.1 nM) and decreased the number of TRAP positive cells with lamellipodia (EC_{50}: 4.2 +/- 1.5 nM). In conclusion, we demonstrated that cultured osteoclasts express functionnal EP_3 and EP_4 receptors, the first implicated in the decrease of lamellipodia and the second decreasing the number of cells presenting actin ring.

SA259

See Friday Plenary number F259.

SA260

Jun Dimerization Protein 2 (JDP2), a Member of the AP-1 Family of Transcription Factor, Mediates Osteoclast Differentiation Induced by RANKL. R. Kawaida*[1], T. Ohtsuka*[1], J. Okutsu*[1], T. Takahashi*[1], Y. Kadono[2], H. Oda[2], K. Nakamura[2], S. Tanaka[2], H. Furukawa*[1]. [1]Biomedical Research Laboratories, Sankyo Co., Ltd., Tokyo, Japan, [2]Department of Orthopaedic Surgery, The University of Tokyo, Tokyo, Japan.

Osteoclasts are multinucleated cells that resorb bones, and are derived from hematopoietic cells of the monocyte-macrophage lineage. Receptor activator of NF-kB ligand (RANKL, also called ODF/TRANCE/OPGL) stimulates both osteoclast differentiation from osteoclast progenitors and activation of mature osteoclasts. However, molecular mechanisms of osteoclast differentiation have yet to be elucidated. To identify genes responsible for osteoclast differentiation, we used a molecular indexing technique. We isolated 10 cDNA clones whose expressions were induced by soluble RANKL (sRANKL) in RAW264.7 cells, a murine myelomonocytic cell line that differentiates to osteoclasts on sRANKL treatment. Sequence comparison analysis revealed that one of them was a mouse homologue of Jun dimerization protein 2 (JDP2), a member of the AP-1 family of transcription factors, containing a basic region-leucine zipper motif. sRANKL-induced up-regulation of this gene was also detected in mouse bone marrow cells during osteoclastogenesis but not in J774A.1 cells which lack oseoclastogenic potential in spite of the fact that they have the same ability to activate the NF-kB pathway as did RAW264.7. To demonstrate the functional role of JDP2 in regulation of osteoclast differentiation, we examined the ability of JDP2 to activate osteoclastogenic pathway. First, infection of mouse primary bone marrow cells with retrovirus expressing JDP2 promoted sRANKL-induced formation of tartrate-resistant acid phosphatase (TRAP)-positive multinuclear osteoclasts. Second, transient transfection experiments of RAW264.7 cells revealed that expression of JDP2 activated promoters for TRAP and cathepsin K genes, which are specific markers for osteoclasts. Our findings suggest that JDP2 may play an important role in the RANK-mediated signal transduction system, especially in osteoclast differentiation.

Disclosures: ***R. Kawaida****, Sankyo Co., Ltd. 3.*

SA261

See Friday Plenary number F261.

SA262

The Transcription Factor AP-1 Regulates RANKL-dependent Differentiation and Survival in Osteoclasts. F. Ikeda[1], T. Matubara*[1], K. Hata*[1], K. Yamashita*[1], T. Watanabe*[2], T. Kukita[2], K. Yoshioka*[3], R. Nishimura[1], T. Yoneda[1]. [1]Dept Biochem, Osaka Univ Grad Sch Dent, Osaka, Japan, [2]Second Dept of Oral Anat, Kyushu Univ Grad Sch of Dent, Fukuoka, Japan, [3]Div of Cell Cycle Regulation, Cancer Res Inst, Kanazawa Univ, Kanazawa, Japan.

RANK ligand (RANKL) plays an important role in the life cycle of osteoclasts through regulating their differentiation and apoptosis. Recent studies show that RANKL activates the transcription factor AP-1 following propagation of JNK and c-Jun in osteoclasts. These results suggest that the AP-1 signaling plays a role in the regulation of the differentiation and apoptosis in osteoclasts. To test this notion, we used a study model in which soluble RANKL (sRANKL) induced the differentiation of RAW264 murine monocytic cells into tartrate-resistant acid phosphatase-positive multinucleated osteoclast-like cells (TRAP(+) MNC) and promoted the transactivation of AP-1 through JNK and c-Jun activation. To examine the role of AP-1 composed of c-Jun and c-Fos, we introduced a dominant-negative mutant of c-Jun (DN-c-Jun) or c-Fos (DN-c-Fos) into RAW264 cells using a newly-engineered adenovirus system. We found that DN-c-Jun or DN-c-Fos markedly inhibited the transactivation of AP-1 and decreased TRAP(+) MNC formation in sRANKL-stimulated RAW264 cells. DN-JNK1 also suppressed sRANKL-induced activation of c-Jun and TRAP (+) MNC formation. Since recent studies suggest an involvement of AP-1 in induction of apoptosis in various types of cells, we next examined whether the AP-1 affects apoptosis in osteoclasts by assessing for active caspase-3 expression and nuclear fragmentation in mature osteoclasts (OCL) which formed in the mouse bone marrow cultures. sRANKL prevented apoptosis in OCL and prolonged their survival, demonstrating anti-apoptotic effects of sRANKL. On the other hand, DN-c-Jun or DN-c-Fos markedly increased apoptosis of mature OCL even in the presence of sRANKL. Since RANKL activates NF-κB as well as AP-1 in osteoclasts, we studied the role of NF-κB in osteoclast differentiation and apoptosis. Consistent with the previous results, suppression of NF-κB activation using an ubiquitin-resistant mutant of Iκ-Bα (Iκ-BαMut) blocked TRAP(+) MNC formation, suggesting a critical role of NF-κB in osteoclast differentiation. In contrast, the Iκ-BαMut did not inhibit sRANKL-stimulated survival, suggesting an involvement of NF-κB in osteoclast apoptosis is unlikely. In conclusion, our results suggest that the transcription factor AP-1 is critical to osteoclast differentiation. In addition, our results also suggest that the AP-1 has anti-apoptotic actions in contrast to other cell systems. Thus, AP-1 plays diverse roles in RANKL-induced events in osteoclasts.

SA263

See Friday Plenary number F263.

SA264

The Express of Fas, Fasl And Nf-kapab in The Process of Osteoclast-like Cell Apoptosis Effected by Sodium Fluoride*. Y. Sun[1], Y. Li*[1], F. Yang*[1], M. Zhu*[2], B. Lu[2], M. Qiu*[2]. [1]Biology, Institute of Radiation Medicine, Chinese Academy of Medical Sciences, Tianjin, China, [2]Endocrinilogy, Tianjin Medical University, Tianjin, China.

Purpose: In the process of bone remolding, absorption of bone depends on the constant recruit of osteoclast. It has now proved that disappear of osteoclast is the result of itself apoptosis. Our previous experiments showed sodium fluoride in tap water drank by rat ad libitum have promoted the process of osteoclast apoptosis in vivo. Fas is the receptor in the membrane of cells and is related to apoptosis. As it binds to its ligand, the signal of apoptosis is transmitted and cell apoptosis happens. Nuclear factor NF- κB may be participated in tumor necrosis factor activating the pathway of apoptosis and prohibits the apoptosis. This paper reports the expression change of apoptosis signals: Fas, FasL and NF-κB in the course of osteoclast-like cells apoptosis effected by sodium fluoride. Method: C57BR/6 mice spleen cells suspension in α-MEM media containing rmIl-3, rhIl-6, BSA, fetal calf serum and agar cultured at 37ºC and 5% CO2 for two weeks and then the colonies suspension re-cultured in theα-MEM media containing rmGM-CSF for two weeks again. Above cells were induced into osteoclast-like cells by 1,25(OH)2VitD3 in theα-MEM solutions. TRAP staining and scanning electron microscope showed these cells were osteoclast-like cell (OLC). OLCs were co-cultured with sodium fluoride at the concentration of 0, 5, 10 and 15mg/L for a week. The expression of Fas, FasL and NF-κB were examined by immuno-histochemistry. 500 cells were checked under microscope. The cells with dark staining were expression positive and counted the percentage of positive cells. Experiments data are treated with statistics software SPSS. Result: The percentage of OLCs that expressed proteins of Fas and FasL increased with the concentrations of sodium fluoride. The percentage of osteoclast-like cells expressing the NF-κB decreased with the concentration of sodium fluoride. Conclusion: In the process of OLC apoptosis induced by NaF, the expression of Fas and FasL increased and the expression of NF-κB decreased. These changes of the expression presented dose-dependent.

*This work was supported by NSFC (39770828, 30070828)

SA265

Prevalence of Osteopenia and Osteoporosis in Hispanic Postmenopausal Females. J. R. Talbot[1], M. Goette-Jaime*[2], F. Cons-Molina[3], O. D. Messina[4], E. Schulz[5]. [1]Pan American Ospeoporosis Foundation (PAOF), Oceanside, CA, USA, [2]Baja California University, Mexicali, Mexico, [3]Unidad de Diagnostico Osteoporosis, Mexicali, Mexico, [4]CIRO, Buenos Aires, Argentina, [5]Loma Linda University, Loma Linda, CA, USA.

The prevalence of osteopenia and osteoporosis in the white-Hispanic population remains controversial. For instance, the NHANES has reported a low 10% prevalence of hip osteoporosis in white-Hispanic females in contrast with a 20 % prevalence observed in white-Caucasian females. However, a higher 36% prevalence of osteoporosis has been estimated by Melton in white postmenopausal females (50 to 80+ years of age) from Rochester Minnesota. Recently, has been reported a 20% prevalence of osteoporosis in white-Hispanic females, but the subjects in this study were 20 to 90 years. However, when only postmenopausal females were evaluated the prevalence of osteoporosis increased to 25 - 30%. The aim of this study was to determine the prevalence of osteopenia and osteoporosis in healthy postmenopausal white-Hispanics females from a relatively homogenous menopause age, and geographical area as is Southern California (USA) and Northern Baja California (Mexico). Lumbar spine (L2-L4) and hip BMD/C were performed with a DEXA-Lunar-DPX densitometer in 369 postmenopausal, healthy white-Hispanic females referred by their physician to a bone densitometry center as part of a routine evaluation. Were included in the analysis of these study only healthy females from Southern and Northern Baja California who had their menopause at age 50 ± 1 years. Were excluded from the study females who had any disease or received any treatment that may affect mineral or bone metabolism, scoliosis, vascular calcifications or any other abnormality that may affect DEXA results. Patients with "normal/high" DEXA due to a non-traumatic vertebral fracture were included as osteoporotic (Fractured vertebras were excluded from the analysis). The preliminary results of the prevalence of osteopenia and osteoporosis in 369 postmenopausal Hispanic females showed a mean age of 61 ± 4 years and mean time in menopause of 14.7 years. BMD t-score: normal 19%, osteopenia 49% and osteoporosis 32 %. [Lunar-DEXA results were adjusted to Hologic standards multiplying BMC/D of lumbar spine by 0.9522 and hip by 0.979]. Our preliminary results suggest similar prevalence of osteopenia and osteoporosis in postmenopausal white-Hispanic and white-Caucasian females.

SA266

Effectiveness of Peripheral DEXA in Predicting Fractures and Targeting Treatment in Women aged 60-80. D. M. Reid[1], R. J. Barr*[2], A. Adebajo*[3], W. D. Fraser[4], J. P. Halsey[5], C. Kelsey*[6]. [1]Medicine & Therapeutics, University of Aberdeen, Aberdeen, United Kingdom, [2]University of Aberdeen, Aberdeen, United Kingdom, [3]Barnsley District Hospital, Barnsley, United Kingdom, [4]Royal Liverpool University Hospital, Liverpool, United Kingdom, [5]Royal Lancaster Infirmary, Lancaster, United Kingdom, [6]Oldchurch Hospital, Romford, United Kingdom.

Purpose To determine the effectiveness of peripheral DXA (PIXI®,GELunar) in the assessment of risk and targeting treatment to prevent future fracture. *Methods* Women aged 60-80 from 5 centres in the United Kingdom attended for a PIXI scan and completed a risk factor questionnaire. Women were designated as high (H), medium(M) or low(L) risk dependent on WHO equivalent T-Scores for the PIXI scanner (T<-1.6 ≈osteoporosis, T<-1 but >-1.6≈osteopenia, T>-1≈normal). 12-24 months later women were followed up by postal questionnaire to determine incident self-reported fractures and treatments for osteoporosis. *Results* Of the initial screened population (n=7604) 74% returned the questionnaire. The proportion of screened women in each risk was H: 24.5%, M: 28.9%, L: 46.6% and this differed significantly from non-responders (H: 26.8%, M: 29.7%, L: 43.5%, $\chi^2 = 7.3$, P=0.026). Of H women 23.4% (n= 323) were on a variety of osteoporosis treatments, including calcium or vitamin D, at baseline(B) rising to 78% at follow-up(F) - see table. More women in the M and L risk groups received treatment at B but the proportions receiving treatment at F changed substantially in the 3 groups ($\chi 2 = 17.71$, P=0.014). Relative risk of all fractures and fractures of hip, wrist and vertebrae were significantly increased in the H and M group compared to L risk. Preliminary analysis did not detect a significant difference in incident total (no treatment -nRx: 8.9%, Rx 8.1%) or hip, wrist and spine fractures (nRx: 3.6%, Rx 3.8%) during 18.6 months follow-up (F). *Conclusions* This study demonstrates that risk assessment by PIXI predicts incident fractures and alters treatment patterns but as yet shows no reduction fracture rates over an 18 month period.

Treatment and Fracture Incidence

	High (n=1377)	Medium (n=1625)	Low (n=2626)
Treatment at baseline (B)	23.4%	25.3%	27.5%
Treatment at follow-up (F)	78.0%	57.2%	17.1%
Never treated (N)	17.4%	33.7%	62.0%
Total Incident Fractures	9.5%	6.1%	3.8%
RR c.f. low (95% CI)	2.5 (1.9 - 3.3)	1.6 (1.2 - 2.2)	
Hip,Wrist, spine only	4.8%	2.7%	1.5%
RR c.f. low (95% CI)	3.2 (2.1 - 4.9)	1.8 (1.1-2.9)	

*Disclosures: **D.M. Reid**, Alliance for Better Bone Health 2, 5; Roche Pharma 5; Merck 5; Eli Lilly 5.*

SA267

Assessment of Bone Mineral Density in an Elderly Population in the City of São Paulo, Brazil. M. B. R. Camargo*[1], G. L. Saraiva*[1], M. Lazaretti-Castro[1], M. Cendoroglo*[2], L. Ramos*[2]. [1]Endocrinology, Universidade Federal de São Paulo, São Paulo, Brazil, [2]Geriatrics, Universidade Federal de São Paulo, São Paulo, Brazil.

This cross-sectional population-based study examined the association of anthropometric parameters with bone mineral density (BMD) in São Paulo, Brazil. This study was conducted as part of the EPIDOSO Study, the first follow-up study of elderly residents in Brazil. The study started in 1991 and approached 1667 elderly people (above 65 years), living in community in the district of Saúde, in the city of São Paulo. BMD was assessed in 294 elderly women (n =197) with a median age of 77 yo (70 -93 yo) and men (n=97), median of 76 yo (70-88 yo), from the population-based EPIDOSO Study, between 1998 and 1999. For women, median weight was 60 kg (37-97 kg) and median height was 152 cm (136-173 cm). BMI ranged from 15,83 to 38,8 kg/m2 (median 26,8 kg/m2). For men, median weight was 71 kg (49-103,9 kg) and median height was 166 cm (152-180 cm). BMI ranged from 19,6 to 36,03 kg/m2 (median 25,89 kg/m2). Total body composition and BMD at the lumbar spine (L), and femoral neck (N) were measured by dual-energy X-ray absorptiometry, using a HOLOGIC 4500 A. Osteopenia and osteoporosis were defined according to the WHO criteria, irrespective to gender. We examined the correlation (Spearman rank order test) between BMD and the factors: age, sex, weight, height, body mass index (BMI), fat-free soft mass index (FFM) (g of lean mass/height in meters squared) and percentage of fat (% fat). The level of significance was set as $P < 0,05$. Osteoporosis has the highest prevalence at N (45% of men and 53% of women) and osteopenia was found in 39% and 38% of men and women, respectively. On the other hand, only 18% of men and 33% of women had osteoporosis at L, and 34% of men and 35% of women had osteopenia at this site, with no correlation with age for both sexes. The strongest correlation was found between N and weight for both sexes (R=0,45 for men and R=0,51 for women), better than with FFM (R=0,25 and 0,37 respectively) or % fat (R=0,24 and R=0,33, respectively), all of them significant. There was also a weak but significant correlation between N and height (R=0,39 for men and R=0,25 for women). Concluding, we found a high prevalence of osteoporosis on femoral neck for men and women, in a rate of 1,2 women for each man. The best predictor of BMD at N was weight. The measurement of BMD at lumbar spine above 70 yo underestimated the prevalence of osteoporosis in both men and women in our studied population.

SA268

Relationship of Radiogrammetry and Bone Mineral Density using DXA in Normal Reference Data. S. Yang[1], S. Ham*[2], S. Lee*[3]. [1]Radiology, Ulsan University Hospital, Ulsan, Republic of Korea, [2]Ulsan University Hospital, Ulsan, Republic of Korea, [3]Kangnam Hospital, Seoul, Republic of Korea.

Digital X-ray Radiogrammetry (DXR) technique from radiographs of the hand estimate forearm BMD without the use of aluminium wedges. It has been shown to have good correlation to DXA and to have very low precision error. We report the results of a correlation between DXR data and DXA for Korean. The system (Pronosco) calculates BMD using a weighted average of cortical and bone width measurements at the second through fourth metacarpal. The output is an absolute BMD estimate called DXR-BMD. A total of 372 Korean women and 140 men were recruited from the Ulsan and Seoul (only men) area. Women and men with a history of bone diseases, medication impacting bone mineral density were excluded, as were those who had undergone prolonged hospitalisation or immobilisation. They had their non-dominant hand radiographed (50 kvp, 8 mA). DXA for the lumbar region was done with Hologic QDR 4500A in Ulsan and Lunar Expert in Seoul. By using the conversion equation, standardized BMD was taken for the analysis. A total of 349 female and 116 male in whom all the data were available is included the analysis. The means for DXR-BMD at the forearm and DXA at L1-4 were:

		DXR-BMD/ DXA (g/cm^2)	
Age	No.F/M	Female Mean ± SD	Male Mean ± SD
20 - 29	64/ 24	0.534±0.044/ 0.956±0.089	0.575±0.040/1.159±0.187
30 - 39	76/ 29	0.554±0.047/ 1.002±0.162	0.593±0.048/1.168±0.143
40 - 49	68/ 15	0.577±0.044/ 1.004±0.109	0.594±0.039/1.120±0.165
50 - 59	57/ 18	0.543±0.055/ 0.876±0.147	0.593±0.052/1.109±0.201
60 - 69	45/ 17	0.470±0.045/ 0.754±0.148	0.577±0.054/1.033±0.168
70 - 79	39/ 13	0.431±0.052/ 0.665±0.154	0.534±0.068/1.062±0.275
All	349/ 116	0.529±0.066/0.905±0.179	0.580±0.052/1.119±0.188

Correlation coefficients between DXR-BMD and DXA were 0.672 in female ($p<0.01$) and 0.448 in male ($p<0.05$).

The results show that relative to the Korean male population, the Korean females have significantly lower DXR-BMD across the age decades as expected. For women DXR-BMD is more closely correlated with DXA of the L-spine than male. This suggests that bone loss in the peri-menopausal women can also be detected by DXR-BMD accurately. Relatively lower correlation between DXR-BMD and L-spine DXA for male population should be elucidated in the future.

SA269

See Friday Plenary number F269.

SA270

Bone Mineral Density in Healthy Asian Indian Women: Development of a Reference Database and Implications for Diagnosis of Osteoporosis in Indian Women living in the United States. P. G. Reddy*[1], A. Mithal[2], D. Rao[1]. [1]Bone & Mineral Metabolism, Henry Ford Hospital, Detroit, MI, USA, [2]Endocrinology, Indraprastha Apollo Hospital, New Delhi, India.

Genetics and ethnicity are the two most important determinants of bone mineral density (BMD), thereby necessitating the establishment of separate reference databases for different ethnic groups. We sought to establish the first BMD reference database for Asian Indian women so that appropriate comparisons can be made in evaluating individuals of Indian origin for osteoporosis in the United States. Two-hundred and thirteen healthy women, age 20-59 years, were recruited both to establish a reference database to calculate ethnic-specific T-scores and to determine the age-related decline in BMD. Measurements were taken at the lumbar spine, hip, and non-dominant forearm by Hologic 4500 dual energy x-ray absorptiometry. Calcium intake was estimated in all subjects and serum 25-hydroxyvitamin D levels were measured in a subset of 41 subjects. In all age categories BMD in Indians was significantly lower than that of U.S. white women at all relevant measurement sites. The expected age-related decline in BMD was seen at all sites. In 75 young women in the 20-29 age range, the peak adult BMD reference group, BMD results for the relevant sites were as follows: lumbar spine (L1-L4): 0.920 ± 0.097, femoral neck: 0.767 ± 0.090, total hip: 0.839 ± 0.095, and forearm (1/3 radius): 0.590 ± 0.050. Dietary intake of calcium in Indians was also significantly lower than that seen in our clinic (491 vs 697 mg/d; $p<0.01$), and the mean serum 25-hydroxyvitamin D level was 10.2 ± 8.1 ng/ml in a small subset of 41 subjects. BMD results at any measurement site were not related to daily calcium intake or age at menarche, but were significantly related to BMI. Conclusions: At all relevant measurement sites, BMD values were significantly lower in Asian Indian women, compared to U.S. white women, although BMI might explain some of this difference. Until BMD-fracture relationship is established in this ethnic group, it is reasonable to use values from the 20-29 age group (peak adult BMD) to calculate T-scores for evaluating Indians living in the United States. Because of distinct cultural, dietary and genetic features of Asian Indians, it is inappropriate to include them with other Asians in studies of ethnic influence on BMD.

SA271

Race Differences in Bone Density, Cross Sectional Geometry and Bone Strength Measured by pQCT in Young Adult Women. H. J. Kalkwarf[1], N. W. Glynn[2], S. R. Daniels*[3], S. Y. S. Kimm[2]. [1]General & Community Pediatrics, Children's Hospital Medical Center, Cincinnati, OH, USA, [2]Family Medicine, University of Pittsburgh School of Medicine, Pittsburgh, PA, USA, [3]Cardiology, Children's Hospital Medical Center, Cincinnati, OH, USA.

Black women have a lower fracture rate than white women. Bone strength is a function of both bone density and bone geometry. The objective of this study was to assess race differences in bone density, cross sectional bone geometry, and bone strength index (BSI) of the radius in a biracial cohort of young women at peak bone mass. We also examined whether race differences in bone measures could be explained by differences in forearm length, muscle area, and grip strength. Subjects were 165 black and 159 white women age 22 ± 1 y. We measured bone density, bone geometry and muscle area of the dominant forearm by pQCT (Norland/Stratec XCT 2000). Measurements were obtained at 2 sites: 4% and 66% from the radial endplate. Total and trabecular bone measurements were obtained at the 4% site. Cortical bone and muscle measurements were obtained at the 66% site. Grip strength was measured by a hand held dynamometer. Black women had greater forearm length (4.2%), muscle area (9.7%) and grip strength (3.4%) than white women ($p<0.05$). At the 4% site, black women had higher total and trabecular BMD. When adjusted for their greater forearm length, muscle area and strength, black women had a smaller bone area. At the 66% site, black women had a greater cortical bone area and thickness, which were due to a greater periosteal circumference. When adjusting for forearm length, muscle area and strength, black women had a smaller endosteal circumference, but there was no difference in periosteal circumference. There was no difference in cortical BMD between black and white women after adjusting for cortical thickness. BSI at the 66% site was greater in black women than in white women, but this difference was no longer evident when adjusting for forearm length, muscle area and strength. These observed racial differences in bone density, geometry and strength may be the underlying factor associated with racial differences in fracture risk later in life.

	Black - White Difference (%)	
Measurement & site	Unadjusted	Adjusted
Trabecular BMD - 4%	14.8*	14.8*
Total bone area - 4%	-2.6	-6.9*
Cortical area - 66%	10.3*	4.4*
Cortical thickness - 66%	9.6*	7.4*
Periosteal circumference - 66%	2.6*	-0.3
Endosteal circumference - 66%	2.8	-6.8*
BSI - 66%	11.2*	0.3

*$p < 0.05$

Disclosures: ***H.J. Kalkwarf****, Procter & Gamble 1.*

SA272

High Parity Is Associated with Greater Bone Size Later in Life. K. S. Wosje*, T. L. Binkley*, B. L. Specker*. EA Martin Program in Human Nutrition, South Dakota State University, Brookings, SD, USA.

Most studies do not find an association between bone health and parity, but there are few studies on the effect of high parity on bone. Female members of the Hutterite Brethren exhibit above normal whole body (WB) and lumbar BMC and bone area (BA) and demonstrate high fecundity. We used cross sectional data to test the hypothesis that high parity is not associated with DXA BMC or pQCT bone parameters among 150 Hutterite women age 30 to 65 y. pQCT measurements were conducted at the 20% and 4% radius sites. 77% of women were estrogen replete. There were 109 women who had previously breastfed (LAC) with average parity 5.5 (range 1 to 10) & 41 women who never breastfed (NoLAC) (n=38 with no live births). LAC and NoLAC were similar in ht, wt, & BMI. WB, lumbar, and hip BMC and BA also were similar between LAC and NoLAC. pQCT 20% radius periosteal & endosteal circumferences and 4% radius total and trabecular densities were similar between LAC and NoLAC. pQCT 20% radius cortical thickness was marginally higher in LAC vs. NoLAC ($p<0.10$) but the effect did not persist in multiple regression models. Cortical density was higher in LAC after controlling for covariates (LSM±SE: 1222±3 vs. 1209±5 mg/cm^3, model $r^2=0.15$, $p<0.05$ for LAC vs. NoLAC). Within LAC, parity was an independent positive predictor of 20% radius periosteal (model $r^2=0.50$, $p<0.05$ for parity) and endosteal (model $r^2=0.37$, $p<0.007$ for parity) circumferences. Adult wt gain {(measured current wt) – (reported wt at age 20-30y)} was marginally higher in LAC compared to NoLAC (14±12 vs. 10±9 kg, $p<0.10$). Parity was positively associated with hip BMC, and WB and hip BA ($P<0.05$ for all), and marginally positively associated with WB BMC and lumbar BA ($p<0.10$) within LAC. Total # months lactating was marginally positively associated with hip BA ($P<0.10$), but not with any other BMC or BA outcomes. In multiple regression, parity independently predicted WB (model $r^2=0.81$, $p<0.001$ for parity), lumbar (model $r^2=0.52$, $p<0.05$ for parity) and hip BA (model $r^2=0.48$, $p=0.01$ for parity). Parity or total # months lactating did not appear in any final regression models predicting BMC. These data show that parity has a positive effect on bone size independently of wt gain or body composition among Hutterite females, but is not associated with BMC or volumetric bone density.

SA273

Bone-Strengthening Medication Use and Low Bone Denisty in Black Elderly Women. D. L. Orwig*[1], N. Brandt*[2], G. Zimmerman*[2], A. L. Smith*[2]. [1]Department of Epidemiology & Preventive Medicine, University of Maryland School of Medicine, Baltimore, MD, USA, [2]University of Maryland School of Pharmacy, Baltimore, MD, USA.

Osteoporosis is a problem that affects approximately 10 million individuals plus 18 million who have low bone mass. One of the common risk factors recognized for osteoporosis is Caucasian or Asian ethnicity; thus, African-Americans are often thought to be at low risk for developing this disease; however, urban residents have been found to have lower bone mass and density due to a variety of reasons such as poorer nutrition (calcium and Vitamin D intake), lower body weight, less active lifestyle, higher consumption of tobacco and alcohol, more frequent use of drugs and higher exposure to environmental pollutants which may put urban black elderly women at particular risk for osteoporosis and its consequences. Very little is known about the use of bone-strengthening medications in the black elderly population and this study examined use of these medications as well as bone mineral density (BMD) in a sample of black elderly women attending one of two managed care sites for older adults dually eligible for Medicare and Medicaid. BMD was measured at the heel using a Lunar PIXI provided by Novartis Pharmaceuticals. Use of bone-strengthening medications was based on the electronic medical records and information was obtained on fracture history and other demographics. A total of 72 elderly black women were assessed with an average age of 77, mean education of 8 years and a mean annual income of $6500. According to the manufacturer's normative database for young adult normal, the mean (BMD) for the os calcis is 0.507 gm/cm2 with each standard deviation equaling 0.09. Using 1.0 and 2.5 standard deviations below the mean as the definition for low bone mass and osteoporosis respectively (0.417 gm/cm2 and 0.282 gm/cm2), 18% of subjects had low bone mass while 30% had osteoporosis. The average BMD for the sample was 0.384 gm/cm2. Thirteen percent of the sample had previous fractures reported in the previous 2 years. Of those with low bone density or osteoporosis, only 30% were taking alendronate and/or calcium and vitamin D. More than half of the sample had low BMD and is at risk of suffering its consequences, yet few were taking any bone-strengthening medication in this managed care setting. Osteoporosis and its treatment in this population is under-recognized and it is important as society ages and as the proportion of the population that is black increases that we take a more preventive role in increasing bone density in this vulnerable population.

SA274

Calcium and Vitamin D Influence Bone Density, but not Fracture Risk, in the Caucasian Population of NORA. J. W. Nieves[1], E. S. Siris[2], E. Barrett-Connor[3], M. Zion*[1], S. Barlas*[4], Y. Chen[4]. [1]Clinical Research Center, Helen Hayes Hospital, West Haverstraw, NY, USA, [2]Columbia University, New York, NY, USA, [3]University Of California, San Diego, CA, USA, [4]Merck & Co., Inc., West Point, PA, USA.

Calcium and vitamin D intake are believed to be related to bone health, although, prospective cohort studies and clinical trials have produced varied results. The purpose of this study is to evaluate the relationship between self-reported lifetime calcium intake and current calcium and vitamin D intake and peripheral bone mass and fracture incidence in the subset (n=75,565) of the NORA cohort of postmenopausal Caucasian women who responded to a dietary questionnaire. Dietary questions focused on consumption of milk, ice cream, yogurt and cheese during four time periods of life: childhood, the teenage years, adulthood, and the current time period. An average daily intake of calcium (mg) was calculated for each of the 4 life periods. Supplemental calcium intake and calcium from fortified juice was added to the current daily intake from foods (61% reported some intake of these additional calcium sources). Vitamin D intake was calculated from the intake of milk, fish and supplements and sunlight exposure. Bone mineral density (BMD) was measured by peripheral SXA/DXA at the forearm, heel, or finger, or by ultrasound of the heel. The impact of calcium and vitamin D intake on risk of osteoporosis based on BMD and fracture incidence were evaluated in logistic regression models controlling for age, years from menopause, body mass index, smoking, estrogen, steroid or diuretic use, exercise, alcohol consumption, caffeine intake, level of education, maternal and personal history of fracture, and machine used for BMD. Mean calcium intake for this population was 655 mg per day and was as high as 960mg/day when supplements were added to current intake. An adequate lifetime calcium intake was associated with a reduction in the risk of osteoporosis (OR=0.727; 0.601, 0.880). Current calcium and vitamin D intake at the recommended intake was also associated with a reduction in the risk of having osteoporosis (OR=0.689; 0.614, 0.773). There were 760 fractures in this cohort during one year of follow-up (114 hip; 196 rib; 306 wrist). Fracture risk in the NORA cohort, analyzed with all fractures combined, and hip, wrist and rib fractures separately, was not related to current calcium or vitamin D intake. There was also no association with calcium and vitamin D intake when analysis was restricted to those over 65 years of age. In conclusion, in Caucasian woman calcium and vitamin D intake influence the risk of osteoporosis, but not fracture during one year of follow-up in the NORA cohort.

SA275

See Friday Plenary number F275.

SA276

Pre-conceptional Predictors of Changes in Maternal Skeletal Status during Pregnancy. M. K. Javaid*[1], S. R. Shore*[1], P. Taylor*[2], H. M. Inskip*[1], K. M. Godfrey*[1], C. Cooper*[1]. [1]Medical Research Council Environmental Epidemiology Unit, Southampton, United Kingdom, [2]Medical Physics and Bioengineering, Southampton University Hospitals NHS Trust, Southampton, United Kingdom.

BACKGROUND: During pregnancy, the fetus acquires 30g of calcium for skeletal growth. To meet this demand, calcium metabolism of the mother undergoes several adaptations, including increasing both intestinal calcium absorption and bone resorption. Previous longitudinal studies have recruited women already pregnant or from selective groups intending to become pregnant. As the lifestyle and anthropometric characteristics of these women are unlikely to be representative, we investigated the magnitude of bone loss and its determinants in a longitudinal study of healthy women who were not pregnant at baseline. METHODS: Between April 1998 and April 2001, 8700 women were interviewed at baseline, from these 340, who became pregnant, were entered into the study. At baseline the women completed a lifestyle questionnaire and had their height, weight and skinfold thickness measured. At 11 and 34 weeks pregnancy, the mothers were interviewed and had their skeletal status measured using a calcaneal quantitative ultrasound instrument (Hologic Sahara). RESULTS: During pregnancy, there was a significant ($p<0.001$) reduction in both speed of sound (SOS) and bone ultrasound attenuation (BUA) at the calcaneus [Table 1]. Ankle oedema led to a mean increase of 12% in heel width during pregnancy; however adjusting for this variable did not alter the changes in QUS during pregnancy. We were unable to identify independent pre-conceptional predictors of BUA at either baseline or during pregnancy. Maternal height, parity and reported physical activity were significantly ($p<0.05$) related to baseline SOS. Low maternal parity ($p=0.001$) and low milk intake ($p=0.01$) were also independently associated with greater bone loss during pregnancy. CONCLUSION: These findings suggest that high maternal milk intake before pregnancy may reduce maternal bone loss during pregnancy, as measured calcaneal ultrasound.

Table 1. Changes in QUS and heel width during pregnancy

Calcaneal	Percentage change	Change as Z score	p
SOS	-0.4%	-0.37	<0.001
BUA	-4.5%	-0.31	<0.001
Width	+12.3%	+0.75	<0.001

SA277

See Friday Plenary number F277.

SA278

Does Tea Drinking Affect Bone Density and Risk of Fractures among U.S. Postmenopausal Women with Different States of Hormone Replacement Therapy? Results from the Observational Study in the Women's Health Initiative. Z. Chen[1], M. B. Pettinger*[2], I. A. Hakim*[1], A. Z. LaCroix[2], J. Robbins*[3], B. J. Caan*[4], D. H. Barad*[5], C. Ritenbaugh*[6]. [1]University of Arizona, Tucson, AZ, USA, [2]Fred Hutchinson Cancer Research Center, Seattle, WA, USA, [3]University of California at Davis, Sacramento, CA, USA, [4]Kaiser Permanente, Oakland, CA, USA, [5]Albert Einstein College of Medicine, Bronx, NY, USA, [6]Kaiser Center for Health Research, Portland, OR, USA.

Tea is a rich dietary source of fluoride, and also contains caffeine and flavonoids, which each may influence bone mass and fracture risk in different ways. It has been suggested that hormone replacement therapy (HRT) in combination with fluoride treatment may induce a synergistic effect on bone mass by dissociating bone formation and resorption in postmenopausal women. In this prospective study, we evaluated the association of tea consumption with bone mineral density (BMD), changes in BMD, and risk of fracture among postmenopausal women with different HRT usage. Study participants (N = 91,465) were women from the Observational Study (OS) in the Women's Health Initiative (WHI). Forty percent of the women had never taken HRT, 15% took HRT in the past, and the remainder were current HRT users at the time of enrollment. The average length of follow-up was 4.1 years. Tea consumption was assessed at the baseline using a questionnaire. Fracture events during the follow-up were self-reported, except for hip fractures, which were confirmed by medical record review. A subgroup of the women (N = 4,979) received total body, total hip and lumbar spine BMD measurements on dual-energy x-ray absorptiometry at baseline and during the follow-up. Results showed that the associations of tea drinking with fracture risk varied by HRT usage and fracture site, but in general were not statistically significant. Baseline BMD was not correlated with tea drinking. Interestingly, total body and spine BMD at year three visit and percent changes of total body and spine BMD between baseline and year three visit were significantly related to tea drinking among current HRT users and past HRT users ($p<0.05$), but not among women who never used HRT. Results of our study suggest that tea drinking does not have significant adverse impact on risk of fracture, and HRT and tea may have a synergistic effect on BMD.

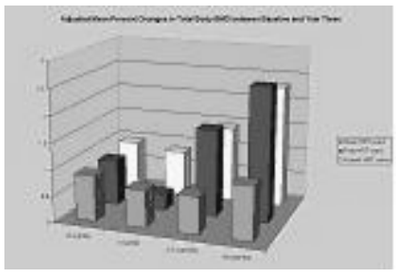

SA279

See Friday Plenary number F279.

SA280

The Effect of Milk and Calcium on the Age at Menarche. K. Ghatge*[1], J. Russell*[2], J. Cadogan*[1], H. Lambert*[3], M. E. Barker*[1], R. Eastell[3]. [1]Centre for Human Nutrition, University of Sheffield, Sheffield, United Kingdom, [2]Corporate Information and Computing Services, University of Sheffield, Sheffield, United Kingdom, [3]Bone Metabolism Group, University of Sheffield, Sheffield, United Kingdom.

Calcium supplementation is known to affect the hypothalamic-pituitary-ovarian axis and fat metabolism. It may therefore influence the age at menarche. We analysed data from two supplementation trials in teenage girls. In the first trial 82, 11-12 year old girls were randomised to 1 pint of milk containing 680 mg of calcium or no supplement, daily, for 18 months. In the second trial, 86, 11-12 year-old girls received 792 mg of calcium in the form of calcium citrate malate (CCM) or no supplement, daily, for 18 months. The difference between the supplemented and the control group in both the trials was tested using Tarone-Ware survival analysis. At the beginning of both the studies, there was no difference between the supplemented and the control groups for the mean age of participants and the Tanner stage of puberty. To study the effect of supplementation (milk or CCM) on menarche, the data was analysed for the mean age at menarche and for the length of time between start of the study and menarche. In the milk supplementation trial, there was no difference between the groups for the mean age at menarche as well as for the length of time between start of the study and menarche. In the CCM supplementation trial, the mean age of menarche was marginally different between the two groups (by 4 months) and the time between start of the study and menarche was significantly different between the two groups, $p<0.05$.

Table 1

	Milk supplementation		CCM supplementation	
	Supplement	Control	Supplement	Control
Age at menarche Mean (S.E.)	13.59 (0.11)	13.74 (0.14)	13.03 (0.12)	13.36 (0.14)
	p = 0.5		p = 0.08	
Time between start of study and menarche Mean (S.E.)	0.90 (0.10)	1.14 (0.14)	1.13 (0.13)	1.57 (0.15)
	p = 0.2		p = 0.03	

The CCM supplementation seems to have a positive effect on the time of puberty. The mechanism of action of milk and CCM are different as CCM suppressed PTH whereas milk did not. The mechanism is unlikely to be an influence by leptin as the body weight gain did not differ significantly between the groups in CCM trial. However, the effect may have been mediated via the hypothalamic-pituitary-ovarian axis. Late menarche is a recognised risk factor for osteoporosis; calcium supplementation in childhood may reduce the risk of fracture in later life by accelerating the onset of the menarche.

SA281

The Osteoporosis Population-Based Risk Assessment Trial (OPRA) Comparing Three Strategies for Fracture Prevention. A. Z. LaCroix[1], D. S. M. Buist*[1], T. A. Abbott[2], S. K. Brenneman[2]. [1]Center for Health Studies, Group Health Cooperative, Seattle, WA, USA, [2]Outcomes Research & Management, Merck & Co., West Point, PA, USA.

The OPRA randomized trial compared 3 strategies for allocating bone density screening in the context of an HMO-based fracture prevention program that provided risk factor assessment, personalized feedback and education for all participants. Women aged 60-80 were eligible if they were not taking HRT or other osteoporosis therapy. In the Universal Screening Group, 1986 randomly sampled women were contacted and all were offered BMD testing; 428 women (21.5%) agreed to participate and were tested. In the SCORE Screening Group, 1940 women were sent the SCORE questionnaire and those scoring ≥ 7 were invited for BMD testing; 597 women (30.8%) completed questionnaires and 425 were tested. In the SOF-based Screening Group, 5342 women were sent a SOF-based risk factor questionnaire and those with ≥ 5 risk factors were invited for BMD testing; 2261 (42.3%) completed questionnaires and 150 were tested. Outcomes were evaluated in all eligible participants using intention-to-treat analysis and included: 1) initiation of osteoporosis therapy; 2) hip and other fracture rates; 3) changes in dietary/lifestyle fracture risk factors; 4) osteoporosis knowledge; and 5) satisfaction with the program. Initiation of osteoporosis therapy was slightly higher in the Universal and SCORE groups (21.1% and 20.2%, respectively; vs. 16.7% in the SOF-based group (p-value vs. Universal=0.04). Hip fracture rates were lowest in the Universal group (3.22/1000) as compared to the SCORE (7.95/1000) and SOF-based groups (8.74/1000) but differences were not statistically significant. Rates of all clinical fracture did not differ among the groups. Initiation of calcium supplements was highest in the Universal group (33%) and slightly lower in the other two groups (27-28%). Average values on an exercise scale were highest in the Universal group and lowest in the SOF-based group ($p<0.003$). Knowledge about osteoporosis risk factors differed dramatically with women in the Universal group reporting 57% correct answers as compared with 53% in the SCORE group ($p=0.02$) and 43% in the SOF-based group ($p<0.0001$). Women in all groups reported a high level of interest in seeing a fracture prevention program like this one incorporated into their routine care (82-93%). The degree to which BMD testing was offered to women in a fracture prevention program significantly affected treatment rates, change in modifiable fracture risk factors and knowledge about risk factors. The benefits of bone density testing must be weighed against the costs and competing priorities for prevention of major chronic disease events in older women.

Disclosures: ***A.Z. LaCroix****, Merck & Co. 2.*

SA282

See Friday Plenary number F282.

SA283

The Modal Distribution of Osteoporotic Vertebral Compression Fracture Types. F. E. McKiernan[1], T. Faciszewski*[2]. [1]Center for Bone Diseases, Marshfield Clinic, Marshfield, WI, USA, [2]Department of Orthopedic Spine Surgery, Marshfield Clinic, Marshfield, WI, USA.

Osteoporotic vertebral compression fractures (VCFs) are distributed bi-modally in the thoracolumbar spine (Osteoporosis Int 3:113, 1993); one peak occurring at the mid-thoracic spine and the other at the thoracolumbar juncture. Recent appreciation of the morphometric variety of osteoporotic VCFs, and in particular the dynamic mobility of many VCFs, led us to consider the possibility that the composition of fracture types of these two modal peaks might differ. Herein we describe the distribution of different fracture types that present for vertebroplasty (VP). Dynamic mobility of osteoporotic VCFs was assessed by comparing preoperative standing lateral X-rays with preoperative supine, cross table-lateral X-rays of the index VCF and was defined as any change in fracture configuration apparent with unaided vision. Non-mobile fractures were considered fixed. Clefts, the gross disruption of cortico-cancellous bone, were sometimes characterized by intravertebral gas on plain radiographs or signal void on short-tau inversion recovery (STIR) sequence magnetic resonance (MR) but were defined as low resistance, confluent reser-

voirs for polymethlymethacrylate (PMMA) at the time of VP. Fifty consecutive patients underwent 56 VP procedures to treat 82 VCFs. There were 33 (66%) women and 17 (34%) men. Twenty-four of 50 patients (48%) had mobile VCFs with clefts. Thirty of their 82 VCFs (34%) were mobile and had clefts. Twenty-two of 30 (73%) mobile, clefted fractures occurred at the thoraco-lumbar junction (T11-L1) whereas only 15 of 52 (29%) fixed fractures occurred at that site ($p< 0.001$). Mobile, clefted VCFs accounted for 59% of all VCFs occurring at the thoracolumbar junction and were infrequent elsewhere (Figure 1). These 82 VCFs were distributed in a bimodal manner characteristic of osteoporotic VCFs. Mobile, clefted VCFs clustered at the thoracolumbar junction whereas fixed VCFs dominated elsewhere in the spine. Thus the composition of the two modal peaks is not homogeneous for fracture type. One peak occurring at the mid-thoracic spine is composed largely of fixed VCFs and is where the concentration of axial load is greatest. The second peak consists largely of mobile, clefted VCFs and occurs at the thoracolumbar juncture where the concentration of dynamic load is greatest.

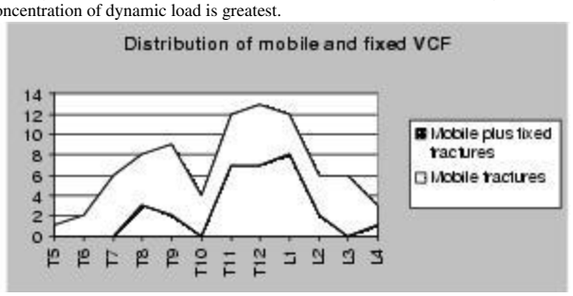

SA284

See Friday Plenary number F284.

SA285

Under Reporting of Vertebral Fractures and the Importance of Standardized Morphometry. S. A. Jackson*[1], L. Robertson*[2], A. Tenenhouse[3]. [1]Nuclear Medicine, University of Alberta, Edmonton, AB, Canada, [2]Radiology, University of Alberta, Edmonton, AB, Canada, [3]McGill University, Montreal, PQ, Canada.

Evidence today indicates that subtle changes within the spine, consistent with a Grade 1, sub clinical fracture of the vertebra can be measured using health related quality of life instruments. The chronic process of osteoporosis leads to posture changes and lifestyle impact at an early stage. Consequently, it is important to detect vertebral changes in order for a suitable therapy to be prescribed and administered. A lateral radiographic series is the primary diagnostic tool. However, the recognition and reporting of vertebral fractures by this technique is subject to considerable observer variability, which may influence the required lifestyle modification. Data presented is derived from the Canadian Multicentre Osteoporosis Study, which is a large population based prospective study of osteoporosis in the Canadian population. The study involves 9424 subjects, both male and female, from nine centers and seven regions of Canada. Each subject completed an extensive interview to obtain medical, demographic and lifestyle information, and was examined by DEXA of the spine and hip, ultrasound of the heel and for subjects over 50 years of age, lateral spine radiographs. Spinal morphometry of the initial radiographs was performed to evaluate the prevalence of vertebral deformity. A method is utilized to extract reference norms for vertebral shape from a subset of the population data, which is then used to categorize any deformity within the whole data set. Radiologists at each center were instructed to report their findings based on a simple definition of 20% height reduction in any of the three vertebral height ratios. One center with specialist expertise acted as the clinical reference. Using the standardized morphometry and 3 standard deviations (Grade 1) as a limit of normality, the male prevalence of 21.5% was similar to the female prevalence of 23.5%. Using 4 standard deviations (Grade 2) this reduced to 7.3% and 9.3%. While our morphometry method agreed with our expert center to within 1%, reporting of fractures from other sites varied between 7% to 35% for a prevalence of Grade 1 fractures and between 1% to 10% for Grade 2. Under reporting of vertebral fractures appears to be a common phenomena, which has implications for clinical studies and patient awareness. The importance of standardized vertebral morphometry, either by radiography or by DEXA is crucial to the early detection of osteoporotic changes within the spine and consistency of radiographic interpretation.

SA286

See Friday Plenary number F286.

SA287

The Impact of Fractures on the Hospital Care System in Italy: Comparison with Other Commonly Admitted Diseases. E. Romagnoli*[1], V. Carnevale*[2], F. Paglia*[1], S. De Geronimo*[1], J. Pepe*[1], E. D'Erasmo*[1], G. Mazzuoli[1], S. Minisola[1]. [1]Dpt. of Clinical Sciences, "La Sapienza" University, Rome, Italy, [2]Dpt. of Internal Medicine, "Casa Sollievo della Sofferenza" Hospital, S. Giovanni Rotondo, Italy.

We investigated the impact of hip, Colles, humeral and vertebral fractures, as compared to other commonly hospitalised diseases, on the health care of the biggest general hospital ("Umberto I") in Rome, Italy. We examined the discharge forms filled in from 1996 to 1999, according to the 9th International Classification of Diseases. Data on fractures were compared to those related to the following diseases: coronary heart disease (CHD), cerebrovascular disorders (CVD), diabetes mellitus (DM), chronic obstructive pulmonary disease (COPD) and breast cancer (BC). Admissions for hip and humeral fractures decreased progressively during the study period, while the number of patients with Colles and vertebral fractures slightly increased. In all groups of patients mean age of females was significantly higher ($p<0.0001$) than that of males. Male patients with hip fractures showed a hospitalisation stay (20.3 ± 20 days) significantly longer than females (14.2 ± 18.9)($p< 0.0001$), while women with Colles fractures showed significantly ($p< 0.02$) higher length of stay (5.5 ± 6.7 vs 4 ± 4). When patients were divided according to age (over or below 60 years), mean hospitalisation length did not differ between younger and older patients in all groups but Colles fractures ($p<0.001$). Hip fracture in older patients showed a striking in-hospital mortality. In the whole period studied hip fractures accounted for the highest annual (more than 1,000,000 of Euro) and per patient (3,500 to 4,500 Euro) costs. In this group of patients, the number of non-invasive procedures increased year by year. The number of female patients with fractures (and obviously breast cancer) was higher, while the opposite applied to the other disorders. Male patients with fractures, CHD, and CVD were significantly younger than females ($p<0.0001$). When deaths percentage (3.6%) was added to that of patients discharged to other institutions (26.3%), fractures showed the poorest outcome of hospitalisation. Global annual costs showed a gradual increase for BC, COPD, CVD, and CHD from 1996 to 1999. Per patient costs were remarkably and progressively higher for CHD (from 4,000 to 6,000 Euro), followed by fractures (average 3,000 Euro). We observed a progressive increase of surgical and diagnostic procedures employed, particularly for patients with fractures and breast cancer. We concluded that fractures represent a growing but often underestimated burden for hospital care in Italy.

SA288

See Friday Plenary number F288.

SA289

Secondary Causes of Osteoporosis in Patients Registered in the Canadian Database of Osteoporosis and Osteopenia (CANDOO). J. P. Brown[1], G. Ioannidis[2], J. D. Adachi[2], A. Petrie*[2], N. Ferko[2], P. Boulos[2], G. F. Stephenson*[3], C. H. Goldsmith*[2], A. Papaioannou[2]. [1]Laval University, Ste-Foy, PQ, Canada, [2]McMaster University, Hamilton, ON, Canada, [3]Procter & Gamble Pharmaceuticals, Toronto, ON, Canada.

The prevalence of causes of secondary osteoporosis varies with the type of population and referral centre. The primary objective of this study was to determine the prevalence of secondary causes of osteoporosis in tertiary referral centers in adults who have experienced a fracture compared to those who have not experienced a fracture. A case-control methodology was conducted utilizing patient information from CANDOO. CANDOO is designed to prospectively compile comprehensive clinical data in multiple centres across Canada and contains data regarding patient demographics, medications and side effects, female reproductive history, diet and quality of life, bone mineral density measurements, fracture history and laboratory investigations. For the current analysis, CANDOO was searched for women and men over the age of 50 years. Data were collected for 5604 women and 561 men with a mean age of 64 years. Approximately 94% of women were postmenopausal at the baseline visit. Of the 1703 (28%) patients with a fragility fracture within 5 years of baseline assessment, 151 had a hip, 539 a wrist, 741 a vertebral, and 281 a rib fracture, respectively. In our cohort, the prevalence of causes of secondary osteoporosis in adults who have experienced a fracture was 45.9% as compared with 40.1% in non-fracture patients ($p<0.001$). 10.1% of fracture patients had vitamin D levels below normal ranges as compared with 5.6% of non-fracture patients ($p<0.001$). Causes of secondary osteoporosis (1 or more) were higher in men, 288/561 (51.3%) than women, 2319/5604 (41.4%)($p<0.001$). Greater use of oral/inhaled corticosteroids is found in men (27.1%), than in women (13.1%) ($p<0.001$). Of patients with osteoporosis, 12.8% had a lung disorder, 3% had a liver disorder, 2% used anticonvulsants, 0.7% had hyperparathyroidism and 1.1% had monoclonal gammopathy. Hypogonadism was not assessed in men. In our cohort, secondary causes of osteoporosis were higher in fracture patients than non-fracture patients. The most prevalent condition associated with secondary causes of osteoporosis was corticosteroid use.

*Disclosures: **J.P. Brown**, Procter & Gamble Pharmaceuticals 2, 5.*

SA290

See Friday Plenary number F290.

SA291

Intervention Thresholds for Osteoporosis. J. A. Kanis*[1], O. Johnell*[2], A. Oden*[3], C. De Laet*[4], A. Oglesby*[5], B. Jonsson*[3]. [1]WHO Collaborating Centre for Metabolic Bone Diseas, University of Sheffield Medical School, Sheffield, United Kingdom, [2]Malmo General Hospital, Malmo, Sweden, [3]University of Stockholm, Stockholm, Sweden, [4]Institute for Medical Technology Assessment, Rotterdam, Netherlands, [5]Lilly Pharmaceuticals, Indianapolis, IN, USA.

With the advent of effective interventions that decrease the risk of fracture, guidance is required to determine who to treat. Against this background, there is an increasing awareness that intervention thresholds should be based on estimates of fracture probability rather than on BMD alone. The aim of this study was to determine the threshold of fracture probability at which interventions became cost-effective. We modelled the effects of a treatment costing $500 per year given for 5 years that decreased the risk of all osteoporotic fractures by 35 percent followed by a waning of effect for 5 years. Sensitivity analyses included a range of effectiveness and intervention costs. Data on costs and risks were from Sweden. Costs included direct costs and costs in added years of life, but exclude indirect costs due to morbidity. A threshold for cost effectiveness of $60,000/QALY gained was used. Cost of added years were excluded in a sensitivity analysis for which a threshold value of $30,000/QALY was used. In the base case, intervention was cost-effective when treatment was targeted to women at average or higher risk at the age of 65 years or older (see Table). In Sweden, this corresponds to a T-score for BMD close to a diagnostic threshold (T< -2.5 SD) in the absence of other risk factors. A less conservative threshold of BMD was cost effective in the presence of strong risk factors where they contribute to a risk that is responsive to intervention (eg a prior fragility fracture).

Age 10 year probability
(years) RR for hip fracture (%)
50 3.9 1.37
60 1.5 3.18
70 <1 5.60
80 <1 13.0

This analysis provides a framework for defining clinical intervention thresholds that can be justified from a health economic perspective. Of particular importance is that elderly women at moderate risk can be offered intervention. Similar analysis should be undertaken in different regions of the world.

SA292

See Friday Plenary number F292.

SA293

A Recent Trend in the Incidence of Hip Fractures in Tottori Prefecture, Japan. H. Hagino, T. Ryota*, H. Katagiri, T. Okano, K. Yamamoto*. Orthopedic Surgery, Tottori University, Yonago, Japan.

[Purpose] Since the growth of the elderly population will be more marked in Asia than in Europe and North America, great increases in osteoporosis-related fractures are predicted in Asia. If an increase in incidence of these fractures is observed, we may expect the more rapid increase in number of patients with fracture in the future than predicted. The purposes of this study were to present the recent trend in the incidence of hip fractures in Tottori Prefecture, Japan. [Methods] Tottori Prefecture is located in mid western Japan. Its population was 616,399 in 1986 and 613,289 in 2000. The percentage of the total population aged 65 years and over was 14.1% in 1986 and 22.0% in 2000. A survey of all fractures in patients 35 years old and over during 1986-88, 1992-94, and 1998-2000 for hip was performed in all hospitals in Tottori Prefecture, Japan. Registration information included name, gender, age, place of residence, date of fracture, type of fracture, and treatment. Patients residing in other prefectures were excluded. Duplication of cases was checked by the patients' name and address. The age- and gender- specific incidence rates (per 100,000 person-years) were calculated based on the population of Tottori Prefecture in each year. [Results] Registered numbers in patients were 272, 287, 359, 464, 404, 480, 604, 671, and 710 in 1986, 1987, 1988, 1992, 1993, 1994, 1998, 1999, and 2000, respectively. The number of women was more than three times the number of men. The mean age- and gender-specific incidence rates (per 100,000 person-years) for men in 1986-1988 were 174.7, 219.3, and 622.3 in the age groups of 75-79, 80-84 and over 84, respectively, and those in 1992-1994 were 235.7, 322.8, and 655.6, and those in 1998-2000 were 227.7, 392.9, and 832.4, respectively. Those for women in 1986-1988 were 474.4, 756.0, and 1266.7, and those in 1992-1994 were 479.9, 934.0, and 1696.5, and those in 1998-2000 were 489.7, 1146.8, and 2088.7, respectively. The incidence rates showed a significant increase with time. [Conclusion] An increase in the incidence rates of hip fractures was observed from 1986 to 2000 in Tottori Prefecture, Japan.

SA294

Management of Osteoporosis in Women Aged 50+ with Osteoporosis-related Fractures. M. J. Gunter*[1], S. K. Brenneman[2], S. J. Beaton*[1], Y. Chen*[2], T. A. Abbott[2]. [1]Lovelace Clinic Foundation, Albuquerque, NM, USA, [2]Merck & Co., Inc., West Point, PA, USA.

Post-menopausal women with a non-traumatic fracture are likely to have low bone mass and are prone to subsequent fractures. Guidelines recommend evaluation and treatment of osteoporosis in post-menopausal women following a fracture. We describe the pattern of diagnosis and treatment of osteoporosis in women age 50+ following an osteoporosis-related fracture. A retrospective cohort study was conducted at a large managed care system located in the southwestern United States. Study subjects were women, age 50+ years, with at least one osteoporosis-related fracture in the calendar years 1996 - 1998 and who were continuously enrolled in the system's health plan for at least 6 months prior to and post fracture. Data were obtained from an administrative claims database. Information on bone-density scans, diagnosis of osteoporosis, and treatment with any FDA-approved medication (including HRT) for osteoporosis was obtained using ICD-9, CPT, and NDC codes.42,041 women ≥ 50 years of age were in the health plan during the study period. 658 continuously enrolled women were identified who had an osteoporosis-related fracture: 189 (29%) hip fractures, 221 (34%) wrist fractures, 127 (19%) vertebral fractures, 116 (18%) rib fractures. In the post-fracture period, 46 (7 %) underwent bone-density testing, 142 (22 %) had a diagnosis of osteoporosis, and 220 (31 %) were treated with at least one of the medications approved for the treatment of osteoporosis. Of the 220 women who had medication claims, 124 (56%) were for HFT and 96 (44%) were for other anti-resorptive agents. Only 80 (16%) were new claims for women who did not have medication claims during the 6 months prior to the fracture. Osteoporosis diagnosis and treatment of postmenopausal-aged women with fractures remain inadequate, despite existing recommendations that osteoporosis be the presumptive diagnosis. There is significant opportunity for improvement in assuring post-fracture follow-up care.

Disclosures: ***M.J. Gunter,*** *Merck & Co., Inc. 2, 5.*

SA295

See Friday Plenary number F295.

SA296

Determining a Clinically Meaningful Difference in a Performance-Based Measure to Assess Recovery from Hip Fracture: The Lower Extremity Gain Scale (LEGS). S. Zimmerman*[1], G. Williams*[2], P. Lapuerta*[2], T. Li*[2], W. Hawkes*[3], D. Orwig[3], L. Wehren[3], J. Hebel*[3], J. Magaziner[3]. [1]University of North Carolina, Chapel Hill, NC, USA, [2]Bristol Myers Squibb, Princeton, NJ, USA, [3]University of Maryland Baltimore, Baltimore, MD, USA.

The Lower Extremity Gain Scale (LEGS) is a validated performance measure of tasks that are often impaired in hip fracture patients. The goal of this analysis is to determine a clinically meaningful difference in LEGS. The analysis used 139 white female patients age 65+ admitted to one of two Baltimore hospitals. Patients were assessed at baseline and 2, 6, and 12 months post-fracture. Average age was 80.2; 55.1% had subcapital fractures. The LEGS score is based on timed performance of 9 activities: walking 10 feet, rising from an armless chair, reaching for an item on the ground, putting on socks, putting on shoes, stepping up and down stairs, and getting on and off a toilet. Each task was scored from 0-4, with higher scores representing better performance. Scores were combined to produce a summary score, ranging from 0-36. Recovery level was determined by the LEGS score, estimated at the point at which the rate of change with time was less than 1% of one standard deviation (SD) of the LEGS. The clinically meaningful difference in the score was evaluated using 2 methods. The anchor-based approach examined the relationships between the LEGS recovery level and age. The LEGS score difference associated with a five year increase in age was considered clinically meaningful. The second, distribution-based, method was determined according to Cohen's effect size. A clinically meaningful difference was defined as a difference in LEGS score with an effect size of .20. According to our model, a difference of approximately 5 years in age corresponded to a difference of 1.6-2.6 points. The SD for LEGS at 12 months was 8.0; thus Cohen's effect size was 0.2-0.32. This suggests a clinically meaningful difference in the LEGS scores for a population in this age range would be 2-3 points. In another anchor-based analysis using by tertiles of grip strength at baseline [<13 kg (weak), >13-18 kg (average), and >18 kg (strong)], the strong group had the best recovery (LEGS score 28.1) in the shortest time (10.1 months). The average group reached a level of 25.4 points in 11.6 months and the weak group reached 22.7 points in 15.5 months. Similar to the age analysis, the strength analysis indicated effect sizes in the range of 0.25-0.3 SD. Both methods suggest that a difference of 2 points in the LEGS score is clinically meaningful. LEGS is the first validated performance measure for use in hip fracture patients and has important potential application in clinical research on interventions to maximize recovery after fracture.

Disclosures: ***J. Magaziner,*** *Bristol Myers Squibb 2.*

SA297

See Friday Plenary number F297.

SA298

Does Having a Fracture Predict Future Fractures in Men Aged 60 Years and Older. B. Ettinger[1], G. T. Ray*[1], A. R. Pressman*[1], O. Gluck[2]. [1]Division of Research, Kaiser Permanente Medical Care Program, Oakland, CA, USA, [2]Arizona Rheumatology Center, Phoenix, AZ, USA.

Background: It is not known whether fractures in elderly men predict future fractures. We hypothesized in elderly men as in elderly women, that fractures of hip, wrist, humerus, and ankle would indicate osteoporosis and skeletal fragility. **Methods:** We examined fracture incidence among male members of a large health plan in Northern California who were aged 60 years and older and who either had no fracture in 1997-1998 (20% sample), or had a hip, ankle, wrist, or humerus fracture during 1997-2001. Fractures were identified using the health plan's electronic databases containing hospitalization, emergency room, and office visit diagnoses. We used proportional hazards models to compare risk of subsequent fractures of hip, ankle, humerus, or wrist between the different groups, after adjusting for age. Recurrences of the same fracture type were excluded from the analyses. **Results:** During an average of 2.4 years follow-up, the percent of persons in the non-fracture control group having a subsequent first fracture of the humerus, hip, wrist or ankle was .21%, .55%, .40% and .50% respectively. Relative to controls, those with prior humerus fractures were almost 4 times more likely to suffer one of the 3 non-hip fractures (either wrist, humerus, or ankle) (RR, CI; 3.7, 2.4-5.6). Those with prior hip or wrist fractures were about twice as likely to fracture (2.4, 1.5-3.8 and 1.9, 1.2-3.0, respectively). In contrast to men with history of osteoporotic-type fractures, those with prior ankle fracture had no greater risk of subsequent fracture than non-fractured controls (0.8, 0.4-1.6). Stratified analyses of men 60-69 and men over 70 yielded similar results. To test for healthy cohort effect, we used as another control group, men 60 years and older who were treated for closed finger fracture. Their subsequent fracture incidence was similar to the non-fractured controls, and using them as the control group produced similar relative risks. **Conclusion:** We conclude that among elderly men, a recent history of humerus, hip, or wrist fracture is a statistically significant and clinically relevant predictor of future osteoporotic fracture risk, but that a history of ankle fracture is not.

Disclosures: ***B. Ettinger****, Merck 2; Eli Lilly 2, 8; Berlex 2.*

SA299

Smoking Is a Risk Factor for Osteoporosis in Men -Longitudinal Study. S. Hagiwara[1], T. Ueda*[2], T. Hayashi*[3], A. Takagi*[2], Y. Mimura*[2], O. Ou*[1]. [1]Matsushita Health Care Center, Moriguchi, Japan, [2]Matsushita Electric Industrial Co.Ltd., Kadoma, Japan, [3]University of Washington, Seattle, WA, USA.

Osteoporosis in men has been focused recently. However, few longitudinal studies are available yet. We evaluated the bone mineral density (BMD) of the heel in Japanese men cross-sectionally and longitudinally. The subject of this study consists of 889 men with the mean age of 41.3 ± 7.5 (SD) years. BMD of the right heel is measured using a Dual X-ray Absorptiometry (DX-2000, Matsushita Industrial Equipment, Japan) at the initiation of this study (Pre) and 5 years thereafter (Post). Smoking habit, alcohol intake in ethanol, and exercise habit are asked using a questionnaire at the time of both examinations. The rate of current smokers is 51.7%, and those with drinking habit and positive exercise habit at Pre are 85.3% and 27.7% of the subject, respectively. The mean alcohol intake is 26.1 ± 24.3 ml in ethanol in a day. Positive exercise habit means that the subjects perform exercise at least 30 minutes in a day per week periodically, regardless of the kind of exercise. The mean BMD at Pre is 0.928 ± 0.093 g/cm^2, and that at Post is 0.910 ± 0.086 g/cm^2. The rate of BMD decrease is -1.8 ± 3.4% for 5 years. As shown in the Table, age, body weight, change of body weight between two measurements, vigorous exercise, daily alcohol intake, and the number of cigarette smoking at Pre are significant determinants for Post BMD ($p<0.001$). The coefficient of determination is 31.6%. In terms of BMD change between two measurements, age, body mass index (BMI) and change of BMI during the observation period are significant factors with the coefficient of determination of 2.6% ($p<0.001$). Cross-sectional analysis also indicates that age, body weight, vigorous exercise, daily alcohol intake, and current smokers are significant determinants for heel BMD ($p<0.001$). The coefficient of determination is 29.7%. These results suggest that smoking is one of the risk factors for heel BMD, and vigorous exercise should be recommended for the prevention of osteoporosis in men.

Multiple linear regression analysis of heel BMD

Independent variables	Regression coefficient	p-value
Age	-0.069	0.029
Body weight	0.543	<0.001
Change of body weight between two measurements	0.066	0.033
Vigorous exercise	0.088	0.004
Daily alcohol intake	0.085	0.008
Number of cigarette smoking	-0.088	0.006
Model R-square	0.316	<0.001

SA300

See Friday Plenary number F300.

SA301

Poor Physical Function Exacerbates the Already Adverse Association between Low Self-reported Physical Activity and BMD in Older Men. J. J. Anderson*[1], D. R. Miller[2], E. A. Krall[1], S. E. Rich*[1], D. P. Kiel[3]. [1]Boston University, Boston, MA, USA, [2]Massachusetts Veterans Epidemiology Resource & Information Center, Boston, MA, USA, [3]Hebrew Rehab Center & Harvard Medical School, Boston, MA, USA.

Both bone density (BMD) and self-reported physical activity decline with age in men over 50, however most previous studies have focused on women. The possible association between physical activity and BMD may also be affected by physical function. We examined the association between self-reported physical activity measured using the Physical Activity Scale for the Elderly (PASE) and BMD at 3 hip sites, adjusting for age and for BMI, in 2 male cohorts: the VA Longitudinal Osteoporosis Research (VALOR) study, and males aged >50 years in the Framingham Osteoporosis Study (FOS). VALOR includes both VA patients (VA-P) and a subgroup of veterans who are not VA patients (non-P). Femoral neck, trochanter and Ward's area BMD were measured using Lunar DPX-L models. In VALOR physical function (pf) was measured using the physical component score (PCS) of the SF-36. In regression analyses (with GEE modeling for VALOR data having up to 3 observations per subject) we assessed associations per population group between PASE (per 50 PASE unit range) and BMD at each site, accounting for age (per 5 year range) and BMI (approximate quintile ranges). We stratified by pf (low pf = PCS <35) within VALOR. The FOS males (n=1126) were aged 50-86 years (median 63) and the VALOR subjects (n=542 VA-P observations, n=522 non-P) were aged 50-91 (median 73). BMI values of 25, 27, 29 and 32 defined approximate quintiles in all groups. FOS and non-P subjects had similar PASE means (157+73, 150+84). VA-P subjects reported less activity (122+83) and also worse pf than non-P (43% vs 10% had low pf). After adjustment for age and BMI categories there were associations between PASE and BMD at all 3 sites among the VA-P (0.7% higher BMD per PASE level, $p<.03$ at each site) and for the FOS subjects (0.6% higher/PASE level at each site, $p=250$ compared with PASE 100-149 by 5-6% per site in FOS, by 3-4% for non-P, and by 2- 4% in VA-P. BMD was lower for PASE <50 compared with PASE 100-149 by 5- 8% across bone sites in VA-P, but did not vary across the lower PASE levels in either non-P or FOS subjects. Among low pf subjects, adjusted BMD was 11-13% lower for PASE <150 vs PASE > 150. These results indicate lower levels of self-reported physical activity are associated with lower hip BMD in older men, and that men with low levels of physical function and lower levels of physical activity have even lower hip BMD, an effect comparable to several decades of normal aging.

SA302

See Friday Plenary number F302.

SA303

Recruitment Design for the Osteoporotic Fractures in Men Study (MrOS). P. E. Mannen[1], J. B. Blank*[2], M. Carrion-Peterson*[3], R. Delay*[4], L. Harper*[5], P. Johnson*[6], E. Mitson*[7], K. L. Stone[1]. [1]Univ of California, San Francisco, CA, USA, [2]Oregon Health and Sciences Univ, Portland, OR, USA, [3]Univ of California, San Diego, CA, USA, [4]Stanford Univ, Palo Alto, CA, USA, [5]Univ of Pittsburgh, Pittsburgh, PA, USA, [6]Univ of Alabama, Birmingham, AL, USA, [7]University of Minnesota, Minneapolis, MN, USA.

The Osteoporotic Fractures in Men Study (MrOS) is a prospective observational study designed to determine risk factors for osteoporosis and fractures in men aged >= 65. Recruitment of participants for this study has recently concluded, and the design of and results from the recruitment strategies will be outlined here. In March and April 2000, recruitment for MrOS began in 6 clinical centers across the US (Univ of Alabama, Birmingham; Univ of Minnesota; Univ of Pittsburgh; Stanford Univ; Oregon Health & Science Univ and Univ of California, San Diego.) The study is directed by an administrative core at OHSU and coordinated by Univ of California, San Francisco. These centers were selected for involvement in this NIH-sponsored investigation based on experience in conducting large, complex studies, and for racial and geographic diversity. At the end of the baseline recruitment period in March 2002, 6,008 participants have been enrolled in the MrOS study, 5% more than the original recruitment goal of 5,700. Minority recruitment has exceeded expectations, as 621 participants (10% of the cohort) listed at least one racial minority background on the study questionnaire (243 African American, 194 Asian). These minority recruitment totals are roughly double the original goals determined at study onset. Recruitment of the "oldest" old, or men age >80, was exceptional, with nearly 18% of the cohort (N=1,060) classified in this age category. All clinical centers completed recruitment on time, with 3 clinics finishing more than 3 months ahead of schedule. Recruitment strategies varied by site, and included DMV, HCFA, voter registration and participant database mailings; community and senior newspaper advertisements; and targeted presentations. A centrally created recruitment brochure enhanced each site's promotional materials. These strategies resulted in an extremely successful recruitment campaign, as response to mass mailings surpassed 10-15% at some sites (compared to a 2-5% expected response rate.) Appointment show rates were an above average 80-90%. Retention so far in the study has been outstanding, as response to one-page follow-up questionnaires mailed every four months has been greater than 99%. Our initial concerns that men would not participate in a study of a "women's disease" were unfounded. Older men, even those over age 80, were enthusiastic about participation. Recruitment for MrOS has been successful.

SA304

See Friday Plenary number F304.

SA305

Femoral Bone Size Among Older Men and Its Relation to Lean and Fat Mass. L. M. Marshall*[1], T. F. Lang[2], J. A. Cauley[3], K. E. Ensrud[4], E. S. Orwoll[1]. [1]Oregon Health & Science University, Portland, OR, USA, [2]University of California, San Francisco, San Francisco, CA, USA, [3]University of Pittsburgh, Pittsburgh, PA, USA, [4]VA Medical Ctr & Univ of Minnesota, Minneapolis, MN, USA.

Bone size, a determinant of bone strength, is a component of fracture resistance. Bone size has been shown to be related to body weight. However, body weight is comprised of fat and lean mass, and the association of bone size with body composition is not well characterized. Thus, we examined whether lean mass and fat mass are independently related to femoral cross-sectional area (CSA). The study population included 835 men ages 65 and older from Minneapolis (n=526) and Pittsburgh (n=309) who are participants in the Osteoporotic Fractures in Men study. At the baseline exam, total fat mass (FM) and lean mass (LM) were obtained from DXA, height (cm) and weight (kg) were measured, and leg power (watts) was assessed on a Nottingham Power Rig. Femoral size, defined as the CSA (cm^2), and volumetric BMD (vBMD) were obtained from quantitative computed tomography (QCT) at the femoral neck, the intertrochanteric plane, and the femoral shaft. We used multiple linear regression to examine the independent relations of LM and FM with CSA. The associations are reported as the change in CSA per 7 kg change in either LM or FM, which is about one standard deviation (sd) in the distribution. The mean age (sd) of the study population was 73.3 (5.7) years. The mean (sd) and inner quartile range (IQR) of each CSA was: femoral neck CSA, 13.9 (1.8), IQR 12.6-15.0; intertrochanteric CSA, 36.0 (4.6), IQR 32.9-38.5; and shaft CSA, 9.1 (1.1), IQR 8.4-9.8. After adjustment for city, age, height, vBMD and FM, LM was independently related to each CSA measure (see table).

Change in CSA (95% Confidence Interval) per 7 kg Change in Variable

Variable	Femoral Neck CSA	Intertrochanteric CSA	Shaft CSA
Lean Mass	0.77 (0.62, 0.91)	1.75 (1.38, 2.11)	0.52 (0.42, 0.63)
Fat Mass	-0.11 (-0.23, 0.004)	-0.21 (-0.49, 0.08)	-0.10 (-0.18, -0.02)

FM was inversely related to CSA, but the association was statistically significant only for shaft CSA. The estimates for LM did not change materially when body mass index (kg/m^2) replaced FM in the models. Adding leg power to the multivariable models did not alter the associations of LM with CSA, and leg power was not associated with any CSA measure. In these cross-sectional data among older men, we observed substantial variation in femoral bone size. In multivariate analyses, CSA was independently related to LM but not to FM. Clarifying the mechanism underlying this association could provide insight into bone size regulation among older men and its relation to fracture risk.

SA306

The Clinical Utility of Laboratory Testing in Women with Low Bone Mineral Density. S. A. Jamal[1], A. M. Bayoumi*[2], R. Wagman[3], S. R. Cummings[3], D. C. Bauer[3]. [1]Endocrinology and Metabolism, University of Toronto, Toronto, ON, Canada, [2]General Internal Medicine, University of Toronto, Toronto, ON, Canada, [3]Epidemiology and Biostatistics, University of California, San Francisco, San Francisco, CA, USA.

Although clinicians often test women with low bone mineral density (BMD) for secondary causes, the utility of routine laboratory testing is unknown. We evaluated the frequency and correlates of abnormal lab tests among 15,371 women from 11 communities in the U.S. who were screened for the Fracture Intervention Trial. Women with femoral neck BMD of 0.68g/cm2 or less (Hologic QDR 2000, Waltham, Mass) had blood drawn for electrolytes, creatinine, urea, complete blood count, alkaline phosphatase, calcium and albumin, random glucose, transaminases, thyroid stimulating hormone and intact parathyroid hormone. Specimen processing was standardized and blood was analyzed at a central laboratory. We classified results outside the reference range as abnormal. The mean age was 69.2 years (± 5.9), and most women (14835 or 97%) were Caucasian. About 1/3 (5381) had normal laboratory tests, 1/3 (5449) had one abnormal result, and the remainder (4541) >2 abnormal laboratory results. The femoral neck T score was <= -2.5 in 5806 (38%) of the women; the remainder had a T score between –1.5 and –2.5. Total body T score was <=-2.5 in 3786 (25%) of the women; the remainder had osteopenia. Compared to women with osteopenia, the prevalence of one or more abnormal laboratory results was slightly higher in women with osteoporosis at the femoral neck (30% vs. 28%; p=0.039) and at the total body (32% vs. 28%; p=0.001). Of the 12,767 women who had spinal radiographs, 2678 (21%) had prevalent vertebral deformities. There was no association between prevalent vertebral deformities and abnormal laboratory results (Odds Ratio [OR]: 1.0; 95% Confidence Interval [CI]: 0.94 to 1.1). Women with osteoporosis at the femoral neck or total body were only slightly more likely to have one or more abnormal laboratory tests (OR: 1.1; 95% CI: 1.0 to 1.2 and OR: 1.3; 95%CI: 1.2 to 1.4) after adjusting for age and weight. Age, weight and the presence of osteoporosis, either at the femoral neck or total body, did not discriminate between women with abnormal and normal laboratory results. Results were similar for women with two or more abnormal test results to women with one or no abnormal test results. We found no clinically important association between abnormalities in a variety of laboratory tests and either low BMD, or vertebral fracture. This suggests that abnormal screening tests in women with osteoporosis are usually incidental findings unrelated to osteoporosis and raises questions about the value of testing for secondary causes in women with osteoporosis.

SA307

See Friday Plenary number F307.

SA308

Computed Posturographic Analysis of Swaying in Aging, Osteoporosis and Degenerative Joint Disease. T. Fujita. Medicine, Calcium Research Institute, Kishiwada, Japan.

Track of the gravity center of the body on standing straight was analyzed by computerized posturography in 136 subjects with osteoporosis and/or degenerative joint disease such as spondylosis deformans and osteoarthritis of the knee. As indices of swaying and postural instability, total length of the track of gravity center (LNG), LNG per unit time indicating sway speed (LNG/T), LNG per unit area estimating sway control mechanism (LNG/A), total area enveloped by the track (ENV), rectangular area covered by the track (REC) and root mean square area of the circle with the radius calculated as a mean of the distance between the center of the track curve and each gravity center (RMS) were measured with the eyes opened and closed by using Gravicorder GS-30 made by Anima Company, Tokyo. For each measurement, the ratio between closed-eye and open-eye values was calculated. Open-eye and closed eye LNG, LNG/T ENv, REC and RMS showed significant positive correlation with age, suggesting an age-bound increase of swaying. While mean lumbar bone mineral density (LBMD) indicating a progress of osteoporosis failed to showed significant correlation with any of these swaying parameters, intraindividual variation of LBMD indicating an advance of spondylotic deformity showed a significant positive correlation with open-eye ENV, REC and RMS and closed-eye RMS. Multiple logistic regression analysis os these swaying parameters on fracture revealed a significant regression of only open-eye REC (p=0.0084,with odd's ratio of 2.87 ; 95% confidence limits : 1.31-6.31). After treatment with 200 mg/day etidronate and 900 mg/day AAA Ca (active absorbable algal calcium), open-eye LNG and close-eye LNG/A, REC and RMS as well as closed-open ratio of LNG, LNG/T, LNG/A, REC and RMS shpwed significant improvements. Aging and spondylotic deformity of the spine is associated with postural instability, whch showed improvement in response to treatment with etidronate and AAA Ca.

SA309

See Friday Plenary number F309.

SA310

Osteoporosis Risk Factors Comparison between Outpatient and Population Screening. A. Defer*. REGO Sachsen/Thüringen, Dresden, Germany.

How do the results of the osteoporosis risk factors analysis differ between women of medical practice and a populations screening? Material and methods: The 11 risk factors of the osteoporosis risk questionnaire of the REGO Saxony & Thuringia were base of the analysis. This questionnaire consists of the following complexes: Bone fractures since the 40^{th} year of life , late menarche , early menopause , low mobility , low consumption of dairy products , falls, abuse of alcohol and nicotine , taking or having taken Cortisone for longer than 6 months , family anamnesis , back pains. 1010 data sets of women were analyzed from the medical practice. These data were subdivided into groups after the bone density diagnosis and into 3 age-groups. Women in the age of 70 to 71 year with an osteoporosis were selected especially for comparison purposes with the population screening analysis. This population screening analysis was carried out in a small town. 50% of the 70-year-old women living there participated with a full risk questionnaire. The percentage frequencies of the data to the 11 risk factors in the different patient groups and in the screening group were compared. Results: Of the 11 risk factors no significant arguments showed Menopause, falls, alcohol and nicotine into relation to the bone density. Clear differences were found at fractures (26% at normal BMD to 50% at osteoporosis) at the menarche (50% to 61%), at the mobility (8% to 17%) and at the milk consumption (10% to 15%) . A positive families case history and back pains are a little more frequent at normal bone density than at osteoporosis (36% to 26% and 95% to85%). Table 1 shows all clear data differences of the comparison in age-groups and between the 70-year-old patients and the 70-year-old women from the screening population analysis. No essential differences were found at the mobility, at falls, at alcohol and nicotine in these groups.

Table 1	Fracture	Menarche	Menopause	Milk	Cortisone	Family	Back pain
Women < 66 years, n=231	39	62	29	11	8	32	88
Women 66-75 years, n=348	55	64	26	16	11	24	86
Women >75 years, n=149	23	28	9	8	5	16	79
Women 70-71 years, n= 75	**47**	**56**	**17**	**16**	**11**	**32**	**92**
women in screening, 70 years, n=86	**26**	**34**	**5**	**2**	**6**	**26**	**65**

Summary: Osteoporosis risk factors can distinguish healthy women from osteoporosis partly. The degree of the distinction possibility is age dependent.

SA311

See Friday Plenary number F311.

SA312

L-Thyroxine Replacement Accelerates Bone Turnover in Patients with Subclinical Hypothyroidism: Results from a Double-Blind Placebo-controlled Study. C. Meier, B. Müller*, M. Christ-Crain*, M. Kunz*, M. Guglielmetti*, J. J. Staub*, M. Kraenzlin. Department of Medicine, Division of Endocrinology, Basel, Switzerland.

Initiation of L-T4 therapy activates bone remodeling with initial loss of bone mineral density in overt hypothyroidism. Data on the effects of L-T4 replacement on bone turnover and bone density in subclinical hypothyroidism (SCH) are scarce. 61 women (mean age 57.1± 1.3 years) with SCH (mean TSH 11.8± 0.9 mU/L, range, 4.7-46.3 mU/L, with normal thyroid hormones) were randomized to receive either L-T4 (mean dose 85.5± 4.3 µg/d; n=31) or placebo (n=30) for 48 weeks. Physiological L-T4 replacement was guaranteed throughout the whole study period by blinded continuous TSH monitoring and adaptation of L-T4 dose. Thyroid hormones, bone mineral density [BMD; DXA], and biochemical markers of bone formation (Osteocalcin [OC], alkaline phosphatase [ALP]) and bone resorption (C-term. telopeptides type I collagen [CTX], deoxypyridinoline [DPD], pyridinoline [PYD]) were measured at 0, 24 and 48 weeks of treatment. At baseline, thyroid hormones, BMD and biochemical markers were identical in both treatment groups. In L-T4 treated patients (TSH 3.1± 0.3 mU/L) markers of bone formation increased progressively: ALP was changed after 24 weeks (p=0.05) and 48 weeks (p=0.004), whereas OC was significantly increased only after 24 weeks (p=0.03). Markers of bone resorption increased significantly after 24 and 48 weeks: PYD (p=0.003, p=0.016 resp.) and DPD (p=0.003, p=0.014 resp.). In contrast, CTX remained unchanged. The increase of bone resorption markers was more pronounced in premenopausal women and women on HRT (n=17). In the L-T4 group BMD decreased by 1.3% (p=0.006) at the lumbar spine, while femoral BMD remained unchanged. During placebo administration no significant changes of these markers were found. L-T4 replacement in SCH is associated with an increase in bone remodeling as documented by significant changes in markers of bone formation and resorption. Consistent with data in patients with overt hypothyroidism, lumbar bone loss was found in the first year of L-T4 treatment. However, the observed reduction in lumbar BMD is smaller and well within the range of precision error of the method and, thus cannot be interpreted as overzealous treatment effect. Based on this placebo-controlled study with physiological L-T4 replacement, we recommend that patients with SCH (e.g. TSH >10 mU/L) should be treated without concern about adverse effects on skeletal integrity.

SA313

Geometry of the Hipin Relation to Age and Sex -a Cross-Sectional Study in Healthy Adults. N. Nissen*[1], E. Hauge*[2], B. Abrahamsen[1], J. E. Bech-Jensen[3], L. Mosekilde[4], K. Brixen[1]. [1]Dept of Endocrinology M, Odense University Hospital, Odense, Denmark, [2]Institute of pathology, Aarhus University Hospital, Aarhus, Denmark, [3]Osteoporosis Research Clinic, Hvidovre, Denmark, [4]Dept of Endocrinology C, Aarhus University Hospital, Aarhus, Denmark.

The age-related bone loss and increased tendency to fall have been demonstrated as the main factors causing hip fracture, however, neither age-related osteoporosis nor the increased risk of falling sufficiently explains the exponential increase in the incidence of hip fracture. It has been suggested that the geometry of the hip is a predictor for hip-fractures independent of bone mineral density (BMD). The purpose of the present study was to investigate the natural variation of the geometry of the hip in relation to age and sex. Using newly developed software, we measured hip-axis-length (HAL), neck-width (NW), neck-shaft-angle (NSA), and femoral head-radius (HR) from DXA-scans performed on a Hologic QDR-1000 densitometer. The study population consisted of 217 healthy adults, aged 18-82 yrs, recruited at libraries, factories, educational institutions, etc. The effects of age and sex on the measured parameters were investigated using multiple regression analysis (SPSS).

	Hip axis length	Neck width	Neck-shaft-angle	Fem. head radius
Male (n=80)	10.9 +/- 0.8	3.9 +/- 0.4	131 +/- 4	2.6 +/- 0.3
Female (n=137)	9.5 +/- 0.6	3.4 +/- 0.7	130 +/- 4	2.3 +/- 0.2

Data are displayed in centimeters or degrees

We found that HAL depended on sex ($p<0.001$, $R^2=0.08$) but not on age. NW depended only on sex ($p<0.001$, $R^2=0.16$) but not on age. A trend towards increasing NW with age ($p=0.09$) was seen in males but not in females. Age and sex were significantly correlated to NSA ($p=0.05$ and $p=0.02$, $R^2=0.047$). HR is also significant correlated to age and sex ($p<0.01$ and $p<0.001$, R^2 0.34). In conclusion, HAL, NW, HR, and NSA differ between genders. Also, age explained a small proportion of the variation in NSA and HR, however, this may be due to a generation-effect. Supporting previous *ex vivo* findings, NW tends to increase with age in males.

Disclosures: ***N. Nissen****, Eli Lilly 2.*

SA314

See Friday Plenary number F314.

SA315

Racial, but not Sex, Differences in Vertebral Body Volumetric Bone Mineral Density in Asian and Caucasian Women and Men. Y. Duan[1], X. F. Wang*[1], C. H. Turner[2], E. Seeman[1]. [1]Department of Medicine, Austin & Repatriation Medical Centre, Melbourne, Australia, [2]Department of Orthopaedic Surgery, The Biomechanics and Biomaterials Research Center, Indianapolis, IN, USA.

Asians have lower vertebral body aBMD than Caucasians. We hypothesized that the prevalence, and perhaps incidence of vertebral fractures in Asians and Caucasians is similar because of scaling; a reduced muscular loading on a commensurately smaller vertebral body in Asians will produce a similar ratio in load/bone strength – ie a similar fracture risk index (FRI). We studied 94 healthy Asians (Chinese ancestry, 58 females, 36 males) and 396 healthy Caucasians (304 females, 92 males) aged 18 to 43 yrs. Vertebral body (VB) cross-sectional area (CSA), aBMD and volumetric BMD (vBMD, excluded posterior elements) were measured by using dual x-ray absorptiometry by postero-anterior and lateral scanning. We calculated vertebral body compressive stress (load/CSA) and FRI during bending forward. Results (mean ± sem). VB aBMD was 20% higher in Asian men than Asian women because CSA was 26% greater in men than women (10.45 ± 0.25 vs 8.29 ± 0.12 cm2); there was no sex difference in vBMD (0.289 ± 0.008 vs 0.274 ± 0.007 g/cm3, NS), stress (329.5 ± 11.0 vs 316.1 ± 6.2 N/cm2, NS), and FRI (0.32 ± 0.01 vs 0.37 ± 0.02, NS). Similar figures were presented in Caucasian men and women. Compared to Caucasians, VB CSA was 13% higher in Caucasian than Asian men and 15% higher in Caucasian than Asian women. VB vBMD was 13% lower in Caucasian men than Asian men, and 9% lower in Caucasian women than in Asian women. There were no different in load per unit CSA between Asian and Caucasians in either gender. However, both Caucasian men and women had higher FRI than Asian men and women, respectively (men 0.41 ± 0.02 vs 0.32 ± 0.01; women 0.42 ± 0.01 vs 0.37 ± 0.02, both $p < 0.01$). In summary and conclusion, (i) The higher aBMD in Asian men than women is due to the larger bone size, vBMD was no different in Asian men and women (this is true for Caucasian men and women). (ii) The load per unit CSA is no different between genders and races, suggesting that the smaller bone is loaded by a proportionally smaller load. (iii) At peak, Asians achieved a smaller bone size but higher vBMD than Caucasians, conferring a lower risk of vertebral fractures. Whether the higher vBMD in Asians than Caucasians is due to the greater trabecular number, thickness or thicker cortical shell are unknown.

SA316

Young-old Differences in Proximal Femoral BMD and Size in Women. M. Meta[1], A. Yu*[1], J. Keyak*[2], J. Li*[1], H. Genant[1], T. Lang[1]. [1]Department of Radiology, University of California, San Francisco, CA, USA, [2]Department of Orthopedic Surgery, University of California, Irvine, CA, USA.

It is thought by some that structural geometry of the femoral neck changes with age to compensate for the age-related loss of bone mineral and that the higher incidence of hip fracture in women may be related to gender differences in these changes. To examine this issue, we have compared groups of young (mean age 41±3 years) and elderly (75±4 years) healthy Caucasian-American women recruited from the San Francisco Bay Area. To compare BMD and geometric parameters, both groups underwent volumetric quantitative computed tomography (vQCT) of the hip (GE 9800Q, 3-mm slice thickness). Images were processed to measure integral (iBMD), trabecular (tBMD) and cortical (cBMD) BMD of the femoral neck and trochanteric regions of the hip. The geometric parameters included the integral volume (iVOL) of the femoral neck and trochanteric regions, the minimum and maximum cross-sectional area (CSA) along the femoral neck axis. The minimum CSA occurred at the thinnest section of the femoral neck, and the maximum CSA occurred at the thickest intertrochanteric plane. We used analysis of covariance to compare measurements between young and old women adjusting for height and weight differences. Mean values (SD) are tabulated below. BMD units are g/cm^3, volume cm^3 and cross-sectional area cm^2.

	iBMD	tBMD	cBMD	iVOL	CSA
Femoral Neck					
Young	0.331*** (0.04)	0.152*** (0.03)	0.518 ns (0.05)	19.7 ns (4.05)	10.0 ns (1.87)
Old	0.264 (0.04)	0.064 (0.05)	0.516 (0.05)	20.1 (5.44)	10.5 (1.76)
Trochanteric					
Young	0.312*** (0.04)	0.140*** (0.03)	0.564** (0.03)	81.7** (2.8)	25.7*** (3.21)
Old	0.250 (0.04)	0.088 0.03)	0.531 (0.05)	89.9 (2.04)	29.7 (3.2)

*** $p<0.001$, ** $p<0.01$, ns $p>0.05$

In the femoral neck, iBMD and tBMD declined with age, but cBMD and the bone size parameters did not change significantly. In the trochanteric region, all BMD parameters declined with age, but the bone size parameters increased. These data are consistent with an absence in women of an increase in femoral neck size to compensate for decreased BMD. However, the age-related decrease observed in all of the trochanteric BMD parameters was accompanied by an increase in iVOL and CSA. This pronounced inter-site difference may be due to differences in how body weight is supported in the different regions as well as the potential effect of muscle forces, given that the trochanteric region, but not the femoral neck, is an important muscle attachment site.

SA317

Endocortical Remodeling in the Human Femoral Neck: Increased Bone Resorption Surfaces Across the 'Neutral Loading Axis' of Hip Fracture Cases. J. Power*[1], N. Loveridge[1], A. Lyon*[1], N. Rushton*[1], M. Parker*[2], J. Reeve*[1]. [1]University of Cambridge, Cambridge, United Kingdom, [2]Peterborough District Hospital, Peterborough, United Kingdom.

Since periosteal expression of alkaline phosphatase was similar between cases and controls, we hypothesised that the mechanism causing the marked femoral neck cortical thinning associated with hip fracture may be raised endocortical bone loss. Twelve female cases of femoral neck fracture (mean age=81±1.5) and 12 age and sex matched post mortem controls (mean age=81.9±1.9) were included in the study. Samples of their femoral neck bone were embedded in methyl methacrylate, sectioned at 10 microns and stained with Solochrome cyanine R and Goldner's trichrome for the detection of osteoid and resorption surfaces respectively. The table shows the % endocortical osteoid (OS/BS) and eroded surfaces (ES/BS) according to quadrantic region. When the data comprising the individual regions were combined OS/BS in cases (9.4±1.8%) were significantly higher than controls (3.7±0.6; P=0.007; Wilcoxon test). Percentage ES/BS was borderline elevated in the cases (5.5±0.9) compared to controls (3.5±0.4; P=0.053). Endocortical %ES/BS could be normalised by log transformation and was modelled using least squares regression analysis with anatomical region nested within disease category (fracture/control). There was a significant interaction of disease and region (P=0.025) for %ES/BS with significant or borderline higher values in the anterior (P=0.006) and posterior (P=0.074) regions. %ES/BS was not significantly raised in those regions (inferior: P=0.29; superior: P=0.77) bisecting the plane of maximum load. We conclude that endosteal bone remodeling (%OS/BS) is elevated in hip fracture cases. Moreover endosteal resorption surfaces are also elevated in those quadrants subjected to minimum stance-related loading.

	Osteoid surface (%OS/BS)		Eroded Surface (%ES/BS)	
Region	Control	Case	Control	Case
Anterior	3.4±0.7	11.0±2.3*	2.8±0.6	5.3±0.7*
Inferior	3.4±1.0	9.9±3.0*	6.4±1.3	8.3±2.1
Posterior	3.2±0.8	9.1±2.3**	2.6±0.4	4.7±1.0
Superior	4.7±1.3	7.9±1.2	3.3±0.5	4.1±1.1

*=P<0.05; **P<0.01. Wilcoxon Test

SA318

Changes in Urinary Sodium and Calcium in Response to a Salt Load in African-American and Caucasian Postmenopausal Women. L. Carbone[1], K. D. Barrow*[1], A. Bush*[2], K. Pitts*[3], K. McFadden*[1], A. Kang*[1], F. A. Tylavsky[2]. [1]Medicine, University of TN, Memphis, TN, USA, [2]Preventive Medicine, University of TN, Memphis, TN, USA, [3]General Clinical Research Center, University of TN, Memphis, TN, USA.

The objectives of this study were to examine the response of 24-hour urine sodium (Na) and calcium (Ca) excretion to a salt load of 270 mmoles/day for six weeks and determine if there were ethnic differences in response to the salt load. The participants were healthy, normotensive, estrogen-deficient African-American (n=20) and Caucasian (n=31) women with no history of renal disease. There were no statistically significant differences between the groups (Caucasians vs. African-Americans) for age (65.3 +/- 6.1 vs. 64.3 +/- 6.3 years (mean +/- SD)), height (161.94 vs. 161.87 cm), weight (76.3 vs. 80.7 kg), or BMI (29.1 vs. 30.8 kg/m2). Bone mineral density (BMD in g/cm2) of the total hip was measured using a Lunar DPX, and 24-hour urine samples were collected at baseline and the end of the six-week salt load. African-Americans had higher BMD of the total hip than the Caucasians (1.01 vs. 0.92, p=0.03) with 10% of the African-Americans and 29% of the Caucasians having a T score <-1 (p=0.11). There were no increases in blood pressure or changes in weight in response to the salt load in either group. Both groups had increases in 24-hour Na and Ca excretion (mmoles/gm/TV) in response to the salt load (p<0.01). The percent change in excretion was similar between the ethnic groups for Na (African-Americans 47.3%, Caucasians 66.9%, p=0.21) and Ca excretion (African-Americans 36.2%, Caucasians 35.6%, p=0.54). The absolute change from pre to post salt load are as follows:

	Pre-Salt Load (Mean +/- SD)	Post-Salt Load (Mean +/- SD)	P
African-Americans			
24-Hour Na excretion	119.59 +/- 37.32	169.88 +/- 56.49	<0.01
24-Hour Ca excretion	2.48 +/- 1.33	3.12 +/- 1.54	0.01
Caucasians			
24-Hour Na excretion	129.67 +/- 33.82	210.01 +/- 65.35	<0.01
24-Hour Ca excretion	3.71 +/- 1.72	4.66 +/- 2.00	<0.01

Despite known differences in calcium metabolism, African-American and Caucasian women have similar increases in calcium excretion in response to a salt load. The relationship of salt intake to bone loss and fracture risk in different ethnic groups requires further study.

Disclosures: ***L. Carbone****, Merck 8; Proctor and Gamble 8.*

SA319

Source of Body Weight Loss Induced by Gastroplasty in Obese Subjects. C. Petracin*[1], J. P. Devogelaer[2], A. Dysseleer*[1], R. Detry*[3], J. P. Thissen*[1]. [1]Department of Endocrinology, St-Luc University Hospital, Brussels, Belgium, [2]Rheumatology Unit, St-Luc University Hospital, Brussels, Belgium, [3]Department of Surgery, St-Luc University Hospital, Brussels, Belgium.

Gastroplasty is now recognized as a successful method for treatment of morbid obesity. This procedure induces a dramatic body weight loss associated with correction of several co-morbidities. However, the nature of the weight loss has been rarely studied, particularly, the effect on bone mineral content (BMC) has been infrequently studied. To investigate the source of weight loss after gastroplasty, we analyzed the changes in body composition in 12 obese (11 females) subjects aged 23-55 years with BMI ranging from 38 to 50 kg/m2. Body compartments were studied by dual energy X-ray absorptiometry (DXA) before, 3 and 12 months (mo) after surgery. Body weight decreased by 32 ± 3 kg (mean ± SEM) at 12 mo ($p < 0.001$ vs time O) and 60 % of this amount was already lost after 3 mo ($p < 0.001$). Fat mass (FM) decreased by 27.1 ± 3.0 kg at 12 mo ($p < 0.001$), with 54 % of this amount lost already after 3 mo ($p < 0.001$). In contrast, fat-free mass (FFM) decreased only by 5.3 ± 1.1 kg ($p < 0.001$), but 91 % of this amount were already lost after 3 mo ($p < 0.05$). The decrease of FFM represented mainly a decrease in lean body mass (LBM) (4.7 ± 0.8 and 5.2 ± 1.0 kg, respectively at 3 and 12 mo; both $p < 0.001$) and secondarily a decrease in BMC (32 ± 10 and 105 ± 31 g, respectively at 3 mo, NS and 12 mo, $p < 0.001$). Appendicular skeletal muscle contributed for most of the loss in LBM (3.7 ± 0.9 kg out of 5.2 ± 1.0 kg). In conclusion, the body weight loss induced by gastroplasty at 12 mo consisted of 83.9 % of fat mass, 15.9 % of lean body mass (11.6 % of skeletal muscle), but only 0.2 % of bone mineral.

SA320

Substituting Soy Protein for Meat Protein did not Affect Calcium Retention in a Controlled Feeding Study of Healthy Postmenopausal Women. Z. K. Roughead. Grand Forks Human Nutrition Research Center, USDA-ARS, Grand Forks, ND, USA.

The Food and Drug Administration has approved a health claim stating that a daily consumption of 25 g of soy protein, as part of a low fat diet, may reduce the risk of heart disease. Recent studies suggest that soy protein may also protect against postmenopausal bone loss. In contrast, the consumption of meat protein is often cited as a risk factor for osteoporosis. In a controlled feeding study, calcium retention was determined from a diet with meat (CONTROL) and a diet in which 25 g of soy protein (SOY; 2.28 mg aglycone/g protein; Dupont Protein Technologies, St Louis, MO) was substituted for 25 g of meat protein. Healthy postmenopausal women (n=13, age:52-69 y; body mass index: 26.0 ± 5.0; femoral neck BMD Z-score: - 0.98 to1.86) consumed the diets (15% protein; 653 and 740 mg calcium/2200 kcal in the CONTROL and SOY diets, respectively), for 8 wk each, in a randomized crossover design. After 4 wk of equilibration, the entire 2-d cycle menu was extrinsically labeled with Ca-47 radiotracer (as $CaCl_2$) and its retention was monitored for 28 d by whole body scintillation counting. The calcium retention data were modeled by the two-component exponential equation: $y = \beta_1 \exp(-k_1 t) + \beta_2 \exp(-k_2 t)$, where y represents Ca-47 retention, as % of the initial dose, t time in hours, and coefficients β_1 and β_2 the turnover of the radiotracer (%) at rates k_1 and k_2, respectively. The retention curves, modeled for each individual on each diet, had coefficients of determination (R^2) of 0.98 to 0.99.
Table: Retention of Ca-47 radio tracer as measured by whole body counting

Variable[1]	CONTROL	SOY
β_1, % dose	77.4 ± 5.8	78.5 ± 5.5
β_2, % dose	22.7 ± 5.7	21.6 ± 5.5
ln (T_1) (days)[2]	0.43 ± 0.30 (1.5)	0.43 ± 0.28 (1.5)
ln (T_2) (days)[2]	3.8 ± 0.5 (44.7)	3.9 ± 0.5 (49.4)
Retention @ day 7, %	24.4 ± 4.7	23.5 ± 5.6
Retention @ day 14, %	18.2 ± 3.8	17.7 ± 4.5
Retention @ day 21, %	15.9 ± 3.5	15.6 ± 4.3
Retention @ day 28, %	14.1 ± 3.2	14.0 ± 4.1

[1]Mean ± SD, n=12; No significant diet effect (P>0.05). [2]Geometric means.

The fractional retention of the calcium tracer was similar between the CONTROL and SOY diets at all time points (P>0.05, Table). On both diets, >75% of the tracer was eliminated rapidly (biological half-life 1.5 d) indicating the excretion of the unabsorbed isotope and early endogenous losses. The remaining tracer (~20%) was eliminated less rapidly with a biological half-life of 45-49 days. In conclusion, a daily substitution of 25 g of a soy protein isolate for meat protein for 8 weeks did not enhance the efficiency of calcium retention in healthy postmenopausal women. Any beneficial effects of soy protein on bone may be due to mechanisms unrelated to dietary calcium retention.

Disclosures: ***Z.K. Roughead****, North Dakota Beef Commission 2.*

SA321

See Friday Plenary number F321.

SA322

Impaired Vitamin D Status in Young Israeli Women. R. Hasid*[1], A. Tamir*[1], B. Raz*[2], E. Segal*[3], S. Ish-Shalom[3]. [1]Technion Faculty of Medicine, Haifa, Israel, [2]Endocrine Laboratory, Rambam Medical Center, Haifa, Israel, [3]Metabolic Bone Diseases Unit, Rambam Medical Center, Haifa, Israel.

Vitamin D is an important regulator of bone metabolism. Vitamin D deficiency was frequently reported in the elderly and correlated with increased hip fracture risk. Lifetime deficiency may affect bone health in later years. The aim of this study was to assess vitamin D status in healthy women of reproductive age and to compare between religious, secular and Arab groups. Fifty five women, aged 20 - 44(mean 25±6.2), 23 secular Jewish women, 24 religious Jewish women, and 8 secular Arab women (with western clothing habits) were enrolled in the study. Sunlight exposure, clothing habits, skin types and dietary history were assessed using previously validated questionnaires. Detailed medical history and routine laboratory examination were performed to rule out any disease that could affect vitamin D or bone metabolism. Serum 25(OH)D3 (^{125}I- radioimmunoassay, DiaSorin, Stillwater, Minnesota, USA), bone specific alkaline phosphatase (BAP) and PTH were assessed in the autumn and the spring. Serum 25(OH)D3 < 10 ng/ml was defined as vitamin D deficiency and between 10 - 15 ng/ml as vitamin D insufficiency. Serum 25(OH)D3 concentration of the religious Jewish women was significantly lower in autumn and spring respectively (8.1±4.7, 7.21±5 ng/ml) than of the secular Jewish women (18.9±10.9, 15.22±9 ng/ml). The mean 25(OH)D3 concentration of the secular Arab women was significantly lower than in two other groups (5. 8±2.3, 4.0±1.6 ng/ml). Nevertheless 43.5 % of secular Jewish women had 25(OH)D3 serum levels <15ng/ml in the autumn and 61.9 % in the spring. Compared with the Jewish and Arab secular women, Jewish religious women were significantly less exposed to sunlight (p< 0.0001). A positive correlation was demonstrated between serum 25(OH)D3 and dietary intake of vitamin D only in the autumn in Jewish religious women (r 0.49; p=0.016) and in the spring in Jewish secular women (r 0.47; p=0.034). 25(OH)D3 serum levels were negatively correlated with PTH serum levels (r - 0.51; p<0.0001) and with BAP serum levels (r -0.32;p=0.024). 25(OH)D3 levels were positively correlated with serum calcium (r 0.34;p=0.01) and serum creatinine levels (r 0.535;p=0.002).We conclude that religious Jewish and secular Arab women have markedly low vitamin D serum levels, that may impair bone metabolism. Vitamin D insufficiency is frequent even in secular young women that reside in the city. The need for routine vitamin D supplementation in young women belonging to vitamin deficient groups, and its impact on bone health deserve further investigation.

SA323

The Effects of Long-Term Dietary Restriction on SENCAR, C57BL/6 and DBA/2 Mouse Bone. E. J. Brochmann*[1], M. E. L. Duarte[2], S. S. Murray[1]. [1]GRECC/Medicine, VAGLA/UCLA, Sepulveda, CA, USA, [2]Universidade Federal do Rio de Janeiro, Rio de Janeiro, Brazil.

Long-term dietary restriction (LTDR) prolongs life and reduces the severity of age-related diseases. However, the effects of DR on bone are controversial, with some reporting that LTDR reduces adult bone size and mineral content, while others report that DR has beneficial effects [e.g., increased trabecular BMD is observed after short-term DR in the SENCAR mouse model of rapid bone growth and early-onset bone loss, while LTDR normalizes calcitropic hormone status and bone metabolism in aging Fisher 344 rats (a model of age-related renal failure and bone loss)]. Animal models vary considerably, and this may underlie the disparity in LTDR study results. We tested the hypothesis that the effects of LTDR are strain-specific. Weanling SENCAR, C57BL/6, and DBA/2 mice (models of elevated, low, and indeterminant rates of free radical generation and aging, respectively) were acclimated to a defined test diet for 5 weeks, then randomly assigned to an *ad libitum*-(AL-) or Ca- and P-normalized LTDR feeding group. Body composition and total, vertebral, and femoral BMD and BMC were determined by PIXImus. Data were analyzed by ANOVA, with post-hoc analysis by Fisher PLSD and Scheffe F-testing. Preliminary results for 8-week old control and 5-month LTDR mice are reported. At 8 weeks of age (t_0), total BMD and BMC were affected by strain, with SENCAR > C57 > DBA (p = 0.0001). Post-hoc analysis indicated that strain-dependent differences were significant for all comparisons between any 2 strains (e.g., C57 vs. DBA, C57 vs. SENCAR, etc.). At t_0, vertebral and femoral BMD and BMC were higher in SENCAR than in C57 and DBA mice (p = 0.001), confirming the robust bone growth in young SENCAR vs. C57 and DBA mice. After 5 months of LTDR with diet normalized for Ca and P, total body, vertebral, and femoral BMD and BMC remained higher in SENCAR mice than in C57 or DBA mice ($p \leq 0.01$). LTDR had no adverse effects on total body or vertebral BMC or BMD in any strain. However, LTDR was associated with a significant (p = 0.0001) reduction in femoral BMD and BMC in SENCAR, but not C57 or DBA, mice. Thus, we validated the hypothesis that the response to LTDR is affected by strain. Of interest are the observations that normalizing dietary Ca and P during LTDR had a protective effect on total body, vertebral, and femoral BMD and BMC in two strains (DBA and C57), but it did not protect the SENCAR mouse from femoral BMD or BMC loss at 5 months of LTDR. Thus, there are strain- and site-specific differences in the effects of LTDR on mice, and dietary Ca and P normalization may provide significant protection against DR-induced decrements in BMD and BMC at specific skeletal sites in some animal models.

SA324

Synchronization of Bone Remodelling and Improvement of Femoral Neck and Lumbar Spine BMD following Normalization of Cortisol Levels in Cushing's Syndrome. K. Godang*, T. Ueland*, C. Kristo*, J. Bollerslev. Section of Endocrinology, National Hospital, Oslo, Norway.

Both endogenous and exogenous glucocorticoid excess has negative effects on bone and collagen turnover, in part by decreasing bone formation and stimulating bone resorption. Thus, secondary osteoporosis is a known complication of endogenous Cushing's syndrome (CS), and although there have been conducted many cross-sectional studies, there are few studies following patients after treament. The present study was designed to account for this by measuring changes in bone dimensions, bone mineral content and biochemical bone markers in 27 CS patients syndrome (19 with pituitary adenoma and 8 with adrenal tumor; 19 woman, mean age 45 ± 12) following normalization of cortisol levels compared to 27 age-,sex- and BMI-matched healthy controls, also assessed longitudinally. Bone mineral content was uniformly reduced in patients at baseline as was total body bone area. Serum levels of CTX-I were increased while osteocalcin was decreased. Following treatment of CS, femoral neck (FN) and lumbar spine (LS) BMD increased (9.4± 8.9% and 4.8± 6.6% respectively, P<0.001 for both), while a slight decrease was found for the total body BMD (-1.1± 2.2%, P=0.043). Similar changes were observed for BMC, only less prominent. Bone area in the FN decreased (-2.7± 4.4%, P=0.004) and increased in the total body (3.5± 6.7%, P=0.044). Furthermore, these changes where significantly larger than those seen in the control population, where no significant longitudinal changes were observed. As for biochemical bone markers, osteocalcin increased markedly following treatment (272± 201%, P<0.001), while no changes where found for CTX-1 (33± 86%). Moreover, while these parameters were uncorrelated prior to treatment (r=0.07), they were significantly correlated following treatment (r=0.83, P<0.001), indicating synchronisation of bone-remodelling. Finally, changes in LS and FN BMD where significantly correlated with the follow-up period (31± 21 weeks?) before measurement (P=0.68, P<0.001 and r=0.55, P=0.005). In summary, cure of CS is associated with a coupling of bone resorption and formation leading to a marked and continuos increase in bone mass.

SA325

See Friday Plenary number F325.

SA326

Medrysone, a Glucocorticoid that Retains Anti-Inflammatory Efficacy, Has Only Modest Effects on Bone Turnover and Remodeling. K. R. Long*[1], P. Hara*[2], J. L. Lee*[1], V. Shen[2], C. Liu[2], H. Zheng*[2], R. Chott*[1], S. Bain[2], L. M. Olson*[1]. [1]Arthritis and Inflammation Pharmacology, Pharmacia Corporation, Chesterfield, MO, USA, [2]Skeletech, Bothell, WA, USA.

Glucocorticoids (GCs) are widely used due to their impressive anti-inflammatory properties but severe side effects, such as osteoporosis, limit long-term use. GC analogs retaining anti-inflammatory efficacy with reduced effects on skeletal tissues would represent a significant advance over current therapeutic modalities. In this study, a murine model of GC-induced osteoporosis was used to compare medrysone (med), a progesterone analog with GC activity, with prednisolone (pred), a GC known to induce osteopenia. Thirteen-week old male Swiss-Webster mice (n=12/group) were treated orally, twice daily with either vehicle, pred (0.5, 1.5, 5.0 mpk) or med (3, 10, 30 mpk) for 4 wk. The doses of pred and med were selected based on their equivalent efficacies in a murine model of LPS-induced endotoxemia. Weekly body weights (wts) and final thymus wts were recorded. Plasma corticosterone was measured as an indicator of HPA axis suppression. The effects on bone turnover were assessed by measuring bone mineral density (BMD), histomorphometry, and serum biomarkers. Weight loss was observed with both GC-treated groups, but pred-treated mice lost significantly more weight than med-treated mice (P<0.01). Mice treated with either GC showed similar reductions in thymus wts and plasma corticosterone, indicating their comparable effects on these two biomarkers. Pred, but not med, caused dose-dependent decreases in serum osteocalcin, a marker of bone formation. Surprisingly, spinal BMD and distal femur BMD were not significantly affected by either GC. In contrast, femoral midshaft BMD was significantly decreased with GC treatment; greater loss occurred in pred-treated mice (7.5% with 5 mpk, P<0.01) than in med-treated mice (4.3% with 30 mpk). Despite the lack of effect of GCs on distal femur BMD, dynamic histomorphometry at both distal and midshaft femoral sites showed greater suppression of bone formation rates (BFRs) with pred than with med treatment (distal BFR/BS, vehicle, 29.16 ± 7.91; 5 mpk pred, 0.64 ± 0.24, P<0.01; 30 mpk med, 13.64 ± 3.02). In sum, oral delivery of GC caused significant suppression of bone formation as indicated by decreased serum OC, reduction of femoral midshaft BMD, and significant suppression of femoral BFRs at both distal and midshaft sites. Despite comparable effects on LPS-induced endotoxemia, thymus wt, and plasma corticosterone levels, med suppressed bone formation less than pred, suggesting that anti-inflammatory properties of GCs may be distinct from their effects on the skeleton.

SA327

See Friday Plenary number F327.

SA328

Low levels of Estradiol Protect Bone Mineral Density in Healthy Young Postmenopausal Women. A. Bagur[1], B. Oliveri[1], M. Belotti*[1], D. Yankelevich*[2], F. Sayegh*[2]. [1]Sección Osteopatías Médicas, Hospital de Clínicas, Universidad de Buenos Aires, Buenos Aires, Argentina, [2]Sección Climaterio, División Ginecología, Hospital de Clínicas, Universidad de Buenos Aires, Buenos Aires, Argentina.

Low levels of endogenous estrogens may play a role in the protection of bone mineral density (BMD) in healthy postmenopausal women (PMP). The aim of this study was to evaluate the role of total and bioavailable estradiol and testosterone in the protection of BMD in healthy PMP. Ninety nine PMP women aged 55 to 75 years were included. The BMD of L2-L4, Total Femur (TF) and Total Skeleton (TS) was measured by DXA (Lunar Prodigy). Serum calcium, bone alkaline phosphatase (BAP), crosslaps (CTX), estradiol, estrona and testosterone and urine calcium were measured. Estradiol was measured with a sensitive assay that detects up to 5 pg/ml. Bioavailable sex hormones were calculated. The population was divided in two groups: <65 (Group 1) and >65 years of age (Group 2). The general characteristics of the groups were (mean ± SD): weight 66 ± 11 vs. 65 ± 9 kg (ns), height 1.57 ± 5 vs. 1.52 ± 0.05 m (p<0.001), BMI 26 ± 4 vs. 27 ± 4 kg/m2 (ns), L2-L4 1.01 ± 0.16 vs. 0.95 ± 0.18 g/cm2 (p<0.08, ns), TF 0.90 ± 0.11 vs. 0.82 ± 0.10 g/cm2 (p<0.001), TS 1.04 ± 0.09 vs. 0.98 ± 0.07 g/cm2 (p<0.001). The Groups were also stratified according to estradiol levels: less and more than 10pg/ml. The only significant differences in BMD were found in Group 1 in which estradiol levels higher than 10 pg/ml protected BMD of L2-L4 (+14%, p<0.05) and TS (+3%, p<0.05). BAP and CTX tended to be lower in Group 1 with more than 10 pg/ml of estradiol. The difference was close to reach statistical significance (p<0.07 for both). The highest positive correlations were found in Group 1: estradiol correlated with L2-L4 (r=0.4, p<0.001), TF (r=0.3, p<0.004) and TS (r=0.4, p<0.001), bioavailable estrogen correlated with L2-L4 (r=0.4, p<0.003) and TS (r=0.4, p<0.001), testosterone correlated with L2-L4 (r=0.6, p<0.001), TF (r=0.4, p<0.01) and TS (r=0.6, p<0.001). CTX correlated negatively with estradiol and bioavailable estradiol (r=-0.3, p<0.01 and r=-0.3, p<0.006 respectively). In conclusion, estradiol levels higher than 10 pg/ml, testosterone and bioavailable estradiol are involved in the maintenance of BMD in healthy postmenopausal women under 65 years of age.

SA329

Correlation of Serum Osteoprotegerin Levels with Age but not Hormone Replacement Status in Elderly Women. J. K. Scariano[1], P. J. Garry*[2], R. N. Baumgartner[3]. [1]Pathology, University of New Mexico School of Medicine, Albuquerque, NM, USA, [2]Pathology, University of New Mexico, Albuquerque, NM, USA, [3]Internal Medicine, University of New Mexico, Albuquerque, NM, USA.

The purpose of this study was to investigate the relationship between serum levels of osteoprotegerin (OPG), biochemical markers of bone turnover, PTH, estrone, leptin and bone mineral density (BMD) measurements made of the total and regional skeleton in 84 healthy, elderly postmenopausal women (61 - 97, mean = 78 years). Circulating OPG levels were directly correlated with the age of the subjects (r = 0.50, p < 0.001), intact parathyroid hormone (r = 0.39, p = 0.008), ICTP (r = 0.31, p = 0.04) and serum NTx levels (r = 0.28, p = 0.01). Inverse correlations were detected between OPG with BMD measured at the femoral neck (r = -0.27, p = 0.01) and total skeleton (r = -0.28, p = 0.01). After adjusting for age, however, all of these correlations were diminished. Although 25 women receiving hormone replacement therapy (HRT) had significantly decreased bone resorption markers and increased BMD at all skeletal regions when compared with the 59 women who were not receiving any type of antiresorptive therapy, levels of OPG were not influenced by HRT or circulating estrone. Multiple regression modeling indicated that the only significant determinant of the serum OPG level in elderly women is age, and its secretion is unaffected by BMD or bone turnover rates.

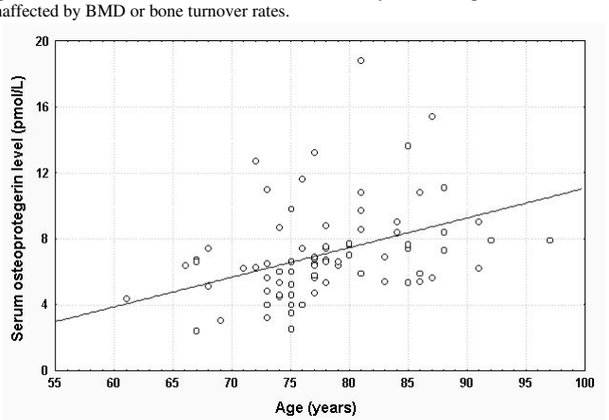

Differences in densitometric, body composition and biochemical parameters in HRT+ or - women

Parameter	HRT + (n=25)	HRT - (n=59)	p value
BMI (k/m^2)	25.7 ± 4.5	25.1 ± 3.0	0. 97
SBMD (g/cm^2)	1.246 ± 0.274	0.981 ± 0.131	< 0.001
FBMD (g/cm^2)	0.833 ± 0.141	0.734 ± 0.024	< 0.01
Estrone (pg/mL)	105.8 ± 131.3	17.3 ± 4.6	0.01
Serum NTx (nmol BCE/L)	14.0 ± 5.6	18.1 ± 11.0	0.009
PINP (μg/L)	33.3 ± 16.1	50.6 ± 25.9	< 0.001
OPG (pmol/L)	7.1 ± 3.6	6.9 ± 3.1	0.55

SA330

See Friday Plenary number F330.

SA331

Elevated Turnover and Osteopenia in Vertebral Bodies of Ovariectomized (OVX) Rabbits. B. L. Pennypacker*[1], P. J. Masarachia[1], M. A. Gentile[1], D. Gilberto*[2], C. Johnson*[2], S. Motzel*[2], G. A. Rodan[1], D. B. Kimmel[1]. [1]Bone Biology and Osteoporosis, Merck Research Laboratories, West Point, PA, USA, [2]Lab Animal Resources, Merck Research Laboratories, West Point, PA, USA.

A non-primate adult animal that displays both Haversian bone remodeling and estrogen deficiency osteopenia would expand opportunities to understand cortical bone behavior in estrogen deficient adult humans. Nine month old New Zealand white rabbits (3.86kg) were ovariectomized (OVX) or Sham-OVXd. OVX rabbits were treated subcutaneously for 26wks with vehicle or 0.2 mg/kg 3X/wk alendronate (OVX+ALN). In-life double calcein labeling (8mg/kg) was done. At necropsy, right femur and second and third lumbar vertebrae (LV) were fixed in 70% ethanol. Bone mineral density (BMD, mg/cm^2) of the central and distal femur and the LV2 and LV3 bodies was measured (dual energy x-ray absorptiometry. 100∝m cross-sections of the mid-femur and 5∝m longitudinal sections of LV3 body were prepared from plastic-embedded specimens. Double labeled surface (MSBS, %) was measured in LV3 cancellous bone. Labeled Haversian canals/mm^2 (lb-HC) were counted in the femur. The three groups were compared (ANOVA with Fisher PLSD). LVBMD was 13% lower in OVX than Sham; LVBMD of ALN-treated OVX rabbits was 79% replete to Sham. No OVX-related differences occurred in the femur. MSBS was ~five-fold higher in OVX than Sham; MSBS of ALN-treated OVX rabbits was 86% replete to Sham. Lb-HC were absent in Sham rabbits, but strongly induced by OVX and strongly suppressed by ALN. Cancellous bone loss occurs in the vertebral body after six months post-OVX in rabbits. This loss is accompanied by increased cancellous and cortical bone turnover. All these changes are suppressed by ALN. Like humans, the adult rabbit has Haversian remodeling of cortical bone and develops estrogen deficiency spinal osteopenia, accompanied by accelerated remodeling of cancellous and cortical bone, all of which are prevented by anti-resorptive therapy.

Group	Sham(N=11)	OVX(N=10)	OVX+ALN(N=12)
LV-BMD	297±34	258±22s	289±29so
LV-MSBS	1.8±2.0	8.8±6.1s	2.8±3.2so
lb-HC	0±0	4.5±4.1s	0.3±0.9so

Mean±SD; s vs. Sham (P<.004); o vs. OVX (P<.02)

SA332

Duration and Severity of the Disease but not Menopausal Status are the Main Risk Factors for Osteoporosis in Primary Biliary Cirrhosis. N. Guañabens[1], A. Parés*[2], I. Ros*[1], L. Caballería*[2], F. Pons*[1], S. Vidal*[1], A. Monegal*[1], P. Peris[1], J. Rodés*[2]. [1]Metabolic Bone Diseases Unit, Hospital Clínic, Barcelona, Spain, [2]Liver Unit, Hospital Clínic, Barcelona, Spain.

Since the clinical spectrum of primary biliary cirrhosis (PBC) has changed in the last years, and the disease is diagnosed usually in postmenopausal women with minor cholestasis, it has been questioned whether PBC itself represents an extra risk for osteoporosis. Therefore this study was carried out to assess the prevalence and risk factors for osteoporosis in an unselected series of 142 women with PBC (age: 54.3 ± 0.8 years) and compared with the prevalence of osteoporosis in the Spanish women. Diagnosis of osteoporosis was established by densitometric criteria (Bone mineral density below –2.5 T-score). Age, duration of PBC, menopausal status, histological stage and severity of liver disease were assessed in all the patients. Prevalence of osteoporosis was significantly higher in PBC (32.4%) than in normal women (11.1%) (RR: 3.83, 95%CI: 2.59 to 5.67, p<0.001). Osteoporosis in PBC was associated with menopausal status (p<0.001), older age (60.2 ± 1.2 vs 51.5 ± 0.9 years, p<0.001), longer PBC duration (4.0 ± 0.6 vs 2.4 ± 0.3 years, p=0.004), advanced histological stage (p<0.001) and high bilirubin (1.96 ± 0.36 vs 1.36 ± 0.29 mg/dl, p=.003), and alkaline phosphatase levels (946 ± 124 vs 634 ± 48 4 u/l),

p=0.005), as well as low albumin (40.9 ± 0.6 vs 42.6 ± 0.4 g/l, p=0.02) and prothrombin index (94 ± 2 vs 99 ± 0.3 %, p<0.001). The stepwise logistic regression analyses identified duration of PBC, age, advanced histological stage and baseline bilirubin > 1.2 mg/dl, but not postmenopausal status as the independent risk factors for osteoporosis. In conclusion, osteoporosis is more prevalent in women with PBC than in general population. Age, duration and severity of the disease but not menopausal status are the main risk factors for osteoporosis in this liver disease.

SA333

See Friday Plenary number F333.

SA334

Skeletal Kinetics at the Lumbar Spine in Postmenopausal Women on Antiresorptive Therapy and Controls Measured by 18F-Fluoride Positron Emission Tomography. M. L. Frost[1], G. J. R. Cook*[2], P. K. Marsden*[1], G. M. Blake[1], I. Fogelman[1]. [1]Radiological Sciences, Guy's, King's and St Thomas' School of Medicine, London, United Kingdom, [2]Department of Nuclear Medicine, Royal Marsden Hospital, London, United Kingdom.

The aim of this study was to compare skeletal kinetics in the lumbar vertebrae in postmenopausal women treated with antiresorptive therapy and controls, measured by 18F-fluoride positron emission tomography (PET). Nineteen women, with a mean age of 65.8 years and a T-score of less than -2 at the spine or hip, had a dynamic PET scan of the lumbar spine after the injection of 180 MBq 18F-fluoride ion. These women were split into two groups: (i) Group 1, women on stable antiresorptive therapy for at least 1 year (n=9); (ii) Group 2, women who were not receiving antiresorptive treatment (n=10). There were no significant differences in mean age, or spine and hip BMD between the two groups. The arterial plasma input function was derived using aorta arterial activity from the PET image. Time activity curves were measured by placing regions of interest over the lumbar vertebrae. A three-compartmental model and non-linear regression analysis were used to calculate the plasma clearance of tracer to bone mineral (K_{bone}) and the clearance of tracer to the whole of the bone tissue (K_{total}). K_{bone} and K_{total} relate to regional mineralisation and formation, and regional blood flow respectively. k2 to k4 were also measured which describe transport between plasma, the ECF compartment and the bone mineral compartment. Mean vertebral K_{bone} was significantly greater in Group 2 (3.35×10^{-2} ml . min^{-1} . ml^{-1}) compared with the mean for Group 1 (2.72×10^{-2} ml . min^{-1} . ml^{-1}), p=0.04. There was no significant difference in K_{total} between Group 1 (1.18×10^{-1} ml . min^{-1} . ml^{-1}) and Group 2 (1.29×10^{-1} ml . min^{-1} . ml^{-1}) p=>0.05. No significant differences were found in k2, k3 or k4. In conclusion, we have shown a direct effect of antiresorptive therapy on skeletal kinetics at the clinically important site of the lumbar spine. The use of 18F-fluoride PET may aid in our understanding of how different treatments for osteoporosis affect regional skeletal metabolism and may provide a useful non-invasive tool to assess novel treatments currently being developed for osteoporosis.

SA335

Effect of Chronic Alcohol Ingestion on Bone Mineral Density in Noncirrhotic Males. Y. Shin*. Endocrinology, Wonju College of Medicine, Wonju, Republic of Korea.

Background: Osteoporosis in men is an important public health problem. Because of the incremental tendency of elderly population and age-specific incidence of fracture, it is evitable that the health burden of fracture will increase. Chronic alcoholism is associated with osteoporosis and other risk factors such as fractures, poor nutrition, leanness, liver disease, malabsorption, vitamin D deficiency, hypogonadism, hemosiderosis, parathyroid dysfunction, and tobacco use. And these risk factors may contribute to the pathogenesis of bone disease in alcoholism. Chronic alcohol intake may reduce bone density but increase bone density. It has been well established that liver disease also induces changes in bone density, and thus it is difficult to distinguish the role of liver disease from that of alcohol itself in bone alterations occurring in patients with chronic alcohol consumption. The purpose of this study is to assess the effect of chronic alcohol consumption on bone mineral density in male chronic alcoholics without liver cirrhosis. **Methods**: We studied 18 chronic heavy drinkers of more than 40 g/day for at least 3 years and age-matched 18 control groups who had drunk alcohol less than 20 g/day. Serum and urinary parameters of bone and mineral metabolism were determined. Bone mineral density(BMD) was measured by dual-energy x-ray absorptiometry at four axial sites(lumbar spine, femoral neck, ward's triangle and trochanter). **Result**: Alcoholic patients drank alcohol 97.6 g/day and control groups drank alcohol 7.2 g/day. Osteocalcin, a marker of bone formation, was slight decreased in alcoholic patients and deoxypyridinoline, a marker of bone resorption, was slight increased but not statistically significant(P>0.05). The levels of free testosterone, estrogen, 25-(OH)-vit D, parathyroid hormone were not different between the two groups. The BMD of ward's triangle and trochanter of femur were significantly lower than controls, and decreased parallel with total alcohol intake amount in lumbar spine of the alcoholics(r=-0.62, P<0.05). **Conclusion**: We suggest that chronic alcohol consumption may induce low bone density on femur ward and trochanter. The large scaled randomized and prospective studies are needed to clarify the pathogenesis of alcohol-induced osteoporosis.

SA336

Individual Course of Trabecular Bone Density in Patients Treated with Alendronate. M. Neff[1], M. A. Dambacher[2], J. Schönbächler*[2], H. Radspieler[3], L. Qin*[4]. [1]Center for Osteoporosis, Zurich, Switzerland, [2]University Clinic Balgrist, Zurich, Switzerland, [3]Center for Osteoporosis, Munich, Germany, [4]Chinese University, Hong Kong, Hong Kong Special Administrative Region of China.

Purpose: Evidenced based medicine is based on studies of thousands of patients (Alendronate, Risedronate, Raloxifen) but in our daily practice we do not treat groups of patients, but individuals. We have evaluated the individual course of trabecular bone density in the first year of treatment with 10mg Alendronate. Methods: For this study we used the trabecular bone density evaluated by the high resolution peripheral quantitative Computed Tomography (hrpQCT), parameters: integral, trabecular and cortical bone density separately, reproducibility ± 0,3% in mixed collectives. Patients: 61 postmenopausal osteoporotic women (WHO definition: > -2,5 SD, T-Score, integral bone density). Results: See graph. After one year of treatment with 10mg Alendronate we found in 38% of the patients an increase of trabecular bone density, in 43% a steady state, in 5% a slow bone and in 14% a fast trabecular bone loss. Conclusions: These densitometric data fits the results of the Alendronate one year studies with a reduction of 50-60% fracture rate in the first year of treatment.

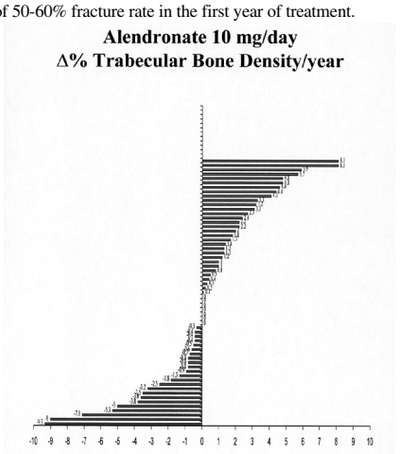

SA337

See Friday Plenary number F337.

SA338

Individual Course of Trabecular Bone Density in Patients Treated with Risedronate. H. Radspieler*[1], M. A. Dambacher*[2], M. Neff*[3], J. Schönbächler*[2], L. Qin*[4]. [1]Center of Osteoporosis Munich, Muenchen, Germany, [2]University Clinic Balgrist, Zurich, Switzerland, [3]Center of Osteoporosis, Zurich, Switzerland, [4]Chinese University, Hongkong, China.

Purpose: Evidenced based medicine is based on studies of thousands of patients (Alendronate, Risedronate, Raloxifen) but in our daily practice we do not treat groups of patients, but individuals. We have evaluated the individual course of trabecular bone density in the first year of treatment with 5mg Risedronate. Methods: For this study we used the trabecular bone density evaluated by the high resolution peripheral quantitative Computed Tomography (hrpQCT), parameters: integral, trabecular and cortical bone density separately, reproducibility 0,3% in mixed collectives. Patients: 32 Postmenopausal osteoporotic women (WHO definition: > -2,5 SD, T-Score, integral bone density with or without vertebral fractures). Results: See graph. After one year of treatment with 5mg Risedronate we found in 71% of the patients an increase of trabecular bone density, in 12,5% a steady state, in 9,5% a slow and in 6% a fast trabecular bone loss. The average increase in trabecular bone density was 3,9% for all 32 patients. Conclusions: These densitometrie data fits the results of the Risedronate studies with a reduction of 50-60% fracture rate in the first year of treatment.

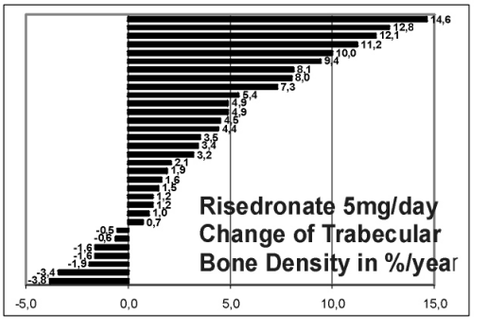

SA339

See Friday Plenary number F339.

SA340

Adherence Profile of Etidronate (ETD), Alendronate (ALD) and Hormone Replacement Therapy (HRT) in Patients Registered in the Canadian Database of Osteoporosis and Osteopenia (CANDOO). A. Papaioannou[1], G. Ioannidis[1], R. J. Sebaldt[1], W. P. Olszynski[2], D. A. Hanley[3], A. Petrie*[1], J. P. Brown[4], R. Josse[5], T. Murray*[5], C. H. Goldsmith*[1], J. D. Adachi[1]. [1]McMaster University, Hamilton, ON, Canada, [2]University of Saskatchewan, Saskatoon, SK, Canada, [3]University of Calgary, Calgary, AB, Canada, [4]Laval University, Ste-Foy, PQ, Canada, [5]University of Toronto, Toronto, ON, Canada.

Therapies for osteoporosis must be taken over the longer-term (years) to be effective and to maintain their benefits over time. Potential barriers to long-term patient adherence to osteoporosis therapies may include the development of side effects, other medical reasons, drug costs, and loss of motivation. The purpose of this prospective observational study was to determine the difference in self reported adherence to ETD, ALD, and HRT in a group of patients registered in CANDOO. CANDOO is an observational database designed to longitudinally capture a standardized and comprehensive set of clinical data in patients referred to and followed by collaborating tertiary care centres. CANDOO was searched for women and men who were receiving either ETD, ALD or HRT. All patients may have also been taking concurrent calcium and vitamin D therapy. Patients were excluded if they did not start osteoporosis therapy on or after their first clinical visit and did not have at least one follow-up visit after initiating therapy. A total of 1196, 477, and 294 men and women with a mean age (standard deviation) of 67.0 (8.6), 66.3 (8.4), 60.1 (7.5) years, initiated ETD, ALD or HRT, respectively. At baseline, approximately 23, 27 and 12% of patients had prevalent vertebral fractures and 45, 48 and 37% of patients had prevalent non-vertebral fractures in the ETD, ALD and HRT groups. A Cox proportional hazards regression model was used to assess differences between treatment groups in the time to discontinuation of therapy (days). Several potential covariates such as anthropometric, medications, illnesses, and lifestyle factors were entered in the model. A forward selection technique was used to generate the final model. Hazard Ratios and 95% confidence intervals (CI) were calculated. Adjusted results indicated that ALD users were 42% (95% CI: 16, 73%) more likely to discontinue therapy as compared to ETD users. No significant differences were found between the HRT group and the two bisphosphonate groups. Potential barriers to long-term patient adherence to osteoporosis therapies should be considered prior to the initiation of treatment.

Disclosures: ***A. Papaioannou****, Procter & Gamble Pharmaceuticals 2, 5.*

SA341

See Friday Plenary number F341.

SA342

Decrease in Bone Resorption Markers in Response to Risedronate: Relationship to Decrease in Estimates of Bone Turnover Using Bone Histomorphometry. R. A. Hannon[1], R. L. Licence*[1], A. A. Chines[2], E. W. Sod[2], E. F. Eriksen[3], R. Eastell[1]. [1]Bone Metabolism Group, University of Sheffield, Sheffield, United Kingdom, [2]Procter & Gamble Pharmaceuticals, Cincinnati, OH, USA, [3]University of Aarhus, Aarhus, Denmark.

Biochemical markers of bone resorption decrease rapidly and to different degrees in response to antiresorptive treatment. It is not known which markers of bone resorption best reflect changes in histomorphometric indices in response to treatment. The aim of this study was to compare changes in bone resorption markers with those in histomorphometric indices in postmenopausal osteoporotic women treated with 5mg risedronate plus 1g calcium per day for 36 months. Histomorphometric indices including activation frequency (AcF), volume-referent bone formation rate (BFR/BV) and bone resorption rate (BRs.R/BV), and mineralised surface (MS/BS) were assessed in bone biopsies obtained at baseline and 36 months from 30 women. Urinary N and C telopeptides of type I collagen (UNTX and UCTX), helical peptide (UHelical) and immunoreactive free deoxypyridinoline (UifDPD) were measured in second morning void urine collected at baseline and 36 months. Change in MS/BS at 36 months correlated (Spearman rank) with change in UNTX ($r = 0.77$, $p = 0.008$) and UHelical ($r = 0.66$, $p = 0.02$). Table shows median percentage changes and 95% confidence intervals at 36 months. The decreases in UNTX, UCTX and UHelical were not significantly different from each other or from changes in AcF, BFR/BV and BRs.R/BV (p=0.3 to 0.7) but were less than the decrease in MS/BS (p=0.02 to 0.07). The decrease in UifDPD was significantly less than the decreases in AcF, BFR/BV, BRs.R/BV and MS/BS ($p = 0.05$ to 0.0002). We conclude that treatment induced changes in dynamic markers such as UNTX, UCTX and UHelical may slightly underestimate the changes in bone histomorphometric indices of bone turnover.

	Median	CI_{upper}	CI_{lower}	n
AcF	-57	-72	-14	12
BFR/BV	-62	-75	0	12
BRs.R/BV	-57	-71	37	10
MS/BS	-74	-87	-37	23
UNTX	-50	-63	-26	20
UCTX	-39	-70	-22	20
UHelical	-48	-73	-18	20
UifDPD	-4	-30	7	20

SA343

See Friday Plenary number F343.

SA344

Risedronate Reduced the Risk of Nonvertebral Fractures as soon as 6 Months in Postmenopausal Osteoporosis. M. L. Brandi[1], T. J. Harrington*[2], I. Barton*[3], L. G. Ste-Marie*[4]. [1]University of Florence, Florence, Italy, [2]University of Wisconsin, Madison, WI, USA, [3]Procter & Gamble Pharmaceuticals, Staines, United Kingdom, [4]University of Montreal, Montreal, PQ, Canada.

Risedronate has been shown to reduce the incidence of clinical vertebral fractures in as early as 6 months. Although vertebral fractures are most commonly associated with osteoporosis, nonvertebral fractures account for a large proportion of all osteoporotic fractures. The purpose of this analysis was to determine the onset of effect of risedronate (RIS) on nonvertebral osteoporotic fractures. The analysis included data from four studies that ranged in length from 12 months to 3 years. Postmenopausal women were enrolled into the clinical trials on the basis of low lumbar spine BMD and/or the presence of vertebral fracture at baseline. Data were analyzed for patients with a lumbar spine T-score<-2.5 (N=1172) regardless of prevalent vertebral fracture status at baseline (42% had no fractures, 25% had one fracture and 33% had >1 fracture). The effect of risedronate on nonvertebral fracture risk was based on a combined endpoint of hip, wrist, pelvis, clavicle, humerus and leg fractures. Nonvertebral fractures were collected as adverse events in 3-month intervals and were subsequently confirmed by radiograph. All patients received 1g/day calcium and either placebo or risedronate daily. Fracture incidence was calculated using Kaplan-Meier estimates and the treatment effect was determined using Cox proportional hazards regression model. The incidence of nonvertebral osteoporotic fracture in women with low lumbar spine BMD was significantly reduced as early as 6 months (p=0.048). There was a 74% reduction at 1 year (4.5% for control vs 1.2% for risedronate, p=0.001) and the effect was sustained over 3 years. Risedronate 5 mg/d significantly reduces the risk of nonvertebral osteoporotic fractures in as early as 6 months in women with postmenopausal osteoporosis. These findings provide additional support for the rapid onset of anti-fracture effect observed with risedronate treatment at both vertebral and nonvertebral sites.

SA345

See Friday Plenary number F345.

SA346

Effect of Whole Body Vibration on Bone and Muscle Performance. S. B. Torvinen*[1], P. S. Kannus*[1], H. T. Sievänen*[2], T. A. H. Järvinen*[3], M. E. Pasanen*[2], S. A. Kontulainen*[2], A. M. Nenonen*[2], T. L. N. Järvinen*[3], T. Paakkala*[4], M. J. Järvinen*[5], M. I. Vuori*[2]. [1]UKK Institute, University of Tampere, Tampere, Finland, [2]UKK Institute, Tampere, Finland, [3]Medical School, Institute of Medical Technology, University of Tampere, Tampere, Finland, [4]Department of Radiology, Tampere University Hospital, Tampere, Finland, [5]Department of Surgery, Tampere University Hospital, University of Tampere, Tampere, Finland.

Recent animal studies have given evidence that vibration loading may be an efficient way to improve mass and mechanical competence of bone thus possessing great potential for preventing and treating osteoporosis. Randomized controlled human studies are, however, lacking. This randomized controlled trial was designed to assess the effects of an 8-month whole body vibration on mass, structure and estimated strength of bones in young adults. In addition, the effects of vibration on muscle performance and body balance were determined. 56 volunteers (aged 19-38 years) were randomly assigned to either the vibration or control group. The vibration intervention consisted of an 8-month whole body vibration (4-min/day, 3-5 times a week), the stimulus being employed by standing on a vertically vibrating platform. During the 4-min vibration program, the platform oscillated in an ascending order from 25 Hz-45 Hz corresponding to estimated, maximum vertical accelerations from 2-8 g (1 g = 9.81 ms-2). Bone mass, structure and strength at the distal tibia and tibial shaft were measured by pQCT at baseline and at 8 months. Bone mineral content was measured at the lumbar spine, proximal femur, calcaneus and distal radius using DXA at baseline and at 8

months. Osteocalcin, CTx, P1NP and TRAP5b were determined at baseline and at 2, 4, 6, and 8 months. Vertical jump, isometric extension strength of the lower extremities, grip strength, shuttle run, and postural sway-tests were performed at baseline and at 8 months. The vibration intervention succeeded well and was safe to perform but had no effect on bone mass, structure or strength at any skeletal site. Instead, at 8 months a 7.8 % net benefit in the vertical jump height was seen for the vibration group (p=0.003). On the other performance or balance tests, the vibration intervention had no effect. An 8-month whole body vibration intervention had no effect on mass, structure or mechanical strength of bones in young, healthy adults. Except for increased vertical jump height, neither muscular performance nor body balance improved due to vibration. Since the results of this randomized clinical trial were not as positive as those of the recent animal investigations, future human studies are definitely needed before any clinical recommendation for vibration exercise.

SA347

The Orthosis Spinomed Improves Posture, Trunk Muscle Strength, and Quality of Life in Women With Vertebral Fractures: Results of a Prospective, Randomized, Cross-over Study. M. Pfeifer, B. Begerow*, H. W. Minne. Institute of Clinical Osteology, Bad Pyrmont, Germany.

Thoracolumbar braces are widely used in the care of patients with vertebral fractures due to osteoporosis. Their usefulness, however, has never been tested under standardized conditions. To our knowledge, this is the first randomized, controlled, prospective, cross-over study to determine the efficacy of an orthosis in the treatment of spinal osteoporosis. In this cross-over study, patients had been randomized into two groups: group A started with an intervention period of six months, while group B served as controls. After 6 months groups changed. Measurements include trunk muscle strength, body sway, angle of kyphosis, pain, and limitations of everyday life and were performed at base-line and every three months thereafter. At base-line, we did not observe any differences between both groups concerning age (p=0.77), height (p=0.90), weight (p=0.84), loss of height (p=0.25) and number of vertebral fractures (p=0.87). Results are presented in Table 1. Spinomed back support improves posture, trunk muscle strength, lung function, body sway, and quality of life in postmenopausal women with osteoporosis and may therefore play an integral part in the rehabilitation process of osteoporotic patients. The efficacy of thoracolumbar braces needs to be further investigated in prospective, randomized and controlled clinical trials.

Initial Values and Changes at 6 Months in 61 Study Subjects

Angle of Kyphosis	Initial Value	Change at 6 Months	P-Value
Group A	74.2 +/- 9.8 (°)	-2.2 +/- 4.1 (°)	0.007
Group B	69.8 +/- 9.9 (°)	+1.4 +/- 4.3 (°)	
Back ext strength	Initial Value	Change at 6 Months	P-Value
Group A	264 +/- 131 (N)	+122 +/- 107 (N)	<0.001
Group B	262 +/- 119 (N)	+ 18 +/- 55 (N)	
Abd flex strength	Initial Value	Change at 6 Months	P-Value
Group A	165 +/- 71 (N)	+66 +/- 61 (N)	0.005
Group N	155 +/- 64 (N)	+25 +/- 41 (N)	
Body Sway	Initial Value	Change at 6 Months	P-Value
Group A	84 +/- 70 (mm)	-14 +/- 45 (mm)	0.045
Group B	78 +/- 37 (mm)	+10 +/- 43 (mm)	
Vital Capacity	Initial Value	Change at 6 Months	P-Value
Group A	83 +/- 21 (%)	+0.5 +/- 13.0 (%)	0.022
Group B	93 +/- 16 (%)	-8.2 +/- 12.9 (%)	
Pain	Initial Value	Change at 6 Months	P-Value
Group A	4.0 +/- 1.1 (Pts.)	-0.9 +/- 1.0 (Pts)	<0.001
Group B	3.9 +/- 1.0 (Pts.)	+0.1 +/- 0.9 (Pts)	
Limi Daily Living	Initial Value	Change at 6 Months	P-Value
Group A	4.8 +/- 1.9 (Pts.)	-1.3 +/- 1.4 (Pts)	0.007
Group B	4.1 +/- 1.7 (Pts.)	+0.2 +/- 0.8 (Pts)	

SA348

See Friday Plenary number F348.

SA349

Daily Activity Triples the Efficacy of PTH on Cortical Bone Formation in Adult Female Rat. Y. Mikuni-Takagaki[1], K. Aoki[2], M. Takahashi*[2], K. Ohya[2], M. Itoman*[3]. [1]Kanagawa Dental College, Yokosuka, Japan, [2]Tokyo Medical and Dental University, Graduate School, Tokyo, Japan, [3]Kitasato University School of Medicine, Sagamihara, Japan.

Controlled clinical trials showed that daily subcutaneous injections of low doses of parathyroid hormone (PTH) reduced incidence of osteoporosis-related fractures. While the ovariectomized rats provide an excellent animal model for postmenopausal osteoporosis, no such models are available for disuse osteopenia. The purpose of this study is to confirm our previous observation in isolated rat osteocytes of synergy between PTH and mechanical loading, *in vivo*. Thirty-week-old female Wistar rats were either housed in cages of limited space (RESTRAINED) or allowed free activity (CONTROL) in the institutional standard cages. Rats were injected subcutaneously with 10 μg/kg human PTH (1-34) (Asahi Chemical Co.) or saline three times a week for 6 weeks. Restrained rats were not apparently stressed judged by their serum cortisol levels. Calcein was injected twice for measuring mineral apposition rate (MAR). After measuring tibial BMD by pQCT, histomophometric analysis was carried out by confocal microscopy. As shown in Table I, MAR of RESTRAINED and PTH groups are significantly different (p<0.001) and the difference, 22.7, is much larger than the added differences between RESTRAINED and CONTROL (5.5, not significant) and RESTRAINED and RESTRAINED + PTH (6.4, not significant). Proximal cortical BMD at 6 weeks also showed a significant difference between the RESTRAINED and PTH (p<0.001) in a similar manner. Also confocal microscope images showed larger numbers of brighter periosteocytic calcein labels in PTH group compared to RESTRAINED rats, suggesting that the osteocytic mineralizing activity was upregulated by combined effects of PTH and daily activity of rats. RT-PCR experiments using cortical bone pulverized by CRYO-PRESS showed a significant difference in messages such as collagenase and IGF-I, reported markers of osteocytic response to mechanical environment. From these results, we suggest the critical role of osteocytes in sensitizing bone to PTH during daily activity and propose the combined use of physical stimulation (exercise) and PTH when treating osteoporoticpatients.

Table I. MARx10 (μm/10 days) in tibial cortical bone at the end of the 6-week experiment.

	Mean	SD	SE
RESTRAINED	16.4	3.8	1.9
CONTROL	21.9	3.9	1.9
PTH	39.1	7.6	3.8
RESTRAINED + PTH	22.8	9.3	4.7

SA350

Functional Outcome of Elderly Patients with Vertebral Compression Fractures. J. T. Lin*[1], E. Myers*[2], S. Backus*[3], M. Peterson*[4], A. Poynton*[5], J. M. Lane[5]. [1]Rehabilitation Medicine, The New York-Presbyterian Hospital, New York, NY, USA, [2]Biomechanics, Hospital for Special Surgery, New York, NY, USA, [3]Rehabilitation Medicine, Hospital for Special Surgery, New York, NY, USA, [4]Statistics, Hospital for Special Surgery, New York, NY, USA, [5]Orthopedics, Hospital for Special Surgery, New York, NY, USA.

The purpose of our study was to assess functional outcome using functional tests in a case-control study of osteoporotic patients with and without vertebral compression fractures. The tests were chosen to reliably identify specific deficiencies such as decreased endurance, flexibility, and functional gait performance. Outcome variables were correlated with the presence of fracture and the age of patients. Thirty-one osteoporotic patients with and without compression fracture physically capable underwent functional evaluation in the motion analysis laboratory, including timed up and go, functional reach, six minute walk, and bilateral single limb stance testing. Age of patients and number of fractures were recorded. Patients without compression fractures vs. patients with compression fractures (range 1-5 fractures) had an average age of 68.4 ± 10.5 years vs. 71.7 ± 7.0 years, timed get up and go 8.63 ± 3.30 seconds vs. 10.32 ± 4.98 seconds, functional reach = 11.38 ± 2.84 inches vs. 10.19 ± 2.71 inches, 6 minute walk = 365.02 ± 98.34 meters vs. 333.43 ± 123.05 meters, average right single limb stance = 10.48 ± 6.61 seconds vs. 7.03 ± 7.73 seconds, and average left single limb stance = 11.2 ± 7.29 seconds vs. 7.14 ± 7.26 seconds, respectively. There was a negative correlation between age and ability to perform six minute walk (Pearson correlation = -0.39, p=0.03), average right single stance (Pearson correlation = -0.485, p=0.019), and left single limb stance (Pearson correlation = -0.573, p=0.04). This suggests that age may represent a confounding variable in our analysis. Our preliminary findings suggest that there may not be direct relationships between presence of compression fracture and functional performance. There may be other variables, including the amount of kyphosis or location of fractures, that significantly impact function. A limitation of this study is that patients with severe pain or physical disability were not evaluated. Thus, the subjects with fracture were possibly a healthier subset of fracture patients. Our data should help identify reliable tests in osteoporotic patients with compression fractures to better direct medically-supervised physical therapy programs and to serve as the foundation for future prospective clinical trials, which will further evaluate the relationship between kyphosis and loss of function/impaired performance in kinesiologic measures.

SA351

Results of the Erlangen Fitness and Osteoporosis Prevention Study (EFOPS) -During Year 2 Exercise Effects Level Off at the Lumbar Spine but not at the Proximal Femur. W. Kemmler*[1], K. Engelke*[1], J. Weineck*[2], W. A. Kalender*[1]. [1]Inst. of Medical Physics, Univ. of Erlangen, Erlangen, Germany, [2]Inst. of Sport Sciences, Univ. of Erlangen, Erlangen, Germany.

Several recent exercise studies using high impact training regimes showed beneficial effects on bone. However, many exercise studies, in particular those with larger sample sizes (>50), did not extend over one year. Here we analyzed 2 year results from EFOPS (Erlangen Fitness Osteoporosis Prevention Study) and investigated whether bone mineral density (BMD) changes leveled off after one year of training, similar to observations in interventions using HRT or Bisphosphonates. EFOPS is an ongoing 3-year controlled exercise trial in 137 early (1 - 8 y) postmenopausal women with osteopenia at the lumbar spine or the hip. 86 women (EG) undergo a vigorous high impact/high intensity regime 2-4 times/week (2 joint, 2 home sessions). 51 non-exercising aged, BMI, and BMD matched women serve as control group (CG). Both groups are individually supplemented with Ca and Vit-D. After 2 years 50 women exercising more than 2 times/week and 33 women of the control group remained in the study. %-changes of isometric strength and BMD (measured by DXA) are shown in the tables (mean ± SD) along with corresponding differences for the two groups. In the EG BMD increased or was stable while in the CG BMD significantly decreased during the two years. However, at the spine BMD changes in the EG during year one (+1.3%) differed significantly from year two (-0.6%). Differences between year one and two were also significant for the trunk extensors in the EG. All other differences between variables shown in the table were non significant. Taken together our results show a significant leveling-off effect on BMD at the LS but not at the proximal femur during year 2.

Isometric Strength of the Trunk

Variable (%-changes)	EG (n = 50)	CG (n = 33)	Difference
Trunk extensors year 1	+31.1 ± 19.0***	-0.6 ± 15.7 n.s.	***
Trunk extensors year 2	+6.3 ± 12.4*	-2.4 ± 14.8 n.s.	*
Trunk flexors year 1	+23.8 ± 19.7 ***	-1.4 ± 15.4 n.s.	***
Trunk extensors year 2	+15.7 ± 18.4 ***	+0.9 ± 15.7 n.s.	***

BMD measured by DXA of the Lumbar Spine (L1-L4) and the Proximal Femur

Variable (%-changes)	EG (n = 50)	CG (n = 33)	Difference
BMD LS for year 1	+1.3 ± 2.6 ***	-1.3 ± 2.2***	***
BMD LS for year 2	-0.6 ± 2.3 n.s.	-1.0 ± 2.4*	n.s.
BMD hip for year 1	-0.2 ± 2.1 n.s.	-0.9 ± 2.5*	n.s.
BMD hip for year 2	-0.1 ± 2.0 n.s.	-1.1 ± 2.2*	*
BMD neck for year 1	-0.6 ± 2.4 n.s.	-1.9 ± 2.6 ***	***
BMD neck for year 2	-0.1 ± 2.6 n.s.	-1.0 ± 2.5*	n.s.

SA352

Influence of Hypogonadism and Hormone Replacement Therapy (HRT) on Bone Mass in Adult Women with Thalassaemia Major. G. B. Rini*[1], M. L. Brandi[2], G. Renda*[1], G. Di Fede*[1], G. Cusumano*[1], N. Napoli*[1], D. Bruno*[1], G. Vitale*[1], E. Carmina*[1]. [1]Clinical Medicine, University of Palermo, Palermo, Italy, [2]Internal Medicine, University of Florence, Florence, Italy.

Osteopenia and/or osteoporosis are major causes of morbidity in adult thalassaemic patients. The purpose of the study was to evaluate the influence of hypogonadism and HRT on bone mass in adult women with thalassaemia major. 30 adult women (mean age 28.5 ± 1.3 years, range 21-41) with thalassaemia major were studied. In all patients and in 10 normal controls of similar age (29.5 ± 1 years) blood levels of estradiol, LH, FSH, PTH, osteocalcin, bone alcaline phosphatase (AP) and type 1 collagen C-telopeptides (T) were determined. Hormones were measured by RIA methods while bone markers were determined by ELISA. Bone mineral density (BMD) of the lumbar spine (L1-L4) and of the femoral neck (F) was determined using dual X-ray absorptiometry. 6 patients (mean age 29 ± 2 years) had normal ovarian function. Compared to controls, they had similar blood levels of PTH (21 ± 3 vs 22.2 ± 5 ng/ml in controls), osteocalcin (16 ± 3 vs 18.4 ± 1.5 ng/ml in controls), AP (13 ± 1 versus 14.3 ± 1.5 µg/L in controls) and T (2958 ± 82 vs 3192 ± 315 pmol/L in controls). Their T score (L1-L4 - 1.33 ± 0.37, femoral neck - 0.64 ± 0.36) was lower than in controls, but the difference was significant ($p < 0.05$) only for L1-L4. 24 patients (mean age 28.2 ± 1.5 years) presented hypogonadism. 11 of these patients were never treated by HRT. Compared to controls, they presented similar blood levels of PTH (24.2 ± 3.5 pg/ml) and osteocalcin (23 ± 3.5 ng/ml) but higher levels of AP (21.6 ± 2.5, µg/L, $p < 0.05$) and T (5380 ± 657, pmol/L, $p< 0.01$). They presented a significantly decreased BMD (T score: L1-L4 - 2.44 ± 0.24, $p< 0.01$ vs controls and $p < 0.05$ vs normogonadic patients; F - 1.8 ± 0.22, $p< 0.01$ vs controls and vs normogonadic patients). 13 thalassaemic patients had been treated from a mean of 11 ± 2 years by HRT (conjugated estrogen 0.625 mg/day or equivalent + progestin). Compared to controls, they presented similar levels of PTH (25.8 ± 2.1 pg/ml), osteocalcin (22.2 ± 3.1 pg/ml) but higher levels of AP (23.6 ± 2.9 µg/L, $p< 0.05$) and T (4548 ± 539 pmol/L, $p< 0.05$). In comparison to both controls and normogonadic patients, their T score was significantly ($p< 0.01$) decreased (L1-L4 - 2.66 ± 0.25, F -1.97 ± 0.31). There was not difference in T score and in bone hormones or markers between hypogonadic patients who were treated or not with HRT. In conclusion: 1. hypogonadism is the major, but not the only, factor in determining bone loss in adult thalassaemic women, 2. Low dose HRT is not sufficient to prevent bone loss in adult thalassaemic women. Probably higher estrogen doses or biphosphonates are needed to prevent bone loss in these patients.

SA353

Bone Mineral Density Changes in a One Year Placebo Controlled Double Blind Randomized Trial of Hormone Replacement Therapy in Postmenopausal Systemic Lupus Erythematosus Patients. H. P. Bhattoa[1], P. Bettembuk[1], A. Balogh[1], G. Szegedi*[2], E. Kiss*[2]. [1]Department of Obstetrics and Gynecology, University of Debrecen, Debrecen, Hungary, [2]3rd Department of Internal Medicine, University of Debrecen, Debrecen, Hungary.

Although there are valid concerns regarding the use of exogenous estrogens in women with SLE, there are also potential health benefits to be considered. Several salutary effects of postmenopausal estrogens assume particular importance in SLE where the risks of osteoporosis, exaggerated by menopause (natural or cyclophosphamide-induced) and glucocorticoids, are substantial. We examined the safety and efficacy of hormone replacement therapy (HRT) in postmenopausal SLE patients. We planned a prospective examination of BMD for a year in a placebo controlled double blind study. Postmenopausal SLE women were randomly allocated to placebo or treatment group (50 microgram trans-dermal estradiol). Both groups received 5 mg continuos oral medroxyprogesterone acetate, 500 mg calcium and 400 IU vitamin D3. The patients confirmed to the ACR SLE criteria, T score < -1.0 and had no other disease influencing bone metabolism. Exclusion criteria were: risk factors for thrombo-embolism, serious liver or kidney disease, vaginal bleeding of unknown origin, breast tumor, endometrial carcinoma, and endometriosis. Follow-up visits took place at 3, 6, 9 and 12 months. From the 43 patients that were screened 32 could be included in the study, of whom 15 were in the treatment group and 17 in the placebo group. There was no significant difference between the two groups at baseline with regards to their mean age, disease duration, body mass index, duration of menopause, SLE disease activity index, SLICC, daily and cumulative corticosteroid dose. At the end of the study, 6 and 14 remained in the treatment and placebo group, respectively. In both the groups we found no statistically significant change in BMD during the study period. There was no statistically significant difference in the femur neck values between the two groups during the study period. There was a significant difference in the change in lumbar spine BMD between baseline and the 6th month visit between the two groups (+3,2% (treatment) vs. -1,0% (placebo); $p < 0.005$). Although the dropout rate was high, none was due to disease activation. Although the high dropout rate makes statistical interpretation at the end of the study period difficult, we conclude that HRT can be safely prescribed to postmenopausal SLE patients under strict medical supervision.

SA354

See Friday Plenary number F354.

SA355

Carborane BE360, One of the Carbon-containing Polyhedral Boron-cluster Compounds, Is A New Type of Selective Estrogen Receptor Modulator. C. Miyaura[1], C. Matsumoto*[1], Y. Endo*[2], A. Ito*[1]. [1]Department of Biochemistry, Tokyo University of Pharmacy and Life Science, Tokyo, Japan, [2]Tohoku Pharmaceutical University, Sendai, Japan.

Carboranes (dicarba-*closo*-dodecaboranes) are a class of carbon-containing polyhedral boron-cluster compounds having exceptional hydrophobicity, and their features may allow a new medical application as a biologically active molecule that interacts hydrophobically with hormone receptors. We designed carborane compounds with an affinity for estrogen receptor (ER) and synthesized these compounds to search for effective agents to treat osteoporosis. Among several carborane compounds, we noted two compounds, BE120 and BE360. BE120 has a carborane structure with one phenol and is the most potent compound bearing a carborane cage exhibiting a binding affinity for ER. Its binding affinity with ERα is 10-fold greater than that of 17β-estradiol (E2). BE360 has a carborane structure with two phenols, and its ER binding affinities are 1.6-fold to ERα and 0.15-fold to ERβ compared with E2. To examine the estrogenic activity of these compounds in bone, ovariectomized (OVX) mice were given BE120, BE360 or E2 subcutaneously for 4 weeks using a miniosmotic pump. Reduced uterine weight in OVX mice was completely restored by not only E2 but also BE120. However, 1000-fold higher doses of BE360 did not increase the uterine weight of OVX mice. Histological analysis also showed that BE360 did not exhibit any estrogenic activity in the uterus. In OVX mice, the trabecular bone volume of the femoral distal metaphysis was reduced markedly, when measured by DEXA and histological analysis. Treatment with BE120 at 1-30 ng/head/day markedly prevented bone loss in OVX mice, and its effective doses in bone and uterus were similar to those of E2. BE360 at 1-30 µg/head/day dose-dependently restored bone loss in OVX mice to a sham level without estrogenic action in the uterus. Therefore, 1000-fold higher does of BE360 were needed to prevent bone loss in OVX mice compared with that of E2 and BE120. To examine the effects of BE360 in bone in castrated mice, male mice were sham-operated or orchidectomized (ORX) and a subgroup of ORX mice was treated with BE360. Treatment with BE360 at 1-30 µg/head/day prevented bone loss in ORX mice without androgenic action on the sex organs. These results indicate that BE360 binds to ERs and exhibits estrogenic action in bone to prevent bone loss without inducing estrogenic action in the uterus, suggesting its possible application to osteoporosis as a new type of selective estrogen receptor modulator.

SA356

See Friday Plenary number F356.

SA357

Effect of Raloxifene on Bone Mineral Density and Bone Markers in Japanese Postmenopausal Women with Osteoporosis. H. Morii[1], Y. Taketani[1], Y. Ohashi*[1], T. Nakamura*[1], M. Fukunaga*[1], A. Itabashi[1], S. Sarkar*[2], K. D. Harper[2]. [1]Japan Clinical Trial Research Group, Tokyo, Japan, [2]Lilly Research Laboratories, Eli Lilly and Co., Indianapolis, IN, USA.

Raloxifene (RLX) is a selective estrogen receptor modulator (SERM) that acts as an estrogen agonist on the skeleton and on cardiovascular risk markers but as an antagonist in the endometrium and the breast. The safety and efficacy of RLX has been studied extensively in large, global clinical trials. Study 301J assessed the safety and efficacy of raloxifene 60 mg/day (RLX60) and 120 mg/day (RLX120) in Japanese postmenopausal women with osteoporosis after one year of therapy. 284 postmenopausal women (mean age, 64 years) with osteoporosis (lumbar spine L2-L4 T-score ≤ -2.5 SD) were enrolled in a multicenter, double-blind study that lasted 52 weeks. They were randomly assigned to receive placebo (PL), RLX60, or RLX120. All treatment groups received calcium 500 mg/day and vitamin D_3 200 IU/day. Lumbar spine bone mineral density (BMD) and markers of bone turnover (osteocalcin, bone-specific alkaline phosphatase, NTx/Cr, and CTx/Cr) were assessed at baseline, 12, 24, and 52 weeks and serum lipids (total cholesterol, LDL-C, HDL-C, and TG) were assessed at baseline, 12, 24, 40, and 52 weeks. Ultrasound examinations of the breast and endometrium were performed at 52 weeks. Routine physiological examinations and safety laboratory tests were performed at each visit. Compared to baseline, women taking RLX60 had significant increases in lumbar spine BMD at week 24 (+3.3%, p<0.001). This increase in BMD remained significant through 52 weeks (+3.5%, p<0.001). At 52 weeks, significant increases in BMD from baseline were also observed in the RLX120 group (+2.9%, p<0.001). No change in BMD from baseline was observed in the PL group (0.0%, p = 0.989). By week 52, among women taking RLX, significant reductions were observed in all markers of bone turnover compared to PL (p<0.001), which is consistent with previous observations (Ettinger et al. JAMA 1999; 282:637-45). Compared to PL, women taking either dose of RLX had significant reductions in total cholesterol and LDL-C (p < 0.05) but no change in HDL-C or TG. Overall, there were no significant treatment differences in the proportion of patients who reported at least one adverse event following randomization (p = 0.851). While no episodes of venous thromboembolism were reported, this is a rare adverse event that may not have been seen in this small sample of patients. The results of this study demonstrate that raloxifene is well-tolerated, is associated with early and sustained increases in lumbar spine BMD and has favorable effects on bone turnover markers and lipids in Japanese postmenopausal women.

SA358

See Friday Plenary number F358.

SA359

The Effects of Raloxifene on Bone Mass and Remodeling are not Mediated by a Modulation of Nitric Oxide Synthesis. M. Diaz-Curiel[1], M. Lefort*[2], C. De La Piedra[2], A. Lopez-Farre*[3]. [1]Medicina Interna, Fundacion Jimenez Diaz, Madrid, Spain, [2]Laboratorio Fisiopatologia Osea, Fundacion Jimenez Diaz, Madrid, Spain, [3]Laboratorio de Investigacion Cardiovascular e Hipertension, Fundacion Jimenez Diaz, Madrid, Spain.

Raloxifene (RLX), a selective estrogen receptor modulator, is used in the prevention and treatment of postmenopausal osteoporosis. Recent works show that nitric oxide (NO) is a regulator of bone remodeling, the fall of NO levels increasing bone resorption. The aim of this work was to study if the administration of RLX to ovariectomised rats, an experimental model of postmenopausal osteoporosis, produced any effects on NO pathway, and if its effects on bone mass and remodeling were changed by the administration of aminoguanidine (AG), and inhibitor of the NO-synthase (NOS). Fifty 15 week-old female Wistar rats were ovariectomised (OVX). Thirteen age-and-sex matched rats were sham operated (SHAM). OVX rats were divided in groups: 1) OVX+RLX: received orally 1 mg/kg/day of RLX analogue (LY 139481.HCl,Lilly); 2) OVX + RLX + AG: received RLX and AG (4 g/L in drinking water); 3) OVX: received vehicle. Treatments were followed during 3 months. BMD was determined in the left femur (f) and lumbar spine (l) by DEXA. Osteocalcin (BGP) and C-terminal telopeptide of collagen I (CTX), biochemical markers of bone remodeling, were determined in serum. Inducible NOS (ions) activity and endothelial NOS (eons) expression by Western blot were analysed. OVX presented a significant decrease in l and f BMD and an increase in BGP and CTX respect to SHAM rats. RLX administration decreased bone remodeling and prevented bone loss in OVX rats, and these protective effects were not influenced by AG. Values of eNOS in group (OVX + RLX) were significantly higher than that of SHAM, OVX or (OVX + RLX + AG) groups, whose eNOS levels were similar. However, iNOS levels were similar in all the studied groups. We can concluded that the beneficial effects of RLX on bone mass and remodeling in OVX rats do not seem to by mediated by a modulation of iNOS activity. On the other hand, although the increase in eNOS expression produced by RLX in OVX rats is annulled by AG, the positive actions of RLX on bone does not seem to be influenced by eNOS levels.

SA360

See Friday Plenary number F360.

SA361

Osteogenic Effects of PTH in Osteoblast-like Cells Is Enhanced by Alendronate Pre-Treatment. D. L. Halladay*[1], T. J. Martin[2], J. E. Onyia*[1]. [1]Gene Regulation, Bone and Inflamation, Eli Lilly & Company, Indianapolis, IN, USA, [2]Saint Vincent Institute of Medical Research, Fitzroy, Australia.

Alendronate (ABP) is a treatment for postmenopausal osteoporosis that has been shown to strongly suppress bone turnover, by inhibiting bone resorption and secondarily reducing bone formation activity. While the direct effects of ABP on osteoclasts is well documented, there is limited information on their actions on osteoblasts that may in part explain their ability to reduce bone formation activity. For example, it is not known if ABP pretreatment of osteoblasts could interfere with their ability to express osteogenic genes and/or respond to an osteogenic stimulus such as PTH. Therefore, we examined directly the actions of 1-100 µM ABP on the expression of bone genes (Runx-2 and osteocalcin) in the human osteosarcoma cell-line SaOS-2. SaOS-2 cells stably transfected with a reporter construct containing the luciferase gene driven by either Runx-2 promoter, 6 copies of Runx-2 binding site (p6OSE2-luc) or osteoclacin promoter were analyzed for activity after ABP treatment. To ascertain possible effects of ABP on an osteogenic response, ABP pre-treated and untreated cells were also sequentially challenged with PTH. After 8h, ABP alone had no effect on expression of any gene. After 24h, ABP at 1-100 µM concentrations had a small but significant inhibitory effect (20-25%) on Runx-2, p6OSE2-luc and osteocalcin expression. PTH treatment resulted in a dose dependent increase in the expression of Runx-2 promoter (170-200%), p6OSE2-luc (500%) and osteocalcin promoter (300%). Simultaneous addition of ABP and PTH did not alter any of the PTH stimulatory effects on these osteogenic genes. In contrast, ABP pre-treatment (24h) followed by PTH resulted in a 1.5-2 fold enhanced expression of p6OSE2-luc (to 700-1000%) and osteocalcin promoter (to 400-600%) over PTH alone treatment. Since PTH regulates these promoters in part via the cAMP-PKA pathway, we further examined the effect of forskolin on ABP treated cells. As with PTH, ABP pre-treatment enhanced forskolin's stimulatory effects (2-3 fold enhancement over forskolin alone) on p6OSE2-luc and osteocalcin promoter. Simultaneous addition of ABP and forskolin did not alter any of the forskolin's stimulatory effects on these osteoblast genes. These data are consistent with a direct effect of ABP on osteoblast function and indicate that ABP pre-treated osteoblast-like cells remain responsive to the osteogenic effects of PTH, which are possibly mediated via the c-AMP-PKA signaling pathway. Taken together, these observations imply that regardless of ABP treatment history, osteoblast-like cells remain responsive to PTH.

Disclosures: ***D.L. Halladay****, Eli Lilly & Company 3.*

SA362

Biological Activity of Recombinant PTH Analog UGL7841. N. M. Mehta[1], J. P. Gilligan[1], B. Stern*[1], M. V. L. Ray*[1], C. P. Meenan*[1], A. P. Consalvo*[1], E. Miranda*[1], X. Peng*[2], A. Vignery[2], V. Ross*[3], J. F. Whitfield[3], P. Morley[4]. [1]Unigene Laboratories, Inc., Fairfield, NJ, USA, [2]Yale University School of Medicine, New Haven, CT, USA, [3]National Research Council, Ottawa, ON, Canada, [4]ParaTecH Therapeutics Inc., Ottawa, ON, Canada.

Recombinant production of a PTH analog was achieved by direct expression of the peptide in *E. coli.* A fermentation protocol was developed where the glycine-extended peptide was secreted into the conditioned growth medium at levels of approximately 1 g/liter. The secreted peptide was partially purified, amidated *in vitro* at the C-terminus using recombinant peptidylglycine α-amidating monooxygenase, and further purified to homogeneity with an overall yield of >50%. The bioactivity of the recombinant peptide was evaluated *in vitro* by its ability to stimulate intracellular cAMP in ROS17/2 osteosarcoma cells. The ED_{50} values of the recombinant peptide, compared to that of the same peptide obtained by chemical synthesis, were determined to be equivalent (4.1×10^{-9} M and 4.2×10^{-9} M, respectively). The *in vivo* anabolic activity of the recombinant peptide was evaluated in an OVX rat model using 3-month old Sprague-Dawley rats. Subcutaneous injections of synthetic or recombinant PTH analog at 0.6 and 2.0 nmol/100 grams body weight were started two weeks after ovariectomy and then given once a day, 6 days a week for 4 weeks. At the end of the experiment distal femurs were removed, fixed and sectioned. The ability of the recombinant or synthetic PTH analog to stimulate trabecular growth in the cancellous bone of the distal femurs was assessed by bone histomorphometry. Both the recombinant and synthetic peptides were shown to give a statistically significant and dose-dependent increase in femoral trabecular volume and trabecular thickness compared to the ovariectomized vehicle-treated controls. This bioactive recombinant PTH analog is currently being evaluated as an oral therapeutic for the treatment of established osteoporosis.

SA363

Intermittent hPTH Administration Increases Bone Strength in Rat Lumbar Vertebral Body after Ovariectomy with Cortical Bone Mass Increase. S. Arita*[1], S. Ikeda*[1], M. Ito*[2], A. Nishida*[2], T. Nakamura[1]. [1]Orthopedic Surgery, University of Occupational and Environmental Health, Kitakyushu, Japan, [2]Nagasaki University School of Medicine, Nagasaki, Japan.

Ovariectomy (ovx) causes significant bone loss and fragility of bone strength in rats, but the varies can be reversed by treatment with human parathyroid hormone 1-34 (hPTH). To clarify the factor to determine the recover of ultimate strength in rat lumbar vertebra after ovx, we compared the results of skeletal measurements by micro-CT, pQCT and ultimate compression load by mechanical tests on the 5th lumbar vertebra. Female Sprague-Dawley rats (n = 204), 16 weeks of age, were divided into 21 groups. Ten rats were killed at day 0 as the baseline control, the others underwent ovx (n = 125) or sham surgery (n = 69). At 6weeks postsurgery, ovx rats were given subcutaneous injections of hPTH three times a week at respective dose of 0 (vehicle group) and 20micro gram/kg body weight (PTH group) for 12 weeks. Sham groups were administered vehicle only. In PTH group, trabecular bone volume (BV/TV) and trabecular thickness (Tb.Th), measured by micro-CT, increased from day 28 compared with vehicle group. The trabecular bone pattern factor (TBPf) and structure model index (SMI) diminished from day 28 compared with vehicle group. The total bone mineral content (BMC), total bone mineral density, cortical BMC, cortical area and cortical thickness measured by pQCT increased from day 28 compared with vehicle group. Ultimate compression loads increased from day 28 compared with vehicle group. In the early period (0-42 days) of PTH treatment, ultimate compression loads increased by 30.3%, and the late period (42-84 days), it increased by 0.02%. In the early period, cortical BMC was the most significant factor that influenced the ultimate load in PTH group, as assessed by stepwise regression analysis (coefficient of determination [R2]=0.663; p<0.0001). These data suggest that increases in cortical bone mass contributes more than that of trabecular bone mass and structure to recovery of bone strength by intermittent hPTH administration in rat lumber vertebral body after ovx.

SA364

See Friday Plenary number F364.

SA365

Human Parathyroid Hormone 1-34 Prevents Bone Loss in Bile Duct-Ligated Rats. R. Dresner Pollak[1], Z. Ackerman*[1], A. J. Foldes[1], M. Weinreb[2]. [1]Hadassah University Hospital, Jerusalem, Israel, [2]Goldschleger School of Dental Medicine, Tel-Aviv University, Tel-Aviv, Israel.

Reduced bone mass and fractures are common manifestations of primary biliary cirrhosis (PBC) in humans. We have previously demonstrated that bile duct-ligated (BDL) male rats develop osteopenia caused by a decreased rate of bone formation (Ackerman et al. Liver, in press). In this study we evaluated whether the administration of the anabolic agent parathyroid hormone (PTH) 1-34 prevents bone loss in BDL rats. Six month-old Sprague-Dawley male rats were divided into 4 groups: Group 1 underwent sham operation and was treated with a vehicle for 4 weeks. Groups 2-4 underwent BDL operation and, beginning on the 8th postoperative day, were treated for 4 weeks with a vehicle, human PTH (1-34) at 80 μg/kg/day and 40 μg/kg/day, respectively. Animals were sacrificed at the end of the fifth postoperative week. Liver cirrhosis and fibrosis were confirmed in all BDL rats by histology. Bone mineral density (BMD) of the femur and tibia was measured ex-vivo by DXA (Hologic QDR 4500A). In addition, femoral bone mass was measured by ashing. BDL rats had significantly lower femoral and tibial BMD compared to sham operated rats (p=0.02 and 0.001 respectively). BMD in animals treated with high dose PTH was not significantly different from BDL rats. Femoral and tibial BMD in animals treated with low dose PTH was significantly higher than in untreated BDL rats (p=0.009 and 0.003, respectively). Femoral and tibial BMD in BDL animals treated with low dose PTH was significantly higher than in animals treated with high dose PTH (p=0.006, p=0.01, respectively), and not significantly different from sham operated rats. The femoral corrected ash weight analysis confirmed that BDL rats were osteopenic (P < 0.03 vs. sham), and that the low dose, but not the high dose PTH restored bone mass to sham-operated levels (P<0.01 vs. BDL group).

	Sham (n=10)	BDL (n=10)	PTH 80 μg /kg/d (n=8)	PTH 40 μg /kg/d (n=6)
Femoral BMD g/cm^2	0.253±0.009	0.239±0.016	0.241±0.011	0.260±0.010
Tibial BMD g/cm^2	0.197±0.007	0.184±0.007	0.185±0.008	0.201±0.012
Femoral ash weight (mg/mm)	13.1±0.6	12.0±1.1	12.0±0.6	13.5±0.7

Data are mean±SD.

In summary, BDL rats develop osteopenia, which is prevented by treatment with PTH (1-34) at 40 but not 80 μg/kg/day. The shift from the published anabolic effect of the high PTH dose may be related to altered PTH metabolism in BDL rats.

SA366

See Friday Plenary number F366.

SA367

Parsimony with PTH: Is a Single Weekly Injection of PTH Superior to a Larger Cumulative Dose Given Daily? D. M. Black[1], C. J. Rosen[2]. [1]University of California, SF, CA, USA, [2]Maine Center for Osteoporosis, Bangor, ME, USA.

While chronic elevations of endogeneous PTH levels in hyperparathyroidism decrease bone mineral density, intermittent daily administration has the paradoxical effect of increasing BMD at the hip and spine. However, the possibility of other than *daily* administration of intermittent PTH has not been fully explored. Some alternatives to daily use have been tested. Hodsman (JCEM, 1997) tested cyclical use of PTH 1-34 (one month out of three) and found an annual spine BMD increase of 7.5%. Fujita (OI, 1999) conducted a randomized trial to explore a single weekly injection of PTH. In this 1 year study (not placebo controlled), 220 women were randomized to 50, 100 or 200 IU of PTH 1-34 (corresponding to about 15, 30 and 60 microgram (ug)) per week. They found surprisingly large increases in spinal BMD: 4% for the 30 ug dose and 8% the 60 ug dose. Bone formation rose during the first 3 months (about 25% with 60 ug) but by 12 months had fallen to below baseline levels. Bone resorption fell slightly. In the table below, we compare weekly to daily administration of PTH. For daily dosing, we interpolated the 12 month change in spine BMD from the 21 month study of Neer (NEJM, 2001) assuming that the BMD change was linear over time. The bone marker results for daily use are derived from a study PTH 1-34 in men (Kurland, JCEM, 2000). These results suggest that weekly administration of PTH might result in larger increases in BMD than much larger cumulative doses given daily. The similarities in BMD changes occur despite very different patterns of changes in bone markers. In conclusion, the weekly use of lower cumulative dose of PTH could potentially dramatically decrease costs, risks and side effects of PTH while maintaining similar efficacy. While these preliminary data have important limitations (e.g., large variations in the biologic activity of the preparations), they strongly support the value of additional studies to directly compare daily and weekly use of PTH and to explore the mechanisms by which PTH reduces fracture risk.

Comparison of weekly and daily use of PTH 1-34

Study Author(s)	Fujita	Fujita	Neer	Neer/Kurland
Total Weekly Dose	30 ug	60 ug	140 ug	280 ug
Administration	Weekly	Weekly	Daily	Daily
% change @ 1 year				
Spine BMD	+4%	+8%	+5%	+7%
Bone formation	-6%	-15%	NA	+150%
Bone resorption	-15%	-20%	NA	+100-300%

Disclosures: ***D.M. Black****, Merck 2, 8; Eli Lilly 5; NPS 5; Novartis 2.*

SA368

A Single Infusion of the Tumor Necrosis Factor-alpha Antibody Infliximab Suppresses Bone Resorption in Patients with Rheumatoid Arthritis. H. P. Dimai[1], T. Mueller*[2], A. Fahrleitner*[1], J. Hermann*[2]. [1]Internal Medicine, Endocrinology and Nuclear Medicine, Graz, Austria, [2]Internal Medicine, Rheumatology, Graz, Austria.

Rheumatoid arthritis (RA) is a chronic inflammatory disease leading progressively to osteoporosis and bone destruction. Treatment with infliximab, a neutralizing anti tumor necrosis factor-alpha antibody, has been shown to completely abrogate the progression of joint destruction in RA. We sought to investigate the hypothesis that infliximab might also be sufficient to inhibit bone resorption, thus preventing development of osteoporosis. 12 patients (7 females and 5 males; mean age 55 ± 11 yrs; disease duration 11 ± 6 yrs) with RA according to the revised ACR-criteria not responding to treatment with methotrexate were included in the study after given informed consent. Blood was drawn two and one day prior, and one and fourteen days after a single infusion of 10 mg/kg of infliximab. Sera were frozen at –70°C until assay. To evaluate the effect of infliximab on bone turnover we measured a marker of bone formation (i.e.osteocalcin) and a marker of bone resorption (i.e. serum beta-CrossLaps). In addition, we determined serum levels of intact parathyroid hormone (iPTH), interleukin-6 (IL-6) and electrolytes. RA disease activity was evaluated using the disease activity score (DAS). The DAS was significantly lower 24 hours, and 14 days after the infusion, respectively. This clinical improvement correlated significantly with a reduction of serum IL-6-levels (data not shown). More importantly, serum beta-CrossLaps levels decreased significantly 24 hours after the infusion. This effect was still significant 14 days after the infusion, albeit less pronounced. Other markers of bone metabolism investigated, such as OC, iPTH and total serum-calcium (tot Ca), did not change throughout the study period.

	visit-2	visit-1	visit+1	visit+2
DAS	6.5 ± 0.3	6.5 ± 0.3	5.7 ± 0.4*	4.9 ± 0.4**
IL-6 (pg/ml)	27.2 ± 8.6	75.4 ± 29.1	17.6 ± 13.0	11.5 ± 5.6**
beta-CrossLaps (pg/ml)	0.30 ± 0.04	0.29 ± 0.04	0.17 ± 0.03**	0.23 ± 0.04*
OC (ng/ml)	16.9 ± 2.7	19.1 ± 2.7	18.4 ± 2.6	19.6 ± 3.4
iPTH (pg/ml)	48.5 ± 5.7	38.4 ± 7.2	36.0 ± 5.7	52.6 ± 10.8
totCa (mmol/L)	2.3 ± 0.03	2.3 ± 0.02	2.3 ± 0.03	2.3 ± 0.02

*p<0.05; **p<0.001

In this study, infliximab treatment ameliorated disease activity in RA patients, as was already demonstrated in prior studies. It also significantly reduced a biochemical marker of bone resorption in these patients. Therefore, infliximab is not only effective to control disease activity and radiological progression of RA, but it may also be sufficient to prevent generalised bone loss in patients with RA.

SA369

See Friday Plenary number F369.

SA370

Short-term Use of Postmenopausal Hormone Replacement Therapy Reduces the Incidence of Osteoporotic Fractures 10 Years after Withdrawal: The PERF Study. Y. Z. Bagger, L. B. Tankó, P. Alexandersen*, P. Ravn*, C. Christiansen. Center for Clinical & Basic Research A/S, Ballerup, Denmark.

Previous studies have shown that a decrease risk of fractures is evident only in women who have received HRT for at least 5 years. In the present study, we investigated whether a previous short-term course of HRT for 2 years had any anti-fracture effect after withdrawal. We followed up a group of 263 early postmenopausal Danish women who participated in various placebo-controlled HRT clinical trials at our center. Participants were re-examined 5, 11 and 15 years after withdrawal of HRT. Age at baseline was 45-59 years. All women included in this study completed the trials and were re-examined in 2000 and 2001. Those currently taking HRT or other drugs known to influence bone metabolisms were excluded from the calculation. Spine BMD and forearm BMC were assessed at baseline, at the end of HRT and 10 years after withdrawal of treatment. Lateral X-ray of the thoracic and lumbar spine was performed. Vertebral deformities from T4 to L4 were assessed by digital measurement. A more than 20% reduction of the vertebral height was considered as a fracture. Non-vertebral fractures were recorded by standard questionnaire. The mean residual effects of 2 years of HRT on bone mass remained 4.9% at the forearm and about 6% at the spine compared to placebo groups after 5-15 years of withdrawal (Table 1). The number of vertebral fractures in the placebo and HRT groups is shown in Table 2. The risk of vertebral fracture was significantly lower in women who had previously received 2 years of HRT as compared to non-users. Furthermore, using HRT for 2 years after menopause reduced the all-osteoporotic fracture incidence to 0.44 (95% CI, 0.25-0.78, p=0.005) as compared to non-users. These results indicate that a short-term course of HRT administered in the early postmenopausal years offers long-lasting benefits in the prevention of osteoporortic fractures.

Table 1. Mean changes in BMC/BMD% at the end of HRT and after withdrawal of HRT

	Δ mean spine BMD%	Δ mean arm BMC%
At the end of 2 years HRT	6.9%	5.3%
10 years after withdrawal of HRT	6.2%	4.9%

Table 2. Odds ratio for vertebral fracture in previous HRT users and non-users

Vertebral fracture	HRT	Placebo	Odds ratio (95% CI)
Yes	18	26	0.41* (0.21-0.80) *p=0.008
No	137	82	

SA371

See Friday Plenary number F371.

SA372

Nasal Calcitonin Increases Spinal Bone Density in Male Osteoporosis without Vertebral Deformity. E. Tóth[1], S. Mészáros*[2], V. Ferencz*[2], E. Csupor*[2], K. Bors*[2], E. V. McCloskey[3], C. Horváth[2]. [1]Rheumatology, Flór Ferenc County Hospital, Kistarcsa, Hungary, [2]1st Department of Medicine, Semmelweis University, Budapest, Hungary, [3]Collaborating Center for Metabolic Bone Diseases, WHO, University of Sheffield, Sheffield, United Kingdom.

The treatment of idiopathic male osteoporosis is still controversial. The aim of our study was to evaluate prospective changes on bone density (BMD) is men with osteoporosis. Patients and methods: Sventy-one men were studied (T score at lumbar spine and femoral neck lower than -2.5) with a mean age of 59±6 years. Men with secondary causes of osteoporosis and vertebral deformity were excluded. 40 patients were randomized to treat with nasal calcitonin (200 IU/day, Miacalcic, Novartis - monthly intermittent doses) plus calcium and Vitamin D replacement while 31 patients were given 1000mg/day calcium and 400NE/day Vitamin D3 only. Bone mineral density of the spine, hip.and forearm was followed by dual energy x-ray absorptiometry (DEXA, LUNAR DPX-L, USA) at baseline and at 18 months of treatment. Results: Calcitonin increased BMD at the spine and hip while no changes were observed in the placebo group. (Tabl. 1). Percent changes of BMD were found as follows (mean ±SD). (Tabl. 2). No fractures occurred in the calcitonin treated group, while 3 patients suffered fractures in the placebo group.Conclusions: Our preliminary results suggest calcitonin to be effective in the management of idiopathic male osteoporosis.

Table 1

ΔBMD mg/cm2	CT (95% CI)	PL (95% CI)	p (CT vs PL)
spine	30 (18-43)	6 (-15-+27)	0,03
hip	23 (11-35)	-8 (-23-+41)	0,001
radius	11 (-17-+81)	11 (-21-+42)	0,99

Table 2

Δ BMD %	CT	PL	p (CT vs PL)
spine	3,5±4,3	0,83±6,4	0,04
hip	3,2±3,9	0,68±5,7	0,004
radius	1,4±8,8	1,4±10,9	0,98

SA373

See Friday Plenary number F373.

SA374

A Therapeutic RANKL Vaccine for the Prevention and Treatment of Degenerative Bone Diseases. T. Bratt*[1], V. Nardi-Dei*[2], L. Sonderbye-Kjaerulff*[1], J. H. Rasmussen*[1], C. Lyngso*[1], S. Tanaka[3], M. Hertz[1]. [1]Pharmexa A/S, Horsholm, Denmark, [2]Pharmexa, Horsholm, Denmark, [3]Department of Orthopaedic Surgery, University of Tokyo, Tokyo, Japan.

The TNF family member Receptor Activator of NFκB Ligand (RANKL) stimulates osteoclast differentiation and activation. RANKL and the soluble receptor for RANKL, osteoprotegerin (OPG), together are the critical regulators of normal bone development. Balance of the RANKL - OPG ratio or overexpression of RANKL can be detected during pathological bone destruction in human diseases such as osteoporosis, rheumatoid arthritis (RA), and bone metastasis. Furthermore, neutralizing RANKL is effective at reducing bone destruction in models of osteoporosis, RA, bone metastasis, periodontal disease and reducing markers of bone turnover in a phase I clinical trial of postmenopausal women. We have previously shown that a murine RANKL vaccine could prevent bone loss in a mouse ovariectomy model and ameliorate bone loss and synovial inflammation in a murine RA treatment model (Hertz, M. et al (2001) J.Bone Miner.Res. 16:S222 and Juji,T. et al. (2001). J.Bone Miner.Res. 16:S150.). Here, we demonstrate that human RANKL vaccines can induce polyclonal antibodies that compete with recombinant OPG for binding of human RANKL *in vitro* and that neutralize *in vitro* osteoclastogenesis. Moreover, these vaccines can prevent bone loss in animal models of bone destruction.

Disclosures: ***M. Hertz****, Pharmexa A/S 1, 3.*

SA375

Effect of Vitamin K^2 on Cancellous Bone in Orchidectomized and Sciatic Neurectomized Rats. J. Iwamoto[1], J. K. Yeh[2], T. Takeda*[1], S. Ichimura*[3]. [1]Department of Sports Medicine, Keio University School of Medicine, Tokyo, Japan, [2]Department of Medicine, Winthrop-University Hospital, Mineola, NY, USA, [3]Department of Orthopaedic Surgery, National Defense Medical College, Saitama, Japan.

We examined the effect of vitamin K_2 on cancellous bone in orchidectomized and sciatic neurectomized rats. Ninety male Sprague-Dawley rats, 3 months of age, were randomized by stratified weight method into nine groups with 10 rats in each group: baseline controls (BLC), age-matched controls (AMC), AMC+vitamin K_2 administration (K), orchidectomy (ORX), ORX+K, unilateral sciatic neurectomy (NX), NX+K, ORX+NX, and ORX+NX+K. Vitamin K_2 (menatetrenone) was administered orally twice a week at dose of 30 mg/kg each. After 10 weeks of feeding, cancellous bone histomorphometry was performed for the proximal tibia. No significant difference in bone volume (BV/TV) was found between the BLC and AMC groups and between the AMC and AMC+K groups. BV/TV was significantly lower in the ORX, NX, and ORX+NX groups by 49.4 %, 58.5 %, and 65.6 %, respectively than in the AMC group. BV/TV loss in the NX and ORX+NX groups was attributable to increased osteoclast number (N.Oc/BS) and eroded surface (ES/BS) and decreased bone formation rate (BFR/BS), whereas BV/TV loss in the ORX group was associated with increased N.Oc/BS, ES/BS, BFR/BS, and BFR/BV. BV/TV was significantly greater in the ORX+K, NX+K, ORX+NX+K groups by 33.1 %, 20.1 %, and 27.3 % as compared to the respective control group without vitamin K_2 administration. This increase in BV/TV by vitamin K_2 administration was primarily due to increased trabecular thickness (TbTh). The protective effect of vitamin K_2 was attributable to decreased N.Oc/BS and ES/BS and increased BFR/BS in the NX+K and ORX+NX+K groups, whereas it was attributable to decreased N.Oc/BS, ES/BS, and BFR/BV in the ORX+K group. The results of the present study suggest that vitamin K_2 could partially prevent cancellous bone loss by suppressing bone turnover in ORX rats and by suppressing bone resorption and stimulating bone formation in NX and ORX+NX rats.

SA376

Alfacalcidol Distributes to Bone Marrow Cells in an Unchanged Form and Converts to Active Forms Locally. N. Hayakawa*, S. Higashi*, A. Shiraishi*, T. Masaki*, E. Hoshino*, S. Matsubara*. Product Research Lab., Chugai Pharmaceutical co., ltd., Tokyo, Japan.

Anti-osteoporosis drug, alfacalcidol [1α(OH)D_3] (ALF), converts to the active form (1α,25$(OH)_2D_3$) at the liver after oral administration. The blood concentration of 1α,25$(OH)_2D_3$ is therefore dominant in the circulation. Recently, we have confirmed that the concentration of pro-drug form (unchanged ALF) was higher in the bone marrow than the plasma and highly distributed in cells on bone surface of adult rats, whereas the 1α,25$(OH)_2D_3$ was dominant in the blood circulation. The distribution of unchanged ALF may be the key to understand the mechanism of the anti-osteoporotic effect. Therefore, in the present study, we examined how bone marrow cells affect on the ALF metabolism in vitro. Bone marrow cells were isolated from femoral bones of male rats (8 weeks old, Wistar-Imamichi) and all the bone marrow cells per femur were seeded in a 35 mm dish with IMDM medium containing [22,23-^{3}H]ALF at a dose of 10^{-8} mol/L. At 4, 24, 48 and 72 h following cultivation, cultured cells were washed and trypsinized to extract radioactivity by 4-5 fold volume of methanol. The radioactivity uptake and the metabolic profiles of ALF were analyzed by liquid-scintillation counting and HPLC analysis, respectively. The radioactivity uptake in the cultured cells reached a maximum after 24 h (about 60 % of dose) and declined up to 72 h (about 40 % of dose). The HPLC analysis of the radioactivity showed that unchanged ALF existed in the cultured cells at the highest ratio during all the time points, while small amounts of 1α,25$(OH)_2D_3$ and some other metabolites were detected. Detailed analysis of the HPLC profiles over the culture period showed that unchanged ALF gradually declined through the all sampling times, whereas 1α,25$(OH)_2D_3$ was evident at 24 h and then maintained its level until 72 h. In summary, the present results demonstrate that, ALF distributed into bone marrow cells might convert to the active form (1α,25$(OH)_2D_3$) gradually and affect bone metabolism for the relatively long period. Therefore, the binding situation between unchanged ALF and vitamin D receptor or the other specific (unknown) binding sites and the induction of converting enzymes in bone marrow cells might be critical.

SA377

Pharmacological Efficacy of Alfacalcidol for the Treatment of Osteoporosis Is Not Achieved by the Use of a Calcium Supplement. A. Shiraishi*[1], S. Higashi*[1], T. Masaki*[1], N. Hayakawa*[1], E. Hoshino*[1], S. Matsubara*[1], M. Ito[2], A. Nishida[2], E. Ogata[3]. [1]Product Research Lab., Chugai Pharmaceutical Co., Ltd., Tokyo, Japan, [2]Department of Radiology, Nagasaki University School of Medicine, Nagasaki, Japan, [3]Cancer Institute Hospital, Tokyo, Japan.

Alfacalcidol [1α(OH)D_3:ALF], the prodrug of calcitriol, has been used for the treatment of osteoporosis in certain countries, including Japan. It is generally agreed that in vitamin D-deficient states, active vitamin D increases bone mass mainly through enhancing intestinal calcium (Ca) absorption. So far, we have reported: 1) ALF has the unique property of suppressing bone resorption while stimulating bone formation in vitamin D-replete rats; 2) ALF acts in bone, at least in part, independently of its effects on calcium absorption and suppression of PTH secretion. In this study, we aimed to assess whether or not a nutritional supply of calcium could be substituted for ALF administration in preventing bone loss due to estrogen deficiency. Eight month-old rats were ovariectomized (OVX) or sham operated. The OVX rats were subjected to ALF administration (0.025, 0.5, 0.1 or 0.2μg/kg, p.o. 5 times a week) or calcium-enriched diets (0.4, 1.4 or 2.5 g/kg, food intake; phosphorus 0.5 g/kg). After 12 weeks of treatment, all rats were sacrificed to harvest the spine, serum, and urine samples. Neither the ALF treatment nor the Ca supplement caused hypercalcemia. Both the ALF administration and the high Ca intake increased the urinary Ca excretion to the maximum level in the same manner, indicating that the intestinal Ca absorption rose to the same extent. In the spine, ALF prevented the decrease in bone mass induced by OVX, and even increased the strength over that of the sham level. Micro-CT analysis also confirmed that the bone-protective effect of ALF was based on an improvement of microstructure in the trabecular bone. In contrast, and of particular interest, with an increase in the Ca intake, there was no change in spinal bone mass and strength despite the range of Ca dosages. In the Ca-treated groups, the dose-dependent changes in urinary deoxypyridinoline excretion and serum osteocalcin level were not observed. Furthermore, excessive Ca intake caused a significant increase in blood urea nitrogen and serum creatinine, and also induced a progressive reduction in urinary excretion of inorganic phosphorus. These results suggested that not only did excessive Ca supplementation have no apparent effect on spinal bone loss in estrogen deficiency, it was also associated with the risk of causing a disorder in the renal function. Consequently, we conclude that ALF has beneficial efficacy for the treatment of osteoporosis, which is not achieved by the use of a Ca supplement.

SA378

Anabolic Effect of Active Vitamin D3 Analog, Alfacalcidol, Is Strongly Related to Bone Strength through Thickening of Transverse Trabeculae. M. Ito[1], S. Higashi[2], A. Nishida[1], A. Shiraishi[2], K. Hayashi*[1]. [1]Radiology, Nagasaki University, Nagasaki, Japan, [2]Product Research Lab. Chugai Pharmaceutical Co., Ltd, Tokyo, Japan.

We previously reported that alfacalcidol (ALF) improves bone strength due to suppression of bone resorption and stimulation of bone formation in ovariectomized (OVX) rats. These pharmacological effects of ALF, however, could not clearly explain the fact that ALF improves bone strength without significantly affecting bone mineral density (BMD). We therefore examined the influence of ALF on microstructure in OVX rats, and investigated the relationship between trabecular microstructure and bone strength. 10-month-old female rats including sham (n=5) and OVX (n=40), were orally administered with ALF at 0, 0.025, 0.05, 0.1mcg/kg BW for 12 weeks. BMD, 3D trabecular microstructure, and bone strength were measured in the lumbar vertebrae, and the histomorphometry was assessed in the femur. We found that 1) Stimulated bone resorption determined by biochemical markers and histomorphometry due to estrogen depletion was dose-dependently inhibited by ALF, and was significantly suppressed at the dose of 0.1mcg/kg. Elevated bone formation markers by OVX did not decrease by ALF treatment and maintained independently of the suppression of bone resorption throughout all the dose range. 2) ALF inhibited decrease in spinal BMD induced by OVX and exerted the maximum effect over the dose range of 0.05-0.1mcg/kg. 3) Bone strength did not increase at the dose of 0.05mcg/kg, but markedly increased at the dose of 0.1mcg/kg. 4) The microstructure dose-dependently improved by ALF. Especially, bone volume (BV/TV) and trabecular thickness (Tb.Th) significantly increased, and trabecular bone pattern factor (TBPf) and structure model index (SMI) significantly decreased. Additionally we found that degree of anisotropy (DA), which determines the ratio of main axes of trabecular direction (vertical and transverse in vertebra) , significantly decreased at the dose of 0.1mcg/kg. To summarize, ALF prevents the loss of trabecular connectivity as indicated by the microstructure indices, such as TBPf and SMI, and, at 0.1mcg/kg, thickens the transverse trabeculae, as evidenced by the decrease of DA. These unique pharmacological effects on trabeculae were considered to be mainly due to the direct anabolic action, while retaining the marked anti-resorptive activity. In conclusion, the anabolic action of ALF appeared to increase bone strength due to thickening transverse trabeculae, in addition to the maintenance of trabecular connectivity due to the suppression of bone resorption. The dose of 0.1mcg/kg ALF markedly improved the trabecular structure and bone strength with minimal increase in BMD.

SA379

Simultaneous Administration of Alfacalcidol and Alendronate at their Subtherapeutic Doses Produces the Inhibition of Bone Loss through Their Synergetic Suppressive Effect on Bone Resorption in Rats. S. Higashi*, T. Masaki*, A. Shiraishi*, N. Hayakawa*, E. Hoshino*, S. Matsubara*. Product Res. Lab., Chugai Pharm. Co., Ltd., Tokyo, Japan.

Both alfacalcidol (ALF) and alendronate (ALN) are reported to prevent estrogen deficiency-induced bone loss by an anti-resorptive effect. The purpose of this study was to clarify the effect of simultaneous administration of ALF with ALN at their threshold doses on bone turnover and OVX-induced bone loss in rats. 40-week-old female Wistar rats, OVX- and sham-operated, were randomized at 12 weeks post-surgery into seven groups (n=5-7); 1) sham+vehicle, 2) OVX+vehicle, 3) OVX+ALF 0.025 μg/kg/day, 4) OVX+ALF 0.1 μg, 5) OVX+ALN 0.3 mg, 6) OVX+ALN 1.0 mg or 7) ALF (0.025 μg) in combination with ALN (0.3 mg). Each drug was administered orally 5 times a week for 12 weeks and thereafter sacrificed. The spinal bone mineral density (BMD) (L2-L4) was measured by dual-energy x-ray absorptiometry every 4 weeks. The rise in urinary excretion of deoxypyridinoline (DPD) induced by OVX was suppressed by both ALF and ALN treatments alone in dose- and time-dependent fashion. The increase in number of osteoclasts determined by histomorphometry of lumbar vertebra (L5) was not ameliorated by ALN but by ALF 0.1 μg/kg ($p < 0.001$ vs OVX) after the 12-week treatment. These results suggest different mechanism of anti-resorption. Moreover, the decrease in DPD excretion by the treatment of ALF 0.025 μg/kg, ALN 0.3 mg/kg, and both administration for 4 weeks were 18% (ns), 24% ($p<0.01$), and 51% ($p<0.001$), respectively, when compared to values of OVX+vehicle group. DPD levels of both-treated group at 4 weeks corresponded to those of ALN 1.0 mg/kg treated group for 4 weeks or of ALN 0.3 mg/kg treated group for 12 weeks. However, elevated bone formation markers by OVX such as serum osteocalcin remained at the same level in either treated group (ns vs. OVX at 4, 8, 12 weeks). The simultaneous administration of ALF and ALN elicited an additive inhibitory effect on bone loss induced by OVX at 12 week, although neither treatment alone elicited obvious effects on spinal BMD. Although doses used in this combination study were below those known to cause severe hypercalcemia and hypocalcemia by ALF and ALN itself, respectively, the decreases in serum calcium (Ca) and urinary Ca excretion in OVX rats were counteracted by the combination therapy and restored to the similar level of sham group. In summary, this study suggests that ALF and ALN are considered to exert additive anti-resorptive activities, and that the simultaneous administration of ALF and ALN at their threshold doses might ameliorate Ca balance and spinal BMD through the prompt beneficial effect on bone turnover.

SA380

Randomized Doubled Blind Twelve Months Study of 1 μg/day of Alphacalcidiol vs Placebo in a High Bone Turnover Postmenopausal Women. G. S. Riera, M. Naressi*, G. Velasquez*, J. Ramos*, B. Herrera*. Medicine, UNILIME. Universidad de Carabobo, Valencia, Venezuela.

Vitamin D metabolites have been used for osteoporosis treatment. Main actions on bone are: mineralization, stimulation of osteoblast and diminish resorption, however available information about action on resorption markers in a prospective double-blind, placebo control trial are scarse. 85 postmenopausal patients with low BMD (T-score between -1 and -3 at L2-L4 or femoral neck) and high turnover (N-telopeptide-NTx-, Tartrate Resistant Acid Phosphatase -TRAP- or Alkaline Phosphatase -AP- 1SD or more above the premenopausal mean) were randomized in a double-blind, placebo control, 12 month trial of 1 μg/day of alphacalcidol vs placebo, according to the principles of the Helsinski Declaration. Exclusion criteria were: secondary osteoporosis, fracture 6 months prior to the study, medication such as TRH, insulin, steroids, diuretics, biphosphonates, calcitonin, raloxifene, antituberculosis drugs and thyroid hormones, allergy to vitamin D. Group A: alphacalcidiol 1μg/day + calcium citrate 500mg/day, Group B: placebo + calcium citrate 500mg/day. Mean age was 61.58 ± 6.69 and 62.4 ± 6.30. Age of menopause was 45.6 ± 5.14 and 46.4 ± 5.5, there were no differences on risk factors between groups. Modest hipercalciuria occurs in 48% (Group A) and 18% (Group B), Calcium supplement was stopped to control this side effect. We did not have hipercalcemia. Drop out rate was 3.5% in the placebo group and

2.4% in the alphacalcidol group. BMD remained stable in both groups. In conclusion the use of alphacalcidiol 1 µg/day during 12 months in postmenopausal women with low BMD and high turnover was very well tolerated and decreased NTx by 27.7%, TRAP by 23.6% and AP by 16%.

	Placebo				Alphacalcidiol			
Marker	Initial	3 m	6 m	12m	Initial	3 m	6 m	12m
AP UI/L	47 ±14	43.2 ±15	43.3 ±12.6	43.2 ±12	48.6 ±15.3	43.1 ±14.7	39.2** ±10.1	40.8** ±10.4
TRAP UI/L	10.2 ±3.3	9 ±2.3	8.4*** ±1.9	8.1*** ±2.2	9.9 ±2.9	8.67 ±12.6	7.4*** ±1.8	7.5*** ±2.3
NTx nMolBCE/ mMolCr	133.5 ±58.3	103.6* ±64	118.5 ±67.5	114.5* ±85.1	128.7 ±67.2	115.2* ±28	102 ±62.8	92.9* ±55.7

* = p<0.05, ** = p<0.01, *** = p<0.001 vs. Initial

Disclosures: ***G.S. Riera****, Ghynoparm. Venezuela 2.*

SA381

See Friday Plenary number F381.

SA382

Senile Defect in the Renal Activation of Vitamin D. C. Horvath[1], E. Hosszu*[2], S. Meszaros*[1], V. Ferencz*[1], K. Bors*[3], E. V. McCloskey[4]. [1]1st Department of Medicine, Semmelweis University, Budapest, Hungary, [2]2nd Department of Pediatrics, Semmelweis University, Budapest, Hungary, [3]Ferencvaros Osteoporosis Center, Budapest, Hungary, [4]WHO Collaborating Centre for Metabolic Bone Diseases, University of Sheffield, Sheffield, United Kingdom.

Vitamin D is formed to active hormone by two steps of activation in the liver and in the kidney. It is supposed that ageing processes of the kidney could deteriorate the vitamin D hydroxylation, too. In our study low-calcium diet was used as a stimulation test estimating the renal vitamin D activating capacity in young and senile people. *Methods:*13 healthy young (between 20-25 ys) and 33 old (70-80 ys) volunteers were involved into the study. They were asked to eat no more than 200 mg calcium daily during 10 days. Serum and urinary calcium, phosphorous, creatinine as well as serum PTH, 25-OHD and $1,25(OH)_2D$ levels were measured before and after the diet period. *Results:*in healthy young people the activated vitamin D level remains normal in a calcium deprivation test (Table, *:p<0,05). Consumption of 25-OHD serum concentration can be observed, however, hypersecretion of parathyroid hormone is not needed to the accomodation. In contrast, elderly people can preserve normal serum level of activated vitamin D only with help of secondary hyperparathyroidism. *Conclusion:* our model suggests that use of activated rather than native vitamin D is rational for supplementation of elder people.

Table

Volunteers	Young	Young	Elder	Elder
Sample	basal	after diet	basal	after diet
se Ca (mmol/l)	2,41	2,44	2,49	2,44
se 25OHD (pg/ml)	25,6	14,9*	23,9	36,4*
se 1,25OHD (pg/ml)	41,2	45,0	41,2	43,2
PTH (pg/ml)	43,4	44,2	47,8	64,5*

SA383

2-Methylene-19-Nor-(20S)-1,25-Dihydroxyvitamin D_3 (2MD), an Analog of 1α,25-Dihydroxyvitamin D_3 (VD) Markedly Increases Bone Mass of Ovariectomized (OVX) Rats. L. Plum*[1], X. Ma*[2], M. Clagett-Dame*[2], N. Shevde[2], L. Fitzpatrick[3], J. W. Pike[2], H. F. DeLuca[2]. [1]University of Wisconsin-Madison/Deltanoid Pharmaceuticals, Inc., Madison, WI, USA, [2]Biochemistry, University of Wisconsin-Madison, Madison, WI, USA, [3]Endo/Metabolism Unit, Mayo Clinic, Rochester, MN, USA.

Sicinski et al. (J. Med. Chem. 41, 4662-4674, 1998) demonstrated that 2MD selectively increases the osteoblastic-mediated mobilization of calcium from bone. We made the assumption that 2MD would also selectively increase all activities of the osteoblast including synthesis of new bone. To test this hypothesis, we obtained retired breeder female rats from Harlan Sprague-Dawley. Groups of 12 rats were either sham-operated (controls) or ovariectomized. Two days prior to initiation of drug administration, the animals were switched to a purified diet containing 0.47% Ca, 0.3% P. The OVX groups were provided with 0, 5 pmol 2MD/day, 7 pmol 2MD/day, 32 pmol 2MD 2X/week, or 500 pmol VD 3X/week orally for a total of 30 weeks. Using DPXα, total body bone scans were performed 5 weeks prior to dose administration and after 13 and 23 weeks. Bone mineral density of the right femurs was determined at week 28. Serum calcium was monitored monthly. Approximately two weeks prior to termination, tetracycline and calcein were given to label the skeleton for histomorphometry. At termination, lumbar vertebrae were scanned ex vivo for mineral density. Vertebrae, femurs and tibias were removed for histomorphometry, bone breaking strength and ash determinations. Serum was collected for measurement of biochemical markers of bone formation and resorption. At both 5 and 7 pmol dose levels, 2MD caused a 5-7% increase in total body bone mineral density by 23 weeks. Daily dosing proved to be more effective in increasing bone mineral density than the 2X week regimen. Preliminary estimates are that there is a 25% increase in trabecular bone and a 25% increase in the cortical bone of femur. This took place in the absence of hypercalcemia. In contrast, VD at 500 pmol 3X week caused no appreciable increase in total body bone mass. Results of ash, histomorphometry and bone strength measurements will be reported. The results strongly suggest that 2MD is an anabolic agent for bone that provides significant promise for the treatment of bone loss diseases such as osteoporosis.

Disclosures: ***L. Plum****, Deltanoid Pharmaceuticals, Inc. 1, 3.*

SA384

Bone Mineral Density Improvement After Two Years of Intravenous Pamidronate Treatment of Patients with Fibrous Dysplasia. M. S. Parisi*, B. Oliveri, C. Mautalen. Sección Osteopatías Médicas, Hospital de Clínicas, Universidad de Buenos Aires, Buenos Aires, Argentina.

Intravenous Pamidronate (APD) has proved to be effective in patients with Fibrous Dysplasia (FD) as shown by its effect on bone pain, markers of bone turnover or radiological changes. We report the effect of two years treatment with intravenous APD (180mg, 60mg/day during 3 days, every 6 months) on BMD of affected bones in 10 patients with FD, 7 women and 3 men (mean age 32 years). Clinical symptoms and markers of bone turnover were evaluated every 3 months. BMD of total skeleton and X-rays of FD areas were performed at baseline and once a year. BMD of FD areas was compared with the contralateral side using the region of interest program on the total skeleton scan. At baseline the average difference in BMD of FD areas was –11.2% compared with contralateral side (a significantly greater difference than that observed between left and right sides in healthy controls –0.7% (p<0.02)). Treatment with intravenous APD improved clinical symptoms and significantly decreased values of bone markers. Mean total skeleton BMD increased 2.7% (p<0.05) after 12 months and 4.4% (p<0.05) after 24months. BDM of FD areas Increased 3.8% after 12 months and 8.2% after 24 months compared with 0.3% and –2.9% changes in contralateral side respectively. Average difference BMD of FD areas diminished to –8.4% after 12 months and –2.6% (p<0.02) after 24 months compared with contralateral side. No radiographics changes were observed in FD lesions. Intravenous APD increased BMD of both the total skeleton and Fibrous Dysplasia affected bones BMD. Densitometric follow-up of these patients is a useful tool to evaluate the efficacy of treatment and is more sensitive to detect early changes than radiology.

SA385

See Friday Plenary number F385.

SA386

Association of Molecular Variants in BMP4 with Ossification of the Posterior Longitudinal Ligament of the Spine. K. Furushima[1], T. Tanaka*[1], T. Nakajima*[2], S. Maeda*[3], S. Toh*[1], I. Inoue*[2]. [1]Department of Orthopedic Surgery, School of Medicine, Hirosaki University, Hirosaki, Japan, [2]Division of Genetic Diagnosis, The Institute of Medical Science,, Minatoku, Japan, [3]Department of Orthopedic Surgery, School of Medicine, Kagoshima University, Kagoshima, Japan.

Introduction; Ossification of the posterior longitudinal ligament of the spine (OPLL), which is characterized by heterotopic bone formation in spinal ligaments, is the leading cause of spinal canal stenosis and myelopathy . Although epidemiological and family studies implicate genetic susceptibility in its pathogenesis, the genetic basis of OPLL remains poorly understood. In the previous study extensive non-parametric linkage studies with 126 affected sib-pairs using markers for 64 candidate genes were performed to identify genetic loci relevant to OPLL. Six genes in them, BMP4, PRG1, TGFb3, osteopontin ,PTHR1, and IGF1, showed evidence of linkage by SIBPAL analysis (P<0.05). Among these genes, only BMP4 showed the evidence of linkage by GENEHUNTER (NPL=2.23). In this study we investigated the association of molecular variants in BMP4 gene with OPLL. Methods; For allelic association study, 268 OPLL cases and 168 non-OPLL controls were collected in Japan. Allele frequencies of single-nucleotide polymorphisms (SNPs) were determined by the direct sequencing for the PCR amplicons covering variant sites. Sequencing was performed with BigDye Terminator cycle sequencing with a 377 ABI Prism automated DNA sequencer. Results; Approximately 7.2kb genomic regions in the BMP4 gene were examined in 12 individuals to discover SNPs. Twelve SNPs were identified in the region and performed typing. Among these SNPs no remarkable significance was shown in association study. Next to begin construction of haplotypes from three SNPs (-1578g/a, +518g/t, +5161t/c), which high-frequency of minor allele, we genotyped 268 OPLL cases and 168 non-OPLL controls. Six haplotypes existed in Japanese population. To evaluate the potential that these haplotypes have for identification of a particular mutation or polymorphism, we compared with the haplotype between OPLL and controls. Haplotype of BMP4 gene with GTC have strong difference association. The haplotype of the OPLL patients were lower frequency compared with non-OPLL population. Discussion; Gene expression may change with osteoblast differentiation by the mutation or polymorphism of BMP4 gene. We detected haplotype, which have strong difference between patients and control. A real mutation or polymorphism may play a protective role in the ectopic ossification process. We are going to keep on further research in order to search a real cause polymorphism.

SA387

See Friday Plenary number F387.

SA388

Osteoclastic Dysfunction Leads to Impaired Mechanical Adaptation of Bone Structure in Pycnodysostosis: Transilical Biopsy Study of Two Patients with Defined Mutations Within the Cathepsin K Gene. A. Valenta*[1], P. Roschger*[2], N. Fratzl-Zelman*[2], A. Nader*[2], B. M. Grabner*[2], B. D. Gelb*[3], P. Fratzl*[1], K. Klaushofer[2]. [1]Austrian Academy of Sciences & University of Leoben, Leoben, Austria, [2]Ludwig Boltzmann Institute of Osteology, 4th Med. Dept., Hanusch Hospital & UKH Meidling, Vienna, Austria, [3]Depts. of Pediatrics and Human Genetics, Mount Sinai School of Medicine, New York, NY, USA.

Pycnodysostosis (Pycno) is an autosomal recessive syndrome resulting from mutations in the gene encoding cathepsin K, the major lysosomal protease responsible for efficient matrix degradation in osteoclasts. While Pycno is genetically (Hou, J Clin Invest, 1999) and clinically (osteosclerosis, bone fragility, short stature) well-characterized, little information is available about the bone phenotype at the tissue and material levels. Transiliacal bone biopsies from two unrelated Pycno patients were studied for cellular activity and histomorphometry (Goldner´s Trichrome and Giemsa staining), mean calcium concentration (Ca_{Mean}) by quantitative backscattered electron imaging (Roschger, Bone, 1998), mean thickness (T-parameter) and alignment of the mineral particles within the bone matrix by small angle X-ray scattering (Rinnerthaler, Calcif Tissue Int, 1999). Alterations of histomophometrical parameters are summarized in the Table. Moreover, broad, demineralized fringes containing collagenous matrix were found adjacent to active osteoclasts (more pronounced in patient A). In both samples, residuals of highly mineralized cartilage were present. Mineral concentration and particle thickness were unaffected, but crystal alignment was disturbed, reflecting a disorder in lamellar organization of the bone matrix. We conclude that the bone phenotype in Pycno is caused by a lack of adaptation to mechanical demands due to osteoclastic dysfunction, resulting in increased fragility.

Patient	A (5 yrs/ male)	B (21 yrs/ female)
Mutation	R312G	G79R and del363(G)
Ob.S./B.S.	3.9 (-54% #)	no Ob.
Oc.S./B.S.	3.7 (+336% #)	0.9 (-13% #)
B.Ar./T.Ar.	28.9 (+63% #)	40.1 (+44% #)
Tb. Th. (microns)	172.8 (+71% #)	207.0 (+35% #)
Ca_{Mean} (wt% Ca)	20.4 (within normal range)	22.5 (within normal range)
T-Parameter (nm)	3.6 (within normal range)	3.8 (within normal range)

compared to age matched normal data from Glorieux, Bone, 2000

SA389

See Friday Plenary number F389.

SA390

Molecular Characterization of Osteopetrosis (OP) Using Nonadherent CD14 Peripheral Monocytes Expanded In Vitro. P. J. Orchard*[1], P. H. Schlesinger[2], H. Blair[3]. [1]University of Minnesota, Minneapolis, MN, USA, [2]Cell Biology and Physiology, Washington University Medical School, St. Louis, MO, USA, [3]Pathology, University of Pittsburgh, Pittsburgh, PA, USA.

Genetic alterations in monocytes can produce, osteoclasts defective in many aspects critical to bone turnover. Disruption of CSF-1 signalling, src, ATP6i, ClC-7, cathepsin K, and RANK-ligand cause OP in transgenic mice. However, except for ATP6i and ClC-7, it has been difficult to characterize the basis for osteoclast dysfunction biochemically because cells cannot be isolated. We developed a method to expand precursor cells from peripheral blood and produce human osteoclasts in vitro. Monocytes from OP children or control donors were recovered on ficoll and purified by antibody binding to removal non-CD14 cells (MACS, Miltenyi Biotec, Auburn CA). Non-adherent cells were cultured in DMEM with kit-ligand, IL-1b, and IL-6, 10 ng/ml each, with 15% monocyte-conditioned human serum for 10 days. These uniformly expressed alpha naphthyl acetate esterase when replated in csf-1. Flow cytometry showed cd11, cd34, and cd64 on these cells at constant but low levels. At 10 days, the cells expanded ~10x (5- >20x) allowing recovery of >500,000 nonadherent pre-osteoclasts from 10 ml of pediatric whole blood. Non-adherent cells, ~90% of cells, replated in CSF-1, 10 ng/ml with RANKL, 20 ng/ml, and 25 um bone fragments, expressed tartrate-resistant acid phosphatase and cathepsin K, with 50% of cells multinucleated and expressing osteoclast markers in 5-7 days. Cells were studied for actin distribution, cathepsin K, TRAP, and acid secretion profiles using fluorescence labeling. Bone particles accelerated and increased osteoclastic markers. In four OP lines and nine controls to date, OP osteoclasts showed reduced or absent acid at the attachment site, determined by labeling acid compartments (Lysotracker Red DND, Molecular Probes, Eugene OR). One OP cell line showed potential attachment defect. The other OP cells were identical to controls in spread area and bone attachment, and cells on glass showed typical lysosomal acid transport patterns although in one case OP cells had inclusions consistent with giant lysosomes. However, unlike controls the OP cells attached to bone did not accumulate acid in any case. We conclude that acid secretion defects in OP patients can be characterized using blood monocyte precursors. Other human OP phenotypes will be examined for differentiation arrest, attachment efects, enzyme secretion, and transport. This will subdivide OP, a syndrome, into specific molecular disorder, some of which may be amenable to therapy other than bone marrow transplant.

SA391

See Friday Plenary number F391.

SA392

Efficacy and Predictors of Response to Treatment of Fibrous Dysplasia of Bone with Intravenous Pamidronate. R. D. Chapurlat, P. Hugueny*, P. D. Delmas, P. J. Meunier. INSERM U403, Lyon, France.

Treatment with intravenous pamidronate has been used for a decade in the treatment of fibrous dysplasia of bone (FD), but efficacy and tolerance in the long run (>5 years), and predictors of response to treatment have been not described so far. We examined a series of 58 patients with FD treated using intravenous pamidronate (180 mg every 6 months) up to 12 years to determine clinical, biological and radiological efficacy of treatment with pamidronate, and predictors of response to treatment. So, we measured intensity of pain and the number of painful localizations. We took repeated radiographs of involved bones and defined radiographic response as a substantial thickening of cortices and/or filling of osteolytic lesions. We also measured biochemical markers of bone turnover (serum total alkaline phosphatase [ALP], urinary CTX) before and after courses of treatment. We used repeated measures techniques to analyze data before and after treatment, and linear and logistic regression analyses to determine predictors of response to treatment. Twenty-eight men and 30 women were followed-up for an average 4 years, with a mean age of 30 at onset of treatment. Thirty-eight percent had a monostotic form of FD. Among the 80% of patients who had pain at baseline, we observed a 70% decrease in intensity of bone pain ($p<0.001$) after the first course of pamidronate. This decrease was maintained throughout follow-up, with 60% of patients classified as complete responders and 24% as partial responders. Forty-five percent of patients had a decrease of at least 30% in total ALP after 1 year of treatment, and this proportion was of 64% for urinary CTX. Fifty-four percent of patients were radiographic responders, similarly distributed between monostotic FD and polyostotic FD. The number of localizations, age, and serum phosphate were not associated with radiological response. Men tended to have a better radiological response, but this was not significant (OR = 2.3 [0.8, 6.6]). Similarly, there was no association between radiographic response and biological response, as assessed by total ALP ($p = 0.9$) and urinary CTX ($p = 0.87$). There was also no association between clinical response and radiographic response ($p = 0.38$). Intravenous pamidronate was well tolerated. Three patients had also mineralization defects, for which the main contributor may have been renal phosphate wasting. We conclude that half of the patients with FD treated with intravenous pamidronate exhibit thickening of cortices and/or filling of osteolytic areas, along with significant reduction in bone pain and bone turnover, but prediction of response to treatment is uncertain.

SA393

Abnormal Phosphate Transport in Hyp-Mouse Osteoblasts May Underlie the Inability to Rescue the HYP Phenotype. A. Bhargava*, R. Aravindan, M. K. Drezner. Medicine, University of Wisconsin, Madison, WI, USA.

Recent studies indicate that PHEX mutations underlie X-linked hypophosphatemic rickets. However, efforts to normalize mineralization and rescue the disease phenotype by *in vitro* transfection of *hyp*-mouse osteoblasts or by creation of transgenic mice over-expressing osteoblast promoter-PHEX gene transcripts have failed. The likely reason for failure is absence of PHEX during osteoblast development, prior to osteocalcin and collagen1A1 expression, and consequent lack of enzyme activity requisite to alter an otherwise immutable osteoblast abnormality, which predisposes to aberrant mineralization. Such an occurrence would impair osteoblast function/mineralization and prove refractory to late PHEX expression. To explore this possibility we studied the immortalized SV40 *hyp*-mouse osteoblasts, used for PHEX transfection, and comparable normal cells. We investigated if sodium dependent phosphate (P) transport, a process likely crucial to mineralization, is abnormal in the mature *hyp*-mouse osteoblast and independent of PHEX expression. We plated 40,000 cells per well in 24 well plates and measured active P transport at 4, 7, 11 and 14 days of culture. P transport in *hyp*-mouse osteoblasts was decreased significantly ($p<0.01$) compared to that in normal osteoblasts at each time point by 48.2±2.3%, 32.9±2.4%, 21.5±3.0% and 19.5±3.1%, respectively. Moreover, comparable alanine transport in the normal and *hyp*-mouse osteoblasts indicated that the defect was specific. Further, Lineweaver-Burke plots documented the defect was due not to an altered Km (0.16±0.04 vs 0.19±0.04) but to an abnormal Vmax (29.4±0.9 vs 16.9±1.0 nmoles/mg/10 min; $p<0.001$). Consistent with the apparent decrease in P transporters, semi-quantitative RT-PCR revealed the sodium-dependent P co-transporter (Npt3) concentration in *hyp*-mouse osteoblasts less than in normal osteoblasts at 4, 7, 11 and 14 days of culture. The PHEX independence of this abnormality was indicated by higher P transport in normal osteoblasts before and after PHEX expression, which occurred at 9 days of culture, and the failure of P transport to decrease in normal cells when exposed to conditioned medium from *hyp*-mouse osteoblasts, which contains PHEX substrate(s). These data indicate that defective mineralization in *hyp*-mouse osteoblasts may occur in part due to abnormal P transport, a PHEX refractory event in mature cells. Thus, the failure to rescue the *Hyp* phenotype, either by PHEX transfection or creation of transgenic animals over-expressing osteoblast promoter driven PHEX transcripts, may be due to failure of this gene to normalize osteoblast P transport early in cell development.

SA394

Evidence That PHEX Has a Role in Normal Mineralization. A. Bhargava*, R. Aravindan, M. K. Drezner. Medicine, University of Wisconsin, Madison, WI, USA.

X-linked hypophosphatemia (XLH) is a genetic disease characterized by impaired bone mineralization and hypophosphatemia. Inactivating PHEX mutations underlie the disorder

and contribute, in part, to defective mineralization, likely by failure to degrade putative phosphatonin(s). Whether the PHEX gene product plays a role in normal mineralization, however, remains unknown. Since previous studies revealed *hyp*-mouse osteoblasts produce a mineralization inhibitor in the absence of PHEX, we investigated if osteoblasts from normal mice produce a similar inhibitory factor, the function of which is dictated by PHEX expression. In these studies we used immortalized osteoblasts from SV40 normal (N) and *hyp*-mice and assessed production of a mineralization inhibitor(s) employing co-culture techniques. We plated 10,000 normal osteoblasts in 6 well plates. After 7 days, inserts containing 40,000 normal or *hyp*-mouse osteoblasts, previously cultured for 0 or 7 days, were placed in the wells. We removed the inserts on the 14th day of culture and determined mineralization of normal osteoblasts in the wells by alizarin red staining and ^{45}Ca incorporation. In this manner normal osteoblasts at 7-14 days of culture, inclusive of the mineralization period, were exposed to secreted products of normal osteoblasts 7-14 (Control) or 0-7 days old and *hyp*-mouse osteoblasts 7-14 or 0-7 days old. Not unexpectedly, co-culture with *hyp*-mouse osteoblasts aged 0-7 or 7-14 days impaired mineralization of normal cells. More importantly, co-culture with normal osteoblasts aged 0-7 days likewise impaired the mineralization of normal osteoblasts. This surprising discovery suggests that normal osteoblasts produce a mineralization inhibitor, the functional expression of which disappears with prolonged culture. Moreover, since PHEX was not expressed in *hyp*-mouse osteoblasts but was expressed in normal osteoblasts only after 7 days of culture, the mineralization inhibitory activity of the *hyp*-mouse and normal osteoblasts correlated with absence of PHEX expression. These observations indicate that osteoblasts routinely produce a mineralization inhibitor(s), the function of which is temporally dependent upon absence of PHEX expression. This mechanism may contribute to the regulation of normal mineralization, playing a role in events that characterize the mineralization process, such as mineralization lag time.

Cells in Insert	PHEX Expression	Alizarin Staining	45Ca Incorporation (cpm/mg protein)
N Osteoblasts 7-14 days (Control)	Present	Normal	247,189±14,245**
N Osteoblasts 0-7 days	Absent	Decreased	77,991±8,726**
Hyp Osteoblasts 7-14 days	Absent	Decreased	65,350±3,354**
Hyp Osteoblasts 0-7 days	Absent	Decreased	92,107±6,112**

**p<0.001

SA395

See Friday Plenary number F395.

SA396

Immunohistochemical Detection of FGF-23 Protein in Tumors that Cause Oncogenic Osteomalacia. T. Larsson*[1], R. Zahradnik*[2], R. Marsell*[1], Ö. Ljunggren[1], J. Lavigne[2], H. Jueppner[3], K. Jonsson[1]. [1]University Hospital, Department of Medical Sciences, Uppsala, Sweden, [2]Immutopics Inc, San Clemente, CA, USA, [3]Endocrine Unit, Massachusetts General Hospital, Boston, MA, USA.

Oncogenic hypophosphatemic osteomalacia (OOM) is a rare disease characterized by hypophosphatemia, inappropriately low levels of circulating 1,25 dihydroxyvitamin D_3 and osteomalacia. The disease is most commonly caused by benign mesenchymal tumors that produce, among several other factors, fibroblast growth factor 23 (FGF-23). FGF-23 has been shown to promote *in vivo* renal phosphate excretion through yet undefined mechanisms. Furthermore, patients with autosomal dominant hypophsophatemic rickets (ADHR), an inherited disorder with clinical and biochemical features similar to those of observed in OOM, carry a mutant FGF-23 gene. Current evidence thus suggest that this protein has an important role in the regulation of phosphate homeostasis. To determine whether OOM tumors expressing FGF-23 mRNA also show readily detectable levels of FGF-23 protein, different polyclonal antibodies were raised in rabbits against three different peptides with sequences derived from human FGF-23: [Cys-70]FGF-23(51-69)amide, [Tyr-223]FGF-23(206-222)amide and [Tyr-224]FGF-23(225-244)amide. After affinity purification, all three antibodies detected recombinant human FGF-23 by Western blot analysis. Through immunohistochemical analysis using the anti-[Tyr-224]FGF-23(225-244)amide antibody and through *in situ* hybridizations using full length antisense FGF-23 cRNA as a probe, we showed that abundant amounts of FGF-23 mRNA and protein are present in certain cells of five different OOM tumors. We therefore conclude that the immunohistochemical detection of FGF-23 in OOM tumors is feasible and may help in establishing the diagnosis of tumor-induced hypophosphatemia through analysis of biopsies or surgical specimens.

SA397

The Effect of Supplementation of Inorganic Phosphorus and 1,25-dihydroxyvitamin D_3 on Bone Density on Sporadic Hypophosphatemic Rickets. Y. Imanishi, K. Nakatsuka, K. Kobayashi*, K. Lee*, H. Tahara, H. Goto, E. Ishimura*, M. Inaba, Y. Nishizawa. Metabolism, Endocrinology and Molecular Medicine, Osaka City University Graduate School of Medicine, Osaka, Japan.

Oncogenic osteomalacia (OOM) is a rare paraneoplastic syndrome that is characterized by hypophosphatemia and low plasma 1,25-dihydroxyvitamin D in association of various types of tumors. Until the responsible tumors were identified and resected, the patients should be treated in combination of pharmacological amounts of inorganic phosphorus and 1,25-dihydroxyvitamin D_3 (1,25-D_3) as sporadic hypophosphatemic rickets. We present two patients with sporadic hypophosphatemic rickets, one was diagnosed as an OOM since the impaired phosphate and vitamin D metabolism completely improved following resection of the responsible tumor (case 1). Another patient was failed to detect any tumors responsible for osteomalacia, and received the combination therapy with inorganic phosphorus and 1,25-D_3 (case 2). Following tumor resection, tubular maximum transport of phosphate (TmP/GFR) was recovered from 0.20 to 1.13 mmol/L, serum phosphate concentration from 0.52 to 1.19 mmol/L on case 1. Suppressed TmP/GFR (0.34 mmol/L) and hypophosphatemia (0.48 mmol/L) were observed at the initiation of the combination therapy on Case 2, and serum phosphate level were kept more than 0.97 mmol/L during the therapy. Bone mineral contents were measured on these patients, before and 1 year after resection of tumor or combined therapy. Lumber spine bone mineral densities were dramatically improved from 0.778 to 1.020 g/cm^2 in case 1, and from 0.448 to 0.962 g/cm^2 in case 2. In conclusion, combination therapy of inorganic phosphorus and 1,25-D_3 is as effective as tumor resection.

SA398

See Friday Plenary number F398.

SA399

False Positive Magnetic Resonance Imaging Skeletal Survey in a Patient with Sporadic Hypophosphatemic Osteomalacia. K. Kobayashi*, Y. Imanishi, K. Nakatsuka, E. Ishimura*, M. Inaba, N. Yoshiki. Metabolism, Endocrinology and Molecular Medicine, Osaka City University Graduate School of Medicine, Osaka, Japan.

We report a case with adult-onset hypophosphatemic osteomalacia due to renal phosphate wasting, known as tumor-induced osteomalacia (TIO). Biochemical evaluation revealed hypophosphatemia, low tubular maximum transport of phosphate (TmP/GFR), low concentration of serum 1,25-dihydroxyvitamin D, and high serum alkaline phosphatase. Bone biopsies also revealed osteomalacia. In an effort to localize the tumor responsible for TIO, we conducted an whole body Magnetic Resonance (MR) survey. MR imaging showed the presence of tumors in a femoral neck. The lesion appeared as a low-intensity and high-intensity mass in T1-weighted spin echo and T2-weighted turbo spin echo sequences, respectively. Resection of the tumor failed to normalize serum phosphate and TmP/GFR, and pathological analysis revealed bone island. In conclusion, MRI screening might not be as specific as previously thought in localizing the responsible tumor of TIO.

SA400

See Friday Plenary number F400.

SA401

Fanconi's Syndrome in HIV Positive Adults: Report of Three Cases and Literature Review. K. Earle*[1], T. Seneviratne*[1], J. Shaker*[2], D. Shoback*[3]. [1]Dept. of Medicine, UCSF, San Francisco, CA, USA, [2]Dept. of Medicine, St. Lukes Medical Center, Milwaukee, WI, USA, [3]Endocrine Research Unit, VA Med Center, San Francisco, CA, USA.

Fanconi's syndrome results from generalized proximal tubular dysfunction and causes increased excretion of amino acids, glucose, urate, bicarbonate, and phosphate. The syndrome includes osteomalacia, metabolic acidosis, polyuria, and dehydration. We report 3 cases of Fanconi's syndrome in HIV positive patients. Case 1 was a 43 year-old HIV positive woman presenting with multiple painful stress fractures on an antiretroviral regimen of tenofovir, ritonivir, lopinavir, and lamivudine. Laboratory abnormalities included hypophosphatemia, hypokalemia, and metabolic acidosis. Urinary studies revealed phosphaturia, glucosuria, and generalized aminoaciduria. She initially received phosphate supplementation, but after tenofovir was discontinued, her laboratory values corrected. Case 2 was a 39 year-old HIV positive man with hypophosphatemia and bone pain whose symptoms began 6 months after initiation of adefovir. He also demonstrated hypokalemia, metabolic acidosis, and glucosuria. After discontinuation of adefovir and supplementation with phosphate and potassium, his symptoms markedly improved. Case 3 was a 48 year-old HIV positive man who presented with tetany and muscle cramping in the setting of mild renal insufficiency. Medications prior to admission included didanosine, ritonavir, saquinavir, nevirapine, and ganciclovir. Nine months prior, he had taken cidofovir for retinitis due to cytomegalovirus. Although serum creatinine values were improving prior to admission, serum calcium, phosphate, and potassium levels declined progressively until frank tetany precipitated hospitalization. All 3 patients exhibited classic features of Fanconi's syndrome, and all were treated with various antiretroviral regimens. In Case 1, Fanconi's syndrome correlated with use of the antinucleoside tenofovir, which has not been previously reported to cause this complication. A similar compound adefovir has been associated with Fanconi's syndrome in HIV positive patients and is the likely etiology in our second patient. The cause of Fanconi's syndrome in the third patient is unknown. Previous use of cidofovir or the recent onset of renal insufficiency, possibly due to drug-induced interstitial nephritis, may have contributed to proximal tubular dysfunction. Although Fanconi's syndrome is a rare complication of HIV disease and antiretroviral therapy, these cases underscore the need for careful clinical and laboratory monitoring of HIV positive patients so that overt tetany, osteomalacia, and fractures are prevented.

SA402

Treatment of Resistant Paget's Bone Disease with Monthly Clodronate Infusion. P. Filipponi[1], S. Cristallini*[1], G. Policani*[1], B. Frediani*[2], M. F. Schifini*[1], P. Garinei*[1], S. Morlunghi*[1]. [1]Umbertide Regional Hospital, Bone & Mineral Research Unit, Umbertide-Perugia, Italy, [2]University of Siena, Institute of Reumatology, Siena, Italy.

Although there is currently no cure for Paget's disease of bone since its etiology is unknown bisphosphonates have been identified as the best therapy option. They induce a substantial reduction in disease activity with the rider that - while some patients go into long-term remission after a single course of therapy (sometimes for several years) - most pagetics experience a biochemical relapse within 1-2 years. In this study we treated 13 pagetics, who had had unsatisfactory results from prior conventional bisphosphonate therapy, with monthly 300 mg clodronate intravenous infusion. Treatment was continued irrespective of the achievement or not of a positive response (that is, a reduction from baseline in excess bone specific alkaline phosphatase of 50% or more). Of the 13 patients, 11 had an average reduction from baseline in excess bAp of more than 50% during the follow-up, which lasted between 30 and 36 months. Response occurred between 3 and 9 months after the beginning of monthly clodronate infusion, the average length of response being 26.7 ± 2.2 months. Of the 11 responders 6 entered remission: the average duration of remission was 20.0 ± 2.9 months, ranging from 9 to 30 months. At the end of the follow-up 3 of these 6 patients were still in remission, while 2 still had a reduction in bAp excess of over 50%. Of the other 5 responsive patients who did not enter remission 2 were relapsing at the 24th and 30th month, while the other 3 were still responding at the end of the follow-up period. The 2 non-responders also showed an average reduction in bone bAp of over 30%. Pain unrelated to osteoarthritic complications was reduced in 7 of the 11 patients who had complained of pain before treatment began: they were usually the pagetics who had a better biochemical response to treatment. No alterations were detected in routine biochemical tests, including white cell count and renal function. One patient had local irritation at the site of infusion. Monthly clodronate administration could be a useful and safe alternative in the treatment of resistant Paget's bone disease. In a large number of patients bone turnover can be suppressed and, in some, returns to within normal range.

SA403

See Friday Plenary number F403.

SA404

Serum Osteoprotegerin and Serum RANKL in Paget's Disease. R. Nuti, G. Martini, R. Valenti*, S. Giovani*, L. Gennari, S. Salvadori*, B. Galli*. Metabolic Disease Unit, University of Siena, Siena, Italy.

Osteoprotegerin (OPG), a secreted member of tumor necrosis factor superfamily, has been identified as a osteoblast-derived regulator of bone resorption: it acts by neutralizing the receptor activator of nuclear factor-kB ligand (RANKL), a cytokine required for osteoclast formation and activation. It has been demonstrated an increase of OPG with age and higher values in females than males. Moreover, serum OPG levels increase in patients with advanced prostate cancer, while a reduction was found in osteolytic multiple myeloma. To better understand the relationships among serum OPG, RANKL and bone metabolism, we studied a group of 30 patients (16 females aged 60-90 years and 14 males aged 47-88 years) with Paget‘s disease of bone. Eleven women with established postmenopausal osteoporosis were used as control group. Sera were assayed for OPG and RANKL using a sandwich enzyme immunoassay (Osteoprotegerin and sRANKL, Biomedica, Vienna, Austria). Precision inter- and intra-assay was lower than 10%. Serum bone alkaline phosphatase (bALP, Ostase-Tandem, Beckman-Coulter, U.S.A.) and serum cross-linked C-telopeptides of type-I collagen (sCTX, Serum CrossLaps, Osteometer, Denmark) were used as markers of bone formation and bone resorption, respectively. Pagetic patients showed the expected significantly higher values of bALP and sCTX compared to osteoporotic women: 64.2 µg/l ± 20 vs 18.6 µg/l ± 17, p<0.01 and 7916 pmol/l ± 4000 vs 4374 pmol/l ± 3187, p<0.05, respectively. In Paget‘s disease we found significantly higher values of OPG and signicantly lower values of RANKL with respect to osteoporotic women (7.81 pmol/l ± 5.2 vs 4.25 pmol/l ± 2.2, p<0.01 and 3.04 pmol/l ± 1.9 vs 7.6 pmol/l ± 6.8, p<0.01, respectively). The relationship between bone markers was statistically significant (r=0.33, p<0.05), while any correlations were found between OPG, sRANKL and indexes of bone formation and resorption. An inverse but not significant relationship was found as regard OPG and sRANKL (r=-0.13, ns). In conclusion, higher values of OPG, considered as an antiresorptive factor, were found in patients with higher bone turnover due to Paget‘s disease of bone: it could indicate an attempt to counteract the increased rate of bone remodeling. The hypothetic explanation of low serum RANKL observed in pagetic patients involves the inhibitory effect of OPG on RANK system. Moreover, the increased sensitivity of osteoclast precursor to the humoral factor like RANKL , justifies persistence of high bone turnover values found in Paget‘s disease.

SA405

See Friday Plenary number F405.

SA406

Use of Intravenously Pamidronate in Paget`s Sarcoma. Z. Man, R. Fiasche. Centro TIEMPO, Universidad Favaloro, Buenos Aires, Argentina.

The bone`s sarcoma in Paget`s Disease (PD) is the worst complication and does not exist any clear protocol of treatment. When the diagnosis is made, the average of life is no longer than a year. We presented the case of a female of 68 years old with PD in left femur, diagnosed radiologically (Rx) after a fall. Laboratory test and other Rx were asked for, and she was dated 20 days later to initiate processing. In this lapse the annoyances attributed to the fall changed to permanent and severe pain. The leg was edematous and the Rx showed rupture of cortical in the area of the Paget`s bone and also the invasion of soft parts. The laboratory findings were: normal serum calcium, phosphorus, creatinine and red and white blood cells counting, and increased erythrocyte sedimentation (ESR) and more than 5 times higher alkaline phosphatase (AP). Surgical cleaning was performed in the patient, and a replace of the pagetic bone with a nonconventional prosthesis took place, that allowed her to walk . Two months before, and also after the surgery, we treated her with monthly infusions of 90 mg of pamidronate (APD) with supplements of calcium and Vitamin D. The first pulmonary metastasis appeared 12 months after the diagnosis, without worsening her quality of life. In the 18th month we observed a local growth, accompanied with a 10 times elevated AP, which forced us to practice another surgical cleaning. We continued with the same medication until completing 24 months. By that time the patient had deterioration of the conscience and passed away one month later. In our casuistry of 5 cases, 4 passed away before the 8 months (range 3-10 months), in a very bad health and without being able to stop the local recurrence nor the pulmonary metastasis. CONCLUSION: We considered that APD IV in doses of 90 mg per month with supplementation with calcium and vitamin D during all the evolution of the disease, contributed to improve the quality of life of this kind of patient

SA407

Trial to Predict Malignancy of Affected Parathyroid Glands in Primary Hyperparathyroidism. Q. Chen*, H. Kaji, R. Nomura*, K. Ikeda, H. Sowa*, M. Yamauchi*, T. Tsukamoto*, T. Yamaguchi, T. Sugimoto, K. Chihara*, M. Kanatani. Endocrinology and Metabolism, Kobe University Graduate School of Medicine, Kobe, Japan.

Primary hyperparathyroidism (pHPT) is included in the common diseases that cause secondary osteoporosis. Parathyroid cancer is rare, but relatively frequent in Japan, compared to Western countries. Surgical parathyroidectomy is the primary choice for the treatment of pHPT, and it is important to distinguish malignant from benign parathyroid tumor in order to determine the surgical indication and operation procedure for pHPT. However, it is not so easy to diagnose parathyroid cancer before the operation. In the present study, we examined the background data, biochemical data and bone mineral density (BMD) of 131 patients with pHPT (111 benign and 20 malignancy) in our institution. BMD of the lumbar spine and mid-radius was measured by dual-energy X-ray absorptiometry. Serum levels of calcium, parathyroid hormone (PTH) and alkaline phosphatase (ALP) were significantly higher in malignant group, compared to benign one. The magnitude of elevation of mid-portion PTH seemed to be greater than that of intact PTH in malignant. Age-, gender- and race-adjusted BMD of mid-radius was significantly decreased in malignant, compared to benign, although that of lumbar spine was not significantly different between two groups, indicating that osteopenia is remarkable in the region which is rich in cortical bone in the patients with parathyroid cancer. On the other hand, serum levels of calcium, ALP and mid-portion PTH as well as age were selected as predictors of malignancy in monovariate logistic regression analysis, although serum level of intact PTH was not selected. In conclusion, mid-radius BMD, which is rich in cortical bone, was lower in malignant, compared to benign in pHPT. Serum levels of calcium, ALP and mid-portion PTH were useful to predict malignancy of affected parathyroid glands in pHPT patients. The fragments of mid-portion or carboxyl-terminal portion of PTH would be predominantly produced from parathyroid cancer.

SA408

See Friday Plenary number F408.

SA409

Lack of Effect of Vitamin D Status on Bone Mineral Density in Italian Female Patients with Primary Hyperparathyroidism. V. Carnevale*[1], S. Minisola[2], A. Scillitani*[3], E. Romagnoli*[2], S. Dionisi*[2], D. Diacinti*[2], E. D'Erasmo*[2], G. Mazzuoli[2]. [1]Dpt. of Internal Medicine, "Casa Sollievo della Sofferenza" Hospital, San Giovanni Rotondo, Italy, [2]Dpt. of Clinical Sciences, "La Sapienza" University, Rome, Italy, [3]Dpt. of Endocrinology, "Casa Sollievo della Sofferenza" Hospital, San Giovanni Rotondo, Italy.

A relative or absolute deficiency of vitamin D is considered a prominent factor determining skeletal damage in patients with primary hyperparathyroidism (PHPT). We investigated the impact of vitamin D status on BMD in PHPT patients. In 62 female PHPT patients we measured serum total and ionised calcium, phosphorus, creatinine, total alkaline phosphatase activity, intact parathyroid hormone (PTH), 25-hydroxyvitamin D (25OHD), together with 24 hour and spot fasting urinary calcium. Bone mineral density (BMD) was measured in 58 patients at lumbar spine and in 56 at femoral neck, Ward’s triangle, great trochanter, intertrochanteric line, and total hip. Patients were studied in the period fron february to june 1999. The associations of all variables with age, 25OHD, and PTH were studied by linear multiple regression analysis, utilising progressively restricted models. Mean 25OHD values of PHPT patients (47.3 ± 2.9 nmol/L) did not significantly differ from those of age-matched healthy women from the same area during winter; 27.4% of patients presented 25OHD values below 30 nmol/L. BMD values showed significant regression with age, 25OHD and PTH (p<0.05 for lumbar spine, femoral trochanter, femoral intertrochanteric line, and total hip; p<0.001 for femoral neck and Ward's triangle). Noteworthy, PTH had a leading role in determining such significance, while no significant regression was found between the parameters studied and 25OHD; this was confirmed by the Pearson’s linear correlation analysis. The progressively restricted models showed sig-

nificant regression of femoral neck, Ward's triangle and total hip BMD with age and PTH ($p<0.05$ to $p<0.01$); significant regression of BMD measured at the intertrochanteric line with PTH ($p<0.05$), and those measured at lumbar spine and great trochanter with age ($p<0.05$ to $p<0.01$)were also found. Our data indicate that the influence of 25-OHD levels on BMD, if any, was overwhelmed by the effects of both PTH excess and age. The latter unequally affected BMD of various measured sites with different composition.

SA410

See Friday Plenary number F410.

SA411

Comparison of Magnesium Metabolism in Patients with Autosomal Dominant Hypocalcemia and Other PTH-Deficient Hypoparathyroidism. S. Watanabe*[1], S. Fukumoto[2], Y. Takeuchi[1], N. Chikatsu[3], R. Okazaki[4], T. Fujita*[1]. [1]Department of Medicine, University of Tokyo, Tokyo, Japan, [2]Department of Laboratory Medicine, University of Tokyo, Tokyo, Japan, [3]Department of Medicine, Hitachi General Hospital, Hitachi, Japan, [4]Department of Medicine, Teikyo University, Ichihara, Japan.

Activating mutations of the calcium-sensing receptor (CaSR) cause autosomal dominant hypocalcemia (ADH). Although patients with ADH are reported to be prone to develop renal dysfunction especially after active vitamin D_3 treatment, there is no clear clinical method to differentiate ADH from other patients with PTH-deficient hypoparathyroidism. Activation of CaSR in kidney inhibits reabsorption of Ca and magnesium (Mg), and hypomagnesemia was reported in patients with ADH. However, it is not clear whether hypomagnesemia is characteristic to ADH. Therefore, to clarify if hypomagnesemia can be a diagnostic marker for ADH, we compared Mg metabolism in PTH-deficient patients with and without mutations in CaSR. Direct sequencing of all coding exons of CaSR and in vitro functional analysis of mutant CaSR detected five patients with ADH (K47N, C131W, P221L, F788E and A843E). In contrast, no mutation was found in other seven patients with PTH-deficient hypoparathyroidism. Serum Mg level was low and fractional excretion of Mg (FE_{Mg}) was high in three of five patients with ADH (C131W, F788E and A843E). In addition, these three patients developed clinical symptoms in or before infancy. On the other hand, serum Mg was normal in two asymptomatic patients with ADH (K47N and P221L) and all seven patients with PTH-deficient hypoparathyroidism without mutations in CaSR. Furthermore, although there was a strong negative correlation between serum Mg and FE_{Mg} in patients with ADH ($r = -0.859$, $p < 0.0001$), this correlation was not significant in patients without mutations in CaSR. These results indicate that serum Mg is not low in all patients with ADH and is mainly determined by tubular Mg reabsorption in patients with ADH. It is suggested that symptomatic patients with more severe activation of CaSR develop hypomagnesemia. Therefore, it is concluded that although lack of hypomagnesemia does not rule out ADH, the presence of hypomagnesemia and high FE_{Mg} in PTH-deficient hypoparathyroidism strongly suggests ADH as a cause of hypocalcemia.

SA412

See Friday Plenary number F412.

SA413

Mast Cells Produce Platelet-derived Growth Factor A (PDGF-A) in Response to Continuous Parathyroid Hormone (PTH). J. D. Sibonga, S. Lotinun, R. T. Turner. Orthopedic Research, Mayo Clinic, Rochester, MN, USA.

Skeletal abnormalities associated with chronic hyperparathyroidism (HPT) are commonly characterized by marrow fibrosis, osteomalacia, and higher indices of bone turnover – including focal bone resorption. A rat model duplicates the histomorphometric traits of HPT following chronic administration of PTH (40 µg/kg) for one week. Lotinun et al. previously reported that a receptor antagonist for PDGF-A, a chemotactic and mitogenic factor for fibroblasts, abrogates the peritrabecular fibrosis and the increase in osteoclast-covered perimeter in this rat model. We performed immunohistochemistry on long bones from this animal experiment to determine the cellular localization of PDGF-A protein in response to continuous PTH. Femora were harvested and fixed in 10% neutral buffered formalin for 18h before decalcification by immersion in 20% EDTA at 4°C. PDGF-A was immunostained using VectorElite peroxidase kit (Burlingame, CA) with a polyclonal antibody (Santa Cruz Biotechnology, Santa Cruz, CA). Mast cells in the bone marrow of rats chronically treated with PTH were intensely positive for PDGF-A. Mast cells were identified by the metachromatic staining of granules with toluidine blue. Rats treated with vehicle alone were largely negative for localization of PDGF-A in mast cells. Continuous PTH increased stem cell factor and histamine H2-gene expression. Stem cell factor is essential to the differentiation of mast cells and the H2 receptor is involved in mast cell degranulation and histamine release. Mastocytosis has been observed both in patients with osteopenia and with chronic renal failure; mast cells are implicated as accessory cells to bone resorption and fibrosis; and PDGF-A gene expression can be induced in cultured mast cells as well as induce mast cell proliferation. These findings suggest that mast cells mediate the fibrosis and focal bone resorption observed in HPT.

SA414

See Friday Plenary number F414.

SA415

Spectrum of Mitochondrial Sequence Variants in Normal and Hyperplastic Parathyroid Glands. J. Costa*, T. Tokura, A. Arnold. Center for Molecular Medicine, University of Connecticut School of Medicine, Farmington, CT, USA.

In the pathogenesis of sporadic parathyroid adenomas, the significance of clonal, homoplasmic mutations of the mitochondrial genome has been strongly suggested by their unusual clustered distribution within genes encoding subunits of the NADH dehydrogenase complex (ASBMR 2001). However, because of the high susceptibility of the mitochondrial genome to mutation, it is unknown whether these somatic mutations might be a frequent occurrence in normal parathyroid cells and perhaps of no direct importance to parathyroid tumorigenesis. Therefore, we performed a rigorous mutational analysis of the mitochondrial genomes of normal and hyperplastic parathyroid glands. Included in this study were 8 independent hyperplastic, apparently polyclonal parathyroids and normal peripheral blood leukocytes from 4 patients, plus 5 normal parathyroid glands and one normal thyroid gland from 5 patients. DNA from each sample was isolated and the entire 16.6kb mitochondrial genome was PCR amplified in overlapping fragments and fully sequenced. The resulting sequences were compared with the standard Anderson public mitochondrial DNA sequence and with the online Mitomap database of previously reported mitochondrial sequence variants. A total of 161 sequence variants were detected, with 36% of changes occurring in the genes encoding subunits of the NADH dehydrogenase complex (which collectively comprise 38.3% of the mitochondrial genome). All sequence variants observed in the hyperplastic parathyroid glands were simultaneously observed in normal control DNA from the same patients and, therefore, were not somatic mutations. Of the nine tumor-specific homoplasmic mutations previously reported in parathyroid adenomas, only one change was represented as a germline base variant; none were found in normal parathyroid DNA. In summary, the mitochondrial sequence variants observed in the normal and hyperplastic parathyroid glands studied were consistent with the typical high level of variability in mitochondrial DNA in human populations. In contrast to observations in parathyroid adenomas, no clustering of sequence variants was observed in normal or hyperplastic parathyroids, nor were somatic mutations found. This genetic evidence supports the potential pathogenetic significance of somatic mitochondrial DNA mutations in parathyroid adenomas.

SA416

Enhanced Osteoclastogenesis in Congenital Pseudarthrosis of the Tibia Mediated by the Expression of RANK Ligand. I. Nakamura[1], N. Haga*[2], K. Aoki[3], A. Fukuda*[4], M. Hamazaki*[2], Y. Kadono[4], K. Ohya[3], R. Shiro*[5], M. Kimiduka*[5], H. Okazaki*[4], H. Oda*[4], S. Tanaka[4], K. Nakamura[4]. [1]Orthopaedic Srugery, Yugawara Kosei-Nenkin Hospital, Kanagawa, Japan, [2]Orthopaedic Surgery, Shizuoka Pediatric Hospital, Shizuoka, Japan, [3]Pharmacology, Tokyo Medical and Dental College, Tokyo, Japan, [4]Orthopaedic Surgery, University of Tokyo, Tokyo, Japan, [5]Orthopaedic Surgery, National Rehabilitation Center for Disabled Children, Tokyo, Japan.

The purpose of this study is to examine the possible pathophysiology of congenital pseudarthrosis of the tibia, one of the most controversial pediatric entities in terms of etiopathogenesis, pathology, and treatment. Eight patients with this disease and seven adult patients with post-traumatic pseudarthrosis as a control were reviewed histologically, using pathologic materials. The area of congenital pseudarthrosis was divided into three parts with different morphological features; a highly cellular, fibromatosis area, a cartilagenous area and an osseous area. Interestingly, a marked number of osteoclasts, tartrate resistant acid phosphatase-positive multinucleated cells were detected on the surface of the bone and cartilage, and even in the fibrous area apart from bone surfaces. Bone histomorphometric analysis revealed that in congenital pseudarthrosis, osteoclast number (N. Oc/BS) and osteoclast surface (Oc. S/BS) were 2.66 +/- 0.92 [/mm](mean +/- SD) and 10.67 +/- 4.86%, respectively, while in the case of adult pseudarthrosis, N. Oc/BS and Oc. S/BS were 0.62 +/- 0.33 [/mm] and 2.28 +/- 1.20%, respectively. Furthermore, immunohistochemical study showed that RANK ligand, an essential factor for osteoclastogenesis, was highly expressed not only in the fibroblastic cells but also osteoclasts themselves in congenital pseudarthrosis. RT-PCR analysis also revealed the higher expression of RANK ligand in congenital pseudarthrosis of the tibia than in post-traumatic pseudoarthrosis. Taken together, the enhanced osteoclastogenesis is at least in part involved in the pathophysiology of congenital pseudarthrosis of the tibia. In addition, RANK ligand, an autocrine and paracrine factor for osteoclast differentiation and activation, might be one of the therapeutic targets for this refractory disease.

SA417

See Friday Plenary number F417.

SA418

Decreased Vitamin D Precursor in Skin Following Burns. G. L. Klein[1], T. C. Chen[2], M. F. Holick[2], C. B. Langman[3], M. M. Celis*[1], D. N. Herndon*[1]. [1]University of Texas Medical Branch and Shriners Burns Hospital, Galveston, TX, USA, [2]Boston University School of Medicine, Boston, MA, USA, [3]Children's Memorial Hospital,Northwestern University Medical School, Chicago, IL, USA.

Children who suffer burns greater than 40 percent total body surface area (TBSA) have chronically low serum levels of 25-hydroxyvitamin D(25D) at 2 and 7 yr post-burn. Serum 1,25-dihydroxyvitamin D (1,25D) is normal at 2 yr post-burn but low in approximately half the patients by 7 yr post-burn (Klein et al J Trauma 2002; 52: 346-50). Because sunlight exposure post-burn is not controlled and vitamin D intake is uncertain, it is difficult to explain why patients exposed to sunlight post-burn are vitamin D deficient. The aim of our study was to see if the skin of burn patients had normal quantities of vitamin D precursor, 7-dehydrocholesterol (7DHC). We studied 6 patients(2M, 4F) burned more than 40% TBSA 6-24mo prior. Skin biopsies 0.6 cm were taken from the burn wound and adjacent normal skin, snap-frozen, and analyzed for 7 DHC by straight-phase high performance chromatography. Lumbar spine bone density was obtained by dual energy x-ray absorptiometry(Hologics 4500A), and 25D and 1,25D were analyzed by radioreceptor assays. There were no differences in 7DHC between burn wound and normal skin. All showed a mean of 545 +/- 364 (SD) ng/cm2, or 23 +/- 15% of the normal level of 2352 +/-320 ng/cm2. Preliminary data from UVB light exposure of skin in one biopsy from one of the patients showed a conversion from 7DHC to pre-vitamin D of 5.7% compared to control skin of similar pigment (20%). Serum 25D was normal in 2 patients and at lower limits of normal in 2 others. S1,25D was normal in all patients. Lumbar spine bone density Z-scores were greater than 1 SD below the mean in 2 of 5 patients (40%) and between 0-1SD below the mean in 2 others. Thus skin has low quantities of 7DHC following severe burn whether wound or unburned skin, suggesting a defect in skin cholesterol biosynthesis. Reduced conversion of 7DHC to pre-vitamin D may also be occurring but more studies must be done to confirm this. There is a need for vitamin D supplementation post-burn.

SA419

See Friday Plenary number F419.

SA420

Pubertal Growth Is Normal in Treated Girls With X-Linked Hypophosphatemic Rickets. O. Makitie*[1], A. Doria*[2], A. Daneman*[2], E. Sochett[1]. [1]Pediatric Endocrinology, University of Toronto, The Hospital for Sick Children, Toronto, ON, Canada, [2]Diagnostic Imaging, The Hospital for Sick Children, Toronto, ON, Canada.

X-linked hypophosphatemic rickets (XLH) is characterized by hypophosphatemia, rickets and impaired growth. Treatment with oral phosphate (Pi) and calcitriol results in resolution of the skeletal changes and improved height gain. However, even with optimal treatment many patients do not achieve normal stature. It is not known to what extent pubertal growth contributes to this height deficit. To assess pubertal growth we have reviewed data for patients with XLH who have been followed in our clinic from diagnosis to adult height. The diagnosis was based on hypophosphatemia, subnormal renal tubular Pi reabsorption, elevated plasma alkaline phosphatase activity and radiologic signs of rickets. All the patients were treated with oral Pi and calcitriol since diagnosis, followed 3-monthly and judged to be in good control. Hospital records were reviewed for growth and pubertal development. Individual growth curves were drawn, heights at every full and half year were interpolated and transformed into SD scores (SDS). Height velocities (HV) (over one year) were calculated at these age points. Final height was defined as height after age 16 years when HV was less than 1 cm/year. Predicted adult heights were calculated by the method of Bayley-Pinneau. There were six females and no males with complete growth data. At treatment onset median age was 2.3 yrs and median height -1.4 SDS (range -3.1 - -0.2 SDS). Median prepubertal (at 3-4 yrs before peak HV) height was -2.2 SDS and HV 4.9 cm/yr. Peak HV was reached at median age of 12.8 yrs and was in average 7.6 cm/yr. Median final height was -1.8 SDS. Height SDS improved during puberty in most patients (Table). Mean age at menarche was 13.3 yrs. Predicted adult heights were calculated based on bone age (BA) films obtained at 9.6-12.0 yrs (median 10.6 yrs). In 4/6 patients BA was delayed for more than 1.0 year (1.2-3.5 yrs) and advanced in none of the patients. The predicted adult heights correlated significantly with the achieved final heights ($r=0.98$, $p<0.001$). Our study suggests that in females with XLH (I) height gain and peak HV are normal during puberty, (II) pubertal growth spurt leads to improved height SD score but does not normalize height, and (III) height predictions based on BA films at 10-12 years are accurate.

Pubertal growth in the six females with XLH

Patient #	Prepub.height (SDS)	Adult height (SDS)	Prepub.HV (cm/y)	Peak HV (cm/y)
1	-2.4	-1.8	4.9	9.0
2	-3.0	-3.1	3.6	6.0
3	-1.7	-1.7	5.5	7.8
4	-2.0	-0.9	4.6	8.8
5	-1.4	-1.2	4.9	6.9
6	-3.0	-2.0	5.6	7.3
Median	-2.2	-1.8	4.9	7.6

SA421

Bone Mineral Density of the Hip and Spine in Patients with Ankylosing Spondylitis Depending on Nutrition. T. Meurer*, H. Franck*. Center of Rheumatology, Oberammergau, Germany.

Introduction: A sufficient alimentation of vitamine D and calcium is essential in the prevention and treatment of osteoporosis. Patients with ankylosing spondylitis have osteoporosis to a various degree. The aim of our study was to look at the influence of nutrition on bone mineral density in our patients with ankylosing spondylitis. Methods: We included 180 patients with ankylosing spondylitis fulfilled the modified New York criteria. The bone mineral density was measured with DEXA (QDR 4500) at the lumbar spine and right hip. Factors of nutrition were examined by a standardized questionnaire. Results: Positive correlations with bone mineral density were only found with wine consumption. Discussion: No significant correlation between milk and cheese intake with bone mineral density was found in patients with ankylosing spondylitis. Dietetic factors do not seem to influence bone mineral density in patients with ankylosing spondylitis. Only wine consumption seems to have a influence on bone mineral density as is correlated positively in our patients with ankylosing spondylitis.

Correlation BMD-hip total (BMD-LS total)

With consumption of milk	N = 180 (180)	r = 0,082 (0,102)	p = 0,277 (0,176)
sausage	N = 180 (180)	r = 0,051 (0,023)	p = 0,051 (0,759)
meat	N = 180 (180)	r = -0,039(-0,018)	p = 0,598 (0,811)
cheese	N = 180 (180)	r = 0,038 (0,004)	p = 0,614 (0,953)
coffee	N = 180 (180)	r =-0,019(-0,001)	p = 0,795 (0,992)
tea	N = 180 (180)	r =-0,120 (-0,081)	p = 0,110 (0,282)
beer	N = 180 (180)	r= 0,118 (-0,018)	p = 0,114 (0,811)
wine	N = 180 (180)	r = 0,217 (0,183)	p = 0,003 (0,014)

SA422

See Friday Plenary number F422.

SA423

Hormone Replacement Therapy and the Development of Knee Osteoarthritis in Elderly White Women. A Case-Control Study. J. Brantus*[1], I. Reading*[2], C. Cooper[2]. [1]Centre Hospitalier, Villefranche sur Saône, France, [2]MRC Environmental Epidemiology Unit, University of Southampton, Southampton, United Kingdom.

The goal of the study was to examine the association of hormone replacement therapy (HRT) with knee osteoarthritis (OA) in a population-based case-control study among 321 female cases and 321 age-and sex- matched controls. A total of 321 women listed for knee surgery because of primary OA over an 24 month period were compared with an equal number of controls selected from the general population and individually matched for age and general practice. Information about reproductive variables was obtained by questionnaire administered at interview. The risk of knee OA was not significantly decreased in women who had undergone oophorectomy (OR 0.6, 95% CI 0.3-1.4) and we observed a non-significantly increased risk of OA in women who had undergone a hysterectomy (OR 1.3, 95% CI 0.7-2.6). After adjustment for body mass index (BMI), presence of Heberden's nodes, previous knee injury (all independent risk factors for knee OA), and for other reproductive variables, there was a non-significantly increased risk of knee OA in the women who used HRT for less than 2 years (OR 1.7, 95% CI 0.4-7.3)and in those who used HRT for more than 2 years (OR 1.3, 95% CI 0.6-3.0). When we divided the group according to whether HRT was started before or after the onset of knee pain, long-term (more than 2 years) HRT use was associated with an non-significantly increased risk of knee OA both in the women whose therapy pre-dated pain (OR 1.2, 95% CI 0.5-3.0) and in the women who started the therapy after the onset of knee pain (OR 1.7, 95% CI 0.2-12.4). Age at menarche, age at menopause, oral contraceptives and number of pregnancies were not significantly associated with risk of knee OA. These data show that HRT after 50 increased the relative risk of knee OA. Our results suggest also that risk of knee OA is decreased among women who have undergone unilateral or bilateral oophorectomy and that there is a non-significant increased risk of OA in women who had undergone a hysterectomy. Studies are required to investigate the mechanisms underlying these associations.

SA424

See Friday Plenary number F424.

SA425

Abnormalities in the Replicative Capacity of Osteoblastic Cells in the Proximal Femur of Patients with Osteonecrosis of the Femoral Head. V. Gangji[1], J. Hauzeur*[1], A. Schoutens*[2], M. Hinsemkamp*[3], T. Appelboom*[1], D. Egrise[2]. [1]Rheumatology, Hôpital Erasme, Brussels, Belgium, [2]Nuclear Medicine, Hôpital Erasme, Brussels, Belgium, [3]Orthopaedic Surgery, Hôpital Erasme, Brussels, Belgium.

Aseptic non traumatic osteonecrosis (ON) of the femoral head is a painful disorder which often leads to femoral head collapse due to subchondral fracture.There are multiple mechanisms postulated for ON but none seems to explain entirely the features seen in ON. We postulated that an alteration of osteoblast function might play a role in the physiopathology of ON. In this study we evaluated the ex vivo proliferation rate and differentiation capacity of osteoblasts derived from the intertrochanteric region of the femur and of the iliac crest of 13 patients with ON and compared it with 8 patients with hip osteoarthritis (OA). Nine patients had ON due to corticosteroid therapy; 2 patients had ON due to alcohol abuse. For 2 patients, no aetiological causes could be found. Their ages at diagnosis ranged from 25-68 years. All patients had a normal bone mineral density. The replicative capacity was assessed by the proliferation rate in secondary culture. The phenotypic characterization was evaluated by the level of alkaline phosphatases activity (APA) and the collagen synthesis. The cell doubling time of the osteoblastic cells calculated between 2 and 7 days was found to be significantly increased (10.9±1.1 days) compared to the iliac crest (6.3±0.8 days) (p=0.003) of patients with ON. In patients with OA the cell doubling time was not statistically different in the femur (6.8±1.0 days) and in the iliac crest biopsies (8.0±1.3 days). The cell doubling time of the osteoblastic cells of the proximal femur was significantly increased in ON patients compared to OA patients (p=0.03). There were no statistical differences in APA or in collagen synthesis between the two sites of biopsies or between ON and OA patients. The altered capacities of proliferation of the osteoblastic cell can be responsible of two different events in the pathogenesis of ON; the appearance of ON and the bone repair that occurs after ON. The decrease of osteoblastic proliferative capacities could reflect the disruption of the mechanosensory role of the osteocyte-canalicular network and explain the evolution from marrow edema to established ON. Secondly, an insufficient repair mechanism due to a decrease in bone formation might explain the evolution to a further stage of ON. In conclusion the present study shows that the replicative capacity of the osteoblastic cell is decreased in the proximal femur of ON due to glucocorticoid therapy or due to other causes suggesting a potential role of osteoblast in the pathophysiology of osteonecrosis of the femoral head.

SA426

A Possible Interaction between 3'UTR of Calcitonin Receptor mRNA and mRNA Degradation Factor AUF1. S. Yasuda*[1], Y. Arao*[2], M. Iitaka*[1], F. Kayama*[2], S. Katayama*[1], S. Wada*[1]. [1]Internal Medicine IV, Saitama Medical School, Iruma-gun, Japan, [2]Dept of Health Science, Jichi Medical School, Tochigi, Japan.

We have studied the mechanism of calcitonin (CT) escape phenomenon and the results indicated that desensitization to CT was associated with the down regulation of CT receptor (CTR). Experiments to explore the molecular basis of the CTR gene expression suggested that decreased stability of CTR mRNA was associated with this down-regulation. In a previous report, we showed that there are several AU rich elements in CTR 3' untranslated region (3' UTR) in various species, which should be crucial to regulate stability of CTR mRNA. In this study, we subcloned the 3' UTR of mouse CTR gene using nested PCR technique from mouse brain cDNA library. UV-cross linking analysis revealed that there are several bands showing interactions between the 32P labelled CTR 3'UTR and nuclear protein extracts form mouse co-culture osteoclasts, RAW-derived osteoclasts, MC3T3E1 and NIH 3T3 cells, respectively. Since AUF1 is well known for its regulatory role of mRNA stability, we examined these extracts by AUF1 specific antibodies using western blotting; the results showed that there are some factors specifically interacted with the antibody. When HA-tagged AUF1 cDNA was transfected to NIH3T3 cells, expression of AUF1 isoforms were only observed on P40 and P45 isoforms. To examine specific interaction of AUF1 and CTR 3'UTR, nuclear extracts of AUF1 transfected cells were co-incubated with CTR 3'UTR, and then immunoprecipitated by HA antibody. RNA was extracted form the mixture and RT-PCR analysis with specific primers of the 3'UTR revealed that CTR 3'UTR was clearly bound to AUF1 P45. Specific binding between AUF1 (P40) and CTR 3'UTR was also supported by the finding that mutant P40 did not interact with CTR 3'UTR. When tetracycline dependent LUC reporter gene was co-inserted with CTR 3'UTR to the vector and then transfected into MCF7, it was found insertion of CTR 3'UTR shortened a half life of LUC activity. We are currently investigating whether certain kinase activators and inhibitors could modify the half life of the LUC activity, since we have shown previously that activation of PKA for mouse and PKC for humans are crucial for the signalling through cell surface CTR.

SA427

What Role Does Calcitonin Play in the Diurnal Regulation of Bone Resorption and Plasma Calcium Homeostasis? L. Klein. Biochemistry & Orthopedics, Case Western Reserve Univ. School of Medicine, Cleveland, OH, USA.

The physiologic function of calcitonin (CT) as a regulator of plasma calcium (Ca) homeostasis is considered relatively minor compared to that of parathyroid hormone (PTH) and vitamin D. It is known that multiple organs (thyroid, lung, liver, thymus, intestine) exist as cellular sources for CT, invalidating the athyroid model for chronic deficiency of CT. Due to efficient conservation of Ca in growing species, young dogs were extensively prelabeled with 45Ca from 6 to 12 weeks of age. Two weeks after labeling, dogs were bled every 4 hours for measuring plasma Ca chemically and isotopically. Previously, we showed that bone 45Ca contributes 2/3 of total blood Ca and intestine (dietary Ca) the remaining 1/3, while the total blood Ca remains constant. Thus, 2 different pools of Ca contributed to blood Ca without changing total level of Ca. During 24 hours blood Ca consists of 70% bone Ca (45Ca) and 30% dietary Ca (40Ca) in the early AM(6-8), and fluctuates daily to 40% bone 45Ca and 60% dietary Ca at 5-7PM while the total Ca and ionizable Ca remain constant. The inverse fluctuating relationship between contibutions of bone and dietary Ca in the presence of constant blood Ca suggests a more sensitive regulation of blood Ca homeostasis than heretofore recognized.

Summary of Experimental Data

Diet	Tx/Rx	Plasma Ca (mg/100ml)	Plasma 45Ca (% of Plasma Ca)	Diurnal Rhythm
Normal	None	12	70	Present
Low Ca	None	12	95	Absent
Normal	TPTX	6	20	Absent
Normal + Ca infus.	TPTX	7	10	Absent
Normal	PTX	10	35	Amplitude 1/2
Normal	TX	12	70	Present
Normal	T/Rx	12	70	Present

The reciprocal changes may require one, two or more hormones. Summary of data (cf. Table) showed 2 protocols (TPTX and Ca deficiency) had lost their diurnal rhythm (DR). These protocols were different, 3 different endocrine tissues were removed from TPTX and no tissues were taken from Ca deficiency. Infusion of supplemental Ca to TPTX dog increased blood Ca without initiating DR. In the PTX dogs (-PTH) on normal diet the amplitude of DR decreased in half but otherwise DR was normal. The removal of thyroid or treatment of thyroid with various anti-thyroid drugs did not affect DR. In 1970 H. Copp and T. Care showed that a Ca deficient state in pigs results in a rapid and complete absence of CT in thyroid blood; not seen after thyroidectomy. Since Ca deficiency yields systemic phenomena it would have a similar deficient affect on all organs and tissues in the body. In normal dogs placed on a Ca deficient diet PTH increases slowly, CT decreases rapidly and DR disappears by 8 to 12 hours in the presence of normocalcemia. CT appears to be the primary hormone for initiating DR because it is very sensitive and rapid in action.

SA428

Calcitonin Gene-Related Peptide Stimulates cAMP Production, Increases Intracellular Calcium Ion, and Hyperpolarizes Em in Human MG63 Cells. T. Kawase*[1], L. Stehno-Bittel*[2], D. M. Burns[3]. [1]Pharmacology, Niigata University Dental School, Niigata-city, Japan, [2]Cell Biology and Physical Therapy, KU Medical School, Kansas City, KS, USA, [3]Research Service and Biochemistry & Molecular Biology, Kansas City VA Med. Ctr. and KU Medical School, Kansas City, MO, USA.

Calcitonin gene-related peptide (CGRP) is a skeletal neuropeptide that acts on stromal osteoprogenitor cells, pre-osteoblasts, and osteoblasts. To expand our understanding of CGRP action in human osteoblastic cells we examined human MG63 pre-osteoblast-like cells with standard assays and laser-scanning confocal fluorescent microscopy. In the presence of 0.5 mM IBMX CGRP stimulated cAMP formation 15-fold in these immature cells, similar to that reported for lining and osteogenic rodent cells. By a semi-quantitative dual-dye fluorescent single-cell method, we demonstrate that CGRP also elicits a strong dose-dependent mobilization of intracellular calcium ion that is followed after 130-150 seconds by a prolonged smaller diltiazem-sensitive increase in calcium ion concentration. Using two different membrane potential-dependent fluorescent dyes, we also demonstrate delayed hyperpolarization of membrane potential (Em). Unlike previous data obtained from rat UMR106 cells, pharmacological challenges indicate that Em hyperpolarization is cAMP-dependent in human MG63 cells. Specific binding assays,either with radioiodinated-CGRP or by fluorescence polarization assay using Fluo-CGRP indicate that 13,200 sites per cell are present with a Kd of approximately 150 pM. Several independent cellular responses could result from a CGRP receptor that couples to multiple G-proteins. Alternatively, MG63 cells may possess two very similar CGRP receptor subtypes.

SA429

RAMP1 and RAMP3 Expressions after Aortic Stenosis. C. Cueille*, E. Pidoux*, R. Ventura-Clapier*, J. GAREL. Hôpital Lariboisière, Unité 349 INSERM, Paris, France.

CGRP receptors are present in bones. Osteoblasts are known to express this receptor,and the peptidic ligand may be released by nerve endings in bones. Vascularisation is of importance for bone growth (endochondral ossification) and bone repair. Thus, it is tempting to speculate that CGRP signaling through its proliferative effect may participate in conjunction with VEGF to bone angiogenesis. CGRP receptors were recently described by Hagner et al.(2002) in capillaries and small arteries. In the present work, as a model, we have studied the effect of a change in blood flow on CGRP receptor expression in the myocardium. Reduction of blood flow was induced in rats by aortic stenosis, and chronic heart failure (CHF) developped as a consequence of aortic stenosis. CGRP and adrenomedullin (ADM) are known as potent vasodilators in humans, and receptors for both CGRP and ADM were already identified by others in heart. Receptor activity-modifying proteins (RAMPs) determine the ligand specificity of the Calcitonin Receptor-Like Receptor (CRLR); co-expression of RAMP1 and CRLR results in a CGRP receptor, whereas the association of RAMP2 or RAMP3 with CRLR gives an ADM receptor. We have used semi-quantitative RT-PCR and Western-blot analysis to detect and quantify the mRNA and the protein of RAMP1 and RAMP3 in both atria and ventricles of failing hearts 6 months after aortic stenosis in rats. For the first time, we showed, an up- regulation of RAMP1 and RAMP3 mRNAs and proteins in this model of cardiac failure.When accurate comparisons between sham and CHF rats were done for ventricles and atria, RAMP1 appeared 3-fold more abundant in CHF than in sham rats. The mRNA level of RAMP3 was 10-fold increased in atria of CHF animals, whereas a 3-fold induction was observed in ventricles. Western-blot detected the same forms both for RAMP1 and RAMP3 in ventricles and atria, the major form for RAMP1 and RAMP3 was the homodimer. A 10-fold increase in RAMP1 homodimer in atria of CHF rats was observed, whereas RAMP3 homodimer was 28-fold induced. In ventricles of CHF rats, a 10-fold induction of RAMP1 homodimer occurred. No change was observed in mRNAs coding for CRLR, RAMP2, RDC1, and ADM.After congestive heart failure in adult rats, an up-regulation of the CGRP1 receptor (by an increase in RAMP1 that is associated with CRLR) in atria and ventricles, and of ADM receptor (by increased RAMP3 expression that is associated with CRLR) in atria are suggested. These findings support a functional role for CGRP and ADM receptors to compensate the chronic heart failure in rats.

SA430

Effect of Salmon Calcitonin on Aorta Connective Tissue in Elastin-Derived Peptides-Induced Experimental Atherosclerosis. J. G. Gminski*[1], K. Siemianowicz*[1], M. Goss*[1], V. Ciszek-Doniec*[2], T. Francuz*[1]. [1]Experimental and Clinical Biochemistry, Silesian Medical Academy, Katowice, Poland, [2]Women Health Promotion, Silesian Medical Academy, Katowice, Poland.

Salmon calcitonin is accepted by FDA for the treatment of postmenopausal osteoporosis.The main medical problem in postmenopausal women is atherosclerosis-related cardiovascular disease. Elastin is one of the most apolar and the most long-lived protein. In healthy adults the turnover of elastin is slow, but it is enhanced during aging, hypertension, diabetes and atherosclerosis. Elastin-derived peptides (EDPs) - products of hydrolysis of insoluble elastin play an important role in regulation of vascular smooth muscle cells proliferation, migration and atherosclerosis development. EDPs act through calcium ions-mobilizing receptor, stimulate respiratory burst, activate proteolytic enzymes and induce immune response. The aim of this study is to evaluate the effect of salmon calcitonin on the metabolism of connective tissue matrix proteins in EDPs-induced experimental atherosclerosis. 30 male New Zealand rabbits were divided into 3 equal groups: C (control) group were injected with compltete Freund's adjuvant (CFA) while two other groups - E (EDPs) and E+CT (EDPs + calcitonin) were received 1.5 mg of EDPs from porcine aorta + CFA. The E+CT group received s.c. injections of salmon calcitonin 0.5 MRC per day. The experiment lasted for 6 months. Statistical analysis was performed using the ANOVA test, followed by the Newman-Keul's test. The aortas from rabbits of E group developed typical advanced atherosclerotic lesions including fragmentation of elastic fibers and calcification. No such atherosclerotic changes were found in rabbits of C and E+CT groups. A statistically significant decrease in the aorta level of insoluble elastin, the rise of salt- and acid-soluble collagens and the increase of the elastase-like activity were found in the E group when compared with C and E+CT groups. Administration of salmon calcitonin (E+CT) prevented the rise of calcium-bound to elastin content found in E group.

Effect of salmon calcitonin on aorta connective tissue parameters (mean values)

	Controls (C)	EDPs (E)	EDPs + Calcitonin (E+CT)
Insoluble Elastin (mg/g of wet tissue)	218	132	196
Acid- + Salt-Soluble Collagens (mg/g of wet tissue)	85	128	103
Aorta Elastase-Like Activity (ng of eq. elastase/g of wet tissue/24 h)	134	204	151
Calcium-Bound To Elastin (micromole/g of insoluble elastin)	37	96	34

SA431

Molecular Cloning and Expression of Equine Calcitonin, Calcitonin Gene-Related Peptide-I, and Calcitonin Gene-Related Peptide-II. R. E. Toribio*[1], C. W. Kohn*[2], G. W. Leone*[3], C. C. Capen[1], T. J. Rosol[1]. [1]Veterinary Biosciences, The Ohio State University, Columbus, OH, USA, [2]Veterinary Clinical Sciences, The Ohio State University, Columbus, OH, USA, [3]Department of Molecular Virology, Immunology and Medical Genetics, The Ohio State University, Columbus, OH, USA.

Abnormal calcium regulation (hypocalcemia and hypercalcemia) is a frequent finding in horses with different pathological conditions (sepsis, endotoxemia, renal failure). In order to investigate the role of the calcitonin gene family in diseased horses we cloned and determined the tissue expression of three transcripts of the equine calcitonin gene family: calcitonin (CT), calcitonin-gene related peptide (CGRP)-I, and CGRP-II. A divergent form of CGRP (CGRP-I) was identified in horses. Equine CT has the greatest homology (>85%) to human, rat and mouse subgroups of calcitonins. Calcitonin carboxyl terminal peptide (katacalcin) homology to other species is low (<38%). Equine CGRP-I (37aa) has low homology (<59%) to CGRPs of other species. The signal and amino terminal peptides for equine CT and CGRP-I were identical, indicating that these peptides are encoded by a gene equivalent to the human *CALC-I* gene. Equine CGRP-II (37 aa) has >80% homology to chicken, human, rat, ovine, swine, and bovine CGRPs. The homology between equine CGRP-I and CGRP-II is low (56%). The high homology of equine CGRP-II and the low homology of equine CGRP-I to CGRP in other species were unexpected findings, because the homology of all known CGRP peptides was reported to be high in mammals. Northern blot analysis revealed that CT mRNA expression was restricted to the thyroid gland; however, RT-PCR revealed that CT mRNA expression was also present in the pituitary gland. CGRP-I and CGRP-II mRNA expression was present in several regions of the nervous system and other tissues of neuroectodermal origin. An unexpected finding was CGRP-I expression in the kidney by both Northern analysis and RT-PCR. Based on these results, CT gene expression in the horse was not restricted to the thyroid gland, and CT may be important in regulating pituitary cell function. CGRPs are widely expressed in tissues of the central and peripheral nervous system. Information from this study will be valuable in developing equine-specific immunoassays to study the role of CT, CGRP-I, and CGRP-II in health and disease, since human assays for serum concentrations of the calcitonin gene family gave variable results.

SA432

Dissociation of Functional Response from Cyclic AMP Stimulation in a Substituted and C-terminally Truncated PTH Peptide. R. J. Murrills, B. M. Bhat, P. V. N. Bodine, Y. Kharode, L. Borella, J. J. Yoon*, R. L. Rupert*, V. E. Coleburn*, R. A. Moran*, J. Marzolf*, F. J. Bex. Women's Health Research Institute, Wyeth Research, Philadelphia, PA, USA.

Selective substitution of several N-terminal amino acids can restore and enhance binding and cyclic AMP activity of PTH peptides whose classical binding domain has been truncated or removed entirely and which would otherwise be weak or inactive (Shimizu et al, 2001, Endocrinology 142:3068). One such modified peptide, [Ala^{3,12}, Nle^{8}, Gln^{10}, Har^{11}, Trp^{14}, Arg^{19}, Tyr^{21}] rPTH(1-21), was created by Gardella's group (JBMR 15 Suppl 1:S566, 2000) and termed modified or MPTH(1-21). We were interested to determine whether MPTH(1-21), which is known to potently stimulate cAMP and bind the PTH receptor, would also be active in animal models of osteopenia and in assays downstream of cAMP in the osteoblast. Initial testing in Saos-2 membrane receptor binding and whole cell cyclic AMP assays confirmed that MPTH(1-21) was indeed almost as potent as PTH(1-34) and induced similar levels of cyclic AMP in Saos-2 cells. However, when tested in OVX osteopenic animals at doses (up to 500ug/kg/day sc in mice, 200ug/kg/day sc in rats) that were up to 20 times higher than those routinely used for PTH(1-34), MPTH(1-21) was completely inactive, as assessed by pQCT. To address this result, we tested MPTH(1-21) in Saos-2 cells that had been stably transfected with 15 copies of the cyclic AMP response element (CRE) linked to a Luciferase reporter. In addition, we tested the peptides in an assay of alkaline phosphatase suppression in a conditionally immortalized human osteoblast cell line, HOB-03-C5, which is sensitive to picomolar (physiological) concentrations of PTH. In both of these downstream assays, MPTH(1-21) was much less potent than would be expected from its binding and cyclic AMP profile.

Assay	PTH(1-34)	MPTH(1-21)
Receptor binding*	0.46nM	0.89nM
Cyclic AMP*	0.65nM	1.19nM
CRE-Luciferase*	1.14nM	28.1nM
Alkaline phosphatase	0.04pM	91pM
OVX mouse	Active @100ug/kg	Inactive at 500ug/kg
OVX rat	Active at 10ug/kg	Inactive at 200ug/kg

*Weighted average EC_{50} value from at least 3 side-by-side determinations.

We conclude that, at the doses tested, MPTH(1-21) was inactive in two animal models of osteopenia. Results from two assays downstream of cAMP suggest a disconnect between cAMP and transcriptional and functional responses that may contribute to this lowered in vivo activity.

SA433

See Friday Plenary number F433.

SA434

Whole PTH Assay Does Not Provide Better Discrimination than the Intact PTH in Patients with Secondary Hyperparathyroidism Due to Renal Failure or Vitamin D Deficiency. P. Glendenning, L. L. A. Laffer*, A. A. Musk*, S. D. Vasikaran. Biochemistry, Royal Perth Hospital, Perth, Australia.

Immunoassays for intact PTH (iPTH) detect the whole PTH molecule (1-84) as well as a mixture of different PTH fragments (2-84 to 7-84). The whole PTH (wPTH) assay has been suggested to be the optimal assay to assess parathyroid function as only whole PTH (1-84), which is the biologically active form of PTH, is detected by this assay. We compared the wPTH to the iPTH assay in 208 patients with secondary hyperparathyroidism to examine if the wPTH assay offered any diagnostic advantage over the iPTH assay. EDTA and serum samples were collected over a 2 month period and stored at -20 degrees C. iPTH was measured by immunochemiluminescence immunoassay (ICMA) on the DPC Immulite 2000 and wPTH was measured by ICMA assay on the Nichols Advantage using EDTA plasma. 25 hydroxy vitamin D (25 OHD) was measured in serum by DiaSorin radioimmunoassay. 18 patient samples were collected in parallel to assess sample stability in EDTA plasma compared to serum. 100 patient samples were collected from patients with advanced renal failure (Cr > 300 umol/L) and 90 samples from patients with vitamin D deficiency (25 OHD < 30 nmol/L) and intact renal function (Cr < 100 umol/L). The correlation coefficient was 0.89 between iPTH and wPTH in both renal failure and vitamin D deficient patient groups. Bland Altman analysis indicated the iPTH result was 75% higher than wPTH in renal failure patients but the difference between both PTH assays was constant across all mean values from 5 to 150 pmol/L. In vitamin D deficient patients, Bland Altman analysis indicated that iPTH result was 60% higher than wPTH but the difference between PTH assays progressively increased to over 80% at mean PTH values above 15 pmol/L. Regression of 25 OHD on iPTH and wPTH in vitamin D deficient patients revealed lack of a relationship with the wPTH assay (P=0.32) but near statistical significance for the iPTH assay (P = 0.06). iPTH was 30% lower in serum than EDTA plasma (P < 0.01). wPTH was 8% lower in serum than EDTA plasma (P > 0.05). The wPTH assay is equally useful compared to the iPTH assay in renal failure patients but may be less useful than the iPTH assay in evaluation of vitamin D deficient patients. However, serum and EDTA plasma give comparable results on the wPTH assay but not with the iPTH assay. Thus there may be pre-analytical reasons but no obvious post-analytical reasons to recommend widespread adoption of the wPTH assay.

SA435

See Friday Plenary number F435.

SA436

A Leader Sequence in the PTH mRNA 5'- Untranslated Region (UTR) Regulates PTH Translation. Y. Moz*, R. Kilav*, J. Silver, T. Naveh-Many. Nephrology, Hadassah Hospital, Jerusalem, Israel.

Computer modeling of the PTH mRNA predicts a stable stem-loop structure of the first 19 nt of the 119 nt long 5'-UTR. Secondary structures in 5'-UTRs often regulate translation of mRNAs. To study the effect of the 5'-UTR on PTH mRNA translation, we performed reticulocyte lysate *in vitro* translation of full-length PTH transcripts or truncated transcripts lacking part of the 5'-UTR. Surprisingly, a full-length transcript was not translated either in this system or in a wheat germ translation system. Truncated transcripts lacking from 9 to 33 nt of the 5'-end of the transcript were translated very efficiently. This suggests that there is a regulatory element in this region that prevented translation. There is no parathyroid cell line, so to study this *in vivo* in cells, we transiently transfected HEK293 cells with plasmids containing the CMV promoter linked to cDNAs for the wild type and truncated transcripts. We then measured the levels of PTH mRNA and PTH secreted into the medium. There was no difference in mRNA levels of the wild type and truncated constructs. However, the truncated constructs resulted in the secretion of large amounts of PTH, while with the wild type full-length PTH construct there was no detectable PTH in the medium. Therefore, both in the *in vitro* translation systems as well as *in vivo* in transfected cells the full-length transcript was not translated. This inhibition could be a result of either sequence or structure that is present in the full-length transcript but not in the truncated transcripts. Point mutations and deletions in the 5'-end of the PTH transcript were subjected to in vitro translation in the reticulocyte lysate system to delineate the mechanism of the translation inhibition by the 5'-UTR 9 nt. Our results show that a sequence/structure in the PTH mRNA 5'-UTR prevents PTH translation. This may be a regulatory mechanism to prevent PTH translation of the large amounts of PTH mRNA that are present in the parathyroid cell. In situations, such as hypocalcemia where increased amounts of PTH are synthesized and secreted, there may be a mechanism whereby the inhibition of PTH translation is overcome. This remains to be tested. In the presence of hypercalcemia up to 90% of the PTH protein may be degraded in the parathyroid. Our results suggest that the individual parathyroid cell is able to regulate the amount of PTH synthesized at a number of levels: PTH gene transcription, mRNA stability, translation and PTH degradation.

SA437

See Friday Plenary number F437.

SA438

Modulation of Parathyroid Hormone Dependent Activation of Phospholipase C. Q. Sun*[1], R. W. Katz[2], J. P. Bilezikian[1]. [1]Medicine, Columbia University College of Physicians and Surgeons, New York, NY, USA, [2]Division of Oral Biology, Columbia University School of Dental and Oral Surgery, New York, NY, USA.

Parathyroid hormone (PTH) can activate Phospholipase C (PLC), which hydrolyzes phosphatidylinositol 4,5-bisphosphate to produce inositol 1,4,5-triphosphate (IP), a second messenger involved in many cell activities. PLC isoforms can be preferentially activated by G protein coupled receptors (PLCβ), by non-receptor tyrosine kinases (PLCγ), and by intracellular Ca^{2+}(PLCδ). We hypothesize that prior modulation of PLC function will alter PTH (1-34)dependent IP production. LLC-PK1 kidney cells overexpressing the rat PTH1 receptor were used in these studies. (1) *Regulation by the G alpha protein subtypes*. Mas-7, a $G\alpha_i/G\alpha_o$ activator, suppressed PTH-dependent IP production by 60%. Pertussis toxin, a $G\alpha_i/G\alpha_o$ inactivator, suppressed PTH IP production by 28%. (2) *Regulation by Ca^{2+}*. Exposure to calcium ionophore A23187 increased basal IP levels over time but one hour pre-exposure did not affect PTH dependent IP. In the presence of EGTA, A23187 reduced PTH IP production by 63%. (3) *Regulation by receptor tyrosine kinases*. Epidermal growth factor, insulin, and platelet-derived growth factor did not affect PTH production of IP. (4) *Regulation by phorbol ester or cAMP analogues*. Adding phorbol-12-myristate-13-acetate overnight reduced the PTH dependent production of IP by 46% but cAMP analogues had no effect of PTH activation of PLC. Our results suggest that PTH receptor signal transduction via the IP second messenger system is affected by alterations in $G\alpha_i/G\alpha_o$ activities, by phorbol ester and by calcium ions, but not by receptor tyrosine kinases or by cAMP. Results provide support for the hypothesis that modulation of PLC activity influences PTH peptide signal transduction.

SA439

See Friday Plenary number F439.

SA440

See Friday Plenary number F440.

SA441

Effect of Low Calcium Diet on Fertility in PTH-Deficient Mice. X. K. Tong*, D. Miao, R. Huo*, D. Goltzman, A. C. Karaplis. Medicine, McGill University, Montreal, PQ, Canada.

We previously reported that targeted disruption of the PTH gene in mice leads postnatally to abnormalities in skeletal development and calcium homeostasis, as well as to decreased fertility in females. $PTH^{-/-}$ mice on a normal diet were hypocalcemic and demonstrated lower serum progesterone level and irregular menstrual cycles. Histological analysis unveiled a marked reduction in the number of corpora lutea present in the ovaries. Here, we examined the effect of a low calcium diet (0.005-0.01%) on the fertility of $PTH^{-/-}$ female mice. On a low calcium diet, animals remained hypocalcemic and were rendered completely infertile. Serum estradiol and progesterone levels were lower than on the regular diet and were associated histologically with uterine hypoplasia, poorly developed ovarian follicles, and complete absence of corpora lutea. Because ovarian follicular and luteal development is dependent on angiogenesis, we next examined the effect of low serum calcium concentration on this process. In the wild type animals, vascular endothelial growth factor (VEGF) and fibroblast growth factor 2 (FGF2) were expressed in the theca layer and in luteal cells, next to the endothelial cells expressing CD31. Wild type animals on a low calcium intake were normocalcemic and showed no change in the expression of VEGF, FGF2 and CD31. In the $PTH^{-/-}$ mice on a normal calcium diet, cells that stained positive for VEGF or FGF2 in the theca layer and in luteal cells were reduced, as were CD31 positive endothelial cells. When $PTH^{-/-}$ mice were placed on a low calcium diet, positive staining for VEGF or FGF2 in luteal cells was completely absent and that in the theca layer was reduced. CD31-positive endothelial cells were also markedly decreased. These findings indicate that a low calcium diet per se has no apparent effect on fertility; however, hypocalcemia reduces fertility in female mice due in part to diminished angiogenic potential of the ovary, a process that is critical for normal follicular and luteal development.

SA442

See Friday Plenary number F442.

SA443

Regulation of OPG/RANK/RANKL by PTHrP Peptides in Human Prostate Cancer Cells. O. A. Ahmadpour, D. W. Burton, S. Tu*, L. J. Deftos. Medicine, University of California and Department of Veterans Affairs, San Diego, CA, USA.

PTHrP is an oncoprotein that regulates the growth and proliferation of many common malignancies. Studies by us and our colleagues have demonstrated that prostatic PTHrP regulates tumor development, growth and progression. We demonstrated previously that PTHrP plays a role in the progression of prostate cancer metastasis to the bone. The identification of the OPG/RANK/RANKL system as the dominant, final mediator of osteoclastogenesis ended a long-standing search for the specific factors produced by preosteoblastic/stromal cells that were both necessary and sufficient for osteoclast development. Since some prostate cancer cells express these proteins, we hypothesized that metastatic prostate carcinomas also utilize the OPG/RANK/RANKL pathway to localize to the bone. We evaluated several prostate cancer cell lines, including 267 B1, 267 B1-XR, DU 145, Dupro-1, PC-3, LNCaP and PPC-1, for the expression of OPG/RANK/RANKL. All cell lines were shown to express these genes by RT-PCR. We next studied the effect of various PTHrP peptides (1-34, 38-64 and 107-139 and 140-173) on the OPG/RANK/RANKL cascade. Using RT-PCR and immunoassays, we demonstrated that PTHrP 1-34 and 140-173 treatment increased OPG expression in 267 B1-XR and PPC-1 cells. PTHrP 38-64 treatment increased OPG expression in PPC-1 cells only. No significant effects on OPG levels by PTHrP peptides were observed in 267 B1, PC-3, DU 145 and Dupro-1 cells. Based on RT-PCR, RANKL expression was increased in PC-3 and 267B1-XR cells with PTHrP 1-34 and 107-139 treatments, respectively. RANKL expression was decreased by PTHrP 1-34 in 267 B1, 267B1-XR, PPC-1 and Dupro-1 cells. No PTHrP peptide treatment effect was demonstrated on RANKL in the other cell lines. RANK expression did not appear to be regulated by PTHrP in the prostate cell lines, with the exception of PTHrP 140-173, which decreased RANK mRNA in 267B1 cells as measured by RT-PCR. In conclusion, these results suggest that PTHrP promotes prostate cancer to spread to bone by regulating the OPG/RANK/RANKL pathway. Future studies may show that PTHrP regulation of the OPG/RANK/RANKL pathway can be used for the treatment of "osteolytic" prostate cancers.

SA444

Two-site Immunoassays for Intact PTHrP Isoforms: Confirmation of Specificity and Measurement of Isoform Expression. L. J. Deftos, C. Chalberg*, K. Smith*, Y. Wang*, S. Tu*, A. Gujral, D. W. Burton. Medicine, University of California and Department of Veterans Affairs, San Diego, CA, USA.

Parathyroid hormone-related protein (PTHrP) is expressed in a wide variety of tissues and has pleiotropic effects on bone minerals and cellular growth and differentiation. Many of these actions have been allocated to specific forms of PTHrP that derive from isoform expression and posttranslation modifications by prohormone convertases to generate peptides of distinct biological function. The development of immunoassays specific to the various forms of PTHrP provides information important to understanding the molecular, cellular, and clinical biology of this oncoprotein. Studies of the human specific and full-length isoforms of PTHrP have been limited by the paucity of specific and sensitive immunoassay for them. In this study, we report the development of two-site immunoassays to measure the intact PTHrP isoforms, including PTHrP 1-141 and PTHrP 1-173. Murine monoclonal PTHrP antibody pairs to PTHrP 1-34 and 109-141 and 1-34 and 140-173 were individually identified by clonal selection, confirmed by tracer binding studies, and purified by affinity chromatography. The antibodies were then configured into a plate-based sandwich assay format that utilized E. Coli produced, recombinant PTHrP 1-141 and PTHrP 1-173 as respective standards. The capture antibodies to PTHrP 109-141 and 140-173 and the biotinylated antibody to PTHrP 1-34 were detected with a streptavidin labeled b-D-galactosidase enzyme reaction using the fluorescent substrate, 4-methylumbelliferyl-b-D-galactopyranoside. The PTHrP 1-141 and PTHrP 1-173 immunoassays appropriately identified the corresponding PTHrP isoforms with sensitivities of 0.08 pmol/L and 0.2 nmol/L, respectively, and dynamic ranges over 3 logs. Other control and test PTHrP species did not react in the assays. The fidelity of the assays was further evaluated by measuring conditioned media and cell extracts from lung, prostate, kidney and pancreatic cancer cell lines that were transfected with PTHrP expression plasmids, including prepro-PTHrP1-87, 1-95, and 1-173. The PTHrP 1-141 and PTHrP 1-173 two-site assays respectively demonstrated increased PTHrP levels in the media and cell extracts of the PTHrP 1-173 group but not in the other groups. Some wild-type cells also expressed specific isoform activity. In summary, we developed high-throughput, non-radioactive, fluorescence immunoassays that specifically measure full-length isoforms of PTHrP. In addition to clinical application, these assays can be especially useful for evaluating the isoform expression and processing of PTHrP.

SA445

Amino-Terminal PTHrP Peptides in Lung Cancer Cell Lines Identified by Mass Spectrometry. R. Miller*[1], B. Schilling*[1], D. W. Burton[2], B. Gibson*[1], R. H. Hastings[3], L. J. Deftos[2], V. H. Hook*[1]. [1]Buck Institute for Age Research, Novato, CA, USA, [2]Medicine, University of California and Department of Veterans Affairs, San Diego, CA, USA, [3]Anesthesiology, University of California and Department of Veterans Affairs, San Diego, CA, USA.

Amino-terminal PTHrP (parathyroid hormone-related protein) peptides are derived from proteolysis of the pro-PTHrP precursor and are secreted from lung tumor cells, resulting in the pathophysiological syndrome of hypercalcemia of malignancy. These amino-terminal PTHrP peptides have largely been identified by immunoassays directed towards synthetic PTHrP(1-34). However, since antibodies may recognize several related peptide forms that resemble standard PTHrP(1-34), the primary sequence identity(ies) of such peptides requires direct determination. In this study, the identification of potential amino acid sequences of peptides detected by anti-PTHrP(1-34) from lung cancer cell lines was accomplished by HPLC and MALDI-TOF mass spectrometry. Acid extracts of BEN (courtesy of T.J. Martin) and A549 cells were subjected to HPLC on a C18 column eluted with an acetonitrile gradient. Fractions were immunoassayed for PTHrP(1-34), and elution positions were compared to synthetic PTHrP(1-34). BEN cells contained PTHrP(1-34) that coeluted with standard PTHrP(1-34). However, the majority of PTHrP(1-34) in A549 cells did not coelute with standard PTHrP(1-34). Identification of the HPLC peaks of PTHrP(1-34) were accomplished by Matrix-Assisted Laser Desorption Ionization Mass Spectrometry. In BEN cells, the mass of the PTHrP(1-34) immunoreactivity, 4015 daltons, corresponded to that of PTHrP(1-34). However, A549 cells contained PTHrP(1-34) immunoreactivity that differed from PTHrP(1-34) and is under further investigation. Production of PTHrP(1-34) would be consistent with cleavage of pro-PTHrP at a Lys-Arg site to generate the NH2-terminus of the peptide, and the C-terminus of PTHrP(1-34) could be generated by cleavage at the monobasic Arg-37 site followed by carboxypeptidase trimming. These results demonstrate the identification by mass spectrometry of peptides included within PTHrP(1-34) from lung cancer that can effect serum calcium.

SA446

See Friday Plenary number F446.

SA447

BIM-44058, A Novel PTHrP Analog, Improves Trabecular Bone Microarchitecture In Old Ovariectomized, Osteopenic Cynomolgus Monkeys. J. Legrand[1], C. Fisch[2], R. Forster[2], B. Koller*[3], J. Z. Dong*[4], C. W. Woon*[4], J. R. Claude*[5], M. D. Culler*[4]. [1]Beaufour-Ipsen, Paris, France, [2]CIT, Evreux, France, [3]Scanco, Bassersdorf, Switzerland, [4]Biomeasure Inc., Milford, MA, USA, [5]Faculty of Pharmacy, Paris, France.

BIM-44058, a novel analog of PTHrP1-34, has been shown to effectively restore bone mineral density (BMD) by stimulating bone formation in both ovariectomized, osteopenic rats, and in old, ovariectomized, osteopenic cynomolgus monkeys, two established models of postmenopausal osteoporosis. In order to study the effect of BIM-44058 on the microarchitecture of trabecular bone, vertebrae from old, ovariectomized (OVX) cynomolgus monkeys, in which established osteopenia had been fully reversed by BIM-44058 therapy, were examined using microcomputed tomography (Micro-CT). Old female monkeys (approx. 4 kg) were either OVX or sham-operated (SHAM), and maintained for 10 months to allow development of osteopenia in the OVX animals. The OVX, osteopenic animals were then treated by daily subcutaneous injection of either saline (n=7) or BIM-44058 at the doses of 1 (n=10) or 10 µg/kg/day (n=8) for 10 months. Upon necropsy, the central portion of the L3 lumbar vertebral bodies were analyzed by high-resolution micro-CT. Total bone volume (TV), trabecular number (Tb.N), trabecular thickness (Tb.Th) and trabecular separation (Tb.Sp) and connectivity density (ConnD) were calculated using standardized methods. The trabecular bone volume, and the number and thickness of the trabecular plates and their separation were identical in all groups. The connectivity density, a 3D index of trabecular connectivity, was higher in animals treated with 10 µg BIM-44058/kg/day when compared with both SHAM ($p<0.05$) and vehicle-treated OVX controls. These results demonstrate that the differences of BMD between the groups are not related to a difference in the cancellous bone volume and suggest that daily treatment with BIM-44058 increases bone mass in osteopenic monkeys by increasing bone mineralization. In addition, treatment with BIM-44058 at 10 µg/kg/day improves the trabecular microarchitecture. Similar observations have been reported in postmenopausal women treated for 36 months with daily injections of human parathyroid hormone 1-34, and suggest that BIM-44058 has the potential to reduce the incidence of spinal fractures in patients with osteoporosis by increasing the bone mineralization and correcting the microarchitectural defects that contribute to skeletal fragility.

SA448

Evidence that Bpa19-modified Parathyroid Hormone-related Peptide (PTHrP) Agonist and Antagonist Analogs Crosslink to Distinct Sites in Transmembrane Domain 2 of the PTH/PTHrP Receptor. R. C. Gensure[1], N. Shimizu*[2], J. C. Tsang*[2], H. Jüppner[2], T. J. Gardella[2]. [1]Endocrine Unit and Pediatric Endocrine Unit, Massachusetts General Hospital and Harvard Medical School, Boston, MA, USA, [2]Endocrine Unit, Massachusetts General Hospital and Harvard Medical School, Boston, MA, USA.

The interaction of parathyroid hormone (PTH) (1-34) and PTHrP(1-36) with the PTH/PTHrP receptor (P1R) is believed to involve two principal components: an interaction between the portion of the ligand spanning residues 15-31 (binding domain) and the receptor's amino-terminal extracellular domain, and an interaction of the amino-terminal portion of the ligand (activation domain, residues 1-14) and the juxtamembrane (J) region of the receptor (the two-domain hypothesis). However, we have recently found that Bpa19-PTHrP(1-36) crosslinks to the P1R within the interval Leu232-Lys240, in transmembrane domain 2 (TM2) of the receptor, with Lys240 being the apparent photo-interaction site, as judged by alanine-scan analysis. Previous studies have indicated that TM2 plays an important role in ligand-dependent and ligand-independent receptor activation, and that mutations at Arg233 in this domain affect the binding of the agonist PTH(1-34) but not the antagonist PTH(3-34). We therefore hypothesized that Bpa19 in an antagonist peptide would crosslink to a different receptor site than would Bpa19 in an agonist peptide. To test this, we prepared the antagonist Bpa19-PTHrP(5-36) and mapped the site of crosslinking to the P1R. This compound crosslinked to the same TM2 interval as did Bpa19-PTHrP(1-36); however, the alanine scan analysis of this interval revealed differences in the effects of the mutations on the crosslinking of the Bpa19-modified agonists and antagonist analogs. The agonist compound crosslinked poorly to the R233A and K240A mutants, whereas the antagonist crosslinked efficiently to these two mutants, but poorly to F238A. Overall, the

data suggest that Bpa19-modified ligands can detect differences between the agonist- and antagonist-occupied states of the P1R; these differences may involve changes in the relative orientation/position of TM2 in active and inactive receptors.

SA449

See Friday Plenary number F449.

SA450

Temporal Regulation of PTH/PTHrP Receptor Coupling to Protein Kinase C Epsilon is Mediated by Changes in Expression of G11-alpha in Chondrocytic Cells. L. P. Lai*, J. Mitchell*. Pharmacology, University of Toronto, Toronto, ON, Canada.

Phospholipase C signaling via the PTH/PTHrP receptor has been shown to be necessary for normal differentiation of chondocytes *in vivo* (Guo, et al., J. Bone Miner. Res. 16:S229, 2001), it is not clear however what role this pathway plays in regulating chondrocyte growth or differentiation. We have examined the ability of PTH to regulate protein kinase C isozymes in the rat chondrocytic cell line CFK2 that progressively express markers of chondrocytic differentiation with time in culture. After nine days in culture the cells express maximal levels PTH receptor mRNA as well as the G proteins $G_s\alpha$ and $G_{11}\alpha$ to which the receptor couples. PTH (10 nM rPTH1-34) stimulates a three-five fold increase in adenylyl cyclase activity and also stimulates the translocation of PKC-α to the plasma membrane and PKC-ε to the nucleus but has no effect on PKC-β1 or PKC-δ. Over the next four days in culture the expression of $G_{11}\alpha$ decreased by 70% but there was no change in the levels of $G_s\alpha$ protein or PTH receptor mRNA. The decrease in $G_{11}\alpha$ was accompanied by a complete loss of the ability of PTH to stimulate PKC-ε translocation, however, adenylyl cyclase activation by PTH was unchanged. The loss of PTH/PTHrP receptor coupling to PKC-ε was accompanied by an increase in inhibition of cell growth and thymidine incorporation by PTH from 15-24% in cells on day 9 to 41-45% on day 13. Stimulation of the cells on both days with the adenylyl cyclase activator forskolin inhibited thymidine incorporation whereas stimulation by the PKC activator PMA increased thymidine incorporation 78-125%. PTH and forskolin both inhibited mRNA encoding collagen type X approximately 36% whereas PMA stimulated the mRNA levels by approximately 30%. These results indicate that the PTH/PTHrP receptor couples to PKC activation through the G protein $G_{11}\alpha$ in CFK2 chondrocytes and similar to chondrocytes *in vivo*, the activation of this pathway modulates PTH regulation of cell growth and differentiation through $G_s\alpha$ and the adenylyl cyclase pathway. Our data also suggest that PTH/PTHrP receptor coupling to the PKC pathway is dependent on $G_{11}\alpha$ expression levels that decrease as the cells progress towards a hypertrophic phenotype.

SA451

See Friday Plenary number F451.

SA452

See Friday Plenary number F452.

SA453

Expression of Type I PTH/PTHrP Receptors in the Rat Osteoclast and Osteoclast-like RAW 264.7 Cells. P. H. Watson[1], M. Kisiel*[2], E. K. Patterson*[3], A. B. Hodsman[1], S. M. Sims*[4], S. J. Dixon[4], L. J. Fraher[1]. [1]Medicine, University of Western Ontario, London, ON, Canada, [2]Lawson Health Research Institute, London, ON, Canada, [3]Biochemistry, University of Western Ontario, London, ON, Canada, [4]Physiology, University of Western Ontario, London, ON, Canada.

One of the basic tenets of parathyroid hormone (PTH) action is that bone turnover is regulated via the osteoblast PTH receptor. However, evidence has accrued over the past 25 years to indicate that mammalian osteoclasts bind and respond to PTH. Recently, PTH receptor mRNA was found in osteoclasts from humans with primary HPT (JBMR 16:448-456, 2001), and both PTH receptor mRNA and immunoreactivity was detected in osteoclasts isolated from the molting deer antler (JBMR 17:455-464, 2002). In an extension of our studies of PTH receptor localization in rat tissues and cultured bone and kidney cell lines, we have used indirect immunofluorescence (IF) to localize the PTH receptor in isolated rat osteoclasts and the mouse monocyte cell line, RAW264.7, which can be induced to form osteoclast-like multinucleate cells in culture. Rat osteoclasts were isolated from the long bones of newborn rats using methods well established in our laboratories. Freshly isolated osteoclasts were allowed to adhere to 22 mm square glass coverslips for 1 hr before fixation in 4% paraformaldehyde and processing for IF. RAW264.7 cells were cultured on glass coverslips in alpha-MEM with 15% FCS in the presence of 100 nM 1,25-dihydroxyvitamin D-3 +/- 50 ng/ml RANKL. Samples were fixed after 48, 96 and 168 hr to follow the development of multinucleated cells. IF was performed using a PTH receptor antibody previously characterized (JBMR 15:1033-1044, 2000). Rat osteoclasts showed a unique pattern of immunoreactivity for the PTH receptor. Distinct rings of fluorescence were apparent around the osteoclast nuclei with some staining observed within the surrounding filamentous network. No cell membrane staining was detected in any osteoclast. Monocytic RAW 264.7 cells exhibited no immunoreactivity for the PTH receptor. After 48 and 96 hours of culture in the presence of 100 nM 1,25-dihydroxyvitamin D-3, multinucleate cells started to appear in the cultures. These cells exhibited PTH immunoreactivity within the cytoplasm which appeared as focal points and clusters of fluorescence. These data suggest that osteoclasts do indeed express the PTH receptor, albeit in a different pattern than that of osteoblasts and other cell types. The appearance of PTH receptor immunoreactivity in cultures of RAW264.7 cells induced to form multinucleate cells suggests that PTH receptor expression may be a normal element of osteoclast development.

SA454

PTH1R Endocytosis Is not Necessary for Resensitization of cAMP Signaling. A. Bisello[1], W. B. Sneddon[2], P. A. Friedman[3]. [1]Medicine, University of Pittsburgh, Pittsburgh, PA, USA, [2]Pharmacology, University of Pittsburgh, Pittsburgh, PR, USA, [3]Pharmacology, University of Pittsburgh, Pittsburgh, PA, USA.

The parathyroid hormone type 1 receptor (PTH1R) undergoes agonist-induced endocytosis. This process involves interaction of the occupied PTH1R with members of the arrestin family (arrestin2 and arrestin3) at the cell membrane, targeting of the agonist/PTH1R/arrestin complexes to clathrin-coated pits and subsequent internalization. Internalized PTH1Rs can then recycle to the cell membrane in a fully functional state (resensitization). In this study, we investigated whether endocytosis is required for resensitization of the PTH1R. We measured the cAMP activity of PTH1Rs in the presence or in the absence of arrestin- and clathrin-mediated endocytosis. In HEK-293 cells, expression of the C-terminal region of arrestin2 (arrestin2(319-418)), which is the clathrin-binding domain and acts as dominant negative inhibitor of clathrin-mediated endocytosis, reduced internalization of radiolabeled PTH(1-34) by 80%. Real-time confocal fluorescence microscopy monitoring of a green fluorescent protein-tagged PTH1R demonstrated that arrestin2(319-418) abolished PTH-stimulated PTH1R endocytosis. Expression of arrestin2(319-418) did not affect basal or acute cAMP accumulation in response to PTH(1-34). Furthermore, desensitization of PTH-stimulated adenylyl cyclase activity was unaffected by expression of arrestin2(319-418), consistent with normal interaction of wild type arrestins with occupied PTH1Rs. Surprisingly however, inhibition of endocytosis did not prevent resensitization of PTH1Rc: following a first stimulation by PTH(1-34), the PTH1R response to a second challenge with agonist was equivalent to the first irrespective of the expression of arrestin2(319-418). In conclusion, our data show that: 1) PTH-stimulated PTH1R endocytosis in HEK cells occurs almost exclusively via clathrin-coated pits; 2) PTH1R endocytosis is not necessary for resensitization of cAMP signaling; and 3) resensitizing events, such as dissociation from agonist and dephosphorylation, may take place at the cell membrane.

SA455

Vitamin D Receptor Null Mice Bone Possesses Increased Potential of Periosteal Bone Formation. N. Inoue*[1], H. Tanaka[1], M. Inoue[1], S. Kato[2], Y. Seino[1]. [1]Okayama University, Okayama, Japan, [2]Tokyo University, Tokyo, Japan.

Vitamin D has been known as an important hormone in bone metabolism, but there is little evidence that shows direct participation of active vitamin D in this process. Vitamin D receptor null mice (VDRKO) have provided lots of information in vitamin D metabolism and the biological roles. VDRKO mice do not show any abnormalities in bone at birth and develop severe rickets after weaning. And calcium supplementation showed apparent cure of rickets. These results suggested that vitamin D may exert its effects on bone via mineral homeostasis and vitamin D might not be essential for bone metabolism. However, even in calcium supplementation, the body fluid environments in VDRKO were not completely normal. For example, they show high serum levels of PTH and $1,25(OH)_2D$. To evaluate the direct function of vitamin D in bone, we previously reported that ectopically implanted VDRKO bone in wild mice showed marked bone formation and this process may involve down-regulation of cbfa1. However, this experimental system is complicated with the contamination of the host cells. Therefore, we confirm our results by implanting bone tissue wrapped with micro-pore filter membrane, and by organ culture experiment in serum-free media. After 2weeks transplantation, both VDRKO femur and calvaria showed significant but less extent increase in bone mineral density compared with wild type bone. This may due to the paucity of blood supply through filter membrane. Therefore, we turned to organ culture experiment. 0-day fetal mouse femora were excised from both VDRKO and wild littermate. Before the start of the culture, we analyzed femora by *f*ÊCT, pQCT and histology. Surprisingly, these analyses clearly demonstrated that there was no difference between VDRKO and Wild type in metaphysis, but in diaphysis and calvaria, bone volume of VDRKO was remarkably increased (1.8 fold) compared to Wild type. And this difference of bone mass was further expanded after 7days culture.Moreover, organ culture in the presence of $1,25(OH)_2D$ (10^{-8} M) showed 86% decrease in bone mineral density in Wild type bone while $1,25(OH)_2D$ did not exert any effects on bone from VDRKO mice. From these results, we conclude that VDRKO bone possesses increased potential of periosteal bone formation and thus vitamin D may play a negative regulating role in periosteal bone formation.

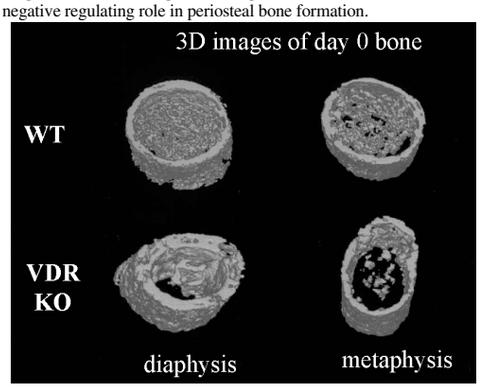

SA456

See Friday Plenary number F456.

SA457

Membrane Effects of 1,25(OH)$_2$D$_3$ Are Intact in VDR(-/-) Mouse Growth Plate Chondrocytes but Effects of 24,25(OH)$_2$D$_3$ Are Modified. B. D. Boyan, V. L. Sylvia, D. D. Dean, Y. Liu*, D. Lopez*, D. B. Dinh*, Z. Schwartz. Orthopaedics, University of Texas Health Science Center at San Antonio, San Antonio, TX, USA.

1α,25(OH)$_2$D$_3$ (1,25) regulates costochondral growth plate chondrocytes via cell maturation-specific membrane-associated mechanisms in addition to classical nuclear vitamin D receptors (1,25-nVDR). Antibodies generated to a 1,25-binding protein isolated from chick enterocyte membranes (Ab99) block membrane-dependent PKC activation and bind a single band on western blots of plasma membranes from 1,25-sensitive cells. Antibodies to 1,25-nVDR or annexin II do not recognize this band, nor is there evidence of the 1,25-nVDR in the membranes. Whereas cells from the growth zone (GC) respond to 1,25, cells from the resting zone (RC) respond to 24R,25(OH)$_2$D$_3$ (24,25), but no 24,25-specific nuclear receptor has been isolated, suggesting that the 24,25-mVDR is sufficient or that the 1,25-nVDR is used in some way by 24,25. This study tested the hypothesis that the 1,25-mVDR and 24,25-mVDR are distinct from the 1,25-nVDR and that they have physiological significance. Fourth passage RC and GC chondrocytes isolated from VDR(-/-) and VDR(+/+) mice were used for these experiments. 1,25 caused a rapid dose- and time-dependent increase in specific activity of PKC and PLC in GC cells from wild type and knockout mice. In VDR(-/-) cells, 10^{-8}M 1,25 increased PKC 10-fold and PLC 4-fold within 9 minutes. 24,25 had no effect on either enzyme in GC cells and 1,25 had no effect on RC cells at any of the times examined. 24,25 caused a dose-dependent decrease in PKC activity of RC cells from VDR(-/-) mice at 9 minutes but had no effect on PKC in VDR(+/+) RC cells. At 90 minutes, however, 24,25 stimulated PKC activity in RC cells from wild type and knockout mice. These results indicate that in chondrocytes there are three distinct receptors that mediate the effects of 1,25 and 24,25. One is the classical 1,25-nVDR and the others are the mVDRs for 1,25 and 24,25. Lack of the 1,25-nVDR had no effect on the membrane-mediated response to 1,25, indicating that the 1,25-mVDR is a unique receptor. However, the lack of 1,25-nVDRs modified the membrane effect of 24,25, indicating cross talk between these receptors.

SA458

See Friday Plenary number F458.

SA459

Ligand-induced Reverse Trafficking of Vitamin D Receptor (VDR) in Avian and Mammalian 1,25(OH)2-Vitamin D3 Target Cells. D. Capiati*, A. M. Rossi*, R. L. Boland*. Biologia, Bioquimica & Farmacia, Universidad Nacional del Sur, Bahia Blanca, Argentina.

1,25-dihydroxy-vitamin D3 [1,25(OH)2D3; calcitriol], the hormonally active form of vitamin D3, exerts its effects through two different modes of action. In addition to regulating gene transcription via its specific intracellular receptor (VDR, vitamin D receptor), 1,25(OH)2D3 induces, rapid, non-transcriptional responses involving activation of transmembrane signal transduction pathways. The stimulation of second messenger systems suggests that a 1,25(OH)2D3 membrane receptor exists. The presence of membrane-bound VDR was investigated in highly purified plasma membranes isolated from chick embryonic skeletal muscle cells (myoblasts/myotubes) and MCF-7 human breast cancer cells, examining the participation of a ligand-induced receptor translocation mechanism. Using a monoclonal antibody against the nuclear VDR (clone 9A7), it has been observed that short-term treatment (5 min) with 1,25(OH)2D3 induces the translocation of the VDR from the nucleus to the plasma membrane in chick muscle cells. The calcitriol-dependent relocation of the VDR is blocked by genistein, herbimycin or colchicine, suggesting that it is mediated by tyrosine kinase/s and microtubular transport. In MCF-7 cells, the hormone also increased the amounts of VDR associated to plasma membrane after 5 min of treatment. These results support the hypothesis that the classic nuclear VDR may be the receptor that mediates, at least in part, the non-genomic effects of 1,25(OH)2D3 in chick muscle and MCF-7 cells.

SA460

See Friday Plenary number F460.

SA461

A Contribution of the Cellular Environment to the Activation of the Vitamin D Receptor by the Tissue-selective Analog, Ro-26-9228. A. Ismail*, C. V. Nguyen*, S. Peleg. Endocrine Neoplasia & Hormonal Disorders, The University of Texas, M.D. Anderson Cancer Center, Houston, TX, USA.

We have recently shown that the vitamin D receptor (VDR)-mediated transcriptional activity of the vitamin D analog Ro-26-9228 was a 100 times greater in human osteoblastic cell lines (MG-63 and hFOB) than in the human colon carcinoma cell line, Caco-2. The events associated with transcriptional activation of the VDR include binding to its ligand, conformational changes that promote heterodimerization with RXR, and recruitment of coactivators of transcription to the VDR-ligand complexes. These events can be reproduced by in vitro synthesized VDR (ivtVDR), but the experiments with Ro-26-9228 suggested a contribution of the cellular environment to these events. To examine this hypothesis we used ivtVDR incubated with ligand in vitro, or VDR extracted from osteoblastic (hFOB) and intestinal (Caco-2) cells after in vivo incubation with either 1,25(OH)2D3 (1,25D3) or Ro-26-9228. The ligand-bound receptors were tested for their abilities to interact with GRIP, RXR or DRIP by pull-down assays. 1,25D3 had similar potencies (1-10 nM) to induce interactions of VDR from all three sources with these partners of transcription. In contrast, analog concentrations of 100-1000 nM induced interaction of ivtVDR with RXR, GRIP and DRIP, and analog concentration of 10 nM induced interaction of osteoblastic VDR with these partners of transcription. Interestingly, VDR from Caco-2 cells did not interact with these proteins even after incubation with analog concentration of 1000 nM. We hypothesized that the subcellular localization of VDR may contribute to differences in its activation in hFOB and in Caco-2 cells. Therefore, VDR distribution between cytoplasm and chromatin was examined in these cells by subcellular fractionation. We found that in hFOB cells, the unoccupied VDR localized exclusively in the cytoplasm, but VDR from analog- or 1,25D3-treated hFOB cells accumulated in the chromatin. In contrast, in Caco-2 cells, VDR was localized in both the cytoplasm and the chromatin, either in absence or presence of ligand. There was some increase in the amount of VDR associated with chromatin in 1,25D3-treated cells but not in chromatin from analog-treated cells. These results suggest that the ligand-bound VDR translocates from the cytoplasm into the nucleus in hFOB cells, but the translocation mechanism is probably defective in Caco-2 cells. We hypothesize that the VDR-analog complexes in Caco-2 cells are probably associated with a repressor that prevents their interaction with RXR, GRIP and DRIP. Translocation into the nucleus may be required for proper activation of the VDR-analog complexes, or for their release from repression.

SA462

Androgen Receptor Isoforms Differentially Regulate Primary Bone and Skin Cell Metabolism. U. M. Liegibel*, I. Boerscoek*, U. Sommer*, P. Nawroth*, C. Kasperk. Dept. of Medicine, Ruprecht-Karls-University, Heidelberg, Germany.

Steroid hormones, including androgens play a crucial role in the regulation of bone metabolism and in the maintenance of normal bone structure. Two isoforms of the androgen receptor (AR-B and AR-A) are expressed in a number of human tissues including bone. AR-A is the N-terminal truncated form of AR-B, produced by translation initiation at the first internal methionine residue (Met-188) of the same gene transcript. To study the distribution of the AR-isoforms in human bone, we examined their expression in primary human osteoblastic cells (HOC). Western blot analysis revealed that AR-A and AR-B are expressed in male as well as female individuals, independently of the donor's age. Transfection studies with HOC and with primary genital skin fibroblasts (GS-540) derived from a patient with testicular feminization (AR$^-$) were aimed to characterize the physiological role of the AR-isoforms in mesenchymal tissues. AR-B induced mitogenic effects in the presence of DHT (100 nM) in GS-540 and HOC, whereas AR-A as well as the combined transfection of AR-B and AR-A did not have such an effect. Differentiated mesenchymal cell function, as measured by collagen type I synthesis, was not significantly affected by either form, although in GS-540, there was a reproducible tendency of AR-A to enhance collagen type I expression. Using electromobility shift assays, we further examined the binding capacity of AR-B to the ARE consensus sequence in the presence of a peptide coding for the N-terminal sequence (AR-N) of AR-B, missing in AR-A. Binding of AR-B to radiolabeled ARE was reduced in the presence of AR-N, presumably due to the competition of the transactivation domains for co-activating proteins required for stable DNA/protein complex formation. These results are in accordance with the lacking capacity of AR-A to stimulate mesenchymal cell proliferation. In summary, this study shows that (1) the activated AR-B isoform exerts mitogenic effects on bone and skin cells and (2) that the mitogenic effect of AR-B is impaired by the presence of the AR-A isoform. In conclusion, the presence of the AR-A isoform limits the androgen-induced mitogenesis in androgen-responsive tissues.

SA463

See Friday Plenary number F463.

SA464

Identification of Estrogen-Regulated Genes of Potential Importance for the Regulation of Trabecular BMD. S. Movérare[1], M. K. Lindberg*[1], A. L. Eriksson*[1], S. Skrtic*[1], H. Gao*[2], K. Dahlman-Wright*[2], J. Å. Gustafsson*[2], C. Ohlsson[1]. [1]Div. Endocrinology, Dept. Internal Medicine, Gothenburg, Sweden, [2]Dept. Medical Nutrition and Dept. BioScience, Karolinska Institute, Novum, Huddinge, Sweden.

Estrogen is of importance for the regulation of trabecular BMD. The aim of the present study was to search for possible mechanisms of action of estrogen on bone in a non-hypothesized driven manner. Ovariectomized mice were treated with 17β-estradiol. Possible effects of estrogen on the expression of 125 different bone-related genes in humerus were analysed using the microarray technique. Estrogen regulated fifteen of these genes, namely two growth factor-related genes, eight cytokines and five bone matrix-related genes. Seven of the fifteen genes are known to be estrogen regulated, while the remaining eight genes are novel estrogen-regulated genes. Six genes, including IL-1ra, IL-1RII, TGFβ, G-CSFR, LIFR and sIL-4R, were selected as probable candidate genes for the trabecular bone sparing effect of estrogen, as the mRNA levels of these genes were highly correlated ($r>0.8$) to the trabecular BMD. The regulation of most of these six genes was predominantly ERα mediated (4/6) while some genes (2/6) were regulated both via ERα

and ERβ. In conclusion, by using the microarray technique, we have identified three previously known and three novel estrogen-regulated genes of potential importance for the trabecular bone-sparing effect of estrogen.

SA465

See Friday Plenary number F465.

SA466

Melatonin Increases Estradiol-Induced Bone Changes in Ovariectomized Rats. M. Ladizesky*[1], V. Boggio*[2], L. Albornoz*[2], P. Castrillón*[2], C. Mautalen[1], D. Cardinali*[2]. [1]Sección Osteopatías Médicas, Hospital de Clínicas, Universidad de Buenos Aires, Buenos Aires, Argentina, [2]Departamento de Fisiología, Facultad de Medicina, Universidad de Buenos Aires, Buenos Aires, Argentina.

Estrogen deficiency induces a high turnover on bone remodeling in wich the accelerated bone resorption and formation simultaneously occur with predominance of the former. Recent data suggest that melatonin has an effect on bone remodeling. Since appropiate circulating estradiol levels could be needed for melatonin effects on bone, the present study was underkaten to assess whether estradiol replacement in Ovx rats prolongs the response to melatonin after Ovx. To asses the effect of melatonin on bone metabolism Ovx rats receiving or not estradiol therapy, melatonin was administered in the drinking water (25 ug/ml water) and estradiol (10 ug/kg BW) or vehicle was given s.c. 5 days/ week for up to 60 days after surgery. Dpyr and circulanting levels of serum bone alkaline phosphatase (BAP), as well as CaS and PS, were measurded every 15 days. BA, BMC, BMD and Total Body Fat (expressed as 100g/BW) were measured by DEXA at the end of the experiment. Main factor analysis in a factorial ANOVA indicated that BW and total body fat augmented after Ovx ($p<0.001$), and decreased after melatonin ($p<0.02$) or estradiol treatment ($p<0.001$). Ovx augmented ($p<0.03$) and melatonin ($p<0.02$) or estradiol lowered ($p<0.0001$) Dpyr excretion. This effect of melatonin and estradiol was seen mainly in Ovx rats ($p< 0.001$). The efficacy of estradiol to counteract Ovx–induced bone resorption was significantly increased by melatonin. Melatonin or estradiol lowered BAP in Ovx ($p<0.02$). SP levels decreases after melatonin administration ($p<0.001$) and augmented after estradiol injection ($p<0.001$), overall, melatonin impaired the increase of SP caused by estradiol . Ovx decreased ($p<0.001$), and estradiol increased SCa levels ($p<0.04$), while melatonin augmented SCa in sham rats only ($p<0.005$). On day 60 after surgery, BMD and BMC decreased after Ovx and augmented after estradiol injection. Melatonin augmented BA of spine ($p< 0.01$) and BMC of whole skeleton and tibia ($p<0.04$). The highest values observed were those of rats treated simultaneously with estradiol and melatonin ($p<0.01$). The presents results indicate that: 1- Melatonin treatmentent restored bone remodeling after Ovx 2- The effect of melatonin needed adequate concentrations of estradiol, 3- Melatonin augmented estradiol effects of bone in Ovx rats. 4- A counterregulation by melatonin of the increase in body fat caused by Ovx was uncovered. The melatonin doses employed were pharmacological in terms of circulating levels, but not necessarily for other fluids or tissues.

SA467

Estrogen Inhibits Class II Transactivator and MHCII Gene Expression in Murine Macrophages: A Mechanism by which Estrogen Suppresses Proliferation of TNF Producing T Cells. O. L. Sierra, S. Cenci, Y. Gao, G. Toraldo*, M. N. Weitzmann, R. Pacifici. Division of Bone & Mineral Diseases, Washington University School Medicine & Barnes-Jewish Hospital, St Louis, MO, USA.

One mechanism by which ovariectomy (ovx) increases the number of TNF producing T cells is by enhancing T cell proliferation. The resulting increased production of TNF is crucial for bone loss induced by estrogen (E2) deficiency. However, ovx induced T cell proliferation is not inhibited by in vitro E2 treatment, thus suggesting that E2 regulates T cells via an indirect mechanism. One such mechanism could be downregulation of activation-induced proliferation via repression of the activity of antigen presenting cells (APC). We found that ovx upregulates macrophage APC activity by decreasing their surface expression of MHC Class II (MHCII), which in turn, was due to an increase in the levels of CIITA, the master gene inducer of MHCII. To determine if E2 represses CIITA gene expression by a direct targeting of macrophages, peritoneal macrophages harvested from sham and ovx mice were stimulated with 0.1-10 U/mL of IFNγ, for 24 hrs. MHCII and CIITA gene expression was then examined by RT-PCR and Northern blot analysis. The expression of both MHCII and CIITA mRNAs was 50% higher in unstimulated macrophages from ovx mice than in those from sham controls. Stimulation with IFNγ increased both MHCII and CIITA mRNA levels in a dose dependent manner, in both sham and ovx macrophages. However, at all doses of IFNγ tested, the increase in MHCII and CIITA mRNA was 2 fold higher in ovx macrophages than in sham cells. These data demonstrate that ovx upregulates the responsiveness of macrophages to IFNγ. To further investigate how E2 regulates CIITA and MHCII expression, RAW 264.7 cells, an ER+ murine monocytic line which expresses CIITA in response to IFNγ, were treated with E2 (10^{-8}M) for 24 hours. We found that E2 decreases the expression of both CIITA and MHCII mRNA by ~50%, further demonstrating a direct E2 targeting of these cells. The CIITA gene has 4 promoter regions which confer cell specific gene expression. Since IFNγ induced expression of CIITA in macrophages is mediated by promoter IV, RAW 264.7 cells were transiently transfected with a full length murine CIITA promoter IV-Luc reporter construct. IFNγ induced a 10 fold increase in CIITA-IV-Luc activity which was reduced by E2 by 50%. In conclusion, our data demonstrate that E2 inhibits CIITA transcription in macrophages via a direct mechanism involving promoter IV. Decreased CIITA gene expression results in blunted MHCII expression, decreased macrophage APC activity and decreased activation induced proliferation of TNF producing T cells.

SA468

See Friday Plenary number F468.

SA469

Identification of a Novel Bone Formation Marker (Periosteal Alkaline Phosphatase) to Detect Bone Activity of Androgens in Short-Term Gonadectomized Rats. W. Y. Chang[1], K. Burnett*[1], D. S. Ramirez*[1], J. N. Miner*[2], F. López*[1], H. Viveros*[1]. [1]Pharmacology, Ligand Pharmaceuticals, Inc., San Diego, CA, USA, [2]Molecular and Cell Biology, Ligand Pharmaceuticals, Inc., San Diego, CA, USA.

Fluoxymesterone (fluoxy) and LGD2226, a first generation androgen receptor modulator, prevented orchidectomy (ORDX)-induced reduction in periosteal bone formation rate in Sprague-Dawley (SD) rat tibiae after daily oral administration for 4 months (The Endocrine Society's 83rd Annual Meeting, 2001:abstract P1-497). The goal of this study was to determine whether the effects of an androgen agonist, fluoxy, could be assessed in bone within a shorter treatment duration utilizing two conventional and one new bone biomarker. Two-months-old male SD rats were orchidectomized or sham-operated, and daily administration with fluoxy (1, 10, and 100 mg/kg/day, *po* or *sc*) or vehicle was initiated and continued for the next 2 weeks. Oral and subcutaneous fluoxy stimulated growth of androgen-responsive organs (ventral prostate, seminal vesicle, levator ani, and preputial gland), while it reduced serum luteinizing hormone levels. At doses that were anabolic for the androgen-sensitive organs, fluoxy suppressed serum osteocalcin (OC) and maintained bone-specific alkaline phosphatase (BSALP) to levels comparable to intact rats. To obtain a direct measurement of anabolic effects in bone, periosteal alkaline phosphatase (PAP) was measured by assaying enzyme activity after collagenase digestion of the tibial periosteum. Fluoxy prevented orchidectomy-induced suppression of PAP (osteoblast activity) in a dose-dependent fashion after only 2 weeks of treatment, while our previous histomorphometric results required 4 months of daily oral administration to document this effect. Fluoxy at 100 mg/kg/day (*po*) was able to maintain PAP at levels comparable to intact rats. To determine whether PAP detected fluoxy effects in females, 2 month-old female SD rats were ovariectomized or sham-operated, and daily administration with fluoxy (1, 3, 10, 30, and 100 mg/kg/day, *sc*) or vehicle was initiated and continued for the next 4 weeks. Fluoxy stimulated clitoral gland growth and suppressed serum luteinizing hormone levels. Ovariectomy raised serum OC and BSALP levels as well as PAP. Fluoxy maintained serum OC at levels similar to intact female rats and did not stimulate serum BSALP or PAP beyond the levels induced by ovariectomy. These results indicate that androgen receptor agonists have pronounced effects on rat bone activity and suggest that PAP may be a useful and direct marker of periosteal bone formation that is valuable in identifying activity of compounds in short-term assays.

Disclosures: ***W.Y. Chang****, Ligand Pharmaceuticals, Inc. 1, 3.*

SA470

Impact of Estrogen and Androgen Receptors on Skeletal Metabolism. T. F. Tözüm*[1], M. Oppenlander*[1], C. Chen*[1], D. M. Robins*[2], L. K. McCauley[1]. [1]Dept. Perio/Prev/Geriatrics, University of Michigan, Ann Arbor, MI, USA, [2]Dept. Human Genetics, University of Michigan, Ann Arbor, MI, USA.

The interaction between estrogens and androgens, with their protective effects in bone, and parathyroid hormone (PTH), with its anabolic and catabolic actions, is complex and largely unclear. The purpose of this study was to; 1) characterize skeletal phenotypes of mice deficient in estrogen receptor alpha (ERα), androgen receptor (AR, mutant *tfm*) or both, and 2) determine if ERα and AR alter osteoblast differentiation and PTH response *in vitro*. Gross skeletal analysis, microradiography, DEXA, histomorphometry, cAMP response to PTH, and osteoblast differentiation assays were performed for mice of all 6 possible homozygous genotypes (n=10-17). Loss of ERα resulted in increased long bone lengths in females, but reduced length in males, suggesting loss of ERα reversed sex steroid dependent skeletal dimorphism. The *tfm* mice had the longest bones and similar to males, lengths were reduced with loss of ERα. Loss of AR and/or ERα resulted in a reduction in bone mineral density (BMD) compared to male WT mice suggesting *tfm* mice follow the female gender for BMD. Loss of AR and/or ERα caused a reduction in cortical width of the tibia compared to male WT mice. Loss of ERα was associated with reduced trabecular bone in tibiae of female and *tfm* mice vs. male littermates, suggesting that *tfm* mice follow the female gender for trabecular bone. Primary calvarial osteoblasts of male WT mice were less responsive to PTH via cAMP levels than all other genotypes, indicating the female gender and/or loss of ERα or AR results in increased sensitivity to PTH. There was no difference in mineralization of cells from any genotypes, suggesting neither ERα nor AR intrinsically alter osteoblast differentiation. In conclusion, *tfm* mice follow the male pattern of appendicular skeletal development, but imitate females in bone density and trabecular bone. Further, loss of ERα and/or AR results in increased osteoblast sensitivity to PTH and may explain actions of PTH noted in hypogonadal humans. Finally, these data underscore that sex steroids impact bone development, composition and metabolism differently.

SA471

WITHDRAWN.

SA472

Decreased Renal Expression of Calbindin-D28k in Aromatase Deficient Mice. O. K. Oz[1], K. Howard*[1], A. Thomas*[1], J. E. Zerwekh[2], C. Y. C. Pak[2]. [1]Radiology, UT Southwestern Medical Center, Dallas, TX, USA, [2]Internal Medicine, UT Southwestern Medical Center, Dallas, TX, USA.

Renal calcium uptake is important for maintenance of normal calcium homeostasis. Most studies of calcium transport in the kidney focus on the roles of the hormones vitamin D3 and parathyroid hormone. However, estrogens are known to regulate calcium transport in tissues, such as the intestines and estrogen deficient states are often associated with abnormal urine calcium levels. The mechanisms are incompletely understood. Aromatase catalyzes the biosynthesis of estrogens from androgen precursors. The protein calbindin-D28k is known to be involved in transcellular calcium transport in the distal convoluted tubule. To determine if estrogen deficiency might cause changes in expression of calbindin-D28k we prepared RNA and protein from kidneys of 10-12 week old wildtype and ArKO female mice. Western blotting demonstrated decreased protein levels in extracts from ArKO kidneys. Relative quantitative RT-PCR demonstrated decreased levels of calbindin-D28k mRNA. These data show suggest that the ArKO mouse maybe useful for understanding the role of estrogen in regulating renal handling of calcium. They suggest estrogen maybe involved in the regulation of transcellular calcium absorption in the kidney via effects on the calbindin-D28k protein.

SA473

See Friday Plenary number F473.

SA474

Anabolic Effects of Testosterone on Bone Require the Presence of a Functional Androgen Receptor in Male Mice. L. Vandenput*[1], S. Boonen[2], R. G. Erben[3], E. Van Herck*[1], J. V. Swinnen*[1], R. Bouillon[1], D. Vanderschueren[1]. [1]Laboratory for Experimental Medicine and Endocrinology, Katholieke Universiteit Leuven, Leuven, Belgium, [2]Leuven University Centre for Metabolic Bone Diseases, Katholieke Universiteit Leuven, Leuven, Belgium, [3]Institute of Animal Physiology, University of Munich, Munich, Germany.

Androgens and estrogens may exert nongenomic effects via activation of both the androgen receptor (AR) and estrogen receptors *in vitro*. In order to investigate the relevance of nonAR-mediated androgen and estrogen action in male skeletal metabolism, we have studied testicular feminized male mice (Tfm), which lack a functional AR due to a single base deletion in the N-terminal region of the AR gene. Eight-week-old orchidectomized (ORX) Tfm mice were treated with either testosterone (T, 167 µg/day), 17beta-estradiol (E2, 25 µg/day) or placebo pellets during 4 weeks. E2 stimulated intramedullary bone formation, resulting in a dramatic increase in trabecular bone density (more than 10-fold) and cortical thickness (+ 20%), compared to placebo-treated ORX mice (as determined by peripheral quantitative computed tomography). Moreover, the effects of E2 were not limited to the appendicular skeleton, but were also observed in the axial skeleton, as evidenced by a 152% increase in distal lumbar vertebrae density (calcium content/volume). This anabolic effect of E2 was associated with a significant increase in both endocortical mineral apposition rate (+ 48%) and bone formation rate (+ 69%), as measured by dynamic histomorphometry on femoral cross-sections. In accordance, serum osteocalcin was also significantly higher in E2-treated compared to placebo-treated ORX mice. Furthermore, growth plate width significantly decreased following E2-treatment of ORX mice whereas femur length and periosteal bone formation were not affected. In contrast, treatment of ORX mice with T affected neither trabecular bone density, nor endocortical and periosteal bone formation, compared to placebo-treated ORX mice. However, growth plate width significantly increased following T-treatment, but femoral length remained unchanged. In conclusion, E2 respectively has anabolic effects on trabecular and endocortical surfaces, no effect on periosteal bone, and an inhibitory effect on the growth plate in male mice. In contrast, the aromatizable androgen T did stimulate neither endocortical nor periosteal bone formation in ORX androgen-resistant male mice. These data indicate that the anabolic bone effects of T in male mice are dependent on the presence of a functional AR.

SA475

Sex Steroid Formation in the Tibial Growth Plate and Metaphyseal Bone of the Rat during Development. B. C. J. van der Eerden[1], J. van de Ven*[2], C. W. G. Lowik[3], J. M. Wit*[1], M. Karperien[3]. [1]Pediatrics, Leiden University Medical Center, Leiden, Netherlands, [2]Laboratory of Endocrinology, University Hospital Utrecht, Utrecht, Netherlands, [3]Endocrinology & Metabolic Diseases, Leiden University Medical Center, Leiden, Netherlands.

Estrogens and androgens can have direct effects on bone but it remains unclear what the source is of these sex steroids. We, therefore, surveyed the presence of several key-enzymes involved in androgen and estrogen biosynthesis in the tibial growth plate and metaphyseal bone of growing female and male rats using *in situ* hybridization. We studied the expression of aromatase, type I and II 17β-hydroxysteroid dehydrogenase (type I and II 17β-HSD), steroid sulphatase (STS) and 5α-reductase in the proximal tibia of 1-, 4-, 7-, 16- and 40-week-old female and male rats. In the growth plate, two age-related mRNA expression patterns were distinguished. Aromatase and type I and II 17β-HSD mRNA expression was low or undetectable at 1 week of age. The expression gradually increased at 4 weeks and reached the highest levels during sexual maturation around 7 weeks of age. Thereafter the expression declined but the mRNAs were still detectable at 16 and 40 weeks of age. In contrast, STS and 5α-reductase were expressed at a relatively constant level in all age groups studied. All enzyme mRNAs were detected in late proliferating and early hypertrophic chondrocytes, which we have previously shown to express estrogen and androgen receptors. These data were supported by measuring enzyme activities in chondrocytes collected from tibial growth plates. Aromatase and type I 17β-HSD bioactivity was low or undetectable, respectively, at 1 week of age and was strongly increased during sexual maturation. STS bioactivity did not change with age. There were no apparent differences in expression and bioactivity of the enzymes studied between the sexes. In the tibial metaphysis, STS mRNA was detected in osteoblasts, osteoclasts and some osteocytes in sexually immature 4-week-old female and male rats during development. In contrast, aromatase, type I and II 17β-HSD and 5α-reductase were first detected at 7 weeks of age and thereafter. Like STS, the mRNA expression of these enzymes was confined to osteoblasts, osteoclasts and occasionally in osteocytes. In conclusion, our findings suggest that sex steroid synthesis occurs in the rat growth plate and the underlying metaphyseal bone. The age-related expression of key enzymes involved in sex steroid metabolism suggests that in contrast to sexually immature animals, locally metabolized sex steroids may play a role in longitudinal growth and bone mass accrual during sexual maturation of the rat.

SA476

In Vivo Adverse Effects of Chronic Glucocorticoid and Mineralocorticoid Administration in Rats. Q. Zeng*, J. Hoover*, R. L. Cain*, A. Harvey*, C. Suen*, H. U. Bryant, M. Sato, A. L. Schmidt*, M. D. Adrian*, Y. L. Ma. Gene Regulation, Bone and Inflammation Division, Eli Lilly Company, Indianapolis, IN, USA.

Glucocorticoids are widely used clinical agents due to their robust effects on anti-inflammatory and immunosuppresion. Unfortunately, a number of serious side effects are seen on the long-term glucocorticoid use patients, which limits the therapeutic utility of glucocorticoids. To examine adverse effects, we treated 11-12 months old, retired breeder male Lewis rats with prednisone (Pred) 0.1, 0.5mg/kg/d *p.o*, dexamethasone (Dex) 0.015, 0.075mg/kg/d *p.o*, cortisone (Cort) 0.5, 2.5mg/kg/d *p.o* or desoxycorticosterone (Doca) 0.5, 2.5mg/kg/mo *im* for 6 weeks. These treatment doses are approximately equal to the typically used clinical doses. When compared to vehicle treatments, there was a dose-dependent decrease in the body weight (13-31%), gastrocnemius muscle (12-37%), whole body lean mass (13-23%), whole body fat mass (17-43%) in Dex-treated rats. No body weight change was observed in other treatment groups. Cort and Doca decreased the whole body lean mass but did not significantly change the fat mass. Serum electrolytes (Na, K, Cl, Ca), BUN, creatine (Creat), creatine phosphokinase (CK) and total protein (TP) were elevated in all the treatment groups at days 3 and 7. By end of the 6 weeks study, with the most of these parameters returned to the vehicle control levels in Corti and Pred groups, some parameters were lower (BUN, Cl, Creat, globulin) or higher (TP, A/G) in Dex group, while CK was lower in Doca group. Serum K was decreased in all the treatment groups after 6 weeks treatment. Dex treatment also increased serum cholesterol (39-91%) and glucose (42-116%), however, glucose was returned to the control levels at end of the study. Although a significant reduction in prostate wet weight was seen only in Dex and Doca groups, serum testosterone was significantly decreased by all the treatments except for Cort. No treatment significantly altered the testicular wet weight. In Dex group, but not other treatments, dose-dependent decreases of serum osteocalcin, whole body BMC and BMD were observed. These data suggest that both mineralocorticoid and glucocorticoid impair the regulation of serum electrolytes and sexual hormone production. Glucocorticoids also have impact on protein, serum lipid, glucose and muscularskeletal metabolism.

*Disclosures: **Y.L. Ma**, Eli Lilly Company 3.*

SA477

Failure to Reduce Glucocorticoid Receptor Expression in Bone Following Burn Injury: Possible Mechanism for Steroid-Induced Bone Loss. G. L. Klein[1], S. R. Beavan[2], J. E. Compston[2], W. G. Williams*[1], D. N. Herndon*[1], D. J. Sherrard[3]. [1]University of Texas Medical Branch and Shriners Burns Hospital, Galveston, TX, USA, [2]Medicine, University of Cambridge, Cambridge, United Kingdom, [3]VAMC and University of Washington School of Medicine, Seattle, WA, USA.

Severely burned children develop abnormalities in bone and calcium metabolism, including reduced bone formation and resorption, and reduced growth velocity. Moreover, they exhibit a systemic inflammatory response reflected by elevated circulating cytokines such as interleukin (IL)-1 b and IL-6.Because all but the cytokine elevation can be side-effects of glucocorticoid exposure, the aim of the study was to detect an effect of glucocorticoids on bone in burn patients by determining if there is down-regulation of glucocorticoid receptor (GR) in bone. We studied 7 patients with burn injury greater than 40% total body surface area, ages 7-14 yr and 4 controls, ages 15-20 yr. We obtained a 24-hr urine for free cortisol and iliac crest bone specimens for histomorphometry and for mRNA analysis 3.7 +/- 1.9 (SD)wks post-burn, range 2-8. Bone tissue was analyzed by reverse transcription polymerase chain reaction (RT-PCR)for mRNA expression of GR alpha (the true receptor), GR beta (a possible inhibitor of GR alpha-induced nuclear transcription), osteocalcin, alkaline phosphatase, mineralocorticoid receptor, and IL-1b, all normalized to glyceraldehyde-3 phosphate dehydrogenase (GAPDH).Histomorphometry revealed markedly reduced bone formation in all 7 burn patients, 1.3 +/- 3.4 mcm2/mm2/d, range 0-9, normal 108-576, while urine free cortisol ranged from 4-12 times normal, 371 +/- 147 mcg/d, range 206-629, upper limit of normal 50 mcg/d. ANOVA failed to reveal any significant differences in mRNA expression between burn patients and controls, although there was an inverse correlation between urine free cortisol and GR alpha mRNA in the burn patients, r=-0.74, p< 0.05 and an inverse correlation between urine free cortisol and type I collagen mRNA, r= -0.64.These data indicate that despite marked reduction in bone formation and a marked increase in endogenous glucocorticoid production, there was no proportionate reduction in GR alpha. While it is possible that the small sample size could not detect a statistically significant change from normal, the modest effect of large quantities of endoge-

nous glucocorticoids on GR alpha may leave bone vulnerable to further injury from corticosteroids.It is also possible that a greater down-regulation of GR alpha mRNA was prevented by the IL-1b that was detected in the bone tissue.

SA478

See Friday Plenary number F478.

SA479

Dexamethasone Decreases Bone Mineral Density and Bone Formation in Mice: A Model for Glucocorticoid-Induced Osteoporosis. P. Clément-Lacroix, D. Minet*, C. Belleville*, L. Lepescheux, R. Baron, M. Resche-Rigon. Proskelia, Romainville, France.

The prolonged administration of glucocorticoids (GC) to patients induces significant bone loss and increases incidence of both vertebral and non vertebral fractures. Glucocorticoid-induced osteoporosis (GIOP) in humans is associated with a profound inhibition of bone formation resulting mainly from inhibition of osteoblastogenesis and from increase in osteoblasts and osteocytes apoptosis. Despite several attempts to establish animal models of GIOP, only ewes have been reported to recapitulate the mechanisms associated with GC-induced bone loss in humans. To determine whether a model of GC-induced osteoporosis could be established in mice, 12 week-old C57bl6/J male mice were treated with dexamethasone (DEX) 1 and 5 mg/kg/d subcutaneously injected 5 days/week for 2 months. Bone mineral density (BMD) at both trabecular and cortical sites was measured using Stratec SA+. Tomodensitometry using SCANCO microCT 20 was used for a two dimensional reconstruction of the right tibia and lumbar vertebra at the end of treatment. In contrast to rats, mice body weight was not affected by glucocorticoid administration. DEX 1 and 5 mg/kg induced significant reduction (-67%) in serum osteocalcin, a marker of terminal osteoblastic differentiation, whereas urinary deoxypyridinolin were only transiently decreased at day15. Despite trends towards decreased indices of bone formation (osteoblasts surface, osteoid volume), trabecular BMD or histomorphometric bone volume remained unchanged in DEX-treated animals. A second experiment was then performed, where 4, 8, and 12 week-old C57bl6/J males were implanted with slow release pellet delivering 5mg/kg/d Dexamethasone for 4 weeks. Trabecular BMD decreased by 27%, 17% and 16% at metaphyseal tibia respectively, in 4, 8, and 12 week-old males after continuous administration of dexamethasone. MicroCT analysis revealed that cortical bone mineral density was also significantly reduced in DEX-treated animals. Bone loss was further confirmed by decreased trabecular bone volume (-37% in 4 week-old mice). As previously observed, osteocalcin but not D-Pyr, were significantly reduced at the end of treatment (-68%, -64% and -84%) respectively, in 4, 8, and 12 week-old males. In addition delayed longitudinal growth was observed in 4 week-old mice. Our data suggest that both young and adult male mice may be valid models for GC-induced bone loss. *Bona fide* reduction in bone formation was consistently observed, leading, at least with slow release of glucocorticoids, in decreased bone mass. The impact of GC treatment on bone resorption needs however further clarification.

SA480

A Glucocorticoid-Induced Leucine Zipper Protein GILZ Inhibits Adipocyte Differentiation. X. Shi, W. Shi*, B. Song*, Q. Li*, M. Wan, X. Cao. Pathology, University of Alabama at Birmingham, Birmingham, AL, USA.

In a previous study we showed that glucocorticoid stimulates human bone marrow stromal stem cells to differentiate into adipocytes, and that this action is mediated by the binding of C/EBPδ to PPARγ2 gene promoter and subsequent up-regulation of its gene transcription. Here we report that a glucocorticoid-induced leucine zipper protein (GILZ) inhibits adipocyte differentiation. Unlike C/EBPδ that binds to PPARγ2 promoter and activates its gene transcription in electrophoretic mobility shift assay (EMSA) and transient transfection assay, respectively, GILZ binds to the promoter of PPARγ2, but it represses PPARγ2 gene transcription. Most importantly, the adipocyte differentiation was blocked in GILZ-expressing stable cell lines of C3H10T1/2 mesenchymal and 3T3-L1 preadipocytes. Northern and Western analyses showed that the levels of both GILZ mRNA and protein were strongly and rapidly induced by glucocorticoid dexamethasone. Transient transfection analyses demonstrated that GILZ significantly represses the luciferase-reporter activity driven by the PPARγ2 promoter. In addition, we have mapped the binding site of GILZ to a 40-base pair PPARγ2 promoter fragment that contains a tandem repeat of C/EBP binding sites. These data indicate that GILZ is directly involved in the regulation of PPARγ2 gene expression and glucocorticoid-induced adipocyte differentiation.

SA481

Cytokine Production by T Cells from Vitamin D Receptor Knockout Mice. P. Pietschmann[1], E. Kallay*[1], P. Hahn*[2], E. Bajna*[1], M. Willheim*[1], K. Mazzucco*[3], S. Kato*[4], H. S. Cross*[1]. [1]Department of Pathophysiology, University of Vienna, Vienna, Austria, [2]Ludwig Boltzmann Institute of Aging Research, Vienna, Austria, [3]Center for Laboratory Animal Care, University of Vienna, Vienna, Austria, [4]Institute of Molecular and Cellular Biosciences, University of Tokyo, Tokyo, Japan.

1,25(OH)2 vitamin D has a major role in the regulation of calcium homeostasis; in addition to the classical effects a multitude of other action sites of the steroid hormone have been discovered. Cells of the immune system are among the nonclassical targets of 1,25(OH)2 vitamin D. Gene targeted knockout animals provide an interesting possibility to investigate complex regulatory systems that cannot be studied in isolated in vitro experiments. We therefore studied cytokine production by T cells in a vitamin D receptor (VDR) knockout mouse model. In knockout mice and wild type animals cytokine production by CD4+ and CD8+ cells was determined by four color flow cytometry. In the knockout animals, the percentage of CD8+ cells in blood was significantly increased when compared to wild type mice. Moreover, in the blood of the knockouts the frequency of CD8+ cells positive for interferon-gamma was significantly higher than in the wild type animals. Also in the thymus the percentage of CD8+ cells positive for interferon-gamma was significantly increased in the knockout animals. In bone marrow, CD4+ cells positive for interleukin-10 were less abundant in the knockout than in wild type animals. In conclusion, lack of the VDR in mice is associated with significant alterations of lymphocyte subsets, in particular CD8+ cells.

SA482

See Friday Plenary number F482.

SA483

Active Vitamin D Reduces c-Fos and Fra-1 Proteins in Osteoclast Precursors, and Inhibits RANKL-induced Osteoclastogenesis *in vivo* and *in vitro*. H. Takasu[1], M. Okazaki*[1], A. Sugita*[1], N. Kubota[1], E. Ogata[2], K. Ikeda[3], Y. Uchiyama[1]. [1]Fuji Gotemba Res. Lab., Chugai Pharmaceutical Co.,Ltd., Shizuoka, Japan, [2]Cancer Inst. Hosp., Japanese Foundation for Cancer Res., Tokyo, Japan, [3]Dept. of Geriatric Res., Natl. Inst. for Longevity Sci., Aichi, Japan.

We have previously demonstrated that active vitamin D inhibits bone resorption and bone loss in estrogen deficient rats and mice (JBMR 2000, Bone 2002, JBMR 2002). In the present study, we examined the effect of active D in OPG KO mice, which exhibit severe osteoporosis and excessive bone resorption due to super-stimulation of RANKL/RANK signaling. Oral administration of $1\alpha,25(OH)_2D_3$ (0.1μg/kg) to OPG KO mice for 2 weeks reduced urinary excretion of deoxypyridinoline, and treatment for 6 weeks caused an increase in bone mineral density at the femur, suggesting that $1\alpha,25(OH)_2D_3$ inhibits bone resorption by interfering with the osteoclastogenic signaling downstream of RANK. Based on these results, the mechanism of action of active D in osteoclast precursors was further examined using bone marrow macrophage (BMM) prepared from *ddy* mice. $1\alpha,25(OH)_2D_3$ inhibited the differentiation of BMM into osteoclasts in the presence of M-CSF and sRANKL markedly and dose-dependently, and this effect was not observed in BMM from VDR KO mice, pointing to a VDR-mediated action. After surveying a number of active D analogs in this osteoclastogenesis assay, we observed that the osteoclastogenesis-inhibitory activity correlates well with their anti-AP-1 activity (R^2=0.78), but not with VDRE-dependent transcription activation function (R^2=0.08), suggesting the involvement of anti-AP-1 activity in the suppression of osteoclastogenesis. Osteoclastogenic signals downstream of RANK involve activation of JNK, p38MAPK, ERK1/2 and IKK. Phosphorylation and activation of these kinases by RANKL was, however, found not to be inhibited by $1\alpha,25(OH)_2D_3$ even at as high as 10^{-7}M. Western blot analyses revealed that the induction of c-Fos and Fra-1 proteins by sRANKL in BMM was completely inhibited by 10^{-7}M $1\alpha,25(OH)_2D_3$. In conclusion, our data suggest that active vitamin D suppresses RANKL-induced expression of c-Fos and Fra-1 proteins, thereby inhibiting osteoclastogenesis. Thus, anti-AP-1 activity may provide a good screening system for developing and selecting a new type of VDR-based drugs for osteoporosis.

SA484

See Friday Plenary number F484.

SA485

Serum sRANKL Levels Are Inversely Correlated with Serum 25OH-Vitamin D. B. P. Lukert, L. Graves. Medicine, University of Kansas School of Medicine, Kansas City, KS, USA.

The purpose of the study was to test the hypothesis that the OPG/RANKL system is influenced by the nutritional status of vitamin D and that the production of RANKL is increased when the levels of 25OHD are low. Vitamin D deficiency plays a role in the etiology of osteoporosis in postmenopausal women. The sequence of events has been presumed to be: vitamin D deficiency causes poor absorption of calcium, which leads to secondary hyperparathyroidism, which in turn induces bone resorption. The OPG/RANKL system plays a major role in the control of osteoclastic bone resorption and may mediate bone loss in vitamin D deficiency. Twenty-six postmenopausal women presenting to the osteoporosis clinic at our institution for evaluation were studied. The patients were not taking hormone replacement, SERMs, bisphosphonates, calcitonin or steroids. They had normal renal and liver function. At their inititial visit blood was drawn for measuring 25OHD, creatinine and N-telopeptide of type I collagen (NTX, a marker of bone resorption). These samples were preserved at -40 degrees centigrade and subsequently used for measuring sRANKL and osteoprotegerin (OPG) using enzyme immunoassay test kits supplied by Biomedica. The correlations between 25OHD, sRANKL, OPG, OPG/sRANKL ratio, and NTX were examined using Pearson's correlation matrix. Correlations were as follows:
25OHD vs sRANKL r= -0.429 p=.032
25OHD vs NTX r= -0.499 p=.041
sRANKL vs NTX r= 0.425 p=.078
25OHD vs OPG r= -.147 p=.483
Serum sRANKL and NTX levels correlate negatively with serum 25OHD; that is, the lower the 25OHD, the higher sRANKL and NTX. This suggests that bone loss in patients with vitamin D insufficiency is due in part to an imbalance of the OPG/RANKL system which favors bone resorption.

Disclosures: ***B.P. Lukert****, Lilly 2, 8; Merck 2, 8; Proctor and Gamble 8.*

SA486

Induction of 25-Hydroxyvitamin D-1alpha-Hydroxylase mRNA by Phosphate Depletion. Y. Taketani[1], M. Nomoto*[1], H. Yamamoto[1], K. Morita[1], M. Isshiki*[2], S. Kato[3], E. Takeda[1]. [1]Clinical Nutrition, University of Tokushima School of Medicine, Tokushima, Japan, [2]Nephrology and Endocrinology, University of Tokyo Faculty of Medicine, Tokyo, Japan, [3]Institute of Molecular and Cellular Biosciences, University of Tokyo, Tokyo, Japan.

25-Hydroxyvitamin D-1alpha-hydroxylase (1alpha-hydroxylase) is a rate limiting enzyme for production of 1,25-dihydroxyvitamin D which is a potent active form of vitamin D. The expression level of 1alpha-hydroxylase is controlled by various hormones or environmental changes. PTH and calcitonin are well-known and well-characterized regulator for the enzyme. On the other hand, phosphate can regulate 1alpha-hydroxylase activity without PTH or calcitonin. However, it has not been clarified how phosphate can regulate the enzyme activity. We investigated the effect of phosphate depletion on the expression of 1alpha-hydroxylase with reference to signal transduction pathway using LLC-PK1 cells. LLC-PK1 cells were cultured with DMEM with 1 mM phosphate and 1% FBS, and then the medium was replaced to DMEM with 0 mM phosphate and 1%FBS. After 2 hours incubation, the cells were subjected to real-time RT-PCR analysis to estimate 1alpha-hydroxylase mRNA level. 1alpha-hydroxylase mRNA level increased after phosphate depletion by 1.3-fold. This effect was abolished in the presence of actinomycin D simultaneously. Furthermore increase of [Ca2+]i by tetraethylammonium chloride also increased 1alpha-hydroxylase mRNA expression. Thus, increase of [Ca2+]i may play an important role in the incuction of 1alpha-hydroxylase. We estimated the elevation of [Ca2+]i after phosphate depletion by modified GFP-based calcium indicator "cameleon" with confocal laser microscopy. After phosphate depletion from 1mM to 0.1 mM, [Ca2+]i was increased by 1.8-fold. This increment was also observed in the absence of extracellular calcium. Thus, phosphate depletion may be involved in the releasing of calcium from intracellular pool. Then we estimated inositol-triphosphate (IP3) production by phosphate depletion. Intracellular IP3 level was also increased by 1.7-fold after phosphate depletion from 1mM to 0.1 mM, by 2-fold from 1 mM to 0 mM. These results suggest that phosphate depletion would be involved in the phospho-inositide hydrolysis and increase of [Ca2+]i from intracellular pool via IP3 receptor to induce 1alpha-hydroxylase gene expression. Furthermore, this phenomenon was observed in opposum kidney cells (OK cells), but not in COS-7 cells. We speculate that phosphate sensor or receptor would exist in the proximal tubular cells and would be coupled with Gq trimeric G-protein.

SA487

Calcitriol Regulates the Expression of Genes Encoding all Three Vitamin D_3-Hydroxylases in the Human Fetal Intestine. C. Theodoropoulos*[1], D. Ménard*[2], C. Demers*[1], E. E. Delvin[1], M. Gascon-Barré[1]. [1]Université de Montréal, Montréal, PQ, Canada, [2]Université de Sherbrooke, Sherbrooke, PQ, Canada.

The human fetal jejunum has been shown to harbour the Vitamin D_3 (D_3) nuclear receptor (VDR_n) and to be responsive to calcitriol (CT) through modulation of proliferation and differentiation processes (Ménard *et al.*, Biol. Neonate, 1995). The aim of the study was to evaluate the presence as well as the effect of CT exposure on the expression levels of the three D_3-hydroxylase gene transcripts (25-hydroxylase, *CYP27A*; 24-hydroxylase, *CYP24*; 1α-hydroxylase, *CYP27B1*) in the human proximal intestine. Specimens from normal fetuses (n=5) ranging from 15 to 20 weeks gestation were obtained following elective termination of normal pregnancies. Intestinal explants were cultured for periods ranging from 6 to 48h with 10^{-7}M CT. All data were compared to those obtained without CT (time 0). Total RNA was extracted and cDNA synthesized by RT-PCR. The cDNA obtained was amplified by radioactive PCR, the signal intensity evaluated by densitometric analyses and expressed in relation to the levels of *GAPDH*. Data indicate that VDR_n and the three D_3-hydroxylases are expressed in all segments of the human fetal small intestine and in the colon. Basal expression levels of VDR_n, and both *CYP27A* and *CYP24* were found to be similar in the proximal, mid and distal jejunum as well an in the proximal and distal colon. In contrast, basal *CYP27B1* expression levels were found to be 65% higher in the colon than in the small intestine ($p<0.05$). *CYP27B1* was also found to be very sensitive to CT with a 31% decrease in its expression levels within 24h of CT exposure to reach a 68% decrease after 48h of incubation in the presence of the hormone ($p<0.05$). Furthermore, CT exposure contributed to a 4 fold increase in the expression of the *CYP24* gene transcript within 24h of exposure whereas ($p<0.05$) the levels of the *CYP27A* gene transcript were decreased by 9% within the first 24h and by 29% after 48h of incubation in the presence of CT ($p<0.03$). VDR_n expression levels were also found to be reduced by 66% 24h following incubation in the presence of CT ($p<0.0006$). These studies clearly show the presence of the D_3-1α and -25-hydroxylase gene transcripts in all segments of the human fetal intestine as well as their regulation by CT. Collectively, the data illustrate that at mid-gestation CT is fully active in the modulation of all D_3-hydroxylases in the human developing intestine.

SA488

See Friday Plenary number F488.

SA489

Post-Transcriptional Defect in the Expression of the Renal 25(OH)D-1alpha-Hydroxylase in Adult Rats. H. J. Armbrecht, M. A. Boltz*, T. L. Hodam*. Geriatric Center, St. Louis VA Medical Center, St. Louis, MO, USA.

The capacity of the kidney to convert 25(OH)D to $1,25(OH)_2D$ declines with age. In addition, the capacity of the kidney to respond to PTH in terms of converting 25(OH)D to $1,25(OH)_2D$ also declines with age. The purpose of this study was to determine whether these age-related changes were due to changes in 1α-hydroxylase mRNA levels. The mRNA levels of the cytochrome P450 component of the rat renal 1α-hydroxylase (CYP1α) were measured by ribonuclease protection assay. Renal $1,25(OH)_2D$ production was measured using isolated renal slices. Studies were performed in young (2 month) and adult (12 month) male F344 rats. In adult rats, serum $1,25(OH)_2D$ levels were decreased, serum PTH levels were increased, and renal production of $1,25(OH)_2D$ was decreased compared to young rats. However, there was no difference in renal CYP1α mRNA levels in the two groups. These basal measurements suggested a refractoriness to PTH in the adult rats. Therefore, the capacity of PTH to increase renal 1α-hydroxylase expression was compared in young and adult rats. Rats of each age group were parathyroidectomized (PTX) and then injected with PTH or vehicle at 48, 24, and 6 hours before sacrifice. PTH significantly increased serum $1,25(OH)_2D$ and renal $1,25(OH)_2D$ production in young rats but not in adult rats. However, PTH increased renal CYP1α mRNA levels to the same levels in both age groups. This was also demonstrated by in vitro studies. In vitro incubation of renal slices from PTXed animals with PTH for 8 hours significantly increased CYP1α mRNA to similar levels in both age groups. However, PTH increased renal $1,25(OH)_2D$ production only in slices from young animals. These studies suggest that the capacity of PTH to increase CYP1α mRNA levels is similar in both young and adult animals. However, the increase in mRNA levels in the adult does not result in an increase in renal $1,25(OH)_2D$ production. This may be due to either a decrease in translation of CYP1α mRNA into protein or else a decrease in functionality of the CYP1α protein in the adult kidney.

SA490

Molecules Mediating the Delivery of Substrate 25-Hydroxyvitamin D to the Mitochondrial 1-Hydroxylase. S. Wu, R. F. Chun, J. S. Adams. The Burns and Allen Research Institute and Division of Diabetes, Endocrinology and Metabolism, Cedars-Sinai Medical Center, UCLA School of Medicine, Los Angeles, CA, USA.

The synthesis of 1,25-dihydroxyvitamin D (1,25-D) from its substrate 25-hydroxyvitamin D (25-D) is mediated by a mitochondrial enzyme, 1-hydroxylase (CPY1*alpha*; 1-OHase). It is not known how 25-D is translocated from cytoplasm to the inner mitochondrial membrane where the 1-OHase is located. We have previously shown that 1-OHase-expressing human kidney cell line HKC-8 shows a significant 2-fold increase in 1,25-D production when stably transfected with the hsc70-related intracellular vitamin D binding protein-1 (IDBP-1; J Bone Miner Res 16:S556, 2001). We now demonstrate that this increase in 1,25-D synthesis occurs in the absence of any increase in expression of the CYP1*alpha* gene. This suggests that the IDBP-1-mediated 1,25-D production increase may be the result of facilitated transportation of substrate 25-D to the inner mitochondrial membrane 1-OHase. Because IDBP-1 bears no mitochondrial targeting sequence, we have hypothesized that IDBP-1 must co-operate with another molecular chaperone which is targeted to mitochondria. One such candidate is the mitochondrial hsp70, grp75. To test our hypothesis, a panel of hsc70 and grp75 cDNA constructs were transiently transfected into HKC-8 cells and the cells were assayed for their 1,25-D synthetic capacity; HKC-8 cells also constitutively express both IDBP-1 and grp75. The cDNAs used in this study were: 1] wild-type IDBP-1; 2] wild-type grp75; 3] a point mutant of IDBP-1 that abolishes its endogenous ATPase activity; 4] a chimeric IDBP-1 that contains the N-terminal mitochondrial targeting sequence from grp75; 5] a truncation mutant of grp75 in which the mitochondrial targeting signal has been deleted. Results showed that 1,25-D production was significantly increased ($p<0.03$) in cells transfected with wild-type IDBP-1, wild-type grp75 and chimeric IDBP-1 carrying the N-terminal mitochondrial targeting sequence with the latter construct showing the highest increase. The ATPase-mutant IDBP-1 and mitochondrial targeting sequence-deleted grp75 mutant showed a significant reduction ($p<0.01$) in 1,25-D production compared to wild-type IDBP-1 and grp75, respectively. Taken together these results suggest that an ATPase-competent, mitochondrially-targeted, hsp70-related protein is required for translocation of substrate 25-D to the kidney 1-OHase.

SA491

1α(OH)D_2 and 1α(OH)D_3 Suppress PTH Secretion by Bovine Parathyroid Cells: Potential Role of Metabolites. A. J. Brown[1], C. S. Ritter*[1], J. C. Knutson[2], S. A. Strugnell[2]. [1]Renal Division, Washington University, Saint Louis, MO, USA, [2]Bone Care International, Madison, WI, USA.

Active vitamin D compounds reduce PTH secretion through a vitamin D receptor (VDR)-dependent repression of PTH gene transcription. 1α(OH)D_3, a vitamin D prohormone with low VDR affinity, was reported to inhibit PTH secretion in cultured bovine parathyroid cells (Nielsen et al, J Am Soc Nephrol 8:578A, 1997), but it was not clear if 1α(OH)D_3 itself or an active metabolite was responsible. In the present study, we have determined the effects of 1α(OH)D_3 and 1α(OH)D_2 on PTH secretion, and examined the metabolism of [^{3}H]1α(OH)D_2 by bovine parathyroid cells. Steady-state rates of PTH secretion were measured after 72-hours of incubation with various concentration of the vitamin D compounds. Both 1α(OH)D_3 and 1α(OH)D_2 suppressed PTH secretion, but at equivalent concentrations were 20 and 40 times less active than 1,25$(OH)_2D_3$, respectively. Incubation of bovine parathyroid cells with [^{3}H]1α(OH)D_2 led to the formation of both 1,25$(OH)_2D_2$ and 1,24$(OH)_2D_2$ as evidenced by co-elution with authentic standards in both normal and reverse phase HPLC systems. The 1,24$(OH)_2D_2$ was detectable at 4 hours, increased to a maximum at 8 hours, and then began to decline. The fall in 1,24$(OH)_2D_2$ was likely due to both: 1) further metabolism by the inducible vitamin D-24-hydroxylase which we have previously characterized in parathyroid cells (Lee et al, Biochemistry 36:9439, 1997; Brown et al, J Cell Biochem 73:106, 1999), and 2) the drop in 1α(OH)D_2 substrate concentration to low levels at which 1,24$(OH)_2D_2$ is not formed efficiently (Strugnell et al, Biochem J 310: 233, 1995). In contrast, 1,25$(OH)_2D_2$ levels in the culture increased linearly with time, suggesting the presence of constitutively active vitamin D-25-hydroxylase not previously reported in parathyroid cells. Whether the suppression of PTH by 1α(OH)D_3 and 1α(OH)D_2 is mediated by these hydroxylated metabolites or through direct effects of the prohormone remains to be resolved.

Disclosures: ***A.J. Brown****, Bone Care International, Inc. 2.*

SU001

Carpal Bone Density Measured by the Norland DXA Scanner to Assess Skeletal Maturation in Chinese Boys and Girls. J. M. Wang*[1], H. W. Zhang*[2], Y. L. Liou*[2], F. W. Guo*[2], T. V. Sanchez[3]. [1]Norland Medical Systems, Beijing, China, [2]Hai Dian Hospital of Beijing, Beijing, China, [3]Norland Medical Systems, Socorro, NM, USA.

The assessment of carpal bone density has been shown to be a precise and effective method of assessing skeletal maturation in Caucasian boys and girls (Braillon, PM, et al. Acta Paediatrica. 67:924, 1998). The present study expanded that work to a population of Chinese boys and girls in the Beijing area. A population of 67 males and 83 females between the ages of 5 and 22 years old from Beijing, China underwent examination of carpal bone density on a Norland XR-36 scanner. All scans were performed using Research Scan Software with a point resolution of 1.0 x 1.0 mm and a scan speed of 45 mm/s. All studies in this report were audited and analyzed by the same factory trained operator (JMW). Carpal bone mineral density showed a significant correlation with chronological age in both male (r = 0.9346) and female (r = 0.9442) subjects. Carpal bone density in boys and girls did not differ between the ages of 5 and 12 years. Beyond the age of 12, Chinese males were shown to have progressively greater carpal bone density than females so that by the age of 21 years, females had 81% of the density seen in males. In conclusion, this report examines the relationship between age and carpal bone density in Chinese males and females. Significant relationships are found between age and carpal bone density in both males and females. Furthermore, males over the age of 12 were found to develop significantly greater carpal bone density than females.

Disclosures: ***J.M. Wang****, Norland Medical Systems 3.*

SU002

Faster Differentiation of Human Osteoblasts Due to Increased Donor Age or High-dose Hydrocortisone Treatment Abrogates Increased Type I Collagen mRNA in Response to High-dose 17-beta Estradiol. D. Ireland*, S. Bord, J. Compston. University of Cambridge School of Clinical Medicine, Cambridge, United Kingdom.

Aging, estrogen deficiency and glucocorticoid excess are well-known conditions that predispose to osteoporosis. Estrogen acts on osteoblasts(OBs) according to their stage of differentiation and estrogen receptor (ER) isoform expression. Both increased donor age and hydrocortisone treatment limit cell proliferation by enhancing differentiation. The aim of this study was to determine whether OBs that differentiate at different rates produce similar increases in type I collagen (COL1) mRNA in response to estrogen. Low-passage, human bone-derived OBs (hOBs) from female donors aged one (Young Donor) and 66 years (Old Donor) were cultured for eleven days on collagen in medium containing 10pM 17-beta estradiol (E2, from human serum) plus 200nM hydrocortisone (HC) and 7.5mM beta-glycerophosphate. After two days, 10nM E2 or carrier was added. mRNA from cells harvested on days four and eleven was assayed by real-time RT-PCR. Changes in mRNA levels with time for ERs, COL1 and ALP reflected the faster differentiation of the OD cells. The ERbeta/ERalpha mRNA ratio rose 300-fold ($p<0.001$) in OD hOBs that formed mineralized nodules but fell three-fold in YD hOBs ($p<0.05$) that did not. OD hOBs produced more COL1 mRNA on day four than YD hOBs but the level fell rapidly. In YD hOBs the level of COL1 mRNA continued to rise over the culture period suggesting greater total COL1 synthesis by these cells. Addition of 10nM E2 to YD hOBs resulted in a two-fold increase in COL1 mRNA on day two of E2 treatment ($p<0.05$) and a two-fold decrease in ERalpha mRNA on day nine ($p<0.05$) compared to controls. No comparable changes were seen in OD hOBs. The effect of increased HC on ERs and COL1 mRNA synthesis was then investigated. OD hOBs were cultured for four days in growth medium supplemented with high-dose hydrocortisone (4mM). The ERbeta/ERalpha mRNA ratio rose 37-fold ($p<0.001$) in treated hOBs compared to untreated controls. When 10nM E2 was added to HC-treated and control cells, only the control cells showed decreased ERalpha mRNA (three-fold, $p<0.05$). Since hOB proliferation increases when ERalpha mRNA levels are reduced, ligand-dependent down-regulation of ERalpha transcription slows the rate of cellular differentiation and allows more total synthesis of type I collagen. Rapidly increasing ERbeta/ERalpha ratios in hOBs from older donors and hOBs treated with high-dose HC prevented this down-regulation of ERalpha transcription. Our results suggest that reduced bone formation seen with increasing age and with glucocorticoid treatment may be due to faster differentiation of osteoblasts.

SU003

Congenital Dislocation of Radial Head. S. Singh*, M. Garg*. Orthopaedics, B.P.Koirala Institute Of Health Sciences, Dharan, Nepal.

Congenital radial head dislocation (CRHD) is a debatable entity. CRHD commonly occurs in association with other congenital anomalies in the same limb or in other parts of the body. We came across a case in which no other associated congenital anomaly was found; hence we found it fit to be reported . **Case Report:** A ten-year old girl presented to us with complaints of deformity of both elbows. There was no history of trauma in recent or distant past. On clinical examination of elbow joints the carrying angle at elbow was 40° in both upper limbs. There was no pain or tenderness around elbow joint, forearm and wrists. The movements at elbow joints were painless, but terminal 10° of flexion was restricted. Extension at elbow and supination - pronation in forearm was full. Detailed physical examination did not reveal any other congenital abnormality. There was not functional limitation because of the deformity. **Discussion:** Non-traumatic dislocation of radial head is the most frequent congenital abnormality around elbow. There are controversies regarding the precise definition of its pathogenesis and nomenclature - congenital or developmental. Merv Letts[1] defined developmental dislocation of radial head as any dislocation that results from maldevelopment of the forearm, and congenital radial head dislocation as an entity in which congenital malformation of the extremity is obvious. We believe that debate on whether the dislocation is congenital or developmental is unnecessary, as both types may be a different expression of same genetic defect. Genetic basis of the CRHD is also supported by the fact that this lesion has been seen in identical twins[2] , and as a familial condition occurring in a patient and her daughter[3]. Because of the benign nature of dislocation of radial head and conflicting reports on the results of surgical management of such cases surgical correction of congenital anterior dislocation of radial head is seldom indicated[6,7]. Pain, cosmesis and restricted range of movements (flexion in anterior type, extension in posterior type and ration especially supination) are the usual indications of surgery. Excision of radial head can be done after skeletal maturity has been achieved[8]. Early excision is undesirable in anterior dislocation as instability of proximal radio-ulnar joint permits the radius to displace further and causing increase in the valgus deformity and instability.

SU004

Does Increased Dietary Calcium Enhance The Exercise Effect at Loaded Sites? A Randomised Controlled Study in Boys. S. L. Bass[1], L. Saxon*[1], S. Iuliano-Burns*[2], G. Naughton*[3], C. Nowson*[1], R. Daly[1], E. Briganti*[4], C. Hume*[1]. [1]School of Health Sciences, Deakin University, Burwood, Australia, [2]Dept. Medicine, Melbourne University, Heidelberg, Australia, [3]The New Childrens Hospital, Westmead, Australia, [4]Dept. of Epidemiology and Preventative Medicine, Monash University, Clayton, Australia.

Combining exercise and increased dietary calcium may produce additive or synergistic effects at loaded sites, thus we conducted a single blind, prospective, randomised controlled study to test the following hypothesis: at the loaded sites, exercise and calcium will produce greater benefits than exercise or calcium alone. Eighty-nine boys aged 9.0 (1.1) years (mean (SD)) of Tanner stages 1 or 2 were randomly assigned to one of four intervention groups: 1 - moderate impact exercise+calcium (n = 20), 2 - moderate impact exercise+placebo (n = 21), 3 - low impact exercise+calcium (n = 22) or 4 - low impact exercise+placebo (n = 26). The 9-mth school-based program consisted of 20 min. of moderate or low impact exercise 3 times/wk. Participants also received ~800 mg/day calcium (milk based calcium-fortified foods) or an equivalent food without additional calcium. Total and regional BMC, anthropometry, sexual maturity, dietary calcium intake using a 3-day food record and physical activity levels (questionnaire) were assessed at baseline and post-intervention. Interaction between exercise and calcium was determined by ANOVA (4-group analysis). The main effects were determined by ANOVA (2 group analysis): exercise (groups 1 & 2 vs groups 3 & 4) and calcium (groups 1 & 3 vs groups 2 & 4). ANCOVA was used to control for baseline confounding factors - BMI, sexual maturity, regional bone mineral content, dietary calcium intake and physical activity level. At baseline, no differences were reported between the intervention groups. There was no significant calcium-exercise interaction on BMC gain at any site. For the unadjusted analysis a main effect of calcium was detected at the femur: additional calcium resulted in a 2.6% greater increase in BMC (mean±SE, 3.9±1.2 g, $p<0.01$). A main effect of exercise was detected at the femur and tibia: moderate impact exercise resulted in a 1.9% and 3.2% greater increase in BMC at the femur (2.5±1.2 g, $p<0.05$) and tibia (2.9±1.4 g, $p<0.05$). There was no effect of additional calcium or moderate impact exercise detected for total, lumbar spine, humerus or radius BMC accrual. Similar results were found after adjusting for baseline confounding variables. In conclusion, in pre- and early pubertal boys greater gains in bone mass at the femur may be achieved with short bouts of moderate impact exercise and increased dietary calcium; the effects however, were not synergistic.

SU005

Quantifying The Relationship Between Mechanical Loading and the Skeletal Response in Pre- and Early- Pubertal Girls: A Randomised Controlled Study. L. Saxon*[1], S. Iuliano-Burns*[2], G. Naughton*[3], R. Daly[1], S. L. Bass[1]. [1]School of Health Sciences, Deakin University, Burwood, Australia, [2]Dept. Medicine, Melbourne University, Heidelberg, Australia, [3]The New Childrens Hospital, Westmead, Australia.

Before exercise prescription for bone health can be recommended the relationship between mechanical loading characteristics and the skeletal response need to be quantified. We asked: i) does moderate impact exercise result in a greater gain in BMC than low impact exercise, ii) what are the loading characteristics associated with a moderate and low impact exercise program and does this differ from non-structured play?, and iii) does loading history affect the osteogenic response to a moderate or low impact program? Sixty-eight pre- and early-pubertal girls (aged 8.9±0.2 yrs) were randomised to take part in a moderate or low impact exercise program 3 time/wk for 8.5 mths (as part of an exercise-calcium intervention). The number and type of loads associated with the exercise classes and non-structured play (recess) were assessed from video footage. The magnitude of loads associated with each activity was assessed using a pedar in-sole mobile system. Hours of moderate and high impact organised sport was assessed from a parental assisted physical activity questionnaire. ANCOVA was used to detect differences in BMC gains between exercise groups, adjusting for baseline BMC, change in bone length and calcium intake. Unpaired t-tests were used to compare the differences in the number and magnitude of loads between the moderate and low impact exercise programs and non-structured play. The moderate and low impact exercise programs consisted of ~400 impacts per class, but the jumping, hopping and dynamic activities performed during the moderate impact program produced forces ranging from 2 to 4 x body weight (BW) compared to ~1 BW for the low impact program. Moderate impact exercise resulted in a 2.7% greater gain in BMC at the tibia compared to the low impact exercise. The moderate impact exercise program consisted of fewer low impacts (1-2 BW) and a higher number of moderate impact (2-4 BW) compared to those typically performed during non-structured play. The number of hours of organised sport outside of school positively correlated with gains in BMC ($r = 0.3$, $p<0.05$). There were greater gains in BMC in subjects participating in the moderate versus the low impact exercise programs who participated in 2 to 3 hours of moderate impact sports outside school (2.5% to 4.5% respectively, $p<0.06$ to 0.01). In conclusion, approximately 400 impacts ranging 2-4 BW, 3 times/wk was enough stimuli to result in an osteogenic response in normally active girls; even in those actively involved in moderate impact sports outside school.

SU006

Influence of Ethnicity and Lifestyle Factors on Bone Mass, Size and Architecture in Pre- and Peri- Pubertal Boys. R. Daly[1], D. Newey*[1], S. Bass[1], L. Saxon*[1], S. Iuliano-Burns*[2], E. Briganti*[3]. [1]School of Health Sciences, Deakin University, Melbourne, Australia, [2]Dept of Medicine, Melbourne University, Melbourne, Australia, [3]Dept of Epidemiology and Preventive Medicine, Monash University, Melbourne, Australia.

A number of factors are known to influence the attainment of peak bone mass, including genetics, ethnicity and various lifestyle factors. While ethnic differences in bone mass during growth have been largely explained by differences in bone size, it is possible that lifestyle factors may also contribute to ethnic differences in bone mass, size and architecture. This study examined the influence of ethnicity and the role of lifestyle factors on bone mass, size, architecture and volumetric BMD (vBMD) in pre- and peri- pubertal boys. We measured anthropometry, sexual maturity, exercise and calcium intake in 75 Caucasian and 20 Asian boys aged 8-10 years. Total body, lumbar spine (L3) and femoral neck BMC, BMD, estimated bone volume and vBMD, and lean mass and fat mass were assessed by DXA; heel BUA and VOS were assessed by ultrasound (CUBAClinical). FN and L3 BMC and bone volume were lower in Asian compared to Caucasian boys ($p<0.05$), but no differences were detected for BMD or vBMD (Table). No ethnic differences were observed for TB BMC (height adjusted), BMD, VOS and BUA, or age, height, weight, sitting height, leg length and fat mass. However, Asian boys had lower lean mass (21.9 ± 2.7 vs 23.3 ± 2.9 kg), were less active (organised sport, 1.6 ± 1.3 vs 2.5 ± 1.6 hr/wk) and had lower calcium intakes (572 ± 189 vs 886 ± 372 mg/day) ($p<0.05$).

	L3		FN	
	Asian	Caucasian	Asian	Caucasian
BMC (g)	4.95 ± 0.89*	5.43 ± 0.94	1.91 ± 0.34*	2.12 ± 0.47
Volume (cm3)	17.4 ± 3.3*	19.4 ± 3.4	5.05 ± 0.85*	5.56 ± 1.34
vBMD (g/cm3)	0.287 ± 0.027	0.282 ± 0.029	0.379 ± 0.038	0.386 ± 0.059

*$p<0.05$ vs Caucasians

Univariate analysis revealed that ethnicity, age, exercise, calcium and BMI were independent predictors of L3 and FN BMC ($p<0.2$). Ethnicity (L3 only), age, Tanner stage, exercise and BMI were independent predictors of L3 and FN volume. In multivariate analysis, ethnicity and BMI accounted for 27.4% and 34.4% of the variance in L3 volume and BMC, whereas BMI and age accounted for ~34% of the variance in FN bone volume and BMC. In summary, lower bone mass reported in Asian boys was largely due to a smaller bone size, and not to differences in exercise or calcium intake. There were no ethnic differences in the structural properties of bone. Since bone size has been reported to be a risk factor for fracture, Asian boys may be at increased risk of fracture due to a smaller bone size and not necessarily lower BMD or architectural differences.

SU007

Effects of Calcium, Vitamin D and Cheese Supplementation on Bone Mass Accrual in 10-12-Year-old Girls During Two-year Follow-up. S. Cheng[1], F. Tylavsky[2], A. Koistinen*[3], M. Kemppinen*[1], M. Kemikangas*[1], P. Salo*[1], R. Korpela*[4], A. Lyytikäinen*[1], A. Mahonen[5], M. Alen*[6], H. Suominen[1], H. Kröger[5]. [1]Univ of Jyväskylä, Jyväskylä, Finland, [2]Univ of Tennessee, Memphis, TN, USA, [3]Central Hospital, Jyväskylä, Finland, [4]Valio Oy, Helsinki, Finland, [5]Univ of Kuopio, Kuopio, Finland, [6]PERUNKA-Medical Rehabilitation Center, Jyväskylä, Finland.

The purpose of this double-blinded randomized intervention study (the CALEX-study) was to evaluate the effect of calcium (Cal), vitamin D (VD) and cheese (Che) supplementation on bone mass accrual during a two-year period. The subjects were 10-12-year-old Finnish girls with Tanner stage I-II and with dietary calcium intake <900 mg/day. In wave I, 104 girls were randomly assigned into four groups of which 91 girls [placebo (Pla, n=24), Cal + VD (n=24), Cal + PlaVD (n=20), and Che (n=21)] completed the intervention. In addition, 20 girls who had dietary calcium intake >900 mg/day served as controls (Con). Bone area and bone mineral content (BMC) of the whole body (WB), total femur (TF), and lumbar spine (LS) were assessed using a Dual-energy X-ray Absorptiometry (Prodigy, GE Lunar Corp.). On average, the subjects increased their BMC for 36% in the WB, 33% in the TF and 47% in the LS during the two-year period. When compared to the other groups, the cheese group had a significantly higher increase in BMC at the LS ($p=0.027$), with a trend for significance in the WB ($p=0.083$) and TF ($p=0.081$). Those with a diet >900 mg/day of calcium appeared to have a similar increase in BMC as the groups with Cal and Cal+VD supplementation. The differences in the increases in bone area between the groups disappeared when controlling for changing in height and weight (Table). Based on our analysis for this first wave, it appears that supplementing the diet with cheese or the consumption of foods high in calcium may provide benefits to the skeleton that is not available from supplements alone. These trends will need to be verified as waves II and III complete the study protocol.

%Change	Con	Pla	Cal+PlaVD	Cal+VD	Che
Area					
WB	22.5	22.9	22.0	22.7	23.9
TF	15.3	16.1	15.6	15.7	15.8
LS	24.0	22.4	23.4	23.3	24.0
BMC					
WB	35.5	34.5	34.1	34.1	36.3
TF	32.1	30.8	33.0	30.9	32.4
LS	47.4	43.6	45.8	44.9	49.8

SU008

Changes in Bone Size and Mass Are Associated with Changes in Fat Free Mass in 10-12-year-old Girls During Two-year Follow-up. H. Kröger[1], F. Tylavsky[2], M. Kemikangas*[3], M. Kemppinen*[3], A. Koistinen*[4], M. Alen*[5], H. Suominen[3], S. Cheng[3]. [1]Univ of Kuopio, Kuopio, Finland, [2]Univ of Tennessee, Memphis, TN, USA, [3]Univ of Jyväskylä, Jyväskylä, Finland, [4]Central Hospital, Jyväskylä, Finland, [5]PERUNKA-Medical Rehabilitation Center, Jyväskylä, Finland.

The purpose of this study was to evaluate the associations between bone growth and changes in body composition over a two-year period in 10-12-year-old Finnish girls. The subjects were 118 girls with Tanner stage I-II, who participated in an intervention study (the CALEX-study). Fat mass (FM), fat free mass (FFM), bone area (BA) and mineral content (BMC) of the whole body (WB), and BA and BMC of the total femur (TF) and lumbar spine (LS) were assessed using dual-energy X-ray absorptiometry (Prodigy, GE Lunar Corp.). During the two-year period, the girls grew on average 11.9 cm in height (HT) and 10.5 kg in weight (WT), and added 486 g to their WB bone mass. Girls who entered the study in Tanner stage I had a higher increase in HT than the girls in stage II (12.9 vs. 11.0 cm, $p<0.001$). We observed a similar % change of the BMC of the WB and TF for those in Tanner stage I and II at baseline. However, there were larger gains in BA for those in Tanner stage I compared to stage II for the WB (25.5 % vs. 21.4%, $p=0.005$), TF (18.8% vs. 13.0%, $p<0.001$). Girls in Tanner stage II had larger increases in BMC of the LS than the girls in the stage I (43.2% vs. 50.9%, $p<0.001$) with no difference in % change of the LS area (24.0% vs. 23.9%). The changes in BA and BMC of the WB, TF and LS are significantly correlated with the changes in the WT, HT and FFM (r-values ranging from 0.42 to 0.74). The WB area and BMC and TF BMC correlated moderately with the FM. Changes in FFM accounted for about 45% of the variation in the changes of the bone area and mass in WB, about 54% in TF and 26-39% in LS. Our data support the hypothesis that muscle mass (estimated by FFM) has an important role in the gain of bone mass in prepubertal girls.

SU009

Ultrasound Assessment of the Calcaneus in Finnish, USA and Chinese Pre-adolescent Children. L. C. Zou*[1], Q. J. Wang*[2], S. M. Cheng*[2], X. D. Zou*[3], F. Tylavsky[4], L. Carbone[4], E. Helkala*[2], S. Cheng[2]. [1]Guang Zhou College of Physical Education, Guang Zhou, China, [2]Univ of Jyväskylä, Jyväskylä, Finland, [3]Nanning Normal School, Nanning, China, [4]Univ of Tennessee, Memphis, TN, USA.

This study investigated whether there were differences in quantitative ultrasond (QUS) assessment of the calcaneus between Finnish, USA and Chinese preadolecscent children. The subjects consist of 544 children aged 8-12-year-old [Finnish white female (FINWF, n=199), USWF (n=69), US white male (USWM, n=30), US black female (USBF, n=12), USBM (n=8), Chinese female from city (ChFci, n=73), ChF from countryside (ChFco, n=46), ChM (n=111)]. QUS assessment was performed using a QUS-2 scanner at the calcaneus (Quidel Corp). Height (in cm) was measured using a stadiometer and weight (in kg) using a calibrated scale. We found that US children had significantly higher BUA values than the Finnish and Chinese children (Figure). There were no differences in BUA between ChM and ChF or between US males and females. However, black males had the highest value compared to other race and gender groups. After controlling for the differences in age, weight and height among the race and gender groups, the significance remained. Our results confirmed that the black has higher BUA than the whit and Chinese in pre-adolescent children which has been reported in adults. The small sample size of US blacks does not provide the power to correctly estimate differences due to gender. However the absence of gender difference in Chinese and whit children is in agreement with findings observed in bone densitometry assessment in pre-adolescent children.

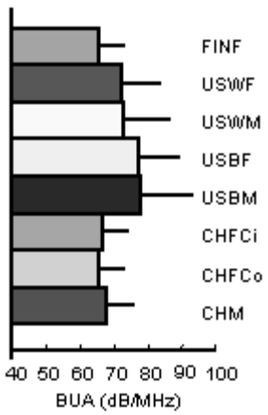

SU010

Microarchitectural Properties of Subchondral Trabecular Bone of Femoral Head in Osteoporosis and Osteoarthritis. G. Lemineur*[1], B. Brunet-Imbault*[1], R. Jennane*[2], F. Peyrin*[3], A. Bonnassie*[3], C. L. Benhamou[1]. [1]Inserm ERIT-M 0101, Orléans, France, [2]Laboratoire d'Electronique Signaux Images, Orléans, France, [3]CREATIS, Lyon, France.

It has been suggested that subchondral bone changes could be early events of osteoarthritis. To investigate this hypothesis, we have studied six femoral heads from osteoarthritis (OA) and eight femoral heads from osteoporosis (OP). The purpose was to quantify microarchitecture of subchondral trabecular bone in OA, either in an area covered by cartilage (n = 6) or in an area where the cartilage had disappeared (n = 6), and to compare them with 8 OP samples. 3R X-Ray microtomographic images were acquired using a synchrotron source at the ESRF. Each 3D image had a size of 6×6×6 mm^3 with an isotropic voxel size of 10.13 µm. 3D characteristics of the trabecular bone microarchitecture were calculated by the Mean Intercept Length method : bone volume fraction (BV/TV), trabecular thickness (Tb.Th), trabecular spacing (Tb.Sp), trabecular number (Tb.N) and degree of anisotropy (DA).

	OA with cartilage n=6	OA without cartilage n=6	OP n=8
BV/TV	0.221 ± 0.063	0.363 ± 0.035	0.181 ± 0.054
Tb.Th (mm)	0.110 ± 0.019	0.158 ± 0.023	0.114 ± 0.023
Tb.Sp (mm)	0.402 ± 0.083	0.280 ± 0.049	0.538 ± 0.113
Tb.N (mm^{-1})	1.992 ± 0.319	2.320 ± 0.326	1.565 ± 0.244
DA	8.584 ± 12.078	4.006 ± 1.763	4.921 ± 2.351

A statistical significant difference was observed concerning all the parameters ($0.002 < p < 0.01$) between OA samples without cartilage and OP samples, except for DA ($p = 0.44$). The comparison between OA samples with cartilage and OP samples showed no statistical difference ($0.07 < p < 0.61$) except for Tb.N ($p = 0.03$). The comparison between OA samples with and without cartilage showed statistically significant differences for all the parameters ($0.001 < p < 0.01$) except Tb.N ($p = 0.07$) and DA ($p = 0.9$). These data suggest that – significant subchondral microarchitectural changes mainly occur in advanced OA, when cartilage has disappeared – there are no or few anisotropy changes in this region in OA. The increase of Tb.N could be an early OA change, or could be due to a decrease of Tb.N in OP.

SU011

Changes in Calcaneal Ultrasound Attenuation Estimate Changes of Bone Mass and Density in Children. H. Suominen, E. Helkala*, S. M. Cheng*, P. Moilanen*, P. H. Nicholson*, S. Cheng. Department of Health Sciences, University of Jyväskylä, Jyväskylä, Finland.

Relatively little is known about the association between changes in quantitative ultrasound (QUS) parameters and changes in bone mineral content (BMC) and density (BMD) in children. We have compared calcaneal broadband ultrasound attenuation (BUA; QUS-2, Quidel Corp) with the BMC and BMD of the whole body (WB), total femur (TF) and lumbar spine (LS) (DXA; Prodigy, Lunar). Subjects (n=91) were girls, aged 10-12 years, who participated in a two-year intervention study to evaluate the effects of calcium, vitamin D and cheese supplementation on the acquisition of bone mass during prepuberty (the CALEX-study). The mean of the CVs for duplicate determinations of BUA was 1.2%. We found that changes in BUA correlated significantly with the changes in BMC of the WB (r=0.317, p=0.002), TF (r=0.276, p=0.009) and LS (r=0.379, p<0.001), and with the changes in BMD of the WB (r=0.583, p<0.001), TF (r=0.460, p<0.001) and LS (r=0.475, p<0.001) during the two-year period. There was also an association between the changes in BUA and the changes in body weight (r=0.279, p=0.007). After controlling the changes in body weight, the correlation remained significant between the changes in BUA and BMD of the WB (r=0.557, p<0.001), TF (r=0.383, p<0.001) and LS (r=0.409, p<0.001). Our study indicates that calcaneal BUA can be used for estimating the bone mass acquisition during growth.

SU012

Effects of Cerivastatin and Parathyroid Hormone on Bone in Male Sprague Dawley Rats. J. Banu[1], D. N. Kalu[2]. [1]Department of Physiology, University of Texas Health Science Center at San Antonio, San Antonio, TX, USA, [2]Dept. of Physiology, University of Texas Health Science Center at San Antonio, San Antonio, TX, USA.

It is well established that age-related bone loss occurs in males. The aim of this study is to determine whether cerivastatin and parathyroid hormone (PTH) will prevent age-related bone loss in the tibia and femur of male Sprague Dawley (SD) rats. Nine months old SD rats were divided into 6 groups. Group 1: Baseline controls; Group 2: Age-matched controls; Group 3: Low dose cerivastatin (0.2 mg/kg b wt/d); Group 4: Medium dose cerivastatin (0.4 mg/kg b wt/d) Group 5: High dose cerivastatin (0.8 mg/ kg b wt/d); Group 6: PTH (80 mg/ kg b wt, 3d/wk). Group 1 was sacrificed at the beginning of the study. Groups 2-6 were treated for 6 months. Cancellous and cortical bones were analyzed using pQCT densitometry at the proximal tibial metaphysis (PTM), the neck of the femur and the tibio-fibula junction. PTM: pQCT analyses were done at the tibia fibula junction in the proximal tibial metaphysis. When compared to the baseline controls, the cancellous bone mineral content (Cn. BMC) of the age-matched controls decreased by 44% (p<0.0001) confirming that male SD rats lose bone with age. The Cn. BMC decreased by 58% (p<0.0001), 58% (p<0.0001) and 60% (p<0.0001) in the low, medium and high doses of cerivastatin groups respectively, when compared to the baseline controls while PTH prevented the bone loss seen in the age-matched controls. When compared to the baseline controls, the cancellous bone mineral density (Cn. BMD) of the age-matched controls decreased by 43% (p<0.0001). The Cn. BMD decreased by 55% (p<0.0001), 56% (p<0.0001) and 58% (p<0.0001) in the low, medium and high cerivastatin groups respectively, when compared to the baseline controls while PTH prevented the bone loss seen in the age-matched controls. In the neck of the femur and the tibio fibula junction cerivastatin also did not prevent age-related bone loss in male SD rats while PTH significantly prevented the age-related bone loss. We, therefore, conclude that cerivastatin, in any of the doses tested, did not prevent age-related bone loss, in male SD rats, in any of the different bone sites studied. On the other hand, PTH prevented age-related bone loss in male SD rats in all the different bone sites studied. These findings are in line with our previous observation that cerivastatin did not prevent age-related bone loss in the lumbar vertebra of male SD rats.

SU013

Effects of IGF-I Overexpression in Muscle on Cortical and Cancellous Bones of Female Mice. J. Banu*[1], L. Wang*[2], D. Kalu[3]. [1]Department of Physiology, University of Texas Health Science Center at San Antonio, San Antonio, TX, USA, [2]Dept. of Physiology, University of Texas Health Science Center at San Antonio, SanAntonio, TX, USA, [3]Dept. of Physiology, University of Texas Health Science Center at San Antonio, San Antonio, TX, USA.

It has been hypothesized that increased muscle mass increases strain on bone resulting in increased bone mass. The aim of this study is to determine the effects of increased muscle mass on bone in female mice. A colony of transgenic FVB mice that overexpresses IGF-I in muscle was established. Overexpression of IGF-I brought about increased muscle mass in the transgenic mice. The offsprings of transgenic animals were screened for their genotype and only the heterozygotes and wild type females were used in this study. The animals were scanned at 1.5, 2.5, 3.5, 4.5, 6, 9 and 12 months of age, using a pQCT densitometer. The tibial diaphysis, distal femoral metaphysis and muscle cross-sectional area were analyzed. Body weight and muscle area: The heterozygous animals maintained a significantly higher body weight when compared to the wild type animals. As expected the muscle area in all the age groups was significantly higher in the heterozygous animals when compared to the wild type animals. Tibial Diaphysis: The cortical bone mineral content (Ct. BMC) did not differ significantly between the two groups in any of the age groups studied. Cortical bone mineral density (Ct. BMD) was significantly higher in the heterozygous animals only at 1.5 (7%, p<0.001), 2.5 (5%, p<0.01) and 3.5 months (2%, p<0.01) of age. Distal femoral metaphysis: The heterozygous animals had increased cancellous bone mineral content (Cn. BMC) in all the age groups studied, but this increase was statistically

significant only in the 2.5 months old animals (21%, p<0.01), when compared to the wild type animals. Cancellous bone mineral density (Cn. BMD) did not show any significant differences between the two groups. In conclusion, overexpression of IGF-I in female mice increased the body weight and muscle cross-sectional area. The increase in muscle cross-sectional area was associated with increased bone mass only in the younger animals. As the animals grew older there was no significant difference in bone between the two groups.

SU014

Exercise During Growth and Young Adulthood is Associated With Reduced Fracture Risk in Old Ages. M. K. Karlsson, H. Ahlborg*, K. J. Obrant, F. Nyquist*, H. Lindberg*, C. Karlsson*. Department of Orthopaedics, University Hospital MAS, Malmo, Sweden.

Exercise during growth is associated with increased peak bone mineral density (BMD). However, fragility fractures occur in old age. We asked: (i) are benefits in peak BMD and skeletal structure derived from exercise during growth retained after age 50? (ii) do former athletes have fewer fractures than controls? We compared the prevalence of fractures in 663 former athletes, mean age 69 years (range 50-93), all on national or international level within impact loaded sports during active career, retired from exercise career mean 34 years (range 1-62), and 943 age- and gender matched controls, randomly selected from the computerised national files. BMD was measured in a sub-cohort consisting of 90 former athletes, mean age 67 (range 50-92), retired from exercise career mean 27 years (range 3-65), and 77 sedentary age- and gender- matched controls, by dual energy X-ray absorbtiometry (DXA) and Quantitative Ultrasound Calcaneus (QUS). Data is presented as mean ± SD. The proportion of subjects with fractures was no lower in former athletes than controls over all [172/663 (25.9%) versus 238/994 (25.2%); NS], higher in the former athletes when they were active and less than 35 years of age [126/663 (19.0 %) vs 130/943 (13.8 %); p <0.01] but lower than controls in adulthood, after the age of 35 years [59/663 (8.9 %) vs 115/943 (12.1 %), p < 0.05]. Additionally, the proportion of subjects with low energy related fragility fractures sustained after age 50 [15/663 (2.3 %) vs 38/994 (4.2 %), p = 0.05] as well as distal radius fractures [5/663 (0.8 %) vs 22/943 (2.3 %), p = 0.01] was lower in former athletes than controls. BMD (g/cm2) was higher in the former athletes than the controls (total body 1.24 ± 0.10 vs 1.16 ± 0.09, p<0.001; spine 1.20 ± 0.13 vs 1.11 ± 0.13, p<0.001; femoral neck 0.93 ± 0.15 vs 0.89 ± 0.14, p=0.08). Additionally, bone size (femoral neck area (cm2) 6.17 ± 0.49 vs 5.98 ± 0.41, p<0.01), lumbar spine width (cm) (3rd lumbar vertebrae 4.78 ± 0.38 vs 4.59 ± 0.45, p<0.01) and skeletal architecture evaluated by QUS (SOS (m/s) 1552.6 ± 42.2 vs 1553.0 ± 34.0, p<0.01; Stiffness index 94.0 ± 18.2 vs 87.5 ± 15.5, p<0.05) was higher in the former athletes than the controls. Fracture rates are lower in former athletes than controls, possibly due to residual benefits in skeletal structure attained by vigorous physical activity during growth. We infer that exercise during growth may reduce the burden of fragility fractures in men.

SU015

Pediatric Whole Body Measurements. T. L. Kelly. Hologic, Inc., Bedford, MA, USA.

We report on the development of an algorithm that dynamically adjusts detection thresholds to optimize performance in pediatric subjects weighing between 10 and 40 kg. The Pediatric Whole Body analysis method performs better than the Adult Whole Body method in young children. However, the Pediatric and Adult Whole Body analysis methods provide different results and it is often unclear which method should be used. Further, longitudinal studies and population based studies such as NHANES may employ both analysis methods, complicating the interpretation of changes and the development of reference data. These issues were resolved with an automatic algorithm that dynamically adjusts bone detection thresholds and soft tissue baseline determinations based upon the subject's weight. The thresholds are set such that the Adult Whole Body analysis is employed in subjects weighing more than 41 kg (90 lbs.), representing more than 98% of U.S. adults. Between 40 kg and 10 kg of body weight, bone detection thresholds and soft tissue baseline values are dynamically adjusted downward to provide technically acceptable bone mapping in all regions of the skeleton. Particular attention was given to the arms, legs, and pelvic region to ensure that bone detection was accurate and reliable. Children 3 to 17 years old were analyzed with the technique and reference databases were developed for bone and body composition results. We conclude that this new whole body analysis method will improve the reliability of pediatric whole body determinations, provide congruent results across all age groups, and obviate the need for an alternative analysis method in young children.

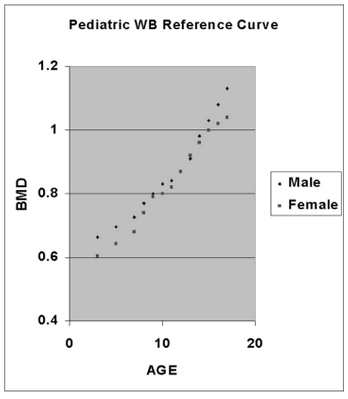

SU016

Age Related Changes in Metacarpal Morphometry and Areal Bone Mineral Density in Children Assessed by Digital X-ray Radiogrammetry (DXR). R. L. Ashby*[1], K. A. Ward[1], Z. Mughal[2], J. E. Adams[1]. [1]Department of Clinical Radiology, The University of Manchester, Manchester, United Kingdom, [2]Central Manchester and Manchester Children's University Hospitals NHS Trust, Manchester, United Kingdom.

The purpose of this cross sectional study was to investigate age related changes in metacarpal morphometry and areal bone mineral density (BMD) from hand radiographs of normal children using DXR. This technique analyses the second, third and fourth metacarpals and gives an assessment of the metacarpal index (MCI), cortical thickness (cm) (CT), outer bone width (cm) (BW) and BMD (g/cm^2). Non-dominant hand radiographs of 119 healthy Caucasian children (70 female, 49 male; mean age 11.32 ± 3.61, range 5.42-18.95 years) were assessed using the Pronosco X-posure system ™ (version 2). Subjects were grouped according to gender, pre-pubertal or pubertal status, chronological age in groups (5-8.99; 9-12.99 and 13-19 years), and Tanner pubertal stage (TS) (females only). Females had a higher mean MCI (mMCI) compared to males (p < 0.001). When grouped according to pubertal status, this difference still existed (pre-pubertal mMCI = 0.353 females, 0.328 males, p < 0.05; pubertal mMCI = 0.462 females, 0.401 males, p < 0.01). TS 2 demonstrated a lower mMCI compared to TS 3 (0.344 vs 0.483, p < 0.001). mMCI increased by age group in females (p < 0.01 to < 0.001) only, although mean CT (mCT) and mean BW (mBW) increased with age in both genders (p < 0.05 to < 0.001). Males demonstrated a higher mBW (p < 0.001) but a lower mCT compared to females (p < 0.05). TS 2 had a lower mCT compared to TS 3 (0.120 cm vs 0.171 cm, p < 0.01). Mean BMD (mBMD) increased with age in males and females (p < 0.001). Males (9-12.99 years) had a lower mBMD compared to females of the same age (0.410 g/cm^2 vs 0.433 g/cm^2, p < 0.05). TS 2 had a lower mBMD compared to TS 3 (0.394 g/cm^2 vs 0.514 g/cm^2, p < 0.01). Chronological age, height, weight, MCI, CT, BW, BMD and grip strength (GS) correlated positively (p < 0.05 to < 0.001) with each other. In pubertal males, MCI did not correlate significantly with GS. The Pronosco X-posure system ™ is a useful tool for the study of age and gender related changes in metacarpal morphometry and BMD in children. Such important information concerning growth parameters in normal children can be applied to the study of paediatric conditions associated with increased fracture risk, such as steroid induced osteoporosis.

SU017

Total Body Bone Mineral Content and Parameters of Bone Strength at the Radius and Tibia in Pre-Pubertal Gymnasts and Sedentary Controls. K. A. Ward[1], J. E. Adams[2], S. Roberts*[3], R. L. Ashby*[2], Z. Mughal[4]. [1]Clinical Radiology, University of Manchester, Manchester, United Kingdom, [2]Department of Clinical Radiology, The University of Manchester, Manchester, United Kingdom, [3]School of Epidemiology and Health Sciences, The University of Manchester, Manchester, United Kingdom, [4]Central Manchester & Manchester Children's University Hospitals NHS Trust, Manchester, United Kingdom.

During the pre-pubertal period, physical activity positively influences bone size, geometry, mass and ultimately bone strength. We hypothesised that, compared to controls gymnasts will have higher total body bone mineral content (TBBMC) and stress strain index (SSI), a measure of bone strength, in the radius and tibia. Bone and muscle cross sectional area (CSA) and SSI were measured at the 50% sites from the distal radius and tibia using peripheral quantitative computed tomography in gymnasts (n=28) and controls (n=33). TBBMC was measured using dual energy x-ray absorptiometry. Bone age was assessed from hand radiographs (Greulich & Pyle). There was no significant difference between the chronological or bone age of the gymnasts' vs. controls (mean age 8.9 SD 1.3: 7.6 SD 1.4 years). Controls were taller than gymnasts (3.6cm, p=0.03); weight and BMI were not significantly different. Weekly median activity was 11 hours in gymnasts and 5-6 hours in controls. After adjustment for bone area, weight, height and sex, gymnasts had higher TBBMC than controls (mean difference = 51.91g, p=0.002). After adjustment for weight and sex gymnasts had higher bone strength (SSI = 60.49mm^3, p=0.01), bone and muscle CSA (15.48mm^2, p=0.002; 181.67mm^2, p=0.06 respectively) than controls at 50% distal tibia. At 50% distal radius, gymnasts had higher bone strength parameters than controls (SSI = 16.61mm^3, p=0.002; bone CSA = 4.76mm^2, p=0.009; muscle CSA = 320mm^2, p<0.001). The appendicular skeleton of pre-pubertal gymnasts has adapted to increased loading in comparison to sedentary controls. The 50% mid-cortical sites at the radius and tibia have adapted to withstand the high forces exerted during activity by increasing the bone and muscle CSA and SSI. If the differences in TBBMC between the two groups persist until the end of the growth period then the gymnasts will have achieved a greater peak bone mass, which may contribute to a lower fracture risk in later life.

SU018

Bone Age Assessment by DXA and Standard Radiographs; Comparison with Chronological Age. R. L. Ashby*[1], I. M. Hodgkinson*[1], E. J. Harrison*[1], K. A. Ward[1], Z. Mughal[2], J. E. Adams[1]. [1]Clinical Radiology, Imaging Science & Biomedical Engineering, University of Manchester, Manchester, United Kingdom, [2]Pediatric Medicine, Central Manchester and Manchester Children's Hospitals, Manchester, United Kingdom.

Bone age (BA) or skeletal maturity assessment is important in the evaluation of children with disorders of growth, and when measuring paediatric bone mineral density (BMD). Hand and wrist radiographs are examined and skeletal maturity is classified as a BA according to the methods of Greulich and Pyle (GP) or Tanner-Whitehouse. We hypothesised that 1) assessment of bone age from hand and wrist images generated by Hologic 4500A DXA (DXAi) would be possible and 2) BA from DXAi and BA from a standard hand and wrist radiograph would not differ significantly from chronological age (CA). 55 healthy children mean age 12.8 years (SD 3.3, range 6.3-18.4 years) were studied. The GP method was used to assess the BA of each individual from postero-anterior radiographs (RADi) and DXAi of the left hand and wrist. A paired samples t-test was used to determine whether there was a significant difference between BA assessed from RADi or DXAi and subject's CA. In the age group 6-11.9 years there was a mean significant difference (-1.40 SD 1.08 years, p<0.001) in BA by DXAi compared to CA; in older children (12-18.4years) there was no significant difference (p=0.47). Comparing BA and CA using RADi there were no significant differences in either of the age groups (p=0.10, 6-11 years and p=0.45, 12-18.9 years). This study confirms the feasibility of estimating BA and BMD from DXA. This may be applied to healthy children who have a CA of 12-18.4 years. The inaccuracy in determining BA from DXAi in younger children is likely to be related to the spatial resolution of DXAi limiting image quality and resulting in partial volume averaging errors.

SU019

Longitudinal Follow-up of Bone Mineral Density in Children and Adolescents with Systemic Lupus Erythematosus (SLE). E. von Scheven*[1], J. Shepherd[2], Y. Chen*[2], H. Genant[2]. [1]Pediatrics, University of California, San Francisco, San Francisco, CA, USA, [2]Radiology, University of California, San Francisco, San Francisco, CA, USA.

Chronic illness such as SLE may affect the acquisition of bone mineral during childhood and adolescence. We utilized Dual X-ray Absortiometry (DXA) to detect BMD change in a longitudinal cohort of youth with SLE. Volumetric methods were utilized to control for underlying changes in body size associated with growth. We performed spine DXA (Hologic QDR 4500) to determine APBMD (areal BMD), APBMAD (volumetric BMD, BMC/AP^1.5), Hologic Lat VolBMD (Lat BMC/vol determined by AP and Lat scan dimensions); and whole body (WB) DXA to determine WB BMD, WB BMC (bone mineral content) and WBMAD (bone mineral apparent density). 17 subjects with pediatric-onset SLE (age 8.8-20.4yrs [mean 13.8], 76% female, 6% Caucasian, 33% Asian, 33% Hispanic, 11% African-American and 17% mixed) were evaluated at baseline and follow-up (1.1-2.4 yrs later, mean 1.9). Healthy controls (n=103, age 7.0-21.9yrs, 75% female, 47% Caucasian, 21% Asian, 29% Hispanic and 3% mixed) were evaluated at baseline only. Changes in height and BMD were annualized. Disease duration ranged from 0.17-8.3 yrs (mean 1.6). Prednisone dose (mg/kg) at baseline ranged from 0.0 -0.39 (mean 0.17) and at follow-up 0.0 -1.2 (mean 0.26). Subject's served as their own control for evaluation of unadjusted BMD values. Controls were used to generate age- and weight-adjusted Z-scores for the non-black female subjects. 35% of subjects demonstrated a loss of bone (g/cm^2) by APBMD and 36% by APBMAD. After adjusting for growth (age and weight) this increased to 75% and 83% respectively, reflecting the importance of age and body size in pediatric analysis. The average annualized change of BMD was 0.14 ± 0.04 g/cm^2 (-0.062 to 0.075 g/cm^2) for APBMD and 0.50 ± 3.5 mg/cm^3 (-5.1 to 8.3 mg/cm^3) for APBMAD. After controlling for age and gender, the change in APBMD was significantly associated with increased height (p=0.003) while change in APBMAD was not. Annualized mean [SD] change of Z-score for non-black females was positive for WBMAD (+0.12 [.22]) but negative for all other measurements: WB BMD ¯ 0.10 [.19]); WB BMC ¯ 0.18 [.29]); APBMAD ¯ 0.25 [.18]); APBMD ¯ 0.26 [.35]); and Hologic Lat VolBMD ¯ 0.43 [.67]. This preliminary study suggests that pediatric SLE may be associated with minimal bone acquisition over time. Although on average absolute values of BMD were maintained, evaluation of age- and weight-adjusted Z-scores suggested deficits in the context of expected gains of BMD. Further subjects are needed to confirm these findings and to determine the best modality for longitudinal studies in this population.

SU020

Correlation between Maximal Effect delivered during Fitness Test and Bone Mineral Density. A 3 Year prospective Study in Children and Adolescents. K. Kramme*[1], L. Mortensen*[2], K. Brixen[1], K. Froberg*[3], H. Beck-Nielsen*[1], P. Charles*[2]. [1]Dept of Endocrinology, Odense University Hospital, Odense, Denmark, [2]Dept of Endocrinology, Aarhus University Hospital, Aarhus, Denmark, [3]Institute of Physical Education and Clinical Biomechanics, University of Southern Denmark, Odense, Denmark.

Previous studies have suggested that exercise may be one of the most important modifyable factors for accretion of bone mass in childhood and adolescence. Studies in adults have reported a positive correlation between VO2max and Bone Mineral Density (BMD). VO2max, however, depends on body weight which in itself is closely related with BMD. Here we aimed to evaluate the association between the maximal effect delivered during fitness test (Vmax-f) and lumbar spine (LS) and whole-body (WB) BMD, and the correlation between Vmax-f and the change in LS BMD in children and adolescents.This prospective study comprised 157 females and 149 males aged 8 to 21 years (median 14 years). Participants were tested on an ergometer bicycle, and BMD subsequently measured using a Norland DXA-scanner. The examinations were repeated after 3 years. The relationship between BMD and Vmax-f, body weight, height, age, and sex was evaluated at start (y0) and after 3 years (y3) using multiple backwards regression analysis. Results are shown in the table as partial correlation coefficients.In conclusion, the maximal effect delivered during exercise test correlates significantly and positively with LS and WB BMD in children and adolescents. The performance in the test was significantly and positively correlated with the change in LS BMD during the subsequent 3 years. Our study supports the idea that exercise positively affects accretion of bone mass during childhood and adolescence.

Table

	BMD LS(y0)	BMD WB(y0)	Change BMD LS(y3-y0)
Sex	0.33***	n.i	n.i
Age	0.46***	0.44***	-0.47***
Body Weight	0.23***	0.55***	n.i
Height	0.17**	n.i	n.i
Vmax-f	0.15*	0.18**	0.19**
Combined model	0.87***	0.89***	0.50***
	* = p<0.05 **= p<0.01	***= p<0.001	n.i= not included in the final model

SU021

Relationships Between High Resolution Computed Tomography for Architectual Characterization of Human Calcaneus and Histomorphometry. B. Cortet[1], D. Chappard[2], N. Boutry*[3], P. Dubois*[3], A. Cotten*[3], X. Marchandise*[3]. [1]Rheumatology, University-Hospital of Lille, Lille, France, [2]University-Hospital of Angers, Angers, France, [3]University-Hospital of Lille, Lille, France.

The present study aimed to characterize the relationships between several variables reflecting bone microarchitecture assessed by both histomorphometry and high resolution computed tomography (HRCT) at the calcaneus. 24 specimens removed from cadavers were studied. There were 12 men and 12 women (mean age: 78 ± 10 years; range: 53-93). 16 axial sections (1 mm in width and 2 mm apart) were selected for HRCT. One core (11 mm internal diameter) was removed from the superoposterior part of the calcaneus and 6 undecalcified sections (7 microns) were analysed. The histomorphometric analysis was performed on a Leica Quantimet Q570 image analyzer. Features measured by both methods were: BV/TV, trabecular thickness (Tr Th), trabecular number (Tr N), trabecular spacing (Tr Sp), interconnectivity index (ICI), node count (NC), free end count (FEC), node-to-node strut count (NNS), node-to-free end strut count (NFS), free end-to-free end strut count (FFS), marrow space star volume (SV), Euler number (EN) and fractal dimension (FD). R values are shown in the table below (*p<0.05). In conclusion the present study suggests that the correlations found for the 2 methods used (HRCT and histomorphometry) vary according to the features measured. Findings also suggests that several features measured by HRCT reflect bone microarchitecture.

BV/TV	Tr Th	Tr N	Tr Sp	ICI
0.69*	0.24	0.86*	0.90*	0.05

NC	FEC	NNS	NFS	FFS
0.47*	0.61*	0.05	0.21	0.14

SV	EN	FD
0.50*	0.43*	0.38

SU022

Medical Conditions in Relation to Bone Mineral Density and Stiffness in Older Men. D. R. Miller[1], E. Krall[2], J. J. Anderson*[3], S. Rich*[1], R. Ferguson*[1], L. Silva*[1]. [1]Chqoer, Veterans Administration, Bedford, MA, USA, [2]Dental Medicine, Boston University, Boston, MA, USA, [3]School of Medicine, Boston University, Boston, MA, USA.

Accelerated bone loss and increased risk of fracture have been associated with a number of common medical conditions in the elderly, including pulmonary, cardiac, metabolic, and gastrointestinal disorders. Generally, these associations have been studied individually and few studies have reported on the independent and compound effects of multiple medical conditions on bone health. This was examined in the VA Longitudinal Osteoporosis Research (VALOR) study using data from 696 male veterans over 50 years of age. Bone mineral density (BMD) at the femur and forearm were measured with dual energy x-ray absorptiometry (model DPX-IQ, Lunar Corp., Madison, WI). Femoral BMD measurements represent averages of right and left hips per subject. Change in BMD with repeat measurements over a period of up to three years are computed as change per year. Bone stiffness at the calcaneus is measured with ultrasonography (Achilles Plus, Lunar). Disease status is determined through self-report of medical diagnoses and diagnostic (ICD-9) codes

from the medical records. General linear modeling was used to estimate associations with various medical conditions, with adjustment for age, body mass index, physical activity, smoking, diet, and other concurrent medical conditions. Femoral BMD was significantly ($p<0.05$) lower (by at least 4%) in men with Crohns disease, rheumatoid arthritis, stroke, transient ischemic attack, congestive heart failure, or cancer. Loss of femoral BMD was also significantly greater in patients with chronic obstructive pulmonary disease. Significantly lower forearm BMD was found in men with these conditions, except for cancer, and was also found in those with diabetes, angina, or syncope. Bone stiffness was lower in men with cardiovascular disease, cancer, Crohns disease, or syncope. The cumulative number of medical conditions was inversely associated with all measures of BMD and bone stiffness, and accounted for a substantial proportion of their variability. Careful examination of the modifying effects of duration of illnesses and their specific pharmacological treatments is in progress. These results document the devastating and independent effects of a number of medical conditions on bone health.

SU023

Long-term Variability of Markers of Bone Turnover in Postmenopausal Women and Implications for their Clinical Utility. The OFELY Study. P. Garnero[1], D. Mulmann*[2], F. Munoz*[3], E. Sornay-Rendu*[3], P. D. Delmas[3]. [1]Synarc, Inserm Unit 403, Lyon, France, [2]INSERM unit 403, Lyon, France, [3]Inserm Unit 403, Lyon, France.

High levels of bone turnover markers is a risk factor for fragility fracture in postmenopausal women, but the variability of their measurement has raised concern about their clinical utility. In this study we investigated the long-term variability of markers in 268 healthy untreated postmenopausal women (1 to 39 yr post menopausal) in the OFELY cohort. A fasting blood sample was collected every yr for 4 yr (5 samples) to measure serum intact osteocalcin (OC) for formation and serum CTX (S-CTX) by automated analyzer for bone resorption. Bone turnover remained stable over 4 years (OC, +1.3%/yr, p=0.003; S-CTX; -0.13%/yr, p=0.7). Women were categorized in tertile (T1, T2 and T3, from lowest to highest) of bone marker levels. Agreement of classification between baseline and 4 yr measurements was moderate (kappa: 0.51 and 0.52, for OC and S-CTX, respectively) with 60% of women remaining in the same group for both markers. However, only 4% and 5% of patients in T3 (high turnover) for OC and S-CTX respectively at baseline were found in T1 (low turnover) after 4 years. Conversely, 10% and 4% of women in T1 for OC and S-CTX respectively were found in T3 after 4 years. Among women in T2 (intermediate bone turnover), 51% and 43% for OC and S-CTX respectively, remained in the same tertile at the second measurement. When the 2 markers were combined, only 2% of women at high turnover at baseline -defined as OC and/or S-CTX in T3- were classified at low turnover 4 years later. We conclude that serum bone turnover markers are stable over 4 years in untreated postmenopausal women. A single measurement of one or two markers accurately classifies most women with a definitively high or low turnover. For those women with intermediate levels (T2), classification may be improved by a second measurement.

SU024

Cyclical Behaviour of Bone Remodelling and Bone Loss in Healthy Women after Menopause: Results of a Prospective Study. G. Mazzuoli*[1], D. Marinucci*[2], E. D'Erasmo*[1], M. Acca*[1], D. Pisani*[1], M. G. Rinaldi*[2], G. Bianchi*[1], D. Diacinti*[1], S. Minisola[1]. [1]Dipartimento Scienze Cliniche, Università La Sapienza, Rome, Italy, [2]Dipartimento Studi Geoeconomici e Statistici, Università La Sapienza, Rome, Italy.

We measured the annual changes of lumbar bone mineral density (BMD) in 238 healthy pre- and postmenopausal women aged 45-74 years providing evidence that bone loss is not monotonic over time but exhibits cyclical damping oscillations. The subjects were divided into groups according to their menstrual status and years since menopause. When the log-linear trend of BMD decrement is transformed into a constant by considering annual percentage changes, the presence of a cyclical component of seven years is evident; by employing a harmonic regression model, the cyclical component is also statistically significant on baseline data. The cyclical behaviour of BMD decrement corresponds to an analogous behaviour of the bone remodelling markers. The results suggest that the lack of oestrogen, acts as a synchronizer on bone remodeling triggering a latent cyclical rhythm of loss of bone persisting throughout the life. The existence of a chronobiological rhythm of bone loss starting after menopause, till now unrecognized, may have important clinical implications.

SU025

Age-related Changes in Cortical Bone Content of Insulin-like Growth Factor Binding Protein (IGFBP)-3, IGFBP-5, and Osteoprotegerin in Postmenopausal Osteoporosis. Possible Connection with Bone Mass. T. Ueland*[1], K. Brixen[2], L. Mosekilde*[3], L. Mosekilde[4], A. Flyvbjerg*[5], J. Bollerslev[6]. [1]Research Institute for Internal Medicine, National University Hospital, Oslo, Norway, [2]Department of Endocrinology C, Aarhus University Hospital, Aarhus, Denmark, [3]Department of Cell Biology, University of Aarhus, Aarhus, Denmark, [4]Department of Endocrinology, Odense University Hospital, Odense, Denmark, [5]Medical Research Laboratory M, Aarhus University Hospital, Aarhus, Denmark, [6]Department of Endocrinology, National University Hospital, Oslo, Norway.

Serum levels of growth hormone (GH), insulin-like growth factor (IGF)-I decline with increasing age, while osteoprotegerin (OPG) increases. IGFs as well as OPG are abundant in bone matrix and are important local regulators of bone metabolism mediating the effects of many upstream hormones (e.g. estrogen). Thus, they may explain some of the decrease in bone mass found in post-menopausal osteoporosis. We measured cortical and trabecular bone content of IGF-I, IGF-II, IGF binding proteins (IGFBP)-3, IGFBP-5, osteoprotegerin (OPG), osteocalcin and total protein in combined extracts obtained after ethylenediamine tetratacetate and guanidine hydrochloride extraction in 60 postmenopausal women aged 46.9 to 74.4 yrs (mean, 63.0 yrs), who had suffered a distal forearm fracture and had low BMD in the spine or hip (z-score < 0). Calcium was determined after HCl hydrolysis. We found significant age-related increases of IGFBP-3 ($r=0.35$, $p<0.01$), IGFBP-5 ($r=0.59$, $p<0.001$) and OPG ($R=0.36$, $p<0.01$) in cortical bone, significantly inversely correlated with femoral neck BMD (IGFBP-5, $r=-0.28$, $p<0.05$; OPG, $r=-0.42$, $p<0.01$). A correlation between age and OPG was also detected in trabecular bone ($r=0.27$, $p<0.05$). No age-related changes were detected for IGF or IGF-II. In conclusion, we found age-related increases in cortical bone matrix levels of OPG, IGFBP-3, and IGFBP-5 in post-menopausal women. These changes could potentially represent both compensatory and inhibitory mechanisms by regulating anabolic actions of IGFs, in addition to IGF-independent effects. As for OPG our findings probably represent compensatory responses to increased osteoclastic bone resorption.

SU026

Cut-Off Value Determined for Osteoporosis in Japanese Women by Using Quantitative Ultrasound. K. Yoh*[1], H. Ohta[2], H. Kishimoto*[3], I. Gorai[4], J. Hashimoto[5], Y. Nakatuka*[6], S. Yosimoto*[7], K. Makita*[8]. [1]Orthopedic Surgery, Hyogo College of Medicine, Nishinomiya, Japan, [2]Tokyo Women's Medical Univ, Tokyo, Japan, [3]Sanin Rosai Hospital, Yonago, Japan, [4]Yokohama city Univ., Yokohama, Japan, [5]Osaka Univ., Osaka, Japan, [6]Osaka City Univ., Osaka, Japan, [7]Hyogo Chuo Hosp., Sanda, Japan, [8]Keio Univ., Tokyo, Japan.

The aim of this study was to evaluate the cut-off value for osteoporosis in Japanese women, by using Quantitative Ultrasound (QUS). The QUS technique is widely used in diagnosis, health check and monitoring of therapy. At present there are more than 2,500 QUS devices installed in Japan. In the case where QUS is used for the purpose of diagnosis and health check as well as dual energy X-ray absorptiometry (DXA), there is a need to consider differences in race and province. For this reason, normative data of speed of sound (SOS) using the handy QUS device (FURUNO CM-100, Japan) was reported in IBMS 2001 by us. A total of 1207 Japanese women aged 20-95 years (mean age: 57) were, after signing an informed consent, enrolled to perform the present study from six centers and three provinces in Japan. They were selected in a random manner with no subject having serious bone metabolism disease. The SOS of all subjects was measured at the right calcareous using the CM-100, and the bone mineral density (BMD) was measured at the lumbar spine (L2-L4) using DXA (Norland: XR-26/36, Hologic: QDR-2000 and Lunar: DPX). After measuring lumbar BMD, we divided the subjects into three categories according to the Japanese diagnostic criterion for osteoporosis proposed the Japanese Society for Bone Mineral Research in 1996. (This criterion defines those people with a BMD value of less than 70% (corresponding to T-score: -2.5SD) of young adult mean (YAM) as having osteoporosis, 70%-80% of YAM as low bone mass and more than 80% (corresponding to T-score:-1.5SD) of YAM as normal, respectively.) According to the cut-off value of lumbar BMD based on the above criterion, 312 of the 1207 women were categorized as osteoporosis, 302 women as low bone mass and 593 women as normal, respectively. Referring to the cut-off value of lumbar BMD, the cut-off value of SOS for osteoporosis, low bone mass and normal corresponded to 1481m/s, 1491m/s and 1506m/s, respectively. As a result of the sensitivity and specificity curve analysis on SOS, the cut-off value of the point of intersection was 1487m/s. This cut-off value, 1487m/s, is equivalent to 72% of YAM of lumbar BMD. This data showed that the cut-off value of SOS using CM-100 is highly compatible with the cut-off value of lumbar BMD using DXA. In conclusion, SOS measurement using the CM-100 gives good performance for diagnosis of osteoporosis as well as DXA. The CM-100 is a useful tool for clinical application.

SU027

Decreased Bone Formation in Ataxia Telangiectasia Mutated (ATM) Knockout Mice. A. Hishiya*[1], M. Ito[2], K. Ikeda[1], K. Watanabe[1]. [1]Dept. Geriatric Res., Natl. Inst. for Longevity Sci., Obu, Japan, [2]Dept. Radiology, Nagasaki Univ. School of Medicine, Nagasaki, Japan.

ATM is a member of PI-3 kinase family proteins, encoded by the gene, Atm, responsible for premature aging syndrome, ataxia telangiectasia (AT). This protein kinase is known to play critical roles in DNA replication and repair. Accelerated carcinogenesis induced by irradiation as well as growth retardation has been observed in Atm knockout (ATMKO) mice. AT is also recognized as a genomic instability syndrome, sharing the symptoms with accelerated senescence in human and mouse. Here, we have found that the bone phenotype of ATMKO is similar to that of bone loss in disuse and/or aging. ATMKO in 129/Sv and its age-matched heterozygous mutant (+/-) and wild-type (+/+) animals were used for experiments. At 10 weeks of age, there is no significant difference in body weight between KO and control (+/- or +/+) mice. Growth retardation of KO mice is pronounced at 14 weeks of age. The fifth lumber vertebra and tibia from these mice were subjected to micro-CT analysis and bone histomorphometry, respectively. Significant decrease in BV/TV was already observed in KO mice at 10 weeks. The difference between KO and control animals was more pronounced at the age of 14 weeks. Furthermore, bone mass was decreased along with aging of KO mice, whereas it was increased in controls. Both BFR/BS and Oc.S/BS were significantly lower in KO mice than in control mice at 10 weeks of age. To determine the cellular basis of the bone phenotype, we employed in vitro osteoclastogenesis and colony formation assays using bone marrow cells from KO and control mice. Although there was no significant decrease in osteoclast formation from M-CSF-dependent bone marrow cells of KO mice, CFU-F, CFU-OB, and CFU-Adip were markedly reduced in KO mice, comparing with bone marrow cells from control mice. These data suggested a possibility that osteopenic phenotype in ATMKO is caused by dysfunction of osteoblast lineage.

SU028

The Design and Baseline Participant Characteristics of Osteoporotic Fractures in Men (MrOS) – a Large Observational Study of the Determinants of Fracture in Older Men. E. Orwoll[1], J. Blank[1], E. Barrett-Connor[2], J. Cauley[3], S. Cummings[4], K. Ensrud[5], C. Lewis[6], P. Mannen*[4], R. Marcus[7], K. Phipps[1], M. Stefanick*[7], K. Stone[4]. [1]Oregon Health & Science University, Portland, OR, USA, [2]University of California, San Diego, San Diego, CA, USA, [3]University of Pittsburgh, Pittsburgh, PA, USA, [4]University of California, San Francisco, San Francisco, CA, USA, [5]VA Medical Ctr & Univ of Minnesota, Minneapolis, MN, USA, [6]University of Alabama, Birmingham, Birmingham, AL, USA, [7]Stanford University, Palo Alto, CA, USA.

Although osteoporosis is common, there is insufficient information concerning the characteristics and risk factors for fracture in men. Osteoporotic Fractures in Men (MrOS), a prospective cohort study, was designed to provide a better understanding of the problem. About 6000 U.S. men ages of 65 years and older were recruited in early 2000 at 6 sites (Birmingham, Minneapolis, Portland OR, Pittsburgh, Palo Alto, San Diego), primarily by mass mailings to population-based lists. Additional participants are being recruited in Sweden and Hong Kong. Study information is collated at a data coordinating center (UCSF). At the baseline examination, each participant completed detailed questionnaires regarding medical history, physical activity, diet, and lifestyle and demographic characteristics. Skeletal assessments are made with DXA, ultrasound, femoral and vertebral QCT, and vertebral radiographs. Serum and DNA has been collected. Data from the baseline examination for 5437 participants is presented here. The mean age is 73 yrs, with 43% $\geq$75 yrs. 10% are minorities, including 210 African Americans, 173 Asians, 100 Hispanics, and 55 American Indians. The population is generally educated (53% completed college) and healthy (86% rated their health as relatively good/excellent). 82% are currently married. There are few current smokers (3%) but 59% smoked previously, and 64% use alcohol at least occasionally. The mean (range) BMI is 26.9 kg/m^2 (17-51), and subjects report a mean weight increase of 10 kg since age 25. 33% have a history of fracture in a parent (father 15%, mother 22%). 17% of the participants reported a non-traumatic fracture since age 50, and 2% reported a fracture within the last 12 months. As measured by DXA, mean (range) total hip BMD is 0.951 gm/cm^2 (0.31 - 2.06) and total spine BMD is 1.06 gm/cm^2 (0.47 - 2.1). Men are followed with brief questionnaires mailed every 4 months to ascertain falls and fractures, and a mid-study questionnaire. After an average of 4.5 years, men will return for a final study visit to assess change since baseline. With this data, the risk of fracture will be examined. MrOS should provide information essential for the understanding and management of osteoporosis in men.

Disclosures: ***E. Orwoll****, Merck 2, 5; Lilly 2, 5; Proctor & Gamble 2, 5; Ligand 5.*

SU029

Periosteal Bone Formation and Resorption are Both Active at the Femoral Neck: Mechanisms for Change in Bone Size. E. Orwoll[1], S. Orwoll[1], S. Kohama*[1], G. Evans[2], R. Turner[2]. [1]Oregon Health & Science University, Portland, OR, USA, [2]Mayo Clinic, Rochester, MN, USA.

The femoral neck is a common site for fracture. It is critical to understand the factors that influence its biomechanical strength. Femoral neck size is a fundamental determinant of fracture resistance and it has recently been appreciated that change in femoral neck size occurs not only during growth but also with aging. The cellular mechanisms involved in mediating change in bone size have not been studied but clearly provide an opportunity to better understand fracture risk and to identify possible methods to change bone size therapeutically. To describe the remodeling events that occur on the periosteal surface of the femoral neck we studied specimens from double tetracycline labeled rhesus macaques. 5 animals of a variety of ages (2-12 yrs) were sacrificed; proximal femurs were carefully removed intact, preserved in 70% alcohol and prepared for histomorphometric analyses. Sections through the femoral neck were examined to determine periosteal osteoblast and osteoclast activity. Bone formation was clearly present on periosteal surfaces in all animals. 3 animals were more completely analyzed. The osteoid surface was 13% (range 8.5-20.7), the extent of double-labeled surface was 5.4% (2.5-7.0) and the mineral apposition rate was 0.5 um/day. At this rate of bone formation, the femoral neck diameter would increase at a rate of ~0.015mm/yr and the cross sectional area would be expected to increase at a rate of ~1%/year. In addition, extensive surface based osteoclastic activity was also apparent. The extent of eroded surface was 15.6% (7.2-24.7). Resorption pits contained multinucleated osteoclasts that stained positively for acid phosphatase. Resorption activity apparently arose on the periosteal surface as there was no evidence that it resulted from extension of intracortical remodeling processes (tunneling). These results document the previously unrecognized presence of surface-based remodeling at the femoral neck in adult non-human primates. In addition to bone formation, bone resorption was an active part of periosteal activity. The rates of bone formation and bone resorption are sufficient to result in biomechanically meaningful changes in femoral neck geometry. In light of the importance of femoral neck geometry in the determination of bone strength, remodeling at this site may play an important role in the determination of fracture risk. Moreover, the presence of both osteoblastic and osteoclastic activity provides the opportunity to target therapies designed to reduce the loss of bone, or to increase bone formation, at the femoral neck and thus to reduce likelihood of fracture.

Disclosures: ***E. Orwoll****, Merck 2, 5; Lilly 2, 5; Proctor & Gamble 2, 5; Ligand 2, 5.*

SU030

Soy Consumption and Bone Mineral Density in Chinese Perimenopausal Women. S. C. Ho[1], J. Woo*[2], S. Lam*[2], Y. Chen*[2], A. Sham*[2]. [1]Department of Community & Family Medicine, The Chinese University of Hong Kong, New Territories, Hong Kong Special Administrative Region of China, [2]CUHK, HK, Hong Kong Special Administrative Region of China.

Recent interest has been shown in the potential beneficial effects of phytoestrogens on bone health. As the early years of menopause are a period of rapid bone loss, and the risk for osteoporosis increases substantially, the habitual intake of soy protein and isoflavones may play a role in the retardation of bone loss in Asian women during the postmenopausal years. This study aims to investigate the relation between soy intake and bone mass in Chinese women within the first 12 years postmenopausal. We estimated the dietary intake of soy foods and other key nutrients, including dietary calcium, using the quantitative food frequency method. Bone mineral density (BMD) was measured with a dual energy x-ray densitometre (Hologic 4500A). Soy isoflavone consumption was categorised as quartiles of intake and related to BMD at different sites. We did not observe differences in BMD among the intake quartiles in women within the first 4 years since menopause. We noted generally higher BMD values with increasing soy protein intake quartiles among women 5 to 12 years postmenopause. Women belonging to the highest intake quartile had a mean intake of 19.8 ± 13.3 g/day with a range from 9.6 to 76.9 g/day. We observed a statistically significant difference between the mean BMD values at the intertrochanter and trochanter areas among women belonging to the highest and lowest soy intake quartiles. The BMD values of women from the first and fourth intake quartiles differed by about 3.5% to 7.1% at the various hip sites, while no difference was observed for the spinal BMD. The chi-square test for trend showed a significant trend ($p < 0.05$) in the increase in mean BMD values at the intertrochanter and the total hip areas among subjects with increasing quartiles of soy intake. The results remained similar after adjusting for body weight and years since menopause in the multiple linear regression analysis. Soy protein intake, together with the two variables, accounted for about 24 to 28% of the variances of the BMD values for the hip and the total body. This study of early Chinese postmenopausal women demonstrated that soy intake had a small but significant effect on the preservation of BMD after the initial years of rapid bone loss. The effects of phytoestrogens on bone health should be further explored in populations with habitual dietary soy intake, taking into account the different stages of menopausal effect.

SU031

Bone Morphogenetic Protein-2 (BMP-2) Induces Distinct Effects on Human Osteosarcoma Cell Proliferation, Differentiation and Apoptosis. E. Haÿ*, D. Modrowski, S. Le Mee*, P. J. Marie. INSERM U349, Paris, France.

We previously showed that BMP-2 promotes normal human osteoblast apoptosis through a Smad-independent, protein kinase C-dependent signaling pathway. In this study, we investigated the effects of BMP-2 on cell proliferation, differentiation and apoptosis in three human osteosarcoma (SaOS2, MG63, OHS4) cell lines. We found that rhBMP-2 (50-1000 ng/ml, Genetics Institute) increased alkaline phosphatase activity (ALP) in SaOS2 and OHS4 cells, but not in MG63 cells, with a maximal effect at 200 ng/ml. Similarly, rhBMP-2 (200 ng/ml) increased the expression of ALP, Cbfa1/Runx2 and N-cadherin mRNA and protein levels in SasOS2 and OHS4 cells, but not in MG63 cells, as shown by RT-PCR and western blot analyses. In contrast, rhBMP-2 inhibited cell proliferation in MG63 and SaOS2 cells, but not in OHS4 cells. More interestingly, rhBMP-2 (200 ng/ml) increased apoptosis in MG63 and SaOS2 cells, but not in OHS4 cells, as demonstrated by TUNEL analysis. In both MG63 and SaOS2 cell lines, rhBMP-2 stimulated caspase-9 and caspases-3, -6, -7 activity, but not caspases-2 and -8 activity. Moreover, the pro-apoptotic effect of BMP-2 in MG63 and SaOS2 cells was inhibited by calphostin C (2 µM), a selective inhibitor of protein kinase C activity, showing that BMP-2 induces apoptosis in responsive human osteosarcoma cells through a PKC-caspase-9-caspase-3, -6, -7 pathway. Transient transfection of MG63 and SaOS2 cells with a vector containing a rat BMP-2 cDNA also increased ALP and Cbfa1/Runx2 mRNA expression and induced pro-apoptotic effects, as found with exogenous rhBMP-2. These data show that 1) BMP-2 induces distinct effects on cell proliferation, differentiation and apoptosis in human osteosarcoma cell lines, depending on their stage of differentiation, 2) BMP-2 promotes apoptosis in responsive osteosarcoma cells by activating PKC and caspase-9 and caspases-3, -6, -7 activities and 3) BMP-2 overexpression reproduces the same effects as exogenous BMP-2 in responsive cells. This study suggests that exogenous BMP-2 or promotion of endogenous BMP-2 by specific agents may be useful to promote cell death of human osteosarcoma cells.

SU032

Regulation of the Cloned Aggrecan Gene Promoter by Osteogenic Protein-1 (OP-1, BMP-7). L. C. C. Yeh*[1], J. C. Lee[2]. [1]Biochemistry (MC7760), University of Texas Health Science Center, San Antonio, TX, USA, [2]Biochemistry (Mail Code 7760), The University of Texas Health Science Center, San Antonio, TX, USA.

Osteogenic Protein-1 is a member of the bone morphogenetic protein subfamily of the transforming growth factor-β superfamily and induces formation of new bone and cartilage. Previous studies have demonstrated that OP-1 stimulates the synthesis of aggrecan, a major extracellular matrix component. To investigate the molecular mechanism of transcriptional regulation of the aggrecan gene by OP-1, we constructed a clone containing a 1 kb region of the 5'-upstream sequence of the mouse aggrecan gene fused to the promoterless luciferase reporter gene in pGL2-Basic vector. Several promoter deletion constructs were also generated by unique restriction endonuclease digestion or by PCR. These DNA constructs were used in transient transfection studies using C2C12 cells. An inhibitory element of the basal transcription activity was detected in the aggrecan promoter. To examine effects of OP-1 on the promoter activity, transfected cells were treated with solvent control

or different concentrations of OP-1 for 24 h. OP-1 stimulated the 1-kb promoter construct in a dose-dependent manner with a maximum stimulation of about 2-fold. Subsequent studies with the various deletion constructs revealed that a 100 bp region was essential for the up-regulation of the aggrecan by OP-1. In summary, we identified an OP-1 response region in the promoter of the mouse aggrecan gene. The information will be useful in additional studies on the nature of transcriptional regulation of the aggrecan gene by BMPs in general and OP-1 in particular.

Disclosures: ***J.C. Lee****, Stryker Biotech 2.*

SU033

Expression of Bone Morphogenetic Proteins and Ectopic Bone Induction by Native and Primary Cultures of Rat Growth Plate Chondrocytes. R. Dhanyamraju*, J. Sipe*, H. H. T. Hsu, H. C. Anderson. Department of Pathology & Laboratory Medicine, University of Kansas Medical Center, Kansas City, KS, USA.

Endochondral bone formation is a very highly coordinated event involving many regulatory factors, which eventually leads to the replacement of cartilage with bone. The maturation of cartilage is thought to be promoted by BMPs, 1,25-OH_2 Vit D_3, retinoic acid, c-myc, ascorbic acid and *Ihh*. In this study, we report the expression of BMPs by primary cultures of rat growth plate chondrocytes. Further, we attribute the osteoinductivity of rat growth plate chondrocytes to the presence of BMPs in them. Chondrocytes were obtained from collagenase-digested tibial and femoral growth plate cartilage of 4 week old rachitic rats. The isolated chondrocytes were plated as monolayers at a density of 0.5 X 10^6 cells/35 mm plate and grown for 17 days in BGJ_b medium supplemented with 10% FBS and 50 µg/ml ascorbic acid. Immunohistochemistry with anti-BMP 2, 4 and 6 showed that BMP expression was associated with maturing hypertrophic central chondrocytes. Expression of BMP-2, 4 and 6 in primary cultures of rat growth plate chondrocytes suggests that BMPs might have a role in the differentiation of chondrocytes. The observation that rat growth plate chondrocytes expressed BMPs *in vivo* and in primary cultures led us to investigate whether these cells would be osteoinductive when implanted subcutaneously in Nu/Nu mice. Soluble bone inducing agent (BIA) was extracted from freeze-dried, native rat growth plate chondrocytes in 4M Gu-HCl and bioassayed for osteoinductivity by subcutaneous implantation in Nu/Nu mice. Our bioassay results showed that freeze-dried extracts of chondrocyte implants were capable of ectopic bone initiation by host mesenchymal cells as revealed by light microscopy and high alkaline specific activity. In conclusion, native and primary cultures of rat growth plate chondrocytes express BMP-2, 4 and 6 and are osteoinductive in subcutaneous implants in mice.

SU034

Effects of Radiation on Ex Vivo Gene Therapy-Directed Osteogenesis. B. Nussenbaum*, R. B. Rutherford, T. N. Teknos*, K. J. Dornfeld*, P. H. Krebsbach. University of Michigan, Ann Arbor, MI, USA.

Craniofacial defects commonly arise from ablative cancer surgery, and autologous bone grafts are used for reconstruction. To avoid donor site morbidity, innovative bone regenerative strategies are being investigated using protein, cell, or gene therapy. Because radiation remains a common post-operative treatment for head and neck cancers, it is critical to determine if these new approaches are effective in healing defects that are challenged by therapeutic doses of radiation. The purpose of this study was to determine if radiation affects the ability of ex vivo gene therapy to heal bone critical sized defects. Dermal fibroblasts derived from Fisher rats were transduced ex vivo using an adenoviral vector containing the cDNA for BMP-7 (AdCMV-BMP-7) for 24 hours at 1000 PFU/cell. Two million cells were loaded onto a 9 mm diameter collagen sponge. Nine mm calvarial defects were created in 200 gm Fisher rats. Either a transduced cell-seeded sponge or an inlay calvarial bone graft was placed in the defect. Two weeks post-operatively, either no radiation or a single 12 Gy radiation dose was delivered to the operated area, and the tissue was harvested 4 weeks later. For the bone graft specimens, histology was used to determine degree of healing at the wound margins. For the gene therapy specimens, histomorphometry was used to determine the defect surface covered with bone, defect area, and percent of defect filled by new bone. Statistical analysis using the unpaired t-test was performed. None of the inlay bone grafts in radiated (n=5) or non-radiated (n=5) rats had gross or histologic evidence of complete healing at the wound margins. For the gene therapy groups, gross estimation revealed near-100% defect healing including the wound margins in the non-radiated defects (n=3), while the radiated defects (n=10) had variable amounts of bone production (30-90%) with incomplete fusion at the margins. Comparison of these 2 groups revealed a statistically significant difference favoring the non-radiated group for mean percentage of defect surface covered by bone (90% vs. 65%, $p<0.02$), and mean percentage of defect area filled by new bone (47% vs. 32%, $p<0.02$). In conclusion, BMP-7 ex vivo gene therapy successfully regenerated bone in rat calvarial critical sized defects despite receiving a therapeutic dose of radiation. Both qualitatively and quantitatively, the defects were not as well healed at 4 weeks post-radiation when compared to the non-radiated rats. The free inlay bone grafts did not heal at the wound margins independent of radiotherapy, which suggests that BMP-7 ex vivo gene therapy was more effective for healing calvarial defects in this defect model.

SU035

Stimulation of BMP Signal in Osteoblasts by Dexamethasone and Testosterone but not by Estradiol. K. Nakayama[1], S. Watanabe*[1], S. Fukumoto[2], Y. Takeuchi[1], T. Fujita*[1]. [1]Department of Medicine, University of Tokyo, School of Medicine, Tokyo, Japan, [2]Department of Laboratory Medicine, University of Tokyo Hospital, Tokyo, Japan.

Steroid hormones, such as glucocorticoid and sex steroids, are involved in bone formation. However it is largely unknown how steroid hormones affect osteoblastic functions at this moment. Bone morphogenetic proteins (BMPs) play a pivotal role for osteoblastic differentiation and bone formation. Thus, it is speculated that there are some interactions between BMP signal and steroid hormones. Since BMPs regulate the transcription of their target genes through Smad proteins, some steroids may affect the transcriptional activity of Smads. We, therefore, investigated actions of glucocorticoids, testosterone and estrogen on BMP signal at the transcriptional level. Because mouse Smad6 promoter has at least one BMP responsive element, we used a reporter plasmid called mS6-lux that has mouse Smad6 promoter in the upstream of Luciferase gene to detect BMP signal. We introduced mS6-lux into mouse osteoblastic MC3T3-E1 cells and treated them with 10 nM dexamethasone (DEX), 10 nM 17β-estradiol (E2) or 10 nM dihydrotestosterone (DHT) for 48 hours in the presence or absence of 100 ng/ml BMP-2, followed by luciferase assay. We also measured alkaline phosphatase (ALP) activity of similarly treated MC3T3-E1 cells. The activities of mS6-lux and ALP in MC3T3-E1 cells induced by BMP-2 were enhanced by DEX and DHT but not by E2. None of them had significant effects in the absence of BMP-2. These results indicate that the stimulatory effect of DEX and DHT on osteoblastic differentiation is at least partially mediated via the enhancement of BMP signal by these steroid hormones. This may explain the reason why physiological amounts of glucocorticoid are essential for the osteoblastogenesis. More importantly, since E2 failed to mimic the positive effect of DHT, androgen receptor (AR) but not estrogen receptor (ER) may be directly involved in the osteoblastogenesis and bone formation. Recent studies demonstrate a crucial role of ER activation by E2 for the suppression of bone resorption both in female and male. However, our observations suggest that testosterone has some stimulatory actions on bone formation via AR activation which may result in the enhancement of the transcriptional activity of BMP-regulated Smads.

SU036

Articular Chondrocyte Maturation Is Induced By Shifting Signaling Pathway Dominance from TGF-β to BMP. M. J. Zuscik, J. F. Baden*, T. J. Sheu*, E. M. Schwarz, R. J. O'Keefe, J. E. Puzas, R. N. Rosier. Orthopaedics, University of Rochester, Rochester, NY, USA.

Maintenance of the articular surface depends on the function of articular chondrocytes (ACs) which produce matrix and are constrained from undergoing terminal maturation. Under unique circumstances, such as in osteoarthritis, these unknown molecular constraints are lost and ACs recapitulate the maturational process that occurs during endochondral ossification. The aim of this study was to identify these unknown suppressive constraints, with the goal of understanding the molecular processes at work during inappropriate stimulation of AC hypertrophy. To address this aim, a novel cell model was developed which utilizes 5-azacytidine (Aza) to induce maturation in cultured ACs. Aza, an s-triazine nucleoside used to treat leukemias, is known to un-mask expression of silenced genes in a number of cell models by replacing cytidine in the DNA, thus blocking the suppressive effect of cytidine methylation on gene transcription. ACs, which do not spontaneously express markers of maturation such as type X collagen (colX), indian hedgehog and alkaline phosphatase, were induced to express these markers by an 8 day treatment with 15 µg/ml Aza. Since it is well established that TGF-β and BMP-2 regulate the respective suppression or induction of chondrocyte maturation, we hypothesized that this Aza-induction of maturation was facilitated via a shift in signaling dominance from TGF-β to BMP. We tested this hypothesis i) by comparing Aza effects with those induced by over-expressing the BMP-2 signaling molecule smad1 or by blocking signaling through the TGF-β smads (2 and 3) using a dominant negative (Δ) approach, ii) by examining the impact of Aza on the expression of the TGF-β smads (2 and 3), the BMP-2 smads (1 and 5), and the ubiquitin E3 ligase smurf2, a protein that initiates the degradation of smad2 and 3, and iii) by using a pulse/chase method to measure the rate of smad2 and 3 degradation following Aza treatment. We found that i) over-expression of smad1, Δsmad2 or Δsmad3 mimicked Aza by inducing expression of the hypertrophic marker colX, ii) Aza-treated ACs displayed less smad2 and 3 protein and increased smad1, smad5 and smurf2 protein, and iii) Aza mimics smurf2 by accelerating smad2 and 3 degradation. These data indicate that Aza induction of AC maturation is facilitated by driving BMP signaling dominance via up-regulation of smad1 and 5 and via increased degradation of smad 2 and 3 by smurf2. We suggest that inappropriate maturation of ACs, such as in osteoarthritis, may be due to dis-regulation of the delicate balance between these pathways leading to the dominance of BMP signals and concomitant maturation.

SU037

Regulation of Osteoblastic Differentiation by BMP Inhibitors. A. Nifuji[1], Y. Ohyama*[1], K. Miyazono*[2], M. Noda[1]. [1]Dept. Molecular Pharmacology, Tokyo Medical and Dental University, Tokyo, Japan, [2]Dept. Molecular Phathology, The University of Tokyo, Tokyo, Japan.

The balance between BMP and BMP inhibitors is crucial for proper skeletal cell differentiation. There are several types of BMP inhibitors including noggin, chordin, tsg, gremlin, Cerberus, Dan, smad6 and smad7. Many of those inhibitors are known to be expressed in the skeletal tissues in development. However, it is not clear whether each BMP inhibitor is functionally equivalent to block skeletal cell differentiation. To address this point, we investigated how and when each BMP inhibitor functions as regulator of osteoblast differentiation by using an adenovirus constructs expressing noggin, smad6 and smad7. When we infected adenovirus expressing noggin into MC3T3 E1 cells at moi250, the increase in alkaline phosphatase (ALP) activity induced by the addition of ascorbic acid and beta glycerophosphate was blocked. Mineralized nodule formation estimated by Von Kossa and Alizarin red staining did not differ between Lac Z-infected and noggin-infected cells at moi 250, suggesting that noggin blocked at the early stage rather than maturation stage of osteogenic differentiation. In contrast to noggin, when we infected adenovirus expressing smad 6, both ALP activity and mineralized nodule formation were blocked when compared with lacZ-expressing adenovirus. Similar results were obtained by using smad 7 expressing adenovirus. These data suggest that the effects of secreted BMP inhibitors on osteoblastic differentiation are not equivalent to those of intra-celluar BMP inhibitors.

SU038

Hoxc-8 C-terminal Domain Sufficiently Inhibits BMP-induced OPG Expression. S. Bai*, M. Wan, X. Cao. Pathology, University of Alabama at Birmingham, Birmingham, AL, USA.

Two transmembrane proteins, RANKL and RANK, mediate the cell-cell contact between osteoblasts and osteoclast precursor cells which is required for osteoclast differentiation and maturation. Osteoprotegrin (OPG) is an osteoblast-secreted decoy TNF receptor. It binds to RANKL, blocks the interaction between RANKL and RANK, and then inhibits osteoclast differentiation and maturation. BMPs stimulate OPG transcription. Previously, Hoxc-8 was identified as a transcriptional repressor on the OPG promoter. Smad1, one of the BMP signal specific effectors, interacts with Hoxc-8, dislodges Hoxc-8 from its binding, and stimulates OPG expression. Hoxc-8 was also identified as interacting with Smad6, one of the inhibitory Smad proteins, through its hexapeptide motif. However, the repressive domain of Hoxc-8 and its transcriptional repressive mechanism remained unclear. To address this question, we mapped Hoxc-8 and identified that the N-terminal domain of Hoxc-8 acts as its transactivation domain while the highly conserved domain within Hox proteins, including its hexapeptide motif, homeodomain and the C-terminal domain (Hoxc-8PHC), mediates its repressive activity. Overexpression of the Hoxc-8 N-terminal domain and the hexapeptide motif (Hoxc-8NP) stimulates OPG promoter activity while Hoxc-8PHC represses OPG promoter activity. Acetylation state of core histones plays a critical role in gene transcription regulation. Hoxc-8 was identified to interact with HDAC-1. To examine the mechanism of Hoxc-8PHC repressive activity, we performed an immunoprecipitation assay and identified that Hoxc-8PHC interacts with HDAC-1, indicating that Hoxc-8PHC recruits HDACs to the OPG promoter to inhibit OPG expression. To test the activity of Hoxc-8PHC on endogenous OPG expression in human bone marrow stromal cells, we generated Hoxc-8PHC expression retrovirus. Overexpression of Hoxc-8PHC inhibited BMP-stimulated endogenous OPG expression in human bone marrow stromal cells. These findings demonstrate that Hoxc-8PHC is the repressive domain of Hoxc-8. In summary, the finding of different functions of Hoxc-8 domains on OPG expression regulation helps us to understand the mechanism of BMP signaling and Hox proteins in bone cell differentiation and will provide us a scientific basis to develop potential clinical therapies.

SU039

Dlx5 Stimulates Osteoblast Differentiation in the Presence of Noggin, an Inhibitor of BMP Signaling. I. Erceg*, I. Marijanovic, M. S. Kronenberg, I. Kalajzic*, T. Tadic*, A. C. Lichtler. Department of Genetics and Developmental Biology, University of Connecticut Health Center, Farmington, CT, USA.

Previous studies from our laboratory and others have demonstrated that the homeodomain protein Dlx5 is present in differentiated osteoblasts, is induced by BMPs, and can induce osteoblastic differentiation. This suggests that Dlx5 may be an important mediator of BMP induction of osteoblastic differentiation. To test this hypothesis, we blocked the function of endogenous BMP in a primary in vitro chick calvarial osteoblast differentiation system using noggin, and supplied exogenous Dlx5 using an unregulated RCAS retroviral expression vector. Our hypothesis predicted that blocking BMP action would inhibit osteoblastic differentiation, as has been demonstrated previously, and that Dlx5 expression would stimulate expression of osteoblastic markers. We used an RCAS vector of subtype A to express noggin, and a subgroup B RCAS vector to express Dlx5. RCAS-noggin alone strongly inhibited differentiation, as expected. Expression of Dlx5 in the presence of noggin consistently induced higher levels of osteocalcin mRNA, although induction was not to the levels observed with Dlx5 alone. Our results suggest that Dlx5 is a significant mediator of BMP induction of osteoblast differentiation. However, it appears that BMPs may induce one or more other factors that cooperate with Dlx5 to induce the full expression of the osteoblast phenotype.

SU040

Mechanisms of BMP2-Induced Heterotopic Bone Formation. A. Davis[1], E. Olmsted-Davis[1], Z. Gugala*[2], K. Moran*[2], R. Lindsey*[2], E. Shore[3], F. Kaplan[3], F. Gannon[4]. [1]Pediatrics/CAGT, Baylor College of Medicine, Houston, TX, USA, [2]Orthopedic Surgery, Baylor College of Medicine, Houston, TX, USA, [3]Orthopedic Surgery, University of Pennsylvania, Philadelphia, PA, USA, [4]Orthopedic Pathology, Armed Forces Institute of Pathology, Washington, DC, USA.

Bone morphogenetic protein 2 (BMP2) belongs to a family of growth factors which induce both orthotopic and heterotopic bone formation, and is currently being developed for clinical use in bone healing. However, little is known about the mechanism by which BMP2 induces this process. We have developed a mouse model to identify the key factors necessary for BMP2 -induced bone formation as well as the initial events that occur upon delivery of the BMP2 protein. In this model, cells transduced to express and secrete BMP2 were injected directly into the muscle and the progression of bone formation was then followed histologically. This model system utilized a novel adenovirus type 5 vector, Ad5F35BMP2, containing a CMV-BMP2 cDNA within the E1 region, but has an adenovirus type 35 fiber replacing the normal adenovirus type 5 fiber. Comparison of this virus to the traditional Ad5BMP2 vector demonstrated enhanced virus uptake and a higher level of BMP2 expression. A correlation was found between bone formation and the level of BMP2 expression. The results also demonstrated that delivery of the BMP2 by mesenchymal stem cells is not required for bone formation since other fibroblastic cells transduced to express similar levels of BMP2 can induce bone formation as effectively. Immunohistochemical analysis using an antibody specific to human cells demonstrated that the majority of cells in the newly forming bone were recruited from the murine host, rather than from the transduced human cells used to deliver BMP2. Histological analysis demonstrated that one of the first events is the appearance of fibroblast-like cells in between the muscle fibers, leading to edema, and eventually new vessel formation in the tissues. This process led to destruction of muscle fibers with subsequent proliferative expansion of both fibroblastic and chondrocytic-like cells outward with eventual engulfment and death of the skeletal muscle. This degeneration of muscle fibers resembled the early phases of fibrodysplasia ossificans progressiva.

SU041

CREB and Smads Interact at the Smad 6 Promoter. A. M. Ionescu*, E. M. Schwarz, J. E. Puzas, R. N. Rosier, R. J. O'Keefe. Orthopaedics, University of Rochester, Rochester, NY, USA.

BMP's are known stimulators of chondrocyte maturation. Smad6, an inhibitor of the BMP signaling, was examined as a potential target for the inhibitory effects of PTHrP on chondrocyte maturation. PTHrP and BMP-2 effects were examined on the 3GC2-lux reporter in embryonic upper sternal chondrocyte cell cultures. This reporter is a 3X repeat of a 22 bp sequence derived from the BMP responsive region of the Smad6 promoter. The promoter contains a Smad binding site with adjacent sequences similar to CRE sites previously described in the osteocalcin and Ubx promoters. BMP treatment caused 4.1-fold and PTHrP a 4.2-fold stimulation of luciferase activity, while in combination, the effects were additive. Mutation of the Smad site abolished BMP responsiveness without altering PTHrP effects, suggesting that PTHrP induces the reporter independent of Smad signaling. PTHrP induction of the Smad6 promoter was blocked with dominant negative CREB (A-CREB), while co-transfections with dominant negatives specific for c-Fos, JunD, ATF-2, and CREB had no effect on reporter activation. Furthermore, gain of function experiments through co-transfection with either wild type CREB, constitutively active CREB or PKA expression vector had a stimulatory effect on the reporter in both control and PTHrP treated cells. EMSA was performed using the Smad6 BMP-responsive promoter oligonucleotide. In cultures transfected with wild type Flag-CREB, binding was enhanced 5 fold as compared with nuclear extracts from control samples. Flag-Creb binding was inhibited by anti-Flag antibody. PKA/CREB signaling was found to enhance BMP signaling; co-transfection with PKA or CREB cdna slightly increased BMP driven luciferase activity while A-CREB decreased the BMP effect from 12.6 to 7.5 fold. The findings demonstrate the requirement of CREB for maximal activation of the Smad6 reporter. However, CREB is not a direct target of BMP signaling since BMP-2 did not increase CREB activity at either of two CREB responsive reporters, one driven by multiple consensus CREs and the other driven by a Gal4 response element sensitive to CREB transactivation. In contrast, PTHrP induced both reporters. The functional importance of CREB in BMP-mediated activation of Smad6 expression was examined. BMP-2 stimulated Smad6 expression 13 fold at two-hours. However, in cultures infected with a replication competent retrovirus expressing ACREB, Smad6 induction was reduced 50% while control viral infection had no effect. The findings demonstrate that CREB acts in association with Smads to induce transcription at the Smad6 promoter. Induction of Smad6 is a potential mechanism involved in the inhibition of differentiation by PTHrP.

SU042

***In Vivo* Retroviral (MLV)-mediated BMP-2/4 Hybrid Gene Therapy Markedly Enhances Callus Formation in the Rat Femoral Fracture Model.** C. H. Rundle, N. Miyakoshi*, Y. Kasukawa, S. T. Chen*, M. H. C. Sheng*, J. E. Wergedal, K. H. W. Lau, D. J. Baylink. J.L. Pettis VAMC, Loma Linda, CA, USA.

Serious injuries, such as bone fractures, constitute a highly significant health problem that is projected to increase over the next several decades. In this study we tested whether 1) a murine leukemia retrovirus (MLV) vector could target transgene expression to the fracture site, and 2) if this application of gene therapy could safely promote fracture healing. Regarding the first hypothesis, because retroviruses transduce proliferating cells and there is a burst of periosteal cell proliferation at the fracture site shortly after bone fracture, MLV vectors should specifically target the fracture site for transgene expression. The transgene we applied was the bone morphogenetic protein (BMP)-2/4 hybrid gene. We chose the BMP-4 gene because it undergoes a considerable increase in expression during normal fracture healing. We found that using the BMP-2 signal sequence significantly enhanced and prolonged the secretion of mature BMP-4 in stromal cells transduced with the BMP2/4 hybrid gene, as compared to the native BMP-4 gene. Twelve week-old male Fischer 344 rats underwent femoral fracture and were divided into groups of 4 animals receiving lateral injections of either 1) MLV-BMP-2/4 transgene, or 2) MLV-B-galactosidase marker transgene (control). Examination by Faxitron and pQCT during healing revealed that BMP-2/4 therapy produced dramatic and significant increases ($p<0.02$) in the cross-sectional areas of calluses at days 7 (1.78-fold), 14 (2.86-fold) and 28 (2.87-fold). These calluses showed significant increases ($p<0.02$) in the bone mineral content at days 14 (5.65-fold) and 28 (3.11-fold). This bone formation suggested successful MLV targeting of BMP-2/4 gene function, and was confirmed by strong immunocytochemical staining for BMP-4 expression at the fracture site. All fractures displayed qualitatively normal bone histology. To examine the long-term response to this therapy, two control and two BMP-2/4 MLV-treated animals were monitored for 70 days. At this time, Faxitron X-rays revealed almost complete remodeling of the new bone in the fracture callus in both groups. Histologic studies showed there were no immune infiltrates in any fracture tissues, suggesting that MLV was nonimmunogenic. PCR analysis of DNA isolated from extraskeletal tissues, including the gonads, failed to detect transgene sequence at any time, indicating that this therapy was safe. In summary, we have demonstrated for the first time that the MLV-based retroviral vector is safe and effective for the introduction of BMP-2/4 gene expression to a fracture site, where it promotes greater fracture callus formation.

SU043

Autocrine Effect of Transgene Affects Bone Healing Elicited By Different Populations of Muscle Derived Cell Transduced With Retroviral Vector Expressing BMP4. H. Peng, A. Usas*, B. Gearhart*, J. Cummins*, J. Huard. Orthopeadics, University of Pittsburgh, Pittsburgh, PA, USA.

Gene therapy has emerged as an effective way to enhance bone repair through delivering osteogenic growth factor, mainly bone morphogenetic proteins (BMPs). A good gene therapy regime consists optimal combination of three components: therapeutic gene or transgene, delivery vector and cellular vehicle. The aim of this study is to determine whether the response of cellular vehicle to the autocrine effect of therapeutic gene product can affect the performance of an ex vivo gene therapy strategy, and to investigate the possible underlining mechanism. We separated different populations of rat muscle-derived cells based on their ability to adhere to collagen type I, and then compared their response to BMP2 and BMP4 stimulation. These initial comparisons led to the selection of two distinguish populations (PP1 and PP6) of rat muscle derived cells: PP1 did not, but PP6 did respond to BMP2 and BMP4 by osteogenic differentiation, as evidence by the expression of an early osteogenic marker, alkaline phosphotase. PP1 and PP6 cells expressed similar level of BMP4 following transduction. When implanted into critical-calvarial defects, transduced PP1 cells expressing BMP4 healed the defect in all animal 7 weeks post implantation. In contrast, PP6 cells expressing BMP4, similar to control cells expressing LacZ, did not heal the defects in all animals even after 14 weeks post implantation. The inability of PP6 cells to heal the defect correlated to their lower rate of proliferation when compared to PP1 cells expressing BMP4 or PP6 cells expressing LacZ. The osteogenic differentiation of rat muscle derived cells correlates conversely with their proliferation potential under BMP4 stimulation. Thus, BMP4 protein directly inhibited proliferation of PP6 cells, but not PP1 cells. BMP4 also induced apoptosis of PP6 cells, but not PP1 cells. Thus, an effective bone gene therapy should use cellular vehicle, such as rat muscle-derived PP1 cells, that does not respond adversely to the autocrine effect of the therapeutic gene.

SU044

Dysregulated BMP4 Signaling in FOP Lymphocytes. L. Serrano de la Peña*, P. C. Billings*, E. M. Shore, F. S. Kaplan. Orthopaedic Surgery, University of Pennsylvania School of Medicine, Philadelphia, PA, USA.

Fibrodysplasia ossificans progressiva (FOP), a devastating disease of bone formation, is characterized by a process of heterotopic endochondral ossification which results in destruction and substitution of ligaments, tendons and skeletal muscle by bone. Bone morphogenetic proteins (BMPs), members of TGF-b superfamily of proteins, are potent osteogenic morphogens and are able to induce ectopic bone formation in animal models. Therefore, it was not surprising to find misregulation of BMP4 mRNA and protein in cultured lymphocytes and pre-osseous fibroproliferative lesional cells obtained from FOP patients. In order to examine downstream components of the BMP4 signaling pathway, we used fluorescence activated cell sorting analysis and observed that levels of BMP receptor type IA (BMPRIA) are 6 fold higher on the surface of FOP cultured lymphocytes compared with cells from unaffected individuals. These results are reproducible in uncultured lymphocytes from fresh peripheral blood. BMP4 downstream signal transmission was analyzed by immunoprecipitation and immuno-blots using antibodies against phosphorylated and unphosphorylated pathway targets. FOP cells exhibit basal hyperphosphorylation and ligand insensitivity of the BMP receptor complex relative to control cells. This insensitivity to exogenous BMP4 protein was confirmed when cells were treated with Noggin, a potent BMP4 antagonist. Following Noggin exposure, the level of BMPRIA phosphorylation remained constant in FOP cells, but decreased in normal cells, as expected. At least two distinct intracellular pathways mediate BMP signals to the nucleus. Although Smad-mediated signaling appears to be the major pathway for BMPs in many cell types, we find a predominant activation of P38 stress-activated protein kinase in lymphocytes. P38 protein, a member of the mitogen-activated protein kinase (MAPK) superfamily, shows the same pattern of chronic activation as BMPRIA in FOP lymphocytes but not in control cells. Our results suggest that FOP lymphocytes exhibit dysregulated BMP signaling, predominantly through the MAPK pathway.

SU045

BMP-2-induced Phosphatidylinositol 3 Kinase (PI 3-K) Regulates GATA-4 and MEF2 Ttranscription Factors During Cardiomyocyte Differentiation. N. Ghosh-Choudhury[1], S. L. Abboud[2], G. Ghosh Choudhury*[3]. [1]Pathology, University of Texas Health Science Center at San Antonio, San Antonio, TX, USA, [2]Pathology, University of Texas Health Science Center, South Texas Veteran's Health Care System, San Antonio, TX, USA, [3]Medicine, University of Texas Health Science Center, GRECC, South Texas Veteran's Health Care System, San Antonio, TX, USA.

BMP-2 plays a pivotal role in cardiac development in mice. BMP-2 induces MEF2C and GATA-4, two critical transcription factors, which regulate cardiac development. In this study, we investigated the role of PI 3-K in cardiomyocyte differentiation using p19CL6 (CL6) cells as model. We used GATA-4 and specially MEF2 as the marker for cardiomyocyte differentiation. Incubation of CL6 cells with BMP-2 increased PI 3-K activity in PI 3-K and antiphosphotyrosine immunoprecipitates. BMP-2 stimulated GATA-4 and MEF-2 expression as determined by immunoblot analysis. Ly294002, a specific inhibitor of PI 3-K, significantly blocked BMP-2-induced expression of both transcription factors. To investigate the role of PI 3-K in MEF-2-dependent transcription, we performed gel mobility shift assay (GMSA) with nuclear extracts from BMP-2-treated CL6 cells using a ^{32}P-labeled DNA element, which recognizes this transcription factor. BMP-2 stimulated protein-DNA complex formation, which was significantly inhibited by 100-fold excess of cold oligonucleotide. Use of MEF2 antibody in supershift analysis showed the presence of this transcription factor in the DNA-protein complex. Ly294002 significantly reduced BMP-2-induced MEF-2-DNA complex formation. To investigate the transcriptional activity of MEF2 in BMP-2-induced cardiomyocyte differentiation, we used a reporter plasmid (MEF2LUC) in which the firefly luciferase gene is driven by 3 copies of the MEF2 DNA binding element. BMP-2 increased transcription of this reporter in CL6 cells. Ly294002 inhibited BMP-2-induced transcription of this reporter gene. Taken together these data demonstrate for the first time that PI 3-K regulates BMP-2-induced GATA-4 and MEF2 expression, two transcription factors necessary for cardiac development. Furthermore our data provide the first evidence that PI 3-K signaling modulates BMP-2-induced transcriptional activation of MEF2 during cardiomyocyte differentiation.

SU046

Local Bone Morphometry - A New Method to Assess Bone Failure. R. Müller, M. Stauber*. Institute for Biomedical Engineering, ETH and University of Zuerich, Zuerich, Switzerland.

Today, it is widely accepted that bone microarchitecture is a significant contributor to trabecular bone strength. Despite the progress in microstructural imaging over the last decade only few approaches have been presented expanding beyond classical 2D bone morphometry. Yet, it is very clear that bone microarchitecture cannot be explained without including direct 3D approaches. Especially, the ability to decompose the bone microarchitecture to extract individual structure features, such as trabecular rods and plates, show high potential to perform local bone morphometry. Local in that sense means that we are now able to quantify individual trabeculae with respect to their volume, thickness, orientation and type of structure. For the purpose of the project, we have scanned a total of 50 human vertebral bone samples (Ø8 mm x 10 mm) using µCT 40 imaging system (Scanco Medical, Switzerland) providing an isotropic resolution of 34 µm. After thresholding, a thinning procedure was applied to the 3D images yielding in a homotopic skeleton. The use of a topological classification algorithm allowed distinction of different point types in the skeleton enabling a complete decomposition of the skeleton in its rods and plates. We then used a dilatation algorithm to identify the volumetric extent of each trabecular rod and plate within the original structure. Subsequently, direct 3D morphometry was used to compute volume, thickness and structure type of each single element. In earlier experimental studies, we have found that bone failure can be predicted best using a “weakest link of the chain” approach. Local bone morphometry allowed identifying such “weak” trabeculae and therefore will improve our predictive power in the determination of bone strength and failure behavior. With upcoming in vivo high-resolution imaging systems, local bone morphometry is likely to become a standard tool not only for the assessment of bone quality in biopsies but also in the living.

SU047

Use of DXA, pQCT, Histomorphometry, and Micro-CT to Explore Bone Changes After Ovariectomy in Old Cynomolgus Monkeys. J. Legrand[1], C. Fisch[2], A. Bécret[2], S. de Jouffrey*[2], J. R. Claude*[3]. [1]Beaufour-Ipsen, Paris, France, [2]CIT, Evreux, France, [3]Faculty of Pharmacy, Paris, France.

The osteopenic, ovariectomized cynomolgus monkey is considered as a model of postmenopausal established osteoporosis in women and used for the assessment of the pre-clinical efficacy and safety of agents intended to prevent or treat this disease. We used dual X-ray absorptiometry (DXA), peripheral quantitative computed tomography (pQCT) and microcomputed tomography (micro-CT) in conjunction with histomorphometric analysis of undecalcified slices to explore changes in the bone structure that take place in vertebrae of old, ovariectomized cynomolgus monkeys. Mature female cynomolgus monkeys from Mauritius, approximately weighing 4 kg, were randomly allocated in two groups. Seven animals were ovariectomized (OVX) and thirteen were sham-operated (SHAM). Twenty months after surgery, bone mineral density (BMD) of the L2-L5 lumbar vertebral block and of the L4 lumbar vertebra were measured in vivo by DXA. The animals received dual bone labeling by alizarin complexone and were euthanized. After necropsy, the BMD of the L4 lumbar vertebra was measured ex vivo by DXA, and by pQCT. The L3 lumbar vertebrae were analyzed by high-resolution micro-CT. Undecalcified sections from the vertebral body of L4 vertebrae were Goldner stained and examined with a light microscope or left unstained and examined with a fluorescent microscope for the determination of histomorphometric parameters for both trabecular and cortical bone. The bone mineral density measurements of the L4 vertebrae obtained by DXA in vivo and ex vivo were highly correlated and were 9% statistically lower in OVX than in SHAM animals. The cortical and trabecular BMD levels measured by pQCT were also statistically 5 to 8% lower in OVX than in SHAM animals depending on the level of the slice. The cortical thickness was identical in both groups, but the cortical porosity was statistically 47% higher in OVX than in SHAM animals. The histomorphometric structural parameters of the trabecular bone did not statistically differ between groups, when measured by micro-CT or histomorphometry. These results suggest that the lower bone mineral density observed in OVX when compared to SHAM animals does not result from a decrease in bone volume but is the consequence of an increased bone remodeling, which induces an increase in cortical porosity and a secondary mineralization deficit.

SU048

Collagen Cross-Link Maturity and Crystallinity Indices Differ Markedly in Recombinant Congenic Mice Having Divergent Calculated Tissue Strength. R. D. Blank[1], M. Kaufman*[2], S. L. Bailey*[3], S. N. Coppersmith*[2], T. H. Baldini*[4], A. L. Boskey[5], P. Demant*[6], E. P. Paschalis[5]. [1]Medicine/Endocrinology, University of Wisconsin, Madison, WI, USA, [2]Physics, University of Wisconsin, Madison, WI, USA, [3]Physics, College of William & Mary, Williamsburg, VA, USA, [4]Biomechanics and Biomaterials, University of Colorado, Boulder, CO, USA, [5]Research Division, Hospital for Special Surgery, New York, NY, USA, [6]Genetics, Netherlands Cancer Institute, Amsterdam, Netherlands.

The structural strength of a bone can be partitioned into architectural and material components. In 3-point bending tests of 6 month old female humeri from the HcB/Dem recombinant congenic series, 2 strains differed markedly in calculated failure stress as summarized in the table. We used Fourier Transform Infrared Spectroscopic Imaging (FTIRI) to determine whether differences in collagen cross-link maturity, crystallinity, or spatial ordering could account for the large difference in calculated tissue strength between these 2 strains with similar mineral content. Cross-link maturity and crystallinity were assayed as the absorbance ratios at 1660:1690 cm^{-1} and 1030:1020 cm^{-1}, respectively. One-dimensional spatial correlation functions were estimated to compare the uniformity of the indices within fields. For HcB/8, the mean cross-link maturity index is 1.654 and the median is 1.641. The mean and median HcB/23 cross-link maturity indices are 1.273 and 1.365, respectively. The difference in cross link maturity is highly significant ($\chi^2 = 1968$, 9 df, $P < 10^{-15}$). For HcB/8, the mean and median crystallinity index are 0.950 and 0.974, respectively. In HcB/23, the corresponding values are 0.840 and 0.909. As for cross link maturity, the difference between the strains is highly significant ($\chi^2 = 400$, 6 df, $P < 10^{-15}$). Cross-link maturity and crystallinity are highly and similarly correlated in both strains, with correlation coeffecients of 0.751 for HcB/8 and 0.758 for HcB/23 ($P < 10^{-16}$ in both strains). We did not find evidence of significant differences between the strains' 1-dimensional spatial correlation functions. The high correlation between cross-link maturity and crystallinity reflects the interdependence of the protein and mineral elements of bone matrix. The data illustrate the usefulness of FTIRI to examine bone quality and relate it to biomechanical performance.

Anatomic and Biomechanical Performance of HcB/8 and HcB/23 Mice

	HcB/8 (N=10)	HcB/23 (N=9)	P value
Body Mass (g)	19.9 ± 1.5	23.5 ± 1.1	$< 10^{-4}$
Humeral Length (mm)	11.1 ± 0.3	11.3 ± 0.2	NS
***I* (mm^4)**	0.041 ± 0.009	0.079 ± 0.011	$< 10^{-6}$
Failure Load (N)	7.9 ± 1.4	8.1 ± 0.9	NS
Structural Stiffness (N/mm)	22 ± 7	23 ± 5	NS
Ash Percentage	68.6 ± 1.0	70.2 ± 1.5	NS
Failure Stress (MPa)	192 ± 36	118 ± 13	$< 10^{-4}$

SU049

Mouse Organ Culture Assay To Identify Bone Anabolic Agents. M. L. Jankowsky*, A. Houghton, R. W. Farmer*, M. Wos*, M. Petrey*, M. W. Lundy. Procter & Gamble Pharmaceuticals, Mason, OH, USA.

Neonatal mice calvaria explants have been used to demonstrate the ability of PGE2 and PTH to increase bone resorption in vitro. Both these agents also increase bone formation and volume when administered parenterally to mice and rats. We investigated whether PGE2, PTH or BMP-2 could also increase bone formation in the mouse calvarial organ culture assay. Calvaria were removed from three-four day old mice, cut in half and incubated overnight in BGJ-b media. Media was changed and test agents added to each calvaria the next day, and three days later. Calvaria were removed on day 7, weighed, processed for paraffin embedding and sections obtained at 0.5 mm intervals. The effects of BMP2 on mineralized bone, osteoid, cellular matrix and cartilage were measured using a) point-count stereology (Cavalieri method) and analyzed using Fishers protected t-test, or b) semi-quantitative methods (graded 0 - 4 with 1 = normal) and analyzed using the Chi-square statistic. In a separate study, BMP2, PGE2 and PTH were evaluated using only the semi-quantitative method. PGE2, PTH and BMP2 all increased calvarial weight, but by increasing the amount of different tissues. PGE2 primarily increased the amount of osteoid, with minimal decreases in the amount of mineralized bone. PTH dramatically increased loss of the mineralized bone, but increased the amount of connective tissue containing osteoblast-like cells and matrix that often stained like osteoid but wasn't adjacent to mineralized bone. BMP2 increased cartilage, without increasing osteoid, as measured by both quantitative and semi-quantitative methods. In the tables below, significance is identified as *p < 0.05, **p < 0.01 or ***p < 0.005 compared to vehicle.

Study A: BMP2 Effects In Calvarial Organ Culture

Treatment (n)	Mineralized Bone	Osteoid	Connective Tissue	Cartilage
Quantitative point count analysis (mm^3)				
Vehicle (4)	0.3 ± 0.3	0.07 ± 0.04	1.0 ± 0.6	0.06 ± 0.07
BMP2-100 ng/ml (4)	0.3 ± 0.02	1.0 ± 0.02	1.2 ± 0.1	***1.3 ± 0.4
Semi-quantitative analysis (1=normal)				
Vehicle (4)	1.0 ± 0.0	2.0 ± 1.4	1.0 ± 0.0	0.5 ± 0.6
BMP2-100 ng/ml (4)	1.0 ± 0.0	2.0 ± 0.08	1.0 ± 0.0	*3.5 ± 0.6

Study B: Comparison of Treatments Using Semi-quantitative Analysis

Treatment (n)	Mineralized Bone	Osteoid	Connective Tissue	Cartilage
Vehicle (4)	1.0 ± 0.0	1.0 ± 0.0	1.0 ± 0.0	1.0 ± 0.0
BMP2-100 ng/ml (5)	1.0 ± 0.0	1.6 ±0.6	1.4 ± 0.6	*3.2 ± 0.5
PGE2-10^{-7} M (5)	0.8 ± 0.5	*2.2 ± 0.5	*2.2 ± 0.5	1.2 ± 0.5
PTH-10^{-11} M (6)	0.5 ± 0.6	*2.3 ± 0.8	1.5 ± 0.6	2.2 ± 1.5
PTH-10^{-7} M (5)	**0.0 ± 0.0	**0.0 ± 0.0	*3.2 ± 0.5	2.2 ± 1.1

In conclusion, this study demonstrated that PGE2 and PTH increase bone matrix formation in mouse calvarial organ culture, while BMP2 primarily increases cartilage.

Disclosures: ***M.L. Jankowsky****, Procter & Gamble Pharmaceuticals 3.*

SU050

Potential Use of a Hydroxyapatite-Collagen Composite in Orthopedics. M. E. L. Duarte[1], A. B. R. Linhares*[2], C. V. M. Rodrigues*[2], M. A. Mello[3], R. Borojevic*[1], M. Farina*[2]. [1]Dept. of Histology and Embriology and PABCAM/HUCFF, Universidade Federal do Rio de Janeiro, RJ, Brazil, [2]Dept. of Anatomy, Universidade Federal do Rio de Janeiro, RJ, Brazil, [3]Nebraska University, Omaha, NE, USA.

The number of materials proposed to be used as bone substitutes is constantly increasing. In dental and orthopedic surgery, the use of biomaterials is intended to replace the loss of mineralized tissue. Collagen has been used as a carrier for demineralized bone matrix (DBM) to improve the managing characteristics and preserve the osteoinductive potential of DBM. However, the biocompatibility of biomaterials is closely associated to cell behavior on contact with them and to cell adhesion to their surface. This study was aimed to examine the viability of culturing human osteoblasts on a hydroxyapatite-collagen composite prepared with cortical bovine bone and type I collagen (1:1). The biomaterial characteristics were determined by scanning electron microscopy (SEM) and X-ray diffraction (XRD). Osteoblasts were obtained from bone chips discarded after orthopedic procedures and plated ($7x10^4$ cells) on the hydroxyapatite-collagen composite surface. XRD results have shown that the bone powder was highly crystalline and composed mainly by hydroxyapatite (HA) particles (average diameter 295.13±112.62µm) with elongated geometries (shape factor 0.016 ± 0.009 and Feret diameter 73.67 ± 22.57). Collagen appeared mainly as locally oriented filaments or irregular networks adhered to bone particles. At day 4 after seeding, a small number of rounded shaped cells with few citoplasmatic projections

were observed on the composite surface. Cell morphology at this time point was suggestive of the beginning of the adhesion process to the composite. At day 11, cells displayed cuboidal morphology characteristic of osteoblasts and were strongly attached to the bone particles surface as well as to the collagen fibers. Cell distribution along the bulk of the composite seemed to follow the same pattern of distribution of the collagen fibers. These results suggest that the biomaterial used in this study, composed by bovine DBM and bovine collagen, was effective in the adhesion process and in the induction of human osteoblastic cell proliferation *in vitro*. Also it was apparent that the cells might have used the collagen fibers as tracks for migration, attachment and spreading throughout the composite surface.

SU051

Murine Calvarial Response in Vitro to IL-1 and PTH Measured with MicroCT. S. R. Stock[1], S. A. Foster*[2], L. A. Forman*[3], P. H. Stern[2]. [1]Institute for Bioengineering and Nanoscience in Advanced Medicine, Northwestern University, Chicago, IL, USA, [2]Molecular Pharmacology and Biological Chemistry, Northwestern University, Chicago, IL, USA, [3]Center for Comparative Medicine, Northwestern University, Chicago, IL, USA.

X-ray microCT, the high resolution variant of clinical CT, allows repeated in vitro observation of bone at spatial resolutions approaching 10 µm (laboratory) or 0.5 µm (synchrotron), and this approach permits the bone in the same specimen to be quantified before and after treatment. This study investigates how microCT (Scanco MicroCT-40) may be effectively employed in in vitro studies of mouse models of bone response to anabolic and other agents. Neonatal mouse calvaria, from individuals of the same litter, were incubated for 96 hours, and the response of control calvaria were compared with that of calvaria in media containing either IL-1 or PTH (all with N=3) using microCT and calcium release (calcein fluorescence titration). Data for 0.1 nM IL-1 treatment illustrate the approach; 3D renderings (constant threshold defining bone) show the 3D bone distribution for control (below left) and treated (below right) calvaria; the graph shows the corresponding calcium release. MicroCT renderings and calcium release show similar correlation for calvaria treated with different levels of PTH: little bone resorption or calcium release with controls, substantial resorption/release with 10 nM PTH and intermediate changes with 1 nM PTH. Bone volume from microCT correlated with the appearance of the renderings, but quantifying the pattern of bone loss in calvarial cultures will require different measures than are typically used in microarchitecture studies of trabecular bone.

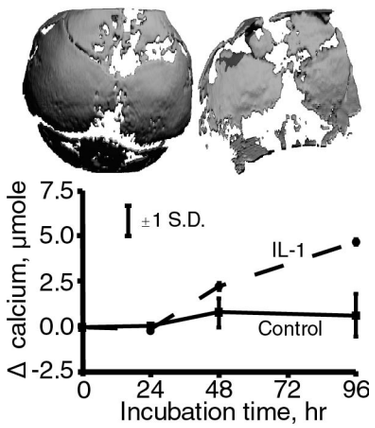

SU052

Preparation of a Polymer Biomaterial (poly (2-Hydroxyethyl Methacrylate)) with an Inter-connected Macroporosity. An X-ray Microtomographic and Histomorphometric Study. R. Filmon*[1], F. Grizon*[1], C. Cincu*[2], M. F. Baslé*[1], M. Audran[1], D. Chappard[1]. [1]LHEA-GEROM, Angers, France, [2]Macromolar chemistry, University Polytehnika, Bucharest, Romania.

Poly (2-hydroxyethyl methacrylate) (pHEMA) is a polymer that has potentially wide biomedical applications: it is hydrophilic, biocompatible and has a hardness comparable to bone when bulk polymerized. Porous biomaterials allow increase bone integration specially when the pores are inter-connected. However, due to the hydrophylicity of the material, it is difficult to prepare large porous blocks that could be used as bone substitutes. We have used three types of water-soluble porogens (sugar fibers, sucrose crystals and urea beads) to prepare macroporous pHEMA. The porogens were embedded in the polymer by bulk co-polymerization at low temperature. They were dissolved by prolonged washing in saline. The different types of porous biomaterials were dried in an oven, and analyzed on a X-ray microtomograph. The polymer cubes obtained had a side measuring 1,5 mm length. 3D measurements of porosity were obtained in a referent space of 950 mm3. In addition, 2D sections were studied by image analysis with algorithms used to measure bone architecture (inter-connectivity indexes, star volumes, fractal dimension). Sucrose crystals, having a high volumetric mass, gave large pores, which were localized on the block sides. Urea beads and sugar fibers provided pores having the same star volume (resp. 2.65 ± 0.46 mm3 and 2.48 ± 0.52 mm3) but which differed by inter-connectivity index, fractal dimension and Euler-Poincaré's number. Urea beads caused non-connected porosity while sugar fibers created a dense and interconnected labyrinth within the polymer. Inter-connectivity was proved by doing a surface treatment of the pHEMA (carboxymethylation in water) followed by a von Kossà staining which detected the carboxylic groups. Carboxymethylated surfaces were observed on the sides of the blocks and on the opened or inter-connected pores. The disconnected pores were unstained. In the blocks prepared with sugar fibers, the surface of all the pores were carboxymethylated even in the very center of the blocks. Macroporous polymers can be prepared with water soluble porogens; X-ray microtomography appears a useful tool to measure porosity and inter-connectedness.

SU053

Quantitative Ultrasound in Bovine Cancellous Bone Does Not Predict Mechanical Damage. R. I. Price[1], T. T. Duong*[1], P. Davey*[1], B. Curtin*[1], R. Day*[2], E. Schwartz*[2], K. P. Singer*[3]. [1]Medical Technology & Physics, Sir Charles Gairdner Hospital, Perth, Australia, [2]Medical Physics, Royal Perth Hospital, Perth, Australia, [3]Department of Surgery, University of WA, Perth, Australia.

Reduced elastic modulus (E), arising from damage induced in human calcaneal cancellous bone by controlled compression, is not predicted by QUS variables Speed of Sound (SOS) or Broadband Ultrasound Attenuation (BUA) (Nicholson & Bouxsein, J Bone Miner Res 2000 15:2467); implying that QUS cannot detect onset of bone fragility in the absence of changes in architecture. The aim of this study was to impose similar mechanical conditioning on bovine cancellous specimens, known to have a higher BMD than the calcaneus, in order to examine whether changes in E were predicted by changes in QUS variables. Sixty cylindrical specimens (15 mm diameter and length) were extracted from bovine femoral condyles using an irrigated diamond coring drill, cleaned with graded alcohol and ether, dried, and hydrated with saline under vacuum. Specimens were randomised to 6 groups and subjected to mechanical testing (Instron 5566) as follows; (a) "preconditioning" phase, 14 compression cycles at 0.4% strain, with measurement of initial E (MPa); (b) "damage" phase (strain rate 0.0004 s-1) for each of 6 strain groups (0.4%, 1.0%, 1.2%, 1.5%, 2.0%, 2.2%); (c) "post-damage" phase, one cycle at 0.4% strain, measuring final E. Measurements were: (i) volumetric BMD (vBMD) using high resolution DXA; (ii) SOS and BUA (dB/MHz/cm) using custom apparatus; before and after mechanical conditioning. SOS was poorly correlated with the predicted "bar wave" velocity, v = SQRT(E/rho), where rho is apparent density (R2 = 0.054, $p<0.05$). vBMD was negatively correlated with BUA (R2=0.37, $p<0.001$) and positively with E (R2=0.13, $p<0.005$). The behaviour of BUA, in contrast to the calcaneus (Nicholson & Bouxsein, 2000) is consistent with its inverse parabolic dependence on BMD (Han S et al. Osteopor Int 1996 64:291) and the higher vBMD of bovine bone. SOS was correlated with vBMD (R2= 0.42, $p<0.001$). With increasing strain in the damage phase, E first fell from the baseline at 0.4% strain (-33.9+/-4.2[SEM]% for 1% strain, -59.0+/-5.3% for 1.20% strain), then rose (-19.0+/-8.1%, +6.9+/-14.1%, +4.35+/-13.6% for 1.5. 2.0 & 2.2% strains, respectively). There was no correlation between changes in E and changes in SOS or BUA, nor between changes in SOS and changes in BUA. It is concluded that the nonlinear response of the elastic modulus (E) in bovine cancellous bone to controlled, increasing strains is more complex than the equivalent response of E in the human calcaneus, but as in the latter case, changes in SOS and BUA do not predict changes in E induced by mechanical damage.

SU054

Cellular Alteration of Growth Plate Chondrocytes Affected by Mechanical Stress. N. Amizuka, Y. Seki*, S. Kenmotsu*, T. Sasaki, T. Maeda*. Niigata University Graduate School of Medical and Dental Sciences, Niigata, Japan.

In order to elucidate the chondrocytic response to the mechanical stress, we have examined the morphological changes of growth plate chondrocytes under similar conditions to hypergravity or microgravity. Mouse tibial epiphyseal cartilage at 17-day-old fetal stage was extracted and then cultured in a continuous centrifuge (5 G) for 16 hours, or in rotation at 15 rpm for 16 hours, enabling putative hypergravity or microgravity, respectively. The stationary culture of the epiphyseal cartilage was employed for a control experiment. The centrifugal force and rotation for 16 hours had no effect on the size of the epiphyseal cartilage and on the expression of PTHrP and FGFR3 that are important for chondrocyte proliferation and differentiation. Although patches of actin filaments, identical to podosomes, were localized evenly along with the cell membranes of the proliferative chondrocytes in the control, chondrocytes affected with the centrifugal force developed the thick layer of actin filaments. Alternatively, chondrocytes in the rotation culture revealed less-developed and uneven distribution of actin filaments along with the cell membranes. Under an electron microscope, chondrocytes subjected to the rotation showed the flattened cell shapes and the ruffling of the cytoplasmic processes, whereas chondrocytes with various cell shapes often made contacts with each other, when affected by the centrifugal force. Thus, the centrifugal force or rotation appeared to distort the chondrocytic columns. In the intracolumnar transverse septa of the control cartilage, the longitudinal lines of electron-dense fibrils were associated with the short cytoplasmic processes of the normal chondrocytes, therefore, connecting adjacent chondrocytes. However, the longitudinal lines of the extracellular fibrils was hardly seen in both the centrifugal and rotation cultures. Thus, the altered distribution of actin filaments, irregular cell shape and the disappearance of longitudinal lines of extracellular fibrils suggest that the hypergravity and microgravity disturb the cell-to-matrix interaction between chondrocytes and peripheral cartilage matrix.

SU055

Pressure-responsive Synthesis of Cytokines by Humam Macrophages in vitro is Inhibited by Anti-TNF Blocking Antibody. C. E. Evans*[1], S. Mylchreest*[2], A. Mee*[3], J. L. Berry*[3], G. Andrew*[4]. [1]Laboratory Medicine Academic Group, University of Manchester, Manchester, United Kingdom, [2]Lmag, University of Manchester, Manchester, United Kingdom, [3]Medicine, University of Manchester, Manchester, United Kingdom, [4]Orthopaedic Surgery, Salford Royal Hospitals Trust, Salford, United Kingdom.

Previous studies showed that physical pressure stimulates cytokine synthesis by human macrophages in vitro in a time-dependent manner. This may be important in osteolysis around loosened joint replacements. This study examined whether blocking macrophage synthesis of TNFα affected synthesis of other cytokines. Monocytes were isolated from human buffy coats by adherence for 1 hour. Cell phenotype after overnight incubation exhibited macrophage markers CD68 & non-specific esterase. Macrophages were incubated with or without 0.05mg/ml blocking antibody to TNFα (AB) overnight (D0) or 7 days (D7), before pressurisation (5psi,1 hour, 2 secs on/off) in our unique pressure jig. Cultures were incubated for a further 23 hours. Control cultures were without AB or pressurisation. AB blocked endogenous TNFα synthesis & pressure stimulus did not overcome this block. Pressurised macrophages (noAB) synthesised more TNFα than controls. Pressurised macrophages synthesised more IL-6 at D0 & D7 than controls & incubation with AB abolished this increase. Levels of IL-1β were often undetectable but appeared to be reduced by incubation with AB. These results suggest that the increase in synthesis of bone-resorbing cytokines seen in pressurised macrophages is dependent upon initial synthesis of TNFα & that without TNFα, IL-1β & IL-6, which we previously showed attain maximum concentration 12 hours after TNFα, are not synthesised in response to pressure. This preliminary finding has implications for treatment of patients with loosened implants and supports the potential use of TNFα blocking antibodies as therapy in this situation.

	Days in vitro	TNFα	IL-1β	IL-6
+AB -Pressure	0	0.46(0.29)	0.73(0.30)	0.88(0.03)
+Pressure	0	1.2 4(0.07)	1.22(0.37)	1.89(0.71)
+AB +Pressure	0	0.48(0.20)	0.70(0.32)	0.88(0.16)
+AB -Pressure	7	0.14(0.17)	N.D.	0.75(0.11)
+Pressure	7	1.44 (0.25)	N.D.	1.78(0.31)
+AB +Pressure	7	0.26 (0.42)	N.D.	0.84(0.21)

Results are expressed as a ratio of test concentration (pg/ml)/control; "no effect' level is 1.0. Results are means of data from four separate experiments ±SD. "N.D.' = below minimum detectable level

SU056

Analysis of Mechanical Stress-induced Changes in Gene Expression Using Differential Display in Cultured Spinal Ligament Cells Derived from Patients with Ossification of the Posterior Longitudinal Ligaments. H. Ohishi*[1], K. Furukawa*[2], K. Ueyama*[1], S. Motomura*[2], S. Harata*[3], S. Toh*[1]. [1]Orthopaedic Surgery, Hirosaki University School of Medicine, Hirosaki, Japan, [2]Pharmacology, Hirosaki University School of Medicine, Hirosaki, Japan, [3]Aomori Prefectural Central Hospital, Aomori, Japan.

Ossification of the posterior longitudinal ligament (OPLL) of the spine is characterized by ectopic bone formation progressing in the spinal ligaments. When the posterior longitudinal ligament of the spine becomes ossified and enlarged, the spinal cord is compressed and myeloradiculopathy occurs. Mechanical stress which acts on the posterior ligaments or ligamentous enthesis of vertebral bodies is thought to be an important factor in the progression of OPLL. To investigate the mechanism of OPLL development, different gene expressions between cells derived from OPLL and non-OPLL patients (OPLL, non-OPLL cells) were identified by RT-PCR differential display technique. Five reproducible differences of the gene expression were detected and one clone had a DNA sequence with 95% homology to human prostacyclin synthase. Prostacyclin is a potent inhibitor of bone resorption and bone modeling and remodeling. To examine the effect of mechanical stress on the expression of prostacyclin synthase, OPLL and non-OPLL cells were subjected to uni-axial stretch (120% in length, 1Hz), and the relative levels of prostacyclin synthase and alkaline phosphatase mRNA on semiquantitative RT-PCR were investigated. In OPLL cells the expression of prostacyclin synthase and alkaline phosphatase were highly expressed at 6 hours, whereas no change was observed in non-OPLL cells. These results suggest that mechanical stress induces onset and progression of OPLL through the production of prostacyclin.

SU057

Application of Mechanical Stress Induces Integrin Signaling in Osteoblasts Cultured on RGD-grafted Surfaces. E. A. Cavalcanti-Adam[1], R. J. Composto*[2], E. Macarak*[3], I. M. Shapiro[4], C. S. Adams[4]. [1]University of Pennsylvania, Philadelphia, PA, USA, [2]Material Science and Engineering, University of Pennsylvania, Philadelphia, PA, USA, [3]School of Dental Medicine, University of Pennsylvania, Philadelphia, PA, USA, [4]Orthopaedic Surgery, Thomas Jefferson University, Philadelphia, PA, USA.

The objective of the investigation was to covalently link RGD peptides to a deformable silicone membrane and to use this substrate to test the hypothesis that mechanical deformation of the membrane is transduced through the integrin signaling pathway. MC3T3E1 cells were grown on silicone membranes grafted with a silane linker to RGDS- or RGES-(control) peptides. We found that RGDS enhanced osteoblast attachment. Cell attachment was integrin mediated. Thus, free RGD peptides as well as αVβ3 antibodies blocked the attachment of osteoblasts to these modified surfaces. Western blot analysis and immunohistochemistry indicated that the grafted RGD peptide upregulated αVβ3 integrin and focal adhesion kinase (FAK) expression; in contrast, the RGES surfaces caused minimal expression of these proteins. When osteoblasts were stretched by applying a dynamic equibiaxial strain to the RGD-surface, the expression of αVβ3 was further increased. Examination of FAK expression indicated that there was upregulation of the phosphorylated protein and that the extent of phosphorylation was dependent on the level of the applied strain. Bad, a protein downstream of FAK, was also modulated by strain application. Following mechanical stretch, phospho-Bad expression was elevated. These results clearly indicate that mechanical stress upregulates osteoblast survival signals. To ascertain if there was a concomitant down regulation of apoptosis, we measured the apoptotic sensitivity of mechanically stressed cells. We noted that serum deprivation killed significantly smaller numbers of mechanically stressed cells than non-stressed controls. It is concluded that the transduction of mechanical force by RGD-integrin interaction promotes bone cell survival, while at the same time inhibiting signals that promote osteoblast apoptosis.

SU058

Mechanical Stress-induced Tooth Movement model in Osteopontin-deficient mice. C. Chung*[1], M. Ishijima[1], M. Morinobu[1], S. Rittling*[2], K. Tsuji[1], K. Soma*[3], A. Nifuji[1], D. T. Denhardt*[2], M. Noda[1]. [1]Molecular Pharmacology, Tokyo Medical and Dental Univ., Tokyo, Japan, [2]Rutger Univ., Piscataway, NJ, USA, [3]Orthodontic Science, Tokyo Medical and Dental Univ., Tokyo, Japan.

When mechanical stress is applied to the tooth, tooth movement occurs in association with the remodeling of underlying alveolar bone. In rodent experimental tooth movement models we can observe bone resorption on the pressure side, and new bone apposition on the tension side according to the direction of the force applied. Osteopontin (OPN), a major noncollagenous bone matrix protein is known to be induced by mechanical stress especially in the pressure sides of experimental tooth movement model in vivo and to have a chemotactic effect on osteoclast precursors in vitro. Recent studies have also reported a difference not only in bone resorption but also in bone formation to mechanical stress in OPN-deficient mice. To elucidate the role of OPN in mechanical stress-induced tooth movement along with the alveolar bone remodeling, we have developed a mice tooth movement model using OPN-deficient mice. By anchoring TiNi closed coil spring to the maxillary incisors, light continuous force (2g, 10g) was applied to the maxillary right first molar for 1~3 weeks. The left side served as an untreated internal control. As days of force application increased, tooth movement and rotation of the treated first molar increased when measured by soft X-ray and micro CT scanning. Both WT and OPN deficient mice showed mesial tooth movement and mesio-palatal rotation of the treated molar compared to the control side. Surprisingly OPN deficiency did not result in a delay in tooth move-

ment, but showed an increased tooth movement as the activation duration proceeded from 1 week to 3 weeks. The periodontal ligament space surrounding the tooth was also measured by micro CT coronal sections of the distobuccal root of the treated molar. In the WT treated group the periodontal ligament space ratio of the tension side (distal periodontal ligament) to the pressure side (mesial periodontal ligament) was significantly greater compared to the KO group ($p<0.05$). Histological examinations of both WT and OPN deficient alveolar complex with treatment showed a reverse pattern in bone remodeling compared to the control. On the pressure side, there was clear presentation of TRAP positive osteoclasts, while in the tension side alkaline phosphatase positive new bone forming cells were observed. However there was no significant difference in TRAP and Alkaline phosphatase positive cells between the WT, OPN deficient group. This indicates OPN deficiency could be backed up by unknown compensating mechanisms for surrounding bone remodeling in the experimental tooth movement in mice

SU059

Osteopontin Deficiency Suppresses New Bone Formation in the Sutures Under Tensile Mechanical Stress in vivo. M. Morinobu[1], M. Ishijima[1], S. R. Rittling[2], K. Tsuji[1], H. Yamamoto*[3], A. Nifuji[1], D. T. Denhardt[2], M. Noda[1]. [1]Dept of Molecular Pharmacology, Tokyo Medical and Dental University, Tokyo, Japan, [2]Rutgers University, Piscataway, NJ, USA, [3]Ehime University, Matsuyama, Japan.

Mechanisms underlying mechanical stress-dependent control of bone remodeling are largely unknown. Mechanical stress enhances osteopontin (OPN) expression in osteoblasts, and OPN deficiency prevents unloading-induced reduction in bone formation (Journal of Exp. Med. 193:399, 2001). Thus, OPN could act as a transducer for mechanical stress. However, the function of OPN in bone formation under mechanical stress is not known. Therefore, we examined the role of OPN in bone formation under tensile mechanical stress in vivo in mice. Sagittal sutures of mice were subjected to expansion by orthodontic springs and bone formation was examined. One week expansion of the sutures resulted in bone formation in the edges of the parietal bones. RT-PCR analysis indicated increase in the levels of OPN mRNA expression in the cells in the wild type calvariae subjected to expansion. In addition, type I collagen mRNA was also expressed in the calvariae under the mechanical stimuli. Immunohistchemical analysis revealed highly abundant expression of OPN protein in the matrix of newly formed bone in the mechanically expanded sutures and on the inner edge of the parietal bone where stress was applied. Osteoblasts forming bone under tensile stress also exhibited high levels of OPN protein expression in the operated mice. In sham-operated mice (without expansion), OPN positive osteoblasts were also observed on the inner edges of parietal bone, however accumulation of OPN protein on the bone matrix was significantly less than expansion group. After the application of mechanical stress, OPN was expressed at low levels in fibroblastic cells in the fibrous interzone. On the primary matrix front, highly OPN positive-oval shaped transchondral cells were observed. Bone formation was clearly observed in the expanded suture area four weeks later in wild type mice. In contrast, reduction in such bone formation in the expanded suture area was observed in the OPN knockout mice. These observations revealed that OPN is required for bone formation under the tensile mechanical stress.

SU060

Skeletal Phenotype of Transgenic Mice Expressing the Beta-1 Integrin Cytoplasmic Tail In Osteoblasts. R. K. Globus[1], M. C. H. van der Meulen[2], C. Damsky*[3], J. B. Kim*[3], D. Amblard*[1], Y. Nishimura*[4], E. Almeida*[1], U. T. Iwaniec[5], T. J. Wronski[5]. [1]NASA Ames Research Center, Moffett Field, CA, USA, [2]Cornell University, Ithica, NY, USA, [3]UCSF, San Francisco, CA, USA, [4]NASA Ames Research Center, Moffett FIeld, CA, USA, [5]University of Florida, Gainesville, FL, USA.

To define the physiologic role of β1 integrin in bone formation and mechanical loading, transgenic mice were generated by expressing the cytoplasmic tail and transmembrane domain of β1 integrin under the control of the osteocalcin promoter. In cultured cells, this truncated fragment of β1 can act as a dominant negative. Previously, the matrix of calvariae was shown to be abnormal in transgenic (TG) compared to wildtype (WT) mice. In this study, we analyzed appendicular bone in TG and WT, male and female mice at 14, 35, 63, 90 and 365 days old (n=8-12/gp). To assess β1 integrin function in mechanical loading, a pilot study using hindlimb unloading by tail suspension was performed. 35d old TG and WT females were hindlimb unloaded for 4 wks (n=3-5). Body mass, bone mineral content, histomorphometric (distal femur) and biomechanical parameters were analyzed. Statistical significance ($P<.05$) was defined by ANOVA using the Tukey-Kramer post-hoc test. We confirmed transgene expression by immunoprecipitating then immunoblotting bone lysates using an antibody against the β1 tail. Body masses of TG mice at 63, 90 and 365d old were greater (16-25%) than WT. Some TG female mice at 365d appeared obese; mean abdominal fat mass was 415% greater in TG than WT mice. Tibiae were longer (5-7%) in TG than WT mice at 63 and 90d. Tibial mineral mass of 35d males was 7% lower in TG than WT mice, but at 63d was 21% higher. The % osteoblast surface in 35d TG mice was 20% higher than WT, and at 63d was 17% lower, while % osteoclast surface did not differ. In 365d mice, cancellous bone volume (125%) and endocortical mineral apposition rate (40%) were greater in TG than WT males but not females. In WT mice, hindlimb unloading caused a reduction in mineral mass of tibiae (-20%) and lumbar vertebrae (-22%) relative to normally loaded controls. Surprisingly, hindlimb unloading also caused a relative reduction (-13%) in humerus mass. The effects of hindlimb unloading on tibia and humerus mass were less obvious in TG than in WT mice. Since hindlimb unloading caused skeletal changes in both loaded and unloaded bones, systemic changes may contribute to bone responses observed using this animal model. In conclusion, transgene expression resulted in marked metabolic changes during growth and in the aged female. Our results demonstrate that expression of the β1 integrin cytoplasmic tail *in vivo* causes gender- and age-specific changes in select morphometric parameters, bone length, and bone mass.

SU061

Demonstration of MAP Kinase Activation in Response to Mechanical Stimulation in a Novel Rat Model of Fracture Healing. N. J. Hubbard*, S. K. Volkman*, S. A. Goldstein, M. R. Moalli. Orthopaedic Research Laboratories, University of Michigan, Ann Arbor, MI, USA.

The MAP Kinase family of threonine and serine kinases is activated in response to diverse extracellular stimuli, and various in vitro studies have demonstrated their responsiveness to mechanical strain. However, the signal transduction mechanisms which cells use to respond to the local strain environment during fracture healing are currently poorly characterized. We have developed the first in vivo model that enables the study of how mechanical stimulation influences the cellular and molecular processes that regulate fracture healing under normal, aged and osteopenic conditions. Using this model we examined the hypothesis that the stage of fracture healing, as well as the local strain environment determine the activation profile of MAPK. Mechanical load-induced MAPK activation was evaluated during the reparative and remodeling stages of fracture healing, which occur at either 8 days or 5 weeks post-operatively in this model, as determined by histological analysis. This study utilized young adult Fischer 344 female rats that received bilateral, 0.6mm, mid-diaphyseal femoral osteotomies. The osteotomies were stabilized with custom four pin external fixators that enabled normal cage activity post-operatively. At either 8 days or 5 weeks post-operatively, a uni-axial compressive load was applied to one fracture site, while the other fracture site was designated as the unloaded control. Due to the predominantly fibroblastic component of the 8 day reparative tissue, the mechanical stimulus was a displacement-controlled force, corresponding to a 15% strain of the fracture tissue. In contrast, due to increased consolidation in the 5 week tissue the mechanical stimulus was a load-controlled force, also corresponding to a 15% strain. Both experimental groups were loaded for 900 cycles at 1Hz. Specimens were harvested immediately after loading, snap frozen and prepared for immunoblot analysis using MAPK and phospho-specific MAPK antibodies. In the 8 day specimens MAPK activation was increased in loaded as compared to the unloaded tissue. Interestingly, MAPK activation was decreased in the loaded as compared to the unloaded tissue of the 5 week specimens. It appears that the viscoelastic nature of the undifferentiated, 8 day repair tissue may be dictating MAPK activation in response to mechanical stimulation. Immunolocalization studies are currently underway to identify the mechanoresponsive cellular phenotypes.

SU062

Use of Predominant Collagen Fiber Orientation for Interpreting Cortical Bone Loading History: Bending vs. Torsion. J. G. Skedros. Dept of Orthop Surg, U of UT, Salt Lake, UT, USA.

Habitual bending appears to be highly conserved in functional loading of appendicular long bones in terrestrial animals. In fact, empirical strain data demonstrate that bending produces the majority (>70%) of longitudinal strains occurring during controlled in vivo activity. Non-uniform patterns of predominant collagen fiber orientation (CFO) in cortical bone are highly correlated with the regional prevalence of tension and compression strain modes. Predominant CFO therefore appears to be highly sensitive and specific for interpreting loading history in a limb diaphysis when strain data are not available. Some bone regions, however, experience habitual torsion. While notable examples include the human femoral neck, and mid diaphyses of the sheep tibia, pigeon humerus, and turkey ulna, only the non-human bones have been verified with in vivo strain measurements. Due to the widely shifting neutral axis that occurs during torsional loading, non-uniform CFO patterns would not be expected in these regions. To test this hypothesis, transverse segments from mid diaphyses of 9 skeletally mature chicken femora were embedded in polymethyl methacrylate and examined for tissue adaptations. In vivo strain gauge studies have demonstrated that this region experiences prevalent torsion (Carrano and Biewener, 1999. J Morph). Undecalcified sections were milled to 100+/-5 microns and viewed under circularly polarized light. CFO is expressed as the mean graylevel in each microscopic field (approx. 2.3mm2) in the mid-cortical region of the cranial (Cr), caudal (Cd), medial (M), and lateral (L) cortices. Graylevels were quantified from pixel histograms obtained from digitized images. Embedded transverse sections from mid shafts of calcanei from a skeletally mature sheep and mule deer, and a horse radius, were used as "control" bones since strain gauge analyses have shown that they have a habitual tension/compression distribution. Results showed no statistically significant CFO differences between any of the chicken femora cortical regions, consistent with the hypothesis of the apparent absence of non-uniform regional CFO patterns in torsional loading. These results are consistent with recently reported findings in mid diaphyses of torsionally loaded mature sheep tibiae and turkey ulnae. It is suggested that the uniform CFO in the chicken femora actually represents adaptation for shear strains produced by torsion. CFO is also uniform in the neutral axes of the control bones where shear stains are prevalent. These observations suggest that predominant CFO is reliable for interpreting strain-mode-specific (tension, compression, shear) adaptations in bending and torsion.

SU063

Increased Dentin Matrix Protein (DMP1) Gene Expression in Osteocytes during Mechanical Loading of Bone. J. Gluhak-Heinrich[1], D. Pavlin*[1], L. F. Bonewald*[2], M. MacDougall*[3], S. E. Harris*[2]. [1]Orthodontoics, UTHSCSA, San Antonio, TX, USA, [2]Oral Biology, University of Missouri at Kansas City, School of Dentistry, Kansas City, MO, USA, [3]Pediatric Dentistry, UTHSCSA, San Antonio, TX, USA.

DMP1 protein has been shown to be expressed in early and mature osteocytes, specifically along their dendritic processes, which implies involvement in osteocyte function. Earlier *in vivo* studies proposed osteocytes to be mechanically responsive cells, but the role of DMP1 in this response is not known. The aim of this study was to examine the effect of mechanical loading on the expression of DMP1 mRNA in the mouse tooth movement model by *in situ* hybridization. The number of osteocytes expressing DMP1 mRNA was determined for various durations of loading between 6 hours to 7 days in 37 loaded and 33 control alveolar bone sites. Expression of DMP1 mRNA in osteocytes increased two-fold as early as 6 hours after loading. After 4 days of loading, DMP1 expression in osteocytes increased to a peak 3.7 fold in the bone formation sites and 3.5 fold in the resorption sites. Osteoblasts responded in the opposite manner, showing a transient 45% decrease of DMP1 mRNA in bone formation sites. A consistent decrease of DMP1 mRNA during the course of loading was observed in bone resorption sites, with maximum inhibition of 67% at day 2. In summary, increased expression in osteocytes and decreased expression in osteoblasts for DMP1 mRNA were observed for both resorption and formation sites. The response of DMP1 to mechanical loading was similar to that of osteopontin observed in our earlier study. These results support the hypothesis that DMP1 has an important role in the responses of osteocytes and osteoblasts to mechanical loading of bone *in vivo*.

SU064

Gravitational Force Alters Intracellular Signaling and Gene Transactivation. C. S. Ontiveros*[1], L. K. McCauley[2], L. R. McCabe[1]. [1]Physiology, Michigan State University, East Lansing, MI, USA, [2]Dept Perio/Prev/Geri, University of Michigan, Ann Arbor, MI, USA.

Changes in gravity affect the cellular and metabolic functions of osteoblasts. During spaceflight, microgravity conditions are thought to lead to decreased bone formation. Histology suggests that changes in osteoblast growth and mineralization are important contributors to this outcome but the specific mechanisms are unclear. Based on evidence demonstrating an important role for AP-1 in regulating growth and differentiation, our studies examined the influence of gravitational force on MAPK and downstream target transcription factor levels and activities in osteoblastic cells. Using a rotating cell culture system, MC3T3-E1 osteoblasts were exposed to simulated microgravity (24 h). To determine if transcriptional activities were influenced by gravitational force, osteoblasts were transfected with an AP-1 luciferase reporter plasmid and luciferase activity measured. Results indicated AP-1 transactivation was decreased under microgravity relative to normal gravity controls and constitutively active CMV reporters. To evaluate AP-1 binding nuclear extracts were obtained from cells cultured in simulated microgravity. AP-1 binding activity correlated with AP-1 transactivation. To evaluate the impact of microgravity on gene expression, AP-1 family members were evaluated by northern analysis to determine whether different AP-1 transcription factors were altered. Levels of cFos and cJun mRNA were decreased in a time dependent manner and correlated with decreases in AP-1 binding and transactivation. Because alteration of specific MAPK members directly influences AP-1 transactivation, intracellular signaling under microgravity was evaluated. Findings demonstrated significant differences in MAPK family member activities compared to normal gravity controls. Some MAPK activities were modulated in a time dependent manner. Next, we hypothesized that osteoblast responsiveness to extracellular cues could be altered under conditions of simulated microgravity. Cells were exposed to simulated microgravity or normal gravity and were treated with 10nM PTH. Interestingly, PTH mediated CRE transactivation was decreased under simulated microgravity when compared to untreated controls suggesting cells under microgravity are less sensitive to the actions of PTH. Taken together, our data demonstrates that alterations in gravitational force cause significant changes in basal and stimulated osteoblast signaling and gene transactivation. Understanding the molecular events leading to changes in signaling and transcription factor activation may facilitate the development of drugs to prevent bone loss.

SU065

Cathepsin K Deficiency in Pycnodysostosis Results in Accumulation of Non-digested Phagocytosed Collagen in Fibroblasts. V. Everts[1], W. Hou*[2], X. Rialland*[3], W. Tigchelaar*[1], P. Saftig*[4], D. Broemme*[2], B. D. Gelb*[2], W. Beertsen[5]. [1]Cell Biology, Academic Medical Centre, Amsterdam, Netherlands, [2]Human Genetics, Mount Sinai Hospital, New York, NY, USA, [3]Pediatrics, Centre Hospitalier Universitaire Angers, Angers, France, [4]Biochemistry, Christian-Albrechts University, Kiel, Germany, [5]Periodontology, Academic Centre for Dentistry, Amsterdam, Netherlands.

The rare osteosclerotic disease, pycnodysostosis, is characterized by decreased osteoclastic bone collagen degradation due to the absence of active cathepsin K. Although this enzyme is primarily expressed by osteoclasts, data indicate that it may also be present in other cells including fibroblasts. Since fibroblasts are known to degrade collagen intracellularly following phagocytosis, we analysed various soft connective tissues (periosteum, perichondrium, dermis, lamina propria of intestine, synovial membrane) from a 13-week-old human fetus with pycnodysostosis for changes in this pathway of collagen digestion. In addition, tissues (periosteum, perichondrium, dermis, synovial membrane) from cathepsin K-deficient and control mice were analysed. The tissues were fixed and processed for electron microscopic examination. Microscopic analysis of the human fetal tissues showed that cross-banded collagen fibrils had accumulated in lysosomal vacuoles of fibroblasts. The highest accumulation was found in connective tissues associated with bone or cartilage; lower amounts were found in the dermal and intestinal lamina propria. In studies of three children with pycnodysostosis (from whom only bone-associated tissues were available), a similar accumulation was seen in periosteal fibroblasts. In biopsies of controls, intracellular collagen was sporadically seen. In contrast to the findings in humans, in fibroblasts of murine cathepsin K-deficient tissues an accumulation of internalised collagen was not apparent. Our observations indicate that in humans with pycnodysostosis, but probably not in the mouse model mimicking this disease, the intracellular digestion of phagocytosed collagen by fibroblasts is inhibited. The data strongly suggest that in human fibroblasts cathepsin K is a crucial protease for this process. Murine fibroblasts may have other proteolytic activities that are expressed constitutively or up-regulated in response to a deficiency of cathepsin K. This may explain why cathepsin K-deficient mice lack some of the dysostotic features, which are prominent in patients with pycnodysostosis.

SU066

In Vivo Impairment of Collagenase Activity Does not Affect Bone Formation in Transgenic Mice Expressing Constitutively Active PTH/PTHrP receptors in Osteoblastic Cells. E. Schipani[1], R. Chiusaroli[2], A. Maier*[1], M. C. Knight*[1], M. Byrne*[3], M. Inada[3], L. Calvi[1], Y. Wang[3], R. Baron[2], S. M. Krane[3]. [1]Endocrine Unit, MGH-Harvard Medical School, Boston, MA, USA, [2]Cell Bio & Orthopedics, Yale University, New Haven, CT, USA, [3]Ciid, MGH-Harvard Medical School, Boston, MA, USA.

Expression of a constitutively active PTH/PTHrP receptor in vivo in cells of osteoblast lineage (Cl2 transgenic mice) causes a dramatic increase in trabecular bone volume and trabecular bone formation, and, conversely, a significant decrease in periosteal mineral apposition rate. Collagenase-3 (MMP-13) is a known downstream target of PTH action. In order to investigate the role of collagenase cleavage in generating the Cl2 bone phenotype described above, we bred Cl2 transgenic animals with mice carrying a mutated col1a1 gene that encodes a protein resistant to digestion by collagenase-3 and other collagenases (rr mice). Adult tibias and parietal bones from 1-month old double mutant animals (Cl2/rr) and from control littermates were analyzed by histology, in situ hybridization and histomorphometry. Trabecular bone volume was higher in Cl2/rr than in Cl2 mice. This increase occurred despite no change in the rate of bone formation, which was equally high in the two animal models. The finding suggests therefore that resorption was impaired in the doubly mutant mice. Interestingly, osteoclast number was not significantly different in Cl2/rr and Cl2 mice. Periosteal mineral apposition rate was similar in the two mutant mice, and significantly lower than in wild type. Serum measurements of ionized calcium and PTH are in progress. In summary, impairment of collagenase activity enhances the increased bone deposition in transgenic mice that express a constitutively active PTH/PTHrP receptor in cells of the osteoblast lineage but does not significantly modify either trabecular bone formation or periosteal mineral apposition rate. Increases in trabecular bone volume in the double mutant mice therefore must result from a deficit in bone resorption.

SU067

Ameloblasts Highly Express Enamel Matrix Serine Proteinase 1 (EMSP1) at Late Stage in Amelogenesis. T. Suzawa, T. Katagiri, R. Kamijo. Biochemistry, School of Dentistry, Showa University, Tokyo, Japan.

Ameloblasts, derived from inner dental epitherial cells, are specialized cells responsible for calcified enamel formation. Mature enamel is the highest calcified tissue among hard tissues in mammals. In early stage of amelogenesis, immature enamel contains large amount of enamel matrix proteins secreted by ameloblasts. In late stage, however, mature enamel contains less amount of enamel proteins due to degradation and removal of the proteins by proteinases. In rodents, ameloblasts are continuously differentiated from an apical loop and further mature into early secretory cells and mature cells. Ameloblasts secrete not only enamel matrix proteins but also proteinases, but the regulatory mechanism is still not known. In order to elucidate the mechanism of amelogenesis, we examined the changes of the expression levels of enamel proteins and proteinases in ameloblast differentiation. An ameloblst-rich cell layer was prepared from a labial side of mandibular incisors of 7-day-old ddY mice. Then, it was divided into three parts; an early secretory, transitional and mature parts, respectively, from an apical loop edge to a gingival margin edge. RT-PCR and Northern blot were used to detect mRNAs of enamel matrix proteins (amelogenin, enamelin, ameloblastin and tafterin) and proteinases (enamelysin and enamel matrix serine proteinase 1 (EMSP1). Expression of amelogenin, enamelin and enamelysin were abundant in early secretory ameloblasts. There was no difference in the pattern of ameloblastin and tafterin expression. In contrast, EMSP1 was highly expressed in mature ameloblasts. Taking together, these results clearly indicate that expression levels of enamel matrix proteins and proteinases in ameloblasts are changed during their differentiation. These changes may be required for removal of enamel proteins at late stage of amelogenesis. It was also suggested that EMSP1 expression is a useful marker for mature ameloblasts.

SU068

Effects of Tetracyclines on Bone and Cartilage Loss in a Rat Model of Rheumatoid Arthritis. P. Pastoureau, N. Moulharat*, V. Renoux*, S. Gaufillier*, M. Sabatini*. Rheumatology Division, Institut de recherches Servier, Suresnes, France.

Inhibition of bone and cartilage degradation *in vitro* is a well-known non-antibiotic effect of tetracyclines (TCs). This is thought to depend on inhibition of matrix metalloproteinases (MMPs) at different levels, including mRNA expression, activation of the proforms, and activity of the mature enzymes. The aim of this study was to examine the effects of doxycycline (Dox), minocycline (Mino) and tetracycline (Tetra), on bone and cartilage degradation induced by inflammation in adjuvant polyarthritis (AP) in the rat. In a parallel assay, we also examined the effects of Dox and Mino on mRNA expression of collagenase (MMP-13) in articular cartilage of AP rats. AP was induced by injection of complete Freund adjuvant into the right hind paw of female Lewis rats. They were then allocated to 4 groups of 12 animals: vehicle (arthritic control), Dox, Mino and Tetra. One extra group was not injected and served as non arthritic control (n=12). Preventive oral treatment started on the day of induction and was continued for 21 days at the same dose of 100mg/kg twice a day, for the three compounds. Pathology was assessed by visual score and paw edema volume. At sacrifice, also measured were bone mineral content of the proximal femur (by DEXA) as well as GAG and OH-Pro content of patellar cartilage (by colorimetric assays) of the non-injected paw. Expression of MMP-13 was analyzed by RT-PCR of mRNA extracted from the tibial cartilage of the non-injected knee, followed by band densitometry. Treated groups were compared to arthritic control and the results, expressed as percent of inhibition of the pathology, are the following:

	Paw edema	BMC	GAG	OHpro	MMP-13 expression
Doxycycline	3 %	48 % ***	58 %	57 %	51 %
Minocycline	53 % ***	53 % ***	47 %	100 % ***	100 %
Tetracycline	3 %	52 % **	18 %	100 % *	not done

n = 12 /group *:p<0.05; **: p<0.01; ***:p<0.001.

The three TCs effectively inhibited bone loss. This effect does not seem to be secondary to anti-inflammatory action, since only Mino significantly decreased paw edema and pathological score. The inhibition of MMP-13 expression by Dox and Mino correlates with the degree of protection against collagen loss in cartilage. Even if we cannot exclude that a) other MMPs contribute to tissue loss and b) TCs inhibit MMPs also by other mechanisms, these results suggest that decrease of MMP expression is at least in part responsible for the protective effects of TCs. This study also confirms the therapeutic potential of TCs in rheumatic diseases.

SU069

Collagenase-3 is induced in human osteoblasts by the synergistic interaction of T cell derived TNF-α, TGF-β and IFN-γ. L. Rifas. Internal Medicine,Division of Bone & Mineral Diseases, Washington University School of Medicine, St. Louis, MO, USA.

Activated T cells secrete multiple osteoclastogenic cytokines which play major roles in the bone destruction associated with Rheumatoid Arthritis (RA). While the role of T cells in osteoclastogenesis has received much attention recently, the effect of T cells on osteoblast activity is poorly defined. In this study, we investigated the hypothesis that in chronic inflammation activated T cells contribute to enhanced bone turnover by regulating human osteoblast (hOB) collagenase-3 production, thus priming the bone for osteoclastic resorption. As a model for RA, we have used activated T cell conditioned medium (ACTTCM) which mimics the *in vivo* cytokine repertoire. We have previously reported (ASBMR 2001) that ACTTCM induces collagenase-3 in human osteoblasts (hOB). Analysis of ACTTCM by specific ELISAs revealed that IFN-γ (23553 ± 2439pg/ml), TGF-β (1142 ± 12pg/ml) and TNF-α (466 ± 8 pg/ml) were major constituents. These cytokines are important regulators of bone turnover and collagenase-3 production. In order to define the role of these three cytokines, hOB were treated with 25% ACTTCM in the presence and absence of neutralizing antibodies to TNF-α, TGF-β or IFN-γ and collagenase-3 measured by specific ELISA. Neutralizing antibodies to TGF-β decreased by 28%, and to IFN-γ approximately 20%, collagenase-3 induction. However, neutralizing antibodies to TNF-α inhibited collagenase-3 by 70%. In order to examine more fully the effect of these three major T cell cytokines on collagenase-3 production, hOB were exposed to recombinant cytokines at their levels present in 25% ACTTCM either individually or in combinations and collagenase-3 production assayed by a specific ELISA. hOB treated with IFN-γ, TNF-α or TGF-β alone or combinations of TNF-α with IFN-γ or IFN-γ and TGF-β did not produce significant amounts of collagenase-3. Combinations of TGF-β and TNF-α induced a small induction. However, when hOB were treated with all three cytokines, collagenase-3 was induced to a level of 10 fold over that induced by TNF-α + TGF-β and 100 fold over control or individual cytokine alone. Furthermore, the combination of all three cytokines induced collagenase-3 to 70% of the level induced by 25% ACTTCM. Taken together, these results demonstrate that in chronic inflammatory diseases such as RA, multiple factors working in concert are responsible for the bone loss observed.

SU070

Prolactin Dependant Expression of RANKL in Mammary Epithelial Cells. S. Srivastava[1], M. J. Mistry*[2], N. D. Horseman*[3]. [1]Mol. and Cellular Physiology, University of Cincinnati, Cincinnati, OH, USA, [2]Mol and Cellular Physiolgy, University of Cincinnati, Cincinnati, OH, USA, [3]Mol. and Cellular Physiolgy, University of Cincinnati, Cincinnati, OH, USA.

Prolactin (PRL) and its immediate target genes are essential for lactation and full development of breast. PRL regulates cyclinD1 expression by activating STAT (STAT 5a) pathway. Mice with disruptions in genes that encode Receptor Activator of NF-κB (RANK) or its ligand RANKL, share similar phenotypes with mice lacking genes that encode PRL, STAT5a or cyclinD1, suggesting that RANKL, RANK or osteoprotegerin (OPG, RANKL decoy receptor) may be direct targets of PRL action. To test this hypothesis, total RNA was extracted from prolactin treated or untreated cells from total mammary gland and from primary mammary epithelial cells (PMEC) and assayed for RANK, OPG and RANKL. We found that untreated and treated PMEC as well as total mammary gland preparation equally expressed the mRNA for RANK and OPG. However, only PRL treated expressed RANKL. Furthermore PRL knockout mice (PRL-/-) failed to express RANKL in mammary epithelial cells, whereas pituitary grafted mice restored RANKL expression in PRL -/- mice. To further confirm that PRL directly regulates the transcription activity of RANKL, we transiently co- transfected RANKL–Luciferase reporter with β-galactosidase reporter constructs in CHO cell line that constitutively express PRL receptor (CHO-D6). CHO-D6 cells treated with PRL induced RANKL reporter activity in a dose dependent manner with maximum induction of 3 fold over untreated controls, demonstrating that RANKL transcription is under the control of PRL. Since PRL expression is developmentally regulated, we examined RANKL expression in virgin, pregnant and lactating mice. We found RANKL mRNA is expressed from mid-pregnancy (day 16) until the end of pregnancy, whereas virgin (6 week) mice failed to express RANKL. In contrast, OPG and RANK were constitutively expressed in mammary gland in all the stages examined. Consistent with this fact PRL receptor knockout mice showed markedly decreased in osteoblast activity and bone formation as compared to wild type littermates (Endocrinology 140:96, 1999), suggesting that the PRL effect is systemic and not restricted to mammary epithelial cells. In summary, we report that mammary epithelial cells express RANK and OPG. In addition, RANKL expression is developmentally regulated. We are currently investigating the link between RANKL expression on mammary epithelial cells and malignancy of breast tumor that leads to bone metastasis.

SU071

Role of CREB Phosphorylation on the Expression of 25-Hydroxyvitamin D-1-alpha-Hydroxylase in Human Prostate Cells. L. Wang*, M. F. Holick, T. C. Chen. Vitamin D, Skin and Bone Research Laboratory, Endocrine Division, Boston University School of Medicine, Boston, MA, USA.

25-Hydroxyvitamin D-1α-hydroxylase (1α-OHase) is expressed in prostate cells. The expression suggests that local production of 1,25-dihydroxyvitamin D could provide an important cell growth regulatory mechanism. However, there is differential expression of 1α-OHase activity among the primary cultures of prostate cells derived from cancerous, benign prostatic hypertrophy and normal tissue, and among normal (PZHPV-7) and various cancer cell lines (PC-3, DU145). No activity was found in cancer cell line LNCaP. Using luciferase reporter gene assay, we further observed a step-wise decrease in the basal promoter activity in two truncated promoter fragments, AN2 (-1100bp) and AN5 (-394 bp), with the highest basal activities found in PZHPV-7 and with loss of promoter activity in LNCaP. In order to understand the mechanism underlying the differential promoter activities among different prostate cells, we investigated the possible role of phosphorylation of cyclic AMP response element binding protein (CREB) on the regulation of 1α-OHase promoter activity in prostate cells. First we compared the levels of CREB phosphorylation among PZHPV-7, DU145, PC-3 and LNCaP cells by western blot analysis using antibody against phosphorylated CREB. We observed that CREB was phosphorylated to a greater extent in PZHPV-7 and DU145 cells than in PC-3 cells. No significant phosphorylation of CREB was found in LNCaP cells. Next, we utilized various activators and inhibitors of protein kinase A (PKA), protein kinase C (PKC), mitogen-activated protein kinase (MAPK) and calcium/calmodulin-dependent protein kinase II (CaMKII) to determine which kinases might be involved in phosphorylating the CREB in PZHPV-7 cells. We demonstrated that forskolin (an activator of PKA) increased the AN2 basal promoter activity 50% ($p< 0.01$), whereas H-89 (an inhibitor of PKA) inhibited the basal and forskolin-stimulated AN2 promoter activity 40 ($p<0.01$) and 70% ($p<0.005$), respectively. We also showed that PD98059 (an inhibitor of MAPK) decreased the AN2 promoter activity 70% ($p< 0.001$). Phorbol 12-myristate 13-acetate (an activator of PKC), GF109203 (an inhibitor of PKC) and KN-93 (an inhibitor of CaMKII) had no effect on AN2 promoter activity in PZHPV-7 cells. Thus, our results suggest that differential phosphorylation of CREB through PKA and MAPK pathways may be involved in the regulation of 1α-OHase promoter activity.

SU072

Androgen Deprivation Causes Bone Loss and Increased Prostate Cancer Metastases to Bone: Prevention by Zoledronic Acid. S. S. Padalecki, M. R. Carreon*, B. Grubbs*, Y. Cui*, T. A. Guise. University of Texas Health Science Center/Institute for Drug Development, San Antonio, TX, USA.

Most patients with advanced prostate cancer have bone metastases. Androgen ablation, a standard treatment for prostate cancer, causes increased osteoclastic bone resorption and bone loss. Bone is a repository for growth factors, which are released as a consequence of osteoclastic bone resorption. As a result, the bones of hypogonadal men should be fertile environment for prostate cancer metastasis to bone. To test the hypothesis that increased osteoclastic bone resorption due to androgen deprivation causes a more fertile environment for bone metastases, we developed a mouse model of prostate cancer bone metastases which mimics the clinical situation of men rendered hypogonadal as a result of treatment for prostate cancer. Surgical castration of male athymic nude mice resulted in reduced trabecular bone volume and increased osteoclast numbers over a 4-week period compared with sham-operated controls. To investigate the role of androgen deprivation in predisposing men with prostate cancer to bone metastases, athymic male nude mice underwent orchiectomy or sham surgery 4 weeks prior to tumor inoculation with PC-3 prostate cancer cells via cardiac inoculation. Mice were treated daily with zoledronic acid or vehicle from the time of surgery. Radiographs, bone mineral density and bone histomorphometry were used to assess bone mass and tumor osteolysis. Hypogonadism resulted in lower bone mineral density compared with sham-controls and this was prevented by zoledronic acid. PC-3 bone metastases were increased in hypogonadal mice treated with vehicle compared to eugonadal controls by x-ray and histology. Zoledronic acid decreased bone metastases in hypogonadal PC-3-inoculated mice and increased survival. Zoledronic acid had no effect on soft tissue metastases. Histomorphometric analysis indicated that tumor area and bone destruction was lower in mice treated with zoledronic acid compared with controls. This work provides in vivo evidence that androgen deprivation therapy causes bone loss and may increase prostate cancer metastases to the skeleton. Treatment with zoledronic acid not only prevented bone loss due to androgen deprivation but also reduced prostate cancer metastases to bone in this model. These data support the hypothesis that increased bone resorption due to androgen deprivation may result in a more fertile environment for the development of bone metastases. Bone resorption inhibitors, such as bisphosphonates, may benefit hypogonadal men with advanced prostate cancer to prevent bone loss as well as skeletal metastases.

SU073

Biochemical and Radiological Assessment of Prostate Cancer Bone Metastases in SCID Mice. S. Peleg[1], D. D. Cody[1], N. Navone*[1], E. Johnson*[1], A. Ismail*[1], G. H. Posner*[2]. [1]The University of Texas, M. D. Anderson Cancer Center, Houston, TX, USA, [2]The Johns Hopkins University, Baltimore, MD, USA.

In man, prostate cancer metastasizes almost exclusively into the bone. The reactions that these malignant cells induce in bone are mixed osteolytic and osteosclerotic responses. We have used intrafemoral injections of two prostate cancer cell lines that induce, preferentially, either osteolytic (PC3) or osteosclerotic (MDA-PCA-2b) response and assessed tumor progression in the bone in the presence or absence of the non-calcemic vitamin D analog JK-1626-2. Injection of MDA-PCA-2b cells into the femur of male SCID mice resulted in the production of detectable serum PSA by 4 weeks after inoculation, which continued to increase after seven weeks. A daily injection of 4 mcg/kg or 10 mcg/kg of JK-1626-2 reduced serum PSA levels by 30% and 45%, respectively, suggesting inhibition of tumor progression by the analog. In spite of the daily administration of high doses of JK-1626-2 for over 7 weeks there was no increase in serum calcium in the analog-treated animals. There was a subtle evidence of change in the tumor-inoculated bones by 2D X-ray imaging, but 3D micro-computed tomography (micro-CT) clearly revealed both loss of trabecular bone and gain of cortical bone in the tumor-bearing femurs. In contrast, intrafemoral injection of the osteolytic prostate cancer cells, PC3, resulted in a rapid bone loss that was evident by x-ray imaging within 18 days. Daily injections of the analog JK-1626-2 (4 mcg/kg and 10 mcg/kg), increased the severity of the bone lesion in the tumor-inoculated femurs by 60%. Furthermore, 3D sample measurements of bone mineral density by micro-CT at the tibias below the tumor-bearing femurs revealed a significant bone loss in the analog-treated animals. This loss of bone was not evident on the contralateral side, suggesting that malignant cells spreading into the tibia below the tumor site induced osteolytic activity. Serum calcium levels in the vehicle-treated tumor-bearing group were slightly but significantly higher than serum calcium in age-matched normal male SCID mice. Interestingly, this increase in serum calcium was more prominent in the analog-treated tumor-bearing animals, findings that were consistent with the observed increases in osteolytic activity in the tumor-bearing bones of these animals. These results indicate that micro CT is a sensitive tool for qualitative and quantitative assessment of bone lesions at early stages of either osteolytic or osteosclerotic metastatic bone disease in mice. Our results also suggest that vitamin D analogs may be useful to treat osteosclerotic metastatic bone disease but may have an adverse effect on advanced osteolytic bone metastases.

SU074

Markers of Bone Turnover Do Not Predict Bone Metastases During Long-Term Follow-Up of Breast Cancer Patients. M. J. Seibel[1], M. Koeller*[2], B. Auler-van der Velden*[2], I. Diel[2], H. W. Woitge[1]. [1]University of Sydney, Sydney, Australia, [2]Univ. of Heidelberg, Heidelberg, Germany.

Markers of bone turnover are often elevated in breast cancer patients with bone metastases (BM). To test whether bone markers could be used as early indicators of developing BM, we prospectively followed 112 postmenopausal women operated for primary breast cancer. At the time of diagnosis/ study inclusion, none of the women had BM, other skeletal disease or bone active drugs. During follow-up (range 0.6 - 4 yrs., median 30 mo.), patients were seen every 3 months and timed blood/ urine specimens were obtained. Eleven patients developed BM (BM+) and each of these were matched to 4 women free of BM (BM-). The markers measured were serum (s) calcium, sTAP, sBAP, sOC, sPICP, urinary (u) PYD, uDPD, uNTX, sNTX, uCTX, sCTX. All analyses were done in single batches after study end. Results: At any given point in time (including baseline), marker levels in the BM+ group did not differ significantly from those in the BM- group. Marker levels at baseline did not predict the later development of BM (OR 0.14 -1.01, all NS). 93% of all changes in bone markers were below the least significant change, as defined in an independent group of similar patients. The remaining 7% of values could not be associated in a consistent pattern with the occurrence of BM. Conclusion: In patients with breast cancer, biochemical markers of bone turnover can not be used to predict or diagnose incident BM. This lack in diagnostic validity is mainly attributable to the high overall and long-term variability of the currently used bone markers.

SU075

Blockade of TGFβ Signaling in Prostate Cancer Cells Exacerbates Osteolytic Metastases. X. Sun, S. Kakonen, T. Oba, B. L. Hill, B. G. Grubbs*, S. Burns*, T. A. Guise, J. M. Chirgwin. Molecular Medicine, U Tx Hlth Sci Ctr, San Antonio, TX, USA.

PC3 prostate cancer cells express abundant PTHrP and cause osteolytic metastases in nude mice. PTHrP production by PC3 cells is increased 4-fold by TGFbeta. Thus, we hypothesized that blockade of TGFbeta signaling in PC3 cells would decrease osteolytic metastases, as was observed with MDA-MB-231 breast cancer cells. Three stable clones of PC3 expressing a dominant negative TGFbeta receptor construct were isolated. 1B2 & 2B2 showed decreased PTHrP production basally and in response to TGFbeta, while 2B4 had unchanged basal production and was stimulated only 1.8X. Growth rates were unchanged in vitro. In the left cardiac ventricle bone metastasis model, these 3 dominant negative clones caused more osteolytic metastases and reduced survival in tumor-bearing mice compared with controls. Mice receiving 2B2 cells survived ~75d ($p<0.0001$ vs empty vector, EV) and 1B2 & 2B4 groups survived ~150 days ($p<0.05$ vs EV), at which time >75% of EV-inoculated animals were still alive. To determine the mechanism for the increased osteolysis caused by the dominant-negative TGFbeta receptor clones, conditioned media +/- TGFbeta were analyzed for osteolytic factors. Dominant negative clones secreted less IL-11, VEGF, and PTHrP than control. These factors could not account for the results seen in vivo. Other factors with actions on bone cells or tumor growth were examined by RT-PCR +/-TGFbeta. Factor mRNAs unchanged by TGFbeta treatment and in clones vs control cells included: osteoprotegerin, RANK ligand, hepatocyte growth factor, tissue inhibitor of metalloproteinase-1, urinary plasminogen activator, plasminogen activator inhibitor-1, IL-18, and its binding protein. However, insulin-like growth factor binding protein (IGFBP) 3 was stimulated by TGFbeta in EV controls and its expression was decreased in the dominant negative receptor clones. IGFs, along with TGFbeta, are abundant components of bone matrix. When released by osteoclastic resorption, IGFs could stimulate tumor growth in bone. This stimulation would normally be limited by IGFBP3 secreted in response to TGFbeta. The effects of TGFbeta signaling blockade on bone metastases may differ between breast and prostate cancer models for 2 reasons: 1) PC3 prostate cells basally secrete very high amounts of PTHrP, even when TGFbeta signaling is blocked; these are higher than those secreted by MDA-MB-231 cells and may be sufficient to stimulate osteolysis. 2) TGFbeta signaling may control prostate cancer cell growth in bone through a paracrine mechanism involving bone-derived IGFs and tumor-produced IGFBPs.

SU076

Effects of RANKL on Breast Cancer Cell Lines. C. Hwang*[1], H. Chung[2], Y. Kang*[1], I. Moon*[1], C. Yim*[2], K. Han[2], H. Jang*[2], W. Park*[2], H. Yoon[2], I. Han[2]. [1]Laboratory of Endocrinology, Samsung Cheil Hospital and Women's Healthcare Center, Seoul, Republic of Korea, [2]Medicine, Samsung Cheil Hospital and Women's Healthcare Center, Seoul, Republic of Korea.

Breast cancer metastasis commonly induces osteolytic bone lesions. This osteolytic metastasis is mediated by the differentiation and activation of osteoclasts through upregulation of RANKL. Breast cancer cells with the capacity to stimulate osteoclastic bone resorption may enrich the bone microenvironment with growth factors that may alter behavior of tumor cells. Therefore, we investigated whether the locally increased RANKL can affect the invasion of breast cancer or have the influence on the change of gene expressions in breast cancer cells. In this study, we showed the NF-κB activation using electrophretic mobility shift assay in breast cancer cell lines (MCF-7 & MDA-MB-231) when they were incubated with soluble RANKL (1 ng/ml-100 ng/ml). Semi-quantitative RT-PCR showed that the expressions of PTHrP, TGFβ mRNA in ratio to internal standard GAPDH mRNA were elevated in RANKL-treated cells(MCF-7, MDA-MB-231) compared with control (respectively; $P<0.05$), but the levels of IL-1β, IL-6, TNF-α, OPG mRNA were not changed. For invasion analysis, we used matrigel invasion assay system. MDA-MB-231 cells supplemented with RANKL for 18 hr in 0.1% BSA/α-MEM dose-dependently showed the high invasiveness (control;16±5 vs 100 ng/ml of RNAKL;146±27). Zymography and RT-PCR analysis of MMP-2, MMP-9 which were correlated with cancer invasion were not changed. In conclusion, these results suggest that the locally increased RANKL in bone microenvironment may activate the invasiveness of breast cancers and enhance the expression of osteolytic factors in tumor cell.

SU077

The Localization of Macrophage and Lymphocytes in Bone Metastasized Lesions. T. Sasaki[1], K. Ono*[2], T. Akatsu*[2], N. Kugai*[2], T. Maeda*[1], N. Amizuka[1]. [1]Division of Oral Anatomy, Department of Oral Biological Science, Niigata University Graduate School of Medical and Dental Sciences, Niigata, Japan, [2]Department of General Medicine, National Defense Medical College, Tokorozawa, Japan.

In order to elucidate the immune-response in bone-metastasis, 4 week-old normal female Balb/c mice were injected with mammary carcinoma cells which were derived from the same strain. After 2 weeks, the tumor-injected mice were fixed with paraformaldehyde solution and then decalcified with EDTA solution. The femurs and tibiae were employed for histochemical and electron microscopic analyses including tartrate resistant acid phosphatase (TRAPase), alkaline phosphatase (ALPase), F4/80 (recognizing macrophage/monocyte lineage), CD45R (recognizing lymphocyte lineage) and CD31 (recognizing endothelial cells). A tumor mass metastasized in the metaphysis showed central necrosis, active proliferation of cells and tumor-derived angiogenesis. ALPase-positive osteoblastic stromal cells surrounded the metastasized lesion. Many TRAPase-possitive osteoclasts were localized on the trabecular surfaces facing to the tumor lesion, associated with ALPase-positive osteblastic cells. In contrast, F4/80-positive macrophages accumulated around the metastasized tumor cells, and often invaded its inner portion. Unlike macrophages, CD45R-positive lymphocytes were located apart from the metastasized tumor lesion; they made contacts with neither the tumor cells nor osteoclasts. Under electron microscope, the macrophages around the tumor lesion showed frequent contacts with the tumor cells by their cytoplasmic processes, and some of them exhibited many secondary lysosomes. Taken together, macrophages but not CD45R-possitive lymphocytes appeared to recognize the metastasized tumor cells in order for the immune-response. Thus, this study suggests that the macrophages play a crucial role in the immune system against the bone-metastasized tumor cells.

SU078

Use of Serum Markers of Tumor Burden and Bone Resorption to Monitor Disease Progression in a Nude Mouse Model of Breast Cancer-Induced Osteolysis. R. NicAmhlaoibh*[1], J. Risteli[2], C. Holst-Hansen*[3], P. Qvist*[1], C. Christiansen[4], N. Brünner*[3], J. Delaissé[1], A. Heegaard[1]. [1]Nordic Bioscience A/S, Herlev, Denmark, [2]Department of Clinical Chemistry, University of Oulu, Oulu, Finland, [3]The Finsen Laboratory, Rigshospitalet, Copenhagen, Denmark, [4]CCBR, Ballerup, Denmark.

Sensitive biochemical markers of cancer-induced osteolytic disease progression and response to therapy are lacking in preclinical models. Using the Arguello model of breast cancer-induced osteolytic disease we have studied the serum levels of cancer markers and bone resorption markers to identify a suitable marker to supplement radiographical evidence of disease and quantitatively follow disease progression and response to therapy. We compared different biochemical markers of tumor burden and bone resorption in 4-week-old nude mice inoculated with a bone-seeking variant of the human MDA-231 breast cancer cell line. Though we have recently found the cytokeratin-associated tissue polypeptide antigen, TPA, to be a very suitable marker for quantification of the tumor burden in extracts of long bones from these mice, and although serum TPA is useful in the clinic to monitor breast cancer progression, human TPA was not detected at significant levels in the serum of mice inoculated with MDA-231 cells. Other human breast cancer serum markers (CA15-3, VEGF, M-CSF) expressed by the MDA-231 cells in vitro, were also not detectable in the serum of diseased mice. Bone resorption markers such as CTX, ICTP, and TRAP5b have been used in the clinic to monitor osteolytic disease progression in patients, and also in the present model their levels were marginally (CTX, ICTP) or significantly (TRAP5b) increased at the late stage of osteolytic disease; however, as expected the basal levels of these markers were high and age-sensitive. In addition, we inoculated the mice with an MDA-231 cell line transfected with E.coli beta-galactosidase (MDA-231/BAG). The concentration of beta-galactosidase in serum from mice with progressive osteolytic lesions was significantly correlated with area of osteolysis and levels of TPA in bone extracts. A particular advantage of beta-galactosidase as a serum marker compared to the bone resorption markers is the negligible basal levels due to its bacterial origin. In conclusion, serum E.coli beta-galactosidase is a useful quantitative serum marker of disease progression in this mouse model of human breast-cancer induced osteolytic lesions.

SU079

Transforming Growth Factor-β Stimulation of Collagenase-3 Expression in Human Breast Cancer Cells. N. Selvamurugan, Z. Fung*, N. C. Partridge. Physiology and Biophysics, UMDNJ-Robert Wood Johnson Medical School, Piscataway, NJ, USA.

TGF (transforming growth factor)-β1, a crucial molecule in metastatic bone cancer, stimulates collagenase-3 (matrix metalloproteinase-13) expression in the human breast cancer cell line, MDA-MB231. Cycloheximide inhibited this stimulation, indicating that *de novo* protein synthesis was essential for this response. In order to analyze the specific response elements involved for TGF-β-stimulated collagenase-3 promoter activity in MDA-MB231 cells, the collagenase-3 promoter constructs having mutations at either the RD/Cbfa or AP-1 sites were used and the effect on CAT activity was assessed in these cells. Mutation of either the distal RD/Cbfa or the proximal RD/Cbfa or the AP-1 sites was enough to cause a significant loss of TGF-β response for collagenase-3 promoter activity in the breast cancer cells. To define the contributions of transcription factors binding to the proximal RD/AP-1 site, gel mobility assays were performed. Proteins in both control and TGF-β-treated nuclear extracts were able to bind to the human collagenase-3 RD/AP-1 site, but significantly more protein-DNA complex was produced when extract from TGF-β-treated cells was used. Further analysis of the proximal RD/AP-1 site-protein complexes identified the presence of both Cbfa1/runx2 and AP-1 factors. The functional role of the RD and AP-1 sites and their transcription factors for TGF-β-stimulated collagenase-3 promoter activity in MDA-MB231 cells was determined by co- transfection of the collagenase-3 promoter construct with either an AML/ETO construct that lacks the transactivation domain of Cbfa/runx and acts as a dominant inhibitor of Cbfa/runx proteins or an antisense-Fra-1 construct. Overexpression of AML/ETO inhibited both the basal and the TGF-β effect suggesting the requirement of the RD/Cbfa site and its transcription factor, Cbfa/runx for collagenase-3 promoter activity. Co-transfection of antisense-Fra-1 plasmid inhibited both the basal and TGF-β-stimulated collagenase-3 promoter activity indicating that the inhibition of Fra-1 expression by antisense-Fra-1 may abolish AP-1 transactivation since Fra-1 forms a complex with c-Jun, JunB or JunD that is necessary for AP-1 transactivation. The specificity of TGF-β-signaling for collagenase-3 promoter activity in MDA-MB231 cells was also determined by co-transfection of the collagenase-3 promoter construct along with either a truncated TGF-β type II receptor or a dominant negative Smad3. Taken together, our results suggest that both the AP-1 and RD sites and their transcription factors along with Smad proteins may account for TGF-β stimulation of collagenase-3 promoter activity in MDA-MB231 cells.

SU080

Gender-specific Role of Endothelin-1 (ET-1) in Pathological Bone Remodeling. K. S. Mohammad[1], J. J. Yin*[1], B. G. Grubbs*[1], Y. Cui*[1], R. Padley*[2], T. A. Guise[1]. [1]Molecular Medicine, UTHSCSA, IDD, CTRC, San Antonio, TX, USA, [2]Abbott, Chicage, IL, USA.

ET-1, a vasoconstrictor, and a potent stimulator of osteoblast activity may play a causal role in osteoblastic metastases. Human breast cancer lines, ZR-75-1, MCF-7 and T47D, all secrete ET-1 and cause osteoblastic metastases in nude mice. Selective ET_A and non-selective $ET_{A/B}$ receptor antagonists, completely inhibited ET-1 and ZR-75-1-mediated new bone formation in mouse calvariae; ET_B antagonist had no effect. In nude mice, an ET_A receptor antagonist (ABT-627, 20mg/kg/day) significantly reduced ZR-75-1 osteoblastic metastases. The data suggest that tumors metastatic to bone cause osteoblastic responses by secreting ET-1, which activates ET_A receptors on osteoblasts. Since ET-1 is expressed in the bone microenvironment, we hypothesized that chronic ET_A receptor blockade would alter normal bone remodeling. We investigated the role of chronic ET_A receptor blockade on bone remodeling in sex steroid-deficient male and female C57 black mice since prostate cancer patients with bone metastases are treated with androgen deprivation therapy. 4 week-old mice underwent orchiectomy, ovariectomy or sham-operation at which time ABT-627 or vehicle was started. BMD was measured at total body, femur, tibia and spine over a 36 week period. Hypogonadal males had significantly lower BMD at all sites compared with intact mice. In hypogonadal males, ABT-627 treatment caused higher BMD at the femur, spine and total body vs. vehicle. In contrast, ABT-627 treatment caused lower BMD at the femur in eugonadal males. Hypogonadal females had lower BMD at the tibia compared with eugonadal controls. In hypogonadal females, ABT-627 treatment caused lower BMD at the femur and spine vs. control treatment. In contrast, eugonadal females treated with ABT-627 had significantly higher BMD at all sites vs. vehicle-treated. Histomorphometric analysis of trabecular bone volume at the femur was consistent with the BMD data in the female mice. In male mice, trabecular bone volume at the femur was consistent with BMD except in eugonadals, where no differences between ABT-627 and control were noted. Taken together, these data indicate that 1) the predominant role of ET-1 in bone remodeling appears to be in pathologic states such as those associated with metastatic bone disease; 2) chronic ET_A receptor blockade has gender-specific differential effects on bone remodeling which depend on the presence or absence of sex steroids. The implications of these findings are: 1) ET_A receptor blockade should benefit those patients with osteoblastic bone metastases and 2) ET_A receptor blockade should not result in bone loss when used to prevent osteoblastic bone metastases in hypogonadal men.

SU081

Prostate Specific Antigen and Human Kallikrein 2 Expression of Prostate Tumor Cells Correlates with the Osteoblastic Response in Prostate Cancer Bone Metastasis. M. P. Roudier[1], S. H. King*[1], S. M. Ott-Ralph[2], R. L. Vessella[1]. [1]Urology, University of Washington, Seattle, WA, USA, [2]Medicine, University of Washington, Seattle, WA, USA.

Prostate cancer (CaP) primarily metastasizes to lymph nodes and bones where it stimulates an osteoblastic response in contrast to other adenocarcinoma bone metastases that are osteolytic. One of the notable differences between CaP and the other adenocarcinomas is the secretion of prostate associated serine proteases such as prostate specific antigen (PSA), human kallikrein 2 (hK2) and prostin. PSA can activate at least 2 main components involved in the osteoblastic response, TGFbeta and IGF. HK2 and prostin can also activate PSA and the bone morphogenetic proteins. These facts provide the rationale to test if PSA and hK2 expression in CaP bone metastases correlates with bone volume. Forty metastatic bone biopsies from eleven androgen independent patients who died from CaP were analyzed for bone volume by histomorphometry using plastic-embedded Goldner's stained sections and the Osteomeasure system. PSA and hK2 were assessed by immunohistochemistry using an avidin-biotin-peroxidase method with antigen retrieval on the following plastic section. Overall expression of PSA and hK2 was low in 2 patients (less than 20% of tumor cells expressing PSA and hK2) and high in the other 9 (greater than 40% of tumor cells expressing PSA and hK2). Overall bone volume was high in 9 patients (mean BV/TV = 49) and low in 2 patients (mean BV/TV = 9). However there was a wide variation of both immunoreactivity of tumor cells and bone volume from one bone site to another in a given patient. Consequently, there was a moderate correlation between the percentage of tumor cells expressing PSA and bone volume (r = 0.5). There was a similar but inverted correlation between the percentage of tumor cells expressing hK2 and the percentage of eroded surface (r = - 0.5). We conclude that PSA and hK2 expression modulates the osteoblastic response in CaP bone metastases. However, further studies are needed to demonstrate that PSA and/or hK2 expression are directly involved with augmenting the osteoblastic response. This will be accomplished in part using our intra-tibia osseous xenograft models that demonstrate osteolytic, osteoblastic and mixed osteolytic/osteoblastic bone responses.

SU082

Histomorphometric Comparison of our Osteolytic PC3 and Osteoblastic LuCaP 23.1 Intra-osseous Mouse Models of Prostate Cancer Bone Metastases with Clinical Specimens. M. P. Roudier*[1], J. E. Quinn*[1], S. M. Ott-Ralph[2], E. Corey[1], R. L. Vessella[1]. [1]Urology, University of Washington, Seattle, WA, USA, [2]Medicine, University of Washington, Seattle, WA, USA.

Although prostate cancer (CaP) bone metastases are typically osteosclerotic, there is also experimental, histological and biochemical evidence of associated increased bone resorption. We have shown that both osteolytic and osteoblastic patterns can be observed in different bone sites of a given patient. To validate our LuCaP 23.1 osteoblastic and PC3 osteolytic intra-osseous mouse models, we compared their histomorphometric data to those of human CaP osteoblastic and osteolytic metastases. LuCaP 23.1 tumors were sampled at early, mid and late stages and after castration, monitored by serum PSA levels (n=8). PC-3 tumors were all sampled after 27 days (n=6). For comparison, we used 10 osteoblastic (mean BV/TV=53.2) and 10 osteolytic (mean BV/TV=9.47) metastatic biopsies taken from autopsies of patients who died from CaP. All bone samples were fixed in buffered formalin, dehydrated and embedded in methylmethacrylate. Analysis was performed on Goldner and TRAP stained sections using the Osteomeasure system. Bone and osteoid volumes, eroded and osteoblastic surfaces, osteoblast and osteoclast numbers were assessed at a magnification 2.5 x on a 9.73 mm^2 total surface in PC3 and LuCap 23.1; at magnification 10 x, on 9.73 mm^2 total surface in a subset of 4 late-stage LuCaP 23.1 and at magnification 10 x on 11.7 mm^2 total surface in human biopsies. The mouse tibial measurements were performed at the injection site including the tibial plateau as a consistent anatomic reference. LuCaP 23.1 showed an increasing osteoblastic pattern (mean BV/TV at late stage = 49.14) while PC-3 showed a consistent lytic pattern (mean BV/TV = 5.91). Statistically there was no significant difference between the mouse and human osteoblastic pattern for bone volume, osteoid volume and eroded surface (p=0.60, 0.39, 0.12 respectively). Similarly there was no difference between the mouse and human bone volume in the osteolytic pattern (p=0.11). In human and mouse osteoblastic lesions, osteoblast cells were not fully differentiated. In both osteolytic lesions, an overall low number of osteoclasts was observed.We conclude that our mouse intra-osseous models reproduce quite well the osteoblastic and osteolytic patterns observed in human CaP bone metastases and can be used to study the mechanisms of CaP bone metastasis.

SU083

Rat Model of Metastatic Bone Disease. B. A. Lechowska, L. C. Dare*, S. J. Hoffman, J. A. Vasko-Moser*, M. W. Lark, G. B. Stroup. Musculoskeletal Diseases, GlaxoSmithKline, King of Prussia, PA, USA.

The injection of human breast cancer cells (MDA-MB-231) into the left heart ventricle of nude mice results in tumor development in the long bones and the spine ultimately causing osteolytic bone lesions closely resembling the human condition of cancer metastasizing to bone. An attempt to develop a similar model in the rat was undertaken because systemic compound profiles are generally more favorable, sample collection (blood, urine) is easier, and bone mineral density (BMD) measurements, an invaluable tool in bone metastases studies, are less variable and also easier in the rat. Hsd:RH-rnu 9-week old female rats were injected with either vehicle or MDA-MB-231 cells at $5x10^5$ (0.5 ml) per rat. Digital x-ray images of the hind limbs were taken at baseline, week 2, 3, and 4. Areal BMD (aBMD) of the lumbar spine and proximal tibia were taken at baseline, week 3, and week 4. Blood was collected at term, [Ca^{++}] was measured and plasma was saved for Ctx analysis. Left tibiae and L3 were excised for pQCT (tibia only) and µCT analysis. Animals were sacrificed at week 4 or at time of onset of hind-limb paralysis. Lesions in long bones were detected in 42% of the inoculated animals as early as week 2 with a mean area of 5.0 mm^2. By week 3, 75% developed lesions with a mean area of 26.9mm^2. No further increase occurred during the fourth week. ABMD of the lumbar spine increased in both groups, but slower in inoculated animals (118% and 113% respectively at week 4). In the proximal tibia, a steady increase in aBMD was observed in vehicle animals (120%, 121% at weeks 3 and 4 respectively), while no change occurred in the other group (101%) during the first three weeks and then a dramatic increase to 125%. This increase in the MDA group between weeks 3 and 4 occurred because at that time only relatively healthy animals remained (most affected ones were euthanized during the previous week due to paralysis). Whole blood Ca^{++} was significantly (p<0.01) higher in inoculated animals (1.47mM) than in Vehicles (1.42mM). Plasma Ctx were slightly higher in inoculated animals (8.6 ng/ml) than in vehicles (7.4 ng/ml). PQCT analysis of the proximal tibia showed that both, total (668.3 mg/cm^3) and trabecular (275.8 mg/cm^3) BMD, was significantly lower in inoculated animals than in controls (728.2 and 343.7 mg/cm^3 respectively). A similar trend was shown by µCT analysis of the same limb. In conclusion, a model of metastatic bone disease has been adapted to the rat. A wider array of analytical tools as well as pharmacokinetic advantages offer a benefit over the mouse model of this disease. This should be a very useful model in evaluating effectiveness of antiresorptive therapies against development and/or growth of osteolytic bone metastases.

SU084

Comparison of Quantitative Heel Ultrasound with Dual Energy X-ray Absorptiometry in Discriminating Fractures in an Elderly Male Population. J. Thomas*[1], S. A. Steel[2], E. Howarth*[3], S. M. Doherty*[4]. [1]Metabolic Bone Disease Unit, Centre for Metabolic Bone Disease, Hull, United Kingdom, [2]Metabolic Bone disease Unit. HS Brocklehurst Building. 220-236 ANLABY ROAD, Centre for Metabolic Bone Disease., Hull, United Kingdom, [3]Medical statistics, Hull University, Hull, United Kingdom, [4]Metabolic bone disease unit, Centre For Metabolic Bone Disease, Hull, United Kingdom.

In this study we compare the ability of BUA of the heel and BMD by DXA of spine and hip to discriminate fractures in an elderly male population over 60 years of age in a UK elderly male population. All the men over the age of 60 years (n=383) in a local general practice of 5,000 were contacted and invited to participate in this study. The subjects were given an appointment to attend the hospital for DXA of lumbar spine, femoral neck (GE-Lunar Expert -XL) and BUA of the heel (McCue CUBA). We report on the BMD results of spine, hip and on BUA and SOS of the heel. We also report on the ability of DXA, BUA and SOS to discriminate fractures, using an unadjusted analysis. As the WHO criteria by BMD for osteopenia and osteoporosis apply only to females we applied a T-score threshold of -2.8 and a BUA threshold of <60 dBMHz-1 for osteoporosis. A total of 198 subjects (52% of the eligible population), aged 60-90 (mean 69) years attended for DXA and BUA. BUA of both heels was obtainable in 112 subjects (57%). BUA and SOS measurements were significantly higher for the right heel compared to the left. The mean (standard deviation) BMD of the spine was 1.29 (0.23) gm/cm2 and 0.96 (0.14) gm/cm2 for hip. Similarly the mean (standard deviation) BUA and SOS measurements for the right heel were 81.66 (16.32) dBMHz-1 and 1619.07 (45.10) m/sec respectively and for the left heel 78.69 (15.45) dBMHz-1 and 1613.25 (39.03) m/sec respectively. Of those attending, 95 subjects (48%) had sustained fractures in the past: 89 (94%) were adult fractures and 18 (19%) followed low trauma. A total of 2 low trauma fracture subjects were osteoporotic by DXA and 2 had BUA<60 dBMHz-1 (5 in this fracture group had a failed BUA). With the above threshold DXA and BUA defined 5.6% and 17.6% as osteoporotic respectively. BUA and SOS are better discriminators of fracture than BMD as BUA and SOS both explained 61% of the overall variation in the model when compared to DXA, which explained only 57% of the variation. At this stage, the basic discrimination between DXA, BUA and SOS is very small. The study is ongoing to determine whether there is greater discrimination between the three methods in predicting future fractures.

SU085

Can the Combination of Two BMD Measurements Ever Improve Fracture Discrimination? R. Patel, G. M. Blake, I. Fogelman. Radiological Sciences, Guy's, King's & St Thomas' School of Medicine, London, United Kingdom.

Intuitively the combination of two or more BMD measurements should improve our ability to identify patients at high risk of an osteoporotic fracture. However, a number of clinical studies have shown that in practice the gains obtained are only modest. We have investigated the effect of combining two BMD measurements using a bivariate gaussian model described by a correlation coefficient r between the two T-score values and individual relative risk values RR_1 and RR_2 for the two measurements. The area under the curve (AUC) for the ROC curve showing the percentage of fracture cases identified plotted against the percentage of the whole population was calculated for: (i) the T-scores of the individual measurements; (ii) the weighted mean T-score ≤ -2.5 (the conventional statistical approach); (iii) either T-score ≤ -2.5 (the conventional approach using the WHO criteria). For approach (ii), when $RR_1 = RR_2$ the two T-scores were weighted equally. When $RR_1 \neq RR_2$ the optimum weighting was used as predicted by the bivariate gaussian model. Results for RR values of 1.5, 2.0 and 2.5 and r = 0, 0.5 and 0.7 are shown in the Table.

		Single Site	Two Sites Weighted Mean T-score ≤ -2.5			Two Sites Either T-score ≤ -2.5		
RR_1	**RR_2**	**AUC**	**AUC**			**AUC**		
			r = 0	r = 0.5	r = 0.7	r = 0	r = 0.5	r = 0.7
1.5	**1.5**	61.3	65.7	63.0	62.2	63.6	62.3	61.8
2.0	**2.0**	68.8	75.6	71.4	70.2	72.4	70.4	69.7
2.5	**2.5**	74.1	82.0	77.3	75.9	78.4	76.0	75.2
1.5	**2.0**		71.5	68.9	68.8	68.5	66.8	66.4
1.5	**2.5**		76.0	74.1	74.1	72.4	70.7	70.4
2.0	**2.5**		79.1	75.0	74.2	75.7	73.5	72.8

The most important conclusion is that the greatest improvement in fracture discrimination is obtained when the two measurements are extremely poorly correlated and have comparable values for RR. While correlations of r = 0.5 seem poor, in practice there is little benefit from combining such measurements. Finally, consistently larger AUC values are obtained using the weighted mean T-score compared with the WHO approach.

SU086

Effect of Patient Positioning Devices on Bone Density Measurements. R. H. Nord, D. L. Ergun, K. G. Faulkner. GE Medical Systems LUNAR, Madison, WI, USA.

DXA bone density measurements are widely used to assist in the detection of osteoporosis and other metabolic bone diseases, and to monitor change longitudinally following treatment. The typical bone density examination evaluates the lumbar spine and the proximal femora. It would be convenient if these scans could be acquired as a single procedure, without repositioning the patient between scans; however the traditional methods for spine and femur acquisitions require different positioning. This study determined the effect on bone density results of departing from traditional patient positioning, exploring the possibility of using the same positioning for both spine and femur acquisitions. 50 volunteer subjects were measured on a Lunar Prodigy densitometer from GE Medical Systems. Subjects included 37 women and 13 men, ages 24 to 83, widely varying in height and weight. Each subject was measured as follows: AP Spine: 2 scans with lower legs elevated in the standard manner, and 4 scans with legs extended straight out on the tabletop. Femur: 3 scans with feet in the standard positioner, and 3 scans with feet simply bound together, toes pointed straight up.

			slope	R sqr.
Spine	Legs Down vs Legs Elevated	L2-L4	1.020	0.990
Femur	Feet Together vs Standard Position	Neck	1.010	0.982
		Trochanter	0.973	0.984
		Total	0.991	0.994

Correlations were excellent between standard and non-standard positioning for all the scan regions investigated. All data sets were fit well by linear regression through the origin. Slopes of the regression lines were very close to unity.

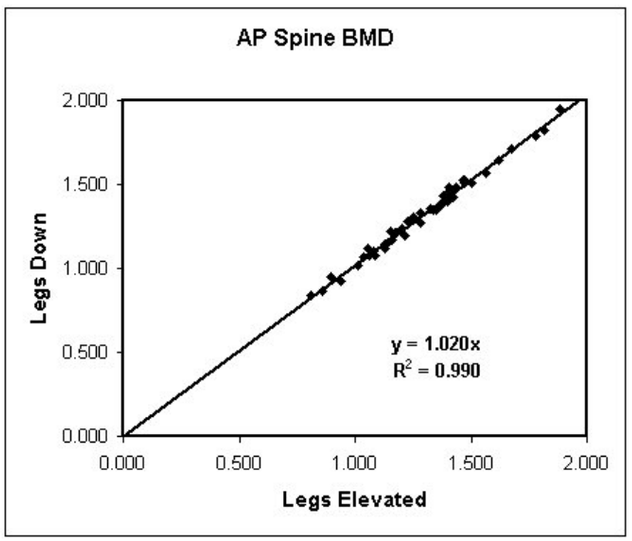

Excellent correlations suggest that reference values acquired with standard positioning could be adjusted for use with alternate positioning, to obtain clinically similar T-score and Z-score values.

Disclosures: ***R.H. Nord****, GE Medical Systems LUNAR 3.*

SU087

Twenty-year Follow-up of Phalangeal Bone Density with Radiographic Photodensitometry and Radiographic Absorptiometry. S. Bonnick[1], N. DiMarco[1], K. Cohlmia*[1], L. Lewis*[1], J. Colvin*[1], L. Al-Dayeh*[2], X. Bi*[2]. [1]Texas Woman's University, Denton, TX, USA, [2]CompuMed Inc., Los Angeles, CA, USA.

Baseline and follow-up radiographic photodensitometry (RPD) films of the left hand of 319 individuals were re-analyzed using a modification of the Osteogram® radiographic absorptiometry (RA) technique. Associations between RA data and baseline and follow-up age were examined and models developed for the prediction of the follow-up RA bone mineral density (BMD) and the change in RA BMD. Between 1950 and 1965 approximately 3000 individuals underwent RPD studies. During a 19-month period in 1979 to 1981, 319 of these individuals (222 women and 95 men) underwent repeat RPD studies. Mean age at baseline was 20.1 years (3 to 79 years). At follow-up, mean age was 43.5 years (16 to 94 years). Mean length of follow-up was 22.5 years (13 to 28 years). A radiographic Look-Up-Table that maps RPD and RA wedge data was used to modify the analysis algorithm of the PC-based software Osteogram® (CompuMed, Inc., Los Angeles, CA). The customized Osteogram® RA technique was applied to RPD x-rays assessing BMD at the middle phalanges of the 2nd, 3rd, and 4th fingers. Mean (SD) baseline RPD and RA BMD was 0.22 (0.03) and 98.04 (16.00), respectively (r=0.397, p<0.01). Mean (SD) follow-up RPD and RA BMD was 0.20 (0.03) and 110.52 (13.63), respectively (r=0.621, p<0.01). The correlation for the change in RPD and RA bone density was 0.486, p<0.01. Pearson correlation coefficients for baseline and follow-up age and RA BMD values are shown in the table. All correlations were significant at p<0.01 (2 tailed).

	Baseline RA BMD	Follow-Up RA BMD	Change in RA BMD
Baseline Age	0.403	-0.657	-0.743
Follow-Up Age	0.444	-0.627	-0.748

Linear regression was performed using SPSS v10 with age and baseline RA BMD as predictors for the dependent variables of follow-up RA BMD and change in RA BMD.
Follow-up RA BMD = 91.014 - [(Baseline Age)(1.439)] + [(Baseline Age)^2 (1.109E-02)] + [(Baseline RA BMD)(0.413)]
Change in RA BMD = 91.014 - [(Baseline Age)(1.439)] + [(Baseline Age)^2 (1.109E-02)] - [(Baseline RA BMD)(0.587)]

Correlations of RPD and RA BMD were statistically significant and similar to that previously reported. RA BMD increased between measurements in individuals who were younger than age 49 at the time of both measurements and declined in individuals older than age 49 at the time of the second measurement.

Disclosures: ***S. Bonnick****, CompuMed Inc. 5; Merck & Co., Inc. 2, 5, 8.*

SU088

Low Bone Density Is a Major Risk Factor for Periprosthetic Bone Loss Following Total Hip Arthroplasty. G. M. Blake[1], A. I. A. Rahmy*[2], A. J. Tonino*[3], W. D. Tan*[2], I. Fogelman[1]. [1]Radiological Sciences, Guy's, King's & St Thomas' School of Medicine, London, United Kingdom, [2]Department of Nuclear Medicine, Atrium Medical Center, Heerlen, Netherlands, [3]Department of Orthopedic Surgery, Atrium Medical Center, Heerlen, Netherlands.

We report a study to investigate the relationship between periprosthestic bone loss following total hip arthroplasty (THA) and the preoperative BMD at the spine, femur and forearm. 51 patients (32F,19M) (mean age 63 y, range 46-75 y) undergoing THA were randomised to one of two cementless hip prostheses, either the Anatomic Benoist Girard (ABG) (Howmedica International, Rutherford, NJ) (n = 24) or the Mallory-Head Porous Hip (Biomet, Warsaw, IN) (n = 27). Preoperative DXA scans (Hologic QDR2000) were performed to measure BMD at the PA and lateral spine, the contralateral femur, and the non-dominant forearm. Postoperative DXA scans were performed to measure BMD in periprosthetic bone at 10 days (treated as baseline for the subsequent follow-up), 6 week, 3 month, 6 month, 1 y, 2 y and 3 y using the standard Gruen zone analysis and the total periprosthetic ROI. 48/51 patients completed the study at 3 y. Statistical analysis confirmed a highly significant relationship between periprosthetic bone loss at 6 month, 1 y, 2 y and 3 y expressed as percent from baseline and the preoperative BMD at the PA spine, trochanter, total hip and forearm. The Table shows the Students-t and p-values for the correlations with the total periprosthetic ROI at each time point. Weaker relationships were also seen for lateral spine, femoral neck and Wards triangle BMD for the 2 and 3 y data. The relationship remained statistically significant when data for the ABG and Mallory prostheses were analysed individually. In conclusion, low bone density at the spine, hip or forearm is a major risk factor for periprosthetic bone loss following THA.

Students t and p-values

	6 months	1 year	2 years	3 years
PA Spine	3.74 (< 0.001)	3.86 (< 0.001)	3.46 (0.001)	3.62 (0.001)
Femoral Neck	1.66 (0.104)	1.72 (0.093)	2.63 (0.012)	2.83 (0.007)
Trochanter	3.42 (0.001)	2.91 (0.006)	3.59 (0.001)	3.81 (< 0.001)
Total Hip	2.81 (0.007)	2.39 (0.021)	2.98 (0.005)	3.26 (0.002)
Ultradistal Forearm	3.20 (0.002)	3.16 (0.003)	3.13 (0.003)	4.35 (< 0.001)
Total Forearm	3.54 (0.001)	3.33 (0.002)	3.85 (< 0.001)	4.86 (< 0.001)

SU089

Retraction of an Overlying Fat Panniculus Is Indicated when Measuring Femur Bone Mass with DXA. D. Krueger[1], N. Vallarta-Ast[2], T. Kawahara-Baccus*[1], K. Elver*[3], N. Binkley[1]. [1]Institute on Aging, University of Wisconsin, Madison, WI, USA, [2]Radiology, Wm. S. Middleton VAMC, Madison, WI, USA, [3]Radiology, UW Health, Madison, WI, USA.

Dual energy x-ray absorptiometry (DXA) is currently the gold standard technique for osteoporosis diagnosis. However, DXA has limitations, including artifacts such as degenerative disease or metallic foreign bodies, which may confound results. It is possible that overlying fat folds may be a currently unappreciated confounder of proximal femur bone mineral density (BMD) measurement. As such, the aim of this study was to evaluate the effect of overlying fat on measured proximal femur BMD. Sixty-eight subjects (31 women/ 37 men) referred for routine BMD measurement at the Wm. S. Middleton VAMC were identified as having a fat fold within the DXA scan field by visual assessment of images obtained utilizing a GE Lunar Expert-XL densitometer. The mean ± SEM age, weight and body mass index (BMI) of these women was 64 ± 0.5 years, 207± 5.8 pounds and 36 ± 0.8; of the men 67 ± 0.6 years, 232 ± 7.0 pounds and 35 ± 0.8. Subsequent to their initial imaging, these 68 individuals were rescanned while retracting their fat panniculus away from the proximal femur scan area without other repositioning between scans. In 65% of the men, and 61% of the women, the femoral neck, total femur and/or trochanteric BMD differed by greater than the least significant change at our facility. In 14 of 68 subjects, the measured BMD differed by >10%. No pattern was observed to predict whether BMD would increase or decrease following fat retraction. Additionally, no relationship between BMI and change in BMD following fat retraction was demonstrated. To evaluate the reproducibility of BMD measurement with panniculus retraction, 25 patients were recruited for a precision study. The mean ± SEM age, weight and BMI of this group was 65 ± 0.7 years, 226 ± 5.2 pounds and 35.3 ± 0.8 respectively. Volunteers were scanned with their panniculus retracted, asked to stand from the table and had a second retracted scan performed. In this group, the total femur BMD least significant change (LSC) was 0.049 g/cm2, which compares favorably with our clinical total femur LSC of 0.033 g/cm2. In conclusion, overlying fat frequently alters BMD values obtained at the total proximal femur, femoral neck and trochanter. This impairs the ability to accurately diagnose low bone mass and monitor osteoporosis therapy in these patients. BMD precision with manual panniculus retraction is acceptable. As such, when fat overlays the proximal femur scan area, its retraction should be part of routine densitometric practice.

SU090

Lead in the Skeleton Interferes with Bone Mineral Density Measurements. E. Puzas[1], J. Campbell*[2], R. J. O'Keefe[1], E. M. Schwarz[1], R. N. Rosier[1]. [1]Orthopaedics, University of Rochester, Rochester, NY, USA, [2]Pediatrics, University of Rochester, Rochester, NY, USA.

Introduction: Two important pieces of data implicate the skeleton as a key tissue for the toxic effects of lead. They are; i) 95% of the body's lead burden resides in bone and ii) lead adversely affects bone cell metabolism. These findings would argue that lead-exposure may be an independent variable for low bone mineral density. In fact, however, no reports have documented osteoporosis (or osteopenia) in lead-exposed humans with DEXA. We believe this is due to a serious artifact created by lead in the measurement of bone density in humans. Methods: one mineral density of bovine bone containing added amounts of lead that mimic human levels was measured with DEXA and ultrasound (US). Also, the calcaneus of 18 human subjects with differing lead-exposure histories were measured with both DEXA and US. The DEXA measurements were performed on both Lunar and Hologic instruments. The ultrasound measurements were performed with a Lunar Achilles instrument. Results: The range of lead levels found in the bone of adult humans causes an artifactual increase in bone mineral density. The artifact ranges from a 4% (10 ug Pb/g bone) to 11% (100 ug Pb/g bone) overestimate of bone density. The overestimate occurred with instruments from both GE/Lunar and Hologic. Ultrasound measurements of the same samples showed no such increase. A ratio of an US measurement to a DEXA measurement at the calcaneus in patients (N=18) showed a statistically significant inverse relationship with blood lead levels. We have used this relationship to calculate a correction factor for bone mineral density based on historic lead-exposure. We believe this effect is due to attenuation of the x-ray beams by the high electron dense lead atoms according to principles of the photo-electric effect. Conclusion: A 4 - 11% overestimate of bone density can alter a patient's t-score by as much as 1.0. Thus, unless one knows the skeletal lead content of their patient, an accurate bone density cannot be determined. If this finding proves to be consistent throughout the population, then a large number of patients are under-treated for their low bone density.

*Disclosures: **E. Puzas**, Merck Pharmaceuticals 8; Proctor and Gamble Pharmaceuticals 8; Lilly Pharmaceuticals 8.*

SU091

Central DXA Reporting: What Do Clinicians Want? N. Binkley, D. Krueger, M. K. Drezner. University of Wisconsin, Madison, WI, USA.

Practicing clinicians reportedly prefer detailed bone densitometry interpretation. However, given the recent emphasis on physician education regarding osteoporosis diagnosis, this may no longer be the case. As such, a survey designed to assess clinician preferences regarding bone densitometry reports was conducted. On review of clinical requests, 212 health care providers were identified who had ordered at least one DXA scan at the University of Wisconsin from May through August 2001. All were requested by mail to evaluate potential elements of a central DXA report. Eleven possible components were listed on a one-page survey and providers were asked to indicate whether they would find each useful in their practice. The survey was anonymous, however different colors were utilized to allow determination of those providers who requested 1-4, 5-8, 9-12 and 13 or more DXA scans during the four-month interval to allow comparison of "low" and "high" users. Of the 212 surveys sent, 118 were returned (56%). There was no difference in response rate between high and low users. BMD values were requested by less than half (48%) of all responding clinicians and T-score by 82%. However, the overwhelming majority requested percentage of young normal and percentage of age-matched controls (91 and 88% respectively). Approximately 75% requested that DXA reports contain determination of need for therapy; interestingly, a similar percentage requested that reports include a recommendation for type of therapy. Enumeration of clinical risk factors for fracture was requested by 65% and fracture risk assessment by 81%. No difference in request for any component was present between the groups ordering 13 or more scans than those requesting 1-4. Twenty-seven responding providers did not request that reports include the T-score values; of these, 22 requested comparison with young normals, 25 with age-matched controls and 21 desired recommendation of need for therapy. In conclusion, a majority of clinicians requesting DXA scans continue to desire detailed reports including need for therapeutic intervention, therapy recommendations and fracture risk estimation. Furthermore, these data may imply that ~20% of health care providers ordering DXA scans may not be familiar with World Health Organization diagnostic criteria and National Osteoporosis Foundation treatment guidelines. A need for ongoing educational efforts persists.

*Disclosures: **N. Binkley**, Merck 8; Eli Lilly 2; Aventis 2; Novartis 2.*

SU092

Use of Densitometric Lateral Vertebral Assessment to Detect Prior Vertebral Compression Fracture. N. Binkley[1], K. G. Faulkner[2], T. Kawahara-Baccus*[1], D. Krueger[1], H. K. Genant[3], M. K. Drezner[1]. [1]University of Wisconsin, Madison, WI, USA, [2]GE Medical Systems, Lunar, Madison, WI, USA, [3]University of California, San Francisco, CA, USA.

Many vertebral fractures are clinically silent, but are associated with increased risk for subsequent osteoporotic fracture. A substantial number of these fractures are demonstrable using Instant Vertebral Assessment with Hologic densitometers[1]. Whether similar recognition is possible using dual-energy Lateral Vertebral Assessment (LVA) with GE Lunar densitometers remains uncertain. Thus, we evaluated the ability of LVA to detect prevalent vertebral fractures compared with conventional spine radiographs in postmenopausal women. In this ongoing study, dual-energy LVA and conventional thoracic and lumbar spine radiographs have been obtained in 32 postmenopausal women. Using an established visual semiquantitative system, vertebral fractures were visually identified individually by two non-radiologist physicians (NB & MKD) from printouts of LVA examinations. These results were compared to semiquantitative evaluations of the spinal radiographs by an expert radiologist (HKG). Study participant mean age ± SEM was 72.8 ± 0.9 (range 61-80) years; their mean lumbar spine BMD T-score was –2.0 ± 0.2 (range –3.9 - +2.7). Using LVA, 97% of the vertebrae from T-7 through L-4 were evaluable, although a majority of vertebrae from T-4 to T-6 were not adequately visualized for fracture assessment. In the evaluable vertebrae, prevalent fractures were identified in 13 vertebral bodies using LVA. Compared to spine radiographs, LVA exhibited a sensitivity of 62%, detecting 13 of 21 vertebral fractures observed on radiographs. Fractures which were undetected by LVA were either mild (grade 1) and/or located in the mid to upper thoracic spine. LVA correctly identified all moderate and severe (grade 2 and 3) vertebral fractures below T-7. On an individual basis, 19 of 32 patients had prior vertebral fractures identified on radiographs. Using LVA, 17 of these individuals were correctly classified as having existing fractures, while the two patients missed by LVA had grade 1 (mild) deformities. All patients without fracture by radiographs were correctly classified by LVA. In conclusion, the low radiation exposure dual-energy LVA technique on GE Lunar densitometers provides a rapid, convenient and economical way for non-radiologists to identify patients with, and without, vertebral fractures. LVA performance is comparable to published results using other DXA systems [1]. This capability should enhance care of osteoporotic patients and may offer an efficient screening technique for osteoporosis clinical trials.
Reference: 1. Rea et al, Osteoporos Int 11:660-668.

*Disclosures: **N. Binkley**, Merck 8; Eli Lilly 2; Aventis 2; Novartis 2.*

SU093

Precision of Single versus Bilateral Hip Bone Mineral Density Scans. J. White*, S. S. Harris*, G. E. Dallal*, B. Dawson-Hughes. Calcium and Bone Metabolism Laboratory, USDA Human Nutrition Research Center on Aging at Tufts University, Boston, MA, USA.

Dual-energy X-ray absorptiometry (DXA) is a precise, fast, and noninvasive method to measure bone mineral density (BMD) and body composition. Software that integrates the results of bilateral DXA hip scans has recently become available. The present study was undertaken to determine and compare the precision of single (left) and bilateral hip BMD measurements and to assess the precision of spine and total body measurements made with a GE-Lunar Prodigy scanner. Six healthy, white postmenopausal women had DXA scans of the femoral neck (left and right), lumbar spine (L2-L4), and total body performed six times each on the same day with repositioning after each scan. Precision was better for the bilateral than for the single hip scans. Specifically, mean % coefficient of variation (%CV) in BMD for single and bilateral hip scans respectively were: 0.70% and 0.57% for the total hip (P=0.028), 1.37% and 0.88% for the trochanter (P=0.028), and 1.38% and 1.00% for the femoral neck (P=0.075). For both single and bilateral hip scans, mean %CV at the total hip was lower than that at the femoral neck and trochanter. Mean %CV was 0.99% for spine BMD (L2-L4), 0.65% for total body BMD, 1.04% for total body bone mineral content, 1.14% for total body fat tissue and 0.74% for total body nonfat soft tissue. In conclusion, precision of DXA hip BMD measurements is improved with bilateral hip scans compared with traditional single hip scans.

SU094

Results of a Follow-up Survey of an Osteoporosis Education and BMD Testing Program for Assisted Living and Skilled Nursing Residents. E. N. Schwartz[1], K. Baird*[1], T. W. Weiss*[2], Y. Chen[2]. [1]Foundation for Osteoporosis Research and Education, Oakland, CA, USA, [2]Outcomes Research, Merck & Co., Inc., West Point, PA, USA.

Osteoporosis remains a largely undiagnosed and untreated disease and its incidence is particularly high in the nursing home population. Here we report the results of follow-up contact with participants of an osteoporosis education and bone mineral density (BMD) testing program in residential communities and assisted living and extended care facilities in 2001. A technologist traveled to individual facilities to conduct BMD testing of the phalanges using an ALARA metriscan™ densitometer. Results were presented to each resident and were sent to their primary care physicians. A one-hour lecture on osteoporosis prevention was also provided to residents. Of the 2042 residents tested, a random sample of 1000 residents was contacted for a follow-up survey at 12 months. The total number of responses was 466 (response rate of 47%). After five responders, aged < 50 years, were excluded from the analysis, the final analysis sample was 461. Baseline demographics (age, gender, and ethnicity) were similar for responders and non-responders. The average age of responders was 78 (range 50, 97); 90% were female and 20% non-Caucasian (Asian 12%; Hispanic 3%; African-American 4%; other 1%). The average T-Score was -2.6 (range 0.97, -5.7); 65% had a T-Score ≤ -2.0 while 50% had a T-Score ≤ -2.5. Responders with T-Scores ≤ -2.0 were much more likely to follow-up with their provider, have follow-up diagnostic tests, have a baseline history of prior fracture after age 55 and have had a recommendation for pharmacologic treatment and/or calcium/vitamin D supplementation (table) since being screened. Osteoporosis testing and education programs that reach elderly residents of residential communities and assisted living and skilled nursing facilities may improve the level of care by increasing disease awareness and appropriate management and treatment.

	T-Score			
	Overall	≤ -2.0 (n=301)	> -2.0 (n=160)	p-value
% follow-up w/provider	58	80	17	< 0.001
% follow-up diagnostic tests	28	36	8	< 0.001
% prior fracture	43	60	13	< 0.001
% osteoporosis treatment recommendation*	31	47	1	< 0.001
% calcium/Vitamin D	59	68	43	< 0.001

* Alendronate, calcitonin, raloxifene, or risedronate.

Disclosures: ***E.N. Schwartz****, Merck & Co., Inc 2, 5, 8.*

SU095

Digital X-ray Radiogrammetry in Assessing Metacarpal Index and Bone Mineral Density in African-American Women. J. A. Shepherd[1], M. Meta[1], A. Rosholm[2], D. Goddard[3], M. Ovalle[4], Y. Sherrer[5], H. K. Genant[1]. [1]Radiology, University of California at San Francisco, San Francisco, CA, USA, [2]Spectra Pronosco A/S, Vedbaek, Denmark, [3]Osteoporosis Center, Brooklyn, NY, USA, [4]Evanston Northwestern Healthcare, Chicago, IL, USA, [5]Center for Rheumatology, Immunology, and Arthritis, Fort Lauderdale, FL, USA.

Bone mineral density (BMD) reference data of non-Caucasians is scarce. This study characterizes normal peripheral bone in African-American women using digital x-ray radiogrammetry and hand radiographs. We recruited 242 healthy African-American women between 20 and 80 years old at four different sites: San Francisco, CA, Fort Lauderdale, FL, Highland Park, IL, and Brooklyn, NY. Radiographs of the non-dominant hand were taken and analyzed using the X-posure System (Pronosco, Version 2. Denmark), a computer-based diagnostic tool that calculates bone status from an X-ray image of the hand. Bone mineral density and metacarpal index (MCI) of the second through fourth metacarpals were automatically calculated as weighted averages across the three bones. We calculated BMD and MCI Z-Scores (Z_{BMD} and Z_{MCI} respectively) from the African-American women BMD and MCI values and the manufacturer's age-matched North American Caucasian reference data. Five subjects were excluded because of either existing bone disease (2) or overexposed x-rays (3). The mean value of Z_{BMD} was 0.43 and of Z_{MCI} was –0.17. Both were significantly different from 0 with a p-value of less than 0.01. There was no statistically significant ($p<0.01$) relationship of either Z value to age, height, or weight. The paradoxical difference in signed between the average Z_{BMD} and Z_{MCI} was explained by an average increased cortical width of 6.5% for the African American women yet comparable cortical thickness. These relationships also held true for the subset of 100 African-American women from 20 to 39 years, the range typically used for T-score calculations. In conclusion, if African-American women are assessed with the Pronosco X-posure device and referenced to North American Caucasian data, it may be appropriate to adjust their T_{BMD} and Z_{BMD} values down by 0.43 and their T_{MCI} and Z_{MCI} values up by 0.17 to accurately reflect their bone status relative to their race-matched peers.

SU096

Urinary Excretion of Type I Collagen Alpha 1 Helical Peptide as a Marker of Bone Resorption in Mice. R. Brommage. Endocrinology, Lexicon Genetics, The Woodlands, TX, USA.

Measurements of the urinary excretion of N- and C-terminal telopeptides of Type I collagen provide a useful index of bone resorption in human studies. A new ELISA assay measuring peptides containing a fourteen amino acid region (620 to 633) within the triple helix of the alpha 1 chains of Type I collagen gives results similar to those obtained with N- and C-terminal telopeptides. Since human and mouse collagen sequences differ by only one amino acid in this region, this helical peptide assay may also be useful in studies of murine bone metabolism. The Quidel Helical Peptide ELISA was employed to explore the ability of this assay to reflect changes in bone resorption in mice. The single amino acid substitution (alanine for proline) did not affect the binding characteristics of mouse collagen peptides for the assay antibody since displacement curves for mouse urine and the human standard were parallel. Urinary creatinine levels, determined by an automated enzymatic assay, were used to normalize urinary helical peptide concentrations to urine volume. Urinary helical peptide excretion in male C57BL/6 mice declined 5-fold between 4 and 10 weeks of age, but remained constant between 10 and 16 weeks of age. This dramatic age-dependence reflects the decrease in bone modeling during the rapid growth phase of young mice. Male C57BL/6 mice treated every second day with subcutaneous injections of 1 mg/kg pamidronate to inhibit bone resorption excreted 38% to 44% less helical peptide in urine at 1, 2, 4 and 6 weeks after treatment initiation. Femur BMD, determined by PIXImus2 DEXA, was increased by 16% compared to vehicle-treated mice after 6 weeks of bisphosphonate treatment (75 vs 65 mg/cm^2). These findings indicate that analyses of the urinary excretion of helical peptide provide a valid index of bone resorption in mice.

SU097

Variability of Serum CTx Measurements in Healthy Male Adults. J. A. Guillemant*[1], C. Accarie*[2], S. E. Guillemant[3]. [1]Biochemistry, Faculté de Médecine Pitié-Salpêtrière, Paris, France, [2]Nutrition Hydrominérale, EPHE, Paris, France, [3]Biochemistry, Faculté de Médecine Pitié-Salpêtrière, EPHE, Paris, France.

Serum C-terminal cross-linked telopeptide (serum CTx) is considered as a sensitive index of bone resorption. In order to assess the utility of serum CTx in monitoring either the acute osteoclastic response to calcium load or the long-term response to therapy, the variability of measurements is to be taken into account. In study 1, fifteen young male adults (23.3 ± 1.2 y) were sampled five times between 07.30 and 08.00 at one week intervals. In study 2, twelve male sportsmen (30.7 ± 4.2 y) were sampled nine times between 08.30 and 09.30. Serum CTx was measured using one step immunoassay (Serum Cross-Laps ; Nordic Bioscience Diagnostics, Denmark). All samples from an individual were assayed in a single analytical batch and the same reference batch was used for the whole study. The within-subject CV (%), including both the analytical variation (CV # 5%) and the biological variation, and the critical difference (= 1.96 x 1.41 x within-subject CV%) were calculated. In study 1, the mean total within-subject CV was 14.2 (range 9-29) and the mean critical difference was 39 (range 25-80). In study 2, the mean total within-subject CV was 12.7 (range 7-19) and the mean critical difference was 35 (range 21-53). These values are substantially lower than those described by Hannon et al. (J Bone Miner Res 1998 ;13 :1124-1133) for urinary CTx in postmenopausal women and argue in favor of using serum CTx rather than urinary CTx for monitoring the effects of therapy . Nevertheless, it should be emphasized that our groups of subjects were very homogeneous and the conditions of sampling (time) very precise. Furthermore they had avoided all calcium-rich meal 12 hours before sampling. By the same token it could be noticed that the between-subject variation is larger (CV = 30%-40%) than the within-subjects variation which suggest that before monitoring the effects of therapy in a single patient its personal CTx variation could be previously measured in order to calculate its own individual critical difference.

SU098

Serum Osteoprotegerin (OPG): Relationship with Age and Dietary Improvement. S. Sankaralingam*[1], J. Cheung*[1], E. Prowse*[2], M. Frost*[2], K. Knapp*[2], I. Fogelman*[2], G. Hampson*[1]. [1]Chemical Pathology, St Thomas Hospital, London, United Kingdom, [2]Nuclear Medicine, Guy's Hospital, London, United Kingdom.

Osteoprotegerin negatively regulates bone resorption by preventing the binding of RANKL to RANK on osteoclasts thus inhibiting osteoclastic differentiation and activity. It is thought that improvement in nutrition may influence bone metabolism by modulating cytokine production. Nutritional intervention could therefore have a positive effect on OPG secretion. We developed and optimised an enzyme linked sandwich immunosorbant assay (ELISA) to measure OPG in serum. Intra and inter - assay CV were 9% and 12% respectively. We assessed circulating levels of OPG in 38 pre-menopausal women and 92 post-menopausal women with normal bone mineral density aged (mean [SEM] years) 36 [1.3] and 65 [1.0] respectively. We also investigated the effect of improvement in nutrition on serum OPG levels in 40 post-menopausal females aged ≥ 70 years with osteoporosis at the hip and a low body mass index (BMI) < 21kg/m2, randomised to two groups (n = 20 in each group). Group 1 received 1 gram of calcium and 800units of vitamin D and group 2 were given, in addition, dietary advice and nutritional supplement. Serial blood samples were taken at base line and at 1, 3, 6, 9 and 12 months following intervention. We observed a significant difference in serum OPG concentrations between pre and post- menopausal women (pre- menopausal 1.67 ng/ml [0.274], post -menopausal 2.54 ng/ml [0.09] $p < 0.0001$). Our results show a significant positive correlation of OPG with age ($r = 0.6$, $p < 0.0001$). There was a trend towards an increase in serum OPG level following intervention in group 2 compared to group1 (Mean [SEM] baseline group1 2.8 [0.147], group 2 2.6 [0.23], 1 month 2.7 [0.128], 2.9 [0.16], 3 months 2.7 [0.122], 3.0 [0.216], 6 months 2.8 [0.131], 3.1 [0.2] * $p < 0.05$, 9 months 2.7 [0.116], 3.1 [0.19]* $p < 0.05$ and 12 months 2.7 [0.10], 3.1 [0.28]. In conclusion, the increase in OPG levels in post menopausal women may be due to compensatory response to increased age related bone resorption. Our findings also support the theory that nutritional improvement may have a positive effect on bone metabolism by increasing OPG production.

SU099

Relationship Between Dental Panoramic Radiographic Findings and Biochemical Markers of Bone Turnover. A. Taguchi[1], M. Sanada*[2], E. A. Krall[3], T. Nakamoto*[1], M. Ohtsuka*[1], Y. Suei*[1], K. Tanimoto*[1], I. Kodama[2], M. Tsuda*[2], K. Ohama*[2]. [1]Oral and Maxillofacial Radiology, Hiroshima University, Hiroshima, Japan, [2]Obstetrics and Gynecology, Hiroshima University, Hiroshima, Japan, [3]Boston University, Boston, MA, USA.

Recent studies suggest mandibular inferior cortical shape and width on dental panoramic radiographs may be useful screening tools for low spine bone mineral density (BMD) or high risk of osteoporotic fracture. However, it is unknown if these measures are associated with bone turnover. We investigated relationships among dental panoramic radiographic findings, spine BMD and biochemical markers of bone turnover in 82 postmenopausal Japanese women aged 46 to 68 years (mean +/- SD, 54.7 +/- 4.9). None used medications that affect bone metabolism. Bone turnover was estimated by serum total alkaline phosphatase (ALP) and urinary N-telopeptide crosslinks of Type I collagen (NTx) corrected for creatinine (Cr). ALP data were missing for 6 patients. Mandibular inferior cortex shape (normal, mild/moderate erosion, severe erosion) and width were evaluated on dental panoramic radiographs. All findings were adjusted for years menopausal and body mass index (BMI). Distributions of spine BMD were 34 normal (T score>-1.0), 31 osteopenic (T -1.0 to -2.5) and 17 osteoporotic (T <-2.5) without spinal fracture. Degree of erosion was significantly related to NTx and ALP levels (Table). Similar NTx and ALP findings were seen among categories of spine BMD. The odds of low spine BMD in women with any cortical erosion were 3.8 (95% confidential interval=1.2 to 12.5). Women with osteoporosis had significantly less mandibular cortical width (mean +/- SE, 3.11 +/- 0.25 mm) than those with osteopenia (4.00 +/- 0.15 mm, P=0.003) or normal BMD (4.30 +/- 0.16 mm, P<0.001). NTx was not significantly correlated to mandibular cortical width but women in the lowest quartile of mandibular cortical width (<3.4 mm) had higher ALP levels (273 +/- 16 IU/L) than those in the upper three quartiles (236 +/- 9 IU/L, P<0.05). Our results suggest that mandibular inferior cortical shape on dental panoramic radiographs may be an indicator of bone turnover and spine BMD in postmenopausal women. Dentists may be able to refer postmenopausal women for bone densitometry by using panoramic radiographs taken for the diagnosis of dental lesions.

Means with matching symbols are significantly different: *P<0.001; #P<0.02; **P<0.01

Dental panoramic findings (n)	NTx (nmol BCE/mmol Cr)	ALP (IU/L)
Normal (47)	51.4+/-4.0*#	229+/-11**
Mild/moderate erosion (29)	77.9+/-5.1*	257+/-14
Severe erosion (6)	80.2+/-10.6#	318+/-28**

SU100

Hypovitaminosis D in Clinical Practice. P. J. Ryan. Osteoporosis Unit, Medway Maritime Hospital, Gillingham, Kent, United Kingdom.

Hypovitaminosis D is a common finding in the elderly and contributes to secondary hyperparathyroidism which is accepted as a major cause of bone loss in the elderly. The value of measuring 25OH Vitamin D in clinical practice is not established. Most patients with osteoporosis especially if elderly would usually be prescribed calcium and vitamin D supplementation as part of their management. This study examined the value of 25OH Vitamin D measurements in a specialised osteoporosis clinic setting. Measurements were made of 25OH Vitamin D, Parathormone, Calcium, Albumin and alkaline phosphatase in 218 patients of average age 61 years (SD15). Patients were investigated for vertebral fractures (22%), Osteoporosis on BMD (23%), Hip Fracture (7%), Wrist Fracture (7%), Other Fracture (13%), Steroid usage (10%), Malabsorption (6%), Renal Failure (3%), Epileptic Drugs (2%), Liver disease (2%), Other (5%). 65 % patients had a T score <-3.0 and Z score of <-1.5 at the lumbar spine or femoral neck. 118/218 (54%)had hypovitaminosis D (<40 nmol/l) and 41 (19%) severe hypovitaminosis D (<20 nmol/l). There was a trend to greater frequency of elevated parathormone measurements with lower 25 OH Vitamin D values. Low vitamin D levels were found across diagnostic categories and were identified in 88 % Hip fractures, 67 % Wrist fractures, 50 % Vertebral fractures, 52 % Other fractures and 46 % Low BMD. All patients had a normal serum calcium. There was no relationship between 25 OH Vitamin D and age. The study demonstrates a high frequency of hypovitaminosis D in a UK specialist bone clinic setting. Many patients were not elderly and the clear need for vitamin D therapy may not have been appreciated without vitamin D measurements.

Vitamin D and Parathormone values

25 OH Vitamin D	Mean age (years)	Normal Parathormone Nos (%)	Upper Tertile Parathormone Nos (%)	Elevated Parathormone Nos (%)
< 20 nmol/l	64	23 (59%)	8 (21%)	8 (20 %)
21-30 nmol/l	61	29 (66%)	7 (16 %)	8 (18 %)
31-40 nmol/l	64	24 (71%)	4 (12 %)	6 (17 %)
>40 nmol/l	58	86 (86%)	8 (8 %)	6 (6 %)

SU101

Evaluation of a Fully Automated Assay for Serum Procollagen Type I N-propeptide in Osteoporosis. P. Garnero[1], P. D. Delmas[2]. [1]Synarc, Inserm Unit 403, Lyon, France, [2]Inserm Unit 403, Lyon, France.

The aim of our study was to evaluate the performances of a new fully automated assay for serum PINP, a marker of bone formation. Serum PINP was measured with a two site immunoassay based on monoclonal antibodies raised against purified intact human PINP and detecting both intact mono and trimeric forms, but not fragments using an automated analyzer (Roche Diagnostics). Results were compared to those of the manual polyclonal based radioimmunoassay (Orion). Intra and inter assay CVs were below 2 % and 3%, respectively. Analytical dilution and recovery ranged from 94 to 118%. Serum PINP levels were stable for up to 24 hours at + 4°C or room temperature and after up to 4 freeze-thaw cycles. The median within person CV% assessed by 3 repeated measurements over 3 months in 15 untreated postmenopausal women was 8.8 %, resulting in a least significant change (LSC) of 17.6 %. In postmenopausal women, automated PINP highly correlated (n=50; r = 0.96, p<0.0001) with the manual RIA. PINP levels increased from a mean 46 ± 14 ng/mL in premenopausal women (n=44) to 63± 17 ng/ml in 33 healthy untreated postmenopausal women (+37 %, p<0.001). After 3 months of treatment with synthetic conjugated estrogens in 35 postmenopausal women, automated PINP decreased by 24% (p<0.0001), a decrease similar to that of PINP by RIA (- 26%, p<0.0001) whereas no significant change was observed with placebo. After 6 months of treatment with bisphosphonate in 31 postmenopausal women with osteoporosis, automated PINP decreased by an average of 55% (p<0.0001) and 30 patients (97%) showed a decrease larger than the LSC. We conclude that the automated assay for serum PINP is highly precise and is a sensitive indicator of the antiresorptive effects of bisphosphonate and estrogens. Because of its convenient use and high throughput this marker should be useful for the investigation of patients with osteoporosis.

SU102

Pronounced Heterogeneity in Long-Term Variability of Bone Turnover Markers in Patients with Breast Cancer. M. J. Seibel[1], M. Koeller*[2], B. Auler-van der Velden*[2], I. Diel[2], H. W. Woitge[1]. [1]University of Sydney, Sydney, Australia, [2]University of Heidelberg, Heidelberg, Germany.

Variability of bone marker measurements remains to be an issue of concern in the clinical application of these parameters. Most studies on marker variability have been performed in healthy subjects and over relatively short intervals of time. As part of a prospective diagnostic study, we evaluated the long-term variability of various bone markers in 113 postmenopausal women diagnosed with primary breast cancer. None of the patients had bone metastasis, other skeletal disease or bone active drugs. During follow-up (range 0.6 - 4.2 yrs., median 30 mo.), patients were seen every 3 months and timed blood/urine specimens were obtained. To minimise analytical variability, all analyses were performed after study end by the same technician, using well documented techniques and a single batch of reagents per analyte. The coefficient of variation was calculated as CV (%) =√Σ(CVi2)/n (CVi= SD/mean x 100; n= n of CVi). The least significant change (LSC) was then LSC (%)= Z x CV x √2. For a 95% confidence interval (LSC95), Z= 1.96. For a 80% confidence interval (LSC80), Z= 1.28. Results are shown in the table below.

.	sTAP	sBAP	sOC	sPICP	uDPD	uNTX	sNTX	uCTX	sCTX	sCa
CV	12.1	14.0	34.4	26.9	38.0	37.3	17.6	55.9	42.0	5.1
LSC 95	33,1	38,8	95,4	74,5	105,3	103,4	48,7	155	116,5	14
LSC 80	22	25,4	62,3	48,6	68,7	67,5	31,8	101,2	76,1	9,2

Conclusions: In this real life study of breast cancer patients, long-term variability varied greatly between markers. For certain markers (e.g. urnary and serum CTX), the LSC was considerably higher than previously reported.

SU103

Comparison of Serum Tartrate-resistant Acid Phosphatase 5b with Other Markers of Bone Turnover in Monitoring Alendronate Therapy. S. L. Alatalo*[1], K. K. Ivaska*[1], S. Cheng[2], H. Schmidt-Gayk[3], K. Uusi-Rasi*[4], A. Nenonen*[4], P. Kannus*[4], H. Sievänen[4], H. K. Väänänen[1], J. M. Halleen[1]. [1]Institute of Biomedicine, Department of Anatomy, University of Turku, Turku, Finland, [2]Department of Health Sciences, University of Jyväskylä, Jyväskylä, Finland, [3]Department of Endocrinology and Oncology, Laboratory group, Heidelberg, Germany, [4]The UKK Institute for Health Promotion Research, Tampere, Finland.

The purpose of this study was to compare the usefulness of serum tartrate-resistant acid phosphatase isoform 5b (TRACP 5b) with other markers of bone turnover in monitoring alendronate therapy. The subjects of this one-year double-blinded intervention trial were 164 healthy postmenopausal women who were within 5 years after onset of menopause and with no previous use of medication related to bone metabolism. The subjects were randomly assigned into two groups, one receiving 5 mg alendronate daily, and the other receiving placebo. All subjects received a daily supplement of calcium and vitamin D. The bone markers, including the resorption markers serum TRACP 5b, total urinary pyridinoline (PYR) and deoxypyridinoline (DPD), and the formation markers serum total osteocalcin (OC), bone-specific alkaline phosphatase (BAP) and procollagen I N-terminal propeptide (PINP) were assessed at baseline and at 3, 6 and 12 months after start of treatment. Bone mineral density (BMD) of the lumbar spine was measured at baseline and at 12 months. Compared with the placebo-group, BMD increased significantly more, and the

markers decreased significantly more in the alendronate-group ($p < 0.0001$ for each parameter). Least significant change (LSC) was determined for each marker based on their analytical and biological variability. Those subjects that showed a decrease of more than LSC were defined as responders for the treatment. Clinical specificity of each marker was determined as the percentage of non-responders in the placebo-group, and clinical sensitivity as the percentage of responders in the alendronate-group. The specificity and sensitivity, respectively, of the markers were: TRACP 5b 89,6% and 81,6%; DPD 90,9% and 60,5%; PYD 84,4% and 59,2%; BAP 93,3% and 55,3%; PINP 83,1% and 86,8%; OC 68,9% and 75,0%. When the specificity of each marker was multiplied with its sensitivity, the results were as follows: TRACP 5b 0,73; DPD 0,55; PYD 0,50; BAP 0,52; PINP 0,72; OC 0,52. The values were clearly higher for TRACP 5b and PINP, indicating that these two were the most specific and sensitive markers for monitoring alendronate treatment.

SU104

An Enzyme Immunoassay for Measurement of 1,25-Dihydroxyvitamin D. M. J. Gardner*, D. Laurie*, A. K. Barnes*, R. T. Duggan. IDS Ltd, Boldon, United Kingdom.

Measurement of 1,25-dihydroxyvitamin D (1,25D) is of clinical importance in determining the cause of disturbances of calcium metabolism such as in malignant hypercalcaemia, renal and parathyroid disease and vitamin D intoxication. Most 1,25D assays require significant technical expertise to perform because they use complex sample extraction procedures usually involving chromatography. Introduction of the IDS 1,25D RIA kit overcame this problem by using simple monoclonal antibody columns to perform immunoextraction of the 1,25D from serum. Extracted samples were reconstituted and then assayed by conventional RIA. We have used this technology to develop a non-isotopic enzyme immunoassay (EIA) with comparable performance to the RIA. Serum samples (500uL) were delipidated and 100uL of clarified sample added to immuno-capsules in duplicate, which were then rotated end over end for 90 min. Following washing to remove serum proteins, the 1,25D was eluted from the immuno-capsule (3 x 150uL ethanol), the solvent was evaporated under nitrogen and the residue reconstituted with assay buffer (100uL). Specific sheep anti-1,25D antibody (100uL) was added, the mixture vortexed and incubated for 15 min. The extract / antibody mixture (150uL) was added to an anti-sheep IgG coated micro-plate, incubated for 90 min (shaken); then 1,25D-Biotin conjugate (100uL) added and incubated for a further 60 min (shaken). The 1,25D-Biotin conjugate competes with the 1,25D for anti-1,25D antibody sites. After a wash, avidin peroxidase (200uL) was added, incubated for 30 min and washed. TMB substrate (200uL) was added and the colour developed for 30 min. After addition of 0.5M HCl (100uL) the absorbance was measured at 450nm. A calibration curve was prepared from the absorbance values for 1,25D buffer standards (8-500pM) using a 4-parameter curve fit. The sensitivity of the assay (mean minus 2SD of "0" calibrator) was less than 6pM. Intra-assay precision was 12.7%, 7.4% and 3.7% for serum controls (n=10) at 18pM, 62pM and 136pM respectively. Inter-assay precision was 14.4%, 8.1% and 6.3% for serum controls (n=6) at 19pM, 59pM and 129pM. Linearity was good with a mean for observed / expected of 119% for 8 samples diluted 1:2, 1:4 and 1:8 with the "0" calibrator. Recovery of spiked calibrator material for 8 samples calculated by observed incremental rise / expected rise was 86% at +25pM and 91% at +100pM. Correlation against the IDS RIA for 91 samples was: EIA = 1.08 x RIA + 2.3pM (R2=0.92). This technology provides a precise and sensitive non-isotopic assay for the measurement of 1,25D, which correlates well with the existing IDS RIA and can be completed within an 8-hour working day.

SU105

Comparison of Biochemical Markers of Bone Turnover in the Ovariectomized Sprague-Dawley Rat. J. Mayer*[1], A. M. Leyshon*[1], P. Qvist*[2], S. Y. Smith[1]. [1]CTBR, Montreal, PQ, Canada, [2]Nordic Bioscience Diagnostics A/S, Herlev, Denmark.

The purpose of this study was to compare RatLaps (C-telopeptide (CTx) of type I collagen), a marker of bone resorption, and N-mid osteocalcin (Rat-MID OC), a marker of bone formation, with free deoxypyridinoline (DPD, resorption marker), intact osteocalcin (OC) and total alkaline phosphatase (ALP, a surrogate formation marker), in a 2-week ovariectomized (OVX) rat model of osteoporosis. Three month-old virgin female rats were randomly assigned to 3 groups. Twenty animals underwent OVX of which 10 were given subcutaneous estradiol pellets (0.5 mg). Ten animals underwent surgery without removal of the ovaries (Sham controls). Blood and urine samples were collected from all animals following a 6-hour daytime fast (food and water deprivation) once prior to surgery and 7 and 14 days following surgery. Serum was harvested and analyzed for Rat-MID OC (NB Diagnostics, ELISA), intact OC (Biomedical Technologies RIA), total ALP (Hitachi 717 enzymatic assay) and CTx (NB Diagnostics RatLaps ELISA). Urine was analyzed for DPD (Immunodiagnostic System Ltd RIA) and CTx (NB Diagnostics RatLaps ELISA) (both corrected for creatinine). Rat-MID OC, intact OC and RatLaps (urine) were significantly increased for OVX controls compared to Sham controls 7 days post-surgery. Relative to baseline values, the percent change (increase) for OVX controls 7 days post-surgery was 39% for Rat MID OC and 78 and 76% for RatLaps serum and urine, respectively, far greater than the 14 to 18% increases observed with OC, ALP and DPD at this time-point. With the exception of DPD, all markers were significantly increased for OVX controls 14 days post-surgery, compared to Sham controls. At 14 days post-surgery RatLaps (serum and urine) showed greater than 2-fold increases for OVX controls relative to baseline levels. Estradiol was noted to effectively prevent the OVX-induced rise in all markers. The use of RatLaps (serum or urine bone resorption marker) and Rat MID OC (serum bone formation marker) permitted the early detection of the OVX-induced increase in bone turnover in this 2-week rat study and will provide sensitive tools for the rapid screening of potential anti-osteoporosis agents.

SU106

Prospective Follow-up Study of Biochemical Markers of Bone Metabolism for Diagnosis of Bone Metastases in Early Breast Cancer. S. Takahashi[1], M. Koizumi*[2], E. Ogata[3]. [1]Dep. of Medical Oncology, Cancer Institute Hospital, Japanese Foundation for Cancer Research, Tokyo, Japan, [2]Dep. of Radiology, Cancer Institute Hospital, Japanese foundation for Cancer Research, Tokyo, Japan, [3]Dep. of Internal Medicine, Cancer Institute Hopsital, Japanese foundation for Cancer Research, Tokyo, Japan.

We have previously shown that the bone metabolic markers, especially serum carboxy-terminal telopeptide of type 1 collagen (ICTP), were useful for diagnosis of bone metastases of breast cancer in a cross-sectional study. ICTP has been reported to derive from collagen degradation by matrix metalloproteases, and represent pathologic bone resorption such as bone metastases, not increase of physiologic bone resorption such as osteoporosis. Sensitivity and specificity of ICTP for diagnosis of bone metastases in our study was about 45% and 97%, respectively. But some reports showed that ICTP is also increased in patients without bone metastases. In this study we prospectively evaluated the efficacy of the bone metabolic markers for diagnosis of bone metastases in patients with early breast cancer. After operation, patients with high risk of bone metastases (stage III or n>3) were prospectively followed for at least 2 years or until bone metastases were detected, and bone metabolic markers were evaluated every 3 months. Urinary free deoxypyridinoline (fDPD, ELISA, Metrabiosystems), serum ICTP (RIA, Orion Diagnostica), procollagen type I C-terminal peptide (PICP, RIA, Orion Diagnostica) and bone-specific alkaline phosphatase (BAP, IMA, Metrabiosystems) were measured. 74 patients were recruited and followed so far. 7 patients have been diagnosed to have bone metastases with radiological diagnostic procedure. Sensitivity of bone metabolic markers at the time of diagnosis of bone metastases were: ICTP, 57%; BAP, 29%; fDPD, 71%; PICP, 29%. False positive rates (rates of patients without bone metastases who showed increase of the markers at least once) during the first year were high: ICTP, 50%; BAP, 42%; fDPD, 84%; PICP, 26%. But false positive rate of ICTP more than 1 year after operation decreased to 6%. In follow-up of patients with early breast cancer, bone metabolic markers seem not very useful for detecting bone metastasis within 1 year after operation, but ICTP might be useful thereafter.

SU107

High Remodeling Turnover in Venezuelan Osteoporotic Patients. G. S. Riera, Y. Cordero*, J. Ramos*, L. Marcano*. Medicine, UNILIME. Universidad de Carabobo, Valencia, Venezuela.

Bone mass is the result of a lifelong balance between bone formation and resorption, and in fact, most metabolic bone diseases including osteoporosis, are consequent to an unbalanced bone turnover. Osteoporotic syndromes are characterized by wide spectrum of bone turnover, ranging from accelerate to reduced remodeling rates. Higher rates of bone remodeling are in general associated to higher rate of bone loss and predict fractures. Biochemical Markers of Bone turnover were measured in 283 women. N-telopeptide: NTx, Osteomark, Ostex,Seattle,USA, Tartrate Resistant Acid Phosphatase: Hydrolysis of paranitrophenyl phosphate at 4.8 pH, Alkaline Phosphatase: Labtest. Roy Modified. Mean age was 57,93 ± 9.6 (30-85). BMD (T-score) at lumbar spine L2-L4 was – 2,36 and -1,6 at femoral neck. Previous fractures were present in 4,5%. Family history of osteoporosis was present in 8%, hypertension in 27.6% diabetes in 7.8%. Surgical menopause in 36.4% and HRT was taken by 35%. Mean values of bone markers were NTx 113,5±69 nMolBCE/mMolCreat, Tartrate Resistant Acid Phosphatase 9.79±3.2 and Alkaline Phosphatase 47.7±21. (Control premenopausal values in our lab are: NTx 40±15 nMolBCE/mMolCreat, TRAP 8.37±2.2 UI/l and AP 35±8.6 UI/l). Cut-off point for 2 and 3 SD above control mean were for NTX 70 and 85, for TRAP 12.77 and 14.9, and for AP 52.2 and 60.8. 62.2% or 55.8% of patient were classified as High Turnover, if the cut-off point is set at 2 or 3 SD above premenopausal mean of NTx. With TRAP values were 16.9% and 7.4% and with AP we found 31.8% and 18.0%. Conclusion. High Turnover osteoporosis (2 SD above the control mean) was present in 62.2% of our Venezuelan osteoporotic patients and 86.5% had resorption over the premenopausal mean according to N-telopeptide determination (NTx), this marker was able to identify more patients with high remodeling state than TRAP or Alkaline Phosphatase

SU108

Fracture Risk Assessment in a Primary Care Setting Using Point-of-Care Technology. S. Twaddle*, T. Mangion*, R. Chandra*, R. Leonard*, C. Moniz. Clinical Biochemistry, Kings College Hospital, London, United Kingdom.

Fracture risk assessment using DXA for community dwelling women over 65 requires different strategies from younger women since the prevalence of low trauma fractures and artefacts resulting in spurious BMDs are common in this age group. We offered an Osteoporosis Nurse led fracture risk assessment service to 755 women over 65 in one large primary care practice using a risk questionnaire, heel ultrasound (HUS) measurements and point-of-care bone biochemical markers. 328 (43%) attended a walk-in service and were classified as low risk (n=53), moderate risk (n=164) or high risk (n=111), based on a heel Stiffness Index T-score measured on a Lunar Achilles Solo machine, of > -1.0, between -1.0 to -2.5 or < -2.5, respectively. All were offered a clinical assessment but 182 were followed within 2 weeks with results of a self-administered fracture risk questionnaire, a point-of-care Crosslaps measurement using Osteosal $^{TM.}$. Subsequently, urine analysis for CTX (Crosslaps ^{TM}) was performed in batch mode in the laboratory at a later date. 44 (23%) had clinical osteoporosis and after excluding secondary causes were prescribed calcium and vitamin D alone or with anti-resorptives. 97 (53%) had no significant risk factors for fracturing and were given life-style advice. 44 (24%) were intermediate and were referred for DXA. Osteosal ^{TM} at baseline was of little value in decision making, but CrossLaps ^{TM} provided increased discriminatory power at a cut-off of 303 µg/mM creat, with 77% sensitivity and 65% specificity (vs 66% and 46% respectively for HUS alone) at a DXA T-score of -2.5. Osteosal ^{TM} correlated with Urinary-CTX (Crosslaps ^{TM}) at baseline and showed a significant reduction of -49% (95.9% CI -67 to -30, range -7 to -86%) in those taking anti-resorptive treatment after 3 months. Fracture prevention in primary care need effective strategies to identify and treat those with incident clinical osteoporosis (approximately 1 in 4 in our series), those who require DXA for management decision making and those who would benefit with life-style modification advice alone. Point-of-care technology such as peripheral bone scanning techniques and risk factor questionnaires can provide a means of making efficient use of resources for fracture risk assessment and bone biochemical markers for indicating bone turnover particularly when monitoring treatment response.

SU109

Urine and Plasma Bone Resorption Markers in Patients with Active Paget's Disease. B. H. Durham, J. J. Dutton*, W. D. Fraser. Bone Disease Unit, Dept of Clinical Chemistry, Royal Liverpool University Hospital, Liverpool, United Kingdom.

We have compared the concentrations of a urinary and a plasma marker of bone resorption in a cohort of elderly patients with active Paget's disease. The urinary marker was free deoxypyridinoline estimated using a HPLC method and normalised for creatinine [f DPD] and for plasma the beta form of the C terminal telopeptide of type 1 collagen [beta-CTX] analysed on the Elecsys automated platform using an ECLIA method [Roche Diagnostics, Germany]. The cohort consisted of 196 patients with Paget's disease who were not on any treatment [99 F, 97M] average age 70 years [range 56-84], the majority [99%]had total alkaline phosphatase [TAP] greater than an age related reference range, [mean 387 range 138-1629]. Blood and a 24hr urine was collected from each patient and the EDTA plasma and an aliquot of the urine was stored at -20oC until analysed. The correlation between f DPD [y] and beta-CTX[x] for all patients was y= 13.99x-0.53, r=0.80, for males y=13.58x -0.37, r=0.85 and for females y= 12.18x+0.38, r=0.77. The top of the reference ranges are 0.50 ng/ml for beta-CTX and 6.4 nmol/mmol Creat for fDPD. In our study 87/196 [44%] had both beta-CTX and fDPD concentrations greater than the top of the reference range , for beta-CTX alone 127/196[65%] and for fDPD 100/196[51%] were elevated. From the results in Paget's patients it appears that beta-CTX is elevated in a greater percentage than fDPD. Each test is reflecting a different component of the resorption process in patients with Paget's disease. The relatively lower elevation of beta-CTX and fDPD compared to TAP may be the result of alteration in beta to alpha CTX ratio and collagen crosslinking in newly formed collagen in Paget's disease.

SU110

Comparison of Changes in Serum Bone Markers for Various Osteoporosis Management Regimens. D. S. Ooi[1], A. B. Cranney[2], J. D. L. Gay[2]. [1]Pathology and Laboratory Medicine, Ottawa Hospital, Ottawa, ON, Canada, [2]Medicine, Ottawa Hospital, Ottawa, ON, Canada.

We (a) compared changes in serum bone-specific alkaline phosphatase (BSAP) and c-telopeptides (CTX) following treatment with raloxifene 60 mg daily (RAL), cyclical etidronate (ICE), alendronate 10 mg daily or 80 mg weekly (ALE) and risedronate 60 mg weekly (RIS), and (b) correlated changes in serum bone markers and bone mineral density (BMD). Serum bone markers were measured prior to and 2-36 months (median 12 months) following initiation or change in regimen in 118 patients attending a specialty clinic; 36 patients (32 females, 4 males) had corresponding BMD data. Serum BSAP was measured using Beckman Access Ostase and CTX by Roche Elecsys CrossLaps. BMD was measured by dual emission x-ray absorptiometry on a Lunar Expert. Median baseline and % change in BSAP and CTX, and % of patients showing either increase or decrease (of >20%) from baseline were:

Regimen (n)	BSAP (ug/L)	Change	% Incr, Decr	CTx (ug/L)	Change	% Incr, Decr
RAL (10)	9.4	+1%	44, 0	0.13	-8%	10, 40
ICE (11)	10.7	-3%	0, 27	0.17	-23%	27, 45
ALE (38)	10.1	-12%	26, 43	0.20	-41%	18, 40
RIS (6)	8.8	+7%	17, 33	0.09	-77%	17, 67
ICE to ALE (42)	9.4	-8%	10, 33	0.17	-43%	17, 46
ALE to RIS (6)	7.4	-19%	33, 50	0.14	-30%	0, 50

Correlations between decreases in BSAP and/or CTX and increases in BMD ($\geq$0.02 g/cm^2) in lumbar spine (LS) or femoral neck (FN) were not statistically significant. Patients with serum BSAP concentrations between 6 and 12 ug/L and CTX concentrations of $\leq$ 0.05 ug/L while on therapy were more likely to have increases in BMD, but did not achieve statistical significance. For CTX, LS increased in 67% vs 52% of patients, FN 42% vs 21%, for BSAP, LS increased in 67% vs 33%, FN 36% vs 25%. We conclude (a) CTX, a bone resorption marker, showed greater decreases with treatment than BSAP, a formation marker, and that the aminobisphosphonates effected the greatest decreases in CTX; (b) BSAP 6-12 ug/L and CTX $\leq$ 0.05 ug/L were more often associated with increases in BMD, however bone marker changes appear to be poorly predictive. This is consistent with the hypothesis that antiresorptives may effect fracture reduction through mechanisms other than increase in bone density such as reduction in bone turnover. In assessing patients on pharmacotherapy, bone markers should be used independently of BMD.

SU111

Is the Bone Marker Response Dependent on the Agent Used to Treat Osteoporosis. M. W. J. Davie, D. E. Powell*, M. Worsfold*, T. Jones*, H. Davies*, H. Williams*. Robert Jones & Agnes Hunt Orthopaedic Hospital, Oswestry, United Kingdom.

Response to osteoporosis therapy may be measured by bone markers or bone density (BMD). Diverse therapies may elicit different responses in different markers. We compared responses of NTX/Cr, DPD/Cr and lumbar spine BMD (L2-4) to treatment with bisphosphonates, HRT or calcium after one year of treatment and investigated whether any marker indicated response at 3 months. Results were expressed as the proportion of patients exceeding the Least Significant Change (LSC) i.e. in excess of the normal variation. Patients were identified by population screening, 145 Patients with osteoporosis (OP,T-score > -2.5) aged 71±6.8 yr treated with HRT (n=12), Bisphosphonates (n=75, 63% Didronel), calcium only (n=7) or not treated (n=48) were compared with non-osteoporotic (NOP) patients treated with bisphosphonates (n=10), HRT (n=3), calcium (n=11) or untreated (n=88). The decision to treat and the agent used were made by the patient's General Practitioner. Markers were measured pre-treatment and at 3, 6 and 12 months and for BMD pre-treatment and at 12 months. Since the distribution of the marker values was positively skewed, the data were log transformed. LSC was calculated from the variance of the values of the non-treated patients over the 4 readings for markers or 2 readings for BMD (LSC= 2.8 x sqrt(variance/mean)). Mann-Whitney was used to compare non-parametric data and Chi squared differences in proportions. Results are presented as mean ± SD. Age matched OP subjects had greater NTX/Cr values compared with NOP (82.4±53.4 vs 60.5±33.4 nM BCE/mM Cr, p<0.001) but similar DPD/Cr (6.69±2.66 vs 6.24±1.78 nM DPD/mM Cr, p=ns). The lower LSC was 60% for NTX and 60.3% for DPD. At month 12 70% of the bisphosphonate OP group responded using NTX, more than calcium (70% vs 29% p<0.05), but HRT showed no difference. The NOP group given bisphosphonate showed 80% exceeding LSC at 12 months (p<0.001). Using DPD/Cr only the HRT OP group showed more responding cf calcium after 12 months (42% vs 0%, p<0.05); in the NOP group there was no response. BMD response at 1yr showed only 33% of patients with OP exceeding LSC in the bisphosphonate group. NTX/Cr showed a response rate of 50% after 3 months in bisphosphonate treated subjects. NTX/Cr shows an earlier response, but even by 12months only 70% show a response to bisphosphonate. This response exceeds that seen with either DPD/Cr or BMD. HRT may however influence the production of DPD from matrix degradation more than NTX though whether this indicates a different effect on the osteoclast awaits elucidation. Bisphosphonates also reduce NTX/Cr in non-osteoporotic subjects suggesting an effect on osteoclasts in normal subjects.

SU112

Stability of C-telopeptides of Type I Collagen During Storage of Serum and Plasma Samples. P. Qvist[1], M. Munk*[1], C. H. Christiansen[2]. [1]Nordic Bioscience Diagnostics A/S, Herlev, Denmark, [2]Center for Clinical & Basic Research, Ballerup, Denmark.

It has recently been demonstrated that variability in bone resorption markers caused by circadian variation was reduced to a level similar to bone formation markers when blood sampling was performed in the morning after an overnight fast (S. Christgau, Clin Chem 46 (2000): 431). However, other pre-analytical parameters influencing variability should likewise be investigated, and the present study was performed to determine the effect of storage temperature on the stability of C-telopeptides of type I collagen (CTX) in serum and plasma. Blood samples from eight premenopausal women (age 27-43 years) and six men (age 28-60 years), were obtained from 8.00 to 10.00 am after an overnight fast. Serum and EDTA plasma were collected, aliquoted and stored at -20ºC, -80ºC, and -150ºC until testing. Circulating levels of C-telopeptides of type I collagen were determined by Serum CrossLaps® ELISA (Nordic Bioscience Diagnostics A/S). No decrease in CTX was observed at either temperature or sample matrix during this storage period as the mean recovery was in the range 98-106%. To further study the stability of CTX at elevated temperatures serum and EDTA plasma samples were obtained from healthy individuals, aliquoted and incubated at either 4ºC or 37ºC until testing. After seven days of incubation at 4ºC approx. 92% of CTX were recovered from serum samples, and after 60 days, 35 and 98% was recovered from serum and EDTA plasma samples, respectively. After incubation for 2 days at 37ºC, 45 and 94% was recovered from serum and EDTA plasma samples, respectively. After 14 days the recovery was 9 and 70%, respectively. These data demonstrate good recovery of CTX in serum samples stored frozen for extended time periods, and more than 90% of CTX could be recovered even after 7 days at 4ºC. Improved stability of CTX was observed in EDTA plasma samples with no detectable decrease even after two months at 4ºC. Therefore EDTA plasma samples might be a useful specimen for measurement of CTX due to the high analyte stability in this matrix. The practical implications of the improved stability of CTX in EDTA plasma samples need to be determined in routine clinical settings.

SU113

Bone Markers Predict Future BMD of Japanese Postmenopausal Osteoporotic Women with Hormone Replacement Therapy (HRT) or Bisphosphonate Treatment. O. Chaki, I. Gorai, K. Kurasawa*, K. Mochizuki*, Y. Arata*, H. Yoshikata*, R. Kikuchi, F. Hirahara*. Yokohama City University, Obstetrics and Gynecology, Yokohama, Japan.

Hormone replacement therapy (HRT) is essential for treating postmenopausal osteoporosis. But thereare some populations who had not received HRT because of complications (i.e.breast cancer, thrombosis etc.). In this study, we assessed the effects of HRT or Bisphosphonate on bone mass and turnover in postmenopausal osteoporotic Japanese population. Seventy one postmenopausal osteoporotic Japanesewomen (62.3+/-7.3 years) were enrolled into this study. Thirty one women were treated with HRT(conjugated estrogens 0.625mg/day, medroxyprogesterone acetate 2.5mg/day; HRT group), 19 women were treated with Etidronate(200mg/day for 2 weeks every 12 weeks; E group) and 21 women were with Alendronate(5mg/day). Lumbar spine bone mineral density(BMD) was determined at the start of the study(0 month) and every 6 months thereafter and biochemical indices, serum alkaline phosphatase(ALP), intact osteocalsin(IOC), urinary deoxypyridinoline(DPD), crosslinked N-telopeptide of type I collagen(NTx) and creatinine were measured at 0, 1, 3 and 6 months. BMD measurement was performed using dual energy X-ray absorptiometry(DXA, QDR2000, Hologic Comp.). There was no differences in each groups in age, years since menopause or BMI. Baseline lumbar spine BMD and biochemical indices did not show any substantial differences in among each groups. There were significant differences in percent changes of BMD(HRT group; 2.6+/-2.3%, E group; 4.0+/-1.5%, A group; 5.2+/-2.3%, A and E group vs. HRT group, $p<0.05$ at 6 months.). NTx and DPD significantly decreased at 3 months in each group from baseline ($p<0.03$). The magnitud of decreasewas grater in E and A group than HRT group(NTx: HRT;-34.1+/-11.5%, E;-38.7+/-10.5%, A;-46.4+/-9.5%). Furthermore, in A group, NTx and DPD significantly decreased at 1 month ($p<0.03$). In conclusion, 1) The bone spearing effect of Alendronate for treatment of postmenopausal osteoporosis appeared earlier and stronger than that of HRT or Etidronate. 2) Biochemical markers of bone resorption were clinically useful in the prediction of future BMD in HRT or Bisphosphonate treated women.

SU114

Assessment of Bone Formation- and Bone Resorption- Markers in Horses. B. Carstanjen[1], N. R. Hoyle*[2], A. Gabriel*[3], J. Detilleux*[4], H. Amory*[1], B. Remy*[5]. [1]Department of Large Animal Internal Medicine, University of Liege, Liege, Belgium, [2]Roche Diagnostics GmbH, Penzberg, Germany, [3]Department of Anatomy, University of Liege, Liege, Belgium, [4]Department of Quantitative Genetics, University of Liege, Liege, Belgium, [5]Department of Physiology of Reproduction, University of Liege, Liege, Belgium.

Various biochemical bone marker assays developed for serum or plasma samples are available in human medicine to monitor bone formation and bone resorption. Collagen breakdown products (β-CrossLaps; β-CTX) are used as indicator of bone collagen degradation and are detected in serum. The serum N-terminal extension peptide of type I procollagen (P1NP) is used as indicator of bone collagen formation. Serum osteocalcin (OC) is used as indicator of osteoblast activity. However, only few species specific assays are available in equine medicine. Aim of this study was to test fully automated ECLIAs for P1NP evaluation (Roche Diagnostics, Penzberg; Germany) and Serum β-CTX evaluation (Roche Diagnostics, Penzberg, Germany) for cross reactivity with horse serum. Additionally, to study the effect of age on bone formation and resorption in horses as determined by the human specific CTX- and P1NP- ECLIA and by a previously described equine specific OC RIA. Venous serum and EDTA plasma samples of 59 healthy horses, aged 1 to 35 years, were obtained between 9 am and 10 am. Horses were divided in 3 age groups. Group 1 (n=22) was composed of 1 to 4 years old horses, group 2 (n=21) of 4.5 to 15 years old horses and group 3 (n=16) was composed of older than 15 years old horses. Gender did not influence serum OC, plasma CTX and plasma P1NP values. Equine serum samples, serially diluted with equine serum free samples, were linear when analyzed with the P1NP- and CTX- ECLIA. Healthy horses showed plasma CTX values in the range from undetectable to 0.297 ng/ml. Plasma P1NP values ranged from undetectable to 3.891 ng/ml and serum OC values ranged from undetectable to 128.80 ng/ml. Group 1 showed highest plasma CTX ($p<0.01$) and serum OC ($p<0.01$) values compared to group 2 and 3. Group 2 showed highest plasma P1NP ($p<0.01$) values compared to group 1 and 3. In conclusion, commercially available human assays for CTX and P1NP quantification in serum/plasma may be a useful tool to monitor bone metabolism changes in horses. Age did influence serum/plasma bone marker concentrations in horses.

Disclosures: ***B. Carstanjen****, Roche Diagnostics 3.*

SU115

Synovial Fluid Analysis of Chlorinated-Peptides for the Early Diagnosis of Osteoarthritis. L. J. Nesti*, P. F. Sharkey*, S. Sastri*, M. J. Steinbeck. Orthopaedic Surgery, Thomas Jefferson University, Philadelphia, PA, USA.

Osteoarthritis is a severely debilitating and degenerative disease that is associated with marked pain and disability. Early detection and therapeutic intervention of arthritic joint diseases is crucial for successful management and treatment; however, there is currently no available biomarker with sufficient sensitivity and specificity for the early diagnosis of osteoarthritis (OA). In seeking to identify biomarkers that will aid in early detection and could be used to monitor the progression of cartilage destruction in OA, our lab has recently demonstrated that neutrophil and macrophage generated reactive oxygen species (ROS), specifically hypochlorous acid (HOCl) and chlorine gas (Cl_2), chlorinate collagen type II (col-II) obtained from human articular cartilage and increases its susceptibility to proteolytic degradation. Based on this unique reaction chemistry and Cl-product formation, we analyzed synovial fluid to determine the presence of Cl-peptides as a sign of cartilage destruction in early OA patients. In this study, we examined synovial fluid samples from 37 knees in 30 patients to identify and profile specific Cl-products that can be used to differentiate early stages of OA. We divided the samples into 3 groups using radiographic and clinical assessment: (1) Control, those patients with some type of acute knee injury with no history of OA and no radiographic evidence of OA; (2) Early OA, patients with a brief history of OA with either normal radiographs or mild arthritic changes seen on radiograph; and (3) Late OA, those patients with a longstanding history of OA and with radiograph evidence of OA. Using a proteomic approach, we identified all Cl-peptides in the synovial fluid samples with mass spectrometry and determined myeloperoxidase (MPO) levels, the enzyme responsible for $HOCl/Cl_2$ production, with a commercially available ELISA. This data was then compared with the OA classification groups. Patients in the control and advanced OA groups demonstrated little elevation in MPO levels and Cl-peptides were undetectable. Patients with early OA demonstrated significantly elevated levels of MPO and Cl-peptides were detected. This data suggests that the presence of Cl-peptides in synovial fluid may serve as a diagnostic marker for the detection of early OA.
Patent Pending STE01-NP001

SU116

Genetic Variations in Cortical and Cancellous Bone Loss Following Ovariectomy in Three Inbred Mouse Strains. C. Li*[1], M. B. Schaffler[1], H. T. Wolde-Semait*[1], C. Hernandez[1], J. Nadeau*[2], K. J. Jepsen[1]. [1]Orthopaedics, Mount Sinai School of Medicine, New York, NY, USA, [2]Center for Computational Genomics, Case Western Reserve University, Cleveland, OH, USA.

The effects of genetic background on the magnitude and rate of post-menopausal bone loss are not fully understood. Inbred mice exhibit differences in bone formation rates during growth leading to variations in morphological and compositional bone traits of adult bone [1]. It is reasonable to expect that inbred mice will also exhibit differences in bone loss. We tested the hypothesis that three inbred mouse strains will show differences in the magnitude and timing of bone loss following ovariectomy. A total of 210 female mice from the C3H/HeJ ("high density"), C57BL/6J ("low density"), and A/J ("intermediate density") strains were examined. Mice were sham-operated or ovariectomized (OVX) at 16-weeks of age (n=10/strain/group) and sacrificed at 4, 8 and 16 weeks post-OVX. Differences in static and dynamic measures of cancellous bone loss in the distal femur were determined from standard histomorphometry of plastic embedded frontal sections. Differences in cortical bone mechanical properties were determined by loading femurs to failure in 4 point-bending. The results of the 4 and 8 week time points revealed significant differences in cortical and cancellous bone loss among the three inbred strains. The "intermediate density" A/J femurs showed no changes in either cortical or cancellous bone. The "low density" B6 femurs showed no change in cancellous bone mass but exhibited a 10% reduction in maximum load at 4 and 8 weeks post-OVX compared to age matched controls. The "high density" C3H mice exhibited a significant reduction (39%) in cancellous bone mass (%B.Ar/T.Ar) as early as 4 weeks post-OVX when compared to the age-matched sham group. This bone loss was accompanied by a 22% decrease in trabecular thickness (Tb.W) and number (Tb.N). The maximum load of C3H femurs was 7-12% lower at 4 and 8 weeks post-OVX compared to age matched controls indicating significant cortical bone changes. These results revealed significant differences in cortical and cancellous bone loss following OVX among three inbred mouse strains indicating that genetic background may play an important role in the magnitude and timing of OVX-induced bone loss. The results also revealed that OVX-induced bone loss was independent of initial "bone density" and that the genes which promote high peak bone mass may not protect against bone loss. [1] Sheng *Bone*, 1999.

SU117

Genetic Variations in the Structural Efficiency of Long Bones May Contribute to Variations in Mineralization Among Inbred Mouse Strains. C. Price*[1], C. Hernandez[1], J. Nadeau*[2], K. J. Jepsen[1]. [1]Orthopaedics, Mount Sinai School of Medicine, New York, NY, USA, [2]Center for Computational Genomics, Case Western Reserve University, Cleveland, OH, USA.

Previous studies revealed that morphological variations between "high density" C3H/HeJ (C3H) femurs, "intermediate density" A/J femurs, and "low density" C57BL/6J (B6) femurs were evident as early as embryonic day E16.5 [1]. Certain aspects of these initial morphological variations were retained in adult femurs suggesting that genetic determinants of peak bone mass may occur early in life. Investigations of adult mouse long bones revealed that understanding the relationship between multiple bone traits was critical to understanding whole bone mechanical function [2]. While morphological variations between inbred strains have been reported [3,4], it remains unclear how the relationship between morphological and compositional traits changed during growth. To explain variations in adult bone traits, we examined how the relationship between morphological traits of A/J, B6, and C3H femurs changed during growth. Variations in post-natal bone morphology were determined by sacrificing 8-10 female A/J, B6, and C3H mice at 1, 4, 7, 14, 28, 56, 105, 182, and 365 days of age. Femoral cross-sectional area (amount of bone), polar moment of inertia (distribution of bone), and other geometric traits were determined from plastic sections. Moment of inertia increased with cortical area in a power law manner ($y=ax^b$) and all three strains showed a similar exponent, b, of 1.48 (A/J), 1.53 (B6), and 1.50 (C3H). However, morphological differences apparent at birth (day 1) lead to significant differences in the constant term, a. A/J and C3H exhibited nearly identical curves. B6 femurs exhibited a greater moment of inertia for a given area indicating that B6 femurs were structurally more efficient than A/J and C3H. The variation in structural efficiency may explain differences in mineralization observed between the 3 strains. The increased mineral content (i.e., increased tissue stiffness) of A/J and C3H femurs may represent an attempt to compensate for the reduced structural efficiency. The results revealed that the relationship between individual bone traits were defined early in life and that genetic background affected the relationship between these traits.

[1] Herman, *Trans ORS* 2001;
[2] Jepsen, *ASBMR* 2001;
[3] Sheng *Bone* 1999;
[4] Richman *JBMR* 2001.

SU118

Double Heterozygosity for Osteogenesis Imperfecta (OI) and Cleidocranial Dysostosis (CCD): Altered Fibroblast Response to Phenol Red and Dexamethasone. Z. Zhang*[1], J. Korkko*[2], J. R. Shapiro[3]. [1]Medicine, Uniformed Services University, Bethesda, MD, USA, [2]Center for Gene Therapy, Tulane University, New Orleans, LA, USA, [3]Osteogenesis Imperfecta Program, Kennedy Krieger Institute, Baltimore, MD, USA.

The proband is a 28 year old Caucasian female who first fractured at age 1 year and later fractured her humeri, radii and femurs. Her clavicles are absent. Her father, grandmother and three uncles have OI. Her mother has CCD and neurofibromatosis. A brother has blue sclerae and cafe au lait lesions but no fractures. A second brother has OI, CCD and neurofibromatosis. Mutation analysis performed by conformation sensitive gel electrophoresis disclosed a COL1A1 IVS 14-2A>G present in the proband, her father and the OI-affected brother. A known CCD mutation, R 225Q (c.674G>A) was found in the mother and brother. We investigated the growth characterstics of the proband's dermal fibroblasts using MTS/PMS (Promega) which by 490 nm absorbance is proportional to the number of living cells in culture. Fibroblasts in passage 9-11, at a concentration of 1000/well, were cultured for 14 days in DMEM containing 10% FCS. Data is reported for day 3. Basal growth rate was decreased in proband cells compared to control ($p =<0.001$). Cells were cultured with estradiol, IGF-1, TGF-b1, basic FGF and in in phenol red (+) and phenol red (-) DMEM media. Basic FGF increased growth rates 8 to 10% ($p=<0.01$) in control and proband cells. Response to IGF-1 was positive, but not significantly different in control vs proband cells. TGF-b1 decreased growth rate 18% in both cell strains. Estradiol increased growth 9% to 12% in control and proband cells. Dexamethasone (10-7 M) increased growth 15% in control fibroblasts but not in proband cells. Phenol red (+) medium increased growth rate in control cells but not in proband cells. This is the first report of double heterozygosity for genes which are essential for normal fibroblast and osteoblast growth and differentiation. Fibroblasts containing a COL1A1 mutation show impaired growth rate responses to dexamethasone and phenol red. Phenol red contains lipophilic agents which has a stimulatory effect on cell growth acting through Na /K cationic channels. This suggests that cationic channels may modulate growth, and/or altered extracellular deposition of bone matrix proteins by OI fibroblasts.

SU119

Expression Profiling of Genes Involved in Osteoporosis using DNA Microarray. S. Kim[1], M. Kim*[2], J. Kim*[2], J. Choi[3], H. Shin*[4], E. Park*[5]. [1]Orthopedic Surgery, Kyungpook National University Hospital, Daegu, Republic of Korea, [2]Immunology, School of Medicine, Kyungpook National University, Daegu, Republic of Korea, [3]Biochemistry, School of Medicine, Kyungpook National University, Daegu, Republic of Korea, [4]Pathology, School of Dental Medicine, Kyungpook National University, Daegu, Republic of Korea, [5]Cell and Developmental Biology, Biomedical Research Institute, Kyungpook National University Hospital, Daegu, Republic of Korea.

Osteoporosis is a common and progressive skeletal disease primarily caused by genetic factors and hormonal imbalances. Alteration of gene expression caused by hormonal imbalances may be one of critical causes for osteoporosis. Although many genes have been implicated to play a role in osteoporosis, systematic studies are necessary to identify genes and to understand their roles in osteoporosis. In an effort to identify differentially expressed genes associated with osteoporosis, we utilized DNA microarray technology. Bone tissues were obtained from young woman of premenopause with high BMD and old woman of postmenopause with low BMD. RNA from cancellous bones was purified, reverse transcribed and labeled with either Cy3-dUTP (nonosteoporotic) or Cy5-dUTP (osteoporotic). Labeled probes were hybridized to the DNA chip containing 3,063 human mesenchymal cell derived genes (http://hair.knu.ac.kr). More than 2 fold in the ratio of Cy-3/Cy-5 was counted for positive signals. We identified 9 genes highly up-regulated in osteoporosis and 10 genes strongly down-regulated. Those up-regulated genes were cell signaling related genes such as IGFBP2 and endoglin, and transcription factors such as transforming growth factor beta inducible early growth response and nuclear factor related to kappa B binding protein. The down-regulated genes were progesterone membrane binding protein, signal transducer and activator of transcription 1, transcriptional adaptor3-like (PCAF histone acetylase complex). We also identified several genes that were not found in GenBank.These results suggest that osteoporosis is followed by fluctuations of expression of genes and the genes identified in this study may play a critical role in osteoporosis in vivo.

SU120

Phenotypic Differences in Bone Morphometry of Inbred Mice with High and Low Bone Density are Gender and Site Specific. D. J. Adams*[1], J. D. Delaney*[2], M. S. Moreau*[1], D. W. Rowe[2]. [1]Orthopaedic Surgery, University of Connecticut Health Center, Farmington, CT, USA, [2]Genetics and Developmental Biology, University of Connecticut Health Center, Farmington, CT, USA.

Inbred strains of female mice exhibiting relatively high (C3H/HeJ) and low (C57BL/6J) bone density have been employed recently to study the genetic regulation of bone mass, structure, and integrity. Female C3H mice demonstrate thicker, more highly mineralized femoral cortical bone than female B6 mice, but substantially less trabecular bone in their vertebrae and proximal femur. The objective of this study was to examine gender differences in cortical and trabecular bone architecture within femora of these two inbred strains as well as the outbred strain CD1. Femora were harvested from male and female inbred (C3H and B6) and outbred (CD1) 4-month old mice (38 mice, 6-7 per group). Cortical and trabecular morphometry were measured at mid-diaphysis and within the distal metaphysis, respectively, from images generated via X-ray computed microtomography. Cortical cross-sectional area, thickness, maximum area moment of inertia, and polar moment of inertia were significantly lower in femora from females than in males for B6 and CD1 mice ($p < 0.05$), but not for C3H mice. Flexural section modulus, a measure of geometrical bending strength, was lower in females than in males for all three strains, although only marginally significant for CD1 ($p = 0.057$). Despite substantial differences in cortical cross-sectional area and thickness, section modulus was the same in female C3H and B6 femora; however, section modulus was significantly lower in B6 males than C3H males ($p = 0.04$). Trabecular volume fraction was significantly lower ($p = 0.004$) in femora from B6 females than in B6 males ($10.7 \pm 0.8\%$ vs. $28.1 \pm 8.4\%$), and significantly higher ($p = 0.01$) in C3H females than in C3H males ($33.5 \pm 4.2\%$ vs. $21.8 \pm 7.4\%$). Femoral trabeculae in B6 females were thinner ($p = 0.008$), fewer in number ($p = 0.002$), and less connected ($p = 0.006$) than in males, whereas the trabeculae in C3H females were significantly thicker than in males ($p = 0.03$). Unlike cortical bone geometry, differences in trabecular bone morphometry between male B6 and C3H mice were minimal, including a small increase in the number of trabeculae ($p = 0.004$) that were otherwise of equal average thickness and not consequential in altering volume fraction ($p = 0.2$). Trabecular number, thickness, connectivity, and volume were substantially lower in B6 females than C3H females ($p < 0.005$). These data demonstrate that phenotypic differences in bone morphometry typically associated with C3H and B6 mice are gender and site specific.

SU121

Linkage Disequilibrium Mapping of Disease Genes with High Allele Frequency and Unknown Mode of Inheritance. G. Gong. Osteoporosis Research Center, Creighton University, Omaha, NE, USA.

Morton, the founder of LOD score linkage analysis, has shown that segregation analysis is unreliable for finding susceptibility genes, which can be identified only by allelic association (linkage disequilibrium) with candidate loci. Recently, Altmül et al. have shown that true linkage is hard to find in mapping complex trait loci with family-based analyses, the future of genetic studies on complex traits such as osteoporosis lies in association analysis. Linkage disequilibrium mapping has been used for mapping rare but not common diseases. As a first step, we investigated whether linkage disequilibrium mapping can be performed under certain conditions seen in common diseases: high disease allele frequency and unknown mode of inheritance. Let n be the total number of subjects who are sampled randomly from the general population, n_D be the number of subjects with the disease, and a, b and c be the numbers of subjects with the disease and marker genotype A_1A_1, A_1A_2 and A_2A_2, respectively. Let p_1 and p_2 be the frequencies of marker allele 1 and 2, respectively, θ be recombination fraction between marker and disease loci, and t be the number of generations passed since the introduction of the mutation. We divide the number of heterozygotes b into two components, m and $(b - m)$. Let $a : m = (b - m) : c$. Thus, $m^2 - bm + ac = 0$, and m is known. Let $n_{DA1} = a + m$. We demonstrated that $(1 - \theta)^t = (n_{DA1} - p_1 n_D)/(p_2 n_D)$. We showed that this equation applies to diseases with high allele frequency. We further showed that this equation applies to diseases with dominant, co-dominant, overdominant, recessive or unknown inheritances. We propose that t be estimated with the ethnic groups in which an association is found: $t = 2{,}050$, when an association found in Asians and Caucasians, or $t = 5{,}000$ when an association is found in Africans and Asians/Caucasians. Here, t is racial divergence time in terms of number of generations. Previously, to find a disease-candidate gene allelic association has been the sole purpose and the end of study

without knowing where the susceptibility genes are exactly located. We show here that association studies become a real mapping tool to locate mutations or DNA sequence variations responsible for common diseases such as osteoporosis.

SU122

Identification of Five Genetic Markers in Mice that Influence Femoral Size and Shape. S. K. Volkman*[1], A. T. Galecki*[2], D. T. Burke*[3], M. R. Paczas*[1], M. R. Moalli[1], R. A. Miller*[4], S. A. Goldstein[1]. [1]Orthopaedic Research Laboratory, University of Michigan, Ann Arbor, MI, USA, [2]Institute of Gerontology, University of Michigan, Ann Arbor, MI, USA, [3]Human Genetics Department, University of Michigan, Ann Arbor, MI, USA, [4]Department of Pathology and Geriatrics Center, University of Michigan, Ann Arbor, MI, USA.

Skeletal fragility has been identified as a factor in more than one million fractures in the United States per year. These fractures are responsible for significant disability and death, and cost the nation more than an estimated ten billion dollars annually. The risk of fracture depends on many factors, including the amount, structural orientation and mechanical integrity of bone, but the extent to which these factors, and their effects on fragility, are regulated by genetic controls is unknown. Previous studies have shown that genetic background affects bone characteristics, particularly bone mineral density, in both mouse and human populations. Much less in known, however, about the specific genetic effect on bone size, shape and mechanical integrity. The purpose of this study was to investigate the genetic determinants of geometric properties of cortical bone in mice. This study utilized 294 female UM-HET3 mice, produced as the progeny of (BALB/cJ x C57BL/6J)F1 females and (C3H/HeJ x DBA/2J)F1 males. This breeding scheme produces a genetically heterogeneous mouse population that can be considered a very large sibship, in that each animal inherits 25% of its genes from each of the same four inbred grandparental strains. The mice were genotyped at 87 polymorphic loci using PCR-based methods and an ALFexpress automated sequence analyzer (Pharmacia, Piscataway, NJ). Animals were humanely euthanized at 18 months of age, at which time right femurs were removed and dissected free of soft tissue. Geometric traits of the femoral cortical bone were assessed with micro-computed tomography. Two genetic markers (D2Mit58 and D3Mit62) were associated with femoral cross-sectional area and cortical thickness, which describe bone size; one marker (D12Mit46) was linked with traits describing bone shape; and two markers (D11Mit83 and D15Mit171) were associated with both size and shape. Our results indicate that the genetic influence on cortical bone geometry is complex and that femoral size and shape may be influenced by different, though overlapping, groups of polymorphic loci.

SU123

Confirmation of Linkage of 17q23 to Bone Size Variation. F. H. Xu, H. Shen, Y. J. Liu, Y. Z. Liu, Q. Y. Huang, H. Y. Deng*, L. J. Zhao, T. Conway*, K. M. Davies, R. R. Recker, H. W. Deng. Osteoporosis Research Center and Biomedical Sciences, Creighton University, Omaha, NE, USA.

Osteoporosis is a major public health problem in the world. Bone size is an important independent determinant of osteoporotic fractures. We conducted a whole-genome linkage scan with 635 individuals from 53 pedigrees to identify genomic regions that may contain QTLs underlying variation in bone area (measured by DEXA). Several genomic regions were identified. To confirm the previous results, we performed an expansion study with both increased samples and denser microsatellite markers within the previously localized regions. Seventy-nine pedigrees were used in this study with 1,816 subjects. The pedigree size ranges from 3 to 423, with a mean (SE) of 23.5 (5.6). A total of 74,498 relatives pairs that are informative for linkage analysis exist in our sample, among which are 3,393 sibling pairs, 316 grandparent-grandchild pairs, and 10,060 first cousin pairs. We genotyped a new set of microsatellite markers which distributed within previously identified genomic regions, with the average inter-marker distance narrowed to ~5cM. Adjusting for age, sex and other significant covariates, we conducted two- and multipoint linkage analysis using software package SOLAR. Some genomic regions previously identified were replicated in this expansion study. For examples, the genomic region 17q23 showed a MLS (maximum LOD score) of 1.18 (p=0.009) for wrist (ultra distal) bone size. Considering that the strength of evidence required for replication of a previously found linkage is different from that in a whole-genome linkage analysis, our results strongly support that the above genomic region may harbor a QTL affecting bone size variation. This study represents our effort in identifying genes and associated etiology for osteoporosis using various important phenotypes and may be one of the first few linkage confirmation studies for complex traits in bone genetic studies.

SU124

A Confirmation Study for Quantitative-Trait Loci for BMD-Related Obesity Phenotypes. Y. J. Liu, F. H. Xu, H. Shen, Y. Z. Liu, Q. Y. Huang, H. Y. Deng, L. J. Zhao, T. Conway, K. M. Davies, R. R. Recker, H. W. Deng. Osteoporosis Research Center and Biomedical Sciences, Creighton University, Omaha, NE, USA.

Bone mineral density (BMD) is a major determinant of osteoporosis. The important indices of obesity such as body mass index (BMI), percentage fat mass (PFM), and body fat mass (FM) are significantly related with BMD. Therefore, study of the determination of obesity phenotypes may shed light on the nature of the determination of osteoporosis. We conducted a whole-genome linkage scan for QTLs for obesity phenotypes. Several genomic regions that may contain obesity-related QTLs were identified. To confirm the previous results, we performed an extension study with both increased samples and denser microsatellite markers within the previously localized regions. The pedigrees used in the study were expanded from 53 to 79, with subjects increased from 630 to 1816. The pedigree size ranges from 3 to 423, with a mean (SE) of 23.5 (5.6). A total of 74,498 relatives pairs that are informative for linkage analysis are included in our sample, among which are 3393 sibling pairs, 316 grandparent-grandchild pairs, and 10,060 first cousin pairs. We genotyped a new set of microsatellite markers which distributed within previously identified genomic regions, with the average genomic distance narrowed to ~5cM. Adjusting for age, sex and other significant covariates, we conducted two- and multipoint linkage analysis using software package SOLAR. Some genomic regions previously identified were replicated in this extension study. For examples, for BMI, on genomic region 1p36, a LOD score of 2.14 (p=0.0008) is achieved near marker D1S468 in twopoint analysis and a MLS of 1.38 (p=0.006) is achieved at the terminal end of short arm on chromosome 1 in multipoint analysis. Considering that the strength of evidence required for replication of a previously found linkage is different from that in a whole-genome linkage analysis, our results strongly support that the above genomic regions may harbor QTLs affecting obesity phenotypes. This study may be one of the first few linkage confirmation studies for complex trait genetic studies. Identification of determinants underlying the variation of phenotypes correlated with BMD such as obesity related phenotypes, should shed light on the determination of susceptibility to osteoporosis.

SU125

Second Stage of Genome Scan for QTLs Influencing BMD Variation. Q. Y. Huang, F. H. Xu, H. Shen, Y. J. Liu, Y. Z. Liu, H. Y. Deng*, L. J. Zhao, V. Dvornyk, K. M. Davies, R. R. Recker, H. W. Deng. Osteoporosis Research Center and Biomedical Sciences, Creighton University, Omaha, NE, USA.

Osteoporosis is a common complex disorder with high social and economic costs. Low bone mineral density (BMD) is a major risk factor for osteoporosis. To identify genomic regions harboring QTLs (quantitative trait loci) contributing to BMD variation, we performed a two-stage genome screen. The first stage involved genotyping of a sample of 53 pedigrees (635 individuals) using 400 microsatellite markers spaced at approximately 10 cM intervals throughout the genome. Genomic regions with multipoint and/or two-point LOD greater than 1.5 were observed in chromosome regions 4q31-32, 7p22, 12q24, 13q33-34, 15p11 for spine BMD, 10q26, 12q13, 17p11 for hip BMD, and 3p26, 4q32, 9p22-24, 17p13 for wrist BMD. In the second stage, 60 microsatellite markers with a mean spacing of about 5 cM were genotyped in these regions in an expanded sample of 79 pedigrees that contain 1,816 subjects. The sample contains a total of 74,498 relative pairs that are informative for linkage analyses, among which there are 3,393 sibling pairs, 316 grandparent-grandchild pairs, and 10,060 first cousin pairs. Each pedigree was ascertained through a proband with extreme BMD at the hip or spine. BMD at the spine (L1-4), hip (the femoral neck, trochanter and intertrochanteric region) and wrist (the ultra-distal region) was measured by DEXA, and was adjusted for age, sex, height, and weight. Two-point and multipoint linkage analyses were performed for each BMD site using a variance component method that is implemented in the computer package SOLAR. Several regions achieved LOD scores in excess of 1 in the second stage follow-up study, in chromosome regions of 10q26, 7p22, 12q13, and 13q33-34. Our strongest evidence for linkage was on 10q26, where we obtained a peak multipoint LOD score (MLS) of 1.65 at 170 cM from peter for hip BMD. Genomic regions homologous to human 10q26 have previously been implicated in mice for BMD (Klein et al. 1998; Beamer et al. 2001). A potential candidate gene was identified in this region. In addition, a multipoint LOD score of 1.62 for spine BMD were achieved on chromosome 7. Further analyses are being conducted. Considering that the LOD score criteria of linkage confirmation for specific genomic regions are different from those in the first-stage whole genome scan, our results provide tentative evidence of confirmation of linkage of several genomic regions to BMD variation. To our knowledge, this is the largest linkage confirmation study in the bone genetics field.

SU126

A Confirmation and Extension Study for Linkage to an Important Complex Trait Related to Osteoporotic Fractures- Height. Y. Z. Liu, H. Y. Deng, J. R. Long, Y. Y. Zhang, S. B. Lu, F. H. Xu, H. Shen, Y. J. Liu, Q. Y. Huang, L. J. Zhao, T. Conway, R. R. Recker, H. W. Deng. Osteoporosis Research Center and Biomedical Sciences, Creighton University, Omaha, NE, USA.

Height is an important complex anthropometric character with high genetic determination (its heritability is more than 50%). It is highly correlated with susceptibility to osteoporotic fracture. Studies of height variation will help identify and understand risk factors underlying susceptibility to osteoporotic fractures. We performed a whole genome scan on 671 subjects from 53 pedigrees. Several genomic regions were suggested to contain QTLs underlying height variation, which included 5q31 (144cM from pter of chromosome 5), 8p22 (16cM from pter of chromosome 8), 17q25 (114cM from pter of chromosome 17), Xp22 (10.1cM from pter of chromosome X), and Xq25 (139.4cM from pter of chromosome X). Based on these results, we performed a confirmation and extension study employing 12 new microsatellite markers concentrating in the above five genomic regions in a expanded sample of 79 pedigrees containing 1,816 subjects. The 79 pedigrees vary in size from 3 to 423 individuals, with a mean of 23.5(SE=5.6). These pedigrees contain 74,498 relative pairs informative for linkage analysis, among which, there are 3,393 sib pairs. Linkage analysis on sex- and age-adjusted height was conducted with SOLAR using a variance component method. We have finished two-point linkage analysis for the markers on the 3 autosomes. Confirmation linkage signals were detected around 146.1 cM from the pter of chromosome 5 (p=0.018) and around 105.7cM from the pter of chromosome 17 (p=0.029). Our preliminary analyses seem to confirm the linkage findings of our previous whole genome scan. Further analysis and experiment will be performed to fine-map the confirmed genomic regions and to identify positional candidate genes for testing for height variation. This study represents our extensive effort beyond initial whole genome linkage scan studies to identify factors underlying the variation of traits related to osteoporotic fractures.

SU127

Linkage Studies of RANK, RANKL and OPG in the Control of Bone Mineral Density. L. J. Miles*[1], E. L. Duncan[1], A. M. Crane*[1], J. A. H. Wass[2], M. A. Brown*[1]. [1]Spondyloarthritis and Bone Disease, Oxford University, Wellcome Trust Centre for Human Genetics, Oxford, United Kingdom, [2]Metabolic Bone Unit, Nuffield Orthopaedic Centre, Oxford, United Kingdom.

RANKL is a tumour necrosis factor ligand family member which together with its receptor, RANK, and its soluble secreted decoy receptor, OPG, comprise an important and novel cytokine system whose interactions regulate osteoclast formation, fusion, activation, survival and apoptosis. Whether genetic polymorphisms of the genes encoding these factors influence bone mineral density in the general population is unknown. To test this hypothesis, we studied 814 family members (330 men, 484 women) belonging to 164 families recruited with probands with extreme low BMD (t-score <-2.5, z-score <-2.0 at either the lumbar spine or femoral neck) from the outpatient services of the Nuffield Orthopaedic Centre, Oxford, UK. Seventeen microsatellite markers lying close to or within the genes of interest were chosen from publicly available databases, and resultant PCR fragments were run on ABI 3700 capillary electrophoresis genotyping machines. Quantitative trait linkage analysis in general pedigrees was then performed using SOLAR [1], controlling for the covariates age, height, gender and ascertainment effects. In agreement with our previously reported findings, weak linkage was observed between the region encompassing RANKL and femoral neck BMD (peak LOD score 0.53), but no significant linkage was observed at any other locus. We are currently studying these genes further for association using SNPs, within the genes themselves, identified by a combination of database searches, denaturing high performance liquid chromatography, and direct sequencing. Preliminary results of these studies will be presented at the meeting.

[1]. Almasy L, Blangero J: Multipoint quantitative-trait linkage analysis in general pedigrees. 1998.

SU128

Lessons From Segregation Analysis for the Ascertainment of Families for Mapping of Osteoporosis Genes. E. L. Duncan[1], L. R. Cardon*[1], J. A. H. Wass[2], M. A. Brown*[1]. [1]Wellcome Trust Centre for Human Genetics, Oxford, United Kingdom, [2]Metabolic Bone Unit, Nuffield Orthopaedic Centre, Oxford, United Kingdom.

Theoretical studies suggest that families ascertained through probands with extreme trait values have greater power to detect quantitative trait loci. To test this hypothesis, we examined the genetic profile of 150 families with 768 individuals recruited with probands with extreme low bone mineral density (BMD, t-score <-2.5, z-score <-2.0). Complex segregation analysis was performed using the Pedigree Analysis Package (1). BMD measured at either the lumbar spine (LS, L1-4) or total hip was expressed either as raw values (g/cm2), or as t-scores or z-scores obtained from the Hologic normative database. Covariates assessed included age, height, gender and menopausal status (premenopausal, early postmenopausal (within 5 years of the menopause), and late postmenopausal (greater than 5 years from the menopause). In all models a major gene effect was observed in addition to a residual polygenic effect. Total heritability ranged at the spine from 0.36 to 0.57, and at the hip from 0.43 to 0.63. Comparing the use of t-scores, z-scores or raw BMD, in all cases heritability was equivalent to or higher when raw BMD was studied. Residual correlation between BMD and age and gender was observed when t- and z-scores were studied. These observations suggest that differences exist between the Hologic database and the population from which these families were drawn, and suggest that maximum power in genetic studies will be achieved by using raw BMD data adjusted for gender and age, rather than using data normalised using external normative databases. We have previously reported that in these families in all male-male comparisions there is greater correlation of the LS BMD than hip, and in female-female comparisons, there is greater hip BMD correlation than LS. This finding remains true for parent-offspring correlations when menopausal status is taken into account. Mother-daughter pairs are more similar at the hip than other parent-offspring pairs (0.45 vs 0.12-0.21, p=0.006), whereas father-son (0.29 vs 0.20-0.24) but not mother-daughter pairs were more similar at the LS. Father-daughter and mother-son pairs were always less correlated than father-son and mother-daughter pairs, supporting a gender specific effect independent of menopause status. This study confirms that whilst osteoporosis is predominantly determined by genes with individually small effects, by studying families drawn from the extremes of the population distribution, a significant major gene effect can be observed.

(1) Hasstedt SJ Genet Epidemiol 1993

*Disclosures: **M.A. Brown**, Arthritis Research Campaign 2.*

SU129

Identification of Genetic Loci that Influences Osteoclastogenesis or Bone Mineral Density in BXD RI Strains of Mice. L. Zhang*[1], X. Xu*[2], H. Hsu*[2], T. R. Nagy*[3], N. Said-Al-Naief*[1], K. J. Ho*[1], P. Yang*[2], J. Li*[3], H. Zhang*[2], J. M. McDonald[1], J. D. Mountz*[2]. [1]Pathology, University of Alabama at Birmingham, Birmingham, AL, USA, [2]Medicine, University of Alabama at Birmingham, Birmingham, AL, USA, [3]Nutrition Science, University of Alabama at Birmingham, Birmingham, AL, USA.

In the present study, C57BL/6 X DBA/2 (BXD) recombinant inbred (RI) BXD strains of mice and their progenitor B6 and D2 strains were utilized to determine the genetic influence on osteoclasts and bone mineral density (BMD) in young (4 mo-old) and aged (13-mo- old) mice. TRAP staining and digital imaging analysis of femur and vertebrae, and in vitro analysis of osteoclastogenesis from bone marrow, showed that there was a significant increase in osteoclast numbers in young D2 compared to young B6 mice. BMD values obtained by dual-energy X-ray absorptiometry showed that there was a significant decrease in BMD in aged mice compared to young mice but there was no difference between B6 and D2 mice. Analysis of in vitro osteoclast differentiation activity and BMD in numerous BXD RI strains showed that there was a genetically dependant strain distribution pattern of these two variables. Nonetheless, there was low correlation between these two variables, suggesting regulation by at least two independent genes. The BMD values from 18 strains of BXD mice were used for Quantitative Trait Loci (QTL) analysis. The genetic locus influencing bone mineral density in BXD mice at 4 month of age was mapped to mouse chromosome 4 (D4Mit186) with a likelihood ratio statistics (LRS) reaching a linkage suggestive value of 18.4 (p = 0.00002). The in vitro osteoclast differentiation values from 11 strains of BXD mice were used for QTL analysis. The genetic locus influencing osteoclastogenesis in BXD mice at 4 month of age was mapped to mouse chromosome 19 (D19Nds1) with a LRS reaching a linkage suggestive value of 13.3 (p = 0.00026). These results suggest that in these mice there are two separated sets of genes that independently regulate osteoclastogenesis and BMD respectively.

SU130

Genotype-by-Sex and Environment-by-Sex Interactions Influence Variation in Serum Bone-Specific Alkaline Phosphatase Levels in Pedigreed Baboons. L. M. Havill, M. C. Mahaney, J. Rogers*. Genetics, Southwest Foundation for Biomedical Research, San Antonio, TX, USA.

While more than 77% of the 10.1 million people in the U.S. with osteoporosis are women, the contributions of genotype-by-sex (G×S) interactions to sex differences in BMD and other osteoporosis risk factors have not been studied. To address this question, we conducted a statistical genetic analysis of serum concentrations of bone specific alkaline phosphatase (BSAP), a highly specific marker of osteoblast function that is elevated in persons with conditions, like osteoporosis, characterized by excessive bone turnover and/or rapid bone loss. We assayed BSAP in frozen serum from 692 pedigreed baboons using a commercially available ELISA kit. Using a maximum likelihood variance decomposition approach, we treated sex as an environmental milieu in which genes influencing BSAP levels are expressed. We modeled the genetic covariance in BSAP between all relative pairs conditional on their sex so that the covariance is the product of the kinship, the genetic correlation between the trait levels in two sexes, and the genetic standard deviations in two sexes. Sex-specific maximum likelihood estimates of residual heritability for BSAP were greater for females than for males (h^2 = 0.44 vs. h^2 = 0.26, respectively), but likelihood ratio tests revealed only a marginally significant difference in sex-specific genetic variances (p = 0.057). In contrast, the between-sex genetic correlation (ρ_G = 0.43) was significantly less than 1 (p = 0.037), and the difference in sex-specific environmental variances was highly significant (p = 0.00006). These results represent the first evidence for the influence of G×S interactions on variation in an osteoporosis risk factor. While the overall contribution of genes to the total phenotypic variance in BSAP may not differ significantly by sex in these baboons, the diminished between-sex genetic correlation implies that different genes influence BSAP levels in the two sexes. Equally interesting, the highly significant differences in environmental variances suggests that unmeasured factors -- including those from the internal, biological environments of the two sexes -- account for a greater proportion of the BSAP variation in females than in males.

SU131

Genotype-by-Age Interactions Influence Normal Quantitative Variation in Spinal BMD in Pedigreed Baboons. M. C. Mahaney, L. M. Havill, L. Almasy*, J. Rogers*. Genetics, Southwest Foundation for Biomedical Research, San Antonio, TX, USA.

The association of decreased bone mineral density (BMD) and increased fracture risk with advancing age are hallmarks of osteoporosis, but the contributions of genotype-by-age (G×A) interactions to variation in BMD have not been investigated directly. To address this question, we conducted statistical genetic analyses of spinal BMD in a nonhuman primate model for age-related changes and pathology in bone in which we previously had estimated heritability and localized QTLs for this trait. We used maximum likelihood variance decomposition methods to analyze data on areal BMD (aBMD, g/cm^2) obtained by DEXA from two projections (anterior-posterior and lateral) at three thoraco-lumbar vertebrae in 692 pedigreed baboons. We modeled G×A interaction for aBMD by defining the additive genetic component of the variance as a function of age. We also modeled the genetic correlation between relative pairs at different ages as an exponential decay function across age values. Through numerical maximization, we simultaneously estimated these two G×A interaction terms plus the mean effects of sex, body weight, crown-rump length, and spinal arthritis severity on each measure of spinal aBMD. Likelihood ratio tests revealed evidence for G×A interaction for arithmetic mean thoraco-lumbar aBMD from both the anterior-posterior (A-P) and lateral (LAT) projections. For both A-P and LAT mean aBMD measures, we observed significant decreases in genetic variance with increasing age (p = 0.000783 and p = 0.002432, respectively). For the mean of LAT aBMD, the genetic correlation between aBMD at different ages differed significantly from 1.0 (p = 0.028). Analyses of aBMD at the three individual vertebral sites scanned from both the A-P and LAT projections, yielded results in complete concordance with those obtained from analyses of the means for each projection. The first observation implies that the magnitude of the effect of genes contributing to variation in aBMD changes with age. The second observation implies that different genes may influence variation in aBMD at different ages in these baboons. These results are consistent with observations by others of possible age-specific genetic effects on BMD in analyses of cohorts with different mean ages. They also may help explain, in part, apparent discrepancies between the results of genetic studies conducted by different researchers with data from subject populations exhibiting dissimilar age profiles.

SU132

Relation of Polymorphism of the COL1A2 and Estrogen Receptor α Gene to the Acquisition of Bone Mass in Prepubertal Finnish Girls. M. M. Suuriniemi*[1], A. Mahonen[2], V. Kovanen*[1], M. Alen*[3], J. Heino*[1], H. Kröger[2], F. Tylavsky[4], S. Cheng[1]. [1]University of Jyväskylä, Jyväskylä, Finland, [2]University of Kuopio, Kuopio, Finland, [3]PEURUNKA-Medical Rehabilitation Centre, Jyväskylä, Finland, [4]Univ of Tennessee, Memphis, TN, USA.

Genetic factors are strongly involved in bone metabolism. The purpose of this study was to evaluate the associations between polymorphism in candidate genes known to be involved in bone metabolism in adult population [COL1A2/PvuII site, estrogen receptor α (ERα)/ PvuII site, vitamin D receptor (VDR)/FokI and TaqI sites, and insulin-like growth factor (IGF)/dinucleotide repeat] and the acquisition of bone mass in prepubertal girls during two-year period. The subjects were 10-12-year-old girls (n=91) with Tanner stage I-II, who participated in an intervention study (the CALEX-study). Genotyping of the four genetic polymorphic sites was performed. Bone mineral content (BMC) and areal bone mineral density (aBMD) of the total body, total femur, and lumbar spine (L2-L4) were measured using dual-energy X-ray absorptiometry (DXA, Prodigy, Lunar). Our results showed that Tanner stage, height, weight, calcium/vitamin D consumption, and physical activity did not differ significantly among girls with different genotypes. The polymorphism of the VDR and IGF gene was not significantly associated with changes (%) of bone mass at different bone sites. The 24-months-change of total femur BMD differed with respect to the PvuII alleles of COL1A2 gene (p=0.031), the PP genotype group achieving the greatest increase in bone mineral density. The 24-months-change of total body and total femur BMC differed with respect to the ERα PvuII alleles (p=0.049 and p=0.046, respectively). There was also a tendency toward greater increase of all bone properties in girls with the PP genotype (both COL1A2 and ERα). In the case of the ERα polymorphism there was a clear gene dosage effect, while the COL1A2 polymorphism showed a homozygote preference. There was no association between the COL1A2 and ERα polymorphism. Our study indicates that the polymorphisms of the COL1A2 and ERα genes are associated with the increase in bone mass during prepubertal and pubertal phases. This may provide valuable knowledge for identifying girls who are at risk for osteoporotic fractures later in life.

SU133

Testing of Association and /or Linkage for the Estrogen Receptor-α Gene with Peak Bone Mass in US Caucasian Nuclear Families. L. J. Zhao, H. Shen, L. Elze*, R. R. Recker, H. W. Deng. Osteoporosis Research Center and Biomedical Sciences, Creighton University, Omaha, NE, USA.

Decades of studies on bone have suggested numerous candidate genes that may regulate bone mineral density (BMD). Among these genes, one that has been studied frequently is the estrogen receptor alpha (ER-α) gene. However, the results of traditional linkage or association studies of the ER-α gene have largely been inconsistent and controversial. The purpose of this study is to test association and /or linkage of the ER-α gene with bone mineral density (BMD) in Caucasian nuclear families. We genotyped two polymorphic markers (Pvu II and Xba I) inside the ER-α gene for 636 individuals from 157 nuclear families with children generally aged 20-50. All these subjects are healthy Caucasians from Midwest of USA. By using the computer program QTDT, we tested for association alone, for linkage alone and for both linkage and association (TDT) between these two polymorphism markers with bone mineral density by specifying a recombination rate between these two markers as 0.0000005. All the raw BMD were adjusted by significant covariates, which include age, sex, weight and height. At the spine, we found marginally significant results for both association and linkage (TDT) between the two markers (Pvu II and Xba I) of ER-α gene and peak BMD (p = 0.0744 for Pvu II and p = 0.0516 for Xba I). In addition, marginally significant results have been observed for the test of linkage between the two markers and spine BMD (p < 0.10), for the test of association between the marker Xba I and Mid-radius BMD (p < 0.10). No population stratification was detected in our sample. We also conducted regular ANOVA test for the phenotype distribution among the genotypes in parents of the nuclear families. ANOVA test revealed that there are significant association between the Pvu II (p = 0.002) and Xba I (p = 0.013) markers and the mid-radius BMD. In conclusion, our preliminary results suggest that the ER-α gene may be one of the genetic factors underlying peak BMD variation in US Caucasians.

SU134

Differentiation of Caucasian and Asian Populations at Six Candidate Loci for Bone Mineral Density. J. R. Long, V. Dvornyk, H. Shen, L. J. Zhao, Y. Y. Zhang, H. W. Deng. Osteoporosis Research Center and Biomedical Sciences, Creighton University, Omaha, NE, USA.

Bone mineral density (BMD) is a characteristic parameter for osteoporosis. It has strong genetic determination and several candidate genes have been studied for their association with BMD within populations of the same ethnicity. We comparatively studied two populations, Chinese and Caucasian, for polymorphism of seven markers of six genes that have been shown to be associated with BMD (Table). 804 and 327 random individuals were recruited in Hunan, China and Omaha, NE, USA, respectively. The Chinese population had significantly lower (p<0.01) total observed heterozygosity (H_o) over all the loci studied and H_o at CASR, AHSG, and PTH loci individually. The populations also manifested striking differences (p<0.01) in the frequencies of alleles and genotypes at all the studied loci, except the ER-*Pvu*II. In the Caucasian population, the overall distribution of the Sp1 alleles (s being the risk allele) was similar to that previously reported for the Caucasians (SS 67%, Ss 28% and ss 5%), while in the Chinese population 78% SS and only 1% ss genotypes were detected. The contrasting genotypic population structure was also observed for the CASR locus. Our data demonstrate that Asian populations have different genotype and allele frequency structure at some BMD candidate gene loci from that in Caucasians. The results have implications for evolutionary differentiation of genetic architecture of complex traits in various human populations, for differential genetic mechanism underlying the racial difference of the risk to osteoporosis, and for some inconsistent results in identifying genes underlying osteoporosis in various populations.

Frequencies of alternative alleles (A and P), H_o and Wright's fixation index (F)

Markers	Chinese				Caucasians			
	A	P	H_o	F	A	P	H_o	F
CASR-*Bsa*HI	0.97	0.03	0.07	-0.03	0.13	0.87	0.23	0.00
Col1A1-Sp1	0.11	0.89	0.21	-0.06	0.81	0.19	0.28	0.11
AHSG-*Sac*I	0.74	0.26	0.36	0.08	0.63	0.37	0.46	0.02
ER-*Pvu*II	0.36	0.64	0.49	-0.05	0.41	0.59	0.49	-0.01
ER-*Xba*I	0.24	0.76	0.41	-0.12	0.31	0.69	0.44	-0.04
VDR-*Apa*I	0.29	0.71	0.42	-0.02	0.58	0.42	0.47	0.04
PTH-*Bstb*I	0.86	0.14	0.25	-0.02	0.42	0.58	0.58	-0.18
Mean	-	-	0.31	-0.03	-	-	0.42	-0.01

SU135

Dinucleotide Repeat (CA) Polymorphisms of the IL-6, TNFR2, and CT Genes and BMD. Y. Y. Zhang, Q. Y. Huang, H. Shen, H. Y. Deng, T. Conway, R. R. Recker, H. W. Deng. Osteoporosis Research Center and Biomedical Sciences, Creighton University, Omaha, NE, USA.

Genetic factors play an important role in determining bone mass. In view of the reported associations between osteoporosis and polymorphisms of the interleukin-6 (IL-6), tumor necrosis factor receptor 2 (TNFR2), and calcitonin (CT) genes, an association study was performed between dinucleotide repeat (CA) polymorphisms at the IL-6, TNFR2, CT genes and BMD in 175 Caucasian nuclear families with 665 subjects. BMD at the spine (L1-4), hip (the femoral neck, trochanter and intertrochanteric region) and wrist (mid region) were measured by DEXA, and were adjusted for age, sex, weight, and height. The QTDT program was employed for analyses. For the IL-6 gene, nine alleles were observed in this population. The allele 8 (130bp) showed strongest association with the spine BMD (p=0.0006) and hip BMD (p=0.048). The alleles 3 (120bp) and 9 (132bp) showed weak association with spine BMD (p=0.0788) and hip BMD (p=0.096), respectively. The allele 2 (118bp) and 7 (128bp) are associated with wrist BMD (p=0.052 and 0.047, respectively). However, population stratification is observed for the alleles 3 (p=0.084) and 6 (p=0.07). For the TNFR2 gene, eight alleles were present in our sample, of which allele 3 (266bp) and allele 8 (276bp) were associated with wrist BMD (p=0.043 and 0.0245, respectively), allele 5 (270bp) with hip BMD (p=0.0669). Allele 1 (260bp) and 5 (270bp) are associated with spine BMD (p=0.0879 and 0.0637, respectively). However, population stratification is observed in allele 5 (p=0.0175) and allele 6 (p=0.098). For the CT gene, we detected six alleles, and only allele 4 (122bp) is weakly associated with hip BMD (p=0.08). Our data are consistent with earlier findings that IL-6 and TNFR2 gene polymorphisms are associated with spine and/or hip BMD. Further studies for linkage and identification of the causative mutation are warranted.

SU136

Osteoprotegerin (OPG) Serum Levels and OPG Polymorphism in Children with Polyarticular Juvenile Idiopathic Arthritis. L. Masi[1], L. Becherini*[1], E. Piscitelli*[1], S. Benvenuti*[2], G. Simonini*[3], F. Falcini*[3], A. Falchetti*[1], A. Tanini[1], R. Imbriaco*[1], M. Brandi[1]. [1]Department of Internal Medicine, University of Florence, Florence, Italy, [2]Department of Clinical Physipathology, University of Florence, Florence, Italy, [3]Department of Pediatrics, University of Florence, Florence, Italy.

Osteoporosis is a common manifestation in children with polyarticular juvenile idiopathic arthritis (JIA). The identification of OPG contributed to a new molecular and cellular concept of osteoclast biology. OPG inhibits differentiation of osteoclasts and it is important for protection of cartilage damage, a critical and irreversible step in the pathogenesis of arthritis. In addition, OPG gene may be a candidate gene in the regulation of bone mass. We have evaluated the levels of serum OPG in a group of 84 (66 female and 18 male) affected by JIA and 21 (11 female and 10 male) controls. The relationship between serum OPG and some disease parameters (PCR, VES and X-ray detectable erosions) was also evaluated. Moreover, a polymorphism of OPG gene was correlated with bone mass in these subjects. Serum OPG was measured using an ELISA method. OPG polymorphism was evaluated by PCR reaction of genomic DNA and digestion of the product by Fok I enzyme. Bone status was evaluated using DXA at the lumbar spine level. We observed that patients affected by JIA had significantly higher levels of serum OPG (60.19±25.9 vs. 39.56±11 pg/ml; p=0.002). In children affected by JIA patients under steroid therapy showed higher serum OPG levels in comparison with patients without therapy (63.19±25 vs. 43.81±20 pg/ml; p=0.001). No significant correlation was found between serum OPG and PCR, VES, and duration of the disease. However, patients with X-ray detectable erosions showed significantly higher OPG levels (72±22 vs. 50±18; p=0.007). CC genotype (76.4%) for the OPG gene was prevalent in the total population and the most frequent in normal children. TC genotype was the most represented in JIA patients (Chi2 test:8.9; df=2; p=0.006). Applying ANCOVA analysis and LSD test to evaluate the L-BMD differences among the OPG genotypes, we observed that patients with CC genotype had a L-BMD 9.4 % higher in comparison with TC genotype subjects (p=0.04). Finally, no significant differences in levels of serum OPG were found between the three genotypes. In conclusion, the increase of serum OPG in patients affected by JIA with erosions could reflect a compensatory response to degeneration of bone and cartilage and circulating OPG levels could predict disease activity but not bone mass changes. Conversely, OPG gene polymorphism may represent marker in the identification of JIA patient with higher risk of bone mass loss.

SU137

Lack of Association of Cdx Polymorphism with Bone Mineral Density in Korean Postmenopausal Women. S. Kim*[1], S. Kim*[1], Y. Rhee*[1], S. Li*[1], J. Jahng[2], S. Lim[1]. [1]Internal Medicine, College of Medicine, Yonsei University, Seoul, Republic of Korea, [2]Orthopaedic Surgery, College of Medicine, Yonsei University, Seoul, Republic of Korea.

The caudal-related homeodomain Cdx-2 played an important role in the intestine-specific transcription of the human vitamin D receptor (VDR) gene. In other previous study, the polymorphism was identified in the core sequence 5'-ATAAAAACTTA-3' in the Cdx-2 binding site in the VDR gene promoter (Cdx-polymorphism). The objectives of this study were to investigate the relationship between Cdx polymorphism and bone mineral density (BMD) in Korean postmenopausal women. Cdx polymorphism was analyzed in 108 Korean postmenopausal women by direct DNA sequence analysis. BMD at the lumbar spine and proximal femur were assessed by dual energy X-ray absorptiometry. Among 108 postmenopausal women, 20 showed genotype A/A (adenine at -3731 nucleotides relative to the transcription start site of human VDR gene 5-ATAAAAACTTAT), 41 showed genotype G/G (guanine at -3731 nucleotide, 5'-GTAAAAACTTAT-3') and 47 showed genotype A/G (heterozygote). The osteoporotic group consisted of 77 women with primary osteoporosis (mean age, 60 ± 5.4 years ; mean Z score at the lumbar spine,-1.80±0.64). There was no difference in prevalence of Cdx polymorphism between the osteoporotic patients and normal control (p=0.293). BMD of the lumbar spine was 0.816± 0.171 g/cm2 in subjects with the AA genotype, 0.900± 0.233 g/cm2 in subjects with the A/G genotype, 1.016± 0.204 g/cm2 in subjects with the GG genotype (p=not significant). There was no significant association between Cdx polymorphism and Z score values of lumbar spine and proximal femur BMD. These data indicate that there are no significant effects of Cdx polymorphism on BMD in Korean postmenopausal women. Our data do not support the idea that Cdx polymorphism has an impact on the bone mass of postmenopausal women.

SU138

Evaluation of Estrogen Receptor Gene and Calcium Sensor Gene Polymorphisms in Patients with Primary Osteoarthritis. I. Szombati*[1], G. Poór[1], A. Tabak*[2], P. Temesvari*[1], P. Lakatos*[2]. [1]National Institute of Rheumatology and Physiotherapy, Budapest, Hungary, [2]1st.Dept.Of Medicine, Semmelweis University, Budapest, Hungary.

The importance of estrogen receptor (ER) gene polymorphism in the pathogenesis of osteoporosis has been well known for years. Recently, several studies were carried out focusing on the calcium sensor gene polymorphism in patients with osteoporosis. A hypothetical relationship has also been suggested between genetic variability of these genes and primary osteoarthritis (OA); however, there are no supporting data available in this field. The present study aimed to examine the theoretical connection between ER gene PvuII and XbaI and CaSR gene A986S polymorphisms and primary osteoarthritis. The authors investigated 44 patients with radiologically and clinically severe osteoarthritis (OA group, mean age: 66.1± 11.4 (SD) years, BMI: 27.8±3.5 kg/m2) and 140 control healthy subjects (C group, aged 55.5 ±5.3 years p<0.001, BMI±4.1 kg/ m2, p7 NS). The genetic evaluation was carried out in all OA cases and in the C group. In the OA group, the ER gene Pp allele was found in 36/41 (87.8 %) cases, the PP allel in 5/41 (12.2%) cases while pp allel was absent in this population. In the C group, significantly (p<0.0001) different results were found: Pp allele in 46/91 (505%), PP in 29/91 (31.9 %), pp in 16/91 (17.6%) cases were detected. The ER gene XbaI genotype frequency in the OA group was the following: Xx: 39/41 (95.1%), XX 2/41 (4.9%), and xx allel was not found in this group. Frequency of the XbaI allele in the healthy control group was significantly different (p= 0.0003): Xx 54/90 (59,3%), XX :16/90 (17.6%), xx: 21/90 (23%). The CaSR gene's alleles frequency in the OA group was: AS: 38/42 (90,5%), AA: 1/42 (2,4%), SS: 3/42 (7.1%). These frequencies were significantly different from the controls: AS: 32 /113 (28.3%), AA: 80/13 (70.8%), SS 1/ 13 (0.9%) (p< 0.0001). There were significant differences between the OA and C group in the studied alleles of the ER and CaSR genes. The authors did not find ER gene xx and pp alleles in patients with osteoarthritis. These findings may suggest that genetic susceptibility might significantly contribute to the developement of osteoarthritis.

SU139

Estrogen-Related Polymorphisms and Their Possible Association with Adult Height, Body Mass Index and Serum Cholesterol. A. L. Eriksson*[1], S. Skrtic*[1], T. Hedner*[2], C. Ohlsson[1]. [1]Div. Endocrinology, Dept. Internal Medicine and Dept. Clinical Pharmacology, Gothenburg, Sweden, [2]Dept. Clinical Pharmacology, Gothenburg, Sweden.

Clinical as well as experimental studies have demonstrated that estrogen is of importance for the regulation of skeletal growth, fat mass and serum cholesterol. We have previously shown that estrogen receptor-α (ERα) deficient mice have a disturbed longitudinal bone growth, are obese and have increased serum cholesterol. The aim of the present study was to investigate if ERα (PvuII) and/or aromatase (A/G, exon 3 of CYP 19) polymorphisms are associated with adult height, body mass index (BMI) or serum cholesterol in a large well-defined clinical cohort. From a subpopulation of the CAPPP cohort (a large hypertension trial conducted in Sweden and Finland) including 364 men and 129 women (age 29-66, mean 56,9), DNA was extracted from the leukocytes. PCR amplification was performed on the regions of interest and the patients were then genotyped with the DASH-technique (Dynamic Allele Specific Hybridisation). The ERα PvuII -polymorphism was not associated with any of the investigated parameters. The aromatase (A/G, exon 3 of CYP 19) polymorphism was associated with serum cholesterol (AA 6,69±0,15, AG 6,32± 0,10 GG 6,26±0,13 mmol/L, p=0,02) while no significant association was found with adult height or BMI. In conclusion, the aromatase (A/G, exon 3 of CYP 19) polymorphism is associated with serum cholesterol as demonstrated by increased levels of cholesterol in the AA-genotype compared with the other genotypes.

SU140

A Single Nucleotide Polymorphism of Interleukin-1-receptor-associated kinase Associate with Bone Mineral Densities of Adult Women. R. Ishida*[1], Y. Ezura[1], H. Yoshida*[2], H. Iwasaki*[1], T. Suzuki*[2], T. Hosoi*[3], S. Inoue[4], M. Shiraki*[5], H. Ito*[6], M. Emi*[1]. [1]Molecular Biology, Institute of Gerontology, Nippon Medical School, Kawasaki, Japan, [2]Dept. Epidemiology, Tokyo Metropolitan Institute of Gerontology, Tokyo, Japan, [3]Internal Medicine, Tokyo Metropolitan Geriatric Hospital, Tokyo, Japan, [4]Geriatric Medicine, University of Tokyo, Tokyo, Japan, [5]Research Institute and Practice for Involutional Diseases, Nagano, Japan, [6]Orthopedics, Nippon Medical School, Tokyo, Japan.

Osteoporosis is a multi-factorial common disease, for which combination of genetic factors regulating bone mineral density (BMD) or bone geometry is assumed in pathogenesis. Interleukin-1 (IL-1) is one of the most potent bone-resorbing factors affecting bone mineral status, and a number of factors acting downstream pathways have been reported to influence bone turnover. In the current study, we focused on IRAK1, an important effecter of IL-1 receptor signaling cascade, by analyzing a correlation between two functional polymorphisms and bone mineral densities (BMD) adjusted by age and body mass index. First, significant correlation between IRAK1+587T/C and adjusted BMD (r=0.21, p=0.0017) was observed in 226 postmenopausal women living in a rural area of northern district of Japan. Consistent correlation was observed in independent subject group with 126 postmenopausal women living in the city area of eastern Japan (r=0.23, p=0.011). Furthermore, the correlation was consistent among randomly selected 21 subjects from outpatient clinic of osteoporosis (r=0.43, p=0.054). There was complete linkage disequilibrium between IRAK1+587T/C and IRAK1+1595C/T in our subjects. Although both IRAK1+587T/C and IRAK1+1595C/T result in amino acid change, functional importance of IRAK1+1595C/T is more likely because it resides in the alternatively spliced sequence of IRAK1b that was shown to have prolonged activation of IL-1 signaling in cultured cells. A significant and consistent correlation between genotypes of IRAK1+1595C/T and adjusted BMD both in general postmenopausal women and in patients indicate a widespread involvement of genetic variance of IRAK1 in bone turnover rate in women, which result in the onset of osteoporosis. Possible involvement of genetic variance in IRAK1 gene may explain, at least in part, the pathogenesis of postmenopausal osteoporosis and may contribute to establish a suitable treatment designs and plans for prevention of the disease.

SU141

The Relationship Between Quantitative Calcaneal Ultrasound and Estrogen Receptor Gene Polymorphism in Korean Premenopausal Women. D. Chung[1], D. Cho*[1], H. Kang*[1], M. Chung*[1], J. Park*[2]. [1]Department of Internal Medicine, Chonnam National University Medical School, Gwangju, Republic of Korea, [2]Department of Forensic Medicine, Chonnam National University Medical School, Gwangju, Republic of Korea.

Peak bone mineral density attained during adulthood is a major determinant of the risk for osteoporosis in later life, and it is largely determined by genetic factors. Quantitative calcaneal ultrasound (QUS) has a significant heritable component, and it is a noninvasive method of estimating bone mineral density (BMD) and bone quality. Estrogen is important for attainment of peak bone mass. In this study, we examined the relationship between the PvuII and XbaI polymorphisms in the estrogen receptor (ER) gene and QUS values at the calcaneus in 69 premenopausal healthy Korean women (mean age; 23.0±6.5years). Genotyping for ER polymorphisms was performed using polymerase chain reaction and RFLP methods. The presence of polymorphic sites at the estrogen receptor gene locus were denoted by p and x, whereas absence of these sites were P and X, respectively. Broadband ultrasound attenuation(BUA) and speed of sound (SOS) were measured at the calcaneus and stiffness index(SI) combining both factors were calculated using Achilles+ (Lunar, Madison, WI, U.S.A.). The frequency distribution of ER genotypes were; PP, 8(11.6%), Pp, 37(53.6%), and pp, 24(34.8%), XX, 3(4.3%), Xx, 23(33.3%), and xx, 43(62.3%). When PvuII and XbaI-RFLPs were combined, the frequencies were as follows; ppxx, 24(34.8%), Ppxx, 18(26.1%), PpXx, 19(27.5%), PPxx, 1(1.4%), PPXx, 4(5.8%), PPXX, 3(4.3%). Subjects with PP and XX genotypes tended to have higher stiffness indices than with pp and xx genotypes, but there were no statistical significances (PP, 91.9±12.6, Pp, 86.0±13.6, pp, 81.9±10.8, XX, 91.2±21.2, Xx, 86.2±14.2, xx, 84.3±11.4). These results suggest that ER gene polymorphisms may not be associated with QUS values at the calcaneus in Korean premenopausal women. However, the number of subjects were too small, further study will be needed with larger sample sizes.

SU142

Influence of Genetic Polymorphisms in VDR and COLIA1 Genes on the Risk of Osteoporotic Fractures in Aged Men. D. Álvarez-Hernández*, M. Naves*, I. Santamaría*, J. B. Díaz-López*, A. Rodríguez-Rebollar*, C. Gómez, J. B. Cannata. Servicio de Metabolismo Óseo y Mineral, Hospital Central de Asturias, Oviedo, Spain.

In the last decade, the likely effect of genetic markers related with the appearance and evolution of osteoporosis has been studied mainly in women, with no categorical results. The aim of this study was to assess the influence of genetic polymorphisms of the VDR and COLIA1 genes on the risk of osteoporotic fractures in men. The study population comprised 156 men, aged 64±9 (50-86), randomly recruited for the *EVOS Study*. They underwent several biochemical markers tests and bone mineral density measurements. Prevalent vertebral fractures and incident non-vertebral fractures were identified (the former, at the beginning of the study and the latter during a period of 10 years), as well as several genetic polymorphisms. According to the Genant classification, all fractures ≥2 were considered prevalent vertebral fractures. The analyzed genetic polymorphisms were located on restriction sites *Bsm*I (*B,b*), *Apa*I (*A,a*) and *Taq*I (*T,t*) in the VDR and Sp1 (*S,s*) in the COLIA1. *Bsm*I and *Taq*I polymorphisms did not show differences between fractured and non-fractured men, neither in the prevalent vertebral fractures nor in the incident non-vertebral fractures. *Apa*I polymorphism showed a slight statistical trend. The *aa* genotype would have a smaller prevalence of vertebral fractures [4% (1/25)], than the *Aa* and *AA* genotypes [14.7% (16/109)], p=0.179. These results were similar when the incident non-vertebral fractures were included. Statistical analysis of COLIA1 polymorphism and fractures (prevalent vertebral and incident non-vertebral) are shown in the table. The percentage of fractures was significantly higher in the *ss* genotype, with relative risk RR=7.64 and confidence interval CI=2.02-28.8 with respect to the other group, *S-*. This risk increased when incident non-vertebral fractures were included (RR=8.56, CI=2.32-31.5).

	PREVALENT VERTEBRAL FRACTURES	PREVALENT VERTEBRAL FRACTURES + INCIDENT NON-VERTEBRAL FRACTURES
GENOTYPE	**FRACTURE FREQUENCY***	**FRACTURE FREQUENCY****
S-	9.8% (12/122)	12.3% (15/122)
ss	45.5% (5/11)	54.5% (6/11)

* p= 0.003 and ** p=0.001

Results from COLIA1 polymorphism did not improve when data from other polymorphisms were added. Additionally, there were no significant differences either in lumbar or in femoral neck densitometry for any genetic polymorphism analyzed. These results show that in men, ss genotype of COLIA1 polymorphism could be the best osteoporotic fracture risk genetic predictor, independently of bone mass values.

SU143

A Common Polymorphism in the Methylenetetrahydrofolate Reductase (MTHFR) Gene Is Associated with Quantitative Ultrasound in Those with Low Plasma Folate. R. R. McLean[1], D. Karasik[1], J. Selhub*[2], K. L. Tucker[2], J. M. Ordovas*[2], S. Friso*[2], L. A. Cupples*[3], P. F. Jacques*[2], D. P. Kiel[1]. [1]Heb Rehab Ctr for Aged and Harvard Med Sch Div on Aging, Boston, MA, USA, [2]USDA Hum Res Ctr, Tufts Univ, Boston, MA, USA, [3]Biostat Dept, BU Sch of Public Health, Boston, MA, USA.

Our previously reported genome search in the Framingham Study using a quantitative ultrasound (QUS) phenotype found suggestive linkage on chromosome 1pter-1p36.3. This region contains several candidate genes for bone status, including the MTHFR gene. MTHFR catalyzes the conversion of 5,10-methylenetetrahydrofolate to 5-methyltetrahydrofolate, which is used for homocysteine methylation to methionine. Studies show that the homozygous form (TT) of the MTHFR C677T polymorphism (alanine-to-valine substitution) is associated with increased plasma homocysteine levels in individuals with inadequate plasma folate. Thus, we examined whether the C677T MTHFR polymorphism is associated with QUS and if it differs by folate status. We evaluated broadband ultrasound attenuation [BUA (dB/MHz)] of the calcaneus, using the SAHARA Bone Sonometer (Hologic), in 1745 men and women (mean age 60, range 32-86) who were members of the Framingham Offspring Study (1996-2001). Participants were genotyped for C677T alleles using standard PCR, digestion with HinfI, and then electrophoretic resolution of fragments to generate genotypes. Genotype frequencies in our sample were 40%, 46% and 14% for CC, CT, and TT, respectively. Plasma folate was measured using an automated chemiluminescence method. Because the homozygous mutation (TT) was of particular interest, participants were classified into two groups: 1) CC+CT and 2) TT. We used analysis of covariance to compare mean BUA between the two groups and tested for an interaction between C677T group and folate. We controlled for gender, age, BMI, smoking, physical activity, alcohol, calcium, and vitamin D intakes, and estrogen use in women. We found no difference in mean BUA between the two C677T groups [Least square means (LSM): CC+CT=75.6, TT=74.7, p=0.4]. Our test for interaction between C677T group and plasma folate was borderline statistically significant at the p=0.07 level. In the CC+CT group, there was no difference in mean BUA between the 71% of persons with high plasma folate (≥4 ng/ml) and the 29% with low folate (<4 ng/ml) (LSM: high=75.6, low=74.7, p=0.4). However, the TT individuals with low folate (61%) had significantly lower mean BUA (LSM: high=78.4, low=73.3, p=0.03). Our findings support the hypothesis that the association between a common mutation in the MTHFR gene and BUA is dependent upon folate status. Further understanding of the underlying mechanisms for these findings in bone is warranted.

SU144

Development of Genetic Screening Assays for Osteoporosis. D. Greene*, K. Walker*, S. Cayabyab*. Human Genetics, Roche Molecular Systems, Alameda, CA, USA.

Osteoporosis is a common chronic disease that is estimated to result in fractures for one out of every two women over the age of 50 and one out of every 8 men. It is a disease that has been increasing worldwide. There are ways to prevent and treat osteoporosis but it has proven difficult to predict who is most at risk for the disease. Given that the heritability for osteoporosis is estimated to be between 65 and 85%, there is tremendous potential to develop a genetic test that would predict disease. Such a test could be used to identify a subset of patients for more intensive screening (DEXA, qC/T) or in conjunction with such radiographic modalities provide a better estimate of risk and thus provide opportunities for earlier pharmacological intervention. The identification of clinically relevant genetic markers requires three major interacting areas of research - 1: candidate genes culled from basic research in bone physiology, from linkage and family studies, and from animal models, 2: large scale population based association studies to assess the effect of variations in these genes on disease and 3: genotyping platforms to efficiently genotype several thousand samples for several hundred possible variants. At Roche Molecular Systems we have developed several genotyping platforms and strategies for genotyping multiple samples for multiple markers. Phenotypes and candidate genes are selected from the research literature - ranging from basic research into bone physiology to linkage and family studies of osteoporosis. Genes are also selected based on genetic research in experimental animals. SNPs in these genes are taken from public databases and from our in house SNP discovery program. Selected SNPs are tested via real time PCR (or kinetic thermal cycling) in individuals and in pools of individuals. These tests provide information as to whether an association may be present and whether it should be pursued further. The SNPs that appear most promising are then put into an immobilized probe linear array assay. These assays, where a multiplex PCR product is hybridized to immobilized probes on nylon membranes, are used to interrogate up to 100 targets simultaneously. The simultaneous genotyping of many candidate SNPs can be achieved quickly and inexpensively.

SU145

Regulatory Polymorphisms of the COLIA1 Gene and Susceptibility to Fracture. F. E. A. McGuigan[1], T. L. Stewart*[1], S. C. Main*[1], N. Garcia-Giralt*[2], A. Diez-Perez*[3], D. Grinberg*[2], S. H. Ralston[1]. [1]Medicine & Therapeutics, University of Aberdeen, Aberdeen, United Kingdom, [2]Genetics, Universitat de Barcelona, Barcelona, Spain, [3]URFOA-IMIM, Hospital del Mar, Universitat de Barcelona, Barcelona, Spain.

Previously we have shown that the Sp1 binding site in the first intron of the COLIA1 gene is important for regulation of the gene. Alterations in this site result in allele-specific differences in transcription of the gene leading to reduced mineralisation and bone strength in some patients. Recently, two novel polymorphisms have been identified in the upstream promoter region of the COLIA1 gene at positions -1663 (T insertion/deletion) and -1997 (G/T substitution). This region of the promoter is known to play an important role in the regulation of COLIA1 expression. In a Spanish study of postmenopausal women, these polymorphisms showed a significant association with BMD. They were also found to be in linkage disequilibrium with the Sp1 polymorphism and all three polymorphisms interacted to predict BMD. The aim of our investigation was to further investigate the role of the promoter and Sp1 polymorphisms in the pathogenesis of osteoporosis using a case-control study of 149 postmenopausal Scottish women with and without vertebral fractures. There was no significant association between -1997 G/T and fracture (p=0.7). There was a non-significant trend towards association between -1663 DelT and fracture, with over-representation of the T7/T7 genotype in fracture cases (p=0.25). We found a significant association between the Sp1 polymorphisms and fracture, with over representation of the G/T and T/T genotypes in fracture cases (p=0.04). Haplotype analysis showed evidence of strong LD between all three polymorphisms (-1997G/T and -1663DelT, (p=0.008) for -1997 G/T and Sp1, (p=0.0081) and for -1663DelT and Sp1, (p<0.0001). Association analysis also showed a highly significant association between Sp1 / -1663 DelT haplotype and fracture, such that individuals carrying -1663T7 and Sp1 "T" alleles were greatly over-represented in the fracture cases (OR 6.1 [2.6-14.1]). In conclusion, this study confirms the allelic association between COLIA1 promoter polymorphisms and fracture and LD between the promoter and Sp1 polymorphisms. Further work is necessary to confirm the relationship between these polymorphisms and COLIA1 gene regulation.

SU146

Allelic Variation at the Insulin-Like Growth Factor I Receptor (IGF1R): Associations With Body Size and Bone Mass in Men. J. M. Zmuda[1], J. A. Cauley[1], M. E. Danielson[1], R. E. Ferrell*[2]. [1]Epidemiology, University of Pittsburgh, Pittsburgh, PA, USA, [2]Human Genetics, University of Pittsburgh, Pittsburgh, PA, USA.

Height is a highly heritable trait, but very little is known about the genetic regulation of height. Insulin-like growth factor I (IGF-I) is a major determinant of linear bone growth and skeletal mass, and IGF-I action is mediated via the IGF-I receptor. In the present study, we tested the hypothesis that common allelic variation at the IGF-I receptor (IGF1R) locus is associated with measures of height and bone mass in 330 community-dwelling Caucasian men (age 66±7 yrs, mean±SD; range, 51-84 yr). BMD was measured at the hip and whole body with dual energy X-ray absorptiometry (Hologic QDR). Men were genotyped for a synonymous G-to-A single nucleotide substitution in exon 16 of the IGF1R gene. We found a significant monotonic increase in reported height at age 25 yr with increasing copies of the A allele (Table). Men with the A/A genotype were 3.2 cm or 0.5 standard deviations taller than men with the G/G genotype (P<0.01), and IGF1R genotype explained 3.2% of the total phenotypic variation in height. Similar results were observed for current standing height measured in the clinic with a stadiometer. In contrast, there was no significant association between this IGF1R polymorphism and femoral neck BMC, area or BMD. We found similar results for femoral neck BMAD, an estimate of volumetric density, and whole body BMD, and similar results after adjusting for age, weight and height (not shown). We conclude that allelic variation at the insulin-like growth factor I receptor locus may contribute in part to the genetic control of linear bone growth among men.

Table. Association between IGF1R Genotype, Height and BMD in Men.

	IGF1R Genotype			
	G/G	G/A	A/A	P (ANOVA)
No. of Men	113	166	51	
Height at age 25 yr (cm)	175.4 (6.3)	176.9 (6.0)	178.6 (4.6)	.005
Current Height (cm)	172.4 (6.8)	174.1 (6.1)	175.2 (5.0)	.016
FN BMD (g/cm^2)	.76 (.13)	.77 (.12)	.79 (.14)	.455

Values are mean (SD).

SU147

Vitamin D Response Element In TNF-alpha Promoter. I. Hakim*[1], Z. Bar-Shavit[2]. [1]Exerimental Medicine, Hebrew University, Jerusalem, Israel, [2]Experimental Medicine, Hebrew University, Jerusalem, Israel.

1,25-Dihydroxyvitamin D3 (VD) has been shown to modulate the synthesis and release of the cytokine TNF-alpha. We examine here if the increased abundance of TNF-alpha mRNA observed following VD treatment is due to increased transcript stability and/or synthesis. Analyses of RNA extracted from murine bone marrow derived macrophages (BMMs) revealed no change in TNF-alpha transcript stability in response to VD treatment. Next, we analyzed the promoter region (1.2 kb) of the TNF-alpha gene for potential vitamin D response elements (VDREs), and identified six sequences which could potentially serve as VDREs. The different core binding sites were spaced by one to six nucleotides (DR1-6, respectivily). To determine whether these potential VDREs are functional, we performed gel shift assays (EMSAs) with nuclear proteins obtained from BMMs. Similar to most characterized VDREs, the DR3-type VDRE (located 1008 to 994 base pairs upstream to transcription initiation) was found to be the most effective. The binding activity to this DR3 was ligand-dependent: an induction was observed following BMMs treatment with VD; while no induction was observed with 9-cis-retinoic acid, this retinoid further enhanced the activity of VD when added together. The specificity of the binding was demonstrated by the effective competition of unlabeled DR3 and of previously characterized VDREs found in the mouse osteopontin or in the rat osteocalcin promoters. A mutataed VDRE sequence from the osteocalcin promoter failed to compete with the DR3. The other potential VDREs found in the cytokine promoter exhibited various degrees of competition. We observed super-shift of the BMMs nuclear extract-DR3 complex in the presence of either antibodies to vitamin D receptor (VDR) or to retinoid X receptor (RXR). Our data suggest that VD increases TNF-alpha transcript abundance in BMMs via a transcriptional mechanism. The receptor complex interacting with the VDRE found in the promoter of the cytokine gene is probably composed of VDR-RXR heterodimer.

SU148

Microarray Analysis of mRNA Gene Expression of the Age-Related Delay in Fracture Healing in Rats. R. A. Meyer, B. R. Desai*, M. H. Meyer. Department of Orthopaedic Surgery, Carolinas Medical Center, Charlotte, NC, USA.

Genes active in the control of fracture healing are not well understood. Young rats heal fractures in four weeks while six-month-old rats require 10 weeks. Thus, genes regulating this process may be identified by their longer up-regulation in adult rats compared to that of young rats. To examine this, 6- and 26-week-old female Sprague-Dawley rats were subjected to mid-diaphyseal femoral fracture with intramedullary fixation. The fracture callus was collected at 0, 1, 2, 4, or 6 weeks after fracture. RNA was extracted and pooled between animals to create one sample for each time point for each age for a total of 10 arrays. cRNA was prepared and hybridized to Affymetrix U34A GeneChip arrays. Of the 8,700 genes on each array, 5,200 genes were scored as absent, and 3,300 as present. Of these, 1,155 were significantly up-regulated, and 927 were significantly down-regulated at 2 weeks after fracture in the adult rats. Up-regulated genes included cytokine and matrix genes for both cartilage and bone. Down-regulated genes included genes related to blood cell synthesis. The hematopoietic marrow may have been displaced by callus. Down-regulated genes also included mitochondrial genes. This may have been caused by the disruption to the local blood supply resulting in an increased anaerobic metabolism in the fracture callus. The data from genes previously studied by RT-PCR (Meyer *et al*., Bone 28: S205, 2001) were similar to the microarray data. Most genes with significantly altered mRNA expression had not been previously identified as participating in fracture healing. Cluster analysis was done with the self-organizing map (SOM) algorithm of the Data Mining Tool (Affymetrix). Clusters were identified with genes more strongly up-regulated in the adult rats than in the younger rats. This suggested partial resistance in the adults and the need for higher levels of expression to effect healing. Other clusters identified genes up-regulated by fracture in the young rats but not in the adults. This suggested loss of function in the adult that may also delay healing. In conclusion, skeletal fracture led to changes in RNA expression in many genes, most of which were not known to participate in the healing process. Cluster analysis revealed differential expression between the two ages that may have contributed to the slowing of the healing process in the adult animals.

SU149

Diverse Effects of Pleiotrophin on Bone Morphogenetic Protein-2 Induced Ectopic Osteogenesis. Y. Sato*[1], H. Takita*[2], N. Ohata*[1], M. Tamura[2], Y. Kuboki*[2]. [1]Department of Oral Functional Science,Graduate School of Dental Medicine, Hokkaido University, Sapporo, Japan, [2]Department of Oral Health Science,Graduate School of Dental Medicine, Hokkaido University, Sapporo, Japan.

Elucidation of molecular mechanisms controlling osteogenesis and growth factors in their processes has been one of the major subjects in bone biology. Pleiotrophin (PTN) is a heparin-binding, developmentaly regulated protein which found in brain, uterus, bone and cartilage. Recently bindings of N-syndecan and RPTP beta/zeta of the transmembrane receptor by PTN has been reported to enhance a migratory response in osteoblasts. We have already isolated PTN from bovine bone and have shown that it stimulated osteoblastic growth and differentiation (Biochem Biophys Res Commun, 186, 1288-1293, 1992). Further details of the function of PTN in bone tissue, however, have not been fully clarified. In this study, we examined the effects of PTN on bone morphogenetic protein (BMP)-induced ectopic osteogenesis. Recommbinant human BMP (rhBMP)-2 (1.2 µg) was combined with a carrier of fibrous glass membrane that had been established as an effective carrier. Various amounts of the purified bovine PTN or rhPTN were added to the rhBMP-2/carrier composites and implanted rats subcutaneously. The amount of bone induced in the system was increased with the addition of 10 µg of purified PTN or rhPTN. Alternatively, the amount of bone decreased with the addition of 50 or 100 µg of purified PTN dose-dependently, as judged by the alkaline phosphatase activity and calcium contents in the retrieved implants. Moreover, soft X-ray examination and histological analyses of the implants revealed that the addition of 10 µg of purified PTN or rhPTN induced more newly bone compared to the control. These findings demonstrated that PTN regulates BMP-induced ectopic osteogenesis and the PTN may be involved the regulation of osteoblastic differentiation and function in bone matrix.

SU150

Differential Mechanisms of IL-6 Induction by PTH and TNFα in Osteoblasts. J. Dai, X. Chen*, E. M. Greenfield. Orthopaedics, Case Western Reserve University, Cleveland, OH, USA.

We have previously shown that PTH and TNFα induce IL-6 mRNA expression and IL-6 protein secretion in MC3T3-E1 cells with distinct kinetics. Thus, while both PTH and TNFα induce IL-6 mRNA and protein rapidly, the effects of PTH are transient and the effects of TNFα are sustained for at least 24 hours. As a result, TNFα induces accumulation of 5-10 fold more IL-6 protein than does PTH after exposure for 24 hours. We have now extended these finding by showing that RANKL mRNA is induced by PTH and TNFα with kinetics similar to that of IL-6 mRNA. We have also further confirmed the relationship between IL-6 mRNA expression and IL-6 protein secretion by examining the effect of PTH in combination with IBMX. As expected, 10 nM PTH plus 100 μM IBMX induces high levels of cAMP (3-5 pmol/2 cm^2 well vs. 0.5-1 pmol/2 cm^2 well) for the duration of the experiment (4 hours). In contrast, IL-6 mRNA and protein are still induced transiently by PTH plus IBMX; however, IL-6 mRNA and protein are potently induced for 2 hours rather than for 1 hour as is observed in response to PTH alone. This increased secretion of IL-6 protein results in a 4-fold increase in the amount of IL-6 that accumulates in the culture media (169 pg/ml vs. 44 pg/ml, $p<0.0001$). Other investigators have shown that stimulation of IL-6 mRNA expression and protein secretion in osteoblasts after 24 hours of exposure to TNFα depends on activation of p38 MAPK. We therefore tested whether the effects of p38 occur during the early, rapid phase and/or the later, sustained phase of IL-6 induction by TNFα. We found that 1-10 μM SB202190, a specific p38 inhibitor, dose dependently blocks induction of IL-6 protein during both the rapid (0-6 hours) and sustained phases (12-24 hours). In contrast, the inactive analogue, SB202474, had much less effect on either phase of IL-6 induction by TNFα. Taken together, our results further characterize the differential mechanisms by which PTH and TNFα induce IL-6 expression in osteoblasts.

SU151

Lactoferrin Is a Potent Osteoblast/Chondrocyte Growth Factor, Inhibits Osteoclastogenesis, and Is Anabolic to Bone *In Vivo*. J. Cornish[1], K. E. Callon[1], T. Banovic*[1], U. Bava*[1], M. Watson*[1], Q. Chen*[1], K. Palmano*[2], N. W. Haggarty*[2], A. B. Grey[1], I. R. Reid[1]. [1]Medicine, University of Auckland, Auckland, New Zealand, [2]New Zealand Dairy Research Institute, Palmerston North, New Zealand.

Lactoferrin is an 80kD iron-binding glycoprotein present in breast milk, epithelial secretions, and the secondary granules of neutrophils. It circulates at 2–7 μg/ml, and has multiple postulated biological roles, including regulation of iron metabolism, immune function and embryonic development. We have demonstrated lactoferrin to be an anabolic factor in bone. *In vitro*, lactoferrin stimulates the proliferation of primary fetal rat osteoblasts, osteoblast-like cell lines and primary ovine chondrocytes at concentrations above 0.1 μg/ml. The magnitude of this effect exceeds that observed in response to other skeletal growth factors such as IGF-1 and TGFβ. DNA synthesis is also stimulated in murine neonatal calvarial organ culture, likely reflecting the proliferation of cells of the osteoblast lineage. Iron-depleted lactoferrin is considerably less potent as an osteoblast mitogen than iron-loaded lactoferrin. Lactoferrin is also a potent osteoblast survival factor. In TUNEL and DNA fragmentation assays, lactoferrin decreased apoptosis induced by serum withdrawal by up to 70%. Lactoferrin activates MAP kinase signaling in osteoblasts in a dose-dependent manner at concentrations of 1-100μg/ml. Lactoferrin also has powerful effects on osteoclastogenesis, decreasing osteoclast development at concentrations >1 μg/ml in a murine bone marrow culture system. However, lactoferrin did not alter bone resorption in calvarial organ culture, suggesting that it does not influence mature osteoclast function. *In vivo*, local injection of lactoferrin in adult mice resulted in increased calvarial bone growth, with significant increases in bone area and dynamic histomorphometric indices of bone formation after only 5 injections. Taken together, these data demonstrate that the naturally-occurring glycoprotein lactoferrin is anabolic to bone *in vivo*, an effect which is consequent upon its potent proliferative and anti-apoptotic actions in osteoblasts, and its ability to inhibit osteoclastogenesis. Lactoferrin may therefore have a physiological role in bone growth, and a potential therapeutic role in osteoporosis.

SU152

A Functional Role for Heat Shock Factors in the Transcriptional Regulation of Human RANK Ligand Gene Expression in Stromal/Osteoblast Cells. J. L. Roccisana*, M. Koide, G. D. Roodman, S. V. Reddy. Medicine, University of Pittsburgh, Pittsburgh, PA, USA.

RANK ligand (RANKL) is a critical osteoclastogenic factor that is expressed on stromal cells and osteoblasts. Most resorption stimuli induce osteoclast formation by modulating RANKL gene expression in stromal/osteoblast cells. In addition, cellular stress has been implicated in osteoclastogenesis. However, it is unclear how these stimuli modulate RANKL gene expression in the bone microenvironment. To characterize the transcriptional control of human RANKL gene expression in stromal/osteoblast cells, we PCR amplified and cloned a 2 kb 5'-flanking sequence of the RANKL gene, using normal human osteoblast derived genomic DNA as a template. Sequence analysis identified the presence of several potential Heat Shock Factor (HSF) responsive elements (HSE) in the human RANKL gene promoter region. Co-expression of HSF-1 or HSF-2 with the RANKL gene promoter-luciferase reporter plasmid in human osteoblastic cells demonstrated a 2-fold and 4.5-fold increase in promoter activity respectively. RT-PCR analysis for HSF-1 and 2 mRNA expression in human bone marrow cells, stromal cells (SAKA) and MG-63 osteoblast cells detected only HSF-2 expression. Expression levels of Heat Shock Proteins (HSP) mRNAs, which modulate HSF activation, were then analyzed. RT-PCR analysis demonstrated HSP-70 and HSP-90 mRNA expression in human bone marrow cells, a normal marrow stromal cell line (SAKA) and MG-63 cells. In contrast, HSP-27 mRNA was not expressed in bone marrow mononuclear cells. However, low levels of HSP-27 mRNA were detected in SAKA cells and osteoblastic cells. These data suggest that activation of HSF may play an important role in modulating RANKL gene expression in stromal/osteoblast cells.

SU153

Effects of IL-1beta and LPS on CTGF Expression in Mouse-derived Odontoblast-like Cells, MDPC-23. W. Sonoyama*, T. Kuboki*, T. Fujisawa*, T. Eguchi*, J. Uehara*, H. Yatani*, M. Takigawa. Okayama University Graduate School of Medicine and Dentistry, Okayama, Japan.

Dental caries is an infection disease that eventually leads to pulp inflammation. To protect the pulp tissue from severe inflammation, acceleration of the dentine matrix formation by odontoblasts takes place toward the pulp cavity. We have previously reported that connective tissue growth factor (CTGF) was up-regulated during reparative dentinogenesis in rat molars pulp. However, the up-regulation mechanisms of this factor are still unknown. The purpose of this study was to investigate the effects of interleukin-1beta (IL-1beta) and Escherichia coli lipopolysaccharide (LPS) on CTGF gene expression in odontoblast-like cells in vitro. MDPC-23, mouse-derived odontoblast-like cells were used in this study (Hanks et al., Connect Tissue Res, 1998). The cells were cultured in alpha-MEM supplemented with 10 % FBS until confluent. Total RNA was isolated from MDPC cells cultured for 12 and 24 hours with IL-1beta (0.1 ng/ml), or LPS (5 microg/ml) in alpha-MEM without FBS. Changes in CTGF and TGF-beta1 genes expression were examined by RT-PCR using each primer set by an unsaturated cycle number of amplification. The amounts of RT-PCR products were compared to that of 18S rRNA, and relative expression ratios were obtained. Next, the cells were cultured with recombinant CTGF (rCTGF, 50 ng/ml) for up to 3 days, and MTT assay was performed to examine the cell proliferation. Then, the cells were cultured under condition for mineralization (with ascorbic acid and beta-glycerophosphate) with or without rCTGF (50 ng/ml), and alkaline phosphatase (ALPase) activity was monitored according to the method described by Bassey et al. (1946) with some modifications. Interestingly, the MDPC-23 cells were expressing CTGF and TGF-beta1 genes. IL-1beta stimulation accelerated the CTGF gene expression to 1.2 and 1.7 times 12 and 24 hours after the stimulation, respectively. On the other hand, the TGF-beta1 gene expression was decreased to 0.4 times after 24 hours from IL-1beta stimulation. LPS stimulation increased the CTGF gene expression to 1.3 times, and decreased TGF-beta1 gene expression to 0.5 times after 24 hours. However, rCTGF had no obvious effects on proliferation and ALPase activity. These results indicate that the odontoblast-like (MDPC-23) cells are expressing CTGF and TGF-beta, and also indicated that both IL-1beta and LPS increased CTGF gene expression and decreased TGF-beta1 gene expression in the odontoblast-like cells within one-day period after stimulation.

Disclosures: ***W. Sonoyama****, Grant-in-Aid for Scientific Research (#12470418) from the Ministry for Education, Science, Sports and Culture of Japan 2.*

SU154

Relationship Between Bone Density and Circulating Leptin Levels in Dietary Restricted Male Rhesus Monkeys. R. J. Colman[1], N. Binkley[2], R. Weindruch*[2]. [1]Primate Research Center, University of Wisconsin, Madison, WI, USA, [2]Department of Medicine, University of Wisconsin, Madison, WI, USA.

There is increasing evidence that leptin, the circulating hormone product of the obese gene, is more than an energy-regulating, body fat-related hormone. It has been implicated in reproduction, endocrine function, angiogenesis, hemopoieses, immune function, and brain development . Moreover, studies have long shown that obesity protects against osteoporosis and both bone mass and peripheral leptin concentration are related to body fat mass. More recently, studies have revealed a relationship between leptin and bone mass independent of body fat mass. As part of a long-term, multidimensional study of the effects of moderate (30%) dietary restriction (which retards the aging process in laboratory rodents) on aging, we explored the relationship between bone density and circulating leptin concentration in adult male rhesus monkeys (Macaca mulatta). At the time of data collection animals were between 13.9 and 20.0 years of age (mean = 15.5 years, sem = 0.4) and had been dietary restricted for 72 months. Animals were divided into control (C, n=14) and restricted (R, n=12), and analyzed for body composition and bone density (of the total body and lumbar spine) by dual-energy x-ray absorptiometry (DXA), and had fasting plasma drawn for leptin analysis. Plasma leptin concentration was 71% lower ($p<0.0001$), and body fat mass 78% lower ($p<0.0001$) in R compared to C animals. Additionally, total body ($p<0.02$) and lumbar spine ($p<0.0005$) BMD were lower in R compared to C animals. Stepwise multiple regression analysis revealed circulating leptin concentration to be a better predictor than body fat for both total body and lumbar spine BMD in C animals. However, circulating leptin concentration was not related to BMD in R animals. The lower body fat, circulating leptin concentration, and BMD associated with dietary restriction is as found previously. However the stronger relationship of leptin concentration than fat mass with BMD in the C animals, with no relationship between leptin and BMD in the R animals is a new finding. Further elucidation of the mechanism(s) involved in these differing relationships may prove informative in understanding the relationship of leptin to bone mass.

SU155

Endothelin-1 Modulates the Expression of Vascular Endothelial Growth Factor Associated with Osteoprogenitor Proliferation and Differentiation. C. J. H. Veillette*, H. P. von Schroeder. Surgery, University of Toronto, Toronto, ON, Canada.

Endothelin-1 (ET-1), a peptide produced by vascular endothelial cells (VECs), is implicated in the signaling between VECs, osteoblasts, and osteoclasts in bone development, remodeling and repair. Vascular endothelial growth factor (VEGF) also plays an important signaling role in these intercellular interactions and osteoblast derived VEGF has been implicated in various paracrine functions including osteoblast differentiation, osteoclast formation and angiogenesis. The goals of the present study were to determine the effect of ET-1 on the mRNA expression and protein production of VEGF isoforms during osteoprogenitor cell proliferation and differentiation in osteoblastic cells derived from fetal rat calvariae. Primary fetal rat calvaria (FRC) cells were seeded at a density of 4000 cells/cm^2 and cultured in the presence or absence of ET-1 (10^{-8}M) with each medium change for up to 18 days. Four, 7, 10, 14 and 18 days after plating, RNA was isolated and reversed transcribed into cDNA. Equal amounts of cDNA from each sample were subjected to PCR using specific primers to amplify the splice variants of rat VEGF-A. VEGF-A protein in the conditioned medium was analyzed using an ELISA. In addition, FRC cells from 7 or 14-days of culture were incubated in serum-free medium with or without ET-1 for up to 36 hours prior to harvesting total RNA and conditioned medium. RT-PCR and ELISA assessed the time and dose dependent responses to ET-1 on VEGF mRNA expression and protein production, respectively. Three VEGF mRNA isoforms were identified in osteoblastic cell populations from FRC cells, corresponding to VEGF120, 165 and 188 isoforms. The predominate isoforms, VEGF 120 and 165, were expressed highest at day 4 and day 18 with a decrease in expression at day 10. ET-1 markedly down-regulated VEGF expression and sustained the down-regulation in long-term cultures over time (ANOVA $p<0.001$). ET-1 inhibited VEGF mRNA expression by up to 2 fold by 3 hours after incubation in 7- and 14- day FRC cells. VEGF-A protein secretion was inhibited by ET-1 in a dose-dependent manner; with a maximal effect at 10^{-7} M. ET-1 (10^{-8}M) inhibited VEGF protein secretion after 24 hours by 5.8 fold ($p<0.01$) and 2.8 fold ($p<0.01$) in 7- and 14- day FRC cells, respectively. Our results show that ET-1 may play an important role in the regulation of osteoblast-derived VEGF and limit the paracrine actions of VEGF on endothelial cells, osteoblasts and osteoclasts during bone remodeling.

SU156

Mechanisms of Calcium Signaling in Human Bone Marrow-Derived Stromal Cells. N. R. Jorgensen[1], S. C. Teilmann*[1], Z. Henriksen*[1], R. Civitelli[2], O. H. Sorensen[1], T. H. Steinberg*[2]. [1]Osteoporosis Research Clinic, Copenhagen University Hospital Hvidovre, Hvidovre, Denmark, [2]Washington University School of Medicine, St. Louis, MO, USA.

In vitro, bone cells propagate intercellular calcium waves (ICW) in response to mechanical stimuli. We have previously demonstrated that osteoblastic cells can propagate these waves by two different mechanisms. One is by autocrine action of ATP on purinergic P2Y receptors and occurs in the osteoblastic cell line UMR 106-01, while the other is dependent on gap junctional communication mediated by connexin 43 (Cx43), and occurs in another osteoblastic cell line, ROS 17/2.8. In human bone marrow-derived stromal cells (BMSC) both mechanisms occur, as these cells express both the gap junctional protein Cx43 and P2Y receptors. In the current studies we investigated the mechanism for the propagation of gap junction-mediated ICW in BMSC. Calcium concentration measurements were performed using video imaging and the Ca^{2+} indicator dye fura-2. ICW were elicited by mechanically stimulating single BMSC in monolayers, which caused fast ICW that spread to many cells. Adding ATP or UTP to the medium elicited calcium transients and also desensitized cells so that mechanical stimulation no longer caused a fast ATP-mediated ICW. Instead, mechanical stimulus caused a slower gap junction-dependent calcium wave that spread to only a few cells, as seen in ROS cells. These ICW required influx of extracellular calcium, but not release of calcium stores, and did not occur after plasma membrane depolarization by addition of extracellular potassium. In addition, low micromolar concentrations of the L-type voltage-gated calcium channel antagonist nifedipine totally blocked the propagation of ICW. To confirm that gap jucntion-dependent ICW in osteoblastic cells are mediated by L-type calcium channels, we performed similar experiments in UMR cells that had been transfected to express Cx43 (UMR/Cx43). After desensitization of P2 receptors, parent UMR cells do not propagate ICW, but UMR/Cx43 cells propagated slow calcium waves which were again inhibited by 1 uM nifedipine. Thus, BMSC propagate intercellular calcium signals in response to mechanical stimuli. These waves are propagated from cell to cell either by autocrine action of ATP on P2 receptors or by Cx43-mediated gap junctional communication and activation of L-type voltage gated calcium channels. These studies highlight the role of L-type calcium channels in the coordination of calcium responses among osteoblasts, and suggest that modulation of channel activity might influence bone turnover.

SU157

Fluid Shear of Very Low Magnitude Stimulates Growth and Improves Anchorage of Human Osteoblastic Cells *in Vitro*. C. Kasperk[1], B. Bundschuh*[1], U. Sommer*[1], B. Schweizer*[2], A. Lieder*[1], L. van den Heuvel*[1], S. Soezeri-Ludwig*[1], M. Holl*[1], P. Nawroth*[1], I. Boercsoek*[1], U. M. Liegibel*[1]. [1]Dept. of Medicine, Ruprecht-Karls-University, Heidelberg, Germany, [2]Institute of Applied Mathematics, Ruprecht-Karls-University, Heidelberg, Germany.

Mechanical loading of bone is crucial for the maintenance of normal bone architecture and may be transmitted to osteoblasts via shear stress by interstitial fluid flow. We applied very small fluid shear stress (1-63 µPa for 10-48 h) to primary human osteoblastic cells (HOC) *in vitro* to characterize proteins involved in translating physical force of low magnitude into a cellular response. The impact of very small fluid shear stress on bone cell metabolism may be of physiological significance in situations with pulsating fluid flow within the Havers‘ channels caused by blood pressure waves within the Havers‘ arteries. Very low shear stress by interstitial fluid shifts also occurs when the hydrostatic pressure within the blood vessels is disturbed by changes of the body position in space or by changes of bone perfusion. We demonstrate that fluid shear of very low magnitude significantly stimulated proliferation of HOC when stress was applied intermittently. Despite stimulating HOC proliferation, very low shear stress also increased differentiated cellular properties such as ALP activity, fibronectin (FN) and fibronectin receptor (FNR) production. TGFβ1+2 neutralizing antibodies and the presence of indomethacine inhibited the mitogenic action of fluid shear on HOC and the positive effects on differentiated functions. Furthermore, TGFβ1+2 dose-dependently increased the production of PGE_2, FN and FNR in HOC cultures. Therefore, the growth factor TGFβ is a physical stress responsive cytokine, regulating HOC proliferation and increasing the production of FN and FNR. In conclusion, fluid shear of very low magnitude possibly induced by arterial pulse waves in enclosed bone compartments or by centrifugal forces enhances osteoblastic proliferation and anchorage of bone cells within the bone matrix.

SU158

Pressure Induces 25-Hydroxyvitamin D 1-Alpha-Hydroxylase Activity in Macrophages: Implications for Disease. J. L. Berry*[1], S. Mylchreest*[1], J. G Andrew*[2], C. E. Evans*[1], A. P. Mee[1]. [1]Manchester University, Manchester, United Kingdom, [2]Salford Royal Hospital's Trust, Salford, United Kingdom.

The active metabolite of vitamin D, 1,25 dihydroxyvitamin D3 (1,25D), plays an essential role in the maintenance of serum calcium homeostasis and bone remodelling. In addition to renal synthesis of 1,25D (due to the actions of the renal 1-alpha-hydroxylase (1OHase) on 25 hydroxyvitamin D3), 1,25D is also produced in extra-renal sites. Activated macrophages are the source of 1,25D in several diseases, including arthritis, sarcoidosis and tuberculosis. In studies to determine the role of macrophages in hip joint replacement implant loosening, we have previously shown that macrophages respond to physical pressure by secretion of a variety of cytokines (IL-1, IL-6, and TNFalpha) that are known to play a role in bone metabolism. We have now used the same pressure system to examine the expression of 1OHase in macrophages. Isolated human peripheral blood monocytes, cultured for 7 days, developed a macrophage phenotype (CD68 and non-specific esterase positive). Macrophages were subjected to 5psi for 1 hour in a custom-built pressure chamber. Cells were then fixed and analysed for 1OHase mRNA and protein expression by in situ hybridisation (ISH) and immunohistochemistry (IHC). Low levels of 1OHase mRNA and protein (Figure 1A) were seen in non-pressurised macrophages. However, an obvious increase in 1OHase levels was seen at both the mRNA and protein (Figure 1B) level in pressurised macrophages.

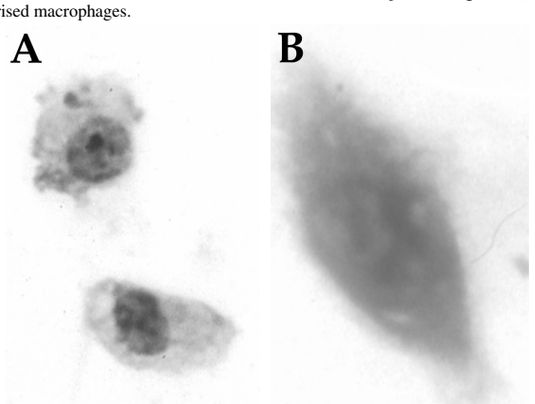

These results show that pressure can induce a dramatic increase in 1OHase expression in macrophages. This has obvious implications for disease states where accumulation of macrophages is associated with local bone remodelling phenomena, such as in joint replacement implant loosening and atherosclerosis.

SU159

The Effects of Different Exercise Modes on the Biomechanical Properties of Growing Bone in Rats. T. H. Huang*[1], R. S. Yang*[1], S. C. Lin*[1], S. S. Hsieh*[2], F. L. Chang*[2], S. H. Liu*[3]. [1]Department of Orthopaedics, National Taiwan University Hospital, Taipei, Taiwan Republic of China, [2]Department of Physical Education, National Taiwan Normal University, Taipei, Taiwan Republic of China, [3]Institute of Toxiology, National Taiwan University, Taipei, Taiwan Republic of China.

During exercising, weight bearing plays an important role in improving the properties of bone material. The effects of non-weight-bearing exercise on bone, such as swimming, are still a controversial issue. In the present study, we designed two typical exercise modes, running and swimming, to investigate their effects on the biomechanical properties of growing bone. Twenty-four rats were randomly assigned into two exercise groups, which were RUN (n=8) and SWIM (n=8), and a control group (CON, n=8). Training program began when the animals were 7 weeks old. During the 8 weeks training session, RUN rats were trained on a level treadmill and the running speed was progressively increased from 12m/min to 22m/min. On the other hand, SWIM rats swam with a weight equivalent to 2%

body weight attached to their tails. The training frequency was 5 days a week. During the training period, exercise groups showed a lower body weight gain. After the end of training session, all the animals were deeply anesthetized and then sacrificed. Femur and tibia were collected for biomechanical three-point-bending testing by using a material testing system (MTS-858). For eliminating the effects of exercise-induced lower body weight gain on bone, one-way analysis of covariance (1-way ANCOVA) was used to compare means among groups and body weight was set as the covariate. In tibial and femoral maximal bending load, two exercise groups were higher than CON group, and SWIM group even showed a significantly higher value in maximal bending load (p= .039) than CON group. However, two exercise groups were significantly lower in tibial yield bending load than CON group (p= .002). In bending stiffness, two exercise groups were lower than CON, though the statistical significance was not reach. Analysis of yield energy showed that two exercise groups were higher in both tibial (p= .031) and femoral (p < .001) yield energy. In conclusion, bone tissues of the two exercise groups showed stronger and more elastic biomaterial properties. Swimming exercise might provide less mechanical loading as weight-bearing exercise so that it usually shows a less effects on improvement of BMD or BMC. However, swimming exercise even show an impressively better maximal load and yield energy in tibia than running exercise in present study. Therefore, non-weight-bearing exercise might have its specially benefits on bone and further study would be valuable to clarify this controversial issue.

SU160

Functional Gap Junctions are Essential for Prostaglandin E_2 (PGE_2) Production by Osteocytes in Response to Mechanical Strain by a Process Independent of Intercellular Channels. X. Wang*[1], E. Sprague*[2], J. X. Jiang[1]. [1]Biochemistry, University of Texas Health Science Center, San Antonio, TX, USA, [2]Radiology, University of Texas Health Science Center, San Antonio, TX, USA.

Connexin 43 (Cx43), a gap junction protein, is highly expressed in osteocytes in bone as well as in the osteocyte-like cell line MLO-Y4 compared to osteoblasts. However, osteocytes are only in contact through their dendritic processes, an extremely small area compared to the total surface area of this cell. These two observations suggest that Cx43 may have other functions in addition to forming intercellular channels between dendritic processes of adjacent osteocytes. Our previous studies using MLO-Y4 cells have shown that shear stress induced by fluid flow increases functional intercellular gap junctions, Cx43 protein, and PGE_2. Furthermore, we have demonstrated that PGE_2 is an essential mediator between mechanical strain and gap junction intercellular communication. However, the importance and role of gap junctions in the production and release of PGE_2 in response to mechanical stress is unknown. In this study, MLO-Y4 cells were plated at various cell densities so that at the lowest densities no cells were physically in contact with adjacent cells thereby preventing the formation of intercellular gap junction channels. These cells were subjected to fluid flow treatment for 2 hrs at 16 dynes/cm^2 and conditioned media assayed for PGE_2. The MLO-Y4 cells with no or few intercellular channels produced significantly more PGE_2 per cell than those at higher density with greater cell to cell contact. PGE_2 production was exponentially increased at the lowest cell density of $1x10^3$ cells/cm^2, compared to the highest cell density of $1.1x10^5$cells/cm^2. β-glycyrrhetinic acid, a specific and reversible gap junction channel blocker that can also block hemichannels, significantly reduced PGE_2 production induced by fluid flow at all cell densities tested, especially cells at the lowest density. Our results suggest that functional gap junctions in the form of hemichannels, instead of intercellular channels, are likely to play an important role in regulating the release of PGE_2 from mechanically treated MLO-Y4 cells. Studies are being performed using Cx43-null MLO-Y4 cells generated using antisense to provide further insight into the potential function of Cx43-formed hemichannels in the response of osteocytes to mechanical stimulation.

SU161

Simulated Microgravity Suppresses Osteoblastogenesis and Decreases Osteoblast Function. M. Zayzafoon, J. M. McDonald. Department of Pathology, University of Alabama at Birmingham, Birmingham, AL, USA.

Space flight is known to induce bone loss of weight-bearing bones. This decrease in bone mass has been attributed to a decline in bone formation without a significant change in bone resorption. Despite numerous studies, the mechanism for this serious condition is still unknown. To determine the effect of microgravity on bone, we utilized the Rotary Cell Culture System (developed by NASA) to simulate microgravity. Calvaria from 5 day old mice were harvested and cultured for 7 days under simulated microgravity. Histologically, we demonstrate a 4-fold decrease in alkaline phosphatase activity and 6-fold decrease in the cortical bone thickness and mineralization in response to simulated microgravity. We also demonstrate that simulated microgravity significantly decreases the expression of alkaline phosphatase (ALP), collagen I and osteocalcin as determined by real time RT-PCR. These results were not due to an increase in osteoblast apoptosis as it is shown by TUNEL staining. To determine the effect of simulated microgravity on osteoblastogenesis we cultured human mesenchymal stem cells (hMSC) grown on plastic microcarrier beads for 7 days in microgravity under osteogenic conditions. A decrease in mineralization was observed with a significant decrease in ALP and collagen I expression. Our preliminary data demonstrate that microgravity decreases the transactivation of Core Binding Factor Alpha 1 (Cbfa1) without any change in its expression in hMSC. Ongoing studies to identify the exact role of Cbfa1 in MSC response to microgravity and the modulation of its target genes are being performed. In conclusion, here we show that osteoblastogenesis in human mesenchymal stem cells and mouse calvaria is decreased in response to microgravity. This results in a decrease in bone mineralization and modulation of osteoblast gene expression. This response is mediated in part by decrease in Cbfa1 activity. Results from this study will increase our understanding of bone biology under microgravity and may lead to developing novel strategies capable of preventing bone loss in future long-term space flights.

SU162

Mechanical Loading and PTH Stimulation of DNA Synthesis. J. A. Barry*, S. J. Tanner*, A. Peyton*, G. R. Haynatzki, D. M. Cullen. Osteoporosis Research Center, Creighton University, Omaha, NE, USA.

Low bone mass that results in osteoporosis causes high morbidity and health care costs. Agents such as mechanical loads or exercise and PTH (parathyroid hormone) have the potential to stimulate bone growth. Although co-treatment with PTH can augment the effects of loading, the mechanism for this interaction is unknown. Our hypothesis was that short term treatment with PTH or loading increases bone cell DNA synthesis, and that combined the effects of loading and PTH are additive. Adult female Sprague-Dawley rats were divided into two injection groups of PTH (80ug/kg, n=4) or Vehicle (n=4). On days 0 and 1, each rat was injected subcutaneously and external loads were applied to the right tibia (35N, 36 cycles, 2 Hz). Bromodeoxyuridine (BRDU 40mg/kg) was administered every six hours throughout the 48-hour treatment period for a continuous label of DNA synthesis. Left (nonloaded) and right (loaded) tibiae were collected, decalcified, embedded in plastic, sectioned, and stained by immunohistochemistry. Differences were analyzed by GLM for repeated measures with significance at P<0.05. In nonloaded legs, PTH compared to vehicle treatment resulted in greater osteoblast and preosteoblast cell numbers and labeling indices. In the vehicle group, loaded legs were 2-3 fold greater than nonloaded legs for osteoblast and preosteoblast cell numbers. Similarly, labeling indices (# BrdU+/total # cells) for osteoblasts and preosteoblasts were 9 and 5 fold greater in loaded than nonloaded legs. There were no differences among loaded legs (PTH vs veh). When treatment was combined with loading, the PTH x Load effect on labeling index was smaller than the Vehicle x Load effects, due to the significant nonloaded leg PTH response. We conclude that individually, loading and PTH are anabolic stimuli for DNA synthesis. After 48 hrs at these loads and doses, the DNA synthesis response was greater for loading than PTH and when combined, PTH did not augment the loading effect. The effects of PTH and loading on preosteoblast DNA synthesis appear redundant.

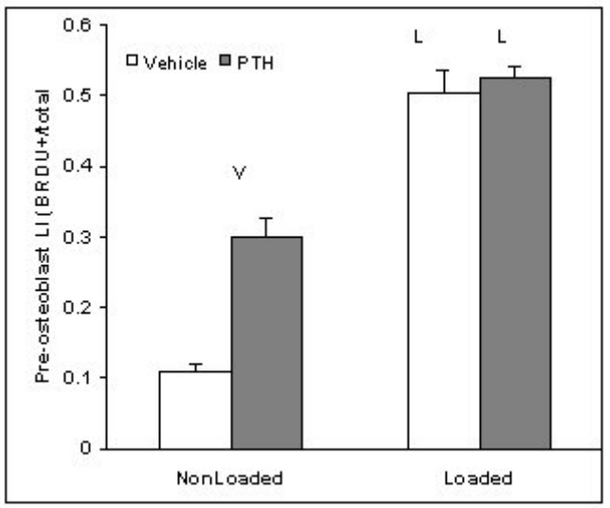

SU163

Suppression of IL1-Stimulated mRNA Expression by Mechanical Shear in Chondrocytes. H. B. Sun*[1], Y. Liu*[2], H. Yokota[2]. [1]Anatomy and Cell Biology, Indiana University School of Medicine, Indianapolis, IN, USA, [2]Biomedical Engineering, IUPUI, Indianapolis, IN, USA.

The specific aims of the current study were (i) to identify the genes whose IL1-stimulated expression in chondrocytes would be suppressed by mechanical shear, and (ii) to build a mathematical model for transcriptional regulation that would help understand the mechanism of suppression of the IL1-induced mRNA expression. A human chondrocyte cell line (C-28/I2) was used in this study and cells were grown under shear at 0-20 dyn/cm2 for 0 – 24 hours in the presence and absence of IL1. We focused on analyzing a family of matrix metalloproteinases (MMPs) together with the proteins expressed in extracellular matrix (ECM), since MMPs play the pivotal role in degeneration of ECM in response to proinflammatory cytokines. The semi-quantitative RT-PCR results show that the mRNA level of MMP-1, MMP-2 and MMP-13 was up-regulated by IL1, and that the elevated mRNA level was decreased by shear stress at 5 dyn/cm2. The effects of shear stress were examined not only at the transcriptional level but also at the proteolytic activity level. The fibril degradation assay using fluorescent substrates for MMPs revealed that collagenase and gelatinase activities were down-regulated by shear stress at 5 dyn/cm2. The shear responses of the family of MMPs in the chondrocyte cells in this study were similar, but not identical, to the shear responses in synovial cells. A higher shear stress was required to alter the expression of MMPs in C-28/I2 chondrocytes than the expression in MH7A synovial cells. The mathematical model for transcriptional regulation predicted involvement of transcription factor motifs such as AP1, AP2, NFkB, NFY, and PEA3 in shear responses as well as IL1 stimulation. The observed suppressive effects of shear stress on MMP expression and activities were additive to the stimulatory effects of IL1. Our study suggested that the molecular mechanism underlying the suppression of MMPs by mechanical shear might contribute to alleviating inflammatory reactions in joint tissue using a signal transduction pathway at least in part independent of IL1 induction.

SU164

Ontogenetic Development of the Ovine Calcaneus: A Model for Examining the Relative Contributions of Genetic, Epigenetic, and Extra-genetic Stimuli. J. G. Skedros, K. J. Hunt, C. L. Sybrowsky*. Dept of Orthop Surg, U of UT, Salt Lake, UT, USA.

Bone morphology may be largely constrained by genetic and epigenetic processes (e.g., via tissue interactions) that govern development along a given growth trajectory. We hypothesize that: 1) structural variations (e.g., trabecular orientation, cross-sectional shape), which dominate in early ontogeny, are primarily genetically/epigenetically derived, and 2) material (e.g., collagen fiber orientation (CFO)) and/or structural variations that appear later in development are primarily environmentally, or "extra-genetically" derived (e.g., as a response to strain transduction or microdamage formation). Because of its highly nonuniform morphologic organization, the ovine calcaneus appears to be a good model for examining mechanisms that mediate the modeling and remodeling processes that produce spatio-temporal developmental variations. Calcanei were obtained from 24 sheep (fetal - adult). In vivo strain data demonstrate that this bone receives relatively simple bending, with prevalent compression in the cranial and tension in the caudal cortex. Geometric measurements included: 1) cranial, caudal, medial, and lateral cortical thickness at 60% 'length', 2) maximum (Imax) and minimum (Imin) 2nd moments of inertia, and 3) cortical area (CA) and total area (TA). Lateral roentgenograms were analyzed for arched trabecular patterns, which may reflect tension/compression stress trajectories. Predominant CFO was determined using circularly polarized light in thin ultra-milled sections. Results showed that although CA/TA and Imax/Imin ratios increased linearly with bone length ($p<0.001$), significant cranial vs. caudal CFO and cortical thickness differences occurred only in the subadult and adult groups. Arched trabecular patterns were identified in fetal bones. The relatively early appearance of preferred trabecular orientation most likely represents programmed development. The 'delayed' temporal development of cross-sectional asymmetry and regional CFO anisotropy probably reflect influences of strain transduction. Mounting evidence suggests that the role of mechanotransduction, especially in the developing skeleton, is to provide the necessary threshold values required for implementation or maintenance of growth patterns that are mediated by modeling processes and guided principally by positional information. In contrast, we speculate that adaptations that are mediated by remodeling activities (e.g., non-uniform CFO patterns) may be more strongly influenced by strain transduction or byproducts of functional loading (e.g., regional or strain-mode-related differences and/or characteristics of microdamage).

SU165

Interactions between Estrogen and Mechanical Strain Effects on Osteoblasts Are not Influenced by Estrogen Receptor Type. T. Thomas[1], F. Lima*[1], M. Lafage-Proust[1], P. van der Saag[2], C. Alexandre[1], L. Vico[1]. [1]Inserm 9901, University Hospital of St-Etienne, Saint-Etienne, France, [2]Netherlands Institute for Developmental Biology, Utrecht, Netherlands.

Estrogens (E) and mechanical strain exert direct effects on osteoblast activity, with good evidence of interactions between their respective effects. Osteoblasts express both forms of estrogen receptors (ER) ERa and ERb, and previous studies have suggested a specific role for each receptor. Therefore, our working hypothesis was that the interactions between E and mechanical strain on osteoblast activity vary depending on which ER is preferentially activated. Using the human osteoblastic cells, U2Os, stably transfected either with ERa or ERb, we evaluated the effects of cyclical cell loading on a F-3000 Flexercell Strain Unit (1.5% elongation, 10 min/day), in presence of estradiol (E2) 10-8 M or not. The U2Os cell lines, either ERa or ERb transfected or the original U2Os cell line which does not express ER, were characterized by low alkaline phosphatase (AP) activity. They expressed all osteoblastic markers but osteocalcin because of a specific gene mutation. In both U2Os-ERa and U2Os-ERb cell lines, mechanical strain induced similar increases in AP activity and gene expression as measured by quantitative RT-PCR (Light Cycler, Roche), and a decrease in type I collagen gene expression. No change in proliferation rate was observed. Strain and E2 had a synergistic effect on AP activity as compared to each stimulus alone. Neither proliferation nor differentiation of the original U2Os cell line, was altered by strain or E2. In summary, the differences observed between the U2Os and the U2Os-ERa or -ERb cell lines are consistent with previous studies suggesting that ER play a critical role in mechanotransduction. However, these data do not support the hypothesis of differing roles for ERa and ERb in these defined experimental conditions. Understanding the mechanisms mediating interactions between estrogens and mechanical strain at the cellular level still requires further investigations.

SU166

Mechanically Related Changes in Gene Expression Using Real Time RT-PCR. M. E. Squire[1], L. R. Donahue*[2], M. Hadjiargyrou[1], C. Rubin[1], S. Judex[1]. [1]Biomedical Engineering, SUNY Stony Brook, Stony Brook, NY, USA, [2]The Jackson Laboratory, Bar Harbor, ME, USA.

Low level mechanical stimuli (<5 microstrain) can be anabolic to bone if induced at high frequencies (30-90 Hz). Conversely, removal of the normal mechanical environment can cause loss of bone tissue. We have recently demonstrated in BALB/cByJ mice that 10 minutes per day of whole body vibration at 45 Hz significantly increased trabecular bone formation rates in the proximal tibia by 34% while hind limb suspension (disuse) decreased bone formation rates by 48%. The identification of key molecular events behind this adaptive process may ultimately lead to the discovery of delivery targets and novel therapeutics for osteoporosis. Using reverse transcription polymerase chain reaction (RT-PCR), we previously characterized the expression of several candidate genes in response to both our anabolic and catabolic stimulus. Here, we tested whether real-time RT-PCR increases the sensitivity of detecting subtle changes in gene expression. Sixteen-week old female BALB/cByJ mice were randomly assigned to control, disuse (tail suspension), and mechanical stimulation groups (n=2 each). Mechanically stimulated mice were placed on a vibrating platform (0.25g, 45 Hz) for 10 min/d, 5 d/wk. After 4 days, RNA was extracted from the whole left tibiae (including bone marrow and cartilage). Real time RT-PCR quantified the expression of the genes coding for collagen type I (α1) and beta-2 microglobulin (beta-2). Mechanical stimulation up-regulated the relative expression (normalized to the housekeeping gene beta-2) of collagen type I by 30% +/- 4.4% (mean +/- SE) while disuse down-regulated the transcriptional levels by 40% +/- 4.8%. These results support our previous findings that collagen type I mRNA levels are rapidly reduced by mechanical unloading. The data also indicate that the expression of the most abundant protein in bone is increased after only 4 days of mechanical vibration, a result that we were unable to observe previously with conventional RT-PCR. Intriguingly, the relative changes in the expression of collagen type I as induced by low level mechanical vibration and disuse accurately reflected the relative changes in trabecular bone formation rates. In summary, this study indicates the superior sensitivity of real time RT-PCR in quantifying small changes in molecular expression levels of bone during the mechanically adaptive process. This sensitivity is currently being utilized for detecting subtle changes in the transcriptional level of genes critical for bone formation, resorption and maintenance.

SU167

Mechanical Properties of the Extracellular Matrix Regulate Fluid Shear-Induced Metabolism of Prostaglandins in Osteoblasts. S. M. Ponik, F. Pavalko. Cellular and Integrative Physiology, Indiana University School of Medicine, Indianapolis, IN, USA.

Fluid shear stress (FSS) resulting from mechanical loading of bone in vivo is a potent stimulus for bone cell metabolism. In this study we tested the hypothesis that FSS-induced cell signaling may be regulated by changing the physical state of the extracellular matrix (ECM) or by modulating expression of integrin adhesion molecules, which link the actin cytoskeleton to the ECM. MC3T3-E1 osteoblasts were cultured on fibronectin or collagen that was adsorbed directly onto untreated glass slides or onto poly-L-lysine coated slides. Cells were allowed to rearrange the matrix for 16 hours and then were subjected to 90 minutes of laminar fluid shear. Following FSS, cells were incubated for 30-minutes during which released prostaglandins were allowed to accumulate in 1 ml of cell culture media. Prostaglandin-E_2 (PGE_2) released into the media was analyzed by enzymeimmunoassay. Integrin expression in cells grown on the different matrix proteins was evaluated by immunoprecipitation of biotin labeled cell surface proteins. Cells grown on either untreated glass or glass coated with fibronectin or collagen expressed both the α5 and αv integrin subunit at the cell surface. However, in response to FSS osteoblasts cultured on fibronectin and collagen released more PGE_2 then cells cultured on untreated glass. The α2 integrin subunit was expressed at the cell surface only in cells cultured on collagen, however, the FSS-induced PGE_2 release was not different between cells grown on fibronectin and collagen. This suggests that cells grown on fibronectin or collagen are more responsive to FSS than cells grown on uncoated glass. To further investigate the role of mechanical properties of the ECM in FSS-induced mechanotransduction, glass slides were first coated with poly-L-lysine prior to adsorption of fibronectin or collagen to immobilize the matrix and decrease the ability of osteoblasts to rearrange the ECM. Interestingly, FSS-induced PGE_2 release from osteoblasts cultured on poly-L-lysine-immobilized fibronectin or collagen was significantly decreased compared to cells cultured on fibronectin or collagen adsorbed to untreated glass. These data suggest that limiting the ability of osteoblasts to reorganize the ECM by immobilizing the ECM proteins decreases the cell's ability to respond to FSS.

SU168

Do Bones Have Memory? Glutamate Receptor Expression in Bone. K. M. Black*, B. L. Theriault*, G. I. Anderson. Pharmacology, Dalhousie, Halifax, NS, Canada.

Learning and memory involve both ionotropic and metabotropic glutamate receptors. Glutamate receptors have been identified in the bones of rat, rabbit, and mouse. Mechanical stimulation elicits changes in glutamate receptor expression. We postulate that glutamate receptors mediate mechanical stimulation to increase bone density in a manner analogous to their role in mediating CNS synaptic plasticity. Estrogen modulates glutamate receptor expression in the CNS: we suggest a similar role in postmenopausal osteoporosis. A mouse osteoclast model is being used to characterize the sensitivity of glutamate receptor expression to mechanical stimulation and estrogen levels. In some cultures, glutamate receptor expression has been seen to decrease or disappear during prolonged culture. To validate the use of our osteoclast culture model, we have verified the expression of the glutamate receptor subtypes and examined their sensitivity to mechanical strain. Bone marrow cells were flushed from the femora and tibiae of 7-week old female CD1 mice using a-minimal essential medium, 8 x 106 cells/35mm well were seeded onto collagen-I coated flexible silastic membranes and cultured for 7 days. Cells were mechanically stimulated (1 Hz, 900 cycles) on days 4, 5, and 6 of culture. The presence of glutamate receptor subunits in the cultured cells was analyzed using immunohistochemistry with mouse hippocampus slices as a positive control. After 7 days of culture, sufficient mature multinucleated osteoclasts differentiated from hematopoeitic progenitor cells to permit analysis. The expression of the following glutamate receptor subunits was confirmed in unstimulated multinucleated osteoclasts: NMDAR1, 2A, 2B, 2C; AMPAR1, 2/3, 4; mGluR1a and 5, but not mGluR2/3. The highest expression levels were observed for NMDAR2B and GluR4, suggesting that they play an enhanced role in the transduction of mechanical strain stimulus. Mechanical stimulation did not appear to alter the expression of NMDAR2B, AMPAR2/3, or AMPAR4, but caused decreases in NMDAR1, NMDAR2A, NMDAR2C, AMPAR1, mGluR1a, and mGluR5 expression. Additionally, we observed marked differences in the distribution of the different receptor subtypes: NMDA receptor subtypes 1, 2A, and 2C were mostly expressed in the periphery where podosomes form, further supporting their role mechanotransduction. We postulate that glutamate receptor subunit expression changes with mechanical stimulation and modulates osteoclast responsiveness to osteoblast glutamate signalling. We are currently tracking the mRNA levels of these immunocytochemically observed changes in glutamate receptor subtype expression induced by mechanical stimulation and the effects of varying estrogen levels in this model.

SU169

Hindlimb Unloading Decreases Osteoprogenitor Cell Number and Bone Formation in the Young Male Rat. N. Basso*, Y. Jia*, C. G. Bellows, J. N. M. Heersche. Faculty of Dentistry, University of Toronto, Toronto, ON, Canada.

Several lines of evidence indicate that the decrease in bone mass observed in humans and rats following space flight or mechanical unloading is primarily caused by a disruption in the development of cells of the osteoblast lineage. Using the NASA model of hindlimb unloading (HU) the effects of 14 days of HU on the number of fibroblastic colony forming units (CFU-F), alkaline phosphatase positive CFUs (CFU-AP), and osteoprogenitors (CFU-O) in cell populations isolated from the proximal femur (decreased loading), calvaria (increased pressure), and proximal humerus (normally loaded) of 6 week old male Fischer 344 rats (n=5) was investigated. Histomorphometry and *in situ* hybridization was performed on the proximal tibia to confirm previously reported changes in bone formation parameters following HU. Control rats were pair-fed. Cell populations were obtained from explant cultures and cultured for either 15 or 21 days in the presence of 10nM dexamethasone. The number of CFU-F in cell populations derived from HU and control rats for the 3 bone sites evaluated were similar. CFU-AP were decreased by 31% (19.2±1.7 vs. 13.3±1.2, $p<0.01$) in cells isolated from femur and increased 2-fold (18.7±1.0 vs. 38.7±1.5, $p<0.01$) in cells isolated from the calvaria of HU rats. CFU-O decreased by 77% (510.1±7.1 vs. 119.2±3.4, $p<0.01$) in cells isolated from femur and increased 1.4 fold (73.0±2.5 vs. 102.0±3.1, $p<0.01$) in cells isolated from the calvaria of HU rats. CFU-AP and CFU-O were not significantly different in cells isolated from humerus from either group. Histomorphometric analysis indicated that the major difference between HU rats and controls was a reduction in trabecular bone volume (BV/TV) which was decreased by 26% and 48% in primary and secondary spongiosa, respectively ($p<0.01$). There were also significant decreases in trabecular thickness (Tb.Th) and number (Tb.N), an increase in trabecular separation (Tb.Sp), and no difference in osteoclast number (Oc.N/BS) or surface (Oc.S/BS) in both regions examined. *In situ* hybridization analysis revealed a marked decrease in collagen mRNA content in the primary spongiosa of the proximal tibia of HU rats. In conclusion, cell culture studies illustrate that the number of osteoprogenitors and therefore osteogenic potential is decreased in cells isolated from the proximal femur, is increased in cells isolated from calvaria, and is not changed in the humerus as a result of HU. Histomorphometric evaluation indicates that in the proximal tibia HU results in a decrease in bone deposition in the primary and secondary spongiosa.

SU170

Inhibition of Fluid Shear-induced ATP Release in MC3T3-E1 Osteoblasts Depends Upon the Extracellular Matrix Proteins. D. C. Genetos[1], R. L. Duncan[2]. [1]Cellular and Integrative Physiology, Indiana University School of Medicine, Indianapolis, IN, USA, [2]Orthopaedic Surgery, Indiana University School of Medicine, Indianapolis, IN, USA.

We have previously demonstrated that 12 dynes/cm^2 of fluid shear stress (FSS) applied to MC3T3-E1 osteoblasts produces a number of biochemical responses, including changes in intracellular calcium ($[Ca^{2+}]_i$) and gene expression. However, the mechanisms through which osteoblasts perceive and transduce mechanical signals into biochemical responses remain unclear. The expression in osteoblasts of ATP-activated P2 purinergic receptors that increase $[Ca^{2+}]_i$ may be one such mechanism We hypothesized that an additional osteoblastic response to FSS is the release of ATP. MC3T3-E1 cells were grown to confluence on either type I collagen- (10μg/cm^2) or fibronectin-coated slides (1μg/cm^2) and subjected to 12 dynes/cm^2 laminar flow. Fluid flow was applied in a parallel plate flow chamber using a flow loop to drive the flow medium through the channel of the flow chamber. Media samples were taken at various time points and ATP levels in the media were determined using an ATP-dependent luciferin/luciferase assay (Roche Biochemical) Static controls exhibited basal ATP release (7.0±0.5nM) that was increased to 27.8±1.6nM within 5 minutes of flow onset and remained elevated for the duration of flow. To determine if Ca^{2+} entry plays a role in ATP release in cells grown on either ECM, we pretreated the cells with either the mechanosensitive channel blocker gadolinium (Gd^{3+}, 10μM) or the L-type voltage-sensitive channel blocker nifedipine (5μM) prior to, and during, shear. Gd^{3+} failed to block ATP release in cells grown on either ECM. However, nifedipine significantly reduced shear-induced ATP release (5.6±2.1nM) in osteoblasts grown on type I collagen, but had no effect on cells grown on fibronectin. Interestingly, pre-treatment of osteoblasts with the chloride transport blocker DIDS (1mM) also significantly decreased ATP release in both static (0.47±0.2nM) and sheared (2.32±0.5nM) cells, independent of the ECM. These data indicate that ATP release is enhanced in osteoblasts subjected to FSS and can be dramatically blocked by the chloride transport inhibitor DIDS, possibly by blocking a mechanosensitive chloride channel that has been previously described in osteoblasts. While nifedipine failed to block ATP release from cells on fibronectin, shear-induced release was blocked to static control levels in cells grown on type I collagen. We have recently shown that inhibition of the L-type VSCC during mechanical loading of rat tibiae significantly reduced the bone formation rate in the loaded limb. The data presented here suggest a possible mechanism for this *in vivo* response

SU171

Modulation of NF-kB Translocation in Osteoblasts in Response to Shear is Mediated Via an ATP-dependent Pathway. D. J. Geist*[1], D. C. Genetos[2], R. L. Duncan[1]. [1]Orthopaedic Surgery, Indiana University School of Medicine, Indianapolis, IN, USA, [2]Cellular and Integrative Physiology, Indiana University School of Medicine, Indianapolis, IN, USA.

We have previously shown that Nuclear Factor-Kappa B (NF-kB) translocates to the nucleus in osteoblasts, subjected to fluid shear stress, within 1 hour. The focus of our present work is to elucidate the signaling mechanisms that influence the activation of NF-kB and the subsequent regulation of COX-2 and prostaglandin synthesis/signaling. MC3T3-E1 cells were grown to confluence in α-MEM media supplemented with 1% Pen/Strep and 10% FBS on fibronectin-coated glass microscope slides and subjected to 12 dynes/cm^2 of laminar flow. Fluid flow was applied in a parallel plate flow chamber using a flow loop with a constant hydrostatic pressure head that drives the media through the chamber in a constant laminar manner. The monolayer of MC3T3-E1 cells were flowed in α-MEM media with 0.2% FBS. Previous studies have demonstrated that the COX-2 gene contains a putative NF-kB binding site in its promoter. When we blocked IkB degradation with Nα-p-Tosyl-L-lysine chloromethyl ketone hydrochloride (TLCK), NF-kB translocation to the nucleus in response to fluid shear was prevented. Consequently COX-2 protein levels were reduced, compared to sheared controls, as shown in Western blot analysis. We have previously demonstrated that NF-kB translocation was dependent upon phospholipase C/IP_3 mediated intracellular Ca^{2+} release. A possible mechanism for PLC activation is via ATP binding to purinergic receptors. Inhibition of purinergic receptors with suramin, a general inhibitor of both P2Y and P2X receptor subtypes, prevented shear-induced NF-kB translocation. Previous reports have suggested that suramin may act to uncouple G-proteins. To ensure that NF-kB translocation is an ATP-mediated event we added apyrase, an enzyme that cleaves exogenous ATP into non-phosphorylated adenosine, to the flow media, and found that shear-induced NF-kB translocation was inhibited. To test whether other signaling mechanisms are involved in NF-kB translocation and COX-2 expression, we exposed cells to laminar flow in the presence of aminoguanidine, an inhibitor of both the constitutive and inducible forms of nitric oxide sythase (NOS). NF-kB translocation was not altered with aminoguanidine, indicating that this translocation was independent of nitric oxide (NO) signaling. These data indicate NF-kB translocation is modulated by shear-induced ATP release and that inhibition of NF-kB translocation reduced COX-2 production.

SU172

Dose Dependence of Bone Formation and Bone Remodeling Elucidated by Dynamic Fluid Flow Stimulation. Y. Qin[1], T. Kaplan*[2]. [1]Biomedical Engineering, SUNY Stony Brook, Stony Brook, NY, USA, [2]SUNY Stony Brook, Stony Brook, NY, USA.

Introduction: Fluid flow that arises from the functional loading of bone tissue has been proposed to be a critical regulator of skeletal mass and morphology. To test this hypothesis, the bone adaptive response to a physiological fluid stimulus, driven by low magnitude, high frequency oscillations of intramedullary pressure (ImP) were examined, in which fluid pressures were achieved without deforming the bone tissue. Methods: The left ulnae of 12 adults, one-year-old male turkeys were functionally isolated via transverse epiphyseal osteotomies. An oscillatory sinusoidal fluid pressure was applied to the ulna with the magnitude of 15mmHg (n=4) (magnitude approximated to the normal marrow blood pressure), 76 mmHg (n=4) (close to 700 peak microstrain induced ImP) and 105 mmHg (n=4) (pressure close to impact loading) at 30 Hz, 10 min/day, for 4 weeks. The adaptive responses of bone were determined through morphometric measurement at the mid-diaphyses. The histomorphometry was analyzed by calculating total area adaptation of periosteal and endosteal new surface bone (NB) formation and intracortical porosity. Results: All animals subjected to fluid flow loading showed a maintenance or gain of total bone mass. While NB formation at the endosteal surface showed no significant difference among applied pressures at 15, 76 and 105 mmHg, it demonstrated dose sensitivity of NB formation at the periosteal surface. This resulted in an increase of NB as a result of an increase of loading pressure, i.e., 2.4±0.3% at 15 mmHg, 5.0±2.0% at 76 mmHg and 8.4±3.7% at 105 mmHg. Disuse induced approximately 3% intracortical porosity. These remodeling experiments have shown nonuniform spatial distribution at endosteal and periosteal surfaces. Interestingly, increasing ImP did not inhibit intracortical porosity rather it activated remodeling in the cortex. Discussion: These data confirmed that fluid flow could significantly elucidate adaptive response if applied at proper fluid pressure and frequency in a short loading duration. The results demonstrated that low magnitudes of ImP can initiate spatial fluid flow in bone and thus stimulate bone adaptive response. At high physiological magnitude, ImP can increase and improve this perfusion process through increasing fluid pressure. Within physiological range, new bone formation is proportional to applied fluid flow stimulation. While pressure applied exceeds the physiological intensity or in the pathologic range, it will trigger extensive remodeling process and even weaken the quality of bone.

SU173

Apoptosis Signal-Regulating Kinase 1 (ASK1) Knockout Mice Revealed Tail Suspension-Induced Bone Loss in C57B6 Background and Reduced Expression of Osterix Gene. H. Kondo*[1], M. Ishijima[1], R. Salingcarnboriboon*[1], M. Morinobu*[1], K. Tsuji1*[1], H. Ichijo*[2], A. Nifuji*[1], M. Noda*[1]. [1]Molecular Pharmacology, Tokyo Medical and Dental University, Tokyo, Japan, [2]Lab. of Cell Signaling, Tokyo Medical and Dental University, Tokyo, Japan.

The mechanisms of bone loss due to unloading have not been fully understood. Hindlimb suspension (HS) is one of the models of unloading-induced bone loss. We have shown that osteopontin deficiency suppresses bone loss due to HS in mice. However, signaling mechanism for unloading-induced bone loss is still not yet fully elucidated. ASK-1 is a MAPKKK, which is involved in stress-induced apoptosis via activation of p38 and JNK. The aim of this paper is to examine whether ASK-1 is involved in certain pathways of unloading-induced bone loss using ASK-1 knockout (ASK-1KO) mice subjected to HS for two weeks. Total of 25 male and 28 female wild and knock out mice with C57BL6 background, which was previously reported to be unresponsive to HS-induced bone loss, were used for the experiments. Micro-CT analysis indicated that basal levels of trabecular bone volume in the tibiae were similar between wild type and ASK-1 KO mice. Further analysis was conduced in four different regions designated as area1, 2, 3 and 4 , which werre within 210, 210/490, 490/770, and 770/2590 micrometer away from the growth plate respectively. In primary trabecular bone (designated as area 1), HS reduced bone volume similarly in wild type and ASK-1 KO male mice. In secondary trabecular bone, HS reduced bone volume in each of the are areas2,3 and 4 in ASK-1KO ($p<0.05$) but not significantly in wild type mice. Female mice did not show as high levels of bone volume as male and although similar tendency was observed in area2 in female, it was less clear. Urinary deoxypyridinoline excretion, mineralized nodule formation and osteolcast-like cell formation in bone marrow cultures were observed in both genotypes. RT-PCR analysis of bone marrow-derived RNA indicated that osterix mRNA levels were reduced by HS in wild type. Basal osterix mRNA levels were less in ASK-1KO than wild type ($p<0.05$). These data indicated that HS induced bone loss similarly in wild type and ASK-1KO mice with C57BL6 background in primary trabeculae while in secondary trabeculae HS reduced bone volume in ASK-1KO but less significantly in wild type mice.

SU174

Sex Steroids, Bone Mass And Markers of Bone Turnover Are Not Related to Stress Fractures in Women Runners. P. K. Korkia[1], O. M. Rutherford*[2]. [1]Sport, Exercise and Biomedical Sciences, University of Luton, Luton, United Kingdom, [2]Guy's, King's and St Thomas' School of Biomedical Sciences, King's College, London, United Kingdom.

The aim of this study was to investigate the role of oestradiol (E2) status, bone mass and bone turnover in runners with a history of a SF. Twenty eumenorrhoeic (EA) and 20 amenorrhoeic (AA) runners without SF and 9 EA and 7 AA with SF, and 10 sedentary controls (Con) were recruited. A lower limb SF had been diagnosed using an x-ray, bone isotope scan or equivalent within the previous two years. Oestradiol (E2), lutenising hormone (LH) and a bone formation marker (bone-specific alkaline phosphatase, BALP) were measured in serum. Bone resorption marker (N-telopeptide; NTx) and creatinine were measured from 24-hour urine samples. In menstruating subjects, samples were taken in the early follicular phase. Spine and tibia/fibula BMD was measured using DEXA (Lunar). The data was analysed using one-way Anova and logistic regression. Measures of serum E2 and LH confirmed that all AA runners were at the low end of normal range. The EA&SF had 40% and AA&SF 28% lower E2 values than their non-SF counterparts. Despite this, E2 was not found to be a significant predictor for SF. No significant differences were found in BMD between the SF and their non-SF menstrual counterparts. The AA had a significantly lower spine BMD compared to all other groups ($p<0.001$). No significant differences were seen in tibia/fibula BMD between any of the running groups, while in the Con were significantly lower after controlling for weight ($p=0.014$). No relationship was found between BMD and SF history. Compared to the Con, there were no significant differences in mean NTx levels in the SF or the non-SF groups. The AA and EA&SF had similar NTx levels and these were significantly greater than in the EA and AA&SF groups ($p<0.001$). Compared to the Con, BALP levels were significantly lower in EA and EA&SF ($p<0.001$) groups but not in the AA groups. The two AA groups had significantly greater BALP levels compared to the EA groups ($p<0.001$). The difference between the EA&SF and AA&SF remained for NTx and BALP after adjustment for the time lag between diagnosis of SF and time of the measurement. An uncoupling index, modified from Eastell et al (Osteoporosis Int.3:255-260,1993) was derived. According to this, resorption and formation was in balance in the EA, AA and Con. The EA&SF had increased resorption while in the AA&SF, formation exceeded resorption. Correction of bone markers for total body BMC did not change any of the conclusions. The results show that lowered E2, spine and tibia/fibula BMD were not related to SF in women runners. Bone turnover is altered in athletes with SF compared to controls and may be associated with reduced E2 status.

SU175

Eccentric Strength But Not Lower Leg Bone Mineral Density or Soft-tissue Composition Is Related to Stress Fractures in Women Runners. P. K. Korkia[1], O. M. Rutherford*[2]. [1]Sport, Exercise and Biomedical Sciences, University of Luton, Luton, United Kingdom, [2]King's College, Guy's, King's and St Thomas' School of Biomedical Sciences, London, United Kingdom.

The aim of the present study was to examine the relationship between tibia/fibula bone mineral density (BMD), bone area, soft-tissue mass and muscle strength in women endurance runners with a history of SF. Twenty eumenorrhoeic (EA), 20 amenorrhoeic (AA) and 9 EA and 7 AA runners with a unilateral lower limb SF were recruited. A lower limb SF had been diagnosed using an x-ray, bone isotope scan or equivalent within the previous two years. Bone mineral density, bone area, lean (muscle) and fat mass in tibia/fibula area were isolated from a total body BMD scan using DEXA (Lunar). Concentric and eccentric quadriceps (Q) and hamstrings (H) actions were measured using isokinetic dynamometry (KinCom 125AP) at 60 and 180 degrees per second (°/s) in a seated position. Concentric plantar flexion (PF), dorsi flexion (DF), inversion (IV) and eversion (EV) strength were measured at 60°/s in a supine position. All measurements of muscle force were done during the early follicular phase in menstruating subjects. For statistical analyses, one-way Anova, independent sample t-tests and logistic regressions were used. Because no significant bilateral or between-group differences were seen in muscle strength, tibia/fibula BMD, bone area, lean and fat mass in any of the groups, the groups were combined to runners with a lower limb SF (n=16) and those without a SF (n=58). There were no muscle strength differences between the affected and non-affected limbs, apart from eccentric Q action at 60°/s, which was weaker on the affected side ($p=0.004$). Group comparisons showed no significant differences in tibia/fibula BMD, bone area or lean and fat mass between the SF and non-SF groups. Similarly, no differences were found for muscle strength. We did find a weak negative link between SF and calf circumference ($p=0.065$) and for SF and the total soft-tissue mass around tibia/fibula ($p=0.062$), but not for fat or lean mass alone. Eccentric quadriceps strength at 180°/s was negatively related to SF ($p=0.027$) while eccentric H strength at 60°/s showed a weak positive relationship ($p=0.04$). The latter finding is somewhat puzzling, but may be reflective of a relative weakness of the quadriceps group in relation to the hamstrings in those with SF. In conclusion, soft-tissue bulk may be more important than actual soft-tissue composition in protecting the lower limb from a SF. The study suggests that eccentric strength around the knee joint, and especially the quadriceps group, may be of practical importance in protecting against SF.

SU176

Bone Sensitivity to Mechanical Loads with the Lrp5 HBM Mutation. D. M. Cullen[1], M. P. Akhter[1], D. Mace*[1], M. L. Johnson[1], P. Babij*[2], R. R. Recker[1]. [1]Osteoporosis Research Center, Creighton University, Omaha, NE, USA, [2]Wyeth Research, Andover, MA, USA.

In humans, the high bone mass (HBM) mutation in the Lrp5 gene results in larger, stronger bones than normal. We hypothesize that this mutation alters bone cell sensitivity to loading such that lower than normal strains stimulate bone adaptation. In this study we tested 4 month old, female HBM transgenic mice (Het) derived from C57BL/6tac mice (Wyeth Research) and their non-transgenic (NTG) littermates. The right tibiae of all mice (30/genotype) were loaded in four-point bending at either 5 or 6 N, 36 cycles, 2 Hz for 5 days. Calcein was injected on day 5 and 12, and tibiae collected on day 15. The loaded (right) and nonloaded (left) legs were measured by standard histomorphometry. Differences due to force, genotype, and leg (right vs. left) were assessed by GLM for repeated measures. Tibial cross-sectional area was greater in Het (1.43±0.21) than NTG (1.13±0.16) mice. Strain or bending is a primary stimulus for mechanical regulation and due to size differences, tibial strains for the same forces were calculated to be 60% greater in NTG tibiae than in Het tibiae. For both genotypes, loading at 5 and 6 N increased periosteal and endocortical formation in loaded compared to nonloaded legs. The load response (loaded-nonloaded) is shown below. Despite large differences in strain, there were no genotype differences for increased periosteal formation surface (FS) or bone formation rate (BFR) with loading. However, endocortical FS responses to loading were greater in Het than NTG mice. Within genotype, only endocortical responses showed significant differences due to applied force. While commonly at least 1000 με is required to initiate a slight bone response, similar strains created large formation responses in the HBM mice. We conclude that less strain is required to stimulate similar or larger bone responses in mice with the HBM mutation than in NTG controls. Increased sensitivity to loading in HBM mice needs to be confirmed over a greater range of strains and forces.

Variable[a]	NTG-5N	NTG-6N	Het-5N	Het-6N
Strain (με)	1721	2065	1083	1300
Peri FS (%)	39 (15)	35 (21)	46 (24)	40 (24)
Peri BFR (um/d)	945 (1010)	2403 (2353)	1506 (2291)	1649 (2438)
Endo FS (%) [b]	14 (15)	18 (18)	16 (18)	25 (19)
Endo BFR (um/d)	52 (18)	137 (126)	77 (91)	105 (148)

[a] Values represent the loading response (loaded-nonloaded (SD)) with loaded legs greater than nonloaded legs for all variables. P<0.001

[b] The loading effect increased with force and was greater in Het than NTG P<0. 01

*Disclosures: **D.M. Cullen**, AHP/ Wyeth 2.*

SU177

Femora of Mice Lacking Myostatin Show Increased Trabecular Bone Density. M. Hamrick[1], G. Njus*[2], D. Ducharme*[2]. [1]Medical College of Georgia, Augusta, GA, USA, [2]Calhoun Research Laboratory, Akron, OH, USA.

Myostatin (GDF-8), a member of the transforming growth factor-β superfamily of secreted growth and differentiation factors, is a negative regulator of skeletal muscle growth. Myostatin-deficient animals show a marked increase in muscle mass compared to normals. We investigated the effects of increased muscle mass on bone modeling by examining cortical and trabecular bone strength and density in mice lacking myostatin function.

The experimental group used in this study included 12 female mice four months of age homozygous for the disrupted myostatin sequence whereas the control group consisted of 12 female wild-type mice also four months of age. The right femur of each mouse was cleaned of all soft tissue and examined using pQCT densitometry. Cross-sectional slices 1 mm thick were scanned at two different locations, the midshaft and the distal metaphysis. The midshaft is primarily cortical bone whereas the distal metaphysis has a high proportion of trabecular bone. The left femur of each individual was stored at -20ºC, thawed to room temperature, and the shaft loaded in four-point anteroposterior bending at a displacement rate of .10 mm/sec. Results show that the myostatin-deficient animals do not differ significantly from normals in bending stiffness (p=.89) or peak failure moment (p=.13). pQCT sections from the femur midshaft show that the myostatin knockouts have slightly (3%) greater cortical bone mineral density than normal mice but lower (10%) section modulus, which explains the similarity in peak failure moment between the two groups. pQCT sections from the distal metaphysis do, however, show that myostatin knockouts have over 20% greater trabecular bone density (p=.02) than normal mice. These data suggest that increased muscle mass resulting from myostatin deficiency may increase trabecular bone modeling in the limb skeleton.

SU178

The Freefall Impact Protocol: A Rodent Model to Assess the Effect of Impact on the Appendicular Skeleton. J. M. Welch*[1], C. M. Weaver[1], C. H. Turner[2]. [1]Foods and Nutrition, Purdue University, West Lafayette, IN, USA, [2]Indiana University Medical School, Indianapolis, IN, USA.

Impact exercise has been shown to have beneficial effects on the proximal femur of growing children. As a tool to further understand what changes this exercise promotes in weight-bearing bones, we developed an in vivo rat model in which rats are dropped from a specified height onto a hard surface. We tested 2 different falling heights and measured differences in the radius among treatment groups. Fischer 344 female rats (n=30), aged 4 weeks, were familiarized with exercise pens and daily handling. At 6 weeks they were randomly assigned to control (n=10) or 1 of 2 freefall groups (n=10 each). Animals assigned to the freefall groups were dropped from heights of either 30 cm or 60 cm. Rats were held horizontally above bare floor and, when released, landed on all four feet. Each rat was dropped every 11 seconds for 10 drops, 5 days a week, for 8 weeks. Additionally, all rats were allowed group exercise in pens 1.0 m in diameter, for the same amount of time daily, and consumed standard rat chow (1.0% Ca). No rat suffered injury or recognizable trauma as a result of this protocol. Upon completion of the 8 weeks of treatment, all rats were euthanized and their left radii removed. The radii were scanned by pQCT at 3 sites: 2.20 mm from the proximal end, midshaft, and 1.35 mm from the distal end. All tomographs were assessed for cross-sectional area (CSA) and volumetric bone mineral density (vBMD). Additionally, maximum and minimum second moments of area (I_{MAX} and I_{MIN}) were measured from the midshaft images. The data were analyzed by Tukey's Honestly Significant Difference Test for differences between groups ($p<0.05$). The vBMD at the proximal site (p=0.03; 5.2%) and distal site (p=0.01; 4.9%) increased over that of the controls in the 60 cm freefall group but not in the 30 cm group. No differences were found in vBMD at the midshaft. The CSA of the 60 cm group increased at both the proximal (p=0.001; 10.3%) and midshaft sites (p=0.002; 8.2%), but not at the distal site. No change in CSA was found in the 30 cm freefall group. Midshaft I_{MIN} increased in both the 30 cm (p=0.01; 18.1%) and 60 cm freefall groups (p=0.004; 21.4%), while I_{MAX} increased in only the 60 cm group (p=0.008; 14.9%). These results indicate that the freefall impact protocol provides a simple and effective new tool to stimulate a weight-bearing appendicular bone in growing rats. Responses in the radius were evident in rats subjected to the 30 cm drop height and improved in rats subjected to the 60 cm drop height.

SU179

Structural Changes in the Rat Humerus as a Result of Freefall Impact. J. M. Welch*[1], C. M. Weaver[1], C. H. Turner[2]. [1]Foods and Nutrition, Purdue University, West Lafayette, IN, USA, [2]Indiana University Medical School, Indianapolis, IN, USA.

Jumping can induce changes in the structure of children's bones. To further determine what structural changes occur as a result of impact loading, we subjected growing rats to a freefall impact protocol. F344 female rats, aged 6 weeks, were dropped 10 times per day, 5 days a week onto a hard surface. Rats in the freefall group (n=10) were dropped from 60 cm, while those in the controls (n=10) were not dropped. After 8 weeks the rats were euthanized and the left humeri removed. Each humerus was scanned by pQCT in 3 locations: (1) proximal site: 2.15 mm from the proximal end, (2) midshaft site, and (3) distal site: 1.15 mm from the distal end. At all sites the volumetric bone density (vBMD) of the total bone (vBMDtot), and both the cortical (vBMDcort) and trabecular (vBMDtrab) fractions were measured. The cross-sectional area of the whole bone (CSAtot), as well as its components, the cortical bone (CSAcort) and trabecular bone (CSAtrab), were also measured. Midshaft scans were analyzed for maximum and minimum second moments of area (I_{MAX} and I_{MIN}). The impact provided by 50 freefall impacts per week resulted in several structural changes in the humerus. At the midshaft, the bone gained CSAtot (p=0.003; 10.0%) due to increases in both the CSAcort (p=0.008; 13.6%) and CSAtrab (p=0.02; 10.5%). Additionally, changes in midshaft geometry were reflected in a greater I_{MIN} in the freefall group ($p<0.0001$; 34.1%). Midshaft I_{MAX} increased by 20.7% but this change was not significant due to variability within the groups. No difference was found in vBMD at the midshaft site. Both the proximal and distal ends of the humerus in the impact group increased in vBMD, with the proximal site reflecting greater changes than that of the distal. The proximal end increased in vBMDtot (p=0.0005; 5.6%) mostly due to an increase in vBMDtrab (p=0.02; 5.6%), while the change in the vBMD of the distal end was smaller (p=0.005; 3.3%), due to a lesser, and nonsignificant increase in both vBMDtrab (2.1%) and vBMDcort (1.5%). No changes were found in CSA at either end sites. These results indicate that the rat humerus gained structural strength in response to impact loading by increasing in all CSA fractions and I_{MIN} at the midshaft, and by responding in the proximal and distal ends by an increase in vBMDtot that was mostly due to an increase in trabecular density. The midshaft changes would attenuate the bending response to impact that is greatest at that site, while the greater trabecular density in the bone ends would result in a greater dissipation of the forces from the impact by distributing them into either more or thicker trabeculae.

SU180

Effect of Long-Term Impact-Loading on Mass, Size, and Estimated Strength of Humerus and Radius of Female Racquet-Sports Players: Aperipheral Quantitative Computed Tomography Study Between Young and Old Starters and Controls. S. Kontulainen*, H. Sievänen*, P. Kannus*, M. Pasanen*, I. Vuori*. UKK Institute, Tampere, Finland.

Bone characteristics were measured from 64 female players and 27 age-, height-, and weight-matched controls with pQCT and DXA. Players were divided into two groups according to the starting age of their tennis or squash training (either before or after menarche) in order to examine the possible differences in the loading-induced changes in bone structure and density. The used pQCT-variables were: bone mineral content (BMC); total cross-sectional area of bone (TotA); area of the marrow cavity (CavA) and that of the cortical bone (CoA); cortical wall thickness (CWT); volumetric density of the cortical bone (CoD) and trabecular bone (TrD); and bone strength index (BSI). BSI was compared to the DXA-derived areal bone mineral density (aBMD) to assess how well the latter represents the effect of mechanical loading on apparent bone strength. At the humeral shaft, the loaded arm's greater BMC (an average 19% gain in young starters and 9% in old starters), was due to a larger CoA (20% and 9%, respectively). The loaded humerus seemed to have grown periosteally (the CavA did not differ between the sites) leading to 26% and 11% gains in BSI in the young and old starters, respectively. CoD was equal between the arms (-1% difference in both player groups). The side-to-side difference in the young starters' BMC, CoA, TotA, CWT and BSI was 8% to 22% higher than that in the controls and 8% to 14% higher than that in the old starters. Old starters' BMC, CoA and BSI side-to-side difference was 6% to 7% greater than that in the controls was. The aBMD difference was 7% and 14% greater in young starters compared to that in the old starters and controls, respectively, whereas the difference between old starters and controls was 6%, in favour of the former. At the distal radius, the player groups differed from controls in the side-to-side BMC, TrD and aBMD differences only: the young starters' BMC difference was 9% greater, TrD and aBMD differences 5% greater than those in the controls, while the old starters' TrD and aBMD differences were both 7% greater than those in the controls. In summary, the structural adaptation of the humeral shaft to long-term loading seemed to be achieved through periosteal enlargement of the bone cortex and this adaptation was clearly greater if playing was started during the growing years. Exercise-induced cortical enlargement was not so clear at the distal radius, but the trabecular density seemed to been modified. DXA-based aBMD detected the intergroup differences but gave smaller estimates of the effect of exercise on the apparent bone strength at humeral shaft, especially in the young starters.

SU181

A Comparison of Cyclic and Rest-Inserted Loading. S. L. Poliachik*, N. Y. Moy*, S. C. Agans*, S. Srinivasan, T. S. Gross. Orthopaedics and Sports Medicine, University of Washington, Seattle, WA, USA.

Insertion of rest periods between each load cycle enables low magnitude loading to become osteogenic. To begin to optimize this stimuli, the current study sought to contrast the osteoblastic response induced by a protocol of strenuous cyclic loading to that achieved by lower magnitude, rest-inserted loading in growing mice. Loading was accomplished via non-invasive application of controlled loads to murine tibia. Sixteen C57Bl/6J mice (female, 16 wk) underwent a 2 week protocol where the right tibiae of the mice were dynamically loaded. Peak normal strains were estimated based upon application of beam theory to strain gage data collected from calibration mice. Animals were randomly assigned to 1 of 4 groups: 1) high magnitude repetitive loading of 100 cycles (peak mid-diaphysis strain of 1600με); 2) low magnitude rest-inserted loading of 10 cycles with 10s rest between cycles (550με peak strain); 3) medium magnitude rest-inserted loading of 10 cycles with 10s rest (1200με peak strain); and 4) medium magnitude rest-inserted loading of 10 cycles with 20s rest (1200με peak strain). Calcein was administered on day 3 and day 12, with the animals sacrificed on day 15. At the periosteal surface, unloaded contralateral control bones displayed minimal bone formation (0.04 ± 0.02 $\mu m^3/\mu m^2/d$). Low magnitude rest-inserted loading with 10s rest did not significantly increase bone formation compared to controls (0.01 ± 0.01 $\mu m^3/\mu m^2/d$, p=0.34). Rest-inserted loading at medium magnitude with 10s rest produced significant bone formation compared to control bones (0.20 ± 0.07 $\mu m^3/\mu m^2/d$, p=0.02). The bone formation for the medium magnitude rest-inserted loading group with 20s rest was similar to the 10s rest group (0.17 ± 0.13 $\mu m^3/\mu m^2/d$), and both medium magnitude rest-inserted groups exhibited greater bone formation than the high magnitude cyclic loading group (0.11 ± 0.07 $\mu m^3/\mu m^2/d$). We conclude that a rest-inserted protocol with only 10 cycles of daily loading induces periosteal bone formation comparable to 100 cycles at higher magnitude loads. One caveat is that the strains were applied in a non-physiologic orientation. If rest-inserted loading proves efficacious when applied in a physiologic orientation, its potential for extension to clinical trials would be greatly enhanced.

SU182

Effect of Physical Activity, Intensity and Length on Dimensions and Mineral Density of Apendicular Skeleton: Study on a Tennis Players Population. L. del Rio[1], P. Bassa*[1], R. Balius*[2], A. Ruiz Cotorro*[2], J. Parra*[2]. [1]Densitometria Osea, CETIR Centre Medic, Barcelona, Spain, [2]Fundacion Blume, Barcelona, Spain.

The aim of this study was to evaluate the effect of physical exercise on the regulation of size and bone density of limbs, as well as the degree of reversibility of such effects after a period with less exercise. **Method***: Bone mineral density measurements*: Global and regional analysis of bone mineral density (BMD) (g/cm2) were obtained using high-resolution DXA (GE-LUNAR, model EXPERT-XL) of both arms (on humerus, radius, ulna). *Osteometric measurements*: Total and sectorial measurements of projected length and width of both upper limb same bones were obtained. **Individuals**: A total population of 144 sportsmen volunteered, including 94 tennis players, which were in turn categorized according to age and physical activity as follows: 36 in growth period, 39 in young adults, 15 active veterans, 5 inactive veterans; the control group included, 50 sportsmen teenagers (24) and young adults (26) with symmetric exercise (martial arts and rowing). **Results**: Significant differences in BMD ($p<0.001$) and size (p: <0.001-005) were found in bones of dominant arm in comparison with non-dominant arm in the tennis players group, with being the region of interest in the upper humerus region the biggest one. Osteometric differences were greater in the projected width than in length, especially at humerus and ulna, and in segments richer in cortical bone. There were no differences in the control group nor the veterans inactive tennis players and the growth period group. **Conclusions**: This study confirmed the effect of physical activity on the regulation and mineralization of appendicular skeleton. Differences shown were small (non significant) in tennis players in growth period, and significant in young adults, with being related to exercise intensity and duration ($r=0.65$). Magnitude of these differences were greater in absorptiometry parameters than anthropometric ones, with the latter being kept in veterans players. Changes in BMD did not follow the same rule, since they were reversed with the lack of exercise.

SU183

The Role of $p57^{Kip2}$ Gene in Bone Metabolism. H. Amano[1], K. Suzuki[1], A. Nara*[2], K. Takahashi*[2], T. Tomita*[2], T. Urano[3], S. Inoue[3], S. Yamada*[1]. [1]Pharmacology, School of Dentistry, Showa Univ., Tokyo, Japan, [2]Biochemistry, School of Pharmaceutical Science, Showa Univ., Tokyo, Japan, [3]Geriatric Medicine, Faculty of Medicine, Tokyo Univ., Tokyo, Japan.

The cyclin-dependent kinase(CDK) inhibitor, $p57^{kip2}$ is a negative regulator of the cell cycle. Mice with a disruped $p57^{Kip2}$gene show cleft palate, endochondral bone ossification defects with incomplete differentiation of hypertrophic chondrocytes. We have also reported that the amount of $p57^{Kip2}$protein increased in rat osteoblasts treated with 1,25 vitamin D_3. However, the role of $p57^{Kip2}$ in bone metabolism is still unknown. In the present study osteoblasts derived from p57null(-/-) mutant calvaria showed increased the proliferation rate and higher alkaline phosphatase activity than that of wild type. In nodule formation assay, mineralization was siginificantly delayed in osteoblasts derived from -/- mice in the absence or presence of 1,25 vitamin D_3. Surprisingly, osteopontin mRNA expression was supressed by the addition of 1,25 vitamin D_3 . However -/-osteoblasts expressed the comparable amount of Vitamin D receptor mRNA to that of wild type. Moreover we have investigated the role of $p57^{kip2}$ on osteoclast formation. Osteoclast formation was also reduced in a co-culture system of -/-osteoblasts and wild type bone marrow cells in the presence of 1,25 vitamin D_3. Taken together, these results may suggest a possible involvement of p57 related to 1,25 vitamin D_3 signaling in the control of both osteoblast proliferation and osteoblast/osteoclast differentiation.

SU184

Increased Sensitivity of Osteoblast-like Cells Against Phosphate-induced Apoptosis Upon Pretreatment with Heparin. H. J. Hausser*, R. Brenner. Division for Biochemistry of Joint and Connective Tissue Diseases, University of Ulm, Ulm, Germany.

Long-term treatment with heparin has been associated with an increased risk of osteoporosis. While the mechanism(s) involved remain to be established, it can be hypothesized that heparin somehow interferes with the normal regulation of bone cells by heparin-binding growth factors. To shed some light on the pathogenesis of heparin-induced osteoporosis, we treated osteoblast-like cells (Saos-2) in monolayer cultures with different concentrations of heparin. After pretreating cells with 0.5 µg/ml heparin for 10 days, we observed a rapid loss of viable cells upon addition of ß-gylcerophosphate (10 mM). Cell death was due to apoptosis, as evidenced by positive TUNEL staining. Interestingly, RT-PCR analysis revealed that heparin treatment led to an increased expression of glypican-3. This glycosylphosphatidylinositol-anchored heparan sulfate proteoglycan which is mutated in Simpson-Golabi-Behmel Syndrome has been shown to induce apoptosis in a cell line-specific manner upon overexpression. Consistent with a possible involvement of this proteoglycan in the increased apoptosis-sensitivity of heparin-treated Saos-2 cells, preliminary data indicate that insulin-like growth factor 2 inhibts the ß-glycerophosphate-induced apoptosis. Our results support a model in which heparin-treatment leads to cellular changes which renders osteoblasts in the remodeling units more sensitive to apoptosis induced by phosphate liberated by active osteoclasts.

SU185

Transient versus Sustained Activation of Extracellular Signal Regulated Kinases (ERKs): A Potential Explanation for the Opposite Effects of Sex Steroids on Osteoblast and Osteoclast Apoptosis. J. R. Chen, S. Kousteni, L. Han, T. Bellido, R. S. Weinstein, C. A. O'Brien, R. L. Jilka, S. C. Manolagas. Division of Endocrinology and Metabolism, Center for Osteoporosis & Metabolic Bone Diseases, Central Arkansas Veterans Healthcare System, U/sity of Arkansas for Medical Sciences, Little Rock, AR, USA.

Estrogens and androgens exert pro-apoptotic effects on osteoclasts but anti-apoptotic effects on osteoblasts, via nongenotropic mechanisms of action of their classical receptors. However, heretofore there is no mechanistic explanation for the diametrically opposite effects of these hormones on the life span of the two cell types. Based on evidence that estrogens or androgens exert their anti-apoptotic effects on osteoblasts via activation of both a Src/Shc/ERK and a PI3K signal transduction pathway, and downregulation of JNK, we have investigated here whether their pro-apoptotic actions on osteoclasts require similar signals. For this purpose osteoclasts were prepared from stromal-cell free cultures in the presence of MCS-F and soluble RANKL and were then pre-treated for 1 hour with either U012345 or PP1, specific inhibitors of ERK and Src phosphorylation, respectively. Cultures were maintained in the presence of 17β-estradiol (E_2) or dihydrotestosterone (DHT) for 24 hours and apoptosis was assayed by monitoring the nuclear morphology of TRAPase positive cells. Both U012345 and PP1 abrogated the pro-apoptotic effects of E_2 and DHT, indicating that as in the case of the anti-apoptotic effects of sex steroids on osteoblasts, their pro-apoptotic effects on osteoclasts are mediated through a Src/ERK signaling pathway. Nonetheless, Western blot analysis of ERK phosphorylation in osteoclasts revealed a dissimilar temporal pattern to that seen in osteoblasts. Indeed, in contrast to a rapid and transient phosphorylation of ERKs in osteoblasts, reaching a peak at 5 minutes and declining thereafter, in osteoclasts both E_2 and DHT induced the phosphorylation of ERKs within 15 min, and the extent of phosphorylation increased progressively thereafter for at least 24-hours. These results indicate that the opposite effects of estrogens and androgens on osteoblast and osteoclast survival are mediated via modulation of the same signaling pathways; and as shown elsewhere in this meeting result from a nongenotropic function of the classical receptors and an interchangeable ligand/receptor interaction in cells from females and males. However, sustained activation of ERKs in osteoclasts as opposed to transient activation of ERKs in osteoblasts may be responsible for the striking difference between stimulation of apoptosis in the former and attenuation of apoptosis in the latter cell type.

SU186

Prevention of Glucocorticoid-Induced Apoptosis in Osteocytes and Osteoblasts by Calbindin-D_{28k}. Y. Liu*[1], A. Porta*[1], R. Donnelly*[1], T. Bellido[2], S. Christakos[1]. [1]UMDNJ - New Jersey Medical School, Newark, NJ, USA, [2]Endo/Metab Center for Osteoporosis and Metabolic Bone Diseases, Central Arkansas Veterans Health Care System,Univ. of Arkansas for Medical Sciences, Little Rock, AR, USA.

Recent studies have indicated that deleterious effects of glucocorticoids on bone involve increased apoptosis of osteocytes and osteoblasts. Since the calcium binding protein calbindin-D_{28k} has antiapoptotic properties in different cell types and in response to a variety of insults, we investigated whether calbindin-D_{28k} could also protect against glucocorticoid-induced cell death in bone cells. Apoptosis was induced by addition of dexamethasone (dex) (10^{-6}M) for 6h to cells transiently transfected with pREP4 vector or vector containing the cDNA for calbindin-D_{28k} together with an expression vector for nuclear green fluorescent protein. Apoptosis was assessed by evaluating nuclear morphology of > 100 transfected (fluorescent) cells. Dex-induced nuclear fragmentation of MLOY-4 osteocytic cells transfected with pREP4 vector (4.0% versus 16.7% apoptotic cells, -dex and + dex respectively). However the proapoptotic effect of dex was blocked in cells transfected with calbindin-D_{28k} cDNA (5.7% apoptotic cells + dex; $p< 0.01$ compared to vector transfected cells + dex). Similar results were observed in UMR osteoblastic cells and in primary murine osteoblastic cells. Dex-induced apoptosis in bone cells was accompanied by an increase in caspase 3 activity. The presence of calbindin markedly attenuated the activity of caspase 3. In vitro assays indicated a concentration dependent inhibition of caspase 3 by calbindin-D_{28k} (0.09 µM - 1.8 µM, K_i =0.22 µM). Calbindin-D_{28k} was found to act as an inhibitor and to bind to caspase 3 but not to act as a substrate for caspase 3. Calbindin inhibits caspase 3 specifically since the activity of caspases 1, 2, 4, 5, 6, 7 and 8 was unaffected by calbindin. Tryptic peptides of calbindin were separated and purified using HPLC and a 6,800 mw fragment was found to be responsible for most of the caspase 3 inhibitory activity. Besides inhibition of caspase 3, the antiapoptotic effect of calbindin in response to dex was also reproducibly associated with an increase in the phosphorylation of extracellular signal regulated kinases 1 and 2 (ERK 1 and 2). Although the mechanism is not known, this finding suggests that calbindin inhibits glucocorticoid-induced apoptosis not only by direct inhibition of caspase 3 but also by activation of survival kinases such as ERKs. This study, which is the first to demonstrate the prevention of glucocorticoid induced bone cell death by calbindin-$D_{28k,}$ has important implications for the therapeutic intervention of glucocorticoid-induced osteoporosis.

SU187

Osteoprotegerin (OPG) Binds TNFα with 2-20 nM Affinity and Regulates TNFα-Induced Apoptosis. R. Bu, C. W. Borysenko*, Y. N. Li*, L. Cao, H. C. Blair. Biochemistry, Pathology and Physiology & Cell Biology, U Pittsburgh, Pittsburgh, PA, USA.

TNF-family proteins are pivotal in the equilibrium of osteoclast and osteoblast activity. Osteoblast apoptosis is driven by cytokines including TNFα, a homolog of RANKL, which drives osteoclast maturation. The decoy receptor OPG modulates two TNFs, RANKL and TRAIL, but other OPG interactions are undefined. Osteoblasts express RANKL and OPG, paradoxically, since OPG neutralizes RANKL. We hypothesized that OPG has additional TNF interactions. We examined effects of OPG apoptosis induced by TNFα using MG63 cells. At 3-10ng/ml, TNFα increased apoptosis in serum free media 10 fold at 2-4h. This was diminished to near control by OPG at 10-30 ng/ml, by annexin V binding or TUNEL. This suggested that OPG protects osteoblasts from TNFα-induced apoptosis. It was, however, unclear whether the mechanism involved reverse signalling by osteoprotegerin bound to RANKL, a transmembrane protein, or an interaction with TNFα. We compared binding of TNFα, RANKL, and TRAIL by immune precipitation and found that OPG binds all of these in PBS at physiological pH. Western blots confirmed specificity of antibodies, with no detectible cross-reaction even with 100 ng of alternate TNF or receptor proteins. Solid phase adsorption, surface plasmon resonance, and carbodiimide crosslinking were used to study these interactions further. Ethyl-3 (dimethylaminopropyl)carbodiimide (EDC) crosslinked human TNFα and OPG efficiently, demonstrating binding in solution, but preventing interaction when TNFa or OPG are crosslinked to dextran support by EDC. However, murine OPG was active after EDC-surface crosslinking for plasmon resonance (Biacore 3000) and showed TNFα binding with dissociation constants 2.4-18 nM. In ELISA, human OPG/TNFα affinity was 2.4-21 nM. Varying binding constants reflected differences with conditions including molar ratios in solution, pH (6.8-8.0), salt concentration, and temperature, which suggest complex physiological interactions. Human RANKL binds both human and mouse OPG-Fc after EDC crosslinking while neither TRAIL nor TNFα did, suggesting that the RANKL interaction involves different OPG sites than binding to TRAIL or TNFα. Numerous other interactions can be studied using plasmon resonance and results include that mouse and human TNFα form heterotrimers. This study suggests that interactions between TNF receptors and TNFs are likely to involve complex interactions including mixed complexes of receptors and heterotrimers of TNFs. Some interactions may be weak, and not of physiological importance, although puzzling interactions such as effects of RANKL on osteoblasts may involve mechanisms related to novel interaction of TNFs and TNF receptors.

SU188

Extra- and Intracytoplasmic Domains of Syndecan-2 Play Distinct Roles in the Control of Osteoblast Proliferation and Apoptosis. D. Modrowski, E. Hay*, S. Le Mee*, P. J. Marie. INSERM U349, Paris, France.

Syndecans are cell surface heparan sulfate proteoglycans that serve as co-receptors and modulate the actions of a large number of extracellular ligands. We previously showed that syndecan-2 (Synd2) modulates the mitogenic activity of GM-CSF in human osteoblastic cells. To further examine the role of Synd2 in osteoblasts we overexpressed Synd2 in MG63 human osteoblastic cells. Full-length Synd2 cDNA was cloned in the expression vector pEGFP-C1 (Synd2-pEGFP). Site-directed mutagenesis was used to obtain a cDNA coding for Synd2 without its carboxyterminal motif (ΔCterSynd2-pEGFP). The cDNA coding for Synd2 lacking for its intracytoplasmic domain (ΔCSynd2-pEGFP) was obtained by PCR. The three constructions or the empty vector (pEGFP) were transfected into MG63 cells for transient or stable expression. Overexpression was confirmed by RT-PCR and Western Blot analysis until 4 days after transfection. Overexpression of Synd2-GFP and ΔCterSynd2-GFP increased cell proliferation for 3 days following transfection when compared with control cells transfected with pEGFP. In contrast to Synd2, transient expression of Synd2 lacking the intracytoplasmic domain (ΔCSynd2-pEGFP) dramatically decreased cell proliferation. Selection with G418 allowed to obtain few clones stably expressing GFP or ΔCterSynd2-GFP, and many clones stably expressing ΔCSynd2-GFP. All clones of cells transfected with Synd2-pEGFP died after 15 days of selection, suggesting induction of apoptosis. We therefore examined whether Synd2 controls apoptosis in MG63 cells. Most Synd2-pEGFP transfected cells were found to be positive for TdT-mediated X-dUTP Nick End Labeling (TUNEL) performed after 11 days of antibiotic selection. In contrast, TUNEL was strikingly decreased in ΔCSynd2-GFP expressing cells compared with control cells or ΔCterSynd2-GFP expressing cells. Accordingly, DNA fragmentation determined on agarose gel was increased in cells that transiently expressed Synd2-GFP and decreased in ΔCSynd2-GFP cells, when compared with GFP or ΔCterSynd2-GFP cells. Consisting with these results, caspases-2 and -9 and effector caspases-3, -6, -7 activities were increased by 40, 57, and 45 %, respectively, in Synd2-GFP expressing cells compared with control cells. The results show that 1) Synd2 controls osteoblastic cell proliferation and apoptosis, 2) the proximal part of Synd2 cytoplasmic domain is required for osteoblastic cell proliferation and 3) overexpression of Synd2 induces apoptosis whereas Synd2 lacking its whole intracytoplasmic domain protects MG63 cells from apoptosis. Thus, extra- and intra-cytoplasmic domains Synd2 play distinct roles in the control of osteoblast proliferation and apoptosis.

SU189

Ionizing Radiation Increases Apoptotic Sensitivity and Cell Cycle Arrest in Cultured Osteoblasts. K. H. Szymczyk*, I. M. Shapiro, C. S. Adams. Orthopaedic Surgery, Thomas Jefferson University, Philadelphia, PA, USA.

While a great deal is known about the effects of ionizing radiation on soft tissue, little is known on its effects on the resident cells of bone. To test the hypothesis that radiation induces bone cells apoptosis, we exposed MC3T3-E1 osteoblast-like cells to gamma-radiation (1.8 to 60 Grays). Cell viability was assessed using the MTT assay. Twenty-four hours post-irradiation, a small decrease in cell viability was noted. TUNEL and TEM analysis revealed that the decrease in viability was not due to the induction of apoptosis. However, there was a dramatic increase in sensitivity to apoptogens. We noted that when irradiated osteoblasts were treated with physiologically relevant apoptogens and chemotherapeutic agents, the number of cells killed by each apoptogen was dependent on the radiation dose. Moreover, the apoptogens and radiation acted synergistically to enhance cell killing. Since the number of surviving cells is dependent on the rate of cell proliferation, we measured osteoblast proliferative response by flow cytometry. Flow cytometric analysis demonstrated that the irradiated osteoblasts underwent cell cycle arrest. In addition, Western blot analysis indicated that p21 and GADD 153 were both elevated in a dose-dependent manner; there was no evidence of p53 activation. It is concluded that irradiation has at two-fold effect on osteoblasts: an increase in apoptotic sensitivity and activation of cell cycle arrest. Studies are in progress to determine if these events occur concomitantly, or are independent of each other.

SU190

Osteoblast Shape, Cytoskeleton and Extracellular Interactions Altered by Hyperosmolarity. S. Botolin*, M. Zayzafoon, L. R. McCabe. Physiology, Michigan State University, East Lansing, MI, USA.

Diabetes mellitus is often accompanied with complications, including bone loss and increased fracture rate. This disease is marked by elevated blood glucose levels and hyperosmolarity. Changes in cell shape and cell volume are important in cell responsiveness and accommodation to a hyperosmotic environment. Therefore, we investigated MC3T3 osteoblast cell shape and expression of proteins involved in shape and volume regulation during acute and chronic hyperosmotic exposure. Exposure to hyperosmotic (320 mOsm) media resulted in significant osteoblast shrinkage. Specifically, osteoblasts developed a more satellite appearance that was clearly evident one hour following treatment. Consistent with this finding, modifications in proteins associated with cell shape were also found and were still evident with long term hyperosmotic exposure. Treatment of osteoblasts daily with media containing an additional 22 mM of glucose, mannitol or contrast dye resulted in an increase in the concentration of heat shock protein HSP27 and osmotic stress protein 94 (Osp94). The induction of these molecular chaperones/cytoskeleton stabilizers is likely a protective response of osteoblasts to chronic exposure to hyperosmotic stress. In addition, levels of connexin 43 and integrin beta 5 were also increased, suggesting that cell-cell and cell matrix interactions are also altered. Taken together, our findings demonstrate that exposure of osteoblasts to hyperglycemic/hyperosmotic conditions associated with poorly controlled diabetes can cause significant changes in osteoblast shape, cytoskeleton and extracellular interactions. Based on our previous findings we hypothesize that these changes contribute to altered osteoblast function.

SU191

CpG Methylation Around Transcription Start Site of RANKL Gene Controls Its Steady-State Expression. S. Kitazawa, R. Kitazawa. Division of Molecular Pathology, Department of Biomedical Informatics, Kobe University Graduate School of Medicine, Kobe, Japan.

Receptor activator of NF-kB ligand (RANKL) is a membrane-bound signal transducer requisite for differentiation and maintenance of osteoclasts. RANKL expression on stromal/osteoblasic cells is tightly regulated to maintain physiological serum calcium levels and bone mass. These stromal/osteoblasic cells, however, comprise a rather heterogeneous population ranging from immature mesenchymal cells to mature osteoblasts and also respond differently to bone resorptive stimuli. In the mouse coculture system, we also have demonstrated the passage-dependent difference of cultured mouse stromal cells in supporting osteoclastogenesis because of altered RANKL gene expression. To address the issue of what molecular mechanism gives the diversity of RANKL gene expression to stromal/osteoblastic cells, we characterized mouse and human RANKL gene promoters. The former promoter contains two CpG clustering regions: one around the transcription start site and the other downstream of the vitamin D response element (VDRE). The latter, on the other hand, containes one CpG clustering region around the transcription start site. Using earlier- and later-passage mouse ST2 cells, we analyzed the CpG methylation status by sodium bisulfite mapping and found that CpG loci around the transcription start site (-66/+246) were predominantly methylated in later-passage ST2 cells. Moreover, earlier- and later-passage ST2 cells transfected with a RANKL promoter construct showed the same steady-state level of luciferase activity and of the inducible effect of 1,25(OH)2D3. Furthermore, the introduction of methylation to the promoter construct silenced promoter activity. Taken together with the fact that DNA methyltransferase (Dnmt) 3b, a de novo DNA methylase, increases in both senescent and immortalized cells, our results suggest that CpG methylation around the transcription start site of the RANKL gene is an important development and a senescence-related epigenetic event, and that its heterogeneity might cause the diversity of the stromal/osteoblastic cells in RANKL gene expression.

SU192

PTH Induction of the Osteocalcin Gene: Requirement for an 82 bp Sequence in the Promoter and Involvement of Multiple Signaling Pathways. G. Xiao, D. Jiang*, R. T. Franceschi. Periodontics/Prevention/Geriatrics, The University of Michigan, Ann Arbor, MI, USA.

Parathyroid hormone (PTH) is an important peptide hormone regulator of bone formation and osteoblast activity. However, its mechanism of action in bone cells is largely unknown. The present study examined the mechanism of PTH regulation of the mouse osteocalcin gene in MC3T3-E1 preosteoblastic cells. PTH stimulated osteocalcin mRNA and promoter activity in a dose and time-dependent manner. Deletion of the promoter sequence from -1316 to -116 caused no change in PTH responsiveness while deletion from -116 to -34 led to complete loss of PTH stimulation. Interestingly, this promoter region does not contain the Runx2 binding site shown to be necessary for PTH responsiveness in other systems. Either H89 or PKI, two specific PKA inhibitors, blocked the PTH response. Forskolin alone, a PKA activator, stimulated OCN expression, but did not increase the PTH response. GF109203X, a specific PKC (protein kinase C) inhibitor, also abolished PTH stimulation. The PTH response is not blocked by U0126, a specific mitogen-activated protein kinase (MAPK) inhibitor. Thus, both PKA and PKC pathways are required for this regulation. Furthermore, phorbol 12-myristate 13-acetate (PMA), an activator of the PKC pathway, dramatically increased the PTH effect although it alone only slightly stimulated gene expression. Interestingly, this synergy was blocked not only by H89, GF109203X, but also by U0126, indicating that MAPK pathway is also required for this regulation. Collectively, these results indicate that PTH stimulation of OCN gene expression requires PKA, PKC, as well as MAPK signaling pathways.

SU193

Transcriptional Profiling of Human Osteoblast Differentiation. J. Billiard[1], R. Moran*[1], K. Gillis*[2], M. Chatterjee-Kishore*[2], E. Brown*[2], L. Sauter*[2], M. Whitley*[2], E. Wilson*[2], B. Komm[1], P. Bodine[1]. [1]Women's Health Research Institute, Wyeth Research, Collegeville, PA, USA, [2]Expression Profiling Sciences, Wyeth Research, Cambridge, MA, USA.

We have developed a collection of human conditionally immortalized cell lines in discrete stages of osteoblast (OB) differentiation. In the present study, we used four cell lines representing preosteoblasts, early and late mature OB, and preosteocytes to analyze changes in gene expression that occur during differentiation. Their respective phenotypes were confirmed by cell morphology and expression of appropriate osteoblastic markers. The mRNA samples from each cell line were subjected to gene chip analysis using the Affymetrix Hu6800 chip (7070 genes) and a custom chip enriched in bone and cartilage cDNAs (3378 genes). The experiment was performed twice on two sets of RNA. A 3-fold change in gene expression between preosteocytic and preosteoblastic stages was considered significant. Overall, 44 genes were found to consistently change in both experiments. Many of the differences reflect expected patterns and support the relevance of our results. These include down-regulation of osteoprotegerin, collagen type I and its processing enzyme, lysyl oxidase, as well as up-regulation of matrix metalloproteinase 1 and plasminogen activator. Other changes have not been reported and offer new insight into the OB differentiation process. Several genes regulating cell proliferation increased with differentiation, among them was the inhibitor of apoptosis, survivin, a member of TNF superfamily CD27L, and the metastasis-promoting S100A4 protein. Cell motility and migration promoting factors including autotaxin, midkine, and CTGF peaked in early and late mature OBs. We also saw changes in mRNAs involved in maintaining the cytoskeleton and extracellular matrix. Actin filament capping protein and α tubulin increased, whereas OB-cadherin and ankyrin decreased during differentiation. Our screen also identified several genes whose role in the differentiation process is uncertain. These include a small ras-related GTPase associated with diabetes that increased with differentiation, an HMG-box transcription factor, SOX4, that was down-regulated, and several components of the complement pathway that decreased with differentiation. The inhibitor of osteoclast formation, follistatin, also decreased with OB differentiation. In summary, this study provides a comprehensive profile of gene expression during human OB differentiation. Gene chip analysis is a powerful tool permitting us to associate genetic changes with OB physiology. With this information the role of the OB in the bone remodeling process will become more completely characterized.

Disclosures: ***J. Billiard****, Wyeth Research 3.*

SU194

Use of Human Genome Data to Identify a DNA Fragment that Completely Recapitulates the Hormone/Cytokine Regulation of the RANKL Gene: A Key Advance Toward Full Elucidation of its Molecular Control. Q. Fu, S. C. Manolagas, C. A. O'Brien. Div. of Endo/Metab, Center for Osteoporosis & Metabolic Bone Diseases, Central Arkansas Veterans Healthcare System, University of Arkansas for Medical Sciences, Little Rock, AR, USA.

PTH, $1,25(OH)_2D_3$, and the gp130 cytokines stimulate osteoclastogenesis and bone resorption primarily by upregulating the expression of RANKL in cells of the stromal/osteoblastic lineage. The mechanisms by which these agents stimulate RANKL expression remain poorly understood. Previous studies using murine RANKL promoter-luciferase constructs containing up to 7 kb of 5'-flanking region have produced inconsistent results with some studies finding a 2-fold stimulation by $1,25(OH)_2D_3$ while other studies find no stimulation by any osteoclastogenic agents. With the ultimate goal of identifying mechanisms involved in RANKL gene expression, we utilized the human genome sequence contig map to identify a bacterial artificial chromosome (BAC) containing a 200 kb fragment of human DNA encompassing the 40 kb RANKL gene flanked on both sides by more than 70 kb. The BAC harboring this fragment was obtained and modified by homologous recombination to contain a Neo cassette and used to stably transfect UAMS-32 cells which express endogenous RANKL in response to cAMP analogs, OSM, or $1,25(OH)_2D_3$. Several clones containing the full-length BAC, as assessed by Southern blot analysis with probes corresponding to regions near either end of the 200 kb fragment, were analyzed for basal and stimulated expression of the human RANKL gene by Northern blot using a human-specific RANKL probe. Seven of 7 clones expressed human RANKL mRNA which was upregulated by dibutyryl-cAMP, $1,25(OH)_2D_3$, or OSM by an average of 10-, 8-, or 4-fold, respectively. The level of basal human RANKL mRNA expression varied among the clones and was not correlated with gene copy number. Dibutyryl-cAMP stimulated transcription, as assessed by nuclear run-on, of both the human RANKL transgene and the endogenous murine RANKL gene. These results indicate that cis- and trans-acting regulators of the RANKL gene are sufficiently conserved between humans and mice such that the human gene can be appropriately expressed in murine cells. Further, cis-acting elements necessary for regulation by osteoclastogenic agents lie within 70 kb of the beginning or end of the human RANKL gene. However, these regions are not sufficient for position-independent or copy-number dependent expression. Identification of the cis-acting sequences necessary for regulation of this construct by osteoclastogenic agents in stromal/osteoblastic cells, and thereby the trans-acting factors that bind them, should provide novel targets for anti-resorptive therapy.

SU195

Overexpression of DLK (delta-like, EGF-like Homeotic Protein) Enhances the Adipogenic Differentiation but Maintain Osteoblastic Differentiation of Human Bone Marrow Stromal Cells. B. M. Abdallah*[1], C. Jensen*[2], G. Leslie*[2], T. Jensen*[3], M. Kassem[1]. [1]Endocrinology, University Hospital of Odense, Odense, Denmark, [2]Immunology, University of Southern Denmark, Odense, Denmark, [3]Genetics, University of Aarhus, Aarhus, Denmark.

The molecular mechanisms of human marrow stromal cells (mesenchymal stem cells, hMSC) differentiation into specific lineages are poorly understood. Dlk (delta-like, also known as pref-1, FA-1) belongs to a family of transmembrane proteins containing epidermal growth factor-like repeat motifs homologus to the notch/delta/serrate. Dlk is involved in the control of several cellular differentiation processes including adipogenesis and it has been reported to inhibit adipocyte differentioation of the preadipocyte 3T3-L1 cell line. As hMSC can differentiate into several cell lineages including adipocytes, the role of dlk in controlling the differentiation processes was examined. Gene expression of dlk was quantitated using a reverse-transcriptase polymerase chain reaction (RT-PCR) and Northern analysis. Normal hMSC obtained from different donors was shown to express constitutively dlk. Furthermore, dlk was expressed in human fetal osteoblast cell line (hFOB) as well as human fetal bones (gestation age 5, 8 and 12 weeks) but was down regulated in adult bone. Full-length DLK cDNA from human liver cDNA library was cloned and subsequently subcloned in a retroviral expression vector (GCsam) that was employed to stably transfect hMSC/TERT$^+$: a human telomerase-immortalized MSC line capable for differentiation into multiple cell types including osteoblasts and adipocytes (Simonsen et al, Nature Biotechnology, 2002 in press).The resultant cell line (hMSC-dlk$^+$) was shown to express high levels of dlk protein in the conditioned media (more than 1.2 μg/ml versus 0.2 μg/ml in control cells) as determined by ELISA and more than 90% of the cells expressed dlk as shown by immunostaining. In contrast to 3T3-L1 cell line, when MSC-dlk$^+$ cells were induced to adipocyte differentiation in a medium containing insulin, dexametasone, IBMX and BRL49653, they formed a larger number of adipocytes as determined by fluorescence-activated cell sorting (FACS) analysis and higher levels of gene expression of PPAR-γ2 and lipoprotein lipase (LPL) compared to control cells. In addition, MSC-dlk$^+$ maintained their osteoblast differentiation potential as estimated by gene expression of osteocalcin, collagen type I and alkaline phosphatase and cytochemical staining for alkaline phosphatase. Our data suggest that dlk signaling does not mediate the adipogenic commitment of hMSC, although dlk overexpression enhances the response of the hMSC to the adipogenic differentiation signals.

SU196

Vitamin D Induces Thrombomodulin Expression in Osteoblasts. A. L. M. Sutton*, D. R. Dowd*, P. N. MacDonald. Pharmacology, Case Western Reserve University, Cleveland, OH, USA.

Vitamin D is critical for the proper development and maintenance of the skeleton. 1,25-dihydroxyvitamin D_3 ($1,25(OH)_2D_3$) is the bioactive metabolite of vitamin D that functions through the vitamin D receptor (VDR), a member of the nuclear hormone receptor family. The $1,25(OH)_2D_3$-VDR complex acts on bone both indirectly, by regulating calcium and phosphate homeostasis, and directly by modulating osteoblast and osteoclast activity. In particular, vitamin D inhibits the proliferation and induces the differentiation of osteoblasts. To characterize novel genes regulated by $1,25(OH)_2D_3$ in MG-63 human osteoblastic cells, we utilized gene expression array analysis. This approach identified several genes that are highly induced following a 6-hour treatment with 10^{-8}M $1,25(OH)_2D_3$. One of these transcripts encodes thrombomodulin, a transmembrane anticoagulant protein. Northern blot analysis shows a time- and dose-dependent induction of thrombomodulin expression by vitamin D treatment in MG-63 cells. Thrombomodulin mRNA is undetectable without vitamin D treatment, but appears after three hours and steadily increases up to 24 hours of treatment with vitamin D. This up-regulation is specific for $1,25(OH)_2D_3$ since another vitamin D metabolite, $24,25(OH)_2D_3$, does not affect thrombomodulin expression. Additionally, cycloheximide treatment only minimally diminishes this response, suggesting that the vitamin D-induced increase in thrombomodulin mRNA does not require *de novo* protein synthesis. Thrombomodulin is a membrane protein known for its anticoagulant effects in the cardiovascular system. However, thrombomodulin is expressed in a variety of other tissues, including the lung, keratinocytes, and developing bone, suggesting that it may have other functions. Since vitamin D regulates cellular differentiation and thrombomodulin is expressed in the developing bone, we hypothesize that thrombomodulin may be involved in vitamin D-mediated differentiation of osteoblasts. Studies are currently underway to elucidate the function of thrombomodulin in osteoblasts and to map the promoter elements responsible for the vitamin D response.

SU197

Gene Expression Profiling Analysis of BMP-2 Induced Commitment Towards the Osteoblast Lineage. E. Balint[1], D. S. Lapointe*[2], H. Drissi*[1], A. J. van Wijnen[1], J. L. Stein*[1], J. B. Lian[1], G. S. Stein[1]. [1]Department of Cell Biology, University of Massachusetts Medical School, Worcester, MA, USA, [2]Information Services, University of Massachusetts Medical School, Worcester, MA, USA.

Runx-2 and BMP-2 are both required for osteogenic lineage commitment and differentiation. To identify gene regulatory mechanisms that drive osteoblast differentiation in response to BMP-2 and in relation to the induction of Runx-2, gene expression microarray analysis was performed. Total RNA was isolated from C2C12 cells at 1, 2, 8, 12 and 16 hours following BMP-2 treatment. Northern blot analysis confirmed suppression of myogenic genes and induction of osteoblast phenotypic genes with Runx-2 mRNA detected by 16 hours in two independent experiments. Gene expression profiling analysis was carried out using hierarchical clustering, SOM analysis and functional clustering. Approximately 900 out of the 13,000 genes showed a minimum change of 1.8-fold throughout the time course. About half of these genes are either activated or repressed during differentiation. Approximately 250 genes were continually upregulated, 450 were continually downregulated, while the remainder exhibited transient elevations during the BMP-2 time course. Functional groups with particular expression patterns including signaling proteins, growth factors, receptors and cell cycle regulators were identified. Among the genes in the functional clusters were known BMP-2 responsive genes, validating the experimental model. Within these clusters we also identified numerous genes with no known function in the bone environment. Consistent with the appearance of the osteoblast phenotype detected by Northern blot analysis, phenotypic, extracellular and cell adhesion proteins begin to exhibit changes in expression at about 8-12-16 hours. In contrast, a representative group of transcription factors (n=62) show sequential patterns of induction or inhibition throughout the time course. A subset (20%) of these transcription factors including both activators and repressors, are acutely induced in response to BMP-2 (1 hour). Subsequent waves of transcription factor induction/repression follows at 2, 8, 12 and 16 hours. The functional clustering method allows predicting functions of genes and EST's clustering together with known genes. Additionally, the functional gene clusters permit identification of common regulators for functionally related groups of genes that exhibit similar expression patterns. This global analysis of expressed genes provides insight to the understanding of the regulatory events that coordinate BMP-2 and Runx-2 activities in osteogenesis.

SU198

A Region of the hBMP-6 Promoter Contributing to Basal and Glucocorticoid-Mediated Effects. Y. Liu[1], G. A. Hair*[1], M. Viggeswarapu[1], M. Nellis*[2], L. Titus[3], S. Voorhees*[1], S. D. Boden[1]. [1]Orthopaedics, Emory University, Atlanta, GA, USA, [2]Atlanta Research and Education Foundation, Decatur, GA, USA, [3]Research, VA Medical Center, Decatur, GA, USA.

The glucocorticoid regulation of osteoblast differentiation is mediated by a 5-8 fold induction of BMP-6 mRNA and protein in secondary rat calvarial cell cultures. To determine the molecular mechanism by which BMP-6 is regulated, we constructed luciferase reporter vectors by inserting the previously characterized hBMP-6 promoter and its 5' flanking region into the pGL3-Basic vector. Transfection of sequential 5' and internal deletion constructs of the reporter vectors along with a GC receptor (GR) expression vector into HeLa cells revealed that the region –869 to –598 is important in mediating both basal and GC-inducible luciferase expression. GC induction was typically 2-3 fold. Luciferase activities of the constructs containing the region –869 to –598 were significantly higher than that of the proximal promoter(-90 to +12) alone. Accordingly, deletion of this region dramatically reduced both basal and GC-induced activities. However, sequence analysis of the region revealed no consensus glucocorticoid responsive element. Further segmentation of the region revealed that a construct containing the 5' end of this region (-869 to -780) retains significant luciferase activity. In order to determine segments of the –869 to –598 region important for transcription factor binding, DNase I footprinting and EMSAs were performed. The primary data demonstrated that nuclear extracts of Hela cells transfected with GR differentially bound to three DNA segments (5'end –869 to –780; midregion –779 to -714 and 3'end –713 to -598) depending on GC treatment. Glucocorticoids increased binding of the nuclear extracts to the 5' end, decreased binding to the 3'end, and did not affect binding to the midregion. We conclude that glucocorticoid can regulate BMP-6 expression at the transcriptional level probably through an indirect mechanism and the region –869 to -598 is critical for both basal and GC-regulated expression.

SU199

Gene Expression Profiles and Transcription Factors Involved in PTH Signaling in Osteoblasts Revealed by Microarray and Bioinformatics. L. Qin[1], P. Qiu*[2], L. Wang*[2], X. Li*[1], P. Tolias*[1], N. C. Partridge[1]. [1]Physiology and Biophysics, University of Medicine and Dentistry of NJ, Piscataway, NJ, USA, [2]Schering-Plough Research Institute, Kenilworth, NJ, USA.

PTH is a major mediator of bone remodeling and an essential regulator of calcium homeostasis having both anabolic and catabolic effects on bone. Prolonged exposure to PTH causes increased bone resorption. The molecular mechanism of PTH signaling in the osteoblast is still largely unknown. UMR 106-01, a rat osteosarcoma osteoblastic clonal cell line, is a model system to study the effects of PTH *in vitro*. The present study was designed to delineate genes and pathways that are regulated by PTH (10^{-8} M) using DNA microarray techniques and bioinformatics approaches. Total RNA, isolated from UMR 106-01 cells collected at 4, 12 and 24 h after treatment with or without 10^{-8} M PTH, was converted into cRNA and hybridized to an Affymetrix rat genomic microarray chip. After stringent filtering, 126 known genes and 30 unknown ESTs were found to have at least 2-fold expression changes in the PTH-treated samples. Most genes previously known to be regulated by PTH were also identified in this screening, such as MMP-13, IGFBP-5, fos, Nurr77, tPA, decorin, fibronectin etc. Real-time quantitative RT-PCR experiments confirmed that about 90% of the genes are indeed regulated by PTH in UMR 106-01 cells and about 50% in primary osteoblasts. Most of these genes belong to the following protein families: hormones, growth factors and their receptors; signal transduction pathway proteins; transcription factors; proteases; metabolic enzymes; structural and matrix proteins; transporters. Analysis of these genes identified several novel biological pathways regulated by PTH, including neurotrophic factor signaling, neurotransmitter signaling, growth factor and cytokine signaling, feedback regulation of signal transduction pathways and glucose metabolism. Next, we designed a computation method to identify the transcription factors involved in PTH signaling. Using human genome sequence, we found human orthologs for 73 genes from the 126 PTH-regulated genes and 61 genes' promoter start site were annotated. The promoter sequences from these genes were matched against a transcription factor database to identify transcription factors that have significantly higher numbers of binding sites within these promoter regions compared to random occurrences. Those transcription factors that are possibly involved in PTH signaling include AP-1, C/EBP, CREB, AP-2, AP-4, myc, SP1, FoxD3 etc. Our data demonstrate that PTH has profound effects on many aspects of osteoblasts through a limited set of transcription factors, suggesting a commonality of signaling pathways.

SU200

The Early Response Gene Epidermal Growth Factor Response Factor (ERF-1) Is Regulated by Parathyroid Hormone and Expressed in Osteoblastic Cells. S. Reppe*[1], O. K. Olstad*[1], J. E. Reseland*[2], E. Rian*[3], V. T. Gautvik*[1], G. J. Kjendlie*[1], K. M. Gautvik[1], R. Jemtland*[4]. [1]Department of Medical Biochemistry, University of Oslo, Oslo, Norway, [2]Institute for Nutrition Research, University of Oslo, Oslo, Norway, [3]Department of Immunology, The Norwegian Radium Hospital, Oslo, Norway, [4]Endocrine Section, Department of Medicine, The National University Hospital, Oslo, Norway.

We have recently identified ERF-1 as one of the genes that are up-regulated by human recombinant PTH(1-84) in human OHS osteoblast-like cells using cDNA expression arrays (Atlas). ERF-1 (also known as butyrate response factor (BRF1), TIS11b, or cMG1) is a member of the TIS11 gene family comprising early response genes that binds DNA through a highly conserved Cys3His binding motif. Northern blot analysis showed that ERF-1 mRNA was up-regulated 3-4 fold in OHS cells treated with hPTH(1-84) for 24h. hPTH(1-84) and hPTH(1-34) (10-9 - 10-10M), but not hPTH(3-84), increased ERF-1 mRNA expression in a time-dependent manner. Forskolin and 8-Br-cAMP duplicated the stimulation of ERF-1 mRNA levels by PTH, while protein kinase C activator TPA was without effect. H89, a protein kinase A (PKA) inhibitor, blunted the stimulatory effects of 8-Br-cAMP or hPTH(1-84) on ERF-1 mRNA expression in OHS cells during co-incubation. These data indicate that PTH increases ERF-1 mRNA levels via activated PTH/PTHrP receptors, where the cAMP-dependent adenylyl cyclase (AC) signaling pathway is important. ERF-1 is also expressed in various human and rodent clonal osteoblast-like cells and ERF-1 mRNA levels are enhanced by PTH(1-84) treatment in primary mouse calvarial osteoblasts cultured for 7d in osteogenic medium. In contrast, treatment of primary osteoblasts with recombinant bone morphogenetic protein 2 (BMP2) caused reduced ERF-1 mRNA levels relative to controls. The expression pattern of ERF1 in differentiating primary human osteoblasts is currently under investigation. This is, as far as we know, the first report to show that ERF-1 is part of the PTH response in osteoblasts via receptor-coupled activation of the cAMP/AC/PKA pathway.

SU201

Gene Expression Regulation During Osteoblast Differentiation of Mesenchymal Stem Cells by Microarray Analysis. W. T. Steegenga*, J. M. A. Hendriks*, W. Olijve, E. J. J. van Zoelen*. Applied Biology and Cell Biology, University of Nijmegen, Nijmegen, Netherlands.

Mesenchymal stem cells are the cells which can, upon receipt of the right triggers, differentiate into osteoblasts. Osteoblast differentiation is a multistep series of events modulated by an integrated cascade of gene expression. To search for new genes involved in the early and late phase of osteoblast differentiation on a large scale, microarray (MA) technology was employed. In a first MA experiment murine C2C12 mesenchymal progenitor cells were induced to differentiate into mature osteoblasts by treatment with bone morphogenetic protein 2 (BMP2). Analysis of the regulated transcripts showed the activation of a number of transcription factors not previously identified as regulators of osteoblast differentiation. We are currently analysing the effects of these genes on Cbfa1 transcription activation. In addition, by means of cluster analysis a large number of potential new late phase bone makers were identified. The bone specificity of the identified late response genes was determined by comparing BMP2-induced expression in C2C12 and MC3T3 osteoblasts with that in NIH3T3 fibroblasts. This resulted in the identification of 9 novel genes and ESTs that were specifically induced in osteoblasts, in addition to the well-known markers alkaline phosphatase and osteocalcin. Expression of three of these putative late phase bone markers was observed *in vivo* in developing bone by *in situ* hybridisation of E16.5 mouse embryos. In a second MA experiment we analysed gene expression regulation during 34 days of osteoblast differentiation of human mesenchymal stem cells on 15 different time points. Results will be presented showing the regulation of a number of well established bone markers and of many previously unidentified transcripts in different phases of the differentiation process. By means of hierarchical clustering, these genes can be grouped by similarities in their expression profiles, resulting in subsets of early, intermediate and late response genes, which are representative of the distinct stages of the osteoblast differentiation process. Analysis of the pathways leading to the regulation of the genes present in the independent clusters is under current investigation.

SU202

Cell-cell Interaction Mediated by Cadherin-11 Selectively Enhances the Mesenchymal Tissue Formation. I. Kii*, A. Kudo. Life science, Tokyo Institute of Technology, Yokohama, Japan.

Cell-cell interaction is an essential event for tissue formation, however, the role of cell-cell adhesion in cell differentiation and tissue formation is unclear. Cadherins form the adherence junction and adhere cells. Recently, it has been suggested that cadherin has abilities to differentiate cells and form several tissues through its adhesion in the embryonic stem cell-derived teratomas; E-cadherin promotes the epithelial tissue formation, and N-cadherin promotes the bone, cartilage and neuroepithilium formation. The osteoblasts were reported to express N-cadherin and cadherin-11, and N-cadherin was indispensable for osteoblasts to induce the alkaline phosphatase activity and form the nodule structures. The targeted disruption of cadherin-11 leads to loss of bone density. Here, we demonstrate that cadherin-11 is widely expressed in the mesenchymal tissues, and cell-cell adhesion mediated by cadherin-11 is responsible for the mesenchymal tissue formation. We examined the localization of cadherin-11 proteins and RNAs in tissues. The immunohistochemical analysis of paraffin sections of the E16.5 mouse embryo head revealed that cadherin-11 proteins were localized in the mesenchymal tissues: osteoblasts, muscle cells, chondrocytes, stromal cells, and vascular pericytes or smooth muscle cells. Whole mount RNA in situ hybridization analysis of the mouse skulls in the stage of E15.5-E18.5 indicated that cadherin-11 was expressed conspicuously in the sutural mesenchyme and pre-osteoblastic cells. To search the function of cadherin-11 in the osteoblastogenesis, the calvarial development of cadherin-11-/- neonatal mice was investigated. Cadherin-11-/- neonatal mice had an ectopic island ossification in the metopic sutural mesenchyme by the side of nasal bone, while the ectopic island ossification was scarcely observed in +/+ neonatal mice, and the smaller one was observed in +/- neonatal mice. These results suggest that cadherin-11 participates in the formation or maintenance of the sutural mesenchyme. Next, we examined the role of cadherin-11 in cell differentiation. The cadherin-11 overexpressed embryonic stem cells were implanted subcutaniously, and teratomas were formed. HE staining showed that the teratomas derived from cadherin-11 overexpressed ES cells produced higher amounts of bone, cartilage and muscle tissues than those from control embryonic stem cells to which the empty vector was introduced. These results demonstrate that cadherin-11 selectively enhanced the mesenchymal tissue formation. In conclusion, cell-cell interaction mediated by cadherin-11 is responsible for the enhancement and maintenance of the mesenchymal tissues containing bone and cartilage.

SU203

Interleukin-6 and Interleukin-11 Modulate Osteoblast Differentiation and RANKL Expression via Activation of JAK-STAT Signal Transduction Pathway. C. Shih, J. F. Shyu. Biology and Anatomy, National Defense Medical Center, Taipei, Taiwan Republic of China.

Interleukin (IL)-6 and IL-11 are members of IL-6 type cytokines which play important roles in normal and abnormal bone remodeling (e.g. postmenopausal osteoporosis) via regulation of cell proliferation and differentiation. IL-6 and IL-11 enhance formation and function of osteoclast via stromal/osteoblastic cells. So far, the effects of IL-6 and IL-11 on Janus kinase (JAK)/signal transducer and activator of transcription (STAT) signal transduction pathway and receptor activator of NF-kB ligand (RANKL) in bone cells are still not well known. The purposes of this study were to investigate 1)which of the JAK/STAT family members or MAP kinase are involved in mediating actions of IL-6 and IL-11 and 2)the relationshop between the activation of IL-6 and IL-11 signal pathways and the biological effects of IL-6 and IL-11 in primary osteoblasts and MG-63 cells. Osteoblasts ($4x10^5$/10 cm Petri dish) were grown to confluence, incubated in low serum (0.5%) and stimulated with different concentrations of IL-6 or IL-11. Cell were lysed in lysis buffer. Lysates were centrifugated and immunoprecipitated with the appropriate antibodies (JAK1/JAK2/TYK2/STAT1/ STAT3/MAPK). Tyrosine phosphorylation was determined by anti-phosphotyrosine Western blotting. Effect of IL-6 or IL-11 (10, 100 or 1000 U/ml) on RANKL expression and osteoblast differentiation were assessed by Western blotting and alkaline phosphatase (ALP) activity assay. Both JAK1 and JAK2 were tyrosine phosphorylated with IL-6 while only JAK1 was tyrosine phosphorylated with IL-11. Moreover, with IL-6 or IL-11, both STAT1 and STAT3 were tyrosine phosphorylated and translocated to the nucleus. Both IL-6 and IL-11 caused a dose-related increases in RANKL expression and stimulated ALP expression in osteoblasts. In conclusion, IL-6 and IL-11 modulate osteoblast differentiation and RANKL expression via the activation of specific members of JAK-STAT pathways.

Disclosures: ***C. Shih****, National Defense Medical Center 3.*

SU204

Expression of Phospholipid Receptors and a Phospholipid Phosphatase in Osteoblast Cells. B. L. Hill, C. Xu*, K. E. Callon, J. Cornish, A. Grey. Medicine, University of Auckland, Auckland, New Zealand.

The naturally occurring phospholipids lysophosphatidic acid (LPA) and sphingosine-1-phosphate (S1P) induce mitogenic and anti-apoptotic responses in a variety of cells. Previously we have described these effects, and characterized the intracellular signaling pathways which subserve them in primary rat osteoblasts and the rat osteoblast cell line UMR-106 treated with either LPA or S1P. The proliferative and anti-apoptotic actions of each phospholipid in osteoblastic cells were sensitive to the Gi protein inhibitor pertussis toxin, implying the involvement of G protein-coupled receptors. In this study we report the expression of specific cell membrane bound receptors for LPA and S1P and a cell membrane associated phospholipid phosphatase in osteoblastic cells. The edg family of G-protein coupled receptors comprise those that bind LPA with high affinity (edg 2, 4 and 7) and those that bind S1P (edg 1, 3, 5, 6 and 8). Both primary rat osteoblasts and UMR-106 cells express the S1P receptors edg 1 and 5 as assessed by RT-PCR but do not express edg 3, 6 or 8. Immunohistochemical analysis of whole fixed primary rat osteoblasts confirmed the presence of edg 1 protein on the surface of these cells. The LPA receptor edg 2 was identified by RT-PCR in primary rat osteoblasts and UMR-106 cells. Membrane-associated phospholipid phosphatases (LPP-1 and LPP-3) are believed to regulate the availability of LPA and S1P for binding to the edg receptors. RT-PCR analysis of primary rat osteoblasts and UMR-106 cells indicates expression of LPP-1 by these cells. We conclude that the mitogenic and anti-apoptotic actions of LPA and S1P on primary rat osteoblasts and the rat cell line UMR-106 are via the interaction of these ligands with their specific edg receptors which are expressed in an osteoblast specific manner. The interaction of LPA and S1P with these receptors is likely to be further regulated by the presence of phospholipid phosphatase on the surface of these cells.

SU205

The P55 TNF Receptor Mediates TNF Inhibition of Osteoblast Differentiation. L. Gilbert*, A. Brantley*, J. Rubin, M. S. Nanes. Division of Endocrinology, Department of Medicine, Emory University and VAMC, Atlanta, GA, USA.

Tumor necrosis factor-α contributes to the pathophysiology of osteoporosis by stimulating bone resorption and inhibiting new bone formation. We have previously shown that TNF is a potent inhibitor of osteoblast differentiation from their pluripotent precursor cells in fetal calvaria, marrow stroma, or in clonal MC3T3-E1 pre-osteoblast cells (Gilbert et al Endocrinology 141:3956 2000). TNF action is mediated by structurally homologous cell surface receptors, p55 and p75, that differ in function. The identity of the TNF receptor type expressed by pre-osteoblasts is unknown since these cells are studied in a mixed culture system. To determine which TNF receptor mediates inhibitory effects on the differentiation of osteoblasts, the effect of TNF was studied in marrow stromal cells obtained from mice genetically deficient in one or both TNF receptors and in control mice matched for the C57BL/6 genetic background. These mice have been reported to be born at the expected Mendelian frequency and to have no overt phenotype. Progression of stromal cells toward the osteoblast phenotype was assessed by monitoring the formation of a mineralizable matrix using the von Kossa stain and by measurement of the secretion of the osteoblast-specific matrix protein osteocalcin. Marrow stromal cells were cultured for 14 days in alpha-MEM supplemented with 10% fetal calf serum, ascorbate, and β-glycerophosphate. Post-confluent control cultures formed mineralized nodules by day 8 and secreted osteocalcin. Treatment of wild type cultures with TNF (10ng/ml) from days 1-14 or 2-14 completely inhibited the formation of mineralized nodules. TNF-treated cells remained viable. In cultures derived from either $p55^{-/-}$ or $p55^{-/-}p75^{-/-}$ mice, TNF treatment had no effect on osteoblast differentiation. Both $p55^{-/-}$ and $p55^{-/-}p75^{-/-}$ cultures appeared indistinguishable from their respective controls whether or not treated with TNF. Osteocalcin levels were (mean±SEM ng/ml): wild type control, 207±6; wild type TNF treated, 2.1±0; p55-/-p75-/- control, 188±8; p55-/-p75-/- TNF treated, 155±33.6; p55-/- control, 192±25.3; p55-/- TNF treated, 215±4. These results support the requirement for the p55 TNF receptor as a mediator of TNF inhibition of osteoblast differentiation.

SU206

Perfusion Culture System Improves Osteogenesis of Rat Bone Marrow-Derived Osteoblastic Cells in Porous Ceramic Materials. Y. Wang*[1], T. Uemura[1], J. Dong[1], H. Kojima[1], T. Tateishi[2]. [1]Tissue Engineering Research Center (TERC), National Institutes of Advanced Industrial Science and Technology (AIST), Tsukuba, Ibaraki, Japan, [2]Biomedical Engineering Laboratory, University of Tokyo, Tokyo, Japan.

Perfusion culture has showed benefits to many cell types in three-dimensional (3D) culture. In this study, we made an attempt to increase bone formation in composites of BMO and β-tricalcium phosphate (β-TCP) by perfusion culture method. For *in vitro* test, BMO/β-TCP composites were cultured in perfusion container (Minucells and Minutissue, Bad Abbach, Germany) with fresh medium delivered at a rate of 2 ml/hr by the peristaltic pump to the perfusion container. ALP activity and osteocalcin (OCN) contents of composites were measured at the end of 1, 2, 3 and 4 weeks of subculture. For *in vivo* test, after subculture for 2 weeks as described above, the composites were implanted into syngeneic rats subcutaneously. These implants were harvested at 4 or 8 weeks after implantation. Then the samples underwent biochemical analysis of alkaline phosphatase (ALP) activity, OCN and histological analysis. ALP activities and OCN contents in the composites of perfusion group were obviously higher than that of the control group both *in vitro* and *in vivo*. Light microscopy and SEM revealed more active bone formation in BMO/β-TCP composites at 4 weeks and 8 weeks after implantation. These data show that application of perfusion culture system during subculture of BMO in porous ceramic scaffold is beneficial to their osteogenesis activity. After differentiation culture *in vitro* by perfusion culture system, the activity of the osteoblastic cells and the consequent bone formation *in vivo* can be significantly enhanced. These results suggest the described perfusion culture system is a valuable and convenient tool for applications in tissue engineering, especially in the generation of artificial bone tissue.

SU207

Melatonin Promotes the Osteoblastic Differentiation and Bone Formation. R. Tokuyama*[1], K. Satomura[1], S. Tobiume*[1], K. Yamanouchi*[2], K. Kume*[1], E. Kitaoka*[1], S. Nishisho*[1], N. Masuda*[1], Y. Hibi*[1], M. Nagayama*[1]. [1]First Department of Oral and Maxillofacial Surgery, School of Dentistry, The University of Tokushima, Tokushima, Japan, [2]Department of Dentistry and Oral Surgery, Tokushima Red Cross Hospital, Tokushima, Japan.

Melatonin is the major hormone secreted by the pineal gland, and its levels are synchronized by environmental light. A number of recent studies demonstrated that melatonin regulated a variety of physiological processes including control of circadian rhythms, regulation of reproductive function, regulation of temperature, sexual development and immune system. Moreover, melatonin is known to influence the release of growth hormone and cortisol in human. These findings suggest that melatonin may have an influence on skeletal growth and bone formation. However, little is known about the influence of melatonin on osteoblasts or bone formation. This study was performed to determine whether melatonin could regulate the proliferation and differentiation of human osteoblasts *in vitro* and mouse bone formation *in vivo*. Reverse transcription-polymerase chain reaction and Western blotting analysis showed that human osteoblasts expressed melatonin 1a receptor and that its expression levels decreased gradually with age of hosts. Melatonin stimulated the proliferation of human osteoblasts in a dose-dependent manner at the concentrations between 50 and 200 μM. In addition, alkaline phosphatase activity of human osteoblasts was enhanced by melatonin at concentrations equal to and more than 10 μM. Melatonin also promotes the expression of mRNA for bone-related genes such as type I collagen, osteopontin, bone sialoprotein and osteocalcin in a dose-dependent manner at concentrations ranging from 1 to 200 μM. Moreover, melatonin stimulated the mineralized matrix formation *in vitro* at the concentration as low as 100 μM. To evaluate the effect of melatonin on bone formation *in vivo*, melatonin was intraperitoneally administered to mice at a dose of 100 mg/kg of body weight. Histological analysis using the labeling with tetracycline and calcein revealed that the volume of newly formed bone of femora increased by the treatment with melatonin. Taken together, these results suggest the possibility that melatonin plays a potential physiological role in bone formation and skeletal growth.

SU208

Tachykinins Stimulate Bone Formation by Rat Calvarial Osteoblasts via the Neurokinin-1 Receptor. T. Goto[1], E. Fukuhara*[2], K. Kometani*[3], S. Kobayashi*[1]. [1]Oral Anatomy, Kyushu Dental College, Kitakyushu, Japan, [2]Oral Surgery, Kyushu Dental College, Kitakyushu, Japan, [3]Orthodontics, Kyushu Dental College, Kitakyushu, Japan.

Tachykinins are neuropeptides that work as neurotransmitters and neuromodulators, and are found throughout the body. Substance P (SP), neurokinin A (NKA), and neurokinin B (NKB) are the major subtypes of tachykinins, and their receptors (neurokinin (NK) -1, -2, and -3 receptors) form the three receptor subtypes. To identify the role of tachykinins in bone formation, we investigated the expression of NK1-Rs in osteoblasts and the effects of SP, NKA, and NKB on bone formation by rat calvarial osteoblasts. Rat calvarial osteoblasts were isolated from the calvariae of three-day-old Wistar rats, and cultured for three weeks in alpha-MEM containing 10% serum, ascorbic acid, dexamethasone, and beta-glycerophosphate. We examined NK1-R expression using RT-PCR, and the binding of fluo-SP to cultured osteoblasts. The effects of SP, NKA, and NKB were investigated by adding these neuropeptides to the culture medium. Furthermore, the effects of blocking these peptides by using SP and NK1-R antagonists were examined. NK1-R mRNA expression and fluo-SP binding were found in 16-day cultured osteoblasts, but not in 8-day cultured osteoblasts or osteoblastic cells ROS. A significant increase in bone formation by cultured osteoblasts was observed with the addition of 10(-7) – 10(-6) M SP or 10(-11) – 10(-9) M NKB, but not NKA. These increases in bone formation with the addition of SP or NKB were inhibited by the addition of SP or NK1-R antagonists. The results indicate that SP and NKB stimulate bone formation by osteoblasts at the late stage of bone formation via NK1-Rs, and that this process is dependent on the expression of NK1-Rs in osteoblasts. These findings suggest that neuropeptides secreted from sensory neurons modulate bone formation following expression of their receptors.

SU209

The Effect of Connective Tissue Growth Factor (CTGF) on Differentiation and Adhesion of MC3T3-E1 Osteoblast-like Cells. R. A. Kanaan*[1], P. Ebrahimpour*[1], S. L. Smock*[2], T. A. Owen[2], S. N. Popoff[1], F. F. Safadi[1]. [1]Anatomy and Cell Biology, Temple University School of Medicine, Philadelphia, PA, USA, [2]Cardiovascular and Metabolic Diseases, Pfizer Global R&D, Groton, CT, USA.

Connective tissue growth factor (CTGF) is a secreted, extracellular matrix-associated signaling protein that regulates diverse cellular functions including adhesion, proliferation and differentiation. We recently showed that osteoblasts *in situ* express CTGF during active growth of the skeleton as well as during fracture repair. Primary osteoblast cultures demonstrated a bimodal pattern of CTGF expression being relatively high during the period of proliferation and reaching peak levels during the period of mineralization. Furthermore, blocking the activity of the endogenous CTGF produced and secreted in these cultures using an anti-CTGF antibody caused a dramatic dose-dependent inhibition of nodule formation and mineralization. In this study, we first examined the effect of CTGF overexpression on osteoblast differentiation by transient transfection of MC3T3-E1 cells with a CMV-CTGF construct. CTGF over-expression resulted in significant increases in alkaline phosphatase activity and calcium deposition (mineralization) compared to control cultures that were treated with transfection reagent alone or transfected with an empty vector. Other studies have shown that specific integrins serve as receptors for CTGF on fibroblasts and endothelial cells. We examined whether MC3T3-E1 cells can adhere to an immobilized CTGF substrate and determined whether specific integrins are involved in this adhesive interaction. MC3T3-E1 cells were plated into culture wells pre-coated with increasing concentrations of recombinant CTGF (rCTGF) with 1% BSA serving as a control substrate. MC3T3-E1 cells adhered to the rCTGF wells in a dose-dependent manner with maximal adherence in wells coated with 5 μg/ml. We then examined whether specific integrins mediate this adhesive interaction by pre-incubating the MC3T3-E1 cells with a panel of anti-integrin antibodies including anti-αvβ3, -αIIbβ3, and -αvβ5. The anti-αvβ5 antibody decreased cell adhesion by 70%, while other antibodies, such as the anti-αvβ3 antibody, had no effect on cell adhesion. These data suggest that the integrin αvβ5 acts as a receptor for CTGF on MC3T3-E1 cells. The induction of distinct signaling pathways mediated by a CTGF/integrin interaction may provide a molecular basis for at least some of the effects of CTGF on osteoblast differentiation.

SU210

Crosstalk between Vitamin C and Vitamin D Signals on the Differentiation of Human Osteoblast-like (MG-63) Cells. R. Hata[1], S. Takamizawa*[2], Y. Maehata*[2], K. Izukuri*[2], Y. Kato*[2], K. Imai*[3], H. Senoo*[3], S. Sato*[4], A. Kimura*[5]. [1]Department of Biochemistry and Molecular Biology, Bioventure Research, Kanagawa Dental College, Yokosuka, Japan, [2]Department of Biochemistry and Molecular Biology, Kanagawa Dental College, Yokosuka, Japan, [3]Department of Anatomy, Akita University School of Medicine, Akita, Japan, [4]Department of Orthodontics, Kanagawa Dental College, Yokosuka, Japan, [5]Department of Molecular Pathology, Medical Research Institute, Tokyo Medical and Dental University, Tokyo, Japan.

In order to investigate mechanisms of human osteoblast differentiation, we employed culture system of MG-63, human osteosarcoma derived cells. The cells were cultured in Dulbecco's modified Eagle's medium with various additives. When the medium was supplemented with L-ascorbic acid 2-phosphate (Asc 2-P, 0.25 to 10 mM), a long-acting vitamin C derivative, growth of the cells was stimulated in the early phase of the culture. Relative rate of collagen synthesis of the cells and alkaline phosphatase (Alk-Pase) activity, a marker for osteoblast differentiation were also increased. The stimulative effects of Asc 2-P on the growth and Alk-Pase activity were attenuated by the co-presence of 0.25 mM azetidine 2-carboxylic acid or 0.2 mM ethyl dihydroxybenzoate, inhibitors for collagen synthesis, suggesting these stimulative effects are dependent on collagen synthesis. Comparison of levels in mRNAs obtained from two culture conditions, cultures in the absence and presence of Asc 2-P, by a gene chip method, indicated that increases in messenger RNA for type III collagen chain is responsible for the increase in collagen synthesis. Addition of 1-alpha, 25-dihydroxycholecalciferol (active vitamin D3, 10 to 100 nM) in the culture medium suppressed growth of the cells but stimulated Alk-Pase activity. Co-presence of Asc 2-P and active vitamin D3 showed synergistic action on the Alk-Pase activity but relatively less effect on the growth of the cells. These data indicate that the presence of crosstalk between vitamin C and vitamin D signals on the expression of Alk-Pase activity, a marker for osteoblast differentiation.

SU211

Effect of Acyl-CoA Binding Protein on Bone Cell Differentiation. H. Si*[1], H. Kim*[1], J. Kim*[1], Y. Kim*[1], Y. Jung*[1], S. Lee*[2], S. Kim[3], H. Ryoo[4], S. Mandrup*[5], R. Park*[1], I. Kim[1], J. Choi[1]. [1]Biochemistry, Kyungpook Natl. Univ. School of Medicine, Daegu, Republic of Korea, [2]Advanced Materials Division, Korea Research Institute of Chemical Technology, Daejeon, Republic of Korea, [3]Orthopedics, Kyungpook Natl. Univ. School of Medicine, Daegu, Republic of Korea, [4]Oral Biochemistry, Kyungpook Natl. Univ. School of Dentistry, Daegu, Republic of Korea, [5]Molecular Biology, Odense University, Odense, Denmark.

Dietary fatty acid has been known as a modulator of the onset and progression of various diseases such as osteoporosis, osteoarthritis, diabetes, obesity and hypertension. The acyl-CoA binding protein(ACBP), intracellular acyl-CoA pool former and transporter of acyl-CoA thioesters, is ubiquitously expressed 10 kDa protein and its gene expression is upregulated during adipogenic differentiation. However, the ACBP function in bone cells remains unknown. The biological activity of ACBP on bone cells was determined by Northern blot analysis, RT-PCR and stable transfection experiment using chondrocyte and osteoblast differentiation models. The expression of ACBP mRNA was the highest at proliferation stage and down regulated at matrix maturation stage and increased again at differentiation stage but less than that of proliferation stage during ATDC5 chondrocyte differentiation. However, the expression of ACBP mRNA was gradually decreased during MC3T3-E1 osteoblast differentiation. To know the loss of function effect, ATDC5 and MC3T3-E1 cells were stably transfected with ACBP antisense or control empty expression vectors. The antisense ATDC5 cells, which expressed ACBP antisense mRNA, showed higher alkaline phosphatase activity and gene expression of osteonectin, type II collagen, and type X collagen than those of control cells. These results indicate that suppression of ACBP gene expression stimulates chondrocyte differentiation. However, the expression of antisense ACBP mRNA in MC3T3-E1 cells showed the inhibition of osteoblastic differentiation. The antisense MC3T3-E1 cells showed lower alkaline phosphatase activity than that of control cells during osteoblast differentiation. Taken together, suppression of ACBP gene expression stimulates chondrocyte differentiation but inhibits osteoblast differentiation. This implicates that lipid metabolism is important in bone cell differentiation.

Disclosures: ***J. Choi****, IBEC of KOSEF of Korean government 2.*

SU212

Differential Growth Factor Regulation of Bone Formation by Human Osteoprogenitor Cells *in vitro*. L. R. Chaudhary[1], A. M. Hofmeister*[2], K. A. Hruska[1]. [1]Pediatrics, Washington University School of Medicine, St. Louis, MO, USA, [2]Earth & Planetary Sciences, Washington University, St. Louis, MO, USA.

The osteogenic factors BMP-7, PDGF-BB, FGF-2 and dexamethasone (Dex) regulate the recruitment of osteoprogenitor cells, their proliferation and differentiation into mature osteoblasts, and play important roles in bone formation. However, their mechanisms of action on osteoprogenitor cell growth, differentiation, and bone mineralization remain unclear. Here, we examined the effects of various osteogenic agents on these parameters with Dex serving as a positive control. Human bone marrow stromal cells were plated in 6-well culture plates ($1x10^5$ cells/well) and treated with BMP-7 (40 ng/ml), PDGF-BB (20 ng/ml), FGF-2 (20 ng/ml), FGF-2 plus BMP-7, or Dex (10^{-7} M) for 28 days in the α -MEM medium containing 10% FBS, 10 mM β -glycerophosphate and 50 μg/ml ascorbic acid. The medium was changed twice weekly with respective treatments. BMP-7 regulated the entire osteoblast differentiation program. It decreased osteoprogenitor proliferation, and stimulated CBFA1 expression, cuboidal morphology, alkaline phosphatase (ALKP) levels and Alizarin Red S positive nodule formation which was shown by Fourier Transform Infrared (FTIR) spectroscopy to be due to hydroxyapatite (HA) deposition into a type I collagen matrix. Dex treated cells appeared elongated and fibroblast like compared to BMP-7 treated cells and BMP-7 effects exceeded those of Dex on the other parameters such as ALKP levels and cell morphology. FGF-2 did not stimulate ALKP, CBFA1 and cell morphology was distorted. PDGF-BB stimulated cell proliferation and had little or no effect on CBFA1, ALKP activity and biomineralization. Alizarin Red S staining of cells indicated that BMP-7, Dex and FGF-2 enhanced calcium mineral deposition, but Alizarin Red S stains all calcium mineral deposits. FTIR spectroscopic analysis of BMP-7 and Dex treated samples demonstrated the formation of HA similar to human bone but no HA formation was observed in control, PDGF-BB and FGF-2 treated samples. Although FGF-2 stimulated a dystrophic calcium mineral deposition. When FGF-2 and BMP-7 were added together, BMP-7 stimulation of ALKP and HA formation was inhibited. Our results demonstrate that BMP-7 has stimulatory effects on the osteoblast differentiation program leading to increased bone formation. The other factors were active at discrete parts of the program and were dystrophic or inhibitory, if present at the wrong stage of osteoblast differentiation.

SU213

hMSCs-Host Interactions in Ectopic Bone Formation. R. A. Dodds*[1], M. Jennings*[1], R. Young*[1], L. Kostura*[1], W. S. Zhou*[2], L. F. Cooper[2]. [1]Osiris Therapeutics, Baltimore, MD, USA, [2]University of NC, Chapel Hill, NC, USA.

In the absence of any stimulation, mesenchymal stem cells (MSCs) remain undifferentiated in culture. Upon attachment to an HA/TCP matrix, the MSC differentiates along the osteoblast (MSC-Ob) lineage and when implanted contributes to ectopic bone formation *in vivo*. The goal of this study was to determine the contribution of host-specific osteoinductive signals associated with osteogenesis supported by HA/TCP adherent MSCs. To achieve this goal, human (h) MSCs adherent to HA/TCP matrices (60/40 fibronectin coated) were subcutaneously implanted in the dorsum of SCID mice for 3-21 days (d), and osteogenesis evaluated at the tissue and molecular level by cytochemistry, immunohistochemistry and RT-PCR. Matrices were loaded with 1.5 x 10^6 hMSC, h-skin fibroblasts (Fb), or were cell free (Cf). Serial sections were reacted for alkaline phosphatase (AP), TRAP, non-specific esterase (monocytes, monos) and expression of h-specific antigen Ok^a. RNA isolated from explants was amplified (Taq polymerase) using species-specific primers for mouse (m) and human (h) BMP2, BMP6, BSP, CD14 (monos) and GAPDH mRNAs. Reactions were evaluated by transillumination of ethidium bromide stained gels. AP activity was evident in human Obs (Ok^a positive) as early as 3d. MSC-Ob differentiation (diff) increased at 14d, and was extensive by 21d. Bone formation apparent at 14d and 21d was associated with both OK^a positive (h-Obs) and Ok^a negative host cells. MSC-Ob diff was absent in the Fb loaded and Cf controls. Monos were evident at the periphery of the matrices in all groups, at all time points. Initial MSC-Ob diff (3-7d) preceded osteoclast (Ocs) diff; by 14-21d TRAP positive Ocs (mono- derived) were observed adherent to the HA/TCP. This association of Ocs with Ob diff is indicative of subsequent coupling between human Obs and mouse Ocs, and osteogenesis. Ocs were not observed in the matrices loaded with Fb or the Cf controls. Thus, Oc diff within the matrices was directly associated with hMSCs. Host-specific m-BMP2 was noted at all time points in all groups; m-BMP6 was expressed 7-21d. The early expression of m-BMP2 and 6 paralleled the expression of m-CD14 mRNA in all groups. At 3d, h-BMP2 and -6 expression was not observed but progressively increased thereafter, peaking at 21d. h-BSP expression was detected at 14d and 21d, paralleling the histological appearance of bone in hMSC containing matrices. From this data, we propose that the expression of m-BMP2 indicates the contribution of host osteoinductive signals at the HA/TCP matrix. When adherent hMSCs were present diff along the Ob lineage occurred, highlighting the importance of providing responsive cells within controlled host tissues to promote bone repair.

SU214

Effects of Cyclooxygenase-2 Gene Disruption on Osteoblastic Cell Growth. Z. Xu*, S. Choudhary*, C. B. Alander, L. G. Raisz, C. C. Pilbeam. Medicine, University of Connecticut Health Center, Farmington, CT, USA.

To study the role of cyclooxygenase-2 (COX-2) in osteoblastic function, we used primary calvarial osteoblasts derived from COX-2 wild type (+/+) and knockout (-/-) mice obtained by mating C57Bl/6x129 COX-2 heterozygote (+/-) mice. Calvariae from 5-8 wk old COX-2 +/+ and -/- mice were sequentially enzymatically digested; cell populations 2-5 were pooled, grown to confluence for 7-8 d and replated for experiments at 5000/cm^2. Similar to previous results in bone marrow stromal cell cultures, alkaline phosphatase (AP) activity was decreased in COX-2-/- cultures relative to COX-2+/+ cultures at 1-2 wk. Differences in AP activity were reversed by adding NS-398 (10^{-7} M), a selective inhibitor of COX-2 activity, to COX-2+/+ cultures or treating COX-2-/- cultures with PGE_2 (10^{-6} M). To determine if differences between COX-2+/+ and -/- cultures were due to differences in cell growth, cells were resuspended and counted by Coulter counter. COX-2-/- cultures had 1.8-fold more cells at day 5 of culture and 2.2-fold more cells at day 7 than COX-2+/+ cultures. Differences could not be accounted for by non-adherent cells since the percent floating cells was the same in COX-2+/+ and -/- cultures at day 5. Culture of COX-2+/+ cells with NS-398 (10^{-7} M) increased cell numbers on days 5 and 7 by 92-95%. Culture of COX-2-/- cells with PGE_2 (10^{-6} M) decreased cell numbers on days 5 and 7 by 57-79%. Measurement of viable cell number using the XTT assay (based on mitochondrial activity) showed 1.5-fold more viable cells in COX-2-/- cultures than in COX-2+/+ cultures at day 7 of culture. To examine differences in DNA synthesis, we measured the incorporation of ^{3}H-thymidine (TdR) during a 2 h pulse on day 4 of culture. TdR normalized to cell number was significantly increased in COX-2-/- cultures relative to COX-2+/+ cultures in 3 separate experiments, with the mean increase being 1.8-fold. In these 3 experiments, some cultures were serum deprived for 24 h to synchronize cells and then given medium with fresh serum (10% FCS) to stimulate cell growth. 48 h after addition of serum cell number had increased 2.7-fold cells in COX-2-/- cultures and 1.8-fold in COX-2+/+ cultures; TdR normalized to cell number was 1.7-fold greater in COX-2-/- cultures. To examine resistance to cell death, we measured the change in viable cell number with the XTT assay following 24 h of serum deprivation on day 4 of culture. COX-2+/+ cell number did not change, while COX-2-/- cell number fell by 77%. We conclude that absence of COX-2 in calvarial osteoblastic cultures decreases early markers of osteoblastic differentiation, increases cell number as a result of enhanced cell proliferation, and may decrease resistance to stress-induced cell death.

SU215

Site-Specific *In Vivo* Response to Osteogenic Induction by Human Bone Marrow Stromal Stem Cells of Different Embryonic Origins. S. O. Akintoye*[1], S. Shi*[1], J. Brahim*[2], M. T. Collins*[1], P. G. Robey[1]. [1]Craniofacial and Skeletal Diseases Branch, National Institute of Dental and Craniofacial Research/National Institutes of Health, Bethesda, MD, USA, [2]Clinical Research Core, National Institute of Dental and Craniofacial Research/National Institutes of Health, Bethesda, MD, USA.

The bone marrow contains a combination of different cell types that secrete various connective tissue components. Because of the osteogenic potential of bone marrow stromal compartment, injection of autologous bone marrow into surgical defect is commonly used to generate bone. Although the craniofacial bones (CF) develop embryologically from neural crest cells while the axial and appendicular bones develop from mesoderm, it is still unclear if there exists site-specific genetic and phenotypic differences in human bone marrow stromal stem cells (hBMSSCs) from these sites. The aim of this study was to investigate differences in bone formation by hBMSSCs of different embryonic origins. Bone marrow samples from CF (specifically, maxilla and mandible), and iliac crest (IC) were obtained from a normal adult female volunteer. hBMSSCs were established in culture using α-MEM (minimum essential medium) containing 20% fetal bovine serum supplemented with or without osteogenic inducers: dexamethasone (10^{-8} M) and ascorbic phosphate (10^{-4} M). Differentiation capacity of the cells was characterized *in vivo* by transplantation of 2 $x10^6$ cells attached to ceramic particles (hydroxyapatite/tricalcium phosphate) into the subcutis of immunocompromised mice. Six populations of cells (IC, maxilla and mandible hBMSSCs with and without osteogenic inducers) were transplanted in duplicates and harvested at different time points: 4, 6, 10 and 12 weeks. Each transplant was fixed, decalcified and hematoxylin/eosin stained sections were prepared for histological analysis. Bone formation was scored using an established system. Without osteogenic inducers, CF formed more bone than IC at each time point. When stimulated by osteogenic inducers, IC was more sensitive than CF by forming bone 2 weeks earlier, and more bone quantitatively. Interestingly bone formed by CF were isolated islands with less hematopoietic marrow compared with IC bone that was more compact and contained more hematopoietic marrow. To our knowledge this is the first time hBMSSCs of different embryonic origins are being compared from the same donor. Further understanding of these site specific differences is needed as it may have an impact on selection of graft materials to repair osseous defects.

SU216

Unfractionated Heparin Enhances IL-11-Induced STAT3 Activation And Leads To Increased Osteoclastogenesis *in vitro*. K. J. Walton*, J. M. Duncan*, M. K. G. Butcher*, P. Deschamps*, S. G. Shaughnessy. Pathology and Molecular Medicine, McMaster University, Hamilton, ON, Canada.

We have previously demonstrated that long-term heparin treatment causes cancellous bone loss in rats due in part to an increase in the number of osteoclasts lining the trabecular bone surface. In the present study, we investigated this phenomenon by examining the ability of heparin to synergistically enhance IL-11-induced osteoclast formation. Treatment of murine calvaria and bone marrow cells with IL-11 was found to induce the formation of tartrate resistant acid phosphatase positive ($TRAP^+$) multinucleated cells (MNCs) in a dose dependent fashion. No effect was seen when co-cultures were treated with heparin alone. However, when co-cultures were treated with both IL-11 and heparin, IL-11's ability to induce $TRAP^+$ MNC formation was enhanced 6-fold. In an attempt to resolve the mechanism responsible for this effect, we examined the ability of heparin to influence IL-11 signaling using murine calvaria cells. Heparin was found to enhance both IL-11-induced STAT3-DNA complex formation and transactivation, without altering either STAT3 tyrosine or serine phosphorylation. Heparin was also found to enhance IL-11's ability to induce the expression of both receptor activator of NF-κβ ligand (RANKL) and glycoprotein (gp)130. When taken together, these findings suggest a plausible mechanism by which heparin may cause increased osteoclastogenesis and therefore bone loss when administered long-term.

SU217

Modulation of the Purinergic Ca2+ Signaling Pathway in Osteoblasts by Olpadronate: Evidence on the Existence of a Bisphosphonate Receptor. G. Santillan*[1], S. Katz*[1], G. Stockman*[1], R. L. Boland*[1], E. Roldan*[2]. [1]Biologia, Bioquimica & Farmacia, Universidad Nacional del Sur, Bahia Blanca, Argentina, [2]Gador S.A., Buenos Aires, Argentina.

We have observed before that in rat osteoblasts (ROS 17/2.8 cells) both olpadronate (OPD) and its R1-aminosubstituted derivative IG-9402 interact with the purinergic calcium signaling pathway, rapidly modulating cytosolic Ca2+ levels by a mechanism implying activation of the PLC/IP3 pathway, release of Ca2+ from IP3-sensitive intracellular stores and influx of extracellular Ca2+. In the present work we have further characterized this interaction. Spectrofluorimetric measurements in Fura-2-loaded ROS 17/2.8 cells showed that stimulation with ATP (5 - 50 μM) in the absence of external Ca2+ induced a fast and transient cytosolic Ca2+ rise. When calcium was added to the medium, Ca2+ influx from the outside through voltage-dependent (VDCC) and store-operated calcium (SOC) channels was observed. Addition of OPD (0.1 - 1 μM) after ATP treatment inhibited Ca2+ entry in the presence of 5μM nifedipine and 5μM verapamil but not in the absence of the VDCC inhibitors. These results suggest that OPD blocks ATP induced calcium influx through SOC but not VDCC channels, acting at the mechanisms which couple inner store depletion and Ca2+ entry. Also, previous radioligand binding studies using [H3]OPD revealed the presence in ROS 17/2.8 cells of a saturable and high affinity binding site for OPD (Kd = 1 μM) which was partially competed by IG-9402 (Kd = 1.5 μM) but not at all by purinergic agonists. We have now observed that etidronate and alendronate compete too for binding to this site (Kd = 2 - 2.5 μM). These results reinforces the notion about the existence of a membrane receptor for bisphosphonates. Such putative receptor may serve as epicenter from which their message is decoded into transmembrane signaling pathways triggering the appropriate cellular response.

SU218

MSP-RON Signalling in Human Osteoblasts Requires Cell Adhesion and Lipid Raft Iintegrity. C. Camerino*[1], M. Santoro*[2], G. Colaianni*[1], G. Mori*[1], G. Gaudino*[2], A. Zallone[1]. [1]Department of Human Anatomy and Histology, University of Bari, Bari, Italy, [2]Department of Medical Science, University of Oriental Piedmont, Novara, Italy.

Ron is a receptor tyrosine kinase that mediates the biological effects of Macrophage Stimulating Protein (MSP). Ron expression has been analyzed in vivo during mouse embryogenesis showing a specific pattern of expression during the development of epithelial, bone and neuroectodermal tissues. We previously evaluated the role of MSP on human Osteoblasts (OBs) demonstrating that this factor plays a role in the differentiative and antiapoptotic pathways of these cells, activating Ca^{2+} mediated signals and triggering different intracellular events mediated by MAPK, AKT and $p70^{S6K}$. Growth, differentiation and survival of anchorage-dependent cells are regulated through signals generated by adhesion to extracellular matrix (ECM). We investigated the role of ECM in the signal pathways activated by MSP. Using Anti-Phosphotyrosine antibodies the phosphorilation state of Ron has been analyzed. In OBs cultured in adhesion condition, binding of MSP to RON induced a rapid phosphorilation of RON 150 kDa β-chain albeit a basal state of phosphorilation was also visible in unstimulated cells. We than speculated if the basal Ron phosphorilation could be due to the adhesion to the ECM that OBs physiologically produce. Indeed in OBs cultured in non adhering conditions, Ron phosphorilation was visible only after MSP stimulation while in unstimulated OBs we can not detect any RON phosphorilated form. Interestingly in non adhering OBs, MSP stimulation failed to activate MAPK and AKT that were activated only in OBs cultured in adhesion condition. These data show that ECM adhesion can lead to RON oligomerization and transphosphorilation, which causes an increase in RON kinase activity above the basal level that initiates the autophosphorilation, however only binding of MSP to RON can turn on the signals responsible for the activation of intracellular pathways like MAPK and AKT. In further experiments we have evidenced that MSP mediated signals require lipid raft integrity. Indeed analyzing the effects of MSP on OBs by single cell fluorometry we detected an intracellular Ca^{2+} increase that was abolished by pretreating the cells with the lipid raft inhibitor methyl-β-cyclodextrin. Similarly in methyl-β-cyclodextrin pre-treated OBs, MSP failed to activate MAPK, AKT and $p70^{S6K}$ that resulted clearly visible in OBs stimulated with MSP but not treated with methyl-β-cyclodextrin.

SU219

ERK Activation is Necessary for RANKL Expression Induced by High Extracellular Calcium. Y. Kim*, S. Kim*, G. Kim, J. Baek. Dept of Pharmacology and Dental Therapeutics, College of Dentistry Seoul National University, Seoul, Republic of Korea.

High extracellular calcium has been implicated in the regulation of osteoclastic bone resorption but the exact mechanism has not been thoroughly elucidated. High extracellular calcium has been shown to stimulate the expression of RANKL, known to be an essential factor for osteoclastogenesis, in osteoblastic cells. In this study, we explored whether the MAP kinase pathway is involved in the regulation of RANKL expression by high extracelluar calcium in mouse calvarial osteoblastic cells. As previously reported, high extracellular calcium induced the RANKL expression in mouse calvarial osteoblastic cells. PD98059, an inhibitor of MEK, an upstream activator of ERK (p44/42), inhibited the RANKL expression induced by high calcium but the inhibition was not complete. U0126, a potent specific inhibitor of MEK, reduced the RANKL induction by high calcium in a dose-dependent manner and completely abrogated at 20 μM. In addition, high extracellular calcium stimulated ERK phosphorylation after 5 min and the ERK activation was maintained after 30 min of high calcium treatment. These results indicate that ERK pathway plays a role in regulating RANKL expression by high extracellular calcium.

SU220

Role of a RGD-peptide in Signalling Pathways in Human Bone Marrow Stromal Cells. S. Pallu*[1], R. Bareille*[2], A. Jonczyk*[3], M. Dard*[4], J. Amedee[2]. [1]INSERM U 443, Bordeaux, France, [2]INSERM U443, Bordeaux, France, [3]Merck Clinical Research, Darmstadt, Germany, [4]Merck Biomaterial GmbH, Darmstadt, Germany.

Osseointegration of bone substitutes can be considerably helped if the implants are cellularized with autologous osteoblastic cells before implantation. Moreover, design of materials with pro-adhesive properties towards osteogenic cells constitutes one of our objectives. Modification of materials by grafting RGD-containing peptides is based on the affinity of integrins to extracellular matrix proteins including in their sequence the RGD sequence. Among the different sequences, the best result in terms of adhesion, has been obtained with a cyclic peptide (cyclo-DFKRG). Here we assessed the function of tyrosine kinase activities (PTK) and the phosphorylation of p125 FAK and MAPK (p42, p44) which could affect cell proliferation, cell differentiation. Human bone marrow stromal cells have been cultured for 15, 30, 60, 90 min in IMDM alone onto different coatings: cyclo-DFKRG (100μM), poly-L-Lysine (PLL) (5%), fibronectin (FN) (10μg/ml) and plastic culture dishes. Total proteins were extracted using a RIPA buffer containing protease and phosphatase inhibitors. PTK activities contained in cell extracts are determined by using a kit provided from PROMEGA. Phosphorylation of p125FAK and MAPK (p42, p44) have been determined by Western blotting using specific antibodies against these proteins and using a monoclonal anti-phosphotyrosine. Products have been quantified using NIH 1.62 and the ratio PY20/p125FAK; PY20/p44; PY20/p42 have been normalized using a-tubulin as control. Culture onto cyclic RGD-peptides induces an increase of PTK activities which reached a maximum after 30 min of culture. Unspecific adhesion as confered by poly-L-Lysine induces a basal PTK activities, contrary to the specific adhesion confered by fibronectin coatings but to a lesser extent than RGD-surfaces. In the same way, adhesion to cyclo DFKRG promotes tyrosine phosphorylation of the p125FAK and MAPK (p42, p44) after 15 to 30 min of cell seeding and then decreased. Fibronectin coatings induce a similar kinetic of phosphorylation according to the engagement of integrins upon adhesion but with a lower extent. Unspecific adhesion confered by poly-L-Lysine induces the lowest level of phosphorylation of these proteins. In conclusion, adhesion of HBMSC onto this cyclic RGD induces activation of several intracellular signal transduction molecules which could be responsible of the stimulation of osteocalcin expression showed by competitive RT-PCR analysis, and to an increase of matrix mineralization. This peptide seems to be a good candidate to modify biomaterials and then to increase its osseointegration.

SU221

Parathyroid Hormone Induces the Nuclear Orphan Receptor NOR-1 in Osteoblasts Primarily through cAMP-PKA Signaling. F. Q. Pirih*, L. Pham*, J. M. Nervina, S. Tetradis. School of Dentistry, UCLA, Los Angeles, CA, USA.

Parathyroid hormone (PTH) regulates osteoblast function by initiating a cascade of gene expression. First to undergo changes in their expression are the primary response genes, whose expression is rapid, transient, and critical for the subsequent molecular events that generate PTH's osteotropic effects. Identifying PTH-induced primary response genes and understanding the molecular signals mediating their function are of fundamental importance in unveiling the mechanisms by which PTH regulates bone metabolism. Among PTH-induced primary response genes are Nurr1 and Nur77, members of the NGFI-B nuclear orphan receptor family. A third NGFI-B gene, NOR-1, is induced in the brain, but to date has not been shown to be regulated in osteoblasts. We report here that PTH induced NOR-1 mRNA in primary mouse osteoblasts (MOB cells) and cultured mouse calvariae mainly through the cAMP-protein kinase A (PKA) signaling pathway. PTH rapidly and transiently induced NOR-1 mRNA levels in MOB cells, with maximal induction at 2 h with 10 nM hormone. PTH binds to the PTHR1 receptor, which is coupled to the PKA, protein kinase C (PKC) and calcium pathways. To determine which pathway(s) mediate PTH-induced NOR-1 induced expression, MOB cells were treated with 10 μM forskolin (FSK, PKA activator), 1 μM phorbol ester (PMA, PKC activator) and 1 μM ionomycin (IO, calcium ionophore). FSK strongly induced NOR-1 mRNA levels, while PMA and IO showed a weaker induction of NOR-1 mRNA levels. In addition, 10 nM PTH (3-34), which does not activate the PKA pathway but activates PKC and calcium pathways, did not induce NOR-1 mRNA levels. Selective pathway inhibitors were tested to further delineate the relative importance of each pathway in mediating PTH-induced NOR-1 expression. A 30 min pretreatment with 30 μM H89 to block PKA inhibited PTH- and FSK-induced NOR-1 mRNA. Overnight pretreatment with 1 μM PMA to deplete PKC did not affect PTH-induced NOR-1 mRNA, but did inhibit PMA-induced NOR-1 mRNA. Finally, PTH induced NOR-1 mRNA maximally at 1 h in cultured neonatal mouse calvariae. Taken together these data indicate that PTH induced NOR-1 mRNA primarily through the cAMP-PKA pathway. PTH-regulated induction of all members of the NGFI-B nuclear orphan receptor family suggests that these genes play an important role in the immediate response of osteoblasts to PTH, with implications for the overall effect of PTH on bone metabolism.

SU222

Parathyroid Hormone Induces NFIL3/E4BP4 Gene Expression in Bone. I. C. Ozkurt*, S. Tetradis. School of Dentistry, University of California at Los Angeles, Los Angeles, CA, USA.

Following binding to its receptor parathyroid hormone (PTH) activates the cAMP/protein kinase A (PKA), protein kinase C (PKC) and calcium signaling pathways and subsequently induces transcription of several osteoblastic primary response genes. Products of primary response genes, subsequently, initiate the cascade of molecular events that mediate osteoblast response to PTH and play a pivotal role in the effects of PTH on bone metabolism. We have performed representational difference analysis and identified the Nuclear Factor regulated by IL-3 (NFIL3)/ adenovirus E4 promoter Binding Protein (E4BP4) as a PTH induced primary gene in osteoblasts. NFIL3/E4BP4 is a basic leucine zipper (bZIP) transcription factor, binds DNA as a dimer and acts either as transcriptional repressor or activator. Osseous localization and PTH induction of NFIL3/E4BP4 have not been reported previously. The objectives of our studies were to characterize the PTH induction of NFIL3/E4BP4 gene expression and to identify the presence of NFIL3/E4BP4 protein in the nucleus where it presumably regulates downstream gene expression. For all our experiments we utilized primary osteoblasts (MOb) derived from 7-day old mouse calvariae. PTH strongly increased NFIL3/E4BP4 mRNA levels MOb cells and in mouse calvariae organ cultures with maximal induction at 2 hours and at 10 nM. Pretreatment with cycloheximide (CHX) superinduced, while pretreatment with actinomycin D inhibited, the PTH induction of NFIL3/E4BP4 mRNA levels. To detect levels of nuclear NFIL3/E4BP4 protein, electrophoretic mobility shift assays (EMSAs) were performed utilizing nuclear extracts from PTH treated MOb cells and a consensus NFIL3/E4BP4 response element (NF3RE) as a probe. PTH induced binding to the NF3RE that peaked at four hours and declined thereafter. A recombinant NFIL3/E4BP4 protein showed a similar binding to the NF3RE. When two mutant NF3REs were used the PTH-induced binding and the binding of recombinant NFIL3/E4BP4 were strongly reduced. CHX significantly reduced the PTH-induced NF3RE binding suggesting that it contains newly synthesized proteins. Finally NFIL3/E4BP4 antibodies supershifted the PTH-induced NF3RE binding complexes suggesting that they contained the NFIL3/E4BP4 protein. In conclusion, PTH induces NFIL3/E4BP4 gene expression in primary osteoblasts and organ cultures. Furthermore, PTH induces specific binding to a consensus NF3RE that contains newly synthesized proteins and is recognized by an NFIL3/E4BP4 antibody. NFIL3/E4BP4 induction could mediate PTH regulation of downstream osteoblastic genes.

SU223

PTHrP Actions in Differentiated Osteoblasts: The Role of the MAPK Pathway. C. Chen*, A. J. Koh*, L. K. McCauley. Perio/Prev/Geriatrics, University of Michigan, Ann Arbor, MI, USA.

Parathyroid hormone-related protein (PTHrP) regulates proliferation and differentiation of osteoblastic cells via binding to the parathyroid hormone receptor (PTH1R). The PKA pathway governs a majority of the effects induced by PTHrP on osteoblasts, but recent evidence also implicates the mitogen-activated protein kinase (MAPK) pathway. To evaluate the role of MAPK in PTHrP-mediated gene expression and regulation of apoptosis, northern analysis, western analysis and cell viability assays were performed. MC3T3-E1 cells were induced to differentiate, pre-treated with U0126 (a MEK inhibitor) for 2h, then treated with PTHrP for different time points. Osteocalcin gene expression was downregulated at 48h by U0126 (7-fold), PTHrP (11-fold), and the combination of U0126 and PTHrP (20-fold). Bone sialoprotein gene expression was downregulated at 48h by U0126 (1.3-fold), PTHrP (1.5-fold) and the combination (3-fold). In contrast, PTHrP downregulated PTH1R gene expression at 48h, but U0126 had no effect and in combination did not alter the PTHrP downregulation. PTHrP induced c-fos gene expression (1h) but U0126 had no effect alone and did not alter the PTHrP induction. Interestingly, U0126 blocked the PTHrP stimulation of fra-2 (2h) and IL-6 (2h) gene expression. We have previously shown that PTHrP induces apoptosis (6h) in differentiated MC3T3-E1 cells and further that PTHrP rapidly decreases phosphorlyation of AKT (an inhibitor of apoptosis in the phosphorylated state). Here, we investigated the role of MAPK and found that a 2h pre-treatment with U0126 before PTHrP treatment partially blocked the pro-apoptotic effect of PTHrP. However, western blot analysis revealed that U0126 had no effect on the PTHrP decrease in phosphorylation of AKT. This suggests that the MAPK pathway is partially responsible for PTHrP mediated apoptosis, but that inhibition of MAPK does not alter the PTHrP effect on AKT phosphorylation. In addition, these data indicate that inactivation of the MAPK pathway by U0126 shows differential regulation of PTHrP stimulated AP-1 members (effecting fra-2 but not c-fos), reduces PTHrP stimulated IL-6 and synergistically downregulates certain osteoblastic markers (BSP, OCN) associated with differentiation. These data confer that the MAPK pathway plays an important role in the actions of PTHrP and suggest that gene expression and apoptosis are regulated by PTHrP via multiple pathways in differentiated osteoblasts.

SU224

Evidence that Activation of Phospholipase D is an Early Event in Downstream Signaling by PTH in UMR-106 Osteoblasts. J. M. Radeff*[1], A. T. K. Singh[1], D. A. Dossing*[1], S. Sebti*[2], P. H. Stern[1]. [1]Molecular Pharmacology and Biological Chemistry, Northwestern University, Chicago, IL, USA, [2]H. Lee Moffitt Cancer Center, University of South Florida, Tampa, FL, USA.

Parathyroid hormone (PTH) activates multiple signaling pathways in osteoblasts, although the precise mechanisms and/or cross-talk between these pathways have not been clearly established. In the current study, we have investigated connections between PTH actions on phospholipase D (PLD), protein kinase C (PKC), expression of the interleukin-6 (IL-6) promoter and receptor activator of NFkB ligand (RANKL) in UMR-106 osteoblastic cells. We have also investigated the potential influence of AC/cAMP/PKA on these pathways. a) Hydrolysis of membrane phospholipids by PLD generates phosphatidic acid, which is converted to diacylglycerol (DAG), a direct activator of PKC, by phosphatidic acid phosphatase. Propranolol was used to inhibit phosphatidic acid phosphohydrolase, demonstrated by an increase in PA and a decrease in DAG. Propranolol prevented the PTH-stimulated membrane translocation (visualized by immunofluorescence) of PKCα and attenuated IL-6 promoter expression, suggesting that PLD pathways contribute to these downstream responses. In contrast, the direct stimulation of PKCα translocation by phorbol dibutyrate, which would not require PLD, was not inhibited by propranolol. b) PTH stimulated membrane translocation of RhoA, but not other small G proteins (RhoB, Rac1, Cdc-42). Dominant negative RhoA (Rho19N), a geranyl geranyl transferase inhibitor (GGTI-2166) and a Rho kinase inhibitor all prevented PLD activity and PKCα translocation by PTH. GGTI-2166 and the Rho kinase inhibitor did not affect phorbol dibutyrate-stimulated PKCα translocation. GGTI-2166 and Rho kinase inhibition also attenuated PTH-stimulated IL-6 promoter expression. c) Although PTH stimulates IL-6 and RANKL expression through both PKC and PKA pathways, forskolin and IBMX failed to promote PKCα translocation. PTH-stimulated PKC translocation was unaffected by the PKA antagonist PKI. These findings establish a pathway from RhoA and Rho kinase to PLD-generated DAG that stimulates PKCα translocation, leading to IL-6 expression. In addition, the AC/cAMP/PKA pathway does not appear to influence these events.

SU225

Ultrastructural Changes in Cathepsin K Deficient Osteoclasts. R. Kiviranta[1], K. Ivaska*[2], J. Risteli[3], H. K. Väänänen[2], E. Vuorio[1], T. Laitala-Leinonen[2]. [1]Department of Medical Biochemistry and Molecular Biology, University of Turku, Turku, Finland, [2]Department of Anatomy, University of Turku, Turku, Finland, [3]Department of Clinical Chemistry, University of Oulu, Oulu, Finland.

Bone resorption is a multi-step process performed by osteoclasts. Cathepsin K is a major protease in resorption of bone matrix molecules. Recent reports indicate that cathepsin K deficient mice develop severe osteopetrosis of long bones due to their inability to degrade organic bone matrix. The aim of our study was to evaluate the cell biological changes in cathepsin K deficient osteoclasts. We chose to generate our own cathepsin K (Ctsk) knockout mice by replacing exons 2 to 5 of the gene with a neomycin resistance gene in embryonal stem cells. Chimeric mice were mated with C57Bl/6J females to get outbred heterozygous Ctsk+/- mice. These mice were subsequently mated to obtain wild type (wt), heterozygous (Ctsk+/-) and homozygous (Ctsk-/-) mice for the inactivated cathepsin K allele. Peripheral quantitative computed tomography (pQCT) was used to confirm the previously published osteopetrotic phenotype at the age of 8 weeks. To study bone resorption in vitro, primary wt and Ctsk-/- osteoclasts were cultured on bovine cortical bone slices for 3 to 4 days. The culture media were analyzed for bone degradation products. Immunofluorescence analysis of various osteoclast and bone matrix proteins was performed to study the morphology of Ctsk deficient osteoclasts. pQCT measurements showed increased bone mineral density in the long bones of Ctsk-/- mice and extensive trabeculation of bone marrow spaces. The amount of medium C-terminal telopeptide of type I collagen (ICTP), degradation products of C-terminal telopeptides of type I collagen (CTX) and bone derived osteocalcin fragments were significantly decreased in the Ctsk-/- cultures. Cathepsin K immunostainings confirmed that Ctsk-/- osteoclasts did not express any detectable cathepsin K protein. Large vesicles containing type I collagen were found in Ctsk-/- osteoclasts while no type I collagen was detected inside the wt cells. Phalloidin staining revealed that a majority of the actin rings were abnormally thick in these osteoclasts, and in most of the cells the actin ring was either partially or totally disrupted into podosomal structures. Also the ruffled border and sealing zone were disorganized. The inner vinculin ring was absent from the vicinity of the disrupted actin structures. This data suggests that the ingestion of large amounts of undegraded type I collagen arrests the bone resorption in Ctsk-/- osteoclasts and leads to disassembly of the sealing zone. Thus cathepsin K deficiency severely impairs osteoclast function.

SU226

Bone Resorption in Osteoclasts Overexpressing Cathepsin K. J. Morko*[1], K. Ivaska*[2], M. Mulari*[2], S. Ylönen*[2], H. K. Väänänen[2], E. Vuorio[1], T. Laitala-Leinonen[2]. [1]Department of Medical Biochemistry and Molecular Biology, University of Turku, Turku, Finland, [2]Department of Anatomy, University of Turku, Turku, Finland.

Bone resorption cycle is a multistep process including osteoclast attachment, polarization, resorption and detachment. The polarization for resorption includes many cytoskeletal changes and formation of distinct plasma membrane domains, namely ruffled border, sealing zone, basal membrane and functional secretory domain. Subsequent resorption includes both the solubilization of crystalline hydroxyapatite and the degradation of demineralized organic matrix. Cathepsin K, a lysosomal cysteine proteinase, has been proposed to be a major proteinase in this degradation process. We have recently developed a transgenic mouse model overexpressing cathepsin K. The present study was designed to study how cathepsin K overexpression affects bone resorption in cultured osteoclasts. Two-day old mice homozygous for the transgene locus and nontransgenic controls were used as a source of osteoclasts, which were cultured on bovine cortical bone slices. Cathepsin K and its transcripts were studied by Western and Northern analyzes, respectively. Other osteoclastic and bone matrix proteins were studied by immunofluorescence stainings. Resorption was analyzed from bone slices, and pits were visualized by field emission scanning electron microscopy. Levels of released degradation products of bone proteins were measured from culture media. Northern and Western analyzes confirmed the overexpression of cathepsin K. Confocal microscopy demonstrated localization of excess cathepsin K near the ruffled border and in numerous intracellular vesicles throughout the osteoclast cytoplasm. These vesicles were positive for Rab7 or Rab9 GTPases indicating that the transport of cathepsin K inside the osteoclasts occurred in

specific endo- and exocytic vesicles. Also the amount of carbonic anhydrase II was slightly increased indicating an enhanced production of protons required for enhanced demineralization. The amount of cathepsin K in the resorption front was increased, and the amounts of type I collagen and osteocalcin in the resorption pits were decreased indicating enhanced degradation of organic bone matrix. This was confirmed with bone slice and culture medium analyzes, where the number of resorption pits, the resorbed area, and the amounts of released degradation products of bone proteins were increased. The current data demonstrates that excessive cathepsin K production leads to increased bone resorption characterized by an enhanced membrane trafficking.

SU227

Osteoblasts Render Osteoclastic Bone Resorption Sensitive to Matrix Metalloproteinase Inhibitors. J. Delaissé, M. T. Engsig*, T. L. Andersen*, K. Henriksen*, T. Kirkegaard*, M. Ovejero*, M. A. Karsdal, C. Christiansen, N. T. Foged*. Nordic Bioscience A/S / CCBR, Herlev, Denmark.

A variety of experiments performed on cultured bone explants have demonstrated that both cysteine proteinases, including cathepsin K, and matrix metalloproteinases (MMP) are rate limiting for osteoclastic bone resorption. However, pit formation by purified osteoclasts is decreased only in the presence of cysteine proteinase inhibitors, not in the presence of MMP inhibitors. Furthermore, the resorption of bone explants from mice lacking the different osteoclastic MMPs is not decreased compared with that of wild types. We thus hypothesized that the MMP responsible for the MMP inhibitor sensitivity of resorbing bone explants is not of osteoclast origin, but instead, may originate from osteoblasts. In order to test this hypothesis, we performed the pit assay with rabbit osteoclasts in the presence of osteoblastic MC3T3 cells at increasing cell densities, thereby mimicking the osteoblastic cell layer lining native bone surfaces. In the absence of osteoblasts, the MMP inhibitors GM6001 and BB94 did not inhibit pit formation. In the presence of osteoblasts, however, pit formation was inhibited by the MMP inhibitors, and the sensitivity to MMP inhibitors increased with increasing cell densities, reaching comparable levels as for bone explant cultures. Next, we investigated systematically the mRNA and protein expressions of MMP-1, -2, -3, -9, -10, -11, -12, -13, and -14 in bone explants, and found a unique localization pattern of MMP-13: the mRNA is highly expressed in mononucleated cells next to resorbing osteoclasts, whereas the protein is not only at the level of these cells, but also further away at the level of osteoclasts, and is particularly abundant in the osteoclastic resorption zone, as assessed in adjacent sections with 5 different antibodies against MMP-13. Finally, we also found that MMP-13 levels are increased in the bones of mice receiving a calcium deficient diet and showing upregulated bone resorption; MMP-13 levels return to normal upon replenishment with a normal diet and normalization of bone resorption to control levels. A key role of MMP-13 in bone resorption is also shown by the decreased resorption of bone explants from mice lacking MMP-13, compared to wild types (S. Krane, J. Bone Min. Res., 161, S149). In conclusion, these data show the type of proteinases involved in bone resorption may depend on the cellular environment of the osteoclast. More specifically, an osteoblastic proteinase of the MMP family, most likely MMP-13, controls osteoclastic bone resorption. MMPs represent thus an additional category of osteoblastic gene products controlling osteoclastic bone resorption.

SU228

Bone in Transgenic Mice Overexpressing Tartrate-resistant Acid Phosphatase (AcP5, TRAP). S. J. Jones[1], A. Boyde[1], A. R. Hayman[2], T. M. Cox*[3]. [1]Department of Anatomy and Developmental Biology, University College London, London, United Kingdom, [2]Division of Molecular and Cellular Biology, School of Clinical Veterinary Science, Bristol, United Kingdom, [3]Dept of Medicine, University of Cambridge, Cambridge, United Kingdom.

Transgenic mice overexpressing tartrate-resistant acid phosphatase (AcP5) were reported to have less trabecular bone than their wildtype, but the mice were examined only as neonates (1). The present study reports on older animals. Wildtype and transgenic mice with either threefold or eightfold overexpression of AcP5 were culled at 10-11 weeks, or at 18 months or 22-23 months. Femurs and tibiae-fibulae, fixed in 70% ethanol, were either embedded in PMMA or opened longitudinally to expose the marrow cavity and cleaned with Tergazyme (Alconox, New York, NY). The embedded specimens were cut and micromilled. All specimens were coated with carbon for SEM using backscattered electrons (BSE). Forelimbs from the older animals were also examined by Piximus DEXA (Lunar). SEM @ 10-11 weeks: male and female femurs of each of the three genotypes showed less than 2% difference in lengths, and internal and external diameters of the bones and extent of trabeculation in distal femur were equal. There was no evidence for increased bone turnover in the transgenic compared with the wildtype mice. SEM @ 18 or 22/23 months: no trabeculae remained in the marrow cavity at either 18 or 22/23 months in any genotype, and the sizes of the bones were similar. Endosteal resorption pits in the bones from mice overexpressing AcP5 did not differ from those in the wildtypes in appearance or distribution, nor were the internal or external diameters of the bones larger. No differences were found from quantitative BSE SEM analysis in either age group. No differences in BMC and BMD were detected by DEXA. There are no differences between the wild type, the 3X and the 8X overexpression phenotypes at the ages examined. The present findings can be explained by assuming that the rate limiting step in osteoclastic bone resorption of mature lamellar bone tissue is that of the acid induced demineralisation prior to organic matrix degradation employing proteolytic enzymes (2). Although lack of AcP5 results in disruption of endochondral ossification and some impairment of resorption leading to a mild osteopetrosis (3), having more AcP5 does not increase bone resorption, because enough is sufficient.

1. Angel et al. J Bone Min. Res. 15, 103-110 (2000)
2. Jones et al.Calcif Tiss Int 56, 554-558(1995)3. Hayman et al. Development 122, 3151-3162 (1996)

SU229

Acid Phosphatase and Oxygen Radical-Generating Activities of Type 5 Tartrate-resistant Acid Phosphatase Are Functionally Independent. S. L. Alatalo*[1], H. Kaija*[2], H. Ylipahkala*[1], Y. Lindqvist*[3], G. Schneider*[3], P. Vihko*[2], H. K. Väänänen[1], J. M. Halleen[1]. [1]Institute of Biomedicine, Department of Anatomy, University of Turku, Turku, Finland, [2]Biocenter Oulu, Research Center for Molecular Endocrinology, University of Oulu, Oulu, Finland, [3]Department of Medical Biochemistry and Biophysics, Karolinska Institutet, Stockholm, Sweden.

Type 5 tartrate-resistant acid phosphatase (TRACP) is an enzyme with unknown biological function that is expressed by bone-resorbing osteoclasts and activated macrophages. Active site of the enzyme contains a binuclear iron center with two irons, one of which is redox-active. In addition to its acid phosphatase (AcP) activity TRACP is also capable of generating reactive oxygen species (ROS) in vitro. Both activities require the redox-active iron in the active site. We have studied the two activities using wild-type and mutated forms of recombinant rat TRACP. Single amino acid mutations were generated by site-directed mutagenesis targeted to the amino acids predicted to be important for the AcP activity. The mutated amino acids were either in the substrate-binding pocket of the enzyme or in the alternative glycosylation sites, but not in the amino acids coordinating the two iron atoms in the active site. The AcP activity was determined using 4-NPP as substrate, and ROS activity either by monitoring the formation of malondialdehyde acetal from degradation products of deoxyribose or by detecting the fluorescence of 7-hydroxycoumarin-3-carboxylic acid (7-OHCCA) after hydroxyl radical attack. The pH-optimum of wild-type recombinant rat TRACP was 4.5 for the AcP activity and 6.5 for the ROS generating activity. All the mutated TRACP enzymes had significantly decreased AcP activity compared to the wild-type enzyme, while the ROS generating activity was decreased, not affected or increased. The changes in the AcP and ROS generating activities did not correlate with each other in individual mutants. These results suggest that not only the substrate availability and specificity, but also the pH of the environment may regulate the function of TRACP. We conclude that the two activities of TRACP may have independent mechanisms and function in different cell types and different intracellular compartments.

SU230

Interleukin-12 Induces Apoptosis of Bone Marrow Cells in Tumor Necrosis Factor-alpha Mediated Osteoclastogenesis. H. Kitaura[1], N. Nagata*[1], M. Tatamiya*[1], N. Yoshida*[1], K. Nakayama*[2]. [1]Department of Orthodontics, School of Dentistry, Nagasaki University, Nagasaki, Japan, [2]Department of Oral Microbiology, School of Dentistry, Nagasaki University, Nagasaki, Japan.

In recent years, much importance has been attached to the relationship between cytokines and bone metabolism. Although RANKL is an essential cytokine for inducing the differentiation of osteoclasts, it has recently been found that the differentiation of osteoclasts is also induced by TNF-alpha. Few studies have clarified the relationship between bone metabolism and Interleukin-12 (IL-12) that plays an important role in immunity. In this study, we investigated the effects of IL-12 on TNF-alpha-mediated osteoclastgenesis. Whole bone marrow cells collected from ddY mice were cultured in the medium containing M-CSF and TNF-alpha with or without IL-12. When bone marrow cells were cultured in the medium without IL-12, a number of osteoclast-like cells were formed. On the other hand, when they were cultured with IL-12, the number of adherent cells decreased in a dose-dependent manner. We found morphological changes such as cell atrophy, and nuclear and cellular fragmentation, and biological changes such as DNA fragmentation in the adherent cells treated with IL-12, indicating apoptosis of these cells. Direct effects of IL-12 on TNF-alpha-inducing osteoclastgenesis were determined using M-CSF dependent bone marrow macrophage (M-BMM) as an osteoclasts precursor (preOC). Apoptotic effects such as cell atrophy were not observed in M-BMM, suggesting that apoptosis would not be induced by a direct effect of IL-12 on preOC, but by a factor formed by IL-12-treated non-preOC cells in whole bone marrow cells. The IL-12-mediated apoptosis was markedly inhibited when bone marrow cells were treated with anti-FasL antibody. FACS analysis revealed that TNF- alpha up-regulated Fas expression on the surface of adherent cells in bone marrow cells culture in the presence of M-CSF, whereas IL-12 could not express Fas in the cells. IL-12 induced FasL on the surface of non-adherent cells in bone marrow cells culture, whereas TNF-alpha could not express FasL in the cells. Taken together, it was found that presence of both IL-12 and TNF-alpha was indispensable for apoptosis in this culture system and the apoptosis was induced by Fas/FasL interaction between adherent and non-adherent cells in bone marrow cells. In summary, we found in this study that a combination of IL-12 and TNF-alpha induced apoptosis of bone marrow cells and that the apoptosis may be caused by interaction of TNF-alpha-induced Fas on the adherent cells and IL-12-induced FasL on the non-adherent cells.

SU231

Human Osteoclasts Secrete TNF-α and IL-6 in Response to IL-1α Stimulation. T. R. Fuson*, R. J. S. Galvin. Gene Regulation, Lilly Research Labs, Indianapolis, IN, USA.

Soluble factors within the bone microenvironment influence osteoclast differentiation and function; however, the role of osteoclasts as autocrine regulators of osteoclast differentiation or resorption has not been well studied. Since IL-1 induces cytokine secretion in numerous cell types and is a critical regulator of osteoclastic bone resorption, we evaluated the effects of IL-1α on IL-6 and TNF-α secretion from cultured human osteoclasts. Delta cultures [suspension culture of cells (1 x 10^6 cells/ml in a T-150 flask) in Iscoves DMEM containing 25% heat-inactivated FBS, 1% antibiotic/antimycotic solution, 20 ng/ml rhIL-3, 20 ng/ml rhGM-CSF, and 10 ng/ml stem cell factor] of human umbilical cord blood cells (purchased from BioWhittaker) served as the source of osteoclast progenitor cells. After 6-16 days in Delta culture, the suspension cells (CD33+) were collected and osteoclast differentiation was induced with rhRANKL and rhM-CSF. The cells were seeded at 2.5 x 10^5 cells/cm^2 in DMEM containing 10% charcoal-stripped FBS, 1% antibiotic/antimycotic, rhRANKL (50 ng/ml) and rhM-CSF (50 ng/ml). After 7 days, large numbers of TRAP-positive multinucleated cells were observed. These *in vitro* generated osteoclasts formed resorption lacunae when cultured on bovine cortical bone slices. The ability of these osteoclasts to secrete IL-6 and TNF-α was evaluated in cells cultured on plastic. The cells were pre-cultured in medium containing 1 mg/ml BSA or 10% FBS (1.5-4 h), and then treated with rhIL-1α (10-100 ng/ml) for 5, 18, 24 or 28 h in the appropriate medium. The medium concentrations of IL-6 and TNF-α were evaluated using a Human Cytokine Linco*plex* Kit (Linco Research Inc.). IL-1α increased the IL-6 concentration a minimum of four-fold following an 18-24 h treatment. A significant increase in IL-6 release to the medium was observed following 5 h of treatment. IL-1α also increased the release of TNF-α into the medium (4-70 fold) following 18-24 h of treatment. Similar results were observed in cultures treated in the presence of FBS or BSA. These results support previous immunohistochemistry studies which demonstrated that human osteoclasts express IL-6 and TNF-α, and suggest that rhIL-1α regulates IL-6 and TNF-α release from human osteoclasts. Furthermore, IL-6 and TNF-α may serve as autocrine regulators of osteoclast differentiation and/or function.

Disclosures: ***R.J.S. Galvin****, Eli Lilly and Company 3.*

SU232

Regulation of Mouse Osteoprotegerin Gene Expression by Steroid Hormones. T. Kondo*, R. Kitazawa, S. Maeda*, S. Kitazawa. Division of Molecular Pathology, Kobe University Graduate School of Medicine, Kobe, Japan.

Glucocorticoid-induced osteoporosis is a common and serious complication of systemic glucocorticoid use. It is generally accepted that glucocorticoids increase bone resorption *in vitro* as well as *in vivo*. In cocultures of ST2 cells and bone marrow macrophages, 1,25 dihydroxyvitamin D_3 supports osteoclastogenesis, and dexamethasone (Dex) administration synergistically stimulates it. To explore the precise mechanism whereby Dex stimulates osteoclastogenesis, we analysed the effect of Dex on cis-acting elements of the mouse osteoprotegerin (OPG) and the receptor activator of NF-κB ligand (RANKL) gene. The 5'-flanking region of the mouse OPG gene was cloned, and a series of deletion constructs ligated with a pGL3-Basic vector plasmid (Luc -116, Luc -697, Luc -1125, Luc -1487) were transfected into ST2 cells and subjected to luciferase assay. Transfected cells were treated with Dex (10^{-7}M) for 48h to assess its effect on the OPG promoter activity. Mirroring Northern blot analysis, Dex reduced the promoter activity of Luc -1487 to 50%. Electrophoretic gel motility shift assay (EMSA) carried out to determine protein-DNA binding on the putative AP-1 binding site (-293/-287, TGACTGA) showed specific binding to the putative AP-1 site and the supershift with an anti c-Jun antibody; the mutation of the putative AP-1 site (TGACTGA to CTCCCTC) nullified the protein-DNA binding. A construct containing the mutated AP-1 binding site (Luc -1487m) showed reduced promoter activity. Moreover, the Luc -1487m construct was resistant to Dex-driven suppression. To assess the inhibitory effect of Dex on the OPG gene at the protein level, the amount of OPG protein secreted by ST2 cells into the culture medium was measured by sandwich enzyme-linked immunosorbent assay (ELISA). The production of OPG protein decreased significantly by the 48-hour treatment with Dex, suggesting that Dex negatively regulates OPG partly by transrepressing OPG promoter activity through the AP-1 site and partly through a posttranscriptional modification process. On the other hand, Dex upregulated RANKL promoter activity to 130%, although only a nominal increase of mRNA was observed by Northern blot analysis. We speculate therefore that glucocorticoids per se promote osteoclastogenesis mostly by inhibiting OPG and partly by concurrently stimulating RANKL reciprocally, thereby enhancing bone resorption.

SU233

Expression of Osteoblast Differentiation Factor in Mature Osteoclasts. N. Udagawa[1], K. Itoh*[2], X. T. Li*[3], H. Ozawa[3], N. Takahashi[3]. [1]Biochemistry, Matsumoto Dental University, Nagano, Japan, [2]Biochemistry, Showa University, Tokyo, Japan, [3]Institute for Dental Science, Matsumoto Dental University, Nagano, Japan.

Previous morphological experiments suggest that osteoclastic bone resorption induces bone synthesis by osteoblasts. This indicates that bone resorption is coupled with bone formation by an unknown factor (coupling factor). The discovery of RANKL elucidates the precise mechanism of osteoclast differentiation and mature osteoclast function regulated by osteoblasts. In this study, we explored the possibility that mature osteoclasts express a factor which induces differentiation of osteoblasts. Osteoclast preparation obtained from cocultures of mouse bone marrow cells and osteoblasts on collagen-gel-coated dish were spot-cultured for 5 h in the center of a single culture well. Then, osteoblastic cells in the spot-culture were removed completely by trypsin-EDTA to purify osteoclasts on the center of the culture well. Mouse stromal cells, MC3T3-G2/PA6, ST2 and C3H10T1/2, all of which are negative for alkaline phosphatase (ALP, a marker enzyme of osteoblasts), were uniformly plated over the culture well. The spot cocultures were performed for 3 days, then fixed and double-stained for tartrate-resistant acid phosphatase (TRAP, a marker enzyme of osteoclasts) and ALP. ALP-positive cells appeared inside or just around the colony of TRAP-positive osteoclasts. No ALP-positive cells were observed outside the colony of osteoclasts. Treatment of the spot coculture with a soluble form of the extracellular domain of BMP receptor type IA (sBMPR-IA) or calcitonin did not inhibit the induction of ALP-positive cells When the contact between stromal cells and osteoclasts was inhibited by a membrane filter, no ALP-positive cells were formed in the spot coculture. ROSA26 transgenic mice express β-galactosidase in various tissues including hematopoietic cells. When osteoclasts obtained ROSA26 mice were spot-cocultured with stromal cells, osteoclasts were positive for β-galactosidase but ALP-positive cells were not, indicating that the osteoclast preparation does not contain progenitors of ALP-positive cells. These results suggest that mature osteoclasts express a membrane-bound factor which induces differentiation of immature stromal cells into ALP-positive osteoblasts.

SU234

Suramin Interacts with RANK and Inhibits RANKL-Induced Osteoclastogenesis. A. Regmi*, T. R. Fuson*, X. Yang*, J. S. Kays*, C. M. Moxham*, E. R. Zartler*, S. Chandrasekhar, R. J. S. Galvin. Lilly Research Labs, Eli Lilly and Company, Indianapolis, IN, USA.

Suramin, a naphthalene trisulfonic acid derivative, has been shown to exhibit numerous activities related to disruption of protein-protein interactions. For example, it has been shown to uncouple G-proteins from their receptors, inhibit cell-surface binding to EGF and PDGF, and dissociate trimeric human TNF-α. With respect to bone, suramin has been reported to inhibit osteoclastic resorption in organ culture and in a rodent model of hypercalcemia. Since RANKL is a member of the TNF- α family of proteins and is essential for osteoclast differentiation and function, we evaluated the effects of suramin on RANKL-induced osteoclast differentiation. Mouse spleen cell cultures were treated with rhRANKL (1.5 nM), mouse M-CSF (2.0 nM) and suramin (0, 1, 3, 10, 30, 100, 300 and 1000 μM) for six days. Osteoclast formation in the presence or absence of suramin was determined by quantification of tartarate-resistant acid phosphatase (TRAP), a marker for osteoclasts. Suramin inhibited osteoclast formation in a concentration dependent manner (IC_{50} = 207 μM). Since RANKL mediated osteoclast activation involves the IkB/NF-kB pathway, we next evaluated the effects of suramin on RANKL-induced signaling. Suramin (100 μM) inhibited rhRANKL (5 nM)-induced IkB-phosphorylation (at 15 min by Western analysis) in spleen-derived pre-osteoclasts and differentiated osteoclasts. To distinguish whether the effects of suramin are on RANK/RANKL binding or on post-receptor mechanism, suramin was also evaluated in a binding assay using rhRANKL (0.1 nM) and rhRANK/Fc chimera (0.2 nM). In this assay, a 40% reduction in rhRANKL binding was observed in the presence of 1 mM suramin. The effects of suramin on binding interactions were also evaluated by surface plasmon resonance technology and Nuclear Magnetic Resonace (NMR). Using a Bioacore 3000 for analysis, suramin was found to interact with immobilized rhRANK/Fc chimera in a concentration dependent manner and this interaction was two-fold greater for rhRANK/Fc compared to IgG_1 Fc. Suramin binding to rhRANK/Fc, but not IgG_1 Fc, was also demonstrated by saturation transfer difference NMR Spectroscopy. Binding of suramin to rhRANKL was barely detectable (at least an order of magnitude weaker than rhRANK/Fc). In the presence of equimolar amounts of RANKL and rhRANK/Fc, suramin still bound, presumably to the rhRANK/Fc. There was no indication of any perturbation in the binding to rhRANK/Fc in the presence of RANKL. In conclusion, suramin appears to inhibit RANKL induced osteoclastogeneis by binding to RANK and blocking the ability of RANKL to induce second messenger signaling.

Disclosures: ***A. Regmi****, Eli Lilly and Company 3.*

SU235

Antisense Oligonucleotide-Mediated Blockade of RANK Inhibits Osteoclast Formation and Enhances Apoptosis in Murine Bone Marrow-Derived Osteoclasts. K. J. Myers*, X. Li*, J. Finger*. Antisense Drug Discovery, Isis Pharmaceuticals, Carlsbad, CA, USA.

RANK is a cell surface receptor expressed on osteoclast precursor cells and mature osteoclasts. RANKL is expressed and secreted from osteoblasts, and engagement of RANK by RANKL is essential for both the differentiation and full functional activity of osteoclasts. We have developed a second generation antisense oligonucleotide specific for mouse RANK mRNA. Isis 181071 was selected from a panel of 48 RANK-specific antisense oligonucleotides as producing the most potent dose-dependent reduction of RANK mRNA, with a 400 nM dose typically inhibiting 80-90% of RANK mRNA expression in undifferentiated RAW 264.7 cells. Isis 181071 also displayed dose-dependent inhibition of RANK mRNA in primary mouse bone marrow-derived osteoclasts and osteoclast precursor cells from bone marrow. Several different control oligonucleotides were without effect at reducing RANK mRNA in RAW cells and primary cells. Isis 181071 potently inhibited TRAP+ multinucleated cell formation from osteoclast precursor cells. This effect was most pronounced when the oligonucleotide was transfected into pre-osteoclasts rather than more differentiated cells, which had already begun to show evidence of polykaryon formation. Isis 181071 was also effective at accelerating apoptosis in mature osteoclasts. This was seen with enhanced caspase-3 activity in RANK antisense-treated cells as well as changes in nuclear morphology visualized by fluorescent microscopy. RANK antisense thus inhibits osteoclast activity through effects on both cell differentiation and also by stimulating apoptosis. These results are consistent with previous reports demonstrating a critical role for RANK in osteoclastogenesis and osteoclast survival.

Disclosures: ***K.J. Myers****, Isis Pharmaceuticals 1, 3.*

SU236

Involvement of RANKL in Osteolytic Loosening of the Prosthesis After Total Hip Replacement. M. Horiki, T. Nakase, A. Myoui, T. Nishii*, N. Sugano*, H. Yoshikawa. Dept of Orthopeadic surgery, Osaka University Graduate School of Medicine, Suita, Japan.

Loosening of the implant is one of the major late complications of joint replacement surgery. Mechanisms of osteolysis have been extensively studied from a histological perspective, and osteoclasts have been shown to play an important role in osteolysis. However, specific molecules involved in this condition yet to be fully elucidated. A potent factor for osteoclastogenesis was recently identified and found to be identical to the ligand for receptor activator of NF-kB, RANKL. Together with M-CSF, RANKL has been shown to support differentiation and maturation of osteoclasts in vitro using mouse, rat, or human cells. Mice with a disrupted RANKL gene exhibited an osteopetrotic phenotype, suggesting RANKL plays an essential role in osteoclastic bone resorption . To investigate the expression and localization of RANKL, a recently purified potent regulator of osteoclastogenesis, in osteolytic loosening. . These recent findings led us to hypothesize that RANKL is involved in osteolysis around artificial implants. We examined fibrogranulomatous tissue interposed between the loosened implant and the host bone by immunohistochemistry and Reverse transcript polymerase chain reaction (RT-PCR). The fibrous tissues obtained seven samples from four patients (5 samples obtained from femurs, 2 samples obtained from acetabulums) during revision surgery. Firstly, we examined expression of RANKL mRNA using the fibrogranulomatous tissue obtained from patients. In all samples, we detected RANKL mRNA by RT-PCR as single bands at the expected molecular weight for human RANKL. Secondly, we examined these tissues by the histologicaly. These tissues were contained numerous macrophage-like mononuclear cells and multinucleated giant cells. Some of these cells contained numerous metal particles and polyetylene particles. In the immunohistochemical demonstrated that RANKL was localized in fibroblast-like cells (positive for PH) negative for CD68 and tartrate-resistant acid phosphatase (TRAP), and in round mononuclear cells and multinucleated giant cells, both of which were positive for CD68 and TRAP. RANKL was expressed by three distinctive types of cells, CD68/TRAP-positive mononuclear histiocytic cells, CD68/TRAP-positive multinuclear giant cells, and PH-positive fibroblastic cells. These cells may contribute to activated osteolysis by acting as bone resorbing effector cells, as well as by supporting osteoclastogenesis via RANKL. And these cells may be activated by particles. The present findings indicate that RANKL may be involved in osteolysis associated with prosthetic loosening.

SU237

TNF-α Downregulates Human Copper-Zinc Superoxide Dismutase Promoter in U-937 Human Promonocytic Cells. V. Afonso*, P. Collin*, A. Lomri. INSERM U349, Paris 10, France.

Proinflammatory cytokines such as TNF-α and IL-1ß; are known modulators of bone remodeling in vitro and in vivo. These cytokines induce the production of nitric oxide (NO) in various cell types, including osteoblasts and osteoclasts and NO has recently been implicated in the regulation of bone resorption and formation. In contrast, superoxide dismutase enzymes (SODs) protect cells from the deleterious effects of reactive oxygen species by scavenging superoxide radicals. Although cytosolic copper-zinc SOD (Cu/Zn-SOD-1) activity has been found modified in some specific situations including hematopoietic cell differentiation, aging and some tumor cells, It has been reported that TNF-α had no effect on SOD-1 expression. In order to determine if TNF-α effects involve Cu/Zn-SOD-1, transient transfection of promoter-reporter gene constructs and RT-PCR analysis were carried out in U-937 human promonocytic cells. We first examined endogenous Cu/Zn-SOD-1 mRNA, protein and activity levels by semiquantitative RT-PCR, Western blot and enzymatic analyses in human osteoblastic and U-937 cell lines. Both human osteoblastic and U-937 cell lines expressed high levels of Cu/Zn-SOD-1 mRNA, protein and activity in basal conditions. Constructs -1499 to -71 displayed basal promoter activity as well as TNF-α repression. In contrast deletion of the regulatory sequences immediately upstream of the TATAA box resulted in total lost of the luciferase activity. TNF-α-inhibited Cu/Zn-SOD-1 promoter activity by 77% ($p<0.01$) after 24 h of treatment and this effect was more pronounced after 48 h (90%, $p<0.01$). It is noteworthy that both basal and TNF-α-inhibited promoter activities gradually decreased following the progressive deletion of 5'-regulatory flanking sequences, indicating the existence of several cis-acting positive regulatory sequences spread along 1.5 kb of the Cu/Zn-SOD-1 promoter proximal region. Both basal and TNF-α-inhibitory elements were mapped to -71 and -29 region of the Cu/Zn-SOD-1 promoter. Sequence analysis of this fragment revealed the presence of different putative transcription factor binding sites (Sp-1, Egr-1, WT1, Krox-20, NF-IL6). In agreement with the transfection results, endogenous SOD-1 mRNA was suppressed by TNF-α (-41%) after 24 h. Our results underline the importance of cytosolic Cu/Zn-SOD as anti-cytotoxic and anti-inflammatory mediator in the osseous microenvironment and might explain partly the observed deficiency of bone formation in inflammatory sites.

SU238

Effects of T Cells on Osteoclast Formation in vitro Depend on the Method of Activation. N. Wyzga*[1], S. Varghese[2], S. Wikel*[3], F. A. Sylvester*[1]. [1]Connecticut Children's Medical Center, Hartford, CT, USA, [2]Saint Francis Hospital and Medical Center, Hartford, CT, USA, [3]University of Connecticut Health Center, Farmington, CT, USA.

T cells are possible regulators of bone mass in chronic inflammatory diseases. Some investigators reported that activation of T lymphocytes results in RANKL-mediated increase in osteoclastogenesis, while others showed that activation leads to interferon-gamma (IFN-γ)-mediated inhibition of osteoclast formation. Because these studies were performed using different methods of T cell activation, we hypothesized that the method of activation determines their effect on osteoclastogenesis in vitro. T cells were harvested from spleen of 5-week-old male C57BL/6J mice using CD90(Thy1.2) magnetic beads. Activation of T cells was performed using anti-CD3e and CD28 antibodies (Antibodies), concanavalin A (Con A), phytohemagglutinin (PHA), and Staphylococcal enterotoxin A (SEA). T cell purity was >90% by flow cytometry. Conditioned media were collected after 4 days, and IFN-γ and RANKL concentrations were determined by ELISA. For osteoclast studies, RAW 264.7 cells (50,000/well) were cultured in α-MEM, containing 10% conditioned media and RANKL at 20 ng/mL. After 5 days, osteoclasts were detected by TRAP staining and a resorption assay. The percent resorbed surface correlated directly with the number of TRAP-positive cells (not shown). The table below summarizes the concentrations of IFN-γ and RANKL in conditioned media and the effects from different methods of activation on osteoclastogenesis (ND = non detectable). As shown, there was an inverse relationship between the concentration of INF-γ and osteoclastogenesis. Adding similar concentrations of IFN-γ to RAW 264.7 cells reproduced this effect. Pre-incubation of conditioned media with an anti-IFN-γ neutralizing antibody restored osteoclastogenesis. We conclude that the effects of T cells on osteoclastogenesis in vitro depend on the method of activation. IFN-γ is a potent inhibitor of osteoclastogenesis that counteracts the effects of RANKL, which may have implications in vivo in chronic inflammatory diseases.

Method	IFN-γ (pg/mL)n = 3	RANKL (pg/mL)n = 2	Osteoclasts
Resting T-cells	ND	ND	+
Antibodies	441,914 ± 2,737	1,068 ± 18	-
Con A	2,282 ± 1,157	7 ± 0.9	+/-
PHA	9 ± 3.4	31 ± 1.9	+
SEA	3,646 ± 969	170 ± 4	-

SU239

Biphasic Effects of Prostaglandin E2 on Osteoclast Formation from Spleen Cells. K. Ono[1], T. Akatsu[2], N. Kugai*[2], C. C. Pilbeam[1], L. G. Raisz[1]. [1]Medicine, University of Connecticut Health Center, Farmington, CT, USA, [2]General Medicine, National Defense Medical College, Tokorozawa, Japan.

Prostaglandin E2 (PGE2) is a potent stimulator of osteoclast (OC) formation through receptor activator of nuclear factor-kB ligand (RANKL) in stromal/osteoblastic cells. PGE2 can also increase OC formation in spleen cells cultured with RANKL and macrophage-colony stimulating factor (M-CSF) in the absence of stromal/osteoblastic cells. In this study, we examined the time course for the effects of PGE2 and selective PGE2 receptor agonists on OC formation in spleen cell cultures treated with RANKL and M-CSF. Spleen cells from C57BL/6 mice were cultured in αMEM containing 10% FCS at 5 x 10^5 cells/well in a 24-well plate (1.0 ml/well) with 10 nM M-CSF and 10 nM RANKL. Cells were cultured with or without 1 μM PGE2, EP2 agonist (EP2A, ONO-AE1-259) or EP4 agonist (EP4A, ONO-AE1-329) for 5-9 d. At the end of culture, adherent cells were stained for tartrate resistant acid phosphatase (TRAP). TRAP-positive cells containing 3 or more nuclei were counted as OC. As shown in the figure, control cultures with only RANKL and M-CSF formed OC at 5 d with the peak at 7 d and subsequently declined. Treatment with PGE2 initially inhibited OC formation but at 8 d there was a significantly greater number of OC than in control cultures at 7 d. EP2A showed an initial inhibition and late peak parallel to PGE2 but with lower OC number. EP4A had no significant effect on OC number compared to control cultures. In a separate experiment OC were counted at 8 d after continuous, 0-4 d or 4-8 d treatment with PGE2, EP2A or EP4A. OC number was less than 2 in a control cultures, cultures treated for 4-8 d with PGE2 or EP2A and all cultures treated with EP4A. 0-4 and 0-8 d treatment with PGE2 or EP2A showed similar significant increases in OC number. We conclude that the effect of PGE2 on OC formation in spleen cell cultures in the presence of M-CSF and RANKL is mediated by the EP2 receptor and consists of an initial inhibition followed by a stimulation of OC formation. These effects are established during the first 4 d of treatment. We speculate that activation of the EP2 receptor produces a transient inhibition of replication of OC precursors followed by an increase in formation and/or survival of mature OC.

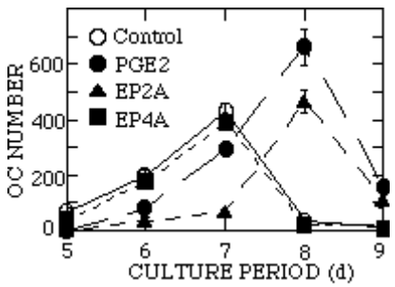

SU240

Lipopolysaccharide Stimulates Osteoclast Formation via RANKL Expression Independent of PGE2 Production. K. Suda*[1], N. Udagawa[2], M. Takami[1], K. Itoh*[1], J. Woo[3], N. Takahashi[4], K. Nagai*[3]. [1]Biochemistry, School of Dentistry, Showa University, Tokyo, Japan, [2]Biochemistry, Matsumoto Dental University, Shiojiri, Japan, [3]Biological Chemistry, Chubu University, Kasugai, Japan, [4]Institute of Dental Science, Matsumoto Dental University, Shiojiri, Japan.

The mechanism of osteoclast formation induced by lipopolysaccharide (LPS) was studied in cocultures of mouse osteoblasts and bone marrow cells. LPS stimulated osteoclast formation and prostaglandin E2 (PGE2) production in the coculture, both of which were inhibited by NS398, an inhibitor of cyclooxgenase-2. LPS stimulated receptor activator of NF-kB ligand (RANKL) mRNA expression, and inhibited osteoprotegerin (OPG) mRNA expression in osteoblasts. NS398 inhibited only down-regulation of LPS-induced OPG mRNA expression, suggesting that LPS-stimulated PGE2 production is important for the down-regulation of OPG in the coculture. Indeed, NS398 failed to inhibit LPS-induced osteoclast formation completely in the coculture with OPG knockout mouse-derived osteoblasts. Among several signal inhibitors examined, calcium/protein kinase C (PKC) inhibitors and PD98059 [an extracellular signal-regulated kinase (ERK) inhibitor] suppressed LPS-induced RANKL mRNA expression in osteoblasts. LPS stimulated phosphorylation of mitogen-activated protein kinase (MAPK) /ERK kinase (MEK), and that of ERK in osteoblasts. LPS-induced phosphorylation of ERK was inhibited by calcium/PKC inhibitors. A23187 (an ionophore) and phorbol-12-myristate-13-acetate (PMA: a PKC activator) but not PGE2 stimulated phosphorylation of ERK in osteoblasts. PD98059, an inhibitor of MEK/ERK, blocked osteoclast formation but not PGE2 production in cocultures treated with LPS. In addition, both PD98059 and NS398 inhibited osteoclast formation induced by interleukin 1 (IL-1) in the coculture, but only PD98059 suppressed IL-1-induced RANKL mRNA expression in osteoblasts. These results suggest that LPS and IL-1 promote osteoclastogenesis through two parallel events: one is enhancement of RANKL expression through calcium/PKC signals followed by MEK/ERK signals, and the other is suppression of OPG production mediated by PGE2.

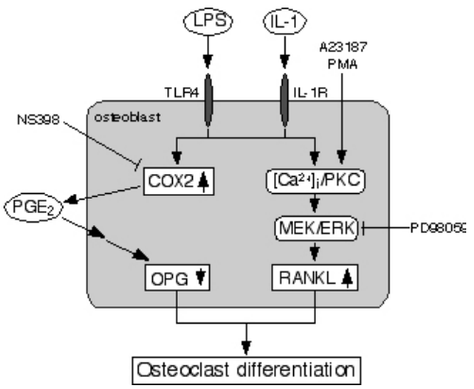

SU241

Bacteral CpG-DNA and Viral Double-stranded RNA Stimulate Osteoclast Formation Through the Induction of RANKL in Osteoblasts. K. Suda*[1], M. Takami[1], N. Udagawa[2], K. Itoh*[1], T. Suzawa[1], J. Woo[3], K. Nagai*[3], N. Takahashi[4]. [1]Biochemistry, Showa University, Tokyo, Japan, [2]Biochemistry, Matsumoto Dental University, Nagano, Japan, [3]Biological Chemistry, Chubu University, Aichi, Japan, [4]Institute for Dental Science, Matsumoto Dental University, Nagano, Japan.

Lipopolysaccharide (LPS), a major constituent of Gram-negative bacteria, is proposed to be a potent stimulator of bone loss in inflammatory diseases such as periodontitis and osteomyelitis. Toll-like receptor 4 (TLR4) has been identified as the signal transducing receptor for LPS. Bacterial DNA, which is enriched in unmethylated CpG motifs, is shown to activate innate immune system. Virus-derived double-stranded RNA (dsRNA), which is produced by viruses during their replication, is also known to induce antimicrobial immune responses. Recent studies have shown that TLR9 and TLR3 are the receptors of CpG DNA and dsRNA, respectively. In this study, roles of bacterial CpG DNA and viral dsRNA in osteoclastic bone resorption were examined, in comparison with those of LPS. (1) RT-PCR analysis showed that primary osteoblasts expressed mRNA of TLR9 and TLR3 as well as TLR4. In contrast, osteoclasts expressed mRNA of TLR4 but not that of TLR9 and TLR3. (2) CpG DNA , polyinosine-polycytidylic acid [poly(I:C), a synthetic analogue of dsRNA] and LPS stimulated the formation of TRAP-positive osteoclasts in cocultures of mouse osteoblasts and bone marrow cells in a dose-dependent manners. GpC DNA (an inactive form DNA) failed to induce TRAP-positive cell formation in the coculture. TRAP-positive cells induced by CpG DNA, poly(I:C) or LPS formed resorption pits on dentine slices. Osteoprotegerin, a decoy receptor of RANKL, completely inhibited osteoclast formation in the cocultures treated with the bacterial and viral products. (3) RT-PCR showed that osteoblasts expressed RANKL mRNA in response to CpG DNA, poly(I:C) or LPS. RANKL mRNA was not induced by GpC DNA in osteoblasts. (4) When osteoblasts were removed from the coculture, almost all the TRAP-positive osteoclasts died within 48 h. LPS supported the survival of purified osteoclasts, but CpG DNA and poly(I:C) did not. Thus, unlike LPS, bacterial CpG-DNA and vial dsRNA failed to act directly on osteoclasts to induce bone-resorbing activity. However, like LPS, CpG-DNA and dsRNA stimulated RANKL expression in osteoblasts, which results in induction of osteoclast formation. These results suggest that together with LPS, bacterial CpG-DNA and viral dsRNA play important roles in osteoclastic bone resorption in inflammatory diseases.

SU242

Signals Mediated by p38 MAP Kinase Are Involved in Differentiation but not Function of Osteoclast Precursors. X. T. Li*[1], N. Udagawa[2], K. Itoh*[3], K. Suda*[3], N. Sato*[2], N. Takahashi[1]. [1]Institute for Dental Science, Matsumoto Dental University, Nagano, Japan, [2]Biochemistry, Matsumoto Dental University, Nagano, Japan, [3]Biochemistry, Showa University, Tokyo, Japan.

[Backgrounds] We previously reported that SB203580, an inhibitor of p38 MAP kinase, inhibited differentiation of bone marrow macrophages (BMMϕ) into osteoclasts in cultures treated with RANKL and M-CSF. However, SB203580 failed to inhibit pit-forming activity of osteoclasts induced by RANKL. Phosphorylation of p38 MAP kinase was induced by RANKL and LPS in BMMϕ but not in osteoclasts. In this study, we further investigated the role of p38 MAP kinase in the differentiation and function of BMMϕ. **[Methods]** BMMϕ were prepared from bon marrow cultures treated with M-CSF for 3 days. osteoclasts were prepared from co-cultures of osteoblasts and bone marrow cells. Activation of JNK, ERK, and p38 MAP kinase was determined by Western blotting in BMMϕ and osteoclasts in response to LPS. Activation of NF-κB was determined by evaluating the degradation of IκB. Production of pro-inflammatory cytokines such as IL-1, TNFα, and IL-6 in BMMϕ and osteoclasts in response to LPS was determined by ELISA. Phagocytic activity of BMMϕ and osteoclasts were determined by the incorporation of latex beads in the presence or absence of SB203580. **[Results]** (1) LPS induced activation of JNK, ERK, and NF-κB in BMMϕ as well as in osteoclasts. LPS stimulated phosphorylation of MAP kinase kinase 3/6 and ATF2, upstream and downstream signals of p38 MAP kinase, respectively, in BMMϕ but not in osteoclasts. (2) LPS stimulated production of IL-1, TNFα, and IL-6 in BMMϕ but not in osteoclasts. SB203580 failed to inhibit the production of these cytokines in BMMϕ treated with LPS. (3) BMMϕ but not osteoclasts showed vigorous phagocytic activity in the presence of M-CSF. SB203580 failed to inhibit the phagocytic activity of BMMϕ. **[Discussion]** SB203580 has been shown to inhibit differentiation of monocytes into dendritic cells induced by GM-CSF and LPS. These results suggest that p38 MAP kinase mediated signals are essentially involved in the differentiation of monocytes/macrophages not only into osteoclasts but also into dendritic cells. In contrast, p38 MAP kinase was not important for macrophage function such as cytokine production and phagocytosis. Signals of upstream and downstream of p38 MAP kinase were completely inactivated in osteoclasts. This phenomenon may be explained by the fact that osteoclast are terminally differentiated cells.

SU243

Osteoclast Progenitors Stimulated by TGF-beta or by RANKL Differ in their Sensitivity to Osteoclastogenesis Inhibitors. J. M. W. Quinn[1], K. D. Häusler*[1], C. Gange*[1], H. Zhou[1], J. S. Rubin*[2], T. J. Martin[1], M. T. Gillespie[1]. [1]St. Vincent's Institute of Medical Research, Fitzroy, Victoria, Australia, [2]NCI, NIH, Bethesda, MD, USA.

Osteoclast formation in vivo and in vitro results from stimulation of hematopoietic progenitor cells by M-CSF and RANKL. This differentiation proceeds in stages in vitro. After initial proliferation, calcitonin receptor and tartrate resistant acid phosphatase are apparent after day 3 of culture while multinucleation and bone resorption are evident after day 5. However, TGFbeta can substitute for RANKL in the initial phases. We previously noted that, in RANKL-dependent osteoclastogenesis assays, inhibitors such as IL-4 and osteoclast inhibitor lectin (OCIL) also act early in the culture period with little effect if added after day 2. We therefore investigated whether inducing the early stage of osteoclast differentiation by TGF-beta rather than RANKL results in a different sensitivity of the osteoclast progenitors to inhibitory factors. M-CSF-stimulated murine bone marrow cells treated with recombinant RANKL (rRANKL; 100ng/ml) for seven days resulted in 3.0±0.3 osteoclasts/ mm2. In contrast osteoclast formation did not occur when rRANKL was added to cells for days 3 to 7 of the culture period, i.e. rRANKL was omitted for days 0 to 3. With TGFbeta 5ng/ml stimulation for days 0 to 3 followed by rRANKL stimulation from days 3 to 7, 3.1±0.3 osteoclasts/ mm2 formed. A similar priming effect was noted with TNF-alpha (day 0 to 3)/rRANKL sequential stimulation (0.5±0.1 osteoclasts/ mm2). We then investigated the action of IL-4, GM-CSF, OCIL and RANKL-binding proteins osteoprotegerin (OPG-Fc), soluble RANK-Fc and secreted frizzled-related protein-1 (sFRP-1). In cultures stimulated only by rRANKL (days 0 to 7) all of these factors blocked osteoclast formation when added for the first three days of culture. However, in TGF-beta-primed cultures only IL-4, GM-CSF and sFRP-1 blocked osteoclast formation while OCIL, OPG-Fc and RANK-Fc had no effect. These results suggest that OCIL, OPG-Fc and RANK-Fc inhibitory action depend on the presence of rRANKL (presumably, in the case of OPG-Fc and RANK-Fc, by sequestering it) or on responses elicited by rRANKL. In contrast, IL-4, GM-CSF and sFRP-1 exerted a rRANKL-independent action. Thus, the sequence of stimuli to which progenitors are exposed may determine their sensitivity to particular inhibitors, an important consideration in investigating anti-osteolytic agents. The in vitro methods we employed may also provide insights into mechanisms of inhibitor action.

SU244

Function of Transcriptional Regulator, OCZF Expressed in Osteoclasts. A. Kukita[1], T. Kukita[2], T. Shobuike*[1], M. M. Rahman*[1], T. Nakamura*[1], O. Kohashi*[1]. [1]Microbiology, Saga Medical School, Saga, Japan, [2]Oral Cellular Molecular Biology, Faculty of Dental Science, Kyushu University, Fukuoka, Japan.

Osteoclast-derived zinc finger (OCZF) gene, which we isolated from osteoclast specific cDNA library, encodes a transcriptional regulatory factor. OCZF protein belongs to a member of POZ Zn finger proteins and has homology in POZ domain with other transcription factors including PLZF which has an important role in monocyte differentiation. In situ hybridization analysis with POZ domain of OCZF as a probe, OCZF mRNA was specifically present in the osteoclasts of rats developed adjuvant induced arthritis. We then examined OCZF expression by RT-PCR analysis using a mouse macrophage cell RAW264 subclone RAW-D which has high potential to differentiate into osteoclasts. RAW-D cell alone expressed OCZF at very low level but treatment of the RAW-D cells with sRANKL for 2 days increased the level of OCZF mRNA. The analysis with polyclonal antibody against OCZF protein also showed that OCZF protein was present in the nuclei of the multinucleated cells of RAW-D cells induced by sRANKL. We then infected RAW-D cells with retroviruses expressing OCZF and OCZF-EGFP fusion proteins. The cells that survived selection were expanded and were shown to express increased levels of OCZF protein by western blotting. These cells proliferated very slowly in comparison with RAW-D cells infected with parental retrovirus. In addition, the adhesive property of the cells expressing OCZF was altered and the aggregation of the cells was occurred. Because other POZ Zn finger transcriptional regulators are involved in the regulation of cell cycle, we then examined the effect of OCZF on transactivation of the cell cycle inhibitors such as $p21^{WAF1}$ and $p27^{KIP1}$ using these inhibitors promoter luciferase plasmids by transient transfection in RAW-D and NIH3T3 cells. We found that OCZF stimulated the transactivation of these plasmids. These results suggest that OCZF is involved in the downstream of RANKL signaling and inhibits growth of the cells by stimulating the expression of cell-cycle inhibitors in differentiated state.

SU245

CD44 Is Not Required for the Development of Bone Marrow Cells Into Actively Resorbing Multinucleated Osteoclasts. T. J. de Vries*[1], T. Schoenmaker*[1], R. van der Neut*[2], W. Beertsen*[3], S. T. Pals*[2], V. Everts[1]. [1]Dept. of Periodontology, ACTA, Dept. of Cell Biology and Histology, AMC, Amsterdam, Netherlands, [2]Dept. of Pathology, AMC, Amsterdam, Netherlands, [3]Periodontology, ACTA, Amsterdam, Netherlands.

Purpose: The role of CD44 in osteoclastogenesis was investigated. *Methods:* Genetically engineered mice were used that express (1) only the standard form of CD44 (CD44s), (2) a splice variant containing variable exons v3-v10 (CD44v3-v10), a splice variant containing variable exons v4-v10 (CD44v4-v10), or (4) no CD44 at all (CD44 k.o.). Bone marrow cells from these mice and wild type mice were cultured in the presence of M-CSF and RANKL to induce osteoclast differentiation. *Results:* Higher numbers of multinucleated TRAP-positive cells were observed in CD44 k.o. cultures, whereas no differences were observed between the other genotypes and wild type controls. Bone resorption was similar for all 5 genotypes. Since wild-type bone marrow only expressed the standard form of CD44 during osteoclastogenesis, further comparisons were performed between wild type and CD44 k.o. mice. Characterization of osteoclasts generated from wild type and CD44 k.o. mice revealed comparable mRNA levels of osteoclast related genes TRAP, cathepsin K and carbonic anhydrase II. The expression of calcitonin receptor proved to be higher in CD44 k.o. cultures. The possibility of a CD44 redundant fusion mechanism was studied by comparing the mRNA levels of proteins involved in macrophage fusion MFR, CD47 and $P2Z/P2X_7$. No difference in expression was observed between the CD44 k.o. and wild type cultures. We further studied the osteoclastogenic potential of wild type and CD44 k.o. marrow in the presence of CD44 blocking antibodies and agents which can compete with CD44 function chondroitin sulphate A and B. All agents used had similar effects on both genotypes, indicating that these effects are CD44 independent. *Conclusions:* Our data clearly demonstrate CD44 is not involved in differentiation of osteoclasts from bone marrow cells. This process differs from the formation of osteoclasts from splenocytes and macrophages, where a requirement for CD44 has been described. recombinant murine RANKL was kindly provided by Amgen Inc, Thousand Oaks, California, U.S.A.

SU246

Lactoferrin Delays Acquisition of the Osteoclast Phenotype. F. Lorget*[1], J. Clough*[1], M. Oliveira*[1], R. Mentaverri*[2], M. Daury*[1], M. Brazier[2], E. A. Offord*[1]. [1]Nutrition, Nestle Research Center, Lausanne 26, Switzerland, [2]Laboratory of Clinical Pharmacy, School of Pharmacy, Amiens, France.

Lactoferrin (LF) is an iron-binding protein found in exocrine secretions of mammals and released from neutrophil granules during inflammation. LF has potent antioxidant and antimicrobial properties due to its iron-chelating ability. In addition, it inhibits activation of macrophages in response to bacterial lipopolysaccharide (LPS) by an iron-independent mechanism. LF interferes with the interaction of LPS with its macrophage cell surface receptor (CD14), and also binds to soluble CD14 found in serum. Binding of LPS to CD14 activates several cytoplasmic kinases resulting in the activation of transcription factors, mainly AP-1 and NFkB. CD14 is expressed on osteoclast precursors derived from cells of the mononuclear-phagocytic lineage. We were therefore interested to know if lactoferrin could influence the bone resorbing process. We first investigated its effect on human osteoclast differentiation. The current experiments were carried out with bovine LF (bLF), which is commercially available and gives comparable bioactivity to human lactoferrin. Blood samples were obtained from healthy male donors less than 60 y. Peripheral blood mononuclear cells (PBMC) or selected CD14 positive cells were differentiated into osteoclasts in the presence of RANKL (25 ng/ml) and M-CSF (30 ng/ml). The osteoclast phenotype was assessed by (i) mRNA expression of calcitonin receptor (CTR) using semi-quantitative PCR and (ii) immunofluorescence labeling for calcitonin and vitronectin receptors (CTR and VNR) and actin ring formation. Bone resorbing ability was evaluated by measuring the resorbed area according to stereological principles. In some PBMC cultures, collagen breakdown products were analyzed by ELISA (CrossLaps™ for culture, Nordic Bioscience A/S). Bovine LF (1 to 100 µg/ml) dramatically stimulated the proliferation of selected CD14 postive cells undergoing osteoclast differentiation. In both CD14 selected and PBMC cells, the number of multinucleated CTR positive cells as well as bone resorbing activity were reduced in the early stages of culture (7 - 14 days) but not in the later stage (at 21 days). Taken together these results suggest that bLF delays acquisition of the osteoclast phenotype. This observation is of particular relevance to inflammatory bone disease, where inflammation and bone loss coexist.

SU247

Modulation of Osteoclastogenesis through Functional Adrenomedullin Receptors Expressed on Osteoclast Precursors, that Is partly Related to Osteoclast Differentiation Antigen. T. Kukita[1], A. Kukita[2], K. Tou*[3], T. Iijima*[3]. [1]Oral Cellular & Molecular Biology, Faculty of Dental Science, Kyushu University, Fukuoka, Japan, [2]Microbiology, Saga Medical School, Saga, Japan, [3]Oral Anatomy & Cell Biology, Faculty of Dental Science, Kyushu University, Fukuoka, Japan.

Fine regulation of osteoclastogenesis is mediated through cell surface molecules expressed on osteoclast precursors. Lines of evidence suggest that peptides regulating the vascular system modulate osteoclast differentiation and function. Adrenomedullin (AM), a member of the calcitonin family peptides, is a potent vasodilator and was shown to be mitogenic to fetal rat osteoblasts. We have previously found a unique cell surface antigen (Kat1-antigen) expressed in rat osteoclasts and their mononuclear precursors, which is involved in the functional regulation of the calcitonin receptor (CTR). Cross-linking of the cell surface antigen by use of the anti-Kat1-antigen monoclonal antibody (mAb Kat1) stimulated osteoclastogenesis under conditions exposed to calcitonin. Here we searched candidates for the natural ligand of the Kat1-antigen. Among factors we have examined, only AM provoked a significant stimulation in osteoclastogenesis in the presence of calcitonin but not in its absence in rat bone marrow culture system. This stimulatory effect mediated by AM was blocked by the addition of the mAb Kat1. ^{125}I-AM binding experiments including autoradiographic studies demonstrated that mononuclear precursors of osteoclasts expressed functional AM receptor and the specific binding of ^{125}I-AM was significantly inhibited by the addition of the mAb Kat1, suggesting a close relationship of the Kat1-Ag with the functional AM receptors expressed on mononuclear osteoclast precursors. Modulation of osteoclastogenesis through AM receptors expressed in osteoclast precursors is supposed to be important in the fine regulation of osteoclast formation.

SU248

Optimal Conditions for Generation of Active Human Osteoclasts In Vitro: Cell Source, Time, and pH. S. Filke, A. F. Schilling, J. M. Rueger, M. Amling. Trauma Surgery, Hamburg University School of Medicine, Hamburg, Germany.

Studying human osteoclast in vitro may lead to major advances in our understanding of osteoclast biology and is of paramount importance to gain insights in osteoclast associated human diseases. We have recently described an in vitro culture system to generate human osteoclasts (OCL) in which human mononuclear cells from either the peripheral blood (PBMC) or the bone marrow (BMMC) differentiate in the presence of M-CSF and RANKL but in the absence of any other supportive cells. Here we modified this human system to improve culture conditions for optimal osteoclast yield and osteoclast function. First we aimed at improving the source of osteoclast precursors. Having demonstrated that PBMC are as potent as BMMC in generating osteoclasts, we show here that 'buffy coats', the generally discarded left over which contains the mononuclear cell fraction when packed red-blood cells are produced, are an ideal cell source for osteoclast cultures. Then we characterized the time course of osteoclast development and function. In human cultures mononuclear cells start to fuse at day 5, and osteoclasts finish their morphological development and express osteoclast associated markers (e.g. TRAP, vitronectin receptor, calcitonin receptor) at day 14. In contrast functional activity only starts at this time with the first resorption pits of single osteoclasts being detected at day 21. Full functional activity of >80% of the osteoclasts formed is detected at day 28. Thus for differentiation assays the read out can be done after 2 weeks of culture, while pit assays for assessment of functional activity require 4 weeks of culture. Finally, we reasoned that an acid milieu might favor osteoclast differentiation and function as pH changes in the microenvironment have been reported for several diseases associated with local bone resorption (e.g. rheumatoid arthritis, implant loosening). Therefore cultures were performed at six different pH values ranging from pH 6.5 to pH 7.5. After 2 weeks the number of TRAP-positive multinucleated OCLs per high power field (magnification 400x) was 3.1 at pH 6.5; 3.4 at pH 6.8; 5.7 at pH 6.9; 5.5 at pH 7.1; 1.6 at pH 7.3; and 1.4 at pH 7.5 (experiments performed in quadruplicate; high power fields per culture n=40). Thus osteoclast development is significantly favored by moderate acid culture conditions with a pH between 6.9 and 7.1 ($p<0.005$).

SU249

Signaling via Gap Junctions Is Important for the Fusion of Human Osteoclasts In Vitro. A. F. Schilling, S. Filke, J. M. Rueger, M. Amling. Trauma Surgery, Hamburg University School of Medicine, Hamburg, Germany.

Precursors of human osteoclasts only start to fuse in vitro at a cell density that allows direct cell-cell contact. This observation led us to reason that cell-cell communication via gap junctions might play a role in the fusion process of human osteoclast precursors. To experimentally test this hypothesis, we first analyzed the expression of connexin 43, a gap junctional hemi-channel, known to be present on rat osteoclasts. Immunolabeling with specific antibodies revealed that connexin 43 is indeed highly expressed by human osteoclast precursors. To further test the functional role of this channel in the process of osteoclast fusion we blocked its activity by heptanol, a known inhibitor of gap junctional communication. Therefore we used an established in vitro culture system to generate human osteoclasts and administered heptanol (at 3 different concentrations) to these cultures in daily intervals. After 4 weeks of culture cells were fixed and labeled for TRAP, a typical marker of osteoclasts. TRAP positive multinuclear cells were counted as osteoclasts and TRAP positive mononuclear cells were counted as unfused osteoclast precursors. Indeed in treated cultures inhibition of gap junctional communication by heptanol led to a significant reduction (>50%) of multinuclear TRAP positive osteoclasts. Consequently also in vitro dentin resorption as assessed in a pit assay was significantly decreased. In contrast the number of TRAP positive mononuclear cells was not affected or even increase by the treatment with heptanol, ruling out the possibility that the decrease in multinucleated osteoclasts was due to toxic effects. These observations indicate that cell-cell signaling via gap junctions plays an important role in the fusion of mononuclear osteoclast precursors to multinuclear osteoclasts in the human culture system.

SU250

TGF-beta Affects the Rate of Formation and Phenotype of Human Osteoclasts Derived from Mobilized CD34$^+$ Cells. M. Wang*, H. Loughrey. SignalGene Inc., Montreal, PQ, Canada.

Human peripheral blood mononuclear cells (PBMC) are a well-established source of osteoclast progenitors. Several groups have shown that various combinations of cytokines induce formation of multi-nucleated tartrate-resistant acid phosphatase (TRAP) positive osteoclasts. These cells were functionally active as shown by bone resorption assays. We were interested in determining whether TGF-beta would enhance the rate of formation of human osteoclasts from mobilized CD34$^+$ cells in a fashion similar to that reported for mouse osteoclasts (1, 2). After adherence selection, human CD34$^+$ cells were treated for up to 11 days with M-CSF and sRANKL, and either with or without TGF-beta. On days 7 and 11 cultures were stained for TRAP and mRNA levels of TRAP and Calcitonin receptor (CTR) were assessed by RT-PCR. With only M-CSF and sRANKL present, TRAP+ multinucleated cells appeared around day 7 ultimately yielding a homogenous mature osteoclast population with increasing numbers detected on day 11. When cells were grown in M-CSF, sRANKL *and* TGF-beta, the rate of formation of osteoclasts was significantly higher than that observed without TGF-beta present. Moreover, two phenotypes were detected on days 7 and 11 in the presence of TGF-beta, in contrast to the homogeneous nature of the mature osteoclast population observed in its absence. The first and most predominant phenotype was the typical TRAP+ multi-nucleated osteoclast. The second phenotype had the appearance of tight cell aggregates that were TRAP positive. RT-PCR studies showed that under both culture conditions TRAP mRNA levels increased over time. However CTR mRNA was detected on day 11 in cells cultured with only M-CSF and sRANKL, but not in those cultured with added TGF-beta at either time point. Thus it is possible that osteoclasts generated in the presence of TGF-beta may not be functionally active. Future work is aimed at determining the nature of TRAP+ cell aggregates and characterizing the bone resorption ability of osteoclasts derived by culturing with TGF-beta.

Fuller K. et al (2000) J Cell Sci 113, 2445-2453.
Yan T et al (2001) J Cell Biochem 83, 320-325.

SU251

Elucidating Differences Between Large and Small Osteoclasts Using the RAW 264.7 Mouse Macrophage Cell Line as a Model System. M. F. Manolson[1], K. Li*[1], H. P. von Schroeder*[2], S. Shorey*[1], D. Chandra*[1], J. N. M. Heersche[1]. [1]Faculty of Dentistry, University of Toronto, Toronto, ON, Canada, [2]University Health Network, University of Toronto, Toronto, ON, Canada.

Increased bone resorption in several bone diseases (e.g. rheumatoid arthritis, Paget's disease, multiple myeloma, periodontal disease) is associated with an increase in the size of osteoclasts in the affected areas, suggesting that an increase in osteoclast size may be related to increased resorptive activity. We found that, as a population, large osteoclasts are more effective resorbers than small osteoclasts, the reason for this being that the proportion of large osteoclasts that are resorbing is much greater than the proportion of small osteoclasts that are resorbing [1, 2]. This could explain why in disease states where there are more large osteoclasts, there is also much more bone resorbed. Our goal is to understand the molecular mechanisms that lead to the differences in resorptive activity between large and small osteoclasts. *In situ* hybridization on cultured rabbit long bone osteoclasts indicates that both the receptor for MCSF, *c-fms*, and the 100 kDa V-ATPase subunit, a3, are both expressed about 2.5 fold higher in large (≥10 nuclei) compared to small (≤5 nuclei) osteoclasts. To look for novel factors using genomic and/or proteomic approaches, we are extending this study by isolating RNA and protein from populations of large and small osteoclasts differentiated from the RAW 264.7 mouse macrophage (RAW) cell line. By titrating the concentration of recombinant soluble Receptor Activator of NFkB (sRANKL), and adjusting the time of incubation and frequency of media changes, two conditions have been established that maximally enrich for populations containing either large (≥10 nuclei) or small (≤5 nuclei) osteoclasts. Using protein isolated from these two populations, preliminary immunoblot studies have shown that cathepsin K and matrix metalloproteinase 9 are expressed at higher levels in large vs small osteoclasts. RNA isolated from large and small osteoclasts are currently being used to screen mouse and human cDNA microarrays to look for additional changes in gene expression. Thus, results using authentic rabbit osteoclasts and osteoclasts differentiated from RAW cells support the view the large osteoclasts differ from small osteoclasts in activation mechanisms, proton transport, and matrix degradation activity. The goal of this work is to selective inhibit the most active osteoclasts, eliminating excessive resorption related to disease while maintaining normal remodeling activity.

1 Lees, R. L. and Heersche, J. N. M (2000) Am J Cell Physiol **279**, C751-C761
2 Lees, R. L., Sabharwal, V. K. and Heersche, J. N. (2001) Bone **28**, 187-94.

SU252

Microarray Expression Profiling of Osteoclast-Like Cells Differentiated with Lipopolysaccharide. H. Saleh*[1], N. Walsh*[1], T. Ravasi*[1], C. Wells*[1], Y. Okazaki*[2], P. Carninci*[2], Y. Hayashizaki*[2], D. A. Hume*[1], A. I. Cassady[1]. [1]Institute for Molecular Bioscience, CRC for Chronic Inflammatory Diseases, University of Queensland, Brisbane QLD, Australia, [2]Genome Research Science Centre, Yokohama, Japan.

Osteoclasts are large multinucleated cells of hematopoietic origin that function specifically to resorb bone. The differentiation of osteoclast progenitor cells into mature osteoclasts in vivo, is tightly regulated by bone-forming osteoblasts through the action of M-CSF and RANKL. The substitution of RANKL with bacterial lipopolysaccharide (LPS) has been shown to induce the differentiation of osteoclast progenitor cells in vitro into osteoclast-like cells (OCL). In pathological conditions, such as periodontal disease, LPS induces elevated osteoclast differentiation and bone resorption. Our aim in this study was to identify novel genes regulated by LPS during this process. We have used RIKEN 40,000 element mouse cDNA microarrays to establish the gene expression profile of LPS-differentiated mouse bone marrow OCL (LPS-OCL) and compared this with mouse co-culture derived osteoclast-like cells (OCL), and mouse bone marrow-derived macrophages (BMM) . We have identified gene clusters that are: (i) highly up-regulated in OCL as compared to BMM and LPS-OCL; (ii) LPS-inducible genes; (iii) down-regulated by LPS relative to BMM and OCL; (iv) shared by OCL and LPS-OCL. Amongst these genes are known osteoclast marker genes as well as many novel genes that have not also been associated with the three different cell populations. Shared osteoclast marker genes with relatively lower level in LPS-OCL implies that LPS-OCL represent "differentiating osteoclasts" under pathological conditions. This cell population has shown more intensive TRAP staining compared to BMM. On the other hand, co-culture derived osteoclast may physiologically represent more mature osteoclasts. We are characterising differentially expressed genes in OCL and LPS-OCL in order to identify novel regulators of osteoclast differentiation and function. These results will help to define our basic understanding of osteoclast differentiation based on the two models of osteoclast-like cells.

Disclosures: ***A.I. Cassady****, AstraZeneca 2.*

SU253

Radicicol Stimulates Osteoclast Differentiation at Low Concentrations. Z. Lee, W. Chung*, H. Kim*. National Research Laboratory for Bone Metabolism, Chosun University, Gwangju, Republic of Korea.

Radicicol, the pharmacological agent that has been shown to exert effects on several enzymes, has been reported to suppress osteoclast function by inhibiting the nonreceptor tyrosine kinase Src. We have examined the effect of radicicol on osteoclast differentiation. At high concentrations (0.1~5 μg/ml) radicicol inhibited formation of multinuclear tratrate-resistant acid phosphatase (TRAP)-positive osteoclasts from mouse bone marrow cells induced by RANKL. This inhibition was due to cytotoxicity. However at low concentrations (10 ng/ml) radicicol significantly enhanced osteoclast differentiation in both bone marrow cell and Raw264.7 cell cultures. As the increase in osteoclast differentiation was similar between cells treated only during the second half of culture period and those treated during the whole period, the effects of radicicol appeared to be after the formation of osteoclst precursors. This effect was accompanied by increased expression of β3 integrin, which was detected by both RT-PCR and FACS analyses. The low concentrations of radicicol also enhanced cell cycle arrest induced by RANKL, which appeared to be mediated by induction of p27 but not that of p21. Radicicol also resulted in a sustained ERK activation at the concentration that enhanced osteoclast formation. Our findings indicate that the pharmacological agent radicicol have diverse effects on osteoclasts depending on treatment concentrations.

SU254

Estrogen Inhibits PTH-Stimulated Osteoclastogenesis through Prevention of PTH-Induced Osteoprotegerin Downregulation in Mouse Marrow Stromal Cells. B. LIU[1], J. Wang*[1], H. Yu*[1], P. Chung*[1], F. Bringhurst[2]. [1]Oral Pathology, National Taiwan University Hospital, and School of Dentistry, National Taiwan University, Taipei, Taiwan Republic of China, [2]Endocrine Unit, Massachusetts General Hospital, and Harvard Medical School, Boston, MA, USA.

Osteoprotegerin (OPG), as a decoy receptor, is well known to inhibit osteoclastogenesis by preventing RANKL from binding to RANK. Recently, we have demonstrated that osteoprotegerin (OPG) is essential for estrogens antagonism of PTH-induced osteoclast formation in a mouse marrow stromal cell (MS1) and spleen cell coculture (Endocrinology 143:627-635, 2002). Although substantial evidence indicates that osteotropic factors such as PTH and estrogen regulate OPG expression in bone cells, its mechanism is not com-

pletely understood yet. In order to determine how OPG expression in PTH-stimulated MS1 cells is regulated by estrogen, we analyzed the effect of estrogen on OPG mRNA expression and protein secretion using semi-quantitative reverse transcript (RT)-PCR and enzyme linked immunoassay (ELISA). MS1 cells was pre-treated with rPTH-(1-34) (10-7 M) for 24 hours then stimulated with various concentrations of 17-beta estradiol (E2) ranging from 10-11 M to 10-8 M. The results indicated that PTH-pretreatment inhibited OPG expression while 24-hour treatment of MS1 cells with E2 significantly increased the OPG mRNA expression with the maximal effect at 10-8 M of E2. Time course studies demonstrated that E2 effect on stimulating OPG expression was detectable at 8 hour after treatment and reached a peak at 24 hour. The ELISA studies demonstrated that PTH-pretreatment inhibited MS1 cell OPG secretion whereas E2-treatment reversed the inhibition in a concentration-dependent manner. Simultaneous treatment of MS1 cells with a pure estrogen receptor antagonist, ICI 182,780, completely abolished the stimulatory effect of E2 on OPG production. Our results suggest that the mechanisms by which E2 inhibits PTH-stimulated osteoclast formation in the mouse coculture model are mediated in part by specifically preventing PTH-induced OPG downregulation.

SU255

Estradiol Down Regulates β3 Integrin Expression on Differentiating and Mature Human Osteoclasts. D. Saintier*, M. C. de Vernejoul, M. E. Cohen-Solal. INSERM U349, Paris, France.

Osteoporosis is related to estrogen deficiency, which induces increased bone resorption. We have previously shown that estradiol inhibits directly osteoclast differentiation and activity from human osteoclast progenitors in vitro. Osteoclast activity is dependent of β3 integrin for osteoclast attachment and further bone resorption. The aim of our study was to evaluate β3 integrin mRNA and protein expressions during human osteoclast differentiation and the effects of estradiol. Human peripheral blood mononuclear cells (PBMC) were allowed to differentiate into osteoclasts in the presence of 10%FCS (C), M-CSF (25ng/ml) and RANK-L (30ng/ml) (C+) for 18 days. Cells were also treated with 10^{-8}M estradiol (E2) or raloxifene (Rlx) from D1 to D18 to assess the effect on osteoclast precursors, from D12 to D18 for the effect on osteoclast differentiating cells, from D18 to D21 on mature osteoclasts. mRNA expression was investigated using nested RT-PCR in cells in 5 samples using Polymerase II as internal standard. Treatment with M-CSF and RANK-L (C+) increased the mRNA expression of β3 integrin compared with control cells (C) at each culture time. Already after 12 days of culture, E2 or Rlx decrease RNA expression of β3. Such a decrease was observed after 18 days of culture when steroids were added at D1 or D12 (for D1-D18: 0.6±0.2 AU for E2, 0.7±0.1 AU for Rlx; for D12-D18: 0.8±0.2 AU for E2, 0.9±0.2 AU for Rlx) compared with C+ (1.8±0.6 AU). When steroids were added to mature osteoclasts from D18 to D21, β3 integrin mRNA was also down regulated (0.6±0.2 AU for E2, 0.3±0.1 AU for Rlx) compared with controls (0.8±0.3 AU). The expression of β3 integrin was also evaluated using immunofluocytochemistry and western blot. The percent of cells labeled with β3 integrin antibody was increased with M-CSF and RANK-L and with culture time suggesting increased expression with osteoclast differentiation. The effect of E2 and Rlx added for 18 days was further assessed using western blot analysis: β3 integrin expression was significantly decreased with E2 (0.7±0.2 AU) and Rlx (0.7±0.3 AU) compared with C+ (1.3±0.6 AU). In conclusion, these data show a decreased β3 expression with E2 or Rlx. They also suggest that the direct inhibitory action of estradiol on bone resorption may be mediated through a down regulation of β3 integrin, which may affect osteoclast attachment.

SU256

Estrogen Receptor α Expression Increases with Osteoclast Differentiation but Is not Regulated by Estradiol and RANK-L. D. Saintier*[1], M. A. Burde*[1], J. M. Rey*[2], T. Maudelonde*[2], M. C. de Vernejoul[1], M. E. Cohen-Solal[1]. [1]Hopital lariboisiere, INSERM U349, Paris, France, [2]hopital A. de Villeneuve, laboratoire de biologie cellulaire, Montpellier, France.

Estrogen is a potent anti-resorbing hormone, which decreases osteoclast differentiation. Both estrogen receptors α (ERα) and β (ERβ) have been shown to be involved in bone loss of ovariectomized mice. Human osteoblasts express both ERα and ERβ. Presence of both ERs in human osteoclasts remains controversial, as well as the regulation by estradiol. Our aim was to study the regulation of ERs and RANK during osteoclast differentiation and estradiol treatment. Human peripheral blood mononuclear cells (PBMC) were cultured in red phenol-free DMEM,10% FCS in the absence (C) or the presence of M-CSF (25ng/ml) and RANK-L (30ng/ml) (C+) for 18 days in 9 samples. 10^{-8}M estradiol (E2) or raloxifene (Rlx) were added from day 1 to day 18. Bone resorption pits of dentine slices were evaluated at day 18. No pits were observed in C cultures. Compared with controls (C+), E2 and Rlx decrease total area of resorption pits (4.7 ±1.3 vs 3±0.9 and 2.3±0.75 respectively, $p<0.05$). mRNA expression of ERs was studied by competitive RT-PCR using HPRT as internal control in cells after Day1 (D1), Day 12 (D12) or Day 18 (D18) of culture. We found no expression of ERβ in our cells at any time and at any culture conditions and in presence of positive controls (SaOS3). In contrast, ERα was detected at all time. In control cultured cells (C), ERα expression was enhanced throughout the time of culture : 0.26±0.12 at D1, 0.32±0.10 at D12 and 0.84±0.15, $p<0.05$. Cells cultured with M-CSF and RANK-L (C+) had an identical increased ERα expression : 0.26±0.12 at D1, 0.53±0.10 at D12, 0.81±0.16 at D18, $p<0.05$, suggesting an increase of ERα expression with monocyte differentiation independent of RANK-L. Expression of ERα was also tested in the presence of E2 and Rlx. At day 12, E2 and Rlx do not regulate ERα expression (0.45±0.09 and 0.41±0.15 respectively) compared with C+ (0.53 ±0.10). No regulation was observed either at D18 (0.74±0.19 for E2, 0.41±0.12 for Rlx, p=NS). Moreover, the regulation of RANK during osteoclast differentiation and under estradiol was assessed by RT-PCR. We found that RANK expression was not regulated by RANK-L and estradiol in human differentiating osteoclasts. In conclusion, ERα expression increased with monocyte differentiation, but RANK-L and estradiol do not regulate RANK and ERα . These results may provide new insights in the mechanism of action of estradiol and pathogenesis of bone loss.

SU257

Secreted Frizzled-related Protein (sFRP-1) Inhibits TNFalpha- or RANKL-Dependent Osteoclast Formation. K. D. Häusler*[1], J. M. W. Quinn[1], N. J. Horwood[1], J. Ellis*[2], C. Lengel*[2], T. J. Martin[1], J. S. Rubin*[2], M. T. Gillespie[1]. [1]St. Vincent's Institute of Medical Research, Melbourne, Australia, [2]National Cancer Institute, NIH, Bethesda, MD, USA.

Wnt signaling is crucial in the processes of organogenesis and limb development, and in cancer metastasis. Moreover, Wnt signaling is crucial for osteoblast differentiation, apoptosis and the development of bone mass exemplified by the point mutations or genetic loss of LRP5, a co-receptor for Frizzled (Fz) family of proteins. Fz proteins can be antagonised by secreted frizzled-related proteins of which there are five members. The sFRPs contain a cysteine rich domain (CRD) with identity to the CRD of Fz proteins, and can bind to Wnt proteins to modulate their activity. We have found that sFRPs are expressed by the osteoblast and that these influence osteoclast formation. Neutralizing antibodies against sFRP-1 enhanced TRAP positive mononuclear and multinuclear osteoclast formation in cocultures of murine osteoblasts with spleen cells treated with PGE2 (10-7M) and 1,25 (OH)2 vitamin D3 (10-8M). Recombinant sFRP-1, or the CRD of sFRP-1, or sFRP-3 was able to dose dependently inhibit RANKL-dependent osteoclast formation in either osteoblast / spleen cocultures, RANKL+M-CSF-treated splenic or bone marrow cultures, or in RANKL-treated RAW264.7 cell cultures. In RANKL-independent osteoclast formation assays using RAW264.7 cells treated with TNFa +TGFb, sFRP-1 also blocked osteoclast formation while OPG did not affect osteoclast formation. The action of sFRP-1 to limit RANKL- or TNFa-induced osteoclast formation may be explained in part by the observation that recombinant sFRP-1 binds specifically to RANKL in an ELISA format. This finding raised the possibility that sFRP-1 limits osteoclast formation by binding directly to these TNF family members, and suggested that sFRP-1 may act as a decoy receptor potentially with dual specificity for RANKL and TNFa. However, a second mechanism is likely. In bone marrow cultures in which TGFb was present during the first three days and RANKL present only during the last three days of culture, sFRP-1 and OPG had different actions when added with TGFb. sFRP-1 inhibited osteoclast formation, while OPG did not effect osteoclast formation. Combined, these findings suggest that sFRP-1 (and possibly sFRP-3) may affect osteoclast formation by binding to TNFa or RANKL as well as through direct action upon hematopoietic cells, presumably interrupting Wnt signaling.

SU258

Mass Spectrometric Proteome Analysis of RANKL-induced Protein Expression in Osteoclast Differentiation. E. Lee*[1], Y. Jin*[1], R. Hwang*[1], Y. Rhee*[2], S. Lim*[2]. [1]Internal Medicine, College of Medicine, Brain Korea 21 Project for Medical Sciences, Yonsei University, Seoul, Republic of Korea, [2]Internal Medicine, College of Medicine, Yonsei University, Seoul, Republic of Korea.

Osteoclasts are highly specified multinucleated bone resorbing cells known as part of the mononuclear phagocyte system. Cytokines macrophage colony stimulating factor (M-CSF) and the receptor activator of NFκB ligand (RANKL) induce differentiation of bone marrow hematopoietic precursor cells and umbilical cord blood cells into bone-resorbing osteoclasts without any requirement for stromal cells. RANKL is a type II membrane protein of the TNF family and plays a critical role in the regulation of osteoclastogenesis. Our aim was to identify and characterize the proteins induced by RANKL that are structurally and functionally undefined. In this study, we attempted to investigate the difference, using proteomics technique, of expression pattern between RANKL-induced cells and those not induced. Briefly, the cells were isolated from bone marrow of mouse femur and tibiae and human umbilical cord blood, respectively, and then were cultured in complete α-MEM media overnight. Next day, the non-adherent cells were removed, and only the adherent cells were further cultured in the presence of M-CSF. After 2 days, the cells were treated with RANKL for 6hr, 24hr, and 72hr respectively. And the obtained cells were subjected to protein purification and subsequent two-dimensional electrophoresis. After visualization of protein spots either by Coomassie or silver nitrate, digital gel images obtained by scanner were analyzed by PDQuest software (Bio-rad, USA) and the results were confirmed visually. The 2D protein pattern of the cells treated with only M-CSF was compared with those treated together with RANKL. As a result, Of thousands of proteins visualized, 32 proteins were increased over three times in amount. Concomitantly, 13 proteins were decreased. Up to now, we identified 26 protein spots using peptide mass spectrometry method by matrix-assisted laser desorption/ionization time-of-flight mass spectrometry (MALDI-TOF MS). Furthermore, to confirm the change of the protein level, we will carry out western blot using specific antibody and differential display polymerase chain reaction. These resulting protein targets offer insights into the mechanisms of osteoclastogenesis in human and mouse and further provide opportunities to find out markers to facilitate early diagnosis of osteoporosis.

SU259

TGF-β Promotes Human Osteoclast Resorption by Increasing Proliferation of Precursors and Down Regulating Their Fusion Through p38 and p44/42 MAP Kinases. M. A. Karsdal*[1], T. Kirkegaard*[1], P. Rasmussen*[1], M. S. Fjording*[2], J. Nielsen*[1], M. Ovejero*[1], H. Lou*[1], M. Stahlhut*[1], P. Boissy*[1], N. T. Foged*[1], P. Qvist*[1], C. Christiansen*[3], K. L. Nielsen*[1], J. Delaissé*[1]. [1]Nordic Bioscience, Herlev, Denmark, [2]LEO Pharmaceuticals, Ballerup, Denmark, [3]Center for Clinical and Basic Research, Ballerup, Denmark.

Although RANK-L is essential for osteoclast formation, factors such as TGF-β are potent modulators of osteoclastogenic stimuli. These secondary stimuli are obviously important for both physiological and pathophysiological bone turnover, and are key points for understanding osteoclast biology. Using cultures of human osteoclasts differentiated from blood monocytes, we have investigated the direct effects of TGF-β on proliferation, fusion, resorption and signalling pathway of osteoclasts and their precursors. Human monocytes were isolated from peripheral blood, and cultured for 3 days with M-CSF. Hereafter, cells were washed extensively, detached by trypsin treatment and re-seeded either on bone slices or plastic and cultured with 25 ng/ml RANK-L and M-CSF for up to 28 days. When TGF-β was added directly after re-seeding for the first 14 days of culture, bone resorption at day 28 was dose-dependently affected in a biphasic curve, and reached a maximum corresponding to a 100% increase at 0.12 ng/ml. Both cell number and TRAP activity were increased to the same extent as resorption. Furthermore, as assessed morphologically, cell fusion was decreased by 50% in the presence of TGF-β. Conversely, TGF-β function blocking antibodies increased cell fusion. However, when TGF-β was present during the entire culture period (Day 1-28), we did not observe stimulatory effects on cell proliferation and resorption, clearly indicating context dependent effects of TGF-β during the different stages of osteoclastogenesis. To further investigate the time dependent effect of TGF-β, we analysed the signal transduction pattern induced by TGF-β in precursor and mature osteoclasts. Interestingly, p38 MAP kinase was activated only in precursor cells, whereas p44/42 and other kinases were activated in both precursor and mature osteoclasts. Furthermore, an inhibitor of p38 MAP kinase (SB203580 10μM) significantly inhibited TRAP activity in osteoclast precursors. These data clearly demonstrate that the presence of TGF-β at a given concentration and at a specific stage of osteoclastogenesis, dramatically influences several steps of this process, i.e. cell proliferation, TRAP expression, fusion, and modulates strongly the bone resorptive activity itself. Furthermore TGF-β acts directly on osteoclast precursors, through stage-specific activation of p38 MAP kinase.

SU260

Mutation of Tyrosine 559 in c-Fms to Phenylalanine Impairs Bone Resorption by Reducing Akt and ERK Phosphorylation. S. Takeshita[1], X. Feng[2], F. P. Ross[1], S. L. Teitelbaum[1]. [1]Pathology, Washington University, St. Louis, MO, USA, [2]Pathology, University of Alabama, Birmingham, AL, USA.

The intracellular signals by which c-fms, the M-CSF receptor, regulates osteoclast (OC) formation and function are unknown. We addressed this issue by retrovirally transducing primary OC precursors, namely bone marrow macrophages (BMMs), with a chimeric cDNA, EpoR/c-fms, containing the extracellular domain of erythropoietin receptor (EpoR) linked to the transmembrane and cytoplasmic domains of c-fms. Transduced cells treated with RANKL and either Epo or M-CSF generate similar OC numbers and bone resorptive capacity. We next transduced EpoR/c-fms cDNAs containing six individual tyrosine (Y) to phenylalanine (F) residues in the cytoplasmic tail (559, 697, 706, 721, 807 and 921) into BMMs and treated the cells with RANKL and either M-CSF or Epo. Cells expressing the c-fms mutations Y559F and Y807F exhibit decreased proliferation, measured by MTT activity and BrdU incorporation, and differentiation, assessed by TRAP solution assay. To determine the role of each mutation on OC function, BMMs bearing wild type and mutant chimeras were treated with M-CSF and RANKL to generate pre-OCs, which were replated on dentin slices. Fresh medium, containing RANKL and either M-CSF or Epo was added, and resorption assessed by Coomassie brilliant blue stain. Cells bearing EpoR/c-fms, with Y559 mutated to F, but not those expressing Y807F, are virtually incapable of resorptive activity, while the remaining four mutants fail to alter OC formation or function. We next examined c-fms-mediated Akt and ERK phosphorylation in BMMs and OCs. Thus, we expressed all individual Y mutations and treated serum- and cytokine-starved cells with Epo or M-CSF. While Akt is activated by the cytokines in both cell types, ERKs are activated only in BMMs. Y559F in the c-fms cytoplasmic domain arrests activation of both Akt and ERKs in BMMs and Akt in OCs. In contrast, Y807F inhibits Akt in BMMs, but has minimal effects in OCs. The kinase inhibitors LY294002 (PI3-kinase, PI3-K) and PP2 (c-Src family) dose-dependently dampen BMM proliferation and mirror the c-fms mutation Y559F, by blocking Akt and ERK activation. In summary residue Y559 in c-fms transmits signals in BMMs, activating both the PI3-K and c-Src pathways. In contrast, c-fms Y807 has limited capacity to signal. Thus, we have detailed, for the first time, Y residues in the c-fms tail which signal in authentic OC precursors. Y559 and Y807 are indispensable for osteoclastogenesis. In contrast, while Y559 is required for the resorptive function of OCs through phosphorylation of Akt and ERKs, Y807 is dispensable.

SU261

The Transcription Factor MITF is a Substrate for the p38 MAP Kinase. K. C. Mansky, M. C. Ostrowski. Molecular Genetics, Ohio State University, Columbus, OH, USA.

The severe osteopetrotic phenotype in microphthalmia (mi) mutant mice is caused by a defect in the terminal differentiation of osteoclasts. Immature mononuclear osteoclasts are present in the mi/mi mice, but these do not fuse or form ruffled borders. Thus the products of the MITF gene, the basic helix-loop-helix zipper (bHLHzip) factor MITF, and the closely related bHLHzip factors TFE3, TFEC and TFEB may be critical regulators of terminal differentiation in this cell type. Because MITF appears to be important for differentiation of osteoclasts, we are interested in understanding extracellular signals that positively regulate the activity of MITF and its partners. One partner of MITF in osteoclasts is PU.1, an ets family factor whose expression is restricted to hematopoietic cells. PU.1 expression is necessary for differentiation of a number of cell types, including osteoclasts. Our lab has previously shown that MITF and PU.1 physically and functionally interact. The RANK receptor a member of the tumor necrosis factor receptor family mediates an essential signal to osteoclast progenitors for their differentiation into osteoclasts. In cells treated with RANKL, p38 mitogen activated protein kinase activity is upregulated. Previously we have shown that there is a p38 phosphorylation site at serine residue 307 in the C-terminal region of MITF. Using a phospho-specific antibody, we were able to show that MITF was phosphorylated at the p38 site upon RANKL stimulation of bone marrow cells. The sustained phosphorylation of MITF correlated with a sustained phosphorylation of p38 MAP kinase and an increase in tartrate resistant acid phosphatase (TRAP) gene expression as measured by Real Time PCR. Activated p38 immunoprecipitated from RAW 264.7 cells and p38 alpha synthesized in vitro were able to phosphorylate MITF but were not able to phosphorylate MITF containing point mutation at serine residue 307. p38 MAP kinase can bind to C-terminal region of MITF (amino acids 217 to 419) and using site directed mutagenesis we are more precisely trying to map the p38 binding site in MITF. To determine the biological significance of the MITF p38 phosphorylation mutant, retroviral vectors containing MITF with the mutation at serine 307 are being used to try and rescue mi/mi osteoclasts. Lastly we have found in transient transfections that MITF co-transfected with a constitutively active MKK6, an upstream activator of p38 MAP kinase, leads to increased functional interaction between MITF and PU.1 and are currently trying to detemine if MITF phosphorylated at seine residue 307 leads to an increase in the physical interaction between MITF and PU.1.

SU262

c-Cbl, but not Cbl-b, Requires Src Phosphorylation to Interact with the p85 Subunit of PI3Kinase. G. DeBlasi, A. Sanjay, T. Miyazaki, W. C. Horne, R. Baron. Yale University, New Haven, CT, USA.

Osteoclasts (OCs) from osteopetrotic Src-/- mice are deficient in both cell migration and bone resorption, and exhibit cytoskeletal changes with altered podosomes and focal adhesions. Engagement of the vitronectin receptor activates Src and Pyk2, a FAK family member present in podosomes, and induces the formation of a tri-molecular complex of Src, Pyk2, and c-Cbl. OCs from c-Cbl-/- mice also exhibit defective migration. c-Cbl interacts with several downstream proteins, including PI3K, whose activity is also required for normal OC function. PI3K is known to bind to c-Cbl via its p85 subunit, a molecular interaction that appears to be necessary for effective translocation of PI3K to the cell membrane. Although recombinant p85-SH3 domains bind c-Cbl, the interaction between c-Cbl and p85 is dependent on phosphorylation of c-Cbl at Y731, suggesting that there is either an additional SH2-mediated interaction between c-Cbl and p85, or that a phosphorylation-dependent conformational change allows the SH3-mediated interaction and thereby the translocation of PI3K to the cell membrane to take place. Our goal was, therefore, to characterize both the molecular nature of the interaction between Cbl family members and the p85 subunit of PI3K, and the role of Src-dependent phosphorylation in these interactions. Mutation of c-Cbl Y731, a known target of Src kinase, to Phe prevents the association of c-Cbl and p85, as does mutation of the Src SH3 binding site on c-Cbl. These results suggest that the interaction of p85 and c-Cbl requires Src binding to and phosphorylating c-Cbl. Indeed, transfection with kinase-dead Src decreased the c-Cbl/p85 interaction in a dose-dependent manner. Given that c-Cbl is a member of a family of proteins and that Cbl-b is also highly expressed in OCs, possibly explaining the mild phenotype in c-Cbl-/- mice, we then determined whether Cbl-b would also interact with PI3K and whether the interaction was governed by the same constraints. In contrast to c-Cbl, over-expression of kinase-dead Src had no effect on the interaction between p85 and Cbl-b. Although highly homologous to c-Cbl, Cbl-b lacks a Tyr residue in a motif homologous to c-Cbl Y731, possibly explaining the independence from Src phosphorylation. This suggests that c-Cbl and Cbl-b bind p85 at different sites and that binding of PI3K to the two Cbl proteins may be regulated differently. In conclusion, the phosphorylation of c-Cbl Y731 by activated Src kinase is necessary for an SH3-mediated interaction with the p85 subunit of PI3K, whereas interaction between Cbl-b and PI3K is independent of Src activity. These differences in Src dependence might explain, at least in part, the phenotypic differences seen in c-Cbl-/- vs Cbl-b-/- mice.

SU263

The Protein-Tyrosine Phosphatase (PTP) Activity of PTP-Oc Is Essential for Both the Differentiation of U937 Cells into Osteoclasts and their Apoptosis. M. Amoui*, S. M. Suhr*, D. J. Baylink, K. H. W. Lau. Musculoskeletal Disease Center, Jerry L. Pettis Mem VAMC, Loma Linda, CA, USA.

Cells of monocyte-macrophage hematopoietic lineage differentiate into osteoclasts. Our past work indicates that once activated, osteoclasts rapidly undergo apoptosis. We also found that the osteoclastic PTP, PTP-oc, is involved in osteoclastic bone resorption. In the present study, we sought to test the hypothesis that the PTP activity of PTP-oc is essential for 1) the differentiation of osteoclasts and 2) their subsequent apoptosis. To test this hypothesis, we evaluated if overexpression of the wild type (wt) and dominant-negative (dn) PTP-oc in human promyelomonocytic U937 cells would affect their differentiation into active osteoclasts and their subsequent apoptosis. The wt PTP-oc expression construct was prepared by inserting the full-length PTP-oc cDNA in frame into our recently developed transposon-based expression vector. The dn PTP-oc construct was constructed by site-directed mutagenesis in which the catalytic cys-325 was mutated to ser. U937 cells were transfected with the wt, the dn PTP-oc, or the empty expression vector to obtain sta-

bly overexpressing cell clones. To test the effect of overexpression of wt or dn PTP-oc on osteoclast differentiation, we have developed a method in which U937 cells were induced by sequential TPA and $1,25(OH)_2D_3$ treatments to form osteoclast-like cells that resorb bone *in vitro*. This treatment converted 29±5% of the vector alone control cells into osteoclast-like cells. The same treatment converted 91±4% (P<0.001) of the U937 cells that were stably overexpressing the wt PTP-oc, but only 14±4% (P<0.001) of the dn PTP-oc stable U937 cell clones formed osteoclast-like cells. To assess the effect of overexpression of wt and dn PTP-oc on the apoptosis, we measured the relative percentage of apoptotic cells in cell pools that stably overexpressed either the wt or the dn PTP-oc by FACS analysis using an apoptotic assay kit and also by a DNA Laddering-based apoptotic assay. About 7-9% of the vector-transduced control cell pools were apoptotic. In contrast, the percentage of apoptotic cells in the cell pools that stably overexpressed the wt PTP-oc was >60% (P<0.001). The percentage of apoptotic cells in cells that stably overexpressed the dn PTP-oc (7-11%) was not significantly different from the control. On the basis of these findings, we conclude that the PTP-oc is a key osteoclastic enzyme which is required not only to promote osteoclast resorption by promoting osteoclast maturation but also to limit the extent of bone resorption by promoting osteoclast apoptosis. We suspect that these two processes can be independently regulated because PTP-oc is an upstream enzyme.

SU264

Glucocorticoid Cooperates With NFAT to Activate the Calcitonin Receptor in Osteoclasts. L. Peng*[1], C. Laplace*[1], S. R. Goldring[1], K. Matsuo*[2], D. L. Galson[1]. [1]NEB Bone & Joint Institute, Dept. of Medicine, Beth Israel Deaconess Medical Center & Harvard Medical School, Boston, MA, USA, [2]Dept. of Microbiology, Keio University School of Medicine, Tokyo, Japan.

During osteoclast differentiation, the calcitonin receptor (CTR) is transcriptionally activated. The osteoclast-specific murine CTR P3 promoter has previously been shown to be responsive to NFATs (Nuclear Factor of Activated T cells) which are activated by calcium signaling. Cotransfection of the –319/+61 P3-reporter (which contains 5 NFAT sites) and a constitutively active NFAT (ΔNFAT3; contains a deletion of the NFAT3 regulatory domain, leading to calcium-signaling independent nuclear localization) into uninduced RAW264.7 cells greatly increased P3-reporter activity above constitutive levels. Sequential 5' deletion of the P3 promoter demonstrated that NFAT sites 1-4 are sufficient for full activity, and that sequential loss of sites 2-4 resulted in a stepwise loss of NFAT-responsiveness. Therefore, we examined the individual and cooperative roles of each site by analyzing individual site-specific mutations of each of the NFAT sites within the –178, –148 and –118 P3 deletions. Although all the sites contribute to maximum ΔNFAT3 activation of P3, it is clear that site 2 (–97 to –93) is absolutely required, no matter how many other sites are present. Site 1 (+17 to +21) is the next most important site, followed in decreasing importance by site 3 (–130 to –126), and then site 4 (–157 to –153). Treatment of osteoclasts with the glucocorticoid dexamethasone (Dex) increases the expression of CTR protein and mRNA. Dex treatment of the P3 5' deletion series demonstrated that P3 is induced, in the absence of ΔNFAT3, by 20-to-40 fold, with the highest induction level observed with the –118 P3-reporter. This implies that the Dex-responsive element in the mCTR-P3 promoter lies between –118 and +61. There is a putative GRE binding site between –40 and –55. However, our results indicate that mutation of NFAT site 2 ablates 90% of the Dex responsiveness, regardless of the number of NFAT sites present. Interestingly, while NFAT site 2 is required for the P3 promoter to respond to cotransfection with ΔNFAT3 in the absence of Dex, P3 constructs with a mutated site 2 regain some responsiveness to ΔNFAT3 in the presence of Dex (~ 7-fold above Dex alone). Additionally, the Dex responsiveness of site 2 mutants is increased by ΔNFAT3. This indicates that the glucocorticoid receptor (GR) and NFAT cooperate to activate the CTR gene through NFAT site 2. This is the first report of GR cooperating with, rather than inhibiting, NFAT action. The precise nature of the Dex-GR interaction with the CTR gene and the mechanism of its cooperation with NFAT remain to be elucidated.

SU265

Functional Assessment Of Specific Gelsolin Peptide Domains In Osteoclast Actin Assembly and Motility. R. S. Biswas[1], D. S. Yuen*[1], K. A. Hruska*[2], M. A. Chellaiah*[1]. [1]Dept. of OCBS, University of Maryland, Baltimore, MD, USA, [2]Department of Pediatrics, Washington University, School of Medicine, St. Louis, MO, USA.

Gelsolin is a critical protein in osteoclast podosome assembly. Gelsolin deficient osteoclasts are devoid of podosomes, hypomotile and partially disabled in bone resorption. A multimolecular signal generating complex assembles on gelsolin in podosomes based on phosphatidyl inositol trisphosphate (PIP3) generated by associated PI 3-kinase and protein-lipid-protein interactions. The complex contains PI 3-kinase, c-Src, and other proteins based on these type of interactions with gelsolin. The primary amino acid sequence of gelsolin consists of six domains. The actin binding sites and activities of gelsolin are correlated with its six repeated (S1-S6) segments. The S1 and S2 domains of gelsolin each contain a phosphoinositides (PI) binding site, and recently, a third site in the C-terminal part of gelsolin was identified. The different segments of gelsolin were cloned in-frame into a bacterial expression vector, pTat-HA, to produce Tat-HA fusion proteins. The proteins were purified and transduced into mouse osteoclasts to study the role of actin- and PI- binding sites on actin assembly. Osteoclasts transduced with full length gelsolin, the N-, and C-terminal actin binding domains, and the PI binding domains, demonstrated an increase in F-actin content. After transduction osteoclasts were immunostained with anti-HA to detect the transduced protein and rhodamine phalloidin to detect F-actin. Osteoclasts transduced with full length and NH-terminal segments of gelsolin demonstrated dot-like structures similar to podosome structures which were stimulated in number by OPN. These osteoclasts were bone resorption competent and responded to stimuli. Thus, the transduced gelsolin or the NH-terminal segment functioned like gelsolin. Transduction of PIP2 binding domains produced larger patches enriched in transduced protein and F-actin, and these cells were bone resorptive disabled in response to stimuli. Thus, the transduced PI binding domain peptides did not function in podosome assembly but accumulated phosphoinositides producing a dominant negative effect of blocking stimulated assembly of the signal generating complex and bone resorption. Our results demonstrate that the PI binding sites in S1 and S2 domains, as well as in COOH- terminal gelsolin have effects on actin dynamics and motility of osteoclasts, and that separating PI binding from actin binding produces a diminished bone resorption in response to stimuli. Thus, gelsolin is an attractive osteoclast target which can be approached by affecting high order phosphoinositide binding.

SU266

A Novel Osteoclast-Specific *cis*-Acting Element Controls Expression of a Mouse Cathepsin K Gene. Y. P. Li, W. Deng*, K. Shimizu*, W. Chen*. The Forsyth Institute, Harvard School of Dental Medicine, Boston, MA, USA.

The osteoclasts, the bone resorbing cells, play a key role both in normal bone remodeling and in the skeletal osteopenia of arthritis, osteoporosis, periodontal disease and certain malignancies. Despite some recent insights from the effects of the targeted deletion of the *c-fos*, *PU.1* and *NF-κB* transcription factor genes on osteoclast differentiation, the mechanisms by which transcription factors control the process of osteoclast differentiation have not been identified. The cathepsin K gene is expressed at high levels only in differentiated osteoclasts. Therefore, it is an excellent marker with which to study the mechanisms of osteoclast-specific gene expression. The purpose of this study was to characterize the *cis*-acting elements required for osteoclast-specific expression of the cathepsin K gene. We reported we have found a novel critical *cis*-element in cathepsin K promoter. The *cis*-acting element required for osteoclast-specific expression has been located in the 5' flanking region of the gene. Osteoclast specific expression of 1.4 kb mouse cathepsin k promoter-CAT construct was verified by comparing CAT activity in osteoclast-like cell (i.e. differentiated MOCP-5 cells) with that in pre-osteoclast cells (MOCP-5) and that in non-osteoclastic cells (e.g. ROS 17/2.8, COS7, and C3H10T1/2 cell lines). In transfected MOCP-5 cells, cathepsin K promoter activity was up regulated about 50 folds by RANKL (OPGL). The deletion and point mutation transfection studies of cathepsin K promoter-CAT constructs defined the core of cis-acting element. Mutation of the core sequence of the *cis*-acting element in cathepsin K promoter resulted in loss of response to RANKL stimulation. The core sequence we defined does not correspond to the binding site of any known transcription factors. Competition-Gel Shift, Super-Gel Shift and DNase1 Footprinting assays revealed a DNA binding protein that bound the *cis*-acting element. Most interestingly, the binding protein was present in osteoclast-like cells, but absent from other non-osteoclastic cell lineage lines and mouse tissues. Therefore, our results suggested that we have characterized a novel *cis*-acting element that was bound by a unknown transcription factor that is restricted to the osteoclastic cell lineage and regulate osteoclast-specific expression of the cathepsin K gene possible through RANKL pathway.

SU267

Trp Channels Regulate Osteoclast Calcium Sensing. B. D. Bennett, K. A. Hruska. Pediatrics, Washington University School of Medicine, St. Louis, MO, USA.

Handling of extracellular calcium, [Ca2+]e, by osteoclasts is important due to the large amount of Ca2+ liberated as these cells resorb bone. Influx of bone derived Ca2+ into osteoclasts may impact the ability of OCs to resorb bone by regulating intracellular Ca2+ pools linked to Ca2+ extrusion. We have hypothesized that [Ca2+]e evoked rises in intracellular calcium, [Ca2+]i , is mediated in part by transient receptor potential channels (trpC) and we have demonstrated that phospholipase C (PLC) activation in OCs is coupled to [Ca2+]e and Ca2+ influx through trpC. We have demonstrated endogenous expression of trp channels in RAW 264.7 macrophage and authentic mouse osteoclasts. Normally PLC activation occurs downstream of heterotrimeric G-protein coupled receptors. To demonstrate that trp channels mediate receptor operated calcium influx in OCs we compared UTP-evoked [Ca2+]i rises in OCs and OCs overexpressing trpC3 and trpC6. UTP stimulation of the G-protein coupled P2Y receptor led to Ca2+ influx that was enhanced in trp3 and trp6 overexpressors, and [Ca2+]e stimulated [Ca2+]i increases were increased by trpC3 and trpC6 overexpression. [Ca2+]e-induced [Ca2+]i rises were inhibited by a trp channel dominant negative construct. Our results demonstrate a role for endogenous trp channel regulation of calcium sensing. To assess the potential role of trp channels in regulating OC handling of the extracellular Ca2+ by intracellular stores, the effect of trp overexpression on Ca2+ loading in intracellular calcium stores was determined. Release of intracellular Ca2+ stores, either by SERCA inhibition or stimulation of intracellular release channels, was increased with trp6 overexpression. Thus, trp regulates Ca2+ content in OC stores. We conclude that trp channels in OCs may form an important feedforward calcium signaling pathway that reports the extracellular Ca2+ load to intracellular stores and may regulate transcytosis of Ca2+ through stored Ca2+.

SU268

p38 MAP-kinase Mediates Glucose-Dependent Transcriptional Regulation of Osteoclast H^+-ATPase Expression. K. I. Larsen[1], L. V. Ponomareva*[2], W. Wang*[2], M. L. Falany*[1], J. P. Williams[2]. [1]Department of Pathology, University of Alabama, Birmingham, AL, USA, [2]Department of Internal Medicine, University of Kentucky, Lexington, KY, USA.

Bone resorption is glucose concentration-dependent and osteoclasts secrete acid via a vacuolar H^+-ATPase heavily expressed in the ruffled membrane. Mechanisms regulating glucose-dependent increases in bone resorption have not been identified. Glucose activates p38 MAP-kinase in other cells and since MAP kinases activate transcription factors, we hypothesized one mechanism mediating glucose-stimulated bone resorption may be increased expression of the H^+-ATPase. Glucose activates osteoclast p38 MAP-kinase in a time-dependent manner as determined by Western analysis with phospho-specific p38 antibody while total p38 levels are unchanged. The $K_{0.5}$ for glucose dependent activation of p38 MAP-kinase is ~2 mM, activation is maximal at 30 minutes and are returning to basal levels by 60 minutes. H^+-ATPase expression increases in a glucose concentration-dependent manner as determined by Western and Northern analysis. The specific inhibitor of p38 MAP-kinase, SB203580, inhibited glucose transport in osteoclasts, as well as glucose concentration-dependent increases in bone resorption and H^+-ATPase A and B subunits. H^+-ATPase expression is transcriptionally regulated since actinomycin D inhibits glucose stimulated increases in mRNA with no effect on G3PDH mRNA. We conclude that glucose transcriptionally regulates osteoclast H^+-ATPase expression by a mechanism likely to involve p38 MAP-kinase.

SU269

Ultrastructure of Osteocyte Process. L. You*[1], S. Weinbaum*[2], S. Cowin*[2], M. Schaffler[3]. [1]Mechanical Engineering, Stanford, Stanford, CA, USA, [2]Mechanical Engineering, City University of New York, New York, NY, USA, [3]Orthopaedics, Mount Sinai School of Medicine, New York, NY, USA.

Osteocytes are believed to be the mechanical sensor cells in bone. One potential mechanism for the mechanosensing process is that osteocytes directly sense the deformation of the substrate to which they are attached. However, tissue level strains in whole bone are typically < 0.2 percent (1), yet many in vitro experiments show that dynamic substrate strains must be at least an order of magnitude larger for intracellular biochemical responses to occur (2, 3). Recently, a novel model was developed (4), which provides a new potential mechanism by which mechanical loading induced fluid flow in lacuno-canalicular system under routine physical activity can produce very large deformations on osteocyte processes that are at least one order of magnitude larger than bone tissue deformations. There are two key assumptions necessary for the model: 1) the presence of the transverse elements bridging the pericellular space surrounding the osteocyte process, which interact with the fluid flow and lead to the outward hoop tension on the process; 2) and the presence of bundled F-actin in the osteocyte processes, which resist the outward hoop deflection. However, morphological data to support these assumptions are scant. In the current studies, 1) transverse tethering elements were observed in the pericellular space surrounding the osteocyte process (Fig. 1),

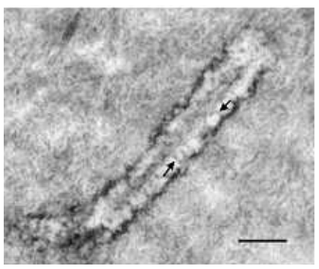

and 2) close packed microfilaments were observed in the center of the cell process (Fig. 2).

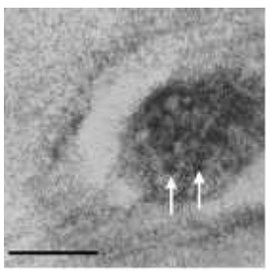

Therefore, the current study provides strong evidence that the fundamental microstructural features needed for local mechanical amplification to function exist in and around osteocytes.

References: 1)Fritton et al. J. Biomech. 33: 317, 2000; 2) Burger, et al. Bone 37 (CRC Press, 1993); 3) You et al. J Biomech Eng 122: 387, 2000. 4) You et al., J Biomech, in press, 2001; 5) Weinger et al. Calcif Tissue Res. 14:15, 1974

SU270

Serotonin Potentiates PTH-induced Collagenase-3 Activity in Osteoblasts and Stimulates Adenylyl Cyclase Activity in Osteocytes. M. M. Bliziotes[1], A. Eshleman*[2], X. Zhang[3], K. M. Wiren[4]. [1]Medicine, Oregon Health and Science University/Portland VAMC, Portland, OR, USA, [2]Pharmacology and Physiology, Oregon Health and Science University/Portland VAMC, Portland, OR, USA, [3]Behavioral Neurosciences, Oregon Health and Science University, Portland, OR, USA, [4]Behavioral Neurosciences, Oregon Health and Science University/Portland VAMC, Portland, OR, USA.

The neurotransmitter serotonin (5-HT) regulates osteoblast signaling pathways. We have demonstrated that 5-HT receptors and 5-HT transporter (5-HTT) are expressed in osteoblasts, and 5-HT increases AP-1 transcription factor activity. 5-HT regulates nitric oxide release by mechanically stimulated osteoblasts. The 5-HT2B receptor is expressed in osteocytes. We demonstrate that 5-HT potentiates the PTH-induced collagenase-3 activity in osteoblasts, and regulates osteocyte cAMP signaling. The clonal osteoblastic cell line UMR 106-01 was transfected with a CAT reporter construct containing the rat collagenase-3 promoter region including the minimal PTH-responsive sequences. Transfected cells were treated with 1 μM 5-HT for 6 hr, then PTH (100 nM) was added for an additional 24 hr. CAT activity was determined on cell lysates. The clonal osteocytic cell line MLO-Y4 was analyzed for the presence of 5-HT receptors by immunblot, and 5-HT transporter expression was analyzed by [^{3}H]5-HT competition uptake and [^{125}I]RTI-55 competition binding experiments. Cyclic AMP levels were determined following 60 min or 6 hr of 1 μM 5-HT treatment, followed by 10 min or 24 hr of 100 nM b(1-34)PTH, respectively. PTH treatment of UMR 106-01 cells induced a 5-fold increase in collagenase-3 promoter activity; 5-HT alone showed no effect. 5-HT potentiated the PTH response by 40%. MLO-Y4 cells express the 5-HT2A, 2B, and 2C receptors. MLO-Y4 cells express the 5-HTT, but not the dopamine or norepinephrine transporters. The Km for 5-HT uptake was 290±100 nM and the Vmax was 6.41±0.41 pmol/mg protein/min. 1 μM 5-HT for 60 min increased cAMP levels in MLO-Y4 cells by 60%, while 24 hr treatment increased levels by 2-fold. The effects were potentiated by PTH. We conclude: 1) 5-HT potentiates the PTH-induced collagenase-3 promoter activity in osteoblasts; this effect may occur by inhibition of a repressor, such as jun-B, which is upregulated by PTH; 2) 5-HT 2A, 2B and 2C receptors are expressed in osteocytes, as is the 5-HTT; 3) 5-HT is positively coupled to adenlylyl cyclase in osteocytes. Thus, 5-HT may have an important role in regulating matrix metalloproteinase activity in osteoblasts, and activates a signaling pathway in osteocytes which has been implicated in protection from apoptosis.

SU271

Pulsed Electromagnetic Fields Affect Phenotype and Connexin 43 Protein Expression in MLO-Y4 Osteocyte-like Cells and ROS 17/2.8 Osteoblast-like Cells. C. H. Lohmann[1], Z. Schwartz[2], Y. Liu*[2], Z. Li[3], S. A. Albert*[2], B. J. Simon[4], V. L. Sylvia[2], D. D. Dean[2], L. F. Bonewald[5], H. J. Donahue[3], B. D. Boyan[2]. [1]Orthopaedics, University of Hamburg-Eppendorf, Hamburg, Germany, [2]Orthopaedics, University of Texas Health Science Center at San Antonio, San Antonio, TX, USA, [3]Orthopaedics, Pennsylvania State University, College of Medicine, Hershey, PA, USA, [4]EBI, L.P., Parsippany, NJ, USA, [5]Oral Biology, University of Missouri, Kansas City, MO, USA.

Osteocytes, the predominant cell type in bone, are postulated to be responsible for sensing mechanical and electrical stimuli, and transducing signals via gap junctions. Osteocytes respond to fluid flow-induced shear by increasing connexin 43 (Cx43) levels, suggesting that they might be sensitive to physical stimuli like low frequency electromagnetic fields (EMF). Others have shown that preconfluent cultures of immature osteoblasts exhibit decreased intercellular communication in response to EMF but no change in Cx43. In the present study we examined if pulsed EMF (PEMF) (0-16 gauss; 15 Hz) modulates physiological responses of terminally differentiated osteocyte-like MLO-Y4 cells or of well-differentiated osteoblast-like ROS 17/2.8 cells. PEMF was applied to confluent cultures for 8 hrs/day for 1, 2, or 4 days for the MLO-Y4 cells and continuously for 1, 2, or 3 days for the ROS 17/2.8 cells. In MLO-Y4 cell cultures, PEMF increased alkaline phosphatase activity but had no effect on cell number or osteocalcin. TGF-β1 and PGE_2 were increased, while NO^{2-} production was differentially affected, depending on treatment time. After 1 day, NO^{2-} production was decreased; after 2 days it was unchanged; and after 4 days it was increased. PEMF's effect on TGF-β1 was via a prostaglandin-dependent mechanism involving Cox-1 but not Cox-2. In ROS 17/2.8 cells, PEMF didn't affect cell number, osteocalcin mRNA or osteocalcin protein. PEMF reduced Cx43 protein in both cells. Longer exposures also decreased Cx43 mRNA. This indicates that cells in the osteoblast lineage, including well-differentiated osteoblast-like ROS 17/2.8 cells and terminally-differentiated osteocyte-like MLO-Y4 cells, respond to PEMF with changes in local factor production and reduced Cx43, suggesting decreased gap junctional signaling. At least some of the effects of PEMF are due to increased prostaglandin production. Differences in cell response to PEMF may be cell-specific as well as signal-specific.

Disclosures: ***C.H. Lohmann****, EBI, L.P. 2.*

SU272

Prostaglandin E_2 Receptor (EP_2) Is Responsible for Increased Intercellular Communication Between Osteocyte-like Cells in Response to Mechanical Strain. B. Cheng*[1], S. Gu*[1], X. Wang*[1], E. Sprague*[2], L. F. Bonewald[3], J. X. Jiang*[1]. [1]Biochemistry, University of Texas Health Science Center, San Antonio, TX, USA, [2]Radiology, University of Texas Health Science Center, San Antonio, TX, USA, [3]Oral Biology, School of Dentistry, University of Missouri, Kansas City, KS, USA.

Osteocytes embedded in the matrix of bone are thought to be mechanosensory cells that translate strain into signals to initiate or regulate bone remodeling. We have previously shown that fluid flow shear stress dramatically induces prostaglandin release and COX-2 mRNA expression in osteocyte-like MLO-Y4 cells, and that prostaglandin E_2 (PGE_2) released by these cells functions in an autocrine manner to modulate gap junction function and connexin 43 (Cx43) expression. In this report, we examined the expression of the subtypes of PGE_2 receptors and potential signaling mechanisms in response to mechanical stimulation. Expression of PGE_2 receptor EP_2 was increased in response to treatment by fluid flow, while EP_1, EP_3, and EP_4 were unchanged. RT-PCR and Northern blot analyses showed that EP_2 receptor mRNA levels were elevated 30 min and further elevated 24 hrs after 2-hours of fluid flow treatment at 16 dynes/cm^2. Application of PGE_2 or conditioned medium from fluid-flow treated cells directly to untreated MLO-Y4 cells stimulated the expression of the EP_2 receptor in a similar fashion to fluid flow. The EP_2 receptor antagonist AH6809 suppressed the effects of all three, suggesting that EP_2 is the functional receptor that responds to fluid flow and to autocrine PGE_2. Conditioned medium from fluid flow treated MLO-Y4 cells and exogenously added PGE_2 stimulated cAMP production and protein kinase A (PKA) activity in untreated MLO-Y4 cells suggesting that PGE_2 released by mechanically stimulated cells is responsible for upregulation of cAMP and PKA. The adenylate cyclase activators, 8Br-cAMP and forskolin, also stimulated cAMP production and PKA activity, suggesting that cAMP activated PKA. The PKA inhibitor H89 blocked the activation of PKA by 8Br-cAMP and forskolin. Both 8Br-cAMP and forskolin enhanced intercellular connectivity, the number of functional gap junctions, and Cx43 protein expression. The increase in Cx43 in response to PGE_2 was attenuated by AH6809 suggesting that the EP_2 receptor mediates the effects of autocrine PGE_2 in the osteocytic response to fluid flow induced shear stress. Hence, the EP_2 receptor, cAMP and PKA are critical components of the biochemical signalling cascade between mechanical strain and gap junction-mediated communication between osteocytes.

SU273

A Potential Role for Osteocytes in Recruiting Osteoclast Precursors to Targeted Bone Sites. S. Ko, S. E. Harris, M. Dallas*, L. F. Bonewald. Oral Biology, University of Missouri-Kansas City, Kansas City, MO, USA.

The mechanism whereby osteoclasts are attracted to specific areas of bone for targeted removal are unknown. It has been hypothesized that the osteocyte, whether unstrained as in immobilization or overstrained as in pathological overload, can send signals indicating which bone should be removed. Osteoclast precursors must be recruited to the site of resorption and must undergo proliferation before fusion and activation. In this study, MLO-Y4 cells were used as a model for osteocytes and RAW264.7 and MOCP-5 were used as models for osteoclast precursors. It has been shown previously that MLO-Y4 cells express RANKL and support osteoclast formation and activation. In addition, these cells and their conditioned media (CM) stimulate proliferation and increase colony size of both RAW 264.7 and MOCP-5 cells. This capacity of MLO-Y4 cells was shown to be due to M-CSF, as anti-M-CSF antibody at 18 μg/ml completely blocked proliferation. MLO-Y4 cells produce large amounts of M-CSF, a factor known to be necessary for osteoclast formation. MLO-Y4 cells and CM are chemotactic for osteoclast precursor cell lines. Transwell membranes (polycarbonate, 8 μm pores) were used in which MLO-Y4 cells or CM were placed in the bottom well and the osteoclast precursor cell lines seeded into the transwell at $5x10^4$ cells per well. MLO-Y4 cells or CM alone increased transmigration of both RAW 264.7 and MOCP-5 cells at 6 hrs. To determine the factor(s) responsible, gene array analysis of MLO-Y4 cells was used. We found 4 factors elevated in MLO-Y4 cells compared to 2T3 osteoblasts, that had previously been described as chemotaxis factors. Two chemokines, MCP-3 and MIP-2α have been described to be chemotactic for monocytes and neutrophils, but their effect on osteoclast precursors was not known. TGF-β and VEGF were also elevated, and are known to induce osteoclast chemotaxis. TGF-β increased transmigration of both osteoclast precursor cell lines, whereas VEGF had no effect. Surprisingly, MCP-3 increased RAW 264.7 cell transmigration, but had no effect on MOCP-5 cells. This suggests that these cell lines may represent different types of precursors or different stages of osteoclast differentiation. Studies using neutralizing antibodies are underway to determine which cytokine(s) made by MLO-Y4 are responsible for osteoclast precursor chemotaxis and if MIP-2α is chemotactic for the osteoclast precursors.

SU274

Neuronal NOS (nNOS) Is Expressed in Human Osteocytes: Multiple Pathways of NO Regulation? A. Caballero[1], V. Das-Gupta*[2], N. Loveridge*[1], A. Pitsillides[2], J. Reeve[1]. [1]University of Cambridge, Cambridge, United Kingdom, [2]Royal Veterinary College, London, United Kingdom.

Until now, eNOS was considered to be the predominant osteocytic NOS isoform in bone and we previously studied the distribution of eNOS protein expression in the human femoral neck because of its possible involvement in the response to load. Studies in rat and human fracture callus have shown that nNOS mRNA is expressed sometime after fracture but no study has yet immunolocalised nNOS in human bone. In this study, we have analysed the density and distribution of both eNOS+ve and nNOS+ve osteocytes in the ilium. Ten micron frozen sections were cut from transiliac biopsies from 8 female osteoporotic patients (range=56-80 y) and incubated overnight in antiserum for eNOS and nNOS followed by peroxidase/VIP substrate detection. We used two separate eNOS antisera directed against different epitopes in the c-terminus. For nNOS three different antisera were used, two binding to different c-terminal epitopes and one binding to a n-terminal epitope. Sections were then incubated in propidium iodide or methyl green to detect all osteocytes. The density (no/mm2 bone) of eNOS and nNOS positive osteocytes and the distances from the nearest bone surface were determined by image analysis (NIH image). The percentage of osteocytes positive for nNOS was higher than that for eNOS (cortical: nNOS 84.04%, eNOS 61.78% $p<0.05$; cancellous: nNOS 82.33%, eNOS 65.21% $p<0.05$). When examined in each BMU the maximum and minimum distances of the eNOS+ve and nNOS+ve osteocytes from bone surface, there was no signicant difference between eNOS+ve and nNOS+ve osteocyte distributions. Only one eNOS antibody was able to detect eNOS epitopes in osteocytes. All three nNOS antibodies detected nNOS epitopes in osteocytes but those directed against the c-terminus had higher detection rates. The present of nNOS protein in osteoblasts and osteocytes was confirmed by western analysis. In conclusion, the nNOS isoform appears present in osteocytes and seems to be more prevalent than the eNOS isoform. The possibility exits that, as with the skeletal muscle, nNOS might contribute to regulating the local blood supply which we showed previously correlates with the corrected mineralisation rate of osteoid.

SU275

Prevalence of Osteoporosis in Rural Postmenopausal Women. J. M. Lappe, K. M. Davies, G. Haynatzki, D. Travers-Gustafson*, R. R. Recker. Osteoporosis Research Center, Creighton University, Omaha, NE, USA.

Women living in farming communities may be perceived as having low risk of osteoporosis since they typically have had more weight bearing activity, well-balanced diets, and sunlight exposure than urban women. In fact, studies consistently show that fracture rates are higher in urban than in rural populations. Also, rural women have less access to DXA measurements. Thus, there is a risk that rural women will be overlooked in the Healthy People 2010 goal to reduce the proportion of adults with osteoporosis. The purpose of this analysis is to estimate the prevalence of osteoporosis in a population sample of rural women. The analysis was conducted on data from 1180 women randomly selected from the population of healthy postmenopausal women over 55 years of age in a nine-county farming area of Nebraska.

Baseline Characteristics

	Mean±SD
Age (yrs)	66.7±7.3
Age at menopause (yrs)	47.3±7.0
Body mass index wt/ht^2	29.0±5.6
Hip BMD (gm/cm^2)	0.862±0.14
Spine BMD (gm/cm^2)	0.944±0.16

Participants were enrolled into an intervention study of vitamin D and calcium. DXA scans and spine radiographs were obtained at baseline. For this analysis, osteoporosis is defined as hip or spine t-score <2.5 or presence of spine fracture on radiographs.

Osteoporosis Criteria	**n**
Hip or spine t-score<2.5	150
Spine fracture	100
t-score <2.5 and fracture	52

Analyses indicated that 26% of this population sample has osteoporosis. This compares with recent estimates by the National Osteoporosis Foundation that 20% of women age 50+ in Nebraska have osteoporosis and with NHANES III estimates that 13-18% of U.S. women over 50 are affected. These findings suggest that the prevalence of osteoporosis is currently underestimated in rural women and underscores the importance of targeting them in prevention and detection programs.

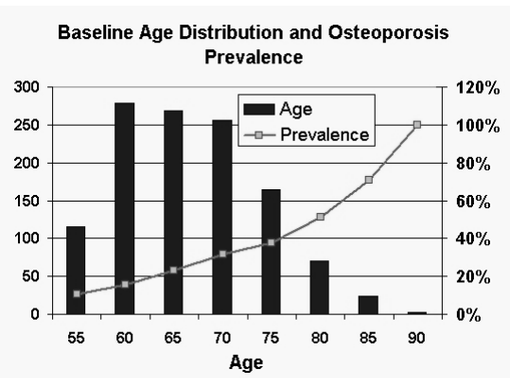

SU276

Racial Differences in the Effect of Early Milk Consumption on Postmenopausal Bone Mineral Density. A. R. Opotowsky*, J. P. Bilezikian. Medicine, Columbia University, New York, NY, USA.

Early milk consumption has been found to influence bone mineral density positively throughout life. Previous studies leading to this finding focused on white women; no data exist to support the view that black women also gain an equivalent benefit from early milk consumption. We hypothesized that there may be a racial difference in the effect of early milk consumption on postmenopausal hip bone mineral density (BMD). Using data from the Third National Health and Nutrition Examination Survey (NHANES III), we analyzed the relationship between reported childhood and teenage milk consumption and current femoral BMD among postmenopausal non-Hispanic white (NHW, n=1,711) and black (NHB, n=742) women. Among NHW women, controlling for age and body mass index (BMI), childhood and teenage milk consumption were positively associated with BMD at two of four sites and all four sites respectively. Early milk consumption, however, was not significantly associated with BMD at any site among NHB women. In fact, NHB women who consumed at least one glass of milk per week as children or teenagers had non-significantly lower BMD than their counterparts who consumed less than one glass of milk per week early in life (Table 1). To test the hypothesis that race modifies the effect of early milk intake on postmenopausal BMD, we evaluated the significance of the interaction between race and historical milk consumption in the overall population. The interaction between race and teenage milk consumption was significant at all sites, while the interaction between race and childhood milk consumption was significant at all sites except the femoral neck. Removing from the analysis subjects previously diagnosed with osteoporosis or who had sustained a hip fracture did little to alter the results. These findings neither challenge the importance of adequate calcium intake for the attainment of peak bone mass, nor demonstrate a detrimental effect of early milk consumption on bone health among black women. They do, however, reveal racial differences in the effect of early milk consumption on postmenopausal BMD. These observations underscore the need to be cautious about extrapolating nutritional relationships seen within one population to another.

Table 1: Effect of teenage milk intake on BMD by race, controlling for age and BMI

	White women		Black women	
	Coefficient	P value	Coefficient	P value
Femoral neck	0.023	0.005	-0.0184	0.22
Intertrochanter	0.032	0.006	-0.016	0.2
Trochanter	0.027	0.002	-0.0114	0.24
Total hip	0.03	0.002	-0.012	0.27

SU277

Environmental and Biologic Factors as Determinants of Peak Bone Mass in a Biracial Cohort. S. Y. S. Kimm[1], N. W. Glynn*[1], H. J. Kalkwarf[2], S. R. Daniels*[3]. [1]Family Medicine, University of Pittsburgh, Pittsburgh, PA, USA, [2]General & Community Pediatrics, Children's Hospital Medical Center, Cincinnati, OH, USA, [3]Cardiology, Children's Hospital Medical Center, Cincinnati, OH, USA.

Primary prevention of osteoporosis includes the achievement of maximal peak bone mass (PBM). Though calcium intake (Ca) and physical activity (PA) are said to affect PBM, their specific roles remain unclear due to a lack of prospectively collected data. We examined the impact of body composition, ethnicity, age of menarche, Ca, PA, smoking, contraceptive use, and pregnancy during the time of PBM accretion in 324 African American (AA) and 282 White (W) women seen annually since ages 9-10 yrs. Ca intake and PA levels were assessed by a validated 3-day food and activity diary. Habitual PA was assessed by a validated questionnaire. Daily Ca intake and PA levels were averaged over a 5 year period from ages 9 to 14. Current oral contraceptive (OC) and Depo-Provera/Norplant use, smoking status and "given birth before age 17" were ascertained. BMD and body composition were assessed at age 22±1 yrs by DXA of the whole body, lumbar spine, total hip and femoral neck. Separate multiple regression models were constructed for each bone site with all of the above as predictors. Lean body mass (LBM) was strongly correlated with BMD at all 4 sites with each kg associated with 0.006-0.008 g/cm^2 greater BMD, P<0.001. AA women had higher (P<0.001) BMD at all sites by 0.05 g/cm^2 (4.8%). Age of menarche was inversely (P<0.05) associated with BMD at all sites except the femoral neck (P=0.07). Each earlier year of menarche was associated with higher BMD by 0.016 g/cm^2 (1.5%) at the spine, 0.009 g/cm^2 (0.85%) at the total hip, and 0.007 g/cm^2 (0.6%) for the whole body. Race interaction with age of menarche was not significant, P>0.4. Ca intake was not (P>0.6) associated with BMD except at the total hip where there was a positive trend, P=0.096. Neither PA measure was associated (P>0.6) with BMD at any site. "Given birth" was marginally (P=0.06) associated with lower BMD at the femoral neck. Contraceptive use was not significant (P>0.25), but OC use showed a positive trend (P=0.1) at the total hip. Smoking was not (P>0.6) associated with BMD for any site. In summary, growth and rate of maturation had the greatest impact on PBM. Other factors, though suggestive for some, may not have sufficient impact to manifest as significant predictors. Though Ca and PA may affect PBM, their relative contributions in multivariate analyses where LBM is dominant may be masked due to the variability of their being self-reported measures. For their maximal effect to be shown, Ca and PA may also need to be evaluated in the context of other potentially mediating factors and other interactions.

SU278

The Effects of Milk Supplementation on Bone Accretion in Chinese Children. E. Lau[1], A. Chan[2], W. Lau*[2], H. Lynn[2]. [1]The Hong Kong Jockey Club Centre for Osteoporosis Care and Control, The Chinese University of Hong Kong, Shatin, Hong Kong Special Administrative Region of China, [2]The Chinese University of Hong Kong, Shatin, Hong Kong Special Administrative Region of China.

The calcium intake of Chinese children is amongst the lowest in the world, and supplementing the diet with calcium may be of tremendous public health significance in enhancing both mass. A randomized controlled clinical trial was conducted to study the effects of supplementing the diet of Chinese children with high calcium milk powder, on the rate of bone accretion. A total of 288 subjects (161 boys and 127 girls) aged 9-10 was randomized into 3 groups: supplementation by 80gm of milk powder containing 1300mg calcium, supplementation by 40gm of milk powder containing 650mg calcium, and no supplementation. Bone mineral density (BMD) was measured at the total body, total hip and the spine at baseline, 6 months, 12 months and 18 months. The percentage change in BMD between the 3 groups were compared by ANCOVA for repeated measures, adjusting for Tanner Staging.

Percentage change in BMD at 18 months

	Total Body	Total Hip	Spine
Boys			
80gm milk	4.1	10.6	10.7**
40gm milk	4.1	11.3	10.6
Control	3.0	9.9	9.0
Girls			
80gm milk	6.9	12.5	18.0
40gm milk	7.4	13.6*	16.4
Control	6.1	11.1	15.9

**P=0.01 and *P=0.06 by ANCOVA for repeated measures, as compared to the control group

Conclusion: There is a statistically non-significant trend that children whose diet is supplemented by milk have a higher gain in BMD.

SU279

High Prevalence of Vitamin D Insufficiency in the Elderly Population in Argentina. B. Oliveri, L. Plantalech, A. Bagur, A. Wittich*, G. Rovai*, E. Pusiol*, J. López Giovanelli*, G. Ponce*, A. Nieva*, A. Chaperón*, M. Ladizesky*, J. Somoza*, C. Casco, S. N. Zeni. Asociación Argentina de Osteología y Metabolismo Mineral, Buenos Aires, Argentina.

Vitamin D insufficiency is common in elderly populations (mainly in subjects living in homes for the elderly) and leads to secondary hyperparathyroidism, high bone resorption, bone loss and osteoporotic fractures. The aim of this study was to evaluate the nutritional status of vitamin D in elderly people living in their own homes in different cities in Argentina. 350 ambulatory subjects older than 65 years (X ± SD)(71.3± 5.2 years),(236 women and 114 men) from 7 cities in Argentina (between latitude 27ºS and 55ºS) were evaluated between the end of winter and beginning of spring (15th August-15th October). None of the subjects was receiving vitamin D or any medication that could affect mineral metabolism. They were grouped in 3 geographical regions: South Region (Bariloche: 41ºS, n=28; Comodoro Rivadavia: 45ºS, n=30; Ushuaia:55ºS, n=32); Mid-region (Buenos Aires 34ºS, n=168; Mendoza:33ºS, n=33) and North Region (Corrientes: 27ºS, n=30; Tucumán: 27ºS, n=30). Two patients were excluded because of primary hyperparathyroidism. Serum levels of calcium (Ca), creatinine (Cre) , bone alkaline phosphatase (BAP), 25(OH)D and mmPTH were measured. The results of 25(OH) D were analyzed as suggested by Mc Kenna (Osteoporosis Int 8, 1998): Deficiency(Def): <10 ng/ml; Insufficiency(Ins): >10-<20 ng/ml. The differences in 25(OH)D were the following: the South Region exhibited the lowest levels (p<0.0001vs North and Mid regions): 14.3± 5.6 ng/ml (Def:13%, Ins:75%), with the highest prevalence of deficiency in the southernmost city Ushuaia: 25%. The highest levels of 25(OH)D were observed in the North (p<0.03 vs Mid, p<0.0001vs South): 20.6 ± 7.4ng/ml (Def:2% Ins:50%). The Mid-region showed intermediate levels, between the South and North 17.8±8 ng/ml (Def:12% Ins:52%). Serum PTH and 25(OH)D were inversely related: r=-0.3, p<0.001). Serum levels of Ca(9.5±0.3mg/dl) BAP(61.0±19UI/l)and Cre(0.9±0.2mg/dl) were within normal limits with no significant differences among regions. Conclusion: The risk of insufficiency increases as latitude augments. The high prevalence of lower winter 25(OH) levels in this elderly urban population suggests the usefulness of vitamin D winter supplementation to reduce osteoporotic fractures.

SU280

Determinants of Circulating Levels of Vitamin D in Elderly People in Buenos Aires City, Argentina. L. Plantalech, B. Oliveri, H. Salerni*, J. Pozzo*, M. Ercolano*, M. Ladizesky*, C. Casco, S. N. Zeni, J. Somoza*, J. Fassi*, A. Bagur. Asociación Argentina de Osteología y Metabolismo Mineral, Buenos Aires, Argentina.

Elderly people, especially those living in overpopulated cities, are a susceptible population to hypovitaminosis D. The aim of this study was to investigate the winter serum level

of 25 OH vitamin D (25OHD) in 169 healthy people aged 71.5 ± 5.4 years (113 women and 56 men), living in Buenos Aires (34°S), and its relationship with exposure to sunlight, vitamin D (D) food (fish) intake, housing, clothing –use of beach-clothes such as short sleeves, shorts, etc– (using a questionnaire adapted from the EURONUT SENECA study), and socioeconomic status (determined by a test provided by the Asociación Argentina de Marketing). 25OHD was measured by Incstar RIA (ng/ml), none of the subjects received treatment with D. Results: Mean 25OHD was :17.5 ± 4.5ng/ml . Forty nine percent of the subjects had no exposure to sunlight; 63% of the study population consumed rich D food. The socioeconomic composition of the study population was: 15.3% high (H), 35.7% middle (M) and 49.0% low(L) level:. Serum 25OHD was higher in people with high exposure to sunlight vs. no exposure (23.3 ± 2.1 vs. 15.3 ± 0.1, p<0.001); who ate D food vs. zero intake (20.5 ± 1.7 vs. 15.2 ± 0.9,p<0.01) ; who lived in a house vs. apartment (19.2 ± 0.9 vs. 17.1 ± 1.3,p<0.05); who wore beach clothes in summer vs. long sleeves(20.9 ± 2.0 vs. 16.7 ± 0.7,p<0.01) and who had a high vs. low socioeconomic level (H: 20.7 ± 2.0 vs. L:.16.7 ± 0.7, p<0.05). A linear correlation was observed between 25OHD and exposure to sunlight (r:0.35, p<0.001). A multistep regression analysis showed that both D food intake and exposure to sunlight are predictors of levels of 25OHD (r2: 0.2, MSE:55.9, p<0.0001). Subjects in the high socioeconomic level had more exposure to sunlight (H: 5.5 ± 1.6 vs. M: 3.3 ± 0.6 vs. L: 1.4 ± 0.6 hours per week, p<0.03) and D food intake (H: 2.6 ± 0.2 vs. M: 1.7 ± 0.1 vs. L: 1.6 ± 0.1 time/week, p<0.0001) than those in the middle or low level. Conclusion: Hypovitaminosis D is found in a high percentage of our elderly population and is associated with low exposure during sunlight and poor D food consumption. It is the people with scant economic resources that are most affected by these factors.

SU281

Factors Related to Bone Health Among Canadian Chinese Immigrants Aged 45+. A. M. Cheung[1], R. Chaudhry*[2], K. Milstead*[2], C. Chan*[2], N. Diaz-Granados*[2], D. Lui-Yee*[2], M. Hamidi*[2], G. Chan*[3], L. Thompson*[4]. [1]Department of Medicine, University Health Network & University of Toronto, Toronto, ON, Canada, [2]University Health Network, Toronto, ON, Canada, [3]Yee Hong Community Centre, Toronto, ON, Canada, [4]University of Toronto, Toronto, ON, Canada.

We conducted a community-based cross-sectional study to examine risk factors for osteoporosis and osteoporotic fractures among Chinese-Canadian immigrants aged 45 and older. Nine hundred and seventy-six (976) participants have been recruited to date through media announcements, health fairs, and community outreach through community centres, shopping centres, churches and libraries which predominantly serve the Chinese community in the Greater Toronto Area. We collected data on demographics, risk factors for osteoporosis and osteoporotic fractures, diet, physical activity, medication use, co-morbid conditions, fall and fracture history, and use of alternative and mainstream preventive health care. We also collected data on height and weight and measured heel bone density (BMD) using Sahara Qualitative Ultrasound (Hologic, Inc). Preliminary analyses were performed for the first 844 individuals recruited (589 women and 255 men, aged 45-95). Immigrants were mainly from Hong Kong (73%) & China (16%), with mean time in Canada of 12.8 years. Population characteristics included: mean age 59.9:63.4 (Female:Male); height 155.0:167.5 cm (F:M); weight 55.2:66.3 kgs (F:M). Dietary assessment showed that 88.5% of our participants consumed dairy products, with a median daily intake of 1.0 serving daily; 96% consumed soya products, median intake of 0.4 servings daily; 98.5% consumed dark green vegetables, median intake of 1.1 servings daily. A total of 167 falls were reported by 123 individuals (range 1-5 per person) in the three years prior to the interview. Of these reported falls, 68% occurred outdoors, 54% occurred during winter, and 23 fractures of various sites were reported. Mean heel BMD was 0.493:0.509 g/cm2 (F:M); mean t-score - 0.782:-0.907 (F:M). 3.9:3.2% (F:M) had t-score below or equal to -2.5, and 41.9:43.3% (F:M) had t-scores between -1 & -2.5. Compared to the North American Caucasian population (USDA, CSFII), this sample of Chinese-Canadian immigrants reported lower intake of dairy products but higher intake of dark green leafy vegetables. The BMD distribution of women and men in our study is similar to that reported in other North American studies (CAMOS, NHANES III). Further analyses are being performed to determine the relationship between the risk factors, BMD and osteoporotic fractures in the Chinese immigrant population recruited for our study.

*Disclosures: **A.M. Cheung**, Eli Lilly 2; Novartis 2; Procter & Gamble 2.*

SU282

Diagnosis of Vertebral Fracture by Instant Vertebral Assessment. J. Damiano*[1], S. Kolta[1], R. Porcher*[2], M. Dougados*[1], C. Roux[1]. [1]Rhumatologie, Hôpital Cochin, Paris, France, [2]Dbim, Hôpital Saint Louis, Paris, France.

Vertebral fractures are the hallmark of osteoporosis. They are independent risk factors for both vertebral and peripheral fractures. Instant Vertebral Assessment (IVA) is a radiographic method using dual energy X-ray absorptiometry (DXA) to assess vertebral deformities. We performed IVA of the spine from T4 to L5 (anteroposterior and lateral views) and BMD (g/cm²) measurement at the lumbar spine and left hip on a Delphi W device (Hologic, Waltham, MA) in 101 post menopausal patients (aged 70.6 ± 8.8 years). They also had lateral and anteroposterior X-rays of the thoracic and lumbar spine. Vertebral fracture was assessed independently by 2 investigators. Weighted kappa statistics vere calculated at the vertebral and the patient levels, adjusted for predefined confounding factors : scoliosis, osteoporosis (T score ≤ 2.5 at either spine or femur) and increased body mass index (BMI, Kg/m²). Sixty one patients had at least one vertebral fracture on X-rays. The percentage of vertebrae not legible was 1 % and 14 % on X-rays and IVA respectively. On IVA, T4 and T5 were not assessable in 42 % of patients. At the patient level, sensitivity and specificity of IVA, as compared to X-rays, were 80 % and 93 % respectively. Inter-reader agreement was good for X-rays (kappa score of 0.77) but moderate for IVA (kappa score of 0.53). At the vertebral level, sensitivity and specificity of IVA were 74% and 98%, and with a good inter-reader agreement (kappa scores of 0.85 and 0.62 for X-rays and IVA respectively). According to the prevalence of vertebral fracture in our sample, negative predictive value of IVA was 97.5% at the vertebral level and 85.3% at the patient level . Conversely, IVA also had a high positive value, 92% at the patient level. In post menopausal women, IVA may avoid unnecessary X-rays.

SU283

Long-Term Prediction of Fracture Incidence in Elderly Men and Women. K. P. Chang*, J. R. Center, T. V. Nguyen, J. A. Eisman. Bone and Mineral Research Program, Garvan Institute of Medical Research, Sydney, NSW, Australia.

The Dubbo Osteoporosis Epidemiology Study is an ongoing longitudinal study of fracture incidence in men and women aged 60 and over. Fractures due to minimal trauma and non-pathological fractures were ascertained by reviewing all radiology reports from the two area radiology services over 12 years. From April 1989 to December 2000, 1055 symptomatic fractures were recorded in 807 persons over 39,357 person-years of observation. Fracture incidence was 3412 and 1632 per 100,000 person years for women and men respectively. The incidence of vertebral, proximal humerus, wrist, hip and pelvis fractures increased exponentially with age in both sexes, typical of osteoporotic fractures. As expected, the risk of subsequent fractures was increased by having any previous osteoporotic fracture; for example, 20% of men and 23% of women with hip and 35% of men and 25% of women with vertebral fractures sustained further fractures. Ankle, hand and foot fractures did not show an exponential age-related increase. However, these "non-osteoporotic" fractures were also predictive of future fractures, particularly in men, with 42% of men and 15% of women with ankle fractures having a subsequent fracture (relative risk: 15.8 [95% CI: 10.3 – 21.4] and 3.5 [95% CI: 0.9 to 7.9], men and women respectively). Similar but lesser increased risks were observed in men and women with prior hand and foot fractures. Although fracture incidence was greater in women than men for all but rib fractures, the female: male ratio decreased with age, particularly in the 80+ age group (e.g. hip 1.8:1, vertebral 1.4:1). Absolute fracture numbers peaked in the 70-79 age group for men (48% of all fractures in men) and in the 80-84 age group in women before declining, due to the smaller 'at risk' population. This is the first long-term study examining fracture incidence over 12 years. Ankle, hand, and foot fractures did not increase with age, but were strong predictors of subsequent osteoporotic fractures, especially in men. The data suggest that fractures traditionally thought not to be osteoporotic do indicate increased risk of future osteoporotic fractures. In addition, the fracture burden for society occurs in younger people than previously recognised, especially in men.

SU284

Incidence of Hip Fractures in Italian Males and Females Aged 45+ Years. P. Piscitelli*[1], S. Maggi*[2], R. Giorgino[3], G. Crepaldi[4]. [1]Epidemiology, Catholic University, Rome, Italy, [2]CNR Aging Center, Padova, Italy, [3]Procter&Gamble Health Care, Rome, Italy, [4]University of Padova, Padova, Italy.

No national-based data on the incidence rates of hip fracture in Italy have been published up to now. This study aims at assessing the incidence rates of hip fracture in Italian males and females aged 45+ years, using the National database available at the Department of Health. We identified codes 820.0 and 820.1 for cervical fractures, codes 820.2 and 820.3 for intertrochanteric fractures, codes 820.8, 820.9 and 821.1 for hip fractures at unknown sites. The most recent data available were for 1999. Census population data from the Italian National Institute of Statistics were used for calculating the incidence rates. The following table shows the rates (per 10,000) of cervical, intertrochanteric and all hip fractures in males and females, by age and sex.

Age	Cervical		Intertrochanteric		All		F:M ratio
	Males	Females	Males	Females	Males	Females	
45-64	1.6	2.9	1.7	1.6	3.6	4.9	**1.4**
65-74	6.1	15.3	6.5	12.3	13.6	30.2	**2.2**
75+	32.4	73.5	34.9	80.1	72.8	163.9	**2.3**

As expected, the incidence rates increase with age, in women the rates are more than double compared to males. We identified a total number of 17,777 hip fractures in men and 60,931 in women. The length of stay in hospital for cervical fractures increased from 14.9 days in the youngest group to 16.2 days in the eldest group in men and from 14.0 days to 17 days in women; for intertrochanteric fractures it ranged from 15.1 days in the youngest group to 16.2 days in the eldest group in men and increased from 14.6 days to 16.3 days in women. This is the first national assessment of hip fracture incidence rates in the Italian population. The rates are consistent with those observed in other Southern European countries. Inspite of the tremendous social impact of hip fracture, the perception of its frequency and severity remains still very low among the general population and also in the medical community, particularly if compared to other conditions considered "very severe", such as myocardial infarction (MI). The same government sources provide a figure of 57,569 MI in age matched men and 28,531 MI in age matched women, but the level of awareness for primary and secondary preventive interventions in this case is very high, while for osteoporotic fractures is virtually null.

SU285

Fractures History and Osteoporosis Drugs Usage: a Population-based National Study. S. Giannini[1], M. Bevilacqua*[2], G. Bianchi[3], S. Gonnelli[4], E. Palummeri*[5], M. Rossini*[6], R. Giorgino[7]. [1]Internal Medicine, University of Padova, Padova, Italy, [2]Endocrinology, Sacco General Hospital, Milano, Italy, [3]Rheumatology, Arenzano General Hospital, Arenzano, Italy, [4]Internal Medicine, University of Siena, Siena, Italy, [5]Geriatrics, Ospedale Galliera, Genova, Italy, [6]Osteoporosis center, Verona, Italy, [7]Procter & Gamble Health Care, Rome, Italy.

The ESOPO study is a national population based study to measure the prevalence of osteoporosis in the Italian general population. This research analyzed the pattern of osteoporosis drugs in subjects according to low trauma fractures history: 83 University and Hospital centers participated to the study. Subjects were randomly invited to participate to the study from 1,536 General Practitioners using their own Patients Directory. A total of 15,992 subjects (11,011 females aged 40-79 and 4,981 males aged 60-79 years) participated to the study. The current use of osteoporosis drugs (namely bisphosphonates, calcium, vitamin D, calcitonin or other drugs used for OP treatment) and HRT was noted. Low-trauma fractures which had occurred after the age of 50 was also recorded. Full data are available for 7,439 women and 4,606 men. The table below shows the age-adjusted proportion of female and male subjects according to fractures history and OP drugs current usage (*p<0.05 **p<0.01 ***p<0.001 vs. pts without fractures).

	Females		Males	
	With Fractures	Without Fractures	With Fractures	Without Fractures
Cases	1326	6133	783	3823
Any drug for OP	26.4%***	13.9%	3.1%**	1.9%
Bisphosphonates	12.7%***	5.6%	1.0%**	0.5%
Calcium	13.3%***	6.6%	2.0%**	0.8%
Vitamin D	10.6%***	4.4%	0.7%*	0.4%
Calcitonin	3.2%**	1.2%	0.4%	0.3%
Other drugs	1.6%	1.8%	0.1%	0.1%
HRT	10.1%	15%		
HRT > 1 year	5.5%	9.1%		

Patients with a history of fractures are more frequently treated with osteoporosis drugs, as predictable. Females are more likely to take a drug than men, which is probably due to higher historical knowledge on postmenopausal osteoporosis among Italian physicians. However, the study demonstrates that only 26% of women and 3% of men with a history of low trauma fractures are currently treated with any OP therapy. Bisphosphonates, calcium and vitamin D usage was higher in females than in males, but still very low: only 1out of 10 of women and 1 out of 100 men with fractures history are treated with bisphosphonates. The use of HRT is limited to early postmenopausal women and is unlinked to fractures history. This large study confirms that osteoporosis is clearly a mistreated disease in women; in men the use of bone active drugs is almost null. Health institutions involvement is mandatory for implementing educational programs to create both patients and physicians awareness on the "silent epidemic" disease.

SU286

Clinical Vertebral Fractures Are Associated with Hip, Rib, and Wrist Fractures in Postmenopausal Women: The Population Based ESOPO Study. O. Di Munno*[1], N. Malavolta*[2], M. Ferraris*[3], F. Silveri*[4], F. Trotta*[5], R. Pellerito*[6], M. Muratore*[7], R. Giorgino[8]. [1]Rheumatology, University of Pisa, Pisa, Italy, [2]S.Orsola Hospital, Bologna, Italy, [3]Rheumatology, S.Andrea Hospital, Vercelli, Italy, [4]Rheumatology, Murri Hospital, Iesi AN, Italy, [5]Rheumatology, S.Anna Hospital, Ferrara, Italy, [6]Rheumatology, Mauriziano Hospital, Torino, Italy, [7]Rheumatology, General Hospital, S.Cesario di Lecce, Italy, [8]Procter & Gamble Health care, Rome, Italy.

The ESOPO study was a national population based study aimed at measuring the prevalence of osteoporosis in the Italian general female population. This research assessed the relationship between the history of clinical vertebral fractures and other osteoporosis related fractures in postmenopausal women. Eighty-three University and Hospital centers located over 18 out of 21 Italian peninsular and insular regions participated to the study. Subjects were randomly invited to participate from 1,536 General Practitioners through their own Patients Directory by a specific randomization protocol: reasons of decline were accurately recorded. Eleven thousands-eleven females aged 40-79 were enrolled for the study. The history of clinical vertebral, hip, rib, wrist and other low-trauma fractures (humerus, pelvis, clavicle, leg) occurred after the age of 50 was recorded. The table below shows the proportion (±SEM) of 7,457 women with and without previous clinical vertebral fractures who had also reported a history either hip, wrist, rib or other low trauma fractures.

	With vertebral fx	Controls	p value	OR	95% C.I.
Cases	146	7313			
Hip fractures	4.1%±1.6%	0.8%±0.1%	0.0003	4.85	2.1-11.4
Rib fractures	15.1%±3.0%	1.8%±0.2%	<0.0001	9.7	5.6-15.8
Wrist fractures	18.5%±3.2%	5.0%±0.2%	<0.0001	4.3	2.8-6.7
Other fractures	17.8%±3.2%	10.2%±0.3%	0.0044	1.9	1.2-2.9

Almost 2% of the study subjects reported a history of clinical vertebral fractures after the age of 50. A very significantly higher number of them reported a history of either hip, rib, wrist or other low-trauma fractures when compared to controls. In particular rib fractures were showed to be very strongly associated with spine fractures by a nearly 10-fold OR increase. This study confirms the high frequency of osteoporotic fractures recurrence in the same subject: rib fractures risk should be taken frequently into account in subjects with osteoporosis. Finally the current spine-hip fracture paradigm should be shifted to a larger spine-hip-wrist-rib fractures circle.

SU287

Underestimation of Vertebral Deformity Prevalence: How Can We Improve Accuracy? N. Napoli*[1], S. Bucchieri*[1], L. Sutera*[1], D. Avila*[1], C. Sferrazza*[1], R. Giorgino[2], G. B. Rini*[1]. [1]Bone Metabolic Disease Unit Dept. II Internal Medicine, Policlinico Giaccone, Palermo, Italy, [2]Procter & Gamble Health care, Rome, Italy.

The prevalence of vertebral deformity is significantly underestimated due to the low frequency of symptoms and mostly the poor attention paid by clinicians and radiologists in the radiographic recognition of vertebral deformity. This study was aimed at measuring the proportion of false negative results for vertebral deformity assessment in an Osteoporosis workout setting based in an University center. Since October 2001 to March 2002 we analyzed 193 consecutive subjects(177 women and 16 men) who referred to the Bone Densitometry unit: all subjects had undergone a X-ray exam of thoracic and lumbar spine in external general radiology centers in the previous 3 months. The presence of vertebral deformity was either not reported or negative in all the original reports. Each film was centrally digitized: T4-L4 vertebral heights ratio was measured from a single physician by a dedicated morphometry software (Spine-X Analyzer, CAM Diagnostics, Milan, Italy). The system is based on a 6-point based recognition of the 3 vertebral heights: the intra-observer CV has been measured, ranging from 2.2% for lumbar to 3.1% for thoracic bodies. The full procedure takes from 5' to 12'. All X-ray films were then blindly evaluated by an expert skeletal radiologist in the University for a visual direct assessment of vertebral body heights. The presence of at least one vertebral deformity was observed in 164 out 188 (87%) of study subjects whose films could be measured by digital computerized morphometry (DCM) and in 124 out 186 (77%) of cases visual manual assessment (VMA) could evaluate. The presence of at least 1 vertebral deformity was concordantly shown by DCM and VMA in 85% of cases: 70% of the subjects showed multiple vertebral deformities according to digital analysis, 57% according to visual assessment. The following table shows the distribution of subjects according to the number of vertebral deformities as measured by DCM and VMA.

N. of vertebral deformities	DCM	%	VMA	%
0	24	12.8%	42	22.6%
1	34	18.1%	38	20.4%
2	36	19.1%	46	24.7%
3	35	18.6%	32	17.2%
4	24	12.8%	14	7.5%
5	16	8.5%	6	3.2%
6	12	6.4%	3	1.6%
7	5	2.7%	4	2.2%
8	2	1.1%	1	0.5%

Our data confirms that the prevalence of vertebral deformities is very largely underestimated in general practice: we propose the use of an easy-to-use computerized morphometry method on digitized films which was shown to dramatically improve diagnostic accuracy.

SU288

Smoking Is Associated with an Increased Fracture Risk in the General Population. L. Rejnmark, P. Vestergaard, L. Mosekilde. Dept. of Endocrinology and Metabolism, Aarhus Amtssygehus, Aarhus, Denmark.

In a cross-sectional design, we studied if smoking is associated with an increased fracture risk. A self-administered questionnaire was issued to 3,600 subjects (age 2-90 years) randomly selected from the general population. The questionnaire concerned prevalence of any fracture in the index subject and smoking habits along with gender, family fracture history, weight, height, age, and alcohol consumption. The adults completed the questionnaire themselves, while the parents completed the questionnaire on behalf of the children. 1637 (54.6%) adults, and 343 children (57.2%) responded. Current smokers had an increased prevalence of fractures compared to never smokers (OR=1.4, 95% CI: 1.1-1.8), while no

significant increase was present in previous smokers (OR=1.2, 95% CI: 0.9-1.6) after adjustment for potential confounders in a logistic regression model. Among potential confounder variables, both a maternal (OR=2.1, 95% CI: 1.6-2.6) and a paternal fracture (OR=1.4, 95% CI: 1.0-1.9) were associated with an increased fracture risk. Also increasing body mass index (OR=1.04, 95% CI: 1.01-1.06 per kg/m2) was associated with an increased fracture risk. Age, gender, and alcohol consumption were not associated with an increased fracture risk in this model. Thus, smoking is associated with an increased risk of any fracture even after adjustment for potential confounder variables. A family history of fracture is also a risk factor for sustaining a fracture.

SU289

Total Body Fat as a Predictor of Hip Fracture. G. El-Hajj Fuleihan[1], M. Badra*[2], A. Tayim*[2], M. Salamoun*[1], N. Afeiche*[2], O. Baddoura*[2], S. Boulos*[2], R. Haidar*[2], S. Lakkis*[2], R. Musharafieh*[2], A. Nsouli*[2], A. Taha*[2]. [1]Internal Medicine, American University of Beirut Medical Center, Beirut, Lebanon, [2]Orthopedics, American University of Beirut Medical Center, Beirut, Lebanon.

Osteoporosis is a major public health problem to-date, with hip fractures incurring a high human and economic toll. Several risk factors for hip fracture have been identified including BMD, age, BMI, height, hip axis length, direction and energy of fall. Hip protectors have been used as a mean to decrease energy of fall and therefore fractures. In this study we hypothesized that total body fat, an index of endogenous hip protection, is a risk factor for hip fractures. This project is part of an on-going institutional project evaluating the epidemiology of hip fractures in our tertiary referral center [JBMR 2001; 16(S1): M337]. As of the summer of 2000, all patients had total body fat measured. Total body BMC, total body fat, and BMD of the hip (contralateral side) were measured in 31 hip fracture patients (17 women,14 men) within one week of their fracture, and 19 controls (18 women,1man). A Lunar DPX-L densitometer was used for the first 8 subjects and a Hologic 4500 A for the last 24. A cross-calibration formula based on 72 subjects measured on both machines allowed calculation of mean total hip BMD and total hip T-scores using the manufacturer's database, expressed in terms of Hologic measurements. Osteoporosis was defined as a T-score<-2.5 using the NHANES database. Numbers expressed as mean (± SD).

Variable	Hip fxs,N=31	Controls,N=19
Age yrs	76(9)	70(6)*
BMI kg/m2	26(3)	31(4)*
Height cms	162(9)	153(8)*
BMD Total hip Hologic gm/cm2	0.65(0.14)	0.73(0.14)*
Total hip T-score NHANES	-2.6(1)	-1.8(1)*
Total body fat kgs	23.2(9.4)	31.1(6.5)*
Total body fat %	34(9)	42(4)*

* p<0.05 hip fractures vs control

BMD in hip fracture patients was significantly lower than controls, identical to Western standards (1-2), and identical in both genders. Significant correlates of hip fractures were age, BMI, height, BMD, total body fat, % body fat, hearing capability and mental status. In conclusion, in addition to confirming known predictors of hip fracture in our population, this is to our knowledge the first study demonstrating that body fat is a predictor of hip fractures. Body fat a known predictor of BMD, may also be a predictor of hip fractures due to mechanical (padding) factors, in addition to recognized hormonal reasons namely increasing circulating estrogen levels, and therefore BMD.

1.Greenspan et al. JAMA 1994; 271: 128-
2.Alonso et al. OI 2000; 11:714-

SU290

Strain Dependent Effects on Bone Fracture Healing in Mice. M. B. Manigrasso*, J. P. O'Connor. Orthopaedics, UMDNJ-New Jersey Medical School, Newark, NJ, USA.

Mice are an optimal mammalian model in which to study genetic and molecular processes that govern osteoporosis and the bone fractures that accompany osteoporosis. Variations in bone mineral density (BMD) have been defined for different inbred strains of mice indicating that genetic differences between inbred mouse strains controls BMD. The purpose of this study was to determine if BMD correlates with fracture healing capacity. To perform this study, a mouse femur fracture model was developed to measure the torsional mechanical properties of healing fractures. Initial experiments involved defining the normal radiographic, histological, and mechanical properties of the healing femur fractures in an outbred mouse strain (ICR). Based upon these initial experiments, three inbred mouse strains with defined BMDs were tested for their ability to heal femur fractures. The three inbred strains tested were C3H (high BMD), DBA/2 (moderate BMD), and C57BL/6 (low BMD). Fracture healing was followed in the inbred mouse strains by weekly radiography and torsional mechanical testing at 4 weeks post-fracture. Only 8-week old female mice were used. Radiography of the fracture calluses clearly indicated that C3H mice formed a larger and more X-ray dense callus than the C57BL/6 mice. The size and X-ray density of the fracture calluses formed by the DBA/2 mice were in between that of the C3H and C57BL/6 mice. These observations appeared to correlate increased fracture callus X-ray density and increased fracture callus size with increased BMD. Fractured femurs and the animals' contralateral unfractured femurs were mechanically tested at 4 weeks post-fracture (C3H: n = 12; DBA/2: n = 16; and C57BL/6: n = 7). Initial experiments with outbred ICR mice showed that fracture bridging occurs between 3 and 4 weeks after fracture. Therefore, fractured femurs from the inbred mouse strains were assayed at 4 weeks post-fracture to measure the initial mechanical properties of the healing callus. Bone and callus dimensions were measured prior to testing. Peak torque and angle at failure were obtained for each femur from its torque-angle deflection curve. From these values, torsional rigidity, shear stress, and shear modulus were calculated based upon a hollow-ellipse model of callus geometry. It was found that the absolute and relative mechanical properties of the DBA/2 fractured femurs were better than those obtained from the C3H and C57BL/6 mice. For instance, the fractured femur shear modulus for the DBA/2 mice (2.1 ± 1.3 GPa) was significantly different from that of the C3H (1.29 ± 0.58 GPa; p = 0.03) and C57BL/6 (0.78 ± 0.57 GPa; p = 0.003) mouse femurs. These results indicate that BMD is not a predictor of fracture healing capacity.

SU291

Morphometric X-ray Absorptiometry In Colles' Fracture Patients. L. del Rio[1], E. Kanterewicz*[2], A. Yáñez*[2], A. Diez[3]. [1]Densitometria Osea, CETIR Centre Medic, Barcelona, Spain, [2]Hospital de Vic, Vic, Spain, [3]Medicina Interna, Hospital del Mar, Barcelona, Spain.

Vertebral morphometry by DXA (MXA) is a research tool developed to evaluate the presence of vertebral deformities although its clinical utility is still limited. OBJECTIVE: The goals of this study were : 1) to know the prevalence of vertebral deformities by MXA in women with Colles' fracture; 2) to determine the correlations between MXA findings and BMD. METHODS: In an incident case-control study, 58 women (mean age 65.8 yrs) with a recent Colles' fracture and 83 population-based control women (mean age 58.7 yrs) were enrolled. Both BMD and MXA were performed by DXA (Lunar Expert). Anterior, middle and posterior heights were measured and wedge (Ha/Hp) and mid-wedge (Hm/Hp) ratios were calculated. A vertebral deformity was defined when at least one ratio fell 3 SD below the reference mean of that ratio at any vertebral level. RESULTS: Mean age of cases was 65,8 yrs and in controls 58,7 (p<0.05). Osteoporosis (T-score <-2.5 SD) was found at lumbar spine in 47% of cases vs 20% of controls (p<0.001) and at total hip in 19% vs 6% (p<0.005). Morphometric vertebral deformities were associated with older age (p<0.05) and were found in 19% of cases against 11% of controls (non-significant). Cases had a lower mid-wedge ratio than controls at each vertebral level (p<0.05) while wedge ratio results were more heterogeneous. When the sample was stratified by age, Colles' fracture show a trend to be associated with vertebral deformity only in the younger (<65 yrs) group. A low but significant coefficient of correlation was found between mid-wedge ratio and BMD mainly at hip level. CONCLUSIONS: A high prevalence of vertebral deformities is detected in Colles' fracture patients using MXA. There is a small positive correlations among MXA deformity ratios and BMD. Although older age is an important risk factor for the presence of vertebral deformities in the whole group, younger Colles' fracture patients showed more vertebral deformities than healthy controls of the same age range.

SU292

Relationship between Fractures of the Extremities and Bone Mineral Density: A 10-year Prospective Study. J. Finigan*[1], D. M. Greenfield*[2], N. F. A. Peel[1], A. Blumsohn[1], R. A. Hannon[1], R. Eastell[1]. [1]Bone Metabolism Group, University of Sheffield, Sheffield, United Kingdom, [2]University of Sheffield, Sheffield, United Kingdom.

Fractures of the feet, hands and skull have been considered to be unrelated to bone mineral density and so not characteristic of osteoporosis. We have carried out a 10-year prospective study of a group of 375 women who were ages 50 to 85 years at baseline. We measured bone mineral density at baseline by dual-energy x-ray absorptiometry (Lunar DPX), pyridinoline to creatinine ratio (PYD) by HPLC, tartrate-resistant acid phosphatase (TRACP) and bone alkaline phosphatase (bone ALP) by enzyme assay, and stiffness of the calcaneus at year 5 by quantitative ultrasound (Lunar Achilles). Details of incident non-vertebral fractures were ascertained from multiple sources including patient questionnaire and review of medical notes, and all were radiologically confirmed. The table shows the relative risk of fracture per standard deviation of bone measurement using a Cox Regression Model (with log transformation for bone markers). We divided the fractures into those of the extremities (hands, feet, skull) and the remaining non-extremity, non-vertebral fractures for comparison.

Measurement	Extremity (n=22)	Non-extremity (n=46)
Femoral neck BMD	2.01**	2.19***
Lumbar spine BMD	1.34	1.56**
Total body BMD	2.09***	1.87***
Achilles Stiffness	2.27**	1.56*
Urinary PYD	1.76**	1.32
Serum TRACP	1.84**	1.22
Serum bone ALP	1.58*	1.16

** p<0.01, *** p<0.001

The relative risks were significant for most measurements for extremity fracture and were of a similar magnitude to those for non-extremity fracture. Interestingly, the sites that best predicted extremity fractures were the total body (a site composed mainly of cortical bone, like the extremities) and the calcaneus (a site close to the foot fractures). The stronger prediction of bone markers for extremity fractures is unexplained. We conclude that fractures of the extremities should be considered to be related to low bone mineral density, and hence to osteoporosis.

SU293

The Radiographic Cleft in Dynamically Mobile Osteoporotic Vertebral Compression Fractures. F. E. McKiernan[1], T. Faciszewski*[2]. [1]Center for Bone Diseases, Marshfield Clinic, Marshfield, WI, USA, [2]Department of Orthopedic Spine Surgery, Marshfield Clinic, Marshfield, WI, USA.

Dynamic mobility refers to a change in configuration of a vertebral compression fracture (VCF) in different postures and implies the gross disruption of cortical and cancellous bone. The radiographic appearance of cortico-cancellous disruption is the intravertebral cleft. Considered a sign of vertebral osseous necrosis (Kummel's sign), clefts are not thought to occur in osteoporotic VCFs. Herein we describe the frequency, radiographic appearance and location of the intravertebral cleft in osteoporotic VCFs presenting for vertebroplasty (VP). Dynamic vertebral mobility was assessed by comparing preoperative standing lateral X-rays with preoperative supine, cross table-lateral X-rays of the index VCF. Dynamic vertebral mobility was defined as any change in fracture configuration apparent with unaided vision. Clefts appeared as intravertebral gas on plain X-ray or signal void on STIR sequence MR but were defined as low resistance, confluent reservoirs for polymethlymethacrylate (PMMA) at the time of VP. Fifty consecutive patients underwent 56 VP procedures to treat 82 VCFs. There were 33 (66%) women and 17 (34%) men. Twenty-four of 50 patients (48%) had intravertebral clefts. Thirty of their 82 VCFs (34%) had clefts. All 30 clefts occurred in mobile VCFs and no mobile VCF was without a cleft. No clefts were appreciated in fixed (non-mobile) VCFs ($p<0.001$). Twenty-two of 30 (73%) clefted fractures occurred at the thoraco-lumbar junction (T11-L1) but only 14 of 52 (27%) fixed fractures occurred at that site ($p< 0.001$). Clefts were appreciated in 4 of 29 (14%) of preoperative standing lateral X-rays, in 18 of 28 (64%) of supine cross-table X-rays and in 25 of 26 (96%) cases by MR. In one case the intravertebral cleft was only appreciated at the time of PMMA injection. Consistent with previous observations the content of the cleft (air or water) was variable and dependent upon time and position. PMMA fill patterns of clefted and non-clefted VCFs were distinct. This radiographic series documents that intravertebral clefts are frequent in osteoporotic VCFs presenting for VP. In many patients clefts can be appreciated on supine cross-table lateral X-rays but are almost always appreciated by MR. Clefts cluster at the thoracolumbar junction and appear to be necessary for dynamic mobility. The relationship between clefted, dynamically mobile VCFs and Kummel's disease needs reconsideration in light of these observations. Technical approaches to VP and clinical outcomes may differ between clefted and non-clefted VCFs.

SU294

The Management of Osteoporosis After Hip Fracture: Have We Improved Our Care? S. Bahl*, P. S. Coates, S. L. Greenspan. Endocrinology, University of Pittsburgh Medical Center, Pittsburgh, PA, USA.

Patients admitted for acute hip fracture are rarely recognized as having osteoporosis or managed appropriately despite the multiple available agents known to prevent fractures. To determine if physicians have improved the recognition and treatment of patients with acute hip fracture, we performed a retrospective analysis to identify the acute hip fractures admitted to the University of Pittsburgh Medical Center, a large tertiary care, academic institution, in the years 1995 and 2000. As a control group, age and sex matched patients with communnity acquired pneumonia were studied. We obtained the patients' demographic data, discharge medications and discharge diagnoses. There were 136 acute hip fractures in 1995 and 117 in the year 2000. Patients in 2000 were more likely to be diagnosed with osteoporosis (18% vs 4%, $p<0.02$), more likely to be discharged on calcium (17% vs 7%, $p<0.02$), and more likely to be discharged on antiresorptive therapy (15% vs 2%, $p<0.001$). Patients with a diagnosis in 2000 were older and more likely to receive antiresorptive agents than those without a diagnosis (29% vs 11%, $p<0.05$). None of the patients received a bone density scan while in the hospital. However in 2000, the patients admitted with pneumonia were just as likely to receive calcium, vitamin D, or antiresorptive agents at the time of discharge, as those with an acute hip fracture. In summary, although there was an improvement in the management of osteoporosis after acute hip fractures from 1995 to 2000, there was no difference in management of patients with hip fracture versus pneumonia in the year 2000. However patients with a "diagnosis" of osteoporosis were more likely to be discharged on appropriate therapeutic options. We conclude that patients identified with the diagnosis of osteoporosis after a fracture are more likely to receive effective management. Further studies are needed to determine the factors needed to target patients for appropriate diagnosis and therapy.

Patients with hip fracture and pneumonia

	Number	Calcium (%)	Vitamin D (%)	Antiresorptives (%)
All Hip Fracture (1995)	136	7	8	2
All Hip Fracture (2000)	117	17*	12	15**
Osteoporosis Diagnosed (2000)	21	24	19	29***
Osteoporosis Not Diagnosed (2000)	96	16	10	11
Pneumonia (2000)	120	20	18	10

*$p<0.02$ 1995 vs 2000 hip fracture patients
**$p<0.001$ 1995 vs 2000 hip fracture patients
***$p<0.05$ 2000 hip fracture patients: osteoporosis diagnosis vs no diagnosis

SU295

A 28 Month Audit of the Efficacy of the Fracture Liaison Service in Offering Secondary Prevention for Patients with Osteoporotic Fractures. A. R. McLellan, M. Fraser*. Medicine & Therapeutics, Western Infirmary, Glasgow, United Kingdom.

The Fracture Liaison Service(FLS), established in 1998, is the first service model of its kind in the world that delivers a comprehensive strategy of assessment (and treatment where appropriate) of osteoporosis for the secondary prevention of osteoporotic fractures to all women and men over 50years who present with 'low trauma' fractures. The FLS is effected by the Fracture Liaison Nurse (FLN), who liaises between secondary care bone metabolism services and the orthopaedic and accident & emergency units to deliver osteoporosis assessment and/or treatment for all appropriate outpatient and inpatient fracture cases. Initial contact with the FLN is designed to raise the patients' awareness of risk of osteoporosis and to apply protocols for the secondary prevention of fractures. For many that requires subsequent attendance at the FLN-DXA clinic, where the DXA result informs the selection of the most appropriate treatment. Other outcomes of the initial assessment by the FLN include a)starting 1000mg calcium carbonate+800I.U.vitaminD or b) review of compliance and use of existing antiresorptive treatments. In the first 28months, the FLS has assessed 3145 fracture cases (2538 women). Fracture sites by decreasing prevalence were wrist (n=992),hip (n=743),humerus (n=460), ankle (n=328), hand or foot (n=226), and at all other sites (n=396); women (age 73.4(SD11.8)yr accounted for between 73% (ankle) and 86% (wrist) of fractures. The table shows the prevalence of osteoporosis and osteopaenia (at lower of spine or total femur)(m/f) in 232m & 1151f who underwent DXA via the FLN-DXA clinic.

Prevalence of osteoporosis and osteopaenia (at spine or total femur)in 232m and 1151f.

Site	number m/f	% o'porosis	% o'paenia
Wrist	71 / 482	28% / 51%	42% / 33%
Hip	23 / 134	87% / 71%	13% / 28%
Humerus	47 / 156	43% / 49%	47% / 37%
Ankle	41 / 148	7%/ 30%	54% / 45%
Hand/foot	19 / 123	21% / 37%	42% / 40%
Other	31 / 108	29% / 52%	45% / 36%

At the 28 month audit of 3145 fracture cases who attended our hospital, overall 71% were assessed (by DXA) or were given treatment for secondary prevention; 10% were awaiting their assessment at the FLN-DXA clinic and 19% either refused assessment or did not attend. Corresponding data for wrist and hip fracture cases were: 67%, 11%, 22% and 84%, 6%, 10% respectively. The FLS is a highly effective model for delivering secondary prevention to inpatients and outpatients presenting to secondary care with incident osteoporotic fractures.

SU296

CANDOO: A Longitudinal Canadian Multi-Center Tertiary-Care Network for Observational Research in Osteoporosis and Osteopenia Using Standardized Clinical Practice Data: 11 Years Of Follow-Up. R. J. Sebaldt[1], J. D. Adachi[1], W. Olszynski[2], J. P. Brown[3], D. A. Hanley[4], R. G Josse[5], T. Murray[5], G. F. Stephenson[6], A. Petrie*[1], A. Mark*[1], C. H. Goldsmith*[7]. [1]Medicine, McMaster University, Hamilton, ON, Canada, [2]University of Saskatchewan, Saskatoon, SK, Canada, [3]Laval University, Ste-Foy, PQ, Canada, [4]University of Calgary, Calgary, AB, Canada, [5]University of Toronto, Toronto, ON, Canada, [6]Procter & Gamble Pharmaceuticals Canada, Inc., Toronto, ON, Canada, [7]McMaster University, Hamilton, ON, Canada.

The CANDOO Project (Canadian Database of Osteoporosis (OP) and Osteopenia) is a collaboration of OP specialists from across Canada for generating new knowledge about long-term outcomes of OP and its treatments and for validating clinical trial results in clinical practice. A comprehensive standardized clinical dataset appropriate to OP subspecialty practice was iteratively evolved by consensus. It has been collected by the CANDOO collaborators as integral part of the clinical care of new and follow-up patients since as early as March, 1990. Dataset updates accommodate new diagnostic and therapeutic options, and a self-administered OP-related quality of life questionnaire (mini-OQLQ) was added in 1995. Data are aggregated anonymously into a central database using standard operating procedures. The 7 collaborators, a biostatistician and a sponsor representative form the steering committee to monitor progress and plan data analyses and publications. By June 1, 2001, 9,855 patients were recorded (86% women (86% postmenopausal)), having at baseline: mean age 59 years, mean t-score at lumbar spine = -2.0, mean number of fractures = 1.3. 38,826 visits (assessments) were recorded, 74% of which were follow-up visits, with a median total patient follow-up of 3.0 years. 80% of patients were last seen within the past 2 years. Over the past 7 years, CANDOO data analyses and publications have confirmed the effectiveness of: (i) etidronate for treatment of corticosteroid-induced OP, (ii) etidronate and alendronate for treatment of male OP, (iii) addition of etidronate or alendronate to stable hormone replacement therapy for treatment of postmenopausal OP, (iv) mini-OQLQ for the demonstration of effect of vertebral and non-vertebral fractures on quality of life. We conclude that aggregate standardized longitudinal clinical practice data can provide valuable information about OP and treatment outcomes under clinical practice conditions.

Disclosures: ***R.J. Sebaldt****, Procter & Gamble Pharmaceuticals Canada Inc. 2; Merck Frosst Canada Ltd. 2; CORRONA Inc. 6.*

SU297

Osteoporotic Fracture: Missed Opportunity for Intervention. L. Port*[1], J. R. Center[2], K. Henderson*[3], R. Cumming*[4], J. A. Eisman[2]. [1]Bone and Mineral Research Program, Garvan Institute of Medical Research, Sydney, NSW 2010, Australia, [2]Bone and Mineral Research Program, Garvan Institute of Medical Research, Sydney, Australia, [3]Curtin University of Technology, Perth, Australia, [4]University of Sydney, Sydney, Australia.

As prior fracture is consistently associated with increased risk of subsequent fracture, subjects with a history of prior fracture represent a high risk group which could be targeted for intervention to reduce future fracture rates. This study aimed to investigate the relationship between hip fractures and treatment patterns following prior osteoporotic fracture. All patients admitted with hip fracture over a twelve month period to two teaching hospitals of the University of NSW, Sydney, Australia, were identified retrospectively from medical records. 380 hip fracture admissions were identified, with 35 exclusions not considered to be osteoporotic fractures or visiting from overseas at the time of fracture. Frequency of prior fractures and treatment status were recorded. Forty four per cent of the 249 women and 31% of the 96 men reported a prior fracture. These were prior hip fractures in 17% of the women and in 7% of the men. Among subjects with prior fractures, 18% of women and 7% of men were on any antiresorptive therapy (HRT, calcitriol or bisphosphonates). Even among those with a prior hip fracture, only 23% of women and none of the men were taking antiresorptive therapy. Calcium supplements were used in 12% of women and none of the men. In this study a high proportion of individuals suffering hip fractures had had prior "signal" fractures yet the majority of these were not receiving any therapy known to reduce the risk of further fractures. Even allowing for the approximate halving of fracture risk with potent antiresorptive therapy, these data indicate that the majority of high risk subjects with fractures do not receive therapy shown to reduce the risk of further fractures, including hip fractures.

SU298

Investigation of Prognostic Factors Relating 1-year Death and Lower Functional Status after Hip Fracture in Japanese Elderly Patients. H. Ishibashi*[1], S. Yamamoto*[1], H. Kawaguchi*[2], H. Fujita*[1], T. Suzuki*[3]. [1]Orthopedic Surgery, Tokyo Metropolitan Geriatric Medical Center, Tokyo, Japan, [2]University of Tokyo School of Medicine, Tokyo, Japan, [3]Tokyo Metropolitan Institute of Gerontology, Tokyo, Japan.

[OBJECTIVE] Hip fracture has been reported to affect both a survival rate and functional status of the elderly patients. Although the treatment method of hip fracture is clinically established, the vital and functional prognosis of the fracture seems to remain unsatisfactory. To improve the prognosis, it is necessary to know what factors would influence it. The objective of this study is to investigate factors relating a 1-year death and lower functional status of elderly patients after hip fracture. [METHODS] The cases for this study were 370 patients (85.3 years old in average) who suffered hip fractures between January 1, 1999 and May 31, 2001. After investigating their vital status, we sent questionnaires in October 2001 to the survivors asking his/her functional status like BADL, IADL and mobility. Also, we gathered the perioperative information like age, gender, type of fracture, mental state, mobility before fracture, comorbidity, waiting period, operation time, volume of hemorrhage. We examined the statistical relationships of the results of the questionnaire and the patientsÅf background. [RESULTS] The ascertained numbers of survivors and deaths were 186 and 64, respectively. To calculate and analyze 1-year death, we extracted patients treated before October 31, 2000. Among them, 166 survivors and 33 deaths within 1 year after treatment were identified. Factors statistically relating 1-year death were male patients, higher age, trochanteric fracture, dementia, lower mobility before fracture, more comorbidity, heart disease and chronic lung disease. The lower functional status of the survivors was statistically correlated by such factors as higher age, dementia and lower mobility before fracture. [DISCUSSION] We should consider how to change the prognosis of this fracture for the better, as well as how to prevent and treat it. In this point, mobility is a good target, because it is one of the factors affecting both 1-year death and functional status and because it could be improved, for example, by the adequate acute-phase and long-term rehabilitation. [CONCLUSION] Investigation of patients after hip fracture revealed the factors relating to 1-year death after fracture and those relating to the lower functional status of the survivors.

SU299

Quality of Life in Postmenopausal Women with a History of Fracture of the Rib, Spine, Wrist, or Hip: Evidence from NORA. L. E. Wehren[1], E. Barrett-Connor[2], E. Barrett-Connor[3]. [1]University of Maryland, Baltimore, MD, USA, [2]University of California, San Diego, La Jolla, CA, USA, [3]University of California San Diego, La Jolla, CA, USA.

The disease burden of osteoporosis includes cost, mortality, and morbidity (functional limitation, loss of independence, pain, and impaired quality of life). Study of health-related quality of life (HRQoL) after fracture has focused on acute after-effects, or on the chronic effect of multiple vertebral fractures. Using data from the National Osteoporosis Risk Assessment (NORA), we examine whether women who report a history of fracture after age 45 of the rib, spine, wrist, or hip have impaired HRQoL as compared to women without this history, and whether deficits are fracture site-specific. HRQoL was measured at baseline using the Short Form-12 (SF-12) Health Survey in a randomly chosen subset of the NORA cohort. Using standard, validated scoring algorithms mean scores for physical (PCS) and mental (MCS) domains were calculated and compared between fractured and non-fractured groups. Linear regression was used to adjust for confounding effects of age. Of 87,060 participants with complete information, 9354 reported a history of fracture. Regardless of the site of the prior fracture, physical HRQoL was negatively affected in women with fracture history, and mental HRQoL was affected in women with a history of fracture of the spine or rib. After adjustment for age, fracture history is associated with lower mean scores in both domains. Prior fracture is associated with lower scores in both physical and mental domains of HRQoL, with greater effects seen in physical functioning. Spine and hip fracture produce the largest decrements. Estimates of the disease burden of osteoporosis may need to account for long-term effects of fracture. In addition, negative effects on HRQoL may directly or indirectly influence risk of future fracture.

Site of Prior Fracture	Physical Composite Score	Mental Composite Score
Spine (n = 970)	-6.85 (0.37)	-1.72 (0.31)
Wrist (n = 5229)	-0.66 (0.16)	-0.52 (0.14)
Rib (n = 3217)	-3.60 (0.20)	-1.68 (0.17)
Hip (n = 1135)	-5.34 (0.34)	-1.29 (0.28)
Any (n = 9354)	-2.43 (0.13)	-1.01 (0.10)

*Disclosures: **L.E. Wehren**, Merck 5, 8; Wyeth 8.*

SU300

Older Men and Women with Kyphotic Posture are at Increased Risk for Mortality: The Rancho Bernardo Study. D. M. Kado[1], M. Huang*[1], E. Barrett-Connor*[2], G. A. Greendale*[1]. [1]Medicine, University of California, Los Angeles, CA, USA, [2]Medicine, University of California, San Diego, CA, USA.

Kyphotic posture is often assumed to be a consequence of vertebral fractures, although several studies report that only about ½ of those with the most severe kyphosis have evidence of spinal osteoporosis. Although vertebral fractures are associated with mortality, the association between kyphotic posture and all-cause mortality is unknown. To test whether older persons with kyphotic posture are at increased risk of subsequent death, we prospectively followed 1173 men and women, aged 50-98 (mean age 73.1 years) enrolled in the Rancho Bernardo Study. At the 1988-1992 clinic visit, kyphotic posture was measured with participants lying recumbent, as the distance from the occiput-to-table (units = 1.7 cm blocks, placed under participant's heads). Mortality was confirmed by review of death certificates after an average follow-up 4.2 years. Kyphotic posture, defined as ≥2 blocks, was present in 21.5% of the population. Cox proportional hazards models were used to assess the association between kyphotic posture and all-cause mortality. In age-adjusted models, persons requiring ≥2 blocks had a 1.75-fold increased risk of mortality compared with those requiring 1 or no blocks (95% C.I. = 1.32 - 2.31, $p < .0001$). After adjusting for potential confounders including age, sex, education, body mass index, spine bone density, clinical vertebral fracture, exercise, smoking, and alcohol use, persons with ≥2 blocks had a 1.49-fold increased risk of mortality (95% C.I. = 1.12 - 2.00, $p = .007$). We conclude that older persons with kyphotic posture have an increased risk of mortality that is independent of age, spine bone density, lifestyle factors, and clinical vertebral fracture. Our data suggest that kyphotic posture may be a clinical indicator of poor health outcomes.

SU301

Osteoporosis Coverage in Selected Women's Magazines and Newspapers, 1998-2001. L. S. Wallace[1], J. E. Ballard[2]. [1]Family Medicine, University of Tennessee Graduate School of Medicine, Knoxville, TN, USA, [2]Health and Kinesiology, University of Texas at Tyler, Tyler, TX, USA.

Mass media is an influential source of medical information and can shape health beliefs and prompt individual decision-making. The purpose of this review was to evaluate the accountability of osteoporosis information available in selected mass-circulating women's magazines (n=8) and a sample of newspapers (n=2) from 1998 through 2001. Osteoporosis articles (n=132) were assessed for sources of information used, incidence/prevalence statistics, risk factors and prevention measures. Expert sources were highlighted in the majority of articles (magazines: n=49, 84.5%; newspapers: n=59, 79.9%), while incidence/prevalence statistics were described in less than half of the articles (magazines: n=16, 27.6%; newspapers: n=32, 43.2%). Risk factors were discussed in 21 (36.2%) magazine and 33 (44.6%) newspaper articles, however much of the information presented was ambiguous and incomplete. Family history of osteoporosis, thin and/or small body frame, use of certain medications (e.g., corticosteroids, anti-convulsants), and Caucasian/Asian race were the most frequently cited non-modifiable risk factors. The most commonly discussed modifiable risk factors included: low dietary calcium consumption, sedentary lifestyle, cigarette smoking, and excessive alcohol consumption. Prevention measures were discussed in 54 (93.1%) magazine and 51 (68.9%) newspaper articles. Regular physical activity and adequate calcium intake were the most commonly discussed primary prevention measures. Of the secondary prevention measures cited, hormone replacement therapy and DEXA screening were the most common. Alendronate (Fosamax) and Raloxifene (Evista) were the most frequently mentioned tertiary measures. It appears that the reporting of osteoporosis in women's magazines and newspapers is not entirely balanced; thus, future coverage should provide greater detail when reporting risks and preventive measures.

SU302

Osteoporosis in Women with Anorexia Nervosa: Is there any Difference in Chinese Patients? S. Y. S. Wong*[1], S. Au*[1], L. Lee*[1], S. Lee*[2], E. M. C. Lau*[1]. [1]Jockey Club Centre for Osteoporosis Care and Control, Chinese University of Hong Kong, Shatin, Hong Kong Special Administrative Region of China, [2]Department of Psychiatry, Chinese University of Hong Kong, Shatin, Hong Kong Special Administrative Region of China.

Previous studies in Caucasians suggested that osteoporosis were frequent in women with anorexia nervosa (AN). To determine whether bone mass is reduced in Chinese patients with AN and to study the risk factors for low bone mass in AN patients, a case-control study was conducted. Bone mineral density (BMD) of the lumbar spine and the hip were measured by dual energy x-ray absorptiometry in 48 patients with AN. Z-scores were calculated by comparison with normative data obtained in the same population. For BMD of the spine, 55.1% had z-score higher than -1, thirty percent of patients had z-score between -1 and -2.49, and 14.3% of patients had z-score less than -2.5. For BMD at total hip, 53.1% of patients had z-score higher than -1, forty percent had z-score between -1 and -2.49 and 6.1% had z-score less than -2.5. In addition, 40.8% of patients had z-score between -1 and -2.49 and 14.3% had BMD z-score lower than -2.5 at either the spine or hip. Current body mass index (BMI) was the only factor found to be significantly associated with BMD at the hip and spine (<0.05) in AN patients. The following risk factors were not found to be significantly associated: duration of AN, lowest BMI, average calcium intake per day and average physical activity per week (p>0.05). It is concluded that Chinese patients with AN are at risk of low BMD. Body mass index was a significant predictor of reduced BMD in Chinese patients with AN.

SU303

Seasonal Variation in Bone Mass in Postmenopausal Women. K. Åkesson[1], P. Gerdhem*[1], H. Mallmin*[2], K. J. Obrant[1]. [1]Malmö University Hospital, Orthopedics, Malmö, Sweden, [2]Uppsala University Hospital, Orthopedics, Uppsala, Sweden.

There may be a seasonal variation in bone metabolism as judged from biochemical markers. Whether such a variation also has an impact on bone mass in postmenopausal and elderly women has yet to be resolved. We investigated seasonal variation in bone mass by cross-sectional designs in three large cohorts of women (n=3742) from two geographical regions in Sweden. One cohort was strictly population based (all 75 years old, n=1044) and two cohorts were patient based (age >54, mean age 67, n=1293 and mean age 69, n=1405). Each woman was assessed once and inclusion for the population-based sample was continuous throughout almost all days of the year, during three consecutive years. Bone mineral density (BMD) of the total body, hip (neck, ward, trochanter) and lumbar spine was determined by means of DEXA. For all three cohorts the BMD was similar in those assessed throughout the summer half year (April-September) compared to those assessed thoughout the winter half year (October-March). This absence of summer/winter difference was evident for all skeletal regions and remained after controlling for small differences in age and weight. On the other hand, when women who had been assessed during spring (January-June) were compared with women assessed during autumn (July-December) we found the BMD to be up to 5% higher during the spring in all skeletal regions in the population-based sample and 4% higher at the wards triangle and the trochanter in one of the patient-based samples but not in the other. After correcting for small differences in age and weight, women who had been assessed throughout the spring still had higher BMD compared with women assessed during autumn at the hip (neck, ward and trochanter) in the population-based sample and at the trochanter in one of the two patient-based samples. If the finding of a spring/autumn difference is true, a hypothetical explanation could be that an increased bone turnover including an initial high osteoclastic activity throughout autumn was triggered off by high vitamin-D levels in summer. In conclusion we firmly believe that we can state that there is no summer/winter variation in bone mass in postmenopausal women. On the other hand, and although our data are not conclusive, we found indications that BMD may be a few percent higher during the spring half year compared to the autumn half.

SU304

Can the SCORE^{tm} Algorithm Reduce the Need for Bone Densitometry? Results from the Danish Osteoporosis Prevention Study. N. Nissen*[1], P. Vestergaard[2], C. L. Tofteng*[3], O. Bärenholdt*[4], O. H. Sørensen[3], S. P. Nielsen[4], L. Mosekilde[2], B. Abrahamsen[1]. [1]Dept of Endocrinology M, Odense University Hospital, Odense, Denmark, [2]Dept of Endocrinology C, Aarhus University Hospital, Aarhus, Denmark, [3]Osteoporosis Research Clinic, Hvidovre, Denmark, [4]Dept of Clinical Physiology, Hilleroed, Denmark.

BMD can be measured quickly and safely, but identifying the appropriate subset of postmenopausal women for densitometry is notoriously difficult as most algorithms predict less than 20% of BMD. Recently, Lydick (Am J Man Care 1998; 4:37) proposed an algorithm (SCORE^{tm}) with high sensitivity and specificity for identifying women with low BMD. The purpose of the present study was to evaluate the performance of this algorithm as a prescreening tool in healthy Danish women with recent menopause. The study population consisted of 2016 healthy women, mean age 50.6 y (SD 2.8), recruited between 3 months and 2y after their last menstrual period. BMD at the spine, hip, forearm and whole body was measured using cross-calibrated Hologic QDR-1000 and -2000 densitometers. BMD was followed longitudinally for 5y. The population had a prevalence of osteopenia/osteoporosis of 34%/4.2% at the spine and 31%/1.3% at the total hip site. The data for SCORE calculation (*race, age, weight, estrogen use, fracture- and rheumatoid arthritis history*) was systematically recorded at the inclusion interview and subsequently retrieved from the study database. The cut-off for the algorithm was set at 6+ pts in accordance with the findings by Lydick et al. Diagnostic performance was as follows:

	Osteopenia(spine)	Osteopenia(hip)	Osteoporosis(spine)	Osteoporosis(hip)
Sens/Spec	66% / 57%	69% / 57%	80% / 50%	80% / 49%
PPV/NPV	44% / 76%	42% / 81%	7% / 98%	2% / 99%

Identifying participants with low BMD (T<-1) or osteoporosis (T<-2½). PPV positive predictive value, NPV negative predictive value).

The algorithm predicted 10% of the variation in BMD by linear regression analysis (p<0.001). 49% of the study population would not be referred to bone densitometry based on the SCORE result. Of these, 24% had spinal osteopenia. In a longitudinal assessment, 5.5% of those with SCORE <6 developed osteoporosis at the spine after 5y compared with 18.6% of those with SCORE 6+ (χ^2 p<0.001). In conclusion, the SCORE algorithm can predict part of the variation in BMD and development of osteoporosis. The algorithm might be useful for selecting patients for clinical trials but the discriminatory performance is too low to rule out osteopenia with confidence in clinical practice.

SU305

The Quality of the Most Recently Formed Osteoid is Altered in both High and Low Turnover Osteoporosis: Implications for Fracture Risk. A. L. Boskey[1], S. B. Doty*[1], E. DiCarlo[2], J. M. Lane[3], J. M. Lane[3], E. P. Paschalis[1]. [1]Research Division, Hospital for Special Surgery, New York, NY, USA, [2]Pathology, Hospital for Special Surgery, New York, NY, USA, [3]Orthopaedics, Hospital for Special Surgery, New York, NY, USA.

In the clinical setting bone mineral density (BMD), has been used as a predictor of fracture risk. But BMD is now recognized as not being the sole predictor of risk. Other factors including the structure and composition of the underlying matrix (mainly collagen) and mineral also contribute. To assess the distribution of collagen cross-links in trabecular bone at ~7um spatial resolution, Fourier transform infrared imaging was used, and the ratio of non-reducible (pyridinoline, (pyr)) and reducible (dehydro-dihydroxy-lysinonorleucine (deH-DHLNL)) cross-links in the collagen of not-previously demineralized stained thin sections of bone from human iliac crest biopsies that showed histomorphometric features of normal bone, low-turnover osteoporosis, and high-turnover osteoporosis (N = 9 per group; age range = 50-75 years old). Measurements were taken at various depths in the bone relative to formative or resorptive surfaces. Distinctive, but complex differences were found in the collagen cross-link ratios at the different depths in the different conditions with osteoporotic bone invariably exhibiting a statistically significant (p<0.01) higher pyr / deH-DHLNL ratio when compared to normals at anatomically equivalent microscopic loci. For example, the ratio 14um from the forming surface was 5.0+/- 0.5 in low turnover osteoporosis, 2.9+/- 0.6 in high turnover osteoporosis, and 0.89+/- 0.34 in controls. Thus even the most recently formed osteoporotic matrix is of different "quality" than normal. At 14um from the resorptive surface the high and low turnover values were similar to each other, but significantly different from controls. The ratio was 10+/- 0.5 in low turnover osteoporosis, 10.1+/- 0.6 in high turnover, and 4.2+/- 0.3 in controls. Because bone mechanical properties are determined in part by the collagen cross-link distribution, this study suggests the importance of such properties towards fracture risk.

SU306

The Role of Standardized Medical History Forms and Set Laboratory Panels in the Routine Diagnosis of Osteoporosis. A. Knauerhase*[1], D. Eska*[2], C. Zingler*[2], G. Tolkemitt*[3], R. Hampel*[2]. [1]Department of Internal Medicine, University of Rostock, Rostock, Germany, [2]University of Rostock, Rostock, Germany, [3]Radiological outpatient´s department, Rostock, Germany.

Is it possible to accurately predict osteoporosis by making use of a correlation between the results of bone density tests and the data collected on standardized medical history forms and/or the values measured in a set laboratory panel? The osteoporosis out-patient clinic at the University of Rostock analyzed the following parameters from 81 women and 59 men (avg. age 58.8, avg. BMI 25.1): height and height loss, weight, degree of pain and localization, previous or existing medical conditions, history of fractures in patient or patient´s mother, gynecological history, dietary factors, physical activity, intoxicants and medications. The laboratory values included serum and urine calcium, bone-specific alkaline phosphatase or osteocalcin, 25-OH Vitamin D, parathyroid hormone, creatinine, phosphate as well as AST and ALT. The bone density of each patient (lumbar spine) was measured with DXA (Hologic QDR 1000) or QCT. The statistical analysis was carried out using SPSS for Windows. For the group as a whole, the average T-score was -3,04 SD and the average bone density was 71,2 mg/cm3. Body weight showed a weak positive correlation with the T-score (r=0,2, p<0,05), whereas age correlated strongly negative to the QCT-value (r=-0,55, p<0,01). Patients without height loss had significantly higher T-scores than those with height loss (T-score -2,8 SD versus -3,2 SD, p=0,017). Patients with pain localized "everywhere" tended to have the lowest T-scores (-3,6 SD). Patients who had "no pain" had average T-scores of -3,1 SD, whereas Patients with "severe pain" had the lowest average T-scores (-4,4 SD). When considering fracture location, patients with either humerus or femur fractures showed the lowest bone densities (T-score -3,3 SD or 52,7 mg/cm3). Moderate alcohol consumption (up to 2 alcoholic drinks per day) tended to correlate to higher bone density when compared to absolute alcohol abstinence or alcohol abuse. Nonsmokers tended to have higher bone densities than smokers. Patients with higher milk consumption (>1l per day) tended to have higher bone densities (T-score -2,6 SD) than drinking no milk (T-score -3,1 SD). The rest of the parameters showed no correlation to bone density. Likewise, it was not possible to drawn a correlation between laboratory values and the results of the bone density test. Certain information concerning anthropometrical features or medical history can be of limited use in diagnosing osteoporosis, but laboratory panels contribute little.

SU307

Risk Stratification Among Caucasian Women with T-score Between -2.5 and -1.0: Results from the National Osteoporosis Risk Assessment. P. D. Miller[1], S. Barlas*[2], S. K. Brenneman*[2], T. A. Abbott[2], Y. Chen*[2], E. Barrett-Connor[3], E. S. Siris[4]. [1]Colorado Center for Bone Research, Lakewood, CO, USA, [2]Merck & Co., Inc., West Point, PA, USA, [3]University of California, San Diego, CA, USA, [4]Columbia University, New York, NY, USA.

Treatment intervention to reduce fractures has largely focused on women whose BMD T-score fall below -2.5. As a consequence, little management guidance is available to the clinician for women with BMD scores in the range -2.5 to -1.0, who are still at increased risk for fracture. Among Caucasian women in the NORA population (n=149,524), 38% (57,421) had baseline T-scores in the range -2.5 to -1.0 and accounted for 50% of the osteoporotic fractures reported during the first year of follow-up. The purpose of this study was to develop a classification algorithm that can be easily used to identify women with T-scores higher than -2.5 who are at the highest risk of fracture within 12 months of BMD testing. We used CART 4.0 (Breiman et al.) to build the optimum tree, taking into account the low incidence of fracture and unequal cost of misclassification (i.e. the cost of misclassification as low risk was set at greater than that for misclassification as high risk). Thirty-two risk factors identified in the literature and available in the NORA database were used to build the tree. The cross-validated optimum tree identified four risk factors including (in order of strength of association with fracture) prior fracture, T-score ≤ -1.8, self-rated health status (one question), and mobility. The algorithm is shown below after accounting for prior fracture, which demonstrated the highest risk for fracture.

High Risk definition for women with T-score -2.5 to -1.0 without prior fracture

If T-score £ -1.8; OR

If T-score > -1.8 AND health status is fair/poor; OR

If T-score > -1.8 AND health status is good/excellent AND mobility is poor.

The algorithm correctly identified most of the women with fractures in the "validation" sample at 82% sensitivity. 55% of the women with T-score > -2.5 were identified as high risk with an overall one-year risk for fracture of 2.4% (range 1.9 - 4.1). Women with prior fracture (first level of the algorithm) had a similar risk of fracture as those with T-score below -2.5 (4.1% and 4.3%, respectively). Women identified at higher risk were over 2 times more likely to have a fracture within one year than women not identified as high risk by the algorithm. A simple easy-to-use algorithm can improve identification of women with T-scores between -2.5 and -1.0 who are at least 2 times greater risk for fracture, and who may also have a risk similar to that of women with T-scores <-2.5.

Disclosures: ***P.D. Miller****, Merck & Co., Inc. 2, 5, 8; Proctor & Gamble 2, 5, 8; Aventis 2, 5, 8; Lilly 2, 5, 8.*

SU308

The National Osteoporosis Foundation (NOF) Guidelines with Peripheral BMD Predict Fractures in Postmenopausal Women Across Ethnic Groups. E. Barrett-Connor[1], S. K. Brenneman[2], Y. Chen*[2], P. D. Miller[3], E. S. Siris[4]. [1]University of California, San Diego, CA, USA, [2]Merck & Co., Inc., West Point, PA, USA, [3]Colorado Center for Bone Research, Lakewood, CO, USA, [4]Columbia University, New York, NY, USA.

National Osteoporosis Foundation (NOF) recommends osteoporosis treatment in women who have T-score < -2.0 or < -1.5 with ≥ 1 risk factor for osteoporotic fracture. We examined the ability of peripheral BMD and four key NOF risk factors (prior fracture, weight < 127 pounds, family history of fracture, and smoking) to predict fracture risk in 5 ethnic groups, African-American, Caucasian, Hispanics, Asian, and Native American, using data from the National Osteoporosis Risk Assessment (NORA). Each participant had BMD measured at baseline at one peripheral site: heel (SXA or US), forearm (pDEXA), and finger (AccuDEXA). Fractures occurring in the subsequent year were identified by self-report. 163,979 women who had baseline BMD data and responded to the follow-up survey reported 2440 osteoporosis-related fractures (hip, rib, wrist/forearm and spine). Fracture rate per 1000 person years and relative risk for fracture by ethnic groups are shown below.

	African American	Caucasian	Hispanic	Asian	Native American
Total N	5841	146486	4411	1256	1281
Mean age (S.D.)	63.5 (8.9)	64.1 (9.0)	64.2 (9.1)	62.6 (8.7)	67.8 (9.5)
% Meeting NOF guidelines	11.7 %	22.6 %	26.8 %	32.8 %	31.1 %
Fx Rate: NOF (95% CI)	12.5 (5.2,19.9)	24.7 (23.2,26.2)	24.8 (17.0,32.5)	8.7 (1.1,16.2)	23.5 (10.4,36.6)
Fx Rate: Non-NOF (95% CI)	5.6 (3.8, 7.5)	8.8 (8.4, 9.3)	9.1 (6.3, 11.9)	3.5 (.07, 6.9)	9.7 (4.0, 15.5)
Relative Risk * (95% CI)	2.22 (1.1, 4.4)	2.79 (2.6, 3.0)	2.69 (1.7, 4.2)	2.33 (0.6, 8.7)	2.39 (1.1, 5.4)

* Based on Cox proportional hazards model adjusted for age

We conclude that low peripheral BMD and one or more of these NOF risk factors are effective in identifying women at increased risk for fracture in all ethnic groups.

Disclosures: ***E. Barrett-Connor****, Merck & Co., Inc. 2, 5.*

SU309

The Influence of Vitamin D Status on Bone and Muscle: The Inchianti Study. D. Maggio*[1], A. Cherubini*[1], R. Giorgino[2], F. Lauretani*[3], C. R. Russo*[3], U. Senin*[1], L. Ferrucci*[3]. [1]Geriatrics, University of Perugia, Perugia, Italy, [2]Procter&Gamble Health care, Rome, Italy, [3]Clinical Epidemiology, INRCA, Firenze, Italy.

The InCHIANTI study is a large population-based study performed in two Italian towns, located in the Chianti area near the city of Florence (Greve in Chianti and Bagno a Ripoli). The study population consisted of a random sample of the population aged of 65+ and a smaller sample of subjects who were randomly selected in each decade between 24 and 64 years. Aim of the study is to evaluate the relationship of vitamin D status with both bone density and muscle area at lower leg level. Peripheral Quantitative Computed Tomography at the right lower leg level was performed in each subject by a Stratec XCT 2000 device. The method allows the measurement of whole, trabecular, and cortical volumetric bone density (mg/cm^3) as well as muscle area (mm^2). 25 (OH)D was measured by RIA method with double antibody and serum intact 1-84 PTH was measured by IRMA method. Subjects aged 50+ were selected for this analysis. Data are available in 488 men and 627 women. The natural logarithm of vitamin D was used because the raw data were not normally distributed. 25 (OH)D levels were significantly associated with cortical bone volumetric density in females independent of age and body mass index (BMI) (β=14.1, SE 5.12; p<0.01) but not in men. 25 (OH)D levels were not associated either with cortical bone area or with trabecular bone volumetric density in either sex. Muscle area was associated with 25 (OH)D levels independent of age and BMI in both sexes (β=181.6, SE=82.2; p<0.05 in men; β=149.3, SE=61.4; p<0.02 in women). This study shows a positive association of vitamin D status with cortical bone density in women and with muscle area in both sexes.

SU310

Vitamin D Status in Old and Very Old Subjects: The Results of the Large Population-Based Italian Inchianti Study. A. Cherubini*[1], D. Maggio*[1], R. Giorgino[2], S. Bandinelli*[3], B. Bartali*[3], U. Senin*[1], L. Ferrucci*[3]. [1]Geriatrics, University of Perugia, Perugia, Italy, [2]Procter & Gamble Health care, Rome, Italy, [3]Clinical Epidemiology, INRCA, Firenze, Italy.

InCHIANTI is a study of the factors contributing to the decline of mobility in late life, which is performed in two Italian towns, located in the Chianti area near the city of Florence (Greve in Chianti and Bagno a Ripoli). The study population consisted of a random sample of the population aged of 65+ and a smaller sample of subjects who were randomly selected in each decade between 24 and 64 years. Each subject underwent a thorough clinical evaluation, a detailed interview (including a validated food frequency questionnaire), and a fasting blood drawing. This research is aimed at evaluating 25(OH)D and PTH levels in the InCHIANTI population. Serum 25 (OH)D was measured by RIA method with double antibody and serum intact 1-84 PTH was measured by IRMA method. Data are available in 564 men and 687 women. The following table shows mean ±SD levels of 25(OH)D and PTH by gender and age group.

	Males (n=564)			Females (n=687)		
Age (years)	N	25(OH)D [nmol/l]	PTH [pg/ml]	N	25(OH)D [nmol/l]	PTH [pg/ml]
<65	128	64.6±35.0	19.9±8.1	141	63.3±34.3	18.5±7.9
65-74	259	64.1±34.9	23.5±25.8	284	49.9±34.6	24.6±12.3
75-84	131	52.3±35.0	27.1±20.4	176	37.5±34.3	27.4±12.7
85+	46	35.7±22.6	35.6±28.3	86	31.8±31.8	38.1±30.3

In subjects aged 65+ years, 25(OH)D levels were negatively associated with age in both sexes (r=-0.32, p<0.0001 in males and r=-0.33, p<0.001 in females), while PTH levels were positively associated with age in both sexes (r=0.23, p<0.0001 in males and r=0.25, p<0.001 in females). The pattern of age related 25(OH)D decline was different between the 2 sex groups. 25(OH)D levels decrease was earlier in women, while the age-related decline of 25(OH) was more evident in the oldest age group in men. Moreover, 25(OH)D levels were significantly associated with Vitamin D dietary intake in women (r=0.09, p<0.05) but not in men (r=0.06, p=NS). In this population-based prospective study including a large sample of old and very old males and females, the analysis of baseline data reveals a sex-dependent pattern of age-related 25(OH)D decline. This suggests that different factors might influence vitamin D status in the two sexes.

SU311

A Longitudinal Study of Low Back Pain and Changes of Spinal Bone Mineral Density in Chinese Perimenopausal Women. S. C. Ho[1], S. Chan*[2], V. Yip*[3], A. Sham*[4], J. Woo*[5]. [1]Department of Community & Family Medicine, The Chinese University of Hong Kong, New Territories, Hong Kong Special Administrative Region of China, [2]CUHK, HK, Hong Kong Special Administrative Region of China, [3]The Polytechnic University, HK, Hong Kong Special Administrative Region of China, [4]Community & Family Medicine, CUHK, HK, Hong Kong Special Administrative Region of China, [5]Medicine & Therapeutics, CUHK, HK, Hong Kong Special Administrative Region of China.

We aim to present data on the association between the report of low back pain and changes of spinal bone mineral density (SBMD) in women undergoing menopausal transition. 438 Chinese women aged between 44 and 55y were recruited through random telephone digit dialing and from the University Family Medicne Clinic. Women on hormone replacement therapy or oophorectomy /hysterectomy were excluded. Women with scoliosis, prolapsed intravertebral disc, spine deformities, ankylosing spondylitis, or leg discrepancy were also excluded. A trained interviewer conducted structured face-to-face interviews. The data included the occurrence of LBP; socio-demographic, menopausal status and lifestyle variables. Women were classifed as pre-, or peri- or postmenopausal according to the WHO definitions of menopausal status. LBP was identified among women who experienced pain for more than one day during the past 12 months, in an area between the lower costal margins and the gluteal folds, with or without radiation into the leg, to below the knee. LBP caused by previous back surgery, cancer, vascular diseases or menstruation alone were excluded. We obtained BMD measurements at baseline, at 9 months (T1) and at 24 months (T2) with the use of dual energy x-ray densitometre (Hologic 4500A). The outcome variable was the percentage change of SBMD over the followup time. Women classified as perimenopausal at baseline or followup, or with a change of menopausal status during followup were categorized as going through menopausal transition. Among the 83 women going through menopausal transition from baseline to T1, and among the 104 women from baseline to T2, 32.5% and 40% respectively complained of LBP at baseline. The mean percentage changes of spinal BMD at T1 were 3.15 % (s.d. = 2.0), and 2.14 % (s.d. =3.12) among women with and without complaints of LBP. The mean spinal BMD changes at T2 were 6.27 % (s.d. = 3.42) and 5.67 % (s.d. = 4.33) respectively. The differences between the mean BMD changes at T1 reached statistical significance after adjustment for body fat. LBP may be a useful predictor of acute spinal bone loss in women going through menopausal transition. The relationship would warrant further investigation.

SU312

The Effect of Tobacco Smoking on Forearm Bone Density in Men and Women - the Nord-Trøndelag Health Study (HUNT), Norway. S. Forsmo[1], A. Langhammer*[1], L. Forsén*[2], B. Schei*[1]. [1]Dept. of Community Medicine and General Practice, Norwegian University of Science and Technology, Trondheim, Norway, [2]National Institute of Public Health, Oslo, Norway.

Smoking is known to be a risk factor of low bone mineral density and fractures. The fracture incidence in Norway is one of the highest in the world. About 30% of the adult population are current smokers. The purpose of this study was to analyse the association between tobacco smoking and forearm bone mineral density (BMD). In 1995-97 all inhabitants aged >19 years were invited to the HUNT study. The participants answered comprehensive questionnaires on demographics, life style, risk factors, symptoms and diseases. Among 92.000 invited subjects a 5 % sample was randomly selected for bone mineral density (BMD) measurement of the non-dominant forearm single X-ray absorptiometry (Osteometer DTX100). From the point of 8 mm distance between radius and ulna, the area 24 mm in proximal direction was identified as the distal area, whilst the area in distal direction to the endplate of radius was identified as the ultradistal site. The non-dominant arm was measured, provided no previous fracture in distal radius. Totally 71 % of the invited participated at the screening, but about 60% of the random sample participated in this substudy, A total of 2779 (1505 women and 1274 men) were eligible for analysis. Mean age for men and women, respectively, was 50.5 and 49.9 years (range 20-97). In men, 29.5% and 32.0% reported present or prior smoking, respectively. In women, 30.6% reported present and 20.3% prior smoking. The percentage of never smokers was highest in men 60 years of age. No difference in mean BMD between present, prior and never smokers was found neither in men nor women < 50 years of age. After the age of 50, BMD decrease was more accentuated in smokers. In bivariate linear regression, a strong statistically significant negative association between packyears of smoking and BMD was found in males (R2=4.0), but not in females. Adjusting for age and body weight, a statistically significant negative association was also found in women at both sites. In male smokers, 50 years or older, weight adjusted odds ratio of being in the lowest age specific BMD tertile, compared to never smokers, was 2.2 (95% CI: 1.4 - 3.5) at distal and 2.6 (95% CI: 1.5 - 3.8) at ultradistal radius. Corresponding OR in female smokers were 1.8 (95% CI: 1.2 - 2.7) and 1.5 (95% CI: 1.0 - 2.3). Adjusting for estrogen therapy and age at menopause did not change the outcome. This study shows that the effect of smoking on the skeleton in both men and women is found after the age of 50 and that the effect is possibly stronger in males.

SU313

Bone Mineral Density and Markers of Bone Remodeling in HIV Infected Patients According to the Treatment. C. Amiel*[1], A. Ostertag*[2], L. Slama*[1], C. Baudoin*[2], T. Nguyen*[1], E. Lajeunie*[3], W. Rozenbaum*[1], M. C. de Vernejoul[2]. [1]Service des Maladies Infectieuses et Tropicales, Hopital Tenon, Paris, France, [2]Hopital Lariboisiere, INSERM U349 et Service de Rhumatologie, Paris, France, [3]Laboratoire de Biologie Endocrinienne, Hopital Lariboisiere, Paris, France.

Osteoporosis has been reported in HIV-infected patients and has been suggested to be related to protease inhibitors treatments (PI). In order to assess this risk, and to investigate its putative link with treatments, we compared the bone density of HIV-infected men (HIV^+), who were treated either with PI(PI^+ n = 49) or without PI (PI^- n=51) or untreated (UT n=48). We included 81 males controls, HIV negative (HIV^-), recruited among hospital employees matched for age with the HIV^+ group (mean ± SD :40 ± 8 years). Bone mineral density adjusted on age (Z-score), was measured by DPX at the lumbar spine (LS) or the femoral neck (FN) using Lunar densitometer. Z-score was decreased in HIV^+ group, at the FN (HIV^+: -0.39± 1.05, HIV^-: 0.25± 0.87, p<0.001) and LS (HIV^+: -1.08± 1.21, HIV^-: -0.06± 1.26, p<0.001). Prevalence of osteoporosis at the LS was 11.5% among HIV^+ and 2.8% in HIV^- (p<0.01). Among HIV^+, the Z-score was not different according to duration of both the disease or the treatment but was correlated to BMI (r= 0.27 at LS and 0.35 at FN). The Z-score did not differ significantly between the treatment groups (at LS: UT: -0.82± 1.15, PI^-): -1.21± 1.41 PI^+: -1.21± 0.99, FN had similar result). UT patients had a lower duration of the disease (4.8± 5.0 years) than PI^+ and PI^-) (10.4± 4.5, p<0.01). BMI and viral load were identical among the 3 HIV^+ groups. After adjustment on age at HIV diagnosis, duration of the disease, BMI and BMI nadir, using multiple regression analysis, there was no significant difference between the 3 HIV^+ groups. Among PI^+ and PI^- groups, Z-score was not different according to the presence of lipodystrophy .
Markers of bone remodeling were measured in the 102 HIV^+ and 42 HIV^- subjects . HIV^+ patients had a decreased bone alkaline phosphatase (9+4 vs 12+4 ng/ml, p<0.01) and increased urinary crosslaps/Cr (3+2 vs 2+1, p<0.01) There was no important difference in the markers among the 3 HIV^+ groups and according to PI treatment. Cortisol was higher and leptin lower in HIV^+ compared to HIV^- subjects. In conclusion: There is a marked decrease in bone density in HIV infected patients that can lead to symptomatic osteoporosis. This osteoporosis is related to an imbalance with high bone resorption and decreased bone formation. Our transversal study does not show a deleterious role of the treatment but points to a decreased bone density before the start of treatment in HIV patients

SU314

Long-Term Effects of Serum Cholesterol over 34 Years on Bone Mineral Density (BMD) in Women and Men: The Framingham Osteoporosis Study. E. J. Samelson[1], L. A. Cupples*[2], M. T. Hannan[3], P. W. F. Wilson*[4], K. E. Broe*[1], Y. Q. Zhang*[4], D. Levy*[5], S. A. Williams*[6], V. Vaccarino*[7], D. P. Kiel[3]. [1]Hebrew Rehab Ctr, Boston, MA, USA, [2]BU Sch Pub Health, Boston, MA, USA, [3]Hebrew Rehab Ctr /Harv Med Sch, Boston, MA, USA, [4]BU Sch Med, Boston, MA, USA, [5]Framingham Study, Boston, MA, USA, [6]AstraZeneca, Wayne, PA, USA, [7]Emory Sch Med, Atlanta, GA, USA.

Low BMD is associated with increased risk of cardiovascular mortality and aortic calcification in postmenopausal women suggesting a possible role for cholesterol in the pathogenesis of both osteoporosis and atherosclerosis. No prospective studies have determined the effect of long-term cholesterol levels on BMD. The purpose of this study was to examine the relation between total serum cholesterol level (TCHOL), averaged over 34 years, and subsequent BMD in women and men in the Framingham Osteoporosis Study. Participants included 1162 cohort members (712 women, 450 men; mean age 76, range 67-98) who obtained hip (femoral neck), spine (L2-L4), and radial shaft BMD measurements using Lunar SP2 and DP3 in 1988-89. TCHOL and information on confounders were collected at study exams conducted every two years since cohort enrollment in 1948. For the present analyses, levels of TCHOL (mg/dL) were averaged over the 34 years of study follow-up prior to BMD measurement. Similar methods were used to obtain mean values of systolic blood pressure (SBP), smoking, alcohol, body mass index (BMI), and diabetes. In women, years of estrogen use were summed over the 34-year follow-up period. Women were also classified according to recent estrogen use (two years prior to BMD). Sex-specific linear regression modeled BMD as a function of TCHOL quartile, adjusted for age, BMI, smoking, alcohol, SBP, diabetes, and in women, duration and recency of estrogen use (Table). Women with higher TCHOL had lower femoral neck BMD than women in lower TCHOL quartiles; however, an inverse trend was not observed at other bone sites. Men with higher TCHOL had lower lumbar spine and radial shaft BMD than men in lower TCHOL quartiles, whereas no relation was observed between TCHOL and femoral neck BMD in men.

Adj. Mean BMD (g/cm^2) by TCHOL Quartile (Q1=Low, Q4=High)

	Q1	Q2	Q3	Q4	Trend, P	Q1	Q2	Q3	Q4	Trend, P
	Women					Men				
Femur	0.73	0.72	0.71	0.71	.07	0.87	0.86	0.90	0.86	.99
Spine	1.07	1.08	1.06	1.08	.96	1.37	1.33	1.35	1.30	.09
Radius	0.51	0.51	0.49	0.51	.61	0.73	0.72	0.72	0.70	.01

While there was some suggestion of an inverse association between TCHOL and BMD, the relation was not consistent for women and men or for all bone sites. In conclusion, cholesterol is not likely to be a significant contributor to the relation between BMD and coronary heart disease.

Disclosures: ***E.J. Samelson****, AstraZeneca Pharmaceuticals LP 2.*

SU315

Relationship between Vitamin D, PTH and Bone Mineral Density in Postmenopausal Women. Preliminary Data. N. Malavolta[1], M. Frigato*[2], R. Mule'*[2], L. Pratelli*[3], S. Gnudi*[4]. [1]Dipartimento di Medicina Interna e dell'Invecchiamento, Azienda Ospedaliera di Bologna, Policlinico S.Orsola-Malpighi, Bologna, Italy, [2]Dipartimento di Medicina Interna e dell'Invecchiamento, Azienda Ospedaliera di Bologna Policlinico S.Orsola-Malpighi, Bologna, Italy, [3]Laboratorio di Patologia Clinica, Istituto Ortopedico Rizzoli, Bologna, Italy, [4]Medicina Interna, Istituto Ortopedico Rizzoli, Bologna, Italy.

To assess the relationship between vitamin D, bone mineral density (BMD) and parathiroid hormone in post-menopause, we studied 96 consecutive postmenopausal women (mean age 62.5±7.2) whose BMD (measured at spine and femoral neck), intact plasma parathiroid hormone (iPTH), serum 25-hydroxy-cholecalciferol (25HD) and serum 1,25 diydroxy-cholecalciferol (1,25DHD) were determined for clinical screening of osteoporosis. A clinical examination was carried out in all subjects to exclude patients with malignancy, long-term immobilization, major rheumatic diseases, chronic renal, hepatic or pulmonary diseases, Paget's disease of bone or long-term treatment with drugs known to affect bone (more than 6 months for estrogen, anabolic steroids, calcitonin or bisphosphonates, or more than 3 months for glucocorticoids or antiepileptic drugs). Mean values of examined parameters were 16.4±10.2 ng/ml for 25HD, 25.2 ± 8.0 pg/ml for 1,25DHD, 58.7±20.3 pg/ml for iPTH, 776.4±129.3 mg/cm² for spine BMD and 639.6±79.2 mg/cm² for femoral neck BMD. 25HD was found to correlate with age (R=0.30, p<0.004), iPTH (R=0.30, p<0.004) and spine BMD (R=0.31, p<0.002) but not with femoral neck BMD. 1,25DHD was not correlated with any of the considered parameters. iPTH was weakly correlated with age (R=0.20, p<0.050). Selecting a cut-off of 15 ng/ml of 25HD as indicative of vitamin insufficiency there was a lower spine BMD (p<0.017) and higher iPTH (p<0.035) in women having their 25(OH)D below the cut-off compared with those above it. There were not differences between groups about age, 1,25DHD and femoral neck BMD. Our data indicate that 25HD status is correlated with spine BMD and iPTH and should be enquired as risk factor for postmenopausal vertebral bone loss.

SU316

Recruitment of Middle-Aged Chinese-Canadian Immigrants for a Study of Bone Health. R. Chaudhry*[1], C. Chan*[1], N. Diaz-Granados*[1], K. Milstead*[1], D. Lui-Yee*[1], G. Chan*[2], A. Cheung[3]. [1]University Health Network, Toronto, ON, Canada, [2]Yee Hong Community Centre, Toronto, ON, Canada, [3]University Health Network & University of Toronto, Toronto, ON, Canada.

We have successfully recruited 976 Chinese-Canadian immigrants, men and women aged 45 and older, for a study of osteoporosis and osteoporotic fractures using convenience sampling methods. Participants were recruited through media announcements, health fairs, and community outreach through community centres, shopping centres, churches and libraries which predominantly serve the Chinese community in the Greater Toronto Area. In order to assess how representative our sample is of the general Chinese-Canadian population, we compared the characteristics of our cohort to that of the Chinese population in the 1998/99 National Population Health Survey (NPHS), a population-based Canadian survey, and the 1996 Census of Canada. The 1998/99 NPHS estimates that there are close to 300,000 men and women of Chinese ethnicity, aged 45 and older, living in Canada; this is similar to what is reported from the 1996 Census of Canada for visible minority Chinese in the same age group. Preliminary analyses were performed for the first 844 individuals recruited to our study (589 women and 255 men). The majority of participants recruited were from Hong Kong (73%) and China (16%), and the rest primarily from Taiwan and Vietnam. We compared our study population to only those individuals in the NPHS, age 45 or older, who responded that either their race or ethnicity was Chinese. The age distribution of women in our cohort is very similar to that of the NPHS (41% are aged 45-54, 24% are aged 55-64, and 35% are aged 65 and older). Males in study are, however, older (27% are aged 45-54, 24% are aged 55-64, and 49% are aged 65 and older). In terms of educational attainment, 43% of women and 60% of men in our study report some post-secondary education. This is a higher proportion than reported in the NPHS, 38% and 51% respectively. Seventy percent of women in our study are married, as compared to 63% in the NPHS, and 92% of men reported being married, as compared to 89% in the NPHS. The Chinese immigrant population recruited to our study through convenience sampling methods appear to be more highly educated than the general Chinese immigrant population in Canada. Women recruited to the study appear to be more representative of the Chinese immigrant population than the males recruited to our study. The NPHS captures data on health indicators, such as height, weight, self-reported health status, smoking, vision and hearing, as well as access to traditional and alternative preventive health care. Further analyses will be reported with respect to these characteristics.

SU317

Balance Characteristics Among Women with Osteoporosis. S. Jaglal[1], B. Maki*[2], G. Hawker[3]. [1]Rehabilitation Science, University of Toronto, Toronto, ON, Canada, [2]Centre for Studies in Aging, Toronto, ON, Canada, [3]Osteoporosis Research Program, Sunnybrook & Women's College Health Sciences Centre, Toronto, ON, Canada.

Persons with osteoporosis, are at increased risk for bone fractures caused by falls. These fractures occur because of a combination of injury and intrinsic bone fragility. In a previous study we determined that 39% of women attending a multidisciplinary osteoporosis clinic (n = 198) with BMD < -2.5 reported a fall in the previous year. Almost half of these patients were under the age of 60 years and did not have the majority of risk factors commonly associated with falling. Lynn et al (1997), suggested that patients with osteoporosis may have balance features that destabilize them, particularly those with kyphosis. We hypothesized, that balance and gait problems may be contributing to a high rate of falls in individuals with osteoporosis. In this preliminary study we tested, three groups of women, those without osteoporosis (n=11), those with osteoporosis who had no history of falls (n=11) and those with osteoporosis who had a history falls (n = 12) to determine their postural balance and gait characteristics, fear of falling and level of physical activity. The first series of balance tests assessed the control of postural sway during quiet, unperturbed stance (platform not moving) under three test conditions, eyes open or closed on a firm or soft surface and while doing a secondary task. To assess balance recovery mechanisms, the subjects performed tests while the platform randomly moved and were instructed to recover balance by taking a single step forward as rapidly as possible. Results: The controls were significantly younger (47.1 $\pm$ 8.3 yrs) than the osteoporotic patients (58.7 $\pm$ 7.2 yrs). Controls reported exercising more than the osteoporosis subjects at a strenuous level. There was no difference between the three groups in the unperturbed stance experiments. However, measures of balance recovery were significantly different for both antero-posterior sway (mean frequency) and medio-lateral sway (average speed) after controlling for age such that the osteoporosis patients who had fallen were significantly different from those who had not fallen and the controls. These comprehensive balance test results suggest that osteoporosis due to low BMD is not associated with poor balance but rather a previous history of falls. We also noted that the majority of falls in this group occurred outdoors whereas most of the literature on fall prevention targets indoor falls. Therefore a fall history noting location should be taken from patients with osteoporosis and appropriate fall prevention strategies should become part of the treatment protocol for this subgroup.

SU318

Bone Density Status of the Elderly in Taiwan - Results of the Nutrition and Health Survey in Taiwan, 1998-1999 by Quantitative Ultrasound Scan. Y. Lin[1], J. Chiu*[2], W. Pan*[1], M. Lin*[3]. [1]Inst. Biomed. Sci., Academia Sinica, Taipei, Taiwan Republic of China, [2]Fooyin Inst.of Technology, Kaohsiung County, Taiwan Republic of China, [3]City Health Dept., Kaohsiung, Taiwan Republic of China.

Osteoporosis has become a growing public health problem as the elderly population expands rapidly in Taiwan in recent decades. The Elderly Nutrition and Health Survey in Taiwan, 1998-1999 was carried out to evaluate the overall nutrition and health status of people aged 65 years and above. The survey was conducted using a multi-stage complex sampling scheme. Townships or city districts in Taiwan were classified into 13 strata. Bone density was measured at heel by quantitative ultrasound (QUS) bone densitometry (CUBA Clinical, McCue). Broadband ultrasound attenuation (BUA, in dB/MHz) was measured, and the corresponding T-score was calculated. 1227 males and 1170 females who had complete physical examination data with ultrasound bone scan were included in the current analysis. All variables were weighted to represent the elderly population in Taiwan. Subjects were grouped by age and gender. Compared to the reference group (65-69.99 y/o group for both genders), elderly women older than 75 y/o had significantly lower weight, BMI, and BUA, and were shorter in height. Men who were 75 y/o and older also had lower weight and BMI, but no significant difference in BUA was observed. Percent of women with BUA T-score in between -1 and -2.5, and below -2.5 significantly increased in those aged 75 y/o and older. Nearly 90% of the women aged 85 y/o and older were classified as having T-score lower than -2.5. In men the distribution of T-score did not change across these age groups. There was no association between the stratification effect and the risk of having low BUA T-score (T-score < -2.5) in either gender. Results of univariate logistic regression analyses showed that in men higher weight and BMI were protective (OR, or odds ratio=0.97 and 0.90, respectively, p<0.0001), whereas in women height was also positively associated with lower risk of having low BUA T-score (OR=0.93, p<0.0001) in addition to weight (OR=0.93, p<0.0001) and BMI (OR=0.87, p<0.0001). These protective effects remained after adjusted for age. Older age (OR=1.11, p<0.0001) as well as longer postmenopausal duration (OR=1.06, p=0.0004) increased the risk in females. The length of time period between menarche and menopause was not related to the status of having low BUA T-score. This is the first island-wide survey with the use of QUS technology as the screening tool to investigate the bone health status of the elderly in Taiwan. The results suggested that there is an overall problem of low bone density in the elderly, especially in women aged 75 years and older.

SU319

Body Composition and Serum Leptin Changes during Hormone Replacement Therapy: A Prospective Study. A. Arabi*[1], C. Roux[1], R. Porcher*[2], C. L. Benhamou[3], P. Garnero[4]. [1]Rhumatologie, Hôpital Cochin, Paris, France, [2]Hôpital Saint Louis, Paris, France, [3]ERIT M0101, Orleans, France, [4]SYNARC, INSERM U403, Lyon, France.

To elucidate the mechanisms underlying the effects of hormone replacement therapy (HRT) on body composition and bone mineral density (BMD), we assessed body composition, serum leptin levels, and the influence of these parameters and of their changes on bone density and bone turnover in 109 healthy postmenopausal women beginning either tibolone 2.5mg (n=29), tibolone 1.25 mg (n=42) or estradiol 2 mg plus norethisterone acetate 1mg (E2+NETA) (n=38), daily for 2 years. At baseline, 1 year, and 2 years, body composition and BMD of the total hip, femoral neck, lumbar spine L2-L4 and the total body were determined by dual energy X-ray absorptiometry (QDR 2000, Hologic), and android fat, gynoid fat, and android obesity index (AOI) were calculated. Serum levels of leptin, bone alkaline phosphatase, osteocalcin and the urinary excretion of type I collagen C-telopeptide (CTX) were measured at the same time points. At baseline, BMD at all sites, lean mass and gynoid fat correlated negatively, whereas android fat and AOI correlated positively, with years since menopause. BMD at all sites correlated with both fat mass and lean mass (r= 0.26, p=0.0066 and r= 0.42, p<10-4 at the total femur). Serum leptin levels correlated positively with total hip BMD: r= 0.26, p= 0.032, and negatively with osteocalcin: r=-0.24, p= 0.043, and CTX: r= -0.4, p= 0.0006.BMD increased at all sites with treatment in all groups with a higher increase of spine BMD in the E2+NETA group(p<10-4). Serum bone alkaline phosphatase, osteocalcin, and urinary CTX decreased by 27%, 36% and 51% respectively without difference between groups. Lean mass increased significantly in all groups (p<10-4), by a mean of 7%, 3% and 6% with tibolone 2.5mg, tibolone 1.25 mg and E2+NETA respectively; android fat and AOI decreased significantly in all groups (p<10-4 and p=0.0023 respectively). The increase in BMD at all sites correlated positively with changes of lean mass at 2 years. No significant changes in leptin levels and no correlation between changes in biochemical bone markers and changes in leptin levels at 2 years were found. In conclusion, 1- both fat mass and lean mass are related to BMD in postmenopausal women, the relation being strongest with lean mass, 2- high serum leptin level are associated with decreased bone turnover and increased hip bone mineral density, 3- serum leptin levels are not affected by HRT, 4- HRT reverses body composition changes occurring with menopause, 5- E2+NETA and tibolone have effects on lean mass which may play a mediating role in their effect on BMD.

SU320

Serum RANK Ligand Levels and Bone Mineral Content in Hyperthyroidism. G. Speer*, Á. Tabák*, É. Bajnok*, I. Takács, Z. Nagy, P. Lakatos. 1st. Dept. of Medicine, Semmelweis University, Budapest, Hungary.

Thyroid hormone-stimulated bone loss is a clinically significant side effect of hyperthyroidism. Its pathomechanism has not yet been fully elucidated. RANKL (receptor activator of nuclear factor kb ligand) is an essential factor in the differentiation and function of osteoclast, produced by osteoblast. Increased production of RANKL has been shown to be associated with increased bone resorption. In the present study, we investigated the serum RANKL levels in hyperthyroidism as well as its relationship with bone mineral density (BMD) and bone quality assessed by bone sonography (QUS) in 40 healthy and 52 hyperthyroid women with osteoporosis. RANKL levels were detected by ELISA. BMD was measured at the lumbar spine and femoral neck using DEXA and at the midshaft radius using SPA method. Bone quality was estimated by QUS at the calcaneus (BUA). There was no difference in RANKL levels between healthy and hyperthyroid subjects. However, we found a significant (p=0.022) inverse correlation between serum RANKL levels (1.34±1.21, mean±SD, pmol/l) and BUA values when all subjects were pooled. The serum levels of RANKL did not correlate with BMD in either group. Our data raise the possibility that RANKL might play a role in the determination of bone quality.

SU321

Quantifying the Relative Influence of Peak BMD, Age-Related Bone Loss and Menopause on the Development of Osteoporosis. C. J. Hernandez[1], G. S. Beaupré[2], R. Marcus[3], D. R. Carter[2]. [1]Orthopaedics Department, Mt. Sinai School of Medicine, New York, NY, USA, [2]RR&D Center, VA Palo Alto Health Care System, Palo Alto, CA, Mechanical Engineering Dept., Stanford University, Stanford, CA, USA, [3]Eli Lilly and Company, Indianapolis, IN, USA.

Because osteoporosis is defined in terms of bone mineral density (BMD), any factor that influences BMD also influences the development of osteoporosis. Factors that determine a woman's BMD include the rate of loss she experiences as she ages (age-related loss), bone loss at menopause and peak BMD. Understanding the relative influence of each of these factors may help identify important preventive treatments and provide new ways to identify women at risk for osteoporosis. In this analysis we utilize a computer model of the bone remodeling process to predict the relative influences of peak BMD, age-related bone loss and menopause on the development of osteoporosis. Bone loss caused by aging is simulated by reducing the focal bone balance so that less bone is formed than is resorbed at each remodeling site. Increases in bone turnover at menopause are based on declines in serum estradiol observed clinically. The delay in the development of osteoporosis (defined as BMD <2.5 S.D. from the young adult mean) caused by modifying peak BMD, age-related bone loss or the age at menopause is quantified. The results suggest that peak BMD has the most influence on when osteoporosis develops. A 10% increase in peak BMD from the population average delays osteoporosis by 10 years while the same change in the age at menopause or the rate of age related bone loss is predicted to delay osteoporosis by approximately 2-3 years (see figure).

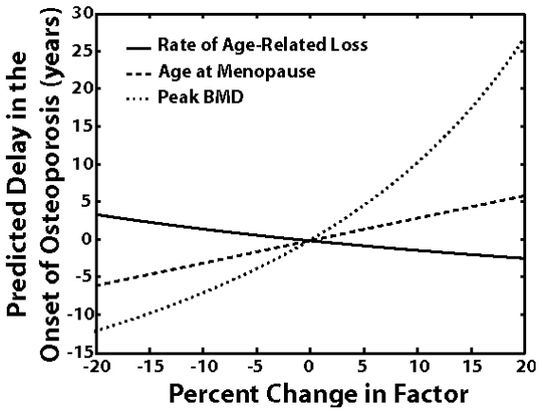

Because peak BMD is determined primarily during growth and maturation our analysis suggests that bone mass in early adulthood may be a more important risk factor for the development of osteoporosis than rates of bone loss later in life. This model is different from previous simulations of bone loss throughout adulthood (Ross et al. 1988 Bone 9:337-347) because it details the bone remodeling process that is responsible for changing bone mass. The bone remodeling description allows the model to describe how multiple factors might magnify or reduce bone loss caused by each other. Further work with this model would be required to predict fracture risk or Remaining Lifetime Fracture Probability.

SU322

Serum OPG Levels and Bone Mineral Content in Healthy, Postmenopausal Osteoporotic and Hyperthyroid Subject. Z. Nagy, Á. Tabák*, É. Bajnok*, I. Takács, G. Speer*, P. Lakatos. 1st Department of Internal Medicine, Semmelweis University, Budapest, Hungary.

Osteoprotegerin (OPG) a member of tumor necrosis factor receptor superfamily. OPG-deficient mice develop severe osteoporosis whereas administration of recombinant OPG to rats results in increased bone mineral density (BMD). Thus,OPG may be important in the aetiology and treatment of osteoporosis in humans. In the present study, we investigated serum OPG in human subjects as well as its relationship with bone mineral density (BMD) and serum beta-crosslaps in 83 healthy, 87 osteoporotic women and 89 hyperthyroid women with osteoporosis. OPG levels were detected by ELISA. BMD was measured at the lumbar spine and femoral neck using DEXA and the midshaft radius using SPA method. There was no difference in OPG levels between healthy, osteoporotic and hyperthyroid subjects.The serum levels of OPG did not correlate with the age, height, BMD and the beta-crosslaps levels in either group. Our data do nat support a passibility that serum OPG might reflect changes in bone metabolism.

SU323

Bone Mineral Density (BMD) of the Dominant and Non-dominant Hip in Postmenopausal Women. R. A. Brownbill, L. G. Tamborini, J. Z. Ilich. School of Allied Health, University of Connecticut, Storrs, CT, USA.

The universal testing sites for osteoporosis are bone density measurements in spine and hip. Recently, a software for successive measurements of both hips was developed, however it is not clear whether both hips need to be tested. The purpose of this study was to determine whether there is a difference in BMD between dominant and non-dominant hip and whether one of them correlates better with other skeletal sites. We also examined whether past physical activity and walking speed affected differently BMD of each hip. Participants were 123 Caucasian women, age 68.9±6.9 years (mean±SD), all healthy and not taking medications known to affect bone. BMD of both hips (in the regions of neck, Ward's, trochanter, and shaft), the total body, spine, and forearm was measured by DPX-MD densitometer. Past activity was assessed by the Allied Dunbar Fitness Survey for older adults and the 8-meter normal- and brisk-pace walking speed was assessed in a straight hallway. Subjects were also divided based on their past activity and walking speed, and subgroup analyses were performed. Pearson r and t-tests were used in analyses. Results showed no statistical difference in any of the measured regions in two hips. Mean % difference for neck, Ward's, shaft, trochanter, and total hip was 0.2, 1.6, 1.3, 1.5, and 0.7, respectively. Non-dominant hip correlated better than dominant and better than average of two with all skeletal sites except spine. In the non-dominant hip, r ranged from 0.502 (with forearm) to 0.793 (with total body) and in the dominant hip from 0.417 (with forearm) to 0.770 (with total body), all p values <0.05. Subjects with higher walking speed had higher neck BMD in the non-dominant hip (p<0.05). There was no difference between BMD in two hips regarding the levels of past activity. Although two hips had similar BMD, the non-dominant hip correlated better with other skeletal sites. We conclude that it might be sufficient to measure BMD in only non-dominant hip.

SU324

A Mid-Region Fragment of Human Parathyroid Hormone (hPTH 28-48) Has no Anabolic Action in Older Mice In Vivo. A. Iida-Klein[1], S. S. Lu[1], K. Yokoyama*[1], D. W. Dempster[1], J. Nieves[2], R. Lindsay[2]. [1]Regional Bone Center, Helen Hayes Hospital, West Haverstraw, NY, USA, [2]Clinical Research Center, Helen Hayes Hospital, West Haverstraw, NY, USA.

During early skeletal development in fetal or neonatal rodents, PTH (28-48) has been shown to stimulate creatine kinase activity and to increase the cortical width of the tibia. However, it has not yet been defined whether PTH (28-48) exhibits a similar anabolic action on the mature murine skeleton. To compare the effects of PTH (28-48) to that of PTH (1-34) in older mice, female C57BL/6 mice at 22 weeks were treated with PTH (28-48) 90 mcg/kg/day (n=9), PTH (1-34) 80 mcg/kg/day (n=9) or vehicle (n=8) 5 days a week (s.c.) for 3 weeks and their bone mineral density (BMD) measured in vivo weekly by dual energy X-ray absorptiometry (DXA). The rate of bone gain at each skeletal site for the initial 3 weeks was calculated by linear regression. From 22 weeks of age, most control animals increased BMD with a mean rate of 0.315, 0.364 and 0.333 mg/cm2/week in the tibia, femur and total body, respectively. In the lumbar vertebrae, however, control animals lost bone (mean -0.131 mg/cm2/week, n=8) between 22 and 25 weeks, suggesting bone loss begins at this site prior to this age. PTH (1-34) increased the rate of initial bone gain by 4-fold ($p<0.01$), 5.7-fold ($p<0.0001$) and 2.9-fold ($p<0.005$) in the tibia, femur and total body bone, respectively, and induced a significant bone gain in the lumbar vertebrae (mean rate changed from -0.131 to +1.605 mg/cm2/week, $p<0.05$). However, PTH (28-48) did not show any anabolic actions on BMD at any sites during 3weeks of treatment with a mean rate of 0.314, 0.386, 0.293 and 0.572 mg/cm2/week for the tibia, femur, total body and lumbar vertebrae, respectively. The appearance of the anabolic action of PTH (1-34) at the long bone sites was somewhat delayed in the older mice as compared to younger mice. These data suggest that the skeletons of mature mice retain responsiveness to the anabolic effect of PTH (1-34), but with age the anabolic activity of PTH (28-48) is lost and a higher dose or longer treatment may be required for the latter being anabolic.

SU325

Age Is a Major Correlation Factor Affecting In Vivo Murine Bone Mineral Density (BMD) for the Longitudinal Studies. K. Yokoyama*[1], S. S. Lu[1], J. Nieves[2], D. W. Dempster[3], R. Lindsay[2], A. Iida-Klein[1]. [1]Regional Bone Center, Helen Hayes Hospital, West Haverstraw, NY, USA, [2]Clinical Research Center, Helen Hayes Hospital, West Haverstraw, NY, USA, [3]Regional Bone Center, Helen Hayes Hopsital, West Haverstraw, NY, USA.

Age and body weight (body size) are important factors, which directly or indirectly affect bone mineral density (BMD) for the longitudinal studies of mouse skeleton, in addition to the experimental conditions such as estrogen-deficiency or treatment with anabolic agents. Although murine models have been intensively utilized for the study of bone metabolism, the database for in vivo murine BMD in normal bone physiology is currently very limited. The present study analyzes in vivo BMD data to determine the factors affecting BMD in mice within one strain. From a total of 136 C57BL/6 female mice between 10 and 23 weeks of age, a total of 532 dual energy X-ray absorptiometry (DXA) scans were analyzed at 4 different skeletal sites (femur, tibia, lumbar spine and total body bone) in correlation to their age and body weight. There are 6 groups analyzed:1) intact mice treated with vehicle (C, n=111), 2) intact mice treated with PTH(1-34) 40 mcg/kg/day (s.c.) 5 days a week for 1 to 7 weeks (P, n=113), 3) sham-operated mice with vehicle (SC, n=78), 4) sham mice treated with PTH (SC, n=80), 5) ovariectomized (Ovx) mice with vehicle (OC, n=76) and 6) Ovx mice with PTH (OP, n= 74). In intact control mice between 10 and 17 weeks, BMD correlated positively with age at all skeletal sites (r = 0.6790, 0.6910, 0.6660 and 0.4283, for total body, femur, tibia and lumbar spine, respectively). The majority of this relationship was related to the continued increase in size of the animals, and body weight was the other important determinant of BMD (r = 0.5828, 0.5052, 0.5438 and 0.4094 for total body, femur, tibia and lumbar spine, respectively). Ovx eliminated the increase in bone density with age in the tibia (r = 0.1600) and lumbar spine (r = -0.1600), and attenuated the relationship in the femur (r = 0.3775) and total body (r = 0.4555). The relationship between body weight and BMD was also reduced by Ovx. Treatment with PTH enhanced the positive relationship between BMD and age at all sites, and in both intact younger animals as well as after Ovx. The present data suggest that age is the most important factor affecting BMD at all sites particularly in younger intact mice, and that body weight may not be a good normalizing factor especially in older operated animals.

SU326

Both Androgen and Estrogen Signalings Contribute to the Maintenance of Bone Mass in Males: Analyses of Male Androgen Receptor Deficient Mice. H. Kawano[1], T. Sato*[2], T. Yamada*[2], T. Matsumoto*[2], H. Kawaguchi[1], S. Kato[2]. [1]Orthopaedics, Univ. of Tokyo, Japan, [2]IMCB, Univ. of Tokyo/ CREST, Japan.

Although testosterone (T), the main androgen, is known to be essential to maintain bone mass in males by the fact that orchidectomy causes bone loss both in animals and humans, the role of androgen signaling on bone in males remains unknown. This is because T activates not only androgen receptor (AR) as T itself or its metabolite dihydrotestosterone (DHT), but also estrogen receptors through aromatization into estradiol (E_2). We recently established an AR deficient mouse (ARKO) line and reported that male ARKO exhibits high turnover osteopenia. Since the T level was markedly decreased due to severe atrophy of genital organs in male ARKO as compared to male wild-type littermates (WT), the decrease in estrogen signaling possibly causes the osteopenia. The purpose of this study was to know the contributions of androgen and estrogen signalings on bone metabolism in males by analyzing ARKO with both disrupted androgen signaling and decreased estrogen signaling. WT and ARKO were orchidectomized (ORX) or sham operated at 3 weeks of age, and implanted subcutaneously with a slow releasing pellet of placebo, T, or DHT (10 mg / 60d). Plain X-ray and 3D-CT features, BMD, and histomorphometric parameters of long bones were compared among 8 experimental groups: WT, WT+ORX, WT+ORX+T, WT+ORX+DHT, ARKO, ARKO+ORX, ARKO+ORX+T, and ARKO+ORX+DHT (each n=8), at 8 weeks of age. WT+ORX, ARKO and ARKO+ORX all showed similar decreases in bone mass (about 15% lower in BMD and 75% lower in BV/TV) and increases in bone formation / resorption parameters than did WT, indicating that testis is the principal source of bone regulatory androgen. Although the serum T level was confirmed to be fully restored to the WT level in the two T implanted groups, bone mass and turnover of ARKO+ORX+T showed about the half restoration (8% lower in BMD and 43% lower in BV/TV than WT) while those of WT+ORX+T showed full restoration to the WT levels. The restored half in ARKO+ORX+T is due to the effect of E_2 converted from the implanted T, whereas the unrestored half indicates the direct effect of androgen through AR. Since the serum E_2 level did not differ between the two groups, bone regulatory E_2 seemed to be converted mainly *in situ* in skeletal tissues. Although ARKO+ORX+DHT showed no restoration of bone mass or turnover by DHT implantation, about half the restoration was seen in WT+ORX+DHT as in WT. This also indicates the contribution of androgen signaling because DHT is not converted to E_2. We therefore conclude that both androgen and estrogen signalings contribute to osteopenia in male ARKO, indicating the involvement of both signalings in the maintenance of bone mass in males.

SU327

Effects of Orchiectomy on Bone Turnover and Bone Mass in the Aged Sprague-Dawley Rat. N. Doyle*[1], J. Jolette*[1], J. Mayer*[1], P. Qvist*[2], R. G Erben[3], S. Y. Smith[1]. [1]CTBR, Montreal, PQ, Canada, [2]Nordic Bioscience Diagnostics A/S, Herlev, Denmark, [3]Ludwig Maximilians University, Munich, Germany.

The purpose of this study was to evaluate the effects of orchiectomy (ORX) on bone turnover measured by biochemical markers and on bone mass as measured by densitometry in the aged Sprague-Dawley rat. Eighteen (18) month-old male rats were randomly assigned to 2 groups by body weight. Thirteen animals underwent ORX and 13 animals underwent Sham surgery. Animals were monitored for 16 weeks. Bones were retained for histomorphometry. Blood and urine samples were collected from all animals following a 6-hour daytime fast pre-surgery and 14, 28, 56, 84 and 112 days following surgery. Serum was analyzed for Rat-MID osteocalcin (OC), total ALP and C-telopeptide (RatLaps). Urine was analyzed for free deoxypyridinoline (DPD) and RatLaps (both corrected for creatinine). Bone densitometry by DXA and pQCT was performed pre-surgery and at 8, 12 and 16 weeks after surgery. DXA scans were obtained for the whole body, femur and lumbar spine. Peripheral QCT scans were obtained at the proximal tibia metaphysis and diaphysis. Body weights were recorded biweekly and seminal vesicle and prostate weights were recorded at necropsy. Ten animals/group survived the four-month observation period. Body weight decreased post-surgery for both groups recovering to pre-surgery weight only for Shams. Seminal vesicle and prostate weights for the ORX group were 23% and 28%, respectively, of the Sham controls. Increases in DPD (x1.6 to 2) were observed at all time-points for the ORX group relative to baseline (and compared to Shams). Urine RatLaps was increased at days 14 and 28 (x1.8) with levels declining to Sham levels thereafter. Increases in OC were noted from day 28 reaching a plateau by day 84 (x2 relative to baseline). Serum RatLaps and ALP showed no consistent differences between groups. Sixteen weeks post-ORX, the distal femur showed the greatest change in BMD measured by DXA with a 15% decrease relative to baseline and 11% compared to Shams. Tibia metaphysis trabecular BMD (pQCT) was decreased 37% relative to baseline and 19% compared to Shams at 16 weeks. The greatest changes in BMD generally occurred during the first 8 weeks post-surgery. An increase in endosteal circumference and decrease in cortical thickness was observed at the diaphysis for the ORX group compared to baseline and Shams. There was no change in periosteal circumference following ORX. ORX in the aged rat induced high turnover osteopenia as measured by biochemical markers and bone densitometry. These data support the use of this androgen-deficient model to evaluate potential anti-osteoporosis agents.

SU328

Androgen Deprivation in Veterans with Prostate Cancer: Implications for Skeletal Health. M. E. Elliott[1], A. J. Wilcox*[2], M. L. Carnes*[3], R. Tobias*[1], H. Baade*[1], E. Stamos*[1], C. D. Counts*[1]. [1]School of Pharmacy, University of Wisconsin, Madison, WI, USA, [2]VA Medical Center, Madison, WI, USA, [3]Department of Medicine, University of Wisconsin Medical School, Madison, WI, USA.

Osteoporosis and fractures are well-recognized complications of androgen deprivation in patients with advanced prostate cancer, and bone loss in these individuals can be reduced by bisphosphonate therapy. The frequency with which skeletal health is assessed and treated in these patients is unclear, however. Accordingly, we have undertaken a retrospective survey of skeletal health assessment and its management in patients undergoing gonadotropin releasing hormone agonist-induced androgen deprivation for prostate cancer at a Veterans Affairs Medical Center (VAMC). Veterans with prostate cancer (but without bony metastases) and receiving leuprolide or goserelin were identified from pharmacy records for the years 1993 through 2001 and included in the study. Hypotheses were: (1) Fracture risk factors in addition to androgen deprivation would be found in most patients; (2) bone mass measurements or vitamin D status would be assessed in a minority; (3) only a minority would receive bisphosphonate therapy or have contraindications for such treatment. The work was approved by the appropriate institutional review boards of the University of Wisconsin and the Madison, Wisconsin VAMC. One hundred and eighty five veterans were identified according to study criteria and included in the project. The median length of androgen deprivation was 18 months (range 1-99). Seventy-six percent of men (95% confidence interval [CI] 70-82%) had other fracture risk factors (13% past history of fracture, 56% current or former tobacco use, 20% documentation of alcohol abuse, 32% body mass index <25 kg/m2, 8% long-term prednisone or antiepileptic drug use). Sixteen percent (CI 11-21%) had received a bone mass measurement, and 6% (CI 3-9%) were assessed for vitamin D status. Only ten percent of men (CI 6-14%) had contraindications to bisphosphonate therapy (swallowing difficulties or inadequate renal function), although only 16% (CI 11-21%) were receiving such therapy. Thus, only a small minority of men had their skeletal health or vitamin D status assessed, and few received specific therapy, despite absence of contraindications. We conclude that the skeletal status of male veterans receiving androgen deprivation for prostate cancer is not adequately evaluated nor treated. Education of clinicians and creation of algorithms may improve long-term care in these patients at high risk for fracture.

SU329

Cortical Bone Loss in Androgen-Deficient Aged Male Rats Is due to Increased Endocortical Bone Remodeling. N. Reim*, K. Stahr*, J. Eberle*, R. G. Erben. University of Munich, Institute of Animal Physiology, Munich, Germany.

Hypogonadism is considered to be one of the major risk factors for osteoporosis in men. However, the mechanisms of bone loss due to androgen deficiency are still unclear. Therefore, we sequentially investigated the effects of androgen deficiency on cortical bone in aged orchiectomized (ORX) rats. Hundred-seventy 13-month-old male Fischer-344 rats were either ORX or sham-operated. Following in vivo fluorochrome labeling, groups of 8 - 15 SHAM and ORX rats each were killed at 2 weeks and at 1, 2, 3, 4, 6, and 9 months postsurgery. As measured by peripheral quantitative computed tomography (pQCT) analysis, total bone mineral density and cortical thickness of the tibial shaft were decreased in ORX rats, beginning from 2 months postsurgery until the end of the study. A consistent decrease in volumetric cortical BMD was seen only beyond 6 months post-ORX. In good agreement with the pQCT data, histological analysis of bone cross-sections at the same bone site revealed cortical bone osteopenia by 2 months postsurgery and at all later time points. Androgen deficiency induced a sustained decrease in periosteal bone formation during the first 4 months post-ORX. Interestingly, this change was reversed at the end of the trial. However, although periosteal expansion of the tibial shaft tended to be slower in ORX rats compared with SHAM controls, the reduction in total cross-sectional area of the tibial shaft in ORX animals reached statistical significance only at 4 months postsurgery. The major mechanism for cortical bone loss in aged ORX rats was a progressive expansion of the marrow cavity, which was associated with an initial increase in endocortical eroded perimeter at 1 and 2 months postsurgery, followed by a sustained increase in endocortical bone formation until the end of the study. At the end of the study, endocortical bone surfaces showed clear evidence of increased bone remodeling in ORX rats, and resorption canals originating from the endocortical surface extended deeply into the underlying cortical bone. All these changes were prevented in aged ORX rats receiving testosterone supplementation. We conclude that androgen deficiency-induced cortical bone loss in aged, non-growing rats is mainly due to augmented endocortical bone remodeling.

SU330

Calciotropic Hormones and Bone Resorption Markers in Healthy Older Men. B. I. Gulanski[1], S. Rettinger*[2], A. L. Arnold*[2]. [1]Internal Medicine, Section of Endocrinology, VA Connecticut Healthcare System, West Haven, CT, USA, [2]Yale University School of Medicine, New Haven, CT, USA.

Osteoporotic fractures are important causes of death and disability in older men, however the mechanisms of age-related bone loss remain uncertain. Conflicting data exists regarding changes in biochemical markers of bone metabolism in older men, and the role of calciotropic hormones in age-related bone loss. We measured calciotropic hormones, gonadal steroids, interleukin-6 (IL-6), bone turnover markers, and bone mineral density (BMD) in healthy community-dwelling men over the age of 50 years without known secondary causes for bone loss and not taking medications known to affect bone metabolism. Seventeen healthy eugonadal subjects (mean age 68; range 50-90 years) were included in the analyses. The majority were Caucasian (94%). Thirty-six percent had either osteopenia or osteoporosis. Mid-molecule PTH values above the upper limit of normal were found in 5/17 (29%) subjects. 1,25 dihydroxyvitamin D (1,25OH2D) levels were widely variable, but all within the normal range. Elevated levels of urinary N-telopeptide (NTX) values were found in 4/17 (24%), however serum osteocalcin was elevated in only 1/17 (6%). The mean value of IL-6 was elevated at 6.3 (± 3.5) pg/ml and was above the normal range in the majority of subjects. Bivariate analyses revealed that PTH and 1,25 OH2D were strongly and significantly correlated with IL-6 (r=0.56 and 0.71 respectively; p values < 0.02) and NTX (r=0.69 and 0.81 respectively; p values <0.002). IL-6 was highly correlated with NTX (r=0.82; p<0.001) but not osteocalcin (r=0.04; p=NS). In conclusion, elevated levels of PTH and NTX were found in roughly one quarter of healthy eugonadal men over the age of 50 years. PTH and 1,25OH2D were strongly and significantly associated with IL-6 and urinary NTX.

SU331

Effects of Ribavirin in Combination with either Interferon alpha or Peginterferon alpha-2b on Calcium and Bone Metabolism in Patients with Chronic Hepatitis C. F. J. S. Fonteles*[1], J. B. A. Paixão*[2], H. S. M. Coelho*[2], M. L. Duarte[3], M. F. Farias[1]. [1]Div. Endocrinology, HUCFF, Federal University of Rio de Janeiro, Rio de Janeiro, Brazil, [2]Div. Gastroenterology, HUCFF, Federal University of Rio de Janeiro, Rio de Janeiro, Brazil, [3]Histology and Embriology / PABCAM, Federal University of Rio de Janeiro, Rio de Janeiro, Brazil.

Combination therapy of Ribavirin with Interferon alpha (R+IFN) is recommended for chronic virus C hepatitis, but a negative impact in calcium metabolism and in bone density has recently been reported. Peginterferon alpha-2b (PegINF) is a new analog, also used in combination with R, but there are no reports on the effects of R+PegIFN on calcium and bone metabolism. Twenty-one female and 16 male patients with chronic virus C hepatitis confirmed by PCR for HCV RNA, persistently elevated alanine amino-transferase and liver biopsy, were enrolled in a prospective study of the comparative effects of R+INF (n=18) and R+PegINF (n=19). All patients were HIV negative. Ribavirin was administered per os according to body weigh, 800-1200 mg/day, in association with either subcutaneous INF 3 million units 3 times a week or subcutaneous PegINF 1.5mcg/kg body weigh once a week. Bone density was evaluated at lumbar spine (LS) and femoral neck (FN) by DEXA, Lunar Coorp. at baseline. Serum calcium, phosphorus and intact PTH (IRMA from DSL, Diagnostic Corp., California) and urinary NTx (ELISA, Osteomark, Ostex International, Seattle, WA) were measured at baseline and after 3 months. Mann-Whitney test was used to compare the 2 groups, and Wilcoxon test was used to evaluate the early effects of therapy. Groups R+INF and R+PegINF did not differ at baseline considering age (50.3+/-5.6 and 46.4+/-10.7 yrs), median Z-scores at LS (-0.4 and -0.7) and FN (-0.4 both groups), serum Ca (8.9 and 9.15 mg/dL) and iPTH (55.5 and 56.9 pg/mL). After 3 months, a significant decrease in serum Ca (-2.7% , p=0.01) and a significant increase in serum iPTH (41,3% , p=0.02) were evident when all patients were considered together, but no difference was found between groups. Serum phosphorus did not change with both therapeutic schedules. Median urinary NTx tended to decrease, but the variation was not significant. Our results confirm the negative influence in calcium balance of Ribavirin in association with INF and also with PegINF, and raises the question whether the secondary elevation in serum iPTH may contribute to the bone loss described with the antiviral therapy

SU332

Mineralization Density Is Correlated with Activation Frequency in Women with Postmenopausal Osteoporosis. S. M. Ott. Medicine, University of Washington, Seattle, WA, USA.

In women with postmenopausal osteoporosis, the reduction in fracture rates after treatment with antiresorbing drugs is not directly related to the changes in bone density measured by radiographic techniques. Other aspects of bone (bone quality) such as bone turnover rate and mineralization density within bone metabolic units, could play a role in determining bone strength. This study examined the relationship between bone turnover and mineralization density in women with postmenopausal osteoporosis. Tetracycline-labelled iliac crest bone biopsies were obtained from 39 women with osteoporosis. Standard bone histomorphometric measurements were made, and mineralization density was determined using a backscattered electron micrograph imaging technique. Bone was scanned at 100x and 20 fields of trabecular bone were imaged per section. Image analysis was done using the NIH image program. The average mineralization density was calculated for each subject. The activation frequency showed a significant negative correlation with the mineralization density (r = 0.49, p=0.004). There was no relationship between mineralization density and formation period or mineral apposition rate, but a significant correlation with the mineralizing surface (r = 0.57, p = 0.0005). Thus, women with higher activation frequency had lower mineralization density. The activation frequency depends on the number of bone metabolic units and on the formation period (the duration of formation at any spot on the bone surface). The mineralization density appears to depend on the number of bone forming units rather than the duration of formation at each unit. An increased number of BMU's could lower mineralization density by replacing older, more mineralized bone with newer, less mineralized bone. Although this study documents a significant relationship between mineralization density and bone turnover in women with osteoporosis, it does not predict the optimum values of these aspects of bone quality.

SU333

Degree of Mineralization and Microdamage Accumulation in Cortacal Bone of Dog Rib. T. Mashiba*, S. Mori, Y. Cao*, J. Li*, S. Komatsubara*, J. Kawanishi*, T. Akiyama*, K. Miyamoto*, H. Norimatsu. Orthopedic Surgery, Kagawa Medical University, Kagawa, Japan.

This study was designed to evaluate the relationship between degree of secondary mineralization and microdamage accumulation in the cortical bone of dog rib. Left 9th rib was harvested from ten beagles aged 4 years old, stained en bloc with basic fuchsin and embedded in MMA. A 100 mcm-thick transverse section was cut for contact microradiograph (CMR) and microdamage analysis. Upon exposure for CMR, each rib section was arranged with calibration aluminum step wedge. An 8-bit gray scale digital image was taken from CMR using a microscope equipped with digital camera, then gray level of each osteon was quantified using NIH image software. Degree of mineralization was measured at X100 in cortical bone of ventral and dorsal side, separately. Microdamage measurement was performed using a same transverse section used for CMR, and the location of damage was examined. New, lower mineralized osteons were observed more frequently in ventral side of rib cortical bone than dorsal side. In contrast, old, highly mineralized osteons were found more frequently in dorsal side of rib cortex. Mean degree of mineralization was significantly higher in dorsal side than in ventral side. Microdamage was observed mainly in ventral side of rib cortical bone, where higher tensile stress is distributed in vivo. This suggests that increased production of microdamage initiate more number of intracortical remodeling as a damage repair process in ventral side, lead to increased population of new, lower mineralized osteons, whereas fewer damage production in dorsal side initiate less remodeling, accumulates the old, highly mineralized osteons.

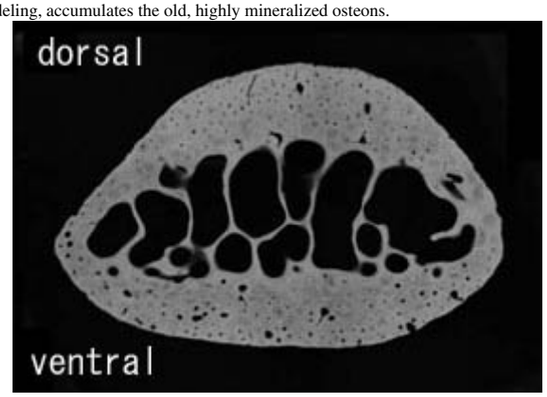

SU334

Are Healthy Premenopausal Women with Asthma and Endometriosis "Normal"? M. F. Delaney[1], S. Hurwitz*[2], N. Glass*[1], M. Hornstein*[3], E. Israel*[4], M. S. LeBoff[1]. [1]Endocrine-Hypertension, Brigham and Women's Hospital, Boston, MA, USA, [2]Harvard Medical School, Boston, MA, USA, [3]Gynecology, Brigham and Women's Hospital, Boston, MA, USA, [4]Medicine, Brigham and Women's Hospital, Boston, MA, USA.

Study recruitment requires the enrollment of volunteers with the disease state to be studied, who are otherwise normal. The baseline screening evaluation may uncover unexpected results. The purpose of the study is to determine the prevalence of undiagnosed medical conditions in a volunteer population of young normal women, as assessed at baseline evaluation in two studies. We reviewed the records of 112 premenopausal women with mild asthma and 27 women with endometriosis (endo) recruited for IRB-approved studies at Brigham and Women's Hospital (BWH). All women were recruited from advertisements, mailings, and physician offices including asthma and gynecology clinics at BWH, Beth Israel Hospital, and affiliated practices. Women included were between the ages 18-46 with a mean of 34.8 yr in the asthma study and a mean of 32.6 yrs in the endo study. Evaluations considered abnormal included calcium intake <600mg/day, vitamin D (25D) ≤15 ng/ml, TSH <0.5 or >5 μU/ml, PTH >65 pg/ml, calcium <8.5 or >10,5 mg/dl, NTX >65 nmol/ BCE/mm, DHEAS <80 μg/mL, and BMI <18.5 or >25 kg/m^2. We included bone density measurements performed on QDR 2000 (Hologic, Waltham, Mass). We found that intact PTH and calcium were normal in both groups. In the asthma group, the mean lumbar spine (LS) Z score was +0.06 (SD 1.03) and total hip (TH) Z score was -0.04 (SD 0.85). The endo group mean LS Z score was -0.1 (SD 0.9) and TH Z score was 0 (SD 0.9). In summary, we found 12% of all normal healthy volunteers were vitamin D deficient, and 15-33% had high bone turnover by NTX, and 26% had a very low DHEAS levels. A low calcium intake was found in 17 of the endo group. Four percent of women had low BMI but we found 26-42% were overweight. In an otherwise healthy group of premenopausal women, these are surprising results. Premenopausal women with endometriosis and asthma and potentially other groups of healthy study participants may have alterations in skeletal homeostasis that are not clinically evident. To identify potential confounding variables on bone in subjects enrolled in clinical studies, a careful baseline evaluation to exclude secondary causes of bone loss should be performed even in the healthiest volunteers.

Abnormal value	Ca intake <600mg/d	25D ≤15	TSH <0.5	TSH >5	NTX >65	DHEAS <80	BMI <18.5	BMI >25
Asthma	0%	12%	0%	5%	15%	-----	4.5%	42%
Endo	17%	12%	8%	0%	33%	26%	4%	26%

SU335

Oral Bisphosphonates for Treatment of Osteoporosis in Elderly Patients with Impaired Renal Function. E. M. Lewiecki, L. A. Rudolph. New Mexico Clinical Research & Osteoporosis Center, Albuquerque, NM, USA.

Background: Elderly patients with osteoporosis are commonly treated with oral bisphosphonates. These patients often have diminished muscle mass, resulting in a serum creatinine that underestimates impairment of renal function. Alendronate and risedronate, the two bisphosphonates approved in the USA for prevention and treatment of osteoporosis, are not recommended in patients with creatinine clearance < 35 ml/min or < 30 ml/min, respectively, due to lack of experience. Since creatinine clearance is not usually measured in clinical practice prior to starting bisphosphonate therapy, some patients with unrecognized impaired renal function may be receiving these medications. Objectives: This study was undertaken to test the hypothesis that some clinical practice patients with impaired renal function are being treated for osteoporosis with oral bisphosphonates, and that serious adverse consequences are unlikely to occur as a result. Methods: A retrospective chart review of female clinical practice patients, age 65 and over, treated with an oral bisphosphonate for osteoporosis or osteopenia during the period 4/7/97 to 7/31/01 was done. Creatinine clearance was estimated from age, body weight, and serum creatinine using the Cockcroft-Gault formula. Adverse outcomes were assessed. Results: 124 women met the inclusion criteria. Of these, 16 (12.9%) had an estimated creatinine clearance < 35 ml/min, and 11 (8.9%) had an estimated creatinine clearance < 30 ml/min. There were no serious adverse events attributed to bisphosphonate therapy in the patients with impaired renal function. Conclusion: Oral bisphosphonates were prescribed to elderly patients with previously unrecognized impaired renal function, without evidence of serious adverse consequences. This may be a common occurrence in clinical practice. Further investigation on the effects of bisphosphonates in patients with impaired renal function is suggested.

Disclosures: ***E.M. Lewiecki****, Merck 2, 5, 8; P&G 2, 5, 8; Aventis 2, 5, 8.*

SU336

How Common Is Loss of Bone Mineral Density in Elderly Clinical Practice Patients Receiving Oral Bisphosphonate Therapy for Osteoporosis? E. M. Lewiecki, L. A. Rudolph. New Mexico Clinical Research & Osteoporosis Center, Albuquerque, NM, USA.

Background: Bone mineral density (BMD) is often measured during bisphosphonate therapy for osteoporosis to monitor for therapeutic effect. Most patients in clinical trials of alendronate and risedronate have an increase or no change in BMD in response to treatment. It is uncertain that clinical practice patients can expect to have the same BMD response to therapy as clinical trial patients. Clinical practice patients may not be as compliant as patients in clinical trials, often have confounding co-morbidities, and may have unrecognized secondary causes of osteoporosis that could impair the therapeutic effect of bisphosphonates. Objectives: This study was undertaken to assess BMD response in elderly clinical practice patients being treated with oral bisphosphonates for osteoporosis. Methods: A retrospective chart review of female clinical practice patients, age 65 and over, treated with an oral bisphosphonate for osteoporosis or osteopenia during the period 4/7/97 to 7/31/01 was done. Subjects for clinical trials, patients referred for consultation, and patients who did not have at least one comparable follow-up DXA were excluded. Each comparable follow-up DXA was evaluated for the presence or absence of a statistically significant change in BMD of the spine or total hip at the 95% confidence level. Least significant change was calculated according to the guidelines of the International Society for Clinical Densitometry. Clinical assessment, confounding co-morbidities, and outcomes of those who lost BMD were reviewed. Results: There were 104 women who met the study criteria. Of these, 10 (9.6%) had a significant loss of BMD at the spine, total hip, or both skeletal sites over a period of at least one year. No patients admitted to non-compliance in drug taking. Laboratory and radiologic work-up of the bone-losers revealed 5 patients (4.8% of the total group, 50.0% of the bone losers) with previously unrecognized contributing factors of clinical significance- vitamin D deficiency, primary hyperparathyroidism, impaired renal function, iatrogenic hyperthyroidism, and cystic bone disease in the hips. Bone-losers typically had multiple co-morbidities and took numerous medications. Conclusion: About one in ten clinical practice patients on bisphosphonate therapy for osteoporosis showed significant bone loss. Evaluation of these bone-losers commonly uncovered previously unrecognized medical conditions that required changes in therapy.

Disclosures: ***E.M. Lewiecki****, Merck 2, 5, 8; P&G 2, 5, 8; Aventis 2, 5, 8.*

SU337

Three-Years Treatment With Risedronate Does Not Alter Bone Mineral Crystallinity In Post-Menopausal Osteoporotic Subjects. E. P. Paschalis[1], R. Phipps[2]. [1]Hospital for Special Surgery, New York, NY, USA, [2]Procter & Gamble Pharmaceuticals, Mason, OH, USA.

Factors such as bone microarchitecture and bone quality as well as bone mineral density (BMD) need to be considered when assessing fracture risk. It has previously been shown that 1- and 3-yr treatment of postmenopausal osteoporotic patients with risedronate reduces vertebral fractures and concomitantly preserves bone microarchitecture as well as increasing BMD. In the current analysis we examined the effects of 3-yr risedronate treatment on mineral crystallinity/maturity, a factor of bone quality, via Fourier transform infrared microscopic imaging (FTIRI). FTIRI allows analysis of bone mineral crystallinity and three-dimensional structures of collagen and other proteins in undemineralized thin tissue sections at the ultrastructural level (each image analyzes a 400 x 400 um^2 area with a spatial resolution of 7 um). Iliac crest biopsies were obtained from nine postmenopausal osteoporotic subjects at baseline and after 3-y treatment with risedronate, 5mg/day orally. The biopsies were embedded in methylmethacrylate, and the trabecular bone region was analyzed by FTIRI in ~4 um thick sections for determination of mineral crystallinity (bone mineral crystallite size in the crystallographic c-axis). Three images (each >2000 pixels)/ section were acquired. Crystallinity was compared before and after treatment for each subject (paired t-test). In the group overall (n=9), risedronate had no significant effect on mineral crystallinity of trabecular bone. Crystallinity before (C_b) and after (C_a) treatment was 0.993±0.104 and 0.924±0.060, respectively (mean ± standard deviation). In one subject however, crystallinity was significantly lower (P<0.01) after treatment (C_b=1.060±0.011 and C_a=0.897±0.015). There was no significant effect in the other 8 subjects. This lack of an increase in mineral crystallinity coupled with increased BMD and preservation of microarchitecture suggests that risedronate suppresses osteoclasts but not osteoblasts. These results contrast to the previously reported increase in mineral crystallinity seen with another bisphosphonate (ibandronate) and with hormonal replacement therapy, and suggest a unique mechanism of action for risedronate.

SU338

Risedronate Treatment of Established Primary and Secondary Osteoporosis in Men: 1-Year Results of a 3-Year Prospective Study. J. D. Ringe, A. Dorst*, H. Faber*, K. Ibach*, J. Preuss*. Medizinische Klinik IV, Klinikum Leverkusen, Akad. Lehrkrankenhaus der Univ. zu Köln, Leverkusen, Germany.

Although osteoporosis is more common in women, approximately one fourth of all hip fractures occur in men. The age-adjusted prevalence of vertebral deformities appears to be similar in men and women. Risedronate sodium has been shown to significantly increase bone mineral density and to reduce the risk of morphometric vertebral fractures in one year and the risk of clinical vertebral fractures after only 6 months of treatment in patients with postmenopausal osteoporosis. In the current study we examine the effects of risedronate on the mean change in lumbar spine, femoral neck and hip BMD in men with primary and secondary osteoporosis. Secondary endpoints include vertebral and non-vertebral fractures, pain, safety, and tolerability. This single center, open label, randomized prospective 3-yr clinical study with yearly examinations enrolled during the first year 102 male patients. They were randomized following their oral consent to receive either (group A) oral risedronate 5 mg daily (plus calcium 1000 mg and 800 IU Vit. D daily; n=51) or (group B) alfacalcidol 1 μg daily (plus calcium 500 mg daily; n=26) or (group C) calcium 1000 mg daily plus 800 IU vitamin D daily (n=25). In group A 19 of 51 patients and in group B+C 19 of 51 patients had secondary OP. In group A 26 of 51 patients and in group B+C 26 of 51 patients had a prevalent vertebral deformity. The patients are seen at baseline and at 12, 24 and 36 months. Bone mineral density (BMD), safety, and tolerability were compared. Spine x-rays are obtained at baseline and yearly thereafter. Men receiving risedronate showed a significant lumbar spine BMD increase of 4.2% compared with a increase of 0.7% in Group B+C patients (p<.0001). The change of total hip BMD was +2.32% in men treated with risedronate and –0.04% in group B+C after 1 year (p<.0001). The corresponding changes in femoral neck BMD were + 1.52% and –0.02% (p=0.0011). Both therapies were well tolerated. A significant reduction of back pain after one year was observed in patients receiving risedronate as compared to group B+C. After 1 year risedronate produced favorable effects on BMD consistent with the results from phase III trials in postmenopausal osteoporosis. The average increase rates were significantly higher than with alfacalcidol or plain vitamin D showing that risedronate is superior in the treatment of men with established primary or secondary osteoporosis. Year 2 and 3 investigations to determine positive long-term Risedronate effects in men with osteoporosis are currently performed.

SU339

Three Year Treatment Results with Alendronate vs. Alfacalcidol in Established Primary Osteoporosis in Men. J. D. Ringe[1], K. Dauhrer*[2], A. Dorst*[1], H. Faber*[1]. [1]Medizin Klinik IV, Leverkusen, Germany, [2]Merck, Sharp & Dohme, Munich, Germany.

Osteoporosis in men is an underdiagnosed and undertreated problem worldwide. Alendronate is the first bisphosphonate studied extensively in men. Our trial was a 3-year prospective, randomized, open-label, active-controlled, randomized clinical study comparing the effects of oral alendronate (ALN), 10 mg daily, and alfacalcidol (1α -D), 1 μ g daily, on bone mineral density (BMD), fracture events, height, back pain, safety and tolerability in 134 males with primary established osteoporosis. All men received 500 mg calcium daily. BMD was measured at the lumbar spine and femoral neck using dual-energy x-ray absorbtiometry (DXA). Spine x-rays were obtained at baseline and every 12 months thereafter, and were evaluated by a radiologist blinded to treatment assignment. At 3 years 1α -D-treated patients showed a significant mean 3.5% increase in lumbar spine BMD, compared with a mean increase of 11.5% in men receiving alendronate ($P < 0.0001$ between groups). The corresponding increases in femoral neck BMD were 2.3% and 5.8% for the alfacalcidol and alendronate groups, respectively ($P = 0.0015$ between groups). Over 3 years, new vertebral fractures occurred in 24.2% and 10.3% of the 1α -D and ALN patients, respectively ($P = 0.040$). ALN-treated patients also had a significantly lower height loss. There were no between-group differences in non-vertebral fractures or changes in back pain. Both therapies were well tolerated, with a compliance rate > 90 %. We conclude that although 1α -D has significant effects on BMD, ALN has greater effects on BMD and fracture efficacy.

Disclosures: ***J.D. Ringe****, J.D. Ringe 2.*

SU340

One Year Treatment With Risedronate Preserves Trabecular Architecture. T. E. Dufresne*[1], P. E. Chmielewski*[1], B. Borah*[1], M. C. Prenger*[2]. [1]Procter & Gamble Pharmaceuticals, Mason, OH, USA, [2]Procter & Gamble Pharmaceuticlas, Mason, OH, USA.

Risedronate has been shown to reduce vertebral and nonvertebral fractures, including hip fractures in osteoporotic postmenopausal women. Morphometric vertebral fractures are reduced by up to 65% in just 1 year in postmenopausal osteoporotic women. Increases in BMD explain these changes only partially. Other factors such as bone turnover and bone architecture play an important role in the anti-fracture efficacy seen with antiresorptives. The objective of the present study was to determine the effect of risedronate treatment on trabecular architecture in postmenopausal women. Paired iliac crest biopsies (baseline and 1 year) from early postmenopausal women were analyzed using three dimensional microcomputed tomography (3D μCT). Women 6-60 months postmenopause were enrolled in a double blind, placebo-controlled study. The primary end point of this previous study was change in LS BMD at 1 year with risedronate treatment. The mean percentage change from baseline in LS BMD at 1 year was 1.4% in the risedronate group and -2.9% in the placebo group. Trabecular architecture degraded significantly in the placebo group (n=12 pairs) as evidenced by a 20% decrease in bone volume, a 13% decrease in direct trabecular number and an 86% increase in marrow star volume compared to baseline values. In the risedronate treated group (n=14 pairs), no significant changes were evident in any of these parameters from baseline. Compared to the risedronate group, the placebo group experienced decreases in BV/TV (p=0.032), trabecular thickness (p=0.061) and trabecular number (p=0.030) and increases in trabecular separation (p=0.019) and marrow star volume (p=0.016). In conclusion, risedronate preserves trabecular bone architecture in postmenopausal women in 1 year. This may contribute to the rapid fracture efficacy seen with risedronate.

SU341

Mineral Binding Affinities and Zeta Potentials of Bisphosphonates. G. H. Nancollas*[1], R. Tang*[1], S. Gulde*[1], F. H. Ebetino[2], R. J. Phipps[2], R. G. G. Russell[3]. [1]SUNY, Buffalo, NY, USA, [2]Procter & Gamble Pharmaceuticals, Mason, OH, USA, [3]University of Oxford, Oxford, United Kingdom.

Different interactions with bone may contribute to differences in pharmacokinetic behavior and in persistence of effect of individual bisphosphonates (BPs). We have previously shown that risedronate has lower kinetic binding affinity for bone mineral (hydroxyapatite or HAP, and octacalcium phosphate or OCP) than does alendronate. The purpose of the present study was to extend these observations to other bisphosphonates, and also to determine bisphosphonate effects on mineral surface phenomena such as zeta potential. BP effects on HAP and OCP crystal growth and dissolution were studied with the constant composition method at ionic strength 0.15 M, 37ºC. Adsorption affinity constants (K_L) were calculated from the kinetic results. Under conditions likely to simulate rate and extent of BP binding onto bone there were significant differences in K_L among the various BPs for HAP growth (pH 7.4, σ = 7) and OCP growth (pH 6.2) with rank order of Zol > Aln > Iban > Ris > Etid > Clod. Affinities were similar for mineral dissolution under conditions likely to prevail during osteoclastic resorption (HAP at pH 4.5 and OCP at pH 6.0). Effects of the various BPs on HAP and OCP growth and on zeta potentials are given below. Zeta potential, the electrical potential near the crystal surface, is a sensitive indicator of the adsorption of bisphosphonates onto the calcium phosphate. These data show that the crystal surface is modified by the adsorption of bisphosphonates with different molecular charges directly related to the proton dissociation of their functional groups. Differences in kinetic binding affinities may contribute to the apparent shorter terminal (bone) half life of risedronate, and to faster clinical off-responses seen with risedronate compared to alendronate and zoledronate.

			HAP Zeta Potential	
BP	K_L HAP Growth (L/mol)	K_L OCP Growth (L/mol)	pH 7.4	pH 5.0
Clodronate	7.20×10^5	2.08×10^6	--	--
Etidronate	1.19×10^6	4.0×10^6	--	+
Risedronate	2.19×10^6	5.3×10^6	--	+
Ibandronate	2.36×10^6	7.69×10^6	++	++
Alendronate	2.94×10^6	8.0×10^6	++	++
Zoledronate	3.47×10^6	1.47×10^7	+	++

SU342

Suppression of Bone Resorption was Restored within Two Months after Quarterly Intravenous Bolus Infusion of Ibandronate in Japanese Osteopenic Women without Vitamin D and Calcium Supplementation. A. Itabashi[1], K. Nemoto[1], M. Tsuboi*[2], N. Nakamichi*[2], H. Orimo[3]. [1]Clinical Laboratory Medicine, Saitama Medical School, Saitama, Japan, [2]NS Clinic, Tokyo, Japan, [3]Tokyo Metropolitan Geriatric Hospital, Tokyo, Japan.

Lowered bioavailability due to food interaction and upper gastrointestinal problems of orally administered bisphosphonates led us to evaluate the efficacy of three monthly intravenous ibandronate injection therapy in postmenopausal osteopenic women. We conducted a phase I placebo-controlled dose-ranging study of intravenous ibandronate in Japan. Fifty otherwise healthy postmenopausal women, aged 60 to 75, with lumbar (L2-L4) BMD between -2.5SD and -1.5SD T-score were enrolled after written informed consent. They were randomly assigned to placebo, ibandronate (BM21.0955) 0.25, 0.5, 1, and 2 mg group (10 subjects for each) and the drug was administered intravenously as a bolus injection (2ml, 30 seconds). The injection was repeated after 13 weeks. No calcium nor vitamin D supplementation were given during the study period. Bone resorption markers (urinary DPD, CTx, NTx) rapidly decreased until 8 days, in a dose-dependent manner, then gradually recovered, returning to the baseline level at 2 months. The second administration showed exactly the same pattern. Osteocalcin and bone specific alkaline phosphatase did not change during the whole period (6 months). No significant gain of lumbar BMD was observed at 6 months. The treatment was well tolerated and no safety concerns were identified. These data suggest that more frequent dosing or higher doses may be necessary to attain an optimal magnitude in efficacy.

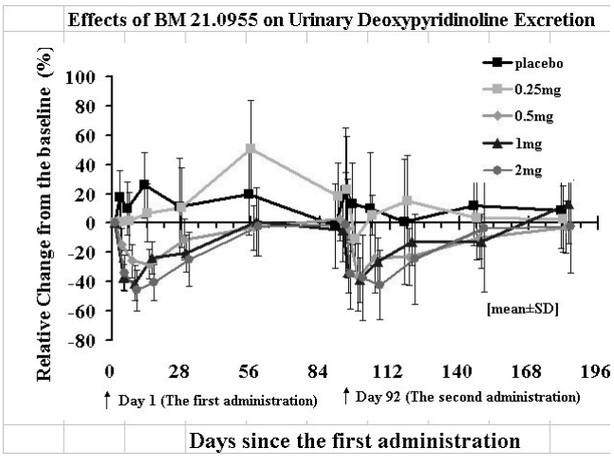

Disclosures: ***A. Itabashi****, Chugai Pharmaceutical Company 5.*

SU343

The Impact of Dropouts on the Efficacy of 5 mg Risedronate: An Assessment Based on an Imputation Analysis. J. D. Adachi[1], K. G. Siminoski[2], G. Cline*[3], J. P. Brown[4], A. B. Cranney[5], D. Goltzman[6], D. A. Hanley[7], A. B. Hodsman[8], R. G. Josse[9], D. L. Kendler[10], L. Ste-Marie[11], W. P. Olszynski[12], A. Tenenhouse[6], Z. Li*[3]. [1]McMaster University, Hamilton, ON, Canada, [2]University of Alberta, Alberta, AB, Canada, [3]Procter & Gamble Pharmaceuticals, Mason, OH, USA, [4]Laval University, Ste-Foy, PQ, Canada, [5]University of Ottawa, Ottawa, ON, Canada, [6]McGill University, Montreal, PQ, Canada, [7]University of Calgary, Calgary, AB, Canada, [8]Western University, London, ON, Canada, [9]Toronto University, Toronto, ON, Canada, [10]University of British Columbia, Vancouver, BC, Canada, [11]University of Montreal, Montreal, PQ, Canada, [12]University of Saskatchewan, Saskatoon, SK, Canada.

Risedronate 5 mg treatment has been demonstrated to reduce the risk of vertebral fractures by 61-65% within 1 year and by 41-49% within 3 years in two large placebo-controlled studies. In these two studies, the pre-specified statistical methods with time-to-event analysis for fracture data were able to include 85% of the maximum person-years. Therefore, about 15% of the person-years were missing due to dropouts. In this analysis, we attempted to assess the impact of dropouts on the efficacy of 5 mg risedronate. Namely, had these dropouts completed the study, what treatment efficacy would have been observed? A logistic regression model was used to determine the important risk factors for dropouts. We used multiple imputation analyses for each treatment group (placebo and risedronate 5.0 mg) with adjustment for important prognostic factors at baseline such as number of prevalent vertebral fractures, baseline BMD values and years since menopause. The treatment effect in fracture risk reduction was estimated based on the Cox's regression model.

	VERT-NA Risk Reduction (95% CI)		VERT-MN Risk Reduction (95% CI)	
	Original	Imputation	Original	Imputation
Yr 0-1	65% (38%, 81%)	68% (46%, 82%)	61% (32%, 78%)	63% (34%, 79%)
Yr 0-3	41% (18%, 57%)	46% (25%, 61%)	49% (27%, 64%)	52% (33%, 66%)

Our analysis indicated that the subjects with severe osteoporosis in the placebo group were more likely to drop out from the study than those subjects in the risedronate 5 mg group. Our imputation analysis suggested that estimates of fracture risk reduction were very robust to the dropouts. A numerically higher fracture risk reduction might have been observed had all subjects completed the three-year study. Therefore, if there was a bias that might have been introduced in the estimates of the anti-fracture efficacy due to dropouts, the bias was unlikely to be in favor of risedronate.

Disclosures: ***J.D. Adachi****, Procter & Gamble Pharmaceuticals 2, 5.*

SU344

Treatment with Alendronate 70-mg Once Weekly† for 3 Months Decreases Biochemical Markers of Bone Turnover in Men with Osteoporosis. P. Miller[1], E. Orwoll[2], M. Czachur*[3], B. MacIntyre*[3], A. Leung[3]. [1]Colorado Center for Bone Research, Lakewood, CO, USA, [2]Oregon Health Sciences University, Portland, OR, USA, [3]Merck Research Laboratories, Rahway, NJ, USA.

This is a 3-month interim analysis of a 12-month, double-blind, randomized, multicenter, placebo (PBO)-controlled study to assess the efficacy of alendronate (ALN) 70-mg once weekly (OW) for the treatment of osteoporosis (OP) in men. The study randomized 167 men, aged 38 to 91 (mean 66.1) years, with idiopathic or hypogonadal OP (defined as lumbar spine or femoral neck [FN] BMD ≥ 2 SD below the normal mean or FN BMD ≥ 1 SD with a prior OP fracture). Fifty-eight received placebo, and 109 received ALN 70-mg OW. All patients received supplementation with open-label calcium (approximately 1000 mg) and vitamin D (approximately 400 IU) daily. No clinically meaningful differences were observed between the treatment groups for any of the baseline characteristics including age, race, weight, height, body mass index, gonadal status, bone-specific alkaline phosphatase (BSAP) or urinary N-telopeptides of type I collagen (NTx). Mean baseline BSAP was 13.6 ng/ml and urinary NTx was 32.8 pmol BCE/µmol creatinine. As shown below, treatment with ALN 70-mg OW for 3 months, significantly decreased urinary NTx and serum BSAP relative to PBO and baseline.

Bone Resorption Marker (urinary NTx) and Bone Formation Marker (serum BSAP) at Month 3

Treatment	N	BL	Mo 3	Percent Change from Baseline ††
Urinary NTx				
Placebo OW	53	33.70	34.66	4.3 (-5.9, 15.6)
ALN 70mg† OW	103	32.23	19.20	-41.4 *** (-46.1, -36.4)
Serum BSAP				
Placebo OW	53	13.21	12.21	-7.4*** (-11.1, -3.6)
ALN 70mg† OW	104	13.71	10.34	-23.5*** (-26.7, -20.1)

†† Transformed from Ln(fraction of baseline).

Within treatment test of mean = 0; ***:$p \leq 0.001$ versus baseline.

Between-treatment group comparison was significant for both NTx and BSAP ($p \leq 0.001$).

These results are consistent with those observed in a previous study of daily ALN 10-mg in 241 men with OP. The results of the primary efficacy analysis of the percent change from baseline in lumbar spine BMD after 12 months of treatment with ALN 70- mg OW will be available upon completion of the trial.

† Manufactured by Merck & Co., Inc., Whitehouse Station, New Jersey

Disclosures: ***A. Leung****, Merck & Co., Inc. 1, 3.*

SU345

Once Weekly Alendronate Produces a Greater Decrease in Bone Resorption Than Does Daily Risedronate. D. Hosking[1], S. Adami[2], D. Felsenberg[3], J. Reginster[4], J. Cannata[5], M. Valimaki*[6], A. Santora[7], S. Suryawanshi*[7]. [1]Nottingham City Hospital, Nottingham, United Kingdom, [2]Ospedale Valeggio, Verona, Italy, [3]University Hospital, Berlin, Germany, [4]Chu de Liege, Liege, Belgium, [5]Hospital Central de Asturias, Asturias, Spain, [6]Helsinki University Central Hospital, Helsinki, Finland, [7]Merck Research Labs, Rahway, NJ, USA.

We report the results of the first head-to-head trial designed to compare the efficacy of alendronate and risedronate for the treatment of osteoporosis. The 3-month, randomized, double-blind, multicenter international study with double-blind extensions for an additional 9 months (12 months in total), enrolled 558 postmenopausal women. Patients were 60-90 years old (mean, 69), with osteoporosis defined by low BMD T-score (either lumbar spine or total hip/femoral neck ≤ -2.5, or ≤ -2.0 at both sites). The primary endpoint was 3-month change in urinary N-telopeptides of type 1 collagen / creatinine (NTx), a marker of bone resorption. Bone specific alkaline phosphatase, BMD (spine and hip), and safety evaluations will be completed after 12 months. Patients maintained a calcium intake of at least 1000 mg daily through food and/or calcium supplements. Patients were randomized into three treatment groups: alendronate 70mg* once weekly using standard am dosing; risedronate 5mg daily dosed 2 hours after a meal and at least 2 hr before the next; or matching placebo for each. Results are based on an intention-to-treat analysis of urinary NTx at Month 3.

Percent Change in Bone Resorption from Baseline at Month 3

	Placebo N= 105		Alendronate N=202		Risedronate N=210	
	Mean	Mean ±SE	Mean	Mean ±SE	Mean	Mean ±SE
Urinary NTx	-10.0*	(-13.8, -6.0)	-55.0***	(-56.7,-53.3)	-35.6***	(-37.7,-33.4)

*** p < 0.001; * p ≤ 0.05; Within-group test of mean percent change=0.
Tests for between treatment comparison of Alendronate Vs Risedronate, Alendronate Vs Placebo, and Risedronate Vs Placebo had p-values <0.001.

In this study, alendronate produced a 50% greater reduction in bone resorption than did risedronate. This difference may be due to the superior anti-resorptive efficacy of alendronate 70 mg once weekly, reduced bioavailability of risedronate resulting from post-meal dosing, or both.
*Manufactured by Merck & Co., Inc., Whitehouse Station, NJ

Disclosures: ***D. Hosking****, Merck & Co., Inc. Rahway, NJ 07065 2.*

SU346

Effect of Etidronate on Three-Dimensional Trabecular Structure of Ovariectomized or Immobilized Rats. A. Nishida[1], M. Ito[1], K. Hayashi*[1], T. Nakayama*[2], T. Tanaka*[2]. [1]Radiology, Nagasaki University, Nagasaki, Japan, [2]Sumitomo Pharmaceuticals Reserch Division, Osaka, Japan.

Etidronate (EHDP) has been reported to prevent bone loss caused by ovariectomy (OVX) or sciatic neurectomy (NX) in rats. The purpose of this study was to determine whether EHDP could prevent the deterioration of three dimensional trabecular structure caused by OVX or NX in rats. Eight-week-old female Lewis rats were subjected to OVX or NX or respective sham operation. They were divided into 6 groups with 10 animals in each group; OVX, its sham operation (sham-OVX), OVX+ EHDP treatment (OVX+E), NX, its sham operation (sham-NX), and NX+ EHDP treatment (NX+E). EHDP at 5 mg/kg or vehicle were injected subcutaneously five days a week from 2 weeks after surgery for 2 weeks. The proximal metaphysis of the tibia was scanned using micro-CT (μCT20, SCANCO Medical, Switzerland) craniocaudally for 150 slices with 13 micron-slice thickness. The region of interest of 50 slices under the growth plate-metaphyseal junction was defined as proximal portion, and 50 slices distal to the proximal portion was defined as distal portion. The proximal and distal portions were analyzed separately. Structural parameters such as bone volume fraction (BV/TV), trabecular number (Tb.N), trabecular thickness (Tb.Th), trabecular separation (Tb.Sp), trabecular bone pattern factor (TBPf), structure model index (SMI), and degree of anisotropy (DA) were assessed. The structural parameters changed in both OVX and NX compared with their respective sham groups. In proximal portion, there was no significant difference in BV/TV between EHDP treated groups and their respective sham groups, which indicates that EHDP prevented bone loss induced by both OVX and NX up to sham level. The greater effect of EHDP on trabecular structure appeared in OVX than in NX; structural parameters of OVX+E improved beyond the OVX-sham level such as SMI (p=0.0031) and TBPf (p=0.0079), while those of NX+E did not improve up to the NX-sham level, such as Tb.N (p=0.0274), Tb.Sp (p=0.0116), and SMI (p=0.0359). The DA significantly increased by OVX, while it decreased by NX. After the treatment with EHDP, DA decreased in both OVX and NX rats. In distal portion, all parameters of OVX+E and NX+E did not improve up to their respective sham groups. In conclusion, EHDP could prevent deterioration of trabecular structure caused by OVX and NX, however the effect of EHDP in NX rats was less than that in OVX rats. These results suggest that the external loading contribute to prevent deterioration of three-dimensional trabecular structure in the treatment with EHDP.

SU347

Effect of Minodronate (ONO-5920) in Adult Rats with Collagen-induced Arthritis. I. Yamane*, D. Yamasaki*, M. Enokida*, T. Okano, H. Hagino, R. Teshima*. Department of Orthopedic Surgery, Faculty of Medicine, Tottori University, Yonago, Japan.

[Purpose] Minodronate (ONO-5920), which contains an imidazol ring, is a newly synthesized third-generation bisphosphonate, and is said to have the most potent inhibitory activity against bone resorption. We investigated the effects of minodronate (ONO-5920), on bone mineral density (BMD), bone microstructure and bone metabolism in adult collagen-induced arthritis (CIA) rats using two different treatment schedules. [Methods] Seven-month-old female Sprague-Dawley rats were grouped into 4 groups: (1)control group (Cont); (2)CIA group (CIA+Veh); (3)CIA + therapeutic treatment group (CIA+The); (4)CIA + prophylactic treatment group (CIA+Pro). In therapeutic treatment, minodronate was orally administered from 2 weeks after sensitization. In prophylactic treatment, this agent was similarly administered from immediately after sensitization. Every 2 weeks until 8 weeks after sensitization, BMD in the proximal metaphysis of the tibia was measured using peripheral quantitative computed tomography (pQCT, XCT-960). After killing, serum osteocalcin (OC) and tartrate-resistant acid phosphatase (TRAP) were measured, and histomorphometric analysis was carried out in the secondary spongiosa of the proximal tibia. [Results] In CIA+Veh, cancellous BMD in the proximal metaphysis of the tibia was significantly decreased compared with that in Cont group. But bone loss in the proximal metaphysis of the tibia in CIA+Pro was inhibited during the experiment. In CIA+Veh, BV/TV and Tb.Th values were significantly lower and ES/BS, N.Oc/BS and BFR/BV values were significantly higher than those in Cont. At any parameters, there were no significant differences between in Cont and CIA+Pro. The value of OC was significantly higher in CIA+Veh than in Cont . The value of TRAP showed no significant difference among four groups. [Discussion] It was considered that minodronate potently inhibited increased osteoclast numbers and bone resorption with accelerated bone turnover related to arthritis, and was effective for inhibiting bone loss and maintaining microstructure of cancellous bone. [Conclusions] It was concluded that minodronate treatment prevented inflammation-induced secondary bone loss and deterioration of bone microstructure by reducing bone turnover related to arthritis to the normal level. In particular, prophylactic treatment was more useful than therapeutic treatment.

SU348

Osteogenesis Imperfecta: Continuous Increment of Bone Mass with Two Years of Cyclical Intravenous Pamidronate following Oral Therapy. C. Tau[1], C. Mautalen[2], O. Brunetto*[3], V. Alvarez*[1], M. Farenga*[1], M. Rubinstein*[4]. [1]Metabolismo Cálcico y Oseo, Endocrinología, Hospital de Pediatría Garrahan, Buenos Aires, Argentina, [2]Centro de Osteopatias, Buenos Aires, Argentina, [3]Endocrinologia, Hospital Pedro Elizalde, Buenos Aires, Argentina, [4]Laboratorio Central, Hospital de Pediatría Garrahan, Buenos Aires, Argentina.

Osteogenesis imperfecta (OI) is an hereditary disease characterized by bone fragility, frequent fractures and progressive skeletal deformities. Bisphosphonate administration improves the quality of life and decreases fractures in children with OI. The aim of this study was to analize the effect of 2 years of cyclical intravenous pamidronate (IV-APD) in 11 children (4F,7M) with OI type I, n=3; OI type III, n=3 and OI type IV, n=5, age (X ±SEM): 7.2±1.4 (range 1.6 to 19.7 y.o.). Every child received IV-APD (provided kindly by Gador Pharmaceutical)at 3-4 months intervals for 2 years, in cycles of 3 consecutive days, (dose 6.5±0.7 mg/kg/year (range 4.8-11.8) the 1st year and 6.8±0.8 (range 2.5-13.1) the 2nd year).Patients also received calcium 0.5 to 1 gr and vitamin D 400-800 IU/day. Prior to intravenous therapy, these patients have received 1 year of oral pamidronate (O-APD). Spine bone mineral density (BMD) was measured by DEXA. Knees X-rays were taken every 6 months. Average basal Height Z-Score (range 0.93 to -5.87) increased, but not significantly: -3.24±0.65 vs -2.85±0.74 the 1st year of IV-APD, and -2.95±0.76 the 2nd year. Basal BMD (0.35±0.04) increased significantly after 1 and 2 years of treatment (0.45±0.03, p<0.02, and 0.51±0.04 gr/cm2, p<0.005, respectively) and Z-Score BMD increased from -3.9±0.2 to -2.5±0.3 and -2.1±0.3, p<0.005, after one and 2 year of treatment respectively. There was an average annual BMD increase of 33±3% (range 1 to 82%) after the 1st and, 12±2% after the 2nd year of therapy. The patients had an annual BMD increase of 27±6% during previous oral therapy. Fractures, between 0.9 to 8/ year before therapy (3.1±0.6), decreased sharply with O-APD (1.4±0.4/year, p<0.02) and continued to diminish with IV-APD (1.2±0.3/year, 1st year, and 0.7±0.2, 2nd year, p<0.0005). As in normals, Z-Score BMD was positively correlated with height after 1 and 2 year of therapy (r: 0.68, p<0.02 and 0.73, p<0.01,respectively. X-rays showed dense lines under growth plates in most patients. Conclusion: Two years of intravenous cyclical pamidronate improved bone mass in children with Osteogenesis Imperfecta with a diminution of the number of fractures and better quality of life. Bone mass had a continuous increment even in patients who had previously augmented the BMD after oral APD.

SU349

Bisphosphonates Enhance Cancellous Bone's Mechanical Properties through Improvement of Three-dimensional Microarchitecture. M. Ding*[1], J. S. Day*[2], D. B. Burr[3], T. Mashiba*[3], T. Hirano*[3], H. Weinans[2], D. R. Sumner[4], I. Hvid*[1]. [1]Orthopaedic Research Lab, Aarhus University Hospital, Aarhus C, Denmark, [2]Orthopaedic Research Lab, Erasmus University Rotterdam, Rotterdam, Netherlands, [3]Departments of Anatomy and Cell Biology, Indiana University School of Medicine, Indianapolis, IN, USA, [4]Departments of Anatomy and Orthopaedics, Rush Medical College, Chicago, IL, USA.

The aim of this study was to investigate the effects of one-year high dose (5-6 times the clinical dose) risedronate (0.5mg/kg/day) or alendronate (1.0mg/kg/day) on the three-dimensional (3-D) microarchitectural and mechanical properties of canine cancellous bone. We hypothesized that the administration of high dose bisphosphonates might significantly change vertebral cancellous bone microarchitecture in addition to increasing bone density and mechanical properties. A high-resolution micro-CT scanner was used to scan cubic specimens (5*5*5 mm3) produced from canine first lumbar vertebrae. Microarchitectural properties of the specimens were calculated directly from the 3-D datasets and the mechanical properties of the specimens were determined. Our data demonstrate significant changes in the cancellous bone microarchitecture after bisphosphonate treatment. The bisphosphonate-treated cancellous bone was typically plate-like, denser, with thicker and more trabeculae compared to those of the controls. Consistent with architectural changes, the Young's moduli of cancellous bone were greater in all three directions with the greatest in medial-lateral direction after bisphosphonate treatment. Our results suggest a bone remodelling-adaptation mechanism stimulated by bisphosphonates that maintains bone volume fraction and trabecular thickness, thus changes trabeculae towards more plate-like, and enhances mechanical properties. The secondary degree of anisotropy contributed significantly to the explained variance in bone strength, and the primary degree of anisotropy improved the explanation of variance for Young's modulus, i.e. 79-83% of strength variances or 83-91% of modulus variances could be explained by the combined anisotropy and bone volume fraction. These significant improvements of cancellous bone architecture provide a rationale for the clinical observation that fracture risk decreased by 50% in the first year of bisphosphonate therapy with only a 5% increase in bone mineral density. We conclude that bisphosphonates enhance mechanical properties and reduce fracture risk through improvement of architectural anisotropy of cancellous bone 3-D microarchitecture.

SU350

The Minipig Is a Good Model for Glucocorticoid-Induced Bone Loss and Shows Efficacy of Ibandronate Treatment for This Disorder. C. C. Glüer[1], K. E. Scholz-Ahrens*[2], W. Timm*[1], R. Barkmann[1], G. Delling*[3], F. Bauss*[4], J. Schrezenmeir*[2]. [1]Medical Physics, Dept. Diagn. Radiol., University Hospital Kiel, Kiel, Germany, [2]Institute of Physiology und Biochemistry of Nutrition, FDRC, Kiel, Germany, [3]Bone Pathology, University Hospital Eppendorf, Hamburg, Germany, [4]Roche Diagnostics GmbH Penzberg and Inst. of Pharmacol and Toxicol Heidelberg University, Mannheim, Germany.

Few large animal models for glucocorticoid (GC) induced osteoporosis have been established. We investigated whether the G÷ttingen Minipig shows trabecular bone loss under glucocorticoid treatment and whether such loss can be recovered by treatment with a bisphosphonate. As part of a larger study, 30 primiparous sows were allocated to 3 experimental groups when they were 15 months old: control group (CTR, n=10), GC treatment for 15 months (GC, n=9), and GC treatment for 15 month plus ibandronate (IBN) treatment for months 8-15 (GC+IBN, n=11). Animals were fed a semisynthetic diet until they were sacrificed. Groups GC and GC+IBN received prednisolon at a daily dose of 1mg/kg body weight for 8 weeks and thereafter 0.5 mg/kg body weight. IBN was administered subcutaneously and intermittently with an integral dose of 2.2mg/kg body weight spread over 22 weeks. Bone mineral density (BMD) of the lumbar spine was assessed in vivo by Quantitative Computed Tomography (QCT) before treatment, after 7 months and after 15 months in 23 animals. Data were analyzed by paired and unpaired t-tests and are given as %mean ± %SEM. BMD was stable in the control group (n=9) both during month 1-7 (-2.5%±2.5%, n.s.) and month 7-15 (-0.5%±1.2%, n.s.), while decreasing in the GC group (n=6) by -13.6%±1.9% (p<0.0005) in the first 7 months and increasing by 2.1%±1.2% (n.s.) in the remaining 8 months. In the IBN-treated group (n=8), the bone loss in the first 7 treatment-free months of -10.9%±1.8% (p<0.0001) was more than recovered by month 15 (+14.8%±1.2%, p<0.0001). During the 8 month treatment period, BMD changes in group GC+IBN were significantly larger by +12.6% (p<0.0001) and +12.7% (p<0.0001) compared to the 8-month changes in the GC group and the CTR group, respectively. Our results demonstrate that minipigs suffer from bone loss induced by GC and that this loss can be more than recovered by 8 month treatment with ibandronate. GC induced bone loss in minipigs can be efficiently monitored in vivo by QCT.

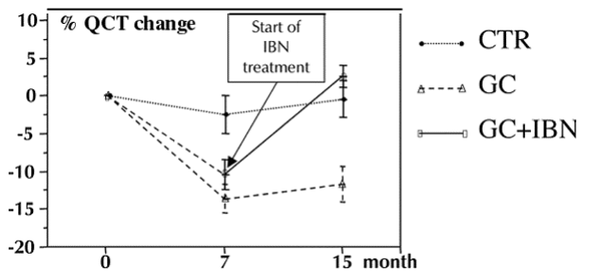

SU351

Not All Calcium Carbonate Supplements Are Equally Absorbable. R. P. Heaney, M. J. Barger-Lux. Creighton University, Omaha, NE, USA.

In the US, calcium supplements are regulated as foods and demonstration of bioequivalency is not required. There seems to be a general presumption of equivalent absorbability across different commercial products using the same calcium salt. This report presents an analysis of data from eight studies that examined the absorbability of calcium carbonate. Each study measured bioavailability of the calcium in a different pharmaceutical formulation of calcium carbonate. The absorbability of each product was compared to plain calcium carbonate that had been prepared without added pharmaceutical ingredients or formulation. The main outcome measures were fractional calcium absorption for products that were intrinsically labeled with a calcium isotope and absorptive calcemia (i.e., area under curve) for marketed products that could not be labeled intrinsically. Subjects were healthy women and men aged 20 to 66 who denied conditions or drugs known or suspected to affect absorptive function. The results showed that two of eight calcium carbonate supplements, one a swallowable and one a chewable tablet, exhibited absorbability comparable to that of plain calcium carbonate. The other six were substantially less bioavailable. The worst performer provided less than half of the calcium predicted for its load size. No product exhibited absorbability superior to plain calcium carbonate. We conclude that pharmaceutical formulation of calcium carbonate supplements has an appreciable effect on absorbability of their calcium. Clinical trials and individual treatment regimens using poorly available calcium sources will produce suboptimal benefits. The industry needs to study this issue and produce products with demonstrated bioequivalency.

*Disclosures: **R.P. Heaney**, Glaxo Smith Kline 2, 5; Dairy Management Inc. 8; International Dairy Foods Assn. 5; General Mills Inc. 2, 5.*

SU352

Isolated Soy Isoflavones Prevent Bone Loss in the Hip in Postmenopausal Women. A. Vincent*[1], L. A. Fitzpatrick[2]. [1]Internal Medicine, Mayo Clinic, Rochester, MN, USA, [2]Endocrine Research Unit, Mayo Clinic, Rochester, MN, USA.

Soy isoflavones have estrogen-like effects on target tissues. Clinical trials that examined the effect of isoflavones on bone density are limited by relatively short duration which is insufficient to detect changes in bone mineral density (BMD).This study investigated the effect of isolated soy isoflavone supplements on bone markers and BMD of the spine and hip. 70 healthy postmenopausal women (mean age 58.3 yr) were randomly assigned to placebo or 2 isolated soy isoflavone tablets containing 110 mg isoflavones for a period of 12 months. The products are commercially available as "Healthy Woman Soy Menopause" a proprietary, standardized tablet made from highly concentrated soy isoflavones and containing 320 mg of soy extract and 55 mg of isoflavone per tablet. Subjects were on an isoflavone poor diet for the entire study period.Groups were matched for age, height, weight and BMI at baseline. Bone markers were measured at baseline, 3 and 6 months. BMD was performed at baseline, 6 and 12 months. We report the results of bone markers in 70 subjects who completed the 6-month time point and BMD in 37 study subjects who completed the 12-month time point. The results were analyzed using the Wilcoxin rank sum test. Between groups, no differences were detected in median changes of serum NTx (p=0.3), Urine NTx (p=0.9), pyridinoline (p=0.12), deoxypyridinoline (p=0.24), bone alkaline phosphatase (p=0.6) or osteocalcin (p=0.4). Compared to placebo, subjects in the soy isoflavone group had smaller losses in hip BMD both at six months (p=0.024) and 12 months (p=0.01). Similarly, smaller non-significant losses of spine BMD were seen in the isoflavone group compared to placebo at 12 months. Serum estradiol and bioavailable estradiol increased in both groups from baseline to six months but the differences were not statistically significant. This is the first reported prospective randomized placebo-controlled trial to see changes in BMD from isolated isoflavones. Women in the isoflavone group had smaller decreases in bone density at the hip when compared to placebo at 6 and 12 months. Though a smaller decrease in bone density was also observed at the spine at 12 months in the isoflavone treated group differences were not statistically significant. This study suggests that isoflavones may preferentially effect cortical bone over cancellous bone. In conclusion soy isoflavone supplementation had a beneficial effect on hip BMD compared to placebo.

*Disclosures: **L.A. Fitzpatrick**, Johnson and Johnson 2; NIH 2; Mayo Foundation 2, 3.*

SU353

Gelatine Hydrolysate Suppresses High Bone Turnover in Pre-menopausal Women. T. Koike[1], Y. Kajiwara*[2], E. Yamashita*[2], Y. Ito*[1], K. Inui[1]. [1]Orthopaedic Surgery, Osaka City University Medical School, Osaka, Japan, [2]Nitta Gelatin Inc., Yao, Japan.

Gelatine has numerous applications, including the pharmaceutical, food and photographic industries. We have developed gelatine-hydrolysates, including the fermented products digested with a pineapple extract to facilitate the function of gelatine. Recently, it has been reported that the ingestion of gelatine has beneficial effects on bone mineral density (BMD) in mice. However, the effects of gelatine hydrolysates on bone metabolism in human have not been studied. This prospective, randomized clinical trial examined the effects of oral gelatine hydrolysates on BMD, biochemical markers of bone turnover, safety, and tolerability in 42 pre-menopausal healthy women. Women before the menopause received either gelatine-hydrolysate 10 g/day (n = 15, 41.3±4.8 years), fermented gelatine-hydrolysates 10 g/day (n = 15, 41.5±4.5 years), or nothing (n=12, 38.8±5.2 years). Urine and serum samples were collected at baseline and at 1, 4, and 8 weeks of administration. To assess bone resorption, we measured the urinary deoxypyridinoline and N-terminal cross-linking telopeptide of type I collagen (NTX), while serum bone alkaline phosphatase and osteocalcin were analysed to assess bone formation. Quantitative ultrasound (QUS) measurement at the calcaneus (A-1000plusII, Lunar) was performed at baseline and at the end of the study. There was no significant difference in bone metabolic markers and QUS values between groups at baseline. All participants who received gelatine products could take a dose every day through the study period and did not show any kinds of adverse events. Generally markers of bone resorption and formation and QUS values did not change in any groups. There were 9 women who showed irregular menstrual cycle and higher urinary NTX (>40 nMBCE/mMCr). Among those higher bone turnover women, urinary NTX decreased significantly only in the fermented gelatine hydrolysates-treated group. These data suggested that short-term (8 weeks) oral gelatine treatment (10 g daily) was well tolerated and might be effective in decreasing higher bone turnover in pre-menopausal women. Longer-term treatment with larger clinical populations is indicated to define more fully the potential efficacy and safety of gelatine therapy.

SU354

Carotts Consumption Prevents Bone Loss in Ovariectomized Rats. C. PUEL*, J. Mathey*, M. Horcajada*, B. Chanteranne*, M. Davicco*, P. Lebecque*, J. Barlet*, V. Coxam. Groupe ostéoporose, INRA, Saint-Genès Champanelle, France.

With increasing life expectancy the implications of osteoporosis are huge and this disease is major public health problem. Diets rich in fruits and vegetables are protective against chronic, degenerative disease. This action could be attributed to the presence of antioxidants like vitamin C, E or β carotene which inhibit free radical production and bone resorption in laboratory studies. The present investigation was carried out to assess the effects of fresh carrots on bone metabolism in ovariectomized (OVX) rats. Thirty 3 month-old Wistar rats were investigated. Twenty were OVX, while the 10 remaining were sham-operated as controls (SH). All the animals were fed a control synthetic diet for 90 days. 15% carrots were added to the diet given to half of the OVX (OVXC). Ovariectomy elicited a marked atrophy of the uterine horns (g) (OVX : 0.25 ± 0.06 ; OVXC : 0.14 ± 0.02 vs 0.61 ± 0.08 in SH ; $p<0.05$). Castration also induced a significant decrease in both total (g/cm2) (OVX : 0.2392 ± 0.0027 vs 0.2536 ± 0.0059 in SH ; $p<0.05$) and metaphyseal femoral mineral density) (OVX : 0.2432 ± 0.0044 vs 0.2617 ± 0.0067 in SH ; $p<0.05$), which was prevented by carrots consumption (OVXC : 0.2534 ± 0.0025 and 0.2561 ± 0.0023, respectively). In the same way, a higher femoral diameter (cm) (OVXC : 3.79 ± 0.03 vs 3.58 ± 0.05 in OVX, $p<0.05$) was associated with a trend towards an improved femoral strength. Moreover, on day 90, urinary deoxypyridinoline (DPD, nmol/mmol creatinine) excretion (a marker for bone resorption) was higher in OVX (99.51 ± 13.05) rats than in OVXC (72.70 ± 8.49) or in SH rats (75.98 ± 4.77). These results indicate that carrots consumption, inhibits ovarectomy-induced trabecular bone loss in rats, by slowing down resorption activity and increasing femoral diameter.

Disclosures: ***C. Puel****, APRIFEL 2.*

SU355

Serum Gla-type Osteocalcin as a Marker for Prediction of Effectiveness of Menatetrenone, a Vitamin K Analog, in Treatment of Glucocorticoid-induced Osteoporosis. I. Tanaka[1], H. Oshima[2]. [1]Department of Biofunctional Research, National Institue for Longevity Sciences, Obu, Japan, [2]Department of Laboratory Medicine, Fujita Health University, Toyoake, Japan.

[Objective] We have shown the effectiveness of menatetrenone, which is an analog of vitamin K and a co-factor for calcium deposition at bone formation, in treatment of glucocorticoid-induced osteoporosis. In this study, we try to clarify clinical usefullness of bone makers in prediction of the effectiveness in glucocorticoid-induced osteoporosis. [Subjects & Methods] Fifty nine patients (47 females and 12 males) with collagen diseases under corticosteroid treatment were enrolled in this prospective study. Subjects were 59 collagen disease patients under corticosteroid treatment. The new incidence of the vertebral compression fracture at two years after the start of corticosteroid therapy was evaluated about the 37 patients among those. The mean of age, daily corticosteroid dosage(prednisolone equivalent), and total corticosteorid dosage were 46 years old, 20.3mg/day, and 6.3g, respectively. Serum Glu type and Gla type osteocalcin (GluOC and GlaOC), and deoxypyridinoline in the urine (DPD) were measured by the ELISA methods. Vertebral compression fractures were evaluated with X-ray photography. [Results] 1) New vertebral compression fracture were revealed in 16 out of 59 cases (27%). 2) Among new corticosteroid(an average dosage of 37mg) medicated patients who were not used anti-osteoporosis agents, GluOC values decreased after four weeks (an average of 54% of pre-value). On the other hand, there was no significant change in GlaOC and DPD values at four weeks after the start of corticosteroid treatment . The use of anti-osteoporosis agents, such as etidronate or active vitamine D3, did not influence the values of the bone markers. 3) A significant negative correlation was found between daily corticosteroid dosages and GluOC values ($p< 0.05$). 4) In the cases who have fractures at the time of bone marker measurements, GluOC and GlaOC values showed significantly higher values ($p< 0.03$, $p<0.03$) compared to those with no fractures. 5) In patients treated with menatetrenone (n=12), GlaOC demonstrated higher values (15.5+/-3.1ng/ml) in 3 cases who had new fractures in the following 2 years than in 9 cases (7.0+/-4.1) having no fracture in that priod ($p<0.03$). [Conclusion] It is suggested that serum GluOC levels decreased in dosage dependent manner after treatment with corticosteroids, and menatetrenone effectively prevented vertebral fractures in patients with low serum GlaOC values.

SU356

Effect of a Diet Low in Cation-Anion Balance on Bone Mineral Density and Skeletal Fragility in Lumbar Vertebrae of Mature Ewes. J. F. Millets*[1], J. M. MacLeay*[2], A. S. Turner*[2], D. L. Wheeler[1]. [1]Mechanical Engineering, Colorado State University, Fort Collins, CO, USA, [2]Clinical Sciences, Colorado State University, Fort Collins, CO, USA.

There is a great need to develop and utilize a practical large animal model to investigate the pathogenesis of osteoporosis and lead to the development of new therapies for this disease. The objective of this study was to determine if significant loss of bone mineral density (BMD) and concurrent increases in skeletal fragility could be induced using a diet low in dietary cation-anion balance (LDCAB) compared to a normal hay diet with a moderate cation-anion balance (MDCAB). Twenty-four adult female sheep were divided into four treatment groups (n=6): No Ovariectomy (Ovx) with MDCAB diet (Control), Ovx with MDCAB (Ovx), No Ovx with LDCAB diet (LDCAB) and Ovx with LDCAB diet (Ovx-LDCAB). The MDCAB diet provided 300Meq/kg dry matter (DM) and the LDCAB diet - 350Meq/kg DM. Dual-Energy X-ray Absorbtiometry (DEXA) scans of the L5 vertebral bodies were taken in vivo at 0-months and 6-months (prior to euthanasia). Axial compression tests were performed on the L3 and L5 vertebral bodies, prepared to have plano-parallel surfaces following removal of dorsal elements, processes and endplates. Specimens were loaded cranially at a displacement rate of 5mm/min to a strain of 20%. Maximum strength and modulus was calculated from load/displacement data obtained during test. Statistical ANOVA and Duncan's comparison tests were performed with a level of significance of 0.05.

Summary of Mean Results

Group	Change in BMD (g/cm2)	Maximum Strength (MPa)	Modulus (MPa)
Control	0.03±0.09 a	60.69±7.09 a	2890.47±1837.40 a
Ovx	0.07±0.05 a	57.27±7.86 a	1865.50±456.38 b
LDCAB	0.08±0.09 a	53.56±8.47 ab	1676.48±482.37 b
Ovx-LDCAB	0.18±0.08 b	48.07±10.44 b	1655.32±452.06 b

Means with the same letter are not different at level of significance=0.05.

The Ovx-LDCAB group had significantly greater change in BMD and lower Maximum Strength than other three treatment groups. The modulus in the control group was significantly greater than other groups. The results of this study show that a LDCAB diet can induce significant decreases in BMD and skeletal fragility over a short period of time. This model shows considerable promise for use in the study of human postmenopausal or senile osteoporosis. Static and dynamic histomorphometry are currently under way to assess the LDCAB effect on bone metabolism.

Disclosures: ***J.F. Millets****, Stryker Biotech 2.*

SU357

Dried Plum Is Beneficial to Bone Health Without Gastrointestinal Side Effects. L. J. Hammond*[1], E. A. Lucas[1], D. A. Khalil[1], A. B. Arquitt[1], M. E. Payton*[2], B. J. Smith[1], B. H. Arjmandi[3]. [1]Nutritional Sciences, Oklahoma State University, Stillwater, OK, USA, [2]Statistics, Oklahoma State University, Stillwater, OK, USA, [3]Nutritional Sciences, Oklahoma State University, Stilwater, OK, USA.

The beneficial effect of dried plum on bone health has been demonstrated in both our animal (JANA, 4:50-56, 2001) and clinical studies (J Womens Health Gend Based Med., 11:61-68, 2002). Dried plum prevented the ovarian hormone deficiency-induced loss of bone mineral density (BMD) in rats as well as reversal of bone loss in osteopenic rats. In a recent clinical study, we demonstrated that three months of daily consumption of 100 g (10 to 12) dried plums significantly increased serum levels of insulin-like growth factor-1 (IGF-1) by 17% and bone specific alkaline phosphatase (BALP) by approximately 6%, suggesting that dried plum may exert positive effects on bone in postmenopausal women. An impediment to the incorporation of dried plums into the diet is due to perceived gastrointestinal side effects. This study investigated the effect of dried plum on bowel habits of postmenopausal women. Fifty-eight healthy postmenopausal women, randomly assigned to receive either dried apple or dried plums daily for 3 months, were asked to assess the bowel habits during the course of the study. Women were asked to fill out questionnaires at baseline, and each month thereafter. Participants were asked to rate consistency, strain, pain, and feeling of constipation based on a 7-point scale with 1 being the least. Reported below are the means ± SE for the dried plum regimen: There were no significant differences in bowel habits for women on either the dried apple or dried plum regimen. These results show that incorporating dried plums into the diet of postmenopausal women can positively affect bone health without the negative gastrointestinal side effects.

	Baseline	Month 1	Month 2	Month 3
Stool Frequency (per week)	11±1	11±1	11±1	12±1
Estimated Fecal Bulk (cups)	8.6±1.0	9.5±1.0	10.8±1.0	9.4±1.1
Consistency	3.4±0.2	3.2±0.2	3.1±0.2	3.0±0.2
Strain	2.6±0.2	2.5±0.2	2.3±0.2	2.1±0.2
Pain	1.5±0.2	1.8±0.2	1.6±0.2	1.5±0.2
Feeling of Constipation	2.0±0.2	2.1±0.2	1.8±0.2	1.8±0.2

SU358

The Combination of Vitamin E and Soy Protein Exerts Added Skeletal Benefits in an Aged Rat Model of Male Osteoporosis. D. A. Khalil[1], M. P. Akhter[2], S. Juma[1], E. A. Lucas[1], D. S. Galloway*[3], L. J. Hammond*[1], D. Soung[1], B. J. Smith[1], R. Recker[2], B. H. Arjmandi[1]. [1]Nutritional Sciences, Oklahoma State University, Stillwater, OK, USA, [2]Osteoporosis Research Center, Creighton University, Omaha, NE, USA, [3]Oklahoma Veterinary and Medical Teaching Hospital, Oklahoma State University, Stillwater, OK, USA.

Studies examining the effects of soy protein or supplemental vitamin E on bone report that these dietary agents may prevent bone loss in animal models of postmenopausal osteoporosis. This study examined the separate and combined effects of vitamin E and soy protein on prevention of bone loss in an aged rat model of male osteoporosis. Sixty, 13-month old F344 rats were randomized into 5 groups and either orchidectomized (ORX; 4 groups) or sham-operated (1 group). Rats were fed a casein- or soy protein-based diet with adequate (75 mg/kg diet) or supplemental vitamin E (750 mg/kg diet) for 180 days. Treatment effects on bone mineral density (BMD), bone mineral content (BMC), and urinary deoxypyridinoline excretion (Dpd) are presented below. Results suggest that the combination of vitamin E and a soy protein-based diet imparts synergistic effects on bone that are not observed with vitamin E or soy protein alone.

	Sham	ORX	ORX	ORX	ORX
Protein Source	Casein	Casein	Casein	Soy	Soy
Vitamin E	75	75	750	75	750
Change in Body BMD, g/cm^2	+0.0062^{ab} (0.0053)	-0.0066^{b} (0.0043)	-0.0095^{b} (0.0061)	-0.0024^{b} (0.0055)	+0.0160^{a} (0.0068)
Tibia BMC, g	0.4033^{a} (0.0071)	0.3552^{bc} (0.0056)	0.3357^{c} (0.0087)	0.3557^{bc} (0.0074)	0.3637^{b} (0.0100)
Tibia BMD, g/cm^2	0.1997^{a} (0.0019)	0.1855^{b} (0.0015)	0.1784^{c} (0.0023)	0.1873^{b} (0.0020)	0.1881^{b} (0.0027)
4th Lumbar BMC, g	0.1579^{a} (0.0031)	0.1265^{bc} (0.0025)	0.1212^{c} (0.0035)	0.1319^{b} (0.0033)	0.1338^{b} (0.0039)
4th Lumbar BMD, g/cm^2	0.2268^{a} (0.0028)	0.2101^{bc} (0.0022)	0.2050^{c} (0.0032)	0.2114^{bc} (0.0029)	0.2177^{b} (0.0036)
Urinary Dpd, nmol/mmol creatinine	71.2 (15.7)	117.5 (13.3)	119.2 (14.3)	97.3 (15.7)	104.1 (14.3)

Values are Mean (SE), n=12. For each parameter, means that do not share the same superscripted letters are significantly different ($P < 0.05$).

SU359

Soy Protein Increases The Bone Mineral Content in Ovariectomy-Induced Osteopenia in Aged Rats. L. Devareddy*[1], V. Hailey-Zitlin*[2], A. Ferris*[1], B. H. Arjmandi[1]. [1]Nutritional Sciences, Oklahoma State University, Stillwater, OK, USA, [2]Food Science and Human Nutrition, Clemson University, Clemson, SC, USA.

Soy protein has been reported to prevent bone loss in ovarian hormone deficiency. However, to what extent soy protein itself or its non-nutritive components, e.g. isoflavones and saponins, exert this bone protective effect requires further investigation. Another objective of this study was to investigate the effects of soy on bone of intact animals. To evaluate the bone protective ability of soy protein with or without its non-nutritive components in intact (sham) or ovariectomized (ovx) rats, 60 eight-month old female Sprague Dawley rats were divided into 3 ovx and 3 sham groups. Animals were fed either a casein- or soy protein-based diet for 90 days Treatment effects on bone mineral density (BMD) of the tibia are presented in table below.

Treatment	Protein Source	Tibial BMD
Sham	Casein	0.2010 ± 0.010 ^{a}
Ovx	Casein	0.1922 ± 0.006 ^{b}
Sham	Isoflavone-deplete soy	0.2037 ± 0.007 ^{a}
Ovx	Isoflavone-deplete soy	0.1974 ± 0.004 ^{ab}
Sham	Soy protein with isoflavones	0.2019 ± 0.006 ^{a}
Ovx	Soy protein with isoflavones	0.1954 ± 0.005 ^{ab}

Values are mean ± SD, n=10; Values with different superscripted letters are significantly different ($P < 0.05$).

Results of this study indicate that bone density of intact rats is unaffected by soy protein compared to casein and that soy protein irrespective of its non-nutritive components exerts bone protective effects in ovarian hormone deficiency.

SU360

Using a Population-Based Evidence-Based Disease Management Program to Prevent and Treat Osteoporosis in Postmenopausal Women. C. J. Metge*[1], C. K. Yuen[2], W. D. Leslie[2], M. Yogendran*[3], B. Kvern*[2], L. Manness*[4]. [1]Faculty of Pharmacy, University of Manitoba, Winnipeg, MB, Canada, [2]Faculty of Medicine, University of Manitoba, Winnipeg, MB, Canada, [3]Manitoba Centre for Health Policy, University of Manitoba, Winnipeg, MB, Canada, [4]Patient Health, Merck Frosst Canada Ltd., Winnipeg, MB, Canada.

A population-based use of an evidence-based disease management program to prevent and treat osteoporosis in post-menopausal women is currently being evaluated by the Maximizing Osteoporosis Management in Manitoba (MOMM) project. This public/private partnership between the University of Manitoba, Merck Frosst Canada Ltd. and Manitoba Health unites a broad coalition of health care stakeholders as active participants and co-investigators. Approximately 6000 Manitoba women at high risk of osteoporosis and/or fracture have been identified through the province-wide administration of a risk factor survey to a random sample of 40,000 women over 50 years of age. During its first year of data collection, MOMM has collected extensive demographic, diagnostic and therapeutic information on 8,681 women (22% response rate). From these, 5,945 women have been identified as being 'high-risk' for fracture and the focus of future interventions. In addition, another 8,018 women with a diagnosed hip fracture (1997/2001) identified through administrative claims files are also being followed for the appropriateness of their post-fracture interventions. The first step in designing population-based interventions is to identify gaps in care. By merging three different data sources [administrative claims, survey-based data and a clinical dataset (bone mineral density results)] this project is better informed about the gaps that need tackling in the designing of population-based interventions. The baseline analysis of data collected through the three data sources has been completed. Our findings to date have found that 53% of Manitoba women 50 years or older are at increased risk of fracture. The rate of clinical investigation for osteoporosis in Manitoba is less than 10% and less than 10% of women with a previous hip fracture are dispensed treatment for osteoporosis. Less than 9% of women at low risk of fracture are obtaining treatment. In conclusion, gaps in the treatment and prevention of osteoporosis in Manitoba women over 50 years of age have been identified. Data responsive interventions are in the conceptual stage and are based on these findings.

Disclosures: ***C.J. Metge****, Merck Frosst Canada Ltd. 2; Bristol-Myers Squibb 2.*

SU361

The Bone Turnover Related Concept for Treating Osteoporosis. M. A. Dambacher[1], M. Neff[2], H. Schwarz*[1], L. Qin*[3]. [1]University Clinic Balgrist, Zurich, Switzerland, [2]Center for Osteoporosis, Zurich, Switzerland, [3]Chinese University, Hong Kong, Hong Kong Special Administrative Region of China.

Purpose: To define a treating concept for osteoporosis related to findings in bone turnover. Methods: We performed measurements of trabecular bone density in patients in Zurich and Hong Kong with an identical device (hrpQCT, Densiscan, Scanco AG, Zürich-Bassersdorf). The reproducibility of this method in mixed populations is ± 0.3%. Results: In early-postmenopausal women the rate of bone loss in peripheral trabecular bone was 4.3% and in axial trabecular bone 4.7%/year (Ito). Approximatly 34% of these women were "fast-loser". In contrast, the proportion of fast-loser in women with very low bone mass (e.g. severe senile osteoporosis) is nearly 75%. "Fast-loser" is a patient losing more than 3%/year of trabecular bone mass in distal radius. The average loss of trabecular bone mass (early-postmenopausal women) in the fast-loser group (only 34%) was 7%/year and 1% in the slow (non) loser (66%). Conclusions: The bone turnover related concept for treating osteoporosis distinguishes between osteoanabolic and antiresorptive agents. Antiresorptive agents are in first line bisphosphonates, only fluorides are currently available as osteoanabolic agents. Although there is still discussion about the vertebral fracture reducing efficacy of fluoride, there is clear evidence, that the vertebral fracture rate is reduced in patients treated for at least two years with 15 to 20 mg F-equivalents /d. The data are shown in the figure. The results of these studies suggest the use of osteoanabolic agents early in the postmenopause where slow-loser situations are dominant and trabecular connectivity is still good. In contrast, antiresorptive agents should be used in severe osteoporosis where the proportion of fast-loser is high.

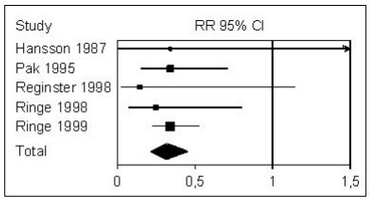

RR and 95% CI for new vertebral fractures in patients treated for 3-4 years with low-dose fluoride

SU362

Improving Management of Glucocorticoid Induced Osteoporosis: A Randomized Controlled Trial of Multifaceted Interactive Education. D. H. Solomon[1], J. N. Katz*[2], A. M. La Tourette*[1], J. Coblyn*[2]. [1]Pharmacoepidemiology and Pharmacoeconomics, Brigham and Women's Hospital, Boston, MA, USA, [2]Rheumatology, Brigham and Women's Hospital, Boston, MA, USA.

Prior work suggests that most patients receive sub-optimal care of glucocorticoid-induced osteoporosis (GIOP).We conducted an RCT of multifaceted interactive education for rheumatologists aimed to improve management of GIOP for their patients with RA taking oral glucocorticoids (GCs). All rheumatologists practicing at one academic medical center were randomized to receive a three part educational intervention or not (control). The intervention included: 1) a 90-minute discussion of GIOP, current practices regarding GIOP at the medical center, and strategies for improving practice; 2) a confidential audit of each rheumatologist's practice with respect to GIOP; and 3) a 1 page handout on treatment for GIOP. We then examined the medical records of patients with RA taking GCs seen by the control or intervention rheumatologists. The structured chart abstraction focused on the 6 months prior to the intervention and the 6 months after. Of the 624 eligible patients identified with RA, 375 patients were taking GCs at their index visit and were included in this study. Patients seen by rheumatologists in the intervention and control groups were similar with respect to age, gender, menopausal status, rheumatoid factor status, duration of RA, proportion taking disease-modifying anti-rheumatic drugs, and rates of comorbid illnesses. Prior to the intervention, 9% of the intervention group underwent bone densitometry (DXA) as did 6% of the control group (P=0.2). Post-intervention DXA rates were 8% for the intervention group and 9% for the control group (P=0.9). Considering pre- and post-intervention periods together, 16% of the intervention group and 13% of the control group underwent DXA (P=0.4). With respect to treatment, prior to the intervention, the rates of prescription osteoporosis medication use (not including HRT) were 26% for the intervention group and 24% for the control group (P=0.5). After the intervention, 27% of the intervention group and 29% of the control group received non-HRT prescription treatment (P=0.8). When we consider pre- and post-intervention periods together, 28% of the intervention group and 30% of the control group received non-HRT prescription treatment (P=0.9). We tested a 3-part interactive educational program in the setting of an RCT and found no increase in rates of DXA and/or use of medications for osteoporosis. We hope that focus groups with these rheumatologists can help inform future interventions.

Disclosures: ***D.H. Solomon****, Merck 2; Pfizer 2; Procter & Gamble 2.*

SU363

The DOMINO Project: To Improve the Compliance of Osteoporotic Patients with Periodic Feedback of Urinary CTX Values. O. Di Munno*[1], M. Mazzantini*[1], V. Braga*[2], S. Adami[2]. [1]Internal Medicine, Rheumatology Unit, University of Pisa, Pisa, Italy, [2]Rheumatologic Rehabilitation, University of Verona, Valeggio sul Mincio (Verona), Italy.

It is well known that discontinuing drug therapy is common in clinical practice. This represents a relevant problem in chronic diseases such as osteoporosis (OP). Recent studies have shown that the compliance in clinical practice is much lower than that in controlled clinical trials. Nearly half of the women starting HRT stopped after a mean of 9 months (Ettinger B, 1996) and about one third of those given alendronate did so after a mean of 8 months (Ettinger B, 1998). Furthermore, many patients may not be compliant with dosing instructions, that are particularly strict in the case of bisphosphonates (BFs). In order to improve patient compliance the use of markers of bone resorption has been proposed. In osteoporotic patients treated with BFs urinary N- or C-telopeptides of type I collagen (uNTX, uCTX) measured by ELISA have been shown to be significantly reduced after 2-3 months. This short-term drop of uNTX or uCTX can predict also the long-term response to therapy in terms of BMD and possibly of fracture risk, thus giving (to both physician and patient) valuable information on treatment efficacy and (to physician) on patient compliance. Recently, a simple and quick diagnostic tool measuring uCTX has been developed (Osteosal™ , Instaquant™): this hand-held multi-path photometer, self-calibrating, generates T-score results of creatinine normalized uCTX, with high correlation with ELISA technique (r = 0.87), and thus it is an effective way to measure uCTX at the point-of-care. The Italian DOMINO project is aimed at testing the possibility to improve the compliance of osteoporotic subjects treated with antiresorptive drugs with a periodic feedback of uCTX values obtained with Osteosal™ and Instaquant™ . Four hundred and fifty physicians have been involved into this project, each enrolling between October 2001 and May 31st 2002 fifty postmenopausal osteoporotic women (total 22.250) planned for antiresorptive once-a-day therapy. The patients are being included into either of two arms: non-CTX arm, in which uCTX will not be measured; and CTX arm, in which uCTX will be measured at baseline, 3 and 6 months and the results will be discussed with the patient. All patients will receive an OP educational sheet together with a diary for the annotation of the days in which the drug has not been taken. Analysis of data collected from the first 700 patients of the CTX arm have shown that uCTX is significantly correlated to age (r = -0.09, p = 0.02), but not with lumbar BMD (r = -0.02, p = ns). Compliance will be assessed by counting the number of patients at control visits and days of therapy in both arms.

SU364

A Survey of Information Needs of Family Physicians for the Management of Osteoporosis. S. Jaglal[1], G. Hawker[2], L. Jaakkimainen*[3], J. Carroll*[3], W. McIsaac*[3], S. Cadarette[4], D. Davis*[5]. [1]Rehabilitation Science, University of Toronto, Toronto, ON, Canada, [2]Medicine, University of Toronto, Toronto, ON, Canada, [3]Family and Community Medicine, University of Toronto, Toronto, ON, Canada, [4]Health Policy, Management and Evaluation, University of Toronto, Toronto, ON, Canada, [5]Continuing Medical Education, University of Toronto, Toronto, ON, Canada.

A survey of a large sample of family physicians in Ontario, Canada was recently conducted as part of a larger study to identify knowledge gaps and barriers to managing osteoporosis in family practice. The mail questionnaire was developed based on the key issues and themes identified in a prior set of focus groups. The findings from these focus groups clearly indicated that the format of the current information available on the management of osteoporosis does not meet the needs of family physicians or their patients in addressing knowledge gaps. The survey was conducted to validate the findings of the focus groups and assist with the development of dissemination and implementation strategies. The survey was mailed to 1000 family physicians between May and June 2001. These physicians were obtained through a computer-generated random sample of active Ontario members of the College of Family Physicians of Canada (CFPC) stratified by urban/rural practice location and male/female physicians. A total of 505 physicians responded (n = 364 eligible surveys; n = 120 no longer practising family medicine and; n = 24 who never see postmenopausal women). Of the 364 eligible respondents; 50% were male, 77% practiced full-time, 35% rural, and 40% graduated more than 15 years ago. Overall, male/female and urban/rural information needs were similar. The majority of respondents (82%) were interested in a guideline/reminder tool for diagnosis and treatment and would like the following information provided on it: an indication of a patient's risk for fracture (97%), an indication of a patient's risk for osteoporosis (95%), a list of potential risk factors that should be considered (95%), and inclusion of a treatment algorithm based on bone densitometry results (95%). Family physicians indicated that the preferred formats were a laminated card (76%), a tear off sheet (63%) and a personal digital assistant program (19%). Preferred dissemination methods were direct mail (86%) and CME events (44%) or group modules (41%). As in the focus groups, patient education material was seen as lacking. The results of our survey also indicate that published guidelines in their present form are not being used. Based on our findings, we will be developing prototypes of tools that can assist family physicians with the management of osteoporosis and will test their implementation in a future study.

SU365

Low Prevalence of Osteoporosis Diagnosis and Treatment on Admission to Nursing Home. R. G. Crilly, M. Kloseck*. Division of Geriatric Medicine, University of Western Ontario, London, ON, Canada.

Osteoporosis is highly prevalent in the long-term care population but much under treated. The purpose of the present study was to ascertain how often osteoporosis appeared as a patient problem at the time of admission to the institution. Charts were randomly selected for review at three nursing homes (skilled nursing facilities). As indicators that osteoporosis might be present, the charts were searched for any mention of osteoporosis or osteoporosis-related fracture in the application form, in the admission history, in any associated documentation, in the medications being taken and in any test results in the chart, especially x-ray reports. Medications listed on the application documentation and those initially prescribed by the admitting physician were reviewed for any bone-active compounds. A total of 169 charts (47 male; 122 female; mean age 82 years + 9.56 S.D.) were audited. Only 13 (7.7%), 12 of which were female, came with a specific diagnosis of osteoporosis, two having had a recent hip fracture and six being on treatment (etidronate with calcium and vitamin D) including the two patients with a hip fracture. Of the 13, two, both with spinal fractures and one also with a hip fracture, had etidronate discontinued at admission. An additional 10 patients (8 female) were admitted with a diagnosis of a recent hip fracture but without a specific diagnosis of osteoporosis. None of these arrived on treatment and in none was treatment started. Etidronate was started in two additional patients who had neither a diagnosis of osteoporosis nor hip fracture. Additionally 11 patients without an osteoporosis diagnosis were on calcium and an additional patient was started on calcium at time of admission. No patient was on alendronate or calcitonin; two were on estrogen for unclear reasons, and a further two without osteoporosis and fractures were prescribed estrogen at admission. In no chart was there an extensive database suggesting that a systematic search for past information had taken place. This applied to all system and disease categories and not just to osteoporosis. This study confirms that few patients in nursing homes are on osteoporosis-related treatments despite the known high prevalence of osteoporosis in this population. A factor underlying this might be the paucity of information available to the admitting physician. However, even when patients arrived with the diagnosis of osteoporosis no additional treatment was begun. There seems to be little or no systematic effort to obtain further information after admission. It appears that the nursing home is part of a continuum of non-care for osteoporosis. An improved strategy for the recognition and treatment of osteoporosis in these patients is needed.

SU366

An Intervention that Educates Wrist Fracture Patients and Their Physicians Can Increase the Detection and Treatment of Osteoporosis – Interim Results of a Controlled Trial. S. R. Majumdar[1], B. H. Rowe*[2], D. Folk*[2], J. A. Johnson*[3], B. H. Holroyd*[2], D. W. Morrish*[1], C. H. Harley*[1], W. P. Maksymowych*[1], I. Steiner*[2], B. Wirzba*[1], D. A. Hanley[4], A. S. Russell*[1]. [1]Medicine, University of Alberta, Edmonton, AB, Canada, [2]Emergency Medicine, University of Alberta, Edmonton, AB, Canada, [3]Public Health Sciences, University of Alberta, Edmonton, AB, Canada, [4]Medicine, University of Calgary, Calgary, AB, Canada.

Fragility fractures of the wrist are the most common symptomatic fracture related to osteoporosis. However, only 10-20% of wrist fracture patients >50 years of age are investigated or treated for osteoporosis in the year post-fracture. The purpose of this study was to use a quality improvement intervention to increase detection and treatment of osteoporosis in older patients with fractures of the wrist treated in the Emergency Department (ED). The intervention included case-finding in the ED; patient counseling (written materials and phone calls about osteoporosis and the importance of follow-up); and primary care physician education (patient-specific one page guidelines recommending BMD testing and evidence-based treatment options, endorsed by local “opinion leaders”). The intervention was compared to usual care controls in a prospective, quasi-randomized, double-blind trial. Patients >50 years with a wrist fracture who were discharged home from the EDs of two large hospitals were eligible; patients already receiving osteoporosis treatment or who were unable/unwilling to give informed consent were excluded. Main outcomes were BMD testing and osteoporosis treatment within 6 months of fracture. Presented results are based on the first planned interim analysis. During the first year, 215 consecutive patients were screened, and 80 patients allocated to intervention (n=44) or control (n=36). Main reasons for exclusion were osteoporosis treatment (n=65) and admission to hospital (n=42). Study patients had a mean age of 67 years (range 50-92 years) and 78% were female. There were no significant differences in important clinical characteristics between intervention and control patients. Using intention-to-treat analyses, 52% of intervention patients had undergone BMD testing compared with only 8% of controls 6 months post-fracture (absolute increase 44%, p<0.001). Furthermore, 27% of intervention patients were started on osteoporosis treatment compared with only 6% of controls (absolute increase 21%, p=0.010). All treated patients were prescribed a bisphosphonate. We conclude that, compared with usual care, an ED-based intervention has the potential to significantly increase the rate of detection and treatment of osteoporosis in older patients with fractures of the wrist.

SU367

An Education Intervention Directed At Healthcare Providers and Patients Improves Attention to Osteoporosis in the Fracture Patient. C. Simonelli[1], J. Morancey*[1], L. Swanson*[1], K. Killeen*[1], T. W. Weiss*[2], Y. Chen[2]. [1]HealthEast, Woodbury, MN, USA, [2]Merck & Co., Inc., West Point, PA, USA.

A pilot project of 301 postmenopausal women hospitalized for a low impact fracture revealed low attention to osteoporosis (Pilot). At one year, only 10% had bone mineral density testing (BMD), 37% were using calcium, and 26% were on osteoporosis medication therapy. We hypothesized that an education program directed toward physicians and nurses and bedside education provided to the patient would increase osteoporosis diagnostic testing and treatment. Staff education was provided in the form of grand round lectures, presentations at staff meetings, mailings and brochures. A general guideline about osteoporosis was placed in the chart of all patients identified with fragility fracture. A geriatric nurse practitioner identified 186 consecutive patients who were hospitalized for low impact fractures during a 6-month period in 2000. Patients were counseled about nutrition, home safety and fall prevention and information about bone density testing and osteoporosis medication was discussed (Educ). Follow-up data were collected by telephone at 6 and 12-months. Results are shown at discharge (D/C) and follow-up. After education intervention, there was a significant increase in bone density testing, and calcium and vitamin D use that persisted through 12 months after intervention. While the use of osteoporosis medication increased, the increase was not statistically significant. This suggests that educational intervention directed at fracture patients and their healthcare providers may increase attention to osteoporosis in this high-risk population and improve quality of care.

	N	% Died	% BMD	% Calcium+	% Vit D+	Osteo. Med*
Pilot D/C	301	n/a	n/a	16	18	17
12-month	227	13	10	37	37	26
Educ D/C	186	n/a	n/a	46^	35^	25++
6-month	153	10	23	68	64	25
12-month	111	17	34^	75^#	75^#	34

*Estrogen, raloxifene, alendronate, risedronate, etidronate, pamidronate, or calcitonin
+ ≥ 500 mg/day; ≥400IU/day
^ $p < 0.001$ compared to pilot phase at same time point
# $p < 0.001$ compared to educational phase baseline
++ $p = 0.02$ compared to pilot phase at baseline

Disclosures: ***C. Simonelli****, Merck & Co., Inc 2, 5, 8.*

SU368

Histomorphometric Evaluation of the Tibio-Fibular Junction after a Long-term Oral Administration of S12911 in Female Rats. V. Shen[1], C. Liu*[1], V. Marque*[2], I. Dupin-Roger*[2], D. Bazot*[3], I. Tupinon-Mathieu*[2]. [1]SkeleTech, Inc., Bothell, WA, USA, [2]Laboratoires Servier, Courbevoie, France, [3]Biologie Servier, Gidy, France.

S12911 (PROTOS®) is a new agent having shown its effectiveness in the treatment of postmenopausal osteoporosis. As the therapeutic use in humans may require prolonged administration, a long-term treatment study was performed in intact Fischer 344 rats. The bone effects at the cortical level were investigated. In this study, cortical bone histomorphometric parameters were measured at the tibiofibular junction of 118 female Fischer rats treated with 0, 225, 450 or 900mg/kg/d of S12911 for 104 weeks. Thirty-micron thick sections were prepared and surface stained with toluidine blue. Results are means ± SEM, ANOVA + Dunnett's test. The treatment with S12911 increased total bone area, cortical area, periosteal perimeter and cortical thickness. At 900mg/kg/d, total bone area, cortical bone area and periosteal bone perimeter were significantly higher than in the control group (+10, +13 and +5%, respectively). After 104 weeks of treatment, the marrow area and endosteal bone perimeter did not show any changes, or even a slight decrease, which is in keeping with the lack of changes seen in endosteal eroded surface. Conversely to what is found in young animals, there was a measurable amount of cortical porosity in a majority of animals. It was not related to treatment since the average percentage of cortical porosity remained the same. In conclusion, cortical bone is improved by a long-term S12911 treatment, as shown by histomorphometric measurements. This confirms previous densitometry and biomechanical findings reported in intact and ovariectomized rats. These results, in addition to those found for trabecular bone, demonstrate that S12911 possesses therapeutic potential by improving both cancellous and cortical bone.

S12911 (mg/kg/d)	Ctrl	225	450	900
Total bone area (mm^2)	3.65 ± 0.03	3.75 ± 0.04	3.75 ± 0.04	4.03 ± 0.04*
Marrow area (mm^2)	0.42 ± 0.04	0.35 + 0.04	0.35 ± 0.03	0.37 ± 0.03
Cortical area (mm^2)	3.23 ± 0.05	3.40 ± 0.06	3.40 ± 0.05	3.66 ± 0.06*
Cortical thickness (mm)	0.73 ± 0.02	0.79 ± 0.03	0.77 ± 0.02	0.80 ± 0.02
Periosteal perimeter (mm)	7.33 ± 0.04	7.46 ± 0.04	7.51 ± 0.06 *	7.70 ± 0.03 *
Endosteal perimeter (mm)	2.28 ± 0.14	2.13 ± 0.14	2.24 ± 0.10	2.22 ± 0.13
Cortical porosity (%)	0.80 ± 0.08	0.91 ± 0.10	0.85 ± 0.06	0.92 ± 0.06

Ctrl: control.* $p < 0.05$ vs. control group.

SU369

Histomorphometric Evaluation of the Proximal Tibia Metaphysis after a Long-term Oral Administration of S12911 in Female Rats. V. Shen[1], B. Robin*[2], D. Bazot*[3], I. Tupinon-Mathieu*[2]. [1]SkeleTech, Inc., Bothell, WA, USA, [2]Laboratoires Servier, Courbevoie, France, [3]Biologie Servier, Gidy, France.

S12911 (PROTOS®) has been shown to reduce the risk of vertebral fracture in postmenopausal osteoporosis. As the therapeutic use of S12911 may require prolonged administration in humans, a long-term treatment study was performed in intact Fischer 344 rats. The long-term effect and safety of the treatment at the trabecular bone level were evaluated. In this study, trabecular bone histomorphometric parameters were measured at the tibia metaphysis of 119 female Fischer rats treated with either 0, 225, 450 or 900mg/kg/d of S12911 for 104 weeks. Five-micron thick sections were prepared and stained with von Kossa stain and McNeal counterstain. Results are expressed as means ± SEM, ANOVA+ Dunnett's statistical tests were performed. Long-term treatment with S12911 significantly and dose-dependently increased (+27 to +41%) cancellous bone volume (BV/TV). The increase in BV/TV was the result of increased trabecular thickness (Tb.Th) and number (Tb.N). Trabecular separation (Tb.Sp) was significantly and dose-dependently decreased at all tested doses. The bone tissue was mainly made of mineralized tissue since osteoid volume (OV/BV) and osteoid thickness (O.Th) were similar between all groups (treated or not). In all groups, O.Th was less than 1.5µm well within the range of physiological levels, indicating no toxicity of this long-term treatment. In conclusion, trabecular bone mass and architecture are improved by long-term S12911 treatment, as shown by histomorphometric measurements. This confirms previous densitometry and biomechanical findings reported in intact and ovariectomized rats. These results, in addition to those found for cortical bone, demonstrate that S12911 possesses therapeutic potential by improving both cancellous and cortical bone.

S12911 (mg/kg/d)	Ctrl	225	450	900
BV/TV (%)	27.0 ± 2.4	34.2 ± 2.7 *	35.0 ± 2.0 **	38.2 ± 1.7 ***
Tb.Th (µm)	74.4 ± 5.3	89.8 ± 6.1 *	82.5 ± 3.8 **	83.5 ± 4.5 **
Tb.N (mm^{-1})	3.5 ± 0.1	3.8 ± 0.1	4.2 ± 0.1 ***	4.6 ± 0.1 ***
Tb.Sp (µm)	216 ± 13	180 ± 9 *	159 ± 8 ***	135 ± 5 ***
O.Th (µm)	1.2 ± 0.3	1.1 ± 0.3	0.7 ± 0.1	1.3 ± 0.3
OV/BV (%)	0.013 ± 0.007	0.011 ± 0.004	0.005 ± 0.003	0.012 ± 0.004

Ctrl: control. *: p< 0.05, **: p< 0.01, ***: p< 0.001 versus control group.

SU370

Bone Anabolic Effects of Subcutaneous Treatment with Basic Fibroblast Growth Factor in Ovariectomized Rats. U. T. Iwaniec, K. A. Magee*, N. G. Mitova-Caneva*, T. J. Wronski. Physiological Sciences, University of Florida, Gainesville, FL, USA.

Although basic fibroblast growth factor (bFGF) is a potent stimulator of bone formation when administered intravenously, less is known regarding the effects of this agent on bone following subcutaneous administration. Therefore, the purpose of this study was to characterize the skeletal response to subcutaneous injection of high doses of bFGF in ovariectomized (ovx) rats. Female Sprague Dawley rats were ovx or sham-operated at 3 months of age and left untreated for 2 months to establish cancellous osteopenia in the ovx group. Rats (7-10/group) were then injected sc with either vehicle or bFGF at a dose of 1 mg/kg/day for 21 days. Blood was drawn at necropsy for determination of hematocrit and serum calcium and phosphorus levels. Lumbar vertebrae were collected and processed undecalcified for quantitative bone histomorphometry. Data were analyzed with the Kruskal-Wallis test followed by a nonparametric posthoc test. The level of statistical significance was set at P<0.05. All data are reported as mean±SD. Treatment of ovx rats with bFGF for 21 days had no adverse effect on body weight, a general index of the health of the animals. At termination of treatment, vehicle-treated sham rats, vehicle-treated ovx rats, and bFGF-treated ovx rats weighed 339±22 g, 353±15 g, and 355±13 g, respectively. The levels of serum calcium and phosphorus were likewise not affected by sc administration of bFGF. However, treatment of ovx rats with bFGF resulted in substantially reduced hematocrit levels in comparison to treatment of ovx and sham rats with vehicle (24±5%, 40±3%, and 39±3%, respectively). Cancellous bone volume was lower in vehicle-treated ovx rats than in vehicle-treated sham rats (31±5% vs. 37±3%, respectively). Although treatment of ovx rats with bFGF had no effect on cancellous bone volume (32±5%) in comparison to treatment of ovx rats with vehicle, osteoid volume was markedly increased in the bFGF-treated animals (8±4% vs. <0.1%). In addition, treatment of ovx rats with bFGF resulted in a 4-fold increase in osteoblast surface and an 8-fold increase in osteoid surface in comparison to treatment of ovx rats with vehicle. Osteoclast surface, an index of bone resorption, was not affected by bFGF treatment. These findings indicate that administration of high doses of bFGF via subcutaneous injection markedly increases bone formation and may be a useful treatment for cancellous osteopenia in the estrogen-deplete skeleton.

SU371

Evidence That Sensitivity to Growth Hormone (GH) is Growth Period and Tissue Type-Dependent: Studies in GH Deficient (lit/lit) Mice. Y. Kasukawa, R. Guo*, D. J. Baylink, S. Mohan. J.L. Pettis VAMC, Loma Linda, CA, USA.

Based on past findings that the magnitude of GH effects on the activation of its intracellular signaling molecule, STAT-5, in liver is age-dependent, we proposed that the effect of GH to increase peak BMD is growth period dependent. To evaluate this hypothesis, the GH-deficient lit/lit mouse, which exhibits deficiency in both endocrine and local IGF-I actions, was used as a model. GH (4 mg/kg body wt./day) or vehicle was administered three times a day during the prepubertal and pubertal (day 7-34), pubertal (23-34), post pubertal (42-56) and adult (day 204-217) periods and their effects on the musculoskeletal system were evaluated by DEXA and pQCT. GH treatment during different periods significantly (P<0.001) increased total body BMC (47-90%), BMD (7-15%), bone area (37-62%) and lean body mass [LBM] (52-85%) and decreased % fat (27-56%) compared to vehicle. As indicated by the range in the brackets, the magnitude of change varied markedly depending on the treatment period. The net gains in total body BMC (5.8 mg/day) and BMD (0.3 mg/cm^2/day) were greatest when GH was administered between days 42-55 compared to other periods. Accordingly, net gain in femur total volumetric BMD (PQCT) was significantly greater (P<0.001) when GH was administered between days 42-55 compared to other growth periods, which was due to greater increase in cortical thickness during this period. The above time-dependent BMD changes imply that the critical metabolic pathways for GH responsiveness are maintained for only a short time during growth. In contrast to changes in BMD, the net loss in % body fat was greatest (-1.3%/day) when GH was administered between days 204-216 and least when GH was administered between days 7-35 (-0.15% day). To determine if GH-induced anabolic effects on musculoskeletal system are maintained after GH withdrawal, we performed DEXA measurements 3-7 weeks after stopping GH treatment. The increases in total body BMC, BMD and LBM but not the decrease in body fat were sustained after GH withdrawal. Summary: 1) GH treatment increased bone accretion and LBM but decreased % body fat in GH deficient mice. 2) The net change in bone accretion was greatest when GH was administered immediately after puberty while net change in % body fat was greatest when GH was administered during adult period. 3) Maintenance of GH-induced changes in target tissues after GH withdrawal was dependent on tissue type. Conclusions: 1) Sensitivity to GH in target tissues is growth period and tissue type-dependent. 2) Continuous GH-treatment is necessary to maintain body fat loss but not BMD gain (Supported by the Department of the Army [DAMD17-97-2-7016] but does not reflect the position/policy of the government).

SU372

Apomine, a Novel Bone Anabolic Agent, Stimulates Bone Formation and Is Hypocholesterolemic in a Mouse Model. Y. Guyon-Gellin*, P. Latin*, P. Villemin*, E. J. Niesor*. Biosciences and Pharmacology, Ilex Oncology Research, Versoix, Geneva, Switzerland.

Apomine is a novel bisphosphonate ester currently in phase II clinical trials. Previous studies have demonstrated that Apomine inhibits cholesterol synthesis *in vitro* and decreases cholesterol levels in various rodent and non-rodent species by increasing the rate of HMG-CoA reductase degradation. Furthermore, Apomine was shown to decrease HMG-CoA reductase mRNA in bone after oral administration in mice. Both statins and nitrogen-bisphosphonates such as risedronate, which inhibit different steps of the mevalonate-isoprenoid -cholesterol (MIC) synthetic pathway, affect bone formation in rodent models. Since the statins have been shown to display bone anabolic activity, Apomine (50, 100, and 200 mg/kg, in the diet) was tested for similar activity in a model of normal mice treated for a 5 weeks period. Changes in bone parameters were measured by pQCT in the right femur to assess the bone anabolic activity of Apomine. Apomine increased trabecular bone mineral content (BMC) by +15%, +33%, and +40% with 50, 100, and 200 mg/kg, respectively. Trabecular density was increased with a similar pattern. In the cortical femur, Apomine increased BMC by +10%, +22%, and +17%. Cortical thickness was increased by +8%, +14%, and +15%, and polar moment of inertia (PMI) was increased by +8%, +20%, and +21% at doses of 50, 100, and 200 mg/kg, respectively. Furthermore, Apomine decreased plasma cholesterol by -22% and -35% with 100mg/kg and 200 mg/kg, respectively. Risedronate (100 mg/kg, in the diet) was used as the reference drug to validate the mice model and was shown to increase trabecular BMC, cortical BMC, cortical thickness, and PMI without hypocholesterolemic activity. These results suggest that Apomine increases bone mass, improves indices of stiffness, and simultaneously lowers plasma cholesterol in mice after a 5 weeks oral administration period.

Disclosures: ***Y. Guyon-Gellin****, Ilex Oncology Research 3.*

SU373

S12911 Treatment Maintains Bone Mineral Crystal Characteristics. S. Cazalbou*, C. Combes*, C. Rey*. Equipe PCP, ENSIACET, CIRIMAT UMR 5085, Toulouse, France.

S12911 (Protos®) is currently being developed as a treatment for osteoporosis. The aim of the present study was to analyze the effect of S12911 treatment on bone mineral characteristics and ionic exchanges at the mineral level. Female *Macaca fascicularis* monkeys were separated into 4 groups, receiving 0, 200, 500, and 1250 mg/kg/day of S12911 (strontium ranelate), respectively. At the end of 52 weeks of treatment, 4 animals were sacrificed in each group, and 2 animals were sacrificed after a 10 week reversibility period. The analysis of bone mineral crystals was performed on powdered samples of the humeral diaphysis and epiphysis using chemical measurements for the Ca, P, Sr, and CO_3 content, X-ray diffraction for determination of crystalline phases and mean size of crystals, and Fourier transform infrared (FTIR) spectroscopy for evaluation of fine structural characteristics. Furthermore, diaphysis

samples underwent an exchange test (bone powder added to a solution of $Ca(NO_3)_2$ for 30 min). Analysis of bone powders before and after exchange was carried out by the three techniques previously described and allowed to obtain a Sr exchange rate. S12911 treatment induced a dose-related increase in the bone Sr content. Preferential Sr uptake (around 2.5 fold) was observed in the epiphysis compared with the diaphysis. After the reversibility period, Sr release was greater in the epiphysis than in the diaphysis. These differences were due to higher bone turnover, higher mineral reactivity due to the amount of labile environment, and better contact with body fluids for the epiphysis than for the diaphysis. Similar Sr content ratios between epiphysis and diaphysis were found in all animals, indicating that Sr incorporation into the different tissues was strongly correlated. Bone Sr incorporation did not lead to any modification of the stoichiometry and crystal size. No modification of the amount of nonapatitic environments of PO_4, CO_3, and HPO_4 was noted by FTIR spectroscopy. The exchange test demonstrated a slight constant exchange rate of 9 to 12% Sr incorporated in the diaphysis. This rate was independent of the treatment dose and bone mineral Sr content, indicating that this easily bone exchangeable Sr was located in labile hydrated nonapatitic environments, on the crystal surface. After the reversibility period, this Sr exchange rate decreased. After the ionic exchanges test, no modification was noted in crystal characteristics. This data, which indicates that Sr incorporation is preferential into bones with high turnover and takes place partly on the crystal surface, demonstrates the safety of S12911 maintaining mineral crystal characteristics during and after treatment.

SU374

Differential Feedback Regulation of HMG-CoA Reductase mRNA in Bone and Liver: Studies with Apomine. M. Montjovent*, D. Masson*, P. Latin*, O. Maurhofer*, Y. Guyon-Gellin*, E. J. Niesor. Biosciences and Pharmacology, Ilex Oncology Research, Versoix, Geneva, Switzerland.

Apomine is a novel bisphosphonate ester that increases the rate of degradation of HMG-CoA reductase in the hepatoma (HepG2) and osteosarcoma (Saos-2) derived cell lines. Furthermore, *in vivo*, Apomine decreases plasma cholesterol and increases bone mineral content and density in mice. Preliminary *in vitro* experiments using microarray technology have shown that the expressions of different genes involved in cholesterol metabolism such as farnesyl diphosphate synthase, isopentenyl-diphosphate delta isomerase, and lanosterol synthase were strongly up-regulated by Apomine treatment of HepG2 cells. In contrast, their expressions did not change in Saos-2 cells, suggesting that liver and bone cells respond differently to inhibition of the mevalonate-isoprenoid-cholesterol (MIC) pathway. The hypothesis was then tested *in vivo* in tissues from mice treated with Apomine. Male mice were administered Apomine (100 mg/kg in diet) for 1, 2, and 3 days. HMG-CoA reductase mRNA was measured in livers and tibiae by quantitative RT-PCR. As expected from the hypocholesterolemic activity, HMG-CoA reductase mRNA was consistently increased in the liver (>100%). Surprisingly, in the same animals, HMG-CoA reductase mRNA was significantly decreased (from -19% to -51%) in bone tissues after 1, 2, and 3 days. The decreased expression of HMG-CoA reductase mRNA in bone was maintained in animals treated for a longer period (2 and 3 weeks), whereas HMG-CoA reductase mRNA in livers of the same animals was significantly increased (+117% to +131%). Thus, liver and bone tissues respond differently, and in an opposite manner, to the inhibition of the MIC pathway produced by Apomine. These results support the hypothesis that bone tissues might not be able to upregulate the MIC pathway and thus might be exquisitely sensitive to inhibitors of various steps of this pathway.

Disclosures: ***M. Montjovent****, Ilex Oncology Research 3.*

SU375

Pharmacological Profile of Apomine, a Bone Anabolic Drug that Induces HMGCoA reductase Degradation. E. J. Niesor[1], D. Masson*[1], M. Montjovent*[1], N. Lameloise*[1], Y. Guyon-Gellin*[1], S. Van Dijk[2], S. Weitman*[2], C. L. Bentzen[3]. [1]Biosciences and Pharmacology, Ilex Oncology Research, Versoix, Geneva, Switzerland, [2]Ilex Oncology, San Antonio, TX, USA, [3]Ilex Oncology Research, Versoix, Geneva, Switzerland.

The Mevalonate-Isoprenoid-Cholesterol (MIC) synthetic pathway plays an important role in the regulation of both osteoclastic bone resorption and osteoblastic bone formation as demonstrated by studies on the mechanism of action of nitrogen bisphosphonates and statins. Apomine a novel tetra-isopropyl bisphosphonate ester, under development, inhibits the MIC pathway in liver (HepG2) and osteoblast (Saos2) derived cells by the unique mechanism of increasing the rate of degradation of HMGCoA reductase. This activity is observed even in the presence of statins and in a statin-resistant cell line, LP-90 (IC50 10nM). Apomine, at hypocholesterolemic doses, was shown to increase bone formation in normal mice. No changes in plasma cholesterol were observed in mice treated with simvastatin or risedronate, which inhibit the MIC pathway at different steps, or by different mechanisms. *In vitro* and *in vivo* studies demonstrated that the inhibition of cholesterol synthesis produced by Apomine triggered the expected positive feedback on enzymes of the MIC pathway (ie HMGCoA red mRNA) in HepG2 cells and in liver tissue from treated animals. Surprisingly, this feedback was not observed in Saos2 cells incubated with Apomine and in bone from mice treated orally with Apomine. Apomine displays both antiproliferative and bone anabolic activities and prevents bone metastasis of breast cancer cell in mice receiving intracardiac injection of MDA-MB-231 cells. The potential bone anabolic activity of Apomine was investigated in Cynomolgus monkeys receiving 25mg/kg/day of Apomine orally for 3 weeks. The plasma marker of osteoblast activity, bone alkaline phosphatase (BAP), was increased by up to 24 % ($P<0.01$). As expected from results previously obtained with the antiresorptive bisphosphonic acids, SR-92D3, the chemically de-esterified derivative of Apomine decreased BAP in this animal model. The unique pharmacological profile and good tolerance of Apomine in preclinical and clinical studies suggest that Apomine may have the potential to become a drug of choice in the treatment on cancer associated bone pathologies and osteoporosis.

Disclosures: ***E.J. Niesor****, Ilex Oncology Research 3.*

SU376

pQCT Analysis of the Anabolic Effects of a Group of Novel Small Peptides on Bone in Intact Adult Rats. G. B. Schneider[1], D. T. Bui*[2], K. J. Grecco*[2]. [1]Basic Medical Sciences, Northeastern Ohio Universities College of Medicine, Rootstown, OH, USA, [2]Division of Basic Medical Sciences, Northeastern Ohio Universities College of Medicine, Rootstown, OH, USA.

We have previously demonstrated that 14 amino acid peptide fragments, based on a human sequence from the third domain of the native serum protein, vitamin D binding protein (DBP) elicit anabolic effects on the skeleton. Intermittent systemic injections of the peptides to intact, newborn and adult rats resulted in significant increases in total bone density within two weeks of treatment. A single, local injection of the same 14 a.a. peptide generated new bone at the site of injection at one week (Schneider et. al., JBMR, 16:S231). In the current study we evaluated peptide fragments ranging in length from 3 - 13 a.a. from the same region of the DBP protein in intact adult rats. Female rats were given subcutaneous injections of saline or peptide (0.4ng/g body wt.) every other day for two weeks; two days after the final injections, the rats were euthanized and the femurs and tibias collected for analysis by peripheral quantatative computerized tomography (pQCT). Specific slices through the metaphysis and mid-shaft of each bone were analyzed from the scans. The proximal tibia metaphysis and midshaft slices were representative of the skeletal responses to the various peptide fragments. The efficacy of the peptide fragments was based on their effect on total bone density. Fragments 12, 11, 10, and 4 amino acids in length demonstrated highly significant ($p < 0.001$) increases in total bone density in the proximal tibia metaphysis. All of these peptides also illustrated the same trends with respect to the other parameters evaluated: increases in cortical/subcortical bone density, decreases in total surface area and decreases in periosteal and endosteal circumferences. The effective peptides also elicited significant increases in bone density of the midshaft, but the other trends were not as prevalent. Those peptide fragments that did not increase bone density did not illustrate any consistent trends with respect to the other parameters measured. The anabolic peptides appear to be increasing bone density and decreasing the diameter and cross-sectional area of the bone. None of the peptides affected bone length, which remained consistent with the saline controls. We hypothesize that the increased bone density may be reflecting better quality bone; the decrease in cross sectional surface area may be in response to this superior quality bone. Biomechanical testing of the bones treated with the effective peptides is planned to test this hypothesis.

SU377

Discovery of Novel Dual Action Src Kinase Inhibitors Demonstrating Anti-Resorptive and Bone Formation Activities In Vitro and In Vivo. L. Xing*[1], Y. Wang*[2], R. Sundaramoorthi*[2], T. Keenan*[2], C. Metcalf*[2], W. Shakespeare*[2], R. Bohacek*[2], M. R. van Schravendijk*[2], T. Yamashita[1], T. Sheu*[1], E. Puzas[1], D. Dalgarno[2], J. Iuliucci*[2], T. Sawyer[2], B. F. Boyce[1]. [1]University of Rochester, Rochester, NY, USA, [2]ARIAD Pharmaceuticals, Cambridge, MA, USA.

Src is a non-receptor tyrosine kinase required for osteoclast (ocl) activation and bone resorption. In addition to its required role in osteoclasts, Src also negatively regulates osteoblast (obl) function. Thus, it is a well-validated therapeutic target for prevention and treatment of postmenopausal osteoporosis and other diseases with bone loss. To this end, we used structure-based drug design to develop a series of novel, potent (low nM IC50s) non-peptide inhibitors of Src tyrosine kinase. These small-molecule Src tyrosine kinase inhibitors incorporate bone-targeting chemical moieties that confer them with high affinity for hydroxyapatite as well as cellular selectivities (ocl and obl). Furthermore, they exhibit significant selectivity (>100-1000 fold) to inhibit Src relative to a panel of more than 30 protein kinases. AP23588 is a promising lead compound from this series of bone-targeted Src tyrosine kinase inhibitors, which possess dual action properties (anti-resorptive and anabolic activities), including: 1) inhibition of ocl resorption in vitro (pit area and number reduced by 55-97% at 1 uM), effects comparable to alendronate; 2) inhibition of PTH-induced hypercalcemia (50-100% inhibition) and bone resorption in vivo; 3) dose-dependent stimulation of alkaline phosphatase activity and mineralized bone nodule formation of fetal rat calvarial cells 2-fold after 5 and 13d treatment, respectively; 4) increased expression of obl genes (cbfa-1 and osteocalcin) detected using real-time PCR and a luciferase reporter assay; and 5) increased periosteal obl numbers and new bone formation in vivo after its injection over the calvaria of normal mice. Our findings provide evidence that these specifically designed bone-targeted Src tyrosine kinase inhibitors prevent bone loss and stimulate bone formation. Thus, they have beneficial action in bone and promising utility for the prevention and treatment of osteoporosis.

Disclosures: ***L. Xing****, ARIAD Pharmaceuticals 2.*

SU378

Has Treatment for Osteoporosis Improved? D. H. Solomon[1], J. Finkelstein[2], H. Mogun*[1], J. Avorn*[1]. [1]Pharmacoepidemiology and Pharmacoeconomics, Brigham and Women's Hospital, Boston, MA, USA, [2]Endocrine, Massachusetts General Hospital, Boston, MA, USA.

Several studies have found that under-diagnosis and under-treatment of osteoporosis is common. These have generally been small surveys conducted at a single clinic or hospital and have not examined trends over time. We examined the rates of osteoporosis treatment before and after hip or wrist fracture in older adults. In a very large continuously enrolled Medicare cohort that also partcipates in a state-run pharmaceutical benefits program, we studied all patients who had undergone a procedure for and/or received a diagnosis of hip or wrist fracture during the period 1995 - 1999. Information regarding filled prescriptions was assessed to determine the proportion of patients using a prescription osteoporosis medication (HRT, calcitonin, etidronate, alendronate, risedronate, raloxifene) in the six months before and after a fracture. During the five year study period, 14,889 persons sustained a hip fracture and 10,216 had a wrist fracture. 8.7% of subjects who experienced a hip fracture filled a prescription for an osteoporosis medication in the six months prior. This increased slightly to 9.5% after the hip fracture. For wrist fracture, 9.1% had filled a prescription in the six months before and 10.8% after the fracture. The frequency of treatment increased significantly over the study period. In 1995, 3.8% of persons with either hip or wrist fracture subsequently filled a prescription for an osteoporosis medication; in 1999, 15.2% filled a prescription (P for trend < 0.001). Patient factors found in adjusted models to be associated with use of a prescription for an osteoporosis medication after a hip fracture include: female gender (OR 4.7; 95% CI 3.3 - 6.7), white race (OR 2.3; 95% CI 1.3 - 4.1), prior fractures (1.2, 95% CI 1.1 - 1.5), fewer comorbid conditions (OR 1.2 ; 95% CI 1.0 - 1.4), and fewer hospitalizations in the prior year (OR 1.5; 95% CI 1.1 - 1.9). In this large community-based cohort, the proportion of persons receiving prescription osteoporosis treatment after hip or wrist fracture is sub-optimal. Trends suggest a slight improvement. Several factors are associated with filling osteoporosis prescriptions. These data can help in the design of quality improvement programs for the management of osteoporosis.

Disclosures: ***D.H. Solomon****, Merck 2; Pfizer 2; Procter & Gamble 2.*

SU379

Risedronate Improves Quality of Life in Women with Osteoporosis After 6 Months: Results from a Prospective Cohort Study. J. Semler*[1], F. Raue[2], A. Grauer[3], S. Eggenweiler*[4]. [1]Immanuel Krankenhaus, Berlin, Germany, [2]Endocrine Practice, Heidelberg, Germany, [3]Procter & Gamble Pharmaceuticals, Geneva, Switzerland, [4]Procter & Gamble Pharmaceuticals, Weiterstadt, Germany.

The impairment of quality of life is an important consequence of osteoporosis. Risedronate has been shown to significantly reduce the risk of morphometric vertebral fractures in one year and the risk of clinical vertebral fractures after only 6 months of treatment in patients with postmenopausal osteoporosis. We conducted a large, prospective cohort study to confirm the efficacy and safety of risedronate 5mg/d therapy for the prevention or treatment of postmenopausal or glucocorticoid-induced osteoporosis. A total of 2739 office-based physicians in Germany enrolled 9188 patients into the study. We report here the results on changes in patients' quality of life during 6 months of risedronate treatment. Patients were asked to submit a completed quality of life questionnaire (short OQLQ)[1] before initiation and after 6 months of treatment. The questionnaire assessed 5 domains of quality of life (symptoms, physical function, activities of daily living, emotional function, leisure) with two questions per domain. A set of seven graded response options per domain was offered to the patients to record their answers. Median age of the patients in the trial was 68.7 years, 3342 (36.4%) of the patients had evidence of vertebral fractures at baseline. 4887 (53.2%) patients completed the first questionnaire, 6394 (69.6%) of the patients completed the second, a total 4413 (45.1%) patients completed both questionnaires and were therefore included in the quality of life analysis. After six months of treatment, there was a significant improvement in the overall quality of life (p<0.001, Wilcoxon-Rank test, two-sided), and in each of the domains individually (p<0.001, Wilcoxon-Rank test, two-sided). The results of this large cohort study show a significant improvement in quality of life parameters after only 6 month of risedronate treatment - the same time period in which a significant clinical vertebral fracture reduction has been demonstrated in clinical trials.

1) Cook et al, Osteoporos Int 10: 207-13 (1999)

SU380

Bone Health Behaviors and Self-Efficacy: An Analysis Based on *Choices* FOR BETTER BONE HEALTH™. S. L. Silverman[1], D. T. Gold[2], M. K. Conditt*[3], B. E. Miller[3]. [1]Cedars-Sinai, Los Angeles, CA, USA, [2]Duke University, Durham, NC, USA, [3]Procter and Gamble, Mason, OH, USA.

Osteoporosis self-management is effective when women adhere to four bone health behaviors (taking medicine, taking calcium and vitamin D, exercising, and managing chronic pain). We studied the self-efficacy (belief that one can do the behavior) for each of these four bone health behaviors using baseline data from 72 ambulatory community dwelling women at four centers nationally participating in the beta and gamma tests of *Choices* FOR BETTER BONE HEALTH™ , an osteoporosis self-management program (mean age= 72.5 yrs ± 7.9). (1) We hypothesized that the belief that a woman could do any health behavior would be strongly correlated with her belief about a second health behavior. This was true for exercise and taking medication (r=0.27, p=0.02), exercise and managing pain (r=0.45, p=0.0001), taking CA/Vit D and taking medication (r=0.33,p=0.005) but was not seen for exercise and taking CA/Vit D (r=0.13, NS). (2) We hypothesized that psychosocial factors influence patients' beliefs that they can do bone health behaviors. Belief that one could cope with negative feelings was significantly correlated with beliefs that one could take medication (r=0.48, p<0.0001), exercise (r=0.27, p=0.02), take CA and Vit D (r=0.29, p=0.015) and manage pain (r=0.45, p<0.0001). (3) We hypothesized that those women who believed that osteoporosis was treatable would also believe that they could do each of the bone health behaviors. Believing that one could make one's bones healthier was significantly correlated with beliefs that one could exercise (r=0.55, p<0.0001), beliefs that one could manage pain (r=0.39, p=0.0036), beliefs that one could take meds (r=0.38, p=0.0005) and beliefs that one could take enough CA and Vit D (r=0.31, p=0.02). (4) In a subset of women (n=17) in the gamma test, we also studied the relationship between beliefs and self-report of the behavior. Correlations varied depending on the behavior: Calcium (r=0.77); Vit D (r=0.22); exercise (r=0.02); and managing pain (r=0.05).We conclude that: (1) Patients who believe they can do one bone health behavior believe they can do most other bone health behaviors,(2) psychosocial factors play an important role in adherence to bone health behaviors such as taking osteoporosis medication, (3) belief that osteoporosis is treatable is significantly correlated to beliefs about ability to do bone health behaviors, and (4) beliefs about a bone health behavior and the report of the performance of the behavior are not always highly correlated. Our study confirms the importance of self-efficacy beliefs in self-management of osteoporosis.

Disclosures: ***S.L. Silverman****, Procter and Gamble 5, 8.*

SU381

Differences and Similarities in Generic HRQoL of Osteoporosis and other Chronic Diseases in Postmenopausal Women in a Population Based Multicenter Study. M. G. Glüer*[1], D. M. Reid[2], C. C. Glüer[3], B. Stampa[4]. [1]Center for Biotechnology and Nutrition, Kiel, Germany, [2]University of Aberdeen, Aberdeen, United Kingdom, [3]University Hospital Kiel, Kiel, Germany, [4]Synarc A/S, Hamburg, Germany.

Although there are now data demonstrating the impact of osteoporosis on Health Related Quality of Life (HRQoL) these data are mostly derived from evaluation studies of osteoporosis specific questionnaires and pharmaceutical trials where patients are selected by distinct criteria. This is to our knowledge the first study that investigates these issues in a population based study (OPUS: Osteoporosis and Ultrasound study) with centers in Germany, Great Britain and France. We investigated in 2374 postmenopausal women (age range 55 to 79 years) self-reported disease and generic HRQoL, employing the SF12 and two items according to the Euroqol thermometer regarding health and HRQoL (0: dead to 100: best HRQoL). We categorized 5 major disorders (Osteoporosis: n=142, Angina Pectoris: n=107, Asthma: n=126, Cancer: n=97, Rheumatoid Arthritis (RA): n=76, total: n=548) according to self reported disease status. Women suffered from only one of the five selected disorders but may have had other health problems in addition. Patients with osteoporosis did not differ from patients with other disease groups in terms of the physical and mental function or with regard to overall Quality of Life and health perception. Except for the Mental Health domain of the SF12, HRQoL of osteoporotic patients was poorer than the rest of the sample ("Other', n=1782). This is particularly interesting because these groups are not necessarily entirely healthy but might suffer from chronic disease other than the five specified.

	SF12 physical	SF12 mental	Euroqol Health	Euroqol QOL
Osteoporosis	41.5±10.6 (n=133)	48.7±9.6 (n=133)	69.8±17.0 (n=137)	65.50±26.1 (n=136)
Cancer	44.6±9.3 (n=91)	51.3±8.9 (n= 91)	73.9±16.9 (n=94)	71.1±25.0 (n=95)
Asthma	42.2±11.0 (n=124)	48.1±10.2 (n=124)	70.7±18.8 (n=124)	69.8±23.4 (n=122)
Angina	41.0±10.5 (n=102)	48.6±10.2 (n=102)	68.9±18.8 (n=104)	67.2±25.8 (n=104)
RA	41.5±10.9 (n=73)	50.2±10.1 (n=73)	69.8±15.1 (n=74)	66.5±23.9 (n=73)
Other	45.7±10.1* (n=1750)	49.9±10.1 (n=1750)	74.1±16.8* (n=1782)	72.5±22.7* (n=1782)

* "Osteoporosis' vs. 'Other' p<0,05

Quality of Life is reduced in women with osteoporosis to a similar degree as in those with cancer, asthma, angina pectoris and RA. It is significantly lower than in study participants without these five disorders. These data need to be confirmed in an independent population database.

SU382

Parathyroid Hormone (PTH) and Alendronate in the Treatment of Osteoporosis: PaTH Trial Update. D. M. Black[1], C. M. Rosen[2], S. Greenspan[3], K. Ensrud[4], J. Bilezikian[5], T. Hue[1], J. McGowan[6]. [1]University of California San Francisco, San Francisco, CA, USA, [2]University of Maine, Bangor, ME, USA, [3]University of Pittsburgh, Pittsburgh, PA, USA, [4]University of Minnesota, Minneapolis, MN, USA, [5]Columbia University, New York, NY, USA, [6]National Institutes of Health, Bethesda, MD, USA.

The PaTH study's primary aim is to evaluate the efficacy of a rhPTH (1-84, 100 microgram/day) and alendronate (10 mg/day) combination therapy for osteoporosis on bone mineral density (BMD) and bone markers. PTH, an anabolic therapy, has been shown to increase BMD and prevent bone loss. PTH 1-34 has recently been shown to reduce fracture

risk. It is not known to what extent combination therapy of an anabolic agent with an anti-resorptive agent, such as alendronate, will be beneficial. Enrollment for PaTH was completed in September 2001. A total of 238 postmenopausal women with low BMD and a risk factor for subsequent fracture, were enrolled in a double-blind, randomized clinical trial, and will be followed for 2 years at 4 clinical centers in the U.S. The women were randomly assigned to 1 of 4 treatment groups: PTH alone, alendronate alone, PTH followed by alendronate and PTH concurrently with alendronate. PTH or its placebo is given only in the first year. The main endpoints include BMD measured by dual energy x-ray absorptiometry and biochemical markers of bone turnover. As of April 1, 2002, the median follow-time is 9 months and 94 (39%) have completed one year of treatment. The last patient will complete the first year in early September 2002. An analysis of the one-year data will be performed at that time and completed by January 2003. Adherence to protocol has been high. 81% of participants are still taking study injections and 88% are still taking study pills. About 97% are still participating in follow-up visits. In addition to the main study endpoints, we have instituted a number of ancillary studies including the effect of PTH/alendronate on spine and hip quantitative computed tomography (QCT) and ultrasound (Sahara). We are also studying the short-term effect of PTH/alendronate on serum calcium and on blood pressure. It is expected that this study will help to answer some of the important clinical questions about the optimal combination of PTH and anti-resorptive therapy.

SU383

Monthly Intravenous Pamidronate Is a Safe and Efficacious Treatment for Patients with Osteogenesis Imperfecta. I. Fujiwara[1], E. Ogawa*[1], Y. Igarashi*[2], K. Kojima*[1], Y. Katsushima*[1], K. Iinuma*[1]. [1]Pediatrics, Tohoku University School of Medicine, Sendai, Japan, [2]Igarashi Pediatric Clinic, Sendai, Japan.

Treatment with bisphosphonates are suggested to increase bone mineral density (BMD) and decrease fracture frequency in patients with osteogenesis imperfecta (OI). Effectiveness of intravenous (IV) pamidronate in cycles of 3 consecutive days with 3 to 4-month intervals is reported, though patients require hospitalization during the treatment. We show efficacy of monthly IV pamidronate at clinics for the period of 6 and 12 months for patients with OI type I/IV and OI type III, respectively. Fourteen patients with OI (7 with type I, 1 with type II, 5 with type III, 1 with type IV) were treated with monthly IV pamidronate (initial dose of 0.6 - 1.1 mg/kg) at the age from 1 month to 13 years (average 6 years and 9 months old). Pamidronate was administered at clinics except newborn patients. Lumbar bone mineral density (BMD) was measured by DXA and serum alkaline phosphatase (ALP) and urinary deoxypyridinoline (Dpyr) were analyzed before and after the treatment. Average fracture rate decreased from 5.3 to 1.1/year after IV pamidronate (p=0.037). Standard deviation (SD) scores of BMD for age significantly increased in both type I/IV (-3.38 to -2.18, p=0.018) and type III (-5.69 to -4.03, p=0.0002) after 6 and 12 months of treatment, respectively. BMD tended to sustain after cessation of the treatment, then they started to decline 12 months (type III) and 18 months (type I) after the therapy. Seven patients were re-treated because of significant decrease in BMD or increased fracture rate 14 to 103 (median 20) months after the cessation of the treatment. Dpyr showed a marked decline 1 week after the first treatment (43.7 % of baseline level [BL]), returned to the BL at 1 month in some patients, and stayed around 70 % of BL. ALP gradually decreased to 60 % of BL at 6 months after the treatment (p=0.026). Transient fever after the initial treatment in 6/14 and hypocalcemia in 2/14 were mild adverse effects observed. Respiratory distress deteriorated after pamidronate in a type II patient. Linear growth was not disturbed by the treatment in type I patients. These data suggested that monthly IV pamidronate at clinics is safe and effective for patients with OI who are without respiratory symptoms.

SU384

Identification of a Novel Splice Site Mutation in RUNX2 Gene causing Korean Cleidocranial dysplasia. H. Kim*[1], M. Hwang*[1], R. Park*[1], I. Kim[1], A. J. Van Wijnen[2], J. L. Stein[2], J. B. Lian[2], G. S. Stein[2], J. Choi[1]. [1]Biochemistry, Kyungpook Natl. Univ. School of Medicine, Daegu, Republic of Korea, [2]Cell Biology, Univ. of Massachusetts Medical School, Worcester, MA, USA.

Cleidocranial dysplasia (CCD) is an autosomal dominant disorder characterized by patent sutures and fontanelles, hypoplasia of clavicles, supernumerary teeth, short stature and other skeletal deficiencies. Haploinsufficiency of the RUNX2 gene results in a CCD. Each mutation of RUNX2 gene in CCD provides an opportunity to understand the pivotal role of RUNX2 gene during bone growth and development. In this study, we analyzed the coding region and 5'- and 3'-untranslated region of RUNX2 gene in five Korean CCD patients using PCR and direct sequencing. Clinical feature was taken by X-ray and photographs of the affected family members. The mutation of three different types was detected. One of them was a novel mutation and others were reported previously. First, we identified a novel exon1 splice donor site mutation (donor splice site GT → AT) at exon1- intron junction. Using RT- PCR, we found that this exon was skipped in affected patient. Second was a heterozygous C- to -T transition in exon7 leading to a translational stop codon in codon 391. Third, was missense mutation at arginine 225 (R225Q; CCG → CTG) in two patients. One case, we could not find any mutation in promoter (up to 755 bp from ATG translation start site), 5'-UTR, coding region and 3'-UTR. There was no difference in severity of phenotypes among patients with identified mutations. The novel splice donor site mutation will provide a useful window to understand how RUNX2 plays its role during bone growth and differentiation.

SU385

Bone Structure and Strength and Muscle-Bone Interactions in 15 Children with Osteogenesis Imperfecta (O.I.). A pQCT Study. E. J. A. Roldán[1], J. L. Ferretti[2], G. R. Cointry*[2], C. Tau[3]. [1]Dept. of Clinical Pharmacology, Gador SA, Buenos Aires, Argentina, [2]CEMFoC, Natl. Univ. of Rosario, Rosario, Argentina, [3]Dept. of Calcium Metabolism, Pediatric Hospital, Buenos Aires, Argentina.

This study analyzes the skeletal status and muscle-bone relationships in 5 boys and 10 girls aged 2-16 years with untreated type I (5), III (5) and IV O.I. (5) and 31 3-21-year controls. The cross-sectional bone area (CSA) and vBMD (attenuation threshold = .710 cm^{-1}), and the moments of resistance and Stress-Strength Indices (SSI's) for bending and torsion of the tibia, and the whole- and fat-free CSA's of the calf muscles were measured by pQCT (XCT-3000, Stratec) at the standard, 66% site of the leg. The vBMD, increasing with age in controls, remained around 900 g/cm^3 showing great dispersion in the O.I. children, corresponding the lowest values to type IV. Bone CSA and SSI's increased with age in controls an more slowly in type I O.I., remaining constantly low in types III-IV. The *"mass/accumulation" curves* between bone CSA (*y*) and vBMD (*x;* usually negative hyperboles) plotted higher for control than O.I. children, these showing no significant slope. Bone CSA and SSI's increased with mobility score, a variable affected by the O.I. type. Both bone CSA and SSI's increased in all groups with the fat-free muscle CSA, more in control than in O.I. children. The whole O.I. group showed single slopes with increasing values of both variables for types IV < III < I. The vBMD of all the O.I. children increased logarithmically with the muscle CSA's, reaching normal values at approximately 600 mm^3 of fat-free muscle CSA regardless of O.I. type. The fat-free/whole muscle CSA ratio decreased in the order: controls > type I O.I. > types III-IV O.I. Fracture incidence rate decreased exponentially with SSI's and mobility score in O.I. children of all types together. This shows that untreated O.I. children (specially types III and IV) are unable to improve compact vBMD, mass and strength with age, presumably because of both, mass/architecture and mineralization defects (low bone formation, enhanced intracortical porosity by disuse-mode remodeling) in proportion with muscle weakness. These effects could be associated with shifts in the mechanostat setpoints for triggering bone modeling and disuse-mode remodeling. Despite that pQCT determinations neglect the mineralization-unrelated, microstructural factors which are affected in O.I., the SSI's predicted adequately the fracture incidence in O.I. children.

SU386

Fracture Repair in Fibrous Dysplasia of Bone: Evidence for Local Segregation and Dynamic Selection of Disease Genotype. M. Riminucci[1], A. Corsi*[1], E. Ippolito*[2], P. Gehron Robey[3], P. Bianco[4]. [1]Medicina Sperimentale, Università dell'Aquila, L'Aquila, Italy, [2]Orthopedics, Universita Tor Vergata, Rome, Italy, [3]Nidcr, csdb, NIH, Bethesda, MD, USA, [4]Medicina Sperimentale e Patologia, Universita La Sapienza, Rome, Italy.

Fibrous dysplasia (FD) is a skeletal disease caused by postzygotic mutations of the Gs alpha gene and characterized by the growth of a pathologic osteogenic tissue at a single (monostotic) or multiple (polyostotic) skeletal sites. In long bones, FD is known to occur as medullary lesions, usually sparing the outer cortical bone. Pathological fractures represent a common complication of FD. We have investigated the repair process at four fracture sites in three patients with FD who underwent corrective surgery at 1, 3, 4 and 12 weeks after a long bone (femur and humerus) fracture. The histology was correlated to mutation analysis separately conducted for different histological components of the samples. The latter consisted in osteotomies depicting the intramedullary FD lesion, the subperiosteal repair reaction, and the periosteum, in an orderly spatial sequence. Reparative changes within the FD tissue proper consisted of an enhanced but dysplastic osteoid-formation activity, whereas reparative changes at subperiosteal sites were indistinguishable from normal ones. Histologically, the periosteal reaction consisted of formation of BSP-enriched lamellar bone deposited by morphologically normal osteoblasts, whereas the repair of fibrous dysplastic bone was noted for an excess deposition of BSP-deprived osteoid by morphologically abnormal osteoblasts. R201 mutations were demonstrated in all samples obtained from the FD lesions proper. In contrast, the disease genotype was not detectable (by DNA sequencing of the relevant PCR product) in the periosteum overlying the fracture, analyzed in 2/4 patients. In one of these, however, the mutation could be detected in the histologically normal subperiosteal bony callus (generated by periosteal cells), and in stromal cells isolated in culture from the callus. Our data show that a) the disease genotype is undetectable by standard methods in the periosteum overlying a mutation-positive FD lesion, indicating a spatial segregation of mutated cells across periosteum vs endosteum of the same bone region, b) proliferative events induced by a fracture, leading to the formation of a subperiosteal callus, positively select mutated cells, without necessarily leading to the deposition of FD bone. These data suggest that dynamic events of local selection of cells carrying the disease genotype are of critical importance in the pathophysiology of FD lesions and their complications.

SU387

Onset of Fibrous Dysplastic Lesions Is Related to the Skeletal Site of Involvement. J. S. Lee[1], N. Ziran*[2], C. Chen*[3], A. I. Leet[1], S. Wientroub[4], P. G. Robey[1], M. T. Collins[1]. [1]Craniofacial/Skeletal Diseases Branch, NIDCR/NIH, Bethesda, MD, USA, [2]Dept Orthopedic Surg, Univ of Rochester, Rochester, NY, USA, [3]Diag Rad/Nuc Med, NIH, Bethesda, MD, USA, [4]Dept of Ped Orthopedic Surg, Dana Children's Hosp, Tel Aviv, Israel.

Fibrous dyplasia of bone (FD) caused by post-zygotic activating mutations of GNAS1 is a slowly progressing skeletal condition. Years of follow-up are required to discern subtle changes in physical appearance. Additionally, unless a fracture in long bones or an expanding cyst associated with FD brings attention to the skeletal problem, detection of skeletal FD may be incidental and detected at a later age, especially in cases of monostotic FD. Thus, it is not clear when FD lesions occur, if a patient is born with lesions and if new lesions occur throughout life. Without question, FD lesions can expand to adjacent bones but understanding the onset of lesions may establish appropriate timing for medical therapy (before onset of lesions and skeletal deformity) or surgical therapy (after lesions stabilize; no new lesions develop). In a unique instance, the opportunity to evaluate patients for FD lesions at an early age occurs when patients are found to have precocious puberty (PP) in the setting of McCune-Albright syndrome (MAS). The aim of this study was to evaluate when and where FD lesions occur in patients with MAS. 9 female patients were included in this study. MAS was detected by onset of PP (menses or development of secondary sex characteristics before age 8); bone scans confirmed presence of FD. Serial bone scans were obtained for at least 4 years. The skeletal system was divided into craniofacial (CF) (8), axial (10), and extremity (18) sites. For the initial bone scan, mean chronological age was 4.7 (2.3-8.4); mean bone age was 7.5 (2.5-12.0). Average number of years between initial and latest bone scans was 11.3 (6.5-18.3). Average number of bone scans per patient was 4 (3-6 scans). In all cases, CF lesions were the earliest detected. When comparing the total number of lesions in the latest bone scans and the age at which the total number was reached, the number of CF lesions was established by the mean chronological age of 10.2 (3.6-20.1). The total number of extremity lesions was established by the mean chronological age of 13.4 (9.9-20.1). Total number of axial lesions was established by the mean chronological age of 15.1 (9.9-21.2). CF FD lesions appear earlier than in other regions, followed by those in extremities, and then in axial bones. In the context of MAS/PP, these results highlight the importance of early screening for skeletal lesions and initiation of appropriate therapy. This study also demonstrates the high occurrence of CF and axial lesions which had previously been considered infrequent.

SU388

Genetic Heterogeneity of Paget Disease of Bone in French-Canadian Families. S. Auger*[1], N. Laurin*[1], J. P. Brown[2], V. Raymond[1], J. Morissette*[1]. [1]Endocrinologie moléculaire et oncologique, Centre de recherche du Centre Hospitalier de l'Université Laval (CHUL), Quebec, PQ, Canada, [2]Groupe de recherche en maladies osseuses, Rhumatologie-immunologie, Centre de recherche du CHUL, Quebec, PQ, Canada.

Paget disease of bone is characterized by focal increases of the bone remodeling process. Genetic factors play a major role in the etiology of the disorder. Seven susceptibility loci have been mapped for the disease. Six are known as *PDB1* to *PDB6*. There is also one, as yet unnamed, locus at chromosome 18q23. We previously reported the mapping of 11 French-Canadian families affected by autosomal-dominant (AD) Paget disease to *PDB3* at 5q35-qter and the linkage of 2 other kindreds to *PDB4* at 5q31. We recently characterized the gene causing Paget disease at *PDB3* as Sequestosome1 (*SQSTM1/p62*). In the present study, we tested 10 additional pedigrees (104 individuals) for linkage at *PDB3*, *PDB4*, *PDB5* (2q36) and *PDB6* (10p13) using a total of 36 microsatellite markers. For linkage analysis, 25 subjects were considered affected, 10 unknown and 69 normal. Two-point and multipoint linkage analyses were performed assuming an AD mode of inheritance with incomplete penetrance. Two markers at *PDB3*, NL5 and D5S2073, showed positive two-point lodscores of 0.53 (θ=0.2) and 0.66 (θ=0.1), respectively. Parametric multipoint analysis, however, revealed lodscore values below -3 across the locus. For *PDB4*, two-point lodscore values below -2 were obtained for all 14 markers spanning 14 cM and multipoint analysis gave values below -4 over the region, showing evidence against linkage. For *PDB5* and *PDB6*, the summated two-point lodscore values were below -2 for 3 of 4 markers spanning 50 cM of each region. Multipoint lodscore values between -1 and -3 were obtained for both regions. These results did not support linkage of our families to any of these regions. When analyzed individually, a few families showed positive lodscore values to one or more region. In the majority of these kindreds, no haplotype cosegregated with the disease phenotype. Some families were too small to show evidence for or against linkage to any specific locus. As linkage to *PDB3* could not be excluded in some families, affected individuals of the 11 pedigrees were screened for mutations in the *SQSTM1/p62* coding region. No mutation segregating with the disease was detected in these families. Our study demonstrated that the *PDB5* and *PDB6* loci do not represent important loci for French-Canadian pagetic families who do not show linkage to *PDB3* or *PDB4*. These data therefore suggest that additional loci may be associated with Paget disease of bone in our population.

SU389

Role of TAF_{II}-17 in the Enhanced 1,25-Dihydroxyvitamin D_3 Responsivity of Osteoclast (OCL) Precursors from Paget's Disease. N. Kurihara[1], S. V. Reddy[1], J. Cornish[2], G. D. Roodman[1]. [1]Medicine, University of Pittsburgh, Pittsburgh, PA, USA, [2]Medicine, University of Auckland, Auckland, New Zealand.

We reported that bone marrow cells from patients with Paget's disease express measles virus nucleocapsid (MVNP) transcripts. Interestingly, expression of the MVNP gene in normal OCL precursors resulted in formation of OCL that shared many characteristics of OCL from Paget's patients (JCI 105, 607-614, 2000), including forming OCL at physiologic concentrations of 1,25-$(OH)_2D_3$, which were 1-2 logs less than required for normal OCL formation. Furthermore, MVNP transduced normal OCL precursors expressed high levels of TAF_{II}-17, a VDR binding peptide. Increased levels of TAF_{II}-17 were also present in pagetic OCL precursors. We hypothesized that the enhanced sensitivity of pagetic OCL precursors to 1,25-$(OH)_2D_3$ results from induction of a specific VDR co-activator by the MVNP gene. To test this hypothesis, RT-PCR analysis of MVNP transduced normal OCL precursors and pagetic bone marrow cells treated with 1,25$(OH)_2D_3$ was performed. TAF_{II}-17 mRNA was highly expressed in both of these cell types compared to other VDR co-activators (SRC-1, CBP/p300, DRIP-205). To determine if the increased levels of TAF_{II}-17 allowed formation of transcription complexes with the vitamin D receptor (VDR) at low concentration of 1,25-$(OH)_2D_3$, CFU-GM transfected with the MVNP cDNA or empty vector (EV) were treated with 10^{-10} to 10^{-8} M 1,25-$(OH)_2D_3$, and then used in GST-VDR pull down experiments. TAF_{II}-17 bound VDR in MVNP transduced cells at very low concentrations of 1,25-$(OH)_2D_3$ (10^{-10} M). In contrast, EV transduced cells required treatment with 10^{-8} M 1,25-$(OH)_2D_3$ for the TAF_{II}-17-VDR complexes to form. Furthermore, when CFU-GM transduced with the MVNP gene or EV were cultured for 14 days in the presence or absence, of a TAF_{II}-17 antisense oligodeoxynucleotide (AS-ODN) and treated with 10^{-11}-10^{-7} M 1,25-$(OH)_2D_3$ to induce OCL formation, AS-ODN decreased the amount of TAF_{II}-17 in MVNP transduced OCL precursors and inhibited OCL formation about 40%. Addition of mismatched AS-ODN to the cultures had no effect on OCL formation or TAF_{II}-17 expression levels. These data suggest that increased expression of TAF_{II}-17 may in part be responsible for the enhanced 1,25-$(OH)_2D_3$ responsivity of pagetic OCL precursors.

SU390

Serum Osteoprotegerin and Receptor Activator Nuclear Factor Ligand (RANKL) in Paget's Disease of Bone. L. Alvarez[1], N. Guañabens[1], P. Peris[2], I. Ros*[2], T. Ferró*[3], F. Pons*[4], X. Filella*[3], A. Monegal*[2], J. Muñoz-Gomez*[2], A. M. Ballesta*[3]. [1]Metabolic Bone Diseases Unit. IDIBAPS, Hospital Clinic, Barcelona, Spain, [2]Service of Rheumatology, Hospital Clinic, Barcelona, Spain, [3]Service of Biochemistry, Hospital Clinic, Barcelona, Spain, [4]Service of Nuclear Medicine, Hospital Clinic, Barcelona, Spain.

Osteoprotegerin (OPG) and receptor activator of nuclear factor k-B ligand (RANKL) have a crucial role in osteoclast formation and activity. However their contribution to the pathogenesis of Paget's disease, a bone disorder characterized by increased bone resorption and bone formation, is unknown. Aims: To evaluate serum OPG and RANKL in patients with Paget's disease of bone and their relationship to disease activity as well as the effect of bisphosphonate therapy on their values. Patients and methods: 31 patients (18 men and 13 women) aged 62.65 ± 2.01 years, with Paget's disease were included. Serum OPG, RANKL, bone alkaline phosphatase and procollagen type I N propeptide as well as urinary N-terminal cross-linking telopeptide of type I collagen were measured at baseline and at 1 month after discontinuation of therapy with tiludronate (400 mg/day/oral x 3 months). The activity of the disease was also evaluated at baseline by quantitative bone scintigraphy. The results were compared with those of a control group of similar age (61.64 ± 1.7 years) and gender (20 men and 19 women). Results: Patients with Paget's disease showed higher mean baseline OPG values compared with those of the control group (4.11 ± 0.39 vs 2.93 ± 0.11 pM/L, p=0.002). Serum OPG concentrations decreased significantly after treatment with tiludronate (3.488 ± 0.226 pM/L, p= 0.032). RANKL values were not significantly different from those of the control group (1.07 ± 0.2 vs 1.10 ± 0.15 pM/L, p=ns). Moreover, they did not change after therapy. No correlation was found between baseline OPG and RANKL levels and bone markers or quantitative scintigraphic indices. There were no differences in bone markers nor scintigraphic indices when patients were classified according to baseline OPG (> 4.1 pM/L vs < 4.1 pM/L) and RANKL (> 0.41 pM/L vs < 0.41 pM/L) values. Conclusions: Serum OPG increases in Paget's disease and decreases after treatment with tiludronate. Serum RANKL does not vary in Paget's disease. Both serum OPG and RANKL are unrelated to the activity of the disease. The increase in serum OPG may reflect a protective mechanism of the skeleton to compensate for increased bone resorption.

SU391

Large Phenotypic Variability of Paget Disease of Bone caused by the P392L Sequestosome1/p62 mutation. N. Laurin*[1], J. Morissette*[1], V. Raymond[1], J. P. Brown[2]. [1]Endocrinologie moléculaire et oncologique, Centre de recherche du Centre Hospitalier de l'Université Laval (CHUL), Quebec, PQ, Canada, [2]Groupe de recherche sur les maladies osseuses, Rhumatologie-Immunologie, Centre de recherche du Centre Hospitalier de l'Université Laval (CHUL), Quebec, PQ, Canada.

Paget disease of bone (PDB) is a common disorder characterized by focal and disorganized increases of bone turnover. Seven loci have been associated with this disorder. Last year, we reported the mapping of the third locus associated with the disorder, *PDB3,* at 5q35-qter. Using 24 French-Canadian families and 112 unrelated pagetic patients, we

recently identified the gene causing Paget disease at *PDB3* as sequestosome1 (*SQSTM1/p62*). A recurrent mutation in *SQSTM1/p62* (P392L) was detected in 11 pedigrees (46%) and 18 sporadic cases (16%). According to our data, the penetrance of this mutation reached 80 % for individuals 60 years old and over. The aim of this study was to assess genotype-phenotype analysis of the P393L mutation. The individual phenotype of 20 patients carrying the P392L mutation (all members of two extended families and including a homozygote) was evaluated. The severity of the disease was assessed by the age at onset, the levels of total serum alkaline phosphatase (SAP) and the bone involvement (number of sites and area of the skeleton affected by PDB calculated by the use of Rénier et al.'s index). A wide range of clinical severity was seen among individuals carrying the P392L mutation. The age at onset varied between 27 to 72 years old and one 77 year-old individual did not show any sign of the disease. The majority of patients from these two families were diagnosed in the scope of this study. The number of affected bones was between 1 to 31 for affected patients and the percentage of affected skeleton between 1 to 64%. These observations are not correlated with the current age or age at diagnosis. The homozygote was severely affected (age at diagnosis 46, 26 affected bones and 31% of the skeleton affected), however, his phenotype is comparable to at least five other family members who are heterozygote for the P392L mutation. The phenotypic expression was highly variable within these two families. However, all patients with the PDB phenotype had the P392L mutation. These observations suggest that there might be other important genetic (background) and/or environmental factors, such as a common viral infection (measles), that could contribute significantly to the variability in the severity of Paget disease of bone. We are currently evaluating the serologies for measles virus in these patients.

SU392

Normalization of Hypercalcemia with the Calcimimetic AMG 073 in a Patient with Metastatic Parathyroid Cancer. M. Peacock. School of Medicine, Indiana University, Indianapolis, IN, USA.

Management of metastatic parathyroid cancer and its associated hypercalcemia is challenging given its resistance to anti-cancer therapy. Progressive morbidity and eventual mortality often result from the hypercalcemia rather than the cancer. The calcimimetic AMG 073 has been shown to reduce serum PTH and normalize hypercalcemia in patients with primary hyperparathyroidism*. This report describes the use of AMG 073 to manage hypercalcemia in a patient with metastatic parathyroid cancer. A 57 year-old woman underwent total parathyroidectomy for parathyroid gland cancer 7 years prior to the study, and subsequently developed neck and lung metastases. Before treatment with AMG 073, serum calcium was 14.0 mg/dL, intact PTH was 785 pg/mL, and she had marked symptoms of hypercalcemia, including lassitude and drowsiness. The hypercalcemia did not resolve with local radiation or bisphosphonate therapy. AMG 073 30 mg bid was initiated, and the dose increased every 2 weeks to achieve a serum calcium ≤ 10.0 mg/dL. Serum calcium began to fall within 1 week of starting therapy and continued to fall as the dose was increased. Hypercalcemia normalized after 14 weeks at a dose of 70 mg tid. The patient was normocalcemic on this dose after 22 weeks (Table). Her symptoms resolved as serum calcium fell, and she returned to normal activities. Plasma PTH decreased from 785 pg/mL at baseline to 686 pg/mL at week 14, was 658 pg/mL at week 22, and 477 pg/mL at week 30. Serum alkaline phosphatase (sALP) decreased and serum phosphorus increased to normal with AMG 073 therapy.

(Normal ranges)	Calcium (8.4-10.3 mg/dL)	PTH (10-65 pg/mL)	Phosphorus (2.2-5.1 mg/dL)	sALP (31-115 U/L)
Baseline	14.0	785	2.2	330
Week 14	10.4	686	3.9	289
Week 22	9.5	658	Not done	Not done
Week 30	10.8	477	2.9	245

The calcimimetic AMG 073 was well-tolerated, reduced PTH, and was highly effective in normalizing hypercalcemia and controlling the associated symptoms in this patient with metastatic parathyroid cancer.

*Peacock M, et al. The calcimimetic AMG 073 reduces serum calcium in patients with primary hyperparathyroidism. *J Bone Miner Res* 2001; 16(Suppl 1): S163.

Disclosures: ***M. Peacock****, Amgen Inc. 5.*

SU393

Expression of *GCMB* by Intrathymic PTH-secreting Adenomas Indicates Their Parathyroid Cell Origin. A. Maret*[1], C. Ding[1], S. S. Kadkol*[2], W. H. Westra*[2], M. A. Levine[1]. [1]Pediatric Endocrinology, Johns Hopkins University, Baltimore, MD, USA, [2]Pathology, Johns Hopkins University, Baltimore, MD, USA.

The *GCMA* and *GCMB* genes encode human orthologs of the *Drosophila* glial cells missing (gcm) gene. *GCMB* is uniquely expressed in developing and mature parathyroid cells and is critical for the development of the parathyroid glands in mice as well as in humans. Mice in which parathyroid glands have been surgically removed or genetically ablated (*Gcm2* knock out) have residual PTH production from a subset of thymic cells that co-express the *Pth*, *Casr,* and *Gcm1* genes. These findings suggest that intrathymic adenomas that produce PTH might be derived from thymic epithelial cells that express *GCMA*. The goal of the present study was to determine the cell-type origin of intrathymic parathyroid adenomas. We obtained paraffin-embedded thymic tissue from normal subjects of varying ages as well as 16 adult patients diagnosed with intrathymic parathyroid adenoma. A eutopic parathyroid adenoma served as a control. Total RNA was extracted from five 10-µm sections of each paraffin block using xylene and digestion with Proteinase K followed by phenol/chloroform extraction. After treatment with DNase I the yield of total RNA was estimated by RT-PCR of 18s ribosomal RNA. Exonic primers that span one intron were designed to amplify *GCMB* and *GCMA* mRNA by RT-PCR, yielding predicted fragments of 120-bp and 182-bp, respectively. RT-PCR analysis of normal human thymus from a fetus and subjects aged 7 days to 21 years showed expression of *GCMA* mRNA (40-60 cycles) but not *PTH* (60 cycles) mRNA or *GCMB* mRNA (60 cycles). All intrathymic parathyroid adenomas and the eutopic parathyroid adenoma revealed a 120 bp fragment for *GCMB* mRNA (41 cycles). No *GCMA* product was seen after the same number of PCR-cycles. The identity of the *GCMB* amplicons was confirmed by direct sequence analysis and slot blot analysis using an internal 21 bp *GCMB* oligonucleotide. In conclusion, our data show that normal human thymus expresses the *GCMA* gene, and that intrathymic parathyroid adenomata express *GCMB.* Thus, intrathymic parathyroid adenomas are not derived from thymic epithelial cells but rather from ectopic parathyroid cells that had likely migrated errantly during embryogenesis.

Disclosures: ***M.A. Levine****, Merck 8; Procter and Gamble 8; Lilly 8.*

SU394

Vascular Stiffness Is Increased in Patients With Primary Hyperparathyroidism. M. R. Rubin, M. S. Maurer*, B. E. Diamond*, L. E. K. Coffin*, J. P. Bilezikian, S. J. Silverberg. Columbia University, College of P & S, New York, NY, USA.

When primary hyperparathyroidism (PHPT) was a more symptomatic disease, it was often associated with increased cardiovascular risk. As the clinical manifestations of the disease have changed to a milder, more asymptomatic disorder, investigation is shifting to more subtle cardiovascular abnormalities. It has been proposed that PHPT increases vascular calcification and stiffness and hence cardiovascular risk. Previous reports on vascular stiffness in PHPT are limited by confounding lipoprotein abnormalities and lack of anthropomorphic data. We measured arterial stiffness in 25 patients (Pts) with mild PHPT (serum calcium 10.6 ± 0.1 mg/dl, PTH 119 ± 19 pg/ml) and in 83 controls (Ctls). Arterial stiffness was measured mathematically with a non-invasive device (Sphygmocor, Australia) as the augmentation index (AI). AI increases as arteries stiffen, resulting in a heightened aortic systolic pressure and increased left ventricular afterload. Pts and Ctls were similar to each other in age and gender. We found no significant difference overall between the groups in AI (Pts 143 ± 4 %, Ctls 137 ± 3 %; p=NS). However, when variables altering vascular stiffness (obesity, height, hypertension, diabetes mellitus, atherosclerosis, and smoking) were controlled for, a significant difference was found (P<0.01 for model). In this model, AI was increased in Pts as compared with Ctls (P<0.05). The increase in AI was positively associated with higher PTH levels (R=+0.505; P=0.01) and negatively associated with radial BMD (R= -0.450; P<0 .05). There was no association between AI and serum or urinary calcium or markers of bone turnover. In summary, vascular stiffness is increased in patients with mild PHPT. The increase is associated with evidence of more active parathyroid disease (higher PTH, lower cortical BMD). It is not known whether increased AI is due to vascular calcification, to direct properties of PTH, or to other factors. The findings of increased vascular stiffness may have important implications for management decisions in asymptomatic PHPT.

SU395

Atypical Adenoma: A New Form of Parathyroid Neoplasia. M. R. Rubin[1], S. J. Silverberg[1], V. L. LiVolsi*[2], B. Bennett*[1], T. P. Jacobs[1], J. P. Bilezikian[1]. [1]Columbia University, New York, NY, USA, [2]University of Pennsylvania Health System, Philadelphia, PA, USA.

When primary hyperparathyroidism (PHPT) presents as a mild, asymptomatic disorder and not accompanied by indications for surgery, conservative monitoring is appropriate. When PHPT presents as a symptomatic disorder accompanied by indications for surgery, operative removal is appropriate. Rarely, some patients in this latter category have parathyroid carcinoma (PCA). It accounts for <1% of patients with PHPT and is cured only by surgery. It is important to determine which symptomatic cases of PHPT are likely to be cancerous. Clinical features which distinguish PCA from benign PHPT include markedly elevated levels of serum calcium and PTH and overt renal and skeletal involvement. Histologic features include capsular or vascular invasion to the thyroid or soft tissues, mitotic figures in tumor parenchymal cells, uniform sheets of cells separated by fibrous trabeculae and metastases. Recently, a new pathologic entity, "atypical adenoma" (AA), has been defined. AA is described by adherence to soft tissues of the neck or thyroid, mitoses, marked cytologic atypia, capsular entrapment and invasion (into but not through the capsule) and intratumoral fibrosis. The clinical features of AA have not yet been defined. We now report 7 patients (Pts) with active PHPT, in whom pre-operative suspicion for PCA was low, but who were all operative candidates. 3 patients were overtly symptomatic (kidney stone, n=1, fractures, n=2). Serum calcium was > 12 mg/dl in 4 of the 7 Pts; PTH was 247 ± 106 pg/ml (range: 74-876; nl: 10-65). Urinary calcium was 260 ± 60 mg/g Cr. All 4 women and 3 men (age: 60.1 ± 3.1 yr) were diagnosed at the time of surgery and initial histology as PCA with capsular invasion (n=3), or atypical cells with nuclear pleomorphism (n=4). However, after more detailed review, 4 samples were interpreted as AA, 1 patient had confirmed PCA and 2 had typical adenoma. There was no recurrent disease during 4 ± 3 years of follow up (range: 1-7), with normal serum calcium (9.3 ±0.2 mg/dl) and PTH (44.9 ±7.5 pg/ml). Bone density improved by approximately 10% (LS T-scores: -2.6 ±0.7 to -1.8 ±0.7; P=0.09). AA may represent a precursor lesion of PCA. However, in this small group, surgical cure of AA and PCA was associated with biochemical and BMD improvements similar to those seen with benign PHPT. In summary, in patients who have clinical features of more active PHPT than usual, but who are not suspected to have PCA, the possibility of PCA or this new pathologic entity, AA, should be considered.

SU396

The Relationship of Serum RANKL to Bone Resorption in States of Acute and Chronic Parathyroid Hormone Excess. I. A. Nakchbandi*[1], U. Masiukiewicz[1], M. Mitnick*[1], R. Lang*[2], B. Kinder*[1], K. L. Insogna[1]. [1]Yale University School of Medicine, New Haven, CT, USA, [2]Osteoporosis Center, Hamden, CT, USA.

It has been previously reported that both acute and chronic elevations in circulating PTH levels are associated with increased serum levels of IL-6 and its soluble receptor (IL-6sR). Blood levels of IL-6 and IL-6sR rise rapidly during short-term PTH infusions and are markedly elevated in patients with primary and secondary hyperparathyroidism. In these patients, both serum IL-6 and IL-6sR correlate with markers of bone resorption and in a recent longitudinal study of patients with primary hyperparathyroidism, serum IL-6sR correlated strongly with rates of femoral bone loss. Since it is now possible to measure serum RANKL and OPG in humans and since PTH regulates RANKL expression, we examined the relationship between serum RANKL/OPG and bone resorption in subjects infused with PTH and in patients with primary hyperparathyroidism. Thirteen postmenopausal women were infused with PTH for 36 hours. PTH induced slight increases in serum RANKL (0.9±0.1→1.3±0.1 pmol/L, nl<1.0) while OPG declined slightly (5.4±0.7→4.5±0.6 pmol/L) during the infusions. Serum RANKL was only weakly correlated with bone resorption markers (urine Dpd; r=0.2, p<0.05). In 29 patients with primary hyperparathyroidism, serum RANKL levels were more significantly elevated at 1.7±0.1 pmol/L while OPG remained within the normal range (5.6±0.3 pmol/L). The elevation in RANKL correlated with both urinary DPD and serum NTX (r=0.5, p<0.005 for DPD; r=0.4, p<0.05 for NTX). Serum RANKL also correlated with serum IL-6sR (r=0.55, p<0.005). Similarly to IL-6sR, RANKL correlated negatively with rates of bone loss at the total femur, r=-0.55, p<0.005. We conclude that circulating levels of RANKL are increased in states of chronic parathyroid hormone excess, and that in hyperparathyroidism, serum RANKL correlates with rates of bone loss at the total femur.

SU397

A Huge Lytic Bone Lesion Prior to and Following Parathyroid Adenoma Excision After 30 Years Follow-up. A. Halabe*[1], M. Harel*[2], D. Gonzalves*[3], M. Lorberboym*[4], G. Gvirtz*[3], R. Shor*[1]. [1]Internal Medicine and Metabolic Bone Diseases, Edith Wolfson Medical Centre, Tel Aviv Israel, Israel, [2]E.N.T., Edith Wolfson Medical Centre, Tel Aviv Israel, Israel, [3]Department of Radiology, Edith Wolfson Medical Centre, Tel Aviv Israel, Israel, [4]Department of Nuclear Medicine, Edith Wolfson Medical Centre, Tel Aviv Israel, Israel.

Bone involvement as a complication of primary hyperparathyroidism is rarely seen nowdays. We present an 82 years old patient who suffered from left kidney stones since 1970 because of primary hyperparathyroidism. The diagnosis was based on the presence of hypercalcemia, hypophosphatemia, lowTmP/GFR and elevated serum iPTH levels. In 1971 she underwent left uretherolithotomy followed one year later by left nephrectomy due to infected kidney stones. A cervical exploration was performed but no adenoma was found and two parathyroid glands were removed. Venous sampling was performed, indicating a venous gradient at the right lower pole of the thyroid gland. A second exploration was performed, and the right pole of the thyroid gland was removed where other normal parathyroid gland was found. Further investigations at N.I.H. included venous sampling, arteriography and a mediastinal exploration but no adenoma was found. She was treated with orally inorganic phosphates controlling her serum calcium around 10-11 mg/dL, 24h-urinary calcium excretion around 300 mg/24h and serum iPTH 100-200 pg/mL. Since 1993 there was a progressive increase in serum PTH up to 3000-4000 pg/mL. A parallel increase in serum alkaline phosphatase from normal up to 900 IU was also observed. Serum calcium 10.8 mg/dL, and creatinine 1.4-1.8 mg/dL remained stable. Two years ago the patient was reported to be bed-ridden for a period of three months, due to severe pain at the left hemipelvis and sacroiliac joint. CT and MRI showed a tremendous osteolytic lesion involving mainly the left sacroiliac joint. A cervical U.S. and MIBI scan showed a parathyroid adenoma located between the common carotid artery and jugular vein on the left side. A third neck exploration was done and a parathyroid adenoma was partially excised. Histological examination demonstrated "chief cell" parathyroid adenoma with fibrous tissue and no mitosis or malignant cells. Following surgery, the patient was given oral calcium 2.0 gr/day and alpha D_3 1.0 ucg/day for a period of 14-months. Serum calcium stabilized around 10.5 mg/dL, PTH levels declined to around 250-340 pg/dL and alkaline phosphatase returned to 250 IU. A repeated CT of the pelvis showed a significant improvement of the bone lesion. This case is unique because of the new bone lesion affecting mainly the sacroiliac joint with clinical and radiological evidence of improvement and the lengthy follow-up of thirty years.

SU398

Genotype-phenotype Relationship in Human Autosomal Recessive Osteopetrosis (arOP) Dependent on Mutations of the ATP6i Gene. A. Taranta, S. Migliaccio, I. Recchia*, M. Caniglia*, M. Luciani*, G. De Rossi*, C. Dionisi-Vici*, R. M. Pinto*, P. Francalanci*, R. Boldrini*, E. Lanino*, G. Dini*, G. Morreale*, D. Del Principe*, F. Cassini*, G. Palumbo*, S. H. Ralston, A. Villa*, P. Vezzoni*, A. Teti. Experimental Medicine, University of L'Aquila, L'Aquila, Italy.

The ATP6i gene encodes for the osteoclast specific a3 V-ATPase subunit and accounts for 50% of patients with arOP. Genotyping of four patients revealed three new allele mutations, also confirmed by RFLP analysis. Patients shared macrocephaly, growth retardation, impaired vision and generalized increase of bone mass. Massive and irregular primary spongiosa with unresorbed cartilage trabecular cores and fibrous tissue featured the bone biopsies. Significant numbers of hypo-functional, but morphological normal, osteoclasts were associated with the trabecular profiles, where shallow Howship lacunae were also observed. Abnormal obvious increase of active osteoblasts was noted, suggesting associated osteosclerosis pattern. Remarkably, patients shared high alkaline phosphatase activity, probably reflecting intense osteoblast activity. Hypocalcaemia was hypothesized to stimulate PTH release, as the PTH serum levels were elevated, and PTH was thought to determine increased osteoclasto- and likely osteoblasto-genesis. Abnormally intense TRAP activity was revealed in bone biopsies and in in vitro osteoclasts. TRAP activity returned to close normal levels in post-bone marrow transplant osteoclasts, suggesting their donor origin, also corroborated by positive outcome and improvement of osteosclerosis. An a3 subunit C terminus-targeted antibody failed to detect the a3 protein and the lymphocyte splice variant, TIRC7, by Western blot, as in our patients these proteins were predicted to be frame-shifted or truncated down-stream the mutations. Immuno-histo and -cytochemistry confirmed this occurrence, providing simple tools for early diagnosis. In vitro analysis of blood-born osteoclasts showed unremarkable cytoskeletal arrangement, podosome pattern, alphavbeta3 integrin, Pyk2 and c-Src distribution, confirming no morphological and/or adhesion/motility anomalies. In contrast, pit analysis demonstrated impaired, but still remarkable bone resorption activity, suggesting partial molecular complementation of the a3 subunit by alternative proton transport mechanisms, and providing a background for potential pharmacological targets to be investigated. In conclusion, we provided evidence suggesting common cellular and clinical features in patients harboring mutations in the ATP6i gene, and suggested potential tools for early diagnosis and pharmacological targeting for this severe disease.

SU399

IV Bisphosphonate Therapy in Children Under 36 months of Age with Osteogenesis Imperfecta. L. A. DiMeglio[1], L. Ford*[2], C. McClintock*[2], M. Peacock[2]. [1]Pediatric Endocrinology, Indiana University, Indianapolis, IN, USA, [2]Medicine, Indiana University, Indianapolis, IN, USA.

Bone mineral density (BMD) and fracture rates in children with osteogenesis imperfecta (OI) improve with oral and intravenous (IV) bisphosphonate therapy. There is limited data available on the efficacy of this therapy in very young children with OI. To examine this, we have instituted a prospective clinical trial of IV bisphosphonate in children under the age of 3. Children (n=8) received cycles of IV pamidronate, 1.5 mg/kg over 3 days every 2 months until the age of 2, then 2.25 mg/kg over 3 days every 3 months until the age of 3, then 3 mg/kg over 3 days over the age of 3. Three children received some infusions via a port or central venous line. The primary outcome was total body (TB) BMD, which was measured at 4-monthly intervals. Secondary outcomes included: biomarkers of bone turnover, fracture incidence, calcium biochemistry, anthropometric measures, dental anomalies, audiologic evaluations, assessment of quality of life, pain measures, and evaluations of gross motor function. Characteristics of 8 children (6 with type III (severe) OI and 2 with type I (mild) OI) are summarized in the table. (Rx = Treatment; ND = not done)

OI Type	Age at Start of Rx	Time of Rx/# of Infusions	Annualized % Change TB BMD	Fractures before/ during Rx
III	1 month	8 months/6	14%	15 / 1
III	2 months	6 months/4	3.2%	5 / 0
III	4 months	29 months/15	28%	9 / 5
III	4 months	6 months/4	33%	1 / 0
I	11 months	27 months/12	14%	2 / 0
III	15 months	14 months/7	-10%	14 / 7
III	32 months	3 months	ND	28 / 0
I	35 months	24 months	14%	3 / 0

The children have demonstrated an increase in BMD beyond expected for age and a decrease in markers of bone turnover on therapy. Radiographs showed discrete dense bands under growth plates corresponding to infusions. Other than fevers following the initial dose of IV bisphosphonate, no adverse effects of therapy have been noted. The children have maintained normal height/length and weight gain. These data confirm that IV bisphosphonate therapy is safe and effective for very young children with OI.

SU400

Abnormal Peri-Pubertal Growth and Development in Girls with Adolescent Idiopathic Scoliosis. W. T. K. Lee*[1], C. S. K. Cheung*[1], X. Guo[2], S. P. Tang*[1], J. C. Y. Cheng*[1]. [1]Orthopaedics & Traumatology, The Chinese University of Hong Kong, Shatin, Hong Kong Special Administrative Region of China, [2]Rehab. Sciences, Hong Kong Polytechnic University, Kln., Hong Kong Special Administrative Region of China.

Adolescent Idiopathic Scoliosis (AIS) is a 3-dimentional deformity of the spine affecting girls in majority between aged 9-16-y. Abnormal pattern of physical growth has been described in AIS patients. Sequential anthropometric development and its variation with pubertal maturation in AIS girls has not been reported. A cross-sectional study was conducted to examine the physical growth of AIS patients *vs.* age and maturity matched normal controls during peri-pubertal period of growth. 582 AIS girls aged 11-16-y and 206 age-matched healthy girls were recruited. Weight (Wt), height (Ht), body mass index (BMI), arm span, sitting height (SH) and Leg length (LL) were evaluated using standard methods. Tanner's staging (Breast stage, BS) was used to grade pubertal maturation. At pre-puberty, AIS girls had significantly shorter arm span, SH & LL than those of controls (Table 1). After the onset of puberty, the reverse relationship was observed. The differen-

tials of arm span and LL gradually increased *with significant differences* between the AIS and control group (Table 1). In addition, Wt and BMI of AIS were found significantly lower than those of controls from BS 2-4 (p= 0.05 - 0.01). Table 1. Percent change in body segments between AIS & Control group using independent t-test

Breast Stage (BS)	Ht	Arm span	LL
	% Difference from the Control group (P-value)		
1	- 4.7 % (0.03)	- 4.3 % (0.04)	- 6.0 % (0.002)
2	- 0.9 % (ns)	+ 1.7 % (0.029)	+ 1.7 % (0.049)
3	- 0.3 % (ns)	+ 1.3 % (0.039)	+ 1.5 % (0.018)
4	+ 1.4 % (0.013)	+ 3.3 % (<0.001)	+ 3.3 % (<0.001)
5	+ 3.9 % (0.003)	+ 5.1 % (0.001)	+ 6.2 % (0.002)

To conclude, body segments: Ht, arm span, SH and LL were significantly shorter in AIS before the onset of puberty. However, body segments of AIS grew significantly longer than those of controls after the onset of puberty, and the discrepancies became larger when the AIS became sexually matured. Results of this large-scale study indicates the presence of abnormal peripubertal anthropometric growth in AIS pointing to likely underlying abnormalities in the regulation of growth and maturation in AIS.

SU401

The Pharmacokinetics and Short-Term Safety of Alendronate in Children and Adolescents with Osteogenesis Imperfecta (OI) Type I. L. M. Ward[1], A. E. Denker*[2], A. G. Porras*[2], S. Shugarts*[2], R. Travers[1], C. Mao*[2], A. Dynder*[2], P. Deutsch*[2], F. H. Glorieux[1]. [1]Genetics Unit, Shriners Hospital for Children, Montreal, PQ, Canada, [2]Merck & Co., Inc., Whitehouse Station, NJ, USA.

Alendronate (ALN) has potential use as a weekly oral agent in pediatric patients with osteoporotic conditions. Our aim was to evaluate the pharmacokinetics and short-term safety of ALN in children with mild OI. Twenty-four children (4-16 yrs) with OI type I received ALN 125 µg IV and oral ALN in a two-period randomized crossover study, with doses separated by a two week washout. The oral dose was 35 mg for patients weighing < 40 kg, 70 mg for ≥ 40 kg. Urine was collected for 24 hrs to determine the total urinary excretion of ALN (TUE-ALN). Patients were monitored for 24 hrs following ALN dosing and phone contact was made 10-14 days after the second dose. Laboratory safety parameters were evaluated pre- and post-study. Twenty-four patients successfully completed the study. 13 subjects received the IV dose and 11 received the oral dose in the first period. The TUE-ALN (dose-adjusted to 1 mg) and bioavailability (%) were as follows:

Dose	LS† Mean TUE-ALN (µg)	SD‡	Bioavailability (%)	95% CI§ for Bioavailability
<40 kg, N=12				
35 mg PO	1.9	1.6	0.43	0.28, 0.64
125 µg IV	441.9	61.0		
≥40 kg, N=12				
70 mg PO	2.4	2.1	0.56	0.36, 0.87
125 µg IV	438.5	90.7		

Root Mean Squared Error = 0.444 (ANOVA model); †LS = Least-Squares (back-transformed from the log scale); ‡SD = Standard Deviation; §CI = Confidence Interval. Comparing adult data from historic studies with results from the pooled pediatric patients, there was no difference in the bioavailability (Geometric mean ratio (GMR) (pediatric/adult)=0.74, 95% CI 0.51,1.07) nor in the TUE-ALN following the IV dose (GMR=1.09, 95% CI 0.96,1.23). Eighteen of the 24 patients reported a total of 44 adverse experiences. All were mild or moderate in intensity, 80% (35/44) occurred within 48 hrs, 91% (40/44) lasted <24 hrs, and 75% (33/44) followed the oral dose. The most common side effects were headache (N=7), nausea (N=7), fever (N=5) and abdominal pain (N=6). Slight decreases were observed in the absolute lymphocyte count and serum alkaline phosphatase at post-study. In conclusion, the bioavailabilities of single oral doses of ALN 35 mg (for children < 40 kg) and 70 mg (for children ≥ 40 kg) were similar to each other and to adults in previous studies. In addition, the TUE-ALN following the IV dose was the same for younger and older children and no different compared to adults, suggesting similar percent distribution to bone regardless of age. The drug was generally well-tolerated.

Disclosures: ***L.M. Ward****, Merck & Co., Inc. 2.*

SU402

Feet in a Family with Type I Osteogenesis Imperfecta (OI). J. Reese*[1], A. L. Burshell[2], W. Coleman*[3]. [1]Medical Student, Tulane University, New Orleans, LA, USA, [2]Section on Endocrinology, Ochsner Clinic Foundation, New Orleans, LA, USA, [3]Orthopedics, Ochsner Clinic Foundation, New Orleans, LA, USA.

Type I OI is the mildest type of OI and is caused by a quantitative defect in Type I collagen. The genetic defect in this large Acadian family is a single base pair substitution in COL1A1 causing one of the two proalpha1 chains not to be expressed. The affected family members have blue sclera, premature hearing loss, frequent childhood fractures, low BMD by DXA, increased flexibility and frequent foot complaints. Ten affected family members (5 women and 5 men) were compared to 16 non-affected non-family (9 women and 7 men) and 2 non-affected family members (1 woman, 1 man). Anteroposterior (AP) and lateral weight bearing X-rays were performed on each foot. Various angles and distances were drawn and measured by 2 observers. Data for each subject was averaged for each foot and observer's measurement, and OI feet compared to controls as well as published references. Lateral radiographs showed that the calcaneal inclination angle was significantly reduced in OI subjects. Additionally, the inferior calcaneal angle was decreased when compared to the 1st metatarsal declination angle, indicating rearfoot collapse. AP radiographs showed the following angles were significantly reduced in OI subjects compared to controls: calcaneus to midfoot, metatarsus adductus and the 2nd-5th intermetatarsal angle. The OI foot collapsed into pronation primarily in the sagittal plane. OI subjects often had a forefoot varus alignment, increased ankle dorsiflexion tested with the knee flexed, narrow foot width, and decreased metatarsal width. The feet of family members affected with OI demonstrate a unique combination of abnormalities. It seems probable that these changes are related to this family's known genetic abnormality of Type I collagen, which may adversely affect the bones, ligaments and tendons. It is unknown whether similar abnormalities are found in other genetic diseases of Type I collagen, including other families with Type I OI, Ehlers Danlos or osteoporosis.

SU403

Differential Diagnostics of Inherited Connective Tissue Diseases. V. Vyskocil. Department of Bone Disease, Charles University Hospital, Plzen, Czech Republic.

The authors followed 318 patients with connective tissue diseases from 1996 to 2001 (Marfan syndrome, Ehlers Danlos syndrome, osteogenesis imperfecta). The cause for that choice is genetic relationship of collagen defect. The studied groups consists of 52 patients with osteogenesis imperfecta OI, 82 children with Ehlers Danlos syndrome ED and 100 patients with Marfan syndrome MS and 84 with familiar joint hyperelasticity. As routine use of molecular genetic methods is impossible in an everyday practice the authors tried to apply the criteria combination for OI, MS and ED so that the validity of particular criteria could be evaluated and then used in diagnostic difficulties among the studied diseases. All 4 groups were examined by densitometry and also the markers of bone metabolism were evaluated (serum Ca, P, PTH, osteocalcin, PICP, telopeptid, in urine Ca, P, crosslinks). In the other 2 groups (ED, MS) the patients with decreased bone density were treated with calcium and vitamin D. Nevertheless the authors stated that in MS osteopenia would improve within 15-18 years even without therapy but in the 2 remaining groups (ED and OI) the treatment is necessary due to abnormal bone density. The present chest deformation was the indication for vital lung capacity measurements and FEV. The authors tried to evaluate the best clinical, radiograph, densitometric and biochemical criteria in diagnostic difficulties. **Conclusions:** In patients with OI the best criteria besides clinical findings were lower stature, asymmetry of the body and densitometry with decrease at least of 15 percent when compared with the other groups. That group has besides fractures the decrease of PICP and the highest levels of osteocalcin and crosslinks. The group of MS had no typical criterium in bone metabolism and densitometry when compared with OI and ED. For Marfan syndrome diagnostics the main criteria are metacarpophalangeal index, the index of arms´expansion to body height, positive ophthalmological findings and body dysproportion. At the same time pulmonary functions were worse in Marfan syndrom than in the groups with OI and ED. Ehlers Danlos syndrome had markedly increased osteocalcin besides basic diagnostic criteria and at the same time lower BMD of the forearm, close to patients with OI. Pes planus had no significance in all 3 groups. The answer to the treatment could be also the method of differential diagnosis in indistinct cases. The best reaction had patients with MS, lower increase of bone density had the patients with ED and the lowest one was in OI. The authors assume that the combination of different diagnostic methods is useful and could differentiate among those 3 groups of patients. Molecular genetics is the definite method in the unclear cases.

SU404

Vitamin D Status of Preterm Infants After Hospital Discharge. W. Koo, M. Hammami*. Pediatrics, Wayne State University, Hutzel Hospital, Detroit, MI, USA.

Preterm infants fed high calcium (Ca) and phosphorus (P) milk during hospitalization can maintain normal vitamin D status with low vitamin D intake. However, all preterm infants receive lower mineral milks after hospital discharge and it is not known whether this affects their vitamin D needs. We measured plasma 25 hydroxy-vitamin D (25 OHD) by radioimmunoassay, Ca and Mg by atomic absorption, and P by spectrophotometric method, at hospital discharge and at 4 and 12 months after hospital discharge, in preterm infants participated in a parallel, randomized, masked study fed milk formulas with either standard or enriched formulation. Ca, P and vitamin D contents per 100 kcal of the former were 73 mg, 56 mg and 60 IU, and for the latter were 105 mg, 62 mg, and 80 IU, respectively. None received additional vitamin D supplementation. Preliminary results from 42 preterm infants (gestational age 28.4 +/- 2.3 wks) showed plasma 25 OHD concentrations in infants fed standard formula were 30.5 +/- 9.8, 33.9 +/- 11.2 and 31.5 +/- 5.0 ng/mL, and in infants fed enriched formula were 23.0 +/- 8.1, 35.1 +/- 9.3 and 34.4 +/- 7.9 ng/mL, respectively. Plasma 25 OHD in the latter group increased with time but there were no significant differences between groups by repeated measures analysis. None of the infants had plasma 25 OHD < 10 ng/mL at baseline and none of the infants had plasma 25 OHD < 19 ng/mL on follow up. Plasma Ca, Mg and P were normal in all infants. We conclude that vitamin D contents in the infant formulas studied are sufficient to maintain normal vitamin D status in preterm infants after hospital discharge.

SU405

Hyperparathyroidism in a Patient with Pseudohypoparathyroidism Type Ib. K. A. Kennel*[1], J. A. van Heerden*[2], R. V. Lloyd*[3], B. L. Clarke[1]. [1]Division of Endocrinology, Mayo Clinic, Rochester, MN, USA, [2]Department of Surgery, Mayo Clinic, Rochester, MN, USA, [3]Department of Laboratory Medicine and Pathology, Mayo Clinic, Rochester, MN, USA.

A 51 year-old female with pseudohypoparathyroidism type Ib developed parathyroid hyperplasia and hypercalcemia. She was diagnosed at age 13 years after years of paresthesias, with hypocalcemia (5.5mg/dL), hyperphosphatemia (8.4mg/dL), increased parathyroid hormone (PTH), and mild osteitis fibrosa on bone biopsy. She had no features of AHO or family history of hypocalcemia. She was given calcium and vitamin D supplementation. Her symptoms resolved, and repeat bone biopsy showed healed osteitis fibrosa. Subsequently, her urine cyclic AMP (cAMP) was found unresponsive to exogenous PTH. Recently, her PTH levels increased dramatically above her baseline level, and her serum calcium became mildly elevated. Her serum calcium was 10.2 mg/dL (8.9-10.1), phosphorus 3.2 mg/dL, and PTH 21 pmol/L (1.0-5.2) on supplemental calcium 1800 mg, 1,25-dihydroxyvitamin D 0.25 mcg, and hydrochlorothiazide 25 mg each day. Baseline urine cAMP was 2.0 nmol/dL glomerular filtrate (1.3-3.7). Her bone mineral density was normal. Neck ultrasound revealed two enlarged inferior parathyroid glands. Parathyroid sestamibi scan confirmed focal uptake in these locations. At surgery, both the right and left inferior parathyroid glands were enlarged. The superior glands were of normal size and appearance. Baseline intraoperative PTH was 43.7 pmol/L. After her right inferior 720-mg gland was removed, her PTH decreased to 31 pmol/L. After her left inferior 130-mg gland was removed, her PTH decreased further to 6.9 pmol/L. Pathology review indicated parathyroid hyperplasia in both glands. Tissue tumor markers Ki-67 and p27 were absent. Her postoperative serum calcium decreased to 8.6 mg/dL, with a PTH nadir of 3.3 pmol/L. She began calcium 2400 mg and 1,25-dihydroxyvitamin D 0.50 mcg daily. By postoperative day three her calcium was normal at 9.2mg/dL. Two weeks later her serum calcium remained normal and her PTH had increased to 16.3 pmol/L (1.3-7.6), indicating function of her remaining parathyroid tissue. Her serum calcium has remained normal on these doses of supplemental calcium and 1,25-dihydroxyvitamin D over two years of follow-up. This patient demonstrates that hyperparathyroidism may occasionally develop in patients with pseudohypoparathyroidism Ib. PTH resistance in this disorder is due to decreased GNAS1 expression in the proximal renal tubules. The patient's documented osteitis fibrosa suggests she had partial skeletal responsiveness to PTH. Chronic stimulation by mild ionized hypocalcemia over many years may have resulted in her parathyroid gland hyperplasia.

Disclosures: ***B.L. Clarke****, Merck and Co., Inc. 2.*

SU406

Height and Weight Development During Long-Term Therapy with Cyclical Intravenous Pamidronate in Children and Adolescents with Osteogenesis ImperfectaTypes I, III and IV. L. M. Zeitlin*[1], F. Rauch[2], H. Plotkin[2], F. H. Glorieux[2]. [1]Genetic Unit, The Shriners Hospitals for Children, Canadial Hospital, Montreal, PQ, Canada, [2]Genetic Unit, The Shriners Hospitals for Children, Canadian Hospital, Montreal, PQ, Canada.

Treatment with pamidronate significantly improves the clinical course in children with osteogenesis imperfecta (OI). However, it is often feared that bisphosphonate therapy might affect longitudinal growth. In this study we analyzed the short-term (1-year) and long-term (4-year) growth effects of 2 to 4-monthly intravenous pamidronate treatment in children and adolescents (age 0.04-15.6 years at baseline) with moderate to severe OI types I, III and IV. At baseline, patients of all OI types were short for age. In the 116 patients who completed one year of therapy height z-scores increased significantly in OI-III (mean±SD, +0.3±0.8, p=0.04; n= 42), but did not change significantly in OI-I (n=29) and OI-IV (n=45). Weight z-scores increased significantly in OI-I (+0.2±0.4, p=0.01). Forty-one patients completed four years of therapy. Mean height z-scores increased significantly for OI-IV (+0.41±0.71; p=0.04; n=12), whereas non-significant trends were found for OI-I (+0.23±0.55; p=0.17; n= 14) and OI-III (+0.42±1.45; p=0.31; n=15). When height was expressed as a percentage of the result expected for untreated patients with the same OI type, long-term pamidronate therapy was associated with a height gain of +5% for OI-I (p=0.03), +11% for OI-III (p=0.01) and +12% for OI-IV (p=0.001). The mean weight of the pamidronate treated patients increased significantly when expressed as a percentage of the expected weight-for-height in untreated patients (OI-I, p=0.002; OI-III, p=0.02; OI-IV, p=0.05). This was due to a few patients with considerable weight gain, whereas most patients followed the curves of untreated patients. In conclusion, 4 years of cyclical intravenous pamidronate treatment led to a significant height gain in moderately to severely affected OI patients. Some children with OI gain weight excessively during pamidronate treatment, which should be closely monitored.

SU407

Bone Formation Following Ischemic Necrosis of the Femoral Head in a Piglet Model. W. Pritchard*, D. Pringle*, H. Kim. Shriners Hospitals for Children, Tampa, FL, USA.

Femoral head deformity after ischemic necrosis can lead to premature degenerative arthritis. Surgically induced femoral head necrosis in piglets was developed as an animal model to study pathogenesis of femoral head deformity. Revascularization begins 2 wks after infarction with later replacement of necrotic bone by fibrovascular tissue, compromising structural integrity of the bony epiphysis. Little is known about bone formation after ischemic necrosis including whether fibrovascular tissue that replaces necrotic bone contains precursor cells capable of osteoblastic differentiation. The purpose was to study bone formation in the piglet model of ischemic necrosis and to determine if fibrovascular tissue contains osteoblast precursors. Ischemic necrosis was induced in 24 piglets by placing a ligature around the femoral neck. Animals were sacrificed at 1,2,3,4,6 and 8 wks after surgery. Contralateral, non-operated sides were used as controls. After gross and radiographic assessments, paraffin sections were prepared for picrosirius,H and E,and immunohistochemistry. Enzyme-linked immunohistochemistry with monoclonal antibodies to markers of osteoblastic differentiation (osteopontin and osteonectin) were used. The infarcted heads deformed over time with resorption of necrotic trabeculae and replacement by fibrovascular tissue. Over the 8 wk period, 3 types of bone formation were observed: endochondral, appositional, and de novo intramembranous. These were observed within the femoral heads at different locations and times. First, endochondral ossification was observed at the periphery of the epiphysis where revascularization had taken place. This produced small centers of ossification. Second, appositional bone formation was observed surrounding some of necrotic trabeculae in bony epiphyses producing thickened trabeculae. Finally, intramembranous de novo bone formation was observed within dense fibrovascular tissue. Intramembranous bone formation was delayed and observed only at 8 wks when deformity was already severe. Immunoreactivity to monoclonal antibodies was observed in mesenchymal cells within fibrovascular tissue prior to intramembranous bone formation. Polarized light microscopy showed woven bone. This study showed bone formation following ischemia of femoral heads occurred through endochondral ossification, appositional formation on existing trabeculae, and de novo intramembranous ossification. Formation of new bone could prevent deformation of the femoral head following ischemia. Further studies are required to define factors that stimulate new bone formation in fibrovascular tissue which can be used therapeutically to prevent femoral head deformity.

SU408

Dietary Phosphate Restriction Therapy for Hypophosphatasia: Preliminary Observations. D. Wenkert[1], M. N. Podgornik*[1], S. P. Coburn*[2], L. M. Ryan*[3], S. Mumm[1], M. P. Whyte[1]. [1]Cntr Metab Bone Dis & Mol Res, Shriners Hosp Child, St. Louis, MO, USA, [2]Ft Wayne St Devel Cntr, Ft. Wayne, IN, USA, [3]Dept Rheumatol, Med Coll WI, Milwaukee, WI, USA.

Hypophosphatasia, an inborn error of metabolism characterized by insufficient alkaline phosphatase (ALP) activity, results from deactivating mutations in the TNSALP gene that encodes the tissue-nonspecific ALP isoenzyme. TNSALP normally functions as an ectoenzyme. Consequently in hypophosphatasia, three phosphocompounds accumulate extracellularly: phosphoethanolamine (PEA), inorganic pyrophosphate (PPi), and pyridoxal 5′-phosphate (PLP). Excess PPi, which inhibits hydroxyapatite crystal growth *in vitro*, could explain the associated rickets. Interestingly, patients with hypophosphatasia have high-normal or elevated circulating inorganic phosphate (Pi) levels due to increased renal reclamation of Pi (&σηψ; TmP/GFR). Recent studies indicate that Pi is an important competitive inhibitor of ALP activity *in vivo* as well as *in vitro*. Accordingly, reductions in extracellular Pi levels might substantially increase endogenous ecto- TNSALP activity in hypophosphatasia. To explore the impact of changes in extracellular Pi levels in hypophosphatasia, 10 affected children were randomized to 3-day regimes of either dietary Pi restriction (1/2 RDA), oral Pi supplementation (21-36 mg/kg/d), or oral vitamin B_6 (pyridoxine) challenge (1/3 mg/kg/d) to assess short-term changes in endogenous TNSALP substrate accumulation. Pyridoxine loading substantially increased the already elevated plasma PLP levels (2.5-4.8 fold), but did not alter urinary PPi levels. Perhaps this is because PLP represents only a small fraction of endogenous phosphocompounds. However, Pi supplementation increased urinary PPi and plasma PLP levels, consistent with relatively large amounts of Pi competitively inhibiting TNSALP endogenously. Dietary Pi restriction successfully lowered urine Pi in only 1 of 3 patients. In this girl, plasma PLP and urinary Pi as well as urinary PPi each decreased by about 50% (no consistent plasma PLP or urinary PPi changes were observed in the other 2 subjects). Our preliminary findings suggest that decreases in extracellular Pi levels may be helpful for hypophosphatasia. Perhaps dietary Pi binders will be an effective medical treatment.

SU409

Bone Mineral Density Assessed by DEXA does not Improve Spontaneously during Puberty in Girls with Untreated Mild Osteogenesis Imperfecta. D. Wenkert[1], M. N. Podgornik*[1], W. H. McAlister*[2], M. P. Whyte[1]. [1]Cntr Metab Bone Dis & Mol Res, Shriners Hosp Child, St. Louis, MO, USA, [2]Mallinckrodt Inst Radiol, Wash Univ Sch Med, St. Louis, MO, USA.

Osteogenesis imperfecta types I and IV are the relatively mild forms of this autosomal dominant, type I collagenopathy. Both types feature osteopenia with recurrent fractures. Blue sclera help to characterize type I disease. It is widely held that the severity of OI (fracture incidence) decreases at the time of puberty. To test this assumption, charts from 12 Caucasian girls with relatively mild OI who had never received pharmacologic therapy were reviewed. Nearly all patients had undergone 3 or more DEXAs (Hologic) between the ages of 10 and 20 years. Nine had type I OI, 3 had type IV OI. Changes in BMD Z-scores (matched by age) were assessed using Hologic software for L_1-L_4 and using a Pediatric Bone Mineral Density Applet (http://www-stat-class.stanford.edu/pediatric-bones/) for total hip and femoral neck. Changes were assessed for sequential determinations. Although fracture frequencies decreased, there was no significant trend for improvement in BMD Z-scores at any of these sites "across" puberty. Decreased fracture frequency in OI at the time of puberty could reflect changes in physical activity, enhanced bone quality, and/or better skeletal geometry, but we find no DEXA evidence for spontaneous improvement in BMD Z-scores.

SU410

Osteoporosis Pseudoglioma Syndrome Caused by a Novel, Homozygous, 2-Base Pair Deletion in The LRP5 Gene. S. Mumm, D. Wenkert, J. Hagen*, M. P. Whyte. Div Bone Miner Dis, Wash Univ Sc Med, Barnes-Jewish Hospt & Center for Metab Bone Dis and Mol Res, Shriners Hospt for Child, St. Louis, MO, USA.

Osteoporosis pseudoglioma syndrome (OPPG) is an autosomal recessive disorder caused by inactivating mutations in the gene which encodes the low density, lipoprotein receptor-related protein 5 (*LRP5*). Clinical features include early-onset blindness (described as retinal dysplasia within the first few months of life, or phthisis bulbi with calcifications and cataract formation diagnosed after 1 year of age), micro-ophthalmia, osteoporosis leading to fractures, wormian bones, hypotonia, and developmental delay. A 1-year-old Caucasian girl of aunt/nephew parentage was found by routine eye exam at 4 days-of-age to have no red reflex. Bilateral retina detachment with persistent fetal retinal vasculature were unexplained. Ophthalmologic surgery preserved light/dark perception. At age 11 months, bilateral distal femur fractures occurred during a fall. She was osteopenic. Our assessment showed microcephaly, micro-ophthalmia, hypotonia, and hyperextensibility of all joints. At age 12 months, after she came out of a spica cast, compression fractures of T_8 were noted. At 13 months compression fractures of T_{10}-T_{12}, L_1, L_2, and L_4 were also noted. Mutation analysis of *LRP5*, including sequencing of exons and intron/exon boundaries, revealed a homozygous 2-base pair deletion (3194_3195delAC) in exon 14. This would cause a frame shift at amino acid 1065 (D1065fs) and addition of 71 missense amino acids. OPPG reveals that *LPR5* acts significantly in bone accrual. In 2002, a single base pair change in exon 3 of *LPR5* was shown to cause a benign phenotype, autosomal dominant high-bone mass trait. Deactivating mutations in *LPR5* cause OPPG syndrome with 6 homozygous disease-causing frame shift and nonsense mutations in *LPR5*, as well as 6 heterozygous putative disease causing missense mutations. These mutations were found in a variety of exons but not exon 14. Our patient has a novel, homozygous, 2-base pair deletion in yet another region of *LPR5* which is, therefore, important for the normal functioning of the gene product.

SU411

Incadronate Disodium Delays and Inhibits Periarticular Bone Atrophy and Joint Destructon in Rat adjuvant-induced Arthritis. T. Akiyama*[1], S. Mori[1], T. Mashiba[1], H. Dobashi*[2], S. Komatsubara*[1], K. Miyamoto*[1], Y. Cao*[1], H. Norimatsu[1]. [1]Department of Orthopaedics, Kagawa Medical University, Kagawa, Japan, [2]Department of 1st. Internal Medicine, Kagawa Medical University, Kagawa, Japan.

Joint detruction of Rheumatoid Arthritis (RA) is accompanied by periarticular bone loss. Bisphosphonates have been used as agents for osteoporosis treatment. In this study we investigated whether bisphosphonate can prevent or delay joint destruction and periarticular bone loss in RA by using rat adjuvant-induced arthritis (AIA) model. Arthritis was induced by injecting 0.1mg of heat-killed Mycobacterium butyricum into the base of tail of female Lewis rats(7 weeks age). Bisphosphonate(incadronate disodium : YM-175, Yamanouchi Pharmaceutical Co., Ltd.) was also administered subcutaneously 3 times per week at a dose of 0.01, 0.1 mg/kg/day. Body weight and hindpaw volume were checked every week. 2 and 4 weeks later, rats were sacrificed and both hindpaws were excised. Joint destruction was evaluated radiologically and histologically. Radiography of ankle (tibiotarsal) joint and tarsal bones were taken by using soft X-ray system. Decalcified saggital sections were cut from ankle joint, stained with toluidine blue and tartrate-resistant acid phosphatase(TRAP). Destruction of articular cartilage and subchondral bone and osteoclasts infiltration were evaluated by using histomorphometry. In arthritic rats body weight decreased and hindpaws swelling was observed at 1 week and 3weeks. At 2 weeks, no changes were observed both ragiolodically and histologically. At 4 weeks, widespread and severe destruction was observed radiographically in tibio-tarsal joint and tarsal bone in arthritic control group, while bone destruction was mild in YM-175 treated groups. Histologically, severe destruction of articular cartilage , numerous osteoclasts infiltration and marked osteopenia of subchondral bone were found in arthritic control group, while these changes were suppressed dose-dependently in YM-175 treated groups. The results show that periarticular bone atrophy and joint destruction were reduced by administering YM-175. However, several destructive changes were observed even in YM-175 treated rats, suggesting that YM-175 suppressed joint destruction by delaying progression of arthritis, rather than preventing arthritis itself. In this study, it is concluded that YM-175 can delay periarticular bone atrophy and joint destruction in rat AIA dose-dependently, but can not prevent them completely.

SU412

Prognostic Value of Serum Bone markers and Hand Bone Densitometry in Very Early Arthritis: Preliminary Results of the VErA Study. A. Daragon*[1], O. Vittecoq*[1], M. Brazier*[2], O. Mejjad*[3], P. Fardellone*[4], K. Krzanowska*[3], P. Boumier*[4], C. Zarnitzky*[5], A. Phan Van*[6], A. Gayet*[3], J. F. Menard*[7], X. Le Loët*[1]. [1]Rheumatology, CHU & INSERM U519, Rouen, France, [2]Biochimie, CHU, Amiens, France, [3]Rheumatology, CHU, Rouen, France, [4]Rheumatology, CHU, Amiens, France, [5]Rheumatology, CHG, Le Havre, France, [6]Rheumatology, CHU, Tours, France, [7]Biostatistics, CHU, Rouen, France.

The aim of the study was to determine the prognostic value of serum bone markers and hand bone densitometry in very early arthritis. From a population-based recruitment, 165 patients with very early (median duration: 4.4 months [1-6 mo]) peripheral arthritis (swelling >= 2 joints for > 4 weeks) were studied. Patients were steroid and DMARDs naive. After a year, patients were classified as RA or non RA. Assessments were performed at entry (T1), after 9 (T2) and 12 (T3) months. Serum bone markers were C telopeptide (sCTX) by ELISA test, pyridinoline (Pyr) and deoxypyridinoline (Dpyr) by HPLC. Other investigation : hand bone densitometry (DEXA), hand and foot X rays. Prognosis was defined as the progression of radiological damage from T1 to T3 (van der Heijde modified Sharp's method). At T3, 42 patients had radiological progressive disease, and 123 no progressive disease. 121/165 patients fulfilled ACR criteria for RA (69% in non progressive group, 86% in progressive group, $p = 0.02$). At T1, no difference was found between progressive group and non progressive group, except for rheumatoid factors more frequent in progressive group ($p < 0,02$). Bone mineral density (BMD) of both hands decreased significantly from T1 to T3 in both groups. However, hand BMD decreased significantly more in the progressive group (- 4.5 % versus - 1.7 %, $p< 0.04$). Levels of sCTX, Pyr and Dpyr at T1 were correlated to the decrease of hand BMD from T1 to T3 ($p< 0.04$). At T1, hand BMD was not different between the 2 groups, but levels of sCTX, Pyr and Dpyr were significantly higher in the progressive group ($p < 0.02$). In patients with early arthritis, a structural bone damage progression after 12 months duration is associated to a decrease of hand BMD. Moreover, decrease of hand BMD and X Rays progression were correlated with levels of serum bone markers at entry. So, sCTX, Pyr and Dpyr could be good predictive factors of the severity of early arthritis assessed by structural damage.

SU413

Biomechanical Properties of the Femoral Head Following Ischemic Necrosis. D. P. Pringle*, T. J. Koob*, H. K. W. Kim. Shriners Hospital for Children, Tampa, FL, USA.

Ischemic necrosis can cause permanent deformity of the femoral head, which can lead to premature degenerative arthritis of the hip. Changes in the biomechanical properties following ischemic necrosis and its role in the pathogenesis of femoral head deformity have not been previously investigated. The purpose of this experiment was to determine the biomechanical properties of the femoral head following ischemic injury in an established animal model. A ligature was placed tightly around the right femoral neck of 18 piglets to disrupt the blood supply to the femoral head. The animals were sacrificed at 2, 4 and 8 weeks post operatively ($n = 6$). Sham operations were performed on 8 piglets, which were sacrificed at 2 and 8 weeks. The load bearing areas of the femoral heads were indented perpendicularly with a 4 mm spherical indenter to a depth of 0.5 mm. Resultant force and indentation depth were measured and indentation stiffness was computed from the force deformation curves. The results were correlated with radiographic and histologic parameters. The left (non-infarcted) femoral heads and sham-operated heads were tested and used as controls. The biomechanical indentation properties of the ischemic heads were significantly reduced in comparison to the controls at 2, 4, and 8 weeks post surgery ($p < 0.001$ at all time periods). At 2 weeks, the average indentation stiffness of the infarcted heads decreased 51% as compared to the controls. The bony epiphysis was necrotic and its growth was arrested, but the heads were not deformed. The average head quotient (height of bony epiphysis divided by the width) was 0.45 which was the same as controls. At 4 weeks, the average indentation stiffness was further decreased to 75%. Small areas of the femoral head had become revascularized. In these areas, necrotic bone had been resorbed and replaced with fibrovascular tissue. Mild head deformity was present (average head quotient was 0.41). At 8 weeks, indentation stiffness was reduced by an average of 74%, which was not significantly different than from the values of specimens obtained at 4 weeks post surgery. All infarcted heads were severely deformed (average head quotient was 0.23). Large areas of revascularization and bone resorption had occurred. In some areas new bone had been laid down but in an irregular manner. There was a significantly large loss of compressive stiffness of the femoral head at the early stage of ischemic necrosis which preceded any radiographic changes other than growth arrest of the bony epiphysis. Our results suggest that from the early stage of ischemic necrosis, the infarcted head is mechanically compromised and institution of load limiting treatment would be clinically beneficial.

SU414

Apoptosis at the Interfacial tissue of Failed Hip Arthroplasty. S. Kim*[1], J. Choi[2], K. Koo*[3], J. Kim*[4], H. Shin*[5], E. Park*[6], Y. Sohn*[7]. [1]Orthopedic Surgery, Kyungpook National University Hospital, Daegu, Republic of Korea, [2]Biochemistry, School of Medicine, Kyungpook National University, Daegu, Republic of Korea, [3]Pathology, School of Medicine, Kyungpook National University, Daegu, Republic of Korea, [4]Microbiology, School of Dental Medicine, Kyungpook National University, Daegu, Republic of Korea, [5]Pathology, School of Dental Medicine, Kyungpook National University, Daegu, Republic of Korea, [6]Cell and Developmental Biology, Biomedical Research Institute, Kyungpook National University Hospital, Daegu, Republic of Korea, [7]Orthopedic surgery, School of Medicine, Gyungsang National University, Jinju, Republic of Korea.

Periprosthetic osteolysis and subsequent loosening are major causes of failure after total hip arthroplasty. In the interface tissue from failed hip after replacement arthroplasty, macrophages express inducible nitric oxide synthase (iNOS) mRNA and iNOS immunoreactivity. Nitric oxide (NO) mediates programmed cell death (apoptosis) in various types of cells. We hypothesized that phagocytic cells in the tissue of aseptic loosening and osteolysis serve as local source of NO and other proapoptotic factors, which will cause DNA damage leading to apoptosis. To investigate this hypothesis, the interface tissues from 18 patients who underwent revision hip arthroplasty due to osteolysis and aseptic loosening were examined. Apoptotic cells were identified using terminal deoxyribonucleotidyl transferase-mediated dUTP nick end labeling (TUNEL) staining. Immunohistochemistry analysis also displayed positive signals for iNOS, p53, Bax (pro-apoptotic signal), Bcl2 (anti-apoptotic siganal), and Ki-67 (proliferative index of cells) in revision hip arthroplasty. Of 18 interface tissues, 16 (89%) samples were positive for iNOS, p53, and Bax. In addition, 12 (67%) samples were positive for Bcl2 and Ki-67. All samples were positive for TUNEL staining. As control, 6 joint capsules were chosen as negative control and 6 herniated nucleosus pulposus materials were chosen as positive control. Of 6 joint capsules, only one (17%) was positive for iNOS, and Bax, respectively and three (50%) tested positive for TUNEL staining. Of six herniated nucleosus pulposus materials, four (67%) tested were positive for iNOS, three (50%) tested positive for Bax, one (17%) tested positive for Bcl2, one (17%) tested positive for Ki-67, and four (67%) tested positive for TUNEL staining. These results indicate that apoptosis inducing factors including nitric oxide, p53 and Bax might be important players in the pathogenesis of aseptic loosening and osteolysis of failed total hip arthroplasty.

SU415

Loss of Resistance to Vascular Invasion and Global Changes in Protein Synthesis with Increasing Severity of Osteoarthritis. J. O. Smith*, R. O. C. Oreffo, N. M. P. Clarke*, H. I. Roach. University Orthopaedics, University of Southampton, Southampton, United Kingdom.

The etiology of osteoarthritis (OA) remains unclear. To better understand the cellular basis, we compared the articular cartilage of human femoral heads from (1) 'controls' with non-OA cartilage, (2) OA samples with low degradation and (3) OA samples displaying high degradation. First, we tested the resistance to vascular invasion by placing pieces of cartilage onto the chorio-allantoic (CAM) membrane of chick embryos and culturing for 3-7 days. The vascular mesenchyme of the CAM will invade any tissue unless prevented by endogenous anti-angiogenic factors. 'Control' cartilage was resistant to vascular invasion, even when the angiogenic factor VEGF or the matrix-degrading enzyme MMP-9 were added to the tissue. In contrast, invasion took place in ~50% of OA samples. VEGF increased the incidence to 70% and MMP-9 further increased vascular invasion to 85% in low degradation and to 100% in high degradation samples. To further define the phenotype of OA chondrocytes, we studied their protein expression by immunocytochemistry. In contrast to 'control' chondrocytes, doublets or quadruplets of cells were present in the superficial layers of samples with low degradation. These chondrocytes had become activated (c-MYC positive) and expressed atypical proteins (e.g. VEGF and MMP-9), whereas single cells of the intermediate zone did not. At the border between the superficial and intermediate zone, we identified asymmetric cell divisions, i.e. divisions that define branch points in lineage commitment. This yielded one "osteoarthritic" chondrocyte (positive for c-MYC and VEGF/MMP-9) and one apoptotic cell. The "osteoarthritic" chondrocytes continued to divide and thus propagated the atypical phenotype so that chondrocytes in samples of severely degraded cartilage were present in clones of up to 32 cells with all cells expressing MMP-9/VEGF. We hypothesize that a global change in gene expression had taken place during the asymmetric cell division in which previously silenced genes, such as VEGF and MMP-9, were activated and constitutively expressed, possibly due to changes in the DNA methylation status of the promoter regions. These studies indicate that an early and significant characteristic of OA cartilage was loss of the normal resistance to vascular invasion and increased susceptibility to exogenous VEGF and MMP-9. In addition, global changes in protein expression occurred resulting in the constitutive expression of "osteoarthritic" chondrocytes (e.g. VEGF/MMP-9), contributing further to the progression of the disease. Delineation of the trigger for these changes has clear therapeutic implications.

SU416

Effect of $_{v}\beta_3$ Integrin Deletion on Inflammatory Arthritis. K. Aya[1], C. Pham*[2], K. Roth*[1], F. P. Ross[1], S. L. Teitelbaum[1]. [1]Pathology, Washington University School of Medicine, St. Louis, MO, USA, [2]Rheumatology, Washington University School of Medicine, St. Louis, MO, USA.

Periarticular osteolysis, reflecting accelerated osteoclast formation and function in face of inflammatory cytokines, is a disabling complication of rheumatoid arthritis.Thus, arrest of osteoclast function holds promise as a means of preventing bone loss in affected patients. The $\alpha_v\beta_3$ integrin is a particularly attractive target, in this regard, because not only is it the major integrin expressed by osteoclasts but is also abundant on stimulated endothelial cells. Thus $\alpha_v\beta_3$ is believed to play a role in neo-angiogenesis which may impact the inflammatory lesion as well as osteoclastogenesis. To determine if $\alpha_v\beta_3$ blockade holds promise as an inhibitor of the bone loss of rheumatoid arthritis we established an experimental paradigm of the disease, namely collage-induced arthritis (CIA) in $\alpha_v\beta_3$ deficient mice. Because the DBA1/J strain is most susceptible to CIA, β_3-/- C57BL6 mice were crossed to this background. The N2 β_3+/- mice whose leukocytes expressed the highest levels of the CIA susceptibility marker, I-A^q, were selected to breed N3. β_3-/- and β_3+/- littermates were injected, intradermally with 100 mg of bovine collagen type 2 (CII) in CFA containing heat-killed *Mycobacterium tuberculosis*. This was repeated 21 days later. The severity of arthritis in each paw was graded from 0 = normal to 3= severe. The sum of all four paws in each mouse was used as clinical score(CS). 2 weeks after the 2nd CII injection, CS in β_3+/-(9.7± 3.3) and β_3-/- (12 ±0) mice were similar as was the increase in hindpaw thickness (IHT) (β_3+/-, 0.76± 0.41; β_3-/-, 0.81± 0.27 mm). At three weeks, β_3+/- CS was 10.3± 2.4 and β_3-/- 12 ±0. IHT in both groups was also similar (β_3+/-, 0.85± 0.35; β_3-/-,0.59± 0.24 mm). All animals had radiographically detectable bony erosions, the severity of which was comparable in the mutant and control arthritic animals. Histological examination of hindpaws also revealed similar magnitudes of inflammation, cartilage damage, and bone erosion. Surprisingly, neo-angiogenesis was not decreased in inflamed joints of β_3-/- mice (PECAM-1(+) capillaries- β_3+/-, 429.2±45.3/mm^2; β_3-/-, 512.6± 78.0) (VEGFR2(+) capillaries- β_3+/-, 342.8±23.9; β_3-/-, 403.0± 78.2/mm^2). We have shown that high dose M-CSF normalizes β_3-/- osteoclast formation and function. In fact we find levels of the cytokine increased 10X by immunoblot, in arthritic paws. Thus, deletion of the $\alpha_v\beta_3$ integrin does not dampen inflammation or bone erosions in experimental rheumatoid arthritis. The aggressive bone resorption extant in these mutants may reflect normalization of β_3-/- osteoclasts by high ambient M-CSF.

SU417

Receptor Activator of the Nuclear Factor Kappa-B Ligand (RANKL) in Serum Is Related to Bone Density, Cartilage Breakdown and Inflammation in Early Active Rheumatoid Arthritis. P. Geusens[1], R. Landewé*[2], D. Chen*[3], C. Dunstan*[3], P. Garnero[4], S. van der Linden*[2], M. Boers*[5]. [1]Rheumatology, Maastricht University, Maastricht, Netherlands, [2]Maastricht University, Maastricht, Netherlands, [3]Amgen, Thousands Oaks, CA, USA, [4]INSERM, Lyon, France, [5]VU University Hospital, Amsterdam, Netherlands.

Bone involvement in rheumatoid arthritis (RA) is characterised by erosions in the joints, and periarticular and generalised bone loss. The final effector of this bone involvement is the osteoclast. As RANKL plays a central role in osteoclast activation, we studied the relation of serum RANKL to bone erosions, periarticular and generalised bone density at baseline in 119 patients with early active RA in the COBRA trial (Lancet 1997; 350:309, Arthritis & Rheumatism 2002; 46:347). Serum RANKL was measured by ELISA with two different monoclonal antibodies directed against the extracellular domain of human RANKL used for capture and detection. Serum RANKL values were logarithmically transformed. Bone mineral density (BMD) was measured in the spine and hip using DXA. Joint damage was scored using the Sharp-van der Heijde index. ESR, CRP and disease activity score (DAS) were used as markers of disease. C-telopeptide fragments of collagen type 1 (CTx-1) and CTx-2 were measured in urine and corrected for creatinine excretion. RANKL was negatively related to BMD in the hip (r=-0.226, p<0.05) and borderline to BMD in the spine (r=-0.188, p=0.07). No significant correlation was found with radiographic joint damage. RANKL was correlated with urinary CTx-2/creatinine (r=0.285, p<0.01) and CTx-1/creatinine (r=0.242, p<0.05). RANKL was related to CRP (r=0.355, p<0.001), ESR (r=0.255, p=0.01) and DAS (r=0.203, p<0.05). RANKL was higher in patients with rheumatoid factor (RF) than in patients without RF (p<0.001). We conclude that in patients with early active RA serum RANKL is related to periarticular BMD (in the hip) and to cartilage breakdown and borderline to generalised bone loss (in the spine). Serum RANKL is related to parameters of inflammation, and is higher in patients with RF. These results indicate that RANKL could play a central role in bone involvement of RA.

SU418

Estrogen Inhibits T Cell-Mediated Arthritis and RANK-Mediated Bone Resorption in Rats with SCW-Induced Arthritis. J. Chen, K. J. Downey*, J. L. Funk. Medicine, University of Arizona, Tucson, AZ, USA.

Streptococcal cell wall (SCW)-induced arthritis, an animal model of rheumatoid arthritis (RA), displays two stages of disease development, a chronic phase that is T cell-dependent and a separate acute phase that is not. Estrogen has previously been shown to inhibit collagen-induced arthritis, an animal model of RA that is also T cell-dependent. If the protective effect of estrogen in arthritis is T cell-mediated, we postulated that estrogen treatment in the SCW model would block the development of chronic arthritis, but not the T cell-independent acute phase. Additionally, we postulated that estrogen treatment would inhibit the bone loss that accompanies T cell-mediated arthritis. To test these hypotheses, a series of experiments were performed using 100g female Lewis rats treated with: (1) vehicle alone (control), (2) 17ß-estradiol (E2, 200-600µg/kg/d sc begun either 1 h or 4 d prior to SCW injection), (3) SCW (25mg/kg ip), or (4) SCW + E2. During the 36 d experiments, SCW-treated animals developed the usual acute phase of arthritis and subsequent nadir in joint swelling, followed by a persistent chronic phase of arthritis. Associated with the development of arthritis, bone mineral density (BMD) decreased in the femur (-19%) and lumbar spine (-13%) (GE Lunar PIXImus 2). Serum pyridinoline (Metra Biosystems), a marker of bone resorption, increased 62% in SCW animals, while osteocalcin (Biomedical Technologies), a marker of bone formation, was unchanged. Bone marrow cells, isolated from femurs and cultured with M-CSF and a RANK activating antibody, showed a 2-fold increase in osteoclast formation in SCW vs. control animals. Treatment of SCW animals with E2, even at doses as high as 600 µg/kg/d begun 4 days prior to SCW injection, did not prevent the acute phase of arthritis, as assessed by Arthritic Index, a standard measure of joint swelling. In contrast, during the chronic phase, E2 inhibited joint swelling by 46% ($p < 0.01$). E2 treatment, while having no effect on BMD in normal animals, inhibited SCW-induced bone loss by 47% and 61%, respectively, in the femur and spine ($p< 0.05$). E2 treatment also inhibited 50% of the increase in serum pyridinoline seen in SCW animals ($p< 0.05$), while having no effect on osteocalcin levels. Consistent with these results, evaluation of osteoclastogenesis in bone marrow cultures revealed a protective effect of E2 treatment in preventing 46% of the increase in RANK-mediated osteoclast formation seen in SCW animals ($p < 0.001$). These results suggest that estrogen treatment only inhibits T cell-dependent joint inflammation in animal models of RA. Moreover, estrogen treatment prevents arthritis-associated bone loss by blocking RANK-mediated bone resorption.

SU419

Synovial Fluid Concentrations of Leptin Increase in Knee Osteoarthritis. S. Juma[1], D. Soung[1], D. A. Khalil[1], C. Pasque*[2], B. H. Arjmandi[1]. [1]Nutritional Sciences, Oklahoma State University, Stillwater, OK, USA, [2]Orthopaedic Surgery and Rehabilitation, Oklahoma University Health Sciences Center, Oklahoma City, OK, USA.

A recent study has demonstrated that human chondrocytes express functional leptin receptors. This receptor is a member of the class I cytokine receptor family that mediates the effects of numerous different cytokines. In osteoarthritis (OA), the balance between cartilage synthesis and degradation is disrupted which, in part, may be due to increased production of pro-inflammatory cytokines and altered sensitivity to growth factors such as insulin-like growth factor-I (IGF-I). The present study explores the possible connection between synovial concentrations of leptin and IGF-I with the incidence of knee osteoarthritis (OA). Synovial fluid specimens were obtained from a total of thirty-four individuals (21 females and 13 males) with and without OA. Specimens were analyzed to determine leptin, IGF-I, and IGF-binding protein-3 (IGFBP-3) concentrations and were normalized to total protein.The synovial fluid levels of leptin, IGF-I, and IGFBP-3 concentrations were significantly higher in women with knee OA, but not in men. The elevated levels of leptin in synovial fluid of osteoarthritic individuals is suggestive of the loss or weakening of signaling pathways by which leptin interacts with chondrocytes to promote or maintain cartilage health. The functional roles of leptin and its receptors in cartilage metabolism in normal and osteoarthritic conditions need to be explored.

Synovial Fluid	F-NOA	F-OA	M-NOA	M-OA
Leptin (ng/mL)	7.89 ± 4.75	34.23 ± 5.54*	15.34 ± 4.12	23.95 ± 7.43
Normalized Leptin (ng/mg protein)	0.62 ± 0.15	2.42 ± 0.28*	1.70 ± 0.64	1.49 ± 0.34
IGF-I (pg/mL)	13.2 ± 5.3	52.5 ± 14.2*	51.8 ± 8.8	66.9 ± 10.4
Normalized IGF-I (pg/mg protein)	1.30 ± 0.24	3.20 ± 0.67*	3.60 ± 0.53	4.51 ± 1.19
IGFBP-3 (ng/mL)	5.0 ± 1.2	53.4 ± 4.0*	58.4 ± 16.9	74.6 ± 3.7
Normalized IGFBP-3 (ng/mg protein)	1.39 ± 0.25	3.90 ± 0.28*	5.47 ± 1.38	5.21 ± 0.68

*Significantly (P<0.05) different from non-OA of the same gender.

SU420

Oral Antiresorptive Therapy Prevents Bone Loss at the Lumbar Spine One Year After Liver Transplantation. P. M. Camacho[1], K. K. Islam*[2], M. I. Peralta*[1], S. D. Creech*[3], N. Bella*[1], F. A. Nabham*[4], G. W. Sizemore[1], D. H. Van Thiel*[2]. [1]Endocrinology and Metabolism, Loyola University of Chicago, Maywood, IL, USA, [2]Gastroenterology, Hepatology and Nutrition, Loyola University of Chicago, Maywood, IL, USA, [3]Oncology Institute, Loyola University of Chicago, Maywood, IL, USA, [4]Medicine, Loyola University of Chicago, Maywood, IL, USA.

Osteoporosis and fractures are known complications of liver transplantation. Previous studies have shown rapid declines in bone mineral density (BMD) in the lumbar spine (LS) and femoral neck (FN) in the post-transplantation period. There is a paucity of data on effective therapy for liver transplant-induced osteoporosis. One study evaluated intravenous pamidronate, and another small study compared calcitonin with etidronate sodium. There is no published study on the use of other oral antiresorptive therapy for prevention of liver transplantation-induced osteoporosis. We retrospectively evaluated pre and one year post-transplantation BMD's of 27 patients who underwent liver transplantation at Loyola University Medical Center from 1998-2000. 14 patients received oral antiresorptive therapy (**Tx group**), including alendronate (11), risedronate (2), estrogen (1). Combination therapy was used in 7/14 patients. 13 patients received no antiresorptive therapy (**no Tx group**). Patients with creatinine above 2 ug/dl, abnormal thyroid stimulating hormone or calcium levels before transplantation were excluded from the study. There were no differences in baseline characteristics (age, sex, weight, height, calcium and creatinine levels, pretransplant liver disease) between the groups. Pretransplant LS BMD was not statistically different but FN BMD was significantly lower in the Tx group (p=.048).

Comparison of Pre and One Year Post-transplant BMD Results

	No Tx Group		Tx Group	
	LS BMD	FN BMD	LS BMD	FN BMD
Baseline	1.234 ± .22	1.067 ± .17	1.147 ± .25	.929 ± .17
One year	1.190 ± .19 (p=.026)	.952 ± .18 (p=.008)	1.120 ± .26 (p=.552)	.844 ± .09 (p=.030)

BMD's are expressed as mean ± SD in gm/cm2. P values compare baseline and post-transplantation BMD using the Wilcoxon Signed-Rank test. At one year, the **no Tx** group had significant bone loss at the LS and FN. The **Tx** group preserved bone at the LS, but lost bone at the FN. Oral antiresorptive therapy appears to diminish bone loss at the lumbar spine one year after liver transplantation.

SU421

One Year Controlled Trial of Pamidronate in the Treatment of Severe Osteopenia After Long Term Renal Transplantation. C. Montilla*, E. Hernandez*, E. Alonzo*, R. Carlini*, A. Arminio*, P. Clesca*, E. Bellorin-Font*, J. R. Weisinger. Division of Nephrology, Hospital Universitario de Caracas, Caracas, Venezuela.

Bone loss, osteopenia and skeletal morbidity after renal transplantation have been well documented. Previous studies from our laboratory have demonstrated that bone alterations can persist many years after a successful renal transplant. Nevertheless, most of the therapeutic efforts have been directed toward the rapid bone loss occurring immediately after the transplant. For these reasons, we decided to conduct a prospective, randomized controlled study on the use of the bisphosphonate Pamidronate in long term male renal transplant patients with evidence of severe osteopenia or osteoporosis as assessed by dual X ray absorptiometry. Twenty-four patients were randomized to receive either oral Pamidronate (200 mg BID) or placebo. Lumbar spine (LS) and femoral neck (FN) bone mineral density (BMD) were similar in both groups at the start of the study. Both groups were similar in age (42.3 ± 6.1 and 37.3 ± 9.1 years), time after transplantation (6.8 ± 2.4 and 5.75 ± 1.91 years), and renal function (serum creatinine of 1.32±0.15 and 1.5±0.2 mg/dL). After one year of treatment, LS BMD increased significantly (6.6 %) in the Pamidronate group (0.927 ± 0.73 to 0.989 ± 0.093 g/cm^2, $p< 0.01$) with an important decrease in the T score (-2.58±0.82 to -2.10±0.87, $p< 0.05$). Similarly, no significant changes were observed in the LS BMD (0.919±0.08 to 0.944±0.09 g/cm^2, NS) or the T score (-2.63±0.65 to -2.44±0.7, NS) in the placebo group. No changes were observed in the femoral neck BMD in both the Pamidronate or placebo groups. Biochemical values including serum calcium, phosphorus and immunoreactive PTH were similar in both groups and did not change after treatment. There was a significant decrease in bone resorption markers (N-telopeptide of collagen cross-links) in the Pamidronate group with no change in the placebo treated patients. No significant side effects were observed in the Pamidronate group when compared to placebo. In summary, this study has shown an important improvement in bone mineral metabolism after 12 months on Pamidronate. The long-term effect of this drug remains to be clarified.

SU422

The Changes of Serum Growth Factor Levels Following Bone Marrow Transplantation: Impact on Bone Turnover Markers and Bone Mineral Density. M. I. Kang, K. H. Baek*, W. Y. Lee*, E. S. Oh*, K. W. Oh*, H. S. Kim*, J. H. Han*, K. W. Lee*, H. Y. Son*, S. K. Kang*, C. C. Kim*. Department of Internal Medicine, The Catholic University of Korea, College of Medicine, Seoul, Republic of Korea.

Loss of bone mass is usually detected after bone marrow transplantation(BMT), especially during the early post-transplant period. We recently reported that enhanced bone resorption following BMT is related to both the steroid dose and the increase in IL-6. We also suggested damage of marrow stromal microenvironment by myoablation partly explains impaired bone formation following BMT. It is well known that some growth factors play an important role in bone growth and osteogenesis. However, there has been no report in which the relationship between serum FGF-2 and IGF-I levels and BMD in human was studied. We have prospectively investigated 110 patients undergoing BMT and have analyzed 36 patients(32.4±1.3 years, 17 men and 19 women) who was measured DEXA before and 1 year after BMT. Serum calcium, phosphorus, creatinine, and biochemical markers of bone turnover were measured before BMT and 1, 2, 3, 4 and 12 wks, 6 Ms, and 1 yr after BMT. Serum FGF-2 and IGF-I levels were measured before BMT and 1, 3, and 12 wks after BMT. The mean bone loss in the lumbar spine and total proximal femur, calculated as the percent change from the baseline to the level at 1 yr was 5.2% ($p<0.05$) and 11.6% ($p<0.01$), respectively. The serum ICTP increased progressively until 4 weeks after BMT. Thereafter, it decreased gradually to reach basal values after 1 year. Serum osteocalcin decreased progressively until 3 wks after BMT. Then it increased transiently and finally returned to basal level at 1 yr. Serum FGF-2 and IGF-I also decreased progressively until 1 wks and 3 wks respectively, then increased to basal values at 3 Ms. There were positive correlation between the percent changes from the baseline BMD of lumbar spine and proximal femur BMD and baseline IGF-I level($r=0.50$, $p<0.05$, $r=0.51$, $p<0.05$). Significant correlation was also found between IGF-I and osteocalcin levels at 3 weeks after BMT. There was a strong positive correlation between the percent change of lumbar spine during post-BMT 1 yr and FGF-2 serum level at 3 wk ($r=0.75$, $p<0.01$), but not proximal femur. In conclusion, there was significant decline in the serum IGF-I and FGF-2 levels at immediate post-BMT period and it was related with decrease in bone formation and decrease of lumbar spine BMD during 1 year following BMT.

SU423

Testosterone Supplementation has Additional Benefits on Bone Metabolism in Cardiac Transplant Recipients Receiving Intravenous Bisphosphonate Treatment: A Prospective Study. A. Fahrleitner[1], G. Prenner*[2], K. H. Tscheliessnigg*[2], G. Leb*[1], C. J. Piswanger-Sölkner*[1], B. Obermayer-Pietsch*[1], H. P. Dimai[1], H. Dobnig[1]. [1]Endocrinology, Medizinische Universitätsklinik, Graz, Austria, [2]Transplantation, Universitätsklinik für Chirurgie, Karl-Franzens University, Graz, Graz, Austria.

Bisphosphonates (BP) are a promising therapeutic option in patients following solid organ transplantation. Hypogonadism is a frequent complication of immunsuppressive therapy. Aim of this study was to evaluate the effects of testosterone supplementation in addition to intermittent intravenous BP treatment on bone metabolism in patients following cardiac transplantation (CTX). Forty-one cardiac transplant recipients (mean age 56 +/- 9) were categorized as either eu- (n=18) or hypogonadal (n=23) based on their free testosterone levels. All patients were treated with 2mg ibandronate intravenously every three months in combination with 1200mg calcium and 800 IU vitamin D daily. Ten of the hypogonadal patients received additional testosterone supplementation (250 mg testosterone enanthate i.m. every 4 to 6 weeks). A laboratory analysis as well as a DXA measurement of the hip was performed at baseline and after 1 year of treatment. Baseline testosterone serum levels showed a positive correlation with bone mineral density (BMD) at the hip (Z-score [neck] and [trochanteric region]: $r=0.35$; $p=0.03$; Z-score [total hip]:$r=0.37$; $p=0.02$) and a negative correlation to the time elapsed since TX ($r= - 0.42$; $p=0.007$). Mean neck-BMD of hypogonadal men was 1 SD lower when compared to eugonadal men ($p<0.001$), whereas patient groups did not differ in age, cumulative prednisolone dosage, renal function, bALP, serum CTX, osteocalcin, iPTH or vitamin D3 levels. ;

	Baseline	delta BMD	delta BMD	CTX changes
	Z-score (neck)	delta Z-neck	delta Z-troch	delta sCTX
Eugonadal (n=18)	- 0.13 +/- 0.27	0.04 +/- 0.03	0.03 +/- 0.04	- 1023 +/- 515
Hypogonadal				
+testosterone (n=10)	-1.79 +/- 0.33*	+0.13 +/- 0.02*	+0.15 +/- 0.04*	- 2359 +/- 803*
-testosterone (n=13)	-1.21 +/- 0.33*	+0.03 +/- 0.02	+0.03 +/- 0.04	-524 +/- 402

*$p<0.05$ vs. baseline and eugonadal patients

A subanalysis of hypogonadal men with vs. hypogonadal men without testosterone supplementation revealed that significant reductions in bone turnover and gains in BMD were confined to testosterone-treated patients (see table).In summary, intermittent ibandronate therapy combined with calcium/vitamin D supplementation independent of gonadal status prevents bone loss in cardiac transplant recipients. Testosterone replaced hypogonadal men show an additional benefit in terms of slowing of bone turnover and increases in BMD.

SU424

The Growth Plate Under Immunosuppressive Therapy. C. P. Sanchez, Y. Z. He*. Pediatrics, UW Medical School, Madison, WI, USA.

Immunosuppressive agents necessary to maintain the renal allograft may affect linear growth in children. There is limited information on the effects of these agents on the growth plate cartilage. Thus, 51 weanling rats, 46± 4 grams, were randomly divided into the following treatment groups: Control (N=13) received saline, Pred (N=12) received prednisone at 3 mg/kg/dose, Rapa (N=13) received rapamycin at 2.5 mg/kg/dose, and CsA (N=13) received cyclosporine at 7 mg/kg/dose. The animals were evaluated after 14 days (N=24) and 28 days of treatment (N=27). All medications were given daily by gavage route at the same volume. Body weight and body length were obtained weekly. All animals were pair-fed to the Rapa group. To measure bone growth, tetracycline was given intraperitoneally 48 and 24 hours prior to sacrifice. Blood was collected for serum calcium (Ca), phosphorus (Phos), IGF-I and PTH at the time of sacrifice. The proximal tibia was obtained for growth plate histomorphometry. Gain in body weight was less in Rapa and Pred groups, 62± 6 and 66± 8 grams, compared to Control and CsA animals, 73± 7 and 77 ±3 grams, $p<0.003$, after 14 and 28 days of therapy. Gain in body length was much less in the Rapa animals, 7.6± 0.6 cm after 14 days and 13±1.2 cm after 28 days, compared to Control animals, 8.6± 0.5 and 16±0.6 cm, $p<0.006$. CsA animals had the largest increase in body length after 14 days of treatment, 9.3± 0.7 cm. Tibial length was shortest in the Rapa group, 3.0 ±0.05 and 3.4±0.09 cm, after 14 and 28 days, compared to Control, Pred and CsA groups, $p<0.05$. Serum Ca, Phos, IGF-I and PTH did not differ in all groups after 14 days of therapy, however, serum Ca, Phos, and PTH levels were lower in the Rapa group, 9.9± 0.1 mg/dl, 10± 0.4 mg/dl, and 31±21 pg/ml, respectively, after 28 days of treatment compared to the other groups, $p<0.05$. After 14 days of therapy, the width of the growth plate was widest in the Rapa animals, 675± 90 um, when compared to the Control, Pred and CsA groups, 499± 29, 498± 43 and 481± 42 um, $p<0.0001$. The area occupied by the hypertrophic chondrocytes was wider, 0.6± 0.02, and the proliferative chondrocytes smaller, 0.4 ±0.05, in the Rapa animals versus the other groups, 0.5 ±0.02, $p<0001$. Bone growth was greater after 14 days of treatment in the CsA treated animals, 312± 131 um/day, and lesser in the Pred animals, 120± 20 um/day, compared to the Control and Rapa animals, 154± 53 and 230± 159 um/day, $p<0.03$. After 28 days of treatment, however, the width of the growth plate and bone growth did not differ in all groups. Thus, rapamycin therapy may adversely affect the growth plate in the younger growing animals, but these changes may not be as evident in older animals. Further studies to evaluate changes in chondrocyte proliferation, chondrocyte hypertrophy and ossification during rapamycin therapy are needed.

SU425

Response of Parathyroid Gland to Human Parathyroid Hormone (1-34) Infusion in Adult Growth Hormone Deficiency Before and During Growth Hormone Replacement. A. M. Ahmad*[1], J. Thomas*[1], M. Hopkins*[1], B. Durham*[2], H. White*[1], J. P. Vora*[1], W. D. Fraser*[2]. [1]Diabetes & Endocrinology, Royal Liverpool University Hospital, Liverpool, United Kingdom, [2]Clinical Chemistry, Royal Liverpool University Hospital, Liverpool, United Kingdom.

Alterations in both parathyroid gland sensitivity to changes in calcium concentration and end-organ response to the effects of PTH play a role in the development of osteoporosis. Since adult growth hormone deficiency (AGHD) is associated with increased prevalence of osteoporosis, we studied the effects of PTH (1-34) infusion on end-organ and parathyroid gland responsiveness. 6 patients with severe AGHD were recruited. All patients were admitted, prior to commencement of GH replacement (GHR), at 1300 h. Venous cannulae were inserted in each arm and ½ hourly blood sampling was commenced at 1400 h. hPTH (1-34) in normal saline was infused at a rate of 0.55 U/ kg/h over 24 h. PTH, calcium and albumin were measured on all samples. GHR was commenced after the baseline visit. The protocol was repeated at 3 and 12 months on GHR. The first 2 samples were averaged and demonstrated a significant increase in adjusted-calcium (ACa) concentration (mmol/L) at 3 and 12 months compared to baseline ($p<0.001$). A significant decrease in PTH (1-84) concentration (pmol/L) was observed at 3 and 12 months ($p<0.01$). Following hPTH (1-34) infusion, ACa concentration increased after 12 h in untreated AGHD patients, whereas, after 12 months on GHR, ACa concentration increased within 6 h. After 12 months on GHR, the percentage increase at 6 h was 3.2 ± 0.60% *vs.* 0.83 ± 0.66% in untreated AGHD patients ($p<0.05$) that remained significantly higher over the 24 h (17.8 ± 2.9% *vs.* 12.6 ± 2.2%, $p<0.05$). There was no significant difference in the maximum PTH (1-84) suppression between 0 (78.2%), 3 (77.3%) and 12 months (79.1%). There was a significant increase in the calcium set-point (the calcium concentration at which the rate of PTH secretion is one half of its maximal value) after 3 (2.50 ± 0.02, $p<0.05$) and 12 months (2.74 ± 0.02, $p<0.001$) compared to baseline (2.38 ± 0.03). We have demonstrated increased end-organ responsiveness to the effects of PTH resulting in a significant increase in calcium concentration in response to PTH (1-34) infusion, following GHR. These findings together with the significant increase in calcium set-point may explain the increase in basal calcium and decrease in PTH concentration following GHR. These results may help understand the mechanisms underlying the genesis of osteoporosis in AGHD.

SU426

Structurally Varied Conformationally Constrained Amino acids Substitutions at Positions 1 and 3 of PTH(1-14) Preserve or Enhance P1R Binding Affinity and cAMP-Signaling Potency. N. Shimizu, T. J. Gardella. Endocrine Unit, Massachusetts General Hospital and Harvard Medical School, Boston, MA, USA.

The structural basis by which the N-terminal residues of PTH contribute to the PTH receptor interaction process is unknown. Recently we found that PTH(1-14) analogs containing the α,α di-substituted amino acid, α-amino-isobutyric acid (Aib) at positions 1 and/or 3, have 10- to 100-fold higher affinities and cAMP signaling potencies than do their counterpart peptides containing alanine at these positions (Shimizu et al. 2001,JBC. 276 pp 49003). These enhancing effects could be due to new receptor contacts provided by the additional methyl group on Aib, or to the conformational constraints imposed by this residue on the peptide backbone, which favor α-helix. To examine these possibilities, we investigated whether other α,α-di-substituted amino acids distinct from Aib would also enhance affinity when introduced at positions 1 and/or 3 of [M]PTH(1-14) (M = $Ala^{1,3,12}$,Gln^{10},Har^{11},Trp^{14}). Three amino acids were chosen: diethylglycine (**B**), cyclopropylglycine (**X**) and cyclopentylglycine (**Z**):

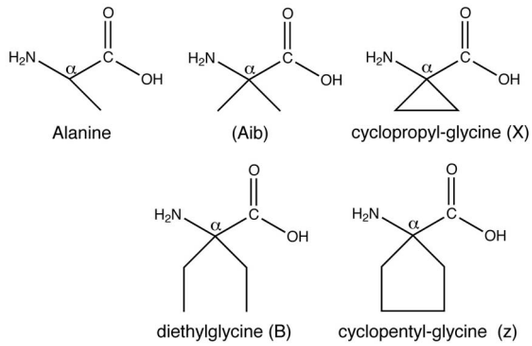

In competition binding assays performed in an LLC-PK1-derived cell line (B28) that stably expresses the hPTH-1 receptor using ^{125}I-[$Aib^{1,3}$,Nle^{8},Tyr^{21},M]PTH(1-21) tracer, the affinities of the B3-, and Z3-containing analogs were comparable to that of [M]PTH(1-14) (IC_{50}s ~ 30 μM); the affinity of X3-containg analog was 14-fold lower than that of [M]PTH(1-14), and the affinities of the B1-, X1- and Z1-substituted peptides were 3- to 50-fold higher than that of [M]PTH(1-14), with the highest affinity exhibited by [Z^{1},M]PTH(1-14) (IC_{50} = 0.6 μM). The analog [Z^{1},Aib^{3},M]PTH(1-14) exhibited the highest binding affinity (IC_{50} = 100 nM) and cAMP potency {EC_{50} = 0.9 nM, compared to 200 nM for [M]PTH(1-14)} of any PTH(1-14) analog studied to date. The finding that several structurally distinct α,α-di-substituted amino acids improve affinity and potency when introduced at positions 1 and 3 of PTH(1-14) suggests that the enhancing effects of these substitutions are not due to specific sidechain contacts with the receptor, but, to the constraining effects that these residues have on the ligand's backbone conformation. The results are further consistent with the hypothesis that the amino-terminal domain of PTH is α-helical when bound to the activation domain of the P1R.

*Disclosures: **N. Shimizu**, Chugai Pharmaceutical Co., Ltd. 3.*

SU427

Role of Residue 19 in PTH(1-20) Analogs: Functional Evidence for Modulation of N-terminal alpha-helical Structure. N. Shimizu[1], J. C. Tsang*[1], J. T. Potts[1], A. Piserchio*[2], D. F. Mierke*[2], T. J. Gardella[1]. [1]Endocrine Unit, Massachusetts General Hospital, Boston, MA, USA, [2]Department of Chemistry and Molecular Pharmacology, Brown University, Providence, RI, USA.

Previous data suggest that residue 19 in PTH and PTHrP (Glu and Arg, respectively) play important roles in binding to the PTH-1 receptor (P1R), but the molecular mechanisms remain unclear. We showed previously that, relative to Glu19, Arg19 increases PTH(1-34) affinity ~10-fold, but does not affect PTH(15-34) affinity, suggesting that the enhancing effect is mediated via the N-terminal portion of the ligand (Gardella et al. 1995 JBC 270 6584). More recently we showed that Aib substitutions at positions 1 and 3 in [M]PTH(1-14) (M = Ala1,3,12,Gln10,Har11,Trp14) increases affinity 10- to 100-fold and increases helicity, as judged by CD spectroscopy (Shimizu et al. 2001 JBC 76 49003). These observations led us to hypothesize that Arg19 and the Aib,1,3 substitutions improve affinity by the same mechanism: e.g. by stabilizing an N-terminal helix, and they would thus be redundant with each other. To test this, we prepared four [M]PTH(1-20) analogs that differed by having either Glu or Arg at position 19, and either Aib or Ala at positions 1 and 3, and we assessed their functional properties in an LLC-PK1-derived cell line (B28) that expresses the hP1R via stable transfection. In competition binding studies performed with 125I-[M,Y21]PTH(1-21) tracer radioligand, the apparent affinity of [R19,M]PTH(1-20) was 41-fold higher than that of [E19,M]PTH(1-20) (IC_{50} = 29±3 nM vs. 1,200±100 nM) whereas the affinity of [Aib1,3,R19,M]PTH(1-20) was only 9-fold higher than that of [Aib1,3,E19,M]PTH(1-20) (IC_{50}s = 7.7±1.7 nM vs. 72±28 nM). Effects on cAMP signaling potency were proportional to these effects on binding affinity, and parallel results were obtained in LLC-PK1 cells that express, via stable transfection, P1R-delNt, which lacks the amino-terminal extracellular domain. The overall results suggest that the enhancing effects of the Arg19 modification and that of the combined Aib1,3 modifications on affinity are largely redundant. Furthermore, in both cases, the effects are mediated via the juxtamembrane (J) region of the receptor. The data are thus consistent with the notion that the enhancing effects of both modifications (e.g. Aib1,3 and R19) are due to stabilization of α-helical structure in the N-terminal portion of the ligand, a conclusion supported by our initial NMR analyses. The preferred agonist structure for productive interaction with the J region of the P1R may thus be a helical segment comprised of PTH residues (1-20).

*Disclosures: **N. Shimizu**, Chugai Pharmaceutical Company 3.*

SU428

Gender Differences in the Response of Mouse Bone to Parathyroid Hormone. Y. Wang*[1], T. Sakata[1], B. P. Halloran[1], W. Beamer[2], C. Rosen[3], H. Z. ElAlieh*[1], S. Majumdar[4], D. D. Bikle[1]. [1]Endocrine Unit, University of California, Veterans Affairs Medical Center, San Francisco, CA, USA, [2]Jackson Laboratory, Bar Harbor, ME, USA, [3]St. Josephs Hospital, Bangor, ME, USA, [4]Department of Radiology, University of California, San Francisco, CA, USA.

Parathyroid hormone (PTH) possesses bi-directional actions, i.e. it is bone-catabolic and anabolic. Studies on the skeletal effects of PTH have seldom considered the effects of gender. Our study was designed to determine whether the response of mouse bone to PTH differed according to sex. As a first step, we analyzed gender differences on bone mass, and structural properties of 4 month control and PTH treated (80 μg/kg bw/day for 2 weeks) male and female mice using fat free weight (FFW), pQCT, μCT and bone histomorphometry. In control mice, FFW of tibia (FFW/BW), cortical bone thickness (C.Th), mean trabecular separation (Tb. Sp), and proximal tibia mineral were significantly less, while bone volume (BV), total bone volume (TV), BV/TV, connectivity density (Conn-Dens), and mean trabecular number (Tb. N) were significantly greater in male than in female mice. PTH significantly increased FFW/BW, periosteal bone formation rate (BFR) and mineral apposition rate (MAR) (30%, 60%, and 44%, respectively), while significantly decreasing BV (30%) in male mice compared with the control, but induced no significant changes in female mice. PTH increased Conn-Dens and decreased C. Th, and mean trabecular thickness (Tb.Th) in female mice, but decreased Conn-Dens and increased C.Th, and Tb.Th in male mice. We then analyzed the gender differences in bone marrow stromal cells (BMSC) from 6 week male and female mice treated with PTH (80 μg/kg BW/day for 1 week). PTH significantly decreased the osteogenic colony number, the total ALP activity on day 14, and the total mineralization on day 28 in BMSCs from female mice, but had less effect on these measurements in BMSCs from male mice. We then analyzed the mRNA levels of RANKL, OPG and bone formation markers in bone tissue (marrow removed) using real-time PCR. PTH increased mRNA levels of RANKL, α1-collagen, ALP, and osteocalcin in both female and male mice, but mRNA levels in female mice were higher than those in male mice. OPG mRNA levels were not affected by PTH in either sex. PTH decreased the mRNA level of IGF-1 in female, but increased it in male mice. Our results indicate that on balance PTH is anabolic on cortical bone but catabolic on trabecular bone in male mice, whereas the reverse trend is found in female mice. This may reflect the greater response to PTH of IGF-I gene expression (affecting primarily cortical bone) in males and/or the greater inhibition of BMSC formation and activity (affecting primarily trabecular bone) by PTH in the females.

SU429

PTH Transcriptionally Regulates ICER Expression via a cAMP-PKA Pathway in MC3T3-E1 Cells. Y. Huang[1], D. Battisti*[2], B. E. Kream[1]. [1]Department of Medicine-Endocrinology, U. Connecticut Health Center, Farmington, CT, USA, [2]Department of Orthodontics, U. Connecticut Health Center, Farmington, CT, USA.

Parathyroid hormone (PTH) regulates serum calcium levels in part by increasing osteoclastic bone resorption, which requires the secretion of several mediators from osteoblastic cells. PTH regulates the expression of many genes via a cAMP-PKA signaling pathway in osteoblasts, including inducible cAMP early repressor (ICER). ICER belongs to the CREM transcription factor family and is transcribed from an internal promoter (P2 promoter) of CREM gene. We previously showed that ICER mRNA is induced by PTH in calvarial organ cultures, in osteoblast cell cultures and in bone in vivo. To study the mechanism by which PTH induces ICER in osteoblastic MC3T3-E1 cells, a fragment of the CREM P2 promoter (-238/+14 bp) was linked to a luciferase reporter (CREMP2-Luc238). The CREM P2 promoter contains 4 CRE-like elements arranged in 2 distinct clusters (CRE1-2 and CRE3-4) that are separated by twelve nucleotides. Constructs with 5' serial deletions were generated to study the involvement of each CRE in the regulation of basal and cAMP inducible promoter activity. CREMP2-Luc constructs were stably transfected into MC3T3-E1 cells and two multi-clonal populations were obtained for each construct. The expression of CREMP2-Luc was measured as luciferase activity. CREMP2-Luc238 expression was induced by 10 nM PTH and 10 μM FSK; activity peaked at 4 h. To study the signaling pathway involved in CREMP2-Luc238 induction, stably transfected cells were treated with various signaling molecules for 4 h: 10 nM PTH(1-34), 10 μM FSK and 3 mM 8-bromo-cAMP significantly induced CREMP2-Luc238 to 205±35%, 494±68% and 369±81 % of control, respectively, whereas 100 nM PMA, 1 μM ionomycin and 100 nM PTH(3-34) were not effective. Deletion of CRE1-2 did not alter FSK inducibility compared to CREMP2-Luc238 (6.4±0.6 vs. 6.2±0.5 fold, respectively). Further deletion of CRE3 significantly reduced both basal activity and FSK inducibility. Electrophoresis mobility shift assays (EMSA) showed that CRE1-2 and CRE3-4 probes formed different protein/DNA binding patterns with nuclear extracts from MC3T3-E1 and primary mouse calvarial cells. These data suggest that the CREM P2 promoter is induced by PTH mainly via a cAMP-PKA signaling pathway. The CRE3 site plays a critical role in mediating the response to cAMP. Lastly, there is differential binding of transcription factors to the CRE clusters of the CREM P2 promoter.

SU430

Evaluation of Agonistic and Antagonistic Signaling Response of Analogs of PTH peptides (1-34), (3-34) and (7-34) in Saos-2 Cells Stably Expressing Multiple Copies of cAMP Response Element (CRE) Reporter System. B. M. BHAT, R. J. Murrills, V. E. Coleburn*, J. Yoon*, R. Rupert*, F. J. Bex. Bone Metabolism and Osteoporosis Group, Women's Health, Wyeth Research, Collegeville, PA, USA.

Several extensive peptide truncation and modification studies have led to a detailed understanding of the functional domains of PTH. These studies have revealed that N-terminal residues mediate mainly adenyl cyclase (AC)-PKA activation and C-terminal residues are involved in PLC-PKC activation. In addition, PTH (3-34), PTH (7-34) and PTHrp (7-34) bind to PTHR1 but act as partial agonists or potent antagonists in binding and cAMP assays. To evaluate the effect of these peptides further downstream in the signaling cascade and specifically on the cAMP response element (CRE), we generated stable Saos-2 cells expressing CRE elements to serve as bone anabolic and pathway specific reporter system. To amplify the signal, the integrated reporter system was designed to contain 15 copies of the CRE sequence upstream of a minimal promoter linked to a luciferase gene. In an overnight assay, PTH (1-34) induced strong CRE-luci expression that ranged between 10- 30 fold above controls with an EC50 of 1.24nM. In comparison, PTH (1-34) was also potent in Saos-2 membrane binding assay (0.3nM EC50) and in a Saos-2 cAMP induction assay (0.65nM EC50). This stable reporter cell line is responsive to other cAMP agonists including Forskolin, Isoproterenol, PGE2, PACAP, and VIP peptide. The specificity of the CRE-reporter system was further evaluated with truncated antagonistic peptides including hPTH (3-34), bPTH (7-34) and analogs with various amino acid substitutions. These studies revealed that at the CRE-activity level, hPTH (3-34) peptide was a more potent antagonist than bPTH (7-34), but it also has partial agonistic activity. Interestingly, bovine PTH (3-34) had substantially less agonistic activity than human PTH (3-34). The residues that are altered in the bovine peptide are Phe7Leu and Ser16Asn. In contrast to bPTH(3-34), bPTH (7-34) was a pure but less potent antagonist. Among four substituted analogs of bPTH/PTHrP (7-34), the Nle 8,18 analog showed the most ideal antagonistic profile; neither suppressing the basal CRE-activity nor showing any partial agonistic activity. These studies demonstrate a good correlation between CRE-related transcription with the known effects of PTH agonists and antagonists on binding and cAMP.

SU431

Molecular Cloning and Phylogenetic Comparison of the cDNAs Encoding the Tuberoinfundibular Peptide of 39 Residues (TIP39) in Several Vertebrate Species. I. A. Hansen*, S. Wortmann*, O. Jakob*, B. Allolio, E. Blind. Dept. of Medicine - Endocrinology, University of Wuerzburg, Wuerzburg, Germany.

The polypeptide TIP39 (tuberoinfundibular peptide of 39 residues), which has been isolated initially from bovine hypothalamus, is a potent activator of the PTH-2 receptor, whereas it acts as a high-affinity antagonist on the PTH-1 receptor. Starting from database search results we cloned the cDNAs coding for the TIP39 protein precursors from man *(homo sapiens)*, mouse *(mus musculus)*, rat *(rattus norvegicus)*, pufferfish *(takifugu rubripes)*, and zebrafish *(danio rerio)* by means of RT-PCR and RACE-PCR. The deduced TIP39 preprohormones have a similar structure consisting of a hydrophobic N-terminal signal peptide, an intercalated peptide followed by a dibasic cleavage site, and the actual TIP39 peptide. The length of the intercalated peptides varied between the various species e.g. 93 amino acids (aa) in zebrafish vs. 31 aa in man and mouse. TIP39 itself had an identical length in all analyzed species. The deduced aa sequences of the peptide TIP39 itself were found to be highly conserved: The sequence was 89% identical between man and mouse and still 55% and 59% identical between man and pufferfish or zebrafish, respectively; between pufferfish and zebrafish, the aa sequence was 87% identical. The relationship was similar for the Pre-Pro-TIP39 peptide, with a 79% identity between man and mouse, and a 60% identity within the fish species (pufferfish vs. zebrafish); the aa identity between mamalians (i.e. man, mouse) and fish (i.e. pufferfish, zebrafish) ranged only between 24% and 32%. Taken together, the presumed amino acid sequence of TIP39 is well conserved over a broad range of vertebrate species suggesting an important, but largely unknown, function of this peptide hormone. These cloned TIP39 cDNAs should allow us to further elucidate the function of this peptide by evaluating stage- and species-specific expression patterns using in-situ hybridization.

SU432

PTH Simulates PI3-Kinase and Its Down Effector AKT/PKB in Intestinal Cells. C. Gentili*, S. Morelli*, A. Russo de Boland*. Biologia, Bioquimica & Farmacia, Universidad Nacional del Sur, Bahia Blanca, Argentina.

Phosphoinositide 3-kinase (PI3K) is a lipid kinase which phosphorylates the D3 position of phosphoinositides and is known to be activated by a host of protein tyrosine kinases. PI3K plays an important role in mitogenesis in several cell systems. However, whether parathyroid hormone (PTH) affects the activity and functional roles of PI3K in intestinal cells remain to be determined. The objective of this study was to identify and characterize the PI3K pathway and its relation to other non-receptor tyrosine kinases in mediating PTH signal transduction in rat enterocytes. PTH dose- and time-dependently increased PI3K activity with a peak ocurring at 2 min. The tyrosine kinase inhibitor genistein, c-Src inhibitor PP1 and two structurally different inhibitors of PI3K, LY294002 and wortmannin, suppressed PI3K activity dependent on PTH. Co-immunoprecipitation analysis showed a constitutive association between c-Src and PI3K which was enhanced by PTH treatment, suggesting that the cytosolic tyrosine kinase forms an immunocomplex with PI3K probably via the N-SH2 domain of the p85α regulatory subunit. In response to PTH, tyrosine phosphorylation of p85α was enhanced, effect that was abolished by PP1, the inhibitor of c-Src kinase. PTH causes a rapid (0.5-5min) phosphorylation of Akt/PKB, effect that was abrogated by PI3K inhibitors, indicating that in rat enterocytes, PI3K is an upstream mediator of Akt/PKB activation by PTH. We report here that PI3K is also requiered for PTH activation of the mitogen-activated protein kinases ERK1 and ERK2, enzymes that regulate intestinal cell proliferation. Taken together, the present study demonstrate, for the first time, that PTH rapidly and transiently stimulates PI3K activity and its downeffector Akt/PKB in rat enterocytes playing c-Src kinase a central role in PTH-dependent PI3K activation and that PI3K signaling pathway contributes to PTH-mediated MAPK activation.

SU433

hPTH-(1-34) and hPTH-(1-31)NH_2 Prevent Phosphate from Killing MC3T3-E1 Preosteoblasts and HKRKB7 Pig Kidney Cells. C. M. Allen*[1], B. Chakravarthy*[1], P. Morley*[2], J. F. Whitfield[1], G. E. Willick*[1]. [1]Institute for Biological Sciences, National Research Council of Canada, Ottawa, ON, Canada, [2]Para TecH Therapeutics Inc., Ottawa, ON, Canada.

During the 1960's Whitfield et al (1) found that inorganic phosphate (Pi) dramatically enhanced x-radiation-induced apoptogenesis of human and rat lymphocytes. Almost 40 years later Meleti et al (2) reported that high concentrations of Pi are apoptogenic for osteoblasts. This suggests that BMU osteoblasts entering osteoclast excavations may face apoptosis-triggering Pi levels. But these osteoblasts may be protected from high Pi by signals from their PTHR1 receptors activated by their autocrine PTHrP. This was tested using MC3T3-E1 murine preosteoblasts and HKRK B7 porcine kidney epithelial cells (LLC-PK1 pig kidney cells expressing 10^6 human PTHR1 receptors/cell). As expected, raising the external Pi concentration between the basal 0.9 mM and 10.9 mM increasingly reduced the survival (as measured colorimetrically with the tetrazolium salt, MTT) of both MC3T3-E1 and HKRKB7 cells during the next 5 days. This killing action of Pi was prevented by adding 3mM PFA (phosphonoformic acid), a potent inhibitor of Pi uptake. While raising Pi to 7.9 mM in the MC3T3-E1 cells' α-MEM medium variably reduced the cells' survival by no less than 50%, this Pi killing was significantly reduced or prevented by adding 1-100 nM hPTH-(1-34) or hPTH-(1-31)NH_2 to the medium. For example, 7.9 mM Pi reduced MC3T3-E1 cell survival to 2.8±3.6% while 1nM hPTH-(1-31)NH_2 increased the survival to 44.0 ± 7.0%. A more detailed study of Pi killing and the effect of PTH on it was carried out with HKRKB7 cells. By 48 h after raising the Pi concentration in their DMEM medium to 10.9mM, for example, the apoptogenic caspase 3-like activity in the HKRKB7 cells had increased 15.7-fold and by 72 h the fraction of Hoechst 33258 fluorochrome-stained cells with apoptotic bodies had risen from 0% to 30%. As expected, PFA prevented the apoptogenic actions of 10.9 mM Pi as did 100nM hPTH-(1-34). In conclusion, it appears that PTHR1receptor signals can shield preosteoblasts and osteoblasts from any high Pi levels they might be exposed to in osteoclast excavations.

1.Whitfield JF et al 1964. Exp Cell Res **36**: 341; 2. Mileti Z, et al 2000. Bone **27**: 359.

SU434

Continued Exposure to PTH Reduces Magnitude of Increased Bone c-fos Expression in vivo Compared to Once Daily PTH, But Does Not Change ex vivo Induction of Osteoclasts. J. Milas, N. Rao*, S. Murthy*, J. Pulcini*, X. Yu*, J. M. Hock. Anatomy & Cell Biology, Indiana University, Indianapolis, IN, USA.

Continued exposure to PTH is associated with the catabolic actions on bone; once daily (anabolic) PTH increases bone formation by stimulating osteoblast differentiation and inhibiting their apoptosis. Our aims were to determine if there were divergent effects of PTH regimen on expression of AP-1 family genes in vivo and bone resorption, and if continued exposure to PTH in vitro modified apoptosis of primary osteoprogenitors. Young C57Bl/6 male mice were treated for 5 days with vehicle or continuous hPTH 1-34 at 40 μg/kg as 6 injections within 6-8 hours/day (which reduces BMD after 12 days, Black et al, JBMR 1994) and terminated 30min after the last injection. Femur metaphyseal RNA was pooled for each group and expression of selected AP-1 genes evaluated by RNAse protection assay. Mice were given BrdUrd to label proliferating cells and calcein to label bone formation. In experiment 2, mice were treated with vehicle or hPTH 1-34 at 40 μg/kg either once daily (intermittent) or with 6 injections/day (continuous) for 6 days to ascertain comparative effects of regimens. Bone marrow and spleen cells were cultured for 7 days with RANKL and M-CSF to assess TRAP+ multinucleated cells (osteoclasts). In experiment 3, apoptosis was measured in cultured primary femur metaphyseal bone cells exposed to hPTH 1-34 at 0-10^{-10}M for 6h, 24h, 48h or 72h. In vivo, although continued exposure to PTH for 5 days was not long enough to decrease bone mass or alter bone shape, the catabolic response was initiated as urinary PYD/creatinine increased 1.4x and osteoclast number increased 1.5x. Immunohistochemistry showed an increase in BrdUrd+ fibroblasts and marrow fibrosis in the trabecular metaphysis of proximal tibia. Once daily and continuous PTH increased RNA expression of c-fos and junB, with little change in c-jun, junD or fra-2. Continuous PTH blunted the increase in c-fos expression by 3-fold. Ex vivo induction of osteoclasts by continuous or once daily PTH increased osteoclasts respectively by 2.2x or 3.6x in bone marrow and by 1.5x or 1.6x in spleen precursors. In vitro, continuous exposure to PTH inhibited apoptotic caspase activity by 60% at 48h and 30% at 72h. Inhibition of osteoprogenitor apoptosis and ex vivo induction of osteoclasts did not correlate with regimen-dependent differences in c-fos expression. Comparisons of catabolic and anabolic PTH regimens suggest that the magnitude of increase in c-fos expression may regulate stromal progenitor cell choice of fate as osteoblasts or fibroblasts.

Disclosures: ***J. Milas****, Eli Lilly & Co 2.*

SU435

Systemic Delivery of PTH Promotes Catabolic and Anabolic Responses in Tissue-Engineered Bone. A. Schneider, J. M. Taboas*, L. K. McCauley, P. H. Krebsbach. School of Dentistry, University of Michigan, Ann Arbor, MI, USA.

Remarkable advances have been made to stimulate bone growth via tissue-engineering strategies. Growth factors, scaffolds and gene therapy have all been used to optimize and support bone regeneration to mimic the native tissue structure and function. However, it remains unknown if tissue engineered bone recapitulates the biology of normal skeletal tissue in response to physiologic cues. Here, we present a tissue engineering strategy in which PTH actions on bone remodeling can be studied in vivo in a well-characterized ectopic bone organ. In this system, ossicles were formed by the differentiation of allogeneic transplanted murine bone marrow stromal cells seeded in gelatin scaffolds. Ectopic ossicles exposed to catabolic doses of PTH (1-34) contained a higher number of TRAP-positive osteoclastic cells per millimeter of bone (3.93 ± 0.7 (PTH) vs. 1.65 ± 0.3 (saline), p<0.01). Higher serum calcium levels were also observed in PTH-treated mice (p<0.02). In contrast, intermittent, low doses of PTH resulted in an anabolic response that significantly altered the ectopic bone microarchitecture. Microcomputed tomographic and histomorphometric analyses revealed a marked increase in percent bone volume (48.2 ± 2.0 % (PTH) vs. 30 ± 3.0 % (saline), p<0.01) and percent trabecular bone area (37.0 ± 7.4 % (PTH) vs. 14.1 ± 2.1 % (saline), p<0.05). No significant differences were observed in the number of osteocytes, cortical width and overall dimensions in ossicles from PTH-treated vs. control mice. Our findings demonstrate that cell-derived, tissue-engineered bone is truly responsive to physiologic stimuli. Catabolic doses of PTH induced an osteoclastic response, whereas anabolic doses of PTH promoted a significant increase in percent trabecular bone volume. These results suggest that systemic PTH may be used therapeutically to augment tissue-engineered bone. Furthermore, because multiple and distinct ossicles can be generated in a single animal, this system can be used to evaluate the effects of a variety of osteotropic agents. This versatile cell transplantation system may also be used to improve our understanding of bone physiology in health and disease and facilitate studies of the: (a) cellular and molecular mechanisms in skeletal regeneration, (b) cell-to-cell interactions in the bone marrow microenvironment and (c) efficacy of pharmacotherapeutic agents that modulate bone turnover in vivo.

SU436

Equine Parathyroid Chief Cells in Vitro: Secretion of Parathyroid Hormone (PTH), PTH and Calcium-Sensing Receptor mRNA Expression, and Effects of IL-1, IL-6 and TNF-alpha. R. E. Toribio*[1], C. W. Kohn*[2], C. C. Capen[1], S. E. Weisbrode[1], T. J. Rosol[1]. [1]Veterinary Biosciences, The Ohio State University, Columbus, OH, USA, [2]Veterinary Clinical Sciences, The Ohio State University, Columbus, OH, USA.

Parathyroid hormone (PTH) is secreted by the chief cells of the parathyroid gland in response to changes in extracellular ionized calcium (Ca^{2+}) concentration. *In vitro* studies on parathyroid cells have advanced our understanding of the physiology and pathophysiology of the parathyroid gland. Several conditions in the horses are associated with abnormal parathyroid gland function; for example, ionized hypocalcemia is present in 75% of horses with sepsis, and half of these horses have an abnormal parathyroid gland function. In the present study we measured PTH secretion, and PTH mRNA and calcium-sensing receptor (CaR) mRNA expression by equine parathyroid chief cell *in vitro*. We also evaluated the effects of interleukin (IL)-1ß, IL-6, and tumor necrosis factor (TNF)-alpha (cytokines known to be increased during sepsis in humans and animals) on PTH secretion, and PTH and CaR mRNA expression. The relationship between PTH and Ca^{2+} *in vitro* was inversely related and sigmoidal. PTH secretion in a low Ca^{2+} (0.8 m*M*) medium decreased from 100% (day 0) to 13% (day 30). PTH mRNA expression declined from 100% (day 0) to 43% (day 5), and to 25% (day 30). CaR mRNA decreased from 100% (day 0) to 31% (day 5), and to 16% (day 30). Chief cells exposed to high Ca^{2+} concentrations had a lower PTH mRNA expression (P<0.05) compared to low Ca^{2+} concentrations. Low and high Ca^{2+} concentrations had no effect on CaR mRNA expression. The inhibitory effect of high Ca^{2+} concentrations on PTH secretion also declined with increasing time in culture. By day 5, higher Ca^{2+} concentrations were required to inhibit PTH secretion and there was a shift (increase) of the Ca^{2+} set-point. After day 10 of culture, there was no significant difference in PTH secretion between low (0.8 m*M*) and high (2.0 m*M*) Ca^{2+} concentrations. IL-1ß (2000 pg/ml) decreased both PTH secretion (75%) and PTH mRNA expression (73%) (P<0.05). IL-1ß concentrations greater than 200 pg/ml resulted in significant (P<0.05) overexpression of CaR mRNA (up to 142%). The effects of IL-1ß were blocked by an IL-1 receptor antagonist (IL-1ra). IL-6 (5 and 10 ng/ml) decreased PTH secretion, but had no effect on PTH and CaR mRNA expression. TNF-alpha (1, 5, and 10 ng/ml) had no effect on PTH secretion, and PTH and CaR mRNA expression. In summary, the decreased responsiveness of parathyroid cells to Ca^{2+} from 0 to 30 days can be explained, in part, by the reduced CaR expression. IL-1 and IL-6 but not TNF-alpha may be important in influencing PTH secretion in the horse with sepsis.

SU437

PTH Analogues can be Defined by their Properties of Signal Transduction and Desensitization. R. W. Katz[1], Q. Sun*[2], E. Dworakowski*[2], S. Morris[3], J. P. Bilezikian[2]. [1]Oral Biology, Columbia University School of Dental and Oral Surgery, New York, NY, USA, [2]Medicine, Columbia University College of Physicians and Surgeons, New York, NY, USA, [3]Aventis Pharmaceuticals, Bridgewater, NJ, USA.

PTH and its biologically active fragments have anabolic effects on bone when administered in low dosage and intermittently. PTH activates osteoblasts through its receptor (PTH1R) and associated G proteins (GP). Deletion of the extreme amino terminal portion of the ligand abrogates receptor activation of adenylyl cyclase (AC) while phospholipase C (PLC) activation is tolerant to more drastic truncations at both amino and carboxyterminal ends of the molecule. Various PTH fragments may show differing effects on cells as a result of differential signal transduction and receptor desensitization, and this may explain their differing *in vivo* properties. Accordingly, we report differences in the properties of PTH (1-34), PTH (1-29) and a substituted PTH (1-21) in terms of AC activation and desensitization, and PLC activation. Maximal activation of AC by Saos-2 membrane homogenates was not different among the PTH peptide fragments. The respective K_as were different, with PTH (1-34) [1.49 x 10^{-8} M] almost four fold greater than PTH (1-21) [5.8 x 10^{-8} M], and almost ten fold greater than PTH (1-29) [1.32 x 10^{-7} M]. PLC activity was measured by inositol phosphate production in LLC-PK1 kidney cells expressing the rat PTH1 receptor. The three PTH peptides demonstrated a similar trend in IP production at 10^{-6} M [PTH (1-34) 5.2 +/- 0.3 fold, PTH (1-21) 3.7 +/- 0.2 fold and PTH (1-29) 2.2 +/- 0.1 fold]. Pretreatment of the Saos-2 cultures with PTH (1-34) at 5 x 10^{-8} M for 2 min suppressed AC activity by 71% but PTH (1-29) pretreatment suppressed activity by only 18% when the cell homogenates were subsequently challenged with PTH (1-34). However, at maximal concentrations PTH (1-34) and PTH (1-29) desensitized equivalently. The results of this study illustrate that fragments that are foreshortened at the carboxyterminal end of PTH (1-34) differed in their effects upon AC, PLC and receptor desensitization. These insights might help to design molecules in which biochemical behavior reflects *in vivo* properties.

Disclosures: ***R.W. Katz****, Wyeth 2.*

SU438

An Amino-Terminal Form of PTH Different from hPTH(1-84) is Detected by a Cyclase-Activating PTH Assay Specific for hPTH(1-84). Clinical Evaluation. P. D'Amour[1], L. Rousseau*[1], J. H. Brossard[1], T. Cantor[2], P. Gao[2]. [1]Département de Médecine, Université de Montréal, Centre de recherche du CHUM, Hôpital Saint-Luc, Montréal, PQ, Canada, [2]Scantibodies Laboratory Inc., Santee, CA, USA.

Intact (I-) or Total (T-) PTH assays recognize PTH molecular forms other than hPTH(1-84), also called non-(1-84) PTH. They account for 15-20% of I-PTH immunoreactivity in normal individuals (NI) and for 40-50% in renal failure (RF) patients. A new Cyclase-Activating (CA) PTH assay has been demonstrated to react with hPTH(1-84) only and not with non-(1-84) PTH. In clinical samples, CA-PTH values are generally lower than I- or T-PTH values but this is not always the case. Furthermore, non-(1-84) PTH values evaluated by HPLC tend to be higher then similar values obtained from the difference between I- or T-PTH and CA-PTH. To investigate this phenomenon, we have analyzed sera from 6 NI, 5 patients with primary hyperparathyroidism (PHP) and 9 patients with terminal RF with both the CA- and T-PTH assays after HPLC separation with a new program which better separates hPTH(1-84) from non-(1-84) PTH. CA-PTH results were lower than T-PTH results in all NI (3.13±0.37 vs 2.29±0.33 pmol/L, p<0.01) but were higher in 3/5 patients with PHP, making the difference between the 2 assays minimal (25.7±26 vs 23.1±24.1 pmol/L, NS). In RF patients, the difference between the 2 assays was more marked and present in all patients (47±35 vs 33.3±26.1 pmol/L, p<0.01). Analysis of HPLC profiles indicated that the CA-PTH assay recognized a peak of PTH immunoreactivity migrating in front of hPTH(1-84) and different from the non-(1-84) peak recognized by the T-PTH assay. This peak represented 8.13±2.45% (range 4.7-12) of CA-PTH immunoreactivity in NI, 24.7±23.3% (range 9-63.3) in PHP patients and 22.2±7.3% (range 17.3-35) in RF patients. This peak of amino-terminal PTH was not recognized by the T-PTH assay suggesting structural modifications interfering with antibody recognition in the region 15-34. These results indicate circulating immunoheterogeneity of the amino-terminal region of PTH particularly in patients with primary and secondary hyperparathyroidism. They also complicate the evaluation of non-(1-84) PTH through the substaction of CA-PTH from T-PTH. More studies will be required to elucidate the exact structure of this new amino-terminal PTH molecule.

SU439

A Comparison of Two Assays Measuring Parathyroid Hormone (PTH) in Plasma in a Normal Population. J. P. Johannesson*, O. S. Indridason*, L. Franzson*, G. Sigurdsson. University Hospital, Reykjavik, Iceland.

Parathyroid hormone (PTH) is in its active form an 84 amino acid polypeptide, 1-84, but inactive fragments are also found in plasma, including 7-84. Most conventional assays measure not only the 1-84 form but also varying amounts of fragments depending on the assay used. A new method has been developed that is believed to measure only the 1-84 form. The purpose of this study was to compare one of the currently used assays to the new one in a large group of healthy individuals of different age. Data from an ongoing population based study of age related changes in calcium and bone metabolism was used. 456 individuals, 209 men and 247 women, age 40-85, from the Reykjavik area were selected. None of them used medications that affect bone metabolism. PTH was measured with two assays, one conventional (PTH elecsys, Roche) and the new one (PTH cap, Scantibodies). We assessed the correlation between the two with the Pearson correlation coefficient and the agreement with regards to normal and abnormal values with the Kappa statistic. We have also examined age related changes and correlation to kidney function. The Pearson correlation coefficient for the two assays was 0.787 (P<0.001) for women and 0.690 (P<0.001) for men. The Kappa statistic was 0.486 (P<0.001) for women and 0.283 (P<0.001) for men. PTH elecsys showed a statistically significant increase with age (P<0.01) but not PTH cap. PTH elecsys also showed a correlation to kidney function parameters (P<0.01) but PTH cap did not. We conclude that the two methods differed significantly in measuring PTH in a normal population. This difference can be explained to some extent by age related reduction in kidney function.

SU440

Residue 19 of Parathyroid Hormone: Structural Insight into the Role in Binding and Activation. A. Piserchio*[1], N. Shimizu[2], T. J. Gardella*[2], D. F. Mierke*[1]. [1]Department of Chemistry and Molecular Pharmacology, Brown University, Providence, RI, USA, [2]Endocrine Unit, Massachusetts General Hospital, Boston, MA, USA.

In the course of establishing a structure-activity relationship for parathyroid hormone (PTH) most attention has been placed on the so called activation domain (the N-terminus, residues 1-7 of the ligand) and the binding domain, consisting of the C-terminus of PTH. Recently an important role has been ascribed to residue 19 of PTH: PTH(1-20) analogs containing R19 are 10- to 100-fold more potent than those containing R19. Here the pharmacological findings are placed onto a structural framework. Using high-resolution NMR methods, two PTH(1-20) analogs, Aib[1]-V-Aib-E-I[5]-Q-L-M-H-Q[10]-Har-A-K-W-L[15]-N-S-M-R-R[20]-NH_2 and Aib[1]-V-Aib-E-I[5]-Q-L-M-H-Q[10]-Har-A-K-W-L[15]-N-S-M-E-R[20]-NH_2 have been structurally characterized in the presence of a lipid vesicle, used as a mimetic of the membrane environment of the PTH receptor. The charge reversal at position 19, E19 vs. R19, leads to distinct conformational differences in the C-terminus. The R19 containing analog is found to adopt a structure consisting of a stable, contiguous α-helix, from V2-R19. In contrast, the E19 containing analog is much less structured in the C-terminus, consisting of an α-helix from ca. V2-L15. These results clearly illustrate the importance of residue 19 in the stabilization of the helical nature of the ligand, an important feature for binding of reduced-size PTH analogs to the PTH1 receptor.

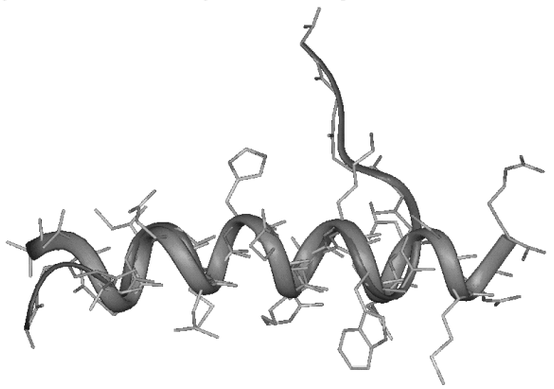

Superposition of the NM derived structures of the R19 (thick ribbon, side chains illustrated) and E19 (thin ribbon) containing PTH analogs.

SU441

The Effect of PTH(1-34) and PTH(2-38) on Mineralized Bone Nodule (MBN) Formation under Different Stage of Differentiation. Y. Lin*, L. J. F. Liu*, T. M. Murray, L. G. Rao. Calcium Research Lab, St. Michael Hospital, University of Toronto, Toronto, ON, Canada.

To investigate the effects of PTH(1-34) and PTH(2-38) on MBN formation at different stages of osteoblast differentiation, SaOS-2 cells were cultured under mineralizing conditions from day 1-18. The number and area of MBN were quantified in von Kossa-stained cells. A single 24 h treatment at day 2 with 10^{-8}M PTH(1-34), a fully effective PTH fragment, inhibited MBN area by 11.2%, while10^{-8}M PTH(2-38) had no effect. With 24 h of treatment at day 7, PTH(2-38), generally thought to be inactive, inhibited MBN area by 24.7%(10^{-8}M). With 6 h out of 48 h intermittent treatment from day 4 -18, PTH(2-38) inhibited MBN area by 20.0% (10^{-9} M) and 43.66% (10^{-8}M). No significant effect on MBN number was observed. However, PTH(1-34) 10^{-10}-10^{-8}M inhibited both MBN area and number at this condition. If PTH(2-38) was added from day 7-18, similar effects were observed. Nevertheless, from day 12-18, with 6 h out of 48 h intermittent treatment, 10^{-8}M PTH (2-38) did not have a significant effect on MBN formation, while, 10^{-8}M PTH(1-34) still inhibited MBN area by 45.3%. With continuous treatment from day 7-18, both fragments inhibited MBN area and number. PTH(1-34) 10^{-10}, 10^{-9} and 10^{-8}M inhibited MBN area by 8.2%, 75.4%, and 99.9%, while the inhibition rates were7.2%, 61.8%, and 99.8% for PTH(2-38). The least differences in effects between these two PTH fragments were observed in this condition compared to all the other conditions. PTH(1-34), at 10^{-10}, 10^{-9} and 10^{-8}M, when added at day 8 for 24 h, inhibited Alkaline Phosphatase(ALP) activity by 13.4%, 19.2% and 22.8%. PTH(2-38) did not affect ALP activity under this condition. PTH(1-34) 6 h out of 48 h intermittent treatment from day 8-16 also dramatically decreased ALP activity. However, PTH(2-38) did not affect ALP activity. PTH(2-38)'s effect on ALP activity was found in a longer treatment, and at the earlier stage of osteoblast development. At 10^{-8}M, continuous treatment from day 5-9 inhibited ALP activity by 30.4%. RT-PCR failed to show any significant change in ALP mRNA level after 1 h treatment of either fragment of PTH. Both PTH(1-34) and PTH(2-38) dramatically increased c-fos mRNA level. At 10^{-8}M, they increased c-fos mRNA by 286.6% and 214.8% after one hour treatment. These data suggested that in vitro, PTH(2-38) might have different effects on osteoblasts from that of PTH(1-34) in some stages of differentiation. Our results also showed that PTH fragments' potency on MBN was generally consistent with previous observations of reduced potency of PTH fragments lacking residue 1 on c-AMP activation. In addition, we observed that the PTH fragments' effects on MBN correlated well with their effects on up-regulating c-fos mRNA level.

Disclosures: ***Y. Lin****, Eli Lilly Inc. 2.*

SU442

PTH Stimulation of Mitogen-Activated Protein Kinases Does not Require PTH/PTHrP Receptor Phosphorylation and Internalization or Phospholipase C Activation. H. A. Tawfeek*, A. B. Abou-Samra. Endocrine Unit, Massachusetts General Hospital, Boston, MA, USA.

Previous studies have demonstrated that binding of PTH and PTHrP to the PTH/PTHrP receptor regulates activity of the mitogen-activated protein (MAP) kinases. The cellular mechanisms underlying MAP kinase regulation by PTH are poorly understood. In the current study, we investigated the role of PTH/PTHrP receptor phosphorylation and internalization and stimulation of phospholipase C (PLC) in the activation of the extracellular signal regulated MAP kinases (Erk1/2). PTH normally stimulated Erk1/2 in two receptor mutants with impaired internalization, a phosphorylation-deficient PTH/PTHrP receptor (PD-PPR), in which 7 serine residues in the carboxy-terminal tail (CT) were mutated to alanine residues, and a tail-less PTH/PTHrP receptor (TL-PPR), in which the CT was truncated at residue 480. Immunoblot analysis revealed that MEK1/2 were also activated by PTH. Further, a specific MEK1/2 inhibitor blocked Erk1/2 activation by PTH; this suggests that MEK1/2 are involved in PTH activation of Erk1/2. To elucidate the role of PLC in PTH activation of Erk1/2, we examined Erk1/2 stimulation by PTH in a cell line expressing a mutant PTH/PTHrP receptor, DSEL, which is defective in PLC signaling. The DSEL mutant did not stimulate Erk1/2 suggesting that PLC stimulation is important for Erk1/2 activation. Alternatively, the DSEL mutant may be defective in signaling through another unknown pathway(s) that is important for PTH stimulation of Erk1/2. To distinguish the two possibilities, Erk1/2 activation by the PTH analog [Gly1,Arg19]hPTH(1-28), which does not stimulate PLC but normally stimulates cAMP accumulation, was examined. [Gly1,Arg19]hPTH(1-28) efficiently activated Erk1/2 in cell lines expressing wild type receptor. Taken together, these data suggest that PTH/PTHrP receptor internalization and stimulation of phospholipase C do not play a major role in PTH activation of Erk1/2. The data also demonstrate that MEK1/2 are involved in the process of PTH stimulation of Erk1/2.

SU443

Identification of Novel Contact Points between Residues in the Mid-Region of PTH(1-34) and the PTH1-Receptor: Refinement of the Model of the PTH--PTH1-Receptor Complex. A. Wittelsberger, M. Corich*, A. Barazza*, R. Yacobi, B. K. Lee*, M. Rosenblatt, J. M. Alexander, M. Chorev. Department of Bone and Mineral Metabolism, BIDMC-Harvard Medical School, Boston, MA, USA.

Parathyroid hormone (PTH) is the major hormone responsible for the regulation of calcium levels in blood and plays a role in bone remodeling. These activities are mediated through its cognate G-protein-coupled receptor, PTH1 Rc, a member of the class II family. Understanding the molecular mechanisms of ligand recognition and signal transduction by the PTH1 Rc may lead to the design of novel hormone analogs as drugs for the treatment of diseases such as osteoporosis, hypercalcemia of malignancy, and hyperparathyroidism. Using the benzophenone-based photoaffinity-crosslinking scanning approach, several contact points, mainly between positions in the N- and C-terminal helical segments of PTH(1-34) and the receptor, were identified previously. The emerging model of the ligand-receptor bimolecular interface includes single contacts between the N-terminal residue of the hormone and Met[425] in the ectopic portion of transmembrane helical domain 6, and between position 13 of the hormone and a site proximal to Arg[186] in the juxtamembrane portion of the N-extracellular domain (N-ECD) of the receptor, and several contact sites between residues at the C-terminal portion of PTH(1-34) and the amino terminal portion of the N-ECD of the receptor. It is very important for the upgrading of the existing model to elucidate additional contact sites between the receptor and residues in the mid-region of the hormone, i. e. in proximity to the putative hinge regions (positions 12 and 19). In this report, we present the design, biological characterization, and photoaffinity crosslinking studies of a series of novel PTH analogs containing the photoreactive *p*-benzoylphenylalanine (Bpa) residue in the mid-region of the hormone sequence, i.e. positions 11, 15, 18, and 21. Preliminary results obtained from restrictive digestion mapping and site-directed mutagenesis studies indicate that while the contact site for position 15 in the ligand lies in close proximity to the C-proximal end of the N-ECD the other positions in the ligand interact with additional extracellular domains of the receptor. Therefore, the novel contact points identified will enable the generation of an enhanced and refined model of the PTH--PTH1 Rc interactions that will be presented.

SU444

Regulation of Gap-Junctional Communication in Bone-Derived Cells by PTH Fragments with Different C Termini. G. D'Ippolito[1], P. Divieti[2], G. A. Howard[1], F. R. Bringhurst[2], P. C. Schiller*[1]. [1]GRECC/Research, VAMC and University of Miami School of Medicine, Miami, FL, USA, [2]Endocrinology, Mass General Hospital/Harvard Medical School, Boston, MA, USA.

Gap-junctional communication (GJC) plays a critical role in bone physiology. We have demonstrated that disturbance of GJC in osteoblasts results in down regulation of osteocalcin and bone sialoprotein gene expression and decreased hormonal responsiveness. Parathyroid hormone (PTH) can increase cell-to-cell GJC among bone cells, via activation of the type 1 PTH/PTHrP receptor (PTH1R). Long fragments of PTH, lacking the N-terminal portion of the hormone, are able to bind to a receptor distinct from the PTH1R and specific for the C-terminal region of PTH, the CPTH receptor (CPTHR). To assess if CPTHR activation is involved in cell-to-cell communication, we studied GJC in bone cells lacking PTH1R but expressing CPTHR. Quantification of GJC was determined utilizing a variation of the “two-dye” and “parachute” techniques in PTH1R-null osteoblastic (F1-14) and osteocytic (OC14) cell lines. After 8 days in culture dye transferred from loaded F1-14 to

F1-14 as well as to OC14 cells. Similarly, loaded OC14 transferred dye to OC14 as well as to F1-14 cells, demonstrating that PTH1R expression is not required for GJC. Subsequently we assessed whether PTH1R-null cells retain the capacity to form functional GJ channels with PTH1R-expressing cells. GJC was assayed between F1-14 or OC14 cells cultured for 8 days and MC3T3-E1 murine or ROS17/2.8 rat osteoblastic cells expressing functional PTH1R. Dye transferred from loaded MC3T3-E1 or ROS17/2.8 cells to PTH1R-null F1-14 as well as to OC14 cells. Similarly, loaded F1-14 or OC14 cells transferred dye to MC3T3-E1 or ROS17/2.8 cells. We then investigated whether PTH fragments, with different C termini, could modulate the extent of GJC among PTH1R-null bone cells and PTH1R-expressing osteoblastic cells. We quantitatively assayed GJC in the presence and absence of PTH (1-34) or PTH (1-84). Interestingly, PTH (1-84) significantly increased GJC among PTH1R-null cells, while PTH (1-34) had no effect in these cells. Moreover, PTH (1-84) increased GJC from loaded ROS 17/2.8 to OC14 or F1-14 cells; however, in this case PTH (1-34) had a stimulatory effect similar to that of PTH (1-84). Our results demonstrate that PTH1R-null cells not only form functional GJ channels among themselves but also with cells expressing PTH1R, and that activation of CPTHR not only increases GJC between PTH1R-null cells but also with PTH1R-expressing osteoblasts. Our data strongly suggest that CPTHR plays a critical role in regulating cell-to-cell communication and maintaining bone homeostasis independent of PHT1R.

SU445

Matabolic Acidosis Up-Regulates PTH/PTHrP Receptors in UMR 106-01 Osteoblast-Like Cells. E. A. Gonzalez[1], S. Disthabanchong*[2], K. J. Martin[3]. [1]Nephrology, Saint Louis University, Saint Louis, MO, USA, [2]Saint Louis University, Saint Louis, MO, USA, [3]Saint Louis University, St. Louis, MO, USA.

Metabolic acidosis results in skeletal demineralization by multiple mechanisms. One of these involves the inorganic phase of bone by which hydrogen ion is buffered by bone carbonate. In addition, the cellular components of bone also participate by the induction and repression of several skeletal genes. Previous studies have suggested that the action of parathyroid hormone (PTH), a major regulator of bone turnover, might be altered by acidosis. The present studies were designed to test directly, in vitro, whether acidosis altered the effects of PTH in UMR 106-01 osteoblast-like cells. Studies were conducted in confluent cultures of UMR 106-01 cells in MEM with 5% FBS at pH values varying from 7.4 to 7.1 by addition of HCl. After time periods of 4-48 hours, cells were tested for cyclic-AMP generation in response to PTH. PTH binding and PTH/PTHrP receptor mRNA levels were determined by radioligand binding assay and Northern analysis respectively. After 48 hours, decreases in pH from 7.4 to 7.1 resulted in a progressive increase in PTH-stimulated cyclic-AMP generation from 1978 +/- 294 to 4968 +/- 929 pmoles/culture/5 minutes($p < 0.05$). Basal cyclic-AMP concentrations were unchanged. PTH binding increased 1.5 to 2 fold. Competitive inhibition of radioligand binding revealed an increase in receptor number which was supported by upregulation of PTH/PTHrP receptor mRNA up to 2 fold from control levels. These findings demonstrate that metabolic acidosis stimulates the response to PTH in UMR 106-01 osteoblast-like cells by a mechanism that involves an increase in the levels of PTH/PTHrP receptor mRNA. Thus, the skeletal response to acidosis which includes an increase in bone resorption may result, at least in part, from an increase in PTH/PTHrP receptors leading to an enhanced effect of PTH on bone. This mechanism could contribute to the spectrum of skeletal abnormalities found in renal osteodystrophy.

SU446

The Putative Membrane Receptor for 1α,25(OH)$_2$-Vitamin D$_3$ Associated with Rapid Biological Responses Is Present in Chick Intestinal Caveolae. C. J. Olivera*[1], F. M. B. Silva*[2], J. E. Bishop[1], A. W. Norman[1]. [1]Univ. California, Riverside, CA, USA, [2]UFSC, Florianpolis, SC, Brazil.

The steroid hormone 1α,25(OH)$_2$-vitamin D$_3$ [125D] exerts its biological activity via distinct receptors that recognize different shapes of the conformationally flexible 125D. These include the nuclear vitamin D receptor (nVDR) associated with genomic responses and a putative membrane receptor (mVDR) linked to rapid, nongenotropic responses. We and others have previously shown that 125D elicits rapid responses including transcaltachia (rapid intestinal Ca^{2+} absorption) and activation of PKC and MAP-kinase in chick intestine. Here we report results from experiments using isolated caveolae (CV) membrane fractions from chronically vitamin D-deficient (-D) chick intestinal cells. CV are 50-100 nm plasma membrane invaginations that in some cells have been shown to be the site of localization of signal transduction molecules. Caveolin-1, a 21 kDa marker protein for CV membrane vesicles, was used for Western analysis to confirm the presence of this key protein in our intestinal CV fractions. Transmission electron microscopy of CV demonstrated the presence of membrane-isolated vesicles similar to those in cells known to possess CV. We have employed the CV fraction as a possible source of the mVDR and studied the *in vitro* saturable binding of [^{3}H]125D (0.05-15 nM) ± 100 fold excess nonradioactive 125D in our standard VDR steroid competition assay. We found that [^{3}H]125D consistently binds to the CV in a saturable fashion; the average KD is 2.0 nM ± 0.7 and the B_{max} is 35 ± 8 fmoles/mg protein; n = 8. Pretreatment of -D chicks with 6.5 nmoles of 125D 2 hrs before isolation of intestinal CV, followed by *in vitro* [^{3}H]125D binding studies, resulted in ~ 35% reduction in B_{max} (n = 3) with no change in KD. We conclude that *in vivo* occupancy of the CV mVDR significantly diminishes the number of binding sites available for *in vitro* CV binding of [^{3}H]125D. Only a low amount of [^{3}H]25(OH)D$_3$ (a measure of vitamin D binding protein contamination) and no [^{3}H]-24R,25(OH)$_2$D$_3$ bound to the CV, thus demonstrating the CV specificity of binding for [^{3}H]125D. Steroid competition assays using conformationally restricted analogs of 125D that are diagnostic for rapid or for genotropic responses indicated that both analog families can compete with [^{3}H]125D for binding to the CV fraction. Further, the process of rapid intestinal Ca^{2+} transport *in vivo* was found to modulate the extent of *in vitro* binding of [^{3}H]125D to CV. Collectively these experiments provide the first evidence for the existence of a binding protein, possibly the mVDR, for 1α,25(OH)$_2$-vitamin D$_3$ in caveolae fractions from chick intestine.

SU447

Evidence for Functional Cooperation between CCAAT/Enhancer-binding Protein Beta and the VDR/RXR Complex in the Regulation of 25-Hydroxyvitamin D$_3$ 24-Hydroxylase Transcription. P. Dhawan*[1], X. Peng*[1], M. Centrella*[2], T. L. McCarthy*[2], S. Christakos[1]. [1]Biochemistry and Molecular Biology, UMDNJ - New Jersey Medical School, Newark, NJ, USA, [2]Yale University Medical School, New Haven, CT, USA.

Relatively few 1,25dihydroxyvitamin D$_3$ (1,25(OH)$_2$D$_3$) regulated genes are known in target tissues maintaining calcium homeostasis. Using gene chip array we found that a gene in addition to 25-hydroxyvitamin D$_3$ 24-hydroxylase (24(OH)ase) and calbindin activated by a factor greater than 50% by 1,25(OH)$_2$D$_3$ in mouse kidney is CCAAT-enhancer-binding protein β (C/EBPβ), an important activator of transcription. Our findings were verified by Northern and Western blot analysis and induction of C/EBPβ by 1,25(OH)$_2$D$_3$ was observed in primary murine osteoblasts, in UMR osteoblastic cells as well as in mouse kidney. Results of Northern analysis indicated that the first significant induction of C/EBPβ mRNA by 1,25(OH)$_2$D$_3$ in UMR osteoblastic cells precedes the induction of 24(OH)ase mRNA (3h compared to 9h), consistent with a possible role of C/EBPβ as a mediator of the 1,25(OH)$_2$D$_3$ response of the 24(OH)ase gene. Since two putative C/EBPβ sites were noted in the 24(OH)ase promoter (at -964/-955 and at -395/-388), this possibility was tested in experiments in which COS-7 cells were transfected with the rat 24(OH)ase promoter (-1367/+74; VDREs at -258/-244 and -150/-136) and the human vitamin D receptor (hVDR) in the presence or absence of C/EBPβ. In dose response studies (0.125 - 5 μg C/EBPβ) we found that suboptimal 1,25(OH)$_2$D$_3$ induction of 24(OH)ase transcription could be enhanced a maximum of 20 fold by C/EBPβ. In the absence of 1,25(OH)$_2$D$_3$ the 24(OH)ase promoter failed to respond to C/EBPβ. C/EBPδ (but not C/EBPα) was also found to enhance the inductive action of 1,25(OH)$_2$D$_3$ on 24(OH)ase transcription. Deletion analysis indicated that enhancement of 1,25(OH)$_2$D$_3$ induced 24(OH)ase transcription by C/EBPβ was observed using the -671/+74 but not the -291/+74 rat 24(OH)ase promoter construct. The C/EBPβ site at -395/-389 (TTGGCAA) differs from the consensus by a single base and mutation of this site within the -671/+74 24(OH)ase promoter construct resulted in a marked attenuation of the response to C/EBPβ. Gel shift analysis indicated the ability of the C/EBPβ protein to interact with this element. These findings establish C/EBPβ as a novel 1,25(OH)$_2$D$_3$ target gene and indicate that C/EBPβ is a major transcriptional activator of the 24(OH)ase gene. In addition, from this study a fundamental role has been established for the first time for cooperative effects and cross talk between the C/EBP family of transcription factors and VDR in 1,25(OH)$_2$D$_3$ induced transcription.

SU448

Comparative Studies on 1α,25(OH)$_2$-vitamin D$_3$ Mediated Ion Channel Rapid Responses in Osteoblasts from Vitamin D Nuclear Receptor Knock-Out and Wild Type Mice. L. P. Zanello, H. L. Henry, J. E. Bishop, A. W. Norman. Univ. California, Riverside, CA, USA.

Osteoblasts are a major target for the steroid hormone 1α,25(OH)$_2$-vitamin D$_3$ [125D] where a primary outcome is a modulation of the bone remodeling process. 125D exerts its physiological effects through both genomic (modulation of gene expression via a nuclear 125D receptor [nVDR]) and rapid, non genomic (at the cell membrane level via a putative membrane receptor [mVDR]) mechanisms. To investigate whether the presence of a functional nVDR is required for a rapid 125D-mediated response(s), we studied the modulation by 125D of ion channel activities in osteoblasts isolated from nVDR knock-out (KO) and wild type (WT) mice calvaria. Whole-cell patch-clamp recordings were performed according to previous protocols (Zanello & Norman, 1997) on primary cultured KO and WT osteoblasts from (PCR) genotyped mice. KO osteoblasts were notably scarce in culture, while WT osteoblasts proliferated abundantly. Both cell types expressed inward and outward currents when subjected to depolarizing potentials between -40 and 80 mV from a holding potential of -50 mV. Our patch-clamp results demonstrated the existence of a 125D-inducible anionic current in the WT and KO osteoblasts, similar to a Cl^- current previously found in an osteoblast-like cell line (Zanello & Norman, 1997). Also a "background" capacitative current was consistently recorded in both WT and KO cells. Whole-cell capacitance measurements carried out in the presence of the hormone showed fluctuations in the range of 0.1-1 pF. This is equivalent to 10-100 _m^2 changes in plasma membrane surface when sampled at 1 sec intervals. We attributed these capacitance changes to the fusion of secretory granules to the cell surface, that is clearly seen with phase contrast microscopy of live cells. In parallel studies, bone tissue from both mice genotypes were separately subjected to mRNA microarray analysis to examine the expression of mRNAs coding for ion channels. There were qualitatively different ion channel profiles for each mouse genotype. More specifically, a Cl^- channel and a series of non-selective cation channels seemed to be preferentially expressed in KO osteoblasts, while mRNA levels for K^+, a capacitative Ca^{2+}, and L-type Ca^{2+} channels were notably below WT levels. We conclude that, as expected from the traditional understanding of 125D modulation of gene transcription, the absence of a functional nVDR in KO mice correlates well with changes in the expression of ion channel molecules (genomic effects). On the other hand, the existence of a 125D-sensitivite anionic current in both KO and WT osteoblasts suggest a common pathway for a rapid response which is independent from a nVDR.

SU449

Microarray Analysis of RNA from Tissues of Vitamin D Receptor Knock-Out and Wild Type Mice Treated with 1α,25(OH)$_2$D$_3$ or 24R,25(OH)$_2$D$_3$. H. L. Henry[1], M. Heim*[2], J. E. Bishop[1], R. Zielinski*[1], H. D. Shah*[1], C. Kwan*[1], I. Bendik*[2], W. Hunziker[2], A. W. Norman[1]. [1]Univ. California, Riverside, CA, USA, [2]Research and Development, Human Nutrition and Health, Roche Vitamins Ltd., Basel, Switzerland.

The vitamin D nuclear receptor null mouse (VDR-KO) offers the opportunity to probe possible VDR-independent responses of cells to the metabolites of vitamin D. We carried out GeneChip DNA microarray analysis of RNA from intestine, kidney and bone from VDR-KO and wild type (WT) mice. Three groups of mice fed a vitamin D deficient diet were given an IP dose of either 1α,25(OH)$_2$D$_3$ (250 ng) or 24R,25(OH)$_2$D$_3$ (500 ng) or vehicle (ethanol/propanediol, 1:1) 8 hours prior to tissue harvest. Total RNA from kidney, bone, and small intestine was isolated from each individual animal and biotin-labeled cRNA was synthesized for hybridization to mouse Affymetrix GeneChip arrays. Only sequences above a minimal level of expression (Average Difference > 150) were used for further analysis. The numbers of transcripts whose expression in vehicle-treated WT mice was at least two-fold greater than in vehicle-treated KO mice were 43, 20, and 98 for bone, intestine, and kidney, respectively. In a separate analysis of the VDR-KO data, 20 transcripts whose expression in bone was up-regulated at least two-fold over vehicle control by 24R,25(OH)$_2$D$_3$ but not by 1α,25(OH)$_2$D$_3$ in VDR-KO mice were identified. The same analysis in kidney and intestine yielded 11 transcripts in each tissue. All but 3 of the 20 24R,25(OH)$_2$D$_3$-regulated bone transcripts were also expressed in WT bone and nine of these were up-regulated by 24R,25(OH)$_2$D$_3$ in that tissue. Approximately half of the 20 transcripts were also expressed in either intestine or kidney, but only one was also up-regulated in one of these tissues (kidney). Of these 20 transcripts that are apparently up-regulated in bone by 24R,25(OH)$_2$D$_3$, 6 have been selected for further confirmatory analysis by RT-PCR. These include transcripts encoding HSP47, a molecular chaperone involved in collagen Type I synthesis, as well as proteins involved in apoptosis and protein phosphorylation. These studies provide evidence that 24R,25(OH)$_2$D$_3$ can alter the pattern of gene expression in a target tissue and confirms that the VDR-KO mouse is a useful model in which to examine elements of the vitamin D endocrine system in the absence of the 1α,25(OH)$_2$D$_3$-VDR complex.

SU450

Novel Interaction of the Vitamin D Receptor with a Mitochondrial Protein, Enoyl CoA Hydratase: Implications with Respect to Vitamin D Function. W. Lutz*[1], E. Frank*[1], M. R. Pittelkow*[2], D. Matern*[3], R. Rinaldo*[3], R. Kumar[1]. [1]Medicine and Biochemistry and Molecular Biology, Mayo Clinic, Rochester, MN, USA, [2]Dermatology, Mayo Clinic, Rochester, MN, USA, [3]Pathology and Laboratory Medicine, Mayo Clinic, Rochester, MN, USA.

The vitamin D receptor (VDR) interacts with co-activator and co-repressor proteins, and steroid hormone receptors to change gene expression. To assess whether the VDR interacts with other biologically relevant proteins, we used the yeast two-hybrid system to identify novel interacting proteins. The Gal4 yeast two-hybrid system was used to screen a kidney cDNA library. Saccharomyces cerevisiae, AH109 cells, were co-transformed with the pACT cDNA library vector and with the pGBKT7 vector expressing the VDR as a fusion protein with the Ga14 DNA-binding domain. Yeast transformants expressing a protein, which interacts with VDR were selected by nutrient auxotrophy and galactosidase activity. A transformant was obtained which expressed enoyl CoA hydratase, short, 1(ECHS1) (Accession # BC008906), a mitochondrial matrix enzyme, which catalyzes the hydration of 2-trans-enoyl CoA intermediates to L-3 hydroxy-acyl CoAs during mitochondrial beta-oxidation of fatty acids. To assess the function consequences of the interaction of the VDR and ECHS1 we compared fatty acid oxidation in primary cultures of skin fibroblasts derived from wild-type mice and VDR-null mutant mice. Beta-oxidation in fibroblasts was evaluated by measuring the concentration of acylcarnitines: C2, C3, C4, C6, C8, C10:1, C10, C12:1, C12, C14:1, C14, C16:1, and C16 in the culture medium by mass spectrometry. Concentrations of all acylcarnitines corrected for protein in the wells were lower in the culture medium from VDR null mutant mouse fibroblasts. The difference was statistically significant ($P < 0.05$) for C5, C8, C10, C14:1, and C16:1 acylcarnitines. As the steady state levels of acylcarnitines is inversely related to the rate of beta-oxidation these results suggest the interaction of VDR and ECHS1 reduces the activity of the enzyme. ECHS1 is encoded by a nuclear gene and is targeted to the mitochondrion by a leader sequence. As the VDR has not been reported to be present in mitochondria it is likely that the receptor and ECHS1 interact in the cytosolic compartment to alter ECHS1 activity by a yet to be defined mechanism. We show that the VDR interacts with enoyl CoA hydratase, a mitochondrial enzyme involved in the beta-oxidation of fatty acids. These results, in part, may explain previous observations in which vitamin D has been shown to alter mitochondrial function.

SU451

Nuclear Localization Sequence of NCoA-62/SKIP and its Colocalization with VDR. C. Zhang*, D. R. Dowd*, P. N. MacDonald. Pharmacology, Case Western Reserve University, Cleveland, OH, USA.

NCoA-62/SKIP is a novel coactivator protein in VDR-mediated transcription, and it functions by binding selectively to the VDR-RXR heterodimer in a ligand-enhanced manner. Little is known of the domains within the NCoA-62/SKIP protein that mediate its coactivator properties. In the present study, we identified a nuclear localization sequence (NLS) in the extreme COOH-terminus of NCoA-62/SKIP. FLAG-tagged NCoA-62/SKIP or a series of NCoA-62/SKIP deletion mutants were transiently expressed in COS7 cells, and the subcellular distribution of the proteins was examined with anti-FLAG antibodies and immunofluorescent microscopy. NCoA-62/SKIP WT showed strict nuclear staining, while NCoA-62/SKIP (1-530), lacking the last 6 amino acids in the COOH-terminus, showed exclusive cytoplasmic staining. These data suggested that residues 530-536 (KKRRKE) of NCoA-62/SKIP comprised a nuclear localization sequence. The sufficiency of the NLS of NCoA-62/SKIP was investigated by fusing this sequence to green fluorescent protein (GFP) at the COOH-terminus. GFP-NCoA (530-536) was located predominantly in nuclei, while GFP alone was equally distributed throughout the cells. To examine colocalization of NCoA-62/SKIP with VDR, we constructed HA-tagged VDR for immunostaining and confocal microscopy. HA-VDR was located predominantly in nuclei with a significant presence in cytoplasm in the absence of ligand. NCoA-62/SKIP WT colocalized with VDR in the nucleus. Importantly, coexpression of VDR transferred NCoA-62/SKIP (1-530) from cytoplasm to nucleus. These results indicate that 1) NCoA-62/SKIP is a nuclear protein; 2) an NLS consisting of 6 amino acids in the COOH-terminus is required and sufficient for nuclear-restricted expression of NCoA-62/SKIP; and 3) VDR expression targets NCoA-62/SKIP (1-530) to the nucleus through a physical interaction between VDR and NCoA-62/SKIP.

SU452

1α,25(OH)$_2$-vitamin D$_3$-Mediated Cross-talk from Rapid to Genomic Responses in Human Leukemic NB4 Cells as Studied by Microarray Analysis and Transfected Reporter Genes. A. W. Norman[1], J. E. Bishop[1], S. Ishizuka[2], H. L. Henry[1]. [1]Univ. California, Riverside, CA, USA, [2]Dept. Bone and Calcium Metabolism, Teijin Institute for Bio-Medical Research, Tokyo, Japan.

The steroid hormone 1α,25(OH)$_2$-vitamin D$_3$ [1α,25(OH)$_2$D$_3$] exerts its biological activity via distinct receptors that recognize different shapes of the conformationally flexible 1α,25(OH)$_2$D$_3$. These include the nuclear vitamin D receptor [nVDR; responsive to the 6-s-*trans* shape of 1α,25(OH)$_2$D$_3$] associated with genomic responses and a putative membrane receptor (mVDR) linked to rapid, nongenotropic responses [responsive to the 6-s-*cis* shape of 1α,25(OH)$_2$D$_3$]. We and others have previously shown that 1α,25(OH)$_2$D$_3$ elicits rapid responses in many cell types including the human leukemic NB4 cell line; these include activation and membrane translocation of PKC and activation of mitogen-activated protein kinase (MAP-kinase). Here we report results in NB4 cells from experiments addressing whether 1α,25(OH)$_2$D$_3$ mediated rapid responses cross-talk to modulate gene expression. We assessed the rapid response contributions to gene expression in the presence of either PD98059 (PD, an inhibitor of MAP-kinase that is known to phosphorylate transcription factors) or 1β,25(OH)$_2$D$_3$ [HL, an analog of 1α,25(OH)$_2$D$_3$ that is an inhibitor of 1α,25(OH)$_2$D$_3$ initiated rapid responses, with minimal effects on genomic responses]. NB4 cells were exposed to 10 nM 1α,25(OH)$_2$D$_3$ ± PD (10 μM for 3 hr) or 10 nM 1α,25(OH)$_2$D$_3$ ± HL (10 nM for 8 hr). Then the total RNA was isolated and biotin-labeled cRNA was synthesized for hybridization to human Affymetrix GeneChip arrays. Only sequences above a minimum level of expression were used for analysis. Of 44 genes that were up-regulated by 3 hr exposure to 1α,25(OH)$_2$D$_3$ (>2-6X), the presence of PD attenuated 20 of these genes (2-5X). Of 128 genes that were up-regulated by 8 hr exposure to 1α,25(OH)$_2$D$_3$ (>2-10X), 79 were attenuated by the presence of HL (13 > 4X; 20 > 3X; 23 > 2X). Comparable results were seen for 1α,25(OH)$_2$D$_3$ mediated down-related genes. In other experiments, NB4 cells were transiently transfected with an osteocalcin promoter [with a 1α,25(OH)$_2$D$_3$ response element, VDRE] linked to a growth hormone reporter and 24 hrs later the cells were exposed for 24 hr to 1α,25(OH)$_2$D$_3$ (10 nM) ± PD (5 μM). The expression of the osteocalcin reporter was inhibited in the presence of PD by 65% ± 7%. A similar result was obtained with the 1α,25(OH)$_2$D$_3$ responsive 25(OH)D$_3$-24-hydroxylase promoter. We conclude that by both microarray analysis or transfection of VDRE containing reporter genes there is evidence for 1α,25(OH)$_2$D$_3$ mediated rapid responses that modulate gene expression.

SU453

Comparative LC-MS/MS Based Metabolic Study of 1α,25(OH)$_2$D$_3$ and 20-methyl-1α,25(OH)$_2$D$_3$ Reveals Reduced Clearance through CYP24-catalyzed C24-oxidation. M. Kaufmann*, S. Masuda, G. Jones. Biochemistry, Queen's University, Kingston, ON, Canada.

CYP24-catalyzed metabolism of 1α,25(OH)$_2$D$_3$ through C24-oxidation results in the excretory form, calcitroic acid (CA). Increased biological activity of side chain substituted analogs of 1α,25(OH)$_2$D$_3$ arises partially from reduced CYP24-mediated target cell clearance, in addition to altered DBP and VDR affinity. The objective of this investigation was to compare the sites and rates of catabolism of 1α,25(OH)$_2$D$_3$ and a model analog, 20-CH$_3$-1α,25(OH)$_2$D$_3$ in human HPK1A-*ras* cells in a time (0-48h) and substrate concentration (100nM-10μM) dependent manner. Capacity of CYP24 to metabolize 1α,25(OH)$_2$D$_3$ and 20-CH$_3$-1α,25(OH)$_2$D$_3$ was assessed by substrate loss and *total* product formation using quantitative diode array [UV$_{265}$] and LC-MS/MS. Mass spectral characterization of metabolites was based upon molecular ions [MH$^+$], dehydration products, and sodium adducts. MS/MS spectra yielded a fragment ion [m/z=135] which formed the basis for highly sensitive and selective metabolite quantitation. 20-CH$_3$-1α,25(OH)$_2$D$_3$ was metabolized through analogous intermediates to 1α,25(OH)$_2$D$_3$ with a similar time-dependent metabolite distribution. At 4-8h time points of 1μM incubations, proximal pathway intermediates 1α,24,25(OH)$_3$D$_3$ [MH$^+$=433/+20-CH$_3$=447] and 24-oxo-1α,25(OH)$_2$D$_3$ [MH$^+$=431/445] predominated, whereas the terminal catabolites tetranor-1α,23(OH)$_2$D$_3$ [MH$^+$=361/375] and CA [MH$^+$=375/389] were the most prevalent at 48h. Analog metabolism differed by reduced production of 23-hydroxylated and side chain cleaved catabolites. Diminished production of 20-CH$_3$-24-oxo-1α,23,25(OH)$_3$D$_3$ over 24-oxo-1α,23,25(OH)$_3$D$_3$ [MH$^+$=461/447] was observed at high substrate concentrations [5-10μM, 24h] and at t=12-48h, 1μM. A similar trend for 20-CH$_3$-tetranor-1α,23(OH)$_2$D$_3$ over tetranor-1α,23(OH)$_2$D$_3$ was also observed at the 1μM time points. The terminal metabolite CA, was produced at t=12-48h, 1μM, and at high efficiency using low substrate concentrations (100-500nM, 24h). In contrast, 20-CH$_3$-CA was observed only at 1μM, 48h and in

lesser quantities than CA. 1α,23,25(OH)$_3$D$_3$ [MH$^+$=433] was observed to be a major product of 1α,25(OH)$_2$D$_3$ at 5-10μM, whereas no 20-CH$_3$ equivalent was found in analog incubations. We have revealed that 20-CH$_3$ substitution of 1α,25(OH)$_2$D$_3$ leads to altered metabolism through CYP24-catalyzed C24-oxidation, characterized by reduced 23-hydroxylation and conversion to water-soluble products. In conclusion, the finding of diminished metabolism of 20-CH$_3$-1α,25(OH)$_2$D$_3$ by CYP24 provides an explanation for increased biological activity for this, and perhaps other analogs.

SU454

Molecular Analysis of the Vitamin D Receptor Interactions with Highly Potent Vitamin D Analogues Using Site-Directed Mutagenesis. T. Okano[1], K. Nakagawa*[1], Y. Sowa*[1], K. Mikami*[2], N. Kubodera[3], K. Ozono[4]. [1]Hygienic Sciences, Kobe Pharmaceutical University, Kobe, Japan, [2]Chemical Technology, Tokyo Institute of Technology, Tokyo, Japan, [3]Chugai Pharmaceutical Co., Ltd., Tokyo, Japan, [4]Developmental Medicine, Osaka University Graduate School of Medicine, Osaka, Japan.

The biologic effects of 1α,25-dihydroxyvitamin D$_3$ [1α,25-D$_3$] are believed to be mediated by the vitamin D receptor (VDR) that acts as a ligand-dependent transcription factor in the nucleus of target cells. Recently, the crystal structure of the human VDR ligand-binding domain (LBD) complexed to 1α,25-D$_3$ has been reported and it was revealed that the 1α-hydroxyl group forms two hydrogen bond with serine-237(H3) and arginine-274(H5), and the residues of lysine-264 and glutamic acid-420 form a salt bridge that stabilizes the conformation of the activation function domain 2 (AF-2) of the VDR. To examine the interactions of highly potent vitamin D analogues with the LBD, especially at the sites of H3, H5 and H12, point-mutations at Ser-237(Ser237Ala, S237A), Arg-274(R274A), and Lys-264(K264A) were generated in the hVDR expression plasmid (pSG5-hVDR) by site-directed mutagenesis using a PCR method. The mutant VDRs were evaluated for in vitro and in situ ligand-binding potency, ligand-dependent transcriptional activity in transfected MG-63 cells utilizing reporter constructs containing either rat 25-hydroxyvitamin D$_3$-24-hydroxylase or human osteocalcin gene promoter, in situ heterodimerization efficiency with retinoid X receptor a (RXRα) and in vitro VDR/RXRα/vitamin D response element (VDRE) complex formation efficiency in the presence or absence of the ligands. The results indicated that the relative binding affinities for 1α,25-D$_3$ were wild-type VDR (100%) = K264A (100%) > S237A (49%) > R274A (0%), while those for 20-epi-1α,25-D$_3$ were wild-type VDR (100%) > K264A (128%) > S237A (213%) > R274A (0%). The mutant VDRs all displayed significantly reduced transcriptional activities and VDR/RXRα heterodimer or VDR/RXRα/VDRE complex formation for 1α,25-D$_3$, while both S237A and K264A displayed similar biological potencies for 20-epi-1α,25-D$_3$ when compared with wild-type VDR. As expected, R274A was totally inactive. These results suggest that Arg-274 in the LBD of the VDR is essential for binding to both 1α,25-D$_3$ and 20-epi-1α,25-D$_3$ and play a vital role to transactivate vitamin D-target genes. In addition, the amino acid residues other than Ser-237 and Lys-264 in the LBD may be involved in the VDR binding of 20-epi-1α,25-D$_3$.

SU455

2,2-Dimethyl Analogues of 1alpha,25-Dihydroxyvitamin D3: The A-Ring Structure of the Ligands Differentiates Activity Profiles of the Natural Hormone. T. Fujishima*[1], A. Kittaka*[1], K. Yamaoka*[2], K. Takeyama[2], S. Kato[2], M. Kurihara*[3], H. Takayama[1]. [1]Faculty of Pharmaceutical Sciences, Teikyo University, Kanagawa, Japan, [2]Institute of Molecular and Cellular Biosciences, University of Tokyo, Tokyo, Japan, [3]National Institute of Health Sciences, Tokyo, Japan.

We have synthesized all possible A-ring stereoisomers of 2-methyl-1,25-dihydroxyvitamin D$_3$, demonstrating that the introduction of a simple methyl group to the A-ring of 1α,25-dihydroxyvitamin D$_3$ (**1**) yields the analogues with unique activity profiles. The eight 2-methyl analogues, which differ in stereochemistry of the methyl group on C2 and the hydroxyl groups on C1 and C3, exhibited cell differentiation- or apoptosis-inducing activity towards HL-60 cells, depending on the A-ring structure. In particular, 2α-methyl-1α,25-dihydroxyvitamin D$_3$ (**2a**) showed 4-fold higher affinity for bovine thymus VDR and 2-fold higher cell differentiation-inducing activity towards HL-60 cells in comparison with **1**, whereas 2β-methyl-1α,25-dihydroxyvitamin D$_3$ (**2b**) showed one-eighth of the affinity of **1**, with a weak apoptosis-inducing activity. In the present work, we have designed 2,2-dimethyl-1α,25-dihydroxyvittamin D$_3$ (**3**) as a hybrid analogue of **2a** and **2b** to investigate how these double methyl groups in the C2 position affect the activity profiles. Synthesis of all four possible stereoisomers of 2,2-dimethyl-1,25-dihydroxyvitamin D$_3$ was carried out by using a convergent method. The A-ring enyne synthon was obtained by a 9-step conversion of methyl hydroxypivalate in excellent yield. The bovine thymus VDR binding affinity of 2,2-dimethyl-1α,25-dihydroxyvittamin D$_3$ (**3**) was 3% of the affinity of **1**. The other three stereoisomers of **3**, which differ in stereochemistry of the hydroxyl groups on C1 and C3, showed rather weak potency. We preliminarily examined interaction of VDR with two coactivaters (SRC-1, TIF2) by the synthesized analogues in mammalian two hybrid assays. The natural hormone **1** induced interaction of VDR with two coactivaters (SRC-1, TIF2). In our preliminary results, the VDR that liganded with the methyl analogues appeared to possess a differentiated potency to recruit these coactivators depending on the A-ring structure. The 2α-methyl analogue (**2a**) induced rather strong interaction of VDR with SRC-1, whereas its 2-epimer, the 2β-methyl analogue (**2b**), showed a preference to TIF2. The 2,2-dimethyl analogue (**3**) exhibited a similar trend of the 2α-methyl analogue (**2a**). Molecular docking studies based upon the X-ray crystal structure of VDR suggested the importance of the 2-methyl substitution in a certain orientation. The detailed biological activities and molecular docking studies of the analogues will be presented.

SU456

The Novel 2alpha-Substituted 1alpha,25-Dihydroxyvitamin D3 Analogues as Superagonists: Evaluation of VDR-Binding and Remarkable Calcemic Activity. A. Kittaka*[1], Y. Suhara*[1], T. Shinki[2], T. Fujishima*[1], M. Kurihara*[3], H. Takayama[1]. [1]Faculty of Pharmaceutical Sciences, Teikyo University, Kanagawa, Japan, [2]School of Dentistry, Showa University, Tokyo, Japan, [3]National Institute of Health Sciences, Tokyo, Japan.

Stereocontrolled syntheses of 1α,25-dihydroxyvitamin D$_3$ (**1**) analogues with a 2α-substituent in three categories (**A** - **C**) have been accomplished in order to investigate the A-ring structure-activity relationships. The representative positive structural motifs at the 2α-position of **1** in VDR binding are the methyl group of the alkyl series (**A**), the 3-hydroxypropyl group in the ω-hydroxyalkyl series (**B**), and the 3-hydroxyalkoxyl group in the ω-hydroxyalkoxyl series (**C**). These analogues were systematically synthesized from the A-ring precursor enyne, derived from D-xylose or D-glucose, and the CD-ring bromoolefin part using Pd-catalyzed coupling reaction. Introduction of one of these positive motifs to the 2α-position of **1** showed ca. 2- to 4-fold higher binding affinity for bovine thymus VDR than that of the natural hormone. Biological activities of these analogues having similar length of the 2α-substituent in each category, i.e., propyl (C3) in **A**, 3-hydroxypropyl (O1C3) in **B**, or 3-hydroxypropoxyl (O2C3) in **C** were studied. In vivo analyses of Northern blot reveal increase in expression of CYP24 mRNA in rat intestine with C3, O1C3, and O2C3, as compared to **1**. The half-life of these analogues, especially O1C3 and O2C3, seems to be much longer than that of **1**; because expression of CYP24 mRNA maintains markedly higher level than that of **1** after 24 hrs. It is also interesting that calcemic activity of C3 in rat serum is almost the same level as **1**, even though VDR affinity of C3 is only 20% of the natural hormone. In the case of O1C3 and O2C3, remarkable calcemic activity continued even after 24 hrs. It would be due to high affinity for VDR and the long half-life of these analogues in rat serum. Some of synthetic analogues of **1** have been clinically used in the treatment of calcium and bone disease, secondary hyperparathyroidism, and skin disorder psoriasis. We believe our novel 2α-manipurated analogues would give important information in structure-activity relationships and contribute to elucidate the molecular mode of action.

SU457

Comparison of the Calcemic Actions of 1α(OH)D$_2$ and 1α(OH)D$_3$ and their Activated Metabolites. A. J. Brown[1], J. L. Finch[1], S. A. Strugnell[2], J. C. Knutson[2]. [1]Renal Division, Washington University, Saint Louis, MO, USA, [2]Bone Care International, Madison, WI, USA.

1α-Hydroxyvitamin D$_2$ (1α(OH)D$_2$ or doxercalciferol), a less calcemic analog than its vitamin D$_3$ counterpart 1α(OH)D$_3$ (alfacalcidol), is currently available for the treatment of secondary hyperparathyroidism in patients with renal failure. Both 1α(OH)D$_2$ and 1α(OH)D$_3$ are prohormones that must be activated to exert their actions. Although both are 25-hydroxylated *in vivo*, in animal and cell culture studies 1α(OH)D$_2$, but not 1α(OH)D$_3$, can be 24-hydroxylated to 1,24(OH)$_2$D$_2$, a metabolite that is much less calcemic than 1,25(OH)$_2$D$_2$ and 1,25(OH)$_2$D$_3$. In the present study, we have examined the calcemic activities of 1α(OH)D$_2$ and 1α(OH)D$_3$ and their dihydroxylated metabolites. 1α(OH)D$_2$ or 1α(OH)D$_3$ were administered IP (1.0 or 2.5 nmol/kg) to vitamin D-replete rats every other day for one week, and serum Ca and P were measured 24 hours after each injection. 1α(OH)D$_2$ was clearly less calcemic and phosphatemic than 1α(OH)D$_3$ even after a single injection. Metabolism and tissue distribution studies showed that in vitamin D-replete rats [^{3}H]1α(OH)D$_2$ was rapidly converted in vivo to both 1,25(OH)$_2$D$_2$ and 1,24(OH)$_2$D$_2$, but 1,25(OH)$_2$D$_2$ was the predominant metabolite both in the circulation and in the intestine and bone. The relative activities of 1α(OH)D$_2$ and 1α(OH)D$_3$ and their dihydroxy metabolites in stimulating intestinal calcium absorption and bone Ca mobilization were compared using vitamin D-deficient rats. The ED50s for stimulation of intestinal Ca absorption were similar for 1,25(OH)$_2$D$_3$ and 1,25(OH)$_2$D$_2$ (0.020 and 0.025 nmol/kg, respectively) but30 times higher for 1,24(OH)$_2$D$_2$ (0.70 nmol/kg). The ED50s for 1α(OH)D$_2$ and 1α(OH)D$_3$ were similar, but the amount of Ca absorption produced by 1α(OH)D$_2$ and 1α(OH)D$_3$ was markedly lower than that produced by the activated metabolites, and the amount of absorption produced by 1α(OH)D$_3$ was less than that produced by 1α(OH)D$_2$. 1α(OH)D$_2$ and 1α(OH)D$_3$ were equipotent in enhancing bone Ca mobilization as were 1,25(OH)$_2$D$_2$ and 1,25(OH)$_2$D$_3$. 1,24(OH)$_2$D$_2$ was less active than 1,25(OH)$_2$D$_3$ and 1,25(OH)$_2$D$_2$, but only at the lowest dose tested (0.01 nmol/kg). In summary, the strikingly disparate calcemic activities of 1α(OH)D$_2$ and 1α(OH)D$_3$ could not be readily explained by differences in their abilities to stimulate intestinal Ca absorption or bone Ca mobilization in vitamin D-deficient rats.

Disclosures: ***A.J. Brown****, Bone Care International, Inc. 2.*

SU458

The Noncalcemic Vitamin D Analogue, EB1089, Downregulates Parathyroid Hormone-Related Protein (PTHrP) Gene Expression in the PC-3 Prostate Cancer Cell Line. V. A. Tovar Sepulveda*, M. Falzon*. Department of Pharmacology and Toxicology, and Sealy Center for Molecular Sciences, UTMB, Galveston, TX, USA.

Parathyroid hormone related protein (PTHrP) contributes to the pathogenesis and progression of prostate carcinoma and the tendency of this tumor to metastasize to bone. In previous studies we demonstrated that (1) PTHrP increases proliferation of the prostate cancer cell line PC-3 through both autocrine/paracrine and intracrine pathways, and (2) 1,25-dihydroxyvitamin D_3 ($1,25(OH)_2D_3$) downregulates PTHrP gene expression in PC-3 cells. $1,25(OH)_2D_3$ is hypercalcemic *in vivo,* and therefore cannot be used clinically. The present study was undertaken (1) to compare the effects of $1,25(OH)_2D_3$ and a noncalcemic analogue, EB1089, on PTHrP gene expression in PC-3 cells; (2) to analyze the mechanism via which $1,25(OH)_2D_3$ and EB1089 regulate PTHrP gene transcription in this cell line; and (3) to investigate whether the observed suppression of PTHrP gene expression has any effect on PC-3 cell growth. Both EB1089 and $1,25(OH)_2D_3$ downregulated steady-state PTHrP mRNA levels, as determined by Northern blot analysis. The two compounds also decreased secreted PTHrP levels, as determined by an immunoradiometric assay. The human PTHrP gene contains a negative vitamin D response element ($nVDRE_{PTHrP}$) analogous to the nVDRE within the human parathyroid hormone gene. Electrophoresis mobility shift assays (EMSAs) demonstrated that this $nVDRE_{PTHrP}$ interacts with the vitamin D receptor (VDR). Both $1,25(OH)_2D_3$ and EB1089 inhibited the reporter activity of a plasmid bearing the $nVDRE_{PTHrP}$ under the control of the SV-40 promoter, as determined by chloramphenicol acetyltransferase (CAT) assays. $1,25(OH)_2D_3$ and EB1089 also produced a significant, dose-dependent decrease in PC-3 cell growth, as determined by direct cell counting. These results suggest that EB1089 suppresses PTHrP gene expression in PC-3 cells by the same mechanism as $1,25(OH)_2D_3$. EB1089 may therefore prove to be therapeutically useful in the treatment of prostate cancer, since it lacks the undesirable hypercalcemic effect of $1,25(OH)_2D_3$.

SU459

CYP24-Null Keratinocytes Demonstrate that CYP24 Is Responsible for Activation and Inactivation of $1\alpha(OH)D_2$. S. Masuda[1], A. Arabian*[2], J. McCaig*[1], M. Kaufmann*[1], S. A. Strugnell*[3], J. C. Knutson*[3], R. St-Arnaud*[2], G. Jones[1]. [1]Biochemistry, Queen's University, Kingston, ON, Canada, [2]Genetics Unit, Shriners Hospital for Children, Montreal, PQ, Canada, [3]Bone Care International, Madison, WI, USA.

CYP24 is postulated to play an important role in the metabolic clearance of $25(OH)D_3$ and $1\alpha,25(OH)_2D_3$. Vitamin D prodrugs require side chain activation by enzymes in the liver and possibly other sites. Previous studies in human keratinocytes incubated with $1\alpha(OH)D_2$ have demonstrated the production of active metabolites and inactive catabolites in a dose- and time-dependent manner. This study examined whether CYP24 is responsible for this target cell activation/ inactivation. Keratinocytes isolated from CYP24 null mice, wild type, and heterozygotic mice were incubated with 50 nM [9,11-^{3}H]$1\alpha(OH)D_2$ and the metabolites characterized by HPLC. No metabolites of [^{3}H]$1\alpha(OH)D_2$ were generated with CYP24-null keratinocytes; most of the radioactivity remained as unchanged substrate. In contrast, wild type and heterozygotic keratinocytes completely converted [^{3}H]$1\alpha(OH)D_2$ into aqueous-soluble metabolites. Mammalian cells transiently transfected with CYP24 and incubated with [^{3}H]$1\alpha(OH)D_2$ produced a series of metabolites similar to those seen in keratinocytes, confirming the central metabolic role of CYP24 established with the mouse keratinocytes. To characterize further the entire set of CYP24-generated metabolites of $1\alpha(OH)D_2$, the human keratinocyte cell line, HPK1A-*ras,* was incubated with 10 μM $1\alpha(OH)D_2$ for 48 h, and the metabolites produced were identified by a combination of diode array and LC-MS detection. Surprisingly, the major metabolite found in the aqueous fraction did not correspond to calcitroic acid, the purported final product of both $1\alpha,25(OH)_2D_3$ and $1\alpha,25(OH)_2D_2$. Its molecular weight of 458 is consistent with the presence of a hydroxy group and a carboxyl group in the side chain. Lack of sensitivity to sodium meta-periodate oxidation indicated that the carboxylated position was C-26(27). The novel metabolite identified as $1\alpha,24\text{-}(OH)_2$, 26-carboxy D_2 is the presumed degradation product of $1\alpha(OH)D_2$, synthesized by CYP24 via successive 24-hydroxylation, 26-hydroxylation and further oxidation at C-26. These findings suggest that CYP24 has the capacity to both activate and inactivate prodrugs in target cells *in vivo* thereby offering the potential for treatment of hyperproliferative disorders such as psoriasis and skin cancer by topical administration of these compounds.

SU460

2-Methylene-19-Nor-(20S)-1,25-Dihydroxyvitamin D_3: A Potent Inducer of Osteoclast Formation through Actions on RANKL. H. Yamamoto, N. K. Shevde, O. Barmina*, L. Plum*, H. F. DeLuca, J. W. Pike. Biochemistry, University of Wisconsin- Madison, Madison, WI, USA.

The two carbon-modified vitamin D_3 analogue 2-methylene-19-nor-(20S)-1,25-dihydroxy-vitamin D_3 (2MD) is a highly potent selective vitamin D receptor modulator (SVDRM). Unlike 1,25-dihydroxyvitamin D_3 ($1,25(OH)_2D_3$) whose physiologic actions are homeostatic, recent studies indicate that 2MD is preferentially anabolic in vivo, leading to the formation of new bone in the rat at concentrations that do not induce hypercalcemia. Despite this, the analogue is a potent transcriptional regulator of osteoblast genes that either induce osteoclast formation (RANKL, OPG) or modulate their function (osteopontin), with peak activity two logs lower than that for $1,25(OH)_2D_3$. This results in the induction of osteoclast formation in either total bone marrow cultures or in coculture assays (ST2 osteoblast cells and either nonadherent hematopoeitic spleen precursors or RAW264.7 cells) at 10^{-10} M. These differences in potency between 2MD and $1,25(OH)_2D_3$ are also observed when the promoters for the human osteocalcin or the 24OHase genes are introduced as luciferase reporter constructs into MC3T3E1 cells and evaluated at concentrations from 10^{-12} to 10^{-7} M. In this context, however, the RANKL promoter (-965) is completely resistant to both ligands. Interestingly, the affinity of recombinant VDR for 2MD is identical to that for $1,25(OH)_2D_3$. We explored this discrepancy using cellular assays and molecular techniques including those involving protease digestion and mammalian two-hybrid interactions. Transcriptional dose response curves under reduced-serum or serum-free conditions for both $1,25(OH)_2D_3$ and 2MD revealed that ligand potency increased proportionately for both vitamin D compounds. This suggested that differences in analogue binding to either serum proteins or DBP were unlikely to explain the potency differences. Interestingly, digestion assays using limited trypsin digestion revealed no differences between $1,25(OH)_2D_3$ or 2MD in their ability to either protect VDR or to alter its pattern of digestion. Interaction technology, however, using the mammalian two-hybrid system revealed that association of VDR with both its RXRalpha partner as well as with the LXXLL domain of comodulator SRC-1 occurred at concentrations of 2MD that were two logs lower than that for $1,25(OH)_2D_3$. These studies suggest that in addition to its classification as a SVDRM, 2MD is a superagonist that stimulates transcription by enhancing interaction between the VDR and at least two protein partners that play key roles in vitamin D-dependent transcriptional activation.

SU461

Cross-linking Analogs of Vitamin D for Prostate Cancer. N. Swamy*[1], R. Ray[2]. [1]Pediatrics, Brown University, Providence, RI, USA, [2]Medicine, Boston Unviersity School of Medicine, Boston, MA, USA.

1,25(OH)2D3 and its analogs are non-tissue specific due to the ubiquitous nature of VDR. Therefore, large doses of these compounds are required to harness any beneficial effect, causing hypercalcemia. Moreover, these analogs are antiproliferative, but not toxic to reduce tumor load. Ideally a vitamin D-related drug should be antiproliferaive and lethal to tumor cells at a dose that does not induce systemic toxicity. We have developed 1,25(OH)2D3-3-BE, a VDR-cross-linking analog and studied its growth-inhibitory effects in keratinocytes (skin cells), MCF-7 (breast cancer cells), LNCaP and PC-3 (prostate cancer cells), and PZ-HPV-7 (papillovirus immortalized normal prostate cells). We observed that 1,25(OH)2D3-3-BE had a stronger antiproliferative effect than 1,25(OH)2D3 in all the cells, but the effect was most pronounced in prostate cells. Furthermore, 1,25(OH)2D3-3-BE appeared to induce apoptosis in prostate cancer cells. FACS analysis of PC-3 and MCF-7 cells, treated with 10-6M of 1,25(OH)2D3-3-BE, revealed apoptosis (81% and 2% of PC-3 and MCF-7 cells respectively) while 1,25(OH)2D3-treated cells showed very little apoptotic effect. Our studies have shown that 1,25(OH)2D3-3-BE can be developed as a therapeutic agent for prostate cancer.

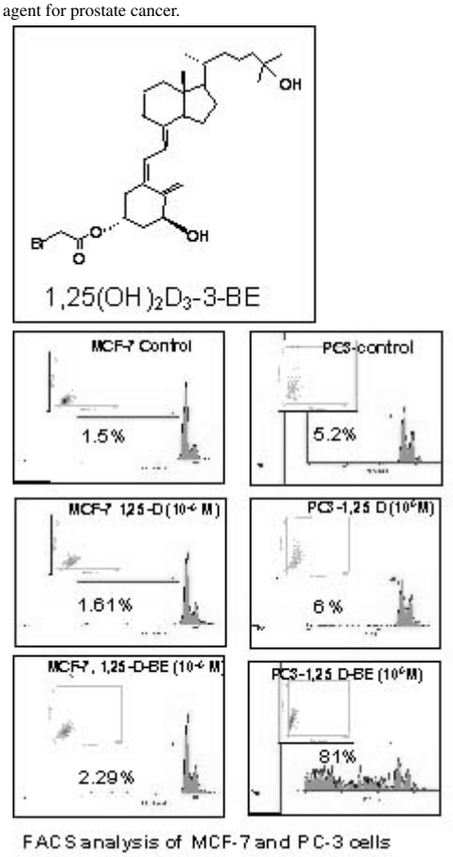

FACS analysis of MCF-7 and PC-3 cells treated With $1,25(OH)_2D_3$ or $1,25(OH)_2D_3$-3-BE

M001

Changes in Vitamin D Status and Bone Mass in Primary Morbidly Obese Adolescents during Weight Reduction. H. Dao*[1], F. Oberlin[1], M. Frelut*[2], D. Porquet[3], G. Pérès*[4], P. Bourgeois*[1]. [1]Pitié-Salpêtrière Hospital, Rheumatology Department, Paris 13, France, [2]Robert Debré Hospital, Gastro-enterlogy Department, Paris, France, [3]Robert-Debré Hospital, Biochemical Laboratory, Paris, France, [4]Pitié-Salpêtrière Hospital, Sports Department, Paris 13, France.

Objective: The increasing prevalence of obesity in childhood and adolescence observed in many countries is currently a major public health concern. The aim of this study is to determine how the vitamin D statut and bone mass vary during weight loss in primary morbidly obese adolescents. Methods: 33 girls and 22 boys, aged 13.4+-3.6 year with BMI 34.6+-3.6 kg/m2 were included in a 7.5+-3.2 months multidisciplinary weight reduction programme including a slight caloric restriction and regular submaximal physical training. Vitamin D statut and bone mass were measured before and after weight loss. Results: Mean weight loss is 23.5+-8.9 kg ($p<0.0001$), growth is 2.7+-1.8 cm ($p<0.01$). Total BMC decreases less (253+-131 g, $p<0.0001$) than bone area (212+-14 cm2, $p<0.0001$) resulting in an increased BMD (0.003+-0.001 g/cm2, p=0.3). BMC Z scores remain higher than that in the reference population (2.7+-1.2 vs 2.5+-1.4 before and after weight loss respectively). Spinal BMC, bone area and BMD increases significantly in both sex ($p<0.001$) while femoral neck BMD only increases in boys ($p<0.01$). 25 OHD concentration increases significantly (12.7+-7.3 vs 16.5+-6.3µg/L, $p<0.003$) while PTH decreases but not significant (34.0+-11.9 vs 28.6+-7.0 pg/mL, p=0.083). 25 OHD <10 µg/L is 36 % before and 12 % after weight loss. The variation of plasmatic and urinary calcium and phophorus is not significant. There is a negative correlation between total BMC and 25 OHD before weight loss in both sex. Conclusion: Within limits of interpretation of DEXA, this multidisciplinary weight loss programme seems to maintain adequate bone mineralization and to improve vitamin D statut in the critical period period of puberty in primary morbidly obese adolescents.

M002

1,25$(OH)_2D_3$ Acts as a Bone Forming Agent in the Hormone Independent Senescence Accelerated Mouse (SAMP6) Model of Osteoporosis. G. Duque[1], N. Dion[2], V. Papavasiliou*[3], L. G. Ste. Marie[2], R. Kremer[3]. [1]Calcium Research Laboratory & Division of Geriatric Medicine, McGill University, Montreal, PQ, Canada, [2]Centre Hospitalier de l'Université de Montreal, Hôpital St. Luc, Montreal, PQ, Canada, [3]Calcium Research Laboratory, McGill University Health Centre, Montreal, PQ, Canada.

Senile osteoporosis is characterized by decreased bone formation rate with concomitant increased bone marrow adipogenesis and osteoblast apoptosis. The P6 strain of senescence-accelerated mice (SAM) is a model of senile osteoporosis with all of the above characteristics. Previous *in vitro* studies indicate that 1,25 dihydroxyvitamin D_3 (1,25 $(OH)_2D_3$) has opposite effects on bone cells by directly stimulating osteoblastic differentiation and mineralized matrix formation, while indirectly enhancing osteoclastic recruitment and differentiation through immature cells of the osteoblastic lineage. In this study, our aim was to determine the effect of 1,25 $(OH)_2D_3$ on bone mass and parameters of bone turnover in the SAMP6 model. Both male and female 4-months old SAMP6 (n=28) were infused continuously with 1,25 $(OH)_2D_3$ (18pmol/24h) or vehicle for a period of 6 weeks. Before and after the infusion period Dual Energy X-ray Absortiometry (DEXA) was performed and mice were then sacrificed. A significant increase in serum calcium levels was observed in the 1,25 $(OH)_2D_3$ treated group but both groups remained normocalcemic for the duration of the experiment. In 1,25 $(OH)_2D_3$ treated animals, histomorphometric analysis showed an anti-resorptive effect of 1,25 $(OH)_2D_3$ as well as a increase in bone formation demonstrated by higher bone volume and higher mineralization in treated bone with a difference of 20% as compared to the non-treated group. DEXA indicated a significant increase in both femora of +20% ($p< 0.001$) and spine bone mineral content of +40% ($p< 0.01$) in 1,25 $(OH)_2D_3$ treated animals as compared to pre-treatment levels. In contrast, non-treated animals indicated a significant decline in bone mineral content in femora (-5%, $p< 0.01$) and in spine (-8%, $p<0.002$) in the same period. Serum bone markers confirmed higher levels of osteoblastic activity in treated animals. Flushed bone marrow cells were separated and plated in osteoblastic differentiation media for a period of 3 weeks and then stained with Alizarin red. The number of bone forming colonies obtained from treated animals was significantly higher ($p< 0.001$) than those obtained from non-treated animals. In summary, our results demonstrate that 1,25 $(OH)_2D_3$ increases bone mass by stimulating bone formation in a mouse model of defective osteoblastogenesis, and suggest its potential usefulness as a therapeutic agent in senile osteoporosis.

M003

Calcium Supplementation Increases Height and Bone Mass of 16-18 Year Old Boys. A. Prentice[1], S. J. Stear*[1], F. Ginty[1], S. C. Jones*[1], L. Mills*[1], T. J. Cole*[2]. [1]MRC Human Nutrition Research, Cambridge, United Kingdom, [2]Department of Paediatric Epidemiology and Biostatistics, Institute of Child Health, London, United Kingdom.

The aim of the study was to investigate the impact of an increase in Ca intake on the growth and bone mineral status of adolescent boys. 150 boys aged 16-18 years were randomised, double-blind to receive 1000 mg Ca/d as the carbonate or a matching placebo for 12 mo (12.7±SD0.5 mo). The recruits were from sixth-form colleges in Cambridge, UK, had mean age 16.8±SD0.5 y and were 103% and 100% of the national average for weight and height at that age. Baseline Ca intake was 1198±SD448 mg/d, range (323-2395 mg/d). Randomisation was stratified according to physical activity level (less or greater than 9 h/wk sport, with or without participation in exercise sessions). Anthropometry and DXA of the whole-body, hip, lumbar spine and forearm (Hologic QDR 1000/w) were performed at baseline and at the end of the intervention. 143 subjects completed the study. Compliance with the calcium supplementation was 65±SD28%. Over the period of the study, the subjects grew in height, gained weight and experienced significant increases in bone mineral content (BMC), bone area (BA), bone mineral density (BMD) and size-adjusted bone mineral content (SA-BMC) at all scan sites. The calcium intervention resulted in a significantly greater BMC of the whole-body (1.3%, p=0.02), lumbar spine (2.5%, p=0.004) and hip (neck 2.1%, p=0.05, trochanter 4.6% p=0.007) but not the forearm. These effects were associated with significantly greater increments in statural height (0.4%, p=0.0004) and in BA at the lumbar spine (1.5%, p=0.003) and trochanter (3.6% p=0.009), but not at the whole-body and femoral neck. The differences in bone mineral were diminished but still evident when data were expressed as BMD but disappeared after size-adjustment, except at the femoral neck (SABMC 1.3%, p=0.05). No significant interaction was detected between the effect of the intervention and baseline Ca intake, tablet compliance or physical activity level. We conclude that calcium supplementation of these adolescent boys led to an increase in bone dimensions, including statural height, and that this resulted in a greater bone mass at the whole-body, spine and hip. Follow-up studies will determine whether this increase reflects a change in the tempo of bone growth in adolescence or represents an effect on skeletal size that persists into adulthood.

Disclosures: ***A. Prentice****, Shire Pharmaceuticals 2; Nycomed Pharma 2.*

M004

Exercise During Growth and Young Adulthood Is Followed by Fewer Fractures in Spite of Increased Bone Loss after Exercise Career. A. H. Gustavsson*[1], E. Giza*[2], P. Nordstrom[1], F. Nyquist*[2], C. Karlsson*[3], M. K. Karlsson*[2]. [1]Department of Surgical and Perioperative Sciences, Sports Medicine Unit, Umea, Sweden, [2]University Hospital MAS, Department of Orthopaedics, Malmo, Sweden, [3]Department of Orthopaedics, University Hospital MAS, Malmo, Sweden.

Exercise during growth is associated with increased peak bone mineral density (BMD). However, fragility fractures occur in old age. We asked: (i) are high peak BMD derived from exercise followed by increased bone loss with reduced activity? (ii) do former athletes have fewer fractures than controls? We measured femoral neck BMD in 55 active male ice hockey players, mean age 18 years (range 16-20) and 58 active male soccer players and weight lifters, mean age 24 years (range 16-35). Thirty-three ice hockey players and 37 soccer players and weight lifters retired during the 4-7 year prospective study. Sixty-three age- and gender- matched volunteers served as controls. We also compared the prevalence of fractures in 454 former soccer and ice hockey players mean age 69 years (range 50-92) and 908 age- and gender matched controls. Data is presented as mean ± SEM. The annual femoral neck BMD (g/cm2/year) loss was higher in both the retired ice hockey players (-0.020 ± 0.004, $p<0.001$) and the controls (-0.001 ± 0.004, $p<0.001$) than in the active ice hockey players (0.010 ± 0.004). The annual femoral neck BMD loss was higher in the retired soccer players (-0.022 ± 0.003) than both the controls (-0.009 ± 0.007, $p<0.05$), and the active soccer players (-0.009 ± 0.002, $p<0.01$). The active ice hockey players had higher BMD than both the controls ($p<0.01$) and the retired ice hockey players ($p<0.05$) and the active soccer players and weight lifters had higher BMD than both the controls ($p<0.01$) and the retired soccer players and weight lifters ($p<0.001$) at follow-up. The proportion of subjects with fractures was not lower in former soccer players than controls over all [111/454 (24.4%) versus 231/908 (25.4%); NS]; it was higher in the former soccer players when they were active and less than 35 years of age [81/454 (17.8 %) vs 127/908 (14.0 %); p = 0.06] and lower than controls in adulthood after the age of 35 years [39/454 (8.6 %) vs 112/908 (12.3 %), $p < 0.05$]. Additionally, the proportion of subjects with fragility fractures was lower in former athletes than controls [9/454 (2.0 %) vs 38/908 (4.2 %), $p < 0.05$]. The higher peak BMD attained by physical activity during growth is followed by increased bone loss with retirement. However, fracture rates are reduced in retired ice hockey and soccer players. It seems that exercise in men during growth may result in fewer fragility fractures later in life.

M005

Osteoporosis Prevention May Begin in Infancy. J. M. Eichenberger Gilmore*[1], J. C. Torner*[2], L. G. Snetselaar*[2], T. L. Burns*[3], E. E. Ziegler*[4], M. C. Willing[4], S. M. Levy*[1]. [1]Preventive and Community Dentistry, University of Iowa, Iowa City, IA, USA, [2]Epidemiology, University of Iowa, Iowa City, IA, USA, [3]Biostatistics, University of Iowa, Iowa City, IA, USA, [4]Pediatrics, University of Iowa, Iowa City, IA, USA.

Development of peak bone mass, a major determinant of osteoporotic risk, occurs primarily during childhood and adolescence. The goals of this project were to assess the influence of early infant feedings on subsequent bone development; and to help understand how early dietary and nutritional factors may relate to bone mass in early childhood. The study population is a cohort of healthy Iowa infants (n=469) recruited at birth. Parents of the infants returned mailed questionnaires and three-day diet diaries at 6 weeks, 3 months, and 6 months. Infant's diets were assessed and categorized by consumption of human milk (dichotomized "any" vs. "none"). The type of feeding and the nutrient content of the feedings was related to growth parameters and bone measurements of the same children at approximately 5 years of age. Linear multiple regression was used to examine the relationship between bone mineral content (BMC) and bone mineral density (BMD) and human milk consumption status. Overall, unadjusted univariate analysis revealed that at age 5 years, boys are taller than girls and have greater whole body, hip and lumbar spine BMC; and whole body and hip BMD ($p < 0.05$) despite similarities in body weight. Human milk consumers (dichotomized) had significantly greater BMC and BMD of the whole body, total hip, femoral neck, trochanter and Ward's triangle ($p < 0.05$) than non-consumers. Statistically significant differences in BMC adjusted for bone area (BA), height, weight and age; and BMD adjusted for height, weight and age were identified. In gender-stratified comparisons, the effect of human milk was evident in pairwise contrasts with diets devoid of human milk particularly among boys. Girls that consumed any human milk exhibited greater BMC and BMD of the Ward's triangle region of the hip ($p < 0.05$); whereas, boys that consumed any human milk exhibited greater whole body and total hip BMC and BMD. The results of this study support the hypothesis that bone mass as measured by BMC and BMD may be influenced by early diet, specifically human milk.

M006

Age Related Changes in Serum Osteoprotegerin Levels and Its Relationship with Biochemical Markers and Bone Mineral Density in a Population Based Sample. O. S. Indridason*, J. P. Johannesson*, L. Franzson*, G. Sigurdsson. University Hospital, Reykjavik, Iceland.

While osteoprotegerin (OPG) seems to be involved in the regulation of bone resorption and theoretically may protect against osteoporosis, its role in bone metabolism remains unclear. The purpose of this study was to examine age dependent changes in serum OPG levels and its relationship with bone mineral density and other markers of bone and mineral metabolism. We are conducting a randomised cohort study on age related changes in bone health in Icelandic subjects aged 40 to 85 years old. For the current study we used data from the first year of the study and excluded subjects who were taking medications affecting bone and mineral metabolism. OPG was measured with an ELISA (Biomedica, Austria). We divided the subjects into 5 age groups; ages 40 and 45, ages 50 and 55, ages 60 and 65, ages 70 and 75, and ages 80 and 85 years old. We used ANOVA to compare the groups with regard to OPG levels and Spearman´s correlation coefficient to assess relationship between OPG and other variables. We have studied 747 subjects to date. After exclusion, 456 subjects, 209 men and 247 women remained for the current analysis. There was a significant, almost linear increase in OPG levels with age; for women from 3.17±1.31 pmol/l in the youngest age group to 5.55±1.66 pmol/l in the oldest age group, and for men from 2.95±0.99 pmol/l in the youngest age group to 5.46±1.22 pmol/l in the oldest age group ($P<0.001$). For women, OPG showed an inverse correlation with BMD (r=-0.4, $P<0.001$) and oestradiol (r=-0.5, $P<0.001$), both of which decreased significantly with age. OPG showed positive correlation with age (r=0.5, $P<0.001$), tartrate resistant acid phsophatase (r=0.3, P=0.003), collagen crosslaps (r=0.35, $P<0.001$), alkaline phosphatase (r=0.32, $P<0.001$), ionised calcium (r=0.28, $P<0.001$), osteocalcin (r=0.36, $P<0.001$), and whole PTH (r=0.2, P=0.001). For men, the correlation between OPG and BMD was weaker than for women (r=-019, $P<0.007$) but also showed a positive correlation with age (r=0.6, $P<0.001$), sex-hormone binding globulin (r=0.38, P=0.001), alkaline phosphatase (r=0.37, $P<0.001$), and whole PTH (r=0.17, P=0.01). We conclude that OPG increases with age and correlates well with markers of bone resorption/turnover. While OPG levels are similar in men and women, the relationship between OPG and BMD is different between the sexes suggesting there may be gender related differences in the role it plays in bone metabolism. With more enrollment, allowing for multivariable analysis, we should be able to better to elucidate this role

M007

Skeletal Development and Calcium Requirements Are the Determinants of Serum PTH Level During Growth. N. E. Badenhop-Stevens*[1], J. D. Landoll*[1], L. A. Nagode*[2], S. L. Mobley*[1], E. Ha*[1], P. Goel*[3], B. Li*[3]. [1]Bone and Mineral Metabolism Laboratory, The Ohio State University, Columbus, OH, USA, [2]Veterinary Pathobiology, The Ohio State University, Columbus, OH, USA, [3]Statistics, The Ohio State University, Columbus, OH, USA.

The relationship between serum PTH and skeletal development has been examined in a cohort of young females, participants of a clinical trial with calcium (Ca) supplementation from childhood to young adulthood. 179 healthy Caucasian young females, age 10.8±0.8 y, in pubertal stage 2 and with Ca intake below threshold level (1480 mg/d) at baseline completed a 7-year long double-blind, placebo-controlled clinical trial (CT) with Ca citrate malate supplementation (Procter & Gamble Co.) of 1000 mg Ca/d. Anthropometry, bone mass measurements of the forearm & whole body by DXA (GE Lunar, DPX-L), nutritional and activity records were obtained every 6 months (m), while blood samples for Ca, PTH, and bone biomarkers were collected every 12 m. Hand X-rays for bone age and radiogrammetry were obtained at ages 11, 15, and 18 y. Serum intact PTH was measured by Nichols kits. Serum was stored in a freezer on -80oC and stability of the PTH was checked by repeated assay on the subsample (n=10) in 1994 and 2000, revealing agreement of 99.1%. Serum PTH levels among the control individuals accustomed to calcium intake of ~850 mg/day/7 years were much higher during the peak skeletal modeling phase of early puberty (~28 pg/ml) with the decline during skeletal consolidation phase (~24 pg/ml) as evidenced by the stabilization of the periosteal envelope of the metacarpal bones by age 15 and with minimal but continuous endosteal apposition of cortical bone by age ~18 y. The PTH values were much lower among the Ca supplemented individuals, however, the trend for the decline with growth was present in them as well. The results of this research indicate the presence of a "hungry bone" syndrome during rapid skeletal expansion when calcium requirements for skeletal development have not been met.As the bone consolidation phase proceeds, calcium requirement declines with concomitant decrease in serum PTH, presumably as a result of the increase in serum ionized Ca. The results of this research may have implications with regard to monitoring the adequacy of Ca nutrition during growth.

M008

Timing of Peak Bone Mass at Various Skeletal Regions of Interest in Young Females: Results of a Seven-Year Follow-up Study. J. D. Landoll*[1], N. E. Badenhop-Stevens*[1], P. Goel*[2], E. Ha*[1], S. L. Mobley*[1], B. Li*[2], V. Matkovic[1]. [1]Bone and Mineral Metabolism Laboratory, The Ohio State University, Columbus, OH, USA, [2]Statistics, The Ohio State University, Columbus, OH, USA.

Timing of peak bone mass at various skeletal regions of interest including the total body has been evaluated in a cohort (n=100) of healthy Caucasian females, participants of a clinical trial with Ca supplementation during growth. The data reported here are only for the control individuals who did not receive extra Ca supplementation and who maintained their baseline Ca intake of about 850 mg/d throughout the seven years of follow-up. Anthropometry and bone mass measurements of the whole body, proximal and distal forearm were done every 6 months from age 11 up to 18 years. Hip and spine measurements were done from age 15 to 18 and radiogrammetry measurements of the metacarpals were done at age 11, 15, and 18 years. Lunar DPX-L was used for bone mass measurements and Pronosco X-posure system was used to evaluate the geometry of the metacarpal bones. Young females reached a plateau in stature by about age 16 y. Periosteal bone expansion has been changing rapidly from age 11 up to 15 years (about 10%) with minimal but continuous apposition thereafter. Most of the bone mass at the other sites have been accumulating by the age of ~16 with continuous accretion at a slower rate thereafter. Bone mineral areal density measurements of the spine (from the whole body scan), femoral neck and trochanter reached a peak by the average age of 17 with a declining trend thereafter. The above results are in agreement with our previously reported cross-sectional data (JCI 93:799-808, 1994) and indicate that timing of peak bone mass is site specific. Understanding the reasons for the early decline in bone mineral density at the hip after reaching its peak may be quite important with regards to primary prevention of hip fractures. Further follow-up of the bone mass in the same cohort seems to be necessary to confirm the observed trends and to understand appropriately bone behavior with age.

M009

Randomized Trial of Physical Activity and Calcium Supplementationon BMC in 3-5 Year Old Healthy Children: The South Dakota Children's Health Study. B. Specker, T. Binkley*, J. Wermers*. EA Martin Program in Human Nutrition, South Dakota State University, Brookings, SD, USA.

Meta-analysis of adult exercise studies and an infant activity trial demonstrate a possible interaction between weight-bearing activity and calcium (Ca) intake. There are no reported studies specifically designed to test whether Ca intake modifies the bone response to activity. This randomized, placebo-controlled, 1-year trial of activity and Ca supplementation was conducted in 239 children aged 3 to 5 years. Children were randomly assigned to participate in either gross motor (GM) or fine motor (FM) activities for 30 min/d, 5d/wk for 12 mo. Within each activity group children were further randomized to receive either Ca (CA; Ca carbonate 1000 mg/d) or placebo (PLAC). Activity programs & supplements were administered and compliance recorded daily by study personnel at childcare centers. Total body BMC using DXA and measurements of the 20% distal tibia using pQCT were obtained at baseline & study completion. 3-d diet records & motion sensor readings were obtained at 0, 6 & 12 months. 178 children completed >38 wk of intervention and were present at the center >50%. Percent time in moderate + vigorous activity were similar at baseline, but higher in GM vs. FM at 6 & 12 mo (both, p=0.01). Total Ca intake was greater in CA vs. PLAC (1354±301 vs. 940±258 mg/d, $p<0.001$). Anthropometric and bone results were similar at baseline. Height increase was less in CA vs. PLAC (6.9±0.2 vs. 7.4±0.2 cm), but was not correlated with compliance within CA group and was not significant when total Ca quartiles were used. The main effects of activity & Ca were not significant for TB BMC or leg BMC. There was an interaction between activity & Ca on leg BMC (p=0.05). The difference in leg BMC gain between GM and FM was more pronounced in children receiving the CA vs. PLAC: among PLAC children there was a similar leg BMC gain in GM vs. FM, but among CA children those in GM had 9.7% greater increase in leg BMC than FM. A similar interaction was observed with activity & Ca quartiles. At study completion, children in GM group had greater periosteal and endosteal circumferences compared to FM ($p<0.05$). There were no differences in cortical thickness & area between PLAC and CA among FM children, but cortical thickness & area were lower in PLAC vs. CA among GM children (interaction, both $p<0.02$). In summary, Ca modifies the bone response to physical activity in young children such that high activity levels in the presence of low Ca may be detrimental to bone.

M010

Collagen-Phosphophoryn Sponge as a Scaffold for Bone Tissue Engineering. D. Iejima[1], T. Saito*[2], T. Uemura*[3], T. Tateishi*[4]. [1]AIST(National Institute of Advanced Industrial Science and Technology), TERC(Tissue Engineering Research Center), Tsukuba, Ibaraki, Japan, [2]Health Science Univ. Hokaido, Hokkaido, Japan, [3]TERC, AIST, Tsukuba, Ibaraki, Japan, [4]Univ. Tokyo, Tokyo, Japan.

Non-collagenous phosphoproteins that interact with type I collagen are thought to nucleate bone mineral into collagen network of mineralized tissues. Previously phosphophoryn cross-linked to collagen type I was reported to be an effective nucleator of apatite (Saito et al. Bone 21, 305 (1997); Saito et al. J.Bone Miner. Res. 13, 265 (1998)). On the other hand, free phosphophoryn molecules inhibit the apatite formation in vitro. On the basis of the above study, we expected that the collagen-phosphophoryn sponge could work as a good scaffold for bone tissue engineering and examined the in vivo bone formation in orthotopically transplanted collagen-phosphophoryn sponge and bone marrow osteoblasts composite in Fisher rats (bone defect model). Osteoblastic primary cells were obtained from the bone shaft of femorae of Fischer 344 male 7-weeks-old rats, according to the method of Maniatopoulos et al. The cell suspension of marrow cells was distributed through a T-75 flask with 15 ml of standard culture medium and incubated at 37oC in a humidified atmosphere containing 95% air and 5% CO2. When culture dishes become near confluent, after 10 days, they were treated with 0.1% trypsin and then concentrated by centrifuge to 106 cells/ml and subcultured onto the synthesized collagen-phosphophoryn sponge and collagen sponge(control). After 14 days culture with standard medium supplemented with 10nM dexamethasone, 10mM b-glycerophosphate, 50mg/ml ascorbic acid, the composites of collagen-phosphophoryn and osteoblastic cells and control composites were transplanted into bone defect sites with 2mm diameter hole of Fischer rats and then the wounds were sutured. The composites were harvested at 1,2,6,8 weeks after implantation, fixed with 4% paraformaldehide and 0.25% glutaraldehyde, decalcified, embedded in paraffin, and stained with hematoxirin and eosin. Results clearly showed that more bone formation was observed in collagen-phosphophoryn sponge and osteoblasts composites than control composites from 1 week to 8 weeks, suggesting that the collagen-phosphophoryn sponge is a good candidate as a scaffold for bone tissue engineering.

M011

BMP-2 Regulation of Calcification is Modulated by Substrate Microtopography. D. D. Dean[1], B. D. Boyan[1], L. F. Bonewald[2], E. P. Paschalis[3], C. H. Lohmann[4], J. Rosser*[2], D. L. Cochran*[5], Z. Schwartz[1], A. L. Boskey[3]. [1]Orthopaedics, The University of Texas Health Science Center at San Antonio, San Antonio, TX, USA, [2]Oral Biology, University of Missouri, Kansas City, MO, USA, [3]Hospital for Special Surgery, New York City, NY, USA, [4]Orthopaedics, University of Hamburg-Eppendorf, Hamburg, Germany, [5]Periodontics, The University of Texas Health Science Center at San Antonio, San Antonio, TX, USA.

Osteoblast physiology in monolayer culture is substrate-dependent; adhesion, differentiation and response to osteogenic agents are enhanced on titanium (Ti) surfaces with a micro-rough topography, while attachment and proliferation are decreased. Here, we tested the hypothesis that substrate microtopography modulates osteoblast physiology in multilayer cultures, and this is regulated by BMP-2 and dexamethasone (dex) in a surface-dependent manner. Fetal rat calvarial (FRC) cells were cultured on three Ti surfaces (PT, R_a=0.6 μm; SLA, R_a=4.0 μm; TPS, R_a=5.2 μm) and treated with rhBMP-2 or dex. At 14 d post-confluence, culture morphology was similar on all surfaces, including multi-layer nodule formation. Cell number decreased with increasing roughness in control and treated cultures, whereas cell layer alkaline phosphatase specific activity increased. BMP-2 caused a further increase in enzyme activity on all surfaces; dex increased activity on SLA and TPS. Von Kossa-positive nodule number and area were affected. Ca and P content in control cultures did not vary with surface roughness; BMP-2 and dex increased Ca on all surfaces; the greatest increase due to BMP-2 was on PT. Dex increased P on rough surfaces, while BMP-2 increased P on all surfaces. A 2:1 Ca/P weight ratio typical of biologic apatite was seen only in BMP-2-treated cultures on rough Ti, corresponding to FTIR imaging showing mineral associated with matrix. All other cultures exhibited dystrophic calcification. This shows that formation of apatite by FRC cells is regulated by both BMP-2 and substrate microtopography. Surface roughness enhanced physiological calcification and worked synergistically with BMP-2. These data suggest that during osteointegration, the implant surface modulates cell attachment, proliferation, differentiation and matrix calcification and that optimal surfaces can be designed for use clinically.

Disclosures: ***D.D. Dean****, ITI Foundation, Waldenburg, Switzerland 2.*

M012

The Plasma Protein Fetuin/a2HS-glycoprotein Is a Physiologic Regulator of Bone Mineralization. P. Catala-Lehnen[1], C. Schäfer*[2], C. Mueldner*[1], M. Amling[1], J. Rueger*[1], W. Jahnen-Dechent*[2], T. Schinke[1]. [1]Trauma Surgery, University Hamburg, Hamburg, Germany, [2]IZKF Biomat, University Hospital Aachen, Aachen, Germany.

The plasma protein fetuin/a2HS-glycoprotein (hereafter refered to as Ahsg) is a major component of the bone extracellular matrix, although it is not expressed by osteoblasts. Ahsg inhibits apatite formation in vitro, and some Ahsg-deficient mice display ectopic calcification of soft tissues. These observations prompted us to ask the question whether Ahsg has an influence on bone mineralization. Therefore we analyzed Ahsg-deficient mice on a C57Bl/6 genetic background compared to their wildtype littermates (n=8 at the age of 4 months). Histomorphometric analysis revealed that Ahsg-deficient bones were indistinguishable from wildtype controls in terms of bone volume as well as osteoblast and osteoclast numbers. Despite the absence of a bone remodeling phenotype we found that Ahsg-deficient bones had improved biomechanical properties in a three-point bending assay (Force to failure was 20.44 +/- 5.03 in Ahsg-/- mice vs. 13.28 +/- 2.16 in wildtype controls, $p<0.001$). This is most likely explained by the fact that Ahsg-deficient bones have an increased bone mineral content (Ash weight as a percentage of dry weight was 59.7 +/- 4.7 vs. 53 +/- 2.76, $p<0.01$) which is consistent with the function of Ahsg as a systemic inhibitor of mineralization. We also found that the calcium to phosphate ratio in the ash of Ahsg-deficent bones was increased compared to wildtype controls (1.72 +/- 0.05 vs. 1.64 +/- 0.03, $p=0.07$) showing that Ahsg has an influence on bone mineral composition. Taken together, these data demonstrate for the first time that Ahsg is a physiologic regulator of bone mineralization. It is therefore the first non-hormonal plasma protein that has a major influence on bone strength. Our data also demonstrate that the biomechanical properties of bone are not solely dependent on bone volume or cortical thickness, but also on the composition of the mineral phase.

M013

Calcium Homeostasis: A Suggested Role for Bone Surface Proteins. R. V. Talmage*[1], G. E. Lester*[2], H. T. Mobley*[3], J. L. Matthews*[4]. [1]Orthopaedics, University of North Carolina, Chapel Hill, NC, USA, [2]National Institutes of Arthritis and Musculoskeletal and Skin Diseases, NIH, Bethesda, MD, USA, [3]Biology, Kilgore College, Longview, TX, USA, [4]Baylor Medical Center, Dallas, TX, USA.

The purpose of this report is to ascribe to bone surface proteins a role in the maintenance of plasma calcium concentration. Presently, the functions of these proteins have been related primarily to bone formation though they also abound in mature bone. The unresolved aspects of plasma calcium control are the processes by which calcium is returned from bone to plasma in quantities sufficient to match that lost to bone surfaces by the established calcium gradient from ECF to bone mineral. Such processes must exist both in the presence and absence of parathyroid hormone (PTH). Recently a new hypothesis has been reported (J. Musculoskel. Neuronal. Interact. 1:121,2000) to explain this calcium movement. The hypothesis suggested the involvement of bone surface proteins as an intermediary step between bone mineral and the ionic calcium of the ECF. In this report, this potential step is studied further. A variety of non-collagenous proteins are found on the surfaces of bone mineral. One of these, osteocalcin, has been described by numerous investigators such as Hauschka. In "The Chemistry and Biology of Mineralized Tissues" (W.T. Butler, Ed, Ebsco Media Inc., Birmingham, Ala. 1985, pp. 149-158), he describes the ability of this protein to fit into the lattice work of hydroxyapatite. Based on this report, it is hypothesized that this and other proteins are able to transfer calcium directly from bone mineral onto the proteins. Subsequently, calcium complexed to these proteins equilibrates with the ionic calcium of the ECF bathing the bone surfaces. The net result is to transfer calcium from bone mineral to the ECF against a calcium gradient moving this ion the opposite direction. The control of plasma calcium levels can then be described as occurring in three continuous and competing steps. (1) The movement of calcium from ECF to bone mineral: (2) The continuous transfer of calcium from bone mineral to surface proteins: and (3) The continuous equilibration between calcium attached to these proteins and the ionic calcium in the ECF. This third step sets the ionic calcium concentration in the ECF. The bulk of this process is not PTH dependent. However, it is suggested that PTH sets a precise calcium concentration by its action on osteocytes and lining cells to determine the amount of calcium complexed to bone surface proteins that is available for equilibration with the ionic calcium of the surrounding ECF.

M014

Association of Serum Osteoprotegerin Levels With the Severity of Coronary Artery Calcification. S. Jono*[1], Y. Ikari*[2], K. Hara*[2], A. Shioi[3], Y. Nishizawa[1]. [1]Department of Metabolism, Endocrinology and Molecular Medicine, Osaka City University Graduate School of Medicine, Osaka, Japan, [2]Division of Cardiology, Mitui Memorial Hospital, Tokyo, Japan, [3]Department of Cardiovascular Medicine, Osaka City University Graduate School of Medicine, Osaka, Japan.

Osteoprotegerin (OPG), a member of the tumor necrosis factor receptor family, has been identified as a regulator of bone resorption. It has been demonstrated that OPG is produced by a variety of tissues including the cardiovascular system as well as bone. OPG-deficient mice develop severe osteoporosis and medial arterial calcification of the aorta and renal arteries. OPG immunoreactivity was demonstrated in the normal blood vessels and in early atherosclerotic lesions. A recent clinical study suggests that there is a significant correlation between elevated serum OPG levels and cardiovascular mortality. It has been demonstrated that coronary artery calcium area correlates with histological coronary atherosclerotic plaque area. We examined whether serum OPG levels are associated with the severity of coronary artery calcification (CAC). This study involved 176 patients who underwent coronary angiography. The study group included 149 men and 27 women, with average age of 63 years. Coronary artery calcification was assessed by radiopacities within the vascular wall on coronary angiography and was classified as ND (not detected calcification), mild (focal radiopacities noted only during the cardiac cycle before contrast injection), moderate (diffuse radiopacities noted only during the cardiac cycle before contrast injection or focal radiopacities noted without cardiac motion), and severe (radiopacities noted only during the cardiac motion before contrast injection generally compromising both sides of the arterial lumen). Serum OPG levels were measured with enzyme-linked immunosorbent assay. Serum OPG levels are positively correlated with age, but other coronary risk factors showed no significant associations with serum OPG levels including male sex, hypertension, diabetes, hyperlipidemia and current smoking. Serum OPG levels were significantly greater in patients with CAC than in those without CAC. Moreover, as the severity of CAC increased, there was a significant increase in serum OPG levels. A similar association between serum OPG levels and the severity of coronary artery disease was found. Multivariate logistic regression analysis revealed that serum OPG levels were significantly associated with the presence of CAC. These data suggest that OPG may be involved in the progression of CAC, and that serum OPG may reflect certain stages of coronary artery calcification.

M015

Overexpression of VEGF induces Bone Formation in the Cultured Bone Transplantation Model. T. Uemura[1], H. Kojima*[2], K. Matsumoto*[2], P. Wang*[3]. [1]TERC(Tissue Engineering Research Center), AIST (National Institute of Advanced Industrial Science and Technology), Tsukuba, Ibaraki, Japan, [2]Terc, AIST, Tsukuba, Ibaraki, Japan, [3]Univ. Tsukuba, Tsukuba, Ibaraki, Japan.

Angiogenesis is quite important for bone tissue regeneration, because formed blood vessels in bone supply oxygen and nutrients to osteoblasts to be differentiated to form new bone. In particular, cultured bone implantation using porous ceramics scaffolds, a kind of bone tissue engineering, needs enough blood vessel formations into central porous area, maintaining osteoblast activities. This is the first report successfully inducing bone formation and showing our application of adenoviral vector carrying angiogenic factor VEGF (vascular endothelial growth factor) for activating osteoblasts to transduce MSC (messenchymal stem cells) in a cultured bone transplantation model. For this purpose, we constructed the recombinant adenoviral vector carrying VEGF cDNA (Adv-VEGF) and confirmed that it worked well by analyzing the proliferation of Adv-VEGF infected HUVEC cells. Then the Adv-VEGF infected MSC / porous ceramic scaffold composite was implanted into subcutaneous sites and orthotropic sites of Fischer rats. In the rat bone defect model, much blood formation were observed at 10 days postimplantation. At three weeks postimplantation, more bone formation was observed in the Adv-VEGF infected group. At five weeks postimplantation, in addition to the induction of bone formation by virus infection, TRAP positive osteoclasts and invasion of bone marrow tissues were observed in the transplanted ceramics showing the remodeling of implanted ceramics. Overexpression of VEGF proved to be effective in inducing bone formation with remodeling in a cultured bone transplantation model.

M016

S12911 Maintains Normal Matrix Mineralization Induced by Murine Calvaria Osteoblasts in vitro. A. Barbara*[1], P. Delannoy*[1], B. Robin*[2], P. J. Marie[1]. [1]INSERM U349, Paris, France, [2]Laboratoires SERVIER, Courbevoie, France.

There is growing evidence that S12911 administration increases bone mass and bone strength in normal and osteopenic animals as well as in humans. We previously reported that S12911, a compound containing two atoms of stable strontium, increases vertebral bone mass in rats by inhibiting bone resorption and stimulating bone formation without altering bone mineralization. We also showed that short term treatment with S12911 enhances osteoblastic cell recruitment and function in rat calvaria cultures. In order to ensure that S12911 does not alter matrix mineralization in long term culture, we analyzed the long term effects of S12911 on matrix mineralization using MC-3T3-E1 calvaria osteoblasts, a murine in vitro model of osteogenesis. Confluent MC-3T3-E1 cells were cultured for up to 14 days in the presence of ascorbic acid (25 µg/ml) and phosphate (3 mM) to induce matrix formation and osteogenesis. Matrix formation was determined by collagen synthesis measured by tritiated proline incorporation into the synthesized matrix. Matrix mineralization was quantified by measuring the number and surface of mineralized nodules using a digital image analyzer. Osteoblast function was determined by alkaline phosphatase (ALP) activity measured biochemically. Treatment with S12911 (1 mM) increased ALP on days 4 and 14 of culture. In this model, treatment with 1,25 (OH)2 vitamin D (1 nM) increased ALP activity on day 4, 8, 10, 12 and 14 of culture. Treatment with S12911 (1 mM) increased collagen synthesis on day 4, 8 and 10 of culture. In contrast, treatment with 1,25 (OH)2 vitamin D (1 nM) inhibited collagen synthesis at 4-14 days of culture. Long term treatment with S12911 (0.1-1 mM) did not alter matrix mineralization, as shown by the ratio of the surface of mineralized nodules to the number of mineralized nodules on day 14 of culture. Thus, long term treatment with S12911 modulates collagen synthesis and ALP activity in MC-3T3-E1 osteoblasts and does not alter matrix mineralization in this model, confirming that S12911 maintains normal bone matrix mineralization, as found in normal and osteopenic animals.

*Disclosures: **A. Barbara**, Laboratoires SERVIER 2.*

M017

Human Aortic Valve Calcification is Accompanied by a Transition to an Osteoblast Phenotype. N. M. Rajamannan*[1], M. Subramanium*[2], D. Rickard*[2], S. Stock*[3], J. L. Donovan*[2], D. Fullerton*[3], T. Orszulak*[2], A. J. Tajik*[2], R. Bonow*[3], T. Spelsberg*[2]. [1]Cardiology, Northwestern University, Chicago, IL, USA, [2]Mayo Clinic, Rochester, MN, USA, [3]Northwestern University, Chicago, IL, USA.

Calcific aortic stenosis is the third most common cardiovascular disease in the USA. Despite the increasing prevalence the mechanism is poorly understood. We hypothesized that the mechanism for aortic valve calcification is similar to skeletal bone formation and that this process is mediated by osteoblast-like cells. To test this hypothesis we examined calcified human aortic valves replaced at surgery (N=22) and normal human valves removed at cardiac transplantation and sudden cardiac death (N=20). Electron microscopy and x-ray dispersive analysis were performed for ultrastructural analysis of the valves. MicroCT was performed to determine the 3 dimensional extent of mineralization. Immunohistochemistry was used to localize osteopontin protein. VonKossa, Goldner's stain and microradiography was performed to localize mineralization fronts. To analyze osteoblast and bone matrix markers, mRNA was isolated from calcified vs normal valves and RT-PCR was performed for a variety of osteoblast specific genes. The distribution of hydroxyapatite coincided with that of calcium as detected by a radiodense pattern using contact microradiography. Energy-dispersive electron microscopy analysis showed that the chemical composition of the calcified valve tissue was hydroxyapatite ($Ca_{10}(P0_4)_6(OH)_2$) interspersed in among the bundles of collagen, the major inorganic component of bone. Mirco-CT analysis identified the distribution of mineralization in the diseased areas. Osteopontin was present in the areas of mineralization by immunogold labeling and immunohistochemistry. RT-PCR of the mRNA from the calcified valves revealed increased levels of mRNA coding for osteopontin, bone sialoprotein, osteocalcin and osteoblast specific transcription factor Cbfa1. These markers indicate the presence of cells with an osteoblast-like phenotype involved in a calcification process analogous to bone formation. These markers were diminished in the normal valves. These findings support the concept that aortic valve calcification is not a random passive, degenerative process, but an active regulated process involving either a transformation of the human aortic valve fibroblast cell to an osteoblast-like phenotype or the recruitment of osteoblast precursor cells in the inflammed area.

M018

Characterization of Mineralized, Honeycombed Sheets Made by MLO-A5 Cells and Comparison with Mineralized Nodules Made by Primary Osteoblasts. C. Barragan-Adjemian*[1], D. Eick*[1], V. Dusevich*[1], M. Dallas*[1], D. Nicolella*[2], L. F. Bonewald[1]. [1]Oral Biology, University of Missouri Kansas City, Kansas City, MO, USA, [2]Southwest Research Institute, San Antonio, TX, USA.

The differentiation and mineralization process of primary osteoblasts and several osteoblast cell lines has been thoroughly characterized. In these cells, proliferation is followed by matrix formation, then mineralization. Expression of various transcription factors and matrix proteins occurs over a 2-3 week time period that includes increases in collagen type 1 production, alkaline phosphatase during the matrix production state and osteocalcin increases with mineralization. Mineralization occurs within multi-layered cells known as nodules that are separated in culture by a non-characterized lawn of cells. The MLO-A5 cell line produces 70 times more osteocalcin than early primary osteoblasts, but similar amounts to mature, mineralizing osteoblasts. MLO-A5 cells mineralize in sheets, not nodules within 3-6 days. The Fourier Transformed Infrared spectroscopy of these *in vitro* cultures is very similar to spectra of rat calvaria. This cell line may represent a particular state in osteoblast differentiation, that of the mineralizing post-osteoblast, pre-osteocyte. These cultures were analyzed using Field Emission, Environmental Scanning Electron Microscopy, in dry mode, to yield secondary images of the culture topography. Honey-combed structures, reminiscent of newly forming trabecular bone, were revealed by using detection of backscattered electrons, a means of identifying mineralized from non-mineralized structures. The location and relative amount of calcium in these structures from 0 to 12 days was identified using Energy Dispersive X-ray Analysis. Cellular processes could be observed curving along the honeycomb structures, suggesting that the cell processes may direct formation of these structures. In non-mineralized areas, at very high magnification (150,000x), collagen bundles and fibers with potential nucleation sites were observed. Using atomic force microscopy to characterize these areas, un-mineralized collagen fibrils exhibiting the characteristic 69 nm banding were observed with clusters of mineral forming at specific locations along the fibrils. Studies are being performed to determine if fluid flow shear stress will modify these structures. These cells are proving to be a useful model to investigate the mechanisms of mineralization.

M019

Bone Origin of the Serum Complex of Calcium, Phosphate, Fetuin, and Matrix Gla Protein: Biochemical Evidence for the Cancellous Bone Remodeling Compartment. P. A. Price, J. M. Caputo*, M. K. Williamson. Division of Biology, University of California, San Diego, La Jolla, CA, USA.

We previously described the discovery of a fetuin-MGP-mineral complex in the serum of rats treated with the bone active bisphosphonate etidronate, and showed that the appearance of this complex in serum correlates with the inhibition of bone mineralization by etidronate (JBC (2002)277:3926). The composition of this high molecular weight protein-mineral complex consists of about 18% mineral, 80% fetuin, and 2% matrix Gla protein (MGP) by weight, and the presence of the complex in serum 6h after an injection of 8mg etidronate/100g body weight elevates calcium by 1.8 fold (to 4.3mM), phosphate by 1.6 fold (to 5.6 mM), and MGP by 25 fold (to 12 µg/ml). In the present study we show that the inhibition of bone resorption by treatment with the hormone calcitonin, the cytokine osteoprotegerin, or the drug alendronate, completely inhibits the generation of the fetuin mineral complex in response to etidronate injection. These observations can best be explained by the bone remodeling compartment (BRC), a recently described cancellous bone compartment in which the concentrations of calcium and phosphate are determined directly by the combined actions of the osteoclast and the osteoblast (JBMR (2001)16:1575). When bone mineralization is acutely inhibited by etidronate, the BRC model predicts that the continuing action of osteoclasts will cause a sharp rise in the concentrations of calcium and phosphate in the aqueous solution of the BRC with the consequent spontaneous formation of calcium phosphate crystal nuclei whose growth could then be arrested by formation of a complex with fetuin. This possibility is supported by the observation that a similar fetuin-mineral complex indeed forms when calcium and phosphate are added to rat serum in vitro. When the inhibition of bone resorption by calcitonin, osteoprotegerin, or alendronate is combined with the acute inhibition of bone mineralization with etidronate, the BRC model correctly predicts that there will no longer be a sharp rise in calcium and phosphate, and therefore no longer be the formation of the fetuin mineral complex. There is evidence that the bone remodeling compartment is also a vascular compartment (JBMR (2001)16:1583), evidence which includes the presence of red blood cells within the compartment and the close association of the compartment with blood vessels. This vascular feature of the BRC could provide an explanation for the observations that the fetuin component of the fetuin-mineral complex is derived from plasma fetuin, and that the fetuin mineral complex appears in plasma within minutes of the inhibition of bone mineralization with etidronate.

M020

Gender – Specific Skeletal vs. Vascular Osteogenic Gene Regulatory Responses in LDL Receptor - Deficient Mice. J. S. Shao*, M. Bidder, A. P. Loewy*, C. Camillo*, M. Moon*, K. T. Bae*, C. F. Semenkovich*, D. A. Towler. Washington University, St. Louis, MO, USA.

Obesity is associated with higher bone mass; however, obesity is also a risk factor for type II diabetes, characterized by increased incidence of arterial calcific vasculopathy. Preliminary analyses of dystrophic human aortic valve specimens indicate that levels of osteopontin (OPN) and Msx2 mRNA track the extent of valve calcification. We identified the elaboration of this early osteogenic gene regulatory program in the calcifying aortas of LDL receptor (LDLR) deficient mice fed diets that induce diabetes with hypercholesterolemia. We wished to characterize effects of this diet -induced dysmetabolic state on orthotopic and heterotopic osteogenic gene regulatory programs, and potential interactions with responses to osteoanabolic agents such as PTH. Therefore 12 week old LDLR -/- mice (weight and gender matched) were fed mouse chow (less than 10 % calories as fat) or Harland Teklad TD 88137 (42% of calories as fat) for 6 weeks. Bone mineral content (BMC) quantified by DXA revealed higher baseline BMC values in males than in females ($p = 0.006$). High fat diets increased BMC in female (389 +/- 67 mg to 450 +/- 54 mg; $p = 0.06$), but not in male (463 + /- 25 mg vs. 450 + /- 27 mg) mice during this treatment period. By contrast, body fat was significantly increased only in male mice (13.0 +/- 1.4% vs. 20.3 +/- 1.3 %; $p = 0.04$). Real-time fluorescence RT-PCR was used to quantify osteogenic gene expression in total RNA isolated from single aortas and hindlimbs (n= 3 to 6 animals per treatment). In aorta, 2.7- fold increases in levels of Msx2 and Runx2 gene expression were observed, but only in male animals; osterix (Osx) was not induced (suppressed). This was associated with marked upregulation of aortic osteopontin (OPN) expression, but only in male animals. Conversely, in bone, Runx2 expression was induced 5-fold by high fat diets, but only in female animals; Osx mRNA increased ca. 2-fold in female bones, and Msx2 was unchanged. We next addressed whether PTH contributed to the regulation of osteogenic gene expression at orthotopic and heterotopic sites in male mice (exhibited robust vascular responses to diet). In 4 weeks, PTH (0.4 mpk s.c. daily) augmented BMC 23% in male LDLR -/- mice fed high fat diets (478 +/- 59 mg vs. 590 +/- 52 mg; $p = 0.01$). While PTH upregulated orthopic expression of Msx2 and OPN in the hindlimbs of male animals, it concomitantly suppressed aortic OPN and Msx2 mRNAs by > 50% ($p < 0.05$). Increases in body fat were not altered by PTH treatment, but glucose levels were lower. These data suggest that gender - specific metabolic signaling cascades differentially control osteogenic gene regulatory responses during orthotopic and heterotopic mineralization.

*Disclosures: **D.A. Towler**, Merck 5; Pharmacia 2.*

M021

Neurotensin and Sortilin/Neurotensin Receptor-3 Promote Extra-Cellular Matrix Mineralization During Osteoblastic Differentiation of Mesenchymal Stem Cells. S. Maeda[1], T. Nobukuni*[2], K. Shimo-Onoda*[1], K. Hayashi*[1], K. Yone*[1], S. Komiya*[1], I. Inoue*[2]. [1]Department of Orthopedic Surgery, Faculty of Medicine, Kagoshima University, Kagoshima, Japan, [2]Division of Genetic Diagnosis, Institute for Medical Science, University of Tokyo, Tokyo, Japan.

Our aim was to understand the mechanisms which divide the fate of human mesenchymal stem cells (hMSCs) to osteoblasts or adipocytes, because it has been shown that bone volume loss associated with osteoporosis and aging is accompanied by a reduced osteoblastic bone formation and an increase in marrow adipose tissue. We compared gene expression profiles of hMSCs between osteoblastic and adipocytic differentiation 24 hours after stimulation using cDNA microarray to detect osteoblastic-specific up-regulated genes. The long-term, day 0 to 11 of differentiation induction, expression patterns of the screened genes were evaluated by quantitative real-time RT-PCR. The 10 genes were up-regulated during osteoblastic commitment, which included sortilin / neurotensin receptor-3. The over-expression of Sortilin using adenovirus vector in hMSCs resulted in acceleration of matrix mineralization during osteogenic differentiation. We tested the effect of lipoprotein lipase (LPL) on osteoblastic differentiation, because LPL had been reported to bind with sortilin and degraded from circulation in vitro. LPL inhibited osteoblastic mineralization in dose dependent manner. Interestingly, this LPL-mediated suppression of matrix calcification was rescued by sortilin-adenoviruses. Sortilin nor LPL had no impact on alkaline phosphatase(ALP) activity. These results and the evidence that LPL is bound on heparan-sulfate ptoteoglycans on the cell surface suggest that LPL has no effect on ostaoblastic differentiation itself of hMSCs but interfere mineralization of extra-cellular matrix by binding on proteoglycans. Sortilin may support mineralization by degrading LPL. Finally, the sortilin ligand neurotensin was tested for its ability to affect osteoblastic differentiation. Neurotensin RNA was up-regulated during early osteoblastic differentiation. Neurotensin promoted osteogenic mineralization, while showed little impact on ALP activity. Moreover, sortilin-adenoviruses enhanced the effect of neurotensin. Our results suggest that neuropeptide neurotensin and receptor sortilin do not affect osteoblast differentiation but may promote bone matrix calcification. Further studies including measuring bone volume of neurotensin knock-out mice or mice centrally injected with the peptide may clarify our hypothesis.

M022

Chondrocyte Differentiation Is Mediated by Inhibition of Cyclin-dependent Kinase 6 Expression as a Downstream Effector of p38 MAPK Pathway. T. Moro[1], T. Ogasawara[1], T. Shimoaka[1], H. Chikuda[1], S. Kamekura*[1], K. Nakamura[1], H. Okayama*[2], H. Kawaguchi[1]. [1]Orthopaedic Surgery, University of Tokyo, Tokyo, Japan, [2]Molecular Biochemistry, University of Tokyo, Tokyo, Japan.

Because cell cycle arrest at the G1 phase is a prerequisite for cell differentiation, cell cycle molecules such as cyclins, cyclin-dependent kinases (CDKs) and CDK inhibitors (CKIs) may possibly regulate not only proliferation but also differentiation of cells. To elucidate the regulation of chondrocyte differentiation by cell cycle molecules, this study investigated the involvement of these molecules in the differentiation of cultured mouse chondrogenic cell line ATDC5 in the presence of insulin. Initially, we analyzed the regulation of cell cycle molecules that are known to affect the G1 phase: cyclin D1, D2, D3, E, CDK2, 4, 6, and CKIs (p18, p21 & p27) during differentiation by Western and Northern blottings. In all of them, both protein and mRNA levels of CDK6 were markedly decreased at 12-24 h of culture and thereafter, while those of other cell cycle molecules did not change throughout the culture period up to 48 h. The protein degradation of CDK6 was not involved in this down-regulation because MG132, a potent proteasome inhibitor, did not reverse the protein level. When inhibitors of p38 MAPK, ERK-1/2 and PI3K: SB203580, PD98059 and LY294002, respectively, were added to the culture, only SB203580 blocked the decrease in the CDK6 protein level, indicating that the CDK inhibition is mediated by p38 MAPK pathway. In fact, p38 MAPK was confirmed by Western blotting to be phosphorylated in advance of the inhibition of CDK6 during differentiation of ATDC5 cells. To further investigate the contribution of CDK6 to chondrocyte differentiation, we established several stable clones of ATDC5 cells transfected with *cdk6* cDNA, and compared the differentiation among the high expressing clones, low expressing clones, and parental cells. All differentiation parameters: type II and type X collagen mRNA levels, alcian blue, alizarin red and alkaline phosphatase stainings, were markedly suppressed in high expressing clones compared with those in low expressing clones and parental cells, indicating that CDK6 expression causes the inhibition of ATDC5 differentiation. However, since cell proliferation determined by BrdU uptake and distribution pattern in the cell cycle phase determined by FACS were not different among the three groups, the inhibitory effect of CDK6 on chondrocyte differentiation was shown to be independent of its effect on the proliferation. We therefore conclude that CDK6 is a key molecule determining the differentiation rate as a downstream effector of p38 MAPK pathway in chondrocytes.

M023

Adenovirus Vector-mediated Alk Gene Transduction To Synovial Cells Induces Chondrogenic Differentiation. H. Seto*[1], H. Hiraoka*[1], M. Fujii*[2], T. Imamura*[2], K. Miyazono*[3], H. Kurosawa*[4], H. Oda*[1], K. Nakamura[1], S. Tanaka[1]. [1]Department of Orthopaedic Surgery, The University of Tokyo, Tokyo, Japan, [2]Department of Biochemistry, The Cancer Institute of the Japanese Foundation for Cancer Research, Tokyo, Japan, [3]Department of Molecular Pathology, Graduate School of Medicine, The University of Tokyo, Tokyo, Japan, [4]Department of Orthopaedic Surgery, Juntendo University, Tokyo, Japan.

We previously reported that the expression of constitutively active forms of bone morphogenetic protein (BMP) type I receptors (BMPR-IA and IB; BMPR-I group) and those of activin receptor–like kinase (ALK)-1 and ALK-2 (ALK-1 group) induced osteoblastic differentiation in mouse myoblast cell line C2C12. Chondrogenic differentiation of ATDC5 cells was induced by the receptors of the BMPR-I group but not by those of the ALK-1 group. Synovium is a thin tissue, which lines the nonarticular surfaces of diarthrodial joints. There is evidence that synovium contains cells with chondrogenic potential, and it was previously reported that synovial cells demonstrated chondrogenesis when treated with TGFβ1. In the present study, we demonstrated that adenovirus vector-mediated ALK-3 or 6 gene expression induced chondrogenic differentiation of synovial fibroblasts. Synovial tissues were obtained from synovial tissues of the knee joints of adult Japanese white rabbits or RA patients at the time of total knee arthroplasty under written informed consents. Synovial cells were isolated from the tissues by enzymatic digestion. After 3-5 passages, subcultured synovial cells are mainly composed of synovial fibroblasts with fibroblastic morphology and free from T cell or macrophage markers. The cells were then infected with adenovirus vectors carrying LacZ (control), HA-tagged constitutively active forms of ALK-3, 5, or 6 genes for 2 hours. Chondrogenic phenotypes of the cells were examined by Northern blotting or RT-PCR of type II,X collagen and aggrecan genes as well as Alcian blue staining. Expression of type I receptors in synovial fibroblasts was confirmed by Westen blotting with anti-HA antibody. After 3 days of infection, dramatic induction of type II and aggrecan genes were observed in rabbit and human synovial cells infected with ALK-3 or 6 virus, while no chondrogenic phenotypes were observed in LacZ or ALK-5-infected cells. Type X collagen expression or calcification was not observed in any types of cultures. These results suggest that adenovirus vector-mediated ALK-3 or 6 gene expression can induce chondrogenic differentiation of synovial fibroblasts, and that they are promising candidates for developing novel cell-based therapeutic approaches for postnatal articular cartilage repair.

M024

The Healing Capacity of Cartilage in vitro. J. P. Petersen[1], W. Dömeland*[1], A. Ruecker*[1], K. Baumbach*[1], P. Adamietz*[2], J. M. Rueger*[1], N. M. Meenen*[1]. [1]Dept. of Trauma Surgery, Hamburg University School of Medicine, Hamburg, Germany, [2]Inst. of Med. Biochemistry and Molecular Biology, Hamburg University School of Medicine, Hamburg, Germany.

The capacity for self-repair of traumatic cartilage injuries is very poor. Lesions do not heal and usually lead to painful arthritis. Although this problem is known for more than 250 years, there is still no sufficient therapy for cartilage repair. One option for correction of chondral defects could be transplantation of tissue engineered cartilage. In this therapeutical option, cartilage generated by autologous chondrocytes in vitro is transplanted into the defect. Although the such generated tissue is biochemically well defined, the healing capacity of this cartilage is still unknown. Therefore, the aim of this study was to investigate the healing capacity of the in vitro tissue engineered cartilage. Cartilage was harvested from the articular surface of adult mini-pig knees. After the cells were isolated and multiplied in monolayer culture, they were seeded in alginate where they form cartilage with its typical extracellular matrix. This tissue engineered cartilage was lesioned with a scalpel and cultivated in medium supplemented with fetal calf serum and growth factors for 21 days. The cartilage was then analysed by histology, immunhistochemistry and by polarization-microscopy to assess the potential for self-repair. Macroscopical and histological analysis showed that the primary cut had healed homogenously. Polarization microscopy revealed that new collagen fibers cross the former cut and show a morphology typical for hyaline cartilage. Immunhistochemical analysis showed that collagen type II is expressed uniformly in the unlesioned cartilage as well as in the dissected area. This study shows that tissue engineered cartilage has the capacity for self repair in vitro, and that this reparation process not only produces scar tissue containing the typical cartilage formation.

M025

The Orphan Receptor, Estrogen Receptor Related Receptor Alpha, ERRa, Is Expressed by Chondrocytes and Reduced in Arthritis. E. Bonnelye[1], V. Kung[2], J. E. Aubin[2]. [1]Department of Molecular and Cell Biology, Ecole Normale Superieure de Lyon, Lyon, France, [2]Department of Anatomy and Cell Biology, University of Toronto, Toronto, ON, Canada.

The orphan estrogen receptor related receptor alpha, ERRa, has been shown to be expressed by osteoblasts and play a functional role in bone formation in the 21 d. fetal rat calvaria (RC) cell model in vitro. We now report that ERRa is also expressed by proliferating chondrocytes and perichondrial precursors but not in hypertrophic chondrocytes in fetal rat growth plate cartilage in vivo. In adult animals, growth plate chondrocytes including those of the hypertrophic zone are also intensely labeled as are articular chondrocytes. To determine whether ERRa expression changes during the chondrocyte developmental sequence, we used a rat chondrocytic cell line, RCJ3.1C518 (C5.18). ERRa mRNA was found by semi-quantitative RT-PCR to be highly expressed at all proliferation/differentiation/maturational stages of chondrocyte development and cartilage nodule formation in vitro. ERRa protein is also expressed at all stages but is highest in maturing and mature chondrocytes associated with cartilage nodules. Notably, ERRa is co-expressed with ERa and ERb in at least some chondrocytes in cartilage nodules. Given these observations, we blocked ERRa in differentiating C5.18 cell cultures using phosphorothioate-modified antisense oligonucleotides. While sense oligonucleotides had a small dose-independent effect, antisense oligonucleotides caused a striking dose-dependent decrease in cartilage nodule formation, i.e., 40% decrease at 1mM and 60% at 2mM. Inhibition of ERRa had effects during both the proliferation and differentiation developmental time windows. Since ERRa is highly expressed in articular chondrocytes, we asked whether ERRa expression levels change in chondrocytes in animal models of arthritis. We used semi-quantitative RT-PCR to assess ERRa levels in samples from a rat and a mouse model of collagen-induced arthritis. Strikingly, no significant change was observed in ERRa expression between control versus arthritic bone samples, but ERRa levels were significantly reduced in arthritic cartilagenous joints. Our findings show that ERRa is highly expressed in chondrocytes where it is co-expressed with ERa and ERb. They also indicate a critical role for ERRa in cartilage formation and integrity. These data suggest that ERRa may serve as a useful diagnostic tool in arthritis and that therapies based on manipulation to increase ERRa levels may be useful in a joint regenerative process.

M026

Regulation of Chondrogenic Differentiation of ATDC5 Cells: A Role for Estrogens? M. Karperien[1], M. Steenvoorden*[2], J. Hoogendam*[2], C. Lowik[1], B. van der Eerden[2], j. Wit*[2]. [1]Endocrinology, LUMC, Leiden, Netherlands, [2]Pediatrics, LUMC, Leiden, Netherlands.

Sex-steroids have profound effects on longitudinal bone growth. They can exert direct effects on growth plate chondrocytes, due to the presence of ERa and ß mRNA and protein. The mechanism of action by which these receptors regulate growth and differentiation of chondrocytes are largely elusive. One possibility is that they influence the activity of the growth restraining PTHrP/IHh-feedback loop which is operational in the prenatal and postnatal growth plate. Indeed, ovariectomy of 3-weeks-old rats reduced PTH/PTHrP-receptor mRNA expression compared to sham as assessed by RT-PCR analysis of tibial growth plate preparations. To study the interactions between sex-steroids and the PTHrP/IHh-feedback loop in more detail, we have started to use the chondrogenic ATDC5 cell line. This cell line differentiates into mineralizing hypertrophic chondrocytes in monolayer in the presence of insulin. Hypertrophic differentiation is enhanced by the addition of BMP4 and can be inhibited by PTHrP. RT-PCR analysis identified the presence of ERa, but not ERß mRNA. In addition, expression of the IGFI-receptor and the Growth Hormone Receptor was found. The expression of ERa was not regulated by differentiation, nor by BMP4 or PTHrP-treatment. Hypertrophic differentiation of ATDC5 cells was dramatically accelerated by inducing cell aggregation when cells were cultured on bacterial dishes. Interestingly, under these culture conditions, insulin was not required for terminal chondrocyte differentiation. In fact collagen X mRNA expression was higher in aggregates cultured in the absence of insulin. However, in the presence of insulin aggregates were larger and their integrity was better maintained. Histological examination demonstrated the presence of alcian blue positive chondrocytes in the center of the aggregates. In addition, swollen cells with a hypertrophic appearance were identified both in the absence and the presence of insulin. The chondrocytes were surrounded by an outer layer of undifferentiated alcian blue negative cells mimicking a perichondrium. Culturing of ATDC5 cells as aggregates in the presence of estrogen reduced terminal chondrocyte differentiation as measured by a decreased mRNA expression of various late stage chondrocyte markers, such as collagen X. In conclusion, hypertrophic differentiation of ATDC5 cells can be accelerated by culturing the cells in aggregates. In addition, cell aggregation appears to be more important for hypertrophic differentiation than treatment with insulin. The ATDC5 cell line appears to be a suitable model to study interactions between sex-steroids and the PTHrP/IHh-feedback loop.

M027

p38 Mitogen-Activated Protein Kinases in Chondrocyte Differentiation. L. Stanton*, S. Sabari*, F. Beier. Physiology, University of Western Ontario, London, ON, Canada.

Chondrocyte differentiation is an important part of bone development. Disturbance of the normal development of these cells can therefore lead to various diseases and conditions, such as osteoarthritis, hypochondrodysplasias and dwarfism. Thus, the activation and tight control of the signaling pathways controlling the physiology of these cells, is crucial. One signaling pathway that has been implicated in chondrogenesis and chondrocyte differentiation is the p38 MAPK signaling pathway. However, the precise role of p38 MAPK and the identity of p38 substrates and downstream transcription factors in the process of chondrocyte differentiation have not been described. We are studying the role of p38 in chondrocyte differentiation using mouse limb bud micromass cultures. Our results demonstrate expression of all four p38 MAP kinases during the chondrocyte differentiation program. We also show the temporal expression profile of these kinases in relation to various well-identified markers of chondrocyte maturation, thereby highlighting p38 MAPK expression at the various distinct stages of chondrocyte maturation. We will also present data on the biochemical roles of p38 in chondrocytes and p38 substrates involved in these processes. Understanding these pathways obviously provides greater insight into possible points of manipulation for disease treatments.

M028

Retinoic acid Induces Expression of Osterix mRNA in Primary Cultures of Chondrocytes. K. Yagi[1], K. Tsuji[1], K. Shinomiya[2], A. Nifuji[1], M. Noda[1]. [1]Medical Research Institute, Tokyo medical and Dental University, Tokyo, Japan, [2]Tokyo Medical and Dental University, Tokyo, Japan.

During endochondral ossification, various local and systemic factors including cytokines and growth factors affect cellular events. Retinoic acid (RA) is one of such factors that regulate proliferation and differentiation of chondrocytes. It has been reported that RA suppressed expression of chondrocyte marker genes such as typeII collagen, aggrecan and Sox9 and that it induced the expression of osteocalcin, osteopontin(OPN) and Cbfa1 in chondrocytes. Thus RA is thought to act as a positive regulator of chondrocyte maturation and ossification. Osterix (Ostx) is a transcription factor that is essential for the bone formation and acts downstream to Cbfa1. We hypothesized that RA may act regulate the expression of Osterix. To elucidate the mechanism of the chondrocyte differentiation, we used the primary chondrocyte cultures derived from costochondral cells of newborn ICR mice. We examined the effects of bone morphogenic protein2 (BMP2), transforming growth factor (TGF)-β, basic fibroblast growth factor (FGF), dexamethasone, vitamin D, RA in the culture medium and evaluated the expression levels of Ostx and OPN mRNA. The expression of Ostx mRNA in chondrocyte cultures was upregulated in the presence of RA. Treatment with RA induced Ostx mRNA in a time-dependent manner. Treatment with BMP, dexamethsone, and vitamin D did not affect the expression of Ostx mRNA, therefore RA effects on Osterix gene expression was specific. RA and FGF, which regulate Ostx mRNA, induced OPN mRNA. FGF effect on OPN mRNA was dose-dependent and suppressed by the addition of U0126, MEK inhibitor. Since Ostx mRNA level was upregulated by RA and this response to RA was not observed at 24 hours but detected in 72 hours, some intermediate factors are involved in this signaling downstream of RA. Furthermore RA and bFGF induced OPN mRNA and bFGF signaling requires the MAPK cascade. In conclusion, RA induced the expression of Ostx mRNA in chondrocyte.

M029

Function of the p21/p53 Pathway in Regulating Chondrocyte Apoptosis and Proliferation in Dwarf Mice. M. Hurley[1], G. Gronowicz*[1], D. Cassarino*[1], S. Clark*[1], N. Sims*[2], R. Baron*[2], M. Amling*[3], D. Brooks*[4], C. Wishcamper*[5], D. Lurie*[5], G. Proetzel*[6], J. D. Coffin[7]. [1]U. Connecticut HSC, Farmington, CT, USA, [2]School of Medicine, Yale Univ., New Haven, CT, USA, [3]Yale Univ., New Haven, CT, USA, [4]Univ. of Montana, Missoula, MT, USA, [5]Univ. of Montana, Missoula, MT, USA, [6]Scil Proteins, Halle, Germany, [7]Pharmaceutical Sciences, Univ. of Montana, Missoula, MT, USA.

Purpose: To characterize the regulatory mechanisms for FGF mediated dwarfism. Methods: Gene expression in TgFGF2 mice and NTg controls was examined using western blots or immunocytochemistry and in situ hybridization on sectioned bones. Results: Fibroblast growth factor-2 (FGF-2) overexpression in transgenic (TgFGF2) mice causes chondrodysplasia and dwarfism. Previous results suggest that excess FGF-2 could alter the chondrocyte transition from the stem cell population to the proliferative and hypertrophic phases, which is thought to involve programmed cell death in the hypertrophy zone. Cell proliferation and apoptosis assays on TgFGF2 and NTg mice reported here show that chondrocytes in TgFGF2 and NTg control mice proliferate at about the same rate, but the TgFGF2 chondrocytes undergo premature and rapid apoptosis causing premature chondrocyte drop-out in the TgFGF2 dwarf mice. Changes in collagen type II (col2), Collagen type X (col10) and Indian hedgehog (IHH) expression support this result. TgFGF2 mediated reductions in parathyroid hormone related peptide (PTHrP) and bcl-2 support a regulatory model where excess FGF2 decreases PTHrP, and down-regulates bcl-2 exposing growth plate chondrocytes in TgFGF2 mice to premature programmed cell death. Concomitant cell cycle regulation involves loss of p21waf expression in a p53 independent mechanism in the TgFGF2 mice. Conclusion: Even though p21waf is allowing entry into the cell cycle, there is not a significant increase in proliferation. Instead the cells enter apoptosis causing chondrocyte drop out in the proliferation and prehypertrophy zones. The mechanism for this is unclear. Overall, the FGF-2 regulatory model derived from TgFGF2 studies suggests that growth factors function to regulate overall stature and the relative proportions of the skeleton.

M030

Effects of Low Oxygen on Chondroinduction by Human Dermal Fibroblasts in 3-Dimensional Culture. S. Mizuno, J. Glowacki. Orthopedic Surgery, Brigham and Women's Hospital, Boston, MA, USA.

In developmental endochondral bone formation, mesenchymal cells condense without vascularity and as a result, cartilage is relatively hypoxic. Low oxygen (O2) has been shown as a potent regulatory factor for maintaining chondrogenesis in monolayer culture (Dev Bio 19:52,1969). Our hypothesis was that chondroinduction in vitro is enhanced by low O2 concentration. In previous studies, we developed a novel chondroinduction system [Exp Cell Res 227:89, 1996] consisting of human dermal fibroblasts (hDFs) cultured with demineralized bone powder (DBP) in a three-dimensional collagen sponge. We evaluated the effects of O2 concentration in perfused medium on matrix accumulation by chondroinduced hDFs. One million cells were seeded onto collagen sponges +/- DBP. A perfusion system was designed with a closed medium reservoir, gas exchange chamber, cylinder pump, and a glass column. As control, bovine articular chondrocytes (bACs) were enzymatically isolated and 3 million cells/sponge were injected into sponges. Sponges were incubated in culture dishes in DMEM/10%FBS for hDF or Ham's F12/10% FBS for bACs. After preincubation (under routine conditions) for 3 days, sponges were suspended in a glass column through which medium was perfused at either 2% O2 or atmospheric (AT) O2 concentration for an additional 5 or 7 days. As measures of chondroinduction and chondrogenecity, sponges were treated with 4 M guanidine and proteoglycan (PG) was precipitated with potassium acetate/alcohol. The accumulation of PG within the sponges was evaluated by ELISA with anti-keratan sulfate, anti-chondroitin 4-sulfate, anti-chondroitin monoclonal antibodies. After 7 days incubation with DBP, metachromatic matrix accumulated in all groups. The content of keratan sulfate in 2% O2 with perfusion (253 ± 39 ng/sponge) was 23% greater than AT O2 with perfusion (205 ± 12 ng/sponge, $P < 0.05$) and 20% greater than AT O2 without perfusion (211 ± 23 ng/sponge). The content of chondroitin 4-sulfate PG was similar in both perfused and non-perfused cultures at AT O2. Content of chondroitin 4-sulfate in 2% O2 with perfusion (167 ± 14 ng/sponge) was 18% greater than AT O2 with perfusion (141 ± 15 ng/sponge, $P < 0.05$) and 24% greater than AT O2 without perfusion (135 ± 27 ng/sponge, $P < 0.05$). In sum, chondrocyte matrix production was suppressed with perfusion and low O2 conditions enhanced chondroinductive and chondrogenic activity.

M031

TNF-α Activation of the Apoptotic Cascade in Articular Chondrocytes Is Accompanied by Induction of Specific, Pro-Resorptive Factors, Metalloproteinases and Angiogenic Factors. T. Cho[1], W. Lehmann[2], C. M. Edgar[3], T. A. Einhorn[3], L. C. Gerstenfeld[3]. [1]Department of Orthopaedic Surgery, Seoul National University College of Medicine, Seoul, Republic of Korea, [2]Department of Trauma and Reconstructive Surgery, University of Hamburg, Hamburg, Germany, [3]Department of Orthopaedic Surgery, Boston University Medical Center, Boston, MA, USA.

TNF-α has been implicated in the progression of rheumatoid arthritis. Therapies that specifically block TNF-α activity have been shown to provide substantive diminishment in the symptoms of rheumatoid arthritis and slow the progression of joint degeneration. In the current studies, we demonstrate that TNF-α induces the expression of multiple mRNAs associated with the apoptotic cascade within murine articular chondrocytes. Furthermore, these mRNAs are directly dependent on the actions of TNF-α as mediated through its receptors, based on comparison of cells from wild type mice and TNF-α receptor deficient ($p55^{-/-}p75^{-/-}$) mice. The induction of the apoptotic cascade was accompanied by the increased expression of multiple factors involved in the regulation of skeletal tissue resorption and a number of specific metalloproteinases and angiogenic factors that promote vessel infiltration. The expression of specific mRNAs that showed quantitative changes from 2 to greater than 10 fold included iNOS, MMP3, VEGFi, VEGF D, VEGE and M-CSF. The dependence of the induction of these mRNAs on TNF-α was confirmed by comparison to the effects of TNF-α on the chondrocytes of receptor null mice. In summary, our findings demonstrate that TNF-α activates a complex array of factors within chondrocytes that contribute to the destruction of joint surfaces independent of its actions on synovial cells. These activities promote the apoptosis of the chondrocytes and the proteolytic destruction of cartilage extracellular matrix, while facilitating the activation of pro-resorptive cells and angiogenesis. Our findings provide a more comprehensive mechanistic understanding on why TNF-α blockade is so effective as a therapeutic in the treatment of rheumatoid arthritis.

M032

Hedgehog Signaling Enhances Expression of Osterix Gene in Chondrocytes. M. Takamoto[1], K. Tsuji[1], T. Komori[2], Y. Taketani*[3], A. Nifuji[1], M. Noda[1]. [1]Molecular Pharmacology, Tokyo Medical and Dental University, Tokyo, Japan, [2]Osaka University, Osaka, Japan, [3]University of Tokyo, Tokyo, Japan.

Hedgehog signaling is considered to play an important role in chondrogenesis. Indian hedgehog (Ihh), expressed in prehypertrophic zone of the growth plate, seems to regulate chondrocyte hypertrophy in a negative feedback loop with PTHrP. Ihh is needed for normal endochondral bone formation. However, downstream molecule of the hedgehog signaling is not fully understood. Osterix is a recently reported novel zinc finger-containing transcription factor, which is required for osteoblast differentiation and bone formation. In Osterix null mice, no bone formation is occurred. In this paper, we examined whether hedgehog signaling has any effect on the expression of Osterix gene. Chondrocytes were prepared from costal cartilage of the newborn mice. Then, chondroctytes were cultured in the presence or in the absence of hedgehog. RT-PCR was performed with Osterix primer. Osterix mRNA was expressed constitutively in these primary chondrocytes, and the expression level was enhanced in the presence of hedgehog signaling. These data indicated that osterix is the target of hedgehog signaling and may play a key role not only in the regulation of bone formation but also in chondrogenesis.

M033

New Calcium Phosphate Scaffolds for Tissue Engineered Osteochondral Implants. Y. Larcher*[1], J. Hendry*[2], D. R. Sindrey[2], R. Hagg*[1]. [1]Millenium Biologix AG, Zurich, Switzerland, [2]Millenium Biologix Inc., Mississauga, ON, Canada.

Mosaicplasty and autologous chondrocyte implantation (ACI) are the most popular methods for repair of articular cartilage injuries. Donor site morbidity is a major concern of mosaicplasty whereas ACI is mainly limited by a relatively long rehabilitation time and its applicability for osteochondral injuries. Novel tissue engineering approaches using scaffolds with capacities to address bone and cartilage formation are believed to overcome existing hurdles. Skelite™ is a new porous calcium phosphate based biomaterial with unique biological activity, which has shown excellent results with respect to new bone formation in animal studies. The aim of this study was to investigate how this new osteoinductive biomaterial qualifies for *in vitro* engineering of osteochondral implants. Porcine articular chondrocytes were enzymatically harvested using a consecutive protease/bacterial collagenase digest. Isolated chondrocytes were seeded onto porous Skelite™ cylinders (7mm dia. x 5mm h). Such 3D high-density cell constructs were incubated in DMEM/F12 medium supplemented with 10% FBS, insulin and ascorbic acid for up to 4 wks. Ground polished sections were toluidine blue stained for assessment of the interface between cartilage and the biomaterial. The newly formed cartilage was further classified by collagen typing via SDS-PAGE and collagen-/proteoglycan quantification by means of H-Proline/DMB-assays. The chondrocytes formed physically palpable tissue with a seamless transition to the underlying Skelite™. The 1.5 mm layer of cartilaginous-like tissue was composed by numerous round to ovoid cells with a vacuolar cytoplasm and with a small round central nucleus, consistent with a chondrocytic phenotype. These cells were embedded in an abundant amorphous lightly metachromatic intercellular matrix having the histological hallmarks of hyaline cartilage. Collagen typing further confirmed that mainly cartilage specific collagen types II, IX and XI were formed when cultured up to 4 wks. Expectedly, due to the short culture period of 4 wks the tissue was still immature and contained only approximately 10-20% of total collagen or proteoglycan amount of native articular cartilage. The connection between biomaterial and cartilage was in all cases relatively tight, as *de novo* cartilage layers could not be removed by applying tensile forces using a forceps. We have demonstrated that Skelite™ not only is a proper scaffold for new bone formation but also supports the formation and attachment of cartilaginous tissue. Our results suggest that a Skelite™ cylinder seeded with chondrocytes could be a promising candidate as carrier matrix for cartilage repair therapy.

Disclosures: ***D.R. Sindrey****, Millenium Biologix Inc. 1.*

M034

Molecular and *In Silico* Analysis of Novel DNAs Expressed During Chondroinduction of Human Dermal Fibroblasts. K. E. Yates. Orthopedic Surgery, Brigham and Women's Hospital, Boston, MA, USA.

Gene expression profiling has emerged as a means to infer biological mechanisms. Interpretation of differential gene expression patterns is confounded when limited information is available on genes of interest. Cloning of additional 5' and/or 3' sequence may be necessary to identify putative functions for novel genes. In this study, an *in silico* approach was combined with molecular techniques to characterize novel genes that are upregulated during postnatal chondroinduction of human dermal fibroblasts (hDFs) by demineralized bone. The purpose was to rapidly screen the novel sequences and prioritize them for further study. Upregulated genes were identified by representational difference analysis of genes expressed in chondroinduced and control hDFs. Novel sequences were defined as those for which a BLAST Sequence Similarity Search of the GenBank database (http://www.ncbi.nlm.nih.gov/Genbank/GenbankSearch.html) found no similar (>90% identity) human DNA sequence. Eleven of 100 clones analyzed were initially identified as novel. Gene expression of all 11 sequences were detected in human DFs, skin, and articular chondrocytes by RT-PCR. A subsequent BLAST search identified matches in GenBank for three human mRNAs and three human genomic clones (Table). Those sequences were aligned to the Human Genome Working Draft sequence using the BLAT algorithm (http://genome.ucsc.edu/cgi-bin/hgBlat?db=hg10) (Table). The Human Genome Browser (http://genome.ucsc.edu/cgi-bin/hgGateway) was used to view known and predicted mRNA sequences at the same genetic loci as the genomic clones. That analysis predicted sequence number 30 was a splice variant of alpha V integrin. Northern hybridization using seq. No. 30 as probe detected a transcript in hDFs similar in size (~8kb) to known alpha V integrin mRNAs. Of the 5 remaining novel sequences, 3 were fully aligned to the Human Genome Working Draft Sequence. Analysis of known and predicted mRNAs at the same genetic loci suggested that one of the novel sequences encodes a kinesin-related protein similar to the murine KIF26B protein. In summary, a putative function was assigned to 45% of DNA sequences initially identified as novel in chondroinduced hDFs. Coupling *in silico* with molecular biology tools expedites analysis of novel DNA sequences and selection of candidate genes for further study.

Identification of novel DNAs in chondroinduced hDFs by comparison to DNA sequence databases

Seq. No.	BLAST Result (GenBank Accession No.)	BLAT Result	Proposed Function
2	FBXO32/atrogin-1 (NM_058229.1)	8q24.13	Ubiquitin ligase
38	RAP2B (XM_003032.1)	3q25.1	GTPase
86B/D	ATP10C (AY029489)	No alignment	ATPase
30	clone RP11-556A11 (AC17101)	2q32.1	Alpha V integrin
11	clone RP5-1175B15 (AL353786)	14q31.3	Unknown
90D	clone CTB-162I23 (AC012613)	5q33.1	Unknown

M035

Expression of *Wnt* and *Frizzled* Genes During Postnatal Chondroinduction of Human Dermal Fibroblasts. K. E. Yates, S. Zhou*. Orthopedic Surgery, Brigham and Women's Hospital, Boston, MA, USA.

Wnt family proteins and their receptors, the Frizzled proteins (Fzd), modulate chondrogenesis during embryonic development. Expression of *wnt* genes may also regulate postnatal chondroblast differentiation and chondrogenesis. In previous studies, we used a novel *in vitro* collagen sponge culture system [1] to identify a pool of genes whose expression was altered in human dermal fibroblasts (hDFs) chondroinduced with demineralized bone powder (DBP) [2]. In this study, we identified *wnt5a* among those genes whose expression was increased (upregulated) in chondroinduced hDFs, and characterized expression of *wnt* and *fzd* genes during chondroinduction of postnatal fibroblasts. A clone containing the *wnt5a* 3' untranslated region was identified among a pool of genes upregulated in hDFs after 3 days of exposure to DBP. Northern hybridization using this clone as a probe detected several *wnt5a* mRNA transcripts (approximate sizes 1.9-, 4.6-, 6.8-, and 8.2-kb) in chondroinduced and control hDFs on day 3. An additional transcript (approximate size 9.0 kb) was transiently expressed only in chondroinduced hDFs. *In situ* hybridization using a probe for the *wnt5a* protein-coding region showed expression in hDFs in DBP/collagen sponges after 4 days, especially in those cells that surrounded the DBP. Expression of other *wnt* and *fzd* genes during chondroinduction (days 3, 7, 14, and 21) was characterized by semi-quantitative RT-PCR. *Wnt5b* mRNA was upregulated in chondroinduced hDFs 2.9-fold over control on day 3; a similar level of expression was observed in chondroinduced hDFs throughout the experiment. *Wnt10b* mRNA was upregulated in chondroinduced hDFs 2.6-fold over control on day 3, 4.8-fold on day 7, and declined thereafter. In contrast, transient suppression of *wnt2B/13* (42% of control) and *fzd7* (55% of control) mRNA levels were observed in chondroinduced hDFs on day 3. Expression levels of *wnt2, wnt3, wnt4,* and *wnt7b* and *fzd1, fzd2* and *fzd3* mRNAs were similar in control and chondroinduced hDFs at all timepoints. In summary, we found modulation of specific *wnt* and *fzd* gene expression during postnatal chondroinduction of dermal fibroblasts by demineralized bone. The results suggest the hypothesis that DBP-mediated changes in expression of Wnt and Fzd contribute to chondroblastic differentiation of postnatal fibroblasts.

[1] Exp Cell Res 227:89, 1996.
[2] Exp Cell Res 265:203, 2001.

M036

Osteoblasts Express Multiple Forms of Laminins - Regulation with the Progression of Differentiation. V. Puche*[1], M. Clerget*[1], P. Rousselle*[2], L. Malaval[1]. [1]U403, INSERM, Lyon, France, [2]Umr 5086, ibcp, CNRS, Lyon, France.

Laminins (LNs) are trimeric molecules of the extracellular matrix which affect cell fate and activity. We have previously shown that LN-1 ($\alpha1\beta1\gamma1$) favors the attachment of osteoprogenitors to the substrate, suggesting a role for these molecules in osteogenesis and/or bone remodeling. Although LN chains are secreted by multiple cell types, only a few studies have focused on their expression by bone cells. To identify the isoforms of LN secreted by osteoblasts, we analysed their expression in a bone nodule forming model of *in vitro* osteogenesis, rat calvaria (RC) cell cultures. A cDNA bank of rat LN chains was generated by RT-PCR and used in Northern blot analysis. mRNA for subunits $\alpha4$, $\beta1$, $\beta2$ and $\gamma1$ were detected in RC cell cultures. The expression of $\beta1$ and $\gamma1$, which was confirmed by immunoprecipitation and Western blot, diminishes with culture time, i.e. the progression of osteogenesis. $\alpha4$ and $\beta2$ are not regulated with culture time but the expression of mRNA and protein is strongly inhibited by Dexamethasone (Dex). Bone nodules are clonal osteoblastic colonies, presenting a differentiation gradient from the periphery to the center. Immunofluorescence analysis of mature nodules shows a strong expression of $\alpha4$, $\beta1$ and $\beta2$, in particular by differentiated osteoblasts in the central part of the colonies. Interestingly, while $\gamma1$ is strongly expressed in peripheral proliferating preosteoblastic cells, labelling is absent in central cells, suggesting the expression of at least one other γ chain by mature osteoblasts. Immunoprecipitation after metabolic labelling with an anti-LN-1 polyclonal antiserum reveals the presence in RC cell cultures of several LN isoforms, whose number and level of expression are regulated with the progression of osteogenesis and under the action of Dex. Immunoprecipitations with specific antibodies show that most of these isoforms contain $\beta1$ and $\gamma1$, and that nidogen, another component of basal laminae, is present in RC cell cultures and is associated with some of the LN variants secreted. In summary, we have shown that multiple LN chains are expressed during osteogenesis *in vitro*, and differentially regulated at successive osteoblast differentiation stages and by Dex, which is a potent osteogenic agent in this model. Specifically, our data are compatible with the presence of LN-8 ($\alpha4\beta1\gamma1$) and/or LN-9 ($\alpha4\beta2\gamma1$) ; however, immunoprecipitation results indicate that other forms, some of which contain long α chains (which may be $\alpha1$, 2 and/or 5), are also secreted. Our data confirm the involvement in osteoblast biology of Laminins, an entirely new family on this scene.

M037

Cellular Distribution and Protein Interactions of Na-dependent Phosphate Transporters in the Osteoclast. M. A. Khadeer*[1], Z. Tang*[1], H. S. Tenenhouse[2], N. Hernando*[3], M. V. Eiden*[4], A. Gupta[1]. [1]University of Maryland, Baltimore, Baltimore, MD, USA, [2]McGill University, Montreal, PQ, Canada, [3]Physiologisches Institut, Universität Zürich-Irchel, Zurich, Switzerland, [4]National Institutes of Mental Health, Bethesda, MD, USA.

We previously demonstrated that inhibition of Na-dependent phosphate transport in osteoclasts led to reduced ATP levels and diminished bone resorption. These findings suggested that Na/Pi cotransporters in the osteoclast plasma membrane provide Pi for ATP synthesis and that the osteoclast may utilize part of the Pi released from bone resorption for this purpose. The present study was undertaken to define the cellular localization of Na/Pi cotransporters in the mouse osteoclast and to identify the proteins with which they interact. Using glutathione S-transferase (GST) fusion constructs, we demonstrate that the type IIa Na/Pi cotransporter (Npt2) in osteoclast lysates interacts with the Na/H exchanger regulatory factor, NHERF-1, a PDZ protein that is essential for the regulation of various membrane transporters. In addition, NHERF-1 in osteoclast lysates interacts with a carboxy terminal Npt2 fragment fused to GST and to a lesser extent with the same Npt2 fragment lacking the PDZ-binding carboxy terminal amino acids TRL, consistent with the interaction of renal Npt2 with NHERF-1. Studies in osteoclasts transfected with green fluorescent protein-Npt2 constructs indicated that Npt2 colocalizes with NHERF-1 and actin at or near the plasma membrane of the osteoclast, and associates with ezrin, a linker protein associated with the actin cytoskeleton, likely via NHERF-1. Furthermore, we demonstrate by RT/PCR of osteoclast RNA and in situ hybridization that the type III Na/Pi cotransporter, PiT1, is also expressed in mouse osteoclasts. To examine the cellular distribution of PiT1, we infected mouse osteoclasts with a retroviral vector encoding PiT1 fused to a double HA epitope tag at the carboxy terminus. We show that PiT1 colocalizes with actin and is present on the basolateral membrane of the polarized osteoclast, similar to that previously reported for Npt2. Taken together our data suggest that association of Npt2 with NHERF-1, ezrin and actin, and of PiT1 with actin, may be responsible for membrane sorting and regulation of these Na/Pi cotransporters in the osteoclast.

M038

Increased Collagen Degradation Is Associated with the Upregulation of Chondrocyte Differentiation Related Genes in Articular Cartilage Explants Induced by a Type II Collagen Peptide. E. V. Tchetina*. Joint Diseases Laboratory, Shriners Hospitals for Children, Montreal, PQ, Canada.

Articular cartilage degeneration in osteoarthritis (OA) involves excessive degradation of extracellular matrix (ECM), including type II collagen and aggrecan. It is also characterized by chondrocyte differentiation (hypertrophy).We hypothesised that destruction of the collagen network in OA is controlled by regulatory mechanisms of ECM resorption that govern chondrocyte terminal differentiation. In human and bovine articular cartilage explants the presence of a type II collagen peptide is capable of inducing collagenase cleavage of type II collagen, measured by ELISA. Examination by semi-quantitative RT-PCR of the expression profiles of genes involved in chondrocyte differentiation revealed

that the increase in collagen cleavage in human or bovine articular cartilage explants induced the collagen peptide was accompanied by the upregulation of terminal chondrocyte differentiation-related genes namely COL10A1, MMP-9, MMP-13, Indian hedgehog and TGFbeta1 as seen in the bovine growth plate. This was preceeded by the transient upregulation of the expression of bFGF and PTHrP. Upregulation of the cytokines IL-1alpha/beta and TNFalpha was also observed. Our results show that a cartilage collagen cleavage product can induce upregulation of the genes involved in chondrocyte terminal differentiation. This may contribute to the pathobiology of articular cartilage degradation in OA.

M039

Microarray Analysis of Human Osteoblast and Cementum-derived Cell. M. Yamamoto[1], T. Nakamura[1], T. Yoshimoto*[1], W. J. Grzesik*[2], H. Sekiya[3], Y. Izumi*[1]. [1]Periodontology, Kagoshima University Dental School, Kagoshima, Japan, [2]Department of Periodontics, School of Dentistry, Dental Research Center, University of North Carolina at Chapel Hill, Chapel Hill, NC, USA, [3]First Department of Oral and Maxillofacial Surgery, School of Dental Medicine, Tsurumi University, Yokohama, Japan.

Teeth are connected to alveolar bone in jaws, with attachment apparatus composed of alveolar bone proper, periodontal ligament, and tooth cementum. Tooth cementum is generally thought to be closely related to bone. Heretofore, numerous previous studies using physiological, anatomical, histology, and biochemical techniques reveal the biological function and characteristics of cementum. However, specific molecular markers or characteristics of cementum are still to be identified. The purpose of this study was to analyze the differences in gene expression between human cementum-derived cell and normal human osteoblast using microarray technique. Radioisotope-labeled cDNA probes were reverse-transcribed with [α33P] dATP from total RNA extracted from cultured normal human osteoblast (NHOst, Clonetics, SanDiego,CA,USA), or human cementum-derived cell clone-10 (HCDC c10) which were isolated from teeth extracted on clinical demands. Side-by-side hybridizations with radioisotope-labeled cDNA probes onto 1176 genes membrane arrays allow the comparison of the expression pattern. Of the known 1176 spotted genes, 21 were unique to NHOst and 37 were distinctive to HCDC. To confirm the differential expression of genes between NHOst and HCDC c10, RT-PCR analyses were performed on 5 genes which were highly expressed in one of the two kind of cells. RT-PCR revealed that IGFBP2 was expressed highly in NHOst, and extremely low in HCDC c10. Further RT-PCR showed that IGFBP2 was expressed abundantly in matured NHOst, alveolar osteoblast and osteocyte isolated from human mandibles, and human osteosarcoma cell lime MG63. On the other hand, HCDC clone-12 did not express the IGFBP2 mRNA, similar to HCDC c10. In summary, these results indicate that IGFBP2 is one of the candidates for markers which are useful to distinguish between cementum-derived cells and other bone cells.

M040

The Genetic Determinants of Bone Strength: Towards the Mapping of Candidate Genes for Bone Turnover. D. Jefferies*, R. Flemming*, C. Farquharson, D. Burt*, C. Whitehead*. Bone Biology Group, Roslin Institute, Edinburgh, United Kingdom.

Bone mineral density is a complex term that includes mineral content, size, trabecular complexity and shape. Bone strength is determined primarily by these variables. In order to characterise the molecular pathways involved in bone formation and resorption it is necessary to determine the genes that contribute to bone strength. Our approach has involved the selection of lines of chickens with high and low bone strength (high and low lines respectively). After 8 generations of bodyweight restricted selection on bone characteristics these lines have tibial breaking strengths that differ by 92% (303.7±12.5 v 157.9±10.9 Newtons: P<0.001), with no significant difference in bodyweight (1625.5±21.14 v 1706.8±36.8 grams). Measurements of mineral apposition rate (12.2±0.7 v 9.6±0.3 mm/day: P<0.001) and serum pyridinoline (0.39±0.03 v 0.46±0.021 pmol/ml: P<0.05) indicate that bone formation is increased and bone resorption is decreased in the high line compared to the low line. Tibial cortical thickness was also significantly greater in the high line (0.42±0.009 v 0.37±0.007 mm: P<0.001). Although the differences were not significant the number of osteoclasts per unit surface area of bone was lower in the high line (1063±101 v 1229±73 per sq. mm) and the serum concentration of carboxylated osteocalcin was higher (285±21.8 v 230±19.1 ng/ml) reinforcing the above trend. No differences were found in the levels of serum ionised or total calcium, or inorganic phosphate. We are currently using these two lines to discover candidate genes for bone strength using a dual approach: 1) Microarray analysis of gene expression in bone cells (osteoblasts and osteoclasts) of the high and low lines to characterise significant changes in gene expression between the lines. 2) QTL analysis of a classical F2 intercross to identify areas of the genome with significant QTL for bone strength. Genes that show significant differences in expression levels between the lines will be mapped initially using human/mouse/chicken comparative gene maps. Known properties of genes from available functional data will be used to prioritise the most likely candidate genes at each QTL. This dual approach will allow us to focus on a limited number of genes important for bone strength for further study.

M041

SFRP-1, a Wnt Antagonist, Is Expressed During Embryonic Development in Bone and Cartilage. J. B. Lian[1], B. Trevant*[1], J. Symons*[1], B. S. Komm[2], P. V. N. Bodine[2], G. S. Stein[1]. [1]Department of Cell Biology, University of Massachusetts Medical School, Worcester, MA, USA, [2]Women's Health Research Institute, Wyeth Research, Collegeville, PA, USA.

Members of the Wnt (wingless) family of secretory proteins have important regulatory roles throughout development in cell-fate determination and inductive tissue interactions, and are involved in many cell functions, including apoptosis. A set of secreted frizzled (FZ) related proteins (SFRPs) interact directly with Wnt factors to block ligand interaction with FZ receptors. Several studies have indicated that members of the Wnt, frizzled receptors, and SFRP families are expressed in osteoblasts and may regulate programmed cell death. Given the importance of apoptosis to regulation of bone development, we examined expression of SFRP-1 in a mouse model in which the beta-galactosidase gene replaced exon1. The LacZ protein, detected by beta-gal activity in whole embryos and cryosections, reflects in situ expression of the endogenous gene in its native context. Knockout of the SFRP-1 gene does not affect embryo development in homozygous mice. At 11.5 dpc beta-gal expression is observed in developing heart, brain, gut, and kidney, consistent with previous in situ hybridization studies and northern blot expression studies in normal mice. Taken together, these studies indicate that absence of functional SFRP-1 protein does not alter regulation of SFRP-1 expression. Beyond 15.5 dpc, beta-gal activity diminished, but was retained in these tissues. At this time, strong SFRP-1 expression becomes evident in connective tissue around developing ribs, but not in the safranin-O positive cartilage tissue forming the rib. From the 16.5-day embryo to the newborn, SFRP-1 is expressed in hyaline cartilage in limbs that have developed epiphyses. Beta-gal activity is observed selectively in regions undergoing joint formation, expansion, and reshaping. In limb bone, ribs, and calvariae, SFRP-1 expression is highest in the mineralizing bone tissue, overlapping alkaline phosphatase positive tissue. Our results support the following conclusions: 1) absence of SFRP-1 regulation of the Wnt pathway is likely compensated by other Wnt inhibitory proteins; 2) SFRP-1 is not expressed in all Wnt regulated developing tissues; and 3) SFRP-1 exhibits a selective expression pattern in the skeleton. We postulate that SFRP-1 is a component of the Wnt pathway operative in the developing skeleton and may be relevant to joint formation, shaping of the epiphyses, and regulating osteoblast populations.

*Disclosures: **J.B. Lian**, Wyeth Research 2.*

M042

Specific Osteoblast Cytosolic Proteins Bind and Stabilize Collagenase 3 RNA. S. Rydziel, A. M. Delany, E. Canalis. Research, Saint Francis Hospital and Medical Center, Hartford, CT, USA.

Collagenase 3 (matrix metalloproteinase 13) degrades collagen fibrils and its activity is critical in the initiation of bone resorption. Glucocorticoid excess causes bone loss, and cortisol increases collagenase 3 synthesis in osteoblasts by increasing its mRNA stability. The collagenase 3 3' untranslated region (UTR) contains AU-rich elements that control transcript stability, and we used RNA electrophoretic mobility shift assay (REMSA) to demonstrate that cortisol increases the interaction of cytosolic proteins from fetal rat calvarial osteoblasts (Ob cells) with collagenase 3 AU-rich elements in the 3' UTR. In contrast, cortisol-dependent protein complexes were not formed with the coding region or the 5' UTR. Transient transfection of Ob cells with CMV-driven collagenase 3 constructs revealed decay of the recombinant transcripts following transcriptional arrest, and mRNA stabilization by cortisol. To confirm that the 3' UTR of collagenase 3, and specifically the AU-rich elements, were responsible for stabilization of its mRNA in osteoblasts, CMV-driven c-fos constructs, where the 3' UTR of the c-fos gene was exchanged with that of collagenase 3 gene, were created. Transient transfections of CMV-driven c-fos in Ob cells revealed a rapid decay ($t_{1/2} < 5$ min) of c-fos mRNA following transcriptional arrest, and stabilization when the 3' UTR was exchanged with that of the collagenase 3 gene ($t_{1/2} > 60$ min). Mutations of AU-rich elements in the collagenase 3 3' UTR sequence resulted in immediate destabilization of chimeric transcripts. Similarly, mutations of AU-rich elements in the 3' UTR of the collagenase gene resulted in immediate destabilization of transfected CMV-driven collagenase constructs, confirming that the AU-rich sequences determined collagenase 3 mRNA stability. A group of collagenase 3 RNA binding proteins was purified from cytosolic extracts of cortisol treated Ob cells by ultracentrifugation, ion exchange chromatography, RNA affinity chromatography, and polyacrylamide gel electrophoresis, and identified by mass spectroscopy. REMSA supershift assays using specific antibodies to each of these proteins demonstrated that vinculin and far upstream element (FUSE) binding protein 2 interacted with the AU-rich collagenase 3 3' UTR sequences. In conclusion, the 3' UTR of collagenase 3 regulates collagenase mRNA stability in osteoblasts. Interactions with cytoskeletal proteins, such as vinculin, and proteins that shuttle from nucleus to cytoplasm, such as FUSE binding protein 2, appear vital to the stability and targeting of transcripts to cytoskeletal polysomes.

M043

Development of Bone-Derived Cell Lines from a Marine Teleost: Establishment of the First In Vitro Model System from Fish Suitable to Analyze Regulatory Pathways of Matrix Gla Protein and Osteocalcin Gene Expression. V. Laizé*, A. R. Pombinho*, M. L. Cancela. Ccmar, Universidade do Algarve, Faro, Portugal.

Recent studies on regulation of bone formation and mineralization in fish have been hampered due to lack of a well-characterized *in vitro* model system. Therefore, while numerous mammalian and avian cell lines, available for decades, have been successfully used for analysis of expression and regulation of genes from bone and cartilage, corresponding mechanisms in lower vertebrates have remained poorly understood. The purpose of this work was to develop bone-derived cell lines from fish origin capable of *in vitro* mineralization and suitable to characterize specific gene expression and regulation. Because of its economical and scientific importance, the teleost fish *Sparus aurata* has been chosen to initiate this work and vertebra-derived primary cell cultures were generated. Two of them (VSa13 and VSa16) were continuously kept in culture for over 100 passages and further characterized. Both cell types exhibited a fibroblast-like phenotype/slow growth when cultured at 22ºC in medium A, and a polygonal phenotype/rapid growth when cultured at 33ºC in medium B and were capable of inducing extracellular matrix mineralization when confluent as detected by von Kossa staining. Mineralization was observed in both cultures grown in medium B but no nodules could be detected when grown in medium A. Nature of the mineral deposits was investigated by X-ray diffraction and by measuring the quantity of calcium and phosphate associated with the matrix. The mineral structure of the deposits was similar to that of hydroxyapatite, a mineral present in mammalian and fish bones. Gene expression and regulation of *S. aurata* (Sa) Matrix Gla protein (MGP) and osteocalcin (BGP) were investigated in both cell types. SaBGP is expressed only in VSa16 cells and is up-regulated during mineralization. In contrast, SaMGP is expressed only in VSa13 cells, is up-regulated by increased extracellular calcium concentration and down-regulated during mineralization. Furthermore, SaMGP gene expression is regulated in VSa13 cells by different hormones, in a temporal and status of mineralized matrix-dependent manner. In this report we describe for the first time the establishment and initial characterization of two cell lines derived from vertebra of a marine teleost fish. Both are capable of mineralizing *in vitro* but they express osteocalcin and matrix Gla protein in a mutually exclusive manner and represent therefore a valuable tool for further studies on expression of genes involved in extracellular matrix mineralization.

M044

Medial Collateral Ligament Insertional Changes (μCT) After Anterior Cruciate Ligament Deficiency. J. M. LaMothe*, M. R. Doschak*, J. R. Matyas, R. C. Bray*, R. F. Zernicke. McCaig Centre for Joint Injury and Arthritis Research, University of Calgary, Calgary, AB, Canada.

The knee anterior cruciate ligament (ACL) has primary responsibility for preventing anterior-posterior translation of the tibia, and ACL disruption leads to increased knee instability. With ACL disruption, the medial collateral ligament (MCL) becomes critical in restraining knee movement, but no studies have investigated the potential influence of joint instability on MCL insertional changes after ACL loss. Loss of joint stability may lead to tissue deterioration affecting all tissues within the joint. Thus, we investigated changes in MCL insertional geometry following ACLX. Skeletally mature female New Zealand White rabbits were separated into two groups: ACLX (n=9) or normal age-matched controls (n=15). The ACLX group underwent unilateral transection of the right ACL followed by 6wk recovery, and the normal age-matched controls did not undergo surgery. Following 6wk recovery, rabbits were euthanized, and femurs were dissected. The medial femoral condyle was sectioned from the femur and scanned with micro computed tomography (μCT-Skyscan 1073). Two-dimensional images generated by scanning were quantified with standardized tracing methods and summated to extract MCL insert-related measurements (Scion image). The University of Calgary Animal Care Committee approved all procedures. There was no significant difference between ACLX and age-matched controls in volume of cortical bone containing the MCL insert. The percentage of cortical bone volume compared to a standardized bone volume surrounding the MCL insert was not significantly different between ACLX and normal controls. MCL insertional volume was significantly greater in the ACLX cohort ($p<0.04$). MCL cross-sectional area increased significantly after ACLX ($p<0.04$). After 6 wk, ACLX periarticular bone mineral density was significantly decreased ($p<0.05$). Thus, an increase in joint instability elicited concomitant changes in joint tissue morphology, and those changes may be associated with changes in joint loading and progression of post-traumatic osteoarthritis.

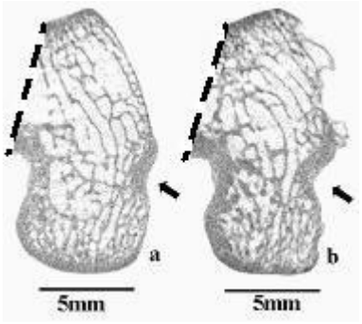

Figure 1. Transverse sections (μCT) of femoral medial condyles illustrating the MCL insert (arrow) in a normal control (a) and 6 wk ACLX (b) animal. Dashed lines denote a sagittal cut dividing distal medial and lateral condyles.

M045

Overcoming the Immune Response to Permit Ex Vivo Gene Therapy for Spine Fusion Using Human Type 5 Adenovirus to Deliver LIM Mineralization Protein-1 (LMP-1) cDNA. M. Viggeswarapu[1], H. Kim*[1], S. D. Boden[1], G. A. Hair*[1], C. Oliver*[1], L. Titus[2]. [1]Orthopaedics, Emory University School of Medicine, Decatur, GA, USA, [2]Medicine, Veterans Affairs Medical Center, Decatur, GA, USA.

Cells transduced with human type 5 Adenovirus containing the osteoinductive LMP-1 cDNA (Ad5-LMP-1) can induce spine fusion in rabbits. Since up to 80% of the human population has been exposed to adenovirus, immune responses to the vector may limit this strategy in humans. Few studies have modeled previous adenoviral exposure and tested strategies to circumvent it. Our goals were: 1) To develop an animal model to simulate previous human adenoviral exposure; 2) To determine the impact of adenoviral pre-exposure on spine fusion induced with ex vivo Ad5-LMP-1; 3) To test strategies to overcome any potential immune response. Adult NZW rabbits were injected with 108 or 109 viral particles of Ad5-LacZ. At 4 weeks or 16 weeks after Ad5 injection, autologous buffy coats were prepared from peripheral blood and 4M cells/side were infected for 10 min with 4 plaque forming units/cell (MOI) Ad5-LMP-1. Cells were implanted on a collagen matrix for posterolateral lumbar arthrodesis. Non-immunized rabbits served as controls. Additional immunized rabbits underwent arthrodesis at 4 weeks with increased cell number (10M), viral dose (MOI=10), or both parameters increased. Rabbits were euthanized at 4 weeks and the spines were assessed by palpation and X-ray. A parallel study was performed in athymic rats using immunized rabbits for the donor cells. All non-immunized rabbits had solid spine fusions. None of the rabbits arthrodesed 4 weeks after Ad5 pre-exposure achieved fusion. At 4 weeks post Ad5 exposure, increasing the MOI to 10 did not overcome the immune response (0/3 fused), but increasing the cell number to 10M (2/3 fused) or increasing both cell number and MOI (3/3 fused) did overcome the immune effects. Delaying arthrodesis until 16 weeks after Ad5 exposure also overcame the immune response (3/3 fused) in rabbits pre-exposed to 108 vp. Similar results were seen in the athymic rat ectopic implant model, suggesting the immune effect was mediated by humoral antibodies rather than a T-cell response. In these studies two model systems were developed which simulate previous exposure to Ad5 and separate the cellular and humoral components of the response. There was a dose-dependent inhibition of spine fusion, probably due to inhibition of ex vivo Ad5-LMP-1 gene transfer to cells from animals previously exposed to Ad5. Data suggest the inhibition of AdV5 infection was due to neutralizing antibodies, rather than a T-cell-based response. Minor modifications in the gene transfer protocol overcame the immune response to allow ex vivo gene therapy

M046

Expression of Small Leucine-rich Proteoglycan Genes During Mineralization by MC3T3-E1 Cells Cultured on Titanium Implant Material. T. Matsuura[1], S. Tsubaki*[1], T. Tsuzuki*[1], M. Yamauchi[2], H. Sato*[1]. [1]Oral Rehabilitation, Fukuoka Dental College, Fukuoka, Japan, [2]Dental Research Center, University of North Carolina at Chapel Hill, Chapel Hill, NC, USA.

It is known that dental/orthopedic titanium implants create a unique microstructure at the bone-implant interface composed of a thin layer of collagen-free/proteoglycan-rich unmineralized matrices (20-50 nm) and a collagenous zone (100-500 nm). The presence of the former appears to be important for successful implants; however, the mechanisms of its formation are unknown. The objective of this study was to investigate the temporal mRNA expression patterns of small leucine-rich proteoglycans (SLRPs), i.e. decorin (DCN), fibromodulin (FM) and lumican (LM), and type I collagen (COL) during mineralization by MC3T3-E1 cells cultured on a titanium implant material (Ti) using a real-time PCR assay. The lysates of the cells cultured on Ti and plastic wells (Pl) for 10 to 50 days were used for calcium and mRNA quantification. The onset of calcium accumulation in the cultures on Ti (30/40 days) was significantly slower than that of Pl (20/30 days). The timings for high mRNA expression for alkaline phosphatase (ALP) and COL were also slower in the former when compared to the latter. However, as mineralization in the cultures proceeded, the temporal mRNA expression for SLRPs showed similar patterns between the two groups. In both cases, DCN mRNA increased up to two-fold, while FM mRNA diminished by almost 95 % at day 50. The latter pattern was similar to those of COL and ALP. The LM mRNA expression level remained essentially the same during mineralization. These results indicate that the temporal expression patterns of these SLRP genes in MC3T3-E1 cells are distinct from one another during mineralization on the Ti surface suggesting their specific roles in this process. The distinct temporal expression of these SLRP genes and their subsequent deposition in the extracellular matrix could be involved in the formation of the unique bone-implant interface structure.

M047

Proteolysis of Human Osteocalcin by MMP's and Cathepsin K. C. M. Gundberg[1], M. Clough*[1], J. S. Mort*[2]. [1]Orthopaedics and Rehabilitation, Yale University School of Medicine, New Haven, CT, USA, [2]Joint Diseases Laboratory, Shriners Hospital for Children, Montreal, PQ, Canada.

Circulating osteocalcin consists of the intact molecule and several smaller fragments. A large N-terminal-mid molecule fragment can be produced by tryptic activity in the circulation and during sample handling. The origin of other fragments is unknown. We have previously shown that the osteoblast can be a source of osteocalcin fragments while others report that fragments are released into the medium when osteoclasts are cultured on human bone slices. We therefore sought to determine if osteocalcin was a substrate for enzymes thought to be involved in the degradation and remodeling of bone matrix. Fully carboxylated (cHOC) or decarboxylated human osteocalcin (dcHOC) was incubated with MMP 1,

2, 3, 9, or 13 and Cathepsin K. An enzyme:substrate ratio of 1:100 (w:w) was used for all incubations. Cathepsin digestions were performed in 20 mM sodium acetate, 2 mM EDTA, 2 mM dithiothreitol, pH 5.0. MMP digestions were performed in 10 mM Tris, 0.2 mM NaCl, 10 mM CaCl2 , 0.05% Brij 35, pH 7.5. All digestions were carried out for 15 hours at 25 C and stopped with either trans-epoxysuccinyl-1-leucylamido-(4-guanidino) butane (E64) (cathepsin K) or 20 mM EDTA (MMP's). Digests were chromatographed on HPLC and peaks subjected to amino acid analysis. Electrospray mass spectrometry was performed to establish the sequence of fragments with potential tryptophan at the N- or C-terminus.There was limited digestion of cHOC by the MMP's whereas dcHOC was extensively fragmented. Cathepsin K degraded both cHOC and dcHOC, resulting notably in a large mid-molecular fragment generated from the carboxylated HOC(table).

Osteocalcin Fragments Produced

Enzymes	Carboxylated HOC	decarboxylated HOC
MMP1	1-4, 5-49	1-4, 5-49
MMP2	1-4, 5-49	1-4, 5-38, 45-49
MMP 3	1-4, 5-14; 42-49	1-4, 5-38, 42-49, 45-49
MMP8	limited (Minor amounts of 1-4, 6-39, 45-49	1-4, 6-39, 5-49, 42-49, 45-49
MMP9	none	1-4,6-39, 45-49
MMP 13	none	1-4,6-39, 45-49
Cathepsin K	1-4,6-39, 45-49	1-3,4-7, 8-17, 10-30, 31-34, 44-49

Even when uncarboxylated, the large mid-molecular fragment is not further degraded by MMPs. This region is in a highly structured section of the molecule and as a consequence may not be accessible to enzymatic cleavage. On the other hand, cathepsin K can cleave carboxylated OC to the large mid-fragment and further degrades it when it is uncarboxylated. The data suggest that a mid-molecular fragment may result from bone resorption. However, mid-molecular fragments may also result from proteolysis of uncarboxylated osteocalcin, which is made in a vitamin K-deficient state.

M048

Analysis of Osteocalcin Fragments Released from Osteoblasts and Osteoclasts in vitro. K. K. Ivaska*, H. Ylipahkala*, T. A. Hentunen, H. K. Väänänen. Institute of Biomedicine, Department of Anatomy, University of Turku, Turku, Finland.

Osteocalcin is the most abundant non-collagenous protein in bone matrix. It is produced by bone-forming osteoblasts and considered as a marker of bone formation both in serum and in cell culture. However, osteocalcin incorporated into bone matrix is also released during osteoclastic bone resorption. We have studied if osteocalcin immunoassays could thus be utilized to monitor both osteoblast and osteoclast cultures. Primary osteoblasts were induced from rat bone marrow cells and vitamin D3 was used to stimulate osteocalcin production. Primary osteoclasts were obtained from rat long bones and cultured on bovine bone slices. Parathyroid hormone (PTH) was used to stimulate resorption. In addition, human osteoclasts differentiated from peripheral blood mononuclear cells (PBMC) were used. Release of osteocalcin into medium during bone formation and bone resorption in vitro was evaluated with several in-house immunoassays for detection of different molecular forms of osteocalcin. For comparison, a commercial osteocalcin assay was used. The heterogeneity of osteocalcin released into medium was determined using reverse-phase HPLC. In bone formation assay, primary osteoblasts produced osteocalcin into culture medium after two weeks and osteocalcin synthesis was significantly upregulated by vitamin D3. All osteocalcin assays recognizing osteocalcin of rat origin were useful for monitoring the activity of rat osteoblasts. In bone resorption assay, primary rat osteoclasts as well as human PBMC-derived osteoclasts released detectable osteocalcin into medium. The amount of osteocalcin was increased in the presence of stimulators of resorption, e.g. PTH, and was decreased in the presence of inhibitors of resorption, e.g. bafilomycin A1 and a cysteine protease inhibitor E64. Osteocalcin level in the medium correlated with the concentration of well-characterized marker of bone resorption, C-terminal telopeptide of type I collagen (CTx), with r-value > 0.9. Several molecular forms of osteocalcin, including intact molecule, were identified in both osteoblast and osteoclast cultures. We conclude that detectable osteocalcin is released from bone matrix during bone resorption as well as it is synthesized by osteoblasts during bone formation. In addition to its conventional use as a marker of bone formation, osteocalcin could also be used as an index of bone resorption in rodent osteoclast and human PBMC-derived osteoclast cultures.

M049

Enhancement of Fibronectin- and Vitronectin-Adsorption to Polymer/ Hydroxyapatite Scaffolds Suppresses the Apoptosis of Osteoblasts. K. M. Woo*, G. Wei*, P. X. Ma*. Biologic & Materials Sciences, University of Michigan, Ann Arbor, MI, USA.

Bone fractures and damage are serious health problems, which result in about 450,000 surgical bone grafts every year in the United States alone. Bone tissue engineering is a promising new approach to replace damaged bones. In this approach, a scaffold (artificial extracelluar matrix) plays a pivotal role. The scaffold is a substrate for cells to attach to, serves as a template for tissue regeneration, and should finally be replaced by the cell-produced extracellular matrix. Bone is a specialized connective tissue for the mechanical support of the body, the protection of vital organs and reservoirs of several ions including calcium. To pursue these functions, bone has high rigidity and strength and is continually remodeled by the cells within it. Thus, an ideal scaffold for bone tissue engineering has mechanical strength, is biodegradable and serves as a three dimensional guide for cell growth and new bone formation. We developed highly porous biodegradable poly(lactic acid)/hydroxyapatite (PLLA/HAP) scaffolds, under the hypothesis that bone-mineral mimicking synthetic HAP could improve the mechanical strength and impart osteoconductivity to PLLA scaffolds. *In vitro* culture showed that better bone nodule formation in the PLLA/HAP scaffolds than in the PLLA scaffolds. We investigated the events leading to this feature and the underlying mechanism. Fifty percent of initially attached cells on the PLLA scaffolds were detached and showed apoptotic cell death within 24 h, while most cells on the PLLA/HAP scaffolds remained. To understand its underlying mechanisms, we examined the protein adsorption onto the scaffold materials. The PLLA/HAP scaffold adsorbed 40% higher and a different profile of serum proteins than the PLLA scaffold did. Serum fibronectin and vitronectin adsorbed with greater affinity to the PLLA/HAP scaffolds, and the pretreatment of the scaffolds with fibronectin and vitronectin increased the cell survival. These results indicate that our highly porous biodegradable PLLA/HAP scaffolds suppress the apoptotic cell death, and suggest that the enhancement of protein adsorption including fibronectin and vitronectin from serum plays an important role.

M050

Uptake and Metabolism of the Cyclin-Dependent Kinase Inhibitor Flavopiridol in Cultured Mouse Osteoblasts: Implications on Therapy. O. Hoffmann[1], B. Hagenauer*[2], P. Haslmayer*[2], T. Thalhammer*[3], W. Jäger*[2]. [1]Pharmacology and Toxicology, University of Vienna, Vienna, Austria, [2]Pharmaceutical Chemistry, University of Vienna, Vienna, Austria, [3]Pathophysiology, University of Vienna, Vienna, Austria.

Flavopiridol (FP) is a novel cyclin-dependent kinase inhibitor currently undergoing clinical development for the treatment of cancer. In combination with doxorubicin it showed pronounced cytotoxicity against SaOs-2 human sarcoma cells lacking a functional retinoblastoma protein and it has been suggested that it would be a useful adjunct therapeutic agent. Although it is known that FP is extensively metabolized by UTP-glucuronosyltransferase (UGT1A9) to the 7-O-ß-glucopyranuronosyl-conjugate (FP-glu) in human liver, its metabolism in other tissues is still unknown. In particular, we focused on whether FP is metabolised in bone, where it might potentially inhibit bone metastatic lesions. Our strategy was to test FP effect, metabolism and transport in osteoblasts (OB). We observed that FP inhibited cellular growth of mouse calvarial OB cultured in αMEM+10% FBS, for 24h (IC50: 0.98µM). In addition, cellular uptake of FP was linear for up to 2h leading to the formation of FP-glu (K_M: 14.9±4.9µM; V_{max}: 0.29±0.036pmol/mg protein), which was rapidly excreted into the medium (K_M: 2.2µM; V_{max}: 2.8±0.36pmol/mg protein) indicating an active transport mechanism. To determine which transporter plays a role in OB, we tested genistein and verapamil, inhibitors of active transport by multi-drug resistance proteins (MRP) and P-glycoprotein (PgP), respectively. We found that 200µM genistein, but not verapamil significantly inhibited efflux by 39.1% and UGT1A9-mediated formation of FP-glu by 86.8%. Furthermore, genistein decreased uptake of FP by 51.4%, indicating that FP and FP-glu are substrates of MRPs rather than of PgPs. To confirm that FP and FP-glu are substrates of MRP1, we analyzed western blots of 5 x 10^6 cultured and FP treated OB and observed strong expression of MRP1 indicating that they are partial substrates of this transporter. These data demonstrate that FP undergoes slow extrahepatic glucuronidation in mouse OB and it diminishes OB proliferation, which may be particularly useful in the treatment of patients with cancers that induce sclerotic bone metastases.

M051

Differential Effects of Amino- and Non-Amino-Bisphosphonates on MMP-9 mRNA and Enzyme Protein Levels: Relevance for Soft and Hard Tissue Metastasis. J. Mandelin[1], H. Valleala*[2], R. Hanemaaijer*[3], S. Santavirta*[4], Y. T. Konttinen*[5]. [1]Institute of Biomedicine, University of Helsinki, Finland, [2]Department of Medicine, Helsinki University Hospital, Finland, [3]Gaubius Laboratory TNO-PG, Leiden, Netherlands, [4]Department of Orthopedics and Traumatology, Helsinki University Hospital, Finland, [5]Institute of Dentistry, University of Helsinki, Finland.

Bisphosphonates (BP) that closely resemble pyrophosphate, like the non-amino BP clodronate, are metabolically converted to nonhydrolysable analogues of ATP, which are able to inhibit ATP-dependent intracellular enzymes. In contrast, nitrogen-containing BPs (N-BP), like pamidronate, inhibit enzymes of the mevalonate pathway/ prevent the biosynthesis of isoprenoid compounds that are essential for the posttranslational modification of small GTPases. These two classes of BPs have differential effects on lipopolysaccharide (LPS)-stimulated, human monocyte-mediated cytokine synthesis and release. Furthermore, non-amino BP reduce skeletal metastasis in breast cancer, whereas N-BPs can increase the soft tissue metastasis. We therefore speculated that these two classes of BPs might have differential effects of MMP-9 production and secretion. ELISA measurements showed that MMP-9 concentrations in non- and LPS-stimulated monocyte culture supernatants at 24 hours were 14 ± 10 and 51 ± 44 ng x ml^{-1}, respectively. Pretreatment for 20-24 hours with clodronate suppressed LPS-stimulated MMP-9 secretion in a dose-dependent manner: inhibition at 30, 100, 300 and 1000 µM was 27 ± 20, 36 ± 11, 62 ± 12 and 87 ± 11, with p-values 0.078, 0.007, 0.002 and 0.0005, respectively. In contrast, N-BP pamidronate had a dual mode of action so that low 30 µM concentrations enhanced MMP-9 secretion to 146 ± 49%. Quantitative RT-PCR confirmed and extended these findings. MMP-9 mRNA levels were stable at various concentrations of clodronate, but again, N-BP had a dual mode of action: low 30 µM concentrations increased the MMP-9 mRNA levels almost 15-fold.Our findings demonstrate that bisphosphonates have a differential action on LPS-stimulated, human monocyte-mediated MMP-9 synthesis and secretion. Non-amino BP clodronate does not affect the MMP-9 mRNA levels, but inhibits MMP-9 synthesis and/or secretion at a post-transcriptional level in a dose-dependent manner. In contrast, N-BP pamidronate has a dual mode of action so that it enhances MMP-9 mRNA and enzyme protein levels at low doses. These findings may in part explain the differential clinical results on soft and hard tissue metastasis obtained with these two classes of BPs in experimental and clinical studies.

M052

A Possible Functional Role of Cadherins to Prevent Osteosarcoma Metastasis. T. Kashima[1], K. Nakamura*[2], J. Kawaguchi*[3], A. Kudo[3], A. E. Grigoriadis[4]. [1]Department of Craniofacial Development, Guy's Hospital, King's College London, London, United Kingdom, [2]Department of Human Pathology, Graduate School of Medicine, University of Tokyo, Tokyo, Japan, [3]Department of Life Science, Tokyo Institute of Technology, Yokohama, Japan, [4]Department of Craniofacial development, Guy's hospital, King's college London, London, United Kingdom.

Osteosarcoma is characterized by aggressive pulmonary metastasis. However, the underlying molecular mechanisms of metastasis in osteosarcoma are still unclear. We have previously shown that N-cadherin (N-cad) and OB-cadherin/cadherin-11 (cad-11) are highly expressed in normal osteoblasts, but are anomalously expressed in human osteosarcomas. In this study, we examined the role of cadherins in osteosarcoma metastasis using an in vivo metastasis model of the mouse osteosarcoma cell line, Dunn, and its highly metastatic subline, LM8. RT-PCR and Western blot analyses demonstrated that Dunn and LM8 cells do not express appreciable levels of several members of the cadherin family, including N-cad and cad-11. We therefore introduced N-cad and cad-11 into LM8 cells and isolated stable subclones for further functional analyses. Immunoprecipitation assays demonstrated that all cadherin-overexpressing clones formed complexes with beta-catenin, whereas control transfectants did not. Overexpression of N-cad or cad-11 in LM8 cells resulted in an inhibitory effect on cell migration, using an in vitro migration assay on uncoated membranes. To clarify the role of N-cad and cad-11 in osteosarcoma metastasis in vivo, we inoculated overexpressing clones subcutaneously into C3H mice. After four weeks, analysis of the lung tissues revealed a reduced total lung weight in mice harboring cadherin-overexpressing cells. In addition, the number of lung metastases were also significantly reduced in all N-cad and one cad-11 transfectants. Measurement of the weight and volume of the primary tumors at the injection site demonstrated an overall inhibition of weight and size of tumors induced by N-cad- and cad-11-overexpressing cells as compared to mock-transfected cells. Western blot analysis of the primary tumors confirmed the expression of the transfected genes. Finally, we have begun to analyze the role of cadherins in osteosarcoma using transgenic mice overexpressing the c-fos proto-oncogene which develop osteosarcomas but do not form any lung metastases. Preliminary expression studies using Northern blot, in situ hybridization and immunohistochemistry analyses revealed that these tumors express both N-cad and cad-11, which is consistent with their inability to metastasize. Taken together, these observations suggest that the absence of N-cad and cad-11 function, i.e. cell-cell adhesion, is important in osteosarcoma metastasis.

*Disclosures: **T. Kashima**, Canon Europe Foundation 2.*

M053

NF-κB Over-expression Protects Growth Plate Chondrocytes from Ionizing Radiation-induced Apoptosis. M. J. D'Souza*[1], M. J. Zuscik[1], R. A. Eliseev*[2], T. E. Gunter*[2], E. M. Schwarz[1], J. E. Puzas[1], R. J. O'Keefe[1], R. N. Rosier[1]. [1]Orthopaedics, University of Rochester, Rochester, NY, USA, [2]Biochemistry and Biophysics, University of Rochester, Rochester, NY, USA.

The use of ionizing radiation as a modality to treat pediatric skeletal carcinomas is known to inhibit bone growth via damage to growth plate chondrocytes (GPCs). This is in contrast to articular chondrocytes (ACs), which display resistance to radiation damage via unknown molecular mechanisms. The purpose of this study was to identify these protective mechanisms/pathways in ACs and to determine if their activation in GPCs can confer radiation resistance. Since there is significant evidence suggesting that the transcription factor NF-κB acts in response to cell stress by suppressing the apoptotic program, we hypothesized that differential activity of this pathway in ACs and GPCs is responsible for the difference in radiation sensitivity of these cell models. To test this hypothesis, initial experiments were performed to compare the amount of basal NF-κB DNA binding and the amount of basal activation of an NF-κB responsive promoter/luciferase reporter (NF-κB-luc) in cultured chick GPCs and ACs. Supporting our hypothesis, gel shift assays using an NF-κB consensus oligo showed that nuclear extracts from ACs possessed 7-fold higher basal NF-κB DNA binding compared to GPCs. Furthermore, using cells transiently transfected with NF-κB-luc, basal promoter function was found to be 100-fold greater in ACs than in GPCs. Since basal NF-κB DNA binding/activation was found to be greater in ACs than in GPCs, we further tested our hypothesis by measuring the effect of ionizing radiation i) on activation of NF-κB-luc in ACs and GPCs, and ii) on activation of apoptosis in GPCs transiently transfected with p65 or the chicken homolog of NF-κB, c-rel. Suggesting that NF-κB was activated post-irradiation in ACs, a 3-fold stimulation of NF-κB-luc was detected following a 10 gray exposure. Conversely, activation of the reporter in GPCs was unaffected by this dose. Furthermore, the robust 15-fold induction of apoptosis by radiation in GPCs, as measured by caspase 3 activity, was reversed by transient transfection of the cells with either p65 or c-rel. This was compared to ACs which did not show caspase 3 activation following radiation, hypothetically due to their robust endogenous NF-κB activity. Collectively, these findings suggest that NF-κB signaling is a key radiation protective signal in ACs that can confer protection to GPCs in p65 and c-rel over-expressing models. We predict that future prophylactic strategies to avoid radiation-induced damage in the growth plate may involve activation of NF-κB signaling prior to radiation therapy.

M054

Myeloma and Lytic Bone Disease: Interdependence of Tumor Growth and Osteoclast Activity. S. Yaccoby*, F. Zhan*, J. Shaughnessy*, B. Barlogie, J. Epstein*. Myeloma Institute for Research and Therapy, University of Arkansas for Medical Sciences, Little Rock, AR, USA.

Multiple myeloma is an incurable B cell neoplasia characterized by accumulation of monoclonal plasma cells. Myeloma tumor growth is restricted to the bone marrow, except in the most advanced stages of plasma cell leukemia. Myeloma growth is associated with severe osteolytic bone disease. We have established *in vivo* and *ex vivo* systems to study the reciprocal relationship between myeloma-induced osteoclastogenesis and tumor growth. *In vivo*, we have exploited the SCID-hu model, in which primary human myeloma cells grow exclusively in and interact with a human microenvironment (*Blood 92:2908, 1998; Blood 94:3576, 1999*), to demonstrate that in medullary, but not in extramedullary disease, survival and growth of myeloma cells depend on osteoclast activity (*BJH 116:278, 2002*). *Ex vivo,* purified myeloma cell-conditioned media from 12 patients increased migration of osteoclast precursors across a 5 μM pore size membrane 1.6-4.2 fold (p=0.001). In cocultures, myeloma cells increased 1.5-10.5 fold from 76±12 in control assays (p=0.002) the differentiation of osteoclast progenitors into mature, multinucleated, bone-resorbing osteoclasts in a stromal cell-free environment, via a RANKL-mediated mechanism. Mature osteoclasts reciprocated by maintaining the viability and proliferative activity of purified myeloma cells, determined by annexin V flow cytometry, BrdU labeling index, and [^{3}H]TdR incorporation, for as long as 50 days. In contrast, control cells cultured alone died rapidly. Quantitative oligonucleotide microarray analyses interrogating 12,000 genes showed ≥ 2 fold baseline changes in the expression of 95 common genes in myeloma cells recovered from 12 independent co-cultures. Similarly, 24 genes were changed in 10 osteoclast samples. Genes with altered expressions in the myeloma cells include oncogenes, chemokines, growth factors, and adhesion molecules, involved in tumor growth, metastases, osteoclastogenesis, and angiogenesis. Osteoclasts from myeloma patients and healthy donors yielded similar results. On hierarchical clustering with 150 myeloma patients, co-cultured myeloma cells fell into two distinct, medullary and extramedullary disease, clusters. The myeloma cell-osteoclast co-culture system that we have developed provides the opportunity to identify genes essential for myeloma cell survival, growth, and bone manifestations. These myeloma cell-osteoclast interactions and the genes involved could identify targets for novel therapeutic approaches for this devastating disease.

M055

Immunofluorescence Co-localization Suggests a Shift in Complex from RANKL:OPG to RANKL:RANK During Osteosarcoma Tumorigenesis. A. M. Deshpande*[1], P. Bhatia[1], D. G. Ammerman*[1], T. Johnson-Pais*[2], D. M. Anderson*[3], K. K. Unni*[4], P. A. Meyers*[5], R. G. Gorlick*[5], R. J. Leach[6], M. F. Hansen[1]. [1]Center for Molecular Medicine, Univ. Connecticut Health Center, Farmington, CT, USA, [2]Dept. Pediatrics, Univ. Texas Health Science Center, San Antonio, TX, USA, [3]Immunex Corp., Seattle, WA, USA, [4]Dept. Pathology, Mayo Clinic, Rochester, MN, USA, [5]Dept. Pediatrics, Memorial Sloan-Kettering Cancer Center, New York, NY, USA, [6]Dept. Cellular & Structural Biology, Univ. Texas Health Science Center, San Antonio, TX, USA.

Receptor activator of NFkB (RANK) and its associated ligand, RANKL, together with Osteoprotegerin (OPG) have been shown to be critical regulators of the bone remodeling process. OPG binds RANKL in normal resting cells/tissues to inhibit activation of RANK and subsequently its downstream pathways. Published data from cultured osteoblasts has shown that, during normal proliferation, the majority of RANKL is bound to OPG. RANK has also found to be expressed in normal osteoblasts at low, but detectable, levels. Previous studies have suggested that a RANK:RANKL interaction may have a stimulatory effect on osteoblasts. We were interested in determining if the normal pattern of RANKL:OPG interaction was altered during osteosarcoma tumorigenesis. Analysis of 49 primary osteosarcoma tumors and 4 tumor cell lines showed an increased expression of RANK while protein levels of RANKL and OPG remained comparable to those seen in the normal osteoblasts. Analysis of co-localization in the tumors showed an increase in co-localization of RANKL and RANK and a decrease in co-localization of RANKL and OPG consistent with a shift in complex formation from RANKL:OPG to RANKL:RANK. This shift in binding to the RANKL:RANK complex, within the tumor cell, has the potential to stimulate cell growth through an autocrine mechanism and may contribute to tumorigenic growth.

M056

The Roles of Integrin $\alpha_v\beta_3$ and Osteopontin in Tumorigenicity of Human Melanoma Cells. M. A. Chellaiah[1], J. Strauss-Schoenberger*[2], K. A. Hruska[2]. [1]Department of OCBS, University of Maryland, Baltimore, MD, USA, [2]Department of Pediatrics, Washington University, School of Medicine, St Louis, MO, USA.

The M21-L cell line is a melanoma cell lacking expression of α_v and thus the $\alpha_v\beta_3$ integrin. We have used this cell line to define the role of α_v in protein association with the $\alpha_v\beta_3$ integrin. M21 cells were generated by overexpressing α_v cDNA in the M21-L cell line. We have reported that generation of cells lacking the α_v cytoplasmic domain (M21-L α_v1-995) resulted in the loss of $pp^{60c\text{-}src}$ association with the integrin, and failure of OPN activation of $pp^{60c\text{-}src}$ kinase. To further investigate the role of the α_v cytoplasmic domain in the integrin interaction with signaling proteins, three synthetic peptides corresponding to the cytoplasmic domain of α_v were constructed: α_v1- 986 to 994; α_v2-995 to 1003; α_v3-1004-1018. Peptides against the β_3 and β_1 cytoplasmic domains were used as controls. Peptides coupled to thiopropyl-sepharose beads were reacted with cell lysates made from

the various M21 cell lines. Proteins bound to the peptides were analyzed by Western analysis. The β-turn peptide of α_v corresponding to amino acids 995-1003 (α_v2) bound to several signaling and cytoskeletal proteins including: talin, paxillin, FAK, pp$^{60c\text{-}src}$, p130 cas and a few uncharacterized proteins. α_v1 and α_v3 did not exhibit lysate protein binding. Because osteopontin (OPN) expression has been implicated in the metastaic potential of melanoma and other tumors, a cDNA encoding full length human OPN was transfected into M21 cells (M21/HOPN). Lysates of these cells exhibited significant differences in the binding pattern of phosphoproteins with the cytoplasmic domain α_v2 peptide compared to M21 cell lysates. Thus, overexpression of an autocrine ligand of $\alpha_v\beta_3$ affected complex formation with the integrin and the signaling mechanisms activated. We then analyzed the impact of altered signaling on the tumorigenic potential of the M21 cell lines by subcutaneous injection of M21-L, M21, and M21/OPN cells. An increase in tumor size was observed in M21 cells as compared to M21-L and M21/OPN cells. The decrease in tumor growth when M21/OPN were injected indicates that the tumorigenic potential of $\alpha_v\beta_3$ is suppressed by over expression of OPN. The M21/OPN cells exhibited increased proliferation rates, cell adhesion, and motility *in vitro*, contrasting with the tumorigenicity data. We conclude that OPN is a unique ligand for $\alpha_v\beta_3$, and that its integrin activation potential produced differential signaling and diminished tumorgenicity in the nude mouse subcutaneous injection model.

M057

Serum Levels of N-Terminal Propetide of Procollagen Type 1 (P1NP) in Patients with Multiple Myeloma or MGUS. K. Brenner*[1], J. Schuster*[1], A. Keck*[1], N. Hoyle*[2], R. Kyle*[3], H. Ludwig*[1], M. Pecherstorfer[1]. [1]I. Department of Medicine and Medical Oncology, Wilhelminenspital, Vienna, Austria, [2]Roche Diagnostics, Penzberg, Germany, [3]Department of Hematology and Internal Medicine, Mayo Clinic, Rochester, MN, USA.

Aim of the present study: To evaluate whether serum concentrations of P1NP differ between patients with multiple myeloma (MM) and those with monoclonal gammopathy of undetermined significance (MGUS). Patients and methods: 132 patients with newly diagnosed and untreated MM, and 111 patients with MGUS were included in the investigation. 38 individuals of the MGUS collective initially presented with MGUS but transformed into overt MM. 35 MGUS patients had had stable disease for at least two years, and a further 38 MGUS patients for at least 10 years. The median age of the population was 65 years and did not differ between the MM patients and the three groups of MGUS patients. P1NP was measured with an electrochemiluminescence immunoassay (Elecsys P1NP, Roche Diagnostics, Penzberg, Germany). Results: The median P1NP serum concentration was significantly higher in patients with MM (64.2 µg/L) than in patients with MGUS stable for 2 years (44.8 µg/L), stable for 10 years (50.4 µg/L) or in patients with initial MGUS later converting to MM (52.5 µg/L) (p< 0.0001). The three groups of MGUS patients did not differ with regard to P1NP levels. In MGUS patients whose disease converted to MM, the initial P1NP level (MGUS state) was a median 52.54 µg/L and, after disease progression (MM state), was 61.5 µg/L (p= 0.0575). Stratification of MM patients according to skeletal status (radiographic evidence of osteoporosis-like changes, lytic lesions, or normal radiographs) showed no differences in P1NP serum concentrations. P1NP did not correlate with age, ß2-microglobulin, the amount of monoclonal protein or serum creatinine levels. At a cut-off level of 64 µg/L, the sensitivity of P1NP in identifying MM was 50%, the specificity in excluding MGUS was 74%. Conclusions: P1NP serum levels, which are regarded as markers of bone formation, are higher in MM patients than in those with MGUS. The progression of MGUS to MM appears to be accompanied by an increase in PINP levels, which would reflect the enhanced bone turnover in this neoplastic disease. Due to the marked overlap of P1NP levels in patients with MGUS and with MM, this marker cannot be used to differentiate between the two plasma cell dyscrasias.

M058

p38 MAP Kinase Is Required For Bone Metastasis, But Not Locally Aggressive Growth, In A Mouse Model of Metastatic Breast Cancer. C. Suarez Cuervo*[1], K. W. Harris*[1], L. Kallman*[1], K. Väänänen[2], K. Selander*[1]. [1]Medicine, UAB, Birmingham, AL, USA, [2]Anatomy, University of Turku, Turku, Finland.

p38 belongs to the family of mitogen-activated protein kinases (MAPKs). p38 is frequently expressed in breast cancer. It is also abundantly expressed in the highly invasive MDA-MB-231 human breast cancer cells, where its activation was shown to be associated with vitronectin-induced urokinase plasminogen activator (uPA) production. This suggested to us that p38 may be important in bone metastasis. To test this hypothesis, we created MDA-MB-231 clones stably expressing dominant negative p38 (p38/AF clones). Unlike the control clones, the p38/AF clones did not up-regulate uPA when cultured on vitronectin. Basal and cytokine-induced levels of interleukin-6 and interleukin-11 were similar in control and p38/AF clones, as measured by ELISA-assays. We have previously shown that the local growth of the p38/AF clone exceeded that of the control clone in an orthotopic mouse model of breast cancer.To test the bone metastasis capacity of the p38/AF clones, a mouse model of breast cancer bone metastasis was utilized. Mice were inoculated with the p38/AF and control clones and bone metastases were allowed to form for 28 days. Histomorphometric analysis of the metastatic tumor area in the long bones of mice revealed that there were significantly less bone metastases in the mice that were inoculated with the p38/AF expressing cells (2.15 +/- 1.2 mm2, mean +/- sem, n=9, p<0.05), as compared to controls (11.9 +/- 2.9 mm2, n=10). In conclusion, expression of dominant negative p38 stimulated the locally aggressive growth of breast cancer in the orthotopic model. In contrast, p38 function was required for bone metastasis. Decreased bone metastasis was not mediated by a decrease in IL-6 or IL-11 production in the p38/AF clone, but may be related to decreased uPA production of these cells in the bone microenvironment.

M059

Opposing Effects of Osteoprotegerin on Bone Metastases: Activation of TGFβ Signaling in Breast Cancer Cells versus Inhibition of Osteolysis. S. M. Kakonen[1], T. Oba[2], B. G. Grubbs*[1], X. Sun[2], R. Sypniewska*[1], S. Burns*[2], T. A. Guise[1], J. M. Chirgwin[2]. [1]Molec Med, Univ Tx Hlth Sci Ctr, San Antonio, TX, USA, [2]Molec Med, Univ Tx Hlth Sci Ctr and VA Research Service, San Antonio, TX, USA.

Osteoprotegerin (Opg) is a secreted member of the TNF receptor gene family. It inhibits bone resorption by neutralizing RANK ligand but also protects tumor cells from apoptosis by neutralizing TRAIL. Previously we expressed full-length mouse Opg in the RANK ligand-negative MDA-MB-231 human breast cancer line, which causes osteolytic metastases, and tested 3 stable clones in an animal model. Clones expressing 24 or 60ng/ml Opg/10^5 cells/48h conferred a 25% survival advantage, compared to nude mice receiving cells expressing 0 or 150ng/ml Opg, by intracardiac inoculation. Opg was secreted by the cells throughout the animal experiment and effectively inhibited osteoclast formation since bone sections adjacent to Opg+ tumors showed significantly decreased [~4X] osteoclast number per mm of tumor-bone interface. Although Opg expression did not affect the growth rate of MDA-MB-231 cells in vitro, the majority of mice inoculated into the mammary fat pad with Opg+ cells (2x10^6) failed to develop tumors, compared to mice receiving empty vector (EV) control cells. The weak effects of Opg to decrease osteolytic metastases and the puzzling effects on growth in the mammary fat pad suggested that Opg may have autocrine regulatory effects on the tumor cells. We tested the effects of TGFβ on Opg+ clones since this factor plays a central role in the regulation of osteolytic metastases. Opg-expressing cell lines, but not controls, were growth inhibited 50% by TGFβ1. Conditioned media were assayed for concentrations of osteolytic factors. PTHrP was increased 3-5 fold both basally and in response to TGFβ in the 3 Opg+ clones compared to EV (p<0.001). The Opg+ clones showed significantly increased TGFβ induction of interleukin (IL)-11 (15-19X; p<0.001), while induction in EV controls was 4X. Compared to EV cells, the Opg+ clones basally secreted 5-10X more vascular endothelial growth factor, and up to 25ng/ml in response to TGFβ. In EV cells IL-6 was <30pg/ml and unresponsive to TGFβ. Basal and TGFβ-induced IL-6 (1.3-2.4X; p<0.01) were substantially increased in the Opg+ clones, reaching 200pg/ml. In summary, osteoprotegerin could promote breast cancer metastases to bone by sensitizing tumor cells to TGFβ, while at the same time opposing bone metastases by inhibiting RANK ligand-stimulated osteolysis. Enhancement by Opg of TGFβ signaling in breast cancer cells suggests that tumor cells may express an unknown receptor for Opg.

M060

Breast Cancer Cell Lines Selected from Bone Metastases Have Greater Metastatic Capacity and Express Increased Vascular Endothelial Growth Factor (VEGF), Interleukin-11 (IL-11), and Parathyroid Hormone-related Protein (PTHrP). S. M. Kakonen[1], Y. Kang*[2], M. R. Carreon*[1], M. Niewolna*[1], R. S. Kakonen*[3], J. M. Chirgwin[1], J. Massague*[2], T. A. Guise[1]. [1]Molec Med, Univ TX Hlth Sci Ctr, San Antonio, TX, USA, [2]Memorial Sloan-Kettering, New York, NY, USA, [3]IDD/CTRC, San Antonio, TX, USA.

Breast cancer frequently metastasizes to bone. Since PTHrP-neutralizing antibodies decrease but do not eliminate bone metastases it is likely that factors in addition to PTHrP contribute to the osteolysis. Possible factors include IL-11 and VEGF, since these stimulate osteoclastic bone resorption and, like PTHrP, their expression in MDA-MB-231 breast cancer cells is increased by TGFβ. We established multiple cell lines that have increased potential to metastasize to bone in a mouse model. We started with a variant of the MDA-MB-231 breast cancer line which had low capacity to cause bone metastases; only 1 of 10 nude mice inoculated into the left cardiac ventricle developed bone metastases over 12 weeks. We harvested bone metastases, established cell lines in culture and repassaged them by inoculation into the left cardiac ventricle of nude mice. We established cell lines from first, second and third passage bone metastases: 7 cell lines were identified which caused more bone metastases sooner than did the parental MDA-MB-231. The capacity of the cell lines to cause increased bone metastases was not due to an increased proliferation since growth at the mammary fat pad was not greater than that caused by parental MDA-MB-231. The production of osteolytic factors PTHrP, IL-11, and VEGF by the cell lines was determined in 48-hour conditioned media ±TGFβ by immunoassay. Basal PTHrP production was significantly increased in a majority of bone metastasis cell lines. The parental MDA-231 cells did not produce IL-11, but the cell lines extracted from bone metastases produced 40-240pg/ml/10^5 cells of IL-11. The lines also produced 2-4-fold more VEGF. TGFβ-induced PTHrP, IL-11 and VEGF were also higher in bone metastases cell lines, but the ratio TGFβ-induced to basal was similar to parental cells. In summary, cell lines extracted from bone metastases express higher levels of TGFβ-responsive osteolytic factors, IL-11, VEGF, and PTHrP, compared to the low-metastatic parental MDA-MB-231. Although the responsiveness to TGFβ is unchanged, the increased expression of these factors suggest that VEGF and IL-11, in addition to PTHrP, stimulate osteolytic bone metastases. TGFβ released as a consequence of bone resorption plays a central role in breast cancer metastases to bone. The data suggest that formation of metastases may involve selection in bone of tumor cells that have increased expression of TGFβ-responsive osteolytic genes.

M061

Three-dimensional Analysis of Trabecular Bone using Synchrotron Radiation Micro-CT in Bone Metastasis from Prostate Cancer. T. Sone[1], T. Tamada*[2], M. Fukunaga[1]. [1]Nuclear Medicine, Kawasaki Medical School, Kurashiki, Japan, [2]Radiology, Kawasaki Medical School, Kurashiki, Japan.

Prostate cancer frequently metastasizes to bone inducing osteosclerotic lesions. However, morphological details of bone metastasis of prostate cancer have not been clarified. The objective of this experiment was to investigate trabecular bone structure and degree of calcification in bone metastasis from prostate cancer using Synchrotron Radiation microcomputed tomography. Small cubes of lumbar vertebrae were excised post mortem, from the sites of metastasis, degenerative osteosclerosis, and the comparative sites of control subjects without skeletal lesion. Three dimensional imaging was performed by taking two dimensional radiographs as the specimens were rotated through 180' in 0.5' increments. The energy was set to 20KeV. The radiographs were reconstructed one slice at a time using a standard Fourier-filtered back projection algorithm. Each reconstructed slice was then stacked, providing data for 750^3 3D images with an isometric voxel size of 6 microns. The 3D images were segmented into bone and marrow fractions, and purified using a cluster labeling algorithm. The trabecular bone was then analyzed for mineral density and morphological parameters. Trabecular bone in metastatic lesions showed highly connected and isotropic network pattern compared with the control cancellous bone. Although the trabecular surface was markedly irregular, the mean trabecular thickness was similar to the control trabeculae. The mineral density of trabeculae in metastatic lesions ranged broader and its mean value was lower than the control. In contrast, trabecular bone in the degenerative sclerotic lesions showed the similar degree of anisotropy and connectivity compared with the control, whereas the trabecular thickness was increased. The mean mineral density shifted toward the higher value concomitantly with an increase of the lowest level of mineral density. The variations of these parameters would make it possible to distinguish significant characteristics, which are useful for understanding the pathophysiology of sclerotic metastasis of bone metastasis.

M062

Parathyroid Hormone Related Protein Neutralization Enhances All-transretonic Acid Induced Apoptosis in Prostate Cancer Cells. F. Asadi*[1], W. Zheng*[1], T. Rosol[2], S. C. Kukreja[1]. [1]Medicine, VA West Side Medical Center, Chicago, IL, USA, [2]Veterinary Pathobiology, Ohio State, Columbus, OH, USA.

In the advanced stages of prostate cancer, the tumor cells become androgen-unresponsive and resist apoptosis. The factors responsible for the increased cell survival in the androgen-resistant state are not known. We have previously demonstrated that PTHrp level is higher in androgen-unresponsive prostate cancer cells (C4-2 LnCaP) as compared to that in androgen-responsive prostate parent LnCaP cell line. In addition we demonstrated that treatment of these cells with PTHrP (1-34) prevented All-trans retinoic acid (tRA)-induced cell death and therefore it is possible that PTHrP contributes, at least partially, to the increased cell survival in the androgen-unresponsive cells. In the present studies, we examined the effects of PTHrP (1-36) neutralization on tRA-induced apoptosis and cell survival in three prostate cancer cell lines. The three cells lines we examined were: 1) androgen-responsive LnCaP-parent, 2) androgen-unresponsive subline C4-2 and 3) androgen- unresponsive and bone metastatic subline C4-2b. Cell survival was assessed by trypan blue exclusion and MTS proliferation assays. Cell apoptosis was examined by TUNEL assay. Baseline cell apoptosis was greater in the LnCaP cells as compared to that in the other two cell lines. Treatment with tRA 5uM resulted in a decrease in cell survival and an increase in apoptosis in all three cell lines. As previously demonstrated PTHrP (1-34) treatment protected against this tRA-induced apoptosis. Addition of PTHrP 1-36 antibodies resulted in a decrease in cell survival under basal conditions. Addition of PTHrP antibodies to the tRA-treated cells further reduced cell survival and increased apoptosis in all three cell lines.

Percent Apoptotic Cells

	LnCaP	C4-2	C4-2b
FBS	13	2	3
tRA+Cont Ab	63	61	57
tRA+PTHrP Ab	88	76	81

FBS=Fetal Bovine Serum; Cont=Control; Ab=antibody

The studies demonstrate that endogenous PTHrP plays a role in increasing cell survival and inhibition of apoptosis and may be one of the factors involved in increased cell survival in androgen-resistant prostate cancer cells.

M063

Radial Shaft Bone Density and Risk of Breast Cancer in White and African-American Women. D. A. Nelson[1], L. Darga*[1], R. K. Severson*[2]. [1]Internal Medicine, Wayne State University, Detroit, MI, USA, [2]Epidemiology, Karmanos Cancer Institute, Detroit, MI, USA.

We measured forearm bone mineral density (BMD) in 220 newly diagnosed breast cancer cases and 196 controls, ages 39-84 (mean = 56.3 + 10.8 years), 50.3% of whom were white and 49.7% African-American. BMD was measured by Norland pDEXA in the distal radius and the radial shaft. Z-scores (age, sex, and ethnicity specific) were calculated using the manufacturer's reference data. There was a significant difference in the radial shaft z-scores for breast cancer cases versus controls (0.45 +1.07 s.d. vs 0.19 + 1.08 s.d., p =0.015), but no significant group difference in the distal forearm (p=0.83). There were no significant ethnic differences in mean z-scores within the cases or controls. We investigated whether having above average radial shaft BMD (z-score > 0) was a significant predictor of breast cancer risk. Using logistic regression analysis with the z-score dichotomized as <=0 or >0, we found that the odds ratio for breast cancer is 1.98 for z-scores >0 (95% C.I. 1.32-2.97). We also evaluated the radial shaft z-score as a continuous variable in a logistic regression model, and the odds ratio for breast cancer associated with a one s.d. increase was 1.25 (95% C.I. 1.04-1.51). We also assessed the potential effect modification and confounding effects of menopause status, age group, body mass index, ever/never use of HRT, and duration of HRT. There were no significant interactions and no appreciable confounding effects of these variables on the relationship between BMD and breast cancer risk. We conclude that an above average radial shaft z-score is a significant risk for breast cancer in white and African-American women. The pDEXA method of BMD measurement is inexpensive, noninvasive, and portable, and can therefore be readily utilized in a clinical setting, with other risk factors, to evaluate breast cancer risk .

M064

Dihydrotestosterone (DHT) Induces Osteoprotegerin (OPG) Gene Expression in an Androgen Responsive Prostate Cancer Cell Line LNCaP. J. Zhang[1], Y. Lu*[2], X. Cao*[3], J. Dai[1], Z. Yao*[2], E. T. Keller[1]. [1]Pathology/ULAM, University of Michigan, Ann Arbor, MI, USA, [2]Department of Immunology, Tianjin Medical University, Tianjin, China, [3]Department of Pathology, University of Alabama at Birmingham, Birmingham, AL, USA.

Prostate cancers (CaP) are initially androgen dependent tumors that become androgen independent and metastasize to bone forming a mixture of osteoblastic and osteolytic lesions. CaP promotes the osteolytic component of metastases through receptor activator of NFkB ligand (RANKL). OPG is a soluble decoy receptor that inhibits RANKL activity. Accordingly, the goal of this study was to determine the regulation of OPG by androgens. We quantified OPG protein levels in cell culture supernatants using ELISA and OPG mRNA levels in cells using real time PCR of several CaP cell lines. The CaP cell lines included LNCaP (an androgen responsive cell line), C4-2B (an androgen non-responsive cell line derived from LNCaP cells), and PC-3 (an androgen non-responsive cell line). Both OPG protein and mRNA levels were greatest in PC-3, followed by C4-2B and least in LNCaP. Treatment of the LNCaP cells with DHT (0.1, 1, 10 and 100 nM) increased OPG protein and mRNA expression at 24 hours; whereas it had no effect in PC-3 and C4-2B cells. To determine if DHT increased OPG mRNA levels through induction of gene transcription, we transiently transfected LNCaP cells with the human OPG promoter (1.1 kb upstream of the 5' transcription initiation site) driving luciferase. DHT induced the promoter activity in a dose dependent manner (by 8 fold). To determine the cis-acting region on the OPG promoter through which DHT mediates its effect, we transiently transfected LNCaP cells with progressively-deleted OPG promoter-luciferase reporter constructs. Responsiveness to DHT was present with deletion of the promoter to -700; however, deletion of the fragment from -700 to -564 resulted in loss of all promoter activity. Taken together, these data demonstrate that DHT regulates OPG at the transcriptional levels. They also suggest that OPG expression is upregulated as CaP progresses and OPG may play an important role in pathophysiology of skeletal metastasis of CaP.

M065

Extract from *Scutellaria baicalensis* Georgi (Huang Qin) Induces Prostate Cancer Cell Apoptosis and Diminishes the Tumor Growth in Murine Bone. Y. Lu*[1], Z. Yao*[1], Z. Zheng*[2], E. T. Keller[3], J. Dai[3], J. Zhang[3]. [1]Department of Immunology, Tianjin Medical University, Tianjin, China, [2]Department of Medicine, University of California-Irvine, Irvine, CA, USA, [3]Pathology/ULAM, University of Michigan, Ann Arbor, MI, USA.

Prostate cancer (CaP) frequently metastasizes to bone forming predominantly osteoblastic lesions with underlined osteolytic components. Because current therapies are generally ineffective in CaP skeletal metastases, patients seek alternative medicines such as herbal medicines, which have been used for many centuries in Asian countries. The purpose of this study was to identify Chinese herbal medicines that may be effective in CaP skeletal metastasis. We first screened 130 Chinese herbs (ethanol extracts) for anti-proliferation effects by non-radioactive cell proliferation assay in LNCaP and C4-2B CaP cells. (C4-2B cells, which form skeletal metastases, are derived from non-metastatic LNCaP cells). We found five extracts with anti-proliferation activity including extract from *Scutellaria baicalensis* Georgi (Huang Qin, HQ), which had the strongest effect. We next evaluated HQ's ability to induce apoptosis of LNCaP and C4-2B cells. HQ, in a dose-dependent manner, induced apoptosis of both cell lines based on DNA fragmentation and TUNEL assay. In addition, HQ induced apotosis-related gene caspase-3 and suppressed bcl-2 expressions in both cell lines. Therefore, we tested if HQ (1mg per mouse three times a week for 8 weeks intraperitoneally) could diminish establishment of skeletal metastases in mice. We injected C4-2B cells into tibia of SCID mice. The animals were randomized into two groups to receive either HQ or vehicle only (n=8/group). At 8 weeks post-tumor injection, mice were sacrificed and tumor establishment in the skeleton was determined using radiography, dual energy x-ray absorptiometry and histology. Radiographic and histological lesions were present in 7/8 vehicle-treated mice and in 6/8 HQ-treated mice. However, the radiographically- and histologically-determined areas of the tumors in the HQ-treated mice were approximately 47% that of the vehicle-treated animals. We conclude that HQ has efficacy for inducing CaP cells apoptosis in vitro and has the ability to diminish growth of CaP in murine bone.

M066

Expression of RANK and RANKL Is Altered in Invasive Carcinoma and Bone Metastasis of Breast Cancer. P. Bhatia[1], M. Sanders*[2], M. F. Hansen*[1]. [1]Molecular Medicine, University of Connecticut Health Center, Farmington, CT, USA, [2]Pathology, University of Connecticut Health Center, Farmington, CT, USA.

Bone is the most common site of metastases by human breast cancer. Most breast cancers form osteolytic metastases, in contrast to tumors such as prostate cancer that form osteosclerotic metastases. Although some evidence suggests that formation of bone metastases by breast cancer cells is mediated by the increased osteoclastogenesis at the target site, a clear controversy exists whether formation of bone metastases is mediated by breast cancer cells directly or by stimulated osteoclasts. To test this we examined the expression of RANK and RANKL, two proteins critical to the bone remodeling signaling pathway, in invasive carcinoma of breast and bone metastases of breast. We observed increased expression of RANK and RANKL in the tumor cells from both the primary and metastatic lesions. Further, in the osteolytic metastases, breast tumor cells were seen directly in contact with the bone in the regions of osteolysis, without any osteoclasts in the vicinity. We suggest that overexpression of RANK and RANKL in breast cancer cells provides a growth advantage to the breast tumor cells, and the tumor cells appear to be directly responsible for the degradation of bone.

M067

Prevalence of Osteopenia and Osteoporosis by Central and Peripheral Bone Mineral Density in Men with Prostate Cancer during Androgen-Deprivation Therapy. J. M. Bruder, M. D. Welch*. Med/Endocrine, UTHSCSA, San Antonio, TX, USA.

Studies have shown that men with prostate cancer treated with androgen-deprivation therapy (ADT) have a lower bone mineral density (BMD) than age-matched controls. We and others have recently demonstrated a significant decrease in BMD after the first year of ADT. The loss of bone density, in some studies, was most pronounced in the radius. We wish to determine the prevalence of osteopenia and osteoporosis by central (spine and hip) and peripheral (radius) BMD in this group of men. We reviewed the charts of patients with prostate cancer seen in the Urology Tumor Clinic from 5/2001-9/2001 and identified 125 patients receiving ADT. Spine and hip BMD results were recorded in 89 patients. Fifty-four patients also had a BMD of the radius. In addition, 33 patients had serum concentrations of 25-hydroxyvitamin D (25-OHD), intact parathyroid hormone (iPTH), and 24-hour urine calcium and N-telopeptide (N-Tx) concentrations measured. The average age of the patients was 77 $\pm$ 7. The race included: 30.3% Hispanic, 58.4% Caucasian, and 9% African-American and 2.2% unknown. Twenty-four out of 89 patients with BMD determinations (26.9%) had osteoporosis of the hip or spine as determined by a T-score of <-2.5. Forty-five patients (50.6%) were designated as osteopenic (T score between -1.0 to -2.5) and 20 patients (22.5 %) were classified as normal. Forty-five of the 54 patients (83.3%) who also had a BMD of the radius measured were categorized as either osteopenia or osteoporosis. The results of the BMD of the radius changed the category of diagnosis (either from normal to osteopenia or osteopenia to osteoporosis) in 22 patients (40.7%). Furthermore, approximately half of the patients with the diagnosis of osteoporosis or osteopenia had an evaluation for secondary causes of osteoporosis. Three (8.8%) patients were classified as Vitamin D deficient with an absolute 25-OHD concentration less than or equal to 15 ng/ml. Fifteen patients (44.1%) had absolute 25-OHD concentration between 16 and 30 ng/ml and were considered insufficient in vitamin D. An elevated iPTH (>50 pg/ml) concentration was found in 11 patients (31.4%). In addition, urinary concentrations of N-Tx were elevated (>38) in 73.3%. The increase was most prevalent and pronounced in patients with osteoporosis (81.3%) compared to patients with osteopenia (64.3%). Men with prostate cancer treated with ADT show a high prevalence of osteopenia and osteoporosis by peripheral and central BMD measurements. The use of peripheral BMD appears to identify more patients with osteoporosis. This data suggest that the BMD of the radius should be obtained in men with prostate cancer receiving ADT in the evaluation of osteoporosis.

M068

The Involvement of LMP-1 in Prostate Cancer Metastasis to Bone. G. A. Hair*[1], L. Titus[2], S. D. Boden[1]. [1]Orthopaedics, Emory University, Atlanta, GA, USA, [2]Research, VA Medical Center, Decatur, GA, USA.

Bone metastases are a common complication in prostate cancer patients and can lead to extensive morbidity and increased mortality. Osteoblastic lesions are a common skeletal manifestation of neoplasia. Both Bone Morphogenetic Protein (BMP)-6 and -7 are involved in membranous bone formation. Their presence has been demonstrated in osteoblastic lesions associated with prostate cancer metastases. In osteoblast (OB) cultures, BMP-6 activity is mediated by several factors, including induction of the intracellular osteoinductive LIM Mineralization Protein-1 (LMP-1) and expression of BMP-7. LMP-1 overexpression is sufficient to induce OB differentiation in culture as well as bone formation in vivo. LMP-1 activity is mediated by the apparent induction of BMP-7 and –4. The goal of these studies was to correlate the effects of LMP-1 with those of BMP-6 and -7 in OB culture as a model for osteoblastic lesions occurring during prostate cancer metastasis to bone. Prostate cancer cells (LNCaP) were grown, and conditioned media (CM) harvested (Day 4 post-confluence) and examined for BMP-6 and –7 expression. Antisense oligodeoxynucleotides (AS-ODN) to BMP-6, BMP-7 or LMP-1 were added (Day 1 post-confluence; 4.0 μM) to inhibit expression of these proteins in LNCaP cells. CMs from untreated and AS-ODN-treated LNCaP cells were applied to multipotent C2C12 cultures to determine their ability to induce an OB phenotype (determined by changes in cell morphology and alkaline phosphatase expression). Here, we confirm that prostate cancer cells (LNCaP) appear to secrete both BMP-6 and –7. The AS-ODN inhibition of either BMP-6 or BMP-7 translation in LNCaP cultures inhibits the production of an osteoinductive CM. Constitutively high expression of the intracellular osteogenic protein LMP-1 is found in LNCaP cells. Furthermore, AS-ODN inhibition of LMP-1 in LNCaP cells inhibits production of an osteoinductive CM. Excess BMP-6 (100 ng/mL;Day 1) added to LNCaP cells cannot overcome LMP-1 AS-ODN inhibition and concomitant loss of osteoinductive activity of the CM whereas this inhibition can be overcome by the addition of suboptimal doses (50 ng/mL) of BMP-7. These data suggest a central role of LMP-1 not only in the differentiation of OBs in normal bone formation but also in producing osteogenic lesions in prostate cancer metastases to bone. These data also suggest a possible sequential relationship between the expression of BMP-6, LMP-1 and BMP-7. Understanding the relationship between BMP-6, BMP-7 and LMP-1 in prostate tumor-induced osteogenesis would have significant relevance in the clinical assessment and treatment of osteogenic lesions formed during prostate cancer metastases to bone.

Disclosures: ***GA. Hair****, Sofamor Danek 7.*

M069

The Proteasome Inhibitor PS-341 Inhibits the Growth of Metastatic Human Prostate Cancer in Bone. P. G. Whang*, R. C. Iglesias*, J. J. Gates*, J. R. Lieberman. Orthopaedic Surgery, UCLA School of Medicine, Los Angeles, CA, USA.

Proteasome inhibitors have been shown to suppress tumor growth by interfering with the NF-κB-mediated degradation of cell cycle regulatory proteins. The purpose of this study is to determine whether the proteasome inhibitor PS-341 inhibits the growth of human prostate cancer cells in a bone metastasis model. Suspensions consisting of $1x10^5$ human prostate cancer cells (PC-3) were injected into the left tibias of SCID mice. PS-341 (1.0 mg/kg) was administered i.v. twice a week according to the following protocols: Pretreatment (1 week of treatment before tibial injection until 4 weeks after); Treatment (4 weeks of treatment); Established Disease (4 weeks of treatment starting 4 weeks after tibial injection); Controls (4 weeks of saline injections). $1x10^6$ PC-3 cells were also injected subcutaneously into the left flanks of SCID mice in order to determine if there is a difference in the efficacy of PS-341 for the prevention of tumor formation in subcutaneous tissue versus bone. PS-341 (1.0 mg/kg) was administered i.v. twice a week as follows: S.C. Treatment (4 weeks of treatment); S.C. Established Disease (4 weeks of treatment once tumors became palpable). Tumor volume was recorded weekly until the time of sacrifice. All animals were euthanized at 8 weeks, at which time radiographs were obtained and both hindlimbs were harvested for histology. Radiographs of the control group demonstrated lytic lesions in bone, and histologic analysis revealed extensive cortical destruction and substantial tumor burden. According to a grading scale based upon the extent of cortical disruption (0 – normal, 1 – scalloping, 2 – 1 cortex disrupted, 3 – 2 cortices disrupted, 4 – complete destruction of the proximal tibia), all the treatment groups showed moderate improvement in the radiographic appearance of PC-3 lesions (Controls – 3.9, Pretreatment – 1.5, Treatment – 1.7, Established Disease – 1.9) with relative preservation of the proximal tibia. However, cortical disruption and tumor burden continued to be present on histologic sections. Administration of PS-341 prevented the formation of subcutaneous PC-3 tumors and decreased the volume of palpable subcutaneous tumors by 49.4%.These findings suggest that PS-341 may inhibit the growth of PC-3 tumors in bone but does not completely eradicate these cells. However, PS-341 does prevent the formation of subcutaneous PC-3 tumors. The attenuated antineoplastic effects of PS-341 against PC-3 tumors in bone may be a result of decreased vascularity and drug bioavailability compared to subcutaneous tissue. Further study is necessary to determine whether PS-341 may be a useful adjunct for the treatment of prostate cancer metastatic to bone.

M070

Mechanisms of Anabolic Action of LNCaP Prostate Cancer Cells on Bone. R. S. Bhattacharyya*, P. H. Stern. Molecular Pharmacology and Biological Chemistry, Northwestern University, Chicago, IL, USA.

Bone metastases are a predominant consequence of late stage prostate cancer. These skeletal metastases tend to be osteoblastic and can promote irregular new bone formation. It has been hypothesized that a soluble factor(s), produced by the prostate cancer cells, is responsible for eliciting this anabolic effect on bone. Our studies have focused on the characterization of prostate cancer cell conditioned media (CM) responses on bone. We have utilized three different bone models, neonatal mouse calvarial bone tissue, MC3T3-E1 osteoblastic cells, and primary osteoblasts isolated from mouse calvaria. The cells or bone tissue were cultured for 24-72 hours and labeled during the final 2 hours of the culture period with ^{3}H-thymidine and ^{14}C-proline to assess cell proliferation and protein/collagen synthesis, respectively. Previous studies from our laboratory have demonstrated that diluted conditioned media (1/18X) from the LNCaP prostate cancer cells generate anabolic responses on ^{3}H-thymidine incorporation with smaller effects on ^{14}C-proline incorporation. The LNCaP CM treatments also produce stimulatory effects on both MC3T3-E1 cells and primary osteoblast cells, increasing both ^{3}H-thymidine and ^{14}C-proline incorporation to a greater extent than observed in the calvaria. In addition to the increase in osteoblast cell proliferation, in both calvarial bone tissue and MC3T3-E1 cells, LNCaP CM treatment elicits a stimulation of the MAP kinase pathway and an increase in the level of phosphorylated p42/44 MAP kinase protein expression. Inhibition of the MAP kinase pathway with the MEK inhibitor, PD98059, also decreases the LNCaP CM stimulated anabolic responses. The MAP kinase pathway has been shown to be involved in multiple proliferative pathways and growth factor responses. One of the many growth factors with proliferative effects on bone is insulin-like growth factor-I (IGF-I). IGF-I treatment stimulates both ^{3}H-thymidine and ^{14}C-proline incorporation in calvarial bone tissue and MC3T3-E1 osteoblastic cells. A neutralizing antibody to the IGF-I receptor blocked the stimulatory effects of LNCaP CM treatment on ^{3}H-thymidine and ^{14}C-proline incorporation in the MC3T3-E1 osteoblastic cells. These results suggest that the MAP kinase pathway and IGF-I may play a role in the effects of LNCaP prostate cancer cell CM on bone.

M071

Musculoskeletal Interactions In Obese, Hyperinsulinemic, Euglycemic Patients. M. R. Ulla[1], J. A. Sánchez*[1], M. Stivala*[2], F. Ghiglione*[2], R. Noriega*[1], G. Cointry*[2], J. L. Ferretti[2]. [1]CEOM, Córdoba, Argentina, [2]CEMFoC, Natl. Univ. of Rosario, Rosario, Argentina.

The aim of this study was to determine whether the metabolic disturbance caused by obesity-related, euglycemic hyperinsulinemia impairs the anthropometric and biomechanical relationships between bones and muscles as determined by the bone mechanostat. We have analyzed the relationships between the DEXA-assessed, whole-body BMC and lean and fat masses (LM, FM) in 30 men and 110 pre- and post-MP women with euglycemic hyperinsulinemia classified according to their fasting plasma insulin (FPI) levels, lower (i) or higher (I) than 15 uUI/ml; body-mass index values, lower (b) or higher (B) than 30, and Insulin Secretion Index (ISI; *Matsuda & DeFronzo 1999*) values, lower (s) or higher (S) than 2.8. The FPI correlated positively with LM and FM but not with BMC. Correlations between BMC and LM were parallel to those found in 300 normal age-matched controls for each group but showed lower intercepts for groups I, B, and S than i, b, and s. After adjusting logarithmically the BMC to a common, 18-kg FM value in order to compensate for the fat interaction with BMC determination, the groups I, B, and S showed significantly lesser intercepts than controls. Those differences were generally more significant for pre-MP women than for post-MP women or men. In these obese patients with fasting euglycemia, relative hyperinsulinemia may have increased FM. Assuming that LM reflects muscle mass, they would have also lowered the BMC/muscle proportion, perhaps reducing the mechanical influence of muscles on the skeleton. This could evidence the induction of a shift in the bone mechanostat setpoint (a typical, ~0.2% bone tissue strain under the maximal customary loads) to a higher level. In addition, the apparent estrogen dependence of the observed differences is congruent with the hypothesis that estrogens interact positively with that homeostatic system.

M072

pQCT Is a Precise and Accurate Tool for Skeletal Analysis of Mice In vivo. M. Priemel[1], C. Schmidt*[2], T. Kohler*[3], J. M. Rueger[1], R. Mueller[3], M. Amling[1], F. Eckstein[2]. [1]Trauma Surgery, Hamburg University School of Medicine, Hamburg, Germany, [2]Anatomy, Munich University, Munich, Germany, [3]Biomedical Engineering, Zurich University, Zurich, Switzerland.

Skeletal research relies extensively on animal models with particular focus on transgenic mice. The standard in characterization of a bone phenotype is histomorphometrical analysis of the skeleton. Micro CT provides additional three-dimensional structural information, but currently cannot be employed in living animals. In contrast peripheral quantitative computed tomography (pQCT) can be applied in anesthesized animals to follow bone changes longitudinally. However, its precision and accuracy in mouse bones has so far not been thoroughly studied. Therefore the specific aim of the current study was to determine the precision (reproducibility) and validity of pQCT in the tibia, femur, and lumbar spine of mice. We examined 27 animals (13 wildtype CL57BL6 mice and 14 leptin-deficient mice with a high trabecular bone volume fraction) at 6 months of age. Axial pQCT images of the tibia, femur and lumbar spine were acquired with a pQCT-M (Stratec, Germany) in quadruplicate. The same bones were subsequently analyzed by µCT imaging at a resolution of less than 10 µm and by histomorphometry after undecalcified embedding. The reproducibility of pQCT was best when analyzing 3 consecutive sections, the precision errors for BMC, area, and density being < 5% in the tibial metaphysis and spine, and < 2% in the femoral metaphysis. Precision errors were smaller at the shaft. The correlation between pQCT (trabecular density) and histomorphometry (BV/TV) was r = 0.89 at all three sites, when choosing small, central regions of interest. The correlation between pQCT and µCT (BV/TV) at the femur was r = 0.97 and that between histomorphometry and µCT r = 0.91. At the shaft, r was > 0.94 for total area, and cortical BMC between pQCT and µCT. Based on these data we conclude that pQCT is an excellent tool for analyzing the density of mouse bones in vivo, its distinct advantage being that living animals can be studied longitudinally.

M073

Precision of Orthopedic Scans Using the GE Lunar Prodigy. C. Simonelli[1], J. J. Monk*[1], H. S. Barden[2], K. G. Faulkner[2]. [1]HealthEast Clinics, Woodbury, MN, USA, [2]GE Medical Systems Lunar, Madison, WI, USA.

We evaluated the precision of bone mineral density (BMD) measurements from orthopedic scans using the Lunar Prodigy. Low precision error is important for measuring changes in periprosthetic bone density with confidence. Total hip replacement, a popular procedure for treating patients with hips damaged by disease or injury, alters the normal stresses applied to weight-bearing bone of the proximal femur. Subsequent redistribution of bone through remodeling, coupled with cell damage caused by wear debris shed from the implant, often results in substantial bone loss surrounding the implant and implant loosening. Both outcomes have a negative impact on prosthesis longevity and can cause difficulties for revision surgery. Dual-energy x-ray absorptiometry (DXA) precisely quantifies bone mineral density (BMD) adjacent to femoral prostheses *in vivo*, and is useful for measuring bone remodeling changes and bone loss longitudinally. Twenty-five subjects with total hip implants were studied. Orthopedic scans were performed twice with interim repositioning with the Lunar Prodigy, a narrow-angle, fan-beam densitometer (GE Medical Systems). Orthopedic analysis software positioned regions-of-interest at the seven Gruen zones around the implant to assess periprosthetic bone loss. Precision of Gruen zone BMD (Table 1) was calculated as the root mean square standard deviation.

Table 1. Precision of Gruen zone BMD measurements

Gruen Zone	Mean BMD (g/cm^2)	SD	%CV
1	1.24	0.03	2.7
2	2.11	0.03	1.6
3	2.21	0.03	1.5
4	2.08	0.03	1.3
5	2.12	0.04	1.7
6	1.83	0.04	2.0
7	1.22	0.04	3.2

Precision of 1% to 3% at all Gruen zones with the Lunar Prodigy was as good as or better than precision of 2% to 5% shown previously with pencil-beam systems [1,2]. Precision errors were considerably less than the BMD loss of 11% to 21% typically seen during the first six months following implantation [1], allowing rapid detection of bone loss in this at-risk population.

1. *J. Arthroplasty* 1996;11:184-193.
2. *Clin Orthop. Res.* 1998; 352:66-74.

Disclosures: ***C. Simonelli****, GE Medical Systems Lunar 2.*

M074

Comparison of Spine BMD Measurements from DXA With and Without Elevated Legs. C. Simonelli, J. J. Monk*. HealthEast Clinics, Woodbury, MN, USA.

Current procedure for measuring lumbar spine bone mineral density (BMD) using DXA requires the legs to be elevated. This position flattens the lower spine, with the intent of yielding more accurate and precise BMD values. In this study we wished to determine if elevating the legs has a significant impact on spine BMD accuracy and precision. Twenty subjects were scanned six times at the lumbar spine using the Lunar Prodigy (GE Medical Systems, Madison WI). Three scans were done using standard positioning, with the legs elevated by the spine block positioner supplied by the manufacturer. The other three scans were done without the spine positioner, with the legs flat on the scan table and feet secured with the dual femur positioner. Subjects were repositioned between scans. Spine BMD (L1-L4) was determined using the manufacturer recommended analysis procedure. L1-L4 BMD was compared using ANOVA to determine the potential influence of leg position. The root mean square precision error (%CV) was determined for the BMD values obtained in each position. There were no appreciable visual differences between the scans performed with the legs up or down. Disc spaces and vertebral bodies appeared identical, despite the positioning difference. There was a small, but statistically significant, difference of 1.1% in spine BMD (L1-L4) between positioner and no positioner values ($p < 0.001$). In 16 cases out of 20, the BMD was higher without the legs elevated. Precision was excellent in both positions, with CV of 0.96% with the positioner in place and 0.92% without positioner.

Table 1. Spine BMD and Precision for Subjects With and Without the Spine Positioner

	Mean L1-L4 BMD (g/cm^2)	SD (g/cm^2)	Precision %CV
Legs Elevated	1.174	0.011	0.96%
Legs Down	1.161	0.011	0.92%

Linear regression analysis (see graph below) confirmed that the BMD measurements with and without the leg positioner were highly correlated (r = 0.99), with slope near unity (1.06), an intercept close to zero (-0.06) and an SEE of 0.021 g/cm^2 or 1.8%. We conclude that elevating the legs has no clinically significant effect on spine BMD accuracy (1%) or precision. In subjects where elevating the legs is difficult, a measurement with the legs down can be used without a significant impact on measurement accuracy or precision.

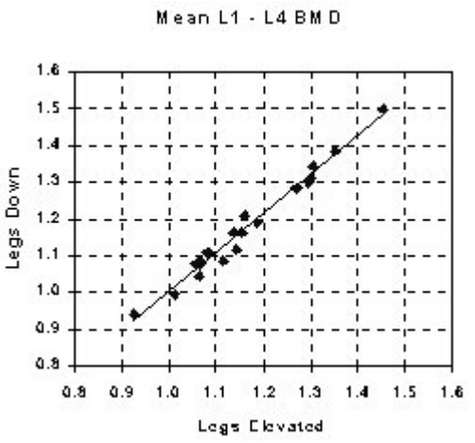

Disclosures: ***C. Simonelli****, GE Medical Systems Lunar 2.*

M075

Evaluation of Bone Mineral Density and Fat-Lean Distribution in Patients with Multiple Myeloma in Long Term Remission. S. Roux[1], C. Bergot*[2], J. P. Fermand*[3], J. Frija*[2], J. C. Brouet*[3], X. Mariette*[1]. [1]Rheumatology, Bicêtre Hospital, Le-Kremlin-Bicêtre, France, [2]Radiology, Saint-Louis Hospital, Paris, France, [3]Immuno-Hematology, Saint-Louis Hospital, Paris, France.

BMD evaluation could be of interest in the follow-up of MM patients, but few data have been published so far. In order to characterize the evolution of BMD in responder patients, BMD was evaluated in 44 MM patients (14F-30M, aged 35-65 years) in long term remission for at least 2 years (35.4±10.5 months) after high-dose chemotherapy and autologous transplantation (HDT) (n=38) or conventional chemotherapy (CC) (n=6) in a retrospective study. Patients never received bisphosphonates before or during the follow-up. All patients underwent a lumbar spine (LS) BMD (n=44) and a whole body (WB) BMD (n=35) before therapy and at least once in the remission period. BMD measurements were performed at interval of 1y (n=29), 2y (n=31) or 3 y (n=32). At baseline, mean LS BMD was 0.863±0,026 g/cm2, mean lumbar Z-score was -1.45 SD (-5 to 2.13). LS BMD increased from baseline by 5±1.8% (P<0.01), 9.3±1.7% (P<0.0001) and 14±1.9% (P<0.0001) at respectively 1y, 2y, and 3y. The number of osteoporotic patients (T-score <-2.5DS) decreased from 39% at baseline, to 28.5% at 1y, 22.5% at 2y and 18.5% at 3y. Compared to baseline, WB BMD decreased by -2.8±0.5% at 1y (P<0.0001), -2.6±0.7% at 2y (P<0.001) and -1.7±0.6% at 3y (P<0.01). When skeletal subregions on WB measurements were analyzed, axial BMD (lumbar and thoracic) increased and appendicular BMD (four limbs altogether) decreased from baseline in each group, with significant correlation between appendicular and WB BMD (r= 0.918), and LS and axial BMD (r= 0.823). Head BMD increased from baseline at 3y (P<0.0001). The pelvis BMD significantly decreased from baseline at 1y and the mean percentage change was -4.5±1% at 1y, -1.6±1% at 2y and -0.2±1.3% at 3y. While the lean compartment did not change, the mean percentage change of the fat compartment from baseline was -9.2 ± 8.4% at 1y, +8.5 ±7% at 2y and +28.4 ± 7.1% at 3y at the trunk, and -6.4 ± 5.5% at 1y, +4.8 ±4.9% at 2y and +17.1 ± 5% at 3y in peripheral areas. In conclusion, in MM patients in remission after HDT or CC, LS BMD progressively increased after a mean follow-up of 3 years. These patients never received bisphosphonates, so this increased was related to the anti-myeloma treatment per se. It is not surprising that the major effect on BMD was observed at the LS which is primarily composed of trabecular bone containing the bone marrow. In areas primarily composed of cortical bone (WB or pelvis), we observed a decrease of the BMD with values that tended to return to baseline at 3 y. Interestingly, a drastic increase of the fat content was also observed.

M076

Assessment of Bone Mineral Density of the Calcaneus in Healthy and Osteoporotic Women by a New DXA Device. G. Martini, R. Valenti*, S. Giovani*, L. Gennari, S. Salvadori*, B. Galli*, R. Nuti. Metabolic Disease Unit, University of Siena, Siena, Italy.

Aim of the study was to analyze the reproducibility and the diagnostic capability of a new portable device (Calscan Dexa-t), able to measuring calcaneus bone mineral density (BMD). The technique is based on the concepts of dual-energy X-ray absorptiometry associated to the measure of heel thickness with laser beam. The population entered the study consists of fourty postmenopausal women (aged 47-82 years) and the following parameters were examined: lumbar spine (postero-anterior L2-L4) and total body-BMD (Lunar DPX), calcaneus imaging quantitative sonography (Lunar-Achilles), and calcaneus-BMD (Calcscan Dexa-t). On the basis of BMD T-score measured by DXA of L2-L4 and using -2.5 as cut-off, twenty women were classified as osteoporotic and twenty women were considered non osteoporotic (5 osteopenic and 15 normal, according to WHO classification). The short-term precision of Calscan was determined from three repeated measurements on the same subject. The coefficient of variation (CV), calculated by expressing the standard deviation as a percentage of the mean, was 2.4%. DXA-BMD of the calcaneus was significantly lower in osteoporotic patients in comparison to non osteoporotic subjects (0.273 g/cm^2 ± 0.40 vs 397 g/cm^2 ± 0.8, p<0.01) as well as DXA-BMC (1.4 g ± 0.2 vs 2.0 g ± 0.4, p<0.01), while no differences were appreciated as regards area and thickness. The diagnostic accuracy of Calscan has been assessed by comparing the agreement with BMD L2-L4 T-score: at Calscan, 16 on 20 osteoporotic women have a T-score <-2.5 and only 4 on 20 women without osteoporotic were misclassified. Sensitivity and specificity were 80% and 80%, respectively. Finally, heel-BMD showed high correlation with ultrasound stiffness (r=0.84), and total body-BMD (r=0.86); the relationship with L2-L4 BMD was lower (r=0.76), but highly significant. In conclusion, the new measuring device Calscan Dexa-t is easy to use; measurement time is relatively short so examinations are rapid; precision is sufficiently good; diagnostic capacity and relationhips with other sites of the skeleton or ultrasound device are excellent.

M077

Precision of Lumbar Spine and Femur BMD Measurements Using Hologic and GE Lunar Fan-Beam Bone Densitometers. S. B. Moody*, P. H. Bowen*. The Emory Clinic, Atlanta, GA, USA.

A low precision error is essential for serial bone density measurements, as skeletal changes associated with osteoporosis are only a few percent a year. Halving of the precision error reduces the time required to detect a statistically significant change in BMD by a factor of 2. In this study, we compared the precision of lumbar spine (L1-L4) and proximal femur BMD from two fan-beam densitometers, the Hologic QDR 4500 and the Lunar Prodigy. Thirty-one women were measured twice with the Lunar Prodigy (GE Medical Systems) and the QDR 4500 (Hologic) at the spine and left proximal femur with repositioning between each scan. Scans were acquired by an ISCD-certified technologist using the standard scan modes for each system: the Prodigy 30-second mode and the QDR 4500 60-second mode. Dual femur measurements that provide average BMD of the two femora were also acquired on the Prodigy. Precision was calculated as the root mean square standard deviation. Pooled precisions (variances) between the Prodigy and QDR 4500 measurements were compared with an F-test. Single femur Prodigy precision was superior to the QDR 4500, with statistically significant differences at all femoral regions (Table 1). Spine precision was comparable between the two systems.

Table 1. Precision of Prodigy and QDR 4500 Spine and Single Femur BMD Measurements

	PRODIGY (30 sec)	QDR 4500 (60 sec)	PRODIGY vs. QDR 4500
Region BMD (g/cm^2)	SD (%CV)	SD (%CV)	p
Femur Neck	0.010 (1.1%)	0.014 (1.8%)	0.03
Ward's	0.011 (1.4%)	0.025 (3.8%)	0.0001
Trochanter	0.007 (0.9%)	0.010 (1.4%)	0.03
Total Femur	0.006 (0.6%)	0.010 (1.2%)	0.002
Spine (L1-L4)	0.013 (1.1%)	0.012 (1.2%)	0.23

Single femur precision errors with the Prodigy 30-second mode were 30% to 60% lower than precision errors with the QDR 4500 60-second scan mode. The left/right average BMD of the Prodigy dual femur measurements further reduced precision error compared to single femur measurements (Table 2).

Table 2. Precision of Prodigy Single and Dual Femur BMD Measurements

Region	PRODIGY Single Femur %CV	PRODIGY Dual Femur %CV
Femur Neck	1.1%	0.7%
Ward's	1.4%	1.3%
Trochanter	0.9%	0.7%
Total Femur	0.6%	0.4%

We conclude that BMD changes from single femur measurements can be detected 30% to 60% faster with the Prodigy compared to the QDR 4500. Average BMD from the Prodigy dual femur scans can detect change 50% to 70% faster than single femur BMD from the QDR 4500.

*Disclosures: **S.B. Moody**, GE Medical Systems Lunar 2.*

M078

Clinical Utility of Combining Calcaneal Bone Mass Measurement with Central DXA in Men. N. Vallarta-Ast[1], D. Krueger[2], N. Binkley[2]. [1]Radiology, Wm S Middleton VAMC, Madison, WI, USA, [2]University of Wisconsin, Madison, WI, USA.

Spinal degenerative disease often elevates measured bone mass in older men. However, peripheral bone mass measurement at the calcaneus is largely unaffected by such artifacts. The purpose of this study was to evalute the utility of calcaneal measurement to detect low bone mass in men. This ongoing study measured lumbar spine (LS), proximal femur (F), forearm (UDR) and calcaneus (Calc) BMD in 66 men age 55-86, referred for clinical DXA. GE Lunar instruments were utilized; Expert-XL (LS, F and UDR DXA), PIXI (Calc DXA) and Achilles Express (Calc ultrasound [US]). Ultrasound stiffness T-scores were derived utilizing the manufacturer's German normal male reference population. World Health Organization diagnostic criteria were arbitrarily applied to data from all instruments. The routine central site combination of LS plus F identified 30 men as osteoporotic; combining LS/F with any peripheral measurement increased ($p < .05$) the number of men identified as osteoporotic; LS/F/UDR = 36, LS/F/PIXI = 36, LS/F/US = 39. It was unexpected that the combination of LS/F with Calc US identified the greatest number, 39 (59%) of this group as osteoporotic. Twenty men had documented prior low trauma fracture; LS/F classified only 10 from this group as osteoporotic. Similar to results in the entire group, addition of US to LS/F diagnosed osteoporosis more frequently (16/20, $p = .03$) in the fracture subgroup than LS/F alone. In conclusion, it is widely accepted that application of WHO diagnostic criteria to calcaneal BMD measurement is inappropriate. However, these data suggest the WHO criteria remain appropriate when used in combination with central measurements. Specifically, combination of central and calcaneal BMD measurements increased osteoporosis classification in these men regardless of whether the calcaneus was measured with DXA or US. This likely reflects the limited utility of LS BMD measurement in this population due to the high prevalence of spinal degenerative disease. Given this situation, monitoring osteoporosis therapy at the calcaneus, a cancellous rich site, may be advantageous. Studies evaluating the feasibility of monitoring osteoporosis treatment at the calcaneus are indicated. The dichotomy of "central measurement" versus "peripheral measurement" may be impairing optimal osteoporosis care.

M079

Should One or More Vertebral Levels Be Used for Fracture Risk Assessment? D. L. Schneider, R. Bettencourt*, E. L. Barrett-Connor. University of California, San Diego, La Jolla, CA, USA.

Fracture risk assessment using dual energy X-ray absorptiometry has been based on 3 or 4 vertebral levels. However, one vertebral level has more bone area than the femoral neck. Is a single vertebral level as predictive of fracture as multiple levels? We examined the minimal number of vertebral levels and fracture risk in 978 community-dwelling ambulatory older women aged 43-97 years. At a 1992-1996 research clinic visit, a standard medical history including clinical fractures was obtained. Bone mineral density (BMD) was measured at the PA lumbar spine using two DXA machines (Hologic QDR 1000, L1-4, and 2000, L2-4). Lateral spine radiographs were read using the semiquantitative method for prevalent vertebral fractures. Osteoporosis was defined by the WHO criteria of T-score =< -2.5 using data from Hologic female normals for spine DXA. Twenty percent of women, mean age 72.2 years, reported clinical fractures and 12% had prevalent vertebral fractures. Results from the two DXA machines were similar. Approximately one in 5 women were identified as osteoporotic using the total spine BMD, and one in 3 women using the single lowest vertebral BMD. The proportion of clinical fractures and prevalent vertebral fractures were similar in women with osteoporosis identified by total or lowest spine BMD. There was no difference in risk of clinical fracture using total spine (OR, 1.68; CI 1.18-2.41) or lowest spine (OR, 1.73; CI 1.24-2.41) and vertebral fractures, total spine (OR, 2.11; CI 1.38-3.24) or lowest spine (OR, 2.18; CI 1.44-3.30). In summary, although fracture risk has been based on total spine BMD, lowest single vertebral BMD level provides a similar but not better predictor of fracture risk. Therefore, the minimum number of vertebra needed for fracture risk assessment is one.

M080

Preliminary Evaluation of the Lexxos 2D Digital DXA Scanner. K. M. Knapp, R. Patel, G. M. Blake, I. Fogelman. Osteoporosis Screening and Research Unit, Guy's Hospital, London, United Kingdom.

The Lexxos (DMS, Perols, France) is the first DXA scanner to utilise a 2D radiographic detector rather than the present convention of a fan beam. This enables faster acquisition times of approximately 2 seconds each for antero-posterior acquisition of the lumbar spine and proximal femur. The aim of this preliminary evaluation was to investigate the cross-calibration of the Lexxos with a Hologic QDR-4500W (Hologic, Bedford, MA), and to calculate the short-term in-vivo precision. A group of 33 patients had BMD measurements performed on both the Hologic and Lexxos scanners. A subgroup of 11 patients had two acquisitions each of the spine and hip performed with repositioning between acquisitions to measure in-vivo short-term precision. The agreement between the Lexxos and Hologic was calculated using linear regression, forcing the line through the origin. The short-term precision results were calculated using the RMS SD and CV% from the duplicate scans.

	n	R	SE(g/cm^2)	Slope
Spine	24	0.93	0.04	1.002
Femoral Neck	31	0.96	0.04	0.993
Total Hip	31	0.96	0.04	1.027

The RMSSD and CV% for the spine (n=9) was 0.02g/cm^2 and 1.8% respectively, for the femoral neck (n=11) was 0.01g/cm^2 and 1.4% and the total hip (n=11) was 0.02g/cm^2 and 1.8% respectively. The BMD values in the spine and hip demonstrate good agreement with the Hologic QDR-4500W. Further data is being obtained to evaluate the precision of the Lexxos scanner.

M081

The Influence of Bone Mineral Density (BMD) Testing on the Treatment of Osteoporosis (OP) in Two Canadian Non-Academic Community Centres. E. A. Papadimitropoulos[1], M. E. Hamel*[2], R. J. Sebaldt[2], J. D. Adachi[2], K. Siminoski[3], C. H. Goldsmith*[4]. [1]Research and Development, Eli Lilly Canada Inc., Scarborough, ON, Canada, [2]Rheumatology, McMaster University, Hamilton, ON, Canada, [3]Department of Radiology, University of Alberta, Edmonton, AB, Canada, [4]Statistics, McMaster University, Hamilton, ON, Canada.

A prospective cohort study with 3 month follow-up was conducted to characterize the patients that Canadian physicians are referring for BMD testing and to assess the impact of the results on subsequent treatment decisions and lifestyle changes. Testing was conducted in two Canadian non-academic centres, which included on-site and mobile dual-energy x-ray absorptiometry (DXA) units. Recruitment for the study consisted of successive patients who were referred for BMD measurements at each of the two BMD testing sites over a 3 month period. Patient questionnaires were used to collect data on demographics, risk factors, medications and lifestyle. The BMD results were used to divide patients into 3 groups; osteoporotic, osteopenic and normal BMD according to WHO criteria. Based on BMD results, 23% of patients were osteoporotic, 46% were osteopenic and 31% had normal BMD. There was a positive correlation between number of risk factors and reduction in BMD from normal values. Application of the Osteoporosis Society of Canada practice guidelines, the National Osteoporosis Foundation guidelines or the Osteoporosis Risk Assessment Instrument, respectively would have eliminated 45%, 13% and 43% of patients without OP that were referred for testing in our study and resulted in BMD testing for 53%, 85% and 78% of the patients with OP in our group. Following BMD testing, there was no significant change in patient-reported calcium intake or excerise, and 34% of patients felt that their knowledge of OP had increased. Three months after BMD testing, 60% of osteoporotic patients, 47% of osteopenic patients and 34% of patients with normal BMD were being treated with calcium, vitamin D or prescription medication. Risk factors and current guidelines are entirely satisfactory in screening patients for BMD referrals. The results of BMD tests influence treatment decisions in the primary care setting although in our cohort of patients did not appear to have a significant effect on patients' lifestyle choices nor result in a reported increase in knowledge about OP in a majority of patients.

Disclosures: ***E.A. Papadimitropoulos****, Eli Lilly and Company 1, 3.*

M082

Short Term DEXA Precision in Children Is Comparable to Precision in Adults. R. P. Green, J. Bartholic*, R. Civitelli. Washington University School of Medicine, St. Louis, MO, USA.

DEXA scans are increasingly being used to evaluate bone health in children at our institution, both for clinical and research purposes. Children may have more difficulty cooperating with positioning, which could result in increased study-to-study variability. Precision error (PE) provides an estimate of study-to-study variability and is used to assess the clinical significance of BMD changes. Therefore, we determined PE for pediatric patients using 15 healthy children, ranging in age 5-14 years. Each child completed three DEXA studies of AP and lateral spine (L-spine), total hip, and whole body (WB), using a Hologic QDR4500 scanner. All studies on each child were performed on the same day. The children left the table and returned for repeat scans. A single technician performed all the studies, including the adult AP spine and hip precision studies included for comparison. No assistance other then verbal instruction was provided to help the children remain still. PE for coefficient of variation (CV) and standard deviation (SD) were obtained using root-mean-square averages of each individual's CV and SD and are shown in the table. L-spine DEXA had a higher PE then any other site or projection. Because difficulty repositioning and maintaining position could contribute to greater variability in younger children, we used regression analysis to determine if there was a relationship between age and the SD or CV of each individual's repeated BMDs. No significant correlation was found at any site, with the exception of WB bone mineral content (BMC), where there was a positive correlation between age and an individual's SD (r^2=0.2797, slope=+1.68 gm/year, p=0.0427). However, no relationship was present between CVs of WB BMC measurements and age (r^2=0, slope=0, p=0.9936). These results indicate that in children between the ages of 5 and 14, DEXA studies at our institution have good precision, comparable to that of adult DEXA studies. Furthermore, younger children do not appear to have greater study-to-study variability, as might be expected if it were more difficult for them to cooperate with the study.

Adult and Pediatric Precision Results

Site	PE SD-Ped	PE CV-Ped	PE SD-Adult	PE CV-Adult
AP Spine BMD	0.0071 gm/cm^2	1.10 %	0.0099 gm/cm^2	0.90 %
L-Spine BMD	0.0222 gm/cm^2	3.89 %	ND	ND
Hip BMD	0.0094 gm/cm^2	1.19 %	0.0070 gm/cm^2	0.80%
WB BMD	0.0087 gm/cm^2	1.03 %	ND	ND
WB BMC	15.99 gm	1.05%	ND	ND

M083

Simulation of the Evolution of Trabecular Bone Structure from High Resolution Magnetic Resonance Imaging: A Preliminary Study Using "Distance to Topological Fracture". L. Pothuaud*, S. Majumdar. Magnetic Resonance Science Center, University of California, San Francisco, San Francisco, CA, USA.

Better knowledge of how a patient's bone is expected to evolve would be very useful for clinicians in increasing the accuracy of predicting risk of fracture in individual subjects. The aim of this work was to explore the utility of image analysis to simulate the evolution of trabecular bone structure. Fifty-seven normal postmenopausal women were recruited in our center following rigorous inclusion / exclusion criterion. High resolution Magnetic Resonance (MR) imaging was used to reconstruct a 3D image of trabecular bone of the ultra-distal radius. The imaging protocol was developed on a 1.5 Tesla clinical scanner, following optimized and standardized conditions, with an in-plane resolution of 156x156 microns2 and a slice thickness of 500 microns. The "apparent" trabecular bone structure was extracted from the gray level MR images by applying a global histogram-based threshold. Bone volume fraction (BV/TV), maximal entropy (ME), and Euler-Poincare characteristic (EPC) were evaluated following previously reported methods. 3D-Line Skeleton Graph Analysis (LSGA) technique was used to segment the 3D trabecular bone structure into elementary trabeculae. Next, a random trabecular deletion process was implemented to simulate bone changes. This process was performed until an ultimate 3D model with EPC = 0 was reached, characterizing the transition state between low-connectivity models and highly disconnected models (i.e., with several clusters of solid). The state reached by simulation and characterized by EPC = 0 was designated "topological fracture". The "distance to topological fracture" (DTF) was then characterized by the absolute differences D-BV/TV and D-ME between the initial structure and the TF model.

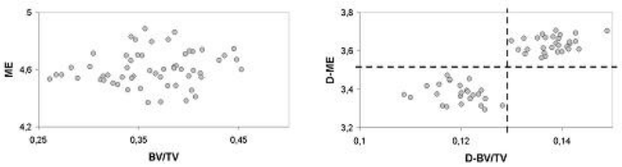

In this preliminary study, we hypothesized that the state EPC=0, reachable by image analysis and simulation, could be related to the bone fracture threshold. In a large group of normal subjects our DTF-based evaluation led to a clustering of the data into two well-separated classes (right). The other parameters used failed to yield such clustering (left). Further analysis will evaluate the meaning of DTF in terms of bone strength, and will determine its usefulness as a tool for predicting the risk of bone fracture in individual subjects.

M084

The Value of Percutaneous Transpedicular Trocar Biopsy for the Diagnosis of Vertebral Body Lesions. R. Kothe*[1], G. Möller[2]. [1]Dept. of Orthopaedics, Hamburg University School of Medicine, Hamburg, Germany, [2]Moosbergstrasse 10, D-64285 Darmstadt, Germany.

Despite the advances in imaging technology a spinal biopsy is often necessary for the diagnosis of vertebral body lesions. Recently, less invasive biopsy techniques using a needle or a trocar have gained increasing popularity. But there still is a lot of controversy if the obtained specimen allow an adequate histologic analysis. We evaluated the safety and accuracy of fluoroscopic guided percutaneous transpedicular trocar biopsies of the spine for the diagnosis of vertebral body lesions. 116 patients with different vertebral body lesions from T1 to S1 were evaluated in a prospective manner. Percutaneous transpedicular trocar biopsies were performed in mild general or local anesthesia. Under fluoroscopic lateral and a.p. C-arm control the specimens were obtained using a Jamshidi trocar with an internal diameter of 3.1 mm. The bone cores were divided in two halves. One was analyzed undecalcified in acrylat, the other decalcified in paraffin. In 112 out of 116 biopsies the quality of the specimen was assessed as good or excellent. No patient required a second biopsy because the obtained tissue was not sufficient. There were 38 malignancies, 32 cases of acute or chronic osteomyelitis, 20 isolated osteoporotic fractures, 3 hemangioma, 1 fibrous dysplasia and 1 chordoma. In 21 cases no pathology could be found. Two postoperative haematoma were the only complications in this series. Percutaneus transpedicular biopsy of the spine using a Jamshidi trocar can be performed safely and efficaciously under fluoroscopic guidance. The obtained specimens provide adequate bone cores for histologic examination with a high diagnostic yield, comparing well with open biopsies.

M085

Biomechanical Examination of Cortical Bone Distribution in the Vertebral Body. H. Tsugeno*[1], B. Goto*[2], T. Fujita[2], M. Nakai*[1], M. Okamoto*[1], T. Yokoi*[1], S. Takata*[1], N. Nishida*[1], K. Ashida*[1], Y. Hosaki*[1], F. Mitsunobu*[1], Y. Shiratori*[3], Y. Tanizaki*[1]. [1]Misasa Medical Center, Okayama University, Tottori, Japan, [2]Calcium Research Institute, Kishiwada, Japan, [3]Department of Medicine and Medical Science, Okayama University Graduate School, Okayama, Japan.

Reductions of radial cortical bone volume and density in osteoporosis were reported by us using peripheral quantitative computed tomography (pQCT). In view of the technical limitations of equipment used in previous studies, which might lead to some inaccuracy in measuring the thin vertebral cortical bone, we used the more precise multi-slice CT Aquilion (Toshiba, Tokyo, Japan) to study deformity-free third lumber vertebra (L3) in 11 postmenopausal women (> 5 years after menopause, mean age; 67.3 years), including 6 patients with osteoporosis and 5 controls. Relative cortical volume (RCV), cortical bone mineral density (BMD) and trabecular BMD in the frontal part of the vertebral body (L3) were calculated. For comparison with those, RCV, cortical and trabecular BMD in the radius were simultaneously measured by pQCT (Stratec XCT960). Both RCV and cortical BMD showed the minimum value at sites close the top and bottom of the vertebral body, and the maximum value at the central part of the vertebral body. RCV, cortical and trabecular BMD in the center of the vertebral body showed significantly lower values (p=0.0039, p=0.0067, p=0.0039) in osteoporosis than those in the controls. RCV, cortical and trabecular BMD of the radius also showed significantly lower values (p=0.0002, p=0.0014, p=0.0047) in osteoporosis than those in the controls. Both cortical bone volume and density were low at sites close the top and bottom in the frontal part of the vertebral body, and these sites may coincide with the fragile part of the vertebral body. In patients with osteoporosis, both cortical bone volume and density in the vertebral body were reduced just like those in the radius.

M086

3-D Synchrotron mCT Allows Unique Insight of Changes in Bone Quality. E. L. Rittman*[1], B. Borah*[2], T. E. Dufresne*[2], R. J. Phipps[2], J. P. Sacha*[1], S. M. Jorgensen*[1], R. T. Turner[1]. [1]Mayo Clinic, Rochester, MN, USA, [2]Procter & Gamble Pharmaceuticals, Mason, OH, USA.

Incidence of bone fracture in people with osteoporosis has been shown to reduce markedly with bisphosphonate treatment. However, the role of bone turnover and its effects on the quality of trabecular bone is relatively unknown. Using a synchrotron CT source, we have developed a unique method to examine mineralization directly in 3-D and correlate it with the underlying trabecular structure. Our study involved micro-CT analysis of 10 pairs of iliac crest biopsies obtained from patients before and after treatment for three years with risedronate therapy. We scanned each biopsy at the Brookhaven National Laboratories' National Synchrotron Light Source X2B beam line micro-CT scanner. Using a novel off-axis rotation of the specimen, followed by a montaging of the full transverse profiles of the sinogram, up to an 8 mm diameter core could be examined without loss of information. Due to the high signal to noise and the monochromatic beam, this technique allows for high resolution (5 μm isotropic voxels) data where the younger less fully mineralized surfaces are clearly discernable from the older fully mineralized bone. Therefore, it is possible to visualize entire remodeled sites spanning broadly across the trabecular bone surface. Such precise delineation of remodeled surfaces is typically not possible with conventional Micro-CT technology, which is used primarily to analyze bone structure only. Preliminary results of histogram-based segmentation of the different density values in the specimens revealed that there was a significant reduction ($p < 0.05$) in less dense bone in the risedronate treated biopsies. This is consistent with previous histology and biomarker data associated with this study. The 3-D visualization of the trabecular surface after segmentation qualitatively confirms this reduction in the 3-year treatment group. This high resolution 3-D imaging method allows for the first time the examination of bone remodeling sites directly in 3-D on human biopsies treated with risedronate. This technique provides data consistent with established histology and will allow for correlation of changes in remodeling activity (size, depth, location) with the underlying trabecular structure (trabecular thickness, orientation, plates/rods, etc).

M087

Comparison of Mechanical Response Tissue Analysis of the Ulna Bone with Quantitative Ultrasound and Dual Energy X-ray Absorptiometry. C. C. Djokoto*[1], S. D. Waldman*[2], M. D. Grynpas[3], A. M. Cheung[4]. [1]Institute of Biomaterials and Biomedical Engineering, University of Toronto, Toronto, ON, Canada, [2]Samuel Lunenfeld Research Institute, Mount Sinai Hospital, Toronto, ON, Canada, [3]Institute of Biomaterials and Biomedical Engineering, University of Toronto and, Samuel Lunenfeld Research Institute, Mount Sinai Hospital, Toronto, ON, Canada, [4]Department of Medicine, University Health Network and University of Toronto, Toronto, ON, Canada.

Mechanical response tissue analysis (MRTA) is a non-invasive technique used to determine the cross sectional bending stiffness (EI) of bone. Previous studies have examined the relationship between ulnar EI determined by MRTA, and bone mineral content (BMC) and bone mineral density (BMD) measured by dual energy x-ray absorptiometry (DEXA) at various anatomical sites. However, the speed of sound (SOS) in bone is related to both the elastic modulus and density, and should provide a better correlation with EI. In this study we correlated MRTA measurements of the ulna bone with quantitative ultrasound (QUS) of the ulna and DEXA measurements of the ulna, radius, hip and spine, to determine if EI correlates with other accepted modalities of bone measurement. A total of 56 healthy subjects (20 men and 36 women) between the ages of 18 and 83 were recruited. The response of the ulna to a low-frequency mechanical vibration was fitted to a 6-parameter model to determine EI. Axial SOS along the ulna bone was determined by QUS (Sunlight Omnisense), and BMC and BMD were determined by DEXA (Hologic QDR 4500A). The projected area of the DEXA ulna region of interest was used to estimate bone width, and BMD and SOS were combined to estimate the elastic modulus of the ulna. EI was found to correlate with DEXA projected area, BMC and BMD. No correlation was found between EI and SOS. EI was most strongly correlated with BMC measured at the site of the ulna bone corresponding to the location of the applied MRTA stimulus ($r = 0.773$, $p<0.001$). There was a weak but significant correlation between EI and estimated elastic modulus ($r = 0.548$, $p<0.001$). The correlations between EI and BMC or BMD are consistent with previous studies examining relationships between densitometry and MRTA. Although axial SOS measurements of the ulna bone alone did not correlate to EI, SOS combined with BMD did. We conclude that MRTA measurements reflect different qualities of bone than either QUS or DEXA alone. Future studies with larger cohorts are needed to further investigate the relationships between these three modalities of bone assessment.

M088

A Mathematical Model of Bone and Applications to Osteoporosis. G. H. Gunaratne[1], S. J. Wimalawansa[2]. [1]Department of Physics, University of Houston, Houston, TX, USA, [2]Department of Medicine, Robert Wood Johnson Medical School, New Brunswick, NJ, USA.

Factors complicating the development of diagnostics for osteoporosis include the anisotropy of porous bone, fraction of trabecular mass, and trabecular thinning. It is extremely difficult to account for these factors and complex interactions between them in clinical studies or in experiments on ex-vivo bone samples. Mathematical models have been used successfully to extract such details in many physical systems. A corresponding analysis of bone can be used to establish the relative importance of mechanical factors that effect bone strength. This information can aid the design of suitable treatment options and help identify accurate non-invasive diagnostic tools. We introduce a mathematical model of a trabecular architecture (TA), which consists of a disordered network of fragile elastic struts. Features such as the preferential growth of regions under high strain (Wolff's Law) are included. Analysis of the model provides a surprising observation on load transmission; an incomplete network can only use a fraction of itself for stress propagation, and this fraction decreases with increasing loss of struts. As a consequence of this inefficiency, bone strength decreases non-linearly with BMD, and a new expression for it has been derived on the basis of our model. This expression was validated using previously published data on samples of human bone (Mosekilde et.al., Bone, 8, 79-85 (1987)). A new diagnostic (Γ) for the ultimate strength of a bone, that is constructed to express changes in the stress carrying backbone of a TA, is proposed. It is the ratio of linear responses of the network to static and periodic external strain, and predicts the ultimate strength of model networks accurately. Anti-resoptive therapies (e.g., bisphosphonates) induce a dramatic reduction of fracture incidence with modest increases of BMD. Analysis of the model system shows that preferential growth of bone at locations under high strain (Wolff's Law) is a possible explanation the reason underlying the efficacy of these agents. Furthermore, it is observed that the efficacy of bone growth is higher in weaker networks, suggesting that therapeutic intervention is more cost-effective in patients with established osteoporosis.

M089

Fan-Beam Hip Axis Length Measurements Predict Hip Fracture. K. G. Faulkner[1], H. S. Barden[1], H. Bui*[1], P. K. Burke[2]. [1]GE Medical Systems Lunar, Madison, WI, USA, [2]Osteoporosis Diagnostic and Treatment Center, Richmond, VA, USA.

Previous studies have shown that a long hip axis length (HAL) is related to an increased risk for hip fracture, independent of age and bone density. However, most of these studies have been performed on older pencil beam densitometers, which are not subject to magnification effects. To evaluate whether fan-beam measurements of HAL are associated with hip fracture risk, we obtained dual-energy x-ray absorptiometry scans (Lunar Prodigy, GE Medical Systems) of the proximal femur on 980 white women aged 70 to 89 years. The Prodigy uses a multi-view fan beam to accurately measure length and area without the need for body size corrections. Measurements of HAL and femoral BMD (neck, upper neck, and total) of the 38 women with previous hip fracture were compared to the same measurements in 942 non-fractured controls of similar age. Results were compared using multiple logistic models, and odds-ratios (OR) were determined for hip fracture per standard deviation change in each measurement. There were no significant differences in age or height between fracture and control subjects. Hip fracture subjects weighed less and HAL was significantly longer in the hip fracture subjects compared to controls (Table 1). HAL was found to be correlated with height ($r = 0.48$, $p<0.001$) and weight ($r = 0.26$, $p<0.001$), but was unrelated to age ($r = 0.05$, $p=0.14$) or BMD ($r=0.03$, $p=0.36$). Each standard deviation (6mm) increase in HAL was associated with a 1.6-fold increase in the risk for hip fracture (OR 1.6, 95% CI 1.1-2.3). The relationship between hip axis length and fracture persisted after adjustment for age, femoral neck density, height, and weight (OR 1.5, 95% CI 1.02, 2.1). Decreasing femoral BMD at all measurement regions was also associated with an increase in hip fracture risk, consistent with previous studies (Table 1). We conclude that hip axis length measured with a multi-view fan beam DXA system predicts hip fractures in elderly Caucasian women, independent of age, height, weight, and bone mineral density. Results showed that HAL in subjects with hip fracture was significantly longer than HAL in subjects without hip fracture. All femur BMD variables were significantly lower in hip fracture subjects compared with subjects without hip fracture. Each standard deviation increase in HAL was associated with a 60% increase in hip fracture risk.

Table 1 (*p<0.05 and **p<0.01 compared to controls)

Measurement	Hip Fracture	Controls	OR per SD (95% CI)
Age (years)	77.5	76.2	NS
Height (cm)	159	158	NS
Weight (kg)	60.7*	64.1	NS
HAL (mm)	107.6**	104.9	1.6 (1.1-2.3)
Neck BMD (g/cm^2)	0.672**	0.747	2.4 (1.6-3.6)
Upper Neck BMD (g/cm^2)	0.519**	0.589	2.6 (1.7-4.2)
Total BMD (g/cm^2)	0.684**	0.787	2.4 (1.7-3.4)

M090

Analysis of Cortical Bone Parameters Extracted Automatically from Lumbar Vertebra CT Images. T. Nagaoka*[1], K. Kondo*[2], H. Honma*[1], K. Ogawa*[2], K. Sakurai[1]. [1]Kitasato University Graduate School of Medical Science, Kanagawa, Japan, [2]Housei University, Tokyo, Japan.

Various parameters were reported as predictive factors for fracture risk other than BMD (bone mineral density). Most of all resulted primarily from image-based analysis focused on the trabecular structure of vertebral bodies. For accurate prediction of fracture risk, we believe, parameters describing the characteristics of the cortical bone are also required. We acquired CT (computed tomography) images by a method similar to quantitative CT, and calculated parameters for cortical bone characteristics automatically from the CT images of lumbar vertebrae (8-bit intensity resolution) for 28 healthy females (50.6±7.5 years), 17 osteoporotic females without spinal compression fracture (69.6±6.2 years), and 11 osteoporotic females with fracture (73.2±3.2 years). In the cortical bone region including the vertebral body and pedicle, automatic extraction was first performed for the contour of the vertebral body by P-tile method, and then for the contour of cancellous bone within the vertebral body and the contour of the vertebral foramen by active contour models (snakes). The center of gravity in the vertebral foramen was then designated a reference point with the posterior of the spine at 0°, angle θ was measured counterclockwise. Three cortical bone regions were designated as an anterior region (AR, 150°-210°), lateral region (LR, 120°-150° and 210°-240°), and pedicle region (PR, 80°-110° and 250°-280°). Parameters based on intensity histograms for each region were the threshold creating a 4:6 ratio of low-intensity area to high-intensity area (T46), and the total frequency of intensity between 80 and 120 divided into four gradations (D80, D90, D100, D110). The maximum intensity value (peak value) along the radial direction was determined for every 1°, and the mean of the peak values within each region (Pmean), the maximum value (Pmax), and the minimum value (Pmin) were also used as parameters. Correlations between age and each parameter of healthy subjects were investigated. The results demonstrated stronger correlations for AR-Pmin, AR-T46, AR-D90, and LR-D80 than for BMD ($r = -0.75$). We deemed these parameters to indicate age-related changes in cortical bone, and we concluded that parameters related to regional cortical bone thickness and regional cortical bone density were extracted successfully. Values for AR-T46 and PR-T46 were also significantly lower in osteoporotic patients with fractures than in patients without fractures, and AR-D90 and PR-D80 values were conversely higher. The results suggest that these parameters are useful for fracture risk prediction.

M091

Analytic Model to Predict Mechanical Behavior of Skeletal Metastasis. A. Nazarian*[1], D. von Stechow[1], M. S. Cordio*[1], R. Mueller[2], B. D. Snyder[1]. [1]Orthopedic Biomechanics Lab, BIDMC, Harvard Medical School, Boston, MA, USA, [2]ETH, Zuerich, Switzerland.

Pathologic fractures occur in up to 30% of patients with skeletal metastases. We have developed a CT based structural analysis method to predict fracture risk based on the hypothesis that bone (normal or pathologic) follows the constitutive relationships established for rigid porous foams: i.e. the strength and modulus of bone depend on both bone tissue density (ρ_{tissue}) and the square of bone volume fraction (Vv_b). The ρ_{tissue} accounts for changes in mineralization, and Vv_b accounts for changes in morphology. However, this hypothesis has never been validated for metastatic bone, and the mechanical properties of skeletal metastases have not been previously described. After obtaining IRB approval and informed consent, 10 patients (7 male, 3 females, 57 ±15 years) underwent excisional biopsy of metastatic prostate, breast, lung, ovarian or colon cancer. The presence of metastatic cancer was confirmed histologically. The biopsy specimens were cored along the predominant trabecular orientation and cut into 24 cylinders. The ρ_{tissue} of each sample was measured using a pycnometer. Mechanical testing was performed using a novel micromechanical device coupled with micro-computed tomographic (μCT) imaging. Progressive step-wise compressive strains were applied to each sample. Each sample was imaged intact and again after the application of each strain step to visualize progressive deformation of the microstructure. The μCT image of each intact sample was divided into 5 equally segmented transaxial subregions and the volume fraction for each transaxial subregion calculated. A bivariate nonlinear regression model (Levenberg-Marquardt) of the form $E, \sigma = A\rho_{tissue}(Vv_b)^2+B$ was fit to the data. In all cases ρ_{tissue} was within the normal range of 1.6 to 2.2 g/cc. The μCT images demonstrated that sample failure occurred predominantly at the weakest subregion with minimum Vv_b. The model accounted for 78% and 88% of the variation in modulus and strength respectively using minimum Vv_b. These results establish a unifying principle that characterizes the mechanical behavior of metastatic bone tissue. In addition, ρ_{tissue} is unaffected by metastatic cancer, and the changes in the mechanical behavior of metastatic bone tissue are primarily caused by localized remodeling of trabecular architecture. This study validates the application of power law functions of bone density and volume fraction to derive the load carrying capacity of bone containing metastatic tumors. These findings suggest that bone itself can be viewed as a substrate undergoing remodeling by osteoclasts and osteoblasts in response to local and/or systemic modulators of their activity.

M092

A New Staining Technique for Undecalcified Bone Sections that Enhances Visualization of Fluorochromes. D. Horn*, P. Rivas*, B. McCluskey*, G. R. Mundy, G. Gutierrez. OsteoScreen, LTD, San Antonio, TX, USA.

Bone histomorphometry (BHM) is an essential tool in basic and clinical research for the assessment of bone micro architecture. It is very useful in determining the cellular activity of the skeleton, since bone is constantly undergoing remodeling. BHM requires that the separate components of the tissue be differentially stained so they can be easily recognized and quantified. Either decalcified or undecalcified sections can be obtained for the analysis of mineralized bone and osteoid. It is also possible to determine not only the structural but also the dynamic changes occurring in bone. The extent and rate of bone formation are usually measured using ultraviolet microscopic analysis of fluorochrome labels in undecalcified sections. Until now however, these measurements have been performed on unstained slides, because the use of the commonly used stains, does not allow visualization of fluorescent dyes. Bone structure is very hard to visualize in unstained sections. For this reason, duplicate slides are usually employed, one stained slide for quantification of bone volume and other parameters, and one unstained slide for assessment of fluorochrome labeling. We have developed a new technique, which allows us to measure static and dynamic parameters using the same slide. We have used this approach in an experiment in which 4-month-old Sprague-Dawley female rats were labeled twice (six days apart) with calcein ip (15 mg/kg/day), and sacrificed 4 days after the last calcein administration. Tibias were excised, cleaned from soft tissue, and placed in 70% ethanol to be processed and embedded in methyl methacrylate. Proximal tibia sections (8 um thick) were obtained and placed directly into a 1% xylene orange solution at room temperature. After 5 minutes, slides were rinsed in DH_20, allowed to dry at room temperature and cover slipped. We were able to obtain very good staining of mineralized bone with xylene orange that allowed us to perform static and dynamic measurements in both cancellous and cortical bone using OsteoMeasure image analyzer linked to a fluorescent microscope. All these measurements were conducted on the same section, eliminating the need for duplication of slides and various staining techniques. Xylene orange has been used as a fluorochrome, but this is the first time that it has been shown to be effective as a staining agent without interfering with calcein labeling. Because this technique is very easy and gives uniform and reproducible results, we believe it is an excellent alternative to the Villanueva staining method, especially in cases where static and dynamic parameters need to be obtained as in models for osteoporosis and other metabolic bone diseases.

Disclosures: ***D. Horn****, OsteoScreen, LTD. 1.*

M093

Outpatient percutaneous Bone Biopsy in a Rheumatology Practice - Methods, Patient Tolerance, and Impact on Disease Management. H. R. Barthel[1], A. Schulz*[2], B. Knoblauch*[2]. [1]Rheumatology Practice, Koenigstein, Germany, [2]Pathology, Justus-Liebig-University, Giessen, Germany.

Introduction: Bone marrow biopsy histology and histomorphometry are important tools in the diagnosis and management of metabolic bone and systemic inflammatory diseases. However, the invasive nature of the biopsy has hampered its widespread use. In addition, most often the procedures are done in inpatient settings only. We describe our experience in an outpatient rheumatology/internal medicine practice. During a time period of 2 years 17 bone biopsies were performed and their indications, tolerability, complications and impact on disease management were evaluated. All patients had full hematol., biochem., radiological, and Dexa or QCT bone density work ups before the bone biopsies were performed. Methods: In all patients the transiliac biopsy approach was chosen. Local infiltration anesthesia was applied to both sides of ileac crest. Biopsy was performed with an 8mm Bordier Trephine or an 1.5mm (11ga) Jamshidi needle at a position approx. 5-10cm dorsal and 3cm caudal of the spina iliaca anterior superior. No general anesthesia or sedation was used. After usage of the Bourdier trephine the skin incision was sutured, which was not necessary with Jamshidi needle technique. 2/3 of biopsies were performed to evaluate metabolic or osteoporotic bone diseases (mostly to evaluate elevated bone turnover by bone resorption markers despite bisphosphonate treatment) 1/3 of biopsies were done to evaluate bone marrow differentiation in syst. inflammatory conditions or to rule out marrow malignancies. Results: Bone biopsy was well tolerated with minimal pain perception by patients, in about 25% a second biopsy approach had to be performed through the same incision site to obtain an adequate specimen. Histol. evaluations obtained good to excellent specimen quality in all cases with adequacy of all core specimens obtained with the 1,5 mm Jamshidi in all cases; therefore this technique was used exclusively later. Although pat. were given pain meds to take home after the procedure less then half reported to have used them. Small hematomas occurred in all cases, to a subst. larger degree with the larger Bourdier Trephine. One (Bourdier) pat. complained of transient upper thigh numbness due to assumed cutaneous femoral nerve compression and needed evaluation with CT to rule out retroperitoneal hematoma. His symptoms subsided after 2 weeks. In about ¼ of cases disease management was changed after obtaining biopsy results. Conclusions: Transiliac bone biopsy can be performed with minimal risks in an outpatient setting. Results help in the management of patients with metabolic, osteoporotic, and inflammation mediated bone diseases.

M094

Nuclear Magnetic Resonance Shows that a Decrease in Cortical Bone Mineralization Parallels an Increase in Osteoid Water. M. A. Fernandez-Seara*[1], S. L. Werhli*[2], M. Takahashi*[1], F. W. Wehrli[1]. [1]Radiology, University of Pennsylvania Medical Center, Philadelphia, PA, USA, [2]NMR Core Facility, Children Hospital, Philadelphia, PA, USA.

Bone strength strongly depends on bone matrix mineralization. Vose and Kubala first showed that an increase in ash of 7% increased static strength threefold. It is also known that an increase in mineral is accompanied by a decrease in osteoid water, since mineralization proceeds by water displacement while volume remains constant. Thus water content may potentially be used as a predictor of bone intrinsic strength. The purpose of this study was to investigate whether water content measured using non-destructive Nuclear Magnetic Resonance (NMR) techniques correlates with mineral content measured by gravimetric methods. Four rabbits (5-6 wk old) were fed a low phosphorus diet (0.09%) to induce hypomineralization of the skeleton. A second group of four rabbits received the same diet supplemented with sodium phosphate to normal phosphorus levels (0.5%). After 8 wks the animals were sacrificed and three cortical bone specimens were cut form the mid-shaft of the harvested tibiae, 2 of which were used to measure water and ash by gravimetric methods. The third one was used to measure water content by means of isotope exchange. Briefly, a proton NMR spectrum of the bone in air was obtained. Thereafter, the specimen was immersed in deuterium oxide and the deuterium-proton exchange was monitored by proton spectroscopy. After 8 hours, the bone was removed from the solution and a second spectrum was acquired in air. These data were used to calculate water content and to measure the diffusion coefficient of water in the bone matrix. In addition, bone volume was measured by MRI. Significant differences in water content measured by drying were observed between control (15.20 ± 0.08 wet weight %) and treatment (15.85 ± 0.07) groups (p=0.002). All treated animals had lower ash content than the controls (65.31 ± 0.11 vs. 67.06 ± 0.12 wet weight %, p=0.0001). Water measured by NMR was higher than the water measured by drying for both, but again significantly different between the control (18.66 ± 0.54 wet weight %) and treatment (21.42 ± 0.47) groups (p=0.02). Water volume fraction was increased in the treatment (40.47 ± 0.01 %) compared with the control group (36.30 ± 0.01 %), (p=0.03). There were significant negative correlations between ash and water measured by both techniques (drying: r2=0.88, p=0.002; NMR: r2=0.71, p=0.02). The results demonstrate a strong correlation between NMR-determined osteoid water and mineral content. Proton NMR has potential as a nondestructive method for indirect assessment of mineralization.

M095

Magnetic Resonance-Based Virtual Bone Biopsy Reveals Architectural Implications of Renal Osteodystrophy. F. W. Wehrli*[1], M. B. Leonard[2], B. R. Gomberg[3], P. K. Saha*[1]. [1]Radiology, University of Pennsylvania, Philadelphia, PA, USA, [2]The Children's Hospital of Philadelphia, Philadelphia, PA, USA, [3]University of Pennsylvania, Philadelphia, PA, USA.

Renal osteodystrophy (ROD) is caused by renal dysfunction that prevents the formation of the active form of vitamin D (calcitriol), leading secondary hyperparathyroidism. A key manifestation of ROD is abnormal bone turnover, accompanied by marrow fibrosis. High-turnover disease (osteitis fibrosa, OF) has been shown by histomorphometry to result in trabecular bone sclerosis and cortical thinning. Here we explore the potential role of the µ-MRI-based virtual bone biopsy (VBB) for quantifying trabecular and cortical bone properties. Localizer image-guided acquisition of transverse 3D MR images of the distal tibia (137x137x420mm3 voxel size) were processed to yield noise-less bone volume fraction maps from which, after subvoxel processing, grayscale images of 69x69x105 µm3 voxel size were obtained. Trabecular thickness was determined with a new method called 'fuzzy distance transform' which provides accurate measurements in the limited spatial resolution regime of in vivo µ-MRI. In addition, 2D spin-echo images were collected at the tibial mid-shaft for measurement of cortical bone parameters at 0.47 mm in-plane resolution and 2 mm slice thickness. Endo and periosteal boundaries were detected with a method based on tracing profiles diagonally across the tibia, from which cortical bone cross-sectional area (CCA) was determined. So far, 24 subjects have been studied but the data from only 17 subjects have been analyzed (10 patients and 7 gender/age matched controls, all African American). Patients had been on dialysis for 840±460 days. All patients except one had abnormally high PTH (672±364µg/l vs. a target level of 200µg/l in dialysis patients and a normal range of 10-65µg/l). The data revealed the following trends: Patients had increased trabecular thickness consistent with trabecular sclerosis, a sparser trabecular network, a thinned cortex, and increased bone area (the area encompassed by the periosteal boundary), the latter suggesting periosteal expansion. These effects were not statistically significant, presumably due to insufficient power at this stage of the study. However, the normalized CCA (CCA/bone area) was significantly smaller in the patients (p=0.05). The present preliminary data corroborate some of the structural features of secondary hyperparathyroidism and indicate that an entirely noninvasive image-based method, the MR-based VBB may have potential to characterize metabolic bone disease, obviating physical bone biopsy.

M096

Directional Measurement of Direct Thickness of Cancellous Bone. T. G. Morgan*, M. C. H. van der Meulen. Sibley School of Mechanical & Aerospace Engineering, Cornell University, Ithaca, NY, USA.

Determining the structure-function relationship for cancellous bone is important for understanding bone diseases, such as osteoporosis, as well as improving outcomes of prosthetic implant surgeries. Trabecular thickness (Tb.Th) is often used as a measure of the architecture of cancellous bone. However, Tb.Th is typically reported as a volume average and does not have any directionality. The goal of this study was to compare direct trabecular thickness measured throughout the volume and along the three primary directions of a cubic cancellous bone sample. A 4x4x4mm cube of cancellous bone from the distal femur of a New Zealand White rabbit was scanned on a micro-computed tomography system (EVS Corp, London ON) and reconstructed with 0.032mm isotropic voxels. The direct thickness (Hildebrand & Ruegsegger 1997) was calculated as the mean diameter of the spheres that fit within the trabecular structure. A single average value was measured for the entire structure, generating a volume-weighted direct thickness. Next the data were skeletonized, producing a one-voxel thick representation located at the midline of the trabecular structure. The nodes, where struts within the trabecular structure met, were removed and each strut's orientation was measured as the angle of a straight line connecting the two endpoints. Trabeculae lying within a 40 degree envelope of the three primary directions of the cube were identified. For each primary direction, the average direct thickness was determined for the individual trabecula identified. From the individual trabecular thicknesses, the overall mean and mean corresponding to each primary direction were determined. The measured direct thickness varied across the different measurement approaches. When the entire sample was considered, the average direct thickness was 0.177mm., and the mean thickness measured only from the trabeculae oriented along the three primary directions was 0.185mm. When the individual directions were considered, the average direct thickness measured in each of the directions was 0.181mm, 0.196mm, and 0.185mm. Measurement of directional direct thicknesses may provide a tool for measuring intraspecimen architecture variation and improve our understanding of the mechanical behavior of cancellous bone.

M097

Characterization of Changes in Trabecular Bone with Age and Disease. E. S. Mittra*[1], W. Lin*[1], B. Gruber[2], C. T. Rubin[1], Y. Qin[1]. [1]Biomedical Engineering, State University of New York, Stony Brook, NY, USA, [2]Allergy and Immunology, State University of New York, Stony Brook, NY, USA.

It is well known that changes in trabecular architecture occur with respect to age and disease and that these changes are related to fracture risk. This preliminary study seeks to elucidate which architectural parameters are most indicative of these properties. A 2 cm^3 section of trabecular bone was harvested from the calcanei of 4 cadavers chosen to be of similar, but advanced age. Physiologic orientation was maintained while harvesting such that the axes of the harvested cube were identical to *in vivo* anatomical axes. Mechanical property data was collected via compression testing and the specimens were subsequently scanned in a μCT machine. Table 1 shows the overall results. The bone volume fraction (BV/TV) gives a general picture of density and clearly identifies the osteopenic individual of the group.

Table . Selected micro-CT parameters showing overall trends.

Age / Sex	TV/BV	Conn. D.	DA	MIL
n/a / male	0.18	3.62	1.68	1.01
86 / female	0.14	4.23	1.64	1.07
85 / female	0.05	0.86	1.72	2.98
85 / female	0.14	5.20	1.58	0.98

The connectivity density (Conn. D.) was chosen to show a representative trend in μCT parameters, and was mimicked by other parameters such as trabecular thickness and trabecular spacing. The degree of anisotropy (DA) gives an indication of overall geometric heterogeneity and the most osteopenic bone had the largest value. In other words, the bone loss is occurring in a very specific manner with regard to geometry. The mean intercept length (MIL) values listed in the table correspond to the largest such values and show that the principal trabecular orientation of the osteopenic individual has a nearly 3-fold stronger effect in comparison to the nearest relatively non-osteopenic individual. An evaluation of the direction associated with these values show an average deviation from the superior-inferior axis of approximately 74º. This is thought to correspond to the physiologic loading direction during gait cycles. Micro-CT parameters seem to provide, therefore, a valuable tool to identify changes in trabecular architecture due to age or disease. In addition, our study provides a validation of the application of Wolff's law in that the principal trabecular orientation is maintained in the direction of principal loading (i.e., gait), and this effect is more pronounced in situations of bone loss.

M098

Computed Tomographic Microscopy in a Rabbit Model of Osteoarthritis. D. L. Batiste*[1], A. Kirkley*[2], S. Laverty*[3], N. L. Ford*[1], M. M. Thornton[4], D. W. Holdsworth[1]. [1]Imaging Research, John P. Robarts Research Institute, London, ON, Canada, [2]Department of Surgery, University of Western Ontario, London, ON, Canada, [3]Dept. de Sciences Cliniques, Universite de Montreal, St. Hyacinthe, PQ, Canada, [4]Enhanced Vision Systems, Corp., London, ON, Canada.

We are interested in the development of quantitative computed tomographic imaging techniques that can be used to study bone density and structure in animal models of osteoarthritis (OA). In this study, we investigate whether it is possible to use micro-computed tomography (micro-CT) to characterize a rabbit anterior cruciate ligament transection (ACLX) model of OA. We have imaged fresh excised tissue from skeletally mature New Zealand White rabbits, including both control animals and those that had undergone ACL transection 4, 8, or 12 weeks prior. All animal surgery was performed within the guidelines of the institutional animal care committee. Hindlimbs were harvested from control animals and imaged in saline, with the soft tissue intact. Specimens were imaged at 80 kVp on a micro-CT system system (Enhanced Vision Systems Corp., London Canada). During data acquisition, 262 digital x-ray projection images were obtained at 0.748 degree intervals. These images were then reconstructed to obtain a 2.5 x 2.5 x 2 cm3 volume of image data, with 0.085 mm isotropic voxel spacing. Example results are shown in the figure, where we compare sagittal sectional views of control (a) and ACLX (b) animals. Precision in the CT data is approximately 85 Hounsfield units, equivalent to about ±5% in bone density. The three-dimensional data format made it possible to characterize joint spacing and bone architecture. We found that joint spacing increased after ACLX, probably due to fluid accumulation. Also visible in the figure is the appearance of poorly mineralized osteophytes in the eight-week post-ACLX animals (arrow). Micro-CT has become a common tool during pre-clinical investigations of new treatments for osteoporosis, but this non-destructive technique is less commonly used during studies related to OA. In this study, we have demonstrated the potential viability of using quantitative high resolution micro-CT to characterize changes in bone architecture and bone density in a rabbit ACLX model of surgically induced osteoarthritis.

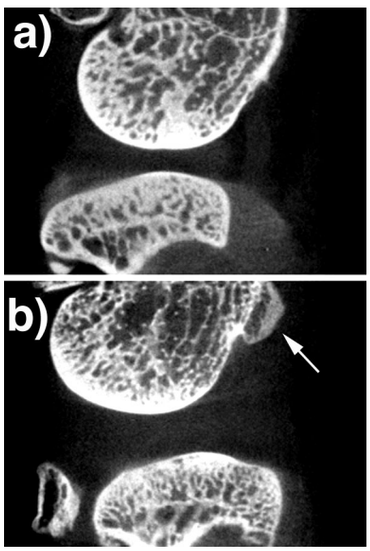

M099

Bone Mineral Density at the Hip And Tibia and Speed of Sound at the Tibia in Spinal Cord Injured Individuals. L. M. Giangregorio*[1], C. E. Webber[2], S. M. Phillips*[1], A. L. Hicks*[1], N. McCartney*[1]. [1]Human Biodynamics, McMaster University, Hamilton, ON, Canada, [2]Nuclear Medicine, McMaster University, Hamilton, ON, Canada.

The aim of the present cross-sectional study was to evaluate the bone mineral density (BMD) at the hip and tibia, as well as the speed of sound (SOS) at the radius and mid-tibia in individuals with a spinal cord injury (SCI). The level of lesion ranged from C4 to T12, the average age of the participants was 32 years old, and average time post-injury was 10.2 years, with a range of 1.17 to 25 years. BMD at the hip was examined in 21 individuals (15 males, 6 females) using dual-energy x-ray absorptiometry (DXA), along with SOS measurements at the radius and mid-tibia with an ultrasonometer. In a sub-group of 14 individuals, tibia BMD was also measured using DXA. Using the WHO criteria for osteoporosis, 11 of 21 subjects were osteoporotic at the hip, 9 were osteopenic and 1 had normal hip BMD. In contrast, only one subject had a tibia SOS T-score of -2 and two subjects had T-scores between -1 and -2. Hip BMD and tibia SOS were moderately correlated ($r = 0.43$, $p0.05$). Hip BMD and tibia BMD were strongly correlated, however ($r = 0.69$, $p<0.005$). Radius SOS T-scores were 0.65 and 0.78 in males and females respectively, and were not correlated with any of the lower limb variables. Lower limb bone mass is reduced in spinal cord-injured individuals, but SOS at the mid-tibia is not. SOS may reflect bone properties other than bone density that may not be reduced in individuals with SCI.

M100

Format of Ultrasound Report Influences Patient Compliance With Treatment and Understanding of Risk. L. Greenwald*[1], A. Bardwell*[2], P. Kushner*[3], J. Maliinak*[4], M. Lewicki[5], S. Silverman[6], M. Greenwald[1]. [1]Desert Medical Advances, Palm Desert, CA, USA, [2]Santa Fe, Santa Fe, NM, USA, [3]Long Beach, Long Beach, CA, USA, [4]La Mesa, La Mesa, CA, USA, [5]Osteoporosis Research, Albuquerque, NM, USA, [6]UCLA, Los Angeles, CA, USA.

A survey of 150 postmenopausal women with no prior bisphosphonate therapy is being conducted in the Southwestern U.S. Postmenopausal women were offered a free bone density with a Sahara ultrasound unit and asked to complete a questionnaire with their primary physician within 30 days. Entry criteria required a unique primary physician for each subject. The women were separated into subgroups above or below age 65 and this report is an interim analysis. For those over 65, the average age was 73 yrs(range 65-84)and insurers were managed care(50%), private(45%),and welfare(5%). Insurance type did not influence follow up with the primary physician. The subject and her physician received by random choice the results of the bone density as a traditional T score provided by Sahara or an absolute risk fracture report. Only 60% of women followed up with their doctor when given the traditional T score Sahara form (many wrote their test was "good' so they didn't need to follow up). Only 20% of these elderly women received a prescription for osteoporosis. In the other group, randomly assigned the absolute fracture report, 70% followed up with their doctor, 40% received a new osteoporosis prescription, and 95% filled the prescription. More women in this elderly group followed up with their doctor and a larger percentage received treatment prescriptions with the absolute fracture risk format for U/S ($p<0.07$). Most concerning was that only 22% of the women under age 65 (avg age 49) followed up with a physician with the traditional T score format. Many women may erroneously assume that there is no osteoporosis risk with the traditional T score U/S report.

M101

Can the WHO Criteria Be Applied to Multi-Site Axial Transmission Quantitative Ultrasound? K. M. Knapp[1], G. M. Blake[1], I. Yaniv[2], T. D. Spector[3], I. Fogelman[1]. [1]Osteoporosis Screening and Research Unit, Guy's Hospital, London, United Kingdom, [2]Sunlight Medical Ltd, Tel Aviv, Israel, [3]Twin Research and Genetic Epidemiology Unit, St Thomas' Hospital, London, United Kingdom.

The WHO criteria defines osteoporosis based on bone mineral measurement as 2.5 or more standard deviations below the young healthy adult mean at the hip, spine or radius. This criteria is widely used for the diagnosis of osteoporosis. However, the use of the WHO criteria may be inappropriate for the diagnosis of osteoporosis using other modalities such as QUS. A previous study by Weiss et al [1] found that different T-score cut-offs were required for SOS measurements of the phalanx, tibia and metatarsal to result in the same prevalence of osteoporosis as a T-score ≤ -2.5 for SOS at the radius. The aim of this study was to investigate the T-score thresholds for the diagnosis of osteoporosis from SOS measurements at the radius, tibia, phalanx and metatarsal compared to BMD measurements at the total hip. A group of 75 women aged 60-69, with no history of drugs or diseases known to affect bone metabolism, low trauma fractures or premature menopause/ prolonged amenorrhoea were recruited. SOS measurements were made at the phalanx, radius, tibia and metatarsal using the Sunlight Omnisense™ (Tel Aviv, Israel) and BMD measurements were made at the proximal femur using the Hologic QDR-4500a (Bedford, MA). The same method was applied as used by Weiss et al [1]. The prevalence of osteoporosis was calculated for BMD at the total hip for the age group 60-69 years. The equivalent T-score required to identify the same percentage of patients as osteoporotic for SOS measurement at the radius, tibia, phalanx and metatarsal was then calculated.

Site	n	Mean T-score	% prevalence	T-score threshold
Radius SOS	71	-1.00	5.6	-2.6
Tibia SOS	75	-1.15	17.3	-3.0
Phalanx SOS	52	-1.80	25.0	-3.0
Metatarsal SOS	49	-0.92	4.1	-2.2
Total Hip BMD	72	-0.60	4.2	-2.5

These results demonstrate that while a T-score cut-off of -2.5 is appropriate for use with Radius SOS, it is inappropriate for use with the other sites. Furthermore, differing T-score thresholds are required for the diagnosis of osteoporosis at different sites using the Sunlight Omnisense™ . Further research is required to verify these T-score thresholds using larger reference populations and possibly different methods for calculating the diagnostic thresholds.

[1] Weiss M. Osteoporosis Int 200 11:688-696

M102

Relationship Between Ultrasonic Backscatter and Trabecular Thickness in Human Calcaneus: Theory and Experiment. K. A. Wear*[1], A. Laib*[2]. [1]Food and Drug Administration, Rockville, MD, USA, [2]Scanco Medical AG, Bassersdorf, Switzerland.

Ultrasonic backscatter from calcaneus is a new diagnostic measurement that may complement existing measurements such as broadband ultrasonic attenuation (BUA), speed of sound (SOS), and bone mineral density (BMD). In addition, the study of scattering from bone elucidates mechanisms underlying attenuation (the combined result of absorption and scattering) and therefore may enhance diagnostic interpretation of BUA measurements. Previously, a model has been developed in which trabeculae are represented as cylinders that are narrow relative to the ultrasonic wavelength. This model predicts frequency dependence of backscatter from calcaneus in close agreement with measurements. Compared with other theoretical models for scattering from trabecular bone (that are also insightful and useful), the cylinder model is somewhat simplistic from a geometric standpoint. However, unlike the other models, it 1) does not require small variations in acoustic properties (material density and sound speed) between trabeculae and the embedding medium (in vivo: marrow or in vitro: water) and 2) allows for propagation within trabeculae of shear waves (which have been demonstrated to occur in cortical bone and therefore are likely to propagate in trabeculae). An approximate formula, derived from the cylinder model, has recently been developed to relate backscatter to four determinants: mean trabecular thickness (Tb.Th), mean trabecular spacing, trabecular mass density, and trabecular longitudinal sound speed. In the realm of expected values of these parameters for trabecular bone, the model predicts that backscatter is approximately proportional to Tb.Th to the nth power where n=2.9. Since volumetric BMD is expected to be proportional to Tb.Th to the power of 2 (rather than 2.9), there is hope that backscatter may convey some information regarding Tb.Th beyond that contained in BMD although recent empirical results, obtained in vitro with a moderate number of samples (Chaffai et al., Bone, 20, 229 - 37, 2002) suggest that this potential added information content is small. To experimentally test the approximate model, ultrasonic backscatter was measured on 43 human calcaneus samples in vitro. In addition, micro computed tomography (voxel size: 30 cubic microns) was performed in order to assess microarchitecture. A power law fit of backscatter coefficient versus Tb.Th produced an estimated exponent of n=2.8 with a 95 percent confidence interval of (1.7, 3.9). In conclusion, backscatter from human calcaneus provides potentially diagnostically useful information regarding mean trabecular thickness consistent with predictions from the cylinder model.

M103

Measurements of Ultrasonic Backscattered Spectral Centroid Shift from Spine In Vivo – Methodology & Preliminary Results. K. A. Wear*[1], B. S. Garra*[2], M. C. Pinet*[2], S. Felker*[2], J. Mai*[2]. [1]Center for Devices and Radiological Health, Food and Drug Administration, Rockville, MD, USA, [2]Radiology Dept., University of Vermont, Burlington, VT, USA.

Previous reports have shown a good correlation between measurements of backscattered ultrasound and bone mineral density (BMD) in the calcaneus. Although measurements in calcaneus are useful, direct measurements in hip and spine would be more valuable since these sites are associated with the clinically most significant osteoporotic fractures. We have developed a technique to measure backscattered ultrasound from lumbar vertebrae using a commercial ultrasound scanner. The method relies on compression of the overlying abdominal tissue to a constant thickness to minimize measurement variability due to attenuation and diffraction effects. Since soft tissue may be approximated as an incompressible fluid, the tissue expands laterally in order to compensate for the longitudinal compression. Therefore attenuation due to overlying tissue between transducer and vertebra remains roughly constant. Radio frequency backscattered ultrasound data are acquired from L3 and/or L4 vertebral bodies using a GE-Vingmed System Five Ultrasound Scanner fitted with a 2.5 MHz phased array ultrasound probe. Data are acquired in both transverse and longitudinal planes after compressing the overlying tissue to a thickness of 3 cm. Correction for instrument gain settings and focusing/diffraction effects is achieved by use of data acquired from a tissue-mimicking calibration phantom (with attenuation coefficient matched to soft tissue) scanned immediately after the human subject using the same settings. The spectral centroid shift between the spine and phantom data is an index of ultrasonic attenuation within the spine. BMD was also measured using a GE-Lunar whole body DEXA system. From measurements from 11 vertebrae in 7 individuals, we have found a correlation coefficient of r = -0.61 between spectral centroid shift and BMD, with a slope of -0.16 MHz/(g/cm2). This negative correlation is expected as denser, more highly attenuating bone would be expected to produce greater downshifts in spectral centroid. In conclusion, 1) acquisition of ultrasonic backscatter data from human spine in vivo is feasible, and 2) spectral centroid shift exhibits a moderate negative correlation with BMD in accordance with expectrations.

M104

***In Vivo* QUS Performance of a Fixed-Array Bone Imaging Ultrasonometer.** W. K. Wacker*, R. F. Morris*, K. L. Morris*, G. F. Mitchelmore*, K. G Faulkner. GE Medical Systems Lunar, Madison, WI, USA.

The Lunar Achilles InSight (GE Medical Systems), a fourth-generation bone ultrasonometer, eliminates 'blind' measurement by displaying a real-time image of the heel prior to and during measurement. A Region-of-Measurement (ROM) circle is superimposed on the image to show the location of the ultrasound measurement. The image is produced using a 2-element coaxial transmit transducer and a 590-element two-dimensional array receiving transducer. Transmission bone ultrasonometry is increasingly accepted as a low cost, effective method to assess and manage osteoporotic patients. We compared the *in vivo* performance of the Achilles InSight to the performance of the Lunar Achilles Express (GE Medical Systems), a previous generation bone ultrasonometer. Measurements were performed on 253 subjects with a wide range of heel densities (Stiffness Index 35 to 149). Stiffness Index was highly correlated (r=0.93) between the two devices. Regression of Achilles InSight Stiffness Index values on Achilles Express values resulted in values for the slope (1.01) and intercept (-1.3) which were not significantly different from identity (α=0.05). We conclude that Stiffness Index values measured with Achilles InSight are equivalent to those measured with previous generation Lunar Achilles bone ultrasonometers.

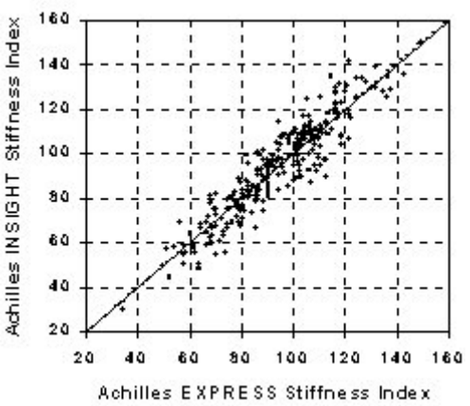

M105

Quantitative Ultrasound for the Evaluation of Skeletal Growth in New-Borns. S. Gonnelli[1], A. Montagnani*[1], L. Gennari[1], C. Cepollaro*[1], S. Martini*[1], D. Merlotti*[1], M. Muraca*[2], S. Perrone*[2], G. Bonocore*[2], F. Bagnoli*[2], C. Gennari[1]. [1]Institute of Internal Medicine, University of Siena, Siena, Italy, [2]Institute of Neonatology, University of Siena, Siena, Italy.

One of the most debated issues in pediatric bone research is the optimal technique for determining bone status in growing children. Quantitative ultrasound (QUS), although being widely used in adults is, by far, scarcely employed in new-borns and in children. This study aimed to evaluate the usefulness of QUS in new-borns and the factors influencing QUS parameters. In 130 healthy new-borns (67 males and 63 females, gestational age range: 32.7-42.1 weeks) QUS parameters were assessed at distal metaphyses of humerus using Bone Profiler (IGEA, Italy), after an appropriate modification of caliper and software. In all subjects we evaluated: AD-SoS (m/s), the characterizing graphic trace parameters (SDy, FWA and BTT) and finally two new indices: SoS (m/s), that is the speed of sound calculated on the first peak and BTT_{1570} (µs), that is the interval time between the first peak of the ultrasound and when this reaches the speed of 1570 m/s. QUS measurements were also performed in all mothers (age range: 24-38 years) who also self-reported a calcium questionnaire. In 30 infants QUS were repeated also after 12 months. In the 130 new-borns we obtained the following results: 1749.8±34.1 m/s for AD-SoS; 879.8±2596.9 mV/µs² for SDy; 1.96±0.73 mV for FWA; 0.23±0.10 µs for BTT; 0.91±0.16 µs for BTT1570 and 1724.8±25.3 m/s for SoS. No differences were found in QUS parameters between the two sexes. Among QUS parameters only BTT and BTT_{1570} correlated with anthropometric indices, such as skull diameter (r=0.18, p<0.05; r=0.39; p<0.01, respectively), the weight (r= 0.20, p<0.05; r=0.37; p<0.01, respectively) and the height (r=0.20; p<0.05 only for BTT1570). The mothers showed a reduction of AD-SoS (T-score: –1.04±0.82), whereas the graphic trace parameters resulted normal as compared to normative data. No correlations were found between mothers and new-borns data. Children, who underwent a second measure after 12 months, showed a reduction of AD-SoS, SDy and FWA, whereas BTT significantly (p<0.001) increased. In conclusion, the present study pointed out that: Bone Profiler is able to perform QUS measurements in new-borns; among all QUS parameters BTT and BTT_{1570} showed the best correlation with anthropometric indices of new-borns; preliminary longitudinal data seem to suggest BTT as the best parameter to monitor the physiological bone growth in pediatric subjects. Therefore, QUS, for its technical characteristics (radiation-free, low cost, portability, rapid scan), offers promise as useful tool for widespread use in pediatrics.

M106

Correlation Between Cut-Off Value Determined by Using Quantitative Ultrasound and Threshold of Fracture in Japanese Women. K. Yoh*[1], K. Makita*[2], H. Kishimoto*[3], H. Ohta[4], I. Gorai[5], J. Hashimoto[6], Y. Nakatuka*[7], S. Yoshimoto*[8], S. Kamae*[9]. [1]Orthopedic Surgery, Hyogo College of Medicine, Nishinomiya, Japan, [2]Keio University, Tokyo, Japan, [3]Sanin Rosai Hosp., Yonago, Japan, [4]Tokyo Women's Univ., Tokyo, Japan, [5]Yokohama City Univ., Yokohama, Japan, [6]Osaka Univ., Osaka, Japan, [7]Osaka City Univ., Osaka, Japan, [8]Hyogo Chuo Hosp., Sanda, Japan, [9]Hyogo College of Medicine, Nishinomiya, Japan.

The aim of this study was to assess the ability of Quantitative Ultrasound (QUS) to identify woman with vertebral fracture. Recently, the QUS technique is becoming available around the world. To diagnosis osteoporosis by using QUS, the correlation between it and dual energy X-ray absorptiometry (DXA) as well as the ability to identify fracture risk needs to be investigated. For this reason, a total of 388 Japanese women, including patients with osteoporosis, were tested, after signing an informed consent. The speed of sound (SOS) of all subjects was measured at the right calcareous using QUS (FURUNO CM-100, Japan), and bone mineral density (BMD) was measured at the lumbar spine (L2-L4) using DXA (Norland: XR26/36, Hologic: QDR-2000 and Lunar: DPX). All subjects also underwent radiographic examination of the thoracic and lumbar spine with the criterion recommended by the Japanese Society for Bone Mineral Research. (This criterion: In the measurement of vertebral bodies, heights of the posterior margin (p), the central portion (c) and the anterior margin (a) of vertebral bodies, fracture and deformity is defined as a/p of less than -25% and c/p as well as c/a of less than –20%.) The result was divided into two categories: 107 women (mean age: 66.0 years) were without vertebral fracture and 281 women (mean age: 61.5 years) were with vertebral fracture. The average value of SOS was 1480m/s without vertebral fracture and 1493m/s with vertebral fracture, respectively. As a result of each sensitivity and specificity curve analysis on SOS, the intersection point was 1484m/s. This SOS value, 1484m/s, is almost the same as the cut-off value for diagnostic of osteoporosis of SOS, 1487m/s, derived from lumbar BMD using DXA. These data showed the high correlation between the cut-off values of SOS derived from with or without vertebral fracture and the cut-off value of SOS derived from diagnostic of osteoporosis based on DXA. In conclusion, SOS measurement can be used to diagnose osteoporosis as well as to predict fracture risk.

M107

Quantitative Ultrasound Measurement at the Femur in Vitro: Feasibility Study, Precision and Relationship Between BUA And BMD. L. Akrout*[1], F. Padilla[1], C. Latremouille*[2], P. Laugier[1]. [1]Lip umr 7623, CNRS - Universite Paris 6, Paris, France, [2]Institut d'Anatomie, Anatomie Broussais Hotel-Dieu, Paris, France.

The goal of this paper is to demonstrate the feasibility of QUS measurements at the femur, and to present relationships between QUS and DXA at the femur. Measurements of broadband ultrasonic attenuation (BUA) represent an established means of skeletal status assessment in osteoporosis, and especially for the prediction of fracture risk at the femoral neck. Today, the preferred site of ultrasound measurement is the calcaneus (heel bone). However, the predictions might be improved if the measurements were performed directly at the site of fracture. Six human femur freshly removed from cadavers have been measured with a pair of 0.5 MHz focused transducers . 2D rectilinear scans were performed and the RF signals were recorded at each measurement point. An appropriate signal processing has been developed to find ROIs were the frequency-dependent attenuation was linear and to compute BUA (slope of the frequency dependent attenuation). 2D BUA images, 6*6 cm2, were obtained, centered on the femoral neck and the great trochanter. Roughly, 20 measurements with reposioning were performed on each sample to determine the reproducibility. The CVs were computed for 4 different ROIs, and were found to vary from 2 to 6% The mean BUA in a ROI centrally located in the great trochanter was compared with BMD (Hologic QDR 4500A) in a site-matched ROI. It resulted in a linear relationship with r^2 = 0.7. In a second step, slices with parallel faces of 2 cm thickness were cut along the sagital axis of two specimens. The same procedure of BUA measurement was followed on 7 ROIs for each slices. The corresponding CVs were found between 2 and 6% Comparison with BMD in site-matched ROIs resulted in a linear relationship with r^2 = 0.9. These data demonstrate in vitro the feasibility of QUS measurements at the femur with reasonable reproductibility. Although, it is not yet possible to conclude on the relationship between QUS and BMD at the femur due to the small number of specimens, our results suggest that BUA could be considered as a surrogate marker of BMD at the proximal femur, which is consistent with data previously shown at the calcaneus.

M108

Assessement of Trabecular Microstructure Using Ultrasonic Statistical Models of Trabecular Bone Microstructure. F. Jenson*, F. Padilla, P. Laugier. Lip umr 7623, CNRS - Universite Paris 6, Paris, France.

The goal of this study is to assess the mean trabecular thickness of trabeculae, in human cancellous bones from ultrasonic backscattering measurements. To address this inverse problem, we propose a model for the ultrasonic frequency-dependent backscatter coefficient in cancellous bone. A weak scattering model is used and the backscatter coefficient is expressed in terms of an autocorrelation function of the medium. The autocorrelation function describes the statistical properties of the fluctuations of the mechanical properties (i.e., density and compressibility) of cancellous bone specimens. Different autocorrelation functions (Gaussian, exponential and dense media) are used to compute the backscatter coefficient. Comparison is made with experimental data obtained on 19 human specimens of calcanei and for frequency ranging from 0.4 to 1.2 MHz. For each specimen a non-linear regression is performed to fit the theoretical predictions to ultrasonic experimental data and the mean trabecular thickness is estimated. Experimental data and modeled theoretical predictions are averaged over the 19 specimens. A good agreement between experimental data and predictions was found for both the magnitude and the frequency dependence of the backscatter coefficient. We also found a good agreement between the experimental mean trabecular thickness (Tb.Th=130±6.5 µm) derived from the analysis of 3D images of bone microarchitecture (very high resolution synchrotron radiation micro tomography) and theoretical predictions (Tb.Th-Gauss=140±10 µm, Tb.Th-exponential=153±12.5 µm and Tb.Th-dense=138±6.5 µm). These results open interesting prospects for the assessment of bone microarchitecture from ultrasonic backscattering measurements.

M109

Assessment of Changes Occurring in Subchondral Bone during Rat Skeletal Maturation using 400 MHz Quantitative Ultrasound. B. Jaffre*[1], K. Raum*[2], J. Brandt*[3], A. Watrin*[4], A. Klemenz*[2], P. Netter*[4], P. Laugier[1], A. Saied[1]. [1]Lab. Imagerie Parametrique, CNRS-Paris 6 UMR 7623, Paris, France, [2]Inst. Med. Physics and Biophysics, Martin Luther University, Halle, Germany, [3]Orthoped. Clinic, Martin Luther University, Halle, Germany, [4]Lab. of Pharmacology, CNRS-UHP UMR 7561, Nancy, France.

High frequency scanning acoustic microscopy is referred to as an acoustic imaging system with a spatial resolution comparable to that of light microscopy. Usually it allows the qualitative characterization of acoustical properties at or close to the surface of flat samples. With the previously described Multi Layer Analysis (MLA) method it is furthermore possible to obtain quantitative acoustic information which can be related to mechanical and structural properties of the tissue under study. We have used this technique to investigate the age-related changes occurring in subchondral bone during rat skeletal maturation. Sixteen patellae of 8 immature (7 weeks old) and 8 mature (11 weeks old) rats were thawed in methanol, frozen in liquid nitrogen and cut in the sagittal plane of the patella using a high precision milling machine. Samples were then imaged in methanol at 400 MHz (3 µm spatial resolution) using an acoustic microscope (KSI SAM 2000). Acoustic impedance (Z) images of each sample were constructed using the local measurement of the reflection coefficient. Results were compared to histology. Qualitative analysis revealed that bone porosity decreases with age and the bone/cartilage interface gets more regular. The mean impedance of mature and immature samples were similar and around 5.0 ± 0.6 Mrayl. However in mature bone, two regions of different reflection coefficients could be distin-

guished on 6 samples out of 8: a region just beneath cartilage where the lower Z (4.5 ± 0.6 Mrayl) could be due to the less mineralized transitional zone between bone and cartilage; and a region of higher reflection coefficient (Z = 5.2 ± 0.7 Mrayl) and probably higher mineralization in the deeper and earlier formed bone. High resolution 400 MHz acoustic microscopy is sensitive to some changes occurring in subchondral bone during the maturation process. Qualitative images enable assessment of changes in bone structural organization and elastomechanical properties at a microscopic scale. Measurements of acoustic impedance are a new means to quantify the observed changes. The study of relationships between QUS microscopy and bulk properties will be the object of further works. QUS microscopy could therefore be a new method to investigate changes occurring in bone during the development of diseases like arthritis and osteoarthritis affecting bone and cartilage.

M110

Quantitative Ultrasound Before And After Heart Transplantation: A Cross-Sectional Study. C. Cepollaro*[1], S. Gonnelli[1], A. Montagnani*[1], M. Breschi*[1], C. Pondrelli*[1], D. Bruni*[1], M. Mangeri*[1], F. Diciolla*[2], M. Maccherini*[2], C. Gennari*[1]. [1]Institute of Internal Medicine, University of Siena, Siena, Italy, [2]Institute of Cardiac Surgery, University of Siena, Siena, Italy.

During the past 2 decades, heart transplantation (HTx) has evolved from an experimental procedure to an accepted life-extending therapy for patient with end-stage heart failure (ESHF). Patients with ESHF awaiting HTx tend to have reduced BMD related to cardiac cachexia with poor nutrition, prolonged physical inactivity and other factors. After HTx, glucocorticoid and immunosuppressive therapy could produce further bone loss. Although DXA is the most used technique for assessing BMD, quantitative ultrasound (QUS) has been explored as an alternative for the assessment of skeletal status. This study aimed to evaluate bone status, by DXA and QUS, before and after HTx. We recruited 30 patients (25 males and 5 females, mean age 55.7±9.0) with ESHF awaiting HTx and 62 patients (48 males and 14 females, mean age 57.3±9.1) who had undergone HTx 12-24 months before. Patients on treatment with bone antiresorptive drugs were excluded. In all patients and in 92 age and sex-matched healthy controls, we performed DXA (Hologic QDR 4500) at lumbar spine (BMD-LS) and at femur (total: BMD-T, neck: BMD-N, trochanter: BMD-Tr, inter-trochanter: BMD-Itr, Ward's triangle: BMD-W) and QUS parameters at calcaneus (speed of sound: SOS, broadband ultrasound attenuation: BUA and Stiffness) by Achilles plus, and at phalanxes (amplitude dependent speed of sound: AD-SoS) by Bone Profiler (Igea, Italy). The T-score values for DXA were: -1.5 for BMD-LS, -1.0 for BMD-T, -1.6 for BMD-N, -1.0 for BMD-Tr, -0.9 for BMD-Itr, -2.0 for BMD-W in the ESHF group and respectively of -1.7, -1.3, -1.9, -1.2, -1.2 and -2.3 in the HTx group. Considering QUS parameters, in the ESHF group, SOS, BUA, Stiffness and AD-SoS showed T-score values respectively of -2.0, -2.2, -2.7 and -1.9; while in the HTx group, the T-score values resulted -2.3, -2.6, -3.0 and -2.2 respectively for SOS, BUA, Stiffness and AD-SoS. In both ESHF and HTx patients, all DXA and QUS parameters resulted significantly lower than incontrols. Instead, the differences in DXA and QUS between ESHF and HTx did not reach the statistical significance. We can conclude that: QUS parameters at calcaneus and at phalanxes, similarly to DXA, are significantly reduced in ESHF; trabecular bone seems to be more affected than cortical bone. QUS, namely at calcaneus, may be a useful tool to assess bone status in heart transplants recipients also in view of some technical advantages, (radiation-free, portability, low cost). However, further longitudinal studies are needed to confirm its usefulness in the management of HTx patients.

M111

Comparison of Ultrasonic Measurements versus DXA in the Course of Osteoporosis Prevention at the Department of Traumatology, University of Vienna Medical School, Austria. N. A. Zobor*[1], M. Greitbauer*[1], D. Mueller*[2], P. Pietschmann*[3], V. Vecsei*[1]. [1]Dept. of Traumatology, University of Vienna, Medical School, Vienna, Austria, [2]University of Vienna, Medical School, Vienna, Austria, [3]Dept. of Pathophysiology, University of Vienna, Medical School, Vienna, Austria.

The purpose of the investigation: comparison of ultrasonic versus DXA measurement in patients who already have suffered a fracture. Method: The bone density was measured in the patients who were of 55 years or older, and have suffered a fracture. The measurements were performed with ultrasonic (on the phalanx, radius and tibia) and by DXA (on the lumbar spine and hip), respectively. From each kind of measurement the worst result was taken for statistical analysis and the patient was treated according to it. Results: In our collective 44 patients could be measured in both ways. The mean age was 76.1 years and we had 87% women and 13% men. According to the DXA measurements 83% of them had osteoporosis and 17% osteopenia, while the ultrasonic measurements showed in 79.4% osteoporosis and 20.6% osteopenia. When comparing the ultrasonic with DXA, the measurements of the phalanx and radius were in 85.7% in good agreement with the DXA results, while on the basis of the tibia measurements only 16% had osteoporosis and 26% osteopenia, and the rest 58% was judged as healthy. Conclusion: In contrast to tibia measurements, in elderly patients with recent fractures ultrasound results at the phalanx and the radius show good agreement with DXA-values.

M112

Concordance of Heel Quantitative Ultrasound and Central DXA in Patients Taking Different Forms of Glucocorticoids. V. I. Petkov*, M. T. Tran*, M. I. Williams*, C. T. McMurtry, R. A. Adler. Endocrinology, McGuire Veterans Affairs Medical Center, Richmond, VA, USA.

Quantitative ultrasound (QUS) may provide information about bone quality not reflected in DXA measurements. The mechanism of bone loss in glucocorticoid-induced osteoporosis differs from most other forms of osteoporosis, as demonstrated by histomorphometry. The goal of this study was to determine if such differences can also be found in the relationship of QUS measurements to central DXA in patients exposed to various glucocorticoid (GC) treatments. We analyzed data from 2 prospective studies conducted in subspecialty clinics at a single Veterans Affairs Medical Center. The participants filled out a questionnaire, which included questions on GC therapy (oral and local), had QUS of the heel (Hologic Sahara), and underwent central DXA (Hologic 4500) within a month. Subjects were divided into 4 groups based on questionnaire responses: ever or currently on oral GC (50%), only intra-articular GC (21%), ever or currently on inhaled GC (16%), and never had GC therapy (13%). ANOVA was used to determine differences between groups and ANCOVA to account for possible confounding by other variables. The relationships among QUS measurements and central DXA (spine, total hip, and femoral neck) in each of the treatment groups were examined. A total of 189 subjects had heel QUS [Speed of sound (SOS), Broadband ultrasonic attenuation (BUA), Quantitative ultrasonic index/Stiffness (QUI), Bone mineral density (BMD), and T-score] and central DXA. The mean (SD) age was 62 (13.6). Nine subjects were women; 2/3 were white men. Mean T-scores were: spine -0.19 (1.8), total hip -0.56 (1.10), femoral neck -1.15 (1.07), and heel -0.57 (1.24). When analyzed by GC treatment group, no significant differences in the QUS measurements were found. However, subjects treated with oral GC had significantly lower spine BMD than those treated with local injectable GC (mean difference from ANCOVA model 7.4%). The correlations among the QUS parameters and DXA at the spine, hip, and femoral neck were similar across the four groups, with one exception. In subjects exposed to oral GC, the correlation of heel SOS with femoral neck or total hip BMD was much less than that of the other heel measurements, suggesting that SOS assessed a characteristic of bone not reflected in the DXA measurements. In patients with pulmonary or rheumatologic disorders, heel QUS and central DXA are generally concordant to a degree reported in other populations. Only the SOS measurement in the oral GC subjects seemed to differ from other QUS parameters. Studies are underway to better quantitate exposure to GC in order to further refine our findings.

M113

Can Heel Ultrasound Bone Mineral Density Plus a Questionnaire Predict Osteoporosis in Rheumatology Patients? M. T. Tran*, V. I. Petkov*, C. Holt*, M. I. Williams*, R. A. Adler. Endocrinology, McGuire Veterans Affairs Medical Center, Richmond, VA, USA.

Rheumatology Clinic patients often need glucocorticoid therapy, and any musculoskeletal disorder that decreases physical activity may be a risk factor for osteoporosis. Ideally patients would be screened with central BMD by dual energy x-ray absorptiometry (DXA). To find a cheaper alternative, we determined whether the combination of heel ultrasound (QUS) BMD and a short questionnaire about risk factors could identify patients at risk for osteoporosis, defined by low central BMD by DXA. Rheumatology Clinic patients completed a simple questionnaire and had heel QUS. Within 1 month, spine, total hip, and femoral neck BMD were tested by DXA. Subjects having previous BMD tests were excluded, including many patients with inflammatory joint disorders. A total of 102 men and 13 women (72 white, 39 black, and 4 other) completed the questionnaire, 111 underwent heel QUS, and 105 had a DXA. Of those with DXA, 21 had a spine, total hip, or femoral neck T-score $\leq$ -2.0. Only 9 patients were taking oral corticosteroids at screening, 31 had a rheumatoid arthritis, and 49 had osteoarthritis. Simple linear regression showed that central DXA correlated significantly with weight and BMI (body mass index) and with all heel QUS parameters. No significant relationships were found between total questionnaire score and any BMD measurement. By stepwise multiple regression analysis, weight, heel BMD, family history of osteoporosis, and race were found to be significant predictors of BMD in the total hip (42% of variance). Similar models for both femoral neck and spine BMD explained less than one-third of variance. Using a DXA T-score of -2 to define central bone loss, a heel T-score of -1 provided a sensitivity of 81%, specificity 71%, positive predictive value of 17%, and negative predictive value of 94%. ROC curve analyses indicated that heel T-score and weight generated a larger area under the curve (0.850, 95% CI [0.756, 0.94]) than did either characteristic alone. In conclusion, heel QUS predicted central BMD in patients enrolled in a Rheumatology Clinic. Though total questionnaire score did not improve predictability, several specific risk factors such as weight, age, race, and family history of osteoporosis did contribute. Thus, heel ultrasound BMD with or without a short questionnaire moderately predicts central BMD in a patient population of primarily white men with degenerative joint disorders and in lesser numbers, rheumatoid arthritis not on glucocorticoids.

M114

Assessment of Bone Quantity and Quality in Human Cadaver Calcaneus Using Scanning Confocal Ultrasound and DEXA Measurements. Y. Qin[1], Y. Xia*[2], W. Lin*[2], A. Chadha*[2], B. Gruber[2], C. Rubin[2]. [1]Biomedical Engineering, SUNY Stony Brook, Stony Brook, NY, USA, [2]SUNY Stony Brook, Stony Brook, NY, USA.

Advents in ultrasound (US) provide a unique method for evaluating bone strength. Using a developing scanning confocal acoustic diagnostic (SCAD) system, we have tested the feasibility of US assessment for bone quality in the real body region. Measurements were performed on 19 human cadaver calcanei age from 66 to 97 years old. The right foot of each cadaver was tested either by confocal scan mode or by plane wave, non-scan mode. The scanning region converged in the middle of the median plane of the calcanei, covering an approximate 40x40 mm2 with 1 mm resolution. The signals transmitted through the bone were processed to calculate broadband ultrasound attenuation (BUA, dB/MHz), the ultrasound energy attenuation (ATT, dB), and the ultrasound velocity (UV, m/sec). A 15x15 grid region of interest (ROI) was chosen. For both scan and non-scan modes, the obtained US properties (ATT, BUA, UV) were correlated with the bone mineral density (BMD, mg/cm2) measured by DEXA (Hologic 4500A, Bedford, MA). A calculated bone BMD data array was generated by combining BUA and UV data for predicting bone density. SCAD generated UV and BUA images demonstrated resolution compatible to X-ray and MR images (Fig)[Top: SCAD BUA, normal (left) and osteoporotic (right); Bottom: corresponding DEXA). Strong correlations were found between BMD and BUA and between BMD and US estimated index (Table. 1). Correlations between BMD and US parameter were significantly improved by using scan mode and selected ROI as compared to non-scan mode, yielding correlations between BMD and scanning US parameters as R=0.43 (ATT), R=0.82 (BUA), R=0.52 (UV) and R=0.86 (scan US est. BMD), as compared non-scan US parameters, R=0.33 (ATT), R=0.66 (BUA), R=0.24 (UV), and R=0.81 (est. BMD). These results suggest that SCAD is feasible for in vivo bone quality mapping. A well-developed system may result in a unique tool for assessing bone quality.

Table 1

Ultrasound Measurement	Scan Mode	Non-scan mode
Parameter	Mean (SD)	Mean (SD)
ATT (dB)	33.1 (8.8)	34.9 (12.1)
BUA (dB/MHz)	55.3 (15.8)	47.7 (19.4)
UV (m/s)	1506 (40)	1554 (47)
BMD (mg/cm2)	0.403 (0.156)	0.403 (0.156)
Est. BMD (mg/cm2)	0.428 (0.141)	0.420 (0.123)

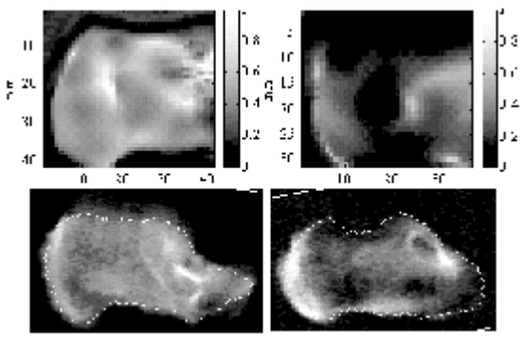

M115

Quantitative Ultrasound of the Heel Does Not Predict Bone Density at the Femoral Neck More Accurately Than Simple Clinical Indices in Postmenopausal Caucasian Women. E. A. Mossman*, N. C. Grinnell*, L. Cole*, K. L. Osborn*, M. R. McClung. Oregon Osteoporosis Center, Portland, OR, USA.

Physicians are confronted with a wide and poorly defined array of clinical diagnostic features upon which to base referral for BMD testing. With the high cost of the DXA procedure to consider and a growing number of aging women potentially at risk, the use of an effective screening tool could significantly reduce the number of patients unnecessarily referred for DXA testing. Quantitative ultrasound sonography (QUS) testing and similar methods of assessing bone at peripheral sites in the skeleton may represent a potential tool with which to select patients for DXA testing. Several index scoring systems based on readily available clinical factors are also available at present, including the Simple Calculated Osteoporosis Risk Estimation (SCORE), the Osteoporosis Risk Assessment Instrument (ORAI), and the Osteoporosis Self-Assessment Tool (OST). These indices may represent attractive alternatives to QUS testing as screening methods for DXA. We compared the performance of these indices with QUS in predicting low DXA bone density at the hip. Femoral neck DXA T-scores ≤ -2 and -2.5 were used as outcome thresholds. Values for each index were calculated using clinical data from the electronic medical records of 656 patients referred for bone density testing at our clinic who had received both DXA (Lunar Prodigy) and QUS (Lunar Achilles) tests. Subjects were postmenopausal Caucasian women with no evidence of DJD, who were not taking oral steroids, anti-resorptive therapy other than estrogen, or anti-seizure medications at the time of the visit. The performance of the screening alternatives in predicting low hip bone density is shown in the table below.

	DXA T-Score ≤-2			DXA T-Score ≤-2.5		
Predictor	Sensitivity	Specificity	Area under ROC curve (95% CI)	Sensitivity	Specificity	Area under ROC curve (95% CI)
QUS	87.8%*	54.6%*	0.802 (0.764-0.841)	92.9%*	49.7%*	0.852 (0.809-0.895)
SCORE†	95.9%	35.0%	0.788 (0.749-0.827)	97.1%	31.1%	0.831 (0.782-0.880)
ORAI	91.2%	43.8%	0.756 (0.713-0.800)	97.1%	39.9%	0.817 (0.769-0.864)
OST	71.4%	66.2%	0.776 (0.736-0.815)	81.4%	62.5%	0.822 (0.774-0.871)

* At threshold QUS T-Score of –1 or lower † n=654 for SCORE analysis

In this referral-based population of postmenopausal Caucasian women, QUS did not predict low DXA bone density at the hip significantly better than any of the three clinical indices. Area under the ROC curve was similar among all 4 diagnostic schemes for both outcome thresholds. The OST index uses only weight and age to predict the likelihood of low bone density, and performed similar overall to QUS testing. Given that the clinical indices are simple, free, and require only clinical data that is likely already collected at the visit, the benefit of QUS screening as a means of selecting patients for DXA tests is dubious.

M116

Effect of the TGF β T869C and the CYP19 TTTA Repeat Polymorphisms on Bone Mineral Density and Prevalent Fracture in Elderly Women. R. L. Prince[1], I. M. Dick[1], A. Devine[1], S. S. Dhaliwal*[2], S. Li*[2], S. Wilton*[3]. [1]Department of Medicine and the Western Australian Institute for Medical Research, University of Western Australia, Perth, Australia, [2]Endocrinology and Diabetes, Sir Charles Gairdner Hospital, Perth, Australia, [3]Australian Neuromuscular Research Institute, University of Western Australia, Perth, Australia.

Osteoporosis is a common disease of bone that is strongly genetically determined. In a population based study of 1337 caucasian women over the age of 70, we have examined genetic polymorphisms in two candidate genes that may influence bone mineral density (BMD) and fracture, the TGF β T869C polymorphism in codon 10 and the Aromatase (Cyp19) tetranucleotide repeat in intron 4. The TGF β C allele was observed in 50.0% of the subjects and was associated with reduced hip BMD at all sites (2.8% total hip, 2.4% femoral neck, 2.6% intertrochanter, 3.4% trochanter) compared to the TGF β TT genotype. The TGF β C allele was also associated with a reduction in the calcaneal quantitative ultrasound (QUS) parameters BUA, SOS and stiffness of 0.87%, 0.26% and 2.4% compared to the TGF β TT genotype. A Cyp19 (TTTA)n > 12 was observed in 63.1% of the subjects and was associated with reduced hip BMD (1.9% total hip, 1.7% femoral neck, 2.0% intertrochanter, 2.3% trochanter) but was not associated with a reduction in calcaneal quantitative ultrasound . After adjustment for weight in an ANOVA model, the effect of the TGF β C allele was no longer significant except at the trochanter but the QUS parameters remained unchanged. The Cyp19 (TTTA)n > 12 effect on BMD remained significant after adjustment for weight.

Odds Ratios for Osteoporosis and Prevalent Fracture

	TGFβ c allele	Cyp19 (TTTA)n>12
O.R. for osteoporosis	2.18 (1.21-3.91	1.63 (0.89-2.99)
O.R. for prevalent fracture	1.37 (1.02-1.85)	1.02 (0.74-1.08)

As indicated above, a TGF β C allele was associated with an increase in osteoporosis (T score < 2.5 S.D. below premenopausal mean) and prevalent fracture. Despite its effect on hip BMD a Cyp19 (TTTA)n > 12 was not associated with osteoporosis or fracture. After adjustment for BMD and QUS stiffness, the association of the TGF β C allele with prevalent fracture was no longer statistically significant (O.R. 1.42, 95% C.I. 0.99-2.0), indicating the association between a reduction in BMD and stifness with fracture. However, the disparate effects of the TGF β C allele and Cyp19 (TTTA)n > 12 on fracture, despite similar effects on BMD in the same population, indicate that the TGF β C allele may be associated with BMD independent, in addition to effects that are dependent on BMD .

M117

The Relationship between Vitamin D Receptor Gene Polymorphisms and the Effect of Hormone Replacement Therapy on Bone Mineral Density in Postmenopausal Korean Women. J. Kim, J. Kim*, S. Kim*, Y. Choi*, S. Moon*, J. Lee*. Department of Obstetrics & Gynecology, Seoul National University Hospital, Seoul, Republic of Korea.

The objective of this study was to investigate whether vitamin D receptor (VDR) gene polymorphisms are associated with the effect of hormone replacement therapy (HRT) on bone mineral density (BMD) in postmenopausal Korean women. The BsmI, ApaI, and TaqI polymorphisms were analyzed by restriction fragment length polymorphism, and poly (A) polymorphism by GeneScan and direct DNA sequencing in 303 postmenopausal Korean women who received HRT for 1 year. HRT was administered by sequential regi-

men of conjugated equine estrogen and medroxyprogesterone acetate. Serum bone alkaline phosphatase (BAP), CrossLaps (CTX), osteocalcin and 1,25 $(OH)_2$ vitamin D_3 levels were measured by immunoassay and BMD at the lumbar spine and femoral neck by dual energy X-ray absorptiometry before and after HRT of 1 year. The BsmI and TaqI polymorphisms were significantly associated with annual percentage change in BMD at the lumbar spine. The bb and TT genotype showed a significantly lower percentage change in BMD of lumbar spine than the Bb and Tt genotype. The bb genotype was more prevalent in HRT-nonresponders (women who lose more than 3 % of bone mass per year) than in HRT-responders, while the Bb gentype was more prevalent in HRT-responders, but the TaqI polymorphism was not distributed differently among HRT-responders and HRT-nonresponders. Combining the BsmI and TaqI genotype reflected only the differences caused by the BsmI polymorphism. No significant association between annual percentage changes in BMD at all skeletal site studied and the ApaI or poly (A) polymorphism was observed. There were no significant differences in the annual percentage changes in 1,25 (OH)2 vitamin D3 or biochemical markers such as osteocalcin, BAP and CTX, among any of the genotypes analyzed. In conclusion, the VDR BsmI polymorphism is associated with the effect of HRT on BMD at the lumbar spine in Korean women.

M118

The Association Study Between the Change in Bone Mineral Density and Serum Estradiol, SHBG Levels and HLA DR2 Type After One Year of HRT. K. Han*[1], I. Moon*[2], H. Choi*[1], C. Yim*[1], H. Chung*[1], H. Yoon*[1], I. Han*[1]. [1]Department of Internal Medicine, Samsungcheil Hospital, School of Medicine, Sungkyunkwan University, Seoul, Republic of Korea, [2]Endocrine Laboratory, Samsungcheil Hospital, Seoul, Republic of Korea.

Estogen acts to prevent osteoporosis by regulating the production of cytokines, including IL-1, IL-6, and TNF. Some studies have shown that the ability to secrete cytokines at the lymphocyte is related to the HLA class II type, and thus, in DR2 type, this finding may be related to the presence of nonresponder group to minor stimulus. This study aims to investigate the relationship between the change in BMD after HRT and the serum sex hormone levels and HLA DR type. The study subjects were 117 women who had received at least one continuous year of HRT, and their mean age at baseline and mean age of menopause were 52.3±4.7 and 47.7±4.7, respectively. To verify the HLA DR2 type, the DR2 specific region in chromosome 6 was selected as a primer, amplified by PCR and observed for the presence of the band. The serum E2 levels at baseline, 3 months, and 1 yr after HRT were 6.3 pg/ml (5.1-8.4), 38.0 (20-60.3), and 41.0 (21.0-60.8) (median IQR), respectively, and the serum SHBG levels increased to 75.0 nmol/l (54.0-104.5), 149.0 (102.8-189.0), and 152.0 (124.0-182.0), respectively. The BMD of spine and femur increased by 3.6% and 1.7% in one year, and the nonresponder group in the spine was 15.4%. The change in spine BMD also was significantly associated with the change in serum E2 and E2/SHBG ratio after HRT, and the correlation coefficients were 0.26 (p=0.01) and 0.27 (p=0.005), respectively. The prevalence of HLA DR2 type was 21.7%, and there were no significant associations between HLA DR2 and clinical parameters. HLA DR2 type did not show significant correlation with baseline BMD and the change in BMD after HRT. However, the baseline deoxypyridinoline level was significantly higher in the HLA DR2 positive group at 8.9±2.6 nmol/mmol Cr compared to the HLA DR negative group at 7.7±1.9. Although not statistically significant, baseline osteocalcin level in the HLA DR2 group also had a tendency to be higher. In conclusion, after HRT, there was no statistically significant correlation between the change in BMD and the serum sex hormone level and the HLA DR2 type, but the HLA DR2 was associated with bone turnover markers and with the rapid bone loss group. This observation is incompatible with the previous reports that HLA DR2 type is associated with the non-responder group to cytokine production, and thus, further in vitro studies need to be conducted to verify these findings in Korean women.

M119

Polymorphisms in the Promoter of the Osteoprotegerin Gene are associated with reduced Perimenopausal Bone Mass. B. L. Langdahl[1], P. Vestergaard[1], B. Abrahamsen[2], C. L. Tofteng[3], N. Kolthoff[4], L. Mosekilde[1]. [1]Endocrinology and Metabolism, Aarhus University Hospital, Aarhus C, Denmark, [2]Endocrinology, Odense University Hospital, Odense C, Denmark, [3]Endocrinology, Hvidovre Hospital, Hvidovre, Denmark, [4]Clinical Physiology, Hillerød Sygehus, Hillerød, Denmark.

Osteoprotegerin (OPG) is a soluble receptor for RANKL and is therefore a competitive inhibitor of osteoclast differentiation and activity. We have previously examined the OPG gene for polymorphisms and found 12 of which 5 were informative. In a case-control study we demonstrated that the rare alleles of the A^{163}-G (G) and T^{245}-G (G) polymorphisms are associated with increased risk of osteoporotic vertebral fractures. In this study we examined the effect of the five polymorphisms: A^{163}-G, T^{245}-G, T^{950}-C, G^{1181}-C and A^{6890}-C on perimenopausal bone mass and early postmenopausal bone loss in 2016 normal women. A^{163}-G: Women with the rare genotypes AG or GG (28.2%) had lower BMD at the lumbar spine (LS): 1.013± 0.131 g/cm^2 versus 1.031± 0.139 g/cm^2 (p<0.05). Perimenopausal bone loss was not affected and BMD(LS) 5 years after menopause was 0.949± 0.144 g/cm^2 in women with AG or GG genotypes versus 0.971± 0.142 g/cm^2 in women with AA genotype (p<0.05). In women treated with HRT, the relative difference between the genotypes was also preserved after 5 years. No significant differences were found at the hip. T^{245}-G: are in strong linkage disequilibrium with A^{163}-G. Women with the rare genotypes TG or GG (9.1%) had reduced BMD(LS): 0.999± 0.134 g/cm^{2}compared with 1.030± 0.137 g/cm^2 (p<0.02). The perimenopausal bone loss tended to be higher in women with TG or GG genotypes: 6.7% versus 5.5% after 5 years (p=0.11) and BMD(LS) after 5 years was 0.932± 0.136 g/cm^2 in women with TG or GG genotypes compared with 0.969± 0.143 g/cm^2 in the women with TT genotypes (p<0.05). Women with different genotypes responded similarly to HRT and the relative difference between the genotypes was preserved after 5 years treatment. No significant differences were found at the hip. None of the other polymorphisms had any effects on perimenopausal bone mass or early postmenopausal bone loss. In conclusion: Two polymorphisms in the promoter of the OPG gene: A^{163}-G and T^{245}-G are in strong linkage disequilibrium. The rare genotypes are significantly associated with reduced perimenopausal bone mass at the lumbar spine. The difference in bone mass was preserved 5 years after menopause independent of whether the women received HRT or not.

M120

Investigation of the Association of dinucleotide Repeats within the Calcitonin and Interleukin 6 Receptor Genes with Low Bone Mineral Density in the Irish Population. C. M. Silke*[1], F. Wynne*[2], K. Quane*[2], M. Daly*[1], F. Shanahan*[2], M. G. Molloy[1], F. Drummond*[2]. [1]Rheumatology, Cork University Hospital, Cork, Ireland, [2]Medicine, Cork University Hospital, Cork, Ireland.

Low bone mineral density (BMD) is a major risk factor for the development of osteoporosis. It is estimated that between 60-80% of variance in BMD is attributable to heredity. Segregation studies have shown that BMD is under the influence of more than one gene. Interleukin 6 (IL6) stimulates osteoclast development and increases bone resorption leading to osteoporosis. Calcitonin (CT) is a calcium-regulating hormone that lowers the calcium level in serum by inhibiting bone resorption. In this study the possible association between dinucleotide (CA) repeat polymorphisms at the IL6 Receptor (IL6R) and the CT locus in 127 postmenopausal Irish women was investigated (mean age 61.31±8.12 years). Participants were recruited from the bone density unit in the Cork University Hospital. IL6R and CT polymorphisms were amplified by PCR and analysed on an ABI 310 Genetic analyzer using genescan software. Regression analysis was used to identify possible confounding factors with BMD at the lumbar spine (LS) and femoral neck (FN) using SPSS v10.0. Significant covariates with BMD identified from stepwise linear regression analysis were used to adjust BMD. Association of these polymorphisms with low BMD was investigated by analysis of variance (ANOVA). Eleven IL6R alleles were found in this population. The most frequent was A1 (151 base pairs) occurring at a frequency of 0.38. This is in contrast with a Japanese population where the frequency for this allele was 0.01. Thus, there appears to be a marked difference between these two racial groups. Nine alleles were found for CT with the most frequent being B5 (121 base pairs). BMD at the LS was adjusted for age and weight, and at the FN was adjusted for age, weight and height. BMD measurements at the FN and LS were compared amongst individuals according to whether they had 0, 1 or 2 copies of A1 (IL6R) or B5 (CT). No association was observed between BMD at the FN or LS and the IL6R A1 allele (p =0.56, p = 0.62, respectively). Similarly, association was not found between the CT B5 allele and BMD at the LS (p=0.35) or the FN (p=0.54), in this population. This is in contrast to a Japanese study which observed significant association between BMD and genetic variations at the CT locus. There was no interaction observed between these genotypes and BMD at either skeletal site when the population was divided into those aged above and below 60 years. We are currently increasing the number of women participating in order to increase the statistical power of our study.

M121

Body Mass Index and Circulating Testosterone Modulate the Effect of Aromatase Gene Polymorphism on Bone in Elderly Men. L. Gennari[1], L. Becherini*[2], D. Merlotti*[3], L. Masi[2], B. Lucani*[3], S. Gonnelli[3], A. Falchetti*[2], N. Dal Canto*[3], R. Nuti[1], C. Gennari[3], M. L. Brandi[2]. [1]Metabolic Disease Unit, University of Siena, Siena, Italy, [2]Department of Internal Medicine, University of Florence, Florence, Italy, [3]Institute of Internal Medicine, University of Siena, Siena, Italy.

Predictors of osteoporosis in men are not clearly defined. Evidence suggest that conversion of testicular androgens into estrogen plays a dominant role in determining bone mineral density (BMD) in men. Recently we demonstrated that a TTTA repeat polymorphism in the CYP19 gene was associated with differences in aromatase activity and lumbar BMD values in elderly males and females. In the present study we longitudinally tested the role of this CYP19 polymorphism on bone loss at different skeletal sites and on vertebral fracture risk in 300 elderly men. Femoral and lumbar BMD (DEXA), bone ultrasound parameters (calcaneous and phalanx), estradiol (E), testosterone (T), sex hormone binding globulin, and bone turnover markers (urinary CTX and serum bone specific alkaline phosphatase) were evaluated for each man at baseline and after 3 years. Six different allelic variants containing respectively 7,8,9,10,11 and 12 TTTA repeats were detected. Circulating E levels positively correlated with body mass index (BMI), T, and the number of TTTA repeats and were significantly higher in subjects with a high repeat genotype (TTTA>9) than in those with a low repeat genotype (TTTA<9). Moreover, men with a low repeat genotype showed higher rates of bone loss at the lumbar spine and Ward's triangle than those with a high repeat genotype. Interestingly an association between CYP19 polymorphism and vertebral fracture risk was observed with a lower incidence of fractures in the high repeat group (RR = 0.20). Finally, a significant interaction with BMI and T was observed. Differences in baseline BMD, bone turnover markers and rates of bone loss between low and high TTTA repeat genotypes were higher when analysis was restricted to subjects with a normal BMI, while progressively decreased in magnitude when overweight or obese men were considered. A similar increased CYP19 genotype effect was observed in subjects with T levels below the median. Taken all together, these results show a major role of CYP19 repeat polymorphism in determining trabecular bone loss and vertebral fracture risk in elderly men and suggest that the CYP19 genetic effect on bone is modulated by circulating androgens and by the amount of body fat.

M122

Intronic Polymorphisms of the Estrogen Receptor Beta Gene Are Associated with Bone Mineral Density: The Framingham Study. D. Karasik[1], A. M. Shearman*[2], L. A. Cupples*[3], K. Gruenthal*[2], D. E. Housman*[2], D. P. Kiel[1]. [1]Hebrew Rehab Ctr for Aged, Harvard School of Medicine, Boston, MA, USA, [2]Ctr for Cancer Research, MIT, Boston, MA, USA, [3]Biostat Dept, BU Sch of Public Health, Boston, MA, USA.

Estrogen exerts its physiological role on bone metabolism via two estrogen-activated transcription factors: estrogen receptor (ER) α and the more recently characterized ERβ. Unlike ERα, few studies have examined variation in the ERβ gene for association with bone mineral density (BMD) and none in large populations that include men as well as women. A single study (Ogawa et al., 2000) has shown association of an ERβ CA repeat polymorphism allele with lumbar BMD in postmenopausal women. Several studies, however, including our own, have reported modest evidence of linkage between BMD and the ERβ region on chromosome 14. The aim of this study was to assess whether silent polymorphisms in ERβ are associated with BMD in men and women. We studied 723 men and 795 women (mean age 60 yrs, range 29-86) from the Offspring Cohort of the Framingham Study. BMD was measured at the femur (neck, trochanter, Ward's area) and lumbar spine (L2-L4) sites. DNA samples were genotyped for three intronic polymorphisms: the previously studied CA repeat and two single nucleotide polymorphisms (SNPs) selected from the National Center for Biotechnology Information SNP database. BMD were adjusted for covariates including age, height, weight, calcium, vitamin D, smoking, alcohol, physical activity, and years since menopause and estrogen therapy in females. For the highly polymorphic CA repeat we subdivided the 15 alleles into two classes at the median number of repeats: small alleles had less than 22 CA repeats, and the remainder were defined as large alleles. In women, but not men, there was a significant association of the CA repeat genotype with Ward's BMD only; women 'homozygous' for the short allele displayed lower BMD than 'heterozygotes' or 'homozygotes' for the large allele (ANOVA p = 0.03 for Ward's BMD). Of the two SNPs, one was very rare and had no significant association with BMD. The second SNP showed an association with BMD at all 4 sites in men (ANOVA p = 0.028 for femoral neck, p = 0.005 for trochanter, p = 0.016 for Ward's area, p = 0.021 for lumbar spine) but not in women (all p>0.1). In conclusion, we identified association of an ERβ CA repeat polymorphism with BMD (Ward's area) in women. The CA repeat had previously given evidence of association with BMD (lumbar spine) in Japanese women. In addition, we have observed significant association of another ERβ polymorphism with BMD (at four sites) in men from the Framingham Study. Variation in the ERβ gene may potentially play a role in BMD and deserves further study.

M123

Polymorphism Analysis of LDL Receptor-Related Protein 5 (LRP5). K. M. Allen[1], A. Anisowicz*[1], M. G. FitzGerald*[2], P. Van Eerdewegh*[1], R. D. Little*[1], T. Keith*[1], R. R. Recker[3], M. L. Johnson[3]. [1]Human Genetics, Genome Therapeutics Corp., Waltham, MA, USA, [2]GenomeVision Services, Genome Therapeutics Corp, Waltham, MA, USA, [3]Osteoporosis Research Center, Creighton University, Omaha, NE, USA.

Mutations in LRP5 have been associated with two extreme bone mineral density (BMD) phenotypes mapped to chromosome 11q13; High Bone Mass (HBM) and osteoporosis pseudoglioma syndrome (OPPG). We previously reported that a single point mutation resulting in a glycine to valine amino acid change (G171V) was responsible for the autosomal dominant high bone mass trait in the HBM kindred and resulted in no clinical bone abnormalities (Little et al. AJHG 70:11, 2002). OPPG, in contrast, is an autosomal recessive disorder characterized by premature osteoporosis that leads to bone fracture and deformities as well as juvenile-onset blindness. Frameshift or nonsense mutations were detected in affected offspring from 9 OPPG families and putative disease-causing missense mutations were detected in another 3 OPPG families. Carriers of the OPPG alleles also had reduced BMD suggesting that OPPG LRP5 mutations can have dominant as well as recessive effects (Gong et al. Cell 107:513, 2001). The occurrence of LRP5 mutations associated with changes in BMD in these two disorders suggests that other allelic forms of LRP5 may contribute to a spectrum of bone density phenotypes. For example, a QTL contributing to normal variation in BMD also maps to 11q12-3 further suggesting that LRP5 may play a role in determining BMD in the normal population (Koller et al. JBMR 13:1903, 1998). To identify polymorphisms in LRP5 that can be tested for their association with BMD we have sequenced the entire coding region (23 exons) as well as intron-exon boundaries in the HBM kindred and in 20 sporadic individuals with elevated BMD (combined hip and spine Z score > 4) as well as 8 random individuals. We observed a total of 42 single nucleotide polymorphisms (SNPs) including 6 missense, 11 silent, and 25 intronic mutations. The HBM G171V was found only in the affected individuals of the HBM kindred. Further analysis is needed to determine if 3 silent mutations identified in the sporadic cases are associated with elevated BMD, since silent mutations can potentially be related to phenotypic variability by influencing splicing accuracy or efficiency. In conclusion, to facilitate the analysis of LRP5 in broader populations, we have identified both coding and intronic SNPs in LRP5 as well as designed primers and PCR protocols for sequencing all exons. Association between polymorphisms in LRP5 and normal variations in BMD and/or segregation with Mendelian forms of extreme BMD could have broad implications in the diagnosis and treatment of osteoporosis.

M124

Testing of Association and/or Linkage for Five Candidate Genes with Peak BMD in US Caucasian Nuclear Families. H. Shen, L. J. Zhao, J. R. Long, Y. Y. Zhang, L. Elze, R. R. Recker, H. W. Deng. Osteoporosis Research Center and Biomedical Sciences, Creighton University, Omaha, NE, USA.

Bone mineral density (BMD) plays an important role in determination of osteoporosis. Studies have shown 50-90% of population variation in BMD is under genetic control. Candidate-gene approach is one of the two major approaches for searching genes that influence BMD. However, traditional linkage or association studies on several candidate genes yield inconsistent and controversial results. Transmission disequilibrium test (TDT) is a robust and powerful approach for testing both linkage and association. It is significant only in the presence of both linkage and association. Here, we studied 636 individuals from 157 nuclear families, in which 62 families have one child, 43 with 2 children and 34 with 3 children, the rest nuclear families have 4 or more children. There are a total of 257 sib pairs in the sample. All these subjects were genotyped with six polymorphic RFLP markers for five candidate genes [*BstU I* inside the Transforming growth factor β1 (TGF), *BsaH I* inside the Calcium-Sensing Receptor (CASR), *Msc I* inside the Collagen type 1 α 1 (COL1A1), *Sac I* and *Nla III* inside the α_2 HS-glycoprotein (AHSG), and *Rsa I* inside the Osteoprotegerin (OPG)]. Spine, hip and mid-radius BMD of all subjects were measured by DEXA. By using the program QTDT, we performed tests for linkage alone, association alone, then for both linkage and association (TDT) between the BMD and the genotypes of these candidate genes. Age, height, weight and sex were adjusted as covariates. For the spine BMD, at the *Sac I* of the AHSG gene, we found marginally significant evidence for association ($p < 0.07$), and for both linkage and association by the TDT ($p < 0.10$). Marginally significant results were also found for association for spine BMD at BsaHI inside CASR gene ($p < 0.10$) and *Msc I* inside the COL1A1 gene ($p < 0.09$). Other unspecified results are generally not significant or only marginally significant. Further extension studies with more nuclear families will be performed to confirm or verify the preliminary results in this study.

M125

Studies of Linkage and/or Association of Estrogen Receptor-α (ER-α), Vitamin D Receptor (VDR) and AHSG Genes with Peak BMD in Chinese Nuclear Families. Y. J. Qin*[1], Q. R. Huang[1], Q. Zhou*[1], J. H. Lu*[1], J. W. He*[1], H. W. Deng[2]. [1]Center for Preventing and Treating Osteoporosis, Shanghai Sixth People's Hospital, Shanghai, China, [2]Osteoporosis Research Center and Biomedical Sciences, Creighton University, Omaha, NE, USA.

Variation of bone mineral Density (BMD) is mainly regulated by genetic factors. Extensive molecular genetics studies have been performed to search for genes underlying BMD variation; however, few studies were performed in Chinese populations. In our previous study among 150 Chinese nuclear families (Qin, 2001), results suggested that the BMD at spine and hip may be modulated by vitamin D receptor (*Apa I*) and estrogen receptor-α (*Pvu II and Xba I*) genotypes. Those results require confirmation with larger samples which may confer reasonable statistical power to test relatively robustly for the importance (linkage and/or association) of these candidate genes to BMD. According to theoretical statistical power analyses, ~400 nuclear families are required for the transmission disequilibrium test (TDT) to detect the presence of both association and linkage for a gene responsible for about 10% of the bone mass variation. In this study, a total of 402 Chinese nuclear families with 1263 subjects with children aged between 25-40 were recruited in the present study. All subjects were genotyped by PCR-RFLP at polymorphic sites of *Apa I* inside the VDR gene, *Pvu II* and *Xba I* inside the ER-α gene and *Sac I* inside the AHSG (α_2 HS-glycoprotein) gene. BMD were measured at lumbar spine (L1-L4) and hip (femoral neck, trochanter, intertrochanteric region). Raw BMD values were adjusted by age, sex, height, and weight as covariates. Using the program QTDT, we detected significant results for association ($p < 0.05$) between spine BMD and ER-α *Xba I* genotypes, but we also detected population stratification for ER-α *Xba I* with spine BMD. Therefore, this association result should be interpreted with caution. For BMD at the hip, at the two markers (*Pvu II* and *Xba I*) inside the ER-α gene, significant ($p < 0.05$) results were generally found for linkage testing and for the testing of both linkage and association (TDT). No significant effect of the VDR and AHSG genotypes on spine or hip BMD was detected. In conclusion, this study indicates the ER-α gene may act as a QTL underlying BMD variation in Chinese population, but VDR and AHSG genotypes were not shown as significant for BMD in our Chinese sample.

M126

Tests of Linkage and /or Association of Genes for COL1A1, PTH, BGP and IL-6 with Peak BMD in a Large Sample of Chinese Han Nuclear Families. X. H. Liu*[1], S. F. Lei*[1], X. G. Zhou*[1], X. Y. Mo*[1], Z. K. Cao*[1], M. Y. Liu*[1], Y. J. Qin*[2], Q. R. Huang[2], Q. Zhou*[2], H. Shen[3], H. W. Deng[3]. [1]College of Life Sciences, HuNan Normal University, Changsha, China, [2]Center for Preventing and Treating Osteoporosis, Shanghai Sixth People's Hospital, Shanghai, China, [3]Osteoporosis Research Center and Biomedical Sciences, Creighton University, Omaha, NE, USA.

Numerous molecular genetic studies have been performed to search genes underlying bone mineral density (BMD) variation. However, few such studies were performed in Chinese populations. In this study, we tested linkage alone, association alone, and linkage and association of the genes for Collagen type 1 alpha 1 (COL1A1), parathyroid hormone (PTH), osteocalcin (BGP) and interleukin 6 (IL-6) with BMD in 1,263 subjects from 402 Chinese Han nuclear families with children aged 25-40. Among these nuclear families, 349 have 1 child, 50 have two children and 3 have 3 children. The RFLP genotypes of COL1A1 (*Msc I*), PTH (*BstB I*), BGP (*Hind III*) and IL-6 (*BsrbI*) in each individual were

determined by PCR-RFLP procedures. For the raw BMD of the spine (L1-L4) and hip (femoral neck, trochanter, intertrochanteric region and Ward's triangle), adjusting for significant covariates of age, sex, height and weight, we performed tests for linkage alone, association alone, and then for both linkage and association using the program QTDT. Associations were found between the COL1A1 marker with the BMD at trochanter (p = 0.01) and Ward's triangle (p = 0.04). Evidences for population stratification were also found between the COL1A1 (*MscI*) with BMD at these two sites. Similar results were detected for association and population stratification between the COL1A1 genotypes with the spine BMD and the combined (femoral neck, trochanter and intertrochanteric region) total hip BMD. Population admixture may interfere with the detection of genetic effects of candidate genes for complex traits. Hence, the significant association results should be interpreted with caution. We also found marginally significant results for linkage alone (p < 0.09), and for linkage and association (p < 0.10) for the marker *Bsrb I* inside the IL-6 gene for the trochanter BMD. Other unspecified results are generally not significant. Compared with earlier studies in non-Chinese populations, our results may suggest population heterogeneity for the genetic effects at candidate genes across populations of various ethnic groups.

M127

Overexpression of FGF2 Protein Isoforms in Osteoblasts: Effects on Proliferation and Differentiation. L. Xiao*[1], P. Liu[2], T. Sobue[1], J. Coffin[3], M. M. Hurley[1]. [1]Medicine, Univ of CT Hlth Ctr, Farmington, CT, USA, [2]Genetics, Univ of CT Hlth Ctr, Farmington, CT, USA, [3]Pharmaceutical Sciences, Univ of Montana, Missoula, MN, USA.

Fibroblast growth factor-2 (FGF2) regulates bone remodeling in vitro and in vivo. There are 3 nuclear isoforms of 22, 23, and 24 kDa and a low molecular wt (LMW) 18 kDa FGF2 protein that is exported from cells. The effect of each isoform on OB function has not been elucidated. To examine the effects of FGF2 isoforms on OB function, a set of expression vectors, called Col3.6-FGF2 isoforms-IRES-GFPsaph, were built by replacing a CAT fragment in previously made Col3.6-CAT-IRES-GFPsaph with individual human FGF2 isoform cDNA between Afe I and Sca I sites. These expression vectors are capable of concurrently overexpressing individual isoforms and GFPsaph from a single bicistronic mRNA. These vectors also harbor a neomycin selection gene. The expression vectors were stably transfected into ROS 17/2.8 cells and the transfected cells were then selected with G418 for a month. Expression of GFP reporter gene in transfectants was detected under fluorescent microscopy. Expression of each FGF2 isoform transgene was demonstrated by Western blot analysis. ROS 17/2.8 cells expressed rodent endogenous FGF2 protein isoforms of 17.5, 19, and 21 kDa, whereas FGF2 transfected cell lines overexpressed the specific human FGF2 isoforms encoded by the respective transgene. To assess the effects of overexpression of different FGF2 isoforms, we compared cell number in ROS17/2.8 cells stably transfected with control (Col3.6-IRES-GFP saph) vs each of the Col3.6-FGF-IRES-GFPsaph constructs. Cells were plated at 5000 cells/well in 96 well dishes in F-12 medium containing G418, (200 μg/ml) and either 1 or 10% FCS. After 96 h cells were harvested and viable cell number was measured by the 3-(4,5-dimethylthiazol-2-yl)-2,5-diphenyltetrazolium bromide (MTT) proliferation assay. In the presence of either 1 or 10% serum, cell number was increased between 28% and 45% in cells harboring the different FGF2 transgenes. To examine OB gene expression and differentiation, ROS 17/2.8 cells were cultured with ascorbic acid and beta-glycerophosphate for 14 days. Northern analysis showed similar expression of Col1a1 or Alkaline phosphatase (ALP) mRNA and similar ALP staining in all cell lines. However, osteocalcin (OC) mRNA expression was 48% higher in cells overexpressing the LMW 18 kDa protein. In summary, overexpression of all isoforms of FGF2 protein increased viable cell number in the presence of low or high concentrations of serum. Overexpression of 18 kDa FGF2 increased OC mRNA, a marker of differentiated OBs. We conclude that differential expression of FGF2 proteins may be important in modulating OB function.

M128

FGF-23 Is a Novel Regulator of Mineral Homeostasis with Unique Properties Controlling Vitamin D Metabolism and Phosphate Reabsorption. T. Shimada*[1], T. Muto*[1], H. Hasegawa*[1], Y. Yamazaki*[1], Y. Takeuchi[2], T. Fujita*[2], S. Fukumoto[3], T. Yamashita[1]. [1]Pharmaceutical Research Labs, KIRIN Brewery Co., Ltd., Takasaki, Japan, [2]Department of Medicine, University of Tokyo School of Medicine, Tokyo, Japan, [3]Department of Laboratory Medicine, University of Tokyo Hospital, Tokyo, Japan.

FGF-23 was identified as a causative factor of tumor-induced osteomalacia. Missesnse mutations in FGF-23 gene were also found to be associated with autosomal dominant hypophosphatemic rickets. Previous reports indicated that FGF-23 can induce hypophosphatemia with increased renal phosphate excretion, inappropriately low serum 1,25-dihydroxyvitamin D [1,25$(OH)_2$D] level and rickets/osteomalacia in vivo. However, it is still unclear how FGF-23 causes these abnormal phosphate and vitamin D metabolism. In the present study, we analyzed acute effects of FGF-23 injection on serial changes of biochemical parameters and expressions of key molecules regulating serum phosphate and 1,25$(OH)_2$D levels. Purified full-length recombinant FGF-23 (5 μg/head) was administered into BALB/c mice intravenously. Reduction of serum phosphate level was first observed after 8 hours. Western blot analysis revealed that the expression of type IIa sodium phosphate cotransporter (NPT2a) was simultaneously decreased. However, changes of serum Ca and PTH levels were not observed. Serum concentration of 1,25$(OH)_2$D was significantly diminished already at 3 hours after the injection. Maximum reduction of 1,25$(OH)_2$D was observed from 8 to 13 hours. Northern blot analysis demonstrated that the administration of FGF-23 reduced the expression of 25-hydroxyvitamin D-1α-hydroxylase (1αOHase) and enhanced the expression of 25-hydroxyvitamin D-24-hydroxylase (24OHase) in kidneys. Because these effects on key enzymes in vitamin D metabolism were observed within 1 hour after the FGF-23 administration, FGF-23 seemed to regulate the expression of these enzymes directly. Such changes of enzyme expression have not been reported in other hormonal factors except for 1,25$(OH)_2$D. In summary, administration of FGF-23 caused rapid suppression of 1αOHase and induction of 24OHase expression, followed by decrease of serum 1,25$(OH)_2$D prior to reduced expression of NPT2a and hypophosphatemia. Although it is not evident at the moment whether reduced expression of NPT2a and hypophosphatemia are mediated by decreased 1,25$(OH)_2$D level, these results indicate that FGF-23 is a novel regulator of mineral homeostasis with unique properties controlling vitamin D metabolism and phosphate reabsorption.

M129

FGF2-stimulated Osteopontin Gene Expression Is Mediated by AP1 Through the Activation of ERK Pathway. H. Kim*[1], H. Park*[1], J. Choi[2], S. Kim*[3], H. Kim[4], H. Ryoo[1]. [1]Biochemistry, School of Dentistry, Kyungpook National University, Daegu, Republic of Korea, [2]Biochemistry, School of Medicine, Kyungpook National University, Daegu, Republic of Korea, [3]Skeletal Genome Research Center, Kyungpook National University, Daegu, Republic of Korea, [4]Pediatric Dentistry, Kyungpook National University, Daegu, Republic of Korea.

Craniosynostosis, characterized by the premature closure of cranial suture, is a congenital disease that is resulted from precocious osteoblast differentiation around suture area. Most of the diseases are resulted from mutations of the fibroblast growth factor receptors, which reflects that FGF/FGFR signaling is indispensable for the osteoblast differentiation. Our previous report showed that osteopontin is an early marker of osteoblast differentiation and strongly expressed in calvarial bones during development. FGF2-soaked bead treatment on osteogenic fronts of mouse calvaria accelerated suture closure and osteopontin gene expression was strongly induced around beads. Specific aim of the present study is illumination of the regulation mechanism of osteopontin by FGF signaling. FGF2-stimulated osteopontin expression required the new protein synthesis. We suspected AP1 in this regulation since FGF2 induced immediately and temporally all the components of AP1 family in osteoblastic cells. Also, EMSA and site directed mutagenesis of AP1 binding site showed that the binding between AP1 and its cis-acting element was crucial for osteopontin induction by FGF signaling. Blocking of ERK pathway by PD98059 completely and specifically abrogated FGF2-induced AP1 gene expression while other MAP kinase or PKC blocker could not. Consistently, the Erk blocking also completely abrogated osteopontin expression around FGF2 beads in mouse calvaria organ culture. Taken together, FGF2-induced osteopontin gene expression is controlled by newly synthesized AP1 transcription factor whose expression is specifically regulated by ERK pathway.

M130

Phenotypic Characterization of Bones of Transgenic Mice Overexpressing Fibroblast Growth Factor-2. T. Sobue[1], L. Xiao[1], Y. Okada[2], Y. Tanaka[2], M. Ito[3], N. Okimoto[2], T. Nakamura[2], J. D. Coffin[4], M. M. Hurley[1]. [1]Univ. of Connecticut Health Ctr, Farmington, CT, USA, [2]Univ. of Occupational & Environmental Health, Kitakyushu, Japan, [3]Univ. of Nagasaki, Nagasaki, Japan, [4]Univ. of Montana, Missoula, MT, USA.

Basic fibroblast growth factor (FGF2) is an important regulator of bone formation and resorption as well as a potent mitogen for osteoblasts. We previously reported that non targeted overexpression of FGF-2 cDNA linked to the phosphoglycerate kinase promoter in transgenic (TgFGF2) mice enhanced apoptosis of chondrocytes in the prehypertrophy zone, premature closure of the growth plate and shortening of bone length of femurs and humeri. In this study, we assessed the effect of overexpression of FGF-2 on bone structure in vivo in TgFGF2 mice harboring the human FGF-2 coding sequence. Hemizygous TgFGF2 males were mated with non-transgenic (NTg) FVB/N females to produce litters of hemizygous TgFGF2 and NTg mice. FGF2 protein levels were assayed by ELISA and were higher in epiphysial bones of TgFGF2 mice age 4 to 230 days old. Structural parameters of trabecular bone were determined by micro-computerized tomography (μCT) of the distal femurs from 1, 3 and 6 months old mice. In 1 month old female TgFGF2 mice, there was a 32% decrease in trabecular bone volume (BV/TV) compared with NTg mice. Trabecular separation (Tb.Sp) was significantly increased compared with NTg mice (0.11 ± 0.01 vs. 0.08 ± 0.01 mm; p<0.01). Trabecular number (Tb.N) and Trabecular thickness (Tb.Th) were not significantly altered. In 3 months old female TgFGF2 mice, BV/TV (13.0 ± 4.3 vs 21.4 ± 0.8 %; p<0.01), Tb.N (4.39 ± 0.43 vs 5.02 ± 0.33 mm-1; p<0.05) and Tb.Th (51.3 ± 5.1 vs. 58.4 ± 4.2 μm; p<0.05) were all significantly reduced compared with NTg mice. In 6 months old male TgFGF2 mice, there were significant reductions in BV/TV (6.6 ± 2.0 vs. 9.7 ± 2.6 %; p<0.05) and Tb.N (1.50 ± 0.35 vs. 2.24 ± 0.51 mm-1; p<0.05). Tb.Sp (0.65 ± 0.14 vs. 0.43 ± 0.11 mm; p<0.05) was significantly increased compared with NTg mice. Bone mineral density (BMD) measured by Piximus DEXA in femurs from 4 week old female mice showed a significant decrease in Tg FGF2 compared with NTg (37.9 ± 1.9 vs. 46.5 ± 2.3 mg/cm2; p<0.05). In summary, FGF2 overexpression in Tg mice decreased bone mass and BMD in both male and female mice. This is consistent with FGF2 overexpression functioning as a negative regulator of bone growth in this animal model. FGF2 mediated apoptosis and chondrocyte drop out could cause decreased deposition of cartilage and matrix; because bone spicules appear to be diminished and disorganized at the epiphysial growth plate in TgFGF2 mice. Defects in osteoblast growth and differentiation combined with chondrocyte deficiencies, likely result in decreased bone density.

M131

ERK Activation in Wounded Osteoblasts Is Mediated by Basic Fibroblast Growth Factor. R. Landesberg, A. B. Burke*, S. Thomas*, R. W. Katz. Columbia University, NY, NY, USA.

The immediate signal transduction response of osteoblasts to acute trauma is poorly characterized. We previously described an in vitro model for osteoblast trauma to investigate the molecular mechanisms of wound healing in bone. Following disruption of a confluent monolayer, "wounded" osteoblasts demonstrated a rapid and transient activation of ERK 1/2. The p38 or SAPK/JNK pathways were not activated by wounding. We hypothesize that growth factors such as bFGF are rapidly released from the cells or surrounding matrix in response to wounding. Previously, we demonstrated that ERK 1/2 could be activated by the media from wounded osteoblasts suggesting that ERK activation was mediated by a soluble factor. In the present report we show evidence that one factor responsible for the activation of ERK 1/2 is basic fibroblast growth factor (bFGF). The osteoblast cell line IRC 10/30 myc 1 was grown to confluence in 100 mm dishes, serum starved, and then wounded. Sham treated dishes served as a control. The media was saved following incubation and concentrated by ultrafiltration through a 3,000 dalton molecular weight cut-off membrane. Equal amounts of concentrated media were analyzed by immunoblotting for bFGF. Experiments were performed with varying concentrations of suramin (an inhibitor of heparin binding growth factors) added to the media one hour prior to wounding. In some experiments dishes of confluent cells were serum starved for six hours in the presence of bFGF (10 ng/ml) or Epidermal Growth Factor (EGF, 50 ng/ml). Following pretreatment the plates received either fresh growth factor or were wounded as described. Phosphorylated ERK 1/2 was assayed by western blot analysis. Media from wounded cells demonstrated increased amounts of bFGF when compared to sham treated dishes. When conditioned media from wounded cells was added to confluent IRC cells, activated ERK 1/2 levels were slightly below that noted in the wounded dishes themselves. This effect was destroyed by boiling and suppressed by the addition of suramin. Finally, the upregulation of phosphorylated ERK 1/2, seen in response to exogenous bFGF or to wounding, was significantly abrogated by pretreatment with bFGF, but not EGF. The data suggest that bFGF is a significant component of the soluble factor(s) responsible for ERK 1/2 activation in wounded osteoblasts.

Disclosures: ***R. Landesberg****, NIH DE 12566 2; RW Katz, NIH DK 52639 2.*

M132

Role of Insulin-like Growth Factors and Fibroblast Growth Factor-2 in TGF-ß Mediated Regulation of Endochondral Bone Formation. A. Mukherjee*, J. Alvarez*, R. Serra*. Molecular and Cellular Physiology, University of Cincinnati, Cincinnati, OH, USA.

Transforming growth factor-ß1 (TGF-ß1) is known to regulate chondrocyte proliferation and hypertrophic differentiation by a perichondrium dependent mechanism, suggesting the involvement of other factors in the process. To begin to determine which additional factors are involved, we studied the effect of Insulin-like Growth Factors (IGF-I, IGF-II) and and Fibroblast Growth actor-2 (FGF2) on metatarsal organ culture. An increase in chondrocyte proliferation and hypertrophic differentiation was observed after treatment with IGF-I. A similar effect was seen after the perichondrium was stripped from the metatarsals suggesting IGF-I acts directly on the chondrocytes. IGF-II added to the metatarsal organ culture also resulted in an increase in BrdU incorporation in the chondrocytes. Furthermore, the treatment of organ cultures with TGF-ß1 down regulated the beta subunit of the IGF-I receptor as determined by immunoprecipitation and immunoblot assays. FGF-2 treatment of the organ cultures resulted in a decrease in bone elongation and hypertrophic differentiation as well as a decrease in BrdU incorporation into chondrocytes and an increase in BrdU incorporation in perichondrial cells, similar to treatment with TGF-ß1. Unlike TGF-ß1, a similar effect was seen with FGF2 after the perichondrium was stripped suggesting FGF2 acts directly on chondrocytes. TGF-ß1 treatment upregulated the FGF receptor 3 expression as determined by immunoprecipitation and immunoblot assays. The data suggest IGF-I stimulates while FGF-2inhibits proliferation and hypertrophic differentiation during bone formation by acting directly on the chondrocytes. Furthermore TGF- ß is involved in the regulation of the IGF receptor and FGF receptor 3, suggesting the possibility of interaction between these three signaling cascades in overall bone development.

M133

Basic Fibroblast Growth Factor has Rapid Bone Anabolic Effects in Ovariectomized Rats. R. A. Power, U. T. Iwaniec, K. A. Magee*, N. G Mitova-Caneva*, T. J. Wronski. Physiological Sciences, University of Florida, Gainesville, FL, USA.

Basic fibroblast growth factor (bFGF) has a strong bone anabolic effect in intact and ovariectomized (OVX) rats. TGFβ and IGF-I may mediate this effect, as osteoblastic immunostaining for TGFβ and gene expression for IGF-I have been reported to be significantly increased in intact and OVX rats treated with bFGF for 1-2 weeks. The purpose of this study was to examine the early effects of bFGF therapy, *in vivo*, on bone formation and gene expression in OVX rats. Animals were OVX at 3 months of age, and maintained untreated for 3 months. At 6 months of age, one group of OVX rats (BSL OVX) and one group of sham-operated rats (BSL SHAM) were euthanized. Additional OVX groups were treated IV with bFGF (Chiron Corp., CA) at a daily dose of 200 µg/kg and euthanized at 1, 2, 3, 6, and 10 days. An additional group of OVX rats was treated IV with vehicle daily for 10 days, then euthanized. At necropsy, lumbar vertebrae were collected for cancellous bone histomorphometry and RNA isolation. RNase protection assays were performed to quantify mRNAs encoding $TGF\beta_1$ and IGF-I. All values listed below are mean±SD. Osteoblast surface (Ob.S/BS; %) and osteoid surface (OS/BS; %) were significantly higher at 1d (12.3±4.5; 10.5±4.0), 2d (17.8±10.8; 15.6±9.9), 3d (21.3±6.5; 18.9 ±6.0), and 6d (21.2±6.5; 27.4±8.0) in bFGF-treated OVX rats than in BSL SHAM (1.4±0.6; 1.3±0.6) and BSL OVX (5.2±2.4; 4.6±2.1) rats; values for Ob.S/BS and OS/BS were significantly higher at 3d and 6d than at 1d. Ob.S/BS and OS/BS were also significantly higher in OVX rats treated with bFGF (25.2±7.8; 26.8±9.8) for 10 days than in OVX rats treated with vehicle (9.3±5.4; 7.8±4.5). Osteoclast surface (Oc.S/BS; %) was significantly higher in BSL OVX rats (0.8±0.2) and at 1d (0.7±0.4) and 2d (0.5±0.4) in bFGF-treated OVX rats than in BSL SHAM rats (0.2±0.1). However, Oc.S/BS was significantly lower at 3d (0.3±0.1) and 6d (0.4±0.2) in bFGF-treated OVX rats than in BSL OVX rats. Oc.S/BS was also significantly lower in OVX rats treated with bFGF for 10 days (0.3±0.3) than in OVX rats treated with vehicle (0.9±0.3). mRNA levels for $TGF\beta_1$ and IGF-I were not significantly different between BSL OVX rats and bFGF-treated OVX rats at 3d. However, mRNA levels for these growth factors were higher in OVX rats treated with bFGF for 10 days than in vehicle-treated OVX rats. The results of this study indicate that the bone anabolic effects of bFGF in OVX rats begin as early as 24 hours post-treatment and increase with time. The growth factors $TGF\beta_1$ and IGF-I do not appear to be associated with initiation of the bone anabolic response to bFGF, but may be necessary to sustain this response.

M134

Basic Fibroblast Growth Factor Stimulates RANKL and Inhibits OPG in Human Bone Marrow Stromal Cells and Microvascular Endothelial Cells via Prostaglandin Independent Pathways. P. Collin-Osdoby, L. Rothe, P. Osdoby. Department of Biology, Washington University, St. Louis, MO, USA.

RANKL is the key signal required for the full development, activation, and survival of resorptive osteoclasts (OC), and its actions are neutralized by binding to OPG. Various osteotropic signals regulate RANKL and OPG expression by osteoblasts (OB) or bone marrow stromal cells (BMSC), thereby influencing OC formation and function. Recently, we showed that human microvascular endothelial cells (HMVEC) also expressed RANKL and OPG, and that inflammatory cytokines (IL-1, TNF) upregulated RANKL/OPG in HMVEC to cause an increase in HMVEC-mediated human OC formation and bone resorption. Basic FGF is an important angiogenic and bone remodeling factor that indirectly stimulates OC recruitment, development and activity in vivo and in vitro. High bFGF levels are linked to excessive vascularity and OC-mediated bone destruction in inflammatory conditions. Therefore, we investigated if bFGF may regulate RANKL or OPG expression in HBMSC or HMVEC to indirectly promote OC formation and bone resorption. HBMSC exposed to bFGF (1 nM, 24 h) exhibited increased RANKL mRNA expression and decreased OPG mRNA levels, leading to a 2-fold rise in the ratio of RANKL/OPG. In HMVEC, bFGF (10 nM, 6 h) also increased RANKL mRNA expression relative to that of OPG, however to a somewhat lesser extent than in HBMSC. In contrast to bFGF, IL-1 (1 nM, 24 h) increased both RANKL and OPG in HMVEC, while it raised RANKL and decreased OPG mRNA expression in HBMSC. To learn whether bFGF upregulated RANKL/OPG expression via an induction of prostaglandins, COX-2 mRNA expression was examined in HBMSC and HMVEC. Whereas IL-1 (1 nM, 24 h) strongly increased COX-2 mRNA expression in HBMSC and did not alter it in HMVEC, bFGF decreased COX-2 mRNA expression in HMVEC and did not alter it in HBMSC. Therefore, the regulation of RANKL and OPG by bFGF in HBMSC or HMVEC may occur via prostaglandin-independent MAPK activation pathways. We conclude that bFGF regulates RANKL and OPG in both HBMSC and HMVEC, via non-prostaglandin mediated mechanisms. Thus, the ability of bFGF to stimulate the expression of RANKL relative to OPG in stromal and vascular endothelial cells present in an inflamed site may contribute to the pathological role of bFGF in promoting OC recruitment, development and bone destruction in inflammatory conditions such as rheumatoid arthritis.

M135

Tgf-ß2 Regulates Fgf2 Signaling and Activity. J. T. Rawlins*, J. R. Sayne*, L. A. Opperman. Biomedical Sciences, Texas A&M University System Health Science Center, Dallas, TX, USA.

FGFR mutations have been linked to premature cranial suture obliteration (craniosynostosis) in humans. In animal models, both Fgf2 and Tgf-ß2 induce cranial suture obliteration, while Tgf-ß2 neutralizing antibodies rescue from obliteration sutures destined to fuse. This study was designed to determine the nature of potential Tgf-ß2 and Fgf2 interactions in regulating coronal suture patency. E19 fetal rat calvaria were cultured serum-free, plus or minus Fgf2 and neutralizing antibodies to Tgf-ß2. Calvaria were harvested and prepared for histological analysis and average suture width determined using digital image capture and Metamorph software. Addition of Fgf2 significantly narrowed coronal suture width, while removal of Tgf-ß2 activity by addition of Tgf-ß2 neutralizing antibodies had no effect on suture width. Addition of Fgf2 and Tgf-ß2 neutralizing antibodies together resulted in wide open sutures, preventing the suture-narrowing effects of Fgf2. Tgf-ß2 has been shown to inhibit Twist expression in sutures, and Twist is a negative regulator of Fgfr expression. Since Tgf-ß2 downregulates Fgfr2 expression in sutures, it is hypothesized that removal of Tgf-ß2 activity results in upregulated Twist expression, followed by down-regulated Fgfr expression and reduced Fgf2 signaling. This is seen morphologically as rescue of Fgf2 treated sutures from obliteration. Studies currently underway are determining if there is a link between Tgf-ß2 regulation of Twist and Fgfr2 expression.

M136

Impaired Fracture Healing in the Absence of TNF-α Signaling. L. C. Gerstenfeld[1], T. Cho[2], T. Kon*[3], T. Aizawa*[4], A. Tsay*[1], G. L. Barnes[1], D. T. Graves*[5], T. A. Einhorn[1]. [1]Department of Orthopaedic Surgery, Boston University Medical Center, Boston, MA, USA, [2]Department of Orthopaedic Surgery, Seoul National University College of Medicine, Seoul, Republic of Korea, [3]Department of Orthopaedic Surgery, Chiba University School of Medicine, Chiba, Japan, [4]Department of Orthopaedic Surgery, Toshoku University School of Medicine, Aiba-ku, Japan, [5]Department of Oral Biology, Boston University School of Dental Medicine, Boston, MA, USA.

Tumor necrosis factor-alpha (TNF-α) is both a major inflammatory factor that is induced during an innate immune response to injury and contributes to the regulatory processes of normal bone resorption. The role of TNF-α during fracture healing was examined in wild type and TNF-α receptor ($p55^{-/-}/p75^{-/-}$) deficient mice. These results demonstrate that TNF-α is a primary regulatory cytokine in postnatal endochondral bone formation and that it plays multiple roles in this process. In the absence of TNF-α signaling, chondrogenic differentiation was delayed by 2 to 4 days but subsequently proceeded at an elevated rate. Endochondral tissue resorption was delayed two to three weeks in the TNF-α receptor ($p55^{-/-}/p75^{-/-}$) deficient mice compared to wild type animals. Functional studies demonstrated that TNF-α mediated both chondrocyte apoptosis and expression of pro-resorptive cytokines that control endochondral tissue remodeling by chondroclasts and/or osteoclasts. While the TNF-α receptor ablated animals showed no overt developmental alterations of their skeletons, these results demonstrated that TNF-α plays an important role in promoting postnatal fracture repair. Our findings indicate that TNF-α signaling is required for normal fracture healing, and they identify essential mechanisms that regulate fracture repair.

M137

Infection with Chlamydia Pneumoniae Stops Development of Peak Bone Density in Growing Male Mice and Is Associated with Increased Levels of Resorptive Cytokines. P. R. Nordström[1], A. H. Gustavsson*[2], O. Nilsson*[3], S. Bergström*[3], A. Waldenström*[4]. [1]Department of Surgical and Perioperative Sciences, Sports Medicine Unit, Umea, Sweden, [2]Department of surgical and perioperative sciences, Sports Medicine Unit, Umeå, Sweden, [3]Department of Clinical Microbiology, Microbiology, Umeå, Sweden, [4]Department of Public Health and Clinical Medicine, Cardiology division, Umeå, Sweden.

Estrogen status, physical activity, and body weight are some of the important determinants of bone density. However, together these factors only explain a small part of the variation in bone density. Infection with Chlamydia pneumoniae (TWAR) is sometimes associated with chronic infections in humans. We investigated whether infection with TWAR in still growing male c57BL/6 mice was associated with decreased peak bone density. Nineteen mice were infected by nasal inoculation with a TWAR containing suspension at ten weeks of age, and 20 mice were sham infected and served as controls. Bone density (mg/mm3) of the distal femur, proximal tibia, and femur diaphysis was measured before and after 16 days of infection using pQCT. Compared to sham infected mice, the infected mice increased significantly less in total bone density of the distal femur (0.4% vs. 9.4%, p=0.01), proximal tibia (-1.6% vs. 9.7%, p=0.001), and cortical bone density of the femur diaphysis (2.7% vs. 5.4%, p=0.006). The relative bone loss was seen in cortical and subcortical bone rather in trabecular bone. The levels of interleukin-6 (56 vs. 39 pg/mL, p=0.02) and interleukin-1b (11 vs. 0 pg/mL, p=0.003) were increased in serum of infected mice. Also levels of osteocalcin (228 vs. 50 pg/mL, p<0.001) were increased in the infected mice. There was no significant difference in weight gain (p=0.53) when comparing infected and sham infected mice. In conclusion, infection with TWAR results in decreased peak bone density and is associated with increased levels of bone resorptive cytokines in male mice.

M138

Modulation of Transcription by Glucose-dependent Insulinotropic Peptide in MG-63 Osteoblastic-like Cells Evaluated by Gene Chip Analysis. Q. Zhong*[1], K. H. Ding*[1], L. Ruan*[1], P. Sridhar*[1], A. Mulloy[2], R. Bollag*[1], C. M. Isales[2]. [1]Institute of Molecular Medicine and Genetics, Medical College of Gerogia, Augusta, GA, USA, [2]Department of Medicine, Medical College of Georgia and the Augusta VAH, Augusta, GA, USA.

Previous reports from our laboratory have demonstrated that Glucose-dependent Insulinotropic Peptide (GIP) increases bone formation both in vivo and in vitro. In view of our results demonstating multiple effects of GIP on osteoblastic proliferation and differentiation we wished to examine the genes activated by GIP in the osteoblastic-like cell line MG-63 using gene microarrays. MG-63 cells were stimulated with the appropiate agonist for 2 hours. GIP 0.1 nM increased 98 genes by at least two fold, the largest change being a 22 fold increase in the gene for the human helix-loop helix protein (Id2). GIP 1 nM increased 119 genes the largest change being a 24.9 fold increase in the expression of mRNA for Fas. GIP 10nM increased the expression of 187 genes and GIP 100nM increased the expression of 415 genes. In contrast PTH 10nM increased the expression of 17 genes the largest change being a 5.5 fold increase in the expression of GLI-Krupple related protein and 1,25 dihydroxyvitamin D 1μM increased the expression of 130 genes. In summary, GIP, is a potent activator of gene expression in osteoblastic-like cells and highlights the potency of this agent as a modulator of osteoblatic cell function.

M139

Effect of Glucose-dependent Insulinotropic Peptide on 3H-Thymidine Incorporation in Osteoblastic-like Cells and its Interaction with other Hormones. K. H. Ding*[1], Q. Zhong*[1], D. Xie*[1], J. Xu*[1], R. Bollag*[1], C. M. Isales[2]. [1]Institute of Molecular Medicine and Genetics, Medical College of Gerogia, Augusta, GA, USA, [2]Department of Medicine, Medical College of Georgia and the Augusta VAH, Augusta, GA, USA.

Glucose-dependent insulinotropic peptide (GIP) has been reported to have an anabolic effect on bone formation. Since GIP likely serves as a hormonal link between nutrient ingestion and bone formation we wished to investigate whether there were any additive or synergistic interactions between GIP and other nutritionally related hormones on osteoblastic cell proliferation. GIP, amylin, insulin and 1,25 dihyroxyvitamin D all significantly stimulated 3H thymidine incorporation into MG 63 osteoblatic-like cells: Control: 10,698+523; GIP 10nM: 14,769+551; Amylin 10nM: 14,333+1748; Amylin 100nM: 14,742+1246; Insulin 10nM: 17,143 +1180; Insulin 100nM: 14,684+877: 1,25 dihydroxyvitamin D 10nM: 16,201+993; 1,25 dihydroxyvitamin D 100nM:17,308+1622 (CPM Mean+SEM). IGF-1 had no effect on thymidine incorporation; IGF-1 10nM: 10,706+158; IGF-1 50nM: 10,097+429 CPM+SEM. If GIP 10nM was added in conjunction to IGF-1 there was now a statistically significant effect on thymidine incorporation: IGF-1 10nM+ GIP 10nM: 14,684+1938; IGF-1 50nM +GIP 10nM: 12,789+426 CPM+SEM. However, concurrent administration of GIP and either amylin, insulin, 1,25 dihyroxyvitamin D or IGF-1 had no statistically significant additive or synergistic effect over addition of GIP by itself. In summary, GIP, amylin, insulin and 1,25 dihyroxyvitamin D all stimulate 3H thymidine incorporation into MG 63 osteoblastic-like cells. However, GIP does not synergize with these other hormones in potentiating the effect of GIP by itself.

M140

Mechanisms for Inflammatory Bone Loss: Catabolic Effects of Chemokines MIP-1α and RANTES via Coordinated Actions on Osteoblasts and Osteoclasts. X. Yu, Y. Huang*, P. Collin-Osdoby, P. Osdoby. Department of Biology, Washington University, St. Louis, MO, USA.

Bone remodeling by osteoclasts (OC) and osteoblasts (OB) is regulated by osteotropic hormones, growth factors, cytokines, and chemokines. Certain chemokines are locally increased at sites of inflammatory bone loss where they function to recruit and activate cells. Recently, OB and OC were also shown to release chemokines at inflammatory sites. Because little is known about chemokine effects on bone metabolism, we analyzed chemokine receptor expression and actions in murine OB, OC, and their precursors. CCR1, CCR3 and CCR5 receptors were detected by multi-probe RPA in mouse OB (generated from newborn mouse calvaria or bone marrow stromal cells) and OC (RANKL differentiated from murine RAW 264.7 or bone marrow cells). CCR1 increased during OB differentiation, beginning at day 6, and was maximal at day 15-18 when ALP activity and mineralization were increased. CCR1 also rose during OC differentiation from RAW or murine bone marrow cells. Thus, we examined if CCR1 ligands (MIP-1α, RANTES, or MCP-3) regulated OB or OC development or function. When OB were differentiated for 3, 9, 15, or 21 days before 48 h treatment with MIP-1α, RANTES or MCP-3, ALP activity was decreased and MMP-2 activity increased by MIP-1α or RANTES with maximal effects at day 15 when CCR1 levels peaked. Because ALP increases in OB differentiation in association with mineralized bone matrix synthesis, while MMP-2 is a matrix-degrading protease, these results suggest that MIP-1α and RANTES exert catabolic effects on OB-mediated bone remodeling. Relative to OC, MIP-1α, RANTES or MCP-3 induced pre-OC (RAW cell) chemotaxis, and MIP-1α increased mature OC (RAW-OC) motility. None of the chemokines affected OC bone pit resorption. Thus, CCR1 may stimulate OC recruitment by inducing pre-OC chemotaxis and mature OC motility, actions that could locally elevate bone resorption. OB and OC also released CCR1 ligands. MIP-1α and RANTES secretion increased in OB differentiation, and were further raised by IL-1 or TNF (maximal at day 9-15 when CCR1 peaked). MIP-1α release was higher (10-60x), and RANTES lower (10-100x), from pre-OC or OC than OB. IL-1 or TNF did not affect RANTES, and only slightly increased MIP-1α release from pre-OC. Thus, OB may be a main source of RANTES in basal or inflammatory conditions, whereas MIP-1α is produced by OB, pre-OC or OC and increased by inflammatory cytokines mainly in OB and pre-OC. These chemokine levels are in the range that exhibit biological actions on OB and OC. Therefore, CCR1 chemokines may exert catabolic effects on bone metabolism via their coordinated autocrine and paracrine actions on OB, OC, and their precursor cells in inflammatory conditions.

M141

Regulation of IL-6 and gp130 Expression by VIP, PACAP-38, Secretin and Glucagon in Mouse Calvarial Osteoblasts. E. Persson*, U. H. Lerner. Oral Cell Biology, Odont. Inst., Umea, Sweden.

Signaling molecules in skeletal nerve fibers have been shown to regulate bone cell activities. The effects of the neuropeptide vasoactive intestinal peptide (VIP) are likely to be due to direct effects on bone cells since osteoclasts and osteoblasts express different VIP receptor subtypes [Ransjö et al. BBRC 274:400, 2000; Lundberg et al. Endocrinology 142:339, 2001]. In the present study, we have investigated the effects of VIP, pituitary adenylate cyclase-activating peptide 38 (PACAP-38), secretin and glucagon, all belonging to the same superfamily of peptides, and the potent bone resorption stimulator IL-1β, on the expression in osteoblasts of IL-6 and the IL-6 intracellular signal-transducing unit glycoprotein 130 (gp130). Mouse calvarial osteoblasts were isolated and incubated in the absence and presence of VIP, PACAP-38, secretin, glucagon and IL-1β for 48 hrs, followed by culture media collection for IL-6 ELISA analysis. In addition, RNA isolation was performed to study the effects of VIP, PACAP-38 and secretin on the mRNA expression of IL-6 and gp130 by using semi-quantitative RT-PCR analysis. The RT-PCR analysis showed that VIP and PACAP-38 both stimulated the mRNA expression of IL-6, whereas secretin had no effect. The results were consistent with the IL-6 ELISA demonstrating that both VIP and PACAP-38 stimulated IL-6 synthesis in a dose-dependent manner, whereas secretin and glucagon had no effect. Furthermore, IL-1β stimulated IL-6 synthesis dose-dependently and the effect was synergistically potentiated by VIP. Both VIP and PACAP-38 decreased the mRNA levels for the IL-6 signal transduction unit gp130, whereas secretin had no effect. These results together indicate that VIP-2 receptors on the osteoblasts mediate the signals affecting IL-6 and gp130, which is in line with the previous findings that osteoblasts express VIP-2 receptors but not VIP-1 receptors. Since osteoclast activity and formation requires the concerted action of several signalling molecules expressed by osteoblast/stromal cells and preosteoclasts/osteoclasts, the importance of the effects of VIP, PACAP-38, secretin and glucagon on IL-6 and gp130 on bone resorption requires further studies. The data further supports the view that neuro-osteogenic interactions are important in bone metabolism and further indicates the possibility of neuro-immune interactions in bone.

M142

The IL-6/IL-6 Soluble Receptor Cytokine System Plays a Role in Mediating PTH-Induced Soluble RANKL Release. M. Mitnick, B. Sun, S. McCarthy*, K. Insogna. Yale University, New Haven, CT, USA.

Recent studies indicate that the interleukin-6/interleukin-6 soluble receptor (IL-6/IL-6sR) cytokine system plays a role in mediating the resorptive actions of PTH. The resorptive response to PTH is markedly attenuated in animals pretreated with neutralizing antibody to IL-6, a finding also observed in IL-6 knock-out animals. RANKL transcript expression is induced by PTH and RANKL is also thought to be critical for mediating the resorbing effects of this hormone. The relationship between the IL-6/IL-6sR and RANKL/OPG cytokine systems is unclear. We therefore infused rats with PTH or vehicle for 5 days and serially measured circulating levels of IL-6/IL-6sR and RANKL/OPG. IL-6 rose significantly within 24 hrs (8.3 pg/ml vs. 4.5 pg/ml, PTH vs. vehicle-infused animals) and was 4-fold elevated at the end of 5 days (21.9 pg/ml vs. 4 pg/ml). Serum RANKL levels did not rise significantly until 72 hrs of infusion (163 vs. 73 pg/ml) but were nearly 5-fold elevated at day 5 (429 vs. 91 pg/ml). This temporal relationship suggested the possibility that IL-6/IL-6sR might play a role in mediating the release of RANKL into the circulation. We therefore examined the effect of neutralizing IL-6 in vivo on PTH-induced changes in circulating RANKL levels. In mice infused with PTH for 5 days, serum RANKL was 2-fold elevated compared to vehicle infused animals. (172±14 vs. 84±15 pg/ml, $p<0.5$). In mice pretreated with neutralizing antibody to IL-6 there was a significant attenuation in the PTH induced increase in serum RANKL (107±5 vs. 142±10 pg/ml, neutralizing antisera vs. control anitbody, $p<0.005$). Serum levels of RANKL were dramatically lower in PTH infused IL-6 knock-out animals than in the wild-type littermates (41±5 vs. 103±8 pg/ml, $p<0.05$) and similar to the value in vehicle infused wild-type animals. To determine whether these changes were also observed at the cellular level, primary human and murine osteoblasts as well as a hepatocyte cell line (HepG-2 cells) were treated with either a control antibody or a neutralizing antibody to IL-6 in the presence of either PTH or vehicle. Neutralizing IL-6 in vitro significantly attenuated the PTH-induced release of RANKL into the culture media. RANKL release was reduced by 50%-60% in the osteoblast cultures and by 40% in the hepatocyte cultures ($p<0.005$ for each). We conclude that the IL-6/IL-6sR cytokine system participates in PTH induced release of soluble RANKL both in vitro and in vivo. The precise mechanism by which this occurs remains unclear but suggests that interdiction of the IL-6/IL-6sR cytokine system may impair PTH-induced resorption in part by diminishing expression of soluble RANKL.

M143

T cells Are Critical Mediators of IL-7 Induced Bone Loss In Vivo. G. Toraldo, C. Roggia, W. P. Qian,*, R. Pacifici, M. N. Weitzmann. Bone and Mineral Diseases, Barnes-Jewish Hospital and Washington University, St. Louis, MO, USA.

Interleukin-7 (IL-7), a powerful lymphopoietic cytokine, is known to induce bone loss in vivo. Recent studies have suggested that IL-7 induces bone loss by stimulating the proliferation of B220+ cells, a population capable of acting as early osteoclast (OC) precursors. However, how IL-7 leads to differentiation of precursors into mature OCs remains unknown. We previously reported that in vitro, IL-7 upregulated T cell derived osteoclastogenic cytokines including Receptor Activator of NFkB Ligand (RANKL). To demonstrate the importance of T cells to the bone wasting effect of IL-7 in vivo we have now examined IL-7 induced bone loss in T cell deficient athymic nude mice. We show that T cell replete mice undergo significant bone loss following IL-7 administration, concurrent with induction of RANKL and TNFalpha (TNF) secretion by splenic T cells. In contrast, T cell deficient nude mice were resistant to IL-7 induced bone loss, and showed no detectable increase in either RANKL or TNF, despite an upregulation of B220+ cells. Importantly, T cell adoptive transfer into nude mice, restored IL-7 induced bone loss, and RANKL and TNF secretion, providing a clear demonstration that T cells are essential mediators of IL-7 induced bone loss in vivo.

M144

WITHDRAWN

M145

The Relationship Between Growth Factor mRNA and Protein Levels in Human Bone. M. H. Bünger*[1], T. Andersen*[1], L. Sørensen*[2], H. Oxlund*[3], M. Lind*[1], E. F. Eriksen[2], C. Bünger*[1], B. Langdahl[2]. [1]Orthopaedic Research Lab., Aarhus University Hospital, Aarhus C, Denmark, [2]Medical Endocrinology Dept. C, Aarhus University Hospital, Aarhus C, Denmark, [3]Department of Anatomy, Aarhus University, Aarhus C, Denmark.

mRNA expression is used for determination of bone cell activity or response to various agents. Few have been concerned whether a measured mRNA expression is followed by a corresponding protein production and thereby effect. We investigated the relation between mRNA and protein levels in human bone. 62 spinal surgery patients (38 males and 24 females, mean age 45, range 13-78) were included. An 8 mm bone biopsy was taken from the posterior iliac crest prior to graft harvesting. 20 of the patients had blood samples taken prior to surgery. RNA isolation was performed using Trizol®-technique. Proteins were isolated by precipitation with acetone and re-dissolved in demineralised water by sonication. mRNA for TGF-β1, IGF-I and II, BMP-2 and 7, FGF-b and LMP-1 were measured by semiquantitative RT-PCR using b-actin as internal standard. Proteins measured were IGF-II(measured as free + bound IGF-II), TGF-β1, both using ELISA kits, and Collagen 1. Collagen 1 content was calculated after further isolation and measurement of hydroxyproline. Protein values were adjusted for the total protein content(measured with the Lowry method). OPG, PINP, IL-6, sCTX concentrations in the serum samples were measured using ELISA kits. PTH, Calcium, Alkaline Phosphatase and Osteocalcin were measured by the clinical chemistry department at the hospital. All values were log-transformed before calculation of the Pearson correlation coefficient. No correlation between mRNA and adjusted protein levels were found for neither IGF-II nor TGF-β1. A positive correlation between TGF-β1 protein levels and mRNA levels for LMP-1 (0.300, $p<0.038$) was found. mRNA levels for IGF-I correlated negatively to TGF-β1 protein levels (-0.353, $p<0.011$). mRNA levels for TGF-β1 and IGF-I were found to correlate negatively to Collagen 1 content in the biopsy (-0.331, $p<0.020$ and -0.530, $p<0.0005$ respectively). BMP-2 mRNA levels were found to correlate negatively to sCTX and IL-6 levels in serum (-0.495, $p<0.026$ and -0.515, $p<0.024$ respectively). TGF-β1 mRNA levels were found to correlate negatively to PINP (-0.423, $p<0.063$) but positively to PTH (0.437, $p<0.054$). These results suggest that mRNA expression in human bone does not directly reflect the concentration of the corresponding protein. Correlations between mRNA and concentrations of other proteins than the corresponding were observed. Surprisingly a connection between mRNA levels for the transcription factor LMP-1 and TGF-β1 protein levels were observed.

M146

The Novel Hormone, Preptin, Is Another Bone-Active Product Of The Pancreatic β-Cell. J. Cornish[1], K. E. Callon[1], U. Bava*[1], A. B. Grey[1], X. Xu*[1], C. M. Buchanan*[2], G. J. S. Cooper*[2], I. R. Reid[1]. [1]Medicine, University of Auckland, Auckland, New Zealand, [2]School of Biological Sciences, University of Auckland, Auckland, New Zealand.

Several hormones that regulate nutritional status also impact on bone metabolism. Preptin is a recently isolated 34-amino acid peptide hormone that is co-secreted with insulin and amylin from the pancreatic β-cells. Preptin corresponds to Asp^{69} - Leu^{102} of proIGF-II. We have assessed preptin's activities on bone. Preptin, like insulin and amylin, dose-dependently stimulates the proliferation (cell number and DNA synthesis), of primary fetal rat osteoblasts and osteoblast-like cell lines at periphysiological concentrations ($>10^{-11}$M). In addition, thymidine incorporation is stimulated in murine neonatal calvarial organ culture, likely reflecting the proliferation of cells from the osteoblast lineage. Preptin does not affect bone resorption in this model. The mitogenic effect of preptin on osteoblasts appears to be dependent upon signaling via p42/44 MAP kinases. Preptin induces phosphorylation of p42/p44 MAP kinases in osteoblastic cells in a dose-dependent manner (10^{-8} -10^{-10} M), as assessed by immunoblotting. The proliferative effects of preptin on primary osteoblasts were blocked when the cells were pre-treated with either of the MAP kinase kinase inhibitors PD-98059 or U-0126. We also assessed preptin's effects on primary osteoblast apoptosis induced by serum deprivation. Apoptotic cells were detected by light microscopy using a modified TUNEL assay. Preptin had anti-apoptotic effects, at 10^{-8} M with treatment/control ratio of 0.78 ± 0.08. In conclusion, preptin is a novel bone-active factor secreted from the pancreatic β-cell that may act in concert with the other β-cell hormones, insulin and amylin, to stimulate bone formation in hyperinsulinemic states, such as obesity. These findings may also be relevant to the high bone mass observed in patients with chronic hepatitis who secrete high levels of proIGF-II.

M147

GH Stimulates Differentiation of Osteochondral Precursor Cells in a Rat Osteotomy Model. M. Huening[1], T. Lindner*[1], H. J. Bail*[1], A. Flyvbjerg*[2], N. P. Haas*[1], M. Raschke*[1]. [1]Trauma and Reconstructive Surgery, Charité, Berlin, Germany, [2]Endocrinology, Komunehospital, Aarhus, Denmark.

GH is an important regulator of cartilage and bone formation which also stimulates bone healing. Purpose of the study was to characterize the cell populations directly involved in the healing process. A total of 48 adult, female SD rats underwent osteotomy of the left femur resulting in an 0,3 mm gap which was subsequently stabilized by a monolateral external fixator. Group I: 3 mg rh-GH subcutaneously /kg body weight /day; Group II: vehicle. 1, 2 and 3 weeks after surgery bones of each group (n=8) were collected, immediately formalin-fixed, decalcified with EDTA and embedded in paraffin. Serial sections were cut and stained alcian-blue. To evaluate the histological stage of healing 3 stains of each animal were scored. Single points were given when bone formation was observed in certain fields of the gap region. To visualize cellular gene expression in situ hybridization was performed on serial sections using Digoxigenin-labelled RNA-probes of extracellular matrix proteins (ECMP). Probes were transcribed from cDNA-clones of mouse type-I collagen (COL1), mouse type-II collagen (COL2), rat osteopontin (OPN) and rat osteocalcin (OC). Histologically Group I animals reached a significant higher score after 1 and 2 weeks. Also gene expression was markedly different between the two groups. After 1 week osteochondral progenitor cells could be detected in the osteotomy gap which were characterized by simultaneous COL1 and COL2 expression. Group I animals showed significantly more such cells.After 2 and 3 weeks COL1-signals were mainly located in deeper layers of the woven bone. In group I a stronger gene expression was noted. At these time points COL2-mRNA was localized in chondrocytes of cartilaginous callus with group II animals showing more of these cells. OC was expressed primarily by mature osteoblasts in the deeper layers of woven bone in both groups at later time points. OPN was mainly observed in osteoblasts and hypertrophic chondrocytes at the ossification front with more signals in group I animals after 1 and 2 weeks. To our knowledge this is the first study demonstrating the influence of GH on ECMP gene expression in bone regeneration. It appeared that gene expression patterns were markedly changed, especially osteochondral progenitor cells were detected more frequently in the early phase. Moreover cartilage formation seemed to be suppressed after 2 and 3 weeks in this model. We conclude that GH may exert its stimulatory effect by promoting the differentiation of precursor cells into osteogenic cells.

Disclosures: ***M. Huening****, Deutsche Forschungsgemeinschaft 2.*

M148

Effect of IGF-I Haploinsufficiency on Growth and Bone Mineral Density in Outbred Male and Female Mice. J. He[1], H. W. Woitge[1], C. J. Rosen[2], L. R. B. Donahue[3], B. E. Kream[1]. [1]Department of Medicine, University of Connecticut Health Center, Farmington, CT, USA, [2]Maine Center for Osteoporosis Research and Education, St. Joseph Hospital, Bangor, ME, USA, [3]Jackson Laboratory, Bar Harbor, ME, USA.

Insulin-like growth factor I (IGF-I) is a key regulator of prenatal and postnatal growth in mice. Many in vitro culture models show that IGF-I is an anabolic growth factor for bone formation, and some human studies demonstrate a positive correlation between serum IGF-I levels and bone mass. An important question is whether IGF-I is a determinant of bone mass throughout life. Mice with a disruption of both Igf1 alleles display a high degree of perinatal lethality in all background strains examined, a feature that precludes a detailed study of their phenotype at various stages of postnatal life. Therefore, as an experimental model, we have chosen to study the influence of IGF-I haploinsufficiency on growth and bone mass in heterozygous Igf1 null (HET) mice, in which one Igf1 allele has been disrupted by the deletion of exon 3 using targeted mutagenesis. These mice are amenable to study as they are healthy and breed normally. In the present study, cohorts of male and female wild-type (WT) and HET mice in the outbred CD-1 background were derived from WT-HET breeding pairs and sacrificed at 1, 2, 4, and 8 months of age. In these initial studies, the number of mice in each group ranged from 6-20. The following measurements were made: body weight, femur length, femoral bone mineral density (BMD) by dual-energy X-ray absorptiometry (DEXA), and serum IGF-I levels by radioimmunoassay. At 1 month, female HET mice had reduced body size, femur length, BMD and serum IGF-I levels compared to female WT mice. Male mice did not show a significant genotype effect at this age, except for serum IGF-I levels; however, male mice showed a tendency toward reduced body size, femur length and BMD. At 2 months, both male and female HET mice had reduced body size, BMD and serum IGF-I levels (femur length was not measured). At 4 and 8 months, male HET mice had reduced body size, femur length, BMD and serum IGF-I levels; female HET mice showed similar changes, but serum IGF-I levels were not significantly different from WT. At 8 months, WT mice showed a significant gender effect: despite their lower body size, female mice had higher femoral BMD and femur length compared to males. In summary, IGF-I haploinsufficiency in outbred male and female mice resulted in reduced body size, femur length, serum IGF-I levels and areal BMD at most ages. Outbred Igf1 heterozygous null mice will provide a useful model to reveal whether IGF-I is a determinant of bone mass during postnatal life.

M149

Evidence that Human Osteoblasts/Skin Fibroblasts Produce an Inhibitor of IGFBP-4 Protease/Pregnancy-associated Plasma Protein-A (PAPP-A). C. Sexton*, S. Mohan, T. Boykin*, S. Kapur*, D. J. Baylink, X. Qin. J.L. Pettis VAMC, Loma Linda, CA, USA.

IGFs play a pivotal role in regulating osteoblast proliferation, differentiation, and apoptosis *in vitro* and bone metabolism *in vivo*. IGFBP-4, the most abundant IGFBP produced by human osteoblasts (hOBs), counter-regulates the activity of IGFs. Importantly, previous studies demonstrated that the effective concentration of the IGFBP-4 in hOB culture is subject to regulation by an IGF-dependent IGFBP-4 protease now known as PAPP-A. Based on the findings that the activity of other proteases are precisely regulated by specific protease inhibitors, and that treatment of hOBs or human skin fibroblasts (hSFBs) with a PKC activator (TPA) resulted in a loss of IGFBP-4 proteolytic activity, we predict that cells which produce PAPP-A may also produce a specific inhibitor of PAPP-A. To test this hypothesis, we determined whether or not the TPA-induced loss of IGFBP-4 proteolytic activity in both hOB and hSFB cultures is mediated through induction of a PAPP-A inhibitor. Treatment of hOBs and hSFBs with 100 nM TPA for 48 hr essentially abolished the IGFBP-4 proteolytic activity in the CM without a profound effect on PAPP-A levels. Addition of excess IGF-II to TPA CM failed to restore the IGFBP-4 proteolytic activity. Addition of TPA CM to control CM dose dependently inhibited IGFBP-4 proteolysis. Moreover, IGFBP-4 proteolysis by control CM was inhibited by PAPP-A immunodepleted CM. The magnitude of inhibition by PAPP-A-depleted TPA CM was greater than that of the PAPP-A-depleted control CM. These data strongly suggest that both hOBs and hSFBs produce a PAPP-A inhibitor which is further up-regulated by activation of the PKC pathway. Since PAPP-A, when covalently linked to proMBP, exhibited a >100 fold reduced IGFBP-4 protease activity compared with the PAPP-A homodimer, we sought to determine if the loss of PAPP-A activity is due to the formation of PAPP-A/proMBP complex. Under non-reducing conditions, PAPP-A/proMBP complex in human pregnancy serum, but not the PAPP-A from either hOB control CM or TPA CM, reacted with proMBP antibody. Additional experiments involving evaluation of the inhibitor activity of proMBP-depleted TPA CM are in progress to determine if the loss of PAPP-A activity in TPA CM is due to non-covalent interaction of PAPP-A with proMBP. In conclusion, these studies demonstrate that: 1) TPA treatment reduced IGFBP-4 proteolysis through induction of a PAPP-A inhibitor rather than reduction of PAPP-A synthesis; and 2) PAPP-A inhibitor may play an important role in regulating the effective concentrations of IGFBP-4 via inhibition of the activity PAPP-A in osteoblasts.

M150

Mathematical Model Predicts that Directed, Random and Pathologically Accelerated Bone Remodeling Are Determined by Osteoclast Autocrine Factors. S. V. Komarova*[1], R. J. Smith*[2], L. M. Wahl*[2]. [1]CIHR Group in Skeletal Development and Remodeling, The University of Western Ontario, London, ON, Canada, [2]Department of Applied Mathematics, The University of Western Ontario, London, ON, Canada.

Bone remodeling involves resorption by osteoclasts, followed by formation of new bone by osteoblasts. Significant contributions to the regulation of bone remodeling derive from interactions between cells of the osteoblastic and osteoclastic lineages. However, experimental approaches to test these interactions are limited. In this study, we employed mathematical modeling to investigate the regulation of bone remodeling. We constructed a model describing the interactions between osteoblasts and osteoclasts and consequent cell population dynamics at a single site of bone remodeling. We included in the model the ability of osteoblasts and osteoclasts to interact with each other (via paracrine factors) as well as their ability to produce factors affecting themselves (autocrine factors). Changes in bone mass were calculated from the difference between rates of formation and resorption, which were proportional to the number of active osteoblasts and osteoclasts, respectively. We investigated how changes in the effectiveness of autocrine and paracrine factors influenced the stability and dynamic behavior of the system. The region of stability for our model included stable nodes, stable foci and centers. Stable nodes, characterized by an individual event of bone remodeling initiated by external stimulus, represented directed bone remodeling. Stable foci and centers, exhibiting intrinsically regulated oscillations, corresponded to random bone remodeling. In addition, unstable behavior resembling pathological bone remodeling seen in Paget's disease was observed. Changes in the effectiveness of osteoclast autocrine factors switched the system among these three different types of behavior. The osteoclast autocrine factor could correspond to a local factor such as TGFβ. The ability of this factor to change the dynamic behavior of the system demonstrated in our model could account for the conflicting observations regarding the effects of TGFβ on bone remodeling. In summary, the mathematical model revealed that interactions between osteoblasts and osteoclasts result in complex system behavior, which cannot be deduced from studies of each cell type alone. The behavior of the system was most sensitive to changes in the osteoclast autocrine factors. The model will be useful in future studies assessing the impact of cytokines and growth factors on the overall process of bone remodeling.

M151

Activations of p42/44 MAPK and JNK by TGF-β Negatively Regulate Smad3-induced ALP Activity and Mineralization in MC3T3-E1 Cells. H. Sowa*, H. Kaji, T. Yamaguchi, T. Sugimoto, K. Chihara*. Endocrinology and Metabolism, Kobe University Graduate School of Medicine, Kobe, Japan.

TGF-β inhibits alkaline phosphatase (ALP) activity and mineralization in mouse osteoblastic MC3T3-E1 cells (MC), while its local administration stimulates bone formation in vivo. We recently demonstrated that Smad3, a critical component of the TGF-β signaling pathway, promotes ALP activity and mineralization in MC (JBMR, in press). Recently, Smad3-knockout mouse showed decreased bone mineral density, indicating that Smad3 plays an important role in the regulation of bone formation. However, why the effects of TGF-β and Smad3 on ALP activity and mineralization are different remains unknown. The purpose of the present study is to clarify the roles of mitogen activated protein kinase (MAPK) in TGF-β- and Smad3-pathways in osteoblast. TGF-β activated p42/44 MAPK, p38 MAPK and c-Jun N-terminal kinase (JNK) in MC. Specific inhibitors of p42/44 MAPK activation (PD98059 and U0126), as well as JNK inhibitors (curcumin and dicumarol) antagonized the inhibitory effects of TGF-β on ALP activity and mineralization, while specific inhibitor of p38 MAPK (SB203580) did not affect them. PD98059 and curcumin promoted Smad3-induced ALP activity and mineralization, while SB203580 inhibited them. In the luciferase reporter assay using 3TP-lux with specific Smad3-responsive element, PD98059 and curcumin enhanced TGF-β - and Smad3-induced transcriptional activity. On the other hand, TGF-β -induced production of type I collagen was antagonized by curcumin, but not by PD98059. The present study indicates that activations of P42/44 MAPK and JNK byTGF-β negatively regulate Smad3-induced ALP activity and mineralization in osteoblast. We propose that Smad3 is a molecule responsible for bone formation, and the local combined administration of Smad3 and inhibitors of p42/44 MAPK might be a novel therapeutic strategy for the stimulation of bone formation.

M152

The Role of Angiogenesis in Distraction Ostogenesis of the Mouse Tibia. R. S. Carvalho*[1], T. Einhorn*[1], C. M. Edgar[1], W. Lehmann*[2], D. M. Pacicca[1], L. C. Gerstenfeld[1]. [1]Orthopedics, Boston University School of Medicine, Boston, MA, USA, [2]Department of Trauma and Reconstructive Surgery, University Clinic Hamburg-Eppendorf, Harburg, Germany.

Distraction osteogenesis is a commonly used technique for limb lengthening. However, the basic mechanisms by which it promotes new bone formation are not well understood. A feature of this process is the observation of robust vascularization of repair tissue both proceeding and during the regenerative process. Therefore, the aim of this study was to investigate the role of angiogenesis in bone regeneration during distraction. In order to test this hypothesis and examine the molecular mechanisms that regulate bone formation we have developed a murine model of distraction osteogenesis. The tibias of Balbc mice 8 to 12 weeks old were fitted with a 6 mm track distractor originally designed for intra-oral bone distraction. Mice were divided into three groups of 6 to 8 animals each for the following experimental phases; 1) latency of 7 days post surgery before the onset of distraction, 2) active distraction of 10 days and 3) post distraction consolidation of 14 days. The rate of distraction was 0.3 mm (2X 0.15mm/day). Samples were processed for standard histology or total RNA was extracted. Micro-arrays containing 96 cDNA fragments from genes associated with the angiogenic process were assayed. In addition, arrays containing more than 20 cDNA fragments from genes encoding signals for proteins with metaloproteinase (MMPs) activity were also used. Finally, the expression of bone extracellular matrix proteins (ECM) and bone morphogenic proteins (BMPs) was studied by ribonuclease protection assays. Validation of this model by histology was evidenced by the induction of new bone formation in the distraction gap with successful bone lengthening. The molecular analysis results indicated that a number of angiogenic and MMP genes were selectively induced during the three separate phases of the distraction protocol. Some of these genes include fibronectin, Hif1A, gelat A and B, SPARC, osteopontin, cyclophilinA, PEDF, VEGFA, TGFb1, endostatin, FGF receptor3, angiopoietin2, MMP2, MMP8, MMP9, MMP13 and MMP14. The expression of ECM genes showed that osteopontin and bone sialoprotein were significantly increased during distraction and expressions of BMP1, BMP3, BMP4, BMP5 and BMP6 were also stimulated. These initial studies start to show the temporal and spatial expression of the angiogenic signals that drive new bone formation during distraction. These experiments represent the first step in defining the molecular mechanisms that regulate bone formation during distraction osteogenesis while testing the functional role of angiogenic regulators in this process.

M153

TGF-β3 Regulation of KC Chemokine Expression in Mouse Mesenchymal C3H10T1/2 and Pre-Osteoblast MC3T3-E1 Cells. D. S. Bischoff*[1], J. H. Zhu*[2], N. S. Makhijani*[1], D. T. Yamaguchi[1]. [1]Research Service, VA Greater Los Angeles Healthcare System, Los Angeles, CA, USA, [2]Research Service, VA Greater Los Angeles Healthcare System, Sepulveda, CA, USA.

Fracture healing is a complex process involving several coordinated steps including hemostasis, inflammation at the fracture site, recruitment and proliferation of mesenchymal cells, cartilage formation followed by replacement of cartilage with bone, and finally bone remodeling. Healing events are mediated by a variety of growth factors and cytokines including members of the TGF-β family. The role of these cytokines is to attract mesenchymal cells to the fracture site that can undergo proliferation and differentiation to form bone. IL-8, a member of the CXC chemokine family is a potent neutrophil chemotactic cytokine. Recently it has become apparent that neither the mouse or rat genome contains a gene that encodes IL-8, although, the genomes do have genes for other CXC chemokines that may be structurally similar to IL-8. Two of these genes, the platelet-derived growth factor-induced KC protein and the macrophage inflammatory protein-2 (MIP-2), have homology to IL-8 and may be functionally equivalent to IL-8 in the mouse. It was found that IL-8-like immunoreactivity was present in the mesenchymal-like cells, macrophages, monocytes, osteoblasts, and pre-chondrocytes in the fracture callus in both young and old rat histologic sections using a polyclonal antibody generated against human IL-8. The role of TGF-β3 on expression of the KC gene in C3H10T1/2, a mouse pluropotent mesenchymal cell line, and MC3T3-E1, a mouse pre-osteoblastic cell line was also explored. RNA was isolated from undifferentiated C3H10T1/2 and MC3T3-E1 cells grown in the absence of ascorbic acid (AA) and β-glycerophosphate (βGP) and treated with 2 ng/ml of TGF-β3 for 0, 3, 6, and 24h. Time points were also taken for all-*trans* retinoic acid (ATRA)-differentiated C3H10T1/2 cells and for MC3T3-E1 cells grown in the presence of AA and βGP at 14 days in culture. Initial northern results for TGF-β3 suggest that KC gene expression is stimulated beginning at 3h post-treatment in ATRA-differentiated C3H10T1/2 cells but not until 24h in undifferentiated cells. KC is also expressed at low levels in MC3T3-E1 cells cultured in the presence or absence of AA and βGP, although, this expression is not stimulated by TGF-β3 treatment. Conclusions: 1) Chemokine IL-8-like immunoreactivity is found in mesenchymal-like cells among other cell types in the fracture callus of old and young rats; 2) KC gene (structurally related murine equivalent to IL-8) is upregulated in the mesenchymal C3H10T1/2 cell line by TGF-β3, and although expressed in MC3T3-E1 cells, is not regulated by TGF-β3 in this cell line.

M154

TGF-β Isoforms Stimulate Chemotaxis But Not Cell Proliferation in the Pluripotent Mesenchymal Stem Cell Line C3H10T1/2. N. S. Makhijani*, D. S. Bischoff*, D. T. Yamaguchi. Research Service, VA Greater Los Angeles Healthcare System, Los Angeles, CA, USA.

Transforming growth factor-β (TGF-β) has been implicated in the promotion of bone repair. Three isoforms of TGF-β, TGF-β1, -β2, and -β3 are expressed in fracture healing, however their specific roles in the repair process are unknown. Proliferation of mesenchymal precursors of chondrogenic and osteogenic cells and migration of these precursors to repair sites are important early steps in bone repair. Differential actions of the TGF-β isoforms on early events of bone repair were explored in the pluripotent mesenchymal precursor cell line, C3H10T1/2. Cell migration or chemotaxis was determined using a modified Boyden chamber in response to concentrations of each isoform from 1 picogram/ml to 1 nanogram/ml while proliferation was assessed by radiolabeled thymidine incorporation and cell counts at concentrations from 0.1 picogram/ml to 10 nanograms/ml. Both TGF-β1 and -β2 demonstrated a similar dose-dependent chemotactic stimulation of C3H10T1/2 cells with maximum chemotaxis demonstrated at 0.1 nanograms/ml of peptide. However, maximal chemotactic response to TGF-β3 occured at 1 picogram/ml with lesser effects at higher concentrations. Twenty-four hour incubation with 3H-thymidine showed that TGF-β2 at concentrations of 0.1 and 1 nanogram/ml significantly enhanced 3H-thymidine incorporation. However, the 3H-thymidine incorporation studies implying cell division were not borne out by cell counts. While it appeared that TGF-β3 was mildly stimulatory for cell proliferation, statistical analysis did not demonstrate significance. Conclusions: 1) while all three TGF-β isoforms stimulate chemotaxis of C3H10T1/2 cells, TGF-β3 appears to be more potent at the lowest concentration tested while the other two isoforms were more potent at higher concentrations; 2) TGF-β isoforms do not appear to stimulate cell proliferation in C3H10T1/2 cells; 3) 3H-thymidine incorporation may not accurately reflect cell proliferation in this cell line.

M155

Cross-talk Between TGFβ Signaling and PPARγ2 Controls the Fate of Mesenchymal Bone Marrow Progenitors. B. Lecka-Czernik, C. Cousins*. Geriatrics, University of Arkansas for Medical Sciences, Little Rock, AR, USA.

Both adipocytes and osteoblasts are derived from a common mesenchymal progenitor and their differentiation is inversely related. The cytokine TGFβ1 controls osteoblast and inhibits adipocyte formation, whereas the transcription factor PPARγ2 plays a critical role in suppressing the osteoblast and inducing the adipocyte phenotype. We have investigated how these opposing activities of TGFβ and PPARγ2 interact with each other and how they contribute to the control of the phenotype of marrow cells. We found that the effect of TGFβ1 on marrow adipocyte differentiation includes the inhibition of PPARγ2 gene expression, which is normally induced during adipogenesis through the autoregulatory mechanism. The PPARγ2 promoter fragment contains a Smad-binding element SBE1 that binds predominantly Smad6 and Smad7, TGFβ signaling proteins. Thus, the effect of TGFβ1 on the regulation of PPARγ2 expression occurs on the transcriptional level and may involve a SBE1 *cis*-acting element. To determine whether, additional TGFβ-mediated mechanisms play a role in the inhibition of the adipocyte phenotype, we used U-33/γ2 cells that were stably transfected with a PPARγ2 expression construct and constitutively express PPARγ2 protein on a level comparable to that seen in marrow adipocytes. We found that TGFβ1 inhibits adipocyte differentiation of these cells by inhibiting the pro-adipocytic activity of PPARγ2 activated with rosiglitazone. This suggests that, in addition to controlling PPARγ2 gene expression, TGFβ1 also controls the activity of PPARγ2 protein. The inhibition of PPARγ2 activity does not require *de novo* protein synthesis. Additionally, we found that the interaction between PPARγ2 protein and the TGFβ1-signaling pathway has a reciprocal character, since PPARγ2 inhibits Smad6 and Smad7 gene expression and modulates the inhibitory effect of TGFβ1 on alkaline phosphatase activity. This effect requires activation of PPARγ2 by rosiglitazone and is not seen in the presence of the PPARγ antagonist GW9662, or in U-33/c cells that do not express PPARγ2. As reported recently, Smad3 may modulate the activity of several transcription factors, among them Runx2/Cbfa1 and PPARγ1, another PPARγ isoform, by physical interaction with these proteins. We postulate that a similar interaction may occur between Smad3 and PPARγ2, resulting in the inhibitory effect of TGFβ1 on the pro-adipocytic activity of PPARγ2 on the one hand, and PPARγ2 inhibitory effect on the TGFβ1 signaling pathway on the other. This possibility is currently under investigation.

M156

Transforming Growth Factor-β1 Selectively Activates p38 Mitogen-activated Protein Kinase and NF-κB upon RANK Stimulation. S. J. Park*, E. J. Chang*, J. S. Ko, H. M. Kim. College of Dentistry and IBEC, Seoul National University, Seoul, Republic of Korea.

Although transforming growth factor-β1 (TGF-β1) is involved in osteoclast differentiation, the intracellular signaling mechanism by which TGF-β1 participates in osteoclastogenesis is still unclear. In this study, we compared the effects of pre-treated with or without TGF-β1 in early stage of osteoclastogenesis to clarify how TGF-β1 regulates RANKL-induced osteoclast differentiation. We pre-treated murine bone marrow cells with TGF-β1 and then stimulate RANK with RANKL after withdrawal of TGF-β1. TRAP-positive multinucleated cell formation was increased by pre-treatment of TGF-β1 in presence of low concentration of RANKL. Treatment of pre-osteoclasts with SB203580 apparently inhibited RANKL-induced osteoclast differentiation in case of the pre-treatment of TGF-β1. Further investigation showed that TGF-β1 reversed the inhibitory effect of SB203580 in RANKL-induced osteoclastogenesis. In contrast, ERK MAPK inhibitor or PI3-kinase inhibitor did not significantly change the effect of TGF-β1. To elucidate the molecular basis of TGF-β involvement in RANK signaling, we observed the effects of TGF-β1 on RANK-derived MAP kinase pathway. Pretreatment of TGF-β1 selectively triggered activation of NF-κB as well as p38 MAPK but not ERK and JNK MAPK upon RANK stimulation. These results indicate that TGF-β1 modulates RANK-derived p38 and NF-κB activation, resulting in promoting osteoclast differentiation.

M157

Bone Morphogenetic Protein Gene Expression Patterns are Altered by Physiological and Pharmacological Regulators of Bone Metabolism. M. Zhang*, A. Maran, G. L. Evans*, A. M. Kennedy*, R. T. Turner. Orthopedic Research, Mayo Clinic, Rochester, MN, USA.

The Bone Morphogenetic Proteins (BMPs), which belong to the transforming growth factor-ß (TGF-ß) super family, have been implicated in bone formation during development, bone regeneration and in the induction of bone formation, as well as non bone related functions. Very few studies have investigated the role of BMPs in normal bone turnover and disease. In this report, we describe the changes in BMP gene expression in rat long bones in the presence of various regulators of bone turnover. BMP expression (BMP 1-7) was measured in the proximal tibial metaphysis by RNAse protection assay. Acute exposure to an estrogen in ovariectomized rats resulted in the down regulation of mRNA levels for several BMP (BMP 1, -2, -3, -4, and -7) family members. Growth hormone selectively increased BMP-1 in hypophysectomized rats while intermittent administration of PTH increased mRNA levels for BMP-1 and -7. Acute (24 hr) exposure to ethanol, an important risk factor for osteoporosis, had no effect but a long-term (2 month) treatment led to an increase in BMP-2 and BMP-4 mRNA levels. Also, alcohol prevented the PTH-induced increase in mRNA levels for BMP-1 and -7. No changes in BMP expression was observed following either hindlimb unloading or spaceflight. These findings demonstrate that BMP expression is influenced by selected physiological and pharmacological regulators of bone turnover in an effector specific pattern. These findings suggest that BMPs may play a role in mediating the skeletal response to some of the most important regulators of bone metabolism.

M158

Lysophospholipids Activate Latent TGF-beta1 and Release Active TGF-beta1 from Extracellular Matrices Produced by Growth Plate Chondrocytes. Z. Schwartz, I. Gay*, V. L. Sylvia, D. D. Dean, B. D. Boyan. Orthopaedics, University of Texas Health Science Center at San Antonio, San Antonio, TX, USA.

Costochondral growth plate chondrocytes produce and store latent TGF-β1 in their extracellular matrix. Several mechanisms allow for the spatial and temporal control of the release of latent TGF-β1 from the matrix and its activation. Activation of matrix vesicle (MV) phospholipase A_2 (PLA_2) by $1\alpha,25(OH)_2D_3$ releases MMP-3 from the organelles, resulting in latent TGF-β1 activation. Here, we tested the hypothesis that lysophospholipids, which are produced by the action of PLA_2, participate in this process. Small latent recombinant human TGF-β1 was incubated with lysophosphatidylcholine (LPC) or lysophosphatidylethanolamine (LPE) [0.6 to 600 μg/ml] and the production of active TGF-β1 measured by ELISA. LPC and LPE caused a biphasic activation of latent TGF-β1, with maximum activation seen in samples treated with 2 μg/ml. Active TGF-β1 was released at incubation times of 9-360 minutes with a peak at 180 minutes. PC and PE, but not choline, also activated latent TGF-β1. However, the effect was much less than that achieved using lysoderivatives of these phospholipids. We verified that the product of the activation was functional TGF-β1 by assessing its ability to enhance [^{3}H]-thymidine incorporation by growth plate chondrocytes. The reaction product significantly enhanced proliferation whereas neither LPC nor LPE was able to do so. Extracellular matrices produced by growth zone (GC) and resting zone (RC) chondrocytes were also incubated with LPC or LPE. Both LPC and LPE stimulated the release of TGF-β1 from the cell free extracellular matrices. Addition of LPC and LPE to GC chondrocyte cultures caused an increase in PKC specific activity of intact cells and matrix vesicles produced by the cells. No increase was observed in plasma membranes, suggesting that the effect was targeted to the extracellular organelles. Moreover, there was a synergistic increase in PKC in cultures co-treated with $1\alpha,25(OH)_2D_3$. In contrast, LPC and LPE inhibited PKC activity in RC cell cultures and partially inhibited the stimulatory effect of $24R,25(OH)_2D_3$. These results suggest that LPC and LPE have an important role in chondrocyte regulation, both directly on MV PKC activity, which is cell maturation dependent, and indirectly by activation of latent TGF-β1 in the matrix.

M159

The Presence of Bone Morphogenetic Proteins (BMPs) in Megakaryocytes and Platelets. J. B. Sipe*, C. A. Waits*, B. Skikne*, M. Imkie*, R. Dhanyamraju*, H. C. Anderson. University of Kansas Medical Center, Kansas City, KS, USA.

Platelets contain various growth factors implicated in the process of bone remodeling and repair, such as Transforming Growth Factor-β (TGF-β), Platelet Derived Growth Factor (PDGF) and Epidermal Growth Factor (EGF), and have been cited as having the ability to induce new bone formation. Recently, we have identified Bone Morphogenetic Proteins (BMPs) 1 through 6 within human fetal megakaryocytes, cells which give rise to platelets, by immunohistochemistry. The possibility of platelets containing BMPs, contributing to their osteoinductive potential, was the focus of this study. Human platelets were isolated from serum, washed and lysed with a buffer containing 2% sodium dodecylsulfate (SDS), to give a lysate of pure platelet proteins. Immunoblotting (Western blotting) technique was performed to identify BMP-2 and BMP-4 within the lysate, using a polyclonal goat-anti-human BMP-2 antibody (Santa Cruz) and a monoclonal mouse-anti-human BMP-4 antibody (NovoCastra), respectively. The proteins were detected using a chemiluminescent detection kit (Amersham-Pharmacia biotech). The use of Western blotting technique revealed the presence of BMP-2 and BMP-4 in isolated human platelets. These findings demonstrate the presence of significant amounts of BMP-2 and BMP-4 in platelets, which may account for their role in bone formation and repair.

M160

Effect of TGFß2 and BMP-3 on Chondrocyte Dedifferentiation in an In Vitro Aggregate Model. B. Han*[1], B. W. Tang*[1], F. Cordoba*[1], M. E. Nimni*[1], B. S. Strates[2]. [1]Departments of Surgery, Biochemistry and Orthopaedics, Keck School of Medicine, University of Southern California, Los Angeles, CA, USA, [2]Departments of Orthopaedics and Rehabilitation, College of Medicine, University of Florida, Gainesville, FL, USA.

Using animal implantation models, we have shown that rhTGFß2 and rhBMP-3, members of the TGFß1 superfamily, are capable of inducing new bone and cartilage formation. To test the hypothesis that chondrocytes are targets of growth factors, we employed an aggregate cell culture system to show that growth factors regulate chondrocyte dedifferentiation. Briefly, cells were obtained from articular cartilage by collagenase digestion (Worthington Biochemicals, Lake Wood, NJ) in monolayer culture using FBS/DMEM + 10-7 dexamethasone after trypsinization. Cells were centrifuged and pellets exposed to various growth factor concentrations, media changed every 4 days, cell aggregates removed at intervals up to 21 days and frozen at -80ºC in OTC medium. Five μm Cryostat sections were fixed in 10% buffered formalin, stained with Alcian blue or fixed in 100% methanol and reacted with type II collagen antibody (Chemicon, Temecula, CA), incubated at 1:40 dilution and fluorescence developed with a second antibody (FITC conujugated goat anti-rabbit IgG). Cells also were homogenized and electrophoresed (SDS-PAGE 4-7%) for Western blots. Chondrocyte progenies from 5th monolayer cultures, without growth factor added, formed a multilayer matrix-rich substratum expressing type II collagen. Addition of rhTGFß2 (0-5 μg) enhanced Alcian blue positive proteoglycan expression in a dose-response manner and expression in a dose-response manner and expression of type II collagen immunohistochemically and by Western blot. Addition of rhBMP-3 at low concentrations also enhanced type II collagen expression that was inhibited at high concentrations. Addition of both growth factors had no synergistic effect. These data indicate that chondrocytes are potential targets of growth factors and may be involved in the regulation of cartilage formation and its repair process.

M161

TGF-β Stimulates Chondrogenesis and Inhibits Adipogenesis of Human Marrow Stromal Cells (hMSCs) *in vitro*: The Role of Wnt-mediated Signaling via LRP5. S. Zhou[1], K. Eid*[2], J. Glowacki[3]. [1]Department of Orthopedic Surgery, Brigham & Women's Hospital & Harvard Medical School, Boston, MA, USA, [2]Department of Orthopedic Surgery, Brigham & Women's Hospital, Boston, MA, USA, [3]Department of Orthopedic Surgery, Brigham and Women's Hospital, Harvard Medical School, Boston, MA, USA.

The decrease in bone volume associated with osteoporosis and age-related osteopenia is accompanied by an increase in marrow adipose tissue. Recent data indicates that Wnt-mediated signaling via LRP5 (LDL receptor-related protein 5) affects bone mass. Wnt signaling inhibits adipogenesis, and stimulates chondrogenesis and/or osteogenesis. TGF-β was reported to enhance chondrogenic/osteogenic differentiation and depress adipogenic differentiation. TGF-β and Wnt signaling pathways can synergistically activate target genes. We tested the hypothesis that TGF-β promotes chondrogenesis and inhibits adipogenesis in human marrow stromal cells, and one of its pathways is Wnt-mediated signals via LRP5. Human bone marrow was obtained from a 58-year-old woman. Adherent stromal cells were expanded and seeded in 3D collagen sponges or were plated in 2D monolayer culture. All cultures included 100 nM dexamethasone with or without 10 ng/ml human TGF-β1 for 35 days. RT-PCR analysis showed that TGF-β up-regulated aggrecan and collagen type II and down-regulated lipoprotein lipase. This was evidence that TGF-β promotes chondrogenesis and inhibits adipogenesis of human marrow stromal cells, but the mechanism was unknown. To investigate the mechanism, we used a human stromal cell line, KM101. KM101 cells were cultured in 2D in phenol red-free α-MEM supplemented with 10% HI-FBS until they reached 80% confluence. The medium was replaced with fresh medium supplemented with 1% charcoal/dextran stripped FBS. After 2 days, when cells were quiescent, 1-5 ng/ml of human TGF-β1 was added to the culture medium. RNA was isolated 6 hours after stimulation. As revealed by RT-PCR, TGF-β up-regulated LRP5, Wnt4, Wnt5a, and Wnt7a, down-regulated Wnt5b, and had no affect on Wnt2, 3, 7b, 10b, 13 and 14 gene expression in KM101 cells. Our results showed TGF-β enhancement of chondrogenesis and inhibition of adipogenesis of hMSCs. TGF-β's regulation of LRP5 and Wnts implies that Wnt-mediated signaling via LRP5 has a role in the effects of TGF-β in chondrogenesis and adipogenesis, either independently or cooperatively with TGF-β signaling pathways.

M162

Relationship Between Hip Bone Density and Calcaneal Stiffness Index Responses to Resistance Training. D. A. Bemben, M. G. Bemben*, S. A. Brickman*. Health and Sport Sciences, University of Oklahoma, Norman, OK, USA.

The purpose of this study was to determine whether changes in total hip BMD in response to resistance training could be detected by changes in calcaneal stiffness index (SI) in older men (n=13) and women (n=18). The 40 week training programs involved 3 sets of 12 isotonic resistance exercises using Cybex® equipment performed 2-3 days/week at either low (40% 1 repetition maximum) or high (80% 1 repetition maximum) intensities. Dual Energy X-Ray Absorptiometry (Lunar DPX-IQ, software version 4.7b) was used to measure BMD of the left proximal femur at baseline, 20 weeks and 40 weeks of training. One the same day as the bone scans, the Achilles+ Ultrasonometer (Lunar Corporation) was used to obtain the SI of the left os calcis. There were no significant (p>.05) gender differences in total hip BMD or calcaneal SI at baseline. There was a significant (p=.001) training effect and a trend (p=.06) for a gender x training effect for calcaneal SI as men increased about 4% from baseline to 40 weeks (82.6±4.7 to 86.2±5.1) while women increased 1% (81.5±4.1 to 82.3±4.0). Total hip BMD increased significantly (p<.05) from baseline to 40 weeks of training for both genders. There were moderate positive correlations (r=.69 to .74, p<.05) between calcaneal SI and total hip BMD at baseline, 20 and 40 weeks of training. However, a low negative correlation (r=-.15, p>.05) was found between calcaneal SI and total hip BMD percent changes from baseline to 40 weeks, indicating that the direction of the total hip BMD response was not matched by the direction of the calcaneal SI response. In conclusion, calcaneal SI and total hip BMD improved in response to resistance training, but the relative changes in calcaneal SI and total hip BMD were not related. Thus, calcaneal SI may not be a valid indicator of the total hip BMD response to an exercise intervention.

M163

Effects of a Mutation in the Lrp5 Gene on Bone Biomechanical Properties. M. P. Akhter[1], D. M. Cullen[1], D. J. Wells*[1], M. L. Johnson[1], P. Babij*[2], G. R. Haynatzki[1], R. R. Recker[1]. [1]Medicine, Creighton University, Omaha, NE, USA, [2]Wyeth Research, Andover, MA, USA.

Identification of the high bone mass (HBM) mutation in the Lrp5 gene has allowed investigators to examine the role of Lrp5 in signaling pathways for bone adaptation to mechanical load. We report the biomechanical strength and mass data in bones from HBM transgenic (HET) mice and their non-transgenic (NTG) littermates. A total of 120 mice (17 wk old, male and female) equally divided into transgenic (HET) and non-transgenic littermates (NTG) were used. Left femurs and ulnae were collected and frozen at -20 C in saline solution for subsequent biomechanical testing. Before testing, femur (FEM) mid shaft anterior-posterior (A-P) widths were measured. Femur shafts were subjected to 3-point bending tests with the lower supports 5mm apart and touching the posterior surface. After testing the femoral shaft, the femoral necks (FN) were tested in bending. All tests were performed using an Instron 5543 at a rate of 3mm/min. Load-displacement curves were analyzed for structural strength properties that included 1) ultimate load (ULT); 2) yield load (YLD); and 3) Stiffness (STIF). Ulnae bone ash weights were measured using standard bone ash technique. Genetic and gender differences in all the measured variables were tested using ANOVA at a significance level of P<0.05. The structural strength properties of both the femur shaft and neck were greater in transgenic (HET) mice as compared to the control (NTG) mice (Table). Femoral shaft anterior-posterior widths in HET mice were also greater than that in the NTG mice. In addition, bone ash content was greater in HET mice than in NTG mice. Femoral neck (FN) stiffness in males were greater than in the corresponding female mice (Table). These data suggest that the HET mice have a larger sized and structurally stronger skeleton. For example, in HET mice the greater size (A-P width) of the femurs resulted in greater structural strength at the femoral shaft and same could be true at the femoral neck site. In addition, greater bone ash weight suggest that HET mice have larger sized ulnae as compared to the NTG mice.

Variables (Mean±SD)	NTG (n=30) Female	HET (n=30) Female	NTG (n=30) Male	HET (n=30) Male
FEM ULT (N)	20.7±3.9	30.7±6.3 [a]	18.8±2.3	28.8±6.8 [a]
FEM YLD (N)	13.1±3.1	18.7±6.3 [a]	13.1±2.1	16.7±3.9 [a]
FEM STIF (N/mm)	138±28	194±39 [a]	125±23	177±34 [a]
FEM A-P width(mm)	0.97±0.11	1.11±0.09 [a]	0.92±0.08	1.04±0.11 [a]
FN ULT (N)	17.84±1.7	27.9±4.5 [a]	18.4±2.0	27.5±4.7 [a]
FN YLD (N)	8.8±1.4	12.6±4.4 [a]	9.6±1.5	13.4±3.6 [a]
FN STIF (N/mm)	149±21	190±49 [a]	171±27 [b]	217±48 [a]
Ash wt (mg)	8.6±0.6	11.6±1.3 [a]	8.2±1.4	11.5±1.7 [a]

[a] different from non-transgenic littermates (NTG) (P <0.05)
[b] different from Females (P <0.05)

Disclosures: ***M.P. Akhter****, Wyeth Research 2.*

M164

Indomethacin Suppresses the Bone Adaptation Response to Mechanical Loading in C57BL/6J Mice. M. P. Akhter, D. M. Cullen, D. J. Wells*, D. L. Mace*, R. R. Recker. Medicine, Creighton University, Omaha, NE, USA.

The bone adaptation mechanism involves a prostaglandin mediated pathway. C57BL/6J (B6) mice have shown a strong bone adaptation response to changes in the loading environment (mechanical stimulus or disuse in tibiae). This project investigated the prostaglandin pathway for bone adaptation to loading in B6 mice through indomethacin treatment to inhibit prostaglandin synthesis. Two groups of mice (n=12/group, 4 mo. old, female, C57BL/6J) were subjected to tibial loading using a four-point bending device at a schedule of 36 cycle per loading session for 3 weeks. Mice were either treated with 2mg/kg of indomethacin or saline (placebo). Indomethacin or placebo was given 3 hours prior to a loading (5N bending load inducing a range of 1500-1600με) session on Monday, Wednesday, and Friday. Standard histomorphometric techniques were used to quantify the net (right leg loaded– left leg nonloaded) loading related bone adaptation response. The load related response was measured in terms of periosteal formation surface (**FS**=(0.5sL+dL+WoS)/ BS), woven bone area (**WoAr**), and bone formation rate (**BFR**). The differences between the placebo and indomethacin treatment in nonloaded legs and in the loading response (loaded-nonloaded) on all the measured variables were compared using one-way ANOVA at a significance level of P<0.05. There were no differences in the nonloaded left leg between placebo and indomethacin treatment. However, the mice treated with indomethacin had a smaller load related bone adaptation response as compared to the placebo treated mice. The increases in FS, WoAr, and BFR were lower in the indomethacin treated mice as compared to the placebo group. Although indomethacin treatment decreased the load related bone formation response it did not eliminate the response completely. These results are similar to those seen in rats exposed to four-point bending. Sensitivity to indomethacin provides an insight into the possible role of PGE_2 in the bone adaptation pathway. These data suggest that the B6 mouse is an excellent model to study the pathways and mechanisms involved in PGE related mechano-transduction signals that are involved in initiating the bone adaptation response to a unique mechanical stimulus.

Variables (Mean±SD)	Placebo	Indomethacin
FS (%)	52±14	38±14 [a]
WoAr (mm^2)	0.029±0.022	0.008±0.011 [a]
BFR ($um^3/um^2/yr$)	296±131	150±48 [a]

[a] different from Placebo treatment group (P <0.05)

M165

Effects of 40 Weeks of Resistance Training on Bone Mineral Density in Older Men and Women. M. G. Bemben*, D. A. Bemben, S. A. Brickman*. Health and Sport Sciences, University of Oklahoma, Norman, OK, USA.

The purpose of this study was to examine the effects of 40 weeks of resistance training on the bone mineral density (BMD) of men (n=49) and women (n=78), aged 60-71 years. The training programs involved 3 sets of 12 isotonic resistance exercises (5 upper body, 7 lower body) using Cybex® equipment performed 2-3 days/week at either low (40% 1 rep-

etition maximum) or high (80% 1 repetition maximum) intensities. Muscular strength was assessed at baseline and at 5 week intervals to determine the rate of progression. Dual Energy X-Ray Absorptiometry (Lunar DPX-IQ, software version 4.7b) was used to measure BMD at the AP lumbar spine (L2-L4), the proximal femur, and for the total body at baseline, 20 weeks and 40 weeks of training. Men had significantly ($p<.05$) higher BMD than women for the trochanter, total hip and total body sites. Both men and women experienced significant ($p<.01$) increases in the trochanter, total hip and spine BMD sites from baseline to 40 weeks of training. There was a significant ($p<.05$) training effect and a trend ($p=.06$) for a gender x training effect for the total body BMD with men tending to decrease from baseline to 20 weeks, while the women increased total body BMD from 20 to 40 weeks of training. There were no significant differences between the low and high intensity programs for effects on BMD. In conclusion, resistance training significantly improved spine and hip BMD in both men and women, and total body BMD in women. The intensity of the exercise did not influence the BMD responses.

BMD Responses to Resistance Training

BMD Site (g/cm^2)	Men (n=49) Baseline	Men 40 Weeks	Women (n=78) Baseline	Women 40 Weeks
Lumbar Spine	1.174±.026	1.195±.026	1.155±.021	1.157±.020
Total Hip	0.991±.023	0.997±.023	0.921±.014	0.928±.014
Total Body	1.239±.012	1.234±.012	1.140±.010	1.143±.010

M166

Remobilization Restores Bone Mass But Not Microarchitecture After Long-term Disuse in Old Adult Dogs. C. Li*, D. Laudier*, M. B. Schaffler. Orthopaedics, Mount Sinai School of Medicine, New York, NY, USA.

Disuse results in not only a dramatic loss of bone mass, but also changes in bone architecture. In cancellous bone, these changes result from a combination of thinning, perforation and ultimately complete loss of trabecular elements. Bone mass that is lost during immobilization can substantially recover with restoration of loading. However, whether bone architecture can recover after long-term disuse is unknown. In the current study, we examined both the bone mass and microarchitectural bases of cancellous bone recovery from long-term disuse osteoporosis. Right forelimbs of 5-7 years old retired breeder Beagle dogs (N=32) were immobilized (IM) for either 3 or 6 months periods, at which time animals were either sacrificed (3IM or 6IM), or remobilized (RM = allowed to resume normal weight-bearing) for an additional 12 months (3IM-12RM and 6IM-12RM). Nonimmobilized age-matched animals were served as control. Changes of cancellous bone were examined using histomorphometry on sections from distal metacarpal metaphyses. At 3 months after IM, there was a marked reduction (-38%) of cancellous bone mass (%Tb.Ar/T.Ar), resulting from a significant decrease in trabecular thickness (Tb.Wi, -45%) and trabecular number (Tb.N, -17%). Bone formation (L.Pm/B.Pm, MAR and BFR/B.Pm), bone turnover (Ac.F) and resorption (E.Pm/B.Pm) were significantly higher in 3IM group compared to control group; these latter results indicate that disuse bone loss at this long-term period is a "high turnover" type process. After 6 months of IM, there was no further decrease in Tb.Wi, but a continued decline in Tb.N. At this time, bone turnover slowed to near control level; however, bone resorption remained elevated. In both 3IM-12RM and 6IM-12RM groups, bone mass was restored to the control level, indicating that bone mass can recover even in older animals. This recovery occurred through thickening of the existing trabeculae. However, bone microarchitecture did not recover from long-term disuse osteoporosis. Trabecular number remained lower in both 3IM-12RM (-12%, $p<0.09$) and 6IM-12RM (-23%, $p<0.002$) groups when compared to the control group. These data indicate that bone mass can recover from long-term disuse osteoporosis, but microarchitectural changes are unreversible. This failure to restore bone microarchitecture may have important implications for determining whether bone can recover adequate mechanical integrity after recovery from osteoporosis.

M167

Attenuation of Disuse Bone Loss by Estrogen and Raloxifene in Mature Male Rats. S. A. Bloomfield[1], M. R. Allen[1], C. Nolan*[2], C. L. Smith[2]. [1]Health & Kinesiology, Texas A&M University, College Station, TX, USA, [2]Molecular and Cellular Biology, Baylor College of Medicine, Houston, TX, USA.

Decreased mechanical usage as experienced during spaceflight, bedrest, and hindlimb unloading (HU) induces loss of bone mass and dramatic reductions in bone formation. Serum testosterone and testes weight is reduced in male rats subjected to HU. Humans and rats with testosterone (TES) and/or aromatase deficiencies experience bone loss, which may be attenuated by 17-β estradiol (E_2) treatment. The objective of this study was to assess the ability of E_2 and the selective estrogen receptor modulator raloxifene (RAL) to minimize deleterious effects of 28 d HU in male rats. Mature adult Sprague-Dawley (6-mo-old) rats were implanted with time-release pellets (Innovative Research of America; Sarasota, FL) containing vehicle (VEH), E_2 (12 μg/d), or RAL (535 μg/d) and were randomly assigned to one of 4 groups: cage-control activity + VEH (CON-VEH; n=12), HU+VEH (n=11), HU+ E_2 (n=10), or HU+RAL (n=12). Peripheral quantitative computed tomography scans (pQCT; Stratec XCT Research M) for bone mineral density (BMD) and geometry were taken *in vivo* at the proximal tibial metaphysis on days 0 and 28; *ex vivo* scans were performed at the distal femur, and proximal and mid-shaft humerus. Serum estradiol, LH, and FSH were measured by RIA. A large reduction in testes mass (-65%) was observed in HU+VEH vs. CON-VEH rats; this reduction was magnified by E_2 treatment, but unaffected by RAL. Serum LH and FSH were elevated by HU, but significantly depressed by E_2 to levels even below those in CON-VEH rats, whereas RAL had little effect on either. Both E_2 and RAL attenuated loss of endocortical bone at the metaphysis in both tibia and femur, reducing the increase in marrow area observed in HU+VEH rats by 50% and 13%, respectively. In the normally loaded humeral metaphysis, HU+ E_2 rats gained bone at the endocortical surface and had an increase in cancellous BMD. RAL prevented and E_2 attenuated the 5% decrease in cancellous BMD in the proximal tibia observed in HU+VEH rats. In conclusion, RAL attenuated loss of endocortical and cancellous bone at metaphyses of unloaded long bones without the deleterious endocrine effects produced by E_2 treatment in these male rats. Hence, RAL may prove useful in attenuating disuse-induced bone loss in males and should be investigated further.

M168

Hip Section Modulus, A Measure of Bending Resistance, Is More Strongly Related To Physical Activity Than BMD. S. Kaptoge[1], N. Dalzell*[1], R. Jakes*[2], N. Wareham*[2], K. Khaw*[3], T. J. Beck[4], N. Loveridge[1], J. Reeve[1]. [1]Department of Medicine, Cambridge University, Cambridge, United Kingdom, [2]Institute of Public Health, Cambridge University, Cambridge, United Kingdom, [3]Clinical Gerontology Unit, Cambridge University, Cambridge, United Kingdom, [4]Department of Radiology, The Johns Hopkins University School of Medicine, Baltimore, MD, USA.

We hypothesized that measures of physical activity would have a closer relationship with section modulus (SM), an indicator of bending resistance, than with BMD because physical activity might expand the bony envelope which reduces BMD. 423 men and 436 women mean age 72yrs (SD=3) were recruited from a prospective population based-cohort study to a study of hip bone loss. Hip BMD was measured on two occasions 2-5 years apart (mean 2.7, DXA - Hologic 1000W). Hip structural analysis (HSA) software was used to calculate structural indices and BMD from the DXA scans on three narrow regions: the narrow neck (NN), intertrochanter (IT) and shaft (S). A physical activity and lifestyle questionnaire was administered at baseline. Multivariate repeated measures analysis of variance was used to model the association between these variables and SM, periosteal diameter (PD) and BMD (4 conventional Hologic regions and 3 narrow regions). In all regions in both genders, body weight was positively associated with SM, PD and BMD ($P<.0001$). Periosteal diameter in 5 of 6 regions, both genders, was associated with lifetime physical activity ($P<0.019$). There was a significant decline of BMD with age at the NN and S regions in women ($P<0.022$) but not SM, or PD which increased. In women, previous fracture history was associated with having lower values of BMD and SM (except for NN, $P<0.017$). Section modulus was positively associated in women with hrs/week recreation (NN, P=0.004), heavy physical activity (NN, P=0.002) and stair climbing (S, P=0.027) whereas NN BMD was the only BMD associate of physical activity in women (P=0.016). In men, section modulus was positively associated with heavy activity (IT and S, $P<0.005$) and moderate activity (IT, P=0.012) while BMD was positively associated with moderate activity (IT and S, $P<0.032$). In conclusion, proximal femur diameter is associated positively with life-long physical activity. If this is mediated through a loading related effect on periosteal expansion, BMD may be an unsatisfactory outcome measure in physical activity studies since it is inversely related to projected bone area. SM in contrast was associated with several measures of recent physical activity.

M169

Site-Specific Effects of Physical Activity and Body Weight on Bone Strength and Geometry: Findings from the Penn State Young Women's Health Study. M. A. Petit[1], T. J. Beck[2], T. L. Oreskovic[2], K. Uusi-Rasi[2], C. Bently*[1], H. Lin*[1], L. Tom[1]. [1]Health Evaluation Sciences, Penn State University, Hershey, PA, USA, [2]Radiology, Johns Hopkins University, Baltimore, MD, USA.

Both body weight and physical activity are known to influence BMD, however little is known about their effects on bone strength and geometry. To explore the effects of these two different types of skeletal loading, we examined proximal femur bone geometry and strength at age 21 using data from the longitudinal Penn State Young Women's Health Study. Participants were enrolled in the study from age 12 and measurements made annually for 10 years. Proximal femur scans at age 21 were analyzed using a hip structural analysis program to assess BMD, subperiosteal width, bone axial strength (cross-sectional area, CSA) and bone bending strength (section modulus, Z) at the femoral neck and femoral shaft regions. Height and weight were measured by standard procedures and body composition taken from DXA total body scans. Data were analyzed in two ways: i) by activity tertile based sports-exercise scores (by questionnaire) from ages 12-18 (inactive n = 19; normal active n = 19; high active n= 20); and ii) by weight tertiles (light n = 20; medium n = 20; heavy n = 18). BMD and bone structural variables at age 21 were compared between groups before and after adjusting for covariates using analysis of covariance. After controlling for body size and lean mass, exercise group differences between the upper and lower tertiles at the femoral neck remained significant for BMD (+10%), section modulus (+12.2%), CSA (+10.2%) and cortical thickness (+10.7%), but not for subperiosteal width. At the femoral shaft, differences remained significant only for BMD (+8.0%) and CSA (+6.5%). When data were divided into weight tertiles differences were significant for all unadjusted variables. However, after adjusting for height and activity, differences decreased and became non-significant at the femoral neck. In the femoral shaft region, differences remained significant with the heaviest girls having greater bone axial strength (CSA +9.1%) and cortical thickness (+15%), but no difference in Z or bone width. Together, these results suggest that loading from high body weight is more likely to influence the long bone axial strength (CSA), while loading from sports-exercise may exert greater benefit to femoral neck bone bending strength (Z).

M170

Patterns of Femoral Neck Bone Loss in Spinal Cord Injury and Spaceflight. J. R. Shapiro[1], T. J. Beck[2], A. LeBlanc[3], V. Schneider[4], B. Mustapha*[5], L. Shakelford*[6], T. Oreskovic*[2], P. Ballard*[5], C. Ruff*[2], J. Toerge*[5], J. Caminis[7]. [1]Uniformed Services University, Bethesda, MD, USA, [2]Johns Hopkins University, Baltimore, MD, USA, [3]Baylor College of Medicine, Houston, TX, USA, [4]NASA, Washington, DC, USA, [5]National Rehabilitation Hospital, Washington, DC, USA, [6]Johnson Space Center, Clearlake, TX, USA, [7]Novartis Pharmaceutical, East Hanover, NJ, USA.

Spaceflight and spinal cord injury (SCI) cause lower limb disuse. SCI is proposed as a model for spaceflight bone loss. Hip DXA scans (Hologic QDR1000) were obtained within 10 weeks of acute SCI and at 3-6 months follow-up in 9 paraplegic and tetraplegic subjects enrolled in a blinded placebo controlled trial of an intravenous bisphosphonate. DXA data were also analysed using the Hip Structure Analysis (HSA) program that measures BMD and geometric properties in narrow regions across the proximal femur. Rates of change were computed as the percent change from baseline or pre-flight/time to follow-up or post-flight for SCI or Cosmonauts.Rates of change in bone parameters at the femoral neck are shown in the figure for pooled SCI and Cosmonauts. BMD, cross-sectional area (CSA), cortical thickness and section modulus (Z) each decrease while buckling ratio (BR) increases and width changes are non-significant in both SCI and microgravity. Rates of change are much greater among cosmonauts although the difference is at least partially due to lack of change expected in some treated SCI subjects. This alteration in geometric properties underlies a decrease in section modulus and an increase in calculated BR that may be associated with increased fracture risk. Conclusions: 1) Bone loss parameters in the femur shaft are similar in SCI and after prolonged spaceflight. 2) Decreased periosteal bone expansion in the presence of endocortical bone resorption suggests a common mechanism operating in both situations. 3) SCI is an appropriate surrogate for modeling the effects of microgravity on bone.

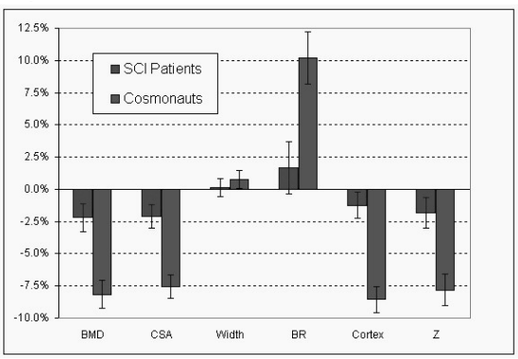

Disclosures: ***J.R. Shapiro****, Novartis Pharmaceutical 5.*

M171

Use of Transgenic Mice Harboring a Collagen Reporter that Reflects Osteoblastic Activity and Responds to Isometric Loading of Long Bone and Spine. J. D. Delaney*, D. Adams*, D. W. Rowe. University of Connecticut Health Center, Farmington, CT, USA.

Bone remodeling reflects the recruitment and regulation of osteo-progenitor cells to preosteoblasts, osteoblasts and osteocytes. Transgenic mice expressing a chloramphenicol acetyl transferase (CAT) marker gene under the control of the rat 3.6 kb COL1A1 promoter (pOBCol3.6) have been previously used as a surrogate marker of the osteoblastic lineage. These mice provide a rather simple and sensitive metric of an activated osteoblastic lineage within intact bone. Our goal is to develop a standardized form of skeletal loading of otherwise mobile mice that is independent of gravity and the volition of the subject. An orbital shaker (Model C10, New Brunswick Scientific) was adapted to contain 16 compartments to exercise the mice uniformly but separately. To determine a rotational force that would elicit a sustainable osteogenic response, 10-12 month old CD-1 mice heterozygous for pOBCol3.6CAT were divided into four groups (n = 6). They were taken through a conditioning phase in which the rotational speed was gradually increased as the mice adapted by "clutching" the stage ultimately achieving a maximum of 250 RPM for 30 minutes a day. The mice were harvested after 1, 2 and 3 weeks of the maximal exercise and compared to control animals who spent 30 min/day in the cages without rotational stimulation. The fact that the mice in all groups lost body weight, femoral trabecular bone volume by µCT (controls 9.29% ± 1.17 and exercised 2.38% ± 0.37%) and failed to increase CAT activity suggested that this vigorous protocol was catabolic for the mice. A second experiment used 8 month old mice that were exercised at 60, 120 and 180 RPM for 30 min every over day (q.o.d.). Relative to control mice, no response in CAT activity was observed in the 60 or 120 RPM group but the femurs from the 180-RPM displayed a four-fold induction of CAT activity after only one week of exercise that returned to a baseline at 2 weeks. Micro-CT data indicated that trabecular bone volume was not being depleted over the course of the experiment, (controls = 13.6% ± 9.0%; 1 week = 14.1% ± 4.5%; 2 weeks = 13.4% ± 8.0%; and 3 weeks = 16.1% ± 9.9%). A third experiment utilizing 5-6 month old mice and the 180 RPM/qod protocol demonstrated a statistically significant (25%) increase in CAT activity in the long bones at 3,7,and 11 days of exercise while the spine samples showed a two-fold increase in CAT activity by 11 days of exercise (all significant to $p < 0.05$). Thus the model does appear to induce new osteogenic activity in which trabecular bone of the spine is particularly responsive. Currently mice transgenic for ColGFP marker genes are being subjected to this protocol to visualize the cellular response to mechanical loading.

M172

Bone and Muscle Recovery after 28 Days of Hindlimb Unloading in Mature Male Rats. M. R. Allen[1], H. A. Hogan[2], S. A. Bloomfield[1]. [1]Health and Kinesiology, Texas A&M University, College Station, TX, USA, [2]Mechanical Engineering, Texas A&M University, College Station, TX, USA.

The purpose of this study was to investigate the response of bone and muscle to hindlimb unloading (HU) and subsequent reambulation. Our working hypothesis was that both tissues would experience significant decrements in mass/strength after 28 days of HU, but that muscle would recover more fully and quickly upon return to cage activity (after 7 & 14 days). Fourteen skeletally mature male Sprague-Dawley rats (6-mo-old) were randomly divided into four groups: baseline control (BC, n=5), 28d HU (HU, n=3), 28d HU + 7d recovery (7REC, n=3) and 28d HU + 14d recovery (14REC, n=3). The results to date are from the first phase of a long-term multi-year study. Longitudinal in-vivo measurements were made using peripheral quantitative computed tomography (pQCT) for bone mineral density (BMD) and cross-sectional geometry of the proximal metaphyseal and mid-diaphyseal tibia on day 0, after 28d HU, and at sacrifice. Hindlimb plantar flexor muscle mass and in-vivo peak isometric torque were obtained on the day of sacrifice. Body mass and plantar flexor muscle mass were lower ($p < 0.05$) in HU compared to BC. Body mass returned to control values in both 7REC and 14REC while muscle mass significantly increased compared to HU but remained lower than BC. Maximum isometric torque was reduced by 15% in HU compared to BC with full recovery for 14REC. Combining data from all unloaded animals after 28d HU (n=9), total and trabecular BMD decreased by 6.5% and 11.8% , respectively, in the proximal tibia metaphysis compared to 0-day values. After 7d of recovery, total and trabecular BMD were non-significantly reduced (-1.6% and -4%, respectively) compared to values after 28d HU, while 14REC also tended to have lower total BMD (-3%) compared to 28d HU. Trabecular BMD of 14REC animals showed a trend of higher values (+6.8%) compared to HU values but lower relative to 0-day values. There were no changes at the mid-diaphysis with respect to BMD or geometry in any group over time. The results confirm that muscle, a very plastic tissue, recovered its unloading-induced force loss after 14d of cage activity, but bone did not. Interestingly, muscle mass did not recover fully, which suggests some alteration in contractile properties of the muscle fibers. Both total and trabecular BMD of the proximal tibia metaphysis were dramatically reduced by HU and failed to recover after 14d of cage activity. These results tend to support the hypothesis, but further work is needed to define the trends more conclusively and to assess if and when BMD returns to baseline values. A large and/or persisting mismatch between bone and muscle strength could very well place the bone at an increased risk of fracture.

M173

The Effects of Nitric Oxide and Titanium Particulate Debris on RANKL Expression and Secretion in Osteoblast . J. T. Ninomiya, M. J. Sytsma*, J. A. Struve. Department of Orthopaedic Surgery, Medical College of Wisconsin, Milwaukee, WI, USA.

Particulate wear debris generated from total joint implants is known to incite the production of a host of pro-inflammatory cytokines and other proteins, ultimately leading to loosening and failure. Recently, the proteins RANKL and its soluble decoy receptor OPG have been shown to have a critical role in the formation of osteolysis. The short-lived free radical nitric oxide (NO) is synthesized in response to specific cytokines and plays a role in the bone remodeling process and we hypothesized that nitric oxide alters osteoclast maturation in response to particulate debris through the regulation of RANKL gene expression and secretion. The roles of NO and titanium particle stimulation on the gene expression and secretion of both RANKL and OPG were investigated in murine osteoblastic MC3T3-E1 cells. Titanium particles in the presence or absence of the nitric oxide donor PAPA NONOate were added to osteoblasts, while controls consisted of unstimulated cells in the absence of particles or NO. Total cellular RNA was isolated and RT- PCR was performed using specific primers for RANKL and OPG, with the results normalized to actin. The effects of particles and NO on osteoclast maturation were assessed using osteoblast whole cell lysates which were collected following incubation. Samples of the cell lysates were added to a murine bone marrow osteoclast maturation assay, and multinuclear TRAP+ cells were counted under light microscopy. Both particulate debris and NO donors alone and in combination increased the gene expression of RANKL, which peaked at 12 hours. However, the combination of titanium particles and NO displayed a significantly higher induction of RANKL transcripts than did titanium or NO alone. In addition, at 12 hours RANKL transcripts demonstrated a significantly higher induction compared to OPG, its soluble decoy receptor, in all three experimental groups. The TRAP assay demonstrated that lysates from MC3T3 E1 cells exposed to titanium for 48, 72, and 96 hours caused a significant increase in the number of TRAP+ cells (osteoclasts) generated from murine bone marrow cultures when compared to lysates from cells that were not exposed to titanium. Also, the addition of an anti-RANKL antibody to a culture containing recombinant RANKL showed a significant decrease in TRAP+ cells when compared to the RANKL protein alone. Our data demonstrate that NO and titanium alone and in combination significantly increase the ratio of RANKL:OPG, resulting in increased osteoclastogenesis. These findings provide important insight into the mechanisms of implant loosening and suggest that nitric oxide modulates bone resorption through a RANKL dependent mechanism.

M174

Influence of Human Osteoblasts on Hematopoietic Stem Cells: Analysis in Coculture on a Synthetic Biphasic Calcium Phosphate Ceramic. N. M. Rochet*[1], N. Tieulie*[2], L. Ollier*[2], A. Loubat*[2], J. M. Bouler*[3], G. Daculsi*[3], G. F. Carle*[1], B. Rossi*[2]. [1]UMR CNRS-UNSA 6549, Nice, France, [2]INSERM U364, Nice, France, [3]INSERM EMI99-03, Nantes, France.

Very little is known about the relationship between bone cells and hematopoietic stem cells (HSC). It has been suggested that human osteoblastic cells could participate to the

survival and/or self-renewal of the CD34 positive hematopoietic stem cells. Using a biphasic calcium phosphate ceramic (BCP), we have studied the influence of normal human osteoblasts on the proliferation and differentiation of CD34 positive cells purified from cord blood, in coculture experiments. This macroporous biomaterial is composed of 60% hydroxyapatite and 40% beta-tricalcium phosphate and has been widely used as a bone substitute in human and rodents. This BCP ceramic mimics partially the three-dimensional structure and the chemical composition of cancellous bone. After one to three weeks of coculture, the hematopoietic cells were counted, analysed morphologically and clonogenic assays were performed to enumerate the CFU-GEMM (Colony Forming Unit - Granular Erythroid Monocyte Megacaryocyte), BFU-E (Burst Forming Unit - Erythroblast) and CFU-GM (CFU - Granular Monocyte). We have demonstrated that human osteoblasts seeded on BCP induce the rapid differentiation of hematopoietic stem cells into both granular and monocyte/macrophage pathways. These results are clearly different from those obtained after coculture on plastic. Indeed, during the first week of coculture on plastic, human osteoblasts induce the proliferation of very immature hematopoietic progenitors (CFU-GEMM). Starting on the second week, we have observed the specific differentiation of these CFU-GEMM into the granular pathway. Using RT-PCR and RNase protection assay, we have shown that the cytokine expression profile of human osteoblasts cultured on BCP is different from that observed on plastic. This finding could explain, as least in part, the differential effects observed on HSC when cocultured on those different surfaces. Additional results suggest that the biomaterial by itself might play a direct role in the differentiation of HSC. In conclusion, we have shown that the nature of the culture substratum must be taken into account when studying the influence of osteoblasts on HSC. Our results suggest that rather than self-renewal, osteoblasts in contact with BCP support the differentiation of HSC in the granular and monocytic pathways leading to osteoclast precursors.

M175

Osteoclasts Produce Inhibitors of Osteoblast Differentiation. J. M. Owens, K. McDermott*, J. Li, J. Wozney, H. Seeherman. Musculoskeletal Sciences, Wyeth Research, Cambridge, MA, USA.

Significant bone formation has been reported in a recombinant human bone morphogenetic protein-2 (rhBMP-2)-stimulated, non-human primate core defect model of intraosseous bone induction, (Seeherman et al ORS, 1998 and 2000). In this animal model, rhBMP-2 treatment induced unexpected, significant, transient bone resorption during the first 2 weeks post-implant, followed by dramatic bone formation present at 4 weeks. Histological analyses revealed that trabecular bone adjacent to the rhBMP-2 implant, was surrounded by numerous osteoclasts resorbing bone. Interestingly, bone surfaces in the rhBMP-2 treated core defects contained only a few osteoblasts during the first 2 weeks post-implant. These findings prompted the hypothesis that activated osteoclasts secrete certain factor(s) that inhibit osteoblastic differentiation. Using the mouse osteoclast-like myeloma cell line RAW264.7 and a mouse osteoblastic cell line (MLB13MYC clone 14, Rosen et al 1994, JBMR 9:1759), we investigated possible roles for osteoclasts in regulating the differentiation of osteoblasts. RAW264.7 cells were treated with 100ng/ml RANKL for 7 days to induce osteoclastic cells (TRAP positive, bone resorbing cells). Fresh medium containing RANKL was added at days 3, 5 and 7. Conditioned medium (CM) samples were collected at time of medium change and transferred onto monolayers of Clone 14 osteoblastic cells. Addition of CM from RAW cells treated with RANKL for 5 to 7 days resulted in significant (up to 80%) inhibition of alkaline phosphatase (alk phos) expression. RANKL at 100ng/ml did not inhibit alk phos expression in Clone 14 cells. Using a similar system, it has recently been shown by others that platelet-derived growth factor (PDGF) is the major inhibitory factor of osteoblastogenesis (JBMR 17:257-265, 2002), where anti PDGF antibody almost completely reversed the inhibitory actions of the CM. In the present study, however, treatment with 2µg/ml PDGF antibody, which completely blocks PDGF-stimulated 3H-thymidine incorporation by NR6R-3T3 fibroblasts, only partially (16%) reversed the inhibitory actions of the CM. This suggests that osteoclasts secrete more than one factor that regulates osteoblast formation and activity and that PDGF may not be the major factor. Our in vitro findings provide further evidence that the induction of numerous osteoclasts in our in vivo model of intraosseous bone formation, may be responsible for the delayed osteoblastic response to rhBMP-2, by their secretion of factor(s) which directly or indirectly suppress osteoblastogenesis.

M176

Decreased Osteoblast Function in RANK-/- Mice. L. Xing[1], E. M. Schwarz[1], R. J. O'Keefe[1], W. C. Dougall[2], B. F. Boyce[1]. [1]University of Rochester, Rochester, NY, USA, [2]Immunex, Inc., Seattle, WA, USA.

A RANKL GST fusion protein was shown last year to stimulate bone formation in vivo and in vitro, suggesting that RANKL/RANK signaling may play a regulatory role in osteoblast (obl) function. To further study this possibility, we examined obl parameters in bones from wild-type (wt) and RANK-/- mice. In both calvarial and long bone sections, RANK-/- mice at three ages (8-day, 3-weeks, and 3-month) have: 1) decreased mineral apposition rate (0.65+/-0.14 um/day vs 1.4+/-0.5 in wt mice) and bone formation rate (0.40+/-0.12 um3/um2/day vs 1.0+/-0.25 in wt mice); 2) decreased obl number (2.9+/-0.5 obls/mm bone surface vs 4.4+/-0.2 in wt mice); 3) flat and irregularly-shaped obls; but 4) normal matrix mineralization (with von Kossa staining) and obl alkaline phosphatase (ALP) staining, despite low blood calcium and high PTH values. Thus, although bone matrix volume is markedly increased in the RANK-/- mice due to osteopetrosis, their obl activity is reduced and the mice do not have osteomalacia. To investigate if the activity of RANK-/- obls is also decreased in vitro, calvarial obl from wt or RANK-/- mice were cultured with or without BMP2. ALP activity and mineralized nodule formation (basal or in response to BMP2) were similar in cultures from wt and RANK-/- mice, and treatment of calvarial osteoblasts with RANKL had no effect on ALP activity. To study the response of RANK-/- obls in vivo to a known stimulator of bone formation, FGF (4 ug/day for 3 days) was injected over the calvariae of RANK-/- mice and their wt littermates. RANK-/- mice formed more new bone after FGF administration than wt mice [51+/-13 new bone (% pre-existing bone) vs 25+/-3% in wt mice]. Because RANK-/- mice have increased blood PTH levels, we hypothesized that continuous PTH treatment would inhibit wt obl function in vitro. We found that PTH (0.1 and 1ug/ml) inhibited both ALP and nodule formation in FRC cells. Our findings indicate that the absence of RANK signaling is associated with reduced basal obl activity in vivo, but not in vitro or in response to BMP2 treatment in vitro, and importantly, they have an increased response to FGF in vivo. This suggests that the reduced obl phenotype in RANK-/- mice may be secondary to a circulating inhibitor, possibly PTH, and that RANK signaling may not be a major direct regulator of obl function.

M177

Effects of PTH on RANK-L and OPG Gene Expression During Osteoblast Differentiation. J. C. Huang[1], T. Sakata[2], M. Bencsik*[2], B. Halloran[2], D. D. Bikle[2], R. A. Nissenson[2]. [1]Growth and Development, University of California San Francisco, San Francisco, CA, USA, [2]Endocrine Research Unit, University of California Veterans Affairs Medical Center, San Francisco, CA, USA.

RANK-L is a critical factor in the induction of osteoclastogenesis. Its decoy receptor OPG is an inhibitory factor that negatively regulates this process. The ratio of the expression of these two proteins is a major determinant of bone turnover. Despite the physiological importance of these genes, the mechanisms by which their expression is regulated by factors that control bone turnover remain incompletely understood. Both genes are expressed in cells of the osteoblast lineage, but the precise relationship between the state of osteoblast differentiation and RANK-L and OPG expression is not clearly defined. In the present study, mouse bone marrow stromal cells isolated from 3-month old male C57Bl/6 mice were cultured for 28 days in the presence of ascorbic acid and beta-glycerophosphate. At specific time intervals (Day 7, 14, 21, and 28), the cells were acutely stimulated with bPTH(1-34) (100 ng/ml, 2 hrs) followed immediately by RNA extraction. Levels of mRNA encoding RANK-L, OPG, alpha-1(Type I) collagen [alpha-1 col] and alkaline phosphatase [Alk. PO4] (early bone markers), and osteocalcin [OC] (late bone marker) were assessed by quantitative real-time RT-PCR. The freshly isolated stromal cells followed a predictable pattern of differentiation, with alpha-1 col and Alk. PO4 expression peaking at 14 day, whereas the osteocalcin gene was maximally expressed after 21 days in culture. OPG reached maximal expression at Day 14 (2.5-fold over Day 7 levels) before tapering off. Conversely, RANK-L established an increased pattern of expression as differentiation occurred, reaching maximum at Day 28 of cell culture. Stimulation with acute PTH caused an inhibition of OPG expression but induced a significant increase in RANK-L expression (relative to control) at the latter stages of cellular differentiation (Days 21 & 28). Acute treatment with PTH did not detectably alter the expression of any of the bone marker genes. By contrast, chronic exposure of cells to PTH (100 ng/ml) starting at the beginning of the culture period resulted in a dramatic decrease in the expression of all of the bone markers, indicating a PTH-induced block in osteoblast differentiation. We conclude: 1) in this model system, maximal sensitivity of the RANK-L gene to PTH occurs relatively late in the process of osteoblast differentiation; and 2) chronic exposure of pre-osteoblasts to PTH can prevent the progression to mature osteoblasts.

M178

Ovariectomy Increases Stromal Cell M-CSF Production via Selection and Expansion of Stromal Cell Lineages Exhibiting Increased Casein Kinase 2 Activity and Resistance to TNF Induced Apoptosis. Y. Gao[1], W. Qian*[1], T. Gianluca*[1], C. Simone[1], N. M. Weitzmann[2], S. Oscar[1]. [1]Division of Bone and Mineral Diseases, Washington University School of Medicine, St. Louis, MO, USA, [2]Division of Bone and Mineral Diseases, Washington University School of Medicine, St. louis, MO, USA.

The increase in TNF induced by ovariectomy (ovx) leads to the selection of bone marrow stromal cells (SCs) with the capacity of producing high levels of M-CSF. The resulting increase in M-CSF level is a key mechanism by which ovx induces bone loss. Ovx SCs exhibit increased casein kinase 2 (CK2) activity which leads to enhanced M-CSF transcription through CK2-induced Egr-1 phosphorylation. Since CK2 is a constitutively active kinase, the ovx induced increase in CK2 activity results from selection and expansion of SCs with intrinsic high CK2 activity. However the mechanism of this selection is unknown. We found that the high levels of TNF characteristic of ovx mice induces apoptosis of SCs with low CK2 activity and low M-CSF production, but not of SCs with high CK2 activity and high M-CSF production. In contrast, SCs with both low and high CK2 activity survive exposure to the lower levels of TNF of sham mice. Furthermore, the specific CK2 inhibitor emodin blocked CK2 activity and abolished the ability of ovx SCs to resist TNF induced apoptosis. Thus, ovx induces the survival and the expansion of SCs with high CK2 activity and high M-CSF production through selective TNF induced apoptosis of SCs with low CK2 activity. Since NFkB, a CK2 substrate, blunts TNF induced apoptosis, we investigated if CK2 blocks TNF induced SC apoptosis by inducing NFkB. We found NFkB activity to be about 2 fold higher in ovx SCs than sham SCs, both unstimulated and TNF stimulated. Ovx SCs possess high levels of the NFkB subunits p50 and p52 while sham SCs have low or undetectable levels of these proteins. In addition, TNF treatment greatly enhanced the expression of p50 and p52 proteins in sham but not in ovx SCs. Thus, the NFkB p50 and p52 are maximally expressed in unstimulated ovx SCs. Conversely, IKBalpha was more abundant in sham than in ovx SCs. Together, these findings demonstrate that ovx upregulates NFkB activity by downregulation of its inhibitor IKBalpha. Furthermore, the CK2 inhibitor emodin blocked TNF induced NFkB activation, confirming that ovx upregulates NFkB through CK2. In summary, the data suggest that elevated levels of CK2 in ovx SCs protect these cells from TNF induced apoptosis by enhancing the anti-apoptotic factor NFkB activity. As a result, the increase in TNF caused by ovx allows the selection of SCs with high M-CSF production and high osteoclastogenic activity.

M179

Protein Kinase C alpha/estrogen Receptor alpha Interaction in Osteoblasts during Differentiation. M. Brama*, M. Longo*, M. Marino*, K. S. Korach*, W. C. Wetsel*, R. Scandurra*, R. Baron, A. Teti, S. Migliaccio. Experimental Medicine, University of L'Aquila, L'Aquila, Italy.

In osteoblast-like cells undergoing confluence-induced differentiation, calcium-dependent protein kinase C (PKC) activity increases, while estrogen receptor alpha (ERalpha) binding and responsiveness to estrogens decrease. We tested the hypothesis that the underlying molecular mechanism requires physical interactions between ERalpha and PKC isoforms. Anti-ERalpha and anti-PKCalpha immunoprecipitates were obtained from rat primary osteoblasts at different confluence conditions, and tested for the presence of PKC isoforms and ERalpha. PKCalpha was found to co-immunoprecipitate with ERalpha both in sub- and post-confluent cells, but to a much greater extent in the latter, where higher levels of the differentiation marker alkaline phosphatase were expressed. All of our anti-ERalpha immunoprecipitates contained a single PKCalpha post-translational variant, *i.e.* its well-known 40 KDa cleavage product PKM alpha, encompassing the catalytic site, with barely detectable amounts of uncleaved protein. Interestingly, only the 66 KDa ERalpha variant was present in input lysates from sub-confluent cells, whereas its newly described 46 KDa splice variant became detectable solely upon differentiation. In rat osteosarcoma cells ROS.SMER #14, stably transfected with ERalpha, we found no significant variation of co-immunoprecipitable PKCalpha levels. In these cells, full-length ERalpha was found to be greatly reduced at post-confluence, but its 46 KDa isoform was unchanged. Both 80 and 40 KDa forms of PKCalpha were readily detectable, but, again, the former was nearly absent in anti-ERalpha immunoprecipitates. As shown by our previous results, c-Src plays an important role in confluence-induced differentiation in osteoblastic cells, and has been found to interact with PKC isoforms. Thus, we analysed c-Src expression and activity in our cells. We observed a significant and transient increase of c-Src expression and kinase activity, which preceded maximal PKC activation. PKCalpha from differentiated osteoblasts induced c-Src phosphorylation *in vitro*. In contrast, c-Src was unable to phosphorylate PKCalpha, although tyrosine phosphorylation was apparent in this PKC isoenzyme and increased in differentiated cells. These data suggest close interactions between PKCalpha, c-Src and ERalpha in osteoblastic cells, which may be crucial for the differentiation process and the related decrease in estrogen responsiveness.

M180

Modulation of Human Estrogen Feceptor alpha *F* Promoter Activity by a Protein Kinase C-dependent Mechanism in Differentiated Osteoblast-like Cells. M. Longo*, V. De Luca*, S. Denger*, G. F. Caselli*, F. Gannon*, A. Teti, S. Migliaccio. Experimental Medicine, University of L'Aquila, L'Aquila, Italy.

The gene for human estrogen receptor alpha (ERalpha) gives raise to six different mRNAs driven, in a tissue-specific manner, by six different promoters (*A* to *F*) and translated into a single protein. The *F* promoter has been described as specifically active in bone cells, but its modulation has not yet been clarified. To elucidate the role of ERalpha promoters in bone physiology and their regulation, we stably transfected human osteoblast-like cells negative for ER (SAOS-2) with expression vectors carrying human *A*, *B*, and *F* ERalpha promoter sequences upstream of the luciferase reporter gene. No luciferase activity was detected in cells containing promoters *A* and *B* relative to cells transfected with empty vectors. In contrast, high basal luciferase activity was found in two clones carrying the *F* promoter. Our previous results have evidenced significant modulations in ERalpha levels and activity, as well as close interactions between ERalpha and PKC isoforms, upon confluence-induced osteoblast differentiation. Thus, we analyzed *F* promoter activity at post-confluence and its possible dependence on PKC isoforms expression and/or activity. *F* promoter activity was evaluated in sub-confluent and post-confluent cells, and found to be constantly up-regulated in the latter. A two/three-fold higher luciferase activity was detectable 24 hr after confluence, with no significant increase up to 96 hr. Again, no such increase could be evidenced in cells carrying the *A* and *B* promoters. Overnight treatment of post-confluent cells with 10^{-7} M 12-O-tetradecanoylphorbol-13-acetate (TPA) nearly abolished PKCalpha protein expression and resulted in a significant decrease of *F* promoter activity, which strongly suggests a PKC-dependent up-regulation of the promoter upon differentiation. We also observed that in sub-confluent cells identical TPA treatment induced a slight increase of *F* promoter activity. In cells treated with calphostin *C*, a compound inhibiting the activity, but not the expression, of most PKCs, no variation in luciferase activity relative to untreated counterparts was observed. In addition, we observed an unchanged Fos family member expression, but a modulated phorphorylation pattern on c-Jun N-terminal serines (63 and 73) in sub- vs. post-confluent cells, either untreated or TPA-treated, suggesting differential confluence-dependent regulation on the AP1-site harboured in the *F* promoter. Collectively, these data strongly suggest tight relationship between intact PKC pathways and *F* promoter regulation, possibly involving kinase activity-dependent and -independent PKC functions.

M181

Potassium Calcium-dependant BK Channel: A Potential Membrane Target of Estrogens and SERMs in Human Osteoblasts. V. Breuil*[1], G. Romey*[2], L. Euller-Ziegler[3], B. Rossi*[1], H. Schmid-Antomarchi*[1]. [1]U 364, INSERM, Nice, France, [2]Institut de Pharmacologie Moléculaire et Cellulaire, CNRS, Nice, France, [3]Rheumatology, University Hospital L'Archet, Nice, France.

Estrogens, and more recently SERMs (Selective Estrogen Receptor Modulators), have been recognized for their positive effects on bone. However, their mechanisms of actions is still only partially resolved. Although it generally is accepted that estrogens act at genomic level by binding to intracellular estrogen receptor, they trigger nongenomic effects mediated by plasma membrane receptor. One of these is to increase activity of BK channel in many cells types (smooth muscle and vascular endothelium), but as never been reported in bone. BK channels are composed of a (encoded by Slo gene) and b subunits. The a subunit forms the K+-selective pore, while b subunits influence the pharmacology, kinetics, and voltage/calcium sensitivity of BK channel. b1 and b4 subunits have been reported to mediate estrogen effects on BK channel. In this study, we show that primary human osteoblasts, and 3 cells lines of human osteosarcoma (MG63, SaOs2, CAL72) express the Slo protein (Western-Blot). Using RT-PCR, we observe in all these cells the expression of the 4 b subunits (b1, b2, b3, b4). In electrophysiology analysis, we observe the typical calcium-induced potassium current of high conductance of BK channel. As expected, b1 subunit expression induce Charybdotoxine and Iberiotoxine (classical inhibitors of BK channel) resistance of BK channel. We investigate the effects of 17b estradiol and Tamoxifen (a SERM) on BK channel activity. In outside-out configuration, 17b estradiol (1-10mM) increase BK channel opening (Npo) in 20% of the cases ; however, we observe no effect in inside-out configuration, suggesting that the target of this effect is located at the extracellular side of the membrane. Interestingly, Tamoxifen (1mM) increase the BK channel activity in 100% of the cases. Our data indicate that estrogen and SERMs can modulate BK channel activity, sheading a new light on nongenomic effects of estrogens and opening new ways for therapeutic development.

M182

Bone Marrow Stromal Cells Express Two Distinct Splice Variants of ER-α that are Regulated by Estrogen. A. Sanyal, B. L. Riggs, T. C. Spelsberg, S. Khosla. Mayo Clinic, Rochester, MN, USA.

The expression of ER-α in reproductive and non-reproductive tissues (such as bone) is regulated by a complex set of promotors. Moreover, splice variants of ER-α appear to be present in different tissues. In addition to the mRNA giving rise to the conventional, full-length, 66 kD receptor, the most common ER-α variant described to date is a 46 kD receptor lacking the AF-1 domain, which arises through alternate splicing of the parent ER-α transcript. While this variant retains responsiveness to estrogen in some tissues, in other tissues it is unresponsive to estrogen and appears to function in a dominant negative manner, at least for actions requiring the AF-1 domain. Since osteoblast differentiation is clearly regulated by estrogen, we sought in the present study to define the ER-α splice variants and their regulation by estrogen in the mouse bone marrow stromal cell line, ST-2, which can be induced to differentiate into mature osteoblasts. By Western blot analysis, ST-2 cells expressed both the 66 and 46 kD forms of ER-α . By analysis of the expressed mRNAs using primers specific for the distinct splice variants giving rise to the two proteins, we also found that ST-2 cells contained the mRNAs for both the 66 kD as well as the truncated, 46 kD receptor. Using primers specific for each of the five 5'-untranslated exons, we found that ST-2 cells utilized only the promoters upstream of exons F and C (in contrast to most reproductive tissues, which utilize promoters upstream of virtually all the five exons). Interestingly, search of the Celera mouse genome database revealed that the exon F promoter contained both an ERE half-site and a consensus AP-1 sequence, suggesting that this promoter may be regulated by estrogen. Consistent with this, estradiol (10^{-8} M) treatment of ST-2 cells markedly diminished levels of the 66 kD ER-α protein (by 78%) as well as the 46 kD variant protein (by 86%). Analysis of the mRNAs revealed that, in ST-2 cells, the mRNA encoding the 46 kD variant arises exclusively via the estrogen responsive, F-promoter, whereas the 66 kD mRNA arises from both the F and C promoters, with only the transcript arising from the F promoter being suppressed by estrogen. In summary, these findings indicate that: (1) bone marrow stromal cells express at least two variants of ER-α; (2) promoter usage in these cells is much more restricted than in classical reproductive tissues; and (3) estrogen downregulates the ER-α message and protein in these cells through effects on one of the two promoters utilized by these cells. These findings have potential implications for understanding the mechanisms by which bone may regulate sensitivity to estrogen under conditions of widely varying estrogen levels, as occur during the estrus or menstrual cycles.

M183

Demonstration of Aromatase Activity in Rodent Bone. U. I. Moedder*, B. L. Riggs, S. Khosla. Mayo Clinic, Rochester, MN, USA.

The aromatization of C19 precursor steroids to estrogens in extragonadal sites such as the breast, vasculature, brain, and bone has been amply demonstrated in higher primates. However, it is generally believed that in rodents, aromatase is present only in the reproductive tissues and in the brain. It has been suggested that the local aromatization of androgens to estrogens may play an important role in regulating bone metabolism (Simpson et al. TEM 11:184, 2000). Since mouse and rat models are used extensively for studies on sex steroid action on the skeleton, the issue of whether C19 steroids can be locally aromatized in bone to estrogens in rodents is clearly important to definitively resolve. Thus, we used a well characterized aromatization assay which measures the conversion of ^{3}H-androstenedione to estrone (Ackerman et al. JCEM 53:412, 1981) to assess aromatase activity in the femurs and tibias from 6 month old mice. Aromatase activity in mouse bone was clearly

detectable (2.28 fmol/h/g bone). Moreover, the specific aromatase inhibitor, 4-hydroxyandrostenedione, markedly reduced aromatase activity in the mouse bone samples to 0.21 fmol/h/g bone, attesting to the specificity of the assay in assessing aromatase activity. Having established the presence of aromatase activity in mouse bone, we next hypothesized that ovariectomy would increase aromatase activity in bone, perhaps as a "protective" local mechanism. However, comparison of both aromatase activity and mRNA levels (by reverse transcriptase polymerase chain reaction) in bones from sham operated versus ovariectomized mice and rats (n = 3 per group) assessed 9-14 days following surgery failed to detect any differences. These findings were confirmed in *in vitro* studies using ROS 17/2.8 cells in which treatment with estradiol (10^{-7} M) had no effect on aromatase mRNA expression. In conclusion, our studies demonstrate that rodent bone does express measurable aromatase activity, but this does not appear to be regulated *in vivo* or *in vitro* by estrogen. While species differences may exist between primates and rodents in terms of the contribution of local aromatization of androgens to estrogens towards skeletal homeostasis, our findings do suggest that rodent models can be used to address this issue.

M184

Raloxifene Stimulates Osteoprotegerin and Inhibits Interleukin-6 Production by Estrogen-Responsive Human Trabecular Osteoblasts. V. Viereck[1], C. Grundker*[1], S. Blaschke*[2], H. Siggelkow[3], K. Frosch*[4], G. Emons*[1], L. C. Hofbauer[5]. [1]Dept Gynecology, Goettingen, Germany, [2]Div Nephrol/Rheumatology, Goettingen, Germany, [3]Div Gastroent/Endocrinology, Goettingen, Germany, [4]Dept Trauma Surgery, Goettingen, Germany, [5]Div Gastroent/Endocrinology, Marburg, Germany.

The selective estrogen receptor modulator (SERM) raloxifene suppresses bone loss and inhibits osteoporotic fractures in postmenopausal women. Its protective skeletal effects following activation of estrogen receptors (ER) are thought to be mediated through paracrine factors that are produced by osteoblastic lineage cells and act on osteoclastic lineage cells. Receptor activator of nuclear factor-kB ligand (RANKL) is an essential factor for osteoclast formation and activation, and enhances bone resorption, while osteoprotegerin (OPG) which is produced by osteoblastic cells neutralizes RANKL, thus preventing bone resorption. Recently, 17b-estradiol and phyto-estrogens were found to stimulate OPG mRNA levels and protein secretion in a human osteoblastic cell line through activation of the ER-a. In this study, we assessed the effects of raloxifene on OPG mRNA steady state levels (by semiquantitative RT-PCR and Northern analysis) and protein production (by ELISA) in primary human trabecular osteoblasts (hOB) which predominantly expressed ER-a. Raloxifene enhanced both ER-a and ER-b gene expression, and induced the gene expression for the estrogen target gene, progesterone receptor by three-fold, respectively. Moreover, raloxifene increased OPG mRNA levels and protein secretion by hOB cells by to two- to four-fold in a dose- and time-dependent fashion with a maximum effect at 10-7 M and following exposure for 48 to 72 h ($P < 0.001$). Co-treatment with the pure ER antagonist ICI 182,780 completely abrogated the stimulatory effects of raloxifene on OPG protein secretion, indicating that the stimulatory effects of raloxifene were specifically mediated through the ER. Analysis of cellular markers of osteoblastic differentiation revealed that raloxifene enhanced type I collagen secretion and alkaline phosphatase activity by three-fold and two-fold, respectively ($P < 0.001$). In addition, raloxifene also inhibited gene expression and protein secretion of the bone resorbing cytokine interleukin (IL)-6 by 25 to 40%, respectively ($P < 0.001$). In conclusion, our data suggest that raloxifene is capable of stimulating OPG production and inhibiting IL-6 production by human osteoblasts, thus favouring an anti-resorptive cytokine milieu. Since OPG production increases with osteoblastic cell maturation, enhancement of OPG by raloxifene could be related to its stimulatory effects on osteoblastic differentiation.

M185

Estradiol and Genistein Stimulate Calcium Deposition and Alkaline Phosphatase Activity in BMP-4 Pretreated MC3T3-E1 Cells. M. Gros-van Hest, A. van Helvoort*, I. Schoenmakers*. Department of Condition and Disease Specific Research, Numico Research B.V., Wageningen, Netherlands.

Estradiol and isoflavones were reported to increase BMD *in-vivo*.To investigate whether the increased BMD can be ascribed to a stimulatory effect of these components on bone formation, the pre-osteoblastic cell line MC3T3-E1 was employed. These cells were pretreated with BMP-4, since BMP-4 was suggested to enhance osteoblastic maturation (Xiao et al., 2002). MC3T3-E1 cells were cultured in phenol red free alpha-MEM supplemented with 10% non-charcoal stripped FCS and ascorbic acid with or without BMP-4 for 3 days. Thereafter, cells were exposed to 17ß-estradiol (E-7M) or genistein (E-6M) in phenol red free alpha-MEM supplemented with 10% charcoal stripped FCS, ascorbic acid and ß-glycerophosphate for 4-11 days. Alkaline phosphatase activity, DNA and calcium depositions were determined. In the absence of BMP-4, 17ß-estradiol slightly, but significantly increased alkaline phosphatase activity and calcium deposition. Cells only formed mineralized bone nodules when pretreated with BMP-4. Preteatment with BMP-4 significantly increased alkaline phosphatase activity and calcium depositions, which could be further stimulated by 17ß-estradiol and genistein. These data suggest that estrogenic components stimulate BMP-4 induced bone formation. This *in-vitro* model is estrogen sensitive, which makes it a valid model to identify estrogenic components stimulating bone formation.

M186

Molecular Mechanisms of Action of the Soy Phytoestrogen Genistein: Emerging Role for its Effects via PPARγ. Z. Dang, S. E. Papapoulos, C. W. G. Lowik. Department of Endocrinology and Metabolic Diseases, Leiden University Medical Center, Leiden, Netherlands.

Interest in soy phytoestrogens for maintenance of health including bone has exploded. However, the molecular mechanisms of action are poorly understood, which frustrates their applications. We used the principal soy phytoestrogen genistein as a model compound to study the molecular mechanisms of action. First, a dose response of genistein showed that osteogenesis in KS483 cells, mouse and human bone marrow cells was stimulated by genistein below 1 μ M but inhibited by micromolar concentrations based on changes in ALP activity, nodule formation, calcium deposition and mRNA expression of Cbfa1, PTH/PTHrP receptor and osteocalcin. In constast, adipogenesis was inhibited by genistein below 1 μ M but stimulated by micromolar concentrations based on changes of adipocyte numbers and mRNA expression of PPARγ 2, aP2 and LPL. The effects of genistein were ER-mediated below 1 μ M but non-ER-mediated in the micromolar range. Second, genistein in the micromolar range binds directly to and activates PPARγ . Concurrently, it inhibited p44 and p42 MAPK activity, leading to stimulation of PPARγ activity. These data indicate that genistein could dully activate PPARγ . Third, cotransfection of PPARγ 2 with ERE-luc into KS483 cells exposed to genistein downregulated its estrogenic transcriptional activity. Our data indicate that activation of PPARγ by genistein in the micromolar range resulted in its antiestrogenic effects. Likewise, cotransfection of ERα or ERβ into KS483 cells exposed to genistein resulted in a decrease of PPRE-luc reporter activity. These findings strongly suggest that biological effects of genistein are concentration dependent and are the result of the balance between activated ERs and PPARγ . Finally, PGC-1 is a common coactivator for PPARγ and ERα in KS483 cells. Interestingly, mRNA expression of ERα , PPARγ 2 and PGC-1 was all downregulated by 1 μ M genistein but upregulated by 25 μ M genistein after 11 days of culture. To test whether there is competition between PPARγ and ERα for PGC-1, we cotransfected ERα or PPARγ 2 or PGC-1 with ERE-luc or PPRE-luc constructs into KS483 cells exposed to genistein. Our results indicate that this is probably not the case. In summary, we define, for the first time, PPARγ as a new target for genistein. Moreover, the biological effects of genistein are determined by the balance between activated ERs and PPARγ , which is concentration dependent. Our findings could have significant physiological implications and can explain diverse action of genistein in different tissues in a way analogus to that of selective estrogen receptor modulators (SERMs).

M187

Development of Inducible Estrogen Receptor-alpha and –beta Osteoblastic Cell Lines to Examine Differential Estrogen Regulation. D. G. Monroe[1], S. A. Johnsen*[1], B. J. Getz*[1], S. Khosla[2], B. L. Riggs[2], T. C. Spelsberg[1]. [1]Biochemistry and Molecular Biology, Mayo Clinic, Rochester, MN, USA, [2]Endocrine Research Unit, Mayo Clinic, Rochester, MN, USA.

Estrogen (i.e. 17-β-estradiol; E2) plays pivotal roles in the function and maintenance of the skeleton, including in the bone-forming osteoblasts (OBs). The functions of E2 are largely mediated through two distinct estrogen receptor isoforms, ERα and ERβ, both of which are coexpressed in OBs. Following E2 binding, the ER can either homodimerize or heterodimerize and regulate gene expression through direct DNA binding of specific elements (i.e. estrogen response elements or EREs) or through indirect DNA binding (i.e. AP1 elements). Although numerous genes are known targets of the ERs in various tissues, little information exists regarding the differential regulation of gene transcription by ERα or ERβ homodimers or the ERα/β heterodimer in OBs. Therefore, to determine whether ERα and ERβ homo- and hetero-dimers can differentially regulate genes in OBs, we developed doxycycline (Dox)-inducible ERα and ERβ stable lines in the U2-OS osteosarcoma model system. Determination of receptor concentrations within these lines using a biopsy nuclear binding assay demonstrated that the ERα (U2OS-ERα) and ERβ (U2OS-ERβ) lines express approximately 8700 and 7300 functional receptors per nucleus, respectively, when treated with Dox. Treatment of the U2OS-ERα and U2OS-ERβ lines with 50 ng/ml Dox and 10 nM E2 resulted in induction of the progesterone receptor (PR) mRNA as analyzed by semi-quantitative RT-PCR, in agreement with previous reports from our laboratory. The induction of PR transcript, and of other genes under study, demonstrates that our ER stable lines function normally to regulate endogenous gene expression. One of these genes, osterix (Osx), is required for the development of mature OBs and is involved in osteoblastic differentiation. Any E2 regulation of the Osx transcript would be of utmost interest. Interestingly, RT-PCR analysis in the U2OS-ERα and U2OS-ERβ lines demonstrated an apparent isoform-specific E2 regulation of Osx. To complement these studies, an ERα/β cell line is being produced in which a constitutive ERα gene is introduced into the U2OS-ERβ line. Treatment of the cells with Dox would trigger the induction of the ERβ gene and therefore result in the formation of ERα/β heterodimers. Current studies involve further analysis of the E2 regulation of Osx gene expression and comparison of the patterns of other E2 regulated genes using microarray analysis in the U2OS-ERα, U2OS-ERβ, and U2OS-ERα/β cell lines. The data generated from these experiments will allow us to identify those genes uniquely regulated by the various ER dimers.

M188

Study of The Aromatase Cytochrome P-450 Gene (CYP19) Promoter Usage in Osteoblasts Cells. A. Enjuanes*[1], N. Garcia-Giralt*[2], D. Grinberg*[2], S. Balcells*[2], A. Supervia*[1], M. Bustamante*[2], L. Mellibovsky*[1], X. Nogues*[1], A. Diez-Perez[1]. [1]Urfoa, IMIM (Institut Municipal d´Investigació Mèdica), Barcelona, Spain, [2]Departament de Genètica, Universitat de Barcelona, Barcelona, Spain.

P-450Arom catalizes the conversion of androgens into estrogens and its presence in bone cells has been documented. Given the incomplete understanding of CYP19 gene regulation in osteoblast cells, we have undertaken a detailed study on the promoter usage of CYP19 gene in a cultured human osteoblast cell line. Several plasmids containing the following CYP19-promoter regions upstream of a luciferase reporter gene were constructed: pA) I.4 promoter region (pr); pB) I.4 pr and exon I.4; pC) I.3 pr; pD) I.3 pr and exon I.3; pE) promoter II, exon I.3, I.3 pr and exon I.6; and pF) promoter II and exon I.3. MG-63 cells were grown in Dulbecco×s modified Eagle medium (DMEM) supplemented with 10% fetal calf serum (FCS). CYP19 promoter vectors and pSVB-Gal control vector were co-transfected in MG-63 cells at 70 % confluency in DMEM without FCS using FuGene Reagent. Six hours after transfection, MG-63 cells were incubated in DMEM without FCS for 24 hours with alternative treatments. One day later, cells were lysed and chemiluminescent assays were performed to mesure luciferase and β-galactosidase activities. Both transfection experiments and chemiluminescent assays were duplicated at each experimental step.Results:

	pA	pB	pC	pD	pE	pF
10% FCS	0.27 (±0.15)	0.39 (±0.14)	0.24 (±0.02)	0.50 (±0.10)	0.36 (±0.03)	0.30 (±0.15)
DEX 100nM	1.71 (±0.35)	2.62 (±0.53)	1.35 (±0.35)	1.34 (±0.16)	1.20 (±0.23)	1.41 (±0.18)
VitD 100nM	1.61 (±0.14)	1.04 (±0.13)	1.63 (±0.14)	2.08 (±0.47)	1.65 (±0.23)	1.28 (±0.48)
VitD + DEX 100nM	2.19 (±0.55)	2.08 (±0.90)	1.69 (±0.13)	1.38 (±0.17)	1.80 (±0.14)	1.69 (±0.20)
17β-estradiol	1.03 (±0.13)	0.63 (±0.10)	0.83 (±0.24)	0.96 (±0.17)	0.85 (±0.40)	1.10 (±0.13)
Testosterone	1.20 (±0.21)	0.77 (±0.09)	0.97 (±0.33)	1.00 (±0.14)	1.00 (±0.37)	1.01 (±0.11)

Values correspond to luciferase activities (normalized by β-galactosidase) expressed respect a reference value of 1 for the basal condition (BSA 0.1%). Mean (sd)

In MG-63 cells, I.4 pr plus exon I.4 mediate the stimulation by DEX, and exon I.4 seems to be important for this stimulation. In contrast, exon I.4 seems to negatively affect the VitD stimulation. Pr I.3 plus exon I.3 mediate the stimulation by VitD and the exon I.3 seems to be relevant for this stimulation. In all cases, FCS inhibit basal expression whereas, 17β-estradiol and testosterone seem to have no effect on these promoters.

M189

Reduced Mineralization by Sera from Women with High Bone Mineral Density: Evidence for Estradiol Control of Mineralization. M. van Driel*, E. M. Colin*, C. J. Buurman*, M. Koedam*, H. A. P. Pols, J. P. T. van Leeuwen. Internal Medicine, Erasmus MC, Rotterdam, Netherlands.

Both a reduced quantity and quality of bone increase the risk for osteoporotic fractures. The elasticity of bone and its resistance to fracture is related to the degree of mineralization. When mineralization reaches too high levels, bone has a decreasing ability to absorb impact energy, becomes more stiff and brittle and more susceptible to fractures. In the present study we analyzed whether there are differences in mineralization between serum from postmenopausal women with a very low or high bone mineral density (BMD). For this purpose sera of 21 women with a femoral neck BMD within the lowest quintile (<0.75 g/cm^2) and sera of 29 women within the highest quintile (≥0.92 g/cm^2) were tested. Hormones and serum/urine markers of bone metabolism were measured. Human fetal osteoblast (SV-HFO) cells, that proceed through different stages of differentiation in culture, including extracellular matrix formation and mineralization, were cultured in medium supplemented with the various sera for 21 days. Mineralization and alkaline phosphatase activity (AP) were measured at 21 days of differentiation. Mineralization was significantly higher in sera of the low BMD group compared to sera of the high BMD group (0.18 ± 0.04 nmol/μ g DNA vs. 0.15 ± 0.04 nmol/μ g DNA, p = 0.02), while at day 21 no difference in induction of AP was observed. There were no differences in serum 1,25-dihydroxyvitamin D_3 and PTH levels between the two groups. Serum 17β -estradiol (E2) levels were significantly lower in women with a low BMD compared to women with a high BMD (17.0 ± 4.6 pmol/l vs. 45.4 ± 6.9 pmol/l, $p < 0.01$). A possible role for E2 was further analyzed by testing the effect of various concentrations E2 on mineralization and AP at multiple time-points during culture. E2 treatment resulted in a 10-20% reduction in calcium deposited during the whole culture period, with most pronounced effects at later time points (days 19-21). In addition, E2 reduced AP activity by 10-20%, with most pronounced effects in the period preceding the peak activity of AP (days 7-14). No effects of E2 on total amount of DNA were observed. In conclusion, serum from postmenopausal women with a high BMD and high E2 level results in a reduced mineralization, which is supported by the direct inhibition of mineralization by E2. Besides the known role in controlling bone turnover via regulation of osteoclast function, on basis of the current data a new role for estradiol can be postulated: control of the extent or set-point of mineralization, which potentially contributes to the quality of bone.

M190

Cloning and Characterisation of the Human Cbfa 1/Runx2 Promoter. S. Gutzwiller*[1], V. Geoffroy*[2], B. Fournier*[1]. [1]Bone Metabolism Unit, Novartis Pharma AG, Basel, Switzerland, [2]Inserm u349, Hôpital Lariboisière, Paris, France.

Runx2 is a transcription factor belonging to the runt domain family, which has been shown to be essential for osteoblast differentiation. Runx2 deficient mice develop to term, their skeleton is characterized by a complete absence of intramembranous and endochondral bone, a consequence of the maturational arrest of hypertrophic chondrocytes and osteoblasts. Three isoforms of the Runx2 gene have been identified that differ in their N-terminal sequence. The Runx2/Osf2 isoform has a novel N-terminus and has been detected exclusively in bone and prostate. Very little is known about the structure of the human Runx2 promoter region to explain this intriguing tissue restricted expression. Therefore we decided to clone the human Runx2 promoter region. Here, we report the cloning of a 12Kb promoter region of the human Runx2 from a PAC library, and the subcloning of 5.3Kb of this region into a luciferase reporter vector. We investigated the activity of the human Runx2 promoter in different cell types and found that its activity is greater in mature osteoblastic cells compared to chondrocytic, pre-osteoblastic, and fibroblastic cells. We studied the regulation of this promoter with two hormones essential for bone metabolism such as PTH (1-34) and 1,25 Dihydroxyvitamin D3. PTH (1-34) was not able to modulate Runx2 promoter activity. In contrast, 1,25 Dihydroxyvitamin D3 dose dependently repressed the promoter activity with a maximum inhibition of 50%. Some transcription factors have been suspected to act upstream of Runx2, these hypotheses were mainly based on in vitro data often coupled with observation of skeletal abnormalities in animal models where these genes were deleted. Very little information is available on the ability of these factors to directly modulate Runx2. We studied the effect of some of these proposed genes on the activity of the human Runx2 promoter. We showed that the homeobox gene Msx2 decreased the activity of the human Runx2 promoter. The Ets1 and 2 transcription factors had no effect on the activity of this promoter despite the presence of perfect consensus site on this promoter. In conclusion, we have identified negative regulators of the human Runx2 promoter activity. The positive regulators of Runx2 remain to be identified.

M191

The Effects of Near Infrared and Visible Light on RANKL and OPG Gene Expression and Secretion in Osteoblasts. J. T. Ninomiya[1], G. S. Takenishi*[1], J. A. Struve[1], E. V. Buchmann*[2], H. T. Whelan*[2]. [1]Department of Orthopaedic Surgery, Medical College of Wisconsin, Milwaukee, WI, USA, [2]Department of Pediatric Neurology, Medical College of Wisconsin, Milwaukee, WI, USA.

The effects of light on wound healing has become an exciting area of research interest, since light emitting diodes (LED) in the near infrared and visible range have been shown to promote rapid healing of ulcers and other skin lesions. We therefore hypothesized that exposure to near infrared (IR) light would have similar effects on bone, promoting enhanced bone turnover. Therefore, we chose to evaluate the effects of LED light on the gene expression and secretion of RANKL and osteoprotegerin, two modulators of osteoclast maturation and ultimately bone resorption. Murine osteoblast MC3T3-E1 osteoblastic cells were stimulated with LED light at specific wavelength and energy densities until confluent. Three stimulatory wavelengths (670, 728, and 880 nm) and energy densities (4 J & 8 J) were utilized. PTH was added as a positive control following the final LED exposure, and after 12 hours of further incubation total RNA was collected. The effects of LED light on the gene expression of RANKL, OPG, and IL-6 were determined by RT-PCR, and were compared to actin controls. A functional osteoclast maturation assay was performed using bone marrow cells extracted from mouse femurs. The effects of whole cell lysates on the maturation of osteoclast precursors were determined by counting the number of TRAP positive multinucleate cells in each sample. Osteoblasts demonstrated wavelength and energy specific responses to LED light. Specifically, exposure to 880 nm at 4 J increased RANKL gene expression and decreased OPG gene expression. The osteoclast maturation assay results confirmed that LED exposure increased RANKL secretion in osteoblast cells, resulting in enhanced maturation of osteoclast precursors. Additionally, the number of multinucleate osteoclast cells was significantly greater in the samples stimulated with LED light alone compared to unstimulated controls. Our studies suggest that near IR and visible light may play an important role in the regulation of bone resorption through alteration of the gene expression and secretion of RANKL and OPG. These studies have important implications in the management of osteoporosis, fracture healing, orthopaedic implant loosening, and the prevention of bone loss due to prolonged space flight.

M192

p300 Requires Runx2/Cbfa1 and the Vitamin D3 Receptor to Regulate Bone Specific Osteocalcin Expression but not its Intrinsic Histone Acetyl Transferase Activity. A. Villagra*[1], J. Sierra*[1], J. Olate*[1], A. van Wijnen[2], J. Lian[2], G. Stein[2], J. Stein[2], M. Montecino[1]. [1]Department of Molecular Biology, University of Concepcion, Concepcion, Chile, [2]Department of Cell Biology, University of Massachusetts Medical School, Worcester, MA, USA.

p300 is a multifunctional transcriptional co-activator that serves as an adaptor for several transcription factors including nuclear steroid hormone receptors. p300 contains an intrinsic histone acetyltransferase (HAT) activity that may be critical for promoting steroid-dependent transcriptional activation. Therefore we addressed p300 control of basal and vitamin D3-enhanced activity of the bone-specific osteocalcin (OC) promoter. In osteoblastic cells, OC gene transcription is principally regulated by the Runx2/Cbfa1 transcription factor and is stimulated in response to vitamin D3 by the Vitamin D3 receptor complex. We find that transient overexpression of p300 results in a significant dose-dependent increase of basal and vitamin D3-stimulated OC gene promoter activity. This stimula-

tory effect requires intact Runx2/Cbfa1 binding sites as well as the Vitamin D responsive element (VDRE). In addition, by co-immunoprecipitation we show that the endogenous Runx2/Cbfa1 and p300 proteins are components of the same complexes within osteoblastic cells under physiological concentrations. The stimulatory effect of p300 on the OC promoter is independent of its intrinsic HAT activity, as a HAT-deficient p300 mutant protein up-regulates expression and cooperates with P/CAF to the same extent as the wild type p300. Based on these results, we propose that within the OC promoter context, p300 interacts with key transcriptional regulators of this phenotype-restricted gene and connects factors bound to distal and proximal promoter sequences.

M193

Translational Regulation of RUNX2 Isoforms: Type-I mRNA Is Translated by Internal Ribosomal Entry Site Mechanism While Type-II mRNA Translation Is Cap-dependent. N. Elango*, Y. Li*, S. Elango*, M. S. Katz. Dept Medicine, Univ Texas Hlth Sci Center and GRECC, VAMC, San Antonio, TX, USA.

RUNX2, a transcription factor implicated in the regulation of osteoblast differentiation and gene expression, is expressed as two isoforms. The two isoforms, type-I and type-II, are encoded by two different mRNAs with distinct 5' untranslated regions (UTRs) (type-I: 1015 nucleotides and type-II: 210 nucleotides). We recently showed that both RUNX2 mRNAs are expressed but dormant in osteoblast precursors and nonosteoblastic cells, and that the expression of both isoforms is regulated at the translational level. In this study we investigated whether the two 5' UTRs function as translational regulators. In vitro transcribed luciferase mRNA containing type-II 5' UTR was translated efficiently in rabbit reticulocyte lysate, whereas luciferase mRNA with type-I 5' UTR was not. In contrast, in transient transfection experiments using clonal osteoblastic cells (UMR-106), translation of luciferase reporter containing type-I 5' UTR was 6 times that of reporter with type-II 5' UTR. Most eukaryotic mRNAs are translated by a cap-dependent ribosome scanning mechanism and are efficiently translated in vitro. The type-I 5' UTR is long and GC-rich, and thus capable of forming stable secondary structures inhibitory to cap-dependent translation. Accordingly, we reasoned that the translation of type-I 5' UTR containing RNA observed in UMR-106 cells might be mediated by an alternative mechanism involving an internal ribosomal entry site (IRES). To investigate this possibility, we performed dicistronic mRNA translation assays using expression vectors containing CAT as the first cistron followed by type-I 5' UTR upstream of luciferase (second cistron); dicistronic constructs in which type-I 5' UTR was replaced by 5' UTRs of β-globin (known to be translated by the cap-dependent mechanism), type-II RUNX2, and luciferase (pGL3-Promoter) mRNAs were used as controls. When UMR-106 cells were transfected with the dicistronic constructs, luciferase activity was detected only in cells transfected with the construct containing type-I 5' UTR. From these results we conclude that translation of type-I RUNX2 mRNA is mediated by an IRES element whereas translation of type-II mRNA is cap-dependent. Interestingly, 40 nucleotides long stem-loop and unstructured sequences inserted near the 5' terminus of the type-I 5' UTR decreased reporter translation by 75% and 90%, respectively. Thus the structural integrity of the type-I 5' UTR appears to be essential for the activity of the IRES element. Translational control of RUNX2 mRNAs by alternate 5' UTR dependent mechanisms may play a role in the regulation of osteoblast differentiation.

M194

Functional Integration of Runx2 and BMP2 Responsive Regulatory Signals at Transcriptionally Active Subnuclear Sites in Osseous and Non-Osseous Cells. S. K. Zaidi, A. J. Sullivan*, A. J. van Wijnen, J. L. Stein*, J. B. Lian, G. S. Stein. Department of Cell Biology, University of Massachusetts Medical School, Worcester, MA, USA.

Runx2/Cbfa1 controls osteogenic lineage commitment and is a transcriptional effector of BMP2 responsive Smad signaling. Genetic defects in the Runx2 and Smad pathways interfere with normal development. The *in situ* localization of Runx2 and Smad proteins must impact the mechanisms by which these proteins function together in gene regulation. To address the significance of the Smad interaction with Runx2 at subnuclear domains, we examined the organization of Runx2-Smad complexes in the nucleus of osseous and non-osseous cells. In response to TGFβ/BMP, Smad enters the nucleus, but does not associate with the nuclear matrix in non-osseous cells lacking Runx2. In osteoblasts, Runx2 recruits either TGFβ responsive Smads 2/3 or the BMP2 related Smads 1/5 to Runx2 subnuclear foci. We show that Smad-Runx2 complexes are associated *in situ* with the nuclear matrix and this association requires the intranuclear targeting signal of Runx2. The convergence of Smad and Runx2 proteins at these sites supports transcription as reflected by BrUTP labeling and functional cooperativity between the proteins. A specific point mutation that abrogates targeting to the nuclear matrix, retains interaction with Smads, but reduces transcriptional activity on a TGFβ responsive promoter. We conclude that the integration of Runx2 and Smad-related signals, which is critical for normal skeletal development, is mediated by *in situ* interactions at specific foci within the nucleus.

M195

Transcriptional Induction of the Osteocalcin Gene During Osteoblast Differentiation Involves Acetylation of Histones H3 and H4. J. Shen*[1], J. B. Lian[1], M. A. Montecino[2], G. S. Stein[1], J. L. Stein*[1], A. J. van Wijnen[1]. [1]Department of Cell Biology, University of Massachusetts Medical School, Worcester, MA, USA, [2]Departamento de Biologia Molecular, Universidad de Concepcion, Concepcion, Chile.

The remodeling of chromatin is required for tissue-specific gene activation to permit interactions of transcription factors and co-regulators with their cognate elements. Here, we investigate the chromatin mediated mechanisms by which the bone-specific osteocalcin gene is transcriptionally activated during cessation of cell growth in ROS 17/2.8 osteosarcoma cells and during normal osteoblast differentiation. Acetylation of histones H3 and H4 at the osteocalcin (OC) gene promoter was assayed during the proliferative and post-proliferative stages of cell growth by using chromatin immunoprecipitation (ChIP) assays with antibodies that recognize different acetylated forms of histones H3 or H4. The results show that the promoter and coding regions of the OC gene contain very low levels of acetylated histones H3 and H4 during the proliferative period of osteoblast differentiation when the OC gene is inactive. However, in mature osteoblasts and confluent ROS 17/2.8 cells, in which the OC gene is actively transcribed, histone H3 and H4 acetylation is observed in the initial 1.1 kbp of the OC gene promoter and the coding region. Histone acetylation at the RUNX2 (CBFA1) locus, which is expressed throughout osteoblast differentiation, is not altered post-proliferatively. We conclude that acetylation of histones H3 and H4 is functionally coupled to the chromatin remodeling events that mediate the developmental induction of OC gene transcription in bone cells.

M196

Regulation of Bone Sialoprotein Gene Expression by the Homeodomain Proteins Msx2 and Dlx5. G. L. Barnes[1], K. Hebert*[1], M. Q. Hassan*[2], A. van Wijen[2], M. F. Young[3], J. B. Lian[2], G. S. Stein[2], L. C. Gerstenfeld[1]. [1]Department of Orthopaedic Surgery, Boston University Medical Center, Boston, MA, USA, [2]Department of Cell Biology and Cancer Center, University of Massachusetts Medical School, Worcester, MA, USA, [3]Craniofacial and Skeletal Diseases Branch, National Institute of Dental Research, NIH, Bethesda, MD, USA.

Bone Sialoprotein (BSP), a phosphorylated and sulfated RGD containing glycoprotein, represents one of the major non-collagenous, extracellular matrix proteins of bone. The expression of BSP is primarily restricted to the mineralized tissues of the skeleton, specifically hypertrophic chondrocytes and osteoblasts. While the restricted nature of BSP expression is well characterized, the molecular regulation of BSP restricted expression remains poorly understood. Recent studies have demonstrated that a homeodomain binding element in the murine BSP promoter is required for the osteoblast-selective expression of BSP and that this element was capable of binding to Dlx5. We have reported similar findings demonstrating that a putative homeodomain element is required for selective expression of both the avian and human BSP promoters in either hypertrophic chondrocytes or osteoblasts. However, our studies do not support the conclusion that Dlx5 acts through direct DNA-binding at this cis-acting element. Furthermore, our results do not support the conclusion that Dlx5 directly modulates BSP expression. Instead, our studies demonstrate that Msx2 represses BSP expression and that Dlx5 acts by antagonizing this repression. Furthermore, our data support the conclusion that the regulation of BSP by Dlx5/Msx2 is not dependent on direct DNA binding at either of the previously described putative homeodomain binding elements in the BSP promoter. This study represents the first report of the regulation of BSP by Msx2 and suggests that the mechanism of regulation of BSP by the combination of Dlx5 and Msx2 factors occurs through a mechanism independent of direct DNA binding similar to that previously described for the osteocalcin gene.

M197

Detection of Jab1-Smad4 Interaction by Both Biochemical Method and AFM. M. Wan[1], W. Hou*[2], X. Shi[1], X. Cao[1]. [1]Pathology, University of Alabama at Birmingham, Birmingham, AL, USA, [2]Biomedical Engineering, CBSE, University of Alabama at Birmingham, Birmingham, AL, USA.

The AP-1 proteins are a family of transcription factors, members of which are essential for bone and cartilage development. Jab1, the Jun activating binding protein, specifically stabilizes complexes of c-Jun or JunD with AP-1 sites, increasing the specificity of target gene activation by AP-1 proteins. Jab1 mRNA expression has been detected in both osteoblast MC3T3-E1 cells and isolated mouse calvaria. Thus Jab1 may represent an important regulator of gene transcription during bone development. Smad4 is the common mediator in the TGF-β/BMP signaling pathway. Previously, we found that Jab1 antagonizes TGF-β function by inducing degradation of Smad4. In this study, we examined the specific interaction of Jab1 with Smad4 in yeast, in vitro, in mammalian cells and by atomic force microscope (AFM). We demonstrated that Jab1 interacts with Smad4, not with Smad1, Smad3, Smad6, or Smad7 in both yeast two-hybrid and pull-down assays. We also performed immunoprecipitation assays. Jab1 was co-immunoprecipitated with Smad4 in 293T cells when both proteins were overexpressed. In addition, we demonstrated that endogenous Jab1 interacts with Smad4 in Mv1Lu cells. More importantly, we could directly view the images of the interaction between these two proteins by AFM. AFM has been recently employed to study the adhesive strength and mechanics of various biomolecular binding interactions, including protein-protein interactions. These measurements rely on measurement of the deflection of an AFM cantilever with a known force constant during retraction of a sample surface from an appropriately modified AFM tip. We demonstrated that both Jab1 and Smad4 alone were present in trimer under AFM. They developed into a ring-shaped hexamer complex when they were mixed together about five minutes later, indicating these two proteins interact with each other and rapidly form a complex. Jab1 is also known as subunit 5(CSN5) in COP9 signalosome regulatory complex (CSN). It is critical to know whether CSN complex is involved in the interaction with Smad4 in vivo. Our result indicates that the complex of CSN may not involved in the interaction with Smad4 by immunoprecipitation assays. In summary, the interaction of Jab1 with Smad4 may provide some novel mechanisms by which Jab1 regulates osteoblast differentiation and bone formation, and may help us find another potential therapeutical approach for bone related diseases.

M198

Homeodomain Protein Interactions at the Bone-Specific Osteocalcin Promoter Regulate Transcription During Osteoblast Differentiation. M. Q. Hassan*, J. Pratap, S. Gutierrez*, A. Javed, J. L. Stein*, A. J. van Wijnen, G. S. Stein, J. B. Lian. Department of Cell Biology, University of Massachusetts Medical School, Worcester, MA, USA.

Developmental expression of the osteocalcin (OC) gene is tightly regulated during osteoblast differentiation. The rat -1.7 OC-CAT transgene is expressed in 13.5 day embryos when the homeodomain(HD) proteins, Msx-2 and Dlx-5 are highly expressed. However, in vitro studies have shown that HD proteins contribute to suppression of OC transcription. In this study, we examined activity of the multipartite OC Box which binds both HD and non-HD proteins. To focus on the mechanism of transcriptional regulation by the OC Box, we constructed a series of point mutations spanning twelve nucleotides of the core OC Box. We identified two mutations, one that selectively abrogated binding of HD complexes, but retained the non HD protein-DNA interaction (mCC1), and the other lost binding of all interacting complexes (J2). In transfection assays in multiple cell types, the CC1 mutant expressed higher than WT, while expression of the J2 mutant was decreased, indicating that both enhancer and repression complexes at the OC Box contribute to basal transcription. To further define activity at the OC Box during osteoblast differentiation, we assayed nuclear extracts from primary rat osteoblasts at three stages of maturation (proliferation, matrix maturation, and mineralization). Modifications in the protein-DNA complexes at the OC Box were observed at each stage of differentiation, further indicating selective binding by distinct classes of factors in relation to OC gene expression. The OC Box is in close proximity to C/EBP and Runx2 enhancer elements. To address the interaction of homeodomain proteins with other regulatory elements, we examined in the ROS 17/2.8 cell line the consequences of Msx-2 and Dlx-5 expression on OC promoter-constructs in which either the C/EBP or Runx site was mutated. As expected, basal activity of the two mutant constructs was significantly decreased from wild type. However, expression of the homeodomain proteins increased basal activity two-fold in constructs carrying the C/EBP or Runx site mutations. These findings suggest promoter context dependent crosstalk among enhancer and repressor domains. Taken together, our results show that the OC Box contributes to regulation of OC transcription and its activity is influenced by neighboring enhancer elements that may contribute to suppression of activity at the OC Box through multimeric regulatory complexes.

M199

Histone Deacetylase (HDAC) 3 Interacts with Runx2 (Cbfa1, AML-3) and Represses Runx2-induced Transcription of the Osteocalcin Promoter. T. M. Schroeder*[1], X. Li*[2], J. J. Westendorf[2]. [1]Biochemistry, Molecular Biology and Biophysics Graduate Program, University of Minnesota, Minneapolis, MN, USA, [2]Orthopaedic Surgery and Cancer Center, University of Minnesota, Minneapolis, MN, USA.

Runx2 (Cbfa1. AML-3) is required for bone formation and cooperates with several oncogenes to induce T cell lymphomas. Runx2 binds the DNA sequence TGPuGGPu to either activate or repress transcription of numerous osteoblast-specific genes. We are interested in defining the molecular mechanisms by which Runx2 represses transcription. We previously demonstrated that Runx factors recruit histone deacetylase containing complexes to regulate tissue-specific gene expression. Histone deacetylases (HDACs) regulate transcription by removing acetyl groups from lysine residues on histone tails and thereby facilitating chromatin condensation and transcriptional inhibition. Our studies indicate that Runx2 contains multiple autonomous repression domains that are sensitive to histone deacetylase inhibitors. Co-immunoprecipitation experiments revealed that HDAC3 interacts with an amino-terminal repression domain of Runx2. To determine the functional significance of the interaction, we tested the effects of HDAC3 on Runx2 transcriptional activity. Runx2 activates the bone-specific osteocalcin promoter by three to five-fold. HDAC3 did not effect the basal activity of the osteocalcin promoter but completely blocked Runx2-dependent activation of this promoter. Thus HDAC3 may interact with Runx2 to regulate osteoblast-specific gene expression.

M200

TWIST Stimulates Osteoblast Type I Procollagen Expression by a Transcriptional Mechanism. T. Yan*[1], D. Strong[2], T. Linkhart[2], S. Flanagan*[3], C. Glackin[3]. [1]Molecular Medicine, Beckman Research Institute City of Hope, Duarte, CA, USA, [2]Loma Linda University and VAMC, Loma Linda, CA, USA, [3]Beckman Research Institute City of Hope, Duarte, CA, USA.

TWIST is a basic helix-loop-helix (b-HLH) transcription factor that is important for cell type determination and differentiation. We have transfected human SaOS-2 osteoblasts with sense or antisense *TWIST* expression vectors to generate stable cell lines that have increased or decreased *TWIST* expression. *TWIST* sense cells (TS) express significantly higher *TWIST* levels and have lower ALP activity compared to parental SaOS-2 cells as evidenced by RT-*PCR*, Northern, and western analyses. *TWIST* antisense cells (TAS) have low *TWIST* and high ALP expression. TS cells have a spindle shaped morphology characteristic of osteoprogenitors, while parental and TAS cells exhibit a cuboidal morphology representing a more differentiated phenotype. To investigate whether other changes in gene expression characteristic of osteoblast differentiation also occurred, we examined mRNA levels of type I procollagen α 2 (ColIA2) in the cell lines. Both RT-*PCR* and northern analyses indicate that TS cells express significantly higher levels of ColIA2 when compared to parental or TAS cells. We hypothesized that the over-expression of *TWIST* may play a role in osteoblast differentiation by regulating the expression of ColIA2 and that the ColIA2 promoter may be a target of *TWIST*. To address this hypothesis, we have performed LM-PCR *in vivo* footprinting on the proximal human (h) ColIA2 promoter (-267 to +1). Automated LM-PCR *in vivo* footprinting is a powerful technique developed in our laboratory that characterizes changes in transcription factor binding to a promoter region in intact cells. Results demonstrate that an E-Box binding site on the ColIA2 promoter are protected in TS cells and not in parental and TAS cells *in vivo*. Transient cotransfection studies with a -276 to +45 hColIA2 pGL3 -luciferase reporter construct and a pcDNA3-Twist expression vector in ROS 17/2.8 cells showed, surprisingly, that *TWIST* over-expression dose dependently and significantly *trans*-activated the hColIA2 promoter (2 fold increase in luciferase activity compared to vector control ($P < 0.05$)). Site-directed mutagenesis of the "E-box' in the promoter sequence abolished *trans*-activation of the ColIA2 promoter by *TWIST*. In summary, these experiments suggest that *TWIST* increases collagen expression by a transcriptional mechanism through an E-box in the hColIA2 promoter. Results from this study provide strong evidence to support the hypothesis that hColIA2 is a target of *TWIST* and that *TWIST* may function to maintain an early osteoblast phenotype by up-regulating ColIA2 expression.

M201

Enhanced *In Vitro* Mineralization of Primary Bone Marrow Stromal Cells Following Runx2/Cbfa1 Overexpression via Retroviral Gene Delivery. B. A. Byers*, A. J. Garcia. Woodruff School of Mechanical Engineering, Georgia Institute of Technology, Atlanta, GA, USA.

We previously demonstrated that forced expression of the osteoblast-specific transcription factor Runx2/Cbfa1 in the MC3T3-E1 osteoblast-like cell line enhanced osteoblastic phenotype expression and upregulated *in vitro* mineralization. In the current study, we investigated sustained Runx2 overexpression in primary bone marrow stromal cells using retroviral gene delivery, hypothesizing that the osteogenic cell population in bone marrow would be highly responsive to exogenous Runx2 expression. Primary bone marrow stromal cells harvested from femora of young adult rats were transduced with Runx2 or empty vector control retrovira and cultured in α-MEM supplemented with 10% FBS, 1% pen-strep, 3 mM β-glycerophosphate, 50 μg/ml ascorbic acid, and with or without 10 nM dexamethasone (dex). Gene expression, including Runx2, osteocalcin (OCN), bone sialoprotein (BSP), alkaline phosphatase (ALP), and osteopontin (OPN), was investigated by real-time RT-PCR, ALP activity was examined by a biochemical assay, and matrix mineralization was quantified by von Kossa staining. Results reported are from three separate donors with two replicates each (n=6). Quantitative PCR revealed significant upregulation in Runx2 (10-fold) and OCN (10-fold) expression in dex-treated, Runx2-infected cultures compared to dex-treated controls ($p<0.001$), while no differences were observed in BSP, ALP, or OPN expression. In the absence of dex, however, Runx2-expressing cultures demonstrated significantly higher transcript levels for all of these osteoblast-specific genes compared to no dex controls ($p<0.0001$). ALP activity was upregulated two-fold in Runx2-infected cultures compared to controls at 7 days ($p<0.005$). Most notably, Runx2-expressing stromal cultures demonstrated upregulated mineralized surface area in the presence or absence of dex at 7 (5-fold), 14 (2-fold), and 21 (1.5-fold) days compared to matched controls ($p<0.001$). FT-IR analysis revealed peaks characteristic of biological mineralization in both Runx2-infected and control cultures. These results demonstrate the *in vitro* response of primary bone marrow stromal cells to Runx2 overexpression and suggest that in the absence of other osteoinductive agents, such as dex, exogenous Runx2 expression upregulates multiple osteoblast-specific genes. Additionally, Runx2 overexpression significantly enhances the *in vitro* mineralized matrix production of primary bone marrow stromal cells. Primary stromal cells overexpressing Runx2 may offer a promising solution to address the clinical need for an osteogenic cell source to be used in the treatment of damaged or diseased bone.

M202

Evidences for a Role of p38 MAP Kinase in Prostaglandin E1 Induced ALP Activity in Osteoblast-like Cells. A. Suzuki[1], J. Caverzasio[2], A. Kakita*[3], M. Kotake*[1], Y. Miura*[3], Y. Oiso*[3], M. Itoh*[1]. [1]Division of Endocrinology, Department of Internal Medicine, Fujita Health University, Aichi, Japan, [2]Division of Bone Diseases, Department of Internal Medicine, University Hospital of Geneva, Geneva, Switzerland, [3]1st Department of Internal Medicine, Nagoya University, Nagoya, Japan.

Prostaglandins are important regulators of bone formation and resorption. Among them, prostaglandin E1 (PGE1) has been reported to stimulate cellular cAMP and induce alkaline phosphatase (ALP) activity, a marker of osteoblastic cell differentiation. Recently, we have shown that p38 mitogen-activated protein (MAP) kinase mediates the stimulation of ALP activity induced by activation of a Gi protein-coupled receptor agonist in mouse osteoblast-like MC3T3-E1 cells. In the present study, we investigated whether p38 MAP kinase is involved in the regulation of ALP induced by PGE1 in MC3T3-E1 cells. PGE1 dose-dependently enhanced ALP activity in the concentration range of 1 nanoM to 1 microM with a maximal effect of 2.3 fold. SB203580 at 10 microM, a specific inhibitor of p38 MAP kinase, decreased the stimulation of ALP activity induced by PGE1 by more than 85%. Immunoprecipitation and Western blotting analysis indicated that PGE1 enhances p38 MAP kinase activity. This effect was mimicked by both Bt2cAMP, a permeable analogue of cAMP, and forskolin, which directly activates adenylate cyclase. H-89, a potent inhibitor of protein kinase A (PKA), significantly reduced the stimulation of p38 MAP kinase induced by PGE1. Taken together, the results of this study strongly suggest that the stimulation of ALP activity induced by PGE1 involves a PKA-dependent activation of p38 MAP kinase. In conclusion, the results of this study suggest the existence of a cAMP-PKA-dependent mechanism of p38 MAP kinase activation by PGE1 in osteoblast-like cells which mediates changes in ALP activity. This observation suggest a significant role of p38 MAP kinase in the regualtion of osteoblastic cell differentiation by calciotropic factors acting through cAMP second messenger signaling.

M203

Cytokine Induced Upregulation of Bradykinin B1 and B2 Receptors in the Human Osteoblastic Cell Line MG-63. A. Bernhold Brechter*, I. Lundgren*, U. H. Lerner. Oral Cell Biology, Odontology, Umeå University, Umeå, Sweden.

The inflammatory mediator bradykinin (BK) has previously been shown to stimulate bone resorption in vitro and to synergistically potentiate the stimulatory effect of IL-1α/IL-1β on bone resorption and prostaglandin biosynthesis. In the present study the effects of a variety of kinins and kinin analogues, on unstimulated and cytokine stimulated prostaglandin biosynthesis, were studied in a human osteoblastic cell line, MG-63. In addition, the effects of different cytokines on BK B1 and B2 receptor expression were assessed using radioligand binding and semi-quantitative RT-PCR. Co-treatment of MG-63 cells with BK and IL-1α, IL-1β or TNFα resulted in synergistic stimulation of PGE_2 and PGI_2 formation. IL-1β induced PGE_2 formation was synergistically potentiated by several kinins and kinin analogues with affinity for BK B1 and B2 receptors. These interactions were specifically inhibited by B1 and B2 receptor antagonists. Pretreatment of MG-63 cells with IL-1β or TNFα resulted in a time- and concentration-dependent enhancement of both B1 and B2 receptor ligand binding. Pretreatment with the B2 receptor agonist BK caused a down-regulation of [^{3}H]-BK binding, whereas pretreatment with the B1 receptor agonist des-Arg^{10}-Lys-BK did not affect the binding of [^{3}H]-des-Arg^{10}-Lys-BK. In cells where B1 and B2 receptor binding sites had been upregulated by pretreatment with IL-1β for 24 hours, B2 receptor agonists caused a rapid burst of PGE_2 formation, whereas B1 receptor agonists caused a delayed PGE_2 response. Semi-quantitative RT-PCR showed that IL-1β and TNFα increased the mRNA expressions of both BK B1 and B2 receptor subtypes. In agreement with radioligand binding data BK decreased B2 receptor mRNA, whereas des-Arg^{10}-Lys-BK did not affect B1 receptor mRNA. The osteotropic cytokines IL-6, IL-11, IL-17, OSM, TGF-β and LIF did not potentiate B1 and B2 receptor induced PGE_2 formation, nor did these cytokines affect B1 and B2 receptor radioligand binding or the mRNA expression for the B1 and B2 receptors. These results show that IL-1 and TNFα synergistically potentiate BK B1 and B2 receptor mediated stimulation of prostaglandin biosynthesis, in MG-63 cells, and that cytokine induced upregulation of B1 and B2 receptor expression seems to contribute to this phenomenon. The mechanism by which B1 receptors activate prostaglandin formation seems to be different from that of B2 receptors as assessed by the large differences in the kinetics. The delayed stimulation of PGE_2 formation caused by B1 receptor ligands is not due to auto- or hetero-induction of B1 receptors.

M204

Inactivation of Menin Inhibits the Commitment of Multipotential Mesenchymal Stem Cell to Osteoblast Lineage. H. Sowa*[1], H. Kaji[1], T. Yamaguchi[1], L. Canaff*[2], G. N. Hendy[2], T. Sugimoto[1], K. Chihara*[1]. [1]Endocrinology and Metabolism, Kobe University Graduate School of Medicine, Kobe, Japan, [2]Department of Medicine, McGill University, Montreal, PQ, Canada.

Menin is the product of MEN1 gene responsible for multiple endocrine neoplasia type1. Although menin is ubiquitously expressed, its physiological roles are not known. We previously demonstrated that menin interacts with the transforming growth factor type β (TGF-β)-receptor-regulated Smad, Smad3 (PNAS 2001), and that Smad3 stimulates alkaline phosphatase (ALP) activity and mineralization in mouse osteoblastic MC3T3-E1 cells (MC) (JBMR, in press). Moreover, homozygous menin knockout mice exhibit cranial and facial hypoplasia, and bone mineral density is decreased in Smad3 knockout mice. We, therefore, investigated the role of menin in osteoblastic differentiation. Menin antisense oligonucleotides (AS) reduced the endogenous menin expression and TGF-β-induced transcriptional activity in mouse mesenchymal stem cell line, C3H10T1/2 cells (10T1/2) and osteoblastic MC. In 10T1/2, AS antagonized ALP activity and the expression of type I collagen, Runx2 and osteocalcin induced by bone morphogenic protein 2 (BMP-2). Control menin sense oligonucleotides did not affect the expression of these genes and AS did not affect retinoic acid-induced ALP activity. In contrast to the effect on osteoblastic markers, AS did not affect adipogenic markers (Oil Red stain and PPARγ) and chondrogenic markers (Alcian Blue stain and the type IX collagen) induced by BMP-2 in 10T1/2. In MC, AS did not affect BMP-2-stimulated ALP activity nor the expression of Runx2 and osteocalcin . Inactivation of menin in MC by stable expression of menin antisense cDNA increased ALP activity, mineralization, and the expression of type I collagen and osteocalcin. In 21-day cultures of MC and BMP-2-treated 10T1/2, endogenous menin expression increased up to day 14 and declined thereafter. In summary, the data indicate that menin inactivation specifically inhibits the commitment of pluripotent mesenchymal stem cells to osteoblast lineage. Menin seems to be important for both early differentiation of osteoblasts and inhibition of their later differentiation.

M205

Effects of Prostaglandin E_2 (PGE_2) and Selective Prostaglandin E Receptor (EP) Agonists on 3',5' Cyclic Adenosine Monophosphate (cAMP) Production in Osteoblastic Cells from Wild Type and EP2 or EP4 Knockout Mice. Y. Sakuma[1], C. C. Pilbeam[1], L. C. Pan[2], L. G. Raisz[1]. [1]Endocrinology, University of Connecticut Health Center, Farmington, CT, USA, [2]Groton Laboratories, Pfizer Global Research and Development, Groton, CT, USA.

PGE_2 can stimulate cAMP production and bone resorption through two prostaglandin E receptor pathways, EP2 and EP4. Selective agonists for these receptors have been developed, Ono-AE1-259 for EP2 (EP2A) and Ono-AE1-329 for EP4 (EP4A). We compared the effects of these agonists with PGE_2 on cAMP production in calvarial osteoblastic cell cultures from wild type mice and mice lacking either EP2 or EP4 receptors (EP2KO or EP4KO). We also examined down-regulation of cAMP responses in primary cultures of osteoblasts after pretreatment with PGE_2, EP2A or EP4A. Cells were cultured for 7 days and serum deprived for 24 hours. In some experiments cells were cultured during serum deprivation and treatment with NS-398 (0.1 μM), a selective inhibitor of inducible cyclooxygenase-2 (COX-2), to block the major source of endogenous prostaglandin production. cAMP was measured by immunoassay after 15 minutes of treatment in the presence of a phosphodiesterase inhibitor (IBMX). In the presence of NS-398, cAMP levels were significantly increased by all three agonists; the mean response to PGE_2, EP2A and EP4A in five experiments were 25-fold, 10-fold and 4-fold, respectively. In the absence of NS398, the cAMP increases were reduced to 19, 7 and 2-fold, respectively. The cAMP responses to PGE_2, EP2A and EP4A were dose-related from 0.01 to 10 μM. In EP4KO cells, the responses to PGE_2 and EP2A were not significantly reduced, but the response to EP4A was abrogated. In EP2KO cells, in the presence of NS-398, PGE_2 responses were reduced by 80% or greater, EP2A responses were abrogated and EP4A responses were still present. In the absence of NS398, EP2A still produced a small stimulation of cAMP in EP2KO cells. In primary osteoblastic cell cultures, pretreatment with PGE_2 or EP2A for 1 hour reduced the cAMP response to PGE_2 by about 50% while pretreatment for 24 hours reduced the response by 80% or greater. Pretreatment with EP4A for 1 hour had little effect, but after 24 hours the response to PGE_2 was reduced by about 50%. We conclude that the cAMP response to PGE_2 in cultured osteoblastic cells is mediated by both EP2 and EP4 receptors with the EP2 pathway predominant. The loss of response in cells lacking the cognate receptors confirms the specificity of EP2A and EP4A as selective agonists. Down-regulation of cAMP responses by pretreatment with PGE_2, EP2A or EP4A is proportional to their initial cAMP effect.

M206

Prostaglandin E EP4 Receptor Agonist Induces the Bone Formation by an Alteration of the Osteoblast and Osteoclast Dynamic State. M. Tanaka*[1], N. Sahara*[2], T. Katayama*[1], K. Yamaguchi*[1], A. Hosoya*[2], N. Mishima*[2], S. Matsuura*[2], H. Ozawa[3]. [1]Fukui Institute for Safety Research, ONO Pharmaceutical Co.,Ltd., Fukui, Japan, [2]Oral Anatomy, Matsumoto Dental University, Nagano, Japan, [3]Dental Science Institute, Matsumoto Dental University, Nagano, Japan.

Recently it has been shown that an activation of EP4, one of prostaglandin E receptor subtype, induced the *de novo* bone formation. To investigate part of the elucidation of the mechanism of the bone formation by activation of EP4, an osmotic pump was implanted to the rats on the back subcutaneous and EP4 agonist (ONO-4819 CD) was administered to rats at dose of 100 ng/kg/min for up to 28 days. Morphology of femur was observed on Day 0, 1, 3, 5, 7, 14 and Day 28. In the ONO-4819 CD-treated rats, proliferation of the osteoclasts in the metaphysis was observed on Day 1. The number of osteoblasts showed an increase from on Day 3. In addition, the endosteal bone formation in the metaphysis and diaphysis was observed from on Day 5 and peaked on Day 28. Serum alkaline phosphatase activity showed a transient decrease on Day 1, and thereafter it showed the increase. The concentration of osteocalcin (Gla) showed an increase from on Day 1. On the other hand, the excretion volume of urinary deoxypyridinoline increased on Day 3, and it showed a transient decrease on Day 5. But it showed an increase from on Day 7. These results indicate that EP4 agonist-induced bone formation is related to an increase of the osteoclast in the early stage and a subsequent increase of the osteoblast. In addition, the adipocyte in the bone marrow was markedly reduced in the EP4 agonist-treated rats as compared with that of the control ones on Day 28.

M207

Analysis of PDE4 Subtype Expression During BMP-2 and Dexamethasone Induced Osteoblastic Differentiation. A. Houghton, M. Jankowsky*, J. Wos*, S. Pikul*, M. W. Lundy. Discovery, Procter & Gamble Pharmaceuticals, Mason, OH, USA.

The cAMP specific PDE4 family is comprised of 4 separate gene products (A-D), which are characterized by their specificity for cAMP and sensitivity to inhibition by Rolipram. Recent literature reports have demonstrated that inhibitors of PDE4 are able to increase bone formation in vivo, however to date the relative expression of all four subtypes during human osteoblast differentiation has not been reported. We therefore analyzed the expression of these subtypes during both BMP-2 and dexamethasone induced osteoblastic differentiation using Taqman. RNA was obtained at various time points from human primary cultures of mesenchymal stem cells (MSCs) induced to undergo osteoblastic differentiation by treatment with either BMP-2 or dexamethasone. Of all the four subtypes PDE4D was the most highly expressed subtype during all stages of osteoblastic differentiation, with significant increases in expression apparent in BMP-2 and dexamethasone treated samples by 48 hours, rising to a maximum level of expression by 72 hours which was sustained until day 14. PDE4A was the second most abundant subtype in the MSC cells however no regulation of expression was observed by either BMP-2 or dexamethasone when compared to untreated controls. PDE4B was the third most abundant mRNA measured in these samples and was increased in the presence of BMP-2 by 72 hours, but no regulation of expression by dexamethasone was observed at any time point. PDE4C was the least abundant subtype expressed, with some small increases in expression noted in response to both agents. Tissue analyses using Taqman demonstrated that PDE4 subtype expression in MSCs was somewhat similar to that seen in brain, liver and heart tissue, however expression of all subtypes in MSCs was significantly less than seen in spleen, stomach, small intestine and lung. In order to determine whether the observed changes in subtype expression regulated MSC responses to PDE4 inhibitors, untreated MSCs and BMP-2 treated MSCs were used to measure the effects of PDE4 inhibitors on PGE_2 stimulated increases in intracellular cAMP. These experiments determined no differences in the potencies of PDE4 inhibitors when tested in untreated or BMP-2 treated MSCs. In conclusion these data demonstrate that PDE4D is the predominantly expressed subtype in human primary osteoblasts, with osteoblastic differentiation regulating the expression of all subtypes except PDE4A. This regulation of expression implies differential modulation of cAMP levels during differentiation and raises the possibility that specific intervention by agents selective for one or more of the PDE4 subtypes might be used to induce bone formation.

*Disclosures: **A. Houghton**, Procter & Gamble Pharmaceuticals 3.*

M208

Mice Deficient in nNOS Have Increased Bone Mass; Possible Indications for a Central Mechanism of Regulation for Bone Turnover. R. J. van 't Hof*, K. J. Armour, S. Penman*, M. H. Helfrich, S. H. Ralston. Medicine & Therapeutics, University of Aberdeen, Aberdeen, United Kingdom.

Nitric Oxide (NO) is a highly reactive molecule synthesized by the nitric oxide synthases (NOS), that plays an important role in bone metabolism. Inducible NOS (iNOS) plays a role in inflammation mediated bone loss, whilst endothelial NOS (eNOS) is important in regulating osteoblast function and bone formation. The third NOS isoform, neuronal NOS (nNOS) is predominantly expressed in the brain and act as a neurotransmitter . The role of nNOS in bone metabolism has so far been little studied. In 2 studies, no nNOS immunoreactivity was observed in bone, while in another study only weak mRNA expression was detected in whole bone RNA extracts. In order to determine whether nNOS plays a role in bone metabolism, we studied bone density in the proximal tibiae of 10-week-old nNOS knockout (nNOS-KO) mice and wild type (nNOS-WT) littermates using a Stratec pQCT machine. Bone density of nNOS-KO mice was 8.4% ($p<0.01$) higher than that of nNOS-WT mice. The difference was particularly pronounced in the trabecular compartment, where bone density was 29% higher in nNOS-KO than in WT controls ($p<0.001$), with a smaller (3%) increase in the cortical bone density ($p=0.02$). In addition, we observed a 10% increase in cortical thickness in the nNOS-KO animals ($p<0.01$). The fact that nNOS influences bone density by such a large amount is quite surprising, as it is expressed at only very low levels by bone cells. This suggests that nNOS deficiency may affect bone metabolism indirectly by a central nervous system (CNS) based relay, as has been suggested for the effects of Leptin on bone metabolism. In summary, we have found that nNOS knockout mice have substantially higher bone density than wild type littermates. As virtually no nNOS is expressed in bone, it is possible that nNOS regulates bone mass by a CNS based mechanism.

M209

Platelet-type 12-Lipoxygenase Expression and Activity in Adult Human Osteoblast-like Cells. M. Pacurari*[1], F. J. Secreto*[1], J. A. West*[1], A. Grover*[1], J. D. Blaha*[2], P. E. Keeting[1]. [1]Biology, West Virginia University, Morgantown, WV, USA, [2]Orthopedics, West Virginia University, Morgantown, WV, USA.

Arachidonic acid (AA) can be metabolized into a variety of hydroxyeicosatetraenoic fatty acids (HETEs) by the action of various lipoxygenases (LOX). The HETEs and the prostaglandins, collectively, comprise a group of bioactive lipids referred to as eicosanoids. At least 18 different LOX sequences have been published, and while the biological actions of many of the LOX products remain uncertain, links with apoptosis, angiogenesis, and mitogenesis have been established in various tissues. In the course of our investigations of arachidonic acid metabolism by adult human osteoblast-like (hOB) cells, we have radiolabeled the cell's glycerophospholipid pools by the addition of [14C]AA, leading to the production of radiolabeled eicosanoids. We have found an hOB cell radiolabeled product that co-migrates with authentic 12(S)-HETE in thin layer chromatographic analyses of extracted cell-conditioned media. The product appears to be formed constitutively, and the application of the osteotropic cytokines TGF-beta, TNF-alpha, or EGF to the cells for 24 hr were without apparent effect on its elaboration. The appearance of the 12-HETE could have been the consequence of cytochrome P450-related monooxygenase activity, or even the spontaneous oxidation of arachidonic acid rather than LOX-dependent generation. Accordingly, an analysis of hOB cell RNA preparations by classical RT-PCR methods was undertaken to determine if these cells expressed the gene encoding one of the 12-LOXs. A band was found in specimens in which intron-exon spanning primers to the human platelet-type 12-LOX were employed following 35 cycles of amplification, using a hybridization temperature of 56 C. Sequencing of the cloned RT-PCR product confirmed its identity as the human platelet-type 12-LOX. Related analyses using primers for the leukocyte-type 12-LOX gave negative results in hOB cell RNA preparations. The biological significance to hOB cells of a possibly constitutively produced 12-HETE remains undetermined.

M210

Zoledronate Is Anabolic for Human Osteoblast-Like Cells. B. Pan*[1], D. M. Findlay[2], L. B. To*[1], G. J. Atkins*[2], A. Evdokiou*[2], A. Labrinidis*[2], S. Bouralexis*[2], A. C. W. Zannettino*[3]. [1]Haematology, Institute of Medical and Veterinary Science, Adelaide, Australia, [2]Orthopaedic Surgery and Trauma, Univeristy of Adelaide, Adelaide, Australia, [3]Haematology, Institute of Medical and Veterinary Science, Adelaide, South Australia, Australia.

Bisphosphonates (BP) exhibit high affinity for the hydroxyapatite mineral in bone and are selectively taken up and adsorbed to mineral surfaces at sites of increased bone turnover. BPs are potent inhibitors of osteoclast (OC)-mediated bone resorption and are used extensively for the treatment of skeletal diseases. BPs inhibit bone resorption by acting directly on OC and indirectly *via* effects on osteoblasts (OB). The newer nitrogen-containing BPs inhibit the mevalonate pathway, with wide ranging cellular effects that include induction of apoptosis in osteoclasts and inhibition of osteoclast formation by osteoblasts. Zoledronate (ZOL), represents a new generation, nitrogen-containing BP and is the most potent inhibitor of bone resorption currently in use. We used an established model of OB-differentiation (Gronthos *et al*, JBMR,1999 14:47) to investigate the effect of ZOL on the molecular expression and and cellular phenotype of cultured human osteoblast-like cells. Human OB-like cells, derived from explants of posterior iliac crest and proximal femoral trabecular bone, were cultured in the presence of ZOL at concentrations ranging from 0.05 to 50μM. At concentrations up to 5 μM, ZOL was strongly cytostatic, blocking cell replication in S and G2/M phase. At higher concentrations, ZOL dose-dependently induced cell death in each of the human OB cultures tested. Using dual colour FACS and CFSE staining, it was shown that cells expressing high levels of the stromal stem cell marker, STRO-1, were more susceptible to ZOL-induced cytostasis and cell death, consistent with the greater proliferative potential of this population. Associated with this loss of STRO-1^+ cells was a concomitant increase in the proportion of cells, which exhibited a more differentiated phenotype. Molecular analysis revealed that the expression of the bone-associated matrix proteins bone sialoprotein and osteocalcin were significantly elevated in cultures treated with ZOL. Consistent with these observations, *in vitro* mineralisation studies showed that ZOL enhanced mineral formation in cultures from all donors, at concentrations in the range of 5-25 μM. Our studies therefore show that in addition to its effects on OC, ZOL also has direct effects on the proliferation and survival of OB-like cells *in vitro*. Our observations support the notion that ZOL is anabolic in bone by increasing the proportion of differentiated OB and enhancing the bone-forming activities of these cells.

M211

A Method to Separate Human Umbilical Vein Endothelial Cells (HUVEC) from Human Bone Marrow Stromal Cells (HBMSC) After Co-culture: Analysis of HUVEC Effects on HBMSC Differentiation. B. Guillotin*[1], F. Villars*[2], S. Pallu*[2], R. Bareille*[2], V. Conrad*[2], J. Amedee[2], O. Chassande*[1]. [1]INSERM U 443, Bordeaux, France, [2]INSERM U443, Bordeaux, France.

Osteogenesis relies on a balanced activity between bone forming cells (osteoblasts) in one hand and bone resorbing cells (osteoclasts) on the other hand, and occurs in striking interaction with angiogenesis. Furthermore, bone formation, remodelling and repair are at least partly regulated not only by growth factors and cytokines that are contained in the mircroenvironment of bone but also by cell-to-cell communication. Thus, numerous studies show that gap junctions, especially composed of connexin43 in bone, participate to the regulation of bone biology. This is why we have been interested for few years in the role of endothelial cells and connexin43 on the differentiation of osteoprogenitor cells. Indeed, our studies on primary cultured cells have shown for the first time that endothelial cells could likely participate to osteogenesis through gap junctions formed of connexin43 between endothelial cells and osteoblasts. Our purpose is now to eventually identify one signaling pathway connexin43-dependent involved in our culture model, and more particularly the function of Cbfa1 in this pathway. To assess the specific effect of HUVEC on osteoblastic gene expression in co-culture, we separated HUVEC from HBMSC after 1, 3, 8 and 24 hours of co-culture with magnetic beads coupled to a CD31 antibody. CD31 is a membrane marker expressed by HUVEC but not by HBMSC. Highly efficient separation is shown by quantitative measure of phosphatase alkaline activity in beads fraction that contains enriched HUVEC population and supernatant fraction that contains enriched HBMSC population. Also, RT-PCR was performed using total RNA extracted from these fractions to study Cbfa1 expression. Our results show a strong amplification of Cbfa1 cDNA in supernatant fraction but a very weak amplification of Cbfa1 in beads fraction. Thus, our data indicate that HUVEC and HBMSC are well separated into two homogenous populations after passage on anti-CD31 coupled magnetic beads. This method will now allow us to answer the following questions. First, are the expression and activity of Cbfa1 regulated in HBMSC or HUVEC in co-culture? Second, are expression and activity of connexin43 regulated in HBMSC or HUVEC in co-culture? Finally, does a signalling link exist between the activation of both connexin43 and Cbfa1?

M212

Lack of Connexin43 (Cx43) Causes Global Osteoblast Dysfunction. F. Furlan, J. Screen, J. Stains, R. Civitelli. Bone and Mineral Diseases, Washington University, St Louis, MO, USA.

Osteoblasts are highly coupled by gap junctions formed primarily by connexin43 (Cx43). Interference with Cx43 expression or function disrupts transcriptional regulation of osteoblast genes, and deletion of the Cx43 gene in the mouse causes skeletal malformations, delayed mineralization, and osteoblast dysfunction. Here, we studied the mechanisms by which genetic deficiency of Cx43 alters osteoblast development using calvarial or bone marrow stromal cells isolated from newborn Cx43 null (Cx43-/-) or wild type (Cx43+/+) mice. In calvarial cultures, the number of mineralized nodules and total mineralized area were lower in Cx43-null osteoblast compared to wild-type cells during the first 3 weeks in mineralization medium (b-glycerophosphate and ascorbic acid). However, after 4 weeks in culture, Cx43-/- cells reached the same degree of mineralization as did Cx43+/+ cultures. Accordingly, alkaline phosphatase activity, which peaks at around day 7 in normal calvarial or bone marrow stromal cell cultures, increased significantly in mutant cells only after 3 weeks, a 2-week delay. Similarly, Cbfa1 and type I collagen mRNA abundance (assessed by real time RT-PCR) was consistently lower in Cx43-/- cells during the first 2 weeks of culture, reaching the levels present in Cx43+/+ cells only after 12-15 days. Furthermore, basal levels of RANK-L mRNA were 3-fold lower in Cx43-/- calvaria or bone marrow stromal cells relative to Cx43+/+ cells whereas OPG mRNA was slightly increased, reflecting a poor support of osteoclastogenesis by Cx43 deficient cells. The number of TRAP-positive multinucleated cells formed in co-cultures with Cx43-/- calvaria cells was 5-fold lower compared to those formed in co-cultures with Cx43+/+ calvaria cells. While cell proliferation rates were similar in osteoblastic cells derived from calvaria of Cx43-null and wild type mice, spontaneous and camphothecin-induced apoptosis rates - assessed by caspase 3 expression - were 5-fold and 3-fold higher, respectively, in mutant compared to wild-type osteoblasts. Therefore, lack of Cx43 leads to a delay in the development of a fully differentiated and functioning osteoblasts. The defect is global, affecting all osteoblast gene products, including those that produce bone matrix and those involved in support of osteoclastogenesis. In addition to regulating gene transcription, Cx43 gap junctional communication favors osteoblast differentiation by inhibiting programmed cell death.

M213

Enhanced Marrow Adipogenesis and Bone Resorption in Estrogen-deprived Rats Treated with the PPARgamma Agonist BRL49653 (Rosiglitazone). M. Kneissel*, V. Sottile*, K. Seuwen*. Bone Metabolism Unit, Novartis Pharma AG, Basel, Switzerland.

Osteoporosis is characterised by loss of bone tissue and increased bone marrow fat content. Since osteoblasts and adipocytes originate from a common mesenchymal precursor cell, it has been proposed that osteoporosis might in part result from a switch of cell differentiation favouring adipogenesis. We tested this hypothesis by evaluating the effect of the thiazolidinedione BRL49653 (Rosiglitazone), a potent stimulator of adipogenesis acting through the nuclear hormone receptor PPARgamma, on bone tissue and marrow of intact and estrogen-deprived female rats. In a first step skeletally mature intact rats were treated for 8 weeks with 5, 10, or 20 mg/kg of BRL49653 or vehicle. Increased body weight and decreased plasma triglyceride levels confirmed the effectiveness of the treatment. No change in bone mass or fat marrow volume was observed as evaluated by DEXA, pQCT, and histomorphometry. However, the study of marrow cultures established at necropsy revealed a significantly higher responsiveness to adipogenic treatment of cultures established from the 10 mg/kg group compared to vehicle control. However, this adipogenic effect appeared disconnected from the osteogenic potential of these marrow cells, since mineral deposition under standard osteogenic stimulation remained evenly high. We then studied rats that had been estrogen-deprived by ovariectomy (OVX). Treatment with the 10 mg/kg dose for 12 weeks resulted in a significantly increased loss of tibial bone mass (+31% based on pQCT), compared to vehicle-treated OVX animals. Ex vivo DEXA measurements demonstrated that bone mass was also significantly reduced in the femur and lumbar spine of treated OVX animals compared to OVX controls. The tibiae were excised at necropsy and histomorphometry of the proximal metaphysis revealed that the fat marrow volume, which had increased 4.6-fold upon OVX compared to sham control, was increased more than 10-fold in the treatment group. Interestingly, osteoblast number was comparable in vehicle and BRL49653-treated OVX animals. Bone resorption parameters, however, were significantly increased in the treatment group (+27% osteoclast number, +30% eroded surface). Our data suggest that the thiazolidinedione BRL49653 did not lead to a measurable decrease in osteoblast number. However, it has the potential to induce marrow adipogenesis and to potentiate bone loss stimulated by estrogen deprivation. TZD-induced increase in sensitivity of marrow cells towards adipogenic signals has hence tangible consequences on the skeleton in a situation of imbalance, as created here by estrogen loss.

M214

Strontium (Sr) Impairs the In Vitro Osteoblast (OB) Differentiation and Hydroxyapatite Formation. S. C. E. Verberckmoes*, M. E. De Broe, P. C. D'Haese*. Nephrology - Hypertension, University of Antwerp, Wilrijk, Belgium.

Recent data from epidemiological studies in dialysis patients together with experimental findings in a chronic renal failure (CRF) rat model established a dose-related multiphasic effect of strontium (Sr) on the bone formation process. To confirm these in vivo findings an in vitro set-up, consisting of mineralizing primary OB cultures derived from 20 day old fetal rat calvaria, was applied. Several Sr concentrations (0.5, 1.0, 2.0, 5.0, 10, 20 and 100 µg/ml) were added to the cultures. Alkaline phosphatase (AP) and calcium (Ca) incorporation, used as an index for mineralization, were determined at various time points in the culture medium. At the end of the experiment, the protein profile was assessed in the medium using 2D-PAGE and the nodule formation (mineralized + unmineralized area) was quantified by means of a digital imaging system. Hydroxyapatite (HA) crystal quality was evaluated using X-ray diffraction (XRD) analysis. A significantly reduced nodule formation in the presence of an intact mineralization was found for the 0.5 and 1 µg/ml doses indicating a defective OB differentiation. No differences were noted for the 2 and 5 µg/ml doses. For the 20 and 100 µg/ml Sr doses a reduced mineralization was noted in the presence of an intact nodule formation. At these concentrations XRD ana1ysis revealed a significant distortion of the crystal lattice. The AP activity fully reflected the multiphasic pattern of the nodule formation while the Ca incorporation correlated well with the multiphasic pattern of the mineralized segments of the formed nodules. No variations in cell proliferation were found, as the total DNA content did not differ between the various groups. Northern blot analysis revealed Sr to interfere with the OB at the level of the mRNA synthesis of various phenotypic parameters. Differential analysis of the 2D-PAGE profile of control cultures versus cultures treated with 1 µg/ml Sr indicated 70 spots out of 250 to be significantly up-regulated and 49 spots to be significantly down-regulated (intensity ratio 1.5; $p<0.05$). Using the proposed in vitro model we confirmed the multiphasic effect of Sr on the bone formation previously shown in a CRF rat model. The presented data allow us to suggest that at low concentrations Sr interferes with the bone formation at the level of the cell differentiation. At high Sr concentrations the disturbed mineralization in combination with an intact nodule formation suggests a physicochemical interaction of the element with the hydroxyapatite formation.

M215

Comparison of Proliferation and Differentiation of Calvarial Osteoblast Culture Derived from Wild Type and Msx2-Deficient Mice. I. Marijanovic[1], M. S. Kronenberg[1], I. Erceg*[1], H. Chin*[1], I. Satokata*[2], R. Maxon*[3], R. Maas*[2], D. W. Rowe[1], A. C. Lichtler[1]. [1]Department of Genetics and Developmental Biology, University of Connecticut Health Center, Farmington, CT, USA, [2]Department of Medicine, Brigham and Women's Hospital and Harvard Medical School, Boston, MA, USA, [3]Department of Biochemistry and Molecular Biology, U.S.C. School of Medicine and Norris Cancer Center, Los Angeles, CA, USA.

Msx2 is a homeodomain-containig protein that has been shown to be involved in regulation of skeletal development. Msx2 protein is expressed in many tissues during different stages of development. Strong expression of Msx2 is found in cells at the extreme ends of the osteogenic fronts of the calvarial sutures. Msx2 knockout mice have defects of skull ossification and persistent calvarial foramen. Our previous studies in cultured chick calvarial osteoblasts suggest that Msx2 inhibits differentiation and stimulates proliferation. To extend these studies into a mammalian system we investigated the proliferation and differentiation of calvarial osteoblast from Msx2 knockout mice. For experiments we used 5-8 days old wild type, heterozygous and knockout animals derived from heterozygous breedings. Cells from calvariae (no sutures) from the three groups were plated at the same density and observed for differences in proliferation and differentiation. Proliferation rate was assessed by counting cell number, BrdU and CalceinAM labeling. Cell number at day 6 in homozygous culture was 20% lower than in wild type. At day 6 wild type culture had 21.6% , heterozygous 20.9% and homozygous 16.8% BrdU labeled cells. CalceinAM marks all living cells so scanning the entire well for fluorescence is a visual way of presenting cell number. Wild type cultures showed higher intensity of fluorescence than homozygous cultures. Differentiation of cell cultures was assessed by several methods. Von Kossa staining showed increased mineralization at later time points (day 14 - day 21) in homozygous cultures. Hybridization of total cell RNA to collagen and osteocalcin probes showed increased collagen message in homozygous knockout cultures when compared to the wild type and heterozygous cultures. After infecting cells with Col2.3 GFP retrovirus, which is induced when osteoblasts differentiate, we observed that GFP comes on earlier in homozygous culture marking more developing nodules. Cultures from heterozygous mice had an intermediate phenotype but were not significantly different from wild type. Based on our experiments we suggest that calvarial osteoblasts derived from Msx2 knockout mice have a lower rate of proliferation and demonstrate increased osteoblastic differentiation compared to cells derived from wild type mice.

M216

Dlx3, 5 and 6 May Have Redundant Effects On Bone Development. I. Marijanovic[1], M. S. Kronenberg[1], I. Erceg*[1], M. L. Stover*[1], W. B. Upholt*[2], A. C. Lichtler[1]. [1]Department of Genetics and Developmental Biology, University of Connecticut Health Center, Farmington, CT, USA, [2]Department of Biostructure and Function, University of Connecticut Health Center, Farmington, CT, USA.

Our previous studies have shown that retroviral overexpression of Dlx5 cDNA has a stimulating effect on chick calvarial osteoblast differentiation. Although Dlx5 knockout mice display significant defects in craniofacial skeletal development, the limbs and axial skeleton are relatively normal. This has led us to investigate the possibility that redundant function of other Dlx genes compensates for the lack of Dlx5. There are six Dlx genes (Dlx1, Dlx2, Dlx3, Dlx5, Dlx6 and Dlx7) and their expression is primarily found in regions undergoing differentiation where they function as homeodomain-mediated transcriptional activators. For our studies we have chosen Dlx6 and Dlx3. The Dlx5 and Dlx6 genes are localized in the same chromosomal locus and are regulated from the same intergenic region. It is reported that Dlx6 has the same expression pattern as Dlx5 but mRNA levels for Dlx6 are lower. Dlx3 is most similar to Dlx5 in terms of protein sequence. Its inactivation in mice resulted in placental failure and a human Dlx3 mutation is responsible for tricho-dento-osseus (TDO) syndrome which is characterized by abnormal hair, teeth and bone. We have detected endogenous Dlx3 mRNA in mouse calvarial osteoblasts and bone marrow stromal cell cultures, which suggests that Dlx3 may have a similar role in bone development as Dlx5. Dlx6 cDNA was amplified by RT-PCR from total RNA extracted from chicken long bone, cloned into an RCAS(A) avian retrovirus vector, and used to infect chick calvarial osteoblast cultures. The effect of Dlx6 overexpression was assessed by alkaline phosphatase and Von Kossa staining through time course of the culture. Von Kossa staining of Dlx6 overexpressing culture showed increased mineralization at a late time point compared to control. By Northern hybridization we showed that Dlx6 is overexpressed by the retrovirus and we observed an increase in mRNA levels of osteoblast differentiation markers such as collagen and osteocalcin compared with cultures infected with RCAS(A) alone. Dlx3 cDNA has also been cloned into an RCAS(A) retrovirus vector, and similar experiments will be performed. In conclusion our data show that Dlx3 is expressed in osteoblasts, and that Dlx6 has similar but less potent effects on osteoblast differentiation than has been previously shown for Dlx5.

M217

Analyses of Osteoblasts Lacking the Vitamin D Receptor. K. Sooy, M. B. Demay. Endocrine Unit, Massachusetts General Hospital, Harvard Medical School, Boston, MA, USA.

Vitamin D is the major steroid hormone that plays a role in mineral ion homeostasis. Its molecular actions are thought to be mediated by the vitamin D receptor (VDR). The development of VDR knockout mice has demonstrated an important physiological role for the VDR. These mice exhibit a variety of defects, including rickets and osteomalacia, which are evident at day 35. These defects can be prevented by normalization of mineral ion homeostasis via dietary means. However, the role of the VDR in bone formation is not completely understood. In order to reconcile the in vivo versus in vitro effects of the VDR on osteoblast development, we isolated calvarial osteoblasts from 3 day old wild type and VDR knockout mice. Osteoblasts isolated from VDR knockout mice form more mineralized matrix as assessed by alizarin red staining than those from wild type mice, with cultures from knockout mice containing 161± 1.4 nodules per 50,000 cells plated versus 44.5 ± 6.4 nodules for wild type mice. This trend of increased alizarin red positive nodules in knockout cultures was observed at all time points from day 18 to day 35 post plating, indicating that the VDR and $1,25(OH)_2D_3$ may play an inhibitory role in osteoblast differentiation or mineralized matrix formation. Studies were also undertaken to examine the effects of ablation of the VDR on bone marrow stromal cells. Mice were weaned at day 18 and fed a diet high in calcium, phosphorus and lactose to eliminate any effects due to hyperparathyroidism or abnormal mineral ion homeostasis. Osteoprogenitor differentiation was evaluated by examining alkaline phosphatase activity and mineralization (von Kossa staining) of nodules. There was a reduction in the number of alkaline phosphatase positive nodules in the VDR knockout mice (22.3 ± 2.5 per 1.5 x 10^6 cells plated versus 31.9 ± 2.3 for the wild type mice). However, there were no differences observed in the mineralization of the nodules isolated from wild type and VDR knockout mice, with 45 ±5% of alkaline phosphatase positive wild type cells being von Kossa positive, while 41 ± 9% of knockout cells were double stained. Further studies will be required to evaluate whether VDR ablation similarly affects other markers of differentiation in the osteoblasts that give rise to intramembranous and endochondral bone.

M218

Developmental Regulation of SOST Gene Expression in Osteogenetic Precursor Cells Derived from Fetal Mouse Cranial Tissues. Y. Ohyama*, Y. Maeda, A. Nifuji, M. Noda. Molecular Pharmacology, Medical Resarch Institute,Tokyo Medical & Dental University, Tokyo, Japan.

Bone morphogenetic proteins (BMP) play a pivotal role in growth and differentiation of skeletal cells. Several BMP inhibitors are expressed in skeletogenesis and are known to modulate intrinsic BMP signals. However, expression and regulation of these BMP inhibitors in osteogenic differentiation are not yet fully understood. To examine if BMP inhibitors function in embryonic osteogenesis, we investigated developmental regulation of BMP inhibitors' expression by using primary osteogenic cells derived from embryonic cranial tissues. We especially focused on SOST, a novel secreted protein, whose mutation causes sclerosteosis in human. At first, we characterized the embryonic osteogenic cells, which we obtained by sequential enzymatic digestion from 15.5dpc fetal mouse cranial tissue. We plated the cells at 10k/cm and added ascorbic acid (AA) and b-glycelophosphate (bGP) after reaching confluency (day 0) to induce differentiation into mature osteoblasts. We analyzed ALP enzymatic activity, osteocalcin (OC) mRNA expression and mineralized nodule formation. ALP level was very low on day 0, and peaked at day 7. We could not detected OC expression on day 0 by RT-PCR. OC expression was induced by the addition of AA and bGP and was increased at least up to day 14. Mineralized nodule formation appeared on day 14, suggesting that the immature cells differentiated into mature osteoblasts at this stage. Then, we examined if BMP inihibitors were expressed in these cell. At confluency, the cells express various BMP inihibitors such as chordin, tsg and gremlin. Expression of another BMP inhibitor, SOST, was observed at low level on day 0, and its level was increased in a time-dependent manner up to day 14 in parallel to OC expression, suggesting that SOST expression was enhanced as the ostogenesis proceeded. Finally, we examined the expression of SOST in fetal mouse embryos by in situ hybridization. In 14.5dpc embryos, SOST was expressed at high level in the central layer of cranial mesenchymal tissues. In summary, during embryonic osteogenesis, BMP inhibitors are expressed and SOST expression increased following osteogenic differentiation. Theses data suggest that embryonic bone formation requires proper levels of BMP activity.

M219

Direct Leptin Exposure and Mechano-stimulation of Human Osteoblastic Cells Promote Proliferation and Differentiation, While Inhibiting Apoptosis. J. O. Gordeladze[1], S. Reppe*[1], K. M. Gautvik[1], C. A. Drevon*[2], J. E. Reseland*[2]. [1]Institute of Medical Biochemistry, University of Oslo, Oslo, Norway, [2]Institute of Nutritional Research, University of Oslo, Oslo, Norway.

We have demonstrated the expression of leptin and its receptor in normal human osteoblasts (hOBs). Furthermore, we have shown that mechano-stimulation of hOBs enhance cell proliferation and de novo collagen synthesis. The present report demonstrates how hOBs and human stromal cells (hSCs) respond to leptin (100 ng/ml) exposure and to mechano-stimulation at 1200 µE. Leptin exposure and mechano-stimulation of hOBs stimulated proliferation, de novo collagen synthesis and mineralisation. Both treatments also enhanced expression of hOB specific differentiation markers (like Cbfa1, ALP and osteocalcin). Leptin also protected against retinoic acid-induced (100 nM) apoptosis, as estimated by DNA laddering patterns, bax-a and bcl-2 mRNA expression, as well as DNA-array analysis of death-associated proteins and transcriptional factors (Stratagene). Leptin facilitated transition of cultured osteoblasts into preosteocytes, as evidenced by a reduction in Cbfa1/CD44 mRNA expression ratio. Leptin also augmented the mRNA levels of both interleukin-6 (IL-6) and osteoprotegerin (OPG). Expression of leptin during hOB differentiation showed marked culture time and donor variation, however, leptin mRNA was markedly enhanced upon mechano-stimulation. Human SCs exhibited less susceptibility to leptin and mechano-stimulation, however, hSCs behaved more like hOBs upon priming with an osteoblast differentiating medium (containing calcitriol and cortisol). Thus, through several factors common to osteoblast and adipocyte differentiation (e.g. PPARg, C/EBPa, and SREBP) leptin may determine their entry into different functional stages, and holds the potential to sustain a certain number of optimally functioning osteoblasts in bone tissue.

M220

Mode of Administration of Human Parathyroid Hormone (hPTH) Determines its Opposing Effects on Osteoblast Growth and Function at the Cellular and Molecular Levels in MC3T3-E1 Osteoblast-like Cells. S. S. Lu[1], K. Yokoyama[2], R. Lindsay[3], A. Iida-Klein[4]. [1]Regional Bone Center, Helen Hayes Hospital, West Haverstraw, NY, USA, [2]Regional Bone Center, Hellen Hayes Hospital, West Haverstraw, NY, USA, [3]Regionl Bone and Clinical Research Centers, Helen Hayes Hospital, Columbia University, West Haverstraw, NY, USA, [4]Regional Bone Center, Helen Haye Hospital, West Haverstraw, NY, USA.

Intermittent administration of PTH exerts a potent anabolic effect on bone in humans and animals in vivo, while hyperparathyroidism in patients or continuous administration of PTH to animals results in active bone resorption, decreased bone formation and reduced bone mass. However, the effects of PTH on osteoblasts in vitro are controversial. To determine whether the mode of exposure of cultured cells to PTH affects osteoblastic cell growth and function, we examined the effects of intermittent and continuous exposures of mouse osteoblast-like MC3T3-E1 cells to PTH on cell proliferation and mineralization, as assessed by 5-bromo-2'-deoxyuridine (BrdU) incorporation and Von Kossa staining in the presence of ascorbic acid and b-glycerophosphate (bGP), respectively. In addition, we also examined mRNA expression of PTH type I receptor (PTH1R), osteoprotegerin (OPG), receptor activator of Nk-B ligand (RANKL), type I procollagen (Col I), and alkaline phosphatase (ALP) by RT-PCR and northern analysis. MC3T3-E1 cells were cultured in a-MEM, and hPTH1-34 (0.1-100 nM) was added, either continuously or by cyclic exposure for 6hr of each 48 hr-cycle. After 2 cycles of treatment (96 hr), continuous PTH inhibited cell proliferation in a dose-dependent manner by 11% (NS), 17 % ($p<0.05$) and 21 % ($p<0.01$) at 0.1, 10 and100 nM, respectively, while intermittent PTH stimulated cell proliferation by 13 % ($p<0.05$) at 0.1 nM. After 6 cycles(288 hr), continuous PTH inhibited cell mineralization by 95 % at 10 n M, while intermittent PTH stimulated cell mineralization by 2-fold at 10 nM. Continuous PTH (10 nM) completely suppressed gene expression of PTH1R, Col I and ALP (all $p<0.01$) and inhibited OPG expression by 34 % ($p<0.05$), but stimulated RANKL gene expression by approximately 2-fold. Conversely, intermittent PTH (10 nM)significantly increased gene expression of PTH1R, OPG, Col I and ALP with decreased RANKL expression. Thus, intermittent PTH in mouse osteoblast-like cells exhibited positive effects on osteoblast proliferation and function, while continuous PTH inhibited on in vitro osteoblast proliferation and function in MC3T3-E1 cells. The present data may explain in part the in vivo actions of PTH; PTH is anabolic when administered intermittently, while PTH is catabolic when administered continuously.

M221

LIF Differentially Regulates the Fate Choice and Differentiation Program of Adipocyte and Osteoblast Progenitor Cells In Vitro. D. Falconi[1], D. Kipp[2], J. Bodnar*[1], J. E. Aubin[1]. [1]Department of Anatomy and Cell Biology, University of Toronto, Toronto, ON, Canada, [2]Department of Nutrition, University of North Carolina at Greensboro, Greensboro, NC, USA.

Osteoblasts and adipocytes derive from a common mesenchymal precursor and their differentiation is often reciprocally affected by particular treatments in vitro and in vivo. We wish to understand how leukemia inhibitory factor (LIF) inhibits osteoblast differentiation stage-specifically in the rat calvaria (RC) cell model. Amongst genes we identified by differential display were four genes involved in lipid metabolism (low-density lipoprotein receptor related protein, Lrp; hormone-sensitive lipase, Lipe; STAT6; and hyaluronan synthase 2, HAS2) that were up-regulated by LIF specifically during the osteoblast inhibition-sensitive period. We therefore asked whether LIF acts, at least in part, by redirecting the fate of osteoprogenitors toward an adipogenic program. RC cells were cultured under osteogenic conditions (50 µg/ml ascorbic acid and 10 mM β-glycerophosphate) and with or without the PPARγ agonist BRL49653 (10^{-6}M). Mature adipocyte (sudan IV-positive lipid-containing cells) foci were induced in RC cells treated with BRL49653 alone, a condition that had no effect on the number of mineralized bone colonies (von Kossa-positive bone nodules), suggesting that osteo- and adipoprogenitors are recruited independently by this treatment. As expected, LIF (5 ng/ml) decreased the number of bone nodules formed, in the presence or absence of BRL49653. However, while LIF alone did not induce adipocytes, combined LIF and BRL49653 increased the number of adipocyte foci but those developing in the presence of LIF stained only faintly with sudan IV, suggesting that they contain immature adipocytes. The total number of adipocyte foci formed was lower than the number of bone nodules in untreated cultures, again suggesting that the adipocyte foci are recruited from committed preadipocytes independently from committed osteoprogenitors. To address this in more detail, we collected and analyzed RNA from discrete developing osteoblast colonies in LIF-treated RC cultures. Strikingly, many LIF-treated osteoblast colonies expressed both osteoblast and adipocyte markers (i.e., alkaline phosphatase, bone sialoprotein, osteocalcin, PPARγ and aP2). We conclude that LIF diverts the fate of at least some osteoprogenitors towards an adipogenic program but alone is not sufficient to induce adipocyte maturation. In addition, LIF blocks the maturation of committed preadipocytes in vitro, an effect dominant over the effects of the PPARγ agonist BRL49653 and consistent with the pro-cachexic effect of the LIF/IL-6 family of cytokines in vivo.

M222

Phenotypic Analysis of Osteoprogenitor (CFU-O) Recruitment, Self-Renewal and Differentiation in Response to Hormone Supplementation. K. A. Purpura*[1], P. W. Zandstra*[1], J. E. Aubin[2]. [1]Institute of Biomaterials and Biomedical Eng., Chemical Eng. and Applied Chemistry, University of Toronto, Toronto, ON, Canada, [2]Department of Anatomy and Cell Biology, University of Toronto, Toronto, ON, Canada.

Depending on concentration and exposure time, hormones such as parathyroid hormone (PTH) and glucocorticoids (e.g., dexamethasone (dex)) either stimulate bone formation or induce bone loss. To develop a greater understanding of these processes, 21 d. fetal rat calvaria (RC) cells obtained by sequential enzymatic digestion were plated at varying densities and maintained in αMEM with 10% FBS, antibiotics, 50 m µg/ml ascorbic acid, 10 mM β-glycerophosphate, and either vehicle control (0.11% ethanol), 10-9M PTH (1-34), or 10-8M dex. Osteoprogenitor cell self-renewal, proliferation and differentiation were functionally and phenotypically examined using the bone nodule/colony (CFU-O) assay and fluorescence activated cell sorting (FACS) analysis of alkaline phosphatase (ALP) and parathyroid hormone/parathyroid hormone related protein receptor (PTH1R). Serial passaging of untreated or hormone-treated RC cells showed that dex-treated cultures exhibited enhanced proliferative capacity compared to vehicle- or PTH-treated cells. CFU-O were detectable for 6-9 subcultures in both vehicle and dex, but a 10-fold expansion in nodules was observed in dex-treated cells re-plated in vehicle and a 6-, 8- or 45-fold expansion was observed for vehicle-, PTH-, and dex-treated cells respectively, re-plated in dex. Similar population cell doubling times (32.1 +/- 0.5 h) amongst the treatment groups indicated that none of the treatments provided a growth advantage. However, the differences in nodule output suggest that the proliferative rates of CFU-O may be different; different fractions of CFU-O may be recruited by the treatments, or a shift between self-renewal and differentiation of CFU-O may occur. To address this further, RC cells were fractionated by cell sorting into ALP-/PTH1R-, ALP+/PTH1R-, ALP-/PTH1R+ and ALP+/PTH1R+ populations. The frequency of CFU-O formation was determined in the sorted fractions and compared to unsorted control cultures. Our results indicate a hierarchy in bone formation capacity such that ALP+/PTH1R+ > ALP+/PTH1R- > ALP-/PTH1R+/- populations. PTH blocked nodule formation reversibly and dex stimulated nodule formation in all fractions. These data suggest that the balance between recruitment, self-renewal capacity and differentiation of CFU-O in RC populations is markedly affected by PTH and dex treatments and that fractionation on the basis of ALP and PTH1R expression is a useful method for marked enrichment of CFU-O.

M223

Lipophilic Statins Increase RANKL and OPG mRNA Levels in Human Osteoblast Cells. G. G. Reinholz[1], M. M. Reinholz*[2], B. Getz*[3], P. C. Roche*[2], T. C. Spelsberg[3]. [1]Department of Orthopedics, Mayo Clinic and Foundation, Rochester, MN, USA, [2]Division of Experimental Pathology, Mayo Clinic and Foundation, Rochester, MN, USA, [3]Department of Biochemistry and Molecular Biology, Mayo Clinic and Foundation, Rochester, MN, USA.

Several reports have suggested that lipophilic statins may modulate bone metabolism and osteoblast cell differentiation. We recently observed that mevastatin decreases human fetal osteoblast (hFOB) cell proliferation and mineralization in culture. Here we examine the effects of statins on bone morphogenetic protein-2 (BMP-2), receptor activated nuclear factor-kB ligand (RANKL) and osteoprotegerin (OPG) mRNA levels in hFOB and MG-63 cells using quantitative real-time PCR. Treatment of hFOB and MG-63 cells with mevastatin or simvastatin, but not pravastatin, increased BMP-2, RANKL and OPG mRNA levels. However, the induction of RANKL mRNA levels was greater than the induction of OPG mRNA resulting in a decrease in the ratio of OPG/RANKL mRNA. The mevastatin-induced increase in BMP-2, RANKL and OPG mRNA was dose-dependent and reversible with mevalonate co-treatment. Interestingly, treatment of hFOB cells with a polyclonal antibody directed against BMP-2 decreased basal RANKL mRNA levels and reversed the mevastatin-induced increase in RANKL mRNA. These results suggest that statins can increase RANKL mRNA levels through BMP-2 induction in human osteoblast cells. In order to determine if the effects of mevastatin on hFOB cell proliferation and mineralization are a result of increased RANKL expression, we treated hFOB cells with mevastatin with or without a polyclonal antibody directed against RANKL (RANKL pAb). As observed previously, mevastatin treatment decreased both hFOB cell proliferation and mineralization. Interestingly, treatment of hFOB cells with RANKL pAb alone increased hFOB cell proliferation and decreased mineralization, suggesting that endogenous RANKL inhibits hFOB cell proliferation and induces differentiation. RANKL pAb also partially reversed the anti-proliferative effect of mevastatin on hFOB cells but further reduced hFOB cell mineralization. Therefore, while the observed mevastatin-induced decrease in hFOB cell proliferation may be in part due to increased RANKL expression, the mevastatin-induced decrease in hFOB cell mineralization appears to be due to other unknown mechanisms. Taken together, these results suggest that the observed effects of statins on the skeleton may involve modulation of RANKL and OPG expression via BMP-2 and support a role for RANKL in the differentiation of osteoblast cells.

M224

Comparison of Bone Induction by Bone Marrow Stem Cells and Subperiosteal Injection of a Cell Growth Factor. B. S. Strates[1], F. Cordoba*[2], M. E. Nimni*[3]. [1]Department of Orthopaedics and Rehabilitation, University of Florida, Gainesville, FL, USA, [2]Departments of Surgery and Biochemistry, University of Southern California, Los Angeles, CA, USA, [3]Departmens of Biochemistry and Surgery, University of Southern California, Los Angeles, CA, USA.

In two preliminary works, we have reported on: (a) endochondral ossification post-injection of a cell growth factor subperiosteally and (b) bone induction by bone marrow (BM) cells. The purpose of this study was to examine the effects on bone induction and ossification of adding hydroxyapatite (HA) to a BM cell culture as compared to the effects of rhTGFß1 + HA. Stromal-enriched BM cells, obtained from long bones post-sacrifice of young-adult lab animals, were seeded at 1 x 106 cells/ml in 10 ml DMEM and cultured as described (Cordoba F et al: Orthop Trans JBJS 17-3:644, 1993-4). Adherent cells with HA were collected and implanted i.m. in filter chambers (MILLIPORE®, 0.3 µm pore diameter) in allogeneic animals. rhTGFß1 (Genetics Institute, Cambridge, MA) + HA were injected subperiosteally with 2 ml buffered saline as described (Kilagbian V et al: Orthop Trans JBJS:16-2:392, 1992-3). The former implants were excised at intervals up to 4 weeks and periosteal implants up to 10 weeks. Bone alkaline phosphatase (bAP) in cultured BM cells and excised implants was determined periodically up to 21 days and all implants were examined radiographically and histologically. In summary, implants of BM cells + HA exhibited bone induction with fibroblast-, chondroblast- or osteoblast-like cells peripherally and a bone-like cell aggregation centrally. Conversely, implants of rhTGFß1 + HA formed mature bone tissue through endochondral ossification. These findings may provide useful clues on the mechanism of bone induction and the bone repair process.

M225

Bone Marrow- Derived Adult Stem Cells: Gene Discovery, Skeletal Tissue Engineering and Stem Cells Plasticity. G. Pelled*, G. Turgeman*, Y. Zilberman, H. Aslan*, I. Bar*, Y. Gafni*, A. J. Domb*, Z. Gazit*, D. Gazit. Skeletal Biotech Lab, Hebrew University-Hadassah Medical Center, Jerusalem, Israel.

Bone marrow-derived stem cells (BMSCs) are multipotent cells that can replicate and differentiate into various lineages. We hypothesized that BMSCs could serve as a powerful tool in three major fields: 1) Novel gene discovery, 2) Skeletal gene therapy and tissue engineering and 3) stem cell plasticity. 1) Novel gene discovery: Adult Mesenchymal Stem Cells (AMSCs), isolated from murine bone marrow were treated in vitro with 17b Estradiol (E2). RNA samples were subjected to robotic high-throughput differential display polymerase chain reaction (RADE) and Gene Chip analysis. Bioinformatic analysis revealed that E2 up-regulated osteogenesis-related genes, and down-regulated adipogenesis-related genes. The novel ESTs are currently being utilized for the discovery of novel genes and their function. In addition, we are currently applying an advanced Gene Chip analysis on samples obtained from a unique in vivo system of engineered AMSCs. 2). Skeletal gene therapy and tissue engineering: We recently published that genetically engineered AMSCs, conditionally expressing rhBMP2, were utilized as a platform for skeletal gene therapy (Mol. Ther. 3:449-461. 2001, J. Gene Med. 3:240-251 2001). We have been able to imply engineered AMSCs for ex vivo skeletal tissue engineering. Based on a novel concept, a hybrid tissue was formed ex vivo, containing primitive capillary network and an osteogenic component originating from genetically engineered AMSCs. Two distinct polymeric scaffolds made of PLA filaments and Arabinogalactan- Chitosan micro-beads, were seeded with engineered AMSCs and endothelial cells, and cultured in a Synthecon rotary bioreactor. The engineered tissue demonstrated a hybrid structure in which osteogenic and angiogenic compartments are combined. Following the ex vivo dynamic culture, in vivo experiments are currently conducted in order to assess capillary and osteogenic tissue functionality. Our novel platform could lead to the ex vivo formation of vascularized matured bone tissue ready for implantation. 3) Stem cell plasticity: We have investigated whether the novel idea of stem cell plasticity could be relevant in skeletal biology. A primitive stem cell population from hematopoietic origin, known as Side Population (SP) cells, was isolated from bone marrow of transgenic mice expressing luciferase under human osteocalcin promoter. The osteogenic potential of these primitive stem cells, expressing luciferase, was shown in vivo. Our study indicates that SP cells can provide an unanticipated avenue for treating bone diseases.

M226

Colony Forming Efficiency of Circulating Skeletal Stem Cells (CSSCs) and Colony Forming Units-Fibroblasts (CFU-Fs) During Fracture and Repair. A. I. Leet, J. S. Lee, N. Ziran*, S. Shi*, S. A. Kuznetsov*, P. G. Robey. Csdb/nidcr, NIH, Bethesda, MD, USA.

Repair of long bone fractures has been well characterized to occur through a process reminiscent of endochondral bone formation during development. However, cell dynamics during this process have not been well defined to date. In this study, we analyzed the colony forming efficiency (CFE) of circulating skeletal stem cells (CSSCs) and colony forming units-fibroblasts (CFU-Fs) at various intervals following fracture in order to determine a potential time frame in which introduction of factors known to enhance osteogenic differentiation of skeletal stem cells may be of clinical benefit. Our model used 3 point fixation to create a closed tibial fracture in adult guinea pigs. After fracture, the animals were splinted for 2 and 6 hrs, and 1, 3 and 6 weeks. At the various intervals, the animals were lethally sedated, arterial and venous blood was sampled by cannulation, and the fractured tibia and opposite tibia were harvested for either histology or determination of CFU-F in the marrow. Blood and bone marrow were plated at a concentration of 10 5 nucleated cells per 75 cm2 flask and were stained for CFE after 11 days. There was no statistically significant difference in CFE of either CSSCs or CFU-F between the time points for either the fractured or opposite-side tibiae, although there was a trend towards an increase in CSSCs in blood of fractured animals, and in CFU-F in marrow of the fractured tibia. The circulating skeletal cells yielded two populations of cells: polygonal and fibroblastic. Counts of both phenotypic cell types were also similar in fractured and unfractured animals, and at different time points following fracture. Our studies indicate that during fracture healing, there is not a significant expansion of either the CSSC or CFU-F populations as had been previously suggested based on histological localization of proliferating cells, and points to other cell types in the marrow and periosteum that contribute to the proliferative phase of fracture healing.

M227

Identification of an Adult Stem Cell for the Osteoblast. E. Olmsted-Davis[1], F. H. Gannon*[2], K. J. A. Jackson*[3], H. D. Shine*[3], K. D. Hirschi*[3], M. K. Brenner*[3], M. A. Goodell*[3], A. R. Davis*[3]. [1]Pediatrics/CAGT, Baylor College of Medicine, Houston, TX, USA, [2]Orthopedic Pathology, Armed Forces Institute of Pathology, Washington, DC, USA, [3]Center for Cell and Gene Therapy, Baylor College of Medicine, Houston, TX, USA.

The purpose of this study was to determine if primitive adult stem cells underlie the production of osteoblasts. Accordingly the "side population" (SP) cells of murine bone marrow were isolated from C57Bl/6-Rosa-Ly5.1 mice based upon their unique ability to efflux Hoechst 33342 dye and transplanted into lethally irradiated C57Bl/6-Ly5.2 mice. Four weeks after transplantation, the percentage engraftment in bone marrow was determined by use of the β-galactosidase marker in the SP cells. Engraftment was typically greater than 80%. Animals then either 1.) remained untreated 2.) were subjected to cranial injury or 3.) were induced to form heterotopic bone in muscle. Thereafter, the long bone of the untreated animals, the calvarium of the injured animals, and the heterotopic bone formed in the animals receiving transduced cells were analyzed for the presence of the β-galactosidase marker in the newly formed bone. In each case the marker was found in osteoblasts as defined by co-staining with the osteoblastic marker osteocalcin. These results indicate that osteoblasts arise from SP cells in each of the three model systems studied. During normal remodeling, osteoblasts in newly formed woven bone rather than osteocytes in lamellar bone were derived from SP cells. In the cranial injury model, osteoblasts derived from SP cells were found at the site of injury.

M228

Perivascular Niche of Postnatal Mesenchymal Stem Cells in Human Bone Marrow and Dental Pulp. S. Shi*[1], P. Bianco[2], P. Gehron Robey[1], S. Gronthos*[3]. [1]Craniofacial & Skeletal Diseases Branch, NIDCR, National Institutes of Health, Bethesda, MD, USA, [2]Dipartimento di Medicina Sperimentale e Pathologia, Universita' La Sapienza, Roma, Italy, [3]Division of Haematology, Institute of Medical and Veterinary Science, Adelaide, South Australia, Australia.

Stem cell populations have been identified in adult bone marrow and dental pulp that upon in vivo transplantation are capable of regenerating the bone and its stroma, and dentin-pulp-like structures, respectively. The maintenance and regulation of these normally quiescent cells is tightly controlled by the local micronenvironment, however, little is known about the anatomical niches that these cells occupy. In this study, we sought to identify these niches using STRO-1, which has previously been shown to recognize bone marrow stromal stem cells (BMSSCs) and dental pulp stem cells (DPSCs). By immunohistochemistry, STRO-1 was found to localize to stromal elements in marrow and to perivascular cells not only in dental pulp, but in other tissues as well. Based on this perivascular localization, freshly isolated STRO-1 positive BMSSCs and DPSCs were tested for expression of the smooth muscle antigens known to be expressed by pericytes (alpha-smooth muscle actin, MUC-18 (CD146) and pericyte-associated antigen, 3G5) by immunohistochemistry, FACS and/or immunomagnetic bead selection. Both BMSSCs and DPSCs expressed alpha-smooth muscle actin and MUC-18, while only DPSCs expressed 3G5. These results strongly suggest that these stem cells are, in fact, pericytes. The finding that BMSSCs and DPSCs share a common perivascular niche, regardless of their diverse ontogeny and developmental potentials, may have further implications in understanding the factors that regulate the formation of mineralized matrices and other associated connective tissues. Furthermore, the data implicates pericytes of other tissues as the source of stem cells that are induced to form mineralised tissue either by addition of exogenous factors or through disease processes.

M229

Oxysterols Promote Osteoblastic and Inhibit Adipogenic Differentiation of Marrow Stromal Cells: Possible New Anabolic Molecules. F. Parhami[1], D. Shouhed*[1], Y. Tintut*[1], T. J. Hahn[2], L. L. Demer*[1]. [1]Medicine, UCLA, Los Angeles, CA, USA, [2]West L.A. VA Medical Center, Los Angeles, CA, USA.

Osteoporosis is still a major cause of morbidity and mortality and is mainly treated by agents that interfere with osteoclastic bone resorption. However, osteoporosis also involves decreased bone formation as a result of reduced osteoblastic cell number and bone forming activity. The mechanism(s) underlying these changes in cellular profile and function in osteoporosis is not clear. We recently reported that the cholesterol biosynthetic pathway of marrow stromal cells (MSC) is important in their osteoblastic differentiation, as demonstrated by the inhibitory effects of HMG-CoA reductase inhibitors, which could be reversed by mevalonate. In the present study we identify several oxysterols as possible products of the cholesterol biosynthetic pathway that are important in mediating osteoblastic differentiation of MSC. Oxysterols are formed by oxygenation of cholesterol in part through the actions of cytochrome P450 enzymes. M2-10B4 (M2) mouse marrow stromal cells undergo osteoblastic differentiation in an osteogenic medium containing fetal bovine serum, ascorbate and ß-glycerophosphate. Treatment of M2 cells with the oxysterols 22(R)-, 22(S)-, and 20(S)-hydroxycholesterols (1-10 μM) significantly enhanced alkaline phosphatase activity, an early marker of osteoblastic differentiation, as early as 2 days post-treatment, and with relative potencies: 20(S)>22(S)>22(R). This enhancement was between 2-10 fold and was persistent up to 12 days. After 10 days of treatment with the oxysterols, mineralization, a late marker of osteoblastic differentiation, was also enhanced 2-5 fold. In contrast, 7-ketocholesterol (1-10 μM) did not have these effects. Furthermore, two other products of the cholesterol biosynthetic pathway, farnesol and geranylgeraniol had no effect or an inhibitory effect, respectively, on markers of osteoblastic differentiation. Osteoporosis is also characterized by increased marrow adipocytes at the expense of osteoblastic cells, and marrow stromal cells undergo adipogenic differentiation in the presence of PPAR-gamma agonist troglitazone. Interestingly, the osteoinductive oxysterols also inhibited troglitazone-induced adipogenesis of M2 cells. Oxysterol-mediated stimulation of osteoblastic bone formation and inhibition of adipogenesis of progenitor cells are potential new strategies for prevention and treatment of osteoporosis.

M230

Evidence for the Maturation-Dependent Expression of an Osteoclastogenic Phenotype in Human Osteoblasts. G. J. Atkins*[1], A. C. W. Zannettino*[2], P. N. Kostakis*[1], B. Pan*[2], A. Farrugia*[2], A. Evdokiou*[1], D. M. Findlay[1]. [1]Orthopaedic Surgery and Trauma, University of Adelaide, Adelaide, Australia, [2]Haematology, IMVS, Adelaide, Australia.

Normal human bone-derived cells (NHBC) are a mixed population of osteoblast (OB)-like cells, separable on the basis of their stage of osteogenic differentiation using the cell surface markers STRO-1 and alkaline phosphatase (AP) (Gronthos et al, J Bone Miner Res 14:47, 1999). We compared the cell surface expression of STRO-1 and AP with that of molecules central to osteoclast (OC) formation, namely RANKL and OPG, to examine the dual functionality of the human osteoblastic stromal cell. NHBC were sorted, using fluorescence activated cell sorting (FACS), into STRO-1bright and STRO-1dull populations. The expression of RANKL and OPG mRNA, as well as the cell surface RANKL expression, was examined in each population in response to 1,25(OH)2vitaminD3 (vitD3) and dexamethasone (DEX). STRO-1bright and STRO-1dull populations were both positive for RANKL mRNA and cell surface RANKL expression. While STRO-1 positivity did not correlate with the basal level of RANKL or OPG mRNA, vitD3 treatment of these populations resulted in an increase in the RANKL:OPG mRNA ratio to a greater extent in the STRO-1bright cells than the STRO-1dull cells. This suggests a greater sensitivity of immature OB to pro-osteoclastogenic factors. Furthermore, vitD3 treatment increased the percentage of immature (STRO-1+/AP-, STRO-1+/AP+) populations over a culture period of 6 days. DEX treatment alone had little effect on the expression of RANKL, downregulated OPG mRNA, and had a profound effect on the maturation of unfractionated NHBC, as indicated by an increase in the percentage of cells expressing AP. The RANKL:OPG mRNA ratio was associated negatively with an increase in the overall maturation of the NHBC cultures in response to DEX. To investigate the effect of hemopoietic cells on human osteoblasts, human PBMC were incubated in co-culture with NHBC. Using the fluorescent dye, CFSE, to label NHBC, we found that human PBMC promoted the proliferation and maintenance of an immature NHBC phenotype. In addition, coculture provoked a vigorous release of PGE2, synthesis of IL-6, and an increase in the RANKL:OPG mRNA ratio that was indomethacin-sensitive. Together, our findings are consistent with the hypothesis that immature OB are more responsive to pro-osteoclastic stimuli than mature OB, and that some of these signals derive from the hemopoietic element in bone. Our data suggest that the dual functionality of OB in supporting OC formation or forming bone is a function of the maturation state of the same lineage of cells.

M231

The Role Of Bone Marrow Adipocytes In BMP-2-Induced Bone Resorption And Formation. J. M. Owens, K. McDermott*, J. Li, J. Wozney, H. Seeherman. Musculoskeletal, Wyeth Research, Cambridge, MA, USA.

Recombinant human BMP-2(rhBMP-2) stimulates significant transient bone resorption, followed by dramatic bone formation in a non-human primate core defect model (Seeherman et al., ORS, 1998 and 2000). Histological analysis indicates rhBMP-2-induced bone resorption is associated with fatty marrow in this model. RhBMP-2-induced de-novo intraosseous bone formation is often initiated in narrow gaps between marrow adipocytes. Numerous spindle cell condensations with associated osteoid matrix production and mineralization are observed in these areas. These findings prompted an investigation to determine whether adipocytes play a role in the response to rhBMP-2. We treated the well-characterized 3T3-L1 mouse pre-adipocyte cell line with 10-8 M 1,25(OH)D3 and 10-6M prostaglandin E2 (PGE2) for 2 days, and observed upregulation of RANKL expression, the factor required for osteoclast differentiation. Addition of 100 ng/ml rhBMP-2 further increased expression of RANKL in these cells. We also examined if rhBMP-2 has similar effects on mature adipocytes. 3T3-L1 cells differentiated into mature adipocytes, under appropriate conditions. Maturation into adipocytes was confirmed by Oil Red O staining. These cells also expressed RANKL, upon stimulation with 1,25(OH)2D3 and PGE2, at levels comparable to those in pre-adipocytes. The addition of 100 ng/ml rhBMP-2 further upregulated expression of RANKL. These results indicate that rhBMP-2 can act on both pre- and mature-adipocytes to increase expression of RANKL which stimulates osteoclastogenesis. We also found that rhBMP-2 suppressed formation of mature adipocyte colonies as assessed by Oil Red O staining. This suggests that rhBMP-2 may block differentiation of adipocytes and/or promote their de-differentiation. Since adipocytes and osteoblasts are derived from common progenitor cells, 3T3-L1 cells were examined for expression of an osteoblastic marker, alkaline phosphatase (ALP). 3T3-L1 cells demonstrated minimal levels of ALP activity. Interestingly however, treatment of 3T3-L1 cells with 100 ng/ml rhBMP-2, in the presence of 1,25(OH)2 D3 and PGE2 for 7 days upregulated ALP activity by 5 fold over control levels. The physiological significance of this rhBMP-2-induced upregulation of ALP in adipocytes is unknown, but the data may imply that adipocytes are involved, either directly or indirectly, in the appearance of numerous osteoblastic cells in our non-human primate core defect model. These results provide further evidence that the in vivo induction of bone resorption and bone formation, stimulated by rhBMP-2, is a complex process that may involve interactions between multiple bone marrow cell types, including adipocytes.

M232

The Isoflavone Genistein Differentially Regulates Osteogenic- and Adipogenic Differentiation of Human Bone Marrow Stromal Cells. M. Heim*[1], O. Frank*[2], N. Sochocky*[1], A. Barbero*[2], G. Kampmann*[1], I. Martin*[2], P. Fuchs*[1], P. Weber[1], W. Hunziker[1], I. Bendik*[1]. [1]Human Nutrition and Health, Roche Vitamins Ltd., Basel, Switzerland, [2]Dept. of Surgery, Research Division, University of Basel, Basel, Switzerland.

There is evidence that dietary phytoestrogens like the isoflavone genistein (Gen) act similarly to17ß-estradiol (E2) by exerting some of their bone-sparing effects via osteoblasts. Currently, not much is known about the function of these estrogens during osteogenic/adipogenic commitment of mesenchymal precursor cells. Therefore, we investigated the transcriptional effects of Gen and E2 on several osteogenic and adipogenic marker genes at various stages of differentiation. Bone marrow samples from six healthy premenopausal donors were expanded with dexamethasone/bFGF. Subsequently, the bone marrow stromal cells (BMSC) were differentiated in osteogenic medium. For the transcriptional profiling the cells were stimulated with DMSO (vehicle), 10nM Gen, 1µM Gen and 10nM E2. Total RNA was harvested at days 3, 7, 11, 15 and 18 postconfluence and reverse transcribed to cDNA. The cDNA samples were tested in multiplex TaqMan real-time quantitative RT-PCR assays. We have previously shown that osteogenic commitment and maturation is associated with the transcriptional activation of BSP-2, osteopontin and BMP-2. These markers were not significantly changed after treatment with Gen or E2, nor were the mRNA levels of other osteoblast markers such as cbfa-1, osteonectin, osteocalcin or collagen type 1 changed. Only alkaline phosphatase mRNA was observed to increase at day 18 of osteogenic differentiation after estrogenic treatment. Interestingly, the expression of OPG and TGFbeta1, which regulates the coupling between osteoblasts and osteoclasts, was up-regulated by Gen and E2 starting from day 11. Furthermore, we showed during the differentiation timecourse that the early adipogenic transcription factors PPARgamma and C/EBPalpha were progressively down-regulated. This suppression was more prominent in the presence of Gen or E2. Using dexamethasone and insulin, BMSC were differentiated to adipocytes and mRNA levels of several adipocyte markers were determined at day 21. Gen and E2 had strong effects on late adipocyte expression markers, whereas the PPARgamma and C/EBPalpha were only mildly affected at this stage. Morphologically, the adipogenic cultures treated with the estrogenic compounds had lower numbers of adipocytes with smaller lipid droplets. Thus, our results give evidence that the soy isoflavone genistein like the natural hormone positively favours the BMSC commitment towards the osteogenic lineage.

M233

Adipose Derived Adult Stem (ADAS) Cells Differentiate into Bone Synthesizing Osteoblasts In Vivo. K. C. Hicok[1], Y. Zhou*[2], Y. Pucilowska*[2], Y. Halvorsen*[1], L. F. Cooper[2], J. M. Gimble[1]. [1]Research, Artecel Sciences Inc, Durham, NC, USA, [2]Department of Prosthodontics, University of North Carolina, Chapel Hill, NC, USA.

The presence in bone marrow of multi-potential cells capable of osteoblastic differentiation is now well established. For reasons of accessibility and low abundance, these cells are also sought in other more "accessible" tissues. Adult subcutaneous fat tissue is an excellent and abundant source of multi-potent cells. In vitro, adipose-derived adult stem (ADAS) cells express bone marker proteins including alkaline phosphatase, type I collagen, osteopontin, and osteocalcin and produce a mineralized matrix as shown by alizarin red staining. In this study, ADAS cell ability to form bone in vivo was determined. ADAS cells isolated from liposuction waste of two different donors and a control osteoblastic cell line, hFOB 1.19, were expanded for 1 week in either DMEM: F12 plus 10% (v/v) FBS or in this media plus an osteoinductive cocktail (10 nM 1,25 dihydroxy-vitamin D_3, 10 nM dexamethasone and 50 µg/ml ascorbic acid). 3 x 10^6 cells were loaded onto either hydroxy-apaptite/ tricalcium phosphate (HA/TCP) cubes or the collagen/ HA/TCP composite matrix, Collagraft®, and were implanted subcutaneously into SCID mice. After 6 weeks, implants were removed, fixed, demineralized and sectioned for hematoxylin and eosin staining. Bone formation was observed in 75% of HA/TCP implants loaded with ADAS cells from both donors. Only 17 % of Collagraft implants were positive for the presence of bone matrix. While 50% of HA/TCP implants loaded with hFOB 1.19 cells formed bone, when Collagraft was loaded with hFOB 1.19 cells, intermatrix spaces displayed a high degree of adipose tissue formation. Immunostaining of serial sections for human nuclear antigen (HNA) demonstrated that cells embedded within and lining regions of bone were of human origin. Little or no bone formation was observed in the control HA/TCP or Collagraft matrices without cells. In summary, the data demonstrates the ability of ADAS cells to form bone matrix in vivo. Because of their abundance and accessibility, ADAS cells may provide an important and renewable source of osteoblasts for tissue engineering based therapeutics of bone injury and disease.

Disclosures: ***K.C. Hicok****, Artecel Sciences Inc. 3.*

M234

Tumor Necrosis Factor Signaling Effects Marrow Stromal Cell Recruitment Into the Osteogenic Lineage. G. L. Barnes, C. Edgar*, K. Hebert*, L. C. Gerstenfeld. Department of Orthopaedic Surgery, Boston University Medical Center, Boston, MA, USA.

Tumor Necrosis Factor alpha (TNFa) is one of the major pro-inflammatory cytokines and has been demonstrated to be an important mediator of bone healing. We have previously demonstrated that TNFa receptor deficient mice (p55-/- /p75-/-) exhibit delayed bone healing and that the delay in healing is primarily due to a defect in removal of the calcified cartilaginous callus. However, examination of these animals also demonstrated a marked absence of the typical intramembranous bone formation that normally occurs on the periosteal surface adjacent to the fracture site in response to the trauma of fracture. In order to independently examine the TNFa effect on direct bone formation, we utilized a bone marrow ablation model system in which repair occurs solely by intramebranous bone formation. TNF-a receptor deficient animals display delayed intramembranous healing in this bone marrow ablation model system. These data suggest that in the absence of TNFa signaling fewer osteogenic precursor cells are present or that these cells are deficient in their response to the inductive signlas directing the induction of osteogenic differentiation. To examine these deficiencies in the absence of TNFa signaling, we examined osteogenic differentiation in a Marrow Stromal Cell (MSC) culture system. Comparison of osteogenesis in MSC cultures from wild type and TNFa receptor null animals demonstrated 50-60% fewer mineralized nodules in the absence of TNFa signaling. This data supports the conclusion that in the absence of TNFa signaling there is a diminished recruitment of mesenchymal stem cells into the osteogenic lineage. In correspondence with the decreased number of osteogenic cells in the TNFa receptor deficient cultures, we observed a decrease in the expression of several osteoblast related matrix genes including osteopontin, bone sialoprotein and osteoclacin (OPN, BSP and OC, respectively). No expression of chondrogenic associated genes, including type II and X collagen, was observed suggesting chondrogenesis does not occur in these cultures. Comparison of the BMP profiles between wild type and TNFa defiecient cultures demonstrates several unique alterations in the BMP profiles of the marrow stromal cells in the absence of TNFa signals including decreased levels of BMPs 1, 2, 3 and 8A and increased expression of BMPs 3B and 5. Our data demonstrate that in the absence of an intact TNFa signaling system fewer mesenchymal stem cells are recruited into the osteogenic lineage and suggest that this decrease may be related to alterations in the expression of specific BMPs.

M235

Characterization of Autologous Rabbit Bone Marrow Stromal Cells for Use in Bone Tissue Engineering. W. Huang, B. Carlsen, G. Rudkin*, M. Berry*, K. Ishida*, D. T. Yamaguchi, T. A. Miller*. VAGLAHS, Los Angeles, CA, USA.

In the search for a synthetic bone graft substitute (BGS) that will be useful in the repair of craniofacial defects, we have explored using autologous rabbit bone marrow stromal cells to establish three-dimensional (3-D) cell cultures on biocompatible scaffolds. Bone marrow was harvested from the iliac crest and nucleated adherent stromal cells were isolated. The isolation technique yielded 80% alkaline phosphatase positive colonies without rhBMP-2 treatment. Unlike human bone marrow stromal cells, rabbit cells showed cessation of growth after three passages in vitro. Osteogenesis, as indicated by alkaline phosphatase activity and mineralization, was significantly enhanced by rhBMP-2. Treatment with rhBMP-2 resulted in a sigmoidal dose response curve with optimal alkaline phosphatase activity at a dose of 50 ng/ml rhBMP-2. Time course studies with rhBMP-2 showed a detectable increase in alkaline phosphatase activity occurred at day 8, and the activity increased steadily through day 16. Mineralization studies, likewise, showed an increase in mineral deposition by von Kossa stain after rhBMP-2 treatment. Interestingly, mRNA level of osteopontin exhibited a significant decrease in first three days of rhBMP-2 treatment and remained low in a course of 2 weeks. Osteonectin, however, remained unchanged during rhBMP-2 treatment. TGF-beta1 exhibited an inhibitory effect on cell growth by cell count studies. Using autologous bone marrow stromal cells, we then established an in vitro 3-D cell culture system, in which cells were cultured within a poly(lactide-co-glycolide) based scaffold. The scaffold is porous, moldable, and absorbable at a rate similar to bone formation when implanted in vivo. Stromal cells were able to attach and proliferate on the surface area inside and outside of the scaffolds. Differentiation of marrow stromal cells was highly responsive to the BMP-2 treatment as indicated by the amount of collagen deposit detected by Masson's Trichrome stain. These cellular scaffolds will be tested in rabbits for their ability to heal a critical-sized cranial defect.

M236

HGF and SCF Support Proliferation of Human Osteoclast Precursors *In Vitro*. H. C. Blair, R. Bu, J. I. Oakley*, S. E. Kalla*. Pathology and Physiology & Cell Biology, University of Pittsburgh, Pittsburgh, PA, USA.

CSF-1 and RANKL are sufficient for osteoclast differentiation. However, osteoclast numbers vary, so a mechanism to expand preosteoclasts must exist. HGF (met ligand) and SCF (kit ligand) stimulate pathways overlapping with CSF-1 and increase osteoclasts in marrow cultures. We hypothesized that HGF or SCF support osteoclast expansion. We compared effects of HGF, SCF, and CSF-1 on growth of preosteoclasts from human blood. Monocytes were recovered on ficoll and purified by CD14 selection (MACS, Miltenyi Biotec). These were plated in DMEM, IL-1β, and IL-6, 10 ng/ml each and serum. This was supplemented with HGF, SCF, or CSF-1, 10 ng/ml, for 10 days. In CSF-1, few cells were nonadherent by 2 d, and proliferation was insignificant. With HGF, ~50% of harvested cells were nonadherent and ~30% were nonadherent with SCF. In SCF or HGF, nonadherent cells grew colonies of 4-~64 cells. Expansion of nonadherent cells from d 2- 10 was ~10 fold in SCF (~5 to >20, n=10) and ~30 fold, in HGF (n=6), although CD14 cells were limited to ~5-6 cell division cycles under conditions tested. In either case, nonadherent cells replated in CSF-1 attached and expressed α-naphthyl acetate esterase. Flow cytometry indicated that the nonadherent cells expressed monocytic markers CD11, CD34, and CD64. Occasional cells with blastic phenotype were seen, <3%. IL-6-R increased nonadherent cells ~50% at 10 days with SCF. IL-3, IL-11, GM-CSF, and 1,25 dihydroxyvitamin D augmented osteoclast differentiation but did not affect colony growth. SCF effects were intermediate between HGF and CSF-1; after four weeks with SCF, ~50% of the cells attached and formed giant cells with weak osteoclast-like phenotype, but very low adherence (<3%) and maturation (TRAP, cathepsin K, or acid lakes) were seen in HGF. However, when nonadherent cells from HGF media were replated on bone in media with TNFα or RANKL and CSF-1, osteoclastic features developed. After 28 d, adherent cells expressed TRAP, with strong secretion onto bone, and produced pits on the dentine slices. To confirm the effect of HGF, nonadherent cells grown in basal medium with SCF were re-sorted using monocytic and size markers and re-plated in SCF or HGF. HGF induced the formation of colonies > 8 cells after culture in SCF, but SCF did not allow re-growth. Re-grown cells also developed osteoclast markers when HGF was removed and CSF-1 plus RANKL was added. These results indicate that HGF and SCF stimulate the proliferation of osteoclast precursors but are not sufficient for osteoclast maturation. HGF had a greater effect on cell number, and SCF weakly replaced CSF-1 in differentiation. These effects appeared to be independent of other factors that augment osteoclastic differentiation.

M237

Nitric Oxide Regulates Acid Secretion Bidirectionally in Human Osteoclasts. G. Hao*[1], Y. N. Li[1], S. E. Kalla*[1], J. I. Oakley*[1], M. Zaidi[2], H. C. Blair[1]. [1]Pathology and Physiology & Cell Biology, U Pittsburgh, Pittsburgh, PA, USA, [2]Medicine and Geriatrics, Mount Sinai School of Medicine, New York, NY, USA.

Nitric Oxide (NO) is an important bone signal, produced by stimulated osteoblasts or macrophage-family cells including osteoclasts. Most NO effects are mediated by the cGMP dependent protein kinase. However, variable and contradictory effects of NO on osteoclasts have been noted, some of which may be related to mixed cell populations. We investigated effects of NO on osteoclasts using CD14-selected circulating monocytes expanded in vitro using a cytokine cocktail, then replated with bone, CSF-1, and RANKL. These cells were devoid of mesenchymal or osteoblastic cells, and express cathepsin K and TRAP, and form acid lakes and pits on bone. These cells were exposed to (±)-S-nitroso-N-acetylpenacillamine (SNAP), an NO donor with a long half life, at concentrations from 3 to 100 μM for periods from zero to 24 hours, monitoring effects on osteoclastic acid secretion using Lysotracker red DND (Molecular Probes, Eugene, OR). Effects on G-kinase were evaluated by anti-kinase antibody binding visualized with Alexafluor 488, and osteoclastic attachment was studied using actin labeling with Alexafluor-568 phalloidin. Cell survival was examined by annexin V binding. We found that at 3 μM SNAP, acid lake intensity decreased within 10 min to near zero, while at concentrations 30-100 μM the effect abruptly switched to increase in acid secretion that lasted 30-60 min. Over longer times (60 min-24 h), at 3 μM, the cells retained other characteristics, but surprisingly, at 100 μM, SNAP, strong acid secretion faded and osteoclast attachment was lost as demonstrated by loss of actin rings and podocytes, which correlated with redistribution of cGMP-dependent kinase from cytoskeletal and cytoplasmic compartments to granular cytoplasmic and nuclear labeling, followed by changes consistent with apoptosis. Time courses showed that cells survived 24 hours in 0-10 μM SNAP, while apoptosis occurred in 30-100 μM SNAP. We conclude that the response of human osteoclasts to NO is distinctly variable, with inhibition of acid secretion at low concentrations, while at higher concentrations NO caused strong acid secretion, but prolonged NO exposure at high concentrations caused redistribution of actin and G-kinase including strong nuclear labeling, followed by cell death. Our findings show that, in cultures without mesenchymal cells, NO at low concentrations inhibits osteoclast acid secretion, possibly a mechanism for osteblastic regulation of osteoclasts by diffusion of NO. In constrast, high NO concentrations, which might result from autocrine NO, increase acid secretion but are proapoptotic if maintained.

M238

Effects of Extremely Low Frequency Pulsed Electromagnetic Field on Osteoclast Formation and Activity. C. Shih[1], W. H. Chang*[2], P. Chu[3]. [1]Biology and Anatomy, National Defense Medical Center, Taipei, Taiwan Republic of China, [2]Biomedical engineering, Chung-Yuan University, Chung Li, Taiwan Republic of China, [3]Nephrology, Tri-Service General Hospital, Taipei, Taiwan Republic of China.

Treatment of osteoporosis has been focused on drug therapies, such as estrogen, calcitonin, bisphosphonates. Alternatives such as physical stimuli are applied to treat osteoporosis whereas cause no adverse effects to other tissues. Previous studies have demonstrated the efficacy of electromagnetic fields in treating and preventing ununion fractures, failed arthrodeses, disuse osteopenia, and osteoporosis. Although there are growing evidences showed that extremely low frequency pulsed electromagnetic fields (ELF-PEMF) could exert significant effects on bone, the effects and possible mechanism of ELF-PEMF on osteoclasts are still not well known. Thus, the purpose of this study was to investigate the effects of ELF-PEMF on osteoclast formation and activity and the underlying mechanism using mouse bone marrow culture system. Bone marrow cells($1x10^6$ cells/well) isolated from 8 week-old ICR male mouse tibiae and femurs were cultured in 10% a-MEM with Vitamin D_3 (10 nM) and prostaglandin E_2(1 000 nM). Multinucleated cells satisfied major criteria of osteoclast, such as TRAP activity, calcitonin receptor, cAMP production in response to salmon calcitonin and the ability to form resorption pit. Secretions of inter-leukin-1, tumor necrosis factor(TNF) were assayed using enzyme-linked immunosorbent assay. TRAP-positive osteoclast formation and activity were significantly enhanced($p<0.05$) in cultures exposed to 0.8 mv/cm electric field and significantly suppressed when exposed to 0.2 mv/cm. In addition, IL-1 and TNF secretion were significantly increased in 0.8 mv/cm and decreased in 0.2 mv/cm as compared to the controls. There was high correlation between osteoclast formation and amount of cytokine secretion. The results of this study demonstrate that ELF-PEMF could enhance and suppress osteoclast formation and activity depending on induced electric intensity. In addition, cytokine secretion may play an important role between osteoclast formation and PEMF exposure.

Disclosures: ***C. Shih****, National Defense Medicak Center 3.*

M239

Truncation Mutants of RANKL Inhibit RANKL-induced Osteoclast Differentiation and Activation. M. H. Zheng*[1], J. W. Tan*[1], C. Wong*[1], J. Li*[2], J. Cornish*[2], J. Xu*[1]. [1]Dept of Surgery (Orthopaedics), University of Western Australia, Nedlands, Australia, [2]Dept of Medicine, University of Auckland, Auckland, New Zealand.

Receptor activator of NF-kB ligand (RANKL) is a key factor necessary for osteoclastogenesis and activation of osteoclasts. We hypothesis that residues or domains of RANKL affect the binding affinity to the decoy receptor OPG and the active receptor RANK; and as a consequence residues or domains of RANKL are involved in biological activity both *in vitro* and *in vivo*. To determine the active ligand domain of the C-terminal extracellular region, a series of overlapping regions of the TNF-like core region were cloned into the bacterial expression vectors pGEX. Soluble forms of recombinant rat RANKL (rRANKL) were affinity-purified and their biological activities were investigated using $RAW_{264.7}$ cell culture and isolated rat osteoclast culture. As expected, GST-rRANKL (aa160-318) containing the full TNF-like core region had the highest capability to induce the formation of osteoclast-like cells from $RAW_{264.7}$ cells whereas GST-rRANKL (aa239-318), (aa160-268), (aa160-291), (aa246-318) had a reduction of osteoclast inductivity. Interestingly, competition studies showed that GST-rRANKL (aa239-318), (aa160-268), (aa160-291), (aa246-318) inhibit RANKL (aa160-318) induced osteoclast formation in various degrees. Among of them RANKL mutant (aa246-318) was the most potent one. Furthermore, RANKL mutant (aa246-318) significantly blocks RANKL (aa160-318) induced osteoclastic bone resorption in isolated rat ostoelcast cultures. An in vitro protein-protein interaction has been carried out to examine the interaction of various RANKL mutants with RANK. Truncated GST-rRANKL (aa239-318), (aa160-268), (aa160-291), (aa246-318) showed efficient binding to Flag tagged RANK in a GST pull down assay. In order to examine the effect of RANKL mutants on activation of NF-kB, a stable Raw cell line expressed a reporter luciferase gene under the control of NF-kB binding site was established. Dose response and time course studies showed that there is a reduced effect on the activation of NF-kB and ERKs by the mutants. In short, these results suggest that truncated mutants of the TNF-like core domain of RANKL can be used to inhibit RANKL induced osteoclast differentiation and activation.

M240

Bone Histomorphometric Analysis of PD-1 Deficient Mice - The Regulation of Tcell Activation and Bone Metabolism. K. Nagahama*[1], K. Aoki[2], K. Nonaka[2], K. Ohyama*[1], K. Ohya[2]. [1]Section of Maxillofacial Orthognathics, Graduate school, Tokyo Medical and Dental University, Tokyo, Japan, [2]Section of Pharmacology, Department of Hard tissue Engineering, Graduate school, Tokyo Medical and Dental University, Tokyo, Japan.

The involvement of lymphocytes in metabolic bone disease and/or local bone destruction has recently been focused. Amgen group showed the decreased bone volume and the increased number of osteoclasts in tibia and femur of the cytotoxic T lymphocyte-associated antigen 4 (CTLA-4/ CD152) deficient mice (Nature 402: 304-309, 2000). CTLA-4 is a negative regulator of T cell activation, and actually the defect of this molecule induces T cell activation. On the other hand, Programmed Death-1 (PD-1) molecule is structurally similar to CTLA-4 working as a negative regulator of T cell activation similarly. The inhibitory mechanism, however, have proved to be different from CTLA-4. We report here the

novel bone phenotype of PD-1 deficient mice, which is quite different from the report of CTLA-4 deficient mice. The trabecular bone mineral density (BMD) of tibia in the 6week-old male PD-1 deficient mice was measured under the anesthesia by pQCT. However, there was no difference between wild type and PD-1 deficient mice. Then we measured it again using the same animals after 6 weeks. Interestingly, the BMD of tibia was significantly increased in the 12 week-old PD-1 deficient mice, which is the opposite phenotype of CTLA-4 deficient mice (see Table 1). The histological and histomorphometric analysis confirmed this phenotype. The primary and the secondary spongiosa of tibia were increased and the long cartilage remnants in the primary spongiosa of tibia was also increased in PD-1 deficient mice relative to wild type mice. The osteoclast number in both cortical and the cancellous regions of tibia were not increased in PD-1 deficient mice, that is different from the report of CTLA-4 deficient mice. T cell activation is not continuously promoted in PD-1 deficient mice, that might be one reason why the different bone phenotype was appeared. Taken together, these results indicate that the structurally related molecules, although those are the same negative regulators of T cell activation, have a different influence on bone metabolism that might depend on the different mechanism regulating T cell activation.

Table 1. The BMD measured by pQCT was significantly increased in the PD-1 deficient mice.

Data were presented as mean ± SD.	Wild type (mg/cm3)	PD-1 KO (mg/cm3)	statistics (compared to wild type)
Cortical BMD of tibial midshaft	1051.6 ± 21.3	1117.3 ± 16.1	$p < 0.005$
Trabecular BMD of proximal tibia	230.8 ± 11.0	288.7 ± 24.8	$p < 0.005$
Total BMD of proximal tibia	329.9 ± 18.8	417.3 ± 47.1	$p < 0.01$

M241

Divergent Effects of Interleukin (IL)-6 and IL-11 on Glucocorticoid Receptor Number in Human Osteoblast-Like Cells. A. Dovio*[1], M. L. Sartori*[1], B. Ceoloni*[1], L. Saba*[1], P. Prolo*[2], F. Chiappelli*[2], A. Angeli[1]. [1]Department of Clinical and Biological Sciences, University of Turin, Orbassano, Italy, [2]Laboratory of Oral and Molecular Immunology, UCLA School of Dentistry, Los Angeles, CA, USA.

Glucocorticoid (GC)-induced osteoporosis is admittedly the most frequent secondary osteoporosis. The pathogenesis still has many unresolved issues. While the effects of GC on cytokine production and action have been extensively studied, little is known on the effects of cytokines on GC action at the target level. Cytokines belonging to the interleukin (IL)-6 or gp130 cytokine family are known as pro-resorptive cytokines, in that they promote osteoclastogenesis. We have previously shown that IL-6 up-regulates GC receptor type II (GR) number, in both an autocrine and a paracrine way. Aim of the present investigation was to study the effects of another gp-130 osteotropic cytokine, IL-11, on GR in two widely used human osteoblast-like cell lines, Saos-2 and MG-63, which have remarkably different constitutive expression of these cytokines and GR as well (Table I). Cytokine secretion was assessed by ELISA; GR number and affinity were determined by radioligand binding assay and Scatchard analysis. When exposed to IL-11 (0.1-100 ng/ml), a significant dose-dependent decrease of GR was observed in MG-63 but not in Saos-2 cells. Incubation with anti-IL-11 monoclonal antibody significantly increased GR in both cell lines. Neither IL-11 addition, nor IL-11 deprivation modified GR affinity. Specific STAT-3 inhibition yielded data compatible with the view that Jak-STAT pathway is involved in the cytokine modulation of the GR. While exerting opposite effects on GR number, neither IL-6 nor IL-11 did significantly modify GC effects on osteoprotegerin (OPG) release, assessed by ELISA. In conclusion, IL-6 and IL-11 have divergent effects on GR in two well-characterized osteoblast-like cell lines. Our data are consistent with the concept of autocrine-paracrine modulatory loops of GC action in bone microenvironment involving pro- and anti-inflammatory cytokines. These loops may have clinical relevance for the dynamics of bone loss in patients given GC and conceivably having high concentrations of these cytokines in the bone microenvironment.

Table I. Functional phenotype of MG-63 and Saos-2 cells

	MG-63	**Saos-2**
IL-6 (pg/10^6 cells)	856 ± 130	4.6 ± 1.2
IL-11 (pg/10^6 cells)	15 ± 1.1	621 ± 40
OPG (pg/10^6 cells)	39273 ± 10912	857 ± 56
GR (binding sites/cell)	110380 ± 4499	31783 ± 1847

Data are expressed as mean ± SE.

M242

Macrophage Colony-Stimulating Factor Suppresses Calcitriol-Induced but Augments Prostaglandin E_2-Induced Osteoclast Formation in Rat Bone Marrow Cell Culture. J. K. Yeh, D. I. Sima*, J. Evans*, J. F. Aloia. Medicine, Winthrop-University Hospital, Mineola, NY, USA.

Macrophage-Colony Stimulating Factor (M-CSF) is a critical early modulator of osteoclastogenesis with a primary action on early monocytic stem cells to induce osteoclast precursor formation. Calcitriol (1,25-D_3) and prostaglandin E_2 (PGE_2) are known to influence osteoclast formation indirectly through their effects on osteoblasts. Evidence indicates that 1,25-D_3 induces the expression of M-CSF which facilitates the formation of osteoclasts. The purpose of the present study is to investigate the effect of $1,25D_3$ at 10^{-8} M and/or PGE_2 at 10^{-7} M in the presence of M-CSF (10 ng/ml) on osteoclast formation in rat bone marrow cell culture. Our data shows that rat bone marrow cells cultured with basal medium (αMEM medium supplemented with 50ug/ml ascorbic acid, 10% fetal bovine serum, antibiotic/antimycotic) developed a few multinucleate osteoclast-like cells with Tartrate-Resistant-Acid Phosphatase (TRAP) positive staining on days 7 through 11 of culture. Treatment with $1,25D_3$ alone resulted in numerous TRAP-positive osteoclast formations. Interestingly, the combined treatment of $1,25D_3$ with M-CSF resulted in an 80±11% suppression of the osteoclast formation at all times as compared to the respective $1,25D_3$ alone group. Treatment with PGE_2 alone also resulted in numerous TRAP-positive osteoclast formations. However, a combined treatment of M-CSF and PGE_2 resulted in a 400±120% increase in the osteoclast formation at all times as compared to the respective PGE_2 alone group. The combined treatment of $1,25D_3$ and PGE_2 had a synergistic effect on osteoclast formation as compared to each treatment alone. Again, in the presence of M-CSF, the formation of osteoclasts was suppressed to less than 20% of the $1,25D_3$ + PGE_2 group. How M-CSF suppresses $1,25D_3$ induction, but augments PGE_2 induction on osteoclast formation is not known, however, the current study results suggest that $1,25D_3$ and PGE_2 induce osteoclastogenesis in rat bone marrow cultures through different mechanisms.

M243

RANKL Regulates Fas Expression and Fas-mediated Apoptosis in Osteoclasts. x. wu[1], G. Pan*[1], M. McKenna[1], J. M. McDonald[2]. [1]Pathology, University of Alabama at Birmingham, Birmingham, AL, USA, [2]University of Alabama at Birmingham, Veterans Administration Medical Center, Birmingham, AL, USA.

Apoptosis of osteoclasts, together with the osteoclast differentiation rate and osteoclast activity determine the rate of bone resorption. The Fas receptor mediates apoptosis in many cells, especially of the immune system. RANKL, which regulates osteoclastogenesis, is a potential cytokine linking the immune system to bone remodeling. Here we investigated the role of RANKL in regulating Fas expression and Fas-mediated apoptosis in osteoclasts. Mouse osteoclasts were generated by treating osteoclast precursors (bone marrow macrophages) isolated from C57bl/6 mice with soluble mouse RANKL and recombinant mouse M-CSF. Osteoclasts generated either from RAW 264.7 cells treated with RANKL or from human peripheral blood monocytes supplemented with human M-CSF and RANKL were also used. Fas expression was determined by flow cytometry, Western analysis and its peripheral location was detected by immunohistochemistry. By flow cytometry, only a small portion of stem cells (6%) isolated from bone marrow had Fas expressed on their surfaces. Fas expression was highly upregulated from 6% positive cells at day zero to 94% positive cells after 6 days of incubation with M-CSF. Most of the increase in Fas expression occurs between day 3 and day 6. Addition of RANKL decreased the peak fluorescence for Fas expression by two logs compared with M-CSF alone. Addition of RANKL decreased Fas expression at both day 3 and day 6. A similar but somewhat less pronounced observation was seen with the RAW cell line. Incubation of RAW cells with M-CSF alone increased Fas expressing cells from 7% at day 3 to 46% at day 6. Addition of RANKL decreased the peak fluorescence by 50%. Flow cytometry results with mouse osteoclasts were confirmed by Western blot. Fas activation induced apoptosis (51%) in osteoclasts generated in the presence of 50ng/ml RANKL; however, cells differentiated in the presence of a higher dose of RANKL (150ng/ml) were resistant to apoptosis induced by Fas antibody. These results demonstrate that in mouse osteoclasts, M-CSF increases Fas expression and RANKL decreases it. RANKL also decreases Fas-mediated apoptosis in osteoclasts by regulating Fas receptor expression. The distribution of RANKL in tissues and its regulation of Fas expression and Fas-mediated apoptosis imply that not only cells of stromal/osteoblast lineage but also of the immune system participate in regulating osteoclast number, therefore regulating the balance between bone resorption and bone formation.

M244

SDF-1 Recruits Osteoclast (OC) Precursors via Inducing MMP 9: A Mechanism Independent from MMP-9 Induction During RANKL-mediated OC Differentiation. X. Yu, Y. Huang*, P. Collin-Osdoby, P. Osdoby. Department of Biology, Washington University, St. Louis, MO, USA.

The directional movement of pre-OC from the circulation into bone occurs via complex mechanisms involving cell surface, matrix, and chemoattractant signals that enable proteinase-dependent transmigration. Although MMP-9 is involved in such pre-OC movement, bone signals that attract pre-OC or regulate MMP-9 are poorly defined. Chemokines direct cell migration, activation, and invasion in normal and pathological states, and are elevated in osteopenic disorders such as periodontal disease, rheumatoid arthritis, or multiple myeloma. Thus, chemokines may aid in the recruitment or formation of OC. To examine this, we analyzed chemokine receptor expression and actions during OC development in murine RAW 264.7 cells (RAW) differentiated by RANKL to yield TRAP+ multinucleated bone-resorptive OC (RAW-OC). CXCR receptor mRNA expression analyzed by multi-probe RPA showed CXCR4 expression in both RAW and RAW-OC, with higher levels in RAW cells that declined as RAW-OC developed. Because SDF-1 is the sole ligand for CXCR4, the key homing signal for hematopoietic cells to the bone marrow, and an activator of MMPs in cell migration, we examined if SDF-1 regulated pre-OC recruitment or differentiation. SDF-1 stimulated pre-OC (RAW) chemotaxis, and increased RAW cell MMP-9 activity (by gelatin zymography) and MMP-9 mRNA levels (by RT-PCR). In comparison, RANKL did not cause RAW cell chemotaxis, although it increased RAW cell MMP-9 activity and mRNA levels. SDF-1 differed from RANKL in evoking a more modest and transient elevation in MMP-9 mRNA expression compared to RANKL. SDF-1 did not further raise high MMP-9 levels in RAW-OC. Consistent with their upregulation of MMP-9, both SDF-1 and RANKL stimulated RAW cell transmigration through collagen-coated transwell membranes via an MMP-dependent process blocked by the general MMP inhibitor GM6001. In contrast to RANKL-mediated RAW-OC formation, SDF-1 did not induce cathepsin K mRNA expression or promote TRAP+ multinucleated bone resorptive RAW-OC formation. Therefore, SDF-1 serves as an important recruitment signal for inducing the directional movement and targeting of pre-OC into and within the bone marrow via chemotactic and MMP-9 stimulated mechanisms. Recruited precursors subsequently decrease CXCR4 and increase MMP-9 in response to RANKL as they develop into bone-resorptive OC. Consequently, MMP-9 induced by SDF-1 or RANKL plays distinct roles in pre-OC and OC: an early SDF-1 regulated role in pre-OC homing and a later RANKL regulated role in bone resorption. Together, SDF-1 and RANKL work in concert to home and target pre-OCs to bone resorption sites for their development and function.

M245

Synergistic Effects of TNF-alpha and RANKL on Osteoclast Differentiation from Bone Marrow Cells of Type-II collagen Induced Arthritis Mice. Y. Azuma[1], E. Ochiai*[1], K. Kaji*[2], K. Kanazawa*[2], T. Kamimura*[1], J. Inoue*[3], A. Kudo[2]. [1]Pharmacological Research Department, Teijin Institute for Biomedical Research, Tokyo, Japan, [2]Depatment of Life Science, Tokyo Institute of Technology, Yokohama, Japan, [3]Facalty of Science and Technology, Keio University, Yokohama, Japan.

The severe local osteolysis in the joint of patients suffered from rheumatoid arthritis associates with up-regulation of osteoclastic bone resorption by the interaction of several inflammatory cytokines. Although TNF-alpha (TNF) synergistically stimulates RANKL-induced osteoclast differentiation from osteoclast progenitor cells, its pathological role has remained unclear. To elucidate the involvement of the TNF-synergy with RANKL in osteoclastogenesis of autoimmune arthritis, we examined the TNF and/or RNAKL-induced osteoclastogenesis by using bone marrow cells (BM-cells) and osteoclast progenitor cells (M-CSF dependent bone marrow macrophages; MDBM cells) from murine type-II collagen induced arthritis (CIA mice). DBA/1J mice were immunized with type II collagen in adjuvant, and the mice were observed for 9 weeks during which time arthritis was scored. Severe inflammation after 5-weeks and the bone destruction of the synovial joints after 7-weeks were observed, respectively. BM cells were obtained from long bone of CIA mice at 1,3,5,7,9 weeks after first immunization, and cultured in the presence of M-CSF. BM-cells were treated with various combinations of TNF and RANKL. The results demonstrated that co-treatment with TNF and RANKL synergistically stimulated the formation of TRAP-positive multinuclear cells (TRAP(+)-MNCs) from BM-cells of both CIA mice and intact mice at all time points. However, at 5, 7 and 9 weeks after immunization, TNF was 2 or 3 times more synergistic with RANKL in BM-cells derived from CIA mice than in that derived from intact mice, suggesting that the high-sensitive population toward the co-treatment with TNF and RANKL increased in the bone marrow cells of CIA mice. Tumor necrosis factor receptor-associated factor (TRAF) 6 is involved in the RANKL and/or TNF-induced osteoclast differentiation from osteoclast progenitor cells, we examined the expression of TRAF6 protein in the TNF-treated MDBM cells. In the process of TNF-induced osteoclastogenesis, the expression of TRAF6 protein increased, suggesting TRAF6 up-regulation by TNF associates with synergistic effects of TNF and RANKL. These results suggest that the up-regulation in the sensitivity toward the co-treatment with TNF and RANKL in the osteoclast progenitor cells involves the local osteolysis in the synovial joints of CIA mice.

M246

ECF-L Is a Critical Co-Factor For RANK Ligand-Induced Osteoclastogenesis. Y. Oba, S. J. Choi*, G. D. Roodman. Medicine, University of Pittsburgh, Pittsburgh, PA, USA.

We produced an osteoclast precursor cell line that formed large numbers of osteoclasts (OCL) and used a subtraction hybridization approach to identify genes upregulated in mature OCL compared to precursors. Using this approach, we recently identified eosinophil chemotactic factor-L (ECF-L) as a novel factor produced by OCL and OCL precursors that enhances OCL formation. Conditioned media from 293 cells transfected with the ECF-L cDNA or recombinant ECF-L significantly increased OCL formation in a dose-dependent manner in mouse and human bone marrow cultures in the presence of low concentrations of 1,25-$(OH)_2D_3$ (10^{-10}M) or RANK ligand (2.5 ng ml) (RANKL),but did not induce significant levels of OCL formation by itself. OCLs induced in mouse marrow cultures treated with ECF-L formed increased pit numbers and resorption area per dentin slice compared to mouse cultures treated with 1,25-$(OH)_2D_3$ alone. Time course studies demonstrated that ECF-L acted at the late stages of OCL formation. Transfection of OCL precursors with an antisense construct to ECF-L inhibited OCL formation in murine marrow cultures. To further examine the role of ECF-L in osteoclastogenesis, osteoprotegerin (OPG), RANK-Fc, or a neutralizing antibody to ECF-L were added to mouse and human bone marrow cultures treated with ECF-L in the presence of 10^{-10}M 1,25$(OH)_2D_3$ or RANKL (10 ng/ml). ECF-L-induced OCL formation was significantly inhibited by OPG and RANK-Fc. Importantly, a neutralizing antibody to ECF-L blocked RANKL (50 ng/ml) or 1,25-$(OH)_2D_3$ (10^{-9}M)-induced OCL formation in mouse bone marrow cultures. RT-PCR and Western blot analyses showed that ECF-L did not enhance RANKL or RANK expression in human or mouse bone marrow cultures. Furthermore, chemotactic assays demonstrated that ECF-L was chemotactic for OCL precursors (TRAP(+) mononuclear cells), and this effect was inhibited by the anti-ECF-L antibody. Taken together, these data suggest that ECF-L is a novel chemoattractant for OCL precursors and appears to be a critical co-factor for osteoclastogenesis induced by RANKL.

M247

The Macrophage Mannose Receptor Is Required for Osteoclastogenesis. S. Wei, S. L. Teitelbaum, F. P. Ross. Pathology, Washington University School of Medicine, St. Louis, MO, USA.

The mannose receptor (MR) is a glycoprotein, which binds to and internalizes high mannose-containing macromolecules. Since the MR is expressed on osteoclast precursors in the form of bone marrow macrophages (BMMs), we examined expression and function of this molecule during OC formation. Using RT-PCR analysis of c-fms positive BMMs treated with M-CSF and RANKL, we find MR levels increase gradually during differentiation, with both RANKL and M-CSF individually enhancing expression. Since MR preferentially recognizes α-linked oligo-mannose with branched rather than linear structures, we used the branched polysaccharide mannan to examine the role of MR in osteoclastogenesis. Mannan blocks OC formation dose-dependently only during the first two days of culture, an effect reversed by withdrawal of the sugar up to five days after initial addition. A second MR inhibitor, BSA with 22 moles of mannose per mole (man-BSA) exhibits the same dose-dependent inhibitory effect on OC formation as mannan. Treatment of BMMs with either mannan or man-BSA enhances cell number, indicating that neither molecule is toxic. Suggesting that inhibitor treatment results in blunting of MR function, BMM-mediated uptake of horseradish peroxidase, an MR ligand, is significantly decreased when the cells are pre-treated with glucosidase inhibitors castanospermine (CAST) or 1-deoxynojirimycin (DNJ). Consistent with this observation, we find that, like mannan and man-BSA, both CAST and DNJ inhibit OC formation dose-dependently. To examine the role of the MR in a more physiological setting we added man-BSA or CAST to a neonatal calvaria whole organ culture treated with RANKL and find that the inhibitors decrease cytokine-induced formation of tartrate-resistant acid phosphatase positive, multinucleated cells by 96% and 99 %, respectively. In addition, we find when OCs are generated on dentin in the presence of mannan, man-BSA, CAST or DNJ, pit area/cell and % resorbing area/field are decreased by about 90% and 85%, respectively, further proving that these agents functionally inhibit osteoclastogenesis. Consistent with the observation that MR is involved in cell-cell fusion in other cell types, mannan, man-BSA and both glucosidase inhibitors dose-dependently inhibit a second form of BMM fusion, interleukin (IL)-4 induced formation of foreign body giant cells (FBGCs). Furthermore, the presence of IL-4 in cultures of BMMs treated with M-CSF and RANKL results in formation of FBGCs and not OCs. In both settings IL-4 treated cell exhibit high MR levels. Thus the MR facilitates fusion of OC precursors during osteoclastogenesis.

M248

Toll-like Receptors Modulate Differentiation and Survival of Osteoclasts. M. Takami, N. Kim*, J. Rho*, Y. Choi*. Department of Pathology and Laboratory Medicine, University of Pennsylvania, Philadelphia, PA, USA.

Immune responses to microbial pathogens are often triggered because various microbial components induce the maturation and activation of immunoregulatory cells such as macrophages or dendritic cells by stimulating Toll-like receptors (TLRs). Since osteoclasts arise from the same precursors as macrophages, we tested whether TLRs play any roles during osteoclast differentiation. Osteoclast precursors prepared from mouse bone marrow cells with M-CSF differentiated into osteoclasts in the presence of TNF-related activation-induced cytokine (TRANCE) and M-CSF. Osteoclast precursors expressed all known murine TLRs (TLR1-TLR9) and had capacities of zymosan-particle incorporation by phagocytosis. However, after differentiating into mature osteoclasts, phagocytic capacities were lost. Peptidoglycan (PGN), double-strand RNA [poly(I:C) RNA], lipopolysaccaride (LPS), and CpG motif of unmethylated DNA (CpG DNA), those are the ligands for TLR2, 3, 4, and 9, respectively induced NF-kB activation and upregulated TNF-alpha mRNA

expression in osteoclast precursors. TLR stimulation of osteoclast precursors by these TLR ligands strongly inhibited their differentiation into multinucleated, mature osteoclasts. Rather, TLR stimulation maintained the phagocytic capacities of osteoclast precursors. Although the intracellular signaling pathways from IL-1 receptors are quite similar to that from TLRs, IL-1 alpha did not inhibit osteoclast differentiation, suggesting that signaling molecules unique to TLR stimulation pathway play roles in the inhibition of osteoclast differentiation. On the other hand, TLR 2 and 4 were prominently expressed in mature osteoclasts. When multinucleated osteoclasts were purified and cultured in the absence of any stimuli, all osteoclasts died within 12 h. However, PGN and LPS but not poly(I:C) RNA and CpG DNA supported the survival of purified osteoclasts. Taken together, these results suggest that TLR stimulation inhibits the differentiation into non-inflammatory mature osteoclasts and simultaneously supports the survival of mature osteoclasts during microbial infection. TLRs are thus likely to regulate the balance of immune responses and bone metabolism during acute attacks of vertebrae hosts by various microbes.

M249

Osteoclastogenesis: Multinucleation Is A True Differentiation Process That Imposes A Major Molecular Stress On Macrophages. J. Zhang[1], J. Li*[2], H. Sterling*[1], G. Peet*[2], R. Barton*[2], A. Vignery[1]. [1]Yale School of Medicine, New Haven, CT, USA, [2]Boehringer Ingelheim Pharmaceuticals, Inc., Ridgefield, CT, USA.

Multinucleated osteoclasts originate from the fusion of cells that belong to the mononuclear phagocyte lineage, and are characterized by a powerful ability to resorb bone. These cells play a central role in osteoporosis and cancer. Yet, despite their potency, their differentiation mechanism remains largely unknown. To study osteoclastogenesis, our laboratory has used primary macrophages isolated from rat lungs, as these cells spontaneously fuse when plated at high density and cultured in the presence of serum (see Int J Exp Pathol 81:291, 2000). This assay has allowed us to clone MFR, and identify its ligand CD47, along with CD44 as surface molecules highly, but transiently induced at the onset of multinucleation. The present study was designed to identify the genes expressed during macrophage multinucleation using oligonucleotide microarray analysis (Affymetrix). To this end, macrophages were either freshly isolated or cultured for 1 h, 24 h or 120 h so as to identify genes expressed in response tissue culture stress, cell-cell fusion, and multinucleation, respectively. Our data revealed limited arrays of genes that were induced in a regulated manner so as to construct the resorption machinery of these cells, yet maintain their intracellular ion homeostasis. Cytokines and chemokines known to activate osteoclast differentiation and activity, such as TNF-a along with growth factors and their receptors, and extracellular matrix proteins were highly and time-dependently up regulated, suggesting auto-regulatory mechanisms and / or control of the microenvironment. The most striking and shared feature was the magnitude with which specific transcripts were up regulated during multinucleation, revealing the role of transcription factors and signaling molecules, and suggesting a high level of stress imposed on the protein synthesis machinery. This was supported by the sequentially up-regulated expression of specific chaperone molecules. This analysis has revealed multinucleation of macrophages as a true and sophisticated differentiation process, and provided important and novel targets to control osteoclastogenesis and bone resorption.

M250

Regulation of OSCAR Gene Expression by the Microphthalmia Transcription Factor. N. Kim*, H. So*, M. Takami, J. Rho*, Y. Choi*. Pathology, University of Pennsylvania School of Medicine, Philadelphia, PA, USA.

Osteoclasts are multinucleated giant cells which resorb bone and differentiated from hematopoietic cells by contact with osteoblasts/stromal cells in response to several osteotropic factors. Two essential factors, M-CSF and the tumor necrosis factor (TNF) family member TRANCE, are well known for osteoclastogenesis. In addition, other factors produced by osteoblast/stromal cells can affect differentiation of osteoclasts. We have recently reported the identification of a novel member of the leukocyte receptor OSCAR (osteoclast-associated receptor) which has two immunogloblin (Ig)-like domains. It has also shown that OSCAR may be an important bone-specific regulator of osteoclast differentiation. We report here that human OSCAR is expressed specifically in osteoclast cells and involved in the differentiation of osteoclasts from PBMC. Five different transcript forms of human OSCAR gene have been identified. To examine the regulation of OSCAR gene, we have analyzed the promoter region of OSCAR. Three PU.1, one NF-kB, and two Mitf binding sites were founded in 1.7 Kb OSCAR promoter region by sequence analysis. Spleen-derived osteoclast cells from mi/mi mutant mice showed 3-fold reduction of OSCAR gene expression compared with osteoclasts derived from normal mice. To examine whether Mitf can directly regulate OSCAR expression, we used reporter assay using the transient transfections into 293T cells with a series of OSCAR promoter constructs. When 1.7 Kb OSCAR fragment was cotransfected with the different amount of wild type Mitf, the luciferase activity was increased in a dose dependent manner, but not by Mitf dominant negative type. The activity of 1.7 Kb OSCAR promoter-reporter gene was increased to 10-fold by wild type Mitf compared with control vector. This induction was totally abolished in mutant type of E-boxes of OSCAR promoter. These results implicate that the relationship between Mitf and OSCAR may be important for osteoclastogenesis. Thus the more studies of regulations between these osteoclast-specific genes may provide a tool for therapeutic approach to treat bone diseases.

M251

RANKL-Induced Osteoclast Formation Is Associated with Upregulation of Connexin 43 Gene Expression and Decreased by a Gap Junction Blocker,Carbenoxolone. M. Ransjö, A. Lie*. Oral Cell Biology, Umeå University, Umeå, Sweden.

Gap junctions are membrane-spanning channels that faciliate intercellular communication by allowing small signaling molecules, such as calcium ions, inositol phosphates and cyclic nucleotides, pass from cell to cell. Connexins (Cx) are the proteins that form gap junctions and more than a dozen different Cx have been identified. It has earlier been demonstrated that osteoblasts are highly coupled by gap junctions formed primarily by Cx43. It is well known that osteoblasts/stromal cells stimulate osteoclast differentiation and activation through cell-cell-contacts. Receptor activator of NF-kB ligand (RANKL) is expressed as a membrane-associated factor on osteoblasts/stromal cells in response to PTH and several other bone resorbing factors. We have recently demonstrated that PTH and forskolin increase Cx43 expression in mouse bone marrow cultures and furthermore, the stimulatory effect on osteoclast recruitment is inhibited by carbenoxolone, a gap junction blocker (paper submitted). In the present study, we wanted to investigate possible interactions between RANKL and gap junction communication on osteoclast recruitment. Mouse bone marrow cells were isolated from 6-9 weeks old CsA mice and cultured for 7-8 days with or without the addition of rmRANKL and in the absence or the presence of different concentrations of carbenoxolone. RANKL (100 ng/ml) significantly increased the number of TRAP-positive multinucleated cells formed in the marrow cultures. RT-PCR analysis demonstrated an upregulation of Cx43 mRNA levels in RANKL-stimulated cultures as compared to control cultures. The expression of mRNA was analysed by semiquantitative measurements performed in the midlinear range of PCR amplification and assessed as the ratio of the optical density of the band normalized to the band of corresponding GAPDH. The gap junction blocker carbenoxolone produced a dose-dependent (10-60 uM) inhibition of the number of TRAP-positive multinucleated cells formed in response to RANKL. These data suggests that gap junction communication may be involved in osteoclastogenesis mediated by RANKL.

M252

Expression of the bHLH Transcription Factor Stra13 Is Up-regulated During Osteoclast Differentiation. B. L. Vincent*, L. Wunderlich*, M. J. Glimcher, K. P. McHugh. Orthopaedic Research, Children's Hospital and Harvard Medical School, Boston, MA, USA.

In the course of expression profiling osteoclasts and their precursors, we have identified Stra13 as a transcription factor that is specifically up-regulated during osteoclast differentiation. Stra13 was originally identified as an induced gene during retinoic acid-dependent neuronal differentiation of P19 embryonic carcinoma cells. Overexpression of Stra13 in P19ec cells leads to expression of neuronal genes and neuronal differentiation. Recently, Stra13 has been shown to mediate inhibition of adipogenesis by hypoxia, as well as to inhibit B lymphocyte activation. Stra13 belongs to the bHLH family of transcription factors and has been shown to function as a repressor of activated transcription in several cell types. Stra13 does not bind canonical bHLH DNA binding motifs, however specific DNA sequences are required for the transcriptional repressor activities of Stra13. We show here, by qualitative RT-PCR, that Stra13 expression is up-regulated during osteoclast differentiation of primary mouse bone marrow macrophages (BMMs), as well as by osteoclastogenic clones of RAW264.7 cells. To further quantify Stra13 expression during osteoclast differentiation, we performed quantitative RT-PCR on RNAs from a time course of BMMs grown with M-CSF, as compared with RNAs from osteoclastogenic cultures grown with M-CSF plus RANKL. After culture with RANKL for 5 days, TRAP, Cathepsin-K, and β_3 integrin are at their maximum expression levels as measured by quantitative RT-PCR. We find that during osteoclastic differentiation Stra13 expression increases while decreasing in cultures grown with M-CSF alone. At 5 days, Stra13 is also expressed at its highest expression level, with a difference in Ct values of 5.25 between osteoclasts and macrophage cultures. This difference in Ct values represents a change in initial PCR target abundance of >32 fold. To demonstrate that the change in message level is reflected by expression of the Stra13 protein, we performed Western blots on osteoclasts derived from BMMs grown with M-CSF plus RANKL, as compared to BMMs grown with M-CSF alone. We find that osteoclastic differentiation enhances Stra13 protein expression. Western blots of osteoclastogenic clones of RAW264.7 cells confirm that Stra13 protein is expressed in a time dependent manner through osteoclast differentiation. In conclusion, Stra13 expression is specifically induced during osteoclastic differentiation at both the RNA message and protein levels. Stra13 may therefore play an important role in osteoclastogenesis, potentially as a transcriptional repressor of macrophage genes.

M253

Microarray, Differential Display, and Northern Analysis of Mouse Bone Cell Gene Expression Early After Cd Gavage. M. H. Bhattacharyya, A. Regunathan*, D. Glesne*. Argonne National Laboratory, Argonne, IL, USA.

We developed an in vivo model for Cd-induced bone loss in which mice excrete bone mineral in feces starting 8 h after Cd gavage. Female mice of 3 strains [CF1; metallothionein-wildtype (MT+); MT1,2-deficient (MT-)] were placed on a low Ca diet for 2 weeks. Each mouse was gavaged with 200 µg Cd or vehicle only. Fecal Ca was monitored daily for 8 days, starting 3 days before Cd gavage, to document the bone response. For CF1 mice, bones were taken from 4 groups: +/- Cd, 2h after Cd; +/- Cd, 4h after Cd. MT+ and MT- strains had 2 groups each: +/-Cd, 4 h after Cd. PolyA RNA was isolated from marrow-free shafts of femura and tibiae, and RNA from each +/- Cd pair was submitted to Incyte Genomics for microarray analysis. To validate the microarray results, the same polyA RNA preparations were subjected to Northern analysis; probes were prepared from 18 clones of genes shown by microarray to be key to the bone response to Cd. Other RNA samples (4 h +/- Cd) were subjected to conventional DDRT-PCR. Fecal Ca results show that the 3 mouse strains differed in amount of bone Ca excreted after Cd (CF1 0.24+0.08 mg; MT+ 0.92+0.22 mg; MT- 1.7+0.4 mg). Differential display results show that 4 cloned bands had Cd down-regulation confirmed by Northern analysis; 2 of the 4 were mitochondrial. One other clone (12-5) displayed 98% identity to integrin linked kinase (Ilk) mRNA; the other was 74% identical to 2 mouse cDNAs of unknown function. Gene microarray results show that nearly all ~8500 arrayed mouse genes were unaffected by Cd. However, MT1 and MT2 had +Cd/-Cd expression ratios >1 in all four groups, while all ratios for MT3 were essentially '1', showing specificity. Both probes for MAPK 14 (p38 MAPK) had expression ratios >1, while no other MAPK responded to Cd. Other genes stimulated by Cd were: vacuolar proton pump ATPase and integrin alpha v (osteoclast genes), transferrin receptor (iron deficiency?), src-like adaptor protein, and two hypothetical proteins. Genes down-regulated by Cd included procollagen type IX and a gene of unknown function. Our validation by Northern analysis included genes expected by microarray results to increase, decrease, or show no change in response to Cd. Results clearly confirmed the above microarray results for all genes except two whose expression levels were too low to effectively quantitate changes by Northern analysis. Recent results in the literature demonstrate that p38 MAPK plays a central role in osteoclast differentiation (Matsumoto et al, JBC, 275:31155-61, 2000; Karsdal et al, JBC, 276:39350-8, 2001, Lee et al, Bone, 30:71-77, 2002). Our results support the hypothesis that Cd stimulates bone demineralization via a p38 MAPK pathway leading to increases in osteoclast-mediated bone resorption.

M254

Runx Factors are Expressed in the Osteoclast and Regulated During Osteoclast Differentiation. Z. Bar-Shavit[1], H. Drissi*[2], A. Javed[2], J. Ribadeneyra*[2], A. J. van Wijnen[2], J. L. Stein*[2], J. B. Lian[2], G. S. Stein[2]. [1]Hebrew University Faculty of Medicine, Jerusalem, Israel, [2]Department of Cell Biology, University of Massachusetts Medical School, Worcester, MA, USA.

Runx factors are obligatory for cellular differentiation. While Runx2 is essential for osteogenesis, Runx1 is required for hematopoiesis. Osteoclasts originate from the hematopoietic lineage. Furthermore, Runx2 increases osteoprotegerin (OPG), an inhibitor of osteoclast differentiation, suggesting that Runx factors may be involved in osteoclast activities. Given the overlap in expression between Runx1 and Runx2 in hematopoietic lineage cells, we addressed whether osteoclasts express Runx factors and if their expression is modulated during osteoclastogenesis. Osteoclast differentiation in vitro was studied using the macrophage like cell line RAW 264.7 (treated with RANKL) and bone marrow mononuclear cells from Balb/c mice (treated with RANKL and M-CSF). At selected times over a 7 day culture period, we examined Runx1 and Runx2 mRNA levels by RT-PCR, protein by in situ immunofluorescence, and DNA-binding activity by EMSA (competition studies and antibody supershift). At the single cell level, using specific antibodies, we observe Runx1 and Runx2 protein in both mononuclear precursors and multinucleated cells. Both Runx factors and the p50 subunit of the NF-κB transcription factor are organized in distinct nuclear domains in all osteoclast nuclei. BrUTP labeling and RNA polymerase II immunoreactivity established that all osteoclasts are transcriptionally active. Expression of Runx factors in mononuclear cells did not change throughout the culture period, while nuclei of osteoclasts exhibited fewer punctate foci by conventional and confocal fluorescence microscopy. TNFα treatment of the osteoclasts resulted in a marked reduction of Runx2 in nuclei. In contrast, transcription factor NF-κB was strikingly increased in osteoclast nuclei in response to TNFα . Expression of Runx proteins was also revealed by gel shift assays. These findings indicate that Runx proteins are present in nuclei of osteoclast lineage cells, form functional DNA binding complexes, and may contribute to the regulation of osteoclast differentiation and/or activity.

M255

The Effects of Pasteurella Multocida Toxin on Osteoclast Differentiation and Activity. D. Harmey[1], G. Stenbeck*[2], A. Lax*[3], A. E. Grigoriadis[1]. [1]Craniofacial Development, King's College London, London, United Kingdom, [2]Bone and Mineral Centre, UCL, London, United Kingdom, [3]Oral Microbiology, King's College London, London, United Kingdom.

Pasteurella multocida toxin (PMT) is a bacterially-produced toxin that causes the porcine bone resorbing disease, atrophic rhinitis. PMT is a potent mitogen and stimulates phospholipase C leading to activation of protein kinase C, and increases in inositol phosphates and intracellular calcium. PMT also induces actin rearrangements via the small GTPase Rho. The mechanisms by which PMT affects bone remodelling are unknown, although we have recently shown that PMT inhibits osteoblast differentiation and gene expression, in part, via a pathway involving Rho and Rho kinase. Here, we aim to determine the effects of PMT on osteoclast differentiation and activity. In co-cultures of primary mouse calvarial osteoblasts (MC) with bone marrow cells, PMT inhibited the number of TRAP-positive multinucleated cells in a dose-dependent manner, with a concomitant decrease in resorption. PMT also affected the morphology of the TRAP-positive mono- and multinucleated cells that formed, inducing a contracted cell morphology. 24h pre-treatment of either the osteoblasts or the haematopoietic cells with PMT prior to co-culture, caused a significant inhibition of TRAP-positive cell number and resorption, suggesting that PMT exerts its inhibitory effects via both populations. To determine the possible mechanism of inhibition, we performed RT-PCR analysis of RANKL and OPG expression. In MC cells PMT caused a decrease in RANKL expression with a concomitant increase in OPG levels. Moreover, addition of exogenous RANKL to PMT-treated cultures partially rescued the block in osteoclast differentiation, suggesting that the effects on osteoblast-mediated osteoclastogenesis are partially mediated by altered RANKL/OPG levels. PMT also dose-dependently inhibited osteoclast differentiation and resorption in stroma-free cultures containing RANKL and M-CSF, and also induced cell contraction. Pulse experiments showed that a 3d pulse at the start of the culture period was sufficient to significantly inhibit differentiation. However, in contrast to differentiation cultures, PMT treatment of mature primary osteoclasts did not significantly inhibit resorption. Surprisingly, preliminary results indicate that PMT disrupted actin ring formation without a parallel decrease in resorption. Taken together, these results demonstrate that PMT inhibits osteoclast differentiation via independent effects on stromal cells and haematopoietic precursors, and causes cytoskeletal changes in primary osteoclasts.

M256

Osteoclastic Differentiation in Primary Mouse Bone Marrow Cultures Is Affected by Addition of Cystatin C. M. Brage*[1], A. Grubb*[2], U. H. Lerner[3]. [1]Oral Cell Biology, Umeå University, Umeå, Sweden, [2]Dept Clinical Chemistry, University of Lund, Lund, Sweden, [3]Dept Oral Cell Biology, Umeå University, Umeå, Sweden.

Osteoclastic bone resorption is dependent on the activity of proteolytic enzymes, among which the cysteine protease chathepsin K has been shown to play a key role in bone matrix degradation. We have previously reported that cystatin C, an inhibitor of papain-like cysteine proteases, inhibits bone resorption in mouse calvariae primarily by inhibiting degradation of bone matrix proteines. This effect is also gained by using a peptide, Arg8-Leu9-Val 10-Gly 11 (RLVG), mimicking part of the cystatin C N-terminal end that binds to the active cleft of cysteine proteinases. We have also reported that not only the activity, but also the formation of osteoclasts is inhibited by addition of cystatin C and Arg8-Leu9-Val10-Gly11. Furthermore, PTH and D3 stimulated osteoclast formation is inhibited also by addition of leupeptin and E64. The present study aims to further elucidate the inhibitory effect of cystatin C on osteoclastic differentiation. In 9 days mouse bone marrow cultures stimulated by PTH and stained for TRAP, the increased number of multinucleated TRAP positive cells caused by PTH treatment was reduced to 40-60% by addition of cystatin C or OPG. The number of osteoclasts was reduced to 90-100% by addition of cystatin C and OPG in combination. The inhibitory effect of cystatin C was found to be exerted at day 4 of culturing. The mRNA expression of OPG was reduced by PTH after 9 days and this reduction was abolished by cystatin C. PTH also reduced the expression of c-fms after both 2 and 9 days and addition of cystatin C abolished PTH-induced down regulation of c-fms. The macrophage cell surface molecule F4/80 was highly expressed in untreated bone marrow cells. PTH treatment totally reduced F4/80 cell population. Addition of cystatin C, together with PTH, abolished this reduction and even increased the number of F4/80 cells. PTH + OPG treated cells were F4/80 negative, whereas PTH + OPG + cystatin C resulted in a great amount of F4/80 positive cells. These data together indicate that the effect of cystatin C on osteoclastogenesis may partly be explained by increased levels of OPG but that other mechanisms also contribute. The CD14 positive OC precursors might, while treated with cystatin C, persist as, and develop towards, macrophages at a specific differentiation stage at day 4 during PTH stimulation.

M257

CamKII Regulates Osteoclastogenesis. L. Zhang*, J. M. McDonald. Pathology, University of Alabama at Birmingham, Birmingham, AL, USA.

Previous work in our laboratory has demonstrated that calmodulin plays an important role in regulating the function of mature osteoclasts. In the present study, we explored the hypothesis that calmodulin is involved in osteoclastogenesis. Mice bone marrow monocytes were isolated and then cultured in the presence of RANKL and M-CSF. Calmodulin antagonists TFP (trifluoperazine), W7 and tamoxifen were added either on the first day or on the fourth day of culturing, then cells were fixed and cytochemically stained for TRAP activity on the fifth day of culturing. Meanwhile, cell lysates from parallel culture plates were obtained to measure TRAP activity in solution. All calmodulin antagonists dose-dependently inhibit osteoclast formation only when added on day 4 but not when added on day 1. IC50s for TFP, W7 and TMX are 3 µM, 5 µM and 1 µM respectively. Inhibition reached 60% for 3 µM TFP, 90% for 10 µM W7 and 80% for 3 µM TMX. These data suggests that calmodulin plays a role in the late stage of pre-osteoclast fusion, resulting in a dramatic reduction of osteoclast formation. To further identify downstream members of the calmodulin signaling pathway that regulate pre-osteoclast fusion, we have treated the cells with cyclosporin A, a specific inhibitor of the calmodulin dependent phosphatase, calcineurin, or KN93, a specific inhibitor for calmodulin kinase II (CamKII). KN93, but not cyclosporin A, inhibited osteoclast formation with an IC50 of ~1 µM (80% maximum inhibition obtained at 2 µM), indicating that CamKII but not calcineurin is involved in the formation of osteoclasts. Studies with a permeable caspase inhibitor, and TUNEL assays showed that apoptosis is not responsible for the action of TFP or KN93 on osteoclast formation. Preliminary electrophoretic mobility shift assays show that KN93 but not TFP blocks RANKL-stimulated NFκB activity. Taken together, our data indicate that CamKII mediates the preosteoclast fusion process, which is a key step in forming multinucleated mature osteoclasts.

M258

M-CSF: Its Role as an Osteoclast Differentiation Factor. R. Faccio[1], J. Chappel*[2], A. Zallone[3], F. P. Ross[2], S. L. Teitelbaum[2]. [1]Human Anatomy, University of Bari, Italy, and Pathology, Washington University, St. Louis, MO, USA, [2]Pathology, Washington University, St. Louis, MO, USA, [3]Human Anatomy, University of Bari, Bari, Italy.

ERK plays an important role in the proliferation of osteoclast (OC) precursors and survival of the mature cells. In this report we show that M-CSF induced ERK signaling, which activates RSK and upregulates c-fos, is also required for OC differentiation. These experiments took advantage of our observation that bone marrow macrophages (BMMs) derived from β_3 integrin knockout mice fail to differentiate into multinucleated OCs in the presence of a concentration (25 ng/ml) of M-CSF which promotes osteoclastogenesis in WT cells. In this study we show that the failure of M-CSF to induce osteoclastogenesis in β3-/- cells is correlated with attenuation of ERK phosphorylation, RSK activation and c-fos expression. Interestingly, high dose M-CSF (100 ng/ml) that rescues β3-/- OC formation, also nomalizes ERK and RSK activation and c-fos expression. Using the ERK inhibitor UO126 we find the ERK signal is required between day 2-3 of OC differentiation. Inhibition of ERK signaling within this time frame, reduces the number of TRAP positive cells by 50%. We next turned to the mechanisms of M-CSF activation of ERK in OC precursors. While M-CSF activates Ras/Raf1, such activation persists for only 15 min. On the other hand, Rap1 and B-Raf activation, which we demonstrate for the first time in OC precursors, mirrors the prolonged ERK phosphorylation, induced by M-CSF, being maintained for at least 2 hrs following cytokine exposure. In contrast to the profound effect of M-CSF on ERK activation, RANKL is a weak agonist. Since c-fos is activated by a prolonged ERK signalling and is required for osteoclastogenesis, we turned to its regulation by M-CSF or RANKL. We find that while M-CSF, alone, has little effect on c-fos expression by BMMs, the level of the proto-oncogene gradually increases during osteoclastogenesis. Interestingly, we find that pre-treatment with RANKL for minimal of 2 hours is indispensable to lead maximal c-fos expression in response to M-CSF alone. In fact RANKL itself is not sufficient to induce c-fos expression in BMMs or OCs. Thus, ERK induction during OC differentiation is principally a product of M-CSF signaling. On the other hand M-CSF maximal induction of c-fos, an event essential to the osteoclastogenic process, requires previous incubation with RANKL. Importantly, these data provide the first insights into the mechanism by which M-CSF promotes OC differentiation.

M259

Anti-SIRPα Inhibits Osteoclastogenesis in Human Osteoclast Progenitors. R. Faccio, F. P. Ross, M. Colonna*, S. L. Teitelbaum, D. V. Novack. Pathology, Washington University, St. Louis, MO, USA.

In the last few years, protocols to obtain human osteoclasts (hOC) from peripheral blood have been developed, but these require long and somewhat variable culture times to obtain mature cells. In this study we used hOC derived from primary human precursors (Cambrex product Poietics # 2T-110), which differentiate into mature bone-resorbing osteoclasts within seven days in the presence of M-CSF and RANKL, with addition of TGFβ during the last four days of the culture. As we have previously observed in OCs derived from other human and murine sources, mature hOCs derived from the Cambrex precursors are TRAP positive and express αvβ3 integrin in the podosome. When plated on dentin slices or an artificial mineral matrix, they show resorptive capabilities. We next examined the signaling capacity of the progenitor cells in response to RANKL stimulation. We found an increase in ERK and JNK phosphorylation, IκBα degradation and NF-κB DNA binding, with a similar timecourse to murine cells. Having established that these hOCs represent a robust model system, we examined the expression of several transmembrane receptors previously found on monocytes. The ILT (Ig-like transcript) family is characterized by 2 or 4 Ig-like extracellular domains. ILT's 2, 3, and 8 are members of a subset with cytoplasmic tails containing ITIMs (immunoreceptor tyrosine-based inhibitory motifs), and can inhibit cell activation via recruitment of phosphatases. ILT2 binds a subset of MHC class I molecules, while the substrates for ILT 3 and 8 are unknown. Signal-regulatory protein α (SIRPα) is a similar transmembrane protein with extracellular Ig-like domains, and a cytoplasmic ITIM. Antibodies to these proteins are available with human, but not murine, specificity. Immunofluorescent staining of hOCs was analyzed by confocal microscopy. ILT2 was expressed more highly on mononuclear cells than on mature hOCs, with a membrane staining pattern. ILT3 and SIRPα showed strong membrane staining in mature hOCs. ILT8 appeared to be intracellular, with a perinuclear distribution. We next attempted to determine whether these proteins modulate osteoclastogenesis by adding supernatants containing antibodies to these proteins, or an Ig control, to hOC cultures at days 0, 2, and 4. Compared to Ig control, only anti- SIRPα had any effect, blocking osteoclastogenesis almost completely. Anti- SIRPα treated cultures fixed and TRAP-stained at day 7 contained no spread multinucleated OCs, and only rare mononuclear TRAP positive cells (<2%). Previous reports have proposed a role for SIRPα as a fusion factor, but the effect of the blocking antibody suggests a more fundamental role at earlier stages of OC differentiation.

M260

RANKL Stimulates iNOS and NO Production in Developing Osteoclasts via NF-kB: An Autocrine Negative Feedback Mechanism to Regulate Osteoclastogenesis and Bone Resorption. H. Zheng, X. Yu, P. Collin-Osdoby, P. Osdoby. Department of Biology, Washington University, St. Louis, MO, USA.

RANKL is the key signal required for the full development, activation, and survival of resorptive osteoclasts (OC), via pathways involving NF-kB activation. Nitric oxide (NO) potently inhibits, while inhibitors of NO production stimulate, OC differentiation and bone resorption both in vivo and in vitro. During studies to examine RANKL-mediated OC formation (RAW-OC) from murine RAW 264.7 cell precursors, we discovered that NO levels (reflected in medium nitrite) became elevated. Thus, RANKL (35 ng/ml) elicited the in vitro development of multinucleated TRAP+ bone pit-resorptive RAW-OC that expressed mRNA for TRAP, MMP-9, cathepsin K, and calcitonin receptor. Concurrently, RANKL stimulated NO release and iNOS mRNA expression in RAW cells in a dose- and time-dependent manner, and these increases were sustained throughout the differentiation of RAW cells into RAW-OC. We therefore examined if autocrine NO production induced by RANKL in differentiating RAW cells had an inhibitory influence on OC formation or function. Aminoguanidine (AG) and L-NIL, selective inhibitors of iNOS-mediated NO release, each blocked RANKL-induced NO rises in the RAW cells and significantly enhanced the differentiation and fusion of RAW cells into TRAP+ multinucleated bone-resorptive RAW-OCs. Consistent with this, RANKL-mediated developmental increases in MMP-9, TRAP, cathepsin K and calcitonin receptor mRNA expression were further raised by L-NIL. Most importantly, bone pit resorption by RAW-OC was significantly potentiated if AG or L-NIL was present during their RANKL-mediated differentiation. Similar results were obtained with primary isolated murine bone marrow cells (MA). Thus, RANKL significantly increased iNOS mRNA expression and NO production throughout the differentiation of MA into TRAP+ multinucleated bone-resorptive OC, and L-NIL augmented bone pit resorption by OC during their RANKL-induced formation in vitro from MA. NF-kB activation was implicated in the signaling pathways by which RANKL both stimulated RAW-OC formation and induced iNOS mRNA and NO production because PDTC, a specific NF-kB inhibitor, blocked each of these RANKL-induced responses. Our results have therefore revealed that a novel mechanism through which NOS inhibitors promote OC differentiation and bone resorption involves their suppression of RANKL induced iNOS-derived NO. RANKL stimulated NF-kB dependent NO production therefore serves as an autocrine negative feedback regulatory signal to buffer osteoclastogenesis and bone resorption.

M261

Hyperlipidemia Enhances Osteoclastic Potential of Bone-Marrow Preosteoclasts. Y. Tintut*[1], B. Saedi*[1], T. Saini*[1], S. Arias-Magaloona*[1], F. Parhami[1], L. L. Demer*[2]. [1]Medicine, UCLA, Los Angeles, CA, USA, [2]Medicine & Physiology, UCLA, Los Angeles, CA, USA.

Emerging evidence suggests that lipid oxidation products, which are increased in tissues of hyperlipidemic subjects, play a role in both vascular calcification and osteoporosis. We previously found that lipid oxidation products have a paradoxical role in vascular and bone tissues: enhancing osteoblastic differentiation in vascular cells but inhibiting osteoblastic differentiation in bone marrow stromal cells as well as preosteoblasts in vitro. In addition, mice fed an atherogenic high fat diet have lower bone density than mice fed a normal chow diet. It is not known whether the decreased bone density was due to decreased osteoblastic function and/or increased osteoclastic function. We recently found that lipid oxidation products enhance osteoclastic potential of bone-marrow preosteoclasts in vitro. In this study, we determined whether hyperlipidemia enhances osteoclastic potential ex vivo. Osteoclastic function was determined in bone marrow preosteoclasts isolated from 1 year-old normolipemic (C57BL/6) and hyperlipidemic (low density lipoprotein receptor (LDLR) null) mice. The non-adherent bone marrow preosteoclasts were cultured in the presence of M-CSF (25 ng/ml) and RANKL (40 ng/ml), and TRAP and resorption assays were determined at 5 and 7 days, respectively. Results showed that LDLR null mice, which had higher triglyceride and total cholesterol levels, had a 3-fold increase in the number of TRAP positive cells and a 6-fold increase in the number of resorption pits compared to those of wild-type C57BL/6 mice. In additional experiments, preosteoclasts from bone marrow cells of LDLR null mice that were fed a high fat diet (which also causes aortic calcification) had increased numbers of TRAP positive cells and increased resorption pits compared with those of C57BL/6 mice. These results suggest that preosteoclasts from hyperlipidemic mice have higher osteoclastic potential than those of normolipemic mice supporting the hypothesis that hyperlipidemia may contribute to osteoporosis.

M262

TWEAK, a Novel TNF Homolog, Induces Osteoclast Differentiation of RAW264.7 Cells. T. C. Polek*, K. Ashikawa*, M. Talpaz*, B. G. Darnay, T. Spivak-Kroizman*. Bioimmunotherapy, U.T. M.D. Anderson Cancer Center, Houston, TX, USA.

TWEAK (TNF-like WEAK inducer of apoptosis) is a new member of the TNF family that has been shown to induce apoptosis in a limited number of cell lines and was implicated in angiogenesis. We describe herein a potential novel function for TWEAK as an osteoclastic factor. We demonstrate that a glutathione-S-transferase (GST)-fusion protein, GST-TWEAK, but not GST alone, induces the differentiation of RAW264.7 cells into large, multinuclear, TRAP positive osteoclasts within four days. RAW cells, a mouse monocyte/macrophage cell line, are often used as a model system to study osteoclastogenesis in response to receptor activator of NF-kB ligand (RANKL), a major osteoclastic factor. Like RANKL, TWEAK induces the differentiation of RAW cells into functional osteoclasts as determined by their ability to resorb an artificial bone matrix. TWEAK-induced differentiation and bone resorption activities are specific, since osteoprotegerin (OPG), a decoy receptor for RANKL, fails to block TWEAK action. Moreover, antagonistic anti-RANKL antibodies had no effect on TWEAK-induced osteoclast formation. TWEAK was less efficient than RANKL in inducing osteoclast differentiation of RAW cells, with its maximal activity reaching about 80% of RANKL activity. Interestingly, TWEAK and RANKL exhibited additive and not synergistic osteoclastic effects when used in combination, suggesting that they both utilize similar signaling pathways. RANKL-induced differentiation of RAW cells involves activation of the NF-kB, ERK1/2, and JNK signaling pathways. We demonstrate that like RANKL, TWEAK also activates these pathways in RAW cells. Using electromobility shift assays, we show that TWEAK induces the binding of the p50/p65 NF-kB heterodimer to DNA. NF-kB activation was accompanied by degradation of its inhibitor, I-kB. Furthermore, we show that TWEAK stimulates the phosphorylation of ERK1/2 and activates JNK in RAW cells. The ability of TWEAK to induce osteoclast differentiation of RAW cells may open new avenues for understanding processes controlling bone homeostasis and pathogenesis.

M263

Microphthalamia Transcription Factor Protein Expression Is Modulated by RANKL in Fusing Osteoclast Precursors. N. Dowland*, K. N. Weilbaecher. Internal Medicine, Washington University School of Medicine, St. Louis, MO, USA.

Microphthalmia transcription factor (Mitf) is a helix-loop-helix factor that plays a critical role in osteoclast(OC) development and fusion. Mitf mutant mice develop osteopetrosis secondary to non-functioning immature mononuclear tartrate resistant acid phosphatase (TRAP) positive osteoclasts. To characterize the regulation of Mitf expression in osteoclasts, we induced osteoclast differentiation using primary bone marrow macrophages stimulated with RANKL and M-CSF. On Day 0, osteoclast precursors are mononuclear and do not express TRAP. Mononuclear TRAP + precursors appear at day 1, by days 2 and 3 in culture the TRAP+ OC precursors begin to fuse and by day 4 large, spread, highly multinucleated osteoclasts develop. Using this primary cell system, we found that Mitf mRNA transcript levels are similar in macrophages and throughout all stages of osteoclast development; however Mitf protein levels were highest in fusing osteoclasts. We found that RANKL stimulation, which plays a critical role in osteoclast fusion, induced a rapid induction of Mitf protein in fusing osteoclasts (days 2 and 3) but not earlier at days 0 and 1. After RANKL stimulation of day 2 and 3 fusing osteoclasts, Mitf protein levels increased within 5 minutes and peak at 30 minutes. We have previously shown that Mitf is rapidly phosphorylated by ERK upon M-CSF stimulation of osteoclasts and that this ERK-mediated Mitf phosphorylation enhances osteoclast fusion. It has been also been shown that ERK mediated Mitf phosphorylation couples Mitf transactivation to proteasome-mediated degradation. Here we demonstrated that blockade of ERK activity by MEK inhibition did not prevent RANKL induction of Mitf levels. Thus, we find that RANKL induces a rapid increase in Mitf protein at a stage of osteoclast differentiation when mononuclear TRAP + osteoclast precursors are fusing. RANKL mediated induction of Mitf protein is not dependent on ERK mediated phosphorylation Mitf. We conclude that the stage specific induction of Mitf protein represents one mechanism by which RANKL could affect osteoclastogenesis.

M264

Effect of PPAR-Agonist on Bone Metabolism. L. Thommesen*[1], B. Theimann*[2], U. Syversen*[3]. [1]Institute of Physiology and Bioengineering Techniques, Norwegian University of Science and Technology, Trondheim, Norway, [2]Faculty of Medicine, Norwegian University of Science and Technology, Trondheim, Norway, [3]Institute of Intraabdominal diseases, Norwegian University of Science and Technology, Trondheim, Norway.

PPARs are nuclear transcription factors controlling the expression of genes involved in lipid homeostasis. PPARs activate transcription in response to a variety of compounds, including fatty acids and hypolipidemic drugs (e.g. Wyeth 14643 and ciprofibrate). We have recently shown that the PPAR-alpha agonist Wyeth 14643 increases bone mineral density (BMD) in female rats. Furthermore, previous studies indicate that supplementation with gamma-linoleic acid and EPA that are natural ligands for PPARs, has a beneficial effect on BMD in elderly patients with osteoporosis. In order to examine if the in vivo effect of PPAR agonists was related to an interference with osteoclast differentiation, we incubated human peripheral blood mononuclear cells (PBMC) with Wyeth 14643, ciprofibrate, gamma-linoleic acid and EPA in addition to osteoclast differentiating factors, RANK-L, MCSF and dexametazone. We found that Wyeth 14643 and ciprofibrate at a concentration of 50 uM reduced osteoclast differentiation by 40 - 50% compared to control. Wyeth 14643 and ciprofibrate also inhibited proliferation of the preosteoclast cell line RAW 264.7 in a dose-dependent manner. A potential cytotoxic effect was measured with MTT-assay, revealing a 20% reduction with the highest concentration used. Generation of osteoclasts from PBMC was inhibited in a dose-dependent manner upon stimulation with gamma-linolenic acid, linoleic acid or EPA. A concentration of 50 uM resulted in 60 -70% reduction of osteoclasts. Gamma-linolenic acid and EPA also increased proliferation of the murine osteoblast cell line MC3T3-E1 in a dose-dependent manner. In conclusion, these studies indicate that Wyeth 14643- and fatty acid-induced increase of BMD may be caused by reduced osteoclastogenesis, mediated by apoptotic and /or anti-proliferative effects on osteoclasts and preosteoclasts.

M265

Src Kinase Activity Is Involved in Osteoclastic Bone Resorption, but Not Their Survival. T. Miyazaki[1], A. Sanjay[1], L. Neff[1], S. Tanaka[2], W. C. Horne[1], R. Baron[1]. [1]Yale University, New Haven, CT, USA, [2]The University of Tokyo, Tokyo, Japan.

It has been reported that the kinase activity of Src is not important for osteoclastic bone resorption and that, in contrast, Akt activation mediated by c-Src kinase is important for osteoclast survival by RANKL. To further examine the role of Src kinase in these two regulatory events of osteoclast function, we constructed an adenovirus carrying kinase-dead Src (Src KD). Src KD was expressed in infected osteoclast-like cells (OCLs) in a dose-dependent manner. Src KD-OCLs do not display the typical rounded appearance of non-infected OCLs, and actin ring formation is disrupted in >90% of Src KD -OCLs. This morphology of Src KD-OCLs is similar to that of Src-/- OCLs. In addition, pit-forming activity was also severely inhibited in proportion to the expression level of Src KD protein. Since the autophosphorylation of Src promotes the adaptation of the fully open active conformation, the SrcKD might not be an effective adaptor, preventing us from concluding whether it is the open conformation or the kinase activity of Src that are required. To rule out this possibility, OCLs were co-infected with AxSrcKD and AxCskKD, which prevents the phosphorylation of the negative regulatory Y527 preventing the closed conformation of Src and promoting the availability of the SH2 and SH3 domains to bind other proteins. Phosphorylation of Tyr-527 in OCLs co-infected with SrcKD and CskKD was decreased to the level seen in the cells infected with CskKD only. The inhibitory effect of AxSrcKD on osteoclast function was not reversed by co-infection with AxCskKD, confirming that c-Src kinase activity, together with the adaptor function of Src, is indispensable for osteoclastic bone resorption., Next, we investigated the role of Src kinase activity in osteoclast survival. Recently, Akt activation mediated by c-Src kinase was reported to be important for RANKL-induced osteoclast survival. On the other hand, it has also been reported that it is the Ras/ERK signaling pathway that is responsible for osteoclast survival, since dominant negative Ras overexpression rapidly induced the apoptosis of OCLs, whereas ERK activation by constitutively active MEK1 (MEKCA) lengthened their survival. To examine the role of c-Src in regulating osteoclast survival, we co-infected OCLs with AxMEKCA and either AxSrcKD, AxCskWT, or AxCskKD. Neither SrcKD, CskWT, nor CskKD had any effect on the survival of OCLs infected with or without AxMEKCA. Interestingly, MEKCA overexpression led to prolonged survival of OCLs infected with AxSrcKD or AxCskWT. These results indicate that c-Src kinase activity is important for cytoskeletal organization and bone-resorbing activity of OCLs, but not for their survival.

M266

The Effect of Gu-Sui-Bu (Drynaria fortunei) on Bone Cell Activity: A Preliminary Study. G. I. Anderson[1], J. Sun*[2], B. L. Theriault*[1]. [1]Surgery/Biomedical Engineering, Dalhousie University, Halifax, NS, Canada, [2]Orthopedics, University of Taipei, Taiwan, Taiwan Republic of China.

Gu-Sui-Bu (Drynaria fortunei), a traditional Chinese herbal remedy, has been widely used as a therapeutic agent for bone disorders. Given the recent popularity of natural products and their increasing use by the Western population, there is concern about the potential toxicity of these herbal medicines, as well as interest in their mechanism(s) of action. In this study, we investigated the biological effects of Gu-Sui-Bu using in vitro bone cell cultures, to investigate a potential mechanism of action. In vitro cell culture – Rabbit osteoclasts and osteoblasts were isolated and cultured with five different concentrations of Gu-Sui-Bu (0.001, 0.01, 0.1, 1, 10 mg/mL) extract. Tartrate-Resistant Acid Phosphatase (TRAP) positive cell counts, and quantitation of osteoclast resorption pits on bovine bone slices were performed. Alkaline Phosphatase (AP) positive cell counts and mineralized nodule formation were established in osteoblast cultures. Mouse osteoclasts were isolated from marrow of long bones and cultured in the same conditions, with determination of TRAP+ multinucleated osteoclast counts and resorption pit formation. Determination of cellular mediators – Osteoclast precursors were harvested from the marrow of mouse long bones and cultured with identical extract doses. Levels of PGE2, M-CSF, OPG and RANKL were evaluated on days 1, 4, 6 and 8 of culture using Enzyme-Linked Immunosorbent Assays (ELISAs). Rabbit and mouse osteoclasts showed an increase in number and size of resorption pits as well as formation of TRAP+ multinucleated osteoclasts over time when treated with the lowest dose of extract (0.001 mg/mL). Rabbit osteoblasts did not show any significant change in number of AP+ colonies or mineralized nodule formation at low doses but were inhibited by 0.1 mg/mL or higher. The highest dose (10mg/mL) inhibited proliferation of all cell types. At lower doses of extract (0.01 and 0.001mg/mL) cultures exhibited increases in RANKL during the culture period. However, OPG levels did not increase at these doses but did at doses >/= 0.1 mg/mL. The higher extract treatment (10mg/mL) produced a marked decrease in PGE2, RANKL and OPG levels, while M-CSF secretion increased. Lower doses of Gu-Sui-Bu have positive effects on osteoclast proliferation, survival and resorptive activity that are possibly mediated by stimulatory action via the RANKL/OPG pathway, and possibly through prostaglandin secretion, while higher doses are potentially detrimental to osteoclast survival. High doses are also effective inhibitors of AP+ cell and bone nodule formation.

M267

Vav1 and Vav 3 Differentially Impact Osteoclast Formation and Function. R. Faccio[1], W. Swat*[2], M. W. H. Wang[2], A. Zallone[3], S. L. Teitelbaum[2], F. P. Ross[2]. [1]Human Anatomy, University of Bari, Italy, and Pathology, Washington University, St. Louis, MO, USA, [2]Pathology, Washington University, St. Louis, MO, USA, [3]Human Anatomy, University of Bari, Bari, Italy.

Osteoclasts (OCs) are motile cells, which must attach to bone and polarize before degrading the matrix. While many signals mediate cell migration, adhesion and polarization, one potential common pathway involves the small GTPase, RhoA, a regulator of cell motility, podosome formation and cytoskeletal re-organization. Activation of RhoA, in turn, is controlled by the Vav family of proteins. By histomorphometric analysis of long bones, Vav1-/- trabecular bone volume (BV/TV) is slightly increased about 38% ($p<.05$). In contrast Vav3-/- BV/TV is enhanced 270% ($p<.01$) and that of mice lacking both Vavs, 340% ($p<.01$). Moreover, radiographic analysis of tibia obtained from same age and sex matched mice confirms the increased trabecular bone of Vav3-/- and Vav1/Vav3 null animals. Despite data in Hela cells regarding the capacity of Vav3 to regulate cell division, M-CSF dependent proliferation of Vav1, Vav3 and Vav1/Vav3 null OC precursors, i.e. bone marrow macrophages (BMMs), is comparable to WT cells from 25ng/ml to 100ng/ml M-CSF. To test the hypothesis that OC formation and/or function are suppressed in mice lacking Vav1 and/or Vav3, we incubated BMMs with RANKL and M-CSF. While the rate of Vav1-/- osteoclastogenesis is delayed approximately 2 days, TRAP positive polykaryons appear by day 5 and function as normal OCs. In contrast, those OCs generated from Vav3 or Vav1/Vav3 null mice have a strikingly abnormal phenotype in that they are smaller, irregular and less spread. Confocal analysis of cells lacking Vav3 or both Vavs reveals dramatic changes in cytoskeletal organization, with failure to form regular actin rings at the cell periphery. Instead, actin is present in clusters of podosome-like structures widely distributed on the cell membrane. As a consequence of the aberrant cytoskeleton, OCs generated from Vav3 and Vav1/3 precursors fail to resorb mineralized matrix or generate pits on dentine slides. Importantly, retroviral transduction of Vav3 completely rescues the morphology and resorptive defect of both Vav3 and Vav1/Vav3 null OCs. Thus, Vav1 and Vav3 differentially impact the OC. Specifically, Vav 1 regulates the rate of OC differentiation and Vav3 the morphology and function of the cell.

M268

Development of a Novel Osteoclast Culture System Using Mouse Mandibular Body. N. Suda, Y. Kitahara*, T. Kuroda*, K. Ohyama*. Maxillofacial Orthognathics, Tokyo Medical and Dental University, Tokyo, Japan.

Mouse bone marrow cell culture, and co-culture of hematopoietic and stromal cells are highly reproducible and widely-used systems to generate osteoclastic cells, in vitro. It is known that osteotropic hormones or growth factors are required for osteoclast formation in these culture systems. Previously, we have reported that high expression of RANKL in dental follicle cells as well as osteoblasts lining on the alveolar bone surface. In addition, we have shown that the organ culture system of mouse tooth germ with surrounding tissues (dental follicle and mandibular alveolar bone) can generate TRAP-positive multinucleated osteoclastic cells without the addition of serum or any additives to the culture. These results suggest that developing mouse tooth germ and its surrounding tissues create a local environment highly inductive for osteoclast formation. To verify this hypothesis and to develop a novel mouse osteoclast culture system not requiring any osteotropic hormones or growth factors, we isolated and cultured primary cells from mandibular bodies. Primary cells were isolated from 9-11 day old mouse mandibular bodies including tooth germs and their surrounding tissues, and cultured in 15% FBS-aMEM. TRAP-positive multinucleated osteoclastic cells started to appear eight days after inoculation and the number continued to increase until day 14 of the culture. This progressive increase in osteoclastic cells is indicative of de novo cell formation. Cathepsin K and calcitonin receptor were localized in these osteoclastic cells, and the pit formation were observed when cells were cultured on dentin slices. The number of osteoclastic cells were significantly suppressed by OPG treatment. When primary cells were isolated from mandibular bodies that were free from tooth germs or their surrounding tissues, TRAP-positive multinucleated osteoclastic cells were not seen in the culture. These results suggest that functional cultured osteoclasts are formed in this culture system via RANK-RANKL. It is shown that tooth gems and the surrounding tissues are essential for the appearance of osteoclast in this system, corroborating our hypothesis that these tissues are creating a local environment highly inductive for osteoclast formation.

M269

Use of Peptide Phage Display to Identify Novel Stromal Cell Surface Molecules that Support Osteoclast Differentiation. P. He*[1], B. Wang*[2], E. M. Greenfield[1]. [1]Orthopaedics, Case Western Reserve University, Cleveland, OH, USA, [2]Medicine, Case Western Reserve University, Cleveland, OH, USA.

We previously identified three peptides from a phage display library that bind to ST2 cells cultured with 10 nM 1,25-D_3 but not to ST2 cells cultured without 1,25-D_3. Peptide #3 inhibits formation of multinucleated TRAP-positive osteoclasts induced by 1,25-D_3 in spleen cell / ST2 cell co-cultures. Maximal effects (~50% inhibition) are induced by 140 nM peptide #3. In contrast, peptides #1 and #2, as well as a scrambled form of peptide #3, have no detectable effect on osteoclast differentiation. We have now identified a fourth phage display peptide that also inhibits formation of multinucleated osteoclasts by ~50%. Peptide #4 is maximally effective at 14 pM, 10,000-fold lower than the maximally effective concentration of peptide #3. Both peptide #3 and #4 inhibit formation of multinucleated osteoclasts without affecting formation of osteoclast precursors (TRAP-positive mononuclear cells). Thus, the effects of peptides #3 and #4 are distinct from those of osteoprotegerin, which inhibits formation of both multinucleated osteoclasts and their mononuclear precusors. To identify extracellular matrix or cell surface molecules that bind to the peptides, we stably expressed Fc-fusion proteins encoding the peptides in HEK293 cells and purified them on Protein G-Sepharose. The Fc-fusion proteins were used to immunoprecipitate binding proteins from lysates of ST2 cells that had been surface biotinylated after culture for six days with or without 1,25-D_3. Western blots of the immunoprecipitated proteins showed that Fc fused to peptide #4 specifically binds to a biotinylated protein of approximately 230 kDa expressed by ST2 stromal cells cultured with 1,25-D_3. This protein is not bound to Fc alone and is not observed in samples from ST2 cells cultured without 1,25-D_3. The 230 kDa protein may be an importantant stromal cell surface molecule that regulates osteoclast differentiation.

M270

Characterization of Commercially Available Cryopreserved Primary Human Osteoclast Precursors. D. E. Greenwalt*, E. Bruno*. R&d, Cambrex, Walkersville, MD, USA.

Use of high-throughput screening techniques in the discovery of new drugs for osteoporosis is limited by both the absence of appropriate assays and the availability of osteoclasts and their precursors in large numbers. We herein report the characterization of a commercially available preparation of cryopreserved primary human osteoclast precursors isolated, after limited expansion, from hematopoietic CD34-positive progenitors. When thawed, 1 million or more osteoclast precursors, with viability at > 90%, were routinely recovered/cryovial. Precursors were resuspended in cell culture medium with supplements and growth factors and immediately seeded in 96-well cell culture plates. In some cases, the precursors were cultured on dentine discs. After 5 to 10 days, the cells were either stained for tartrate-resistant acid phosphatase or analyzed for CD61 expression (plates) or stained with Toluidine Blue to quantify resorption pits (discs). No changes of culture medium were required. The presence of M-CSF and soluble RANK ligand were required for osteoclast differentiation. M-CSF and sRANKL optimal concentrations were determined to be 25 ng/ml for each factor. It was found that addition of TGF-beta 1 (1 ng/ml) at day 3 of culture enhanced cell differentiation. The optimal seeding density was found to be 10,000 cells/well, which, on day 7 of culture, produced as many as 500 multinucleated TRAP-positive cells/well. Differentiated cells contained from 2 to >10 nuclei/cell. Bone resorption increased dramatically from day 7 to day 10. Interferon gamma dramatically inhibited differentiation of the precursors. The number of osteoclasts obtained from precursors isolated from three different donors varied less than 20%. The availability of large numbers of osteoclast precursors is required for high-throughput screening efforts. For example, 1 million cells are required to seed a 96-well bone resorption plate for subsequent assay by a robotic image analysis system. The primary human osteoclast precursors are available in large numbers and offer convenience of a cryopreserved product. The relatively minor variation observed due to donor sources insures screen-to-screen consistency. In addition the biological relevance offered by use of human cells decreases the occurrence of false negatives that might otherwise occur as a result of species-specific receptor binding. The osteoclast precursors will be of use in both the characterization of lead compounds that target osteoporosis and in high-throughput screening efforts in drug discovery programs.

M271

Application of Laser Capture Microdissection for the mRNA Analysis of Cultured Bone Marrow Cell. M. Nakamura, Q. Yang*, K. Takeda*, T. Hisamatsu*, Y. Nakamura*, I. Mori*, K. Kakudo*. Pathology, Wakayama Medical University, Wakayama, Japan.

Laser capture microdissection (LCM) is a new tool useful for recovering small amount of tissue samples and enables us to collect even individual cells from tissue sections. This method facilitates the separation of histologically different cells so that proteins, DNA, or RNA from these cells can be analyzed in isolation from the surrounding cells. Whether this method is applicable for culture cells is still unknown. The purpose of this study is to establish a method of dissecting single cultured bone marrow cell and test it captured cells are available for mRNA analysis. Bone marrow cells and spleen cells were obtained from 8 to 10 weeks-old male C57BL/6 mice. Both the cells were co-cultured on the LCM film (Leica Microsystems Co.) in α-MEM supplemented with 10% fetal calf serum and 10-8 M $1,25(OH)_2$ D for 6 to 8 days at 37 ºC. Cells were fixed on the film for 1 min by ethanol and stained for 3 min by filtrated hematoxylene followed by washing with sterilized water and air-dried for 10 min. 50-100 cells of osteocalsts or osteoblasts were captured from cultured cells using Application Solutions Laser Mycrodissection System (Leica Microsystems Co.). Total RNA was extracted from LCM captured cells using TRIzol LS Reagent. The SUPERSCRIPT TM One-Step RT-PCR with PLATINUM *Taq* (Invitrogen life technologies Co.) was used to synthesize cDNA and PCR. β-actin, calcitonin receptor, and receptor-activity-modifying-proteins (RAMP) primers were used for RT-PCR analysis. All PCR products were detected by above method. This approach will allow us to study single group cultured in various conditions.

M272

Osteoclastic Potential of Human Cord Blood Mononuclear Cells and Derived CFU-GM: Effects of M-CSF, GM-CSF and IL-3. J. M. Hodge*[1], M. A. Kirkland*[2], C. J. Aitken*[1], D. E. Myers*[1], G. C. Nicholson*[1]. [1]Department of Clinical and Biomedical Sciences, The University of Melbourne, Geelong, Australia, [2]Douglas Hocking Research Institute, Barwon Health, Geelong, Australia.

Osteoclasts (OC) and dendritic cells differentiate from hematopoietic cells of the monocyte/macrophage lineage. However, how and when their precursor cells diverge from this lineage is unclear. To further investigate OC lineage commitment we performed progenitor assays of human umbilical cord blood mononuclear cells (CBMC) followed by *in vitro* studies of osteoclastogenesis. CBMC were cultured in semi-solid media containing GM-CSF, IL-3 and stem cell factor. Pooled colonies or individual colonies identified as CFU-GM or CFU-M were harvested following 14 days of culture and transferred into 96-well plates containing dentine slices in the presence of RANKL and human M-CSF for a further 6 days. The efficiency of OC formation, calculated by dividing the number of nuclei resulting within mature OC by the initial seeding density, was 20% for CBMC and increased to 37% when precursors were obtained from pooled colonies. OC formation from precursors derived from CFU-GM was further increased by 88% and resorption by 45% compared to pooled colonies. However, more committed cells derived from CFU-M were very poorly osteoclastogenic. Pre-treatment of pooled colonies with M-CSF for 7 or 14 days prior to RANKL exposure for 14 days decreased OC size by 41% and 52% and resorption by 26% and 51%, respectively. In contrast, pre-treatment with IL-3 (plus M-CSF) for 7 days reduced OC number by 96%, and in the case of GM-CSF (plus M-CSF) completely inhibited OC formation in favour of TRAP-negative cell clusters indicative of dendritic cell activation. These results demonstrate that (i) clonal expansion of CFU-GM progenitors from human CBMC markedly increases osteoclastogenic potential. More committed CFU-M-derived progenitors appear to have lost their capacity to form OC; (ii) exposure of pooled colonies to M-CSF prior to RANKL only moderately reduces osteoclastogenic potential; (iii) exposure of pooled colonies to GM-CSF or IL-3 prior to RANKL stimulus completely inhibits osteoclastogenesis, directing cells instead towards dendritic cell differentiation.

M273

Transforming Growth Factor-β Induced Osteoclasts Survive by Activating Divergent Survival Pathways. A. Gingery[1], G. A. Gorny*[2], M. J. Oursler[3]. [1]Biochemistry and Molecular Biology, University of Minnesota, Duluth, MN, USA, [2]Biology, University of Minnesota, Duluth, MN, USA, [3]Biology, Biochemistry and Molecular Biology, Medical Microbiology and Immunology, University of Minnesota, Duluth, MN, USA.

Transforming Growth Factor - β (TGF-β) is a multifunctional growth factor that can either stimulate apoptosis or promote survival, depending on the target cell. During elevated bone resorption, osteoclasts release active TGF-β from the bone matrix. TGF-β has been reported to induce osteoclast apoptosis, yet there is no evidence of increased osteoclast apoptosis when bone resorption is elevated. Since osteoclasts differentiate in the presence of TGF-β within the bone environment, we investigated how the presence of TGF-β during in vitro differentiation influences osteoclast apoptosis. Once mature, osteoclasts were either maintained or withdrawn from TGF-β treatment for up to 24 hours. We observed that osteoclasts maintained in TGF-β survived longer than withdrawn cells. For this reason we have explored the mechanism of this survival. The second messenger PI3K has been implicated in survival in a number of cell types. We therefore examined two PI3K inhibitors with differing inhibitory mechanisms, LY294002 and wortmannin, for impacts on osteoclast survival. Wortmannin, but not LY294002, inhibited TGF-β withdrawn osteoclast survival whereas both the PI3K inhibitors inhibited TGF-β maintained osteoclast survival. PI3K activates multiple survival signals, including AKT and Raf/MEK/ERK. We have examined these pathways. There was increased AKT phosphorylation in the TGF-β maintained but not in the withdrawn osteoclasts. Using an inhibitor to MEK1/2 (U0126) we found that survival decreased in both the TGF-β maintained and withdrawn osteoclasts when MEK was blocked. MEK1/2 and ERK1/2 were phosphorylated in TGF-β maintained and withdrawn osteoclasts, providing evidence of MEK and ERK activation in these cells. Raf inhibition with Geldanamycin resulted in decreased survival of TGF-β maintained osteoclasts while it had no impact on survival of TGF-β withdrawn osteoclasts. We conclude from these data that osteoclast that are differentiated in the presence of TGF-β and at maturity are either maintained or withdrawn from TGF-β have divergent survival pathways. In particular, TGF-β maintained osteoclasts appear to activate the survival pathways AKT and Raf/MEK/ERK. In contrast, TGF-β withdrawn osteoclast survival, although requiring PI3K and MEK, do not require Raf activation. The increased understanding of survival signals for osteoclasts should provide future benefit in terms of both understanding normal osteoclast activity and pathological conditions of excess bone loss.

M274

Roles of NO for TNF-α Stimulation of Osteoclast Survival. S. Lee*[1], Z. Lee[2], H. Kim[3]. [1]National Research Laboratory for Bone Metabolism, Chosun University, Gwangju, Republic of Korea, [2]NRL for Bone Metabolism, Microbiol.&Immunol., Dental School, Chosun University, Gwangju, Republic of Korea, [3]Research Center for Proteineous Materials, Microbiol.&Immunol., Dental School, Chosun University, Gwangju, Republic of Korea.

Tumor necrosis factor α (TNF-α) has been shown to potently stimulate the survival of osteoclasts. We have previously demonstrated that the phosphatidyl inositol 3 kinase (PI 3-kinase)/Akt and the extracellular signal-regulated kinase (ERK) signaling pathways function for the TNF-α-promoted survival of osteoclasts. In the present study we investigated what downstream targets of PI 3-kinase/Akt and ERK are involved in the survival mechanisms. Treatment of mature osteoclasts with TNF-α did not induce cIAP-1, cIAP-2, XIAP, $Bcl X_L$, genes known to be antiapoptotic. Neither a change in phosphorylated Bad nor tBid, reported to regulate apoptosis, was detected. However TNF-α stimulation was found to cause induction of iNOS gene expression in purified mature osteoclasts. Blocking the generation of NO with the NOS inhibitor L-NAME suppressed the TNF-α-induced survival of osteoclasts, whereas treatment with SNP, a NO donor, stimulated osteoclast survival. Our findings suggest that NO produced by iNOS plays an important role in osteoclast survival by TNF-α.

M275

Inhibition of Protein Prenylation by Risedronate Causes Activation of Rac and PAK. J. E. Dunford*, F. P. Coxon, M. J. Rogers. Medicine & Therapeutics, University of Aberdeen, Aberdeen, United Kingdom.

Nitrogen-containing bisphosphonates drugs (N-BPs), such as risedronate (RIS), act by inhibiting farnesyl diphosphate synthase in osteoclasts. This prevents the synthesis of isoprenoid lipids required for prenylation of small GTPases, such as the Rho family proteins (Rho, Rac and Cdc42). Prenylation is essential for the correct function of small GTPases since it enables their interaction with specific subcellular membranes, where they can be activated by exchange of GDP for GTP. We therefore sought to confirm that N-BPs affect the activity of Rho family GTPases in J774 macrophages. In these cells, like osteoclasts, RIS treatment causes apoptosis. The activity of Rho GTPases was measured using a pull-down assay utilising agarose beads conjugated to the GTPase-binding domain of an effector molecule (Rhotekin or p21 activated kinase/PAK) that specifically binds the active, GTP-bound form of Rho, Rac or Cdc42. Precipitated, GTP-bound Rho, Rac or Cdc42 was then quantitated by western blotting. Surprisingly, treatment of J774 cells for 20 hours with 100μ M RIS caused an increase in the amount of GTP-Rac but had no effect on the amount of GTP-Cdc42 or GTP-Rho. Inhibition of Rac geranylgeranylation by 10μM GGTI-298 also caused an increase in active, GTP-Rac, but 1mM clodronate (a bisphosphonate that does not inhibit protein prenylation) had no effect. We next examined whether the active, GTP-bound Rac in RIS-treated J774 cells was prenylated or unprenylated. Cells were metabolically labelled with [14C]mevalonate in the absence or presence of RIS. GTP-Rac was then precipitated from lysates of RIS-treated cells using PAK-agarose. When lysates from untreated cells were incubated with GTPγS to maximally activate small GTPases, the precipitated GTP-Rac was radiolabelled and hence in the prenylated form. However, precipitated GTP-Rac from RIS-treated cells was not radiolabelled and hence was in the unprenylated form. To determine whether the active, unprenylated Rac that accumulated in RIS-treated cells was capable of activating downstream pathways, the activity of the Rac effector PAK was analysed using a [32P]-kinase assay with PAK immunoprecipitated from cell lysates. Treatment for 20 hours with 100μM RIS or 10μM GGTI-298 caused an increase in the kinase activity of PAK. These studies demonstrate that, in J774 cells, inhibition of protein prenylation by RIS causes activation rather than inhibition of Rac. The unprenylated, activated form of Rac can stimulate downstream PAK activity. Since prolonged Rac activation can cause apoptosis in some cell types, RIS may cause J774 apoptosis as a result of inhibition of prenylation and hence activation of Rac.

Disclosures: ***J.E. Dunford****, Procter & Gamble Pharmaceuticals 2.*

M276

Possible Involvement of Proapoptotic BH3-only Protein Bim in Osteoclast Apoptosis. T. Akiyama*[1], T. Inaba*[2], T. Okada*[3], P. Bouillet*[4], A. Strasser*[4], H. Oda*[1], K. Nakamura*[1], S. Tanaka*[1]. [1]Department of Orthopaedic Surgery, The University of Tokyo, Tokyo, Japan, [2]Department of Molecular Oncology, Hiroshima University, Hiroshima, Japan, [3]Departments of Molecular Biology, Jichi Medical School, Tochigi, Japan, [4]The Walter and Eliza Hall Institute of Medical Research, Melbourne, Australia.

The anti- and pro-apoptotic members of the Bcl-2 protein family play a central role in the signaling events leading to apoptosis in various types of cells. The BH3-only subfamily members are pro-apoptotic molecules, which trigger apoptosis via interaction with anti-apoptotic Bcl-2 members. A number of BH3-only proapototic molecules have been identified in mammals, including Blk, Bad, Bik, Hrk, Bid, Bim, Noxa, Puma, and Bmf, and it has been revealed that pathways to apoptosis induced by different damage signals involve distinct BH3-only proteins in their initiation. In an attempt to identify a key initiator of osteoclast apoptosis, we examined the expression of BH3-only proteins in osteoclasts. Osteoclast-like cells (OCLs) generated in co-cultures of mouse osteoblasts and bone marrow cells are subjected to rapid apoptosis in the absence of supporting cells or stimulatory cytokines. Interestingly, the apoptosis stimuli caused rapid increase in the protein level of Bim in the cells as determined by Western blotting, while the expression of other members did not show such dramatic changes. This increase appears to be due to the posttranscriptional regulation because Bim mRNA level did not change after the stimuli as determined by RNase protection assay and RT-PCR. Immunohistochemical analysis showed the time-dependent translocation of Bim to the mitochondrial membrane, which corresponded to the cytochrome *c* release to the cytosol. To further elucidate the role of Bim in osteoclast apoptosis, we utilized adenovirus vector expression system and Bim -/- mice. We constructed the adenovirus vector carrying Bim gene and successfully overexpressed Bim protein in OCLs. Adenovirus vector-induced overexpression of Bim induced rapid apoptosis in OCLs, which was inhibited by co-expression of anti-apoptotic Bcl-2 family protein, Bcl-xL. We finally compared the phenotypes of OCLs generated from Bim-deficient mouse bone marrow cells with those of wild type OCLs. OCLs differentiated from Bim -/- bone marrow cells showed remarkable resistance to the apoptosis stimuli, and about 100% cells survived after 48hrs of cytokine withdrawal compared to 0% survival in wild type OCLs. These results demonstrate that proapoptotic BH3-only protein Bim plays an essential role in osteoclast apoptosis

M277

Regulation of Osteoclast Survival by Nitric Oxide: Possible Involvement of NMDA-R. R. Mentaverri*, S. Kamel, M. Brazier. Laboratoire de Pharmacie Clinique, Amiens, France.

Nitric oxide (NO) has been shown to play a biphasic activity on osteoclast. At concentration greater than 10 μM, it was responsible for an inhibition of osteoclastic bone resorption while lower concentrations seem to be necessary to normal bone resorption. It is now clearly established that osteoclasts express inducible NO synthase (iNOS) which is upregulated by proinflamatory cytokines and produce large amount of NO. However, little is known about constitutive NOS isoenzymes which product small amounts of NO in osteoclast. In this work, using RT-PCR amplification, we demonstrate for the first time that mature osteoclasts prepared from 10-day-old rabbit express mRNA encoding for both endothelial and neuronal NOS suggesting that these two enzymes could be involved in production of low output of NO. In order to precise the possible involvement of constitutive NO in bone resorption process we assessed the effect of carboxy-PTIO, a NO scavenger, on osteoclast survival. Our results have shown that addition of carboxy-PTIO (10 - 100μM) induced osteoclast apoptosis in a dose dependent manner. After 18h of culture, the rate of apoptosis was three fold increased in osteoclasts treated with 100 μM of Carboxy-PTIO compared to untreated cells. The carboxy-PTIO-induced apoptosis was dependent of caspase 3 activity (measured with Ac-DEVD-AMC as substrate). These results suggest that basal concentration of NO is necessary to osteoclast survival. It has been recently demonstrated that osteoclasts express functional N-Methyl-D-Aspartate receptors (NMDA-R). In central nervous system, this receptor was involved in NO biosynthesis through a physical coupling with the calcium dependent neuronal NOS (nNOS). Therefore in this study, we tested the hypothesis that NMDA-R could be implicated in NO production in osteoclast. We first demonstrated that blockade of NMDA-R with MK-801 or DEP, two non-competitive specific NMDA-R channel blockers, leads to a rapid decrease in intracellular calcium concentration monitored by Ca2+-sensitive fluorescence dye (Fura2-AM). Concurrently, we observed a decrease in osteoclast survival in the same extent as those observed with carboxy-PTIO and that SNAP, a NO donor, was able to partially prevent the MK-801-induced osteoclast survival inhibition. Taken together, these results suggest strongly that in osteoclast, calcium entry throughout the NMDA-R channel could be involved in nNOS activation. In turn the NO production by this way may be important for the regulation of osteoclast survival.

M278

RANK Signaling through Calcineurin and Protein Kinase C Accelerates NF-κB Activation in Osteoclasts. S. V. Komarova*, S. J. Dixon, S. M. Sims*. CIHR Group in Skeletal Development and Remodeling, The University of Western Ontario, London, ON, Canada.

The binding of RANK ligand to its receptor RANK stimulates bone resorption by increasing osteoclast formation and activity. RANK activates the transcription factor NF-κB resulting in translocation of NF-κB from the cytoplasm to the nuclei. We have previously shown that RANK ligand activates phospholipase C in rat osteoclasts, leading to transient elevation of cytosolic free calcium, which in turn accelerates nuclear translocation of NF-κB. The purpose of this study was to investigate the mechanism underlying the effect of cytosolic calcium on NF-κB activation. Osteoclasts were isolated from neonatal rat long bone and nuclear translocation of NF-κB was assessed using immunofluorescence. Soluble RANK ligand (100 ng/ml) induced transient translocation of NF-κB from the cytosol to the nuclei, with maximal translocation at 15-30 min and reversal within 60 min. We examined the role of two calcium-sensitive effectors known to contribute to activation of NF-κB in other systems -- the calcium-calmodulin-dependent phosphatase, calcineurin, and protein kinase C (PKC). The calcineurin inhibitors, cyclosporin A (CsA, 1 μM) or FK-506 (10 nM) applied 30 min before addition of RANK ligand, suppressed initial NF-κB translocation (7 min), with no significant effect at later times (15-30 min). This finding is consistent with transient activation of calcineurin secondary to RANK ligand-induced elevation of cytosolic calcium. The PKC inhibitor bisindolylmaleimide I (BI, 100 nM), but not the inactive control bisindolylmaleimide V (BV, 100 nM) applied 30 min before addition of RANK ligand suppressed NF-κB translocation at 7 and 15 min, with no significant effect at 30 min. This finding is consistent with a role for PKC, activated following stimulation of phospholipase C by RANK ligand. The effects of calcineurin inhibitors and BI were additive at 7 min, however calcineurin inhibitors had no additional effect at 15 min. Taken together, these data indicate that calcineurin and PKC are downstream effectors of RANK that accelerate activation of the key transcription factor NF-κB. The kinetics of NF-κB translocation may be critical for controlling the transcription of genes regulated by NF-κB in concert with other factors. Moreover, these heretofore unrecognized signaling events may help explain the complex effects of immunosuppressants such as cyclosporin A on osteoclastic resorption.

M279

P38 Mediates RANKL-Induced NF-kB Activation and Osteoclastogenesis. S. Abbas*, Y. Abu-Amer. Orthopaedics & Cell Biology and Physiology, Washington University School of Medicine, St. Louis, MO, USA.

Receptor activator of NF-kB ligand (RANKL) is essential for differentiation of marrow macrophages into bone resorbing osteoclasts. RANKL binds to the cell surface receptor RANK and triggers several down stream signal transduction pathways, most of which have been shown to be involved in the osteoclastogenic process. Two such pathways are NF-kB activation pathway and the p38 MAP kinase pathway. Activation of these factors can be blocked by specific inhibitors. In this regard, earlier studies from our group as well as others documented that blockade of either pathway attenuates osteoclast development. Thus, we asked if these two pathway intersect throughout the osteoclast differentiation process. In the current study we have utilized purified marrow macrophages. In the presence of soluble RANKL, these cells form giant multi-nucleated osteoclasts that express tartrate-resistant acid phosphatase and resorb bone. First we show that administration of dominant-negative (DN) IkB, which blocks NF-kB activation, and selective inhibitor of p38, namely SB203580, significantly block osteoclastogenesis. We next examined if DN-IkB affects P38 status. P38 kinase activity which was induced by RANKL, appeared unaffected by DN-IkB, so as protein levels of the kinase. In contrast, we find that SB203580 dose-dependently inhibits osteoclastogenesis, which coincides with diminished NF-kB activity. Specifically, SB203580 at 0.1 - 10 microM blocked over 75% of NF-kB-DNA binding activity (by EMSA), and virtually inhibited entire osteoclastogenesis. These effects were reversible upon SB203580 withdrawal from the media, thus excluding cytotoxicity. Using co-imunoprecipitation studies, no direct physical interactions were observed between p38 and NF-kB, suggesting other co-factor(s) may be mediating this event. Supershift analysis was then employed to determine which NF-kB subunits are affected by p38 inhibition. Our data indicate that at least p65 NF-kB subunit is inhibited in the presence of p38 kinase inhibitor. We conclude that p38 participates and may be required for RANKL-activation of NF-kB in marrow macrophages and differentiating osteoclasts. Thus, inhibitory strategies targeting p38 may impede NF-kB-fueled inflammatory osteolysis.

M280

Mutation of the Src SH3 Binding Site on Cbl Reduces Src-Cbl Interaction, Cbl Phosphorylation and Bone Resorption in Osteoclasts. A. Sanjay, T. Miyazaki, W. C. Horne, R. Baron. Yale University, New Haven, CT, USA.

c-Cbl (Cbl) is a substrate of the non-receptor tyrosine kinase Src. Cbl is phosphorylated downstream of integrins in osteoclasts (OC) and like Src is involved in the regulation of OC motility. Cbl also negatively regulates Src kinase activity either by binding to the autophosphorylated tyrosine within the Src kinase domain or by ubiquitinating the activated Src kinase. We have found two distinct interactions between Src and Cbl, the first between the SH3 domain of Src and the proline-rich region (PR, aa 481-690) of Cbl and the second between the phosphorylated tyrosine 416 of Src and the phosphotyrosine binding domain (PTB) of Cbl. Mutation of the PTB domain did not prevent the interaction of Src and Cbl indicating that it is primarily due to the binding of the Src SH3 domain and the PR of Cbl. Using an in vitro peptide-binding assay we demonstrated that 540RDLPPPPPPPDRP binds to the Src SH3 domain. The binding of Src to a mutant c-Cbl protein in which these six prolines were replaced by alanines (Cbl6PA) was reduced in 293 VnR cells and in adenovirus-infected osteoclast like cells (OCLs). Cbl6PA phosphorylation was also reduced. Consistent with the role of Cbl as negative regulator of Src kinase, co-expression of Cbl and constitutively activated Src in 293 VnR cells led to a 80% decrease in Src kinase activity. This inhibition was partially prevented (55 %) by the co-transfection of Cbl 6PA indicating that the Src SH3/PR interaction is required for the inhibition of Src kinase activity. Interestingly, the pit forming activity of OCLs infected with Cbl 6PA was also significantly albeit moderately inhibited (25% decrease). This data supports our hypothesis that Cbl's interaction with Src, which is largely dependent on the SH3/PR binding and regulates the Src kinase activity and, thereby, bone resorbing activity. Thus, the interaction of Cbl with Src, which leads to phosphorylation of Cbl and the down regulation of Src kinase activity, is important for osteoclastic bone resorption.

M281

Inhibition of p38 MAPK Inhibits Bone Resorption Associated with Inflammation. G. Mbalaviele, A. L. Jones*, G. Anderson*, P. De Ciechi*, S. Settle*, J. Portanova*. Arthritis and Inflammation, Pharmacia Corporation, St. Louis, MO, USA.

MAPKs are proline-directed kinases, which include the insulin/mitogen-regulated extracellular signal-regulated kinase (ERK), the stress-activated protein kinases/c-Jun NH_2 terminal kinases (JNK) and the p38 kinases (p38). The ERK family is typically strongly stimulated by growth factors while the JNK/p38 pathways are activated by cellular stresses and inflammatory cytokines. Recent data indicate that TNF-α and IL-1β, potent activators of MAPKs are involved not only in inflammation, but also in bone resorption, in synergy with RANKL. These observations suggest that blockade of production and/or signaling of these cytokines is important to protect bone from destruction in inflammatory diseases such as rheumatoid arthritis. Thus, this study was designed to test this concept by using a novel selective p38 inhibitor, known to block inflammatory cytokine production. Human bone marrow $CD34^+$ hematopoietic stem cells and murine RAW 264.7 cells expressed p38α, but not p38β, p38δ and p38γ isoforms. Exposure of these cells to RANKL resulted in a rapid phosphorylation of p38, heat shock protein (HSP-27, downstream of p38), ERK, c-Jun (downstream of JNK) and IκB-α (NF-κB pathway). This inhibitor blocked 100% RANKL-induced HSP-27 phosphorylation, but not c-Jun and IκB-α phosphorylation in RAW 264.7 cells and $CD34^+$ cells. This inhibitor also decreased RANKL-induced DNA binding activity of transcription factor, myocyte-enhancing factor 2 (MEF2C, downstream of p38) as determined by electrophoretic mobility shift assay. To determine the role of p38 in bone resorption, human $CD34^+$ cells, murine bone marrow cells or RAW 264.7 cells were treated with p38 inhibitor (0-10 μM) and RANKL alone or in combination with TNF-α in the presence of M-CSF. RANKL and TNF-α-dependent osteoclast (Ocl) formation and activity were blocked in a dose-dependent manner up to 100% by the inhibitor. Finally, the role of p38 in bone resorption *in vivo* was tested in streptococcal cell wall-induced rat arthritis. In this model, p38 inhibitor prevented joint swelling (up to 80%), Ocl numbers and bone destruction assessed by radiography, micro-computed tomography and histomorphometry. While this inhibitor had no effect *in vivo* on OPG, MMP-3 mRNA expression, it did block ~ 95% RANKL, TRAP, MMP-9, -13, IL-6, and IL-1β mRNA , and DNA binding activity of MEF2C. In conclusion, these data demonstrate that p38 regulates the expression and signaling of osteoclastogenic factors, and selective inhibition of this pathway is sufficient to inhibit bone resorption associated with inflammation

M282

Protein Kinase C Affects Activities of a Voltage-gated Proton Channel in Murine Osteoclasts. H. Mori*[1], H. Sakai[2], H. Morihata*[3], M. Kuno[1]. [1]Physiology, Osaka City University Graduate School of Medicine, Osaka, Japan, [2]Orthopedic Surgery, Osaka City University, Osaka, Japan, [3]Neurology, Osaka City University, Osaka, Japan.

Osteoclasts, bone resorbing multinucleated giant cells, were differentiated from mononuclear preosteoclasts originated from the monocyte-macrophage lineage of hematopoietic stem cells. Osteoclasts attach to bone surface, form bone resorption pit sealed at clear zone, and then secrete a great amount of proton (H^+) ions and proteolytic enzymes into the pit to absorb bone mineral and matrix. Although the H^+ secretion is mediated mainly by a vacuolar type H^+-ATPase, osteoclasts are equipped with various pH regulating mechanisms, such as, $Cl^-/HCO3^-$ exchangers, Na^+/H^+ exchangers and a voltage-gated H^+ channel. The voltage-gated H^+ channel is opened at the membrane potential positive to the reversal potential determined by the pH gradient through the membrane. As the H^+ channel can extrude massive H^+ ions rapidly, the channel activation may induce drastic changes in intracellular and extracellular pH environments of osteoclasts. In this study, we have examined effects of protein kinase C (PKC) on the H^+ channel activity, because PKC activity is reported to modulate osteoclast functions. The whole cell H^+ currents were recorded from murine osteoclasts generated in the presence of a soluble form of receptor activator of nuclear factor kappa B ligand (sRANKL). The H^+ current density varied greatly among cells: generally, the current density was much larger in osteoclasts with < 5 nuclei than those with ≥ 6 nuclei. When cells were pretreated with a strong activator for PKC, phorbol 12-myristate 13-acetate (PMA; 1 μg/ml) for 30 min - 2 hrs, the current density and the activation rate in cells with < 5 nuclei were almost same to those in non-treated cells. In cells with ≥ 6 nuclei, the current-density and the activation rate tended to be enhanced by PMA and decreased by a PKC inhibitor, staurosporin (10 nM), but the changes were not significant. To evaluate the amount and temporal pattern of the effects of PMA in individual cells, the H^+ current was recorded in the permealized patches, where the intracellular machinery required for activation of PKC was preserved. In cells with small current density in control, PMA increased the current density up to 500 - 600% and decreased the activation time constant to less than 30 - 40% within 10 - 20 min. In cells with the large H^+ current activity, the effects of PMA were only slight. These results suggest that PKC is an activator for the voltage-gated H^+ channel in osteoclasts, although its efficacy may alter among cells dependently on the activation status of the channel.

M283

The Role of Postural Sway in the Maintenance of Bone Mass. K. J. McLeod*[1], J. P. Ryaby[2], J. M. McCabe*[3]. [1]Department of Bioengineering, Binghamton University, Binghamton, NY, USA, [2]Exogen Products, Smith & Nephew, Inc., Somerset, NJ, USA, [3]McCabe Research Associates, White Plains, NY, USA.

Osteoporosis is a common occurrence in the aged, but a similar pattern of bone loss also develops during extended bed rest, cast immobilization, and exposure to microgravity. These observations, and the established role of fluid flow in mediating bone formation and resorption led us to hypothesize that postural sway activity (resulting in enhanced bone fluid flow and skeletal muscle pump activation) should be associated with greater bone mass in individuals of comparable age. To address this question, we measured postural sway, bone mineral density, and blood pressure response to orthostatic stress, in a relatively homogeneous group of 13 post-menopausal women (mean age 76 ± 5 years). Bone density was assessed by DEXA, with duplicate measurements. Response to orthostatic stress was assessed by blood pressure and heart rate changes following three minutes of quiet standing. Postural sway was measured by recording the angular acceleration of a balance platform on the axis of medial lateral sway of the subjects. Acceleration recordings were converted to the frequency domain by Fast Fourier analysis, then converted to displacements, which were plotted on a log-log scale as a function of frequency. Postural sway was defined as the peak sway at 1 Hz, as obtained by linear regression. Postural sway measurements were repeated five times for each subject over the five month study period. Postural sway was observed to be highly correlated to bone density in the femoral neck region (R^2=0.72; P=0.0005). While increasing age was found to be associated with decreased postural sway (R^2=0.49; p=0.01), indicating a prevalence to a more rigid stance with advancing age, stepwise linear regression showed that neither age, body mass, or other body size indices were significant predictors of bone density in this group of women. Blood pressure changes in response to orthostatic stress also demonstrated significant correlations to both postural sway (p=0.005) and bone mineral density (p=0.04). We interpret these findings as indicating that postural sway provides a dominant stimulus for the maintenance of bone mass through its influence on blood flow and interstitial fluid flow in the lower appendicular and axial skeleton. We suggest that therapies which assure both adequate filtration through maintenance of normal capillary pressure, and adequate blood and lymphatic return through skeletal muscle pumping, will provide the most successful approaches to the prevention and treatment of osteoporosis.

Disclosures: ***K.J. McLeod****, Smith & Nephew, Inc. 2.*

M284

Modifiable Lifestyle Factors Associated with BMD in Adolescent Women. D. Scholes[1], A. Z. LaCroix[1], L. E. Ichikawa*[1], W. E. Barlow*[1], S. M. Ott[2]. [1]Center for Health Studies, Group Health Cooperative, Seattle, WA, USA, [2]Dept. of Medicine, University of Washington, Seattle, WA, USA.

Maximizing peak bone mass is essential for prevention of future morbidity from osteoporosis. Heritable factors predominate, but identification of modifiable risk factors offers opportunities for interventions aimed at improving bone health. We conducted a cross-sectional evaluation of lifestyle factors (6 dietary factors, physical activity, and current smoking) for their association with BMD in a population-based cohort of 174 adolescent women ages 14-18. Participants were enrollees of a Washington state HMO who were selected using the HMO's computerized databases. Data on risk factors were collected via exam and health and food frequency questionnaires. BMD was measured at the hip, spine and whole body using DEXA. After adjustment for the effects of age, height, weight, ethnicity, number of periods in the past year, and hormonal contraception, lifestyle factors most significantly and consistently associated with bone density at one or more anatomic sites were higher dietary intake of magnesium (positively associated) and consumption of caffeinated cola beverages (negatively associated). Current smoking and higher calcium and protein intake were also marginally significant in the expected directions (0.10≤adj. p≤0.13) for at least two anatomic sites. Factors examined but not significantly associated with bone density were weight-bearing physical activity, alcohol (drinks/mo., and g/day) and total caffeine (any, and mg/day) consumption.

Variable	Adjusted BMD (g/cm2)		
	Hip	Spine	Whole body
Magnesium (mg/d)	0.958	0.962	1.066
<180	0.952	0.976	1.072
180-<360	0.999	1.058	1.169
360+	adj. p=0.29	adj. p=0.04	adj.p=0.002
Cola drinks (drinks/day)	0.969	0.985	1.095
0-1	0.938	0.978	1.053
2+	adj. p=0.12	adj. p=0.72	adj. p=0.01

Consistent with other studies of this age group, two dietary factors-magnesium intake and cola drinking-were significantly associated with BMD and offer possible avenues for intervention. However, most of the lifestyle factors examined were not significantly associated with BMD in this cohort of healthy adolescent women. When compared to inherited and hormonal influences, these exposures may have relatively modest effects on bone density and peak bone mass attainment.

M285

Vitamin A Intake and Bone Mineral Density in Postmenopausal Women. P. B. Rapuri[1], J. C. Gallagher[1], V. Haynatzka*[2]. [1]Bone Metabolism Unit, Creighton University, Omaha, NE, USA, [2]Creighton University, Omaha, NE, USA.

The association between excess vitamin A intake and bone mineral density (BMD) is not clear. Some studies suggest that ingestion of excess vitamin A leads to accelerated bone loss and increase the risk of fracture while others found no association. In a population of 205 postmenoupausal women aged 55-72 years participating in a nutritional study, we examined at baseline the relationship between the total vitamin A intake (including both the dietary and supplemental vitamin A, expressed as retinol equivalents(RE)) and BMD at the spine, femoral neck, total body and mid-radius.Dietary vitamin A intake was assessed by 7-day food diary and information about the use of vitamin A supplements was also obtained from the subjects. The BMD at multiple skeletal sites were analyzed by quartiles of total vitamin A intake and also according to quartiles of dietary vitamin A intake after controlling for confounding factors (age, weight, smoking, alcohol intake, calcium and caffeine intake). There was no significant association between the BMD at all skeletal sites tested and vitamin A intake (both total and dietary).

Bone Mineral Density by Quartiles of Total Vitamin A Intake

quartiles (RE)/ variable	spine BMD	femoral neck BMD	trochanter BMD	total body BMD
1 (<6350)	1.10±0.14	0.88±0.10	0.76±0.10	0.92±0.12
2 (6350-10035)	1.06±0.16	0.84±0.09	0.73±0.09	0.87±0.09
3 (10035-13114)	1.13±0.19	0.87±0.11	0.76±0.11	0.92±0.12
4 (>13114)	1.07±0.15	0.89±0.10	0.75±0.10	0.90±0.10

values are mean±SD

M286

High Prevalence of Vitamin D Deficiency and Hyperparathyroidism in Elderly Population from the City of São Paulo, Brazil. G. L. Saraiva*[1], M. S. Cendoroglo*[2], J. R. Ramos*[2], L. M. Quirino*[2], I. Kunii*[1], V. A. Lui*[1], V. C. Z. Borba*[1], J. G. Vieira*[1], M. Lazaretti-Castro[1]. [1]Endocrinology, Unifesp, São Paulo, Brazil, [2]Geriatric, Unifesp, São Paulo, Brazil.

Osteoporotic fractures, mainly at the hip are events of high morbi-mortality in elderly population. European and American studies show correlation between these fractures with vitamin D deficiency and secondary hyperparathyroidism. In Brazil, a sunny country, vitamin D deficiency was never thought to be a medical problem. Intending to check the real situation of calcium metabolism in our elderly population, this study is being made. We evaluated 352 patients, 172 (118 women and 54 men) living in geriatric hospitals for at least 6 months (group A) with a median age of 77 y.o. (60 and 100 y.o), and 180 patients (129 women and 51 men) who live in their own houses (group B) with median age of 79 y.o (61-93 y.o.). A third group (C) of young healthful volunteers (median 32 y.o.) were analyzed to compare biochemistry values. We excluded recent bedfast patients or those with renal or hepatic insufficiency. Fasting blood samples were collected and intact PTH (normal range (NR): 10-70 pg/mL), 25-hydroxivitamin D3 (25OHD) (NR: 16-74 ng/mL) and ionized calcium (Cai) (NR: 1.12-1.32 mM) were analyzed. All patients had a quantitative calcaneus ultrasound measurement (USQ- Sahara, Hologic). The statistics analysis were made using Mann Whitney test and Spearman correlation and if p<0,05 it was considered significant. The median values of 25OHD were different in groups A, B and C (10.5; 18.8; 35.6 ng/mL, respectively), the PTH were also different in three groups (95.0; 80.0 and 42.0 pg/mL; respectively) and the Cai also differ in the three groups (1.29; 1.25 e 1.20 mM, respectively). We find the presence of 19 cases (11%) in group A and 9 cases (5%) in group B of hypercalcemia in association with inadequate PTH levels. The PTH in group A> group B (p=0,02) > group C (p<0,0001). The 25OHD in group A< group B (p=0,04) < group C (p<0,0001) and in group A 54% and in group B 35.5% of the patients showed vitamin D values below normal range. Using the A plus B group, age and calcium have positive correlation (p=0.01), PTH and 25OHD show positive correlation (p=0.003) and 25OHD and BUA also show a positive correlation (p=0.05); when these parameters were checked in each group, no correlation was found. The BUA (broad ultrasound attenuation) were lower in group A when compared with group B (p<0,0001). This study shows a high prevalence of vitamin D deficiency and hyperparathyroidism in brazilian population and it were more intense in the institutionalized patients. The elderly population may have benefits with vitamin D treatment but caution is recommended because of high prevalence of hypercalcemia.

M287

Fruit and Vegetable Intake Is an Independent Predictor of Bone Mass in Early-Pubertal Children. F. A. Tylavsky[1], K. Holliday*[2], R. K. Danish[1], C. Womack[1], J. Norwood*[1], K. M. Ryder*[1], L. D. Carbone[1]. [1]University of Tennessee, Memphis, TN, USA, [2]University of Memphis, Memphis, TN, USA.

Adequate intake of fruits (F) and vegetables (V) is recommended for optimum growth and development in children. The objective of this study was to determine if the consumption of 3-5 servings of fruits and vegetables is beneficial to bone mass in children. 58 white females in Tanner stage II recorded dietary intake on 3 independent days. The number of servings of fruits and vegetables were recorded for each day, tallied and divided into 2 groups for analysis. 21 participants reported consuming < 3 servings of F & V a day (4.5 ± 0.3 (mean ± SD)) with 37 reporting ≥ 3 per day (11.5 ± 0.5). Bone area (BA), bone mineral content (BMC) and density (BMD) of the whole body (WB), and lumbar spine (LS) were assessed using a QDR 2000 (Hologic, Inc). 24-hour urine samples were analyzed for the excretion of calcium (Ca) and sodium (Na). There were no differences between the low and adequate groups with respect to age (10.3 ± 0.3 vs. 9.9 ± 0.2) or BMI (19.5 ± 0.7 vs. 18.8 ± 0.5). Bone area, BMC and BMD for the WB and LS, and Na and Ca excretion were compared between the consumption groups, adjusting for age and BMI. Means (SD) for the dependant variables are reported in table 1.

Table 1 Mean (SD)

F & V intake	WB Area	WB BMC	WB BMD	Urine Na	Urine Ca
(N)	cm2	g	g/cm2	mmol/liter	mmol/liter
Low (21)	1189 (32)	957(41)	0.799(0.012)	146 (11.9)	3.8 (0.4)
Adequate (37)	1322 (25)	1099(28)	0.828(0.008)	142 (9.0)	2.2 (0.3)
% Diff (Adeq. vs. Low)	11.2	14.8	3.6	-2.7	-42.1
P value	0.02	0.03	0.32	0.78	0.002

Those with adequate F & V intake also had higher Area (p=0.03), BMC (p=0.10), and BMD (0.49) for the LS. Nutrient analysis showed that those with low F & V intake had lower calcium, potassium, vitamin A, and vitamin C intake (p<0.01). There were no differences in kilocalories, protein, fat, carbohydrate, magnesium or vitamin D intake between the consumption groups. Multivariate analysis showed the relationships between F& V consumption and WB Area and BMC remained after adjusting for calcium, potassium, vitamin A and vitamin C intake. Our data suggests that adequate F & V intake is an independent predictor of bone size and BMC of the total body in early-pubertal children. The increased excretion of calcium in the urine by those with low F & V intake is consistent with the acid-ash hypothesis that the consumption of F & V intake produces an alkaline diet and conserves the loss of calcium.

M288

Dairy Products Effects on Body Fat and Bone Composition in Children. T. P. McNaught*, G. M. Chan. Pediatrics, University of Utah, Salt Lake City, UT, USA.

Dietary calcium (Ca) may play a beneficial role in controlling body fat. Calcitropic hormones in a low Ca state may stimulate fat cells. In children, a critical time of fat development is between 4 and 8 years. It is hypothesized that children with additional dietary Ca from products will have low body fat. To test this hypothesis, 50 healthy children with low Ca intakes (< 800 mg/day) aged 2.5-8.8 years with mean age of 6±2 years (± SD) were studies for 6 months. The children were randomly divided into a dairy (14 females, 11 males) or control (15 females, 10 males) group. The dairy group was supplemented to 1200 mg Ca or four servings of dairy foods daily. Weight, height, and 2 day dietary records were recorded at the start, 3, and 6 months. Bone mineral content (BMC) and body fat determinations by dual energy X-ray absorptiometry body scans were recorded at the start and 6 month. Weights and heights were similar between the dairy and control groups at start, 3, and 6 month visit. At the start, total body fat between the two groups was similar. By 6 months, the controls had gained more body fat, 9.1±3.8 to 10.6±4.7 kg (paired t, P<0.001), while the dairy group's body fat was similar during the study 9.3±4.4 to 9.6±4.3 kg (NS). Bone mineral mass was similar between the two groups during the study. Daily dietary intakes of total calories, total fats, saturated fats, sodium, and carbohydrates were similar between the two groups during the study. At the start, Ca, protein, and vitamin D were similar between the two groups. By 6 months, the dairy group had higher daily Ca intakes (1317±233 vs. 753±426 mg, P<0.001), protein (66±15 vs. 48±20 g, P<0.001), and vitamin D (7.6±2.5 vs. 2.0±1.5 mcg, P<0.0001). In conclusion, children supplemented with additional Ca from dairy product gain less body fat than controls.

M289

Environmental Risk Factors and Quantitative Ultrasound Parameters in French Canadian Menopausal Women. S. Dodin[1], C. Blanchet*[1], M. Dumont*[2], N. Laflamme*[3], F. Rousseau*[4]. [1]Centre Ménopause Québec, Québec, PQ, Canada, [2]Nuclear Medecine Department, HSFA, Québec, PQ, Canada, [3]Signalgène, Montréal, PQ, Canada, [4]Research Unit in Human and Molecular Genetics, Québec, PQ, Canada.

The purpose of the study was to evaluate the prevalence of environmental risk factors among 3466 healthy French Canadian menopausal women (age : 60.5 ± 8.0 years, weight : 66.0 ± 12.1 kg, height : 157.1 ± 6.0 cm and body mass index (BMI) : 26.3 ± 4.8). Bone parameters of the right calcaneus, such as broadband ultrason attenuation (BUA; mean : 109.8 ± 10.1), speed of sound (SOS; mean : 1539 ± 30.7), and stiffness index (SI; mean : 84.0 ± 13.8), were measured by a AchillesTM ultrasound bone densitometry (QUS). All women answered a detailed questionnaire and anthropometry measurements were recorded. In order to identify the risk factors associated with QUS parameters, we performed Pearson correlation. Age, BMI, current hormone replacement therapy (HRT) use, smoking habits and history of family fracture were positively associated with bone mass assessed by ultrasound parameters. Then, a multiple linear regression model was built with stepwise removal of non-significant independent variables. The independent predictors of stiffness were age, BMI, leisure physical activity, current HRT users, smoking habits, history of family fracture, dairy product intake, and wrist fracture. These variables accounted for 20% of the variance in the stiffness(r2 = 0.1996). Similar models were built with BUA and SOS as dependent variables. In conclusion, many environmental risk factors are associated with QUS parameters, and these associations remains significant after controlling for potential confounding factors.

M290

Hypovitaminosis D in an Urban European Population. J. L. Sackrison*[1], J. J. Body[2], D. L. Ersfeld*[1], J. S. Fenske*[1], H. Cheblal*[2], C. M. Van Patten*[1], A. B. Miller*[1], M. Calleri*[3], G. D. MacFarlane[1]. [1]Research and Development, DiaSorin Inc, Stillwater, MN, USA, [2]Institut Jules Bordet, Brussels, Belgium, [3]DiaSorin s.r.l., Saluggia, Italy.

Serum 25 OH vitamin D (25 OH D) concentrations generally vary with latitude, season, and the composition of the populations studied. There is growing recognition that rather than seasonal specific decline in serum 25 OH D, a significant proportion of the population may exhibit asymtomatic subclinical vitamin D insufficiency. Vitamin D insufficiency has been described in populations at risk, such as nursing home residents and the homebound elderly. We assessed a population of normal, apparently healthy volunteers at a single European urban center for 25 OH vitamin D sufficiency. All samples were drawn in accordance to the Declaration of Helsinki. Serum 25 OH D concentrations were determined using an automated LIAISON® 25 OH Vitamin D assay (DiaSorin, Stillwater, MN). For the purposes of this study, vitamin D insufficiency was defined as a serum 25 OH D concentration of < 15 ng/ml. Of the total population (n = 126) 34% exhibited 25-OH D concentrations of < 15 ng/ml. The mean (±SD) serum 25 OH Vitamin D concentration among the total, sufficient, and insufficient populations was 19.4 ± 7.7, 23.6 ± 6.4, and 12.1 ± 2.3 ng/mL. Intact PTH, as assessed by the LIAISON® N-tact® PTH assay (DiaSorin, Stillwater, MN) showed no difference between the sufficient and insufficient populations (means = 34.4 pg/mL *vs.* 35.6 pg/mL respectively). From these data, we conclude that 25 OH D insufficiency is more common than previously thought, and is not restricted to high-risk groups such as the homebound elderly.

Disclosures: ***J.L. Sackrison****, DiaSorin Inc 3.*

M291

Risk Factors for Hip Fracture in Men. S. Muraki*[1], S. Yamamoto*[2]. [1]Orthopedics, Tokyo Metropolitan Geriatric Hospital, Tokyo, Japan, [2]Tokyo Metropolitan Geriatric Hospital, Tokyo, Japan.

Risk factors for hip fracture in elderly men with hip fracture were studied and compared with those found in elderly women with hip fracture. As subjects for this study, 1376 patients with hip fracture aged 65 years or older, who were admitted to Tokyo Metropolitan Geriatric Hospital from June in 1989 to May in 2001, were enrolled. At admission, risk factors for osteoporosis and accidental falls were examined. Risk factors for osteoporosis included diabetes mellitus (DM), chronic lung disease, chronic liver disease, chronic renal disease, a history of gastrectomy, a history of colonectomy, hyperthyroidism, rheumatoid arthritis, a history of uterectomy or ovarectomy before menopause (only female), a history of steroid administration, excessive smoking, and excessive alcohol intake. Risk factors for accidental falls included hemiplegia, Parkinson disease or syndrome, dementia, psychosis, and visual disorders. Among risk factors for osteoporosis, complication rates for excessive smoking, chronic lung disease, excessive alcohol intake and diabetes mellitus in elderly men with hip fracture was high, while, chronic lung disease and diabetes mellitus exhibited the same complication rates in elderly women. Among the aforementioned four factors, complication rates for all of them, except for diabetes mellitus, were significantly higher in elderly men with hip fracture than in elderly women with hip fracture. Among the risk factors for accidental falls, the complication rates for dementia, hemiplegia and visual disturbance was high in elderly men with hip fracture and the same in elderly women with hip fracture. Among the aforementioned three factors, the complication rate for hemiplegia was significantly higher in elderly men with hip fracture than in elderly women with hip fracture. The number of risk factors for osteoporosis in each patient was significantly larger in elderly men than in elderly women. Moreover the number of risk factors for hip fracture, which are risk factors for osteoporosis and risk factors for accidental falls, was significantly larger in elderly men with hip fracture than in elderly women with hip fracture. In elderly men with hip fracture, about 90% of all patients were complicated with more than one risk factor for hip fracture. Most risk factors could likely be prevented, however, systematic social efforts are required to do this, which is a problem to be solved.

M292

Use of Instant Vertebral Assessment in an Internal Medicine Practice. D. Greenblatt*[1], L. A. Jones*[2], K. E. Wilson[2]. [1]Internists of Fairfield, Fairfield, OH, USA, [2]Hologic, Inc., Bedford, MA, USA.

This study looked at the prevalence of vertebral fractures with respect to age and BMD status in patients referred for osteoporosis evaluation from within a multi-specialty internal medicine group. The patients had total AP spine, total hip, and femoral neck BMD measurements and an Instant Vertebral Assessment (IVA) exam. IVA is a low-dose, 10 s, single-energy, lateral X-ray exam of T4-L4. All measurements were performed using a Hologic Inc. QDR Delphi densitometer. The practice consisted of 4 internists, 2 rheumatologists, 2 pulmonologists and 2 nurse practioners, all of whom could refer patients for osteoporosis assessment. A number of the patients referred were undergoing care for chronic conditions, including those whose pathology or treatment are known to affect skeletal health. For this analysis, only female patients over the age of 50 years were considered. There were 172 patients (mean age 68.2 ± 9.8 years, maximum age 91). The subjects were classified by the lowest BMD T-score of the three measured sites and the WHO criteria. The IVA exams were read using the Genant's semi-quantitative method. The patients were also stratified into age decades.

Age	Total	# with fractures	% with fractures
50 - 59	42	2	5%
60 - 69	54	11	20%
70 - 79	54	24	44%
80 - 91	22	9	41%

The percentage of patients with fractures between ages 60-64 (5 of 22) was not statistically different from the number of fractures between the ages of 65-69 (6 of 32).

WHO	Mean age	Total	# with fractures	% with fractures
Normal	64.1	37	6	16%
Osteopenia	67.9	83	19	23%
Osteoporosis	71.4	52	21	40%

In this study population, the presence of Normal or Osteopenic BMD did not rule out the possibility of a prevalent vertebral fracture. 20% of the women in the age range of 60-69 and >40% of the women over the age of 70 had a prevalent vertebral fracture.

Disclosures: ***D. Greenblatt****, Hologic, Inc. 2.*

M293

Prevalence and Severity of Vertebral Fractures Among Patients with Chronic Obstructive Pulmonary Disease (COPD) in Canada. N. Ferko*[1], A. Papaioannou[2], J. D. Adachi[2], G. Ioannidis[2], E. Jurrianans*[2], L. Probyn*[2], G. Cox*[2], W. Parkinson[3], G. Stephenson[4]. [1]Clinical Health Sciences, McMaster University, Hamilton, ON, Canada, [2]Dept. of Medicine, McMaster University, Hamilton, ON, Canada, [3]School, Rehabilitation Sciences, McMaster University, Hamilton, ON, Canada, [4]Procter & Gamble Pharmaceuticals Canada Inc., Toronto, ON, Canada.

The severity of vertebral fractures has been correlated with reduced quality of life and chronic pain. The purpose of this study is to determine 1) the prevalence of vertebral fractures among patients with COPD admitted to acute care settings compared to age-matched controls and 2) the extent to which COPD patients with vertebral fractures were discharged on osteoporosis therapy and 3) the severity of fractures experienced by those with COPD. The design is a case-controlled study of 149 COPD patients identified by ICD-9 codes and 145 sex-and age matched controls, 50 years of age and over who were randomly identified from admissions in 1999 to acute care hospitals in Hamilton, Ontario. Outcomes were established using a chart review to identify diagnosis, medication use, and chest radiograph interpretations. The sample included 154 women and 140 men with a mean age of 72.2 (SD 12.2) and 71.9 (SD 8.2), years respectively. 246 chest radiographs were available for radiology review. Two radiologists blinded to the diagnosis applied Genant's criteria yielding disease severity in three categories: grade 1 (mild), grade 2 (moderate) and grade 3 (severe) deformities. Radiology review of chest radiographs indicates the prevalence of any type of vertebral fracture to be 38/124 (30.6%) in the COPD patients and 30/122 (24.5%) in the control patients, p=0.2834. The prevalence of grade 1 fractures was found to be 43/122 (35.3%) in the COPD patients and 39/124 (31.5%) in the control patients, p>0.5. The prevalence of grade 2 fractures was found to be higher for COPD patients, 19/124 (15.3%) and 8/122 (6.5%) for control patients, p=0.003. Similarly, the prevalence of grade 3 fractures is higher in COPD patients being 24/124 (19.3%) than in control patients, 4/122 (3.3%), p=0.0001. Of all patients with vertebral fractures, 7/18 (38.8%) had a diagnosis of osteoporosis indicated in their medical records. This study demonstrates an increased severity of vertebral fractures in those with COPD. This high-risk group should be targeted for the prevention and treatment of osteoporosis related fractures.

M294

Different Risk Factors of Forearm Fractures and Hip Fractures in 113.000 Scandinavian Women. The Scandos Study. M. G. Stenstrom[1], J. Stakkestad*[2], A. Skaag*[3], E. Öijfjord*[2], O. Johnell[4], D. Mellstrom[5]. [1]Geriatric Medicine, Goteborg University, Goteborg, Sweden, [2]University of Bergen, Center of Osteoporosis, Bergen, Norway, [3]Universty of Bergen, Center of Osteoporosis, Bergen, Norway, [4]Dep of Orthopedic Surgery, Malmoe University, Malmoe, Sweden, [5]Dep of Geriatric Medicine, Goteborg University, Goteborg, Sweden.

Scandinavian women have the highest known risk for hipfracture and vertebral fracture. A former fracture is a major risk factor to experience a new fracture. The question is if risk factors are the same for fracture in forearm and hip? A postal enquiry about issues concerning osteoporosis was answered by 113.000 women (aged 50-80 years) in the western part of Norway and Sweden. Mean age was 63.6 years. The prevalence of forearm fractures was14.472 and 2.482 women had sustained a hip fracture. A multivariat model showed that increased age and body height were risk factors and late menopause and higher body weight were protective factors for both forearm and hip fractures. Cortisone treatment (OR 1.965) and smoking (OR 1.241) were signifikant risk factors only for hip fracture. Daily walking was a protective factor against hip fracture (OR 0.749) and a risk factor for forearm fracture (OR 1.131). Estrogen treatment was only protective against forearm fracture (OR 0.697). This study showes that there are different risk factors for hip fractures and forearm fractures. Daily walking was a risk factor for forearm fracture and protective against hip fracture. Smoking and cortisone treatment were risk factors for hipfracture exclusively.

M295

Fracture Risk and Low Bone Mass: The Relationship Holds for Women Aged 80+. E. S. Siris[1], S. K. Brenneman*[2], T. W. Weiss*[2], S. Barlas*[2], Y. Chen*[2], P. D. Miller[3], E. Barrett-Connor[4]. [1]Columbia University, New York, NY, USA, [2]Merck & Co., Inc., West Point, PA, USA, [3]Columbia University, Lakewood, CO, USA, [4]University of California, San Diego, CA, USA.

Current knowledge of the risk factors for fracture is based largely on cohorts of women aged 60-79. Few studies have enrolled enough women age 80+ to specifically evaluate the association of fracture risk with bone mineral density (BMD). NORA enrolled 200,160 postmenopausal women aged 50 years and older. Baseline BMD was measured at the heel, forearm, or finger. In the current analysis, we included 163,935 NORA subjects who completed a one-year follow-up survey containing questions regarding incident fractures (wrist/forearm, rib, spine, hip) since baseline. Of these, 8517 were aged 80+, representing the largest known osteoporosis study cohort of this age group. Women were categorized into 3 age groups: 50-64 (53%), 65-79 (41%) and 80+ (5%). The prevalence of low BMD (T-score ≤ -2.0) was 6 % in those aged 50-64, 22 % in the age 65-79 group, and 47 % among those aged 80+. 2439 (1.5%) osteoporosis-related fractures were reported. Using logistic regression, the constellation of risk factors (i.e., BMD, years since menopause, education, health status, fracture history, race/ethnicity, BMI, glucocorticoid use, estrogen use, smoking status, exercise, and alcohol use) was predictive of fracture risk across age groups. Adjusted for these risk factors, older age was associated with greater risk for fracture. The relationship between low bone mass and increased fracture risk was statistically significant and comparable for each age group. (Table).

	50 - 64	**65 - 79**	**80+**
N	86690	66289	8517
# Fractures (%)	904 (1.0)	1206 (1.8)	329 (3.7)
Risk per age category (reference 50 - 64 years)	1.00	1.04 (.9, 1.2)	1.56 (1.2, 2.1)
Risk per 1 SD decrease in T-score (95% CI)	1.4 (1.3, 1.5)	1.4 (1.3, 1.5)	1.3 (1.1, 1.5)
Risk per T-score category (reference category >-1.0)			
-2.0 to -1.0 (95% CI)	1.7 (1.5, 2.0)	1.5 (1.3, 1.8)	1.5 (1.0, 2.2)
<= -2.0 (95% CI)	2.5 (2.0, 3.1)	2.4 (2.1, 2.8)	2.2 (1.5, 3.2)

In a large cohort of postmenopausal women, the relationship between BMD and fracture risk persisted regardless of age group. In women age 80+, fracture risk continued to be significantly associated with low BMD, after adjusting for other risk factors. The strength of the association was comparable with those of their younger counterparts.

Disclosures: ***E.S. Siris****, Merck & Co., Inc. 5, 8; Lilly 2, 5, 8; Aventis 2; Proctor & Gamble 8.*

M296

Hearing Acuity and the Risk of Incident Fracture in Older Women: The Study of Osteoporotic Fractures. E. L. Purchase-Helzner*[1], J. A. Cauley[1], E. Talbott*[1], S. Pratt*[2], J. Zmuda[1], M. Hochberg*[3], K. L. Stone*[4]. [1]University of Pittsburgh, Pittsburgh, PA, USA, [2]Universtiy of Pittsburgh, Pittsburgh, PA, USA, [3]University of Maryland, Baltimore, MD, USA, [4]University of California, San Francisco, CA, USA.

Hearing acuity may be related to bone health. Demineralization of the cochlear capsule and/or the internal auditory canal has been associated with hearing loss, and demineralization may be linked to osteoporosis. Hearing loss may also result in balance problems that may influence fracture risk by increasing the risk of falling. The purpose of this study was to test the hypothesis that hearing loss is related to decreased bone mineral density and increased risk of incident fracture in 6,718 older women (GE 65 years) from the Study of Osteoporotic Fractures. Hearing acuity at 25 and 40 decibels (dB) at 1000 and 2000 Hz was ascertained in both ears via screening audiometry. Women were classified as having normal hearing (passed screening at 25 and 40 dB); mild hearing loss (failed screening at 25dB only) or significant hearing loss (failed screening at both 25 and 40 dB), according to a modification of AAO guidelines. Classification was based on performance in the better ear. Incident non-spine fractures were ascertained every four months and confirmed by radiographic report. ANCOVA was used to assess the relationship between hearing loss and hip and calcaneal BMD, adjusting for age, BMI and estrogen use. Adjusted mean calcaneal BMD (g/cm^2) was 0.379 in the normal hearing group, 0.374 in the mild loss group, and 0.371 in the significant loss group (p=0.043). No significant difference in total hip BMD was seen across the hearing loss categories. Cox Proportional Hazards regression was used to evaluate the relationship between hearing loss and fracture risk over an average of 6.7 years, using women with normal hearing as the referent group (See Table 1). Based on age-adjusted models, women with mild or significant hearing impairment had no increase in all fracture risk, hip fracture risk and wrist fracture risk compared to women with normal hearing. In conclusion, preliminary results indicate only modest differences in BMD at the calcaneus across hearing loss categories, and results do not support the hypothesis that hearing impairment is a risk factor for fracture.

Table 1

Hearing Loss Category	Fracture Type	# women with Fracture	Hazard Ratio (95% CI)
Mild Loss (n=1764)	All non-spine, non-trauma	435	1.00 (0.89, 1.12)
	Hip	135	1.13 (0.91, 1.40)
	Wrist	87	0.96 (0.74, 1.24)
Significant Loss (n=937)	All non-spine, non-trauma	246	0.95 (0.92, 1.10)
	Hip	78	0.98 (0.75, 1.28)
	Wrist	48	0.94 (0.68, 1.31)

M297

Knowledge of Osteoporosis in a Fracture Population. R. K. Wilson*[1], V. Stas*[1], R. Ridout[1], N. Mahomed*[2], A. Gross*[3], A. M. Cheung[1]. [1]Department of Medicine, University Health Network & University of Toronto, Toronto, ON, Canada, [2]Department of Orthopaedics, University Health Network, Toronto, ON, Canada, [3]Department of Orthopaedics, Mount Sinai Hospital, Toronto, ON, Canada.

Osteoporosis places a substantial burden on patients, their social supports, and the health care system, and is an increasing public health concern as our population ages. It is known that patients with previous fragility fractures are at increased risk of future fractures. This study was designed to assess the knowledge of osteoporosis among fracture patients and to identify what social factors, health behaviours, and other characteristics determine this level of knowledge. Fracture patients aged 40 and over attending fracture clinics at two academic hospitals in Toronto were approached to fill out a questionnaire based on the "Facts on Osteoporosis Quiz" (FOOQ) [1], which has true/false/don't know questions on risk factors for osteoporosis as well as prevention and treatment. Our questionnaire included the FOOQ, which has a content validity of 0.92 and a reliability of 0.83, as well as a few additional questions. Of 259 eligible fracture patients, 204 (78.8%) agreed to participate. Respondents were predominantly (63.7%) female. Just over half (56.8%) of respondents were between 40 and 60 years of age, and most of them (84.8%) were Caucasian. The mean number of correct responses was 16.5 out of 30 (54.8%). There were no differences between the two hospitals with respect to level of knowledge or patient characteristics. We found that women had a higher level of knowledge than men (p<0.001) and that post-menopausal women taking estrogen therapy knew more than those who did not (p=0.030). Other characteristics associated with a greater number of correct responses were English as the first language (p=0.004), having a post-graduate education (p=0.004), taking calcium supplements (p=0.001), having had a BMD test previously (p<0.001), having osteoporosis (p=0.007), knowing someone with osteoporosis (p<0.001), and having received information about osteoporosis (p=0.001). The level of osteoporosis knowledge in the fracture population in our study seems inadequate, as the average score of 54.8% represents a fairly low level of knowledge. More needs to be done to educate fracture patients about osteoporosis risk factors, prevention and treatment. This study has also highlighted certain groups that should be targeted for osteoporosis educational initiatives, so as to appropriately reduce the risk of future fractures in this population.

References 1. Ailinger RL, Harper DC, Lasus HA (1998) Bone up on osteoporosis. Development of the Facts on Osteoporosis Quiz. *Orthop.Nurs.* 17:66-73

M298

Associations of Number and Type of Vertebral Deformities with Back Pain among Japanese Women. H. Kitahara[1], K. Aoyagi[2], P. D. Ross*[3]. [1]Nagasaki University, Dept of Surgery, Nagasaki, Japan, [2]Dept of Public Health, Nagasaki, Japan, [3]Merck & Co.,Inc, Rahway, NJ, USA.

Vertebral deformity is a classical hallmark of osteoporosis. Three types of vertebral deformity are often described: crush, wedge and endplate. However, there are few data concerning the descriptive epidemiology of the individual deformity types, and the relative clinical impact in Japanese women. We examined the associations of number and type of vertebral deformity with back pain among 584 Japanese women ages 40 to 89 years. Lateral spine radiographs were obtained and radiographic vertebral deformities were assessed by quantitative morphometry, defined as vertebral heights more than 3 SD below the normal mean. Vertebrae which met this criterion for the posterior height were classified as crush; among the remaining vertebrae, those that had an anterior height reduction were called wedge, and those that only had a central height reduction were called endplate. A self-administered questionnaire was used to survey participants about back pain in the previous one month. The overall prevalence of back pain was 30% and was relatively constant after age 50. Endplate (84 vertebrae) and wedge (82 vertebrae) were the most frequent types of deformity, and there were 50 vertebrae with crush deformity. The prevalence of deformity was highest in the T12-L4 region, with a smaller peak centered at T8. In an age-adjusted logistic regression model, the odds of back pain was 2.3 (95% CI: 1.2-4.4) times higher for women with a single wedge deformity, and 5.0 (95% CI: 1.7-14.1) times higher for women with 2 or more wedge deformities, compared to women with no wedge deformity. Both a single any deformity (odds ratio, OR: 2.6, 95% CI: 1.3-5.1) and 2 or more any deformities (OR: 2.4, 95% CI: 1.3-4.6) were associated with back pain, independent of age. Separate analyses of endplate and crush deformities yielded associations that were smaller in magnitude, and were not significant. Additional adjustment for body mass index and number of other painful joints did not alter these findings. These data suggest that vertebral wedge and endplate deformities are more common than crush deformity, and that wedge deformities may be more strongly associated than endplate or crush deformities with back pain in Japanese women.

M299

Hip, Wrist, and Lower Extremity Fractures Predict the Development of Future Hip Fractures. B. J. Edwards[1], A. Bunta*[2], L. Fitzpatrick[3], M. Bolander*[4], C. Simonelli[5]. [1]Medicine, Northwestern University, Chicago, IL, USA, [2]Orthopaedic Surgery, Northwestern University, Chicago, IL, USA, [3]Medicine, Mayo Clinic, Rochester, MN, USA, [4]Orthopaedic Surgery, Mayo Clinic, Rochester, MN, USA, [5]Medicine, Health East, Minneapolis, MN, USA.

The Fracture Intervention Work group was established in 2000, with the goal of developing and establishing clinical algorithms for the evaluation and treatment of osteoporosis-related hip fractures between. All subjects admitted with low trauma hip fractures between 1999-2001were assessed. High-speed trauma, known metastatic cancer or metabolic bone disease were excluded. Clinical data such as patient demographics, co-morbid medical conditions, prior fractures, location of prior fractures, prior diagnosis and treatment for osteoporosis were analyzed. Statistical analysis was performed with SPSS using t-test and chi square. A total of 638 patients were assessed Age: 80 ± 12 yrs. for females, and 73 ± 12 years for males (p=0.002). Predominant ethnic origin was white (> 90%) and a female : male ratio of 4:1. Female weight 61 ± 16 Kgs., and males 78 ± 18 Kgs. (p=0.001). 263 patients (41%) with current hip fractures had presented a prior minimal trauma fracture, in (7) 3% of cases these were multiple fractures. Prevalence of prior fractures was highest at Northwestern University with 62%, and comparable at Health East and Mayo Clinic at 40 and 41%. The sites of previous fracture included: hip (101) 38%, wrist (84) 32%, lower extremity : femur, tibia, fibula, ankle, foot (55) 21%, vertebral (27) 10% and pelvis fractures (9) 3%. Among the lower extremity fractures ankle fractures were the most common (29) 50%. Individuals were cognitively impaired in (10) 9% of the Northwestern cohort while this increased to 25% of the Health East and Mayo Clinic subjects. In a similar fashion nursing home residence was lowest at Northwestern (11%) while higher at Health East and Mayo Clinic. The presence of a prior minimal trauma fracture increased the likelihood of osteoporosis being diagnosed (p< 0.05) However, in spite of a diagnosis of osteoporosis, these individuals were no more likely to receive osteoporosis treatment than those without this diagnosis (<15%) Gait disorders were present in 61% and 55% of subjects at Northwestern University with or without prior fractures. (p= NS) Our results suggest that although prior fractures are common in patients who subsequently develop hip fractures, the presence of such does not increase the likelihood of being diagnosed or ttreated for osteoporosis.

Disclosures: ***B.J. Edwards****, Merck Pharmaceutical 2, 5, 8; Procter and Gamble 5, 8; Eli Lilly 8; Wyeth Ayerst 8.*

M300

Validity of Self-Report of Fractures among a Postmenopausal Multiethnic Cohort ---Results from the Women's Health Initiative. Z. Chen[1], C. Kooperberg*[2], M. B. Pettinger*[2], T. Bassford*[1], J. A. Cauley[3], A. Z. LaCroix[2], C. E. Lewis[4], S. Kipersztock*[5], M. C. Borne*[6], R. D. Jackson[7]. [1]University of Arizona, Tucson, AZ, USA, [2]Fred Hutchinson Cancer Research Center, Seattle, WA, USA, [3]University of Pittsburgh, Pittsburgh, PA, USA, [4]The Universityof Alabama at Birmingham, Birmingham, AL, USA, [5]University of Florida, Gainesville, FL, USA, [6]UCLA Medical Center, Los Angeles, CA, USA, [7]The Ohio State University Medical Center, Columbus, OH, USA.

The purpose of this study is to examine the validity, and factors associated with the accuracy, of self-reported fractures. This study was conducted in Women's Health Initiative (WHI) Clinical Trial (CT) and Observational Study (OS) cohorts. All women were postmenopausal at the time of enrollment; populations included American Indian, Asian/pacific islander, black, Hispanic, and non-Hispanic white. The average time of follow-up was 4.4 years. Self-reported hip fractures were adjudicated by reviewing medical records, while non-hip fractures were only confirmed for all participants in the CT and OS participants in the three WHI bone mineral density (BMD) centers. We included 160,703 women (67,838 were CT participants and 92,865 were OS participants) in the analyses for hip fracture. Non-hip fractures were studied among 74,989 women from the CT and the three BMD centers. Multiple fractures from a single event were not included in this report, and only the first self-reported fracture for each woman was counted here. Of the 623 self-reported hip fractures, 78.2% were confirmed by medical records, and 2.5% were adjudicated as other fractures. Among the non-hip fractures, the overall accuracy of self-report was high for arm fractures (83-86%) and lower leg fractures (77.8-83%). About half (52%) of self-reported spine fractures had a confirmed fracture at the exact or an adjacent skeletal site. Confirmation of reported tailbone fractures was low (46%). Results of the multivariate analysis indicated several factors were significantly related to the accuracy of self-report of fractures. Minorities, except Hispanic women, were more likely to over-report fractures than non-Hispanic whites. Large body mass index, history of osteoporosis, history of fracture, more than three falls in the last 12 months, high physical activity level, depression and living in the midwest or south region of the United States were associated with lower accuracy of self-reported fractures. In conclusion, results of our study suggest that some osteoporotic fractures (hip, lower arm) are reported with high accuracy whereas other types of fractures (spine, tailbone) have unacceptably low rates of confirmation. The validity of self-report of fractures may be affected by multiple factors.

M301

Maternal Hip Fracture and Current Smoking Are not Associated with Hip Fracture Risk in Elderly Women in the UK. S. K. Bal*[1], K. Kayan[1], A. Richards*[1], S. Vasireddy*[1], J. Cliffe*[1], A. Hinch*[1], C. McGurk*[1], T. Jalava*[2], M. Beneton*[1], J. A. Kanis[1], E. V. McCloskey*[1]. [1]University of Sheffield, Sheffield, United Kingdom, [2]Leiras Oy, Helsinki, Finland.

An assessment tool for fracture risk, developed from the SOF study, has been tested in an elderly French female population. In French women, fracture risk was underestimated compared to US women suggesting that some risk factors may not have the same relevance in different populations. For this reason, we studied the value of risk factors identified in the SOF study to women in the UK. We studied 4347 community dwelling women aged ≥ 75 years selected randomly from Sheffield and the surrounding area who were enrolled subsequently to a randomized placebo-controlled study of bisphosphonate treatment. At entry, each woman underwent a detailed assessment of their health including questions and measurements similar to that in the SOF tool for risk assessment (age, prior fracture, maternal history of hip fracture, low weight, current smoking, difficulty in sit-to-stand and DXA-measured total hip BMD). The gradients of risk for incident hip and all osteoporotic fractures were computed from univariate logistic regression analysis and all factors were entered to a multivariate forward conditional regression to determine their independent contribution, if any, to fracture risk. During a median follow-up of 4 years, one or more incident osteoporotic fractures occurred in 454 women (10.4%) including hip fractures in 131 women (3%). With regard to hip fracture risk, only 4 of the 7 assessments were significantly associated with increased risk of fracture in univariate models. Maternal history of hip fracture (OR and 95%CI, 1.2, 0.5-2.7), prior fracture after age 50 years (1.1, 0.7-1.5) and current smoking (0.8, 0.3-1.9) were not significant predictors of risk. In multivariate analyses, body weight (<57 Kg) was only significant in models that excluded total hip BMD T-score. For all osteoporotic fractures, maternal history and current smoking were again not significantly associated with fracture risk in univariate models (1.2, 0.7-1.9 and 0.7, 0.5-1.2 respectively). In multivariate models, age was not a significant independent contributor to fracture risk and, similar to the observation for hip fracture alone, weight was only a significant predictor in the model excluding hip BMD. We conclude that maternal history of hip fracture and current smoking are not significantly associated with the risk of osteoporotic fractures in elderly women in the UK. Caution is required in accepting the utility of risk factors derived from one region to another. There is a need therefore for international validation of putative risk factors before they can be applied globally.

Disclosures: ***E.V. McCloskey****, Leiras Oy, Helsinki, Finland 2.*

M302

Determinants of Bone Mass, Size, Architecture and Distribution in Middle Aged and Older Men. R. Daly[1], M. Brown*[1], S. Bass[1], C. Nowson*[1], E. Briganti*[2]. [1]School of Health Sciences, Deakin University, Melbourne, Australia, [2]Dept of Epidemiology and Preventive Medicine, Monash University, Melbourne, Australia.

Osteoporosis represents a major public health problem in men. Many factors may contribute to an individual's risk of developing osteoporosis and subsequent fracture, but bone mass is a primary determinant. While bone mass is related to bone strength, bone size (cross-sectional area, CSA), architecture and the structural distribution of bone (cross-sectional moment of inertia, CSMI) also influence bone strength. However, little is known about the determinants of these parameters in older men, and it is uncertain whether risk factors for bone mass are the same as for CSA, architecture and CSMI. To investigate determinants of parameters related to bone strength in middle aged and older men (n=144) aged 49 to 87 years (mean ± SD, 61.8 ± 7.6 yrs), we measured femoral neck BMC, BMD, CSA and CSMI (DXA, hip strength analysis), as well as heel BUA. Explanatory variables included age; height, weight, fat mass and lean mass; exercise, smoking, and calcium, tea, coffee and alcohol intake; history of fracture after the age of 45 years, hypertension, diabetes, asthma and arthritis; use of antihypertensives, thiazide diuretics, diabetes and lipid lowering agents, antidepressants and corticosteroids; and family history of osteoporosis. BMD T-scores indicating osteopenia (-1.0 to -2.5 SD) and osteoporosis (below -2.5 SD) were found in 34.7% and 6.2% of the men, respectively. The initial regression model included explanatory variables with a P-value <0.20 on univariate analysis. The final model was determined by purposeful backward stepwise regression using the log likelihood ratio test, with a P-value <0.10 considered significant (Table). The total variance for FN bone traits explained by these models ranged from 17-34%.

Beta-coefficients	BMC g	BMD g/cm^2	CSA mm^2	CSMI mm^4	Heel BUA dB/MHz
Weight, per kg	+0.050	+0.005	+1.5	-	-
Height, per cm	-	-	+0.6	+183.4	-
Fat mass, per kg	-0.040	-0.004	-1.3	-	-
Lean mass, per kg	-	-	-	+276.2	-
Hypertension	-0.409	-0.061	-16.5	-	-
Fx history	-	-0.056	-	-	-
Use of antihypertensives	-	-	-	-	-5.89
Daily coffee intake, per cup	-	-	-	-	+1.58
Adjusted R^2	31.3%	16.7%	31.5%	34.3%	4.3%

In summary, hypertension, fat mass and weight were important determinants of bone mass and size, while history of fx was associated only with bone mass and height only with bone size. In contrast, only lean mass and height were associated with the structural distribution of bone. These results indicate that different parameters related to FN bone strength may be affected by different clinical risk factors. The role of hypertension as a determinant of bone strength parameters requires greater attention.

M303

Body Composition Correlates of Total Hip Bone Mineral Density in Afro-Caribbean Men: Tobago Bone Health Study. D. D. Hill*[1], J. A. Cauley[1], A. Patrick*[2], J. M. Zmuda[1], V. Wheeler*[2], C. H. Bunker*[1]. [1]Epidemiology, University of Pittsburgh, Pittsburgh, PA, USA, [2]Scarborough Regional Hospital, Scarborough, Trinidad and Tobago.

Body weight is a strong determinant of bone mineral density (BMD). Body weight consists of several components, including fat mass and lean mass. The relative contribution of lean mass and fat mass to BMD is uncertain, particularly among men and non-Caucasian populations. To test the hypothesis that lean mass and fat mass are independently correlated with BMD in men of African ancestry, we studied the relationship between body composition (lean mass and fat mass) and BMD in a cohort of 2,076 Afro-Caribbean men, aged 40 and over, who were enrolled in the Tobago Bone Health Study. Body composition and BMD were measured with a Hologic QDR 4500W densitometer. The mean age and height of men were 59.2 ± 11.2 years and 82.8 ± 14.6 kilograms, respectively. Both lean mass (r = 0.46) and fat mass (r = 0.26) were correlated with total hip BMD. In models considering lean mass or fat mass separately, both were independently related to hip total BMD. We then analyzed mean total hip BMD across quintiles of lean mass, fat mass, and lean mass + fat mass interaction, adjusting for age and height using ANCOVA. There was no association between fat mass and total hip BMD. Total hip BMD increased across increasing quintiles of lean mass (Table 1). Within each fat mass quintile, total hip BMD increased across quintiles of lean mass and was 14-22% higher in men with the greatest lean mass. Similar results were observed for femoral neck BMD and BMAD. In this population, lean mass was a significant independent contributor to total hip BMD. These results emphasize the relative importance of lean mass as a correlate of BMD in men of African ancestry.

Table 1. Adjusted Mean Total Hip BMD (g/cm^2) across Quintiles of Lean Mass and Fat Mass[a]

Lean Mass	Fat Mass				
	1	2	3	4	5
1	1.01	1.05	1.05	1.06	1.04
2	1.09	1.09	1.11	1.11	1.09
3	1.14	1.17	1.14	1.14	1.14
4	1.18	1.17	1.19	1.18	1.18
5	1.29	1.27	1.23	1.23	1.26

[a] Controlling for age and height;
p (lean mass) <0.0001
p (fat mass) = 0.95
p (lean mass x fat mass) = 0.15

M304

The Usefulness of an Osteoporosis Risk Profile for Men in Three Racial/ Ethnic Groups. D. L. Broussard*, J. H. Magnus. Tulane University Health Sciences Center, New Orleans, LA, USA.

Risk factor profiles for low bone mineral density (BMD) have been determined in White women and men to indicate when BMD measurement is needed. The purpose of this study was to determine if a risk factor profile for White men identifies low BMD in African-American (AA) and Mexican-American (MA) men. Only three risk factors were found to be consistent for White men in published population-based, longitudinal and cross-sectional studies; body mass index (BMI), cigarette smoking, and calcium intake. This profile was evaluated among 574 AA, 554 MA, and 1274 White men, between the ages of 50 and 79 years, who participated in the household interview and BMD measurement of the Third National Health and Nutrition Examination Survey (NHANES III). Osteoporosis T-scores were calculated for each race/ethnic group as ≥2.5SD below the young male adult (20-35 years) mean BMD for the total femur using NHANES III data. Osteopenia T-score was defined as between 1 and 2.5SD below the race/ethnic group-specific young male adult mean. Low BMD was defined as BMD below 1SD of the race/ethnic relevant young adult mean. The sensitivity, specificity, and positive and negative predictive values (PPV and NPV) of individuals with total femur osteoporosis based on T- scores were calculated. Based on the race specific T-scores, the overall prevalence of osteoporosis in this NHANES III population was 4.9%, 4.0%, and 3.8%, respectively, for AA, MA, and White men. The presence of two risk factors identified osteoporosis with a sensitivity and specificity of 61% and 78% in AA men, and 50% and 77% in MA men, respectively. The NPVs across all race/ethnic groups were approximately 97% and the PPVs ranged from 8-12%. Osteopenia was present in 35.9%, 31.1%, and 32.2% of AA, MA, and White men, respectively. Between 47% and 59% of men reporting two risk factors were classified with low BMD. In all race/ethnic groups, more subjects with low BMD reported two risk factors ($p<0.0001$). As expected, sensitivity and NPVs decreased while the PPV values increased when low BMD was assessed. Among AA men, the sensitivity and specificity for low BMD were 35% and 83%. Logistic regression analyses revealed statistically significant associations between the presence of two risk factors and osteoporosis, osteopenia, and low BMD in all race/ethnic groups. The age adjusted relative risks for low BMD given two risk factors were 2.6 (95% CI, 1.8-4.0) for AA men, 2.2 (95% CI, 1.5-3.3) for MA men and 1.9 (95% CI, 1.5-2.4) for White men in this population. These results suggest that AA, MA, and White men with any of the two risk factors studied are more likely to be osteoporotic or osteopenic. The usefulness of this as a screening tool in a clinical setting needs further investigation.

M305

The OST Risk Tool Is Valid in American Men. R. A. Adler, M. T. Tran*, V. I. Petkov*. Endocrinology, McGuire Veterans Affairs Medical Center, Richmond, VA, USA.

The simple-to-administer OST risk tool was first developed to identify Asian postmenopausal women at increased risk of osteoporosis. It has been validated in Caucasian women. The calculated risk index is based on self-reported age and weight: [(weight in kg - age) X 0.2, truncated to an integer]. Does the OST risk tool work in men? We used data from two prospective studies conducted among patients enrolled in Pulmonary and Rheumatology clinics at a single Veterans Affairs Medical Center. The studies evaluated the usefulness of screening methods to predict osteoporosis as defined by central DXA (Hologic 4500). Only those patients who did not have a previous DXA were eligible to participate. The OST- tool index was calculated, and ROC curves were constructed. Sensitivity and specificity were determined at different cut-offs of the risk index. One hundred and eighty men (132 white, 64 black, 4 other) filled out a questionnaire and within a month underwent central DXA (total hip, femoral neck, and lumbar spine). The mean (SD) age was 63.3 (13.1) years, and the mean weight was 91.1 (21.4) kg. The OST risk index ranged between - 5 and 25, (mean 5 ± 5). By DXA, 15.6% of the men had a T of ≤-2.5 and 33.9% had a T of ≤-2 at one of the measured sites. The OST-tool index yielded areas under the ROC curves of 0.837, 95% CI [0.749, 0.925] and 0.816, 95% CI [0.747, 0.885] for T≤-2.5 and T≤-2, respectively. As shown in the table, the OST-tool index was categorized as low risk ≥ 4, moderate risk from -1 to 3 and high-risk ≤ -2. Defining osteoporosis as a T-score of ≤-2.5, an OST cut-off of 3 provided sensitivity of 93%, specificity of 66%, positive predictive value of 33%, and negative predictive value of 98%. Similar results were obtained when white and black men were analyzed separately. In conclusion, we found the OST-tool to be valid in male veterans from 2 specialty clinics. We will extend the study to general practice clinics to determine if the results can be applied to other groups of American men. The simple OST-tool appears to be an excellent method to identify men at high and low risk for osteoporosis.

Prevalence of osteoporosis in veteran men by risk tool categories and central DXA T-score

OST Category	T-score ≤-2.5	T-score ≤-2.0
≥ 4 (Low Risk)	2.0% (2/102)	15.7% (16/102)
-1 to 3 (Moderate Risk)	26.9% (18/67)	52.2 (35/67)
≤ -2 (High Risk)	72.7% (8/11)	90.9% (10/11)

M306

Serum Leptin Concentrations and Bone Mass: Differential Association Among Obese and Non-Obese Men. M. Lee, J. M. Zmuda, S. Wisniewski*, S. Krishnaswami*, R. W. Evans*, J. A. Cauley. Epidemiology, University of Pittsburgh, Pittsburgh, PA, USA.

Recent animal studies suggest that the adipocyte derived hormone, leptin, may be a potent and centrally acting inhibitor of bone formation. In clinical studies, however, leptin has been inconsistently related to bone mass. In the present study, we further evaluated the relationships among body composition, serum leptin levels, and bone mineral density (BMD) in a cohort of community-dwelling older men. Total fat and lean mass and hip BMD were measured with a Hologic QDR-2000 densitometer. Men with a history of osteoporosis and those taking glucocoticoids or medications known to alter sex steroid hormone metabolism were excluded from analyses. The final sample consisted of 297 men aged 58 - 91 yrs (Mean ± SD; 73 ± 7 yrs). In the total cohort, serum leptin levels were not significantly related to femoral neck BMD (r_s=0.03, p =0.64) after adjusting for age, height and body composition. To further evaluate the association between serum leptin levels and BMD, we stratified the sample into obese (BMI >30 kg/m^2; n=78) and non-obese (BMI <30 kg/m^2; n=219) men. As expected, obese men had markedly higher serum leptin levels than non-obese men (12.2 ±1.7 ng/ml *vs* 5.7 ± 1.6 ng/ml; P<0.01). In analyses adjusting for age, height and body composition, serum leptin levels were inversely correlated with femoral neck BMD among obese men (r_s= -0.26, $p<0.05$) but not among non-obese men (r_s= 0.05, p=0.44). Multiple regression analysis revealed that serum leptin levels explained 4.6% of the variation in femoral neck BMD among obese men. Similar results were observed for femoral neck bone mineral apparent density (BMAD). Our results suggest that serum leptin may be differentially associated with bone mass among obese and non-obese men.

M307

Bone Mineral Density (BMD) in HIV Patients on Stable First Line Treatment. S. Azriel*[1], M. Torralba*[2], G. Martínez*[1], E. Jódar*[1], R. Rubio*[2], F. Hawkins[1]. [1]Endocrinology Service, Hospital Universitario 12 de Octubre, Madrid, Spain, [2]HIV Unit, Hospital Universitario 12 de Octubre, Madrid, Spain.

Several studies have reported osteopenia and osteoporosis in HIV infected patients. Antiretroviral therapy and HIV infection itself may be involved as aetiological factors. Our goal was to describe osteoporosis/osteopenia prevalence in HIV patients who had been treated with the same antiretroviral drugs since they started therapy and to investigate the possible relationship between low bone mass and lipodystrophy syndrome. Observational cohort of 65 HIV patients who were treated with the same antiretroviral drugs at least 12 months. Severity of body changes was scored as: 0=no changes; 1= mild; 2= moderate and 3 =severe. Body changes were considered to be present if both physician and patient agree with lipodystrophy and at least score 2 was present in one of them. Dual X Ray Absorptiometry (DXA) of the lumbar spine and femoral neck was done. 67% of subjects were males. Median age of patients was 38 years (36-42 IQR). Weight was 68 kg (60-76 IQR) with BMI 23.7 Kg/m^2 (21,65-26,64 IQR), and waist 87,5 cm (81-93,75). Median CD4 cells/ml were 549 and 94% of the patients had VL < 500 copies/ml. The median-time of treatment was 41 months (26-53 IQR). 25% were treated with nuclease-reverse transcriptase inhibitor bitherapy (NRTI). 19% were treated with 2 NRTI plus non-nuclease-reverse transcriptase inhibitor (NNRTI) and 57% with NRTI plus PI (highly active antiretroviral therapy, HAART). Body shape abnormalities were detected in 45% patients (lipoatrophy: 38%, lipohypertrophy: 17% and mixed:11%). According to WHO definitions using T score, 62% of patients in the whole group had osteopenia and 11% were osteoporotic. Males were more severely affected: 71% had osteopenia and 14% osteoporosis. Premenopausic women presented osteopenia in 43% and osteoporosis in 5% of cases. There was no statistical association between lipodistrophy and osteopenia. However low bone mass was less frequently found in NRTI cohort (31,3%) than in HAART (62,2%) (p=0.033). There is a high prevalence of low bone mineral density as well as of body shape abnormalities in a cohort of HIV patients who never have switched treatment. Association between osteopenia and body shape abnormalities have not been found. Osteopenia is less prevalent in NRTI bitherapy regimens.

M308

Intra-uterine and Early Postnatal Growth Influence Proximal Femoral Geometry and Mechanical Strength in Late Adulthood. S. Lekamwasam*[1], M. K. Javaid*[2], E. M. Dennison*[2], H. E. Sydall*[2], N. Loveridge*[1], J. Reeve*[1], T. J. Beck*[3], C. Cooper[2]. [1]Medicine, Addenbrooke's Hospital, Cambridge, United Kingdom, [2]Medical Research Council Environmental Epidemiology Unit, Southampton, United Kingdom, [3]Radiology, Johns Hopkins University, Baltimore, MD, USA.

The proximal hip is the most important site of osteoporotic fracture in terms of morbidity, mortality and healthcare costs. Both femoral geometry and bone mass are independent predictors of hip strength and fracture. While growth in early life is known to influence adult bone mass, its effect on hip geometry is not known. We therefore investigated the relationship between intra-uterine and early postnatal growth and hip geometry/ strength in a sample of men and women, aged 60- 75 years, who have been characterised for both birthweight and weight at one as well as current anthropometry, diet and lifestyle factors. Hip geometry was derived from proximal femur images (Hologic QDR1000). The images were analysed using the Hip Strength Analysis software. Women had significantly ($p<0.001$) lower femoral width, cross-sectional moment of inertia (CSMI) at all sites and shorter femoral neck lengths than men. Despite these gender differences, there were significant ($p<0.002$) relationships between weight at age one year and measures of femoral width (intertrochanteric [IT] and femoral neck) as well as IT CSMI, among both men and women. Relationships with birhweight were less pronounced. There was no association between weight in infancy and femoral axis length. The relationships with measures of femoral width but not CSMI remained after adustuting for adult body weight and for lifestyle correlates of bone mass (smoking, alcohol consumption, dietary calcium intake and physical activity). These results support the hypothesis that different patterns of growth in utero and during the first year of life lead to persisting differences in proximal femoral geometry and mechanical strength thereby mediating the effects of early growth on risk of hip fracture.

Relationship between femoral geometry and birthweight and weight at one year

Birthweight	Birthweight		Weight at one year	
	Unadjsuted	Adjusted*	Unadjusted	Adjusted*
Men (n=178) Femoral neck length	-0.03 (0.67)	-0.06 (0.47)	0.12 (0.11)	0.08 (0.33)
IT width	0.22 (0.003)	0.18 (0.02)	0.37 (<0.001)	0.31 (<0.001)
IT CSMI	0.14 (0.06)	0.06 (0.41)	0.23 (0.002)	0.11 (0.15)
Women (n=155) Femoral neck length	0.05 (0.50)	0.03 (0.73)	0.08 (0.31)	0.04 (0.65)
IT width	0.19 (0.02)	0.11 (0.21)	0.40 (<0.001)	0.32 (<0.001)
IT CSMI	0.19 (0.02)	0.05 (0.54)	0.28 (<0.001)	0.14 (0.09)

Figures are correlation coefficients with p values.
*adjusted for adult weight and lifestyle factors.

M309

Genetic and Hormonal Influences in Bone Mass of Postmenopausal Women. M. E. Muñoz-Torres[1], P. Mezquita-Raya*[1], F. Lopez-Rodriguez*[1], J. M. Quesada*[2], F. Luque-Recio*[2], G. Alonso*[1], J. D. Luna*[3], B. Torres*[1], F. Escobar-Jiménez*[1]. [1]Bone Metabolic Unit. Endocrinology Division, University Hospital San Cecilio, Granada, Spain, [2]Endocrinology Division, University Hospital Reina Sofía, Cordoba, Spain, [3]Biostatistics Department, School of Medicine, Granada, Spain.

Bone mass and its mineral content are under genetic and hormonal control. Genetic factors are now recognized to be one of the most important determinants of bone mineral density (BMD). Also, several studies have shown that bone mass is under diverse hormonal influences. However, the relationship between genetic and hormonal factors in postmenopausal bone mass is not well established. **AIMS:** to examine the association of the COLIA1, VDR and ER genotypes, IGF-I and 25OHD with bone mineral density in postmenopausal women.**SUBJECTS AND METHODS:** We determined anthropometric parameters, lifestyle factors, serum levels of IGF-I and 25OHD, the COLIA1 (MlsI), VDR (BsmI, FokI) and ER (Xba, Pvu) polymorphisms by PCR and BMD by dual X-ray absorptiometry in 141 ambulatory postmenopausal spanish women (61±7 yrs). **RESULTS:** there was a significant overrepresentation of the "s" allele in osteoporotic women ($p=0.009$). After controlling for all other variables, lumbar spine BMD was found to be significantly associated with 25OHD, IGF-I, COLIA1, body mass index (BMI) and years after menopause ($R2=0.347$; $p<0.001$). For femoral neck, significant independent predictors of BMD were 25OHD, IGF-I, COLIA1, body mass index (BMI) and years after menopause ($R2=0.4$; $p<0.001$). None of the remaining genotypes entered the multiple linear regression models.**CONCLUSION:** our study shows that COLIA1 polymorphism, 25OHD and IGF-I concentrations are associated with bone mineral density independently of anthropometric parameters and lifestyle factors.

M310

Bone Mineral Density in Young Adults with Cystic Fibrosis. O. Lamy*[1], I. Pache*[1], E. Udry*[2], P. Burckhardt[2], A. Sauty*[1]. [1]Internal Medicine, Centre Hospitalier Universitaire Vaudois, Lausanne, Switzerland, [2]Centre Hospitalier Universitaire Vaudois, Lausanne, Switzerland.

Aims: To determine the bone mineral density (BMD) and its relation with body mass index (BMI), 25-OH-vitamin D (25-OH-D) level, calcium and vitamin D supplementation, and pulmonary function tests, in young adults with cystic fibrosis (CF). Methods: 25 adult patients with a stable disease or on a waiting list for lung transplantation. Results: The mean age at the first BMD was 26.4 + 5.8 years. 12 (48%) patients had osteoporosis on > 1 site, 8 (32%) had osteopenia on > 1 site and only 5 (20%) had a normal BMD. The site where we most frequently found a low BMD were the lumbar spine (90%) and the femoral neck (85%). Seven out of 8 patients waiting for lung transplantation had osteoporosis and one had osteopenia on three different sites. Calcemia, phosphatemia and alkaline phosphatase values were similar in all patients. 25-OH-D values were also similar with 79% of the patients having a level < 25mmol/l. Only 50% of the patients with low BMD received calcium and vitamin D supplementation before this evaluation. 25-OH-D values were not higher in patients under 800 UI oral vitamin D supplementation. None of the patients with normal BMD had been prescribed long term steroids. No difference in the frequency of steroids administration was found between the patients with osteoporosis compared with those with osteopenia. Patients with a low BMI had a significantly lower BMD ($p=0.04$). Low BMD was more prevalent in patients with low forced expiratory volume in 1 second (FEV1) and low forced vital capacity (FVC), $p<0.02$. We did not found any relationship between the presence or absence of colonisation with Pseudomonas aeruginosa and BMD. Conclusions: Low BMD is a frequent problem in young adults with CF and is more prevalent in patients with low FEV1 and FVC. The first bone evaluation occurred rather lately in the life of these patients and only half of them received a calcium and vitamin D supplementation before densitometry assessment. In order to prevent complications related to osteoporosis or graft-induced osteoporosis, such as vertebral fractures, more attention should be given to the bone status of these patients. Earlier bone evaluation would lead to a better prevention of osteoporosis.

M311

Pregnancy Associated Decrease of Skeletal Integrity Assessed by Phalangeal Ultrasonometry. P. Hadji[1], C. Wüster[2], L. Hellmeyer*[1], S. Schmidt*[1], V. Ziller*[1], K. Schulz*[1]. [1]Dept. of Obstetrics and Gynecology, Philipps-University of Marburg, Marburg, Germany, [2]Dept. of Endocrinology, University of Heidelberg, Heidelberg, Germany.

Due to the substantial transfer of calcium from mother to fetus during pregnancy, reproductive factors such as parity have been associated with osteoporotic fractures in later years. This study was aimed to elucidate skeletal integrity by phalangeal ultrasonometry during pregnancy. Quantitative ultrasonometry (QUS) of the phalanges (digits II to V) was performed by using the DBM Sonic 1200 (IGEA, Italy). The device measures the Amplitude dependent Speed of Sound (Ad-SoS), the graphic trace of the ultrasound wave which is highly correlated to bone structure and calculates the Ultrasound Bone Profile Index (UBPI). We performed a cross-sectional study including 128 pregnant women (mean ±SD age, 28.7 ± 5.9 years) in whom diseases and drug treatments known to affect bone metabolism had been excluded. The ultrasonometry variables Ad-SOS and the UBPI were assessed in accordance to the week and trimenon of pregnancy. The results showed a decrease of Ad-SOS and the UBPI during pregnancy, however the results did not reach statistical significance (fig. 1&2). The additional multiple linear regression analysis did not show any significant influence of pregnancy on QUS variables. There was no significant decrease of phalangeal ultrasonometry variables during prgnancy. Since QUS does not require exposure to radiation, is easily accessible, fast, portable and cheap, QUS seems to be especially useful for evaluation of skeletal integrity during pregnancy. Further longitudinal studies are need to improve our understanding of the mechanism of bone changes during pregnancy.

M312

The Influence of Age, Testosterone and Estrogen on Quantitative Ultrasonometry (QUS) of Bone in Healthy German Men. P. Hadji, U. Saeger*, K. D. Schulz*. Dept. of Obstetrics and Gynecology, Philipps-University of Marburg, Marburg, Germany.

The aim of this study was to evaluate the influence of age, testosterone and estrogen levels on quantitative ultrasonometry (QUS) of the os calcis in a large sample of healthy German men. 484 healthy men aged 20 to 80 years (mean age, 54.4 ± 15.4 years) not on medication known to effect bone metabolism were randomly recruited. Before entry to the study, all men had answered a detailed questionnaire on important risk factors. Speed of sound (SOS), broadband ultrasound attenuation (BUA) and stiffness index (SI) of the os calcis were measured using the Achilles ultrasonometer (GE/Lunar). Additionally, serum testosterone and estrogen levels were determined. BUA, SOS and SI decreased continuously from age 20. The total age-related decline was 17% for BUA, 2.4% for SOS and 17.4% for SI ($p<0.001$). This occurred over a 47-year period. The annual decrease derived from age regressions was -0.4% for BUA, -0.05% for SOS, and -0.39% for SI. There was a significant decrease of serum testosterone with age ($p<0.001$), while estrogen showed no such association. There was a significant correlation of testosterone to SOS and SI ($p<0.01$), but non of estrogens to QUS variables. This significant correlation diminished after performing a multiple linear regression analysis. Hereby only age remained as a significant predictor of QUS variables. Like in women, men show a significant age related decline of QUS variables. In contrast to women, the QUS variables decline continuously from the age of 20 years. There is no age-independent influence of testosterone or estrogens on QUS variables.

M313

Premenopausal Women with Type 1 Diabetes Have Poor Bone Quality Assessed by Quantitative Ultrasound (QUS). E. S. Strotmeyer, J. A. Cauley, J. S. Dorman*. Epidemiology, University of Pittsburgh, Pittsburgh, PA, USA.

Little is known about bone quality in women with type 1 diabetes compared to women without diabetes before or after the menopausal transition. Bone quality was assessed in premenopausal women, with type 1 diabetes (n=60) and without diabetes (n=143) by heel QUS using broadband ultrasound attenuation (BUA) and the speed of sound (SOS) (Sahara System, Hologic Inc.). Type 1 diabetes registry cases and non-diabetic community controls were enrolled in the ProHealth Study to evaluate their menopausal transition. Mean diabetes duration for cases was 31 years and mean HbA1C was 8%. Hormone use (HRT, OC), smoking status, fracture history and menstrual data were collected by questionnaire. Mean age was lower in cases vs. controls (42±4 vs. 44±4 years; p<0.001). Cases were similar to controls in current smoking (26% vs. 20%; ns) and any current hormone use (14% vs. 18%; ns). Both cases and controls had 29 mean days between their last two menstrual cycles (ns). Weight (69±14 vs. 73±20 kg; p=0.16) was slightly lower and waist-hip ratio (WHR) (0.81±0.06 vs. 0.79±0.06; p=0.03) was higher for cases. Mean clinical Michigan Neuropathy Screening Instrument (MNSI) score was 1.8±1.4 for cases vs. 0.9±1.0 for controls (p<0.001). More cases reported fractures after age 20 years (30% vs. 18%; p<0.05). Cases had lower mean BUA (68±18 vs. 83±19 dB/MHz; p<0.001) and SOS (1555±34 vs. 1574±34 m/s; p<0.001), indicating a much poorer bone quality. Multiple linear regression analyses were performed with BUA (dependent variable) and variables described above. Type 1 diabetes was (p<0.001) negatively related to BUA (R^2=0.133; p<0.001). Using the same modeling for SOS, type 1 diabetes (p<0.01) and current smoking (p=0.01) were both negatively related to SOS (R^2=0.097; p<0.001). Considering only women with diabetes, and adding duration and HbA1C to the model, increased weight (p=0.002) and decreased cycle length (p=0.05) were related to lower SOS (R^2=0.135; p<0.01). In conclusion, type 1 diabetes was strongly associated with poorer bone quality in premenopausal women. Menstrual cycle length, possibly as a marker of perimenopause, and weight may affect poor bone quality for women with type 1 diabetes. Type 1 diabetic women may be at high risk of osteoporosis. Appropriate screening and preventive efforts may be warranted.

M314

Osteoporosis in Patients with Depression. J. Menczel[1], Y. Gelfin*[2], B. Shapira*[2]. [1]Institute of Osteoporosis, Herzog Hospital, Jerusalem, Israel, [2]Schonbaum Depression Department, Herzog Hospital, Jerusalem, Israel.

Osteoporosis and depressive disorders (MDD) are major health problems affecting a large proportion of the population. The prevalence of osteoporosis increases with age; MDD has a rate of incidence between 10 to 25% for women and 5-12% in men. Higher prevalence of osteoporosis in patients with depression has been reported, but not confirmed, by others. A greater incidence of falls and fracture of the neck of femur was observed in these patients. Twenty-five patients with major depression were examined and Bone Mineral Density (BMD) with a Lunar Prodigy Dual Photon Absorptiometer (Dexa) were performed. BMD of lumbar spines and both hips were measured. Hamilton, depressive scale ratings, were performed in all patients. The Hamilton score ranged between 13 and 31. Of the 25 patients with major depression, 12 had definite osteoporosis (48%), 14 of them were females and 11 males. The BMD of the neck of femur ranged from t = -1.6 to -4.3, and L2 - L4, from -0.6 to -3.8. Only patients who had a t lower than minus 2.5, either of the neck of femur or L2 - L4, were included. Seven were females and 5 were men. The ages of the 25 patients ranged between 42 to 84 years and 13 were under the age of 64. Osteopenia, defined as a BMD measurement with a t of one of the sites between -1 to -2.5, was found in 5 patients. All 5 patients were females and their ages ranged from 26 to 73 years. It can be deducted that 48% of the patients with major depression had a loss of bone mass greater than expected. Five who had a t lower than -2.5 were over 75 years. Each patient underwent an interview and risk factors for osteoporosis and fractures were recorded. Two of the patients with a low BMD had a body mass index (BMI) below 20, being underweight. Ten had a normal weight with a BMI between 20 to 25, 10 were overweight with a BMI between 25 to 30, and 2 of these were obese and osteopenic. High BMI has a protective influence against bone loss due to peripheral estrogen production by adipose tissue. We do not have a matched control group of the same age and sex, and the results were compared to published prevalence figures. A higher incidence of osteoporosis was found. Taking into consideration the higher prevalence of a low bone mass in patients with major depression disorders, and that they suffer from falls, preventive and therapeutic measures should be started to avoid fractures, especially of the neck of femur.

M315

Correlation of Height Loss with Fracture History and Bone Mineral Density (BMD). R. D. Pathak*, A. L. Burshell. Section on Endocrinology, Ochsner Clinic Foundation, New Orleans, LA, USA.

Multiple vertebral compression fractures markedly increase the risk of future fractures. We studied self reported, greater than or equal to 2 inches height loss and its association to BMD and self reported fractures. Data were analyzed from 2571 subjects who completed a BMD evaluation and clinical questionnaire at Ochsner Clinic Foundation from July 2001 to March 2002. Most patients were postmenopausal women with risk factors for osteoporosis, but a minority were premenopausal or men. Subjects completed 20 questions via computer or paper forms and underwent both hip and lumbar BMD performed on Hologic Delphi SN 70045 scanner. Subjects were divided into 4 groups on the basis of height loss, positive or negative (HL+), (HL-) and fracture history (Fx+), (Fx-) and femoral neck and total hip BMD were measured. HL+ was present in 11% of the subjects and BMD was lower in this group. Fx+ defined as any fractures were present in 39% of the subjects, 52% of HL+ and 37% of HL- subjects. The combination of HL+, Fx+ was associated with the lowest femoral neck and total hip BMD. HL+, Fx- group had a lower BMD than Fx+, HL-. Self reported history of 2 inches or greater height loss is associated with low hip BMD and together with fracture history may help identify very high risk patients for fractures.

BMD and Clinical Data

No of Subjects	149	135	857	1430
Height Loss	HL+	HL+	HL-	HL-
Prior Fracture(s)	Fx+	Fx-	Fx+	Fx-
Mean Femoral Neck BMD (gm/cm2)	0.624	0.681	0.705	0.741
Mean of Total Hip BMD (gm/cm2)	0.751	0.819	0.853	0.893
Weight (kg)	67.6	67.2	73.0	72.4

M316

Public Release of Data from the Study of Osteoporotic Fractures: Design of the Website. D. Kimmel*[1], S. Ewing*[1], K. Stone[1], C. Fox*[1], J. Cauley[2], K. Ensrud[3], M. Hochberg[4], T. Hillier[5], M. Nevitt[1], S. Cummings[1]. [1]The Study of Osteoporotic Fractures Research Group, Univ of California San Francisco, San Francisco, CA, USA, [2]Univ of Pittsburgh, Pittsburgh, PA, USA, [3]Univ of Minnesota, Minneapolis, MN, USA, [4]Univ of Maryland, Baltimore, MD, USA, [5]Kaiser Permanente Center for Health Research, Portland, OR, USA.

The multi-center Study of Osteoporotic Fractures (SOF) has 16 years of prospective data about osteoporosis that has served as the basis for many findings about osteoporosis and aging in women ≥ age 65. In addition to adjudication of fractures, SOF has tracked cases of incident breast cancer, stroke, and total and cause-specific mortality. The data include serial measures of bone mineral density, measurements of sex and calcitropic hormones, tests of strength and function, cognitive exams, use of medication, health habits and much more. We are introducing a public website and process for releasing SOF anonymized data to the broader research community. Through dynamic internet technology, the website provides interactive documentation on 6,000 variables collected over seven principal visits of this unique cohort of nearly 10,000 older women. Users can browse variables by category or perform variable searches, viewing search results in a convenient longitudinal format of variable availability across visits. Users may link to the study data collection forms, as well as view descriptive statistics (e.g., means or frequency distributions). We expect that investigators in many fields will use the website to formulate and submit analysis plans of the dataset. The website facilitates online submission of these plans as well as the means to search for and view previously submitted plans by other researchers. Over 170 publications, 40 of which by external researchers, have already been published using SOF data. We hope that the dataset will prove increasingly fruitful by providing online access to new investigators who may propose unique research topics to be studied in SOF. Furthermore, as the trend continues toward mandatory public release of data from NIH-funded studies, this website will serve as a template for future data releases from our other studies. We hope our web-based applications can serve as a model for others as they address this important need. We encourage investigators in osteoporosis to discuss the website and processes with us and make use of this valuable public resource.

M317

Osteoporosis Perceived Vulnerability, Worry and Stress in Healthy Women. I. Vered[1], P. Werner*[2], D. Olchovsky*[3]. [1]Endocrinology, Sackler School of Medicine, Tel Aviv University, Sheba Medical Center, Tel Hashomer, Israel, [2]Department of Gerontology, Faculty of Social Welfare & Health Studies, University of Haifa, Haifa, Israel, [3]Department of Medicine, Sackler School of Medicine, Tel Aviv University, Sheba Medical Center, Tel Hashomer, Israel.

The relationship between perceived vulnerability and worries about a specific disease and preventive behaviors has been established for several diseases such as breast cancer, prostate cancer and AIDS. However, little attention has been paid to these relationships regarding osteoporosis, and no studies have yet examined the correlates of these variables. The aim of the present study was to assess predictors of perceived vulnerability, worry and stress about developing osteoporosis in healthy women. Two-hundred and forty one women (mean age = 53.94; 71.4% Jewish and 28.6% Arab) were interviewed regarding their perceived likelihood to develop osteoporosis, their perceived concern about developing the disease, and their perceived stress should they develop the disease. Background variables (age, marital status, ethnic group, education, and income), health variables (being menopausal, taking hormone replacement therapy and having a first-degree relative suffering from osteoporosis), and cognitive variables (knowledge about osteoporosis and health locus of control, i.e., internal, powerful others and chance locus of control) were also assessed. Seventy percent of the women were menopausal, a fifth of them were taking HRT, and a fifth reported having a family member diagnosed as suffering from osteoporosis. The participants had a relatively low level of knowledge about osteoporosis, (mean score of 11 points in an osteoporosis quiz with a maximal score of 23). Higher scores were reported in the internal and powerful others' dimensions than in the chance dimension. The participants reported moderate levels of vulnerability and moderate to strong levels of concerns about developing osteoporosis. Results of path analyses indicated that having a family member suffering from osteoporosis, higher knowledge, lower internal beliefs, and higher powerful others locus of control, were associated with higher perceived vulnerability. Additionally, higher feelings of vulnerability were associated to greater worries, which were associated with greater stress. The results have implications for the construction of educational programs designed to acknowledge feelings of osteoporosis worries and stress.

M318

Evaluation of the Sensitivity and Specificity of Screening Tools for Referring Women for Bone Densitometry. S. K. Brenneman[1], A. Z. LaCroix*[2], D. S. M. Buist*[2], Y. Chen*[1], T. A. Abbott[1]. [1]Merck & Co., Inc., West Point, PA, USA, [2]Center for Health Studies, Group Health Cooperative of Puget Sound, Seattle, WA, USA.

Low bone mineral density (BMD) is a strong predictor for fracture related to osteoporosis. However, BMD testing of all postmenopausal women is not standard practice. This study examines the diagnostic properties of 2 screening tools for selecting women for BMD testing and subsequent intervention: Simple Calculated Osteoporosis Risk Estimation (SCORE: 6 weighted risk factors) and a Study of Osteoporotic Fracture (SOF)-based screening tool (SOF-based: prior fracture or ≥ 5 of 17 risk factors). Women aged 60+ without previous osteoporosis diagnosis were randomly selected from a managed care population and invited to receive a BMD test. 416 women participated in the study. Women were classified using 3 different intervention strategies: WHO diagnostic criteria (t-score <-2.5), NOF criteria (t-score < -2.0 or < -1.5 with ≥ NOF 1 risk factor), and the SOF-based criteria (prior fracture or age 60-64: t-score <-2.5 or age ≥ 65: z-score <-0.43 and ≥ 5 risk factors). The percentage of women identified for BMD testing were 82% by SCORE and 26% by the SOF-based tool. Sensitivity, specificity and area under the receiver operating characteristic (AUROC) curve are shown below.

	Sensitivity (95% CI)	Specificity (95% CI)	AUROC (SE)
NOF intervention guidelines: N=275 (66%)			
SCORE	89.8 (79.9, 99.6)	34.8 (23.7, 45.8)	.73 (.03)
SOF-based	30.2 (22.1, 38.9)	80.9 (72.9, 89.4)	.56 (.03)
WHO (t-score ≤ -2.5): N=126 (30%)			
SCORE	93.7 (88.3, 99.1)	23.8 (9.6, 38.0)	.73 (.03)
SOF - based	31.8 (26.6, 38.6)	75.9 (63.5, 88.6)	.54 (.03)
SOF-based intervention: N=115 (28%)			
SCORE	98.3 (92.7, 100.4)	24.3 (9.7, 38.8)	.68 (.03)
SOF - based	85.2 (77.8, 91.9)	96.0 (89.0, 102.6)	.90 (.03)

For NOF and WHO criteria, SCORE demonstrates better utility to discriminate high vs. low risk women for intervention compared to the SOF-based screening tool. In general, SCORE correctly identified more high-risk women for intervention, whereas the more restricted SOF-based screening tool correctly ruled out more low-risk women. The appropriate selection of a screening tool depends upon the objective for intervention and trade-off between not identifying women for BMD testing who are at high-risk and identifying more women who are at low-risk.

M319

Validation of a Patient Questionnaire, 'Osteoporosis and You,' Designed to Assess Osteoporosis-related Attitudes, Knowledge and Behavior. S. K. Brenneman[1], E. M. Blau*[2], Y. Chen*[1], T. A. Abbott[1]. [1]Merck & Co., Inc., West Point, PA, USA, [2]Kaiser Permanente, San Diego, CA, USA.

The questionnaire, "Osteoporosis and You", is a 20-item self-report questionnaire designed to assess the attitude, knowledge and behavior of women about osteoporosis. The items are grouped to form three sections hypothesized to assess different domains: Knowledge, Attitude/Actions related to Osteoporosis, and Health Behavior. This study examined the validity of the questionnaire in a patient population. 500 women over the age of 20 were recruited consecutively during January 2001 until there were 100 women in each age cohort (under 40, 40-49, 50-59, 60-69, and 70+). Validity was examined by item analysis, internal consistency, confirmatory factor analysis, and hypothesized relationships between responses and demographics. Of the 500 respondents, 76% were Caucasian, 9% Hispanic, 6.4% African-American and 5.4% Asian. The responses to the Knowledge items indicated overall awareness and knowledge of osteoporosis. Response distribution varied across age groups. The Action section showed a hierarchical pattern consistent with increasing level of intervention. Greater than 50% of respondents were concerned that she might get/have osteoporosis and only 6% were prescribed medication for osteoporosis. The item responses for the Behavior section were distributed across the scale. Good internal consistency was found (Cronbach's alpha = 0.75). Confirmatory factor analysis supported the division of the questionnaire into the 3 sections. Hypothesized relationships among responses and demographics were supported. Results show significant differences in Knowledge and Behavior by age group. Women < 50 years were less knowledgeable and demonstrated fewer behaviors than women 60+ years of age. There were also differences in Knowledge and Behavior related to the level of response to Action items. The results of this study support the use of the questionnaire to obtain information about current knowledge of women about osteoporosis, from which educational interventions could be customized. Confirmation of the findings in populations of different characteristics merits further investigation.

M320

Standardized Documentation of Osteoporosis Patients in Germany. K. Abendroth[1], M. A. Dambacher[2], A. Defer*[3], E. Bitzer*[4], B. Birkner*[5], K. Wawra*[6]. [1]Regional Experts Groups Osteoporosis (REKO), Jena, Germany, [2]Regional Experts Groups Osteoporosis (REKO), Konstanz, Germany, [3]Regional Experts Groups Osteoporosis (REKO), Dresden, Germany, [4]Institute for Social Medicine, Epidemiology and Health Systems Research (ISEG), Hannover, Germany, [5]Quality Management, Gastroenterology Practice, Munich, Germany, [6]Procter&Gamble Pharmaceuticals, Weiterstadt, Germany.

Osteoporosis is an under-diagnosed and under-treated disease in Germany. The handling of the disease by many different medical specialties complicates improvements in osteoporosis care. As one step for improvement, a standardized documentation of the diagnostic and therapeutic options in osteoporosis care was designed by the REKO (Regional Expert Groups Osteoporosis) in Germany. In a pilot phase the documentation with the standardized data set was tested for practicability and delivery of meaningful data in daily practice. Data from 2649 patients, with possible or known osteoporosis, were gathered by 78 office-based physicians throughout Germany. The data was then centrally analyzed. 86.8% of the patients were women, 13.2% men, mean age 63.9 years. Based on densitometry findings (WHO definition), 51.5% of the patients had osteoporosis, 29% had osteopenia, and 19.4% had normal bone density. For analysis, 95%-confidence intervals (CI) and effect-tests at the multiple 5%-level were used. Selected results of risk factors and clinical findings are shown in the table below. The use of the standardized documentation in daily practice delivers meaningful data. It is a practical tool for giving insights into the status of osteoporosis care in Germany.

	Osteoporosis	Osteopenia	Normal Bone Density	Effect-test
History: Fracture after age of 40	35.9% (CI:33.4-38.5)	24.1% (21.0-27.0)	18.7% (15.3-22.0)	p<0.05
Back pain	66.2% (63.2-69.2)	61.0% (57.6-64.5)	50.0% (45.7-54.3)	p<0.05
Estrogen exposition < 30y	24.5% (22.2-26.8)	19.9% (17.0-22.7)	21.0% (17.5-24.5)	n.s.
Clinical findings: Kyphosis	47.5% (44.8-50.1)	29.8% (26.6-33.0)	22.7% (19.1-26.3)	p<0.05
Localized back pain	66.2% (63.7-68.7)	61.5% (58.1-65.0)	51.3% (47.0-55.6)	p<0.05
Decrease in height (cm)	3.1cm (2.9-3.2)	1.8cm (1.6-2.0)	1.6cm (1.4-1.8)	p<0.05
Radiological findings: Vertebral fracture	29.5% (27.1-31.9)	17.0% (14.4-19.7)	11.1% (8.4-13.8)	p<0.05

Disclosures: ***K. Wawra****, Procter&Gamble Pharmaceuticals 3.*

M321

What Occult Disorders Should Be Screened in a Patient with Osteoporosis. R. B. Wagman[1], S. R. Cummings[2], R. Marcus[1]. [1]Division of Endocrinology, Gerontology, and Metabolism, Stanford University Medical Center, Stanford, CA, USA, [2]Departments of Medicine and Epidemiology and Biostatistics, University of California, San Francisco, CA, USA.

While hyperthyroidism and hyperparathyroidism have demonstrated causality in the development of osteoporosis, systematic review has not been performed to describe other potential occult causes of skeletal fragility. We conducted a MEDLINE and PubMed search, reviewing all articles published in the English language since 1966 using the search terms Cushing's syndrome, hypercortisolism, diabetes mellitus, pernicious anemia/aenemia, vitamin B12 deficiency, celiac/coeliac disease, sprue, systemic mastocytosis, osteoporosis, and fracture. We collected data on the following: 1) number of patients enrolled, 2) use of a control group, 3) type of bone densitometry equipment, 4) anatomical site measured, and 5) change in bone mineral density (BMD). We found 85 studies, many of which demonstrated methodological problems. We found reasonable evidence for association between osteoporosis and Cushing's syndrome, diabetes mellitus Type 2, and mastocytosis. Patients with active Cushing's syndrome had an average 16-20% decrease bone density in the lumbar spine and 15-17% decrease in the femoral neck than controls. While patients with diabetes mellitus Type 2 demonstrated increased bone density than controls, concomitant increased fracture incidence was found in the hip, proximal humerus, and foot. In patients with mastocytosis, the prevalence of osteopenia by spine radiograph was 14-100% with a fracture prevalence of 36-100%. We found weaker associations between skeletal fragility and celiac disase and diabetes mellitus Type 1, and an indeterminate association with pernicious anemia. We conclude that it is worth screening a patient with low bone density or fragility fracture for Cushing's syndrome in the context of clinical and/or biochemical stigmata, as well as diabetes mellitus Type 2. Our review indicates inconsistent value of screening for celiac diase and insufficient data to recommend screening for pernicious anemia. The rarity of mastocytosis makes it difficult to recommend routine screening.

M322

Performance of a Simple Clinical Tool (FOSTA) for Identifying Japanese Women with Osteoporosis based upon Heel Bone Density. K. Aoyagi[1], P. D. Ross[2]. [1]Public Health, Nagasaki University, Nagasaki, Japan, [2]Merck & Co., Inc., Rahway, NJ, USA.

The Female Osteoporosis Self-assessment Tool for Asians (FOSTA) has been validated in numerous Asian and (with slight modification) Caucasian populations for classifying the risk of osteoporosis based on spine and femoral neck bone mineral density (BMD). However, central site (hip or spine) BMD measurements are not available in all communities. Heel BMD performs at least as well as central BMD measurements for predicting the risk of vertebral and nonvertebral fractures. We therefore evaluated the performance of the FOSTA tool among postmenopausal Japanese women in a population-based study (Mitsugi Bone and Joint Study (MBJS)) using peripheral (heel) BMD to define osteoporosis (T < -2.5). The subjects were 315 women aged 40 years and older (average age 64±8.1 years) with heel BMD measurements between 1994 and 1995. The index achieved 99% sensitivity and 30% specificity, which was similar to previous findings using femoral neck BMD in Japanese women. Using three previously-reported risk categories, 22% of all women were categorized as high risk (FOSTA -1). Physicians might be advised to consider treating women with osteoporosis. Almost all (86%) of the high risk patients had osteoporosis (heel BMD T-score < -2.5). Among women with low risk (18% of all women), only 2% had osteoporosis, and BMD measurements are probably not necessary. Approximately 40% of the moderate risk women had osteoporosis; BMD measurements are useful in this group to determine which individuals have osteoporosis, and which individuals do not. In summary, the FOSTA tool performed well for classifying the risk of osteoporosis based on heel BMD, as has been reported previously using femoral BMD. This free and simple tool could help clinicians actively assess osteoporosis and determine the need for BMD measurements to assess fracture risk and initiate appropriate intervention before fractures occur.

M323

Validation of a Simple Questionnaire of Risk Factors to Identify Postmenopausal Osteoporosis. M. Diaz-Curiel, M. Garcés*, A. Rapado. Internal Medicine, Fundación Jimenez Diaz, Madrid, Spain.

Bone densitometry is the best option to detect osteoporosis in postmenopausal women, although its use may be limited by the availability of equipment and cost. The aim of this study, which was completed at our Outpatient Clinic, was to validate a simple questionnaire of the risk factors for low bone mass and to assess the predictive character of osteoporosis of each factor. A cross-sectional population-based study was completed on 105 postmenopausal women, aged between 41 and 86. The questionnaire included details of the patient's height and weight, drug history, years of menopause, existence of early menopause, oophorectomy, fracture history - after the age of 50, or family history of osteoporosis, physical activity, symptoms of dementia, smoking or alcohol consumption, and low calcium intake. BMD of the lumbar spine and femoral neck were measured using dual-energy X-ray absorptiometry (DXA Hologic 4500), which classified the women as "normal' or "abnormal' (osteopenia and osteoporosis), based on the WHO criteria. Univariate analysis was used to exclude factors that did not show a relationship with BMD (p>0.3). Multivariate stepwise forward logistic regression analysis, using BMD values as the dependent variable, were performed to identify the remaining factors, these being the most predictive factors of low bone density at the lumbar spine, and at the femoral neck. Sensitivity, specificity and predictive values, by receiver operating curves (ROC) analysis, were also analysed. A simple scoring system was devised based on a regression model: more than ten years of menopause (5), prior fracture (4), osteoporosis family history (2), weight (<55kg:3; 55-60kg:2; >60:1) and age (70 or >70:3; 60-69:2; 50-59:1). The cut-off score, to discriminate between normal and osteopenic women, was 5: (Sensitivity 91.4%; specificity 42.9% at lumbar spine, and 87.9% and 41.9% respectively, at the femoral neck). The cut-off score, to discriminate between normal and osteoporotic women, was 8: Sensitivity 61.9%; specificity 85.7% at lumbar spine, and 65.1% and 76.2% respectively, again at the femoral neck. The use of a simple questionnaire, to score for risk factors of low bone mass, could be useful to facilitate the diagnosis of osteopenia or osteoporosis. However our questionnaire should be further validated on a larger sample of the postmenopausal population.

M324

Osteoporosis in COPD Patients. I. Holme*[1], L. Henriksen*[1], V. Petersen*[1], V. Backer*[1], P. Schwarz[2]. [1]Respiratory unit Department of Internal Medicine, Bispebjerg Hospital, University Hospital of Copenhagen, Copenhagen, Denmark, [2]Department of Endocrinology, Hvidovre Hospital, Copenhagen, Denmark.

Purpose: Evaluation of the incidence of osteoporosis in patients with COPD. Methods:Out-patients from the espiratory unit with COPD, FEV1 less than 1,3 L., and age between 50-70 years were included. All had a questionnaire concerning smoking habits, sun exposure and medication taken (steroids, calcium and Vitamin D). A blood sample were drawn for specific analysis and furthermore a spirometry (FEV1 and FVC), a 5 minutes exercise-test, X-ray of the thoratic-lumbal spine and a DXA-scan of the femur and lower back (L2-L4). Results: Of 181 invited patients, 71 patients were included of who 54 were females (93% post menopausal). All had symptoms of COPD and had a severe airflow limitation with a mean (sd) FEV1 0,9 (0,4) L, mean daily dietary intake of calcium was 500 mg of vitamin D 5 micrograms. We found 7 patients had secondary hyperparathyroidism. In 16 patients X-ray showed not previously known compression fracture, DXA-scan showed osteoporosis in 37 patients including the 16 with X-ray diagnosed osteoporosis. Furthermore 14 patients had osteopenia defined from DXA-scan. Conclusions: A high frequency (72 %) of unknown osteoporosis or osteopenia was found among COPD patients. The present study indicates that many patients receiving corticosteroid treatment need osteoporosis prophylaxis. Prospective studies of prophylactive treatment are though urgently needed, as the current population at risk for developing corticosteroid-induced fractures is of major economic interest, since 15 % of the adult population in Denmark suffer from COPD.

M325

Hip Geometry and Bone Mineral Density in Postmenopausal Women. R. A. Brownbill, C. Lindsey, J. Z. Ilich. School of Allied Health, University of Connecticut, Storrs, CT, USA.

Both femoral neck strength (FNS) and hip axis length (HAL) have been shown to influence hip fracture, although these relationships are not always clear due to different radiological tools used to calculate these values and different study conditions. Our objective was to obtain both FNS and HAL values from left and right femurs scanned by DXA and evaluate their relationship with femoral BMD. Participants were 136 Caucasian women, (age range 57.4-88.6 y), all healthy and not taking medications known to affect bone. The dual hip measurements were performed using DPX-MD bone densitometer (GE Medical Systems, LUNAR Corp. Madison, WI). HAL was determined automatically by software. FNS analysis uses femoral geometry to calculate stresses at the femoral neck for two loading conditions: Safety Factor Index (SF) indicates risk of fracture for forces generated during a one-legged stance, and Fall Index (FI) indicates risk of fracture for forces generated during a fall on the greater trochanter. As both these values get closer to "1", the risk of fracture increases. Multiple regression analyses with regions of hip as dependent variables and corrected for height, weight, and age were used to determine predictive ability of HAL, SF, and FI for respective BMD values. Results showed that longer HAL values of the left hip were negatively related to neck, trochanter, shaft and total hip BMD with R square (adjusted) ranging from 0.27 to 0.33 (p less than 0.05). HAL was not significantly associated with any of the right hip BMD regions. FI was significantly associated with all sites of the hip BMD with R squared (adjusted) ranging from 0.24 to 0.39 (p less than 0.05),while SF was associated with neck and wards BMC with R squared (adjusted) ranging from 0.35 to 0.49 (p less than 0.05). We conclude that having a longer HAL is associated with lower BMD, and higher FI values are associated with higher bone mass. It appears HAL, SF and FI all play a key role in estimating fracture risk and should be assessed along with BMD when using DXA.

M326

Bone Changes in Ovariectomized (OVX) Rats Evaluated by DXA and Micro-CT. P. J. Masarachia, S. Adamski*, G. A. Rodan, D. B. Kimmel. Bone Biology and Osteoporosis, Merck Research Laboratories, West Point, PA, USA.

Micro-computed tomography (M-CT) may provide new information about bone changes in OVX rats. Six month old S-D rats were OVXd or Sham-OVXd. OVX rats were treated orally for 6wks with 0 or 0.6 mg/kg/d ethinyl estradiol (OVX+EE). At necropsy, right femora were fixed in 70% ethanol. Bone density was measured by dual energy x-ray absorptiometry (BMD-X, mg/cm^2) (DXA) in a uniform cylindrical volume (Table 1) containing cortical and cancellous bone. A 0.02mm resolution tomographic reconstruction of the distal 16mm of all femurs was obtained (EVS Corp; London, Ontario; CAN). The metaphyseal region of most marked cancellous bone loss was identified by qualitatively comparing OVX and Sham images. A uniform cylindrical volume (Table 1) containing only cancellous bone and representing that region was identified. M-CTBMD (mg/cc) and bone volume (M-CTBVTV, %) were computed. The three groups were compared (ANOVA with Fisher PLSD). Group coefficients of variation (CV) were computed. BMD-X was 20% lower in OVX than Sham; BMD-X of OVX+EE rats was 96% replete to Sham. M-CTBMD was 67% lower in OVX than Sham; M-CTBMD of OVX+EE rats was only 33% replete to Sham. M-CTBVTV and M-CTBMD data were similar. CV's were higher for M-CT endpoints than BMD-X (20-50% vs. 7-10%). In EE-treated OVX rats that show BMD equal to intact rats by DXA, M-CT discloses marked differences in bone mcroarchitecture. Though CVs of the M-CT endpoints are greater than BMD-X, the larger OVX-related difference seen by M-CT suggests that M-CT can increase power of OVX rat studies.

Table 1. DXA and M-CT Volumes of Interest

Dimensions	DXA	M-CT
Distal*	5	5
Proximal*	10	8
Diameter (mm)	6	1.5
Volume (mm3)	141	5.3

*mm from distal end of femur

Table 2. DXA and M-CT Endpoints

Group	N	BMD-X	M-CTBMD	M-CTBVTV
Sham	9	186.7±16.2	303±56	20.6±5.4
OVX	9	149.0±10.8s	99±33s	4.7±2.2s
OVX+EE	11	185.3±19.2o	166±88so	11.9±5.3so

Mean±SD; s vs. Sham (P<.001); o vs. OVX (P<.01)

M327

Iliac Three-Dimensional Trabecular Microarchitecture in Premenopausal Healthy Women and Postmenopausal Osteoporotic Women with and without Fracture. J. Zhao[1], Y. Jiang[1], R. R. Recker[2], M. W. Draper[3], H. K. Genant[1]. [1]Oarg, University of California, San Francisco, CA, USA, [2]Osteoporosis Research Center, Creighton University, Omaha, NE, USA, [3]Lilly Research Laboratories, Indianapolis, IN, USA.

Capturing true 3D trabecular microstructural information may help understand the pathophysiology of osteoporosis and estimate fracture risk as bone mechanical competence is a function of its density and 3D distribution. In histomorphometry based on 2D sections using the parallel plate model assumption, whether trabecular thinning or disappearance occurs with aging and/or menopause remains unresolved. We scanned bone biopsies from the iliac crest of healthy premenopausal women (Pre, n=20, age mean ± SEM, 49 ± 1 years), and osteoporotic postmenopausal women without fracture (Post, n=20, 56 ± 1 years) and with vertebral osteoporotic fracture (Post+Fx, n=20, 70 ± 2 years), using a Scanco micro CT with isotropic resolution of 17 $\propto m^3$. 3D trabecular microstructure was directly measured without stereological model assumptions. Among the 3 groups (Table), ANOVA showed significant differences in 3D trabecular bone volume fraction (BV/TV, %), trabecular number (Tb.N, 1/mm) and thickness (Tb.Th, ∝m) and separation (Tb.Sp, ∝m), structure model index (SMI, values 0 or 3 represent a perfect plate or rod structure, respectively), degree of anisotropy (DA), and connectivity density (CD, $1/mm^3$). Adjusted for age, most odds ratios (OR) discriminated fracture. The annual percentage change was greater from Pre to Post in Tb.Th (-3) and SMI (18) than from Post to Post+Fx (Tb.Th -0.1, SMI 1), and greater in CD from Post to Post+Fx (-5) than from Pre to Post (-3). Thus, dual phases were observed: deterioration of all 3D parameters in the initial years of osteoporotic postmenopausal women without fracture, and further deterioration of 3D connectivity in the later years with fracture. In the initial years, trabecular thinning does occur. Trabeculae dramatically shift from a plate-like structural type to a rod-like type, and become more isotropic. In the later years, the remaining trabeculae are more widely separated and less connected, and some mechanically significant trabeculae may undergo compensatory thickening and reinforcing, resulting in an increase in trabecular anisotropy. Changes in 3D trabecular microstructure play important roles in osteoporotic fracture.

	Pre	Post	Post+Fx	OR (95% CI)
BV/TV	22.2±1.7	16.3±1.3	9.1±1	3.9 (1.7-9.5)
Tb.N	1.61±0.03	1.46±0.04	1.12±0.06	1.5 (1.3-1.9)
Tb.Th	166±9	137±5	136±6	1.1 (0.2-5.5)
Tb.Sp	615±12	694±23	929±47	1.9 (1.3-4.6)
SMI	1.06±0.12	2.34±0.08	2.63±0.07	1.7 (1.1-3.2)
DA	1.41±0.03	1.32±0.03	1.48±0.03	2.4 (1.3-4.6)
CD	5.50±0.33	4.38±0.37	1.23±0.18	2.6 (1.5-7.2)

M328

The Effect of Ovariectomy on Bone Changes Differs between the Edentulous and the Dentate Mandible. E. S. Elsubeihi*. Faculty of Dentistry, University of Toronto, Toronto, ON, Canada.

Whether postmenopausal osteoporosis in humans is associated with decreased bone mass in either the dentate or the edentulous mandible or both is unclear at the present. We have shown previously that ovariectomy (OVX) in rats reduced bone mineral density (BMD) of the edentulous mandible but not of the dentate mandible. Whether OVX affects alveolar ridge resorption and/or cancellous bone volume of the edentulous mandible still needs to be resolved. To accomplish this, we first investigated the healing process of mandibular extraction sockets of molars and the incisor on one side of the mandible of adult female rats at 2, 4, 8, 12 and 16 weeks after extraction. After having established that complete healing of the extraction sockets occurred 4 months after extraction, we next ovariectomized animals 4 months after teeth extraction to investigate the effect of OVX on bone changes in the edentulous and dentate mandible at 6 weeks, 6- and 9-months after ovariectomy. Bone changes were assessed using BMD, backscattered electron microscopy and light and fluorescent microscopy. The results show that extraction of teeth resulted in a 16% reduction of the residual ridge 4 months after extraction. The decrease in residual ridge height of edentulous mandible of control animals reached to about 35% at 10 months after extraction. OVX did not increase residual ridge resorption. However, BMD and bone volume measurements showed that OVX resulted in significant bone loss in the edentulous but not in the dentate mandible. Static and dynamic parameters of bone formation and resorption indicated that there was a significant increase in mineralizing surfaces (2 fold P=0.039) as well as eroded (1.9 fold P=0.012) and osteoclast (2 fold, P=0.0073) surfaces and bone formation rate (2 fold, P=0.03) together with loss of cancellous bone volume (18%, P=0.006) in the edentulous mandible of OVX as compared to control animals at 6 months post-OVX. There were no significant differences between dentate mandibles of OVX and control animals. In summary, teeth extraction caused significant reduction in residual ridge height, and OVX did not affect the residual ridge height of the edentulous mandible. Furthermore, OVX caused a significant reduction in cancellous bone volume of the edentulous mandible but not of the dentate mandible. We also established that bone loss in the edentulous mandible of ovariectomized animals is the result of an increase in bone turnover, and that masticatory force controls the rate of bone turnover in the dentate mandible.

M329

Inverse Relationship between Osteoporosis and Spondylosis in Postmenopausal Women. N. Miyakoshi[1], E. Itoi*[2], H. Murai*[2], I. Wakabayashi*[2], H. Ito*[2], T. Minato*[2]. [1]Orthopedic Surgery, Akita University School of Medicine, Alita, Japan, [2]Orthopedic Surgery, Akita University School of Medicine, Akita, Japan.

The literature contains both studies that have demonstrated an inverse relationship between osteoporosis and spondylosis, as well as those in which insufficient support for such a relationship has been documented. However, in these previous studies, only limited-range grading systems (e.g., grades 1 to 4) were used to evaluate the severity of spondylosis. Therefore, the purpose of this study was to examine the possible inverse relationship between osteoporosis and spondylosis by evaluating the association between bone mineral density (BMD) and osteophyte formation or intervertebral disc narrowing using a semi-quantitative scoring system. A total of 104 postmenopausal women aged over 60 underwent BMD measurement of the lumbar (antero-posterior, lateral, and mid-lateral) and proximal femur (femoral neck, trochanter, and Ward's triangle) using dual-energy X-ray absorptiometry. Raw data representing semi-quantitative osteophyte score and disc score, as well as the number of vertebral fractures, was obtained using spinal X-ray. Correlation between each BMD and radiologic variable was then analyzed. Significant negative correlation was found between all BMD data and the number of vertebral fractures ($p<0.05$). Moderate and positive correlations were observed between osteophyte score and BMD data, as well as between disc score and BMD data ($p<0.05$). Based on the finding that in postmenopausal women, spondylotic changes exhibited positive correlation with not only lumbar BMD but also with remote site BMD, such as at the proximal femur, this study supports the view that osteoporosis has an inverse relationship with spondylosis.

M330

The Dynamic Mobility of Vertebral Compression Fractures. F. E. McKiernan[1], T. Faciszewski*[2]. [1]Center for Bone Diseases, Marshfield Clinic, Marshfield, WI, USA, [2]Department of Orthopedic Spine Surgery, Marshfield Clinic, Marshfield, WI, USA.

Vertebroplasty is a minimally invasive procedure that relieves vertebral compression fracture (VCF) pain but is not thought to restore lost vertebral height. We have observed that many VCFs are dynamically mobile and that significant height recovery and sagittal realignment can be achieved during vertebroplasty with careful patient positioning alone. Herein we report the frequency and magnitude of osteoporotic vertebral fracture mobility. This is a retrospective radiographic analysis of 41 consecutive patients with 65 VCF who underwent vertebroplasty. Preoperative standing and supine cross-table lateral radiographs were evaluated to assess dynamic vertebral fracture mobility. Postoperative standing lateral radiographs were evaluated to assess restoration of height and vertebral area and reduction of kyphotic angle. Restorations are reported as percent of original, pre-vertebroplasty fracture dimensions. Dynamic fracture mobility was demonstrated in 44% of patients and 35% of treated vertebrae. In mobile fractures, average posterior, middle and anterior vertebral height restorations were 15%, 93% and 106% respectively. Mean lateral vertebral area increased from 48% to 80% of normal and kyphotic angle decreased 40%. This radiographic series documents the surprising frequency and substantial mobility of many osteoporotic vertebral compression fractures. Dynamic VCF mobility must be considered when performing vertebroplasty and when reporting and interpreting the significance of vertebral height restoration. The definition and epidemiology of VCF, the pathophysiology of vertebral fracture healing and the distinction between Kummel's disease and severe, dynamically mobile VCFs need reconsideration in light of these observations.

M331

Methods for Enhancing Depth of Field and Information Content in Scanning Electron Microscopic Imaging of Porotic Bone. A. Boyde. Dept of Anatomy and Developmental Biology, University College London, London, United Kingdom.

The scanning electron microscope (SEM) is an ideal tool box for imaging macerated trabecular bone specimens, which holds more methods than are generally employed in the bone research field, but there are problems with the instrument and the samples. Commonly, the secondary electron (SE) signal is used because it is strong and the collection efficiency great, so that an acceptable depth of field can be obtained by using a small beam defining aperture and a long working distance. However, the depth of field is limited, and this becomes more of a problem as trabecular bone becomes overtly porotic. Further, SE images give little clue as to bone composition and SE collection has little directionality, so they are poor at encoding surface slope. Further, it is difficult to prevent the untoward effects of electrostatic charging with dried samples (and 'wet' SEMs can give only a very small field of view at a very short working distance). Charging is greatly reduced if only fast backscattered electrons (BSE) are employed, and these have straight, line-of-sight paths to appropriate detectors. Here, a greater beam current is required for a reasonable signal level, implying the use of a larger beam defining aperture at a shorter working distance and a consequent reduction in the depth of field. The present work aims to exploit the directionality of BSE paths and detectors and to enhance the depth of field in the resultant image. Direction and slope of the surface generate false color when assigning each of three separate detectors as red, green or blue in a composite image. The detectors may be symmetric or asymmetric with respect to the normal electron beam path. Admixture of color enhances both information content and interest in morphologic SEM images, which, of course, exceed the resolution possibilities of any other current bone imaging technique which gives contextual cues. The problem of depth of field has been overcome by recording series of images taken at different mechanical focus distances of the sample, and using computer image processing to extract the best in-focus (high frequency) component at each XY patch in the Z stack. Inevitably, we are considering wide field images and therefore a

perspective projection. This is turn necessitates a correction of scale for each separate image plane because magnification also varies with distance in this projection. Finally, we have the first in-focus, 3D color images of stunning beauty and meaning, which illustrate key features of bone micro-anatomy and pathology.

M332

Histomorphometry and Micro-Computed Tomography on Human Bone Biopsies: Comparison Insight Measurements. D. Chappard, E. Legrand, M. Audran, M. F. Baslé*. LHEA-GEROM, Angers, France.

Osteoporosis due to a decrease in bone mass associated with a deterioration of the trabecular bone architecture. Bone histomorphometry is used to explore the various metabolic bone. The technique is done on then microscopical two dimensional (2D) and several methods have been proposed to extrapolate 2D measurements to the 3D dimension. X-ray micro-computed tomography (microCT) is a recently developed imaging tool to appreciate 3D architecture. Recently the use of 2D histomorphometric measurements have been shown to provide discordant results when compared with 3D values obtained directly. 96 human bone biopsies were removed from patients prententing metabolic bone diseases. Complete bone biopsies were examined with the SkyScan-1072 microCT. Bone volume (BV/TV), Tb.Th and Tb.Sp were measured on the 3D models reconstructed from X-ray scanned sections. Thichness were measured by a method based on the sphere algorithm. In addition, 6 scanned images (separated by 100 µm) were transferred to an image analyzer and bone volume (B.Ar/T.Ar-x) and trabecular characteristics were measured after thresholding of the images. Bone cores were embedded undecalcified; histological sections were prepared and measured by routine histomorphometric methods providing B.Ar/T.Ar-h and trabecular characteristics. Comparison between the differents methods were done by using regression analysis, Bland and Altman plots and Passing-Bablock plots. Correlations between BV/TV and B.Ar/T.Ar-h were highly significant (r=0.94) but the microCT overestimated bone volume by about 5-15%. Using the mineralized bone volume instead of total bone volume did not improved the results. Overestimation may be due to the less potent methods available in 3D to remove artefactual particles. Also the countours of the trabeculae are often more difficult to threshold on X-ray scans than on highly contrasted histologic sections. BV/TV and B.Ar/T.Ar-x were also highly correlated (r=0.96) and similar findings were obtained with B.Ar/T.Ar-h and B.Ar/T.Ar -x (r=0.96). Correlations between Tb.Th values obtained by 3D or 2D-x or 2D-h measurements were lover (r=0.70) and 3D analysis always overestimated thickness by about 50%. In clinical practice, microCT appears to be an interesting method providing reliable morphometric results in less time than conventional histomorphometry (about 2-3 h vs 15 d).

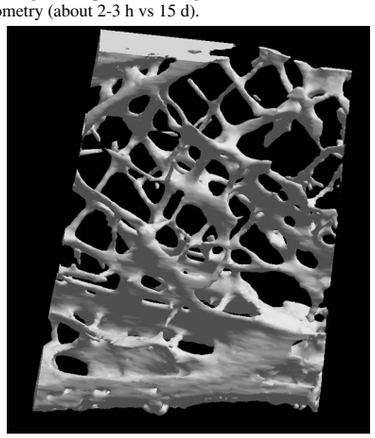

M333

Relationship between Dietary Intake and Bone Mineral Density in Postmenopausal Women: A 20-Year Study. N. M. DiMarco, S. L. Bonnick, A. J. Cox*, E. DeVries*. Institute for Women's Health, Texas Woman's University, Denton, TX, USA.

The relationship between dietary intake variables and bone mineral density (BMD) in postmenopausal women was examined to determine if dietary intake can predict BMD and if significant differences in dietary intakes and BMD over a 20-year period exist. Thirty postmenopausal women were selected from a population of 352 men and women who completed a 20-year study of phalangeal and radial bone density conducted between 1950 and 1981. The mean age at 20-year follow-up was 67 years (34 to 91). Thirteen had a natural menopause and 17 had a surgical menopause. Carbohydrate, protein, fat, calcium, vitamin D, phosphorus, and total kilocalorie intakes were determined using a 7- and 3-day dietary record and analyzed using Nutritionist V, version 5.0 software (N-Squared Computing, San Bruno, CA). Only documented dietary intakes were used with no inclusion of vitamin or dietary supplements. At both the initial and 20-year follow-up, a questionnaire was used to obtain demographics, medications, reproductive history, recreational habits, and fracture history. Descriptive statistics were performed on each variable. Pearson product moment correlation was used to determine if there was a significant relationship between dietary intake variables and BMD. Multiple regression analyses were used to determine which diet variables were significantly correlated with BMD values. Paired t-tests were used to detect differences between mean dietary intake variables, and mean BMD measures at the two time points. There was a significant correlation between protein intake at baseline and RG of the second metacarpal region (r=0.39;p=0.04). There was also a significant correlation between baseline fat intake and SPA (r=0.42;p=0.02). BMD results are shown in the table. There were no significant dietary predictors of BMD at baseline or 20-year follow-up. There were no significant differences between dietary intake variables at baseline or 20-year follow-up. There were significant differences between baseline and 20-year follow-up BMD measurements for RPD and RG.

BMD changes over 20 years

	Baseline	20-year Follow-up	p value
RPD 5-2, mm Al/mm bone	0.22 (0.004)	0.17 (0.004)	0.000
RG 2nd metacarpal, um	0.58 (0.017)	0.52 (0.016)	0.002
RG 3rd metacarpal, um	0.51 (0.015)	0.48 (0.015)	0.02
SPA, g/cm2	NA	0.40 (0.015)	

M334

The Relationship between Urinary Sodium Excretion and Bone Mineral Metabolism of Climacteric Women in Korea. K. W. Oh[1], E. S. Oh*[1], S. W. Kim*[1], D. C. Lee*[2], S. I. Roh*[3], S. H. Song*[3], M. I. Kang[4]. [1]Internal Medicine, Miz Medi Hospital, Seoul, Republic of Korea, [2]Family Medicine, Miz Medi Hospital, Seoul, Republic of Korea, [3]Obstetrics and Gynecology, Miz Medi Hospital, Seoul, Republic of Korea, [4]Internal Medicine, Catholic University of Korea, College of Medicine, Seoul, Republic of Korea.

High oral intake of sodium is known to increase urinary calcium excretion in experimental animals and humans, and there is well-documented correlation between urinary sodium and calcium excretion in 24-hour urine collections from normal subjects and postmenopausal women. To investigate relationship between urinary sodium excretion and bone mineral metabolism of climacteric women, we measured 24-hour urinary sodium, calcium, and creatinine level; serum osteocalcin level, serum alkaline phosphatase (ALP) level, serum follicular stimulating hormone (FSH) level; urine deoxypyridinoline (DPD) level; and bone mineral density (BMD) in 430 climacteric women in Korea (331 postmenopausal and 99 premenopausal women). The postmenopausal women had higher ($p <$ 0.05) value for mean urinary sodium to creatinine ratio of 0.225±0.078 mmol/mg vs. 0.209±0.061 mmol/mg and higher ($p < 0.001$) value for mean urinary calcium to creatinine ratio of 0.261±0.125 mg/mg vs. 0.209±0.081 mg/mg than the premenopausal women. Significant positive correlation was noted between urinary sodium to creatinine ratio and urinary calcium to creatinine ratio (r =0.426, $p < 0.001$). Negative correlation was found between urinary sodium to creatinine ratio and femur neck BMD (r = -0.099, $p < 0.05$). Although urinary sodium to creatinine ratio was not significantly correlated to serum FSH level (r = 0.066, p = 0.088), serum ALP level (r = 0.067, p = 0.083), urine DPD level (r = 0.077, p = 0.056), and lumbar bone mineral density (r = -0.067, p = 0.083), but there is a weak trend in it. There is not only an increase in urinary calcium excretion at postmenopausal women, but also an increase in the urinary sodium excretion. It seems that subjects with a high urinary sodium excretion show a higher urinary calcium excretion that may have some effect on bone mineral metabolism. However, further studies are required to establish whether urinary sodium excretion have a direct effect on bone mineral metabolism of climacteric women in Korea.

M335

First Morning Urine Measured With pH Paper Strips Reflects Acid Excretion. S. J. Whiting[1], J. Bell*[1], S. E. Brown[2]. [1]College of Pharmacy and Nutrition, University of Saskatchewan, Saskatoon, SK, Canada, [2]605 Franklin Park Drive, Osteoporosis Education Project, East Syracuse, NY, USA.

Net acid excretion (NAE) is implicated in bone loss, as increased calcium loss is seen with a high net acid excretion. Dietary protein is identified as a significant producer of acid whereas fruit and vegetable may counteract this effect through the production of metabolizable organic anions which buffer acid. Determination of NAE is important in recognizing the effect diet may have on bone. Most commonly, a 24-hour urine collection is obtained for measurement of NAE where NAE is measured as titratable acidity minus bicarbonate (TA-bicarb) plus ammonium (NH_4^+). However, this measurement can be inconvenient and pH measured on first morning urine with semi-quantitative paper strips may be a practical estimator of NAE. We recruited 23 (4M, 19F) healthy subjects age 20-50 y who recorded dietary intake for a day during which they collected urine from approximately 7 am to 11 pm in one container (“day”) and approximately 11 pm to 7 am (“overnight”,ON) in a separate container. The first morning void contained ON urine. Subjects also provided a two-hour fasting urine at 9 am. pH paper strips (colorpHast ®, EM-Reagents, range 4-7) were used to measure pH of the ON urine, as would be done in practice. A second set of strips (pH range 6.5-10) was used if initial pH read high. Although measurement with pH paper strips was not significantly correlated with 24-hr NAE, there was a significant correlation with 24-hour TA-bicarb (r= -0.466, p<0.025). Further, pH strip measures were significantly correlated with ON NAE (r= -0.710, p<0.005). We noted that ON NAE was correlated with total NAE (r=0.504, p<0.014). We conclude there is useful information is measuring first morning urine pH (which provides pH of urine formed overnight) to obtain an estimate of acid excretion. pH paper strips appear to be useful in the absence of longer (more invasive) urine collections.

M336

The Effect of Low-Fat Dietary Intervention on Bone Turnover. L. E. Ryan*, D. Zaqqa*, H. N. Nagaraja*, R. D. Jackson. The Ohio State University, Columbus, OH, USA.

Osteoporosis affects more than 25 million women and is a major cause of excess morbidity due to the functional impact of fractures on quality of life. In postmenopausal women, estrogen deficiency is an important factor contributing to the development of accelerated bone loss and risk of fracture. Recent epidemiologic data suggest that postmenopausal women with estradiol (E2) levels less than 5 pg/ml have lower bone mass and a higher fracture risk than women with higher E2 values. Studies have suggested that a low-fat diet can result in a decrease in E2 by an average of 17%. We hypothesized that low-fat dietary intervention in postmenopausal women might have an adverse effect on osteoporosis by increasing markers of bone turnover due to the effect of lowering E2 levels. Sixteen postmenopausal women without osteoporosis were recruited and completed a 9 mo low-fat dietary intervention study. Each woman served as her own control. After a 3 mo washout period, all participants began a dietary intervention which included reduction of fat intake to $\leq$ 20% of daily calories; dietary change was maintained for 6 mo. At baseline, after a 3 mo washout period, and after 3 and 6 mo on dietary intervention, serum E2, osteocalcin (OC), bone-specific alkaline phosphatase (BSAP), and N-telopeptide (NTx) levels were measured. All participants significantly decreased their daily fat intake from baseline (mean decrease of 56.36 %); 88% of the women reached the intervention goal. In response to the lowered fat intake, the E2 significantly decreased by 23% (p= 0.001) from baseline and was maintained. There were no significant changes in any of the bone turnover markers (OC, BSAP, or serum or urine N-Tx) between baseline and after 3 or 6 months on a low-fat diet. Subgroup analyses also failed to show any significant change in turnover markers in those participants who dropped their E2 levels below 5 pg/ml after dietary intervention. In conclusion, in our group of postmenopausal women, despite successful reduction in dietary fat intake with a corresponding significant reduction in E2, there was no change in bone turnover markers. These findings suggest that a diet low in fat will likely not adversely affect bone metabolism.

M337

Comparative Effects of Dietary Omnivore and Vegan Protein on Calcium Homeostasis. R. H. Raphael*[1], J. E. Kerstetter[1], C. M. Svastisalee*[1], K. O. O'Brien*[2], D. E. Wall*[3], M. M. Mitnick*[3], D. M. Caseria*[3], K. L. Insogna[3]. [1]School of Allied Health, University of Connecticut, Storrs, CT, USA, [2]Bloomberg School of Public Health, Johns Hopkins University, Baltimore, MD, USA, [3]School of Medicine, Yale University, New Haven, CT, USA.

In adults, a low-protein diet (from omnivorous sources) leads to hypocalcuria and secondary hyperparathyroidism (2^0 HPT). Using dual stable isotopic methods, it was reported that low-protein diets decrease intestinal Ca absorption, which in part, explains the 2^0 HPT. The impact of vegan proteins on Ca absorption and circulating levels of parathyroid hormone is unknown. The purpose of this study was to directly compare vegan sources of dietary protein (primarily soy) with omnivorous protein on Ca homeostasis. Sixteen healthy women (8 premenopausal and 8 postmenopausal) were studied. The protocol consisted of 2 weeks of a well-balanced diet containing moderate amounts of Ca, Na, and protein followed by 4 days of an experimental diet. Subjects randomly received all 4 experimental diets (high-protein vegan, low-protein vegan, high-protein omnivore, low-protein omnivore). The high-protein diet contained 2.1 g protein/kg and the low-protein diet contained 0.7 g protein/kg. In the low and high vegan diets, soy supplied 22$\pm$1 g and 89$\pm$3 g of the total daily protein, respectively. Experimental diets consisted of ordinary foods that were prepared in a metabolic kitchen and contained controlled amounts of Ca (800 mg), P (1100-1500 mg), Na (2400 mg), and energy (2200 kcal). Caffeinated beverages were limited to one a day and alcohol was not allowed. The isoflavone content of all diets was very low (<35 mg/d). Within 4 days of the low-protein omnivore diet, 2^0 HPT developed in all women as evidenced by a 2.6-fold rise in PTH, 1.3-fold rise in $1,25(OH)_2$ vitamin D, and a 1.2-fold rise in NcAMP in comparison to baseline (p<0.0001). At day 4 of the low-protein diet, serum PTH was higher during the vegan in comparison to omnivore diet (57$\pm$2 vs. 46$\pm$1 nleq/ml, p<0.00001), as was serum $1,25(OH)_2$ vitamin D (59$\pm$1 vs. 54$\pm$1 pg/ml, p<0.00001) and NcAMP (2.10$\pm$0.05 vs. 1.87$\pm$0.03, nmol/100 ml GF, p<0.0001). Hypercalciuria was greater during the high-protein omnivore diet compared to the high-protein vegan diet. These data clearly demonstrate that vegan proteins are changing Ca homeostasis differently than protein from omnivorous sources. Whether this difference is due to an effect on Ca absorption or bone turnover or a combination of effects is currently under investigation. The more pronounced 2^0 HPT and blunted calciuric response are consistent with, but do not prove, reduced Ca bioavailability from vegan protein sources.

M338

Factors Modifying the Degree of Secondary Hyperparathyroidism in Hypovitaminosis D. J. A. Pasco*[1], M. J. Henry*[1], M. A. Kotowicz[1], E. Seeman[2], G. C. Nicholson[1]. [1]Clinical and Biomedical Sciences, Barwon Health, The University of Melbourne, Geelong, Australia, [2]Medicine, The University of Melbourne, Heidelberg, Australia.

There is an inverse relationship between serum 25-hydroxyvitamin D (25OHD) and parathyroid hormone (natural log transformed, lnPTH). However, elevated PTH is not observed in all persons with low 25OHD. To characterise women with low vitamin D status for factors associated with PTH, fasting serum samples were analysed for 721 women (aged 20-92 yr) who were free from drugs and diseases known to influence calcium metabolism, recruited at random for the Geelong Osteoporosis Study. Serum 25OHD was measured by RIA (Incstar; precision 6% intra, 15% inter-assay), intact PTH by ICMA (Immulite; precision 5% intra, 5% inter-assay), and total calcium and phosphate by standard techniques. Dietary calcium intake was estimated using a food frequency questionnaire. We confirmed the inverse relationship between 25OHD and lnPTH in the entire group and identified 105 women (median age 64.1 yr, range 21-90) with low 25OHD (<38 nmol/L), for whom mean lnPTH (±SD) was 1.71 (±0.51). There was a logarithmic relationship between PTH and age, the largest single predictor identified, contributing 17.9% of the variance in PTH. Women with PTH levels above compared with below mean PTH for age had lower dietary calcium intakes (576±294 vs 697±451 mg/d, p=0.1), lower serum calcium (2.25±0.11 vs 2.29±0.1 mmol/L, p=0.04) and lower serum phosphate (1.01±0.14 vs 1.08±0.14 mmol/L, p=0.01) levels. Age-adjusted lnPTH was inversely related to dietary calcium intake (partial r^2=0.02; p=0.1) and serum calcium (partial r^2=0.04; p=0.03). A similar association was observed for serum phosphate (p<0.001), probably reflecting the phosphaturic effect of PTH at the kidney. These provisional data suggest that secondary hyperparathyroidism in the face of low vitamin D can be offset by calcium supplementation and so may reduce the increased cortical bone remodeling and bone loss accompanying secondary hyperparathyroidism associated with hypovitaminosis D.

M339

Effect of Atrophic Gastritis on Bone Mineral Density. C. B. Lee*[1], Y. C. Jeon*[2], I. K. Park*[3], Y. S. Park*[4], D. S. Kim*[5], W. H. Choi*[6], Y. H. Ahn*[4], T. W. Kim*[6]. [1]Internal Medicine, Hanyang University Hospital, Kuri, Republic of Korea, [2]Hanyang University Hospital, Kuri, Republic of Korea, [3]Clinical Pathology, Hanyang University Hospital, Kuri, Republic of Korea, [4]Hanyang University Hospital, Kuri, Republic of Korea, [5]Hanyang University Hospital, Seoul, Republic of Korea, [6]Hanyang University Hospital, Seoul, Republic of Korea.

Hydrochloric acid has been demonstrated to be important for the absorption of calcium in intestinal mucosa, and the bone loss is often seen in human after total gastrectomy. The observations that gastric acid secretion decreases with aging in Asian were in contrast to those from many Western countries. One of causative mechanisms of impairment of gastric acid secretion has been attributed to a higher prevalence of H pylori infection in Asian countries. And also it is well known that H pylori causes atrophic damage to secretory tissue of stomach mucosa. The aim of our study was to document the change of calcium and bone metabolism in the patients with decreased capacity of gastric acid secretion like chronic atrophic gastris. The study sample consisted of chronic atrophic gastritis group and control group. Chronic atrophic gastritis group was 20 post-menopausal females (age: 60.3 ±5.1 yr) who was confirmed by gastroscopic biopsy, demonstrating atrophic change of gastric mucosal secretory tissue. Control group had 21 healthy females (age: 58.7 ±6.5 yr) with normal gastroscopic biopy results. Serum levels of calcium, phosphorus, total alkaline phosphatase, intact PTH, and bone mineral density (Delphi, Hologic, USA) were monitored in all the patients in both group before medication. There were no significant differences of calcium (8.9 ±0.9 vs 8.8 ±1.4 mg/dL, p > 0.05), phosphorus (3.2 ±1.5 vs 3.5 ±0.9 mg/dL, p > 0.05), total alkaline phosphatase (72.5 ±24.5 vs 60.3 ±22.4 U/L, p > 0.05) and intact PTH (29.3 ±5.1 vs 27.2 ±3.8 pg/ml, p > 0.05) between chronic atrophic gastritis group and control group. Bone mineral density showed decreased average value in atrophic gastritis group comparing control group (0.78 ±0.27 vs 0.85 ±0.31 g/cm2, p = 0.09). H pylori micro-organism was detected in 10 cases in the atrophic gastritis group and 6 cases in control group. In conclusion, chronic atrophic gastritis which have lower capacity of gastric acid secretion may cause decrease of bone mineral density. And this mechanism may be one of the pathogenesis of senile osteoporosis.

M340

Rate of Weight Loss Influences Calcium Absorption. S. A. Shapses[1], M. Cifuentes*[1], R. Sherrell*[2], C. Riedt*[1]. [1]Nutritional Sciences, Rutgers University, New Brunswick, NJ, USA, [2]Inst. Marine Coastal Sci., Rutgers University, New Brunswick, NJ, USA.

Weight loss (WL) is associated with reduced bone mass and an increased fracture risk, but mechanisms regulating calcium metabolism are not clear. In this study we assessed the effect of 6 weeks of WL at 2 levels of calcium intake (normal intake, NCa; and high intake, HCa) on true fractional calcium absorption (TFCA) and bone-regulating hormones in overweight (BMI of 28.4±1.8 kg/m2) postmenopausal women. Average WL was 0.5±0.3 kg/wk. Due to a wide range of loss (0.1-1.3 kg/wk), we divided the subjects into faster (>0.5kg/wk F-WL, n= 24) and slower (<0.5kg/wk, S-WL, n=18) WL groups. Total calcium intake was lower in the NCa intake (957±213 mg/d) compared to HCa (1794±206 mg/d) group and in the slower compared to faster WL group (p<0.05). Baseline TFCA for all women was 25±8%. The rate of WL affected TFCA differently in normal compared to high calcium subjects (interaction, p<0.05; Table). This interaction notwithstanding, a faster rate of WL decreased total calcium absorbed more than slower WL (p<0.05; Table). Multiple regression analysis showed that none of the measured variables explained the variance in TFCA in the HCa group. However, in the NCa group, the changes in parathyroid hormone (PTH) and 25-hydroxy-vitamin D together accounted for 42% of the variance in TFCA. It is suggested that 1 g/d calcium intake during WL does not meet calcium demands and the body compensates by activating the calcium-PTH axis to absorb more calcium. These results support and extend previous findings that supplemental calcium intake suppresses serum PTH levels during wt loss (1-2). In addition, these data suggest that a slower rate of moderate wt loss in overweight postmenopausal women may preserve calcium stores and bone mass. (1)Ricci et al. JBMR 1998 (2) Jensen et al. JBMR 2001. Supported by NIH AG12161.

% Change in Ca Intake & Absorption

	NCa S-WL	NCa F-WL	HCa S-WL	HCa F-WL
Ca Intake	30±51	-6±25	114±45	87±39
TFCA	-13±20	2±23	-12±16	-28±12
Ca absorbed	19±69	-5±34	85±37	37±40

M341

Effect of Alendronate Withdrawal on Bone Mineral Density (BMD) in a Comunity Clinic. C. L. Smith. Department of Medicine, Division of Nephrology, Hennepin County Medical Center, Minneapolis, MN, USA.

Following withdrawal of estrogen or calcitonin there is a resurgence of bone loss from the skeleton. This may not be true of the bisphosphonates as one study has shown that BMD can remain stable for some time after discontinuation of alendronate (Am J Med 103:291 [97]). Another study, however, suggested that bone loss resumes after alendronate is withdrawn (J Clin Endoc & Metab 85:1492 [00]). Patients seen in the clinic are given the option of discontinuing alendronate when the BMD has stabilized (usually at three years). We reviewed the BMD data on eleven patients who had discontinued alendronate. There was one male and ten females with a mean age of 55±10 years (range 35-72 years) who had taken 20mg of alendronate per day for three years. BMD was measured using dual energy x-ray absorptiometry at the spine, femoral neck and the 33% and ultradistal sites of the radius. Measurements were obtained prior to alendronate and at yearly intervals for five years: three years on alendronate and two years off alendronate. Serum osteocalcin and urine deoxypyridinoline were obtained at years three through five. BMD data are expressed as the mean ± SEM of the percent change from baseline. There was no significance difference between year 1, 2 or 3 and year 4 or 5 at any site (Table). No significant changes in osteocalcin or deoxypyridinoline were present from year 3 to 5. BMD and bone cell markers remained stable in these patients for up to 2 years after withdrawal of alendronate.

Percent Change in BMD During Three Years of Alendronate Treatment and Two Years of Withdrawal

Time	Spine	Femoral Neck	33%	Ultradistal
1 year	6.2±1.5	1.5±1.3	0.06±0.03	2.0±1.3
2 year	8.1±2.1	1.8±3.6	0.06±0.54	1.7±1.4
3 year	10.0±1.7	1.6±2.5	0.28±0.73	2.8±1.5
4 year	9.2±1.5	3.5±3.0	0.1±0.94	4.4±3.0
5 year	8.8±1.9	5.1±3.2	-0.58±1.24	8.0±3.3

M342

A Randomized Controlled Trial with ONO-5920 (Minodronate/YM529) in Japanese Patients with Postmenopausal Osteoporosis. H. Morii, Y. Nishizawa, Y. Taketani, T. Nakamura, A. Itabashi, H. Mizunuma, H. Hagino, M. Fukunaga, T. Miki, K. Yamazaki, T. Nakamura, T. Matsumoto, T. Minamide, T. Makita. ONO-5920 Phase II Osteoporosis Treatment Research Group, Osaka, Japan.

ONO-5920 is a recently developed bisphosphonate which has 200-fold effectiveness in increasing bone mineral density (BMD) and 10,000-fold activity in suppressing osteoclastic function in in vitro study compared with etidronate. Written informed consents were obtained from postmenopausal women with ages between 40 and 75 years who were diagnosed as having osteoporosis accoriding to Japanese criteria of diagnosis. Subjects were those who have fragility vertebral fracture with BMD of L2-4 less than 80 % of YAM (Young Adult Mean) or those with BMD of L2-4 less than 70 % of YAM and without vertebral fracture. They were classified into 4 groups to each of which 0.5, 1.0 and 1.5 mg of ONO-5920 or placebo was administered for 36 weeks at 24 facilities. To placebo group as well as other groups calcium lactate was prescibed at a daily dose of 0.8 g. Among 352 patients registered number of PPS (Per Protocol Set) was 323 and that of FAS (Full Analysis Set) was 345. Number of patients for safety analysis was 351. Primary endpoint was the percentage change of BMD. The percentage change of L2-4 BMD was 100.72 % in placebo group, 105.65 % in 0.5 mg, 106.42 % in 1.0 mg and 105.93 % in 1.5 mg group recpectively. Latter 3 groups showed significant increases compared with placebo group. There were significant decreases of urinary deoxypyridinoline/creatinine and NTX/creatinine at 4 weeks of treatment with 3 doses of ONO-5920 compared with the placebo group. There were significant decreases of serum bone specific alkaline phosphatase at 12 weeks of treatment with 3 doses. Incidence of adverse drug reactions (ADRs) was 13.2 %, 23.3 %, 22.9% and 27.3 % in placebo, 0.5 mg, 1.0 mg and1.5 mg group recpectively. Although the incidence of gastrointestinal ADRs was 0 %, 12.6 %, 6.3 % and 11.1 % in placebo, 0.5 mg, 1.0 mg and 1.5 mg group recpectively, serious adverse events have not been reported. In conclusion ONO-5920 is a new bisphosphonate which shows the efficacy and safety in patients with osteoporosis.

Disclosures: ***H. Morii****, Chugai Pharmaceutical Co., Ltd 5.*

M343

Alendronate Reverses Methotrexate Associated Osteopenia without Adverse Effect on Longitudinal Growth in Skeletally Immature Animal Model. J. A. Spadaro, T. A. Damron*, R. Chen*, D. A. Clemente*, J. Feak*, B. Margulies*, J. Horton*, I. Cherrick*. Upstate Medical University, Syracuse, NY, USA.

Bisphosphonates have yet to be rigorously evaluated to prevent chemotherapy induced osteopenia during childhood. The hypothesis was that in a growing animal model methotrexate (MTX) would decrease BMD and longitudinal growth while concurrent treatment with alendronate (ALD) would prevent this effect without further adverse effect on growth. Twenty-four 5 week old male Sprague-Dawley rats were divided into 4 groups. The ALD group received alendronate, 0.30 mg/kg SC once per week for 6 weeks. The CTL and MTX groups received IP injection of either vehicle or methotrexate 0.75 mg/kg/day, respectively, in a 2-cycles (5 d on/9 d off/5 d on). The MTX+ALD group had both regimens as above. After 6 weeks the bone density was studied by pQCT (vBMD) and DXA (aBMD). Hind limb bone lengths were measured and histological sections examined. The MTX group showed an 11% decrease in aBMD of the femur, a 3% decrease in whole body aBMD, and 3% shortening vs. controls (Table 1). ALD with MTX treatment resulted in a 19% greater femoral aBMD than CTL and 7.5% greater whole body aBMD. Cross sectional area in the MTX+ALD femurs was greater than CTL, especially distally near the more active growth plate. Femoral length remained less than CTL in the MTX+ALD animals. ALD and MTX+ALD groups were similar in all endpoints, suggesting that ALD overwhelmed the effect of MTX. Striking transverse hyperdense banding corresponding to the weekly ALD in both ALD and MTX+ALD groups was seen in radiographs and microscopically in growth areas of the skeleton. Femoral lengths for the ALD group were NS different from CTL. ALD administered in a pulsed dose fashion more than reverses the effects of MTX on aBMD in growing areas, but with little effect on the minor growth losses induced by MTX. ALD had no additional significant independent adverse effect on growth. Bisphosphonates such as ALD may be useful in prevention of treatment associated osteopenia in patients with pediatric malignancies.

Table 1: % Difference from Controls. ns = p>0.05

	MTX	MTX+ALD	ALD
aBMD whole body (DXA)	-2.8 %	+7.5 %	+7.3 %
aBMD entire femur (DXA)	-10.9 %	+19.2 %	+11.1 % (ns)
vBMD distal femur (pQCT)	+1.3 % (ns)	+43.0 %	+47.1 %
vBMD prox. femur (pQCT)	+4.3 % (ns)	+8.7 %	+2.4 % (ns)
section area, distal femur (pQCT)	-6.3 % (ns)	+26.8 %	+44.6 %
Section area, prox. Femur (pQCT)	-5.9 % (ns)	+0.8 % (ns)	+9.2 % (ns)
Femur length	-3.0 %	-2.2 %	-1.2 % (ns)

M344

The Effect of Three-years Treatment of Incadronate Disodium on Accumulation of Microdamage, Microarchitecture and Strength in Dog Vertebra. S. Komatsubara*[1], S. Mori[1], T. Mashiba*[1], M. Ito*[2], J. Kawanishi*[1], T. Akiyama*[1], K. Miyamoto*[1], Y. Cao*[1], H. Norimatsu[1]. [1]Department of Orthopaedic Surgery, Kagawa Medical University, Kagawa, Japan, [2]Department of Radiology, Nagasaki University, School of Medicine, Nagasaki, Japan.

This study aimed to investigate the effect of long-term suppression of bone resorption by bisphosphonate on microstructure, accumulation of microdamage and mechanical properties of trabecular bone. 29 beagles (15 males, 14 females), 1year old were divided into three groups. The control (CNT) was treated daily with vehicle, and the other two groups were treated with incadronate at a dose of 0.3 mg/kg/day (LOW) or 0.6 mg/kg/day (HIGH) orally for 3 years. After sacrifice, the second thoracic vertebra was scanned with micro-CT. The left side of second thoracic vertebra was stained with Villanueva bone stain for histomorphometry. The right side was stained en block with basic fuchsin for microdamage measurement. Fourth lumbar vertebra was mechanically tested in compression. Incadronate concentration in bone was measured in eleventh thoracic vertebra using high performance liquid chromatography (HPLC). Micro-CT analysis demonstrated the plate-like trabecular structure and increased concave surface of trabeculae in the thoracic vertebra of incadronate treated groups. Three years incadronate treatment significantly suppressed activation frequency by 56% in LOW and by 67% in HIGH without impairment of mineralization, and increased microdamage accumulation in both treated groups. Trabecular bone volume was significantly increased in both LOW (31%) and HIGH (31%), and vertebral strength was significantly increased in HIGH when compared with CNT. However, no significant differences were found among groups in any intrinsic material property. Regression analysis showed a significant linear relationship between suppressed bone remodeling and increased microdamage accumulation. Incadronate concentration in bone was dose dependent. There was significant linear relationship between increased incadronate concentration in bone and reduced Ac.f. Also significant linear association was found between increased incadronate concentration in thoracic vertebra and increased Cr.Dn and Cr.S.Dn. This study suggested that long-term suppression of bone remodeling increased microdamage accumulation, but this was not necessarily associated with vertebral fragility because of compensated increase of bone mass and improved microarchitecture.

M345

One-year Alendroante Administration Is Effective to Prevent Bone Loss and Decline of Bone Strength in Severe Osteoporotic Patients -A pQCT Study. P. C. Or*[1], W. S. Chan*[2], L. Qin[2], M. A. Dambacher*[3], E. Lau[1], P. C. Leung*[1]. [1]The Jockey Club Osteoporosis Centre for Care and Control, The Chinese University of Hong Kong, Hong Kong, Hong Kong Special Administrative Region of China, [2]Department of Orthopaedics and Traumatology, The Chinese University of Hong Kong, Hong Kong, Hong Kong Special Administrative Region of China, [3]Universitätsklinik Balgrist, Zürich, Switzerland.

High risk patients with established osteoporosis should be treated for the prevention of further fractures. Antiresorptive drugs have been developed and shown to be effective treating Caucasians in western countries and we want to test the same drugs for Asians. In this study, we evaluated the treatment effects of Alendronate in 120 postmenopausal Chinese women aged between 55 to 83, with history of vertebral fracture. After randomization, patients received either oral administration of 10mg/day Alendroante or placebo for one year. Daily supplemental of 1200mg calcium was given to both groups. Baseline and follow-up multislice pQCT measurement (Densiscan 2000) was performed in the non-dominant distal radius. 42 patients in alendronate group and 43 patients in placebo group completed one-year follow-up. Results in table 1 showed that alendronate was effective to prevent both trabecular and cortical bone loss as compared with placebo. In addition, the alendronate might be effective to prevent bone resorption on the surface of shaft marrow cavity (positive changes in shaft cross-sectional area (CSA) in alendronate treated group as compared with placebo group). This might result in significant protective effects on the decline of bone shaft strength as shown in the non-invasive bone strength index (BSI) of distal radial cortical bone. Since osteoporosis is a systemic bone health problem and oral alendronate has systemic antiosteoporotic effects, the benefits of alendronate shown in distal radial shaft BSI might also positively influence the femoral neck, which could not be measured in the current study due to methodological limitations. Long-term follow-up is needed to reveal the benefits of alendronate treatment in reducing osteoporotic fractures in Chinese population.

Comparison of percentage changes in BMD, CSA, CSMI and BSI for different parts of distal radius

Measured Region in Distal Radius			Percentage Changes (%) (Mean ± SD)		p-value
			Alendronate (n=42)	Placebo (n=43)	
Ultradistal	**BMD**	**tBMD**	0.06 ± 4.04	-3.48 ± 6.21	0.003*
		iBMD	1.13 ± 8.35	-2.25 ± 7.54	0.053
	CSA	**tCSA**	1.04 ± 15.06	2.93 ± 12.26	0.526
		iCSA	0.87 ± 11.74	1.91 ± 9.13	0.649
Distal Shaft	**BMD**	**cBMD**	0.85 ± 3.31	-0.25 ± 1.05	0.041*
		iBMD (iBMC/iCSA)	0.55 ± 1.57	-1.38 ± 2.00	<0.001*
	CSA	**cCSA**	0.80 ± 3.49	-1.01 ± 1.46	0.002*
		iCSA	0.57 ± 4.05	-0.13 ± 2.42	0.336
	CSMI	**cCSMI**	0.74 ± 5.65	-0.69 ± 4.56	0.202
		iCSMI	0.71 ± 6.49	-0.10 ± 5.41	0.531
	BSI	**cBSI**	1.67 ± 7.96	-1.86 ± 6.95	0.033*

t-trabecular; c-cortical; i-integral (average of trabecular and cortical bone) CSA-cross sectional area; CSMI-cross sectional moment of inertia; BSI-bone strength index (BSI=BMDxCSMI)

M346

Etidronate Retards Radiological Disease Progression And Prevents Axial And Appendicular Bone Loss in Rheumatoid Arthritis (RA) – A Randomaized Controlled Study. M. Ide[1], Y. Suzuki[2], G. Itoh*[1], R. Uehara[1], Y. Ohsone*[3], Y. Okano*[4], Y. Matsuoka*[3], M. Akizuki*[4], Y. Ichikawa*[5], S. Ozaki*[1]. [1]Rheumatology, St. Marianna Univ. School of Med., Kawasaki, Japan, [2]Rheumatology, Tokai Univ., Isehara, Japan, [3]Internal Medicine, Kawasaki Municipal Hosp., Kawasaki, Japan, [4]Internal Medicine, Yokohama Municipal Hosp., Yokohama, Japan, [5]Internal Medicine, St. Joseph Hosp., Yokosuka, Japan.

Etidronate, an analog of inorganic pyrophosphate, its main biologic effect is the inhibition of bone resorption by suppression of osteoclast function. Recently, favorable effects of etidronate was reported on bone loss in RA. On the other hand, it was suggested that osteoclast like cell derived from synovium of RA patient was participated with joint destruction in RA. We focus on whether etidronate influences progression of joint destruction and prevents bone loss in RA. **Methods.** Twenty eight women with active rheumatoid arthritis (defined by a level of serum CRP >1mg/dl, and/or an erythrocyte sedimentation rate >20 mm/h) enrolled for this study. The patients were randomly allocated into one of two treatment group; etidronate group (400mg/day, 14 days/3 months) or control group (calcium lactate 1g/day). We measured lumbar and radial bone mineral density (periarticular region and 33% distal shaft) by DXA at baseline and 1 year later. Furthermore, the radiological development of erosions and joint space narrowing on hands were scored using Sharp method modified by van der Heijde et al. at the same time as DXA. **Results.** 1) The parameters of RA activity, age, administration of DMARDs, and bone mineral density were similar in 2 groups at baseline. 2) The lumbar BMD at 1 year later was significantly lower than at baseline in control group (1.056 vs 1.013 g/cm^2, mean±SEM, p <0.05). On the other hand, the lumbar BMD in etidronate group at 1 year later was significantly higher than at baseline (1.023 vs 1.058, p <0.05). 3) The periarticular and 33% distal shaft BMD at 1 year later in control group were significantly lower than at baseline (0.337 vs 0.323, 0.596 vs 0.562, p <0.05), whereas the both BMD were maintained as well as at baseline in etidronate group (0.342 vs 0.343, 0.530 vs 0.529, NS). 4) Although the change of serum CRP in both groups was similar, the progression score in etidronate group was significantly smaller than in control group (2 vs 7, p <0.05). **Conclusion.**These results suggest that etidronate is not only prevents bone loss but retards progression of joint destruction in RA .

M347

Three-Monthly 2mg Intravenous Ibandronate Injections Restore Bone Turnover to Premenopausal Levels. S. Adami[1], C. Christiansen*[2], A. Burdeska*[3], K. Coutant*[3], P. Mahoney*[3]. [1]University of Verona, Verona, Italy, [2]CCBR, Ballerup, Denmark, [3]F. Hoffmann-La Roche Ltd, Basel, Switzerland.

For some patients, oral bisphosphonates (BPs) have limitations that may reduce compliance. Intravenous (i.v.) administration avoids these problems, thereby potentially enhancing acceptability. Less frequent dosing may further improve compliance. A pivotal phase III fracture study of 3-monthly ibandronate (0.5mg and 1.0mg) i.v. injections showed suboptimal increases in BMD and suppression of bone turnover, such that the fracture reduction did not reach significance (Recker R, et al. Osteoporos Int 2000;11: abstract 565). Preliminary results from a trial examining the impact of increasing dose (Adami S, et al. IOF World Congress on Osteoporosis 2002; abstract O36) support the conclusion that insufficient dose was a key reason for this finding. This double-blind, parallel-group phase III study of 1mg versus 2mg ibandronate i.v. injection every 3 months as treatment of PMO enrolled 520 postmenopausal women (aged 55-75 years, at least 5 years since menopause onset) with established osteoporosis (mean BMD T-score at the lumbar spine <-2.5 SD). Patients were randomized to receive either 1mg (n=131) or 2mg (n=261) ibandronate or placebo (n=128), plus daily calcium (500mg) and vitamin D (400IU). The primary endpoint was the relative change in lumbar spine BMD. Secondary endpoints included change in the rate of bone turnover, as measured by assessing serum C-telopeptide (CTx) concentration, urinary CTx excretion (ratio of CTx/creatinine) and serum osteocalcin concentration at baseline, and every 3 months thereafter (before injection). Three-monthly 2mg i.v. ibandronate provided greater increases in lumbar spine BMD versus 1mg after 1 year (5% vs 3%, respectively; p<0.0001), with no increase in the placebo group. These BMD gains were associated with a significant reduction in markers of both bone resorption and bone formation after 12 months, relative to placebo. The effects on bone turnover were more pronounced in the 2mg versus 1mg ibandronate group: serum CTx levels, urinary CTx excretion and serum osteocalcin levels were reduced by 60.4% versus 44.1%, 60.9% versus 42.0% and 52.7% versus 47.9%, respectively, after 12 months. This study provides evidence that increasing the ibandronate dose to 2mg effectively reduces biochemical markers of bone turnover to premenopausal levels and provides more sustained suppression of bone turnover and significant increases in BMD that could translate into fracture benefit. This study also underscores the importance of examining bone marker patterns in conjunction with BMD increases.

M348

Dose Dependent Effects on Bone Resorption and Formation, on a Group and an Individual Level, of Intermittently Administered Intravenous Ibandronate. A. Moelgaard*[1], S. Christgau*[2], P. Qvist*[2], L. Wieczorek*[3], N. Hoyle*[3], C. Christiansen[1]. [1]Center for Clinical & Basic Research A/S, Ballerup, Denmark, [2]Nordic Bioscience A/S, Herlev, Denmark, [3]Hoffmann-La Roche Ltd., Basel, Switzerland.

To delineate in detail the dose-dependent effects of intermittent intravenous (iv.) ibandronate treatment on markers of bone turnover. The study included 73 healthy postmenopausal women with a spinal BMD between -5 and -1 T-score. Two groups received an intravenous injection every three months of either 1 mg or 2 mg ibandronate and one group served as control. Study duration was 168 days and treatment was administered on day 0 and day 84. Serum CTx and NMid were measured on samples drawn on 19 occasions. Three (3) days after drug administration s-CTx in the 1 mg and 2 mg groups had decreased by -70% and -83%. At day seven (7) nadir was reached with a decrease of -81% and -90%, respectively. Two weeks after drug administration s-CTx started to rise again in both the 1 mg and 2 mg groups reaching -16% and -20% at day 84 i.e. immediately before the second drug administration. The 1 mg and 2 mg curves were parallel, but the 2 mg curve was consistently and significantly (p<0.001) lower than the 1 mg curve. S-NMid had completely different dynamics with a steady decrease that reached a nadir of -35% after 5 months (140 days) of treatment. The 1 mg and 2 mg doses resulted in parallel curves. On group level, the suppression of bone resorption was greater or equal to the suppression of bone formation at all time points. On the individual level, however, the different dynamics of resorption and formation in response to the iv. ibandronate treatment resulted, in several time points where more individuals had higher resorption than formation, suggesting that bone loss resumed periodically. This tendency became worse with increasing treatment time.The data suggests that the reasons why a 3-year fracture study using 1 mg and 0.5 mg iv. ibandronate every 3 months yielded a sub-optimal effect on bone mineral density and failed to show a significant reduction in the incidence of vertebral fractures, can be found in both the timing of the drug administration and the dose. Furthermore, it demonstrates that the analysis of bone marker data on an individual level may be at least as important as the conventional evaluation on a group basis.

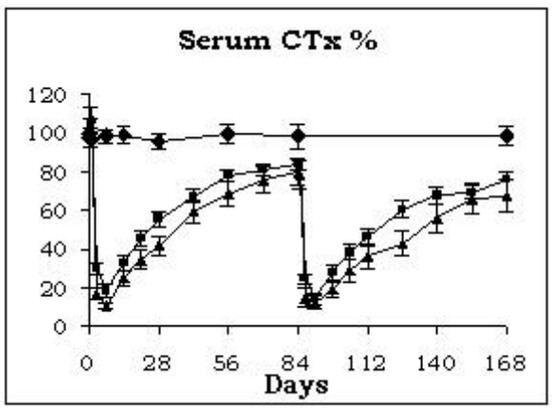

M349

The Efficacy of 12-month Oral Ibandronate Treatment in Postmenopausal Osteoporosis When Taken 30 min Versus 60 min Before Breakfast. L. B. Tankó*[1], M. R. McClung[2], R. C. Schimmer*[3], P. Mahoney*[4], C. Christiansen[1]. [1]CCBR A/S, Ballerup, Denmark, [2]FACE, Oregon Osteoporosis Center, Portland, OR, USA, [3]F.Hoffmann-La Roche Ltd, Basel, Switzerland, [4]Roche Products Ltd, Welwyn Garden City, United Kingdom.

The purpose of the study was to demonstrate comparable efficacy of oral ibandronate 2.5 mg daily to increase bone mineral density (BMD) and suppress bone turnover when the post-dose fasting period is reduced from 60 to 30 min. Forty-eight week, multi-center, open-label, randomized non-inferiority study. Subjects (n=184) were postmenopausal women 55-80 years old with lumbar spine BMD T-score ≤-2.5. All participants received a daily dose of 2.5 mg ibandronate supplemented with 500 mg calcium and 400 IU of vitamin D. Subjects were randomly assigned to take ibandronate exactly 30 or 60 min before breakfast. Time of drug intake with reference to breakfast was registered in diaries. Change in spine BMD (L1-L4) and proximal femur (trochanter, femoral neck, total hip) from baseline was measured by DEXA, whereas changes in markers of bone turnover (serum osteocalcin and urinary CTx excretion) were assessed by ELISA. Baseline efficacy parameters were similar between the intervention groups. Both groups adhered tightly to the dosing regimen, with a more narrow distribution in the 30-min fasting group. After 48 weeks of treatment, the increase in spine BMD from baseline was lower in the 30-min (3.1%) compared to the 60-min group (5%) to an extent that the pre-specified non-inferiority criteria were not met. Similar results were found at the trochanter, femoral neck and total hip, although the magnitude of the difference between the treatment groups at these sites was smaller than at the lumbar spine (Figure 1). Less suppression of the markers of bone turnover, assessed by the mean change from baseline of creatinine-corrected urinary CTx (-48.49% versus -61.75%) and serum osteocalcin concentration (-34.77% versus -43.78%) was observed in the 30-min compared to the 60-min group, respectively. Ibandronate was well-tolerated in both treatment groups. A reduction of the fasting interval following drug intake decreases the efficacy of treatment. Intermittent dosing regimens, currently under clinical testing, are expected to further improve the convenience and compliance of oral treatment with bisphosphonates.

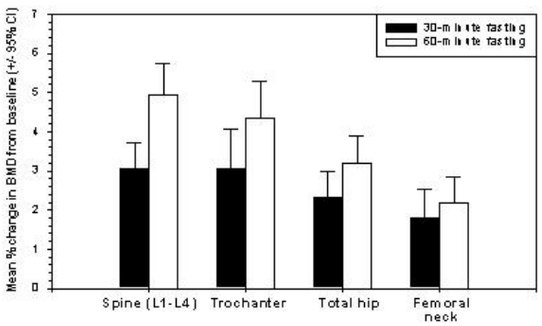

M350

Upper GI Tolerability of Once-Weekly Alendronate 70 mg with Concomitant NSAID Use. A. E. de Papp, J. Palmisano*, G. P. Geba*. Clinical Development, Merck & Co., Inc., West Point, PA, USA.

Safety assessments of oral bisphosphonates have focused on upper gastrointestinal (GI) adverse events (AEs), because of the known potential for bisphosphonates to irritate the upper GI mucosa. Similarly, nonsteroidal anti-inflammatory drugs (NSAIDs) may induce gastric mucosal damage, and are frequently used by the same patient population that is prescribed bisphosphonates. In order to determine the rate of clinical adverse GI events with exposure to once-weekly alendronate 70 mg (ALN), and NSAIDs, we performed an analysis on a subgroup of 257 patients who received both medications concomitantly during a 12 week, randomized, placebo controlled osteoporosis trial. Survival analysis was performed using Kaplan Meier estimation, and significance was assessed using the log rank test. Logistic regression was used to assess the effect of treatment, NSAID exposure and interaction on the rate of upper GI AEs. 450 women and men with osteoporosis, from 48 US sites were randomized to treatment with once-weekly ALN, or placebo (PBO) in a 1:1 ratio. 60.2% (135/224) of ALN patients, and 53.9% (122/226) of PBO patients, reported concomitant use of NSAIDS or aspirin during the study. In the analysis of upper GI AEs of the "all patients treated" population, 25 ALN patients and 30 PBO patients reported one or more upper GI AEs, (11% and 13% respectively; p= NS). In the subgroup of patients taking NSAIDs concomitantly, 15 ALN patients, and 14 PBO patients reported upper GI AEs (11.1 % vs 11.6% respectively; p = NS). Logistic regression revealed no significant interaction between once-weekly ALN and concomitant NSAID use.

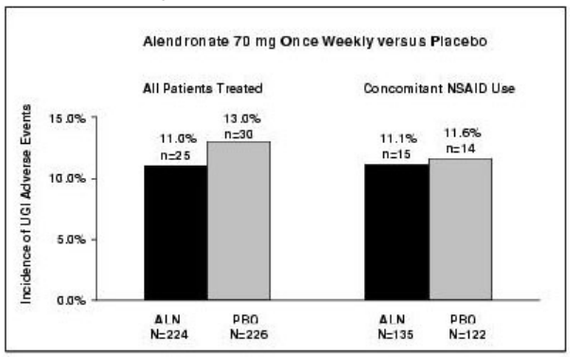

We conclude that once-weekly alendronate 70 mg was generally well tolerated, and when used concomitantly with NSAIDs, did not increase the rate of upper GI AEs relative to placebo over a 3 month study period.

*Disclosures: **A.E. de Papp**, Merck & Co., Inc. 3.*

M351

Effect of Pamidronate and Alendronate on Bone Mineral Density in Osteoporotic Patients - A Control Matched Study. R. M. Noord*[1], R. Minkowitz*[2], P. Maid*[1], J. M. Lane[1]. [1]Hospital for Special Surgery, New York, NY, USA, [2]Weill Medical College of Cornell University, New York, NY, USA.

A substantial fraction of osteoporotic patients cannot be treated with alendronate due to treatment failure or gastrointestinal contraindication. Therefore, date are needed regarding the bone mineral density (BMD) increases achieved with alternative bisphosphonate regimens compared to those provided by alendronate. This study aims to investigate the efficacy of IV pamidronate, compared to alendronate, in increasing BMD in patients with low BMD. The experimental group consisted of 28 consecutive, pamidronate-treated (30mg IV q 3 months), osteoporotic (27) or severely osteopenic (1) patients from an office orthopaedic practice. Included were 2 males with a history of a fragility fracture, 11 females without fracture history and 15 females with a fracture history. Experimental patients were matched to a control patient treated with alendronate (10mg qd). Control patients were of similar sex, fracture history and bone mineral density before treatment. Dual-energy x-ray absorptiometry was used to measure patients' BMD both before and after treatment. Overall, 81% of patients treated with pamidronate experienced an increase in lumbar spine (LS) BMD, with a mean age of +2.40%/year. In comparison, 85% of patients treated with alendronate had an increase in LS BMD, with a mean change of +3.00%/year. In the femoral neck (FN), 60% of patients experienced improved BMD in the pamidronate group, with a mean change of +.22%/year, and 61% of patients in the alendronate group had an increase in FN BMD, with a mean change of +.12%/year. In females without fracture history, 64% of those treated with pamidronate increased LS BMD (mean change of +.95%/year), and 64% increased FN BMD (mean change of +.52%/year). In similar females treated with alendronate, 90% had a LS BMD increase (mean change of +3.30%/year), and 54% had an increase in FN BMD (mean change of +.72%/year). In females with a fracture history, 93% of those treated with pamidronate incresed LS BMD (mean change of +3.19%/year), and 66% increased FN BMD, with a mean change of +.68%/year. In the alendronate group, 80% of females with a fracture history had increased LS BMD (mean change of +2.64%/year), and 60% increased FN BMD (mean change of -.69%/year). In conclusion, data shows no statistical difference between the effects of pamidronate patient and alendronate matched patient on the overall study population's lumbar spine or femoral neck bone mineral densities.

*Disclosures: **R.M. Noord**, Novartis 8; Merck 2, 8.*

M352

Alendronate Reduces Risk of Vertebral Fracture in Women with BMD T-scores Above -2.5: Results from the Fracture Intervention Trial (FIT). D. Black[1], D. Thompson[2], S. Quandt[3], L. Palermo[1], K. Ensrud[4], O. Johnell[5]. [1]University of California, San Francisco, CA, USA, [2]Merck & Co., Inc., West Point, PA, USA, [3]Wake Forest University, Winstom-Salem, NC, USA, [4]University of Minnesota, Minneapolis, MN, USA, [5]Malmo General Hospital, Malmo, Sweden.

Alendronate has been shown to be effective in reducing risk of non-vertebral, hip and vertebral fractures among women with BMD T-scores below -2.5. However, several studies have suggested that bisphosphonates are less effective in reducing risk of non-vertebral and hip fractures among women with BMD above -2.5. The question of whether reductions in vertebral fractures depend on initial BMD has not been fully explored. We performed an analysis of data from FIT in order to examine whether reductions in vertebral fractures were larger in those with lower BMD. FIT was a randomized trial of 6459 women with femoral neck T-scores below -1.6 of whom 2027 had existing vertebral fractures. In this analysis, we combined data from women with and without existing vertebral fracture. Women were assigned to alendronate (5 mg for first two years, then 10 mg) or placebo and followed for an average of 3.8 years. We stratified the population according to initial femoral neck T-score into those with T-scores at or below -2.5 and those with T-scores above -2.5. We analyzed the effect of alendronate on incidence of morphometric and clinical vertebral fractures within those strata.

	FN BMD T≤-2.5 (n=2715)		FN BMD T>-2.5 (n=3741)	
Type of Fracture	N	RR (aln vs. pbo)	N	RR (aln vs. pbo)
Morph. Vertebral	214	0.50 (0.37, 0.67)	130	0.57 (0.39, 0.82)
Clinical Vertebral	78	0.62 (0.39, 0.98)	41	0.41 (0.21, 0.80)

We found no significant differences between the two groups in reductions of morphometric vertebral fractures or clinical vertebral fractures. We conclude that alendronate is effective in reducing the risk of both morphometric and clinical vertebral fracture in women with BMD T-scores above -2.5. There is no evidence that the effect of alendronate on vertebral fractures is different in those with lower BMD.

Disclosures: ***D. Thompson****, Merck & Co., Inc. 3.*

M353

Upper GI Tolerability of Alendronate (FOSAMAX) 70 mg Once Weekly Is Similar to Placebo. J. Eisman[1], R. Rizzoli[2], K. A. Gaines*[3], N. Verbruggen*[3], M. E. Melton[3]. [1]St. Vincent's Hospital, Sydney, Australia, [2]University Hospital Geneva, Geneva, Switzerland, [3]Merck & Co., Inc., Whitehouse Station, NJ, USA.

Alendronate has established efficacy for treatment of osteoporosis whether given daily or in a more convenient once weekly regimen. To further investigate the tolerability of once weekly alendronate, this study examined the overall and upper gastrointestinal (GI) tolerability profiles of alendronate given in a 70-mg once weekly regimen as compared to placebo. In 19 countries representative of Europe, the Americas and Asia-Pacific, 449 men and women with osteoporosis were recruited for this study. Subjects were randomized to either alendronate 70 mg or placebo once weekly for 12 weeks and advised to take the tablets using standard morning dosing. The incidence of any adverse experience was evaluated. Upper GI adverse experience and discontinuation of therapy due to a drug-related upper GI adverse experience between groups were assessed using Kaplan-Meier estimation at week 12 for the time-to-first-event data. The change from baseline in urinary NTx/Cr was also assessed. The subjects were aged 64 +/- 9 years, 94% women, 66% Caucasian, 18% Asian and 12% Hispanic. Urinary NTx/Cr excretion decreased significantly in the group receiving alendronate (-43%) compared to placebo (+8%, P<0.001 alendronate vs. placebo). Overall safety and tolerability was similar between groups, with similar proportions of subjects reporting an adverse experience in each group (alendronate 40%, placebo 38%). A similar proportion of alendronate and placebo subjects reported an upper GI adverse experience (9.8% and 9.4%, respectively) and a similar proportion of subjects discontinued therapy due to a drug-related upper GI adverse experience (2.7% and 2.2%, respectively). Neither these proportions nor the time-to-first event differed significantly between the alendronate and placebo groups. Thus, similar to results from an earlier US study (Greenspan et al., JBMR 2001;17(Suppl 1):S405), alendronate 70 mg once weekly significantly decreased bone turnover and had an upper GI and overall tolerability profile indistinguishable from placebo.

Disclosures: ***J. Eisman****, Merck & Co., Inc. 2, 5.*

M354

Effect of Bisphosphonates in Osteoporosis Secondary to LHRH Analogs for Prostate Cancer. S. Yaturu[1], C. DePrisco[2], S. DjoDjo*[3]. [1]Endocrinology, Overton Brooks VAMC/LSUHSC, Shreveport, LA, USA, [2]Endocrinology, LSUHSC, Shreveport, LA, USA, [3]LSUHSC, Shreveport, LA, USA.

Prostate Carcinoma is the most common visceral malignancy in men. Treatment with Leutinizing Hormone Releasing Hormone (LHRH) analogs improves survival. Therapy with LHRH analogs decreases bone mineral density and increases the risk of osteoporotic fractures in men with prostate cancer. Several in vitro studies have shown the benefit of bisphosphonates in the prostate cancer cell lines. Our main goal is to compare the effect of alendronate on patients with osteoporosis secondary to prostate cancer on GnRH analogs compared to the age matched patients with osteoporosis in men. We compared the changes in the bone mineral densities of 12 patients with osteoporosis secondary to LHRH analogs in comparison to 27 patients without prostate cancer and have osteoporosis. The changes in the bone mineral density at lumbar spine and both hips were measured by dual energy x-ray absorptiometry in both groups over one year on bisphosphonates.The data is expressed as mean plus or minus standard error.

Mean Changes

	Group1(n=12)	Group2(n=27)	*p*
Spine	-0.75±2.4	0.98±2.3	0.65
Right Hip	-5.06±1.74	-0.47±0.60	0.158
Left Hip	-3.77 ±1.7	0.05±0.44	0.007

Mean changes in bone mineral density differed significantly between the two groups (P<0.05) at the left hip but not at the lumbar spine and total hip. This data suggest that bisphosphonate therapy is beneficial at spine and effective for patients with prostate cancer.

M355

Medroxyprogesterone Augments Positive Bone Mineral Density Effects of Cyclic Etidronate in Menopausal Women. J. C. Prior, C. L. Hitchcock*. Endocrinology/Medicine, U of British Columbia, Vancouver, BC, Canada.

The purpose of this study is to determine whether co-therapy of medroxyprogesterone (MP) with intermittent cyclic etidronate (ICE) has a more positive effect on bone mineral density (BMD) change than ICE alone. Progesterone and progestins cause osteoblast-related bone formation *in vitro* (Tremollieres, 1992; Ishida, 1997). Premenopausal bone change is positively related to luteal lengths and progesterone levels (Prior, 1990; Sowers, 1998). A prospective cohort control study showed greater effects of MP with estrogen versus estrogen alone (Grey, 1996). Increased bone formation from PTH therapy reduces vertebral and non-vertebral fragility fracture rates (Neer 2001). **Design:** Retrospective clinical cohort study using randomly sampled charts of women with osteopaenia or osteoporosis from a single endocrinology practice. 263 charts were randomly selected and reviewed, of which 19 were eligible. These data were compared with published data, because insufficient numbers were available on ICE alone from this practice. **Inclusion criteria**: women past menopause, full dose therapy with MP (10mg/d) or oral micronized progesterone (OMP; 300mg/d) as well as ICE, BMD baseline data within 6 months of starting therapy and 1-4 y later. Diseases or steroid use were not exclusion criteria. **Cohort Characteristics:** These 19 menopausal women were 58.3 y (SD 5.6) at baseline, with BMI 23.5 (3.35). All were taking at least 500 mg supplemental calcium and 400 IU vitamin D/d. Baseline spine (LS) BMD was 0.786 (0.114) g/cm^2 and femoral neck (FN) 0.673 (0.126) g/cm^2. **Results:** LS BMD change on MP plus ICE was LS: 6.99% (SD 5.76, n=16) and FN 2.71% (SD 6.41, n=16) over 2.7 (95% CI: 2.3,3.1) y. A comparable clinical study of ICE alone over 2 y (Crilly, OI, 2000) showed BMD changes of LS: 5.20 (7.39)%; FN: 1.40 (7.50)%). MP plus ICE produced a 1.79% greater increment in LS (t_{224} = 12.95, P < 0.0001) and 1.31% greater gain in FN BMD (t_{253}=9.17, P <0.0001) than ICE alone. MP plus ICE BMD changes (7% spine and 2.7% FN) are also greater than from a meta-analysis of ICE clinical trials (4.1% and 2.4% respective increments over placebo)(Cranney, OI, 2001). **Conclusion:** These data suggest MP and OMP increase bone formation in menopausal women and, combined with anti-resorptive agents, may improve fracture prevention. Randomized, controlled trial data are needed.

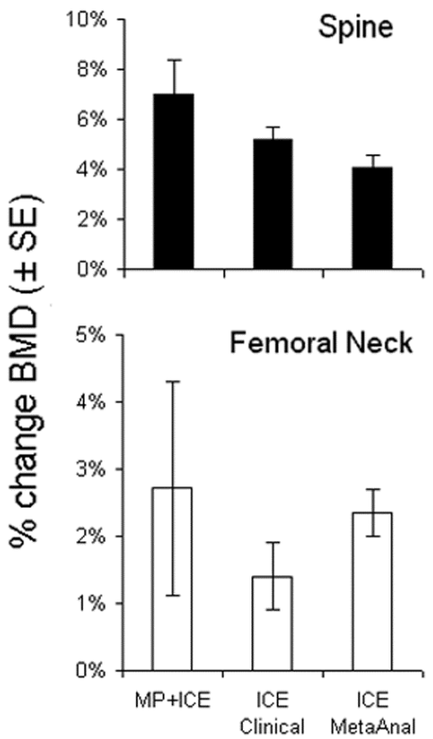

M356

Ibandronate Decreases Femoral Head Flattening in a Piglet Model of Ischemic Necrosis of Femoral Head. H. K. W. Kim[1], D. Pringle*[1], D. Hunter*[1], W. Pritchard*[1], F. Bauss[2]. [1]Shriners Hospital for Children, Tampa, FL, USA, [2]Roche Diagnostics GmbH, Penzberg, Germany.

Ischemic necrosis of growing femoral head, as seen in children with Legg-Calve-Perthes disease, is associated with development of permanent deformity of femoral head and premature degenerative arthritis in adulthood. A piglet model of ischemic necrosis has been shown to reliably produce progressive flattening of the femoral head by 6 wks, and radiographic and histopathologic changes resembling Perthes disease. An imbalance of bone resorption and formation following revascularization has been identified as one of the mechanisms of femoral head deformity. We hypothesized that anti-resorptive agents, such as bisphosphonates, will minimize the deformity following ischemic necrosis by decreasing bone loss and allowing time for new bone formation. Purpose of the study was to determine the effects of ibandronate on femoral head deformity following ischemic necrosis in the piglet model. Ischemic necrosis was induced surgically in 12 male piglets by tightly placing a ligature around the femoral neck. The animals were assigned to one of 4 groups (3 animals per group): Grp 1: Ibandronate started 1 wk prior to ischemia (prophylactic grp), Grp 2: 1wk post-ischemia, Grp 3: 3wks post-ischemia, and Grp 4: saline only (control). Ibandronate was administered subcutaneously 3X per wk and total dose was 1.5 mg/kg. All animals were sacrificed at 6 wks following surgery. Histologic and radiographic assessments were performed. Radiographically, the infarcted heads from Grp 1 (prophylactic grp) animals had no flattening. Mild flattening with small areas of bone resorption was observed in the infarcted heads from Grp 2 animals. The infarcted heads from Grp 3 and 4 animals showed severe flattening and large areas of bone resorption. Histologically, all groups of animals showed revascularization of the infarcted marrow space of the femoral head. However, the presence of osteoclasts and bone resorption was most prominent in the infarcted heads from Group 3 and 4 animals, whereas, it was limited in the infarcted heads from Grp 1 and 2 animals. To our knowledge, this is the first study of the role of bisphosphonate in a large animal model of ischemic necrosis. The results suggest that it is feasible to minimize the femoral head deformity using an anti-resorptive agent, ibandronate, in the piglet model. However, early treatment (started 1 wk post-ischemia at least) is required to minimize the deformity in this model. We conclude that further studies are required to determine the optimal dose and treatment regimen of ibandronate to prevent femoral head deformity following ischemic necrosis.

M357

Loading Doses of Bisphosphonates: A New Concept to Enhance the Efficacy of Bisphosphonates on BMD, and to Expedite Fracture Reduction in Osteoporosis. S. J. Wimalawansa. Department of Medicine, Robert Wood Johnson Medical School, New Brunswick, NJ, USA.

Efficacy of bisphosphonates in enhancing the bone mineral density (BMD) and decreasing the fracture rates is now well-established. However, the absorption of bisphosphonates is usually less than 1% of that of the orally administered dose (e.g., alendronate, risedronate, etidronate, tiludronate, etc.). Therefore, generally it may take several months or up to a year or more to get an adequate amount of a bisphophonate incorporated into bone, to be highly effective in the reduction of bone turnover and the reduce fracture incidence. This is also true for the standard doses of bisphosphonate administered intravenously (pamidronate, ibandronate and zolendronate). We hypothesized that if we could get adequate amount of the bisphosphonate into bone earlier in the course of a treatment, then one would expected to see a rapid response, and also enhance the beneficial effects on BMD and fracture reduction. We have been examining the effectiveness of loading doses of oral and intravenously administered bisphosphonates on BMD in comparison with the standard doses of the same agent. We have compared the effects of loading doses of alendronate, risedronate and pamidronate with their standard recommended doses for osteoporosis over a one-year period. Results demonstrated a significant increase of BMD in both oral and intravenously administered agents with in 3-6 months (with significant decrease of biomarkers within the first 4-8 weeks), in comparison with the 6-12 months for the standard therapy. If the fracture efficacy of an anti-resorptive drug is depends on the rapidity of the reduction of bone turnover and enhancement of the BMD, then this new approach of administration of bisphosphonates should significantly enhance the fracture reduction with bisphosphonate therapies. This novel approach with bisphosphonates (and some other osteoporosis therapies as well) should be particularly beneficial for the patients with high bone turnover, and also those who are with established osteoporosis.

M358

Improvement in Nutrition Reduces Bone Resorption in Elderly Women with Osteoporosis and Low Body Mass Index : A Randomised Controlled Trial. G. Hampson[1], F. C. Martin*[2], K. Moffat*[3], S. Vaja*[1], G. Blake*[4], I. Fogelman*[4]. [1]Chemical Pathology, St Thomas Hospital, London, United Kingdom, [2]Elderly Care Unit, St Thomas Hospital, London, United Kingdom, [3]Dietetics, St Thomas Hospital, London, United Kingdom, [4]Nuclear Medicine, Guy's Hospital, London, United Kingdom.

Malnutrition is a risk factor for osteoporosis and hip fractures. We investigated the effects of dietary advice and nutritional supplementation on bone metabolism in 71 women aged ≥70 years with a low BMI(kg/m^2) (mean [SD] 20.1 [1.9]) and osteoporosis at the hip. They were randomised to 2 groups; Group 1 (n=36) received 1 gram of calcium and 800 units of cholecalciferol only, Group 2 (n=35) also received dietary advice and nutritional supplements to increase their BMI by ≥$1kg/m^2$ over 12 months. Bone mineral density (BMD), body composition (DXA), calciotrophic hormones, biochemical markers of bone remodelling and dietary intakes were assessed. No significant difference was seen at baseline between the 2 groups. At the end of the intervention period, Group 2 increased their weight significantly (mean [SD] Group 2 : 2.42 [2.82] kg, Group 1: 0.15 [2.45] kg, $p < 0.01$). There was an increase in fat mass (Group 2 : 1894 [1754] g, Group 1: -266 [1865], $p < 0.0002$). Although there was a trend towards an increase in lean body mass (LBM) and body mineral content (BMC) in Group 2, this was less marked than the gain in fat mass (LBM Group 2: 478 [944] g, Group 1 : 241 [1063], BMC Group 2 : 28.9 [54.9] g, Group 1: 5.5 [70] g). No significant difference was seen in the one - year percentage change in BMD at the spine, femoral neck and total hip (%), although we observed a positive trend at the total hip in Group 2 (Total hip Group 2 : 1.33 [3.23], Group 1 : 0.27 [5.72]). A significant reduction in serum C-terminal telopeptides of Type 1 collagen (CTx) (pM), a marker of bone resorption was seen in Group 2 compared to Group 1 at 1, 3, 9 and 12 months (change from baseline :1 month Group 2 : -583 [721], Group 1 : -269 [387] p= 0.036, 3 month: -774 [878], -208 [824] p= 0.009, 6 month : -554 [1211], -184 [633] p= 0.12, 9 month: -526 [930], - 4.1 [705] p= 0.015, 12 month: -525.4 [1120], 174 [717.9] p= 0.005). We observed an increase in serum osteocalcin (ng/ml) in Group 2 at 6, 9, and 12 month (6 month Group 2 : 2.0 [2.7], Group 1 : -0.2 [2.3] p=0.024, 9 month: 2.2 [3.0], 0 [1.7] p=0.022, 12 month: 2.3 [3.0], -0.7 [2.9] p=0.011). There was no significant difference in serum PTH and 25 (OH) D_3 between the 2 groups. A higher proportion of subjects in Group 2 reported feeling better at the end of the study (Group 2 : 48%, Group 1 : 20% p=0.029). Dietary improvement in elderly underweight women is associated with a reduction in bone resorption with a 'net' positive effect on bone formation. This may have a favourable impact on fracture risk.

M359

Effects of Long-term L-Arginine Supplementation on Bone Metabolism. N. Kamps*[1], R. Gerzer*[1], E. Schoenau[2], M. Heer[1]. [1]DLR-Institute of Aerospace Medicine, Cologne, Germany, [2]University Children´s Hospital, Cologne, Germany.

In the present study we aimed at the effect of oral L-Arginine supplementation on bone metabolism in healthy postmenopausal women. As Nitric Oxide (NO), synthesised from the nonessential amino acid L-Arginine, is an important regulator of bone turnover in humans exerting an anabolic effect on bone cell activity, oral supplementation with L-Arginine might be highly potential to effect bone cell activity via NO synthesis from L-Arginine. Thirty healthy, postmenopausal women took part in the study. Fifteen (mean body weight (BW): 66.3 ± 10.5 kg; mean age: 54.5 ± 4.1 years) received a six months oral supplementation with 18 g L-Argininehydrochlorid. Another fifteen volunteers (mean body weight (BW): 64.2 ± 9.1 kg; mean age: 55.3 ± 4.4 years) received a placebo of 18 g Dextrose for six month. Physical activity was documented in an activity protocol. To calculate protein, fat and carbohydrate as well as calcium and L-Arginine intake a food frequency questionnaire (FFQ) was chosen. To eliminate side effects the volunteers were asked not to change their activity or eating behaviour during the six months of the study. For the analyses of IGF 1, bone formation markers PICP, bAP, osteocalcin, the bone resorption marker CTX, calcium and PTH blood was drawn at baseline and after 2, 4 and 6 months. 24 hour urinary excretion of nitrogen was analysed during two days of each study period at baseline and after two, four and six months. The volunteers did not change protein (mean intake 66,8 ± 7,4 g), fat (mean intake: 89.4 ± 13.2 g) and carbohydrate (mean intake: 213.7 ± 22.4 g) intake during the six months of intervention. Moreover calcium (mean intake: 1128.0 ± 143.9 mg) and L-Arginine (mean intake: 3.7 ± 0.43 g) intake remained constant. The volunteers physical activity was unchanged during the investigation. Nitrogen excretion, as an indicator for compliance, rose from 448.2 ± 30.92 µmol/min during baseline to 635.9 ± 24.1 µmol/min during treatment in the L-Arginine group. In contrast, nitrogen excretion remained constant in the placebo group (443.7 ± 36.6 during baseline 419.6 ± 25.7 µmol/min during placebo application). Contrary to our hypothesis our results showed neither a change in bone formation markers nor in bone resorption marker. PTH, IGF 1 and transformed calcium concentrations were unchanged as well. We conclude from these results that mere L-Arginine supplementation does not have an effect on overall bone cell activity.

M360

Bicarbonate in Mineral Water Inhibits Bone Resorption. P. M. Burckhardt[1], S. Waldvogel Abramowski*[1], J. M. Aeschlimann*[2], M. J. Arnaud*[3]. [1]Internal Medicine, University Hospital, Lausanne, Switzerland, [2]Nestle Research Center, Lausanne, Switzerland, [3]Nestle Water Institute, Vittel, France.

Not only nutritional Calcium, but also a nutritional alcaline load seems to lower bone resorption and urinary Calcium (Ca) excretion. Oral bicarbonate positivated Ca-balance in postmenopausal women (Sebastian et al NEJM 1994). Therefore, bicarbonate in mineral water could serve as a natural inhibitor of bone resorption. Three groups of 10 healthy young women (20-38 yrs) drank 1.5 L/day of one of 3 mineral waters during 4 weeks on a free diet aiming at 1g Ca, 6g NaCl, and 80 g proteins/day, which was evaluated 1 week before, and 1 week after the beginning of the study, by 24 hrs recall and food frequency questionnaire. Blood and urine (fasting and 24 hrs) were examined at time 0,1,2 and 4 weeks, for Ca, Na, K, C-telopeptides, alk.phosphatase (ALP), osteocalcine, pH, bicarbonate. For this presentation the results from weeks 1,2,4 are pooled. But they were analysed for variance by ANOVA. Nutritional intake was not different in the 3 groups. Ca intake was ±806 mg before and ±1040 mg after the first week of the test, and increased with the mineral water to ±1340 mg in A and C, to ±1850 mg in B. Blood Ca and bicarbonate, ALP and osteocalcine did not change. Urine pH (fasting and 24 hrs) increased slightly in A, and decreased in B and C (n.s.). 24 hour-urine Na/creatinine increased slightly with A; K/creatinine decreased slightly with C (both n.s.). 24 hour-urine Ca/creatinine increased by ±31% in B,as expected, and by ±24% in C, and remained unchanged in A. Fasting serum C-telopeptides decreased slightly in A and increased slightly in B and C (n.s.). Fasting urine C-telopeptides / creatinine decreased by ±25% in A, at week 4 by -41%, significantly different from B (ANOVA p<0.05), and remained unchanged in B and C. Increased intake of bicarbonate as mineral water lowers bone resorption independently of the concomitant intake of Calcium.

Table

Mineral Water.....: A:Quezac... B:Contrex.... C:San Pellegrino
Bicarbonate mg/1.5L.... 2643.....605.....330
Calcium - K mg/1.5L... 378-78..... 728-5.....312-5

M361

Interaction of Nutritional Calcium and HRT in Prevention of Postmenopausal Bone Loss. J. Sirola*[1], H. Kröger[2], R. Honkanen[3], L. Sandini*[2], M. Tuppurainen[4], J. S. Jurvelin*[5], S. Saarikoski*[6]. [1]University of Kuopio, OSTPRE Study Group, Kuopio, Finland, [2]Dpt of Surgery, Kuopio University Hospital, Kuopio, Finland, [3]Research Institute of Public Health, University of Kuopio, Kuopio, Finland, [4]University of Kuopio, Clinical Research Center, Bone and Cartilage Research Unit, Kuopio, Finland, [5]Dpt of Clinical Physiology & Nuclear Medicine, Kuopio University Hospital, Kuopio, Finland, [6]Dpt of Obstetrics and Gynaecology, Kuopio University Hospital, Kuopio, Finland.

The aim of the study was to investigate the interactive effects between nutritional calcium intake and intermittent HRT on bone loss. The study population, 937 women who had undergone natural menopausal transition before or during the follow-up, was selected from a random sample (n=2025) of the OSTPRE-study cohort. Out of them, 545 women had never used HRT whereas 392 women reported use of intermittent HRT during the follow-up (mean 6 years). Women were divided into tertiles according to self reported dairy nutritional calcium intake (mg/day, mean of baseline and follow-up report): <648 (1st), 648-927 (2nd), >927 (3rd). BMD at lumbar spine (LS) and femoral neck (FN) was measured with DXA absorptiometry at baseline in 1989-91 and at five year follow-up in 1994-97. In analysis of variance there were no statistically significant differences in bone loss rate between calcium intake tertiles in HRT never users. In intermittent HRT users the bone loss was significantly lower in the third tertile than in the second (p<0.05) and first (p<0.001) tertile at FN in contrast to no differences at LS. In linear regression model high calcium intake significantly predicted lower FN bone loss (p<0.001) in intermittent HRT users in contrast to no effect in HRT never users. At LS the corresponding linear calcium effect was weak in HRT users and of borderline significancy (p=0.063). In addition, at FN the difference in bone loss rate between HRT users/non-users was found statistically significant (p<0.001) only among women in the third calcium intake tertile whereas at LS this difference was significant in all tertiles but was greater in second (p<0.01) and third (p<0.001) tertile than in the first one (p<0.05). Analysis of interaction between HRT use and calcium intake showed statistically significant effect on bone loss at FN only (p<0.003). Adjustment for baseline age, baseline weight, baseline BMD, duration of menopause, bone affecting diseases/medications and use of calcium supplements did not change any of these results. In conclusion, nutritional calcium intake seems to improve the bone protective effects of even intermittent HRT, more clearly at FN than LS, and low nutritional calcium intake seems to be a significant risk factor for no response to HRT.

M362

Dietary Potassium Conserves Calcium After Menopause. K. M. Davies[1], R. P. Heaney[2], K. A. Rafferty*[1]. [1]Osteoporosis Research Center, Creighton University, Omaha, NE, USA, [2]John A. Creighton University Professor, Creighton University, Omaha, NE, USA.

Data from 8-day inpatient balance studies of healthy white women (Omaha Nuns) in the age range from 50 to 70, median age 59, all at or after the year of menopause, were analyzed for the effect of diet potassium on urinary calcium excretion. 208 data sets from 122 women were treated as independent because multiple visits were 5 years apart. Characteristics are in the Table. Based on their excellent correlation (Regression: $y = 0.9192x$; $R^2 = 0.8255$), we used Urinary K as a surrogate for Dietary K. Diet Calcium (Diet Ca) was obtained by ash-weight analyis of the actual diet. Calcium Absorbed (Ca Absrb) was determined by a tracer method. In stepwise regression, Na fails to enter as a variable, probably because of its uniformly low level. Expressed in terms of standardized coefficients, Ca Absrb (0.533 ± 0.061 SE, P<0.0001) is offset by Urinary K (-0.163 ± 0.061 SE, P<0.01) in the ratio 3/10. Conclusion: Potassium offsets excretion of Absorbed Ca . Eating one medium baked potato or one large banana can conserve about 60 mg of Ca.

Component (mmol)	average	St. Dev.
Urinary K	60.01	13.89
Diet Ca	20.59	9.16
Ca Absrb	4.70	2.01
Urinary Ca	3.60	1.44
Urinary Na	97.93	29.53

M363

Dairy Calcium Intervention Prevents Total Hip and Spine Bone Loss in Young Oral Contraceptive Users. P. A. Legowski*[1], C. W. Gunther*[1], R. M. Lyle*[2], G. P. McCabe*[3], C. M. Weaver[1], D. Teegarden[1]. [1]Foods and Nutrition, Purdue University, West Lafayette, IN, USA, [2]Health and Kinesiology, Purdue University, West Lafayette, IN, USA, [3]Statistics, Purdue University, West Lafayette, IN, USA.

This study examined the % change in total hip bone mineral density (BMD) and spine BMD among oral contraceptive users (OCont: n=57) and non-users (non-OCont: n=76) who were participating in a one year dairy calcium intervention trial. Healthy women (20.2 yr, range: 18-30) with initial calcium intakes <800 mg/day were randomized into control (n=43), recommended calcium (RecCa, 1000 mg/day, n=43) or high calcium (HiCa, 1250 mg/day, n=47) intake groups, achieved by increased dairy product intake. Hip and spine BMD were measured at baseline and 12 months (Lunar DXA). Baseline calcium intake was similar between calcium intervention groups (mean of groups =702±274 mg/day) and between OCont groups. While calcium intake in the control group did not change, calcium intake increased to 1046±307 and 1191±361 mg/day, respectively, in RecCa and HiCa groups by 3 months and remained similar over the year. Hip and spine BMD were not different between groups at baseline. Calcium intervention group assignment significantly predicted % change hip BMD (p=0.03). However, the effect of calcium intervention group assignment on % change hip BMD was noted in OCont users only (p=0.02, Figure 1); not non-OCont users (p=0.64). One year % change spine BMD was predicted by a model which included age, baseline weight, OCont use and interaction of OCont use by calcium intervention group assignment (p=0.009). Similar to hip BMD, calcium intervention group assignment predicted % change spine BMD, when controlled for age and weight, in OCont users only (p=0.001, Figure 1); but not non-OCont users (p=0.17). Adjustment for energy intake and physical activity did not affect results. Dairy calcium supplementation at 1000 mg/day or greater, protected the hip and spine BMD from loss observed in young healthy women with low calcium intakes who were taking OCont.

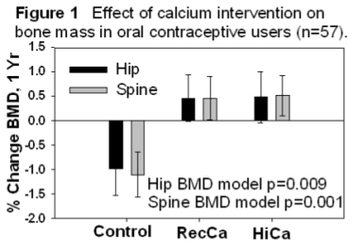

Figure 1 Effect of calcium intervention on bone mass in oral contraceptive users (n=57).

M364

Changes in Bone Turnover in Patients with Anorexia Nervosa during one Year of Dietary Treatment. C. Mika*[1], I. Grzella*[2], B. Herpertz-Dahlmann*[2], M. Heer*[1]. [1]DLR, Institute of Aerospace Medicine, Cologne, Germany, [2]Department of Child and Adolescent Psychiatry, Technical University, Aachen, Germany.

Anorexia nervosa (AN) is a common chronic eating disorder with an estimated prevalence of 0.5 to 1 % in female adolescents and young women. The restrictive eating pattern is associated with profound metabolic complications such as amenorrhea, growth hormone resistance, increased plasma cortisol, low production of insulin-like growth factor 1 (IGF1) and decreased leptin concentrations. One of the most important long-term somatic complications of AN is the decrease in bone mineral density, which often leads to spontaneous fractures. The aim of our study was to verify if dietary treatment including calcium intake of >2000 mg/d and 400 IU vitamin D/d in combination with an individually defined hypercaloric diet improves bone metabolism in patients with AN compared to a control group. We studied 19 female patients (age 14.13 ± 1.35 years; body weight 38.87 ± 5.04 kg; BMI 14.18 ± 1.38 kg/m2) with AN (ICD-10: F50.0, F 50.1) and a healthy control group (n=19, age 15.14 ± 2.25 years; body weight 56.28 ± 7.67 kg; BMI 20.80 ± 1.92 kg/m2) for 1 year. After a basal examination in the first week in hospital, 2000 mg calcium and 400 IU vitamin D were administered with the volunteers diet. Blood was drawn during BDC and at eight definite times (five times for the control group) in the following year for analyzing serum calcium, parathyroid hormone (PTH), bone formation (bone alkaline phosphatase (bAP) and C-terminal procollagen-I-propeptide (PICP)) and resorption markers (serum C-terminal telopeptide (CTX)),

leptin, IGF1, sexual hormones and cortisol. Comparing the two groups we found different baseline values for the bone formation marker PICP (p=0.0001), for BMI (p<0.0001), IGF1 (p<0.0001) and Leptin (p<0.0001), respectively. After 15 weeks of dietary treatment the patient group had still lower BMI values than the control group (p<0.0001). At that time we found an adjustment of the other parameters PICP, IGF1 and leptin for the two groups. At the end of the study levels of BMI (p<0.0001) and leptin (p<0.0001) were different between the two groups. There were no distinctions between anorexic patients and controls in bAP and CTX in the course of treatment. We summarized that for the patient group there were at least 15 weeks of high energy intake necessary in order to reach levels of bone formation of healthy adolescents. Bone resorption however remained unchanged. This underlies the importance of nutrition on bone turnover in anorectic patients.

M365

Vitamin K1 Supplementation Retards Bone Loss in Postmenopausal Women between 50 and 60 Years of Age. L. A. J. Braam*[1], M. H. J. Knapen*[1], P. Geusens[2], F. Brouns*[3], K. Hamulyak*[2], M. J. W. Gerichhausen*[4], C. Vermeer*[1]. [1]Biochemistry, Maastricht University, Maastricht, Netherlands, [2]Internal Medicine, Maastricht University, Maastricht, Netherlands, [3]Human Biology, Maastricht University, Maastricht, Netherlands, [4]Novartis Nutrition Research AG, Neuenegg, Switzerland.

The effect of vitamin K1 supplementation on bone mineral density (BMD) has never been studied, although many observational studies have shown an association between vitamin K-status and BMD. In a randomized placebo-controlled intervention study the potential synergistic effect of vitamin K1 and a mineral + vitamin D supplement was investigated on postmenopausal bone loss. 181 healthy postmenopausal women between 50 and 60 years old were recruited via newspaper advertisements and eventually 155 women completed the study. For three years they received daily either a placebo (n=60) or a supplement containing calcium, magnesium, zinc and vitamin D (MD-group, n=58), or the same supplement with additional vitamin K1 (MDK-group, n=63). The main outcome measure of this study was the change in BMD of the femoral neck and lumbar spine after three years, as measured by DEXA. The data were analysed according to intention-to-treat. The group receiving the supplement containing additional vitamin K1 showed reduced bone loss of the femoral neck. The differences in % BMD loss from baseline between the MDK-group and placebo [1.7%] (95% CI: 0.35 to 3.44) and between the MDK- and the MD-group [1.3%] (95% CI: 0.10 to 3.41) were statistically significant after three years (p<0.05) after adjustment for baseline BMD, age, BMI, and years since menopause. After three years, there was no significant difference in the % change from baseline in femoral neck BMD between the MD-group and placebo (mean difference: 0.4%, 95% CI: -1.51 to 1.79). Differences between the three groups with respect to change of BMD at the site of the lumber spine did not reach the level of statistical significance. In this study we have shown that a supplement containing minerals, vitamins D and K has a long-term beneficial effect on the prevention on bone loss in healthy postmenopausal women. Although the supplement used in this study did not result in a complete halt of bone loss, the rate of bone loss was substantially decreased. If this effect sustains during longer periods of intake, it may result in postponement of osteoporosis to later ages, and thus to a reduction of osteoporotic fractures.

M366

Soy Isoflavones May Enhance Bone Formation in an Aged Rat Model of Male Osteoporosis. M. P. Akhter[1], D. A. Khalil[2], E. A. Lucas*[2], D. S. Galloway*[3], L. J. Hammond*[2], B. J. Smith*[2], R. Recker[1], B. H. Arjmandi[2]. [1]Osteoporosis Research Center, Creighton University, Omaha, NE, USA, [2]Nutritional Sciences, Oklahoma State University, Stillwater, OK, USA, [3]Oklahoma Veterinary and Medical Teaching Hospital, Oklahoma State University, Stillwater, OK, USA.

Soy isoflavones have been reported to exert estrogen-like protective effects on the female skeleton. Since estrogen is also important in the maintenance of male bone health, we examined the effects of two doses of soy isoflavones (Iso) in the context of soy protein or casein on bone histomorphometry in aged orchidectomized rats. Thirteen-month old male F344 rats were either orchidectomized (ORX; 5 groups) or sham-operated (sham; 1 group). One ORX group served as control and was fed a casein-based diet whereas the remaining ORX groups received either a casein- or soy protein-based diet each with two levels of Iso (593 and 1186 mg/kg diet) for 180 d. Calcein was injected at 8 and at 1 day before necropsy and the proximal tibial metaphysis was assessed for bone histomorphometry. Treatment effects on trabecular separation (TbSP), trabecular numbers (TbN), bone volume as a percentage of tissue volume (BV/TV), mineralizing surface (MS/BS), and bone formation rate (BFR/BS) are presented below. Overall, results indicate that soy isoflavones irrespective of protein source exert beneficial effect on bone of male rats by preventing the orchidectomy-induced increase in TbSp and decrease in TbN and BV/TV without suppressing bone formation as evidenced by effects on MS/BS and BFR/BS.

	Protein Source	**Iso** (ppm)	**BV/TV** (%)	**TbSp** (µm)	**TbN** (mm^{-1})	**MS/BS** (%)	**BFR/BS** (mm^2/ mm/yr)
Sham	Casein	-	8.5±1.2	1504±480	0.94±0.13	10.3±3.0	0.03±0.01
ORX	Casein	-	3.5±1.2*	3110±480*	0.48±0.13*	19. 9±3.2*	0.06±0.01
ORX	Casein	593	5.9±1.2	1329±480†	0.84±0.13†	13.0±3.0	0.04±0.01
ORX	Casein	1186	6.0±1.2	1527±480†	0.75±0.13	20.7±3.2*	0.07±0.01*
ORX	Soy	593	5.8±1.2	1398±480†	0.83±0.13	16.7±3.2	0.05±0.01
ORX	Soy	1186	6.9±1.2	1426±480†	0.88±0.13†	16.1±3.0	0.05±0.01

Values are mean ± SE, n=7 for histomorphometric parameters, *ORX groups different from Sham controls (P<0.05); †ORX groups different from ORX controls (P<0.05).

M367

Calcium and Vitamin D in the Prevention of Hip and Other Fractures: An Update on the Women's Health Initiative CaD Trial. J. A. McGowan[1], R. D. Jackson[2], J. A. Cauley[3], A. Z. LaCroix[4]. [1]National Institute of Arthritis and Musculoskeletal and Skin Diseases, Bethesda, MD, USA, [2]Ohio State University, Columbus, OH, USA, [3]University of Pittsburgh, Pittsburgh, PA, USA, [4]Fred Hutchinson Cancer Research, Seattle, WA, USA.

Several observational studies and randomized trials support a role for calcium and vitamin D in reducing bone loss and preventing fractures. The Calcium-Vitamin D (CaD) trial component of the WHI is a large, randomized controlled trial in a diverse population of healthy postmenopausal women designed to test the primary hypothesis that women who are randomized to receive calcium and vitamin D supplementation (500mg CaCO3 and 200 IU of Vitamin D, twice daily) will have a lower risk of hip fractures and secondarily, a lower risk of all fractures than women receiving the corresponding placebo. Over 36,000 postmenopausal women between the ages of 50 and 79 have been recruited at 40 clinical centers across the country and will be followed for about 7 years for ascertainment of hip and all fractures. Baseline measures include anthropometrics, lifestyle and nutritional habits, medical/medication status, fall history, personal and family fracture history, and bone density by Dual Energy X-Ray Absorptiometry (at 3 WHI clinics only). Analyses of the baseline characteristics by factors known to be associated with osteoporotic fracture indicate a relatively low risk population at the onset of the study. The mean age of the CaD trial cohort is 62.3 years with 37.5% aged 50-59, 45.2% aged 60-69, and 17.4% aged 70 and older. 17% are minorities, including 9% Black, 4% Hispanic, 2% Asian, 1% American Indian and 1% other/unspecified. There are few current smokers (7.7%) but 40 % smoked previously, and 72% use alcohol at least occasionally. The average calcium intake in the diet is 750 mg per day and 54% use some kind of calcium supplement. The majority of the trial cohort are overweight and the mean BMI is 29.1. A non-traumatic fracture has occurred in 12% of the subjects since age 55 but 40% have a parental history of fracture. The prevalence of osteoporosis based on the World Health Organization cut points was low: 4.5%, 2.7% and 0.35% of non-Hispanic white women, Hispanic, and black women respectively. However, as expected both osteoporosis and osteopenia were common in the women over seventy: 9.3% were osteoporotic and 56% were osteopenic. The WHI CaD Trial is the largest randomized clinical trial with the longest duration of exposure and follow-up (~7 years) focusing on the impact of calcium plus vitamin D supplementation on the incidence of hip and all fractures. All participants will complete intervention in March, 2005.

M368

Impact of an Educational Intervention for the Prevention and Treatment of Osteoporosis: A Health Plan's Perspective. P. Paccione*[1], R. Powell*[1], J. O'Neill*[1], T. W. Weiss*[2]. [1]HealthNow, Albany, NY, USA, [2]Merck & Co., Inc., West Point, NY, USA.

In the fall of 1999, Blue Shield of Northeastern New York initiated an ongoing health management program for their members who were found to be potentially at risk for osteoporosis and those already diagnosed with osteoporosis. The purpose of the program was to improve the diagnosis and management of members with osteoporosis. The program involved both interventions to members and their physicians. The member targeted intervention group was women aged 40+ years and men aged 65+ years. The physician targeted intervention group was the primary care physician and any physician who prescribed osteoporosis-related medications (including estrogens). Member interventions included NOF brochures with a cover letter encouraging them to schedule an appointment with their PCP to discuss getting a DEXA scan (a covered benefit), informal focus groups, the NOF newsletters, and 'Boning Up on Osteoporosis' booklet via free NOF membership. Members were also encouraged to visit a Rite Aid pharmacy for an Osteoporosis Education Day that included free heel US and pharmacist counseling. The physician interventions included practice guidelines along with NOF pocket guide, DEXA scan/QCT profile for targeted members, medication non-compliance profile, a CME credited seminar for PCPs, and BMD/medication reminder stickers. Within one year, these interventions demonstrated the ability to increase the percent of at-risk members screened, diagnosed, and compliant with osteoporosis medication (table). Conclusion: a health plan can implement a health management program to substantially improve the diagnosis and treatment compliance of its members with osteoporosis.

	Baseline (Jan-Dec '99)	Re-measurement (Jan- Dec '00)	% Change
DEXA scan/QCT usage*	51 per 1000	104 per 1000	104%
Osteoporosis Diagnosis*	47 per 1000	90 per 1000	92%
Medication Compliance**	45%	71%	58%

* Based on billing codes submitted

** Compliance was defined as filling prescriptions for osteoporosis medications at least 80% of the time

Disclosures: ***P. Paccione****, Merck & Co., Inc 2, 5.*

M369

Antiresorptive and Sex Steroid Therapies: Impact on Circulating Osteprotegerin. A. Rogers[1], P. M. Mah*[2], A. M. Braga de Castro Machado*[1], C. A. Pereda*[1], R. Eastell[1], A. Blumsohn[1]. [1]Bone Metabolism Group, University of Sheffield, Sheffield, United Kingdom, [2]Dept of Endocrinology, University of Sheffield, Sheffield, United Kingdom.

Osteoprotegerin (OPG) is a potent inhibitor of osteoclastogenesis and bone resorption *in vivo*. OPG production by osteoblasts *in vitro* is modulated by sex steroids, and by bisphosphonates. Assays for serum OPG are now available which may be useful for monitoring response to antiresorptive therapy. The aim of this study was to determine the effect of estrogen and bisphosphonate therapy on serum OPG in postmenopausal women and of testosterone therapy in men. We evaluated the change in bone turnover and serum OPG in response to: **1)** subcutaneous estradiol implant (25 mg implant replaced 6-monthly for two years) in postmenopausal women (n=10, ages 60 to 75 years). **2)** testosterone patch (6mg/day for 6 or 12 months) in men with hypogonadism (n=34, ages 40 to 77 years). **3)** alendronate (10mg/day for 6 months) in postmenopausal women with osteoporosis (n=15, ages 50 to 78 years). Serum OPG was determined using two assays, a commercial ELISA (Biomedica, Austria) and an in-house sandwich ELISA. Bone alkaline phosphatase (bone ALP), osteocalcin (OC) and urine N-telopeptides of type I collagen (UNTX) were measured using commercially available assays. Serum estradiol increased fourfold by the first month after implant and sixfold at 24 months (67± 3pmol/L at baseline to 422± 46 pmol/L at 24 months). Serum testosterone increased twofold over the course of treatment (8.2± 0.5 to 16.6± 2.1 nmol/L). There was a significant decrease in bone turnover in the estradiol and bisphosphonate treated models. However there were no significant changes in serum OPG using either OPG assay in any treatment model. (Table shows % change from baseline at the end of treatment ± SEM).

	UNTX	OC	Bone ALP	OPG
Estradiol	-47± 3**	-14± 4*	-12± 4*	-6± 4
Testosterone	-14± 5	-4± 3	-6± 3	+2± 3
Alendronate	-71± 5***	-34± 4***	-44± 5***	+1± 3

* P<0.05, ** P<0.01, *** P<0.001.

We conclude that circulating OPG is unlikely to be useful to monitor antiresorptive therapy in postmenopausal women and is also unresponsive to testosterone therapy in men. The tissue origin of serum OPG is uncertain, and measurements made in serum may be unlikely to reflect changes in OPG activity within the bone microenvironment.

M370

Prevention and Treatment of Osteoporosis by Postgraduate Resident Physicians. L. Graves[1], G. Smith*[2], B. P. Lukert[1]. [1]Internal Medicine, University of Kansas School of Medicine, Kansas City, KS, USA, [2]Internal Medicine, University of Missouri-Kansas City School of Medicine, Kansas City, MO, USA.

Previous survey studies of practicing physicians have revealed inadequate prevention, diagnosis and treatment of osteoporosis. The purpose of this study was to assess resident physicians in training for their level of understanding of osteoporosis, current practices in prevention and treatment, and their assessment of the curriculum in osteoporosis they received in medical school and residency. This survey canvassed post-graduate residents at two mid-western universities. Residents in the fields of internal medicine (IM), obstetrics and gynecology (Ob-Gyn), family medicine (FM) and orthopedics (OR) received a one page, two sided survey by mail, followed by one reminder phone call at 8-10 weeks. This survey took place between 1999-2000. Responses were received from 151 out of 404 residents surveyed (37%). 25-37% of IM, FM, and Ob-Gyn residents did not know their institution had the capability to perform bone densitometry (BMD). Less than 40% utilized BMD for diagnosing osteoporosis. Most residents estimated 10-30 outpatient encounters per week and estimated 40-60% being postmenopausal women, however, less than 50% reported ordering a bone density in the previous 3 months. The remaining residents reported ordering less than 5 BMD studies in the previous 3 months. In a series of case scenarios, hormone replacement therapy was selected most commonly for prevention and treatment of osteoporosis. In severe osteoporosis bisphosphonate therapy was chosen in less than 40% of responses. Calcitonin and raloxifene were chosen for prevention or treatment in less than 10% of responses. The majority of responders rated training in osteoporosis in medical school and residency as minimal. Greater than 60% of responders desired more training in indications, and interpretation of BMD and in the treatment of osteoporosis. Residents rated pharmaceutical programs and journals outside of their respective field as least important sources of information. Didactic conferences and journals within their specialty field were rated as important information sources. The majority of residents rated observation of faculty practice as the single most important information source. Current understanding and practice in prevention and treatment of osteoporosis is inadequate in this group of postgraduate residents. This important health problem should be adequately reflected in medical school and residency curriculum.

Disclosures: ***L. Graves****, Merck 2; Merck 8.*

M371

Effect of Inliximab on Markers of Bone Metabolism in Patients with Rheumatoid Arthritis. M. Vis*[1], G. J. Wolbink*[2], R. M. van Soesbergen*[2], M. C. Lodder*[1], R. J. v.d. Stadt*[3], B. A. C. Dijkmans[1], W. F. Lems[1]. [1]Rheumatology, Vrije Universiteit medical center, Amsterdam, Netherlands, [2]Rheumatology, Slotervaart Hospital, Amsterdam, Netherlands, [3]Jan van Breemen institute, Amsterdam, Netherlands.

We studied the effect of infliximab (Remicade) on markers of bone metabolism in patients with rheumatoid arthritis (RA).All consecutive patients with active RA, who were treated with infliximab were included. Infliximab is a specific inhibitor of tumor necrosis factor (TNF), that significantly reduces disease activity in RA. Infliximab (3mg/kg) was administered intravenously at 0, 2 and 6 weeks. At all visits disease activity was measured by swollen-, tender joint counts, ESR and visual analogue scale for disease activity. From these 4 variables the disease activity score (DAS-28) was calculated. Blood samples were collected prior to each infusion and stored at -70°C. Serum markers of bone formation, (osteocalcin and aminoterminal propeptide of type I collagen (PINP)) and bone resorption (ß-isomerized c-terminal cross-linked telopeptide of type I collagen (ß-CTx) and crosslinked carboxyterminal telopetide of type I collagen (I-CTP)) were determined to evaluate bone metabolism. Bone markers at the 3 time points were compared by means of a paired t-test and by Wilcoxon signed rank test where appropriate. A total of 68 patients were enrolled. 79 % of the patients were female, mean (SD) age 55 years (13), median (range) disease duration of RA 10 years (0-59). At baseline all patients had active disease with a DAS-28 ≥ 3.2. Mean (SD) DAS-28 at baseline was 5.9 (1.4) and decreased significantly to 4.7 (1.4) after 2 weeks and to 4.1 (1.5) after 6 weeks. Both osteocalcin and PINP showed a significant increase when compared to baseline. Both markers of bone resorption seemed to decrease but only I-CTP was decreased significantly at 6 weeks when compared to baseline. (table)However in the subgroup of responders (DAS-28 decrease ≥ 1.2) both ß-CTx and I-CTP were significantly decreased after 6 weeks when compared to baseline. (p <0.05) The study suggests that infliximab has a favourable effect on bone metabolism, since in the early phase of treatment bone formation increases while bone resorption seems to decrease. Whether long-term treatment with infliximab has a positive effect on bone metabolism and subsequently on bone mineral density needs to be further investigated.

	T = 0 weeks	**T = 2 weeks**	**T = 6 weeks**
Formation mean (SD)			
Osteocalcin ng/ml	21.2 (11.4)	23.0* (11.7)	23.9* (11.4)
PINP µg/ml	43.9 (21.3)	50.6* (23.7)	50.1* (21.1)
Resorption median (range)			
I-CTP µg/ml	8.9 (3.5-38.3)	8.6 (3.9-39.7)	7.8* (3.3-32.1)
β-CTx ng/ml	0.32 (0.01-1.08)	0.29 (0.03-0.89)	0.29 (0.01-1.12)

** p<0.001, compared to T = 0 weeks*

M372

A Two-Year Randomized Controlled Trial of Hormone Replacement Therapy, Etidronate, Calcitonin, Vitamin D, or Vitamin K, in Women with Postmenopausal Osteoporosis. Y. Ishida, S. Kawai*. Department of Orthopaedic Surgery, Yamaguchi University School of Medicine, Yamaguchi, Japan.

Although a number of medications are now available for the treatment of osteoporosis, there are few comparative treatment studies. This study was conducted to assess the effectiveness of various pharmacologic therapies on bone mineral density (BMD), biochemical bone markers and new fracture incidence in postmenopausal women and to identify predictors of changes in BMD after 2 years of treatment. Three hundred thirty-seven postmenopausal women, aged 45 to 75 years, attending metabolic bone disease outpatient clinics with established osteoporosis were randomly allocated into one of six treatment groups: control (no treatment); hormone replacement therapy (HRT); etidronate; calcitonin (CT); vitamin D3; and vitamin K2. BMD of distal 1/3 radius was measured every 3 months by dual energy X-ray absorptiometry, along with biochemical markers of bone turnover [serum bone specific alkaline phosphatase (BAP), serum osteocalcin (OC), urinary N-telopeptide of type I collagen (NTx) and urinary deoxypyridinoline (D-pyr)]. The occurrence of new vertebral fractures were determined by radiographs taken every 3 months. Over 2 years, the new vertebral fracture incidence in HRT, etidronate, CT, vitamin D3 and vitamin K2 groups was reduced by 70%, 47%, 62%, 34% and 35% relative to control, respectively. The control group showed a significant decrease in BMD from baseline after 2 years of treatment (-3.3%, p<0.001) while the HRT group showed a significant increase (+2.2%, p<0.001). Other treatments, etidronate, CT, vitamin D3 and vitamin K2 produced -1.4%, +1.9%, -3.6% and -1.9% changes in BMD from baseline, respectively. Logistic regression analysis revealed that changes in BMD at 3 months predicted changes in BMD after 2 years of treatment (odds ratio, 2.4; p=0.01). The associations between biochemical markers and BMD were too weak to allow for a valid individual estimation of future BMD changes based on the changes in biochemical markers. In contrast, the biochemical markers (NTx and D-pyr) were shown as valid tools for monitoring and prediction of treatment effect of antiresorptive medications (HRT, CT and etidronate). As a whole, groups of patients who gained more BMD experienced greater fracture protection, although the relationship was not clear on the individual level. In conclusion, antiresorptive medications (HRT, CT and etidronate) reduce bone turnover, increase BMD and produce a significant reduction in the incidence of vertebral fractures in postmenopausal osteoporosis, in which HRT is most potent. The data suggest that vitamin D3 and vitamin K2 can reduce the fracture incidence without significant rise of BMD.

M373

Characteristics of Non-responders to 5-years of Hormone Replacement Therapy. The Danish Osteoporosis Prevention Study (DOPS). L. Rejnmark[1], P. Vestergaard[1], C. L. Tofteng*[2], N. Kolthoff*[3], L. S. Stilgren[4], K. Brixen[4], L. Mosekilde[1]. [1]Dept. of Endocrinology and Metabolism, Aarhus Amtssygehus, Aarhus, Denmark, [2]The Osteoporosis Research Centre, Hvidovre Hospital, Hvidovre, Denmark, [3]Dept. of Clinical Physiology and Nuclear Medicine, Hilleroed Hospital, Hilleroed, Denmark, [4]Dept. of Endocrinology, Odense University Hospital, Odense, Denmark.

A nested case control study was performed to characterize perimenopausal women not responding to hormone replacement therapy (HRT) with an increase in bone mineral density (BMD). In the Danish Osteoporosis Prevention Study (DOPS), 2016 women three months to two years after menopause were allocated to a HRT- (n=723) or to a control-group (n=1293). After 5-years, 543 women had been treated continuously with HRT. Among these, paired DEXA-scans had been performed at baseline and after five years in 466 women receiving HRT. We defined densitometric non-responders as women on HRT, who had a decrease in BMD over 5-years similar to or grater than the mean bone loss in the control group. Baseline characteristics were used as exposures. In the control group, femoral-neck and lumbar spine BMD decreased by 6.3±0.2% (mean±SD) and 6.4±0.2%, respectively. In the HRT group, 10.7% and 6.0% were classified as non-responders according to their changes in femoral-neck and lumbar spine BMD, respectively. 2.6% were classified as non-responders at both measurement sites. Baseline measures of body weight, age, BMD, daily calcium- and vitamin D intake, smoking status, and biochemistry (urinary hydroxyproline, bone-specific alkaline phosphatase, 25-hydroxyvitamin D) did not differ between responders and non-responders to HRT at the femoral-neck, lumbar spine, or at both sites. Thus, only a small proportion of perimenopausal women who begin HRT do not benefit from the treatment as assessed by DEXA. However, non-responders are difficult (impossible?) to identify at the time of initiation of treatment.

M374

Osteoporosis Fracture Tracking Study: Medical Care Is Often Delayed for Patients of Orthopaedic Surgeons. J. G. Skedros. Utah Bone and Joint Center; Dept of Orthop Surg, U of UT, Salt Lake City, UT, USA.

Patients with osteoporotic fractures typically do not receive subsequent medical treatment for osteoporosis. We hypothesized that even if patients with osteoporotic fractures were specifically referred to their primary care providers (PCPs), the majority would not be treated within 84 days (12 weeks) of fracture. We evaluated the effectiveness of 14 surgeons in facilitating a timely PCP visit for their patients. Participating orthopaedic surgeons received remuneration for each patient completing the study. Patients who qualified were >50 years old, had an apparent osteoporotic (low-energy) fracture, and had no prior treatment for osteoporosis. Two letters requesting a PCP appointment were sent: the first letter within 10 days of fracture, and the second letter 3-10 weeks after fracture. Patients were also: 1) informed that they may have osteoporosis and may be at risk for subsequent fracture, and 2) instructed to make a PCP appointment for possible further work-up and treatment. Results showed that of 55 patients (48 females, 7 males: avg. age 70.8, range 51-90), 23 (42%) were not seen by a PCP within 84 days. 32 (58%) patients saw a PCP within 84 days, but osteoporosis was not addressed in 4 patients (avg. days to PCP, 38: range 7-71days). Of patients seen within 84 days, pharmacologic treatment (e.g., estrogen, bisphosphonate, etc.) was started in 19 (59 %), but typically not within 37 days of fracture. Of the 14 participating orthopaedic surgeons, five were non-compliant and six were inconsistent in their participation, forgetting to send the letters and to inform their patients to make a PCP appointment. These results indicate that standing discharge hospital orders (for medications, PCP follow up, bone density scanning, etc.) may be more effective in achieving timely medical treatment for patients with osteoporotic fractures.

M375

Subsidizing Medications Does Not Ensure the Use of Potent Osteoporosis Drugs Following Low-Impact Fractures. Y. Liel*[1], H. Castel*[2], D. Y. Bonneh*[3]. [1]Endocrinology, Soroka Medical Center, Beer Sheva, Israel, [2]Medicine, Soroka Medical Center, Beer Sheva, Israel, [3]Southern District, Clalit Health Services, Beer Sheva, Israel.

Recently, potent anti-resorptive drugs (a bisphosphonate, and a SERM) were introduced into the National Health Basket in Israel for treatment of all osteoporotic women and for men with glucocorticoid-related osteoporosis. We carried out the present study to evaluate the effect of subsidizing osteoporosis drugs on the use of osteoporosis drugs in patients following low-impact fractures. Hospital charts of women and men age 50 and older with new fractures due to low or moderate impact treated in the emergency room (mostly peripheral bone fractures), orthopedic surgery and rehabilitation departments (mostly proximal-hip fractures), were reviewed. Notation of osteoporosis as contributing cause for the fracture, and treatment recommendations were abstracted from the records. In addition, we took advantage of the centralized pharmacy database of the largest health maintenance organization (HMO) in the area to follow dispensation of osteoporosis drugs in the community following fracture incidents. The cumulative data from the period of January and February of 2000 and 2001 ("post-basket") was compared with the cumulative data from January and February of 1998 and 1999 ("pre-basket"). Our results revealed a significant, approximately 2-fold increase in the baseline rate of dispensation of osteoporosis drugs between the pre- and post-basket periods. The rate of patients treated after a fracture incident also increased significantly 1.6 fold in the post-basket period. However, even in the post-basket period two-thirds of the patients remained untreated following a fracture incident and most of those treated received only calcium and vitamin D. Only about 15% received any of the potent osteoporosis drugs. Men were considerably less likely to be treated than women. In a univariate analysis, younger age, female gender, being treated in the emergency room, incident of fracture in the post-basket period and being treated for osteoporosis before the fracture incident, were significantly correlated with treatment following the fracture. In a multivariate model, age lost its effect and treatment before the fracture incident emerged as the far most influential variable. Subsidizing has a significant positive effect on osteoporosis drugs utilization. However, other factors are important. There is an ongoing need to increase awareness and encourage the use of potent pharmacological means for primary and secondary prevention of osteoporotic fractures.

M376

Phytoestrogen-Rich Herbal Formula For Prevention Of OVX Induced Bone Loss In Rats. L. Qin*[1], G. Zhang*[2], W. Y. Hung*[3], M. A. Dambacher[4], P. C. Leung*[5]. [1]Orthopaedics & Traumatology, Chinese University of Hong Kong, Hong Kong, Hong Kong Special Administrative Region of China, [2]Suguang Hospital, Shanghai University of Chinese Medicine, Shanghai, China, [3]Dept. of Orthopaedics and Traumatology, The Chinese University of Hong Kong, Hong Kong, Hong Kong Special Administrative Region of China, [4]University Clinic of Balgrist, Zurich, Switzerland, [5]Institute of Chinese Medicine, The Chinese University of Hong Kong, Hong Kong, Hong Kong Special Administrative Region of China.

The purpose of this animal experimental study was to investigate a phytoestrogen-rich herbal formula (genistein and daidzein at 250mAU) and calcium supplementation for prevention of OVX induced bone loss. In this study, tis phytoestrogen-rich herbal formula Xianlingubao (XLGB) with Epimedium Leptorhizum as the main component was developed and studied in 45 eleven-months old female Wistar rats, that were randomly grouped according to their body weight. These included one sham-operated (Sham) and four OVX subgroups, i.e. OVX along, OVX with XLGB, OVX with calcium, and OVX with HLGB and calcium (Table 1). Daily oral administration of XLGB (250 mg/kg) and/or element calcium (25 mg/kg) started immediately after OVX for 12 weeks before scarifying the animals. Left femur was prepared for BMD measurements at both proximal femur and femoral diaphysis using DXA. (XR36) for data comparison. BMD measurement results showed that osteoporosis was established in trabecular bone rich proximal femur but not in cortical bone dominant disphysis in the OVX rats as compared with Sham group. XLGB, calcium, and XLGB with calcium intervention all showed preventive effects against OVX induced bone loss in proximal femur. The mean BMD of proximal femur in OVX rats treated with both XLGB and calcium administration was higher than that of treated with XLGB along or with calcium along, however, without statistical significance (Table 1: *: $p<0.05$; **: $p<0.01$, as compared with OVX group). In conclusion, the phytoestrogen rich herbal formula HLGB was effective for prevention of OVX induced bone loss in the high turnover trabecular bone rich proximal femur. The additional calcium supplementation did not reveal additive effects in prevention of bone loss or in increase of BMD.

Table 1: Phytoestrogen-rich herbal formula and/or dietary calcium in prevention of OVX induced bone

Groups (n=9, each)	BMD measured by DXA (mg/cm2)	
	Proximal femur	Femoral diaphysis
Sham	191±10**	179±6
OVX	166±7	177±6
OVX+XLGB	184±11**	177±8
OVX+Calcium	176±11*	177±4
OVX+XLGB+Calcium	185±4**	178±5

*Disclosures: **L. Qin**, Hong Kong RGC grant 2001 2.*

M377

PremPro vs. FemHRT in Cynomolgus Monkeys. C. J. Lees. Pathology, Wake Forest University School of Medicine, Winston-Salen, NC, USA.

Women use FemHRT® (ethinyl estradiol and norethindrone) and PremPro® (conjugated equine estrogens and medroxyprogesterone) for the prevention of postmenopausal osteoporosis. The effects of these two treatment modalities on bone were examined in ovariectomized cynomolgus monkeys (*Macaca fasicularis*). Sixty female cynomolgus monkeys were imported from Indonesia, ovariectomized and randomized into 3 groups: 1) placebo (OVX), 2) FemHRT® (human equivalent of 1 mg norethindrone and 5 micrograms ethinyl estradiol) and 3) PremPro® (human equivalent of 2.5 mg medroxyprogesterone and 0.625 mg conjugated equine estrogens). Treatment lasted 1 year. Serum alkaline phosphatase (ALP) levels and fibular bone mineral density and cortical thickness (determined by pQCT) were measured at 12 months. Both PremPro® and FemHRT® groups had significantly lower ALP levels compared to OVX (OVX - 181 ± 9, FemHRT® - 117 ± 9, PremPro® - 97 ± 10, $p < 0.0001$). PremPro® treated monkeys had greater fibular cortical density (CRTDEN 1080 ± 12) and cortical thickness (CRTTHKC 1.54 ± 0.03) compared to OVX CRTDEN 1029 ± 12 ($p < 0.02$) and OVX CRTTHKC 1.44 ± 0.02 ($p < 0.02$). FemHRT® treated animals did not differ from either OVX or PremPro® treated animals in CRTDEN (1060 ± 12) or CRTTHKC (1.49 ± 0.02). PremPro® had a positive effect on bone mass in monkeys. Although, FemHRT® treatment suppressed ALP levels, FemHRT® did not induce significant changes in bone mass.

*Disclosures: **C.J. Lees**, Pfizer 2.*

M378

Effect of Time on Estrogen (E) Therapy and of E Therapy Begun at Menopause Vs. Delayed Onset of E Therapy on the Prevalence of Low Bone Mineral Density (BMD). G. Ding*, J. Javier*, D. J. Baylink, K. Jolley*, C. Libanati. J.L. Pettis VAMC, Loma Linda, CA, USA.

We report on the prevalence of low BMD at the spine & hip in a population of 355 postmenopausal females (F) (mean age= 67.9 ± 5.7 y/o, range 60-80) currently receiving HRT. To determine if the effect of HRT was similar in younger & older F, we divided the group into those F younger than 71 years (groups A and B, n=242), and those older than 70 years (groups C and D, n=113). Additionally, to examine the effect of onset time of HRT in relation to menopause, younger and older groups were evaluated based on continuous HRT use since menopause (groups A and C,) vs. delayed HRT use (groups B and D, HRT started >5 years post menopause).

Table 1: BMD and T-Scores at the spine, femoral neck (FN) & total hip (T Hip) for each group (G).

			BMD (in mg/cm2)			Mean T-Score		
G	**n**	**Age**	**Spine**	**FN**	**T Hip**	**Spine**	**FN**	**T Hip**
A	160	64.2±3.2	1016	743	891	1.02±0.2	-0.96±1	-0.43±1
B	82	65.2±3.1	896*	666*	820*	-1.4±1.4*	-1.65±0.8*	-1.0±0.9*
C	61	74.8±2.6	1005	719	879	-0.38±1.6	-1.4±2	-0.8±2.3
D	52	75.1±2.8	921*	646*	775* †	-1.19±0.2*	-1.65±1.3*	-1.4±1* †

* = p<0.001 compared to continuous users, † = p<0.05 compared to younger group.

Table 2: Percent prevalence of normal (N) & low BMD [osteopenia (P) & OP] at each skeletal site.

	Spine %			Femoral Neck %			Total Hip %		
Group	**N**	**P**	**OP**	**N**	**P**	**OP**	**N**	**P**	**OP**
A	69	26	5	47	48	5	69	29	2
B	37*	40*	23*	17*	62*	21*	52*	46*	2
C	62	28	10	34	56	10	65	33	2
D	42*	37*	21*	23*	54	23*	33*	61*	6*

* = p<0.001 compared to age matched group receiving continuous estrogen replacement.

In summary: a) younger & older postmenopausal F receiving HRT had similar BMD suggesting that age dependent bone loss is effectively attenuated by E and, b) continuous HRT since menopause (versus delayed onset) conferred maximum benefit against low BMD at all skeletal sites. Only 10% of F older than 70 who had received continuous HRT since menopause had OP. In conclusion: E therapy is effective in preventing bone loss up to 80 yrs of age but it must be continuous.

M379

Prevention of Ovariectomy-Induced Changes in the Sprague-Dawley Rat by the Selective Estrogen Receptor Modulator HMR 3339. S. Y. Smith[1], J. Jolette*[1], A. M. Leyshon*[1], C. H. Turner[2], M. Gaillard-Kelly[3], J. M. Vidal*[3], R. Baron[4]. [1]CTBR, Montreal, PQ, Canada, [2]Indiana University, Indianapolis, IN, USA, [3]Aventis Pharma, Romainville, France, [4]Proskelia, Romainville, France.

The purpose of this study was to determine the effects of 12 months of treatment with HMR 3339 on bone mass, strength and architecture in the ovariectomized (OVX) Sprague-Dawley rat. Twenty, 6-month old virgin females were randomly assigned to each of five groups: Sham Control, OVX Control, 3 OVX groups treated with HMR 3339 at 0.01, 0.1 or 0.5 mg/kg/day. Vehicle or test article was given daily by oral gavage. Blood and urine were evaluated for markers of bone turnover (osteocalcin (OC), free deoxypyridinoline, (DPD)). BMD by DXA was determined *in vivo* for the lumbar spine, femur and whole body. Histomorphometry was done for 10 animals per group at the tibia and lumbar vertebra (L3). Biomechanical strength testing was performed for the femur in 3-point bending, femoral neck shear and lumbar vertebra (L4) in compression for 10 animals per group. HMR 3339 dose-dependently prevented the OVX-induced rise in OC and DPD and decreases in BMD. BMD at the lumbar spine and femur was essentially maintained at pre-OVX levels at the mid and high doses with a partial preservation at the low dose. HMR 3339 preserved cancellous bone architecture (BV/TV) at the proximal tibia and L3 for the mid and high doses with a partial effect at the low dose. Reduction of bone turnover as measured by mineralized surface accounted for the preservation of bone architecture at these sites. HMR 3339 dose-dependently prevented the OVX induced expansion of the medullary area and total tissue area in the tibial diaphysis by decreasing bone turnover as measured by the labeled surface on the periosteal and endocortical envelopes. Peak load for all HMR 3339-treated groups was slightly greater than, or similar to Sham controls for the femur 3-point bending test and for the mid and high dose groups for L4 in compression. For treated groups, peak load was not significantly different from Sham controls at the femoral neck. In conclusion, treatment of aged OVX Sprague-Dawley rats with the SERM HMR 3339 at 0.01, 0.1 or 0.5 mg/kg/day for 12 months resulted in a treatment-related preservation of bone mass, strength and architecture at clinically relevant axial and appendicular skeletal sites.

M380

Equivalence of the Skeletal, but not the Reproductive, Actions of Estrogens and Androgens in Female and Male Mice. S. Kousteni, J. R. Chen, L. Han, A. M. Vertino, A. A. Ali, T. Bellido, R. S. Weinstein, C. A. O'Brien, R. L. Jilka, S. C. Manolagas. Division of Endocrinology and Metabolism, Center for Osteoporosis & Metabolic Bone Diseases, Central Arkansas Veterans Healthcare System, U/sity of Arkansas for Medical Sciences, Little Rock, AR, USA.

In contrast to reproductive tissues, the sex specificity of the skeletal effects of estrogens and androgens is seemingly relaxed. To document this phenomenon and elucidate its cellular basis in an amenable experimental model, mature Swiss Webster mice (8 month old), n=8-10 per group, were sham-operated or gonadectomized (GNDX). The GNDX animals were then left untreated or were treated with slow release pellets containing 17β-estradiol (E_2) or dihydrotestosterone (DHT), at doses corresponding to physiologic replacement, as determined by restoration of uterine weight in the females and seminal vesicle weight in the males, respectively. Six weeks later, we determined BMD in live animals, osteoblastogenesis and osteoclastogenesis in ex vivo bone marrow cultures, osteoblast apoptosis in histologic sections of the vertebrae, serum osteocalcin, and wet uterine or seminal vesicle weight. Ovariectomy (OVX) or orchidectomy (ORX) caused upregulation of osteoclastogenesis, osteoblastogenesis and osteoblast apoptosis as well as the loss of BMD. All these changes were effectively prevented by either E_2 or DHT replacement, irrespective of the sex of the mouse. Further, E_2 or DHT prevented the increase of serum osteocalcin in females. DHT prevented the ORX-induced increase in serum osteocalcin, but E_2 was ineffective in this respect. In contrast to the equivalence of the skeletal actions of E_2 and DHT, E_2 administration to ORX males failed to restore seminal vesicle weight; however, DHT administration to OVX females did restore wet uterine weight, probably because of the 300-fold higher dose of DHT as compared to E_2; a uterotrophic effect of high DHT doses has been demonstrated previously by others in the rat. These findings establish that unlike their actions in reproductive tissues, skeletal actions of estrogens and androgens in adult female and male mice are equivalent and result from the same cellular changes. As shown elsewhere in this meeting, such equivalence results, at least in part, from interchangeable ligand/receptor interactions in bone cells from either sex. Elucidation of the differences in the sex specificity of the actions of sex steroids in non-reproductive tissues, like bone, versus reproductive ones, suggest novel means of preserving the beneficial effects of sex steroids on non-reproductive tissues during post-reproductive life, while minimizing or eliminating effects that are no longer needed (and are often harmful) on reproductive tissues.

M381

Effect of Menatetrenone Administration on Bone Mineral Density during Gn-RH Agonist Treatment for Endometriosis. K. Aisaka[1], S. Obata*[1], M. Kaibara*[2], H. Mori*[2]. [1]Obstetrics & Gynecology, Hamada Hospital, Tokyo, Japan, [2]Obstetrics & Gynecology, Teikyo University, Tokyo, Japan.

Objective: Gn-RH agonist therapy is widely used for treatment of endometriosis. However, it is well known that there are some side effects due to too much suppress of plasma estrogen levels. To prevent these problems, so-called the add back therapy using estrogen progestogen (EP) preparations is attempted and many reports show that the add back therapy is useful for prevention hypo-estrogenic symptoms. It is reported that estrogen suppresses osteolysis, while menatetrenone (vitamin K2) promotes osteogenesis. Present study was performed to elucidate whether menatetrenone administration with add back therapy could prevent bone loss more effectively during Gn-RH agonist treatment. Subjects and Methods: Twenty-six patients of endometriosis who were undertaken Gn-RH agonist treatment (Luprorelin, 1.88mg/month) were subjected. They were divided into two groups; add back therapy with EP preparations (Sophia-A, mestranol 0.05mg + norethisterone 1mg/day) only, 14 cases, group A, and EP add back with menatetrenone (Gra-K, 45mg/day), 12 cases, group B. Then, bone mineral density (BMD) of the lumber spine was examined before and 6, 12 months after the treatment. The biomarkers of the bone metabolism (urinary deoxy-pyridinoline (d-Pyr) and plasma intact osteocalcin (OC) levels) were also measured in the same time to evaluate the effects of these medications. The same examinations were also done in 6 cases of endometriosis who did not take the add back therapy during Gn-RH agonist treatment for the control (group C, treated for 6 months only). Results: There was a significant increase in BMD values of the group A and B during the treatment compared to those in the group C (A: 0.93+/-0.35, B: 7.34+/-1.26, C: -3.77+/-0.72 % increase from basal value, p<0.01). Urinary d-Pyr levels in the group C tended to increase during Gn-RH agonist treatment (before: 4.2+/-1.9, 6 months after: 5.5+/-2.7m mol/mol.cre), however, there were no changes in the group A and B. Plasma OC levels increased significantly in the group B (8.8+/-2.8) and C (8.2+/-2.5) compared those in the group A (7.3+/-2.4ng/dl, p<0.02). Conclusion: From these results, it was concluded that there was a beneficial effect for the BMD values during Gn-RH agonist treatment by the combination add back method of menatetrenone and EP preparations. And it was suggested that menatetrenone increased the BMD values through its osteogenic mechanism.

M382

The Decrease in Bone Mineral Mass and in Bone Strength induced by Ovariectomy in Adult Rats is corrected by the New Selective Estrogen Receptor Modulator HMR 3339. P. Ammann[1], F. Brunner[2], M. Gaillard*[2], J. M. Meyer*[3], R. Rizzoli[1]. [1]Department of Internal Medicin, Division of Bone Diseases, Geneva-14, Switzerland, [2]Aventis, Romainville, France, [3]Scholl of Dentistry, Geneva-14, Switzerland.

The selective estrogen receptor modulator (SERM) raloxifene (RAL) has been shown to prevent vertebral fracture. However, there is a need for SERMs with optimal profile, which could restore mechanical competence and reduce the risk of fractures at multiple sites. We investigated the effects of a new steroidal SERM, HMR 3339, on bone mineral density (BMD; mg/cm2) and bone strength (U St; N) at the level of the proximal tibia (PT), lumbar spine (LS) and femur in ovariectomized (OVX) osteoporotic rats, and compared these effects to those of RAL. Eight weeks after OVX, 8-month old rats were allocated to 5 groups (n=8) and given orally HMR at 0.03/0.1/0.3, or RAL at 3.0 mg/kg BW x day or the vehicle for 16 weeks. Changes from baseline are expressed as means±SEM; * indicates p<0.05 vs OVX and º vs baseline by ANOVA.

	PT BMD	PT U St	LS BMD	LS U St
Baseline		132.8±8.5		171.7±14.6
SHAM	1.9±0.7	173.4±11.1	-3.3±1.8	190.4±16.8
OVX	1.3±1.3	134.7±12.0	-6.8±2.3	162.3±14.1
OVX HMR 0.03	3.0±1.2	194.7±17.4º*	1.0±1.7*	214.8±13.6º*
OVXHMR 0.1	6.8±1.7*	211.9±14.0º*	3.9±2.1*	221.5±14.7º*
OVXHMR 0.3	3.5±1.3*	189.5±11.5º*	4.7±1.4*	221.1±12.3º*
OVX RAL 3.0	4.0±0.6*	178.2±9.4º*	1.7±2.6*	195.4±13.9

In OVX rats, HMR increased BMD and ultimate strength at the level of lumbar spine and proximal tibia. Similar results were obtained at the level of the midshaft tibia and of femoral neck. Serum IGF-I measured at the end of the study was 495±31, 556±26, 672±21*, 732±31*, 765±54* and 610±41 in SHAM, OVX, HMR 0.03/0.1/0.3 and RAL. HMR increased IGF-I plasma levels above those of OVX, an effect not observed with RAL. This might account for the differences in response to HMR and RAL. In conclusion, HMR 3339 increased not only bone mineral mass, but also restored bone mechanical strength at multiple sites in aged osteoporotic rats, acting in a curative way.

M383

The New Selective Estrogen Receptor Modulator HMR 3339 Prevents Ovariectomy-Induced Bone Loss and Alteration of Bone Strength in Adult Rats. P. Ammann[1], S. Bourrin*[1], F. Brunner[2], M. Gaillard*[2], J. M. Meyer*[3], R. Rizzoli[1]. [1]Department of Internal Medicin, Division of Bone Diseases, Geneva-14, Switzerland, [2]Aventis, Romainville, France, [3]School of Dentistry, Genenva-14, Switzerland.

Prevention of bone loss after menopause with estrogen replacement therapy is not accepted by all women due to the fear of cancer. Thus, there is a need for alternative therapy like selective estrogen receptor modulators (SERMs) which could prevent bone loss and decrease bone fragility, while preventing breast cancer and lacking side effects on genital tract. We investigated the effects of a new steroidal SERM, HMR 3339, on bone mineral density (BMD; mg/cm2) and bone strength (US; N) as evaluated at the level of the tibia, and spine in ovariectomized (OVX) rats and compared its effects to those of raloxifen (RAL). Bone histomorphometry was investigated at the level of the proximal tibia. At the end of the study serum IGF-I was measured. Immediately after OVX, 6-month old rats were given orally HMR at 0.03/0.1/0.3, or RAL at 3.0 mg/kg BW x day for 16 weeks. The SHAM and OVX controls received the vehicle. Values are means±SEM and were all obtained at the level of the proximal tibia ;* indicates p<0.05 vs OVX and º vs RAL by ANOVA.

	BMD	US	BV/TV	Tb.N
SHAM	319.6±3.0	179.39±19.7	17.2±2.5	4.45±0.45
OVX	293.2±2.6	146.6±9.2	5.6±1.1	1.58±0.26
OVX HMR 0.03	312.1±3.3*	175.7±10.2	14.0±1.8*	3.56±0.33*
OVXHMR 0.1	315.6±1.9*	199.1±14.9*º	15.3±1.3*	3.91±0.26*
OVXHMR 0.3	322.9±3.7*	181.1±10.7*	16.0±2.3*	3.97±0.44*
OVX RAL 3.0	312.1±3.3*	161.7±4.25	13.2±0.8*	3.57±0.18*

Serum IGF-I measured at study completion was 506±24, 691±35, 694±35*, 778±38*, 725±37*º and 688±34 in SHAM, OVX, HMR 0.03/0.1/0.3 and RAL. Uterus weight was 462±23*, 93±16, 140±15, 115±14, 142±20 and 119±23 mg, respectively in the same groups. HMR prevents the decrease of BMD and maintains ultimate strength. Similar results were obtained at the level of the midshaft tibia, spine and femoral neck. Decrease of trabecular bone volume (BV/TV, %) and of trabeculae number (Tb.n, 1/mm) was also prevented. Combining all parameters, the optimal effect was obtained at a dose of 0.1mg/kg. HMR increased IGF-I plasma levels above those of OVX, an effect not observed with RAL. Uterus weight were not different from OVX control in HMR treated rats. In conclusion, HMR 3339 prevents OVX-induced bone loss and alteration of mechanical properties at multiple sites without significant increment of uterus weight in aged rats.

M384

Estrogen in the Establishment of Peak Bone Mass. J. E. Mulder[1], C. A. Sklar*[2], A. Klibanski[3], J. P. Bilezikian[1]. [1]Columbia University, New York, NY, USA, [2]Memorial Sloan-Kettering Cancer Center, New York, NY, USA, [3]Massachusetts General Hospital, Boston, MA, USA.

Advances in combination chemotherapy, radiation therapy, surgery, and bone marrow transplantation have resulted in markedly improved survival rates for many patients with cancer. These advancements in therapy, however, have led to new problems, namely, long-term consequences of effective treatments. Not infrequently, for example, men and women treated for cancer suffer the premature loss of gonadal function. Premature ovarian failure (POF) places women at great risk for bone loss and osteoporosis. The issues raised in this study, however, differ from usual considerations of age-related menopausal ovarian failure and the accelerated bone loss that ensues. This more typical clinical event follows well after the establishment of peak bone mass. The young women to be investigated in this study have become estrogen deficient before achieving peak bone mass. We will determine the importance of estrogen in achieving optimal peak bone mass in this setting. Other potential contributing factors, such as androgen deficiency, growth hormone deficiency, chemotherapeutic agents, nutritional, and other metabolic parameters will be evaluated. 26 female survivors of childhood cancer with POF and 10 female cancer survivors (age- and weight-matched) with normal ovarian function will be recruited from 2 centers. The main goals of the study are to characterize the skeletal profile of these young women, and then to determine the dosage of estrogen required to establish peak bone mass optimally in the subset of women with POF. The young women must be between 16-25 years of age. After the initial characterization, the young women with POF will be randomized to one of two treatment groups and followed for 2 years. Regimen I consists of "standard" replacement with estradiol 0.5 mg daily, plus micronized progesterone (MP) 200mg daily for 14 days. Regimen II (higher dose) consists of estradiol 2.0 mg daily, plus MP 200 mg daily for 14 days. Primary outcomes include individual percent change in BMD at the lumbar spine and hip by DXA. Other endpoint measurements include changes in BMD at peripheral sites (1/3 radial, phalangeal sites, as measured by peripheral DXA, and calcaneal site as measured by ultrasound) and changes in markers of bone remodeling. As of April 1st, 297 potential subjects have been identified from searching 2 different databases. It is expected that enrollment will proceed, and we will reach our recruitment goals over the next year.

M385

Evidence That Estrogen Receptor AF-1 Activity Prevents Bone Loss: Results From Selective Estrogen Receptor Modulator (SERM) Therapy In OVX Mice. D. von Stechow[1], N. Quibria*[2], S. Fish*[2], J. M. Alexander[2]. [1]Orthopedic Biomechanics Laboratory, BIDMC/Harvard Medical School, Boston, MA, USA, [2]Bone and Mineral Metabolism Unit, BIDMC/Harvard Medical School, Boston, MA, USA.

The aim of this *in vivo* mouse study was to compare estrogen (E2) replacement therapy with the effects of two SERMs, tamoxifen (Tam) and ICI 178,180, on bone in an ovariectomized (OVX) mouse model of osteoporosis. Previous *in vitro* data have determined that tamoxifen acts as a partial E2 antagonist by selectively inhibiting the AF-2 ligand binding domain of ER, while ICI is a pure anti-estrogen that inhibits both the AF-1 amino-terminal activation function and AF-2 domains of the ER. In this study, three-month-old Swiss-Webster mice underwent 5 weeks of treatment with either E2, Tam, or ICI (500 mcg weekly, *sc* injection) or vehicle. Animals were sacrificed after five weeks (Sham and OVX-vehicle controls, along with 3 treated groups). Femoral bones were analyzed by micro-computed tomography. Morphometric indices, such as bone volume density (%BV/TV), trabecular number (Tb.N), and trabecular thickness (Tb.Th) were quantitatively assessed at the distal metaphysis. In addition, marrow volume (%MV/TV) and cortical thickness (Ct.Th) were measured at the femoral diaphysis using direct 3D morphometry. OVX vehicle-treated control mice showed an 83% loss of metaphyseal trabecular bone compared to sham animals. This loss was associated with marked decreases in Tb.N and Tb.Th. E2-treated mice exhibited a significant increase in trabecular %BV/TV over vehicle-treated mice, largely through increased Tb.Th. While Tam treatment was protective for bone loss, ICI treatment had no protective effect, with ICI-treated mice showing bone loss comparable to OVX-vehicle treated mice. At the diaphysis, %MV/TV decreased significantly after E2 and Tam treatment, indicating cortical endosteal bone formation in both groups. E2 treatment caused a 13.5% increase in Ct.Th, but there were no significant differences observed in Ct.Th in Tam-treated versus Sham operated mice. ICI-treated mice were not significantly different from OXV-vehicle mice in any of the parameters measured in this study. We conclude that E2 treatment resulted in significant bone formation, while Tam, similar to its effect in other E2-sensitive tissues, has partial estrogenic activity in bone and is protective against OVX-induced bone loss. Conversely, ICI, a pure anti-estrogen, does not prevent OVX-induced bone loss. Therefore, our findings in OVX mice suggest that the protective effect of E2 and Tam in bone is mediated in part via the AF-1 domain of the estrogen receptor.

Disclosures: ***J.M. Alexander****, Millennium Pharmaceuticals Inc. 2.*

M386

Influence of BMI on Changes in Bone Density After Treatment With Multiple Doses of Conjugated Equine Estrogens (CEE) and Medroxyprogesterone Acetate (MPA) in Early Postmenopausal Women. R. Lindsay[1], J. Gallagher[2], M. Kleerekoper[3], R. Northington*[4], K. Qi*[4], J. H. Pickar*[5]. [1]Internal Medicine, Helen Hayes Hospital, West Haverstraw, NY, USA, [2]Bone Metabolism Unit, Creighton University School of Medicine, Omaha, NE, USA, [3]Division of Endocrinology, Wayne State University School of Medicine, Detroit, MI, USA, [4]Clinical Biostatistics, Wyeth Research, Philadelphia, PA, USA, [5]Clinical Research and Development, Wyeth Research, Philadelphia, PA, USA.

Body mass index (BMI) is an important determinant of bone mineral density (BMD). Whether BMI influences the BMD response to hormone replacement therapy (HRT) has not been well studied. The Women's Health, Osteoporosis, Progestin, Estrogen (Women's HOPE) study included a 2-year substudy of 749 women to evaluate the effects of different doses of CEE, either alone or with one of two doses of MPA, on BMD. Postmenopausal women 40-65 years were randomized to receive a daily dose of CEE 0.625 mg, CEE 0.625/MPA 2.5 mg, CEE 0.45 mg, CEE 0.45/MPA 2.5 mg, CEE 0.45/MPA 1.5 mg, CEE 0.3 mg, CEE 0.3/MPA 1.5 mg, or placebo. All women also received calcium carbonate (600 mg elemental calcium daily). At enrollment, women were between 1 and 4 years post menopause and were within 20% of normal body weight range. Lumbar spine (L2-L4) and total hip BMD and total body bone mineral content (BMC) were measured using a Lunar DPX-L. Correlation analyses between BMI and BMD or BMC changes from baseline at 1 year and 2 years were performed for all treatment groups. Statistical significance was set *a priori* at $P<.05$. Increases in BMD ranged from 1.7%-3.9% at the spine and 2.0%-3.1% at the hip, and total body BMC increased from 0.6%-2.3% at 2 years of active treatment; all doses of CEE and CEE/MPA produced significant increases ($P<.05$) in BMD and BMC relative to placebo. Placebo-treated patients lost 2.7 ± 3.3% (mean ± SE) of spine BMD and 0.9 ± 3.4% of hip BMD over 2 years; the loss of total body BMC averaged 2.8 ± 2.8%. Mean BMI (24.4 kg/m^2) was similar among groups and individual values ranged from 16.9-31.7 kg/m^2. Pearson correlation coefficients (r) for the relation between BMI and the percent change from baseline in BMD or BMC for all groups ranged from -0.24 to 0.19; no correlations were significant at year 1 or 2. These data indicate that BMI does not influence the beneficial effect of CEE, alone or combined with MPA, on BMD or BMC in early postmenopausal women who are within 20% of normal body weight range.

Disclosures: ***R. Lindsay****, Pfizer, Inc. 2; Proctor & Gamble Company 2, 5; Eli Lilly and Company 5; Wyeth Pharmaceuticals 2, 5.*

M387

Estrogen Replacement Therapy and Tibial Bone Structure and Physical Performance in Postmenopausal Women. A. O. Heinonen*[1], H. Sievänen*[1], K. Uusi-Rasi*[2], I. Vuori[1]. [1]UKK Institute for Health Promotion Research, Tampere, Finland, [2]Johns Hopkins Outpatient Center, Baltimore, MD, USA.

Osteoporotic fractures are a common and increasing public health problem. Hormone replacement therapy (HRT) is one of the commonly recommended means for preventing osteoporosis and related fractures due to its ability to increase bone mineral density (BMD). However, BMD is only one factor affecting bone fragility. Also bone size, shape and architecture play a role. It has also been suggested that HRT may have anabolic effects and it might have a role in improving muscle strength or balance. The purpose of this cross-sectional study was to focus on factors associated with bone structure of lower limbs, and physical performance after menopause. Eighty non-smoking, healthy postmenopausal women participated in the study. They were classified into two groups by their use of hormone replacement therapy (HRT), either to the current users [n=43, age: 62 (SD 1) yrs, height: 161.0 (4.8) cm, weight: 68.2 (11.0) kg] or never or discontinued users [n=37, 62 (1) yrs, height: 161.3 (5.4) cm, weight: 73.9 ± 14.9 kg]. The tibial shaft and distal tibia were scanned with pQCT (Norland /Stratec XCT3000; Norland/Stratec, Pforzheim, Germany). For the shaft region, cortical density (CoD, g/cm^3), cortical area (CoA, mm^2) and section modulus (BSI, mm^3) were determined. For the distal part, the evaluated variables were ratio of cortical to total area (CoA/ToA), trabecular density (TrD, g/mm^3) and BSI. Isometric and dynamic muscle strength of the leg extensors, dynamic and static balance, and cardiorespiratory capacity (VO_2max) were measured. Between-group differences were evaluated with analysis of covariance body weight as a coavariate. Unadjusted values for all bone variables were slightly higher in the HRT-users compared to non-users, with the exception of TrD with no difference. After controlling for body weight, the mean differences (95% confidence interval) remained significant for CoD of the tibial shaft and BSI of the distal tibia only, the mean between group differences being 1.5% (95% CI 0.4 to 2.5%) and 23.0% (7.1 to 41.3%), respectively. No differences existed between two study groups for lower limb isometric or dynamic power, cardiorespiratory capacity or balance. These results suggest that HRT results in apparently stronger bone structure in tibia but its role in improving physical performance is not evident.

M388

Simvastatin Given Twice Daily Increases Cortical Bone Formation and Strength in OVX Rats. H. Oxlund[1], T. T. Andreassen[2]. [1]Department of Connective Tissue Biology, Institute of Anatomy, Aarhus, Denmark, [2]Department of Connective Tissue Biology, Institute of anatomy, Aarhus, Denmark.

Some of the statins possess bone anabolic properties. Statin increased expression of the BMP-2 gene in osteoblasts resulting in increased cancellous bone volume and a minor decrease in osteoclast number of 3-month-old rats (Mundy et al, Science 286, 1946-1949, 1999). Simvastatin increased the vertebral cancellous bone mass and compressive strength of one-year-old female rats (Oxlund et al., Calcif Tissue Int 69:299-304, 2001). In the present study the effects of statin on tibia cortical bone of OVX (ovariectomized) rats were studied. Sixty Wistar female rats, 4 months old, were allocated to 4 groups: 1. Baseline control, 2. Sham + placebo group, 3. OVX + placebo, 4. OVX + simvastatin. Simvastatin MSD (20 mg/kg) or placebo were given twice daily at 9 a.m. and at 3 p.m. by a gastric tube for 3 months. The rats were injected with tetracycline i.p. at day 11 and calcein i.p. at day 4 before sacrifice of the 7 months old rats. The mechanical properties of the tibia diaphysis were studied by a 3-point-bending test. The breaking strength of the OVX + statin group (111.2 +/- 2.1 newton, mean +/- SEM) was increased ($2p<0.02$) compared with the OVX group (102.4 +/- 2.8 newton), and increased ($2p<0.001$) compared with the sham + placebo group (97.5 +/- 2.2 newton). Cross-sections were cut and mineral apposition rates (MAR) at the different aspects and in different regions of the tibia were calculated from the fluorescent labels. In the upper part of the tibia diaphysis for example, the endosteal MAR of the OVX + statin group (1.7 +/- 0.1 micrometer/day) was increased ($2p<0.001$) compared with the OVX group (1.0 +/- 0.1 micrometer/day), and increased ($2p<0.0001$) compared with the sham + placebo group (0.4 +/- 0.1 micrometer/day). In conclusion, simvastatin given perorally twice daily increased the bending strength of the tibia diaphysis of OVX rats. The mineral apposition rates were increased in OVX rats given simvastatin. The new cortical bone exhibited a normal lamellar structure. Simvastatin increases bone formation, but seems to respect the regional pattern of bone resorption, formation and drift.

M389

Effects of Oral DHEA on Bone Density in Young Women with Anorexia Nervosa. C. M. Gordon[1], E. Grace*[1], S. J. Emans*[1], H. Feldman*[1], E. Goodman*[2], K. Becker*[1], C. J. Rosen[3], C. M. Gundberg[4], M. S. LeBoff[5]. [1]Children's Hospital, Boston, MA, USA, [2]Children's Hospital, Cincinnati, OH, USA, [3]St. Joseph Hospital, Bangor, ME, USA, [4]Yale-New Haven Hospital, New Haven, CT, USA, [5]Brigham & Women's Hospital, Boston, MA, USA.

Young women with anorexia nervosa (AN) have subnormal levels of dehydroepiandrosterone (DHEA) and estrogen that may be mechanistically linked to the bone loss commonly seen in this disease. The purpose of this study was to compare the effects of a 1-year course of oral DHEA treatment vs. conventional hormonal replacement therapy (HRT) in young women with AN. Sixty-one young women were randomly assigned to receive DHEA (50 mg/d) or HRT (20 mcg ethinyl estradiol/0.1 mg levonorgestrel). Anthropometric, nutrition and exercise data were acquired every 3 months, and bone mineral density (BMD) and body composition were measured by dual energy x-ray absorptiometry (DXA) every 6 months over 1 year. Serum samples were obtained for hormones, proresorptive cytokines, and bone formation markers, and urine for bone resorption markers at each visit. Total hip BMD increased significantly and similarly (+1.7%) in both groups. In those receiving DHEA, hip BMD increases were positively correlated with increases in IGF-I ($r=0.44$, $P=0.030$) and the bone formation marker, BSAP. There was no significant change in lumbar BMD in either treatment group. Both bone formation markers, BSAP and osteocalcin, increased transiently at 6-9 months in those patients receiving DHEA compared to the HRT group ($p<0.05$). Both DHEA and HRT significantly reduced levels of the bone resorption markers, NTx. There was a positive correlation between changes in IGF-I and changes in weight, percentage body fat and estradiol for both groups. In addition, patients receiving DHEA exhibited significantly lower scores ($p<0.05$) on 3 psychological instruments (Eating Attitudes Test, Anorexia Nervosa Subtest and Spielberger Anxiety Inventory), reflecting clinical improvement. Both DHEA and HRT resulted in significant increases in hip BMD. Maintenance of spinal BMD was seen, but there was no significant increase over 1 year. DHEA appeared to have anabolic effects, evidenced by the positive correlation between increases in hip DXA measurements and IGF-I, and the significant increase in bone formation markers seen in those subjects receiving DHEA. In both groups, IGF-I appeared to be nutritionally dependent, correlating with weight and percentage body fat. Both therapies significantly decreased bone resorption. As has been reported in the elderly, DHEA resulted in improvements in specific psychological parameters in these young women.

M390

Amylin(1-8) and a Stable Analog Are Anabolic after Local but not Systemic Administration in Rodents. J. A. Gasser, M. Heidl*, T. Buhl*, T. Petcher*, R. Beerli*. Arthritis & Bone Metabolism, Novartis Pharma AG, Basel, Switzerland.

Work in rodents indicates that amylin(1-8) may be anabolic for bone after local and systemic administration. We investigated the anabolic properties of amylin(1-8) and a stable octapeptide analog on the mineral apposition rate (MAR) after their direct administration to the calvaria surface in mice. In addition, eight-month old estrogen replete and ovarietcomized rats were treated daily s.c. for 4 weeks with 0.5 or 5mg/kg of the analog to investigate its bone anabolic and/or antiresorptive effects after systemic administration. Cancellous and cortical bone parameters were measured non-invasively by pQCT in the proximal tibia metaphysis at baseline, 2 and 4 weeks after the start of treatment. In mice treated for 5 consecutive days with local injections of 1, 10 or 100nM amylin(1-8), MAR increased significantly in a concentration dependent manner. The stable analog was more potent than the natural fragment and was therefore chosen for daily injections over 4 weeks at 0.5 or 5mg/kg to estrogen-replete and OVX rats. PTH(1-34) injected s.c. at 5µg/kg served as a positive control. In estrogen replete animals, PTH(1-34) increased total- and cancellous bone mineral density (10.3 and 11.6%, both $p<0.01$) and cortical thickness (40.8%, $p<0.01$). In contrast, no effect on any parameter was seen in rats treated with 0.5 or 5mg/kg of the amylin analog (all parameters NS vs sham-op). OVX-rats showed significant cancellous bone loss (17.0%, $p<0.01$) and cortical thinning (19.8%, $p<0.01$). PTH was fully protective on all parameters and increased cortical thickness by 5% (NS). The amylin analog reduced cancellous bone loss to 13.9% (NS vs OVX) and 11.8% ($p<0.05$ vs OVX) but did not show any significant protective effect on cortical thinning at 0.5mg/kg (22.9%, NS vs OVX) or 5mg/kg (18.1%, NS vs OVX). Our data suggests that the N-terminal amylin fragment or the stabilised octapeptide analogue is anabolic when administered directly to the bone surface in mice and rats. However, no anabolic effect was observed in rats after 'systemic' s.c. administration to estrogen replete animals and only mild but significant protective effects were seen in the OVX-prevention study. All effects of amylin or the analog were less pronounced compared to the anabolic agent PTH(1-34). The reasons for the discrepancy between the result of local and systemic administration of the amylin analogue is not known at this point.

M391

Agonist of the VEGF Receptor R1/flk-1/KDR Prevents Unloading-Induced Trabecular Bone Loss in the Rat by Increasing Osteoblastic Activity. M. H. Lafage-Proust[1], O. Barou*[1], V. David*[1], T. Thomas[1], P. Ruegsegger*[2], J. Plouët*[3], C. Alexandre[1], L. Vico[1]. [1]EM-INSERM 9901, St-Etienne, France, [2]ETH, Zurich, Switzerland, [3]GDR CNRS 1927, Toulouse, France.

There is growing evidence that a functional relationship links bone remodeling to angiogenesis. Hence, we postulated that unloading-induced bone loss is, at least in part, related to bone vascularisation alterations. Using the tail-suspended rat model, we first showed a concurrent decrease in both capillary number and bone formation rate (BFR) in tibia metaphysis after 7 days of unloading preceding bone loss. Moreover, we observed an early dramatic decrease in mRNA expression of the potent angiogenic factor VEGF in the bone marrow, metaphysis and periosteum of the unloaded tibia. Conversely, none of these changes occurred in normally loaded humeri. We next tested the effects of anti-idiotypic anti-VEGF receptor Kdr antibodies (KdrAb) administration in this model. KdrAb dimerises the receptor and mimics the VEGF pro-angiogenic effects,(Ortega et al, Am J Pathol. 1997,151:1215-24). 300g Wistar male rats were divided in 4 groups of 7 animals: tail-suspended rats (Susp) treated with intra-peritoneal KdrAb (5µg/kg bw) or vehicle (V), on days 0, 4, 7 and 11 ; non-suspended rats (Ctr) similarly treated with KdrAb or V. Trabecular bone volume (BV/TV, %), trabecular linear attenuation coefficient (LAC) (correlate of bone mineral density) and cortical area (mm^2) were assessed longitudinally (at days 0, 7 and 14) with micro-computerized tomodensitometry (VivaScan) on femur metaphysis. After sacrifice, at day 14, osteoclastic (OcS/BS) and osteoblastic activities (mineral apposition rate, MAR and mineralising surfaces, MS/BS) were measured with quantitative bone histomorphometry on tibia metaphysis secondary spongiosa. Results are given as mean ± SD.

Results

	Ctr V	Ctr KdrAb	Susp V	Susp KdrAb
BV/TV, %	9.5±1.8	10.4±1.9	5.6±2.2 a	7.5±3.2
LAC	0.745±0.021	0.760±0.032	0.653±0.054 a	0.700±0.071
Cortical Area	5.93±0.09	5.81±0.09	5.1±0.16 a	5.23±0.17 a
OcS/BS,%	15.7±2.5	14.4±3.6	14.9±3.3	14.4±2.9
MAR, µm/d	2.60±0.12	2.61±0.17	2.15±0.12 b	2.63±0.12
MB/BS, %	18.4±1.8	20.1± 5.9	11.7±1.3 b	13.5±3.3 b

Significant difference: a vs baseline (repeated measures ANOVA), b vs Ctr-V (Mann-Whitney).The unloading-induced decrease in growth plate and primary spongiosa width was not prevented by KdrAb treatment. Thus, KdrAb prevented unloaded-induced trabecular bone loss through an increase in osteoblastic activity. Whether KdrAb effects on bone were mediated through endothelial cells, direct osteoblastic stimulation or both remains to be elucidated.

M392

A Non-Prostanoid EP4 Receptor Selective Prostaglandin E2 (PGE2) Agonist Stimulates Bone Formation and Restores Bone Mass and Strength in Ovariectomized Rats. H. Z. Ke, D. T. Crawford*, H. QI, M. Li, V. M. Paralkar, T. A. Owen, L. C. Pan, T. A. Brown, K. O. Cameron*, B. A. Lefker*, P. DaSilva-Jardine*, B. Lu*, W. A. Grasser, H. A. Simmons, L. J. Yu*, D. O. Scott*, D. D. Thompson. Pfizer Global Research and Development, Groton, CT, USA.

PGE2 stimulates bone formation, increases bone mass and strength. However, the mechanism of PGE2's bone anabolic effects is not known. PGE2 binds to all four receptor subtypes, EP1-EP4. We hypothesized that the EP4 receptor plays an important role in the bone anabolism of PGE2. CP-A is a newly identified EP4 receptor selective agonist. CP-A binds selectively to the EP4 receptor with an IC50 of 54 nM, while it did not bind to EP1, EP2, EP3 and other prostanoid receptors including DP, FP, IP, and TP. CP-A stimulates the EP4 receptor to initiate signaling by the cAMP pathway with an EC50 value of 32.5 nM. CP-A increases osteogenesis in vitro as demonstrated by a dose-dependent increase in mineralized nodule formation in rat bone marrow cell cultures with an EC50 of 1 micromolar. The maximum effect of CP-A in this assay is equivalent to those of PGE2. Daily subcutaneous injection of CP-A at 3, 10, or 30 mg/kg was given for 4 weeks to 5.5-month-old rats that had been ovariectomized (OVX) for 5 weeks prior to the beginning of treatment. PQCT analysis of the distal femoral metaphysis (DFM) showed that CP-A dose-dependently increased total content (up to +16%), total density (up to +24%), cortical content, cortical thickness, and cortical area in OVX rats as compared with OVX controls. Proximal tibial metaphyseal (PTM) cancellous bone histomorphometric analysis showed that CP-A significantly and dose-dependently increased trabecular bone volume (up to +97%), thickness, number, mineralizing surface, mineral apposition rate, and bone formation rate in OVX rats. All bone mass and structural parameters in DFM and PTM in OVX rats treated with CP-A at 30 mg/kg did not differ from sham controls, indicating the complete restoration of bone mass in the OVX rats. Further, the indentation test of DFM and the compression test of the 5th lumbar vertebral body showed that CP-A dose-dependently restored ultimate strength back to level of sham controls in vertebral body and above the level of sham controls in DFM in the OVX rats. In summary, we report for the first time that a non-prostanoid EP4 receptor selective agonist increases osteogenesis in vitro and completely restores bone mass and strength to the levels equal to or greater than sham controls in the established osteopenic, OVX rat model by stimulating bone formation. Thus, EP4 receptor agonists may provide therapeutic potentials for prevention and treatment of skeletal disorders including osteoporosis and it related fractures.

*Disclosures: **H.Z. Ke**, Pfizer inc. 3.*

M393

Novel, Non-steroidal Selective Androgen Receptor Modulators (SARMs) Have Bone Anabolic Activity in Adult Osteoporotic Rats. K. Hanada*, K. Furuya*, N. Yamamoto*, H. Nejishima*, K. Ichikawa*, S. Amano*, Y. Sumita*, N. Oguro*, M. Miyakawa*, T. Nakamura*. Drug Discovery Research Department, Kaken Pharmaceutical, Co.,Ltd.,, Kyoto, Japan.

We successfully generated novel, non-steroidal small compounds as selective androgen receptor modulators (SARMs), which showed strong androgen receptor (AR) binding affinity and bone-selective agonistic activity. The Compounds showed AR-selective binding and therefore did not cross-reaction to AR-related nuclear receptors, progesterone and glucocorticoid receptors. When the Compounds were administrated into orchiectomized (ORX) rats, bone mineral density (BMD) of femoral diaphysis (cortical bones) assessed by dual energy X-ray absorptiometry (DEXA) was dose-dependently increased as same potency as androgen steroids, testosterone propionate (TP) and dihydrotestosterone (DHT). In contrast, their virilizing effects manifested by weight of ventral prostates were reduced in comparison with TP and DHT. These results strongly suggested that the Compounds were SARM candidates, which had unique tissue selectivity with high potency for bone formation and lower impact upon prostate. Current studies were undertaken to confirm the direct bone anabolic activities of the Compounds in osteoporotic animal models. Firstly, to exclude the possibility that the Compounds stimulate bone formation indirectly by enhancement of muscle strength, ORX rats were further subjected to sciatic neurectomy (NX). After 4-week s.c. injection with 30mg/kg of Compound N1, one of our lead compounds, BMD of immobilized tibia was significantly increased as compared with that of vehicle-treated NX+ORX rats, irrespective of severe muscle atrophy of hind limb. These data suggest that the Compound has direct bone anabolic activity. Moreover, Compound N1 did not elevate prostate weight above the normal level, confirming the diminished virilizing activity of it. We next investigated bone formation activity of the Compound N1 in ovariectomized (OVX) rats. The Compound N1 (10 and 30mg/kg) was given sc to OVX rat for 2 months and BMD of femurs was measured. The Compound significantly increased BMD of femoral diaphysis as well as DHT and TP, whereas estrogen, anti-bone resorptive hormone, did not. Combined administration of the Compound N1 and estrogen further increased BMD of femoral diaphysis as compared with single administration of the Compound. In addition, the Compound N1 significantly enhanced mechanical strength of cortical bones of femurs in 3-point bending experiments. Collectively, these results indicated that the Compounds had high potency of bone anabolic activity distinct from anti-resorptive agents. Bone histomorphometric analyses are now in progress.

M394

Effect of Nandrolone Decanoate on Bone Mineral Density and Vertebral Fracture in Osteoporotic Elderly Women: A Double-Blind, Randomized, Clinical Trial. A. Frisoli*[1], M. Pinheiro*[2], W. Braga*[2], V. Szejnfeld[2]. [1]Rheumatology and Geriatric Division, Universidade Federal de Sao Paulo, Sao Paulo, Brazil, [2]Rheumatology, Universidade Federal de Sao Paulo, Sao Paulo, Brazil.

A double blind, randomized, clinical trial was performed, for two years, to evaluate the effect of nandrolone decanoate(ND) on bone mineral density(BMD) of lumbar spine, femoral neck, trochanter, lean body mass and vertebral fracture rate. Sixty-five osteoporotic women aged 70 years old or more were divided in two groups: one, with 32 patients who took injections of 50mg nandrolone decanoate every 3 weeks, plus 500mg calcium tablets daily. The second group with 33 patients who took injections of placebo every 3 weeks, plus 500mg calcium tablets daily. Significant positive changes from baseline in BMD at the lumbar spine (3,4±6,0 e 3,7%±7,4; p<0,05) and femoral neck (4,1%± 7,3 e 4,7%±8,0; p<0,05) were observed in the first and second year in the nandrolone decanoate group. BMD of trochanter showed significant positive changes from the base line only in the first year (4,8%±9,3 e 3,1%±10,2; p>0,05). Otherwise, there was no significant difference between BMD of the lumbar spine of two groups. A significant statistical difference in the trochanter BMD of ND group and placebo group was observed between the first (p=0,003) and second year (p=0,02). Also for femoral neck BMD a difference between the two groups over the two years was observed (p=0,01). Lean body mass of ND group showed considerable increase from baseline, not only in first (6,2% ±5,8; p<0,00004), but also in the second year (11,9%±29,2; p<0,0001). New vertebral fractures were significantly lower in the ND group (21%; p<0,05), than in placebo group (43%). We conclude that treatment with nandrolone decanoate does increase the bone mineral density of proximal femur and lean body mass, and reduce the vertebral fracture of elderly women.

M395

Discovery of CP-533536: an EP2 Receptor Selective Prostaglandin E2 (PGE2) Agonist That Induces Local Bone Formation. B. A. Lefker*, K. O. Cameron*, D. T. Crawford*, P. Dasilva-Jardine*, S. L. Deninno*, H. Gao*, W. A. Grasser, D. R. Healy*, N. C. Elliott*, H. Z. Ke, M. Li, B. Lu*, T. A. Owen, V. M. Paralkar, H. Qi, D. D. Thompson, C. M. Tjoa*, A. S. Wright*, L. J. Yu*, M. P. Zawistoski*, R. L. Rosati*, C. F. Ebbinghaus*. Cardiovascular and Metabolic Diseases, Pfizer Global Research and Development, Groton, CT, USA.

PGE2 stimulates bone formation in humans and animals when dosed systemically or locally. Of the four PGE2 receptor subtypes (EP1-EP4), EP2 and EP4 have been envisaged as the two receptors most likely to be responsible for PGE2's actions on bone. As part of a drug discovery program to identify agents that would induce local bone, we sought a non-prostanoid, subtype selective PGE2 agonist. We initiated our search by screening known PGE2 analogs most likely to be selective for EP2 and/or EP4. An in house compound, CMP-1, was identified as a mixed EP2/EP4 agonist (rEP2=27 nM, rEP4=219 nM) with good selectivity vs. other prostanoid receptors. CMP-1 was locally injected into the bone marrow of the proximal tibial metaphysis of 6-week-old male rats. A single 3 mg/kg injection was given on day 1, and the rats were necropsied on day 7. The injected tibia was analyzed using peripheral quantitative computerized tomography (PQCT), bone histomorphometry, and biomechanical testing. CMP-1 dose-dependently increased new bone formation in the injected site of the marrow cavity. Having confirmed that a mixed EP2/EP4 selective agonist was active in vivo in this model, we sought subtype selective agonists. CMP-2, reported previously, was characterized in our labs as a weak but selective EP2 agonist. The benzylic alcohol derivative, CMP-3, had similar potency and selectivity. In the local injection model, CMP-3 increased local bone formation to a similar extent as observed with the EP2/EP4 agonist, CMP-1. A range of aliphatic bottom chains, acid linkers, and alkyl and aryl sulfonamides were explored. This chemistry optimization led to the identification of a more potent and highly selective agonist, CP-533536 (50 nM IC50 for rEP2, 0.31 nM EC50 for rEP2, > 3200 nM IC50 for rEP4). Upon local injection, CP-533536 dose-dependently increased new bone formation in the injected site of the marrow cavity. At a dose of 3 mg/kg, CP-533536 increased total bone content by 54% and total mineral density by 28%. In summary, we have identified potent, EP2 selective agonists which produce significant new bone after a single local injection into the marrow cavity of young male rats. These agents have potential clinical utility as local bone healing agents.

Disclosures: ***B.A. Lefker****, Pfizer 3.*

M396

Effect of Simvastatin on Bone Turnover and Bone Density in Postmenopausal Hypercholesterolemic women: A 1-year longitudinal Study. A. Montagnani*, S. Gonnelli, C. Cepollaro*, S. Mondillo*, S. Pacini*, C. Caffarelli*, M. S. Campagna*, M. B. Franci*, B. Lucani*, C. Gennari. Institute of Internal Medicine, University of Siena, Siena, Italy.

Experimental evidence has shown that the statins increase bone formation and some observational studies have reported a lower risk of osteoporotic fracture in hypercholesterolemic patients treated with statins. However longitudinal studies on the effects of statins on bone turnover and on bone mass are lacking. The aim of the present study was to evaluate BMD and bone turnover changes in hypercholesterolemic women after one-year treatment with simvastatin. From a large number of patients who attended the outpatient clinics of the Institute of Internal Medicine at University of Siena for atherosclerotic risk evaluation, 30 consecutive postmenopausal hypercholesterolemic women (61.2±4.8 years) were selected and treated for 12 months with simvastatin 40 mg/day. Thirty normocholesterolemic age-matched postmenopausal women provided control data. We made sure (by a validated questionnaire given a 6-month intervals) that dietary calcium intake was stable and of at least 1200 mg/day during the study period. In all subjects, at baseline and at 3-month intervals, serum lipids, calcium, phosphate, total and bone alkaline phosphatase (TALP and BALP) and carboxy-erminal fragment of type I collagen (CTx) were measured in a fasting blood sample. At baseline and after 6 and 12 months bone mineral density was measured at lumbar spine (BMD-LS) and at femur (BMD-F) by DXA (Hologic QDR 4500). In simvastatin treated-group TALP and BALP significantly (P<0.05) increased by 9% and 16% and by 3.7% and 9.3%, respectively at the sixth and the twelfth month. Instead, serum CTx showed a weak increase over study period without reaching the statistical significance. In treated women BMD-LS and BMD-F increased by 1.1% and by 0.4% at month 6 and by 2.8% and by 1.1% at month 12. In controls BMD-LS and BMD-F at the end of the study period decreased by 1.1% and 1.2%, respectively. At month 12 the difference between controls and simvastatin-treated patients was significant (p<0.05) for both BMD-LS and BMD-F. In conclusion our results, although obtained from a small sample of subjects, suggest that in postmenopausal hypercholesterolemic women, 1-year treatment with simvastatin 40 mg daily is able to moderately stimulate bone formation and to induce an effect on BMD, which is significant in comparison with the control group.

M397

Discovery of Highly Selective EP4 Receptor Prostaglandin E2 (PGE2) Agonists Which Stimulate New Bone Formation and Restore Bone Mass in Ovariectomized Rats. K. O. Cameron*, B. A. Lefker*, D. T. Crawford*, P. DaSilvaJardine*, S. L. DeNinno*, W. A. Grasser, H. Z. Ke, B. Lu*, T. A. Owen, V. M. Paralkar, H. Qi, D. O. Scott*, D. D. Thompson, C. M. Tjoa*, M. P. Zawistoski*. Cardiovascular and Metabolic Diseases, Pfizer Global Research and Development, Groton, CT, USA.

PGE2 stimulates bone formation and increases bone mass and strength in pre-clinical animal models of bone loss. Of the four PGE2 receptor subtypes (EP1-EP4), EP2 and EP4 have been delineated as the two receptors responsible for PGE2's anabolic actions on bone. We sought to identify EP-4 selective agonists that would promote bone formation with minimal side effects. Our initial screens identified, CP-1, a mixed EP2/EP4 agonist (rEP2 IC50=27 nM, rEP4 IC50=219 nM) with good selectivity vs. other prostanoid receptors. When dosed subcutaneously at 10 mg/kg in an ovariectomized (OVX) rat model, CP-1 produced significant increases in trabecular bone density (+30%) as compared with vehicle-treated OVX controls when measured by peripheral quantitative computerized tomography (PQCT). Having confirmed that bone anabolic effects were achievable with a mixed EP2/EP4 selective agonist, we sought specific EP-4 subtype selective agonists to test whether systemic bone anabolism could be achieved with an EP4 selective agonist. High throughput screening led to the identification of CP-A, an EP4 selective agonist with reasonable potency (rEP2 IC50 = >3200 nM, rEP4 IC50 = 54 nM, EC50 for rEP4 cAMP production = 32.5 nM). Chemical optimization of CP-A led to the identification of a more potent EP4 agonist, CP-B(rEP2 IC50 = >3200 nM, rEP4 IC50=21 nM, EC50 for rEP4 cAMP production =13.2 nM). Administration (subcutaneously at 1, 3, 10, and 30 mg/kg) of CP-B in an osteopenic rat model (5 weeks post-OVX) showed dose dependent increases in total bone content (up to 32.5%), total density (up to 23.7%), cortical content (up to 57.7%), cortical thickness (up to 124%), and cortical area (up to 67%) as compared with vehicle treated OVX controls as measured by pQCT. In summary, we have identified potent, EP4 selective agonists which produce significant new bone in an osteopenic rat model. These agents have potential clinical utility for the treatment of skeletal disorders such as osteoporosis.

Disclosures: ***K.O. Cameron****, Pfizer 3.*

M398

Evidence of Altered Bone Homeostasis in Patients after Gastric Bypass Surgery. A. M. Novy*[1], H. J. Sugerman*[2], R. W. Downs[1], E. J. DeMaria*[2], J. M. Kellum*[2], L. G. Wolfe*[2], D. M. Biskobing[1]. [1]Medicine, Virginia Commonwealth University, Richmond, VA, USA, [2]Surgery, Virginia Commonwealth University, Richmond, VA, USA.

Surgery for obesity has become accepted therapy since it results in long-term weight loss in the majority of patients. In the past, jejunoileal bypass was known to be associated with fat soluble vitamin deficiencies such as vitamin D which may lead to osteomalacia. Current surgeries have been developed to produce less malabsorption in hopes of avoiding nutritional deficits. However, little data has been published on long-term effects on calcium homeostasis and bone status of these patients. Over the last 20 years, more than 2100 patients have undergone proximal gastric bypass surgery (PGBP) at the Medical College of Virginia. We reviewed the patient database for evidence of bone disease occurring at post-operative years one and five. 198 patients (182 women and 16 men) had laboratory follow-up at year one and year five. Overall, the frequency of hypocalcemia rose from 11% of patients at year one, to 23% at year five, (p=0.0039). In women, the frequency of hypocalcemia rose from 10% at year one to 20 % at year five, and corrected serum calcium levels decreased from 9.39 mg/dl +/-0.03 at year one to 9.18 mg/dl +/-0.03 at year five, (nl 8.9-10.5mg/dl, p<0.0001). In men, the frequency of hypocalcemia rose from 12.5% at year one to 62.5% at year five, (p<0.0005), and corrected serum calcium levels decreased from 9.46+/- 0.23 mg/dl at year one, to 9.02+/- 0.39 mg/dl at year five, (nl 9.2-10.7mg/dl, p<0.0001). The frequency of hypophosphatemia was 1.3% at one year and 3.8% at 5 years, (p=0.0170). The average serum phosphorus decreased from 3.87 +/- 0.05 mg/dl at year one to 3.57 +/-0.05 mg/dl at year five, (nl 2.5-4.6 mg/dl, p<0.0001). Alkaline phosphatase was elevated in 12% at year one and elevated in 20% at year five, (p =9.460E-08). The average serum alkaline phosphatase rose from 88.27 +/- 2.42 mg/dl at year one to 96.77 +/- 3.25 mg/dl at year five, (nl <115,p<0.0001). The average serum magnesium decreased slightly but was not clinically significant. These results show that hypocalcemia becomes more prevalent over time in patients after GBP surgery. Neither 25-OH vitamin D nor PTH are

routinely measured in GBP patients and were therefore not available. However, the decrease in calcium in conjunction with phosphorus suggests a nutritional deficiency of either calcium or vitamin D, or both. Over many years, this may result in deleterious effects on bone which could increase fracture risk. Further investigations of calcium metabolism in patients after PGBP surgery will be necessary to further characterize effects on bone to establish appropriate guidelines for follow up, treatment and prevention.

M399

Gastric Bypass Surgery for Morbid Obesity Leads to Increased Bone Turnover. P. S. Coates[1], R. Satyawadi*[2], M. H. Fernstrom*[1], P. R. Schauer*[1], S. L. Greenspan[1]. [1]University of Pittsburgh Medical Center, Pittsburgh, PA, USA, [2]Mercy Hospital, Pittsburgh, PA, USA.

Obesity is a growing problem worldwide associated with increased morbidity and mortality. Roux-en-Y gastric bypass achieves long-term weight loss of 60-70% excess body weight, and many morbidly obese patients are opting for this procedure. Very little is known about the effects of this surgery and subsequent weight loss on calcium metabolism and the skeleton. To examine these effects, we compared patients who underwent prior gastric bypass surgery with morbidly obese patients before the procedure. Age, gender and menopausal status were similar between the two groups. The postoperative patients had lower weight and BMI. Calcium and vitamin D intake was significantly higher in the postoperative group, reflecting prescription of supplements. However, 24-hour urinary calcium was not increased in these patients, suggesting that calcium absorption may be impaired after gastric bypass. Although vitamin D levels were higher in the postoperative patients, levels remained low normal and PTH levels remained high in this group, suggesting continuing vitamin D insufficiency. Markers of bone turnover were significantly increased in the postoperative patients. Radius BMD and heel ultrasound BUA did not differ between the pre-and post-operative patients. These results suggest that obese patients are at risk of reduced calcium absorption and increased bone loss after gastric bypass surgery. Longitudinal studies are needed to further characterize the effects of this procedure on the skeleton.

	Pre-operative	Post-operative
N	28	25
Mean ± SD Age	49 ± 10	51 ± 8
Weight	135 ± 20	92 ± 16***
BMI	49 ± 7	31 ± 5***
Calcium intake (mg/day)	1227 ± 1150	1783 ± 714*
Vitamin D intake (IU/day)	400 ± 257	693 ± 396**
24 hour urine calcium (mg)	193 ± 105	160 ± 94
25-hydroxy vitamin D (ng/ml)	17 ± 7	22 ± 7*
PTH (pg/ml)	68 ± 39	67 ± 26
Urine NTX (nM BCE/nM Cr)	24 ± 12	91 ± 40***
Osteocalcin (ng/ml)	12 ± 7	23 ± 7***

*p<0.05, **p<0.01, ***p<0.001 compared to preoperative group.

M400

Intravenously Pamidronate in Bone Lesions of Gaucher`s Disease. Z. Man*, N. Chamoles*, A. Copquin*, J. Roel*, J. Falcon*. Centro TIEMPO, Universidad Favaloro, Buenos Aires, Argentina.

The pure bone form of Gaucher´s Disease is not so frequent and its processing is not clear. A man of 44 years old, that 10 years ago was diagnosed with idiopathic osteoporosis, after a fracture of right femoral neck caused by a minimum trauma, received processing with oral pamidronate (APD) (300 mg/d) and later, oral alendronate 10 mg, during this years, with few changes in the BMD. Two years ago, he presented aseptic necrosis in left femoral neck and a few months later a crisis of severe bone pain with the finding by MNR of a litic injury in distal left femur. He was treated with 90 mg of APD (IV infusion of 250 cc of dextrose 5% in two hours) and very high doses of morphine. A biopsy revealed Gaucher´s Disease. The existence of this pathology was certified itself with the seric determination of kitotriosidase 70.0 mU/ml (n v 0,05 to 1) and the reduction of the beta glucosidase in sanguineous leukocytes. The genotype was N37OS/N370S that corresponds to a heterozigote for the mutant gene with low enzymatic level, being the only member of his family who suffers this disease. The only affection of Gaucher´s Disease in this patient, were bone lesions. Then, he received processing with alglucerase (CEREDASE - Genzyme) (extracted enzyme of human placenta) during six months and afterwards, and still in treatment, with imiglucerase (CEREZYME- Genzyme) (recombinant enzyme) every 15 days (60 U/kg = 500 U). By digestive intolerance to oral alendronate, it was decided to administer 60 mg APD IV in quarterly form. At the end of the first year of treatment, the BMD increased (3% in spine and 5% in hip), being one of the most important results the fact that he didn`t display again a new crisis of bone pain. **Conclusion:** We considered that 60 mg APD IV every 3 months constitutes a valid alternative in Gaucher`s Disease with bone commitment and digestive intolerance to other bisphosphonates.

M401

Effects of Bacteroides forsythus on MG-63 Cell Cultures In Vitro. P. M. Loomer, R. Smith*, C. Hoover*. Stomatology, University of California, San Francisco, San Francisco, CA, USA.

Specific oral microorganisms have been implicated in the etiology and pathogenesis of periodontal diseases. Bacteroides forsythus, an oral bacterium, is considered to a putative periodontal pathogen largely based on data showing its presence in elevated proportions at diseased sites. However, the specific effects of its metabolic products on cells of the periodontium, including osteoblasts, are less known. Therefore, this study was undertaken to evaluate the effects of extracts of B. forsythus on osteogenesis in vitro. Cultures of B. forsythus were grown under anaerobic conditions and sonicate extracts were prepared after 7 days. Sonicate concentrations of 0, 0.01, 0.1, 1, 10, 100 ug/ml tissue culture media were subsequently added to confluent cultures of MG-63 cells, a human osteosarcoma cell line. The effects of bacterial extracts on parameters of osteogenesis were evaluated at days 2, 4, 6 and 14 by measuring alkaline phosphatase (AP) activity and mineral production (inorganic phosphate and calcium.) The results showed the extracts stimulated bone formation at concentrations of 10 and 100 ug/ml. AP activity increased 15-fold in 2-day cultures ($p<0.001$), 6-fold in 4-day cultures ($p<0.001$) and 2.7-fold in 14 day cultures ($p<0.001$), in comparison to controls. Comparable results were found for mineral content. Extracts from Porphyromonas gingivalis, another putative periodontal pathogen, showed similar increases in osteogenic activity of MG-63 cells. While previous studies have shown that extracts of these microorganisms inhibit bone formation in other in vitro culture systems, these results show they may also play a role in stimulating bone formation. This suggests that these bacteria exhibit both inhibitory and stimulatory effects on bone formation and thus may play a role in bone remodeling in periodontal diseases.

M402

Effect of Growth Hormone (GH) on Cortical Bone Remodelling in Adult GH-deficiency - A 12 Month Double-blind Placebo Controlled Study. K. E. Koroma*[1], E. M. Hauge[2], H. Brockstedt*[3], J. S. Christiansen*[4], T. B. Hansen*[1], F. Melsen*[2], C. Hagen*[1], K. Brixen[1]. [1]Dept. of Endocrinology, Odense University Hospital, Odense, Denmark, [2]Dept. of Pathology, Aarhus University Hospital, Aarhus, Denmark, [3]Dept. of Endocrinology, Aarhus University Hospital, Aarhus, Denmark, [4]Dept. of Pathology, Rikshospitalet, Oslo, Norway.

Fracture incidence is increased and bone mineral density (BMD) reduced in patients with adult-onset GH-deficiency (GHD). Short-term GH-treatment decreases whereas long-term treatment increases BMD. It has been suggested that this initial decrease in BMD is explained by an increase in the remodelling space.(1)In this study we examined the changes in cortical bone remodelling. Twenty-nine patients with adult-onset GHD, aged 21-61 (mean 45.5)years (19 men and 10 women) were randomized to treatment with GH (Norditropin, Novo-Nordic, Denmark)2.0IU/m2/day or placebo. None of the patients had previous acromegaly. Substitution with other hormones than GH were continued unchanged throughout the study. GHD was defined as a maximal GH-peak of < 10 mg/l during insulin-tolerancetest (blood glucose < 2.0 mmol/l). Bone biopsies were obtained from the iliac crest before and after 12 months of treatment. Twenty-four paired biopsies were available for determination of cortical porosity (Ct.po),absolute cortical width (A.Ct.Wi), quiscent(QSi), formative (FSi),and eroded (ESi) cortical osteons, core width (C.Wi), fractional cortical width (F.Ct.Wi)and osteoid width (O.Wi). Moreover osteonal diameter (On.Dm), wall width (W.Wi), Haversian canal width (H.Ca.Dm) in quiscent (q) and formative (f) osteons, respectiveley, were measured as previously described (2). Results are shown intable 1. QSi decreased ($p=0.04$) and FSi tended to increase ($p=0.07$).1)Brixen, K et. al. J. Bone Miner. Res. 2000;15:293-300 2)Brockstedt H et. al.:Bone 1996;18:67-72

	Placebo (n=12)		GH-treatment(n=12)	
	Before after	After	Before and after	After
Ct.po(%)	5.8 (0.6)	8.0 (0.6)	5.6 (0.6)	7.3 (0.9)
A.Ct.Wi (mm)	1.5 (0.1)	1.3 (1.0)	1.1 (0.1)	1.1 (0.1)
QSi (%)	88.9 (2.6)	89.7 (1.8)	91.9 (2.7)	85.7 (2.0)(*)
FSi (%)	8.9 (2.7)	7.6 (1.8)	6.3 (2.5)	11.0 (1.4)(*)
ESi(%)	2.2 (0.6)	2.6 (0.8)	1.8 (0.5)	3.3 (1.0)
On.Dm (um)(q/f)	199 (11)/201 (11)	183 (8)/189 (12)	179 (7)/185 (19)	179 (7)/178 (7)
H.Ca.Dm (um)q/f)	74 (4)/54 (8)	71 (3)/47 (5)	68 (3)/ 51(9)	69 (3)/47 (2)
W.Wi (um) (q/f)	53 (3)/65 (4)	43 (3)/64 (7)	46 (3)/61 (7)	53 (3)(**)/56 (4)
O.Wi (um) (f)	17 (4)	10 (1)	15 (4)	11 (1)

M403

Mesenchymal Stem Cell Therapy for Osteoarthritis. F. Barry*[1], M. Murphy*[1], K. Kavalkovich*[1], R. Young*[1], B. Koller*[2], A. Laib*[2], R. Kapadia[2], R. A. Dodds*[1]. [1]Osiris Therapeutics, Baltimore, MD, USA, [2]Scanco Medical AG, Bassersdorf, Switzerland.

Meniscal injury significantly increases the risk of developing osteoarthritis (OA), a joint disease involving articular cartilage degeneration, and thickening of the subchondral and trabeculae bone. Mesenchymal stem cells (MSCs) differentiate to tissues such as bone, cartilage and tendon. In this study the ability of allogeneic MSCs to impact meniscal regeneration and influence OA progression in a goat model was studied. Bone marrow-derived MSCs were injected into the joint as a suspension in hyaluronan (HA). The MSCs were retrovirally transduced to express green fluorescent protein (GFP). 20 goats, unrelated to the donors, were randomized into 4 groups (n=5/group) and total unilateral medial meniscectomy was performed. After 1 or 6 weeks the operated joint was treated by injection of 1 x 10^7 MSCs in 5 ml of HA (4 mg/ml) or HA alone. Two weeks post-surgery, the goats were exercised daily until sacrifice (12 weeks). Knee joints were macroscopically and histologically assessed for meniscal regeneration and cartilage degradation. 3D microCT analysis determined changes to subchondral and trabecular bone structure in the central medial condyle. Parameters quantified were: subchondral bone thickness (Sb.Th), BV/TV, Tb.N, Tb.Th, Tb.Sp and ConnDens. Results were analyzed by ANOVA and ANCOVA (including contralateral femurs). Gross evaluation demonstrated regenerated neomeniscal tissue associated with the medial compartment in MSC treated animals. In goats injected with cells 1 week post-surgery the amount of neomeniscal tissue was significantly larger compared to knees treated with HA alone. Neomeniscal tissue sections demonstrated a dense, cellular matrix containing GFP positive cells (peripheral) positive for type I and II collagen and proteoglycan. Analysis of the cartilage on the medial femoral condyle and tibial plateau determined less degradation in cell-treated joints. Menisectomy caused thickening of the subchondral and trabecular bone in the medial femoral condyle. For the ANCOVA, the covariate was significant for Sb.Th ($p<0.002$), ConnDens ($p=0.013$), Tb.N ($p<0.005$) and Tb.Sp ($p<0.003$). The effect of MSC treatment compared to treatment with HA alone approached statistical significance for Tb.N ($p=0.066$) and Tb.Sp ($p=0.07$ ANOVA); there was no significant effect on Sb.Th. Tb.N was lower and Tb.Sp was higher in MSC-treated animals. The effect of time of administration was not significant for any parameter. Injection of allogeneic MSCs into OA joints resulted in regeneration of meniscus with concomitant chondro- and osteoprotective effects. This data suggests the therapeutic benefit of injected MSCs in the OA joint.

M404

The Kidney and the Calcium Endocrine System of One-year-old Dahl Salt-sensitive and Salt-resistant Male Rats. S. B. Arnaud[1], S. Cephas*[2], A. De Paoli*[3], P. Sayavongsa*[2], S. Locklear*[1], M. Thierry-Palmer[2]. [1]Life Sciences Division, NASA Ames Research Center, Moffett Field, CA, USA, [2]Dept of Biochemistry, Morehouse School of Medicine, Atlanta, GA, USA, [3]Pathology, IDEXX Veterinary Services, Sacramento, CA, USA.

Dahl salt-sensitive (S) rats become hypertensive with age when fed standard rat chow (J Lab Clin Med 98:599, 1981; Biol Trace Element Res. 31:199, 1991). To determine the effect of age on the kidney and the calcium endocrine system we maintained Dahl S and salt-resistant (R) rats on standard diets (1% salt) for 12 months in vivarium cages. We then divided S and R rats into low (0.3%) and high (2%) salt diet groups and transferred them to metabolic cages for periodic urine collections 3 weeks before euthanasia. Renal histopathology, urine volume, calcium, sodium, protein, and creatinine clearance were compared in S and R rats. Plasma parathyroid hormone (PTH) concentration was assayed by ELISA, 25-hydroxyvitamin D (25-D) and 24,25-dihydroxyvitamin D (24,25-D) concentrations by protein binding assay, and 1,25-dihydroxyvitamin D (1,25-D) concentration by receptor binding assay. Renal changes in 11 S rats were characteristic of moderate to severe nephrosclerosis associated with hypertension; 14 R rats showed minimal changes consistent with the nephropathy of aging. Differences in dietary salt groups were confined to urinary sodium and 1,25-D; both higher in the high than low salt groups. Estimates of renal function revealed mean (±SD) urine volumes, calcium, and protein to be higher and creatinine clearances lower (108±41 vs. 152±33 ml/min/1/73m^2, $p<0.01$) in S compared with R rats. Salt sensitivity significantly affected total plasma calcium (2.22±0.13 vs. 2.35±0.03 nmol/L, $p=0.002$), 25-hydroxyvitamin D (6±3 vs. 27±10 nmol/L $p<0.001$), 24,25-dihydroxyvitamin D (1.4±0.7 vs. 19±15 nmol/L, $p=0.002$), and parathyroid hormone (316±94 vs 109±41 pg/mL, $p<0.001$). The modest decrease in plasma calcium, three-fold increase in PTH, low 25-D and 24,25-D but normal 1,25-D, are the principle differences in the calcium endocrine systems of aged S and R male rats. In spite of long term normal salt diets, S rats develop moderate to severe nephrosclerosis and impaired renal function with age. This is associated with changes in the calcium endocrine system of S rats that are characteristic of nutritional vitamin D deficiency. The metabolic processes that lead to apparent vitamin D deficiency remain to be elucidated.

M405

Beneficial Impact of Calcium Supplementation on Gestational and Lactational Bone Loss: A Case Study. K. Kent[1], B. Wipfler*[2], R. Marcus[2]. [1]Musculoskeletal Research Laboratory, Stanford University and VA Medical Center Palo Alto, Menlo Park, CA, USA, [2]Stanford University, Stanford, CA, USA.

We report here the experience of a 35 year old, highly physically active, Caucasian densitometry technician with documented bone loss from spine, hip and whole body (DXA, Hologic 1000W) during each of 2 prior episodes of pregnancy and lactation. When a 3rd pregnancy was diagnosed, she increased dietary calcium to 800-1100mg/d and instituted calcium supplementation, 1500 mg/d as carbonate (ViactivTM). When this pregnancy was determined to be twins, her physician insisted she terminate all recreational exercise and also restricted her to bed rest for the last 9 weeks of gestation. BMD was measured 10d post-delivery of healthy full-term girls and again after 11 months of breast-feeding. BMD losses during the two earlier, non-supplemented, pregnancies were 10.4 and 6.8% (spine), 10% (hip), and 3.3 and 1.9% (Whole Body). Given twin pregnancy and profoundly decreased activity, even greater loss was predicted for the 3rd pregnancy. Contrary to expectation, gains in BMD of 4.1, 2.7, 4.9, and 1.5% (spine, total hip, femoral neck, Whole Body) were observed. Body weight and composition did not differ from values after the second pregnancy. After 11 months of lactation, despite continued calcium supplementation and restoration of exercise, BMD decreased by 11.6, 3.4, 5.7, and 3.6%, giving net losses of 8, 0.8, 1.1, and 2.2%. These did not differ from those of her earlier single infant delivery and lactation periods. These findings suggest that increased calcium supplementation effectively maintains BMD during pregnancy despite extraordinary fetal demands and reduced physical activity. In addition, supplemental calcium appears to have partially mitigated the increased bone loss expected from nursing two infants.

M406

Myostatin Gene Polymorphisms and Age-related Sarcopenia in the Italian Population. L. Masi[1], A. Gozzini*[1], A. M. Corsi*[2], A. Tanini[1], A. Falchetti*[1], M. L. Brandi[1], L. Ferrucci*[2]. [1]Department of Internal Medicine, University of Florence, Florence, Italy, [2]Department of Geriatric, I. N. R. C. A., Florence, Italy.

It has been hypothesized that the genetic variation of myostatin, a TGF-beta superfamily member, plays an important role in age-associated sarcopenia. Variants of the human myostatin gene have been originally reported in literature (Ferrell RE et al. Genomics 1999). Two polymorphisms of the encoding region, specifically an A to G change at codon 55 in the exon 1 (A55T) and an exon 2 (K153R), have been described. In particular, the K153R polymorphism was reported to be overrepresented in persons who did not show substantial increments in muscle mass after strength training. These findings were confirmed by Seibert MJ et al (J Am Geriatr Soc 2001), who found that older African-American women with an 153R allele tended to have low muscle strength. Using data from the InCHIANTI project, a large population-based epidemiological study of the causes and course of mobility/disability in older persons, we tested the hypothesis that myostatin polymorphisms may account for part of the variability in muscle mass and strength that is often found in older persons. From the original cohort, we selected a random sample of 450 subjects (mean age: 69.5+15.2 years, range: 22-96 years, 189 men and 261 women) and searched for myostatin gene polymorphisms. The A to G missense substitution at residue 55 in the exon 1 (A55T) was analyzed by PCR amplification followed by AluI enzymatic digestion and A to G substitution in exon 2 was studied by PCR amplification followed by direct sequencing in 120 DNA samples. Of the 450 DNA samples only two individuals showed an A55T polymorphism. Among the 120 DNA samples, analyzed for K153R variant, 6 K153R heterozygous, 1 R153R and 113 K153K homozygous individuals have been found. The presence of a 153R allele was associated with lower muscle strength (153R+: 18.8+2.2 Kg; 153R: 26.5+ 1.0 Kg; P=0.05). Our preliminary findings confirm those reported by Seibert et al. and suggest that the K153R genotype may be associated with accelerated sarcopenia. We are currently characterizing the entire InCHIANTI population for the K153R polymorphism.

M407

Association of Oral Exostosis with Higher Bone Mineral Density of Elderly Women. T. Yoda*[1], M. Yamaguchi*[1], H. Amano[2], H. Orimo[3], T. Hosoi[4]. [1]Department of Dentistry and Oral Surgery, Tokyo Metropolitan Geriatric Medical Center, Tokyo, Japan, [2]Department of Pharmacology, School of Dentistry Showa University, Tokyo, Japan, [3]Tokyo Metropolitan Geriatric Medical Center, Tokyo, Japan, [4]Endocrinolgy Section, Tokyo Metropolitan Geriatric Medical Center, Tokyo, Japan.

Osteoporosis is a systemic pathological condition, in which bone formation is overcome by bone resorption. On the other hand, oral exostosis, also prevalent in the elderly, is a disease of unknown origin and may be caused by an interplay of genetic and environmental factors. Then we hypothesized that the patients with oral exostosis may have higher bone mineral density (BMD) compared to those without exostosis. We recruited randomly the patients who visited the dental and oral surgery department of Tokyo Metropolitan Geriatric Medical Center (average age 77.5 years). We examined exostosis by a digital examination and measured the extent of elevation from the bone surface using study models. BMD of lumbar spine, femoral neck, and radius was measured by dual-energy X-ray absorptiometry (DXA, DPX-L IQ, Lunar Co.). Z score was used to analyze the data of BMD, which is a deviation from the weight-adjusted average BMD of each age. We compared the BMD in z scores between the subjects with palatal or mandibular exostosis and those without exostosis. As a result, the female subjects with palatal exostosis (n=9) had higher BMD than those without (n=24) at femoral neck (0.671+0.53 vs. 0.129+0.78, $p=0.03$) but not at lumbar spine and radius. The female subjects with mandibular exostosis (n=4) had higher lumbar spine and femoral neck BMD than those without (n=24) (1.225+ 1.15 vs.-0.529+1.01, $p=0.02$, 1.000+0.73 vs. 0.122+0.66, $p= 0.03$, respectively). On the other hand, no association was found between the presence of oral exostosis and radius BMD. There was not any association between oral exostosis and BMD measurements in male patients. Our results suggest that common mechanisms may increase the BMD of the elderly and cause oral exostosis. The effects of exostosis on BMD were restricted to the so-called loading bones, spine and femur. We speculate that the pathophysiology of oral exostosis may reflect the higher sensitivity to the mechanical stress resulting in excessive bone formation. Elucidation of the molecular mechanisms in oral exostosis would provide us a novel way for the prevention and treatment of osteoporosis.

M408

Circulating Levels of Fetal Fibronectin Correlate with the Decrease in Markers of Bone Formation in Non-Alcoholic Liver Disease. I. A. Nakchbandi, P. Feick*, A. Geursen*, M. V. Singer*. Medicine II, University of Heidelberg at Mannheim, Mannheim, Germany.

Hepatic osteodystrophy contributes significantly to the decrease in the quality of life of those affected. Previous research has established that hepatic osteodystrophy results mainly from decreased bone formation. The production of the cellular isoforms of fibronectin is markedly elevated in hepatocytes and stellate hepatic cells treated with toxins. It is known that the interaction between osteoblasts and matrix fibronectin is required for osteoblast differentiation, and that inhibitors of this interaction such as fragments encompassing the RGD sequence result in decreased osteoblast differentiation. We therefore hypothesized that an increase in cellular fibronectin (with defining domains close to the RGD sequence) in patients with autoimmune liver disease will inhibit the interaction between osteoblasts and matrix fibronectin and result in decreased osteoblast differentiation. We examined cellular fibronectin and osteocalcin in the blood of 20 patients with autoimmune liver disease without bilirubin elevation or vitamin D deficiency and compared them with 20 age-, sex-, BMI-, and menopausal age-matched controls. We found a statistically significant negative correlation between fetal fibronectin (by ELISA) and osteocalcin in the whole group as well as in the patients (all subjects: r= - 0.382, p<0.05; patients: r= - 0.488, p<0.05). We further found that circulating fetal fibronectin was elevated in patients as compared to controls albeit not statistically significantly so. (Results are expressed as Mean±SEM, patients: 4.0±0.56 ug/ml, controls: 3.0±0.22 ug/ml, p=0.14). Based on these data, we propose that the increase in fetal fibronectin production and release in the circulation directly contributes to the decrease in bone formation seen in autoimmune liver disease.

M409

Biochemical, Densitometric and Histomorphometric Changes in an Experimental Model of Uremic Bone Disease: Possible Beneficial Effect of Bisphosphonates. S. N. Zeni[1], A. Tomat*[1], A. Gamba*[2], P. Mandalunis*[3], M. C. De Grandi*[1], J. Somoza*[1], S. Friedman*[2]. [1]Sección Osteopatías Médicas, Hospital de Clínicas, Buenos Aires, Argentina, [2]Cátedra de Bioquímica General y Bucal, Facultad de Odontología, Buenos Aires, Argentina, [3]Cátedra de Histología. Facultad de Odontología., Universidad de Buenos Aires, Buenos Aires, Argentina.

Rats with reduced renal mass are used as a model to assess pathophysiological aspects of bone metabolism in chronic renal failure. Bisphosphonates (BPs) are potent antiresorptive agents used successfully in several bone diseases associated with high bone resorption. The present experimental study was undertaken to determine changes in bone makers, bone mineral density (BMD) and histomorphometric parameters in rats with moderately impaired renal function. The effect of olpadronate (OPD) was also evaluated. Sixteen male Wistar rats, aged approximately 100 day old were 2/3 nephrectomized and divided into two groups. After 1 week (To), one group received placebo (Nx) (n=8) and the other, 16 ug OPD/100 g rat (Nx+ODP) (n=8), both, intraperitoneally once weekly for 4 weeks (Tf). A group of aged-matched SHAM rats (n=8) served as control (C). At To and Tf, BMD (Lunar DPX), blood and 24hs-urine samples were assayed. The tibia was evaluated histomorphometrically at Tf. At the end of the experimental time: serum calcium and phosphorus were significantly higher in the Nx group than in Nx+OPD and C rats; Deoxypyridinoline/Creatinine ratio (X±DS) was similar in Nx and C groups (1692±141 vs. 1661±318 nM/mM) but Nx+ODP rats attained the significantly lowest value (542±99nM/mM, p<0.0005). OPD treatment prevented the 21% decrease in tibia BMD observed in Nx rats. During the study, tibial BMD increased 8% in C group (CV=4%) compared to a 6% increase in Nx+OPD group (ns). Histomorphometrical studies showed the highest trabecular bone volume in Nx+OPD treated group. TRAP positive cell number was significantly higher in Nx compared to Nx+OPD rats (p<0.05). Conclusions: Although further consideration is necessary, bisphosphonates like ODP, may provide an attractive tool to manage high bone turnover associated to renal disease.

M410

Bone Mineral Density After Renal Transplantation: Implications For Prophylaxis. E. A. O'Shaughnessy*, D. C. Dahl*, B. L. Kasiske*, C. L. Smith. Division of Nephrology, Hennepin County Medical Center, Minneapolis, MN, USA.

Most studies showing a loss of bone density after renal transplantation have given mean values for the population. Since some have advocated giving all patients prophylactic bispohosphonates to prevent bone loss, we decided to examine individual logitudinal data to understand better the significance of universal prophylactic treatment. We examined data from 18 patients (12 men and 6 women) who received BMD studies as part of the transplant protocol. The protocol called for patients to receive a BMD within one month of transplant and again at 6 months. From April, 2000 through April, 2001 23 out of 96 patients fulfilled this protocol. Five female patients were on estrogen at the time of transplant and were excluded leaving 18 patients. All but one had been on dialysis (average 28 months) and none had had a prior transplant. The BMD at the lumbar spine (LS) and proximal femur (trochanter and femoral neck) were measured with DEXA. Osteopenia (OPe) and osteoporosis (OPo) were defined by the WHO criteria. Reproducibility in our lab is such that a 3% change at the LS and 6% at the femur are significant. At the lumbar spine baseline values showed 11 patients to be normal, 5 with OPe, and 2 with OPo. At 6 months, 9 patients (50%) had lost >3% of bone density. Five of these patients were within the normal range at baseline and remained in this category. One patient declined from OPe to OPo. Three patients increased their bone density and 6 remained stable. At the trochanter 5 patients were normal, 10 OPe, and 3 OPo. At 6 months 3 lost >6%, 1 gained and 14 remained stable. One patient changed from OPe to OPo. At the femoral neck 5 patients were normal, 13 had OPe and 0 had OPo. At 6 months 5 patients lost >6% with only one patient changing to OPo. Thirteeen patients had stable BMD. There were two fractures in this group of 18 patients and both of these could be identified as being at increased risk with the baseline study. The majority of renal transplant patients are not OPo at 6 months. An individualized approach based on baseline and followup BMD studies may be preferable to routine prophylaxis.

M411

Increased In Vitro Stimulation of Osteoblastic Cells in Non-Azotemic Nephrotic Syndrome (NS). M. Freundlich*[1], E. Alonzo*[2], E. Bellorin-Font*[2], J. R. Weisinger*[2]. [1]Department of Pediatrics, University of Miami, Miami, FL, USA, [2]Division of Nephrology, Hospital Universitario de Caracas, Caracas, Venezuela.

Diminished bone mass and altered bone histology have been reported in patients with NS even when GFR is normal. However, the osteomalacia and hyperparathyroidism noted by some investigators in adults and by us in children seldom correlate with the prevailing serum concentrations of PTH and vitamin D metabolites. Since other circulating factors affecting bone remodeling may be present in these patients, we cultured a normal human osteoblast (OB) cell line (NHost) in the presence of sera (N=27) obtained from 15 children, age 9.2±5.4 yr., with NS [urinary protein/creatinine (up/c) 4.2 ± 8.5 mg/mg, normal < 0.2] and normal GFR (127±27 ml/min/1.73 m2), and 4 normal controls. OB were incubated for 24 or 48 hours in the presence of increasing concentrations of sera (0,10 and 20%). Alkaline phosphatase (ALP) activity was determined in cell lyzates using nitrophenylphosphate as the substrate. Results are expressed as units of enzymatic activity per L per mg protein. ALP activity obtained from OB cultures in the presence of NS sera was increased when compared to OB incubated with normal control sera (11,826±13,889 vs 218±132, and 12,011±14,475 vs 764±865, for incubations with 10% and 20% serum, respectively). In 6 NS patients studied prospectively during both relapse and remission, ALP activity in remission declined by 33 ± 48% from relapse values. Furthermore, there was a significant correlation between up/c and ALP activity (r= 0.5, p<0.05) throughout both clinical stages. Treatment with corticosteroids did not affect significantly ALP activity (9,098±11,655 vs 7,085±9,94, before and during corticosteroid treatment, respectively). Neither serum bone-specific alkaline phosphatase nor osteocalcin concentrations correlated to ALP activity. Slot-blot of cell lyzates demonstrated increased RANK-L expression during relapse of the NS with decreased expression during the remission period. In summary, serum from NS patients increased human OB activity in vitro which correlates with the degree of proteinuria. These observations suggest that OB activation may play a role, independent of corticosteroids, in the pathogenesis of the bone alterations observed in patients with NS and normal GFR.

M412

Spectrum of Renal Bone Disease and Diagnostic Value of Biochemical Markers in ESRF. A. R. J. Bervoets*[1], G. Spasovski*[2], G. J. S. Behets*[1], M. E. De Broe[1], P. C. D'Haese*[1]. [1]Nephrology-Hypertension, University of Antwerp, Antwerp, Belgium, [2]Nephrology, University of Skopje, Skopje, The former Yugoslav Republic of Macedonia.

We assessed the spectrum of renal bone disease and the diagnostic value of various biochemical markers in an unselected population of 84 Macedonian patients with end-stage renal failure (ESRF) from one geographical region just before entering a dialysis programme. None of the patients took vitamin D whilst the only phosphate binder used in this population was calcium carbonate (70%). In all patients we performed a bone biopsy for histological and histodynamic examination. Bone histology was correlated with several biochemical serum markers of bone turnover. Aluminum (Al) and strontium (Sr) levels in serum and bone were not elevated. 38 % of the patients still had normal bone histology, 23 % had adynamic bone disease (ABD), 18 % manifested a mixed lesion, 12 % showed osteomalacia (OM) and only 9 % presented with hyperparathyroidism (HPTH). Patients in the group of OM tended to be older, whilst patient characteristics associated with ABD were male gender, later referral and diabetes. There was no difference in underlying renal diagnosis. Routine blood analysis and serum creatinine did not differ between groups. Significant (p<0.005) differences between groups were noted for some biochemical markers of bone turnover: intact parathyroid hormone (iPTH), total and bone alkaline phosphatase (TAP and BAP) and osteocalcin (OC). We could not find a difference for (deoxy)pyridinolines. For the diagnosis of ABD versus all other groups of ROD, OC had the best diagnostic performance showing a sensitivity of 83 % and a specificity of 68 % at a cut off value of 41.0 ng/l. By combining both these parameters the specificity could be increased up to 89 %. ABD and normal bone taken as one group versus all other types of ROD could best be detected by BAP and TAP, showing sensitivities of 72 and 88 % and specificities of 76 and 60 % at a cut off value of 25 U/l and 84 U/l respectively. As a conclusion, data of the present study show 62 % of the ESRF patients to have an abnormal bone histology before entering a dialysis programme. In the absence of Al or Sr overload the relatively high prevalence of OM is rather surprising. Although bone biopsy remains the golden standard for diagnosis of bone disease, OC, TAP and BAP can contribute to the non-invasive diagnosis of ABD/normal bone versus the other types of renal osteodystrophy.

M413

Development of Lumbar Bone Mineral Density in the Late Course Following Kidney Transplantation. V. M. Brandenburg*[1], W. J. Fassbender[2], M. Ketteler*[1], J. Floege*[1], T. H. Ittel*[1]. [1]Dept. of Nephrology, University Hospital Aachen, Aachen, Germany, [2]Medical Dept. I, Endocrinology, University Clinic Frankfurt, Frankfurt am Main, Germany.

Rapid bone loss is a frequent finding early after kidney transplantation. Only limited data are available on the bone mineral density (BMD) in long-term kidney transplant recipients. In 26 unselected kidney transplant recipients (13 men, 13 women; mean age 45.3+/-12.3 years) serum biochemical markers of bone metabolism and the BMD at the lumbar vertebrae L2-L4 were prospectively evaluated in three serial examinations (E1, E2, E3; method: dual-energy X-ray absorptiometry). Examinations were performed at 47+/-2 months (E1), 59+/-2 months (E2) and 71+/-2 months (E3) after renal transplantation. All patients received standard dual or triple immunosuppression including prednisolone (median daily dosage 7.5 mg). Over the study period the mean lumbar BMD was significantly lower ($p<0.05$) than in sex-matched young controls: T-score was -1.43+/-1.49 (E1), -1.39+/-1.40 (E2) and -1.44+/-1.30 (E3). The BMD did not change significantly from E1 to E3 (delta BMD-0.5+/-5.9%). No significant gender-related differences in BMD or delta BMD were seen. Multiple regression analysis did not show significant correlations between delta BMD and biochemical parameters or prednisolone dosage. No new lumbar vertebral fracture occurred. The mean intact parathyroid hormone (iPTH) was 110.1+/-97.5 (E1), 121.0+/-102.7 (E2) and 134.5+/-128.6 ng/l (E3). Serum creatinine (CREA) was measured as 127+/-40, 127+/-42 and 128+/-62 µmol/l. 10 patients (38.5%) showed an increase of BMD from E1 to E3 (+5.7+/-3.2%), 15 patients (57.7%) showed a decrease of -4.7+/-3.2% ($p<0.0001$). Both groups were different in T-scores at E1 (-2.29+/-1 vs. -0.88+/-1.5); iPTH, CREA, vitamin D levels or prednisolone dosage were not significantly different. Lumbar BMD is reduced in long-term kidney transplant recipients. However, during our 24 months observation period, overall lumbar BMD remained stable.

M414

Predictors of Bone Mineral Density in Patients on Hemodialysis. G. El-Hajj Fuleihan[1], D. Zayour*[1], M. Daouk*[2], W. Medawar*[2], M. Salamoun*[2]. [1]Internal Medicine, American University of Beirut Medical Center, Beirut, Lebanon, [2]American University of Beirut Medical Center, Beirut, Lebanon.

Renal osteodystrophy is a universal complication of uremia, and renal failure patients are at risk for low bone mineral density (BMD) and fractures. Parathyroid hormone (PTH) plays a pivotal role in the pathophysiology of uremic bone disease. Histomorphometric studies suggest that the maintenance of PTH levels between two -four times the upper limit of normal is associated with the least prevalence of two common forms of osteodystrophy: osteitis fibrosa cystica, and adynamic bone disease. The purpose of this study was to investigate whether the above recommendation for PTH levels in dialysis patients corresponds to a more optimal BMD, with a special emphasis on diabetic versus non-diabetic subjects. Twenty-eight patients with chronic renal failure on hemodialysis had serial measurement of PTH levels, and BMD at the lumbar spine, hip and forearm. They were divided into three groups based on a mean PTH level over two years: <120 pg/ml, 120-250 pg/ml, >250 pg/ml. A substantial proportion of patients on dialysis had osteoporosis.

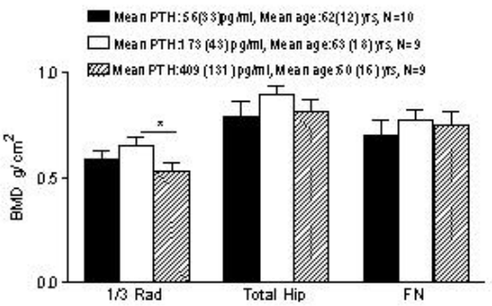

Predictors of BMD were gender, duration on hemodialysis, diabetes, and PTH levels less than 120 pg/ml (12.7 pmol/L) or greater than 250 pg/ml (26.5 pmol/L). Our study therefore supports the histomorphometry-based studies suggesting that the maintenance of intact PTH levels two-four times the upper limit of normal is associated with better skeletal health in uremic patients on hemodialysis.

M415

Effects Of Sevelamer on Bone Histology in Comparison with Lanthanum Carbonate in a Chronic Renal Failure Rat Model. G. J. S. Behets*, M. Gritters*, G. Dams*, M. E. De Broe, P. C. D'Haese*. Dept. of Nephrology - Hypertension, University of Antwerp, Wilrijk, Belgium.

Both lanthanum carbonate and sevelamer (Renagel ®) have recently been proposed as new phosphate binding agents. Previous studies have shown that high La2(CO3)3 doses (1000 and 2000 mg/kg/day) may lead to a mineralisation defect in CRF rats (5/6 nephrectomy), which was suggested to be due to the induction of a phosphate depletion, in combination with a disturbed vitamin D metabolism. In the present study, the effects of La2(CO3)3 on bone are compared with those of sevelamer. Sevelamer is a non metal-containing polymeric compound, which is virtually not gastro-intestinally absorbed and thus does not accumulate in bone. Twenty-one male Wistar rats underwent a 5/6 nephrectomy and were treated with sevelamer (500 or 1000 mg/kg/day), La2(CO3)3 (1000 mg/kg/day) or vehicle only by oral gavage during 12 weeks. At sacrifice, bone histology showed the development of an impaired mineralisation in 1 of 5 (20%) of the La2(CO3)3 treated animals, and in 4 of 7 (57%) of the animals treated with sevelamer at 1000 mg/kg/day. Vehicle and sevelamer at 500 mg/kg/day did not induce any mineralisation defect. During the 12-week loading period, a clear decrease in phosphaturia was noted in all treatment groups. Animals receiving La2(CO3)3 showed a statistically decreased phosphaturia already after 2 weeks of treatment. Sevelamer showed decreased phosphaturia after resp. 4 and 6 weeks of treatment with 1000 and 500 mg/kg/day. The hypophosphaturia was observed in the absence of any hypophosphatemia. Interestingly, 1,25-(OH)2 vit D was dose-dependently reduced in the sevelamer treated animals, whilst this was not the case for the La2(CO3)3 treated group. In conclusion, these results confirm our hypothesis that the previously observed mineralisation defect after treatment with La2(CO3)3 and in the present study with sevelamer is secondary to a phosphate depletion resulting from the pharmacological actions of the phosphate binding agents, rather than being due to a direct toxic effect of these substances on bone. Further investigations on the effects of sevelamer on vitamin D and bone metabolism are needed. Furthermore, these results demonstrate that in this animal model, phosphate depletion can occur despite normal serum phosphorus levels.

M416

Importance of the Bone in Severe Absorptive Hypercalciuria. H. J. Heller, J. E. Zerwekh, C. Y. C. Pak. Center for Mineral Metabolism and Clinical Research, UT Southwestern, Dallas, TX, USA.

Absorptive hypercalciuria (AH), a stone-forming condition in which calcium is excessively absorbed from the intestine, is paradoxically associated with low bone mass. We hypothesized that in patients with severe AH, bone formation is impaired and the relative excess bone resorption contributes to hypercalciuria. Each subject without other causes of bone loss underwent bone biopsy after tetracycline labeling. They were placed on a stone-prevention diet for 3 weeks followed by baseline inpatient evaluation on a constant metabolic diet. On the same diet, provocative tests were used to probe the relative contribution of intestinal calcium absorption (sodium cellulose phosphate 5 g with meals X 3 days; S) and bone resorption (alendronate 10 mg/d X 2 weeks; A) to urinary calcium. Age ranged from 40 to 53. Bone volume and connectivity were markedly decreased and out of proportion to the osteopenia demonstrated by bone mineral densitometry. Relative to the controls, we found impaired bone formation in AH patients. Bone resorption was also lower than controls but to a lesser degree. There was no evidence of osteomalacia in AH patients. The mean decrement in urinary Ca was greater after S (-128 mg/d) than after A (-6 mg/d). However, fasting urinary Ca fell with both agents- S (-63%), A (-38%). PTH rose more with A (+58%) than with S (+12%). Intestinal calcium absorption and 1,25-(OH)2 D tended to increase with A, and bone resorption markers decreased. Thus, although 24-h urine Ca did not change with A, it appears that the greater quantity of absorbed calcium replaced some of the calcium derived from the bone. We conclude that severe AH is associated with low bone formation and that treatment with A, by reducing fasting renal calcium while increasing intestinal calcium absorption, may improve calcium balance in the short term.\

Cancellous Bone Parameters	AH Man (n=1)	AH Premenopausal Women (n=2)	Controls (mean±SD)
BV/TV, %	9.4	16.3, 8.8	23.2±4.4
OV/TV, %	0.06	0.10, 0.01	0.32±0.19
Tb. Th, mcm	98	94, 84	133±22
OS/BS, %	3.4	7.4,0.7	12.1±4.6
Ob.S/BS, %	1.6	1.8,0.1	3.9±1.9
ES/BS, %	2.0	4.1,1.8	4.1±2.3
BFR/BS, mcm3/mcm2/yr	0.001	0.005,0.002	0.011±0.006

M417

Elevated 14-3-3 Protein in Proliferating Cells of Uremic Rat Parathyroid Glands. C. S. Ritter*, S. Pande*, I. Krits*, Z. Huang*, E. Slatopolsky, A. J. Brown. Renal Division, Washington University School of Medicine, St. Louis, MO, USA.

Secondary hyperparathyroidism (2^{o}HPT) associated with chronic renal failure is characterized by hypersecretion of parathyroid hormone (PTH) and parathyroid (PT) cell hyperplasia. Control of hyperphosphatemia, the primary pathogenic factor for 2^{o}HPT, can both prevent and arrest development of the condition, but the precise cellular and molecular mechanisms of this regulation remain unclear. The 14-3-3 proteins are a family of isoforms that, through interactions with other proteins, modulate a number of cellular processes including regulation of the cell cycle and stimulation of calcium-dependent exocytosis. The involvement of 14-3-3 in these cellular functions in the PT gland is unknown. We investigated the expression of 14-3-3 in normal and hyperplastic rat PT tissue. PCR analysis of parathyroid tissue from normal rats revealed the presence of the beta, gamma, epsilon, zeta, theta and eta 14-3-3 isoforms. Gene array analysis (Clontech rat Atlas array) revealed increased 14-3-3 zeta in uremic rats fed a high phosphate diet (which promotes 2^{o}HPT) versus uremic rats fed a low phosphate diet (which prevents 2^{o}HPT). Immunohistochemical analysis using a pan-14-3-3 antibody showed that elevated levels of 14-3-3 were consistently found in the PT glands from uremic rats fed a high phosphate diet compared to normals. In addition, the 14-3-3 staining pattern in the hyperplastic PT glands was heterogeneous. Further analysis revealed that the areas of increased 14-3-3 immunostaining were associated with areas of PT cell hyperplasia (as detected by PCNA immunostaining). In conclusion, 14-3-3 gene and protein expressions were upregulated in hyperplastic parathyroid tissue in uremic rats, and up-regulation of the protein was associated with areas of cell proliferation. The exact role of 14-3-3 and control of cell proliferation, and possibly PTH hypersecretion, is currently being investigated.

M418

Hormonal Replacement Therapy in Chronic Renal Failure and Ovariectomy: Histomorphometric Study. A. Rodríguez-Rodríguez*, M. Naves*, M. Serrano*, A. González-Carcedo*, C. Díaz-Corte*, J. L. Fernández-Martín*, J. B. Cannata. Servicio de Metabolismo Óseo y Mineral, Hospital Central de Asturias, Oviedo, Spain.

The main goal of the renal osteodystrophy treatment is to control the secondary hyperparathyroidism, avoiding the induction of low-bone turnover. There are few studies focussed on the treatment of estrogens and calcitriol in postmenopausal women with chronic renal failure (CRF). The aim of this study was to compare the histomorphometric changes produced by the hormonal replacement therapy in rats with both CRF and ovariectomy. Six-month old female Sprague-Dawley rats were studied (n=31). All rats were ovariectomized and nephrectomized (7/8). One week after surgery, the rats were divided in 4 experimental groups: placebo, 17-β-estradiol at 45 mg/kg/day (E-45), calcitriol (CT) at 10 ng/Kg/day, and CT+E-45. A group of animals without any manipulation was used as control group. The rats were sacrificed after 8 weeks of treatment. All the treatment groups recovered the trabecular bone volume (BV/TV), 29.2±6.8 % vs to 15.4±5.5 % observed in the placebo group. The value of this histomorphometric parameter was in the range of the results observed in the control group. As table shows, treatment with E-45 alone, with CT alone, or with both E-45 and CT combined, decreased the osteoid surface (OS/BS). In addition, the E-45 group decreased both osteoclast surface (Oc.S/BS) and eroded surface (ES/BS). The antiresorptive effect of estrogens decreased with the addition of calcitriol. Despite dynamic studies with tetracyclines were not included in the study, the results from CT+E-45 group demonstrated the combined therapy achieved the highest bone-forming rate, similar to the control group (data not showed). They showed the highest level of osteoblasts surface (Ob.S/BS), a normal resorption rate (Oc.S/BS and ES/BS) and the lowest osteoid surface (OS/BS).

Treatment Groups	OS/BS (%)	Oc.S/BS (%)	ES/BS (%)	Ob.S/BS (%)
Placebo (n=7)	33.3 ± 7.6	18.9 ± 6.8	12,8 ± 3,1	27.6 ± 7.2
E_2-45 (n=5)	**6.7 ± 2.1[a]**	**11.4 ± 4.2[cd]**	**10,1 ± 3,3[d]**	28.0 ± 14.3
CT (n=7)	**3.8 ± 0.5[a]**	20.2 ± 4.9	13,4 ± 3,4	23.3 ± 3.0
CT+E_2-45 (n=7)	**3.3 ± 1.3[ab]**	20.0 ± 4.2	16,6 ± 2,8	**35.0 ± 9.4[c]**

[a,b,c,d] *p<0.05* with respect to placebo, E-45, CT and CT+E-45 respectively.

The histomorphometric study shows that the combination of CT+E-45 was the most effective therapy in rats with CRF and ovariectomy. The relationship between forming and resorbing parameters (some data not shown) were more equilibrated in this group of treatment. The addition of CT to E-45 seems to increase bone resorption, but at the same time it may increase bone formation enhancing osteoblast activity and mineralization.

M419

Acidosis-Induced Alteration in Bone Bicarbonate and Phosphate. D. A. Bushinsky[1], S. B. Smith*[1], J. M. Chabala*[2], K. L. Gavrilov*[2], R. Levi-Setti*[2]. [1]University of Rochester School of Medicine, Rochester, NY, USA, [2]Fermi Institute, University of Chicago, Chicago, IL, USA.

During an acute fall in systemic pH, clinically termed metabolic acidosis, there is an influx of hydrogen ions into the mineral phase of bone, which buffers the decrement in pH. We have previously shown that when bone is cultured in medium modeling metabolic acidosis, there is an influx of hydrogen ions coupled to a reduction of bone bicarbonate and phosphate. These ionic fluxes would be expected to result in buffering the excess protons and increasing the pH toward normal. We hypothesize that the surface of bone would respond to the increased concentration of hydrogen ions in a different manner than the interior of bone. In the current study we utilized a high resolution scanning ion microprobe with secondary ion mass spectroscopy to localize the changes in bone bicarbonate and phosphate and determine their relative contribution to the buffering of hydrogen ions during acute metabolic acidosis. Neonatal mouse calvariae were incubated in control medium (pH ~ 7.44, [HCO3-] ~ 27 mM) or in medium acidified by a reduction in bicarbonate concentration (pH ~ 7.14, [HCO3-] ~ 13). Compared to control, after a 3 hr incubation in acidic medium there is a 5 fold decrease in surface bicarbonate with respect to C2 (carbon-carbon bond) and a 3 fold decrease in surface bicarbonate with respect to CN (carbon-nitrogen bond) with no change in cross-sectional bicarbonate. Compared to control, after a 3 hr incubation in acidic medium there is a 10 fold decrease in cross-sectional phosphate with respect to C2 and a 10 fold decrease in cross-sectional phosphate with respect to CN with no change in surface phosphate. On the bone surface there is a 4 fold depletion of bicarbonate in relation to phosphate and in cross-section a 7 fold depletion of phosphate in relation to bicarbonate. Thus acute hydrogen ion buffering by bone involves preferential dissolution of surface bicarbonate and of cross-sectional phosphate.

Disclosures: ***D.A. Bushinsky****, NIH 2; Renal Research Institute 2; AMGEN 5.*

M420

CLX-0921, A Novel Thiazolidinedione Prevents Loss Of Cancellous Bone In Adjuvant Induced Arthritis (AIA) Rats. N. Lane[1], W. Yao[1], A. Burghardt*[1], S. Majumdar*[1], A. Sen*[2], C. Gross[2]. [1]Departments of Medicine and Radiology, University of California at San Francisco, San Francisco, CA, USA, [2]Calyx Therapeutics, Hayward, CA, USA.

Inflammatory arthritis results in significant peri-articular bone loss due to activation of cytokines that increase osteoclast activity. Thiazolidinediones (TZD) are insulin senstitizing agents that may inhibit TNFa production, an important factor leading to bone loss in the inflammatory arthritis. The purpose of this investigation was to determine if the CLX-0921, a TZD, and Etanercept (p55 TNF soluble receptor) would prevent bone loss in AIA rats. Arthritis was induced in male Lewis rats (Harlan, weight 150 g) by immunizing them with Freund's Complete Adjuvant containing Mycobacterium Butyricum (500ug) at the base of the tail. When the arthritic symptoms began to appear (by day 13), the animals were randomized to one of the four groups and treated from day 13-24: Group I: Sham + Vehicle (20% PEG-400 in water, p.o.), Group II: AIA + Vehicle, Group III: AIA + CLX-0921 (50 mg/kg, p.o.), Group IV: AIA + Etanercept (1.67 mg/kg, i.p.). Four joints per animal were individually scored from 0 (normal) to 4 (marked arthritis with swelling, erythemia, nodules, deformation, rigidity) by an observer blinded to the treatment groups. On day 24, AIA rats were sacrificed and the right femur + tibias harvested and the cancellous bone volume and microstructure of the proximal tibiae were accessed by MicroCT (mCT-20, Scanco Medical, Bassersdorf, Switzerland). Results: Body weights decreased 4.6% in the vehicle treated group and increased 2-4% in the CLX-0921 and Etanercept groups. Mean arthritic paw score (range 0-16) from day 13 to day 24 in the vehicle group was 1.9±0.5 to 5.9±4.2, in the CLX-0921 was 1.8±1.2 to 2.7±2.9 (p<0.02 from vehicle day 24) and in the Etanercept was 1.5±0.5 to 2.0±3.5 (p<0.01 from vehicle day 24). Cancellous bone mass and architecture changes were shown in the table. In summary, significant cancellous bone loss and microarchitecture changes occurred in AIA rats. However, in this AIA model, nearly 50% less cancellous bone was lost in animals treated with either CLX-0921 or p55 TNF soluble receptor; Etanercept. Therefore, CLX-0921 may be effective in reducing bone loss in inflammatory arthritis.

Micro-CT Changes

Groups	BV/TV (%)	Tb.N (1/mm)	Conn.Dens (1/mm3)	SMI (0-3)	C.Th (um)
Sham+Vehicle (n=7)	21.4±2.6	4.5±0.4	70.5±14.9	2.3±0.9	250±24
AIA+Vehicle (n=9)	6.2±4.0*	2.0±0.4*	10.3±15.3*	3.5±0.3*	167±27#
AIA+CLX-0921 (n=9)	13.7±4.7	2.6±0.5	38.3±19.7	2.8±0.3	186±25
AIA+Etanercept (n=9)	12.9±5.2	2.8±0.5	31.9±19.7	2.8±0.4	198±25

*=p<0.05 from all other groups; #=p<0.05 from Sham and Etanercept group.

M421

Bone Mineral Density (BMD) and Bone Biochemical Markers (BBM) in Lupus (*L*) and Control (*C*) Women (*W*) Stratified by Menopause Status. A. Bongu[1], C. Langman[2], S. Manzi*[3], S. Spies*[1], R. Ramsey-Goldman[1]. [1]Northwestern University, Chicago, IL, USA, [2]Childrens' Memorial Hospital, Chicago, IL, USA, [3]University of Pittsburgh, Pittsburgh, PA, USA.

Over the past 2 decades improved survival of *LW* lead researchers to focus on minimizing morbidity associated with disease and its treatment. Of the various complications facing *LW*, osteoporosis remains a problem. The goal of this study was to determine if BMD correlated with BBM in *LW* & *CW* matched by age +/- 4 yrs, race, and menopause status. In this cross-sectional study, data collected included: a lifestyle questionnaire and medication survey, BMD of the hip, spine, and distal forearm, urine for N-telopeptide (NTx), and blood for osteocalcin (OC), bone alkaline phosphatase (BAP). The mean age of *LW* & *CW* was 44.1yrs and 43.9 yrs respectively; the mean disease duration for *LW* was 9.7 yrs. 65 pairs were studied, of which 28 were post menopausal (PM) with a mean age of menopause in *LW* & *CW*, 41.6yrs and 44.3yrs respectively. When stratified by menopause status: BMD was lower in menstruating (M) *LW* vs. *CW* at the hip (0.913 vs. 0.940 gm/m^2) and spine (1.015 vs. 1.046 gm/m^2), and in PM *LW* vs. *CW* the BMD was lower at the spine (0.939 vs. 0.975 gm/m^2) and wrist (0.639 vs. 0.673 gm/m^2).

Median BBM in LW and CW Stratified by Menopause Status

BBM	MLW	MCW	PMLW	PMCW
NTX nM/mM	33.0	30.5	29.0	38.0
BAP U/L	13.4	13.8	17.7	19.7
OC ng/ml	7.0	6.6	6.3	7.4

There were no significant differences in median BBM between *LW* & *CW* stratified by menopause status. In PM *LW*: higher NTx correlated with lower BMD at the hip (r= -0.540, p= 0.003) and spine (r= -0.395, p= 0.038), higher BAP correlated with lower BMD at the hip (r= -0.424, p= 0.025), and wrist (r= -0.436, p= 0.029), and higher OC correlated with lower BMD at the hip (r= -0.545, p=0.003), spine (r= -0.381, p= 0.045), and wrist (r= -0.450, p= 0.024). In PM *CW*, higher NTx (r= -0.534, p= 0.005), BAP (r= -0.584, p= 0.002), and OC (r= -0.503, p= 0.009) correlated with lower BMD at one site, the wrist. In M *LW*, higher NTx correlated with lower BMD at the spine (r= -0.347, p= 0.035), and wrist (r= -0.396, p= 0.020), and higher OC correlated with lower BMD at the hip (r= -0.343, p= 0.038). Whereas, in M *CW*, only higher BAP correlated with lower BMD at the spine (r= -0.404, p= 0.012). In conclusion, there may be higher bone turnover in M & PM *LW* vs. *CW*. Thus, BBM may have a potential role in identifying *LW* at risk for low BMD and a high bone turnover state. Future studies include longitudinal follow up of subjects' to assess baseline BBM and BMD to predict subsequent BMD.

M422

The Relationship Between Osteoprotegerin (OPG) and Receptor Activator of NF-kB and Bone Mineral Density (BMD) in Lupus (L) and Control (C) Women (W). A. Bongu, S. Cole*, R. Pope*, E. Shamiyeh*, S. Spies*, R. Ramsey-Goldman. Northwestern University, Chicago, IL, USA.

In an inflammatory illness such as SLE, the balance between bone formation and bone resorption may be altered. However, the mechanisms driving the effect of the inflammatory process on bone metabolism is not clearly understood. Multiple hormones and cytokines regulate skeletal health; the final two effectors in osteoclast regulation are OPG and receptor activator of NF-κB or RANK ligand (RANK-L). The goal of this study was to determine if BMD correlated with OPG and RANK-L in LW & CW. In this cross-sectional study, all study subjects completed a lifestyle questionnaire and a medication survey; BMD was measured at the hip, spine, and distal forearm; and serum measured for OPG and RANK-L using Elisa kits from BioNet, Inc. Each Elisa sample was run in duplicate. The standard error of the mean was 2.6 for OPG and 0.81 for RANK-L. There were 146 LW and CW in which 55 LW and 45 CW women were postmenopausal (PM). The mean age of LW and CW was 41.4yrs and 41.8yrs respectively; with mean disease duration of 8.2yrs. The mean age of menopause in LW was 40.9 yrs vs. 44.0yrs in CW.

Mean BMD in LW and CW Stratified by Menopause Status

BMD Site g/m^2	M LW	M CW	PM LW	PM CW
Hip	0.911	0.953	0.872	0.882
Spine	0.999	1.051	0.953	1.006
Distal Forearm	0.687	0.695	0.649	0.679

BMD was lower at all sites in LW vs. CW regardless of menopause status but only differed significantly at the spine (p= 0.02) in menstruating (M) LW vs. CW and at the wrist (p= 0.04) in PM LW vs. CW.

Median OPG and RANK-L Levels Stratified by Menopause Status

Menopause Status	LW	CW
M OPG pg/ml	74.4	75.5
PM OPG pg/ml	93.4	78.9
M RANK-L pg/ml	6.1	4.0
PM RANK-L pg/ml	4.6	2.5

LW compared to CW had higher levels of OPG and RANK-L regardless of menopause status. OPG was significantly higher in PM LW vs. CW (P= 0.03). In M LW, higher RANK-L correlated with lower BMD at the wrist (r= -0.262, p= 0.02). Higher OPG correlated with higher BMD at the wrist in PM CW (r= 0.348, p= 0.02). In conclusion, M LW have lower BMD at the spine and PM LW have lower BMD at the wrist when compared to CW. Higher RANK-L was associated with lower BMD at wrist in M LW suggesting increased bone resorption. In contrast,higher OPG was associated with higher BMD at the wrist of PM CW, suggesting a protective effect on bone. LW are at an increased risk for osteopenia, identifying those who may benefit from prevention strategies.

M423

Fall Risk and Bone Density in Older Women with Rheumatoid Arthritis. S. Patel[1], D. Johnson*[1], H. Kaz Kaz*[1], U. Chinappen*[2], K. Tweed*[1]. [1]Department of Rheumatology, St Helier Hospital, Surrey, United Kingdom, [2]Department of Rheumatology, St George's Hospital, London, United Kingdom.

Previous studies suggest that the risk of hip fracture is doubled in patients with rheumatoid arthritis (RA). This is in part due to patients with RA having lower bone density at the hip compared to aged matched non-RA controls. However the risk of hip fracture occurring in an individual is determined by both hip bone density and the risk of falling. Although studies have been carried out of hip bone density in RA patients there are no studies of fall risk. The risk of falls may be higher in patients with RA because of lower limb joint disease, muscle weakness due to disuse and steroids. Visual acuity may also be affected in steroid treated patients due to cataract formation. The aim of this study was to determine whether fall risk was increased in women with RA and to determine high risk sub groups at risk of hip fracture. We performed a case control study examining fall risk and bone density in older women (aged > 65 yrs) with rheumatoid arthritis. The cases were recruited from a single centre treating patients with rheumatoid arthritis. The controls were women without rheumatoid arthritis or steroid use referred by their primary care physicians for bone densitometry. We recruited 99 RA patients and 198 controls matched for age to within 2 years. Cases and controls provided a history and underwent tests of falls risk previously shown to predict hip fracture. These were measurement of binocular corrected visual acuity (VA), tandem gait (EPIDOS grading) and ability to do 5 standups from a chair without arm use. Bone density was measured at the lumbar spine and femoral neck by DXA. Mean age of the patients and controls was 74 yrs (range 65 to 87). Ability to perform tandem gait normally was 39% in the controls versus only 18 % in the RA patients ($p < 0.05$), inability to perform standups was 10 % in the controls versus 32 % in the RA patients ($p < 0.05$). However VA was similar in the two groups. RA patients with poor functional status and high tender joint counts were more likely to have impairment of tandem gait and inability to perform standups. The prevalence of FN osteoporosis was 24 %, FN osteoporosis and abnormal tandem gait was 13 %, FN osteoporosis and inability to do standups 16 %, FN osteoporosis and VA < 0.5 was 7 %. These data suggest that fall risk is increased in women with RA, and is a major contributor to the increased risk of hip fracture associated with RA. Management of osteoporosis in patients with RA should include assessment of fall risk as well as drug treatment for osteoporosis.

M424

Intramedullary Spinal Tuberculoma - A Case Report. M. Garg*, S. Singh*. Orthopaedics, B.P.Koirala Institute Of Health Sciences, Dharan, Nepal.

Intramedullary tuberculoma is a rare form of central nervous system tuberculosis. A case report of intramedullary spinal tuberculoma detected on magnetic resonance imaging (MRI) is presented. Excellent results were obtained on medical therapy aloneconfirmed by MRI normalization. **Introduction :** Intramedullary spinal tuberculoma is an extremely rare disease entity. Early detection might help in reducing the morbidity associated with this benign and curable lesion. We present a case a intramedullary spinal tuberculoma detected on MRI and treated by antitubercular chemotherapy alone. **Case report :** A 18-year-old girl with no family history of tuberculosis presented with bilateral lower extremity weakness and numbness and bladder incontinence for the past two months. Neurologic examination revealed paraparesis (grade 3) with hyperactive deep tendon reflexes, positive Babinski sign and no clonus. There was sensory deficit to pin prick and light touch below D8 level with loss of superficial lower abdominal reflexes. Laboratory investigations revealed elevated ESR. X-rays of the chest, dorsal and dorso lumbar spine were normal. MRI of the dorsal spine revealed a ring enhancing intramedullary mass at D6 - D7 level with focal cord enlargement and oedema(fig.1.1) .A cerebrospinal fluid (CSF) analysis showed an elevated protein level of 100mg/dl glucose level of 40 mg/dl. Red blood cell count of $8/mm^3$ and white blood cell count of $18/mm^3$ (15 % polymorphs, 85% monocytes). CSF acid - fast bacillistains were positive and cultures grew M. tuberculosis. The lesion was diagnosed as an intramedullary tuberculoma. The patient was started on antitubercular chemotherapy with isoniazid, rifampicin, ethambutol and pyrazinamide. At three months follow-up, the neurologic improvement was satisfactory. The ATT (Isoniazid and rifampicin) was continued for another 15 months. At five months follow-up, patient showed significant neurologic improvement. Repeat MRI of the dorsal spine showed significant reduction in the size of the lesion with modular enhancement and minimal focal cord enlargement (fig. 1.2) . There was complete neurologic recovery after fourteen months of antitubercular therapy and MRI revealed small nonenhancing intramedullary isointense focus at D6-D7 level (fig. 1.3) .

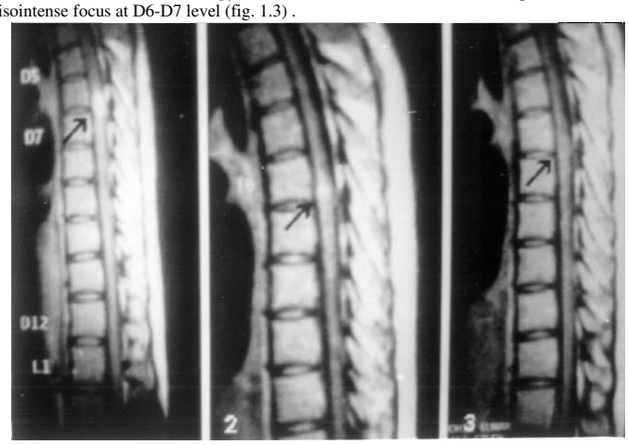

M425

Acceleration of Autoimmune Arthritis in MRL/*lpr* Mice Transferred with RANKL-stimulated Dendritic Cells. T. Izawa*[1], K. Moriyama[1], Y. Hayashi*[2]. [1]Department of Orthodontics, School of Dentistry, University of Tokushima, Tokushima, Japan, [2]Department of Pathology, School of Dentistry, University of Tokushima, Tokushima, Japan.

Receptor activator of NF-kB ligand (RANKL) is a regulator of the immune system and of bone development. In vitro, RANKL promotes the survival of mature dendritic cells (DCs), and induces the production of proinflammatory cytokines, such as IL-1 and IL-6, and cytokines that stimulate and induce differentiation of T cells. The aim of this study was to analyze the effect of transfer of DCs stimulated with RANKL on the development of autoimmune arthropathy in MRL/*lpr* mice, and to evaluate the possible relationship between RANKL-mediated osteoclastogenesis. (Methods) Freshly isolated bone marrow cells were stimulated with IL-4 and GM-CSF for seven days and induced differentiation into DC (BMDC) by further stimulation of RANKL and type II collagen (CII) for three days. BMDC ($1x10^6$) activated with RANKL were subcutaneously injected into inguinal region. The mice were sacrificed after eight weeks and were histopathologically examined. We further analyzed various factors including surface markers on T cells, proliferation assay, anti-CII antibody, rheumatoid factors (RF), cytokine production, and osteoclast activation. (Results and Discussion) Acceleration of autoimmne arthritis accompanied by bone destruction of knee was observed in DC-transferred mice compared with age-matched controls. We detected an significant increase in T cells bearing memory type and DCs expressing MHC class II ($I\text{-}A^k$). In addition, an increased osteoclast formation, and the bone resorption pits cultured from bone marrow cells were observed in DC-transferred mice, suggesting that RANKL induce osteoclast formation by direct activation of osteoclast progenitors. These results indicate that RANKL pathway play a crucial role on acceleration of autoimmune arthropathy for promoting DCs and activation of osteoclastogenesis in a murine model for RA.

M426

Uni-Axial Cyclic Stretch Induces Core Binding Factor Alpha 1 (Cbfa1) in Spinal Ligament Cells Derived from Patients with Ossification of the Posterior Longitudinal Ligament. K. Iwasaki*[1], K. Furukawa*[2], M. Tanno*[1], T. Kusumi*[3], K. Ueyama*[4], S. Harata*[5], S. Motomura*[2], S. Toh*[1]. [1]Orthopaedic Surgery, Hirosaki University School of Medicine, Hirosaki, Japan, [2]Pharmacology, Hirosaki University School of Medicine, Hirosaki, Japan, [3]Second Department of Pathology, Hirosaki University School of Medicine, Hirosaki, Japan, [4]Orthopaedic Surgery, Hirosaki Memorial Hospital, Hirosaki, Japan, [5]Orthopaedic Surgery, Aomori Prefectural Central Hospital, Aomori, Japan.

Ossification of the posterior longitudinal ligament of the spine (OPLL) is characterized by ectopic bone formation in the spinal ligaments. In some cases ossification enlarges in the spinal canal and compresses the spinal cord resulting in serious neurological damage. Mechanical stress, which acts on the posterior ligaments, is thought to be an important factor in the progression of OPLL. To elucidate this mechanism, we investigated the effects of in vitro cyclic stretch (120% peak to peak, at 1 Hz) on cultured spinal ligament cells derived from OPLL (OPLL cells) and non-OPLL (non-OPLL cells) patients. The mRNA expressions of type I collagen, alkaline phosphatase (ALP) and core binding factor alpha 1 (Cbfa1), an osteoblast- specific transcription factor, were increased by cyclic stretch in OPLL cells, whereas no change was observed in non-OPLL cells. The effects of cyclic stretch on the spinal ligament tissues derived from OPLL and non-OPLL patients were also analyzed by immunohistochemistry using an antibody against Cbfa1. The expression of Cbfa1 was increased by cyclic stretch at both the center and the enthesis of the spinal ligament tissues of OPLL patients, whereas no change was observed in tissues of non-OPLL patients. These results suggest that the mechanical stress which acts on the spinal ligaments or spinal ligament cells plays an important role in the progression of OPLL through an increase in Cbfa1 expression.

M427

Association of Analgesic Effects of the Bisphosphonate Zoledronic Acid with Its Anti-Osteoclast and Anti-Inflammatory Action. M. Nagae*, T. Hiraga, K. Iwata*, T. Yoneda. Dept Biochemistry and Oral Physiology, Osaka Univ Grad Sch Dent, Osaka, Japan.

Bone pain is one of the major causes of increased morbidity in patients with bone disorders including osteoporosis and skeletal metastasis. Although the mechanism of bone pain is totally unknown, large bodies of clinical studies have reported that bisphosphonates (BPs), which are potent and specific inhibitors of osteoclasts, have significant analgesic effects on bone pain. Moreover, it has been recently reported that osteoprotegerin, which is another specific inhibitor of osteoclasts, suppresses tumor-induced bone pain. These results raise the possibility that BP decreases bone pain by its anti-osteoclast action. To test this notion, we established an animal model in which a subcutaneous injection of complete Freund's adjuvant (CFA) into the hind paw of ddY mice induced inflammatory hyperalgesia with increased osteoclastic bone resorption in underlying bone. One day after the CFA injection, mice received either a bolus intravenous or intrathecal injection of or an orthotopic subcutaneous administration of the BP zoledronic acid (ZOL) (2.5, 25, 250, 2,500μg/kg). The analgesic effects of ZOL were evaluated by measuring paw withdrawal latency in response to thermal stimuli using the electronic clock circuit and a microcomputer. The intravenous and subcutaneous injection of ZOL significantly reduced the CFA-induced hyperalgesia in a dose-dependent manner, whereas the intrathecal administration of ZOL showed no effects, suggesting that the effects of ZOL are peripheral rather than central. No effects of ZOL were observed in the untreated right hind paws in the same animals. Histological examination revealed that ZOL inhibited CFA-induced bone resorption with reduced TRAP-positive osteoclasts and increased apoptotic osteoclasts. We next conducted the hind paw withdrawal experiments in c-src-deficient mice which had osteoclast dysfunction. We found that the CFA-induced hyperalgesia was significantly impaired in conjunction with reduced bone resorption in these c-src-deficient mice compared with wild-type mice. Since the CFA-induced hyperalgesia is primarily caused by local inflammatory reactions, we next examined whether ZOL exhibited anti-inflammatory effects. We found that a bolus intravenous injection of ZOL significantly suppressed CFA-enhanced vascular permeability determined by Evans Blue dye extravasation test to a similar extent with indomethacin. In summary, our data show that ZOL suppresses CFA-induced hyperalgesia, bone resorption and local inflammatory reactions. These results suggest that analgesic effects of ZOL on bone pain are associated with its anti-osteoclastic and anti- inflammatory actions.

M428

Risedronate Conserves Periarticular Bone and Ligament Mechanical Properties in Early Osteoarthritis. M. R. Doschak*, G. R. Wohl*, D. A. Hanley, R. C. Bray*, R. F. Zernicke. McCaig Centre for Joint Injury and Arthritis Research, University of Calgary, Calgary, AB, Canada.

Periarticular loss of bone mineral density (BMD) early after anterior cruciate ligament (ACL) rupture in the knee has been well documented. The influence of periarticular BMD loss on joint function and osteoarthritic progression, however, has yet to be determined. The purpose of this study was to assess in an osteoarthritis (OA) model whether antiresorptive therapy altered periarticular bone and collateral ligament biomechanics and OA progression. We surgically transected the ACL in two groups of 15 rabbits. The first group was dosed (0.01 mg/kg s.c.) daily with Risedronate, a commercially available bisphosphonate (BP) for 6 wk. The second group was untreated for 6 wk and served as age-matched ACL-transected (ACLX) controls. A third group of 10 age-matched, normal (unoperated) controls was also evaluated. We measured distal femoral BMD (Dual Energy X-ray Absorptiometry: DEXA), medial collateral ligament (MCL) laxity, and bone mechanical function (bone cores mechanically tested in compression) 6 wk after ACLX. We also examined (micro computed tomography) bone mineral changes at the distal femoral insertion of the MCL. These measures were compared to cartilage/joint gross morphology and histology for evidence of early OA. The University of Calgary Animal Care Committee approved all procedures. BMD by DEXA in 6 wk ACLX animals was 18% less than normal controls ($p<0.01$). BP dosing conserved BMD; Risedronate-treated rabbits had distal femoral BMD only 5% less than normal controls. When the same bone cores were compressed to failure, both ACLX and BP-dosed animals were significantly weaker than normal controls ($p<0.05$). Blocking bone resorption with BP did not reduce capsular thickening or inflammatory angiogenesis, which were elevated in both untreated and BP-treated ACLX joints compared with normal controls ($p<0.05$). However, MCL-complex laxity was significantly less in BP-dosed animals (1.2 times that of normal controls) compared to untreated ACLX animals (1.7 times that of normal controls; $p<0.05$). Early loss of periarticular bone mineral after ACLX included significant loss at the MCL insertion ($p<0.02$). The loss of MCL insertional bone was less with BP dosing and was similar to normal control animals. Thus, compared to the untreated ACLX condition, administering BP immediately after ACL damage conserved periarticular bone and collateral ligament-bone properties in an early OA model.

M429

Bone Mineral Density in Rheumatoid Arthritis: Disease Related Variables Associated with Low Bone Mineral Density. M. C. Lodder*[1], Z. de Jong*[2], P. J. Kostense*[3], E. T. H. Molenaar*[1], K. Staal*[4], A. E. Voskuijl*[1], J. M. W. Hazes*[5], B. A. C. Dijkmans*[1], W. F. Lems[1]. [1]Rheumatology, VU University Medical Center, Amsterdam, Netherlands, [2]Rheumatology, LUMC, Leiden, Netherlands, [3]Clinical Epidemiology and Biostatistics, VU University Medical Center, Amsterdam, Netherlands, [4]Endocrinology, VU University Medical Center, Amsterdam, Netherlands, [5]Rheumatology, University Hospital, Rotterdam, Netherlands.

To examine the frequency of osteoporosis and variables associated with bone mineral density (BMD) in patients with rheumatoid arthritis (RA). 373 patients participating in 2 research projects were investigated. The first project was the RAPIT trial, a study after the effect of frequent weight-bearing exercise versus usual care. The second project concerned a cohort of patients in clinical remission. Demographic and clinical data were collected and bone mineral density (BMD) was measured by means of dual X-ray absorptiometry (DEXA). Associations between demographic and clinical measures on the one hand and BMD on the other were investigated in single and multiple regression analyses. The mean age (standard deviation (SD)) of the patients was 54 (12) years. 77% were female of whom 73% were premenopausal. The median (range) disease duration was 7 (1-50) years, 66% was rheumatoid factor positive. 83% never used corticosteroids. The median Larsen score of hands and feet, reflecting radiographic joint damage, was 27 (0-155). The mean BMD at the spine (L1-4) was 0.99 (0.16) g/cm2, at the femoral neck the BMD was 0.78 (0.13) g/cm2. 7 % of the patients had osteoporosis of the hip and 13 % osteoporosis of the spine (T score $\leq$ -2.5 SD). High age, female sex, and low BMI are related to low BMD at the hip and spine. Participation in the RAPIT trial and a high Larsen score were significantly associated with low BMD at the hip. Data on BMD in patients with RA are presented, demonstrating an association between radiological RA damage and low BMD at the hip.

M430

Amino-terminal and Mid-molecule PTHrP Peptides Stimulate Lung Phosphatidylcholine after Silica Injury. R. H. Hastings[1], R. A. Quintana*[1], R. Sandoval*[1], Y. Rascon*[1], D. W. Burton[2], L. J. Deftos[2]. [1]Anesthesiology, VA San Diego, San Diego, CA, USA, [2]Endocrinology, VA San Diego, San Diego, CA, USA.

PTHrP 1-34 stimulates synthesis and secretion of phosphatidylcholine, the major lipid in pulmonary surfactant, by cultured alveolar type II epithelial cells. This study investigated whether PTHrP regulates lung phosphatidylcholine levels in silicosis, an injury state marked by profound alveolar phospholipidosis. Silica lung injury was produced by intratracheal instillation of 10 mg Min-U-Sil silica in PBS per rat with or without 15 μg PTHrP peptide (1-34, 38-64, 67-86 or 107-138). Animals also received daily subcutaneous injections of 5 μg of the same peptide. Bronchoalveolar lavage liquid (BAL) phospholipids were extracted after four days and measured by phosphorus assay or TLC. Studies were approved by the IACUC. Type II cell proliferation was assessed by proliferating cell nuclear antigen (PCNA) immunostaining and type II cell numbers were evaluated after alkaline phosphatase or surfactant apoprotein C staining. In additional rats, lung PTHrP expression was assessed by immunostaining at 7, 14 and 28 days after silica. Primary cultures of rat type II cells were assayed for the effects of PTHrP peptides and neutralizing PTHrP antibodies on incorporation of tritiated choline into phosphatidylcholine. cAMP levels with and without PTHrP treatment were assayed by ELISA and inositol phosphate production was measured by incorporation of tritiated myo-inositol. The PTHrP 1-34 and PTHrP 67-86 treatment groups demonstrated a two-fold increase in BAL phosphatidylcholine compared to no treatment in silica-injured rat lung ($P < 0.05$). Other peptides had no effect. PCNA immunoreactivity and numbers of alkaline phosphatase positive cells did not increase after PTHrP 1-34 or 67-86 treatments. In cultured type II cells, PTHrP 67-86 caused a dose dependent increase in phosphatidylcholine synthesis, while PTHrP antibodies caused a significant 50% decrease in phospholipid production. PTHrP 1-34 and PTHrP 67-86 significantly stimulated cAMP and inositol phosphate levels by about 50%. PTHrP 67-86 immunoreactivity fell in silica injured lungs seven days after injury, but rebounded and surpassed baseline levels at 14 and 28 days, coinciding with the period of maximum alveolar phospholipidosis. Thus, increased PTHrP levels at 14-28 days may contribute to the phospholipid accumulation with silica injury. These data indicate that exogenous and endogenous PTHrP 1-34 and 67-86 stimulate phosphatidylcholine production and that PTHrP 67-86 may act through an as yet unrecognized G-protein coupled receptor in alveolar type II cells.

M431

Inhibition of Metastasis in Melanoma Following Targeted Disruption of the PTHrP Gene: Enhanced Visualization of the Invasion Process with Green Fluorescent Protein. D. C. Huang, R. Kremer. Medicine, Royal Victoria Hospital, Mcgill University, Montreal, PQ, Canada.

Tumoral production of parathyroid hormone-related peptide (PTHrP) is frequently elevated in advanced metastatic cancer associated with hypercalcemia. However, there is yet no direct evidence of PTHrP role in tumor invasion and metastasis. In this study we used a highly metastatic cancer cell line, the human amelanotic melanoma cell line A375, which expresses high levels of PTHrP (Abdaimi *et al.*, *Am J Physiol Cell Physiol* 279: C1230-C1238, 2000) and metastasizes to liver, lung, lymph nodes and bone. In order to evaluate the role if any of PTHrP in invasion and metastasis we inactivated both alleles of the PTHrP gene by targeted disruption and compared the metastatic potential of the knockout (KO A375) cell line to its parent cell line transfected with the vector alone (WT A375). To precisely determine the time course and the extent of the metastatic process, green fluorescent protein (GFP) transduced KO A375 and WT A375 cells were implanted into the left ventricle of nude mice. Mice were sacrificed at timed intervals and disseminated tumor cells expressing GFP were visualized by fluorescence microscopy. Survival and tumor progression was determined by histology and high sensitivity X-ray analysis of bone osteolytic lesions. Metastasis was visualized on a single cell basis by GFP expression and the kinetic of tumor cell dissemination demonstrated that trafficking of tumor cells via blood and lymph vessels was substantially reduced in animals injected with KO A375 cells. Furthermore the total number of metastasis and the % of animals with metastasis in each organ analyzed was drastically reduced in nude mice receiving KO A375 as compared to WT A375 cells (lung 4/14 vs 12/14, $p<0.01$; liver 5/14 vs 10/14, $p<0.01$; lymph node 3/14 vs 10/14, $p<0.05$ and bone 4/14 vs 9/14, $p<0.05$). Kaplan-Meier analysis revealed a highly significant survival benefit in nude mice injected with KO A375 cells as compared to WT A375 cells. Overall, our study provides the first direct evidence that PTHrP plays a major role in tumor invasion and metastasis and suggests that agents aimed at suppressing PTHrP may be beneficial in advanced metastatic cancer.

M432

Stability of Parathyroid Hormone-Related Protein mRNA Isoforms and its Regulation by TGF-beta. R. S. Sellers*[1], A. I. Luchin*[1], H. Iguchi*[2], T. J. Rosol[1]. [1]Veterinary Biosciences, The Ohio State University, Columbus, OH, USA, [2]National Kyushu Cancer Center, Fukuoka, Japan.

Humoral hypercalcemia of malignancy (HHM) is one of the most frequently occurring paraneoplastic syndromes and results in muscle weakness, cardiac arrhythmias, bone loss, and life-threatening renal failure. Parathyroid hormone-related protein (PTHrP) is the primary mediator of HHM. Alternative splicing at the 3'-end of PTHrP mRNA results in three different mRNA isoforms that encode three different peptides. These isoforms share the majority of the coding region, but differ in the 3'-end of the coding region and have completely different 3'-untranslated regions (UTRs). The 1-139 and 1-141 isoforms are relatively unstable, with half-lives ranging from 90 to 120 min and 45 to 90 min, respectively. The 1-173 isoform is much more stable with a half-life of 4 hr or more. It was previously reported that PTHrP mRNA is stabilized by TGF-beta, which may be an important determinant for the ability of cancer to induce hypercalcemia. The effect of TGF-beta on the stability of separate PTHrP mRNA isoforms has not been well studied. We utilized an in vitro mRNA stability assay containing cell extracts and radiolabeled PTHrP mRNAs to show that the half-life of the 1-141 isoform was increased 2-3-fold by TGF-beta- from 45 to 90 min in a canine oral squamous carcinoma cell line (SCC2/88) and from 90 min to 4.5 hr in a human lung squamous carcinoma cell line (HARA). TGF-beta, however, had no detectable effect on the stability of the 1-139 and 1-173 isoforms of PTHrP mRNA. The differences can most likely be attributed to different regulatory elements present in the 3'-UTRs of PTHrP mRNA. We also attempted to address the mechanism of stabilization of 1-141 isoform by TGF-beta. We previously reported the binding of the three unknown proteins, p27, p31 and p33 to the coding region of PTHrP mRNA in the canine SCC2/88 cell line. This binding was significantly reduced by TGF-beta (Sellers et al., Molecular and Cellular Endocrinology, 2002). We observed binding of the proteins to PTHrP mRNA with similar mobility in human HARA and HeLa cells lines. In addition, we observed binding of the three proteins (35-25 kDa) in S35-labeled cytoplasmic extracts from HARA cells. In conclusion, we demonstrated the selective regulation of stability of different isoforms of PTHrP mRNA by TGF-beta. This is most likely to be due to a different regulatory elements present in the 3'UTRs of PTHrP mRNA. We also identified three proteins that are possibly involved in the regulation of the stability of the PTHrP 1-141 isoform by TGF-beta.

M433

Parathyroid Hormone-related Protein (PTHrP) Regulatory Interactions with Cytokines and Chemokine Receptor Expression in Pancreatic Cancer Cell Lines. M. Bouvet[1], R. Nassirpour*[1], O. A. Ahmadpour*[2], D. W. Burton[2], L. J. Deftos[2]. [1]Surgery, University of California and Department of Veterans Affairs, San Diego, CA, USA, [2]Medicine, University of California and Department of Veterans Affairs, San Diego, CA, USA.

PTHrP regulates the function and growth of many normal and malignant tissues, notably breast and prostate cancer. These growth-regulating effects are mediated by cytokines. For example, IL-6 (Interleukin-6) and IL-8 regulate cancer growth by angiogenic activity and growth-promoting effects. We have demonstrated regulatory interactions of PTHrP and cytokine expression in growth regulation of prostate cancer and pancreatic cancer. Recently, chemokine receptors, especially CCR-7, have been implicated in breast cancer metastasis, a PTHrP dependent process. Therefore, we sought to investigate the functional relationship of PTHrP, cytokines and chemokines in pancreatic cancer. Eight human pancreatic cancer cell lines demonstrated constitutive expression of PTHrP and IL-8, and 4 of the lines also showed expression of IL-6. We investigated the effect of PTHrP 1-34, PTHrP 67-86, PTHrP 107-138, PTHrP 140-173, and PTHrP140-173 scrambled (negative control) synthetic peptides on the production of IL-6 and IL-8 by pancreatic carcinoma cells and correlated PTHrP expression with chemokine receptor levels. The pancreatic cell lines were treated with each of these different PTHrP peptides at 1, 10, and 100 nM concentrations. After 48 hours of incubation, the media were collected and immunoassayed for IL-8 and IL-6. PTHrP 1-34 significantly stimulated IL-8 secretion in BxPC-3 pancreatic cell line in a dose-dependent manner. However, PTHrP140-173 inhibited the secretion of IL-8 in BxPC-3. In 50% of the pancreatic cell lines that secrete IL-6, PTHrP140-173 had inhibitory effects and in 75% of the cells, PTHrP1-34 stimulated IL-6 secretion. PTHrP 67-86 and 107-138 exhibited mostly inhibitory effects on IL-6 and IL-8 secretion. Differential expression of the chemokine receptors in pancreatic cancer cells was noted by RT-PCR. For example, MIA PaCa-2, a high expressing PTHrP cell line, also highly expressed the chemokine receptor CCR-7. In contrast, PANC 28, a low PTHrP expressor, had a lower relative expression of CCR-7 than MIA PaCa-2. These results establish a regulatory pathway among PTHrP, cytokine expression, and chemokine receptor activity in pancreatic cancer. These pathways serve to extend the growth regulatory effects of PTHrP from prostate and breast cancer to tumors of the pancreas. Further characterization of these molecular interactions can help to elucidate the regulatory pathways that PTHrP utilizes in mediating cell growth.

M434

Parathyroid Hormone Related Protein (PTHrP) Production in the Lamprey Geotria Australis: Developmental and Evolutionary Perspectives. M. K. Trivett*[1], I. C. Potter*[2], G. Power*[2], D. L. Macmillan*[3], T. J. Martin[1], J. A. Danks[1]. [1]St Vincent's Institute of Medical Research, Fitzroy, Australia, [2]School of Biological and Environmental Sciences, Murdoch University, Murdoch, Australia, [3]Department of Zoology, University of Melbourne, Parkville, Australia.

Parathyroid hormone-related protein (PTHrP) is a mediator of humoral hypercalcemia of malignancy in humans. It has been previously demonstrated in the tissues and circulation of both bony and cartilaginous fish. The origins of these jawed vertebrates, lies somewhere among the extinct jawless fish. The lampreys and hagfish, collectively called cyclostomes, are the only representatives of this group that survive today. This study examined the distribution of PTHrP antigen and mRNA in jawless fish. The animals used were the Southern Hemisphere lamprey, Geotria australis. This species which undergoes a radical metamorphosis to produce a juvenile adult that migrates downstream to the sea. The adult ultimately re-enters the rivers and migrates back upstream to spawning areas The tissue distribution of PTHrP was examined in larval lampreys, downstream migrants and upstream migrants. The different developmental stages were examined for the presence of PTHrP, by immunohistochemistry using antisera to human PTHrP (1-14). Positive and negative controls were included in each assay and all samples were assayed in duplicate. Sites of PTHrP mRNA production were demonstrated by in situ hybridization with a digoxigenin labeled riboprobe to Exon VI of the human PTHrP gene. A panel of positive and negative controls were included in every experiment. The results revealed widespread distribution of the PTHrP antigen and its mRNA in sites similar to those described in mammalian and avian species. In addition, novel sites of localization were demonstrated, such as in the gill and notochord. Some differences in PTHrP localization were noted between animals in different stages of the lamprey life cycle, indicating that the distribution of parathyroid hormone-related protein, and possibly its roles, change with the stage of development in this species. The widespread distribution of PTHrP in Geotria australis implies that parathyroid hormone-related protein may have diverse physiological roles in this animal. The presence of PTHrP in the lamprey, a representative of the oldest group of vertebrates, suggests that parathyroid hormone-related protein is of ancient origin.

M435

PTHrP Regulates Expression of DNA Repair Genes and Modulates Apoptotic Response. N. Ilievska*, R. J. Thomas*, T. J. Martin, M. T. Gillespie. St. Vincent's Institute of Medical Research, Melbourne, Australia.

Parathyroid hormone-related protein (PTHrP) is widely expressed in breast tumors and its production promotes osteolysis in bone. In addition, PTHrP affects cellular functions including differentiation, proliferation and apoptosis. To determine the potential roles of PTHrP within breast cancer cells, we have examined the effect of overexpressing PTHrP in the MDA-MB-231 and MCF7 cell lines. The growth rate, cell cycle parameters apoptosis rate and changes in gene expression were assessed in the PTHrP overproducing cells with respect to the parental cells. PTHrP overproduction had no demonstrable effect on cellular proliferation or cell cycle profiles. However, an enhancement of UV-induced apoptosis was noted in cells overexpressing PTHrP; this contrasts to previous reports that establish PTHrP to diminish apoptosis. To determine which genes altered their expression in response to PTHrP, we used differential display of mRNA comparing the mRNA fingerprints of overexpressing cells relative to the parental. Several candidate PTHrP-regulated genes were identified then subsequently confirmed by Northern analysis or RT-PCR. PTHrP was found to regulate genes involved with DNA repair (XPG, BRCA1, BRCA2 and Rad51), cell cycle (p21 and p53), and apoptosis-related genes such as Bcl-2: each is a UV-induced gene. PTHrP peptides (107-111 or 107-139 at 100 nM) encompassing osteostatin (TRSAW: 107-111) upregulated the expression of mRNA levels for these genes within 4 to 24 hrs in MCF-7 or MCF-10A cells, and changes were also noted in protein levels. A mutant form of osteostatin (PRSAW) or PTHrP peptides 1-34, 1-108, 106-139 or 122-139 did not effect mRNA or protein levels for these target genes. To determine the signal transduction pathway(s) involved in osteostatin-induced regulation of DNA repair genes, MCF-10A cells were treated with the NFkB inhibitor (N-acetyl-L-cystine), PKA inhibitor (H89) or PKC inhibitor (chelerythrine chloride) with and without TRSAW (100nM). Of these three inhibitors, only H89 was able to block the effects of TRSAW on DNA repair or cell

cycle genes. In contrast, N-acetyl-L-cystine blocked osteostatin induction of Bcl-2 implicating NFkB signaling for this action. Finally, since PTHrP and these DNA repair genes may attain nuclear / nucleolar localisation, the subcellular distribution of PTHrP and BRCA1 were analysed by green fluorescent protein constructs or by immunohistochemistry using confocal studies which identified that PTHrP and BRCA1 colocalised within the nucleolus. These studies indicate a potential role for PTHrP in DNA repair.

M436

Role of Cell Cycle Factors in Regulating Chondrocyte Proliferation, and Mediating PTHrP Action, *In Vivo*. H. E. MacLean, C. J. Paller*, H. M. Kronenberg. Endocrine Unit, Massachusetts General Hospital/Harvard Medical School, Boston, MA, USA.

We are investigating the role of positive and negative cell cycle factors in regulating chondrocyte proliferation and mediating PTHrP action during embryonic mouse development. We have previously shown that *in vivo*, absence of the cyclin dependent kinase (cdk) inhibitor (CKI) p57, or the Rb-related pocket proteins p107 and p130, causes increased chondrocyte proliferation and delayed differentiation; and loss of p57, or p107 and p130, also normalizes the PTHrP-null chondrocyte phenotype in the ulna, ribs, sternum and vertebrae. We have performed Western analysis on crude protein lysates from limbs of E18.5 wild-type and p57-null embryos, and observe increased levels of the hyper-phosphorylated form of p130 in the p57-null samples, consistent with loss of p57 causing increased cdk activity. This finding is currently being confirmed by using collagen-II-GFP expressing mice to isolate pure chondrocyte populations. We have examined the role of other cell cycle regulators during embryonic chondrocyte development, using *in situ* hybridization and immunohistochemistry. p21 and p27 mRNA and protein are expressed at very low levels in hypertrophic chondrocytes, and levels are unchanged in p57-null and PTHrP-null embryos. At E15.5 – E18.5, p21-null long bones are phenotypically normal, and p21/p57 double knockouts are indistinguishable from p57 single knockouts, suggesting p21 plays little role in regulating chondrocyte cell cycle exit during development. Cyclin D1 mRNA and protein are virtually undetectable in chondrocytes pre-natally, whereas cyclin D2 and D3 proteins are expressed widely in both proliferative and hypertrophic chondrocytes. Cyclin A protein is expressed in only a sub-set of chondrocytes in the proliferative zone. There is an increased percentage of cyclin A-positive chondrocytes in both p57 knockout and p107/p130 double knockout embryos, consistent with the elevated proliferation observed in these bones. There was no detectable difference in the levels of cyclin A, D1, D2 or D3 protein in PTHrP-null long bones compared to wild-type, suggesting little regulation of these factors by PTHrP *in vivo* during embryonic development. We examined the bone morphology and chondrocyte proliferation *in vivo* from cyclin D1-null embryos at E18.5. At this developmental stage, bones are morphologically normal, and chondrocyte proliferation rate is normal, indicating that in late embryonic stages, absence of cyclin D1 has no effect on chondrocyte function. We are currently investigating the potential redundancy of D-type cyclins in chondrocyte development.

M437

Altered Set-Point for Calcium-Stimulated Calcitonin Release in Calcium Sensing Receptor Gene-Ablated Mice. N. J. Fudge*, L. L. Chafe*, C. S. Kovacs. Faculty of Medicine, Memorial University of Newfoundland, St. John's, NF, Canada.

The calcium sensing receptor (CaR) regulates serum calcium by suppressing parathyroid hormone; it also regulates renal tubular calcium excretion. Inactivating mutations of CaR raise serum calcium and reduce urine calcium excretion. Apart from parathyroids and kidney tubules, thyroid C-cells (which make calcitonin) also express CaR. Consequently, CaR might regulate calcitonin synthesis and secretion by C-cells. Since calcium stimulates release of calcitonin, the higher blood calcium caused by inactivation of CaR should increase serum calcitonin, unless CaR mutations alter the responsiveness of calcitonin to calcium. To demonstrate regulatory effects of CaR on calcitonin physiologically, we studied calcitonin responsiveness to calcium challenge in CaR ablated mice. In this model, heterozygous (het) mice have hypercalcemia and hypocalciuria, and live normal life spans. Homozygous (null) mice have severe hypercalcemia and die within three weeks of birth. Since fetal and neonatal mice were too small for the proposed studies, the comparisons were made between wild-type (wt) and het adults. 20 wt and 20 het mice, all first degree relatives, were studied. Ionized calcium was measured. Each mouse then received 500 µmol/kg injection of elemental calcium or an equal volume (500 µl) of normal saline. After 10 minutes, ionized calcium and serum calcitonin were measured. In wt, ionized calcium was 1.28 ± 0.02 mmol/l and rose to 1.34 ± 0.02 mmol/l after calcium ($p<0.02$). In het, ionized calcium was 1.45 ± 0.02 mmol/l and rose to 1.52 ± 0.02 mmol/l after calcium ($p<0.02$). In wt and het, ionized calcium was unchanged by saline. In wt, calcitonin was 13.3 pg/ml and rose to 41.2 ± 17.8 following calcium ($p<0.008$). In het, calcitonin was 11.2 pg/ml and rose to 60.0 ± 17.8 pg/ml following calcium ($p<0.003$). The peak responses of wt and het were not significantly different. Wt and het mice had the same calcitonin level at baseline, and similar peak calcitonin responses, despite a significantly higher blood calcium in het vs wt both before and after calcium injection. Calcitonin levels of het were consistently lower than predicted by their higher ionized calcium. Moreover, wt mice achieved a calcitonin level of 41.2 pg/ml at an ionized calcium level of 1.34 mmol/l, significantly higher ($p<0.002$) than the calcitonin level (11.2 pg/ml) of het mice at a higher baseline ionized calcium of 1.45 mmol/l. These results indicate that the sensitivity for calcitonin release in response to calcium is shifted to the right in het mice, resulting in lower calcitonin concentrations than expected. This confirms that the CaR is a physiological regulator of calcitonin.

M438

Two Novel Mutations in the Calcium-Sensing Receptor Gene in Familial Hypocalciuric Hypercalcemia and Neonatal Severe Hyperparathyroidism. L. D'Souza-Li[1], M. B. D. Silva*[2], M. T. Grande*[2], D. Carvalho*[2], G. Guerra*[3]. [1]Center for Investigation in Pediatrics, State University of Campinas, Campinas, Brazil, [2]Boldrini Children´s Hematological Investigation Center, Campinas, Brazil, [3]Department of Pediatrics, State University of Campinas, Campinas, Brazil.

Neonatal severe hyperparathyroidism (NSHPT) is a rare disorder. In many cases, homozygous inactivating mutations of the calcium-sensing receptor (CASR) gene have been identified. Most heterozygous are clinically asymptomatic but manifest as familial hypocalciuric hypercalcemia (FHH). We report a 10-year old girl who presented with progressive growth of a mass in left maxilla. During the neonatal period, the child's hypotonia, failure to thrive and poor feeding were attributed to congenital toxoplasmosis. The child evolved with bone deformities, rachitic changes, mental retardation, intestinal obstipation and malnourishment. Physical evaluation revealed a wheelchair bound child with 11 kg, with a mass on the left maxilla and on the right knee. In the course of investigation, the biochemical profile showed serum Ca^{++} 18.3 mg/dl, ionized Ca^{++} 2.79 mmol/L, renal calcium clearance 0.0004, Phosphorus 2.04 mg/dl, Mg^{++} 3.37 mg/dl, serum alkaline phosphatase 2,268 IU/L and PTH 671 pg/ml. Several calcifications in pancreatic region and multiple osteolytic lesions on the metaphysis and the diaphysis of left tibia, right femur, left humerus were seen on radiographic images. The cranial CT showed multiple intracranial calcifications and an expansive mass eroding the left maxilla measuring 6.5 x 5.5 x 6.1 cm and invading the nasal and oral cavity, the maxillary sinus, ethmoid bone and the left orbital plate. Biopsy of the tumor was compatible with brown tumor. There is no consanguinity in the family. Serum Ca^{++} is normal in the mother (9.4 mg/dl) and above the higher limit in the father (10,7 mg/dl) with calcium clearance < 0.01. Sequencing of the CASR gene revealed a novel heterozygous point mutation c.1913.G>T [R638L] and also a silent mutation c.2244.C>G in the DNA from the proband and the mother. These mutations were not present in the DNA sample from the father. Due to the severe clinical manifestation in the child, she is probably a compound heterozygous and we are currently searching for another mutation in the father's and in the proband´s DNA samples. This is the first family with mutations in the CASR gene described in Brazil. Common associated factors contributed to the delay in the diagnosis and the irreparable damage to the patient.

M439

Severe Hypercalcemia in a 9-year-old Brazilian Girl Due to a Novel Inactivating Mutation (L13P) of the Calcium Sensing Receptor. K. Miyashiro*[1], T. D. Manna*[2], H. M. Filho*[2], H. Kuperman*[2], D. Damiani*[2], O. M. Hauache[1]. [1]Laboratório de Endocrinologia Molecular, Escola Paulista de Medicina - UNIFESP, São Paulo, Brazil, [2]Unidade de Endocrinologia Pediátrica, Instituto da Crianca - FMUSP, São paulo, Brazil.

Familial hypocalciuric hypercalcemia (FHH) and neonatal severe hyperparathyroidism (NSHPT) are consequent to inactivating mutations of the calcium sensing receptor (CaR) gene. FHH is usually associated with heterozygous inactivating mutations of the CaR gene, whereas NSHPT is usually due to homozygous inactivation of the CaR gene. FHH is generally asymptomatic and is characterized by mild to moderate hypercalcemia, relative hypocalciuria and normal intact PTH. In this study, we report a novel mutation (L13P) in the exon 2 of the CaR gene, identified in a Brazilian patient. The proband was a 9-year-old girl born to consanguineous parents who came to our attention complaining of severe headaches and vomits that started 6 months ago. Laboratorial evaluation revealed hypercalcemia [total calcium:14.1 mg/dL (reference values: 8.2-10.2 mg/dL); ionized calcium: 2.1mmol/L (reference values:1.12-1.32 mmol/L], hypophosphatemia [P: 2.1 mg/dL (reference values: 2.6-6.0 mg/dL)], intact PTH levels varied between 50-110 pg/mL (reference values: 11-62 pg/mL) and relative hypocalciuria (calcium to creatinine clearance ratio = 0.0042). Total parathyroidectomy was performed and revealed parathyroid hyperplasia. Direct sequencing of the CaR gene from this patient showed a novel homozygous mutation (L13P) in exon 2. In this context, nucleotide sequence analysis identified a T → C point mutation at nucleotide 38, resulting in the conversion of CTC (leucine) to CCC (proline) at codon 13 of the CaR gene. This mutation was confirmed by restriction endonuclease analysis using the enzyme *Ban* I. The T → C transition creates a *Ban* I restriction enzyme site (G↓GCACC) so that in the mutant sequence, the digestion results in 2 products of 189 and 61 base pairs (bp). The proband´s parents, who had mild asymptomatic hypercalcemia, showed the same mutation in the heterozygous form. The mutation described in this study is the inactivating missense mutation which is present at the most N-terminal end among the known CaR missense mutations. This study reinforces the fact that patients with homozygous inactivation of the CaR gene may present with severe hypercalcemia in different phases of life.

M440

NF-kappaB Mediates Transcriptional Up-regulation of the Human Calcium-Sensing Receptor Gene by Interleukin-1beta and Tumor Necrosis Factor-alpha. L. Canaff, G. N. Hendy. Medicine, McGill University, Montreal, PQ, Canada.

The calcium-sensing receptor (CASR), expressed in parathyroid gland and kidney tubule, is essential for maintenance of calcium homeostasis. Transcription of the human CASR gene is driven by two promoters (P1 and P2) yielding transcripts having alternative 5' untranslated regions, but encoding the same receptor protein. We have characterized functional vitamin D responsive elements in both promoters (Endocrine Society Meeting, 2002), but other cis-acting elements remain to be identified. Hypocalcemia is common in critically ill patients although the underlying causes are not known. Circulating pro-inflammatory cytokines are increased in such patients, interleukin-1β (IL-1β) increases CASR mRNA levels in cultured bovine parathyroid fragments, and following burn injury in sheep the expression of the parathyroid gland CASR is increased. This would reduce the set-point for PTH suppression by extracellular calcium likely leading to the observed hypocalcemia and hypoparathyroidism. We have investigated whether pro-inflammatory cytokines, via NF-κB activation, upregulate transcription of the CASR gene thereby providing a mechanism for the above observations. Human CASR promoter/luciferase reporter gene constructs were transfected into human proximal tubule kidney (HKC) cells. IL-1β or tumor necrosis factor-α (TNF-α) (5 ng/ml) stimulated transcriptional activity of both P1 and P2 promoters 2-fold over basal. Several potential NF-κB responsive elements are in the human CASR gene promoters. One is in promoter P1, one in exon 1A, one in promoter P2, and one in exon 2. Cotransfection of CASR promoter/luciferase gene constructs with exogenous NF-κB proteins into HKC cells led to increased transcriptional activity with p65 only and the p50/p65 combination but not with p50 only. This is fully consistent with the p65/p65 homodimer and p50/p65 heterodimer being transcriptionally active whereas p50/p50 homodimers are not. Co-transfection with inhibitor I-κB abrogated the responsiveness of the CASR gene promoters to cytokines and exogenous NF-κB proteins. In electrophoretic mobility shift assay with in vitro transcribed/translated p50 and p65, complexes comprising p65/p65 homodimers and to a lesser extent p50/p65 heterodimers, formed on three of the putative NF-κB elements in the following order of intensity, exon 1A>P2>exon2. In conclusion, NF-κB elements in the CASR gene promoters mediate transcriptional up-regulation to pro-inflammatory cytokines. This is likely to contribute, in part, to the hypocalcemia in critically ill patients.

M441

CASRdb, Calcium Sensing Receptor Locus-Specific Database for Mutations Causing Familial (Benign) Hypocalciuric Hypercalcemia, Neonatal Severe Hyperparathyroidism and Autosomal Dominant Hypocalcemia. S. Pidasheva*[1], L. D'Souza-Li*[1], D. E. C. Cole*[2], G. N. Hendy[1]. [1]McGill University, Montreal, PQ, Canada, [2]University of Toronto, Toronto, ON, Canada.

Familial hypocalciuric hypercalcemia (FHH) is caused by heterozygous loss-of-function mutations in CASR, in which the lifelong hypercalcemia is generally asymptomatic. Affected individuals from some FHH kindreds may experience pancreatitis, gallstones or chondrocalcinosis. Homozygous loss-of-function CASR mutations manifest as neonatal severe hyperparathyroidism (NSHPT), a rare disorder characterized by extreme hypercalcemia and the bony changes of hyperparathyroidism which occur in infancy. Activating mutations in the CASR gene have been identified in several families previously diagnosed with autosomal dominant hypocalcemia (ADH), autosomal dominant hypoparathyroidism, or hypocalcemic hypercalcemia. ADH affected individuals may have mild hypocalcemia, and relatively few symptoms. Seizures can occur, especially in younger patients, and these often happen during febrile episodes due to intercurrent infection. Parathesias, tetany and laryngospasm - other symptoms of hypocalcemia - are uncommon. The human CASR gene was cloned in 1993 and so far 80 naturally occurring mutations in it have been published. To have a better understanding of the mutations causing defects in the CASR gene and to define specific regions relevant for ligand receptor interaction and other receptor functions, the data on mutations was collected and the information was centralized in the CASRdb (http://data.mch.mcgill.ca/casrdb). It is easily and quickly accessible by search engine in several Internet servers for search and retrieval of specific information. The information can be searched by mutation, genotype/phenotype, clinical data, *in vitro* analyses and authors of published mutations. CASRdb is regularly updated for new mutations and it also provides a mutation submission form to insure up to date information. The home page of this database provides links to different web pages, which are relevant to the CASR, as well as disease clinical pages, sequence of the CASR gene exons, and position of mutations in the CASR. The CASRdb will help to better understand and analyze the mutations, and aid in structure-function analyses.

M442

Functional Characterization of a Novel CaR Missense Mutation in an Italian Kindred with Familial Hypocalciuric Hypercalcemia. F. Cetani[1], E. Pardi*[1], S. Borsari*[1], E. Morabito*[1], G. Dipollina*[2], A. Pinchera*[1], C. Marcocci[1]. [1]Dipartimento di Endocrinologia & Metabolismo, Università di Pisa, Pisa, Italy, [2]Dipartimento di Endocrinologia e Metabolismo, Università di Pisa, Pisa, Italy.

We describe two unrelated Italian kindreds with familial hypocalciuric hypercalcemia (FHH), an autosomal dominant disease mostly caused by heterozygous inactivating mutations of the Ca^{2+} receptor (CaR). In the proband of family A direct sequencing of the entire coding region of the CaR revealed a novel heterozygous Y218C missense mutation in exon 4. The same mutation was identified in the affected, but not in the unaffected family members, and in any of the 50 unrelated Italian controls. Transient expression of the Y218C CaR in COS-7 cells revealed a blunted Ca^{2+}-evoked accumulation of inositol triphoshates, indicating that the Y218C is a loss-of-function mutation. Cotransfection experiments showed that the mutant receptor had no impact on the function of the wild type receptor, suggesting that a reduced expression of the normal CaR, rather than a dominant negative effect, account for the functional impairment. In the proband of Family B an already described heterozygous P55L missense mutation in exon 2 of the CaR gene was found. The same mutation was identified in the affected family members. In conclusion, we described the two FHH kindreds with loss-of- function mutations of the CaR gene and identified a novel heterozygous mutation (Y218C) characterized by a blunted response to Ca^{2+} stimulation compared to the WT receptor and no interference with the function of the WT CaR.

M443

L-Amino Acids promote Ca2+-sensing Receptor Activity and Inhibit PTH Secretion from Human Parathyroid Cells. A. D. Conigrave*[1], L. Delbridge*[2], E. M. Brown[3], S. J. Quinn*[3]. [1]School of Molecular and Microbial Biosciences, University of Sydney, Sydney, Australia, [2]Department of Surgery, Royal North Shore Hospital, St Leonards, NSW, Australia, [3]Endocrine-Hypertension Division, Brigham and Womens Hospital, Boston, MA, USA.

We previously demonstrated that L-amino acids are allosteric activators of the human calcium-sensing receptor (CaR) stably expressed in HEK-293 cells (1,2). These data led to the prediction that aromatic and aliphatic, but not branch chain or basic L-amino acids, would activate parathyroid CaRs and acutely suppress PTH secretion. In the current study, CaR activation was assessed in collagenase-dispersed normal and adenomatous human parathyroid cells. CaR-induced intracellular Ca2+ mobilization was assessed in fura-2 loaded cells exposed to the CaR agonists Ca2+ and spermine in the presence or absence of L- or D-amino acids. PTH secretion was determined from separate parathyroid cell incubations (37 °C, 30 min) and, after storage of samples at –80 °C, intact PTH was measured using an autoanalyser. We confirmed that the aromatic amino acids L-Phe, L-Trp and the aliphatic amino acid L-Ala (0.3 – 10 mM), but not L-Leu, L-Ile or L-Arg stereoselectively activated parathyroid CaRs in the presence, but not the absence, of submaximal concentrations of the CaR agonists Ca2+ or spermine. Furthermore, active amino acids left-shifted the concentration-dependence curves for both Ca2+ and spermine. Similar behavior was observed in normal and adenomatous cells, however, the responses exhibited greater sensitivity in normal parathyroid cells. In addition, L-Phe stereoselectively inhibited intact PTH secretion from normal and adenomatous cells in acute 30 min incubations at 37 °C. This effect exhibited a leftward shift in the extracellular Ca2+ concentration dependence at lower amino acid concentrations (<= 3 mM) and a suppression of baseline PTH secretion at higher amino acid concentrations (10 mM). Acute activation of parathyroid CaRs by aromatic and aliphatic L-amino acids may contribute to the phenomena of high protein diet induced hypercalciuria (3) and/or low protein diet induced secondary hyperparathyroidism (4,5) in humans.

1. Conigrave, A. D., Quinn, S. J., and Brown, E. M. (2000) Proc. Natl. Acad. Sci. USA 97, 4814-4819
2. Kobilka, B. (2000) Proc. Natl. Acad. Sci. USA 97, 4419-4420
3. Johnson, N. E., Alcantara, E. N., and Linkswiler, H. (1970) J. Nutr. 100, 1425-1430
4. Kerstetter, J. E., Caseria, D. M., Mitnick, M. E., Ellison, A. F., Gay, L. F., Liskov, T. A. P., Carpenter, T. O., and Insogna, K. L. (1997) Am. J. Clin. Nutr. 66, 1188-1196
5. Kerstetter, J. E., Svastisalee, C. M., Caseria, D. M., Mitnick, M. E., and Insogna, K. L. (2000) Am J Clin Nutr 72, 168-173

M444

Calcium-Sensing Receptor Stimulates PTHrP Secretion by PKC Dependent p38 Pathway. J. Tfelt-Hansen*, R. J. MacLeod*, N. Chattopadhyay*, E. M. Brown. Endocrine-Hypertesion Division and Membrane Biology Program, Brigham and Women's Hospital, Boston, MA, USA.

PTHrP is the main mediator of Humoral Hypercalcemia of Malignancy (HHM).The xenotransplantable rat leydig cell cancer, H-500, is a well established model for HHM. Previously, we showed that activating the calcium-sensing receptor (CaR) increases PTHrP secretion from these cells. We show CaR activation upregulates PTHrP transcripts assessed by Northern analysis, because elevated extracellular calcium (Ca2+o) (8.0 mM) upregulated PTHrP mRNAs within 6 h. In order to understand the signaling mechanisms underlying the CaR-mediated increase in PTHrP secretion, we studied the involvement of various MAP kinase (MAPK) pathways by using specific pharmacological inhibitors. We found that a pan-PKC inhibitor, GF109203X (1 uM), inhibited PTHrP secretion in response to high Ca2+o (8 mM) by 30% of the control value while having no effect on basal (Ca2+o = 0.5 mM) PTHrP secretion. A similar pattern of inhibition was observed using the p38 MAPK inhibitor, SB-203580 (10 uM). Both PKC and p38 MAPK inhibitors together had no additive effect on the inhibition of PTHrP secretion in response to high Ca2+o, suggesting PKC-dependent activation of p38 MAPK by the CaR. In this study SB203580 and GF109203X inhibited high Ca2+o-stimulated PTHrP secretion by 67% of control, but had no effect on basal PTHrP secretion. Furthermore, we observed 77% and 63% attenuation of PTHrP secretion in response to 8 mM Ca2+o by the MEK inhibitor PD098059 (10 uM) and the JNK inhibitor, SP-625 (20 uM), respectively. However, basal PTHrP secretion was inhibited 49% and 61%, respectively, by these two inhibitors. Therefore, our data show that although PKC-dependent activation of p38 MAPK is the major mediator of CaR-stimulated PTHrP secretion, involvement of ERK1/2 and JNK pathways can not be overruled. Given the availability of the p38 MAPK inhibitor for in vivo use, these results may impact the therapeutic strategies available for treatment of HHM.

M445

$1,25(OH)_2D_3$ Regulates PKC via Two PLA_2-dependent Pathways: Lysophospholipid and PLC-beta v. Arachidonic Acid and PGE_2. V. L. Sylvia, Z. Schwartz, D. Shaked*, R. R. Hardin*, D. D. Dean, B. D. Boyan. Orthopaedics, The University of Texas Health Science Center at San Antonio, San Antonio, TX, USA.

Phospholipid metabolism is critical to the regulation of protein kinase C (PKC) and PKC-dependent chondrocyte differentiation by $1\alpha,25\text{-}(OH)_2D_3$ (1,25). 1,25 causes rapid changes in arachidonic acid (AA) turnover and metabolism, as well as production of inositol 1,4,5-trisphosphate (IP3) and diacylglycerol (DAG) in chondrocytes from the prehypertrophic and upper hypertrophic zones of the costochondral cartilage growth plate. This implicates phospholipase A_2 (PLA_2) and phospholipase C (PLC) in the mechanism of PKC activation. Here, we examined if PLC-dependent PKC is regulated via PLA_2 in costochondral chondrocytes and determined which isoform of PLC is involved. 1,25 (10^{-10}-10^{-8}M) stimulated PLC and PKC activity in a dose-dependent manner. Increases were observed within 0.5 min and peak activity was at 9 min. $1\beta,25(OH)_2D_3$, $24R,25(OH)_2D_3$ and $24S,25(OH)_2D_3$ had no effect on either enzyme, demonstrating the specificity of the response. Activation of PLA_2 by mastoparan increased both PLC and PKC and inhibition of PLA_2 by quinacrine blocked the effect of 1,25 on both enzymes. However, AA and its metabolite PGE_2 only affected PKC. Moreover, PGE_2 (EP) receptor agonists only affected PKC. This suggests that lysophospholipid may mediate the PLA_2-dependent effect on PLC. To test this, cells were treated with lysophosphatidylcholine (LPC) and lysophosphatidylethanolamine (LPE), both of which activated PLC and augmented the effects of 1,25. The effects of PLA_2 stimulation on PLC and PKC, and of AA and PGE_2 on PKC were mediated by Gq protein. GDPβS blocked basal and 1,25-stimulated PLC and PKC, whereas the Gi inhibitor pertussis toxin did not. RT-PCR showed that the cells express PLC-β1a, PLC-β1b, PLC-β3 and PLC-γ1 isoforms. Antibodies to PLC-β1 and PLC-β3 blocked the stimulatory effect of 1,25 on PLC activity whereas antibodies to PLC-δ and PLC-γ had no effect. These results indicate that 1,25 regulates costochondral chondrocytes via two parallel membrane-mediated pathways. One pathway is through PLA_2-dependent production of lysophospholipid, activation of PLC, and DAG-dependent activation of PKC. The other is via PLA_2-dependent production of AA and PGE_2, which then activate PKC.

M446

Comparative Effects of Repletion with Calcium or Calcitriol in Chronically Hypocalcemic Vitamin D Depleted Rats on Bone Formation and Resorption Parameters. N. Dion, C. Deschênes*, G. Mailhot*, M. Gascon-Barré, L. G. Ste-Marie. Hôpital Saint-Luc, CHUM Research Centre, Montréal, PQ, Canada.

Adequate dietary intake of vitamin D (D) and calcium (Ca) are essential to ensure normal bone formation, mineralization and growth. To study the role of Ca and calcitriol (CT) in bone metabolism, non-rachitic rats with severe hypocalcemia secondary to D and Ca depletions (Ca-D-) were subjected to repletion protocols containing either a high dietary Ca content (Ca+) for 14 d or physiological i.p. concentrations of calcitriol (CT+) for 7 d or 14 d. Ca-D- rats matched for age and weight were also studied. Normocalcemic rats paired for weight served as controls (C). Histomorphometric measurements were performed on trabecular bone at the secondary spongiosa of proximal tibiae. Structural parameters (BV/TV, Tb.Th, Tb.Sp, Tb.N) were found to be similar in all groups. Ca-D- rats showed hyperosteoidosis (OV/BV $p<0.05$; OS/BS $p<0.01$; O.Th $p<0.001$) when compared to C. Although no tetracycline labeling (TL) was observed in the metaphysis, a few were seen in the epiphysis suggesting that some mineralization occurred in this group. Repletion with CT+ induced at 7d and 14d a significant normalization of static bone formation parameters to a level similar to that of C. The presence of linear TL confirmed ongoing mineralization but, at a slower rate than C as indicated by the absence of double TL. Moreover, in CT+14d rats, there was a significant reduction of the bone resorption parameter, ES/BS, compared to Ca-D- and C ($p<0.05$ and $p<0.001$, respectively). In addition, CT+14d showed a significant reduction of osteoclast number (N.Oc/B.Pm)compared to C. These changes in bone resorption parameters were dependent on time exposure as CT+7d rats were not significantly different from Ca-D- and C groups. In contrast, Ca+ rats tended to have lower static bone formation parameters than Ca-D- although they were found to be higher than in CT+ and C groups. Absence of well defined TL confirmed a severe mineralization defect despite the normalization of serum Ca and secondary hyperparathyroidism. Significant widening of the growth plate in Ca+ rats ($p<0.001$ compared to all groups) was mainly due to higher hypertrophic chondrocytes with intense alkaline phosphatase activity. The data indicate that chronic Ca and D depletions in the rat induces hyperosteoidosis with some impairment of bone mineralization. Calcitriol repletion alone induces normalization of bone formation and mineralization allowing bone recovery after Ca and D depletion diet. Despite normalization of serum Ca and reduction of trabecular osteoidosis, Ca+ repletion induces hypophosphatemia leading to the development of rickets and severe impairment of bone mineralization.

M447

NfκB Suppression of VDR Transactivation Is not due to Competition for p160 Nuclear Proteins. X. Lu*[1], H. W. Sepp*[1], X. He*[1], P. Farmer[2], J. Rubin[1], M. S. Nanes[1]. [1]Division of Endocrinology, Department of Medicine, Emory University and VAMC, Atlanta, GA, USA, [2]Department of Pathology, Emory University, Atlanta, GA, USA.

Vitamin D-stimulated gene transcription requires binding of a liganded VDR to DNA and assembly of a protein complex that modifies histone and activates RNA Polymerase II. The modification of histone may occur by acetylation (HA) or de-acetylation (HDAC). Multiple nuclear proteins participate in transcriptional activation, including the p160 co-activators CBP/p300 and also SRC-1, which contain intrinsic HA activity. We have previously shown that vitamin D-stimulated transcription is suppressed by the inflammatory cytokine TNF-α and that the suppression of VDR activity is due to activation of the transcription factor NfκB. Furthermore, NfκB suppression of VDR can be localized to the p65 subunit of NfκB. To determine if NfκB-p65 suppressed VDR transactivation by stimulating a histone de-acetylase (HDAC), ROS 17/2.8 cells were transiently transfected with a VDRE-luciferase reporter and treated with 1,25(OH)2D3 (vitD) in the presence or absence of the HDAC inhibitors trichostatin A (TCA) or sodium butyrate (NaBut). Forced expression of p65 inhibited vitD-stimulated transcription >90%, as expected. Treatment with either TCA or NaBut alone increased vitD-stimulated transcription but failed to prevent the p65 inhibition. These results showed that p65 did not suppress VDR function by activation of a HDAC and suggested that p65 may compete for HA or other accessory proteins. To determine if p65 competed with the VDR or RXR for binding to CBP or SRC-1, GST-VDR or GST-RXR fusion proteins were used in pull-down assay with in vitro translated 35S-CBP or 35S-SRC-1. 35S-CBP failed to bind VDR or RXR with or without their cognate ligands (vitD or 9-cisRA). VitD stimulated binding of the VDR to SRC-1 and this interaction was enhanced by addition of RXR. However, the addition of in vitro translated p65 failed to block VDR (or RXR) interaction with SRC-1. Additionally, in vitD-treated ROS 17/2.8 cells, p65 inhibition of the VDRE-luciferase reporter activity was not reversed by forced expression of CBP or SRC-1. These results suggest that NfκB suppression of VDR function is not due to competition for the p160 coactivators. NfκB may act on other accessory proteins, pre-initiation factors, or RNA Polymerase itself to inhibit vitamin D action.

M448

Regulation of CaT1 and ECaC1 mRNA Levels by Calcitriol in the Duodenum and Kidney of Mice. Y. Song*, J. C. Fleet. Interdepartmental Program in Nutrition, Purdue University, West Lafayette, IN, USA.

The calcium channels ECaC1 and ECaC2 (i.e. CaT1) have been proposed to play a role in calcium (Ca) transport in duodenum and kidney but their regulation has not been systematically studied in whole animals. Here we examined the regulation of CaT1 and ECaC1 mRNA levels by diet and calcitriol injection in mice. Calbindin D_{9k} (CaBP9k) mRNA was examined for comparison. Animals were raised on chow diet until 90 days of age. In study I, mice were fed a normal Ca (0.5% Ca, AIN76A base), high Ca (2% Ca), or low Ca diet (0.02% Ca) for 7 days. At day 97, duodenal scraping and kidney were harvested for mRNA analysis, and duodenal Ca absorption was measured by in *situ* ligated loops (2 mM Ca, 10 min incubation). Plasma calcitriol levels were decreased 83% on the high Ca diet, and increased 81% on the low Ca diet; duodenal Ca absorption was strongly correlated with plasma calcitriol levels (r^2=0.8). Duodenal CaBP9k, CaT1 and ECaC1 mRNA levels were reflective of changes in serum calcitriol and correlated with Ca absorption. Duodenal CaBP9k, CaT1 and ECaC1 mRNA were significantly decreased by 56%, 87% and 66% on the high Ca diet, and increased 120%, 100% and 160% on the low Ca diet, respectively. Renal CaBP9k mRNA was decreased by 53% on the high Ca diet and increased 50% on the low Ca diet while renal CaT1 and ECaC1 mRNA were not affected by diet. In study II, mice were given a 0.8% strontium diet for 7 days (to reduce serum calcitriol), injected with calcitriol (200 ng/100g body weight, s.c.), and tissues were harvested at 0, 1, 3, 6, and 16 hours after injection. The pattern of regulation was different among the genes in duodenum and kidney suggesting distinct regulatory mechanisms. Duodenal CaT1 and ECaC1 mRNA accumulation was rapid (peak induction of 12X and 11X at 3 h, respectively) and suggests transcriptional regulation. CaBP9k mRNA was gradually increased along the time course in duodenum (6X at 16 h) and kidney (3X at 16 h). Renal CaT1 and ECaC1 mRNA peaked at 6 hours (2X) and maintained this level to 16 h. This suggests that the renal CaT1 and ECaC1 as well as duodenal and renal CaBP9k mRNA levels may be regulated post-transcriptionally (e.g. by mRNA stabilization). In conclusion, our data show that CaT1 and ECaC1 mRNA levels are strongly regulated by calcitriol in vivo but that the mechanism of regulation is different in duodenum and kidney.

M449

Down-Regulation of the Gene for the cAMP-Dependent Protein Kinase Inhibitor: Requirement for the VDR and Analysis of the Promoter Region. B. Holmquist, R. Zielinski*, H. Shah*, H. L. Henry. Biochemistry, University of California, Riverside, CA, USA.

The seco-steroid hormone 1α,25-dihydroxyvitamin D_3 (1α,25$(OH)_2D_3$) is the major biologically active metabolite of vitamin D. The primary mechanism by which 1α,25$(OH)_2D_3$ generates biological responses is alteration of the expression of target genes through binding of the ligand-activated vitamin D receptor (VDR). These changes can be regulated both tissue-specifically and developmentally. Ligand activated VDR has been shown to increase gene transcription through binding as a heterodimer with the 9-cis retinoic acid receptor (RXR) to a vitamin D response element (VDRE) in the promoter region of 1α,25$(OH)_2D_3$ targeted genes. We have studied the tissue-specific regulation by 1α,25$(OH)_2D_3$ of the endogenous inhibitor of cyclic AMP-dependent protein kinase (PKI) in chick kidney. Treatment with 1α,25$(OH)_2D_3$ decreases PKI activity in primary cultures of chick kidney cells and also decreases steady state levels of chick kidney PKI mRNA both in vivo and in cell culture. In the present studies, we show by quantitative competitive RT-PCR that in the mouse, in which three separately encoded forms of PKI, designated α, β, and γ, have been identified, it is PKIα that is down-regulated by 1α,25$(OH)_2D_3$ in the kidney. Furthermore, down-regulation of PKIα does not occur in mice genetically homozygous for the absence of the VDR, providing confirmation that this is a VDR-mediated process. To further study the molecular mechanism of transcriptional repression of the PKIα gene, the chick genomic clone was obtained through library screening with the PKI cDNA. A putative negative VDRE (nVDRE) was found in the PKI promoter sequence within 50 bp of the TATA box along with an unusually large (363nt) 5'-untranslated region. We have established a functional assay for 1α,25$(OH)_2D_3$ –mediated down-regulation of this promoter region using various constructs of the PKI promoter linked to the secreted alkaline phosphatase (SEAP) reporter. Plasmid constructs were transiently transfected into primary cultures of chicken kidney cells and exposed to either 1α,25$(OH)_2D_3$ or vehicle. Using this assay we have found that the 5'-untranslated region is essential for reporter gene expression. Down-regulation of reporter expression by 1α,25$(OH)_2D_3$, which is consistently to approximately 50% of control levels, requires the 105bp immediately upstream of the transcription start site. Further analysis will focus on the relative contributions of sequence and position of this nVDRE to effective down-regulation of PKIα.

M450

1,25(OH)2-vitamin D3 Activates Muscle Cell PLC gamma through the Tyrosine Kinase c-Src and PI3-quinase. C. Buitrago*[1], V. Gonzalez Pardo*[1], A. Russo de Boland*[2]. [1]Dept. Biologia, Bioquimica & Farmacia, Universidad Nacional del Sur, Bahia Blanca, Argentina, [2]Biologia, Bioquimica & Farmacia, Universidad Nacional del Sur, Bahia Blanca, Argentina.

We have previously demonstrated that the steroid hormone 1α,25(OH)2-vitamin D3 [1α,25(OH)2D3] stimulates the production of inositol trisphosphate (IP3), the breackdown product of PIP2 by phospholipase C (PI-PLC), and activates the cytosolic tyrosine kinase c-Src in skeletal muscle cells. In the present study we examined whether 1α,25(OH)2D3 induces the phosphorylation and membrane translocation of PLCgamma and the mechanism involved in this isozyme activation. We found that the steroid hormone triggers a significant phosphorylation on tyrosine residues of PLC gamma and induces a rapid increase in membrane-associated PLC gamma immunoreactivity with a time course that correlates with that of phosphorylation in muscle cells. Genistein, a tyrosine kinase inhibitor, blocked the phosphorylation of PLCgamma. Inhibition of 1α,25(OH)2D3 -induced c-Src activity by its specific inhibitor PP1 or muscle cell transfection with an antisense oligodeoxynucleotide directed against c-Src mRNA, prevented hormone stimulation of PLCgamma tyrosine phosphorylation. The isozyme phosphorylation is also blocked by both wortmannin and LY294002, two structurally different inhibitors of phosphatidyl inositol 3-kinase (PI3K), the enzyme that produces PIP3 known to activate PLCgamma isozymes specifically by interacting with their SH2 and PH domains. The hormone also increases the physical association of c-Src and PI3K with PLCgamma and induces a c-Src-dependent tyrosine phosphorylation of the p85 regulatory subunit of PI3K. The time course of hormone-dependent PLCgamma phosphorylation closely correlates to the time course of its redistribution to the membrane, suggesting that phosphorylation and redistribution to the membrane of PLCgamma are two interdependent events. 1α,25(OH)2D3-induced membrane translocation of PLCgamma was prevented to a great extent by c-Src and PI3K inhibitors, PP1 and LY294002. Taken together, the present data indicates that the cytosolic tyrosine kinase c-Src and PI3-kinase play indispensable roles in 1α,25(OH)2D3 signal transduction cascades leading to PLCgamma activation.

M451

Daily Skin Dose of Vitamin D_3 in Healthy Men with Intensive Summer Sun Exposure. M. J. Barger-Lux[1], R. P. Heaney[1], T. C. Chen[2], M. F. Holick[2]. [1]Creighton University, Omaha, NE, USA, [2]Boston University, Boston, MA, USA.

We report here the results of work to determine daily input of vitamin D_3 among outdoor workers with intensive summer sun exposure. Subjects were 30 healthy men who had just completed a summer of extended outdoor activity (e.g., landscaping, construction work, farming, or recreation). We estimated duration and extent of sun exposure as total daytime hours outdoors and body surface area exposed by usual outdoor attire, and measured serum 25(OH)D twice, to mark the end of summer sun exposure (Aug. 3 to Sept. 2) and the end of winter sun deprivation (Feb. 1 to Mar. 20). Between-visit intervals for the 26 subjects who completed both visits ranged from 158 to 227 days. Median seasonal difference in 25(OH)D was 48.6 nmol/L. In earlier work carried out during winter, we examined the dose-response relationship between oral vitamin D_3 and serum 25(OH)D in healthy men. For every μg of vitamin D_3 given daily, serum 25(OH)D settled at an equilibrium level that was higher by about 0.70 nmol/L. We used this relationship to estimate the daily skin dose of vitamin D_3 among the subjects of the present study. The median effect of summer sun exposure among our subjects was equivalent to an oral dose of 69.5 μg/d (2780 IU/d) of vitamin D_3. Over the winter, the median daily rate of decrease in 25(OH)D was 0.2758 nmol/L, and 25(OH)D of more than half of the subjects fell below 80 nmol/L. In general terms, a level of at least 80 nmol/L at the end of winter could be expected if serum 25(OH)D was at least 128 nmol/L in late summer. However only 12 of 26 (46%) of our subjects achieved late summer levels this high. If duration and extent of an individual's summer sun exposure are known, our data could be used to predict summer 25(OH)D increment. For example, a typical gardening hobbyist might accrue roughly 112 hours of summer sun exposure (i.e., 7 hr/wk for 16 wks) while exposing about 41% of body surface area (e.g., attired in a short-sleeved shirt, shorts, and a hat). These conditions predict a summer 25(OH)D increment of only about 6 nmol/L. This estimate is probably low, since cholecalciferol synthesis is greater in pale skin than in tanned. Nevertheless, casual sun exposure at mid latitudes is not sufficient to ensure optimal 25(OH)D levels year round.

Disclosures: ***M.J. Barger-Lux****, Dairy Council of Nebraska 5.*

M452

Dahl Salt-sensitive Rats Excrete 25-Hydroxyvitamin D into Urine. M. Thierry-Palmer[1], A. Doherty*[1], M. A. Bayorh*[2], K. Griffin*[1]. [1]Biochemistry, Morehouse School of Medicine, Atlanta, GA, USA, [2]Pharmacology, Morehouse School of Medicne, Atlanta, GA, USA.

Plasma 25-hydroxyvitamin D concentration of Dahl salt-sensitive rats (S) is markedly decreased in response to high salt intake (J. Steroid Biochem. Molec. Biol. 66: 255-61, 1998). Exogenous 25-hydroxycholecalciferol, administered by osmotic pumps, did not increase plasma 25-hydroxyvitamin D concentration, suggesting a higher rate of metabolism and/or clearance of 25-hydroxyvitamin D when S rats are fed a high salt diet (J. Steroid Biochem. Molec. Biol. 67: 193-9, 1998). We have conducted studies to determine whether excretion into urine is a mechanism for the decrease in plasma 25-hydroxyvitamin D concentration of S rats during high salt intake. Dahl S and salt-resistant (R) female rats (120-130 g) were fed low (0.3%) or high salt (8%) diets for two weeks. Urine was collected at baseline and weekly. 25-Hydroxyvitamin D, purified from three ml of urine by HPLC, was determined by protein binding assay. 25-Hydroxyvitamin D binding activity in urine was determined by binding to tritiated 25-hydroxycholecalciferol (10,000 dpm) in the presence and absence of 200-fold unlabeled 25-hydroxycholecalciferol. Female S rats excreted 11 ± 3 ng 25-hydroxyvitamin D /24 hr into urine at week 2 of low salt intake, whereas excretion by female R rats was non-detectable. Female S rats excreted 104 ± 16 ng 25-hydroxyvitamin D/24 hr at week 2 of high salt intake. This level was five times that of female R rats at week 2 of high salt intake (20 ± 6 ng/24 hr) and nine times that of S rats at week 2 of low salt intake. The calculated 25-hydroxyvitamin D binding activity in the 24 hr urine of female S rats was 79 ± 11 pmol/hr at week 2 of high salt intake, two times that in the urine of S rats at week 2 of low salt intake (33 ± 10 pmol/hr) and greater than 35 times that in the urine of female R rats at week 2 of low (1.5 ± 1.4 pmol/hr) or high salt intake (2.1 ± 1.5 pmol/hr). We conclude that S rats excrete 25-hydroxyvitamin D and 25-hydroxyvitamin D binding activity into urine during low salt intake, and that this excretion is markedly increased during high salt intake. It has not yet been determined whether altered cubilin/megalin delivery of vitamin D binding protein/25-hydroxyvitamin D to the kidney of S rats explains the loss of 25-hydroxyvitamin D and 25-hydroxyvitamin D binding activity into urine during low salt intake.

M453

1,25-Dihydroxyvitamin D_3 Modulates Voltage Sensitive Calcium Channel Expression and Function in Murine Osteoblastic Cells. J. J. Bergh*, E. Puente*, M. C. Farach-Carson. Department of Biological Sciences, University of Delaware, Newark, DE, USA.

The balance of osteoblast/osteoclast activity maintains bone density. Osteoclastogenesis is regulated by signals generated by osteoblastic cells responding to environmental cues. As serum Ca^{2+} levels decrease, an elevation in 1,25-dihydroxyvitamin D_3 (1,25$(OH)_2D_3$) production occurs. 1,25$(OH)_2D_3$ triggers secretion of receptor activator of NF kappa B ligand (sRANKL). sRANKL stimulates osteoclast maturation, leading to bone resorption and liberation of stored Ca^{2+}. The mechanism by which the osteoblastic response to 1,25$(OH)_2D_3$ stimulates sRANKL production and secretion remains unknown. We previously have shown that, within millisecs of exposure to 1,25$(OH)_2D_3$, an increase in Ca^{2+} influx across the osteoblast plasma membrane occurs via activation of L-type voltage-sensitive calcium channels (VSCCs). This elevation in intracellular Ca^{2+} initiates downstream signaling cascades, including secretion of various proteins, a process known as excitation-secretion coupling. Longer exposure to 1,25$(OH)_2D_3$ leads to changes in gene expression, including decreasing expression of the dihydropyridine (DHP)-sensitive α_1 subunit of the L-type VSCC ($Ca_V1.2$), previously shown to modulate plasma membrane permeability to Ca^{2+} in the proliferating osteoblast. Functional data show, however, that the DHP-sensitive current is replaced in the 1,25$(OH)_2D_3$-treated osteoblast with a novel Ca^{2+} current that is not sensitive to DHP. To identify the source of this current, we used real-time RT-PCR, confocal microscopy, and $^{45}Ca^{2+}$ flux assays to measure the changes in expression and activity of the α_1 subunit of different families of VSCCs. We find that as $Ca_V1.2$ expression decreases, there is a concomitant increase in the expression and activity of the T-type channel $Ca_V3.2$. We conclude that Ca^{2+} permeability of the osteoblast treated with 1,25$(OH)_2D_3$ is maintained through the up-regulation of $Ca_V3.2$, a process that we believe necessary to maintain a secretory state. We are currently examining how changes in the VSCC expression affect sRANKL secretion along with that of its regulatory partner, osteoprotegerin (OPG). (Supported by DE12641, to MCF-C).

M454

The Effect of Differentiation on Nuclear Vitamin D Receptor (VDR) Function in Human Intestinal Cells. A. Klopot*[1], K. Hance*[1], L. Wang*[1], J. Barsony[2], J. C. Fleet[1]. [1]Foods and Nutrition, Purdue University, West Lafayette, IN, USA, [2]National Institutes of Health, Bethesda, MD, USA.

$1,25(OH)_2$ vitamin D_3 (calcitriol) regulates intestinal calcium absorption through VDR-mediated gene expression. We examined the effect of enterocyte differentiation on calcitriol-mediated transcriptional (25-hydroxyvitamin D-24-hydroxylase (CYP24) mRNA levels) and post-transcriptional actions (calbindin D9k (CaBP9k) mRNA levels) in proliferating (2d cultures), post-proliferative (8d) and differentiated (15d) Caco-2 cells. The induction of CYP24 mRNA by calcitriol (8h, 10 nM) was 15X higher in 8d cultures and 25X higher in 15d cells compared to 2d cells. In contrast, calcitriol (48h, 100 nM) increased CaBP9k mRNA levels by 2-fold at all stages of culture while CaBP9k mRNA levels increased 300X from 2 to 15d. These findings suggest that enterocyte proliferation is associated with blunted calcitriol-mediated transcription. VDR protein levels increase 2X between 2 and 15d cells and do not fully explain our observations. Using confocal microscopy, we examined whether cell stage influenced calcitriol-induced nuclear translocation of VDR in the BBe clone of Caco-2 using cells transiently transfected with a GFP-VDR expression vector. In 2d and 15d cultures, GFP-VDR distribution was 60% nuclear:40% cytoplasmic and evenly distributed from the basolateral to the apical membrane. Fluorescence recovery after photobleaching (FRAP, 8 mm2, 100% power, 10 sec) was used to assess GFP-VDR redistribution kinetics in response to 100 nM calcitriol. In both 2d and 15d cells, calcitriol induced a rapid translocation of GFP-VDR to the nucleus (2-fold above control at 2.5 min) that was complete within 15 minutes. This suggests that the resistance to calcitriol in proliferating cells is not due to a defect in nuclear translocation. DNA microarray analysis of BBe cell differentiation reveals that steroid receptor coactivator-1e mRNA levels increase 75% from 2d to 8d and 300% from 2d to 15d in culture. Future studies will be required to determine whether reduced coactivator levels or impaired VDR-protein or VDR-DNA interactions lead to lower vitamin D-mediated gene transactivation in proliferating Caco-2 cells.

M455

1,25-dihydroxyvitamin D Downregulates Cell Membrane and Nuclear Growth Promoting Signals by the Epidermal Growth Factor Receptor. J. Cordero*[1], M. Cozzolino*[1], Y. Lu*[1], E. Sltopolsky[1], M. Vidal*[1], P. Stahl*[2], A. Barbieri*[2], A. S. Dusso[1]. [1]Renal Division, Washington University, St. Louis, MO, USA, [2]Cell Biology and Physiology, Washington University, St. Louis, MO, USA.

The severity of parathyroid (PT) hyperplasia in renal failure correlates with PT expression of transforming growth factor-α (TGF-α), a ligand for the epidermal growth factor receptor (EGFR). Since 1,25-dihydroxyvitaminD$_3$ [$1,25(OH)_2D_3$], the hormonal form of vitamin D, effectively suppresses PT growth, this study examined $1,25(OH)_2D_3$ regulation of TGFα/EGFR growth signals. Due to the lack of a PT cell line, we used human epidermoid A431 cells, which mimic hypeplastic PT cells in overexpressing TGF-α and EGFR. $1,25(OH)_2D_3$ inhibited autocrine and EGF-induced A431 cell proliferation. In the absence of exogenous ligand, $1,25(OH)_2D_3$ changed cellular EGFR localization from the plasma membrane to early endocytic compartments, leading to a reduction in ^{125}I-EGF-specific binding to cell surface EGFR. Consequently, $1,25(OH)_2D_3$ inhibited EGF-dependent activation by tyrosine-phosphorylation of EGFR and the downstream MAPK, ERK1/2. The cytosolic TGF-α/EGFR co-localization in $1,25(OH)_2D_3$-treated cells suggests that the sterol also impairs EGFR activation by the endogenous ligand. This is further supported by a marked reduction in phosphorylated ERK1/2 in the nucleus, an index of autocrine TGFα/EGFR signaling. However, not only is $1,25(OH)_2D_3$ inhibition of autocrine A431 growth more potent than that of saturating concentrations of a TGF-α neutralizing antibody, but simultaneous treatment with $1,25(OH)_2D_3$ and anti-TGF-α exerts additive inhibition of A431 growth. In fact, $1,25(OH)_2D_3$ also impairs nuclear translocation of activated EGFR and its binding to AT-rich DNA sequences, known to mediate EGFR-transactivation of cyclin D1. These results demonstrate that $1,25(OH)_2D_3$, alters EGFR trafficking, reducing its levels at the plasma membrane and in the nucleus, thus shutting down autocrine proliferation signals and impairing further EGFR activation by exogenous ligand.

M456

Vitamin D Stimulates the Expression of Interleukin-1 Receptor Antagonist in Mouse Keratinocytes. J. Kong*, Y. Li. Medicine, University of Chicago, Chicago, IL, USA.

Interleukin-1 (IL-1) is a key mediator in inflammatory reactions. Keratinocytes are the largest source of pro-IL-1, and excessive production of IL-1 by keratinocytes has been implicated in psoriasis and other inflammatory and hyperproliferative skin diseases. One important cytokine that modulates the biologic effect of IL-1 is IL-1 receptor antagonist (IL-1Ra), which specifically binds to both type I and II IL-1 receptors to antagonize IL-1 signaling. Therefore, IL-1Ra regulates the activity of both IL-1a and IL-1b. Two isoforms of IL-1Ra resulted from alternative splicing of two distinctive first exons have been identified, and keratinocytes mainly express the intracellular isoform (icIL-1Ra). It is known that 1,25-dihydroxyvitamin D3 [1,25(OH)2D3] has immunosuppressive activity, and has been used to effectively treat psoriasis; therefore, we investigated the effect of vitamin D on icIL-1Ra expression in primary keratinocytes derived from 3-day old mice. Northern blot analyses showed that treatment of keratinocytes with 1,25(OH)2D3 stimulates icIL-1Ra mRNA expression in a dose- and time-dependent manner. The maximal stimulation (3 to 5-fold) was seen after 24-hour treatment with 10-8 M of 1,25(OH)2D3. Similar induction was also detected at the icIL-1Ra protein level. The increase of icIL-1Ra mRNA expression was abolished by cycloheximide, suggesting that new protein synthesis is required for icIL-1Ra stimulation. Moreover, 1,25(OH)2D3 had no effect on icIL-1Ra expression in VDR(-/-) keratinocytes derived from VDR null mice, but the stimulation was restored in keratinocytes derived from VDR(-/-) mice that specifically express human VDR in the skin, indicating that VDR is required to mediate the effect of 1,25(OH)2D3 on icIL-1Ra expression. When keratinocytes were transfected with a reporter plasmid containing 4.5 kb 5'-flanking sequence of human icIL-1Ra gene, the promoter activity was increased 3-fold by 1,25(OH)2D3 treatment. Thus it is concluded that 1,25(OH)2D3 increases icIL-1Ra gene transcription. These results suggest that vitamin D can suppress IL-1 activity and cutaneous inflammatory reactions through stimulation of IL-1Ra expression in keratinocytes.

M457

Vitamin D-Induced Artery Calcification and Calciphylaxis Are both Inhibited in the Same Rat by Doses of Ibandronate that Inhibit Bone Resorption. P. A. Price, N. Omid*, T. Nguyen*, M. K. Williamson. Division of Biology, University of California, San Diego, La Jolla, CA, USA.

The present experiments were carried out to test the hypothesis that all ectopic calcifications induced by treatment with toxic doses of vitamin D are linked to bone resorption. In previous studies we showed that lethal doses of vitamin D cause extensive calcification of arteries, lungs, kidneys, and cartilage, and that doses of the amino bisphosphonate ibandronate that inhibit bone resorption completely inhibit each of these soft tissue calcifications and prevent death (ATVB (2001)21:817-824). In the present experiments we have examined the effect of ibandronate on an entirely different type of ectopic calcification, the calciphylaxis induced by administration of a challenger to rats previously treated with sublethal doses of vitamin D. The present studies show that ibandronate doses that inhibit bone resorption completely prevent artery calcification as well as, in the same rat, the Alizarin red-staining for calcification at sites of calciphylactic challenge by either subcutaneous injection of 300μg $FeCl_3$ or intrascapular epilation. Chemical analysis further showed that the level of calcium was increased by 40-fold at the $FeCl_3$-induced calciphylaxis site and by 100-fold at the skin epilation-induced calciphylaxis site, and that concurrent treatment with ibandronate reduced calcium to control levels at both sites. Since vitamin D treatment dramatically increased levels of bone resorption, and concurrent treatment with ibandronate normalized resorption, these results support the hypothesis that all soft tissue calcifications in the vitamin D treated rat may be linked to bone resorption. This hypothesis is also supported by the present observation that the effect of vitamin D dose on bone resorption activity, artery calcification, and caliphylaxis in the same animal are essentially identical. The underlying biochemical mechanism responsible for the linkage between bone resorption and ectopic calcifications is presently unknown. Since serum calcium levels in animals treated with vitamin D plus ibandronate are not significantly different from the elevated levels seen in animals treated with vitamin D alone, the ectopic calcifications induced by vitamin D-treatment cannot be caused by hypercalcemia per se. It is possible, however, that all vitamin D-induced ectopic calcifications are caused by the recently described fetuin mineral complex, a complex that is generated at sites of enhanced bone resorption and is found in blood (JBC (2002)277:3926).

M458

Calbindin D28K Interacts with RanBPM and Undergoes a Large Ca2+-Induced Change Between Two Ordered Conformations. R. A. Venters*[1], L. M. Benson*[2], W. Lutz*[3], T. A. Craig*[3], K. H. Paul*[4], J. Bagu*[4], R. Thompson*[4], S. Naylor*[5], J. Cavanaugh*[4], R. Kumar[3]. [1]Duke University Medical Center, Durham, NC, USA, [2]MN, USA, [3]Mayo Clinic, Rochester, MN, USA, [4]North Carolina State University, Raleigh, NC, USA, [5]Beyond Genomics, Waltham, MA, USA.

Calbindin D_{28K} is a vitamin D-dependent EF-hand calcium-binding protein found in the central and peripheral nervous system, kidney, and intestine. There is a paucity of information concerning the mechanism of action calbindin D_{28K} and the effect of calcium on calbindin D_{28K} structure. Using yeast two-hybrid screening studies we show that calbindin D_{28K} interacts with Ran-binding protein M (RanBPM). Saccharomyces cerevisiae, AH109 cells, were co-transformed with pACT brain-derived cDNA library and the pGBKT7 vector expressing rat brain calbindin D_{28K} as a fusion protein with the Gal4 DNA binding domain. Yeast transformants expressing interactive proteins were selected by nutrient auxotrophy and galactosidase activity. This interaction between calbindin D_{28K} and RanBPM was verified by co-immunoprecipation experiments. We used NMR and electrospray ionization mass spectrometry (ESI-MS) to investigate calcium-induced conformational changes of calbindin D_{28K}, and we show that apo-calbindin D_{28K} has an ordered tertiary structure that transforms into a disordered intermediate as levels of Ca^{2+} increase. This disordered intermediate transitions into a different ordered tertiary structure upon a further increase in Ca^{2+} concentrations. This form of the protein continues to load calcium and persists until fully loaded. Our studies, therefore, identify two ordered calbindin D_{28K} conformations existing under differing calcium concentration levels partitioned by a state of conformational exchange. Our results suggest that calbindin D_{28K} has characteristics of both a calcium-sensor and buffer. We thus show conclusively that calbindin D_{28K} not only binds calcium as a buffer but also acts as a sensor to bind other intra-cellular proteins and we identify RanBPM as an important target.

M459

Antagonism of the RAR Signaling Pathway Induces Osteoblast Differentiation and Bone Formation. A. V. Sampaio*[1], R. A. S. Chandraratna*[2], T. M. Underhill[3]. [1]Physiology, University of Western Ontario, London, ON, Canada, [2]Retinoids Research Group, Allergan Inc., Irvine, CA, USA, [3]Faculty of Medicine and Dentistry, University of Western Ontario, London, ON, Canada.

The vitamin A metabolite retinoic acid has been shown to have various effects on the development and remodeling of bone. Retinoic acid functions through activation of the retinoic acid receptor (RAR), a member of the nuclear hormone receptor superfamily of transcription factors. The purpose of this study was to delineate the role of retinoid signaling in osteoblast differentiation and matrix synthesis. Combinations of molecular and pharmacological approaches were used to manipulate the retinoid signaling in either MC3T3-E1 (immortalized murine osteogenic cell line), primary cultures derived from 1 day-old rat calvaria, and *in vivo* studies. The consequences on the osteoblast phenotype were assessed using reporter gene analysis, histological analyses, proliferation and cell death assays, real-time PCR, northern blotting analysis, and bone mineral density (BMD) quantification by dual x-ray absorptiometry (DEXA) scans of bones. Pre-treatment of osteoblast cultures with 10nM $1,25(OH)_2$ vitamin-D_3 followed by treatment with 1000nM all-*trans* retinoic acid stimulated apoptosis to a greater extent than either ligand alone as measured by TUNEL assay and propidium iodide staining. Thus, it appears that $1,25(OH)_2$ vitamin-D_3 enhances retinoic acid-mediated cell death. Moreover, this synergistic effect also extended to bone nodule formation, as nodules were completely absent in cultures co-treated with retinoic acid and $1,25(OH)_2$ vitamin-D_3. Interestingly, the addition of an RARα-selective antagonist (AGN194301) or expression of a dominant-negative version of RARα ameliorated the effects of $1,25(OH)_2$ vitamin-D_3 on cell death and bone nodule formation and mineralization. Treatment with AGN194301 alone was found to cause precocious expression of osteocalcin and alkaline phosphatase activity and at low concentration (10 nM) induced a ~3-fold increase in matrix mineralization. Treatment of ovariectomized mice with AGN194301 for 4 weeks increased bone mineral density by ~15%. Further, antagonism of the retinoid-signaling pathway increased Cbfa1 activity. Together, these findings reveal novel and unexpected roles for $1,25(OH)_2$ vitamin-D_3 and retinoic acid in regulating the osteoblast phenotype–inhibition of osteogenesis by $1,25(OH)_2$ vitamin-D_3 involves stimulation of apoptosis through an RAR-dependent pathway, and abrogation of retinoid signaling is required for expression of the osteoblast phenotype.

M460

Retinoids Induce Envelope-specific Changes in Adult Endochondral Bone Resulting in Cortical Bone Destruction and Suppressed Cancellous Bone Turnover. M. Kneissel*[1], M. Susa[1], A. Boyde[2]. [1]Bone Metabolism Unit, Novartis Pharma AG, Basel, Switzerland, [2]Anatomy, University College, London, United Kingdom.

Retinoids play important and complex roles in the shaping of endochondral bone by mediating perichondrial invasion of the cartilage rudiment, promoting osteogenic differentiation, cartilage maturation and mineralization (1). Furthermore retinoid action can influence endochondral bone beyond development. We aimed to contribute to the understanding of this action by short-term application of the retinoid Ro 13-6298 to young and aged adult rats and determining its bone-envelope specific effects. Ro 13-6298 (30 microg /day sc. for 4 days) induced bone loss in the hind limbs of 12- and 56-week-old Wistar rats as detected by DEXA, plasma TRAP and calcium levels. This loss could be blocked by a bisphosphonate but not by estradiol. In vivo pQCT measurements demonstrated that bone mass decline was due to rapid subperiosteal bone loss in both age groups, reducing cortical bone mineral content, whilst cancellous bone mineral density was preserved and bone length unaffected over this short experimental period. Histomorphometric evaluation revealed that this cortical bone destruction was due to increased subperiosteal osteoclastic resorption (+73%). Conversely, bone resorption was suppressed (by 60%) in the entire cancellous bone compartment. The latter observation is in line with our in vitro finding that the retinoid suppressed osteoclastogenesis (dose-dependently: 1, 10, 100 nM, up to 50%) and pit formation (area, up to 90%) when added to osteoclast cultures stemming from the bone marrow of 21-week-old C57Bl/6J mice. Bone forming surfaces were significantly decreased at the subperiosteal cortex and in the secondary spongiosa, while the primary spongiosa was unaffected. Furthermore, quantitative back-scattered electron imaging revealed that the short-term retinoid treatment was sufficient to accelerate significantly cartilage mineralization (+17%). Thus retinoids have a complex impact on endochondral bone beyond embryonic stages. It has previously been shown that retinoids increase bone resorption and decrease bone formation in vivo in a generalised manner, but published in vitro results are multifaceted and conflicting. Our data suggest that in vivo effects also vary greatly between different bone envelopes and are partially opposing. The finding that the retinoid triggers principally subperiosteal cortical bone destruction in adult endochondral bone is interesting in the context of the finding that high intake of vitamin A, as retinol, is associated with an increased risk of hip fracture (2).
(1) Jimenez et al., JCB 2001; (2) Feskanich et al., JAMA 2002;

M461

Phosphorylation of the Human Retinoid X Receptor α Inhibits the Signal Transduction Mediated by its Heterodimeric Partners. M. Macoritto*, R. Kremer. Medicine, Mcgill University, Montreal, PQ, Canada.

Via its heterodimeric association with numerous members of the nuclear receptor superfamily, the retinoid X receptor α (RXRα) defines itself as a necessary factor in a variety of signaling pathways. The RXRα affects the DNA binding and transcriptional activity of the vitamin D receptor (VDR), the thyroid receptor (TR), the peroxisome proliferator-activated receptor (PPAR) and the retinoic acid receptor (RAR). In *ras* transformed keratinocytes, the serine 260 of RXRα is phosphorylated by the *ras-raf*-map kinase cascade, resulting in the inhibition of signaling through VDR-RXR heterodimers. (Solomon, C., White, J. H., and Kremer, R. K. (1999) J. Clin. Inv. **103**, 1729-1735) The purpose of the present study is to determine whether the phosphorylation of serine260 of RXRα in *ras* transformed keratinocytes (HPK1A*ras*) inhibits signaling through PPAR-RXR, TR-RXR and RAR-RXR heterodimers as well as RXR homodimers. To determine whether the RXR heterodimers were able to recognize and bind DNA response elements, electrophoretic mobility shift assays were performed using nuclear extracts from the keratinocytes. TR-RXR, PPAR-RXR, RAR-RXR heterodimers and RXR-RXR homodimers were able to bind labeled oligos containing their cognate DNA response elements. To define the effects of the phosphorylation on transcriptional activity, reporter constructs bearing the cognate response elements for the receptors were transiently transfected into the HPK1A*ras* keratinocytes as well as the control immortalized keratinocytes (HPK1A). Treatment of the cells with increasing amounts of the receptors' respective ligand revealed that the phosphorylation of the RXRα resulted in an inhibition of the transcriptional activities of these receptors. Addition of a map kinase inhibitor, PD98059, reversed this transcriptional inhibition. Simultaneous transfection of a non-phosphorylatable mutant RXRαser260ala also reversed the inhibition. The ability of all trans retinoic acid (ATRA), a ligand of the RAR, to inhibit the growth of keratinocytes was significantly reduced in the HPK1A*ras* cells as compared to the control cell line HPK1A, but was restored with the addition of PD98059. HPK1A*ras* cells showed complete resistance to ATRA at 10^{-7}M, but pretreatment with PD98059 resulted in significant growth inhibition at 10^{-9}M. With the RXR synthetic ligand LG1069, HPK1A*ras* cell growth was significantly inhibited at 10^{-7}M, but pretreatment with PD98059 resulted in significant inhibition at 10^{-10}M. These results indicate that the *ras-raf*-MAPK cascade phosphorylation of RXRα impairs signaling through all its partners and suggests an important role in tumor biology.

ADULT BONE AND MINERAL WORKING GROUP

WG1

Relationship Between Disease Specific Symptoms and Indices of Disease in Patients with Primary Hyperparathyroidism (PHPT): A Pilot Study in a Referral Center. I. Paek[1], L.Boboc[2], D. S. Rao[2], [1]Brown University School of Medicine, Providence, RI, USA, [2]Henry Ford Hospital, Detroit, MI, USA.

Patients with PHPT have symptoms that are specific (i.e., traditionally attributed to hypercalcemia) and those that appear to be non-specific (i.e., those not traditionally attributed to hypercalcemia). The latter symptoms are often used to recommend surgery in the absence of specific symptoms. Accordingly, we conducted a pilot study to ascertain the relationship between symptoms and indices of the disease (serum Ca and PTH). We hypothesized that polydipsia, polyuria, nausea, vomiting, dry mouth, and metallic taste (specific symptoms) would be related to serum Ca levels since they occur in all varieties of hypercalcemia and respond to treatment with some consistency. In contrast, fatigue, muscle weakness, headache, irritability, depression, lack of concentration, and memory problems (non-specific symptoms) would be related to serum PTH levels. 142 consecutive patients with PHPT completed a questionnaire consisting of the 14 questions. Physician input was sought when in doubt since a categorical answer was required. The relationship between the prevalence of various symptoms and disease indices was determined based on serum Ca and PTH levels, the two most important determinants of disease severity. We arbitrarily divided the patients with serum Ca < or > 11 mg/dl and serum PTH < or > 100 pg/ml. The latter was chosen based on our previous work with mild asymptomatic PHPT. For the entire study group the mean (SD) of Ca was 10.8 (0.6) mg/dl and PTH was 123 (68) pg/ml. Results (%) are shown in the Table.

Variable	Ca <11 mg/dl	>11 mg/dl	PTH <100 pg/ml	>100 pg/ml
Specific Symptoms (?Ca Related)				
Polydipsia	24	44	34	37
Polyuria	45	55	50	50
Nausea	12	17	16	11
Vomiting	3	8	16	11
Dry Mouth	39	49	45	50
Mettalic Taste	13	9	12	10
Constipation	35	37	35	36
Non-Specific Symptoms (?PTH Related)				
Fatigue	56	71	60	64
Muscle Weakness	33	38	37	33
Headache	26	29	26	31
Irritability	20	32	24	28
Depression	34	39	32	40
Lack of Concentration	30	35	34	30
Memory Problems	42	43	46	38

There appeared to be a trend for the specific symptoms related more to serum Ca than to PTH levels. However, with the exception of fatigue no consistent trend was seen in non-specific symptoms and PTH or Ca levels. This may partly relate to the fact that Ca and PTH levels are significantly correlated. Further studies are needed to confirm our preliminary results.

WG2

Hepatitis C Associated Osteosclerosis. S. Ortolani, R. Cherubini*, P.J. Meunier, E. Galbiati, S. Saraifoger*, M.L. Bianchi, Istituto Auxologico Italiano IRCCS, Milan, Italy and Hôpital E. Herriot, Lyon, France.

A new syndrome of acquired generalized osteosclerosis associated with hepatitis C virus infection (HCAO) has been firstly described in 1992 and ten cases have been reported since then. We present radiological, densitometric, histomorphometric and biochemical features of a new case of HCAO, with 1 year follow-up without treatment. A 65-yr-old women with hepatitis C virus infection from blood transfusion more than ten years earlier was referred in January 2001 for increasing pain of thighs, legs and upper arms, requiring high doses of analgesic and significantly reducing her walking ability. Radiographs showed diffuse osteosclerosis, with marked cortical and trabecular thickening involving all the skeleton, except the cranium. Bone morphology and structure was otherwise normal. Total body scan demonstrated diffusely increased radionuclide uptake. Consistent with bone scan, serum alkaline phosphatase, serum osteocalcin and urinary NTx were markedly increased, respectively 12, 4 and 20 times the upper normal limit. Intact PTH was moderately elevated, with serum calcium, 25-hydroxy-vitamin D and 1,25-dihydroxy-vitamin D within the normal range. BMD was measured at multiple skeletal sites by DXA (Hologic QDR 2000) resulting well above the expected values not only for the same age and sex, but also when compared to young normals, as indicated by T- and Z-scores, that were respectively +5.0 and +6.8 for lumbar spine, +5.3 and +6.7 for total hip, +1.7 and +3.3 for whole body. Moreover, whole body bone densitometry showed elevated values for all the skeletal sub-regions, except the head. Iliac crest bone histomorphometry demonstrated high remodeling osteosclerosis, lamellar bone texture and normal haematopoietic cells. Cancellous bone volume was 73% (normal 15.3±4.6%), eroded surfaces were 15.0% (3.6±1.1%), osteoid volume and osteoid surfaces were respectively 13% (1.6±0.7%) and 67% (8.6±3.9%), but osteoid thickness index was normal at 19.4 (18.5±2.5). Mineralization rate was slightly increased: 0.88 µm/day (0.72±0.12). One year later BMD was reassessed and showed marked increases at all skeletal sites: lumbar spine +10.5%, total hip +12.3% and total body +16.3%. This is the first case of HCAO reported from Europe and confirms the major landmarks described in the very few previous cases. Noteworthy, as in some of the other cases, cranium appears not to be much affected by this bone disorder, suggesting that the unknown pathogenetic mechanism should incorporate some interaction with mechanical stimuli, as cranium is the less weight-bearing bone of the skeleton. The good lamellar bone quality and the impressive increases in bone density observed in our case during the one year follow-up confirm that, although speculative, elucidation and control of the pathogenetic mechanism could result in effective treatment of osteoporosis.

WG3

Osteoporosis in patients with Turner's Syndrome - Presentation of two cases. S. Levy, G. Edelson, William Beaumont Hospital, Royal Oak, MI, USA.

The etiology and presentation of bone loss in women with Turner's Syndrome is still not fully understood. Also it is not clear to what extent does the estrogen deficiency contribute to the bone loss. Here we present two women who developed significant osteopenia. One was and one was not on estrogen replacement prior to the development of bone loss. Case1. S.E. is a 55 year old Caucasian with a past medical history significant for Hashimoto's thyroiditis and the diagnosis of Turner's Syndrome at the age of twenty. The patient was treated with hormone replacement therapy since the time of diagnosis. Currently is on Estradiol 0.1 mg/day (Vivelle patch) and Synthroid 0.075mg/day. The patient consumed 1000mg of calcium per day and was active physically (4 miles/day walking.) No bone loss risk factors identified. Patient had never been pregnant. At 55 years of age the patient presented with a complaint of height loss which was not quantitated. DEXA revealed L1 T score (Ts) -1.8, L2 -1.2 and Femoral Neck (FN) -1.3. Two years later, the patient had a repeat DEXA scan with a L1 Ts -2.6, L2 -1.2, FN -1.3. The patient was started of Fosamax 70mg/week and a year later her DEXA scan values were L1 Ts -1.5, L2 -1.1 and FN -0.8. Case2. M.H. is a 71 year old caucasian women who was found to have severe osteopenia. DEXA test L1-L3 Ts -1.64, FN -1.86. Because of short stature, wide carrying angle of the upper extremities and 0-1 fingerbreadth distance between rib cage and pelvic brim bilaterally, the patient karyotype was done and was found to be XO confirming Turner's Syndrome. The patient did not have known bone loss risk factors, and her estimated calcium consumption was 800 mg /day. The patient was never on estrogen replacement therapy and was never pregnant. The patient was started on Fosamax treatment. Repeat DEXA is still pending. These 2 cases support the notion that Turner's Syndrome associated osteopenia can not be solely attributed to estrogen deficiency. Though both patients are currently treated with Fosmax the efficacy of this treatment on the osteopenia seen in Turner's Syndrome is not clear.

WG4

Dysregulated Expression of BMP5 in a Patient with Deformed Helices, Axial Skeletal Defects, and Heterotopic Ossification: A Clue from the Short-Ear Mouse. G.J.Feldman[1], R.Patel[1], P.C.Billings[1], D.M.Kingsley[2], E.M.Shore[1], F.S.Kaplan[1], [1]Department of Orthopaedic Surgery, University of Pennsylvania, Philadelphia, PA, USA, [2]Department of Developmental Biology, Howard Hughes Medical Institute and Stanford University School of Medicine, Stanford, CA, USA.

Bone morphogenetic proteins (BMPs) play critical roles in embryonic patterning and skeletal formation and in adult skeletal repair and maintenance. The biological importance of the BMPs is highlighted by the fact that these genes have been conserved over a wide variety of species from worms to humans. Mutations in the protein coding region and in the downstream regulatory elements of the BMP5 gene cause a complex syndrome characterized by short ears and a broad range of axial skeletal malformations in the mouse (Kingsley et al Cell 71:399-410,1992). We examined a child, reminiscent of the short ear mouse, who has abnormally small external ears and multiple malformations of the axial skeleton as well as progressive heterotopic bone formation in the back and neck. We hypothesize that she has a mutation either in the BMP5 gene or in another gene that regulates BMP5 expression. We have examined the DNA sequence of the BMP5 gene in this patient and 800 bp of the 5'flanking sequence but identified no mutations. The possibility of mutations in regulatory regions further upstream or downstream of the examined region is currently being investigated. The mRNA expression of BMP2, BMP4 and BMP5 was examined by RT-PCR using a lymphoblastoid cell line established from the patient. We detected elevated levels of BMP5 and BMP4, but not BMP2 mRNA in this patient's cells relative to the levels detected in 14 unaffected individuals. To determine if this elevated BMP5 mRNA leads to increased production of secreted BMP5 protein, we performed immunoblot analysis using medium conditioned by the patient's cell line and an antibody against BMP5. BMP5 protein was detected in the patient's sample but was absent in 4 unaffected controls. Our data suggest that dysregulated expression of the BMP5 gene may be associated with an array of axial skeletal abnormalities in this patient.

WG5

Prevalence of Low Bone Mass (LBM) in Adult Celiac Disease (ACD): A Pilot Study in an Urban ACD Support Group Population. M.J. Scheafer[1], L. Teasdale[2], E.R. Phillips[2], D. S. Rao[2], [1]University of North Dakota School of Medicine, Grand Forks, ND, USA, [2]Henry Ford Hospital, Detroit, MI, USA.

Malabsorption of calcium and vitamin D is common in ACD and results in significant morbidity in patients with ACD. However, the prevalence of low bone mass, a known risk factor for fractures, is unknown. The recognition of ACD as a cause of osteoporosis in the US appears to be far from satisfactory. We have presented our experience on metabolic bone disease in patients with ACD, but the study involved only patients referred for evaluation based on symptoms, abnormal laboratory tests or low bone mineral density (BMD). To the best of our knowledge no systematic study of BMD in ACD has been reported from the US. Accordingly, we ascertained the status of bones in a group of individuals with established ACD. Study subjects were recruited during at a monthly meeting of the ACD support group in an urban community. All participants had an established diagnosis of ACD either by serologic tests and/or intestinal biopsy, and were following a gluten free diet for at least one year. BMD was measured by broadband ultrasound attenuation using Sahara bone densitometer (Hologic Inc). T-scores were calculated from the manufacturer's database. Low bone mass was defined as T-score <1.5 SD, although exact cut off criteria for low bone mass by ultrasound technique is yet to be defined. All subjects completed a questionnaire that included relevant information such as height, weight, menopausal status, hormone replacement therapy (HRT), smoking and fractures. Results (mean ± SD or %) are shown in the Table.

Variable	Total Group	Pre Menopausal	Post Menopausal	
			On-HRT	No-HRT
Number	59	11	24	24
Age (y)	58 ± 13	40 ± 7	60 ± 9	56 ± 16
BMI (kg/m^2)	24.4 ± 4.4	24.1 ± 5.2	23.5 ± 2.5	24.3 ± 5.0
BMD (g/Cm^2)	0.54 ± 0.14	0.63 ± 0.14	0.54 ± 0.13	0.53 ± 0.16
T-Score (SD)	-0.40 ± 1.22	0.43 ± 1.30	-0.38 ± 1.14	-0.44 ± 1.42
<-1.0 (%)	25	9	29	29
H/O Fx (%)	29	18	38	25
Calcium (%)	68	45	92	54
Vit.D (%)	36	27	29	46

Despite knowledge about ACD and adherence to a gluten free diet, the prevalence of low bone mass is high among individuals with ACD. As expected, there was an age-related decline in BMD. The proportion of individuals with a history of fracture was also high and the proportion taking supplemental calcium and vitamin D was disappointingly low. Conclusions: Prevalence of low bone mass and history of fractures is high among apparently "well informed" patients with ACD. Further studies are needed to establish the scope of the problem and to explore the impact of ACD on BMD and fracture.

WG6

Severe Osteoporosis and Persistent Bone Loss Leading to Late Diagnosis of Celiac Disease. M.L. Bianchi, M.T. Bardella*, E. Galbiati*, S. Saraifoger*, R. Cherubini*, S. Ortolani. Bone Metabolic Unit, Istituto Auxologico Italiano IRCCS and Gastroenterology Department, Università di Milano; Milano, Italy.

Two women of 62 and 64 years with severe osteoporosis, multiple fractures and persistent bone loss notwithstanding therapy were separately referred to our Bone Metabolic Unit. Both were caucasian, of normal weight, in menopause (at 52 and 53 yrs), with normal dietary calcium intake (1.2 and 1 g/day), doing regular physical activity, and with no other disease except osteoporosis. *Case 1 (62 yrs):* first fracture (D10) at 58 yrs; after fracture, spine BMD was measured (T-score -3.2) and alendronate (10 mg/day) was started; at 60 yrs, second fracture (L1); BMD decreasing (-2.3% yearly); alendronate was continued and a calcium supplement was added (500 mg/day); we first saw her at 62 yrs, one year after a third fracture (D11). *Case 2 (64 yrs):* first fracture (left foot) at 56 yrs (while on HRT); after a second fracture (left wrist) at 59 yrs, alendronate (10 mg/day) was started; third fracture (right wrist) at 61 yrs; BMD T-score -4.1 at spine, -4 at hip. At 64 yrs, after she broke her right humerus, with a BMD still decreasing (-2.5% yearly), she was sent to our attention. At admission, case 1: severe back pain and kyphosis; case 2: pain and functional impairment of right arm. No other signs/symptoms. Bone metabolism parameters (s = serum; u = urinary):

	sCa (mg/dl)	*sAP (U/l)*	*sPTH (pg/ml)*	*s25-OHD (ng/ml)*	*uNTx (nMBE/mMCr*
normal range	(8.1-10.4)	(50-300)	(13-54)	(9-47)	(29-58)
case 1	8.6	312	81	8	178
case 2	8.7	287	75	12	99

Case 1 had a slight increase in GOT (51 U/l) and GPT (58 U/l). Case 2 had moderate anemia (red-cell count 3.670.000/mm^3; Hb 11 g/dl; serum iron 32 mcg/dl). BMD: case 1, T-score -4.1 at spine and -3.9 at hip; case 2, T-score -4.5 at spine and -4.2 at hip. The persistent decrease in bone mass and the presence (case 1) of transaminase increase (not related to previous hepatitis) or (case 2) of hypochromic anemia, induced us to test the serological markers of celiac disease. In both cases, anti-endomysium antibodies were positive. Upper gastrointestinal tract endoscopy confirmed the diagnosis. A gluten free diet was started. Alendronate was maintained and calcifediol was added (35 - 50 mcg/day). In 4 months, a normalization of AP, PTH, NTx and an increase in calcium and 25-OH D were observed in both cases. After 2 years or more, BMD was persistently increasing: case 1: + 6.7% at spine and +5.6% at hip yearly; case 2: + 6% at spine and +5% at hip yearly. The patients did not have new fractures and pain was significantly decreased. In conclusion, even in the absence of specific intestinal signs and in advanced age, the progressive worsening of osteoporosis (bone loss plus fractures) notwithstanding therapy requires a thorough evaluation of the possible causes of secondary osteoporosis, among them celiac disease. In such cases, a gluten free diet and an over-correction of hypovitaminosis D can radically change the bone response.

WG7

Association Between Height, Weight, Body Mass Index and Discordant Regional Bone Mineral Density. R.L. Munasinghe, V. Botea, G.W.Edelson. Department of Medicine, Sinai-Grace Hospital, Wayne State University, Detroit, MI, USA.

Patients with osteoporosis have a body mass index (BMI) that is significantly lower than patients with normal bone mineral density (BMD). This study was conducted to study the associations between age, height, weight and body mass index in patients with discordant regional BMD. For the purpose of this study, discordant regional BMD was defined as having a BMD result that is in the osteoporotic range at one site while being normal at the other sites. Data from 7,095 qualifying bone densitometry scans from a suburban Detroit osteoporosis testing center were analyzed. A patient was classified as having generalized osteoporosis if the t score was less than –2.5 at the lumbar spine, femoral neck and distal radius and normal if the t score was greater than –1 at the same three sites. Patients were determined to have discordant lower BMD when the t score was less than –2.5 at one site while the t score was greater than –1 at the same three sites. Patients were determined to have discordant low BMD when the t score was less than –2.5 at one site while the t score was greater than –1 at the same three sites. Patients with generalized osteoporosis were older (mean age 72 vs. 54, *P*<.001), shorter (height 153 vs. 161 cm, *P*<.001) and had lower BMI (23.7 vs. 28.6 Kg/m2, *P*<.001) compared to patients with normal BMD. The distal radius was the site where discordant osteoporosis was most prevalent (64 patients, 0.9%). Patients with isolated low distal radius BMD were similar in age (mean age 70.5 vs. 72.2 years, *P*=NS), but were taller (height 158 vs. 153 cm, *P*<.001)and had BMI values that were significantly higher (BMI 28.9 vs. 23.7 Kg/m2, *P*<.001) than patients with generalized osteoporosis. Patients with discordant BMD at the distal radius have anthropometric characteristics that are significantly different from patients with generalized osteoporosis. These differences may represent differences in the etiology of osteoporosis and differential effects on cortical versus trabecular bone.

WG8

Association Between Age, Height, Weight and Bone Mass Index with Discordant Changes in Bone Mineral Density Detected on Sequential Bone Densitometry Scans. R. Munasinghe, V. Botea, G. Edelson. Department of Medicine, Sinai-Grace Hospital, Wayne State University, Detroit, MI, USA.

Osteoporosis is a systemic disease with age related concordant decline in bone mineral density at most major skeletal sites. Low body weight is another important risk factor for osteoporosis. In some patients detrimental change in BMD is discordant and limited to one skeletal site. This study was done to compare the anthropometric characteristics of patients with concordant and discordant changes in BMD on sequential bone densitometry scans. Data from 1180 patients with sequential bone densitometry scans were analyzed to evaluate changes in BMD at the lumbar spine, femoral neck and distal radius. Two methods were used to identify discordant and concordant change in BMD. In the first, changes in BMD were compared relative to the median rate of change for the entire cohort. In the second method absolute gain or loss of BMD from the first to the second scan were used. A patient was determined to be concordant for detrimental change in BMD when changes in BMD were detrimental at all three sites and discordant for a particular skeletal site when the detrimental change was limited to that site. The mean age, height, weight and body mass index (BMI) of these groups were compared. Discordant detrimental change in BMD was most prevalent at the distal radius independent of the method used to determine detrimental change in BMD. When defined using changes relative to the group median, patients with discordant detrimental change in BMD at the radius were significantly older (mean age 63.3 vs. 61.2, P<.05), shorter (mean height 157 vs. 159 cm, P<.01) and heavier (mean weight 65.1 vs. 63.5 Kg, P<.05, BMI 26.2 vs. 25.0 Kg/m2, P<.001) than patients with concordant detrimental change in BMD. The results were similar when the absolute changes in BMD were used to define discordancy. The differences in anthropometric characteristics between patients with concordant and discordant changes in BMD may represent differential effects on bone related to the etiology or treatment of osteoporosis, weight bearing and mechanical loading properties, or due to differential effects of these factors on cortical and trabecular bone.

WG9

Hypocalcemia in a Male with Polyglandular Failure in Association with an Antibody to the Calcium Sensing Receptor. M.S. LeBoff[1], O. Kifor[2], E. M. Brown[1]. [1]Skeletal Health and Osteoporosis, Brigham and Women's Hospital, Harvard Medical School, Boston, MA, USA, [2]Endocrine Hypertension Division, Brigham and Women's Hospital, Harvard Medical School, Boston, MA, USA.

Autoimmune-mediated hypoparathyroidism is a feature of polyglandular failure type I in children but not polyglandular failure type II. We describe a male who presented with hypocalcemia in the presence of adrenal crisis. PM is a 25 yo male admitted with 6 months of progressive fatigue, weight loss, vomiting, and salt craving, and hyperpigmentation over 2 years. The patient was hypotensive on admission with a Na 124 mmol/L, K 5.9 mmol/L, calcium 8.0 mg/dl, albumin of 4.4 mg/dl, and ionized calcium of 1.10 mmol/L (1.13-1.32). Past medical history revealed hypothyroidism for which he was treated with synthroid 100 mcg/d. Family history was positive for celiac disease (cousin). Laboratory evaluation revealed a PTH of 20 pg/ml and 25-hydroxyvitamin D level of 18.5 ng/ml. ACTH stimulation resulted in cortisol levels of a 0.2 and .5 mcg/dl at 0 and 60 minutes, respectively. The patient was treated with stress-dose hydrocortisone and fluid resuscitation. TPO antibody was 120 (0-20 IU) and an antiendomysial antibody was negative. In vitro studies to assess the presence and functional activity of antibodies to the calcium sensing receptor (CaR) showed:

- Positive Western blots of bovine parathyroid gland extracts.
- Positive ELISA against a peptide within the CaR's amino-terminal region.
- Stimulation of inositol phosphate generation compared to control serum in HEK cells transfected with the calcium sensing receptor.
- Inhibition of PTH release from dispersed human parathyroid cells compared with control serum.

In summary, this is an unusual case of a male with hypocalcemia, autoimmune-mediated hypothyroidism, presenting with adrenal crisis, a setting in which the calcium is expected to be elevated. Detailed analysis of his serum showed a normal 25-hydroxyvitamin D and PTH = 20 ng/ml in the presence of low calcium levels. In vitro studies revealed a functional antibody to the calcium sensing receptor that activates inositol phosphate generation and inhibits PTH release in association with hypocalcemia. These data indicate that hypocalcemia and antibodies to the CaR may represent a new feature of polyglandular failure Type II.

PEDIATRIC BONE AND MINERAL WORKING GROUP

WG10

I-cell Disease Presenting as Severe Neonatal Hyperparathyroidism. S. Unger[1], D.E.C Cole[1,2]. [1]Division of Clinical and Metabolic Genetics, Hospital for Sick Children, Toronto, Canada, [2]Departments of Pathobiology and Medicine, University of Toronto, Toronto, Canada.

I-cell disease (mucolipidosis II) is an autosomal recessive disorder of enzyme targeting that presents between 6 and 12 months of age with a clinical phenotype resembling Hurler syndrome and a radiographic phenotype of dysostosis multiplex. When I-cell disease is so severe as to be detected in the newborn period, its radiographic changes have been previously described as similar to hyperparathyroidism or rickets. The biological basis of these radiographic findings has not been explored and few biochemical measurements have been recorded. We describe a newborn with radiographic features of severe hyperparathyroidism including osteopenia, bent long bones due to in utero fracturing, metaphyseal fraying and expansion, and sub-periosteal cloaking. The first PTH measurement on day 12 of life was 876 ng/L (normal:10-65 ng/L) and PTH peaked at 1176 ng/L with subsequent resolution to normal by one month of age (39 ng/L). The alkaline phosphatase level followed a similar but delayed course: in the immediate newborn period it was dramatically increased and reached a peak value of 2883 U/L (normal: 185-555 U/L) at one month of age. However, the calcium level remained normal throughout (2.32mmol/L on day 4), while the phosphate was low (1.12 mmol/L) and 1,25(OH)2 D was normal (100 pmol/L -- reference range, 40-140 pmol/L). At 3 months of age, markedly elevated lysosomal enzymes in plasma established I-cell disease as the primary diagnosis. With normalization of PTH, the osteopenia, metaphyseal cupping and periosteal cloaking resolved and the typical changes of dysostosis multiplex became more obvious. We speculate that severe I-cell disease can be accompanied by hyperparathyroid bone disease early in life. The mechanism of the prenatal stimulation of the parathyroid glands and its spontaneous resolution remain unknown. However, one possible explanation would be that the enzyme targeting defect underlying I-cell disease resulted also in an uncoupling between the calcium sensing receptor (CASR) and PTH, but the maintenance of normocalcemia in spite of highly elevated PTH is unexplained.

WG11

Osteoporosis in Mucopolysaccharidosis type II (Hunter's syndrome) D. Rigante[1], G. Segni[1], R. Ricci, A. Di Stasio[1], P. Caradonna[2]. [1]Department of Pediatrics, Universita Cattoilca Sacro Curoe, Rome, Italy, [2]Department of Internal Medicine, Università Cattolica Sacro Cuore, Rome, Italy.

Mucopolysaccharidosis (MPS) type II or Hunter's syndrome is an X-linked recessive lysosomal storage disorder due to iduronate sulphatase deficiency displaying a wide spectrum of clinical severity. Skeletal involvement is constant in MPS type II: osteoporosis is a substantial cause of morbidity because of fracture risk. We have submitted two patients with MPS II to dual energy X-ray absorptiometry (DEXA, Hologic QDR 2000) in order to assess bone mineral density (BMD) and determine its relationship with disease severity. The features of our two patients and the results of our investigation, expressed in Z-scores calculated on the basis of the respective ages of normal males, are shown in the following table.

	Age	Bone storage	Onset	BMI	Deambulation	Puberty	Epilepsy	L-BMD	Z-score	F-BMD	Z-score
1	22 ys	present	3.5 ys	15.3	absent	absent	present	0.401	-6.49	0.281	-6.29
2	21 ys	present	5 ys	17.0	absent	present	absent	0.454	-4.73	0.638	-4.34

Patients with MPS type II may present restricted growth, mental/physical disability and a wide spectrum of functional bone impairment due to bone storage of undegraded mucopolysaccharides, inadequate body weight, malabsorption of calcium, decreased serum 25-hydroxyvitamin D, absent physical exercise and sex hormone deficiency. Lumbar and femoral neck BMDs were found to be very severely reduced in the two patients, with differences attributable to hypogonadal state and use of antiepileptic drugs altering vitamin D metabolism. Bone integrity needs to be overlooked in order to ameliorate the quality of life of these patients: dietary supplements (calcium, vitamin D) can slow the process of skeletal demineralization and physiotherapy can contribute to the construction of bone substance and pain alleviation. We conclude that DEXA determinations have a great utility for screening patients with disorders electively involving the skeleton at risk for osteoporosis.

A

Acetylcholinesterase, F048
Achondroplasia, 1206
Acidosis, metabolic, M419, SA178, SU445
Acid phosphatase, SU229
Actin-related protein 2/3 complex, F223
Activator of Nongenotropic Estrogen-Like Signaling (ANGELS), 1058
Activator protein-1, F058, F186, M129, SA262
Activin receptor-like kinase-3 or -6, M023
Acyl-CpA binding protein, SU211
α-Adaptin C, SA057
Adenosine triphosphatase, SU170
Adipocytes, M221, M231
Adipogenesis, 1100, 1184, SA480
Adipose-derived adult stem cells, M233
A Disintegrin and Metalloprotease-9 (ADAM-9), F150
A Disintegrin and Metalloprotease (ADAMs) domain, 1195
ADO2 gene characterization, 1081
Adolescents, SU020. SEE ALSO *Puberty*
- Abnormal growth with idiopathic scoliosis, SU400
- BMD with SLE, SU019
- Bone geometry and body composition in women, SA002
- Bone turnover with idiopathic scoliosis, SA005
- Calcium supplementation, F003, M003
- Head and neck osteosarcoma, SA072
- Lifestyle factors and BMD in women, M284
- Obese, vitamin D status and bone mass during weight reduction, M001
- Osteopenia with idiopathic scoliosis, SA004
- Skeletal variations in female peak bone mass, M008

Adrenomedullin receptors, SU247
Adult growth hormone deficiency, F433, M402, SU425
Aged. SEE ALSO *Osteoporosis, postmenopausal; Postmenopausal women*
- Anthropometric parameters and BMD, SA267
- BMD after resistance training, M162
- BMD and gene encoding sclerostin, 1222
- Hip fracture prognosis, SU298
- IGFBP-2 and BMD, F307
- IGF-I gene promoter polymorphism and fracture risk, 1221
- Kyphosis and mortality risk, SU300
- PTH (28-48) anabolic action, SU324
- PTH serum levels and VDR, F414
- RANKL and OPG expression, SA010
- Rest-inserted loading, 1046
- Skeletal response to intermittent PTH, 1180
- Vertebral compression fractures, SA350
- Vitamin D, SU310
- Vitamin D activation, SA382
- Vitamin D/calcium supplementation, 1137
- Vitamin D deficiency in Argentina, SU279, SU280
- Wrist fractures and osteoporosis detection and treatment, SU366

Age determination by skeleton, SU001, SU018
Age factors
- *Bax* deficiency and bone quality, 1219
- BMD variation between hips, 1115
- Hip geometry, SA313
- Intervertebral disc degeneration, F009
- Kidney function and PTH assays, SU439
- Milk and calcium at menarche, SA280
- Myostatin gene polymorphisms and sarcopenia, M406
- OPG and bone resorption/remodeling, M006
- OPG levels, SU098
- Subchondral bone changes in rat maturation, M109
- Trabecular bone changes, M097
- *In vivo* murine BMD, SU325
- Young-old differences in femoral neck, SA316

Aggrecan, SU032
Akt. SEE *Protein kinase B*
Alcohol drinking, SA117, SA335
Alendronate
- Administration and dosage, M353, SA379, SU345
- BMD in osteoporotic postmenopausal women, 1039
- Bone turnover reductions and fractures, F106
- Discontinuation, 1037, M341
- Efficacy and safety, 1059
- Exercise in ovariectomized rats, F165
- Fracture repair in ovariectomized rats, F373
- Gene microarray analysis of bone formation markers, 1135
- Heart transplantation, 1042
- Hypercalciuria, absorptive, M416
- Male osteoporosis, 1007, SU339, SU344
- Methotrexate-associated osteopenia, M343
- NSAIDs and once-weekly, M350
- Osteogenesis imperfecta, SU401
- Osteoporosis prevention, F345
- Osteoporosis treatment monitoring with biochemical markers, SA105
- Pamidronate *versus,* M351
- Postmenopausal osteoporosis in Chinese women, M345
- Primary hyperparathyroidism, 1169
- PTH for osteoporosis, SU382
- PTH in osteoblast-like cells, SA361
- Trabecular BMD, SA336
- TRACP 5b *versus* bone resorption markers, SU103
- Turner's syndrome, WG3
- Vertebral fractures with BMD above -2.5, M352

Alfacalcidol. SEE ALSO *1-Hydroxylase; 25-Hydroxyvitamin D-1α-hydroxylase; 25-Hydroxyvitamin D_3 1 α-hydroxylase*
- Administration and dosage, SA379
- Bone marrow, SA376
- Bone strength, SA378
- Calcium supplementation, SA377
- Male osteoporosis, SU339
- Postmenopausal women, SA380

Alkaline phosphatase, SU130
Alveolar bone, F184
Ameloblasts, SU067
AMG 073, SU392
Amino acid peptides, SU376
L-Amino acids, M443
Amylin(1-8), M390
Analgesics, M427
Anastrozole, 1170
Androgen-deprivation therapy, 1128, M067, SA112, SU072, SU328
Androgen receptor, SA202, SA462, SA470, SA474
Androgens
- Elk-1 transcription factor inhibition, F203
- Endocortical bone remodeling in aged male rats, SU329
- Formation in growth plate and metaphyseal bone, SA475
- Ligand/receptor interactions, 1032
- Signaling and male bone mass, SU326
- Skeletal actions, M380

Anemia, pernicious, M321
Angiogenesis, 1192, M152
Angiogenic factors, SA065
Angioplasty, 1102
ANK, F024
Ankylosing spondylitis, SA090, SA421
Anorexia nervosa, M364, M389, SU302
Anterior cruciate ligament, M044
Anticonvulsants, 1214
Antiretroviral therapy, M307
Aorta connective tissue, SA430
Aortic stenosis, SA429
Aortic valve calcification, M017
AP23451 Src kinase inhibitor, 1145
Apomine, 1095, SU372, SU374, SU375
Apoptosis
- Calbindin-D_{28k} and glucocorticoid-induced, SU186
- Chondrocytes, SA030
- Crovidisin in ROS 17/2.8 osteosarcoma cells, SA174
- ERK and JNK effects, 1190
- ERK/cPLA2/cytochrome C pathway and, SA172
- Hip arthroplasty, SU414
- Osteoblasts, GSK-3 signaling and FGF-2, SA138
- Osteoclasts, Bim effects, M276
- Osteoclasts, Rac1 effects, 1150
- Osteoclasts, sodium fluoride effects, SA247, SA264
- PTHrP modulation, M435
- Sustained *versus* transient ERKs activation, SU185
- VDR and hypertrophic chondrocytes, 1030

Apoptosis signal-regulating kinase 1 (ASK1), SU173
Arachidonic acid, M445
L-Arginine, M359
Arm bones, SU182
Aromatase, 1116, M183, SA127, SA472. SEE ALSO *CYP19*
Arrestins, 1062, F451
Arthritis, 1114, M425, SU412. SEE ALSO *Osteoarthritis; Rheumatoid arthritis*
- Collagen-induced, M245, SA257, SU347

Arthritis, inflammatory, M420
Arthritis, polyarticular juvenile idiopathic, SU136
Asthma, SU334
Ataxia telangiectasia, SU027
ATDC5 cells, M026
Atherosclerosis, SA027, SA430
Athletes, professional, M004
ATP61 gene, SU398
AUF1 (mRNA), SA426

B

B6.C3H congenic mice, 1217, 1220
Baboons, SU130, SU131
Back pain, SA305
Bacterial artificial chromosome, SU194
Bacteroides forsythus, M401
Bad, F173
Basic fibroblast growth factor, 1061, M131, M133, M134, SU370
Bax, 1219
Bazedoxifene, F371
Bicarbonate, M360, M419
BIG-3 (BMP-2 Induced Gene 3kb) gene, F038
Biglycan, 1067, 1068, 1194
Bim, M276
BIM-44058, SA447
Bioinformatics, SU199
Biopsy, bone, M084, M093, M095, M332
Bisphosphonates. SEE ALSO *Alendronate; Apomine; Clodronate; Etidronate; Ibandronate; Incadronate; Minodronate; Olpadronate; ONO-5920; Pamidronate; Risedronate; Zoledronate*
- Administration and dosage, M357
- Amino-/non-amino and metastasis, M051
- Bone resorption markers, SU113
- Breast cancer, 1091
- Cancellous bone 3-D microarchitecture, SU349
- Elderly with impaired renal function, SU335
- Giant cell tumor, SA076
- Luteinizing hormone releasing hormone for prostate cancer, M354
- Nitrogen-containing, F249, SA251, SA255
- Osteocyte viability and bone strength, 1133
- Osteogenesis imperfecta, SU399
- Pharmacokinetics, SU341

Bisphosphonates. SEE ALSO *Alendronate; Apomine; Clodronate; Etidronate; Ibandronate; Incadronate; Minodronate; Olpadronate; ONO-5920; Pamidronate; Risedronate; Zoledronate* (Continued)
Prostate cancer and apoptotic bone disease, 1094
Resistance to, F248
Unrecognized secondary osteoporosis causes, SU336
Uremic bone disease, M409
Urinary CTx and treatment compliance, SA340
BK channels, M181
Body composition, M075, M303, SA002, SU289, SU319
Body height, M003, SA127, SU126, SU139, WG7
Loss, 1129, F284, F302, M315, M330
Body mass index, 1134, M121, M386, SU139, WG7
Body weight, 1115, M169, SU406, WG7. SEE ALSO *Weight loss*
Bone and Cartilage Stimulating Peptide, synthetic (P30), SA147
Bone formation. SEE ALSO *Bone formation, in vitro studies; Bone formation markers; Bone reconstruction; Cranial development; Distraction osteogenesis; Fracture healing*
Apomine, SU372
Bacterial infection and OP-1, SA017
Biglycan, 1194
BMP-1, SA022
BMP-2, SU040
Bone marrow side population cells, M227
Calcineurin Aα, 1018
Cbfb, 1004
CGI-135 effects, F210
Chlorobenzene effects, SA049
Collagenase and PTH/PTHrP receptors expression, SU066
CP-533536, M395
Ectopic, mesenchymal stem cells in, SU213
FHL2, 1017
Fluid shear stress dose dependence, SU172
GATA-1 and p45 BF-E2 effects, 1014
IGF-I promoter 2 gene transcription in C3H/HeJ mice, SA152
IL-10, F146
Integrins, SU060
Ischemic necrosis of femoral head in piglet, SU407
Low amplitude vibration in mouse ulna, SA164
Melatonin, SU207
Microdamage in cortical bone of dog rib, SU333
Osteopontin deficiency and mechanical stress, SU059
Oxysterols, M229
P2X7 receptor, 1107
Periosteal, in VDR knockout mice, SA455
Pleiotrophin effects, SU149
Prostaglandin E EP4 receptor agonist, M206
PTH and FGF2, 1061
PTH and L-type voltage-sensitive calcium channels, F155
PTH and osteopontin deficiency, F442
PTH(1-34) and PTH(2-38), SU441
Runx2, 1112
Sclerostin, 1077
Simvastatin, M388
Src kinase inhibitors, SU377
Tachykinins and neurokinin-1 receptor, SU208
Unloading effects, SU169
VEGF overexpression, M015
Bone formation, *in vitro* studies
BMP-2 regulation, M011
Culture substratum effects, M174
Growth factor regulation, SU212
MLO-A5 cells, M018
Runx2/Cbfa1 overexpression, M201
sFRP-3 effects, 1183
Bone formation, *in vitro* studies (Continued)
Strontium effects, M214
Zoledronate effects, M210
Bone formation markers, 1035, 1135, SA469, SU105, SU114
Bone grafts, M049, M235, SU215
Bone histomorphometry. SEE ALSO *Bone morphometry*
Bone microarchitecture, SU021
Micro-computed tomography on bone biopsies, M332
Outpatient transiliac biopsy, M093
Percutaneous transpedicular trocar biopsy of spine, M084
Programmed Death-1 deficient mice, M240
Skeletal analysis of mice *in vivo,* M072
Staining for undecalcified bone sections, M092
Bone implants, SA047. SEE ALSO *Bone substitutes*
Bone markers. SEE ALSO *Bone formation markers; Bone remodeling markers; Bone resorption markers*
Arthritis, SU412
Bone disease diagnosis in end-state renal failure, M412
Bone metastasis in early breast cancer, SU106
Breast cancer-induced osteolysis, SU078
Calcium supplementation in adolescent boys, F003
In periodontal ligament cells, SA035
Teriparatide and prior antiresorptive therapy, 1136
Vertebral fracture risk with raloxifene, F356
Bone marrow
Alfacalcidol metabolism, SA376
Bone induction, M224
IL-12-induced apoptosis, SU230
Laser capture dissection for mRNA analysis, M271
MET and estrogen-induced transcription, 1119
Scanning and transmission electron microscopy studies, SA219
Bone marrow stromal cells
Calcium signaling, SU156
Different embryonic origins for, SU215
Dlk overexpression in, SU195
ER-α spice variants regulated by estrogen, M182
Genistein regulation, M232
Human, Runx2/Cbfa1, SA217
Perivascular niche of, M228
RGD peptides in signaling pathways, SU220
Telomerase expression, F218
TNF-α signaling, M234
Umbilical vein endothelial cells and, M211
Bone marrow transplantation, SU422
Bone mass. SEE ALSO *Bone mass, peak; Bone mineral density; Bone size*
Adult celiac disease, WG5
Aged orchiectomized rats, SU327
Alcohol drinking by rats, SA117
Bone formation in ovariectomized rats, M397
Calcium supplementation and dairy products in young females, 1200
Calcium supplementation in adolescent boys, M003
Estrogen and androgen in castrated aromatase-knockout mice, 1116
Estrogens and dietary calcium with IL-6 genetic variation, 1060
Female adolescent changes, SA002
Fracture risk in elderly women, M295
Fruit and vegetable intake by children, M287
Genetic and hormonal influences in postmenopausal women, M309
HMR 3339, M382
IGF1R allelic variation in men, SU146
LRP5 G171V mutation, F119
Male androgen receptor deficient mice, SU326
Men of African heritage, F304
Bone mass. SEE ALSO *Bone mass, peak; Bone mineral density; Bone size* (Continued)
Neuropeptide Y Y4 and Y2 receptors regulation, 1125
OF45 knockout mice, SA053
Osteogenesis imperfecta, SU385
Perimenopause and OPG gene polymorphisms, M119
PGE2 agonist in ovariectomized rats, M392
Postural sway, M283
Prepubertal girls, SU008
Rat heritability, SA121
Remobilization after disuse, M166
Sex steroids in elderly men, 1166
Vibration exercise, SA346
Bone mass, peak
Cadherins, 1184
Environmental and biologic determinants in women, SU277
ER-α association in nuclear families, SU133
Estrogen, M384
Genetic variations, SU117
Skeletal variations in young females, M008
Young women and aromatase gene variations, SA127
Bone metastasis
Amino-/non-amino bisphosphonates, M051
β3 integrin, F075
Bone markers and breast cancer, SU074, SU106
Bone sialoprotein, F052
Breast cancer and clodronate, F083
Breast cancer and OPG, 1092
Breast cancer and RANK/RANKL expression, M066
Flavopiridol effects, M050
Fracture risk prediction, M091
Macrophages and lymphocytes, SU077
Osteoprotegerin, M059
p38 MAP kinase and breast cancer, M058
Prostate cancer, F085, M068, SA082, SA088, SU073
Rat model, SU083
TGFβ signaling blockade in prostate cancer, SU075
3-D trabecular microarchitecture in prostate cancer, M061
Bone mineral content (BMC), SA007, SU320, SU337, SU359, SU373
Bone mineral density (BMD)
Activation frequency in postmenopausal osteoporosis, SU332
Age differences in men, F011
Age factors in murine models, SU325
Alendronate discontinuation, 1037, M341
Alendronate treatment and trabecular, SA336
Algorithm for low measures, SU304
Ankylosing spondylitis and nutrition, SA421
Asian *versus* Caucasian vertebral, SA315
Bone marrow transplantation, SU422
Calcium/vitamin D influences on osteoporosis risk, SA274
Candidate genes influencing peak, M124
Cdx polymorphism in postmenopausal women, SU137
Chlamydia pneumoniae, M137
Cholesterol, SU314
Concordant *versus* discordant changes in osteoporosis, WG8
Cystic fibrosis in young adults, M310
Dietary intake of postmenopausal women, M333
Dietary phytoestrogens, F279
Dominant *versus* non-dominant hip, SU323
DXR correlation with DXA, SA268
In elderly and gene encoding sclerostin, 1222
Elderly men with medical conditions, SU022
Elderly population, SA267
ER-β gene intronic polymorphisms, M122
Estradiol control, M189

Bone mineral density (BMD) (Continued)
Estrogen-regulated genes regulation of trabecular, SA464
Extremity fractures, SU292
Factor score with ultrasound for genetic studies, SA125
Fra-1 polymorphism in women, SA135
Fracture risk and peripheral, SU308
Fracture risk stratification, SU307
Gastritis, atrophic, M339
Genetic and hormonal influences in postmenopausal women, M309
Genetic loci in BXD RI mice, SU129
Genome scan for QTLs influencing variation, SU125
Heel in Japanese women, M322
Hemodialysis, M414
Hip and body composition, M303
HIV, SU313
HIV and antiretroviral therapy, M307
Leptin levels, SU154
Lifestyle factors in adolescent women, M284
Liver transplantation and antiresorptive therapy, SU420
Loading bisphosphonate doses, M357
Long term care, 1087
LRP5 polymorphisms, M123
Lumbar spine after kidney transplantation, M413
Lunar Prodigy scans, M073
Lupus and OPG/RANKL, M422
Maternal history of osteoporosis, 1088
Menopause and MTHFR polymorphism, SA131
MEPE/PHEX expression effects, F400
Microdamage in cortical bone of dog rib, SU333
Multiple myeloma in remission, M075
Nandrolone decanoate, M394
OPG levels, SU322
Oral corticosteroids, 1213
Oral exostosis in elderly women, M407
Ovariectomized rats and 2MD, SA383
Overlying fat folds and DXA accuracy, SU089
Patient positioning devices for DXA scans, SU086
Peak, osteoporosis development, SU321
Postmenopausal hypercholesterolemic women, M396
Primary hyperparathyroidism and vitamin D status in women, SA409
QTL at 1p36 and 3p21, F124
QTL differentiation in Caucasians and Asians, SU134
QTL for obesity phenotypes, SU124
QTL for spine, 1079
Quantitative ultrasound of elderly Taiwanese, SU318
Rheumatoid arthritis, M429
Smad1C, F206
Spinal and genotype-by-age in baboons, SU131
Spinal and low back pain in premenopausal women, SU311
Testing and osteoporosis treatment, M081
Two-site measurement, SU085
Ultrasonic backscatter data of spine, M103
Ultrasound and foot loading, SA110
Variation between hips, 1115
VDR gene polymorphisms in Japanese women, SA134
Vitamin B_{12}, 1214
Vitamin D, SU309
Young-old differences in femoral neck, SA316
Bone morphogenetic protein-1 (BMP-1), SA022
Bone morphogenetic protein-2 (BMP-2). SEE ALSO *Placental growth factor*
Bone formation, SU040
Calcification and substrate microtopography, M011
Cartilage formation, SU049
CIZ deficiency, 1006
Bone morphogenetic protein-2 (BMP-2). SEE ALSO *Placental growth factor* (Continued)
COX2-dependent PGE2 in osteoblast differentiation, F044
GATA-4 and MEF2 in cardiomyocyte differentiation, SU045
Gene expression by NF-κB in growth plate chondrocytes, F016
Gene expression profiling analysis, SU197
Integrins, F020
Osteosarcoma cells, SU031
PDE4 expression, M207
Recombinant human, bone marrow adipocytes and, M231
Recombinant human, osteoblast differentiation and, M175
Runx2/Cbfa1 regulation, SA196
In situ interactions and signaling, M194
Bone morphogenetic protein-2 inducible kinase (BIKe), SA193
Bone morphogenetic protein-3, M160
Bone morphogenetic protein-4 (BMP-4), SA386, SU043
Bone morphogenetic protein-5 (BMP-5), WG4
Bone morphogenetic protein-6 (BMP-6), 1076, SU198
Bone morphogenetic protein-7, 1140, F018, SU212. SEE ALSO *Osteogenic protein-1*
Bone morphogenetic proteins (BMPs)
Chondrocyte maturation, SU036
Gene expression, M157
Growth plate chondrocytes, SU033
Inhibitors, SU037
Megakaryocytes and platelets, M159
Prostate cancer osteoblastic metastasis, F085
SOST gene expression and, M218
Bone morphometry, SA285, SU046, SU120. SEE ALSO *Bone histomorphometry*
Bone neoplasms, SA086
Bone reconstruction, SA021, SU034
Bone remodeling
Adult-onset growth hormone deficiency, M402
Aged orchiectomized rats, SU327
Candidate genes and bone strength, M040
Celiac disease, SA175
Chondromodulin-I, F046
Chronobiological rhythm of, SU024
CXC chemokine receptors, SU204
Endocortical in androgen-deficient aged male rats, SU329
FGFR3 signaling, M012
Fluid shear stress dose dependence, SU172
Hip fractures, SA317
IL-11 receptor signaling, 1073
Low-fat diet, M336
Mathematical model, M150
Melatonin and estradiol, SA466
Multiple myeloma, SA068
nNOS regulation, M208
OPG and bone turnover in human pregnancy and lactation, 1132
Osteoporosis and elevated, SU107
Osteoporosis treatment concept, SU361
Ovariectomized rabbits, SA331
Postmenopausal hypercholesterolemic women, M396
Postmenopausal osteoporosis and antiresorptive medications, M372
Preptin, M146
Seasonal modulations, SA103
Thyrotropin receptor, 1054
Bone remodeling markers, F109, SU174, SU313, SU422
Bone resorption
Bicarbonate in mineral water, M360
Calciotropic hormones in men, SU330
Calcitonin effects, SA427
Cathepsin K, F064, SU226
Chlamydia pneumoniae, M137
Compound A of $\alpha_v\beta_3$ integrin, F246
Bone resorption (Continued)
Dietary calcium and elevated osteoblastic VDR, F460
Familial idiopathic hyperphosphatasia, 1057
Inflammation and p38 kinase, M281
Integrins, 1033
P2X7 receptor, 1107
PGEα, SA235
Protein undernutrition-induced, F321
RANKL, 1009, SA238, SU396
SHIP, F403
Src kinase inhibitors, SU377
Y residues in c-fms tail, SU260
Bone resorption markers
Bone metastasis in breast cancer patients, SU074
Breast cancer-induced osteolysis, SU078
Changes with various osteoporosis treatments, SU110
Collagen type Iα1, SU096
Dental radiography, SU099
First morning urine test with pH paper strips, M335
Horses, SU114
HRT or bisphosphonates, SU113
Ibandronate, M348
Long-term variability, SU023, SU102
Ovariectomized rats and RatLaps, SU105
Paget's disease, SU109
Risedronate, SA342
TRACP 5b *versus,* SU103
Bone sialoprotein, F052, M196
Bone size
Age differences in men, F011
Bone formation/remodeling of femoral neck, SU029
High parity, SA272
IGF1R allelic variation in men, SU146
Lean and fat mass and older male femur, SA305
Prepubertal girls, SU008
QTL 17q23 linkage, SU123
Strength index, 1163
Young-old differences in femoral neck, SA316
Bone stiffness, F297, M162, SA116, SU022
Bone strength
Alfacalcidol, SA378
Bisphosphonates and osteocytes viability, 1133
Bone turnover candidate genes, M040
Collagen cross-link maturity and crystallinity, SU048
Femoral neck of Japanese-American women, 1207
Fetuin/a2HS-glycoprotein, M012
HMR 3339, M382, M383
Intermittent PTH, SA363
Intrauterine and postnatal growth, M308
Mouse model, SA060
Older men, M302
OPG during spaceflight, F369
Osteogenesis imperfecta, SU385
Osteoid water, M094
PGE2 agonist in ovariectomized rats, M392
Physical activity and body weight, M169
Racial differences in young adult women, SU299
Radiographic texture analysis, SA096
Reduction during rapid growth, SA163
Simvastatin, M388
Strength index, 1163
Bone substitutes, SU050, SU052
Bone surface proteins, M013
Bone turnover. SEE *Bone remodeling*
Boys, 1201, SU004, SU006. SEE ALSO *Children*
Bradykinin B1 and B2 receptors, M203
Breast cancer
Anastrozole and/or tamoxifen, 1170
Bisphosphonates, 1091
Bone metastasis and bone markers, SU074, SU106
Bone metastasis and clodronate, F083

Breast cancer (Continued)
Bone metastasis and OPG, 1092
Bone metastasis and p38 MAP kinase, M058
Bone metastasis and RANK/RANKL expression, M066
Bone metastasis cell lines, M060
Bone resorption markers, SU102
Estrogen receptor-α, SA084
IL-8 regulation of RANKL, F079
Metastatic and non-metastatic, SA080
Minodronic acid effects, SA245
NF-κB and osteoclastogenesis, F087
Osteolysis and bone markers, SU078
Osteopontin, 1196, F081
Radial BMD and risk, M063
RANKL, F151
Rat model of bone metastasis, SU083
TGF-β stimulation of MMP-13, SU079
Broadband ultrasound attenuation (BUA), M107, SA114, SU011, SU084. SEE ALSO *Ultrasound, quantitative*
Burns, SA418, SA477

C

C3H10T1/2 cells, M153, M154
C3H/HeJ mice, 1216, 1220, SA152, SU120
C57BL/6J (B6) mice, 1012, 1220, M164, SA323, SU120
C57BL/6 X DBA/2 (BXD) recombinant inbred mice, SU129
C282 mutation HFE gene homzoyg**oty,** SA120
C677T. SEE *Methylenetetrahydrofolate reductase (MTHFR) gene*
Ca^{2+} receptor. SEE *Ryanodine receptor*
CAAT/enhancer-binding proteins-β (C/EBPβ), 1109
Caco-2 cells, M454
Cadherins, 1184, M052, SU202
Calbindin-D_{28k}, M458, SA472, SU186
Calcaneus. SEE ALSO *Heel*
Broadband ultrasound attenuation and osteoarthritis, SA114
Calscan Dexa-t for BMD measurement, M076
Ontogenetic development ovine, SU164
Population-based quantitative ultrasound reference data, F113
Quantitative ultrasound and ER gene polymorphism, SU141
Quantitative ultrasound and fracture history in men, F115
Quantitative ultrasound in androgen-deprivation therapy, SA112
Radiographic texture analysis, SA096
SCAD system and DEXA measurements, M114
Stiffness index after resistance training, M162
Ultrasonic backscatter *versus* trabecular thickness, M102
Calcification, arterial, M014, M457. SEE ALSO *Vascular stiffness*
Calcineurin, M278
Calcineurin Aα, 1018
Calciotropic hormones, SU330
Calciphylaxis, arterial, M457
Calcitonin
Calcium-sensing receptor regulation, M437
Dinucleotide repeat polymorphisms and BMD, SU135
Dinucleotide repeats and low BMD, M120
Diurnal bone resorption and plasma calcium homeostasis, SA427
Expression of cloned equine, SA431
Nasal, for male osteoporosis, SU333
Pyk2 effects, SA226
Salmon, SA430
Calcitonin gene-related peptide (CGRP), SA428
Calcitonin receptor, 1175, F263, SA426, SU264
Calcitriol, 1026, 1042, F381, M446, M448, SA078. SEE ALSO *1α,25-Dihydroxyvitamin D_3*
Calcium. SEE ALSO *Fetuin-MGP-mineral complex*
Bone formation and resorption in hypocalcemic vitamin D-depleted rats, M446
Bone mass acquisition in girls, SU007
Endocrine system in Dahl salt-sensitive rats, M404
Fracture prevention with vitamin D, M367
Homeostasis, M013
Metabolism after gastric bypass, M398
Omnivore *versus* vegan protein diet, M337
Primary hyperparathyroidism, F104, WG1
Signaling in bone marrow stromal cells, SU156
Weight loss and absorption, M329
Calcium-binding domain, SA039
Calcium channels, F155, M448, M453
Calcium-dependant potassium current, SA229
Calcium, dietary. SEE ALSO *Calcium supplementation*
Age at menarche, SA280
Body fat and bone composition in children, M288
Bone loss during pregnancy, SA276
Bone loss in ovariectomized rats, M376
Bone resorption with elevated osteoblastic VDR, F460
Calcitonin effects, SA427
Chinese children, SU278
$1,25(OH)_2D_3$ in PTH-deficient mice, F439
Exercise in boys, SU004
Fertility in PTH-deficient mice, SA441
HRT and postmenopausal bone loss, M361
Oral contraceptives in young healthy women, M363
Postmenopausal BMD, SU276
Stress in IGF-I knockout mice, F151
Calcium, extracellular, F261, SU219, SU267
Calcium phosphate ceramic culture, biphasic, M174
Calcium phosphate scaffolds, M033
Calcium-sensing receptor *(CasR)*
L-Amino acids, M443
Calcitonin release, M437
GCM2-deficient mice studies, 1181
Gene mutations, M438
Gene polymorphisms in osteoarthritis, SU138
Hypocalcemia in male with polyglandular failure, WG9
Inactivating mutation and hypercalcemia, M439
Locus-specific mutations database, M441
Mutation and idiopathic hypercalciuric nephrolithiasis, 1008
NF-κB transcriptional up-regulation, M440
PTHrP secretion by PKC dependent p38 pathway, M444
Calcium supplementation, SU351. SEE ALSO *Calcium, dietary*
Alfacalcidol efficacy, SA377
Bone markers in adolescent boys, F003
Bone mass in young females, 1200
Bone response to exercise in children, M009
Dietary protein and bone mass in boys, 1201
Exercise and prepubertal bone accretion, 1043
Gestational and lactational bone loss, M405
Growth and bone mass in adolescent boys, M003
PTH and skeletal development, M007
Calmodulin kinase II (CamKII), M257
Calpains, SA231
Calscan Dexa-t, M076
Canadian Database of Osteoporosis and Osteopenia, SA289
Cancellous bone
Bisphosphonates and 3-D microarchitecture, SU349
Bovine, quantitative ultrasound and mechanical damage prediction, SU053
Cbfa1 gene dosage, 1111
Directional direct thickness measurement, M096
Cancellous bone (Continued)
Genetic effects on bone loss after ovariectomy, SU116
MicroCT scanner and anesthetized rats, F099
Remodeling compartment, M019
Teriparatide (rhPTH (1-34)), 1041
Vitamin K_2, SA375
CAN/Nup214, F484
Carbenoxolone, M251
Carborane BE360, SA355
Cardiomyocytes, F446, SU045
Carrots, SU354
Cartilage, 1065, 1078, M024
Cartilage, articular, M038, SA025, SA059
Cartilage oligomeric matrix protein (COMP), SA039
Cas interacting zinc finger protein (CIZ), 1006
β-Catenin, 1015, F042, SA160
Cathepsin K
Fibroblasts in pycnodysostosis, SU065
Gene mutations and pycnodysostosis, SA388
Inhibitors, F064
Osteocalcin degradation, M047
Osteoclast function, SU225
Osteoclast-specific *cis*-acting element, SU266
Overexpression, bone resorption and, SU226
Cbl, 1149, M280, SA232, SU262
CCAAT/enhancer binding proteins (C/EBPs), SA211, SU447
CD14 peripheral monocytes, nonadherent, SA390
$CD34^+$ cells, SU250
CD38 gene promoter, SA215
CD44, 1148
CD44 surface expression, F236
Cd gavage, M253
Celiac disease, SA175, WG5, WG6
Cementum, F024
Cementum-derived cells, M039
Cerivastatin, SU012
c-Fos, 1024, SA483
CGI-135 (chromatin remodeling protein complex), F210
Chemokines, M140, SA143. SEE ALSO *Interleukin-8*
Children. SEE ALSO *Boys; Girls; Infants*
Age-related changes in metacarpal morphometry and BMD, SU016
BMC and bone strength in prepubertal gymnasts, SU017
BMD and maximal effect during fitness test, SU020
BMD with SLE, SU019
Bone age *versus* chronological age, SU018
Calcaneal BUA for bone acquisition estimates, SU011
Calcaneal ultrasound and ethnicity, SU008
Carpal bone density, SU001
Dietary calcium effects on body fat and bone composition, M288
Dietary calcium for Chinese, SU278
Duchenne muscular dystrophy, F419
Exercise and calcium supplementation, M009
Fracture risk with oral corticosteroids, 1199
Fruit/vegetable intake and bone mass, M287
Growth plate under immunosuppressive therapy, SU424
I-cell disease, WG10
Pediatric Whole Body analysis, SU015
Polyarticular juvenile idiopathic arthritis, SU136
pQCT of tibia, F006
Precision error of DEXA scans, M082
Prepubertal bone accretion, 1043
PTH, skeletal development and calcium requirements, M007
Quantitative ultrasound, M105
Whole body DXA of cortical bone, 1202
Chinese herbal extracts, M065, M266
Chlamydia pneumoniae, M137

Chloramphenicol acetyl transferase (CAT) marker gene, M171
Chloride channel 7 (ClCN7), 1081
Chlorinated-peptides, SU115
Chlorobenzene, SA049
Cholesterol, F241, SA027, SU139, SU314, SU372
Chondrocyte differentiation
  Adenovirus vector-mediated ALK-3 or 6 gene expression, M023
  Apoptosis, SA030
  Cyclin-dependent kinase 6 inhibition, M022
  Estrogens regulation, M026
  MEK1 expression, 1070
  NFAT and p38 MAP kinase regulation, F033
  Oxygen effects, M030
  p21 MRNA, SA034
  p38 MAP kinases, M027
  RANKL/RANK/NF-κB signaling, 1153
  Runx1, 1110
  Sox9, 1071
  TGFβ2 and BMP-3, M160
  TGFβ2 during embryonic development, F139
Chondrocytes. SEE ALSO *Growth plate*
  β-Catenin, F042
  Cell cycle factors, M436
  CTGF/Hcs24 effects, F031
  Estrogen receptor-related receptor-α, 1114
  IL-1 gene expression in, SU163
  Mechanical stress response, SU054
  MMP-13 internalization by, SA032
  Osteopontin and TNF-α-mediated cytotoxicity of, 1156
  Sprouty2 and IGF-I signaling, 1204
  SRF expression, SA041
  Stretch-activated calcium influx pathways, SA156
  TRENDIC and CTGF gene expression, SA043
  VDR(-/-) mouse, SA457
Chondrocytes, articular, SU036
Chondromodulin-I, F046
CHOP, SA211
Chromosome 1q, F122
Chromosome 3, SA123
Chromosome 4, F168
Chromosome 14, 1218
Chromosome 15, 1218
Chromosome 19, SA123
Chromosome 19q, 1079
Chromosome 21q, 1079
Chronic obstructive pulmonary disease, M293, M324
Circulating skeletal stem cells, M226
cis-acting element, F435, SU266
Cleft, intravertebral, SU293
Cleidocranial dysplasia, 1004, SU118, SU384
Clinical practice, SU100, SU296, SU336
Clinical trials, 1040, SU343
Clodronate, F083, SA092, SA402. SEE ALSO *Bisphosphonates*
CLX-0291, M420
Collagen, 1197, M038
Collagenase 3. SEE *Matrix metalloproteinase-13*
Collagenase-3 promoter, F186, SU270
Collagen cross-link maturity and crystallinity, SU048
Collagen fiber orientation, SU062
Collagen-phosphophoryn sponge, M010
Collagen type I, M145, SA105, SU002
Collagen type Iα1, M126, SA012, SU096, SU142, SU145
Collagen type Iα2, 1160, M200, SU132
Collagen type I-green fluorescent protein, 1186
Colles' fracture, SU291
Colony forming unit-fibroblastic cells, M226, SA224
Colony forming unit osteoprogenitors, M222
Colony-stimulating factor-1 (CSF-1). SEE *Macrophage colony-stimulating factor (M-CSF)*
Computed tomographic microscopy, M085, M086, M098, SA008, SU021. SEE ALSO *Micro-computed tomography; Peripheral quantitative computed tomography*
Congenic mice
  B6.C3H, 1217, 1220
Conjugated equine estrogens and medroxyprogesterone, M377, M386
Connective tissue diseases, inherited, SU403
Connective tissue growth factor, SA043, SU153, SU209
Connective tissue growth factor/hypertrophic chondrocyte-specific gene product 24, F031, SA028, SA037
Connexin43, 1158, M212, M251, SU160
Connexin45, F182
Contraception, M363. SEE ALSO *Dehydroepiandrosterone (DHEA)*
Copper, dietary, SA148
Copper-zinc superoxide dismutase enzyme promoter, SU237
Cord blood mononuclear cells, M272
Core binding factor A1 (Cbfa1)
  Inhibited by BMP-2 inducible kinase, SA193
  Locally delivered for periodontal bone repair/regeneration, F184
  OSEBF1 expression, 1003
  Ossification of posterior longitudinal ligament, M426
  Osteoblastic differentiation, 1111
  Osteogenic lineage allocation, 1015
Core binding factor b (Cbfb), 1004
Cortical bone
  Biomechanical examination of spinal distribution, M085
  Collagen fiber orientation in loading interpretation, SU062
  Genetic effects on bone loss after ovariectomy, SU116
  Genetic markers influence on mouse femur, SU122
  Remodeling in adult-onset growth hormone deficiency, M402
  Teriparatide (rhPTH (1-34)), 1041
Corticosteroids, oral, 1199, 1213. SEE ALSO *Glucocorticoids*
CP-533536, M395
CpG clustering regions, SU191
CpG-DNA, bacterial, SU241
Cranial development, F048
Craniofacial implants, SA047
CRM1/exportin1 (nuclear exporter), 1161
Crovidisin, SA174
Cushing's syndrome, M321, SA324
CXC chemokine receptors, SU204
Cyclase-activating parathyroid hormone (1-84), SU438
Cyclic adenosine monophosphate (cAMP), SA432, SA454
Cyclic AMP response element (CRE), SU430
Cyclic AMP response element binding (CREB) protein, SU041, SU071
Cyclin-dependent kinase 6, 1148, M022
Cyclooxygenase-2, F437, SA244, SU214
Cyclooxygenases, F311
CYP3A4, F488
CYP19, M116, M121, M188, SA127, SA128
CYP24, SU459
Cyproterone acetate, 1027
Cystatin C, M256
Cystic fibrosis, M310
Cytokines, SA143, SA145, SU055

D

Dach1, F139
Dahl salt-sensitive rats, M404, M452
DBA/2 mice, 1012, SA323
DD045, F201
Decorin, 1068
Dehydroepiandrosterone (DHEA), M389
Densitometry. SEE ALSO *Dual energy X-ray absorptiometry; Dual X-ray absorptiometry; Fan-beam bone densitometry; Morphometric X-ray absorptiometry; Phase-contrast X-ray imaging; Radiographic absorptiometry*
  Screening postmenopausal women, M318
Dental matrix protein 1 (DMP1), SA190
Dental pulp stem cells, M228
Dentin matrix protein (DMP1), SU063
Depression, M314
Dermal fibroblasts, M034
Dexamethasone, M207, SA153, SA479, SU035, SU118
Diabetes mellitus, M313, M321, SA023, SA237, SU190
Diet
  Anorexia nervosa and bone turnover, M364
  Bone mass in children, M287
  Bone remodeling and low-fat, M336
  Bone resorption in elderly osteoporotic women, 1134
  Carrots and ovariectomy-induced bone loss, SU354
  Long-term restrictions, SA323
  Omnivore *versus* vegan protein diet, M337
  OPG levels, SU098
  Vitamin D depletion, F277
Digital X-ray radiogrammetry (DXR), F091, SA092, SA268, SU016, SU095
Dihydrotestosterone, M064
1,25-Dihydroxyvitamin D, F456, SU104
25-Dihydroxyvitamin D, SA485
1,25-Dihydroxyvitamin D_3
  Calcium channel expression, M453
  Dietary calcium in PTH-deficient mice, F439
  Epidermal growth factor receptor signaling, M455
  Ion channel responses in osteoblasts, SU448
  Membrane effects in VDR(-/-) mouse growth plate chondrocytes, SA457
  Membrane receptor, SA459
  Muscle cell phospholipase Cγ, M450
  Osteoblasts and 2MD analogue, 1120
  PHEX gene expression, F385
  Renin-angiotensin system, 1049
  Senescence accelerated mouse osteoporosis model, M002
  Signaling and $p57^{Kip2}$ gene, SU183
  Sporadic hypophosphatemic rickets, SA397
1α-Dihydroxyvitamin D_3. SEE *Alfacalcidol*
1α,25-Dihydroxyvitamin D_3
  Cross-talk in leukemic NB4 cells, SU452
  CYP24-catalyzed C24-oxidation, SU453
  2,2-Dimethyl analogues, SU455
  Gene microarray analysis of VDR-KO mouse, SU449
  Membrane receptor in chick intestinal caveolae, SU446
  2,α-Substituents as superagonists, SU456
24,25-Dihydroxyvitamin D_3, 1082, SA457
24R,25-Dihydroxyvitamin D_3, SU449
Diskectomy, interlaminar for degenerated disk lesions, SA062
Distraction osteogenesis, F256, M152, SA167
Disuse osteoporosis, 1047, M166, M167
Diurnal modulations, bone remodeling markers, F109
Dlk (delta-like, EGF-like homeotic protein) overexpression, SU195
Dlx3 genes, M216
Dlx5 homeobox gene, 1159, M196, M216, SU039, SU208
Dlx6 genes, M216
Dmp-1, 1005
cDNA microarray system. SEE *Gene chip microarray analysis*

Dual energy X-ray absorptiometry (DEXA)
- Bone quality assessment, M114
- BUA or SOS of heel *versus,* SU084
- Femur bone mass and overlying fat folds, SU089
- Mechanical response tissue analysis, M087
- Precision error with children, M082
- Single *versus* bilateral hip bone BMD scans, SU093
- Skeletal lead effects, SU090
- Standardized vertebral morphometry, SA285

Dual X-ray absorptiometry (DXA). SEE ALSO *Morphometric X-ray absorptiometry*
- Ankylosing spondylitis, SA090
- BUA of femur *versus,* M107
- Calcaneal bone mass and lumbar spine BMD in men, M078
- Calscan Dexa-t, M076
- Central measurements and glucocorticoids, M112
- Central reports for physicians, SU091
- Childhood bone age *versus* chronological age, SU018
- Factor score with ultrasound for genetic studies, SA125
- Fan-beam of hip axis length, M089
- Hip areal BMD, 1131
- Lateral vertebral assessment, SU092
- Lexxos 2D radiographic detector, M080
- Ovariectomized rats, M326
- Patient positioning devices and BMD, SU086
- Peripheral, in postmenopausal women, SA266
- pQCT for BMD *versus,* SA093
- Radiogrammetry and BMD, SA268
- Socioeconomic factors in primary care referral, F269
- Spinal BMD and leg elevation, M074
- Ultrasonic measurements of fractures *versus,* M111
- Whole body of cortical bone in children, 1202

Dwarfism, 1072, M029. SEE ALSO *Growth retardation*

Dynamin, SA232

E

Ears, BMP5 expression and, WG4

EB1089, SU458

Ehlers Danlos syndrome, SU403

Elastic modulus, SU053

Electromagnetic fields, M238, SU271

Elk-1 transcription factor, F203

Embryonic stem cells, 1186

Embryo, TGF-β2 regulation, F139

Enamel matrix serine proteinase 1, SU067

Endochondral bone, 1066, 1154, M132, M460, SA051

Endometriosis, SU334

Endothelin-1, SU080, SU155

Enoyl CoA hydratase, SU450

Enzyme immunoassay, SU104

Eosinophil chemotactic factor-L, M246

Epidermal growth factor receptor, M455

Epidermal growth factor response factor (ERF-1), SU200

Estradiol
- Aromatase gene polymorphisms in postmenopausal women, SA128
- BMD changes with HRT, M118
- BMD of older postmenopausal women, 1164
- BMD of young postmenopausal women, SA328
- BMP-4 induced bone formation, M185
- ERα and osteoclast differentiation, SU256
- HRT in elderly women, F358
- Integrin expression on osteoclasts, SU255
- Melatonin and bone remodeling, SA466
- Mineralization control, M189
- Postmenopausal osteoporosis and circulating OPG, M369

17β-Estradiol, SU254

Estrogen receptor-α
- Breast cancer, SA084
- Gene polymorphisms, SA132, SU132, SU139
- Gene transcription and ER-β, F465
- Osteoblastic response to loading, 1010
- Osteoclast differentiation, SU256
- Peak BMD linkage in nuclear families, M124
- Peak bone mass linkages in nuclear families, SU133
- Protein kinase Cα in osteoblast differentiation, M179
- Skeletal metabolism effects, SA470
- Splice variants in bone marrow stromal cells, M182
- Transcription repression and Smad4, F473

Estrogen receptor AF-1, M385

Estrogen receptor-α F promoter, M180

Estrogen receptor-β, 1031, F465, M122

Estrogen receptor-related receptor-α, 1114

Estrogen receptors, F468, M187, SA202
- Gene polymorphisms, SU138, SU141

Estrogens
- Bad phosphorylation, F173
- Chondrocyte differentiation, M026
- Disuse bone loss in rats, M167
- Formation in tibial growth plate and metaphyseal bone, SA475
- Fracture repair in ovariectomized rats, F373
- Gene polymorphisms and menstruation, F130
- IGF-I and peak bone acquisition, 1080
- Ligand/receptor interactions, 1032
- Peak bone mass, M384
- Sex differences and loading, 1048
- Skeletal actions, M380
- Streptococcal cell wall-induced arthritis, 1156
- TNF-producing T cells proliferation, SA467

Ethinylestradiol, F371. SEE ALSO *FemHRT*

Ethnic-racial groups
- Anorexia nervosa and osteoporosis, SU302
- BMD in older men, F300
- Bone mass in men, F304
- Bone strength in young adult women, SU299
- Calcaneal ultrasound in children, SU008
- Early milk consumption and postmenopausal BMD, SU276
- Femoral neck strength, 1207
- Growth and hip fracture risk, 1167
- Hip bone loss, 1085
- Hip fractures, SA293
- Metacarpal DXR and BMD references, SU095
- Osteopenia and osteoporosis in Hispanic postmenopausal women, SA265
- Osteoporosis reference database of Asian Indian women, SA270
- Osteoporosis risks and fractures, SU281
- Osteoporosis risks for men, M304
- Peak bone mass in women, SU277
- Peripheral BMD and fracture risk, SU308
- QTL for BMD, SU134
- Quantitative ultrasound cut-off value and fracture threshold for Japanese women, M106
- Recruitment for bone health study, SU316
- Salt load and urinary sodium/calcium, SA318
- Structural properties of bone in boys, SU006
- Vertebral BMD, SA315

Etidronate, M346, M355, SU346

Euglycemia, M071

Evidence-based medicine, SU360

Exercise. SEE ALSO *Impact exercise; Loading; Resistance training; Running; Stress, mechanical; Swimming; Vibration exercise*
- Alendronate in ovariectomized rats, F165
- Back muscles and vertebral fracture risk, F288
- BMD and maximal effect during fitness test, SU020
- BMD in older men, SA301
- Bone strength and geometry, M169

Exercise. SEE ALSO *Impact exercise; Loading; Resistance training; Running; Stress, mechanical; Swimming; Vibration exercise* (Continued)
- Bone structure and density in women athletes, SU180
- Calcium supplementation and prepubertal bone accretion, 1043
- Calcium supplementation in children, M009
- Dietary calcium in boys, SU004
- Fracture risk in old age, SU014
- During growth *versus* professional, M004
- Hip section modulus *versus* BMD, M168
- Lumbar spine and proximal femur effects, SA351
- Preterm infants, F001
- Rat model of freefall impact, SU178
- Tennis player forearms, SU182
- Weight-bearing *versus* non-weight-bearing, SA170, SU159

Exostosis, oral, M407

Extracellular matrix, M021, M147, SA194, SA204, SU167, SU170

Extracellular signal-regulated kinases (ERKs)
- Apoptosis regulation, 1190
- CTGF/Hcs24, SA028
- Cytoplasmic-restricted signaling by, 1161
- Extracellular calcium and RANKL expression, SU219
- FGF2-induced osteopontin gene expression, M129
- Flow shear strain-induced human osteoblast proliferation, F161
- Sustained *versus* transient activation, SU185

F

Fall prevention, 1137, F381, M423, SU317

Family practice, SU364

Fan-beam bone densitometry, M077, M089

Fanconi's syndrome, SA401

Farnesyl diphosphate synthase, SA251, SA255

Far upstream element (FUSE) binding protein, M042

Fas, M243

Fat vascularized pedicle, SA021

Feet, SA110, SU402

FemHRT (ethinylestradiol and norethindrone), M377

Femoral head, M356, SA025, SA425, SU407, SU413

Femoral neck
- BMD and hip fracture risk, 1086, 1104
- Bone formation/remodeling and geometry, SU029
- Calcaneal quantitative ultrasound to predict BMD, M115
- Cortisol normalization in Cushing's syndrome, SA324
- Long-term bone loss in elderly women, SA014
- Magnetic resonance imaging, F295
- Spinal cord injury and spaceflight, M170
- Strength in Japanese-Americans, 1207
- Young-old differences in women, SA316

Femur
- BUA *versus* DXA measurements, M107
- Exercise effects, SA351
- Genetic factors in peak bone mass, SU117
- Genetic markers influencing size and shape in mice, SU122
- Intrauterine and postnatal growth, M308
- QTL linkages to chromosomes 3 and 19, SA123
- Trabecular bone density with myostatin deficiency, SU177

Fetal intestine, 1026

Fetuin. SEE *α2-HS-glycoprotein gene*

Fetuin-MGP-mineral complex, M019

Fibroblast growth factor, F139. SEE ALSO *Basic fibroblast growth factor*

Fibroblast growth factor 2
GSK-3 signaling, SA138
Overexpression, M130
Overexpression in osteoblasts, M127
p21/p53 pathway in dwarfism, M029
TGF-β2 regulation of signaling and activity, M135
TGF-β mediated regulation of endochondral bone formation, M132
Fibroblast growth factor 2 receptor, F137, F197, SA136
Fibroblast growth factor 3 receptor , 1204, M012, SA140
Fibroblast growth factor 23
Endocrine response to phosphate supplementation in men, 1144
Gene expression, F395
Humoral hypercalcemia of malignancy and primary hyperparathyroidism, 1108
Hyperphosphatemia and growth retardation, 1182
Oncogenic hypophosphatemic osteomalacia, F398
Oncogenic osteomalacia, SA396
Oncogenic osteomalacia and X-linked hypophosphatemic rickets, 1139
Tumor-induced osteomalacia, 1143
Vitamin D and phosphate regulation, M128
Fibrodysplasia ossificans progressiva (FOP), F417, SU044
Fibronectin, M049, M408
Fibrous dysplasia of bone, SA384, SA392, SU386, SU387
Filamin, F263
Fischer 344 rats, SA055, SU368
Fish, M043. SEE ALSO *Lamprey Geortira australis*
Flavopiridol, M050
Flt-1 tyrosine kinase, F144
Fluid shear stress. SEE ALSO *Loading; Pulsatile fluid flow*
ATP release in MC3T3-E1 cells, SU170
Bone adaptive response, SU172
β-Catenin translocation, SA160
ERKs and osteoblast proliferation, F161
Low magnitude and osteoblasts, SU157
NF-κB response modulation, SU171
Prostaglandin E_2 receptor and intercellular communication, SU272
Prostaglandin metabolism in MC3T3-E1 cells, SA162
Prostaglandin metabolism in osteoblasts, SU167
Fluorochrome, M092
Folate, plasma, SU143
Foraminotomy, SA062
Forearm, SA098, SU182. SEE ALSO *Radius; Ulna* Fractures, F094
DFosB, 1097
ΔFosB, 1097
Four and a half lim protein 2 (FHL2), 1017
14-3-3 protein, M417
Fra-1, SA135, SA200, SA483
Fracture healing. SEE ALSO *Fractures*
Circulating skeletal stem cells during, M226
Colony forming units-fibroblasts during, M226
Estrogen, raloxifene, and alendronate effects, F373
Fibroblast-based gene therapy, F018
Fibrous dysplasia of bone, SU386
Gene expression of age-related delay, SU148
Id1/Id3 double gene for angiogenesis, 1192
Lower Extremity Gain Scale, SA296
Mechanical stimulation and MAP kinase activation, SU061
MMP and angiogenic fracture expression, SA065
Molecular mechanism, SA045
NSAIDs, 1171
PP6 rat muscle-derived cells, SU043
Retrovirus-mediated BMP-2/4 hybrid gene therapy, SU042
Fracture healing. SEE ALSO *Fractures* (Continued)
Strain dependent effects, SU290
Synthetic Bone and Cartilage Stimulating Peptide, SA147
TNF-α signaling, M136
Fracture prediction, M089, M091, M106, SA298, SU283
Fracture risk
Calcium/vitamin D intake in Caucasian women, SA274
Exercise during growth and young adulthood, SU014
Hearing acuity in older women, M296
Inflammatory bowel disease, F282
Low *versus* high turnover osteoporosis, SU305
Magnesium intake in women, 1089
Racial differences, 1167
Renal transplantation, 1211
Sleep disorders in postmenopausal women, F290
Smoking, SU288
Two-site BMD measurement, SU085
Ultrasound comparison in elderly women, 1130
Vertebral levels for assessment, M079
Fractures. SEE ALSO *Hip fractures; Stress fractures; Vertebral fractures; Wrist fractures*
Blood-borne mesenchymal stem cells, SA221
Celiac disease, WG5, WG6
Children on oral corticosteroids, 1199
COLIA1 promoter polymorphisms, SU145
Extremities and BMD, SU292
Fragility, osteocyte density and, F314
Future fracture prevention therapy, SU297
Hip fracture risk, M299
Hospital care in Italy, SA287
Ibandronate, 1038
IGF-I gene promoter polymorphism in elderly, 1221
Male study recruitment strategies, SA303
Orthopedic surgeons, M374
Osteoporosis drugs, SU285
Osteoporosis education for health personnel, SU367
Osteoporosis knowledge questionnaire, M297
Osteoporotic and drug subsidization, M375
Peripheral and axial densitometry measurements, F094
Postmenopausal osteoporosis management, SA294
Postmenopausal women, SU286
Prevention strategies, SA281
Prevention with alendronate, F106
Prevention with calcium and vitamin D, M367
Risedronate, SA344
Risk assessment in primary care using point-of-care technology, SU108
Risk stratification and BMD, SU307
Secondary prevention, SU295
Self-report validity in postmenopausal women, M300
Stiffness index in postmenopausal women, F297
Traumatic, 1212
Ultrasonic measurements *versus* DXA, M111
Frizzled proteins, M035
Frizzled-related protein 4 (FRP-4), 1142
Frzb1, 1012

G

Gait, M097
Gap junctions, F182, SU249, SU444
Gαq-mediated signaling, 1051
Gastric bypass, M398, M399
Gastritis, atrophic, M339
Gastroplasty, SA319
GATA-1, 1014
Gaucher's disease, M400
GCNB, SU393
Gelatin hydrolysate, SU353
Gelsolin, SA228, SU265
Gender differences. SEE *Sex differences*
Gene chip microarray analysis. SEE ALSO *Quantitative trait loci*
Age-related delay in fracture healing, SU148
Bone loss after Cd gavage, M253
Candidate genes for IGF-I QTL affecting bone mass, 1106
1α,25$(OH)_2D_3$ or 24R,25$(OH)_2D_3$-treated tissue, SU449
Gene expression regulation in mesenchymal stem cells, SU201
Glucose-dependent insulinotropic peptide in MG-63 cells, M138
Leukocytes for skeletal response to PTH, F440
Mineralization in mesenchymal stem cells, SA185
Osteoblast differentiation, SU193
Osteoclast-like cells differentiated with lipopolysaccharide, SU252
Osteoporosis profiling, SU119
Placental growth factor, SA015
PTH signaling in osteoblasts, SU199
Gene expression profiling, M034
Gene therapy
Anti-proliferative mutant of PTHrP, 1102
BMP-2/4 hybrid for fracture healing, SU042
Fibroblast-based for bone repair, F018
Mesenchymal stem cells, M225
Radiation and bone reconstruction, SU034
Spine fusion and Ad5-LMP-1 gene transfer, M045
Genistein, M185, M186, M232
Genome, human, 1106, SU125, SU194
Giant cell tumor, SA076
Girls. SEE ALSO *Children*
Abnormal bone turnover with scoliosis, SA005
Abnormal growth with scoliosis, SU400
Age at menarche and dietary calcium, SA280
Bone mass acquisition, SU007, SU132
Hypercalcemia, M439
Mechanical loading and skeletal response, SU005
Prepubertal bone size and mass changes, SU008
Pubertal growth with X-linked hypophosphatemic rickets, SA420
Skeletal variations in peak bone mass, M008
Spinal BMC during puberty, SA007
Tibia assessment with ultrasound, SA100
Glial cells missing, 1064
Glial cells missing2, 1181
Glucagon, M141
Glucocorticoid-induced leucine zipper protein (GILZ), SA480
Glucocorticoid receptors, F478, M241, SA477
Glucocorticoids. SEE ALSO *Corticosteroids; Osteoporosis, glucocorticoid-induced*
Anabolic effects in bone, 1026
BMP-6 expression, SU198
Bone formation markers, 1035
Calcitonin receptor in osteoclasts, SU264
Chronic administration in rats, SA476
Duchenne muscular dystrophy in children, F419
Heel QUS and central DXA concordance, M112
Medrysone, SA326
Osteoprotegerin gene expression, SU232
Overexpression and BMD and strength loss, 1025
Sex steroids in men, F327
Vertebral fracture risk, F325
Withdrawal after kidney transplantation, 1141
Glucose-dependent insulinotropic peptide (GIP), M138, M139
Glucose, dietary, 1165
Glutamate receptor expression, SU168
Glutamine synthetase, SA187
Glycogen synthase kinase-3, SA138
Glycosaminoglycans, SA242
GNAS1 mutations, 1083, F387, F389
Gn-RH agonist therapy, M381

gp130, 1123, F176
G protein α subunit, F387, F389
G protein-coupled receptors (GPCRs), F452
G protein 11α, SA450
G proteins, 1065
Granulocyte/macrophage colony stimulating factor, M161
Green fluorescent protein, 1185, F191, SA207
Growth, exercise and future fractures, M004
Growth factors, M145
Growth hormone, M147, SA118, SU371
  Adult-onset deficiency, F433, M402, SU425
Growth plate. SEE ALSO *Chondrocytes*
  BMP-2 regulation by NF-κB, F016
  BMPs expression, SU033
  Chondrocyte response to mechanical stress, SU054
  Immunosuppressive therapy, SU424
  Lysophospholipids and TGF-β1, M158
  MMP-13 and collagen breakdown, F066
  Remnant removal after bolus zoledronic acid in growing rabbits, 1203
  Sex steroid formation, SA475
  Tumor suppressor gene VHL, 1152
Growth retardation, 1182. SEE ALSO *Dwarfism*
Gu-Sui-Bu (Drynaria fortunei), M266

H

Halogenic hydrocarbons, SA049
Hand, SU087, SU412
Health care costs, F286, SA291
Health education, osteoporosis, M368, SU362. SEE ALSO *Patient education*
Health personnel, SU367
Health plan, M368
Hearing, M296
Heart transplantation, 1042, M110, SU423
Heat shock factors, SU152
Heel. SEE ALSO *Calcaneus*
  BMD in Japanese women, M322
  Quantitative ultrasound and glucocorticoids, M112
  Radiographic texture feature analysis for vertebral fracture risk prediction, SA102
  Ultrasound BMD for osteoporosis prediction in rheumatoid arthritis, M113
HEK 293T cells, 1064
Hematopoietic stem cells, 1053
Hemochromatosis, SA120
Hemodialysis, M414, SA023, SA107. SEE ALSO *Kidney failure*
Heparin, SU184, SU216
Hepatitis C-associated osteosclerosis, WG2
Hepatocyte growth factor (HGF), M236
Heterogeneous nuclear ribonucleoprotein K (hnRNP K), SA183
Hip
  Age and sex factors in geometrical measurements, SA313
  Areal BMD *versus* volumetric spinal BMD, 1131
  BMD after resistance training, M162
  BMD and chromosomes 14 and 15, 1218
  BMD and long-duration spaceflight, SA166
  BMD in dominant *versus* non-dominant, SU323
  BMD in postmenopausal women, M325
  BMD in spinal cord injury, M099
  Fracture prediction with fan-beam DXA scan of hip axis length, M089
  Section modulus *versus* BMD with exercise, M168
  Single *versus* bilateral BMD scans, SU093
  Soy isoflavone supplementation and BMD, SU352
  Structural geometry and teriparatide, F364
Hip arthroplasty, SA129, SU088, SU236, SU414. SEE ALSO *Joint prosthesis*
Hip fractures
  Body fat as predictor, SU289
  Bone remodeling, SA317
  Femoral neck BMD, 1086
  Higher BMD T-scores in women, F292
  Hip protectors, F348
  Italian males and females, SU284
  Japan, SA293
  Male risks, M291
  Maternal, current smoking and risk, M301
  Mortality prevention, 1090
  Osteoporosis management after, SU294
  Peripheral and axial densitometry measurements, F094
  pQCT cross sectional images, SA101
  Prevention with calcium and vitamin D, M367
  Prior fractures, M299
  Recovery performance measure, SA296
  Risk assessment in institutionalized elderly, F111
  Risk *versus* radius fractures, M294
  Survival and functional status in elderly, SU298
Hip protectors, F348
Histone deacetylase-2 (HDAC2), 1118
Histone deacetylase-3 (HDAC3), M199
Histones H3 and H4, M195
HIV, M307, SA401, SU313
HLA DR2, M118
HMG-CoA reductase mRNA, SU374
HMR 3339, M379, M382, M383
Hologic QDR 4500, M077, M080
Hormone replacement therapy
  Abdominal fat and BMD, F354
  BMD changes and estradiol, SHBG, and HLA DR2, M118
  Body composition and leptin, SU319
  Bone resorption markers, SU113
  Chronic renal failure and ovariectomy, M418
  Dietary calcium and postmenopausal bone loss, M361
  Estradiol levels in elderly women, F358
  Hypogonadism in women with thalassaemia major, SA352
  Knee osteoarthritis, SA423
  Non-responder characteristics, M373
  Sex neutral, 1058
  Short-term use in postmenopausal women, SA370
  Tea and BMD, SA278
  Tibial bone structure/performance in postmenopausal women, M387
  VDR gene polymorphisms and BMD in postmenopausal Koreans, M117
Hormone supplementation, M222
Horses, SA116, SA431, SU114, SU436
Hoxc-8, SU038
α_2-HS-glycoprotein gene (AHSG), M012, M124
Humerus, F094, SU179, SU180
Humoral hypercalcemia of malignancy, M432
Hunter's syndrome, WG11
Hydrocortisone, SU002
Hydroxyapatite, M224
Hydroxyapatite-collagen composite, SU050
12(S)-Hydroxyeicosatetraenoic fatty acids (12(S)-HETE), M209
24-Hydroxylase, 1082. SEE ALSO *25-Hydroxyvitamin D_3-24-hydroxylase*
1-Hydroxylase, substrate 25-$(OH)_2$D, SA490. SEE ALSO *Alfacalcidol*
11β-Hydroxysteroid dehydrogenase, 1026
25-Hydroxyvitamin D, F482, M452, SA490
25-Hydroxyvitamin D-1α-hydroxylase, 1029, SA163, SA486, SA489, SU071. SEE ALSO *Alfacalcidol*
1α-Hydroxyvitamin D_2, SA491, SU457, SU459
1α-Hydroxyvitamin D_3, SA491, SU457
25-Hydroxyvitamin D_3 1 α-hydroxylase, 1028. SEE ALSO *Alfacalcidol*
25-Hydroxyvitamin D_3-24-hydroxylase, SU447. SEE ALSO *24-Hydroxylase*
Hypercalcemia, 1172, M439, SU392
Hypercalcemia, humoral, 1108
Hypercalcemia, hypocalciuric, M438, M441, M442
Hypercalciuria, absorptive, M416
Hyperinsulinemia, M071
Hyperlipidemia, M261
Hyperparathyroidism, M286, SA413, SU396, SU405
Hyperparathyroidism, neonatal severe, M438, M441, WG10
Hyperparathyroidism, primary
  Alendronate, 1169
  Atypical parathyroid adenoma, SU395
  Diagnostic tools, F104
  FGF-23, 1108
  Forme fruste, 1172
  Lytic bone lesion, SU397
  Parathyroid glands malignancy, SA407
  Parathyroid hormone (7-84) molecule, F408
  Symptoms and indices relationship, WG1
  3-D trabecular architecture, 1173
  Trabecular bone density, F412
  Vascular stiffness, SU394
  Vitamin D status and BMD in women, SA409
Hyperparathyroidism, secondary, F410, M338, M417, SA434
Hyperphosphatasia, familial idiopathic, 1057
Hyperphosphatasia, idiopathic, 1056
Hyperphosphatemia, 1182
Hyperthyroidism, SA132, SU320
hyp mouse, 1205, SA393
Hypocalcemia, M398, M440, M441, SA411, WG9
Hypogonadism, 1209, SA352
Hypoparathyroidism, PTH-deficient, SA411
Hypophosphatasia, SU408
Hypophosphatemia, familial, F456, SA397
Hypophosphatemia, X-linked, 1139, SA420
Hypothyroidism, subclinical, SA312
Hypovitaminosis D, M290, SU100
Hyp phenotype, F391

I

Ibandronate
  Administration and dosage, 1038, F339, M347, M348, M349, SU342
  Heart transplantation and testosterone, SU423
  Ischemic necrosis of femoral head, M356
  Oral daily in postmenopausal women without osteoporosis, 1138
  Vertebral fractures, F341
  Vitamin D-induced artery calcification and calciphylaxis, M457
I-cell disease, WG10
Iliac crest, F360, M086, M093, M327
Immediate-early genes, SA213
Immobilization. SEE *Unloading*
Impact exercise, freefall, SU178, SU179
Incadronate, SA379, SU411
Indian hedgehog, 1154, F208, M032, SA140
Indinavir, F333
Indomethacin, M164
Inducible cAMP early repressor, SU429
Infants, M005, M105, SU399
Infants, preterm, F001, SU404
Inflammation, F422, M140, M281, SU246
Inflammatory bowel disease, F282
Infliximab, M371, SA368
Inhibin B, 1168
Insulin-like growth factor(s), M132
Insulin-like growth factor I (IGF-I)
  Dietary copper and bone strength, SA148
  Estrogen and peak bone acquisition, 1080
  Gene polymorphisms and fracture risk in elderly, 1221
  Genomic scanning for QTL controls, 1106
  Haploinsufficiency effects, M148
  LNCaP prostate cancer cell-conditioned medium and bone, M070

Insulin-like growth factor I (IGF-I) (Continued)
Low dietary calcium stress, 1167
Overexpression in muscle on cortical and cancellous bones, SU013
Prostate cancer release, 1096
Unloading-induced insulin resistance, F159
Vertebral trabecular architecture, SA118
Insulin-like growth factor I receptor (IGFIR), SU146
Insulin-like growth factor II (IGF-II), M145
Insulin-like growth factor binding protein 2, M039
Insulin-like growth factor binding protein 2 (IGFBP-2), F307
Insulin-like growth factor binding protein-4 (IGFBP-4), M149, SA153
Insulin-like growth factor binding protein 5, 1121, F149
Insulin-like growth factor binding proteins, SU025
Integrin-linked kinase, F029
Integrins
BMP-2, F020
Bone remodeling, F239
Compound A and bone resorption, F246
Estradiol regulation, SU255
Extracellular, RGD-binding site, F227
Mechanical stress effects, SU057
Ovariectomy-induced bone loss, 1033
Programmed cell death in osteoclasts, 1022
Signaling proteins in melanoma cells, M056
Interferon-α, SU331
Interferon-α2b, SA171
Interferon-γ, F234, F330
Interleukin-1, SA142, SU051, SU163
Interleukin-1β, SU153
Interleukin-1 receptor antagonist, M456
Interleukin-1-receptor-associated kinase, SU140
Interleukin-3, M161
Interleukin-6
Dinucleotide repeat polymorphisms and BMD, SU135
Expression in osteoblasts, SU150
Genetic variations and estrogen and dietary calcium effects, 1060
Glucocorticoid receptors in osteoblast-like cells, M241
IL-1α effects on osteoclasts, SU231
JAK-STAT pathways, SU203
Peak BMD linkage in nuclear families, M126
Raloxifene inhibition of, M184
Interleukin-6/interleukin-6 soluble receptor cytokine system, M142
Interleukin-6 receptor, M120
Interleukin-7, M143
Interleukin-8, F079
Interleukin-10, F146
Interleukin-11, 1036, F058, M060, M241, SU203
Interleukin-11 receptor, 1073
Interleukin-12, SU230
Intracellular estradiol binding protein, F463
Ion channels, SU448
IRAK1, SU140
Iridoid glucosides, SA209
Ischemic necrosis of femoral head, M356, SU407, SU413
Italy, fractures and hospital care, SA287

J

J777 cells, F248
Jab1, M197
JAK/STAT1 pathway, F234
JAK-STAT pathways, SU203
JNK, 1124, 1190, M151
Joint prosthesis, SA143. SEE ALSO *Hip arthroplasty*
Jun dimerization protein 2, SA260

K

Kaliotoxin, F422
Kallikrein 2, SU081
Kdr antibodies, M391
Kidney, 1205, M404, SA489, SU439. SEE ALSO *Nephrolithiasis; Nephrotic syndrome; Renal*
Kidney failure, M412, M415, M418, SA050
Kidney failure, chronic, 1140
Kidney insufficiency, F385
Kidney transplantation, 1141, 1211, M410, M413, SU421
Knees, SA423
Knockout mice
Ataxia telangiectasia mutated, SU027
$\alpha_v\beta5$ integrin, F239
β3 integrin, F075
Bax, 1219
Bmp6, 1076
c-Cbl-/- *versus* Cbl-b-/-, 1149, SU262
Dmp-1, 1005
Fgf2, 1061
Gcm2-CasR, 1181
GH-deficient lit/lit, SU371
Id1/Id3 double gene, 1192
IGF-I, M148
Male androgen receptor, SU326
Msx2, M215
MyoD/Myf5, 1193
Pax5, 1098
Proline-rich transcript of brain, F036
PTHrP, 1052
RANK -/-, M176
SFRP-1, 1001
WASp, F230
KRN1493, F410
KS483 cells, F208
Ku antigen complex, 1114
Kummell's sign, SU293
Kyphosis, 1208, SU300

L

Laboratory tests, M335, SU306
Lactation, 1063, 1132, M405
Lactoferrin, SU151, SU246
Laminins, M036
Lamprey Geortira australis, M434
Lanthanum carbonate, M415
Laser capture dissection, M271
Latent transforming growth factor-β binding protein-1, F056
LDL receptor-related protein, M020
LDL receptor-related protein 1, 1198
LDL receptor-related protein 5 (LRP5), M123
G171V mutation transgene expression in mice, F119
High bone mass mutation and loading, M163, SU176
Osteoporosis pseudoglioma syndrome, SU410
Wnt-mediated signaling, 1002, F214, M161
Lead, and DEXA/ultrasound bone measurements, SU090
Leptin, M219, M306, SA172, SU154, SU319, SU419
Leucine-rich proteoglycan genes, M046
Leukemia inhibitory factor, M221
Leukocytes, F440
Lewis rats, SA055
Lexxos 2D radiographic detector, M080
Light, near infrared and visible, M191
LIM mineralization protein-1 (LMP-1), M068
Linkage disequilibrium mapping, SU121
LIP, in mesenchymal stem cells, 1109
Lipopolysaccharide, SU153, SU240, SU252
Lipoproteins, F241. SEE ALSO *LDL receptor-related protein*
Lipoxygenases, M209
Liver, SA152
Liver cirrhosis, biliary, SA332, SA365
Liver diseases, M408, SU335
Liver transplantation, SU420
Loading. SEE ALSO *Exercise*
Calcium-influx pathways in chondrocytes, SA156
Chloramphenicol acetyl transferase marker gene and osteogenic activity, M171
Collagen fiber orientation for interpretation of, SU062
Cyclic *versus* rest-inserted, SU181
DMP1 gene expression in osteocytes, SU063
Gender and estrogen effects, 1048
LRP5 high bone mass mutation, M163, SU176
MyoD/Myf5 knockout mice, 1193
Osteocyte process ultrastructure, SU269
PTH and cortical bone formation, SA349
PTH stimulation of preosteoblast DNA synthesis, SU162
Rest-inserted and aged skeleton, 1046
Skeletal mechanosensitivity gene in mouse, F168
Skeletal response in girls, SU005
Long term care, 1087, F111, SA273, SU094, SU365
LuCaP 23.1 mice, SA088, SU082
Lumbar spine
BMD, F122, M078, M413, SA324
Cortical bone parameters with computed tomography, M090
Exercise effects, SA351
18F-Fluoride positron emission tomography, SA334
Interlaminar diskectomy and foraminotomy for degenerated disk lesions, SA062
Lunar Achilles InSight, M104
Lunar Prodigy, M073, M077
Lung cancer cells, SA445
Lupus erythematosus, systemic, M421, M422, SA353, SU019
Luteinizing hormone releasing hormone, M354
Lymphocytes, F417, SU044, SU077
Lysophospholipids, M158, M445

M

M21-cells, M056
α2Macroglobulin, F150
Macrophage colony-stimulating factor (M-CSF)
Bone marrow stromal cells, M178
Cord blood mononuclear cells, M161
Op/op mouse, 1122
Osteoclast differentiation, 1084, M258, SA240
Osteoclast formation, M242
Macrophage inflammatory protein-1α, F073
Macrophages, M249, SA163, SU055, SU077
Macrophage stimulating protein, 1189
Macrophage stimulating protein kinase (MAPK) pathway, 1070, SU061, SU223
Magnesium, dietary, 1089, SA411
Magnetic resonance imaging, F295, M095, M424, SA399
High resolution, M083
Mammary epithelial cells, 1063, SU070
Mandible, M268, M328, SA158
Mannose receptor, M247
MAP kinases, M070, SU442. SEE ALSO *p38 MAP kinase*
Marfan syndrome, SU403
Mast cells, SA413
Mastocytosis, M321
Mathematical models, M088, M150
MATRIGEL-coated dentin slices, SA067
Matrix extracellular phosphoglycoprotein (MEPE), F400, SA053, SA063
Matrix Gla protein, M043. SEE ALSO *Fetuin-MGP-mineral complex*
Matrix metalloproteinase-9, SU415

Matrix metalloproteinase-9 antisense phosphorthiorate oligodeoxynucleotide, SA067
Matrix metalloproteinase-13
Collagen accumulation and bone formation, 1197
Collagen breakdown for cartilaginous epiphysis excavation, F066
Internalization by chondrocytes, SA032
LRP1 and collagenase-3 specific receptor, 1198
Osteoblast cytosolic proteins, M042
Spondyloepimetaphyseal dysplasia, Missouri variant, 1215
T cell derived TNF-α, TGF-β, and IFN-γ, SU069
TGF-β in breast cancer, SU079
Matrix metalloproteinases, M047, SA065, SU227
MC3T3-E1 cells
Cell population density and proliferation of, SA204
Connective tissue growth factor effects, SU209
Cox-2 and prostaglandin release, SA162
Fluid shear-induced ATP release, SU170
Hyperosmolarity effects, SU190
Mineralization on titanium implant material, M046
PTH administration, M220
Radiation effects, SU189
McCune-Albright syndrome, SU387
MDA-231 cells, SA080
MDA-MET cells, SA080
Mechanical loading/unloading. SEE *Loading; Unloading*
Mechanical response tissue analysis, M087
Mechanical strain. SEE *Stress, mechanical*
Medial collateral ligament, M044
Medial collateral ligament cells, SA019
Medical history, SU306
Medroxyprogesterone, M355
Medrysone, SA326
Megakaryocytes, M159
MEK1, 1070
Melanoma, F054, M431
Melatonin, SA466, SU207
Memory, glutamate receptor expression in bone, SU168
Men. SEE ALSO *Osteoporosis, male; Sex differences*
Age differences in bone density and size, F011
Age, testosterone and estrogen, M312
BMD in genetic hemochromatosis and C282 mutation HFE gene homozygoty, SA120
BMD in noncirrhotic, SA335
Body size/bone mass and IGF1R allelic variation, SU146
Bone mass and leptin, M306
Bone strength, M302
Calcaneal bone mass and lumbar spine BMD, M078
Calcaneal quantitative ultrasound and fracture history, F115
Calciotropic hormones and bone resorption, SU330
CTx variability, SU097
DXA of spine/hip *versus* BUA or SOS of heel, SU084
DXA of vertebral fractures in women *versus,* F013
Endocrine response to phosphate supplementation, 1144
Exercise and BMD, SA301
Femoral bone size and body mass, SA305
Fracture prediction, SA298, SU283
Fractures study design and baseline characteristics, SU028
Fractures study recruitment strategies, SA303
Glucocorticoids and sex steroids, F327
Hip fracture risk, M291
Hypocalcemia with polyglandular failure and CasR antibody, WG9
Men. SEE ALSO *Osteoporosis, male; Sex differences* (Continued)
Hypogonadism, 1209
Medical conditions and BMD/stiffness, SU022
Osteoporosis self-assessment tool, SA095
Racial differences in BMD, F300
Sex hormones and bone mass/loss, 1166
Testosterone and body mass index and aromatase gene polymorphism, M121
VDR and COLIA1 genetic polymorphisms and osteoporotic fracture risk, SU142
Vitamin K status and BMD, F275
Menatetrenone, M381, SU355. SEE ALSO *Vitamin K_2*
Menin, M204
Menopause, M289, SA131. SEE ALSO *Perimenopause; Postmenopausal women; Premenopause*
Menstruation, F130
Mesenchymal stem cells
Androgen receptor regulation of, SA462
Blood-borne, after fractures, SA221
Cadherin-11, SU202
Ectopic bone formation, SU213
Fra-1 overexpression, SA200
Gene expression, SA185, SU201
Gene therapy, M225
LIP and C/EBPβ, 1109
Menin inactivation, M204
Osteoarthritis, M403
Tendon, F220
TGFβ signaling and PPARγ2, M155
Thrombospondin-2 effects, 1069
Metacarpal cortical index, F091, SA092, SU016, SU095
Metastasis. SEE *Bone metastasis*
Methotrexate, M343
2-Methoxyestradiol, SA070
20-Methyl-1α,25-dihydroxyvitamin D_3, SU453
2-Methylene-19-nor(20S)-1,25-dihydroxyvitamin D_3 (2MD), 1120, SA383, SU460
Methylenetetrahydrofolate reductase (MTHFR) gene, SA131, SU143
MET stimulation of estrogen-induced transcription, 1119
Mevalonate-isoprenoid-cholesterol (MIC) synthetic pathway, SU375
Mevastatin, 1191
MG-63 (osteoblast) cells, M138, M203, M401, SA428, SU210
Microarray analysis. SEE *Gene chip microarray analysis*
Micro-computed tomography, F099, M096, M326, M332, SU051. SEE ALSO *Computed tomographic microscopy; Peripheral quantitative computed tomography; 3-D computed tomography*
Microdamage, F061, SA379, SU333
Microphthalmia transcription factor, M250, M263
Microtubules, 1189
Mim-1, 1126
Mineralocorticoids, SA476
Minipig, Göttingen, SU350
Minodronate, M342, SU347. SEE ALSO *Bisphosphonates*
Minodronic acid, SA245
MITF transcription factor, SU261
MLO-A5 cells, M018
MLO-Y4 osteocyte-like cells, SU271, SU273
MOCP-5 cells, SU273
Monkeys, cynomolgus, M377, SA447, SU047
Monoclonal gammopathy of undetermined significance (MGUS), M057
Monocytes, SA222
Morphometric X-ray absorptiometry, SU291
Msx2, 1114, M196
mTOR/S6 kinase, 1146
Mucilipidosis II, WG10
Mucopolysaccharidosis type II, WG11
Multiple myeloma
BMD and fat-lean distribution, M075
Bone remodeling, SA068
Cellular interplays with bone cells, SA077
MIP-1α expression, F073
OPG-Fc-fusion protein, 1093
Osteoclast interactions, M054
Procollagen type I N-propeptide, M057
Proteasome inhibition, SA071
Runx2 and osteogenesis, F069
Muscle, M172, M406, SA346, SU013, SU309
Muscle, smooth, vascular, SA145
Muscle strength, SA126, SU175, SU385
Muscular dystrophy, Duchenne, F419
Myostatin, M406, SU177

N

Nandrolone decanoate, M394
Natriuretic peptides, C-type, 1206
NB4 cells, SU452
NCoA-62/SKIP, SU451
Nephrolithiasis, idiopathic hypercalciuric, 1008
Nephrotic syndrome, non-azotemic, M411
Net acid excretion, M335
N-Ethyl-N-Nitrosourea mutant mice, 1216
Neurofibromatosis type 1, F040
Neurokinin-1 receptor, SU208
Neuropeptide Y Y4 and Y2 receptors, 1125
Neurotensin, M021
Newspapers and magazines, osteoporosis coverage, SU301
New World primates, F463
NFAT, SU264
Nicotine, SA167. SEE ALSO *Smoking*
Nitric oxide
NMDA receptors, M277
Osteoclastic acid secretion, M237
Osteoclast survival by TNF-α, M274
Raloxifene effects on bone mass and remodeling, SA359
RANKL expression and osteoclastogenesis, M173
RANKL-stimulated NF-κB-dependent production, M260
Nitric oxide synthase
Endothelial, 1101, 1191
Neuronal, M208, SU274
Nkx 3.2, 1160
N-Methyl-D-Aspartate (NMDA) receptors, M277
Noggin, 1075, SA198, SU039
Nonsteroidal anti-inflammatory drugs (NSAIDs), 1171, F311, M350
Northern analysis, M253
Notch 1, F199
Npt2, M037
Npt IIa, F252
Nuclear factor-κB
Autoimmune rheumatoid arthritis, 1155
BMP-2 regulation in growth plate chondrocytes, F016
Breast cancer and osteoclastogenesis, F087
CASR up-regulation to pro-inflammatory cytokines, M440
Chondrogenesis regulation, 1153
Cyclin-dependent kinase 6, 1148
Fluid shear stress response modulation, SU171
OPN regulation in bone marrow cells during unloading, 1044
Radiation therapy for skeletal carcinomas, M053
VDR transactivation suppression and p160 coactivators, M447
Nuclear factor of activated T cells (NFAT), F033
Nuclear factor-regulated by IL-3/adenovirus E4 promoter, SU222
Nuclear orphan receptor (NOR-1), SU221
Nutrition. SEE *Diet*

O

Obesity
- Body weight loss by gastroplasty, SA319
- Bone turnover after Roux-en-Y gastric bypass, M399
- Musculoskeletal interactions with hyperinsulinemia and euglycemia, M071
- QTL for BMD-related phenotypes, SU124
- Vitamin D status and bone mass during weight reduction, M001

Octreotide, 1165
OF45. SEE *Matrix extracellular phosphoglycoprotein*
OK cells, F137
Olpadronate, 1105, M409, SU217
ONO-5920, M342, SU347. SEE ALSO *Minodronate*
Oophorectomy, 1103
Orchiectomy, SU327
Ossification of posterior longitudinal ligament, M426, SA386, SU056
Osteoactivin, 1188
Osteoarthritis
- Calcaneal broadband ultrasound attention, SA114
- Computed tomographic microscopy, M098
- ER gene and calcium sensing receptor gene polymorphisms, SU138
- HRT effects, SA423
- Knee, leptin in synovial fluid, SU419
- Mesenchymal stem cell therapy for, M403
- Risedronate, M428
- Subchondral trabecular bone changes, SU010
- Synovial fluid analysis of chlorinated-peptides, SU115
- Vascular invasion and protein synthesis, SU415

Osteoblast differentiation
- Acyl-CpA binding protein, SU211
- Adipose-derived adult stem cells, M233
- Biglycan and BMP-4-stimulated, 1067
- BMP inhibitors, SU037
- COX2-dependent PGE2 and BMP-2, F044
- CTGF/Hcs24 and gene expression, SA037
- DD045, F201
- Early BMP2-Dlx5 functions, 1159
- Estrogen and androgen receptors expression, SA202
- FGFR2 signaling with Apert mutation, F197
- Gene expression, SU193
- Glucocorticoid receptor function, F478
- Green fluorescent protein experimental models, SA207
- IGFBP-5, 1121
- Lactoferrin, SU151
- LIF effects, M221
- Melatonin, SU207
- Microtubule assembly, 1189
- Mim-1, 1126
- Msx2 knockout mice, M215
- Noggin, 1075
- Osteoactivin, 1188
- Osteocalcin box transcriptional regulation, M198
- Osteogenic lineage allocation, 1015
- p55 TNF receptor, SU205
- PGTI0306 effects, 1187
- PKCα and ERα interaction, M179
- PPARγ activation, SA205
- PTH(1-34) or PTH(2-38) and bone formation, SU441
- Retinoic acid receptor signaling, M459
- Runx1, 1110
- Spaceflight, SU161
- Tensile stress-inducible α-adaptin C, SA057
- Tob (transducer of ErbB2), 1034

Osteoblasts
- ADAM-9 and α2Macroglobulin, F150
- Biglycan and decorin, 1068

Osteoblasts (Continued)
- β-Catenin, F042
- Cell signaling, eNOS and, 1101
- Connexin43 effects, M212
- COX-2 effects, SU214
- ERα and ERβ homo- and heterodimers, M187
- ER-α and loading, 1010
- ERKs and fluid shear stress-induced proliferation, F161
- Estrogen and mechanical strain effects, SU165
- FGF2 overexpression, M127
- Gene expression in spaceflight, SU161
- Glutamine synthetase in, SA187
- gp130-mediated signals, F176
- Laminins, M036
- Leptin and mechano-stimulation, M219
- Loading response in mandible, SA158
- LPA and S1P expression in, SU204
- Matrix metalloproteinase inhibitors, SU227
- Maturation-dependent expression of osteoclasts, M230
- 2-Methylene-19-nor(20S)-1,25$(OH)_2D_3$, 1120
- Mineralization inhibitor(s) and PHEX, SA394
- Near infrared and visible light effects, M191
- Nephrotic syndrome, M411
- Osteonectin, 1151
- Phosphate transport in *hyp*-mouse, SA393
- Proliferation/anchorage with fluid shear, SU157
- Proliferation and $p57^{Kip2}$ gene, SU183
- PTH protection from phosphate in, SU433
- RANK expression in Paget's disease, F412
- Runx2/Cbfa1 and PTH, 1176
- Statins effects on RANKL and OPG gene expression, M223
- Steroid hormones, SU035
- Syndecan-2 effects, SU188
- Unloading effects on signaling and gene transactivation, SU064
- Vitamin D receptor ablation, M217

Osteoblast-specific cis-acting element binding factor 1 (OSEBF1), 1003
Osteocalcin
- Bone resorption, M048
- CT element, F182
- Gene expression and PTH induction, SU192
- Gene expression, *in vitro* model from fish, M043
- Gene transcription in bone cells, M195
- Gla-type and menatetrenone effects, SU355
- HDAC3 and Runx2 regulation, M199
- MMPs and cathepsin K, M047
- MSX and, 1114
- Peak BMD linkage in nuclear families, M126
- Stress in Lewis and Fischer 344 rats, SA055

Osteocalcin box, M198
Osteocalcin promoter, SA183, SA193
Osteoclast-associated receptor (OSCAR), M250
Osteoclast-derived zinc finger gene, SU244
Osteoclast differentiation factor (ODF), SU233
Osteoclast differentiation/osteoclastogenesis
- 2MD actions on RANKL, SU460
- Adrenomedullin receptors, SU247
- Calmodulin kinase II, M257
- CD44 effects, 1148
- c-Fos overexpression, 1024
- Congenital pseudarthrosis of tibia, SA416
- COX-2 activity, SA244
- Cystatin C, M256
- Genetic loci in BXD RI mice, SU129
- IL-11-induced STAT3 activation, SU216
- Lactoferrin, SU151
- Lipopolysaccharide-induced, SU240
- Mannose receptor, M247
- Mass spectromic proteome analysis of RANKL-induced protein expression in, SU258
- M-CSF, M242, M258
- M-CSF and gene expression, SA240
- Multinucleation, M249
- p38 MAP kinase, M279, SU242
- $p57^{Kip2}$ gene, SU183

Osteoclast differentiation/osteoclastogenesis (Continued)
- Pasteurella multocida toxin (PMT), M255
- PPAR-α agonist Wyeth 14643, M264
- Pulsed electromagnetic fields effects on, M238
- Radicicol, SU253
- RANK antisense-treated cells, SU235
- RANKL-induced, chimeric receptor studies, 1019
- RANKL-induced, eosinophil chemotactic factor-L, M246
- RANKL-induced, Jun dimerization protein 2 and, SA260
- RANKL/-RANK-induced and PTH/PTHrP receptor, 1177
- RANKL truncation mutants inhibition of, M239
- Ruffled border regulation by PYK2, 1147
- Runx factors, M267
- sFRP-1 inhibition, SU257
- Stra13 transcription factor, M252
- Suramin, SU234
- T cells effects, SU238
- TGF-β through p38 and p44/42 MAP kinases, SU259
- TMC-315B2 inhibition of, F254
- Toll-like receptors, M248
- TWEAK, M262
- Vav1 and Vav3, M267
- *In vitro* studies, M272, SU248

Osteoclast inhibitory lectin, SA242
Osteoclastogenesis. SEE *Osteoclast differentiation/osteoclastogenesis*
Osteoclast precursors
- 1,25-$(OH)_2D_3$ responsivity in Paget's disease, SU389
- Commercially available cyropreserved, M270
- HGF and SCF support *in vitro,* M236
- Human, anti-SIRPα effects, M259
- Hyperlipidemia, M261
- Mitf modulation by RANKL, M263
- Monocytes effects, SA222
- PTH(7-84) inhibition, 1178
- SDF-1, M244
- TNF-α and CD11b+, 1021

Osteoclasts
- Arp2/3 complex, F223
- Calpain regulation of attachment and spreading, SA231
- Cathepsin K-deficient, SU225
- Cell movement and spreading, SA229
- Cell swelling, F261
- Gelsolin peptide domains in actin assembly and motility, SU265
- Gu-Sui-Bu (Drynaria fortunei) effects, M266
- H+ transport, SA253
- Integrins and programmed cell death, 1022
- Iridoid glucosides and inhibition of, SA209
- Large *versus* small, SU251
- Mandibular bodies culture system, M268
- Mature, ODF expression, SU233
- mTOR/S6 kinase signaling, 1146
- Multiple myeloma cellular interplays, SA077
- Myeloma cells interactions, M054
- Nitric oxide regulation of acid secretion, M237
- Osteoblast maturation-dependent expression, M230
- Osteocalcin, M048
- Osteopontin and tumor cell invasion, F054
- Periosteal, OPG and, 1020
- PTH continuous exposure, SU434
- PTH(7-84) inhibition, 1178
- PTH/PTHrP receptors type 1 expression, SA453
- RhBMP-2 and osteoblast differentiation, M175
- Src kinases, M265
- TGF-β-induced, M273
- *In vitro* studies, gap junction signaling, SU249

Osteocytes
- Bisphosphonates and bone strength, 1133
- DMP1 gene expression during loading, SU063
- Formation during rapid growth, SA163

Osteocytes (continued)
Fragility fractures, F314
Loading response in mandible, SA158
Mechanical loading model, SU269
Microcrack matrix strain, F061
NNOS expression, SU274
Serotonin (5-HT), SU270
Osteogenesis, F069. SEE ALSO *Bone formation*
Osteogenesis imperfecta
Alendronate pharmacokinetics, SU401
Bisphosphonates in children under 3 years, SU399
Differential diagnostics, SU403
Fibroblast response to phenol red and dexamethasone, SU118
Olpadronate, 1105
Pamidronate, SU348, SU383, SU406
Skeletal status and muscle-bone relationships, SU385
Untreated, BMD Z-scores in puberty, SU409
Osteogenesis imperfecta type I, SU402
Osteogenic protein-1, SA017, SA019, SU032. SEE ALSO *Bone morphogenetic protein-7*
Osteomalacia, oncogenic, 1139, 1143, SA396
Osteomalacia, oncogenic hypophosphatemic, F398
Osteomalacia, sporadic hypophosphatemic, SA399
Osteonecrosis of femoral head, F424, SA425
Osteonectin, 1151
Osteopenia
Dietary calcium and adolescent idiopathic scoliosis, SA004
Gαq-mediated signaling, 1051
Ibandronate administration and dosage, SU342
IL-10, F146
Indinavir effects, F333
Ovariectomized rabbits, SA331
Pamidronate after kidney transplantation, SU421
Pax5 deficient mice, 1098
Raloxifene therapy monitoring in postmenopausal women, 1127
Treatment adherence, SA340
Osteopetrosis, 1122, SA390
Autosomal dominant type II, 1081
Autosomal recessive, SU398
Osteopontin
Bone nodule formation and pulsatile fluid flow, SA154
CD44 surface expression, F236
Deficiency and mechanical stress-control of remodeling, SU059
Deficiency and mechanical stress-induced tooth movement, SU058
Deficiency and PTH effects on bone formation, F442
FGF signaling regulation, M129
Kidney failure and bone remodeling, SA050
Melanoma invasion into bone marrow, F054
Neurofibromatosis type 1, F040
Regulation by TGF-β in breast cancer, 1196
Signaling proteins in melanoma cells, M056
TNF-α-mediated cytotoxicity in chondrocytes, 1156
Unloading and gene expression in bone marrow cells, 1044
Unloading and osteocyte stress, 1165
Osteoporosis. SEE ALSO *Osteoporosis, animal models; Osteoporosis, glucocorticoid-induced; Osteoporosis, male; Osteoporosis, postmenopausal*
Activation frequency of BMD, SU332
Attitudes, knowledge and behavior questionnaire, M319
Bisphosphonates in elderly with impaired renal function, SU335
BMD testing and treatment, M081
Body mass index, height, weight and BMD, WG7
Bone resorption markers and various treatments, SU110, SU111
Osteoporosis. SEE ALSO *Osteoporosis, animal models; Osteoporosis, glucocorticoid-induced; Osteoporosis, male; Osteoporosis, postmenopausal* (Continued)
Bone turnover-related treatment, SU361
Celiac disease diagnosis, WG6
Chinese-Canadian immigrants risk factors, SU281
Clinical practice patients with co-morbidities, SU336
COLIA1 promoter polymorphisms, SU145
Concordant *versus* discordant BMD changes, WG8
COPD, M324
Depression, M314
Drug subsidization, M375
Dual X-ray absorptiometry of vertebral fractures, F013
Early infant feedings, M005
Fracture prevention strategies, SA281
Gene chip microarray analysis, SU119
Genetic screening assays, SU144
Genetic segregation analysis, SU128
High bone remodeling, SU107
Hip fractures, SU294
Intervention thresholds, SA291
Linkage disequilibrium mapping of DNA sequences, SU121
Liver cirrhosis, biliary, SA332
Long term care, SU365
Long term care education and BMD testing, SU094
Low *versus* high turnover, SU305
Maternal history and femur BMD, 1088
Mathematical models, M088
Mucopolysaccharidosis type II, WG11
Newspapers and magazines, 1998-2001, SU301
Occult disorders, M321
Postural analysis, SA308
Prescription treatment, SU378
Prevention with alendronate, F345
Primary care resident evaluation of chronic conditions, F309
Procollagen type I N-propeptide automated assay, SU101
Quantitative ultrasound cut-off value for Japanese women, SU026
Reference database of Asian Indian women, SA270
Resident physicians' prevention and treatment, M370
Risk instrument validation, SA089
Risk tool in American men, M305
Secondary causes, SA289
Sodium-phosphate type IIa cotransporter gene mutations, 1055
Standardized documentation in Germany, SA293
Standardized medical history forms and set laboratory panels, SU306
Subchondral trabecular bone changes, SU010
Traumatic fractures, 1212
Treatment adherence, SA340
Treatment after fractures, SU285
Turner's syndrome, WG3
Website of study data, M316
Osteoporosis, animal models
Aging and ER-β, 1031
Diet low in cation-anion balance, SU356
Glucocorticoid-induced, SA479
Göttingen minipig, SU350
1,25-$(OH)_2D_3$ and bone formation, M002
Ovariectomized cynomolgus monkeys, SU047
RANKL vaccines, SA374
SARM Compound N1, M393
Soy isoflavones and bone formation in males, M366
Osteoporosis, glucocorticoid-induced
Gla-type osteocalcin as marker of menatetrenone effects, SU355
Göttingen minipig and ibandronate, SU350
IL-11, 1036
RANKL/OPG and bone turnover markers with hPTH(1-34), F366
Rheumatologist interactive education program, SU362
Osteoporosis, male
Alendronate and bone turnover markers, SU344
Alendronate *versus* alfacalcidol, SU339
Body height loss and risk, F302
Calcitonin and spinal BMD, SU333
Fractures study design and baseline characteristics, SU028
PTH and/or alendronate and BMD, 1007
Risedronate, SU338
Risk index, SA095
Risks for ethnic-racial groups, M304
Risk tool among veterans, M305
Smoking, SA299
VDR and COLIA1 genetic polymorphisms, SU142
Osteoporosis, postmenopausal
Alendronate in Chinese, M345
Algorithm for low BMD, SU304
Antiresorptive medications, M372
Clodronate monitoring by DXR and metacarpal cortical index, SA092
Combination therapy, 1040
Edentulous and dentate mandible bone changes, M328
Evidence-based management, SU360
Fall prevention strategies, SU317
Genetic polymorphisms, M116
IGFBP-3, IGFBP-5, and OPG changes, SU025
Iliac crest microarchitecture, M327
Instant vertebral fracture assessment, SU282
Laboratory testing, SA306
Oral exostosis and BMD, M407
Peak BMD influence, SU321
Post-fracture management, SA294
PTH and alendronate, 1039
Raloxifene, SA357
Risedronate, SU340
Risk factors between outpatients and general population, SA310
Risk questionnaire, M323
Rural women, SU275
Self-efficacy in self-management, SU380
Spondylosis, M329
Ultrasound report format and patient treatment compliance, M100
Osteoporosis pseudoglioma syndrome, SU410
Osteoprotegerin (OPG)
Age and bone resorption/remodeling markers, M006
Age and hormone replacement status in women, SA329
Age and nutrition effects, SU098
Antiresorptive and sex steroid therapies, M369
bFGF expression of RANKL and inflammation, M134
Bone loss in postmenopausal women, SA012
Bone mass in postmenopausal osteoporosis, SU025
Bone mineral density, SU322
Bone strength and osteopenia prevention during spaceflight, F369
Bone turnover in human pregnancy and lactation, 1132
Breast cancer metastases to bone, 1092, M059
Coronary artery calcification, M014
DHT and gene expression in androgen-responsive prostate cancer cells, M064
Estrogen and PTH-stimulated osteoclastogenesis, SU254
Familial idiopathic hyperphosphatasia and bone resorption, 1057

Osteoprotegerin (OPG) (Continued)
Gene expression and steroid hormones, SU232
Gene mutations and idiopathic hyperphosphatasia, 1056
Gene polymorphisms and perimenopausal bone mass, M119
Hoxc inhibition, SU038
Juvenile Paget's disease, F405
Linkage studies in BMD control, SU127
Osteoclastogenesis in aging, SA010
Overexpression and breast cancer growth in bone, F081
Paget's disease, SA404, SU390
Parathyroid hormone effects, M177
Periosteal osteoclasts in normal bone growth, 1020
Polyarticular juvenile idiopathic arthritis, SU136
Prostate cancer bone metastasis, SA088
Raloxifene stimulation of, M184
Spaceflight changes in mouse bone, 1045
Systemic lentiviral delivery, 1134
TNF-α-induced apoptosis, SU187
Osteoprotegerin-Fc-fusion protein, 1093
Osteosarcoma
BMP-2 effects, SU031
Cadherins effects, M052
Head and neck, SA072
2-Methoxyestradiol inhibition of, SA070
RANKL:RANK and tumor growth, M055
Osteosclerosis, 1100
Hepatitis C-associated, WG2
Osteotesticular protein tyrosine phosphatase, SA189
Osterix, 1016, M028, M032, SU173, SU208
Ovariectomy
Aging and ER-β, 1031
Alendronate and exercise, F165
Alendronate and fracture repair, F373
BMD and 2MD, SA383
Bone remodeling, SA331
Bone resorption markers, SU105
Cancellous bone and cortical bone loss, SU116
Carrots and bone loss, SU354
Integrins and bone loss, 1033
Kidney failure and HRT, M418
Phytoestrogens and bone loss, M376
Prostaglandin E_2 agonists and bone formation, M392, M397
Raloxifene and hPTH with osteopenia, F371
SERM therapy, M385
Soy products and BMC, SU359
Swimming, SA169
TNF-α and M-CSF, M178
Oxygen, chondrogenesis and, M030
Oxysterols, M229

P

P2X7 receptor, 1107
p20C/EBpβ, 1162
p21 mRNA, SA034
p38 MAP kinase
Alkaline phosphatase regulation, M202
BMP-2 activation, 1124
Bone resorption with inflammation, M281
Breast cancer bone metastasis, M058
Chondrocyte differentiation, M027
Chondrogenesis, F033
CTGF/Hcs24, SA028
MITF effects, SU261
Osteoclast differentiation, SU242
Osteoclast H^+-ATPase expression, SU268
RANKL activation of NF-κB and osteoclastogenesis, M279
TGF-β1 activation, M156
p42/44 MAP kinase, M151
p45 BF-E2, 1014
p55 TNF receptor, SU205
$p57^{Kip2}$ gene, SU183
p300, M192
P392L sequestosome1/p62 mutation, SU391
P-450 gene promoter, M188
Paget's disease
Bone sarcoma and pamidronate, SA406
Clodronate, SA402
Genetic heterogeneity, SU388
Juvenile, OPG deficiency, F405
OPG and RANKL, SA404, SU390
P392L sequestosome1/p62 mutation, SU391
RANK expression in osteoblasts, F412
SHIP osteoclasts, F403
TAF_II-17 and 1,25-$(OH)_2D_3$ responsivity of osteoclast precursors, SU389
Urine and bone resorption markers, SU109
Pain, M427
Pamidronate
Alendronate *versus,* M351
Fibrous dysplasia of bone, SA384, SA392
Gaucher's disease, M400
Osteogenesis imperfecta, SU348, SU383, SU406
Osteopenia after kidney transplantation, SU421
Paget's sarcoma, SA406
Pancreatic cancer cells, M433
Parathyroid hormone (1-20), SU427, SU440
Parathyroid hormone (1-34)
Adult growth hormone deficiency, SU425
Bile duct-ligated rats, SA365
Bone resorption markers in glucocorticoid-induced osteoporosis, F366
Intermittent administration, SA363
PTH1-receptor contact points, SU443
Parathyroid hormone (1-84), SU438, SU439
Parathyroid hormone (7-84), 1178, F408
Parathyroid hormone (28-48), SU324
Parathyroid hormone (PTH). SEE ALSO *Teriparatide*
Adhesion in osteoblastic precursors, SA224
Administration and dosage, M220, SA367
Adult growth hormone deficiency and calcium, F433
Agonists and antagonists and CRE-related transcription, SU430
Alendronate for osteoporosis, SU382
L-Amino acids, M443
Amino-terminal domain and P1R, SU426
Analogues' signal transduction and desensitization, SU437
β-Arrestin2, 1062
BMD in osteoporotic postmenopausal women, 1039
Bone formation, F155, SU049
Bone mass maintenance with zoledronate, F337
Bone tissue engineering, SU164
Cerivastatin in male rats, SU012
c-fos expression and stromal progenitor cell choice of fate, SU434
COX-2 and calvarial response to, F437
C-terminally truncated peptide and cAMP stimulation, SA432
1α-$(OH)D_3$ and 1α-$(OH)D_2$ suppression, SA491
Dietary calcium and 1,25$(OH)_2D_3$, F439
ERF-1 regulation in osteoblasts, SU200
Fertility and dietary calcium, SA441
Gap junctional communication, SU444
GCMB transactivation of, 1064
GFP-marked osteoblast culture for osteoblastic differentiation, 1185
ICER expression regulation, SU429
IL-6 expression in osteoblasts, SU150
Intact *versus* whole assay in secondary hyperparathyroidism, SA434
Intermittent and skeletal response in elderly, 1180
Intrathymic parathyroid adenomas, SU393
Loading and cortical bone formation, SA349
Male osteoporosis, 1007
Parathyroid hormone (PTH). SEE ALSO *Teriparatide* (Continued)
MAP kinases, SU442
Murine calvarial response measured with microCT, SU051
NFIL3/E4BP4 gene expression, SU222
Nuclear orphan receptor in osteoblasts, SU221
Octreotide, 1165
Osteoblast-like cells and alendronate pre-treatment, SA361
Osteocalcin gene expression, SU192
Peak BMD linkage in nuclear families, M126
Phospholipase C activation, SA438
Preosteoblast DNA synthesis, SU162
Primary hyperparathyroidism, F104, WG1
Proteasome and Runx2/Cbfa1, 1013
RANK-L and OPG expression, M177
RANKL release and Il-6/Il-6 soluble receptor cytokine system, M142
Recombinant analog UGL7841, SA362
Runx2/Cbfa1 and osteoblast apoptosis, 1176
Sex differences in mouse bone, SU428
Skeletal development and calcium requirements, M007
Skeletal response and peripheral leukocyte gene analysis, F440
Synthesis regulation, SA436
Vitamin D and BMD in postmenopausal women, SU315
Parathyroid hormone mRNA 3'-untranslated region calcium and phosphate responsive element, F435
Parathyroid hormone mRNA 5'-untranslated region, SA436
Parathyroid hormone/parathyroid hormone-related peptide (PTH-PTHrP) receptor
Bpa19-modified PTHrP agonist, SA448
Collagenase activity impairment and bone formation, SU066
Endochondral development signaling, 1066
$G_{11}α$ expression in chondrocytes, SA450
Hematopoiesis in bone marrow stromal cells, 1053
Metabolic acidosis in osteoblast-like cells, SU445
Signaling in RANKL/RANK-induced osteoclastogenesis, 1177
Parathyroid hormone/parathyroid hormone-related peptide (PTH-PTHrP) receptor Type 1, SA453
Parathyroid hormone receptor, F452, SU426
Parathyroid hormone receptor type 1, F449, F451, SA140, SA454, SU443
Parathyroid hormone-related peptide (PTHrP)
Amino terminal in lung cancer cells, SA445
Anabolic effects in bone, 1052
Angioplasty gene therapy, 1102
Bpa19-modified and crosslinks to PTH/PTHrP receptor, SA448
CaR-stimulated secretion, M444
25-Hydroxyvitamin D-3 1 α-hydroxylase in melanoma cells, 1028
Melanoma metastasis inhibition, M431
OPG/RANK/RANKL regulation in prostate cancer, SA443
Two-site immunoassays, SA444
Parathyroid hormone-related protein (PTHrP)
All-trans retinoic acid apoptosis in prostate cancer cells, M062
Breast cancer metastasis cell lines, M060
Cardiomyocyte function, F446
Cell cycle factors, M436
Cytokines, chemokine receptor activity in pancreatic cancer cells, M433
DNA repair genes and apoptotic response, M435
Gene expression in prostate cancer cells and EB1089, SU458
Lamprey Geortira australis, M434
MAPK pathway, SU223

Parathyroid hormone-related protein (PTHrP) (Continued)
RANKL gene transactivation, SA216
TGF-β regulation of, M432
Parathyroid neoplasms
AMG 073 and hypercalcemia, SU392
Atypical adenoma, SU395
Intrathymic, *GCNB* expression, SU393
Lytic bone lesion, SU397
Mitochondrial sequence variants, SA425
Primary hyperparathyroidism, SA407
Parity, SA272
Pasteurella multocida toxin (PMT), M255
Patient education, M368, SU094
PC3 mice, SU082
Pediatrics. SEE ALSO *Adolescents; Boys; Children; Girls; Infants, preterm*
Pediatric Whole Body analysis, SU015
Peginterferon-α-2b, SU331
Peptide phage display, M269
Perfusion culture system, SU206
Perimenopause
Fra-1 polymorphism and BMD, SA135
HRT non-responders, M373
Inhibin B and bone turnover, 1168
Low back pain and spinal BMD, SU311
OPG gene polymorphisms and bone mass, M119
Soy consumption and BMD, SU030
Periodontal ligament cells, SA035
Periosteal alkaline phosphatase, SA469
Peripheral quantitative computed tomography (p-QCT). SEE ALSO *Computed tomographic microscopy*
Amino acid peptides in bone, SU376
DXA for BMD *versus,* SA093
Hip fractures *versus* matched controls, SA101
Skeletal analysis of mice *in vivo,* M072
Tibia in children, F006
Peroxisome proliferator-activated receptor-α agonist, M264
Peroxisome proliferator-activated receptor γ (PPARγ), M186, SA205
Peroxisome proliferator-activated receptor γ-2 (PPARγ2), M155
Peroxisome proliferator-activated receptor γ agonist BRL49653, M213
PGTI0306 (secreted protein), 1187
Phase-contrast X-ray imaging (PCI), SA047
Phenol red, SU118
Phex. SEE *Phosphate-regulating gene with homologies to endopeptidases on X chromosome (Phex)*
Phosphate. SEE ALSO *Fetuin-MGP-mineral complex*
False positive MRI in sporadic hypophosphatemic osteomalacia, SA399
FGF-23, M128
FRP-4 infusion and renal excretion *in vivo,* 1142
25-Hydroxyvitamin D-1α-hydroxylase, SA486
MEPE/PHEX expression effects, F400
Metabolic acidosis, M419
PTH protective effects in osteoblasts and preosteoblasts, SU433
Phosphate, dietary, 1205, SU408
Phosphate-regulating gene with homologies to endopeptidases on X chromosome (Phex), F385, F391, F400, SA063, SA394
Phosphatidylcholine, lung, M430
Phosphatidylinositol 3 kinase (PI 3-K), SU045
Phosphatonin, 1144
Phosphodiesterases-4, M207
Phosphoinositide 3-kinase (PI3K), SU432
Phospholipase C, SA438
Phospholipase Cg, M450
Phospholipase D, SU224
Phospholipid receptor lysophosphatidic acid , SU204
Phosphorus, inorganic, SA397
Physical activity. SEE *Exercise*
Physician's practice patterns
Central DXA reports, SU091
Instant vertebral assessment, M292
Osteoporosis education, M368
Osteoporosis fracture tracking, M374
Osteoporosis management, SU364
Standardized documentation in Germany, SA293
Phytoestrogens, F279, M376. SEE ALSO *Genistein*
Pituitary adenylate cyclase-activating peptide 38 (PACAP-38), M141
Placental growth factor (PlGF), SA015
Plasma cell glycoprotein-1 (PC-1), 1011
Plasma, CTx stability in storage, SU112
Platelet-derived growth factor A (PDGF-A), SA413
Platelets
BMPs, M159
Pleiotrophin, SU149
Plums, dried, SU357
pOBCol3.6GFP transgene, SA192
Point-of-care technology, SU108
Poly (2-hydroxyethyl methoacrylate) (pHEMA), SU052
Poly(lactic acid)/hydroxyapatite scaffolds, M049
Positron emission tomography, 18F-fluoride, SA334
Postmenopausal women. SEE ALSO *Menopause; Osteoporosis, postmenopausal*
Alendronate efficacy and safety, 1059
Alfacalcidol, SA380
Algorithm for low BMD, SU304
Anticonvulsants and hip bone loss, 1214
L-Arginine supplementation, M359
Bone loss and OPG, COLIA1 and VDR gene polymorphisms, SA012
Bone mass and fracture risk, M295
Bone-strengthening medication for elderly African Americans, SA273
Bone turnover markers, SU023
Calcaneal quantitative ultrasound and femoral neck BMD, M115
Cdx polymorphism and BMD, SU137
Densitometry screening, M318
Dietary intake and BMD, M333
Dietary potassium, M362
Dried plums and bone health, SU357
Estradiol and aromatase gene polymorphisms, SA128
Femoral neck BMD and hip fracture risk, 1104
Fracture prediction, SU283
Genetic and hormonal bone mass influences, M309
Genetic polymorphisms and bone quality, SA133
Hip bone loss in African-American *versus* Caucasian, 1085
Hip fracture and higher BMD T-scores, F292
Hip geometry and BMD, M325
Hispanics with osteopenia and osteoporosis, SA265
HRT and iliac crest microarchitecture, F360
HRT and lupus erythematosus, SA353
HRT and tibial bone structure/performance, M387
HRT onset and BMD, M378
HRT, short-term, SA370
Hydrocortisone and type I collagen, SU002
25(OH)D and bone resorption, F482
Ibandronate without osteoporosis, 1138
Instant vertebral fracture assessment, SU282
Long-term bone loss, SA014
Low BMD and dinucleotide repeats in calcitonin and IL-6 receptor genes, M120
Older, estradiol and bone loss, 1164
Oophorectomy and fracture risk, 1103
OPG and age, SA329
Postmenopausal women. SEE ALSO *Menopause; Osteoporosis, postmenopausal* (Continued)
Osteoporosis risk factors, SA310
Osteoporosis risk instrument validation, SA089
Peripheral dual X-ray absorptiometry, SA266
Quality of life after fracture, SU299
Quality of life with osteoporosis, SU381
RANKL mediation of bone resorption, 1009
Seasonal bone mass variation, SU303
Self-report of fractures validity, M300
Soy protein and calcium retention, SA320
Stiffness index and fractures, F297
Urinary sodium and bone metabolism, M334
VDR gene polymorphisms and HRT effects on BMD, M117
Vitamin A and BMD, M285
Vitamin D, PTH, and BMD, SU315
Vitamin K_1 and bone loss retardation, M365
Young, estradiol and BMD, SA328
Posture, M283, SA308
Potassium, dietary, M362
PP6 (rat muscle-derived cells), SU043
Pregnancy, 1132, M311, M405, SA142, SA276
Pregnancy-associated plasma protein-A (PAPP-A), M149, SA153
Premenopause, F122, M313, SU334, SU353
PremPro (conjugated equine estrogens and medroxyprogesterone), M377
Preptin, M146
Primary care, F269, F309, SU108
Procollagen type I N-propeptide, M057, SU101
Programmed Death-1 deficient mice, M240
Progressive osseous heteroplasia, F387
Prolactin, SU070
Proline-rich transcript of brain, F036
Proline-rich tyrosine kinase 2 (PYK2), 1147, F225, SA226, SA228
Prostaglandin E_1, M202
Prostaglandin E_2, F044, M205, SA235, SU049, SU239
Prostaglandin E_2 agonists, M392, M395, M397
Prostaglandin E_2 receptor, SU272
Prostaglandin E_2 receptor subtype EP_2 agonist, M205
Prostaglandin E_2 receptor subtype EP_3, SA258
Prostaglandin E_2 receptor subtype EP_4, SA258
Prostaglandin E_2 receptor subtype EP_4 agonist, M205, M206
Prostaglandins, M164, SA136
Prostate cancer
All-trans retinoic acid apoptosis, M062
Anabolic action on bone, M070
Androgen-deprivation therapy and osteopenia, 1128
Androgen-deprivation therapy and osteopenia/osteoporosis, M067, SU328
Apoptotic bone disease and bisphosphonates, 1094
BMPs and osteoblastic metastasis, F085
Bone metastasis in SCID mice, SU073
Castration in mice and C4-2 bone metastasis, SA082
Cross-linking vitamin D analogs, SU461
DHT and OPG gene expression, M064
EB1089 and PTHrP gene expression, SU458
IGF-1 release, 1096
LMP-1 in bone metastasis, M068
Luteinizing hormone releasing hormone with bisphosphonates, M354
Mouse models of osteoblastic and osteolytic metastasis, SU082
Osteoblastic response of bone metastasis, SU081
Proteasome inhibitors, M069
PTHrP regulation of OPG/RANK/RANKL, SA443
Scutellaria baicalensis Georgi, M065
TGFβ signaling blockade, SU075
3-D trabecular bone analysis of metastasis, M061

Prostate specific antigen, SU081
Proteasome, 1013, F071, M069
Protein, dietary, 1201
Protein kinase 2, cGMP-dependent, 1072
Protein kinase A, SA216
Protein kinase B, F029, SU432
Protein kinase C
  Calcitriol regulation of, M445
  ER-α F promoter activity in osteoblast-like cells, M180
  Gαq-mediated signaling, 1051
  NF-κB activation, M278
  Prostaglandins and FGF receptor gene expression, SA136
  RANKL gene transactivation, SA216
  Voltage-gated proton channel, M282
Protein kinase Cα, M179
Protein kinase C, DNA-dependent, 1118
Protein kinase D, SA212
Protein kinase D inhibitor Go6976, 1124
Protein kinase inhibitor 166, SA074
Protein kinase inhibitor-α, M449
Protein kinase inhibitor-γ, SA213
Protein lysine 6 oxidase, SA051
Protein prenylation, M275
Protein-tyrosine phosphatase, SA189, SU263
PS120 cells, F449
PS-341 proteasome inhibitor, M069
Pseudarthrosis of tibia, congenital, SA416
Pseudohyperparathyroidism type IA, F389
Pseudohyperparathyroidism type Ib, 1083, SU405
Puberty, M001, SA420, SU409. SEE ALSO *Adolescents*
  Precocious, SU387
Pulsatile fluid flow, SA154. SEE ALSO *Fluid shear stress*
Pycnodysostosis, SA388, SU065
Pyrophosphate, 1011

Q

Quality of life, SU299, SU379, SU381
Quantitative trait loci. SEE ALSO *Gene chip microarray analysis*
  BMD, F124
  BMD differentiation in Caucasian and Asian populations, SU134
  BMD-related obesity phenotypes, SU124
  Body height variations, SU126
  Bone size and 17q23 linkage, SU123
  Genome scan for BMD variation, SU125
  IGFBP5 in F2 mice, F149
  Paget's disease, SU388
  Spondyloepimetaphyseal dysplasia, Missouri variant, 1215
Questionnaires
  Osteoporosis knowledge, M297
  Osteoporosis prediction in rheumatoid arthritis, M113
  Osteoporosis-related attitudes, knowledge and behavior, M319
  Postmenopausal osteoporosis risk, M323

R

Rac, M275
Rac1, 1150
Radiation, M053, M346, SU034
Radiation, ionizing, SU189
Radicicol, SU253
Radiographic absorptiometry, SU087
Radiographic photodensitometry, SU087
Radiographic texture feature analysis, SA102
Radiography, dental, SU099
Radius. SEE ALSO *Arm bones; Forearm*
  BMC and bone strength in prepubertal gymnasts, SU017
  BMD and breast cancer risk, M063
  BMD and smoking, SU312
Radius. SEE ALSO *Arm bones; Forearm* (Continued)
  Congenital dislocation of radial head, SU003
  Fractures, M294
  3-D computed tomography, SA098
Raloxifene
  Bone markers and vertebral fracture risk, F356
  Disuse bone loss in rats, M167
  Fracture repair in ovariectomized rats, F373
  Gene microarray analysis of bone formation markers, 1135
  hPTH in ovariectomized rats with osteopenia, F371
  Nitric oxide synthesis, SA359
  Osteoporosis treatment monitoring with collagen type I biochemical markers, SA105
  Osteoprotegerin stimulation and IL-6 inhibition, M184
  Postmenopausal osteoporosis, SA357
  Treatment adherence and persistence, 1127
RAN-binding protein M, M458
RANK-associated inhibitor (RAIN), 1099
RAW264.7 cells, M262, SU251, SU273
Reactive oxygen species (ROS), SA078, SU229. SEE ALSO *ROS 17/2.8 cells*
Receptor activator of NFκB (RANK)
  Antisense oligonucleotide-mediated blockade, SU235
  Breast cancer bone metastasis, M066
  Linkage studies in BMD control, SU127
  Osteoblast function, M176
  Osteoblasts in Paget's disease, F412
  TRAF6 interaction, 1023
Receptor-activator-of-NFκB-associated inhibitor (RAIN), 1099
Receptor activator of NFκB ligand (RANKL)
  2MD actions and osteoclast formation, SU460
  AP-1 regulation, SA262
  Autoimmune arthritis, M425
  bFGF stimulation of expression of, M134
  Bone resorption, SA238, SU396
  Breast cancer, F151
  Breast cancer bone metastasis, M066
  Chondrogenesis regulation, 1153
  Congenital pseudarthrosis of tibia, SA416
  CpG methylation, SU191
  Extracellular calcium, SU219
  Fas regulation, M243
  Heat shock factors, SU152
  Human vaccines, SA374
  Hyperthyroidism, SU320
  iNOS and NO production in osteoclastogenesis, M260
  Linkage studies in BMD control, SU127
  Mass spectromic proteome analysis in osteoclast differentiation, SU258
  Metabolic acidosis and gene expression, SA178
  Osteoclast differentiation with collagen-induced arthritis, M245
  Osteoclastogenesis in aging, SA010
  Osteoclastogenesis inhibitors, SA483, SU243
  Osteolytic loosening after total hip replacement, SU236
  Osteosarcoma tumorigenesis binding to RANK, M055
  Paget's disease, SA404, SU390
  Parathyroid hormone effects, M177
  PTH and Il-6/Il-6 soluble receptor cytokine system, M142
  Rheumatoid arthritis, SU417
  Truncation mutants and osteoclast differentiation and activation, M239
  Vitamin D deficiency, SA485
  W9 effects, SA250
Receptor activator of NFκB ligand (RANKL) promoter, SA177
Receptor activity-modifying protein-1 (RAMP1), SA429
Receptor activity-modifying protein-3 (RAMP3), SA429
Renal cell carcinoma, SA074
Renal osteodystrophy, M095, SA107
Renin-angiotensin system, 1049
Resident physicians, F309, M370
Resistance training, M162
Retinoic acid. SEE *Tretinoin*
Retinoic acid receptor, M459
Retinoids, M460
Retinoid X receptor α, M461
Reverse transcription polymerase chain reaction, SU166
RGD peptides, F052, SU220
Rheumatoid arthritis
  Autoimmune, NF-κB effects, 1155
  BMD, M429
  Disease activity *versus* trabecular texture at wrist, SA097
  Estrogen inhibition of streptococcal cell wall-induced, 1156
  Etidronate, M346
  Fall risk and bone density, M423
  Incadronate and adjuvant-induced arthritis in rats, SU411
  Infliximab and bone metabolism markers, M371
  Infliximab and bone resorption, SA368
  Osteoporosis prediction with heel ultrasound BMD and questionnaire, M113
  RANKL, SU417
  Tetracyclines effects on bone and cartilage loss, SU068
  TNF-α blockade, M031
Rheumatologists, SU362
Ribavirin, SA171, SU331
Rickets. SEE *Hypophosphatemia, familial; Hypophosphatemia, X-linked*
Risedronate. SEE ALSO *Bisphosphonates*
  Administration and dosage, SU345
  Apomine *versus,* 1095
  Bone mineral crystallinity, SU337
  Bone remodeling markers and response to, F109
  Bone resorption markers, SA342
  Clinical trial dropouts, SU343
  Male osteoporosis, SU338
  Nonvertebral osteoporotic fractures, SA344
  Osteoarthritis, M428
  Quality of life with osteoporosis, SU379
  Rac and PAK activation, M275
  Trabecular architecture, SU340
  Trabecular BMD, SA338
  Vertebral fractures, F343
dsRNA, viral, SU241
Ro-26-9228, SA461
Ron, 1189
ROS 17/2.8 cells, SA174, SU271
Rosiglitazone, M213
Running, SA170, SU159, SU174, SU175
Runt domain binding (RD/Cbfa), F186
Runt domain factor 1 (Runx1), 1110, M254
Runt domain factor 2 (Runx2)
  Cell growth regulatory role, 1112
  Cleidocranial dysplasia, SU384
  Dlx5 expression, SU208
  ΔFosB effects, 1097
  DFosB effects, 1097
  Gene expression profiling analysis, SU197
  Multiple myeloma patients, F069
  Osteoclast differentiation, M254
  In situ interactions and signaling, M194
  Translational regulation of, M193
Runt domain factor 2/core binding factor 1 (Runx2/Cbfa1)
  BMP-2 regulation of, SA196
  Bone marrow stromal cells, M201
  Cloning and characterization of, M190
  Human bone marrow stromal cells and, SA217
  p300 and osteocalcin expression, M192
  PTH and osteoblast apoptosis, 1176
  PTH and proteasome, 1013

Runt domain factor 2/core binding factor 1 (Runx2/Cbfa1) (Continued)
Smurf1 effects, 1157
Translational control in expression of, F180
Runt domain factor 2/core binding factor 1/osteoblast-stimulating factor 2 (Runx2/Cbfa1/Osf2), 1114
Ryanodine receptor, M442

S

S12911, M016, SU368, SU369, SU373
Salt load, in postmenopausal women, SA318
Saos-2 cells, M180, SU184, SU430
Scanning confocal acoustic diagnostic (SCAD) system, M114
Scanning electron microscope (SEM), M331
Sclerostin, 1077, 1222
Scoliosis, adolescent idiopathic, SA004, SA005, SU400
Scutellaria baicalensis Georgi, M065
SDF-1, M244
Seasonal modulations, SA007, SA103, SU303
Secreted and membrane-bound proteins (secretome), SA195
Secreted frizzled-related protein (SFRP)-1, 1001, M041, SU257
Secreted frizzled-related protein (sFRP)-3, 1183
Secretin, M141
Secretome, SA195
Selection bias
Chinese-Canadian immigrants for bone health study, SU316
Selective androgen receptor modulators (SARMs), 1027, M393
Selective estrogen receptor modulators (SERMs), M181, M385. SEE ALSO *Bazedoxifene; Carborane BE360; HMR 3339; Raloxifene*
Self-efficacy in postmenopausal osteoporosis self-management, SU380
SENCAR mice, SA323
Serotonin (5-HT), SU270
Serum alkaline phosphatase, F400
Serum response factor, 1160, SA041
Sevelamer, M415
Severe combined immunodeficient (SCID) mice, SU073
Sex differences
Endothelin-1 in pathological bone remodeling, SU080
Estrogen and loading, 1048
Hip geometry, SA313
IGF-I quantitative trait locus, 1080
LDL receptor related-protein deficient mice, M020
Osteoporosis reference database of Asian Indian women, SA270
PTH effects on mouse bone, SU428
Vitamin D, SU310
Shear stress, SU163. SEE ALSO *Fluid shear stress*
Sheep, SU164, SU356
SHIP (SH2-containing inositol-5-phosphatase), F403
Short-ear mouse, WG4
Side population cells, M225
Signal-regulatory protein α (SIRPα), M259
Silica injury, M430
Silico data mining, 1106
Simvastatin, M388, M396
Single nucleotide polymorphisms (SNPs), SU144
Skeletal genetics, rat models, SA121
Skeleton
Development and SFRP-1, M041
Estrogens and androgens, M380
Skin, vitamin D deficiencies after burns, SA418
Sleep disorders, F290
Smad1C, F206
Smad3, M151
Smad4, F473, M197
Smads, SU041
Smoking, M301, SA299, SU288, SU312
Smurf1, 1157
Socioeconomic factors
Hypovitaminosis D, M290
Primary care referral to DXA scanning, F269
Sodium-dependent phosphate transporters, M037
Sodium fluoride, SA247, SA264
Sodium-hydrogen ion exchanger regulatory factor 2, F449
Sodium-phosphate transporters, F026
Sodium-phosphate type IIa cotransporter, 1055, F137
Inhibitors, F252
Sodium, urinary, M334
Sortilin/neurotensin receptor-2, M021
SOST, M218
Sox9, 1071
Soy products. SEE ALSO *Genistein*
BMD in Chinese perimenopausal women, SU030
Bone formation in aged, orchidectomized rats, M366
Bone mineral content in ovariectomized rats, SU359
Calcium homeostasis, M337
Calcium retention in postmenopausal women, SA320
Isoflavone supplementation and hip BMD, SU352
Vitamin E in aged, orchidectomized rats, SU358
SP-1 binding site, SA179
Spaceflight, 1045, F369, M170, SA166, SU161
Speed of sound, M087. SEE ALSO *Ultrasound, quantitative*
Sphingosine-1-phosphate, SU204
Spinal cord injury, M099, M170
Spinal fusion, M045
Spine. SEE ALSO *Lumbar spine; Ossification of posterior longitudinal ligament; Vertebral deformities; Vertebral fractures*
BMD measured by DXA with and without leg elevation, M074
Cortical bone biomechanical examination, M085
Percutaneous transpedicular trocar biopsy, M084
Quantitative trait loci, 1079
Ultrasonic backscatter data, M103
Volumetric BMD *versus* areal hip BMD, 1131
Spinomed thoracolumbar brace, SA347
Spleen cells, SU239
Spondylitis, ankylosing, SA090
Spondyloepimetaphyseal dysplasia, Missouri variant, 1215
Spondylosis, M329, SA308
Sprague Dawley rats, M379, SU012, SU327
Sprouty2, 1204
Src kinases
AP23451 inhibitor, 1145
Cbl interaction, M280, SU262
Inhibitors, SA086, SU377
Osteoclastic bone resorption, M265
Pyk2-dependent recruitment to adhesion structures, F225
Stanniocalcin 1, F026
Statins, M223. SEE ALSO *Cerivastatin; Mevastatin; Myostatin; Simvastatin*
Stem cell factor (SCF), M236
Stra13 transcription factor, M252
Stress, M317
Stress fractures, SU174, SU175
Stress, mechanical. SEE ALSO *Loading*
AP-1/IL-11 transcriptional cascades, F058
Bone size effects, SA060
Cellular alteration of growth plate chondrocytes, SU054
Connexin43 and PGE_2 production by osteocytes, SU160
Fracture healing, SU290
Stress, mechanical. SEE ALSO *Loading* (Continued)
Integrin signaling in osteoblasts, SU057
Ossification of posterior longitudinal ligament, SU056
Osteoblasts and estrogen receptor type, SU165
Tooth movement in osteopontin-deficient mice, SU058
Stromal cells, M269, SA198
Strontium, M016, M214
Subchondral bone, M109
Sun exposure, M451
Suppressors of cytokine stimulation (SOCS), F259
Suramin, SU234
Sutures, SA057
Swimming, SA169, SA170, SU159
Syndecan-2, SU188
Synovial fluid, SU115

T

Tachykinins, SU208
TAF_{II}-17, SU389
Tamoxifen, 1170
Tartrate-resistant acid phosphatase (TRAP), F243, SU262
Tartrate-resistant acid phosphatase type 5 (TRACP), SU229
Tartrate-resistant acid phosphatase type 5a, SA108
Tartrate-resistant acid phosphatase type 5b, SA107, SA108, SU103
T cells
Activation regulation and bone metabolism, M240
Cytokine production in VDR knockout mice, SA481
IL-7-induced bone loss, M143
Interferon-γ and class II transactivator, F330
MMP-13 induction by TNF-α, TGF-β, and IFN-γ, SU069
Nitrogen-containing bisphosphonates, F249
Osteoclast formation, SU238
TNF-production, SA467
Tea, dietary, SA278
Teeth, SU058
Telomerase, F218
C-Telopeptide (CTx), SA340, SU097, SU112
Tendon, F220
Teriparatide (rhPTH (1-34)), 1041, 1136, 1179, F364
Testosterone, M121, M369, SA474, SU035, SU423
Tetracyclines, SU068
Thalassaemia major, SA352
Thiazide-sensitive sodium chloride co-transporter (NCC), SA194
Thiazolidinediones, M420
Thoracolumbar braces, SA347
3-D computed tomography, SA098
Three-dimensional cell cultures, M235
3-D synchrotron computed tomography, M086
3-D trabecular microarchitecture. SEE ALSO *Trabecular bone*
Bone metastasis from prostate cancer, M061
Iliac crest in postmenopausal women, F360
Local bone morphometry, SU046
Multi-detector computed tomography of human vertebra, SA008
Primary hyperparathyroidism, 1173
Ultrasonic statistical backscatter model, M108
Thrombomodulin, SU196
Thrombospondin-2, 1069
3H-Thymidine, M139
Thyroid hormones, SA132, SA233
Thyroid-stimulating hormone, F389
Thyrotropin receptor, 1054
L-Thyroxine, SA312
Tibia, F006, M099, M387, SA475, SU017, SU369
Tissue engineering, bone, M010, M033, M174, SU206, SU435
Tissue engineering, cartilage, M024

Tissue nonspecific alkaline phosphatase (TNAP), 1011
Titanium implant material, M046, M173
TMC-315B2 (non-peptide small molecule), F254
TNFRSF11B, F405
Tob (transducer of ErbB2), 1034
Toll-like receptors, M248
Toothless mutation in rat CSF-1 gene, 1084
Trabecular bone. SEE ALSO *3-D trabecular microarchitecture*
  Calcaneal thickness *versus* ultrasonic backscatter, M102
  Changes with age and disease, M097
  Estrogen-regulated genes BMD regulation, SA464
  Evolution simulation, M083
  Flt-1 tyrosine kinase, F144
  Genetic and GH/IGF-I effects on vertebral, SA118
  Genetic compensation mechanism for unloading, 1047
  gp130, 1123
  Myostatin deficiency, SU177
  Porotic, depth of field and information content in scanning electron microscopy, M331
  Primary hyperparathyroidism, 1174
  Rheumatoid arthritis *versus* trabecular texture at wrist, SA097
  Risedronate, SA338
  SFRP-1 effects, 1001
  Skeletal site-specific genetic regulation, 1217
  Ultrasonic statistical backscatter model, M108
  Unloading recovery, M172
Transforming growth factor-β
  Bone matrix degradation, F056
  C3H10T1/2 cells expression, M154
  Chondrocyte maturation, SU036
  LRP5 and Wnt regulation, M161
  MMP-13 in breast cancer, SU079
  Osteoclastogenesis inhibitors, SU243
  Osteoclast progenitors and, SU250
  Osteoclast survival, M273
  p38 and p44/42 MAP kinases, SU259
  p38 MAP kinase, M156
  PPARγ2 and mesenchymal stem cells, M155
  PTHrP regulation, M432
  SOCS expression, F259
  T869C polymorphism and postmenopausal osteoporosis, M116
Transforming growth factor-β1, M145, M158
Transforming growth factor-β2, M135, M160
Transforming growth factor-β3, M153
Transforming growth factor-β inducible early gene (TIEG), 1016, SA179
Transforming growth factor-β type II receptor, 1078
Transgenic animals
  11β-HSD2, 1025
  40 T-antigen gene, SA035
  Autofluorescent transgenes, F191
  FGF2 overexpression, M130
  P20C/EBpβ, 1162
  pOBCol3.6GFP, SA192
  RANKL overexpression, SA238
  TRAP overexpression, SU262
  In vivo estrogen receptor imaging, F468
Transient receptor potential channels (trpC), SU267
Transmission disequilibrium test, M124
Transplant osteoporosis. SEE *Bone marrow transplantation; Heart transplantation; Kidney transplantation; Liver transplantation*
Trauma, M131
TRENDIC (transcription enhancer dominant in chondrocytes), SA043
Tretinoin, M028
Tuberculoma, intramedullary spinal, M424
Tuberoinfundibular peptide of 39 residues (TIP39), SU431
Tumor necrosis factor-238A promoter allele, SA129
Tumor necrosis factor-α (TNF-α)
  Apoptosis and osteoprotegerin regulation, SU187
  Bone marrow stromal cells, M234
  CD11b+ osteoclast progenitors, 1021
  IL-1α effects on osteoclasts, SU231
  IL-6 expression in osteoblasts, SU150
  M-CSF after ovariectomy, M178
  Nitric oxide in osteoclast survival, M274
  Osteoblasts and osteoclasts in diabetes, SA237
  Osteoclast differentiation with collagen-induced arthritis, M245
  Protein undernutrition-induced bone resorption, F321
  Rheumatoid arthritis, M031
  Signaling and fracture healing, M136
Tumor necrosis factor-α converting enzyme (TACE), 1195
Tumor necrosis factor-α (TNF-α) promoter, SU147
Tumor necrosis factor receptor 2, SU135
Tumor necrosis factor receptor-associated factor 6 (TRAF6), 1023
Tumor suppressor gene VHL (Von Hippel Landau), 1152
Turner's syndrome and osteoporsis, WG3
TWEAK (TNF-like WEAK inducer of apoptosis), M262
Twin studies, F124, F354
TWIST, 1113, M200

U

U-937 cells, SU237, SU263
UGL7841 (recombinant PTH analog), SA362
Ulna, M087. SEE ALSO *Forearm*
Ultrasound, quantitative. SEE ALSO *Broadband ultrasound attenuation (BUA); Scanning confocal acoustic diagnostic (SCAD) system; Speed of sound*
  Age, testosterone and estrogen in men, M312
  Ankylosing spondylitis, SA090
  Backscattered spectral centroid shift, M103
  Backscatter *versus* calcaneal trabecular thickness, M102
  Biomechanical validation, SA116
  BMD and foot loading, SA110
  BMD in elderly, SU318
  Calcaneus and ER gene polymorphisms, SU141
  Calcaneus and femoral neck BMD, M115
  Calcaneus and fracture history in men, F115
  Cut-off value and fracture threshold in Japanese women, M106
  DXA measurement of fractures *versus,* M111
  Factor score with DXA for genetic studies, SA125
  Genetic polymorphisms and bone quality in postmenopausal women, SA133
  Heart transplantation, M110
  Heel measurements and glucocorticoids, M112
  Hip-fracture risk assessment in institutionalized elderly, F111
  Infants and children, M105
  Mechanical damage in bovine cancellous bone, SU053
  Mechanical response tissue analysis, M087
  Menopause and environmental risk, M289
  Methylenetetrahydrofolate reductase (MTHFR) gene, SU143
  Osteoporosis diagnosis in Japanese women, SU026
  Osteoporotic fracture risk in elderly women, 1130
  Phalangeal, during pregnancy, M311
  Population-based calcaneal, F113
  Real-time fixed-array bone imaging, M104
  Report format and patient treatment compliance, M100
Ultrasound, quantitative. SEE ALSO *Broadband ultrasound attenuation (BUA); Scanning confocal acoustic diagnostic (SCAD) system; Speed of sound* (Continued)
  Statistical backscatter model of trabecular microstructure, M108
  Subchondral bone changes during rat skeletal maturation, M109
  T-score thresholds at multi-site axial transmission, M101
Umbilical vein endothelial cells, human, M211
UMR-106 osteoblasts, SU224
Unloading. SEE ALSO *Spaceflight*
  Articular cartilage, SA059
  Bone and muscle recovery after, M172
  Genetic compensation mechanism, 1047
  Insulin resistance to IGF-I, F159
  β1 Integrins, SU060
  Intracellular signaling and gene transactivation, SU064
  Osteopontin and osteocyte stress, 1165
  Osteoprogenitors and bone formation, SU169
  Osterix gene expression in ASK1 knockout mice, SU173
  VEGF receptor Kdr antibodies, M391
Uremic bone disease, M409
Urine tests, M335, SU109
Urolithiasis, 1055

V

Vacuolar H^+-ATPase (V-ATPase), SA253, SU268_
Vascular endothelial growth factor, M015, M060, SU155, SU415
Vascular endothelial growth factor receptor 1 (Flt-1), F144
Vascular endothelial growth factor receptor 1 (Flt-1) agonists, M391
Vascular stiffness, SU394. SEE ALSO *Calcification, arterial*
Vasoactive intestinal peptide (VIP), M141
Vav1 and Vav3, M267
Vertebrae, F009, M079, M085, SA008, SA118
Vertebral deformities, SA305, SU287, SU291
Vertebral fractures. SEE ALSO *Fractures*
  Alendronate and BMD above -2.5, M352
  Body height loss, 1129, F284
  Body height loss and BMD, M315
  Compression types, SA283
  COPD, M293
  Densitometric lateral vertebral assessment, SU092
  Dual X-ray absorptiometry of women and men, F013
  Dynamically mobile compression, SU293
  Dynamic mobility and height restoration, M330
  Elderly function with compression-type, SA350
  Health care costs, F286
  Hip, rib, and wrist fractures in postmenopausal women, SU286
  Ibandronate effects, F341
  Instant assessment, M292, SU282
  Nandrolone decanoate, M394
  Peripheral and axial densitometry measurements, F094
  Risedronate, F343
  Risk prediction with glucocorticoid treatment, F325
  Risk prediction with metacarpal cortical index, F091
  Risk prediction with radiographic texture feature analysis *versus* BMD, SA102
  Risk reduction with back exercises, F288
  Standardized morphometry, SA285
  Thoracic kyphosis, 1208
  Thoracolumbar braces, SA347
Vertebrates, SU431
Vibration exercise, SA164, SA346, SU166
Vinculin, M042

Viral delivery systems, 1134
Vitamin A, M285
Vitamin B_{12}, 1214
Vitamin C, SU210
Vitamin D
  Aging and activation of, SA382
  BMD and muscle, SU309
  Bone mass acquisition in girls, SU007
  Cross-linking analogs for prostate cancer, SU461
  Depletion, F277
  Elderly in urban Argentina, SU279, SU280
  FGF-23, M128
  Fracture prevention with calcium, M367
  Hyperparathyroidism in elderly in Brazil, M286
  Hyperparathyroidism, secondary, M338
  IL-1 receptor antagonist expression in keratinocytes, M456
  Osteoclast formation through RANKL induction, SA233
  Preterm infants, SU404
  Primary hyperparathyroidism and BMD in women, SA409
  PTH and BMD in postmenopausal women, SU315
  Sex-dependent, age-related decline, SU310
  Skin deficiencies after burns, SA418
  Thrombomodulin expression in osteoblasts, SU196
  Vitamin C crosstalk signaling in osteoblast differentiation, SU210
  Young Israeli women, SA322
Vitamin D_3, M451
Vitamin D receptor
  $1,25(OH)_2D_3$-induced transcription, SU447
  Activation by Ro-26-9228, SA461
  Age and PTH serum levels, F414
  CAN/Nup214 regulation of, F484
  CYP3A4 induction, F488
  Cytokine production from T cells, SA481
  Differentiation in human intestinal cells, M454
  Enoyl CoA hydratase interaction, SU450
  Gene polymorphisms and bone loss in postmenopausal women, SA012
  Gene polymorphisms and HRT effects on BMD in postmenopausal Koreans, M117
  Gene polymorphisms and muscle strength, SA126
  Gene polymorphisms and osteoporotic fracture risk in elderly men, SU142
  Gene polymorphisms in Japanese women, SA134
  Hypertrophic chondrocyte apoptosis, 1030
  Mutation and rickets without alopecia, F456
  NCoA-62/SKIP, SU451
  Osteoblast development, M217
  p160 nuclear proteins and NF-κB suppression, M447
Vitamin D receptor (Continued
  p300 and osteocalcin expression, M192
  Peak BMD linkage in nuclear families, M124
  Periosteal bone formation, SA455
  Reverse trafficking in $1,25(OH)_2D_3$ target cells, SA459
  Vitamin D gene repression and, 1118
  Vitamin D regulation of skeletal and calcium homeostasis, 1029
  WINAC transactivation, 1050
  Wnt expression in cortical bone formation, 1117
Vitamin D receptor B1, F458
Vitamin D receptor ligand binding-domain, SU454
Vitamin D response element, M449, SU147
Vitamin E, SU358
Vitamin K, F275
Vitamin K_1, M365
Vitamin K_2, SA375. SEE ALSO *Menatetrenone*
Vitronectin, M049
Voltage-gated H^+ channel, M282
Vulnerability perception, M317

W

W9, osteoclast-induction stimuli, SA250
Water, M094
WD-40 proteins, F038
Website, osteoporosis study data, M316
Weight-bearing exercise, SA170, SU159
Weight loss, M329. SEE ALSO *Body weight*
Williams syndrome transcription factor (WSTF) including nucleosome assembly complex (WINAC), 1050
Wiskott Aldrich Syndrome protein (WASp), F230
Wnt, 1117, M035
  LRP5 signaling and, 1002, F214, M161
Wnt-11, 1113
Women, M421, SA322, SU180, SU275. SEE ALSO *Osteoporosis, postmenopausal; Perimenopause; Postmenopausal women; Premenopause; Sex differences*
World Health Organization, M101
Worry, M317
WP9QY peptide, SA257
Wrist fractures, SU366

X

Xylene orange, M092

Y

Y559F (c-Fms tyrosine residue), SU260
Y807F (c-Fms tyrosine residue), SU260
YM529, M342, SA245. SEE ALSO *Minodronate*
Young adults, cystic fibrosis and BMD, M310

Z

Zoledronate, F337, M210
Zoledronic acid
  Analgesic effects, M427
  Androgen deprivation and prostate cancer metastasis, SU072
  Distraction osteogenesis repair, F256
  Growth plate remnant removal in growing rabbits, 1203
  Osteonecrosis of femoral head, F424

A

Abbas, S. M279
Abbott, T. A. SA281, SA294, SU307, M318, M319
Abboud, S. L. 1122, SU045
Abbs, I. C. 1141
Abdallah, B. M. SU195
Abdelmagid, S. M. 1188
Abe, E. 1018, 1054, 1075, SA215
Abe, M. SA077
Abendroth, K. M320
Abou-Samra, A. B. SU442
Abrahamsen, B. SA131, SA313, SU304, M119
Abu-Amer, Y. 1155, M279
Acca, M. SU024
Accarie, C. SU097
Achenbach, S. J. 1103, 1168, 1211
Ackerman, Z. SA365
Ackert-Bicknell, C. 1080, 1217, SA152
Ackert-Bicknell, C. L. 1106, SA060
Adachi, J. D. 1129, F284, SA097, SA284, SA289, SA340, SU296, SU343, M081, M293
Adami, S. SU345, SU363, M347
Adamietz, P. M024
Adamo, M. L. SA152
Adams, C. 1135
Adams, C. S. SU057, SU189
Adams, D. M171
Adams, D. J. 1026, SU120
Adams, G. B. 1053
Adams, J. F091, SA091, SA092
Adams, J. E. 1170, 1174, SU016, SU017, SU018
Adams, J. S. F463, SA463, SA490
Adams, M. A. F009, SA009
Adamski, S. M326
Addesso, V. 1042
Adebajo, A. SA266
Adler, R. A. M112, M113, M305
Adrian, M. D. SA476
Aeschlimann, J. M. M360
Afeiche, N. SU289
Afonso, V. SU237
Afzal, F. 1101
Agans, S. C. 1046, SU181
Ahlborg, H. SU014
Ahlborg, H. G. 1163
Ahmad, A. M. F433, SA433, SU425
Ahmadpour, O. A. SA443, M433
Ahmed, M. M. 1169
Ahn, H. SA045
Ahn, Y. H. M339
Aihara, K. F046, SA046
Aisaka, K. M381
Aitken, C. J. M272
Aizawa, T. M136
Akatsu, T. SU077, SU239
Akatsuka, H. F201, F254, SA201, SA254
Åkesson, K. SU303
Akhter, M. P. SU176, SU358, M163, M164, M366
Akintoye, S. O. SU215
Akiyama, H. 1071
Akiyama, T. 1150, F373, SA373, SU333, SU411, M276, M344
Akizuki, M. M346
Akrout, L. M107
Akune, T. 1072
Al-Dayeh, L. SU087
Alam, I. SA117
Alam, M. I. SA164
Alander, C. B. SU214
Alatalo, S. L. SU103, SU229
Albagha, O. M. E. SA135
Albert, S. A. SU271
Albornoz, L. SA466
Alen, M. SU007, SU008, SU132
Alexander, J. M. F227, SA227, SU443, M385
Alexandersen, P. SA370
Alexandre, C. M391, SU165
Ali, A. A. 1032, 1058, 1176, M380
Allen, C. M. SU433
Allen, H. C. 1144, 1165
Allen, K. M. M123
Allen, M. R. 1194, M167, M172
Alles, C. M. 1117
Allolio, B. SU431
Almasy, L. SU131
Almeida, E. SU060
Aloia, J. F. M242
Alonso, G. M309
Alonzo, E. SU421, M411
Alos, N. F419, SA419
Alsop, C. 1174
Altmann, E. F064, SA064
Alvarez, J. 1078, M132
Alvarez, L. SU390
Alvarez, V. SU348
Álvarez-Hernández, D. SU142
Alvarez-Pinera, J. 1074
Amaar, Y. 1183, F150, F151, SA150, SA151
Amagasa, T. F220, SA220, SA257
Amano, H. SU183, M407
Amano, S. M393
Amblard, D. SU060
Amedee, J. SU220, M211
Amiel, C. SU313
Amin, S. F307, SA307
Amizuka, N. SU054, SU077
Amling, M. 1171, F036, SA036, SU248, SU249, M012, M029, M072
Ammann, P. F321, SA321, M382, M383
Ammerman, D. G. F412, SA072, SA412, M055
Amory, H. SU114
Amoui, M. SU263
An, C. S. SA172
Ancoli-Israel, S. F290, SA290
Andersen, T. M145
Andersen, T. L. SU227
Anderson, D. M. M055
Anderson, G. M281
Anderson, G. I. SU168, M266
Anderson, H. C. 1011, SU033, M159
Anderson, J. J. F302, SA301, SA302, SU022
Andreassen, T. T. M388
Andrew, G. SU055
Andrew, J. G. SU158
Angeli, A. M241
Anisowicz, A. M123
Aoki, K. SA250, SA257, SA349, SA416, M240
Aoyagi, K. M298, M322
Appelboom, T. SA425
Arabi, A. SU319
Arabian, A. F029, SA029, SU459
Arai, H. SA134
Arao, Y. SA426
Arata, Y. SU113
Aravindan, R. SA393, SA394
Arden, N. K. F282, SA282
Arias-Magaloona, S. M261
Arita, S. SA363
Arjmandi, B. H. SU357, SU358, SU359, SU419, M366
Armbrecht, H. J. SA489
Arminio, A. SU421
Armour, K. E. 1191
Armour, K. J. 1191, M208
Arnaud, C. D. F366, SA366
Arnaud, M. J. M360
Arnaud, S. B. M404
Arnold, A. SA415
Arnold, A. L. SU330
Arp, P. P. 1222
Arquitt, A. B. SU357
Asadi, F. M062
Asahina, I. SA021
Asano, T. F087, SA087
Ashby, R. L. SU016, SU017, SU018
Ashford, R. F091, SA091
Ashida, K. M085
Ashikawa, K. M262
Ashley, S. F083, SA083
Aslan, H. M225
Asma, G. F348, SA348
Asuncion, F. J. 1020
Atkins, G. J. M210, M230
Atkinson, E. J. F307, SA307
Atula, S. F083, SA083
Au, S. SU302
Aubin, J. E. F026, F210, SA026, SA210, M025, M221, M222
Audoly, L. P. 1107
Audran, M. SU052, M332
Auger, S. SU388
Auler-van der Velden, B. SU074,z SU102
Auluck, J. SA147
Avila, D. SU287
Avorn, J. SU378
Aya, K. SU416
Ayres, J. A. F139, SA139
Azriel, S. M307
Azuma, Y. M245

B

Baade, H. SU328
Babij, P. F119, SA119, SU176, M163
Backer, V. M324
Backus, S. SA350
Baddoura, O. SU289
Baden, J. F. SU036
Badenhop-Stevens, N. 1200
Badenhop-Stevens, N. E. M007, M008
Badra, M. SU289
Bae, K. T. M020
Baek, J. SU219
Baek, K. H. SU422
Bagger, Y. Z. SA370
Bagnoli, F. M105
Bagu, J. M458
Bagur, A. SA328, SU279, SU280
Bahl, S. SU294
Bai, S. F473, SA473, SU038
Bai, X. F391, SA391
Bail, H. J. M147
Bailey, S. L. SU048
Bain, S. SA326
Baird, K. SU094
Bajna, E. SA481
Bajnok, E. SA132
Bajnok, É. SA133, SU320, SU322
Baker, S. U. K. 1117
Bakewell, S. J. F075, SA075
Bal, S. K. F091, SA091, M301
Balcells, S. M188
Baldini, T. H. SU048
Baldock, P. A. 1117, 1125, F256, F424, F460, SA256, SA424, SA460
Balduino, A. SA171
Balint, E. 1110, SU197
Balius, R. SU182
Ball, S. D. F001, SA001
Ballard, J. E. SU301
Ballard, P. M170
Ballesta, A. M. SU390
Balling, R. F414, SA414
Balogh, A. SA353
Bandinelli, S. SU310
Banovic, T. 1057, SU151
Banu, J. SU012, SU013
Bar, I. M225
Bar-Shavit, Z. SU147, M254
Barad, D. H. SA278
Barazza, A. SU443
Barbara, A. M016
Barbero, A. M232
Barbieri, A. M455
Bardella, M. T. SA175, WG6
Barden, H. S. M073, M089
Bardwell, A. M100
Bareille, R. SU220, M211
Bärenholdt, O. SU304
Barger-Lux, M. J. SU351, M451
Barker, M. E. 1144, SA280
Barkmann, R. F113, SA113, SU350
Barlas, S. SA274, SU307, M295
Barlet, J. SU354
Barley, C. F056, SA056
Barlogie, B. M054
Barlow, W. E. M284
Barmina, O. SU460
Barnes, A. K. SU104
Barnes, G. L. M136, M196, M234
Barnett, B. SA255
Baron, R. 1002, 1027, 1097, 1100, 1149, F176, F225, F263, SA176, SA225, SA231, SA232, SA257, SA263, SA479, SU066, SU262, M029, M179, M265, M280, M379
Barou, O. M391
Barr, R. J. SA266
Barragan-Adjemian, C. M018
Barrett-Connor, E. SA274, SU028, SU299, SU299, SU300, SU307, SU308, M295
Barrett-Connor, E. L. M079
Barrow, K. D. F311, SA311, SA318
Barry, F. M403
Barry, J. A. SU162
Barsony, J. M454
Bartali, B. SU310
Barthel, H. R. M093
Bartholic, J. M082
Bartlett, W. A. 1035
Barton, I. SA344
Barton, R. M249
Baslé, M. SA068
Baslé, M. F. SU052, M332
Bass, S. SU006, M302
Bass, S. L. SU004, SU005
Bassa, P. F013, SA013, SU182
Bassford, T. 1089, M300
Bassilana, F. SA015
Basso, N. SU169
Bastepe, M. 1065
Bataille, R. SA068
Bateman, T. A. 1045, F369, SA369
Batiste, D. L. M098
Battisti, D. SU429
Baudoin, C. SU313

Bauer, D. C. 1212, F106, F115, F290, F311, SA106, SA115, SA290, SA306, SA311
Bauer, R. L. 1079
Baumbach, K. M024
Baumgartner, R. N. SA329
Bauss, F. SU350, M356
Bava, U. SU151, M146
Baxter, I. F269, SA269
Baylink, D. J. 1183, 1216, F149, F150, F151, F161, SA060, SA149, SA150, SA151, SA161, SU042, SU263, SU371, M149, M378
Bayorh, M. A. M452
Bayoumi, A. M. SA306
Bazot, D. SU368, SU369
Beamer, W. SU428
Beamer, W. G. 1080, 1106, 1217, 1220, F168, SA060, SA118, SA152, SA168
Beaton, S. J. SA294
Beaupré, G. S. SU321
Beavan, S. R. SA477
Bech-Jensen, J. E. SA313
Becherini, L. SU136, M121
Beck, T. J. 1088, 1167, F364, SA002, SA364, M168, M169, M170, M308
Beck-Nielsen, H. SU020
Becker, K. M389
Bécret, A. SU047
Beerli, R. M390
Beertsen, W. SA222, SU065, SU245
Begerow, B. SA347
Behets, G. J. S. SA050, M412, M415
Beier, F. M027
Beil, F. T. 1171
Belcredito, S. F468, SA468
Belknap, J. K. 1012
Bell, J. M335
Bell, O. F435, SA435
Bella, N. SU420
Belleville, C. SA479
Bellido, T. 1013, 1032, 1058, 1161, 1176, 1190, F173, SA173, SU185, SU186, M380
Bellorin-Font, E. SU421, M411
Bellows, C. G. SU169
Belotti, M. SA328
Bemben, D. A. M162, M165
Bemben, M. G. M162, M165
Bemis, K. 1135
Bencsik, M. M177
Bendik, I. SU449, M232
Bendre, M. F079, SA079, SA080
Beneton, M. F091, SA091, M301
Benezra, R. 1192
Benhamou, C. 1043
Benhamou, C. L. SU010, SU319
Bennett, B. SU395
Bennett, B. D. SU267
Bennett, J. F003, SA003
Benoist-Lasselin, C. SA140
Benson, L. M. M458
Bentley, C. SA002
Bently, C. M169
Bentzen, C. L. SU375
Benvenuti, S. SU136
Bergh, J. J. M453
Bergot, C. M075
Bergow, C. F414, SA414
Bergström, S. M137
Berndt, T. J. 1142
Bernhold Brechter, A. M203
Berry, J. E. F024, SA024
Berry, J. L. SU055, SU158
Berry, M. M235
Bervoets, A. R. J. SA050, M412
Bessette, M. 1187
Betschart, C. F064, SA064
Bettembuk, P. SA353
Bettencourt, R. M079
Bevilacqua, M. SU285
Bex, F. 1001, F119, SA119
Bex, F. J. F371, SA371, SA432, SU430
Bhargava, A. SA393, SA394
Bhat, B. F119, SA119
Bhat, B. M. 1112, SA432, SU430
Bhatia, P. F412, SA072, SA412, M055, M066
Bhattacharyya, M. H. M253
Bhattacharyya, R. S. M070
Bhattoa, H. P. SA353
Bi, L. X. SA219
Bi, X. SU087
Bi, Y. 1068
Bianchi, G. SU024, SU285
Bianchi, M. L. SA175, WG2, WG6
Bianco, P. SU386, M228
Bidder, M. M020
Bikle, D. D. F159, SA159, SU428, M177
Bilezikian, J. SU382
Bilezikian, J. P. 1169, 1172, 1173, SA438, SU276, SU394, SU395, SU437, , M384
Billiard, J. SU193
Billings, P. C. F417, SA417, SU044, WG4
Binkley, N. SU089, SU091, SU092, SU154, M078
Binkley, T. M009
Binkley, T. L. SA272
Biondo, C. 1155
Bird, D. SA110, SA114
Birkner, B. M320
Bischoff, D. S. M154, M153
Bisello, A. F451, F452, SA451, SA452, SA454
Bishop, J. E. SU446, SU448, SU449, SU452
Bishop, N. 1199
Biskobing, D. M. M398
Biswas, R. S. F236, SA236, SU265
Bitzer, E. M320
Blacher, R. F400, SA400
Black, D. M352
Black, D. M. 1131, F106, F292, SA106, SA292, SA367, SU382
Black, K. M. SU168
Black, R. A. 1195
Blackwell, T. L. 1214
Bladbjerg, E. M. SA131
Blaha, J. D. M209
Blair, H. 1054, SA390
Blair, H. C. 1018, SU187, M236, M237
Blake, G. M358
Blake, G. M. SA334, SU085, SU088, M080, M101
Blakely, A. C. F279, SA279
Blakley, G. SA055
Blanchet, C. M289
Blank, J. SU028
Blank, J. B. SA303
Blank, R. D. SU048
Blaschke, S. M184
Blau, E. M. M319
Bledsoe, S. E. 1168
Blind, E. SU431
Bliziotes, M. M. SU270
Blobel, C. P. 1195
Bloomfield, S. A. 1194, M167, M172
Blumsohn, A. 1035, 1132, 1144, 1165, F109, SA103, SA109, SU292, M369
Blundell, M. P. F230, SA230
Bobec, L. WG1
Boden, S. D. SU198, M045, M068
Bodine, P. 1001, F119, SA119, SU193
Bodine, P. V. N. F371, SA187, SA371, SA432,k M041
Bodnar, J. M221
Body, J. J. 1094, M290
Boercsoek, I. SU157
Boers, M. SU417
Boerscoek, I. SA462
Bogado, C. E. F364, SA364
Boggio, V. SA466
Bohacek, R. 1145, SU377
Boisdet, J. SA120
Boissy, P. 1195, SU259
Boland, R. L. SA459, SU217
Bolander, M. M299
Boldrini, L. SA171
Boldrini, R. SU398
Bollag, R. M138, M139
Bollerslev, J. SA324, SU025
Bologna, M. SA086
Boltz, M. A. SA489
Bonaventure, J. SA140
Bone, H. 1059
Bonewald, L. 1005
Bonewald, L. F. F056, F061, SA056, SA061, SU063, SU271, SU272, SU273, M011, M018
Bongiovanni, S. SA240
Bongu, A. M421, M422
Bonjour, J. P. 1201
Bonnassie, A. SU010
Bonneh, D. Y. M375
Bonnelye, E. M025
Bonnick, S. SU087
Bonnick, S. L. M333
Bonocore, G. M105
Bonow, R. M017
Boonen, S. SA474
Booth, S. L. F275, SA275
Borah, B. SU340, M086
Borba, V. C. Z. M286
Bord, S. SU002
Borella, L. 1001, SA432
Borne, M. C. M300
Borojevic, R. SA171, SU050
Bors, K. SA372, SA382
Borsari, S. M442
Borysenko, C. W. SU187
Boskey, A. L. SU048, SU305, M011
Bostock, J. SA092
Botea, V. WG7, WG8
Bothwell, A. L. M. 1098
Botolin, S. SU190
Bouillet, P. M276
Bouillon, R. SA474
Bouler, J. M. M174
Boulos, P. SA289
Boulos, S. SU289
Boumier, P. SU412
Bouralexis, S. M210
Bourgeois, P. M001
Bourrin, S. M383
Bouter, L. M. F348, SA348
Boutry, N. SU021
Bouvet, M. M433
Bouxsein, M. F119, SA119
Bouxsein, M. L. 1014, 1062, 1080, 1180, 1217, 1220, SA118, SA125
Bowen, P. H. M077
Bowl, M. R. 1008
Bowman, P. J. 1214
Boyan, B. D. SA457, SU271, M011, M158, M445
Boyce, B. F. 1021, 1024, 1145, 1153, F016, SA016, SU377, M176
Boyde, A. SA025, SU228, M331, M460
Boykin, T. M149
Boyle, W. J. 1009
Braam, L. A. J. M365
Braga, V. SU363
Braga, W. M394
Braga de Castro Machado, A.M. M369
Brage, M. M256
Brahim, J. SU215
Brama, M. SA084, M179
Brandenburg, V. M. M413
Brandi, M. SU136
Brandi, M. L. SA344, SA352, M121, M406
Brändström, H. SA126
Brandt, J. M109
Brandt, N. SA273
Brantley, A. SU205
Brantus, J. SA423
Bratt, T. SA374
Braut, A. SA190
Bray, R. C. M044, M428
Brazier, M. SU246, SU412, M277
Brenneman, S. K. SA281, SA294, SU307, SU308, M295, M318, M319
Brenner, K. M057
Brenner, M. K. M227
Brenner, R. SU184
Breschi, M. M110
Breuil, V. M181
Brewer, A. J. F385, SA385
Briand, S. I. SA244, SA258
Brickman, S. A. M162, M165
Briganti, E. SU004, SU006, M302
Bringhurst, F. SU254
Bringhurst, F. R. 1053, 1177, 1178, F176, SA176, SU444
Bringhurst, R. F. 1066
Briody, J. N. 1203, F256, SA256
Britschgi, T. B. 1222
Brixen, K. SA131, SA313, SU020, SU025, M373, M402
Brochmann, E. J. SA323
Brockstedt, H. M402
Brodt, M. D. F403, SA403
Broe, K. E. 1087, F275, SA275, SU314
Broemme, D. SU065
Brommage, R. SU096
Brooks, D. M029
Brossard, J. H. SU438
Brouet, J. C. M075
Brouns, F. M365
Broussard, D. L. M304
Brousseau, Y. F419, SA419
Brown, A. J. SA491, SU457, M417
Brown, E. SU193
Brown, E. M. 1063, M443, M444 WG9
Brown, J. P. SA289, SA340, SU296, SU343, SU388, SU391
Brown, M. M302
Brown, M. A. SU127, SU128
Brown, S. E. M335
Brown, T. A. 1031, SA053, M392
Brownbill, R. A. SU323, M325
Bruder, J. M. M067
Bruna, P. SA030
Brunet-Imbault, B. SU010
Brunetto, O. SU348
Bruni, D. M110

(Key: 1001-1222 = Oral, F = Friday Plenary poster, SA = Saturday poster, SU = Sunday poster, M = Monday poster, WG = Working Group Abstract)

Brunkow, M. E. 1222
Brunner, F. M382, M383
Brünner, N. SU078
Bruno, D. SA352
Bruno, E. M270
Brunstetter, V. L. F001, SA001
Brusadelli, A. F468, SA468
Brusse, L. S. F282, SA282
Bruzzaniti, A. SA232
Bryant, H. 1135
Bryant, H. U. 1179, SA476
Bu, R. SU187, M236
Bucchieri, S. SU287
Buchanan, C. M. M146
Buchmann, E. V. M191
Buckendahl, P. E. SA055
Buckwalter, K. A. 1081
Buford, W. L. SA219
Buhl, K. M. 1185
Buhl, T. F064, SA064, M390
Bui, D. T. SU376
Bui, H. M089
Buijs, J. 1091
Buist, D. S. M. SA281, M318
Buitrago, C. M450
Bundschuh, B. SU157
Bünger, C. M145
Bünger, M. H. M145
Bunker, C. H. F304, SA304, M303
Bunta, A. M299
Burckhardt, P. 1130, M310
Burckhardt, P. M. M360
Burde, M. A. SU256
Burdeska, A. 1138, M347
Burghardt, A. M420
Burke, A. B. M131
Burke, D. T. SU122
Burke, G. SA221
Burke, P. K. M089
Burnett, K. SA469
Burns, D. M. SA428
Burns, S. SU075, M059
Burns, T. L. M005
Burr, D. B. F155, SA155, SU349
Burshell, A. L. SU402, M315
Burt, D. M040
Burton, D. W. SA443, SA444, SA445, M430, M433
Bush, A. SA318
Bushby, A. J. SA025
Bushinsky, D. A. SA178, M419
Bustamante, M. M188
Butcher, M. K. G. SU216
Buttery, L. D. K. 1101
Buurman, C. J. M189
Byers, B. A. M201
Byrne, M. SU066
Byrne, M. H. 1197, 1198

C

C. B. M. B. 1129, F284, SA284
Caan, B. J. SA278
Caballería, L. SA332
Caballero, A. SU274
Cadarette, S. SU364
Cadarette, S. M. SA089
Cadogan, J. SA280
Caffarelli, C. M396
Cain, R. L. SA476
Caldwell, N. J. 1173
Callander, N. S. F073, SA073
Calle, Y. F230, SA230
Calleri, M. M290
Callon, K. E. SU151, SU204, M146
Calvi, L. SU066
Calvi, L. M. 1053
Camacho, P. M. SU420
Camargo, M. B. R. SA267
Camerino, C. SU218
Cameron, K. O. M392, M395, M397
Camillo, C. M020
Caminis, J. M170
Campagna, M. S. M396
Campagna, S. 1166
Campbell, J. SU090
Canaff, L. F385, SA385, M204, M440
Canalis, E. 1121, 1151, F199, SA198, SA199, SA211, M042
Cancela, M. L. M043
Candeliere, G. A. F026, F210, SA026, SA210
Caniglia, M. SU398
Cannata, J. SU345
Cannata, J. B. SU142, M418
Cantor, T. F408, SA408, SU438
Cao, J. F159, SA010, SA159
Cao, L. 1049, SU187
Cao, X. 1017, F206, F473, SA206, SA473, SA480, SU038, M064, M197
Cao, Y. F373, SA373, SU333, SU411, M344
Cao, Z. K. M126
Capen, C. C. SA431, SU436
Capiati, D. SA459
Cappellen, D. SA240
Cappuccio, F. P. 1008
Caputo, J. M. M019
Caradonna, P. WG11
Carbone, L. SA318, SU009
Carbone, L. D. F311, SA311, M287
Cardinali, D. SA466
Cardon, L. R. SU128
Carle, G. F. M174
Carlini, R. SU421
Carlos, A. S. 1012
Carlsen, B. M235
Carlson, C. S. SA189
Carmina, E. SA352
Carn, G. 1081
Carnes, M. L. SU328
Carnevale, V. SA287, SA409
Carninci, P. SU252
Caron, R. F417, SA417
Carr, L. G. SA117
Carreon, M. R. SU072, M060
Carrion-Peterson, M. SA303
Carroll, J. SU364
Carstanjen, B. SU114
Carter, D. R. SU321
Carter, H. SA194
Carvalho, D. M438
Carvalho, R. S. M152
Casco, C. SU279, SU280
Caselli, G. F. M180
Caseria, D. M. M337
Cassady, A. I. SU252
Cassarino, D. M029
Cassinelli, H. 1056
Cassini, F. SU398
Castel, H. M375
Castrillón, P. SA466
Castro, C. 1158, 1184
Catala-Lehnen, P. M012
Cattini, L. SA188
Cauley, J. 1089, SU028, M316
Cauley, J. A. 1085, 1131, 1138, 1212, F115, F292, F304, F311, SA115, SA292, SA304, SA305, SA311, SU146, M296, M300, M303, M306, M313, M367
Cauley, J. C. F290, SA290
Cavalcanti-Adam, E. A. SU057
Cavanaugh, J. M458
Caverzasio, J. 1124, SA212, M202
Cayabyab, S. SU144
Cazalbou, S. SU373
Cecchini, M. 1091
Celis, M. M. SA418
Cenci, S. F330, SA093, SA330, SA467
Cendoroglo, M. SA267
Cendoroglo, M. S. M286
Center, J. R. 1086, 1104, SA014, SU283, SU297
Centrella, M. SU447
Ceoloni, B. M241
Cephas, S. M404
Cepollaro, C. M105, M110, M396
Cetani, F. M442
Chabala, J. M. M419
Chaboissier, M. C. 1071
Chabot, G. F419, SA419
Chadha, A. M114
Chafe, L. L. M437
Chaki, O. F130, SA130, SU113
Chakravarthy, B. SU433
Chalberg, C. SA444
Chalès, G. SA120
Chambers, T. F230, SA230
Chambers, T. J. F259, SA224, SA259
Chamoles, N. M400
Chan, A. SU278
Chan, C. SU281, SU316
Chan, E. F252, SA252
Chan, G. SU281, SU316
Chan, G. M. M288
Chan, J. F016, SA016
Chan, S. SU311
Chan, W. S. M345
Chandra, D. SU251
Chandra, R. SU108
Chandraratna, R. A. S. M459
Chandrasekhar, S. 1135, SU234
Chang, E. J. M156
Chang, F. L. SA170, SU159
Chang, K. P. SU283
Chang, W. H. M238
Chang, W. Y. SA469
Chanteranne, B. SU354
Chao, T. SA107
Chaperón, A. SU279
Chappard, D. SA068, SU021, SU052, M332
Chappel, J. M258
Chapurlat, R. D. SA392
Charles, P. SU020
Charlesworth, D. F091, SA091
Charlton-Kachigian, N. 1114
Charmley, P. 1222
Chase, C. C. F279, SA279
Chassande, O. M211
Chatterjee-Kishore, M. SU193
Chattopadhyay, N. M444
Chaudhary, L. R. SU212
Chaudhry, R. SU281, SU316
Cheblal, H. M290
Chellaiah, M. A. F236, SA236, SU265, M056
Chen, C. SA470, SU223, SU387
Chen, D. 1005, 1093, 1157, 1189, F016, F042, F071, SA016, SA042, SA071, SU417
Chen, H. F463, SA463
Chen, J. 1017, F184, SA184, SU418
Chen, J. R. 1032, 1058, SU185, M380
Chen, P. 1135
Chen, Q. F056, SA056, SA407, SU151
Chen, R. M343
Chen, S. F040, F218, SA040, SA218
Chen, S. T. F161, SA161, SU042
Chen, T. C. SA418, SU071, M451
Chen, W. SU266
Chen, X. 1067, 1068, SA017, A213, SU150
Chen, X. D. 1194
Chen, Y. SA274, SA294, SU019, SU030, SU094, SU307, SU308, SU367, M295, M318, M319
Chen, Z. 1049, 1089, SA278, M300
Cheng, B. SU272
Cheng, D. M. F275, SA275
Cheng, J. C. Y. SA004, SA005, SU400
Cheng, S. 1015, 1184, SA100, SU007, SU008, SU009, SU011, SU103, SU132
Cheng, S. L. 1017, 1114, F020, SA020, SA172
Cheng, S. M. SU009, SU011
Cheng, Y. Y. SA076
Chennareddy, K. 1019
Chenu, C. SA229
Cherrick, I. M343
Cherubini, A. SU309, SU310
Cherubini, R. WG2, WG6
Chesnut, C. 1138
Cheung, A. SU316
Cheung, A. M. SU281, M087, M297
Cheung, C. S. K. SA004, SA005, SU400
Cheung, J. SA128, SU098
Chevalley, T. 1201
Chhabra, A. F309, SA309
Chiano, M. F124, SA124
Chiappelli, F. M241
Chiba, M. SA035
Chihara, K. F325, SA156, SA325, SA407, M151, M204
Chikatsu, N. SA411
Chikazu, D. 1148
Chikuda, H. 1072, M022
Childs, L. 1153
Chin, H. M215
Chinander, M. R. SA096, SA102
Chinappen, U. M423
Chines, A. A. SA342
Chirgwin, J. M. SU075, M059, M060
Chiu, J. SU318
Chiusaroli, R. 1100, 1149, SU066
Chmielewski, P. E. SU340
Cho, D. SU141
Cho, J. Y. 1083
Cho, T. SA065, M031, M136
Choi, H. M118
Choi, J. 1112, SU119, SU211, SU384, SU414, M129
Choi, J. Y. SA172
Choi, S. J. F073, SA073, M246
Choi, W. H. M339
Choi, Y. M117, M248, M250
Chong, B. 1056
Choong, P. F. M. F081, SA081
Chorev, M. F227, SA227, SU443
Chott, R. SA326
Choudhary, S. SU214
Choudhury, I. 1198, SA032
Chow, G. 1092
Chow, J. F230, SA230
Christ-Crain, M. SA312
Christakos, S. SU186, SU447
Christgau, S. M348
Christiansen, C. 1037, 1195, SA370, SU078, SU227, SU259, M347, M348, M349
Christiansen, C. H. SU112

(Key: 1001-1222 = Oral, F = Friday Plenary poster, SA = Saturday poster, SU = Sunday poster, M = Monday poster, WG = Working Group Abstract)

Christiansen, J. S. M402
Christie, P. T. 1008, 1215
Chu, P. SA107, M238
Chu, P. H. 1017
Chun, R. F. SA490
Chung, C. SU058
Chung, D. SU141
Chung, H. SU076, M118
Chung, L. 1096
Chung, M. SU141
Chung, P. SU254
Chung, S. SA226
Chung, U. 1065, 1066, 1072, 177, 1186, F176, SA176
Chung, W. SU253
Chung, Y. 1183
Churchill, G. 1106
Chusho, H. 1206
Ciana, P. F468, SA468
Cianciosi, M. C. 1115
Cifuentes, M. M340
Cincu, C. SU052
Ciszek-Doniec, V. SA430
Civitelli, R. 1015, 1158, 1184, F182, SA182, SA183, SU156, M082, M212
Clack, G. 1170
Clagett-Dame, M. 1120, SA383
Clapp, D. W. F040, SA040
Clark, P. A. F456, SA456
Clark, S. M029
Clarke, B. L. 1211, SU405
Clarke, N. M. P. SU415
Clarkin, C. E. 1191
Claude, J. R. SA447, SU047
Claustrat, B. 1209
Clemens, T. L. F446, SA446
Clement, J. G. SA047
Clément-Lacroix, P. 1027, SA479
Clemente, D. A. M343
Clerget, M. M036
Clesca, P. SU421
Cliffe, J. M301
Cline, G. 1129, F284, SA284, SU343
Clough, J. SU246
Clough, M. M047
Clowes, J. A. 1127, 1165, F094, SA094
Coady, C. 1180
Coates, P. S. 1128, SA112, SU294, M399
Coblyn, J. SU362
Coburn, S. P. SU408
Cochran, D. L. F184, SA184, M011
Cody, D. D. SU073
Coelho, H. S. M. SU331
Coffin, J. 1061, M127
Coffin, J. D. M029, M130
Coffin, L. E. K. SU394
Cohen, S. 1038
Cohen-Solal, M. E. SU255, SU256
Cohlmia, K. SU087
Cointry, G. M071
Cointry, G. R. SU385
Coker, M. 1056
Colaianni, G. SU218
Colbert, M. C. F446, SA446
Cole, D. E. C. M441, WG10
Cole, H. W. 1179
Cole, L. M115
Cole, S. M422
Cole, S. A. 1079
Cole, T. J. F003, SA003, M003
Coleburn, V. E. SA432, SU430
Coleman, W. SU402
Colin, E. M. M189
Colley, S. M. 1076, 1119
Collin, P. SU237
Collin-Osdoby, P. M134, M140, M244, M260
Collins, D. A. F288, SA288
Collins, M. T. SU215, SU387
Colman, R. J. SU154
Colonna, M. M259
Colussi, G. F398, SA398
Colvin, J. SU087
Combes, C. SU373
Composto, R. J. SU057
Compston, J. SU002
Compston, J. E. F360, SA360, SA477
Conditt, M. K. SU380
Conigrave, A. D. M443
Conneally, P. M. 1218, F122, SA122, SA123
Conrad, V. M211
Cons-Molina, F. SA265
Consalvo, A. P. SA362
Conway, T. SU123, SU124, SU126, SU135
Cook, G. J. R. SA334
Cooper, C. 1199, 1213, F282, F286, F339, SA276, SA282, SA286, SA339, SA423, M308
Cooper, G. J. S. M146
Cooper, L. F. SU213, M233
Cooper, M. S. 1035
Coppersmith, S. N. SU048
Copquin, A. M400
Cordero, J. M455
Cordero, Y. SU107
Cordio, M. S. M091
Cordoba, F. M160, M224
Corey, E. SA082, SA088, SU082
Corich, M. SU443
Cormier, C. F104, SA104
Cormier, S. SA140
Cornish, J. 1057, SU151, SU204, SU389, M146, M239
Cornuz, J. 1130
Correa-Rotter, R. 1059
Corsi, A. SU386
Corsi, A. M. M406
Cortet, B. SU021
Costa, J. SA415
Cotten, A. SU021
Counts, C. D. SU328
Courteix, D. 1043
Courtney, J. SA047
Cousins, C. M155
Coutant, K. M347
Couzens, M. 1125
Cowin, S. SU269
Cox, A. J. M333
Cox, G. M293
Cox, T. M. SU228
Coxam, V. SU354
Coxon, F. P. M275
Cozzolino, M. M455
Craig, T. A. M458
Crane, A. M. SU127
Crane, J. L. F389, SA389
Cranney, A. B. SU110, SU343
Crans, G. 1136
Crans, G. G. F356, SA356
Crawford, D. T. 1031, 1107, M392, M395, M397
Crawford, J. A. 1025
Creech, S. D. SU420
Crepaldi, G. F297, SA297, SU284
Crilly, R. G. SU365
Cristallini, S. SA402
Cristino, S. SA188
Cross, H. S. SA481
Csupor, E. SA372
Cueille, C. SA429
Cui, Y. SU072, SU080
Culbert, A. SA089
Cullen, D. M. SU162, SU176, M163, M164
Culler, M. D. SA447
Cumming, R. SU297
Cummings, S. M316, SU028
Cummings, S. R. 1085, 1131, 1208, 1212, F290, SA290, SA306, M321
Cummins, J. SU043
Cundy, T. 1056, 1057
Cupples, A. L. 1060
Cupples, L. A. F275, SA125, SA275, SU143, SU314, M122
Curley, A. J. 1008
Curtin, B. SU053
Cusumano, G. SA352
Cuzick, J. 1170
Czachur, M. SU344

D

D'Amour, P. SU438
D'Avola, G. F297, SA297
D'Erasmo, E. SA287, SA409, SU024
D'Haese, P. C. SA050, M214, M412, M415
D'Ippolito, G. SU444
D'Souza, M. J. M053
D'Souza-Li, L. M438, M441
Daculsi, G. M174
Daems, M. F327, SA327
Dahl, D. C. M410
Dahlgren, J. SA142
Dahlman-Wright, K. F465, SA464, SA465
Dai, J. F085, SA085, SA213, SU150, M064, M065
Dal Canto, N. M121
Dalgarno, D. 1145, SU377
Dallal, G. E. SU093
Dallas, M. SU273, M018
Dallas, S. L. 1005, F056, SA056
Daly, M. M120
Daly, R. SU004, SU005, SU006, M302
Dalzell, N. M168
Dambacher, M. A. SA098, SA336, SA338, SU361, M320, M345, M376
Damiani, D. M439
Damiano, J. SU282
Damron, T. A. M343
Dams, G. M415
Damsky, C. SU060
Daneman, A. SA420
Dang, Z. M186
Daniels, S. R. SA271, SU277
Danielson, M. E. SU146
Danilenko, D. M. 1020
Danish, R. K. M287
Danks, J. A. M434
Dann, P. R. 1063
Dao, H. M001
Daouk, M. M414
Daragon, A. SU412
Dard, M. SU220
Dare, L. C. SU083
Darga, L. M063
Dargie, R. F269, SA269
Darnay, B. G. 1023, 1099, M262
Das-Gupta, V. SU274
DaSilva-Jardine, P. M392, M395
DaSilvaJardine, P. M397
Dauhrer, K. SU339
Daury, M. SU246
Davey, P. SU053
Davicco, M. SU354
David, V. M391
Davie, M. W. J. SU111
Davies, A. S. 1010
Davies, H. SU111
Davies, J. SA224
Davies, K. M. SU123, SU124, SU125, SU275, M362
Davies, M. 1174, SA092
Davies, M. R. 1140
Davies, T. F. 1054
Davis, A. SU040
Davis, A. R. M227
Davis, D. SU364
Dawson-Hughes, B. F275, SA275, SU093
Day, J. S. SU349
Day, R. SU053
De Bacquer, D. F327, SA327
De Broe, M. E. SA050, M214, M412, M415
De Ciechi, P. M281
de Crombrugghe, B. 1070, 1071
De Geronimo, S. SA287
De Grandi, M. C. M409
de Jong, Z. M429
de Jouffrey, S. SU047
De La Piedra, C. SA359
De Laet, C. 1090, SA291
De Luca, V. M180
De Paoli, A. M404
de Papp, A. E. M350
De Rossi, G. SU398
de Vernejoul, M. C. SU255, SU256, SU313
de Vries, T. J. SU245
De-Brum Fernandes, A. J. SA244, SA258
Dean, D. 1160
Dean, D. D. SA457, SU271, M011, M158, M445
Dearlove, A. 1215
Debiais, F. SA138
DeBlasi, G. SU262
Dedhar, S. F029, SA029
Defer, A. SA310, M320
Deftos, L. J. SA443, SA444, SA445, M430, M433
Del Principe, D. SU398
del Rio, L. F013, SA013, SU182, SU291
Delaissé, J. SU078, SU227, SU259
Delaisse, J. M. 1195
Delaney, J. D. SU120, M171
Delaney, M. F. SU334
Delannoy, P. M016
Delany, A. M. 1151, F199, SA199, SA211, M042
Delay, R. SA303
Delbridge, L. M443
Delezoide, A. L. SA140
Delling, G. SA143, SU350
Delmas, P. 1038
Delmas, P. D. 1209, F106, SA106, SA392, SU023, SU101
DeLuca, H. F. 1120, SA383, SU460
Delvin, E. F419, SA419
Delvin, E. E. SA487
Demant, P. SU048
DeMaria, E. J. M398
Demay, M. B. 1030, F038, SA038, M217
Demer, L. L. M229, M261
Demers, C. SA487
Dempster, D. W. 1173, SU324, SU325
Deng, H. W. SU123, SU124, SU125, SU126, SU133, SU134, SU135, M124, M125, M126
Deng, H. Y. SU123, SU124, SU125, SU126, SU135

Deng, W. SU266
Denger, S. M180
Denhardt, D. T. 1044, F054, F236, F442, SA054, SA154, SA236, SA442, SU058, SU059
Deninno, S. L. M395, M397
Denker, A. E. SU401
Dennison, E. M. M308
DePrisco, C. M354
deRosier, A. F252, SA252
Desai, B. R. SU148
Deschamps, P. SU216
Deschênes, C. M446
Deshpande, A. M. SA072, M055
Desphande, A. M. F412, SA412
Detilleux, J. SU114
Detry, R. SA319
Deugnier, Y. SA120
Deutsch, P. SU401
Devareddy, L. SU359
Devine, A. M116
Devogelaer, J. P. SA319
DeVries, E. M333
Dey, A. SA092
Dhaliwal, S. S. M116
Dhanyamraju, R. SU033, M159
Dhawan, P. SU447
Di Fede, G. SA352
Di Munno, O. SU286, SU363
Di Stasio, A. WG11
Diacinti, D. SA409, SU024
Diamond, B. E. SU394
Díaz-Corte, C. M418
Diaz-Curiel, M. SA359, M323
Diaz-Granados, N. SU281, SU316
Díaz-López, J. B. SU142
DiCarlo, E. SU305
Diciolla, F. M110
Dick, I. M. M116
Dickason, A. SA200
Dickson, J. D. F184, SA184
Diel, I. SU074, SU102
Diez, A. SU291
Diez-Perez, A. SU145, M188
Dijkmans, B. A. C. M371, M429
Dimai, H. P. SA368, SU423
DiMarco, N. SU087
DiMarco, N. M. M333
DiMeglio, L. A. SU399
Ding, C. 1064, 1083, F389, SA389, SU393
Ding, G. M378
Ding, K. H. M138, M139
Ding, M. SU349
Ding, N. SA219
Dinh, D. B. SA457
Dini, G. SU398
Dion, N. M002, M446
Dionisi, S. SA409
Dionisi-Vici, C. SU398
Dipollina, G. M442
Disthabanchong, S. SU445
Divieti, P. 1053, 1178, SU444
Dixon, L. B. SA096, SA102
Dixon, S. J. SA453, M278
DjoDjo, S. M354
Djokoto, C. C. M087
Dobashi, H. SU411
Dobnig, H. F111, SA111, SU423
Dodds, R. A. SU213, M403
Dodin, S. M289
Doetschman, T. 1061
Dogan, S. F191, SA191
Doherty, A. M452
Doherty, S. M. SU084
Doi, H. SA037
Doi, M. SA185
Dolan, P. F009, SA009
Dolgilevich, S. 1054
Domb, A. J. M225
Dömeland, W. M024
Donahue, H. J. SU271
Donahue, L. 1047
Donahue, L. R. 1080, 1106, 1217, 1220, SA118, SA152, SU166
Donahue, L. R. B. M148
Dong, J. SU206
Dong, J. Z. SA447
Donnelly, R. SU186
Donohue, M. M. 1030
Donovan, J. L. M017
Doran, P. 1093, 1134
Doria, A. SA420
Dorman, J. S. M313
Dornfeld, K. J. SU034
Dorst, A. SU338, SU339
Doschak, M. R. M044, M428
Dossing, D. A. SU224
Doty, S. B. SU305
Doucet, M. SA074
Dougados, M. SU282
Dougall, W. C. 1024, 1153, M176
Dovio, A. M241
Dow, E. 1135
Dowd, D. R. SU196, SU451
Dowland, N. M263
Dowland, N. R. F075, SA075
Downey, K. J. SU418
Downs, R. W. M398
Doyle, N. SU327
Draper, M. W. M327
Dresner Pollak, R. F146, SA146, SA365
Drevon, C. A. M219
Drezner, M. K. SA393, SA394, SU091, SU092
Drissi, H. 1110, SU197, M254
Drummond, F. M120
Drummond, F. J. SA012
Drysdale, I. P. SA110, SA114
Du, K. 1023, 1099
Du, Q. SA228
Duan, Y. 1167, SA315
Duarte, M. E. L. SA171, SA323, SU050
Duarte, M. L. SU331
Dubé, J. F419, SA419
Dubois, P. SU021
Dubois, S. J. 1169
Ducharme, D. SU177
Ducy, P. 1097
Dufresne, T. E. SU340, M086
Duggan, M. E. F246, SA246
Duggan, R. T. SU104
Dumon, J. C. 1094
Dumont, M. M289
Duncan, E. L. SU127, SU128
Duncan, J. M. SU216
Duncan, R. L. F155, SA155, SU170, SU171
Dunford, J. SA255
Dunford, J. E. SA251, M275
Dunn, F. 1002
Dunstan, C. SU417
Dunstan, C. R. 1020, 1045, 1092, 1134, F081, F369, SA081, SA369
Duong, L. T. 1147, F246, SA246
Duong, T. T. SU053
Dupin-Roger, I. SU368
Duque, G. M002
Durant, D. 1121
Durham, B. F433, SA433, SU425
Durham, B. H. SU109
Dusevich, V. M018
Dusso, A. S. M455
Dutton, J. J. SU109
Duysen, E. F048, SA048
Dvorak, M. M. SA194
Dvornyk, V. SU125, SU134
Dworakowski, E. SU437
Dynder, A. SU401
Dysseleer, A. SA319

E

Eagleton, A. C. F109, SA103, SA109
Earle, K. SA401
Eastell, R. 1035, 1127, 1132, 1144, 1165, 1170, F094, F109, F113, SA094, SA103, SA109, SA113, SA129, SA280, SA342, SU292, M369
Ebbinghaus, C. F. M395
Eberle, J. SU329
Ebert, D. SA200
Ebetino, F. H. SA251, SA255, SU341
Ebrahimpour, P. SU209
Eckstein, F. M072
Economides, A. N. SA198
Econs, M. 1139
Econs, M. J. 1081, 1218, F122, F398, SA122, SA123, SA398
Edgar, C. M234
Edgar, C. C. SA065
Edgar, C. M. M031, M152
Edelson, G. WG3, WG7, WG8
Edwards, B. J. M299
Eggenweiler, S. SU379
Eghbali-Fatourechi, G. 1009
Egrise, D. SA425
Eguchi, T. SA043, SU153
Eichenberger Gilmore, J. M. M005
Eichhorst, K. R. F488, SA488
Eick, D. M018
Eid, K. M161
Eiden, M. V. M037
Einhorn, T. M152
Einhorn, T. A. SA065, M031, M136
Eisman, J. M353
Eisman, J. A. 1086, 1104, 1117, 1203, F256, F458, F460, SA014, SA256, SA458, A460, SU283, SU297
Ejiri, S. SA057
El-Hajj Fuleihan, G. SU289, M414
ElAlieh, H. Z. F159, SA159, SU428
Elango, N. M193
Elango, S. M193
Eliseev, R. A. M053
Elliott, M. E. SU328
Elliott, N. C. M395
Ellis, J. SU257
Elloitt, J. F081, SA081
Elsubeihi, E. S. M328
Elver, K. SU089
Elze, L. SU133, M124
Emans, S. J. M389
Emi, M. 1044, SU140
Emkey, R. 1059, F339, F341, SA339, SA341
Emons, G. M184
Encinas Dominguez, C. F488, SA488
Endo, Y. SA355
Engelbert, R. 1105
Engelke, K. SA351
Engsig, M. T. SU227
Enjuanes, A. M188
Enokida, M. SU347
Enriquez, R. F. 1117, 1125
Ensrud, E. R. 1214
Ensrud, K. 1138, F011, SA011, SU028, SU382, M316, M352
Ensrud, K. E. 1085, 1208, 1214, F290, SA290, SA305
Epstein, J. M054
Epstein, S. 1018
Erben, R. G. F414, SA414, SA474, SU327, SU329
Erceg, I. SU039, M215, M216
Ercolano, M. SU280
Ergun, D. L. SU086
Eriksen, E. F. 1041, SA342, M145
Eriksson, A. L. SA464, SU139
Ernst, M. 1073, 1123
Ersfeld, D. L. M290
Escobada, A. F400, SA400
Escobar-Jiménez, F. M309
Eshleman, A. SU270
Eska, D. SU306
Eskridge, T. F277, SA277
Espinosa, L. SA229
Ettinger, B. 1136, SA298
Ettinger, M. F341, SA341
Euller-Ziegler, L. M181
Evans, A. F203, SA203
Evans, A. E. SA202
Evans, C. E. SU055, SU158
Evans, G. SU029
Evans, G. L. M157
Evans, H. SA166
Evans, J. M242
Evans, R. W. M306
Evans, W. E. 1081, F398, SA398
Evdokiou, A. M210, M230
Evenson, K. F069, SA069
Everts, V. SA222, SU065, SU245
Evron, T. F048, SA048
Ewing, S. F106, F115, SA106, SA115, M316
Ewing, S. K. F290, SA290
Ezura, Y. 1044, SU140

F

Fabbro, D. SA086
Faber, H. SU338, SU339
Facchini, A. SA188
Faccio, R. M258, M259, M267
Faciszewski, T. SA283, SU293, \ M330
Fahrleitner, A. F111, SA111, SA368, SU423
Falany, M. L. SU268
Falchetti, A. SU136, M121, M406
Falcini, F. SU136
Falcon, J. M400
Falconi, D. M221
Falzon, M. SU458
Fan, X. 1096, SA177
Farach-Carson, M. C. M453
Fardellone, P. SU412
Farenga, M. SU348
Farias, M. F. SU331
Farias, M. L. F. SA171
Farina, M. SU050
Farkas, A. SA049
Farmer, C. K. T. 1141
Farmer, P. M447
Farmer, R. W. SU049
Farquharson, C. SA163, M040
Farrugia, A. M230
Fassbender, W. J. M413
Fassi, J. SU280
Faulkner, K. G. SU086, SU092, M073, M089, M104
Favus, M. 1059
Favus, M. J. SA096
Fawkner, M. 1056
Feak, J. M343
Fedarko, N. S. F052, SA052
Feick, P. M408
Feldman, D. F456, SA456
Feldman, G. J. WG4

Feldman, H. M389
Felker, S. M103
Felsenberg, D. F113, F343, SA113, SA343, SU345
Feng, J. Q. 1005, F016, F042, SA016, SA042
Feng, X. 1019, F243, SA228, SA243, SU260
Fenske, J. S. M290
Ferencz, V. SA372, SA382
Ferguson, R. F302, SA302, SU022
Ferguson, V. L. 1045, F369, SA025, SA369
Ferko, N. SA289, M293
Fermand, J. P. M075
Fernández-Martín, J. L. M418
Fernandez-Metzler, C. F246, SA246
Fernandez-Seara, M. A. M094
Fernstrom, M. H. M399
Ferrari, S. 1201
Ferrari, S. L. 1060, 1062
Ferraris, M. SU286
Ferrell, R. E. SU146
Ferretti, J. L. SU385, M071
Ferris, A. SU359
Ferró, T. SU390
Ferrucci, L. SU309, SU310, M406
Festuccia, C. SA086
Fiasche, R. SA406
Fiaschi-Taesch, N. M. 1102
Fidler, I. J. SA074
Filella, X. SU390
Filho, H. M. M439
Filiatreault, M. F419, SA419
Filipponi, P. SA402
Filke, S. SU248, SU249
Filmon, R. SU052
Finch, J. L. SU457
Findlay, D. M. M210, M230
Finger, J. SU235
Finigan, J. SU292
Finkelstein, J. 1039, SU378
Finkelstein, J. S. 1007
Finnegan, P. M. F405, SA405
Fisch, C. SA447, SU047
Fish, S. M385
Fisher, J. E. F246, SA246
Fisher, J. L. F081, SA081
Fisher, L. W. F052, SA052, SA154
FitzGerald, M. G. M123
Fitzgerald, S. F387, SA387
Fitzpatrick, L. SA383, M299
Fitzpatrick, L. A. 1173, SU352
Fjording, M. S. SU259
Flanagan, J. L. F458, SA458
Flanagan, S. M200
Flanagan, S. D. 1113
Fleet, J. C. M448, M454
Flemming, R. M040
Floege, J. M413
Flores, R. H. F300, SA300
Flynn, A. 1119
Flyvbjerg, A. SU025, M147
Foged, N. T. SU227, SU259
Fogelman, I. 1141, SA128, SA334, \ SU085, SU088, SU098, M080, M101, M358
Foldes, A. J. SA365
Foldspang, A. 1137
Folk, D. SU366
Fong, C. F458, SA458
Fonteles, F. J. S. SU331
Ford, L. SU399
Ford, N. L. M098
Forman, L. A. SU051
Foroud, T. 1081, 1218, F122, SA121, SA122, SA123
Forsén, L. SU312
Forsmo, S. SU312
Forster, R. SA447
Fortier, I. SA258
Fortunati, D. SA175
Foster, B. L. F024, SA024
Foster, S. A. SU051
Fournier, B. SA196, M190
Fowler, S. F381, SA381
Fox, C. M316
Fox, S. W. F259, SA259
Fraher, L. J. SA453
Francalanci, P. SU398
Franceschi, R. T. SU192
Franci, M. B. 1166, M396
Francis, R. SA092
Franck, H. SA090, SA421
Francuz, T. SA430
Frank, E. SU450
Frank, O. M232
Franzson, L. SU439, M006
Fraser, D. G. 1134
Fraser, M. SU295
Fraser, R. B. 1132
Fraser, W. D. F433, SA266, SA433, SU109, SU425
Fratzl, P. SA388
Fratzl-Zelman, N. SA388
Frediani, B. F297, SA297, SA402
Frelut, M. M001
French, M. R. F279, SA279
Freundlich, M. M411
Frick, K. K. SA178
Friedlander, G. 1055
Friedman, P. A. F451, F452, SA451, SA452, SA454
Friedman, S. M409
Frigato, M. SU315
Frija, J. M075
Friso, S. SU143
Frisoli, A. M394
Froberg, K. SU020
Froelich, C. J. F087, SA087
Frolik, C. A. 1135
Frosch, K. M184
Frost, M. SA128, SU098
Frost, M. L. SA334
Fu, Q. 1176, SU194
Fu, W. M. SA174
Fuchs, P. M232
Fuchs, R. K. F165, SA165
Fudge, N. J. M437
Fueg, M. 1201
Fujii, M. M023
Fujikawa, K. SA059
Fujiki, R. 1050
Fujisawa, T. SU153
Fujise, N. SA238
Fujishima, T. SU455, SU456
Fujishiro, M. F087, SA087
Fujita, H. SU298
Fujita, K. F137, SA137
Fujita, M. SA205
Fujita, T. 1118, 1143, 1182, SA156, SA205, SA308, SA411, SU035, M085, M128
Fujiwara, I. SU383
Fukagawa, M. F408, SA408
Fukuda, A. 1150, SA416
Fukuhara, E. SU208
Fukumoto, S. 1143, 1182, SA205, SA411, SU035, M128
Fukunaga, M. SA169, SA357, M061, M342
Fuller, K. F230, SA230
Fullerton, D. M017
Fung, Z. F186, SA186, SU079
Funk, J. L. SU418
Furlan, F. M212
Furukawa, H. SA260
Furukawa, K. SU056, M426
Furushima, K. SA386
Furuya, K. M393
Furuya, Y. F410, SA410
Fuson, T. R. SU231, SU234

G

Gabay, C. F321, SA321
Gabel, C. A. 1107
Gabriel, A. SU114
Gaddy-Kurten, D. 1168, F079, SA079, SA080
Gafni, Y. M225
Gagnon, D. R. F275, SA275
Gaillard, M. M382, M383
Gaillard-Kelly, M. 1027, M379
Gaines, K. A. M353
Galbiati, E. WG2, WG6
Galecki, A. T. SU122
Gálfi, M. SA049
Galindo, M. 1112
Gallacher, S. J. F269, SA269
Gallagher, J. M386
Gallagher, J. C. 1164, F358, F381, SA358, SA381, M285
Galli, B. SA404, M076
Galloway, D. S. SU358, M366
Galmozzi, F. SA022
Galson, D. L. 1175, SU264
Galvin, R. J. S. SU231, SU234
Gamba, A. M409
Gamse, R. F064, SA064
Gandolini, G. F297, SA297
Gange, C. SA242, SU243
Gangji, V. SA425
Gannon, F. SU040, M180
Gannon, F. H. F417, SA417, M227
Gao, H. F465, SA464, SA465, M395
Gao, P. F408, SA408, SU438
Gao, Y. F330, SA093, SA330, SA467, M178
Garcés, M. M323
Garcia, A. J. M201
Garcia, I. F321, SA321
Garcia-Giralt, N. SU145, M188
Gardella, T. J. SA448, SU426, SU427, SU440
Gardiner, E. M. 1117, 1125, 1203, F256, F458, F460, SA256, SA458, SA460
Gardner, M. J. SU104
Garel, J. SA429
Garg, M. SA062, SU003, M424
Garinei, P. SA402
Garman, R. 1047
Garnero, P. 1209, F106, SA106, SU023, SU101, SU319, SU417
Garra, B. S. M103
Garrett, I. R. F071, SA071
Garrett, R. F400, SA400
Garry, P. J. SA329
Gascon-Barré, M. M446, SA487
Gasser, J. A. F064, F099, SA064, SA099, M390
Gates, J. J. M069
Gathings, B. F473, SA473
Gatto, S. F297, SA297
Gaudino, G. SU218
Gaufillier, S. SU068
Gaumond, M. 1187, SA195
Gautvik, K. M. SU200, M219
Gautvik, V. T. SU200
Gavrilov, K. L. M419
Gay, I. M158
Gay, J. D. L. SU110
Gayet, A. SU412
Gazit, D. M225
Gazit, Z. M225
Gazzerro, E. SA198
Gearhart, B. SU043
Geba, G. P. M350
Gehron Robey, P. SU386, M228
Geist, D. J. SU171
Gelb, B. D. SA388, SU065
Gelb, N. F146, SA146
Gelbert, L. 1135
Gelczer, R. F288, SA288
Gelfin, Y. M314
Geller, A. 1178
Genant, H. SA166, SA316, SU019
Genant, H. K. 1041, 1212, F343, F360, F403, SA343, SA360, SA403, SU092, SU095, M327
Genetos, D. C. SU170, SU171
Genever, P. F048, SA048
Geng, Z. 1045, F369, SA369
Gennari, C. 1166, M105, M110, M121, M396
Gennari, L. 1166, SA404, M076, M105, M121
Gensure, R. C. SA448
Gentile, M. A. F246, SA246, SA331
Gentili, C. SU432
Gentzsch, C. SA143
Geoffroy, V. M190
George, A. F300, SA190, SA300
Gerdhem, P. SU303
Gerichhausen, M. J. W. M365
Germain-Lee, E. L. F389, SA389
Gerstenfeld, L. C. SA065, M031, M136, M152, M196, M234
Gerzer, R. M359
Gesicki, M. 1171
Getz, B. M223
Getz, B. J. M187
Geursen, A. M408
Geusens, P. SU417, M365
Ghatge, K. SA280
Ghayor, C. 1124, SA212
Ghiglione, F. M071
Ghosh Choudhury, G. SU045
Ghosh-Choudhury, N. 1122, SU045
Giangregorio, L. M. M099
Gianluca, T. M178
Giannini, S. SU285
Gibson, B. SA445
Giger, M. L. SA096, SA102
Gilbert, L. SU205
Gilberto, D. SA331
Gilbride, J. F341, SA341
Gillespie, M. T. 1073, 1123, F081, SA081, SA242, SU243, SU257, M435
Gilligan, J. P. SA362
Gillis, K. SU193
Gimble, J. M. M233
Gingery, A. M273
Gingras, R. 1187
Ginty, F. F003, M003, SA003
Giorgino, R. F297, SA297, SU284, SU285, SU286, SU287, SU309, SU310
Giovani, S. SA404, M076
Givol, D. 1070
Giza, E. M004
Glackin, C. M200
Glackin, C. A. 1113
Glantschnig, H. 1146
Glass, N. SU334
Glatt, M. 1123
Glatt, V. 1062
Glendenning, P. SA434
Glesne, D. M253
Glimcher, M. J. M252
Globus, R. K. SU060
Glorieux, F. H. SU401, SU406

(Key: 1001-1222 = Oral, F = Friday Plenary poster, SA = Saturday poster, SU = Sunday poster, M = Monday poster, WG = Working Group Abstract)

Glowacki, J. SA167, M030, M161
Gluck, O. SA298
Glüer, C. C. F113, SA113, SU350, SU381
Glüer, M. G. SU381
Gluhak-Heinrich, J. SU063
Glynn, N. W. SA271, SU277
Gminski, J. G. SA430
Gnudi, S. SU315
Goad, M. 1001
Godang, K. SA324
Goddard, D. SU095
Goddard, P. E. 1035
Godfrey, K. M. SA276
Godin, É. 1187
Godin, E. SA195
Goel, N. F309, SA309
Goel, P. 1200, M007, M008
Goemaere, S. J. A. F327, SA327
Goette-Jaime, M. SA265
Gold, D. T. SU380
Goldring, S. R. 1175, SU264
Goldsmith, C. H. SA289, SA340, SU296, M081
Goldstein, S. A. 1173, SU061, SU122
Goltzman, D. 1028, 1029, 1052, 1154, F391, F439, SA141, SA391, SA439, SA441, SU343
Gomberg, B. R. M095
Gomelsky, M. F006, SA006
Gómez, C. SU142
Gong, G. SU121
Gonnelli, S. 1166, SU285, M105, M110, M121, M396
Gonzalez, E. A. SU445
Gonzalez Pardo, V. M450
González-Carcedo, A. M418
Gonzalez-Macias, J. SA127
Gonzalves, D. SU397
Goodell, M. A. M227
Goodman, E. M389
Gorai, I. F130, SA130, SU026, SU113, M106
Gordeladze, J. O. M219
Gordon, C. M. M389
Gordon, S. A. F249, SA249
Gori, F. F038, SA038
Gorlick, R. G. M055
Gorny, G. A. M273
Goss, M. SA430
Goto, B. M085
Goto, H. SA397
Goto, M. SA156
Goto, T. SU208
Gozzini, A. M406
Grabner, B. M. SA388
Grace, E. M389
Grandchamp, B. 1055
Grande, M. T. M438
Grant, W. 1100
Grasser, W. A. 1107, M392, M395, M397
Grassi, F. SA188
Grauer, A. SU379
Graves, D. T. M136
Graves, L. SA485, M370
Grecco, K. J. SU376
Green, J. R. F064, SA064
Green, R. P. M082
Greenblatt, D. M292
Greendale, G. A. 1207, SU300
Greene, D. SU144
Greene, M. I. SA257
Greenfield, D. M. SU292
Greenfield, E. M. SA213, SU150, M269
Greenspan, S. SU382
Greenspan, S. L. 1040, 1128, SA112, SU294, M399
Greenwald, L. M100
Greenwald, M. M100
Greenwalt, D. E. M270
Greiner, S. M. 1093
Greitbauer, M. M111
Grenet, O. SA240
Grey, A. SU204
Grey, A. B. SU151, M146
Griffin, K. M452
Grigoriadis, A. E. M052, M255
Grinberg, D. SU145, M188
Grinnell, N. C. M115
Gritters, M. M415
Grizon, F. SU052
Gronowicz, G. M029
Gronowicz, G. A. F437, SA437
Gronthos, S. F218, SA218, M228
Gros-van Hest, M. M185
Gross, A. M297
Gross, C. M420
Gross, T. S. 1046, F157, SA157, SU181
Grover, A. M209
Grubb, A. M256
Grubbs, B. SU072
Grubbs, B. G. SU075, SU080, M059
Gruber, B. M097, M114
Gruenstein, E. F446, SA446
Gruenthal, K. M122
Grundberg, E. SA126
Grundker, C. M184
Grynpas, M. D. 1219, M087
Grzella, I. M364
Grzesik, W. J. M039
Gu, H. 1149
Gu, R. SA192
Gu, S. SU272
Guañabens, N. F013, SA013, SA332, SU390
Gubrij, I. 1176
Guerra, G. M438
Guess, H. A. 1208
Gugala, Z. SU040
Guggenbuhl, P. SA120
Guglielmetti, M. SA312
Guido, V. SA118
Guillemant, J. A. SU097
Guillemant, S. E. SU097
Guillotin, B. M211
Guise, T. A. SU072, SU075, SU080, M059, M060
Gujral, A. SA444
Gulanski, B. I. SU330
Gulde, S. SU341
Gunaratne, G. H. M088
Gundberg, C. M. 1180, M047, M389
Gunter, M. J. SA294
Gunter, T. E. M053
Gunther, C. W. M363
Guo, D. 1159
Guo, F. W. SU001
Guo, J. 1066, 1177
Guo, R. F151, SA063, SA151, SU371
Guo, X. SA004, SA005, SU400
Guo, Y. SA051
Gupta, A. F071, SA071, M037
Gupta, J. 1059
Gurley, K. F024, SA024
Gustafsson, J. Å. F465, SA464, SA465
Gustavsson, A. H. M004, M137
Guthrie, J. F056, SA056
Gutierrez, G. 1189, M092
Gutierrez, S. M198
Gutzwiller, S. M190
Guyon-Gellin, Y. 1095, SU372, SU374, SU375
Gvirtz, G. SU397

H

Ha, E. M007, M008
Ha, H. SA209
Haas, N. P. M147
Haase, V. 1152
Haberland, M. 1171
Hadji, P. M311, M312
Hadjiargyrou, M. F036, SA036, SA045, SU166
Haga, N. SA416
Hagen, C. M402
Hagen, J. SU410
Hagenauer, B. M050
Hagg, R. M033
Haggarty, N. W. SU151
Hagino, H. SA293, SU347, M342
Hagiwara, S. SA299
Hahn, P. SA481
Hahn, T. J. M229
Haidar, R. SU289
Haigh, C. F091, SA091, SA092
Hailey-Zitlin, V. SU359
Hair, G. A. SU198, M045, M068
Hajime, O. F144, SA144
Hakim, I. SU147
Hakim, I. A. SA278
Halabe, A. SU397
Halczenko, W. F246, SA246
Halladay, D. L. 1135, SA361
Halleen, J. M. SA108, SU103, SU229
Halleux, C. SA196
Halloran, B. M177
Halloran, B. P. F159, SA010, SA159, SU428
Halsey, J. P. SA266
Halstead, L. 1158
Halstead, L. R. 1017
Halvorsen, Y. M233
Ham, S. SA268
Hamazaki, M. SA416
Hamel, M. E. M081
Hamersma, H. 1077
Hamidi, M. SU281
Hammami, M. SU404
Hammond, L. J. SU357, SU358, M366
Hampel, R. SU306
Hampson, G. 1139, 1141, SA128, SU098, M358
Hamrick, M. SU177
Hamulyak, K. M365
Han, B. M160
Han, I. SU076, M118
Han, J. H. SU422
Han, K. SU076, M118
Han, L. 1032, 1058, 1190, F173, SA173, SU185, M380
Hanada, K. M393
Hance, K. M454
Hanemaaijer, R. M051
Hankenson, K. D. 1069
Hanley, D. A. F343, SA340, SA343, SU296, SU343, SU366, M428
Hannan, M. T. 1087, 1210, F275, SA125, SA275, SU314
Hannon, R. A. 1170, SU342, SU292
Hans, D. 1201
Hansen, B. F165, SA165
Hansen, I. A. SU431
Hansen, M. F. F412, SA072, SA412, M055, M066
Hansen, T. B. M402
Hao, G. M237
Hara, K. M014
Hara, P. SA326
Harata, S. SU056, M426
Hardin, R. R. M445
Harding, B. 1008, 1215
Harel, M. SU397
Harley, C. H. SU366
Harmey, D. M255
Harper, K. D. F356, SA356, SA357
Harper, L. SA303
Harrington, T. J. SA344
Harris, F. 1131
Harris, K. W. M058
Harris, M. A. 1159
Harris, S. E. 1005, 1159, F016, F042, SA016, SA042, SU063, SU273
Harris, S. S. SU093
Harris, S. T. 1212
Harris, T. 1131
Harris, T. B. F311, SA311
Harrison, D. 1162
Harrison, E. J. SU018
Harrison, J. R. 1026, 1162
Hartman, G. D. F246, SA246
Harvey, A. SA476
Hasegawa, H. 1182, M128
Hashimoto, J. SU026, M106
Hashimoto, N. 1196
Hashimoto, S. F254, SA254
Hashimoto, T. SA077
Hasid, R. SA322
Haslmayer, P. M050
Hassan, M. Q. M196, M198
Hastings, R. H. SA445, M430
Hata, K. 1109, SA262
Hata, R. SU210
Hathway, G. F150, SA150
Hattori, T. SA028
Hauache, O. M. M439
Hauge, E. SA313
Hauge, E. M. M402
Häusler, K. D. SU243, SU257
Hausser, H. J. SU184
Haussler, C. A. F488, SA488
Haussler, M. R. F488, SA488
Hauzeur, J. SA425
Havill, L. M. SU130, SU131
Hawker, G. F339, SA339, SU317, SU364
Hawker, G. A. F279, SA089, SA279
Hawkes, W. SA296
Hawkins, F. M307
Haÿ, E. SU031
Hay, E. SU188
Hayakawa, N. SA376, SA377, SA379
Hayashi, K. SA378, SU346, M021
Hayashi, T. SA299
Hayashi, Y. M425
Hayashizaki, Y. SU252
Hayes, A. 1007, 1039
Hayes, T. 1077
Hayman, A. R. SU228
Haynatzka, V. M285
Haynatzki, G. 1164, F358, F381, SA358, SA381, SU275
Haynatzki, G. R. SU162, M163
Hazes, J. M. W. M429
He, B. 1052
He, J. SA192, M148
He, J. W. M125
He, P. M269
He, X. M447
He, Y. Z. SU424
Healy, D. R. M395
Heaney, R. P. SU351, M362, M451
Hebel, J. SA296
Hebela, N. F387, SA387
Hebert, K. M196, M234
Hedner, T. SU139

Heegaard, A. 1194, SU078
Heer, M. M359, M364
Heersche, J. N. SA153
Heersche, J. N. M. SU169, SU251
Hefferan, T. E. F440, SA440
Hegde, M. 1056
Heidl, M. M390
Heim, M. SU449, M232
Heino, J. SU132
Heinonen, A. O. M387
Helfrich, M. H. 1191, M208
Helgason, C. D. F403, SA403
Helkala, E. SU009, SU011
Heller, H. J. M416
Hellmeyer, L. M311
Henderson, J. E. 1154, SA141
Henderson, K. SU297
Hendriks, J. M. A. SU201
Hendry, J. M033
Hendy, G. N. 1029, F385, SA385, M204, M440, M441
Henriksen, K. SU227
Henriksen, L. M324
Henriksen, Z. SU156
Henry, H. L. SU448, SU449, SU452, M449
Henry, M. J. M338
Hentunen, T. SA108
Hentunen, T. A. M048
Herbert, A. G. 1060
Hermann, J. SA368
Hernandez, C. SU116, SU117
Hernandez, C. J. SU321
Hernandez, E. SU421
Hernando, N. M037
Herndon, D. N. SA418, SA477
Herpertz-Dahlmann, B. M364
Herrera, B. SA380
Hertz, M. SA374
Herzog, H. 1125
Hessle, L. 1011
Hesslein, D. G. T. 1098
Hewison, M. 1035
Hibi, Y. SU207
Hicks, A. L. M099
Hicok, K. C. M233
Higashi, S. SA376, SA377, SA378, SA379
Higashio, K. SA238
Hill, B. L. SU075, SU204
Hill, D. 1020
Hill, D. D. M303
Hill, J. F277, SA277
Hillier, T. 1085, M316
Hillier, T. A. 1212, F290, F292, SA290, SA292
Hilton, R. M. 1141
Hinch, A. M301
Hinkley, H. J. SA110, SA114
Hinsemkamp, M. SA425
Hippomène, V. 1027
Hiraga, T. M427
Hirahara, F. F130, SA130, SU113
Hirai, H. 1006
Hiraki, Y. F046, SA046
Hirano, T. SU349
Hiraoka, H. M023
Hirata, K. F018, SA018
Hirschi, K. D. M227
Hisamatsu, T. M271
Hishiya, A. SU027
Hitchcock, C. L. M355
Hiura, K. F197, SA077, SA197
Hixson, J. E. 1079
Ho, A. Y. Y. 1169
Ho, J. SA209
Ho, K. J. SU129
Ho, S. C. SU030, SU311
Hoang, D. 1019
Hochberg, M. F106, SA106, M296, M316
Hochberg, M. C. 1085, F292, F300, SA095, SA292, SA300
Hock, J. M. F040, SA040, SU434
Hodam, T. L. SA489
Hodge, J. M. M272
Hodgkinson, I. M. SU018
Hodsman, A. B. SA453, SU343
Hofbauer, L. C. M184
Hoffman, S. J. SU083
Hoffmann, O. M050
Hofmeister, A. M. SU212
Hogan, H. A. M172
Holdsworth, D. W. M098
Holick, M. F. SA418, SU071, M451
Holl, M. SU157
Holliday, K. M287
Holliday, L. S. F223, SA223
Holmäng, A. SA142
Holme, I. M324
Holmquist, B. M449
Holroyd, B. H. SU366
Holst-Hansen, C. SU078
Holt, C. M113
Hong, J. S. SA172
Honkanen, R. M361
Honma, H. M090
Hoogendam, J. M026
Hook, V. H. SA445
Hoover, C. M401
Hoover, J. SA476
Hoover, J. L. 1179
Hopkins, M. F433, SA433, SU425
Horcajada, M. SU354
Horiki, M. SU236
Horn, D. F016, SA016, M092
Horne, W. 1097
Horne, W. C. 1100, F225, F263, SA225, SA231, SA257, SA263, SU262, M265, M280
Horner, A. F139, SA139
Hornstein, M. SU334
Horowitz, M. C. 1014, 1098
Horseman, N. D. SU070
Horst, R. L. 1028
Horton, J. M343
Horton, L. G. 1220
Horvath, C. SA092, SA132, SA133
Horváth, C. SA372
Horvath, C. SA382
Horwood, N. J. SU257
Hosaki, Y. M085
Hoshi, K. 1072
Hoshi, M. SA238
Hoshino, E. SA376, SA377, SA379
Hosking, D. 1037, SU345
Hosoi, T. SU140, M407
Hosoya, A. M206
Hosoya, M. SA021
Hosszu, E. SA382
Hou, W. SU065, M197
Houghton, A. SA200, SU049, M207
Housman, D. E. M122
Houwing-Duistermaat, J. 1221
Howard, G. A. SU444
Howard, K. SA472
Howard, T. F239, SA239
Howarth, E. SU084
Hoyle, N. F109, SA109, M057, M348
Hoyle, N. R. SU114
Hruska, K. A. F236, SA236, 1140, SU212, SU265, SU267, M056
Hsieh, S. S. SA170, SU159
Hsu, H. SU129
Hsu, H. H. T. SA027, SU033
Hu, B. F463, SA463
Huang, D. C. 1028, M431
Huang, H. 1005
Huang, J. C. M177
Huang, L. SA076
Huang, M. 1207, SU300
Huang, P. L. 1101
Huang, Q. R. M125, M126
Huang, Q. Y. SU123, SU124, SU125, SU126, SU135
Huang, S. 1135
Huang, T. H. SA170, SU159
Huang, W. F234, SA234, M235
Huang, X. F239, SA239
Huang, Y. SU429, M140, M244
Huang, Z. M417
Huard, J. SU043
Huart, V. 1055
Hubbard, N. J. SU061
Hue, T. SU382
Huening, M. M147
Hughes, C. 1138
Hugueny, P. SA392
Hui, C. 1154
Hui, S. L. 1218, F122, SA122, SA123
Hume, C. SU004
Hume, D. A. SU252
Humphries, R. K. F403, SA403
Hung, W. Y. M376
Hunt, K. J. SU164
Hunter, D. M356
Hunziker, W. SU449, M232
Huo, R. 1029, 1154, F439, SA439, SA441
Huq, N. 1140
Hurley, M. M029
Hurley, M. M. 1061, SA136, M127, M130
Hurst, I. R. F223, SA223
Hurtig, M. B. SA116
Hurwitz, S. SU334
Hussain, N. F309, SA309
Hutchinson, J. H. F246, SA246
Hvid, I. SU349
Hwang, C. SU076
Hwang, M. SU384
Hwang, R. F337, SA337, SU258

I

Ibach, K. SU338
Ichida, F. 1109
Ichijo, H. SU173
Ichikawa, K. M393
Ichikawa, L. E. M284
Ichikawa, Y. M346
Ichimura, S. SA059, SA375
Ichinose, S. SA021
Ide, M. M346
Iejima, D. M010
Igarashi, Y. SU383
Iglesias, R. C. M069
Iguchi, H. M432
Iida-Klein, A. SU324, SU325, M220
Iijima, T. SU247
Iinuma, K. SU383
Iitaka, M. SA237, SA426
Ikari, Y. M014
Ikeda, F. 1109, SA262
Ikeda, K. SA407, SA483, SU027
Ikeda, M. SA134
Ikeda, S. SA363
Ikegame, M. SA057
Ilich, J. Z. M325, SU323
Ilievska, N. M435
Imai, K. SU210
Imai, S. SA008
Imai, Y. F201, SA201
Imamura, T. M023
Imanishi, Y. 1139, SA397, SA399
Imbriaco, R. SU136
Imkie, M. M159
Inaba, M. SA397, SA399
Inaba, T. M276
Inada, M. 1197, F130, SA130, SU066
Indridason, O. S. SU439, M006
Inkson, C. A. F048, SA048
Inoue, D. 1036, F058, SA058, SA077
Inoue, H. SA037
Inoue, I. SA386, M021
Inoue, J. M245
Inoue, M. SA455
Inoue, N. SA455
Inoue, S. SU140, SU183
Inoue, T. SA023
Inskip, H. M. SA276
Insogna, K. 1180, F214, SA214, M142
Insogna, K. L. SU396, M337
Inui, A. 1125
Inui, K. SU353
Inui, T. SA067
Ioannidis, G. SA289, SA340, M293
Iolascon, G. F297, SA297
Ionescu, A. M. SU041
Iozzo, R. V. 1068
Ippolito, E. SU386
Ireland, D. SU002
Isales, C. M. M138, M139
Ish-Shalom, S. SA322
Ishibashi, H. SU298
Ishibashi, O. SA057, SA067
Ishida, K. M235
Ishida, R. SU140
Ishida, Y. M372
Ishihara, H. F064, SA064
Ishijima, M. 1044, 1156, F442, SA442, SU058, SU059, SU173
Ishikawa, I. 1034, SA250
Ishimura, E. SA023, SA397, SA399
Ishizuka, S. SU452
Islam, K. K. SU420
Ismail, A. SA461, SU073
Israel, E. SU334
Isshiki, M. SA486
Itabashi, A. SA357, SU342, M342
Ito, A. 1116, SA355
Ito, H. SU140, M329
Ito, M. 1061, SA363, SA377, SA378, SU027, SU346, M130, M344
Ito, Y. 1036, SU353
Itoh, G. M346
Itoh, K. SU233, SU240, SU241, SU242
Itoh, M. M202
Itoi, E. F288, SA288, M329
Itoman, M. SA349
Ittel, T. H. M413
Ittenbach, R. F006, SA006
Iuliano-Burns, S. SU004, SU005, SU006
Iuliucci, J. 1145, SU377
Ivaska, K. SU225, SU226
Ivaska, K. K. SU103, M048
Iwamoto, J. SA375
Iwaniec, U. T. SU060, SU370, M133
Iwasaki, H. SU140
Iwasaki, K. M426
Iwata, K. M427
Izawa, T. M425
Izukuri, K. SU210
Izumi, Y. M039

J

Jaakkimainen, L. SA089, SU364
Jackson, K. J. A. M227
Jackson, R. D. 1089, M300, M336, M367
Jackson, S. A. SA285
Jacobs, T. P. SU395

Jacques, P. 1210
Jacques, P. F. SU143
Jaffre, B. M109
Jaffré, C. 1043
Jäger, W. M050
Jagger, C. F230, SA230
Jaglal, S. SU317, SU364
Jaglal, S. B. SA089
Jahnen-Dechent, W. M012
Jahng, J. SU137
Jain, A. F052, SA052
Jaiswal, N. SA200
Jakes, R. M168
Jakob, F. 1082
Jakob, O. SU431
Jalava, T. F091, SA091, SA092, M301
Jamal, S. A. SA306
James, L. J. F184, SA184
Jan de Beur, S. M. 1083, F387, SA387
Janckila, A. J. SA107, SA108
Jang, H. SU076
Jankowsky, M. M207
Jankowsky, M. L. SU049
Jansen, M. 1105
Jarvinen, M. 1048
Järvinen, M. J. SA346
Järvinen, T. A. H. SA346
Jarvinen, T. L. N. 1048
Järvinen, T. L. N. SA346
Javaid, M. K. F282, SA276, SA282, M308
Javed, A. 1004, 1110, M198, M254
Javier, J. M378
Jee, W. S. S. 1031, 1107, F206, SA206
Jefcoat, S. C. F186, SA186
Jefferies, D. M040
Jelinek, D. F073, SA073
Jemtland, R. SU200
Jenkins, B. J. 1073, 1123
Jennane, R. SU010
Jennings, M. SU213
Jensen, C. SU195
Jensen, T. SU195
Jenson, F. M108
Jeon, Y. C. M339
Jepsen, K. J. SU116, SU117
Jerome, C. P. F064, SA064
Jesudason, D. R. F482, SA482
Ji, X. F206, SA206
Jia, D. SA153
Jia, Y. SU169
Jiang, D. SU192
Jiang, J. X. SU160, SU272
Jiang, Y. 1041, F360, F403, SA360, SA403, M327
Jilka, R. L. 1013, 1032, 1058, 1176, 1190, F173, SA173, SU185, M380
Jin, Y. SU258
Jing, X. F137, SA137
Jinnai, K. SA156
Jódar, E. M307
Johannesson, J. P. SU439, M006
Johansson, H. 1090
John, R. F113, SA113
Johnell, O. 1090, 1163, F286, SA286, SA291, M294, M352
Johnsen, S. A. 1016, SA179, M187
Johnson, C. SA331
Johnson, D. M423
Johnson, E. SU073
Johnson, J. A. SU366
Johnson, K. A. 1011
Johnson, M. L. 1081, SU176, M123, M163
Johnson, P. SA303
Johnson, R. S. 1152
Johnson, T. D. F343, SA343
Johnson-Pais, T. M055
Johnston, C. C. 1218, F122, SA122, SA123
Jolette, J. SU327, M379
Jolley, K. M378
Jonczyk, A. SU220
Jones, A. L. M281
Jones, G. SU453, SU459
Jones, G. E. F230, SA230
Jones, J. L. F405, SA405
Jones, L. A. M292
Jones, S. C. F003, SA003, M003
Jones, S. J. SU228
Jones, T. SU111
Jono, S. SA145, M014
Jonsson, B. 1090, SA291
Jonsson, K. SA396
Jonsson, K. B. 1139
Joo, J. SA045
Joo, Y. SA169
Jorgensen, N. R. SU156
Jorgensen, S. M. M086
Josse, R. SA340
Josse, R. G. SU296, SU343
Journé, F. 1094
Jover, L. F013, SA013
Judex, S. 1047, SU166
Jueppner, H. 1139, SA396
Juhász, A. SA049
Juma, S. SU358, SU419
Jung, Y. SU211
Juppner, H. 1065
Jüppner, H. 1178, SA448
Jurisicova, A. 1219
Jurrianans, E. M293
Jurutka, P. W. F488, SA488
Jurvelin, J. S. M361

K

Kaban, L. B. SA167
Kacena, M. A. 1014
Kadkol, S. S. SU393
Kado, D. M. 1208, SU300
Kadono, Y. 1150, SA260, SA416
Kadowaki, A. SA207
Kahan, A. F104, SA104
Kahler, R. A. F069, SA069
Kaibara, M. M381
Kaija, H. SU229
Kaiser, E. A. SA143
Kaji, H. SA407, M151, M204
Kaji, K. M245
Kajiwara, Y. SU353
Kakita, A. M202
Kakitani, M. 1182
Kakonen, R. S. M060
Kakonen, S. SU075
Kakonen, S. M. M059, M060
Kakudo, K. M271
Kalajzic, I. 1186, SA190, SU039
Kalajzic, Z. SA192
Kalender, W. A. SA351
Kalidas, M. 1023
Kalkwarf, H. J. SA271, SU277
Kalla, S. E. M236, M237
Kallay, E. SA481
Kallman, L. M058
Kalu, D. SU013
Kalu, D. N. SU012
Kamae, S. M106
Kamekura, S. M022
Kamel, S. M277
Kamijo, R. SU067
Kamimura, T. M245
Kammerer, C. M. 1079
Kampmann, G. M232
Kamps, N. M359
Kanaan, R. A. SU209
Kanatani, M. SA407
Kanazawa, K. M245
Kang, A. SA318
Kang, H. SU141
Kang, M. I. SU422, M334
Kang, S. K. SU422
Kang, Y. SU076, M060
Kanis, J. F083, SA083
Kanis, J. A. 1090, F091, F286, SA091, SA092, SA286, SA291, M301
Kannno, T. SA238
Kannus, P. 1048, SU103, SU180
Kannus, P. S. SA346
Kansagor, J. N. 1012
Kanterewicz, E. SU291
Kantor, S. F354, SA354
Kapadia, R. M403
Kaplan, F. SU040
Kaplan, F. S. F387, F417, SA387, SA417, SU044, WG4
Kaplan, T. SU172
Kaptoge, S. M168
Kapur, S. F161, SA161, M149
Karadag, A. F052, SA052
Karagrigoriou, E. F186, SA186
Karamohamed, S. 1060
Karaplis, A. C. 1052, F391, F439, SA391, SA439, SA441
Karasik, D. 1060, SA125, SU143, M122
Karkkainen, T. SA100
Karlamangla, A. S. 1207
Karlsson, C. SU014, M004
Karlsson, M. K. 1163, SU014, M004
Karmeli, F. F146, SA146
Karperien, M. 1077, F208, SA208, SA475, M026
Karsdal, M. A. SU227, SU259
Karsenty, G. 1003, 1181, F184, SA184
Kartsogiannis, V. SA242
Kashima, T. M052
Kasiske, B. L. M410
Kasperk, C. SA462, SU157
Kassem, M. SU195
Kasugai, S. 1177
Kasukawa, Y. 1183, F151, SA151, SU042, SU371
Katagiri, H. SA293
Katagiri, M. 1148
Katagiri, T. SU067
Katayama, S. SA237, SA426
Katayama, T. M206
Kato, S. 1036, 1050, F046, SA046, SA205, SA455, SA481, SA486, SU326, SU455
Kato, Y. SU210
Katou, N. SA245
Katsushima, Y. SU383
Katz, J. N. SU362
Katz, M. S. M193
Katz, R. W. SA438, SU437, M131
Katz, S. SU217
Kaufman, J. M. F327, SA327
Kaufman, M. SU048
Kaufman, S. 1020
Kaufmann, M. SU453, SU459
Kaup, S. F006, SA006
Kaur, A. 1037, F345, SA345
Kavalkovich, K. M403
Kawaguchi, H. 1051, 1072, 1148, F046, SA046, SA235, SU298, SU326, M022
Kawaguchi, J. M052
Kawahara-Baccus, T. SU089, SU092
Kawai, A. SA037
Kawai, E. F201, SA201
Kawai, S. M372
Kawai, T. F422, SA422
Kawaida, R. SA260
Kawanishi, J. SU333, M344
Kawano, H. 1072, F046, SA046, SU326
Kawano, K. 1072, F254, SA254
Kawase, T. SA428
Kawashima, H. SA057
Kawashima, K. SA034
Kawata, T. F410, SA410
Kawawaki, J. SA253
Kayama, F. SA426
Kayan, K. M301
Kaymakci, B. F354, SA354
Kays, J. S. SU234
Kaz Kaz, H. M423
Kazanecki, C. C. SA154
Ke, H. Z. 1031, 1107, M392, M395, M397
Kearns, A. E. SA193
Keck, A. M057
Keenan, T. 1145, SU377
Keeting, P. E. M209
Keith, T. M123
Keller, E. T. F085, SA082, SA085, SA088, M064, M065
Keller, H. SA196
Keller, H. J. SA015
Kellum, J. M. M398
Kelly, P. L. 1162
Kelly, T. L. SU015
Kelsey, C. SA266
Kemikangas, M. SU007, SU008
Kemmler, W. SA351
Kemppinen, M. SU007, SU008
Kendler, D. L. SU343
Kenmotsu, S. SU054
Kennedy, A. M. 1215, SA070, M157
Kennel, K. A. SU405
Kenrali, J. SA092
Kent, K. M405
Kerstetter, J. E. M337
Ketteler, M. M413
Keyak, J. SA316
Khadeer, M. A. M037
Khalil, D. A. SU357, SU358, SU419, M366
Khan, A. A. 1169
Kharode, Y. 1001, F119, SA119, SA432
Kharode, Y. P. F371, SA371
Khaw, K. M168
Khedoumi, N. 1094
Khosla, S. 1009, 1093, 1103, 1134, 1168, F307, SA217, SA307, M182, M183, M187
Kidder, L. S. SA017
Kido, S. 1036, F058, SA058, SA077
Kiefer, J. A. SA088
Kiel, D. P. 1060, 1087, 1210, F275, SA125, SA275, SA301, SU143, SU314, M122
Kifor, O. WG9
Kii, I. SU202
Kikuchi, K. SA008
Kikuchi, R. F130, SA130, SU113
Kikuchi, T. SA059
Kilav, R. F435, SA435, SA436
Kilbride, J. 1038
Killeen, K. SU367
Kim, C. SA209
Kim, C. C. SU422
Kim, D. S. M339
Kim, E. S. SA172

Kim, G. SU219
Kim, G. S. SA172
Kim, H. SA181, SU211, SU253, SU384, SU407, M045, M129, M129, M274
Kim, H. K. W. SU413, M356
Kim, H. M. M156
Kim, H. S. SU422
Kim, I. SU211, SU384
Kim, J. SU119, SU211, SU414, M117, M117
Kim, J. B. SU060
Kim, M. SU119
Kim, N. M248, M250
Kim, S. F337, SA337, SU119, SU137, SU137, SU211, SU219, SU414, M117, M129
Kim, S. W. SA172, M334
Kim, T. W. M339
Kim, Y. SA181, SU211, SU219
Kimiduka, M. SA416
Kimm, S. Y. S. SA271, SU277
Kimmel, D. F239, SA239, M316
Kimmel, D. B. F246, SA246, SA331, M326
Kimura, A. SU210
Kimura, H. SA021
Kinder, B. SU396
Kindermans, C. F104, SA104
Kindmark, A. SA126
King, S. H. SU081
Kingsley, D. M. F024, SA024, WG4
Kinosaki, M. SA238
Kipersztock, S. M300
Kipp, D. M221
Kirilov, M. F478, SA478
Kirkegaard, T. 1195, SU227, SU259
Kirkland, M. A. M272
Kirkley, A. M098
Kishimoto, H. SU026, M106
Kisiel, M. SA453
Kiss, E. SA353
Kiss-Toth, E. SA129
Kitagawa, H. 1050
Kitahama, S. SA237
Kitahara, H. M298
Kitahara, K. F442, SA442
Kitahara, Y. M268
Kitaoka, E. SU207
Kitaura, H. SU230
Kitazawa, R. SA216, SU191, SU232
Kitazawa, S. SA216, SU191, SU232
Kittaka, A. SU455, SU456
Kiviranta, R. SU225
Kizu, A. SA145
Kjendlie, G. J. SU200
Klaushofer, K. SA388
Kleerekoper, M. M386
Klein, G. L. SA418, SA477
Klein, L. SA427
Klein, R. 1080
Klein, R. F. 1012
Klemenz, A. M109
Klibanski, A. M384
Klopot, A. M454
Kloseck, M. SU365
Kluczyk, B. F066, SA066
Knapen, M. H. J. M365
Knapp, K. SA128, SU098
Knapp, K. M. M080, M101
Knauerhase, A. SU306
Kneissel, M. M213, M460
Knight, M. C. 1053, 1152, SU066
Knoblauch, B. M093
Knopp, E. A. 1180
Knutson, J. C. SA491, SU457, SU459
Ko, J. S. M156
Ko, S. SU273
Kobayashi, K. SA397, SA399
Kobayashi, N. F410, SA410
Kobayashi, S. SU208
Kobayashi, T. 1152, F176, SA059, SA176
Kocisko, M. 1081
Kodama, I. SU099
Koedam, M. M189
Koeller, M. SU074, SU102
Koffman, G. 1141
Kogawa, M. SA237
Koh, A. J. SU223
Koh, J. M. SA172
Kohama, S. SU029
Kohashi, O. SU244
Kohler, T. M072
Kohn, C. W. SA431, SU436
Kohno, J. F254, SA254
Koide, M. SU152
Koike, T. SU353
Koistinen, A. SU007, SU008
Koitabashi, E. F254, SA254
Koizumi, M. SU106
Kojima, H. SU206, M015
Kojima, K. SU383
Kojima, T. SA257
Kok, D. 1105
Koller, B. SA447, M403
Koller, D. L. 1081, 1218, F122, SA121, SA122, SA123
Kolta, S. SU282
Kolthoff, N. M119, M373
Komarova, S. V. M150, M278
Komatsu, Y. 1206, SA233
Komatsubara, S. F373, SA373, SU333, SU411, M344
Komeda, K. 1072
Kometani, K. SU208
Kometani, M. F064, SA064
Komiya, S. M021
Komm, B. 1001, SU193
Komm, B. S. F371, SA371, M041
Komori, T. 1111, 1112, F018, SA018, M032
Kon, S. 1156
Kon, T. M136
Kondo, H. 1177, SU173
Kondo, K. M090
Kondo, S. F031, SA031, SA043
Kondo, T. SU232
Kondoh, T. SA158
Kong, J. 1049, M456
Konttinen, Y. T. M051
Kontulainen, S. SU180
Kontulainen, S. A. SA346
Koo, K. SU414
Koo, W. SU404
Koob, T. J. SU413
Kooperberg, C. M300
Korach, K. S. M179
Koren, R. SA078
Korkia, P. K. SU174, SU175
Korkko, J. SU118
Koroma, K. E. M402
Korpela, R. SU007
Korsmeyer, S. J. 1219
Koshiyama, H. 1139
Kostakis, P. N. M230
Kostense, P. J. M429
Kostenuik, P. J. 1045, 1092, F369, SA369
Kostura, L. SU213
Koszewski, N. J. 1126
Kotake, M. M202
Kothe, R. M084
Kotowicz, M. A. M338
Kousteni, S. 1032, 1058, 1190, F173, SA173, SU185, M380
Koutoku, H. SA245
Kouzmenko, A. P. F458, SA458
Kovacs, C. S. M437
Kovanen, V. SU132
Kowalewski, R. F186, SA186
Koyama, H. SA145
Kraenzlin, M. SA312
Krall, E. SU022
Krall, E. A. F302, SA301, SA302, SU099
Kramme, K. SU020
Krane, S. M. 1197, 1198, SU066
Kream, B. SA192
Kream, B. E. 1026, SU429, M148
Krebsbach, P. H. SU034, SU435
Kremer, R. 1028, M002, M431, M461
Krieg, M. A. 1130
Krishnadasan, D. SA072
Krishnaswami, S. M306
Krishnaswamy, A. 1159
Kristensen, S. R. SA131
Kristo, C. SA324
Kritchevsky, S. B. F311, SA311
Krits, I. M417
Kröger, H. M361
Kroger, H. SA101
Kröger, H. SU007, SU008, SU132
Kronenberg, H. M. 1053, 1065, 1066, 1177, F176, F446, SA176, SA446, M436
Kronenberg, M. S. SU039, M215, M216
Krueger, D. SU089, SU091, SU092, M078
Krystal, G. F403, SA403
Krzanowska, K. SU412
Kubodera, N. SU454
Kuboki, T. F031, SA031, SA043, SU153
Kuboki, Y. SU149
Kubota, M. SA035, SA134
Kubota, N. SA483
Kubota, S. F031, SA031, SA043
Kudo, A. 1113, SU202, M052, M245
Kudo, I. SA235
Kugai, N. SU077, SU239
Kukita, A. SU244, SU247
Kukita, T. SA262, SU244, SU247
Kukreja, S. C. M062
Kumagai, Y. F400, SA400
Kumar, R. 1108, 1142, SU450, M458
Kume, K. SU207
Kumta, S. M. SA076
Kundu, M. 1004
Kung, A. W. C. 1169
Kung, V. M025
Kunii, I. M286
Kuno, M. F261, SA253, SA261, M282
Kunz, M. SA312
Kuperman, H. M439
Kurasawa, K. SU113
Kurihara, M. SU455, SU456
Kurihara, N. SU389
Kuroda, T. M268
Kurosawa, H. 1044, F442, SA442, M023
Kushner, P. M100
Kusumi, T. M426
Kuznetsov, S. A. M226
Kveiborg, M. 1097, 1100
Kvern, B. SU360
Kvetnansky, R. SA055
Kwan, C. SU449
Kyle, R. M057

L

La Tourette, A. M. SU362
Labrinidis, A. M210
Lacey, D. L. 1009, 1020, 1045, 1092, F369, SA369
Lacour, B. F104, SA104
LaCroix, A. 1089
LaCroix, A. Z. SA278, SA281, M284, M300, M318, M367
Ladizesky, M. SA466, SU279, SU280
Lafage-Proust, M. SU165
Lafage-Proust, M. H. M391
Laffer, L. L. A. SA434
Laflamme, N. M289
Lagneaux, L. 1094
Lai, C. F. 1017, F020, SA020
Lai, F. M. SA076
Lai, L. P. SA450
Laib, A. M102, M403
Laidlaw, A. F003, SA003
Laitala-Leinonen, T. SU225, SU226
Laizé, V. M043
Lajeunie, E. SU313
Lakatos, P. SA132, SA133, SU138, SU320, SU322
Lakkakorpi, P. T. 1147
Lakkis, S. SU289
Lam, S. SU030
Lambert, A. 1001
Lambert, H. SA280
Lameloise, N. 1095, SU375
Lamothe, B. 1023, 1099
LaMothe, J. M. M044
LaMotta, A. 1059
Lamplugh, L. F066, SA066
Lamy, O. M310
Lan, L. F354, SA354
Lanctot, C. 1187, SA195
Landesberg, R. M131
Landewé, R. SU417
Landoll, J. 1200
Landoll, J. D. M007, M008
Lane, J. M. SA350, SU305, SU305, M351
Lane, N. F239, F366, SA239, SA366, M420
Lane, N. E. F440, SA440
Lang, R. SU396
Lang, T. 1131, SA316
Lang, T. F. F011, SA011, SA166, SA305
Langdahl, B. M145
Langdahl, B. L. M119
Langdown, M. F124, SA124
Langhammer, A. SU312
Langman, C. M421
Langman, C. B. 1008, SA418
Lanino, E. SU398
Lankford, J. F061, SA061
Lanske, B. F446, SA446
Lanyon, L. E. 1010
Laplace, C. 1175, SU264
Lapointe, D. S. SU197
Lappe, J. M. SU275
Lapuerta, P. SA296
Larcher, Y. M033
Lark, M. W. SU083
Larsen, E. R. 1137
Larsen, K. I. SU268
Larsson, T. 1139, SA396
Laska, B. 1161
Lasmoles, F. SA138
Latham, J. A. 1077, 1222
Latin, P. 1095, SU372, SU374
Latremouille, C. M107
Lattmann, R. F064, SA064
Lau, E. SU278, M345
Lau, E. M. C. SU302
Lau, K. H. W. F161, SA161, SU042, SU263
Lau, W. SU278
Laudier, D. M166

Laugier, P. M107, M108, M109
Lauretani, F. SU309
Laurie, D. SU104
Laurin, N. SU388, SU391
Laverty, S. M098
Lavigne, J. 1139, SA396
Lawrence, F. 1135
Lawson-Body, E. F104, SA104
Lax, A. M255
Lazaretti-Castro, M. SA267, M286
Le Loët, X. SU412
Le Mee, S. SU031, SU188
Leach, R. J. F412, SA412, M055
Leb, G. F111, SA111, SU423
Lebecque, P. SU354
LeBlanc, A. SA166, M170
Leblond, C. P. F066, SA066
LeBoff, M. S. SU334, M389, WG9
Lecanda, F. F182, SA182, SA183
Lechowska, B. A. SU083
Lecka-Czernik, B. M155
Lee, B. K. SU443
Lee, C. B. M339
Lee, D. C. M334
Lee, E. SU258
Lee, E. R. F066, SA066
Lee, J. M117
Lee, J. C. SA019, SU032
Lee, J. L. SA326
Lee, J. S. SU387, M226
Lee, J. Y. 1162
Lee, K. SA397
Lee, K. C. L. 1010
Lee, K. W. SU422
Lee, L. SU302
Lee, M. SA181, M306
Lee, S. SA268, SU211, SU302, M274
Lee, S. K. M. SA005
Lee, W. T. K. SA004, SA005, SU400
Lee, W. Y. SU422
Lee, Z. SU253, M274
Lees, C. J. M377
Leet, A. I. SU387, M226
Lefevre, G. SA138
Lefker, B. A. M392, M395, M397
Lefort, M. SA359
Legault, S. F083, SA083
Legeai-Mallet, L. SA140
Legowski, P. A. M363
Legrand, E. M332
Legrand, J. SA447, SU047
Lehmann, W. SA065, M031, M152
Lei, S. F. M126
Lekamwasam, S. M308
Lemineur, G. SU010
Lemonnier, J. 1124, SA212
Lems, W. F. M371, M429
Lengel, C. SU257
Lenhard, T. R. 1195
Leonard, M. B. 1202, F006, SA006, M095
Leonard, R. SU108
Leone, G. W. SA431
Leong, G. M. F458, SA458
Lepescheux, L. SA479
Lerner, U. H. M141, M203, M256
Leslie, G. SU195
Leslie, W. D. SU360
Lespessailles, E. 1043
Lester, G. E. M013
Leu, C. F246, SA246
Leufkens, H. G. M. 1199, 1213, F282, SA282
Leung, A. SU344
Leung, P. C. M345, M376
Levi-Setti, R. M419
Levine, M. A. 1064, 1083, F387, F389, SA387, SA389, SU393
Levy, D. SU314
Levy, S. WG3
Levy, S. M. M005
Lew, W. D. SA017
Lewicki, M. M100
Lewiecki, E. M. SU335, SU336
Lewis, C. SU028
Lewis, C. E. M300
Lewis, L. SU087
Leyshon, A. M. SU105, M379
Li, B. 1200, M007, M008
Li, C. F387, SA387, SU116, M166
Li, G. 1005, SA221
Li, J. 1020, F011, F155, SA011, SA155, SA316, SU129, SU333, M175, M231, M239, M249
Li, K. SU251
Li, M. 1107, M392, M395
Li, P. 1021, 1024
Li, Q. F206, SA206, SA480
Li, S. SU137, M116
Li, T. SA296
Li, T. K. SA117
Li, X. 1175, F069, F149, F473, SA069, SA149, SA473, SU199, SU235, M199
Li, X. T. SU233, SU242
Li, Y. 1049, 1054, SA247, SA264, M193, M456
Li, Y. N. SU187, M237
Li, Y. P. SU266
Li, Z. SU271, SU343
Lian, J. 1001, 1004, M192
Lian, J. B. 1110, 1112, SU197, SU384, M041, M194, M195, M196, M198, M254
Liang, S. F137, SA137
Libanati, C. M378
Liberman, U. A. SA078
Libouban, H. SA068
Licence, R. L. SA342
Lichter, J. F124, SA124
Lichtler, A. C. 1159, 1186, F191, SA191, SU039, M215, M216
Lie, A. M251
Lieberman, J. R. M069
Lieder, A. SU157
Liegibel, U. M. SA462, SU157
Liel, Y. M375
Lim, S. F337, SA337, SU137, SU258
Lima, F. SU165
Lin, C. SA226
Lin, H. M169
Lin, J. T. SA350
Lin, M. SU318
Lin, S. C. SU159
Lin, W. M097, M114
Lin, Y. SA107, SU318, SU441
Lind, M. M145
Lindberg, H. SU014
Lindberg, M. K. F465, SA464, SA465
Lindner, T. M147
Lindqvist, Y. SU229
Lindsay, R. 1173, SU324, SU325, M220, M386
Lindsey, C. M325
Lindsey, R. SU040
Linhares, A. B. R. SU050
Linkhart, T. 1160, M200
Linnala-Kankkunen, A. SA187
Linton, O. F186, SA186
Liou, Y. L. SU001
Lipfert, L. F246, SA246
Lips, P. F286, F348, SA286, SA348
Lisignoli, G. SA188
Little, D. G. 1203, F256, F424, SA256, SA424
Little, R. D. M123
LIU, B. SU254
Liu, C. SA326, SU368
Liu, C. Z. SA174
Liu, G. SA123
Liu, H. SA141
Liu, J. 1060
Liu, L. J. F. SU441
Liu, M. Y. M126
Liu, P. 1004, M127
Liu, S. 1049, SA063
Liu, S. H. SA170, SU159
Liu, X. SA255
Liu, X. H. M126
Liu, Y. F243, SA243, SA457, SU163, SU186, SU198, SU271
Liu, Y. J. SU123, SU124, SU125, SU126
Liu, Y. Z. SU123, SU124, SU125, SU126
Liu, Z. F206, F473, SA206, SA473
LiVolsi, V. L. SU395
Ljunggren, Ö. 1139, SA126, SA396
Lloyd, R. V. SU405
Lloyd, T. SA002
Lo, S. 1042
Locklear, S. M404
Lockridge, O. F048, SA048
Lodder, M. C. M371, M429
Loewy, A. P. 1114, M020
Lohmann, C. H. SU271, M011
Lombardi, A. F345, SA345
Lombardo, F. SA045
Lomri, A. SU237
Long, J. R. SU126, SU134, M124
Long, K. R. SA326
Longo, M. SA175, M179, M180
Looker, A. C. 1088
Loomer, P. M. M401
Lopez, D. SA457
López, F. SA469
López Giovanelli, J. SU279
Lopez-Farre, A. SA359
Lopez-Rodriguez, F. M309
Lora, M. SA244
Lorberboym, M. SU397
Lorenzo, J. A. 1098
Lorget, F. SU246
Lostritto, K. 1180
Lotinun, S. SA413
Lotz, O. 1178
Lou, H. SU259
Loubat, A. M174
Loughrey, H. SU250
Love, D. 1056
Loveridge, N. SA101, SA163, SA317, SU274, M168, M308
Löwik, C. 1091
Lowik, C. F208, F468, SA208, SA468, M026
Lowik, C. W. G. 1077, SA475, M186
Lu, B. SA247, SA264, M392, M395, M397
Lu, C. F206, F473, SA206, SA473
Lu, J. H. M125
Lu, M. 1018, SA215
Lu, S. B. SU126
Lu, S. S. SU324, SU325, M220
Lu, X. M447
Lu, Y. 1005, SA166, M064, M065, M455
Lucani, B. M121, M396
Lucas, E. A. SU357, SU358, M366
Luchin, A. I. M432
Luciani, M. SU398
Luckey, M. M. F345, SA345
Ludvigson, J. 1093
Ludwig, H. M057
Luegmayr, E. B. F241, SA241
Lui, L. 1085
Lui, L. L. 1212
Lui, V. A. M286
Lui-Yee, D. SU281, SU316
Lukaski, H. C. SA148
Lukert, B. P. SA485, M370
Lumeng, L. SA117
Luna, J. D. M309
Lund, R. J. 1140
Lundgren, I. M203
Lundy, M. W. SU049, M207
Luong-Nguyen, N. SA240
Luque-Recio, F. M309
Lurie, D. M029
Lutz, W. SU450, M458
Lyle, R. M. M363
Lyngso, C. SA374
Lynn, H. SU278
Lyon, A. SA317
Lyytikäinen, A. SU007

M

Ma, L. 1135, F373, SA373
Ma, P. X. M049
Ma, X. SA383
Ma, Y. L. 1179, SA476
Maas, R. M215
Macarak, E. SU057
Maccherini, M. M110
MacDonald, P. N. SU196, SU451
MacDougall, M. SU063
Mace, D. SU176
Mace, D. L. M164
MacFarlane, G. D. M290
MacIntyre, B. SU344
MacIntyre, N. J. SA097
MacKay, A. R. SA086
MacLean, H. E. 1152, M436
MacLeay, J. M. SU356
MacLeod, R. J. M444
Macmillan, D. L. M434
Macoritto, M. M461
Madsen, J. S. SA131
Maeda, N. F026, SA026
Maeda, S. SA386, SU232, M021
Maeda, T. SU054, SU077
Maeda, Y. 1192, M218
Maehata, Y. SU210
Magaziner, J. SA296
Magee, K. A. SU370, M133
Maggi, A. F468, SA468
Maggi, S. SU284
Maggio, D. SU309, SU310
Magnus, J. H. M304
Mah, P. M. M369
Mahaney, M. C. SU130, SU131
Mahomed, N. M297
Mahon, M. J. F449, SA449
Mahonen, A. SA187, SU007, SU132
Mahoney, P. 1038, 1138, F339, F341, SA339, SA341, M347, M349
Mai, J. M103
Maid, P. M351
Maier, A. SU066
Mailhot, G. M446
Main, S. C. SU145
Mainous, E. SA219
Majumdar, S. SU428, M083, M420
Majumdar, S. R. SU366
Mak, Y. T. SA128
Makhijani, N. S. M153, M154
Maki, B. SU317
Makino, T. F325, SA325
Makita, K. SU026, M106

(Key: 1001-1222 = Oral, F = Friday Plenary poster, SA = Saturday poster, SU = Sunday poster, M = Monday poster, WG = Working Group Abstract)

Makita, T. M342
Makitie, O. SA420
Maksymowych, W. P. SU366
Malaval, L. M036
Malavolta, N. SU286, SU315
Maliinak, J. M100
Malkasian, G. D. 1103
Mallmin, H. SA126, SU303
Malloy, P. J. F456, SA456
Man, Z. SA406, M400
Mancini, D. 1042
Mandalunis, P. M409
Mandelin, J. M051
Mandrup, S. SU211
Manduca, P. SA022
Mangeri, M. M110
Mangion, T. SU108
Manhart, M. D. F343, SA343
Manigrasso, M. B. SU290
Manna, T. D. M439
Mannen, P. SU028
Mannen, P. E. SA303
Manness, L. SU360
Manolagas, S. C. 1013, 1025, 1032, 1058, 1133, 1161, 1176, 1190, F173, SA173, SU185, SU194, M380
Manolson, M. F. SU251
Mansky, K. C. SU261
Mansolf, A. SA053
Mansour, S. L. F036, SA036
Mansur, J. L. 1115
Mantz, A. M. 1037
Manzi, S. M421
Mao, C. SU401
Maran, A. SA070, M157
Marcano, L. SU107
Marchand, F. 1209
Marchandise, X. SU021
Marchetti, L. SA136
Marcocci, C. M442
Marcus, R. SU028, SU321, M321, M405
Maret, A. 1064, SU393
Margerison, C. F354, SA354
Margulies, B. M343
Marians, R. 1054
Marie, P. J. SA138, SU031, SU188, M016
Mariette, X. M075
Marijanovic, I. F191, SA191, SU039, M215, M216
Marino, M. M179
Marinucci, D. SU024
Mark, A. SU296
Marks, S. C. 1084
Marque, V. SU368
Marrony, S. SA015
Marsden, P. K. SA334
Marsell, R. SA396
Marsh, D. SA221
Marshall, L. M. F292, SA292, SA305
Martin, B. SA055
Martin, F. C. M358
Martin, I. M232
Martin, J. F. 1071
Martin, K. J. SU445
Martin, T. J. 1073, 1123, F081, SA081, SA361, SU243, SU257, M434, M435
Martínez, G. M307
Martini, G. 1166, SA404, M076
Martini, S. M105
Martins, H. S. H. SA171
Maruoka, Y. SA021
Marzia, M. SA231
Marzolf, J. SA432
Marzolf, J. T. F371, SA371
Masaki, T. SA376, SA377, SA379
Masarachia, P. J. SA331, M326
Mascarelli, F. SA138
Masellis, A. M. F069, SA069
Mashiba, T. F373, SA373, SU333, SU349, SU411, M344
Masi, L. SU136, M121, M406
Masinde, G. F149, SA149
Masiukiewicz, U. SU396
Mason, R. S. F395, SA395
Massague, J. M060
Masson, D. 1095, SU374, SU375
Masters, S. 1102
Masuda, N. SU207
Masuda, S. SU453, SU459
Materazzi, S. SA136
Matern, D. SU450
Mathey, J. SU354
Matkovic, V. 1200, M008
Matsubara, S. SA376, SA377, SA379
Matsubara, T. 1109
Matsuda, K. SA235
Matsui, D. 1050
Matsumoto, C. 1116, SA355
Matsumoto, K. M015
Matsumoto, T. 1036, 1050, F058, SA058, SA077, SU326, M342
Matsuo, K. SU264
Matsuoka, Y. M346
Matsuura, S. M206
Matsuura, T. M046
Matthews, J. L. M013
Matubara, T. SA262
Matyas, J. R. M044
Maudelonde, T. SU256
Maugeri, D. F297, SA297
Maurer, M. S. SU394
Maurhofer, O. SU374
Mauro, L. J. SA189
Mautalen, C. SA384, SA466, SU348
Maxon, R. M215
Maybaum, S. 1042
Mayer, J. SU105, SU327
Mayhew, P. SA101
Mazzantini, M. SU363
Mazzucco, K. SA481
Mazzuoli, G. SA287, SA409, SU024
Mbalaviele, G. 1015, M281
McAlister, W. H. F405, SA405, SU409
McCabe, G. P. M363
McCabe, J. M. M283
McCabe, L. R. SU064, SU190
McCaig, J. SU459
McCarthy, J. T. 1211
McCarthy, S. M142
McCarthy, T. L. SU447
McCartney, N. M099
McCauley, L. K. 1032, 1176, SA470, SU064, SU223, SU435
McClintock, C. SU399
McCloskey, E. F083, SA083, SA092
McCloskey, E. V. F091, SA091, SA372, SA382, M301
McClung, M. 1037, 1138
McClung, M. R. M115, M349
McCluskey, B. M092
McCulloch, C. A. G. F184, SA184
McDermott, K. M175, M231
McDonald, J. M. M243, M257, SA228, SU129, SU161
McDonald, R. F339, SA339
McDougall, K. E. 1076
McEvoy, A. 1203, F256, F424, SA256, SA424
McFadden, K. SA318
McGill, P. F269, SA269
McGowan, J. SU382
McGowan, J. A. M367
McGuigan, F. E. SA135
McGuigan, F. E. A. SU145
McGurk, C. M301
McHugh, K. P. M252
McIsaac, W. SU364
McIsaac, W. J. SA089
McKee, M. D. F391, SA391
McKenna, M. M243
McKiernan, F. E. M330, SA283, SU293
McKinney, S. 1070
McLean, R. R. F275, SA275, SU143
McLellan, A. R. F269, SA269, SU295
McLeod, K. J. M283
McLoughlin, P. 1017
McMurtry, C. T. M112
McNally, D. S. F009, SA009
McNaught, T. P. M288
McNearney, T. F309, SA309
Medawar, W. M414
Medich, D. L. SA112
Mee, A. SU055
Mee, A. P. SU158
Meenan, C. P. SA362
Meenen, N. M. M024
Mehta, N. M. SA362
Mei, L. SA228
Meier, C. SA312
Mejjad, O. SU412
Mellibovsky, L. M188
Mello, M. A. SU050
Mellstrom, D. M294
Melsen, F. M402
Melton, L. J. 1103, 1211, F286, F307, SA286, SA307
Melton, M. E. M353
Menaa, C. F087, SA087
Ménard, D. SA487
Menard, J. F. SU412
Menczel, J. M314
Menghi, G. SA136
Menghi, M. SA136
Mentaverri, R. SU246, M277
Mentrup, B. 1082
Merlotti, D. 1166, M105, M121
Messina, O. D. SA265
Mészáros, S. SA372
Meszaros, S. SA382
Meta, M. SA316, SU095
Metcalf, C. 1145, SU377
Metge, C. J. SU360
Meunier, P. J. SA392, WG2
Meurer, T. SA090, SA421
Meyer, J. M. M382, M383
Meyer, M. H. 1205, SU148
Meyer, R. A. 1205, SU148
Meyers, P. A. M055
Mezquita-Raya, P. M309
Miao, D. 1029, 1052, 1154, F391, F439, SA391, SA439, SA441
Michalska, D. SA105
Michigami, T. F484, SA484
Middleton-Hardie, C. A. 1057
Mieling, G. SA255
Mierke, D. F. F227, SA227, SU427, SU440
Migliaccio, S. SA084, SA086, SA175, SU398, M179, M180
Mika, C. M364
Mikami, K. SU454
Miki, T. M342
Mikuni-Takagaki, Y. SA156, SA158, SA349
Milas, J. F040, SA040, SU434
Miles, L. J. SU127
Miles, R. R. 1135
Millán, J. L. 1011
Miller, A. B. M290
Miller, B. E. SU380
Miller, D. R. F302, SA301, SA302, SU022
Miller, P. SU344
Miller, P. D. SU307, SU308, M295
Miller, R. SA445
Miller, R. A. SU122
Miller, T. A. M235
Millets, J. F. SU356
Mills, L. M003
Milstead, K. SU281, SU316
Mimura, Y. SA299
Mina, M. SA190
Minamide, T. M342
Minato, T. M329
Miner, J. N. SA469
Minet, D. 1027, SA479
Minisola, S. SA287, SA409, SU024
Minkowitz, R. M351
Minne, H. W. SA347
Mirams, M. F395, SA395
Miranda, E. SA362
Mishima, N. M206
Mishina, Y. 1005
Missbach, M. F064, SA064
Mistry, M. J. SU070
Mitani, H. SA035
Mitchell, B. D. 1079
Mitchell, J. SA450
Mitchelmore, G. F. M104
Mithal, A. SA270
Mitlak, B. H. 1041
Mitnick, M. F214, SA214, SU396, M142
Mitnick, M. M. M337
Mitova-Caneva, N. G. SU370, M133
Mitson, E. SA303
Mitsunobu, F. M085
Mittra, E. S. M097
Miura, M. SA233
Miura, Y. M202
Miyakawa, M. M393
Miyakoshi, N. M329, SU042
Miyamoto, K. F373, SA134, SA373, SU333, SU411, M344
Miyashiro, K. M439
Miyata, K. SA245
Miyata, S. F410, SA410
Miyauchi, A. 1139, SA156, SA158
Miyauchi, Y. F484, SA484
Miyaura, C. 1116, 1197, SA355
Miyazaki, T. F225, SA225, SU262, M265, M280
Miyazawa, T. 1206
Miyazono, K. SU037, M023
Mizokami, A. F085, SA085
Mizukami, J. F254, SA254
Mizuno, A. F018, SA018, SA238
Mizuno, S. M030
Mizunuma, H. M342
Mo, X. Y. M126
Moalli, M. R. SU061, SU122
Mobley, H. T. M013
Mobley, S. L. M007, M008
Mochizuki, K. SU113
Modrowski, D. SU031, SU188
Moe, S. M. F398, SA398
Moedder, U. I. M183
Moelgaard, A. M348
Moffat, K. M358
Moffat, P. SA195
Moffatt, P. 1187
Mogun, H. SU378
Mohammad, K. S. SU080
Mohan, S. 1183, 1216, F149, F150, F151, SA149, SA150, SA151, SU371, M149
Moilanen, P. SA100, SU011
Molenaar, E. T. H. M429
Möller, G. M084

(Key: 1001-1222 = Oral, F = Friday Plenary poster, SA = Saturday poster, SU = Sunday poster, M = Monday poster, WG = Working Group Abstract)

Molloy, M. G. M120, SA012
Mon, T. F079, SA079, SA080
Mondillo, S. M396
Monegal, A. F013, SA013, SA332, SU390
Moniz, C. SU108
Monk, J. J. M073, M074
Monroe, D. G. M187
Montagnani, A. 1166, M105, M110, M396
Montecino, M. M192
Montecino, M. A. M195
Montilla, C. SU421
Montjovent, M. SU374, SU375
Moody, S. B. M077
Moon, I. SU076, M118
Moon, M. M020
Moon, S. M117
Moonga, B. S. 1018
Morabito, E. M442
Moran, K. SU040
Moran, R. F119, SA119, SU193
Moran, R. A. SA432
Morancey, J. SU367
Moreau, M. SA068
Moreau, M. S. SU120
Moreira, R. O. SA171
Morelli, S. SU432
Morgan, T. G. M096
Mori, G. SU218
Mori, H. F261, SA253, SA261, M282, M381
Mori, I. M271
Mori, S. F373, SA373, SU333, SU411, M344
Morihata, H. F261, SA253, SA261, M282
Morii, H. SA357, M342
Morinaga, H. F130, SA130
Morinobu, M. 1006, SU058, SU059, SU173
Morissette, J. SU388, SU391
Morita, K. SA486
Moriyama, K. F197, SA077, SA197, M425
Morko, J. SU226
Morley, P. SA362, SU433
Morlunghi, S. SA402
Moro, T. M022
Morony, S. 1045, 1092, F369, SA369
Morreale, G. SU398
Morris, K. L. M104
Morris, R. F. M104
Morris, S. SU437
Morrish, D. W. SU366
Morrison, C. F269, SA269
Mort, J. S. F066, SA066, M047
Mortensen, L. SU020
Mosekilde, L. 1137, SA131, SA313, SU025, SU025, SU288, SU304, M119, M373
Moses, K. 1160
Mossman, E. A. M115
Motagally, Z. 1169
Motomura, S. SU056, M426
Motzel, S. SA331
Moulharat, N. SU068
Mountz, J. D. SU129
Movérare, S. F465, SA464, SA465
Moxham, C. M. SU234
Moy, N. Y. 1046, F157, SA157, SU181
Moyer-Mileur, L. J. F001, SA001
Moz, Y. SA436
Mueldner, C. M012
Mueller, D. M111
Mueller, R. M072, M091
Mueller, T. SA368
Muenke, M. 1004
Mughal, Z. SU016, SU017, SU018
Mukherjee, A. 1074, 1078, M132
Mukudai, Y. SA043
Mulari, M. SU226
Mulder, J. E. M384
Mule', R. SU315
Mullan, B. P. F288, SA288
Müller, B. SA312
Müller, R. 1217
Muller, R. SA118
Müller, R. SU046
Mulloy, A. 1059, M138
Mulmann, D. SU023
Mumm, S. F405, SA405, SU408, SU410
Munasinghe, R. L. WG7, WG8
Mundy, G. R. 1157, 1189, F016, F042, F071, F400, SA016, SA042, SA071, SA400, M092
Munk, M. SU112
Munoz, F. 1209, SU023
Muñoz-Gomez, J. SU390
Muñoz-Torres, M. E. M309
Muraca, M. M105
Murai, H. M329
Murakami, A. SA238
Murakami, M. SA235
Murakami, S. 1070
Muraki, S. M291
Murali, R. SA257
Murata, K. SA008
Muratore, M. SU286
Murphy, G. F066, SA066
Murphy, M. M403
Murphy, T. C. 1096, SA177
Murray, D. SA163
Murray, S. S. SA323
Murray, T. SA340, SU296
Murray, T. M. SU441
Murrills, R. J. SA432, SU430
Murthy, S. F040, SA040, SU434
Musharafieh, R. SU289
Musk, A. A. SA434
Mustapha, B. M170
Muto, T. M128
Myers, D. E. M272
Myers, E. SA350
Myers, K. J. SU235
Mylchreest, S. SU055, SU158
Myoui, A. SU236
Myskowski, S. M. F488, SA488

N

Nabham, F. A. SU420
Nadeau, J. SU116, SU117
Nader, A. SA388
Nagae, M. M427
Nagahama, K. M240
Nagai, K. SU240, SU241
Nagano, A. SA185
Nagano, N. F410, SA410
Nagaoka, T. M090
Nagaraja, H. N. M336
Nagata, N. SU230
Nagayama, M. SU207
Nagode, L. A. M007
Nagy, R. M. F246, SA246
Nagy, T. F206, SA206
Nagy, T. R. SU129
Nagy, Z. SA132, SA133, SU320, SU322
Nakagawa, K. SU454
Nakai, M. M085
Nakajima, M. SA034
Nakajima, T. SA386
Nakamichi, N. SU342
Nakamichi, Y. F046, SA046
Nakamoto, T. 1006, SU099
Nakamura, I. SA416
Nakamura, K. 1072, 1148, 1150, SA235, SA260, SA416, M022, M023, M052, M276
Nakamura, M. M271
Nakamura, T. 1061, F144, SA144, SA357, SA363, SU244, M039, M130, M342, M342, M393
Nakamura, Y. SA185, M271
Nakanishi, T. F031, SA028, SA031, SA037
Nakao, K. 1206, SA233
Nakasato, Y. R. SA108
Nakase, T. SU236
Nakata, E. SA037
Nakatsuka, K. SA397, SA399
Nakatuka, Y. SU026, M106
Nakayama, K. SA205, SU035, SU230
Nakayama, T. SU346
Nakchbandi, I. A. SU396, M408
Namba, N. F403, SA403
Namerow, P. 1042
Namgung, R. F337, SA337
Nancollas, G. H. SU341
Nanes, M. S. 1096, SA177, SU205, M447
Naot, D. 1057
Napoli, N. SA352, SU287
Nara, A. SU183
Narayanan, A. SA190
Nardi-Dei, V. SA374
Naressi, M. SA380
Naski, M. C. F033, SA033, SA041
Nassirpour, R. M433
Naughton, G. SU004, SU005
Naveh-Many, T. F435, SA435, SA436
Naves, M. SU142, M418
Navone, N. SU073
Nawroth, P. SA462, SU157
Naylor, K. E. 1132, SA103
Naylor, S. M458
Nazarian, A. M091
Need, A. G. F482, SA482
Neer, R. 1039
Neer, R. M. 1007
Neff, L. F225, F263, SA225, SA231, SA232, SA263, M265
Neff, M. SA098, SA336, SA338, SU361
Negishi, Y. SA034
Nejishima, H. M393
Nellis, M. SU198
Nelson, A. E. F395, SA395
Nelson, D. A. M063
Nelson, J. B. 1128, SA112
Nemoto, K. SU342
Nemoto, Y. F054, SA054
Nenonen, A. SU103
Nenonen, A. M. SA346
Nervina, J. M. SU221
Nesti, L. J. SU115
Netter, P. M109
Neustadt, D. H. SA108
Nevalainen, J. F083, SA083
Nevantaus, A. F083, SA083
Neville, M. C. 1063
Nevitt, M. F011, SA011, M316
Nevitt, M. C. 1208
Newey, D. SU006
Ng, K. W. 1073, SA242
Nguyen, C. K. 1171
Nguyen, C. V. SA461
Nguyen, T. SU313, M457
Nguyen, T. V. 1086, 1104, SA014, SU283
NicAmhlaoibh, R. SU078
Nicholson, G. C. M272, M338
Nicholson, P. H. SU011
Nicholson, P. H. F. SA100
Nicolella, D. M018
Nicolella, D. P. F061, SA061
Nielsen, J. SU259
Nielsen, K. L. 1194, SU259
Nielsen, S. P. SU304
Niesor, E. J. 1095, SU372, SU374, SU375
Nieva, A. SU279
Nieves, J. SU324, SU325
Nieves, J. W. SA274
Niewolna, M. M060
Nifuji, A. 1006, 1034, 1044, 1156, F054, F220, F442, SA054, SA220, SA442, SU037, SU058, SU059, SU173, M028, M032, M218
Niida, S. F144, SA144
Nilsson, C. SA142
Nilsson, O. M137
Nimni, M. E. M160, M224
Ninomiya, J. T. M173, M191
Nishida, A. SA363, SA377, SA378, SU346
Nishida, N. M085
Nishida, T. F031, SA028, SA031, SA037
Nishii, T. SU236
Nishimura, R. 1109, 1204, SA262
Nishimura, Y. SU060
Nishio, M. F254, SA254
Nishisho, S. SU207
Nishizaki, Y. F046, SA046
Nishizawa, Y. SA023, SA145, SA397, M014, M342
Nissen, N. SA313, SU304
Nissenson, R. A. M177
Niu, M. 1154
Niwa, S. SA067
Njus, G. SU177
Nobukuni, T. M021
Nociti, Jr., F. H. F024, SA024
Noda, M. 1006, 1034, 1044, 1111, 1156, 1192, F054, F220, F442, SA054, SA220, SA442, SU037, SU058, SU059, SU173, M028, M032, M218
Noda, T. SA057
Noguchi, S. F408, SA408
Nogues, X. M188
Nohadani, M. 1101
Nokubi, T. 1109
Nolan, C. M167
Nolli, S. 1095
Nomoto, M. SA486
Nomura, R. SA407
Nonaka, K. SA257, M240
Noord, R. M. M351
Nord, R. H. SU086
Nordin, B. E. C. F482, SA482
Nordstrom, P. M004
Nordström, P. R. M137
Noriega, R. M071
Norimatsu, H. F373, SA373, SU333, SU411, M344
Norman, A. W. SU446, SU448, SU449, SU452
Norman, M. 1119
North, T. 1110
Northington, R. M386
Norvell, S. SA162
Norvell, S. M. SA160
Norwood, J. M287
Notoya, K. SA156
Novack, D. V. 1033, M259

Novy, A. M. M398
Nowson, C. F354, SA354, SU004, M302
Nsouli, A. SU289
Nuckolls, G. 1004
Nuckolls, G. H. F139, SA139
Nussenbaum, B. SU034
Nuti, R. 1166, SA404, M076, M121
Nyquist, F. SU014, M004

O

O' Keefe, R. F234, SA234
O'Brien, C. A. 1013, 1025, 1032, 1058, 1176, 1190, F173, SA173, SU185, SU194, M380
O'Brien, K. O. M337
O'Connell, S. L. SA047
O'Connor, J. P. SU290
O'Keefe, R. F044, SA044
O'Keefe, R. J. 1021, 1153, SU036, SU041, SU090, M053, M176
O'Loughlin, P. D. F482, SA482
O'Neill, J. M368
O'Shaughnessy, E. A. M410
Oakley, J. I. M236, M237
Oba, K. 1139
Oba, T. F073, SA073, SU075, M059
Oba, Y. M246
Obana, S. F410, SA410
Obata, S. M381
Oberg, A. L. 1103, 1211, F307, SA307
Oberlin, F. M001
Obermayer-Pietsch, B. F111, SA111, SU423
Obinata, M. SA035
Obrant, K. J. SU014, SU303
Obrecht, S. E. F405, SA405
Ochiai, E. M245
Oda, H. 1150, SA260, SA416, M023, M276
Oda, M. SA021
Oden, A. 1090, SA291
Odgren, P. R. 1084
Odman, A. M. SA082, SA088
Offord, E. A. SU246
Ogasawara, T. 1148, M022
Ogata, E. 1118, SA377, SA483, SU106
Ogata, N. 1051
Ogawa, E. SU383
Ogawa, K. M090
Ogawa, Y. 1206
Oglesby, A. SA291
Oguro, N. M393
Oh, E. S. SU422, M334
Oh, K. W. SU422, M334
Ohama, K. SU099
Ohashi, Y. SA357
Ohata, N. SU149
Ohguma, A. 1182
Ohishi, H. SU056
Ohlsson, C. F465, SA142, SA464, SA465, SU139
Ohsone, Y. M346
Ohta, H. SU026, M106
Ohtsuka, M. SU099
Ohtsuka, T. SA260
Ohya, K. SA250, SA257, SA349, SA416, M240
Ohyama, K. M240, M268
Ohyama, Y. F054, SA054, SU037, M218
Öijfjord, E. M294
Oiso, Y. M202
Ojeda, C. SA229
Okabe, K. SA156
Okada, T. M276
Okada, Y. 1061, SA134, M130
Okamoto, M. M085
Okano, T. SA293, SU347, SU454
Okano, Y. M346
Okayama, H. 1148, M022
Okazaki, H. SA416
Okazaki, M. SA483
Okazaki, R. 1143, SA411
Okazaki, T. 1118
Okazaki, Y. SU252
Okimoto, N. 1061, M130
Okuno, E. F137, SA137
Okuno, Y. SA145
Okutsu, J. SA260
Ola, E. SA089
Olate, J. M192
Olchovsky, D. M317
Olijve, W. SU201
Oliveira, M. SU246
Oliver, C. M045
Olivera, C. J. SU446
Oliveri, B. SA328, SA384, SU279, SU280
Olkku, A. SA187
Ollier, L. M174
Olmsted-Davis, E. SU040, M227
Olson, D. A. 1012
Olson, D. P. 1053
Olson, L. M. SA326
Olstad, O. K. SU200
Olszynski, W. SU296
Olszynski, W. P. SA340, SU343
Omid, N. M457
Omizo, M. 1037
Omura, K. SA021
Ono, K. SU077, SU239
Onodera, S. SA169
Ontiveros, C. S. SU064
Onyia, J. E. 1135, SA361
Ooi, D. S. SU110
Opotowsky, A. R. SU276
Oppenlander, M. SA470
Opperman, L. A. M135
Or, P. C. M345
Orchard, P. J. SA390
Ordovas, J. M. SU143
Oreffo, R. O. C. SU415
Orellana, S. A. SA213
Oreskovic, T. M170
Oreskovic, T. L. F364, SA002, SA364, M169
Orimo, H. SU342, M407
Orloff, J. F106, SA106
Ornitz, D. M. SA141
Ortolani, S. WG2, WG6
Orszulak, T. M017
Orwig, D. SA296
Orwig, D. L. SA273
Orwoll, E. 1080, F011, SA011, SU028, SU029, SU344
Orwoll, E. S. 1012, F115, F292, SA115, SA292, SA305
Orwoll, S. SU029
Osborn, K. L. M115
Oscar, S. M178
Osdoby, P. M134, M140, M244, M260
Oshima, H. SU355
Oshima, T. SA077
Osinska, H. F446, SA446
Ostertag, A. SU313
Ostrowski, M. C. SU261
Ott, S. F106, SA106
Ott, S. M. SU332, M284
Ott-Ralph, S. M. SU081, SU082
Ottestad, L. F083, SA083
Ou, O. SA299
Oursler, M. J. M273
Ovalle, M. SU095
Ovejero, M. SU227, SU259
Ovejero, M. C. 1195
Owen, T. A. 1188, SU209, M392, M395, M397
Owens, J. M. M175, M231
Oxlund, H. M145, M388
Oyajobi, B. F042, SA042
Oyajobi, B. O. F071, SA071
Oz, O. K. SA472
Ozai, M. F410, SA410
Ozaki, S. SA077, M346
Ozasa, A. 1206, SA233
Ozawa, H. SU233, M206
Ozkurt, I. C. SU222
Ozono, K. F484, SA484, SU454

P

Paakkala, T. SA346
Paccione, P. M368
Pache, I. M310
Pacicca, D. M. M152
Pacifici, M. F417, SA417
Pacifici, R. F330, SA093, SA330, SA467, M143
Pacini, S. M396
Pacurari, M. M209
Paczas, M. R. SU122
Padalecki, S. S. SU072
Padilla, F. M107, M108
Padley, R. SU080
Paek, I. WG1
Paeper, B. W. 1222
Paglia, F. SA287
Paixão, J. B. A. SU331
Pajamaki, I. 1048
Pajevic, P. F176, SA176
Pajunen, M. F083, SA083
Pak, C. Y. C. SA472, M416
Palamakumbura, A. H. SA051
Palermo, L. M352
Paller, C. J. M436
Pallu, S. SU220, M211
Palmano, K. SU151
Palmer, G. F321, SA321
Palmisano, J. M350
Palnitkar, S. F314, SA314
Pals, S. T. SU245
Palumbo, G. SU398
Palummeri, E. SU285
Pan, B. M210, M230
Pan, G. M243
Pan, L. C. M205, M392
Pan, W. SU318
Panda, D. F391, SA391
Panda, D. K. 1029
Pande, S. M417
Pannett, A. A. J. 1215
Papadimitropoulos, E. A. M081
Papaioannou, A. SA289, SA340, M293
Papapoulos, S. 1091
Papapoulos, S. E. 1077, M186
Papavasiliou, V. M002
Paralkar, V. M. 1107, M392, M395, M397
Pardi, E. M442
Pardi, S. 1042
Parés, A. SA332
Paret, L. G. SA229
Parfitt, A. F314, SA314
Parfitt, A. M. 1133
Parhami, F. M229, M261
Parikh, N. F277, SA277
Parisi, M. S. SA384
Parisien, M. 1173
Park, E. SU119, SU414
Park, H. M129
Park, I. K. M339
Park, J. SU141
Park, R. SU211, SU384
Park, S. J. M156
Park, W. SU076
Park, Y. S. M339
Parker, M. SA101, SA317
Parker, R. A. 1040
Parkinson, W. M293
Parra, J. SU182
Partridge, N. C. 1198, F186, SA032, SA186, SU079, SU199
Pasanen, M. SU180
Pasanen, M. E. SA346
Paschalis, E. P. SU048, SU305, SU337, M011
Pasco, J. A. M338
Pasque, C. SU419
Pastoureau, P. SU068
Patel, P. 1019
Patel, R. SU085, M080, WG4
Patel, S. M423
Paterson, A. F083, SA083
Pathak, R. D. M315
Pathmanathan, D. F412, SA412
Paton, L. M. F354, SA354
Patrick, A. M303
Patrick, A. L. F304, SA304
Patterson, E. K. SA453
Paul, K. H. M458
Pavalko, F. SA160, SA162, SU167
Pavlin, D. SU063
Pavo, I. 1136
Pawlotsky, Y. SA120
Payton, M. E. SU357
Peacock, M. 1218, F122, F398, SA122, SA123, SA398, SU392, SU399
Peat, R. A. 1203, F256, F424, SA256, SA424
Pecherstorfer, M. M057
Peel, N. F. A. 1127, F094, SA094, SU292
Peet, G. M249
Peet, N. M. 1193
Peleg, S. SA461, SU073
Pelled, G. M225
Pellerito, R. SU286
Peng, H. SU043
Peng, L. F456, SA456, SU264
Peng, X. SA362, SU447
Peng, Y. SA102
Penman, S. M208
Pennypacker, B. F246, SA246
Pennypacker, B. L. SA331
Pepe, J. SA287
Peralta, M. I. SU420
Perdriger, A. SA120
Pereda, C. A. M369
Pereira, R. C. SA211
Pereira, R. M. R. 1121
Pérès, G. M001
Perez, G. I. 1219
Perez, R. 1079
Perez, S. SA222
Peris, P. F013, SA013, SA332, SU390
Perrone, S. M105
Perrott, D. SA167
Perry, M. J. 1076
Persson, E. M141
Persy, V. P. SA050
Peschon, J. 1195
Petcher, T. M390
Petersen, D. N. 1031, SA053
Petersen, J. P. M024
Petersen, V. M324
Peterson, J. W. F275, SA275
Peterson, M. SA350
Peterson, W. J. SA204

(Key: 1001-1222 = Oral, F = Friday Plenary poster, SA = Saturday poster, SU = Sunday poster, M = Monday poster, WG = Working Group Abstract)

Petit, M. A. SA002, M169
Petkov, V. I. M112, M113, M305
Petracin, C. SA319
Petrey, M. SU049
Petri, A. SA049
Petrie, A. SA289, SA340, SU296
Pettinger, M. B. SA278, M300
Peyrin, F. SU010
Peyton, A. SU162
Pfeifer, M. SA347
Pflugh, D. L. 1098
Pham, C. SU416
Pham, L. SU221
Phan Van, A. SU412
Philbrick, W. M. 1100
Phillips, E. F277, SA277
Phillips, E. R. WG5
Phillips, S. M. M099
Phipps, K. SU028
Phipps, R. SA255, SU337
Phipps, R. J. SU341, M086
Pi, M. 1181
Piacentini, A. SA188
Pickar, J. H. M386
Pidasheva, S. M441
Pidoux, E. SA429
Pierroz, D. 1062
Pietschmann, P. SA481, M111
Pike, J. W. 1023, 1099, 1120, SA177, SA383, SU460
Pikul, S. M207
Pilbeam, C. C. F437, SA437, SU214, SU239, M205
Pinchera, A. M442
Pinet, M. C. M103
Pinheiro, M. M394
Pinto, R. M. SU398
Pirih, F. Q. SU221
Pisani, D. SU024
Pischon, N. R. SA051
Piscitelli, E. SU136
Piscitelli, P. SU284
Piserchio, A. SU427, SU440
Piswanger-Sölkner, C. J. F111, SA111, SU423
Pitsillides, A. SU274
Pittelkow, M. R. SU450
Pitts, K. SA318
Planelles, G. 1055
Plantalech, L. SU279, SU280
Plawinski, E. SA147
Plotkin, H. SU406
Plotkin, L. I. 1013, 1161, 1176, 1190
Plouët, J. M391
Plum, L. 1120, SA383, SU460
Plutat, J. SA143
Poblenz, A. 1023, 1099
Podgornik, M. N. F405, SA405, SU408, SU409
Poeppelmeier, O. 1082
Pohorecky, L. SA055
Polak, J. M. 1101
Polek, T. C. M262
Poliachik, S. L. 1046, SU181
Policani, G. SA402
Pollintine, P. F009, SA009
Pols, H. SA095
Pols, H. A. 1221
Pols, H. A. P. 1222, M189
Pombinho, A. R. M043
Ponce, G. SU279
Pondrelli, C. M110
Ponik, S. SA162
Ponik, S. M. SU167
Ponomareva, L. V. 1126, SU268
Pons, F. SA332, SU390
Poole, R. SA141
Poór, G. SU138
Pope, R. M422
Popoff, S. N. 1084, 1188, SU209
Porcher, R. SU282, SU319
Porquet, D. M001
Porras, A. G. SU401
Port, L. SU297
Porta, A. SU186
Portanova, J. M281
Posner, G. H. SU073
Pothuaud, L. M083
Potter, I. C. M434
Potter, O. F040, SA040
Potts, J. T. SU427
Powell, D. SA152
Powell, D. E. SU111
Powell, R. M368
Power, G. M434
Power, J. SA317
Power, R. A. M133
Powers, C. C. 1133
Powles, T. F083, SA083
Poynton, A. SA350
Pozzo, J. SU280
Pratap, J. 1112, M198
Pratelli, L. SU315
Pratt, S. M296
Preissner, C. M. 1108
Prenger, M. C. SU340
Prenner, G. SU423
Prentice, A. F003, SA003, M003
Prentis, D. 1165
Pressman, A. R. SA298
Preuss, J. SU338
Price, C. SU117
Price, J. SA074
Price, J. E. 1023
Price, P. A. M019, M457
Price, R. I. SU053
Prié, D. P. 1055
Priemel, M. F036, SA036, M072
Priest, L. SA198
Prince, R. L. M116
Pringle, D. SU407, M356
Pringle, D. P. SU413
Pringle, G. SA072
Prior, J. C. M355
Pritchard, W. SU407, M356
Probyn, L. M293
Proetzel, G. M029
Proll, S. 1222
Prolo, P. M241
Prowse, E. SA128, SU098
Prud'homme, J. F029, SA029
Prueksaritanont, T. F246, SA246
Pruijs, H. 1105
Puche, V. M036
Pucilowska, Y. M233
Puel, C. SU354
Puente, E. M453
Pulcini, J. SU434
Purchase-Helzner, E. L. M296
Purpura, K. A. M222
Pusiol, E. SU279
Puzas, E. F044, SA044, SU090, SU377
Puzas, J. E. F234, SA234, SU036, SU041, M053
Pylkkänen, L. F083, SA083

Q

Qi, H. 1031, 1107, M392, M395, M397
Qi, K. M386
Qian, J. F446, SA446
Qian, W. F330, SA330, M178
Qian,, W. P. M143
Qiao, M. 1157, 1189
Qin, L. SA336, SA338, SU199, SU361, M345, M376
Qin, X. M149
Qin, Y. SU172, M097, M114
Qin, Y. J. M125, M126
Qiu, M. SA247, SA264
Qiu, P. SU199
Qiu, S. F314, SA314
Quandt, S. M352
Quane, K. M120
Quane, K. A. SA012
Quarles, L. D. 1181, F180, SA063, SA180
Que, I. 1091, F468, SA468
Quesada, J. M. M309
Quibria, N. M385
Quinlan, E. 1110
Quinn, J. E. SA082, SA088, SU082
Quinn, J. M. W. 1073, 1123, SA242, SU243, SU257
Quinn, S. J. M443
Quintana, R. A. M430
Quirino, L. M. M286
Qvist, P. SU078, SU105, SU112, SU259, SU327, M348

R

Rabaia, N. A. F157, SA157
Rachmilewitz, D. F146, SA146
Radeff, J. M. SU224
Radspieler, H. SA336, SA338
Rafferty, K. A. M362
Raggatt, L. J. 1198, SA032
Rahman, M. M. SU244
Rahmy, A. I. A. SU088
Raisz, L. G. F437, SA136, SA437, SU214, SU239, M205
Rajamannan, N. M. M017
Ralston, S. H. 1191, SA135, SU145, SU398, M208
Ramirez, D. S. SA469
Ramos, J. SA380, SU107
Ramos, J. R. M286
Ramos, L. SA267
Ramsey-Goldman, R. M421, M422
Ransjö, M. M251
Rao, A. 1007, 1039
Rao, D. F277, F314, SA270, SA277, SA314
Rao, D. S. WG1, WG5
Rao, L. G. SU441
Rao, N. SU434
Rao, S. SA055
Rapado, A. M323
Raphael, R. H. M337
Rapuri, P. B. 1164, F358, SA358, M285
Raschke, M. M147
Rascon, Y. M430
Rasmussen, J. H. SA374
Rasmussen, K. SA179
Rasmussen, P. SU259
Rauch, F. SU406
Raue, F. SU379
Raum, K. M109
Ravasi, T. SU252
Ravid, A. SA078
Ravn, P. 1037, SA370
Rawadi, G. 1002, 1097
Rawlins, J. T. M135
Ray, G. T. SA298
Ray, M. V. L. SA362
Ray, R. SU461
Raymond, V. SU388, SU391
Raz, B. SA322
Reading, I. SA423
Reaney, L. F091, SA091, SA092
Recchia, I. SA086, SU398
Recker, R. 1038, 1138, SU358, M366
Recker, R. R. SU123, SU124, SU125, SU126, SU133, SU135, SU176, SU275, M123, M124, M163, M164, M327
Reczek, D. 1142
Reddy, P. F119, SA119
Reddy, P. G. SA270
Reddy, S. V. SU152, SU389
Redline, S. F290, SA290
Reed, P. W. F124, SA124
Reese, J. SU402
Reeve, J. SA101, SA317, SU274, M168, M308
Reginster, J. SU345
Regmi, A. SU234
Regunathan, A. M253
Rehman, Q. F440, SA440
Reid, D. F113, SA113
Reid, D. M. SA135, SA266, SU381
Reid, I. 1059
Reid, I. R. 1057, SU151, M146
Reim, N. SU329
Reinhold, M. I. SA041
Reinholz, G. G. M223
Reinholz, M. M. M223
Rejnmark, L. SU288, M373
Remy, B. SU114
Renda, G. SA352
Renoux, V. SU068
Reppe, S. M219, SU200
Resche-Rigon, M. 1027, SA479
Reseland, J. E. SU200, M219
Resnick, N. M. 1040
Reszka, A. A. 1146, F241, SA241
Rettinger, S. SU330
Rey, C. SU373
Rey, J. M. SU256
Rhee, Y. F337, SA337, SU137, SU258
Rho, J. M248, M250
Rialland, X. SU065
Rian, E. SU200
Riancho, J. A. SA127
Rianon, N. SA166
Ribadeneyra, J. M254
Ribich, J. 1128, SA112
Ribom, E. SA126
Riccardi, D. SA194
Ricci, J. F186, SA186
Ricci, R. WG11
Ricevuto, E. SA084
Rich, S. SU022
Rich, S. E. F302, SA301, SA302
Richards, A. M301
Rickard, D. M017
Ridout, R. M297
Riedt, C. M340
Riera, G. S. SA380, SU107
Rifas, L. SU069
Rigante, D. WG11
Riggs, B. L. 1009, 1093, 1103, 1134, F307, SA217, SA307, M182, M183, M187
Riminucci, M. SU386
Rinaldi, M. G. SU024
Rinaldo, R. SU450
Ringe, J. D. SU338, SU339
Ringel, M. F389, SA389
Rini, G. B. SA352, SU287
Risteli, J. SU078, SU225
Ritenbaugh, C. SA278
Ritter, C. S. SA491, M417
Rittling, S. F054, SA054, SU058
Rittling, S. R. 1044, 1156, F236, F442, SA236, SA442, SU059
Rittman, E. L. M086
Rivadeneira, F. 1221

Rivas, P. M092
Rizzoli, R. 1201, F321, SA321, M353, M382, M383
Roach, H. I. SU415
Robb, L. 1073
Robbins, J. SA278
Roberts, S. SU017
Robertson, E. J. 1076
Robertson, L. SA285
Robey, P. G. F218, SA218, SU215, SU387, M226
Robin, B. SU369, M016
Robin-Jagerschmidt, C. 1027
Robins, D. M. SA470
Robinson, B. G. F395, SA395
Robinson, J. F119, SA092, SA119
Robinson, J. A. 1112
Robling, A. G. F168, SA117, SA168
Roccisana, J. L. SU152
Roche, P. C. M223
Rochet, N. M. M174
Rodan, G. A. 1146, 1147, F241, F246, SA241, SA246, SA331, M326
Rodan, S. B. F246, SA246
Rodés, J. SA332
Rodrigues, C. V. M. SU050
Rodriguez, J. P. F345, SA345
Rodríguez-Rebollar, A. SU142
Rodríguez-Rodríguez, A. M418
Roel, J. M400
Rogers, A. 1132, M369
Rogers, J. SU130, SU131
Rogers, M. SA255
Rogers, M. J. 1191, F248, F249, SA248, SA249, SA251, M275
Roggia, C. F330, SA093, SA330, M143
Roh, S. I. M334
Roldan, E. SU217
Roldán, E. J. A. SU385
Rolland, Y. SA120
Romagnoli, E. SA287, SA409
Roman Roman, S. 1002
Romey, G. M181
Roodman, G. D. F073, SA073, SU152, SU389, M246
Ros, I. SA332, SU390
Rosati, R. L. M395
Roschger, P. SA388
Rosen, C. SU428
Rosen, C. J. 1061, 1080, 1096, 1106, 1217, 1220, SA007, SA118, SA152, SA367, M148, M389
Rosen, C. M. SU382
Rosenberg, I. 1210
Rosenblatt, M. F227, SA227, SU443
Rosenqvist, K. F083, SA083
Rosholm, A. SU095
Rosier, R. F044, F234, SA044, SA234
Rosier, R. N. SU036, SU041, SU090, M053
Rosol, T. M062
Rosol, T. J. SA431, SU436, M432
Ross, F. 1019
Ross, F. P. 1022, 1033, F239, F333, F403, SA239, SA333, SA403, SU260, SU416, M247, M258, M259, M267
Ross, P. D. M298, M322
Ross, V. SA362
Rosser, J. M011
Rossi, A. M. SA459
Rossi, B. M174, M181
Rossini, G. 1189
Rossini, M. SU285
Roth, K. SU416
Roth, S. I. 1051
Rothe, L. M134
Roudier, M. P. SU081, SU082
Roughead, Z. K. SA148, SA320
Rousseau, F. M289
Rousseau, L. SU438
Rousselle, P. M036
Roux, C. F113, SA113, SU282, SU319
Roux, S. M075
Rovai, G. SU279
Rowe, B. H. SU366
Rowe, D. SA190, SA192
Rowe, D. W. 1185, 1186, F191, SA191, SU120, M171, M215
Rowe, G. 1097
Rowe, P. S. N. F400, SA063, SA400
Rozenbaum, W. SU313
Ruan, L. M138
Rubin, C. 1047, SU166, M114
Rubin, C. T. SA045, M097
Rubin, J. 1096, SA177, SU205, M447
Rubin, J. S. SU243, SU257
Rubin, M. 1169
Rubin, M. R. SU394, SU395
Rubinstein, M. SU348
Rubio, R. M307
Rucci, N. SA084, SA086
Rudkin, G. M235
Rudolph, L. A. SU335, SU336
Ruecker, A. M024
Rueger, J. M012
Rueger, J. M. 1171, F036, SA036, SA065, SU248, SU249, M024, M072
Ruegsegger, P. M391
Rüegsegger, P. SA098
Ruesink, T. J. 1016
Ruff, C. M170
Ruiz Cotorro, A. SU182
Runciman, R. J. SA116
Rundle, C. H. SU042
Rupert, R. SU430
Rupert, R. L. SA432
Rushton, N. SA101, SA317
Russell, A. S. SU366
Russell, J. SA280
Russell, R. G. G. SA255, SU341
Russell, S. J. 1093, 1134
Russo, C. R. SU309
Russo de Boland, A. SU432, M450
Rutherford, O. M. SU174, SU175
Rutherford, R. B. SU034
Ryaby, J. P. M283
Ryan, L. E. M336
Ryan, L. M. SU408
Ryan, P. J. SU100
Ryder, K. M. M287
Rydziel, S. SA198, M042
Ryoo, H. SA181, SU211, M129
Ryota, T. SA293

S

Saarikoski, S. M361
Saba, L. M241
Sabari, S. M027
Sabatakos, G. 1097, 1100
Sabatini, M. SU068
Sabbieti, M. G. SA136
Saboia, F. J. S. SA171
Sacha, J. P. M086
Sackrison, J. L. M290
Sacks, S. H. 1141
Saedi, B. M261
Saeger, U. M312
Saegusa, M. SA235
Safadi, F. F. 1084, 1188, SU209
Saftig, P. SU065
Saggar, A. K. 1008
Saha, P. K. M095
Sahara, N. M206
Said-Al-Naief, N. SU129
Saied, A. M109
Saini, T. M261
Sainsbury-Salis, A. 1125
Saintier, D. SU255, SU256
Saito, T. M010
Saji, M. F389, SA389
Sakaguchi, K. F137, SA137
Sakai, A. F144, SA144
Sakai, H. F261, SA253, SA261, M282
Sakata, T. F159, SA159, SU428, M177
Sakkers, R. J. B. 1105
Sakuma, Y. M205
Sakurai, K. M090
Sakurai, N. F201, F254, SA201, SA254
Sakuta, K. F261, SA261
Salamoun, M. SU289, M414
Saleh, H. SU252
Salerni, H. SU280
Salingcarnboriboon, R. F220, SA220, SU173
Salo, P. SU007
Salois, P. 1187, SA195
Salvadori, S. SA404, M076
Samadfam, R. SA244
Sambrook, P. N. F345, SA345
Samelson, E. J. SU314
Sampaio, A. V. M459
San Martin, J. A. 1136
Sanada, M. SU099
Sanchez, C. P. SU424
Sánchez, J. A. M071
Sanchez, T. V. SU001
Sanders, K. M. F295, SA295
Sanders, M. M066
Sanders, M. M. SA072
Sandini, L. M361
Sandoval, R. M430
Sanjay, A. 1149, F225, SA225, SA232, SU262, M265, M280
Sankaralingam, S. SU098
Sankuratri, S. F252, SA252
Santamaría, I. SU142
Santana, R. B. SA051
Santavirta, S. M051
Santillan, G. SU217
Santora, A. 1037, 1059, SU345
Santoro, M. SU218
Sanyal, A. M182
Sanyal, B. SA193
Saraifoger, S. SA175, WG2, WG6
Saraiva, G. L. SA267, M286
Sarfati, E. F104, SA104
Sarkar, S. F356, SA356, SA357
Sarrazin, P. SA258
Sartori, M. L. M241
Sasaki, T. SU054, SU077
Sastri, S. SU115
Sato, H. M046
Sato, M. 1135, 1179, F364, F373, SA364, SA373, SA476
Sato, N. F254, SA254, SU242
Sato, S. SU210
Sato, T. F046, SA046, SU326
Sato, Y. SU149
Satokata, I. M215
Satomura, K. SU207
Satyawadi, R. M399
Sauter, L. SU193
Sauty, A. M310
Sawyer, T. 1145, SU377
Saxon, L. SU004, SU005, SU006
Sayavongsa, P. M404
Sayegh, F. SA328
Sayne, J. R. M135
Scadden, D. T. 1053
Scandurra, R. M179
Scariano, J. K. SA329
Schafer, B. W. 1017
Schäfer, C. M012
Schaffler, M. SU269
Schaffler, M. B. SU116, M166
Schatz, D. G. 1098
Schatzman, R. C. 1222
Schauer, P. R. M399
Scheafer, M. J. WG5
Schedl, A. 1071
Schei, B. SU312
Schiavi, S. C. 1142
Schifini, M. F. SA402
Schiller, P. C. SU444
Schilling, A. F. SU248, SU249
Schilling, B. SA445
Schimmer, R. 1038, F339, F341, SA339, SA341
Schimmer, R. C. M349
Schinke, T. 1003, F036, SA036, M012
Schipani, E. 1053, 1152, SU066
Schlesinger, P. H. SA390
Schmid-Antomarchi, H. M181
Schmidt, A. 1179
Schmidt, A. H. SA017
Schmidt, A. L. SA476
Schmidt, C. M072
Schmidt, S. M311
Schmidt-Gayk, H. SU103
Schneider, A. 1075, SU435
Schneider, D. L. F106, F115, SA106, SA115, M079
Schneider, G. SU229
Schneider, G. B. SU376
Schneider, J. L. 1079
Schneider, V. M170
Schoenau, E. M359
Schoenmaker, T. SU245
Schoenmakers, I. M185
Schohe-Reiniger, C. 1082
Scholes, D. M284
Scholz-Ahrens, K. E. SU350
Schönbächler, J. SA336, SA338
Schoutens, A. SA425
Schrezenmeir, J. SU350
Schroeder, T. M. M199
Schuetze, N. 1082
Schulten, A. J. M. SA167
Schultz, K. L. 1217
Schultz, N. SA143
Schulz, A. M093
Schulz, E. SA265
Schulz, K. M311
Schulz, K. D. M312
Schuster, J. M057
Schütz, G. F478, SA478
Schwartz, E. SU053
Schwartz, E. N. SU094
Schwartz, Z. SA457, SU271, M011, M158, M445
Schwarz, E. F044, F234, SA044, SA234
Schwarz, E. M. 1021, 1024, 1153, SU036, SU041, SU090, M053, M176
Schwarz, H. SU361
Schwarz, P. M324
Schweitzer, D. 1105
Schweizer, B. SU157
Schwindinger, W. F. F389, SA389
Sciaudone, M. P. F199, SA199
Scillitani, A. SA409
Scott, D. O. M392, M397
Screen, J. F182, SA182, M212
Sebaldt, R. J. SA340, SU296, M081

(Key: 1001-1222 = Oral, F = Friday Plenary poster, SA = Saturday poster, SU = Sunday poster, M = Monday poster, WG = Working Group Abstract)

Sebti, S. SU224
Seck, T. F263, SA263
Secreto, F. J. M209
Seedor, J. G. F246, SA246
Seeherman, H. M175, M231
Seeman, E. 1167, SA315, M338
Segal, E. SA322
Segni, G. WG11
Segre, G. V. 1051, F449, SA449
Seibel, M. J. SU074, SU102
Seidel, J. 1056
Seino, Y. 1204, SA455
Seki, Y. SU054
Sekiya, H. SA158, M039
Selander, K. M058
Selby, P. L. 1174, F091, SA091, SA092
Selhub, J. 1210, SU143
Selim, A. 1188
Sellckau, R. SA143
Sellers, R. S. M432
Sellin, K. 1187, SA195
Selvamurugan, N. F186, SA186, SU079
Semenkovich, C. F. M020
Semler, J. SU379
Sen, A. M420
Seneviratne, T. SA401
Senin, U. SU309, SU310
Senoo, H. SU210
Sepp, H. W. M447
Serra, R. 1074, 1078, M132
Serrano, M. M418
Serrano de la Pena, L. F417, SA417
Serrano de la Peña, L. SU044
Seto, H. M023
Seto, K. SA158
Seton, M. F412, SA412
Settle, S. M281
Seuwen, K. SA015, M213
Severson, R. K. M063
Sexton, C. M149
Sferrazza, C. SU287
Shackleton, C. H. 1035
Shah, H. M449
Shah, H. D. SU449
Shaked, D. M445
Shakelford, L. M170
Shaker, J. SA401
Shakespeare, W. 1145, SU377
Shalhoub, V. 1045, 1092
Sham, A. SU030, SU311
Shamiyeh, E. M422
Shanahan, F. M120
Shane, E. 1042, 1173
Shao, J. S. 1114, M020
Shapira, B. M314
Shapiro, I. M. SU057, SU189
Shapiro, J. R. SU118, M170
Shapses, S. A. M340
Sharkey, P. F. SU115
Sharma, M. F463, SA463
Shaughnessy, J. M054
Shaughnessy, S. G. SU216
Shea, M. F165, SA165
Shearman, A. M. M122
Sheikh, S. 1015, 1158, 1184
Shen, H. SU123, SU124, SU125, SU126, SU133, SU134, SU135, M124, M126
Shen, J. M195
Shen, V. SA326, SU368, SU369
Shen, Z. 1006
Sheng, M. H. C. SA060, SU042
Shepherd, A. J. F309, SA309
Shepherd, J. SU019
Shepherd, J. A. SU095
Sheppard, D. F239, SA239
Sher, L. B. 1026
Sherrard, D. J. SA477
Sherrell, R. M340
Sherrer, Y. SU095
Sheu, T. SU377
Sheu, T. J. SU036
Shevde, N. SA383
Shevde, N. K. 1023, 1099, 1120, SU460
Shi, D. 1002
Shi, L. F373, SA373
Shi, M. F124, SA124
Shi, S. F218, SA218, SU215, M226, M228
Shi, W. F206, SA206, SA480
Shi, X. F206, SA206, SA480, M197
Shi, Y. 1117
Shi, Z. F243, SA243
Shibasaki, K. SA245
Shibata, H. SA077
Shibata, M. 1143
Shibata, O. SA238
Shibata, Y. F018, SA018, SA207
Shih, C. SU203, M238
Shimada, T. 1182, M128
Shimizu, K. SU266
Shimizu, N. SA448, SU426, SU427, SU440
Shimo-Onoda, K. M021
Shimoaka, T. 1072, M022
Shimomura, J. SA057
Shin, C. 1184
Shin, H. SU119, SU414
Shin, H. I. F176, SA176
Shin, Y. SA335
Shindo, M. F046, SA046
Shine, H. D. M227
Shinki, T. SU456
Shinomiya, K. M028
Shioi, A. SA023, SA145, SA253, M014
Shioyasono, A. SA077
Shipp, K. M. 1208
Shiraishi, A. SA376, SA377, SA378, SA379
Shiraki, M. SU140
Shiratori, Y. M085
Shirley, D. SA221
Shiro, R. SA416
Shoback, D. SA401
Shobuike, T. SU244
Shoji, S. SA023
Shor, R. SU397
Shore, E. SU040
Shore, E. M. F387, F417, SA387, SA417, SU044, WG4
Shore, S. R. SA276
Shorey, S. SU251
Shouhed, D. M229
Shugarts, S. SU401
Shui, C. SA217
Shukunami, C. F046, SA046
Shulman, D. I. F398, SA398
Shults, J. 1202
Shultz, K. L. 1080, 1106, 1220, F168, SA118, SA168
Shum, L. F139, SA139
Shyu, J. SA226
Shyu, J. F. SU203
Si, H. SU211
Sibonga, J. D. SA413
Siemianowicz, K. SA430
Sierra, J. M192
Sierra, O. F330, SA330
Sierra, O. L. SA467
Sievanen, H. 1048
Sievänen, H. SU103, SU180, M387
Sievänen, H. T. SA346
Siggelkow, H. M184
Sigurdsson, G. SU439, M006
Sijmons, B. 1091
Silke, C. M. M120
Silva, A. B. 1220
Silva, F. M. B. SU446
Silva, L. SU022
Silva, M. B. D. M438
Silva, M. J. F403, SA403
Silve, C. M. 1055, SA140
Silver, J. F435, SA435, SA436
Silverberg, S. J. 1169, 1172, 1173, SU394, SU395
Silveri, F. SU286
Silverman, S. M100
Silverman, S. L. SU380
Sima, D. I. M242
Siminoski, K. 1129, F284, SA284, M081
Siminoski, K. G. SU343
Simmons, H. A. 1031, M392
Simon, B. J. SU271
Simone, C. M178
Simonelli, C. SU367, M073, M074, M299
Simonet, W. S. 1020
Simonini, G. SU136
Simpson, L. G. F180, SA180
Sims, N. M029
Sims, N. A. 1073, 1123, F176, SA176
Sims, S. M. SA453, M278
Simske, S. J. 1045, F369, SA369
Sinaki, M. F288, SA288
Sindrey, D. R. M033, SA147
Singer, K. P. SU053
Singer, M. V. M408
Singh, A. T. K. SU224
Singh, R. 1108
Singh, S. 1023, SA062, SU003, M424
Sipe, J. SU033
Sipe, J. B. M159
Sips, H. F208, SA208
Siris, E. S. SA274, SU307, SU308, M295
Sirola, J. M361
Sizemore, G. W. SU420
Skaag, A. M294
Skedros, J. G. SU062, SU164, M374
Skerry, T. M. 1193
Skikne, B. M159
Sklar, C. A. M384
Skrtic, S. F465, SA464, SA465, SU139
Slama, L. SU313
Slatopolsky, E. M417
Slattery, E. 1078
Slosman, D. 1201
Sltopolsky, E. M455
Small, C. F119, SA119
Smit, J. H. F348, SA348
Smith, A. L. SA273
Smith, B. J. SU357, SU358, M366
Smith, C. 1132
Smith, C. L. M167, M341, M410
Smith, E. J. 1203, F256, F424, SA256, SA424
Smith, G. M370
Smith, I. F083, SA083
Smith, J. O. SU415
Smith, K. SA444
Smith, R. M401
Smith, R. J. M150
Smith, S. B. M419
Smith, S. Y. SU105, SU327, M379
Smock, S. L. 1188, SU209
Sneddon, W. B. F451, F452, SA451, SA452, SA454
Snetselaar, L. G. M005
Snodgrass, S. 1037
Snow, C. M. F165, SA165
Snyder, B. D. M091
So, H. M250
Sobue, T. 1061, M127, M130
Sochett, E. SA420
Sochocky, N. M232
Sod, E. W. SA342
Soegiarto, D. W. F414, SA414
Soezeri-Ludwig, S. SU157
Sohn, P. 1078
Sohn, Y. SU414
Solanki, P. 1217
Solomon, D. H. SU362, SU378
Soma, K. SU058
Somerman, M. J. F024, SA024
Sommer, U. SA462, SU157
Sommerfeldt, D. W. F036, SA036
Somner, J. SA128
Somoza, J. SU279, SU280, M409
Son, H. Y. SU422
Sonderbye-Kjaerulff, L. SA374
Sone, T. SA169, M061
Song, B. SA480
Song, S. H. M334
Song, Y. M448
Sonoyama, W. SU153
Sooy, K. M217
Sorensen, E. S. SA154
Sørensen, L. M145
Sorensen, O. H. SU156
Sørensen, O. H. SU304
Soreq, H. F048, SA048
Sornay-Rendu, E. SU023
Sottile, V. M213
Souberbielle, J. F104, SA104
Soung, D. SU358, SU419
Sowa, H. F325, SA325, SA407, M151, M204
Sowa, Y. SU454
Spadaro, J. A. M343
Sparks, A. 1089
Spasovski, G. M412
Speck, N. A. 1110
Specker, B. M009
Specker, B. L. SA272
Spector, T. D. F124, SA124, M101
Speer, G. SA132, SA133, SU320, SU322
Spelsberg, T. M017
Spelsberg, T. C. 1016, SA179, SA217, M182, M187, M223
Spies, S. M421, M422
Spivak-Kroizman, T. M262
Sprague, E. SU160, SU272
Sprague, S. M. F087, SA087
Squire, M. 1047
Squire, M. E. SU166
Sridhar, P. M138
Srinivasan, S. 1046, F157, SA157, SU181
Srivastava, A. 1216
Srivastava, A. K. 1183
Srivastava, S. SU070
St-Amant, N. 1187
St-Armant, N. SA195
St-Arnaud, R. F029, SA029, SU459
Staal, K. M429
Stahl, P. M455
Stahlhut, M. SU259
Stahr, K. SU329
Stains, J. M212
Stains, J. P. 1015, F182, SA182, SA183
Stakkestad, J. M294
Stakkestad, J. A. 1038
Stallings, V. F006, SA006

(Key: 1001-1222 = Oral, F = Friday Plenary poster, SA = Saturday poster, SU = Sunday poster, M = Monday poster, WG = Working Group Abstract)

Stallings, V. A. 1202
Stamos, E. SU328
Stampa, B. SU381
Standish, T. I. 1169
Stanton, L. M027
Stark, S. F165, SA165
Staron, R. 1042
Stas, V. M297
Staub, J. J. SA312
Stauber, M. SU046
Ste-Marie, L. SU343
Ste-Marie, L. G. SA344, M446
Ste. Marie, L. G. M002
Stear, S. J. F003, SA003, M003
Steegenga, W. T. SU201
Steel, S. A. SU084
Steenvoorden, M. M026
Stefanick, M. SU028
Stehno-Bittel, L. SA428
Stein, G. 1001, 1004, M192
Stein, G. S. 1110, 1112, SU197, SU384, M041, M194, M195, M196, M198, M254
Stein, J. M192
Stein, J. L. 1110, 1112, SU197, SU384, M194, M195, M198, M254
Steinbeck, M. J. SU115
Steinberg, T. H. SU156
Steiner, I. SU366
Stenbeck, G. M255
Stenstrom, M. G. M294
Stepan, J. J. SA105
Stephenson, G. M293
Stephenson, G. F. SA289, SU296
Sterling, H. M249
Stern, B. SA362
Stern, P. H. SU051, SU224, M070
Sternlight, D. 1062
Stevens, P. SA200
Stewart, A. F. 1102
Stewart, C. E. 1087
Stewart, P. M. 1035
Stewart, T. L. SU145
Stilgren, L. S. SA131, M373
Stirling, D. F003, SA003
Stivala, M. M071
Stivers, C. 1160
Stock, S. M017
Stock, S. R. SU051
Stockman, G. SU217
Stockwell, J. D. 1106
Stone, K. M316, SU028
Stone, K. L. 1085, 1212, 1214, F290, SA290, SA303, M296
Stover, M. 1186, SA190
Stover, M. L. M216
Strasser, A. M276
Strates, B. S. M160, M224
Strauss-Schoenberger, J. M056
Stride, B. F478, SA478
Strong, D. M200
Strong, D. D. 1160
Strotmeyer, E. S. M313
Stroup, G. B. SU083
Strugnell, S. A. SA491, SU457, SU459
Struve, J. A. M173, M191
Stuart, W. D. F446, SA446
Su, M. 1107
Suarez Cuervo, C. M058
Subramaniam, M. 1016, SA179
Subramanium, M. M017
Suda, K. SU240, SU241, SU242
Suda, M. SA233
Suda, N. M268
Suda, S. SA237
Suei, Y. SU099
Suen, C. SA476
Sugano, N. SU236
Sugerman, H. J. M398
Sugimoto, T. 1139, F325, SA156, SA325, SA407, M151, M204
Sugita, A. SA483
Suhara, Y. SU456
Suhr, S. M. SU263
Sullivan, A. J. M194
Sullivan, S. S. SA007
Sumita, Y. M393
Sumner, D. R. SU349
Sun, B. 1180, M142
Sun, C. F206, SA206
Sun, F. SA027
Sun, H. B. SU163
Sun, J. M266
Sun, L. 1018, SA215
Sun, Q. SA121, SA438, SU437
Sun, X. SU075, M059
Sun, Y. SA247, SA264
Sun, Z. F463, SA463
Sundaramoorthi, R. 1145, SU377
Sung, J. SA181
Sunn, K. L. F458, SA458
Suominen, H. SU007, SU008, SU011
Supervia, A. M188
Suryawanshi, S. SU345
Susa, M. SA086, M460
Susa, M. M. SA196, SA240
Sutera, L. SU287
Sutton, A. L. M. SU196
Suuriniemi, M. M. SU132
Suva, L. J. F079, SA079, SA080
Suzawa, M. SA205
Suzawa, T. SU067, SU241
Suzuki, A. M202
Suzuki, K. SU183
Suzuki, T. SU140, SU298
Suzuki, Y. SA250, M346
Svastisalee, C. M. M337
Swamy, N. SU461
Swanson, L. SU367
Swat, W. M267
Swinnen, J. V. SA474
Swolin-Eide, D. SA142
Sybrowsky, C. L. SU164
Sydall, H. E. M308
Syed, Z. A. 1169
Sylvester, F. A. SU238
Sylvia, V. L. SA457, SU271, M158, M445
Symons, J. M041
Sypniewska, R. M059
Sytsma, M. J. M173
Syversen, U. M264
Szegedi, G. SA353
Szejnfeld, V. 1158, M394
Szombati, I. SU138
Szulc, P. 1209
Szymczyk, K. H. SU189

T

Taaffe, D. 1131
Tabak, A. SA132, SU138
Tabák, Á. SU320, SU322
Tabata, T. SA023
Taboas, J. M. SU435
Tachiki, K. H. SA204
Tadic, T. SU039
Taguchi, A. SU099
Taha, A. SU289
Tahara, H. SA397
Tajik, A. J. M017
Takacs, I. SA132, SA133
Takács, I. SU320, SU322
Takada, M. SA008
Takagi, A. SA299
Takagi, T. F201, SA201
Takagi, Y. SA156
Takahashi, K. SU183
Takahashi, M. SA349, M094
Takahashi, N. SU233, SU240, SU241, SU242
Takahashi, S. SU106
Takahashi, T. SA260
Takami, M. SU240, SU241, M248, M250
Takamizawa, S. SU210
Takamoto, M. M032
Takane, K. K. 1102
Takano-Yamamoto, T. SA028
Takasu, H. SA483
Takata, S. M085
Takato, T. 1148
Takayama, H. SU455, SU456
Takeda, E. SA134, SA486
Takeda, K. M271
Takeda, T. SA375
Takenishi, G. S. M191
Takeshita, S. 1019, F403, SA403, SU260
Taketani, Y. SA357, SA486, M032, M342
Takeuchi, Y. 1143, 1182, SA205, SA411, SU035, M128
Takeyama, K. SU455
Takigawa, M. F031, SA028, SA031, SA037, SA043, SU153
Takita, H. SU149
Talbot, J. R. SA265
Talbott, E. M296
Talmage, R. V. M013
Talpaz, M. M262
Tamada, T. M061
Tamborini, L. G. SU323
Tamir, A. SA322
Tamura, M. SU149
Tamura, N. 1206
Tan, H. 1092
Tan, H. L. 1045
Tan, J. W. M239
Tan, W. D. SU088
Tanaka, H. 1204, SA455
Tanaka, I. SU355
Tanaka, K. F130, SA130, SA233
Tanaka, M. M206
Tanaka, S. 1148, 1150, F144, F225, SA144, SA225, SA245, SA260, SA374, SA416, M023, M265, M276
Tanaka, S. M. SA164
Tanaka, T. SA386, SU346
Tanaka, Y. 1061, M130
Tang, B. W. M160
Tang, C. H. SA174
Tang, J. F184, SA184
Tang, R. SU341
Tang, S. P. SA005, SU400
Tang, Z. M037
Tanimoto, K. SU099
Tanimoto, Y. F197, SA077, SA197
Tanini, A. SU136, M406
Taniwaki, H. SA023, SA145
Tanizaki, Y. M085
Tankó, L. B. SA370, M349
Tanner, S. J. SU162
Tanno, M. M426
Taranta, A. SA175, SU398
Tatamiya, M. SU230
Tateishi, T. SU206, M010
Tau, C. 1056, SU348, SU385
Taubman, M. A. F422, SA422
Tawfeek, H. A. SU442
Tawfik, O. SA027
Tayim, A. SU289
Taylor, P. SA276
Taylor, T. 1008
Tchetina, E. V. M038
Teasdale, L. WG5
Teegarden, D. M363
Teilmann, S. C. SU156
Teitelbaum, S. L. 1019, 1022, 1033, F333, F403, SA333, SA403, SU260, SU416, M247, M258, M259, M267
Teknos, T. N. SU034
Temesvari, P. SU138
Tenenhouse, A. SA285, SU343
Tenenhouse, H. S. F385, SA385, M037
Teno, N. F064, SA064
Terkeltaub, R. 1011
Terpstra, L. F029, SA029
Teshima, R. SU347
Teti, A. SA084, SA086, SA175, SU398, M179, M180
Tetradis, S. SU221, SU222
Tfelt-Hansen, J. M444
Thakker, R. V. 1008, 1215
Thalhammer, T. M050
Theimann, B. M264
Theodoropoulos, C. SA487
Theriault, B. L. SU168, M266
Thierry-Palmer, M. M404, M452
Thissen, J. P. SA319
Thomas, A. SA472
Thomas, G. 1187, SA195
Thomas, G. P. 1117, F460, SA460
Thomas, H. F. F184, SA184
Thomas, J. F433, SA433, SU084, SU425
Thomas, R. J. F081, SA081, M435
Thomas, S. M131
Thomas, T. SU165, M391
Thommesen, L. M264
Thompson, D. F106, SA106, M352
Thompson, D. D. 1031, 1107, M392, M395, M397
Thompson, G. F150, SA150
Thompson, K. F248, F249, SA248, SA249
Thompson, L. SU281
Thompson, L. U. F279, SA279
Thompson, P. D. F488, SA488
Thompson, R. M458
Thornton, M. M. M098
Thrasher, A. F230, SA230
Throndson, R. T. SA219
Tibba, J. 1171
Tidy, A. F083, SA083
Tieulie, N. M174
Tigchelaar, W. SU065
Tiku, M. L. SA032
Tilly, J. L. 1219
Timm, I. A. 1194
Timm, W. SA103, SU350
Timonen, J. SA100
Tintut, Y. M229, M261
Titus, L. SU198, M045, M068
Tjoa, C. M. M395, M397
To, L. B. M210
Tobias, J. H. 1076, 1119, F009, SA009
Tobias, R. SU328
Tobiume, S. SU207
Toda, K. 1116
Toerge, J. M170
Tofteng, C. L. SU304, M119, M373, SA131
Toh, S. SA386, SU056, M426
Tokura, T. SA415
Tokuyama, R. SU207
Tolias, P. SU199
Tolkemitt, G. SU306
Tom, L. M169
Tomat, A. M409

(Key: 1001-1222 = Oral, F = Friday Plenary poster, SA = Saturday poster, SU = Sunday poster, M = Monday poster, WG = Working Group Abstract)

Tomita, M. F033, SA033
Tomita, T. SU183
Tomiya, M. SA059
Tomizuka, K. 1182
Toneguzzi, S. SA188
Tong, X. K. 1052, F439, SA439, SA441
Tonino, A. J. SU088
Toraldo, G. F330, SA093, SA330, SA467, M143
Toribio, R. E. SA431, SU436
Toriyama, K. F064, SA064
Torner, J. C. M005
Torralba, M. M307
Torres, B. M309
Torvinen, S. B. SA346
Tóth, E. SA372
Tou, K. SU247
Tovar Sepulveda, V. A. SU458
Towler, D. A. 1017, 1114, F182, SA182, SA183, M020
Toye, K. F327, SA327
Tözüm, T. F. SA470
Trackman, P. C. SA051
Tracy, J. K. F300, SA095, SA300
Tran, M. T. M112, M113, M305
Trauernicht, A. F071, SA071
Travers, R. SU401
Travers-Gustafson, D. SU275
Trevant, B. M041
Trivett, M. K. M434
Troiano, N. 1180
Tronche, F. F478, SA478
Trotta, F. SU286
Trump, D. L. 1128, SA112
Tsai, A. D. SA019
Tsang, J. C. SA448, SU427
Tsay, A. M136
Tsay, A. W. SA065
Tscheliessnigg, K. H. SU423
Tschesche, H. F150, SA150
Tschon, M. SA188
Tsubaki, S. M046
Tsuboi, M. SU342
Tsuchiya, Y. 1156
Tsuda, E. SA238
Tsuda, M. F254, SA254, SU099
Tsugeno, H. M085
Tsuji, K. 1006, 1034, 1044, 1111, 1156, F220, F442, SA220, SA442, SU058, SU059, M028, M032
Tsuji1, K. SU173
Tsukamoto, T. SA407
Tsukazaki, T. F018, SA018, SA207
Tsuzuki, T. M046
Tu, Q. 1181
Tu, S. SA443, SA444
Tucker, K. L. 1210, SU143
Tuckermann, J. P. F478, SA478
Tuji, K. F054, SA054
Tulchinsky, M. SA002
Tupinon-Mathieu, I. SU368, SU369
Tuppurainen, M. M361
Turbov, J. F087, SA087
Turgeman, G. M225
Turner, A. S. SU356
Turner, C. H. 1163, 1217, F155, F168, SA117, SA121, SA155, SA164, SA168, SA315, SU178, SU179, M379
Turner, J. J. O. 1008
Turner, R. SU029
Turner, R. J. 1012
Turner, R. T. F440, SA070, SA413, SA440, M086, M157
Tuukkanen, J. 1048
Tuysuz, B. 1056
Twaddle, S. SU108
Tweed, K. M423
Tylavsky, F. 1131, SU007, SU008, SU009, SU132
Tylavsky, F. A. F311, SA311, SA318, M287

U

Uchida, S. F144, SA144
Uchino, S. F408, SA408
Uchiyama, Y. F130, SA130, SA483
Udagawa, N. SU233, SU240, SU241, SU242
Udry, E. M310
Ueda, K. 1204
Ueda, T. SA299
Uede, T. 1156
Uehara, J. SU153
Uehara, R. M346
Ueland, T. SA324, SU025
Uemura, T. SU206, M010, M015
Ueno, N. 1125
Ueyama, K. SU056, M426
Ui, N. SA034
Uiterwaal, C. 1105
Uitterlinden, A. G. 1221, 1222
Ulla, M. R. M071
Underhill, T. M. M459
Unger, S. WG10
Unni, K. K. F412, SA072, SA412, M055
Upholt, W. B. M216
Urano, T. SU183
Usas, A. SU043
Usui, M. 1034
Uusi-Rasi, K. F364, SA002, SA364, SU103, M169, M387

V

V.E.R.T. Study Group 1129, F284, SA284
v.d. Stadt, R. J. M371
Väänänen, H. K. SU103, SU225, SU226, SU229, M048
Väänänen, K. M058
Vaccarino, V. SU314
Vaja, S. 1141, M358
Valenta, A. SA388
Valenti, R. SA404, M076
Valimaki, M. SU345
Valkusz, Z. SA049
Vallarta-Ast, N. SU089, M078
Valleala, H. M051
Valverde, P. F422, SA422
Valverde-Franco, G. SA141
Van Bezooijen, R. L. 1077
van de Ven, J. SA475
van den Heuvel, L. SU157
van der Eerden, B. M026
van der Eerden, B. C. J. SA475
van der Horst, G. F208, SA208
van der Klift, M. SA095
van der Linden, S. SU417
van der Meulen, M. C. H. SU060, M096
van der Neut, R. SU245
van der Pluijm, G. 1091
van der Saag, P. SU165
van der Wee-Pals, L. 1077
Van Dijk, S. SU375
Van Dongen, A. 1105
van Driel, M. M189
Van Duijn, C. M. 1221
Van Eerdewegh, P. M123
van Heerden, J. A. SU405
van Helvoort, A. M185
Van Herck, E. SA474
Van Hul, W. 1084
van Leeuwen, J. P. T. M189
van Meurs, J. B. J. 1222
Van Patten, C. M. M290
van Schoor, N. M. F348, SA348
van Schravendijk, M. R. 1145, SU377
van Soesbergen, R. M. M371
van Staa, T. P. 1199, 1213, F282, SA282
Van Thiel, D. H. SU420
Van Wesenbeeck, L. 1084
van Wijen, A. M196
van Wijnen, A. M192
van Wijnen, A. J. 1110, 1112, SU197, SU384, M194, M195, M198, M254
van Zoelen, E. J. J. SU201
van't Hof, R. J. 1191, M208
Vanasse, M. F419, SA419
Vandenput, L. SA474
Vanderschueren, D. SA474
VanHouten, J. N. 1063
Varghese, S. SU238
Vartanian, K. A. 1012
Vasikaran, S. D. SA434
Vasireddy, S. F091, SA091, M301
Vasko-Moser, J. A. SU083
Vassiliadis, J. 1142
Vautour, L. 1211
Vayssière, B. 1002
Vecsei, V. M111
Vedi, S. F360, SA360
Vegeto, E. F468, SA468
Veillette, C. J. H. SU155
Velasquez, G. SA380
Venters, R. A. M458
Venton, L. L. SA010
Ventura-Clapier, R. SA429
Verberckmoes, S. C. E. M214
Verbout, A. 1105
Verbruggen, N. M353
Vered, I. M317
Vermeer, C. M365
Vertino, A. M. 1032, 1058, M380
Vessella, R. L. SA082, SA088, SU081, SU082
Vestergaard, P. SU288, SU304, M119, M373
Vetró, O. SA049
Vezzoni, P. SU398
Vico, L. SU165, M391
Vidal, J. M. M379
Vidal, M. M455
Vidal, S. SA332
Vieira, J. G. M286
Viereck, V. M184
Viggeswarapu, M. SU198, M045
Vignery, A. SA362, M249
Vihko, P. SU229
Villa, A. SU398
Villagra, A. M192
Villars, F. M211
Villemin, P. 1095, SU372
Vincent, A. SU352
Vincent, B. L. M252
Vis, M. M371
Visser, A. 1077
Vitale, G. SA352
Vittecoq, O. SU412
Vitti, R. 1110
Viveros, H. SA469
Vogt, M. T. F292, SA292
Vokes, T. SA102
Vokes, T. J. SA096
Vokrouhlicka, J. SA105
Volkman, S. K. SU061, SU122
Volta, C. SA022
von Scheven, E. SU019
von Schroeder, H. P. SU155, SU251
von Stechow, D. M091, M385
Voorhees, S. SU198
Vora, J. P. F433, SA433, SU425
Voskuijl, A. E. M429
Voznesensky, O. S. F437, SA437
Vradii, D. 1112
Vuohelainen, T. 1048
Vuori, I. M387, SU180
Vuori, M. I. SA346
Vuorio, E. SU225, SU226
Vyskocil, V. SU403

W

Wacker, W. K. M104
Wactawski-Wende, J. 1089
Wada, M. F410, SA410
Wada, S. SA237, SA426
Waddington, D. SA163
Wagman, R. SA306
Wagman, R. B. M321
Wagner, J. 1128, SA112
Waguespack, S. G. 1081
Wahl, L. M. M150
Wahner, H. W. F288, SA288
Wainwright, S. A. F292, SA292
Waits, C. A. M159
Wakabayashi, I. M329
Wakley, G. K. F009, SA009
Walczak, T. S. 1214
Waldenström, A. M137
Waldman, S. D. M087
Waldvogel Abramowski, S. M360
Walker, K. SU144
Wall, D. E. M337
Wallace, L. S. SU301
Walsh, N. SU252
Walters, N. J. SA110, SA114
Walton, K. J. SU216
Wan, M. SA480, SU038, M197
Wang, B. M269
Wang, C. Y. F218, SA218
Wang, J. SA226, SU254
Wang, J. M. SU001
Wang, L. SU013, SU071, SU199, M454
Wang, M. SU250
Wang, M. W. H. F333, SA333, M267
Wang, O. 1041
Wang, P. M015
Wang, Q. SA100, SA228
Wang, Q. J. SU009
Wang, W. 1126, SU268
Wang, X. F036, SA036, SU160, SU272
Wang, X. F. 1167, SA315
Wang, Y. 1145, 1197, F159, SA159, SA444, SU066, SU206, SU377, SU428
Wang, Y. H. 1185
Wanke, C. SA240
Ward, K. A. SU016, SU017, SU018
Ward, L. M. SU401
Warden, S. J. SA121
Wareham, N. M168
Wark, J. D. F354, SA354
Warmington, K. 1092
Warmington, K. S. 1045, F369, SA369
Wasnich, R. 1037
Wasnich, R. D. 1138, F345, SA345
Wass, J. A. H. SU127, SU128
Watanabe, K. SU027
Watanabe, S. F408, SA205, SA408, SA411, SU035
Watanabe, T. SA262
Watanuki, M. F144, SA144
Watkins, J. 1141

Watrin, A. M109
Watson, M. SU151
Watson, P. H. SA453
Watson, S. SA047
Wawra, K. M320
Wear, K. A. M102, M103
Weaver, C. M. SU178, SU179, M363
Webber, C. E. SA097, M099
Weber, K. F414, SA074, SA414
Weber, P. M232
Weber, T. 1038
Wehren, L. SA296
Wehren, L. E. SU299
Wehrli, F. W. M094, M095
Wei, G. M049
Wei, M. 1049
Wei, S. F333, SA333, M247
Weilbaecher, K. N. F075, SA075, M263
Weinans, H. SU349
Weinbaum, S. SU269
Weindruch, R. SU154
Weineck, J. SA351
Weinreb, M. F146, SA146, SA365
Weinstein, L. 1065
Weinstein, R. S. 1025, 1032, 1058, 1133, SU185, M380
Weisbrode, S. E. SU436
Weisinger, J. R. SU421, M411
Weiss, T. W. SU094, SU367, M295, M368
Weitman, S. SU375
Weitsman, G. SA078
Weitzmann, M. N. F330, SA093, SA330, SA467, M143
Weitzmann, N. M. M178
Welch, J. M. SU178, SU179
Welch, M. D. M067
Wells, C. SU252
Wells, D. J. M163, M164
Wenkert, D. SU408, SU409, SU410
Wergedal, J. E. 1216, F151, SA060, SA151, SU042
Werhli, S. L. M094
Wermers, J. M009
Werner, P. M317
Wesolowski, G. F239, F246, SA239, SA246
West, J. A. M209
Westendorf, J. J. F069, SA069, M199
Westmore, M. S. F373, SA373
Westra, W. H. SU393
Wetsel, W. C. M179
Whan, G. SA116
Whang, P. G. M069
Wheeler, D. L. SU356
Wheeler, V. M303
Wheeler, V. W. F304, SA304
Whelan, H. T. M191
White, D. SA045
White, H. F433, SA433, SU425
White, J. SU093
White, K. E. 1081, 1139, F398, SA123, SA398
Whitehead, C. M040
Whitfield, G. K. F488, SA488
Whitfield, J. F. SA362, SU433
Whiting, S. J. M335
Whitley, M. SU193
Whitworth, T. 1076
Whybro, A. 1144
Whyte, M. P. 1215, F405, SA405, SU408, SU409, SU410
Widrick, J. F165, SA165
Wieczorek, L. M348
Wientroub, S. SU387
Wierzbicki, A. S. SA128
Wikel, S. SU238
Wilcox, A. J. SU328
Wilde, N. 1132
Wilkinson, J. M. SA129
Willheim, M. SA481
Williams, B. SA163
Williams, G. SA296
Williams, H. SU111
Williams, J. P. 1126, SU268
Williams, M. I. M112, M113
Williams, P. F071, SA071
Williams, P. R. F424, SA424
Williams, S. 1198, SA032
Williams, S. A. SU314
Williams, W. G. SA477
Williamson, M. K. M019, M457
Willick, G. E. SU433
Willing, M. C. M005
Willis, D. M. 1114
Wilson, A. G. SA129
Wilson, E. SU193
Wilson, K. 1180, F339, SA339
Wilson, K. E. M292
Wilson, K. M. 1014
Wilson, P. D. F300, SA300
Wilson, P. W. F. 1210, F275, SA275, SU314
Wilson, R. K. M297
Wilson, S. G. F124, SA124
Wilton, S. M116
Wimalawansa, S. J. M088, M357
Winkler, D. 1077
Wipfler, B. M405
Wiren, K. M. F203, SA202, SA203, SU270
Wirzba, B. SU366
Wise, L. M. 1219
Wishcamper, C. M029
Wisniewski, S. M306
Wit, j. M026
Wit, J. M. SA475
Witte, D. F446, SA446
Wittelsberger, A. F227, SA227, SU443
Wittich, A. SU279
Wodtke, J. SA143
Wohl, G. R. M428
Woitge, H. W. 1026, SU074, SU102, M148
Wolbink, G. J. M371
Wolde-Semait, H. T. SU116
Wolfe, L. G. M398
Wollan, P. F288, SA288
Womack, C. M287
Wong, C. M239
Wong, M. F356, SA356
Wong, S. Y. S. SU302
Woo, J. SU030, SU240, SU241, SU311
Woo, K. M. M049
Woodruff, K. 1122
Woon, C. W. SA447
Worsfold, M. SU111
Wortmann, S. SU431
Worton, L. E. 1117
Wos, J. M207
Wos, M. SU049
Wosje, K. S. SA272
Wozney, J. M175, M231
Wozney, J. M. SA181
Wright, A. S. M395
Wronski, T. J. SU060, SU370, M133
Wu, H. 1023
Wu, L. F473, SA473
Wu, M. 1037, 1097, 1100
Wu, S. SA490
Wu, X. SA228, M243
Wu, X. B. 1018, 1054, 1075
Wu, Y. F206, F417, SA206, SA417
Wunderlich, L. M252
Wüster, C. M311
Wynick, D. 1119
Wynne, F. M120, SA012
Wysolmerski, J. J. 1063
Wyzga, N. SU238

X

Xi, Y. 1098
Xia, Y. M114
Xiao, G. SU192
Xiao, L. 1061, M127, M130
Xiao, Z. F180, SA180
Xie, D. M139
Xie, Y. SA228
Xing, L. 1021, 1024, 1145, 1153, F016, SA016, SU377, M176
Xiong, W. C. SA228
Xu, C. SU204
Xu, F. H. SU123, SU124, SU125, SU126
Xu, J. M139, M239
Xu, M. F387, F437, SA387, SA437
Xu, R. F456, SA456
Xu, T. 1067, 1068
Xu, X. SU129, M146
Xu, Z. SU214

Y

Yaccoby, S. M054
Yacobi, R. SU443
Yagi, k. M028
Yahalom, D. F227, SA227
Yam, J. F099, SA099
Yam, L. T. SA107, SA108
Yamada, S. SU183
Yamada, T. F046, SA046, SU326
Yamagami, E. 1204
Yamaguchi, A. 1109, F018, SA018, SA207
Yamaguchi, D. T. SA204, M153, M154, M235
Yamaguchi, K. SA238, M206
Yamaguchi, M. M407
Yamaguchi, T. F325, SA325, SA407, M151, M204
Yamamoto, A. 1148, 1150
Yamamoto, H. 1006, 1120, SA486, SU059, SU460
Yamamoto, K. SA293
Yamamoto, M. M039
Yamamoto, N. M393
Yamamoto, S. SU298, M291
Yamamoto, T. 1034, 1139
Yamamoto, Y. F046, SA046
Yamanaka, Y. 1204
Yamane, I. SU347
Yamanouchi, K. SU207
Yamaoka, K. SU455
Yamasaki, D. SU347
Yamashita, E. SU353
Yamashita, H. F408, SA408
Yamashita, K. 1109, SA262
Yamashita, T. 1024, 1143, 1153, 1182, SU377, M128
Yamauchi, M. F325, SA325, SA407, M046
Yamazaki, K. M342
Yamazaki, Y. 1143, 1182, M128
Yan, T. 1113, M200
Yan, X. F137, SA137
Yanagisawa, J. 1050
Yanaka, N. F201, SA201
Yáñez, A. SU291
Yang, F. SA247, SA264
Yang, H. 1019, F243, SA243
Yang, P. SU129
Yang, Q. M271
Yang, R. S. SA170, SA174, SU159
Yang, S. SA268
Yang, X. 1003, SU234
Yang, Y. 1004, F186, SA186
Yaniv, I. M101
Yankelevich, D. SA328
Yano, K. SA238
Yao, G. F214, SA214
Yao, L. F137, SA137
Yao, W. F239, F366, SA239, SA366, M420
Yao, Z. M064, M065
Yasoda, A. 1206
Yasuda, H. SA238
Yasuda, S. SA237, SA426
Yatani, H. SA043, SU153
Yates, K. E. M034, M035
Yaturu, S. M354
Yaworsky, P. F119, SA119
Ye, L. 1005
Yeh, J. K. SA375, M242
Yeh, L. C. C. SA019, SU032
Yim, C. SU076, M118
Yin, J. J. SU080
Yip, V. SU311
Ylipahkala, H. SU229, M048
Ylönen, S. SU226
Yoda, T. M407
Yogendran, M. SU360
Yoh, K. SU026, M106
Yokoi, T. M085
Yokota, H. SU163
Yokote, H. F137, SA137
Yokoyama, K. SU324, SU325, M220
Yokozeki, M. F197, SA197
Yone, K. M021
Yoneda, T. 1109, 1196, SA262, M427
Yoon, H. SU076, M118
Yoon, J. SU430
Yoon, J. J. SA432
Yoshida, H. SU140
Yoshida, N. SA207, SU230
Yoshida, S. SA134
Yoshida, Y. 1034
Yoshihara, Y. SA059
Yoshikata, H. SU113
Yoshikawa, H. SU236
Yoshiki, N. SA399
Yoshiko, Y. F026, F210, SA026, SA210
Yoshimoto, S. M106
Yoshimoto, T. M039
Yoshimoto, Y. SA156
Yoshimura, K. F046, SA046
Yoshioka, K. SA262
Yoshitake, H. F220, SA220
Yoshizawa, T. SA057
Yosimichi, G. F031, SA028, SA031
Yosimoto, S. SU026
You, L. SU269
Young, B. F417, SA417
Young, J. T. 1207
Young, M. 1067
Young, M. F. 1068, 1194, M196
Young, R. SU213, M403
Yu, A. F011, SA011, SA316
Yu, H. SU254
Yu, K. F214, SA214
Yu, L. J. M392, M395
Yu, X. F040, SA040, SU434, M140, M244, M260
Yuen, C. K. SU360
Yuen, D. S. F236, SA236, SU265
Yuksel, B. 1056
Yumoto, K. 1156
Yunker, L. A. SA189
Yusuke, H. SA039
Yuyama, H. SA245

(Key: 1001-1222 = Oral, F = Friday Plenary poster, SA = Saturday poster, SU = Sunday poster, M = Monday poster, WG = Working Group Abstract)

Z

Zahradnik, R. 1139, SA396
Zaidi, M. 1018, 1054, 1075, SA215, M237
Zaidi, S. K. 1112, M194
Zallone, A. SU218, M258, M267
Zamurovic, N. SA196
Zanchetta, J. R. F364, SA364
Zandstra, P. W. M222
Zanello, L. P. SU448
Zannettino, A. C. W. M210, M230
Zanotti, S. SA022
Zaqqa, D. M336
Zarifa, G. SA089
Zarnitzky, C. SU412
Zarrabeitia, A. L. SA127
Zarrabeitia, M. T. SA127
Zartler, E. R. SU234
Zawistoski, M. P. M395, M397
Zayour, D. M414
Zayzafoon, M. SU161, SU190
Zeitlin, L. M. SU406
Zeitz, U. F414, SA414
Zemel, B. S. 1202, F006, SA006
Zeng, Q. SA476
Zeng, Q. Q. 1179
Zeni, S. N. SU279, SU280, M409
Zernicke, R. F. M044, M428
Zerwekh, J. E. SA472, M416
Zhan, F. M054
Zhang, C. SU451
Zhang, G. M376
Zhang, H. SU129
Zhang, H. W. SU001
Zhang, J. 1005, F016, F042, F085, SA016, SA042, SA082, SA085, SA088, M064, M065, M249
Zhang, L. 1110, SU129, M257
Zhang, M. M157
Zhang, Q. 1031, 1107
Zhang, X. 1018, 1061, F044, SA044, SA215, SU270
Zhang, X. W. F203, SA202, SA203
Zhang, Y. SA219
Zhang, Y. Q. SU314
Zhang, Y. Y. SU126, SU134, SU135, M124
Zhang, Z. SU118
Zhao, H. 1022, 1033
Zhao, J. 1041, F360, SA360, M327
Zhao, J. J. F403, SA403
Zhao, L. J. SU123, SU124, SU125, SU126, SU133, SU134, M124
Zhao, M. 1157, 1189, F016, F042, F071, SA016, SA042, SA071
Zhao, W. 1001, F119, SA119
Zheng, H. SA326, M260
Zheng, M. H. SA076, M239
Zheng, W. M062
Zheng, Z. M065
Zhong, Q. M138, M139
Zhou, H. SA242, SU243
Zhou, Q. M125, M126
Zhou, S. M035, M161
Zhou, W. S. SU213
Zhou, X. G. M126
Zhou, Y. M233
Zhu, J. H. M153
Zhu, L. 1096, SA177
Zhu, M. SA247, SA264
Zhu, W. 1117
Ziegler, E. E. M005
Zielinski, R. SU449, M449
Zikan, V. SA105
Zilberman, Y. M225
Ziller, V. M311
Zimmer, W. 1160
Zimmerman, G. SA273
Zimmerman, S. SA296
Zingler, C. SU306
Zion, M. SA274
Ziran, N. SU387, M226
Zmuda, J. M296
Zmuda, J. M. F304, SA304, SU146, M303, M306
Zobor, N. A. M111
Zou, L. C. SU009
Zou, X. D. SU009
Zucker, M. 1042
Zuo, J. F223, SA223
Zuscik, M. J. SU036, M053